

THE PROCEEDINGS OF THE PHYSICAL SOCIETY

Section A

VOL. 66, PART 1

1 January 1953

No. 397A

EDITORIAL

The 1952 Volumes of the *Proceedings of the Physical Society* were about 7% smaller in size than those of 1951, although the number of papers published increased by some 5%. In the Editorial of January 1952 the need for greater conciseness was stressed, and this, together with the patience and vigilance of referees, may account for the reduction in the average length of papers.

The Papers Committee considered during the year an analysis of the papers published in 1950 and 1951. It was reported that the average time required to publish papers in 1950 was $6\frac{1}{2}$ months. This had decreased to $5\frac{1}{2}$ months in 1951, and it is pleasing to record that a preliminary analysis for 1952 shows a further decrease to 5 months. Nevertheless the Committee feels that this is too long—even for the average—and steps are in hand which, it is hoped, will reduce this period. Authors can help greatly in this matter by paying attention to the preparation of manuscripts, and by submitting duplicate copies of the text together with three copies of the abstract and rough copies of diagrams.

A small sub-committee considered, and reported on, the quality of Letters to the Editor. The position was considered to be reasonably satisfactory and no action called for.

Beginning in January 1953, it is proposed to accept Research Notes for publication. These should be shorter in form than a Paper, and are intended for the communication of results where the work reported does not need a full paper.

During the latter part of the year Dr. E. P. George has resumed his work for the Society in assisting me in the consideration of papers submitted for publication in the *Proceedings*. Professor S. Devons continued to act as Chairman of the Papers Committee.

H. H. HOPKINS,
Honorary Papers Secretary.

Determination of the Surface Energy of a Metal by Molecular Orbitals

By G. R. BALDOCK

University of Liverpool

Communicated by C. A. Coulson; MS. received 7th April 1952, and in final form 5th September 1952

ABSTRACT. The electronic binding energy of a monovalent metal is calculated by means of the molecular approximation for the simple cubic lattice in one, two and three dimensions, and for the body-centred cubic lattice, in terms of the resonance integral β . The corresponding surface energy is deduced in each case. The effects of various improvements in the approximation are estimated, namely the inclusion of the overlap integral, the inclusion of next-nearest-neighbour interaction, and the modification of the coulomb terms of surface atoms due to their special environment. The bond orders in the neighbourhood of the surface are determined and the relation between them and the binding energy is discussed. Numerical values of the surface tensions of the alkali metals are calculated and compared with previous results. It is found that the theory underestimates the surface tension by a factor of about 2, and it is concluded that the coulomb term modification is the most important of the corrections studied.

§1. INTRODUCTION

BRAGER and Schuchowitzsky (1946) calculated the surface energy of a metal by assuming that the metal could be represented as an assembly of free non-interacting electrons in a potential well of infinite depth, obtaining results two to three times the experimental value for monovalent metals. This error factor was reduced to about 1.5 by Huang and Wyllie (1949) who included a term due to the fact that the potential barrier at the surface of the metal is finite. The height of this barrier was derived from the experimental cohesive energy. They also calculated the small correction due to the electric double layer. Huntington (1951) has obtained surface energies about one half of the experimental values by assuming a strictly square-cut barrier, and has shown that even lower results may be derived by considering a barrier potential whose form depends on the wave vector.

These results are independent of the crystal structure, since the free-electron model used takes no account of the positions of the various nuclei. In this respect the tight-binding (molecular-orbital) approximation has an advantage. It is the purpose of this paper to investigate what contribution this approach can make to the problem. As we shall be using the theory in its simplest form (neglecting the electronic interactions except in averaged form) we cannot calculate the energy directly, but only in terms of the resonance integral β . The numerical results will be obtained by estimating β from the experimental cohesive energy. Until recently theoretical estimates of β have been most unsatisfactory, and values calculated on purely theoretical grounds have differed widely from those necessary to give agreement with experiment. But in the last few years, thanks to the work of Mulliken (1949), Griffing (1947), van Dranen (1951), van Dranen and Ketelaar (1949, 1950) and Altmann (1952), improved calculations have been made which agree closely with the values required both for the cohesive energy and the electronic excitation of small molecules. It is true that this encouraging situation does not yet apply to crystals. But very recently Löwdin (1951) has used the refined form of the method, in which the electron correlations are more

properly included, to calculate the cohesive energy of sodium, obtaining a figure very close to the experimental value. In the light of these successes the tight-binding approximation, despite its well-known deficiencies, deserves further study.

We assume that the motion of each conduction electron is described by a single-electron wave function of the form

$$\psi = \sum_{r=1}^N c_r \phi_r,$$

where ϕ_r is the wave function of a conduction electron moving in the field of ion r only, and N is the total number of atoms in the crystal. Let

$$\alpha_r = \int \phi_r^* H \phi_r d\tau, \quad \beta_{rs} = \int \phi_r^* H \phi_s d\tau, \quad S_{rs} = \int \phi_r^* \phi_s d\tau,$$

where H is the one-electron Hamiltonian corresponding to the periodic potential.

By minimizing the energy E of the orbital ψ with respect to the coefficients c_r the following set of secular equations is obtained:

$$(\alpha_r - E)c_r + \sum_s (\beta_{rs} - ES_{rs})c_s = 0, \quad (r = 1, 2, \dots, N)$$

where the summation extends over all $s \neq r$.

When the problem is formulated in this way the actual potential in which the electrons move is left unspecified, so that we shall not obtain results which correspond to the separate terms in the surface energy in the treatment of Huang and Wyllie. But surface peculiarities in the potential may be represented approximately by modifications of the appropriate α_r , and we shall consider this effect in §2.

From the secular equations we obtain N values of E , and N corresponding orbitals, each of which can accommodate two electrons. For a monovalent metal there is one conduction electron per atom, so the energy of the ground state will be twice the sum of the lowest $\frac{1}{2}N$ values of E .

If all the atoms are equivalent and the atomic orbitals ϕ_r are effectively of the s -type (that is, not specifically directed towards any neighbouring atom), then we may put $\alpha_r = \alpha$ for all r and $\beta_{rs} = \beta$, $S_{rs} = S$ for all nearest neighbours.

In general we neglect β_{rs} and S_{rs} for all except nearest neighbours, but we consider next-nearest-neighbour interaction in §3(ii).

It is convenient to define the following quantities: a = distance between nearest neighbours; $\gamma = \beta - \alpha S$, $\epsilon = E - \alpha$, $x = \epsilon/(\gamma - S\epsilon)$; \mathcal{E} = twice the sum of the lowest $\frac{1}{2}N$ values of ϵ ; N_f = number of atoms in the face f of the crystal.

When N is large we shall find that \mathcal{E} may be expressed in the form $\mathcal{E}/\gamma = h_e N - \sum_f h_a(f) N_f$ where the summation extends over all the crystal faces and the constants h_e and h_a have the following interpretations: $-\gamma h_e$ = binding energy per electron, $-\gamma h_a(f)$ = surface energy per surface atom in the face f . We also define \bar{p} = average bond order, $\bar{p}_s(f)$ = average bond order of bonds in the face f , $\bar{p}_n(f)$ = average bond order of bonds connecting atoms in the face f to atoms in the interior. These bond orders are not directly connected with the surface energy, but they furnish a measure of the lattice distortions to be expected near the surface; these would have a local effect on integrals like S and β .

The quantities h_e , h_a , \bar{p} , \bar{p}_s , \bar{p}_n are calculated (neglecting overlap) for the following models: (i) the one-dimensional linear chain, (ii) the two-dimensional square lattice, (iii) the simple cubic lattice, (iv) the body-centred cubic lattice. The effect on h_e and h_a of the inclusion of the overlap integral is calculated for

models (i) and (ii). In model (i) we also correct for the coulomb term modification at the ends of the chain, and in model (ii) we consider interactions between second-nearest neighbours.

§2. LINEAR CHAIN

(i) *Overlap*

The energy \mathcal{E} for a linear chain of m atoms was calculated by Brager and Schuchowitzsky (1946). Hoffmann and Kónya (1948) calculated the effect of including the overlap integral S . It is easy to show that, for $S < \frac{1}{2}$,

$$h_e = \{\pi - 2(1 - 4S^2)^{-1/2} \cos^{-1} 2S\} / \pi S; \quad h_a = (1 + 2S)^{-1} - \frac{1}{2}h_e.$$

These functions of S are illustrated in fig. 1. (The faces in this model are the two

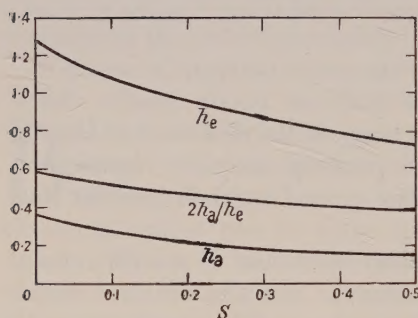


Fig. 1.

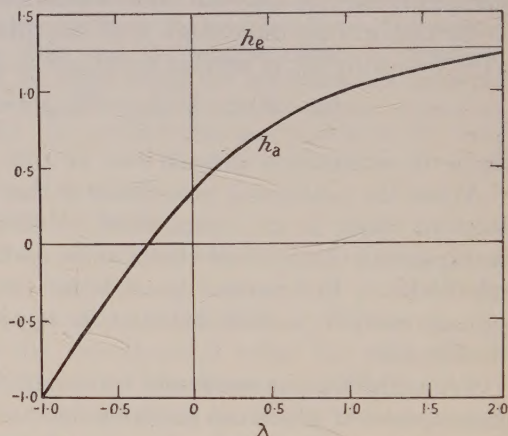


Fig. 2.

ends of the chain, each containing just one atom.) When $S=0$,

$$h_e = 4/\pi \quad \text{and} \quad h_a = 1 - 2/\pi. \quad \dots\dots(1)$$

Also the order of the bond between the r th and the $(r+1)$ th atoms from one end is $p_{r,r+1} = 2\{1 - (-1)^r/(2r+1)\}/\pi$ (Coulson 1939). In particular $\bar{p} = 2/\pi$ and $\bar{p}_n = 8/3\pi$.

(ii) *End Corrections*

We suppose that the coulomb term for the end atoms of the chain is $\alpha - \lambda\beta$. We expect λ to be positive since the absence of a neighbour on one side of the end atom effectively decreases its electron affinity, but our calculations would be unaffected if it turned out that λ were negative. To simplify the calculations we take $S=0$.

Let the number of atoms in the chain be $2m+1$, numbered from $-m$ to $+m$. The secular equations are

$$\begin{aligned} xc_r &= c_{r-1} + c_{r+1}, & r &= 0, \pm 1, \pm 2, \dots, \pm(m-1). \\ (\lambda + x)c_m &= c_{m-1}, & (\lambda + x)c_{-m} &= c_{-(m-1)}. \end{aligned}$$

The wave functions must be either symmetrical or antisymmetrical about the centre of the chain. For the symmetrical solutions we substitute $x = 2 \cos \theta$, $c_r = \cos r\theta$, giving

$$\cos(m+1)\theta + \lambda \cos m\theta = 0. \quad \dots\dots(2)$$

Similarly for the antisymmetrical solutions we put $c_r = \sin r\theta$, which gives

$$\sin(m+1)\theta + \lambda \sin m\theta = 0. \quad \dots\dots(3)$$

When $\lambda = 0$, the solutions of these equations are $\theta = \phi = j\pi/2(m+1)$, $j = 1, 2, \dots (2m+1)$. Odd values of j give solutions of (2) and even values give solutions of (3).

When $\lambda > -1$, the effect of λ is to alter each root of (2) and (3) by a small quantity, except the roots corresponding to $j = 2m$ and $j = 2m+1$, which become imaginary if $\lambda > 1$ (Goodwin 1939). Since we are only interested in the lowest $m+1$ values of θ we can assume $\theta = \phi + \delta$, where δ is small. Equations (2) and (3) both give

$$\delta = \frac{1}{m} \tan^{-1} \frac{\lambda \sin \phi}{1 + \lambda \cos \phi} + O(m^{-2}).$$

Hence $\mathcal{E}/\beta = 4\Sigma^+ \cos \theta = 4\Sigma^+ \cos \phi - (4/m)\Sigma^+ \sin \phi \tan^{-1} \{\lambda \sin \phi / (1 + \lambda \cos \phi)\}$,

where Σ^+ denotes summation over the occupied orbitals. The first term is given by the expressions (1). Since the values of ϕ in the second summation occur at intervals of $\pi/2(m+1)$ in the range 0 to $\pi/2$, we can convert the sum into an integral. Thus

$$\mathcal{E}/\beta = \frac{4}{\pi} (2m+1) - 2 \left(1 - \frac{2}{\pi}\right) - \frac{8}{\pi} \int_0^{\pi/2} \sin \phi \tan^{-1} \frac{\lambda \sin \phi}{1 + \lambda \cos \phi} d\phi + O(m^{-1}),$$

so that $h_e = 4/\pi$ and

$$h_a = 1 - \frac{2}{\pi} + \frac{4}{\pi} \int_0^{\pi/2} \sin \phi \tan^{-1} \frac{\lambda \sin \phi}{1 + \lambda \cos \phi} d\phi = 1 + \lambda - \frac{2}{\pi} \left(\lambda + \frac{1}{\lambda} \right) \tan^{-1} \lambda.$$

This formula is true for all λ greater than -1 , and the same result is obtained for an even number of atoms in the chain. If $\lambda < -1$ an extra term arises from the roots of (2) and (3) corresponding to $j = 1$ and $j = 2$, which become imaginary. The dependence of h_a on λ in the range $-1 < \lambda < 2$ is illustrated in fig. 2.

§3. SQUARE LATTICE

(i) Overlap

The secular equations for a rectangular array of $m \times n$ atoms may be written in the form $xc_{rs} = c_{r,s-1} + c_{r,s+1} + c_{r-1,s} + c_{r+1,s}$, together with the boundary conditions $c_{r0} = c_{0s} = c_{m+1,s} = c_{r,n+1} = 0$. The solutions are $x = 2 \cos \theta + 2 \cos \phi$, where

$$\theta = j\pi/(m+1) \quad (j = 1, 2, \dots, m)$$

and

$$\phi = k\pi/(n+1) \quad (k = 1, 2, \dots, n),$$

and the corresponding normalized coefficients are

$$c_{rs} = 2\{(m+1)(n+1)\}^{-1/2} \sin r\theta \sin s\phi. \quad \dots\dots(4)$$

Hence $\epsilon = 2\gamma (\cos \theta + \cos \phi) / (1 + 2S \cos \theta + 2S \cos \phi)$. The denominator of this expression is always positive, since the matrix of the overlap integral must be positive definite, which implies that $S < \frac{1}{4}$. Larger values of S are permissible only if non-nearest-neighbour interaction is included.

In the ground state the occupied orbitals are those for which $\cos \theta + \cos \phi \geq 0$, so that we have to sum ϵ over all values of θ and ϕ lying inside the triangle whose vertices are $(0, 0)$, $(\pi, 0)$ and $(0, \pi)$.

Let \iint^+ represent integration over this area. By suitably subdividing the area into small rectangles and considering the values of ϵ at the boundary we can show that, to the first order of small quantities,

$$\iint^+ \frac{\epsilon}{2\gamma} d\theta d\phi = \frac{\pi^2}{(m+1)(n+1)} \sum^+ \frac{\epsilon}{2\gamma} + \frac{\pi}{2} \left(\frac{1}{m} + \frac{1}{n} \right) \int_0^\pi \frac{1 + \cos \theta}{1 + 2S(1 + \cos \theta)} d\theta.$$

Hence
$$\frac{\mathcal{E}}{\gamma} = \frac{4(m+1)(n+1)}{\pi^2} \iint^+ \frac{\epsilon}{2\gamma} d\theta d\phi - \frac{2(m+n)}{\pi} \int_0^\pi \frac{1 + \cos \theta}{1 + 2S(1 + \cos \theta)} d\theta,$$

so that
$$h_e = \frac{4}{\pi^2} \iint^+ \frac{\cos \theta + \cos \phi}{1 + 2S(\cos \theta + \cos \phi)} d\theta d\phi \quad \dots\dots (5)$$

and
$$h_a = \frac{1}{\pi} \int_0^\pi \frac{1 + \cos \theta}{1 + 2S(1 + \cos \theta)} d\theta - \frac{1}{2} h_e = \frac{\{1 - (1 + 4S)^{-1/2}\}}{2S} - \frac{1}{2} h_e.$$

The expression (5) can be reduced to the following form, which involves a single integration of an elliptic integral:

$$h_e = \frac{1}{S} - \frac{4 \cos^{-1}(4S) K(4S)}{\pi^2 S} - \frac{8}{\pi^2} \int_0^{\pi/2} F^2(4S, \alpha) \sin \alpha d\alpha,$$

where $F(k, \alpha) = \int_0^\alpha \frac{d\phi}{(1 - k^2 \sin^2 \phi)^{1/2}}$ and $K(k) = F(k, \frac{1}{2}\pi)$; h_e and h_a are shown as functions of S in fig. 3. When $S=0$, we have

$$h_e = 16/\pi^2 \quad \text{and} \quad h_a = 1 - 8/\pi^2. \quad \dots\dots (6)$$

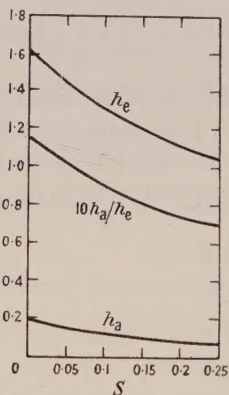


Fig. 3.

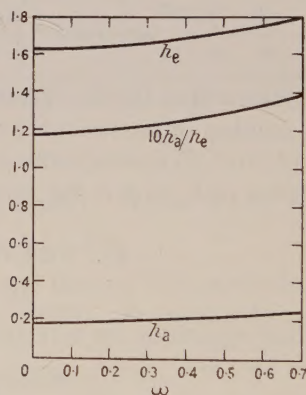


Fig. 4.

From (4) it may be deduced that for large m and n the bond order

$$\begin{aligned} p_{rs}; r+1, s &= 8\pi^{-2} \iint^+ \sin r\theta \sin (r+1)\theta \sin^2 s\phi d\theta d\phi \\ &= 4\pi^{-2} \{1 - (2r+1)^{-2} + (4s^2 - 1)^{-1} + [(2r+1)^2 - 4s^2]^{-1}\}. \end{aligned}$$

Hence $\bar{p} = 4/\pi^2$, $\bar{p}_s = 16/3\pi^2$, $\bar{p}_n = 32/9\pi^2$.

(ii) Next-Nearest-Neighbour Interaction

The next-nearest-neighbour distance is $\sqrt{2}a$, and we should therefore not expect the corresponding resonance integral to be negligible in comparison with β . We denote it by $\omega\beta$. Then the secular equations (neglecting overlap) are

$$\alpha c_{rs} = c_{r, s-1} + c_{r, s+1} + c_{r-1, s} + c_{r+1, s} + \omega(c_{r-1, s-1} + c_{r-1, s+1} + c_{r+1, s-1} + c_{r+1, s+1})$$

together with the boundary conditions $c_{r0} = c_{0s} = c_{r, n+1} = c_{m+1, s} = 0$. The solutions are $x = 2(\cos \theta + \cos \phi + 2\omega \cos \theta \cos \phi)$ and $c_{rs} \propto \sin r\theta \sin s\phi$, where

$$\theta = j\pi/(m+1) \quad (j=1, 2, \dots, m)$$

and

$$\phi = k\pi/(n+1) \quad (k=1, 2, \dots, n).$$

The derivation of expressions for h_e and h_a is tedious and we shall not reproduce it. The method is similar to that used in §4, and the results are as follows:

$$h_e = 4\pi^{-2}(1+2\omega)^{1/2} \int_{\mu_0}^1 (1+2\omega\mu)^{-1/2}(1+\mu+2\omega\mu)K(k) d\mu,$$

$$h_a = 1 + (1+2\omega)\{(1-\alpha_0/\pi) \cos \alpha_0 + \pi^{-1} \sin \alpha_0\} - \frac{1}{2}h_e.$$

Here $k^2 = (1-\mu)(3-2\omega+\mu+2\omega\mu)/4(1+2\omega\mu)$, $\alpha_0 = \cos^{-1} \mu_0$ and μ_0 is defined so that $\int_{\mu_0}^1 (1+2\omega\mu)^{-1/2} K(k) d\mu = \frac{1}{2}\pi^2(1+2\omega)^{-1/2}$. h_e and h_a are shown as functions of ω in fig. 4.

§4. SIMPLE CUBIC LATTICE

The secular equations for a cubical block of $m \times n \times p$ atoms are $xc_{rst} = c_{r-1, st} + c_{r+1, st} + c_{r, s-1, t} + c_{r, s+1, t} + c_{rs, t-1} + c_{rs, t+1}$ together with the boundary conditions $c_{0st} = c_{m+1, st} = c_{r0t} = c_{r, n+1, t} = c_{rs0} = c_{rs, p+1} = 0$. The solutions are

$$x = 2 \cos \theta + 2 \cos \phi + 2 \cos \psi \quad \dots\dots (7)$$

where

$$\theta = j\pi/(m+1) \quad (j=1, 2, \dots, m)$$

$$\phi = k\pi/(n+1) \quad (k=1, 2, \dots, n)$$

$$\psi = l\pi/(p+1) \quad (l=1, 2, \dots, p)$$

and the normalized coefficients are

$$c_{rst} = 2^{3/2}\{(m+1)(n+1)(p+1)\}^{-1/2} \sin r\theta \sin s\phi \sin t\psi. \quad \dots\dots (8)$$

Neglecting overlap, we have from (7)

$$\mathcal{E}/4\beta = \Sigma^+ (\cos \theta + \cos \phi + \cos \psi),$$

Let $I = \iiint_V (\cos \theta + \cos \phi + \cos \psi) d\theta d\phi d\psi$, where V is the volume within the cube $0 \leq \theta \leq \pi$, $0 \leq \phi \leq \pi$, $0 \leq \psi \leq \pi$, in which $\cos \theta + \cos \phi + \cos \psi \geq 0$. Then, to the first order of small quantities,

$$I = \pi^3 \{(m+1)(n+1)(p+1)\}^{-1} \Sigma^+ (\cos \theta + \cos \phi + \cos \psi) + \frac{1}{2}\pi(m^{-1} + n^{-1} + p^{-1}) \{ \iint^+ (1 + \cos \phi + \cos \psi) d\phi d\psi + \iint^+ (\cos \phi + \cos \psi - 1) d\phi d\psi \},$$

where \iint represents integration over the area within the square $0 \leq \phi \leq \pi$, $0 \leq \psi \leq \pi$, in which the integrand is positive.

Let $J = \iint^+ (\cos \phi + \cos \psi - 1) d\phi d\psi$. Then

$$\begin{aligned} \iint^+ (1 + \cos \phi + \cos \psi) d\phi d\psi &= \int_0^\pi \int_0^\pi (1 + \cos \phi + \cos \psi) d\phi d\psi \\ &\quad - \iint^+ (1 + \cos \phi + \cos \psi) d\phi d\psi = \pi^2 + J. \end{aligned}$$

Hence $\mathcal{E}/4\beta = \pi^{-3}Imnp - (\frac{1}{2} + J/\pi^2 - I/\pi^3)(np + pm + mn)$, so that $h_e = 4I/\pi^3$ and $h_a = 1 + 2J/\pi^2 - \frac{1}{2}h_e$.

There are approximately $3mnp$ bonds, so that according to the formula of Coulson and Longuet-Higgins (1947) the average bond order $\bar{p} = \mathcal{E}/6mnp\beta = h_e/6$.

From (8) it follows that the contribution to the bond order $p_{1st; 1, s+1, t}$ from the orbital for which $\epsilon = 2\beta(\cos \theta + \cos \phi + \cos \psi)$ is

$$16\{(m+1)(n+1)(p+1)\}^{-1} \sin^2 \theta \sin s \phi \sin (s+1) \phi \sin^2 t \psi.$$

For large m, n, p the average of this quantity over all the values of s and t is $4 \sin^2 \theta \cos \phi / mnp$. Adding the terms for the bonds parallel to the t direction, we find that the average partial bond order in the surface $r=1$ is $2 \sin^2 \theta (\cos \phi + \cos \psi) / mnp$. Hence $\bar{p}_s = 2L/\pi^3$, where $L = \iiint_V \sin^2 \theta (\cos \phi + \cos \psi) d\theta d\phi d\psi$.

Similarly $\bar{p}_n = 8M/\pi^3$, where $M = \iiint_V \sin^2 \theta \cos \theta d\theta d\phi d\psi$. We now have to evaluate the integrals I, J, L and M .

Let the section of V by the plane parallel to $\theta=0$ which passes through the point $(\pi-\theta, 0, 0)$ have an area A_θ . Then the area of the section by a parallel plane through the point $(\theta, 0, 0)$ is $\pi^2 - A_\theta$. We now define the function $A(v)$ as the area in the (ϕ, ψ) -plane cut off between the axes and the curve $\cos \phi + \cos \psi = 1 - v$. If $v = -\cos \alpha$, this curve meets the axes at the points $(\alpha, 0)$ and $(0, \alpha)$. Hence

$$A(v) = \int_0^\alpha \cos^{-1}(1 + \cos \alpha - \cos \phi) d\phi.$$

Then $dA/dv = \int_{-v}^1 \{(1-x^2)(v+x)(2-v-x)\}^{-1/2} dx$, where $x = \cos \phi$. This integral can be simplified by means of the substitution

$$x = \{2 - (2-v)(1+v)y^2\} / \{2 - (1+v)y^2\}$$

and we obtain $dA/dv = K'(k)$, where $k = \frac{1}{2}(1-v)$. Hence

$$A(v) = \int_{-1}^v K'(k) dv = 2 \int_{(1-v)/2}^1 K'(k) dk,$$

that is, $A_\theta = A(1 - \cos \theta) = 2 \int_{\frac{1}{2} \cos \theta}^1 K'(k) dk$ (9)

In particular $A_{\pi/2} = A(1) = 2 \int_0^1 K'(k) dk = \pi^2/2$.

Now by symmetry we have

$$\begin{aligned} I &= 3 \iiint_{V_1} \cos \theta d\theta d\phi d\psi = 3 \int_0^{\pi/2} (\pi^2 - A_\theta) \cos \theta d\theta - 3 \int_0^{\pi/2} A_\theta \cos \theta d\theta \\ &= 3 \int_0^{\pi/2} (\pi^2 - 2A_\theta) \cos \theta d\theta. \end{aligned}$$

Substituting for A_θ from (9) we obtain

$$\begin{aligned} I &= 12 \int_0^{\pi/2} \cos \theta \int_0^{\frac{1}{2} \cos \theta} K'(k) dk d\theta = 12 \int_0^{1/2} K'(k) \int_0^{\cos^{-1} 2k} \cos \theta d\theta dk \\ &= 12 \int_0^{1/2} K'(k) (1 - 4k^2)^{1/2} dk. \end{aligned}$$

Alternatively we may write $I = \frac{3}{2} \iiint_V (\cos \phi + \cos \psi) d\theta d\phi d\psi$, from which it is easily shown that $I = 3 \int_0^{\pi/2} \int_{A_\theta} (\cos \phi + \cos \psi) d\phi d\psi d\theta$. Now

$$\begin{aligned} \int_{A_\theta} (\cos \phi + \cos \psi) d\phi d\psi &= \int_0^{A_\theta} (1-v) dA = \int_{-1}^{1-\cos \theta} K'(k) (1-v) dv \\ &= 4E'(\tfrac{1}{2} \cos \theta) - \cos^2 \theta K'(\tfrac{1}{2} \cos \theta). \end{aligned}$$

Hence $I = 12 \int_0^{\pi/2} \{E'(k) - k^2 K'(k)\} d\theta$, where k now means $\frac{1}{2} \cos \theta$. This reduces to

$$I = 24 \int_0^{1/2} (E' - k^2 K')(1 - 4k^2)^{-1/2} dk. \quad \text{Similarly we obtain}$$

$$L = 16 \int_0^{1/2} (E' - k^2 K')(1 - 4k^2)^{1/2} dk \quad \text{and} \quad M = \frac{4}{3} \int_0^{1/2} K'(k)(1 - 4k^2)^{3/2} dk.$$

To evaluate J we note that the area of integration is A_0 . Hence

$$J = \int_0^{A_0} (-v) dA = - \int_{-1}^0 v K'(k) dv, \quad \text{where } k = \frac{1}{2}(1 - v).$$

This simplifies to $J = 4E'(\frac{1}{2}) - K'(\frac{1}{2}) - \frac{1}{2}\pi^2 + 2 \int_0^{1/2} K'(k) dk$.

Numerical values of I , J , L and M can now be found by using the series expansions of K' and E' and integrating term by term. The resulting series converge rapidly. The calculated energies and bond orders are given in table 1.

§5. BODY-CENTRED CUBIC LATTICE

By suitably numbering the atoms we can calculate the surface energies associated with the (100) and (110) type faces. Let the face $r = 1$ be (100) and the faces $s = 1$ and $t = 1$ be of the (110) type. Then the secular equations take the form

$$\begin{aligned} xc_{rst} = & c_{r-1, s, t-1} + c_{r-1, s, t+1} + c_{r-1, s-1, t} + c_{r-1, s+1, t} \\ & + c_{r+1, s, t-1} + c_{r+1, s, t+1} + c_{r+1, s-1, t} + c_{r+1, s+1, t} \end{aligned}$$

together with the boundary conditions

$$c_{0st} = c_{m+1, st} = c_{r0t} = c_{r, n+1, t} = c_{rs0} = c_{rs, p+1} = 0.$$

$$\text{The solutions are} \quad x = 4 \cos \theta (\cos \phi + \cos \psi) \quad \dots\dots (10)$$

$$\text{and} \quad c_{rst} = 4\{(m+1)(n+1)(p+1)\}^{-1/2} \sin r\theta \sin s\phi \sin t\psi, \quad \dots\dots (11)$$

where $\theta = j\pi/(m+1)$, $\phi = k\pi/(n+1)$, $\psi = l\pi/(p+1)$ (j, k, l integers).

Now if the point (1, 1, 1) represents an atom, the lattice points occupied by atoms are those for which $r+s+t$ is odd, so that for even m, n, p there are $\frac{1}{2}mnp$ atoms altogether. By inspection of equations (10) and (11) we see that a complete set of independent solutions is given by

$$j = 1, 2, \dots, \frac{1}{2}m; \quad k = 1, 2, \dots, n; \quad l = 1, 2, \dots, p.$$

Then the occupied orbitals are those for which $\cos \phi + \cos \psi > 0$ and $0 < \theta < \frac{1}{2}\pi$, so that the binding energy is obtained by a summation of x over values of θ, ϕ and ψ lying within a triangular prism. We obtain $\mathcal{E}/8\beta = \Sigma^+ \cos \theta (\cos \phi + \cos \psi)$. This summation is performed with the help of the expressions (1) and (6), and the result is

$$\mathcal{E}/\beta = 32\pi^{-3}mnp - 4\pi^{-1}(1 - 8\pi^{-2})m(n+p) - 16\pi^{-2}(1 - 2\pi^{-1})np.$$

$$\text{Hence } h_e = 64\pi^{-3}, \quad h_a(100) = 16\pi^{-2}(1 - 2\pi^{-1}), \quad h_a(110) = 4\pi^{-1}(1 - 8\pi^{-2}).$$

As in the case of the square lattice, the general expression for the order of the bond between any two neighbours is easily deduced:

$$\begin{aligned} p_{rst; r+1, s+1, t} = & 8\pi^{-3}\{1 - (-1)^r(2r+1)^{-1}\} \\ & \times \{1 - (2s+1)^{-2} + (4t^2 - 1)^{-1} + [(2s+1)^2 - 4t^2]^{-1}\}. \end{aligned}$$

$$\text{Hence } \bar{p} = 8/\pi^3, \quad \bar{p}_n(100) = 32/3\pi^3, \quad \bar{p}_n(110) = 64/9\pi^3, \quad \bar{p}_s(110) = 32/3\pi^3.$$

§6. DISCUSSION

The effect of the overlap integral on h_e and h_a in the linear and square lattice models is shown in figs. 1 and 3 respectively. In both cases h_e and h_a decrease as S increases. But γ , which depends on S , cannot be computed directly on the basis of the present approximation, so that it has to be estimated from the experimental binding energy. Hence h_a/h_e becomes the relevant measure of the surface energy. The diagrams show that this quantity decreases by about 40% as S increases from zero to its maximum value. For the three-dimensional models h_e and h_a can be expressed as power series in S (Hoffmann 1950), but the series converge slowly and the calculation of sufficient terms would be tedious.

The effect of next-nearest-neighbour interaction in the square lattice (fig. 4) is to increase h_e and h_a , but it is evidently less important than the overlap integral. It is unlikely that ω exceeds $\frac{1}{2}$, so that the alteration of h_a/h_e will be less than about 10%. This interaction would have more effect in the body-centred cubic lattice, where each atom has six next-nearest neighbours at a distance $2a/\sqrt{3}$, so that we might expect ω to be as much as $\frac{3}{4}$. However, the smallness of the effect in the case of the square lattice suggests that the neglect of ω in the three-dimensional calculations should not produce large errors.

As far as the surface energy is concerned, the effects we have just discussed are probably outweighed by the surface corrections, some idea of which is given in fig. 2, for the linear model. If, as Goodwin (1939) supposed, we should take λ greater than unity, then our estimate of the surface energy may be in error by a factor of 3. Although it is unlikely that λ is so large, it is certainly not negligible, and we must conclude that little significance can be attached to any calculation of surface energy which does not take into account the particular environment of the surface atoms. This conclusion applies also in the case of the free-electron model, as has been shown by Huntington (1951), who found that the surface energy depended critically on the shape as well as the height of the surface potential barrier.

From what we know of the effects of S , ω and λ we can reasonably assume that they are much the same for the different models, so that the comparative results given in table 1 have some significance. The table shows that the binding

Table 1. Energies (h) and Bond Orders (p) for Various Metal Lattices

	Chain	Square	Simple cubic	Body-centred cubic	
				(100)	(110)
h_e	1.273	1.621	2.005	2.064	
h_a	0.363	0.189	0.173	0.589	0.241
\bar{p}	0.637	0.405	0.334	0.258	
\bar{p}_s	—	0.540	0.367	—	0.344
\bar{p}_n	0.849	0.360	0.359	0.344	0.229
$h_e - P_s$	0.424	0.180	0.179	0.688	0.229

energy per atom in the body-centred lattice is almost equal to the same quantity for the simple cubic. The surface energy is much larger, however, and there is a marked difference between its values for the (100) and (110) type faces. As we should expect, the (110) face has the lower surface energy, being the face of highest reticular density.

The deviations of \bar{p}_s and \bar{p}_n from \bar{p} show that the nearest-neighbour distance at the surface will be different from its average value. This produces a change

in β in the neighbourhood of the surface, so that the secular equations ought to be modified accordingly. The resulting adjustment of the energy levels would give rise to a contribution to the surface energy. This contribution can be estimated, but it is unprofitable to include it until we can choose numerical values of S and λ with some confidence for any specific crystal.

The quantity P_s in the lowest row of table 1 is the sum of the average bond order of all the bonds joining a surface atom to its neighbours. For an interior atom the corresponding quantity is equal to h_e . If the surface energy is supposed to be the excess of the binding energy of an interior atom over the binding energy of a surface atom then we should expect $h_a = h_e - P_s$. Table 1 shows that this is approximately the case, and we infer that results based on the above relation are valid. Such an assumption has been made by Harkins (1942) in calculating the surface energy of diamond.

The integral β can be roughly estimated from the heat of sublimation and the lattice constant. Using the values of these quantities given by Seitz (1940), together with the entropy terms F_S calculated by Huang and Wyllie (1949), the surface tensions σ of the (100) and (110) surfaces of crystals of the alkali metals at their melting points can be obtained. Values of β and σ are given in table 2.

For the hydrogen molecule the quantity analogous to $-\beta$ is about 4 ev (Mulliken 1949), and for π -electrons in conjugated hydrocarbons it is about 1 ev. Table 2 shows that somewhat lower values are appropriate to the alkali metals.

Table 2. Surface Energy for Alkali Metals

	Li	Na	K	Rb	Cs
$-\beta$ (ev)	0.82	0.54	0.42	0.40	0.39
$-F_S$ (erg cm ⁻²)	66	34	25	21	18
σ (100) (erg cm ⁻²)	579	252	118	98	84
σ (110) (erg cm ⁻²)	307	132	58	48	41
σ (experimental)	—	290	300*	—	—

* (± 100)

Like the results of Huntington's 'square-cut barrier' calculations, our surface tensions σ (110) are about one third of the values obtained by Huang and Wyllie. Thus our model agrees with Huntington's in producing results well below the measured surface tensions. The theoretical values are increased if we admit that the surface contains a proportion of (100) faces and faces of higher energy, but this correction would by no means close the gap. Evidently the neglected parameters S and ω , and particularly λ , should be included. Finally it must be emphasized that the method, in common with previous treatments, ignores the electronic interactions, except in so far as they are averaged in setting-up the one-electron Hamiltonian. It is quite likely that their inclusion would produce more satisfactory results, although at present the experimental material on alkali metals is insufficient to provide a thorough comparison.

Table 3 shows how the bond orders vary near the corner of the two-dimensional lattice. The quantity tabulated is $p_{rs; r+1, s}$ and its variation gives a rough measure of the effective thickness of the surface. This table suggests that all atoms below the fourth layer from the surface may be regarded as interior atoms, but that above this layer we should expect appreciable distortions due to the varying

strengths of the bonds. This conclusion may reasonably be extended to three dimensions, but it seems that the actual manner of variation of bond order with position is different for the different models. For example, table 1 shows that $\bar{p}_n > \bar{p}$ for the linear chain and the simple cubic, and body-centred cubic (100) faces, but $\bar{p}_n < \bar{p}$ for the square lattice and the body-centred (110) face. This result does not have an obvious physical explanation.

Table 3. Bond Orders near a Corner of a Square Lattice
The table shows p_{rs} ; $r+1, s$

$r \backslash s$	1	2	3	4	∞
1	0.577	0.329	0.357	0.359	0.360
2	0.543	0.461	0.364	0.385	0.389
3	0.541	0.436	0.440	0.375	0.397
4	0.541	0.434	0.421	0.431	0.383
∞	0.540	0.432	0.417	0.412	0.405

ACKNOWLEDGMENTS

I should like to thank Professor C. A. Coulson for valuable discussions relating to this work, and for bringing to my notice some unpublished calculations on the cubic lattice by himself and Dr. D. E. Rutherford. I am also indebted to Dr. T. A. Hoffmann of Budapest for an interesting correspondence concerning the integral I .

REFERENCES

- ALTMANN, S. L., 1952, *Proc. Roy. Soc. A*, **210**, 327, 343.
 BRAGER, A., and SCHUCHOWITZKY, A., 1946, *Acta Physicochimica, URSS*, **21**, 13.
 COULSON, C. A., 1939, *Proc. Roy. Soc. A*, **169**, 413.
 COULSON, C. A., and LONGUET-HIGGINS, H. C., 1947, *Proc. Roy. Soc. A*, **191**, 39.
 VAN DRANEN, J., 1951, *Thesis* ('s Gravenhage Excelsior).
 VAN DRANEN, J., and KETELAAR, J. A. A., 1949, *J. Chem. Phys.*, **17**, 1338; 1950, *Ibid.*, **18**, 1125.
 GOODWIN, E. T., 1939, *Proc. Camb. Phil. Soc.*, **35**, 205.
 GRIFFING, V., 1947, *J. Chem. Phys.*, **15**, 421.
 HARKINS, W. D., 1942, *J. Chem. Phys.*, **10**, 268.
 HOFFMANN, T. A., 1950, *J. Chem. Phys.*, **18**, 989.
 HOFFMANN, T. A., and KÓNYA, A., 1948, *J. Chem. Phys.*, **16**, 1172.
 HUANG, K., and WYLLIE, G., 1949, *Proc. Phys. Soc. A*, **62**, 180.
 HUNTINGTON, H. B., 1951, *Phys. Rev.*, **81**, 1035.
 LÖWDIN, P. O., 1951, *J. Chem. Phys.*, **19**, 1570.
 MULLIKEN, R. S., 1949, *J. Chim. Phys.*, **46**, 497.
 SEITZ, F., 1940, *The Modern Theory of Solids*, Chap. 1 (New York: McGraw-Hill).

"The Range-Energy Relation for Protons and Alpha-Particles in Diluted Ilford G5 Emulsions

By C. F. LEES, G. C. MORRISON AND W. G. V. ROSSER

Department of Natural Philosophy, University of Glasgow

MS. received 5th August 1952

ABSTRACT. An account is given of the experimental determination of the range-energy relations for protons and alpha-particles in diluted Ilford G5 emulsions. The results are compared with those calculated by a method described by Webb. The range-energy relations for protons in the energy range from 2.5 mev to 9 mev can be represented by the empirical formulae $E=0.227R^{0.602}$, $E=0.221R^{0.595}$, $E=0.220R^{0.583}$ for Ilford G5, G5 $\times 2$ and G5 $\times 4$ emulsions respectively, where E is in mev and R in microns.

§ 1. THE RANGE-ENERGY RELATIONS FOR PROTONS

(i) Method

ILFORD G5 $\times 2$ and G5 $\times 4$ (Dodd and Waller 1951) plates were exposed under vacuum conditions to protons produced by the bombardment of Li and B by 550 kev deuterons. The plates were kept *in vacuo* for one hour before the exposure. The energies of the proton groups entering the diluted emulsions were determined by exposing Ilford G5 emulsions under identical conditions. The measured ranges of the protons in the G5 plates could then be related to their kinetic energies by use of experimental curves of Rotblat (1950, 1951) for this emulsion. The method used for track measurement was that of Lattes, Fowler and Cuer (1947).

(ii) Results

The experimental results are given in tables 1 and 2, the quoted range in all cases being the arithmetic mean. The calculated values of the range were also obtained, using a method described by Webb (1948). The atomic constitutions used in this calculation are given in table 3; they correspond closely to vacuum conditions for the emulsions.

Table 1. Ranges of Protons in Ilford G5 Emulsions

Reaction	Exptl. range (μ)	Energy (mev)	Calc. range (μ)
(i) $\begin{matrix} {}^2_1\text{H} + {}^2_1\text{H} \rightarrow {}^3_1\text{H} + {}^1_1\text{H} \\ {}^{12}_6\text{C} + {}^2_1\text{H} \rightarrow {}^{13}_6\text{C} + {}^1_1\text{H} \end{matrix}$	67.6 ± 0.2	2.84	67.5
(ii) $\begin{matrix} {}^6_3\text{Li} + {}^2_1\text{H} \rightarrow {}^7_3\text{Li}^* + {}^1_1\text{H} \\ {}^6_3\text{Li} + {}^2_1\text{H} \rightarrow {}^7_3\text{Li} + {}^1_1\text{H} \end{matrix}$	130.9 ± 0.3	4.27	129.0
(iii) $\begin{matrix} {}^6_3\text{Li} + {}^2_1\text{H} \rightarrow {}^7_3\text{Li} + {}^1_1\text{H} \\ {}^{10}_5\text{B} + {}^2_1\text{H} \rightarrow {}^{11}_5\text{B}^\dagger + {}^1_1\text{H} \end{matrix}$	152.6 ± 0.3	4.68	150.5
(iv) $\begin{matrix} {}^{10}_5\text{B} + {}^2_1\text{H} \rightarrow {}^{11}_5\text{B}^\dagger + {}^1_1\text{H} \\ {}^{10}_5\text{B} + {}^2_1\text{H} \rightarrow {}^{11}_5\text{B} + {}^1_1\text{H} \end{matrix}$	283.0 ± 0.9	6.81	284
(v) $\begin{matrix} {}^{10}_5\text{B} + {}^2_1\text{H} \rightarrow {}^{11}_5\text{B} + {}^1_1\text{H} \\ {}^{10}_5\text{B} + {}^2_1\text{H} \rightarrow {}^{11}_5\text{B} + {}^1_1\text{H} \end{matrix}$	444.0 ± 0.8	8.90	446

* excited state of 440 kev

† excited state of 2.14 mev

The agreement between the calculated and experimental values in tables 1 and 2 is always within 2%; this is satisfactory considering the approximations made in the calculations. The calculated ranges, however,

are about 2% shorter than the experimental ones for all values in the $G5 \times 4$ emulsion. This appears to be a systematic difference and may be because the figures given in table 3 do not correspond to the actual constitution of the $G5 \times 4$ emulsion under our experimental conditions.

Table 2. Ranges of Protons in Ilford $G5 \times 2$ and $G5 \times 4$ Emulsions

Energy (mev)	2.84	4.27	4.68	6.81	8.90
Experimental range in $G5 \times 2$ (μ)	75.3 ± 0.2	144.6 ± 0.3	169.0 ± 0.3	316 ± 1.4	498 ± 0.9
Calculated range in $G5 \times 2$ (μ)	75.0	145	169	319	506
Experimental range in $G5 \times 4$ (μ)	82.9 ± 0.2	161 ± 0.4	188 ± 0.3	361 ± 1.0	565 ± 0.8
Calculated range in $G5 \times 4$ (μ)	81	158	185	354	562

Table 3. Constitutions of Emulsions used in Calculating Range-Energy Relations

Element	Amount (g/cm ³)		
	G5	$G5 \times 2$	$G5 \times 4$
Silver	1.85	1.31	0.82
Bromine	1.36	0.96	0.60
Iodine	0.024	0.026	0.016
Carbon	0.27	0.36	0.46
Oxygen	0.27	0.31	0.37
Nitrogen	0.067	0.106	0.145
Sulphur	0.010	0.008	0.005
Hydrogen	0.056	0.062	0.072
Total	3.91	3.14	2.49

The experimental results for protons shown in tables 1 and 2 can be represented by the following empirical formulae with errors of less than 1%:

$$E = 0.227 R^{0.602} \text{ for } G5 \text{ emulsions} \quad \dots\dots(1)$$

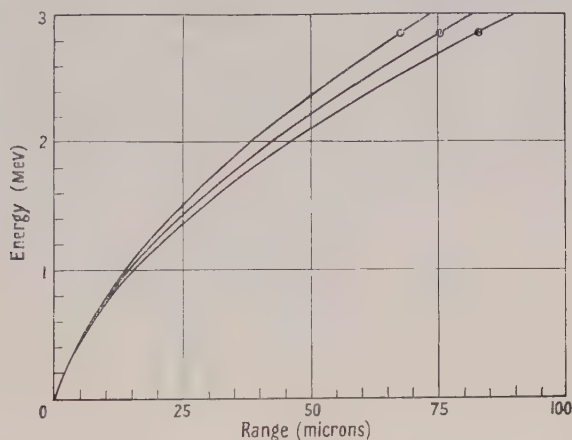
$$E = 0.221 R^{0.595} \text{ for } G5 \times 2 \text{ emulsions} \quad \dots\dots(2)$$

$$E = 0.220 R^{0.583} \text{ for } G5 \times 4 \text{ emulsions} \quad \dots\dots(3)$$

where E is in mev and R in microns. For energies below 2.5 mev the empirical formulae deviate from the calculated range-energy curves by as much as 10%. The empirical formulae, therefore, cannot be used in this energy range. In the figure the range-energy relations calculated by the method described by Webb are shown. The calculated values for $G5 \times 4$ emulsions are renormalized to allow for the systematic difference between experimental and calculated values discussed previously. These curves should be used for energies below 2.5 mev. In §2 results for thorium C' and polonium α -particles are presented. These show that the range-energy relations in the figure are satisfactory for protons of energies as low as 1.4 mev.

The results presented above are valid for plates exposed under vacuum conditions. If exposed under normal atmospheric conditions the ranges are longer due to the water absorbed by the gelatine of the emulsion. The increase in range at a relative humidity at 60% has been calculated for proton energies

of 2 and 10 mev. For G5 emulsion the amount of water absorbed per cm^3 at various relative humidities is known (Wilkins 1951). If it is assumed that the amount of water absorbed by an emulsion is proportional to the amount of gelatine in that emulsion, and that the volume of the emulsion increases by the amount of water absorbed, then the atomic constitutions can be recalculated. The increases in range were then derived using Webb's method. The results are shown in table 4.



Calculated range-energy curves for protons in G5, G5 \times 2, G5 \times 4 emulsions reading from left to right respectively.

Table 4. Calculated Increase in Range at 60% Relative Humidity

Emulsion	G5		G5 \times 2		G5 \times 4	
Proton energy (mev)	2	10	2	10	2	10
% increase in range at 60% relative humidity	3.3	4.0	3.6	4.5	4.2	5.0

§ 2. THE RANGE-ENERGY RELATIONS FOR ALPHA-PARTICLES

The residual ranges of protons and alpha-particles are connected by the following expression (Wilkins 1951):

$$R_p(E) = 1.0069R_\alpha(3.973E) - c \quad \dots\dots(4)$$

where c is a constant which we have taken to be 1.5μ for the G5 emulsion, 1.65μ for the G5 \times 2 emulsion and 1.8μ for G5 \times 4 emulsion. With this formula the energy of an α -particle can be determined from its range using either the empirical formulae given by eqns. (1), (2) and (3) for α -particle energies greater than 10 mev or the curves presented in the figure for α -particle energies less than 10 mev. In order to check the procedure below 10 mev measurements

Table 5. Ranges of α -particles in Ilford G5, G5 \times 2 and G5 \times 4 Emulsions

			Calculated	
		Experimental	Vacuum condns.	60% R.H.
G5	Polonium	22.88 ± 0.04	21.85	22.84
	Thorium C'	47.87 ± 0.08	46.5	47.7
G5 \times 2	Polonium	24.86 ± 0.06	23.6	24.7
	Thorium C'	52.8 ± 0.13	51.2	52.6
G5 \times 4	Polonium	26.63 ± 0.06	25.3	26.5
	Thorium C'	58.29 ± 0.15	56.0	58.2

were made on the ranges of polonium and thorium C' α -particles of energies 5.3 and 8.78 mev respectively, using Ilford G5, G5 \times 2 and G5 \times 4 emulsions. The results are shown in table 5. The calculated results were obtained from the figure using eqn. (4) for α -particles with energies of 5.3 and 8.78 mev.

In the present experiment the α -particle tracks were obtained by dipping the plates in radioactive solution and drying quickly to normal atmospheric conditions, the plates being kept under the same conditions until developed. The experimental ranges are, as a result, longer than those calculated for vacuum conditions due to the absorption of water vapour. The values calculated, assuming a relative humidity of 60%, are also shown in table 5, and give good agreement with those obtained experimentally. This justifies the use of the calculated range energy relations presented in the figure for proton energies below 2.5 mev.

ACKNOWLEDGMENTS

The authors wish to thank Dr. H. Muirhead for many stimulating discussions and for his help in all possible ways. We are also grateful to Mr. R. Anderson, Dr. J. Rutherglen and Dr. R. D. Smith for carrying out the deuteron exposures. Finally, we would like to thank Dr. C. Waller of Messrs. Ilford, Ltd., for supplying the information in table 3. One of us (G. C. M.) is grateful to the Department of Scientific and Industrial Research for the award of a grant which enabled him to carry out the research.

REFERENCES

- DODD, E. C., and WALLER, C., 1951, *Photographic Sensitivity* (London: Butterworths Scientific Publications), p. 266.
LATTES, C. M. G., FOWLER, P. H., and CUER, P., 1947, *Proc. Phys. Soc. A*, **59**, 883.
ROTBLAT, J., 1950, *Nature, Lond.*, **165**, 387; 1951, *Ibid.*, **167**, 550.
WEBB, J. H., 1948, *Phys. Rev.*, **74**, 511.
WILKINS, J. J., 1951, Atomic Energy Research Establishment Report G/R 664.

The Effect of the Tensor Force on the Binding Energy of the Alpha-Particle*

By J. IRVING

Department of Mathematics, University of Southampton

Communicated by R. E. Peierls; MS. received 18th August 1952

ABSTRACT. The binding energy of the ${}^4\text{He}$ nucleus is calculated by the variation method, assuming charge-independent neutral two-body forces, using Yukawa wells, not necessarily of the same range, for the central and tensor parts of the interaction. The wave function chosen represents a mixture of the principal ${}^1\text{S}_0$ and the principal ${}^5\text{D}_0$ states, the radial wave functions being of a simple exponential type. With the nuclear parameters adjusted to fit the deuteron energy and quadrupole moment, and other low-energy data, it is found that the introduction of the tensor force greatly reduces the large value of the ${}^4\text{He}$ energy, obtained in the purely central force case. Whereas equal ranges yield a very small binding, the unequal ranges, which according to Pease and Feshbach fit the triton, give reasonable values for ${}^4\text{He}$. Thus it seems possible that a phenomenological two-body interaction of the above type may give consistent results in the two-, three-, and four-body problems.

For the triton the same type of wave function gives rather poor results, compared with another exponential function, used previously.

§ 1. INTRODUCTION

IT is well known that a purely central two-body interaction, containing a set of parameters compatible with the energies of the ground and virtual states of the deuteron, the low-energy scattering data, and the binding energy of the triton, yields too large a binding energy for the alpha-particle. Since the existence of the quadrupole moment of the deuteron necessitates the introduction of some type of non-central force in the two-body interaction, it is of importance to determine the effect of such a force on the binding energies of the three- and four-particle nuclei. Several calculations with an interaction consisting of a mixture of central and tensor forces have already been made for the triton (Gerjuoy and Schwinger 1942, Feshbach and Rarita 1949, Clapp 1949, Hu and Hsu 1951, Pease and Feshbach 1951) with varying degrees of success. Only one previous calculation has so far been made on the ${}^4\text{He}$ nucleus with non-central forces (Gerjuoy and Schwinger 1942), a square-well potential being used for the central and tensor forces. The calculations yielded roughly half the required energy. As scattering data at higher energies indicates some preference for the long-tailed potential, it is of interest to investigate the binding energy of the alpha-particle for such a case. However, for this type of well the gaussian type wave functions used by Gerjuoy and Schwinger generally give poor results, so that it is necessary to use a wave function which has a more accurate asymptotic behaviour. Such a wave function is used in this calculation.

A phenomenological nuclear interaction potential consisting of central and tensor forces of the form

$$V(r) = -V_0 \left[\left\{ 1 - \frac{1}{2}g + \frac{1}{2}g(\sigma_1 \cdot \sigma_2) \right\} \frac{\exp(-r/r_c)}{r/r_c} + \gamma S_{12} \frac{\exp(-r/r_t)}{r/r_t} \right] \dots\dots(1)$$

* A brief summary of the results of the calculations discussed in this paper has already been published (Irving 1952).

has been found to be satisfactory for a description of low-energy scattering processes and, in accounting for the properties of the deuteron (Feshbach and Schwinger 1951), for certain values of the central and tensor force range parameters r_c and r_t respectively. Furthermore, such an interaction also yields a reasonable value for the binding energy of the triton for an appropriate choice of these ranges (Hu and Hsu 1951, Pease and Feshbach 1951). In this paper the binding energy of the helium nucleus is calculated for an interaction of the type given in eqn. (1). The neutral interaction is used in preference to the charged or symmetric type, since, in a nucleus no heavier than the alpha-particle, the difference between forces of different exchange character is likely to be very slight; the neutral potential is also easier to handle.† The results of a similar calculation for the triton are also mentioned.

The standard variation method is employed with a ground state wave function representing a mixture of the principal 1S_0 and the principal 5D_0 state. All the six D-states, which appear in first approximation will make some contribution to the energy; since, however, the symmetry properties indicate that one of these states is more important than the others, it alone is considered in detail in this paper. The radial wave functions are of an exponential type (cf. eqn. (7)); these yield a large excess binding energy in the purely central force case (Irving 1951), suggesting that they may be a good approximation to the correct wave functions, because they have the correct asymptotic behaviour.* It is shown in this paper that the selected wave functions give rise to an exceedingly simple mathematical analysis, no approximations being necessary in the evaluation of the integrals involved, even in the tensor force case. It may be remarked that wave functions of the same type may be extended to apply to nuclei of more than four particles. The general method of calculation can in fact be used for such nuclei.

It is found that the introduction of the tensor force is very effective in reducing the binding energy of the alpha-particle as compared with the purely central force case. Indeed, if equal ranges are assumed for the central and tensor forces, very little binding energy is obtained. It is, of course, to be expected that contributions from other states—in particular, some of the D-states referred to—will increase the value of the binding energy, but it is hardly conceivable that anything like the experimental value will be obtained for the equal range case. This is in contrast with Hu and Hsu's result for the triton, namely that the triton energy may be obtained for equal central and tensor force ranges. They use a ground-state wave function with many parameters, representing a mixture of many states.

On the other hand, Pease and Feshbach obtain reasonable values for the triton binding energy, using unequal central and tensor force ranges, though their wave function, which is of the same radial form as that of Hu and Hsu, does not contain quite so many variation parameters. With these ranges and

* Recently, Morpurgo (1952) has found in an elegant way the best wave functions, which are functions of the sum of the squares of the interparticle distances, for the triton and the alpha-particle for purely central forces of the gaussian type. He finds that this type of wave function is as good as a gaussian wave function with a large number of variation parameters.

† Note added in proof. Recent calculations carried out at Southampton have verified that the Pease-Feshbach interaction, converted to a symmetric interaction with the same ranges, differs little in effect, in the case of the alpha-particle, from the neutral interaction. However, a calculation carried out for a heavier nucleus (^9Be) using the neutral Pease-Feshbach interaction yielded a large excess binding energy (unpublished work of E. H. Kronheimer using single particle wave functions).

the corresponding values of the nuclear parameters, the binding energies obtained for the alpha-particle in this paper are smaller than the experimental value, but, allowing for the contributions from additional states, they suggest the possibility of fitting the energies of the three- and four-particle nuclei with the same two-body interaction, which also accounts for the deuteron properties.

The value of the kinetic, potential and coulomb energies are given explicitly and it is found that the kinetic energy has a much more reasonable value than in the case where central forces alone are used.

A calculation of the binding energy of the triton with the same type of wave function as that used for the alpha-particle has also been made, assuming a mixture of the principal ${}^2S_{1/2}$ and the principal ${}^4D_{1/2}$ states for the ground state wave function. This is not discussed in detail as the method of calculation is exactly the same as for the case of ${}^4\text{He}$.

A second calculation of the binding energy of the triton has been carried out with the same type of wave function used by other authors (Pease and Feshbach 1951, Hu and Hsu 1951) for the same mixture of states, since the value of the energy for this case is not given by these authors. It is found that the latter wave function yields much better results. This is discussed in § 4.

§ 2. CONSTRUCTION OF THE GROUND STATE WAVE FUNCTION

Since the assumed interaction (1) is neutral, there is no advantage in introducing the isotopic spin formalism. The wave function representing the ${}^4\text{He}$ system has to be constructed so that it is anti-symmetrical for interchange of the two neutrons and the two protons respectively. Now the ground state of ${}^4\text{He}$ is of even parity and has a total angular momentum $J=0$, so that the classification of possible states can be made using the rules for compounding angular momenta, subject to the limitation that the maximum total spin is $S=2$. Gerjuoy and Schwinger (1942) have listed the possible states in operator form. A mixture of the states 1S_0 , 3P_0 and 5D_0 is possible. In the absence of the spin-orbit coupling due to the tensor force, the ground state of ${}^4\text{He}$ is 1S_0 . The introduction of a tensor interaction gives a term of the form

$$\sum_{i>j}^4 J(r_{ij}) S_{ij}$$

where $J(r_{ij})$ defines the shape of the well and

$$S_{ij} = 3(\boldsymbol{\sigma}_i \cdot \mathbf{r}_{ij})(\boldsymbol{\sigma}_j \cdot \mathbf{r}_{ij})/r_{ij}^2 - \boldsymbol{\sigma}_i \cdot \boldsymbol{\sigma}_j \quad \dots\dots(2)$$

in the Hamiltonian, and the application of this to a 1S_0 wave function produces only 5D_0 wave functions, so that the 3P_0 wave functions will appear only as a second approximation. Of the six independent 5D_0 states appearing in first approximation, the state with maximum symmetry in the tensor operators has no radial nodes and may be taken to be the principal 5D_0 state. Its angular and spin part has the form

$${}^5D_0^{(1)} = \left\{ \sum_{i>j}^4 D(r_{ij}) \right\} \chi \quad \dots\dots(3)$$

where $D(r_{ij}) = r_{ij}^2 S_{ij}$ and $\chi = \frac{1}{2}(\chi_1^+ \chi_2^- - \chi_1^- \chi_2^+)(\chi_3^+ \chi_4^- - \chi_3^- \chi_4^+)$ is the spin wave function; 1, 2 denote the neutron and 3, 4 the proton coordinates; S_{ij} is the operator given by eqn. (2).

Since the tensor operator vanishes when it acts on a singlet spin state, the expression for ${}^5D_0^{(1)}$ becomes, from eqn. (3),

$$D(r_{13}) + D(r_{14}) + D(r_{23}) + D(r_{24}). \quad \dots\dots(4)$$

Introducing the coordinate system

$$\rho_1 = r_2 - r_1, \quad \rho_2 = r_4 - r_3, \quad r = \frac{1}{2}(r_4 + r_3 - r_2 - r_1) \quad \dots\dots(5)$$

(4) assumes the more compact form

$$3(\sigma_1 \cdot \rho_1)(\sigma_3 \cdot \rho_2) + 3(\sigma_1 \cdot \rho_2)(\sigma_3 \cdot \rho_1) - 2(\rho_1 \cdot \rho_2)(\sigma_1 \cdot \sigma_3). \quad \dots\dots(6)$$

It might be mentioned that the remaining five D states appearing in first approximation are obtained by writing down all the expressions of the form (6) from the vectors ρ_1 , ρ_2 and r , including the cases where two identical vectors are chosen. The complete D-state wave functions are then formed by multiplying the angular spin part with a spatial radial function with the appropriate symmetry. For the radial wave functions in the spatially symmetric case we adopt the form

$$\phi = N^{1/2} \exp \left\{ -\alpha \left(\sum_{i>j}^A r_{ij}^2 \right)^{1/2} \right\} \quad \dots\dots(7)$$

$N^{1/2}$ being a normalization factor, and A the number of nucleons.

This type has proved very satisfactory in the central force case (Irving 1951). Similarly, the principal 5D_0 state will be assumed to have a radial part of the form given in eqn. (7).

Though the contributions from other D-states are not calculated in this paper, it may be of interest to mention how the formalism is extended for this case. For any such D-state, the correct symmetry properties are obtained by multiplying ϕ of eqn. (7) by a factor such as $\rho_1 \cdot r$, $\rho_2 \cdot r$ or $\rho_1 \cdot \rho_2$. The complete D-state wave functions obtained in this way are independent, but are not mutually orthogonal. As it is difficult to construct a mutually orthogonal set of D-state wave functions, it is more convenient to build up the complete wave function for the system out of a linear combination of the D-states, and to take account of their lack of orthogonality in the evaluation of the energy matrix elements.

The principal ${}^5D_0^{(1)}$ term will make the most important contribution to the energy and its calculation is treated in detail here. The complete wave function, representing a mixture of the 1S_0 and ${}^5D_0^{(1)}$ states, where ${}^1S_0 = \chi$, may then be written in the form

$$\psi = \{\psi_S + C\psi_{D^{(1)}}\} / (1 + C^2)^{1/2} \quad \dots\dots(8)$$

where C^2 determines the amount of D-state in the mixture, assuming ψ_S and $\psi_{D^{(1)}}$ to be normalized to unity, so that ψ is then normalized to unity. The radial parts of ψ_S and $\psi_{D^{(1)}}$ are of the form given in eqn. (7), with $A=4$, but are assigned different variation parameters, α and β respectively.

The integrals appearing in the calculation are most simply evaluated in the coordinate system

$$\rho_1 = \sqrt{2}\mathbf{v}, \quad \rho_2 = \sqrt{2}\mathbf{w}, \quad r = \mathbf{u}, \quad \mathbf{R} = \frac{1}{4}(\mathbf{r}_1 + \mathbf{r}_2 + \mathbf{r}_3 + \mathbf{r}_4). \quad \dots\dots(9)$$

In this system the radial wave function ϕ of eqn. (7), with $A=4$, assumes the simple form

$$N^{1/2} \exp \{ -2\alpha(u^2 + v^2 + w^2)^{1/2} \}. \quad \dots\dots(7')$$

§ 3. METHOD OF CALCULATION

The energy W of the four-particle system, apart from the coulomb energy which is treated as a perturbation, is given by

$$W = \int \psi^* H \psi d\tau \quad \text{.....(10)}$$

where the Hamiltonian is given by

$$H = -(\hbar^2/2M) \sum_{i=1}^4 \Delta_i + \sum_{i>j}^4 V(r_{ij}). \quad \text{.....(11)}$$

Δ_i is the Laplace operator acting on the coordinates of the particle whose position vector is \mathbf{r}_i ; $V(r_{ij})$ is of the form given in eqn. (1) and represents the interaction between the particles i and j .

When W is minimized with respect to the variation parameters, the variation principle yields the result that $W \geq E$ the experimental energy provided the interaction is correct.

From eqns. (8) and (10), and the orthogonality of the S- and D-states it follows that

$$\begin{aligned} (1 + C^2)W = & \int \psi_S^* \left\{ -\frac{\hbar^2}{2M} \sum_{i=1}^4 \Delta_i \right\} \psi_S d\tau + C^2 \int \psi_{D^{(w)}}^* \left\{ -\frac{\hbar^2}{2M} \sum_{i=1}^4 \Delta_i \right\} \psi_{D^{(w)}} d\tau \\ & + \sum_{i>j}^4 \left[\int \psi_S^* V_c(r_{ij}) \psi_S d\tau + C^2 \int \psi_{D^{(w)}}^* V_c(r_{ij}) \psi_{D^{(w)}} d\tau \right. \\ & \left. + 2C \int \psi_S^* V_t(r_{ij}) \psi_{D^{(w)}} d\tau + C^2 \int \psi_{D^{(w)}}^* V_t(r_{ij}) \psi_{D^{(w)}} d\tau \right] \quad \text{.....(12)} \end{aligned}$$

where $V_c(r_{ij})$ and $V_t(r_{ij})$ are the central and tensor parts of the two-particle interaction of the form given in eqn. (1).

The first two terms on the right-hand side of (12) represent the kinetic energy of the system, the others the potential energy.

The coulomb energy of the alpha-particle is

$$E_{\text{coul}} = e^2 \left\{ \int \psi_S^* (1/r_{34}) \psi_S d\tau + C^2 \int \psi_{D^{(w)}}^* (1/r_{34}) \psi_{D^{(w)}} d\tau \right\} / (1 + C^2). \quad \text{.....(13)}$$

The third and fourth terms of eqn. (12) are of the same type, and their values together with those of the first terms of eqns. (12) and (13) may be obtained from a previous paper (Irving 1951). The second kinetic energy integral of eqn. (12) is simply transformed to

$$(\hbar^2/2M)C^2 \int \phi_{D^{(w)}}^* \sum_{i=1}^4 (\nabla_i \phi_{D^{(w)}})^2 \langle {}^5D_0^{(1)*} | {}^5D_0^{(1)} \rangle d\tau. \quad \text{.....(14)}$$

In the coordinate system of eqn. (9)

$$\sum_{i=1}^4 (\nabla_i \phi_{D^{(w)}})^2 = (\nabla_{\mathbf{u}} \phi_{D^{(w)}})^2 + (\nabla_{\mathbf{v}} \phi_{D^{(w)}})^2 + (\nabla_{\mathbf{w}} \phi_{D^{(w)}})^2 + \frac{1}{4} (\nabla_{\mathbf{R}} \phi_{D^{(w)}})^2.$$

$\phi_{D^{(w)}}$ the radial part of the D-state wave function is of the form given in eqn. (7'), and $\langle {}^5D_0^{(1)*} | {}^5D_0^{(1)} \rangle$ denotes the matrix element obtained by summation over the spins of the four particles. This spin matrix element also appears in the second term of the coulomb energy in eqn. (13). The remaining potential energy integrals in eqn. (12) involve the spin matrix elements $\langle {}^1S_0^* | S_{ij} | {}^5D_0^{(1)} \rangle$ and $\langle {}^5D_0^{(1)*} | S_{ij} | {}^5D_0^{(1)} \rangle$. The method of evaluation of spin matrix elements is described in the Appendix and their respective values are given.

The evaluation of the energy integrals is most simply accomplished in the coordinate system given in eqn. (9). The method of evaluation is now illustrated for a typical case, namely the energy matrix element

$$2C \sum_{i>j}^4 \int \psi_S^* V_t(r_{ij}) \psi_{D^{\omega}} d\tau \quad \dots\dots(15)$$

where $V_t(r_{ij}) = -\gamma V_0 S_{ij} \{\exp(-r_{ij}/r_t)\}/(r_{ij}/r_t)$. The expression (15) may be written as

$$-8\gamma C V_0 \int \phi_S^* \phi_{D^{\omega}} [\{\exp(-r_{13}/r_t)\}/(r_{13}/r_t)] \langle {}^1S_0^* | S_{13} | {}^5D_0^{(1)} \rangle d\tau \quad \dots\dots(16)$$

in the notation used above. Now, from eqn. (4) of the Appendix,

$$\langle {}^1S_0^* | S_{13} | {}^5D_0^{(1)} \rangle = \{18(\mathbf{r}_{13} \cdot \mathbf{p}_1)(\mathbf{r}_{13} \cdot \mathbf{p}_2)/r_{13}^2 - 6(\mathbf{p}_1 \cdot \mathbf{p}_2)\}. \quad \dots\dots(17)$$

Since, also, the value of the expression (16) is unaltered by interchanging \mathbf{r}_1 and \mathbf{r}_4 , the integral becomes

$$-8\gamma C V_0 \int \phi_S^* \phi_{D^{\omega}} [\exp(-r_{34}/r_t)/(r_{34}/r_t)] \{18(\mathbf{r}_{43} \cdot \mathbf{r}_{42})(\mathbf{r}_{43} \cdot \mathbf{r}_{31})/r_{43}^2 - 6(\mathbf{r}_{42} \cdot \mathbf{r}_{31})\} d\tau.$$

That is,

$$-8\gamma C V_0 N_S^{1/2} N_{D^{\omega}}^{1/2} \times \int [\exp\{-\delta(u^2 + v^2 + w^2)^{1/2} - \kappa'_t w\}/(\kappa'_t w)] f(\mathbf{u}, \mathbf{v}, \mathbf{w}) d\mathbf{u} d\mathbf{v} d\mathbf{w} \quad \dots\dots(18)$$

where $\delta = 2(\alpha + \beta)$, $\kappa'_t = \sqrt{2}/r_t$ and $N_S^{1/2}$, $N_{D^{\omega}}^{1/2}$ are the normalization coefficients for the ψ_S and $\psi_{D^{\omega}}$ states respectively in the \mathbf{u} , \mathbf{v} , \mathbf{w} coordinate system; $f(\mathbf{u}, \mathbf{v}, \mathbf{w})$ is the expression

$$\left[18 \left\{ \frac{(\mathbf{w} \cdot \mathbf{u})^2}{w^2} - \frac{(\mathbf{w} \cdot \mathbf{v})^2}{2w^2} - \frac{1}{2} w^2 \right\} - 6 \left\{ u^2 - \frac{1}{2}(v^2 + w^2) \right\} \right]. \quad \dots\dots(19)$$

The expression (18) can then be evaluated, after integration over the angles, using the transformation $u = R \sin \theta \cos \phi$, $v = R \sin \theta \sin \phi$, $w = R \cos \theta$. For example, consider the term $18(\mathbf{w} \cdot \mathbf{u})^2/w^2$ in expression (19). The corresponding integral in expression (18) then becomes

$$6 \cdot 2^6 \pi^3 \int_0^{\pi/2} \cos^4 \phi \sin^2 \phi d\phi \int_0^{\pi/2} \sin^7 \theta \cos \theta d\theta \int_0^\infty R^9 e^{-\mu R} dR$$

where $\mu = \delta + \kappa'_t \cos \theta$. This reduces to

$$\{12(9!) \pi^4 / \kappa_t'^{11}\} \int_0^1 \frac{u(1-u^2)^3}{(u+e)^{10}} du$$

where $e = \delta / \kappa_t'$ and $u = \cos \theta$. The other terms in $f(\mathbf{u}, \mathbf{v}, \mathbf{w})$, (eqn. (9)), are evaluated in a similar way. Hence the expression (18) reduces to the form $+ \{3 \cdot 2^6(9!) \pi^4 / \kappa_t'^{11}\} \gamma C V_0 N_S^{1/2} N_{D^{\omega}}^{1/2} F(e)$ where $F(e)$ denotes the integral

$$\int_0^1 \frac{u^3(1-u^2)^2}{(u+e)^{10}} du.$$

The other energy matrix elements may be reduced in a similar way to single integrals. These single integrals are of an elementary type and are listed in § B of the Appendix. W is then given by the formula

$$\begin{aligned} (1 + C^2)W = & \{\hbar^2/(4Mr_c^2)\} \{c_1^2 + C^2 c_2^2\} - (315/32) V_0(1-g) c_1^9 A(c_1) \\ & + C\gamma V_0(63\sqrt{6}/8)(r_t/r_c)^{11} c_1^9 c_2^{13/2} F(e) \\ & - C^2 V_0(231/256) c_2^{13} \{20B(c_2) + (25/4)C(c_2) + 4D(c_2)\} \\ & + C^2 \gamma V_0(231/256) d_2^{13} \{28B(d_2) + 8D(d_2)\} \quad \dots\dots(20) \end{aligned}$$

where r_c, r_t represent the central and tensor force ranges respectively, $c_1 = 2\sqrt{2}\alpha r_c$, $c_2 = 2\sqrt{2}\beta r_c$, $d_2 = (r_t/r_c)c_2$, $e = (r_t/r_c)(c_1 + c_2)/2$, C is a parameter measuring the amount of D-state; A, B, C, D, F are the integrals listed in § B of the Appendix.

It is thus evident that the analysis yields a relatively simple form for the energy W . Minimization is carried out numerically with respect to the three parameters c_1, c_2 and C . Since C appears only quadratically, C can be eliminated and the secular equation obtained. However, the energy of the system is not very sensitive to the D-state parameter, it is more convenient to estimate C and carry out the minimization with respect to c_1 and c_2 by an iteration method. When c_1 and c_2 have been determined in this way, the minimization with respect to C can then be carried out, and the process repeated. The minimum can be ascertained very quickly in this way. The coulomb energy, which has the form

$$E_{\text{coul}} = \{7e^2/512r_c\}\{20c_1 + 11C^2c_2\}/(1 + C^2) \quad \dots\dots(21)$$

is then added as a perturbation.

§ 4. RESULTS AND CONCLUSIONS

The binding energy of the alpha-particle was calculated from eqns. (20) and (21) for various central and tensor force ranges, with corresponding values of the nuclear parameters. The results are given in tables 1, 2, 3 and 4, the value of the triton binding energy as calculated by Pease and Feshbach, and Hu and Hsu being quoted for the appropriate ranges. The set of nuclear parameters given in tables 1 and 2 is consistent with the sets determined by Feshbach and Schwinger (1951) to give a reasonable fit to the deuteron data. From table 1 it is seen that the binding energy of 24.2 meV for the alpha-particle corresponds to a binding energy of 8.5 meV for the triton. The former value is obtained from a ground state wave function representing a mixture of only two states, namely, the principal S- and D-states respectively. The latter value arises from a ground state wave function representing a mixture of one S-state and three D-states. The inclusion of additional D-states in the wave function for the alpha-particle will undoubtedly increase the binding energy value, so that a value nearer the experimental value of 28.2 meV may be obtained. This is at present being investigated.

In the case of the triton, the author has calculated the binding energy for the set of parameters of table 1, using a wave function consisting of the principal S- and the principal D-state. Two forms for the radial wave functions were chosen, namely that given by eqn. (7), with $A=3$, and the form

$$\phi = \exp\{-\alpha(r_{12} + r_{23} + r_{31})\} \quad \dots\dots(22)$$

which has been used by previous authors (Hu and Hsu 1951, Pease and Feshbach 1951), but the energy corresponding to the two-state mixture has not been quoted by them for the ranges in question. The calculation yields 6.5 meV of binding energy for the wave function (22), but only 3.0 meV for the wave function (7). From Pease and Feshbach's results it is thus evident that the additional D-states in the triton wave function contribute about 2 meV to the binding energy. The wave function (7) yields rather poor results. This is, in fact, evident from the central part of the interaction alone, as the better wave function (22) gives approximately an additional 2 meV binding energy for this case.

This conclusion does not necessarily invalidate the calculations on the photoelectric disintegration of the triton, where the wave function (7) has been

used, because of its greater simplicity (Gunn and Irving 1951), since such calculations are sensitive to the asymptotic form and the functions (7) and (22) are very similar in that respect.

Table 1. ${}^4\text{He}$ Energy for one set of Pease-Feshbach Nuclear Parameters

Nuclear parameters and ${}^3\text{H}$ energy	${}^4\text{He}$ energy terms	Variation parameters for ${}^4\text{He}$
$r_c = 1.184 \times 10^{-13}$ cm	S-S K.E. = 115.3 mev	
$r_t = 1.67 \times 10^{-13}$ cm	D-D K.E. = 6.8 mev	$c_1 = 4.0$
$V_0 = 46.1$ mev	S-S P.E. = -134.1 mev	$c_2 = 6.0$
$\gamma = 0.54$	S-D P.E. = -12.0 mev	$C = -0.162$
$g = -0.004$	D-D P.E. = -1.5 mev	
	E (coulomb) = 1.3 mev	
$E({}^3\text{H}) = -8.5$ mev*	E (${}^4\text{He}$) = -24.2 mev	

Table 2. ${}^4\text{He}$ Energy for second set of Pease-Feshbach Nuclear Parameters

Nuclear parameters and ${}^3\text{H}$ energy	${}^4\text{He}$ energy terms	Variation parameters for ${}^4\text{He}$
$r_c = 1.184 \times 10^{-13}$ cm	S-S K.E. = 104.0 mev	
$r_t = 1.58 \times 10^{-13}$ cm	D-D K.E. = 6.5 mev	$c_1 = 3.8$
$V_0 = 42.7$ mev	S-S P.E. = -118.2 mev	$c_2 = 5.7$
$\gamma = 0.69$	S-D P.E. = -12.1 mev	$C = -0.167$
$g = -0.044$	D-D P.E. = -1.0 mev	
	E (coulomb) = 1.3 mev	
$E({}^3\text{H}) = -7.5$ mev*	E (${}^4\text{He}$) = -19.5 mev	

* Calculated by Pease and Feshbach.

In the case of the alpha-particle, it is not possible to make a similar comparison of wave functions. Calculations with a wave function of type (22) for the ${}^4\text{He}$ nucleus can only be carried out numerically and are extremely tedious, as the central force calculations indicate (Fröhlich, Huang and Sneddon 1947). However, even if a better wave function than that given by eqn. (7) can be constructed and consequently yields a larger binding energy, this may be offset, if need be, by a reduction of the tensor range—a conclusion which follows from the results given in tables 1, 2, 3 and 4.

Table 3. ${}^4\text{He}$ Energy for Hu and Hsu's Nuclear Parameters

$$r_c = r_t = 1.36 \times 10^{-13} \text{ cm}, \quad \gamma = 1.80, \quad V_0 = 25.56 \text{ mev}, \quad g = -0.191$$

$$E({}^3\text{H}) = -6.7 \text{ mev}^\dagger, \quad E({}^4\text{H}) = -7.0 \text{ mev}$$

† Calculated by Hu and Hsu.

From table 2, it is seen that the binding energy of 19.5 mev for the alpha-particle corresponds to a triton energy of 7.5 mev. In this case, it appears improbable that the effect of additional D-states will be great enough to give

an excess binding energy for the alpha-particle, which is the difficulty that arises when purely central forces are used. Table 3 gives the very low binding energy of 7.0 Mev for the alpha-particle, corresponding to an energy of 6.7 Mev for the triton, for equal tensor and central force ranges. Lastly, table 4 gives the large value of 36.1 Mev for the alpha-particle energy, corresponding to a rather long tensor force range. It is obvious from Pease and Feshbach's calculations that this set of nuclear parameters would also yield an excess energy for the triton. It is evident, of course, that increasing the tensor force range relative to that of the central force is equivalent to reducing the strength of the tensor forces.

From the above calculations, it seems reasonable to conclude that the binding energies of both the triton and alpha-particle may be fitted, using a two-body interaction which accounts for the low energy and deuteron data, provided unequal central and tensor force ranges are chosen, the magnitudes of the ranges being of the order of those given in tables 1 and 2.

Table 4. ^4He Energy for one set of Feshbach and Schwinger's Nuclear Parameters

Nuclear parameters	^4He energy terms	Variation parameters for ^4He
$r_c = 1.184 \times 10^{-13}$ cm	S-S K.E. = 146.9 Mev	
$r_t = 2.121 \times 10^{-13}$ cm	D-D K.E. = 6.0 Mev	$c_1 = 4.5$
$V_0 = 54.59$ Mev	S-S P.E. = -179.2 Mev	$c_2 = 6.5$
$\gamma = 0.2305$	S-D P.E. = -9.1 Mev	$C = -0.140$
$g = +0.074$	D-D P.E. = -2.2 Mev	
	E (coulomb) = 1.5 Mev	
	E (^4He) = -36.1 Mev	

In principle the same method with similar wave functions can be employed to calculate the ground state and some excited state energy levels of other light nuclei, such as ^6Li , ^7Li , etc.

ACKNOWLEDGMENTS

Part of this work was carried out at the Institute of Theoretical Physics, Copenhagen, and at the Department of Natural Philosophy in the University of Glasgow. The author wishes to thank Professor Bohr for his hospitality and the Nuffield Foundation for the award of a Fellowship and a grant which made possible the visit to Copenhagen.

APPENDIX

§ A. SPIN MATRIX ELEMENTS

Since the alpha-particle D-states are constructed in an operator form involving the spin-vectors it is convenient to have a systematic method of evaluating the more complicated spin matrix elements. These operators act on the singlet spin state χ , so that a projection operator of the form $S = (1 - \sigma_1 \cdot \sigma_2)(1 - \sigma_3 \cdot \sigma_4)/16$ must be introduced to reduce the spin summations to the trace of an operator. Consider any two states, represented by $P\chi$ and $Q\chi$, P and Q being operators

involving the spin vectors. The spin matrix element $\langle (P\chi)^* | O | Q\chi \rangle$ where O is the operator for the interaction, is then given by

$$\text{trace}_{1,2,3,4} POQS \quad \dots\dots (1)$$

the trace being taken in the spin-space of the particles 1, 2, 3, 4.

As an illustration of the method, the spin matrix element

$$\langle {}^1S_0^* | S_{13} | {}^5D_0^{(1)} \rangle \quad \dots\dots (2)$$

is evaluated. From expression (1), eqn. (2) becomes

$$\begin{aligned} \text{trace}_{1,2,3,4} \{ & 3(\sigma_1 \cdot r_{13})(\sigma_3 \cdot r_{13})/r_{13}^2 - (\sigma_1 \cdot \sigma_3) \} \\ & \times \{ 3(\sigma_1 \cdot \rho_1)(\sigma_3 \cdot \rho_2) + 3(\sigma_1 \cdot \rho_2)(\sigma_3 \cdot \rho_1) - 2(\rho_1 \cdot \rho_2)(\sigma_1 \cdot \sigma_3) \} \\ & \times \{ 1 - \sigma_1 \cdot \sigma_2 - \sigma_3 \cdot \sigma_4 + (\sigma_1 \cdot \sigma_2)(\sigma_3 \cdot \sigma_4) \} / 16. \quad \dots\dots (3) \end{aligned}$$

In the evaluation of expression (3) and the similar expressions arising from the other spin matrix elements, use is made of the following elementary results:

$$(\sigma \cdot A)(\sigma \cdot B) = A \cdot B + i\sigma \cdot A \wedge B$$

$$\text{Trace } (\sigma \cdot A) = 0$$

$$\text{Trace } (\sigma \cdot A)(\sigma \cdot B) = 2(A \cdot B)$$

$$\text{Trace } (\sigma \cdot A)(\sigma \cdot B)(\sigma \cdot C) = 2i(A \wedge B) \cdot C$$

$$\text{Trace } (\sigma \cdot A)(\sigma \cdot B)(\sigma \cdot C)(\sigma \cdot D) = 2[(A \cdot B)(C \cdot D) - (A \cdot C)(B \cdot D) + (A \cdot D)(B \cdot C)]$$

where σ is the usual spin vector with eigenvalues ± 1 and A, B, C, D are vectors which commute with σ .

From the form of expression (3), it is evident that only the first term in the third bracket gives a non-zero contribution. The other matrix elements have similar simple features and the evaluation is straightforward. Multiplying out the first two brackets of the expression (3), keeping the terms in their correct order, the traces of the separate terms are then evaluated. The matrix element (2) has the value

$$\langle {}^1S_0^* | S_{13} | {}^5D_0^{(1)} \rangle = \{ 18(r_{13} \cdot \rho_1)(r_{13} \cdot \rho_2)/r_{13}^2 - 6(\rho_1 \cdot \rho_2) \}. \quad \dots\dots (4)$$

The matrix elements $\langle {}^1S_0^* | S_{14}, S_{23}, S_{24} | {}^5D_0^{(1)} \rangle$ are easily deduced from eqn. (4).

The following matrix elements are used in the text:

$$\begin{aligned} \langle {}^1S_0^* | {}^1S_0 \rangle &= 1, & \langle {}^5D_0^{(1)*} | {}^5D_0^{(1)} \rangle &= 18\rho_1^2\rho_2^2 + 6(\rho_1 \cdot \rho_2)^2 \\ \langle {}^5D_0^{(1)*} | S_{12} | {}^5D_0^{(1)} \rangle &= \langle {}^5D_0^{(1)*} | S_{34} | {}^5D_0^{(1)} \rangle = -\{ 18\rho_1^2\rho_2^2 + 30(\rho_1 \cdot \rho_2)^2 \}. \\ \langle {}^5D_0^{(1)*} | S_{13} | {}^5D_0^{(1)} \rangle &= \{ 42(\rho_1 \cdot \rho_2)^2 - 18\rho_1^2\rho_2^2 - 72(r_{13} \cdot \rho_1)(r_{13} \cdot \rho_2)(\rho_1 \cdot \rho_2)/r_{13}^2 \\ &\quad + 54[\rho_1, r_{13}, \rho_2]^2/r_{13}^2 \} \end{aligned}$$

with similar expressions for the matrix elements $\langle {}^5D_0^{(1)*} | S_{14}, S_{23}, S_{24} | {}^5D_0^{(1)} \rangle$.

§ B. ELEMENTARY INTEGRALS OCCURRING IN THE ENERGY MATRIX ELEMENTS

The normalization integrals for ψ_S and $\psi_{D\omega}$ are easily evaluated in u, v, w space and yield

$$N_S^{1/2} = c_1^{9/2} / \{ \sqrt{3} \cdot 2^{15/4} \pi^2 r_c^{9/2} \}, \quad N_{D\omega}^{1/2} = c_2^{13/2} / \{ 5 \cdot 3^2 \cdot 2^{25/4} \pi^2 r_c^{13/2} \}$$

$c_1 = 2\sqrt{2}\alpha r_c$; $c_2 = 2\sqrt{2}\beta r_c$, α and β being the S- and D-state radial wave function parameters respectively.

The following integrals appear in the calculation:

$$\begin{aligned}
 A(a) &\equiv \int_0^1 \frac{u(1-u^2)^2}{(u+a)^8} du = \frac{35a^3 + 47a^2 + 25a + 5}{210a^6(a+1)^5} \\
 B(a) &\equiv \int_0^1 \frac{u^3(1-u^2)^3}{(u+a)^{12}} du = \frac{231a^4 + 312a^3 + 186a^2 + 56a + 7}{9240a^8(a+1)^8} \\
 C(a) &\equiv \int_0^1 \frac{u(1-u^2)^4}{(u+a)^{12}} du = \frac{231a^5 + 593a^4 + 686a^3 + 434a^2 + 147a + 21}{2310a^{10}(a+1)^7} \\
 D(a) &\equiv \int_0^1 \frac{u^5(1-u^2)^2}{(u+a)^{12}} du = \frac{231a^3 + 159a^2 + 45a + 5}{13860a^6(a+1)^9} \\
 F(a) &\equiv \int_0^1 \frac{u^3(1-u^2)^2}{(u+a)^{10}} du = \frac{21a^3 + 19a^2 + 7a + 1}{504a^6(a+1)^7}.
 \end{aligned}$$

REFERENCES

- CLAPP, R. E., 1949, *Phys. Rev.*, **76**, 873.
 FESHBACH, H., and RARITA, W., 1949, *Phys. Rev.*, **75**, 1384.
 FESHBACH, H., and SCHWINGER, J., 1951, *Phys. Rev.*, **84**, 194.
 FRÖHLICH, H., HUANG, K., and SNEDDON, I. N., 1947, *Proc. Roy. Soc. A*, **191**, 61.
 GERJUOY, E., and SCHWINGER, J., 1942, *Phys. Rev.*, **61**, 138.
 GUNN, J. C., and IRVING, J., 1951, *Phil. Mag.*, **42**, 1353.
 HU, T., and HSU, K., 1951, *Proc. Roy. Soc. A*, **204**, 176.
 IRVING, J., 1951, *Phil. Mag.*, **42**, 338; 1952, *Phys. Rev.*, **87**, 519.
 MORPURGO, G., 1952, *Nuovo Cim.*, **9**, 461.
 PEASE, R. L., and FESHBACH, H., 1951, *Phys. Rev.*, **81**, 142.

Some Features of the Deuteron Stripping Process*

By R. H. DALITZ

Department of Mathematical Physics, University of Birmingham

Communicated by R. E. Peierls; MS. received 25th August 1952

ABSTRACT. The stripping model of Butler is presented in a simpler, more intuitive form which is used to show that the outgoing nucleons are unpolarized, and to calculate the statistical matrix of the final nucleus, from which the angular distribution of later radiation may be calculated by the method of Spiers.

It is now well known that the stripping mechanism (Serber 1947) is sufficient to explain the outstanding features of the angular distributions found in (d, p) and (d, n) reactions, when deuterons of moderate energy are incident on light and medium weight nuclei, provided that due consideration is given to the requirements of conservation of angular momentum and of parity in the process (Butler 1951, Bhatia, Huang, Huby and Newns 1952). According to this mechanism, only one nucleon of the incident deuteron joins with the target nucleus to form a compound state, a consequent feature of great practical importance being that it is possible in this way to form compound states from which the re-emission of the absorbed nucleon is not energetically possible. The purpose of the present note is to discuss several further features of the stripping process, presenting a more intuitive picture of this process, which depends on the same physical assumptions as were made by Butler and from which his final result may be simply derived. For definiteness we will refer always to (d, p) reactions, it being understood that the same conclusions apply also to (d, n) reactions.

Apart from the neglect of coulomb interactions and of compound state formation in which the whole deuteron is absorbed, Butler's main assumption is that, for a neutron distance $r_n > r_0$ (r_0 is an essentially arbitrary radius, most suitably chosen equal to the Gamow nuclear radius) the neutron and proton interact only between themselves, forming a free deuteron plane wave†, whilst, for $r_n < r_0$, the neutron interacts with the nucleons of the initial nucleus, the proton being free from all interactions. Thus for $r_n > r_0$ the wave function of the system is

$$\exp \{i\mathbf{K} \cdot (\mathbf{r}_n + \mathbf{r}_p)/2\} \phi(\mathbf{r}_n - \mathbf{r}_p) \chi^{ms} \psi_{jm}, \quad \dots\dots (1)$$

where \mathbf{K} is the momentum of the deuteron, χ^{ms} its spin wave function, ϕ its space wave function (which is a spin operator when the D-state of the deuteron

* Since the completion of this work, the author has learnt of unpublished papers by R. Huby, by F. Friedman and W. Tobocman, and by L. C. Biedenharn, K. Boyer and R. A. Charpie, each of whom have independently arrived at this simple viewpoint, which is, however, developed by each in a different manner and for differing purposes.

† Note that the interaction between the proton and the tail of the wave function representing the neutron during its interaction with the initial nucleus is neglected in Butler's treatment. This neglect is probably responsible for the singular behaviour of Butler's angular distribution (Bhatia *et al.* 1952) in cases when the binding energy of the neutron in the final nucleus is small, when this neutron tail is appreciable. Similarly, for $\epsilon < 0$, when neutrons are re-emitted, the interaction between outgoing neutron and proton needs consideration, as has been found the case in the π -meson production process $p + p \rightarrow \pi^+ + p + n$ (Foldy and Marshak 1949). The extreme case where outgoing neutron and proton are bound together, i.e. (d, d') scattering, has been considered in Born approximation by Huby and Newns (1951).

is included) and ψ_{jm} represents the initial nucleus. For $r_n < r_0$ the wave function consists of the sum of products of a proton plane wave and the wave function of the corresponding compound state formed by absorption of the neutron, the latter being found by joining smoothly the wave functions in the regions $r_n \geq r_0$ at the boundary $r_n = r_0$. Consider now, for a final proton momentum \mathbf{k} , the Fourier component \mathbf{k} of these wave functions, taken with respect to the proton coordinate only. This component of the incident wave is $\exp(i\mathbf{q} \cdot \mathbf{r}_n) f_D(\mathbf{Q}) \chi^{m_s} \psi_{jm}$, where $\mathbf{q} = \mathbf{K} - \mathbf{k}$, $\mathbf{Q} = (\mathbf{K} - 2\mathbf{k})/2$, and $f_D(\mathbf{Q})$ is the Fourier transform of ϕ . Clearly the problem is solved when the amplitude is known for the formation of a compound state Ψ_{nJM} by absorption of a plane neutron wave of momentum \mathbf{q} by a nucleus (jm), energy $-\epsilon = K^2/2M_d - k^2/2M_p - \Delta$ being associated with this neutron wave (Δ being the binding energy of the deuteron, M_d , M_p the reduced masses of deuteron and outgoing proton): denote this amplitude by $\langle nJM | U(\mathbf{q}) | jm, \frac{1}{2}m_n \rangle$, $U(\mathbf{q})$ being the operator transforming initial spin states to the final spin states. The method of calculating this amplitude is well known (Kapur and Peierls 1938) and its explicit form will be briefly obtained in the Appendix. To use this, it is now convenient to make use of the triplet state projection operator and to represent the incident wave by $\exp(i\mathbf{q} \cdot \mathbf{r}_n) f_D(\mathbf{Q}) \frac{1}{4}(3 + \boldsymbol{\sigma}_n \cdot \boldsymbol{\sigma}_p) \chi^{m_s} \psi_{jm}$ so that all later summations may proceed over all four spin states of the neutron-proton system. Hence the basic spin states may be chosen to be products of neutron and proton spin states, and the incident wave is then taken to be

$$\exp(i\mathbf{q} \cdot \mathbf{r}_n) f_D(\mathbf{Q}) \frac{1}{4}(3 + \boldsymbol{\sigma}_n \cdot \boldsymbol{\sigma}_p) u_{m_n} v_{m_p} \psi_{jm}. \quad \dots\dots(2)$$

For the final system of compound state and proton (momentum \mathbf{k}) the state formed is

$$\sum_n \sum_J \Psi_{nJM} \langle nJM | U(\mathbf{q}) f_D(\mathbf{Q}) \frac{1}{4}(3 + \boldsymbol{\sigma}_n \cdot \boldsymbol{\sigma}_p) | jm, \frac{1}{2}m_n \rangle v_{m_p}. \quad \dots\dots(3)$$

The characteristics of the decay of Ψ_{nJM} are known, so that the later course of the reaction can at once be deduced.

In most cases at present of physical interest, interference between compound states does not occur, and generally only one compound state is of interest. This compound state, formed by absorption of the neutron beam \mathbf{q} , will not be isotropic in general, but will be aligned along the direction \mathbf{q} . Its statistical matrix* will be diagonal when \mathbf{q} is chosen as axis of quantization and its form is specified by $P(M)$, the relative probability of formation of the substate of angular momentum component M along \mathbf{q} . Clearly

$$P(M) = \frac{1}{4(2j+1)} \sum_{m, m_n} \text{Trace} [\langle nJM | U f_D \frac{1}{4}(3 + \boldsymbol{\sigma}_n \cdot \boldsymbol{\sigma}_p) | jm, \frac{1}{2}m_n \rangle \langle jm, \frac{1}{2}m_n | \frac{1}{4}(3 + \boldsymbol{\sigma}_n \cdot \boldsymbol{\sigma}_p) f_D U^\dagger | nJM \rangle],$$

* The statistical matrix U has the general form :

$$U = (1 + J_i P_i^{(1)} + J_i J_j P_{ij}^{(2)} + J_i J_j J_k P_{ijk}^{(3)} + \dots) / (2J+1),$$

where $P_i^{(1)}$, $P_{ij}^{(2)}$, $P_{ijk}^{(3)}$. . . are the $2J$ totally symmetric irreducible tensors which characterize the polarization properties of the system (Dalitz 1952). In the present situation, \mathbf{q} is the only vector available, so that $P_{ijk}^{(n)}$. . . is proportional to

$$\left(q_i q_j q_k q_l q_m \dots - \frac{1}{(2n-1)} \sum \delta_{ij} q_k q_l q_m \dots + \frac{1}{(2n-1)(2n-3)} \sum \delta_{ij} \delta_{kl} q_m \dots - \dots \right).$$

For odd n , $P^{(n)}_{ijk\dots}$ is then zero, since all $P^{(r)}_{ijk\dots}$ must remain unchanged on reflection of the axes. Hence U is an even polynomial in $\mathbf{J} \cdot \mathbf{q}$ and is diagonal when \mathbf{q} is the axis of quantization.

where the operation 'Trace' carries out the summations of initial and final proton spin states. This becomes

$$P(M) = \frac{1}{4(2j+1)} \text{Trace} [\langle nJM | U f_{D\frac{1}{2}} (3 + \boldsymbol{\sigma}_n \cdot \boldsymbol{\sigma}_p) f_D U^\dagger | nJM \rangle] \dots\dots (4)$$

$$= \frac{3}{8(2j+1)} f_D^2 \langle nJM | U U^\dagger | nJM \rangle, \dots\dots (5)$$

when the D-state of the deuteron is neglected.

The effect of the D-state of the deuteron may be included by using the operator form for ϕ_D (Rarita and Schwinger 1941):

$$\phi_D^{ms}(r) = \left\{ \phi(r) + \zeta(r) \left(\frac{3\boldsymbol{\sigma}_n \cdot \mathbf{r} \boldsymbol{\sigma}_p \cdot \mathbf{r}}{r^2} - \boldsymbol{\sigma}_n \cdot \boldsymbol{\sigma}_p \right) \right\} \chi^{ms},$$

so that f_D is then

$$\left\{ f(Q) + g(Q) \left(\frac{3\boldsymbol{\sigma}_n \cdot \mathbf{Q} \boldsymbol{\sigma}_p \cdot \mathbf{Q}}{Q^2} - \boldsymbol{\sigma}_n \cdot \boldsymbol{\sigma}_p \right) \right\}.$$

Use of this expression modifies (5) only by replacing f_D^2 by $f(\mathcal{Q})^2 + 6g(\mathcal{Q})^2$. It is clear therefore that in the stripping model the D-state of the deuteron can play no essential role.

According to eqn. (A2), the explicit form of $\langle nJM | U(\mathbf{q}) | jm, \frac{1}{2}m_n \rangle$ is

$$\sum_l (\sum_{S=j-\frac{1}{2}}^{j+\frac{1}{2}} c_{jm\frac{1}{2}m_n}^{SM} c_{SMl0}^{JM} \alpha_{Sl}^{nJ}), \dots\dots (6)$$

where, from eqn. (A2), α_{Sl}^{nJ} is given by $\frac{i^l (2l+1)^{1/2} (j_l' - f_l^c j_l)}{N_{nJ} (W_{nJ} + \epsilon - E_j)} \frac{\hbar^2}{2M} \cdot \lambda_{Sl}^{nJ}$. Hence,

$$\begin{aligned} P(M) &= \frac{3}{8(2j+1)} f_D^2 \sum_{l,l'} \sum_{S,S'} \sum_{mm_n} c_{jm\frac{1}{2}m_n}^{SM} c_{jm\frac{1}{2}m_n}^{S'M} c_{SMl0}^{JM} c_{S'M'l'0}^{JM} \alpha_{S'l'}^{nJ*} \alpha_{Sl}^{nJ} \\ &= \frac{3}{8(2j+1)} f_D^2 \sum_{S=j-\frac{1}{2}}^{j+\frac{1}{2}} (\sum_{l,l'} c_{SMl0}^{JM} c_{S'M'l'0}^{JM} \alpha_{S'l'}^{nJ*} \alpha_{Sl}^{nJ}). \dots\dots (7) \end{aligned}$$

The angular distribution of any consequent radiation in coincidence with protons \mathbf{k} may now be written down at once, using the results of Spiers (1949) for the angular distribution of the decay products of a state JM . This distribution will have \mathbf{q} as an axis of rotational symmetry and will be unchanged on reflection in a plane perpendicular to \mathbf{q} . Its complexity will be limited not only by the values of J and of l_r , the highest orbital angular momentum of the outgoing radiation, but also by the allowed l for the absorbed neutron, which the requirements of angular momentum and parity conservation severely limit. Interference between terms of different l , where several are allowed, may be expected to be of greater importance in the angular distribution of later radiation than has been found the case in the study of the proton angular distributions.

The differential cross section for the (d, p) reaction with emission of a proton \mathbf{k} is then

$$\begin{aligned} d\sigma(\mathbf{k}) &= \frac{1}{3} \frac{M_d}{K} [\sum_M P(M)] k M_p dE_p d\Omega_k \\ &= \frac{k}{K} \frac{M_d M_p f_D^2}{8(2j+1)} (\sum_l (\alpha_{j-\frac{1}{2},l}^{nJ})^2 + (\alpha_{j+\frac{1}{2},l}^{nJ})^2) dE_p d\Omega_k, \end{aligned}$$

using (7). After integration over the resonance $E_p = E_d + E_j - E_{nJ} - \Delta$, assuming

this to be of negligible width, this becomes

$$d\sigma = \frac{k}{K} [f^2(Q) + 6g^2(Q)] (\Sigma_i N_{Ji} (\mathcal{J}'_i - f_i \mathcal{J}_i)^2) d\Omega_k,$$

in agreement with the result of Butler.

It has recently been proposed (Holt 1952) that observation of the polarization of the outgoing protons might also lead to useful information on the nuclear states involved. However, the stripping model predicts this polarization to be zero, for, since the proton spin is coupled only to the neutron spin, there could be a preferred spin direction for the outgoing protons only if there is a preferred spin direction for the absorption of a neutron, which is well known not to be the case. More formally, the polarization \mathbf{p} is given by (Dalitz 1952)

$$\begin{aligned} \mathbf{p}(\text{Trace } \Sigma_M \langle nJM | U f_{D\frac{1}{2}} (3 + \sigma_n \cdot \sigma_p) f_D U^\dagger | nJM \rangle) \\ = \text{Trace } \Sigma_M \langle nJM | \sigma_p U f_{D\frac{1}{2}} (3 + \sigma_n \cdot \sigma_p) f_D U^\dagger | nJM \rangle \\ = \frac{1}{2} \Sigma_M \langle nJM | U \left\{ \sigma_n (f - 4g)^2 + \frac{\sigma_n \cdot \mathbf{Q}\mathbf{Q}}{Q^2} 6g(f - g) \right\} U^\dagger | nJM \rangle, \end{aligned}$$

of which the right-hand side is a homogeneous linear function of

$$\Sigma_M \langle nJM | U \sigma_n U^\dagger | nJM \rangle.$$

This quantity is a pseudovector and depends only on \mathbf{q} : however, it is not possible to construct a pseudovector from \mathbf{q} , so that $\mathbf{p} = 0$.

It must be emphasized that these conclusions will need modification owing to defects in the treatment of deuteron waves of low angular momentum l_d in the stripping model and to the related neglect of compound nucleus formation involving the whole deuteron. This will be particularly the case when the outgoing protons have a direction for which the stripping model predicts zero intensity.

APPENDIX

In this section we will briefly outline the derivation of the amplitude $\langle nJM | U(\mathbf{q}) | jm, \frac{1}{2}m_n \rangle$, following the method of Kapur and Peierls (1938). The wave function representing the compound system with angular momentum J, M may be expanded in terms of the various conceivable modes of disintegration, e.g. for the emission of a neutron of energy $p^2/2M_n = -\epsilon$:

$$\Psi_{JM} = \sum_j \sum_{lm_l m m_n} \psi_{jm} u_{m_n} Y_{lm_l} \phi_{JMjlm_l m m_n}(r_n) / r_n.$$

For sufficiently large r_n , $\Phi = \phi_{JMjlm_l m m_n}(r_n) Y_{lm_l} / r_n$ satisfies the equation $(\nabla^2 + p^2)\Phi = 0$. For given l it is convenient to define two radial solutions of this equation, $\phi_l^+ = (\frac{1}{2}\pi pr)^{1/2} H_{l+\frac{1}{2}}^{(1)}(pr)$, $\phi_l^- = (\frac{1}{2}\pi pr)^{1/2} H_{l+\frac{1}{2}}^{(2)}(pr)$, which represent an outgoing and an ingoing neutron wave respectively, each normalized to unit amplitude at large distances. If $\epsilon > 0$, so that neutron emission is not energetically possible, p is to be replaced by ip' in these expressions (where $\epsilon = (p')^2/2M$), so that ϕ_l^+ shows an exponential decay, ϕ_l^- an exponential rise, for large r_n . Denote $f_l = [(d/dr)(\log \phi_l^+)]_{r_n=r_0}$, and following Kapur and Peierls, define the compound eigenstates JM by imposing the condition $[l(d/dr_n) - f_l] \phi_{JMjlm_l m m_n}(r_n) |_{r_n=r_0} = 0$ on the neutron channel, similar conditions being also imposed on all other channels of disintegration, to ensure that the

compound state contains only outgoing waves. By these conditions the set of states Ψ_{nJM} is defined, with complex eigenvalues $W_{nJ} = E_{nJ} - \frac{1}{2}i\gamma_{nJ}$.

A neutron wave $\exp(i\mathbf{q} \cdot \mathbf{r}_n)u_{m_n} = \sum_{l=0}^{\infty} i^l (2l+1)^{1/2} \mathcal{J}_l(qr_n) Y_{l0} u_{m_n}/r_n$ is incident on a nucleus ψ_{jm} . $[\mathcal{J}_l(qr) = (\pi r/2q)^{1/2} J_{l+\frac{1}{2}}(qr)]$. The compound state formed with angular momentum JM will have wave function $\sum_n a_{nJM} \Psi_{nJM} + X_{JM}$, where X_{JM} vanishes on all boundaries except that of the ingoing channel $r_n = r_0$. In this neighbourhood $X_{JM} = \sum_{lm_l m_n} \psi_{jm} u_{m_n} Y_{lm_l} \chi_{JMjmlm_n}(r_n)/r_n$ and χ_{JMjmlm_n} is required to satisfy the condition

$$[\chi'_{JMjmlm_n} - f_l \chi_{JMjmlm_n}]_{r_n=r_0} = i^l (2l+1)^{1/2} \delta_{0m_l} [\mathcal{J}_l' - f_l \mathcal{J}_l]_{r_n=r_0} \dots\dots (A1)$$

which reduces to eqn. (78) of Kapur and Peierls in the case $p=q$.

The function χ is necessary since all wave functions in the internal region contain only outgoing waves whilst the wave function in the external region contains both ingoing and outgoing waves. It is possible later to take each function χ_{JMjmlm_n} to be everywhere as small as we like, provided only that condition (A1) is satisfied. Then, following Kapur and Peierls, the required amplitude is

$$\langle nJM | U(\mathbf{q}) | jm_{\frac{1}{2}} m_n \rangle = a_{nJM} = \sum_l i^l (2l+1)^{1/2} \frac{\hbar^2}{2M} \frac{\phi_{JMjml0m_n}(r_0) (\mathcal{J}_l' - f_l \mathcal{J}_l)_{r_n=r_0}}{N_{nJ} (W_{nJ} + \epsilon - E_j)}, \dots\dots (A2)$$

where $\phi_{JMjml0m_n}(r_0)$ must have the form $\sum_S c_{SMl0}^{JM} c_{jm_{\frac{1}{2}} m_n}^{SM} \lambda_{Sl}^J$, the λ_{Sl}^J being constants characteristic of the state Ψ_{nJM} .

REFERENCES

- BHATIA, A. B., KUN HUANG, HUBY, R., and NEWNS, H. C., 1952, *Phil. Mag.*, **43**, 485.
 BUTLER, S. T., 1951, *Proc. Roy. Soc. A*, **208**, 559.
 DALITZ, R. H., 1952, *Proc. Phys. Soc. A*, **65**, 175.
 FOLDY, L. F., and MARSHAK, R. E., 1949, *Phys. Rev.*, **75**, 1493.
 HOLT, J. R., 1952, Report of the International Physics Conference (Copenhagen, June 1952), p. 8.
 HUBY, R., and NEWNS, H. C., 1951, *Phil. Mag.*, **42**, 1442.
 KAPUR, P. L., and PEIERLS, R. E., 1938, *Proc. Roy. Soc. A*, **166**, 277.
 RARITA, W., and SCHWINGER, J. S., 1941, *Phys. Rev.*, **59**, 436.
 SERBER, R., 1947, *Phys. Rev.*, **72**, 1008.
 SPIERS, J. A., 1949, *Directional Effects in Radioactivity* (National Research Council, Chalk River, Canada, April 1949).

A Search for Irregularities in the Absorption of Cosmic Rays in Lead

By G. R. HEYLAND AND W. E. DUNCANSON

Physics Department, University College, London

MS. received 17th March 1952, and in final form 20th August 1952

ABSTRACT. The integral absorption curve of cosmic rays has been examined at sea level up to a thickness of 365 cm of lead. In the first place, the absorption curve was examined in sections using a control telescope method to reduce the effects of atmospheric variation. It was found, to an accuracy of within about 1%, that there was no deviation from a monotonically decreasing curve. By a second method two regions of the curve, namely 0–30 cm and 71–193 cm, were examined in greater detail. Five Geiger–Müller counter telescopes were employed so that five consecutive points on the absorption curve were determined simultaneously. No irregularities in the absorption curves for these two regions were found, and it was also shown for the 0–30 cm region that this was true whether the absorber was wholly above or wholly within the telescope. The fact that no irregularities were found in the 71–193 cm region (corresponding to a momentum range of about 1–3 kmev/c for μ -mesons) indicates that the irregularities in the meson momentum spectrum suggested by Blackett, and by Glaser, Hamermesh and Safonov are probably due to poor statistics.

§ 1. INTRODUCTION

SEVERAL reports have been published of irregularities in the absorption curve of cosmic rays in lead at sea level. Blackett (1937) and Glaser, Hamermesh and Safonov (1950) have suggested the possibility of an anomaly in the momentum distribution for mesons in the region between 2 and 4 kmev/c (corresponding to a range in lead between 125 cm and 250 cm), but apparently more definite irregularities have been found in the absorption curve between 0 and 30 cm of lead.

Clay, Venema and Jonker (1940), using ionization chambers, obtained three maxima at 1.5, 17 and 25 cm respectively. These maxima disappeared when a Geiger–Müller counter telescope was employed and the absorber placed within the telescope. With the absorber above the telescope two rather extended maxima appeared at about 15 and 30 cm. Clay associates these with maxima observed in the absorption curve for showers. Chandrashekhar Aiyar (1944) determined the absorption curve for the hard component only, and found an abrupt drop in the intensity between 21 and 24 cm. Apart from this discontinuity, the curve was of constant slope over the range 5–30 cm of lead. The absorber was all placed above the counter telescope. George and Appapillai (1945) have used a counter telescope with the absorber placed within it, and find at most, a plateau region at about 10–17 cm. Swann and Morris (1947) find the slope of the absorption curve is greater at latitude 7° S than at 51° N, but find no evidence for plateaux or maxima. More recently Fenyves and Haiman (1950) have obtained pronounced maxima in the absorption curve at 17 and 25 cm. They used counter telescopes and determined two consecutive points simultaneously. (The position of the absorber is not mentioned.) George, Jánossy and McCaig (1942) report that the second maximum in the shower curve is instrumental and not real, unless it be very small.

Kellermann and Westerman (1949) have examined the integral and the differential absorption curves in the region 0–30 cm of lead. Their integral absorption curve, corrected for atmospheric pressure changes (cf. Duperier 1944), exhibits several changes of slope, with a short plateau region at about 10 cm of lead. The differential absorption curve obtained by these authors, using the anti-coincidence method, does not corroborate their irregular integral absorption curve. Their statement that the anti-coincidence method gives 'more definite information' is certainly correct, but we cannot agree that this is due to the 'influence of scattering being greatly diminished'. We are of the opinion that the usual corrections applied to the integral absorption curve to account for variations in the composition, intensity and energy spectrum of the cosmic-ray beam are first-order corrections only, and that the remaining irregularities in the absorption curve, which are often outside the statistical fluctuations, are mainly due to incomplete correction for atmospheric variations. In some experiments the irregularities in the integral absorption curve may have been inadvertently introduced by bad placing of the absorbers. Unless corrections are applied for scattering it is advisable to build up the absorber progressively, from a fixed level, when the corrections for scattering, though not necessarily known, will increase regularly. The importance of this procedure is discussed in the following paper (Heyland and Duncanson 1953).

It is doubtful whether any significance can be attached to small variations which appear in the absorption curve, when determined by the simple telescope method. To illustrate this point we quote the following example. With 10 cm of lead absorber, we recorded counting rates of 530.1 ± 4.4 per hour and 505.5 ± 4.6 per hour (24-hour runs) on two different days, i.e. a difference of more than five times the standard error, and a change in intensity equivalent to an extra absorber of 5 cm of lead. If one of these rates were the average rate, it would take a run of about a month on this point to 'iron out' the effect of the other.

The experiments now to be described consist of a search for irregularities in the absorption curve for cosmic rays in lead, up to a thickness of 365 cm (corresponding to a meson momentum of 6 kMeV/c). The two methods used were both designed to eliminate the effect of atmospheric changes.

§ 2. FIRST METHOD

The first method involved the use of a control telescope whose readings were taken simultaneously with those of the main telescope. Its use can be illustrated with reference to fig. 1 (inset). The counter trays 1, 2, 3 constituted the control telescope and, for a given experiment, the amount of absorber within this telescope was kept constant and in a fixed position. The coincidences N_{123} , N_{124} and N_{1245} were recorded simultaneously, varying the thickness of absorber only in the region below tray 3. The counting rate N_{123} was a measure of the cosmic-ray intensity capable of penetrating absorber I. The absorption curve was obtained by plotting the ratio N_{124}/N_{123} (or N_{1245}/N_{123}) against the absorber thickness; this should then be independent of atmospheric changes as long as the total thickness of lead in the main telescope is not too much greater than that in the control telescope.* To avoid having too great a difference between these two thicknesses the absorption curve was examined in sections; the thickness of absorber I in the control

* We are of the opinion that the usual method of correcting the cosmic-ray intensity for atmospheric fluctuations is inadequate.

telescope was kept constant for any one section. Attention could be transferred to another section of the curve by altering the thickness of absorber I. The counter tray 5 was included to enable two sections of the curve to be examined simultaneously, thus saving time and also providing a check.

This type of experiment was carried out with three different counter telescopes capable of containing 150 cm, 225 cm, and 365 cm of lead respectively.* The absorption curve between 18 cm and 365 cm of lead was obtained in six overlapping sections A-F, shown in fig. 1. For the larger thicknesses of absorber, i.e. sections

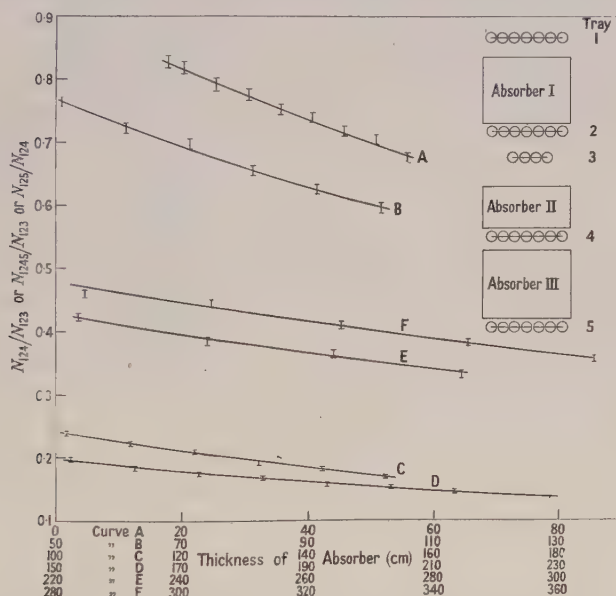


Fig. 1. Absorption curve in six sections A-F, covering the range 17-365 cm of lead. Inset. Arrangement of counter trays 1, 2, 3, 4, 5 and absorbers I, II, III.

E and F, the telescope 124 was used as the control telescope, and the absorber III only was varied. The ratio N_{125}/N_{124} was then used as ordinate. The standard deviation for each point was about 1%, and it is seen that each section consists of a smoothly falling curve. It will be noticed that the slope of the curve for the same absorber thickness on successive sections does not always correspond. This discrepancy is due to the fact that no corrections have been made for accidentals, showers and scattering, or for the changes in angular aperture of the telescopes. The 50% change of slope which occurs at 100 cm of absorber is mainly due to scattering, the position of the variable absorber II in this region being such as to cause large scattering effects.

§ 3. SECOND METHOD

In the second method a telescope of square cross section was used, with counter trays and absorbers so arranged that five neighbouring points on the absorption curve were determined simultaneously with approximately the same accuracy.

* Absorber thicknesses are quoted in centimetres though, in fact, the absorber dimensions correspond to inch units.

The apparatus is shown in fig. 2 (inset), and consisted of seven Geiger-Müller counter trays each having a sensitive area of $30 \times 30 \text{ cm}^2$. The triple coincidences 123, 124, 125, 126 and 127 were recorded simultaneously; the counting rates being denoted by N_3, N_4, N_5, N_6 and N_7 respectively. The main absorber, which was included in all five telescopes, was divided into two parts A and B, where $A + B = d$, to give more effective screening against showers. By inserting equal thicknesses of lead in positions C, D, E, and F, five consecutive points on the absorption curve could be determined simultaneously. All counts were normalized to those of telescope 127 by recording the counting rates with no

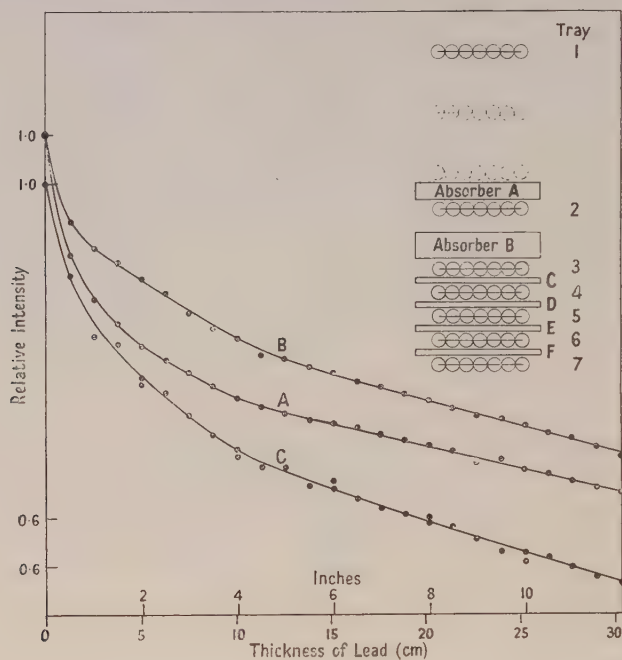


Fig. 2. Curve A. Absorption curve obtained by fitting together the successive sections of the absorption curve, using appropriate multiplying factors. Mean semi-angular aperture of telescope $= 6.3^\circ$.

Curves B and C. Smoothed curves similar to A for mean semi-angular apertures of 9.6° and 18.25° respectively. The ordinates for the three curves are normalized at zero thickness, and for curve C are displaced downwards, for clarity.

Inset. Arrangement of counter trays 1, 2, 3, 4, 5, 6, 7 and absorbers A, B, C, D, E, F.

absorbers in positions C, D, E and F. The normalizing factors were sensibly constant for all values of d , except for $d=0$. (A small correction is needed for $d=0$, and is discussed later).

Two sections of the curve were chosen for more careful examination by this method: firstly, the region between 71 cm and 193 cm of lead, corresponding to a momentum range of 1 to 3 kmec/c for μ -mesons, and secondly, the region between 0 and 30 cm of lead. (These two ranges cover regions where earlier work has indicated possible irregularities.) In the first case the distances between the five lower trays were sufficient to allow 10.16 cm (4 in.) of lead to be placed in each of the positions C, D, E and F. In this manner the five overlapping sections, 71–111.6 cm, 91.3–132 cm, 111.6–152.3 cm, 132–172.6 cm and 152.3–193 cm, were examined separately. The results showed that each section was a smooth curve,

confirming the fact that there are no anomalies greater than 1% in the absorption curve in the range 71–193 cm of lead.

To examine the second selected region (0–30 cm of lead) the telescope was closed up so that the mean semi-angular aperture of telescope 123 was 6.3° , with the distances between the lower trays just sufficient to accommodate 1.27 cm ($\frac{1}{2}$ in.) of lead in positions C, D, E and F. Five points were recorded simultaneously in each of the sections 0–5 cm, 2.5–7.5 cm, 5–10 cm... 25–30 cm. There was no evidence in any of the sections of a deviation from a smoothly falling curve, and when all the sections were fitted together* a continuous smooth curve was obtained as shown in fig. 2 (curve A). For $d=0$ the normalizing factors are smaller than the mean values. This effect is partly due to the larger absorption of the soft rays in the supporting material between trays 3 to 7 (it has been assumed that when absorbers C, D, E and F are absent no particles stop between trays 3 to 7), and partly due to the ignoring of the scattering corrections. The effect of using the mean values of the normalizing factors has been to make the slope of the absorption curve between 0–5 cm too large.

As it has been suggested that the magnitude of the anomalies which some observers have found in the absorption curve varies with the aperture of the telescope, the experiment was repeated with the mean semi-angular aperture of the 123 telescope increased to 9.6° (curve B), and again to 18.25° (curve C). In each case the results were similar.

A further point to be considered in this low-energy region is that an anomaly may exist whose position depends on atmospheric conditions, and that measurements over an extended period of time would tend to smooth it out. The experiment with the 18.25° telescope helped to resolve this point, since the greatly increased counting rates (2000 to 5000 counts per hour) permitted a rapid survey of the whole curve. A run of one hour on each section enabled the whole absorption curve from 0–30 cm to be examined in six hours. This experiment was repeated several times and, although the statistical fluctuations were somewhat larger than in the previous cases, no systematic deviation from the smooth absorption curve was found. A typical result is shown in fig. 2 (curve C).

It is desirable to make a few comments on this method for determining the position of five points on the absorption curve simultaneously.

(i) The relative statistical error of neighbouring points is small. For curves A and B of fig. 2, at least 50 000 particles were counted by each telescope for each point on the curve. If these were independent observations the standard deviation of a point would be about 0.5%. However, since at least 80% of the particles counted by one telescope are also counted by the neighbouring telescope, the relative standard deviation for neighbouring points is about 0.2%, since the relative error is zero for the common particles. The relative standard deviations are too small to be indicated on the absorption curve.

(ii) It will be seen that the slopes of the curves of fig. 2 appear to increase with increasing aperture of the telescope. Kellermann and Westerman (1949) point out that the slope of the absorption curve in this region, as determined by many observers, varies by a factor of about two. Much of this variation may be due to the different geometry of the telescopes employed. Another important factor is scattering. It is shown in the following paper (Heyland and Duncanson 1953)

* Owing to fluctuations in the cosmic-ray intensity neighbouring sections of the curve did not necessarily link up and had to be fitted together by appropriate multiplying factors.

that the correction for scattering for a triple coincidence telescope is largest when the absorber is in the middle of the telescope. A little consideration will show that part of the increase in slope from curve A to curve C of fig. 2 is due to neglecting the increasing scattering corrections.

(iii) The method is valuable in that it reveals instrumental errors which may lead to false irregularities in the absorption curve; for example a change in the performance of any particular telescope subsequent to a determination of the normalizing factors is readily seen in this type of experiment as the irregularity it may produce appears in the corresponding position in each set of points.

This experiment is suitable for examining the absorption curve for irregularities, but is not suitable for determining the slope of the curve accurately.

§ 4. ABSORBER ABOVE THE TELESCOPE

As some experimenters have reported anomalies in the absorption curve when the absorber is placed above the detecting apparatus a further experiment was undertaken to test this point. It is not possible to use the previous method of determining several points on the curve simultaneously, but it is possible to make simultaneous counts for the same absorber thickness, (*a*) with the absorber within the telescope, and (*b*) with the absorber above it. Having shown that there are no irregularities with the absorber within the telescope, any irregularity in the absorption curve with the absorber above the telescope would be indicated by a change in the ratio of the counts for (*a*) and (*b*) as the thickness of the absorber was changed progressively.

The apparatus consisted of four equally spaced counter trays. For convenience, fig. 1 (inset) may be referred to, ignoring tray 3, and regarding the apparatus as comprising trays 1, 2, 4 and 5. Each tray has a sensitive area of $30 \times 30 \text{ cm}^2$. The triple coincidence counting rates for telescopes 124 and 245, N_1 and N_2 respectively, were recorded simultaneously (i) with the absorber in position II, for absorber thicknesses 5, 10 and 20 cm respectively, and (ii) with the absorber in position I, for thicknesses of absorber from 2.5 to 25 cm in steps of 2.5 cm (absorber I was sufficiently wide to ensure that all particles accepted by telescope 245 passed through it).

From (i), the ratio of the counting rates $N_2/N_1 = f$ was determined; f is the geometrical factor which enabled the counting rates of the 124 and 245 telescopes to be compared for the same absorber thickness when both telescopes contain the absorber within them. It was found that f was sensibly independent of the absorber thickness, and its value was 0.8714 ± 0.001 .

From (ii), the quantity fN_1/N_2 was determined for each absorber thickness. Any irregularity in the absorption curve for the 245 telescope which does not exist in the curve as determined by the 124 telescope would reveal itself by a change in the quantity fN_1/N_2 . It was found that within the accuracy of the experiment — within about 0.5% — the value of this quantity remained constant at 0.9835 for all absorber thicknesses between 5 and 25 cm. Thus it is evident that, to this accuracy, the absorption curve in this range is independent of whether the absorber is above or within the telescope. The fact that fN_1/N_2 is slightly less than unity is due to scattering: scattering tends to reduce the value of f when the lead is in position II, and when the lead is in position I it tends to reduce the ratio N_1/N_2 . Hence the effects of scattering in both parts of the experiment tend to reduce the value of fN_1/N_2 below unity.

The low value of $fN_1/N_2 = 0.940$ which was obtained for 2.5 cm of absorber is partly due to scattering, but mainly due to the effects of non-ionizing radiation in the soft component. Non-ionizing rays which produce ionizing secondaries in the absorber when in position I will be recorded by the 245 telescope but not by the 124 telescope. This effect is well known and needs no further discussion.

§ 5. CONCLUSION

It is concluded from these experiments (with the possible exception of the case with an absorber of about 2.5 cm of lead above the telescope) that there are no significant anomalies in the absorption curve between 0 and 365 cm of lead, as determined by Geiger-Müller counter telescopes.

Although no corrections have been made for scattering, the conclusions drawn from these experiments are not affected. In order to obtain the true absorption curve the scattering corrections to be applied to the absorption curve must be determined. Experiments to do this are described by Heyland and Duncanson (1953) and consideration is also given to the separation of the electronic and penetrating components, to enable the momentum spectra of the various components to be determined.

REFERENCES

- BLACKETT, P. M. S., 1937, *Proc. Roy. Soc. A*, **159**, 1.
 CHANDRASHEKHAR AIYA, S. V., 1944, *Nature, Lond.*, **153**, 375.
 CLAY, J., VENEMA, A., and JONKER, K. H. J., 1940, *Physica*, **7**, No. 8.
 DUPERIER, A., 1944, *Nature, Lond.*, **153**, 529.
 FENYVES, E., and HAIMAN, O., 1950, *Nature, Lond.*, **165**, 244.
 GEORGE, E. P., and APPAPILLAI, V., 1945, *Nature, Lond.*, **155**, 726.
 GEORGE, E. P., JÁNOSSY, L., and MCCAIG, M., 1942, *Proc. Roy. Soc. A*, **180**, 219.
 GLASER, D. A., HAMERMESH, B., and SAFONOV, G., 1950, *Phys. Rev.*, **80**, 625.
 HEYLAND, G. R., and DUNCANSON, W. E., 1953, *Proc. Phys. Soc. A*, **66**, 40.
 KELLERMANN, E. W., and WESTERMAN, K., 1949, *Proc. Phys. Soc. A*, **62**, 356.
 SWANN, W. F. C., and MORRIS, P. F., 1947, *Phys. Rev.*, **72**, 1262.

Momentum Distribution for Cosmic Ray Mesons up to 6 kmev/c

BY G. R. HEYLAND AND W. E. DUNCANSON

Physics Department, University College, London

MS. received 17th March 1952, and in final form 20th August 1952

ABSTRACT. The absorption curve and differential absorption curve have been determined for cosmic rays at sea level up to 365 cm (144 in.) of lead. Since similar curves were obtained for the differential absorption both by differentiating the absorption curve and by an anti-coincidence method, the absorption curve was corrected for accidentals, showers and scattering and used for subsequent determinations. The scattering correction is shown to be important. After subtraction of the soft component contribution from the absorption curve the momentum distribution for μ -mesons is determined by making use of the range-momentum relation. This curve rises above the Rossi curve for momenta below 0.4 kmev/c reaching a rather sharp maximum at about 0.16 kmev/c. It is suggested that there are several factors contributing to this difference: (i) the soft component may not have been separated out completely and may be making a small contribution to the present curve at the low end, (ii) in the present work the proton component has not been separated out and will make an effective contribution just in the region of the maximum and (iii) the effect of scattering may mean that the Rossi curve is rather low in this region.

§ 1. INTRODUCTION

THE preceding paper (Heyland and Duncanson 1953, to be referred to as I) was mainly concerned with establishing the fact that the absorption curve for cosmic rays at sea level exhibits no significant irregularities in the range 0–365 cm of lead. However, the experimental methods adopted were not so suitable for determining the absolute intensities and the momentum distributions of the various ionizing components. The present paper is concerned with these two problems, the satisfactory solution of which requires a suitable geometrical arrangement, a means of separating the contributions made by the several components (e.g. electrons, mesons and heavier charged particles), and corrections applied for scattering and a number of ‘background’ effects.

A number of workers (Blackett 1937, Blackett and Brode 1936, Caro, Parry and Rathgeber 1950, Glaser, Hamermesh and Safonov 1950, Hall 1944, Hughes 1940, Jones 1939, Künze 1932, Mylroi and Wilson 1951, Sarabhai 1944, Wilson 1946) have made measurements on the momentum spectrum of the hard component extending up to about 80 kmev/c. There is general agreement that there is an excess of positive particles of the order of 20% at sea level, and much of the work is consistent with the existence of an extended maximum in the momentum spectrum in the region between 0.1 and 1 kmev/c as shown by Rossi’s (1948) composite curve. Certain criticisms of this portion of the curve can be made, but will be postponed to the discussion at the end of the paper.

§ 2. EXPERIMENTAL PROCEDURE

Both anti-coincidence and coincidence methods were used for determining the differential absorption curve, and experiments were also performed to correct it for scattering and to separate the electronic and penetrating components.

The anti-coincidence apparatus is shown in fig. 1 (inset). Trays 1 and 2 each had a sensitive area of $50 \times 37 \text{ cm}^2$ and tray 3 of $40 \times 30 \text{ cm}^2$. The anti-coincidence tray A had a sensitive area of $50 \times 41 \text{ cm}^2$ and contained a double layer of Geiger-Müller tubes (all connected in parallel) so that any particle traversing the 123 telescope certainly triggered at least one Geiger-Müller tube in tray A unless it stopped in absorber III. The anti-coincidence circuit was not 100% efficient which resulted in a rather high background rate. Absorber III was kept at 10.16 cm (4 in.) of lead and the main absorber was varied from 0 to 267 cm in steps of 10.16 cm or 20.32 cm, starting at the bottom and building upwards.*

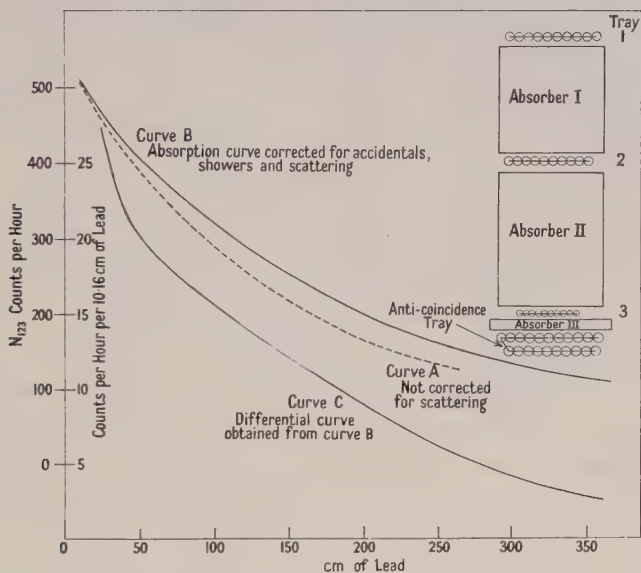


Fig. 1. Curve A. Absorption curve uncorrected for scattering. Ordinate N_{123} is the number of counts per hour.

Curve B. Absorption curve corrected for accidentals, showers and scattering.

Curve C. Differential curve obtained by differentiating curve B. Ordinate is the number of counts per hour per 10.16 cm of lead.

Inset. Arrangement of counter trays 1, 2, 3, A and absorbers I, II, III.

The counting rates N_{123} and N_{123A} were recorded simultaneously at each step, a background count also being recorded at several points with absorber III removed. The difference between the counts N_{123A} with and without the absorber III then gives the number of particles stopping in this absorber, i.e. in 10.16 cm of lead. This difference is given in column (4) of the table. Column (1) of the table gives the extreme limits of the range of the particles, while column (2(a)) gives the total number of counts per hour (corrected for accidentals and showers) corresponding to the absorber thickness in column (1(a)); columns (2(b)) and (1(b)) are similarly related. Column (3) is the difference between (2(a)) and (2(b)).

The absorption curve obtained by plotting N_{123} against the absorber thickness is shown in fig. 1 curve A. Differentiating this curve for each 10.16 cm of lead should give values in agreement with the anti-coincidence counts (corrected for background) in column (4) of the table. In fact they were about three counts per hour greater than the anti-coincidence counts, cf. columns (3) and (4) of the table.

* The absorbers used were in 1 inch and 2 inch units, but all thicknesses are given in centimetres.

This discrepancy is due to the fact that the anti-coincidence background count has been over-estimated. This is mainly due to inefficiency of the anti-coincidence tray, caused by the dead time following every counter discharge. This inefficiency is increased when absorber III is removed, since the background counting rate of the anti-coincidence counters is then increased.

(1) Absorber thickness (cm)*		(2) N_{123} (counts/hr)		(3) ΔN_{123} (counts/hr)	(4) N_{123A} (counts/hr)
(a)	(b)	(a)	(b)		
10.2	20.3	506	470	36	30.4
20.3	30.5	470	438	32	24.8
30.5	40.6	438	410	28	23.2
50.8	61.0	386	364	22	20.1
71.1	81.3	342	322	20	17.0
91.4	101.6	303	286	17	14.7
111.8	121.9	270	255	15	13.2
142.2	152.4	226	213	13	10.0
172.7	182.9	191	180	11	7.1
203.2	213.4	161	153	8	5.2
233.7	243.8	141	135	6	4.6
266.7	276.9	126	120	6	4.5

* Values quoted for absorber thickness are rounded off to the first decimal place but the difference between columns (1(b)) and (1(a)) always corresponds to 10.16 cm (= 4 in.).

§ 3. CORRECTION FOR SCATTERING

We have shown above that the anti-coincidence method gives a smooth differential absorption curve in agreement with that obtained from the integral absorption curve. As the corrections for accidentals and showers for the integral absorption curve vary but slowly with absorber thickness, and are only small corrections, and further, since the differential absorption curve as determined by the anti-coincidence method is also subject to a correction for inefficiency, it is more satisfactory to correct the integral absorption curve for scattering. The method adopted for this is given in the Appendix. The integral absorption curve corrected for accidentals, showers and scattering is shown in fig. 1 curve B, while curve C is the differential absorption curve deduced from curve B. These curves extend up to 365 cm of lead; the portion above 267 cm for the integral absorption curve was taken from I, fig. 1, and fitted to the corrected curve B at this point. This is justified, firstly because the scattering at high energies is small, and secondly because in the experiment in question the curve between 267 cm and 365 cm was obtained by varying the absorber in the lowest position, where the additional scattering is negligible.

§ 4. SEPARATION OF THE ELECTRONIC COMPONENT

The low-energy region of the absorption curve will be a compound of the penetrating component and the electronic (soft) component. The complete separation of these two components is not easy, and the results now presented are intended merely to indicate the trend of the curve for the penetrating particles of low energy. More precise experiments are projected.

The method adopted for separating the two components is that used by Hall (1944) modified by the addition of an anti-coincidence tray to permit the measurement of the differential absorption curve. A diagram of the apparatus is shown

in fig. 2 (inset). The object of the 1.27 cm ($\frac{1}{2}$ in.) absorber I is to convert to showers as high a proportion as possible of the electronic component, and its vertical position is adjusted for maximum shower detection by trays 2 + 3 in which alternate counters are connected in parallel.

The coincidence counts, 1, 2+3, 4; 1, 2+3, 4, A; and 1, 2, 3, 4, A were recorded. 1, 2+3, 4 gives the counting rate of all events passing through the telescope together with accidentals* and side-showers. 1, 2+3, 4, A gives the counting rate of all events passing through the telescope and failing to reach A. This will be made up of single particles stopping in absorber III, together with showers of particles passing through the telescope, some or all of which stop in III, the remainder in any case missing A.

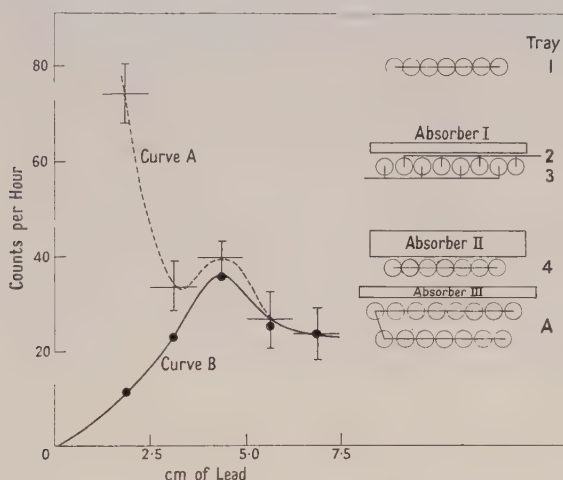


Fig. 2. Differential absorption curve for non-electronic component.

Curve A. Experimentally determined curve.

Curve B. Differential absorption curve derived from curve A after correction for inefficiency of apparatus in separating out the electronic component. Vertical limits are standard deviations for many readings on each point, fluctuations being due to atmospheric changes.

Inset. Diagram of apparatus for measuring electronic and non-electronic components.

This shower group is represented by count 1, 2, 3, 4, A. The more efficient the conversion of electrons to showers and the more efficient the shower detection, the more nearly will this count represent the total electronic component and therefore the more nearly will the difference between counts 1, 2+3, 4, A and 1, 2, 3, 4, A represent the non-electronic component. We shall denote this difference by N_p .

This method of separation is not very satisfactory for not only is the efficiency of shower production and detection, in general, less than 100% but it decreases rapidly with decreasing energy. The first experiment was performed under a concrete roof of 12.5 g/cm² (equivalent to about 1 cm of lead) with a mean semi-angular aperture of 6°, and the second experiment was performed out of doors (with less than 1 g/cm² above the apparatus) with the counter trays of larger area with a mean semi-angular aperture of 13.5°. Although the resolving power of this second arrangement is not so great, the results obtained are more reliable because of the

* These 'background' events will contribute to all counts and will not be mentioned explicitly each time. Further, all anti-coincidence counts must be corrected for background counts with absorber III removed as explained earlier.

much faster counting rates. The curves given in fig. 2 are for this second experiment and are in general agreement with those obtained in the first experiment. The dotted curve represents N_p uncorrected for the shower-detection inefficiency of the apparatus. The vertical lines on each point do not denote the statistical fluctuations which are much smaller, but are the standard deviations calculated from many readings taken on each point, the fluctuations being due to atmospheric changes—a matter which does not lend itself so readily to correction at the low-energy end of the spectrum. The full curve in fig. 2 is the differential curve for the non-electronic component after correction for inefficiency in shower production and detection. The correction involves estimating the efficiency of absorber I in converting electrons into showers, the efficiency of tray 2 + 3 in detecting showers which fall on it, and the probability that an electron of given energy will be detected as a shower producing particle and that the shower will have a range between d cm and $d + 1.27$ cm of lead. It is unnecessary to give a detailed account of the method of correction as it cannot be estimated with great accuracy, but it does verify the existence of a maximum in the non-electronic component in the region between 3.75 cm and 5.0 cm of lead, a maximum of which there is already evidence in the uncorrected curve. The curves in fig. 2 have not been corrected for scattering, but it is immediately obvious from the arrangement of the apparatus that most of the scattering will be due to the 1.27 cm of lead of absorber I. The corrections for scattering due to absorber I will require a steadily increasing positive correction to the differential absorption curve with decreasing total absorber thickness. This correction will not change appreciably either the general shape of the curve or the position of the maximum.

§ 5. MOMENTUM DISTRIBUTION AND DISCUSSION

In order to deduce the momentum spectrum from the differential absorption curves of figs. 1 and 2, it is necessary to make an assumption about the nature of the penetrating particles. The full-line curve of fig. 3 is a plot of the momentum distribution deduced from figs. 1 and 2, *on the assumption that all the particles contributing to these curves are μ -mesons*. This conversion was made with the range-momentum curve given by Halpern and Hall (1948). The above assumption is only correct if the electronic component has been eliminated and if the contribution from charged particles of mass greater than that of μ -mesons is negligible. These points will be discussed later.

The dotted curve of fig. 3 is the composite curve by Rossi (1948), combining all results up to 1948 and including the results of Sands (1950). Later work tends to be in general agreement with this curve. Above 1 kmev/c, the Rossi curve is based on absorption measurements under water and underground, by Ehmert (1937), Wilson (1938) and others, and is confirmed by the cloud chamber-magnetic field method. The present work is substantially in agreement with the Rossi curve in this region, and needs no further comment. Below 1 kmev/c, the Rossi curve is based on absorption measurements using coincidence, anti-coincidence and delayed coincidence methods, and on the cloud chamber-magnetic field method.

Before comparing the results of the present work with the Rossi curve below 1 kmev/c, we will consider the experiments on which it is based and also discuss subsequent work.

It has been pointed out in I that the coincidence method is unsuitable for the low momentum region, unless a control telescope is employed and corrections are

made for scattering. Most of the early absorption experiments do not fulfil these requirements, and the plateaux and irregularities which were found in the absorption curve below 30 cm of lead, i.e. suggesting a sudden drop (or a zero) in the momentum spectrum around 0.5 kmev/c, are spurious.

The anti-coincidence method is preferable to the coincidence method, but is still subject to a scattering correction. We are of the opinion that Kellermann and Westerman (1949) have not made adequate corrections for the scattering of the low momentum particles.

The delayed coincidence method used by Kraushaar (1949) and Sands (1950) definitely selects μ -mesons, and should give reliable results provided the fraction of positive to negative mesons is known as a function of momentum, and the correction for scattering is applied. Unlike the coincidence and anti-coincidence methods, the delayed coincidence method is only suitable for comparative measurements, as the detection efficiency of the delayed coincidence events can only be approximately assessed.

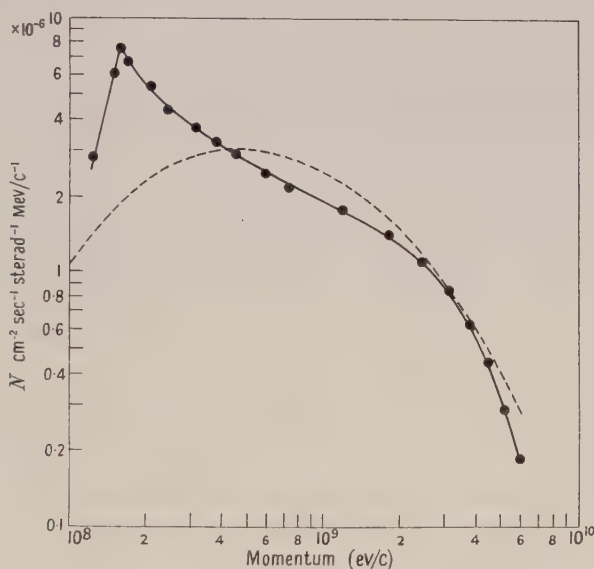


Fig. 3. Momentum distribution of penetrating component. Full line curve is derived from present experimental results assuming all the penetrating particles are μ -mesons. Broken line curve is that given by Rossi for the meson component.

The cloud chamber-magnetic field measurements are subject to a cut-off correction which increases with decreasing particle momentum, and is generally only approximately determined. Further, when control counters are used to trigger the apparatus, scattering corrections may be necessary when any absorbers are used.

Using a magnetic spectrograph Caro, Parry and Rathgeber (1950) have confirmed the Rossi momentum spectrum. The rather sudden drop below 0.4 kmev/c may be partly due to scattering, as most of the slow particles are thrown to the edge of the telescope. Further, the correction for magnetic cut-off in this region must be large.

Finally, York (1952 a), using a cloud chamber without a magnetic field, but with several absorber plates within the chamber, states that his results are not

inconsistent with the Rossi curve, but a decrease in the intensity below 0.4 kmev/c is not conclusive from his work. On the other hand, it can also be stated that the results of a number of the experiments discussed above, are not inconsistent with some rise in the curve below 0.4 kmev/c, but not rising to a peak as sharply as shown in the present results.

The only significant divergence between the results of the present work and the Rossi curve is the sharp rise from the Rossi curve below 0.4 kmev/c, and the pronounced maximum at 0.16 kmev/c. There are two factors which might contribute to this divergence. In the first place, it is possible that the electron component has not been completely eliminated. This is possible for the region below 7.5 cm of lead (corresponding to about 0.2 kmev/c for μ -mesons) and may account to a small extent for the sharp maximum, but we do not believe that this contribution can be large. Furthermore, the sudden drop below 4.5 cm of lead (approximately 0.16 kmev/c) may not be as rapid as indicated, as the two lowest points are subject to a large error, being obtained as the difference of two large quantities. However, a maximum at 4.5 cm (0.16 kmev/c) appears to be quite definite, and is apparent even before the correction for inefficiency of detection of the soft component is made (see fig. 2).

The second factor which may contribute to the pronounced peak in our results below 0.4 kmev/c is the presence of protons in the penetrating component. If we assume, for the sake of discussion, that the whole of the difference between our curve and the Rossi curve below 20 cm of lead (i.e. below 0.4 kmev/c for μ -mesons) is due to protons (which would imply a proton component of at least 6.6% of the total penetrating component), then the momentum distribution curve for these protons would fall in the region 0.5–1.2 kmev/c (considering ionization loss only). The present results would then agree everywhere with the Rossi curve to within 25%.

There is considerable doubt as to the magnitude of the proton component at sea level. Germain (1950), using a cloud chamber containing several lead plates and controlled by a counter telescope, "identified very few protons", although they would not easily be distinguished from mesons by this method in the region examined. Goldwasser and Merkle (1951), using two cloud chambers to measure momentum and range respectively, identified 72 protons to 161 μ -mesons, but in this case the lead absorber was placed above the controlling counter telescope and, as the authors point out, many of the protons were probably produced by neutrons in the lead absorbers. Mylroï and Wilson (1951) using the magnetic spectrograph, came to the conclusion that protons with momentum exceeding 1 kmev/c contribute about 1% to the penetrating component and, using the value for the proton component at about 0.5 kmev/c as determined by Rochester and Bound (1940), assumed that there are very few protons below 1 kmev/c. This assumption is not in agreement with the results of York (1952 a) which do not indicate a rapid decrease in intensity for low-energy protons. However, York (1952 b) has recently indicated that the point obtained by Rossi (1948), based on the data of Rochester and Bound (1940), has been placed much too low, partly due to a misprint in Rossi's paper. The corrected value is in reasonable agreement with the results of York and of other investigators, but the more recent results favour a higher proton flux.

As a consequence of the above discussion it is not improbable that protons with momentum greater than 0.5 kmev/c, should account for at least 2% of the total penetrating component at sea level.

§ 6. CONCLUSIONS

It is seen from the preceding work that considerable care must be taken to correct for the scattering of mesons by the absorbing material and that this varies with the position and shape of the absorber. The result of the present work, after this correction is made, is to give a momentum spectrum for mesons differing considerably from that given by Rossi in the region below 0.4 kmev/c. It is suggested that part of this difference is to be expected because the proton component is included in the present work and that there may also be a small electron component which was not completely eliminated. The remaining difference is more probably due to the care taken in the present work to correct for scattering. Nevertheless, it is quite definite that the present results indicate that the momentum distribution curve in the region below 0.4 kmev/c lies above that given by Rossi, but the sharp peak in fig. 3 may quite likely disappear if the proton component were subtracted.

APPENDIX

SCATTERING CORRECTION

As scattering may have considerable effect on the slope of the absorption curve it is important to record in some detail the method adopted for applying the scattering correction.

To enable a correction factor for scattering to be calculated the following experiment was made: The counter telescope of fig. 1 was used with the absorber III retained at 10 cm of lead; absorber II was kept fixed at 10 cm of lead; absorber I was replaced by an absorber S (the scatterer) whose vertical height within the telescope could be varied.

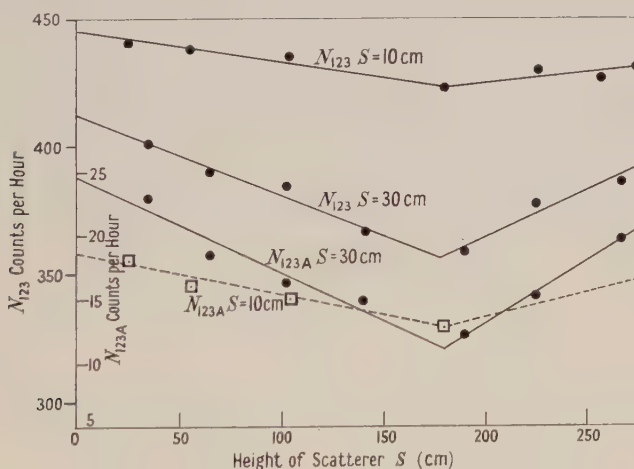


Fig. 4. Curves showing the plot of number of particles recorded against position of absorber within the telescope. The two upper curves show the variation of the total count for scatterers of thickness 10.16 cm and 30.48 cm respectively. The two lower curves show the corresponding variation for particles with ranges in lead between 20.32 cm and 30.48 cm and between 40.64 cm and 50.8 cm respectively.

In fig. 4 the counting rates N_{123} and N_{123A} are plotted against the height of the midpoint of S above the anodes of the counters in tray 3. Curves are given for

both $S = 10$ cm and $S = 30$ cm of lead, N_{123} being corrected for both accidentals and showers and N_{123A} for background, so that the variations in these counts are due solely to scattering. The minimum in these scattering curves can be understood if it is remembered that scattering out of the telescope will be small when S is near tray 3, and scattering into the telescope will be most effective when S is at its maximum height, that is, just below tray 1. These two effects when taken together will tend to give a minimum count at some point intermediate between the two extreme positions of S .

To use these results to calculate the scattering correction to be applied to the experimental results, the following assumptions were made.

Assumption 1. That for a given thickness of S the scattering correction was zero at zero height, increased linearly with height up to a height of 183 cm, then decreased linearly to zero at the maximum height of 335 cm in accordance with results in fig. 4, and that this was true for particles of all energies.

Assumption 2. That the scattering by a thick absorber took place abruptly in steps of 10 cm and that all the scattering took place at its horizontal medial plane.

Assumption 3. That these partial scattering corrections were additive.

Assumption 4. That the net fraction of mesons scattered out of the telescope by a 10 cm scatterer, i.e. the excess of those scattered out over those scattered in, within an incident momentum interval p to $p + \Delta p$ is proportional to $\Delta p/p$.

Assumption 5. That the net number of mesons scattered out of the telescope by 10 cm of lead at a height of 183 cm and whose range lies between 40 cm and 50 cm of lead is 2.80 per hour.

The justification for these assumptions is fairly obvious; assumption 4 derives from the theory of multiple scattering and assumption 5 is the experimental result.

The numerical procedure necessary to calculate the correction to be applied to the absorption curve is straightforward and will not be reproduced here.

REFERENCES

- BLACKETT, P. M. S., 1937, *Proc. Roy. Soc. A*, **159**, 1.
 BLACKETT, P. M. S., and BRODE, R. B., 1936, *Proc. Roy. Soc. A*, **154**, 573.
 CARO, D. E., PARRY, J. K., and RATHGEBER, H. D., 1950, *Nature, Lond.*, **165**, 689.
 EHMERT, A., 1937, *Z. Phys.*, **106**, 751.
 GERMAIN, L. S., 1950, *Phys. Rev.*, **80**, 616.
 GLASER, D. A., HAMERMESH, B., and SAFONOV, G., 1950, *Phys. Rev.*, **80**, 625.
 GOLDWASSER, E. L., and MERKLE, T. C., 1951, *Phys. Rev.*, **83**, 43.
 HALL, D. B., 1944, *Phys. Rev.*, **66**, 321.
 HALPERN, O., and HALL, H., 1948, *Phys. Rev.*, **73**, 477.
 HEYLAND, G. R., and DUNCANSON, W. E., 1953, *Proc. Phys. Soc. A*, **66**, 33.
 HUGHES, D. J., 1940, *Phys. Rev.*, **57**, 592.
 JONES, H., 1939, *Rev. Mod. Phys.*, **11**, 235.
 KELLERMANN, E. W., and WESTERMAN, K., 1949, *Proc. Phys. Soc. A*, **62**, 356.
 KRAUSHAAR, W. L., 1949, *Phys. Rev.*, **76**, 1045.
 KÜNZE, P., 1932, *Z. Phys.*, **79**, 203.
 MYLROI, M. G., and WILSON, J. G., 1951, *Proc. Phys. Soc. A*, **64**, 404.
 ROCHESTER, G. D., and BOUND, M., 1940, *Nature, Lond.*, **146**, 745.
 ROSSI, B., 1948, *Rev. Mod. Phys.*, **20**, 543.
 SANDS, M., 1950, *Phys. Rev.*, **77**, 180.
 SARABHAI, V., 1944, *Phys. Rev.*, **65**, 250.
 WILSON, J. G., 1946, *Nature, Lond.*, **158**, 414.
 WILSON, V. C., 1938, *Phys. Rev.*, **53**, 337.
 YORK, C. M., 1952 a, *Phys. Rev.*, **85**, 998; 1952 b, *Proc. Phys. Soc. A*, **65**, 558.

Some Aspects of the Altitude Variation of Extensive Air Showers.

By A. L. HODSON*

The Physical Laboratories, University of Manchester

Communicated by P. M. S. Blackett; MS. received 21st August 1952

ABSTRACT. γ , the exponent of the density spectrum of extensive air showers, is found to increase from 1.445 ± 0.014 at sea level to 1.549 ± 0.018 at 26 000 ft. The values quoted are mean values for the density range 50–500 particles per square metre. The increase is considerably less than that predicted by cascade theory on the primary electron hypothesis. It is suggested that the discrepancy may be explained by the formation of secondary cascade showers in a nucleon cascade process.

Extensive air showers recorded by a fixed experimental arrangement show a maximum frequency at about 26 000 ft. (8000 m). At that altitude the shower rate is found to be 42 times the rate at sea level. The barometer coefficient of extensive air showers at sea level is found to be $-(9.0 \pm 1.1)\%$ per cm Hg.

Details are given of the quenching and hodoscope circuits used with the counters.

§ 1. INTRODUCTION

Cocconi, Loverdo and Tongiorgi (1946a) and others have shown that the frequency of extensive air showers incident on a given small area with a density greater than Δ particles per square metre can be expressed by a power law: $I(\Delta) = B\Delta^{-\gamma}$ where B and γ are constants to a first order of approximation, $B \sim 620 \text{ m}^{-2} \text{ h}^{-1}$ and $\gamma \sim 1.45$ at sea level. This empirical law has been widely used to calculate the rate at which extensive air showers discharge various arrays of Geiger-Müller counters. The assumptions usually made to facilitate such a calculation are (a) that the extent of the apparatus is sufficiently small compared with the average spread of extensive showers for the particle density to be regarded as uniform over the apparatus, and (b) that the particles are randomly distributed in a horizontal plane.

The rate at which extensive air showers are recorded by counter trays of areas F_1, F_2, \dots, F_n in n -fold coincidence is then given by

$$R(F_1, F_2, \dots, F_n) = B\gamma \int_0^\infty \{1 - \exp(-F_1\Delta)\} \dots \{1 - \exp(-F_n\Delta)\} \frac{d\Delta}{\Delta^{\gamma+1}}.$$

Such integrals may readily be evaluated by the method of Broadbent and Jánosy (1948).

Two of the methods commonly used for the determination of γ will now be considered.

Method A. Suppose we have $n+1$ trays of counters of equal area F and we record $(n+1)$ -fold coincidences, M_{n+1} , and n -fold coincidences, M_n . If the above assumptions are made the ratio of the two coincidence rates may be expressed as a function of γ only (Cocconi and Tongiorgi 1949):

$$\frac{M_{n+1}}{M_n} = \frac{{}^{n+1}C_1 - {}^{n+1}C_2 2^\gamma + {}^{n+1}C_3 3^\gamma - \dots}{{}^nC_1 - {}^nC_2 2^\gamma + {}^nC_3 3^\gamma - \dots}.$$

* Now at the Palmer Physical Laboratory, Princeton University, New Jersey, U.S.A.

Method B. Cocconi *et al.* (1946 a), Daudin (1947) and others have shown that the rate of coincidences between counter trays of areas $\alpha F_1, \alpha F_2, \dots \alpha F_n$ is given by

$$R(\alpha F_1, \alpha F_2, \dots \alpha F_n) = \alpha^\gamma R(F_1, F_2, \dots F_n).$$

Thus if the areas of the counter trays are simultaneously varied by a factor α the counting rate varies by a factor α^γ .

The results of previous investigations at low altitudes (Cocconi *et al.* 1946 a, Treat and Greisen 1948, Loverdo and Daudin 1948) show that Method A usually gives appreciably higher values of γ than Method B (~ 1.55 – 1.65 and ~ 1.45 , respectively, at sea level). Broadbent *et al.* (1950) have shown that Method A is particularly sensitive to density gradients in the showers and, as a result, tends to give too high a value of γ . However, on the reasonable assumption that all extensive showers at a given altitude possess a similar structure it can be shown that Method B is insensitive to density gradients in the showers (Ise and Fretter 1949) and yields a reliable value of γ . In the present work the main emphasis is therefore placed on results obtained by this method.

§ 2. THE EXPERIMENTAL ARRANGEMENT

Three trays of copper-in-glass argon-ether Geiger-Müller counters were arranged as shown in fig. 1. Trays E_I and E_{II} each contain three counters of 'unit area' ($45 \text{ cm} \times 3 \text{ cm}$, sensitive area $\sim 119 \text{ cm}^2$) and one counter of 'half-unit area' ($23.5 \text{ cm} \times 3 \text{ cm}$, sensitive area $\sim 60 \text{ cm}^2$). Tray E_{III} contained seven counters of unit area and three of half-unit area. The counter boxes were of dural, 0.7 mm thick.

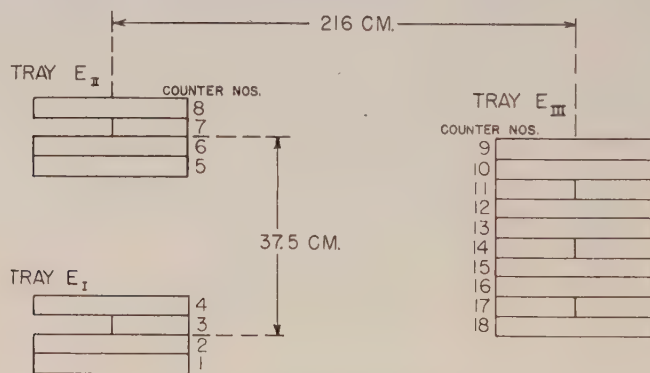


Fig. 1. Plan view of trays.

The discharges of each counter were rapidly quenched by $10\text{-}\mu\text{sec}$ single-shot multivibrators, the effective insensitive time of the counters thereby being considerably reduced (see Appendix). Whenever a threefold coincidence occurred between trays E_I , E_{II} and E_{III} a 'master pulse' was applied to a 'mixing stage' associated with each counter. Those counters which had been discharged were then identified by flashes in a row of neon lamps, the flashes being recorded photographically on a continuously moving film. Details of the hodoscope circuit are given in the Appendix.

The apparatus was installed in the rear compartment of an R.A.F. Mosquito aircraft under a roof of 0.5 g/cm^2 of plywood and in a region free from dense

local material. Flights were made at various altitudes between 15 000 ft. and 33 500 ft. At sea level the equipment was operated in a laboratory with a light roof and the geometrical arrangement of the counter trays was identical with that used for the flights.

In analysing the hodoscope records it is necessary to assume that the counters considered in any particular shower are discharged by different particles, i.e. that no single shower particle can strike more than one counter. If the counters in a tray are sufficiently near together for single inclined shower particles to discharge two or more of them with an appreciable frequency, the number of high density showers will be over-estimated. The result will be that the value of γ deduced from the hodoscope records will be too low.

In an ideal hodoscope arrangement for recording showers the counters in a tray are therefore placed sufficiently far apart for the effect of inclined shower particles to be negligible. Unfortunately this was not possible in the present experimental arrangement owing to lack of space in the aircraft. The same hodoscoped counter trays were used for an experiment on extensive penetrating showers (Hodson 1952). This necessitated the use of as large counter areas as possible, and the available space was therefore fully occupied by counters placed close together. However, in the analysis of the hodoscope records for extensive air showers only alternate counters were considered together, so that the minimum distance between any two counters considered was one counter diameter, i.e. 3 cm. In order to discharge two counters with this separation a particle had to be incident at an angle greater than 63° to the vertical. The counters were divided into two groups, group A consisting of counters Nos. 2, 4, 6, 8, 10, 12, 16, 18 and group B consisting of the alternate counters Nos. 1, 3, 5 . . . 17 (see fig. 1). The two groups were then analysed separately. A minimum requirement in the number of counters discharged in either group was one counter in each of the trays E_I , E_{II} and E_{III} . Although a high density shower could thus be recorded as a shower discharging both group A and group B shower sets, this type of event presented a sufficiently small fraction of the shower rate of either group ($\sim 35\%$) for the two groups to be regarded as independent shower sets.

It will be shown later that with the counters of a group at least 3 cm apart the effect of inclined shower particles is small even at the highest altitudes reached in the present experiments.

§ 3. THE DETERMINATION OF γ BY THE METHOD OF VARIATION OF AREAS

3.1. *Theoretical Discussion of the Method*

We now describe a method of analysis of the hodoscope record which is essentially the method of 'variation of areas' (Method B above). The method will be described in a general form before being applied to the particular experimental arrangement used here.

Suppose that we have three trays A, B, C containing N_A , N_B , N_C counters, respectively, and that the counters are each of unit area. Consider now particular sub-groups (each of area n) of counters in the three trays. Suppose that the core of an incident air shower containing N particles falls at a distance r_1 from the first sub-group, r_2 from the second, and r_3 from the third. The densities at these sub-groups will then be $\Delta_1 = Nf(r_1)$, $\Delta_2 = Nf(r_2)$ and $\Delta_3 = Nf(r_3)$,

where $f(r)$ is the structure function of the shower. The probability that this shower will be recorded is

$$\{1 - \exp(-n\Delta_1)\}\{1 - \exp(-n\Delta_2)\}\{1 - \exp(-n\Delta_3)\}.$$

The rate of threefold coincidences $R(n, n, n)$ between the three sub-groups n is obtained by integrating this expression over a horizontal plane and over all showers. Assuming that the (integral) size spectrum of extensive showers follows a power law $KN^{-\gamma_N}$ and that all the showers possess a similar structure, we have (cf. Ise and Fretter 1949)

$$R(n, n, n) = 2\pi\gamma_N K \int_{N=0}^{\infty} \int_{r=0}^{\infty} \int_{\theta=0}^{\pi/2} \frac{2}{\pi} \{1 - \exp(-n\Delta_1)\}\{1 - \exp(-n\Delta_2)\} \\ \times \{1 - \exp(-n\Delta_3)\} \frac{dN}{N^{\gamma_N+1}} r dr d\theta \quad \dots\dots(1)$$

It can be shown that $R(\alpha n, \alpha n, \alpha n) = \alpha^{\gamma_N} R(n, n, n)$. Method B thus yields γ_N , the exponent of the size spectrum of the showers. γ_N may therefore be identified with γ , the exponent of the density spectrum, and in future we shall not distinguish between the two.

The principle of the method consists in observing the change in the coincidence rate as the area n of the sub-groups is varied. Obviously, one method of obtaining $R(n, n, n)$ would be to choose three particular groups of counters and scan the hodoscope record, picking out those showers which discharged the three groups simultaneously. However, there are many ways of choosing such groups out of the three trays. To make the most use of the data available on the hodoscope record would necessitate scanning the record for each possible combination of sub-groups, a formidable task with a large number of hodoscoped counters. Further, the results for different combinations of sub-groups would not be strictly independent.

These difficulties are avoided in the following way. We first relate expression (1) to the distribution of neon flashes observed when showers are recorded by the three trays A, B and C.* Consider a *particular* area n of one of the trays. The probability that a shower of density Δ_1 at this tray discharges this area is $P(n) = \{1 - \exp(-n\Delta_1)\}$, and this may be expressed as the sum of the probability that the area n is discharged, but not the remaining area $N-n$ of the tray, and the probability that both the areas n and $N-n$ are discharged; here and in the equations below N is written for N_A if tray A is considered, etc. We may thus write

$$P(n) = \{1 - \exp(-n\Delta_1)\}[\exp\{-(N-n)\Delta_1\} + 1 - \exp\{-(N-n)\Delta_1\}]. \quad \dots\dots(2)$$

We may also write

$$1 - \exp(-n\Delta_1) = {}^nA_1 {}^nP_1 + {}^nA_2 {}^nP_2 + \dots + {}^nA_s {}^nP_s + \dots + {}^nA_n {}^nP_n,$$

where nP_s is the probability that (exactly) s counters out of the area n are discharged and nA_s is the number of ways in which we can select s counters out of the area n . The second bracket in (2) may be expressed in a similar manner. We thus have

$$P(n) = ({}^nA_1 {}^nP_1 + {}^nA_2 {}^nP_2 + \dots + {}^nA_s {}^nP_s + \dots + {}^nA_n {}^nP_n) \\ \times [{}^{N-n}A_0 {}^{N-n}P_0 + {}^{N-n}A_1 {}^{N-n}P_1 + \dots + {}^{N-n}A_s {}^{N-n}P_s + \dots \\ + {}^{N-n}A_{N-n} {}^{N-n}P_{N-n}]. \quad \dots\dots(3)$$

* We are indebted to Prof. L. Jánosy and Mr. D. Broadbent for suggesting this approach to the problem.

Similarly for the other trays $1 - \exp(-n\Delta_2) = Q(n)$ and $1 - \exp(-n\Delta_3) = R(n)$.

$$\text{Then } R(n, n, n) = 2\pi\gamma K \int_{N=0}^{\infty} \int_{r=0}^{\infty} \int_{\theta=0}^{\pi/2} \frac{2}{\pi} P(n)Q(n)R(n) \frac{dN}{N^{\gamma+1}} r dr d\theta. \dots\dots(4)$$

For a given experimental arrangement the terms in this integral may readily be expressed in terms of the distribution of neon flashes observed for trays A, B and C. This can be seen by considering the present experimental arrangement.

Counter Group A. Let us consider counter group A (two counters of unit area in each of the trays E_I and E_{II} , and four counters of unit area in tray E_{III}), and let us first evaluate $R(1, 1, 1)$. Considering tray E_I we have $N=2$ and $N-n=1$. Then (by definition of ${}^n P_s$)

$$P(n) = P(1) = {}^1 A_1 {}^1 P_1 \times ({}^1 A_0 {}^1 P_0 + {}^1 A_1 {}^1 P_1) = {}^1 P_1 ({}^1 P_0 + {}^1 P_1) = {}^2 P_1 + {}^2 P_2$$

Similarly for tray E_{II} $Q(1) = {}^2 Q_1 + {}^2 Q_2$. For tray E_{III} we have $N=4$ and $N-n=3$. Therefore $R(1) = {}^4 R_1 + 3{}^4 R_2 + 3{}^4 R_3 + {}^4 R_4$ and

$$R(1, 1, 1) = 2\pi\gamma K \int_{N=0}^{\infty} \int_{r=0}^{\infty} \int_{\theta=0}^{\pi/2} \frac{2}{\pi} ({}^2 P_1 + {}^2 P_2) ({}^2 Q_1 + {}^2 Q_2) \\ \times ({}^4 R_1 + 3{}^4 R_2 + 3{}^4 R_3 + {}^4 R_4) \frac{dN}{N^{\gamma+1}} r dr d\theta.$$

$$\text{A typical term in } R(1, 1, 1) \text{ is thus: } (\text{const})\gamma K \int_{N=0}^{\infty} \int_{r=0}^{\infty} \int_{\theta=0}^{\pi/2} {}^2 P_p {}^2 Q_q {}^4 R_r \frac{dN}{N^{\gamma+1}} r dr d\theta.$$

But this is just the number of showers in which a *particular* set of p counters are discharged in tray E_I , a particular set q in tray E_{II} , and a particular set r in tray E_{III} . Denote this number by (p, q, r) . Then

$$R(1, 1, 1) = (1, 1, 1) + 3(1, 1, 2) + 3(1, 1, 3) + (1, 1, 4) \\ + (1, 2, 1) + 3(1, 2, 2) + 3(1, 2, 3) + (1, 2, 4) \\ + (2, 1, 1) + 3(2, 1, 2) + 3(2, 1, 3) + (2, 1, 4) \\ + (2, 2, 1) + 3(2, 2, 2) + 3(2, 2, 3) + (2, 2, 4). \dots\dots(5)$$

Each term (p, q, r) may be found in the following way. If the number of ways of choosing the particular sets p, q, r of counters is W_{pqr} and if F_{pqr} denotes the number of showers in which any p counters in tray E_I , any q in E_{II} and any r in E_{III} are discharged we have $(p, q, r) = F_{pqr}/W_{pqr}$. The first step in the analysis of the hodoscope record is thus to classify each shower according to the number of counters discharged in the three trays. Hence F_{pqr} is obtained. Since W_{pqr} is a constant which may readily be written down for any given experimental arrangement (p, q, r) may be found immediately.

(For example, the number of ways of choosing one counter in tray E_I , one in E_{II} and two in E_{III} in counter group A is $W_{112} = 2 \times 2 \times 6 = 24$. Thus if 65 showers are observed in which one counter is discharged in E_I , one in E_{II} and two in E_{III} , $F_{112} = 65$ and $(p, q, r) = 65/24$.)

Having obtained the terms (p, q, r) , $R(1, 1, 1)$ is easily found from expression (5) above. Expressions for $R(2, 2, 2)$ and $R(1, 1, 2)$ may be deduced in a similar way to that used above for $R(1, 1, 1)$.

For counter group A the total number of showers recorded is equal to $R(2, 2, 4)$.

$$\text{Now} \quad R(2, 2, 2)/R(1, 1, 1) = 2^\gamma \quad \dots\dots (6)$$

$$\text{Similarly} \quad R(2, 2, 4)/R(1, 1, 2) = 2^\gamma \quad \dots\dots (7)$$

Counter Group B. The second group of counters consisted of one counter of unit area and one of half unit area in each of the trays E_I and E_{II} , together with three counters of unit area and two of half unit area in tray E_{III} . Using the method of analysis described above, expressions for $R(\frac{1}{2}, \frac{1}{2}, \frac{1}{2})$, $R(1, 1, 1)$ and $R(1\frac{1}{2}, 1\frac{1}{2}, 1\frac{1}{2})$ may be obtained in terms of the observed neon distribution. Then

$$R(1, 1, 1)/R(\frac{1}{2}, \frac{1}{2}, \frac{1}{2}) = 2^\gamma, \quad \dots\dots (8)$$

$$R(1\frac{1}{2}, 1\frac{1}{2}, 1\frac{1}{2})/R(\frac{1}{2}, \frac{1}{2}, \frac{1}{2}) = 3^\gamma, \quad \dots\dots (9)$$

$$\text{and} \quad R(1\frac{1}{2}, 1\frac{1}{2}, 1\frac{1}{2})/R(1, 1, 1) = (1.5)^\gamma \quad \dots\dots (10)$$

The reason for using different arrangements of counters in groups A and B will now be clear; by introducing some counters of half unit area into group B, γ is determined in a rather different way. This is useful in checking the consistency of the method of analysis.

3.2. Corrections Applied to the Experimental Data

Two corrections to the observed neon distribution at high altitudes have to be considered.

Firstly, we must discuss the effect of inefficiency of the counters at the high background rates obtaining at high altitudes. As described in the Appendix, each counter in the trays E_I , E_{II} and E_{III} was connected to a quenching unit which reduced its insensitive time from its normal value of about $300 \mu\text{sec}$ to an effective value of $42 \pm 9 \mu\text{sec}$. The inefficiency of a single $45 \text{ cm} \times 3 \text{ cm}$ counter at 33 500 ft. is then only 0.5%; without the quenching circuit it would be 3.4%. The importance of using counters of high efficiency in work of this nature may be shown by considering the effect of counter inefficiency on the observed neon distribution. For example, with the normal insensitive time 24°_0 of the events F_{224} (two counters discharged in each of the trays E_I , E_{II} and four counters in tray E_{III}) would be missed (cf. 3.7% with the quenching units). Some of the F_{224} events missed would appear as spurious F_{124} , F_{223} events, etc. Although the observed neon distribution can in principle be corrected for these perturbations, it is very undesirable to have to make such large (and rather uncertain) corrections. In order to eliminate any errors due to the small residual inefficiency the neon distribution has been carefully corrected at the two highest altitudes (33 500 ft. and 30 000 ft.). The correction at other altitudes was then easily estimated.

The effect of accidental coincidences on the neon distribution has also been studied. Threefold coincidences of independent particles were found to be of less importance than accidental coincidences of a genuine twofold event and a single independent particle. Using a short resolving time in the hodoscope ($1.2 \mu\text{sec}$) the corrections were sufficiently small to be estimated accurately.

With these precautions the total corrections due to residual counter inefficiency and accidental coincidences then amounted to only -1% in γ at the highest altitude reached.

3.3. The Statistical Error in γ

Due to the limited number of showers recorded, the value of γ which is obtained from any of the above formulae has a certain statistical error (standard deviation), $\Delta\gamma$ obtained by differentiating the formulae.

3.4. The Relative Sensitive Areas of the Counters

In eqns. (8), (9) and (10) it was tacitly assumed that the counters of 'half unit area' had sensitive areas which were exactly half that of the 'unit area' counters. Although the dimensions of the counters were nominally chosen so that this should be so, the uncertainty in the end corrections made it unlikely that this ratio was achieved accurately. We now describe a method of eliminating this uncertainty.

Let the accurate sensitive area of the 'half unit area' counters be a fraction β of that of the 'unit area' counters. Equations (8), (9) and (10) may then be rewritten as follows:

$$R(1, 1, 1)/R(\frac{1}{2}, \frac{1}{2}, \frac{1}{2}) = (1/\beta)^\gamma, \quad \dots\dots(11)$$

$$R(1\frac{1}{2}, 1\frac{1}{2}, 1\frac{1}{2})/R(\frac{1}{2}, \frac{1}{2}, \frac{1}{2}) = \{(1+\beta)/\beta\}^\gamma, \quad \dots\dots(12)$$

$$R(1\frac{1}{2}, 1\frac{1}{2}, 1\frac{1}{2})/R(1, 1, 1) = (1+\beta)^\gamma. \quad \dots\dots(13)$$

We have thus two independent equations which may be solved graphically for β and γ . At sea level we obtain $\gamma=1.45$ and $\beta=0.514$. The mean solution at high altitudes is $\gamma=1.56$ and $\beta=0.511$. The two values of β are not significantly different because of the statistical errors in $R(\frac{1}{2}, \frac{1}{2}, \frac{1}{2})$ etc.

It is important to know accurately the relative sensitive areas of the counters. An error of 1% in β , i.e. an error of only 2 mm in the effective length of a 20 cm counter, gives an error of 0.022 in the value of γ derived from eqn. (13). A determination of the relative sensitive areas by the usual direct method (Greisen and Nereson 1942) to the required accuracy would be very laborious.

3.5. The Experimental Results

The values of γ determined from eqns. (6), (7), (11), (12) and (13) at each altitude are given in table 1. γ_A and γ_B represent the best values of γ obtained with the two counter groups A and B. It is seen that the various methods of determining γ are consistent, allowing for the statistical errors. However, it should be noted that the two methods used to determine γ using counter group A are somewhat interdependent since the calculation of $R(2, 2, 2)$, $R(2, 2, 4)$, etc., partly involves the same data (p, q, r), etc. The same is true of the results obtained using counter group B. This fact has been taken into account when estimating the errors in γ_A and γ_B . The weighted mean of γ_A and γ_B is given at the bottom of table 1 and plotted against atmospheric depth in fig. 2. Since the statistical errors at particular altitudes are rather large, more significant values are obtained by considering all the high-altitude showers together. The results may then be taken to correspond to a mean atmospheric depth of 366 g/cm^2 (26000 ft.). A small but definite increase of γ with altitude is found; the ground-level value is 1.445 ± 0.014 and the value at the mean depth of 366 g/cm^2 is 1.549 ± 0.018 . These results are based on the analysis of some 4000 showers observed at high altitudes and over 7000 at ground level.

3.6. *The Average Density of the Showers Recorded*

The average densities of the showers contributing to the rates $R(n, n, n)$ are given in table 2. The values of γ shown in fig. 2 may be taken as mean values for the density range 50–500 particles per square metre. The variation of counting area which is possible with the present experimental arrangement is too small to give any significant information on the variation of γ with density.

Table 1. γ by Method B

Counter Group A					
Altitude (ft)	No. of showers	γ from $\frac{R(2, 2, 2)}{R(1, 1, 1)}$	γ from $\frac{R(2, 2, 4)}{R(1, 1, 2)}$	γ_A	
33500	220	1.55 ± 0.09	1.57 ± 0.08	1.56 ± 0.07	
30000	668	1.56 ± 0.05	1.54 ± 0.04	1.55 ± 0.04	
27000	335	1.56 ± 0.07	1.55 ± 0.06	1.55 ± 0.05	
25000	195	1.56 ± 0.09	1.52 ± 0.08	1.54 ± 0.07	
23000	495	1.55 ± 0.06	1.51 ± 0.05	1.53 ± 0.04	
22000	150	1.51 ± 0.10	1.56 ± 0.09	1.53 ± 0.08	
20000	174	1.69 ± 0.10	1.64 ± 0.09	1.66 ± 0.08	
All flights together	2293	1.556 ± 0.027	1.537 ± 0.024	1.546 ± 0.021	
Sea level	4085	1.442 ± 0.020	1.446 ± 0.018	1.444 ± 0.016	

Counter Group B					
Altitude (ft)	No. of showers	γ from $\frac{R(1, 1, 1)}{R(\frac{1}{2}, \frac{1}{2}, \frac{1}{2})}$	γ from $\frac{R(1\frac{1}{2}, 1\frac{1}{2}, 1\frac{1}{2})}{R(\frac{1}{2}, \frac{1}{2}, \frac{1}{2})}$	γ from $\frac{R(1\frac{1}{2}, 1\frac{1}{2}, 1\frac{1}{2})}{R(1, 1, 1)}$	γ_B
33500	155	1.43 ± 0.27	1.47 ± 0.16	1.55 ± 0.18	1.49 ± 0.13
30000	518	1.55 ± 0.15	1.58 ± 0.09	1.64 ± 0.10	1.60 ± 0.07
27000	246	1.76 ± 0.22	1.65 ± 0.13	1.47 ± 0.14	1.60 ± 0.10
25000	150	1.47 ± 0.28	1.56 ± 0.17	1.70 ± 0.18	1.60 ± 0.13
23000	355	1.61 ± 0.18	1.59 ± 0.11	1.56 ± 0.12	1.58 ± 0.09
22000	122	1.12 ± 0.31	1.30 ± 0.19	1.59 ± 0.20	1.38 ± 0.15
20000	110	1.85 ± 0.33	1.67 ± 0.20	1.37 ± 0.21	1.58 ± 0.15
All flights together	1698	1.560 ± 0.083	1.559 ± 0.050	1.557 ± 0.054	1.558 ± 0.038
Sea level	3092	1.450 ± 0.060	1.450 ± 0.035	1.448 ± 0.038	1.449 ± 0.028

Altitude (ft)	Final value of γ	Altitude (ft)	Final value of γ	Altitude (ft)	Final value of γ
33500	1.55 ± 0.06	25000	1.55 ± 0.06	20000	1.64 ± 0.07
30000	1.55 ± 0.03	23000	1.54 ± 0.04	All flights together	1.549 ± 0.018
27000	1.56 ± 0.05	22000	1.50 ± 0.07	Sea level	1.445 ± 0.014

3.7. *The Effect of Inclined Showers*

The hodoscope records of counters Nos. 1, 4, 5, 8, 9, 12, 15, 18 (counter group C) were analysed in a manner exactly similar to that used for counter group A. The spacing of adjacent counters in group C is 6 cm instead of the

3 cm spacing in group A; otherwise the two groups are similar. A single particle can only discharge two counters in group C if it is inclined at more than 73° to the vertical (cf. 63° for group A). The values of γ obtained from group C are given in table 3. These values show no significant difference from those obtained

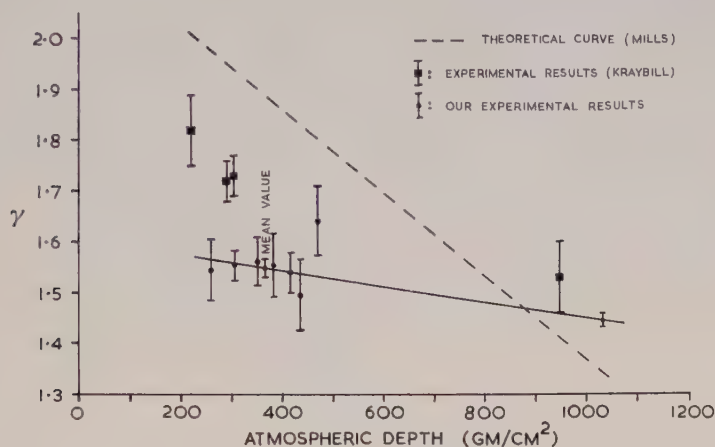


Fig. 2. The altitude variation of γ .

Table 2. Average Shower Densities (particles/m²)

	$R(\frac{1}{2}, \frac{1}{2}, \frac{1}{2})$	$R(1, 1, 1)$	$R(1\frac{1}{2}, 1\frac{1}{2}, 1\frac{1}{2})$	$R(2, 2, 2)$
Sea level	470	240	160	120
High altitudes (~ 26000 ft)	380	190	130	100

Table 3. γ from Counter Group C by Method B

Altitude (ft)	Number of showers	γ from $\frac{R(2, 2, 2)}{R(1, 1, 1)}$	γ from $\frac{R(2, 2, 4)}{R(1, 1, 2)}$	γ_c
33500	203	1.46 ± 0.09	1.48 ± 0.08	1.47 ± 0.07
30000	721	1.62 ± 0.05	1.59 ± 0.04	1.60 ± 0.04
27000	328	1.52 ± 0.07	1.52 ± 0.06	1.52 ± 0.05
25000	202	1.62 ± 0.09	1.59 ± 0.08	1.61 ± 0.07
23000	535	1.59 ± 0.06	1.56 ± 0.05	1.57 ± 0.04
22000	161	1.56 ± 0.10	1.56 ± 0.09	1.56 ± 0.08
20000	189	1.64 ± 0.10	1.62 ± 0.09	1.63 ± 0.08
All flights together	2406	1.575 ± 0.027	1.557 ± 0.024	1.566 ± 0.021
Sea level	4194	1.462 ± 0.020	1.464 ± 0.018	1.463 ± 0.016

from group A (γ_A in table 1). The error in γ_A due to the effect of particles inclined between 63° and 73° to the vertical is thus small. We conclude that the final values of γ given in the last column of table 1 are not seriously in error because of inclined showers.

§ 4. THE DETERMINATION OF γ BY METHOD A

The hodoscope record has also been analysed for γ by Method A. The counters were considered as four groups: Group I, counters Nos. 1-4; Group II, counters Nos. 5-8; Group III, counters Nos. 9-12; Group IV, counters Nos. 15-18 (fig. 1). Threefold coincidences (I, II, III) and (I, II, IV), and also fourfold coincidences (I, II, III, IV) were picked out. We then have

$$\frac{\text{average number of threefold coincidences}}{\text{number of fourfold coincidences}} = \frac{4 - 6 \cdot 2^\gamma + 4 \cdot 3^\gamma - 4^\gamma}{3 - 3 \cdot 2^\gamma + 3^\gamma}.$$

This equation is best solved graphically. The values of γ thus obtained are given in table 4. As expected, the ground level value (1.584 ± 0.015) is considerably higher than that obtained by Method B (1.445 ± 0.014). Broadbent *et al.* (1950) have ascribed the high values of γ which are obtained by Method A at sea level to density gradients in the showers. It is interesting to note that the present results confirm this interpretation. For at high altitudes (i.e. at lower pressures) the average spread of a shower is larger than at sea level. The effective separation of the counters in a fixed experimental arrangement thus decreases with increasing altitude and the shower density is then more likely to be uniform over the extent of the apparatus. At high altitudes the value of γ obtained by Method A may therefore be expected to approach asymptotically the true value obtained by Method B. The mean value of γ found by Method A at high altitudes (1.559 ± 0.020) is, in fact, in excellent agreement with that found by Method B (1.549 ± 0.018). Since the value of γ obtained by Method A shows no increase with altitude, the effect produced by density gradients in showers apparently is sufficient to mask the true increase with altitude.

Table 4. Determination of γ by Method A

Altitude (ft)	4-fold coinc. (I, II, III, IV)	3-fold coinc. (I, II, III)	3-fold coinc. (I, II, IV)	γ (method A)
33500	209	312	323	1.41 ± 0.07
30000	650	1055	1112	1.61 ± 0.04
27000	333	515	527	1.50 ± 0.05
25000	207	321	333	1.52 ± 0.07
23000	500	802	832	1.59 ± 0.04
22000	159	250	245	1.49 ± 0.08
20000	168	281	286	1.65 ± 0.07
Total*	2286	3634	3756	1.559 ± 0.020
Sea level	4010	6522	6537	1.584 ± 0.015

* All high altitude results together (mean altitude 26000 ft.)

§ 5. DISCUSSION OF RESULTS AND COMPARISON WITH PREVIOUS WORK

While the present flights were in progress, Kraybill (1949) reported measurements of γ at altitudes up to 12000 m. The only other investigations made at aeroplane altitudes are those of Maze, Fréon and Auger (1948) at 6700 m. In both these investigations only Method A was used. Maze *et al.* observed a lower value of γ at 6700 m than at sea level, while Kraybill found γ to increase with altitude. The data for sea level and mountain altitudes are similarly inconsistent. Using Method A, Auger and Daudin (1945) found γ

lower at mountain altitudes than at sea level, while with Method B Cocconi, Loverdo and Tongiorgi (1944, 1946 b) found an increase with altitude. Cocconi and Tongiorgi (1949) combined results obtained by Methods A and B and found no significant change between 260 m and 3260 m. The reasons for these inconsistencies have been discussed by Broadbent *et al.* (1950).

The most significant results for comparison with those of the present work are the high altitude results of Kraybill (1949). Our results by Method A show no significant change with altitude, whereas Kraybill, by the same method, obtained an increase. The discrepancy probably arises because the sets respond differently to variations in shower density. With the present experimental arrangement counter groups III and IV only required uniform density over 30 cm. Kraybill required uniform shower density over about 4 m. Although we expect the values of γ by Method A to be everywhere rather higher than those by Method B, it is somewhat difficult to understand why Kraybill's increase in γ by Method A is higher than the increase found here by Method B, the reverse being expected. However, the results may not be incompatible when the statistical errors of the two experiments are taken into account.

Table 5

Altitude (m)	720	9200	9500	11000-12000
Theoretical value of γ	1.41	1.94	1.95	2.01

Since we have no reason to suspect the validity of Method B we conclude that γ shows a small increase with altitude.

Mills (1948, quoted by Kraybill 1949) has calculated theoretically the value of γ expected at various altitudes assuming electrons incident at the top of the atmosphere with a power law energy spectrum of the form $E^{-1.8}$ (table 5). (See also Wolfenstein (1945), Cocconi (1947) and Cocconi and Tongiorgi (1949).)

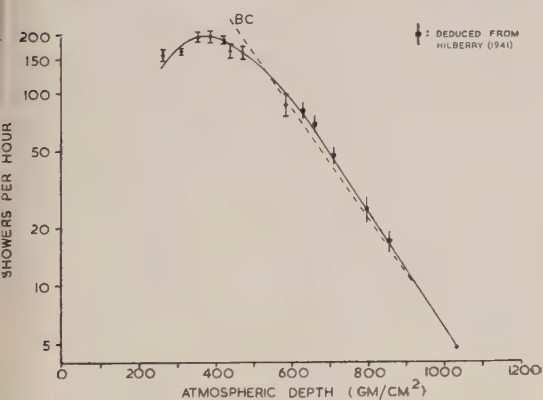
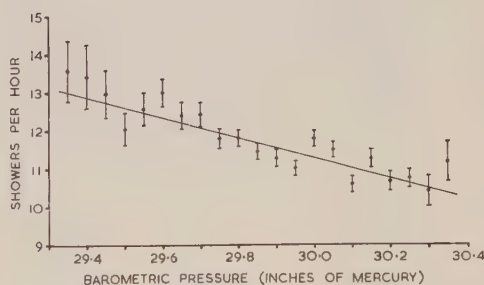


Fig. 3. The altitude variation of extensive showers.

Fig. 4. The barometer effect of extensive showers E_I, II, III .

Although Kraybill (1949) observed a smaller increase in γ than that predicted theoretically on the above hypothesis he did not consider the difference to be significant. However, if we also take into account the present data it seems that there is a real discrepancy between the theoretical and experimental values of γ at high altitudes (fig. 3). This discrepancy is not surprising as it is unlikely that extensive showers develop as pure electron cascades. If we consider instead the

more likely picture of extensive showers originating from neutral mesons emitted in successive nuclear interactions we can see qualitatively that a smaller variation in γ would be expected. Many of the showers recorded are probably secondary showers originating a few kilometres above the apparatus. The effect of these secondary showers must be to smooth out to some extent the variation of γ which is predicted on the hypothesis of single cascades starting near the top of the atmosphere.

§ 6. THE ALTITUDE VARIATION OF EXTENSIVE AIR SHOWERS

6.1. *Experimental Results*

We have described the recording of extensive showers by the following arrangements: threefold coincidences (I, II, III) and (I, II, IV), (§ 4); fourfold coincidences (I, II, III, IV), (§ 4); threefold coincidences $R(2, 2, 4)$, (§ 3.1). The counting rates of these arrangements at various altitudes are given in table 6. It is seen that the altitude variations of all the counting rates are very similar. The rate of fourfold coincidences (I, II, III, IV) is plotted against atmospheric depth in fig. 3. The number of showers recorded passes through a broad maximum at about 26000 ft. (8000 m). At the maximum the shower rate is some 42 times the sea-level value.

Table 6. The Altitude Variation of Extensive Air Showers
(The ratios of the counting rates at high altitudes to those at sea level are given in brackets)

Altitude (ft)	Atmospheric depth (g/cm ²)	Recording time (hours)	Hourly rate of coincidences		
			3-fold (I, II, III) and (I, II, IV)	4-fold (I, II, III, IV)	3-fold $R(2, 2, 4)$
33500	261	1.31	237 ± 11 (31)	159 ± 11 (34)	168 ± 12 (34)
30000	307	3.90	273 ± 7 (36)	166 ± 7 (35)	170 ± 7 (35)
27000	351	1.69	305 ± 11 (40)	197 ± 11 (42)	198 ± 11 (40)
25000	383	1.05	310 ± 15 (41)	197 ± 14 (42)	186 ± 13 (38)
23000	418	2.62	310 ± 9 (41)	191 ± 9 (40)	189 ± 8 (38)
22000	436	0.95	259 ± 14 (34)	167 ± 13 (35)	158 ± 13 (32)
20000	470	1.02	276 ± 14 (36)	164 ± 13 (35)	170 ± 13 (35)
15000	583	0.68	143 ± 12 (19)	88 ± 11 (19)	82 ± 11 (17)
Sea level	1033	427	7.64 ± 0.11	4.73 ± 0.11	4.92 ± 0.11

6.2. *The Barometer Coefficient of Extensive Air Showers at Sea Level*

A continuous record of the air shower rate $E_{I, II, III}$ at ground level for the five months period April to September 1950 was analysed for changes in the barometric pressure. Some 37000 showers were recorded in 3240 hours of operation. Hourly readings of the number of showers recorded were classified into equal pressure intervals of 0.05 in. Hg. The mean shower rate for the

mean pressure of each interval is shown graphically in fig. 4. The variation of air-shower rate with barometric pressure may be taken as linear over the pressure range considered. An analysis of the results by the method of least squares gave the barometer coefficient of extensive showers as $-(9.0 \pm 1.1)\%$ per cm Hg at 76 cm Hg. There is good agreement between this value and that found by Daudin and Daudin (1949) at sea level, $-(9.2 \pm 2)\%$ per cm Hg. These sea-level values are not significantly different from the barometer coefficient found at 2860 m by Daudin and Daudin (1949), i.e. $-(10.2 \pm 2)\%$ per cm Hg.

6.3. Discussion

Expressing the barometer coefficient $-(9.0 \pm 1.1)\%$ per cm Hg in g/cm^2 we find that the gradient of the curve of shower rate plotted against atmospheric depth should be $-(0.66 \pm 0.08)\%$ per g/cm^2 at sea level. Assuming that this variation is maintained, the altitude variation of the shower rate at low altitudes is of the form $\exp\{-x/(151 \pm 18)\}$, where x is the atmospheric depth in g/cm^2 . This law is shown in fig. 3 (line BC). It is in good agreement with the shower rate observed at 15000 ft and with the results of Hilberry (1941). (Hilberry's data have been normalized to our counting rate at sea level.) Only above 15000 ft. is there significant deviation from the exponential law.

At high altitudes the results are in substantial agreement with those of Kraybill (1949). At 30000 ft. (9200 m) Kraybill found the rate to be 28 times greater than at 750 m for showers detected by counters of 2.8 m spread and 24 times greater with counters of 13 m spread. Extrapolating to sea level, the factors of increase are found to be 51 and 43 respectively. Both these factors are higher than the increase of approximately 38 times found in the present experiment with counters of 2.2 m spread.

§ 7. APPENDIX

7.1. The Quenching and Hodoscope Circuits

The necessity of using Geiger-Müller counters of very high efficiency in trays E_I , E_{II} and E_{III} has been discussed in § 3.2.

It was found (Hodson, reported by Smith 1948) that if the anode of a counter is given a 250 v negative pulse of $10\mu\text{sec}$ duration after each discharge the insensitive time of the counter is considerably reduced. This may be explained as follows: Each discharge is confined to a short length of the anode wire, leaving the rest of the counter free from positive-ion space charge and therefore sensitive to further incident ionizing particles. Since only part of the counter remains insensitive after each discharge we may define an 'effective insensitive time' T such that the overall efficiency of the counter is $\epsilon = (1 + NT)^{-1}$, where N is the rate of arrival of ionizing particles on the counter (cf. Blackman and Michiels 1948).

In the present experiments each counter in trays E_I , E_{II} and E_{III} was therefore quenched rapidly by a $10\mu\text{sec}$ single-shot multivibrator, valves V_1 and V_2 (fig. 5 (a)). Valves V_3 - V_6 constitute the mixing and indicating units associated with each counter. The mixing circuit has a resolving time of $1.2\mu\text{sec}$, achieved in the following manner. When valve V_1 becomes conducting a voltage 'ring' is produced across coil L_1 , the voltage of the point A' (fig. 5) swinging in the negative direction during the first half cycle. Coil L_2 is coupled inductively to L_1 in such a way that, but for the diode V_3 , a voltage 'ring' of the

opposite phase would be produced across it (fig. 6, curve (C)). The effect of the diode V_3 is to damp out the oscillation of coil L_2 after the first positive half cycle (fig. 6, curve (D)). The inductances and distributed capacities of L_1 and L_2 are such that the control grid of valve V_4 receives a positive pulse of about $1 \mu\text{sec}$ duration. If this is coincident with a positive 'master pulse' on the suppressor grid of V_4 a negative pulse is obtained from the anode of V_4 . After being lengthened this pulse cuts off valve V_5 , which flashes a neon lamp for about $\frac{1}{50}$ second.

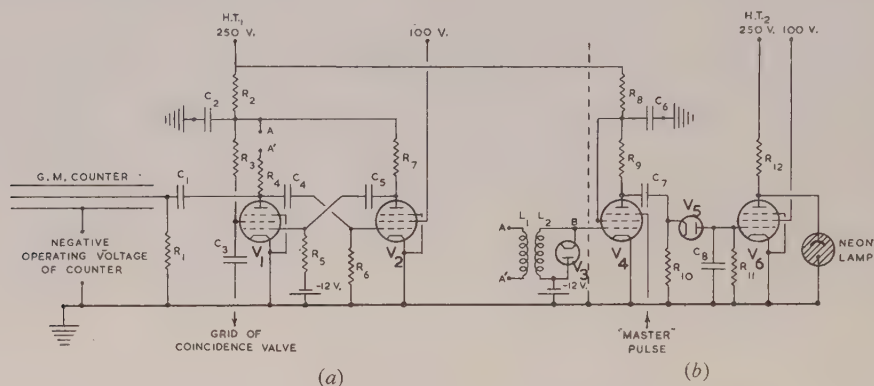


Fig. 5. (a) The quenching circuit. (b) The hodoscope circuit.

R_1 1 M Ω , $\frac{1}{2}$ w	R_7 68 k Ω , 1 w	C_1 0.025 μF	C_5 25 μF
R_2 5.6 k Ω , $\frac{1}{2}$ w	R_8 5.6 k Ω , $\frac{1}{2}$ w	C_2 1 μF	C_6 0.5 μF
R_3 4.3 k Ω , $\frac{1}{2}$ w	R_9 100 k Ω , $\frac{1}{2}$ w	C_3 25 μF	C_7 0.005 μF
R_4 68 k Ω , $\frac{1}{2}$ w	R_{10} 100 k Ω , $\frac{1}{2}$ w	C_4 10 μF	C_8 0.001 μF
R_5 300 k Ω , $\frac{1}{2}$ w	R_{11} 10 M Ω , $\frac{1}{2}$ w	Valves V_1, V_2, V_4, V_6 Mullard EF 50	
R_6 100 k Ω , $\frac{1}{2}$ w	R_{12} 68 k Ω , 1 w	Valves V_3, V_5 Mullard EA 50.	
		Neon lamp, Siemens L 9	

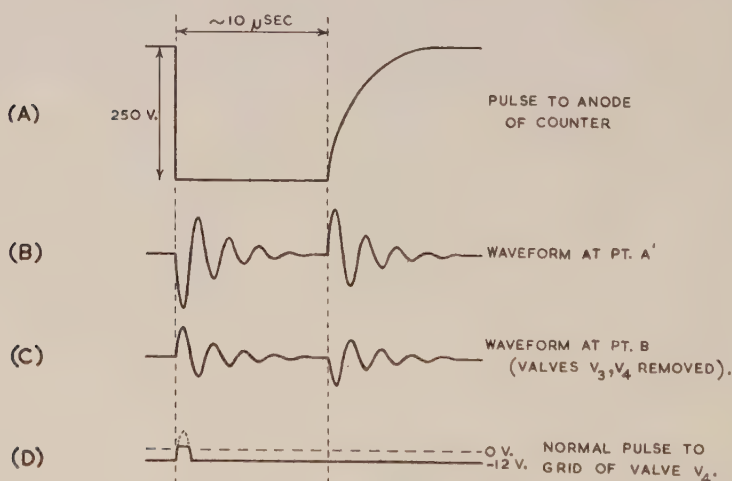


Fig. 6. Waveforms of the circuits shown in fig. 5.

Extensive showers in which at least one counter is discharged in each of the trays E_I , E_{II} , E_{III} are selected by a threefold Rossi coincidence circuit in the following manner. Each time one of the counters is discharged a negative pulse is obtained from the non-decoupled screen-grid resistance R_3 of the valve V_I

of its quenching unit (see fig. 5(a)). The screen-grid pulses of all the counter-units in one tray may be coupled together directly to the grid of one coincidence valve. For coincidence purposes counters so coupled are effectively in parallel. However, the quenching units still operate independently since they are insensitive to negative pulses on the screen of valve V_1 . 'Master pulses' ($\sim 1 \mu\text{sec}$ long) are produced whenever threefold coincidences are recorded.

7.2. The Determination of the Effective Insensitive Time of the Counters

The effective insensitive time of a counter and its associated quenching circuit was determined in the following manner. Trays E_I and E_{II} (for this purpose each containing four counters, $45 \text{ cm} \times 3 \text{ cm}$) were turned into a vertical plane. Counters in tray E_{III} were not operated, but counter No. 1 (tray E_I) was connected to a quenching unit belonging to tray E_{III} . Threefold master pulses were then produced whenever counter No. 1 (see fig. 1), at least one of the counters 2, 3, 4, and at least one of the counters 5, 6, 7, 8 were discharged simultaneously.

From the hodoscope record events were picked out in which (a) all eight counters in trays E_I and E_{II} were discharged and (b) seven of these counters were discharged, the one not discharged being one of the four inner counters of the telescope, Nos. 3, 4, 5 or 6. (Anticoincidences of this type were mainly due to inefficiency of one of these counters.) The average inefficiency of counters 3, 4, 5 and 6 was then

$$\eta' = \frac{\text{no. of anti-coincidences}}{4 \times (\text{no. of 8-fold coincidences})}.$$

η' was determined at various background counting rates of counters 3, 4, 5 and 6, the counters being stimulated uniformly along their length by radon needles contained in a long tube S. The results are given in table 7.

Table 7

Mean counting rate N' (per sec)	No. of 8-fold coincidences	No. of anti- coincidences	Observed inefficiency (%)*
7.8	1663	41	0.62 ± 0.10
55	503	24	1.19 ± 0.24
77	521	15	0.72 ± 0.19
109	525	18	0.86 ± 0.20
184	1365	74	1.36 ± 0.16
241	486	34	1.75 ± 0.30

* Including geometrical inefficiency.

If N' is the average counting rate of one of the counters under test, the inefficiency due to the insensitive time T is very nearly $N'T$. If the average inefficiency is plotted against N' we obtain T as the slope of the best straight line given by the experimental points: $T = (42 \pm 9) \mu\text{sec}$. The inefficiency which is found for $N' = 0$ ($\sim 0.6\%$) is attributed to a slight geometrical inefficiency in the telescope.

The quenching circuit described here thus achieves results similar to the circuit of Hodson (1948 a) in which the counter potential was reversed after each discharge. One advantage of the present circuit is that it avoids putting the high operating voltage of the counter on the anode of the quench valve V_1 .

ACKNOWLEDGMENTS

It is a pleasure to thank Professor P. M. S. Blackett and Dr. H. J. J. Braddick for their interest in this work. Thanks are also due to the Air Ministry for permission to make the aeroplane flights and to Squadrons 109 and 139 for their assistance and cooperation. I also wish to thank Dr. D. Jakeman for several helpful discussions.

REFERENCES

- AUGER, P., and DAUDIN, J., 1945, *J. Phys. Radium*, **6**, 233.
 BLACKMAN, M., and MICHIELS, J. L., 1948, *Proc. Phys. Soc.*, **60**, 549.
 BROADBENT, D., and JÁNOSSY, L., 1948, *Proc. Roy. Soc. A*, **192**, 364.
 BROADBENT, D., KELLERMANN, E. W., and HAKEEM, M. A., 1950, *Proc. Phys. Soc. A*, **63**, 864.
 COCCONI, G., 1947, *Phys. Rev.*, **72**, 964.
 COCCONI, G., and TONGIORGI, V. C., 1949, *Phys. Rev.*, **75**, 1058.
 COCCONI, G., LOVERDO, A., and TONGIORGI, V., 1944, *Nuovo Cim.*, **2**, 14; 1946 a, *Phys. Rev.*, **70**, 841; 1946 b, *Ibid.*, **70**, 846.
 DAUDIN, J., 1947, *J. Phys. Radium*, **8**, 301.
 DAUDIN, J., and DAUDIN, A., 1949, *J. Phys. Radium*, **10**, 394.
 GREISEN, K., and NERESON, N., 1942, *Phys. Rev.*, **62**, 316.
 HILBERRY, N., 1941, *Phys. Rev.*, **60**, 1.
 HODSON, A. L., 1948, *J. Sci. Instrum.*, **25**, 11; 1952, *Proc. Phys. Soc. A*, **65**, 702.
 ISE, J., Jr., and FRETTER, W. B., 1949, *Phys. Rev.*, **76**, 933.
 KRAYBILL, H. L., 1949, *Phys. Rev.*, **76**, 1092; 1952, *Phys. Rev.*, **86**, 590.
 LOVERDO, A., and DAUDIN, J., 1948, *J. Phys. Radium*, **9**, 134.
 MAZE, R., FRÉON, A., and AUGER, P., 1948, *Phys. Rev.*, **73**, 418.
 SMITH, P. B., 1948, *Rev. Sci. Instrum.*, **19**, 453.
 TREAT, J. E., and GREISEN, K., 1948, *Phys. Rev.*, **74**, 414.
 WOLFENSTEIN L., 1945, *Phys. Rev.*, **67**, 238.

Note added in proof. Since this paper was written, Kraybill (1952) has briefly reported measurements of γ up to 33 000 ft. which are in agreement with the results given here. Kraybill has also kindly supplied us with more complete data on the altitude variation of γ , as calculated by Mills, than is reproduced in table 5. This shows that the theoretical curve in fig. 2 should be slightly concave upwards over the range shown. The linear interpolation shown in fig. 2, deduced from the data of table 5, is approximately 0.7 too high at an atmospheric depth of 500 gm/cm². The difference is not sufficiently great to affect our conclusions.

Penetrating Particles in Extensive Air Showers

By A. L. HODSON*

The Physical Laboratories, University of Manchester

Communicated by P. M. S. Blackett; MS. received 22nd August 1952

ABSTRACT. Extensive penetrating showers observed under a transition layer of lead 10 cm thick are approximately 300 times more frequent at 30 000 ft. than at sea level. A tentative analysis of their altitude variation suggests that the mean attenuation length in air of the N-component of extensive showers is of the order of 200 g/cm². It is shown that in extensive showers at 30 000 ft. the fraction of particles which are penetrating is of the same order as at sea level.

§ 1. INTRODUCTION

IT is now recognized that penetrating particles associated with extensive air showers are of two types: (i) incident penetrating particles, mainly μ -mesons (Coconi *et al.* 1949), and (ii) highly interacting particles which produce groups of penetrating particles in local absorbers (Broadbent and Jánossy 1948, Ise and Fretter 1949, Brown and McKay 1949). The energetic interacting particles responsible for these events are generally referred to as the 'N-component' of extensive air showers.

Some information about the altitude variation of the N-component may be derived from the altitude variation of penetrating showers which are associated with air showers, data on which are given by Hodson (1952, to be referred to as I). The experimental arrangement, consisting essentially of a Jánossy-type penetrating shower detector operated in coincidence with various unshielded counter trays, is described in detail in that paper (§§ 2 and 3). In this paper an attempt is made to analyse the observed altitude variation of extensive penetrating showers. Some experimental data on penetrating particles in extensive air showers at 30 000 ft are also presented.

§ 2. THE OBSERVED ALTITUDE VARIATION OF EXTENSIVE PENETRATING SHOWERS

The data on extensive penetrating showers to be considered here are given in table 1 of I.

First we consider a few general arguments for believing that most of the observed coincidences represent true extensive penetrating showers. The resolving time for coincidences between the penetrating shower set and counters in the unshielded trays was $1.2\mu\text{sec}$; the accidental coincidence rate was thus very small. There remains the possibility that stray particles emitted from penetrating showers produced locally in the P-set occasionally discharged the unshielded trays. However, the hodoscope record for counters in trays E_I , E_{II} , E_{III} shows that on the average several (see table 1), and occasionally all, of these counters were discharged simultaneously with the P-set. It is clear that very few of the coincidences with the trays E_I , E_{II} or E_{III} can be attributed to spurious extensive penetrating showers arising in the way suggested above.

* Now at the Palmer Physical Laboratory, Princeton University, New Jersey, U.S.A.

Tray E_B was much nearer to the P-set than trays E_I , E_{II} , E_{III} and was thus more liable to be discharged by such stray particles. However, the solid angle subtended by tray E_B at the P-set is quite small and we believe that even in this case most of the coincidences were due to true extensive penetrating showers. In support of this we note that the altitude variations of coincidences (P , E_B), (P , E_R) and (P , $E_{I\ II\ III}$) are very similar (I, table 1). Although tray E_B recorded coincidences with the P-set more frequently than the more distant trays E_I , E_{II} , E_{III} , we believe that this was most likely due to a decoherence effect and to cascade effects in the duralumin bomb case containing tray E_B and the P-set.

Table 1. Average Number of Counters discharged in the Events (P , E_R)

	$\Sigma=0$	$\Sigma=10$ cm of lead
Average number discharged at high altitudes	$5.9 + \frac{1}{2}(1.7) + 0.83E_B$	$3.4 + \frac{1}{2}(1.0) + 0.85E_B$
	(23 showers)	(13 showers)
Average number discharged at sea level	$5.9 + \frac{1}{2}(1.9) + 0.89E_B$	$4.9 + \frac{1}{2}(1.2) + 0.74E_I$
	(28 showers)	(45 showers)

$(n + \frac{1}{2}m + E_B)$ denotes an extensive penetrating shower in which n counters of 'unit area' ($45\text{ cm} \times 3\text{ cm}$) and m counters of 'half unit area' are discharged in trays E_I , E_{II} , E_{III} , together with at least one counter in tray E_B ($n \leq 13$; $m \leq 5$).

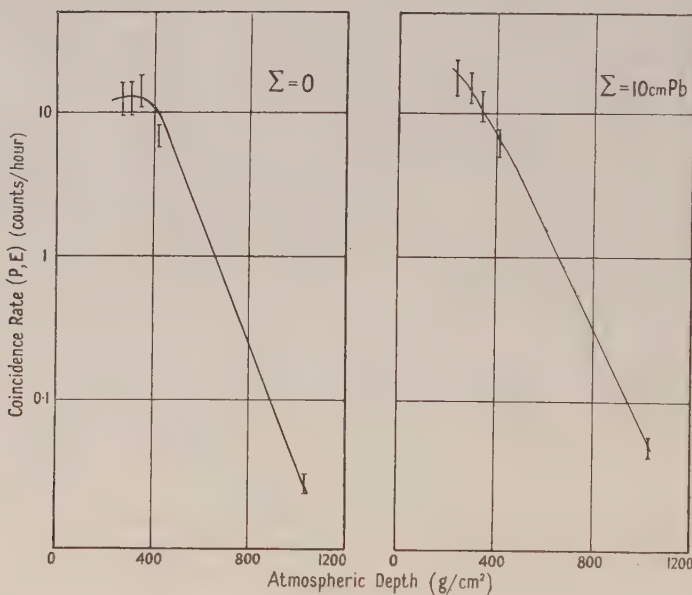


Fig. 1.

There is a slight indication from the rates of coincidences (P , E_B), (P , E_R), (P , $E_{I\ II\ III}$) and (P , E), (I, table 1), that the extensive penetrating showers observed with $\Sigma=0$ have a maximum frequency at about the altitude of the maximum of all extensive showers (Kraybill 1949). The altitude variation of coincidences (P , E) is shown in fig. 1.

Tinlot (1948) observed that up to 4260 m the rate of extensive penetrating showers was between 5% and 10% of the rate of local penetrating showers. Tinlot and Gregory (1949), using a detector with a definite bias against recording dense air showers, found this ratio to be about 1% at 4260 m. In both these investigations very small unshielded trays were used. In a cloud chamber experiment at 3027 m Fretter (1949) found almost as many extensive penetrating

showers as local showers. The actual ratio is clearly rather dependent on the experimental arrangement. However, the altitude variations observed with a given arrangement should be of greater significance. Fretter (1949) found that the frequency of extensive penetrating showers increases by a factor 7.2 ± 2.0 between sea level and 3027 m (713 g/cm²). By interpolation from the present results with $\Sigma = 10$ cm Pb, we deduce a factor 12.7 ± 2.0 between these altitudes. George and Jason (1950), using a penetrating shower detector similar to that used here, but much larger, have found that the coincidence rates $(P, E)_{\Sigma=0}$ and $(P, E)_{\Sigma=10 \text{ cm Pb}}$ increase by factors of 15 ± 2 and 10 ± 2 respectively between sea level and the Jungfraujoch (3457 m, 675 g/cm²). The corresponding factors deduced from fig. 1 are 24.5 ± 6 and 17 ± 3 . At high altitudes no previous data on extensive penetrating showers appear to be available.

§ 3. ANALYSIS OF THE ALTITUDE VARIATION OF EXTENSIVE PENETRATING SHOWERS

We consider separately the extensive penetrating showers observed with $\Sigma = 10$ cm of lead and with $\Sigma = 0$.

(i) $\Sigma = 10$ cm of lead. It will be shown later that the majority of the coincidences (P, E) must be attributed to groups of penetrating particles produced locally (in Σ) by the N-component.

Suppose that at a given atmospheric depth the N-component forms a fraction k_N of all the particles in extensive showers. Then if the density spectrum of extensive showers at that depth is of the form $I(>\Delta) = B\Delta^{-\gamma}$, the rate of events $(P, E)_{\Sigma=10 \text{ cm Pb}}$ is given by

$$(P, E)_{\Sigma=10 \text{ cm Pb}} = \beta B \gamma \int_0^\infty \{1 - \exp(-k_N S \Delta)\} \{1 - \exp(-E \Delta)\} \frac{d\Delta}{\Delta^{\gamma+1}}, \dots (1)$$

where S is the effective area of the P-set, E is the total area of the unshielded trays and β is the probability that the N-particle interacts and discharges the P-set. Now the above integral is linear in k_N over a range sufficiently wide for us to write $\beta k_N = k_{NP}$, where k_{NP} is to be interpreted as the fraction of shower particles which discharge the P-set. Thus

$$(P, E)_{\Sigma=10 \text{ cm Pb}} = B \gamma \int_0^\infty \{1 - \exp(-k_{NP} S \Delta)\} \{1 - \exp(-E \Delta)\} \frac{d\Delta}{\Delta^{\gamma+1}}. \dots (2)$$

In order to eliminate the constant B of the density spectrum we consider the ratio of this rate to the rate of fourfold coincidences between unshielded counter trays of area F . The rate of fourfold coincidences is

$$R(4\text{-fold}) = B \gamma \int_0^\infty \{1 - \exp(-F \Delta)\}^4 \frac{d\Delta}{\Delta^{\gamma+1}}.$$

As will be described elsewhere, fourfold coincidences between trays E_I , E_{II} and two groups of counters in tray E_{III} (fig. 2) were recorded in the same series of flights. Evaluating the integrals by the method of Broadbent and Jánossy (1948) we have therefore

$$\frac{(P, E)_{\Sigma=10 \text{ cm Pb}}}{R(4\text{-fold})} = \left(\frac{E}{F}\right)^\gamma \left\{ \frac{1 + (k_{NP} S/E)^\gamma - (1 + k_{NP} S/E)^\gamma}{4 - 6 \cdot 2^\gamma + 4 \cdot 3^\gamma - 4^\gamma} \right\}, \dots (3)$$

where $E = 3035$ cm², $F = 417$ cm², and $S = 303$ cm² (assuming that the effective area of the P-set is equal to the area of one of the trays). Experimentally this ratio is 0.0105 at sea level and 0.092 at 30 000 ft. From experiments to be published elsewhere we find $\gamma = 1.445$ at sea level and $\gamma = 1.559$ at 30 000 ft. Equation (3) then gives $k_{NP} = 7.6 \times 10^{-4}$ at sea level and $k_{NP} = 5.0 \times 10^{-3}$ at

30 000 ft. k_{NP} thus increases by a factor 6.5 between sea level and 30 000 ft. Thus if the soft component of extensive showers increases by a factor n between these levels, the N-component increases by a factor $6.5n$. We now determine n .

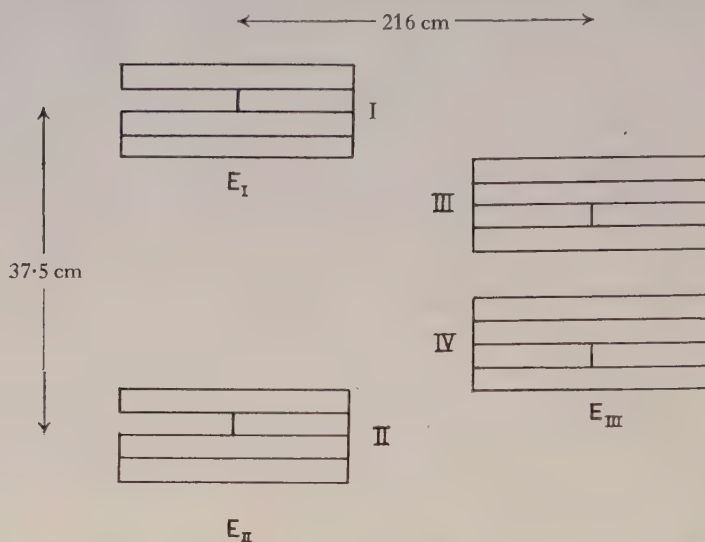


Fig. 2.

Consider an experimental arrangement in which fourfold coincidences are recorded between counter trays each of area Ap_0^2 square cascade units (measured at sea level, pressure p_0), i.e. of area $Ap_0^2X_0^2$ square metres. Let the number of showers at sea level which contain more than N particles and whose cores fall within an area of one square cascade unit (measured at sea level) be $C_0N^{-\gamma_0}$ per hour. The sea-level coincidence rate is then given by (cf. Ise and Fretter 1949)

$$\begin{aligned}
 R(4\text{-fold})_{sl} &= 2\pi\gamma_0 C_0 \int_{N=0}^{\infty} \int_{r=0}^{\infty} \int_{\theta=0}^{\pi/2} \frac{2}{\pi} [1 - \exp \{-Nf_0(r_1 p_0) Ap_0^2\}] \dots \\
 &\quad \times [1 - \exp \{-Nf_0(r_4 p_0) Ap_0^2\}] \frac{dN}{N^{\gamma_0+1}} r dr d\theta \\
 &= 2\pi\gamma_0 C_0 p_0^{2\gamma_0} \int_{N=0}^{\infty} \int_{r=0}^{\infty} \int_{\theta=0}^{\pi/2} \frac{2}{\pi} [1 - \exp \{-Nf_0(r_1 p_0) A\}] \dots \\
 &\quad \times [1 - \exp \{-Nf_0(r_4 p_0) A\}] \frac{dN}{N^{\gamma_0+1}} r dr d\theta, \quad \dots (4)
 \end{aligned}$$

where $f_0(r)$ is the structure function of the showers at sea level.

Let the number of showers at altitude x (pressure p) which contain more than N particles and whose cores fall within an area of one square cascade unit (measured at pressure p) be $CN^{-\gamma}$ per hour. If $f(r)$ is the structure function of the showers at altitude x the coincidence rate there is

$$\begin{aligned}
 R(4\text{-fold})_{alt} &= 2\pi\gamma C \int_{N=0}^{\infty} \int_{r=0}^{\infty} \int_{\theta=0}^{\pi/2} \frac{2}{\pi} [1 - \exp \{-Nf(r_1 p) Ap^2\}] \dots \\
 &\quad \times [1 - \exp \{-Nf(r_4 p) Ap^2\}] \frac{dN}{N^{\gamma+1}} r dr d\theta \\
 &= 2\pi\gamma C p^{2\gamma} \int_{N=0}^{\infty} \int_{r=0}^{\infty} \int_{\theta=0}^{\pi/2} \frac{2}{\pi} [1 - \exp \{-Nf(r_1 p) A\}] \dots \\
 &\quad \times [1 - \exp \{-Nf(r_4 p) A\}] \frac{dN}{N^{\gamma+1}} r dr d\theta. \quad \dots (5)
 \end{aligned}$$

The ratio of the two integrals in eqns. (4) and (5) may be expressed in terms of α_0 and α , the exponents of the decoherence curves at sea level and at altitude.

We finally obtain

$$\frac{R(4\text{-fold})_{\text{alt}}}{R(4\text{-fold})_{\text{sl}}} = \frac{\gamma C}{\gamma_0 C_0} \frac{p^{2\gamma-\alpha}}{p_0^{2\gamma_0-\alpha_0}}. \quad \dots\dots(6)$$

(The factor $p^{2\gamma}/p_0^{2\gamma_0}$ arises because the trays are effectively a factor $(p/p_0)^2$ smaller at altitude than at sea level and the factor $p^{-\alpha}/p_0^{-\alpha_0}$ arises because the trays are effectively nearer together.)

Now suppose that the number of particles in an extensive shower at sea level is (on the average) a fraction $1/n$ of the number of particles in the shower at altitude. The number of showers which contain more than N particles at sea level and whose cores fall in an area of one square *metre* is then equal to the number of showers which contain more than nN particles at altitude x and whose cores fall in an area of one square *metre*. Since the size spectra at 30 000 ft and at sea level are very similar ($\gamma=1.56$ and $\gamma_0=1.445$) we thus write

$$\frac{C_0 N^{-\gamma'}}{X_0^2} = \frac{C(nN)^{-\gamma'}}{X_0^2 (p_0/p)^2}, \text{ where } \gamma' \text{ is the mean of } \gamma \text{ and } \gamma_0,$$

giving

$$C/C_0 = n^{\gamma'} (p/p_0)^{-2}. \quad \dots\dots(7)$$

From (6) and (7) we have

$$\frac{R(4\text{-fold})_{\text{alt}}}{R(4\text{-fold})_{\text{sl}}} = \frac{\gamma}{\gamma_0} n^{\gamma'} \frac{p^{2\gamma-2-\alpha}}{p_0^{2\gamma_0-2-\alpha_0}}. \quad \dots\dots(8)$$

Now $\alpha \sim 0.2$ and $\alpha_0 \sim 0.1$ (cf. Kraybill 1949) and the coincidence rate at 30 000 ft is 38 times that at sea level. Equation (8) then gives $n=12.4$.

The N-component in these extensive showers therefore increases on the average by a factor $6.5 \times 12.4 = 81$ between sea level and 30 000 ft. Assuming that the increase is exponential this corresponds to an apparent attenuation length in air λ_N of about 170 g/cm². (We use the term 'apparent attenuation length' in the sense defined in I, i.e. the attenuation length uncorrected for the effect of inclined primaries.)

We now show that our assumption that the P-set is mainly discharged by the N-component is justified. In order to discharge the P-set a minimum of two penetrating particles is required, together with an additional particle on the top tray T. The third particle required at the top tray may be either another penetrating particle or a cascade particle which emerges below Σ . An upper limit to the rate at which the P-set is discharged by randomly associated μ -mesons in air showers is obtained by assuming that all the penetrating particles in air showers are μ -mesons. Suppose that these form a fraction $k_\mu (=0.02)$ of all the shower particles. Now the soft component which penetrates 10 cm of lead (Σ) is a fraction $k_s = 0.03$ of the incident shower density (Greisen 1949). The total density of particles under 10 cm of lead is thus a fraction $k' = k_\mu + k_s = 0.05$ of the incident shower density.

In a shower of density Δ the probability that μ -mesons discharge both groups of counters in the bottom tray B of the P-set is $[1 - \exp\{(-kS\Delta)/2\}]^2$. The probability that a μ -meson or a cascade particle discharges a counter group in the top tray is $1 - \exp\{(-k'S\Delta)/3\}$. An upper limit to the rate of (P, E) $_{\Sigma=10 \text{ cm Pb}}$ events due to μ -mesons is obtained by assuming that the μ -mesons which discharge tray B also discharge tray M and the other two groups of the top tray T. The upper limit is then given by

$$R = B\gamma \int_0^\infty \{1 - \exp(-kS\Delta/2)\}^2 \{1 - \exp(-k'S\Delta/3)\} \{1 - \exp(-E\Delta)\} \frac{d\Delta}{\Delta^{\gamma+1}}. \quad (9)$$

Evaluating the integral in the usual manner we find that R is equal to 19% of the observed $(P, E)_{\Sigma=10 \text{ cm Pb}}$ rate at sea level. The actual rate of (P, E) events due to associated μ -mesons will be less than R because some of the μ -mesons which discharge the tray B will fail to discharge the required groups in trays T and M. From a careful consideration of showers in which more than the minimum number of particles strike the P-set and of the geometry of the counter trays we estimate that not more than 10% of the observed rate of $(P, E)_{\Sigma=10 \text{ cm Pb}}$ events at sea level can be attributed to incident μ -mesons in air showers. At high altitudes the fraction must be even smaller.

(ii) $\Sigma=0$. The altitude variation of coincidences $(P, E)_{\Sigma=0}$ is related to that of the N-component but in a more complicated way than in the case considered above ($\Sigma=10 \text{ cm Pb}$). With $\Sigma=0$ most of the penetrating showers will be produced in the lead between trays T and M. A simple expression for the counting rate (cf. eqn. (1)) does not obtain, for in a satisfactory analysis we must note that the requirements to be satisfied by the air shower at tray T are modified. (a) according to whether the penetrating shower is produced by a neutral or a charged particle, (b) by the discharge of counters in tray T by back-scattered particles from the penetrating showers, (c) by back-scattered particles from cascade showers occurring in the lead below tray T, and (d) by cascade multiplication in local material above the P-set (in particular in the 4.6 cm thick dural beam of the bomb case which contained the P-set). (c) and (d) increase the probability of the air shower discharging counters in tray T.

The complicated nature of factors (b), (c), (d) means that coincidences $(P, E)_{\Sigma=0}$ are much less amenable to analysis than coincidences $(P, E)_{\Sigma=10 \text{ cm Pb}}$. Our estimate of the altitude variation of the N-component of air showers is therefore based only on the analysis of the events $(P, E)_{\Sigma=10 \text{ cm Pb}}$.

§ 4. PENETRATING PARTICLES IN AIR SHOWERS

It has been shown by Chaudhuri (1948) and others that when an extensive shower strikes an absorber the density of shower particles observed underneath the absorber is a fraction k of the incident shower density Δ where k is independent of Δ to a first approximation. We now describe measurements of k at sea level and at 30 000 ft.

(i) *The experimental arrangement.* In this experiment the counters in the bottom tray B of the P-set were connected in parallel. This tray was then operated in coincidence with threefold master pulses produced by extensive showers discharging trays E_I , E_{II} , E_{III} . The other counter trays of the P-set were not operated. Measurements were made only with $\Sigma=0$: the tray B was thus shielded vertically by 22 cm of lead, the shielding being sufficiently complete to ensure that, in the main, this tray was not discharged by electrons or low-energy photons (Greisen 1949).

(ii) *The experimental results.* One flight was made with the above arrangement. The hodoscope record was examined and the following events picked out: (a) fourfold coincidences between the unshielded counter groups I, II, III, IV (fig. 2), (b) fivefold coincidences between the unshielded counter groups I, II, III, IV, and the shielded tray B. The results obtained in this flight and at ground level are given in table 2. Let F represent the sensitive area of each of the unshielded counter groups I, II, III, IV and S that of the shielded tray B. Using

integrals of a type similar to those above, the ratio of fivefold coincidences to fourfold coincidences may be expressed as a function of kS/F . Solving the function graphically (cf. Cocconi *et al.* 1949) for the experimental ratios at 30 000 ft. and sea level and taking $F=417 \text{ cm}^2$ and $S=303 \text{ cm}^2$ we find $k=0.029 \pm 0.008$ at 30 000 ft and $k=0.0161 \pm 0.0013$ at sea level (for an average shower density ~ 90 particles/ m^2). The sea-level value is in agreement with recent results of Jakeman and Hakeem (private communication) for showers of similar mean density (~ 50 particles/ m^2). These workers find $k=0.019 \pm 0.001$ under 15 cm of lead (after correcting for the effects of low-energy photons) and $k=0.016 \pm 0.003$ under 30 cm of lead.

Table 2

Altitude (ft.)	Recording time (h)	4-fold coinc. (I, II, III, IV)	5-fold coinc. (I, II, III, IV, B)	Ratio 5-fold/4-fold
30000	1.68	303	17	0.056 ± 0.014
(Total for flight)		(512)	(28)	(0.055 ± 0.010)
Ground level	1076	5020	191	0.038 ± 0.003

The results of McCusker (1950) and also some unpublished work by Jakeman and Hakeem suggest that the N-component constitutes some 20–40 per cent of the penetrating particles in extensive showers at sea level. An approximate calculation shows that if this is so and if the N-component has an apparent attenuation length λ_N of the order of 170 g/cm^2 the expected ratio $k_{30\,000}/k_{sl}$ is of the same order as that observed experimentally. If λ_N were equal to the apparent attenuation length for fast nucleons which are unaccompanied by air showers ($\sim 116 \text{ g/cm}^2$) we should expect the ratio $k_{30\,000}/k_{sl}$ to be of the order of 8 to 16. Such a large ratio is quite outside even the large statistical errors of the present experiment. This is further evidence for a high value of λ_N .

Cocconi, Tongiorgi and Greisen (1949) found that k at 3260 m is 0.47 of the value obtained at 260 m whereas we find that k at 30 000 ft. is about 1.8 times the sea-level value. Although the accuracy of our value at 30 000 ft. is not very good it is sufficient to show that a continued decrease of k with altitude at altitudes greater than 3260 m is very unlikely. Rather better statistical evidence on the value of k at high altitudes is obtained by taking all the counts observed in the flight, i.e. those obtained during the ascent and descent as well as those at 30 000 ft. (table 2).

We expect k to decrease slightly with increasing altitude up to about 15 000 ft. and then to increase fairly rapidly. At low altitudes μ -mesons predominate over the N-component and since they increase with altitude less rapidly than the soft component of extensive showers, k at first decreases with altitude. However, due to the fairly rapid increase with altitude of the N-component this should eventually predominate over the μ -meson component and k should then increase with altitude. The values of k found by Cocconi *et al.* at 260 m and at 3260 m and the present value at 30 000 ft. are consistent with such a picture.

§ 5. CONCLUDING REMARKS

It is realized that the type of analysis used in this paper over-simplifies the physical situation in extensive showers. For example, it deals only with average ratios of the various components and also neglects the effects of possible

differences in the lateral distributions of the N-component, μ -mesons and electrons.

The analysis suggests that the altitude variations of extensive penetrating showers and of k are consistent with a mean apparent attenuation length of the N-component of the order of 170 g/cm². This value may be compared with the apparent attenuation length (~ 116 g/cm² of air) found for fast nucleons which are unaccompanied by air showers. If the N-component consists mainly of nucleons as seems likely since a large fraction is neutral radiation (Sitte 1950, Greisen *et al.* 1950), the longer attenuation length may be readily interpreted on the basis of very energetic nucleon cascades in air showers. The primary particles which produce extensive penetrating showers are of higher average energy than those which give rise to local penetrating showers. The attenuation of the N-component of air showers is therefore less rapid than that of nucleons which are unaccompanied by an appreciable density of soft component.

After making the appropriate corrections for the effect of inclined primaries (cf. I, §3) we find that the mean attenuation length of the N-component of extensive air showers is of the order of 200 g/cm².

ACKNOWLEDGMENTS

The author wishes to thank Dr. H. J. J. Braddick, Professor J. G. Wilson and Dr. D. Jakeman for their interest in this work and for helpful discussion. He is greatly indebted to Mr. D. Broadbent for many valuable comments and for pointing out one factor which had not been sufficiently well considered in the original draft of this paper.

REFERENCES

- BROADBENT, D., and JÁNOSSY, L., 1948, *Proc. Roy. Soc. A*, **192**, 364.
 BROWN, W. W., and MCKAY, A. S., 1949, *Phys. Rev.*, **76**, 1034.
 CHAUDHURI, B., 1948, *Nature, Lond.*, **161**, 680.
 COCCONI, G., TONGIORGI, V. C., and GREISEN, K., 1949, *Phys. Rev.*, **75**, 1063.
 FRETTER, W. B., 1949, *Phys. Rev.*, **76**, 511.
 GEORGE, E. P., and JASON, A. C., 1950, *Proc. Phys. Soc. A*, **63**, 1081.
 GREISEN, K., 1949, *Phys. Rev.*, **75**, 1071.
 GREISEN, K., WALKER, W. D., and WALKER, S. P., 1950, *Phys. Rev.*, **80**, 535.
 HODSON, A. L., 1952, *Proc. Phys. Soc. A*, **65**, 702.
 ISE, J., Jr., and FRETTER, W. B., 1949, *Phys. Rev.*, **76**, 933.
 KRAYBILL, H. L., 1949, *Phys. Rev.*, **76**, 1092.
 MCCUSKER, C. B. A., 1950, *Proc. Phys. Soc. A*, **63**, 1240.
 SITTE, K., 1950, *Phys. Rev.*, **78**, 721.
 TINLOT, J., 1948, *Phys. Rev.*, **74**, 1197.
 TINLOT, J., and GREGORY, B., 1949, *Phys. Rev.*, **75**, 520.

Spark Counters for Short Time Interval Cosmic Ray Measurements

By E. ROBINSON*

The Physical Laboratories, University of Manchester

Communicated by P. M. S. Blackett; MS. received 27th August 1952

ABSTRACT. An original design of parallel plate spark counter, developed especially for use in cosmic-ray experiments involving the measurement of millimicrosecond time intervals, has a stable and trouble-free performance over many months of continuous operation. Distinctive features of the construction are the comparatively large sensitive areas and the sealed-off type of assembly in glass. The counter time resolution obtainable under normal operating conditions is 5 μ sec. By using statistical methods it is possible to resolve time intervals down to 1 μ sec. An illustration of this is afforded by measurements of the mean velocity of cosmic-ray particles in the sea-level flux.

§ 1. INTRODUCTION

A PLATE spark counter consists essentially of a uniformly narrow, overvolted gap, the sensitive volume of which is bounded by two plane or curved electrodes. When the gap is suitably adapted so as to break down by the formation of a filamentary, streamer-type spark, it will record the passage of an ionizing particle with a time resolution of less than 10^{-8} sec. Experimental tests which confirmed the feasibility of high resolution particle detection by this means were first carried out by Keuffel (1948 a, b) and Madansky and Pidd (1948, 1949 a). Since that time counters of this type have been under development and construction in these laboratories, and in the past two years they have been employed in a number of cosmic-ray experiments to measure millimicrosecond time intervals. The designs which have been evolved meet the requirements of these experiments, which are for stable, efficient counters of appreciable area and good geometry, having a reasonable life and the highest possible resolving time.

§ 2. DESIGN CONSIDERATIONS

Though developed independently the present designs bear a structural resemblance to those developed by Keuffel (1949). Other known designs have geometries which are unsuitable for cosmic ray work, as well as being either too restricted in their sensitive area (Madansky and Pidd 1949 b, 1950) or difficult to produce in quantity (Hudson 1951). The new features embodied in the present designs, and which are desirable for cosmic-ray work, are the sealed-off type of assembly in glass and the comparatively large 50 cm² sensitive areas. The latter is a compromise figure. Larger individual areas, though preferable, would cause a loss in counter efficiency of more than 2%, due solely to the relatively long dead time ($\frac{1}{50}$ sec) which has to be imposed after each count. Again, with larger areas the self-capacity of a counter (30 pF), and hence the energy going into each spark, would be increased: this is undesirable in view of the difficulty of quenching the heavy ionization. Large sensitive areas have been employed by grouping numbers of counters into a tray (K. R. Keep of

* Now at Nelson Research Laboratories, English Electric Co. Ltd., Stafford.

these laboratories) as is the established practice with Geiger-Müller counters.

In spark counters the time resolution depends on the gradient of the electric field and inversely on the gas pressure. Hence for a given pressure and gap (the latter is usually 2 mm), the higher the operating potential the better the resolution. For this reason absolute alcohol is thought to be preferable to other organic quenching vapours of lower vapour pressure, since the latter usually cause a greater reduction of the starting potential for spark counting. In the present counters the threshold occurs at about 2200 v, the normal operating point being some 500 v higher than this, which point is almost half way up the usable portion of the plateau of the counting curve characteristic.

Experience gained in counter design has shown that electrodes consisting of evaporated metal films on glass are unsatisfactory. The reason for this is thought to be the destruction of the metal film in the region of the spark crater, leaving localized regions of poor conductivity which cannot lose their charge quickly enough and which cause spurious counts. Accordingly the counter plates are still made from metal sheet, since with the present construction technique a satisfactory reliability of counter operation is consistently obtained. When used to record the sea-level cosmic-ray flux, periods of continuous operation of at least three months are usual before the stability begins to deteriorate. Refilling is normally all that is required to extend the counter life.

§ 3. CONSTRUCTION

The counter plates are cut from $\frac{1}{16}$ inch copper sheet to a rectangular shape of size 11.5 cm by 4.5 cm. The corners are rounded off and the edges smoothed to a half-round profile. The plates are eventually held apart by three glass distance pieces, two at the blank end of the glass counter container tube and the third at the other end near the tungsten-Pyrex seals and the filling stem (fig. 1). For this purpose three 3 cm legs of $\frac{1}{16}$ inch copper tubing are hard-soldered to

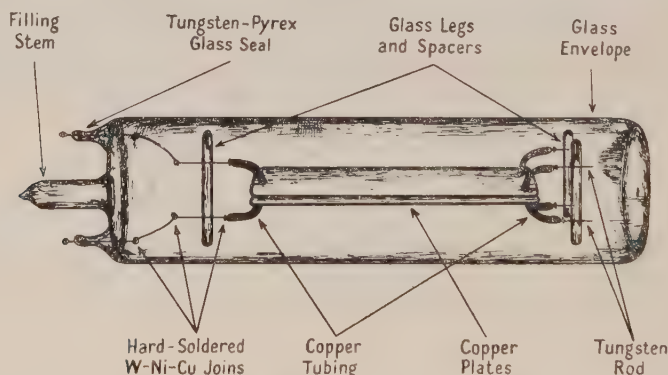


Fig. 1. Diagram showing parallel plate spark counter construction.

one side of each plate, so as to jut out at the ends. Lengths of tungsten rod are inserted in the copper tubing so that 1 cm protrudes: a hard solder join is then made between the two via an intermediate binding of nickel wire. These plate units are now given a rough polish on their free surface by means of emery cloth. Since the impurities in commercial copper sheet have been found to cause spurious counts a $\frac{1}{1000}$ -inch thick deposit of pure copper is then electroplated on

to all surfaces in an acid bath. When dry a final light polish and careful smoothing with finest emery cloth ensures that no scratches or points remain.

The electrodes are taken in pairs and clamped, sandwich fashion, on either side of a ground steel flat, which acts as a temporary spacer of the chosen gap dimension (2 mm). The ends of the glass legs are then melted on to the tungsten rods to complete the plate structure and the steel spacer removed. Connecting wires of copper joined to tungsten-Pyrex seals are attached to the tungsten rods at that end of the counter where there is only one glass spacer. The plate assembly can now be slid into a Pyrex tube of 55 mm bore, one end of which has previously been closed square and fitted with a central filling and holding stem of 10 mm bore. The seals are next fused into holes which have been prepared on either side of the filling stem. Closure of the blank end of the containing tube completes the construction.

By a chemical cleaning process the copper oxide films formed by the glass-blowing operations are removed, liquids being admitted through the filling stem. A succession of rinses with filtered, distilled water and methylated spirits follow and the interior of the containing tube is then pumped dry. At this stage a close inspection of the gap is made to see if any minute dust particles remain on the electrode surfaces. Failure to remove these by further rinsing inevitably results in a counter which operates with a continuous point discharge. The counters are now sealed by the filling stem on to a glass filling system and evacuated by a mercury diffusion pump. Although the assembly is designed to withstand baking to a temperature of 450°C this practice is unnecessary if the electrodes are free from oxide. The gas filling comprises a saturation pressure of dry absolute alcohol and 98% pure argon introduced in that order (see Keuffel 1949, who suggests that a film of organic droplets acts as a protective coating). The alcohol supply is warmed to about 40°C before being introduced into the counters in order that a visible film will condense on the electrode surfaces. Argon is then admitted till the total pressure is approximately 60 cm Hg. The counters are finally sealed off the filling system and stored with plates horizontal.

§ 4. TIME RESOLUTION

The subsidiary performance characteristics of parallel plate spark counters have been adequately treated in the references already given. The present designs, when employed to count the sea-level flux of cosmic-ray particles, show no radical departure from these either as regards their efficiency (98%), the length and slope of the plateau of the counting curve characteristic (1000 v, 4% per 100 v), or the minimum dead time (10 msec, electronically imposed) and the pulse rise time ($\sim 5 \times 10^{-9}$ sec over 500 v). Since only the counter time resolution is of importance from the point of view of short time interval measurements this characteristic alone will be treated fully.

The time lag associated with each counter pulse is here taken to mean the time interval beginning with the passage of an ionizing particle across the gap and ending with the rise of the output pulse of voltage to a predetermined level. For the purpose of time interval measurements the important parameter which requires to be known for each counter is not so much the time lag but the random lag variation. It is not easy to ascertain this in an experiment employing only a single counter, since the instant of passage of particles through that counter must be determined with the aid of a second. At best, therefore, one can only

hope to measure the difference in the random lag variation occurring in a pair of counters traversed by the same particle. In the present investigations twofold coincidences, due to the passage through two counters in succession, of single particles in the sea-level cosmic-ray flux, were recorded and the time intervals between the output pulses measured oscillographically.

The cathode-ray tube employed was of the three stage post-deflection accelerator kind (G.E.C. type 1608 BBCA operated at 10 kv). It enabled single sweep traces of 0.1 microsecond duration over 10 cm screen to be easily recorded on Ilford 5G91 film using a Wray f/1 lens. Each counter pulse was differentiated directly into two transmission lines, one of 2 m length and the other of approximately 20 m length. One of the short line pulses was used to trigger the time base circuit (Prime and Ravenhill 1950) and the second a gating pulse circuit on the modulator grid of the cathode-ray tube, which caused a momentary increase in the beam current. Thus a coincidence of the two counter pulses within 10^{-7} sec resulted in a visible trace. The long lines were used to convey the two display signals to the Y_1 and Y_2 deflecting plates respectively, their lengths being unequal by an amount which caused the pulses to be positioned conveniently apart on the trace. Both the time base and gating pulse circuits had starting delays of approximately 5×10^{-8} second.

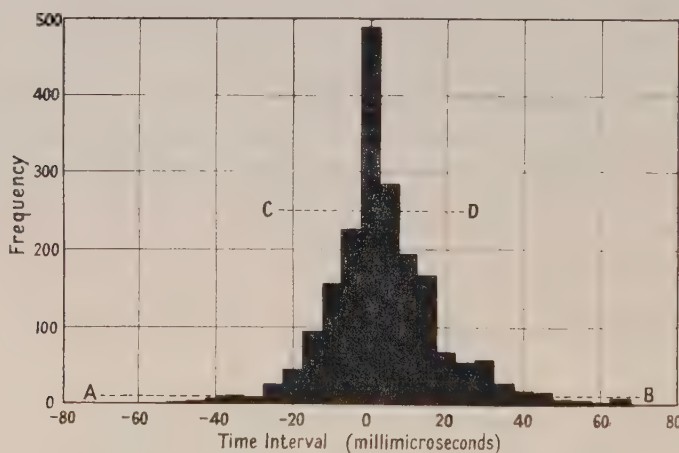


Fig. 2. Time-interval histogram for counter resolution.

Measurements of the pulse separation, and hence of the time interval, were facilitated by registering on the same film as the pulses a standard 50 Mc/s. calibration signal. The order of accuracy of any one such time interval measurement was to within 10^{-10} second. In fig. 2 some typical time interval data are reproduced in the form of a histogram, the measurements being grouped into intervals of 5×10^{-9} second. The data is for two counters, with their plates horizontal, in coincidence for single cosmic rays and separated vertically by a distance of 6 cm. A total of 2000 events was recorded. Both counters were operated at 500 v overvoltage.

The important parameter of the histogram is the half-width, in time, of the half-maximum point of the distribution: this is taken as the resolving time of a counter. Before fixing the half-maximum point it is necessary to correct for a small number of spurious contributions to the data due to showers, knock-on

electron events and in particular associated pairs of penetrating particles (Robinson 1953). The latter give rise to relatively long time delays and consequently give the histograms the appearance of having a much greater spread in time interval values than would otherwise be the case. The correction consists in drawing a new base line A . . . B for the histogram (see fig. 2) in such a position that the spurious contributions fall below it. The half-maximum point C . . . D of the distribution lying above this point can now be established: at this point an imaginary, smooth distribution curve would have a half-width of $5\text{ m}\mu\text{sec}$, and this is taken as the resolving time of a single counter. A gradual reduction of this value may be obtained by going to higher overvoltages, as has been shown by Keuffel (1949). For cosmic-ray purposes, however, it is undesirable to operate counters at these higher overvoltages, since the performance becomes much less stable and the useful life considerably shortened.

§ 5. APPLICATION TO TIME OF FLIGHT MEASUREMENTS

Spark counters have been employed in these laboratories recently in a number of investigations to ascertain the 'time structure' or time coherence of cosmic rays. This involves measuring time delays at sea level between certain particles in a group, for example the delays of electrons on each other in extensive air showers, the delays of the penetrating component in these showers on the electrons, and similarly for the so-called 'associated pairs of particles' the delay of one penetrating particle on another. One further application is described now, in detail, since it has a bearing on the limiting value of the time interval resolution obtainable with the present counters.

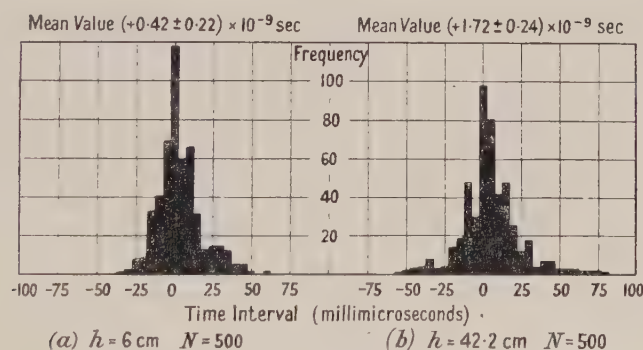


Fig. 3. Time-interval histograms for vertical counter separation h .

If spark counters under normal operating conditions have a time resolution of 5×10^{-9} sec, then it should be possible to detect time intervals of the order of 10^{-9} sec, by means either of a shift in the mean value of a frequency distribution or a broadening of a distribution along the time axis, as measured by a significant increase in the standard deviation. As an illustration of the former attempts have been made to measure the mean sea-level velocity of cosmic rays over a vertical distance of 36 cm. This was done by taking the difference of the mean time delays for a pair of counters traversed by single cosmic-ray particles and separated by two successive vertical spacings, namely 6 cm and 42.2 cm. If β for the cosmic-ray particles were equal to unity then the time shift of the mean value would amount to 1.21×10^{-9} second.

The two histograms compiled from the results are shown in fig. 3 (a) and (b). In going from one setting to the other the variance is seen to vary too, the larger separation giving a broader distribution. This is due, as previously, to a small number of long delays from associated pairs of particles, these being detected in greater proportion at the larger vertical separation. The extreme values of these distributions are accordingly omitted from the following measurements: only the central truncated portions are used, in such a way that the same range of values is covered in each distribution. The mean time interval values of the distributions together with the standard error values, are as follows:

Separation	6 cm	42.2 cm
Mean time interval value	$(+0.42 \pm 0.22) \times 10^{-9}$ sec	$(+1.72 \pm 0.24) \times 10^{-9}$ sec

The time difference, or shift in the mean value, is $(1.30 \pm 0.33) \times 10^{-9}$ second. Combining this with the path length of 36.2 cm gives a mean velocity value of $\beta = 0.93 \pm 0.25$. The important result here is not the actual value of β but the fact that the standard errors involved in it, and in the time interval, are only about one-quarter of the values they qualify. In fact, the ratio: difference of means/standard error difference is 6.2, i.e. three times greater than the value usually accepted as conferring statistical certainty on a difference value.

In some previously reported measurements on the time of flight of sea-level mesons, Officer (1951) used trays of Geiger counters separated by a distance of 5.45 m. The mean velocity obtained for 288 particles was $\beta = 0.96 \pm 0.25$, the resolution of the trays of overlapped counters being approximately 7×10^{-8} second. The standard error in the β -value is almost the same as that obtained from the present measurements where the distance used was some fifteen times shorter. As a consequence the spark counters have shown themselves to have a time resolution which is about fifteen times better than the optimum arrangement of Geiger counters, as may also be gauged from the relative figures for the respective resolving times. In addition the spark counter measurements confirm the feasibility of measuring time intervals of the order of 10^{-9} sec with statistical certainty.

ACKNOWLEDGMENTS

The author wishes to record his appreciation to Professor P. M. S. Blackett for the encouragement and the facilities he has afforded this work, and to Professor J. G. Wilson for his helpful advice. Acknowledgment is also due to Mr. K. R. Keep for his assistance in constructing some of the counters.

REFERENCES

- HUDSON, D. E., 1951, *Rev. Sci. Instrum.*, **22**, 849 (note only).
 KEUFFEL, J. W., 1948 a, *Phys. Rev.*, **73**, 531 (A); 1948 b, *Ibid.*, **74**, 1562 (A); 1949, *Rev. Sci. Instrum.*, **20**, 202.
 MADANSKY, L., and PIDD, R. W., 1948, *Phys. Rev.*, **73**, 1215 (L); 1949 a, *Ibid.*, **75**, 346 (A); 1949 b, *Ibid.*, **75**, 1175; 1950, *Rev. Sci. Instrum.*, **21**, 407.
 OFFICER, V. C., 1951, *Aust. J. Sci. Res. A*, **4**, 526.
 PRIME, H. A., and RAVENHILL, P., 1950, *J. Sci. Instrum.*, **22**, 7, 192.
 ROBINSON, E., 1953, *Proc. Phys. Soc. A*, **66**, 79.

Short Time Interval Measurements on Pairs of Associated Cosmic Ray Particles

By E. ROBINSON*

Physical Laboratories, University of Manchester

Communicated by P. M. S. Blackett: MS. received 27th August 1952

ABSTRACT. Twofold coincidence rates for associated pairs of cosmic-ray particles have been measured at sea level as a function of their (small) horizontal separation. The parallel plate spark counters used had a time resolution of 5×10^{-9} second. Simultaneously with the rates, measurements of the time intervals between the arrival of the two particles at a given horizontal plane were made, both for counters in air and under 18 cm Pb.

When allowance is made for the effect of spurious phenomena it is found that the coincidence rate falls off rapidly with increasing counter separation, that the particles forming the pairs are penetrating and that they have a mean delay between them which is significantly greater than the resolving time of the counters.

§ 1. INTRODUCTION

THE present results point to the existence of comparatively long time delays between pairs of penetrating particles in the sea-level cosmic-ray flux. The nature of these particles, and the significance of their association, is not understood at present: for example, it is not known whether the penetrating particles being observed occur with multiplicities in excess of two, or whether they are connected in any way with normal extensive air showers. For these reasons the method of presentation adopted here is phenomenological, possible related work and a discussion of the results being deferred till the end.

§ 2. EXPERIMENTAL AIMS

The investigations to be described arose out of some incidental features of the results shown in fig. 3 of the previous paper (Robinson 1953, to be referred to as I). There it was noted that the distribution of fig. 3(a) appeared to be slightly, and symmetrically, broadened along the time axis, as compared with the distribution of fig. 3(b), although little statistical weight could be attached to this observation. One explanation of such a broadening effect is that a small proportion of the total number of events could be caused by the non-simultaneous arrival, in the neighbourhood of the apparatus, of pairs or groups of associated particles, i.e. two different particles triggering the two counters, instead of, as in the majority of cases, a single particle traversing them in succession. Experiments were, therefore, undertaken in order to corroborate the existence of such an effect, to measure it in a quantitative manner, and to test the validity of various explanations.

§ 3. RESULTS

By disposing the two parallel plate spark counters close together on the same horizontal plane it was possible to reduce the number of coincidence counts due to single cosmic-ray particles (travelling almost horizontally) to negligible proportions. Because of its flat geometry the sensitive counter area presented to such particles was only 3 cm^2 (i.e. about 6% of that presented to the vertical radiation). Hence it was possible to search for events giving rise to comparatively

* Now at Nelson Research Laboratories, English Electric Co. Ltd., Stafford.

long time delays and, after taking into account minor corrections due to knock-on electrons and showers, to establish the existence of an effect with statistical certainty.

3.1. Associated Pair Rates

The twofold coincidence rates for two parallel plate spark counters, each of 50 cm^2 area, and separated horizontally by distances of 8.8, 15 and 21 cm respectively are tabulated in the table. The rate of accidental coincidences was

Twofold Coincidence Rates (per hour)

Horizontal separation s	8.8 cm	15 cm	21 cm	2 m
In air	6.43 ± 0.32	3.30 ± 0.07	1.71 ± 0.13	0.70
Under 18 cm Pb	3.73 ± 0.20	1.43 ± 0.09	0.12 ± 0.02	—

less than 10^{-3} counts per hour. At each separation the measurements were carried out in air (6 ft below a roof of about 100 g cm^{-2} concrete) and under 18 cm Pb (the counter plates being 6 cm below the bottom surface of the lead). For the measurements in air the rate of triggering of two counters by normal extensive air showers is given, the same figure being obtained both by calculation and by experiment. For these shower measurements the counters were separated by a distance of approximately 2 metres. It is seen that in air the rate of coincidences for close separations is more than ten times greater than this value.

3.2. Time Interval Histograms

Simultaneously with the rate measurements time interval measurements were made for each of the six experimental arrangements and the corresponding histograms are shown in fig. 1 (*a*) to (*f*). For comparison purposes the histograms have been normalized so that the total number of events in each is approximately 165. The actual number of observations N , and the horizontal separation s between the counters, is shown in each case. It is obvious that all these distributions due to two particles have a spread which is greater than that observed in fig. 3(*a*) of the previous paper, where the results for vertical coincidences due to single particles are given. The long and symmetrical tails to each distribution seem, therefore, to represent genuine delays elapsing between the arrival of the first and second particle of an associated pair, since some of the time intervals are much longer than can be accounted for by the resolving times of the counters themselves.

§ 4. CONCLUSIONS

The rate and time interval data shown in the table and fig. 1 respectively are diluted by unwanted types of events, principally knock-on electrons and showers. Under lead, and to a lesser extent in air, the knock-on electron and penetrating shower contributions to the rate will be most effective at the smaller separations; in air there will be an additional spurious contribution from extensive air showers. The total frequency of these spurious contributions has been estimated, but in no case has it been found to amount to more than 20% of the rate, even for the smallest counter separation used. The true rates in air are still seen to be significantly greater than the statistical uncertainties, whilst under lead, where there can be no contribution from extensive air showers, a very appreciable coincidence rate persists. This result in particular is difficult to understand on the basis of the present knowledge of cosmic-ray phenomena.

From the data of the table, and making allowance for the extensive air shower correction, it is evident that the effect of 18 cm Pb is to reduce the rate by a factor of only about one half at the two smaller separations, and by a factor of about one eighth at the 21 cm separation: this latter figure is statistically uncertain and therefore is best disregarded. Assuming that the same type of event is being measured under the lead as in air, it is evident that the particles involved must be as penetrating as μ -mesons. (At sea level the flux of single μ -mesons is reduced in intensity by a factor of approximately two thirds by 18 cm Pb.) Hence, although nothing can be deduced as to their nature, the associated pairs of particles which are capable of penetrating 18 cm Pb together may be classed as 'penetrating'. In order to justify the assumption that the air and under lead measurements refer to the same type of event, it is only necessary to notice the

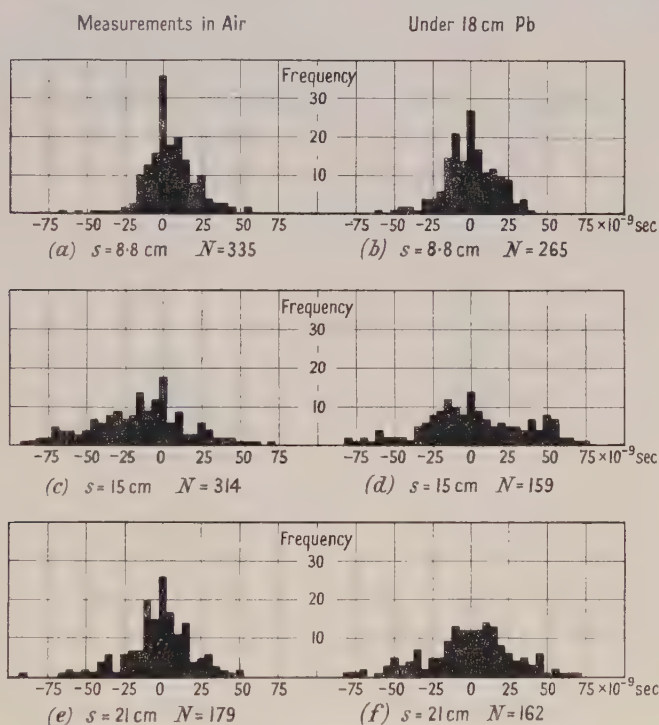


Fig. 1. Time-interval histograms for horizontal counter separation s .

similarity between the corresponding time interval data and their marked difference from the data obtainable from the vertical coincidence measurements. The similarity of the decoherence effect in air and under lead adds confirmation to this view.

The time interval data of fig. 1, which is of prime importance in the present investigations, is summarized in fig. 2. Here the data of fig. 3 (a) of I for single particles are reproduced alongside a composite histogram for pairs of particles, compiled from the data of fig. 1 (c), (d), (e) and (f), and normalized to the same total number of observations $N = 500$. The data of fig. 1 (a) and (b) are disregarded, for this purpose, on account of the relatively high contribution due to knock-on

electron events. From fig. 2 below it is apparent that the mean time delay between the pairs of particles is of the order of 2.0×10^{-8} second. Unless some decay process is involved this time interval must represent the mean delay of the second particle of an associated pair or group on the first. For the results under lead neither knock-on electron nor local penetrating shower events could give rise to the longer time delays recorded, no matter what combination of path difference from a common point of origin, or what velocity difference for the two particles, is considered. We thus have confirmation of the fact that the rate data are attributable not to these spurious agencies but to some other associated particle phenomena.

The 'decoherence' effect detectable in the rate data reproduced in the table is such that, both in air and under lead, there is a decrease in the rate by a factor of approximately 10 as a result of increasing the mean horizontal separation of the two counters from 8 cm to 21 cm. At separations in excess of 25 cm the associated pair rate in air falls to a value which is comparable with the extensive air shower rate; within these limits the coincidence rate increases rapidly. Similar effects have been noticed by other workers employing extensive air shower

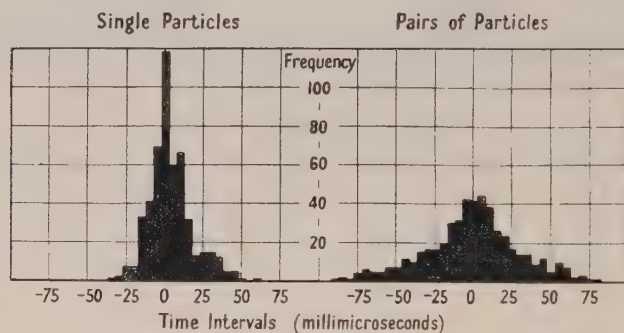


Fig. 2. Time-interval histograms for single and pairs of particles.

detecting arrangements, the phenomenon being attributed to the so-called 'narrow showers'. It is rarely the case, however, that the sensitive areas of the counters or counter trays employed are as small as those used in the present investigations, with the result that it would be difficult to detect any strong decoherence effect with them at separations as small as 10 cm. In addition the present measurements reveal the persistence of the strong decoherence effect under 18 cm Pb, a result which throws considerable doubt as to whether some of the 'narrow shower' effects in air are in fact due to soft groups of particles at all.

To obtain a true measure of the decoherence the rate data should be further corrected to allow for the finite sensitive areas of the counters. The separations quoted are only mean values, it being possible for pairs of particles with separations differing from the mean by as much as -4.0 cm and $+6.0$ cm to be counted. The correction is small, however, and does not greatly affect the actual value of the decoherence, which need only be represented by an order of magnitude, bearing in mind that this is the effective accuracy of the other principal measurements carried out on the penetration and delay properties of the pairs of particles.

§ 5. POSSIBLE RELATED WORK

Similar conclusions to the above may be deduced from incidental evidence obtained in a number of other recent cosmic-ray investigations. None of the methods is based on time interval measurements, however, and there is one further point of difference: the counter arrangements used operate in coincidence circuits for which the resolving times are always longer than 10^{-6} second. The spark counter data, on the other hand, have been obtained with a coincidence resolving time which is always shorter than 10^{-7} second.

In his experiments on knock-on electrons Clay (1947) observed twofold coincidences due to the production of knock-on electrons by μ -mesons in absorbers. In addition he obtained a background effect which he attributed to pairs of associated penetrating particles. These were detected with rates roughly comparable with those quoted in the table. The decoherence of the effect was, however, less marked in his measurements, which were made with Geiger counters shielded with up to 10 cm thickness of lead.

Associated penetrating particles in the cosmic-ray flux underground have been studied extensively by Braddick, Nash and Wolfendale (1951) both with cloud chambers and Geiger counter arrangements. They have also observed similar effects at sea level, but it is not known whether the two types of phenomenon are identical. At sea level there is, however, a definite rate of parallel, penetrating particles which is well above the spurious rate.

In several recent investigations on penetrating showers McCusker and his co-workers (McCusker, Messel, Millar and Porter, to be published) have observed pairs of penetrating particles and have attempted to measure their barometer coefficients. Groups of penetrating particles with multiplicities up to at least twelve were recorded but the twofold events have a distinctive behaviour in that their barometer coefficient showed a change with the amount of water above the apparatus. They also exhibit a strong decoherence effect.

It is thought that further evidence may lie in the recent contributions to the knowledge of narrow air showers (Maze *et al.* 1949, Hamelin 1952, Northrop 1951, Wei and Montgomery 1950). In these events several penetrating particles are thought to co-exist, but here, as elsewhere, it is not always possible to correlate these events with ordinary extensive air showers.

§ 6. DISCUSSION

The restricted sensitive areas of the counters employed in the present investigations, though not without some advantages from the point of view of the decoherence measurements, have precluded the possibility of getting high rates for the associated pairs of particles. If much higher rates were obtained investigations of the possible association of the phenomena with extensive air showers or with a third or even more penetrating particles could be made, and also the barometric coefficient obtained. In the absence of any evidence on these points it is difficult to formulate an adequate explanation of the facts already ascertained, which is consistent with the established views concerning the sea-level flux of cosmic-ray particles. The most significant of these facts is the relatively long mean delays revealed by the time interval data.

To explore one possible explanation in detail we can suppose that the delays may be attributed either to pairs of particles of very dissimilar energy, and therefore of velocity, coming to the apparatus from several metres distance, or to two

particles of roughly equal velocity which have travelled distances of several kilometres together. It seems unlikely that a flux of pairs of particles, occurring with rates as high as those quoted in the table, would be composed of particles other than those already known to exist at sea level. Further, in view of their penetrating property, it is natural to suppose that they are comprised chiefly of μ -mesons. In this event the particle momenta must exceed 350 MeV/c and as a consequence their velocities cannot be dissimilar, as both will arrive at sea level with velocities in excess of 0.96c. Before reaching sea level the particles will have lost energy rapidly as a result of ionization, so that their velocity difference above the apparatus would not be greater than about one per cent. From this we may conclude that in order to give rise to delays of the order of magnitude of 2.0×10^{-8} sec the two particles would have to come from a distance in excess of 1 km above sea level.

From this conclusion it would seem, therefore, that we might be dealing with pairs or small groups of penetrating particles of roughly equal energy coming from the upper atmosphere, possibly from that region at the top which is responsible for the production of extensive air showers. According to Cocconi (1950), see also Clay (1951), there is a qualitative similarity between the hard component and the extensive air shower type of event at sea level. Hard showers at sea level, which are devoid of any accompanying soft particles, may be caused by primary events occurring at such a height in the atmosphere that the electronic component is absorbed by the time sea level is reached. However, to make this picture conform to the decoherence effect observed in the present measurements would require that the root mean square scattering angle, for particles travelling distances of the order of a kilometre, and also the angular separation of the two particle trajectories at the point of formation, be less than 10^{-2} degree. Neither of these conditions can be fulfilled. The r.m.s. scattering angle, under these conditions, would still exceed 1 degree for energies up to approximately 5 kMeV; so also would the angular separation of two shower secondaries formed by a primary nucleon for which the ratio of its incident energy to the rest energy is less than 50.

We see, therefore, that apart from non-ionizing path linkages it is improbable that a shower of penetrating particles, formed at a height of the order of a kilometre above sea level, would give rise to a strong decoherence effect. The alternative explanation, based on pairs of particles coming to the apparatus from several metres distance, has already been discounted, for the case where the particles have very different velocities. It is possible, however, that this type of event may be connected with some decay process, in which case the necessity for a large velocity difference does not arise.

ACKNOWLEDGMENTS

It is a pleasure to thank Professor P. M. S. Blackett for his interest and support, and Professor J. G. Wilson for helpful discussions.

REFERENCES

- BRADDICK, H. J. J., NASH, W. F., and WOLFENDALE, A. W., 1951, *Phil. Mag.*, **42**, 1277.
 CLAY, J., 1947, *Physica*, **13**, 433; 1951, *Phys. Rev.*, **81**, 645 (L).
 COCCONI, G., 1950, *Phys. Rev.*, **79**, 1006.
 HAMELIN, J., *J. Phys. Radium*, 1952, **13**, 11-14.
 MAZE, R., FREON, A., DAUDIN, J., and AUGER, P., 1949, *Rev. Mod. Phys.*, **21**, 14.
 NORTHROP, J. A., 1951, *Phys. Rev.*, **84**, 83.
 WEI, J. N. P., and MONTGOMERY, C. G., 1950, *Phys. Rev.*, **80**, 480 (L).

Nuclear Magnetic Resonance Line Width Transition in Aluminium

By E. F. W. SEYMOUR

Clarendon Laboratory, Oxford

Communicated by B. V. Rollin; MS. received 16th May 1952, and in final form 24th September 1952

ABSTRACT. The nuclear magnetic resonance absorption line due to ^{27}Al in the metal exhibits a line width transition centred at 330°C . The connection with diffusion processes is discussed.

§ 1. INTRODUCTION

NUCLEAR magnetic resonance lines in solids commonly have a width of several gauss, due to the local magnetic field at a resonating nucleus produced by its neighbours. It is well known that sufficiently rapid motion of the nuclei can reduce the effective value of the local field, so that onset of such motion can be observed as a reduction in line width. There may also be a marked effect on the spin-lattice relaxation time. In a metal, where the possibility of any rotational motion is excluded, the motion is presumably connected with a diffusion process.

Line width transitions in solid metallic sodium and lithium have been reported by Gutowsky (1951), and have been interpreted as due to self-diffusion. The self-diffusion coefficient of sodium has also been calculated by Norberg and Slichter (1951), from measurements of the related quantity, the spin-spin relaxation time. Their result was in satisfactory agreement with results of radioactive tracer measurements. Norberg (1952) has deduced a value for the diffusion coefficient of hydrogen in palladium, from the temperature variation of the proton spin-lattice relaxation time. When the coefficient is written in the form $D = D_0 e^{-E/RT}$ the constants D_0 and E are lower than the averages obtained by other methods. The author suggests that the low values may be due to diffusion along internal 'short-circuit' paths.

In the present paper a line width transition in metallic aluminium is reported. If this is interpreted in terms of self-diffusion, values of D_0 and E are obtained which are lower than the expected values (Nowick 1951).

§ 2. EXPERIMENTAL METHOD

The resonance absorption due to ^{27}Al was observed at 4 Mc/s in a magnetic field of about 3600 gauss, at temperatures between 15°C and 440°C . Resonance was detected by means of a radio-frequency bridge. The magnetic field at the sample was modulated at 200 c/s with an amplitude small compared with the line width. The derivative of the absorption curve was traced by a recording milliammeter, connected to the output of a phase-sensitive amplifier.

The bridge circuit is shown in fig. 1. It is similar to that described by Grivet, Soutif and Buyle (1949). It is characterized by low input and output

impedances, a property which makes it relatively insensitive to changes in capacity resulting from microphonic shaking of the leads. Best results are obtained if the sample coil L and the condensers C are mounted rigidly, and together, so that the high impedance regions are subject to the minimum microphonic movement. The condensers were connected to the remainder of the circuit by short lengths of coaxial cable. Tuning was accomplished by varying the frequency and the resistance R . Standard low-inductance dial resistance boxes were found to be sufficiently non-reactive at the frequency used, so that the two adjustments were nearly independent. A resistive unbalance was always used so that the absorption curve was observed, since this condition led to least microphonic noise. The signal was fed to the radio-frequency amplifier through a tuned step-up transformer.

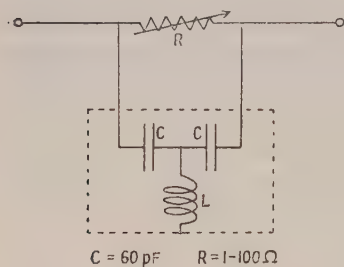


Fig. 1.

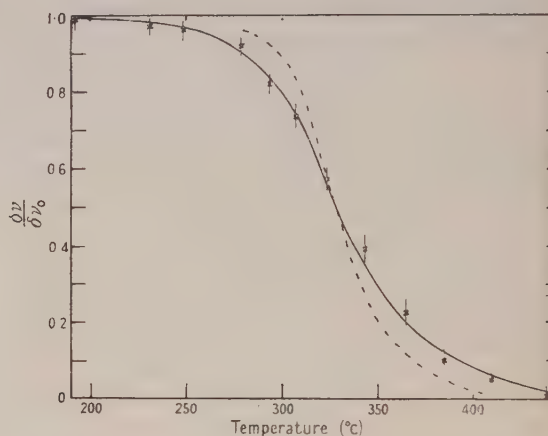


Fig. 2.

Resonances were observed at constant frequency, by slow variation of the magnet exciting current. Due to hysteresis effects the rate of change of magnetic field with current could not be obtained directly. Instead it was calculated from a subsidiary experiment in which the consequent shift in resonant frequency of protons was measured.

The specimen consisted of foil, stated by the makers to be 99.99% pure, cold rolled to a thickness of about 10μ , which is comparable with the skin depth at 4 Mc/s. Layers of foil were separated by mica slips. After annealing at 640°C for an hour, the grain size was of the order of 0.05 mm.

The specimen with its coil was mounted rigidly inside a brass tube, which acted as a radio-frequency shield, and also carried an electric heater. The whole assembly fitted between the magnet poles. To avoid oxidation of the metal an atmosphere of hydrogen was maintained in the furnace. Two copper-constantan thermojunctions were embedded in the specimen, one near its centre and one near its surface, and connected so as to measure both the temperature and any gradient within the specimen. In this way the temperature inhomogeneity was found not to exceed 1°C .

§ 3. RESULTS

The second moment (Van Vleck 1948) of the resonance line, measured at room temperature, was 11.2 gauss^2 . The value calculated for magnetic dipole

broadening in the rigid lattice is 7.5 gauss². There should be no contribution due to the nuclear quadrupole moment. This discrepancy has been observed by Gutowsky (1951) for a number of metals including aluminium and sodium.

The quantity which was measured as a function of temperature was the separation between maxima of the absorption derivative curve. The corresponding interval on a frequency scale, $\delta\nu$, will be referred to as the line width. Between room temperature and about 200°C the line width was constant at 9.8 kc/s. Above this temperature the width decreased as shown in fig. 2. The points represent the experimental results after a correction has been applied for the inhomogeneity of the field of the magnet. For fractional widths greater than about 0.5, the main inaccuracy was in estimating the positions of the broad flat maxima. For sharper lines the uncertainty arose mainly from the manner of allowing for the residual width due to the magnet.

The amplitude of the signal increased as the width decreased, showing that the mechanism responsible for the narrowing affected the majority of the nuclei.

§ 4. DISCUSSION

The decrease in line width provides strong evidence for internal motions. Bloembergen, Purcell and Pound (1948) derive a general expression for the line width when relative motion of the nuclei, of any sort, takes place, in terms of the Fourier components of the local field spectrum. The components are effective up to a frequency of the order of the observed width $\delta\nu$. If one assumes that the motion is a random one, and is isotropic on the average, the theory gives the relation

$$(\delta\nu)^2 = \frac{2}{\pi} (\delta\nu_0)^2 \tan^{-1} (4\pi\tau\delta\nu),$$

where $\delta\nu_0$ is the width characteristic of the static lattice. τ is a correlation time which may be regarded as the average time for the interaction between two neighbours to change appreciably.

The full curve in fig. 2 is a theoretical one calculated from the above equation with $\tau = 10^{-13} e^{21000/RT}$ sec.

It is natural to attempt to interpret this motion as self-diffusion. τ would then be the average time for an atom to make a jump to a neighbouring lattice point, assuming diffusion by the vacancy or place-exchange mechanisms. The self-diffusion coefficient would be given by $D = \frac{1}{6}\delta^2/\tau$ where δ is the distance between nearest lattice sites, 2.8 Å. The result obtained is

$$D = 10^{-3 \pm 1} e^{-(21000 \pm 2000)/RT} \text{ cm}^2/\text{sec.}$$

It should be emphasized that the errors indicated here are experimental, and do not take into account the approximate nature of the theory.

Unfortunately the self-diffusion coefficient of aluminium has not so far been measured. However there are good grounds (see, for instance, Nowick 1951) for believing that it will be found to be of the order of $D = 0.45 e^{33000/RT} \text{ cm}^2/\text{sec.}$ The broken line in fig. 2 has been calculated using an activation energy 33 kcal/mole, with an approximate value for D_0 of 10 cm²/sec, chosen to cause line narrowing in this temperature range. This curve lies outside the estimated experimental error.

It is known that diffusion by 'short-circuit' paths can lead to low values of D_0 and E . Since the signal observed in this experiment was evidently due

to the majority of the nuclei, and dipole-dipole interactions have an effective range of only two or three lattice distances, the density of lattice imperfections would have to be correspondingly large to produce any effect on the signal. Such an effect is thus likely to be a small one.

The result could be in error if the motion affected dipole-dipole interactions, and other unidentified interactions which apparently contribute to the low temperature line width, differently. It should be remarked, however, that the above treatment has proved satisfactory in the case of sodium (Norberg and Slichter 1951), and it is not clear in what significant respects the two cases differ.

It is concluded that, although the numerical result should be treated with some reserve, the line narrowing must almost certainly be attributed to self-diffusion.

ACKNOWLEDGMENTS

The author is indebted to Dr. B. V. Rollin for suggesting this work, and for advice in the course of it, and to the Department of Scientific and Industrial Research for a maintenance grant.

REFERENCES

- BLOEMBERGEN, N., PURCELL, E. M., and POUND, R. V., 1948, *Phys. Rev.*, **73**, 679.
GRIVET, P., SOUTIF, M., and BUYLE, M., 1949, *C.R. Acad. Sci., Paris*, **229**, 113.
GUTOWSKY, H. S., 1951, *Phys. Rev.*, **83**, 1073.
NORBERG, R. E., 1952, *Phys. Rev.*, **86**, 745.
NORBERG, R. E., and SLICHTER, C. P., 1951, *Phys. Rev.*, **83**, 1074.
NOWICK, A. S., 1951, *J. Appl. Phys.*, **22**, 1182.
VAN VLECK, J. H., 1948, *Phys. Rev.*, **74**, 1168.

Antiferromagnetism by the Spin Wave Method III: Application to more Complex Systems

By J. M. ZIMAN
Clarendon Laboratory, Oxford

MS. received 25th July 1952

ABSTRACT. The formulae developed in previous papers by the author are applied to body-centred and face-centred cubic lattices, with various ratios of next-nearest to nearest-neighbour antiferromagnetic interactions between the spins. Luttinger's results for the ground states of the corresponding Ising models are obtained by a simplification of his method. The face-centred cubic lattice with only nearest-neighbour interactions is shown not to be antiferromagnetic. In other cases the Curie temperatures are calculated and are found to be proportional to $S(2S+1)$, where S is the spin of the magnetic ion. The experimental values of θ/T_c can be explained only if superexchange between next-nearest neighbours is greater than the nearest-neighbour interaction in compounds like MnO , but is negligible, or favours parallel spins, in MnF_2 and FeF_2 .

§ 1. INTRODUCTION

IN previous papers by the author (Ziman 1952 a, b—to be referred to as I and II) a general treatment of the antiferromagnetic state has been given, using the spin wave method. It was shown that the antiparallel ordered state is a good approximation to the ground state of the system, and that formulae could be obtained for magnetic susceptibility at temperatures below the Curie point. This treatment was applied to the case of the simple cubic (S.C.) lattice with nearest-neighbour (N.N.) interactions, which, although it does not exist in nature, is a useful standard model for a qualitative comparison with experiment and with other theories. But the analysis was not restricted to this simple case, and is capable of dealing, without modification, with models of much greater complexity.

Real antiferromagnetic substances differ from the standard model in two main respects: the lattice structure is usually more complex, and the interactions are not always restricted to nearest neighbours. It has been shown by Anderson (1950 a, b) that in a large class of antiferromagnetic compounds, having either body-centred (B.C.) or face-centred (F.C.) lattices, the next-nearest-neighbour (N.N.N.) interaction may be very strong, owing to superexchange. This has been confirmed by neutron diffraction experiments (Shull, Strauser and Wollan 1951). In the present paper the spin wave method has been applied to systems of this type and estimates obtained of the Curie temperature. For the sake of brevity the notation of the earlier papers, I and II, is used without redefinition.

§ 2. THE BASIC ARRAY

To use the spin wave method we must know the 'basic array', that is, the ordered antiparallel arrangement, of minimum energy, of an array of Ising dipoles with the prescribed lattice structure and the given interactions. This

problem has been solved, in all the cases we consider here, by Anderson (1950 b) and, more rigorously, by Luttinger (1951). But the basic array has usually been described in terms of sets of ordered, simple cubic, sublattices, which are interleaved to construct the whole complex lattice, whereas we require the whole lattice to be generated by integral displacements along the three basic vectors, $\mathbf{u}_1, \mathbf{u}_2, \mathbf{u}_3$, the ordering being prescribed by the vector \mathbf{w} as in I, §2.

The appropriate vectors $\mathbf{u}_1, \mathbf{u}_2, \mathbf{u}_3$ are easily constructed for the B.C. and F.C. cases, and the value of \mathbf{w} may be discovered by inspection of the known solutions. It is easy, for example, to show that the arrangements found by Luttinger and Tisza (1946) for dipole-dipole interactions can all be generated using simple values of \mathbf{w} , which provides, perhaps, the most compact prescription for such arrangements.

But it is also possible to solve these problems directly, by a generalization of the method of Luttinger. For if, instead of using cubic axes, we use the basic vectors $\mathbf{u}_1, \mathbf{u}_2, \mathbf{u}_3$ for position vectors, i.e.

$$\mathbf{R}_l = l_1 \mathbf{u}_1 + l_2 \mathbf{u}_2 + l_3 \mathbf{u}_3,$$

and the reciprocal set $\mathbf{v}_1 = (\mathbf{u}_2 \times \mathbf{u}_3) / (\mathbf{u}_1 \cdot \mathbf{u}_2 \times \mathbf{u}_3)$, etc. as basic vectors in the reciprocal space, $\mathbf{x} = \kappa_1 \mathbf{v}_1 + \kappa_2 \mathbf{v}_2 + \kappa_3 \mathbf{v}_3$, and carry out the Fourier transformation by expanding in the form

$$\begin{aligned} f(l) &= \sum_{\mathbf{k}} C_{\mathbf{k}} \exp(i\mathbf{x} \cdot \mathbf{R}_l) \\ &= \sum_{\mathbf{k}} C_{\mathbf{k}} \exp\{i(\kappa_1 l_1 + \kappa_2 l_2 + \kappa_3 l_3)\}, \end{aligned}$$

the argument used by Luttinger in the S.C. case can be followed through, without further modification, in all cases, and \mathbf{w} is just that value of \mathbf{x} that minimizes the energy.

The results of this investigation may be summarized as in table 1. Here r measures the ratio of N.N.N. to N.N. interactions; $\mathbf{i}, \mathbf{j}, \mathbf{k}$ are vectors (not necessarily of unit length) along the cubic axes.

Table 1. Data for Basic Arrays

Lattice	Basic vectors	N.N. at origin	N.N.N.	r	\mathbf{w}
B.C. cubic	$\mathbf{u}_1 = \mathbf{j} + \mathbf{k} - \mathbf{i}$ etc.	(1, 1, 1) etc. (1, 0, 0) etc.	(1, 1, 0) etc.	$\left. \begin{array}{l} < \frac{2}{3} \\ > \frac{2}{3} \end{array} \right\}$	$\left. \begin{array}{l} -\pi(\mathbf{v}_1 + \mathbf{v}_2 + \mathbf{v}_3) \\ \pm \frac{1}{2}\pi(\mathbf{v}_1 + \mathbf{v}_2 + \mathbf{v}_3)^* \end{array} \right\}$
F.C. cubic	$\mathbf{u}_1 = \mathbf{j} + \mathbf{k}$ etc.	(1, 0, 0) etc. (1, -1, 0) etc.	(1, 1, -1) etc.	$\left. \begin{array}{l} < \frac{1}{2} \\ > \frac{1}{2} \end{array} \right\}$	$\left. \begin{array}{l} -\pi(\mathbf{v}_1 \pm \frac{1}{2}\mathbf{v}_2 \mp \frac{1}{2}\mathbf{v}_3)^* \\ \text{etc.} \\ -\pi(\mathbf{v}_1 \mp \mathbf{v}_2 - \mathbf{v}_3) \\ -\pi\mathbf{v}_1 \text{ etc.} \end{array} \right\}$

§ 3. COMPLEX ARRAYS

In certain cases (marked *), $\exp(i\mathbf{w} \cdot \mathbf{R}_l)$ is not always real. It is then necessary to use the formula $\sigma_l = \frac{1}{2}(1+i)\exp(i\mathbf{w} \cdot \mathbf{R}_l) + \frac{1}{2}(1-i)\exp(-i\mathbf{w} \cdot \mathbf{R}_l)$ for the sign of the spin on the l th site. It is quite possible to carry through the analysis in these cases by substituting σ_l for $\exp(i\mathbf{w} \cdot \mathbf{R}_l)$ in I (14) and (15), and writing $\sigma_{lm} = \sigma_l \sigma_m$ for I (16). The Fourier transformations can be performed without difficulty, but the results are rather more complicated than in the simpler case.

In the absence of a magnetic field it turns out that we obtain almost the same formulae as previously, e.g. $\mu_\lambda = (A_\lambda^2 - |B_\lambda|^2)^{1/2}$, where

$$A_\lambda = g\beta H_A + \sum S J_h [\cos(\mathbf{w} \cdot \mathbf{R}_h) - \frac{1}{2}\{1 + \cos(\mathbf{w} \cdot \mathbf{R}_h)\} \cos(\mathbf{K}_\lambda \cdot \mathbf{R}_h)],$$

$$B_\lambda = -\sum S J_h \{1 - \cos(\mathbf{w} \cdot \mathbf{R}_h)\} \exp(-i\mathbf{K}_\lambda \cdot \mathbf{R}_h).$$

The energy of the ground state and the correction factor ϕ_0 may be calculated, just as in I § 5, II §§ 4, 5; but when a magnetic field is present the eigenvalues μ_λ are the roots of an equation of the fourth degree in μ_λ^2 , and it is very difficult to discuss the susceptibility. Fortunately, the cases considered in this paragraph are just those which are believed not to occur naturally, and are therefore not of great practical interest.

One important theoretical point should be mentioned. Li (1951) has shown that the F.C. cubic system should not be antiferromagnetic if there are only N.N. interactions. This we can verify. Suppose we calculate ϕ as a function of temperature, using II (30). Then we must approximate to the sum by means of an integral, i.e.

$$\phi = 1 - (32S\pi^3)^{-1} \int \int \int_{-\pi}^{\pi} \left\{ \coth \left(\frac{\phi \mu_\lambda}{2kT} \right) \frac{A_\lambda}{\mu_\lambda} - 1 \right\} d\mathbf{K}_\lambda.$$

Near $K_\lambda = 0$, $\mu_\lambda \rightarrow 0$, and the integral converges only if $\int \int \int \frac{A_\lambda}{\mu_\lambda^2} d\mathbf{K}_\lambda$ converges.

But for the F.C. lattice, using the above formulae, we have

$$\begin{aligned} \mu_\lambda^2 = & 2S|J| [4 - 2\cos K_1 - 2\cos(K_2 - K_3) - 2r\{1 - \sum \cos(K_1 + K_2 - K_3)\}] \\ & \times [4 + 2\sum \cos K_1 + 2\sum \cos(K_1 - K_2) - 2r\{1 - \sum \cos(K_1 + K_2 - K_3)\}] \end{aligned}$$

where $|J|$ is the magnitude of the N.N. interaction and the sums are over cyclic permutations of 1, 2, 3. When $r=0$, μ_λ vanishes along the line $K_1=0$, $K_2=K_3$, and it is easy to show that the integral diverges logarithmically. That is to say, ϕ cannot be calculated. But ϕ measures the average value of $(1 - u_i/2S)$, which must be near unity if the system is in an ordered antiferromagnetic phase. Thus this special type of system should not be antiferromagnetic. It will be seen that if $r \neq 0$, i.e. there is any appreciable N.N.N. interaction, μ_λ vanishes only at isolated points and the integral converges. But it should be noted that there must be a similar instability at points where the ordering changes from one type to the other, that is, when $r = \frac{2}{3}$ in the B.C. case, or $\frac{1}{2}$ in the F.C. case.

§ 4. CURIE TEMPERATURE

Once we have obtained the basic array, the calculations for the remaining cases are straightforward (although the numerical integrations are tedious) and require no special discussion. The detailed susceptibility curves are so similar in shape to those already published (II, fig. 2) that we need not give them in detail.

In II § 7 the question of defining the Curie point is discussed. The suggested extrapolation from a high-temperature solution obtained by the Bethe-Weiss method is not applicable when there are N.N.N. interactions, and we use the simple condition that the parallel and perpendicular susceptibilities should become equal at the Curie temperature.

In each case, then, we have $\chi_c = \chi_\perp = Ng^2\beta^2 S/2VA_0$, where $A_0 = 16S|J|$ for B.C., $r < \frac{2}{3}$; and $A_0 = 12S|J|(1+r)$ for F.C., $r > \frac{1}{2}$.

The critical temperature depends on the value of S . It turns out, to a reasonable degree of accuracy, that $kT_c/S|J| \propto (2S+1)$. This is not, apparently, a direct consequence of the equations, in the sense that it is explicitly evident by inspection, but comes out of the detailed numerical computation. It is, perhaps, not unexpected that the factor should be just the multiplicity of the state, yet no algebraic argument for it has been found.

In fig. 1 the critical temperature is plotted as a function of the ratio r .

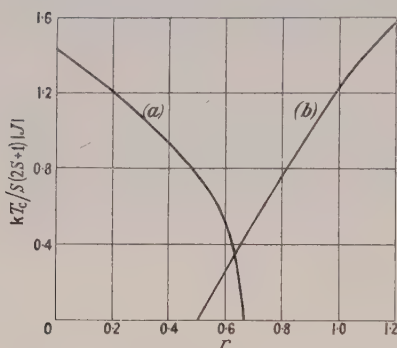


Fig. 1. Critical temperature as function of ratio of N.N.N. to N.N. interaction. (a) B.C. cubic, (b) F.C. cubic.

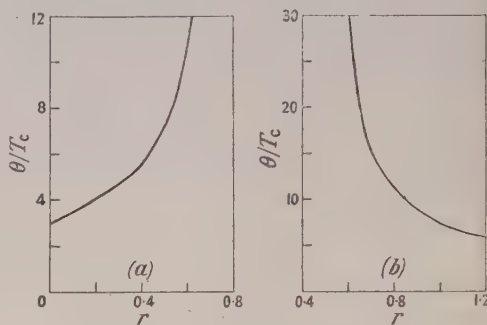


Fig. 2. θ/T_c as function of ratio of N.N.N. to N.N. interaction. (a) B.C. cubic, (b) F.C. cubic.

A more useful way of expressing these results is to calculate θ/T_c where θ is the constant in the Curie-Weiss law $\chi = C/(T+\theta)$, since this can be measured directly. Unfortunately we have no very exact theory from which to obtain θ . If, however, we use the simplest internal-field theory, it is easy to show that

$$\frac{k\theta}{2S|J|} = \frac{2}{3}(S+1)(4+3r) \quad (\text{B.C.});$$

$$\frac{k\theta}{2S|J|} = (S+1)(4+2r) \quad (\text{F.C.}),$$

and using these formulae we obtain fig. 2. Here the curves are not independent of S , and θ/T_c must be multiplied by $2(S+1)/3(S+\frac{1}{2})$ when $S \neq \frac{1}{2}$.

For comparison, in table 2 are quoted experimental data as compiled by Anderson (1950 b) and Smart (1952).

Table 2. Experimental Values of θ/T_c

Compound	Lattice	θ/T_c
MnF ₂	B.C. tetragonal	1.57
FeF ₂	"	1.48
MnO	F.C. cubic	5.0
MnS	"	3.1
MnSe	"	~3
FeO	"	2.9
NiO	"	3.8
CoO	"	0.96

§ 5. DISCUSSION

The calculations were made for values of r covering the range of values proposed by Anderson to account for the experimental data. It will be seen that none of these results can be fitted, by the present theory, between these limits. The experimental values are all too small, even allowing for the spin factor (whose minimum value, when $S=5/2$, is $7/9$). To fit these data we should evidently require that the N.N.N. interaction should be negative in the B.C. case, and very much larger than the N.N. interaction in the F.C. case.

The labour of calculating a single point on the curves of fig. 1 is rather heavy, but it is easy to extrapolate approximately by simple arguments. Thus we may obtain the asymptotic form of the function plotted in fig. 2(b) by remembering that for very large r we should have, in effect, four sets of independent S.C. sublattices. For these $kT_c/2S|J| \sim 1.30r(S + \frac{1}{2})$, and using the formula for θ it is easy to show that as $r \rightarrow \infty$, $\theta/T_c \rightarrow 2.3$, which lies below all the measured values for F.C. compounds (except CoO). The curve in fig. 2(b) must then certainly pass through these values for some large value of r , so that the observations can be fitted by a structure in which the N.N. interaction is small compared with the N.N.N. superexchange. If we take, for example, $\theta/T_c = 3$ we get $r \sim 5.7$.

For the B.C. case, on the other hand, we can see that θ vanishes when $r = -4/3$, whereas T_c increases slowly as r decreases, and we can extrapolate θ/T_c backwards nearly linearly to zero; $\theta/T_c = 1.5$ then corresponds to $r \sim -0.5$.

Although such an interpretation is not impossible, our estimates are not sufficiently accurate to make precise predictions. The value of θ comes from a simple approximate theory, which is not reliable anywhere near the critical region (where θ is actually measured). It is true that Li (1951) has obtained better approximations to θ for the S.C. and B.C. cases without N.N.N. interaction, but it turns out that these are larger (by factors of 1.13 and 1.19, respectively) than the values we have used, and merely worsen the agreement. Our estimates for T_c are even more suspect, since they involve a mathematically unjustified extrapolation from a low-temperature theory. Referring back to fig. 2 of II, if we assume that our theory is accurate at low temperatures we see that a better fit with the experimental results would be obtained if our curve did not bend upwards so rapidly at higher temperatures, thus increasing the estimated value of T_c . Again, the definition of T_c is somewhat arbitrary, and if we chose to define it as the maximum temperature at which the equation for ϕ , II (30), has a solution we should again obtain a larger value.

Nevertheless it does seem reasonable to suppose that the true critical temperature does not differ from our estimate by more than a factor of 2. That is to say, the curves in fig. 2 are reliable in shape, if not in scale. The value $r = 0.5$ suggested by Anderson for MnO becomes quite impossible; it must be at least 0.8, if not larger. For the other F.C. compounds r must be somewhat greater still, so that superexchange does indeed play a dominant role in these substances. The case of CoO, however, is quite anomalous. Smart (1952) has suggested that it might be explained by taking a small *ferromagnetic* N.N. interaction, whilst retaining the large *antiferromagnetic* N.N.N. coupling, thus reducing θ without seriously affecting T_c . Indeed, remembering that such a system is effectively a set of antiferromagnetic S.C. sublattices whose interaction is small, we can set $kT_c/2S|J| \sim -1.3r(S + \frac{1}{2})$, whilst $k\theta/2S|J| = -(S + 1)(4 + 2r)$, which leads to $r \sim -3.5$, perhaps not so surprising as the value -75 proposed by Smart.

The question of the fluorides is more complicated, since, in the tetragonal lattice, all the N.N.N. sites are not at the same distance from the origin, and we should, strictly speaking, introduce another interaction for them, thus adding another parameter to the theory. There is no difficulty in doing this, but without some independent experimental datum it would be impossible to fix the ratios of the N.N.N. interactions uniquely. Some further arbitrary assumption would need to be made, and the simplest procedure is to assume that the N.N.N. interaction is about the same in every direction, making the system equivalent, mathematically, to a B.C. cubic array. In any case these substances are stabilized by the N.N. interaction, and two different N.N.N. interactions are probably roughly additive in their effects on θ/T_c , so that the assumption of cubic symmetry will give an estimate of their arithmetic mean. However, it does seem that the N.N.N. interaction is either negligible or negative. The former is perhaps to be expected, since the fluorine ions F^- will not part with electrons nearly so readily as O^{2-} , and they do not lie on the lines between N.N.N. magnetic ions, the conditions which Anderson (1950 a) has shown to be essential for super-exchange.

REFERENCES

- ANDERSON, P. W., 1950 a, b, *Phys. Rev.*, **79**, 350, 705.
 LI, Y.-Y., 1951, *Phys. Rev.*, **84**, 721.
 LUTTINGER, J. M., 1951, *Phys. Rev.*, **81**, 1015.
 LUTTINGER, J. M., and TISZA, L., 1946, *Phys. Rev.*, **70**, 954.
 SHULL, C. G., STRAUSSER, W. A., and WOLLAN, E. O., 1951, *Phys. Rev.*, **83**, 333.
 SMART, J. S., 1952, *Phys. Rev.*, **86**, 968.
 ZIMAN, J. M., 1952 a, b, *Proc. Phys. Soc. A*, **65**, 540, 548.

An Investigation of the Neutron Groups from the Reactions $^{12}\text{C}(\text{d}, \text{n})^{13}\text{N}$, $^{16}\text{O}(\text{d}, \text{n})^{17}\text{F}$ and $^{32}\text{S}(\text{d}, \text{n})^{33}\text{Cl}$

By R. MIDDLETON, F. A. EL-BEDEWI* AND C. T. TAI†
 Nuclear Physics Research Laboratory, University of Liverpool

Communicated by H. W. B. Skinner; MS. received 8th August 1952

ABSTRACT. The experimental arrangement and method of investigation by the photographic plate technique of (d, n) reaction at a deuteron bombarding energy of 8 mev are described. The positions are reported of some of the energy levels of the residual nuclei ^{13}N , ^{17}F and ^{33}Cl . It has also been possible to determine spins and parities of the corresponding levels from measurements of the angular distributions of some of the neutron groups. A comparison of the mirror nuclei $^{13}\text{C}^{13}\text{N}$, $^{17}\text{O}^{17}\text{F}$ and $^{33}\text{S}^{33}\text{Cl}$ is made.

§ 1. INTRODUCTION

SEVERAL authors (Roberts and Abelson 1947, Falk, Creutz and Seitz 1949 and Ammiraju 1949) have measured the angular distributions of the neutrons emitted by various thick targets when bombarded by 10 to 20 mev deuterons. They reported in all cases a pronounced maximum in the forward direction which they were unable to explain on the assumption that the reactions were proceeding via a compound nucleus stage (Weisskopf 1937, Wolfenstein 1950). Since Serber's stripping theory (1947) had successfully accounted for the narrow cone of neutrons observed in the forward direction at about 200 mev deuteron energy, it appeared likely that stripping might also be occurring at these energies. Attempts were made to fit the observed distributions with theoretical curves based on the Serber stripping theory. In some cases good agreement was obtained but the rate of increase of the half-width of the neutron peak with atomic number was definitely not in agreement with this theory. More recent thick target neutron angular distribution measurements (Hughes 1951, Falk 1951) showed that the maximum did not always occur in the forward direction but frequently at some small angle. The Serber stripping theory, however, always predicts a maximum in the forward direction.

Recently several authors (Holt and Young 1950, Burrows, Gibson and Rotblat 1950, Rotblat 1951 a, b) have investigated the angular distributions of the proton groups from various light elements bombarded by 4 to 8 mev deuterons. These measurements were not extended to angles much less than about 20° due to the high intensity of the elastically scattered deuterons at small angles. However, in all cases there was evidence of a large peak either in the forward direction or at some small angle. In an attempt to explain these observations Butler (1951) has proposed a stripping theory for relatively low deuteron energies (~ 10 mev). The shapes of the angular distribution curves at small angles predicted by this theory are very sensitive to the angular momentum transferred by the absorbed neutron (or proton) to the initial nucleus. In each of the above-mentioned cases good agreement has been obtained with just one of the

* Now at the University of Alexandria, Egypt.

† Now at the Academia Sinica, Peking, China.

possible theoretical curves. However, since the most characteristic portions of the theoretical curves occur at angles less than 30° , it is important that the experimental observations should be extended to the forward direction. As previously mentioned it is rather difficult to measure the protons in the forward direction due to the intensity of the elastically scattered deuterons but in the case of the neutrons this difficulty is avoided. It was therefore desirable to measure the angular distributions of separate neutron groups.

The use of thin targets to resolve the neutron groups has been mostly confined to relatively low deuteron energies. Except in the cases of the mono-energetic neutrons from the $D + D$ reaction and the recent investigation of the neutrons from oxygen bombarded by 3.1 mev deuterons (Ajzenberg 1951), no angular distributions of separate neutron groups have been reported. We employed the 8 mev deuteron beam of the Liverpool University 37 in. cyclotron to investigate the energy spectra and the angular distributions of some neutron groups emitted from the bombardment of various light nuclei. In this communication the experimental arrangement used for the investigation and the results of the measurements of the neutron groups from the reactions $^{12}\text{C}(d, n)^{13}\text{N}$, $^{16}\text{O}(d, n)^{17}\text{F}$ and $^{32}\text{S}(d, n)^{33}\text{Cl}$ are described. Preliminary results of the former two reactions have been published recently (El-Bedewi, Middleton and Tai 1951).

Attempts have been made to fit the observed angular distribution with the theoretical curves calculated on the Butler theory and also on a stripping theory based on the Born approximation (Bhatia, Huang, Huby and Newns 1952). The latter theory, though differing widely in the theoretical derivation, generally gives a very similar result to that of the Butler theory.

Since the shapes of the angular distribution curves are characterized by the angular momentum transferred by the absorbed proton, it has been possible to make certain predictions concerning the spins and parities of the levels of the residual nuclei knowing the spins and parities of the initial nuclei. In this investigation the spins of the initial nuclei were all zero and thus the number of possible predicted values was reduced.

§ 2. APPARATUS

The principle difficulties encountered in the investigation of (d, n) reactions are the low efficiency of neutron detectors in general and the high neutron background encountered close to a cyclotron tank. To overcome these difficulties it is necessary to increase the neutron yield either by using thicker targets or by increasing the intensity of the incident deuteron beam. The former method is not very satisfactory since it entails a reduction in the neutron energy resolution. The latter method was successfully applied by magnetically focusing the deuteron beam emerging from the cyclotron. This also possesses the advantage that it permits very effective shielding to be made since the position of the focus is usually about 12 to 20 feet from the tank, leaving plenty of space in which to build a thick shielding wall.

In this investigation photographic plates have been used as neutron detectors. This method possesses the advantage that the neutrons can be detected simultaneously at all angles, thus eliminating the errors associated with a monitor which must be used in conjunction with a counter system to correlate the observations at various angles. It also has the advantage that it is relatively

insensitive to γ -rays and can therefore be used close to a cyclotron tank without taking any special precautions. The neutron energy resolution is at least as good as that of any known neutron detector in current use and is limited only by the percentage straggling of the recoil protons in the emulsion which is very nearly the same as in air at energies greater than about 1 mev. These advantages coupled with the economy made in cyclotron running time and the simplicity of the method render it suitable for the investigation of neutron angular distributions.

A schematic drawing of the experimental arrangement is shown in fig. 1. The focusing magnet was placed about 6 feet from the exit port of the cyclotron tank and was designed to produce a focus a further 6 feet away. The horizontal divergence of the cyclotron beam was restricted to about 10° by the slits S_1 and S_2 prior to entering the focusing chamber. A third slit S_3 positioned mid-way between the magnet and focus served to limit the vertical divergence of the beam caused by the fringing field of the focusing magnet. Also shown in the figure is the location of the neutron screening wall which was built from boxes of whale fat.

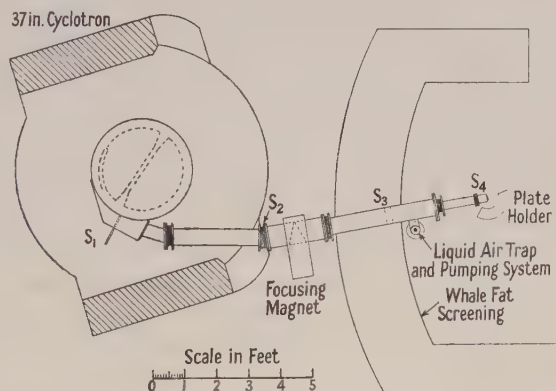


Fig. 1. Diagram of general experimental arrangement.

A sectional drawing of the target chamber is shown in fig. 2. It consisted essentially of 4 in. long section of 3 in. diameter brass tube of $\frac{1}{32}$ in. wall thickness which bolted on to the extension tube system but was insulated from it by a polythene intermediate flange. The targets which were backed by thick gold discs were mounted behind an aperture in the end of the chamber. It was necessary to cool the targets and this was achieved by allowing water to flow from an insulated reservoir through a thin cell behind the target. A gold slit S_4 containing a circular aperture was cut vertically into two segments and mounted as indicated in the figure about 2 in. in front of the target.

Each segment was electrically insulated and connected to a sensitive microammeter such that a slight lateral drift of the focus was indicated by a current reading in one of the meters. Thus by making small adjustments to the focusing magnet current to keep the meter reading at a minimum the focus was maintained centrally on the target.

The relative intensities of exposures were measured by a current integrator (Collinge and Tai 1951) connected to the target chamber. A large leakage

resistor connected between the chamber and the input of the integrator provided a +500 volt bias to suppress secondary electrons.

Twenty pieces of Ilford C₂ 400 μ or 600 μ emulsions of size 2 in. \times 2 in. were mounted radially about the target with the planes of their emulsions vertical and contained in an arc-shaped plateholder. Grooves milled in the top and bottom of the plateholder accommodated the plates at angles ranging from -5° to $+125^\circ$ with respect to the direction of the incident deuteron beam

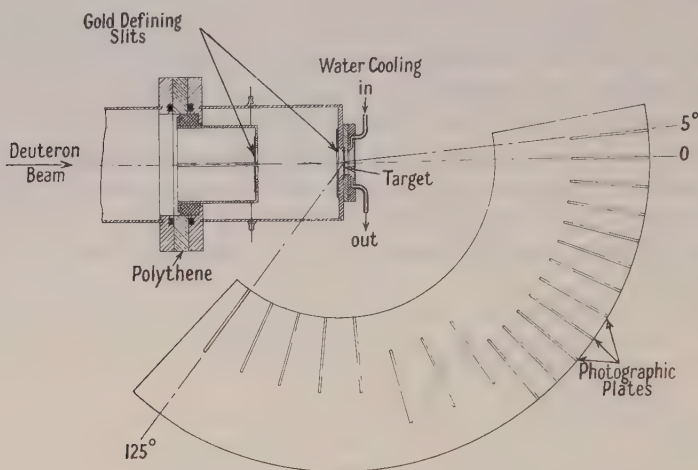


Fig. 2. Detail of target assembly and photographic plateholder.

(fig. 2). Since rapid fluctuations in the neutron angular distributions were expected at small angles the plates were spaced at 5° intervals up to angles of 55° and the remainder at 10° intervals. The distance of the inner edge of the plate from the target varied between 15 cm at small angles to 10 cm in the backward direction.

§ 3. PROCEDURE

(i) *Alignment.* The alignment of the extension tubes, the target chamber and plateholder was carried out step by step, allowing the beam to pass out into the air through an aluminium window at the end of each section and observing its position on a fluorescent screen. These observations, together with geometrical considerations, allowed us to locate the direction of the beam within 0.5° .

(ii) *Energy of Deuteron Beam.* The energy of the deuteron beam was measured at 1 cm intervals across its width of 10 cm at a position just before entering the focusing chamber. A fast shutter was used to give a photographic plate inclined at a small glancing angle a brief exposure. The energy was then determined from the measurements of the ranges of the deuteron tracks in the emulsion. The extreme variation of the energy across the entire width of the beam was observed to be about 0.1 mev and the mean energy determined to be 8.13 ± 0.05 mev. This method gives only an instantaneous measure of the beam energy and since small fluctuations in the energy are to be expected, this value can only be used as approximate. Whenever possible the known Q -value of the reaction being investigated was used to calculate the beam energy.

(iii) *Geometry of Focus.* The effective size of the focus was determined by bombarding a halide target and by directly measuring the extent of the discoloured portion. It was found to be 1 cm wide and 1.4 cm high. From geometrical considerations the horizontal convergence of the beam at the focus was calculated to be $\pm 1.2^\circ$ and the vertical divergence $\pm 0.3^\circ$.

(iv) *Targets.* The targets consisted of thin layers (0.5 to 4 mg/cm²) of various light elements deposited on thick gold backing discs. The oxygen target was prepared by smearing a suspension of analytically pure lead dioxide in distilled water on to the gold backing. By trial and error two fairly uniform targets were prepared and the thickness calculated to correspond to an energy loss of 40 and 140 kev respectively for 8 Mev deuterons. The former thin target was used to investigate the neutron energy spectrum and the latter to measure the angular distributions of the neutrons corresponding to the formation of ¹⁷F in the ground and first excited states.

The carbon target was prepared by collecting soot on a gold backing disc from the burning of camphor. The thickness of the layer was estimated to correspond to an energy loss of 30 kev. The sulphur target was prepared in a similar manner by subliming the sulphur on to a gold backing. Its thickness was estimated to correspond to an energy loss of 100 kev.

(v) *Exposure Technique.* Before each exposure, a trial exposure of four plates of 100 μ emulsion thickness placed at angles 0°, 30°, 60° and 90° was made. From preliminary measurements of the track density in these plates an estimate of the required exposure for 400 μ or 600 μ emulsions was made. The main exposure was then carried out in two parts. All the plates were given about one-third to one-half the total exposure and then the plates in the forward direction ranging up to and including 35° were removed. A new plate was then placed at angle 35° and the additional exposure given to the remaining plates. The purpose of this operation was to ensure a convenient track density in the plates exposed at all angles.

(vi) *Shrinkage Determination.* Four plates from each batch exposed were further exposed to a collimated source of 'ThC' alpha-particles for the purpose of shrinkage calibration. This method of determining the shrinkage factor depends upon a comparison of the angles of entry (30° and 45°) of the alpha-particles with the observed angles of inclination of the tracks after processing. The shrinkage factor was determined to be 2.3 ± 0.1 .

(vii) *Processing.* The plates were processed by a temperature development method (Dilworth *et al.* 1948) similar to that developed in the H. H. Wills Physics Laboratory (Dainton *et al.* 1951). The temperature and duration of development were adjusted to ensure the minimum number of background grains while retaining the clear cut appearance of the beginning of long-range tracks.

(viii) *Measurement.* All measurements were made with Cooke, Troughton and Simms binocular microscopes with $\times 10$ eyepieces and $\times 45$ fluorite objectives. Measurements of the recoil protons were confined to a strip of emulsion centred about the line joining the centres of the target and plate and were commenced 8 mm from the inner edge of the plate. This strip was usually 5 mm wide and extended 1 to 3 mm along the centre line in a direction away from the target. For the angular distribution measurements, tracks were recorded which subtended a horizontal angle of less than or equal to 10° with the centre line and

had an angle of dip (after shrinkage correction) of less than or equal to 10° . The range, horizontal angle and dip were measured and recorded for all recoil proton tracks fulfilling the above criterion. The corresponding neutron energy was then evaluated from simple geometrical consideration and using the range-energy relation of El-Bedewi (1951).

§ 4. INTERPRETATION OF MEASUREMENTS

Since the n-p scattering differential cross section is known to be very nearly isotropic in the centre-of-mass system at neutron energies less than about 10 Mev and the condition of acceptance of the recoil tracks is rigidly defined, it is apparent that a constant fraction of the total number of recoil protons for small neutron energies was recorded. A correction was applied to the number of recoil protons at each angle for the variation of the total n-p scattering cross section with energy (Adair 1950). The relative intensity of the neutron group at each angle was then calculated from (i) the relative number of observed recoil protons belonging to the group, (ii) the volume of emulsion scanned, (iii) the distance of the emulsion from the target, and (iv) the ratio of exposures for plates exposed at angles less than or larger than 35° .

Since the Q -values of the ^{12}C , ^{16}O and $^{32}\text{S}(\text{d}, \text{n})$ reactions are small it was possible to use 400μ emulsions while still keeping the number of escape tracks within the acceptance criterion small. For the longest range proton recoil groups, the fraction of escape tracks was calculated in a manner similar to that used by Richard (1941) to be about 5%. Since this correction factor varies little over a neutron angle of emission range of 0° to 60° and is in itself small, it has been neglected in the present results.

In the above considerations we have assumed the hydrogen content of the emulsions used for one exposure to be the same. This condition is more or less realized since the plates used for a particular exposure were all selected from one packet and would therefore be subjected to the same humidity conditions.

No correction has been applied to the results for the attenuation of the intensities of the neutron groups in passing through the intermediate materials between the target and emulsion. This was considered justifiable since neither the distance traversed nor the neutron energy changes appreciably over the small angular range measured.

§ 5. RESULTS

(i) *Neutron Background.* A 'blank' exposure was made, with plates of 400μ emulsion thickness, to the neutrons emitted by a thick gold target (typical target backing disc). Figure 3 shows the measured energy spectrum of the neutrons from the plate exposed at an angle of emission of 15° . Also shown in this figure is the energy spectrum of the neutrons from the bombardment of a 30 kev thick carbon target at the same angle normalized to the same intensity of exposure and volume of emulsion. It is to be noted that in the figure the neutron spectrum from gold is magnified ten times with respect to that from the carbon target. Comparison of the two spectra shows the contribution from the gold backing to be very small, particularly at neutron energies greater than 3 Mev.

At larger angles of emission, the contribution due to gold may be significant since the neutron intensity from light elements usually exhibits a more pronounced forward maximum (Allen *et al.* 1951). Since the neutron groups

whose angular distributions have been investigated possess energies greater than 3 MeV, it is clear from fig. 3 that even when taking this fact into consideration the background is insignificant at all angles of emission. In the analysis of the energy spectra the neutron background at low energies was of the order of the statistical uncertainty of the observations and was therefore neglected.

(ii) *Investigation of the Reaction $^{12}\text{C}(d, n)^{13}\text{N}$.* A total of about 4000 tracks was measured from plates exposed at different angles ranging from -5° to 55° with respect to the direction of the incident deuterons. A representative histogram at angle 15° is shown in fig. 3. From an analysis of the histograms the existence

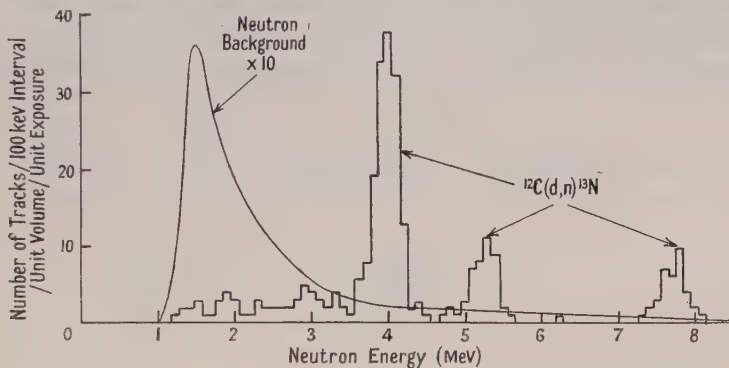


Fig. 3. Neutron energy spectrum at angle 15° from the reaction $^{12}\text{C}(d, n)^{13}\text{N}$, also showing the neutron background.

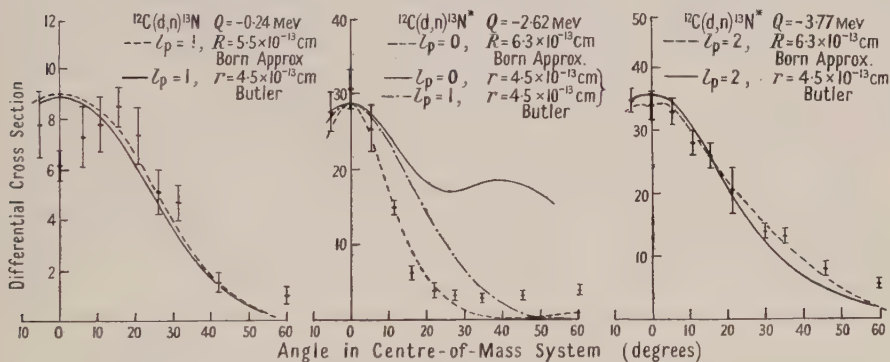


Fig. 4. Angular distributions of the neutron groups corresponding to the ground and excited states of ^{13}N at 2.38 and 3.53 MeV.

of three neutron groups corresponding to the transitions to the ground and two excited states of ^{13}N at 2.38 ± 0.05 MeV and 3.53 ± 0.05 MeV were established. These results are in agreement with those of previous investigators (Grosskreutz 1949, Van Patter 1949).

The angular distributions of the neutron groups corresponding to the formation of ^{13}N in the ground, first and second excited states were determined as described in the preceding section and are shown in fig. 4. The experimental errors shown in the figure are the statistical standard deviations.

(iii) *Investigations of the Reaction $^{16}\text{O}(d, n)^{17}\text{F}$.* Measurements of the complete neutron energy spectra were made at angles of emission of 0° , 30° , 85° and 125° for the plates exposed to the thin lead dioxide target. Two intense

neutron groups were observed which were well separated from the remainder of the spectrum, corresponding to the ground and an excited state at 0.53 ± 0.06 Mev of ^{17}F . The value for the first excited state is in agreement within the experimental error with that reported by Ajzenberg (1951) of 0.536 ± 0.010 Mev. There was also evidence for the existence of several levels at an excitation energy greater than about 3 Mev, but, due to the complexity of the neutron spectrum at small neutron energies, it was impossible to locate them accurately.

Measurements were made of the angular distributions of the two neutron groups corresponding to the formation of ^{17}F in the ground and first excited states over an angular range of -5° to 55° with respect to the incident deuteron beam. Since these two groups were well separated from the remaining groups measurements were confined to all tracks of range greater than those corresponding to the formation of ^{17}F in its second excited state. From intensity considerations it was more convenient to use the plates exposed to the thicker (140 kev) oxygen target. In fig. 5 are shown the experimental angular distribution curves, together with the theoretical curves which will be discussed in § 6.

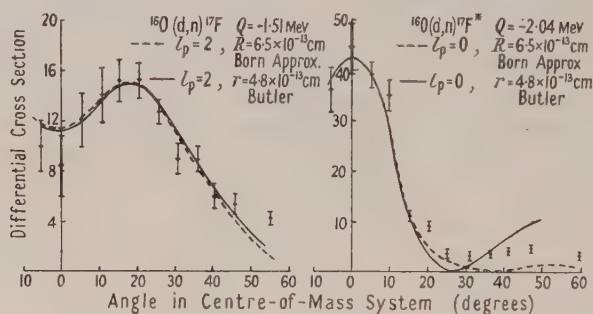


Fig. 5. Angular distributions of the neutron groups corresponding to the formation of ^{17}F in the ground and first excited states.

(iv) *Investigation of the Reaction $^{32}\text{S}(d, n)^{33}\text{Cl}$.* The neutron energy spectra were measured at angles ranging from -5° to 55° with respect to the incident deuteron direction and from an analysis of the histograms energy levels were established at 0.76 ± 0.07 , 2.84 ± 0.06 and 4.22 ± 0.08 Mev in the residual nucleus ^{33}Cl . A rather weak neutron group was also observed at certain angles of emission which corresponded to an energy level in ^{33}Cl at about 1.89 Mev. There was also evidence for the existence of several levels of excitation energy greater than 4.22 Mev but these were too closely spaced to be resolved by the present experimental arrangement. In fig. 6 are shown the experimental angular distributions of the four neutron groups corresponding to the formation of the residual nucleus ^{33}Cl in the ground and excited states at 0.76, 2.84 and 4.22 Mev respectively.

§ 6. COMPARISON OF THE EXPERIMENTAL AND THEORETICAL ANGULAR DISTRIBUTIONS

Attempts have been made to fit the experimental angular distribution curves with those based on the nuclear stripping theories of Butler (1951) and Bhatia, Huang, Huby and Newns (1952). The shapes of the angular distribution curves predicted by these theories are dependent upon the angular momentum transferred by the absorbed proton and also to a lesser extent upon the radius of interaction. From an analysis of ten experimental curves Bhatia *et al.* (1952)

report the most satisfactory radius of interaction to be the Gamow radius in the case of the Butler theory, whereas a somewhat larger radius is required by the Born approximation theory, namely the Gamow radius plus about 2×10^{-13} cm. In the present communication we have used the Gamow radius in calculating all the Butler curves, but in the case of the Born approximation theory we have made slight adjustments to the radius of interaction in order to obtain better agreement.

(i) Angular Distribution of Neutron Groups from $^{12}\text{C}(d, n)^{13}\text{N}$

In the case of the angular distribution of the neutron group corresponding to the transition to the ground state of ^{13}N the general appearance suggests the angular momentum transferred by the absorbed proton $l_p = 2$. Agreement

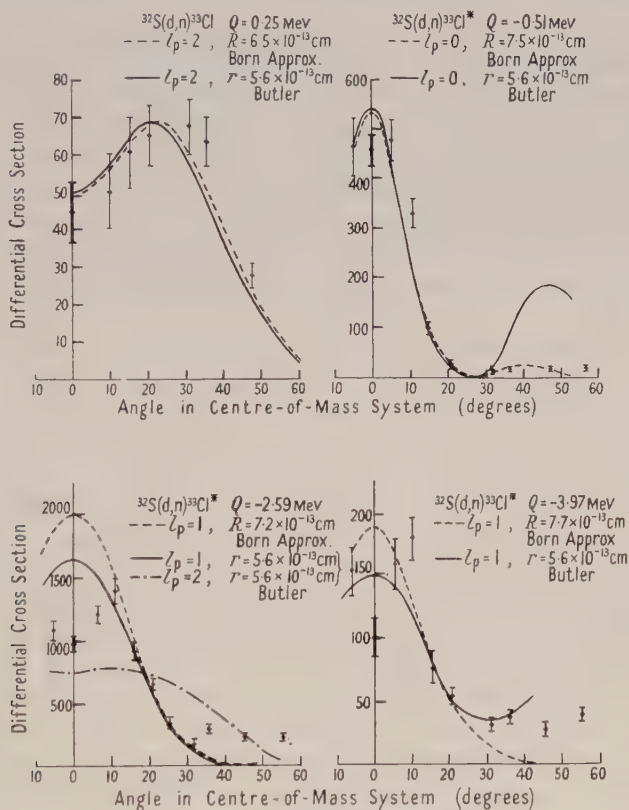


Fig. 6. Angular distribution of the neutron groups corresponding to the ground and excited states of ^{33}Cl at 0.76, 2.84 and 4.22 MeV.

however could be obtained with either theory only by assuming a radius of interaction considerably larger than those indicated above. Some measure of agreement was obtained as shown in fig. 4 by assuming $l_p = 1$ using the Gamow radius and the Gamow radius plus 1.0×10^{-13} cm in the cases of the Butler and Born approximation theories respectively. This would then determine the ground state of ^{13}N to be a $P_{1/2}$ or $P_{3/2}$ state. Since the ground state of the mirror nucleus ^{13}C is known to be a $P_{1/2}$ state (Rotblat 1951a, Jenkins 1948) and also the shell model (Mayer 1950) predicts the ground state of ^{13}N to be a $P_{1/2}$ state the assumption of $l_p = 1$ is justified.

For the angular distributions corresponding to the first and second excited states good agreement was achieved by assuming $l_p=0$ and 2 respectively and a radius of interaction of 6.3×10^{-13} cm using the Born approximation theory. The Butler theory, however, though giving good agreement with the angular distribution corresponding to the second excited state was in serious disagreement with that corresponding to the first excited state. As can be seen from the figure, the Butler curve corresponding to an angular momentum transfer of one unit resembles more closely the experimental angular distribution than the one corresponding to $l_p=0$.

Since the first excited states of both ^{13}N and its mirror nucleus ^{13}C have been reported to be $S_{1/2}$ states (Jackson and Galonsky 1951, Rotblat 1951 a) it is evident for this particular Q -value and deuteron energy that the Butler theory is incorrect.

(ii) *Angular Distribution of Neutron Groups from $^{16}\text{O}(d, n)^{17}\text{F}$*

In fig. 5 are shown the experimental angular distribution curves corresponding to the ground and first excited states of ^{17}F , together with the theoretical curves calculated using the Butler and Born approximation stripping theories. Good agreement was obtained in both cases with either theory by assuming $l_p=2$ and 0 respectively. These results are consistent with the ground state of ^{17}F being a $D_{5/2}$ or a $D_{3/2}$ state and the first excited state an $S_{1/2}$ state. The same conclusions were inferred from the angular distributions of the two neutron groups as obtained by Ajzenberg (1951) using 3.1 mev bombarding energy. These results are confirmed to some extent by the prediction made by the Mayer shell model that the ground state of ^{17}F is probably a $D_{5/2}$ state and also the observation that the first excited state of the mirror nucleus ^{17}O is an $S_{1/2}$ state (Burrows, Gibson and Rotblat 1950).

(iii) *Angular Distribution of Neutron Groups from $^{32}\text{S}(d, n)^{33}\text{Cl}$*

For the angular distributions corresponding to the ground and first excited states of ^{33}Cl fairly good agreement was obtained with the theoretical curves corresponding to $l_p=2$ and 0 respectively based on both the Butler and Born approximation stripping theories. As previously stated, the Gamow radius was used in the Butler calculations but the best agreements with the Born approximation were obtained when using radii of interaction of 6.5×10^{-13} cm and 7.5×10^{-13} cm respectively. The assumption that $l_p=2$ in the transition to the ground state of ^{33}Cl indicates that it is a $D_{5/2}$ or a $D_{3/2}$ state. This is consistent with the prediction of a $D_{3/2}$ state from the Mayer shell model and also the measured spin value of 3/2 for the mirror nucleus ^{33}S (Mack 1950). It may also be noted that, from observations of the angular distributions of the protons from the reaction $^{32}\text{S}(d, p)^{33}\text{S}$, Holt and Marsham (to be published) have shown that the ground state of the mirror nucleus ^{33}S is a $D_{5/2}$ or a $D_{3/2}$ state and also the first excited state is an $S_{1/2}$ state.

In the cases of the remaining angular distributions corresponding to the formation of ^{33}Cl in excited states at 2.84 and 4.22 mev agreement could not be achieved by using either of the stripping theories. Both the experimental distributions exhibit a fairly sharp minimum in the forward direction which is not predicted by either theory assuming $l_p=1$ or 2. As shown in fig. 6 the theoretical curves corresponding to $l_p=1$ are in fair agreement with the experimental points at angles larger than about 10° , but below this angle the

theoretical curves deviate from the experimental points and rise to a maximum. A similar discrepancy, but to a lesser extent, also exists in the ground state angular distribution of $^{12}\text{C}(\text{d}, \text{n})^{13}\text{N}$ reaction reported in this present communication. This discrepancy may possibly be due to the effect of the coulomb field which has been neglected in both theories. This would account for the effect being more pronounced for sulphur since it has a larger charge than the other elements so far investigated. Also it may be noted that both these excited states have high negative Q -values. If it is assumed that one unit of angular momentum is transferred in the transition to these two states, then it follows that they are both either $\text{P}_{3/2}$ or $\text{P}_{1/2}$ states. But, on account of the poor agreement of the theories at small angles, we cannot have much confidence in these predictions.

(iv) Summary

(1) In several cases, the predicted spins and parities found by the use of the Butler or the Born approximation theories agree with those found from other sources.

(2) In one case, $^{12}\text{C}(\text{d}, \text{n})^{13}\text{N}^*$ with a Q -value of -2.62 mev, the Born approximation theory gives the known value for the spin correctly, but the Butler theory gives an incorrect value. This is possibly associated with the fact that the Butler theory has a singular behaviour in the region of negative Q s equal to the binding energy of the deuteron (2.3 mev). Figure 7 illustrates the behaviour of the Butler curves for $l_p=0$ and various Q -values in the case of $^{12}\text{C}(\text{d}, \text{n})^{13}\text{N}$.

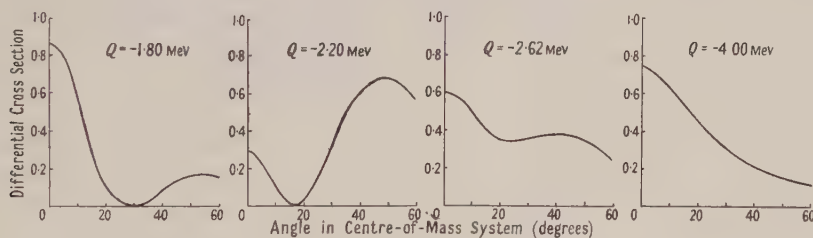


Fig. 7. The theoretical angular distribution curves calculated from the Butler theory for the reaction $^{12}\text{C}(\text{d}, \text{n})^{13}\text{N}$ assuming $l_p=0$ and Q -values of -1.80 , -2.20 , -2.62 and -4.00 mev.

(3) Several of the curves found experimentally, namely $^{12}\text{C}(\text{d}, \text{n})^{13}\text{N}$ ($Q=0.24$ mev), $^{32}\text{S}(\text{d}, \text{n})^{33}\text{Cl}^*$ ($Q=-2.59$ mev) and $^{32}\text{S}(\text{d}, \text{n})^{33}\text{Cl}^*$ ($Q=-3.97$ mev), show a minimum in the forward direction where none is predicted either by the Butler or the Born approximation theories. There is certainly a definite discrepancy, but it would appear that the l_p values for the reactions can be correctly obtained from the points on the curves at angles greater than about 15° . This discrepancy is possibly associated with the omission of the coulomb force from either set of calculations, an assumption which may be supported by its greater magnitude in the case of sulphur. It appears, however, only in cases where $l_p=1$.

(4) It will be noticed that in several of the cases we have given, the theories give a maximum cross section at 0° when l_p is not zero. This behaviour is associated with high negative Q -values, and makes the interpretation of the experimental curves less direct than in the case of positive Q -values. In spite of these difficulties, it seems that in general we can use the theories to predict spins and parities correctly.

§7. COMPARISON OF MIRROR NUCLEI

In fig. 8 is shown a comparison of the energy levels of the mirror nuclei $^{13}\text{C}^{13}\text{N}$, $^{17}\text{O}^{17}\text{F}$ and $^{33}\text{S}^{33}\text{Cl}$. The ground and first excited states of ^{13}C have been reported by Rotblat (1951a) from an investigation of the angular distributions of the protons from the reaction $^{12}\text{C}(\text{d}, \text{p})^{13}\text{C}$ to be $\text{P}_{1/2}$ or $\text{P}_{3/2}$ and $\text{S}_{1/2}$ states respectively, which agrees with the results obtained by the authors for the mirror nucleus ^{13}N . Since the spin of the ground state of ^{13}C is known to have the value $\frac{1}{2}$ (Jenkins 1948) it follows that it must be a $\text{P}_{1/2}$ state. The shell model predicts both ground states of ^{13}C and ^{13}N to be $\text{P}_{1/2}$ states, and therefore it is likely that the ground state of ^{13}N is also a $\text{P}_{1/2}$ state. From an analysis of Goldhaber and Williamson's data for elastic proton scattering from ^{12}C Jackson and Galonsky (1951) have reported the first excited state of ^{13}N to be an $\text{S}_{1/2}$ state and the second excited state to be a closely spaced doublet of a $\text{P}_{3/2}$ state at 3.503 mev and a $\text{D}_{5/2}$ state at 3.550 mev. In a later communication Rotblat

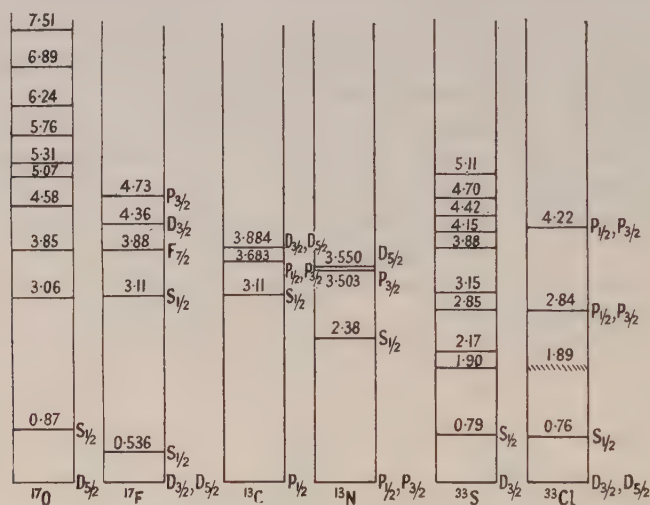


Fig. 8. Comparison of the mirror nuclei $^{13}\text{C}^{13}\text{N}$, $^{17}\text{O}^{17}\text{F}$ and $^{33}\text{S}^{33}\text{Cl}$.

(1951b) reported the existence of two similar levels in the mirror nucleus ^{13}C at 3.683 and 3.884 mev and from angular distribution measurements concluded the former to be a $\text{P}_{1/2}$ or a $\text{P}_{3/2}$ state and the latter a $\text{D}_{3/2}$ or a $\text{D}_{5/2}$ state.

The positions of the energy levels of ^{17}O have been accurately determined by Burrows, Powell and Rotblat (1951) from an investigation of the reactions $^{16}\text{O}(\text{d}, \text{p})^{17}\text{O}$ and $^{19}\text{F}(\text{d}, \alpha)^{17}\text{O}$, and as shown in the figure exhibit a similarity to those of ^{17}F . Also from the angular distribution measurements of the protons from the former reaction Burrows, Gibson and Rotblat (1950) report the ground and first excited states to be $\text{D}_{3/2}$ or $\text{D}_{5/2}$ and $\text{S}_{1/2}$ states respectively, and since the spin of ^{17}O is known to be $5/2$ (Alder and Yu 1951) the ground state must be $\text{D}_{5/2}$. Again from the similarity between ^{17}O and ^{17}F and the fact that the shell model predicts both ground states to be probably $\text{D}_{5/2}$ states it is likely that the ground state of ^{17}F is also $\text{D}_{5/2}$. The positions, spins and parities of the third, fourth and fifth excited states of ^{17}F indicated in the figure were determined by Laubenstein and Laubenstein (1951) from an analysis of the yield of elastically scattered protons from ^{16}O .

It is of interest that the first excited states of ^{33}S and ^{33}Cl almost exactly coincide and both are probably $S_{1/2}$ states. The energy levels of ^{33}S shown in the figure were reported by Davison (1949) and the spins and parities of the ground and first excited states were determined by Holt and Marsham (private communication) from the measurement of the angular distributions of the protons from the $^{32}\text{S}(d, p)^{33}\text{S}$ reaction. They obtained angular distributions compatible with angular momenta transfers of 2 and 0 respectively in the transitions corresponding to the formation of ^{33}S in the ground and first excited states. Since the spin of ^{33}S is known to be $3/2$ (Mack 1950) the ground state must be a $D_{3/2}$ state and the first excited state an $S_{1/2}$ state.

ACKNOWLEDGMENTS

The authors are extremely indebted to Professor H. W. B. Skinner for his encouragement and many helpful suggestions during the present investigation. Our thanks are due to Dr. R. Huby, Mr. H. C. Newns and Mr. T. S. Green for assistance in calculating the theoretical angular distribution curves, and also to Dr. J. R. Holt and Mr. T. N. Marsham for making known the results of their investigation of the $^{32}\text{S}(d, p)^{33}\text{S}$ reaction. We would also like to thank Mr. E. C. Hewitt for processing the nuclear emulsions and also Miss B. Anderson and Mr. E. C. Hewitt for assistance in the microscope work.

REFERENCES

- ADAIR, R. K., 1950, *Rev. Mod. Phys.*, **22**, 249.
 AJZENBERG, F., 1951, *Phys. Rev.*, **83**, 693.
 ALDER, F., and YU, F. C., 1951, *Phys. Rev.*, **81**, 1067.
 ALLEN, A. J., NECHAJ, J. F., SUN, K. H., and JENNINGS, B., 1951, *Phys. Rev.*, **81**, 536.
 AMMIRAJU, P., 1949, *Phys. Rev.*, **76**, 1421.
 BHATIA, A. B., HUANG, K., HUBY, R., and NEWNS, H. C., 1952, *Phil. Mag.*, **43**, 485.
 BURROWS, H. B., GIBSON, W. M., and ROTBLAT, J., 1950, *Phys. Rev.*, **80**, 1095.
 BURROWS, H. B., POWELL, C. F., and ROTBLAT, J., 1951, *Proc. Roy. Soc. A*, **209**, 478.
 BUTLER, S. T., 1951, *Proc. Roy. Soc. A*, **208**, 559.
 COLLINGE, B., and TAI, C. T., 1951, *J. Sci. Instrum.*, **28**, 58.
 DANTON, A. D., GATTIKER, A. R., and LOCK, W. O., 1951, *Phil. Mag.*, **42**, 396.
 DAVISON, P. W., 1949, *Phys. Rev.*, **75**, 757.
 DILWORTH, C. C., OCCHIALINI, G. P. S., and PAYNE, R. M., 1948, *Nature, Lond.*, **162**, 102.
 EL-BEDEWI, F. A., 1951, *Proc. Phys. Soc. A*, **64**, 1079.
 EL-BEDEWI, F. A., MIDDLETON, R., and TAI, C. T., 1951, *Proc. Phys. Soc. A*, **64**, 756, 1055.
 FALK, G. E., 1951, *Phys. Rev.*, **83**, 499.
 FALK, G. E., CREUTZ, E., and SEITZ, F., 1949, *Phys. Rev.*, **76**, 322.
 GROSSKREUTZ, J. C., 1949, *Phys. Rev.*, **76**, 482.
 HOLT, J. R., and YOUNG, C. T., 1950, *Proc. Phys. Soc. A*, **63**, 833.
 HUGHES, J., 1951, *Proc. Phys. Soc. A*, **64**, 797.
 JACKSON, H. L., and GALONSKY, A. I., 1951, *Phys. Rev.*, **83**, 876.
 JENKINS, F. A., 1948, *Phys. Rev.*, **74**, 355.
 LAUBENSTEIN, R. A., and LAUBENSTEIN, M. J. W., 1951, *Phys. Rev.*, **84**, 18.
 MACK, J. E., 1950, *Rev. Mod. Phys.*, **22**, 64.
 MAYER, M. G., 1950, *Phys. Rev.*, **78**, 16.
 RICHARD, H. T., 1941, *Phys. Rev.*, **59**, 796.
 ROBERTS, R. B., and ABELSON, P. H., 1947, *Phys. Rev.*, **72**, 76.
 ROTBLAT, J., 1951 a, *Nature, Lond.*, **167**, 1027; 1951 b, *Phys. Rev.*, **83**, 1271.
 SERBER, R., 1947, *Phys. Rev.*, **72**, 1008.
 VAN PATTTER, D. M., 1949, *Phys. Rev.*, **76**, 1264.
 WEISSKOPF, V., 1937, *Phys. Rev.*, **52**, 295.
 WOLFENSTEIN, L., 1950, *Phys. Rev.*, **78**, 322.

An Investigation of the Reaction $^{14}\text{N}(\text{d}, \text{n})^{15}\text{O}$ at 8 mev Deuteron Energy

BY W. H. EVANS, T. S. GREEN AND R. MIDDLETON
Nuclear Physics Research Laboratory, University of Liverpool

Communicated by H. W. B. Skinner ; MS. received 21st August 1952

ABSTRACT. The neutrons emitted from a nitrogen gas target bombarded by 7.7 mev deuterons have been investigated using the photographic plate technique. The existence of six excited states of ^{15}O has been established and certain predictions about the spins and parities of these levels have been made by comparing the observed angular distributions of the corresponding neutron groups with those based on a nuclear stripping theory.

§ 1. INTRODUCTION

THE energy levels of ^{15}O have been investigated above an excitation energy of about 7.5 mev by Duncan and Perry (1950) using the reaction $^{14}\text{N}(\text{p}, \gamma)^{15}\text{O}$. The lower levels, however, cannot be determined by this method, though some measurements have been made in this region using the $^{14}\text{N}(\text{d}, \text{n})^{15}\text{O}$ reaction at low deuteron energies. Stephens, Djanab and Bonner (1937) and more recently Hudspeth and Swann (1949) have reported a Q -value for the reaction of about 5.1 mev and also a suspected energy level in ^{15}O at about 4.0 mev. However, Gibson and Livesey (1948), while confirming the Q -value did not observe a low energy neutron group corresponding to the 4.0 mev level. It therefore seemed desirable to investigate this reaction further at a larger deuteron energy (~ 8 mev).

Furthermore, it appeared desirable to investigate the angular distributions of some of the neutron groups from this reaction in order to make comparisons with the theoretical distributions based on a nuclear stripping theory (Butler 1951, Bhatia *et al.* 1952), thus enabling certain predictions to be made concerning the spins and parities of the levels of ^{15}O .

§ 2. EXPERIMENTAL TECHNIQUE

The photographic plate technique as described by Middleton, El-Bedewi and Tai (1953, to be referred to as I) was used to measure the energy and the angular distributions of the neutron groups. A slight modification of the target assembly and method of orientation of the photographic plates as described by the above authors was necessary due to the use of a gaseous target.

A simplified diagram of the gas cell and the arrangement of the plates is shown in fig. 1. The gas cell consisted of a thin brass cylinder closed at one end and was bolted on to the target chamber in place of the solid target (see fig. 2 of I). A thin platinum window of approximately 14 mg/cm^2 isolated the nitrogen gas from the cyclotron vacuum system. It was mounted behind an aperture of diameter 1 cm in a thick gold disc and would withstand a maximum pressure difference of about 30 cm Hg. For this particular exposure, analytically pure nitrogen gas at a pressure of 22 cm Hg was used. The volume of the target was defined by the aperture in the gold disc and by the 2.0 cm length of the cell. To minimize

the neutron background the brass walls of the cell were lined with gold foil sufficiently thick to stop the deuterons.

The photographic plates were mounted radially about the centre of the window of the gas cell with the planes of their emulsions vertical and facing the axis of the deuteron beam. With this arrangement, most of the neutrons entered the emulsions at a small glancing angle and scattering in the glass backings was minimized.

The mean energy of the incident deuteron beam at the centre of the gas cell was determined from the value of 8.13 ± 0.05 MeV for the direct beam energy determined by Middleton *et al.* (1953), corrected for the stopping power of the platinum window and nitrogen gas (Bethe 1937). This gave a value of 7.69 ± 0.06 MeV.

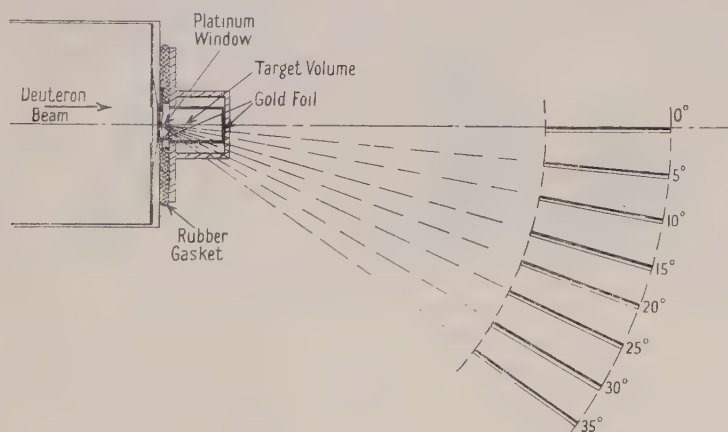


Fig. 1. Gas target assembly and plate-holder.

As described in I, proton recoils were recorded only when observed to lie within the angular acceptance criterion of 10° with respect to the neutron direction in the horizontal and vertical planes. For neutrons entering parallel to the plane of the emulsion the dip criterion after correction corresponds very nearly to 8μ in 100μ measured relative to the horizontal plane. However, for neutrons entering at a glancing angle as in this case, the criterion must be changed to $(8 - \delta)\mu$ up and $(8 + \delta)\mu$ down, where δ is calculated from the glancing angle and the shrinkage factor, in order to maintain symmetry about the neutron direction. Since δ depends upon the glancing angle of the neutrons, which varies with the angle of emission, the dip criterion was slightly different for each plate measured.

§ 3. RESULTS

The neutron energy spectra have been measured at angles ranging from 0° to 35° and at intervals of 5° . At each angle about 1000 tracks were recorded in a volume of about 2 mm^3 of emulsion and in fig. 2 is shown a typical histogram at angle 15° . Due to the low intensity of the neutron groups corresponding to the transitions to the ground, first and second excited states, a considerably larger volume of emulsion had to be scanned for these tracks. The histogram shown in the figure has not been normalized to the same volume of emulsion or corrected for the variation of the n-p cross section with energy.

From an analysis of the histograms the existence of seven neutron groups was established corresponding to transitions to the ground and excited states of ^{15}O . In the table are listed the Q -values of these groups and also the energies of the corresponding levels. The Q -value of the reaction agrees within the experimental errors with those reported by Gibson and Livesey (1948), Hudspeth and Swann (1949) and Rose, Hudspeth and Heydenburg (1952). There was no indication of the 4.0 meV level reported by Gibson and Livesey, the first excited state being observed at 5.29 ± 0.17 meV. This value is not in very good

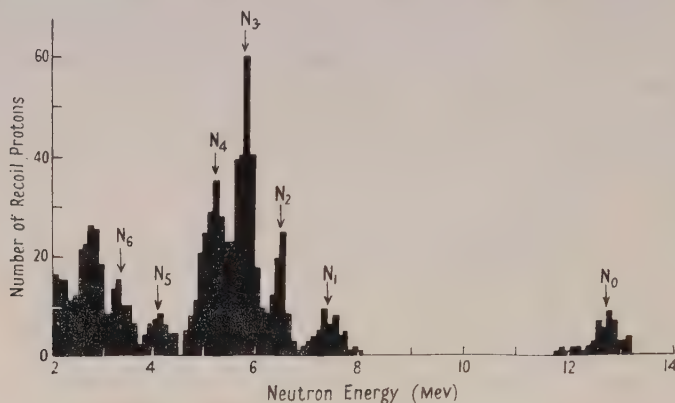


Fig. 2. Histogram at 15° for $^{14}\text{N}(\text{d}, \text{n})^{15}\text{O}$.

agreement with that of approximately 4.9 meV given by Rose *et al.*, but agrees well with the value 5.25 ± 0.08 meV deduced by Johnson, Robinson and Moak (1952) from observations of γ -rays from the reaction $^{14}\text{N}(\text{p}, \gamma)^{15}\text{O}$. They also observe γ -rays consistent with levels at 6.21 ± 0.05 meV and 6.85 ± 0.05 meV which agree well with our observations of levels at 6.19 ± 0.16 meV and 6.84 ± 0.16 meV.

Group No.	Q -value (meV)	Energy level (meV)	l_p	Parity	Spin
N_0	5.15 ± 0.16	0	1	—	$5/2, 3/2, \text{ or } 1/2$
N_1	-0.14 ± 0.11	5.29 ± 0.17	2	+	$7/2, 5/2, 3/2 \text{ or } 1/2$
N_2	-1.04 ± 0.06	6.19 ± 0.16	1	—	$5/2, 3/2 \text{ or } 1/2$
N_3	-1.69 ± 0.08	6.84 ± 0.16	0	+	$3/2 \text{ or } 1/2$
N_4	-2.33 ± 0.09	7.48 ± 0.16	1	—	$5/2, 3/2 \text{ or } 1/2$
N_5	-3.27 ± 0.09	8.42 ± 0.16	1	—	$5/2, 3/2 \text{ or } 1/2$
N_6	-3.91 ± 0.07	9.06 ± 0.16	1	—	$5/2, 3/2 \text{ or } 1/2$

The angular distributions of these neutron groups have also been measured and are shown (fig. 3) plotted in the centre-of-mass system. The unit of intensity for the various groups is the same, corrections having been applied for the volume of emulsion scanned and the variation of the n-p cross section with energy (Adair 1950).

In each case an attempt has been made to fit the experimental points with the theoretical angular distributions calculated from the nuclear stripping theories of Butler (1951) and Bhatia, Huang, Huby and Newns (1952).

For the ground state distribution good agreement was achieved by assuming that the angular momentum l_p transferred by the absorbed proton was one unit

for both theories and by choosing radii of interaction of 4.7×10^{-13} cm and 7.0×10^{-13} cm respectively. These values for the radii are in agreement with those suggested by Bhatia *et al.* (1952) namely the Gamow radius for use with the Butler theory and the Gamow radius plus 2×10^{-13} cm for use with their own theory.

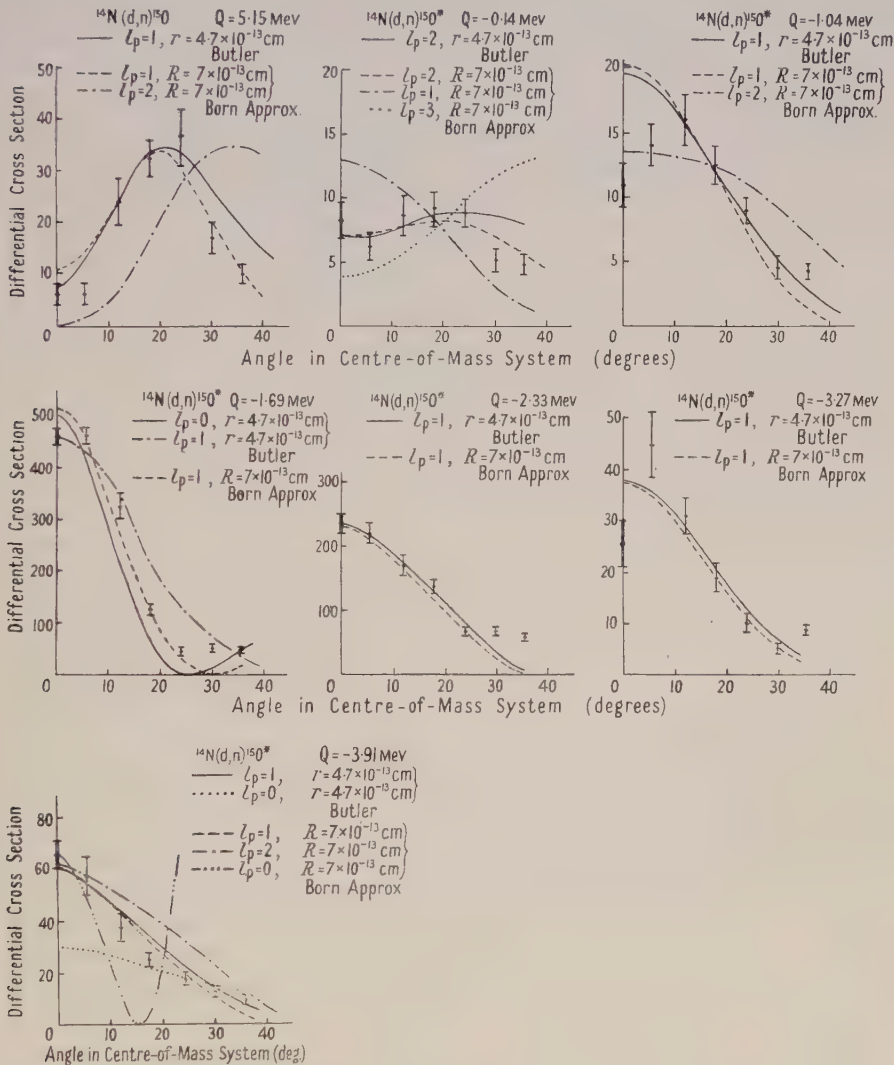


Fig. 3. Angular distributions of the neutron groups from the reaction $^{14}\text{N}(\text{d}, \text{n})^{15}\text{O}$.

In this case the Q has a large positive value and as usual for such values the agreement is good; for the rest of the states the Q -values are negative and, as suggested in I, the theories cannot be applied with the same degree of confidence.

The angular distribution of the first excited state is unusually flat and, at first sight, would not appear to fit into the types of curves given by the theories. However, calculation shows that it can be so fitted with L_p equal to 2. On the other hand the corresponding state of the mirror nucleus ^{15}N has been resolved

into a close doublet of 29 kev spacing by Malm and Buechner (1950) (fig. 4). If a corresponding doublet is assumed to exist in ^{15}O then a flat curve could be obtained by the superposition of two curves of different l_p values. Therefore, the fit we obtain for $l_p=2$ must be considered probably fortuitous.

For the neutron groups corresponding to transitions to the third, fourth and sixth excited states good agreement was obtained between the experimental and theoretical angular distributions by assuming $l_p=0, 1$ and 1 respectively.

	l_n		l_p
9.2		9.06	1(?)
8.3		8.42	1(?)
7.34		7.48	1(?)
7.16		6.84	0
6.33		6.19	1(?)
5.31		5.29	2(?)
5.28			
^{15}N	1	^{15}O	1

Fig. 4. A comparison of the mirror nuclei ^{15}N and ^{15}O .

As Middleton *et al.* have shown the angular distribution curve for $l_p=0$ in the region of $Q = -2.0$ Mev given by the Butler theory is very sensitive to the exact value of Q and the agreement between the experimental points and the Butler curve is possibly not significant. The angular distribution predicted by the Born approximation theory in this region of Q -values is not so sensitive to the exact value of Q and we feel justified in assigning a value of $l_p=0$ for the transition to the third excited state.

The angular distributions corresponding to transitions to the second and fifth excited states, though exhibiting the characteristics to be expected for $l_p=1$ in the case of positive Q -values, cannot in fact be fitted to either theory for any value of l_p . The best fit is for $l_p=1$ but this does not give the observed minimum in the forward direction. On the other hand the fourth and sixth excited states have been found to agree with the curves for $l_p=1$ without showing any such forward minimum.

Middleton *et al.* (1953) have reported several cases of angular distributions corresponding, above 15° , to the theoretical curve for $l_p=1$ but with a pronounced forward minimum. The levels concerned are formed in the reactions $^{12}\text{C}(\text{d}, \text{n})^{13}\text{N}$,

$Q = -0.24$ mev, $^{32}\text{S}(d, n)^{33}\text{Cl}$, $Q = -2.59$ mev and -3.97 mev. They also found that the maximum of the curve moved closer to zero the higher the (negative) value of Q . On the other hand they did not find any case for $l_p = 1$ agreeing with theory.

We therefore have two types of angular distributions both fitting best to the case of $l_p = 1$. One of these agrees with the theories, but the other does not. A study of the possible theoretical curves shows that the distribution with a minimum could not be fitted with any superposition of two theoretical curves with different values of l_p corresponding to a doublet state, so this angular distribution appears certainly not to be one predicted by the theories. We also cannot definitely state that the observed distributions of the fourth and sixth excited states may not be due to the superposition of the type of curve observed in the cases of the second and fifth excited states and a curve of some other value of l_p . However, this is improbable and it may be that we have to accept two different curves, one agreeing with the theories and the other not doing so, for the case of $l_p = 1$. From a formal point of view, this is not impossible in the case of a nucleus such as nitrogen, which has a non-zero total angular momentum.

In the case of nitrogen $j = 1$ and this vector can add to the l_p vector so as to give three values, either 1, 2 or 0. The value 1 implies the addition of the vectors at an angle whilst in the other cases they are added in parallel directions. On the other hand, when the j of the initial nucleus is zero, we have only one case, and it is possibly significant that in the work of Middleton *et al.* who dealt entirely with such cases, only one type of curve was found for $l_p = 1$. They suggested that the disagreement of their type of curve with the theories might be due to the neglect of the coulomb interaction, but our present results perhaps indicate a more complicated state of affairs.

In this region of negative Q -values the assignment of a value of $l_p = 1$ to an angular distribution must be treated with reserve.

§ 4. COMPARISON OF THE ENERGY LEVELS OF THE MIRROR NUCLEI

A comparison of the levels of the mirror nuclei ^{15}O and ^{15}N is shown in fig. 4, the most striking feature being the almost equal large separation of the ground and first excited states. The positions of the energy levels of ^{15}N in the figure are those reported by Malm and Buechner (1950). The spin of the ground state of ^{15}N is that determined by Krüger (1939) and Wood and Dieke (1940), whilst the value of the angular momentum transfer is that observed by Gibson and Thomas in the reaction $^{14}\text{N}(d, p)^{15}\text{N}$.

By assuming that the ground state of ^{14}N has unit spin and even parity (Rotblat 1951, Bromley and Goldman 1952) the spins and parities of the ground and excited states of ^{15}O were determined from the selection rules (angular momentum of final state equal to the vector sum of the angular momentum of the initial state, the orbital angular momentum of the absorbed proton and the proton spin; parities of the initial and final states the same or different according as l_p is even or odd). The values are listed in the table.

The shell model predicts the ground state of ^{15}O as $P_{1/2}$, which is determined by a single neutron hole in a complete shell of eight neutrons. For this ground state we obtain $l_p = 1$, which gives on vector addition the possible nuclear spins of $1/2$, $3/2$ or $5/2$ for the ^{15}O nucleus. Our result is therefore consistent with that given by the shell model.

There have been no other experimental determinations of the spins and parities of the excited states of ^{15}O with which to compare the above values. The angular momentum transfer values for the proton groups in the reaction $^{14}\text{N}(\text{d}, \text{p})^{15}\text{N}$ have been determined by Gibson and Thomas (1952). Unfortunately their observations were not extended much below 20° so that the behaviour of the distributions in this region, which critically affects the assignment of values of angular momentum transfer, is not known. This seems to us to make their predictions of the spins and parities of the levels of ^{15}N unreliable, except perhaps for the ground state.

ACKNOWLEDGMENTS

The authors' thanks are due to Professor H. W. B. Skinner for his encouragement and advice and also to Mr. E. C. Hewitt and Miss B. Anderson for assistance in the microscope work. One of us (W. H. E.) wishes to make grateful acknowledgment to the Imperial Chemical Industries for a Research Fellowship, and another (T. S. G.) is grateful to the Department of Scientific and Industrial Research for a research grant.

REFERENCES

- ADAIR, R. K., 1950, *Rev. Mod. Phys.*, **22**, 249.
BETHE, K. A., 1937, *Rev. Mod. Phys.*, **9**, 272.
BROMLEY, D. A., and GOLDMAN, L. M., 1952, *Phys. Rev.*, **86**, 796.
BHATIA, A. B., HUANG, K., HUBY, R., and NEWNS, H. C., 1952, *Phil. Mag.*, **43**, 485.
BUTLER, S. T., 1951, *Proc. Roy. Soc. A*, **208**, 559.
DUNCAN, D. B., and PERRY, J. E. Jr., 1950, *Phys. Rev.*, **80**, 136.
GIBSON, W. M., and LIVESSEY, D. L., 1948, *Proc. Phys. Soc.*, **60**, 523.
GIBSON, W. M., and THOMAS, E. E., 1952, *Proc. Roy. Soc. A*, **210**, 543.
HUDSPETH, E. L., and SWANN, C. P., 1949, *Phys. Rev.*, **76**, 464.
JOHNSON, C. H., ROBINSON, G. P., and MOAK, C. D., 1952, *Phys. Rev.*, **85**, 931.
KRÜGER, H., 1939, *Z. Phys.*, **111**, 467.
MALM, R., and BUECHNER, W. W., 1950, *Phys. Rev.*, **78**, 337.
MIDDLETON, R., EL-BEDEWI, F. A., and TAI, C. T., 1953, *Proc. Phys. Soc. A*, **66**, 95.
ROSE, W. B., HUDSPETH, E. L., and HEYDENBURG, N. P., 1952, *Phys. Rev.*, **87**, 382.
ROTLAT, J., 1951, *Nature, Lond.*, **167**, 1027.
STEPHENS, W. E., DJANAB, K., and BONNER, T. W., 1937, *Phys. Rev.*, **52**, 1079.
WOOD, R. W., and DIEKE, G. H., 1940, *J. Chem. Phys.*, **8**, 351.

RESEARCH NOTES

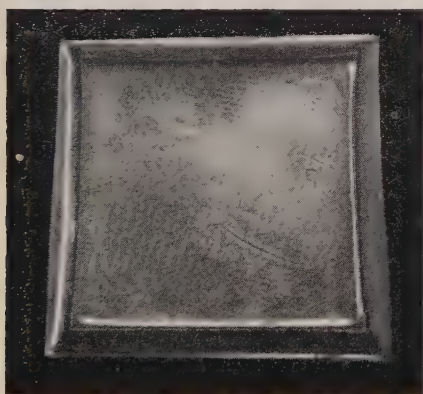
The Reduction of Distortion in Nuclear-Research Emulsion

By A. J. HERZ AND M. EDGAR

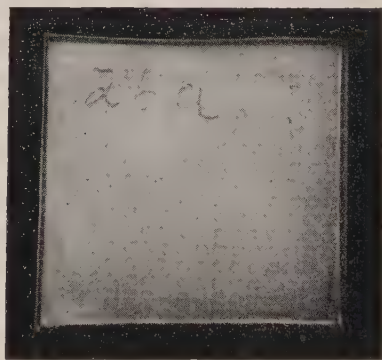
Imperial College, London S.W.7

Communicated by E. P. George; MS. received 30th October 1952

ONE of the most important sources of error in making scattering measurements on the tracks of particles in nuclear-research emulsion, is emulsion distortion. Much work has, therefore, been done in attempts to reduce distortion, and a number of precautions have been suggested in particular by Bonetti, Dilworth and Occhialini (1951). These authors, as most other workers in the field, used the temperature-cycle method (Dilworth, Occhialini and Vermaesen 1950) in which the developer is soaked into the emulsion at low temperature (5°C) and the plates are subsequently taken out of the solution and warmed to between 20° and 30°C to complete development. As the developer does not have access to the emulsion during this so-called 'dry' warm stage, excessive swelling is prevented, and an even distribution of developer throughout the emulsion is ensured. However, even after the



(a)



(b)

- (a) Shows how the edges of the emulsion are drawn inwards when a warm stage has been used.
- (b) Shows a plate which was developed without a warm stage and the edges are distorted only slightly.

suggested precautions have been applied, an appreciable amount of distortion is quite often found, and it is important to make further efforts to prevent it. It is the purpose of this note to draw attention to a source of trouble which appears to have been overlooked so far, and to describe methods by which the resulting distortion may be reduced.

During experiments on the behaviour of developers when used in the temperature-cycle method, it was found that plates which had been processed

entirely at low temperature (about 5° c) showed much less distortion than those which had been given a warm stage. How striking the effect is can be seen from the figure which shows photographs of two sample plates, coated with 1000 μ Ilford G5 emulsion. Both samples were cut from the same (larger) plate, and they were processed together at approximately 5° c with the exception that a dry warm stage (27° c, 30 min) was given to one of them. The two samples are quite typical and it is thus certain that, in the temperature-cycle method of processing, a considerable part of the distortion found in the finished plates is caused by changes occurring during the warm stage.

The exact mechanism by which a *dry* warm stage can cause distortion is not known. Clearly, this type of distortion cannot be due to excessive swelling, for swelling is not possible during the warm stage when the plate has been removed from the solution. The experimental facts which appear relevant at the moment may be summarized in the following way: (i) When the wet emulsion is warmed it loses its elasticity, and becomes dough-like and sticky. If stresses are present, it appears likely that they are released at this stage. (ii) During drying, an emulsion which has undergone a warm stage has a much greater tendency to shrink in a direction parallel to the glass base than one which has been kept at a low temperature throughout. One is thus led to the conclusion that some kind of 'annealing' takes place during a warm stage, and that the properties of the emulsion in the final drying process are changed as a result. To give a rough picture, one might say that the emulsion, as manufactured, tends to shrink and swell mainly in a direction at right angles to the glass base. This directional property is removed by annealing, with the result that shrinkage parallel to the glass surface occurs during drying.

A further reduction in distortion is probably obtained by carrying out the whole of the processing at low temperature. This considerably reduces the swelling during fixing and washing, and the emulsion remains firm and resistant to mechanical damage throughout. Changes in temperature which might give rise to distortion are also avoided.

Up to the time of writing, the developers which have been used in our experiments on low-temperature development have, unfortunately, not given results which are satisfactory in all respects. It is well known that development without a warm stage is possible, especially if amidol-bisulphite developers are used (Herz 1952). However, in the absence of a warm stage, the ratio between the grain density of minimum-ionization tracks and the background density has been found to be rather low with the developers tested so far. It is most important that this disadvantage should be overcome, and work is in progress in an attempt to find more suitable developers.

REFERENCES

- BONETTI, A., DILWORTH, C. C., and OCCHIALINI, G. P. S., 1951, *Bull. Cent. Phys. Nuc. Univ. Libre Bruxelles*, No. 13b.
DILWORTH, C. C., OCCHIALINI, G. P. S., and VERMAESEN, L., 1950, *Bull. Cent. Phys. Nuc. Univ. Libre Bruxelles*, No. 13a.
HERZ, A. J., 1952, *J. Sci. Instrum.*, **29**, 60.

LETTERS TO THE EDITOR

Note on the Fluctuation Problem of Cascades

In a recent paper (Jánossy 1950) a general method for the mathematical treatment of cascade showers was given. An erroneous expression occurs in that paper which will be corrected here.

The distribution of particles in a cascade is derived from a generating function $G(E_0, E, x, u)$, where

$$G(E_0, E, x, u) = \sum_{\nu=0}^{\infty} u^{\nu} \Phi_{\nu}(E_0, E, x),$$

and $\Phi_{\nu}(E_0, E, x)$ is the probability that a primary of energy E_0 should give rise to a cascade which contains at a depth x exactly ν particles with energies exceeding E . The diffusion equation for the G can be obtained as follows. Denote by $\phi(E, x)$ the probability that a primary of energy E should travel a distance x without catastrophic collision. Denote further by $W(E; E', E'') dE' dE'' dx$ the probability that a primary of energy E should suffer a collision along dx resulting in loss of energy such that after the collision the primary is found in an interval E', dE' , and the secondary in an interval E'', dE'' .

Apart from catastrophic collisions we admit also the possibility that the particles should lose energy more or less continuously (as for example is the case for ionization loss). The latter type of loss can be described by $dE/dx = -O(E)$, where $O(E) = \beta = \text{const.}$ is an approximation often used.

The diffusion equation. When a shower containing ν (>1) particles with energies greater than E arises, then the primary must suffer a first catastrophic collision in some interval $d\xi$ giving rise there to two particles, one with energy E' and another with energy E'' ; the latter particles can be regarded as primaries of two secondary showers and these together must provide the final ν particles. We have thus

$$\Phi_{\nu}(E_0, E, x) = \sum_{\nu_1 + \nu_2 = \nu} \int_0^x \int_0^E \int_0^E \phi(E_0, \xi) W[E_0(\xi); E', E''] \Phi_{\nu_1}(E', E, x - \xi) \times \Phi_{\nu_2}(E'', E, x - \xi) dE' dE'' d\xi, \quad \nu > 1. \quad \dots\dots (1)$$

In the above equation $E_0(\xi)$ is the energy to which a primary of energy E_0 is reduced along a path ξ by continuous loss alone.

The above equation is *not valid* for $\nu \leq 1$, since in the latter case we have to add the probabilities for processes where *no collision occurs at all*. In case of no collision, there are two possibilities. Firstly, $E_0(x) > E$; in this case we are left with one particle with energy greater than E at the depth x , namely the primary. Alternatively if $E_0(x) \leq E$, then the primary continuously loses so much energy that no particle with energy greater than E can arrive at the depth x . Including these terms we have to write instead of (1)

$$\Phi_{\nu}(E_0, E, x) = \{\Delta_{\nu}[E, E_0(x)] + \Delta_{\nu-1}[E_0(x), E]\} \phi(E_0, x) + \sum_{\nu_1 + \nu_2 = \nu} \int_0^x \int_0^E \int_0^E \phi(E_0, \xi) W[E_0(\xi); E', E''] \Phi_{\nu_1}(E', E, x - \xi) \times \Phi_{\nu_2}(E'', E, x - \xi) dE' dE'' d\xi, \quad \nu \geq 0, \quad \dots\dots (2)$$

where

$$\Delta_{\nu}(E_1, E_2) = \begin{cases} 1 & \text{if } \nu = 0 \text{ and } E_1 > E_2 \\ 0 & \text{otherwise.} \end{cases}$$

Multiplying (2) by u^{ν} and summing over ν from 0 to ∞ we get

$$G(E_0, E, x, u) = \{\Delta_0[E, E_0(x)] + u\Delta_0[E_0(x), E]\} \phi(E_0, x) + \int_0^x \int_0^E \int_0^E \phi(E_0, \xi) W[E_0(\xi); E', E''] G(E', E, x - \xi, u) \times G(E'', E, x - \xi, u) dE' dE'' d\xi. \quad \dots\dots (3)$$

The first term on the right-hand side was omitted by mistake in the corresponding formula of the original paper (Jánossy 1950, eqn. (6), p. 242).

That this term is indeed important can be seen by putting $x=0$ into (3); the second term vanishes for $x=0$, but owing to the first term we have, since $E_0(0)=E_0$, $\phi(E_0, 0)=1$

$$G(E_0, E, x=0, u) = \begin{cases} 1 & \text{for } E > E_0 \\ u & \text{for } E \leq E_0 \end{cases} \quad \dots\dots (3a)$$

as it must be.

In spite of this error no wrong results were derived from the original formula for the following reason. Provided $O(E)=\beta=\text{const.}$, we may write $E_0(x)=E_0-\beta x$ and in the latter case we have

$$\phi(E_0, x) = \exp \left\{ - \int_0^x \alpha(E_0 - \beta x) dx \right\} \quad \text{with} \quad \alpha(E) = \int_0^E \int_0^E W(E; E', E'') dE' dE''.$$

A simple calculation shows that (3) can be transformed into

$$\left(\frac{\partial}{\partial x} + \beta \frac{\partial}{\partial E_0} + \alpha(E_0) \right) G(E_0, E, x) = \int_0^{E_0} \int_0^{E_0} W(E_0; E', E'') G(E', E, x) G(E'', E, x) dE' dE''. \quad \dots\dots (4)$$

The latter equation could also be derived from the imperfect G -equation of the previous paper, in which we made use only of the correct equation (4) and not of the incorrect equation corresponding to (3).

The fact that the correct equation (4) could be derived from an imperfect G -equation seems surprising at first. However, this is explained easily as follows. Equation (3) determines the G -function fully and no initial condition can be added to (3). Because of the differentiation with respect to x , eqn. (4) admits solutions which are not solutions of (3); the solution of (3) is that solution of (4) which satisfies the initial condition (3a). Now omitting the first term of (3) we still arrive at eqn. (4) from this imperfect equation (3); the extra term in (3) affects only the initial condition which has to be imposed on the solution of (4) to make it satisfy (3). In the previous paper we introduced with the help of physical considerations the correct initial condition for the G and did not notice that the correct equation thus obtained did not satisfy the imperfect integro-equation from which it was originally derived.

A more detailed derivation and a considerable generalization of the G -equations will be published soon (Jánossy 1953).

Department of Cosmic Rays,

Hungarian Academy of Sciences,

Central Research Institute for Physics, Budapest.

20th October 1952.

L. JÁNOSY.

JÁNOSY, L., 1950, *Proc. Phys. Soc. A*, **63**, 241; 1953, *Acta Phys., Hung.*, **2**, in the press.

Paramagnetic Resonance in Four Double Nitrate Salts

Double nitrates of the type $3\text{Mg}(\text{NO}_3)_2 \cdot 2\text{Bi}(\text{NO}_3)_3 \cdot 24\text{H}_2\text{O}$ form an isomorphous series in which either a divalent ion of the 3d transition group or a trivalent ion of the 4f group, or both, can be included in place of the magnesium and bismuth respectively. Such paramagnetic salts are fairly dilute and of considerable interest for adiabatic demagnetization work below 1°K and for nuclear alignment. A number of them have therefore been investigated by means of paramagnetic resonance at 3 cm wavelength, using about 1% paramagnetic impurity in magnesium bismuth nitrate. This forms trigonal crystals of which the detailed structure is not known. The results given for 90°K are less accurate than those at 20°K where proton resonance was used to measure the magnetic field.

Manganese bismuth nitrate showed two magnetically distinct types of ion in unit cell. Since the spectrum of the first type was twice as intense as the spectrum of the second it was assumed that there are two ions of type X and one ion of type Y in unit cell. Each spectrum had a fine structure of five components each of which was divided into six hyperfine lines. The constants in the formulae given by Bleaney and Ingram (1951a) were evaluated from measurements with the magnetic field parallel and perpendicular to the crystal axis. The absolute signs of the constants were found from the relative intensities of the lines at 20°K .

Cobalt bismuth nitrate also showed two types of ion in unit cell. Each spectrum of eight hyperfine lines was measured with the magnetic field parallel and perpendicular to the crystal axis and the constants evaluated using the formulae quoted by Bleaney and Ingram (1951b). However, exact numerical calculation of the energy levels was necessary in the case of the Y type of ion perpendicular to the axis as perturbation theory is not sufficiently accurate. No effect due to B could be detected giving a value of $|B|$ of $1 \times 10^{-4} \text{ cm}^{-1}$ or less.

Copper bismuth nitrate shows a radical change in its spectrum between 90°K and 20°K in a similar manner to certain other copper salts (Bleaney and Bowers 1952). Measurements on the single nearly isotropic spectrum at 90°K were made parallel and perpendicular to the axis of the crystal. At 20°K the spectrum was of three ions in unit cell and measurements were made parallel and perpendicular to the axis of symmetry of each ion. In the spectrum perpendicular to the axis at 20°K the lines corresponding to changes of ± 2 in the nuclear quantum number m were of almost equal intensity to the $\Delta m = 0$ lines (Bleaney 1951). An electric quadrupole interaction term of magnitude $10 \times 10^{-4} \text{ cm}^{-1}$ was assumed (Bleaney, Bowers and Ingram 1951) in evaluating the constant B from this spectrum, since the lines due to the two isotopes 63 and 65 were not resolved.

Gadolinium magnesium nitrate gave a single spectrum, indicating that there was one type of ion in unit cell, with lines of half width 2 gauss, compared with a half width of 5 gauss in the other three salts. No hyperfine structure could be seen although each of the seven main lines was flanked by two unexplained satellites of about one-tenth the intensity. Measurements at 90°K and 20°K were fitted with the constants given in the formulae quoted for gadolinium ethyl sulphate (Bleaney, Elliott, Scovil and Trenam 1951). The term in A_6^6 produces first-order changes in the spectrum varying as $\cos 6\phi$ from which the magnitude of A_6^6 can be deduced. (The sign is indeterminate unless the direction $\phi = 0$ is specified.) The absolute signs of the other constants were found from intensity measurements at 20°K using cerium magnesium nitrate as a dilutant, since the spectrum using bismuth magnesium nitrate as a dilutant showed strong saturation effects at 20°K . The cerium ions have a very short relaxation time, and the magnetic interaction between them and the gadolinium ions reduces the relaxation time of the latter.

Type of Ion	Temp.	g_{\parallel}	g_{\perp}	a	D	A	B
Mn^{2+} X	90°K	1.98 ± 0.02	2.00 ± 0.02	+10	-64	-88	-90
	20°K	1.998 ± 0.003	1.996 ± 0.003	+10	-80	-90	-90
Mn^{2+} Y	90°K	1.98 ± 0.02	2.00 ± 0.02	+ 8	-211	-90	-89
	20°K	1.998 ± 0.003	1.996 ± 0.003	+ 8	-215	-90	-89
Co^{2+} X	20°K	4.108 ± 0.003	4.385 ± 0.003			85	103
Co^{2+} Y	20°K	7.29 ± 0.01	2.338 ± 0.004			283	(≤ 1)
	90°K	2.219 ± 0.003	2.217 ± 0.003			27	26
Cu^{2+}	20°K	2.454 ± 0.003	2.096 ± 0.003			110	17

Type of Ion	Temp.	g_{\parallel}	g_{\perp}	$3A_2^0$	$60A_6^0$	$1260A_6^0$	$1260A_6^6$
Gd^{3+}	90°K	1.990 ± 0.004	1.992 ± 0.004	+124	+0.9	+0.6	12
	20°K	1.992 ± 0.003	1.992 ± 0.003	+124	+0.9	+0.6	12

a , D , A , B , A_2^0 , A_4^0 , A_6^0 , and A_6^6 , are all in units of 10^{-4} cm^{-1} . Where errors are not given the number is correct to ± 1 in the last digit.

Work is in progress on the copper salt in an endeavour to grow crystals from heavy water with narrower lines. The better resolution obtainable should make this salt very suitable for measurements on the quadrupole moments of copper.

The author wishes to record his gratitude to Dr. B. Bleaney for generous help and advice.

Clarendon Laboratory,
Oxford.

R. S. TRENAM.

10th November 1952.

BLEANEY, B., 1951, *Phil. Mag.*, **42**, 441.

BLEANEY, B., and BOWERS, K. D., 1952, *Proc. Phys. Soc. A*, **65**, 667.

BLEANEY, B., BOWERS, K. D., and INGRAM, D. J. E., 1951, *Proc. Phys. Soc. A*, **64**, 758.

BLEANEY, B., ELLIOTT, R. J., SCOVIL, H. E. D., and TRENAM, R. S., 1951, *Phil. Mag.*, **42**, 1062.

BLEANEY, B., and INGRAM, D. J. E., 1951a, *Proc. Roy. Soc. A*, **205**, 336; 1951b, *Ibid.*, **208**, 143.

Inelastic Neutron Scattering in Iron

A method has been developed for the measurement of the excitation function of inelastic neutron scattering by studying the gamma radiation from the excited states so formed, and preliminary results have been obtained for iron. The neutrons were produced by the $T(pn)^3\text{He}$ reaction in a tritium gas target attached to the Harwell Van de Graaff machine. The detector was a naphthalene-anthracene crystal $1\frac{3}{4}$ in. in diameter and $1\frac{1}{4}$ in. thick, used in conjunction with an EMI photomultiplier type VX5045. The iron scatterer was an annular ring, $2\frac{1}{4}$ in. inside diameter, $4\frac{1}{2}$ in. outside diameter and $1\frac{1}{2}$ in. thick, closely surrounding the crystal. A polythene cone 6 in. long was arranged to shield the crystal from neutrons coming direct from the target.

The spectrum of pulses produced in the crystal was recorded on a thirty-channel kicksorter. At a given neutron energy a spectrum was taken first with the iron scatterer in position and then with it removed, the neutron flux being monitored by a boron trifluoride

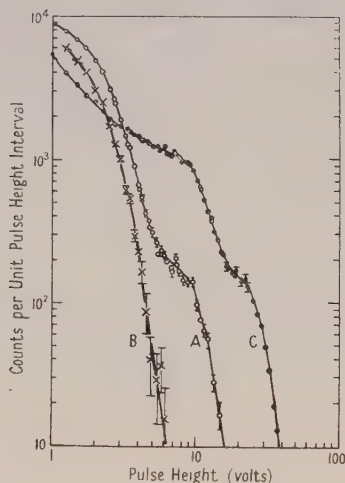


Fig. 1. Curves A and B: the distribution of pulses due to the iron and phosphorus scatterers respectively for an initial neutron energy of 1.05 mev. Curve C: the distribution due to γ -radiation from ^{56}Mn .

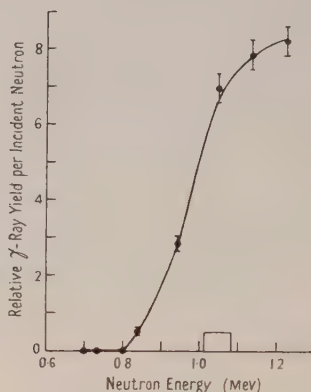


Fig. 2. The excitation function for the γ -rays following inelastic neutron scattering in iron. The rectangle indicates the neutron energy spread.

counter. The total counting rate with the iron ring in position was about twice that without it. The difference curve obtained by subtracting the two spectra then corresponded to the pulses due to various processes occurring in the iron. A typical difference curve is shown in fig. 1, curve A, where two groups of pulses may be distinguished. The higher energy group, with a knee at 9.5 volts pulse height, is attributed to γ -rays following inelastic neutron scattering, and the lower energy group, with no very well defined knee, is attributed principally to elastically scattered neutrons, on the following evidence.

A group similar in pulse height distribution to the lower energy group was obtained either when a phosphorus or a lead scatterer was substituted for the iron (fig. 1, curve B), or when the crystal was exposed to neutrons coming straight from the target; in neither case was the higher energy group of pulses observed over the range of neutron energies used. The higher energy group could be reproduced by irradiating the crystal with γ -rays from ^{56}Mn , which decays by β -emission to several excited states of ^{56}Fe , including the first known excited state at 0.83 mev (Mitchell 1950). The pulse spectrum C, fig. 1, shows the group due to the 0.83 mev γ -rays together with a higher energy group produced by unresolved 1.81 and 2.06 mev γ -rays. By comparison of the spectra obtained from ^{56}Mn and from ^7Be , which emits a γ -ray of energy 0.478 mev, it was possible to establish that the γ -ray energy corresponding to the high energy group of curve A was within 5% of that of the low energy component from ^{56}Mn .

The excitation function of the γ -rays following inelastic scattering was obtained from the difference curves taken at a number of neutron bombarding energies, the neutrons at the scatterer having an energy spread of 70 kev. The relative γ -ray intensity at each energy was determined by adding together all counts between 7 and 14 volts pulse height, a correction being made, where necessary, for a small contribution from the lower energy group. The results are given in fig. 2. It will be observed that the threshold for the reaction is close to the value of 0.81 mev expected for the neutron energy spread used.

An approximate estimate of 0.4 barn for the absolute cross section for inelastic scattering at a neutron energy of 1.23 mev was obtained by calculating the crystal efficiency and assuming spherical symmetry of the γ -radiation. This value is believed to be correct to a factor of two.

We thank the Director, Atomic Energy Research Establishment, for permission to publish this work.

Atomic Energy Research Establishment,
Harwell, Didcot, Berks.
28th October 1952.

B. ROSE.
J. M. FREEMAN.

MITCHELL, A. C., 1950, *Rev. Mod. Phys.*, **22**, 36.

Electron Spin in Semiconductors

In a recent paper Landsberg (1952) contrasts two techniques for determining electron distributions in semiconductors. In one approach, which I shall call the 'thermodynamic', one first obtains a formula for the free energy as a function of possible distributions and then minimizes. In the other approach, which I shall call the 'direct', one writes down the equilibrium distribution in terms of the absolute activity (or the Fermi level) without any mention of the free energy or entropy. In the simple cases hitherto dealt with the two approaches are mathematically equivalent and if used correctly must lead to the same results, whereas Landsberg states that the thermodynamic approach "is to be preferred".

Amongst the best known texts on the theory of semiconductors that by Mott and Gurney (1948) uses the thermodynamic approach and gives formulae which correctly take account of electron spin. Most of the other authoritative texts, such as those by Wilson (1936), Fowler (1936), Seitz (1940) and Shockley (1950) use the direct approach. None of them examines the effect of electron spin in sufficient detail to avoid all possibility of ambiguity. Landsberg implies that the direct approach is unsuitable for taking account of electron spin. In fact it can do so more powerfully and more concisely than the thermodynamic approach. It is the object of the present note to demonstrate this.

I shall treat a system sufficiently general to include as special cases practically all types of semiconductors that have previously been considered. Formulae for the number n_e of electrons per unit volume in a nearly empty conduction band and for the number n_h of electrons per unit volume missing from an almost full valence band need not be re-derived since they are well known and not controversial. They are

$$n_e = 2\lambda(2\pi m^- kT/h^2)^{3/2} \exp(-E_c/kT), \quad \dots\dots (1)$$

$$n_h = 2\lambda^{-1}(2\pi m^+ kT/h^2)^{3/2} \exp(E_v/kT), \quad \dots\dots (2)$$

where m^- denotes the effective mass of the electron and m^+ that of a 'hole'; E_c denotes the energy of the bottom of the conduction band and E_v the energy of the top of the valency band. The first factor 2 takes account of electron spin. In both these formulae λ is the absolute activity (Fowler and Guggenheim 1939) of the electrons and is related to Gibbs' potential μ or to the Fermi level E_F by $\lambda = \exp(\mu/kT) = \exp(E_F/kT)$. It is fundamental that at equilibrium λ has the same value in all expressions, whether relating to the conduction band or the valency band or electronic states at donor and acceptor sites. The remaining task is to express the number of electrons on the various kinds of sites in terms of this

same parameter λ . The value of λ is then always determined by equating the sum of the number of electrons in each kind of band or site to the total number of electrons in the system.

The system may contain several kinds of impurity sites, some donors, others acceptors, but only one set of sites need be considered explicitly, since the formula obtained will apply to *any and every set*. It is assumed that one of these sets consists of N sites, which are independent; that is to say the manner of occupation of each site is independent of the manner of occupation of every other site. It is also assumed that at most only the following (and in practice not all these) manners of occupation of each site need be considered :

- a 1S state of energy E_0 containing no electrons (other than inner shell electrons which are ignored throughout);
- a $^2S_+$ state of energy E_1 containing one s electron with a positive spin;
- a $^2S_-$ state of energy E_1 containing one s electron with a negative spin;
- a 1S state of energy E_2 containing two s electrons with opposite spins.

The number of sites occupied in these manners will be denoted by n_0, n_+, n_-, n_2 respectively. In fact $n_+ = n_-$, but it is preferable initially to preserve the separate symbols.

Since the four specified manners of occupation are *non-degenerate*, we are not troubled with weighting factors, and according to the most general principles of Fermi-Dirac statistics

$$n_0 : n_+ : n_- : n_2 = \exp(-E_0/kT) : \lambda \exp(-E_1/kT) : \lambda \exp(-E_1/kT) : \lambda^2 \exp(-E_2/kT) \dots (3)$$

The four expressions on the right are just terms in the grand partition function (Fowler 1938) for one of the sites. If there are several kinds of impurity levels, this formula will apply to every such set of sites with, of course, the appropriate values of the energies.

This general treatment includes two specially simple examples which are familiar.

- (i) Donor centres with unpaired s electrons (or acceptor centres for unpaired s electrons).

E_2 is so great that n_2 is effectively zero, and from (3) we have $n_0/N = \{1 + 2\lambda \exp(-E_d/kT)\}^{-1}$ where $E_d = E_1 - E_0$.

- (ii) Acceptor centres for paired s electrons (or donor centres with paired s electrons). E_0 is so great that n_0 is effectively zero, and from (3) we have $n_2/N = \{1 + 2\lambda^{-1} \exp(E_a/kT)\}^{-1}$ where $E_a = E_2 - E_1$.

The technique here described is completely reliable as long as every degenerate state is resolved into its non-degenerate component states. This procedure can readily be extended to take account of orbital degeneracy of p electrons.

I am grateful to Dr. A. H. Wilson for drawing my attention to this problem and for stimulating correspondence.

Department of Chemistry,
University of Reading.
21st October 1952.

E. A. GUGGENHEIM.

- FOWLER, R. H., 1936, *Statistical Mechanics*, 2nd edn. (Cambridge : University Press), §§ 11.6 and 11.61; 1938, *Proc. Cam. Phil. Soc.*, **34**, 382.
FOWLER, R. H., and GUGGENHEIM, E. A., 1939, *Statistical Thermodynamics* (Cambridge : University Press), p. 66.
LANDSBERG, P. T., 1952, *Proc. Phys. Soc. A*, **65**, 604.
MOTT, N. F., and GURNEY, R. W., 1948, *Electronic Processes in Ionic Crystals*, 2nd edn. (Oxford : University Press), p. 157.
SEITZ, F., 1940, *The Modern Theory of Solids* (New York : McGraw-Hill), p. 186.
SHOCKLEY, W., 1950, *Electrons and Holes in Semiconductors* (New York : Van Nostrand), p. 240.
WILSON, A. H., 1936, *The Theory of Metals* (Cambridge : University Press), p. 70.

The Asymptotic Solution of an Equation Occurring in Scattering Theory

The purpose of the present note is to provide a useful generalization of a well known theorem in scattering theory. We consider the equation

$$\mathbf{M}\psi = [\nabla^2 + k^2 - U(\mathbf{r}) + \mathbf{K}]\psi(\mathbf{r}) = F(\mathbf{r}), \quad \dots\dots (1)$$

which differs from a similar equation discussed by Mott and Massey (1949) by the inclusion of a term involving the operator \mathbf{K} , which is assumed to be Hermitian. The particular case which we have in mind is that which arises when exchange distortion is allowed for in a scattering problem, see for example, Bransden and Burhop (1950), Erskine and Massey (1952), Massey and Mohr (1952), Seaton (1953). \mathbf{K} is then a Hermitian integral operator, defined by a relation of the form

$$\mathbf{K}\psi(\mathbf{r}) = \int K(\mathbf{r}, \mathbf{r}')\psi(\mathbf{r}') d\tau'. \quad \dots\dots (2)$$

It is assumed that \mathbf{M} and $F(\mathbf{r})$ are such that there exists a unique solution ψ of (1) which is bounded at the origin and has asymptotic form

$$\psi(\mathbf{r}) \sim f(\theta, \phi)e^{ikr}/r. \quad \dots\dots (3)$$

The theorem to be proved then states that

$$f(\theta, \phi) = -\frac{1}{4\pi} \int \mathcal{F}^*(\mathbf{r}', \Theta)F(\mathbf{r}') d\tau', \quad \dots\dots (4)$$

where $\mathcal{F}(\mathbf{r}, \theta)$ is that solution of the homogeneous equation

$$\mathbf{M}\mathcal{F} = 0 \quad \dots\dots (5)$$

which is bounded at the origin and has asymptotic form

$$\mathcal{F}(\mathbf{r}, \theta) \sim \exp(ikr \cos \theta) + g(\theta)e^{ikr}/r \quad \dots\dots (6)$$

and where Θ in (4) is the angle between \mathbf{r} and \mathbf{r}' .

In the absence of the operator \mathbf{K} , the theorem can be proved by letting r tend to infinity in a Green's function solution of (1), as is done by Mott and Massey (1949); but when an integral operator \mathbf{K} such as (2) is included, \mathbf{M} is no longer a point operator and the usual theory of the Green's function ceases to be applicable. This difficulty can be overcome by direct evaluation of the integral in (4). Using (1) we can write

$$\int \mathcal{F}^*(\mathbf{r}', \Theta)F(\mathbf{r}') d\tau' = \int [\mathcal{F}^*(\mathbf{r}', \Theta)\mathbf{M}\psi(\mathbf{r}') - \psi(\mathbf{r}')\mathbf{M}^*\mathcal{F}^*(\mathbf{r}', \Theta)] d\tau',$$

since (5) ensures that $\mathbf{M}^*\mathcal{F}^* = 0$. Using the Hermitian property of \mathbf{K} , we find that the only terms that do not cancel are those arising from the ∇^2 part of \mathbf{M} , giving

$$\int \mathcal{F}^*F d\tau' = \int [\mathcal{F}^*\nabla^2\psi - \psi\nabla^2\mathcal{F}^*] d\tau' = \lim_{R \rightarrow \infty} \int_R \left[\mathcal{F}^* \frac{\partial\psi}{\partial r'} - \psi \frac{\partial\mathcal{F}^*}{\partial r'} \right] R^2 \sin \theta' d\theta' d\phi',$$

where the integration is over the surface of a large sphere of radius R with centre at the origin. Over this surface we replace ψ and \mathcal{F} by their asymptotic forms (3) and (6), thus obtaining an integral of a type which has already been evaluated by Dirac (1947), giving the required result: $\int \mathcal{F}^*(\mathbf{r}', \Theta)F(\mathbf{r}') d\tau' = -4\pi f(\theta, \phi)$.

A one-dimensional form of this theorem states that, if the integro-differential equation

$$\mathbf{L}y = \left[\frac{d^2}{dr^2} + k^2 - U(r) \right] y(r) + \int_0^\infty K(r, r')y(r') dr' = F(r),$$

with $K(r, r') = K(r', r)$, has a solution y such that $y(0) = 0$, $y(r) \sim \beta e^{ikr}$, then

$$\beta = -\frac{1}{k} e^{i\eta} \int_0^\infty u(r')F(r') dr',$$

where $u(r)$ is that solution of $\mathbf{L}u=0$ which satisfies $u(0)=0$, $u(r) \sim \sin(kr+\eta)$. This can be proved by essentially the same method as was used for the three-dimensional case.

We would like to thank Professor H. S. W. Massey for his interest in this problem.

Department of Physics,
University College, London.
21st November 1952.

G. A. ERSKINE.
M. J. SEATON.

BRANDSEN, B. H., and BURHOP, E. H. S., 1950, *Proc. Phys. Soc. A*, **63**, 1337.

DIRAC, P. A. M., 1947, *Quantum Mechanics* (Oxford: University Press) 3rd edn., p. 191.

ERSKINE, G. A., and MASSEY, H. S. W., 1952, *Proc. Roy. Soc. A*, **212**, 521.

MASSEY, H. S. W., and MOHR, C. B. O., 1952, *Proc. Phys. Soc. A*, **65**, 845.

MOTT, N. F., and MASSEY, H. S. W., 1949, *The Theory of Atomic Collisions* (Oxford: University Press) 2nd edn. Chap. VI, § 3.

SEATON, M. J., 1953, *Phil. Trans. Roy. Soc. A*, in the press.

REVIEWS OF BOOKS

Cosmology, by H. BONDI. Pp. ix + 179. (Cambridge: University Press, 1952.) 22s. 6d.

This book is a remarkable feat of exposition. It is a comprehensive survey of the whole of modern cosmology. Its comprehensiveness is achieved within its modest length by skilful arrangement of the material and by keeping attention fixed upon general principles and upon the underlying coherence of the developments in the subject. The result is an extremely readable account for the non-specialist as well as an invaluable summing-up for those with some specialist interest in the work.

It can be said without exaggeration that the book will do much to enhance the scientific status of the subject. Strictly speaking, the subject ought not to stand in need of any such aid to its enhancement. There is, however, a tendency to regard cosmology as a field for somewhat fruitless speculation and controversy in which other scientists find difficulty in recognizing the achievement of definite progress. Actually, the situation could be matched by that of other important developments at roughly analogous stages in the past. One thinks, for instance, of the developments concerning evolution in biology and concerning stellar constitution and stellar energy generation in astrophysics. Mr. Bondi now presents "cosmology as a branch of physics in its own right". His book makes its appearance when there is ample ground for the view implied; the character of his book is calculated to win general recognition for this view.

W. H. MCCREA.

Conformal Mapping, by Z. NEHARI. Pp. viii + 396. 1st edn. (New York: McGraw-Hill, 1952.) \$7.50. 64s.

In this book, the third in the International Series in Pure and Applied Mathematics, the author aims at bridging the gap between the pure mathematician and the applied mathematician, physicist or engineer concerned with conformal mapping. In general, however, the treatment is of such a nature that it is likely to appeal mainly to the pure mathematician. The methods described and the results obtained do, nevertheless, provide a most valuable reference for the non-specialist. The first four chapters, which constitute nearly half the book, serve as an introduction to those parts of potential theory, the Green's function, boundary value problems and complex variable theory which are a necessary preliminary to the study of mapping problems. The treatment is fairly rigorous but, although forming an admirable summary for the more advanced student, would hardly be suitable for one unfamiliar with these topics.

The next two chapters deal with the mapping of simply-connected domains, including a detailed discussion of the bilinear transformation, Riemann's mapping theorem, the Schwarz-Christoffel transformation, domains bounded by circular arcs and nearly circular domains, and with the mapping properties of some common special functions. The clearness of exposition and the wealth of information contained here leave little to be desired.

The last chapter, which contains an up-to-date account of the mapping of multiply-connected domains, will be of interest mainly to the specialist in this field.

Each topic is followed by an appropriate set of exercises, in all nearly 400 problems being provided.

A. N. GORDON.

Concepts and Methods of Theoretical Physics, by R. B. LINDSAY. Pp. x + 515. (London: Macmillan, 1952.) 52s. 6d.

This book is an attempt to outline the main features of theoretical physics in its broadest sense; it covers the whole field of classical physics and a good deal of quantum theory. The treatment is elementary, and not free from elementary mistakes. The book has also philosophic pretensions, and this is unfortunately its greatest weakness. What should one think of a philosophy of science which ignores not only the idea of complementarity, but even the correspondence principle, and accordingly describes the fundamental ideas of quantum mechanics as 'cook-book recipes'?

The plan of the book seems indeed inspired by the philosophical outlook of the past rather than the present century. The author takes as his main principle of classification the subdivision into particle and field physics; thus he puts together the mechanics of fluid and deformable media and the electromagnetic theory, as if the common use of the continuum conception in the two cases had more than a formal significance nowadays. Another disastrous result of this mistaken dichotomy is that it obviously leaves no natural place for quantum theory, which is arbitrarily squeezed into the 'particle physics' compartment. In this way the fundamental fact that quantum theory represents the dialectical synthesis of the contradictory concepts of particle and field is not only ignored, but hopelessly confused.

From the point of view of typography, the book consists of a photographic reproduction of a typescript, executed without regard to even modest aesthetical requirements. The text is legible enough, but the formulae are unduly clumsy. This poor production is not offset by a low price.

L. ROSENFELD.

Die praktische Behandlung von Integralgleichungen, by H. BÜCKNER. Pp. vi + 127. (Berlin: Springer, 1952.) DM. 18.60.

The practical solution of integral equations forms a relatively new branch of numerical mathematics. But the development of numerical methods of solving Fredholm's integral-equation

$$y(s) = f(s) + \lambda \int_a^b K(s, t)y(t) dt$$

or the corresponding homogeneous equation

$$y(s) = \lambda \int_a^b K(s, t)y(t) dt$$

has now reached the stage when a connected account of the mathematical theory of these methods is desirable. This is the object of the present monograph, the first of a new series published by Springer under the title *Ergebnisse der angewandten Mathematik*.

The fundamental problem is to determine the eigenvalues, that is the values of the constant λ for which the homogeneous equation has solutions other than $y \equiv 0$. An excellent account is given of the theory of the various techniques available for their approximate numerical determination. Yet the problems to which the methods are applied all seem rather trivial. The book, despite its title, is theoretical not practical. This may be unavoidable as the subject of integral-equations still awaits its 'Piaggio'.

The only equations discussed are of the Fredholm type. Of recent years integral equation formulations of diffraction problems have become increasingly important. In many cases, the equations are not capable of solution in closed form, and recourse must be had to some method of numerical solution. Such work is nowhere mentioned although the variational techniques of Levine and Schwinger probably form the most important advances in the practical applications of integral equations.

E. T. COPSON.

Oeuvres scientifiques de Jean Perrin. Pp. xii+408. (Paris: Service des Publications du Centre National de la Recherche Scientifique; London agents, H. K. Lewis, 1950.) In paper cover 33s., bound in cloth 40s.

It is already a sign of belonging to the older generation of physicists to be able to recall the thrill of reading Perrin's *Les Atomes* and in finding there set out visible, almost tangible, proof of the real existence of these still rather hypothetical entities. Jean Perrin belonged to that small and happy band of adventurers in thought and experiment who built and secured the bridge between classical and modern physics. The publication of his scientific papers thanks to the initiative of the Centre National de la Recherche Scientifique which he helped to found, is a welcome addition to the literature of that heroic episode. It is an example that might well be imitated here.

The book is a slim one for a life's work, but this is deceptive: Perrin belongs to the great tradition of French lucidity and brevity. Seldom has more thought been concentrated into a smaller number of words. From the very beginning of his career he had the genius of seizing on the essential point and focusing his enquiry on the decisive experiment. His greatest discovery, the negative charge of the cathode rays, was the result of his very first research at the age of twenty-four, a record only equalled by Pasteur's discovery of molecular asymmetry at the same age, on graduating from the same school, the Ecole Normale Supérieure. That was in 1895, the year $X-1$ of the modern era.

Immediately x-rays were discovered, Perrin was one of the foremost to study their properties, particularly ionization and the photo-electric effect. His doctoral thesis of 1897 though only thirty pages long, is packed with more new observations and deductions than a dozen of the hundred page theses of today. Indeed Perrin had discovered independently in those two years, many of the effects which J. J. Thomson and Rutherford were establishing at the same time at Cambridge. It was in this work that Perrin established that close and friendly relation with his great colleague Langevin, which was to last for the rest of their lives and, through him, established contacts with the English school of physics.

This first phase of Perrin's research, which fits into the main line of electron and nuclear physics, was not to be followed up but before he left it altogether he was to enunciate, twelve years before it was to be definitely established by Rutherford, the positive nuclear theory of the atom. On 16th February 1901 in a Popular Lecture we find him saying "Chaque atome serait constitué, d'une part, par une ou plusieurs masses très fortement chargées d'électricité positive, sorte de soleils positifs dont la charge serait très supérieure à celle d'un corpuscule et, d'autre part, par une multitude de corpuscules, sorte de petites planètes négatives. L'ensemble de ces masses gravitant sous l'action des forces électriques, et la charge négative totale équivalant exactement à la charge positive totale, en sorte que l'atome soit électriquement neutre" (p. 166). He even calculated the time of revolution of such a planetary corpuscle (electron) and found it to be of the order of 10^{-15} sec, of the same order as the periods of the spectral emission. Although the quantum theory was absolutely necessary to justify and make fully quantitative the planetary hypothesis of atomic structure, Perrin's inspired guess deserves a place in the history of physics.

In 1898, Perrin became a lecturer at the Sorbonne and his scientific work took a different turn. Theoretical considerations on the implication of thermodynamics led him in the direction of Physical Chemistry. Influenced by the school of Ostwald he strove to remould the exposition of physics in terms of one observable energy. This was the basis of his *Principes* (1903), later elaborated in *Les Elements de la Physique* (1930). He found however that the continuum of thermodynamics was difficult to reconcile with hypothetical and, still more, with real atoms of absolute and determinable weights. This difficulty was to lead him to the study of visible atom models, to the Brownian movement and to the field of colloid chemistry. The results are summed up in *Les Atomes* (1913), but the series of papers in which they were first published form the bulk of this volume. Reading through them, how many of the phenomena of colloids—the double layer, the effects of ions, electro-osmosis—that were afterwards to be of much importance, were clearly appreciated and explained by Perrin?

Like most of the physicists of his generation, Perrin's work was interrupted by the first world war. When peace returned he had once again changed his field of work to that of photochemistry and fluorescence. That this later work does not stand out in the same manner as his earlier researches is due to the fact that now, with the emergence of the quantum theory, many new and younger workers were in the field, but here again Perrin's intuition led him to foresee the significance of phenomena such as those of activated molecules, whose importance was only recognized long afterwards.

In his last years Perrin turned more and more to the practical task of the administration, the teaching and popularization of science in France. Despite inertia and opposition, he was largely responsible for the preservation of the spirit and activity of French science, whose achievements he displayed so brilliantly in the 'Palais de la Découverte' which will remain his monument in showing the beauty as well as the utility of science.

J. D. BERNAL.

Mechanical Properties of Metals at Low Temperatures. National Bureau of Standards Circular 520. Pp. iv + 206. (Washington, D.C.: U.S. Department of Commerce, 1952.) \$1.50.

This book is based on nine lectures read at a Symposium held in May 1951 at the National Bureau of Standards in Washington. Although all the papers contain much that must be of interest to the metallurgist, they vary somewhat in their usefulness to the low temperature physicist; this is partly due to the broad interpretation of the term 'low temperatures'. For example, one paper is called 'Application of metals in aircraft at low temperatures', and another 'Brittle fractures in ship plates'. On the whole, however, 'low temperatures' means the temperatures of liquid air and liquid hydrogen and there is even a mention of some work done at 1°K . Among the more interesting papers is one dealing with the properties of copper and nickel and their alloys and three others on the properties of different kinds of steel.

Considered as a whole, the book is written in metallurgical jargon which sometimes makes difficult reading for the physicist and there is an excess of experimental detail in many of the papers. However, the discriminating and patient reader will be able to extract much useful information. The profusion of different units is irritating, particularly in the case of temperatures which are expressed in $^{\circ}\text{F}$, $^{\circ}\text{C}$ and $^{\circ}\text{K}$ according to the whim of the author. Apart from the absence of an index, the book is well produced; it is also lavishly illustrated.

A. J. CROFT.

Application de la notion d'échauffement relatif à l'étude de la convection forcée de la chaleur, by EDOUARD ROCHE. Pp. iii + 78. (Paris: Publications Scientifiques et Techniques du Ministère de l'Air (No. 267), 1952.) 750 fr.

Time and Universe for the Scientific Conscience, by MARTIN JOHNSON. (The Sixth Arthur Stanley Eddington Memorial Lecture.) Pp. v + 42. (Cambridge: University Press, 1952.) 2s. 6d.

Tables of the Bessel Functions $Y_0(x)$, $Y_1(x)$, $K_0(x)$, $K_1(x)$, $0 \leq x \leq 1$. National Bureau of Standards Applied Mathematics Series 25. Pp. ix + 60. (Washington, D.C.: U.S. Department of Commerce, 1952.) 40 c.

Contribution à l'étude de la sursaturation du fer en hydrogène cathodique, by JEAN DUFLOT. Pp. 58. (Paris: Publications Scientifiques et Techniques du Ministère de l'Air, 1952.) 1000 fr.

CONTENTS OF SECTION B

	PAGE
Editorial	1
Mr. A. N. STROH. The Mean Shear Stress in an Array of Dislocations and Latent Hardening	2
Dr. DOROTHY FISHER. Crystal Structures of Gutta Percha	7
Prof. F. LLEWELLYN JONES and Dr. G. C. WILLIAMS. Collisional Processes and Similarity in High-Frequency Discharges in Helium	17
Dr. K. J. LE COUTEUR. Perturbations in the Magnetic Deflector for Synchro-Cyclotrons	25
Mr. L. W. DAVIES. Spectroscopic Study of Caesium Discharges in a Magnetic Field	33
Dr. C. HENDERSON, Mr. F. F. HEYMANN and Dr. R. E. JENNINGS. Phase Stability of the Microtron	41
Dr. P. C. BANBURY. Carrier Injection and Extraction in Lead Sulphide	50
Mr. G. LINDSTRÖM, Dr. K. SIEGBAHN and Mr. A. H. WAPSTRA. A Precision Measurement of the ^{137}Cs γ -Line	54
Letter to the Editor :	
Mr. J. J. DOWD and Mr. R. L. ROUSE. Distribution Coefficient of Indium in Germanium on Crystallization	60
Reviews of Books	61
Corrigenda	63
Contents of Section A	64

Quantum Electrodynamics with Auxiliary Fields

By SURAJ N. GUPTA

Physical Laboratories, University of Manchester

Communicated by L. Rosenfeld; MS. received 3rd July 1952

ABSTRACT. A consistent scheme of quantum electrodynamics with auxiliary fields of photons and electrons of infinitely large masses is developed. The auxiliary fields are introduced from the very beginning in the Lagrangian density, but it is ensured by means of suitable initial conditions that these fields are completely unobservable. For some of the auxiliary photon fields the usual sign of the Lagrangian density is reversed, while for some of the auxiliary electrons fields the usual statistics of the field is reversed. For such fields it is found necessary to use an indefinite metric.

It is shown that the present treatment provides us with a well-defined procedure for the evaluation of divergent integrals in quantum electrodynamics. As an application, the self-energy of the photon is evaluated and shown to vanish for a free photon.

§ 1. INTRODUCTION

SEVERAL devices of integration have been proposed in recent years to evaluate the divergent integrals in quantum electrodynamics in an unambiguous way. One of these devices is the method of auxiliary masses or regularization, which has been introduced by Feynman (1949) and by Pauli and Villars (1949). The method of auxiliary masses is certainly a very useful one, and it is probably the most reliable method of integration which is available at present. However, as Pauli and Villars have shown, the regularization of divergent integrals has to be carried out according to certain rules, but so far no clear justification for these rules has been given. It has also not been shown how the auxiliary masses are to be introduced in the basic equations of quantum electrodynamics in a consistent way.

The aim of the present paper is to develop a systematic scheme of quantum electrodynamics with auxiliary fields of particles of infinitely large masses. The auxiliary fields will be introduced from the very beginning in the Lagrangian density, but it will be ensured by means of suitable initial conditions that these fields are completely *unobservable*. As we shall see, the present treatment will provide us with a well-defined procedure for the evaluation of divergent integrals in quantum electrodynamics.

In this paper, as far as possible, we shall follow the notation of Schwinger (1948, 1949) and Dyson (1949), and we refer to their papers for the meaning of the various symbols to be used here.

§ 2. THE PERTURBATION THEORY AND CONSERVATION OF ENERGY

It is well known that the perturbation theory requires that in any collision process the energy in the final state of a system should be equal to the energy in the initial state. We shall discuss the meaning of this statement more closely, because an essential argument in the present paper is based on it.

It can be easily seen that for any collision process, in which there are m particles in the initial state and n particles in the final state, the contribution of the S -matrix reduces to the form

$$S_{fi}' = \int_{-\infty}^{\infty} dt F \exp \{i(E_1' + E_2' + \dots + E_n')t\} \exp \{-i(E_1 + E_2 + \dots + E_m)t\}, \dots (1)$$

where E_1, E_2, \dots, E_m are the eigenvalues of the Hamiltonian of the particles in the initial state, E'_1, E'_2, \dots, E'_n are the eigenvalues of the Hamiltonians of the particles in the final state, and the quantity F is independent of t . The above equation shows that the contribution of the S -matrix vanishes, unless

$$E_1 + E_2 + \dots + E_m = E'_1 + E'_2 + \dots + E'_n \quad \dots\dots(2)$$

or

$$E_i = E_f, \quad \dots\dots(3)$$

where E_i and E_f are the *eigenvalues* of the Hamiltonian of the system in the initial and the final states respectively. Hence, from any initial eigenstate in a collision process a system can make transitions only to those final eigenstates, in which the eigenvalue of the Hamiltonian of the system remains unchanged. It is important to note that (3) involves the *eigenvalues* of the Hamiltonian and not simply the expectation values.

The result (3) holds even when one is using an indefinite metric, which only modifies the relation between the probability of finding the system in the final state and the quantity S_{fi} , given by (1).

§ 3. THE AUXILIARY PHOTON FIELDS

Let us assume that the electrons interact not only with the usual photon field but also with one or more auxiliary photon fields of very large masses. It will be explained in § 5 how many of these auxiliary fields are to be used in practice. In this section we shall only show how the auxiliary fields can be treated in such a way that the auxiliary particles remain completely unobserved. We shall discuss below two kinds of auxiliary photon fields, which will be called the normal and the abnormal ones.

(i) Normal Auxiliary Photon Field

We take the Lagrangian density for the normal auxiliary photon field as

$$L = -\frac{1}{2} \left\{ \left(\frac{\partial A_\mu}{\partial x_\nu} \right)^2 + \kappa^2 A_\mu^2 \right\}, \quad \dots\dots(4)$$

where κ , the rest mass of the auxiliary photons, is a very large constant, which ultimately tends to infinity. We then obtain for the field equation and the Hamiltonian density in the usual way

$$(\square^2 - \kappa^2)A_\mu = 0, \quad \dots\dots(5)$$

$$H = \left(\frac{\partial A_\mu}{\partial t} \right)^2 + \frac{1}{2} \left\{ \left(\frac{\partial A_\mu}{\partial x_\nu} \right)^2 + \kappa^2 A_\mu^2 \right\}. \quad \dots\dots(6)$$

We also find the commutation relation

$$[A_\mu(x), A_\nu(x')] = i\delta_{\mu\nu}\Delta(\kappa, x - x'). \quad \dots\dots(7)$$

As in the case of the radiation field (Gupta 1950, to be referred to as I), we regard A_μ as a self-adjoint quantity, and expand it as*

$$A_\mu(x) = \sum_{\mathbf{k}} (2k_0)^{-1/2} [a_\mu(\mathbf{k}) \exp \{i(\mathbf{k} \cdot \mathbf{x} - k_0 t)\} + a_\mu^\dagger(\mathbf{k}) \exp \{-i(\mathbf{k} \cdot \mathbf{x} - k_0 t)\}] \quad \dots\dots(8)$$

$$\text{with} \quad k_0 = (k^2 + \kappa^2)^{1/2}, \quad \dots\dots(9)$$

where a dagger denotes an adjoint. Substituting the Fourier expansion (8) in (7), we get

$$[a_\mu(\mathbf{k}), a_\nu^\dagger(\mathbf{k})] = \delta_{\mu\nu}. \quad \dots\dots(10)$$

* We are using the expansion (8) for A_μ for the sake of simplicity. But, in order to establish the Lorentz invariance of our treatment we can express A_μ in terms of four scalar fields, as we have done in I. Then we can carry out the Fourier expansions of the scalar fields and follow the above treatment with practically no other change.

Further, substituting the expansion (8) in (6), using the commutation relation (10), and omitting the zero-point energy, we obtain for the Hamiltonian of the auxiliary field

$$\int H d\mathbf{v} = \sum_{\mathbf{k}} k_0 \{ a_1^\dagger(\mathbf{k}) a_1(\mathbf{k}) + a_2^\dagger(\mathbf{k}) a_2(\mathbf{k}) + a_3^\dagger(\mathbf{k}) a_3(\mathbf{k}) - a_0^\dagger(\mathbf{k}) a_0(\mathbf{k}) \}. \quad \dots (11)$$

We now have four types of auxiliary photons, which will be referred to as the a_1 -, a_2 -, a_3 - and a_0 -auxiliary photons. As explained in I, we treat the a_0 -auxiliary photons by means of an indefinite metric, while we treat the other types of auxiliary photons in the ordinary way. Then the operators $a_1(\mathbf{k})$, $a_2(\mathbf{k})$, $a_3(\mathbf{k})$ and $a_0(\mathbf{k})$ are all absorption operators, while their adjoints are all emission operators. Moreover, all the four types of auxiliary photons have *positive eigenvalues* for their Hamiltonians, though the states containing an odd number of a_0 -auxiliary photons have a negative normalization.

The interaction of the auxiliary photons with the electron field can be taken into account in the usual way by adding the term $A_\mu j_\mu$ to the Lagrangian density (4). For practical purposes it is most convenient to use the interaction representation, which presents no difficulty in the present case. For, since the use of an indefinite metric for the scalar auxiliary photons ensures that all components of $A_\mu^{(+)}$ contain the absorption operators, the state of vacuum satisfies the relation

$$A_\mu^{(+)} \Psi_0 = 0, \quad \dots (12)$$

where $A_\mu^{(+)}$ denotes the positive frequency part of A_μ . Using the vacuum condition (12) and the commutation relation (7), we easily obtain

$$\langle \{ A_\mu(x), A_\nu(x') \} \rangle_0 = \delta_{\mu\nu} \Delta^{(1)}(\kappa, x - x'), \quad \dots (13)$$

$$\langle P \{ A_\mu(x) A_\nu(x') \} \rangle_0 = \frac{1}{2} \delta_{\mu\nu} \Delta_F(\kappa, x - x'), \quad \dots (14)$$

where it is to be noted that the indefinite metric operator η , as defined in I, is simply equal to unity for the state of vacuum. It follows from (14) that in any 'graph' the contribution of an internal auxiliary photon line will be given by $\Delta_F(\kappa, k)$ apart from numerical factors, whereas the corresponding contribution for an ordinary internal photon line is known to be $D_F(k)$.

The above treatment involves four types of auxiliary photons of positive energy. We now have to ensure that these auxiliary photons always remain completely unobserved. For this, we assume that there are no auxiliary photons in the initial state, which can be expressed in the interaction representation by the initial condition

$$A_\mu^{(+)} \Psi_i = 0. \quad \dots (15)$$

Moreover, since the rest-mass κ ultimately tends to infinity, by choosing κ to be sufficiently large we can always make the energy of an auxiliary photon greater than the energy of the given system in the initial state. Hence, on account of the condition (3) the auxiliary photons will never appear in any final state of the system, though they can of course appear in virtual states.

(ii) Abnormal Auxiliary Photon Field

For the abnormal auxiliary photon field we choose the Lagrangian density

$$L = \frac{1}{2} \left\{ \left(\frac{\partial A_\mu}{\partial x_\nu} \right)^2 + \kappa^2 A_\mu^2 \right\}, \quad \dots (16)$$

which differs from (4) by a negative sign. We then again obtain the field equation (5), but the Hamiltonian density for the abnormal field is

$$H = - \left(\frac{\partial A_\mu}{\partial t} \right)^2 - \frac{1}{2} \left\{ \left(\frac{\partial A_\mu}{\partial x_\nu} \right)^2 + \kappa^2 A_\mu^2 \right\}. \quad \dots (17)$$

We also find in the usual way the commutation relation

$$[A_\mu(x), A_\nu(x')] = -i\delta_{\mu\nu}\Delta(\kappa, x - x'). \quad \dots\dots(18)$$

We can now follow with slight modifications the same treatment as has been applied to the normal auxiliary photon field. Thus, using the expansion (8), we obtain from (18) and (17) respectively

$$[a_\mu(\mathbf{k}), a_\nu^\dagger(\mathbf{k})] = -\delta_{\mu\nu}, \quad \dots\dots(19)$$

$$\int H dv = \sum_{\mathbf{k}} k_0 \{ -a_1^\dagger(\mathbf{k})a_1(\mathbf{k}) - a_2^\dagger(\mathbf{k})a_2(\mathbf{k}) - a_3^\dagger(\mathbf{k})a_3(\mathbf{k}) + a_0^\dagger(\mathbf{k})a_0(\mathbf{k}) \}. \quad \dots\dots(20)$$

We again have four types of auxiliary photons. But now we have to treat a_{1-} , a_{2-} , and a_{3-} auxiliary photons by means of an indefinite metric, while we treat the a_0 -auxiliary photons in the ordinary way, so that the operators $a_1(\mathbf{k})$, $a_2(\mathbf{k})$, $a_3(\mathbf{k})$ and $a_0(\mathbf{k})$ are all absorption operators. Moreover, all the four types of auxiliary photons have *positive eigenvalues* for their Hamiltonians, though some of these states have a negative normalization according to the relation

$$\Psi^\dagger\Psi = (-1)^{n_1+n_2+n_3}, \quad \dots\dots(21)$$

where n_1 , n_2 , n_3 are the numbers of the a_{1-} , a_{2-} and a_{3-} auxiliary photons in the state Ψ .

The interaction of the abnormal auxiliary photons with the electron field can be taken into account by adding the term $A_\mu j_\mu$ to the Lagrangian density (16). We can then pass over to the interaction representation in the usual way, and obtain

$$\langle P\{A_\mu(x)A_\nu(x')\} \rangle_0 = -\frac{1}{2}\delta_{\mu\nu}\Delta_F(\kappa, x - x'). \quad \dots\dots(22)$$

Hence, in the present case the contribution of an internal auxiliary photon line is minus times the corresponding contribution in the normal case.

In order to ensure that the abnormal auxiliary photons appear only in virtual states, we again impose the initial condition (15). We also note that all the abnormal auxiliary photons have positive eigenvalues for their Hamiltonians, and κ is a large constant tending to infinity. Then, as in the case of the normal auxiliary photons, it follows that the abnormal auxiliary photons will never appear in any final state of the system due to the condition (3).

§ 4. THE AUXILIARY ELECTRON FIELDS

In addition to the auxiliary photon fields discussed in the last section, we now introduce auxiliary electron fields of very large masses, which interact with photons in the usual way. For an auxiliary electron field we choose the Lagrangian density

$$L = -\frac{1}{2}(\bar{\psi}\gamma_\mu\frac{\partial\psi}{\partial x_\mu} - \frac{\partial\bar{\psi}}{\partial x_\mu}\gamma_\mu\psi) - M\bar{\psi}\psi \quad \dots\dots(23)$$

$$\text{with} \quad \bar{\psi} = \psi^\dagger\gamma_4, \quad \dots\dots(24)$$

where the rest mass M is a large constant ultimately tending to infinity, and ψ^\dagger is the adjoint of ψ according to the definition[†] given in I. From (23) we obtain the field equations

$$\gamma_\mu\frac{\partial\psi}{\partial x_\mu} + M\psi = 0, \quad \frac{\partial\bar{\psi}}{\partial x_\mu}\gamma_\mu - M\bar{\psi} = 0, \quad \dots\dots(25)$$

and the Hamiltonian density

$$H = \frac{1}{2}\left(\frac{\partial\bar{\psi}}{\partial x_4}\gamma_4\psi - \bar{\psi}\gamma_4\frac{\partial\psi}{\partial x_4}\right) = \frac{1}{2}\left(\frac{\partial\psi^\dagger}{\partial x_4}\psi - \psi^\dagger\frac{\partial\psi}{\partial x_4}\right). \quad \dots\dots(26)$$

[†] This definition of the adjoint of ψ should not be confused with the quantity $\psi^*\gamma_4$, which is often referred to as the adjoint of ψ .

In accordance with (25) we carry out the usual expansions

$$\left. \begin{aligned} \psi(x) &= \sum_{\mathbf{p}} \sum_{r=1,2} [a_r(\mathbf{p})u_r(\mathbf{p}) \exp \{i(\mathbf{p} \cdot \mathbf{x} - p_0 t)\} + b_r^\dagger(\mathbf{p})v_r^*(\mathbf{p}) \exp \{-i(\mathbf{p} \cdot \mathbf{x} - p_0 t)\}] \\ \psi^\dagger(x) &= \sum_{\mathbf{p}} \sum_{r=1,2} [a_r^\dagger(\mathbf{p})u_r^*(\mathbf{p}) \exp \{-i(\mathbf{p} \cdot \mathbf{x} - p_0 t)\} + b_r(\mathbf{p})v_r^*(\mathbf{p}) \exp \{i(\mathbf{p} \cdot \mathbf{x} - p_0 t)\}] \end{aligned} \right\} \dots\dots(27)$$

$$\text{with} \quad p_0 = (\mathbf{p}^2 + M^2)^{1/2}, \quad \dots\dots(28)$$

where an asterisk denotes the Hermitian conjugate, and the spinor amplitudes occurring in (27) are normalized to satisfy the relations

$$u_r^*(\mathbf{p})u_s(\mathbf{p}) = \delta_{rs}, \quad v_r^*(\mathbf{p})v_s(\mathbf{p}) = \delta_{rs}. \quad \dots\dots(29)$$

Substituting the expressions (27) in (26), and using (29), we obtain for the Hamiltonian of the auxiliary electron field

$$\int H dv = \sum_{\mathbf{p}} \sum_{r=1,2} p_0 [a_r^\dagger(\mathbf{p})a_r(\mathbf{p}) - b_r(\mathbf{p})b_r^\dagger(\mathbf{p})]. \quad \dots\dots(30)$$

We shall now describe two kinds of auxiliary electron fields, which will be called the normal and the abnormal ones. The normal auxiliary field will be treated according to the Fermi-Dirac statistics in the usual way, while the abnormal field will be treated according to the Bose-Einstein statistics.

(i) Normal Auxiliary Electron Field

According to the Fermi statistics, the commutation relation for the auxiliary electron field is

$$\{\psi_\alpha(x), \bar{\psi}_\beta(x')\} = -iS_{\alpha\beta}(M, x - x'). \quad \dots\dots(31)$$

Using (27) and (29), we obtain from (31)

$$\{a_r(\mathbf{p}), a_s^\dagger(\mathbf{p})\} = \delta_{rs}, \quad \{b_r(\mathbf{p}), b_s^\dagger(\mathbf{p})\} = \delta_{rs}. \quad \dots\dots(32)$$

The second relation in (32) enables us to write (30) as

$$\int H dv = \sum_{\mathbf{p}} \sum_r p_0 [a_r^\dagger(\mathbf{p})a_r(\mathbf{p}) + b_r^\dagger(\mathbf{p})b_r(\mathbf{p})], \quad \dots\dots(33)$$

where we have omitted the zero-point energy.

We now treat the auxiliary electrons in the usual way by using a positive definite metric, so that we have

$$a_r^\dagger(\mathbf{p}) = a_r^*(\mathbf{p}), \quad b_r^\dagger(\mathbf{p}) = b_r^*(\mathbf{p}). \quad \dots\dots(34)$$

In this way $a_r(\mathbf{p})$ and $b_r(\mathbf{p})$ are the absorption operators for the two types of auxiliary electrons, $a_r^\dagger(\mathbf{p})$ and $b_r^\dagger(\mathbf{p})$ are the emission operators, and the eigenvalues of the Hamiltonian are positive. In fact, the normal auxiliary electron field is simply an ordinary Dirac field with a very large rest mass M , which tends to infinity.

The interaction of the auxiliary electron field with the photon field can be treated in the usual way by adding the term $A_\mu j_\mu = ieA_\mu \bar{\psi} \gamma_\mu \psi$ to the Lagrangian density (23). Then, using the interaction representation and the vacuum conditions

$$\psi^{(+)}\Psi_0 = 0, \quad \bar{\psi}^{(-)}\Psi_0 = 0, \quad \dots\dots(35)$$

$$\text{we obtain} \quad \langle [\psi_\alpha(x), \bar{\psi}_\beta(x')] \rangle_0 = -S_{\alpha\beta}^{(1)}(M, x - x'), \quad \dots\dots(36)$$

$$\epsilon(t, t') \langle P(\psi_\alpha(x) \bar{\psi}_\beta(x')) \rangle_0 = -\frac{1}{2} S_{F, \alpha\beta}(M, x - x'), \quad \dots\dots(37)$$

according to which the contribution of an internal auxiliary electron line can be obtained from the contribution of an ordinary internal electron line on replacing the electron mass m by the auxiliary mass M .

As in the last section, we now assume that there are no auxiliary electrons in the initial state, which can be expressed by the initial conditions

$$\psi^{(+)}\Psi_i=0, \quad \bar{\psi}^{(-)}\Psi_i=0. \quad \dots\dots(38)$$

Then, on choosing M to be sufficiently large, it follows from the argument of the last section that the auxiliary electrons will never appear in any final state.

(ii) Abnormal Auxiliary Electron Field

If we assume that the auxiliary electron field obeys the Bose statistics[†], the commutation relation (31) has to be replaced by

$$[\psi_\alpha(x), \bar{\psi}_\beta(x')] = -iS_{\alpha\beta}(M, x-x'), \quad \dots\dots(39)$$

which gives on account of (27) and (29)

$$[a_r(\mathbf{p}), a_s^\dagger(\mathbf{p})] = \delta_{rs}, \quad [b_r(\mathbf{p}), b_s^\dagger(\mathbf{p})] = -\delta_{rs}. \quad \dots\dots(40)$$

Using the second relation in (40), and omitting the zero-point energy, we can write (30) as

$$\int H dv = \sum_{\mathbf{p}} \sum_r p_0 [a_r^\dagger(\mathbf{p}) a_r(\mathbf{p}) - b_r^\dagger(\mathbf{p}) b_r(\mathbf{p})]. \quad \dots\dots(41)$$

Thus, we have two types of auxiliary electrons, which we call the a - and the b -electrons. We now use a positive definite metric for the a -electrons, while we treat the b -electrons by means of an indefinite metric, so that we have

$$a_r^\dagger(\mathbf{p}) = a_r^*(\mathbf{p}), \quad b_r^\dagger(\mathbf{p}) = -b_r^*(\mathbf{p}). \quad \dots\dots(42)$$

In this way, as in the normal case, the eigenvalues of the Hamiltonian are positive, $a_r(\mathbf{p})$ and $b_r(\mathbf{p})$ are the absorption operators, and $a_r^\dagger(\mathbf{p})$ and $b_r^\dagger(\mathbf{p})$ are the emission operators.

The interaction of the abnormal auxiliary electron field with the photon field can be taken into account by adding the term $ieA_\mu \bar{\psi} \gamma_\mu \psi$ to the Lagrangian density. Then, passing over to the interaction representation, and using the vacuum conditions (35), we obtain from (39)

$$\langle \{\psi_\alpha(x), \bar{\psi}_\beta(x')\} \rangle_0 = -S_{\alpha\beta}^{(1)}(M, x-x'), \quad \dots\dots(43)$$

$$\langle P\{\psi_\alpha(x), \bar{\psi}_\beta(x')\} \rangle_0 = -\frac{1}{2}S_{F, \alpha\beta}(M, x-x'). \quad \dots\dots(44)$$

The S -matrix for the interaction of photons and abnormal auxiliary electrons can be investigated by following the analysis of Dyson (1949). It is then found that the contribution of any graph in the present case differs from the contribution of the corresponding graph in the normal case only by a factor $(-1)^l$, where l is the number of electron loops in the graph.

Finally, by imposing the initial conditions (38), we can again ensure that the abnormal auxiliary electrons will never appear in any final state of the system.

§ 5. REGULARIZATION WITH THE AUXILIARY FIELDS

We shall now consider the effect of introducing an arbitrary number of auxiliary electron and photon fields in quantum electrodynamics assuming that all the electron fields can interact with all the photon fields. For this purpose we shall follow the Feynman-Dyson treatment, according to which the contribution of

[†] Such a possibility for an ordinary electron field has recently been investigated and found unacceptable by Pauli (1950). However, the difficulty pointed out by him does not arise in the present case. For, as we shall see, the auxiliary electrons appear only in virtual states.

the S -matrix for any physical process can be represented by means of graphs. For future use, we note that the functions $D_F(x)$, $\Delta_F(\kappa, x)$ and $S_F(m, x)$, occurring in the last two sections, are given by

$$D_F(x) = \frac{1}{(2\pi)^4} \int dk e^{ikx} D_F(k) = \lim_{\epsilon \rightarrow +0} \frac{-2i}{(2\pi)^4} \int dk e^{ikx} \frac{1}{k^2 + \lambda^2 - i\epsilon} \quad \dots\dots(45)$$

$$\Delta_F(\kappa, x) = \frac{1}{(2\pi)^4} \int dk e^{ikx} \Delta_F(\kappa, k) = \lim_{\epsilon \rightarrow +0} \frac{-2i}{(2\pi)^4} \int dk e^{ikx} \frac{1}{k^2 + \kappa^2 - i\epsilon} \quad \dots\dots(46)$$

$$S_F(m, x) = \frac{1}{(2\pi)^4} \int dk e^{ikx} S_F(m, k) = \lim_{\epsilon \rightarrow +0} \frac{-2i}{(2\pi)^4} \int dk e^{ikx} \frac{i\kappa\gamma - m}{k^2 + m^2 - i\epsilon} \quad \dots\dots(47)$$

Here it proves convenient to introduce an invariant quantity λ of the dimensions of mass in (45), remembering that in every result of physical interest we must ultimately put $\lambda=0$. Further, in practice we can ignore the infinitesimal quantity ϵ in the above integrals, if, following Feynman (1949), we always regard the masses λ , κ and m as having infinitesimal negative imaginary parts.

Now the effect of the auxiliary photon fields in the S -matrix can be easily investigated. In ordinary quantum electrodynamics the contribution of an internal photon line is (Dyson 1949)

$$D_F(k) \quad \dots\dots(48)$$

apart from some numerical factors. In a similar way it follows from the treatment of § 3 that the effect of introducing the auxiliary photon fields is to replace (48) by

$$R[D_F(k)] \equiv D_F(k) + \sum_i C_i \Delta_F(\kappa_i, k), \quad \dots\dots(49)$$

where Σ denotes summation over all the auxiliary photon fields, and C_i is equal to $+1$ or -1 according to whether the field is normal or abnormal. Denoting $D_F(k)$ by $f(\lambda^2, k)$, we can also write (49) as

$$R[f(\lambda^2, k)] = f(\lambda^2, k) + \sum_i C_i f(\kappa_i^2, k). \quad \dots\dots(50)$$

We next consider the effect of the auxiliary electron fields. For this, we first observe that in ordinary quantum electrodynamics all the electron lines in a graph occur in the form of one or more chains. Each of these chains forms either a closed loop or an open chain with its two ends representing two external electron lines. Similarly, an auxiliary electron field will give rise to graphs involving one or more chains of auxiliary electron lines. But, since the auxiliary electrons cannot exist in real states, the auxiliary electron lines can only form closed loops. Hence the effect of introducing auxiliary electron fields in quantum electrodynamics is to give rise to new graphs, in which one or more loops of ordinary electron lines are replaced by similar loops of auxiliary electron lines in all possible ways. It follows from the treatment of § 4 that if the contribution of any electron loop in ordinary quantum electrodynamics is given by*

$$\int g(m^2, k) dk, \quad \dots\dots(51)$$

the effect of introducing the auxiliary electron fields is to replace $g(m^2, k)$ by

$$R[g(m^2, k)] \equiv g(m^2, k) + \sum_i C_i g(M_i^2, k), \quad \dots\dots(52)$$

where Σ denotes summation over all the auxiliary electron fields, and C_i is equal to $+1$ or -1 according to whether the auxiliary field is normal or abnormal.

* In practice it is slightly more convenient to regard the contribution of an electron loop as a function of m^2 rather than of m .

So far the number and masses of the auxiliary fields have been kept arbitrary, except that all the auxiliary masses ultimately tend to infinity. We now observe that our aim in introducing the auxiliary fields is to evaluate the divergent integrals in quantum electrodynamics in an unambiguous way. In order to achieve this purpose, we shall now describe a general method of choosing the number and masses of our auxiliary fields in such a way that all integrals in the resulting theory will be convergent over the momentum-energy space.

Let us first consider any divergent integral in ordinary quantum electrodynamics, which involves $D_F(k) = f(\lambda^2, k)$ as a factor representing the contribution of an internal photon line. Let us denote the first, second and n th derivatives of $f(\lambda^2, k)$ with respect to λ^2 by $f'(\lambda^2, k)$, $f''(\lambda^2, k)$ and $f^{(n)}(\lambda^2, k)$ respectively. It is obvious from (45) that, for large values of k , $f'(\lambda^2, k)$ is of lower order than $f(\lambda^2, k)$, $f''(\lambda^2, k)$ is of still lower order, and so on. Therefore the given integral can be made convergent over the momentum-energy space, if we can replace $f(\lambda^2, k)$ by some suitable derivative $f^{(n)}(\lambda^2, k)$. We now note that

$$(-1) \int_0^{\xi^2} dz_1 f'(\lambda^2 + z_1, k) = f(\lambda^2, k) - f(\lambda^2 + \xi^2, k), \quad \dots\dots (53)$$

$$(-1)^2 \int_0^{\xi^2} dz_1 \int_0^{\xi^2} dz_2 f''(\lambda^2 + z_1 + z_2, k) = f(\lambda^2, k) - f(\lambda^2 + \xi^2, k) - f(\lambda^2 + \xi^2, k) + f(\lambda^2 + 2\xi^2, k), \quad \dots\dots (54)$$

and so on. It follows that by a suitable choice of the number and masses of the normal and abnormal auxiliary photon fields, we can express (50) in the form

$$R[f(\lambda^2, k)] = (-1)^n \int_0^{\xi^2} dz_1 \int_0^{\xi^2} dz_2 \dots \int_0^{\xi^2} dz_n f^{(n)}(\lambda^2 + z_1 + z_2 + \dots + z_n, k), \quad \dots (55)$$

where ξ , which is a large constant of the dimensions of mass, ultimately tends to infinity. According to (55), we can always make the given integral convergent over the momentum-energy space by a suitable choice of n .

Let us now consider the contribution of an electron loop, which gives rise to a divergent integral of the form (51). Let us also denote the first derivative of $g(m^2, k)$ with respect to m^2 by $g'(m^2, k)$, the second derivative by $g''(m^2, k)$, and so on. Since $g(m^2, k)$ is a product of factors of the form $S_F(m, k)$, it is obvious from (47) that, for large values of k , $g'(m^2, k)$ is of lower order than $g(m^2, k)$, $g''(m^2, k)$ of still lower order, and so on. Therefore, as in the case of the auxiliary photon fields, we choose the number and masses of the normal and abnormal auxiliary electron fields in such a way that (52) can be expressed in the form

$$R[g(m^2, k)] = (-1)^n \int_0^{\eta^2} dz_1 \int_0^{\eta^2} dz_2 \dots \int_0^{\eta^2} dz_n g^{(n)}(m^2 + z_1 + z_2 + \dots + z_n, k), \quad \dots (56)$$

where η ultimately tends to infinity. With a suitable choice of n , (56) will always enable us to make the integral

$$\int R[g(m^2, k)] dk \quad \dots\dots (57)$$

convergent over the momentum-energy space.

We have shown that by introducing the auxiliary fields in quantum electrodynamics, the expressions $f(\lambda^2, k)$ and $g(m^2, k)$ can be replaced by $R[f(\lambda^2, k)]$ and $R[g(m^2, k)]$ according to the relations (55) and (56). This replacement will be briefly referred to as *regularization*. In principle we can choose any value of n in (55) or (56) such that the given integral becomes convergent over the

momentum-energy space. But, of course, in practice it will be convenient to choose n as small as possible. In fact, it will always be found sufficient to take $n=1$ in (55) and $n=2$ in (56).

§ 6. THE SELF-ENERGY OF THE PHOTON

As an application of the present treatment, we consider the well-known problem of the self-energy of the photon. The second order contribution of the S -matrix to the photon self-energy is

$$S_{\text{photon}} = -\frac{e^2}{8} \int_{-\infty}^{\infty} dx \int_{-\infty}^{\infty} dx' A_{\mu}(x) \text{tr} [S_F(x-x') \gamma_{\mu} S_F(x'-x) \gamma_{\nu}] A_{\nu}(x'). \quad \dots (58)$$

Putting $A_{\nu}(x') = A_{\nu}(q) \exp(iqx')$,

and using (47), we obtain in the momentum-energy space

$$\begin{aligned} S_{\text{photon}} &= \frac{e^2}{2(2\pi)^4} \int_{-\infty}^{\infty} dx \int dk A_{\mu}(x) \text{tr} \left[\frac{ik\gamma - m}{k^2 + m^2} \gamma_{\mu} \frac{i(k+q)\gamma - m}{(k+q)^2 + m^2} \gamma_{\nu} \right] A_{\nu}(q) e^{iqx} \\ &= -i \int_{-\infty}^{\infty} dx A_{\mu}(x) J_{\mu\nu}(q) A_{\nu}(q) e^{iqx}, \end{aligned} \quad \dots (60)$$

where $J_{\mu\nu}(q) = \frac{ie^2}{2(2\pi)^4} \int dk \frac{\text{tr} [\{ik\gamma - m\} \gamma_{\mu} \{i(k+q)\gamma - m\} \gamma_{\nu}]}{[k^2 + m^2][k^2 + q^2 + 2kq + m^2]} \dots (61)$

We can easily evaluate the trace in (61), and combine the denominators with the help of Feynman's identity (Feynman 1949)

$$\frac{1}{ab} = \int_0^1 \frac{du}{[a + (b-a)u]^2}. \quad \dots (62)$$

Then we get

$$J_{\mu\nu}(q) = \frac{2ie^2}{(2\pi)^4} \int dk \int_0^1 du \frac{k^2 \delta_{\mu\nu} - 2k_{\mu} k_{\nu} + kq \delta_{\mu\nu} - k_{\mu} q_{\nu} - k_{\nu} q_{\mu} + m^2 \delta_{\mu\nu}}{[k^2 + 2ukq + uq^2 + m^2]^2}. \quad \dots (63)$$

The first derivative of the above expression with respect to m^2 is still divergent over the k -space, but the second derivative is convergent. Therefore, we can regularize (63) with the help of (56) taking $n=2$. Thus

$$\begin{aligned} J_{\mu\nu}(q) &= \frac{4ie^2}{(2\pi)^4} \int dk \int_0^1 du \int_0^{\eta^2} dz_1 \int_0^{\eta^2} dz_2 \left\{ -\frac{2\delta_{\mu\nu}}{[k^2 + 2ukq + uq^2 + m^2 + z_1 + z_2]^3} \right. \\ &\quad \left. + 3 \frac{k^2 \delta_{\mu\nu} - 2k_{\mu} k_{\nu} + kq \delta_{\mu\nu} - k_{\mu} q_{\nu} - k_{\nu} q_{\mu} + (m^2 + z_1 + z_2) \delta_{\mu\nu}}{[k^2 + 2ukq + uq^2 + m^2 + z_1 + z_2]^4} \right\}. \end{aligned}$$

Since the above integral is convergent over the momentum-energy space, we can shift the origin of the k -space as $k_{\mu} \rightarrow k_{\mu} - uq_{\mu}$, which gives after some simplification

$$\begin{aligned} J_{\mu\nu}(q) &= \frac{4ie^2}{(2\pi)^4} \int dk \int_0^1 du \int_0^{\eta^2} dz_1 \int_0^{\eta^2} dz_2 \{ k^2 \delta_{\mu\nu} - 6k_{\mu} k_{\nu} + 3(1-2u)kq \delta_{\mu\nu} + 3(2u-1) \\ &\quad \times (k_{\mu} q_{\nu} + k_{\nu} q_{\mu}) + 5(u^2-u)q^2 \delta_{\mu\nu} + 6(u-u^2)q_{\mu} q_{\nu} + \delta_{\mu\nu}(m^2 + z_1 + z_2) \} \\ &\quad \times [k^2 - u^2 q^2 + uq^2 + m^2 + z_1 + z_2]^{-4}. \end{aligned} \quad \dots (64)$$

We can now carry out the integration over the k -space symmetrically with respect to the origin, so that

$$\int k_{\mu} f(k^2) dk = 0, \quad \int k_{\mu} k_{\nu} f(k^2) dk = \int \frac{1}{4} \delta_{\mu\nu} k^2 f(k^2) dk, \quad \text{etc.} \quad \dots (65)$$

Further, by contour integration

$$\int \frac{dk}{(k^2 + \Delta)^3} = \frac{i\pi^2}{2\Delta}, \quad \dots\dots (66)$$

from which we can easily deduce, by differentiating with respect to Δ ,

$$\int \frac{dk}{(k^2 + \Delta)^4} = \frac{i\pi^2}{6\Delta^2}, \quad \int \frac{k^2 dk}{(k^2 + \Delta)^4} = \frac{i\pi^2}{3\Delta}. \quad \dots\dots (67)$$

Using (65) and (67), we integrate (64) over the k -space, and get

$$\begin{aligned} J_{\mu\nu}(q) &= \frac{e^2}{4\pi^2} \int_0^1 du \int_0^{\eta^2} dz_1 \int_0^{\eta^2} dz_2 \frac{(u-u^2)(q^2\delta_{\mu\nu} - q_\mu q_\nu)}{[uq^2 - u^2q^2 + m^2 + z_1 + z_2]^2} \\ &= \frac{e^2}{4\pi^2} \int_0^1 du (u-u^2)(q^2\delta_{\mu\nu} - q_\mu q_\nu) \{ -\log(uq^2 - u^2q^2 + m^2 + 2\eta^2) \\ &\quad + 2\log(uq^2 - u^2q^2 + m^2 + \eta^2) - \log(uq^2 - u^2q^2 + m^2) \}. \quad \dots\dots (68) \end{aligned}$$

Since η tends to infinity, we can neglect the finite terms compared with η^2 within the log terms in (68), which gives

$$\begin{aligned} J_{\mu\nu}(q) &= \frac{e^2}{4\pi^2} \int_0^1 du (u-u^2)(q^2\delta_{\mu\nu} - q_\mu q_\nu) \left\{ \log \frac{\eta^2}{2m^2} - \log \left(1 + \frac{uq^2 - u^2q^2}{m^2} \right) \right\} \\ &= \frac{e^2}{24\pi^2} (q^2\delta_{\mu\nu} - q_\mu q_\nu) \log \frac{\eta^2}{2m^2} \\ &\quad - \frac{e^2}{4\pi^2} (q^2\delta_{\mu\nu} - q_\mu q_\nu) \int_0^1 du (u-u^2) \log \left(1 + \frac{uq^2 - u^2q^2}{m^2} \right) \quad \dots\dots (69) \end{aligned}$$

where the first term is logarithmically divergent and the second term is convergent.

For a free photon the expression (69) vanishes on account of the field equation and the supplementary condition. On the other hand, in the case of a virtual photon with $q^2 \neq 0$ eqn. (69) represents the gauge-invariant effect of the so-called polarization of vacuum.

In conclusion, we may add that the treatment of this paper can be easily extended to the meson fields. In fact, corresponding to any field we can introduce an appropriate number of normal and abnormal fields. The normal field can be treated in exactly the same way as the ordinary field. On the other hand, for the abnormal field we have to reverse either the usual sign of the Lagrangian density or the usual statistics of the field according to our requirements.

REFERENCES

- DYSON, F. J., 1949, *Phys. Rev.*, **75**, 486, 1736.
 FEYNMAN, R. P., 1949, *Phys. Rev.*, **76**, 769.
 GUPTA, S. N., 1950, *Proc. Phys. Soc. A*, **63**, 681.
 PAULI, W., 1950, *Prog. Theor. Phys.*, **5**, 526.
 PAULI, W., and VILLARS, F., 1949, *Rev. Mod. Phys.*, **21**, 434.
 SCHWINGER, J., 1948, *Phys. Rev.*, **74**, 1439; 1949, *Ibid.*, **75**, 651.

Isotopic Spin and Coulomb Forces

By L. A. RADICATI

Department of Mathematical Physics, University of Birmingham*

Communicated by R. E. Peierls; MS. received 25th August 1952

ABSTRACT. The importance of the coulomb forces in mixing states with a different isotopic spin T is investigated assuming charge independence of the specific nuclear forces. It is found that for two and four nucleons outside a closed shell in the state $T=0$ this mixing is very small (less than 0.25%, taking into account interconfigurational mixing). It can therefore be concluded that the coulomb forces have very little importance in destroying the validity of the isotopic spin selection rules for β and γ transitions and for collisions, which result from the assumption of the charge independence of nuclear forces.

§ 1. INTRODUCTION

THE experimental evidence on the nucleon-nucleon scattering at low energies seems to favour the assumption that the nuclear forces are charge independent apart from the coulomb repulsion between protons (Rosenfeld 1948). This assumption is also in agreement with the ordering of levels in neighbouring isobars such as ${}^6\text{He}$, ${}^6\text{Li}$, ${}^6\text{Be}$; ${}^{14}\text{C}$, ${}^{14}\text{N}$, ${}^{14}\text{O}$, etc. (see for instance Sherr, Meuthner and White 1949). In fact, the comparison of the level schemes of such nuclei shows that it is possible to establish a correspondence between the levels of the nuclei with neutron excess $A-2Z = \pm 1$, and those of the nucleus with $A-2Z=0$.

On the other hand, in the nuclei with $A-2Z=0$ there are levels which have no counterpart in the neighbouring isobars.

Using the concept of isotopic spin T (see for example Rosenfeld 1948, § 10.12) we can say that the levels which appear only in the $A-2Z=0$ nucleus have $T=0$ (singlet charge states), while the levels extending over the three isobars have $T=1$ (charge triplet), with a third component given by $2T_3 = A-2Z$.

As a consequence of the charge independence of nuclear forces there exist certain selection rules for electromagnetic and β transitions. For β transitions Wigner (1939) has proved that the selection rule is

$$\Delta T = 0, \pm 1. \quad \dots\dots(1)$$

The same rule holds also for γ transitions (Radicati 1952), with the additional restriction

$$T=0 \rightarrow T=0 \text{ forbidden for electric dipole.} \quad \dots\dots(2)$$

However, one knows that the charge independence of nuclear forces is at best a good approximation to the actual situation owing to the difference between the masses of protons and neutrons, and to the existence of the coulomb repulsion between the protons. Therefore the selection rules resulting from the charge independence of the specific nuclear forces are expected to be only approximate.

* On leave of absence from the Istituto di Fisica, Politecnico di Torino, Torino, Italy.

As for the mass difference it is easy to see that this cannot have any influence on the isotopic spin of the nuclear states and therefore on the selection rules. In fact the operator corresponding to the mass difference is

$$H_m = \frac{1}{2} \sum_i \{ (1 - \tau_3^{(i)}) m_p + (1 + \tau_3^{(i)}) m_n \}$$

which commutes with T^2 .

The situation is more complicated in the case of the coulomb forces. The coulomb energy ($H^c = \frac{1}{4} \sum_{ij} (1 - \tau_3^{(i)})(1 - \tau_3^{(j)})/r_{ij}$ does not commute with T^2 ($\tau_3 = \pm 1$ for protons and neutrons respectively; r_{ij} is the distance between the i th and the j th nucleon). This means that each nuclear state is no longer a pure T state, but is in general a mixture of states with different T values.

It is the purpose of this paper to investigate quantitatively the amount of mixing between states of a different T introduced by the coulomb forces in order to get an idea of their influence on the validity of isotopic spin selection rules.

To be more precise let T be the isotopic spin of a nuclear level which one would expect if the specific nuclear forces were strictly charge independent, and let $\Psi(T)$ be the corresponding wave function. Considering the coulomb forces as a first order perturbation, the actual wave function Φ can be written in the form

$$\Phi = \Psi(T) + \sum_{T'} \frac{H_{TT'}}{E_T - E_{T'}} \Psi(T') = \Psi(T) + \sum_{T'} \alpha_{T'}(T') \Psi(T') \quad \dots\dots(3)$$

where $H_{TT'}$ is the matrix element of the coulomb potential between the states $\Psi(T)$, $\Psi(T')$ with energies E_T , $E_{T'}$, and the summation is over all states of isotopic spin T' . We will assume the square of the coefficient $\alpha_{T'}(T')$ as a measure of the proportion of the state $\Psi(T')$ introduced in the state $\Psi(T)$ by the coulomb forces. $\alpha_{T'}(T')$ will be calculated under the following assumptions: (i) we will use a shell model of the nucleus, (ii) we disregard the influence of the coulomb forces on the isotopic spin of the core, that is to say, we disregard the possibility of excitation of the core, (iii) we will consider only the case $T=0$ since this case seems to be more suitable for an experimental test of the results (see §4), (iv) only the cases of two and four nucleons outside a closed shell will be considered.

§ 2. TWO NUCLEONS OUTSIDE A CLOSED SHELL

If the two nucleons are both neutrons or both protons, the system can only exist in the state $T=1$ because the third component of T must be ± 1 respectively. If on the other hand, the two nucleons are different, there is the possibility of two states: $T=0$, or $T=1$, with $T_3=0$ in both cases. According to Feenberg and Wigner (1937), and Feenberg and Phillips (1937), the ground state of such nuclei must have an angular momentum $J=1$ which is in accord with the experimental values for ${}^6\text{Li}$, ${}^{14}\text{N}$, ${}^{18}\text{F}$, The theory predicts in addition $T=0$. We will consider the admixture of charge triplet states produced by the coulomb field of the core. (There is in this case obviously no electrostatic interaction between the two particles outside the core.)

Let $\psi(TSL, J)$ be those combinations of one-particle wave functions for the two nucleons outside the core which belong to total spin S and total orbital angular momentum L . In the case of the $(1p)^2$ configuration (${}^6\text{Li}$, ${}^{14}\text{N}$) the possible wave functions with $J=1$ are

$$\psi(010, 1), \quad \psi(012, 1), \quad \psi(001, 1), \quad \psi(111, 1). \quad \dots\dots(4)$$

These are coupled by non-central forces, and if the ground state has $J=1$, $T=0$, the wave function is a linear combination of the first three functions (4).

Now since L^2 , S^2 commute with H^c , the electrostatic interaction will have no matrix component between states with different L and S . Therefore the coulomb forces cannot mix the wave function for $T=1$, $\psi(111, 1)$, with any of the wave functions corresponding to $T=0$. A similar result can be shown to hold also for the configurations $(1d)^2$, $(2s)^2$, $(1f)^2$.

There remains the possibility that the coulomb forces produce a mixing between the singlet charge state of the configuration $(1p)^2$, $(1d)^2$, etc., and a charge triplet state belonging to a different configuration. Since the electrostatic potential commutes with the parity operator there is interaction only between configurations of the same parity such as $(1p)^2$, $(1d)^2$, $(2s)^2$, $1p1f$, $1p2p$, . . .

However, it is easy to see that, for example, the configurations $(1p)^2$ and $(1d)^2$ cannot interact through the field of the core because they differ by more than an individual set of quantum numbers (Condon and Shortley 1951, §5⁶).

As for the $(1p)^2-(1p1f)$ interaction, this is also zero, as can be seen from formula 6⁸ 17 of Condon and Shortley (1951). We are left therefore only with the possibility of the $(1p)^2-(1p2p)$ interaction. The only state in the configuration $1p2p$ that can be mixed with the state $\psi(010, 1)$, which is expected to constitute the major part of the ground state $J=1$, $T=0$ (Feenberg and Wigner 1937), is a state $T=1$, $S=1$, $L=0$. The detailed calculation of H_{10}^c depends on the precise knowledge of the excitation energy for the configuration $1p2p$ and on the explicit calculation of the matrix element H_{10}^c . Using for a crude estimate of the excitation energy a square well of infinite depth, one would obtain for ^{14}N an energy of about 66 mev (Bethe and Bacher 1936) which reduces to approximately 40 mev for a finite depth of 18.6 mev (Feenberg and Motz 1938). For sake of argument we will use $E_0 - E_1 \simeq 40$ mev. Since the matrix element H_{10}^c is of the order of 2 mev, we have therefore $\alpha_0^2(1) \simeq 2.5 \times 10^{-3}$.

§ 3. FOUR NUCLEONS OUTSIDE A CLOSED SHELL (2 NEUTRONS AND 2 PROTONS)

There are two nuclei of this type, ^8Be , ^{20}Ne ; and ^{12}C , ^{30}A can be added to these as they have four holes in the $1p$ or $1d$ shell. The angular momentum of such nuclei is $J=0$ and the isotopic spin predicted is $T=0$, both in ' LS -coupling' (Feenberg and Phillips 1937, Jahn 1950) and in ' jj -coupling' (Flowers 1952).

We consider the $1p$ shell in detail (^8Be , ^{12}C) adding only a few remarks for the case of the $1d$ shell. The possible states for the $(1p)^4$ configuration are listed in the table (Feenberg and Phillips 1937, see also Rosenfeld 1948, p. 207). According to the LS -coupling approximation, the ground state is $[4]^{11}\text{S}$ (i.e. symmetric in space). Since H^c commutes with L^2 and S^2 , the only state that can be mixed with $[4]^{11}\text{S}$ is the state $[22]^{51}\text{S}$. We first consider the mixing caused by the electrostatic interaction between the four nucleons outside the core.

To evaluate such mixing one must calculate the matrix element

$$H_{20}^c(p^4) = \langle p^4[4]000 | H^c | p^4[22]200 \rangle \quad \dots\dots(5)$$

between the two states $\psi(p^4[4]T=0, S=0, L=0)$ and $\psi(p^4[22]T=2, S=0, L=0)$ (in the following the values of T, S, L will always be written in this order).

Using Racah's (1943) method, the matrix element (5) can be calculated from the formula (see Racah 1943, eqn. (33 *a*) apart from obvious modifications)

$$\begin{aligned} H_{20}^c(p^4) = & 6 \sum_{\alpha_1 T_1 S_1 L_1} \langle p^4[4]000 | p^2(\alpha_1 T_1 S_1 L_1)_1 p^2(\alpha_2 T_2 S_2 L_2)_2 000 \rangle \\ & \times \langle p^2(\alpha_1 T_1 S_1 L_1)_1 p^2(\alpha_2 T_2 S_2 L_2)_2 \rangle p^4[22]200 \rangle \\ & \times \langle p^2 T_2 S_2 L_2 | H^c | p^2 T_2 S_2 L_2 \rangle. \quad \dots\dots(6) \end{aligned}$$

The fractional parentage coefficients $\langle \dots \{ \} \dots \rangle$ in eqn. (6) between the configurations p^4 and p^2 are obtained from those calculated by Jahn and van Wieringen (1951) with formula (32) of Racah (1943).

One gets in this way

$$H_{20}^e(p^4) = \frac{\sqrt{10}}{9} \{ \langle p^2 100 | H^e | p^2 100 \rangle - \langle p^2 102 | H^e | p^2 102 \rangle \} = \frac{\sqrt{10}}{9} \{ \mathcal{H}_D - \mathcal{H}_S \} \quad \dots\dots(7)$$

where \mathcal{H}_S and \mathcal{H}_D are the coulomb energies in the ^{31}S and ^{31}D states for 6Be and ^{14}C according as we are interested in 8Be or in ^{12}C . Using Feenberg and Phillips (1937) calculations one gets $\mathcal{H}_S - \mathcal{H}_D \simeq 0.084$ mev. The difference $\mathcal{H}_S - \mathcal{H}_D$ is the same for 6Be and ^{14}C . We therefore obtain from (7)

$$H_{20}^e(p^4) \simeq 0.03 \text{ mev.} \quad \dots\dots(8)$$

For obtaining $\alpha_0(2)$ (i.e. the proportion of admixture of the state $T=2$) we must know the energy difference $E_2 - E_1$ between the charge quintet and singlet. No quintet state is experimentally known in light nuclei, so we will use the (lower) energy of the triplet charge state. For ^{12}C , $E_1 - E_0$ is of the order of 15 mev. We obtain in this way from (8)

$$\alpha_0^2(2) \simeq 4 \times 10^{-6}. \quad \dots\dots(9)$$

We have not yet taken into account the interaction between the four external nucleons and the coulomb field of the core. However, it can easily be shown that this interaction cannot cause any mixing between the charge quintet and singlet states. In fact, the interaction with the central field is represented by the operator

$$K^c = \frac{1}{2}(Z-2)e^2 \sum_i (1 - \tau_3^{(i)})/r_i$$

where r_i is the distance between the i th nucleon and the core. Now it is well known that such a linear function of the vector components has no matrix component between states for which $\Delta T > 1$.

[4]	^{11}S	^{11}D	^{11}G					
[31]	^{13}P	^{31}P	^{13}F	^{31}F	^{33}P	^{33}F		
[22]	^{11}S	^{11}D	^{15}S	^{51}S	^{15}D	^{51}D	^{33}S	^{33}D
[211]	^{13}P	^{31}P	^{33}P	^{55}P				

The letters S, P, ..., have the ordinary spectroscopic meaning. The superscripts indicate the charge and spin multiplicity; e.g. ^{15}D means charge singlet, spin quintet, $L=2$. The number in brackets denotes the space symmetry of the wave function with respect to the permutation group.

We will now investigate the possibility of mixing between the $[4]^{11}S$ state of the configuration $(1p)^4$ and a state with $T \neq 0$ in a different configuration. Taking into account only configurations of even parity and disregarding the excitation of the core, the lowest excited configuration for ^{12}C is $(1p)^6 (1d)^2$ (Feenberg and Motz 1938). In this configuration there are two triplet charge states ^{31}S , namely,

$$\psi(p^6[42]100, d^2[2]100; 100), \quad \text{and} \quad \psi(p^6[42]102, d^2[2]102; 100) \quad \dots\dots(10)$$

which can be mixed with the ^{11}S state of the $(1p)^8$ configuration. The two states in (10) arise from coupling the ^{31}S or ^{31}D state in the $(1p)^6$ configuration to the

^{31}S or ^{31}D state in the $(1d)^2$ configuration in such a way as to obtain a ^{31}S state with space symmetry [31]. We disregard other triplet charge states with a different symmetry since they will correspond to a greater excitation energy.

To evaluate the amount of mixing of the states (9) we must calculate

$$H_{10}^c(p^6d^2) = \langle p^8[44]000 | H^c | p^6[42]100, d^2[2]100; 100 \rangle \\ + \langle p^8[44]000 | H^c | p^6[42]102, d^2[2]102; 100 \rangle.$$

The calculation can be performed using formula (33c) of Racah (1943); we obtain in this way two-particle matrix elements between the $(1p)^2$ and $(1d)^2$ configurations. The problem is therefore reduced to the evaluation of one G_1 and one G_3 integral (Condon and Shortley 1951, §8⁶). These were calculated using the same radial wave function as Feenberg and Phillips (1937), i.e. oscillator wave function, and gave the result $H_{10}^c(p^6d^2) \simeq 0.1$ mev. In the case of ^8Be the result is of the same order of magnitude.

With $E_1 - E_0 \simeq 15$ mev we obtain therefore

$$\alpha_0^2(1) \simeq 5 \times 10^{-5}. \quad \dots\dots(11)$$

Also in this case the coulomb field of the core cannot give rise to any mixing, since the configurations $(1p)^6(1d)^2$ and $(1p)^8$ differ by the individual quantum numbers of two particles.

We have therefore proved (eqns. (9) and (11)) that the coulomb interaction is very inefficient in mixing states with $T \neq 0$ to the state ^{11}S .

In the case of the d shell, we will point out only that, as for the p shell, the only state that can be mixed to the ^{11}S state is a state with $T=2$. It can therefore be argued that the situation will be similar to the p shell case, although the interconfigurational mixing is now probably more important.

§ 4. CONCLUSIONS

In §§ 2 and 3 we have shown, assuming the validity of the shell model, that if the specified nuclear forces are charge independent, the isotopic spin of the ground states of the nuclei considered is almost unaffected by the presence of the coulomb forces.

We have considered only the case $T=0$ because this seems to present the possibility of an experimental test of the main assumption on which the calculations rest, namely the charge independence of the specific nuclear forces. In fact, since the present calculation indicates that $T=0$ is a very good quantum number, the selection rule (2) for electric dipole transitions is almost unaffected by the coulomb forces.

Therefore, if some instances are found which violate this rule, one would question the assumption of the charge independence of nuclear forces. On the other hand, if it were possible to prove that electric dipole radiation is absent between states with $T=0$, when it would be allowed by angular momentum and parity conditions, the charge independence hypothesis would be somewhat strengthened.

The selection rule (1) for β and γ transitions does not seem very restrictive since no state with $T=2$ is known experimentally. Of course eqn. (1) would provide a much more decisive test of the charge independence hypothesis since it holds for electromagnetic transitions of any multipolarity.

Finally we wish to point out two obvious instances in which the ordinary rules of vector addition allow us to determine uniquely the isotopic spin of a nuclear state:

(i) The excited states produced by the collision of an α particle or a deuteron have the same T value as the initial nucleus. For instance, the states of energy 4.47 and 9.7 Mev in ^{12}C which arise from $^{14}\text{N} + d$ must have $T=0$.

(ii) Conversely, a state which decays into two fragments, one of which is an α -particle or a deuteron, has the same T as the other fragment. For example, the 16.11 Mev state in ^{12}C decays into $^8\text{Be} + \alpha$, and is therefore a singlet charge state; in ^{10}B the 8.76 Mev state decays in $^6\text{Li}^* + \alpha$. If it is possible to prove that the excited state in ^6Li is the homologue of the ground state of ^6He (Day and Walker 1952), in which case it must have $T=1$, we can conclude that the parent state in ^{10}B has $T=1$.

ACKNOWLEDGMENTS

The author wishes to thank Professor R. E. Peierls and Mr. B. H. Flowers for many useful comments and suggestions, and Professor R. E. Peierls for granting him facilities to work in his Department. This work was completed while the author was holding a Research Fellowship of the Italian Consiglio Nazionale delle Ricerche, whose financial support is acknowledged.

REFERENCES

- BETHE, H. A., and BACHER, R. F., 1936, *Rev. Mod. Phys.*, **8**, 82.
 CONDON, E. U., and SHORTLEY, G. H., 1951, *The Theory of Atomic Spectra* (Cambridge: University Press).
 DAY, R. B., and WALKER, R. L., 1952, *Phys. Rev.*, **85**, 582.
 FEENBERG, E., and MOTZ, L., 1938, *Phys. Rev.*, **54**, 1055.
 FEENBERG, E., and PHILLIPS, M., 1937, *Phys. Rev.*, **51**, 597.
 FEENBERG, E., and WIGNER, E., 1937, *Phys. Rev.*, **51**, 95.
 FLOWERS, B. H., 1952, *Proc. Roy. Soc. A*, **212**, 248.
 JAHN, H. A., 1950, *Proc. Roy. Soc. A*, **201**, 516.
 JAHN, H. A., and VAN WIERINGEN, J. S., 1951, *Proc. Roy. Soc. A*, **209**, 502.
 RACAH, G., 1943, *Phys. Rev.*, **63**, 367.
 RADICATI, L. A., 1952, *Phys. Rev.*, **87**, 521.
 ROSENFELD, L., 1948, *Nuclear Forces* (Amsterdam: North-Holland).
 SHERR, R., MEUTHER, H., and WHITE, M., 1949, *Phys. Rev.*, **75**, 282.
 WIGNER, E., 1939, *Phys. Rev.*, **56**, 519.

Certain Exact Solutions of the Equations of General Relativity with an Electrostatic Field

By W. B. BONNOR

Department of Applied Mathematics, University of Liverpool

MS. received 12th August 1952, and in amended form 3rd November 1952

ABSTRACT. Certain exact solutions of the field equations of general relativity for empty space containing an electrostatic field are derived, and a physical interpretation is attempted. The canonical cylinder coordinates of Weyl are used, and all the solutions in which the electrostatic potential depends on only one of the two variables are obtained. Some of these are special cases of a class of solutions previously obtained by Weyl and they are shown to correspond either to a uniform electric field or to the field of a line-charge. Two of the solutions are not members of Weyl's class, and in these the electric field has no analogue in classical electrostatics and possesses the property of generating an orthogonal gravitational field.

§ 1. INTRODUCTION

IN the general theory of relativity the field equations for regions containing electromagnetic fields but no matter are (Eddington 1924, Chap. VI, § 77)

$$G_{\mu\nu} = -8\pi E_{\mu\nu}, \quad \dots\dots(1.1)$$

$$E_{\mu}^{\nu} = -F^{\nu\alpha}F_{\mu\alpha} + \frac{1}{4}g_{\mu}^{\nu}F^{\alpha\beta}F_{\alpha\beta}, \quad \dots\dots(1.2)$$

$g_{\mu\nu}$ being the metric tensor, $G_{\mu\nu}$ the contracted Riemann-Christoffel tensor, and $F_{\mu\nu}$ the electromagnetic field tensor. This last tensor satisfies Maxwell's equations if we write

$$F_{\mu\nu} = \kappa_{\mu,\nu} - \kappa_{\nu,\mu}, \quad \dots\dots(1.3)$$

$$\mathfrak{F}^{\mu\nu}_{,\nu} = \mathfrak{Z}^{\mu}, \quad \dots\dots(1.4)$$

where κ_{μ} is the four-potential, and \mathfrak{Z}^{μ} is the charge-and-current density which may be put equal to zero in a region free of matter.

Weyl (1917) has found a class of solutions of the above equations corresponding to certain axially symmetric electrostatic fields. In such fields the potential has only one non-vanishing component κ_4 (denoted hereafter by $\frac{1}{2}\pi^{-1/2}\phi$). Weyl's solution is for the axially symmetric case where there is a functional relation between g_{44} and ϕ of the form

$$g_{44} = A + B\phi + \phi^2 \quad \dots\dots(1.5)$$

where A and B are arbitrary constants.

Majumdar (1947) and Papapetrou (1947) have considered solutions of eqns. (1.1) to (1.4) when no spatial symmetry is assumed, and have given the general solution when there is a relationship between g_{44} and ϕ of the form

$$g_{44} = (C + \phi)^2 \quad \dots\dots(1.6)$$

where C is a constant. Majumdar has also proved that (1.5) is the only possible functional relationship between g_{44} and ϕ , whether or not there is spatial symmetry.

With the above-mentioned exception, the only exact electrostatic solutions reported appear to be special cases of Weyl's solution. Among the latter are the following: the well-known solution for a charged mass-point (see, for example, Eddington 1924, § 78), the axially symmetric solution of Curzon (1925) for several charged mass-points when the relation (1.6) exists between g_{44} and ϕ , the case of an

electric field of uniform direction studied by McVittie (1929), the solution of Mukherji (1938) for a charged line-mass, and a solution corresponding to a particular uniform electric field given by Papapetrou (1947).

In this work we study in some detail certain axially symmetric electrostatic solutions of the field equations for empty space. We use the 'canonical' cylinder coordinates introduced by Weyl, and give complete sets of solutions in these coordinates for two types of field: first, that in which the electric field is parallel to the axis of symmetry, called a longitudinal field; and secondly, that in which there is no component along this axis, called a radial field. These two types of field are the relativistic analogues of the uniform field, and of the field of a line-charge, in classical theory. Some of the solutions which we give are special cases of Weyl's form, but two of them are not of this type.

§ 2. THE SOLUTIONS

In canonical coordinates the line element for a field with axial symmetry is

$$ds^2 = -e^{\lambda}(dx_1^2 + dx_2^2) - e^{-\rho}x_2^2 dx_3^2 + e^{\rho} dx_4^2, \quad \dots\dots(2.1)$$

where the origin of coordinates 0 is on the axis of symmetry $0x_1$, x_2 is a radial coordinate, x_3 is an angular coordinate and x_4 is time-like. λ and ρ are functions of x_1 and x_2 only. The equations (1.1) to (1.4), with $\mathfrak{F}^\mu = 0$, yield the following set which has previously been given by Curzon (1925):

$$\lambda_{11} + \lambda_{22} + \rho_1^2 + \lambda_2/x_2 = 2e^{-\rho}(\phi_1^2 - \phi_2^2), \quad \dots\dots(2.2)$$

$$\lambda_{11} + \lambda_{22} + \rho_2^2 - \lambda_2/x_2 - 2\rho_2/x_2 = -2e^{-\rho}(\phi_1^2 - \phi_2^2), \quad \dots\dots(2.3)$$

$$\rho_1\rho_2 - \rho_1/x_2 - \lambda_1/x_2 = 4e^{-\rho}\phi_1\phi_2, \quad \dots\dots(2.4)$$

$$\nabla\rho = 2e^{-\rho}(\phi_1^2 + \phi_2^2), \quad \dots\dots(2.5)$$

$$\nabla\phi = \rho_1\phi_1 + \rho_2\phi_2. \quad \dots\dots(2.6)$$

A suffix 1 or 2 after an unknown function means partial differentiation with respect to x_1 or x_2 , and ∇ denotes the Laplacian operator in cylindrical coordinates, i.e.

$$\nabla = \frac{\partial^2}{\partial x_1^2} + \frac{\partial^2}{\partial x_2^2} + \frac{1}{x_2} \frac{\partial}{\partial x_2}.$$

Adding (2.2) and (2.3) to twice (2.5), we have

$$2(\mu_{11} + \mu_{22}) + \rho_1^2 + \rho_2^2 = 4e^{-\rho}(\phi_1^2 + \phi_2^2), \quad \dots\dots(2.7)$$

where $\mu = \lambda + \rho$. Subtracting (2.3) from (2.2) we obtain

$$\rho_1^2 - \rho_2^2 + 2\mu_2/x_2 = 4e^{-\rho}(\phi_1^2 - \phi_2^2). \quad \dots\dots(2.8)$$

Further, (2.4) gives

$$\rho_1\rho_2 - \mu_1/x_2 = 4e^{-\rho}\phi_1\phi_2. \quad \dots\dots(2.9)$$

It is easily verified from (2.8) and (2.9) that, given (2.5) and (2.6) $\mu_{21} = \mu_{12}$ so that the condition for the integrability of eqns. (2.8) and (2.9) is satisfied; further, (2.7) is easily shown to be consistent with (2.8) and (2.9) subject only to (2.5) and (2.6). Hence λ is determined except for an additive constant, and the problem reduces to finding solutions of (2.5) and (2.6).

Weyl's solution may be written as follows:

$$e^{\rho} = A + B\phi + \phi^2, \quad \dots\dots(2.10)$$

$$\int \frac{d\phi}{A + B\phi + \phi^2} = \psi, \quad \dots\dots(2.11)$$

where

$$\nabla\psi = 0. \quad \dots\dots(2.12)$$

We shall later consider special cases of this, so we give here the integral (2.11). There are two cases:

$$(i) \quad A = \frac{1}{4} B^2, \quad \phi = -\frac{1}{2} B - \psi^{-1}, \quad \dots\dots(2.13)$$

$$(ii) \quad A - \frac{1}{4} B^2 = D^2 \text{ (where } D \text{ may be real or imaginary), } \phi = -\frac{1}{2} B + D \tan D\psi. \quad \dots\dots(2.14)$$

(a) *Longitudinal fields.*

To obtain the solutions corresponding to the longitudinal fields we take

$$\phi \equiv \phi(x_1) \quad \dots\dots(2.15)$$

so that (2.5) and (2.6) reduce to

$$e^e(\rho_{11} + \rho_{22} + \rho_2/x_2) = 2\phi_1^2, \quad \dots\dots(2.16)$$

$$\phi_{11} = \rho_1 \phi_1. \quad \dots\dots(2.17)$$

From (2.17) we have

$$\rho = \log \phi_1 + u(x_2), \quad \dots\dots(2.18)$$

where $u(x_2)$ is a function to be determined. Substituting from (2.18) in (2.16) and neglecting the trivial case where ϕ is constant, we find

$$e^u \left(\frac{\phi_{111}}{\phi_1} - \frac{\phi_{11}^2}{\phi_1^2} + u_{22} + \frac{u_2}{x_2} \right) = 2\phi_1. \quad \dots\dots(2.19)$$

From (2.15) we evidently must have either that u is constant or that ϕ_1 is constant. In the former case both ϕ and ρ are functions of x_1 only and therefore there must be a functional relationship between them, which, by Majumdar's work must be of the form (2.10). Hence if u is constant, ϕ must be given by (2.13) or (2.14) with $\psi = Cx_1 + E$ where C, E are arbitrary constants. Calculating e^e from (2.10), and e^A from (2.8) and (2.9) we find that the solutions in this case are

$$\left. \begin{aligned} e^A &= K(Cx_1 + E)^2, & e^e &= (Cx_1 + E)^{-2}, \\ \phi &= -\frac{1}{2} B - (Cx_1 + E)^{-1}; \end{aligned} \right\} \quad \dots\dots(2.20)$$

and

$$\left. \begin{aligned} e^A &= K \exp \{D^2 C^2 x_2^2\} \cos^2 \{D(Cx_1 + E)\}, \\ e^e &= D^2 \sec^2 \{D(Cx_1 + E)\}, \\ \phi &= -\frac{1}{2} B + D \tan \{D(Cx_1 + E)\}, \end{aligned} \right\} \quad \dots\dots(2.21)$$

where K is another arbitrary constant.

We now revert to the remaining possibility in (2.19), viz. $\phi = Cx_1 + E$, which reduces (2.19) to

$$e^u(u_{22} + u_2/x_2) = 2C. \quad \dots\dots(2.22)$$

Putting $w = 2 \log x_2 - u$, $t = \log x_2$, (2.22) becomes

$$d^2 w / dt^2 = -2C e^w. \quad \dots\dots(2.23)$$

Solving (2.23) and transforming back to the original variables, it is found that the only solution which gives a positive value for g_{44} is

$$\left. \begin{aligned} e^A &= K x_2^{k(k-2)/2} (1 + b^2 x_2^k)^2, \\ e^e &= C^2 k^{-2} b^{-2} x_2^{2-k} (1 + b^2 x_2^k)^2, \\ \phi &= Cx_1 + E, \end{aligned} \right\} \quad \dots\dots(2.24)$$

where K, k and b are arbitrary constants ($k \neq 0$).

(b) *Radial fields.*

Taking now $\phi \equiv \phi(x_2)$ eqns. (2.5) and (2.6) become

$$e^e(\rho_{11} + \rho_{22} + \rho_2/x_2) = 2\phi_2^2, \quad \dots\dots(2.25)$$

$$\phi_{22} + \phi_2/x_2 = \rho_2 \phi_2. \quad \dots\dots(2.26)$$

Equation (2.26) gives $\rho = \log \phi_2 x_2 + v(x_1)$ (2.27)

Inserting (2.27) in (2.25) and neglecting the case when ϕ is constant, we find

$$x_2 e^v \left(v_{11} + \frac{\phi_{222}}{\phi_2} - \frac{\phi_{22}^2}{\phi_2^2} + \frac{\phi_{22}}{x_2 \phi_2} \right) = 2\phi_2, \quad \text{..... (2.28)}$$

which requires either that v is constant, or that

$$\phi_2 = Cx_2 \quad \text{and} \quad e^v v_{11} = 2C \quad \text{..... (2.29)}$$

where C is an arbitrary constant.

If v is constant the solutions are special cases of Weyl's solution in which g_{44} and ϕ are functions of x_2 only, and they are obtained by substituting $\psi = C \log(x_2/a)$ in (2.13) and (2.14). They are found to be as follow :

$$\left. \begin{aligned} e^\lambda &= K \{C \log(x_2/a)\}^2, & e^e &= \{C \log(x_2/a)\}^{-2}, \\ \phi &= -\frac{1}{2}B - \{C \log(x_2/a)\}^{-1}; \end{aligned} \right\} \quad \text{..... (2.30)}$$

$$\left. \begin{aligned} e^\lambda &= Kx_2^{-2C^2D^2} \cos^2\{DC \log(x_2/a)\}, \\ e^e &= D^2 \sec^2\{DC \log(x_2/a)\}, \\ \phi &= -\frac{1}{2}B + D \tan\{DC \log(x_2/a)\}, \end{aligned} \right\} \quad \text{..... (2.31)}$$

where K is an arbitrary constant.

Continuing with the case where v is not constant, we solve (2.29) and find for the complete solution :

$$\left. \begin{aligned} e^\lambda &= K \exp\left\{-\frac{1}{4}h^2x_2^2\right\} \cosh^2\left(\frac{1}{2}hx_1+k\right), \\ e^e &= 4C^2h^{-2}x_2^2 \cosh^2\left(\frac{1}{2}hx_1+k\right), \\ \phi &= \frac{1}{2}Cx_2^2 + E, \end{aligned} \right\} \quad \text{..... (2.32)}$$

where K, h, k and E are arbitrary constants.

The expressions (2.20), (2.21), (2.24), (2.30), (2.31), (2.32) give all the solutions of the field equations for the electrostatic case when the line element assumes the form (2.1) and when the potential depends on only one of the canonical cylinder coordinates x_1 or x_2 . Of these, (2.24) and (2.32) are solutions not of Weyl's type.

§ 3. DISCUSSION OF THE SOLUTIONS

We shall later use Gauss' theorem on the gravitational flux in its relativistic form given by Whittaker (1935). For a line element of the type (2.1) the gravitational force measured by an observer at rest (i.e. whose space coordinates x_1, x_2, x_3 are constant) is the three-vector

$$g^i = \frac{1}{2} \frac{g^{ii}}{g_{44}} \frac{\partial g_{44}}{\partial x_i}, \quad (i=1, 2, 3). \quad \text{..... (3.1)}$$

The relativistic form of Gauss' gravitational theorem states that

$$\begin{aligned} & - \iint \left\{ g^1 \frac{\partial(x_2, x_3)}{\partial(u, v)} + g^2 \frac{\partial(x_3, x_1)}{\partial(u, v)} + g^3 \frac{\partial(x_1, x_2)}{\partial(u, v)} \right\} (-g)^{1/2} du dv \\ & = 8\pi \iint \left(T_4^4 - \frac{1}{2}T \right) (-g)^{1/2} dx_1 dx_2 dx_3, \end{aligned} \quad \text{..... (3.2)}$$

where the integration is taken over any simple closed surface S in the instantaneous space of the observer, and where u and v are any two parameters which specify the position of points on S . The right-hand side of (3.2) is proportional to the quantity which in relativity plays the part of gravitational mass in classical

mechanics, and we shall denote the left-hand side of (3.2) by $4\pi M$, and speak of M as the gravitational mass. In our case, it includes the contribution which arises from the electrostatic field, and we shall try to distinguish this where necessary.

Gauss' electrostatic theorem can be adapted in a natural way to electrostatic fields in general relativity if the electric flux density across the surface $x_i = \text{constant}$ is taken as $-F^{4i}(-g)^{1/2}$ (see Synge 1936). In our case F^{43} is zero and we have

$$-F^{4i}(-g)^{1/2} = \frac{1}{2}\pi^{-1/2}e^{-\phi}\phi_i x_2, \quad (i=1, 2). \quad \dots\dots(3.3)$$

If the solution is of Weyl's type, this becomes $\frac{1}{2}\pi^{-1/2}\psi_i x_2$ so that the electric flux density is proportional to that of the field represented by the classical potential ψ .

We may now begin the detailed examination of the solutions given in §2.

(a) Longitudinal fields.

From (3.3) we find that the electric flux density across the surface $x_1 = \text{constant}$ is in the solutions of Weyl's type (2.20) and (2.21) simply $\frac{1}{2}\pi^{-1/2}Cx_2$, and the electric flux across an element of this surface is $\frac{1}{2}\pi^{-1/2}Cx_2 dx_2 dx_3$. We are therefore justified in regarding these solutions as corresponding to uniform electric fields.

Applying to solution (2.21) the transformation

$$D \tan \{D(Cx_1 + E)\} = Cx_1' + b, \quad x_2 = x_2', \quad x_3 = x_3', \quad x_4 = x_4',$$

and adjusting the values of certain arbitrary constants, one finds

$$\left. \begin{aligned} ds^2 &= -\exp \{C^2(1-b^2)x_2'^2\} [X^{-3} dx_1'^2 + X^{-1} dx_2'^2] - x_2'^2 X^{-1} dx_3'^2 + X dx_4'^2, \\ \phi &= -\frac{1}{2}B + Cx_1' + b, \end{aligned} \right\} \quad (3.4)$$

where $X = 1 + 2Cbx_1' + C^2x_1'^2$, $b \geq 0$, $b^2 \neq 1$, in which the electric potential has the classical form for a uniform field. The properties of the solution (3.4) are in general what would be expected if the field is considered to arise from point infinite charges at infinity as in the case of the classical uniform field, and we confine ourselves to a statement of the main results, without detailed proof.

If the constant Cb in (3.4) is taken to represent mass it is found from (3.1) that the gravitational force g^1 due to the mass is repulsive at $x_1' = +\infty$ and attractive at $x_1' = -\infty$ (or vice versa, according to the sign of Cb), so that the solution requires the existence of negative mass, unless $b=0$. At large x_1' the gravitational force due to the charge predominates, corresponding to the fact that in the line element for a charged mass-point, viz.

$$ds^2 = -\left(1 - \frac{2m}{r} + \frac{e^2}{r^2}\right)^{-1} dr^2 - r^2 d\theta^2 - r^2 \sin^2\theta d\phi^2 + \left(1 - \frac{2m}{r} + \frac{e^2}{r^2}\right) dt^2, \quad \dots(3.5)$$

the term e^2/r^2 predominates at the origin. The singular region for finite x_1' which occurs in (3.4) if $b^2 > 1$ corresponds to that in (3.5) when $m > |e|$.

In (3.4) we may abolish either the mass, by putting $b=0$ (in which case the solution contains no singularity* except at infinity), or the charge, by letting C tend to zero and b tend to infinity in such a way that Cb remains finite. In the latter case the solution represents a uniform gravitational field.

Turning now to the solution (2.20), we find that if we put $K=1$ and make the transformation $Cx_1 + E = (Cx_1' + 1)^{-1}$, $x_2 = x_2'$, $x_3 = x_3'$, $x_4 = x_4'$, we have (3.4) with $b^2 = 1$. In this form the solution has been given by Papapetrou (1947). It has properties similar to those of the solution already discussed. (The corre-

* Here and in what follows we shall not count as a singularity the zero in g_{33} which occurs on the rotation axis.

sponding case of (3.5) is where $m = |e|$.) The electric field of uniform direction given by McVittie (1929) can be obtained from it by a transformation.

We shall now consider the very different field represented by the solution (2.24). We notice that unless $k = 2$ there is a singularity along Ox_1 which, since ϕ and ϕ_1 are finite there, must be attributed to a mass source and not to the presence of electric charge. If we put $m = \frac{1}{2}(1 - \frac{1}{2}|k|)$ and choose K appropriately we find

$$\left. \begin{aligned} e^\lambda &= \left(\frac{x_2}{a}\right)^{4m(2m-1)} \left[1 + \frac{C^2 a^2}{(2-4m)^2} \left(\frac{x_2}{a}\right)^{2-4m} \right]^2, \\ e^o &= \left(\frac{x_2}{a}\right)^{4m} \left[1 + \frac{C^2 a^2}{(2-4m)^2} \left(\frac{x_2}{a}\right)^{2-4m} \right]^2, \end{aligned} \right\} \dots\dots (3.6)$$

where a is arbitrary and $m \neq \frac{1}{2}$ because $k \neq 0$. The canonical form of the line element for a line-mass of density m per unit length without electrostatic field is (Levi-Civita 1919)

$$ds^2 = - \left(\frac{x_2}{a}\right)^{4m(2m-1)} (dx_1^2 + dx_2^2) - x_2^2 \left(\frac{x_2}{a}\right)^{-4m} dx_3^2 + \left(\frac{x_2}{a}\right)^{4m} dx_4^2, \dots\dots (3.7)$$

$m \neq \frac{1}{2}$. From (3.6) it is seen that the line element in the present solution tends to (3.7) as x_2 tends to zero so the solution corresponds to a line-mass along Ox_1 , of mass m per unit length, in a certain electric field. The electric flux across the area bounded by the intersection of the surfaces $x_1 = \text{constant}$, $x_2 = R$ is found to be

$$\pi^{1/2} \frac{Ca^{4m}R^{2-4m}}{2-4m} \left[1 + \frac{C^2 a^2}{(2-4m)^2} \left(\frac{R}{a}\right)^{2-4m} \right]^{-1}, \dots\dots (3.8)$$

which tends to the finite limit $\pi^{1/2} (2-4m) C^{-1}$ as R tends to infinity.

It is clear from (3.8) that the electric field, although of constant direction and independent of x_1 , is certainly not a uniform one in the classical sense. If it is abolished by putting C equal to zero, the line element reduces to that of a line-mass (3.7). The solution has the remarkable property that the radial gravitational field is modified by the axial electric field, which, however, produces no component of gravitational field parallel to itself. Indeed, by a comparison of the form of the line element at $x_2 = 0$ and at $x_2 = \infty$ it appears that the gravitational effect of the whole electric field is equivalent to that of an additional line-mass along Ox_1 , of density $1 - 2m$ per unit length. We may put $m = 0$ in (3.6) and so abolish the line-mass; in this case the line element has no singularities for finite x_2 yet the gravitational field at infinity is that of a line-mass along Ox_1 of unit density. All the components of the Riemann-Christoffel tensor for the solution (3.6) tend to zero as x_2 tends to infinity so that the space-time tends to flatness.

(b) Radial fields.

The electric flux across unit length of the cylinder $x_2 = \text{constant}$ for the solutions (2.30) and (2.31), which are of Weyl's type, is $\pi^{1/2}C$ so that the electric field may be considered to arise from a line-charge along Ox_1 of density $\frac{1}{2}\pi^{-1/2}C$ per unit length.

In the case of (2.30) the application of Gauss' theorem in the form (3.2) yields for the mass inside unit length of the cylinder $x_2 = R$ the expression $M = -\frac{1}{2}[\log(R/a)]^{-1}$ which tends to zero as R tends to zero or infinity. Since, however, g_{ik} , ϕ and M all become singular when $x_2 = a$, the most reasonable procedure seems to be to cut off the field at this radius (i.e. to allow x_2 to range only from a to infinity), regarding it as the radius of the line-charge. It is then necessary

to regard the electrostatic energy of the whole field (per unit length of Ox_1) outside $x_2 = a$ as corresponding to infinite gravitational mass but as being counteracted by an infinite negative mass inside the singularity $x_2 = a$, so that the mass appears to be zero at large x_2 . The singularity at $r=0$ when $m < |e|$ in (3.5) may be considered in a rather similar manner as a source of infinite negative mass (see Papapetrou 1947).

If in (2.31) D is taken as real it does not seem possible to derive any solutions of physical significance. If D is taken as imaginary the gravitational field at large x_2 is that of a line-charge of negative mass $-\frac{1}{2}|CD|$ per unit length. No solution appears to exist for a line-charge with positive mass.

Considering now the last solution (2.32) we observe that g_{33} does not contain x_2 so that x_3 cannot be taken as an angular coordinate. The solution does not appear to correspond, strictly speaking, to a radial field, but the g_{ik} and ϕ have the same values on every surface $x_3 = \text{constant}$, and there is symmetry about the surfaces $x_2 = 0$ and $x_1 = -2k/h$.

The electric field in this solution has its only component in the direction of x_2 , and the electric flux across an element of the surface $x_2 = \text{constant}$ is

$$\frac{1}{8}\pi^{-1/2}h^2C^{-1}\text{sech}^2(\frac{1}{2}hx_1+k)dx_1dx_3.$$

Hence the electric field is of uniform direction but the magnitude of the electric flux at a point depends on x_1 .

The gravitational flux across an element of the surface $x_2 = \text{constant}$ is simply $-dx_1dx_3$, which implies a uniform gravitational field in the direction of x_2 ; but there is also a component of the flux in the direction of x_1 , which is

$$-\frac{1}{2}h \tanh(\frac{1}{2}hx_1+k)x_2dx_2dx_3.$$

This flux depends on x_1 and must arise from the electric field, so that, as in the case of the other solution (3.6) which is not of Weyl type, the electric field produces a component of gravitational field orthogonal to itself.

The solution contains two significant arbitrary constants, h and C , and both seem to refer to the electric field, rather than to mass sources. The sources of both mass and charge appear to be wholly at infinity.

If in (2.32) we let h and C tend to zero so that h/C remains finite the solution may be reduced to $ds^2 = -(dx_1^2 + dx_2^2 + dx_3^2) + x_2^2 dx_4^2$, for which all components of the Riemann-Christoffel tensor vanish identically, showing that the electric field and permanent gravitational fields have been abolished.

§ 4. CONCLUSION

The four solutions (2.20), (2.21), (2.30) and (2.31) are particular cases of Weyl's general class and arise from a classical electrostatic potential ψ as shown in eqns. (2.10) to (2.12). In solutions of this type the electric flux density is proportional to that of the classical field arising from ψ so that the problem of identifying the relativistic and the classical electric fields presents no difficulty. Thus (2.20) and (2.21) represent the relativistic analogue of the classical uniform electric field, and (2.30) and (2.31) are analogous to the classical field of a line-charge.

When we consider the associated gravitational fields we find that the electric field alters the gravitational field of the matter present but only in a direction parallel to itself. In the case of the uniform electric field (2.20) and (2.21), the gravitational field is not unexpected if the electric field arises from two charged mass-points at infinity. Unless both masses are zero one of them is required to be

negative. Of the solutions (2.30) and (2.31), the former corresponds to a line-charge without mass, and the latter to a line-charge whose mass per unit length must, rather surprisingly, be negative, whatever the sign of the charge.

The most interesting solutions are (2.24) and (2.32) which are not of Weyl's type and which do not correspond to a classical potential. The solution (2.32) is not axially symmetrical but its line element can be expressed in the canonical form so it has been considered here. The electric fields in these solutions are quite different from any classical electrostatic fields, though both are of uniform direction. They have the property of producing an orthogonal gravitational field, and in the case of (2.24) the field so produced is, at large x_2 , equivalent to that of an additional line-mass along Ox_1 .

It therefore appears that whereas the axially symmetric solutions which are of Weyl's general type may be capable of explanation in terms of classical electrostatics together with relativity gravitation theory, the solutions which are not of this form may be expected to require a quite different mode of interpretation. If examples of the latter can be found in which the sources are wholly within a finite region, and in which the line element tends to its Galilean form at infinity, further light may be thrown on this problem, and it may be possible to predict effects of a non-classical nature which can be measured experimentally.

REFERENCES

- CURZON, H. E. J., 1925, *Proc. Lond. Math. Soc.*, **23**, 477.
 EDDINGTON, A. S., 1924, *The Mathematical Theory of Relativity* (Cambridge : University Press).
 LEVI-CIVITA, T., 1919, *Atti Accad. Lincei, Rendiconti*, **28**, 101.
 MAJUMDAR, S. D., 1947, *Phys. Rev.*, **72**, 390.
 McVITTIE, G. C., 1929, *Proc. Roy. Soc.*, **124**, 366.
 MUKHERJI, B. C., 1938, *Bull. Calcutta Math. Soc.*, **30**, 95.
 PAPAPETROU, A., 1947, *Proc. Roy. Irish Acad.*, **51**, 191.
 SYNGE, J. L., 1936, *Proc. Roy. Soc.*, **157**, 434.
 WEYL, H., 1917, *Ann. Phys., Lpz.*, **54**, 117.
 WHITTAKER, E. T., 1935, *Proc. Roy. Soc. A*, **149**, 384.

The Statistical Aspect of Boltzmann's H-Theorem

BY D. TER HAAR AND C. D. GREEN

Department of Natural Philosophy, University of St. Andrews

MS. received 24th April 1952, and in amended form 1st October 1952

ABSTRACT. The statistical aspect of the second law of thermodynamics is illustrated by a discussion of two simple models. In both cases the most probable behaviour, and the mean life and the average time of recurrence of different states of fluctuation are obtained and discussed.

§ 1. INTRODUCTION

It is well known that among the fundamental problems of statistical mechanics two are closely connected. These are the justification of the use of statistical methods in describing an actual system and especially the use of ensemble theory, on the one hand, and the apparent contradiction between microscopic reversibility and macroscopic irreversibility, or the statistical counterpart of the second law of thermodynamics, on the other hand.

It is relatively easy to prove that for practically all systems of physical interest it does not make any difference whether one uses as the representative ensemble a micro-canonical ensemble, a macro-canonical ensemble, or even a grand ensemble (see, for example, Gibbs 1902) and the first problem mentioned is thus reduced to a proof that averages taken over a representative micro-canonical ensemble are the same as the time averages with which we have to deal in actual circumstances. This proof is usually called the (quasi-) ergodic theorem, and as far as classical statistical mechanics is concerned, it was given by von Neumann (1932) and Birkhoff (1931). They showed that the time average taken over an infinite period is equal to the average taken over the representative micro-canonical ensemble, provided the appropriate phase space is metrically transitive. As far as we are aware, nobody has ever shown that in the case of an actual system this condition is fulfilled, even though Oxtoby and Ulam (1941) have proved the existence of metrically transitive manifolds. Even if one could prove the metrical transitivity of phase spaces corresponding to actual systems there remains the point that one still must prove the identity of the long-time averages, calculated by ensemble theory, with the short-time averages which are of physical significance (Fowler 1936).

As regards the second problem, it was originally thought that Boltzmann's *H*-theorem (1872) had given a proof of the second law of thermodynamics. Boltzmann's function *H*, which was especially introduced for this purpose, is essentially the negative of the entropy in the case of equilibrium and can be considered to be a generalization of the thermodynamic entropy in non-equilibrium situations. The *H*-theorem consisted in showing that (a) *H* is minimum in an equilibrium situation, and (b) *H* always decreases in the case of a non-equilibrium situation. It was only afterwards realized that the *H*-theorem was not the rigorous proof Boltzmann thought it to be, but that one had to use the so-called Stosszahlansatz in order to derive it. This meant that one had to make certain plausible assumptions regarding the number of collisions per

unit time. We do not wish to enter here into a detailed history of the H -theorem, and we refer to existing critical discussions (Ehrenfest and Ehrenfest 1911, Chandrasekhar 1943, ter Haar 1953). All difficulties seemed finally to disappear when the Ehrenfests (1911) pointed out the following facts: (i) instead of considering H as a function of a continuous variable one should consider the so-called H -curve which one obtains by plotting the values of H at the times $n\Delta t$ where Δt is a time interval small compared with macroscopic, but large compared with microscopic time intervals, (ii) the H -theorem is a *probability* statement regarding the H -curve. Its content is as follows: (a) if H' is a value of H much larger than the equilibrium value H_{eq} , the H -curve will practically always go downwards from H' , (b) this will be true whether we read the H -curve from $t = -\infty$ to $t = +\infty$ or vice versa, (c) the H -curve is practically always in the immediate neighbourhood of H_{eq} and (d) values of H different from H_{eq} will be reached over and over again, but the greater the difference between H and H_{eq} the longer will be the time interval before recurrence.

From the considerations of the preceding paragraph it is obvious that although the H -curve is essentially symmetrical with respect to a reversal of the time direction, it still remains true that H will practically always decrease from an appreciably higher value towards H_{eq} . Furthermore, we must bear in mind that any actual observations on a system will always take place within finite time intervals and we may thus conclude with Smoluchowski (1912, see also Chandrasekhar 1943) that a process will appear irreversible, or reversible, if the initial state is characterized by an average time of recurrence which is long, or short, compared with the periods available for experimental observations. This recurrence of an apparent irreversibility has been the subject of many detailed discussions in the case of Brownian motion. We may refer the reader once more to Chandrasekhar's review (1943) where one can also find an extensive bibliography. It was realized by the Ehrenfests that it would be necessary to discuss in detail the fluctuations occurring in a gaseous system in order to justify the second law of thermodynamics. With this end in view they gave in their paper (1911) a programme for future investigations of the statistical aspect of the H -theorem. It is the purpose of the present paper, and of work still in progress, to pursue the Ehrenfests' programme by considering in detail some simplified models, since such an investigation has, as far as we know, not yet been made.

If the extended H -theorem were proved, we should be able not only to derive from it the quasi-ergodic theorem, but at the same time see in how far short-time averages and long-time averages are equal. On the other hand, once the quasi-ergodic theorem is proved, it follows in the same way as in the old ergodic theorem that the second law of thermodynamics must hold. In that case, however, we should not yet have obtained detailed information regarding fluctuations.

In the present paper we consider two different models. The first model, discussed in §2, is the urn model introduced by Ehrenfest and Ehrenfest (1907) and Kohlrausch and Schrödinger (1926). The second model, discussed in §3, is a simplified version of the wind-wood model of the Ehrenfests (1911). In both cases we shall introduce a quantity Δ which measures the departure from equilibrium. We can then calculate (i) the probability $w(\Delta)$ of the occurrence of a given value of Δ , (ii) the probability $w(\Delta', \Delta'')$ that during a time interval τ the value of Δ has changed from Δ' to Δ'' , (iii) the average value Δ_{av} of Δ ,

(iv) the average rate of change of Δ , (v) the average lifetime $T(\Delta)$ of a state characterized by Δ , and (vi) the average time of recurrence $\Theta(\Delta)$, that is, the average time between two consecutive occurrences of a state characterized by Δ . We shall discuss the results obtained in §§2 and 3 in §4.

§ 2. THE URN MODEL

Let N balls numbered from 1 to N be distributed over two urns A and B. For the sake of simplicity, we shall assume N to be even. Let there also be a box containing N tickets numbered from 1 to N . At regular intervals, $\frac{1}{2}\tau$ apart, a ticket is drawn and the ball whose number is drawn is removed from the urn in which it lies into the other urn and stays there until such time as its number is drawn again. The ticket is returned to the box and the process is repeated. At each draw the probability of drawing any particular number is $1/N$.

Let N_A and N_B be respectively the number of balls in A and B. If we denote by Δ the difference between the numbers of balls in the two urns, we have

$$\Delta = N_A - N_B, \quad N = N_A + N_B. \quad \dots\dots(1)$$

From symmetry considerations it follows—as we shall verify presently—that $\Delta=0$ is the equilibrium value of Δ and that thus $|\Delta|$ measures the departure from equilibrium.

The probability $w(\Delta)$ is most easily calculated by remarking that a situation with given N_A and N_B can be imagined to have been obtained by the tossing of a coin, heads entailing putting a ball in A and tails putting a ball in B. As there are N balls, $w(\Delta)$ is equal to the probability of getting $N_A (= \frac{1}{2}N + \frac{1}{2}\Delta)$ heads from N throws, or,

$$w(\Delta) = \left(\frac{1}{2}\right)^N \binom{N}{\frac{1}{2}N + \frac{1}{2}\Delta}, \quad \dots\dots(2)$$

where $\binom{a}{b}$ is the binomial coefficient $\frac{a!}{b!(a-b)!}$. \dots\dots(3)

As eqn. (2) is the formula for a Bernoulli distribution, we have

$$\left(\frac{1}{2}N + \frac{1}{2}\Delta\right)_{av} = \frac{1}{2}N, \quad \text{or} \quad \Delta_{av} = 0 \quad \dots\dots(4)$$

and the dispersion $\sigma(\Delta)$ is given by the equation

$$\sigma(\Delta) \equiv [(\Delta_{av} - \Delta)^2]_{av} = (\Delta^2)_{av} = \frac{1}{4}N. \quad \dots\dots(5)$$

When $N \gg 1$, eqn. (2) can be written to a fair approximation in the following gaussian form,

$$w(\Delta) = (2\pi N)^{-1/2} \exp(-\Delta^2/2N). \quad \dots\dots(6)$$

If the situation at time t is characterized by Δ , the situation at $t + \frac{1}{2}\tau$ is characterized by either $\Delta - 2$ or by $\Delta + 2$, and the situation at $t + \tau$ by one of the three possibilities $\Delta - 4$, Δ , or $\Delta + 4$. Starting from Δ at t the probabilities $p(\Delta, \Delta - 2)$ and $p(\Delta, \Delta + 2)$ that respectively $\Delta - 2$ or $\Delta + 2$ are realized at $t + \frac{1}{2}\tau$ are easily seen to be given by the equations

$$p(\Delta, \Delta - 2) = (N + \Delta)/2N, \quad p(\Delta, \Delta + 2) = (N - \Delta)/2N. \quad \dots\dots(7)$$

The transition probabilities $w(\Delta, \Delta - 4)$, $w(\Delta, \Delta)$ and $w(\Delta, \Delta + 4)$ are given by the equations

$$\left. \begin{aligned} w(\Delta, \Delta - 4) &= p(\Delta, \Delta - 2)p(\Delta - 2, \Delta - 4), \\ w(\Delta, \Delta + 4) &= p(\Delta, \Delta + 2)p(\Delta + 2, \Delta + 4), \\ w(\Delta, \Delta) &= p(\Delta, \Delta + 2)p(\Delta + 2, \Delta) + p(\Delta, \Delta - 2)p(\Delta - 2, \Delta), \end{aligned} \right\} \dots\dots(8)$$

and we get, using eqns. (7),

$$\left. \begin{aligned} w(\Delta, \Delta - 4) &= (N + \Delta)(N + \Delta - 2)/4N^2, \\ w(\Delta, \Delta + 4) &= (N - \Delta)(N - \Delta - 2)/4N^2, \\ w(\Delta, \Delta) &= (N^2 + 2N - \Delta^2)/2N^2. \end{aligned} \right\} \dots\dots(9)$$

It is seen immediately that any $w(\Delta', \Delta'')$ for which $\Delta' - \Delta''$ is not equal to -4 , 0 , or $+4$ vanishes.

From eqns. (9) we get for the average value Δ'_{av} at $t + \tau$, if we start at t from Δ , the equation

$$\Delta'_{av} = (\Delta - 4)w(\Delta, \Delta - 4) + \Delta w(\Delta, \Delta) + (\Delta + 4)w(\Delta, \Delta + 4) = \Delta - 4\Delta(N - 1)/N^2, \dots\dots(10)$$

and we get for the average rate of change

$$(d\Delta/dt)_{av} = (\Delta'_{av} - \Delta)/\tau = -4\Delta(N - 1)/\tau N^2. \dots\dots(11)$$

We shall leave a discussion of eqns. (4), (5), (9), (10) and (11) to § 4.

We can now easily calculate the average life time $T(\Delta)$ and the average time of recurrence $\Theta(\Delta)$ by using the method employed by Chandrasekhar (1943) in his discussion of Brownian motion. Let $\phi_\Delta(k)$ be the probability that starting at t_0 from a situation characterized by Δ , Δ is realized on $k - 1$ consecutive occasions (at $t_0 + \tau$, $t_0 + 2\tau$, . . . , $t_0 + (k - 1)\tau$) while on the k th occasion (at $t_0 + k\tau$) a value different from Δ is realized. In terms of $w(\Delta, \Delta)$ we have clearly

$$\phi_\Delta(k) = w^{k-1}(\Delta, \Delta) [1 - w(\Delta, \Delta)]. \dots\dots(12)$$

The mean life $T(\Delta)$ is defined by the following translucent equation

$$T(\Delta) = \Sigma k\tau\phi_\Delta(k), \dots\dots(13)$$

where the summation is over k from zero to infinity. From eqns. (12) and (13) we then have easily

$$T(\Delta) = \tau/[1 - w(\Delta, \Delta)]. \dots\dots(14)$$

In the same way it is possible to express $\Theta(\Delta)$ in terms of $w(\Delta, \Delta)$ and $w(\Delta)$. We shall not give the detailed derivation of the result, since it is essentially the same as the derivation given by Chandrasekhar (1943). The final result is

$$\Theta(\Delta) = T(\Delta)[1 - w(\Delta)]/w(\Delta). \dots\dots(15)$$

Again, we shall postpone discussion of eqns. (14) and (15) to § 4.

§ 3. THE ONE-DIMENSIONAL WIND-WOOD MODEL

As an extremely simplified model of an actual gas the Ehrenfests (1911) introduced a two-dimensional model containing two kinds of molecules. One kind was fixed in the plane and scattered the other kind elastically, while collisions between molecules of the same kind were supposed not to occur. It may be remarked in passing that this model is actually more closely related to a metal than to a gas. We hope to discuss it in a subsequent paper, limiting ourselves meanwhile to the discussion of an even simpler model consisting of the one-dimensional counterpart of the Ehrenfests' model.

Consider a line segment of unit length in the x -direction on which N point particles are moving. We assume that these particles do not interact with each other and they are all moving with the same speed c , part of them in the positive and part in the negative x -direction. On the line segment n 'screens' are

randomly distributed. These screens have fixed positions and they have the property that a point particle colliding with a screen has a probability α of being reflected back and a probability $1 - \alpha$ of passing through, in both cases without change in speed.

Let f_1 and f_2 be the number of particles moving respectively in the positive and in the negative x -direction and let the difference between f_1 and f_2 be denoted by Δ so that we have

$$\Delta = f_1 - f_2, \quad N = f_1 + f_2. \quad \dots\dots(16)$$

The probability $w(\Delta)$ is again a Bernoulli distribution and given by eqn. (2) or by eqn. (6), if $N \gg 1$. Equations (4) and (5) for the average value and the dispersion of Δ also hold again.

In order to obtain $w(\Delta', \Delta'')$ we must calculate the rate of change of f_1 and f_2 . Let x_1 and x_2 be respectively the number of particles which during a time interval τ change their directions from the positive to the negative direction or vice versa. If we neglect end effects and the possibility that a particle may change its direction more than once during τ , we have clearly

$$df_1/dt = (x_2 - x_1)/\tau, \quad df_2/dt = (x_1 - x_2)/\tau, \quad d\Delta/dt = 2(x_2 - x_1)/\tau. \quad \dots\dots(17)$$

From these equations it follows that we must first of all obtain the probabilities $p(x_1)$ and $p(x_2)$ for the occurrence of given values of x_1 and x_2 . It is essential *not* to put

$$x_i = gf_i, \quad \text{where } g = \alpha n c \tau, \quad \dots\dots(18)$$

as we shall discuss presently, but to introduce straight away the appropriate Bernoulli distributions,

$$p(x_i) = \binom{f_i}{x_i} g^{x_i} (1-g)^{f_i-x_i}. \quad \dots\dots(19)$$

Equation (18) assumes that the number of collisions is always equal to its average and this equation would thus correspond to a Stosszahlansatz for our model. We shall assume that $N \gg gN \gg 1$ and in that case we may approximate $p(x_i)$ by the gaussian distribution

$$p(x_i) = (2\pi gf_i)^{-1/2} \exp [-(x_i - gf_i)^2 / 2gf_i]. \quad \dots\dots(20)$$

From eqn. (17) we find easily that $w(\Delta', \Delta'')$ is given by the equation

$$w(\Delta', \Delta'') = \sum p(x_1) p(x_2), \quad \dots\dots(21)$$

where the summation extends over all values of x_1 and where x_2 is related to x_1 by the equation

$$x_2 = x_1 + \frac{1}{2}(\Delta'' - \Delta'). \quad \dots\dots(22)$$

Bearing in mind that Δ is a discrete variable, we see that once the $w(\Delta', \Delta'')$ are calculated, $T(\Delta)$ and $\Theta(\Delta)$ follow from eqns. (14) and (15).

From the fact that the $p(x_i)$ are normalized it follows that

$$\sum w(\Delta', \Delta'') = 1, \quad \dots\dots(23)$$

where the summation extends for fixed Δ' over all possible values of Δ'' .

The average value Δ'_{av} follows from the equation

$$\Delta'_{av} = \sum \Delta' w(\Delta, \Delta') = \sum \sum p(x_1) p(x_2) \Delta', \quad \dots\dots(24)$$

where the summations extend over both x_1 and Δ and where x_2 is given by eqn. (22). Using for the $p(x_i)$ eqn. (20) and replacing the sums by integrals (from $-\infty$ to $+\infty$) we find

$$\Delta'_{av} = \Delta + 2g(f_2 - f_1) = (1 - 2g)\Delta, \quad \dots\dots(25)$$

and for the average rate of change of Δ we find, as we might have expected,

$$(d\Delta/dt)_{av} = (\Delta'_{av} - \Delta)/\tau = 2g(f_2 - f_1)/\tau = -2g\Delta/\tau. \quad \dots\dots(26)$$

Before we discuss the results of the present section we shall derive an expression for $w(\Delta', \Delta'')$. This is done by using eqns. (20) to (22) and replacing the sum by an integral (from $-\infty$ to $+\infty$). The final result is

$$w(\Delta, \Delta') = (2\pi Ng)^{-1/2} \exp[-g\Delta^2/2N - 2gz(z + \Delta)/N], \quad \dots\dots(27)$$

where we have introduced the abbreviation

$$z = (\Delta' - \Delta)/4g, \quad \dots\dots(28)$$

and we have especially for $w(\Delta, \Delta)$ the formula

$$w(\Delta, \Delta) = (2\pi gN)^{-1/2} \exp(-g\Delta^2/2N). \quad \dots\dots(29)$$

§ 4. DISCUSSION

In the preceding two sections we have collected all the formulae which we need to illustrate the points mentioned in § 1. As can be seen on inspection the two models which we have discussed are very similar in nature and it is thus possible to discuss them simultaneously. In both cases we introduce a quantity Δ to measure the departure from equilibrium and we are thus concerned with a Δ -curve rather than with an H -curve. If we wish to compare our model with a real system, we may assume N to be large compared to 1. In order to fix our ideas we shall take $N = 10^{19}$ which is of the order of magnitude of the number of gas atoms per unit volume under normal circumstances, and we shall take $\tau = 1$ second. From the results of the preceding sections we reach now the following conclusions:

(ia) From eqns. (9) we see that, if Δ is positive, the probability $w(\Delta, \Delta - 4)$ is so much larger than $w(\Delta, \Delta)$ or $w(\Delta, \Delta + 4)$ that the average change of Δ , which is given by eqn. (10), is always in the direction of $\Delta = 0$, that is towards equilibrium. Moreover, the rate of change of Δ is greater, the larger the absolute magnitude of Δ (see eqn. (11)).

(ib) A similar situation arises in the model studied in § 3. From eqn. (27) we see that $w(\Delta, \Delta')$ is largest, when z and Δ have opposite signs. The actual maximum of $w(\Delta, \Delta')$ occurs for the value of Δ' given by eqn. (25). Again we see a preference for an approach to equilibrium. From eqn. (26) we see furthermore that this approach to equilibrium is the faster, the larger $|\Delta|$.

(ii) It can easily be verified that the following relation holds

$$w(\Delta)w(\Delta, \Delta') = w(\Delta')w(\Delta', \Delta) \quad \dots\dots(30)$$

for both models. This ensures symmetry with respect to past and future.

(iii) From eqns. (9), (29) and (14) we see that $T(\Delta)$ is always of the order of magnitude of τ and practically independent of Δ .

(iv) It follows from (iii) that the time averages of Δ and of Δ^2 are practically the same as Δ_{av} and $(\Delta^2)_{av}$ and thus given by eqns. (4) and (5). We see thus that Δ is, indeed, practically always in the neighbourhood of Δ_{av} . More quantitatively, the average departure from equilibrium, which can be measured by the quantity $|f_1 - f_2|_{av}/N$, is only of the order of $N^{-1/2}$.

(v) From (iii) and eqns. (15) and (6) it follows that $\Theta(\Delta)$ is essentially equal to $\tau/w(\Delta)$ as could have been expected from elementary considerations. In order to verify that the times of recurrence of observable fluctuations are extremely

long we can use eqn. (6). If $\Delta^2 = (\Delta^2)_{av}$, $\Theta = 10^{10}$ sec = 300 years. If $|f_1 - f_2| N = 10^{-8}$, a departure from equilibrium by only one-millionth of one per cent, $\Theta \sim 10^{200}$ years !!

(vi) In conclusion, we wish to consider briefly eqn. (26). If we had not taken into account the fact that eqns. (18) would only give us the average values of the x_i , but not necessarily their actual values at any given moment, we should have started by writing down eqn. (26) from which a uniform approach to equilibrium follows. This would have corresponded to the unrestricted *H*-theorem which was based on the Stosszahlansatz. In the same way eqn. (26) can be derived in a straightforward manner by using eqn. (18). We see here also why one should carefully distinguish between the Stosszahlansatz and the assumption of molecular chaos—as was done by Jeans and the Ehrenfests. All our calculations in § 3 are based on the assumption of molecular chaos, since it is only possible to use for the $p(x_i)$ eqn. (19) if the positions of the various point particles are unrelated.

In the future we plan to extend our considerations to more realistic models both in the way of more dimensions and by introducing velocity distributions instead of a single value of c .

ACKNOWLEDGMENT

We would like to thank Professor R. E. Peierls for a discussion which clarified the connection between the *H*-theorem and the quasi-ergodic theorem.

REFERENCES

- BIRKHOFF, G. D., 1931, *Proc. Nat. Acad. Sci., Wash.*, **17**, 650, 656.
 BOLTZMANN, L., 1872, *S.B. Akad. Wiss. Wien*, **66**, 275.
 CHANDRASEKHAR, S., 1943, *Rev. Mod. Phys.*, **15**, 1.
 EHRENFEST, P., and EHRENFEST, T., 1907, *Phys. Z.*, **8**, 311 ; 1911, *Enzykl. Math. Wiss.*, Vol. 4, part 32 (Leipzig : Teubner).
 FOWLER, R. H., 1936, *Statistical Mechanics* (Cambridge : University Press), p. 8.
 GIBBS, J. W., 1902, *Elementary Principles in Statistical Mechanics* (New Haven : Yale University Press).
 TER HAAR, D., 1953, *Elements of Statistical Mechanics* (New York : Rinehart), Appendix I (in course of publication).
 KOHLRAUSCH, K. W. F., and SCHRÖDINGER, E., 1926, *Phys. Z.*, **27**, 306.
 VON NEUMANN, J., 1932, *Proc. Nat. Acad. Sci., Wash.*, **18**, 70, 263.
 OXToby, I., and ULAM, S., 1941, *Ann. Math. Princeton*, **42**, 874.
 VON SMOLUCHOWSKI, M., 1912, *Phys. Z.*, **13**, 1069.

East-West Asymmetry of Moderate-Energy Neutrons in the Cosmic Radiation

By J. C. BARTON*

Birkbeck College, University of London

Communicated by E. P. George; MS. received 16th September 1952

ABSTRACT. An anticoincidence counter arrangement showed no significant asymmetry in the arrival of moderate-energy neutrons at sea level. It is concluded that these neutrons do not maintain the same direction as the primary cosmic-ray particles which give rise to them.

§1. EXPERIMENTAL METHOD AND RESULTS

EXPERIMENTS with an anticoincidence arrangement of counters (Barton 1951) have shown that the penetrating non-ionizing component of the cosmic radiation consists chiefly of neutrons with energies of a few hundred million electron volts. The apparatus which was used to determine the zenith angular distribution of these particles has since been modified so that their East-West asymmetry could be measured. This was done by mounting the counter system on a turntable and enlarging the lead screen so that the counter system could be rotated inside it, as shown in figs. 1 (a) and (b). The arrangement of the

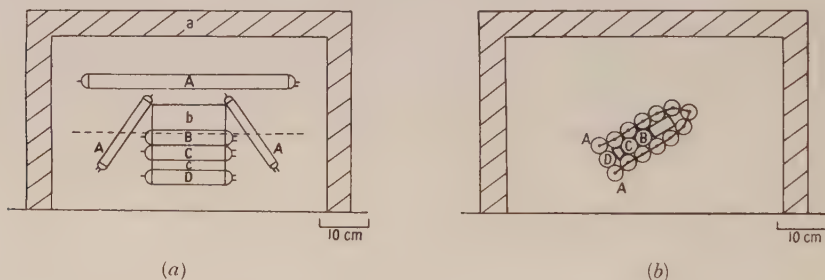


Fig. 1.

(a) Longitudinal section (counter system vertical). (b) Transverse section (counter system at 60°).

counters was the same as before: a threefold counter telescope BCD, surrounded by a close-fitting screen of counters A. The coincidences BCD are caused by the flux of charged cosmic ray particles at sea level, filtered by 5 cm Pb + 5 cm C. It has been shown previously (Barton 1951) that the anticoincidences BCD-A are mostly due to neutrons of moderate energy giving rise to charged secondary particles in the absorber 'b'. During the present experiment the zenith angle of the counter system was fixed at 60° . The observations were carried out on the roof of the University of London Senate House.

The following results were obtained with absorber $a = 5$ cm Pb, $b = 5$ cm C, $c = 0$. (In all cases the errors given are the statistical standard deviations, or estimates of this quantity.)

* Now at University College of the West Indies.

	Telescope pointing E	Telescope pointing W
Rate B + C + D	$114.2 \pm 0.3/\text{hour}$	$115.9 \pm 0.3/\text{hour}$
Rate - A + B + C + D	$1.39 \pm 0.04/\text{hour}$	$1.32 \pm 0.04/\text{hour}$

From these figures we find the asymmetry $(I_W - I_E)/\frac{1}{2}(I_W + I_E)$ to be $+1.5 \pm 0.4\%$ for the coincidence rate BCD and $-5 \pm 4\%$ for the anticoincidence rate BCD-A. The former of these values is a measure of the E-W asymmetry of the total ionizing radiation under 5 cm of lead; it is consistent with the figure of $+2.2 \pm 0.9$ found by Johnson (1935) under similar conditions. The asymmetry for the anticoincidence events, which are due to moderate-energy neutrons is seen to be not significantly different from zero.

§ 2. DISCUSSION

If the neutrons that are detected in this experiment maintained the same direction as the primary cosmic ray which produced them, then only primaries with energy greater than 13.5 kMeV could be responsible for them; for this energy is the minimum required for a primary particle arriving from the East at 60° , whereas one from the West only requires 1.6 kMeV (e.g. Alpher 1950). This would mean that the neutrons were produced by latitude insensitive primaries. No measurements of the latitude effect of this component have so far been reported but we can consider instead the results obtained for the low-energy neutrons that are detected by boron counters; according to Tongiorgi (1949) these low-energy neutrons are produced locally by nucleons whose energy is comparable with that which is necessary for a particle to be detected by the present apparatus. It has been found by Adams and Braddick (1951) and Gill and Curtiss (1951) that the latitude effect for low-energy neutrons at sea level is much larger than it is for the total ionizing radiation. This shows that the neutrons cannot be the descendants of latitude insensitive primaries and we conclude that the assumption of collimation between the observed neutrons and the cosmic-ray primaries was unwarranted. It seems more likely that the neutrons have been ejected at comparatively large angles from nuclear disintegrations which are produced by particles arriving from directions near the zenith. This conclusion is consistent with the earlier observations of the zenith angular distribution (Barton 1951) in which it was shown that the neutrons have a broad distribution in angle at sea level.

ACKNOWLEDGMENT

I am indebted to Dr. E. P. George for suggesting this experiment and for valuable discussions.

REFERENCES

- ADAMS, N., and BRADDICK, H. J. J., 1951, *Z. Naturforsch.*, **6A**, 592.
 ALPHER, R. A., 1950, *J. Geophys. Res.*, **55**, 437.
 BARTON, J. C., 1951, *Proc. Phys. Soc. A*, **54**, 1042.
 GILL, P. S., and CURTISS, L. F., 1951, *Phys. Rev.*, **84**, 591.
 JOHNSON, T. H., 1935, *Phys. Rev.*, **48**, 287.
 TONGIORGI, V. C., 1949, *Phys. Rev.*, **76**, 517.

Domains of Reverse Magnetization

By L. F. BATES AND D. H. MARTIN

University of Nottingham

MS. received 18th August 1952

ABSTRACT. An experimental study by the powder deposit technique has been made of interesting domains of reverse magnetization which arise when an initially saturated crystal of silicon-iron is demagnetized. Two cases have been studied with the crystal (*a*) as perfect as possible, and (*b*) with an artificial defect made at one end to provide controlled demagnetization effects. They show that imperfections in the surface are very important in determining the observed demagnetization phenomena. The surfaces of the crystal may themselves act as imperfections.

§ 1. INTRODUCTION

IN this communication we report experiments made on a single crystal of 3.0% silicon-iron cut so that each surface of the specimen is a true {100} plane, with the long axis parallel to a [100] direction along which the magnetic field was applied. We desired to know how the domain structure changed as the initially saturated crystal was demagnetized, and in particular how the one single domain of the saturated state broke down. The latter problem was considered theoretically by Brown (1945), who stated that he could find no reason why a perfect crystal when once saturated should change its domain structure except when an appreciable reverse field was applied to it, the field being considerably greater than the coercivity of the material. A similar problem in the case of permalloy under stress was tackled by Dijkstra (1950) who envisaged the formation of domains of reverse magnetization by the rotation of the magnetization vectors in regions of ellipsoidal shape. The application of Dijkstra's treatment to the case of silicon-iron gives results similar to those of Brown.

§ 2. EXPERIMENTAL DETAILS

The specimen was of rectangular shape, 8 mm × 2 mm × 1.5 mm. It was placed with its long axis between the pole faces of a simple electromagnet and it was first saturated by the application of a field of some 200 oersteds. An examination by the powder deposit technique (cf. Bates and Neale 1950), showed by the absence of powder patterns upon the surface that the crystal was a single domain. The applied magnetic field was thereupon slowly reduced to zero and then increased again in the reverse sense. The domain structure recorded by powder patterns on the surface of the specimen was examined as the half-cycle of magnetization was traversed.

§ 3. EXPERIMENTAL RESULTS

(i) *The Role of Surface Imperfections*

The first indication of departure from the single domain condition was the appearance of closure domains at imperfections in the surface. At first they were very small, but they increased in size as the field was reduced until, when the effective field acting in the crystal was approximately zero, they were of the

size generally recorded in the literature, as for example, by Bates and Mee (1952). They consisted entirely of domains magnetized at 90° to the original direction of saturation. Closure domains had formed, in some cases at what appeared to be extremely small imperfections, so small that the latter were revealed only by the clouds of colloid which always collect at surface imperfections. Further growth of closure structures occurred when the effective field was reversed. The subsequent changes in domain structure as the cycle was further traversed were photographed, and selected pictures are reproduced in fig. 1 (Plate I).

Figure 1(a) shows the closure structure at a large imperfection when a small reverse field acted. Figure 1(b) shows how the structure increased in size with increase in the reverse field. On still further increasing this field a new phenomenon, shown clearly in 1(c), was recorded. It is seen that a breakdown of a 90° closure domain has occurred with the formation of a new structure running upwards from one side of a closure domain, and it is obvious from the nature of the powder deposits that the new structure is magnetized in the opposite sense to the initial saturation direction. Incidentally, the new structure is found in a region of some slight surface imperfection. A small increase in the field brought about considerable growth of the reverse domain, as we shall now call this structure, and (d) together with the composite photograph 1(e) show the changes which occurred for an increase in field of only an oersted or so. In the upper part of 1(e) other reverse domains are seen, including the base of a very large one situated in the upper left-hand corner.

The sudden break-up of a pattern such as that of fig. 1(b) following upon a very small increase in the reverse field and, when the pattern has reformed, the appearance of a structure similar to that in 1(c) seem to indicate that an irreversible process is concerned in the creation of reverse domains.

On increasing the field from that of fig. 1(e), one finds that two or three reverse domains fuse and that the one large domain so formed gradually extends along the length of the crystal and pushes its boundaries sideways. The remaining domains of reverse magnetization decrease in size and finally disappear as the boundaries of the large reverse domain approach them. Eventually the whole crystal surface becomes one domain except for a few closure structures which persist at imperfections. Further increases in the field cause the latter domains to diminish in size and finally to disappear, when we then have the specimen saturated in the reverse direction.

Experiments were also made upon a specimen in which the demagnetizing field was deliberately made non-uniform. This was done by cutting a niche in one corner of the crystal as shown in fig. 2. The patterns now obtained were more simple, and in our view showed the process of formation rather more clearly. The crystal was magnetically saturated as before, and on reducing the magnetizing field the first breakdown in the domain structure occurred at the imperfections around the cut edge, although the field for the rest of the specimen was still of appreciable magnitude. These patterns grew fairly rapidly as the half-cycle was further traversed, and they spread well into the rest of the crystal surface and were there markedly developed before closure structures around 'local' imperfections in the main surface became of appreciable size. Figure 2 shows in a diagrammatic way how these large closure structures spread from the edge. They contained only domains magnetized at 90° to the direction of initial saturation.

In fig. 3 (Plate II) are given a number of photographs which represent these phenomena and the subsequent appearance of reverse domains. Starting with 3(a), which shows the large closure domains in the main surface, we pass to 3(b), where on the right-hand side the formation of a domain of reversed magnetization is noted. This is seen as a trapezium-shaped figure; a small reverse field was acting when this picture was obtained. Figure 3(c) shows how the reverse domain grew with additional increase in field. 3(d) shows a further breakdown of a 90° closure domain on the left-hand side of the picture.

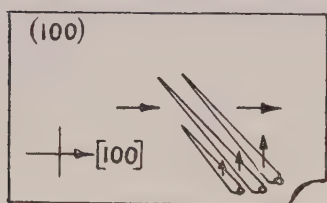


Fig. 2. Illustrating origin of large closure domains.

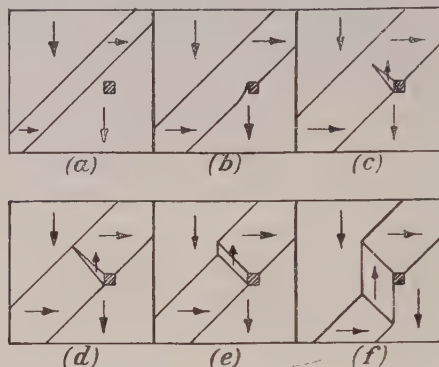


Fig. 5. Suggested mode of formation of domains of reverse magnetization.

A large-scale breakdown has occurred outside and to the left of photograph 3(e) so that the boundary of the resulting large reverse domain is seen in the photograph. Finally, 3(f) shows a further increase in the size of this domain, and one notes the rather clear-cut 180° boundary running almost from top to bottom of the picture.

(ii) *The Role of the End Faces and the Edges of the Crystal*

(a) *The end faces.* At an early stage in the half-cycle of magnetization 90° closure domains appear at both ends of the crystal, which thus act as the boundaries of large imperfections. The type of structure as seen on the surface under observation is illustrated in fig. 4(a), and it acts as a source of reverse domains in a similar way to the 90° closure structures at imperfections as described in §2(i) above.

The 'zigzag' boundaries which are seen in those parts of the surface near the ends of the crystal, particularly when the specimen is magnetically on open circuit, i.e. with gaps between pole faces and specimen, are believed to be associated with 90° closure domains which originate as shown in fig. 4(c) within the end faces of the crystal. The 'zigzag' boundaries photographed in fig. 4(b) ought then to arise from the creation of subsidiary closure domains when the 90° closure structures, growing with change of field in the usual way, reach a surface of the specimen as depicted in fig. 4(c). It will be seen that the subsidiary closure domains are in fact reverse domains, but except when the crystal is on pronounced open circuit, i.e. with large gaps between pole faces and specimen, they are too few in number to play a major role in the demagnetization process.

(b) *The edges.* Some of the 90° closure domains, of the type considered in §2(i), which form at imperfections around the lateral edges of the surfaces,

strike the edges when they grow with change in field, and presumably form subsidiary closure domains like those drawn in fig. 4(d). This would explain the occasional appearance of 'zigzag' boundaries close to the lateral edges of the surface under observation; and, indeed, the fusing of several large reverse domains, as described in §2(i), does in general take place very close to a lateral edge, where the reverse domains described in §2(i) occur in the two adjacent surfaces as well as the type of reverse domain described in this section.

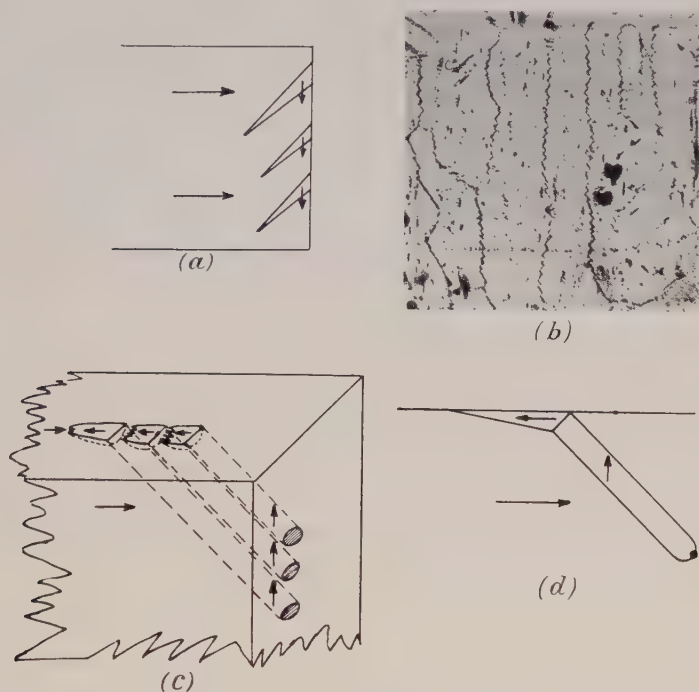


Fig. 4. The role of the end faces and edges of a crystal (diagrams not to scale).

§ 4. DISCUSSION OF RESULTS

The question at once arises, do any large reverse domains form within the body of the crystal? One can only say that it appears improbable, in the absence of any effect on the surface patterns. The next question which arises is, how deep are those domains whose patterns are observed in the surface? The closure domains which form at imperfections must be surface phenomena, and the reverse domains when they first appear are part of these surface structures. As these reverse domains increase in length and breadth, however, it is reasonable to assume that they also increase considerably in depth, eventually to occupy the whole crystal. We intend to repeat these experiments with a crystal of pure iron and to attempt to measure changes in magnetization at the same time as we observe the changes in domain structure. This will then provide a better experimental answer to the questions posed above.

The mechanism of the formation of closure domains around imperfections is perhaps fairly well known, but we must now attempt to explain how reverse domains are initially formed. The true method of formation is not sufficiently clear from the photographs owing to the difficulty of recording the rapid processes which apparently take place when a domain of reverse magnetization is created.

A tentative scheme of formation is put forward in fig. 5. Diagram 5(a) represents a closure domain similar to those in fig. 3(a). This closure domain expands on increase in the reverse field; its boundary encounters an imperfection and is momentarily held up as shown in 5(b). A further increase in field results in the situation depicted in (c) with the irreversible creation of a domain of reverse magnetization at the imperfection. Under the action of the (reverse) field this domain grows rapidly as shown in (d), (e) and (f). Comparison may be made with the structures in fig. 3, especially with those near the left-hand edge of 3(c).

An alternative method of formation could be that pictured by Dijkstra if we suppose that the critical field necessary to initiate the rotation is considerably reduced in the neighbourhood of an imperfection. The stray fields in the vicinity of a boundary of a closure domain, due to the presence of some free poles on these boundaries, may supplement the reverse field to provide the necessary critical field. In fig. 3, photographs (d) and (e) show in the upper right-hand corner the formation of a new reverse domain apparently starting from a small imperfection close to, but independent of, a large closure domain.

§ 5. CONCLUSIONS

It is therefore seen that surface imperfections play an extremely important part in domain formation. We have known for a long time of their importance in the formation of purely closure domain structures, but in this communication is stressed their importance in the formation of domains of reverse magnetization which permit a specimen to be demagnetized by very small fields. In other words the difficulties which Brown encountered in trying to explain how an ideal, saturated crystal could eventually become demagnetized do not exist in the case of a crystal in which there are surface imperfections. It is interesting, if not profitable, to speculate what degree of imperfection is necessary to provide a material with minimum hysteresis loss. For the problem considered here is but one example of domain processes which cannot be described in terms of simple boundary displacement and rotation of domain magnetization vectors alone. The creation of new domains, a process which appears to be necessary in each of these cases, might well be expected to contribute to hysteresis effects.

ACKNOWLEDGMENTS

One of us (D. H. M.) is indebted to the Department of Scientific and Industrial Research for a maintenance grant which made this work possible. The crystal was cut from an ingot kindly provided by Dr. Shoenberg of the Cavendish Laboratory.

REFERENCES

- BATES, L. F., and MEE, C. D., 1952, *Proc. Phys. Soc. A*, **65**, 129.
- BATES, L. F., and NEALE, F. E., 1950, *Proc. Phys. Soc. A*, **63**, 374.
- BROWN, W. F. JR., 1945, *Rev. Mod. Phys.*, **17**, 15.
- DIJKSTRA, L. J., 1950, *Thermodynamics in Physical Metallurgy* (Cleveland: American Society for Metals), p. 271.

Further Measurements of the Ionization by Energetic Cosmic-Ray μ -Mesons

By B. T. PRICE*, D. WEST*, J. BECKER†, P. CHANSON†,
E. NAGEOTTE† AND P. TREILLE†

* Atomic Energy Research Establishment, Harwell, Berks.

† Centre National de la Recherche Scientifique, France

Communicated by W. J. Whitehouse; MS. received 22nd October 1952

ABSTRACT. The most probable specific ionization of energetic μ -mesons has been measured as a function of momentum, using proportional counters filled with a neon-methane mixture. The results confirm previous measurements, and are in good agreement with the theoretically predicted increase of specific ionization at high momenta.

§ 1. INTRODUCTION

THE experiment described below is a continuation of the work, on the ionization of relativistic μ -mesons, already reported by Becker *et al.* (1952, to be referred to as I). In that article the problems of using proportional counters for such measurements were discussed at some length. In particular, the difficulties caused by the existence of fluctuations in the rate of ionization (Landau 1944) were considered, and a summary was given of a method (Behrens 1951) which had been found useful in the statistical treatment of the results.

The aim of the present experiment (which, like the previous work, was performed at the Aiguille du Midi laboratory), was to extend the technique of ionization measurement by means of proportional counters to something approaching its practical limit. Considerable changes were therefore made in details, although the main layout of the earlier experiment was retained. The experiment consisted of measuring simultaneously the momenta and ionization of cosmic-ray mesons, using a cloud chamber in a magnetic field and proportional counters respectively. The rate at which information was collected was increased by having four separate counters, each giving an independent measurement for every particle. A change was made in the filling of the counters, since very large ionization fluctuations had been observed in the krypton counters used for the earlier work. There were reasons for expecting these fluctuations to be smaller—and the ionization resolution to be correspondingly better—in counters filled with light gases (I; Rothwell 1951). A neon-methane mixture was therefore used in the present experiment and was found to give a worth while increase in accuracy. Finally, an anti-coincidence array was installed around the proportional counters to minimize the effect of side showers.

The net effect of these modifications was to increase the accuracy of measurement by a factor of about 2.5.

§ 2. EXPERIMENTAL ARRANGEMENT

The apparatus used is sketched in fig. 1. A lead filter, to cut out the soft component, was placed above the apparatus, and the beam of cosmic-ray particles was defined by counter trays A, B and C. Between A and B the four rectangular proportional counters were mounted in a vertical stack in such a way that the beam passed through all of them. The effect of the accidental passage through the counters of any unwanted particles which happened to be coincident with an $(A+B+C)$ event was minimized by two rows of guard counters G. Events of the type $(A+B+C+G)$ were rejected.

The cloud chamber, situated between trays B and C, was in the field (3000 gauss) of a large electromagnet, the curved coilformers of which are shown. This assembly enabled momenta of up to 5×10^9 ev/c to be measured. Both the operation of the cloud chamber and the recording of the counter pulses were controlled by triple coincidences of the telescope.

The dimensions of the counters were as follows: useful length 25 cm, mean internal depth in the direction of the beam 7.0 cm, width 9 cm (the width of the beam being 7 cm). They were filled with a mixture of 20.5 cm Hg of neon, 20.5 cm Hg of methane and 1.6 cm Hg of krypton (at 20°C), the trace of krypton being added to facilitate calibration with x-rays.

Energy calibrations of the counters were regularly carried out, using x-rays from radio-isotopes (Rothwell and West 1950). Particular reliance was placed on the calibration given by the K x-rays from ^{51}Cr , since the energy (5.0 kev) was close to the most probable energy loss measured in the course of the experiment.

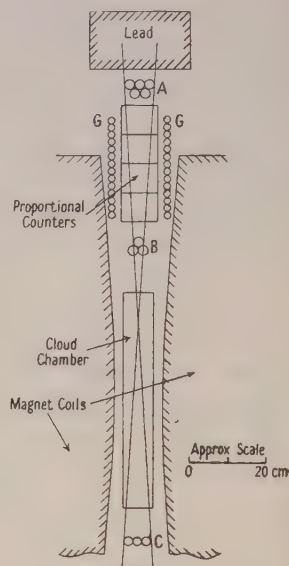


Fig. 1. Experimental arrangement.

§ 3. SELECTION OF PARTICLES

Of the particles classified as $(A+B+C-G)$ events, only those were selected which appeared from the cloud-chamber photographs to be unaccompanied by other coincident particles, and, of these, the negative particles only were used for those momenta ($p > 550$ mev/c) where the presence of protons might affect the result. (It was not, of course, possible to make such a selection for the unresolved group of high-energy particles.) The particles were grouped into the six momentum categories indicated in the table (§ 5).

The majority (85%) of the particles finally selected were μ -mesons (I). The remainder were mostly π -mesons, which since they do not differ greatly in ionization properties from μ -mesons, introduce an error of less than one per cent.

§ 4. OBSERVATIONAL UNCERTAINTIES

(i) Ionization Measurement

The principal uncertainty in the measurement of the most probable ionization is due to the large fluctuations in the rate of ionization from point to point along the track of the particle (I; Landau 1944, Blunck and Leisegang 1950). As a result of these fluctuations, measurements in the same counter, of particles of the same nature and energy, show a broad distribution, which

has a 'tail' on the high-energy side. The histograms of fig. 2 show the effect very clearly for the six momentum groups.

Because of the width of the distribution, the rather small number of observations, and the small effect being investigated, it is necessary to use some objective statistical method for evaluating the most probable ionization for each group. Use was again made of Behrens' method (see I) by which a peaked curve can be fitted to the histograms*, allowing the position of the maximum, and hence the most probable ionization, to be determined with considerable accuracy. The curves used for this purpose were those given by Rothwell (1951) for the energy loss of 2 Mev electrons in krypton, neither experimental nor theoretical values for the distribution in a neon-methane mixture being available. However, the method allows both the position of the maximum, and the horizontal scale (determining the width of the curve) to be independently varied to give the best fit. The position of the maximum is, in fact, very insensitive to the exact shape of the curve which is fitted to the observations.

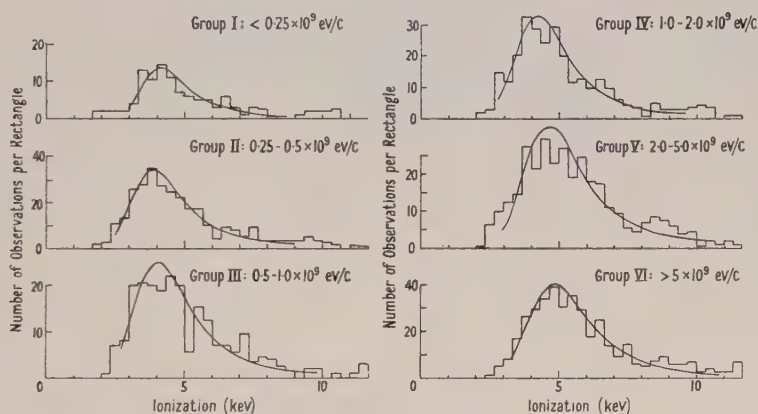


Fig. 2. Experimental ionization distributions for the six momentum groups.

This method of curve-fitting makes use not only of observations close to the peak, but also those lying in the high-energy tail. However, with the gain setting necessary to observe the peak satisfactorily, saturation in the apparatus limits the extent to which this tail can be observed; relatively more is observable the smaller the value of the most probable ionization. Thus, if all the observations—up to the saturation value—were used for the computation of the most probable ionization for each group, the result would be to reduce the apparent increase of ionization with momentum. To avoid introducing an effect of this kind we have applied a cut-off at a value 2.4 times the most probable ionization for each group. This figure is the ratio of the saturation ionization to the most probable ionization of the highest momentum group (VI). (The most probable ionization was in each case determined by successive approximation.) Computations made with this restriction should then yield the correct relative values of the most probable ionization for the various groups, provided the shape of the distribution is the same for each; within the rather

* The widths of the histogram rectangles were chosen so that no appreciable error was introduced by the grouping of the results.

poor statistical accuracy this appears to be true. The correction introduced by this procedure is largest for Group II (minimally ionizing mesons), for which it amounts to 1.1% (43 ev). It decreases with increasing ionization, becoming zero for Group VI.

Since the errors in the measurement of the ionization are small, the final accuracy of the experiment depends almost entirely upon the accuracy of the curve-fitting procedure. The approximations dealt with above may have introduced a small but regular shift of the maximum from the true position; this possibility should be borne in mind when comparing the experimental values with the theoretical curves.

(ii) *Momentum Measurement*

The error in the determination of the momentum p of an individual particle was such that the standard deviation of $1/p$ was 0.2, when p was in units of 10^9 ev/c. Examination of the effect of such errors on the grouped results shows that they are unimportant except in the case of the 'unresolved group' (VI), for which the effective momentum is calculated to be approximately 6.5×10^9 ev/c. This value was obtained by first calculating what was the real momentum spectrum of the particles 'observed' as having momenta greater than 5×10^9 ev/c; a theoretical ionization distribution for the group was then synthesized, and was found to have a most probable value equal to that assumed for monoenergetic μ -mesons of true momentum 6.5×10^9 ev/c. The assumptions used in this calculation were that the true momentum followed the sea-level distribution, and that effects due to the polarization plateau were unimportant. Both these assumptions would tend to make the value found for the effective momentum an overestimate, but the error cannot be large, since the corresponding calculation for Group V gave good agreement with the observed mean momentum.

§ 5. RESULTS

The following table gives the results obtained from the histograms of fig. 2 by the curve-fitting procedure.

(1)	(2)	(3)	(4)	(5)	(6)	(7)
I	< 0.25	0.185	+, -	(a) 33 (b) 113	4.15 ± 0.12	48 ± 6
II	0.25-0.50	0.39	+, -	(a) 85 (b) 298	3.92 ± 0.07	57 ± 4
III	0.50-1.0	0.75	-	(a) 63 (b) 226	4.07 ± 0.09	60 ± 4
IV	1.0-2.0	1.38	-	(a) 80 (b) 290	4.25 ± 0.08	55 ± 4
V	2.0-5.0	3.05	-	(a) 98 (b) 323	4.65 ± 0.08	56 ± 4
VI	> 5.0	(See § 4 (ii))	+, -	(a) 115 (b) 397	4.89 ± 0.08	52 ± 4

(1) Group number; (2) limits of observed momenta (10^9 ev/c); (3) mean observed momentum for group (10^9 ev/c); (4) sign of particles; (5) number of (a) particles, (b) ionization observations included in histograms; (6) Δ (kev); (7) percentage width of distribution at half height.

In the above table Δ is the most probable ionization, determined as described in § 4 (i), produced by the particles in the 7 cm path length in the counters. The errors given in the last two columns are standard deviations.

The average of the widths given in the last column is smaller by a factor of 1.5 than that for the krypton-filled counter used in earlier experiments; in both cases approximately the same energy—4 kev for minimally ionizing mesons—was expended in the counters.

§ 6. COMPARISON OF RESULTS WITH THEORY

A theoretical value of the most probable ionization has been given for pure gases by Landau. The authors are indebted to J. S. Bell (private communication) for an extension of Landau's work covering the case of mixtures; we reproduce his result for the convenience of readers. For a mixture of gases the most probable energy loss by ionization Δ_0 is given in electron volts by the equation

$$\Delta_0 = \sum_i \eta_i (c/v)^2 \{ \log [5.5 \times 10^5 \eta / (13.5 Z_i)^2 (1 - v^2/c^2)] + 1 - v^2/c^2 \}$$

where $\eta_i = 1.54 \times 10^5 \mu_i Z_i / A_i$; $\eta = \sum_i \eta_i$ and μ_i is the mass per unit area of the i th constituent. This formula differs from a straightforward addition of the most probable values of the energy loss in the individual components of the mixture by having the term η under the logarithm instead of η_i .

Below 10^{10} ev/c polarization corrections to this formula (Swann 1938, Fermi 1940) should be unimportant. It has therefore been used in calculating the full line curve of fig. 3, in which the theoretical values are compared with the experimental results. The broken curve in the same figure was obtained by substituting for the value of $13.5 Z_i$ ev used by Landau for the average ionization potential I of atomic electrons, values based on the work of Bakker and Segrè (1951). These authors quote experimental results for a number of elements, including carbon and hydrogen; their results show a fairly regular

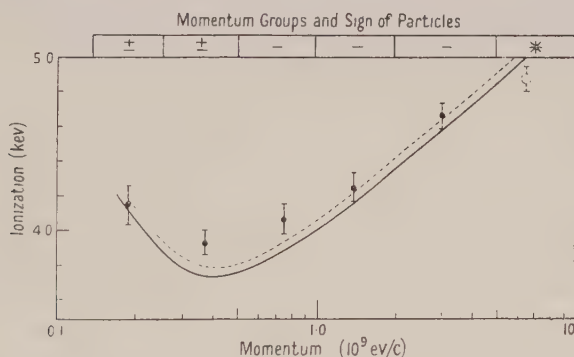


Fig. 3. Comparison of experimental results with theory. Solid curve: calculated from Landau's theory; Dotted curve: obtained by substituting in Landau's theory experimental values for average ionization potential (§ 6).

* The effective momentum for the unresolved group was obtained by calculation (§ 4 (ii)). For the other groups the points are plotted at the mean observed momenta.

dependence on Z so that, although no value is given for neon, a reasonably accurate figure can be obtained by interpolation between carbon and aluminium. The use of the more recent values for the average ionization potential gives better agreement between theory and experiment.

The dotted curve and the experimental points (excluding that for Group VI, for which the momentum accuracy is poor) have been compared by means of the χ^2 test. A probability of 0.29 was obtained, which is within the limits (0.1 to 0.9) usually regarded as denoting satisfactory agreement. We conclude, therefore, that Landau's formula, with the modification mentioned above, gives the correct value for the most probable ionization for relativistic μ -mesons.

This conclusion, like that of our earlier experiment, is supported by the recent work of Ghosh, Jones and Wilson (1952), of Kupperian and Palmatier (1952) and of Carter and Whittemore (1952).

ACKNOWLEDGMENTS

The authors wish to thank Mr. W. J. Whitehouse, Dr. H. G. Hereward, and Mr. D. J. Behrens for the benefit of their advice, and M. M. Reposeur and Mr. F. Bradley for their assistance in the laboratory. Two of us (B. T. P. and D. W.) are indebted to Professor LePrince-Ringuet for his invitation to collaborate in the work, and to Sir John Cockcroft (Director, Atomic Energy Research Establishment), Dr. E. Bretscher and Dr. J. V. Dunworth for making the collaboration possible.

REFERENCES

- BAKKER, C. J., and SÈGRÈ, E., 1951, *Phys. Rev.*, **81**, 489.
BECKER, J., CHANSON, P., NAGEOTTE, E., TREILLE, P., PRICE, B. T., and ROTHWELL, P., 1952, *Proc. Phys. Soc. A*, **65**, 437.
BEHRENS, D. J., 1951, A.E.R.E. Report T/M 50 (H.M.S.O. code 70-674-0-42).
BLUNCK, O., and LEISEGANG, S., 1950, *Z. Phys.*, **128**, 500.
CARTER, R. S., and WHITTEMORE, W. L., 1952, *Phys. Rev.*, **87**, 494.
FERMI, E., 1940, *Phys. Rev.*, **57**, 485.
GHOSH, S. K., JONES, G. M. D. B., and WILSON, J. G., 1952, *Proc. Phys. Soc. A*, **65**, 68.
KUPPERIAN, J. E., and PALMATIER, E. D., 1952, *Phys. Rev.*, **85**, 1043.
LANDAU, L., 1944, *J. Phys., U.S.S.R.*, **8**, 201.
ROTHWELL, P., 1951, *Proc. Phys. Soc. B*, **64**, 911.
ROTHWELL, P., and WEST, D., 1950, *Proc. Phys. Soc. A*, **63**, 541.
SWANN, W. F. G., 1938, *J. Franklin Inst.*, **226**, 598.

Electron Capture

II: Resonance Capture from Hydrogen Atoms by Slow Protons

By A. DALGARNO* AND H. N. YADAV†

* Department of Applied Mathematics, Queen's University, Belfast

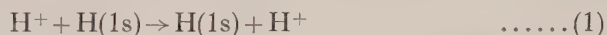
† University College, London (now at Department of Physics, Patna University, India)

Communicated by D. R. Bates; MS. received 9th September 1952

ABSTRACT. The cross sections for resonance electron capture from hydrogen atoms by protons of incident energy up to 100 kev are calculated theoretically using the Perturbed Stationary State method and a comparison is made with the results of the Born approximation both with and without neglect of momentum transfer.

§ 1. INTRODUCTION

LITTLE quantitative information is available on the cross sections associated with the various types of heavy particle collisions though many of these are important for an understanding of a wide range of atmospheric and discharge tube phenomena. In paper I (Bates and Dalgarno 1952) one of the simplest of such processes, resonance capture



was investigated using the Born approximation. There are no experimental data with which a reliable comparison can be made so that to determine the range of applicability of the approximation it is desirable that the reaction be examined using a theoretical treatment designed specifically for low energy collisions. The Perturbed Stationary States method (P.S.S. method) is the most suitable (cf. Mott and Massey 1949a) for such collisions giving reliable results for velocities up to at most the orbital velocity of the bound electron. It is used in the present paper to evaluate the cross section of the reaction (1) for incident protons in the energy range 0–10 kev.

§ 2. THEORY

A detailed description of the P.S.S. method has been given recently by Bates, Massey and Stewart (1952) so that only a brief account will be presented here. Essentially the system is regarded as being in equilibrium with the two protons at rest and the relative motion of these is then introduced as the perturbation causing the charge transfer transition. If $\Psi(\boldsymbol{\rho}, \mathbf{R})$ is the wave function of the system, $\boldsymbol{\rho}$ being the position vector of the electron and \mathbf{R} that of one proton relative to the other, then taking account of only the two states which result from the initial states of the atoms when the two approach each other adiabatically, we may expand

$$\Psi(\boldsymbol{\rho}, \mathbf{R}) = X^+(\boldsymbol{\rho}, \mathbf{R})F^+(\mathbf{R}) + X^-(\boldsymbol{\rho}, \mathbf{R})F^-(\mathbf{R}) \quad \dots\dots(2)$$

where X^+ and X^- are wave functions describing the behaviour of the electron when the two protons are at a fixed distance R apart, the former being symmetrical,

the latter antisymmetrical in the nuclei. Substituting the expansion (2) in the Schrödinger equation for the entire system, two coupled equations for F^+ and F^- are obtained

$$\left. \begin{aligned} \{\nabla_R^2 + k^2 - \epsilon^+(\mathbf{R})\} F^+(\mathbf{R}) &= -\nabla_R F^-(\mathbf{R}) \int X^{+*}(\boldsymbol{\rho}, \mathbf{R}) \nabla_R X^-(\boldsymbol{\rho}, \mathbf{R}) d\boldsymbol{\rho} \\ \{\nabla_R^2 + k^2 - \epsilon^-(\mathbf{R})\} F^-(\mathbf{R}) &= -\nabla_R F^+(\mathbf{R}) \int X^{-*}(\boldsymbol{\rho}, \mathbf{R}) \nabla_R X^+(\boldsymbol{\rho}, \mathbf{R}) d\boldsymbol{\rho} \end{aligned} \right\} \dots\dots (3)$$

where \mathbf{k} is the wave vector of the initial relative motion and $\epsilon^+(R)$, $\epsilon^-(R)$ are the interaction energies of the $1s\sigma$ and $2p\sigma$ states of the H_2^+ molecule described respectively by the wave functions X^+ and X^- . We require solutions of eqns. (3) with asymptotic forms

$$\begin{aligned} F^+(\mathbf{R}) &\sim \frac{1}{\sqrt{2}} [\exp(i\mathbf{k}\mathbf{n} \cdot \mathbf{R}) + R^{-1} f^+(\Theta) \exp(ikR)] \\ F^-(\mathbf{R}) &\sim \frac{1}{\sqrt{2}} [\exp(i\mathbf{k}\mathbf{n} \cdot \mathbf{R}) + R^{-1} f^-(\Theta) \exp(ikR)] \end{aligned}$$

Θ being the angle through which the direction \mathbf{n} of relative motion is turned by the impact. The cross section for elastic scattering with charge exchange is

$$Q = \frac{1}{4} \int \int |f^+ - f^-|^2 \sin \Theta d\Theta d\Phi.$$

Bates, Massey and Stewart (1952) have shown that the coupling terms on the right-hand sides of eqns. (3) may be neglected so that we may take

$$Q = \frac{\pi}{k^2} \sum_{l=0}^{\infty} (2l+1) \sin^2(\eta_l^+ - \eta_l^-) \dots\dots (4)$$

where η_l^+ and η_l^- are such that the asymptotic forms of the solutions g_l^+ , g_l^- of the equations

$$\frac{d^2}{dR^2} g_l^{+-} + \left(k^2 - \frac{2M}{\hbar^2} \epsilon^{+-}(R) - \frac{l(l+1)}{R^2} \right) g_l^{+-} = 0$$

which are zero at the origin are given by

$$g_l^{+-} \sim k^{-1} \sin(kR - \frac{1}{2}l\pi + \eta_l^{+-}).$$

Determination of the Phase Shifts and Summation of the Series

Accurate values of $\epsilon^+(R)$ and $\epsilon^-(R)$ for R up to $9a_0$ are known from the work of Bates, Ledsham and Stewart (1952).^{*} Though some values for greater R have been calculated by Hylleraas (1931) these are at irregular and rather wide intervals so that it is inconvenient to use them. Instead we adopted the Heitler-London approximation (Heitler and London 1927) which gives

$$\epsilon^{+-}(R) = \frac{2}{R} + \frac{-2/R + 2\{e^{-2R}(1+1/R) - e^{-R}(1+R)\}}{1 + e^{-R}(1+R+R^2/3)} \dots\dots (5)$$

to which was added the second-order perturbation term (Coulson 1941)

$$-\frac{9}{4R^4} - \frac{15}{2R^6} - \frac{213}{4R^7} - \frac{7755}{64R^8} - \frac{1773}{2R^9} - \frac{86049}{16R^{10}} - \dots\dots (6)$$

the energy being measured in rydbergs. A comparison between the values given by the sum of (5) and (6) and the accurate values of Bates *et al.* and of Hylleraas is made in table 1. It is apparent that the error entailed by the use of the

^{*} Our thanks are due to Professor D. R. Bates, Mrs. K. Ledsham and Mr. A. L. Stewart for allowing us the use of their results before publication.

approximate values for R greater than $9a_0$ is trivial, noting that it is the difference between $(\epsilon^-)^{1/2}$ and $(\epsilon^+)^{1/2}$ which is of importance for the determination of the cross section.

The phase shifts were computed using Jeffreys' formula with the Langer modification (cf. Mott and Massey 1949 b)

$$\eta_l^{+,-} = \int^{\infty} \left\{ k^2 - \frac{2M}{\hbar^2} \epsilon^{\pm}, (R) - \frac{(l + \frac{1}{2})^2}{R^2} \right\}^{1/2} dR - \int^{\infty} \left\{ k^2 - \frac{(l + \frac{1}{2})^2}{R^2} \right\}^{1/2} dR$$

where the lower limit of each integral is at the zero of the integrand. The accuracy of this approximation should be ample especially since in $\eta_l^+ - \eta_l^-$ the errors of the individual phases should partially cancel.

Table 1. The Interaction Potentials of the $1s\sigma$ and $2p\sigma$ States of H_2^+ (in rydbergs)

$1s\sigma$			$2p\sigma$		
$R (a_0)$	Accurate	Approximate	$R (a_0)$	Accurate	Approximate
7.0	-0.01119	-0.01032	7.0	0.00745	0.00619
8.0	-0.00514	-0.004703	8.0	0.00279	0.00229
9.0	-0.00239	-0.002218	9.0	0.00091	0.000711
9.043	-0.00169		9.053	0.00084	
10		-0.001076	10		0.000117
11		-0.000565	11		-0.000082
11.039	-0.00059		11.041	-0.00008	
12		-0.0003233	12		-0.0001288
13		-0.0002017	13		-0.0001241
13.034	-0.00020		13.035	-0.00012	
14		-0.0001358	14		-0.0001050
15		-0.0000971	15		-0.0000849

The number of phase shifts that contribute to the cross section ranges from about one hundred to several thousand as the energy of the incident proton increases from 1 eV to 10 keV. The series expression (4) for Q was evaluated by splitting it into two parts, averaging the first part and replacing the second part by an integration (cf. Buckingham and Dalgarno 1952).

§ 3. RESULTS AND DISCUSSION

The cross sections for electron capture derived by the P.S.S. method are given in table 2 for energies up to 100 keV, the value at the highest energy being obtained by extrapolation (assuming the third difference to be zero). As is usual for such reactions the cross section at low energies is rather larger than the gas-kinetic cross section.

Table 2. Cross Section for Electron Capture derived by the P.S.S. Method (in units πa_0^2)

$\log (\text{energy}) (\text{eV})$	0	1	2	3	4	5
$Q (\pi a_0^2)^*$	53.7	40.7	29.1	18.8	9.8	2.1†

* $\pi a_0^2 = 8.8 \times 10^{-17} \text{ cm}^2$

† The value of 2.1 was obtained by extrapolation

In table 3 the values of the impact parameter p for which the probability of electron transfer (cf. Bates, Massey and Stewart 1952) first attains the values 1 , $\frac{1}{2}$ and $\frac{1}{4}$ are given. It is noteworthy that as the incident energy increases the probability of electron transfer for other than head-on collisions steadily decreases.

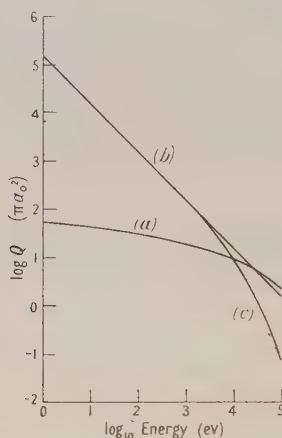
A comparison of the P.S.S. values with those obtained using the Born approximation (Bates and Dalgarno 1952) both with and without neglect of momentum transfer is made in the figure. As would be expected the P.S.S. curve lies below the less accurate Born curve at small energies. It may be

Table 3. The Largest Parameters* p for which the Probability of Electron Transfer is 1, $\frac{1}{2}$, $\frac{1}{4}$

Energy of incident proton (ev)		1	10	100	1000	10000
		p (in units of a_0)				
Probability of electron transfer	{ 1	8.5	7.2	5.7	3.9	2.0
	{ $\frac{1}{2}$	9.3	7.9	6.6	5.0	3.2
	{ $\frac{1}{4}$	9.9	8.3	7.1	5.5	3.7

* For values of the impact parameters between zero and the values for a probability of unity given in the table the probability of electron transfer oscillates rapidly between 0 and 1.

mentioned that the cross sections obtained by Brinkman and Kramers (1930) from a simplified Born approximation (in which one term of the interaction is neglected) are larger, and therefore more seriously in error than the cross sections obtained from the true Born approximation.



Curve (a) : Q derived by the P.S.S. method.

Curve (b) : Q derived by the Born approximation ignoring momentum transfer.

Curve (c) : Q derived by the Born approximation taking account of momentum transfer.

The considerable importance at high energies of momentum transfer, ignored by the P.S.S. method, in reducing cross sections is clearly shown by curves (b) and (c) of the figure. These curves which differ only in that (b) (like the P.S.S. method) neglects, whilst (c) includes, momentum transfer begin to diverge at energies of some 2 kev. This is therefore the upper limit to the energy for which the P.S.S. method gives accurate results.

It may be shown by an analysis similar to that indicated by Bates, Massey and Stewart (1952) for direct scattering that if the interaction between the colliding particles is sufficiently weak the P.S.S. method reduces for high energies, in the case of exchange scattering, to the Born approximation with neglect of momentum transfer. From examination of the figure it appears likely that the P.S.S. curve and the curve obtained using the Born approximation

ignoring momentum transfer do tend to the same values at high energies indicating that the effective interaction is sufficiently weak for the true Born approximation, taking account of momentum transfer, to be useful for incident energies above about 10 keV and to be reliable for incident energies above about 100 keV.*

ACKNOWLEDGMENTS

We are greatly indebted to Professor D. R. Bates and to Professor H. S. W. Massey for their encouraging interest in this work.

REFERENCES

- BATES, D. R., and DALGARNO, A., 1952, *Proc. Phys. Soc. A*, **65**, 919.
 BATES, D. R., MASSEY, H. S. W., and STEWART, A. L., 1952, *Proc. Roy. Soc. A*, in the press.
 BATES, D. R., LEDSHAM, K., and STEWART, A. L., 1952, in the press.
 BRINKMAN, H. C., and KRAMERS, H. A., 1930, *K. Wet. Amst.*, **33**, 973.
 BUCKINGHAM, R. A., and DALGARNO, A., 1952, *Proc. Roy. Soc. A*, **213**, 506.
 COULSON, C. A., 1941, *Proc. Roy. Soc. Edin. A*, **61**, 20.
 HEITLER, W., and LONDON, F., 1927, *Z. Phys.*, **44**, 455.
 HYLLERAAS, E., 1931, *Z. Phys.*, **71**, 739.
 MOTT, N. F., and MASSEY, H. S. W., 1949 a, *Theory of Atomic Collisions*, 2nd edn. (Oxford: Clarendon Press), p. 153; 1949 b, *Ibid.*, p. 127.

* When the energy of the incident proton is 10 keV and 100 keV, the velocity of relative motion is respectively about 0.5 and 1.5 times the orbital velocity of the electron.

The Theory of the Thomas-Fermi Electron Density*

By J. S. PLASKETT

H. H. Wills Physical Laboratory, University of Bristol

Communicated by N. F. Mott; MS. received 3rd September 1952

ABSTRACT. A new modification of the Thomas-Fermi formula is derived which is similar to Weizsäcker's; this provides what is claimed to be a more plausible proof than usual of the Thomas-Fermi method. The method is applied to give a non-divergent relativistic approximation for $Z < 137/2$ and is used to demonstrate the incorrectness of the Thomas-Fermi-Dirac equation based on Foch's equations. Slater's approximation to Foch's equations is used to derive a Thomas-Fermi equation with exchange only differing from Dirac's by a change in Z . The solutions of this equation are re-interpreted and shown to be not unique, though always giving a positive electron density.

§ 1. INTRODUCTION

THE Thomas-Fermi method has been used to obtain approximate values for the electron density, the total energy, and the momentum distribution function, of many-electron problems. It is possible to regard the method as being based on two fundamental assumptions.

(1) A classical approximation to quantum mechanics, e.g. equal volumes of phase space are equally probable (Thomas 1927, Fermi 1928), position and momentum commute (Dirac 1930), the introduction of cells with impenetrable walls (Lenz 1932), the use of hydrostatic considerations (Chandrasekhar 1934), or the use of B.W.K. wave functions inside the classical region (Brillouin 1934).

(2) Reduction of the many-electron problem to a one-electron problem, for instance by Hartree's symmetrized equations, i.e. the equations obtained when it is assumed that an electron moves in its own field as well as in the field of the other electrons, or by Foch's equations. These are non-relativistic approximations; similar relativistic approximations are possible.

The necessity for assumption (2) is that the classical approximation of assumption (1) can only deal with one-electron problems—at any rate in the first instance.

The original consequence of assumption (1) (cf. for example Thomas's assumption 3) is what we shall call the simple Thomas-Fermi formula:

$$\sum |\psi_i|^2 \simeq \frac{1}{h^3} \frac{4\pi}{3} [2m(E' - V)]^{3/2},$$

if $(-h^2/2m)\nabla^2\psi_i + V\psi_i = E_i\psi_i$, where the sum is over the lowest N states and E' is adjusted so that the integral of the approximate $\sum |\psi_i|^2$ is N . The application of this formula to the various self-consistent equations of assumption (2) now leads to various 'Thomas-Fermi equations': The 'Thomas-Fermi' equation (Thomas 1927, Fermi 1928) from Hartree's symmetrized equations (cf. Thomas's assumption 4), the Thomas-Fermi-Dirac equation (Dirac 1930) from Foch's equations, and the relativistic Thomas-Fermi equation (Chandrasekhar 1934).

* Most of the subject matter of this paper formed part of a University of London Ph.D. thesis.

In addition to these an attempt has been made by Fermi and Amaldi (1934) to give a Thomas-Fermi equation corresponding to Hartree's unsymmetrized equations, and Gombás (1943) has given a Thomas-Fermi equation that is alleged to take some account of the correlation between the positions of electrons besides that included by the use of antisymmetric wave functions.

The simple Thomas-Fermi formula for $\Sigma |\psi_i|^2$ is not the only possible consequence of assumption (1). Weizsäcker (1935) has given another approximate formula for $\Sigma |\psi_i|^2$ in the form of a differential equation that he has claimed to be more accurate than the simple Thomas-Fermi formula. Of course the 'Thomas-Fermi-Weizsäcker formula' can be applied to any of the self-consistent equations of assumption (2) to give a corresponding 'Thomas-Fermi-Weizsäcker equation'.

It is interesting to make a digression to examine the reason for Weizsäcker's extension of the simple Thomas-Fermi formula. Weizsäcker wanted to calculate the surface energy of nuclei (read nucleons for electrons above), but the surface energy by the Thomas-Fermi formula is zero (there is a Thomas-Fermi formula for ΣE_i just as there is for $\Sigma |\psi_i|^2$) and if this is made self-consistent the energy is lowered, so giving a negative surface energy. Weizsäcker believed that this curious result was caused by the pooriness of the simple Thomas-Fermi formula near the surface, where the potential changes very rapidly, and in particular he thought that the simple Thomas-Fermi formula underestimated the kinetic energy. Exactly the same problem arises in the calculation of the surface energy of solids and Samoilovich (1945) has used Weizsäcker's formula to solve it, but there is another explanation of the negative result of the simple Thomas-Fermi formula, namely that the formula is found by replacing a summation over the eigenvalues by an integral. To illustrate the procedure consider a one-dimensional box with infinite potential walls. The wave functions are proportional to $\sin n\pi x/L$, where n is an integer and L is the length of the box. The eigenvalues are $\hbar^2 n^2 \pi^2 / 2mL^2$ and the simple Thomas-Fermi formula for their sum is

$$\int_0^N \frac{\hbar^2}{2m} \frac{n^2 \pi^2}{L^2} dn = \frac{\hbar^2}{2m} \frac{N^3 \pi^2}{3L^2} = \frac{\hbar^2}{24m} \frac{N^3}{L^3} L = \int \frac{\hbar^2}{24m} \rho^3 dx$$

where N is the number of occupied wave functions and ρ is the electron density N/L . The accuracy of the above Thomas-Fermi formula for the sum of the eigenvalues is increased by adding to it the term $\hbar^2 N^2 \pi^2 / 4mL^2$ that comes from the Euler-Maclaurin sum formula (cf. eqn. (5)). This term (suggested by Brager and Schuchowitzky 1946) is quite adequate to make the surface energy positive without introducing Weizsäcker's correction (see Huang and Wyllie 1949).

The original proofs of the simple Thomas-Fermi formula were very poor involving as they did classical assumptions (1). Weizsäcker's attempt to improve the formula can be questioned for the same reason and also because the approximation of sums by integrals may in some cases be just as important. In §2 we attempt to overcome both these difficulties by giving a proof of a new Thomas-Fermi formula for the electron density, which we claim to be more accurate than the simple Thomas-Fermi formula. This new formula consists of a differential equation for the electron density, which is very similar to Weizsäcker's. The approximations made in the derivation of the differential equation are more of a mathematical than of a classical nature, and the Euler-Maclaurin sum formula is used explicitly. An approximate solution of

the differential equation—good when the electron density varies slowly—is the electron density given by the simple Thomas–Fermi formula.

An approximate form of the new Thomas–Fermi formula is applied to the Klein–Gordon relativistic equation in §3 and leads to the relativistic Thomas–Fermi formula given by Chandrasekhar, but with a correction that removes the divergence of his method for atoms with Z less than $137/2$, above which atomic number the Klein–Gordon equation itself is rather peculiar.

In §2 the Thomas–Fermi formula is proved for a Schrödinger equation in which the potential is a function of the energy. This is applied in §4 to an approximate form of Foch’s equation in which the exchange operator is replaced by a potential that is a function of the energy (Brillouin 1934, Dirac 1930). It is shown that the resulting Thomas–Fermi–Dirac equation is not an equation for the electron density, but for a related and quite useless quantity. This is due to the fact that the potential is a function of the energy, and so in §5 the Thomas–Fermi formula is applied to Slater’s (1951) approximate form of Foch’s equations in which the exchange operator is replaced by a potential that is independent of the energy. This leads to the usual Thomas–Fermi–Dirac equation for the electron density, only with Z appearing in a different way. An examination of the equation shows that it is impossible to obtain negative electron densities, so contradicting the usual belief, which belief has led Corson (1951), for example, to suggest that the simple Thomas–Fermi equation is only less inconsistent fortuitously. On the other hand it is shown that the Thomas–Fermi–Dirac equation has not a unique solution, a fact which does not appear to have been previously noticed.

It has only been found possible to prove the new Thomas–Fermi formula in one dimension, or in three if the Schrödinger equation is separable, e.g. if it is spherically symmetrical.

§ 2. AN EXTENSION OF THE THOMAS–FERMI FORMULA

It is convenient, but does not constitute a generalization, to consider from the start the Sturm–Liouville equation rather than the simpler Schrödinger equation. This will save us repetition later on and is no more difficult. With another generalization, to cover the case of a non-linear energy term (as in the Klein–Gordon equation), this differential equation is

$$-\frac{\hbar^2}{2m} \frac{d}{dx} \left[f(x) \frac{d\psi}{dx} \right] - g(x, E) \psi(x) = 0, \quad \dots\dots (1)$$

where f , which nowhere vanishes, and g are supposed to be real functions. Following Young (1931) we find two real functions $A(x, E)$ and $P(x, E)$ such that

$$A(x) \cos \frac{1}{\hbar} \int_x^\infty P(\xi) d\xi \quad \text{and} \quad A(x) \sin \frac{1}{\hbar} \int_x^\infty P(\xi) d\xi$$

are both solutions of the differential equation (1). In other words $A \exp \{ (i/\hbar) \int P d\xi \}$ must satisfy the equation and, equating real and imaginary parts to zero, we find that A and P must satisfy the simultaneous equations:

$$\begin{aligned} -\frac{\hbar^2}{2m} \left[\left(\frac{d^2 A}{dx^2} - \frac{1}{\hbar^2} A P^2 \right) f + \frac{dA}{dx} \frac{df}{dx} \right] - A g &= 0 \\ 2 \frac{dA}{dx} P f + A \frac{dP}{dx} f + A P \frac{df}{dx} &= 0, \end{aligned}$$

The integral of the second equation is $A^2Pf = \text{constant}$, and eliminating A from the first equation gives for P the equation

$$\frac{1}{2m} P^2 f - g - \frac{\hbar^2}{2m} P^{1/2} f^{1/2} \frac{d}{dx} \left[f \frac{d}{dx} (P^{-1/2} f^{-1/2}) \right] = 0. \quad \dots\dots(2)$$

If f and P do not vary too rapidly a good solution of this is

$$P \simeq (2mgf^{-1})^{1/2}, \quad \dots\dots(3)$$

just giving the B.W.K. approximation (i.e. neglecting \hbar^2).

We now prove that Pf can never become infinite (so that A is never zero). This shows that the nodes in the wave function can only be at the zeros in the trigonometric part. The proof depends on finding an interesting expression for P due to Milne (1930). Suppose ψ_1 and ψ_2 are two independent solutions of (1) with Wronskian W , then $Wf = \psi_2 f d\psi_1/dx - \psi_1 f d\psi_2/dx$ is a non-zero constant. Define $w(x)$ as $(\psi_1^2 + \psi_2^2)^{1/2}$, then we may easily show that $w(x)$ satisfies the equation

$$-\frac{\hbar^2}{2m} \frac{d}{dx} \left(f \frac{dw}{dx} \right) - gw + \frac{\hbar^2}{2m} \frac{W^2 f}{w^3} = 0,$$

which enables us to make the identification

$$P/\hbar = W/w^2 = W/(\psi_1^2 + \psi_2^2). \quad \dots\dots(4)$$

From (4) we see that since Wf is a constant Pf cannot become infinite except where ψ_1^2 and ψ_2^2 are both zero, an impossibility since $Wf \neq 0$. Clearly by a suitable choice of ψ_1 and ψ_2 any solution of the equation for P can be put in the form (4). Notice that P can consist of a sequence of δ functions as $\psi_1 \rightarrow \psi_2$, or can be quite smooth if ψ_1 and ψ_2 have their nodes properly spaced.

Since an arbitrary solution of the equation (1) can be written

$$\psi \propto P^{-1/2} f^{-1/2} \sin \{ \hbar^{-1} \int^x P d\xi + \gamma \},$$

where γ is an arbitrary phase factor, the solution which vanishes at $\pm \infty$ must be

$$P^{-1/2} f^{-1/2} \sin \frac{1}{\hbar} \int_{-\infty}^x P d\xi, \quad \text{where} \quad \frac{1}{\hbar} \int_{-\infty}^{+\infty} P d\xi = n\pi$$

fixes the eigenvalues, P being a function of E .

Next we normalize the wave function by a method due to Furry (1947). Consider two solutions of the differential equation (1), ψ_1 and ψ_2 with energies E_1 and E_2 respectively (not necessarily eigenvalues); multiplying the two equations by ψ_2 and ψ_1 and subtracting we find

$$-\frac{\hbar^2}{2m} \frac{\partial}{\partial x} \left[\psi_2 f \frac{\partial \psi_1}{\partial x} - \psi_1 f \frac{\partial \psi_2}{\partial x} \right] - [g(E_1) - g(E_2)] \psi_1 \psi_2 = 0.$$

Now let E_1 and E_2 tend to some E , and imagine that ψ_1 and ψ_2 are the two values of a differentiable function of E , then performing the limit and integrating with respect to x we find

$$\int_a^b \frac{\partial g}{\partial E} \psi^2 dx = -\frac{\hbar^2}{2m} \left[\psi \frac{\partial}{\partial E} \left(f \frac{\partial \psi}{\partial x} \right) - \frac{\partial \psi}{\partial E} f \frac{\partial \psi}{\partial x} \right]_a^b.$$

If g were the usual $E - V(x)$ this would enable us to determine the integral of ψ^2 in terms of the value of ψ at the end points. We now evaluate the right-hand side of this expression when $\psi = A \sin \hbar^{-1} \int^x P d\xi$ and a and b are nodes of ψ . We find the identity

$$\int_a^b \frac{\partial g}{\partial E} \psi^2 dx = \left[\frac{\hbar^2}{2m} \frac{A^2 P f}{\hbar^2} \int_a^x P_E d\xi \right]_a^b = \frac{1}{2m} \int_a^b P_E d\xi$$

if we take $A^2 P f = 1$, where $P_E = \partial P / \partial E$. If ψ is an eigenfunction it has nodes at $\pm \infty$, and so the identity will give the normalization integral in terms of the integral of P_E from $-\infty$ to $+\infty$. The identity also gives a very useful average value for $\psi^2 \partial g / \partial E$, namely $P_E(E, x) / 2m$. That the word average is not being used unreasonably is shown by the identity, which proves that the integral of the average value between two nodes is equal to the integral of $\psi^2 \partial g / \partial E$ between the nodes. We shall indicate this average by means of a bar, i.e.

$$\overline{\frac{\partial g}{\partial E} \psi^2(E, x)} = \frac{1}{2m} P_E(E, x).$$

Thus the total average electron density is

$$\sum_{n=1}^N \overline{\frac{\partial g}{\partial E} \psi_n^2(x)} = \sum_{n=1}^N P_E(E_n, x) \bigg/ \int_{-\infty}^{+\infty} P_E(E_n, x) dx$$

assuming that the eigenfunctions ψ_n with energies E_n are normalized according to the equation

$$\int_{-\infty}^{+\infty} \frac{\partial g}{\partial E} \psi_n^2(x) dx = 1.$$

It will be recalled that the eigenvalues E_n are given by the equation

$$\frac{1}{\hbar} \int_{-\infty}^{+\infty} P(E, x) dx = n\pi.$$

This expression for the total average electron density would not be too difficult to use since, as Milne (1930) has pointed out, P is (or at least can be) a smooth function and so easy to obtain by numerical integration. However, by making one further approximation a tremendous simplification is brought about: viz. by using the Euler-Maclaurin sum formula to replace the sum over the eigenvalues by an integration over the energy with a density of states function. The density of states is found by differentiating the equation for the eigenvalues with respect to E :

$$\frac{dn}{dE} = \frac{1}{\pi \hbar} \int_{-\infty}^{+\infty} P_E dx,$$

which cancels the normalization factor and gives

$$\sum_{n=1}^N \overline{\frac{\partial g}{\partial E} \psi_n^2} = \frac{2}{\hbar} P(E_N) - \frac{2}{\hbar} P(E_1) + \frac{1}{2} \frac{P_E(E_N)}{\int_{-\infty}^{+\infty} P_E dx} + \frac{1}{2} \frac{P_E(E_1)}{\int_{-\infty}^{+\infty} P_E dx} + R. \quad \dots (5)$$

The asymptotic form for the remainder is

$$R \sim \frac{B_1}{2!} \frac{\hbar}{2} \left[\frac{1}{\int P_E dx} \left\{ \frac{P_{EE}}{\int P_E dx} - \frac{P_E \int P_{EE} dx}{(\int P_E dx)^2} \right\} \right] - \frac{B_2}{4!} \frac{\hbar^3}{8} \left[\dots \right];$$

this can be regarded as an expansion either in ascending powers of \hbar , or in ascending derivatives of P with respect to E . It would be advisable in any actual example to compute the error involved in omitting the remainder.

Another approximation can now be made which makes it unnecessary to calculate $P(E_1)$, $P_E(E_1)$ and $P_E(E_N)$: that is to set

$$\sum_{n=1}^N \overline{\frac{\partial g}{\partial E} \psi_n^2} = \frac{2}{\hbar} P(E_N) + R'; \quad \dots (6)$$

the three terms in (5) which have been transferred to R' to obtain this formula do, it is true, cancel out on the average from $-\infty$ to $+\infty$ (just as R does), but the effect of the cancellation is to put too much charge in the ground state at

the expense of the most energetic state. Notice of course that the substitution of (3) for P immediately gives the usual Thomas-Fermi formula, or if we are just interested in the Schrödinger equation

$$\sum_{n=1}^N \overline{\psi_n^2} \simeq \frac{2}{\hbar} [2m(E_N - V)]^{1/2}.$$

It is interesting to compare the formula (6) applied to the Schrödinger equation (without the remainder term) with the expression given by Weizsäcker for the electron density. The prescription for finding Weizsäcker's density is to minimize

$$\int \left(\frac{\hbar^2}{24m} \rho^3 + \rho V + \frac{\hbar^2}{8m} \frac{\rho'^2}{\rho} \right) dx$$

subject to the condition $\int \rho dx = N$. Euler's equation for this variational problem is

$$\frac{\hbar^2}{8m} \rho^2 + V - \frac{\hbar^2}{4m} \frac{\rho''}{\rho} + \frac{\hbar^2}{8m} \frac{\rho'^2}{\rho^2} = E',$$

where E' is the Lagrange multiplier. Putting $f=1$ and $g=E-V$ in (2) gives the following equation for $\rho = \Sigma \overline{\psi^2}$ from (6):

$$\frac{\hbar^2}{8m} \rho^2 + V + \frac{\hbar^2}{4m} \frac{\rho''}{\rho} - \frac{3\hbar^2}{8m} \frac{\rho'^2}{\rho^2} = E_N. \quad \dots\dots(7)$$

Before going on we use (5) to prove a theorem due to Friedel (1952) on the accumulation of electrons over a potential well. The potential is zero for large x and is arbitrary for small x ; the boundary conditions are that the wave function should be zero for x equal to 0 and X , a large x . For large x the wave function is of the form $A \sin(px/\hbar + \eta)$, A and η being independent of x , although the phase shift η is a function of the energy. The number of electrons in the interval $(0, x)$, due to all states up to energy E , is

$$\int_0^x \frac{2}{\hbar} P(E) d\xi = \frac{1}{\pi} \left(\frac{1}{\hbar} px + \eta(E) \right),$$

while if the potential were everywhere zero the number of electrons would be $px/\pi\hbar$, so the accumulation of electrons is $\eta(E)/\pi$. Notice that this result does not depend on the type of boundary condition at X .

The Invariance of the Formula

An essential requirement of an accurate expression for the electron density is that it should be invariant to a change of variables in the Schrödinger equation. As an illustration let us consider the ordinary Thomas-Fermi formula: it gives

$$\Sigma \overline{\psi^2} \simeq \frac{2}{\hbar} [2m(E' - V(r))]^{1/2}, \quad \text{when} \quad -\frac{\hbar^2}{2m} \frac{d^2\psi}{dr^2} + [V(r) - E]\psi = 0.$$

Suppose now we change the variables in this differential equation to u and x : $\psi = A(x)u(x)$, $r = C(x)$; then we obtain the following equation for u :

$$-\frac{\hbar^2}{2m} \frac{d}{dx} \left(\frac{A^2}{C'} \frac{du}{dx} \right) + \left\{ (V-E)A^2C' - \frac{\hbar^2}{2m} \left(\frac{AA''}{C'} - \frac{AA' C''}{C'^2} \right) \right\} u = 0.$$

Now let us apply the Thomas-Fermi formula, which we have just proved (eqns. (6) and (3)), to this new equation; we find

$$\Sigma A^2 C' u^2 \simeq \frac{2}{\hbar} (2m)^{1/2} \left\{ (E' - V)C'^2 + \frac{\hbar^2}{2m} \left(\frac{A''}{A} - \frac{A' C''}{A C'} \right) \right\}^{1/2},$$

with u normalized so that $\int A^2 C' u^2 dx = 1$, i.e. $\int \psi^2 dr = 1$, i.e.

$$\Sigma \psi^2 \simeq \frac{2}{h} \left\{ 2m(E' - V) + \hbar^2 \left(\frac{A''}{A} - \frac{A'}{A} \frac{C''}{C'} \right) \frac{1}{C'^2} \right\}^{1/2};$$

which is not the usual Thomas–Fermi formula for the electron density with which we started.

The fact that the Thomas–Fermi formula is not invariant under this type of transformation means that it may be possible to choose a set of variables such that the Thomas–Fermi formula, expressed in these variables, is more accurate than the formula in the original variables. Since the Thomas–Fermi formula is proved by means of the B.W.K. approximation, it is clear that those variables should be chosen for which the B.W.K. approximation is best. Langer (1937) has shown that for the radial wave equation

$$-\frac{\hbar^2}{2m} R_l'' + \left[V(r) + \frac{\hbar^2}{2m} \frac{l(l+1)}{r^2} - E \right] R_l = 0$$

the variables should be changed to x and u : $R_l = e^{x/2} u$, $r = e^x$. The Thomas–Fermi formula now gives

$$\Sigma R_l^2 \simeq \frac{2}{h} \left\{ 2m \left[E' - V(r) - \frac{\hbar^2}{2m} \frac{l(l+1)}{r^2} \right] - \frac{\hbar^2}{4r^2} \right\}^{1/2},$$

which is an expression for the radial electron density for states with angular momentum l , E' being adjusted so that the expression gives the correct number of electrons with quantum number l (cf. Hellmann 1936, who does not give the correction $\hbar^2/4r^2$). The total electron density is just

$$\Sigma_l \frac{2l+1}{4\pi r^2} \Sigma R_l^2 \simeq \frac{1}{h^3} \frac{4\pi}{3} \left[2m \left(E' - V - \frac{1}{4r^2} \frac{\hbar^2}{2m} \right) \right]^{3/2} \dots\dots (8)$$

if we use the Euler–Maclaurin formula to evaluate the sum over l ; in addition to omitting the remainder we have assumed E' to be independent of l . Equation (8) is the usual Thomas–Fermi formula for three dimensions, apart from the last term; this only makes an appreciable difference near the nucleus, where the electron density is now zero instead of infinite like $r^{-3/2}$.

An advantage of our new formula (6) for the electron density can now be seen: this formula gives the same electron density no matter what the functions $A(x)$ and $C(x)$ are, as can easily be proved, i.e. this formula is invariant. We may therefore suppose that it gives the electron density more accurately than the ordinary Thomas–Fermi formula no matter what coordinates are used. For example the electron density given by the new formula will decrease exponentially (as is obvious from (4)) and not like r^{-6} as in the ordinary Thomas–Fermi equation.

§ 3. THE RELATIVISTIC THOMAS–FERMI APPROXIMATION

It is important to take relativistic effects into account for the inner electrons of heavy atoms and those collapsed stars known as white dwarfs. These electrons are moving at speeds comparable with that of light.

Chandrasekhar (1934) has given a modified Thomas–Fermi formula which he claims corresponds to the relativistic case; Eddington (1935) has disputed this, maintaining that the relativistic and non-relativistic formulae are identical. We will not attempt to weigh the relative merits of these two schools of thought, but merely apply eqn. (6) to the Klein–Gordon equation.

The Klein-Gordon equation in one dimension, with zero vector potential, is $-\hbar^2 \mathbf{c}^2 d^2 \psi / dx^2 + \mathbf{m}^2 \mathbf{c}^4 \psi = (E - \mathbf{e}\phi)^2 \psi$ and the electron density is

$$\rho = -\frac{\hbar}{2\mathbf{m}\mathbf{c}^2 i} \left(\Psi^* \frac{\partial \Psi}{\partial t} - \Psi \frac{\partial \Psi^*}{\partial t} \right) - \frac{\mathbf{e}\phi}{\mathbf{m}\mathbf{c}^2} \Psi \Psi^*.$$

With $\Psi = \psi \exp(-iEt/\hbar)$ this becomes $\rho_n = (\mathbf{m}\mathbf{c}^2)^{-1} (E - \mathbf{e}\phi) |\psi_n|^2$. Equation (6) gives the total electron density

$$\Sigma \frac{1}{2\mathbf{m}\mathbf{c}^2} \frac{\partial}{\partial E} (E - \mathbf{e}\phi)^2 \psi_n^2 = \Sigma \bar{\rho}_n = \frac{2}{\hbar} P + R'$$

and using the B.W.K. approximation for P , namely (3), we find

$$2[(E' - \mathbf{e}\phi)^2 - \mathbf{m}^2 \mathbf{c}^4]^{1/2} / \hbar \mathbf{c}$$

for the simple Thomas-Fermi formula in this case.

We can extend this to a three-dimensional spherically symmetrical problem for which the Klein-Gordon relativistic equation is

$$-\hbar^2 \mathbf{c}^2 \frac{d^2 R}{dr^2} + \mathbf{m}^2 \mathbf{c}^4 R + \hbar^2 \mathbf{c}^2 \frac{l(l+1)}{r^2} R = (E - \mathbf{e}\phi)^2 R,$$

so that the total electron density using Langer's (1937) correction is

$$\rho \simeq \Sigma_l \frac{2}{\hbar \mathbf{c}} \left[(E' - \mathbf{e}\phi)^2 - \hbar^2 \mathbf{c}^2 \frac{l(l+1)}{r^2} - \mathbf{m}^2 \mathbf{c}^4 - \frac{\hbar^2 \mathbf{c}^2}{4r^2} \right]^{1/2} \frac{2l+1}{4\pi r^2},$$

and integrating over l gives

$$\rho \simeq \frac{4\pi}{3} \frac{1}{\hbar^3 \mathbf{c}^3} \left[(E' - \mathbf{e}\phi)^2 - \mathbf{m}^2 \mathbf{c}^4 - \frac{\hbar^2 \mathbf{c}^2}{4r^2} \right]^{3/2}.$$

This is Chandrasekhar's result apart from the term $\hbar^2 \mathbf{c}^2 / 4r^2$. In an atom $\phi \rightarrow -Ze/r$ near the nucleus and so ρ would diverge like r^{-3} were it not for this term; however the Langer correction ensures convergence provided $Z < \frac{1}{2} \hbar \mathbf{c} / \mathbf{e}^2 \simeq 137/2$. This is very satisfactory, for the Klein-Gordon equation itself becomes peculiar for Z greater than this—if the s wave function is like r^{λ} for small r then the indicial equation for λ has the solutions $2\lambda = 1 \pm (1 - 4Z^2/137^2)^{1/2}$ for the Klein-Gordon equation, but has the solution $\lambda = \pm (1 - Z^2/137^2)^{1/2}$ for the Dirac equation.

§ 4. THE THOMAS-FERMI EQUATION WITH EXCHANGE (DIRAC)

It is clearly of importance to obtain a Thomas-Fermi approximation based on Foch's equations. This would, for example, probably make it possible to find the electron densities of negative ions—almost an impossibility with the symmetrized Hartree equations. Even our general equation (1) is not general enough for this purpose, since Foch's equations contain an integral operator, i.e. the exchange operator. It has been customary therefore to replace this operator by a potential (cf. Dirac 1930, Brillouin 1934) to which it approximates, namely

$$D = \frac{\mathbf{e}^2}{\hbar} \left[2p' + \frac{p'^2 - p^2}{p} \log \frac{p' + p}{p' - p} \right], \quad \dots (9)$$

where p is the scalar magnitude of the momentum of the electron being considered and is of course a function of \mathbf{r} (e.g. $[2\mathbf{m}(E - V(x))]^{1/2}$ in one dimension), while p' is the momentum of the highest filled state.

In order to illustrate the subsequent details of the proof of the Thomas-Fermi-Dirac approximation it is simplest just to consider the one-dimensional case (for example the radial equation): Foch's equations are now approximately

$$-\frac{\hbar^2}{2m} \frac{d^2\psi}{dx^2} + [V(x) - D(x, E)]\psi = E\psi.$$

As indicated D is a function of x and E . If the Thomas-Fermi formula is applied to this equation, disregarding till the last moment the fact that D is a function of E , we find

$$\Sigma\psi^2 \simeq \frac{2}{\hbar} \{2m[E' - V(x) - D(x, E')]\}^{1/2} = \frac{2}{\hbar} p'.$$

$D(x, E')$ is what is obtained from (9) when $p \rightarrow p'$, namely $2e^2 p' / \hbar$. This is just the formula given by Dirac and Brillouin.

However this proof is not correct. Applying our equations (3) and (6) we find

$$\Sigma \left(1 + \frac{\partial D}{\partial E}\right) \psi_n^2 \simeq \frac{2}{\hbar} \{2m[E' - V(x) + D(x, E')]\}^{1/2}, \quad \dots\dots(10)$$

where ψ is normalized so that

$$\int \left(1 + \frac{\partial D}{\partial E}\right) \psi_n^2 dx = 1. \quad \dots\dots(11)$$

Clearly the Thomas-Fermi-Dirac formula is not giving the electron density. It is interesting that this flaw is not uncovered in the cellular (Lenz 1932) type of proof either—the $(1 + \partial D / \partial E)$'s cancelling each other in (10) and (11)—although Brillouin's proof could demonstrate it.

§ 5. THE THOMAS-FERMI EQUATION WITH EXCHANGE (SLATER)

It was due to the fact that the potential was a function of the energy that we were unable to obtain the electron density by the Thomas-Fermi formula in the last paragraph. If then we wish to replace the exchange operator by a potential in order to be able to use the Thomas-Fermi formula this 'potential' must be independent of the energy. Slater (1951) has suggested such a potential and his equation for an atom is

$$-\frac{\hbar^2}{2m} \nabla^2 \psi + \left[-\frac{Ze^2}{r} + e^2 \int \frac{2\Sigma |\psi|^2}{|\mathbf{r} - \mathbf{r}'|} d\mathbf{r}' - 3e^2 \left(\frac{3}{4\pi} \Sigma |\psi|^2 \right)^{1/3} \right] \psi = E\psi. \quad \dots\dots(12)$$

The Thomas-Fermi solution of this is (8), neglecting Langer's correction,

$$2\Sigma |\psi|^2 = \rho \simeq \frac{2}{\hbar^3} \frac{4\pi}{3} \left\{ 2m \left[E' + \frac{Ze^2}{r} - e^2 \int \frac{\rho(\mathbf{r}')}{|\mathbf{r} - \mathbf{r}'|} d\mathbf{r}' + 3e^2 \left(\frac{3}{8\pi} \rho \right)^{1/3} \right] \right\}^{3/2}. \quad \dots\dots(13)$$

Notice that this is the usual Thomas-Fermi-Dirac equation except that the last term is $3e^2(3\rho/8\pi)^{1/3} = 3e^2 p' / \hbar$ instead of $2e^2 p' / \hbar = D(x, p')$; the maximum value of the exchange potential is $4e^2 p' / \hbar = D(x, 0)$.

In order to simplify this equation it has been customary to take its two-thirds power immediately (Dirac 1930, Brillouin 1934, Corson 1951) if not before (Gombás 1949). However, by squaring one loses the fact that the radical on the right-hand side of (13) must always be taken with the positive sign according to the Thomas-Fermi formula. Another fact to be remembered about the formula is that $\rho \simeq 0$ if the term inside the curly brackets is negative.

Notice the fact that the variational approach to this problem, now so much in vogue (cf. Gombás 1949), starts directly from (13) to the two-thirds power. We will postpone this squaring as long as possible.

We make the usual change of variables in (13)

$$E' + \frac{Ze^2}{r} - e^2 \int \frac{\rho(r')}{|\mathbf{r}-\mathbf{r}'|} d\mathbf{r}' = \frac{Ze^2\phi}{r}$$

and $r = \mu x$,

$$\mu = \left[\frac{32\pi^2 e^2}{3\hbar^3} (2m)^{3/2} \right]^{-2/3} (Ze^2)^{-1/3};$$

whereupon the equation becomes

$$\frac{\phi''}{x} = + \left\{ \frac{\phi}{x} + 3\beta \left(\frac{\phi''}{x} \right)^{1/3} \right\}^{3/2}, \quad \dots\dots(14)$$

with $\beta = (3/32\pi^2 Z^2)^{1/3}$. We recall once more that this equation is not valid if $\phi/x + 3\beta(\phi''/x)^{1/3} < 0$: the correct equation is then

$$\phi''/x = 0. \quad \dots\dots(15)$$

Combining the inequality with (14) we see that ϕ'' can never become negative.

Next we solve (14) for ϕ''/x by taking the two-thirds power, and find on solving the quadratic

$$\frac{\phi''}{x} = \left\{ \frac{3}{2} \beta \pm \left(\frac{9}{4} \beta^2 + \frac{\phi}{x} \right)^{1/2} \right\}^3. \quad \dots\dots(16)$$

To decide on the sign of the radical we substitute this value for ϕ''/x into (14) and make sure that it satisfies (14); we find on taking the cube root

$$\frac{3}{2} \beta \pm \left(\frac{9}{4} \beta^2 + \frac{\phi}{x} \right)^{1/2} = + \left\{ \frac{\phi}{x} + 3\beta \left[\frac{3}{2} \beta \pm \left(\frac{9}{4} \beta^2 + \frac{\phi}{x} \right)^{1/2} \right] \right\}^{1/2}.$$

Notice, as is obvious from the way in which we obtained (16) from (14), that this is an identity when it is squared, independently of the sign of the radical. The left-hand side of this supposed identity is a double valued function of ϕ/x say f_+ and f_- , with its branch point at $\phi/x = -9\beta^2/4$. The right-hand side is more complicated: if we had included the minus sign as well as the plus sign it would have been two double valued functions, say $\pm g_+$ and $\pm g_-$ each with its branch point at $\phi/x = -9\beta^2/4$, and $\pm g_-$ having a branch point at $\phi/x = 0$; however by forcing the plus sign the function on the right is g_+ or $|g_-|$, the modulus sign on g_- being necessary since otherwise on passing through $\phi/x = 0$ it would change sign. To make the position clear we give the expansions of the left and right-hand sides for small ϕ/x

$$\begin{array}{l} \text{L.H.S.} \quad \left\{ \begin{array}{l} f_+ = 3\beta + \frac{1}{3\beta} \frac{\phi}{x} - \frac{1}{27\beta^3} \frac{\phi^2}{x^2} + \dots \\ f_- = -\frac{1}{3\beta} \frac{\phi}{x} + \frac{1}{27\beta^3} \frac{\phi^2}{x^2} - \dots, \end{array} \right. \\ \\ \text{R.H.S.} \quad \left\{ \begin{array}{l} g_+ = 3\beta + \frac{1}{3\beta} \frac{\phi}{x} - \frac{1}{27\beta^3} \frac{\phi^2}{x^2} + \dots \\ |g_-| = \frac{1}{3\beta} \left| \frac{\phi}{x} \right| - \frac{1}{27\beta^3} \left| \frac{\phi}{x} \right| \frac{\phi}{x} + \dots \end{array} \right. \end{array}$$

We know that $(f_+)^2 = (g_+)^2$ and $(f_-)^2 = (g_-)^2$, or that $f_+ = \pm g_+$ and $f_- = \pm g_-$; the correct relations are

$$\begin{aligned} f_+ &= g_+ & \text{for all } \phi/x \geq -9\beta^2/4, \\ f_- &= -g_- & \text{for all } \phi/x \geq 0, \\ f_- &= +|g_-| & \text{for all } 0 \geq \phi/x \geq -9\beta^2/4. \end{aligned}$$

The positive sign in (16) is therefore correct for $\phi/x \geq -9\beta^2/4$, while the negative sign is only correct for $-9\beta^2/4 \leq \phi/x \leq 0$.*

We now consider the types of solution of (14), i.e. (16) with the condition on the sign of the radical just given, that represent possible physical solutions of (13). The first requirement is that ρ (or ϕ''/x) should not have any δ functions in it. This implies that ϕ and ϕ' must be continuous. We might make the further requirement that the electron density should be continuous, implying the continuity of ϕ'' . This however makes it impossible to find any solution. The continuity of ϕ and ϕ' makes it appear that we should continue a solution of (14) to $x = \infty$, but this is not true since in any interval of x we may replace (14), or (16), by (15) provided ϕ/x is negative. In such an interval the electron density is zero. This possibility of breaking off the solution at a more or less arbitrary point introduces considerable ambiguity into the Thomas-Fermi-Dirac method which is not present in the Thomas-Fermi method. Another cause of ambiguity is that ϕ''/x is not determined uniquely from ϕ/x by (14) if ϕ/x is negative—in this event either sign of the radical may be used in (16), see figure.

Taking any permissible ϕ , in the sense just described, we must calculate ρ from it:

$$\rho = \frac{1}{4\pi e^2} \nabla^2 \frac{Ze^2\phi}{r} = \frac{Z}{4\pi r} \frac{d^2\phi}{dr^2}.$$

This is then to be inserted in the right-hand side of (13) and E' determined, if possible, to make it equal to the left-hand side. In other words we must make sure we have lost nothing by differentiating, in passing from the integral equation (13) to the differential equation (14). The question is whether we can determine an E' such that

$$E' + \frac{Ze^2}{r} - \frac{Ze^2}{4\pi} \int \frac{\phi''(r')}{r'|\mathbf{r}-\mathbf{r}'|} d\mathbf{r}' = \frac{Ze^2\phi}{r}.$$

The integral can be easily evaluated and is found to be

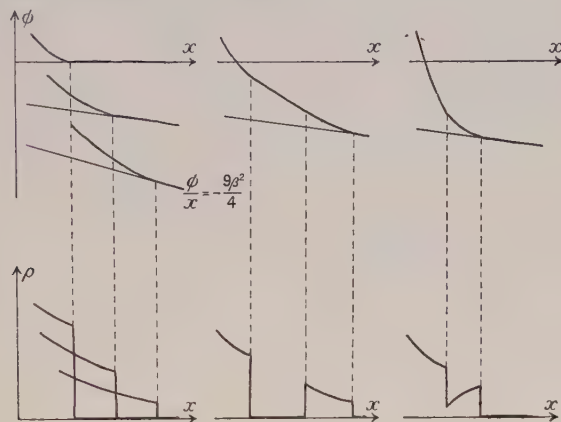
$$- \frac{Ze^2}{4\pi} \left[-4\pi \frac{\phi(r)}{r} + 4\pi \frac{\phi(0)}{r} + 4\pi\phi'(\infty) \right]$$

since $\phi'(r)$ is continuous. Thus we must have $\phi(0)=1$ and then we find that $E' = Ze^2\phi'(\infty)$, so answering our question in the affirmative and determining the value of E' .

* The sign for the radical in (16) has usually been obtained by the following argument: near the nucleus the Thomas-Fermi-Dirac method must reduce to the Thomas-Fermi method implying the positive sign for large ϕ/x , and this must be maintained unless ϕ/x goes through the branch point at $-9\beta^2/4$. The last part of this argument seems to be quite wrong.

Knowing now that any solution of (14) will do (with $\phi(0) = 1$), we have sketched in the figure a number of possible solutions for the neutral atom. To enable a large scale to be used we have omitted the central part of the atom.

The explanation of the ambiguity in the solution of the Thomas-Fermi formula applied to Slater's equations (12) is quite clear: if the electron density is suddenly made zero then the potential is suddenly made repulsive and so provides a reason for the electron density becoming zero. Alternatively, if in a region where previously the density was zero, it is now made non-zero, then this will produce a potential hole which will increase the electron density.



A number of different solutions of ϕ for a neutral atom of given Z and the corresponding electron densities ρ or ϕ''/x below them. When ϕ is negative either sign of the radical in (16) may be taken or (15) may be used. The only requirement is that since this is a neutral atom ϕ must eventually be tangent to a straight line passing through the origin and having a negative slope. We may continue the solution of (16) right up to this line as shown in the left hand figure, but since any line between $\phi=0$ and $\phi = -9\beta^2 x/4$ will do this allows a whole range of possible solutions, the two extremes and an intermediary of which are shown. In the middle figure, ϕ is made to satisfy (15) for a region of x , then (16), and then become tangent to the line through the origin. This gives a shell of electrons separated from the main body of the atom. In the right-hand figure, (16) with the negative sign of the radical has been used for a range of x . This gives a shell of increasing electron density.

It seems that Slater's equation has the potentiality of producing many different solutions. Notice however that the Thomas-Fermi formula accentuates this possibility by the fact that it makes the electron density follow changes of potential immediately, whereas the correct electron density only follows changes of potential with an exponential lag. Our modification of the Thomas-Fermi formula (eqn. (6)) is not subject to this fault.

ACKNOWLEDGMENTS

I am indebted to Professor H. Jones for introducing me to the Thomas-Fermi method and for a number of valuable discussions on the subject when I was at the Imperial College. I have received both a grant and an award from the Department of Scientific and Industrial Research during the research.

REFERENCES

- BRAGER, A., and SCHUCHOWITZKY, A., 1946, *J. Chem. Phys.*, **14**, 569.
BRILLOUIN, L., 1934, *Actual. Sci. Industr.*, **160**.
CHANDRASEKHAR, S., 1934, *Mon. Not. R. Astr. Soc.*, **95**, 207.
CORSON, E. M., 1951, *Perturbation methods in the Quantum Mechanics* (London : Blackie).
DIRAC, P. A. M., 1930, *Proc. Camb. Phil. Soc.*, **26**, 376.
EDDINGTON, A. S., 1935, *Mon. Not. R. Astr. Soc.*, **95**, 194 ; *Proc. Roy. Soc. A*, **152**, 253.
FERMI, E., 1928, *Z. Phys.*, **48**, 73.
FERMI, E., and AMALDI, E., 1934, *Mem. Acc. Italia*, **6**, 117.
FRIEDEL, J., 1952, *Phil. Mag.*, **43**, 153.
FURRY, W. H., 1947, *Phys. Rev.*, **71**, 366.
GOMBÁS, P., 1943, *Z. Phys.*, **121**, 523 ; 1949, *Die Statistische Theorie des Atoms* (Vienna : Springer).
HELLMANN, H., 1936, *Acta Physicochimica, U.R.S.S.*, **4**, 225.
HUANG, K., and WYLLIE, G., 1949, *Proc. Phys. Soc. A*, **62**, 180.
LANGER, R. E., 1937, *Phys. Rev.*, **51**, 669.
LENZ, W., 1932, *Z. Phys.*, **77**, 713.
MILNE, W. E., 1930, *Phys. Rev.*, **35**, 863.
SAMOILOVICH, H., 1945, *Acta Physicochimica, U.R.S.S.*, **20**, 97.
SLATER, J. C., 1951, *Phys. Rev.*, **81**, 385.
THOMAS, L. H., 1927, *Proc. Camb. Phil. Soc.*, **23**, 542.
VON WEIZSÄCKER, C. F., 1935, *Z. Phys.*, **96**, 431.
YOUNG, L. A., 1931, *Phys. Rev.*, **38**, 1612.

LETTERS TO THE EDITOR

Ultra-Violet Bands associated with Germanium

The spectra of several diatomic molecules containing germanium such as Ge_2 , GeC , GeH , GeN , have yet to be discovered, and it seemed possible that some of these species might be observed in absorption in a King furnace. Experiments in search of Ge_2 , GeC and GeN have had no definite success, but ultra-violet bands have been photographed which may be tentatively assigned to GeH .

In the search for Ge_2 and GeC the pure element was heated in carbon-tube furnaces at about 2000°C ; in some experiments the furnace-chamber was evacuated, in others a slow current of purified helium at 100 mm pressure was maintained within it. Although absorption lines of GeI appeared strongly, no new bands were observed in the range 2000–7000 Å. For GeN the experiment was repeated at a pressure of 1 atmosphere of nitrogen, with negative results. It may be that experiments with longer paths and/or higher temperatures will be profitable.

In the presence of 1 atmosphere of hydrogen absorption bands were found in the region 2400–2600 Å at temperatures around 1800°C . Blank experiments showed that the bands are truly associated with the presence of Ge. They have been photographed on a Hilger E.478 quartz Littrow instrument. They are degraded to longer wavelengths: measurements of the most prominent heads are given below:—

λ_{air} (Å)	2454.18	2463.96	2510.49	2519.03	2565.89	2580.15
ν_{vac} (cm^{-1})	40734.5	40572.8	39820.9	39685.9	38961.2	38745.9
Intensity	8	10	9	10	2	4

The outstanding feature of the spectrum is the group of four strong, rather diffuse, heads which occur in pairs separated by about 900 cm^{-1} . The incompletely resolved rotational structure shows variations in sharpness from place to place, suggestive of an isotope effect. This structure is somewhat more open than that of GeO .

The simplest interpretation of these results seems to be that the absorbing molecule is GeH . Consideration of the data for the other hydrides of this group indicates that the ground-state of GeH will be $^2\Pi_r(a)$, with $A \sim 920$, $B \sim 6.0$, $\omega \sim 1700\text{ cm}^{-1}$ (Howell 1945). The most likely transitions are $^2\Delta(b) - ^2\Pi(a)$ or $^2\Sigma - ^2\Pi(a)$, and in either case the head-forming branches in a red-degraded system will be $^8R_{21}$, $R_1 + ^8Q_{21}$, R_2 and $Q_2 + ^8R_{12}$. If the assumption is now made that the four strong heads arise from the (0, 0) band as follows: 8R 40734.5, R_1 40572.8, R_2 39820.9, Q_2 39685.9, it can be tested by a rough calculation of B' from the head-separations ($^8R - R_1 = \Delta\nu_1$, $(R_2 - Q_2) = \Delta\nu_2$, using $\Delta\nu_1 = 2B'B_1''/(B_1'' - B')$ and $\Delta\nu_2 = 2B'B_2''/(B_2'' - B')$, with $B_1'' = B''(1 - B''/A)$, $B_2'' = B''(1 + B''/A)$. Taking $B'' = 6.00$, $A = 920\text{ cm}^{-1}$, we find $B' = 5.54\text{ cm}^{-1}$ from the sub-band presumed to arise from $^2\Pi_{3/2}$, and $B' = 5.55\text{ cm}^{-1}$ from $^2\Pi_{1/2}$.

Thus the head-separations are consistent with the assumption that the transition is $^2\Delta(b) -$ or $^2\Sigma - ^2\Pi(a)$, where the $^2\Pi(a)$ state has values of A and of B about those expected for the ground-state of GeH . Some further support for

this view comes from the fact that the two longest wavelength bands in the table may reasonably be identified as the ^8R and R_1 heads of the (0, 1) band, with $\Delta G''_{0,1} \sim 1825 \text{ cm}^{-1}$. It therefore appears that the assignment of the new bands to GeH is at least feasible: confirmation, or otherwise, must await the measurement of high resolution spectrograms.

There is evidently, as in the case of Sn (Garton 1951), a considerable field for investigation here, requiring the use of higher temperatures and longer paths. This work has been begun by one of us (W. R. S. G.).

Physical Chemistry Laboratory,
The University, Oxford.
Physics Department,
Imperial College, London S.W.7
28th November 1952.

R. F. BARROW.
G. DRUMMOND.
W. R. S. GARTON.

GARTON, W. R. S., 1951, *Proc. Phys. Soc. A*, **64**, 591.
HOWELL, H. G., 1945, *Proc. Phys. Soc.*, **57**, 44.

Some Comments on the Resolution of Scintillation Spectrometers

There have been a number of papers published on the statistical spread in the pulse height distribution from the scintillation spectrometer. An expression has been deduced similar to that of other workers (Garlick and Wright 1952) but it was found that a small term usually neglected can be included in such a manner as to demand further consideration. The expression is

$$\sigma^2 = \frac{1}{N} \left(\frac{\delta_0^2}{N} - 1 \right) + \frac{1}{N} \cdot \frac{1}{fpq} \left[1 + \frac{\delta_1^2}{m_1^2} + \frac{\delta^2}{m_1 m (m-1)} \right]$$

where σ^2 is the fractional variance in the pulse height distribution. δ_0^2 is the variance in the number N of photons emitted by the phosphor. δ_1^2 and δ^2 are the variances in the secondary emission ratios m_1 and m of the first and succeeding stages respectively. f is the fraction of light transmitted to the photocathode, p is the photocathode quantum efficiency, and q is the fraction of photoelectrons transmitted to the first dynode.

It can be shown that statistical variations introduced by losses between the dynodes can be automatically included if we define m_1 and m as the stage gain instead of the secondary emission ratio. A binomial distribution was assumed in calculating the effects of the factors f , p and q and the expression is approximated to the case of a large number of dynode stages.

If we assume that the production of a photon neither determines the following history of the ionizing particle nor was determined by the particle's previous history, then it follows that the photon emission follows a Poisson distribution. For this distribution $\delta_0^2 = N$ and the expression reduces to $\sigma^2 = F/fpqN$.

We see that the statistical spread in the pulse height distribution depends solely on the number of photoelectrons entering the multiplier, apart from the constant factor F , and is independent of the phosphor.

Garlick and Wright (1952) show a plot of σ^2 against $1/fpqN$ (actually the square of the full width at half-maximum against the reciprocal of pulse height)

for different flawless crystals and the points all lie on a straight line passing through the origin. They also show a number of points on the same graph obtained from crystals containing flaws and these lie scattered above the line suggesting that the first term is now no longer zero. Garlick has informed the author that by taking such a crystal and varying the factor f artificially with neutral filters a straight line is obtained which cuts the ordinate above the origin.

It is doubtful whether reasoning on the above lines can be carried very much further. It would be attractive to assume $\delta_0^2 = aN$ where a is a factor which determines the deviation from a Poisson distribution but evidence seems to show that the spread would not be explained satisfactorily by this procedure. The spread is more likely to be due to variations in the mean number of photoelectrons between successive scintillations.

Swank and Buck (1952) describe an experiment in which they measured the variation of σ obtained by changing the distance of the source from the photocathode. They plotted σ against the reciprocal square root of the pulse height. The curve was extrapolated to the ordinate and it was concluded that the source has an intrinsic resolution of 20 200 (their definition of resolution is $R = 1/\sigma^2$). If the form of the expression is as quoted here then it would be necessary to plot σ^2 against the reciprocal of the pulse height. Re-plotting the results taken from their graph the line of best fit is $\sigma^2 = 4.5 \times 10^{-4} + 0.589/H$. This gives an intrinsic resolution of approximately 2200.

The expression shows the importance of achieving good optical contact between the phosphor and the photocathode and of obtaining a photomultiplier tube with a high quantum efficiency. Both the quantities m_1 and q increase with increasing cathode to first dynode potential and hence it is usual to operate the first stage at a higher potential than each of the other stages. Kurrelmeyer and Hayner (1937) have shown that for a beryllium surface the distribution in the number of secondary electrons deviates from a Poisson distribution for increasing values of the secondary emission ratio. This may also apply to the antimony-caesium surface and hence a large m may in fact be compensated by an increase in δ^2 .

We have found it convenient to replace the first resistance in the dynode chain by a low current neon. This makes it possible to vary the potential across the other stages and so vary the gain over a wide range, without affecting the statistical spread. It can be seen that the contribution to the spread from the stages beyond the first is small.

An examination with our instruments of the 662 kev gamma-ray from ^{137}Cs using a NaI(Tl) phosphor and an EMI VX5052 tube gave $\sigma^2 = 1/760 E(\text{mev})$. By expressing the equation in this form the number 760 represents the effective number of photoelectrons entering the multiplier per mev. This makes it possible to compare the resolution obtained by different workers without making any assumption about the values of f , p , q , δ , etc.

Looking back at some earlier investigations of Hopkins (1951) on the linearity in the response of anthracene to electrons, we find that he plots a^2 against E , where a is the half-width of the distribution at $1/e$ maximum and E is the energy of the incident electron beam as obtained from a single lens β spectrometer. The line drawn cuts the ordinate below the abscissa and makes the intercept meaningless. If, however, an expression of the form $\sigma^2 = \sigma_0^2 + 1 \cdot KE$ is assumed,

then $a^2/2E^2$ must be plotted against $1/E$. Hopkins' results plotted in this way gave the line $\sigma^2 = 1.4 \times 10^{-3} + 1/440 E (\text{mev})$. This gives an effective number of 440 photoelectrons entering the multiplier per mev and a spread due to the lens spectrometer and other causes of 3.7% (fractional standard deviation) or 8.7% for the half-height width.

Birks (1950) stated that he had resolved the ^{114}In internal conversion lines using anthracene as a phosphor. If we assume that the lines must be separated by at least $2\sigma E$ for resolution, we get $\sigma^2 = 1/1440 E (\text{mev})$ a result in disagreement with Hopkins. This also disagrees with measurements by Taylor *et al.* (1951) who showed that the ratio of the pulse heights from NaI(Tl) and anthracene for 1 mev electrons, is approximately 1.7.

Physics Department,
St. Mary's Hospital Medical School, London W.2,
and University College, London W.C.1.
28th November 1952.

P. W. ROBERTS.

BIRKS, J. B., 1950, *Proc. Phys. Soc. A*, **63**, 1294.

GARLICK, G. F. J., and WRIGHT, G. T., 1952, *Proc. Phys. Soc. B*, **65**, 415.

HOPKINS, J. I., 1951, *Rev. Sci. Instrum.*, **22**, 29.

KURRELMAYER, B., and HAYNER, L. J., 1937, *Phys. Rev.*, **52**, 952.

SWANK, R. K., and BUCK, W. L., 1952, *Nucleonics*, **10**, No. 5, 51.

TAYLOR, C. J., JENTSCHKE, W. K., REMLEY, M. E., EBY, F. S., and KRUGER, P. G., 1951, *Phys. Rev.*, **84**, 1034.

Excitation Functions for the (γp) and (γT) Reactions in Lithium-7 for Energies up to 24 Mev

Photographic plate evidence for the $^7\text{Li}(\gamma p)^6\text{He} - 10.1$ mev reaction (Titterton 1950 a) and the $^7\text{Li}(\gamma T)^4\text{He} - 2.54$ mev reaction (Titterton 1950 b) induced by γ -rays from the 440 kev $^7\text{Li}(p\gamma)$ resonance has already been given. Crude preliminary excitation functions for the two reactions were presented at the Harwell Conference (Titterton 1950 c). The results given in this communication represent the continuation of that work to obtain improved statistics.

In the experiments Ilford type E1 emulsions, 200μ thick and loaded with lithium sulphate, were exposed to the 24 mev bremsstrahlung from the Atomic Energy Research Establishment synchrotron and were processed to obtain good low energy discrimination between particles of charges one and two units. The plates were searched and events identified as described in the earlier communications. In all 338 complete (γT) events and 118 complete (γp) events were found in the course of the work. The number-energy histograms, plotted in $\frac{1}{2}$ mev intervals, were corrected for geometrical losses (assuming in each case that the reaction products were isotropic about the incoming γ -ray direction) and converted to cross sections as a function of energy assuming a spectrum of the shape given by Heitler's theory. The energy dependence of the cross sections is shown in fig. 1 (a) and (b), where the points derived from the histogram and the corresponding statistical standard deviations are shown. A slow neutron background from the machine leads to the presence of events in the emulsion from the reaction $^6\text{Li}(n\alpha)^3\text{H}$ which are identical in character with (γT) events

produced by γ -rays of 7.18 MeV energy. To correct the distribution for these events the slow neutron flux in the vicinity of the plate at the time of the experiment was determined using boron-loaded plates (Titterton and Calcraft 1950).

A curve drawn through the points of fig. 1 (a) shows four peaks suggestive of the resonance absorption of γ -rays at energies corresponding to levels of the ${}^7\text{Li}$ nucleus each leading to disintegration into an α -particle and a triton. The first of these at 9.3 MeV is clearly resolved, the others at 16.7, 21.5 and 23.5 MeV are not so certain. This behaviour, strongly suggestive of the formation of a compound nucleus, is similar to that observed recently by Haslam *et al.* (1952) for the reaction ${}^{16}\text{O}(\gamma, n)$, by Goward and Wilkins (1952) in the case of ${}^{12}\text{C}(\gamma, 3\alpha)$ and ${}^{16}\text{O}(\gamma, 4\alpha)$, and by Livesey and Smith (1952) also for the reaction ${}^{16}\text{O}(\gamma, 4\alpha)$.

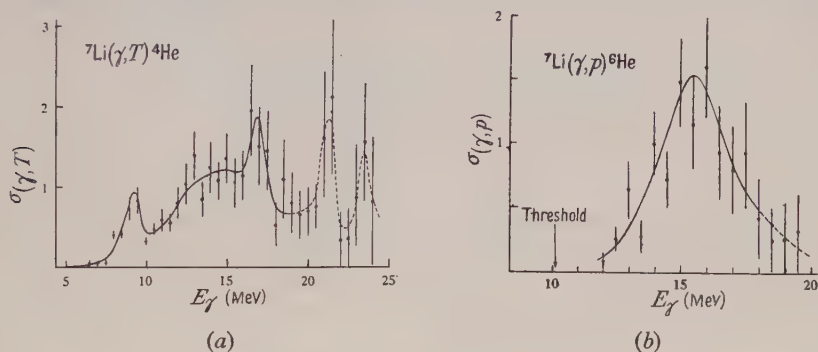


Fig. 1.

In the case of the (γp) reaction, although there is some scatter of points which may be due to unresolved fine structure, with the present statistics and resolution one can only justify drawing a smooth curve showing the general trend of the cross section as a function of energy. The complication also arises that ${}^6\text{He}$, unlike ${}^4\text{He}$, is expected to have low lying levels which, if they should de-excite by γ -ray emission, would lead to events being assigned an incorrect gamma-ray energy calculated from $E_\gamma = (E_p + E_{{}^6\text{He}} + 10.1)$ MeV. This could produce a smearing of fine structure if it were present.

Research School of Physical Sciences,
Australian National University,
Canberra.

18th November 1952.

E. W. TITTERTON.
T. A. BRINKLEY.

- GOWARD, F. K., and WILKINS, J. J., 1952, A.E.R.E. G/M127.
HASLAM, R. N. H., KATZ, L., HORSLEY, R. J., CAMERON, A. G. W., and MONTALBETTI, L., 1952, *Bull. Amer. Phys. Soc.*, **23**, No. 3, Abstract H4.
LIVESY, D. L., and SMITH, C. L., 1952, *Proc. Phys. Soc. A*, **65**, 758.
TITTERTON, E. W., 1950 a, *Proc. Phys. Soc. A*, **63**, 1297; 1950 b, *Ibid.*, **63**, 915; 1950 c, Harwell Conference Report, A.E.R.E. G/M68.
TITTERTON, E. W., and CALCRAFT, M. E., 1950, *Brit. J. Radiol.*, **23**, 465.

The Production of Bremsstrahlung in Electron-Electron Collisions

In a recent paper, Katzenstein (1950) has given a formula for the cross section for the production of bremsstrahlung in electron-electron collisions, in the limit of sufficiently high electron energy, and sufficiently low photon energy.

His result for the cross section is:

$$\Phi = 512 \Phi_0 E k^{-2} dk. \quad \dots\dots(1)$$

Φ_0 is the 'natural cross section' $\alpha^3 \lambda^2$, where α is the fine structure constant and λ the Compton wavelength of the electron. E and k are the energy of one of the electrons and of the emitted photon respectively, as seen from the centre-of-mass frame.

The k^{-2} spectrum obtained by Katzenstein has recently aroused some interest in connection with a possible mechanism for the production of radio noise in intergalactic space (Wilkinson, private communication).

It is the purpose of this note to point out that Katzenstein's result is in error, and that the low-frequency spectrum is, in fact, of the form $k^{-1}(a + b \ln k)$ rather than k^{-2} .†

Katzenstein derives his spectrum from a differential cross section (eqn. (30) in his paper) which contains two errors: (a) the Møller denominators have been incorrectly expanded in powers of k/E , and (b) a factor two is omitted in front of the third term in the radiation bracket.

After correcting these two mistakes, and generalizing the result to arbitrary electron energy, one obtains for the integrated cross section for radiation of a photon with energy in the range k^* to $k^* + dk^*$ as seen from the laboratory frame, in the limit as $k^* \rightarrow 0$, the result:

$$\begin{aligned} \Phi = \Phi_0 \frac{dk^*}{k^*} & \left[\frac{2}{3} \frac{(E^2 + p^2)^2}{E^5 p^5} \{3U + Ep(8p^4 + 2p^2 - 3)\} \ln \left(\frac{4p^2 E}{k^*} \right) \right. \\ & - \frac{2(E^2 + p^2)}{E^3 p^3} \left(2 + \frac{1}{4E^2 p^2} \right) \left\{ 4U \ln E + F \left(\frac{2p}{p+E} \right) \right. \\ & \left. - F \left(\frac{2p}{p-E} \right) + 2F \left(\frac{p}{p-E} \right) - 2F \left(\frac{p}{p+E} \right) \right\} \\ & + \frac{4}{p^2} \left\{ 4 \ln 2 \ln E + \ln^2 \left(1 + \frac{p}{E} \right) + \ln^2 \left(1 - \frac{p}{E} \right) + 2F \left(\frac{1}{2} - \frac{p}{2E} \right) \right. \\ & \left. + 2F \left(\frac{1}{2} + \frac{p}{2E} \right) - \frac{\pi^2}{3} + 2 \ln^2 2 \right\} \\ & + \frac{2U}{E^5 p^5} \left(\frac{4}{3} + \frac{57}{9} p^2 + \frac{10}{3} p^4 - \frac{62}{3} p^6 - \frac{92}{3} p^8 - \frac{32}{3} p^{10} \right) \\ & \left. + \frac{16U^2}{E^4 p^2} \left(1 + 2p^2 + p^4 \right) - \frac{4}{E^4 p^4} \left(\frac{2}{3} + \frac{23}{9} p^2 + \frac{4}{9} p^4 - \frac{41}{9} p^6 - \frac{28}{9} p^8 \right) \right] \quad \dots\dots(2) \end{aligned}$$

where E and p are the energy and momentum respectively of one of the electrons referred to the centre-of-mass system, measured in natural units

$$(\hbar = m = c = 1), \quad U = \sinh^{-1} p \quad \text{and} \quad F(x) = - \int_0^x y^{-1} \ln |1-y| dy,$$

is the 'Spence' function, which has been extensively tabulated by Mitchell (1949).

† This has been noted independently by J. Hamilton (private communication).

The non-relativistic limit of this formula is:

$$\Phi \simeq 8\Phi_0 \frac{dk^*}{k^*} \left[\frac{4}{5} \ln \left(\frac{4p^2}{k^*} \right) - 1 \right]. \quad \dots\dots(3)$$

The extreme relativistic limit, referred to the centre-of-mass frame for direct comparison with Katzenstein's result is:

$$\Phi \simeq 8\Phi_0 \frac{dk}{k} \left[\frac{16}{3} \ln E + \frac{1}{9} + \frac{8}{3} \ln \left(\frac{2}{k} \right) \right]. \quad \dots\dots(4)$$

I am grateful to Professor H. S. W. Massey for drawing my attention to this problem.

Physics Department,
University College, London.
21st November 1952.

M. L. G. REDHEAD.

KATZENSTEIN, J., 1950, *Phys. Rev.*, **78**, 161.
MITCHELL, K., 1949, *Phil. Mag.*, **40**, 351.

On the Motion of Electrons in Non-sinusoidal Periodic Fields

Morse (1930) has applied Hill's solution (1886) for the generalized Mathieu equation to the problem of electronic states in a crystal where the potential may be expressed as a Fourier series in each of the rectangular coordinates. An actual numerical solution for the energy bands was computed by Morse for a purely sinusoidal field only. It was decided to study quantitatively the effects of certain simple deviations from the sinusoidal potential that would bring the field represented mathematically closer to the actual field in a crystal. For small deviations, perturbation theory is applicable, but for the substantial modifications that are usually required, it would be more satisfactory to work fairly rigorously with a general solution of the Morse-Hill type. Hence, this solution was used exclusively at this preliminary stage of an investigation of electronic band structures for metals and alloys.

Two of the potential fields studied to date are those formed by adding to the fundamental sinusoidal field of period a , (a) a harmonic component of period $\frac{1}{2}a$, and (b) a subharmonic component of period $2a$. The ratios of the amplitudes of the harmonic and of the subharmonic to the amplitude of the fundamental were both set at 0.4. It is evident from fig. 1 that the two resultant periodic potentials are approximations to two different physical situations. The one shown in (a) is a definite improvement over the pure sinusoid as a representation of the periodic field of an electron in a monatomic chain, while that of (b) is a cruder approximation for a diatomic chain.

The amplitudes of both fundamental components were given the value chosen by Morse in his numerical solution of the sinusoidal field problem. The first few energy bands calculated for the non-sinusoidal potentials of figs. 1 (a) and (b) are represented by the solid curves of figs. 2 (a) and (b) respectively. For comparison, the energy bands for the sinusoidal potential considered by Morse are shown in both parts of fig. 2 (broken curves). The ranges of E_x in these figures are those for which the approximation made in the evaluation of the Morse-Hill infinite determinant is valid to within $\frac{1}{2}\%$. These ranges are adequate, however, for the purposes of the following discussion.

That the modifications of the band structure caused by the introduction of the harmonic and subharmonic potential components are so vastly different in *type* in the two cases can be readily understood in terms of the difference in the periodicities of the two resultant non-sinusoidal potentials. It is, however, the difference in *magnitude* of these modifications in the two cases that is of particular interest here. The small effect of the harmonic component and the pronounced effect of the subharmonic component on the band structure (the amplitudes of the two components being equal) would appear to allow a first approximation of the potential field in an ordered alloy in terms of only the main sinusoidal components and their subharmonics, even though the harmonics, actually present, be comparable in amplitude with the subharmonics.

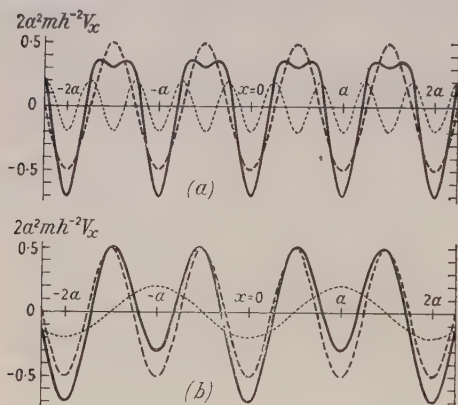


Fig. 1. The electronic potential V_x as a function of position in the idealized crystal.

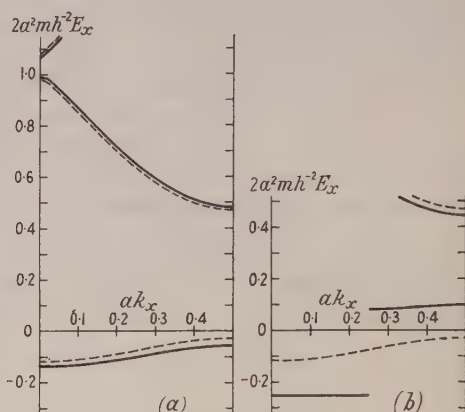


Fig. 2. The electronic energy E_x as a function of the reciprocal lattice parameter k_x . The diagrams are folded over at $ak_x=0.5, 1.0$, and 1.5 in the usual manner.

Incidentally, Slater (1952) recently considered by perturbation theory methods the energy bands for the same two types of non-sinusoidal periodic fields. From his calculated results, he concluded that contrary to an assumption often made in the theory of alloys, no one-to-one correspondence exists between the Fourier components of potential and their effect on the band structure. It may be noted that the energy gap at $ak_x=0.5$ in fig. 2 (a) of the present paper has been broadened by the introduction of the harmonic potential component, yet this component, if considered as the total potential field, would cause no energy gap at all at this k_x value; precisely the reverse situation occurs at $ak_x=1.0$ in fig. 2 (a) and at $ak_x=0.5$ in fig. 2 (b). Hence, Slater's conclusion is clearly supported by the present work.

I am grateful to Professor Stoner and Dr. Hoare of this Department for many encouraging discussions.

Department of Physics,
University of Leeds.

J. S. KOUVELITES.

26th November 1952.

HILL, G. W., 1886, *Acta Math.*, **8**, 1.
MORSE, P. M., 1930, *Phys. Rev.*, **35**, 1310.
SLATER, J. C., 1952, *Phys. Rev.*, **87**, 807.

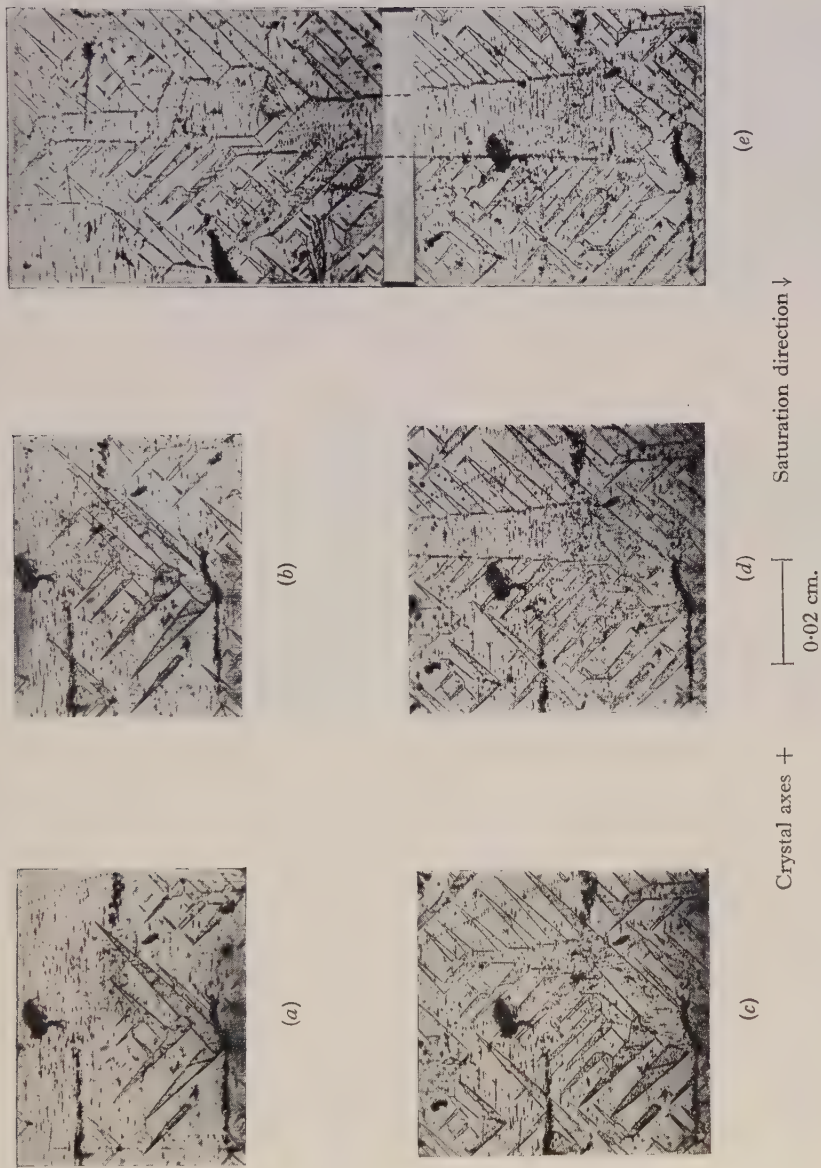


Fig. 1. Appearance of domains of reverse magnetization.

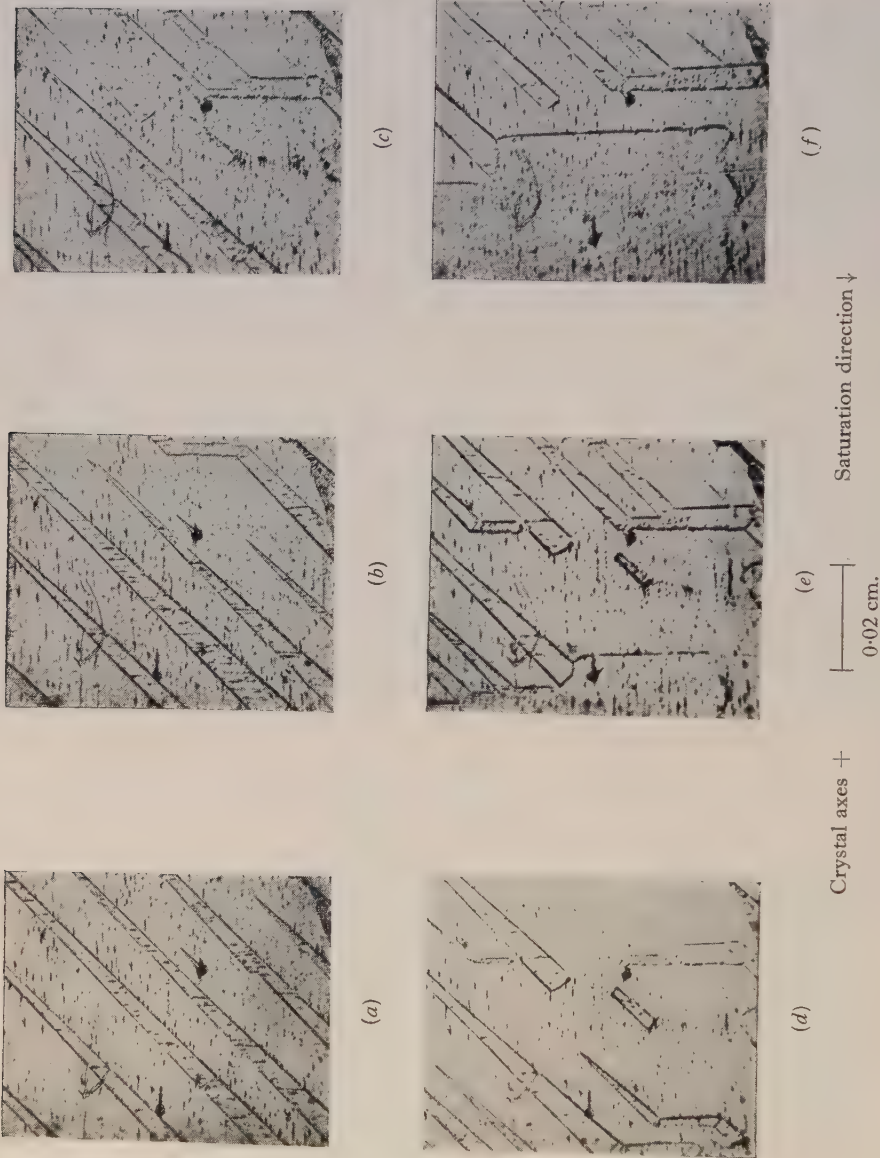


Fig. 3. Appearance of domains of reverse magnetization. (Non-uniform demagnetizing field.)

BOOK REVIEW

The Principles of Quantum Mechanics, by W. V. HOUSTON. Pp. viii + 288. (London : McGraw-Hill, 1951.) 51s.

This book by Professor Houston is a valuable addition to the expanding literature of quantum mechanics. It is written principally for graduate students studying modern theoretical physics and is based, we are told by the author, on many years' experience of teaching students of this type. Although this is certainly not a book for the beginner, unless exceptionally gifted, there are several chapters which an industrious undergraduate could study with profit to himself.

The book opens with a chapter entitled Experimental necessity for the quantum theory, which deals, in addition to other things, with the energy distribution in black-body radiation, the photoelectric and the Compton effects, and also with the diffraction of electrons, a phenomenon not discovered until after the establishment of wave mechanics. The next few chapters unfold the story of wave mechanics. The author makes no attempt to 'derive' the basic principles from experimental data, but prefers to state these principles in the form of concise postulates on the basis of which the theory is constructed. A most commendable feature of the book is the careful treatment of the theory of atomic spectra, including the theory of two electron systems. This is not usually dealt with so extensively in books on general Quantum Mechanics, and the present account provides a most useful introduction to this difficult subject. The theory of the electronic states in metals, including the elements of Brillouin zone theory, also receives more attention than is customary in such books. In spite of this the book is not a large one; the limitation in size is achieved partly by the economical use of mathematics, which, although always precise and sufficient, is perhaps just a trifle too condensed for comfortable reading.

Inevitably in a book of this size there are important omissions, even on matters of general theory. There is, for instance, little on matrix mechanics; radiation theory is allowed relatively little space, and there is no mention of Dirac's relativistic wave equation.

There are one or two minor points which call for comment: When most of us have become accustomed—perhaps one should say resigned—to the hybrids 'eigenfunction' and 'eigenvalue', it is rather disconcerting to find these quantities referred to as characteristic functions and characteristic values, thereby placing an additional burden on a word already overworked in mathematical literature. Again in the chapter on the solid state we find what is usually known as Bloch's theorem referred to as Floquet's theorem, a change not fully justified by the much earlier date of the latter's work since the content of Bloch's theorem extends far beyond the treatment of the case of a single independent variable. These are, however, small points and do not affect the value of this admirable book which deserves to be widely used by a variety of students as well as by those engaged in the teaching of the subject. To the latter the excellent selection of problems attached to each chapter will be particularly welcome.

H. JONES.

CONTENTS OF SECTION B

	PAGE
Dr. A. J. GOSS. The Effect of Added Metallic Impurity and of Closed Moulds on the Growth from the Melt of Single Crystals of Tin	65
Mr. J. H. CALDERWOOD and Dr. R. COOPER. Variation of the Electric Strength of KCl and NaCl Crystals with Temperature	74
Prof. J. B. BIRKS and Mr. J. W. KING. The Luminescence of Air, Glass and Quartz under α -Particle Irradiation	81
Dr. D. W. GOODWIN and Mr. K. A. MACFADYEN. Electrical Conduction and Breakdown in Liquid Dielectrics	85
Dr. J. H. PIDDINGTON. Thermal Theories of the High-Intensity Components of Solar Radio-Frequency Radiation.	97
Mr. R. B. BANERJI. Some Studies on Random Fading Characteristics	105
Dr. S. THORNTON. The Measurement of the Absolute Viscosity of Anomalous Fluids—I: The Measurement of the Time-dependence of Viscosity of Thixotropic Materials	115
Dr. S. THORNTON and Dr. D. RAE. The Measurement of the Absolute Viscosity of Anomalous Fluids—II: A Comparison of Absolute Viscosity Measurements on Instantaneously Thixotropic Fluids	120
Dr. H. R. THIRSK. The Structure and Orientation of Calomel formed on Liquid Mercury by Anodic Polarization	129
Dr. D. G. AVERY. The Optical Constants of Lead Sulphide, Lead Selenide and Lead Telluride in the $0.5\text{--}3\mu$ Region of the Spectrum	134
Dr. T. S. MOSS. Inter-Relation between Optical Constants for Lead Telluride and Silicon	141
Dr. E. H. LINFOOT and Dr. E. WOLF. Diffraction Images in Systems with an Annular Aperture	145
Letter to the Editor :	
Dr. T. R. KAISER and Dr. J. S. GREENHOW. On the Decay of Radio Echoes from Meteor Trails	150
Book Notices	151
Contents of Section A	152

Effect of the Fermi Energy on the Stability of Superlattices

By J. F. NICHOLAS *

Division of Tribophysics, Commonwealth Scientific and Industrial
Research Organization, Melbourne, Australia

MS. received 29th July 1952

Abstract. When an alloy develops an ordered structure, new Brillouin zone boundaries are formed corresponding to the extra Bragg reflections. It is shown that, in this process, the Fermi energy is lowered, and this tends to stabilize the superlattice. The theory is applied to the superlattices in CuPt, CuAu and Ag_3Mg , where the ordered structures do not follow from the simple principle of lattice-strain relief.

§ 1. INTRODUCTION

MANY superlattice structures are characterized by a tendency for the solute atoms to surround themselves with solvent atoms as nearest neighbours. This has been explained by Hume-Rothery and Powell (1935) in terms of the strain produced in the lattice when solute atoms, having a diameter different from that of the solvent atoms, are introduced into the structure. The energy associated with this distortion is a minimum, and the structure therefore most stable when the strain is distributed as uniformly as possible throughout the lattice, i.e. when similar atoms are as far apart from each other as possible. However, there are certain superlattices, notably CuPt, for which this principle does not hold. Recently, Slater (1951) has suggested that the explanation in these cases may follow from a consideration of the change in Fermi energy on ordering since the stability of the superlattice must clearly depend on the total energy of the structure, i.e. the energy of the ionic core, as considered in the lattice-strain theory, plus the energy of the free electrons.

Muto (1938) seems to have been the first to recognize the fact that, in a superlattice, new Brillouin zone boundaries are formed corresponding to the extra Bragg reflections. However, little further attention had been given to this until Lipson (1950) and Slater (1951) pointed out that the depression of the energy levels just below such new boundaries could lower the Fermi energy and hence help to stabilize the ordered structure. Lipson discounts the importance of this effect after a consideration of Cu_3Au , CuZn and the Fe-Al superlattices in all of which the effects of lattice-strain relief may swamp the Fermi energy effect. Slater, however, suggests that the electronic energy is the dominant factor in the disorder-order transformation in CuPt and in the tetragonal-orthorhombic change in CuAu, but as his ideas are based on an analogy with a one-dimensional model, further consideration is needed before they can be applied in three dimensions.

In this paper, it is shown that ordering may cause a significant decrease in the Fermi energy. The theory is then applied to the CuPt and CuAu cases mentioned above and also to the superlattice in Ag_3Mg (Clarebrough and Nicholas 1950).

* Now at H. H. Wills Laboratory, University of Bristol.

§ 2. THEORY

If we define $N(E)dE$ as the number of possible energy states per unit volume with energies between E and $E+dE$, we can find the maximum Fermi energy E^* by the condition that $\int N(E)dE$ from zero to E^* is equal to the number of free electrons per unit volume in the alloy. The total energy per unit volume is then given by

$$W = \int_0^{E^*} EN(E) dE.$$

Strictly, these formulae will only apply at the absolute zero of temperature but they will not be seriously in error at room temperature as the degeneracy temperature is very much higher. We will use subscripts *d* and *o* to denote the disordered and ordered states respectively. Then, we will assume that the number of free electrons does not change on ordering so that we have the relation

$$\int_0^{E_d^*} N_d(E) dE = \int_0^{E_o^*} N_o(E) dE.$$

As a general case, we will assume that, in the disordered structure, the first Brillouin zone lies well outside the Fermi surface which may therefore be taken as spherical. The $N_d(E)$ curve (fig. 1, curve *a*) will be parabolic for low energies with a peak at some value greater than E_d^* . If, now, inside the original first

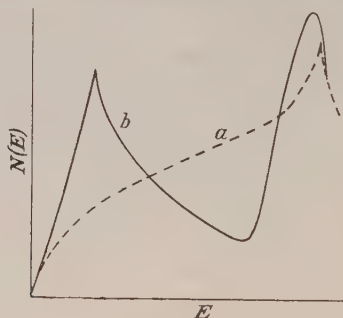


Fig. 1. Schematic diagram of the $N(E)$ curves for: *a*, the disordered structure; *b*, the ordered structure.

Brillouin zone, a new zone is produced by an ordering process, then the effect of the new boundaries is to raise the energy levels just outside the zone and lower those just inside it. The $N_o(E)$ curve will therefore be of some shape such as that shown in fig. 1, curve *b*, where we are now concerned with two or more zones having overlapping energy levels.

The decrease in total Fermi energy per unit volume on ordering will be

$$W_d - W_o = \int_0^{E_d^*} EN_d(E) dE - \int_0^{E_o^*} EN_o(E) dE$$

and, if this is positive, it will have a stabilizing influence on the superlattice. The full expression for the stability will involve entropy terms as well, but the effect of these can be neglected at sufficiently low temperatures. It is important to note that, depending on the shapes of the $N(E)$ curves and the number of available electrons, it is possible to have $W_o > W_d$ with $E_o^* < E_d^*$ and conversely. Therefore a decrease in E^* , which is the energy at the Fermi surface, is *not* the criterion for stability.

If a new zone boundary is well within the original Fermi surface, it is generally assumed that it has no effect on either E^* or W and this imposes conditions on the shape of the $N_o(E)$ curve. However, the calculation of the shape of the complete $N_o(E)$ curve will usually be very complicated, for not only are the magnitudes of the energy gaps uncertain but the number of zone boundaries crossing the Fermi surface may be quite large. Therefore, a general argument is used here to show that W_o is less than W_d in simple cases.

We assume that some of the new zone boundaries cut through the original Fermi surface without penetrating deeply and then consider the effect on the total Fermi energy. At first, we suppose that the distribution of electrons (in \mathbf{k} -space) is not altered by the introduction of the new zone. Then, there will be more occupied states close to, but just below, the boundary than close to and just outside the boundary. Provided the energy discontinuity at the boundary is made up of approximately equal depressions and elevations of the energy of states adjacent to the boundary (the usual assumption), then the introduction of the boundary will lower the energy of the system as a whole. In the one-dimensional case this is the only effect of the introduction of the boundary but, in three dimensions, a second process will now take place since with the new system of energy levels the original Fermi surface is no longer a surface of constant energy. Therefore, there will be a readjustment of the electron distribution to produce the new Fermi surface, the major effect being a transfer of electrons from the high energy levels outside the zone boundary to previously unoccupied levels inside the boundary. This must involve a further reduction in the total Fermi energy so that introduction of the new boundary does tend to stabilize the superlattice.

It should be noticed that both Lipson and Slater implicitly assume that this change in energy will be significant only when the new Brillouin zone has a volume very close to that required to accommodate all the free electrons. However, the above argument depends only on the existence of a zone having some boundaries intersecting, or even approaching closely, the original Fermi surface. Obviously, the closer the correspondence between the original Fermi surface and the new Brillouin zone the greater will be the energy decrease, but quite significant changes can appear even when the zone has a volume very different from that necessary to hold all the free electrons of the alloy (for example, the case of CuPt in §3). If all the electrons did go into a new zone of exactly the correct volume, there would of course be a catastrophic decrease in the electrical conductivity, as the energy gaps across the new boundaries are far greater than thermal energies. However, the formation of new zones as described above, no zone being completely full, will only cause small changes in the number of electrons near the Fermi surface, and therefore will not have a great effect on the conductivity.

At first sight, the above argument resembles that used in the general case of stability of alloy structures (e.g. Jones 1937) but the superlattice case has several distinctive features. In the general case, the Fermi energy is calculated for several possible structures as a function of electron concentration, and hence the ranges of electron concentration for which each structure is the most stable are found. In these comparisons, cases where the zones have overlapping energy levels are not considered. For the superlattice, however, the comparison is between structures at a fixed value of electron concentration and, in general, one structure (disordered) has non-overlapping levels while in the other there are two or more partly filled zones. In this case, too, the new peaks in the $N(E)$

curve correspond to much lower values of electron concentration than are ever considered in the ordinary case.

§ 3. APPLICATION TO CuPt

In CuPt, the disordered structure is face-centred cubic and the first Brillouin zone is the well-known truncated octahedron. Platinum, being a transition element, is taken into the solid solution as a neutral atom so that the alloy contains 0.5 free electrons per atom. The Fermi surface, therefore, lies well within the Brillouin zone and the electrons can be considered as free. The corresponding values of maximum and total Fermi energy are given in the table.

Fermi Energies in CuPt

	Fermi energy	
	Maximum (ev)	Total (ev/atom)
Disordered structure	4.05	1.22
Superlattice : spherical energy levels	4.52	1.27
Superlattice : cylindrical energy levels	3.87	0.97

In the superlattice, the Cu and Pt atoms are arranged on alternate (111) planes (Johansson and Linde 1927). The face-centred cubic cell is not now a unit cell for the structure but a convenient choice of unit cell is the cube which contains $2 \times 2 \times 2$ of the original face-centred unit cells. This has rhombohedral internal symmetry. Referred to this cell (of side length $2a$), the lowest angle x-ray reflections are 111 (superlattice line), $3\bar{1}\bar{1}$ (superlattice line) and 222 (main lattice

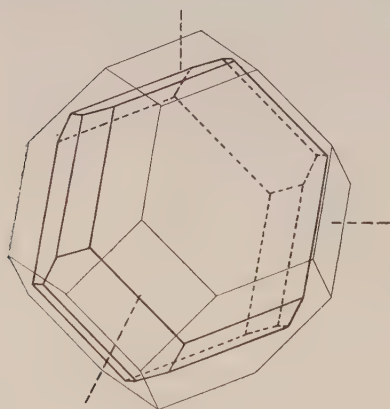


Fig. 2. First Brillouin zone of ordered CuPt. Thin lines show the first zone of the disordered structure.

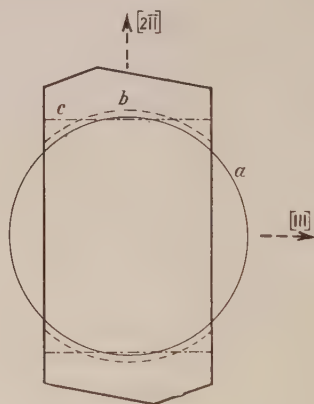


Fig. 3. Section through the first Brillouin zone of ordered CuPt, showing the positions of the Fermi surface for: *a*, the disordered state; *b*, the ordered state with spherical energy levels; *c*, the ordered state with cylindrical energy levels.

line). The symmetry of the cell allows interchange of indices for all reflections but the only change of sign possible for the superlattice reflections is $hkl \rightarrow \bar{h}\bar{k}\bar{l}$. The first Brillouin zone, which is bounded by planes corresponding to these reflections, is shown in fig. 2. The volume of this zone is $2/a^3$, corresponding to 1 electron per atom, but the inscribed sphere contains only 0.17 electron per atom.

Using a formula due to Jones (1934), the energy gaps across the (111) and ($\bar{1}\bar{1}\bar{1}$) planes are $6SeV$ (S =long range order parameter). For the fully ordered

alloy we assume that this is sufficient to keep all the electrons within the new first zone. To find upper bounds for both E^*_0 and W_0 , we will assume that the energy levels within the new zone are undisturbed by the zone boundaries. Then the energy surfaces are still spheres or portions of spheres and the values of E^*_0 and W_0 found on this assumption are given in the table. Since the maximum energy is still less than the energy gap in the fully ordered state, the assumption that no overlap occurs is justified. These values must provide upper bounds to the true values as no allowance has been made for the depression of the levels just inside the zone boundary.

Figure 3 shows a section through the new zone, the shape of the zone being almost a surface of revolution about $[111]$ as axis. We expect the energy depression to be 2-3 ev at the boundary and less towards the centre of the zone. The formerly spherical outer energy surfaces, therefore, become almost cylindrical with generators parallel to $[111]$. Another approximation to E^*_0 and W_0 is therefore found by taking *all* energy surfaces to be cylindrical, the energy on any cylinder being equal to the energy of a free electron at a point on the cylinder midway between the (111) and $(\bar{1}\bar{1}\bar{1})$ planes. This implies that the energies of the levels at the boundary are lowered by 2 ev. The most serious errors in this assumption will occur for the low energy levels where, however, the number of states is also low, so that the contribution to the total energy is small. The values of E^*_0 and W_0 found on this approximation are given in the table and these should be closer to the correct values than those found by the spherical approximation. The significance of the decrease in total energy can be judged by comparing it with the heat of transformation of CuPt found by Weibke and Matthes (1941), viz. 0.04 ev/atom (1.82 kcal/mol).

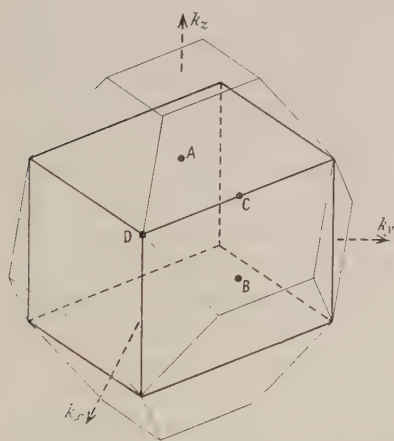


Fig. 4. First Brillouin zone of the tetragonal superlattice in CuAu. Thin lines show the first zone of the disordered structure.

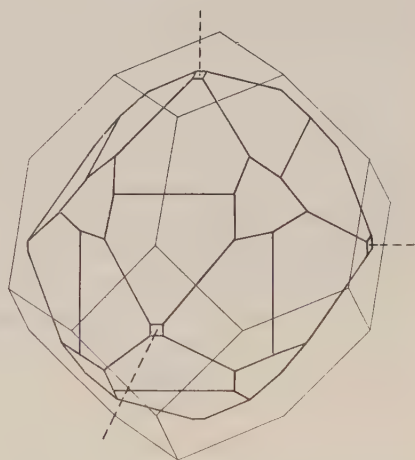


Fig. 5. First Brillouin zone of ordered Ag_3Mg . Thin lines show the first zone of the disordered structure.

On the other hand, as Slater points out, the lattice-strain theory predicts little or no energy decrease since, in both the ordered and disordered structures, the nearest neighbours of each atom are six like and six unlike atoms (in the disordered case, this is true only on the average, of course). It should be noted that, in the superlattice, the angles between the $[100]$, $[010]$ and $[001]$ directions are actually 91° but this slight distortion of the basic lattice has been neglected in the foregoing calculations.

It must also be pointed out that the above reasoning does not explain why CuPt should order in this rhombohedral structure rather than into the structure of, say, CuAu. All it shows is that the rhombohedral superlattice is likely to have a significantly lower Fermi energy than the disordered structure and, therefore, should be the more stable at sufficiently low temperatures.

§ 4. APPLICATION TO CuAu

For CuAu, the disordered structure is again face-centred cubic and the number of free electrons per atom is one. In the superlattice the Cu and Au atoms are arranged on alternate (001) planes and a tetragonality develops so that $c/a=0.93$ (Johansson and Linde 1925). The ordered structure can still be described in terms of the face-centred unit cell (now tetragonal) and the new inner Brillouin zone bounded by {001} and {110} planes is shown in fig. 4. The volume of the zone is $2/a^2c$ corresponding to 1 electron per atom while the inscribed sphere can contain only 0.26 electron per atom. In the ordered state the energy gaps are $6S$ and $4.4S$ eV across the {001} and {110} planes respectively while the free electron energies at A, B, C and D (fig. 4) would be 2.8, 4.8, 7.6 and 12.0 eV respectively. Therefore, it seems likely that overlap will occur across at least the {001} planes. The general picture will be as described in § 2 and a lowering of the Fermi energy is to be expected. In this case, of course, the lattice-strain theory also predicts a lowering of energy since each atom is now surrounded by eight unlike atoms and four like atoms. The two effects will be cumulative, but we will not attempt here to compare their relative magnitudes.

Under certain conditions, a further ordering process occurs in which the unit cell becomes an orthorhombic one containing ten of the original tetragonal cells (Johansson and Linde 1935). The number of like nearest neighbours is still four for each atom so that lattice-strain theory cannot account for the transformation. The effect on the x-ray pattern is that the 001 reflection is split into a number of reflections, the strongest being 011 and $0\bar{1}1$ (the second index now referring to an axis of length approximately $10a$) and the 110 reflection is split into 1 9 0, 1 11 0, etc. The new Brillouin zone structure formed by the planes corresponding to these reflections is similar to the zone shown in fig. 4 except that the boundaries are now a closely spaced series of small energy gaps. The total volume enclosed is slightly larger and the outer boundary at points such as A and B is displaced further from the origin so that the overlap is reduced. The complete pattern is naturally very complicated, but the general effect of this extra ordering will be that more electrons are near to, but just below, energy gaps so that the total energy is reduced.

It is not clear why the periodicity of ten cells is the stable one but the following considerations may be relevant. In both the rhombohedral CuPt and the tetragonal CuAu a doubling of the periodicity interval caused a halving of the volume of the innermost Brillouin zone, but in the orthorhombic CuAu case there is no Brillouin zone having one-tenth the volume of the first disordered Brillouin zone. Instead, there is an inner zone of volume less than one-half the original volume surrounded by the series of neighbouring planes of small energy discontinuity, the total volume enclosed being just over one-half the original volume. If the length of the orthorhombic cell were slightly different, say eleven elementary cells long, the zone structure would be very similar though the total Fermi energy might be markedly different for this particular electron concentration.

However, a small change in electron concentration could suffice to stabilize this extended structure relative to the ten-cell one. This could account for the varying lengths of cell that have been reported, since Raynor (1949) has pointed out that, although the nominal valency of gold is one, its value in alloys varies considerably.

§ 5. APPLICATION TO Ag_3Mg

In the case of Ag_3Mg , the disordered structure is again face-centred cubic but this alloy has 1.25 free electrons per atom. Lattice-strain theory would predict the ordered structure as being of the Cu_3Au type with every Mg atom surrounded by twelve Ag atoms. However, x-ray evidence shows that this does not occur. Mathieson (private communication) has shown that the unit cell of the superlattice consists of $4 \times 4 \times 4$ elementary face-centred cubic cells, but the arrangement of the atoms within this cell has not yet been determined. Referred to this cell, the x-ray reflections which determine the inner Brillouin zone structure are: (a) 444, 800-main lattice reflections, (b) 400, 440-'normal' superlattice reflections (as would occur in an alloy of the Cu_3Au type), (c) 410, 430, 450-'extra' superlattice reflections. (In all these reflections the indices and signs may be interchanged.) The energy gaps across the corresponding Brillouin planes are approximately 8 eV for the main reflections and 1 eV for all the superlattice reflections.

The main reflections lead, of course, to the normal first Brillouin zone of the face-centred cubic lattice, while the addition of the (b) reflections subdivides this zone into four smaller zones (for diagrams of these, see Brillouin 1946). The outer boundary of the second zone is a dodecahedron bounded by {440} planes and the enclosed volume can contain one electron per atom; this zone is the most important one for Cu_3Au (Lipson 1950), for which alloy, however, the main contribution to the energy decrease would come from the relief of lattice-strain. When the (c) reflections are considered, this zone is modified by the {430} and {450} planes in a similar way to that described above for orthorhombic CuAu . Therefore, the Brillouin zone structure is again complex, but the boundaries which have most influence are those corresponding to the {450} reflections. These form a twenty-four-sided polyhedron which is truncated by {444} and {800} planes to give the zone shown in fig. 5. This zone is nearly spherical (ratio of maximum to minimum diameter = 1.25), the inscribed sphere can contain 1.09 electrons per atom and the whole zone can contain 1.32 electrons per atom. Therefore, the 1.25 electrons per atom will probably be accommodated inside it without overlap but the Fermi surface will be close to the zone boundary throughout, so that a large energy depression will result. If the ordering process had been of the Cu_3Au type, the inner dodecahedral zone would have held as a maximum 1 electron per atom and therefore considerable overlap would have resulted and the reduction in total energy due to the new zone boundaries would have been much less.

§ 6. CONCLUSIONS

On the basis of the above results, it seems probable that the Fermi energy plays a significant part in determining the stability of a superlattice structure. The effect is complementary to that of the lattice-strain energy, the relative magnitude of the two effects varying from case to case. Thus, it seems that the

reduction of strain energy in the lattice is the dominant factor in such alloys as Cu_3Au and CuZn , while the reduction in Fermi energy determines the stability of the ordered structures in CuPt and Ag_3Mg .

REFERENCES

- BRILLOUIN, L., 1946, *Wave Propagation in Periodic Structures* (London and New York : McGraw-Hill), p. 152.
- CLAREBROUGH, L. M., and NICHOLAS, J. F., 1950, *Aust. J. Sci. Res. A*, **3**, 284.
- HUME-ROTHERY, W., and POWELL, H. M., 1935, *Z. Kristallogr.*, **91**, 23.
- JOHANSSON, C. H., and LINDE, J. O., 1925, *Ann. Phys., Lpz.*, **78**, 439; 1927, *Ibid.*, **82**, 449; 1935, *Ibid.*, **25**, 1.
- JONES, H., 1934, *Proc. Roy. Soc. A*, **144**, 225; 1937, *Proc. Phys. Soc.*, **49**, 250.
- LIPSON, H., 1950, *Progress in Metal Physics II* (London : Butterworths Scientific Publications), pp. 47-50.
- MUTO, T., 1938, *Sci. Pap. Inst. Phys. Chem. Res., Tokyo*, **34**, 377.
- RAYNOR, G. V., 1949, *Progress in Metal Physics I* (London : Butterworths Scientific Publications), p. 9.
- SLATER, J. C., 1951, *Phys. Rev.*, **84**, 179.
- WEIBKE, F., and MATTHES, H., 1941, *Z. Elektrochem.*, **47**, 421.

The Ultra-Violet Absorption Spectrum of Nitric Oxide

By L. H. SUTCLIFFE AND A. D. WALSH

Department of Chemistry, University of Leeds

Communicated by R. W. B. Pearse; MS. received 3rd September 1952, and in final form 19th December 1952

Abstract. New photographs of the absorption spectrum of nitric oxide have been obtained. Three red-degraded bands between 1711 and 1676 Å resemble the β bands and plausibly represent the $v'=14, 15, 16$ members of the β system. An intensity and spacing anomaly between the $v'=13$ and $v'=14$ members is probably connected with the diffuseness and disturbance in position of the $v'=2$ member of the δ system and the failure of the $v'=3$ member of that system to appear; and can be accounted for in terms of a crossing of the $B^2\Pi$ and $C^2\Sigma^+$ potential energy curves. The β system suffers a further disturbance when the $B^2\Pi$ curve cuts the $D^2\Sigma^+$; the $v'=17$ member of the β system appears to be replaced by the $v'=3$ member of the ϵ system. There is no need to introduce a hypothetical repulsive curve to explain the perturbations of the various systems; they all appear to be explicable in terms of successive crossings of the $^2\Sigma^+$ curves by the $B^2\Pi$ potential curve. All the states A, C, D and E involve extra-valency shell (Rydberg) orbitals. Plausible interpretations of these states are given.

§ 1. INTRODUCTION

THERE are five well known excited states of the NO molecule. In order of increasing excitation these are $A^2\Sigma^+$, $B^2\Pi$, $C^2\Sigma^+$, $D^2\Sigma^+$, $E^2\Sigma^+$. Transitions between the ground state and the first four of these excited states give rise to the γ , β , δ and ϵ systems respectively. Absorption bands due to transitions between the ground and $E^2\Sigma^+$ states have recently been recorded (Tanaka, Seya and Mori 1951). A further upper state, labelled B' and giving rise to a β' system of bands on transition to the ground state has recently been reported from emission studies (Baer and Miescher 1951). Another recent communication (Baer and Miescher 1952) has proved, by the study of the emission spectrum of $^{15}\text{N}-\text{O}$, that the ϵ and γ bands really do belong to separate systems. We desire to make a number of contributions.

§ 2. THE β SYSTEM

The absorption bands of NO as far as 1296 Å were first measured by Leifson (1926), using a hydrogen continuum as background and low dispersion. Careful comparison of his measurements with the known bands of the above systems shows that all but four of Leifson's bands of wavelength longer than 1645 Å are now accounted for. These four lie at 1740.0, 1709.4, 1690.1 and 1677.7 Å. The 1740.0 Å band is almost certainly the $v'=13$ member of the β bands. These have previously been reported in absorption up to $v'=12^5$.*

* Measurements of the β bands have also been given by Migeotte and Rosen (1950). These authors suggest that the 1740.0 Å and 1621.1 Å bands of Leifson may be successive bands of a system other than the β . The fact that these bands are red-degraded appears to be decisive evidence against this, for the suggested new system has $\omega' > \omega''$.

1740.0 Å band is faint but just visible on plates we have taken using a Lyman continuum as background and a dispersion of approximately 8 Å/mm.

The bands at 1709.4, 1690.1 and 1677.7 Å can be clearly distinguished (see Plate). They are double-headed and red-degraded, looking very like the β bands. They therefore almost certainly belong to a ${}^2\Pi \leftarrow {}^2\Pi$ system. Our measurements of the heads are compared with Leifson's measurements of band centres in table 1. The agreement of the separations between the two sets of measurements is very good. The separations are not constant, but the bands are

Table 1

v'	v''	Present authors		Leifson	
		λ (Å)	ν (cm $^{-1}$)	λ (Å)	ν (cm $^{-1}$)
n	0	1710.50	58462	1709.4	58500
		1707.70	58558		
$n+1$	0	1691.04	59135	1690.1	59168
		1688.38	59228		
$n+2$	0	1678.34	59583	1677.7	59605
		1676.08	59663		

670

668

437

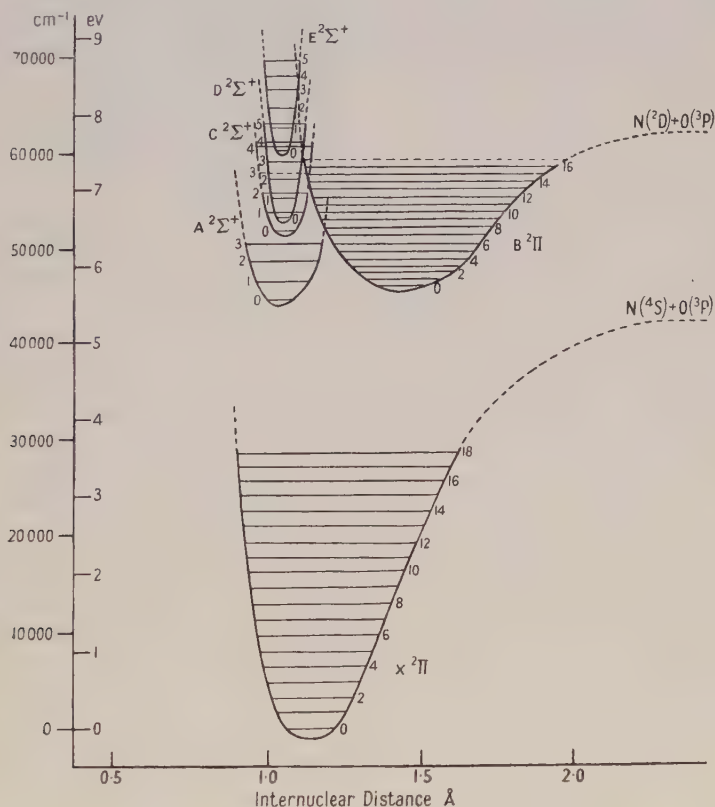
435

so similar that they almost certainly represent successive vibrational bands of a single electronic system. The separation of the two heads of a particular band is virtually the same as that reported by Tanaka (1949) for the β bands. It is possible that the bands represent a further fragment of the β series, being the $v'=14, 15 \dots$ members. If so, there is an intensity and spacing anomaly between the $v'=13$ and $v'=14$ members. This is possible, for it is known that the δ series of bands is cut off sharply after the $v'=2$ member at 1750 Å. Tanaka (1949) has already commented on the strength of the δ bands in absorption and how the intensity increases from the $v'=0$ to the $v'=1$ and $v'=2$ members, but that the $v'=3$ member fails to appear, at any rate in the expected position and with the expected intensity. Our plates confirm his comment. In place of the $v'=3$ member appear the red-degraded bands $v'=n+1$ and $v'=n+2$ of table 1. It is probable that the potential energy curves of the $B^2\Pi$ and $C^2\Sigma^+$ states cross and suffer a mutual disturbance at an energy corresponding to a wavelength between 1740 and 1670 Å.

§ 3. THE $B^2\Pi$ - $D^2\Sigma^+$ PERTURBATION

The $(n+1, 0)$ band of table 1 is considerably stronger than the $(n, 0)$, while the $(n+2, 0)$ and $(n+1, 0)$ bands have about the same strength. It is therefore surprising that the $(n+3, 0)$ member is not readily visible. In its expected place occurs the $v'=3$ member of the ϵ system, which is weaker than the $(n+2, 0)$ band of table 1. A glance at the potential energy curves (see figure) for the various states of NO (cf. Tanaka 1949, Gaydon 1947) shows (i) that the $B^2\Pi$ and $C^2\Sigma^+$ curves will cross at about the $v'=3$ level of the latter state, in agreement with what we have said in § 2, (ii) that the $B^2\Pi$ and $D^2\Sigma^+$ curves will cross at about the $v'=3$ level of the latter state. It is plausible therefore to

ascribe the failure to appear of the $(n+3, 0)$ member of the bands of table 1 to a crossing of the $B^2\Pi$ and $D^2\Sigma^+$ curves; the $(n+3, 0)$ band is simply replaced by the $v'=3$ member of the $D^2\Sigma^+$ system, just as the $v'=3$ member of the $c^2\Sigma^+$ system is simply replaced by the $(n+1, 0)$ or $(n+2, 0)$ band of table 1. The failure of the $(n+3, 0)$ member to appear and the fact that its energy height is just about that at which the $B^2\Pi$ and $D^2\Sigma^+$ curves cross strengthens our belief that the bands of table 1 represent a further fragment of the β series. The rapid convergence of the supposed β bands in table 1 may be due to perturbation of the $B^2\Pi$ curve by the c and $D^2\Sigma^+$ curves and/or to the bands lying close to the dissociation limit of the $B^2\Pi$ state.



§ 4. THE β' SYSTEM

The list of bands given by Baer and Miescher (1951, 1952) for the new β' emission series includes three for which $v''=0$, v' being 1, 2, 3. These bands are visible on our plates between 1634 Å and 1575 Å. There is no sign of the $(0, 0)$ band (which was also not observed by Baer and Miescher) but the $v'=4$ band is visible. Our measurements are compared with those of Baer and Miescher in table 2. Our measurements refer to the shortest wavelength head which appears to consist of two lines close together. The agreement of the separations between the two sets of measurements is good. The $(1, 0)$ and $(3, 0)$ bands shade into the violet-degraded $(0, 0)$ and $(1, 0)$ bands respectively of the $E^2\Sigma^+$ system reported by Tanaka, Seya and Mori (1951). The $(2, 0)$ band overlaps the $(4, 0)$ of the $c(D^2\Sigma^+)$ series. Table 2 includes also what we think are the corresponding

bands measured by Leifson. The bands are red-degraded and therefore Leifson's measurements of band centres are at longer wavelengths than are ours of band heads. Leifson's measurements are also subject to a possible inaccuracy which is not less than $\pm 1 \text{ \AA}$.

Table 2

v'	v''	Baer and Miescher]		Present authors		Leifson	
		λ (Å)	ν (cm ⁻¹)	λ (Å)	ν (cm ⁻¹)	λ (Å)	ν (cm ⁻¹)
0	0	—		—		—	
1	0	1633.83	61205.9	{ 1633.70 61211 1633.24 61228 }	1149	1642.3	60890
2	0	1603.70	62355.8			{ 1603.58 62360 1603.20 62375 }	1605.6
3	0	1575.43	63474.7	{ 1575.41 63476 1575.10 63488 }	1116	1552.1	64429
4	0	—					

§ 5. THE $B^2\Pi-C^2\Sigma^+$ PERTURBATION

With the above identifications, every band but one measured by Leifson at wavelengths longer than 1600 \AA can be accounted for in terms of the known bands of the known systems. The one exception is at 1621.1 \AA . Our plates show this band to be moderately strong in absorption, violet-degraded and multiple-headed. It is possible that it represents the $v'=4$ band of the δ series, the $v'=3$ band being missing. It is in about the position expected for the $v'=4$ band. Our measurements of the four main heads are shown in table 3 (a); the separations are similar to those given by Tanaka (1949) for the earlier δ bands. Table 3 (b) shows the separation of the band from the $v'=2$ member compared with the separations of the $v'=0$, $v'=1$ and $v'=2$ members as given by Tanaka

Table 3

(a)		(b) Longest wavelength heads		
$\lambda (\text{\AA})$	$\nu (\text{cm}^{-1})$	v'	v''	$\nu (\text{cm}^{-1})$
1623.15	61609	0	0	52221.0
1622.65	61628	1	0	54533.1
1620.09	61725			
1619.57	61746	2	0	56958.0
		3	0	—
		4	0	61609

(1949). Tanaka has already pointed out that the separation of the $v'=1$ and $v'=2$ members is greater than that of the $v'=0$ and $v'=1$ members. This is presumably other evidence of the perturbation referred to in §2, which causes the $v'=3$ member not to appear. That the $v'=2$ member is disturbed is indicated not only by its position but also by its diffuseness.

§ 6. THE $B^2\Pi-A^2\Sigma^+$ PERTURBATION

Various authors have discussed a perturbation of the γ system between $v'=3$ and 4. Herzberg and Mundie (1940) supposed that the ϵ system of bands was simply a continuation of the γ system, an intensity anomaly resulting at $v'=3$ or 4 from a perturbation supposed due to a crossing of the $A^2\Sigma^+$ potential energy curve by that of a repulsive $^2\Sigma$ state. Tanaka (1949) followed them. It is now definite that the ϵ and γ systems have separate upper states (Baer and Miescher, 1952, Migeotte and Rosen 1950, Gaydon 1947). This means that there is a disturbance of the γ system after $v'=3$, though not necessarily one due to a repulsive $^2\Sigma$ curve. Higher members of the system simply do not appear. Kaplan (1931) failed to obtain the β bands in emission above $v'=4$ and therefore supposed there was a predissociation just above $v'=4$ for the β system. Gaydon (1947), however, observed bands up to $v'=6$ in emission, and Tanaka (1949) observed bands up to $v'=12$ in absorption but was unable to observe any intensity anomaly at about $v'=4$. Instead, Tanaka observed a perturbation at about $v'=8$. This perturbation is not altogether certain because of overlapping bands (Migeotte and Rosen 1950). Migeotte and Rosen report an abnormal intensity for $v'=9$ of the β system and suggest that the bands with $v'>10$ really belong to a system other than the β , but the slight evidence they give in favour of this might be equally well interpreted simply as due to a disturbance of the $B^2\Pi$ curve above $v'=8$ or 9. Now the $B^2\Pi$ curve probably crosses the $A^2\Sigma^+$ curve at just about $v'=8$ for the former and $v'=3$ or 4 for the latter (see figure). The two perturbations can therefore be ascribed to a single cause, the crossing of the two potential energy curves. There is no need to suppose a repulsive $^2\Sigma$ potential curve as was done by Herzberg and Mundie (1940) and by Tanaka (1949). Tanaka similarly assumed that the cutting off of the δ system after $v'=2$ was due to crossing of the $C^2\Sigma^+$ potential curve by the potential curve of this supposed $^2\Sigma$ repulsive state. Again this is unnecessary. The disappearance of the $v'=3$ band is connected with the disturbance of the β system at the same wavelengths.

§ 7. CONCLUSIONS FROM §§ 2-6

To sum up, when the $B^2\Pi$ curve cuts each of the curves $A^2\Sigma^+$, $C^2\Sigma^+$ and $D^2\Sigma^+$ a disturbance is caused. Its crossing of the $A^2\Sigma^+$ curve is shown by the cutting off of the γ system above $v'=3$ and by a disturbance of the β system at about $v'=8$. Its crossing of the $C^2\Sigma^+$ curve is shown by the failure of the $v'=3$ member of the δ bands to appear, by a disturbance in position and diffuseness of the $v'=2$ member, and by a disturbance of intensity and spacing in the $v'=13$ to 15 members of the β system. The β bands simply replace the $v'=3$ δ band. The crossing of the $B^2\Pi$ and $D^2\Sigma^+$ curves is shown by the failure of the $v'=17$ member of the β system to appear. It would be most surprising if a repulsive $^2\Sigma$ curve ran through each of the points of intersection of the $B^2\Pi$ and $A^2\Sigma^+$, $C^2\Sigma^+$ and $D^2\Sigma^+$ curves. Economy of hypothesis is strongly in favour of not introducing any supposed repulsive curve to explain the observed effects. The figure shows the crossings of the various curves.

§ 8. RYDBERG TRANSITIONS

With three exceptions every band measured by Leifson at wavelengths longer than 1500\AA can now be accounted for. The three exceptions are at $1599\cdot5$, $1593\cdot8$ and $1502\cdot2\text{\AA}$. The first two of these are very faint indeed on

our plates. The third is weak, but clear. A few further weak or faint bands not reported by Leifson are visible on our plates between 1575 and 1500 Å. Really strong bands begin just below 1500 Å. The dissociation energy of $(\text{NO})^+$ is known to be some 4.1 eV greater than that of NO. It is practically certain therefore that the internuclear distance will be markedly less in the ground state of $(\text{NO})^+$ than in that of NO. It follows that, although the strong bands below 1500 Å probably belong to Rydberg transitions, they represent transitions to fairly high vibrational levels of the Rydberg states. Each Rydberg transition will have much vibrational structure (the vibration frequencies presumably being greater than in the ground state of NO). The overlapping of the vibrational bands and the crowding of the Rydberg levels as they approach the ionization potential (given by electron impact work as about 9.4 ± 0.2 eV (Hagstrum 1951)) is responsible for the confused appearance of the spectrum in the 1500–1300 Å range, and makes analysis extremely difficult. A few definite statements concerning Rydberg transitions may however be made.

The first Rydberg transition expected to occur (see Walsh, to be published) is

$$\dots (\sigma 3s), {}^2\Sigma^+ \leftarrow \dots (\bar{\pi}), {}^2\Pi \dots (1)$$

$(\sigma 3s)$ stands for an orbital built by the in-phase overlap of a 3s orbital on the N atom and another 3s orbital on the O atom. It corresponds to the $(\sigma_g 3s)$ orbital of O_2^+ . The contribution from the O atom is greater than that from the N atom, so that the orbital may be said to be largely a 3s orbital on the O atom. The transition should cause a strengthening of the NO bond in the excited state, since the electron excited comes from the anti-bonding $(\bar{\pi})$ orbital. The latter orbital corresponds to the $(\pi_g 2p)$ orbital of O_2^+ . It is more localized on the N than on the O atom. The quantum defect of the term value of the transition is expected to be approximately 1.1. Its expected term value is approximately $30\,398\text{ cm}^{-1}$. The actual term value, based on an ionization potential of 9.4 ± 0.2 eV, is likely to be greater rather than less than $30\,398\text{ cm}^{-1}$ since electron impact ionization potentials are expected and generally found to be a little greater than Rydberg series limits. The first member of a molecular Rydberg series is expected to be shifted somewhat relative to its calculated position, but in this case probably not by more than one or two thousand cm^{-1} . Table 4 shows that the $\text{A}^1\Sigma^+$ state is the only one that can well be identified as the first Rydberg level. The next nearest ${}^2\Sigma^+$ state is c which is 7000 cm^{-1} away from the

Table 4

Term Values of ${}^2\Sigma^+$ States assuming an Ionization Limit of $75835 \pm 1614\text{ cm}^{-1}$

State	$\text{A}^2\Sigma^+$	$\text{c}^2\Sigma^+$	$\text{D}^2\Sigma^+$
Term value (cm^{-1})	31784 ± 1614	23614 ± 1614	22700 ± 1614

expected position and on the short wavelength side. The N–O binding in the A state is known to be strengthened relative to the ground state, in agreement with our expectation. It appears virtually certain that A is to be identified with the upper state of transition (1). Mulliken (1932) has earlier concluded that the $\text{A}^2\Sigma^+$ state arises by promoting an electron from the $(\bar{\pi})$ orbital to a σ orbital derived from the 3-quantum shell; and has pointed out that the σ orbital is probably analogous to a σ_g orbital in O_2^+ since no corresponding transition is known for O_2^+ , in agreement with a $\dots (\sigma_g), {}^2\Sigma_g^+ \leftarrow \dots (\pi_g), {}^2\Pi_g$ transition being forbidden.

Gaydon (1947) has supposed $A^2\Sigma^+$ to correlate with the $^2\Sigma^+$ state that can be built from the ground state atoms $N(^4S)$ and $O(^3P)$. However, since the $A^2\Sigma^+$ state probably involves an extra-valency shell orbital, it probably leads 'originally' (i.e. before the effects of the non-crossing rule are considered) to dissociation products that are not both ground-state atoms. The probable ground state configuration of the NO molecule may be written

$$KK'(\sigma)^2(\sigma)^2(\pi)^4(\sigma)^2(\bar{\pi}), ^2\Pi$$

or, perhaps

$$KK'(\sigma)^2(\sigma)^2(\sigma)^2(\pi)^4(\bar{\pi}), ^2\Pi.$$

The lowest excited configurations should be

$$KK'(\sigma)^2(\sigma)^2(\pi)^4(\sigma)(\bar{\pi})^2 \quad \dots\dots(2)$$

and

$$KK'(\sigma)^2(\sigma)^2(\pi)^3(\sigma)^2(\bar{\pi})^2. \quad \dots\dots(3)$$

Expression (3) almost certainly represents the $B^2\Pi$ state, the internuclear binding being greatly reduced as expected. Expression (2) can give rise to a $^2\Sigma^+$ state but, by analogy with the corresponding configurations and states of N_2 and CO, it is unlikely to have a strengthened internuclear binding relative to the ground state. It is unlikely that any of the known $^2\Sigma^+$ states of NO are to be supposed to arise from configuration (2); or indeed from any intra-valency shell configuration. It appears therefore that an intra-valency shell $^2\Sigma^+$ state of NO remains to be discovered. By analogy with the corresponding transition in N_2 ($^1\Pi_g \leftarrow ^1\Sigma_g^+$ at about 1450 Å; cf. also O_2 and O_2^+), we should expect transition from the ground state to configuration (2) to lie at a wavelength shorter than that (c. 2270 Å) of the transition to the $A^2\Sigma^+$ state. The operation of the non-crossing rule and the expectation that the $^2\Sigma^+$ state will have an internuclear distance markedly greater than that of the ground state make it probable that the actual $A^2\Sigma^+$ curve must possess a maximum of considerable width. The observation of stable vibrational levels of the $A^2\Sigma^+$ state above 5.29 eV (Gaydon 1947) cannot therefore be taken as evidence against the value of $D(NO)=5.29$ eV; though it is also compatible with $D(NO)=6.49$ eV. The value 5.29 eV (corresponding to $D(N_2)=7.38$ eV) has been favoured by Herzberg (1950) and by Hagstrum (1951); that of 6.49 eV (corresponding to $D(N_2)=7.76$ eV) is implicitly favoured by Douglas (1952), Thomas, Gaydon and Brewer (1952), Kopineck (1952) and Kistiakowsky, Knight and Malin (1952).

In addition, as Mulliken (1932) has pointed out, a $^4\Pi$ state corresponding to configuration (3) should lie below $B^2\Pi$. In this connection it is of interest to note that Goodeve and Katz (1939) refer to an excited state of NOCl which arises from a hitherto unknown level of NO. The height of this unknown level is approximately 8000 cm^{-1} (i.e. transitions to it from the ground state would occur around 12000 Å).

The position of the $E^2\Sigma^+$ state makes it possible that transition to this state represents the second member of the Rydberg series beginning with transition (1). It should be noted that the internuclear distance in the A and E states is almost identical. Possible assignments for states C and D are as upper levels for two of the transitions

$$\dots (\bar{\sigma}3s), ^2\Sigma^+ \leftarrow \dots (\bar{\pi}), ^2\Pi$$

$$\dots (\sigma 3p), ^2\Sigma^+ \leftarrow \dots (\bar{\pi}), ^2\Pi$$

$$\dots (\bar{\sigma}3p), ^2\Sigma^+ \leftarrow \dots (\bar{\pi}), ^2\Pi.$$

The ($\bar{\sigma}3s$) orbital is largely localized on the N atom and should correspond to the (σ_u3s) orbital of O_2^+ . The anti-bonding power of such a highly excited orbital may be only slight. The meanings of the ($\sigma3p$) and ($\bar{\sigma}3p$) orbitals should be clear.

ACKNOWLEDGMENTS

We are indebted to the Royal Society and the Chemical Society for grants in aid of equipment, to Dr. W. C. Price for the generous loan of a diffraction grating, and to the Department of Scientific and Industrial Research for financial support to one of us (L. H. S.).

REFERENCES

- BAER, P., and MIESCHER, E., 1951, *Helv. Phys. Acta*, **24**, 331; 1952, *Nature, Lond.*, **169**, 581.
DOUGLAS, A. E., 1952, *Canad. J. Physics*, **30**, 302.
GAYDON, A. G., 1947, *Dissociation Energies* (London: Chapman and Hall), p. 136.
GOODEVE, C. F., and KATZ, S., 1939, *Proc. Roy. Soc. A*, **172**, 432.
HAGSTRUM, H. D., 1951, *Rev. Mod. Phys.*, **23**, 185.
HERZBERG, G., 1950, *Spectra of Diatomic Molecules*, 2nd edn. (New York: van Nostrand).
HERZBERG, G., and MUNDIE, L. G., 1940, *J. Chem. Phys.*, **8**, 263.
KAPLAN, J., 1931, *Phys. Rev.*, **37**, 1406.
KISTIAKOWSKY, G. B., KNIGHT, H. T., and MALIN, M. E., 1952, *J. Chem. Phys.*, **20**, 876.
KOPINECK, H. J., 1952, *Z. Naturforsch.*, **7(a)**, 22, 314.
LEIFSON, S. W., 1926, *Astrophys. J.*, **63**, 73.
MIGEOTTE, P., and ROSEN, B., 1950, *Bull. Soc. Roy. Liège*, **19**, 343.
MULLIKEN, R. S., 1932, *Rev. Mod. Phys.*, **4**, 51.
TANAKA, Y., 1949, *J. Sci. Res. Inst., Tokyo*, **43**, 160.
TANAKA, Y., SEYA, M., and MORI, K., 1951, *J. Chem. Phys.*, **19**, 979.
THOMAS, N., GAYDON, A. G., and BREWER, L., 1952, *J. Chem. Phys.*, **20**, 369.

The Thermal Conductivity of Superconducting Tin below 1°K

By B. B. GOODMAN

Royal Society Mond Laboratory, Cambridge

Communicated by A. B. Pippard; MS. received 10th September 1952

Abstract. An account is given of measurements on the thermal conductivity of superconducting tin below 1°K, made by observing the conduction of heat along a tin rod joining two pills of paramagnetic salt. Measurements were made on specimens of widely differing purities and a comparison of the results for the several specimens enabled an estimate to be made of the separate contributions, from the electrons and from the lattice, to the conductivity of each specimen. The electronic contribution to the thermal conductivity is in agreement with calculations due to Heisenberg and Koppe. The significance of this is discussed and it is tentatively suggested that the thermodynamic properties of the superconducting state may be determined by an energy gap of order kT_c in the spectrum of energy levels available to the electrons.

§ 1. INTRODUCTION

ON the two fluid picture of the superconducting state the electric and magnetic properties are related directly to the fraction ω of the conduction electrons that constitute the ordered, superconducting phase. The remaining conduction electrons, which constitute the normal phase, play no part in determining the low frequency electric and magnetic properties owing to the short circuiting effect of the superconducting electrons, which are able to move through the ionic lattice without resistance. At frequencies higher than about 10^9 c/s the inertia of the superconducting electrons causes their short circuiting effect to be imperfect, and measurements in this frequency range have been used to study the normal electrons, notably by Pippard. The normal electrons may also be studied from their contributions to the electronic thermal conductivity and the electronic specific heat of a superconductor. At temperatures well below the transition temperature ω is close to unity, and in common with the properties to which only the superconducting electrons contribute, its temperature dependence is very slight. In contrast, $1 - \omega$ is markedly temperature dependent, and therefore the properties which it is interesting to study in this temperature range are those involving the normal electrons. In the present paper measurements on the thermal conductivity of superconducting tin below 1°K are described; since the superconducting electrons constitute an ordered phase it is possible that they do not contribute to this property at all, but it may be noted that for the electronic specific heat there is an additional contribution proportional to $d\omega/dT$, arising from the transfer of electrons between the normal and superconducting phases. Valuable information on the thermal conductivity of superconductors has already been obtained from experiments in the helium range by Hulm (1950) and others, but the only previous measurements below 1°K

were those briefly reported by Daunt and Heer (1949). The present measurements were reported briefly at the Oxford Conference on Low Temperature Physics in 1951 (Goodman 1951).

§ 2. OUTLINE OF THE EXPERIMENTAL METHOD

The thermal conductivity of tin below 1°K was measured using an arrangement in which two pills of paramagnetic salt at slightly different temperatures were in thermal contact through a tin rod. At each end the tin rod was fused to a copper foil insert around which a pill of salt, chromium potassium alum, was pressed. The system was suspended in an evacuated chamber standing in liquid helium in the usual manner. The temperature of each pill of salt was deduced from magnetic susceptibility measurements (Kurti and Simon 1935). The susceptibility measurements actually consisted of observations on the mutual inductance between a pair of measuring coils placed around each pill of salt, made with a 40 c/s Hartshorn bridge. The contribution to the mutual inductance of a pair of coils from the pill of salt inside it was approximately $(200/T)\mu\text{H}$, and contributions from one pill to the mutual inductance between the coils around the other were negligible.

The characteristics of each pill of salt were determined in the normal way, but because of the effect on the readings of the superconducting transition in the tin specimen only readings below the transition temperature were included. The normal procedure for magnetic cooling was then carried out, and by arranging for the pills of salt to be in different magnetic fields while the helium exchange gas was being pumped away the pills were cooled to different temperatures on demagnetizing.

For the measurements below 1°K an alternating magnetic field of 0.3 gauss r.m.s. was used. The resulting heating of the cold system by eddy currents in the metal inserts and by losses in the paramagnetic salt was about 0.4 erg sec^{-1} ; under these circumstances the bridge could be set to within $0.1\mu\text{H}$. Because of the finite setting time of the bridge uncertainties of up to $1\mu\text{H}$ were encountered in measuring the varying mutual inductances resulting from the conduction of heat between the pills of salt.

At each temperature investigated a temperature difference was established between the two pills of salt and the approach to thermal equilibrium was observed. The quantity directly deduced from the observations, the thermal conductance between the two pills of salt q is given by

$$m_1 c_1 \frac{dT_1}{dt} = -m_2 c_2 \frac{dT_2}{dt} = q(T_2 - T_1), \quad \dots\dots(1)$$

where m_1 , m_2 , c_1 , c_2 , T_1 and T_2 are respectively the masses, specific heats and temperatures of the two pills of salt. When the temperature difference is small, so that c_1 and c_2 can be replaced by their mean value c , the approach to thermal equilibrium is exponential, with a time constant τ given by

$$\tau = m_1 m_2 c / q(m_1 + m_2). \quad \dots\dots(2)$$

Values of q for the tin specimen superconducting will be denoted by q_s and values of q for the tin specimen normal, in the presence of a magnetic field greater than critical, will be denoted by q_n ; similarly it will be convenient to distinguish τ_s and τ_n . Since in the temperature range studied the metal is a much better thermal conductor in the normal than in the superconducting state τ_n is much less than τ_s .

The observations followed one of two patterns according as the value of τ_s was greater or less than about 100 seconds. For the longer relaxation times, which obtained below about 0.6°K , measurements were made on T_1 and T_2 alternately, in the absence of a magnetic field. Sets of simultaneous values of T_1 , T_2 , dT_1/dt and dT_2/dt obtained from graphs of T_1 and T_2 against time were then used to deduce q_s by using eqn. (1). By applying a magnetic field greater than critical to the tin specimen for a short interval after each three or four observations on each of T_1 and T_2 and determining the changes in T_1 and T_2 which took place while the field was on, it was possible to determine q_n in the same way. Since it was not possible to measure T_1 or T_2 with the magnetic field applied to the specimen the values of T_1 and T_2 at the beginning and at the end of the time interval were deduced by extrapolating the measurements made in the absence of a magnetic field. For values of τ_s less than about 100 seconds it was not possible to obtain a sufficient number of alternate readings of T_1 and T_2 to make use of eqn. (1), either for determining q_s or q_n . Instead the exponential temperature change of one salt only was studied and q_s was deduced from eqn. (2). Because measurements were not possible in the presence of a magnetic field q_n could not be determined when τ_s was less than about 100 seconds.

In each sequence of observations initial temperature differences of up to 0.1°K were employed and the average temperature of the cold system remained fairly constant during the approach to thermal equilibrium. After each sequence of observations the temperature difference was re-established. This was achieved by applying a non-uniform magnetic field of order 500 gauss to the cold system; since the tin specimen was rendered normal by the field thermal equilibrium was quickly established, and on removing the non-uniform field the two pills of salt were cooled to different temperatures.

§ 3. DETAILED CONSIDERATIONS

(i) The Inserts

The two copper inserts for providing thermal contact between each end of a specimen and a pill of salt were of a type already described (Mendoza 1948, Goodman and Mendoza 1951). Each consisted of a mushroom shaped copper part with strips of copper foil hard soldered to its flat surface. The tin specimens were first fused at each end to the stem of an insert and a cylindrical pill of salt 1.6 cm in diameter and about 5 cm long was then pressed around the inserts at each end of the specimen. Mendoza's expression $1/\zeta T^2$ for the effective thermal resistance inside each salt insert system was verified in the present experiments, but the value $\zeta = 4 \times 10^4 \text{ erg deg}^{-3} \text{ sec}^{-1}$ obtained was a few times larger than that given by Mendoza.

(ii) Choice of Shape of the Specimens

The effective thermal resistance $1/q$ between the pills of salt is the sum of the thermal resistance of the tin rod and the thermal resistance inside each pill of salt :

$$\frac{1}{q} = \frac{l}{KA} + \frac{2}{\zeta T^2}. \quad \dots\dots(3)$$

Here l is the length of the rod, A is its cross-sectional area and K is its thermal conductivity. In order that K should be measurable it is necessary for three

conditions to be fulfilled: (a) in eqn. (3) l/KA must be the dominant term in $1/q$ in order that the correction for the thermal resistance inside the pills of salt shall be small; (b) the heat flow between the pills of salt, given by $q(T_2 - T_1)$, must be large compared with the natural warming; this was most difficult to achieve below 0.3°K where the thermal conductivity in the superconducting state reached very low values; (c) at temperatures near 1°K it is desirable to keep q_s small because the small specific heat of the salt tends to result in values of τ_s which are too short to allow measurements to be made.

In order to ensure that K was measurable over a wide range it was therefore necessary to compromise between the large values of l/A required by conditions (a) and (c) and the small values required by condition (b). In most of the specimens K_s/K_n was very small and it was impossible to choose a value of l/A which would have ensured that K_s and K_n were both measurable in the same specimen; in very pure tin at 0.2°K K_s/K_n was about 5×10^{-4} . In practice l/A was chosen to give the optimum conditions for measurement of K_s . It was assumed, on the strength of Hulm's measurements, that K_n could be calculated using the Wiedemann-Franz law:

$$K_n = L_0 T / \rho_0 \quad \dots\dots(4)$$

for all the specimens below 1°K . For the three purest specimens the thermal resistance in the normal state was small and the insert-salt thermal resistance was in fact studied using the values of q_n for these specimens.

(iii) The Specimens

The characteristics of the tin specimens are given in the table. The values of the diameters will be useful in discussing the contribution of the lattice to the total conductivity. The ratio l/A needed in calculating K for each specimen was obtained by a resistance measurement, and was usually known more accurately than the diameter.

The Characteristics of the Specimens

	% weight impurity	ρ_0/L_0 (watt unit)	diameter (mm)
Sn II	spec. pure	0.217	1.3
Sn III	" "	0.133	0.7
Sn IV	~ 0.3	6.8	2.8
Sn IX	~ 3	63	2.8
Sn X	~ 3	91	2.8

The specimens were all prepared by casting into a clean glass tube which was afterwards cracked away. Indium was chosen as the impurity to be added, and because the limit of its solubility in tin, 4%, was not reached, it was assumed that the specimens were homogeneous. For the three purest specimens no effort was made to control the size of the crystals making up the specimen, but for the specimens with an impurity content of 3% it was interesting to see whether the lattice conductivity could be made to depend on the average size of the crystals in the specimen. Differing crystal sizes were obtained by varying the rates at which the specimens were allowed to solidify. All the specimens except Sn X were made up of crystals of the order of the diameter of the specimen in size, but in Sn X the crystals were only a fraction of the diameter in size.

(iv) *The Specific Heat of Chromium Potassium Alum*

All the thermal conductivity measurements depend for their interpretation on a knowledge of this quantity. The values given in the literature (Bleaney 1950, Garrett 1948, Casimir, de Klerk and Polder 1940) show a spread of about 15% at all temperatures between 0.2°K and 1.0°K and an average curve of specific heat against temperature was used in the present calculations. In interpreting measurements made at 1.15°K the small additional contribution to the specific heat due to the lattice was assumed to be the same as for ferric ammonium alum, and therefore for the present salt only a few per cent of the whole.

(v) *Natural Warming of the Pills of Salt*

Because of the natural warming of the pills of salt, of order 3 erg sec^{-1} for each, eqn. (1) is not exactly true, but if the natural heat input were equally divided between the pills of salt the equation

$$\frac{1}{2} \left(m_1 c_1 \frac{dT_1}{dt} - m_2 c_2 \frac{dT_2}{dt} \right) = q(T_2 - T_1) \quad \dots\dots (5)$$

would be valid. In fact it appeared that the natural heat input was not equally divided between the pills of salt, thus giving rise to an apparent flow of heat between them, of order 1 erg sec^{-1} , which in eqn. (5) corresponds to an approximately constant extra term. Each set of observations by the long time constant method yielded pairs of values of the quantity on the left-hand side of eqn. (5) and the quantity $T_2 - T_1$, and therefore q could be determined from the gradient of a linear plot of these quantities. It can be seen that this procedure also eliminated the effect of small systematic errors in $T_2 - T_1$ arising from small errors in the determination of the characteristics of the two pills of salt. At high temperatures, where the method of observation for long relaxation times could not be used, the natural warming was unimportant in comparison with the observed flow of heat owing to the much larger values of q .

(vi) *Secondary Effects due to the Magnetic Field applied during Measurements of q_n*

The probable effect of this magnetic field, of order 350 gauss, on the thermal conductivity of normal tin could be estimated from the work of Hulm (1950). This suggested that the effect of this magnetic field on the thermal conductivity was only appreciable in the very pure specimens Sn II and Sn III. Since with these specimens the value of q_n was mainly controlled by the thermal impedance inside the pills of salt it is unlikely that the magneto-conductivity effect in normal tin was a significant factor in the experiments.

The effect of the magnetic field on the pills of salt was also considered, taking into account the reversible warming effect and the effect of the field on the specific heat of the salt. The necessary correction to the values of q_n was of order 10%.

§ 4. THE RESULTS

The experimental values of K_s for the specimens are plotted against temperature logarithmically in fig. 1. The chain lines represent the behaviour of K_n , calculated from eqn. (4). It will be seen that there is a large scatter in the experimental points, but this is not inconsistent with the estimated errors, of order 10% to 25%, in the individual values of K_s . Since K_s proved to be a very rapidly varying function of T this large scatter was not serious.

§ 5. DISCUSSION OF THE ELECTRONIC AND LATTICE CONTRIBUTIONS TO THE THERMAL CONDUCTIVITY

Comparatively little was known about the thermal conductivity of either normal or superconducting metals at liquid helium temperatures, until the recent experiments by Hulm (1950), and his work forms a useful basis for a discussion of the present results. Hulm measured the thermal conductivity of specimens of several superconductors, both in the normal state, in the presence of a magnetic field, and in the superconducting state; the results for the normal state are discussed first, in the light of theoretical ideas presented by Makinson (1938), and the conclusions reached will be useful in the discussion of the superconducting state results which will follow.

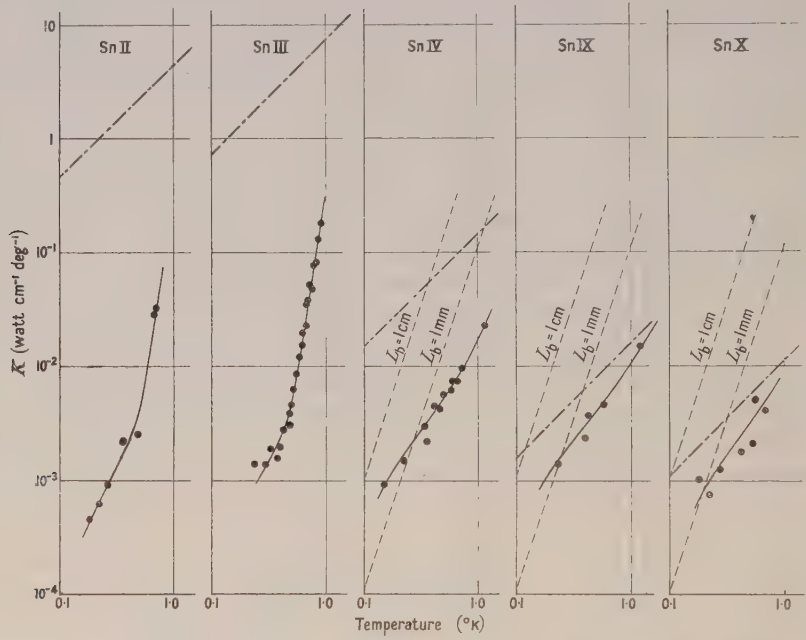


Fig. 1. Thermal conductivity of the five tin specimens, plotted against temperature logarithmically.

- Measured values of K_s .
- - - - - K_n deduced from eqn. (4).
- K_g deduced from eqn. (10).

(i) The Behaviour of Normal Metals

Makinson pointed out that the thermal conductivity of a normal metal K_n could be separated into two parts, the normal electronic conductivity K_{en} and the normal lattice conductivity K_{gn}

$$K_n = K_{en} + K_{gn} \quad \dots\dots (6)$$

K_{en} was expected to be dominant in all but very impure specimens.

Now K_{en} and K_{gn} are each limited by a number of scattering processes, and the corresponding impedances $1/K_{en}$ and $1/K_{gn}$ can be written, in Hulm's notation, as sums of a number of terms, each corresponding to one scattering process. At

temperatures very much lower than the Debye temperature

$$\frac{1}{K_{\text{en}}} = \alpha T^2 + \frac{\rho_0}{L_0 T} \quad \dots\dots (7)$$

and

$$\frac{1}{K_{\text{gn}}} = \frac{A}{T^2} + \frac{B}{T^3 L_b} \quad \dots\dots (8)$$

Here αT^2 represents the scattering of conduction electrons by thermal vibrations of the crystal lattice, $\rho_0/L_0 T$ represents the scattering of conduction electrons by impurities and small scale lattice defects, A/T^2 represents the scattering of lattice waves by conduction electrons, $B/T^3 L_b$ represents the scattering of lattice waves by crystal boundaries. L_0 is the Lorenz constant $\frac{1}{3}(\pi k/e)^2$, ρ_0 is the residual electrical resistivity of the specimen, L_b is the mean free path of the lattice waves (phonons) for crystal boundary scattering and α , A and B are constants of the metal. No term is included in eqn. (8) corresponding to the scattering of lattice waves by impurities because the average size of the impurity scattering centres is very small compared with the average wavelength of the phonons responsible for thermal conduction at helium temperatures ($\sim 10^{-4}$ cm).

From Hulm's experiments, carried out on a total of twelve specimens, of tin, mercury, indium and tantalum, it appeared that all the four processes represented in eqns. (7) and (8) did in fact occur, and by comparing specimens with different purities and crystal sizes it was possible to estimate the relative importances of the four processes in each specimen. The expression for mechanism (ii) was found to be valid to within a few per cent. The expressions for mechanisms (i) and (iii) were only in rough agreement with experiment. Mechanism (iv) was identified in one specimen, but in the absence of an accurate estimate of L_b no close comparison with theory was possible.

(ii) The Behaviour of Superconducting Metals

The specimens investigated by Hulm in the normal state were also investigated in the same temperature range in the superconducting state and he found that eqns. (6), (7) and (8) for the normal state could be replaced by

$$K_s = K_{\text{es}} + K_{\text{gs}}, \quad \frac{1}{K_{\text{es}}} = \frac{\alpha T^2}{g} + \frac{\rho_0}{f L_0 T}, \quad \frac{1}{K_{\text{gs}}} = \frac{A}{h T^2} + \frac{B}{j T^3 L_b} \quad \dots\dots (9)$$

for the superconducting state, where f , g , h and j were characteristic functions of T/T_c only. For all specimens for which the same conduction mechanism dominated in both states the ratio K_s/K_n was simply given by the appropriate characteristic function of T/T_c .

Of the four characteristic ratio functions only two have received any theoretical treatment. The j ratio function was expected to be unity at all temperatures, since it was difficult to see how conduction by lattice waves scattered by crystal boundaries could depend on the electronic state of the metal. In the only specimen examined by Hulm where this was thought to be the dominant lattice conduction mechanism $K_{\text{gs}}/K_{\text{gn}}$ was in fact close to unity over the whole temperature range investigated. The f ratio function has been considered by Heisenberg, and much of the rest of this paper will be devoted to a discussion of the experimental evidence on its behaviour.

The present measurements of the thermal conductivity of superconducting tin have been analysed according to the characteristic ratio function hypothesis

proposed by Hulm, the validity of which has not been extensively tested outside the range of specimens and temperatures which he described. An adequate test of this hypothesis below 1°K would involve an extensive series of measurements on a number of superconductors; in the absence of such results we can hardly do better than take Hulm's hypothesis on trust.

(iii) *The Results for the Lattice Thermal Conductivity*

The results presented in fig. 1 represent a range of values of ρ_0 in which the largest value is about 700 times the smallest. At high temperatures the effect of increasing ρ_0 is seen to be a marked reduction in K_g , but below about 0.5°K it appears that K_g is not sensitive to changes in purity. Since the lattice conductivity is believed to be independent of impurity content at very low temperatures this suggests that in all five specimens K_{gs} was the dominant term in K_s below about 0.5°K . Using Hulm's assumption that K_{es} at a given temperature is proportional to the residual electrical conductivity in the normal state, it is readily seen from the results for Sn II and Sn III that K_{es} contributes only to a negligible extent to K_s in the three less pure specimens (except for Sn IV near 1°K). After applying the necessary small correction for K_{es} the curves for Sn IV, Sn IX and Sn X therefore represent the behaviour of K_{gs} .

The results for K_{gs} may be compared with the values expected for conduction predominantly due to lattice waves scattered by crystal boundaries

$$K_g = L_b T^3 / B. \quad \dots\dots(10)$$

The constant B is related to the lattice specific heat and the velocity of lattice waves in the metal, and a reasonable estimate of its magnitude may be derived from the constants of the metal. In estimating B allowance was made for the separate contributions from transverse and from longitudinal waves. On the graphs in fig. 1 showing the measured values of K_s for Sn IV, Sn IX and Sn X the broken lines represent eqn. (10) for $L_b = 1\text{ cm}$ and 1 mm respectively. The probable actual values of L_b for these specimens, obtained by visual examination of the etched specimen, were of order 2 mm for Sn IV and Sn IX, and of order 0.5 mm for Sn X. It can be seen that, for each of these three specimens, the estimated value of L_b just accounts for the value of K_{gs} observed at about 0.2°K , and it is therefore possible that at this temperature crystal boundaries were the only important scattering mechanism for lattice waves. At successively higher temperatures, for each of the three specimens the estimated value of L_b leads to values of K_{gs} which are increasingly larger than those observed, and the presence of some other scattering mechanism for the lattice waves must therefore be assumed. It is reasonable to identify this mechanism with electronic scattering of lattice waves. Unfortunately no estimate of the h ratio function, the value of K_{gs}/K_{gn} for electronic scattering of the lattice waves, could be obtained for the temperature range below 1°K because K_{gn} was not known, but an extrapolation of Hulm's measurements of K_{gn} in the helium range suggests that h may be several times unity at 0.5°K in tin.

Hulm's measurements suggest that h is approximately equal to $(T/T_c)^1$ down to $T/T_c = 0.5$, and qualitatively he attributed these results to less effective electronic scattering of lattice waves in the superconducting state, compared with the normal state, arising from the condensation of conduction electrons into the ordered, superconducting phase. On this hypothesis values of h large

compared with unity may be expected at very low temperatures, owing to the greatly reduced number of normal electrons available for scattering the lattice waves.

(iv) *The Results for the Electronic Thermal Conductivity*

Unlike the measurements of K_s for the three less pure specimens, the measurements of K_s for Sn II and Sn III are interesting for the information they give about the behaviour of K_{es} . For these specimens K_{es} has been deduced from eqn. (9), K_{gs} being estimated for each specimen using the values of K_{gs} for the three less pure specimens and taking into account the probable values of L_b . In fig. 2 the results are plotted in the form of a graph of K_{es}/K_{en} against T/T_c . The probable limits of error indicated by the lengths of the lines representing the results arise both from experimental uncertainties and from uncertainties in estimating K_{gs} . A smooth curve has been fitted to the results.

Since the conduction electrons are scattered only by impurities the smooth curve represents the f ratio function proposed by Hulm and already investigated by him down to $T/T_c = 0.4$. In fig. 3 f is plotted logarithmically against $(T/T_c)^{-1}$; the reason for plotting the curves in this way will become clear later. It will be seen that the results obtained by Hulm and the present results, which cover the temperature range between $T/T_c = 0.24$ and $T/T_c = 0.12$, both agree quite well with the theoretical curve deduced by Heisenberg, to whose theory we now turn our attention.

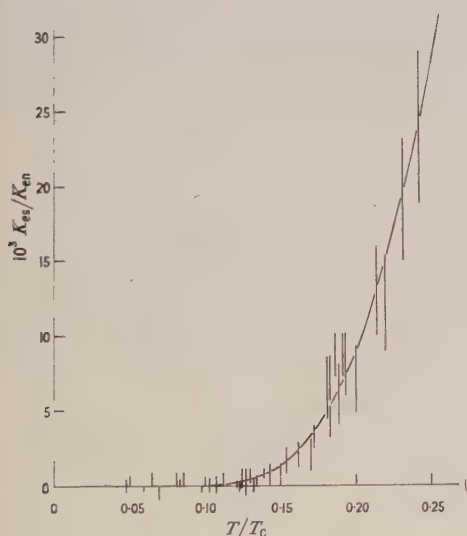


Fig. 2. Ratio of superconducting to normal electronic thermal conductivity for Sn II and Sn III, plotted against reduced temperature.

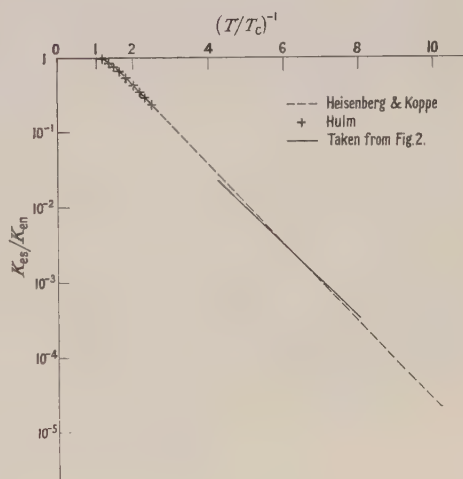


Fig. 3. Ratio of superconducting to normal electronic thermal conductivity for scattering by impurities, plotted logarithmically against $(\text{reduced temperature})^{-1}$.

§ 6. HEISENBERG'S THEORY OF SUPERCONDUCTIVITY

The theoretical work on the thermal conductivity of superconductors due to Heisenberg (1948) made use of calculations by Koppe (1947) which were, in turn, based on Heisenberg's theory of superconductivity (Heisenberg 1947, 1949), and resulted in an expression for the f ratio function which can be seen in fig. 3 to be in agreement with experiment over a wide range of temperature.

Much criticism however has been directed against the fundamental principles of Heisenberg's theory and it is therefore of interest to discover whether there is any essentially correct feature of the calculations of Heisenberg and Koppe to which this agreement can be attributed.

In discussing the thermal conductivity due to the electrons in a superconductor Heisenberg made use of the familiar equation $K = \frac{1}{3} \lambda u c$ for the conductivity K of a perfect gas. Here λ is the mean free path, u is the average molecular velocity and c is the specific heat per unit volume at constant volume. In a metal the modification of K_e by a superconducting transition was attributed to modifications in λ and c for the electrons, while u , the electron velocity at the surface of the Fermi sphere, was considered to remain constant; f was therefore given by

$$f = \lambda_s c_s / \lambda_n c_n, \quad \dots\dots(11)$$

where λ_s and c_s , and λ_n and c_n refer to the superconducting and normal states respectively, at a common temperature. c_s is not the total specific heat due to the electrons in a superconductor, but only the part due to the electrons taking part in the conduction process.

From fig. 3 it can be seen that between $T = T_c$ and $T = 0.1 T_c$ f falls from unity to less than 10^{-4} . This is clearly not due to the dependence of c_n on temperature. Nor, according to Heisenberg, is it due to the behaviour of λ_s/λ_n , which he represented by

$$\lambda_s/\lambda_n = (1 - \frac{1}{2}\omega)^{-1}. \quad \dots\dots(12)$$

Because ω , the fraction of superconducting electrons, can only take values between zero and unity λ_s/λ_n can only change by a factor of two over the whole temperature range. Therefore, so far as the calculations of Heisenberg and Koppe are concerned, the rapid variation of f with T/T_c must be due to similar behaviour in c_s .

In the temperature range investigated by Hulm f is given quite closely by the approximate form of Heisenberg's (1949) formula

$$f = \frac{2(T/T_c)^2}{1 + (T/T_c)^4}. \quad \dots\dots(13)$$

This relation however does not agree with experiment below $T/T_c = 0.4$, as had already been noticed by Darby *et al.* (1951). They found that for a lead specimen at 0.2°K K_s/K_n was certainly less than $1/60$ of the value expected from eqn. (13); f was smaller still but it was not possible to estimate by how much.

From fig. 3 it can be seen that except near the transition temperature the relation between $\log f$ and $(T/T_c)^{-1}$ is linear. Over this temperature range in fact the empirical equation

$$f = a \exp(-bT_c/T) \quad \dots\dots(14)$$

holds, where a and b are constants both of the order of unity. It therefore seems probable that the behaviour of c_s in the calculations of Heisenberg and Koppe is governed by the same or a similar exponential term, and a detailed investigation of the calculations shows that this is so.

This type of exponential dependence of specific heat on temperature may be recognized as being characteristic of a certain type of physical assembly, for which an energy gap exists between the ground state and the lowest excited state available to members of the assembly. An energy gap of ϵ leads to an expression for the specific heat usually dominated by the term $\exp(-\epsilon/kT)$ at sufficiently low temperatures. In Koppe's calculations the energy ϵ per electron which determines the thermodynamic properties of the electron assembly is temperature

dependent, rising from zero at the transition temperature to $1.283kT_c$ at 0°K . The value $1.20kT_c$ obtained by fitting eqn. (14) to the linear part of fig. 3 is close to the latter value. It is possible that an energy gap of order kT_c per electron which plays a crucial part in determining the thermodynamic properties of the superconducting state is in fact the essentially correct feature of the calculations of Heisenberg and Koppe.

It has been assumed so far that the very rapid variation of f with T/T_c is due to c_s in eqn. (11) and not to λ_s . It should be possible to test this assumption experimentally by measuring the specific heat of a suitable superconductor down to very low temperatures. Although the total electronic specific heat is larger than c_s , as already pointed out, its behaviour is expected to be similar and therefore measurements of this quantity should give some indication of the extent to which the very rapid variation of f with T/T_c is attributable to c_s . Furthermore, if the detailed assumption represented by eqn. (12) is correct then the electronic specific heat should be in agreement with Koppe's calculations. These are already known to be in agreement with experiment down to temperatures of about $0.3T_c$, where the electronic specific heat has the form $3\gamma T^3/T_c^2$. At temperatures below $0.3T_c$ an exponential fall in the electronic specific heat is predicted, but until recently no measurements which would have revealed this effect had been reported. Preliminary measurements on niobium by Brown, Zemansky and Boorse (1952) now suggest that below $0.3T_c$ this departure of the electronic specific heat from a T^3 law does in fact take place. If, as it appears likely, this departure in the electronic specific heat from a T^3 law can be shown to be associated with an exponential fall in the electronic specific heat at still lower temperatures, then the arguments in favour of the existence of an energy gap in the superconducting state will be considerably strengthened.

ACKNOWLEDGMENTS

I should like to thank Dr. J. Ashmead and Dr. D. Shoenberg for suggesting the present problem, and for their valuable encouragement and advice while the work was being carried out. I should also like to thank Dr. A. B. Pippard for much helpful discussion during the preparation of the paper. For financial assistance I am indebted to the Department of Scientific and Industrial Research.

REFERENCES

- BLEANEY, B., 1950, *Proc. Roy. Soc. A*, **204**, 216.
 BROWN, A., ZEMANSKY, M. W., and BOORSE, H. A., 1952, *Phys. Rev.*, **86**, 134.
 CASIMIR, H. B. G., DE KLERK, D., and POLDER, D., 1940, *Physica*, **6**, 737.
 DARBY, J., HATTON, J., ROLLIN, B. V., SEYMOUR, E. F. W., and SILSBEE, H. B., 1951, *Proc. Phys. Soc. A*, **64**, 861.
 DAUNT, J. G., and HEER, C. V., 1949, *Proceedings of the International Conference on the Physics of very Low Temperatures*, M.I.T., p. 64.
 GARRETT, C. G. B., 1948, *Cérémonies Langevin-Perrin* (Paris), p. 43.
 GOODMAN, B. B., 1951, *Proceedings of the International Conference on Low Temperature Physics*, Oxford, p. 129.
 GOODMAN, B. B., and MENDOZA, E., 1951, *Phil. Mag.* [7], **42**, 594.
 HEISENBERG, W., 1947, *Z. Naturforsch.*, **2a**, 185; 1948, *Ibid.*, **3a**, 65; 1949, *Two Lectures*, 1st edn. (Cambridge: University Press).
 HULM, J. K., 1950, *Proc. Roy. Soc. A*, **204**, 98.
 KOPPE, H., 1947, *Ann. Phys., Lpz.* (6), **1**, 405.
 KURTI, N., and SIMON, F. E., 1935, *Proc. Roy. Soc. A*, **151**, 610.
 MAKINSON, R. E. B., 1938, *Proc. Camb. Phil. Soc.*, **34**, 474.
 MENDOZA, E., 1948, *Cérémonies Langevin-Perrin* (Paris), p. 53.

The Anomalous Specific Heat of Ferrous Ammonium Sulphate

BY R. W. HILL AND P. L. SMITH

The Clarendon Laboratory, Oxford

Communicated by F. E. Simon; MS. received 24th October 1952

Abstract. The specific heats of ferrous and zinc ammonium sulphates have been measured from 2 to 30°K; the difference between these gives the anomalous contribution of the ferrous ion. Two maxima are found in this latter quantity, these occurring at 3.8 and 20.3°K. A scheme of energy levels capable of explaining the anomaly is put forward and the question of its uniqueness discussed.

§ 1. INTRODUCTION

THE behaviour of paramagnetic ions in crystals is usually studied either by infra-red or radio-frequency spectroscopy; both of these are powerful techniques, but neither can at present be used to measure the separations of energy levels between about 1 and 100 cm⁻¹. Ions whose energy levels are of this type can only be studied by measuring the susceptibility or specific heat, since these properties will change markedly at temperatures where the thermal energy kT is comparable with the separations of the energy levels. From this point of view, 1 cm⁻¹ corresponds to a temperature of 1.4°K so that the appropriate temperatures are low but not inaccessible. Lattice specific heats are generally small in this temperature range, so that anomalous specific heat behaviour due to the paramagnetic ion is clearly seen.

One common ion of this type is the ferrous ion. The ground state of the free ion is ⁵D₄, which has a twenty-five-fold degeneracy; the ion being divalent, Kramer's rule does not apply, and the whole of this degeneracy can be removed by the combined effects of a crystalline electric field of cubic symmetry and spin-orbit coupling. The effect of the electric field alone will be to raise two of the orbital states to energies which must be considered inaccessible from the present point of view, but it is to be expected that up to 15 levels should exist at energies low enough for investigation. The only published information as to the location of these levels is contained in Lyon and Giauque's (1949) measurements on ferrous sulphate heptahydrate, which show specific heat anomalies at 2 and 15°K. The usefulness of these measurements is limited by the fact that this salt is a concentrated one from the magnetic point of view, since the paramagnetic ions are sufficiently close to interact appreciably. The present measurements on ferrous ammonium sulphate hexahydrate were therefore undertaken; in this salt the ions are well separated, and the crystal structure and morphology are well known (Tutton 1913).

One disadvantage of using a salt of this dilution is that the lattice specific heat will become large compared with the anomalous specific heat at quite low temperatures. It is therefore necessary to obtain quite accurate values for the lattice specific heat alone, which can best be done by means of measurements on

the most similar diamagnetic salt. Zinc ammonium sulphate was chosen for this purpose, and its specific heat was measured throughout the temperature range of the investigation.

§2. EXPERIMENTAL

The samples were prepared by crystallization from a solution of either zinc or ferrous sulphate and ammonium sulphate in stoichiometric proportions. Crystals prepared in this manner should have the compositions $\text{Fe}(\text{NH}_4)_2(\text{SO}_4)_2 \cdot 6\text{H}_2\text{O}$ and $\text{Zn}(\text{NH}_4)_2(\text{SO}_4)_2 \cdot 6\text{H}_2\text{O}$ respectively, both belonging to the well known class of Tutton salts. That the crystals were in fact of this type was checked by measuring the angles between faces of a number of crystals; these angles were in perfect agreement with those given by Tutton, and this was considered a sufficient test that ferrous and zinc sulphates had not been prepared.

About 40 g of each substance was prepared, the average linear dimension of the crystals being about 2 mm. After careful drying at room temperature the crystals were sealed into a calorimeter of the type described by Parkinson, Simon and Spedding (1951); with this type of calorimeter the process of sealing does not involve undue heating of the specimen and consequent loss of water of crystallization. The apparatus used was essentially similar to that described by Parkinson, and no further account need be given here.

§3. RESULTS

The first experiments were carried out on the ferrous salt, the range of temperatures being 2 to 20°K. A maximum in the specific heat was found at 4°K, but these results could not be analysed in detail, due to the rapidly rising lattice specific heat. It was found that the total specific heat was far from cubic in temperature in the 15 to 20°K range, so that the lattice contribution could not be obtained without further study. The specific heat of zinc ammonium sulphate was therefore measured over the appropriate temperature range. The values obtained fell everywhere lower than those for the ferrous salt, the difference being still some 20% at 20°K. Measurements were therefore extended up to 30°K, at which temperature the difference is less than 10%. The accuracy of measurement was not better than within 2 or 3% at the highest temperatures, owing to the very poor thermal conductivity of these salts, and it was not considered profitable to extend the measurements to higher temperatures.

The results for the two salts are shown in fig. 1. The difference between the two, which is assumed to be the magnetic contribution of the ferrous ions, is plotted in fig. 2, where it may be seen that there are two maxima, centred around 4 and 20°K. Entropy values calculated from the anomalous specific heat are listed as a function of temperature in the table, which also contains smoothed specific heat values.

§4. INTERPRETATION OF RESULTS

The interpretation of overlapping specific heat anomalies is not an easy matter, but we may proceed on the following lines. A specific heat anomaly of the Schottky type rises exponentially with temperature, while at sufficiently high temperatures it decreases as $1/T^2$. It therefore follows that the influence of the higher anomaly on the height of the maximum of the lower

one will be small, while that of the lower on the higher may be appreciable. Starting, then, with the lower anomaly, we observe that its maximum height is $0.86 \text{ cal deg}^{-1} \text{ mole}^{-1}$, in good agreement with the value of $0.872 \text{ cal deg}^{-1} \text{ mole}^{-1}$ corresponding to the case of two energy levels of equal degeneracy. The temperature of the maximum is 3.8°K , corresponding to a splitting of 9.4°K or 6.5 cm^{-1} , from which we may calculate the magnitude of the anomaly at all temperatures. When this quantity has been subtracted from the total anomaly, there remains a peak at 20.3°K , this being $1.20 \text{ cal deg}^{-1} \text{ mole}^{-1}$ high, a value which may be associated with a triplet level above a doublet. If the two levels discussed above are treated as a degenerate doublet, we may then calculate the energy separation of the triplet from the doublet, obtaining a value of 52°K , or 56°K (38 cm^{-1}) above the ground state.

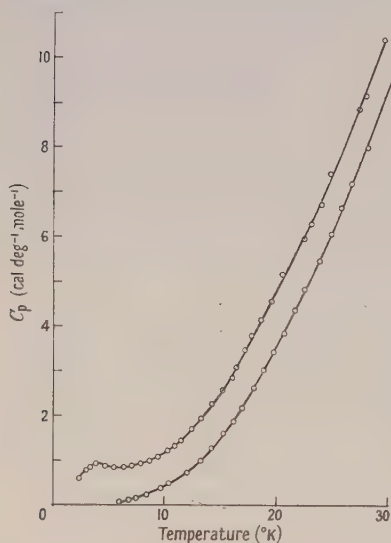


Fig. 1. The specific heats of ferrous ammonium sulphate (upper curve) and zinc ammonium sulphate (lower curve).

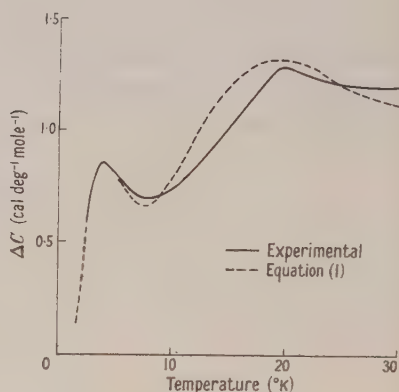


Fig. 2. The anomalous specific heat of ferrous ammonium sulphate.

Having thus arrived at an approximate level scheme, which is shown in fig. 3, the next step is to calculate the total anomalous specific heat from it without the simplifying assumptions made above. The appropriate partition function is $Z = 1 + \exp(-\theta_1/T) + 3 \exp(-\theta_2/T)$ with $\theta_1 = 9.4^\circ$ and $\theta_2 = 56^\circ$. Proceeding in the usual way, the following expression for the specific heat is deduced:

$$C = R \left\{ \frac{(\theta_1/T)^2 \exp(-\theta_1/T) + 3(\theta_2/T)^2 \exp(-\theta_2/T) + 3\{(\theta_2 - \theta_1)/T\}^2 \exp\{-(\theta_1 + \theta_2)/T\}}{1 + \exp(-\theta_1/T) + 3 \exp(-\theta_2/T)} \right\} \quad \dots\dots(1)$$

This rather awkward expression has been evaluated for suitable values of T , and the results are shown in fig. 2 together with the experimental ones. It is at once clear that this calculation is on the right lines, but the detailed agreement is far from perfect. It is equally clear that a better choice of θ_1 and θ_2 will not improve the agreement substantially, for the maxima occur at very nearly the

right temperatures. The defect in the calculations undoubtedly lies in the assumption that there exists a degenerate triplet at the top of the pattern, rather than a doublet and singlet or even three singlet levels. To proceed further with this analysis without theoretical guidance would be a formidable task, since the calculation of the specific heat of any assumed pattern of five levels takes a long time. Many such calculations would have to be performed to find the scheme which fits the data best, since the problem cannot be generalized. Furthermore, since the experimental values have only a finite accuracy it cannot be assumed that there exists a unique energy scheme which will explain them. It may be noted, for example, that the energy levels shown in fig. 4 give rise to a single anomaly whose height is almost exactly that of the 4°K anomaly, though the

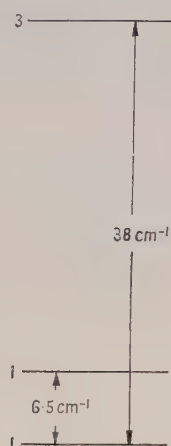


Fig. 3. Proposed energy levels for Fe^{2+} in ferrous ammonium sulphate.

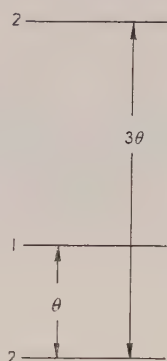


Fig. 4

Smoothed Specific Heat and Entropy Values

(°K)	$C_p(\text{F})^*$	$C_p(\text{Z})^*$	ΔC	ΔS	(°K)	$C_p(\text{F})^*$	$C_p(\text{Z})^*$	ΔC	ΔS
2.5	0.59		0.59	0.21†	14	2.13	1.19	0.94	1.55
3	0.75	0.01	0.74	0.33	16	2.88	1.82	1.06	1.68
3.5	0.84	0.01	0.83	0.45	18	3.82	2.59	1.23	1.82
4	0.88	0.02	0.86	0.57	20	4.76	3.47	1.29	1.95
5	0.85	0.04	0.81	0.75	22	5.72	4.47	1.25	2.08
6	0.82	0.07	0.75	0.90	24	6.74	5.52	1.22	2.18
7	0.84	0.13	0.71	1.01	26	8.00	6.75	1.25	2.27
8	0.91	0.20	0.71	1.10	28	9.10	7.95	1.15	2.36
10	1.14	0.40	0.74	1.26	30	10.3	9.25	1.05	2.44
12	1.56	0.71	0.85	1.41					

The thermal unit is the calorie per mole throughout.

* F=ferrous ammonium sulphate; Z=zinc ammonium sulphate. † Extrapolated value.

detailed shape of the curve and the entropy of the anomaly are slightly different. By a judicious arrangement of the higher levels it may well be possible to obtain an energy scheme which fits the experimental facts as well as does that of fig. 3. Considerations of entropy should throw some light on this matter, but some estimate must first be made of the contribution to be expected above the highest temperature of measurement. If it is assumed that, in this temperature range,

the anomalous specific heat is proportional to $1/T^2$, it is easily shown that this extra contribution is 0.6 E.U. Adding this to the experimental value at 30°K, the total entropy becomes 3.04 E.U., a value which may be expected to be too low rather than too high, since the anomalous specific heat decreases with temperature less rapidly than $1/T^2$ up to the highest temperature of measurement. The failure of the experimental curve to fall as rapidly as the theoretical one may be due to experimental error, to the over-simplification of the theory or to the existence of higher levels; in no case should the extrapolated value be wildly wrong. The entropy of the simplest energy scheme is $R \log 5$ or 3.2 E.U., and the agreement may be considered adequate. If all fifteen levels are invoked with the more complicated scheme, the total entropy would be $R \log 15/2$ or 4.0 E.U., but better agreement can be obtained on the assumption that a few of the higher levels are at inaccessibly high energies. It is concluded, then, that a somewhat modified version of fig. 3 is the simplest, but not necessarily the only energy scheme which is consistent with the experimental facts.

In view of the fact that the accuracy of the ΔC values decreases with rising temperature, it will be appreciated that the temperature of the higher maximum cannot be fixed very accurately, resulting in a corresponding uncertainty in the value of 38 cm^{-1} given for the larger splitting. Since it is most unlikely that the highest level is truly degenerate, the value quoted only indicates the order of magnitude of the energy at which levels should exist; as such its relative inaccuracy is not of great importance.

§ 5. CONCLUSIONS

As a result of these measurements it is concluded that the ground state of the ferrous ion in ferrous ammonium sulphate is probably split into two levels of equal degeneracy n with a separation of 6.5 cm^{-1} , above which a further group of $3n$ levels exists, these being centred some 38 cm^{-1} above the lowest level. The value of n cannot be predicted, apart from the fact that it cannot be greater than three, nor can any information be obtained about possible fine structure of these levels. These points can in principle be settled by paramagnetic resonance experiments, provided the transitions are not forbidden, and it is hoped that the present work may be useful in the interpretation of such experiments.

ACKNOWLEDGMENTS

The authors would like to express their gratitude to Dr. B. Bleaney for suggesting the problem and for assistance with the preparation of the samples, and to Professor F. E. Simon for advice and encouragement. They are also indebted to the University of Oxford for the award of an Imperial Chemical Industries Fellowship and the Department of Scientific and Industrial Research for a research grant respectively.

REFERENCES

- LYON, D. N., and GIAUQUE, W. F., 1949, *J. Amer. Chem. Soc.*, **71**, 1647.
PARKINSON, D. H., SIMON, F. E., and SPEDDING, F. H., 1951, *Proc. Roy. Soc. A*, **207**, 137.
TUTTON, A. E. H., 1913, *Proc. Roy. Soc. A*, **88**, 361.

Damping Corrections in the Photo-Meson Process

By G. R. ALLCOCK

Department of Theoretical Physics, University of Liverpool

Communicated by K. J. Le Couteur; MS. received 5th September 1952

Abstract. An examination is made of the effect of damping on the photo-production of pseudoscalar charged and neutral π -mesons from protons, ignoring all self-energy effects. In the case of pseudoscalar coupling the damping corrections are large, but do not greatly remedy the disagreement of second order perturbation theory with experiment; while for pseudovector coupling damping effects are unimportant.

§ 1. INTRODUCTION

THE lowest order weak-coupling approximations to the cross sections for production of charged and neutral π -mesons by γ -rays incident on protons (Araki 1950, Brueckner 1950) are not in good accord with experiment (Steinberger and Bishop 1952, Panofsky *et al.* 1952, Silverman and Stearns 1951). PS and PV coupling are equivalent for this process in lowest order, and in particular predict that the cross section for production of π^0 is small compared to that for π^+ . For example, the differential cross sections in the laboratory coordinate system at 90° to γ -rays of energy 300 Mev are predicted to be in a ratio of about 1:8, whereas the actual ratio is of order 1:2. The angular distribution of the π^+ between 45° and 150° in the centre-of-mass system also appears to be too flat, while that of the π^0 shows a backward peak, in contrast to the experimental results so far obtained, which indicate a slight forward peaking.

Various attempts have been made to take account of the higher order processes, and much better agreement with experiment has been obtained. In the case of PS coupling the finite corrections remaining after renormalization are large (Koba *et al.* 1951, Minami 1952).

In the case of PV coupling a semi-classical phenomenological analysis is made possible by the introduction of a finite sized nucleon (Brueckner and Case 1951, Drell 1951). The relativistic properties of the theory are thereby sacrificed. The Wigner-Eisenbud resonance theory can also be applied advantageously (Brueckner and Watson 1952). Alternatively, renormalization can be carried out to fourth order for this process, though not without difficulties of principle (Koba *et al.* 1951, Minami 1952).

A simpler approach to the problem has been effected (Kaplan 1951, Aidzu *et al.* 1951) by including in the interaction Lagrangian a Pauli term to represent the experimentally observed anomalous magnetic moments (hereafter referred to as A.M.M.). This considerably increases the neutral cross section, though the angular distributions are still at fault.

The object of the present investigation is to find out the effect of damping; that is to say, we take account of those higher order processes which can be considered as a succession of real scatterings in which both energy and momentum are conserved. The intermediate states containing a meson and a nucleon are far more

important than those containing a photon and a nucleon. The charge exchange scattering tends to equalize the two cross sections. Some effects of the damping have been calculated by Hamilton and Peng (1944), but in their calculation the recoil of the nucleon was ignored, and only a charged meson field was considered. An examination of the matrix elements for the photo-production process shows that the recoil must be taken into account to obtain neutral mesons in the absence of A.M.M. and also that the recoil effects are very important in the positive meson process.

Damping and self-energy effects are not separated out in the Feynman-Dyson rules for writing down the elements of the S matrix, but a discussion of the relativistic formulation of damping theory has recently been given by Pirenne (1952).

In the following, Heitler's original prescription for the treatment of damping effects is used, namely the interaction Hamiltonian compound matrix element is replaced by its first finite term.

§ 2. CONCLUSIONS

We summarize below the conclusions reached.

(1) The charge exchange effect does not increase the $\pi^0:\pi^+$ ratio sufficiently, so that inclusion of A.M.M. is still necessary.

(2) In the case of PS coupling the damping effects are considerable because the pion scattering cross section is large even at zero energy: charged + neutral theory has been used, as this gives large charge exchange effects, while symmetric theory gives mainly pure damping on each process separately, and is therefore of less interest. The large backward peak in the π^0 -cross section, produced by the A.M.M., is much reduced by the damping, and the angular distribution of the π^+ is improved (fig. 1). However, recent experiments by Anderson *et al.* (1952a) on the scattering of pions by protons are in complete disagreement with the predictions of PS(PS) theory (Ashkin *et al.* 1950) in second or fourth order weak coupling approximation. Photo- π production without damping necessitates $g^2/4\pi \sim 60$; using this value the predicted second order pion scattering cross sections are about 10 to 20 times too large and decrease with increasing pion energy. Such a state of affairs cannot be remedied by including damping alone.

(3) Photo-meson production with PV coupling indicates a coupling parameter $f^2/4\pi \sim \frac{1}{3}$; this value with charge symmetric theory gives low energy pion scattering cross sections of the correct order of magnitude and energy dependence (Ashkin *et al.* 1950), though the angular distributions and absolute magnitudes of the cross sections are by no means in good agreement with experiment (Anderson *et al.* 1952b).

At the energies of the photo-production experiments the damping corrections turn out to be as small as the probable experimental error, as illustrated by the angular distributions (fig. 2) which have been calculated taking account only of the charge exchange scattering. Weak coupling PS(PV) theory with damping is not therefore adequate, and this is even more the case when one considers the scattering of π^+ on protons.

(4) The theoretical (PS or PV coupling) excitation function for π^+ production rises steeply near threshold and is markedly concave downwards, while the observed excitation function is only slightly concave downwards. The introduction of damping can only make this situation worse.

§ 3. THE DAMPING EQUATION

Rationalized natural field units are used; thus, for example, $e^2/4\pi = 1/137$. The four-momentum of a Fermion is denoted by $p = (E, \vec{p})$, and of a Boson by $k = (\omega, \vec{k})$. The masses of a meson and a nucleon are denoted by μ and M . In Feynman's notation $p^\nu \gamma_\nu = \not{p}$ and $\not{p}u = Mu$, where u is the four-component spinor of a nucleon. The total unperturbed energy of the system is represented by W , and $k^\nu p_\nu = k \cdot p = \omega E - \vec{k} \cdot \vec{p}$.

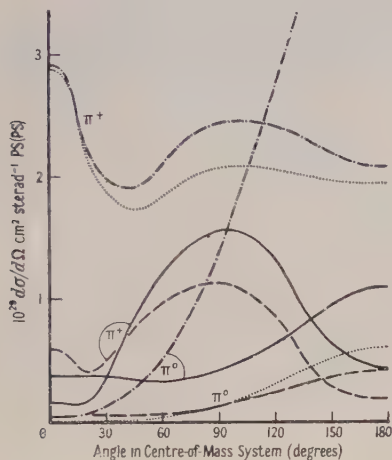


Fig. 1. PS(PS) $g_p = g_N = g = \sqrt{(60 \times 4\pi)}$; all damping due to π scattering accounted for.

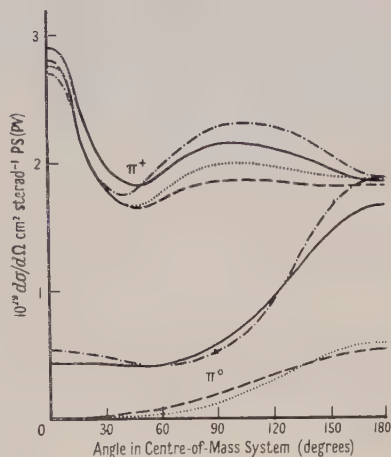


Fig. 2. PS(PV) $f_p = -f_N = f = \sqrt{(4\pi/3)}$; only charge exchange damping accounted for.

The angular distributions of the mesons in the centre-of-mass system evaluated for a meson momentum $4\mu/3$, corresponding to a γ -ray of energy 295 mev in the laboratory.

———— with A.M.M. and damped — . — . — . with A.M.M., undamped
 - - - - - without A.M.M. and damped without A.M.M., undamped

Referred to a set of eigenstates of the unperturbed Hamiltonian, Heitler's equation on the energy shell $W_a = W_b$ reads

$$F_{ab} = K_{ab} - i\pi \sum_c K_{ac} \delta(W_b - W_c) F_{cb} \quad \dots\dots (1)$$

where K_{ab} is the perturbation matrix between states b and a .

In order to write (1) in a covariant form, neglecting intermediate states c containing more than 1 Boson, we use the simple connection between the Feynman matrix element \mathfrak{K}_{ab} and the Hamiltonian matrix element K_{ab} referred to a unit box,

$$\mathfrak{K}_{ab} \left(\frac{M}{E_a} \frac{M}{E_b} \frac{1}{2\omega_a} \frac{1}{2\omega_b} \right)^{1/2} = K_{ab}, \quad \dots\dots (2)$$

and replace the summation by an integration. Defining a matrix \mathfrak{F} which bears the same relation to F as does \mathfrak{K} to K we obtain an obviously covariant form for Heitler's equation (1):

$$\mathfrak{F}_{ab} = \mathfrak{K}_{ab} - \frac{iM}{16\pi^2} \sum_c \iint \frac{d^3\vec{k}_c}{\omega_c} \frac{d^3\vec{p}_c}{E_c} \mathfrak{K}_{ac} \delta^4(p_c + k_c - p_b - k_b) \mathfrak{F}_{cb} \quad \dots\dots (3)$$

where the integrations are carried out over the surfaces $k_c^2 = \mu^2$, $\omega_c > 0$ and $p_c^2 = M^2$,

$E_c > 0$, and Σ_c denotes a sum over spins and over intermediate states of different types. In the centre-of-mass system (3) reduces to

$$\mathcal{F}_{ab} = \mathcal{K}_{ab} - \frac{iM}{16\pi^2 W} \Sigma_c |\vec{k}_c| \int \mathcal{K}_{ac} d\Omega_c \mathcal{F}_{cb}. \quad \dots\dots(4)$$

With indices to represent the type of Boson in initial and final states the matrix elements are denoted by

$$\begin{aligned} \bar{u}_a f_{ab}^{0\gamma} u_b \quad \text{and} \quad \bar{u}_a k_{ab}^{0\gamma} u_b \quad \text{for} \quad P + \gamma \rightarrow P + \pi^0, \\ \bar{u}_a k_{ab}^{+0} u_b \quad \text{for} \quad P + \pi^0 \rightarrow N + \pi^+, \text{ etc.} \end{aligned}$$

The damping due to intermediate states c containing photons is ignored.

The reader is referred to Kaplon (1951) for the matrix elements \mathcal{K} for photo- π production, and to Ashkin *et al.* (1950) for the meson scattering matrix elements (apart from a factor $-i$).

Replacing $|\vec{k}_c|/32\pi^2 W$ by r , the integral equations to be studied become

$$f_{ab}^{+\gamma} = k_{ab}^{+\gamma} - ir \int d\Omega_c \{k_{ac}^{++}(\mathbf{p}_c + M)f_{cb}^{+\gamma} + k_{ac}^{+0}(\mathbf{p}_c + M)f_{cb}^{0\gamma}\} \quad \dots\dots(5)$$

together with a similar equation obtained by interchanging 0 and $+$.

§ 4. SOLUTION OF THE DAMPING EQUATION

Non-relativistic approximations to the photo-production \mathcal{K} matrices are inadequate; fortunately, however, one can simplify the meson scattering matrices in the low energy region. The main features of the modes of solution of (5) are given below.

PS Coupling

The partial angular dependence of the denominators in the meson scattering matrices is ignored as $|\vec{k}_a|$ is fairly small. In charge symmetric theory k^{0+} almost vanishes, and as $k^{00} \sim 2k^{++}$ the ratio of cross sections will be made worse by the damping, at any rate without the A.M.M. Approximately we may write in charged $+$ neutral theory $2k_{ac}^{++} \sim k_{ac}^{00} \sim k_{ac}^{0+} \sim k_{ac}^{+0} \xrightarrow{\sim} g^2 \mathbf{k}_a / E_a \omega_a$, which, it should be noted, is entirely independent of the direction of \vec{k}_c . An estimate of the order of magnitude of the damping is provided by the consideration that

$$4\pi(2M)r k^{00} \sim 5 \quad \text{if} \quad |\vec{k}_a| \sim \mu \quad \text{and} \quad g^2/4\pi \sim 60.$$

$2M$ represents the projection operator $\mathbf{p}_c + M$, and 4π the solid angle. The correction is comparable to the undamped matrix element, and indeed the solution found cannot be expressed as a power series in g^2 except for very low values of $|\vec{k}_a|$.

Denote by \tilde{f}_b^{+} the quantity $\int (\mathbf{p}_c + M) f_{cb}^{+\gamma} d\Omega_c$, then, after integration, (5) becomes

$$\left. \begin{aligned} \tilde{f}_b^{+} &= \tilde{k}_b^{+} - iB(C + D\gamma_0)(\frac{1}{2}\tilde{f}_b^{+} + \tilde{f}_b^0) \\ \tilde{f}_b^0 &= \tilde{k}_b^0 - iB(C + D\gamma_0)(\tilde{f}_b^0 + \tilde{f}_b^{+}) \end{aligned} \right\} \quad \dots\dots(6)$$

where $B = g^2 r / E_a \omega_a$, $C = 4\pi \{E_c \omega_c + (\vec{k}_c \cdot \vec{\gamma})^2\} = 4\pi \hat{p}_a \cdot \mathbf{k}_a$ and $D = 4\pi M \omega_a$.

It is now a simple matter to solve (6) for the \tilde{f}_b in terms of the \tilde{k}_b ; we then substitute the \tilde{f}_b into the right-hand side of (5) to obtain the f_{ab} .

PV Coupling

The meson scattering matrices consist of large terms, some of which are angle dependent, and which almost cancel each other. An approximation to the difference of these terms cannot in general be found.

In charge symmetric theory ($f=f_P=-f_N$) a fairly good approximation to \mathbf{k}^{0+} or \mathbf{k}^{+0} is $2\vec{k}_a \cdot \vec{k}_c f^2 \mathbf{k}_a / \mu^2 \omega_a^2$ provided $\mu \lesssim |\vec{k}_a| \lesssim 2\mu$.

If the direct scattering is neglected altogether, the resulting integral equations can be solved exactly. To obtain an estimate of the damping effect on $\mathbf{f}_{ab}^{0\gamma}$ one evaluates

$$2Mr(4\pi/3)(2f^2|\vec{k}_a|^2/\mu^2\omega_a^2)\omega_a \sim \frac{1}{3},$$

taking $|\vec{k}_a| \sim 4\mu/3$ and $f^2/4\pi \sim \frac{1}{3}$. (The factor $4\pi/3$ results from integration over $d\Omega_c$ of the angle dependent $\vec{k}_a \cdot \vec{k}_c$). Thus one expects to obtain $\mathbf{f}^{0\gamma} \sim \mathbf{k}^{0\gamma} + \frac{1}{3}i\mathbf{k}^{+\gamma} + \dots$ and after averaging over spin directions $|\mathbf{f}^{0\gamma}|^2 \sim |\mathbf{k}^{0\gamma}|^2 + \frac{1}{9}|\mathbf{k}^{+\gamma}|^2 + \dots$. The estimate is of the correct order of magnitude, though a little high.

Since the correction is small (this applies equally if all the damping effects are included) two iterations give a good solution. At higher energies iteration is not possible. The accurate mode of solution of the simplified equation follows the same lines as in the (PS) theory, but is somewhat complicated by the angular dependence of \mathbf{k}^{0+} .

ACKNOWLEDGMENTS

I should like to express my thanks to Dr. K. J. Le Couteur for proposing this investigation, and for many helpful discussions. I am also indebted to the Department of Scientific and Industrial Research for financial support.

REFERENCES

- AIDZU, K., FUJIMOTO, Y., and FUKUDA, H., 1951, *Prog. Theor. Phys.*, **6**, 193.
 ANDERSON, H. L., FERMI, E., LONG, E. A., LUNDBY, A., MARTIN, R., NAGLE, D. E., and YODH, G. B., 1952 a, *Phys. Rev.*, **85**, 934, 935, 936.
 ANDERSON, H. L., FERMI, E., NAGLE, D. E., and YODH, G. B., 1952 b, *Phys. Rev.*, **86**, 793.
 ARAKI, G., 1950, *Prog. Theor. Phys.*, **5**, 641.
 ASHKIN, J., SIMON, A., and MARSHAK, R., 1950, *Prog. Theor. Phys.*, **5**, 634.
 BRUECKNER, K. A., 1950, *Phys. Rev.*, **79**, 641.
 BRUECKNER, K. A., and CASE, K. M., 1951, *Phys. Rev.*, **83**, 1141.
 BRUECKNER, K. A., and WATSON, K. M., 1952, *Phys. Rev.*, **86**, 923.
 DRELL, S. D., 1951, *Phys. Rev.*, **83**, 555.
 HAMILTON, J., and PENG, H. W., 1944, *Proc. Roy. Irish Acad. A*, **49**, 197.
 KAPLON, M. F., 1951, *Phys. Rev.*, **83**, 712.
 Koba, Z., KOTANI, T., and NAKAI, S., 1951, *Prog. Theor. Phys.*, **6**, 849.
 MINAMI, S., 1952, *Prog. Theor. Phys.*, **7**, 69.
 PANOFSKY, W. K. H., STEINBERGER, J., and STELLER, J., 1952, *Phys. Rev.*, **86**, 180.
 PIRENNE, J., 1952, *Phys. Rev.*, **86**, 395.
 SILVERMAN, A., and STEARNS, M., 1951, *Phys. Rev.*, **83**, 853.
 STEINBERGER, J., and BISHOP, A. S., 1952, *Phys. Rev.*, **86**, 171.

The Elastic Scattering of Neutrons by Tritons at 14 Mev

By P. SWAN

Physics Department, University College, London

*Communicated by H. S. W. Massey; MS. received 20th June 1952,
and in amended form 10th September 1952*

Abstract. The theory of neutron-triton scattering has been worked out, using Wheeler's resonating group structure method, and applied to a neutron energy of 14 Mev for four types of nuclear interaction: an ordinary force, an exchange force of Majorana-Heisenberg type, a symmetrical exchange force, and the Serber exchange mixture. The nuclear potential is taken in the gaussian form $V_0 \exp(-\mu r^2)$ and the corresponding two body ground state wave function as $N_0 \exp(-\frac{1}{2}\lambda r^2)$. The resulting integro-differential equations for scattering are solved by variational methods.

The symmetric and Majorana-Heisenberg forces give the right general shape for the angular distribution of scattering, but the ordinary and Serber forces give a rather higher peak of back scattering than indicated by the experiments of Coon, Bockelman and Barschall at 14 Mev. The measurements appear to favour forces of a symmetrical exchange type as against an ordinary force type.

§ 1. INTRODUCTION

THE investigation of the collisions of neutrons with tritons offers an opportunity to extend the knowledge of nuclear forces already gained by the study of neutron-deuteron scattering, and also is a step towards finding methods of calculating the interaction of nucleons with light nuclei. Detailed calculations and comparison with experiment (Buckingham, Hubbard and Massey 1952) of the collisions of neutrons with deuterons, employing Wheeler's resonating group structure method, have strongly favoured an exchange type of force, so it is of interest to see whether exchange forces are also necessary to explain neutron-triton scattering.

The triton with its binding energy 8.2 Mev is a more compact structure than the deuteron (binding energy 2.2 Mev), so that one might expect any polarization effect to be rather smaller for neutron-triton scattering than for neutron-deuteron scattering. As calculations on neutron-deuteron collisions have always neglected this effect, and have yet obtained good agreement with experiment except for neutron energies below 3 Mev for which the polarization effects would be most important, we may conclude that the same approximation for neutron-triton collisions would be valid to a rather greater degree. In the same way as for the deuteron, the size of the triton means that incident neutrons of several Mev energy and with one unit of quantized angular momentum should pass close enough to the triton structure to interact strongly, resulting in a p phase contribution to scattering and a consequent departure from the isotropic scattering distribution found for neutron-proton collisions at the same energy.

In this paper the scattering of neutrons by tritons is calculated at 14 Mev, and compared with the experiments of Coon, Bockelman, and Barschall at the same

energy. The basic assumption is that the method of resonating group structure due to Wheeler is at least approximately valid. As the interaction involves four bodies, it cannot be treated as accurately as in the case of neutrons incident on deuterons, and so use has had to be made of approximate wave functions and a nuclear force shape, the mathematical properties of which allow computations to be made which would otherwise be not practicable.

§ 2. GENERAL FORMULATION

We take the triton as consisting of neutrons 1 and 2, and proton 3, with a neutron 4 incident on it. To obtain the total wave function $\Psi_j(123, 4)$ of the system, we employ the method of resonating group structure, so that the identity of particles 1, 2 and 4 requires us to write $\Psi_j(123, 4)$ as the linear sum of terms totally antisymmetric in any pair of 1, 2 and 4. Thus

$$\begin{aligned}\Psi_j(123, 4) &= 6^{-1/2}[\Phi_j(123, 4) + \Phi_j(243, 1) + \Phi_j(413, 2) - \Phi_j(213, 4) \\ &\quad - \Phi_j(143, 2) - \Phi_j(423, 1)], \\ &= 6^{-1/2}(1 - P_{12})(1 - P_{14} - P_{24})\Phi_j(123, 4), \quad \dots\dots(1)\end{aligned}$$

where P_{mn} is an operator interchanging both space and spin coordinates of particles m and n .

Following the usual method of group structure, we take the final wave function $\Phi_f(123, 4)$ as equal to the initial wave function $\Phi_0(123, 4)$ in the form

$$\Phi_0(123, 4) = \psi_0(123)F(123, -4)\chi_{1-4}(\sigma_{1-4}) = \phi_0(123, 4)\chi_{1-4} \quad \dots\dots(2)$$

where $\psi_0(123)$ is the spatial part of the triton ground state wave function, assumed symmetrical in any pair of the particles 1, 2, 3. $F(123, -4)$ is the spatial wave function of the incident neutron relative to the centre of mass of the triton, $\chi_{1-4}(\sigma_{1-4})$ is an appropriate spin function, and $\phi_0(123, 4)$ is the total spatial wave function for the group. This treatment neglects any polarization effect.

To obtain the appropriate spin functions χ_{1-4} , we see that the triton must be in its doublet 2S ground state with its spin function symmetrical in the deuteron particles 2 and 3. (We here regard the triton as built up from a deuteron in its ground state plus a spare neutron.)

$$\text{Triton ground state} \begin{cases} {}^2\Box_{1/2} = 6^{-1/2}(\alpha_1\alpha_2\beta_3 + \alpha_1\beta_2\alpha_3 - 2\beta_1\alpha_2\alpha_3), \\ {}^2\Box_{-1/2} = 6^{-1/2}(2\alpha_1\beta_2\beta_3 - \beta_1\beta_2\alpha_3 - \beta_1\alpha_2\beta_3). \end{cases} \quad \dots\dots(3)$$

For the corresponding four-particle system, the required spin functions correspond to a singlet and a triplet state and are as follows:

$$\text{Triplet} \begin{cases} {}^3\chi_1 = {}^2\Box_{1/2}\alpha_4, \\ {}^3\chi_0 = 2^{-1/2}({}^2\Box_{1/2}\beta_4 + {}^2\Box_{-1/2}\alpha_4), \\ {}^3\chi_{-1} = {}^2\Box_{-1/2}\beta_4. \end{cases} \quad \dots\dots(4)$$

$$\text{Singlet} \quad {}^1\chi_0 = 2^{-1/2}({}^2\Box_{1/2}\beta_4 - {}^2\Box_{-1/2}\alpha_4). \quad \dots\dots(5)$$

If we write

$$\sigma_4 = \chi(123, 4) - \chi(213, 4), \quad \sigma_1 = \chi(243, 1) - \chi(423, 1), \quad \sigma_2 = \chi(413, 2) - \chi(143, 2) \quad \dots\dots(6)$$

the total wave function $\Psi_0(123, 4)$ becomes

$$\Psi_0(123, 4) = 6^{-1/2}[\sigma_4\phi(123, 4) + \sigma_1\phi(243, 1) + \sigma_2\phi(413, 2)], \quad \dots\dots(7)$$

where we have assumed the spatial wave function $\phi(123, 4)$ to be symmetrical in any pair of the triton particles 1, 2, 3. For the two cases we find

Triplet :

$$\sigma_4 = 2^{-1/2}(\alpha_1\beta_2 - \beta_1\alpha_2)\alpha_3\alpha_4, \quad \sigma_1 = 2^{-1/2}(\alpha_2\beta_4 - \beta_2\alpha_4)\alpha_1\alpha_3, \quad \sigma_2 = 2^{-1/2}(\alpha_4\beta_1 - \beta_4\alpha_1)\alpha_2\alpha_3. \quad \dots\dots(8)$$

$$\text{Singlet: } \left. \begin{aligned} \sigma_4 &= \frac{1}{2}(\alpha_1\beta_2 - \beta_1\alpha_2)(\alpha_3\beta_4 - \beta_3\alpha_4), \\ \sigma_1 &= \frac{1}{2}(\alpha_2\beta_4 - \beta_2\alpha_4)(\alpha_3\beta_1 - \beta_3\alpha_1), \\ \sigma_2 &= \frac{1}{2}(\alpha_4\beta_1 - \beta_4\alpha_1)(\alpha_3\beta_2 - \beta_3\alpha_2). \end{aligned} \right\} \quad \dots\dots(9)$$

§ 3. THE WAVE EQUATION

The wave equation describing the interaction of triton and neutron is

$$[T + \mathcal{V}(12) + \mathcal{V}(23) + \mathcal{V}(31) + \mathcal{V}(14) + \mathcal{V}(24) + \mathcal{V}(34)]\Psi = (E_n + E_T)\Psi, \quad \dots(10)$$

where E_T is the triton binding energy, E_n is the incident neutron energy in the centre-of-mass system ($E_{c.m.} = \frac{3}{4}E_{lab}$). T is the kinetic energy operator:

$$T = -(\hbar^2/2M)(2\nabla_{23}^2 + \frac{3}{2}\nabla_{23-1}^2 + \frac{4}{3}\nabla_{123-4}^2). \quad \dots\dots(11)$$

Here ∇_{23}^2 , ∇_{23-1}^2 and ∇_{123-4}^2 are the Laplacian operators of 3 relative to 2, 1 relative to the centre of mass of 2 and 3, and 4 relative to the centre of mass of the triton respectively.

It is our objective to deduce from (10) the integro-differential equation describing the scattering in terms of $F(123, -4)$, the spatial wave function of the incident neutron.

Following Buckingham and Massey (1942), we write for the exchange potential

$$\mathcal{V}(12) = (mM_{12} + hH_{12} + bB_{12} + w)V(12), \quad \dots\dots(12)$$

where M is the Majorana spatial exchange operator, H is the Heisenberg operator exchanging both space and spin coordinates, B is the Bartlett spin exchange operator. m , h , b and w are the coefficients of Majorana, Heisenberg, Bartlett and ordinary forces respectively, such that $m + h + b + w = 1$. If we substitute (7) and (11) in (10), and use the wave equation for the binding energy of the triton

$$[-(\hbar^2/2M)(2\nabla_{23}^2 + \frac{3}{2}\nabla_{23-1}^2) + \mathcal{V}(12) + \mathcal{V}(23) + \mathcal{V}(31)]\psi_0(123) = E_T\psi_0(123), \quad \dots\dots(13)$$

and also the relation

$$\left. \begin{aligned} (2\nabla_{23}^2 + \frac{3}{2}\nabla_{23-1}^2 + \frac{4}{3}\nabla_{123-4}^2) &= (2\nabla_{423-1}^2 + \frac{3}{2}\nabla_{23-4}^2 + \frac{4}{3}\nabla_{23}^2) \\ &= (2\nabla_{143-2}^2 + \frac{3}{2}\nabla_{43-1}^2 + \frac{4}{3}\nabla_{43}^2) \end{aligned} \right\} \quad \dots\dots(14)$$

then by multiplying both sides by $\sigma_4^*\psi_0(123)$, performing the exchange operations, and integrating over \mathbf{r}_{23} and \mathbf{r}_{23-1} space we find

Triplet :

$$\begin{aligned} (\nabla^2 + k^2)F(\mathbf{r}) &= (9/8)^3(M/\hbar^2)\left\{ \frac{3}{2}(-m - 2h + 2b + 3w)\iint\psi_0^2(123)V(14)d\mathbf{R}d\mathbf{r}' \right\} F(\mathbf{r}) \\ &+ (9/8)^3(M/\hbar^2)\left\{ -3(m + w)\iint\psi_0(123)\psi_0(234)V(12)F(\mathbf{r}')d\mathbf{R}d\mathbf{r}' \right. \\ &+ \frac{3}{2}(3m + 2h - 2b - w)\iint\psi_0(123)\psi_0(234)V(14)F(\mathbf{r}')d\mathbf{R}d\mathbf{r}' \\ &+ \frac{3}{2}E_n\iint\psi_0(123)\psi_0(234)F(\mathbf{r}')d\mathbf{R}d\mathbf{r}' \\ &\left. + (9/8)^3\iint\psi_0(123)\nabla_{\mathbf{r}'}^2\{\psi_0(234)F(\mathbf{r}')\}d\mathbf{R}d\mathbf{r}'. \right\} \quad \dots\dots(15) \end{aligned}$$

Singlet:

$$\begin{aligned} (\nabla^2 + k^2)F(\mathbf{r}) = & (9/8)^3 (M/\hbar^2) \left\{ \frac{3}{2}(-m-2h+3w) \iint \psi_0^2(123) V(14) d\mathbf{R} d\mathbf{r}' \right\} F(\mathbf{r}) \\ & + (9/8)^3 (M/\hbar^2) \left\{ 3(-m+h+b-w) \iint \psi_0(123) \psi_0(234) V(12) F(\mathbf{r}') d\mathbf{R} d\mathbf{r}' \right. \\ & + \frac{3}{2}(3m-2b-w) \iint \psi_0(123) \psi_0(234) V(14) F(\mathbf{r}') d\mathbf{R} d\mathbf{r}' \\ & + \frac{3}{2} E_n \iint \psi_0(123) \psi_0(234) F(\mathbf{r}') d\mathbf{R} d\mathbf{r}' \} \\ & + (9/8)^3 \iint \psi_0(123) \nabla_{\mathbf{r}'}^2 \{ \psi_0(234) F(\mathbf{r}') \} d\mathbf{R} d\mathbf{r}', \end{aligned} \quad \dots (16)$$

$$\text{where } \left. \begin{aligned} k^2 = (3/2)(M/\hbar^2)E_n, \quad \mathbf{r} = \mathbf{r}_{123-4} = \frac{1}{3}(\mathbf{r}_1 + \mathbf{r}_2 + \mathbf{r}_3) - \mathbf{r}_4, \\ \mathbf{R} = \mathbf{r}_{23} = \mathbf{r}_2 - \mathbf{r}_3, \quad \mathbf{r}' = \mathbf{r}_{234-1} = \frac{1}{3}(\mathbf{r}_2 + \mathbf{r}_3 + \mathbf{r}_4) - \mathbf{r}_1, \end{aligned} \right\} \dots (17)$$

We have here transformed one of the integration variables from \mathbf{r}_{23-1} to $\mathbf{r}' = \frac{1}{3}(8\mathbf{r}_{23-1} - 3\mathbf{r})$. It is now necessary to symmetrize the last expression in (15) and (16). Using Green's theorem, one finds

$$\iint \psi_0(123) \nabla_{\mathbf{r}'}^2 \{ \psi_0(234) F(\mathbf{r}') \} d\mathbf{R} d\mathbf{r}' = \iint \nabla_{\mathbf{r}'}^2 \{ \psi_0(123) \psi_0(234) \} F(\mathbf{r}') d\mathbf{R} d\mathbf{r}'. \quad \dots (18)$$

We take $\mathbf{r}_{23-1} = \mathbf{u}$, $\mathbf{r}_{23-4} = \mathbf{t}$, so that

$$\mathbf{u} = \frac{3}{8}(\mathbf{r} + 3\mathbf{r}'), \quad \mathbf{t} = \frac{3}{8}(3\mathbf{r} + \mathbf{r}'). \quad \dots (19)$$

$$\text{Then} \quad \nabla_{\mathbf{r}'}^2 = \frac{9}{64} \left\{ 9\nabla_{\mathbf{u}}^2 + \nabla_{\mathbf{t}}^2 + 6 \left(\frac{\mathbf{u} \cdot \mathbf{t}}{ut} \right) \frac{\partial^2}{\partial u \partial t} \right\}. \quad \dots (20)$$

We now need to express $\psi_0(123)$ and $\psi_0(234)$ in terms of u , t and R , and to do this in simple closed form and also to perform the \mathbf{R} integrations in (15) and (16), we assume the triton ground state wave function $\psi_0(123)$ as equal to the product of three deuteron wave functions of gaussian radial dependence

$$\psi_0(123) = v(12)v(23)v(31),$$

$$\text{where} \quad v(r) = \exp(-\frac{1}{2}\lambda r^2). \quad \dots (21)$$

$$\text{Using} \quad \left. \begin{aligned} \mathbf{r}_{12} = -\mathbf{u} - \frac{1}{2}\mathbf{R}, \quad \mathbf{r}_{23} = \mathbf{R}, \quad \mathbf{r}_{31} = \mathbf{u} - \frac{1}{2}\mathbf{R}, \\ \mathbf{r}_{34} = \mathbf{t} - \frac{1}{2}\mathbf{R}, \quad \mathbf{r}_{24} = \mathbf{t} + \frac{1}{2}\mathbf{R}, \end{aligned} \right\} \quad \dots (22)$$

$$\text{we find} \quad \psi_0(123)\psi_0(234) = v^2(u)v^2(t)v^3(R). \quad \dots (23)$$

From (18), (20) and (23), then

$$\begin{aligned} \nabla_{\mathbf{r}'}^2 \{ \psi_0(123) \psi_0(234) \} = & \frac{9}{64} \left[9\psi_0(234) \nabla_{\mathbf{u}}^2 \psi_0(123) + \psi_0(123) \nabla_{\mathbf{t}}^2 \psi_0(234) \right. \\ & \left. + 6 \left(\frac{\mathbf{u} \cdot \mathbf{t}}{ut} \right) v^2(u)' v^2(t)' v^3(R) \right] \\ = & -\frac{9}{32} [9\psi_0(234) \sigma_1^* \nabla_{\mathbf{u}}^2 \psi_0(123) \sigma_4 + \psi_0(123) \sigma_4^* \nabla_{\mathbf{t}}^2 \psi_0(234) \sigma_1] \\ & + \frac{27}{32} \left(\frac{\mathbf{u} \cdot \mathbf{t}}{ut} \right) v^2(u)' v^2(t)' v^3(R), \end{aligned} \quad \dots (24)$$

as $\sigma_1^* \sigma_4 = \sigma_4^* \sigma_1 = -\frac{1}{2}$ for both triplet and singlet from (8) and (9). Now the triton function $\psi_0(123)$ satisfies (13), which may be generalized to include spin thus

$$[-(\hbar^2/2M)(2\nabla_{\mathbf{R}}^2 + \frac{3}{2}\nabla_{\mathbf{u}}^2) + \mathcal{V}(12) + \mathcal{V}(23) + \mathcal{V}(31)] \sigma_4 \psi_0(123) = E_{\text{T}} \sigma_4 \psi_0(123). \quad \dots (25)$$

On multiplying both sides of (26) by σ_1^* , one obtains expressions for the part involving potentials

Triplet:

$$\begin{aligned} \sigma_1^* [\mathcal{V}(12) + \mathcal{V}(23) + \mathcal{V}(31)] \sigma_4 \psi_0(123) = & [\frac{1}{2}(-m-w+h+b)V(12) \\ & - \frac{1}{2}(m+w)V(23) - \frac{1}{2}(m+w+h+b)V(31)] \psi_0(123). \end{aligned} \quad \dots (26)$$

Singlet:

$$\sigma_1^*(\mathcal{V}(12) + \mathcal{V}(23) + \mathcal{V}(31))\sigma_4\psi_0(123) = [\frac{1}{2}(-m-w+h+b)V(12) + \frac{1}{2}(-m-w-2h-2b)V(23) + \frac{1}{2}(-m-w+h+b)V(31)]\psi_0(123) \dots (27)$$

with similar expressions involving $\psi_0(234)$. On substituting (26) and (27) in (25), and using the result to eliminate the Laplacian factors from (24), we find

Triplet:

$$\begin{aligned} & \iint \nabla^2_{\mathbf{r}\mathbf{r}'} \{\psi_0(123)\psi_0(234)\} F(\mathbf{r}') d\mathbf{R} d\mathbf{r}' \\ &= (M/\hbar^2) \iint \psi_0(123)\psi_0(234) \left\{ \frac{27}{8}(m+w)V(12) + \frac{15}{8}(m+w)V(23) \right. \\ & \quad \left. + \frac{3}{8}(m+w)V(24) \right\} F(\mathbf{r}') d\mathbf{R} d\mathbf{r}' - \frac{15}{8}(M/\hbar^2) E_T \iint \psi_0(123)\psi_0(234) F(\mathbf{r}') d\mathbf{R} d\mathbf{r}' \\ & \quad + \frac{3}{8} \iint \psi_0(123)\psi_0(234) \left[9 \left(\frac{\mathbf{u} \cdot \mathbf{t}}{ut} \right) \frac{v'(u)v'(t)}{v(u)v(t)} - 5 \frac{\nabla_R^2 \psi_0(123)}{\psi_0(123)} \right] F(\mathbf{r}') d\mathbf{R} d\mathbf{r}'. \end{aligned} \dots (28)$$

Singlet:

$$\begin{aligned} & \iint \nabla^2_{\mathbf{r}\mathbf{r}'} \{\psi_0(123)\psi_0(234)\} F(\mathbf{r}') d\mathbf{R} d\mathbf{r}' \\ &= (M/\hbar^2) \iint \psi_0(123)\psi_0(234) \left\{ \frac{27}{8}(m+w-h-b)V(12) + \frac{15}{8}(m+w+2h+2b)V(23) \right. \\ & \quad \left. + \frac{3}{8}(m+w-h-b)V(24) \right\} F(\mathbf{r}') d\mathbf{R} d\mathbf{r}' - \frac{15}{8}(M/\hbar^2) E_T \iint \psi_0(123)\psi_0(234) F(\mathbf{r}') d\mathbf{R} d\mathbf{r}' \\ & \quad + \frac{3}{8} \iint \psi_0(123)\psi_0(234) \left[9 \left(\frac{\mathbf{u} \cdot \mathbf{t}}{ut} \right) \frac{v'(u)v'(t)}{v(u)v(t)} - 5 \frac{\nabla_R^2 \psi_0(123)}{\psi_0(123)} \right] F(\mathbf{r}') d\mathbf{R} d\mathbf{r}'. \end{aligned} \dots (29)$$

Substitution of (28) into (15) and (29) into (16) gives

Triplet:

$$\begin{aligned} (\nabla^2 + k^2)F(\mathbf{r}) &= \frac{3}{2}(-m-2h+2b+3w)U(\mathbf{r})F(\mathbf{r}) \\ & \quad + \int \left[\frac{3}{8}(m+w)Q(\mathbf{r}, \mathbf{r}') + \frac{3}{2}(3m+2h-2b-w)T(\mathbf{r}, \mathbf{r}') + \left(\frac{E_n}{E_T} - \frac{5}{4} \right) N(\mathbf{r}, \mathbf{r}') \right. \\ & \quad \left. + P(\mathbf{r}, \mathbf{r}') + \frac{3}{8}(m+w)S(\mathbf{r}, \mathbf{r}') + \frac{15}{8}(m+w)R(\mathbf{r}, \mathbf{r}') \right] F(\mathbf{r}') d\mathbf{r}'. \end{aligned} \dots (30)$$

Singlet:

$$\begin{aligned} (\nabla^2 + k^2)F(\mathbf{r}) &= \frac{3}{2}(-m-2h+3w)U(\mathbf{r})F(\mathbf{r}) \\ & \quad + \int \left[\frac{3}{8}(m+w-h-b)Q(\mathbf{r}, \mathbf{r}') + \frac{3}{2}(3m-2b-w)T(\mathbf{r}, \mathbf{r}') + \left(\frac{E_n}{E_T} - \frac{5}{4} \right) N(\mathbf{r}, \mathbf{r}') \right. \\ & \quad \left. + P(\mathbf{r}, \mathbf{r}') + \frac{3}{8}(m+w-h-b)S(\mathbf{r}, \mathbf{r}') + \frac{15}{8}(m+w+2h+2b)R(\mathbf{r}, \mathbf{r}') \right] \\ & \quad \times F(\mathbf{r}') d\mathbf{r}'. \end{aligned} \dots (31)$$

where

$$U(\mathbf{r}) = (9/8)^3 (M/\hbar^2) \iint \psi_0^2(123) V(14) d\mathbf{R} d\mathbf{r}', \dots (32)$$

$$Q(\mathbf{r}, \mathbf{r}') = (9/8)^3 (M/\hbar^2) \iint \psi_0(123)\psi_0(234) V(12) d\mathbf{R}, \dots (33)$$

$$T(\mathbf{r}, \mathbf{r}') = (9/8)^3 (M/\hbar^2) \iint \psi_0(123)\psi_0(234) V(14) d\mathbf{R}, \dots (34)$$

$$N(\mathbf{r}, \mathbf{r}') = \frac{3}{2} E_T (9/8)^3 (M/\hbar^2) \iint \psi_0(123)\psi_0(234) d\mathbf{R}, \dots (35)$$

$$P(\mathbf{r}, \mathbf{r}') = \frac{3}{8} (9/8)^3 \iint \psi_0(123)\psi_0(234) \left[9 \left(\frac{\mathbf{u} \cdot \mathbf{t}}{ut} \right) \frac{v'(u)v'(t)}{v(u)v(t)} - 5 \frac{\nabla_R^2 \{v^3(R)\}}{v^3(R)} \right] d\mathbf{R}, \dots (36)$$

$$S(\mathbf{r}, \mathbf{r}') = (9/8)^3 (M/\hbar^2) \iint \psi_0(123)\psi_0(234) V(24) d\mathbf{R}, \dots (37)$$

$$R(\mathbf{r}, \mathbf{r}') = (9/8)^3 (M/\hbar^2) \iint \psi_0(123)\psi_0(234) V(23) d\mathbf{R}. \dots (38)$$

§ 4. EVALUATION OF THE SCATTERING

Solutions of eqns. (30) and (31) are needed having the asymptotic form

$$F(\mathbf{r}) \sim e^{ikz} + r^{-1}g(\theta)e^{ikr}.$$

The angular distribution $I(\theta)$ for scattering is then given by

$$I(\theta) = \frac{3}{4} |g_T(\theta)|^2 + \frac{1}{4} |g_S(\theta)|^2, \quad \dots\dots(39)$$

where the suffixes T and S denote triplet and singlet respectively, and θ is the angle of scattering in the centre-of-mass system. The total cross section for elastic scattering is

$$\sigma = \int_0^\pi I(\theta) \sin \theta d\theta. \quad \dots\dots(40)$$

To obtain $g(\theta)$ we expand in spherical harmonics

$$F(\mathbf{r}) = r^{-1} \sum_l f_l(r) P_l(\cos \theta), \quad Q(\mathbf{r}, \mathbf{r}') = \sum_l \frac{(2l+1)}{4\pi r r'} P_l(\cos \vartheta) q_l(r, r'),$$

$$\text{where} \quad q_l(r, r') = 2\pi r r' \int_0^\pi P_l(\cos \vartheta) \sin \vartheta d\vartheta Q(\mathbf{r}, \mathbf{r}'), \quad \dots\dots(41)$$

$$\cos \vartheta = (\mathbf{r} \cdot \mathbf{r}') / (r r'),$$

with similar expressions for $T(\mathbf{r}, \mathbf{r}')$, $N(\mathbf{r}, \mathbf{r}')$, $P(\mathbf{r}, \mathbf{r}')$, $S(\mathbf{r}, \mathbf{r}')$, $R(\mathbf{r}, \mathbf{r}')$ in terms of $t_l(r, r')$, $n_l(r, r')$, $p_l(r, r')$, $s_l(r, r')$ and $r_l(r, r')$ respectively, and vice versa. Here $Q(\mathbf{r}, \mathbf{r}')$ is a function only of r, r' and ϑ , because central forces only are assumed.

By use of the orthogonal properties of spherical harmonics, eqns. (30) and (31) may then be reduced to the radial form

$$\left[\frac{d^2}{dr^2} + k^2 - \frac{l(l+1)}{r^2} \right] f_l(r) = \alpha U(r) f_l(r) + \int_0^\infty \left[\beta q_l(r, r') + \gamma t_l(r, r') + \left(\frac{E_n}{E_T} - \frac{5}{4} \right) n_l(r, r') \right. \\ \left. + p_l(r, r') + \beta s_l(r, r') + \delta r_l(r, r') \right] f_l(r') dr'. \quad \dots\dots(42)$$

As all terms on the right-hand side of (42) approach zero for large r , the asymptotic solution is the usual form

$$f_l(r) \sim \sin(kr - \frac{1}{2}l\pi + \delta_l). \quad \dots\dots(43)$$

Hence one finds (Mott and Massey 1949)

$$g(\theta) = \frac{1}{2ik} \sum_l (2l+1) \{ \exp(2i\delta_l) - 1 \} P_l(\cos \theta). \quad \dots\dots(44)$$

§ 5. THE LAWS OF FORCE

Four cases of the general interaction operator (12) were considered. These are

I Ordinary force: $m = h = 0$, $w = \frac{1}{2}(1+x)$, $b = \frac{1}{2}(1-x)$,

II Majorana-Heisenberg force: $w = b = 0$, $m = \frac{1}{2}(1+x)$, $h = \frac{1}{2}(1-x)$,

III Symmetric force: $m = 2b = \frac{1}{3}(1+3x)$, $h = 2w = \frac{1}{3}(1-3x)$,

IV The Serber mixture: $m = w = \frac{1}{4}(1+x)$, $h = b = \frac{1}{4}(1-x)$.

Here $x \sim 0.6$ is the ratio of singlet to the triplet neutron-proton interaction. The expression 'ordinary force' is here used to include Bartlett forces.

Values of the constants α , β , γ , δ occurring in the wave equation (42) are given in table 1.

Table 1

Nuclear force Law	Spin state	α	β	γ	δ
I	triplet	$\frac{3}{4}(5+x)$	$\frac{3}{16}(1+x)$	$\frac{3}{4}(-3+x)$	$\frac{15}{16}(1+x)$
	singlet	$\frac{9}{4}(1+x)$	$\frac{3}{8}x$	$\frac{3}{4}(-3+x)$	$\frac{15}{32}(3-x)$
II	triplet	$\frac{3}{4}(-3+x)$	$\frac{3}{16}(1+x)$	$\frac{3}{4}(5+x)$	$\frac{15}{16}(1+x)$
	singlet	$\frac{3}{4}(-3+x)$	$\frac{3}{8}x$	$\frac{9}{4}(1+x)$	$\frac{15}{32}(3-x)$
III	triplet	$\frac{3}{8}(-1+3x)$	$\frac{3}{16}(1+x)$	$\frac{1}{4}(-1+27x)$	$\frac{15}{16}(1+x)$
	singlet	$\frac{3}{4}(-1-x)$	$\frac{3}{8}x$	$\frac{3}{4}(1+5x)$	$\frac{15}{32}(3-x)$
IV	triplet	$\frac{3}{4}(1+x)$	$\frac{3}{16}(1+x)$	$\frac{3}{4}(3x-1)$	$\frac{15}{16}(1+x)$
	singlet	$\frac{3}{2}x$	$\frac{3}{8}x$	$\frac{3}{2}x$	$\frac{15}{32}(3-x)$

The gaussian potential used is that derived by Hoisington, Share and Breit (1939) from analysis of low energy proton-proton scattering

$$V(r) = -V_0 \exp(-\mu r^2), \quad \dots\dots (45)$$

where $V_0 = 45$ mev, $\mu = 21.59 Mmc^2/\hbar^2 = 2.669 \times 10^{25}$, $r_0 = 1/\sqrt{\mu} = 1.936 \times 10^{-13}$ cm. With this definition and a corresponding form for our two-body wave function $v(r) = N_0^{1/3} \exp(-\frac{1}{2}\lambda r^2)$, the volume integrals (32)–(38) may be evaluated analytically, and from them the corresponding expressions (41) for $q_l(r, r')$, $t_l(r, r')$, $n_l(r, r')$, $p_l(r, r')$, $r_l(r, r')$ and $s_l(r, r')$.

To find the constant λ involved in the wave function $v(r)$, one computes the variation integral for the binding energy of the triton, using the trial function (21). Evaluation of the expectation energy yields the result

$$E_T = \frac{9}{2} \left(\frac{\hbar^2}{M} \right) \lambda + 3^{5/2} (m+w) V_0 \frac{\lambda^{3/2}}{(3\lambda + 2\mu)^{3/2}}. \quad \dots\dots (46)$$

On minimizing this expression, one obtains two equations for μ , λ in terms of V_0 and the binding energy E_T , the first being eqn. (46), and the second (47)

$$\frac{(3\lambda + 2\mu)^{5/2}}{\lambda^{1/2}\mu} + 6\sqrt{3}(m+w) \frac{M}{\hbar^2} V_0 = 0. \quad \dots\dots (47)$$

As $(m+w) = \frac{1}{2}(1+x)$ has the same value for all the forces I, II, III and IV, substitution of the given values of V_0 and μ leads in each case to the result $\lambda = 1.436 \times 10^{25}$, $E_T = -5.49$ mev. This variational binding energy compares with the experimental value of -8.3 mev, but the theoretical value must be employed together with the given λ . As scattering calculations are not sensitive to small variations in binding energy, no appreciable error will be introduced by the employment of the theoretical binding energy.

§ 6. NUMERICAL CALCULATIONS

The potential function $U(r)$ and the kernels q_l , t_l , n_l , p_l , s_l , r_l may all be evaluated analytically, and for their interpretation it is convenient to define a function $\mathcal{J}(x)$ thus:

$$\mathcal{J}_{l+1/2}(x) = (\pi x/2)^{1/2} J_{l+1/2}(ix). \quad \dots\dots (48)$$

The first two values for $l=0, 1$ are then $\mathcal{J}_{1/2}(x) = \sinh x$, $\mathcal{J}_{3/2}(x) = (\sinh x/x) - \cosh x$. This function has the property $\mathcal{J}_{l+1/2}(x) = (1/x)\mathcal{J}_{l-1/2}(x) - \mathcal{J}'_{l-1/2}(x)$. The kernels

may then be written in the following form:

$$\left. \begin{aligned} U(r) &= A_0 \exp(-\gamma_0 r^2), \\ q_i(r, r') &= A_1 \exp\{-\gamma_1 r^2 - \gamma_5 r'^2\} \mathcal{J}_{l+1/2}(\kappa_1 r r'), \\ t_i(r, r') &= A_2 \exp\{-\gamma_2(r^2 + r'^2)\} \mathcal{J}_{l+1/2}(\kappa_2 r r'), \\ n_i(r, r') &= A_3 \exp\{-\gamma_3(r^2 + r'^2)\} \mathcal{J}_{l+1/2}(\kappa_3 r r'), \\ p_i(r, r') &= A_4 \exp\{-\gamma_4(r^2 + r'^2)\} \\ &\quad \times \left[\left(3r^2 + 3r'^2 + \frac{160}{27\lambda} \right) \mathcal{J}_{l+1/2}(\kappa_4 r r') - 10rr' \mathcal{J}'_{l+1/2}(\kappa_4 r r') \right], \\ s_i(r, r') &= A_5 \exp\{-\gamma_5 r^2 - \gamma_1 r'^2\} \mathcal{J}_{l+1/2}(\kappa_5 r r'), \\ r_i(r, r') &= A_6 \exp\{-\gamma_6(r^2 + r'^2)\} \mathcal{J}_{l+1/2}(\kappa_6 r r'), \end{aligned} \right\} \dots\dots (49)$$

where

$$\begin{aligned} A_0 &= 27 \left(\frac{M}{\hbar^2} V_0 \right) \frac{\lambda^{3/2}}{(9\lambda + 2\mu)^{3/2}}, & \gamma_0 &= \frac{9\lambda\mu}{(9\lambda + 2\mu)}, \\ A_1 &= \frac{81}{2} \left(\frac{3}{\pi} \right)^{1/2} \left(\frac{M}{\hbar^2} V_0 \right) \frac{\lambda^2}{(6\lambda + \mu)^{1/2}(3\lambda + 2\mu)}, & \gamma_1 &= \frac{9}{16} \lambda \left(\frac{15\lambda + 4\mu}{6\lambda + \mu} \right), \\ & & \kappa_1 &= \frac{27}{8} \lambda \left(\frac{3\lambda + 2\mu}{6\lambda + \mu} \right), \\ A_3 &= \frac{81}{8} \left(\frac{2}{\pi} \right)^{1/2} \left(\frac{M}{\hbar^2} E_T \right) \lambda^{1/2}, & \gamma_3 &= \frac{90}{64} \lambda, & \kappa_3 &= \frac{27}{16} \lambda, \\ A_4 &= \left(\frac{9}{8} \right)^4 \left(\frac{8}{\pi} \right)^{1/2} \lambda^{5/2}, & \gamma_4 &= \frac{90}{64} \lambda, & \kappa_4 &= \frac{27}{16} \lambda, \\ A_5 &= \frac{81}{2} \left(\frac{3}{\pi} \right)^{1/2} \left(\frac{M}{\hbar^2} V_0 \right) \frac{\lambda^2}{(6\lambda + \mu)^{1/2}(3\lambda + 2\mu)}, & \gamma_5 &= \frac{9}{16} \lambda \left(\frac{15\lambda + 16\mu}{6\lambda + \mu} \right), \\ & & \kappa_5 &= \frac{27}{8} \lambda \left(\frac{3\lambda + 2\mu}{6\lambda + \mu} \right), \\ A_6 &= \frac{81}{4} \left(\frac{6}{\pi} \right)^{1/2} \left(\frac{M}{\hbar^2} V_0 \right) \frac{\lambda^2}{(3\lambda + 2\mu)^{3/2}}, & \gamma_6 &= \frac{90}{64} \lambda, & \kappa_6 &= \frac{27}{16} \lambda. \dots\dots (50) \end{aligned}$$

It is not possible to solve analytically the resulting integro-differential equations (42) using the kernels (49), and so to find the S and P phases, the kernels $q_0, q_1; t_0, t_1; n_0, n_1; p_0, p_1; s_0, s_1; r_0, r_1$ were plotted as contour representations, and the triplet and singlet wave equations solved numerically using the variation methods due to Hulthén (1944) and Kohn (1948). The higher phases, namely for $l=2, 3$, were obtained by the Born approximation, in some cases improved using a correction due to Pais (1946), although in no case did this correction amount to more than 5%.

The variational wave function for S-wave scattering was taken as

$$f_0(r) = \{1 - A \exp(-0.3r^2)\} \sin kr + \{M - B \exp(-0.3r^2)\} \{1 - \exp(-0.3r^2)\} \cos kr, \dots\dots (51)$$

where we have taken the unit of length as 10^{-13} cm.

The corresponding function for P-wave scattering is

$$\begin{aligned} f_1(r) &= \{1 - A \exp(-0.3r^2)\} \left(\frac{\sin kr}{kr} - \cos kr \right) + \{M - B \exp(-0.3r^2)\} \\ &\quad \times \{1 - \exp(-0.3r^2)\} \left(\frac{\cos kr}{kr} + \sin kr \right). \dots\dots (52) \end{aligned}$$

A and B are two arbitrary parameters, while $M = \tan \delta$, as can be seen from the asymptotic behaviour of f_0 and f_1

$$f_0(0) = f_1(0) = 0, \quad f_0(r \rightarrow \infty) \sim \sin kr + M \cos kr, \\ f_1(r \rightarrow \infty) \sim \left(\frac{\sin kr}{kr} - \cos kr \right) + M \left(\frac{\cos kr}{kr} + \sin kr \right). \quad \dots\dots (53)$$

The factor 0.3 in $\exp(-0.3r^2)$ corresponds to a 'mean range' of the kernels.

Hulthén's variational method employs the integral

$$I = \int_0^\infty f^* L f dr, \quad \dots\dots (54)$$

where

$$L f = \left\{ \frac{d^2}{dr^2} + k^2 - \frac{l(l+1)}{r^2} - \alpha U(r) \right\} f_l(r) - \sum_{n=1}^6 \int_0^\infty \phi_{ln}(r, r') f_l(r') dr' \quad \dots\dots (55)$$

and $\phi_{ln}(r, r')$ represents the kernels involved, their sum being symmetrical in r and r' . The wave function $f(r)$ is found from the conditions

$$I(A, B, M) = 0, \quad \partial I / \partial A = \partial I / \partial B = 0. \quad \dots\dots (56)$$

These lead to a quadratic equation for $M = \tan \delta$. Kohn's linear method uses the equations

$$\frac{\partial I}{\partial A} = \frac{\partial I}{\partial B} = 0, \quad \frac{\partial I}{\partial M} = -k, \quad \delta = \arctan \left(M + \frac{I}{k} \right). \quad \dots\dots (57)$$

This leads to a linear equation in M .

The success of the variational methods depends largely on choosing the correct form for the wave functions (51) and (52), and so four simple cases were tried

(a) $A = B = 0$, (b) $A \neq 0, B = 0$, (c) $A = 0, B \neq 0$, (d) $A \neq B \neq 0$.

Now Kato (1950) showed that Hulthén's and Kohn's methods are exactly equivalent if the variational conditions (56) and (57) are satisfied, which holds only

Table 2. Phases for Scattering of Neutrons by Tritons at 14 mev

Spin state	I (ordinary)	II (exchange)	III (symmetric)	IV (Serber)
triplet δ_0	1.22	1.29	1.27	1.13
δ_1	-0.59	-0.60	-0.60	-0.49
δ_2	(0.14)	(0.044)	(0.073)	(0.096)
δ_3	(-0.031)	(-0.016)	(-0.005)	(-0.023)
singlet δ_0	1.28	1.25	1.24	1.24
δ_1	-0.64	-0.52	-0.56	-0.45
δ_2	(0.11)	(0.026)	(0.038)	(0.061)
δ_3	(-0.017)	(-0.012)	(-0.002)	(-0.014)

The δ_0 and δ_1 phases were found by variational methods. The δ_2 and δ_3 phases in brackets were derived by Born's approximation.

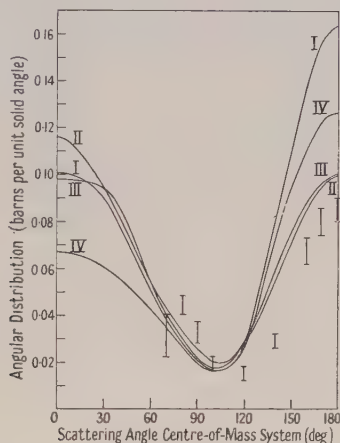
for a good choice of $f(r)$; hence our method is to work out Hulthén's and Kohn's methods for cases (a), (b), (c) and (d) for each of the exchange forces I, II, III and IV, and to choose the trial function which gives good agreement, say within 2%, between the phases obtained by the two methods. The use of Kohn's method further enables one to differentiate between the two alternative phase values given by Hulthén's method. In each case the phase value given by the latter method was chosen, as atomic calculations by Massey and Moiseiwitsch (1951) have shown that Hulthén's method tends to be more accurate than that of Kohn.

The above technique was applied to the elastic scattering of neutrons by tritons at 14 mev, the resulting phases being given in table 2.

The evaluation of the integral I in (54) was carried out by numerical integration, steps of 0.4×10^{-13} cm being used out to a distance of five times the well range, that is about 10×10^{-13} cm, beyond which the tail of the kernels becomes quite negligible. A check on the variational phases was carried out by iteration of the trial function in several cases, and the phase was found to be given an order more correct than the wave function, but the phase was not altered by more than 2%.

§ 7. COMPARISON WITH EXPERIMENT

The angular distribution at 14 meV is shown in the figure for the four forces considered, and is compared with the scattering experiments at the same energy by Coon, Bockelman and Barschall (1951).



Theoretical and experimental angular distributions for neutron-triton collisions at 14 meV; curve I, ordinary forces; curve II, Majorana-Heisenberg exchange forces; curve III, symmetric exchange forces; curve IV, Serber exchange forces. The experimental angular distribution $\sigma(\theta)$ is subject to an absolute error of $\pm 20\%$.

The latter's experimental curve is characterized by a scattering minimum at about 110° – 120° in the centre-of-mass system, and a sharp peak of back-scattering, but the results do not extend reliably below 80° . The total error in the absolute values of $\sigma(\theta)$ was estimated at $\pm 20\%$.

Table 3. Total Cross Sections for Scattering at 14 meV

Ordinary	=0.64 barn	Symmetric exchange	=0.62 barn
Majorana exchange	=0.61 barn	Serber mixture	=0.49 barn

The symmetric and Majorana exchange type forces give almost identical results, with large peaks of forward and back scattering, and minima at about 105° . The scattering at large angles is greater than that obtained by experiment, although part of the difference may be explained by the above experimental error in $\sigma(\theta)$. The ordinary curve, however, gives a much larger peak of back scattering than experiment, while the Serber exchange mixture lies intermediate between the ordinary and exchange curves in this respect. Thus the evidence appears to favour a force of symmetric exchange type rather than an ordinary force.

The total scattering cross section for the four forces has been calculated and is shown in table 3. This compares with an experimental neutron-proton cross section at 14 meV of 0.64 barn.

Coon, Bockelman and Barschall, whose experiments do not extend below 70° (c.m.), point out that integration of the experimental curve from 90° to 180° gives a value of only 0.17 barn, and if, as might be expected, the total cross section of tritium turns out to be greater than that of hydrogen (0.64 barn), there must either be a large peak of forward scattering, or a disintegration process contributing a large fraction to the total cross section, although it is not strictly necessary that the n-T cross section be greater than the n-P cross section.

If we disregard the second possibility in the absence of any evidence for disintegration protons in the above experiments, the absence of a peak of forward scattering sharp enough to give a cross section larger than that of hydrogen in the above calculations may be understood if we remember that the approximate two-body ground state wave functions used have gaussian radial dependence, whereas the true wave functions are more nearly exponential in shape. Consequently, outside the well-range our wave functions fall off too quickly, and therefore any calculations should underestimate the small angle scattering. However, the quantitative importance of the effect is not known, but one might expect it to be important at energies less than the binding energy of the triton.

Further work is being carried out at lower energies than 14 mev, and it is hoped to extend calculations to cover the scattering of protons by tritons.

ACKNOWLEDGMENTS

I would like to express my sincere thanks to Professor H. S. W. Massey, for his advice and encouragement in this work, and to thank the Department of Scientific and Industrial Research for the provision of a Research Assistantship.

REFERENCES

- BUCKINGHAM, R. A., HUBBARD, S. J., and MASSEY, H. S. W., 1952, *Proc. Roy. Soc. A*, **211**, 183.
 BUCKINGHAM, R. A., and MASSEY, H. S. W., 1942, *Proc. Roy. Soc. A*, **179**, 123.
 COON, J. H., BOCKELMAN, C. K., and BARSCHALL, H. H., 1951, *Phys. Rev.*, **81**, 33.
 HOISINGTON, L. E., SHARE, S. S., and BREIT, G., 1939, *Phys. Rev.*, **56**, 884.
 HULTHÉN, L., 1944, *K. Fysiogr. Sällsk. Lund, Förh.*, **14**, 1.
 KATO, T., 1950, *Phys. Rev.*, **80**, 475.
 KOHN, W., 1948, *Phys. Rev.*, **74**, 1763.
 MASSEY, H. S. W., and MOISEWITSCH, B. L., 1951, *Proc. Roy. Soc. A*, **205**, 483.
 MOTT, N. F., and MASSEY, H. S. W., 1949, *the Theory of Atomic Collisions* (Oxford: University Press.)
 PAIS, A., 1946, *Proc. Camb. Phil. Soc.*, **42**, 45.
 WHEELER, J. A., 1937, *Phys. Rev.*, **52**, 1107.

An Investigation of (d, p) Stripping Reactions

I: Apparatus and Results for Aluminium

By J. R. HOLT AND T. N. MARSHAM

Nuclear Physics Research Laboratory, University of Liverpool.

MS. received 10th October 1952

Abstract. An apparatus is described which enables angular distribution measurements to be carried out within the angular region -5° to $+140^\circ$ on disintegration particles of long range. The differential range spectrum is measured at each angle by the use of a triple proportional counter of novel design.

Measurements are reported for the two proton groups of longest range produced in the reaction $^{27}\text{Al}(d, p)^{28}\text{Al}$ with a deuteron energy of 8 Mev and the results discussed in the light of the theories of the stripping process.

§ 1. INTRODUCTION

THEORIES of the nuclear reactions in which a deuteron with energy of the order of 10 Mev is the bombarding particle and a proton or neutron is emitted have been formulated recently by Butler (1951) and by Bhatia, Huang, Huby and Newns (1952) on the basis of a stripping process. These theories lead to angular distributions of intensity of the emitted protons or neutrons which show maxima at small angles relative to the incident beam. The position and shape of these maxima depend on the energy of the bombarding deuterons, the Q -value for the reaction, the orbital angular momentum l taken into the nucleus by the captured member of the pair of particles in the deuteron and a quantity related to the radius at which the particle is captured. Experimental measurements of such angular distributions enable the value of l to be determined and hence yield information about the spin and parity changes involved in the reactions.

Measurements of this type have been carried out by a number of workers for both proton and neutron emission (Bromley and Goldman 1952, Burge *et al.* 1952, El-Bedewi *et al.* 1951, Gibson and Thomas 1952, Gove 1951, Holt and Young 1950, Parkinson *et al.* 1952, Rotblat 1951 a, b). In general the main features of the experimental distributions are in accord with theory and whenever the spin change in the reaction is known the value of l determined from the distribution is the expected one. However, most of the measurements on protons emitted in the (d, p) reactions suffer from the disadvantage that they do not extend to angles smaller than about 20° with respect to the direction of the incident beam, and this is often the most critical region. The neutron measurements, although they extend down to 0° , are of lower statistical accuracy.

The apparatus to be described here was designed to enable intensity measurements to be made on proton groups of long range within the angular region -5° to $+140^\circ$. In this and subsequent papers the results of measurements with a variety of target elements will be presented.

§ 2. APPARATUS

(i) *Target Chamber*

The target chamber is similar to that described by Holt and Young. The beam of 8 mev deuterons from the Liverpool cyclotron was roughly focused at the centre of the target chamber by means of a magnet and collimated by circular apertures S_1 and S_2 (fig. 1) having diameters 5 mm and 3 mm respectively, placed 27 cm apart. The beam current entering the target chamber was about $\frac{1}{50} \mu\text{A}$. The target had a thickness equivalent to 1 or 2 cm of air and was either a self-supporting foil or a layer deposited on thin gold or platinum. The target holder T was a vertical brass sheet having a hole over which the target foil was mounted. This was attached to the centre of the lid of the target chamber and could be rotated externally. For measurements on protons emitted at angles between 0° and 100° the plane of the target holder was usually at an angle of 45° , as shown in fig. 1, but for measurements at larger angles this plane was rotated through 90° .

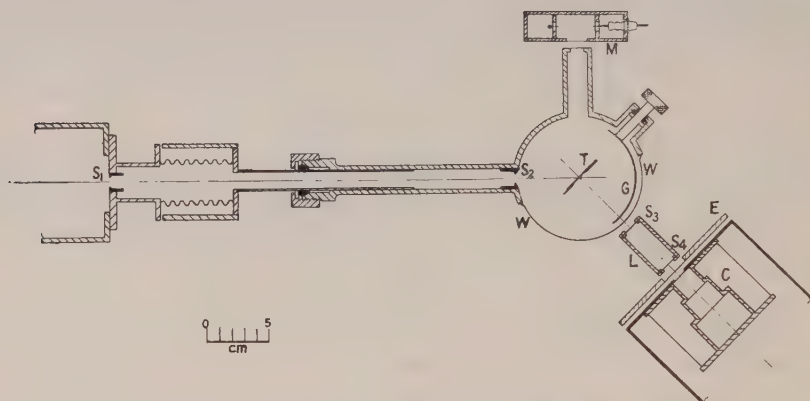


Fig. 1. Apparatus for the measurement of the angular distribution of disintegration particles.

After passing through the target the deuteron beam encountered a curved strip of gold G of just sufficient thickness to stop the beam. With 8 mev deuterons the yield of protons from the gold was quite negligible. Those protons which had ranges greater than that of the deuteron beam and which were emitted from the target at angles near the forward direction, passed through the gold and out of the target chamber through a window of 'Cellophane' WW. This had a thickness of 4.5 mg cm^{-2} and was sealed with Armstrong Cement over a long slit of width 8 mm in the side of the target chamber. The curved strip G was so mounted that it could be swung out of the way and replaced by a much smaller gold beam catcher. The protons were detected with the triple proportional counter C described below and the range spectrum was measured using a variable pressure air cell L and a wheel E holding absorbers of aluminium foil which had been carefully selected for uniformity of thickness. This detecting arrangement was mounted on a turn-table concentric with the target to allow measurements to be made at various angles. Circular stops could be fitted to either end of the air cell (S_3 and S_4) to define the solid angle for the collection of particles from the target. The intensity of

the deuteron beam was monitored by counting deuterons scattered elastically from the target at an angle of 90° using the proportional counter M.

(ii) Triple Proportional Counter

A diagram of the counter is shown in fig. 2. It consists of three proportional counters (A, B and C) sealed within the same container. The counters are short cylinders arranged with their axes along the direction of the incident particles which enter through the window W. The diameters increase from one counter to the next to reduce the chance of particles which are scattered in the aluminium absorbers from striking the walls, while keeping the volume of the counters as small as possible. The wires are of tungsten having a diameter of 0.1 mm and pass across the diameters of the cylinders through holes in their walls. Each wire is attached at one end only, the attached end being shielded by a glass tube and the free end by a glass bead. During the design of the counter tests were carried out using a well collimated beam of α -particles to determine the gas amplification at different points along the length of the wire. By adjusting the positions of the glass hood and the glass bead with respect to the holes in the cylinder it was found possible to make the gas amplification constant to within 10% along that portion of the wire which was used. The gas filling was of argon with 4% of carbon dioxide at a total pressure of 26 cm Hg.

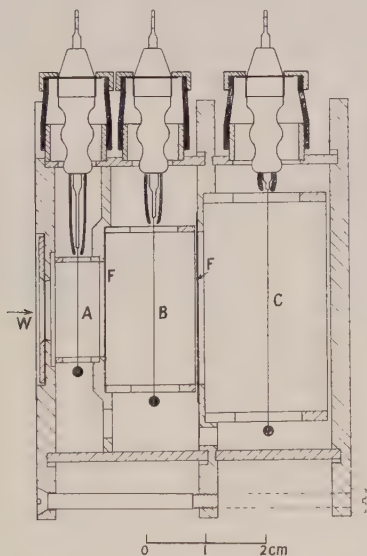


Fig. 2. Triple proportional counter.

The sensitive volumes of the counters are separated by aluminium foils F whose thicknesses determine certain properties of the arrangement. The foils can be changed by breaking the joint in the centre of the container which is sealed with soft vacuum wax.

The pulses from the three counters are fed through separate channels of conventional amplifiers and discriminators into a coincidence unit. This unit records coincident pulses from counters A and B not accompanied by a pulse from C. Thus the arrangement counts particles which pass through counter A into B but do not reach counter C.

In fig. 3 curve *a* shows the variation in the height of the pulse produced at the output of amplifier A by a proton which enters counter A with the residual range indicated on the horizontal scale. Similar curves *b* and *c* show the pulse heights produced at the outputs of the amplifiers B and C by protons entering A with various residual ranges. The amplification was adjusted so that the size of the pulses corresponding to the maxima of the curves was the same in the three channels. Representative working levels of the pulse amplitude discriminators associated with each of the three counters are shown at X, Y and Z. The effective counting depth is given by the horizontal distance between Y and Z, providing that the level Y is below the level of the intersection of the vertical line through Z with the curve *b*. With this arrangement the counting depth is then fixed mainly by the thickness of the absorber between counters B and C and is not sensitive to small changes in discriminator level, circuit amplification or counter voltage. For example, a 10% change in the discriminator level of

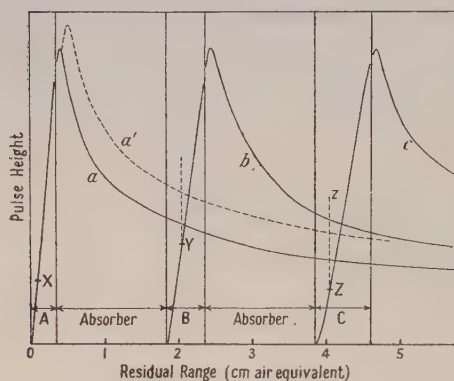


Fig. 3. Curves *a*, *b* and *c* show how the size of the pulse produced in counters A, B and C by a proton depends on the residual range of the proton when it enters counter A. Curve *a'* is the corresponding curve for counter A relating to deuterons.

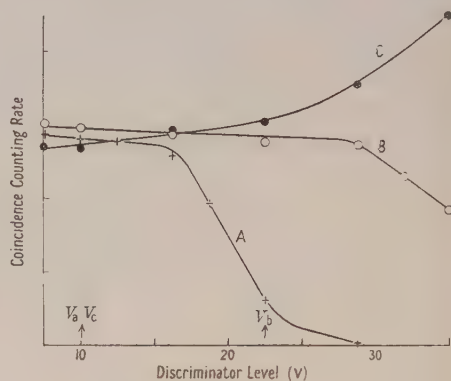


Fig. 4. Discriminator bias curves for the three channels, A, B and C with protons entering the counter.

counter B produces only a 1% change in the counting depth. Curve *a'* shows the variation in the height of pulses in counter A produced by deuterons. Similar curves could be drawn for counters B and C, and in each case the slope of the curve near the origin is nearly the same as that of the proton curve. Thus the counting depth is nearly the same for protons and deuterons. This is also true for other types of heavy charged particles. This feature allows direct comparison of the intensities of two groups of particles of different kinds. In order to distinguish between the different kinds of particles the discriminator level of counter A can be varied. When the level X rises above the intersection of Zz with curve *a* the counting depth for protons starts to decrease while that for deuterons remains constant until the level X rises above the intersection of Zz with curve *a'*. In this way it was found possible with our counter to achieve almost complete discrimination between protons and deuterons and partial discrimination between deuterons and tritons. Alpha-particles could be counted to the complete exclusion of single-charged particles. The discrimination between

particles of different kinds can be improved by decreasing the thickness of absorber between B and C or by increasing that between A and B. The former cannot be made much smaller than the natural width of the peaks in the range spectrum without serious loss of intensity. An increase in the latter increases the minimum energy which a particle must have in order to be detected. The thicknesses chosen appeared to provide a good compromise between the various requirements.

Characteristic bias curves for the counting system are shown in fig. 4. These were obtained while the counter was detecting protons at the peak of a group which was broad compared with the counting depth. The coincidence counting rate is here plotted as a function of the discriminator voltage for each counter in turn, the discriminator levels of the remaining two counters being kept at their normal values. The normal operating levels are V_a , V_b and V_c and the curves show how insensitive the counting properties of the arrangement are to alterations in these. It was found desirable to make V_b as large as possible since this reduced the background rate of the counter. Figure 5 shows how the arrangement discriminates between different types of particles. Curve *a* shows the effect of altering the discriminator level of channel A when a mixture of protons, tritons and α -particles are entering the counter. Curve *b* shows the corresponding curve for deuterons.

Boyer *et al.* (1951) have used a triple proportional counter of different design to determine range spectra and to discriminate between different types of charged particles. The method of using the counter was different from that employed in the present work.

§ 3. PROCEDURE

The angular distributions of charged particles were obtained by plotting the differential range spectrum at various angles. The number of particles in a certain group which are emitted into the solid angle defined by a stop placed at S_3 or S_4 is proportional to the area enclosed by that group in the differential range spectrum. Measurements could be made at angles down to 0° on proton groups which had sufficient energy to penetrate the gold absorber G and the various windows. In our case such protons were those emitted in reactions having *Q*-values greater than zero. The angular distributions of groups of long range were measured in two parts. Near the forward direction measurements were made on protons which had passed through the gold absorber but at angles greater than 11° the small beam catcher was used. At these larger angles measurements could also be made on proton groups of shorter range which did not have to pass through the gold. When measurements were made through the gold the number of protons reaching the counter was reduced by scattering in the gold. The amount of this reduction depends on the proton energy and the geometry of the detecting system. Since the variation in energy of any one group of protons is small within the angular range involved, the scattering introduced no appreciable distortion of the angular distribution. To fit together the two parts of the angular distribution it was necessary to make two measurements of intensity at some angle greater than 11° , first with and then without the gold absorber in position. The two parts of the distribution were then normalized to the same value at this angle.

The angular resolution of the apparatus was fixed by the dimensions of the area of intersection of the beam with the target and the diameter of the stop

placed at S_3 or S_4 , together with its distance from the target. For measurements without the gold absorber it was desirable that S_4 should be the defining aperture. With the gold absorber in position the angular resolution was determined mainly by S_3 owing to the scattering of the protons by the gold. When necessary a correction was made to the measured angular distributions to allow for the effect of the finite angle of acceptance of the detector. In most cases, however, this correction was negligible compared with the experimental errors.

§4. RESULTS

The Reaction $^{27}\text{Al}(d, p)^{28}\text{Al}$. Angular distributions of certain proton groups from the reaction $^{27}\text{Al}(d, p)^{28}\text{Al}$ have previously been measured (Holt and Young 1950, Gove 1951) but the measurements did not extend to angles smaller than about 20° . We have measured the variation of intensity with angle down to 0° for the two proton groups of longest range from this reaction. The target was of aluminium foil 1.5 mg cm^{-2} in thickness. The diameter of the deuteron beam at the target was 2 mm and the solid angle for collection of the emitted protons was defined by the stop S_3 , with a diameter of 2 mm, at a distance of 4.5 cm from the target. Proton counting rates up to 4000 per minute were observed with a background rate of 10 per minute.

In fig. 6 the measured region of the range spectrum is shown for an angle of observation of 1° . The two proton groups are designated p_0 and p_1 . Within the resolving power of the arrangement they appeared to be single groups, well

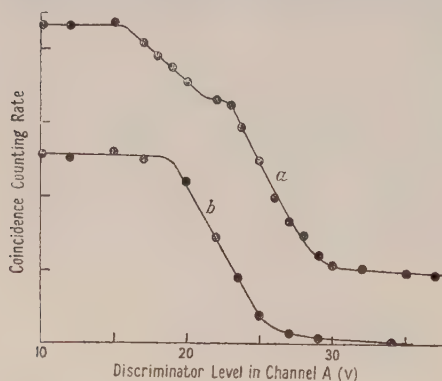


Fig. 5. Discriminator bias curves for channel A with a mixed beam of protons, tritons and α -particles entering the counter (curve a) and with deuterons entering the counter (curve b).

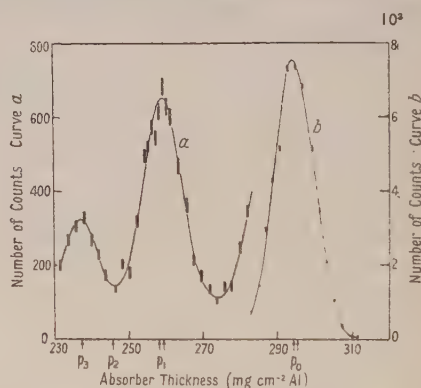


Fig. 6. Proton spectrum of the reaction $^{27}\text{Al}(d, p)^{28}\text{Al}$ at an angle of observation of 1° .

separated from each other. This was the case over the whole range of angles investigated which extended to 60° . Since the half-width of the peaks was observed not to change with angle the angular distributions were determined by reading off the heights of the peaks at each angle and subtracting the background rate of the counter.

The distribution for the group p_0 is shown in fig. 7 in which the experimental points are corrected for the effect of finite acceptance angle and plotted with centre of mass coordinates. In the case of the distribution of the group p_1 the

correction for finite acceptance angle was negligible compared with the experimental error. The experimental points plotted with centre-of-mass coordinates are shown in fig. 8.

Estimates of the absolute cross sections for the transitions involving the two proton groups were made by comparing the intensities of the groups with the intensity of the deuterons scattered elastically from the target at an angle of 50° . On the assumption that Rutherford scattering is responsible for the whole cross section in the latter case, the differential cross sections for the groups p_0 and p_1 at 0° have the values $2.2 \times 10^{-25} \text{ cm}^2$ and $1.9 \times 10^{-26} \text{ cm}^2$.

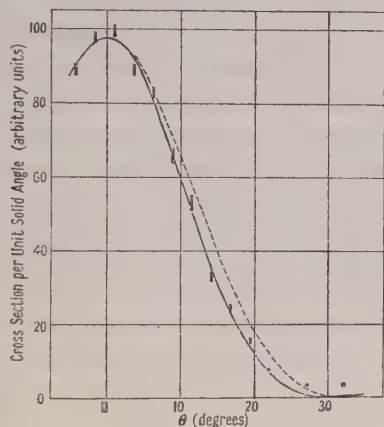


Fig. 7. Angular distribution in the centre-of-mass system of the proton group p_0 .

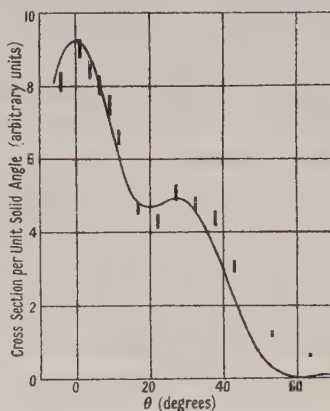


Fig. 8. Angular distribution in the centre-of-mass system of the proton group p_1 .

§ 5. DISCUSSION

A magnetic analysis of the present reaction has been carried out by Enge *et al.* (1952) with deuterons having an energy of 2.0 mev. This shows that the ground state of ^{28}Al is a doublet with a spacing of 31 kev, and the first excited state at 1.0 mev is a doublet with a spacing of 41 kev. Thus it is likely that both the proton groups p_0 and p_1 in our case are mixtures of protons corresponding to both members of each doublet. The arrows at the bottom of fig. 6 indicate the expected ranges of protons corresponding to the energy levels found by Enge. The double arrow corresponding to the ground state was adjusted to coincide with the position of the maximum of group p_0 . It will be seen that there is no indication of a group at the position of the arrow p_2 , and this is so over the whole angular range investigated. With the bombarding energy used in this experiment the intensity of this group must be less than 15% of that of group p_1 .

In fitting theoretical curves to the experimental angular distributions the values of two adjustable parameters have to be decided. These are the orbital angular momentum l with which the neutron is captured in the stripping process and a length r defining the radius at which the neutron is captured by the target nucleus. The latter quantity should be approximately the 'geometrical' radius of the nucleus. A useful empirical formula for this radius is the one given by Gamow and Critchfield (1949) on the basis of attenuation experiments with fast neutrons, namely $R = (1.7 + 1.22A^{1/3}) \times 10^{-13} \text{ cm}$. From the comparisons between

theory and experiment which have so far been carried out it appears that this value of r is a good one to use in the theory of Butler, while the theory of Bhatia *et al.* requires a value greater than this by about 2×10^{-13} cm.

The theoretical differential cross section for the formation of a certain nuclear state can be considered as the product of two terms. The first is proportional to the probability of the neutron within the deuteron arriving at the surface of a nucleus with the correct energy and orbital momentum to be captured into the particular nuclear state in question. This term contains the factors which depend on the direction of emission of the stripped proton and its value at the most favourable angle of emission decreases by a factor of about 5 as l increases by one unit, assuming a positive Q -value for the reaction of about 4 mev. The second term is proportional to the probability for capture of the neutron by the nucleus. No calculations are available for the magnitudes of the neutron capture probabilities but one may hope to obtain some hints regarding the structure of nuclear states by comparing their relative values for different transitions. In the paper by Bhatia *et al.* it is suggested that final states having similar constitution should be associated with similar values of the neutron capture probability. We have used the quantity $\Lambda/(2j_i + 1)$ in their formula as a measure of the neutron capture probability and derived its values from the measured differential cross sections.

In fig. 7 the full curve was drawn according to the theory of Butler with values of r and l chosen to give the best fit with the experimental points, these being $r = 6.15 \times 10^{-13}$ cm and $l = 0$. A practically identical curve was obtained using the theory of Bhatia *et al.* with the values $r = 7.4 \times 10^{-13}$ cm and $l = 0$. The broken curve was drawn using Butler's theory with the value $r = 5.4 \times 10^{-13}$ cm given by the Gamow-Critchfield formula.

The experimental points for the group p_1 could not be fitted by any theoretical curve employing only one value of l . However, a good fit could be obtained by adding together two theoretical curves, one having $l = 0$ and the other having $l = 2$. The curve shown in fig. 8 was drawn according to Butler's theory by adding two such curves whose maximum values were adjusted to be in the ratio 1.85 and with $r = 6.15 \times 10^{-13}$ cm. A similar agreement with experiment could be obtained using the theory of Bhatia *et al.*

The results have been briefly discussed in a previous communication (Holt and Marsham 1952). Since then more complete information has been published regarding the results of the magnetic analysis of this reaction (Enge *et al.* 1952) and it now appears that the first excited state of ^{28}Al is a close doublet, whereas in the previous note we assumed it to be single. The ratio of the intensities of the proton groups corresponding to the two members of the doublet emitted at an angle of 90° in the (d, p) reaction at a bombarding energy of 2.0 mev is about 8:1. A complete interpretation of the angular distributions obtained in the present investigation would require a magnetic analysis of the reaction at a bombarding energy of 8 mev and at some angle within the range examined. Failing this, a number of alternative conclusions are possible.

In the case of the group p_0 either one or both members of the doublet are formed by capture of neutrons with zero orbital momentum. If one member of the doublet were formed by capture of neutrons with a value of l greater than 1, this might not be evident from the distribution, because the component of the angular distribution having $l = 0$ is expected, from the theory of the process, to

have a peak value at least twenty times greater than that due to such a higher value of *l* if we assume that the neutron capture probability is the same in each case. Thus we conclude that one or both members of the doublet have spin 2 or 3 and the same parity as ^{27}Al , since the spin of ^{27}Al is 5/2.

In the case of the group p_1 there is also ambiguity in the interpretation of the results since we do not know whether both members of the doublet contribute to the measured differential cross section for the stripping process. It is possible that one member of the doublet is associated with a relatively small differential stripping cross section owing to the neutron capture probability being small or to the *l*-value being greater than 2. Then the interpretation given in the previous note (Holt and Marsham 1952) would still apply. However, the most plausible assumption is that the two components of the angular distribution having *l*=0 and *l*=2 are associated with the two members of the doublet. Then the spin of one is restricted to 2 or 3, while the other may have any integral spin between 0 and 5 units. The neutron capture probabilities for the transitions having *l*=0 and *l*=2 have the values 0.6 and 6.7 in arbitrary units. That calculated for the group p_0 is 6.3 in the same units. According to the Mayer shell model (Mayer 1950) the ground state of ^{28}Al is formed from ^{27}Al by adding a neutron in an s-orbit. This is consistent with the value *l*=0 which was found for the proton group p_0 . Since the group p_0 and the component of the group p_1 which has *l*=2 have similar neutron capture probabilities, it seems reasonable to suppose that the corresponding transitions are of a similar nature. The much smaller neutron capture probability for the component of the group p_1 with *l*=0 would suggest a more complicated mode of formation of the final state in this case.

ACKNOWLEDGMENTS

We are grateful to Professor H. W. B. Skinner for helpful discussions and to Dr. R. Huby and Mr. H. C. Newns for information regarding the theories of the stripping process. One of us (T. N. M.) thanks the Department of Scientific and Industrial Research for a maintenance grant.

REFERENCES

- BHATIA, A. B., HUANG, K., HUBY, R., and NEWNS, H. C., 1952, *Phil. Mag.*, **43**, 485.
BOYER, K., GOVE, H. E., HARVEY, J. A., DEUTSCH, M., and LIVINGSTON, M. S., 1951, *Rev. Sci. Instrum.*, **22**, 310.
BROMLEY, D. A., and GOLDMAN, L. M., 1952, *Phys. Rev.*, **86**, 790.
BURGE, E. J., BURROWS, H. B., GIBSON, W. M., and ROTBLAT, J., 1952, *Proc. Roy. Soc. A*, **210**, 534.
BUTLER, S. T., 1951, *Proc. Roy. Soc. A*, **208**, 559.
EL-BEDEWI, F. A., MIDDLETON, R., and TAI, C. T., 1951, *Proc. Phys. Soc. A*, **64**, 756, 1055.
ENGE, H. A., BUECHNER, W. W., and SPERDUTO, A., 1952, *Phys. Rev.*, **88**, 963.
GAMOW, G., and CRITCHFIELD, C. L., 1949, *Theory of the Atomic Nucleus* (Oxford: University Press), p. 11.
GIBSON, W. M., and THOMAS, E. E., 1952, *Proc. Roy. Soc. A*, **210**, 543.
GOVE, H. E., 1951, *Phys. Rev.*, **81**, 364.
HOLT, J. R., and MARSHAM, T. N., 1952, *Proc. Phys. Soc. A*, **65**, 763.
HOLT, J. R., and YOUNG, C. T., 1950, *Proc. Phys. Soc. A*, **63**, 833.
MAYER, M. G., 1950, *Phys. Rev.*, **78**, 16.
PARKINSON, W. C., BLACK, E. H., and KING, J. S., 1952, *Phys. Rev.*, **87**, 387.
ROTLAT, J., 1951 a, *Phys. Rev.*, **83**, 1271; 1951 b, *Nature, Lond.*, **167**, 1027.

An Investigation of (d, p) Stripping Reactions II : Results for the Isotopes of Magnesium

BY J. R. HOLT AND T. N. MARSHAM

Nuclear Physics Research Laboratory, University of Liverpool

MS. received 10th October 1952

Abstract. Angular distribution measurements have been carried out on a number of proton groups from the bombardment with 8 meV deuterons of targets of natural magnesium and of ^{25}MgO and ^{26}MgO . Spins and parities have been assigned to various states of the product nuclei on the basis of the theory of the stripping process. These are given herewith, the excitation energy of each state in meV being followed by the possible spin values and the parity in brackets:

^{25}Mg : ground state (5/2, 3/2+), 0.582(1/2+), 0.976(5/2, 3/2+), 1.957(5/2, 3/2+), 3.405(3/2, 1/2-).

^{26}Mg : 1.825(3, 2+ and 5, 4+), 2.972(3, 2+), 3.969(3, 2+), 4.353(3, 2+), 6.147(3, 2+).

^{27}Mg : ground state (1/2+), 0.887(5/2, 3/2+), 3.50(1/2+).

The following new energy levels have been observed:

^{25}Mg : 4.62 ± 0.05 , 5.05 ± 0.08 , 5.49 ± 0.05 and 6.40 ± 0.05 meV.

^{26}Mg : 7.29 ± 0.06 and 8.28 ± 0.06 meV. ^{27}Mg : 3.50 ± 0.05 meV.

§ 1. INTRODUCTION

THE apparatus described in the preceding paper (Holt and Marsham 1953, to be referred to as I) has been used to measure angular distributions of some of the proton groups emitted from the three magnesium isotopes when bombarded by 8 meV deuterons.

The proton spectra from these reactions at a bombarding energy of 2 meV have been analysed magnetically by Endt, Haffner and Van Patter (1952) and by Endt, Enge, Haffner and Buechner (1952). The results of these measurements have been found very useful in the interpretation of the range spectra obtained in the present investigation.

§ 2. TARGET PREPARATION

Natural magnesium consists of three isotopes with mass numbers 24, 25 and 26 having abundances in the ratios 77.4:11.5:11.1. For the present work the separated isotopes were available as metallic layers containing a few milligrams of the isotope on a stainless steel backing. For use as targets the magnesium was transferred to a thin support of platinum foil which had a thickness equivalent to 4.5 cm of air. This was done by converting the magnesium to oxide in the following way. The magnesium layer was dissolved in a drop of dilute hydrochloric acid and the drop transferred to a piece of platinum foil using a micro-pipette. A drop of ammonium hydroxide was added and the platinum heated gradually to about 300°C to drive off the ammonium chloride,

leaving a layer of magnesium hydroxide. After cooling, some more ammonium hydroxide was added and the procedure repeated to make sure of eliminating all the chloride. Finally a drop of water was added to the magnesium hydroxide, the suspension stirred to aid the formation of a uniform layer and the platinum gradually heated to redness to convert the hydroxide to oxide. In this way fairly uniform layers were obtained about 0.5 cm^2 in area and about 1 mg cm^{-2} in thickness; thicker layers tended to peel off.

The target was mounted with its surface at an angle of 60° to the direction of the incident beam, with the oxide layer facing the oncoming deuterons. No protons could be detected from the platinum foil. The presence of the oxygen interfered with measurements on the short range proton groups. To avoid this and also to make feasible the use of a thicker target, measurements on the most abundant isotope ^{24}Mg were carried out with natural magnesium. This target was a self-supporting foil having a thickness equivalent to 1.9 cm of air.

§ 3. RESULTS

(i) Spectra of Proton Ranges

The differential range spectrum of the protons from the target of natural magnesium is shown in fig. 1 for an angle of observation of 31° . The horizontal scale indicates the total range of the emitted protons in aluminium and the vertical scale shows the proton count. The arrows at the bottom of the figure

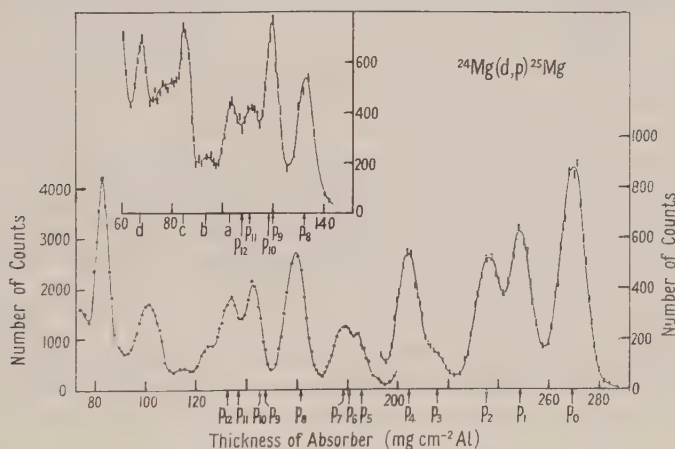


Fig. 1. Range spectrum of protons at an angle of observation of 31° resulting from the deuteron bombardment of a target of natural magnesium. The inset shows a portion of the spectrum at an angle of 90° .

show the expected positions of proton groups as calculated from the Q -values given by Endt *et al.* for the reaction $^{24}\text{Mg}(d, p)^{25}\text{Mg}$. The energy of the bombarding deuterons was derived from the measured range and known Q -value of the proton group p_0 . This energy was 8.21 mev . It can be seen that most of the peaks in the range spectrum can be identified from the positions of the arrows, although in some cases the resolution is insufficient to separate neighbouring groups of protons. Angular distribution measurements were made on peaks p_0 , p_1 , p_2 , p_3 , p_4 and p_8 . The possibility of contributions to the

spectrum from the less abundant isotopes of magnesium is considered during the discussion of the angular distributions.

The region of the spectrum below a range of about 130 mg cm^{-2} has not previously been investigated and we have examined this region at several angles between 15° and 90° . The plot at 90° is shown as an inset in fig. 1. Several prominent groups are visible and their ranges, intensities and alteration of range with angle indicate that they originate in magnesium and not in a possible contamination of oxygen or carbon. The excitation energies of the levels in ^{25}Mg corresponding to the proton groups designated a, b, c and d in fig. 1 are 4.62 ± 0.05 , 5.05 ± 0.08 , 5.49 ± 0.05 and 6.40 ± 0.05 mev. Toops *et al.* (1952) from an analysis of the reaction $^{27}\text{Al}(d, \alpha)^{25}\text{Mg}$ report levels in ^{25}Mg at 4.12 ± 0.04 , 4.87 ± 0.03 , 5.56 ± 0.03 , 5.93 ± 0.03 and 6.98 ± 0.03 mev.

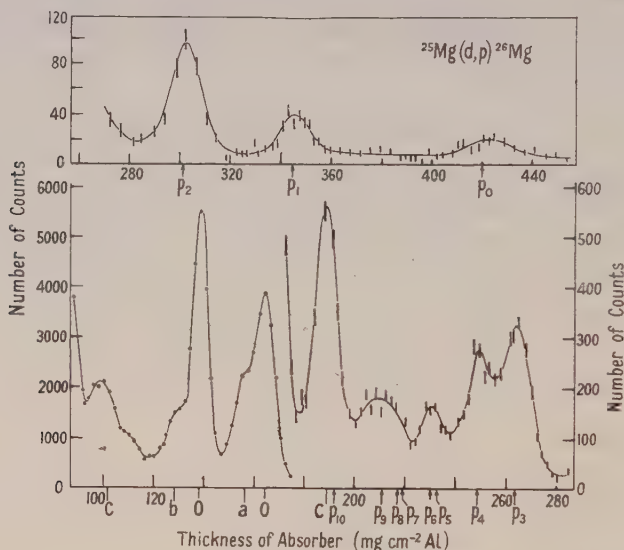


Fig. 2. Range spectrum of protons at an angle of observation of 21° resulting from the deuteron bombardment of a target of ^{25}MgO .

The differential range spectrum of the protons from the target of ^{25}MgO is shown in fig. 2 for an angle of observation of 21° . The arrows indicate the expected positions of the proton groups calculated from the Q -values given by Endt *et al.* using the group p_2 to obtain the deuteron energy, which had the value 8.19 mev. The expected positions of groups due to oxygen and carbon are indicated by the lines marked O and C. Two oxygen peaks are very prominent in the range spectrum. Adjacent to these at a and b are two peaks which we ascribe to magnesium. These have not previously been observed and the corresponding excitation energies in ^{26}Mg are 7.29 ± 0.06 and 8.28 ± 0.06 mev. Angular distribution measurements were made on peaks p_1 , p_2 , p_3 , p_4 and p_{10} . The intensity of peak p_0 was too small for such measurements to be made.

The differential range spectrum of the protons from the target of ^{26}MgO is shown in fig. 3 for an angle of observation of 31° . The value of the deuteron beam energy in this case was 8.05 mev as derived from the range and known Q -value of the prominent peak due to oxygen. Arrows indicate the positions of the groups p_0 and p_1 corresponding to the formation of the ground state and the

first excited state of ^{27}Mg according to the Q -values given by Endt *et al.* The expected positions of groups due to oxygen and carbon are indicated as before. A new peak ascribed to magnesium can be seen adjacent to one of the oxygen peaks and is marked 'a' in fig. 3. The inset in this figure shows the region of the spectrum in question at an angle of 21° . The excitation energy in ^{27}Mg corresponding to this group is 3.50 ± 0.05 mev. Angular distribution measurements were made on this group and on the groups p_0 and p_1 .

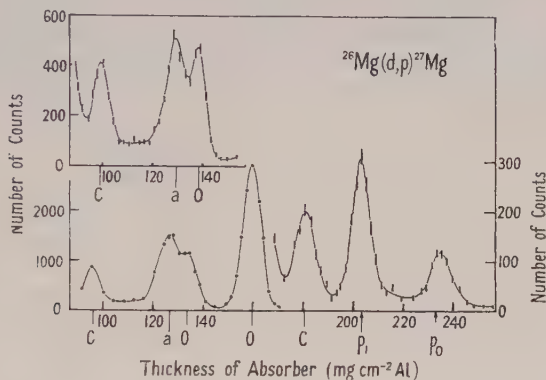


Fig. 3. Range spectrum of protons at an angle of observation of 31° resulting from the deuteron bombardment of a target of ^{26}MgO . The inset shows a portion of the spectrum at an angle of 21° .

(ii) Angular Distributions

The angular distributions of the various groups of protons were obtained from the range spectra either by determining at a number of angles the proton count at the peak of the group or by finding the area enclosed by the group. In the former case a correction was made, where necessary, for any change in the half width of the peak with variation of angle. In cases where there was overlapping of neighbouring groups separation was achieved by fitting curves having the shape of an isolated group. The resulting angular distributions are shown in figs. 5 to 12, in which the coordinates refer to the centre-of-mass system. The errors shown on the experimental points include the statistical counting errors together with an allowance for any drifts in the apparatus and, where necessary, for the uncertainty introduced by the overlapping of neighbouring peaks. The curves drawn in each case have been calculated using the theory of Butler (1951) with a radius of interaction $r = 5.3 \times 10^{-13}$ cm as given by the formula of Gamow and Critchfield (1949). Comparisons were also made with the theory of Bhatia, Huang, Huby and Newns (1952).

The Reaction $^{24}\text{Mg}(d, p)^{25}\text{Mg}$. The angular distribution of the proton group p_0 resulting from the formation of the ground state of ^{25}Mg is shown in fig. 4. The theoretical curve was drawn using a value of 2 for the amount of orbital angular momentum l taken into the nucleus by the captured neutron. There may be some slight distortion of the experimental distribution at very small angles due to the fact that the range of the proton group p_3 from the ^{25}Mg constituent of the target has a range only 6 mg cm^{-2} different from that of the group p_0 from ^{24}Mg . The angular distribution of the former has a sharp

maximum at 0° and will have a negligible effect on the distribution of the group p_0 at angles greater than 20° .

The angular distributions of the groups p_1 and p_2 , which were not completely resolved in the range spectrum, were obtained by plotting the double group at the required angles and obtaining the separate contributions graphically. Figure 5 shows the experimental angular distribution of the group p_1 . The theoretical curve was drawn using $l=0$.

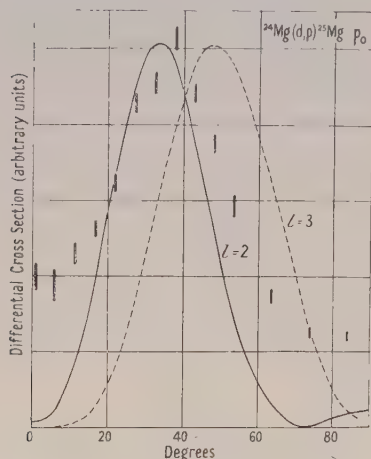


Fig. 4. Angular distribution of the proton group p_0 from $^{24}\text{Mg}(d, p)^{25}\text{Mg}$.

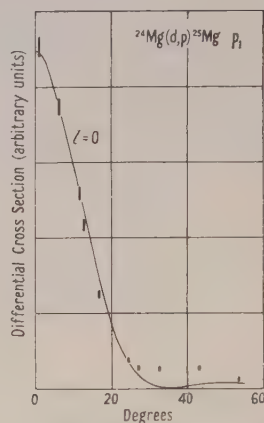


Fig. 5. Angular distribution of the proton group p_1 from $^{24}\text{Mg}(d, p)^{25}\text{Mg}$.

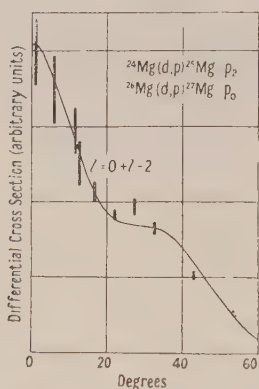


Fig. 6. Total angular distribution of the two proton groups p_2 from $^{24}\text{Mg}(d, p)^{25}\text{Mg}$ and p_0 from $^{26}\text{Mg}(d, p)^{27}\text{Mg}$.

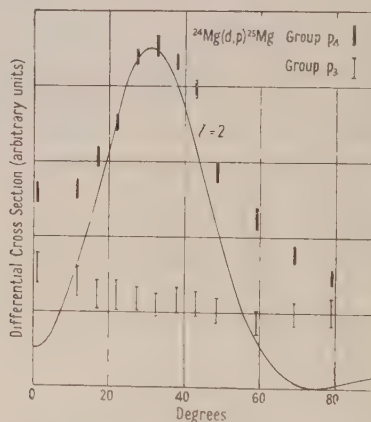


Fig. 7. Angular distributions of the proton groups p_3 and p_4 from $^{24}\text{Mg}(d, p)^{25}\text{Mg}$.

The angular distribution of the protons in group p_2 is shown in fig. 6. The experimental points could be fitted theoretically only by adding together two curves, one having $l=0$ and the other $l=2$, the ratio of the maxima being 2.5:1. The component having $l=0$ is considered to be due to the proton group p_0 from the ^{26}Mg constituent of the target which has a range only 3 mg cm^{-2} greater than that of the group ^{24}Mg and would not be resolved from it. The component with $l=2$ must be due to the proton group from ^{24}Mg .

The angular distributions of groups p_3 and p_4 were obtained by plotting the combined group and determining the separate contributions graphically. Figure 7 shows the measured angular distributions for these two groups, the vertical scale being the same for both. Group p_3 does not exhibit the pronounced peak in the distribution characteristic of stripping reactions. The experimental angular distribution of the group p_4 is fitted by a theoretical curve having $l=2$.

It was not possible to resolve the three close groups of protons corresponding to the formation of the 5th, 6th and 7th excited states of ^{25}Mg , but the large increase in intensity of this composite group at very small angles indicates that at least one of the levels is to be associated with $l=0$.

Figure 8 shows the experimental distribution of the protons corresponding to the formation of the 8th excited state of ^{25}Mg . The theoretical curve was drawn for $l=1$.

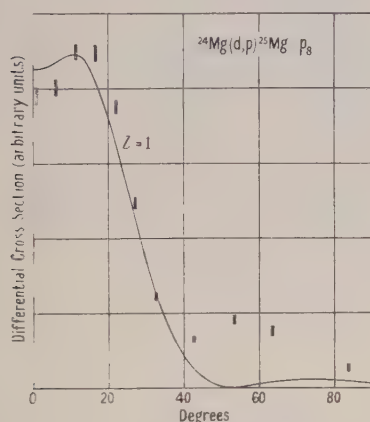


Fig. 8. Angular distribution of the proton group p_8 from $^{24}\text{Mg}(d, p)^{26}\text{Mg}$.

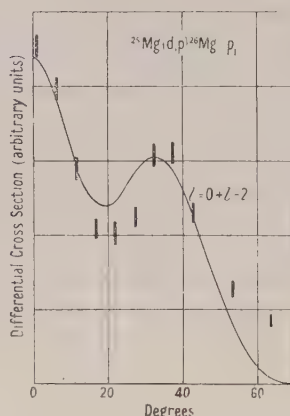


Fig. 9. Angular distribution of the proton group p_1 from $^{25}\text{Mg}(d, p)^{26}\text{Mg}$.

The Reaction $^{25}\text{Mg}(d, p)^{26}\text{Mg}$. The angular distribution of the protons in group p_1 is shown in fig. 9. A reasonably good fit with theory could be obtained only by combining two curves, one with $l=0$ and the other with $l=2$. In the figure such a curve is shown having components in the ratio 1.5:1 at their maximum values. Both components must be ascribed to the group p_1 of ^{25}Mg since the Q -value of the group (7.05 mev) is higher than that of any likely target contaminant.

The angular distribution of group p_2 was very similar to that shown in fig. 5 and characteristic of the value $l=0$.

Measurements were made at angles of 0° , 10° , 20° and 30° on the region of the spectrum which includes the proton groups p_3 to p_9 . These showed that groups p_3 and p_4 are both associated with the value $l=0$ and that the remainder probably have higher values of l .

The angular distribution of the group p_{10} shown in fig. 10 is complex. Since the carbon group p_0 has almost the same range as that of the magnesium group and the presence of carbon was suspected, the distribution was analysed into two components, one of which had the shape previously determined for the carbon group. The remaining component, due to magnesium, has a shape characteristic of the value $l=0$.

The Reaction $^{26}\text{Mg}(d, p)^{27}\text{Mg}$. The angular distribution of the proton group p_0 from the target of ^{26}MgO was fitted by a theoretical curve having $l=0$. The distribution of the group p_1 is shown in fig. 11, together with a theoretical curve having $l=2$.

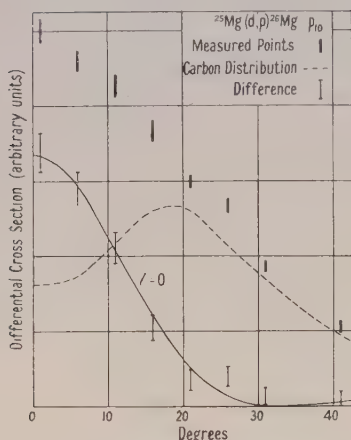


Fig. 10. Angular distribution of the mixed proton group p_{10} from $^{26}\text{Mg}(d, p)^{26}\text{Mg}$ and p_0 from $^{12}\text{C}(d, p)^{13}\text{C}$.

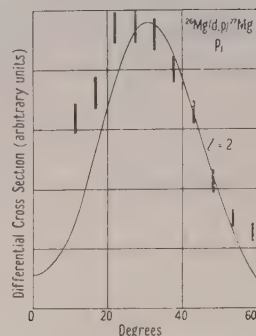


Fig. 11. Angular distribution of the proton group p_1 from $^{26}\text{Mg}(d, p)^{27}\text{Mg}$.

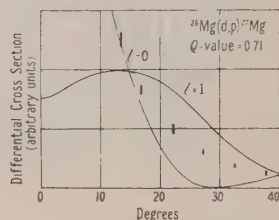


Fig. 12. Angular distribution of the proton group a (excitation = 3.50 mev) from $^{26}\text{Mg}(d, p)^{27}\text{Mg}$.

The only other group in the range spectrum which can be ascribed to magnesium is that with a range of 127 mg cm^{-2} . The prominent group at a range of 181 mg cm^{-2} is at the position expected for the carbon group p_0 and must be mainly, if not entirely, due to carbon contamination of the target. This was indicated by the form of the angular distribution of the group, which could be fitted theoretically only by using a value $l=1$, the known one for the carbon transition, and by reducing the radius of interaction r to $4 \times 10^{-13} \text{ cm}$, which is close to that expected for carbon.

Measurements were made on the magnesium group of range 127 mg cm^{-2} at a number of angles greater than 12° . In fig. 12 theoretical curves for $l=0$ and $l=1$ are shown for comparison with the experimental points. Bearing in mind that the experimental points at larger angles usually lie above the theoretical curve there seems no doubt that the appropriate value of l is 0.

(iii) Measurement of Cross Sections

The relative differential cross sections for the transitions leading to the emission of the various groups of protons in the spectrum of each isotope were measured by comparing the areas enclosed by the groups in the range spectrum at one angle. These relative values were then expressed in terms of the differential

cross section at the maxima of the angular distributions of the groups. In the case of the measurements with ^{24}Mg these cross sections could be expressed on an absolute scale by comparison with the cross section for elastic scattering of the deuterons from magnesium, since the target was a self-supporting one. The comparison was made at an angle of 16° and it was assumed that the cross section for the elastic scattering was, to a good approximation, that given by the Rutherford formula. The measurements with the targets of ^{25}MgO and ^{26}MgO were related by assuming that both targets contained the same proportion of oxygen and by comparing the measured intensities for the oxygen groups in the two cases. A rough conversion to the absolute scale was carried out by making use of the angular distribution of the mixed group p_2 from the natural magnesium target to estimate the relative intensities of the components due to ^{24}Mg and ^{26}Mg . The results of the cross section measurements are given in the table. The absolute values of the cross sections given for the reaction $^{24}\text{Mg}(d, p)^{25}\text{Mg}$ may be in error by $\pm 15\%$. The relative cross sections for each of the reactions $^{25}\text{Mg}(d, p)^{26}\text{Mg}$ and $^{26}\text{Mg}(d, p)^{27}\text{Mg}$ have an estimated error of the same amount, but the error in the absolute cross sections may be $\pm 50\%$.

§ 4. DISCUSSION

In the table are collected the *l*-values assigned to the various transitions and the corresponding alternative values for the spins of the final states. These were obtained from the known spins of the target nuclei, namely 0 for ^{24}Mg and ^{26}Mg and $5/2$ for ^{25}Mg (Crawford, Kelly, Schawlow and Gray 1949). The parities are given on the assumption, based on the shell model, that the parities of ^{24}Mg , ^{25}Mg and ^{26}Mg are all even. In column 5 of the table are given the values of the differential cross sections at the maxima of the angular distributions. The numbers in the last column are proportional to the values of the quantity $\Lambda/(2j_i + 1)$ in the expression given by Bhatia *et al.* for the differential cross section. Each of these was obtained by making use of the measured differential cross section at the maximum of the angular distribution and assuming that this was due entirely to the stripping process. This quantity is proportional to the probability of capture of a neutron which arrives at the nuclear surface with those values of energy and orbital momentum required for the formation of the final state.

The value $l=2$ for the transition from ^{24}Mg to the ground state of ^{25}Mg is consistent with the Mayer shell model (Mayer 1950), since, according to this, the lowest vacant neutron orbit in ^{24}Mg is a d-orbit. The *l*-values for the formation of the ground state and the first two excited states of ^{25}Mg are the same as those assigned by Goldberg (private communication) to the corresponding states in the mirror nucleus ^{25}Al produced in the stripping reaction $^{24}\text{Mg}(d, n)^{25}\text{Al}$.

The ground state of ^{27}Mg is formed from ^{26}Mg by capture of a neutron with zero orbital angular momentum. According to the shell model the 14 neutrons in ^{26}Mg completely fill the levels up to and including the $1d_{5/2}$ level. Our result indicates that the next neutron level to be filled is the $2s_{1/2}$ level. It is already known from the fact that the spin of ^{31}P is $1, 2$ that the 15th proton goes into the $2s_{1/2}$ level.

The intensity of the protons in the group p_0 from the target of ^{25}MgO was too small for the measurement of its angular distribution. However, according to the shell model the captured neutron is expected to go into a d-orbit and thus

the l -value for the transition should be 2. On this assumption and using the measured cross section, a rough value for the neutron capture probability was obtained, and this is shown in brackets in the last column of the table.

No conclusions can be drawn at present from the values of l and the spins assigned to the various excited states. One noteworthy feature of the results, however, is the similarity in the magnitudes of most of the neutron capture probabilities given in the table. According to Bhatia *et al.* different final states of similar constitution should be associated with similar neutron capture probabilities.

(1)	(2)	(3)	(4)		(5)	(6)
			$^{24}\text{Mg}(\text{d}, \text{p})\ ^{25}\text{Mg}$			
p_0	0	2	5/2, 3/2	Even	1.7×10^{-26}	15.4
p_1	0.582	0	1/2	Even	2.3×10^{-25}	6.2
p_2	0.976	2	5/2, 3/2	Even	9.3×10^{-27}	6.2
p_3	1.612	Isotropic	—	—	3.6×10^{-27}	—
p_4	1.957		5/2, 3/2	Even	8.9×10^{-27}	5.5
p_5	2.565		—	—	—	—
p_6	2.742	0	1/2	Even	—	—
p_7	2.806		—	—	—	—
p_8	3.405	1	3/2, 1/2	Odd	1.4×10^{-25}	8.7
			$^{25}\text{Mg}(\text{d}, \text{p})\ ^{26}\text{Mg}$			
p_0	0	[2]	0	Even	1.6×10^{-27}	[2.1]
p_1	1.825	0	3, 2	Even	1.7×10^{-26}	0.65
		2	5, 4, 3, 2, 1, 0	Even	1.1×10^{-26}	12.3
p_2	2.972	0	3, 2	Even	1.6×10^{-25}	5.7
p_3	3.969	0	3, 2	Even	1.7×10^{-25}	6.1
p_4	4.353	0	3, 2	Even	1.9×10^{-25}	5.6
p_{10}	6.147	0	3, 2	Even	1.2×10^{-25}	3.3
			$^{26}\text{Mg}(\text{d}, \text{p})\ ^{27}\text{Mg}$			
p_0	0	0	1/2	Even	1.1×10^{-25}	2.8
p_1	0.887	2	5/2, 3/2	Even	8.7×10^{-27}	4.6
—	3.50	0	1/2	Even	—	—

(1) Proton group; (2) excitation* (mev); (3) l -value; (4) spin and parity of final state; (5) maximum differential cross-section (cm^2); (6) Neutron capture probability (arbitrary units).

* According to Endt, Enge *et al.* (1952) and Endt, Haffner *et al.* (1952).

The neutron capture probability for the component having $l=0$ of the mixed transition p_1 in the reaction $^{25}\text{Mg}(\text{d}, \text{p})\ ^{26}\text{Mg}$ is smaller by a factor of 19 than that of the component having $l=2$. The angular distribution of the proton group associated with this transition is remarkably similar to that of the proton group p_1 in the reaction $^{27}\text{Al}(\text{d}, \text{p})\ ^{28}\text{Al}$ reported in I. The neutron capture probabilities of the two components in each case also have similar values. The possible interpretations given previously (Paper I and Holt and Marsham 1952) apply equally to the present case. The group may correspond to a close doublet in which the spins of the two components are respectively 2 or 3, and an integral value between 0 and 5. Such a doublet was not revealed by the magnetic analysis carried out by Endt, Haffner and Van Patter (1952). Another possible interpretation is that the level is single but is so constituted that it can be formed by the addition of a neutron with either 0 or 2 units of orbital angular momentum. In this case the final spin is limited to 2 or 3.

The angular distribution of the proton group p_3 in the reaction $^{24}\text{Mg}(d, p)^{25}\text{Mg}$ is interesting because it is nearly isotropic. This suggests that the reaction proceeds mainly by the formation of a compound nucleus. The small value of the differential cross section for the stripping process may be due to the required value of l being greater than 3, or the l -value may be less than this and the neutron capture probability for the transition unusually small.

In the fitting of theoretical curves to the experimental angular distributions no ambiguity in the assignment of an l -value has been encountered when Butler's theory was used with a radius given by the formula of Gamow and Critchfield. Generally the fit was good only in the neighbourhood of the prominent peak in a distribution. The general impression is that the characteristic stripping distribution, as given by theory, is superimposed on a roughly isotropic background. This may be due to the alternative process in which the reaction proceeds through the formation of a compound nucleus.

Using the theory of Bhatia *et al.* some difficulty was encountered in the choice of the value of R , the parameter corresponding to the radius of interaction r in Butler's theory. To obtain some information regarding the correct choice of this parameter, having found for each distribution the value of l by using Butler's theory, we determined the value of R which was required in each case to give the best agreement between the theory of Bhatia *et al.* and the experimental distribution. A range of values of R between 5.5×10^{-13} cm and 7.4×10^{-13} cm was required. The higher values were needed to fit those distributions having $l=0$ and the lower values to fit those having $l=2$. This variation in R is outside the range suggested in the paper of Bhatia *et al.* namely $(7.3 \pm 0.5) \times 10^{-13}$ cm, and a choice of radius within the latter range did not always lead to an unambiguous determination of the l -value. With a suitably chosen value of R a curve was obtained in each case which agreed well with that obtained using Butler's theory.

ACKNOWLEDGMENTS

We are grateful to Professor H. W. B. Skinner for helpful discussions and to Dr. R. Huby and Mr. H. C. News for information regarding the theories of the stripping process. One of us (T. N. M.) thanks the Department of Scientific and Industrial Research for a maintenance grant.

We wish also to thank the Director and Dr. R. H. Dawton of the Atomic Energy Research Establishment, Harwell, for the supply of the separated magnesium isotopes.

REFERENCES

- BHATIA, A. B., HUANG, K., HUBY, R., and NEWS, H. C., 1952, *Phil. Mag.*, **43**, 485.
 BUTLER, S. T., 1951, *Proc. Roy. Soc. A*, **208**, 559.
 CRAWFORD, M. F., KELLY, F. M., SCHAWLOW, A. L., and GRAY, W. M., 1949, *Phys. Rev.*, **76**, 1527.
 ENDT, P. M., ENGE, H. A., HAFFNER, J. W., and BUECHNER, W. W., 1952, *Phys. Rev.*, **87**, 27.
 ENDT, P. M., HAFFNER, J. W., and VAN PATTEN, P. M., 1952, *Phys. Rev.*, **86**, 518.
 GAMOW, G., and CRITCHFIELD, C. L., 1949, *Theory of the Atomic Nucleus* (Oxford: University Press), p. 11.
 HOLT, J. R., and MARSHAM, T. N., 1952, *Proc. Phys. Soc. A*, **65**, 763; 1953, *Ibid.*, **66**, 249.
 MAYER, M. G., 1950, *Phys. Rev.*, **78**, 16.
 TOOPS, E. C., SAMPSON, M. B., and STEIGERT, F. E., 1952, *Phys. Rev.*, **85**, 280.

The Application of Variational Methods to Scattering by Ions I: The Elastic Scattering of Electrons by Helium Ions

BY B. H. BRANSDEN* AND A. DALGARNO†

* Department of Physics, Queen's University, Belfast

† Department of Applied Mathematics, Queen's University, Belfast

Communicated by D. R. Bates; MS. received 18th August 1952

Abstract. The variational method is used to investigate the elastic scattering of slow electrons by the positive helium ion. Zero order phases and wave functions found by this method are shown to agree, in general, with those found by numerical integrations of the wave equation, both when the wave function is of the 'one-body' type and when it is of the correct symmetry. The inclusion in the trial wave function of a term involving the distance between the two electrons is found to lead to smaller phases. Detailed results are given for energies of the incident electron in the range 3–60 eV.

§ 1. INTRODUCTION AND THEORY

METHODS have been developed by a number of writers (Hulthén 1944, 1945, Kohn 1948, 1951, Kato 1950, 1951) that allow the approximate determination of the phases describing a collision process by a variational procedure. These methods have been most extensively applied to the elastic scattering of slow electrons by hydrogen atoms (Huang 1949, Massey and Moisewitsch 1951, Kato 1951) and to the elastic scattering of neutrons by deuterons (Verde 1949, Verde and Troesch 1951, Clemental 1951). Such collision processes are characterized by the asymptotic form of the associated wave function, which is the sum of an incident plane and an outgoing spherical wave:

$$\Phi(r) \sim e^{ikz} + r^{-1}f(\theta, \phi)e^{ikr}.$$

There is a large class of collisions for which the scattering potential is of the coulomb type at large distances. In these circumstances a different form of asymptotic wave function must be used,

$$\Phi(r) \sim \exp[i\{kz + \alpha \log k(r - z)\}] + r^{-1} \exp\{i(kr - \alpha \log 2kr)\}f(\theta, \phi). \quad \dots\dots(1)$$

The purpose of the present paper is to study a collision process of this class, choosing as an example the elastic scattering of slow electrons by normal positive helium ions. Zero order phases and wave functions computed by the variational method have been compared with the results of direct integration of the wave equation, and the effect of the inclusion in the wave function of terms depending on the relative distance of the two electrons has been investigated.

The wave function $\Psi(\mathbf{r}_1, \mathbf{r}_2)$ for an electron moving in the field of a helium ion satisfies the Schrödinger equation (expressed in Hartree units)

$$(\nabla_1^2 + \nabla_2^2 + k^2 - \kappa^2 + 4/r_1 + 4/r_2 - 2/r_{12})\Psi(\mathbf{r}_1, \mathbf{r}_2) = 0 \quad \dots\dots(2)$$

where $\mathbf{r}_1, \mathbf{r}_2$ are the position vectors of the electrons 1 and 2 relative to the nucleus, r_{12} denotes $|\mathbf{r}_1 - \mathbf{r}_2|$, $-\kappa^2$ is the binding energy of the ion and \mathbf{k} is the wave vector of the incident electron.

In solving the equation (2) various approximations may be made. If the identity of the electrons is ignored, a 'one-body' solution may be derived by writing the wave function as the product

$$\Psi(\mathbf{r}_1, \mathbf{r}_2) = \chi(\mathbf{r}_1) \Phi(\mathbf{r}_2), \quad \dots\dots(3)$$

in which $\chi(\mathbf{r}_1)$ is the ground state wave function of the helium ion satisfying $(\nabla_1^2 + 4/r_1 - \kappa^2) \chi(\mathbf{r}_1) = 0$ and $\Phi(\mathbf{r}_2)$ has (1) as its asymptotic form.

Inserting (3) into (2) and expanding $\Phi(\mathbf{r}_2)$ so that

$$\Phi(\mathbf{r}_2) = \sum_{l=0}^{\infty} (2l+1) i^l r_2^{-1} g_l(r_2) P_l(\cos \theta),$$

equations for the $g_l(r_2)$ are obtained:

$$\left(\frac{d^2}{dr^2} + k^2 + \frac{2}{r} + V_{00} - \frac{l(l+1)}{r^2} \right) g_l(r_2) = 0 \quad \dots\dots(4)$$

with $V_{00} = (4 + 2/r) e^{-4r}$.

The required solutions are bounded at the origin, and at large r tend to $F_l(r) + a_l G_l(r)$, $F_l(r)$ and $G_l(r)$ being the regular and irregular coulomb functions of order l for an attractive field, defined by

$$\left(\frac{d^2}{dr^2} + k^2 + \frac{2}{r} - \frac{l(l+1)}{r^2} \right) \begin{cases} F_l(r) \\ G_l(r) \end{cases} = 0 \quad \dots\dots(5)$$

$$F_l(r) \sim \sin(kr + k^{-1} \log 2kr + \eta_l - \frac{1}{2}l\pi)$$

$$G_l(r) \sim \cos(kr + k^{-1} \log 2kr + \eta_l - \frac{1}{2}l\pi)$$

and $\eta_l = \arg \Gamma(1 + l - ik^{-1})$.

If ρ_l is the phase shift associated with the l th partial wave then $\rho_l = \eta_l + \tan^{-1} a_l$ where η_l is the corresponding phase shift for scattering by a unit positive charge, so that $\tan^{-1} a_l$, which will be denoted by μ_l , gives a measure of the departure from coulomb scattering.

The scattering amplitude $f(\theta)$ is related to the phases by the standard formula (Mott and Massey 1949)

$$f(\theta) = \frac{1}{2ik} \sum_{l=0}^{\infty} (2l+1) \{ \exp(2i\rho_l) - 1 \} P_l(\cos \theta)$$

and the differential cross section for scattering into a solid angle $d\Omega$ is $I(\theta) d\Omega = |f(\theta)|^2 d\Omega$.

A further approximation taking account of the identity and spin properties of the electrons may be obtained by writing the wave functions as a combination possessing definite symmetry,

$$\Psi(\mathbf{r}_1, \mathbf{r}_2) = \chi(\mathbf{r}_1) \Phi(\mathbf{r}_2) \pm \chi(\mathbf{r}_2) \Phi(\mathbf{r}_1), \quad \dots\dots(6)$$

the + sign being taken for singlet and the - for triplet spin states. It is easily shown that the $g_l^{\pm}(r)$ now satisfy the integro-differential equations

$$\left(\frac{d^2}{dr^2} + k^2 + \frac{2}{r} + V_{00} - \frac{l(l+1)}{r^2} \right) g_l^{\pm}(r) = \mp 32 \exp(-2r) r \phi^{\pm}(r)$$

where

$$\begin{aligned} \phi^{\pm}(r) = & \int_0^{\infty} (k^2 + 4) g_l^{\pm}(r_1) r_1 \exp(-2r_1) dr_1 - 2 \int_r^{\infty} g_l^{\pm}(r_1) \exp(-2r_1) \left(\frac{r}{r_1} \right)^l dr_1 \\ & - 2 \int_0^r g_l^{\pm}(r_1) \exp(-2r_1) r \left(\frac{r_1}{r} \right)^{l+1} dr_1 \quad \dots\dots(7) \end{aligned}$$

and that

$$\begin{aligned} g_l^+(r) &\sim F_l(r) + a_l^+(r) G_l(r) \\ g_l^-(r) &\sim F_l(r) + a_l^-(r) G_l(r). \end{aligned}$$

Clearly the differential cross section becomes

$$I(\theta) d\Omega = \left[\frac{1}{4} |f^+(\theta)|^2 + \frac{3}{4} |f^-(\theta)|^2 \right] d\Omega.$$

It is convenient to express results in the form of the ratio of the actual scattering into a solid angle $d\Omega$ in the direction θ to that produced by the coulomb field that would arise if the nucleus were fully screened by the bound electron (i.e. the field for which the F_l and G_l defined above are radial wave functions). If $R(\theta)$ is this ratio then

$$R(\theta) = \frac{1}{4} R^+(\theta) + \frac{3}{4} R^-(\theta)$$

$$\text{where } R^\pm(\theta) = \left| 1 + f_c^{-1}(\theta) \frac{1}{2ik} \sum_n \exp(2i\eta_n) \{ \exp(2i\mu_n^\pm) - 1 \} (2n+1) P_n(\cos\theta) \right|^2$$

$$\text{and } f_c = \frac{1}{2k^2} \operatorname{cosec}^2 \frac{1}{2}\theta \exp[ik^{-1} \log \sin^2 \frac{1}{2}\theta + 2i\eta_n + i\pi].$$

Variational methods may be used to compute the parameters a_l , a_l^\pm without resorting to the integration of the equations (4) or (7). The procedure is based on a consideration of the integral

$$J = \int \Psi_t^* (H - E) \Psi_t d\tau$$

where Ψ_t is some trial function satisfying the proper boundary conditions. In the energy range concerned (up to 60 eV) the incompleteness of the screening by the bound electron may be neglected except for S states so that $R^\pm(\theta)$ may be simplified to

$$R^\pm(\theta) = |1 + ik \sin^2 \frac{1}{2}\theta \exp(ik^{-1} \log \sin^2 \frac{1}{2}\theta) \{ \exp(2i\mu_0^\pm) - 1 \}|^2.$$

Since Ψ_t must have the asymptotic form

$$\Psi_t \sim \chi(r_1) \{ F_0(r_2) + a_t G_0(r_2) \}$$

and must be finite when either r_1 or r_2 is zero, it follows (Hulthén 1945, Kohn 1948) that $\delta J = 4\pi k \delta a_t$, and that if Ψ_t is a function of n parameters b_n , besides a_t , then b_n , a_t and μ_0 may be found from either the equations

$$\frac{\partial J}{\partial b_n} = 0, \quad J = 0, \quad \tan \mu_0 = a \quad (\text{Hulthén})$$

$$\text{or } \frac{\partial J}{\partial b_n} = 0, \quad \frac{\partial J}{\partial a} = 4\pi k, \quad \tan \mu_0 = a - J/4\pi k \quad (\text{Kohn}).$$

§ 2. THE TRIAL WAVE FUNCTIONS

If trial functions separable in the coordinates r_1 , r_2 of the forms (3) and (6) are chosen, the variational method is equivalent to the determination of the phase by the integration of equations (4) or (7) respectively. However, a trial function of greater flexibility may be chosen by the addition of a term containing the coordinate r_{12} . Such a term allows partially for the instantaneous, as distinct from the averaged, repulsion between the electrons, that is for the distortion or polarization of the ion by the incident beams and of the corresponding effect produced on the incident beam by the ion.

In principle the scattering cross section may be calculated to any degree of accuracy by replacing the terms $\chi(\mathbf{r}_1) \Phi(\mathbf{r}_2)$ in (6) by the series

$$(\Sigma + \int) \chi_n(\mathbf{r}_1) \Phi_n(\mathbf{r}_2), \quad \dots\dots\dots (8)$$

where the summation is over the complete set of helium ion wave functions, and solving the set of coupled integro-differential equations for as many of the Φ_n as prove important. Such a procedure is in general outside the possibilities of present mathematical techniques, but a variational method using trial functions allowing for polarization may be expected to provide a solution that is equivalent to the inclusion of some of the more important terms $\chi_n \Phi_n$ in the series.

The following forms of trial function were chosen.

A. The 'One-Body' Approximation

$$\begin{aligned} \Psi &= \chi(r_1) r_2^{-1} g_0(r_2) \\ \text{with } \chi(r_1) &= \left(\frac{8}{\pi}\right)^{1/2} \exp(-2r_1) \\ g_0(r_2) &= F_0(r_2) + \{a + b \exp(-2r_2)\} \{1 - \exp(-2r_2)\} G_0(r_2). \end{aligned} \quad \dots\dots (9)$$

B. The 'Exchange' Approximation

$$\begin{aligned} \Psi &= r_2^{-1} [\chi(r_1) g_0^\pm(r_2) \pm \chi(r_2) g_0^\pm(r_1)] \\ g_0^\pm(r_2) &= F_0(r_2) + \{a^\pm + b^\pm \exp(-2r_2)\} \{1 - \exp(-2r_2)\} G_0(r_2). \end{aligned} \quad \dots\dots (10)$$

Kato (1950) and Massey and Moiseiwitsch (1951) have shown that similar trial functions depending on one parameter b , apart from the phase parameter a , are capable of giving accurate values for the phase (except perhaps for the singlet exchange case) within the limitations imposed by the assumption that only the first term in the series (8) is of importance.

C. The Inclusion of 'Polarization'.

Any additional term containing r_{12} must satisfy the conditions of finiteness at the origin of both r_1 and r_2 and also it must vanish for $r_1, r_2 \rightarrow \infty$. The antisymmetry of the wave function for the triplet state implies that the two electrons are not found close together, so that polarization would not therefore be expected to make a large contribution to the integral J (and hence to the phase). In view of this the r_{12} term was given a form which made its effect vanish except in the case of the singlet state. The trial functions taken were:

(a) Polarization approximation

$$g_0^P = g_0 + c r_2 r_{12} \exp(-2r_2). \quad \dots\dots (11)$$

(b) Exchange polarization approximation

$$g_0^{P\pm} = g_0^\pm + c r_2 r_{12} \exp(-2r_2). \quad \dots\dots (12)$$

With the forms A, B, and C for Ψ_t the calculation of J is elementary but somewhat lengthy, since many of the integrals that occur have to be evaluated by numerical methods.

§ 3. THE COMPUTATION OF THE COULOMB FUNCTIONS $F_0(r)$, $G_0(r)$

The regular and irregular coulomb functions for a repulsive field have been extensively investigated and practical formulae developed for their calculation by Breit and his collaborators (1936). For the attractive field formulae have been given by Hargreaves (1929), valid only in the limit of small energies. The formulae in the latter case without energy restriction are outlined below.

It was found convenient to integrate the differential equation for F_0 and G_0 by a method due to Fox and Goodwin (1949). Care must be taken, however, to guard

against the accumulation of errors. A check on the accuracy of the integration is provided by observing that the Wronskian relation

$$F_0'(r) G_0(r) - F_0(r) G_0'(r) = k$$

is satisfied.

To start the integration and to check its initial accuracy several values of the regular and irregular functions F_0 and G_0 were computed from the following series expansions:

$$F_0(r) = (2\pi k)^{1/2} \{1 - \exp(-2\pi k^{-1})\}^{-1/2} \sum_{j=0}^{\infty} a_j r^j$$

with $a_j = (-2a_{j-1} - k^2 a_{j-2}) j^{-1} (j-1)^{-1}$ $a_1 = 1, a_0 = 0.$

$$G_0(r) = \left(\frac{k}{2\pi}\right)^{1/2} \{1 - \exp(-2\pi k^{-1})\}^{1/2} \sum_{j=0}^{\infty} b_j r^j - \frac{1}{\pi} \{1 - \exp(-2\pi k^{-1})\} \\ \times (\log 2kr + q) F_0(r)$$

with $b_j = [-k^2 b_{j-2} - 2b_{j-1} + 2(2j-1)a_j] j^{-1} (j-1)^{-1},$ $b_0 = 1, b_1 = 0$

$$q = \gamma - 1 + k^{-2} \sum_{n=1}^{\infty} n^{-1} (n^2 + k^{-2})^{-1}$$

$$\gamma = 0.5172157 \text{ (the Euler-Mascheroni constant).}$$

§ 4. RESULTS AND DISCUSSION

The Phases μ_0

The values for the phases μ_0 obtained by the use of the various trial wave functions A, B, C in the variational methods of Hulthén and Kohn are given in table 1.

Table 1. Approximate Phases μ_0 derived by the Variational Methods of Hulthén and Kohn*

Energy of incident electron (ev)		3.28	8.25	15.74	24.90	48.84	65.49
One-body approximation (9)		H, K	0.571	0.554	0.531	0.509	0.443
Exchange approximation (10)	μ_0^+	{H	0.419	0.404	0.365	0.333	0.307
		{K	-0.281	0.038	0.073	0.110	0.226
		H, K	0.959	0.824	0.807	0.762	0.604
Polarization approximation (11)	$b=0$	{H, K	0.534	0.519	0.495	0.482	0.422
	$b \neq 0$	{H	0.570	0.534	0.522	0.502	0.443
		{K	0.571	0.549	0.530	0.510	0.443
Exchange-polarization approximation (12)	$b=0$	{H			0.254	0.280	0.292
		{K			0.254	0.282	0.293
	$b \neq 0$	{H			0.291	0.321	0.293
		{K			0.315	0.356	0.314

* All phases are given in radians.

H=Hulthén's method, K=Kohn's method.

Those based on the one-body function (9) are approximations to the phases determined by the differential equation (4), and those based on the exchange functions (10) are approximations to the phases determined by the integro-differential equations (7). Solutions of these equations have been computed for

energies of 48.84 and 65.49 eV, and in table 2 a comparison is made of the accurate phases found from them and the approximate phases.

Table 2. Comparison of Phases calculated in the One-Body and Exchange Approximations by Numerical Integration and by Variational Methods*

Electron energy (eV)	One-body approximation		Exchange approximation			
	μ_0		μ_0^+		μ_0^-	
	N	V(H&K)	N	V(H)	V(K)	N V(H&K)
48.84	0.468	0.460	0.288	0.315	0.240	0.648 0.645
65.49	0.443	0.443	0.283	0.307	0.226	0.604 0.604

* All phases are in radians.

N=by numerical integration; V=by variational methods; H=Hulthén; K=Kohn.

It will be seen that for the one-body and the antisymmetric exchange approximations the variational methods give identical results and that these are in excellent agreement with the accurate values. For the symmetric exchange for which the trial wave function is probably not sufficiently flexible the accord is less good, the values derived by Hulthén's method being closer to the accurate phases than those obtained by Kohn's method. Reference to table 1 shows that Kohn's method gives values which become negative at low energies and are clearly incorrect. Thus it appears that when the two methods give differing results, Hulthén's is to be preferred. This is in harmony with the conclusions of Massey and Moiseiwitsch (1951) and Massey and Erskine (1952).

Inclusion of a term involving the inter-electronic separation in the trial wave function when exchange is ignored makes very little difference. The sense of the effect is always to reduce the phase, this being the opposite to and smaller than that found for elastic scattering by neutral hydrogen (Massey and Moiseiwitsch 1951) and may be typical of attractive coulomb fields. A possible reason is that for such a field there is comparatively great overlap between the two electron clouds, so that the repulsion between the electrons when near the nucleus may be of more importance than the increased attraction (due to polarization) when the incident electron is far from the nucleus. The inclusion of the parameter b as well as c in the polarization approximation may have a marked influence on the phase, indicating that it is occasionally very sensitive to the type of trial wave function adopted.

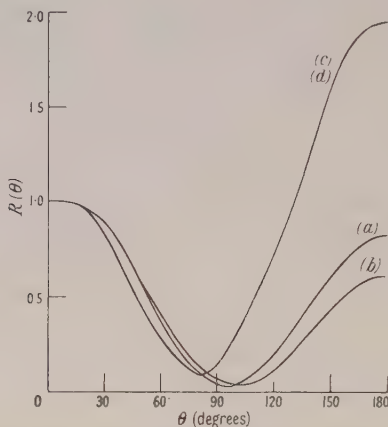
It was noted earlier that, because of the form of the term chosen, its inclusion in the trial function has no effect in the antisymmetric exchange-polarization approximation.

For the symmetric case the additional parameter improves the agreement between the higher energy phases derived by the two methods. At the lower energies, however, the conditions $J=0$, $\partial J/\partial b=0$ and $J=0$, $\partial J/\partial b=0$, $\partial J/\partial c=0$ cannot be satisfied by a real phase parameter.† Further, Kohn's method is also unreliable at these energies as the correction term is large compared to a . It follows that to represent adequately a symmetric scattering function at low energies it is necessary to use a more flexible trial wave function.

† This is analogous to the work of Morse, Young and Haurwitz (1935) on the binding energy of the 2^1S state of He, where the use of an apparently reasonable trial wave function did not lead to a minimum for the energy.

The Differential Scattering Cross Section

The figure illustrates for an energy of 48.84 eV the ratio $R(\theta)$ as a function of θ obtained by substitution of the phases obtained by Hulthén's method in the one-body, polarization, exchange and exchange-polarization approximations in the formulae for $R(\theta)$ given earlier. For this energy, curve (d) should be the most accurate, but no experimental data are available for comparison.



$R(\theta)$, the ratio of the scattering intensity at angle θ of electrons by positive helium ions to that of electrons by a nucleus of unit positive charge. Energy 48.84 eV.

Curve (a) one-body, (b) one-body with polarization, (c) exchange, (d) exchange with polarization.

Curves (c) and (d) are indistinguishable on the scale shown.

The Wave Functions

A check on the reliability of the wave functions obtained by applying Hulthén's variational method in the one-body and exchange approximations is provided by the fact that the exact expression for the phase μ_0 satisfies in the one-body case

$$\sin \mu_0 = k^{-1}(1 + a^2)^{-1/2} \int_0^\infty F_0(r) V_{00}(r) g_0(r) dr$$

and in the exchange cases

$$\sin \mu_0^\pm = k^{-1}(1 + a^2)^{-1/2} \left\{ \int_0^\infty F_0(r) V_{00}(r) g_0^\pm(r) dr \pm 32 \int_0^\infty e^{-2r} r F_0(r) \phi^\pm(r) dr \right\}$$

where $\phi^\pm(r)$ is the function occurring in (7).

Table 3 illustrates the accuracy with which the integral equation for $\sin \mu_0$ is satisfied by the wave functions derived by Hulthén's method for the one-body and exchange approximations. As will be observed, the accuracy is high for the one-body and antisymmetric cases, but rather lower for the symmetric exchange approximation.

Direct comparisons of the exact and approximate wave functions of the one-body and exchange equations are made in tables 4, 5 and 6. The agreement of the wave functions obtained by Hulthén's method with those by numerical integration is clearly excellent in the one-body and antisymmetric exchange cases and by no

means poor in the symmetric exchange case even though the condition involving the integral equation for the phases is not here fulfilled at all well. One may conclude that continuum wave functions constructed by a variational procedure may be used with some confidence for the evaluation of matrix elements associated

Table 3. The accuracy with which the integral equation for $\sin \mu_0$ is satisfied by the variational wave functions derived by Hulthén's method in the one-body and exchange approximations*

Electron energy (ev)	One-body approximation		Exchange approximation			
	$\sin \mu_0$	integral	$\sin \mu_0^+$	integral	$\sin \mu_0^-$	integral
3.28	0.540	0.546	0.415	0.553	0.819	0.805
8.25	0.526	0.531	0.407	0.511	0.734	0.739
15.74	0.506	0.511	0.357	0.429	0.722	0.729
24.90	0.487	0.491	0.327	0.405	0.690	0.693
48.84	0.444	0.447	0.310	0.347	0.601	0.614
65.49	0.429	0.432	0.302	0.330	0.568	0.575

* A wave function derived by Kohn's method is constructed so that it satisfies the integral equation.

Table 4. Comparison of the wave functions $r\Phi(r)$ for the relative motion of an electron in the field of a positive helium ion calculated in the one-body approximation by numerical integration and by the variational methods of Hulthén and Kohn

Energy=48.84 ev, $r\Phi(r) \sim \sin(kr + k^{-1} \log 2kr + \rho_0)$					Energy=65.49 ev		
r (A.U.)	N		V		V		
			H	K		H	K
0.02	0.094		0.086	0.089	0.101	0.094	0.097
0.04	0.181		0.170	0.176	0.194	0.184	0.191
0.08	0.334		0.324	0.334	0.358	0.349	0.361
0.12	0.460		0.455	0.469	0.491	0.489	0.505
0.16	0.561		0.563	0.580	0.598	0.603	0.621
0.20	0.641		0.648	0.667	0.680	0.690	0.710
0.3	0.753		0.768	0.792	0.789	0.804	0.825
0.4	0.764		0.777	0.807	0.781	0.792	0.814
0.6	0.565		0.568	0.611	0.515	0.508	0.525
0.8	0.192		0.186	0.242	0.065	0.048	0.081
1.0	-0.231		-0.240	-0.178	-0.407	-0.424	-0.364
1.5	-0.912		-0.916	-0.901	-0.931	-0.934	-0.944
2.0	-0.573		-0.578	-0.645	-0.184	-0.184	-0.241
2.5	+0.374		+0.368	+0.279	+0.811	+0.811	+0.777
3.5	0.599		0.605	0.674	-0.198	-0.198	-0.136

N=by numerical integration; V=by variational methods; H=Hulthén; K=Kohn.

with various atomic transitions, although it may be remarked that the functions obtained by the variational methods did not provide very good initial approximations for the solution by iterative methods of the corresponding symmetric integro-differential equations.

Table 5. Comparison of the wave functions $r\Phi(r)$ for the relative motion of an electron in the field of a positive helium ion calculated in the symmetric exchange approximation by numerical integration and by the variational methods of Hulthén and Kohn.

r (A.U.)	Energy = 48.84 ev, $r\Phi(r) \sim \sin(kr + k^{-1} \log 2kr + \rho_0^+)$			Energy = 65.49 ev.		
	N	V		N	V	
		H	K		H	K
0.02	0.092	0.077	0.071	0.100	0.084	0.071
0.04	0.176	0.152	0.140	0.191	0.165	0.140
0.08	0.325	0.290	0.268	0.352	0.315	0.268
0.12	0.449	0.413	0.379	0.485	0.446	0.378
0.16	0.550	0.518	0.472	0.593	0.557	0.467
0.20	0.630	0.605	0.545	0.677	0.649	0.535
0.3	0.750	0.818	0.647	0.796	0.792	0.612
0.4	0.776	0.801	0.645	0.805	0.825	0.573
0.6	0.617	0.672	0.410	0.581	0.625	0.249
0.8	0.265	0.338	0.098	0.159	0.205	-0.219
1.0	-0.158	-0.083	-0.408	-0.316	-0.277	-0.636
1.5	-0.958	-0.875	-0.907	-0.972	-0.941	-0.778
2.0	-0.754	-0.681	-0.344	-0.348	-0.313	+0.213
2.5	+0.211	+0.236	+0.602	+0.711	+0.731	+0.950
3.5	0.756	0.820	0.362	-0.044	-0.066	-0.576

N=by numerical integration; V=by variational methods; H=Hulthén; K=Kohn.

Table 6. Comparison of the wave functions $r\Phi(r)$ for the relative motion of an electron in the field of a positive helium ion calculated in the antisymmetric exchange approximation by numerical integration and by the variational methods of Hulthén and Kohn

r (A.U.)	Energy = 48.84 ev, $r\Phi(r) \sim \sin(kr + k^{-1} \log 2kr + \rho_0^-)$			Energy = 65.49 ev.		
	N	V		N	V	
		H	K		H	K
0.02	0.090	0.088	0.117	0.097	0.095	0.102
0.04	0.174	0.174	0.230	0.186	0.186	0.200
0.08	0.319	0.330	0.448	0.341	0.353	0.378
0.12	0.438	0.461	0.597	0.467	0.492	0.525
0.16	0.534	0.566	0.722	0.567	0.601	0.640
0.20	0.606	0.644	0.809	0.641	0.683	0.724
0.3	0.700	0.739	0.896	0.730	0.773	0.816
0.4	0.691	0.716	0.844	0.702	0.664	0.700
0.6	0.454	0.440	0.525	0.400	0.391	0.428
0.8	0.060	0.028	0.104	-0.066	-0.094	-0.056
1.0	-0.357	-0.400	-0.306	-0.523	-0.549	-0.516
1.5	-0.909	-0.932	-0.934	-0.908	-0.899	-0.925
2.0	-0.422	-0.400	-0.546	-0.041	-0.032	-0.110
2.5	+0.528	+0.524	+0.291	+0.896	+0.884	+0.843
3.5	0.454	0.456	0.674	-0.347	-0.347	-0.266

N=by numerical integration; V=by variational methods; H=Hulthén; K=Kohn.

ACKNOWLEDGMENT

The authors wish to thank Professor D. R. Bates for many interesting discussions.

REFERENCES

- BREIT, G., WHEELER, J. A., and YOST, F. L., 1936, *Phys. Rev.*, **49**, 174.
CLEMENTAL, E., 1951, *Nuovo Cim.*, **8**, 185.
FOX, L., and GOODWIN, E. T., 1949, *Proc. Camb. Phil. Soc.*, **45**, 373.
HARGREAVES, J., 1929, *Proc. Camb. Phil. Soc.*, **25**, 75.
HUANG, S. S., 1949, *Phys. Rev.*, **76**, 477, 1878.
HULTHÉN, L., 1944, *K. fysiogr. Sällsk. Lund. Forh.*, **14**, No. 21; 1945, *Ibid.*, **15**, No. 22.
KATO, T., 1950, *Phys. Rev.*, **80**, 475; 1951, *Prog. Theor. Phys.*, **6**, 394.
KOHN, W., 1948, *Phys. Rev.*, **74**, 1763; 1951, *Ibid.*, **84**, 495.
MASSEY, H. S. W., and ERSKINE, G. A., 1952, *Proc. Royal. Soc. A*, **212**, 521.
MASSEY, H. S. W., and MOISEWITSCH, B. L., 1951, *Proc. Roy. Soc. A*, **205**, 483.
MORSE, P. M., YOUNG, L. A., and HAURWITZ, E. S., 1935, *Phys. Rev.*, **48**, 948.
MOTT, N. F., and MASSEY, H. S. W., 1949, *Theory of Atomic Collisions*, 2nd edn. (Oxford University Press).
VERDE, M., 1949, *Helv. Phys. Acta*, **22**, 339.
VERDE, M., and TROESCH, A., 1951, *Helv. Phys. Acta*, **24**, 39.

Thermal Diffusion of Gas Mixtures and Forces between Unlike Molecules

BY B. N. SRIVASTAVA AND M. P. MADAN

Department of Physics, University of Lucknow

MS. received 22nd September 1952, and in final form 10th November 1952

Abstract. The Chapman-Enskog formulae for thermal diffusion in a mixture of gases have been utilized to interpret the data on several gas mixtures at different temperatures but having the same composition. Assuming the Lennard-Jones 12:6 interaction potential also for unlike molecules, the minimum mutual potential ϵ_{12} for interaction between two unlike molecules has been calculated from the temperature dependence of the thermal diffusion ratio k_T . These determinations are expected to provide the most accurate value for this interaction as thermal diffusion is far more sensitive to the laws of interaction than the other transport properties which have been hitherto used to estimate ϵ_{12} . The distance r_{12} at which the potential vanishes is calculated from the experimental data on the inter-diffusion coefficient D_{12} by utilizing these values of ϵ_{12} . Thus ϵ_{12} and r_{12} are determined purely from experimental data. Equations have been developed to correlate ϵ_{12} and r_{12} with ϵ_{11} , ϵ_{22} and r_{11} , r_{22} , and these relations have been tested with the help of the experimental values. It is found that our theoretical relations give much better agreement than the assumed geometric mean relation for ϵ_{12} and the arithmetic mean relation for r_{12} . Equations have also been developed for μ_{12} and λ_{12} and their theoretically obtained values compared with the experimental results.

§ 1. INTRODUCTION

FOLLOWING the discovery of the phenomenon of thermal diffusion by Enskog and Chapman, much theoretical and experimental work has been done which has been conveniently summarized by Chapman and Cowling (1939). The experimental work with gases has been carried out either with isotopes of a single gas using the tracer technique or with mixtures of different gases. As is well known, the coefficient of thermal diffusion is far more sensitive to the type of molecular interaction than the three elementary gas coefficients. It follows therefore that a determination of the laws of molecular interaction from thermal diffusion will be much more accurate and useful than their determination from viscosity, diffusion and virial coefficients, which is usually done. With this idea we have already investigated from the available thermal diffusion data the law of force and the force constants for argon and a few other isotopic gases (Srivastava and Madan 1953) and have obtained some interesting results. In the present paper we propose to examine the available data on thermal diffusion of gas mixtures and deduce therefrom the law of interaction between unlike molecules and the force constants for different pairs of gases.

§2. THEORY AND FORMULAE

The Chapman-Enskog theory of non-uniform gases expresses the transport properties in terms of a set of collision integrals (Chapman and Cowling 1939) which depend on the law of interaction between the colliding molecules. These integrals have been evaluated for various molecular models but, as shown by Hirschfelder, Bird and Spotz (1948, 1949) and others, the Lennard-Jones 12:6 model

$$E_{ij}(r) = \lambda_{ij}r^{-12} - \mu_{ij}r^{-6} = 4\epsilon_{ij}[(r_{ij}/r)^{12} - (r_{ij}/r)^6] \quad \dots\dots (1)$$

is more in accord with the observed properties of gases than any other model. We shall therefore assume the validity of the 12:6 potential and use it to calculate the intermolecular force constants from the thermal diffusion and inter-diffusion data on various gas mixtures. The previous workers on thermal diffusion of gas mixtures, viz. Hirschfelder *et al.* (1949), Grew (1949) and Winter (1950), on the other hand, assume, in addition to the 12:6 potential, the values of the force constants ϵ_{12} and r_{12} derived from certain empirical formulae of doubtful validity and compare the calculated values with the experimental data on thermal diffusion. Our calculations do not suffer from any such approximate assumptions and yield the force constants within the limits of accuracy of the experimental data, subject only to the validity of the 12:6 potential energy function.

As the second approximation to the thermal diffusion ratio k_T for a mixture of two gases 1, 2 involves very complicated algebra, only the first approximation formulae will be employed here. We have (Hirschfelder *et al.* 1949)

$$[k_T]_1 = 5y_1y_2(C-1)a, \quad \dots\dots (2)$$

where $a = (S_1y_1 - S_2y_2)/(Q_1y_1^2 + Q_2y_2^2 + Q_3y_1y_2)$

$$S_1 = \frac{M_1}{5} \left(\frac{r_{11}}{r_{12}} \right)^2 \left[\frac{2(M_1 + M_2)^3}{M_2} \right]^{1/2} \left[\frac{W^2(2; kT/\epsilon_{11})}{W^1(1; kT/\epsilon_{12})} \right] \\ - 3M_2(M_2 - M_1) - 4AM_1M_2$$

$$Q_1 = \frac{1}{5} \left(\frac{r_{11}}{r_{12}} \right)^2 \left[\frac{2(M_1 + M_2)^3}{M_2} \right]^{1/2} \left[\frac{W^2(2; kT/\epsilon_{11})}{W^1(1; kT/\epsilon_{12})} \right] \\ \times [6M_2^2 + (5 - 4B)M_1^2 + 8AM_1M_2]$$

$$Q_3 = 3(M_1 - M_2)^2(5 - 4B) + 4AM_1M_2(11 - 4B) \\ + \frac{4}{25} \left(\frac{r_{11}r_{22}}{r_{12}^2} \right)^2 \left[\frac{(M_1 + M_2)^3}{(M_1M_2)^{1/2}} \right] \left[\frac{W^2(2; kT/\epsilon_{11})W^2(2; kT/\epsilon_{22})}{\{W^1(1; kT/\epsilon_{12})\}^2} \right]$$

with similar expressions for S_2 and Q_2 . M_i is the molecular weight of the i th species, y_i is the mole fraction, A, B, C are functions of kT/ϵ_{12} while $\epsilon_{11}, \epsilon_{22}$ and ϵ_{12} , the minimum potential energy (taken as positive) for pairs of like and unlike molecules, and r_{11}, r_{22} and r_{12} the low-velocity collision diameters. Equation (2) shows that $[k_T]_1$ is a complicated function of the masses, concentrations and the force fields of the molecules. The effect of the force field enters in the 'collision' integrals $W^l(n; kT/\epsilon_{ij})$ and the functions A, B, C , all of which have been tabulated by Hirschfelder *et al.* (1948), and also in the values of r_{11}, r_{22}, r_{12} . Equation (2) is only a first approximation, and the error involved in taking this approximation cannot be definitely stated as the accurate expression for k_T has not been given for the 12:6 potential. For the Lorentzian case with inverse power repulsion, the repulsive force index being 13, the error involved is found from accurate calculations to be 15%, while for molecules of the same mass it is likely to be less

than 3%. In the absence of any exact knowledge for the case of 12:6 potential, it may be assumed that the error is of the same order and therefore negligible.

The early calculations of k_T were made for molecules interacting with inverse power repulsion, for which k_T from theory comes out to be independent of temperature. Since the experimental investigations showed that k_T varies with temperature, Jones (1940, 1941) calculated the values of k_T for molecules which have an attractive field superposed on a repulsive field, viz. the 8:4 model, while Hirschfelder and others calculated for the 12:6 model, but no expression has been given for generalized values of the force indices.

The first approximation for the coefficient of interdiffusion is given by

$$[D_{12}]_1 = \frac{0.00092916 T^{3/2} [(M_1 + M_2)/M_1 M_2]^{1/2}}{p(r_{12})^2 W^1(1; kT/\epsilon_{12})} \text{ cm}^2 \text{ sec}^{-1}, \quad \dots\dots (3)$$

where p is the pressure in atmospheres and M_i represents the molecular weight. The expression for the second approximation is

$$[D_{12}]_2 = [D_{12}]_1 / (1 - \Delta); \quad \dots\dots (4)$$

where Δ is found to be a small quantity, usually less than 0.03. As the experimental errors in the measurement of D_{12} are of this order, we shall use only the first approximation formula for D_{12} .

Equation (2) will be utilized to give ϵ_{12} . This, when substituted in eqn. (3), gives r_{12} .

§ 3. CALCULATION OF THE FORCE CONSTANTS ϵ_{12} AND r_{12}

Equation (2) shows that if the thermal diffusion ratio k_T is experimentally measured at different temperatures, but with the same fixed composition, it is possible to calculate ϵ_{12} , since C is a function of kT/ϵ_{12} . Assuming provisionally that the term a does not vary sensibly with temperature, the observed variation of k_T is to be attributed solely to the variation of C with temperature, and the latter variation, as stated above, depends on the value of ϵ_{12} . Hence from the observed variation of k_T with temperature the variation of C with temperature can be deduced, and from this the value of ϵ_{12} can be determined. The procedure is explained below.

A graph of $C-1$ against arbitrarily assumed values of x , where $x = kT/\epsilon_{12}$ is plotted, using the values of C tabulated by Hirschfelder *et al.* (1948) for the 12:6 model. From this another graph, in which the value of the ratio $(C-1)_2/(C-1)_1$ for $x_2/x_1=2$ is plotted (fig. 1) against the initial value $(C-1)_1$. Next a graph of k_T against T is drawn and $(k_T)_2/(k_T)_1$ for $T_2/T_1=2$ is found for different initial values T_1 of the temperature. Now since

$$(k_T)_2/(k_T)_1 = (C-1)_2/(C-1)_1$$

we can look for any observed value of $(k_T)_2/(k_T)_1$ on the $(C-1)_2/(C-1)_1$ graph and read for this value of the ordinate the corresponding $(C-1)_1$. This value of $(C-1)_1$ corresponds to T_1 , and by reference to the $(C-1, x)$ graph the corresponding value of $x_1 = kT_1/\epsilon_{12}$, and hence of ϵ_{12} , is found.

To test the correctness of the simplifying assumption that a does not vary with temperature, values of this function were calculated at different temperatures by using the values of ϵ_{12} obtained by the above method, and the other quantities ϵ_{11} , ϵ_{22} , r_{11} , r_{22} from the data on pure gases; r_{12} was assumed to be the arithmetic mean of r_{11} and r_{22} . It was found (see table 3) that this function remains sensibly

constant; the slight variation observed hardly shows any definite trend and is itself liable to uncertainties on account of errors in the assumed values of the various ϵ_{ij} and r_{ij} . Hence the assumption of k_T varying as $C-1$ is justified for all practical purposes. This, then, provides a simple and elegant method of finding ϵ_{12} for different gas mixtures.

§ 4. EVALUATION FROM EXPERIMENTAL DATA

The experimental measurement of the thermal diffusion constant has been carried out by a number of workers, some of them aiming at finding out its variation with concentration and others its variation with temperature. The former set of data cannot yield ϵ_{12} , as is evident from the form of eqn. (2). In the latter set we have the investigations of Ibbs (1925), Ibbs, Grew and Hirst (1929), Blüh and Puschner (1937), Bastick, Heath and Ibbs (1939), Grew (1947), van Itterbeek *et al.* (1947) and others. Of these the data of Grew (1947) on inert gas mixtures and of Ibbs *et al.* (1929) on H_2-O_2 , H_2-A , N_2-A , H_2-N_2 , H_2-CO are fairly extensive, that of Grew (1947) being most reliable. Ibbs and Grew keep the

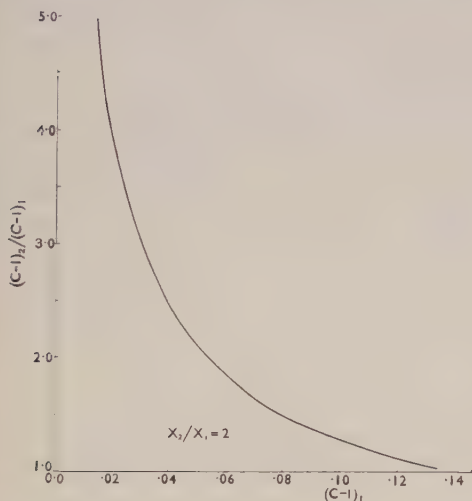


Fig. 1.

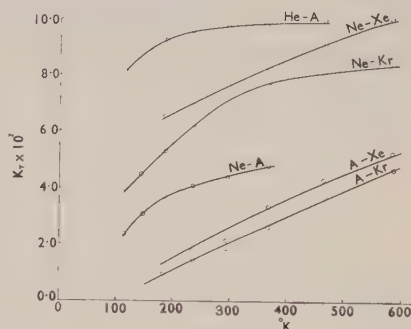


Fig. 2.

temperature of one bulb fixed and measure the separation $s = y_1' - y_1$ for different temperatures T' of the other bulb, y_1 being the concentration at the temperature T . They calculate k_T at the temperature T' with the help of the relation

$$ds = dy_1' = k_T d(\log T') \quad \dots\dots (5)$$

by determining the slope of the curve of separation plotted against $\log(T'/T)$ and obtain k_T at different temperatures. This derivation, however, assumes that k_T is independent of the composition of the mixture, while eqn. (2), as well as the experiments of Atkins, Bastick and Ibbs (1939), show that it is not so. Grew has therefore corrected these k_T values to obtain k_T for the same composition at all temperatures by utilizing the experimental results of Atkins *et al.* (1939). For our purpose we want the values of k_T for the same concentration of the gases but different temperatures, and hence these values of Grew have been used directly. The data of Ibbs *et al.* (1929), however, are not corrected for the change in composition. As these data refer to only a few concentrations (in the case of

H₂-O₂ mixture only for one concentration), it is not possible to correct their k_T values for the change in composition. An error of about 5% in the values of k_T is likely to be produced for this reason. These authors have tabulated some k_T values, while others have been calculated by us using eqn. (5).

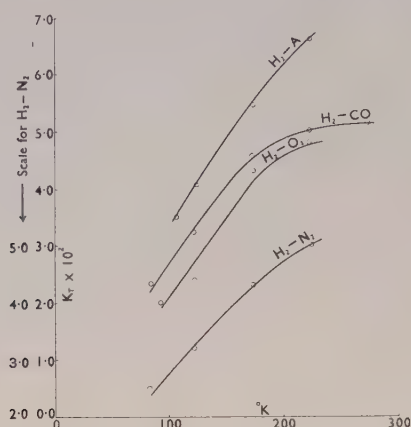


Fig. 3.

The R_T values given by Grew (1947) were converted into k_T values, which are plotted in fig. 2, while those obtained from the data of Ibbs *et al.* (1929) are plotted in fig. 3. Then, as explained earlier, the experimental values of $(k_T)_2/(k_T)_1$ for the ratio $T_2/T_1=2$ at different initial values of T_1 were used to obtain ϵ_{12} (tables 1(a) and 1(b)).

Table 1(a)

Gas pair	Temp. range ($^{\circ}\text{K}$)	Calc. ϵ_{12}/k	Mean ϵ_{12}/k
H ₂ -N ₂	90-180	45.0	46.53
	100-200	48.07	
H ₂ -O ₂	100-200	57.48	59.81
	110-220	62.15	
H ₂ -CO	90-180	51.42	52.02
	100-200	52.62	
H ₂ -A	110-220	56.41	56.41

Table 1(b)

Gas pair	Temp. range ($^{\circ}\text{K}$)	Calc. ϵ_{12}/k	Mean ϵ_{12}/k
He-A	125-250	26.04	26.65
	150-300	27.27	
Ne-A	125-250	56.82	56.92
	150-300	57.03	
Ne-Kr	125-250	59.53	62.09
	150-300	64.66	
Ne-Xe	200-400	64.51	69.01
	250-500	73.52	
A-Kr	150-300	125.0	144.1
	200-400	140.8	
	250-500	166.5	
A-Xe	250-500	163.4	166.5
	275-550	169.7	

These values of ϵ_{12} were used to calculate a , as explained in § 3. For this purpose the values of ϵ_{ii} and r_{ii} employed are given in table 4. The values of a

thus obtained are given in table 2. It will be seen that a does not vary appreciably with temperature, and thus the assumption of k_T varying as $C - 1$ is found to be justified.

Table 2. Values of a

T ($^{\circ}\text{K}$)	Ne-A	He-A	Ne-Kr	Ne-Xe	A-Kr	A-Xe
100	0.320	0.590	0.549		0.316	
200	0.357	0.560	0.500	0.597	0.305	0.469
300	0.363	0.592	0.515	0.585	0.300	0.458
400				0.586		0.453

As a further check these numerical values of a were substituted in eqn. (2) and $k_T a$ was plotted against the corresponding temperature and ϵ_{12} calculated to a second approximation, almost in the same manner as explained previously. For comparison the first and second approximation values in the case of neon-argon mixture are given in table 3. It will be seen that for practical purposes it is needless to work to the second approximation. Therefore only the first approximation values have been calculated for the different pairs of gases.

Table 3. Ne-A

Temp. range ($^{\circ}\text{K}$)	125-250	150-300
ϵ_{12}/k (first approx.)	56.82	57.03
ϵ_{12}/k (second approx.)	56.56	56.82

Knowing ϵ_{12} , the intermolecular separation r_{12} for the zero interaction energy can be calculated from eqn. (3), when the data on D_{12} are available. For this purpose the data listed by Hirschfelder *et al.* (1949) were used. The values of r_{12} thus obtained for a few pairs of gases are given in table 5, column 5.

§ 5. THEORETICAL FORMULAE FOR FORCES BETWEEN UNLIKE MOLECULES

The values of ϵ_{12} and r_{12} determined experimentally, as explained above, can be used to find correct interaction between unlike molecules. Assuming for unlike molecules also the Lennard-Jones interaction potential in the form (1), it follows that

$$\mu_{ij} = 4\epsilon_{ij}r_{ij}^6, \quad \text{and} \quad \lambda_{ij} = \mu_{ij}r_{ij}^6 = 4\epsilon_{ij}r_{ij}^{12}. \quad \dots\dots(6)$$

Thus from the values of ϵ_{12} and r_{12} the values of μ_{12} and λ_{12} can be determined with the help of eqn. (6). These are given in columns 2 and 4 of table 6.

It is of great interest to find how the force constants μ_{12} and λ_{12} or ϵ_{12} and r_{12} depend on the force constants μ_{11} , μ_{22} , λ_{11} , λ_{22} , etc., for like molecules. For this it is necessary to examine the nature of the intermolecular forces. The forces between two molecules at large distances are attractive and have been discussed in detail by London (1937) and Margenau (1939). They are, for non-polar molecules, due to the so-called dispersion effect, first noted by Wang (1927) and fully interpreted by London (1930). Even for polar molecules it is found that the attractive energy due to the orientation and induction effects is usually much less than the dispersion energy, and can be ignored. The dispersion energy arising from the mutual perturbations of the electron clouds of the two atoms or molecules gives rise to the so-called London forces, and has been treated on the classical, as well as the quantum-mechanical model of the atom. It is found to be connected with the polarizability of the atom. By the methods of perturbation

theory the quantum theory of dispersion yields, for the polarizability α of an atom in its ground state (denoted by subscript $_0$), the expression

$$\alpha(\nu) = (e^2/4\pi^2 m) \sum_l f_l / (\nu_l^2 - \nu^2), \quad \dots\dots(7)$$

where $\nu_l = (\epsilon_l - \epsilon_0)/h$ and f_l denotes the oscillator strength which may be derived from the intensities of the corresponding spectral lines.

The quantum-mechanical expression for the dispersion energy (London 1930) is

$$E(r) = 3\hbar e^4 / 32\pi^4 m^2 r^6 \sum_{l, \lambda} \frac{f_l f_\lambda}{\nu_l \nu_\lambda (\nu_l + \nu_\lambda)}, \quad \dots\dots(8)$$

where the subscripts l and λ denote stationary quantum states of atom 1 and 2 respectively with energy level ϵ_l and ϵ_λ . If the absolute intensities of all spectral lines of the two atoms be known, the dispersion energy can be precisely calculated from eqn. (8), but unfortunately this knowledge is not available. We have, therefore, to determine f_l, f_λ from the observed polarizability with the help of eqn. (7). Since the index of refraction r is connected with the polarizability α by the relation

$$\frac{r^2 - 1}{r^2 + 2} = \frac{4\pi}{3} \frac{N}{V} \alpha, \quad \dots\dots(9)$$

measurements of the values of r over a large range of frequencies can be correlated to give values of f_l, f_λ . In many instances this correlation can be done with sufficient accuracy in the measured range of r by using a single f . If, then, we assume only one term dispersion formula, eqn. (7) yields for the static polarizability α_0

$$f_l = 4\pi^2 m \nu_l^2 \alpha_0 / e^2, \quad \dots\dots(10)$$

and eqn. (8) yields, with the help of eqn. (10),

$$E(r) = \frac{3}{2r^6} \frac{\hbar \nu_l \nu_\lambda (\alpha_0)_l (\alpha_0)_\lambda}{\nu_l + \nu_\lambda}, \quad \dots\dots(11)$$

where $\hbar \nu_l$ is to be identified with the ionization potential. Equation (11) is the first order term in the dispersion energy, which in general can be expressed in the form

$$E(r) = -\mu r^{-6} - \mu' r^{-8} - \mu'' r^{-10} - \dots, \quad \dots\dots(12)$$

but the higher order terms can be generally neglected.

The explanation of the repulsive forces between molecules was given by Heitler and London (1927), and is based on the Pauli exclusion principle. This repulsion becomes important when the two charge distributions for the two molecules overlap appreciably. This repulsive energy can be calculated from the perturbation theory of quantum mechanics, but the mathematical difficulties involved are great, and detailed calculations have been carried out only for a few molecules. In all these treatments highly approximate wave functions have been employed to obtain tractable results, and still the results are very complicated. It is however found that a simple exponential relation of the form

$$E(r) = A e^{-r/\rho} \quad \dots\dots(13)$$

reproduces the numerical values satisfactorily for r greater than 1 \AA . The constant ρ seems to have roughly the same value for most atoms, but the factor A varies from atom to atom and is not easily predictable. If we write the above expression in the form

$$E(r) = \lambda r^{-n} \quad \dots\dots(14)$$

it follows that λ also cannot be predicted. Thus in the absence of any theoretical relation for λ_{ij} it is not possible to obtain a relation for λ_{12} in terms of λ_{11} and λ_{22} . We have therefore only to depend upon the theoretical relationship for μ_{ij} for correlating μ_{12} with μ_{11} and μ_{22} .

Equation (11) can be written as

$$E(r) = -\frac{3}{2} \frac{\alpha_1 \alpha_2}{r^6} \frac{I_1 I_2}{I_1 + I_2}, \quad \dots\dots(15)$$

where I_1, I_2 denote the ionization potentials of the two molecules. For the case of two identical molecules eqn. (15) gives

$$E(r) = -\frac{3}{4} \alpha^2 I / r^6. \quad \dots\dots(16)$$

Comparing with eqn. (1), eqn. (15) gives

$$\mu_{12} = 4\epsilon_{12} r_{12}^6 = 3\alpha_1 \alpha_2 I_1 I_2 / 2(I_1 + I_2). \quad \dots\dots(17)$$

Similarly

$$\mu_{11} = 4\epsilon_{11} r_{11}^6 = \frac{3}{4} \alpha_1^2 I_1 \quad \text{and} \quad \mu_{22} = 4\epsilon_{22} r_{22}^6 = \frac{3}{4} \alpha_2^2 I_2, \quad \dots\dots(18)$$

for interaction between identical molecules. Combining eqns. (17) and (18), we obtain

$$\epsilon_{12} r_{12}^6 = 2(\epsilon_{11} \epsilon_{22} r_{11}^6 r_{22}^6)^{1/2} (I_1 I_2)^{1/2} / (I_1 + I_2) \quad \dots\dots(19)$$

and

$$\mu_{12} = (\mu_{11} \mu_{22})^{1/2} 2(I_1 I_2)^{1/2} / (I_1 + I_2). \quad \dots\dots(20)$$

Again, from eqns. (6) and (20)

$$\lambda_{12} = (\lambda_{11} \lambda_{22})^{1/2} \{r_{12} / (r_{11} r_{22})^{1/2}\}^6 2(I_1 I_2)^{1/2} / (I_1 + I_2). \quad \dots\dots(21)$$

In general $I_1 \neq I_2$, so that $2(I_1 I_2)^{1/2} / (I_1 + I_2) < 1$, hence

$$\epsilon_{12} < (\epsilon_{11} \epsilon_{22})^{1/2} \{(r_{11} r_{22})^{1/2} / r_{12}\}^6. \quad \dots\dots(22)$$

Several workers have assumed that $\epsilon_{12} = (\epsilon_{11} \epsilon_{22})^{1/2}$ and $r_{12} = (r_{11} + r_{22})/2$, but there is no theoretical justification for these assumptions. The assumption regarding r_{12} seems plausible for hard rigid molecules, but will certainly not be applicable in the general case, when eqn. (19) or the inequality (22) should hold.

§ 6. COMPARISON OF THE THEORY WITH EXPERIMENTAL RESULTS

For testing eqns. (19) to (22) the experimental data given in table 4 have been used. The low temperature values of ϵ_{ii} and r_{ii} have been selected since the experimental data on thermal diffusion given in table 1 usually refer to low temperatures. The data given in group I were obtained by us from thermal diffusion data and the viscosity data for the range 100°K to 300°K (Srivastava and Madan 1953). The values of ϵ_{ii} and r_{ii} given in group II are the mean of our values obtained from thermal diffusion and those given by Hirschfelder *et al.* (1949) from viscosity, while those given in group III are taken from Hirschfelder *et al.* from viscosity measurements. From these values of ϵ_{ii} and r_{ii} the force constants μ_{ii} and λ_{ii} were calculated with the help of eqn. (6), and are recorded in table 4.

Equation (19) was used to calculate ϵ_{12} for different pairs of gases by using the data for individual gases given in table 4, and the r_{12} values determined experimentally from interdiffusion data and given in column 5 of table 5. The ionization potentials of the gases were taken from Margenau (1939). These theoretically calculated values of ϵ_{12} are recorded in column 3 of table 5 and are seen to agree with the experimentally determined values (column 2). The table shows further that

eqn. (19) gives better agreement than the hitherto assumed geometric mean relation for ϵ_{12} which will be approximately obeyed if $(r_{11}r_{22})^{1/2}/r_{12} \simeq 1$. It is true that the error in the value of ϵ_{12} given in columns 2, 3, 4 is of the order of $\pm 5\%$, so that for all cases except $\text{H}_2\text{-CO}$, $\text{H}_2\text{-A}$ the discrepancies between columns 3 and 4 lie within the limits of that error. It is however precisely these cases of $\text{H}_2\text{-CO}$ and $\text{H}_2\text{-A}$ where $(r_{11}r_{22})^{1/2}/r_{12}$ differs appreciably from unity that should be employed to test eqn. (19), and these prove conclusively the superiority of eqn. (19) over the geometric mean formula.

Table 4

	Gas	ϵ_{ii}/k ($^\circ\text{K}$)	r_{ii} (\AA)	$\mu_{ii} \times 10^{60}$ (erg cm ⁶)	$\lambda_{ii} \times 10^{104}$ (erg cm ¹²)
I	Argon	124.9	3.424	110.4	17.77
II	Oxygen	110.6	3.444	101.3	16.90
	Nitrogen	87.10	3.701	122.8	31.53
	CO	99.46	3.646	128.1	30.09
III	Hydrogen	33.3	2.968	12.48	0.854
	Helium	6.03	2.70	1.28	0.050
	Neon	35.7	2.80	9.44	0.455
	Krypton	190	3.61	230.6	51.04
	Xenon	230	4.051	556.9	246

Table 5

Gas pair	ϵ_{12}/k exp.	ϵ_{12}/k theor.	ϵ_{12}/k (geom. mean)	r_{12} (\AA) exp.	r_{12} (\AA) theor.	r_{12} (\AA) (arith. mean)
$\text{H}_2\text{-N}_2$	46.53	51.42	53.86	3.339	3.395	3.334
$\text{H}_2\text{-O}_2$	59.81	56.99	60.67	3.194	3.168	3.206
$\text{H}_2\text{-A}$	56.41	58.21	64.47	3.241	3.258	3.196
$\text{H}_2\text{-CO}$	52.02	50.28	57.55	3.364	3.345	3.307
He-A	26.65	27.04	27.45	3.041	3.049	3.062

Table 6

Gas pair	$\mu_{12} \times 10^{60}$ (erg cm ⁶)		$\lambda_{12} \times 10^{104}$ (erg cm ¹²)		$\frac{2(I_1 I_2)^{1/2}}{I_1 + I_2}$
	Exp.	Theor.	Exp.	Theor.	
$\text{H}_2\text{-N}_2$	35.4	39.1	4.91	5.43	0.9994
$\text{H}_2\text{-O}_2$	34.8	35.5	3.69	3.77	0.9994
$\text{H}_2\text{-A}$	35.8	37.0	4.15	4.28	0.9956
$\text{H}_2\text{-CO}$	41.4	40.0	5.99	5.80	0.9997
He-A	11.6	11.7	0.91	0.89	0.9860

A comparison of the r_{12} values is however not sufficiently conclusive of the accuracy of our equation (19), since r_{12} is much less sensitive to changes in ϵ_{12} , as eqn. (19) shows. However, for the sake of comparison the experimental values of ϵ_{12} are substituted in eqn. (19) to yield r_{12} (theoretical), which is given in table 5, column 6, and may be compared with r_{12} (experimental) and r_{12} (arithmetic mean). Here also it will be seen that the large discrepancies between r_{12} (experimental) and r_{12} (arithmetic mean) are considerably minimized by the use of eqn. (19).

Equations (20) and (21) could be best tested if I_1 , I_2 were very different. Unfortunately most of the data on thermal diffusion refer to gases for which values of I are not very different and the values of $2(I_1 I_2)^{1/2}/(I_1 + I_2)$ are greater than 0.986. We have, however, calculated the values of μ_{12} and λ_{12} from eqns. (20) and (21) and recorded them in table 6, together with the experimental values. The

agreement is fairly satisfactory. These calculations show that the geometric mean rule for ϵ_{12} or μ_{12} , λ_{12} will apply fairly closely if the I and r values for the two types of molecules are not very different, but is not applicable in the general case. The values given in columns 2 and 4 are liable to an error of $\pm 5\%$.

ACKNOWLEDGMENT

We record our thanks to the Government of Uttar Pradesh for the award of a research grant.

REFERENCES

- ATKINS, B. E., BASTICK, R. E., and IBBS, T. L., 1939, *Proc. Roy. Soc. A*, **172**, 142.
BASTICK, R. E., HEATH, H. R., and IBBS, T. L., 1939, *Proc. Roy. Soc. A*, **173**, 543.
BLÜH, G., BLÜH, O., and PUSCHNER, M., 1937, *Phil. Mag.*, **24**, 1103.
CHAPMAN, S., and COWLING, T. G., 1939, *The Mathematical Theory of Non-Uniform Gases* (Cambridge : University Press).
GREW, K. E., 1947, *Proc. Roy. Soc. A*, **189**, 402; 1949, *Ibid.*, **62**, 655.
HEITLER, W., and LONDON, F., 1927, *Z. Phys.*, **44**, 455.
HIRSCHFELDER, J. O., BIRD, R., and SPOTZ, E. L., 1948, *J. Chem. Phys.*, **16**, 968; 1949, *Chem. Rev.*, **44**, 205.
IBBS, T. L., 1925, *Proc. Roy. Soc. A*, **107**, 470.
IBBS, T. L., GREW, K. E., and HIRST, A. A., 1929, *Proc. Phys. Soc.*, **41**, 456.
VAN ITTERBEEK, A., VAN PAEMEL, O., and VAN LIERDE, J., 1947, *Physica*, **13**, 231.
JONES, R. C., 1940, *Phys. Rev.*, **58**, 111; 1941, *Ibid.*, **59**, 1019.
LONDON, F., 1930, *Z. Phys. Chem. B*, **11**, 222; 1937, *Trans. Faraday Soc.*, **33**, 8.
MARGENAU, H., 1939, *Rev. Mod. Phys.*, **11**, 1.
SRIVASTAVA, B. N., and MADAN, M. P., 1953, *J. Chem. Phys.*, in the press.
WANG, S. C., 1927, *Phys. Z.*, **28**, 663.
WINTER, E. R. S., 1950, *Trans. Faraday Soc.*, **46**, 81.

Inelastic Collisions of Electrons in Helium and Townsend's Ionization Coefficient

BY I. ABDELNABI AND H. S. W. MASSEY

University College, London

MS. received 5th August 1952

Abstract. It is pointed out that the accuracy of the cross sections observed by Maier-Leibniz for the excitation of helium by slow electrons may be tested by using them to calculate the Townsend ionization coefficients α and comparing the results of such calculations with observed values. Information about the reliability of the difficult measurements of excitation cross sections is essential to check attempts made to develop a satisfactory theory. To carry out this test it is necessary to extend and to some extent refine the work of Smit on the velocity distribution of electrons in helium diffusing under the action of a uniform electric field F when inelastic collisions are allowed for. This has been done and numerical results have been obtained for $F/p=10$ and 20 v/cm/mm Hg. The ionization coefficient has been measured for the higher values of F/p and agrees quite well with that calculated when Maier-Leibniz's cross sections are used. The sensitivity of this test of the cross sections was examined by calculating α assuming that Maier-Leibniz's values were respectively twice and one-half the correct value. It was found that the calculated value of α is nearly proportional to the size of the assumed excitation cross section (it was assumed throughout that the ionization cross section is given correctly from Smit's observations). It is concluded that the observations of Maier-Leibniz may be used for checking theoretical determination of excitation cross sections in helium.

§ 1. INTRODUCTION

IF a swarm of electrons of low concentration is diffusing through a gas at pressure p (containing n atoms/cm³) under the influence of a uniform electric field of strength F there will always be a finite fraction of the electrons which possess sufficient kinetic energy to ionize the gas atoms. If in diffusing through a distance δx in the direction of the field, $n\alpha\delta x$ ionizing collisions occur, then α is known as the Townsend ionization coefficient. For a particular gas α/p is a function of F/p . If $f(\mathbf{v})d\mathbf{v}$ is the fraction of the electrons which have velocities between \mathbf{v} and $\mathbf{v}+\delta\mathbf{v}$, $Q_i(v)$ is the cross section for ionization of the gas atoms by electrons of speed v and E_i is the ionization energy of the gas, then

$$\alpha = \frac{\int n Q_i v f(\mathbf{v}) d\mathbf{v}}{\int \xi f(\mathbf{v}) d\mathbf{v}}, \quad \text{where } Q_i = 0 \text{ for } v < (2E_i/m)^{1/2}. \quad \dots\dots (1)$$

ξ is the component of the velocity in the direction of the field. Q_i can be measured directly for any particular gas. The velocity distribution function $f(\mathbf{v})$ for $v > (2E_i/m)^{1/2}$ will depend strongly on the probability of the electrons undergoing inelastic collisions involving excitation as well as ionization. It follows that, if

$f(\mathbf{v})$ can be obtained when the cross sections for elastic (Q_0) and inelastic (Q_{in}) collisions are known, then α may be calculated. Alternatively, if the cross sections for elastic and ionizing collisions are known accurately but those for excitation only imperfectly it should be possible to obtain further information about the latter from the relation (1), using observed values of α and Q_i and velocity distributions calculated for different assumptions about Q_{in} . In this paper an account is given of an application of this procedure to obtain information about the reliability of experimental data on the cross sections for excitation of the 2^1S and 2^3S levels of helium by slow electrons.

Very considerable interest attaches to a knowledge of the absolute values of the cross sections for excitation of the low-lying excited states of helium atoms by electron impact, particularly when the electron energy is not greatly in excess of the threshold. This is largely because of the usefulness of such data in checking the range of validity of theoretical methods of calculating inelastic cross sections. A satisfactory theory exists when the exciting electron possesses a kinetic energy greatly exceeding that required for the excitation concerned, but for many applications it is the cross section near the threshold which is important. To determine which factors play the dominant role in such collisions it is necessary to extend the theory in various ways. These extensions are difficult except for the simplest atoms, hydrogen and helium. For obvious reasons very few measurements of cross sections for excitation of atomic hydrogen have so far been carried out, so that it is necessary to rely on observations made with helium for providing a check on new theoretical methods. Especial interest attaches to the excitation of the 2^1S and 2^3S levels by slow electrons. Unfortunately the observed data are meagre and often unreliable. They have been discussed in detail by Bates, Fundamirsky, Leech and Massey (1950).

The most complete observations are those of Maier-Leibnitz (1935). Using these, Smit (1936) has already calculated, with certain approximations, the function $f(\mathbf{v})$ for electrons in helium with F/p up to 10 v/cm/mm Hg. Using this function, Dunlop (1949) has calculated α/p for these values of F/p , but at present α/p has only been measured for values of F/p between 12 and 100 v/cm/mm Hg. We have extended the calculations in various ways. They have been carried out for $F/p = 20$ v/cm/mm Hg for which experimental measurements of α/p are available. Certain of the approximations made by Smit which are less valid at the higher value have not been made, and the sensitivity of the results to the absolute magnitude of the cross sections for excitation has been examined by varying the size of these cross sections. It is found that the calculated value of α/p is quite sensitive to the excitation cross sections assumed and that Maier-Leibnitz's observations lead to values of α/p in quite good agreement with observation.

§ 2. CALCULATION OF THE VELOCITY DISTRIBUTION FUNCTION

When a swarm of electrons is diffusing in the direction of a uniform electric field and producing ionization, the distribution function for the electrons will be a function of the displacement x in the direction of the field as well as of the electron velocity vector \mathbf{v} . To a high degree of approximation, however, the distribution function may be written as the product of two factors $g(x)f(\mathbf{v})$ where $f(\mathbf{v})$ is independent of x and $g(x)$ allows for the increase in the number of electrons due to ionization as the stream diffuses.

To calculate $f(\mathbf{v})$ we use an extension of the method of Morse, Allis and Lamar (1935) on the lines indicated by Druyvesteyn and Penning (1940). The function is expanded in spherical harmonics in the form

$$f(\mathbf{v}) = \sum \sum f_n(v) P_n^{lm}(\cos \omega) e^{im\psi},$$

where ω and ψ are the usual polar angles specifying the direction of the velocity vector \mathbf{v} . If the electric field is in the x -direction, the distribution possesses axial symmetry about Ox , so that only zonal harmonics appear in the expression. Furthermore, as the dependence of $f(\mathbf{v})$ on ω arises from the finiteness of F/p it is reasonable to assume that for small F/p only the first term in the harmonic expansion which depends on ω is important. We then have

$$f(\mathbf{v}) = f_0(v) + P_1(\cos \omega) f_1(v) = f_0(v) + (\xi/v) f_1(v), \quad \dots (2)$$

where ξ is the component of velocity in the x -direction and $f_1(v) \ll f_0(v)$.

The distribution must be such that the number of electrons whose representative points enter an element $d\gamma (= d\xi d\eta d\zeta)$ of velocity space in a time δt is equal to the number leaving it. Thus if a, b denote the numbers leaving, per unit volume of velocity space, due to elastic and inelastic collisions respectively, c and d the corresponding numbers entering due to these respective collisions and e the number leaving due to the action of the electric field, we must have

$$a + b + e = c + d. \quad \dots (3)$$

a, c and e have been calculated by Morse, Allis and Lamar (1935) and are given by

$$a = nv \int_0^\pi \int_0^{2\pi} I_0(v, \theta) f(v, \xi) \sin \theta d\theta d\phi, \quad \dots (4)$$

$$c = nv \int_0^\pi \int_0^{2\pi} \left\{ I_0(v, \theta) f(v, \xi') \left[1 + \frac{4m}{M} (1 - \cos \theta) \right] + \frac{m}{M} (1 - \cos \theta) v \frac{\partial}{\partial v} [I_0(v, \theta) f(v, \xi')] \right\} \sin \theta d\theta d\phi, \quad \dots (5)$$

$$e = \frac{eF}{m} \frac{\partial f}{\partial \xi}. \quad \dots (6)$$

In these expressions $I_0(v, \theta) \sin \theta d\theta d\phi$ is the differential cross section for elastic scattering of electrons of velocity v into the solid angle $\sin \theta d\theta d\phi$ about (θ, ϕ) , m is the mass of an electron of charge e , M is the mass of a gas atom and n is the number of atoms per cm^3 . Terms of order $(m/M)^2$ have been neglected in calculating c . ξ' is given by

$$\frac{\xi'}{v} = \cos \omega \cos \theta + \sin \omega \sin \theta \cos (\phi - \psi). \quad \dots (7)$$

If $I_{\text{in}}^s(v, \theta) \sin \theta d\theta d\phi$ is the differential cross section for an inelastic collision in which the electron loses an amount of energy $\frac{1}{2}mv_s^2$ we have

$$b = nv \sum_s \int_0^\pi \int_0^{2\pi} I_{\text{in}}^s(v, \theta) f(v, \xi) \sin \theta d\theta d\phi = nv Q_{\text{in}}(v) f(v, \xi), \quad \dots (8)$$

where $Q_{\text{in}}(v)$ is the total cross section for inelastic collisions.

Electrons whose representative points enter the element $d\gamma$ due to inelastic collisions in which an amount of energy $\frac{1}{2}mv_s^2$ is lost, accompanied by a deflection through an angle θ , must previously have possessed a velocity of magnitude $v_{1s} = (v_s^2 + v^2)^{1/2}$ and x -component ξ_{1s} where

$$\frac{\xi_{1s}}{v_{1s}} = \cos \omega_{1s} = \cos \omega \cos \theta + \sin \omega \sin \theta \cos (\phi - \psi). \quad \dots (9)$$

We have then from these collisions

$$d_s = \frac{n}{v} \int \int I_{\text{in}}^s(v_{1s}, \theta) v_{1s}^2 f(v_{1s}, \xi_{1s}) \sin \theta \, d\theta \, d\phi.$$

The total contribution from all inelastic collisions Σd_s can be written in the form

$$d = \frac{n}{v} \int \int I_{\text{in}}(v_1, \theta) v_1^2 f(v_1, \xi_1) \sin \theta \, d\theta \, d\phi, \quad \dots\dots (10)$$

where v_1, ξ_1 are suitable mean values of v_{1s}, ξ_{1s} and $I_{\text{in}} = \Sigma_s I_{\text{in}}^s$. In practice there is no difficulty in choosing v_1 as it is close to the minimum value of v_{1s} for which I_{in}^s is appreciable.

Using now the approximate form (2) for $f(v, \xi)$ we find from (3), (4), (5), (6), (7), (8), (9) and (10) that

$$\begin{aligned} \frac{m}{Mv} \frac{d}{dv} [Q_d(v) v^4 f_0(v)] + v_1^2 Q_{\text{in}}(v_1) f_0(v_1) - v^2 Q_{\text{in}}(v) f_0(v) \\ - \cos \omega \{v^2 f_1(v) [Q_d(v) + Q_{\text{in}}(v)] - v_1^2 f_1(v_1) Q_{\text{in}}^c(v_1)\} \\ = \frac{eF}{nM} \left[\frac{1}{3v} \frac{d}{dv} \{v^2 f_1(v)\} + v \cos \omega \frac{d}{dv} f_0(v) \right], \end{aligned}$$

where

$$Q_d(v) = 2\pi \int_0^\pi (1 - \cos \theta) I_0(v, \theta) \sin \theta \, d\theta, \quad Q_{\text{in}}^c(v) = 2\pi \int_0^\pi \cos \theta I_{\text{in}}(v, \theta) \sin \theta \, d\theta.$$

Equating separately the terms independent of, and proportional to, $\cos \omega$ respectively we have

$$\frac{eF}{nm} \frac{d}{dv} f_0(v) = -v f_1(v) [Q_d(v) + Q_{\text{in}}(v)] + \frac{v_1^2}{v} f_1(v_1) Q_{\text{in}}^c(v_1),$$

$$\frac{m}{Mv} \frac{d}{dv} [Q_d(v) v^4 f_0(v)] + v_1^2 Q_{\text{in}}(v_1) f_0(v_1) - v^2 Q_{\text{in}}(v) f_0(v) = \frac{eF}{3nmv} \frac{d}{dv} [v^2 f_1(v)].$$

It is convenient to change from the velocity v to the kinetic energy E as independent variable to give

$$\frac{eF}{n} \frac{d}{dE} f_0(v) = -f_1(E) [Q_d(E) + Q_{\text{in}}(E)] + \left(1 + \frac{E_0'}{E}\right) f_1(E + E_0') Q_{\text{in}}^c(E + E_0') \quad \dots\dots (11)$$

$$\begin{aligned} \frac{eF}{3n} \frac{d}{dE} [E f_1(E)] = -E Q_{\text{in}}(E) f_0(E) + (E + E_0') Q_{\text{in}}(E + E_0') f_0(E + E_0') \\ + \frac{2m}{M} \frac{d}{dE} [E^2 Q_d(E) f_0(E)], \quad \dots\dots (12) \end{aligned}$$

where E_0' is approximately equal to the threshold energy for inelastic collisions, and $E + E_0' = \frac{1}{2} m v_1^2$.

The Cross Sections Q_d , Q_{in} and Q_{in}^c

The diffusion cross section Q_d can be taken as equal to the observed total cross section—up to energies of 40 eV the main contribution to the observed cross section comes from elastic collisions in which the scattered intensity does not depend on the angle of scattering. The observed values are closely fitted by taking for Q_d the convenient analytical form

$$\left. \begin{aligned} nQ_d &= aE_a^{-1/2}, & E \leq E_a = 5.6 \text{ eV} \\ &= aE^{-1/2}, & E \geq E_a \end{aligned} \right\} \quad \dots\dots (13)$$

where n is taken as the number of atoms per cm^3 at 1 mm Hg pressure and 15°C ; $a=50$ if Q_d is measured in cm^2 and E in eV. The same approximation was made by Smit except that for higher energies ($E \geq 19.8$ eV) he used, for analytical convenience, the form

$$\frac{1}{Q_d} \frac{d}{dE} Q_d = -0.02.$$

The difference from (13) is not important.

Smit has provided a convenient schematic representation of the total inelastic collision cross section as measured by Maier-Leibniz. It is

$$\left. \begin{aligned} nQ_{\text{in}} &= 0, & 0 \leq E < E_0 = 19.8 \text{ eV} = \text{threshold energy}, \\ &= b_1(E - D_1)E^{-1/2}, & E_0 \leq E \leq E_1 = 23.7 \text{ eV}, \\ &= b_2(E - D_2)E^{-1/2}, & E \geq E_1. \end{aligned} \right\} \dots\dots (A)$$

In terms of the same units as employed for nQ_d , we have taken $b_1 = 0.174$, $D_1 = 17.2$ eV, $b_2 = 0.358$ and $D_2 = 20.5$ eV.

For E greater than E_1 the cross section includes a contribution from ionization. The ionization cross section has been accurately measured by Smith (1930). One of the main objects of the present investigation is to test the accuracy of the total *excitation* cross section measurements of Maier-Leibniz. Two alternative forms for Q_{in} were therefore used, in one of which the total excitation cross section was taken to be approximately twice, and in the other approximately one half, that of Maier-Leibniz. In both the ionization cross section remained that given by Smith. Convenient analytical expressions of these cases were found to be

$$\left. \begin{aligned} nQ_{\text{in}} &= 0, & 0 \leq E < E_0 \\ &= 0.451(E - 18.2)E^{-1/2}, & E \geq E_0 \end{aligned} \right\} \dots\dots (B)$$

$$\left. \begin{aligned} nQ_{\text{in}} &= 0, & 0 \leq E < E_0 \\ &= 0.08 (E - 16.6)E^{-1/2}, & 19.8 \leq E \leq 24.1 \\ &= 0.269(E - 21.9)E^{-1/2}, & E \geq 24.1 \end{aligned} \right\} \dots\dots (C)$$

in terms of the same units as for (A).

There remains Q_{in}^e . The main excitation processes, involving excitation of the 2^1S and 2^3S states, are associated, for electron energies near the threshold, with a nearly isotropic angular distribution so that Q_{in}^e is very small compared with Q_{in} under these conditions. It is only when ionizing collisions become important that Q_{in}^e will be comparable with Q_{in} .

Calculation of f_0

The technique used in all three cases is covered by that for case (A) which we shall alone describe.

For $E < E_0$, $Q_{\text{in}} = 0$. Except for very small values of E , $(E + E_0')f_1(E + E_0')$ will be small compared with $Ef_1(E)$. For these values of E , $Q_{\text{in}}^e(E + E_0')$ will be small compared with $Q_{\text{in}}(E + E_0')$ which is itself small compared with $Q_d(E)$. It is therefore legitimate to replace (11) by

$$\frac{df_0}{dE} = - \frac{nQ_d}{eF} f_1. \dots\dots (14)$$

The second equation, (12), may be expressed in a convenient form by integration with respect to E from E to ∞ . This gives

$$\frac{1}{3}eFEf_1(E) - \frac{2m}{M}nQ_d(E)E^2f_0(E) = n \int_{E_0}^{E+E_0'} Q_{in}(E)Ef_0(E)dE.$$

No important error is made by extending the upper limit of the right-hand integral to ∞ and replacing E_0' by the threshold energy E_0 , giving

$$\begin{aligned} \frac{1}{3}eFEf_1(E) - \frac{2m}{M}nQ_d(E)E^2f_0(E) &= n \int_{E_0}^{\infty} Q_{in}(E)Ef_0(E)dE \\ &= \frac{1}{3}eFA_1, \text{ say.} \end{aligned} \quad \dots\dots(15)$$

The right-hand side is now a constant which vanishes when inelastic collisions are neglected.

With the form (13) for Q_d these equations may be solved without difficulty to give

$$\begin{aligned} 0 \leq E \leq E_a \quad (=5.6) \\ \left. \begin{aligned} f_0 &= \exp\left(-\frac{3mE^2}{ME_i^2}\right) \left\{ B_1 + \frac{A_1}{E_i} \int_{E_a}^E \exp\left(\frac{3mE^2}{ME_i^2}\right) \frac{dE}{E} \right\} \\ f_1 &= \frac{6mE}{ME_i} f_0 - \frac{A_1}{E}. \end{aligned} \right\} \dots\dots(16) \end{aligned}$$

$$\begin{aligned} E_a \leq E \leq E_0 \\ \left. \begin{aligned} f_0 &= \exp\left(-\frac{6mE}{Md^2}\right) \left\{ B_2 + \frac{A_2}{d} \int_{E_a}^E E^{-3/2} \exp\left(\frac{6mE}{Md^2}\right) dE \right\} \\ f_1 &= \frac{6m}{Md} E^{1/2} f_0 - \frac{A_2}{E}, \end{aligned} \right\} \dots\dots(17) \end{aligned}$$

where $E_i = eFE_a^{1/2}/a$, $d = eF/a$.

For $E > E_0$ the terms involving $f_1(E + E_0')$, $f_0(E + E_0')$ may be neglected in (11) and (12). There is no difficulty then in eliminating f_1 from these two equations to give

$$\begin{aligned} \frac{d^2 f_0}{dE^2} + \left\{ \frac{d}{dE} \log\left(\frac{E}{nQ_d}\right) + \frac{6mn^2 Q_d^2 E}{Me^2 F^2} \right\} \frac{df_0}{dE} \\ - \left\{ \frac{3n^2 Q_{in} Q_d}{e^2 F^2} - \frac{6mn^2 Q_d}{M^2 e^2 F^2 E} \left(\frac{d}{dE} (Q_d E^2) \right) \right\} f_0 = 0, \end{aligned} \quad \dots\dots(18)$$

where we have neglected $Q_{in}(E)$ compared with $Q_d(E)$.

Taking the analytical approximations for Q_d and Q_{in} as in (13) and (A) where $nQ_d = aE^{-1/2}$, $nQ_{in} = b(E - D)E^{-1/2}$, (18) takes the form

$$\frac{d^2 f_0}{dE^2} + \left(\frac{3}{2E} + 2\alpha \right) \frac{df_0}{dE} - \left(\beta - \frac{\gamma}{E} \right) f_0 = 0, \quad \dots\dots(19)$$

with $\alpha = \frac{3ma^2}{Me^2 F^2}$, $\beta = \frac{3ab}{e^2 F^2}$, $\gamma = \frac{3abD + 9ma^2/M}{e^2 F^2}$.

The substitution $f_0 = \exp[-\{\alpha + (\alpha^2 + \beta)^{1/2}\}g_0]$ \dots\dots(20)

with $2(\alpha^2 + \beta)^{1/2}E = x$ reduces this equation to the standard form

$$x \frac{d^2 g_0}{dx^2} + \left(\frac{3}{2} - x \right) \frac{dg_0}{dx} - \left(\frac{3}{4} - k \right) g_0 = 0, \quad \dots\dots(21)$$

of which the general solution is

$$g_0 = C_{11} F_1\left(\frac{3}{4} - k, \frac{3}{2}; x\right) + D_1 E^{-1/2} {}_1F_1\left(\frac{1}{4} - k, \frac{1}{2}; x\right), \quad \dots\dots(22)$$

where ${}_1F_1$ is the confluent hypergeometric function

$${}_1F_1(p, q; x) = 1 + \sum_{s=1}^{\infty} \frac{p(p+1) \dots (p+s-1)}{q(q+1) \dots (q+s-1)} \frac{x^s}{s!}$$

and $k = (2\gamma - 3\alpha)/4(\alpha^2 + \beta)^{1/2}$.

Alternatively, the substitution

$$f_0 = E^{-3/4} e^{-\alpha E} h_0 \quad \dots\dots(23)$$

in place of (20) leads to the equation

$$\frac{d^2 h_0}{dx^2} + \left(-\frac{1}{4} + \frac{k}{x} + \frac{\frac{1}{4} - m^2}{x^2} \right) h_0 = 0; \quad m^2 = \frac{1}{16}, \quad \dots\dots(24)$$

of which the general solution is

$$h_0 = C_2 W_{k, m}(x) + D_2 W_{-k, m}(-x) \quad \dots\dots(25)$$

in terms of the Whittaker functions $W_{\pm k, m}$.

For the solution in a region extending to infinity it is more convenient to use the form (25). As $W_{k, m} \sim e^{-x/2} x^k$, $W_{-k, m} \sim e^{x/2} (-x)^{-k}$ only the first is an acceptable solution and we must take, for $E > E_1$, in (25), putting $\alpha_2^2 + \beta_2 = \lambda_2^2$,

$$f_0 = C_2 E^{-3/4} \exp(-\alpha_2 E) W_{k_2, 1/4}(2\lambda_2 E),$$

$$f_1 = \frac{F}{a} C_2 E^{-1/4} \exp(-\alpha_2 E) \left[\{ \alpha_2 + \lambda_2 - (k_2 - \frac{3}{4})/E \} W_{k_2, 1/4}(2\lambda_2 E) \right. \\ \left. - \{ (k_2 - \frac{1}{4})(k_2 - \frac{3}{4})/E \} W_{k_2-1, 1/4}(2\lambda_2 E) \right],$$

the appropriate values of a , b_2 and D_2 being used to obtain α_2 , β_2 and k_2 . The form for f_1 follows from the relations (14) and

$$\frac{d}{dx} W_{k, m}(x) = \left(-\frac{1}{2} + \frac{k}{x} \right) W_{k, m}(x) + \frac{(k - \frac{1}{2})^2 - m^2}{x} W_{k-1, m}(x).$$

In the region $E_0 \leq E \leq E_1$ it is most convenient to use the form (22) as the functions ${}_1F_1$ are rather easier to calculate than the $W_{k, m}$ when the asymptotic expansion of the latter is not applicable. We have then, putting $\alpha^2 + \beta = \lambda^2$,

$$f_0 = \exp\{-(\alpha + \lambda)E\} \{ C_1 E^{-1/2} {}_1F_1(\frac{1}{4} - k, \frac{1}{2}; 2\lambda E) + D_1 {}_1F_1(\frac{3}{4} - k, \frac{3}{2}; 2\lambda E) \}.$$

$$f_1 = (F/a) \exp\{-(\alpha + \lambda)E\} \left[\{ (\alpha + \lambda + 1/2E) {}_1F_1(\frac{1}{4} - k, \frac{1}{2}; 2\lambda E) \right. \\ \left. + (4k - 1)\lambda {}_1F_1(\frac{5}{4} - k, \frac{3}{2}; 2\lambda E) \} C_1 + \{ (\alpha + \lambda) E^{1/2} {}_1F_1(\frac{3}{4} - k, \frac{3}{2}; 2\lambda E) \right. \\ \left. + (\frac{4}{3}k - 1)\lambda {}_1F_1(\frac{7}{4} - k, \frac{5}{2}; 2\lambda E) \} D_1 \right], \quad E_0 \leq E \leq E_1,$$

the appropriate values of a , b and D being used to obtain α , β and k .

The form for f_1 follows by use of the relation

$$\frac{d}{dx} {}_1F_1(p, q; x) = \frac{p}{q} {}_1F_1(p+1, q+1; x),$$

in connection with (14).

To complete the solution the constants A_1 , B_1 , A_2 , B_2 , C_1 , D_1 and C_2 are determined by the conditions that f_0 and f_1 should be continuous at $E = E_0$, $E = E_0$ and $E = E_1$ and that

$$4\pi \int_0^\infty f_0(v) v^2 dv = 1.$$

The procedure adopted by Smit differs from the above for $E > E_0$. The equation (18) may be written

$$\frac{d}{dE} \left(F_0 \rho + F_1 \frac{d\rho}{dE} \right) = n E^{1/2} Q_{\text{in}} \rho \quad \dots\dots(26)$$

where $\rho = E^{1/2}f_0$, $F_0 = -\frac{F_1}{2E} + \frac{2m}{M}E^{3/2}nQ_d$ and $F_1 = \frac{F^2e^2E^{1/2}}{3nQ_d}$. Smit assumes now that

$$\left| \rho \frac{dF_0}{dE} + \frac{d\rho}{dE} \frac{dF_1}{dE} \right| \ll \left| F_0 \frac{d\rho}{dE} + F_1 \frac{d^2\rho}{dE^2} \right|, \quad \dots\dots(27)$$

so that (26) reduces to

$$\frac{d^2\rho}{dE^2} + \frac{F_0}{F_1} \frac{d\rho}{dE} = \frac{nE^{1/2}Q_{in}\rho}{F_1} = \frac{b(E-D)\rho}{F_1}.$$

It is further assumed that F_0 and F_1 are constants for $E > E_0$ so that for $E_0 \leq E \leq E_1$,

$$\rho = x^{1/2} \exp \{ -F_2(E-D) \} [G_1 i^{1/3} J_{-1/3}(\frac{2}{3}ix^{3/2}) - H_1 i^{-1/3} J_{1/3}(\frac{2}{3}ix^{3/2})],$$

where $x = F_3^{1/3}(E-D) + F_2^2 F_3^{-2/3}$, $F_2 = F_0/2F_1$ and $F_3 = b_1/F_1$.

For $E > E_1$ the same formula is obtained with D_1 , b_1 , G_1 and H_1 now replaced by D_2 , b_2 , G_2 and H_2 respectively. In order that ρ should tend to 0 as $E \rightarrow \infty$, $G_2 = H_2$. At this stage Smit introduced the further approximation of assuming also that $G_1 = H_1$ although the values of these constants should have been derived from the continuity of f_0 and f_1 at $E = E_0$ and $E = E_1$.

The error made in the assumption (27) is probably the largest involved in Smit's calculations. For $F/p = 10$ v/cm/mm Hg and $E = 19.8$ ev the left-hand side of (27) is about one quarter of the right. It is likely to be relatively larger for larger F/p and larger E as the derivatives $d\rho/dE$ and $d^2\rho/dE^2$ will be relatively smaller under these circumstances. As in the calculation of Townsend's ionization coefficient it is important that the distribution should be accurate for $E > 24.5$ ev and $F/p = 20$ v/cm/mm Hg it was considered undesirable to employ Smit's approximations in the present calculations.

§ 3. RESULTS OF CALCULATIONS

Calculations of the velocity distribution functions were carried out for $F/p = 10$ and 20 v/cm/mm Hg assuming inelastic cross sections (A), and for the higher value of F/p assuming also the inelastic cross sections (B) and (C). The confluent hypergeometric functions occurring in the formulae were calculated numerically either from the series or asymptotic expansions at each point required. Using these distribution functions the Townsend coefficient α was calculated from (1), (2) together with the approximate averages $\bar{\xi} = 0$ and $\bar{\xi}^2 = \frac{1}{3}v^2$. α then takes the form

$$\alpha = \frac{3 \int_{E_1}^{\infty} nQ_1 E f_0(E) dE}{\int_0^{\infty} E f_1(E) dE}.$$

The results are given in table 1.

It will be seen that the observed value of α/p for $F/p = 20$ v/cm/mm Hg agrees quite well with that calculated on the assumption that the total inelastic cross section observed by Maier-Leibnitz is correct. The sensitivity of the calculated value to the magnitude of this cross section is manifest from a comparison of the results obtained with the assumed cross sections (A), (B) and (C). In fact over this range the calculated α/p is roughly inversely proportional to the magnitude assumed for Q_{in} . It seems very likely that the absolute magnitude found by

Maier-Leibniz for Q_{in} is not far from the correct value, and can be used with some confidence as a check on theoretical results.

Table 1. Calculated Values of the Townsend Ionization Coefficient α in Helium

F/p (v/cm/mm Hg)	10	10	20	20	20	20
Method of calculation of velocity distribution	Smit	—————Present paper—————				Observed value
Assumed inelastic cross sections	(A)*	(A)	(A)	(B)	(C)	—
α/p (ions/cm/mm Hg) at 15° C	0.044	0.036	0.17	0.081	0.31	0.19

*Maier-Leibniz.

Table 2 gives the distribution functions f_0 and f_1 , in units of $m^{3/2}/4\sqrt{2\pi}$, calculated using the observed cross section Q_{in} for the two F/p values.

Table 2

F/p (v/cm/mm Hg)	10		20	
E (ev)	f_0	f_1	f_0	f_1
0	∞	∞	∞	∞
1.12	0.07407	0.01090	0.06582	0.02018
2.24	0.05580	0.005592	0.04922	0.01016
3.36	0.04480	0.003844	0.03945	0.006822
4.48	0.03675	0.002972	0.03246	0.005156
5.6	0.03032	0.002443	0.02699	0.004155
7.02	0.02403	0.001975	0.02173	0.003328
8.44	0.01936	0.001656	0.01784	0.002776
9.86	0.01571	0.001422	0.01482	0.002381
11.28	0.01277	0.001242	0.01239	0.002083
12.70	0.01035	0.001098	0.01037	0.001850
14.12	0.00831	0.000980	0.00867	0.001663
15.54	0.00658	0.000881	0.00721	0.001508
16.96	0.00509	0.000795	0.00594	0.001379
18.38	0.00380	0.000722	0.00482	0.001268
19.80	0.00266	0.000657	0.00383	0.001173
20.58	0.00213	0.000562	0.00334	0.001079
21.36	0.00168	0.000474	0.00290	0.000986
22.14	0.00132	0.000394	0.00251	0.000896
22.92	0.00102	0.000325	0.00216	0.000811
23.7	0.00078	0.000266	0.00185	0.000731
26.33	0.00028	0.000118	0.00105	0.000485
29.63	0.00007	0.000033	0.00048	0.000258
33.86	0.00001	0.000005	0.00016	0.000101
39.5	0.00000	0.000000	0.00004	0.000025
47.40	0.00000	0.000000	0.00000	0.000003

REFERENCES

- BATES, D. R., FUNDAMINSKY, A., LEECH, J. W., and MASSEY, H. S. W., 1950, *Phil. Trans. Roy. Soc. A*, **243**, 93.
 DRUYVESTEYN, M. J., and PENNING, F. M., 1940, *Rev. Mod. Phys.*, **12**, 87.
 DUNLOP, S. H., 1949, *Nature, Lond.*, **164**, 452.
 MAIER-LEIBNIZ, H., 1935, *Z. Phys.*, **95**, 499.
 MORSE, P. M., ALLIS, W. P., and LAMAR, E. S., 1935, *Phys. Rev.*, **48**, 412.
 SMIT, J. A., 1936, *Physica*, **3**, 543.
 SMITH, P. T., 1930, *Phys. Rev.*, **36**, 1293.

The Angular Correlation of the Protons and γ -Radiation from the Reaction ${}^6\text{Li}(\text{d}, \text{p}){}^7\text{Li}^*\gamma{}^7\text{Li}$

By A. J. SALMON AND E. K. INALL*

Research Laboratory, Associated Electrical Industries Ltd., Aldermaston, Berks.

Communicated by D. R. Chick; MS. received 7th January 1952 and in final form 5th November 1952

Abstract. In order to provide information on the first excited state of ${}^7\text{Li}$ the angular correlation between the protons and the γ -radiation from the reaction ${}^6\text{Li}(\text{d}, \text{p}){}^7\text{Li}^*\gamma{}^7\text{Li}$ has been studied. An isotropic angular correlation was observed. The angular correlations, predicted theoretically, for the most likely transitions in this reaction have been determined. It is shown that an isotropic angular correlation indicates that, very probably, $J = \frac{1}{2}$ for this state.

§ 1. INTRODUCTION

FALKOFF and Uhlenbeck (1950), and others (Spiers 1950), have shown that when two radiations are emitted in successive nuclear transitions there is an angular correlation between their directions of emission which depends only on the angular momentum quantum numbers involved in the transitions. In certain cases the observation of an angular correlation has been a powerful method of identifying the quantum states involved in a reaction (Barnes, French and Devons 1950, Thorion 1951). Recently the total angular momentum of the first excited state in ${}^7\text{Li}$ has been widely discussed, the splitting ratio of the reaction ${}^{10}\text{B}(\text{n}, \alpha){}^7\text{Li}$ which favours the first excited state (Wilson 1941) suggested that $J = 5/2$ (Hanna and Inglis 1949), but the isotropic angular correlation between the alpha-particles and the γ -rays from the reaction ${}^{10}\text{B}(\text{n}, \alpha){}^7\text{Li}^*\gamma{}^7\text{Li}$ (Rose and Wilson 1950) strongly favours the assignment of $J = \frac{1}{2}$. In order to provide further evidence on the total angular momentum of this state the angular correlation between the protons and the γ -radiation from the reaction ${}^6\text{Li}(\text{d}, \text{p}){}^7\text{Li}^*\gamma{}^7\text{Li}$ has been studied.

§ 2. EXPERIMENTAL METHOD

A target of separated ${}^6\text{Li}$, supplied by the Atomic Energy Research Establishment, was bombarded with 410 kev deuterons. The target thickness was about $55 \mu\text{g cm}^{-2}$, deposited on a 0.005 inch silver foil supported by water-cooled tubes. The plane of the target was inclined to the direction of the incident deuterons to give a greater effective target thickness. A liquid nitrogen oil-trap was mounted between the target chamber and the main accelerator tube; the pressure in the tube was kept below 10^{-5} mm Hg. A thermocouple was used to measure the target temperature, and the flow of cooling water adjusted to maintain a target temperature of 150°C to 200°C .

* Now at the Department of Physics, Australian National University, Canberra, Australia.

Both detectors were scintillation counters, using E.M.I. 5311 photomultipliers. An anthracene crystal, with a 5000 Å thick aluminium reflector, was the phosphor in the proton detector. The γ -ray detector phosphor was a NaI (Tl) crystal, 1 cm thick, contained in paraffin oil. The angular resolution required ($\pm 5^\circ$) limited the absolute detection efficiency of each counter to within about 0.1%.

The proton counter detected the protons from the reaction to the ground state of ${}^7\text{Li}$, as well as the shorter range protons to the first excited state. The γ -ray counter detected the γ -rays from the reaction ${}^6\text{Li}(d, n){}^7\text{Be}^* \gamma {}^7\text{Be}$, these were almost of the same energy as the γ -rays from ${}^7\text{Li}^*$; it also detected some of the neutrons produced in the ${}^6\text{Li}(d, n)$ reactions. These two conditions of low absolute efficiency and many background counts meant that, even with a fast coincidence circuit, counting had to be continued at one angle for more than two hours to obtain a statistical accuracy of $\pm 2.5\%$.

Because of fluctuations in the counting rate due to changes in beam intensity, wandering of the beam across its defining slits, and changes in target thickness, the random coincidence count could not be estimated directly and was measured by using a coincidence unit with a delay of 95×10^{-9} sec, which was greater than the resolving time inserted in one input (Littauer 1950 a). True coincidences were therefore not recorded by this unit, whereas random coincidences, say R_1 , were recorded. Another coincidence unit, without a delay, recorded both true and random coincidences, say $T + R_2$. Now $R_2/R_1 = \tau_2/\tau_1$, where τ_1 and τ_2 are the resolving times of the first and second units respectively. Thus, with τ_2/τ_1 known, R_2 could be calculated and hence, by subtraction, the number of true coincidences recorded could be found. The standard error $\sigma(T)$ of each true coincidence count thus obtained was calculated from the equation

$$[\sigma(T)]^2 = [\sigma(T + R_2)]^2 + [\sigma(R_1 \tau_2/\tau_1)]^2,$$

where $\sigma(T + R_2)$ is the standard error of the count $T + R_2$ and is equal to $(T + R_2)^{1/2}$. A check was kept on the ratio of the resolving times of the two units: this ratio was known to $\pm 1.5\%$ and was constant, to this accuracy, throughout the observations.

The individual γ -rays and protons were counted at each angle, as well as the coincident counts in each fast coincidence unit which were similar in design. The photomultipliers were operated at 2400 v to ensure rapidly rising pulses; these pulses were shaped, at the inputs of the coincidence units, so that their duration was about 19×10^{-9} sec for the γ -ray pulses and about 7×10^{-9} sec for the proton pulses. The resolving time of the coincidence units was about 15×10^{-9} sec, this was determined by arranging each counter to detect a separate source and measuring the individual counts and random coincidence counts. The resolving time and operation of a unit were checked by observation of the p- γ coincidence rate by inserting additional known delays in each input. The distribution of counts versus delay time showed a peak due to true coincidences, at zero delay time for the unit recording both true and random coincidences, whereas the other unit, normally recording random coincidences only, showed a peak when an additional delay of 95×10^{-9} sec at Z, fig. 1, cancelled the fixed delay previously mentioned. This indicated that during the experiment this unit was recording only random coincidences. The width of a peak was equal to the combined resolving times of both inputs of that particular coincidence unit.

The peak in each of the two distributions was shown to be due to true coincidence events by placing an aluminium foil before the proton counter so that the

short-range, but not the long-range, protons were absorbed. The counting rates of both coincidence units were thereby reduced to a value that did not vary with changes in delay time.

Two fast coincidence unit designs were used. The first was a modified version of the circuit described by Garwin (1950); this operated satisfactorily for some time but eventually one of the units became unstable and the circuit was discarded. One series of observations was made with this design. The second design employed CG1C diode valves only and operated satisfactorily throughout the rest of the experiment.

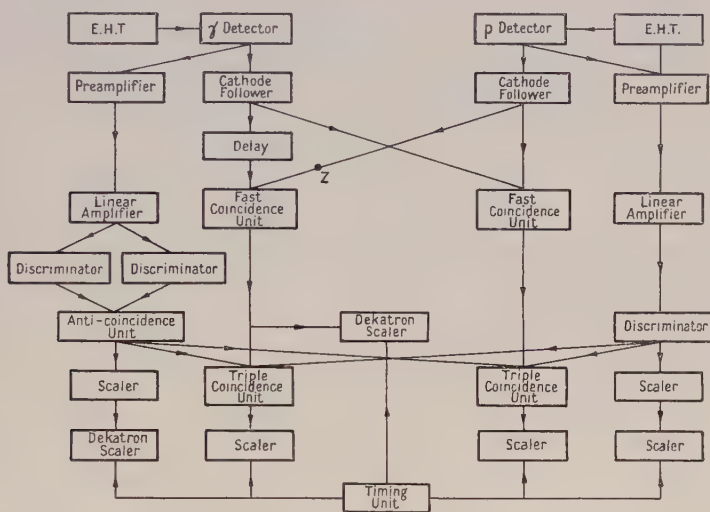


Fig. 1. Block diagram of complete recording apparatus.

In the first series of observations two further triple coincidence units were used (see fig. 1) each detecting coincidences between the output of one fast coincidence unit and the two single channels. The bias in each of the single pulse channels was set so that the only counts recorded were those capable of operating the fast coincidence units. These triple coincidence units were not used in the second series of observations and variations in the sensitivity of the coincidence units during an observation could not be controlled. The greater dispersion of the second series of observations is probably due to such variations in sensitivity.

The proton counter was fixed at 116° to the incident deuterons, and the γ -ray counter was rotated about the target in the plane of the deuteron beam and the proton counter. Aluminium foil was placed in front of the proton counter to absorb all but the protons from the ${}^6\text{Li}(d, p)$ reactions. With a beam current of $20\mu\text{A}$ the true coincidence rate was about equal to the random coincidence rate, each being approximately one per second. The individual counting rates were approximately 5000 protons per second and 12000 γ -rays per second. At the bombarding energy of 410 keV the percentage of long-range protons from the reaction was 75%. This estimate was made from the absorption curves taken during the experiment and is in good agreement with previous results (Dunbar and Hirst 1951).

§ 3. RESULTS

The number of $p\text{-}\gamma$ coincidences per 4×10^7 proton counts was determined at different angles in the range $5^\circ \leq \theta_2 \leq 95^\circ$, where θ_2 is the angle between the γ -detector and the incident beam. The mean number of true coincidences in this angular range was 8700; in all about 10^5 true coincidences were detected. At a deuteron energy of 410 kev the velocity of the centre of mass is so small that the conversion from laboratory to centre-of-mass coordinates introduces a negligible correction. The results are shown in fig. 2. Measurements were made with the γ -detector on both sides of the beam and for the same values of θ_2 the numbers of

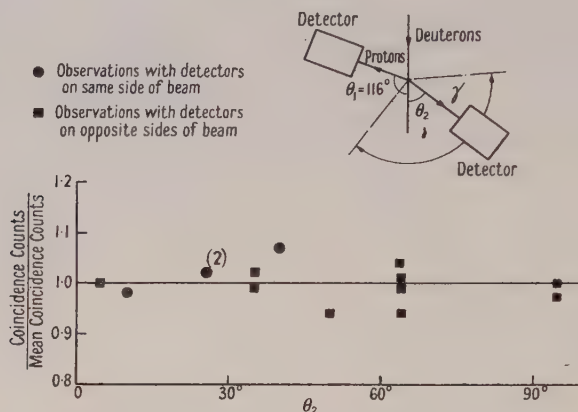


Fig. 2. Plot of observations showing no significant variation of the coincidence rate with change in angle θ_2 .

true coincidences were equal thus providing a check that scattering of the γ -rays was negligible. The accuracy of each point is limited to a standard deviation of about 2.5% by the number of counts recorded. There is also a systematic error of $\pm 1.5\%$ in the ratio of the resolving times of the delayed and undelayed coincident circuits; this however produces only a second order effect on the plotted ratio. The variance of the two sets of observations obtained with the different recording circuits was consistent with the hypothesis that they belong to the same normal population. Both sets were therefore treated as one population and a function of the form $1 + A \cos^2 \theta$ was fitted. The value of $|A|$ was less than 0.01. The standard deviation of the observations was 2.8% which was consistent, at the 5% level according to Snedecor's F test, with the hypothesis that the dispersion was only due to the random nature of the coincident counts which limited the statistical accuracy to 2.5%. From these results it was concluded that the angular correlation is isotropic.

§ 4. PREDICTION OF ANGULAR CORRELATIONS

The radiations emitted in this reaction are a proton and then a γ -ray; the results given below are for this particular case, when one particle with spin and then a γ -ray are successively emitted. If the reaction is produced by particles with zero orbital angular momentum then the magnetic sub-states of the compound nucleus are equally populated and the correlation is of the form derived by Spiers. Assuming that the transitions are between three states with total angular momentum and magnetic quantum numbers $(J_0 M_0)$, $(J_1 M_1)$, and $(J_2 M_2)$ and a particle is

emitted with spin (s, s'), orbital angular momentum l_1 , and total angular momentum (j_1, m_1), followed by a γ -ray of multipolarity 2^{l_2} we have :

$$W(\theta) = \sum_{M_0 M_1 M_2 s' p = \pm 1} \sum_{p = \pm 1} |(J_1 j_1 M_1 M_0 - M_1 | J_0 M_0) (l_1 s m_1 - s' s' | j_1 m_1) Y_{l_1}^{m_1 - s'}(\theta)|^2 \\ \times |(J_2 l_2 M_2 M_1 - M_2 | J_1 M_1) D_{M_1 - M_2, p}^{l_2}(\theta)|^2, \quad \dots\dots (1)$$

where θ is the polar angle between the two directions of emission, the dihedral angle being zero. The elements of the spatial rotation group $D_{mp}^l(\theta)$ are discussed by Goertzel (1946), who gives expressions for them when $l=1$. $(J_1 j_1 M_1 M_0 - M_1 | J_0 M_0)$ is the transformation coefficient for the addition of the angular momenta $\mathbf{J}_1 + \mathbf{j}_1 = \mathbf{J}_0$ (Condon and Shortley 1935). It has been shown that $W(\theta)$ is a polynomial in $\cos^2 \theta$ and the maximum degree of $\cos^2 \theta$ is not greater than the least of l_1, J_1 , and l_2 . The above assumes that only one value each of j_1 and l_2 is involved in the reaction. If more than one value of j_1 is possible then interference between the different partial waves may occur; similarly if various multipoles are possible with comparable relative intensities interference between them may occur (Ling and Falkoff 1949).

If the reaction is produced by particles with non-zero orbital angular momentum l then the correlation becomes more complicated than expression (1) since there is unequal weighting of the magnetic substates of the compound nucleus and the sum over M_1 becomes coherent. The theory has been discussed by Biedenharn, Arfken and Rose (1951) for the case in which two particles without spin are emitted successively. The correlation is now a function of θ_1 and θ_2 , the polar angles of the first and second radiation respectively with respect to the incident beam. If their expression is extended to the case when the first emitted radiation has spin it becomes

$$W(\theta_1 \theta_2) = \sum_{M_0 M_2 s' p = \pm 1} |A(S)|^2 (l S o M_s | J_0 M_0)^2 \\ \times \left| \sum_{M_1} (J_1 j_1 M_1 M_0 - M_1 | J_0 M_0) (l_1 s m_1 - s' s' | j_1 m_1) Y_{l_1}^{m_1 - s'}(\theta_1) \right. \\ \left. \times (J_2 l_2 M_2 M_1 - M_2 | J_1 M_1) D_{M_1 - M_2, p}^{l_2}(\theta_2) \right|^2, \quad \dots\dots (2)$$

the beam and both emitted radiations being coplanar. S is the 'channel spin' and $A(S)$ is some complex quantity, usually unknown, representing the probability that that particular value of S will be formed. Biedenharn, Arfken and Rose showed that the cross products in the sum over M_1 could be removed by making θ_1 or θ_2 equal to zero or π radians. We could not do this with our experimental arrangement as with θ_1 or θ_2 equal to zero soft x-rays were detected from the top of the accelerator tube which greatly increased the random coincidence counting rate.

The prediction of explicit coefficients in an angular correlation between two particles emitted from a nuclear reaction is possible if certain conditions are fulfilled. These are :

(a) The intensities of the channel spin components should be known, or only one value of channel spin should be operative. The latter condition is fulfilled when the target nucleus has zero intrinsic spin, when the reaction is produced by S-wave particles, or when a chance combination of quantum numbers makes only one value possible.

(b) Each of the emitted particles should have only one possible value of j ; if more than one value is possible then the ratio of their intensities and their phase relationship must be known. Only one value of j is possible if the emitted particle has zero intrinsic spin.

(c) Only one value of orbital angular momentum for the incident particles should be operative. If only one level of the compound nucleus is taking part in the reaction then at low energies all except one partial wave can usually be neglected.

(d) Only one level in the compound nucleus should be effective. If more than one is effective then the above conditions should hold and also the relative intensities and phase relationships of the effects due to the various levels should be known.

If these conditions are fulfilled the coefficients can be calculated using expressions (1) and (2) or extensions of them; otherwise, as is usual, simplifying assumptions have to be made so that the expressions can be used directly, inferences are then made from the results.

§ 5. INTERPRETATION

An isotropic correlation between the emitted radiations has also been observed in a plane containing the beam by Class and Hanna (1952). Newton (1951) has observed an isotropic correlation in the plane perpendicular to the beam. The angular distribution of the protons with respect to the incident beam in this reaction has also been studied; Dunbar and Hirst (1951) have compared the results obtained, which are not self-consistent particularly at low energies. It appears probable, from these results, that at a deuteron energy of 400 kev both S and P deuterons are taking part in the reaction, and in this case two states in ^8Be of opposite parity must be involved. However Whaling and Bonner (1950) find an isotropic angular distribution in which case: S deuterons alone could produce the reaction, or a state in ^8Be with $J=0$ might be involved, or S-wave protons could be emitted.

If $J=\frac{1}{2}$ for the first excited state in ^7Li then whatever other states are involved in the reaction the angular correlation will be isotropic. If $J=5/2$, which is the other possibility, then the angular correlation could be isotropic or anisotropic dependent upon the particular quantum numbers involved. We have calculated for the most probable quantum numbers the angular correlations for S deuterons incident using expression (1), and for P deuterons incident using expression (2). The results are shown in the table with the main quantum numbers given in the form $J_0 j_1 J_1 l_2 J_2$. When two values of j_1 are possible they are shown as (j_1', j_1'') , and they have been assumed to be incoherent and of equal probability. In the reactions produced by P-waves we have assumed $|A(S)|^2$ is constant for all values of S . In all the reactions magnetic dipole γ -radiation is assumed to be emitted as is indicated by the results of Elliot and Bell (1948).

S deuterons incident.

Transition.	0,5/2,5/2,1,3/2	1,3/2,5/2,1,3/2	2($\frac{1}{2}$,3/2),5/2,1,3/2
$W(\theta)$	$1 - 0.5 \cos^2 \theta$	$1 - 0.37 \cos^2 \theta$	$1 + 0.03 \cos^2 \theta$

P deuterons incident.

Transition.	0,5/2,5/2,1,3/2	1(3/2,5/2),5/2,1,3/2	2, $\frac{1}{2}$,5/2,1,3/2
$W(116^\circ, \theta_2)$	$1 + 0.46 \cos^2 \theta_2$	$1 + 0.46 \cos^2 \theta$	Isotropic
Transition.	2(3/2,5/2),5/2,1,3/2	3, $\frac{1}{2}$,5/2,1,3/2	3(3/2,5/2),5/2,1,3/2
$W(116^\circ, \theta_2)$	$1 + 0.01 \cos^2 \theta$	$1 - 0.34 \cos^2 \theta_2$	$1 - 0.20 \cos^2 \theta$

If the angular distribution of the protons with respect to the beam is isotropic then S deuterons alone could produce the reaction and an almost isotropic angular correlation would be observed if the transitions were 2($\frac{1}{2}$,3/2),5/2,1,3/2. If for some reason $j_1=\frac{1}{2}$ only was operative in this scheme then an isotropic angular

correlation would be observed, even though the protons are emitted with $l_1 = 1$. The scheme $2, \frac{1}{2}, 5/2, 1, 3/2$ would also give an isotropic angular correlation and an isotropic angular distribution as the protons are emitted with $l_1 = 0$. If the angular distribution is anisotropic then the reactions produced by P deuterons only all give anisotropic angular correlations with relatively large coefficients, except the transitions $2(3/2, 5/2), 5/2, 1, 3/2$ which has an almost isotropic angular correlation. The correlation in this latter case is also almost isotropic if $\theta_1 = 0$, the experimental arrangement of Class and Hanna, although if either $j = 3/2$ or $j = 5/2$ only is operative the anisotropy would be easily detectable. The angular distribution appears to involve terms in $\cos \theta$, thus both S and P deuterons are probably taking part in the reaction. In this case the angular correlations are unpredictable precisely; but as will be seen from the table, the only simple scheme which will give an almost isotropic correlation involves both S and P deuterons reacting through states in ${}^8\text{Be}$ with $J = 2$. However, in this case the several conditions must be satisfied that the various values of j involved, and the effects of the two levels, are incoherent, and the various values of $A(S)$ are approximately equal; also the emission of the protons with $l = 2$ must be favoured with respect to the most probable value of $l = 0$ allowed by angular momentum considerations. The observed isotropic angular correlation is thus more probably due to the first excited state of ${}^7\text{Li}$ having a total angular momentum J of $\frac{1}{2}$. This is in agreement with the observed isotropic angular correlation of the alpha-particles and γ -radiation from the reaction ${}^{10}\text{B}(n, \alpha) {}^7\text{Li}^* \gamma {}^7\text{Li}$ which strongly suggests that $J = \frac{1}{2}$ (Rose and Wilson 1950), and with the isotropy of the γ -radiations in the reactions ${}^7\text{Li}(p, p') {}^7\text{Li}^*$ (Littauer 1950 b) and ${}^6\text{Li}(d, p) {}^7\text{Li}^*$ (Class and Hanna 1952) which would be unlikely if $J = 5/2$ but certain if $J = \frac{1}{2}$.

ACKNOWLEDGMENTS

The authors are indebted to Dr. T. E. Allibone for permission to publish this paper. They wish to thank Mr. D. Hancock for making some of the apparatus, Miss J. McCann and Miss P. Rush for assistance in computing the angular correlations, and Mr. D. R. Chick for his continued interest in the work.

REFERENCES

- BARNES, C. A., FRENCH, A. P., and DEVONS, S., 1950, *Nature, Lond.*, **166**, 145.
 BIEDENHARN, L. C., ARFKEN, G. B., and ROSE, R., 1951, *Phys. Rev.*, **83**, 586.
 CLASS, C. M., and HANNA, S. S., 1952, *Phys. Rev.*, **87**, 247.
 CONDON, E. U., and SHORTLEY, G. H., 1935, *Theory of Atomic Spectra* (Cambridge: University Press).
 DUNBAR, D. N. F., and HIRST, F., 1951, *Aust. J. Sci. Res. A*, **4**, 278.
 ELLIOT, L. C., and BELL, R. E., 1948, *Phys. Rev.*, **74**, 1869.
 FALKOFF, D. L., and UHLENBECK, G. E., 1950, *Phys. Rev.*, **79**, 323.
 GARWIN, R. L., 1950, *Rev. Sci. Instrum.*, **21**, 569.
 GOERTZEL, G., 1946, *Phys. Rev.*, **70**, 897.
 HANNA, S. S., and INGLIS, D. R., 1949, *Phys. Rev.*, **75**, 1767.
 LING, D. S., and FALKOFF, D. L., 1949, *Phys. Rev.*, **76**, 1639.
 LITTAUER, R. M., 1950 a, *Rev. Sci. Instrum.*, **21**, 750; 1950 b, *Proc. Phys. Soc. A*, **63**, 294.
 NEWTON, J. O., 1951, *Proc. Phys. Soc. A*, **64**, 938.
 ROSE, B., and WILSON, A. R. W., 1950, *Phys. Rev.*, **78**, 68.
 SPIERS, J. A., 1950, *Phys. Rev.*, **80**, 491.
 THORION, J., 1951, *Comptes Rendus*, **233**, 37.
 WHALING, W., and BONNER, T. W., 1950, *Phys. Rev.*, **79**, 258.
 WILSON, R. S., 1941, *Proc. Roy. Soc. A*, **177**, 382.

Photoelectric Absorption in Lithium Vapour

BY J. TUNSTEAD Physics Research Laboratory, University of Reading

Communicated by R. W. Ditchburn; MS. received 4th December 1952

THE continuous absorption of light in lithium vapour for wavelengths in the region near the series limit has been measured using methods previously described (Ditchburn, Tunstead and Yates 1942). The principal difference was the use of a steel absorption tube to withstand the higher temperature required to vaporize the lithium. The atomic and molecular absorptions were separated by plotting the absorption coefficient at each wavelength against the concentration of the vapour and extrapolating to zero concentration, as explained in the paper quoted. The best value for the absorption cross section at the series limit (corresponding to the emission of electrons with zero kinetic energy) is $2.5 \times 10^{-18} \text{ cm}^2$.

Under the conditions of this experiment, accurate photographic photometry is difficult and an uncertainty of $\pm 15\%$ must be assigned to errors in photometry and in temperature measurement. The vapour pressure was calculated from a formula given by Ditchburn and Gilmour (1941) based on a review of the experimental evidence. Ditchburn and Gilmour estimate that the vapour pressure may be in error by $\pm 30\%$. The total error in absorption cross section is thus about $\pm 40\%$ and the value lies between 1.5 and $3.5 \times 10^{-18} \text{ cm}^2$. There is a possibility of a systematic error due to the vapour attacking the steel absorption tube. An error of this type would make the observed value too low. Certain tests indicate that no very large error is due to this cause. The absorption cross section has been calculated by Hargreaves (1929) who obtains the value $3.7 \times 10^{-18} \text{ cm}^2$, which is just above the upper limit of the observed value and considerably above the best value. Recent recalculation (Seaton 1951) of the corresponding quantity for sodium has reduced the theoretical value from 3.1 to $1.0 \times 10^{-19} \text{ cm}^2$, bringing it into agreement with the experimental value for sodium (Ditchburn and Jutsum 1950). A recalculation for lithium appears desirable.

On the short wavelength side of the series limit (from 2300 \AA to 1850 \AA) the absorption is approximately proportional to $\lambda^{3.5}$. This agrees well with the calculations of Trumphy (1928). The maximum on the short wavelength side of the limit predicted by Hargreaves (1929) is not observed.

The exact shape of the absorption curve in the neighbourhood of the series limit has been investigated. There is a fairly steep increase over a range of 5 \AA on the long wavelength side of the limit to a maximum value at 2299.6 \AA . This wavelength agrees with the value calculated from the convergence of the series lines. The absorption cross section for the Li_2 molecule at 2500 \AA is estimated to be of order 5×10^{-16} .

This work was carried out at Trinity College, Dublin, as part of a programme initiated by Professor Ditchburn. I wish to acknowledge receipt of a maintenance grant from the Department of Industry and Commerce, Eire.

REFERENCES

- DITCHBURN, R. W., and GILMOUR, J. C., 1941, *Rev. Mod. Phys.*, **13**, 310.
DITCHBURN, R. W., and JUTSUM, P. J., 1950, *Nature, Lond.*, **165**, 723.
DITCHBURN, R. W., TUNSTEAD, J., and YATES, J. G., 1943, *Proc. Roy. Soc. A*, **181**, 386.
HARGREAVES, J., 1929, *Proc. Camb. Phil. Soc.*, **35**, 75.
SEATON, M. J., 1951, *Proc. Roy. Soc. A*, **208**, 418.
TRUMPHY, B., 1928, *Z. Phys.*, **47**, 804.

LETTERS TO THE EDITOR

Nuclear Spin and Magnetic Moment of Radioactive Cobalt 57

From the hyperfine structure observed in a paramagnetic resonance spectrum, the nuclear spin of ^{57}Co has been determined as $7/2$, and the magnetic moment as 4.6 ± 0.2 nuclear magnetons.

The ^{57}Co , together with some ^{56}Co and ^{54}Mn , was made by the reaction $^{56}\text{Fe}(d, n)^{57}\text{Co}$ using 18 mev deuterons produced in the Birmingham cyclotron. The target consisted of a strip of 'Specpure' iron soldered to a copper cooling-tube; after bombardment the iron was dissolved in concentrated hydrochloric acid, the copper and solder having been waxed to prevent their dissolution. When most of the radioactive material had dissolved, the bulk of the iron was removed by two ether extractions. The aqueous layer was evaporated to a small volume and placed in a narrow band across a strip of Whatman's No. 1 filter paper previously washed with 2N hydrochloric acid.

Separation of the elements present was then effected by using a conventional paper-chromatographic technique (see, for example, Burstall *et al.* 1950). The solvent used was ethyl methyl ketone containing 8% by volume of concentrated hydrochloric acid. After 24 hours the paper was dried and the positions of the ^{54}Mn and $^{56, 57}\text{Co}$ bands were determined by measurement of their radioactivity. The paper containing the radio-cobalt was cut out and washed with dilute hydrochloric acid until free of activity. A little cobalt-free zinc sulphate was then added and the solution was evaporated to dryness and ignited to remove ammonium salts and filter particles. The residue was dissolved in sulphuric acid, evaporated to dryness and dissolved in heavy water containing cobalt-free zinc potassium sulphate. All reagents used were 'Analar' materials which had been twice distilled in an all-glass apparatus.

A single crystal of mass about 30mg of $\text{ZnK}_2(\text{SO}_4)_2 \cdot 6\text{D}_2\text{O}$ containing about 60% of the radioactive cobalt was grown from a solution in 1 cm^3 of heavy water. At 20 K the paramagnetic resonance spectrum showed a set of eight nearly equally spaced lines, whose angular variation of spacing and g -value confirmed that they were due to cobalt. At $1\frac{1}{4}\text{ cm}$ wavelength the signal/noise ratio of these lines displayed on an oscilloscope was about 20 : 1 while at 3 cm wavelength, using a narrow band amplifier, it was 100 : 1. There was no trace of a second contiguous spectrum which might be due to another cobalt isotope. The spacing of the hyperfine structure was the same, as nearly as could be determined, as that due to the stable isotope ^{59}Co , which also shows eight lines, corresponding to a nuclear spin of $7/2$ (Bleaney and Ingram 1951). An accurate comparison was impossible, as the high anisotropy makes it necessary to determine the direction of the external magnetic field relative to the crystal axes to within 1° , and the faces of the active crystal were not recognizable.

At this point three possible explanations of this result seemed possible: (a) the spectrum observed was entirely due to ^{57}Co , which therefore has $I=7/2$, and a magnetic moment close to but not necessarily identical with that of ^{59}Co ; (b) the spectrum was entirely due to ^{59}Co , present as impurity, and the ^{57}Co spectrum was too weak to be seen; (c) ^{59}Co and ^{57}Co were present in comparable quantities, but the two isotopes have the same spin and almost identical magnetic

moments. Two independent measurements of the activity, using scintillation counters to discriminate between the gamma-rays due to ^{57}Co and ^{56}Co , showed that the amount of ^{57}Co in the crystal was at least $0.5\text{ }\mu\text{g}$, and more if there is considerable internal conversion. Comparison of the intensity of the spectrum with that of a crystal estimated to contain $3.0\text{ }\mu\text{g}$ (subsequent chemical analysis gave $2.6\text{ }\mu\text{g}$) suggested that the active crystal contained about $1.5\text{ }\mu\text{g}$ of Co, but variation of the intensity with angle because of the high anisotropy made this comparison rather unreliable. This evidence thus favoured (c) but could not be considered conclusive.

The crystal was regrown from a solution to which $\frac{1}{2}\text{ }\mu\text{g}$ of stable ^{59}Co had been added. Once more only a single spectrum could be observed, and intensity comparison with another crystal again showed that the total cobalt of the active crystal was about $1.5\text{--}2\text{ }\mu\text{g}$. This eliminated (a), and chemical analysis (using nitroso-R salt) of the active crystal then showed that its total cobalt content was $2.4 \pm 0.1\text{ }\mu\text{g}$. Thus the ratio $57:59$ was at least $0.5:1.9$ and (b) could also be eliminated. The intensity of all eight lines was equal within 5% , thus eliminating the possibility of the spin of ^{57}Co being other than $7/2$, though with the same gyromagnetic ratio as ^{59}Co . No trace of broadening could be detected on the outermost lines showing the gyromagnetic ratios must be equal within $\pm 5\%$.

Our thanks are due to the Nuffield Cyclotron team of Birmingham University, who carried out the irradiation, and to Dr. M. A. Grace and Dr. J.R. Prescott, who determined the radioactivity of the crystal.

Clarendon Laboratory,
Oxford.
18th December 1952.

J. M. BAKER.
B. BLEANEY.
K. D. BOWERS.
P. F. D. SHAW.
R. S. TRENAM.

BLEANEY, B., and INGRAM, D. J. E., 1951, *Proc. Roy. Soc. A*, **208**, 143.

BURSTALL, F. H., DAVIES, G. R., LINSTEAD, R. P., and WELLS, R. A., 1950, *J. Chem. Soc.*, 516.

Measurements of the Energy Loss Distribution for Minimum Ionizing Electrons in a Proportional Counter

The energy spent in matter by relativistic charged particles over a length of track short compared with their range is subject to large fluctuations due to delta-rays. These fluctuations impose a serious limitation on the amount of information which can be derived from specific ionization measurements with counters. The fluctuation problem has been treated by Landau (1944) and by Blunck and Leisegang (1950). Measurements of the energy loss distribution for relativistic electrons were made by Rothwell (1951), who found, in argon and krypton, distributions broader than Landau's theory would suggest but narrower than predicted by Blunck and Leisegang. The present experiments

are an extension of Rothwell's to a greater variety of gases and to a wider range of pressures, using the same experimental method.

Minimum ionizing electrons of energy 1.3 mev selected by a β -spectrometer pass through a proportional counter fitted with two thin windows at opposite ends of a diameter. An end window Geiger counter is placed opposite the 'exit' window of the proportional counter. A coincidence between pulses from the proportional and the Geiger counters operates a gating unit which allows the proportional counter pulse to pass to a four-channel pulse analyser. Two cylindrical brass proportional counters, fitted with aluminium windows 1 cm diameter and 0.001 in. thick, were used. The effective depth, i.e. the distance between the windows, was 4.61 cm in one counter and 7.19 cm in the other. Pulse size distributions were measured in the two counters separately over a range of pressures of filling gas. Energy calibrations were made with K x-rays of energies 4.95 kev and 8.05 kev from ^{51}Cr and ^{65}Zn .

It was noticed that a significant variation in the width of the distribution occurred as the pressure of filling gas, and therefore the energy spent, was varied.

(1)	(2)	(3)	(4)	(5)	(6)	(7)
Ne 58.0, CH ₄ 3.2	4.61	2.79	0.86	76.3	72.3	}† 2.11 } 2.26 } 2.42 } 3.18 }
Ne 36.6, CH ₄ 4.0	7.19	2.79	0.83	72.8	68.2	
Ne 63.5, CH ₄ 5.0	4.61	3.26	0.86	70.4	67.0	
Ne 54.2, CH ₄ 4.2	7.19	3.94	0.79	64.4	59.5	
A 30.0, CH ₄ 1.9	4.61	2.39	0.90	89.0	84.7	} 1.07 } 2.13 } 3.52 } 6.9 }
A 36.8, CH ₄ 4.1	7.19	4.99	0.90	67.7	64.5	
A 36.4, CO ₂ 2.7	7.19	5.06	0.90	67.3	63.9	
A 57.5, CO ₂ 2.65	4.61	5.14	0.94	66.5	63.6	
A 63.7, CH ₄ 4.1	7.19	8.64	0.89	58.2	56.4	
A ~150, CH ₄ 7	7.19	17.9	—	50.9	49.6	
Kr 21.9, CH ₄ 1.6	4.61	2.95	0.87	96.0	93.4	} 0.76 } 1.30 } 2.31 } 3.63 }
Kr 37.5, CH ₄ 2.7	4.61	5.61	0.91	84.8	82.4	
Kr 67.0, CH ₄ 3.8	4.61	11.0	0.95	68.3	67.2	
Kr 67.6, CH ₄ 3.8	7.19	16.8	0.88	59.4	58.1	
CH ₄ 36.7, Kr 1.7	4.61	2.34	0.90	62.7	57.6	} — } — }
CH ₄ 32.9						
Ne 33.0, Kr 4.2	4.61	4.10	0.91	62.2	59.2	—

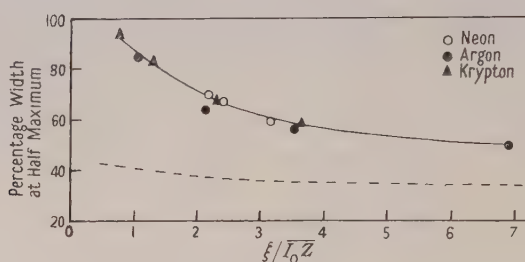
(1) Filling (cm Hg at 0°C); (2) counter depth (cm); (3) Δ_0 (exp) (kev);
(4) Δ_0 (exp)/ Δ_0 (Landau); (5) % width at half height; (6) corrected width (%); (7) $\xi/\overline{I_0 Z}$.

* Mean 64.0. † Mean 70.2.

This was investigated for the gases krypton, argon and neon. The results are given in the table. Columns (3) and (4) give the experimentally determined most probable energy loss Δ_0 (exp) and the ratio of the experimental to the theoretical (Landau) values of this quantity. In column (6) the experimental width of the energy loss distribution, expressed as a percentage of the most probable energy loss, has been corrected for the line width of the proportional counter corresponding to a monokinetic radiation of energy Δ_0 (exp).

The widths for each of the gases when plotted against Δ_0 (exp) lie on separate smooth curves. However, the points for the three gases neon, argon and krypton

can be made to lie on the same curve by plotting the widths against a function of I_0Z , the mean ionization potential of electrons in an atom of atomic number Z , and a parameter ξ . This last quantity is an energy such that, on the average, one delta ray of energy greater than ξ is produced in the length of track examined. Delta rays of energy approximately equal to ξ are mostly responsible for the spread in the distribution (Cranshaw 1952). The value of ξ in electron volts is given by $\{1.54 \times 10^5 / (v/c)^2\} \{\sum \mu_i Z_i / A_i\}$ where μ_i is the mass per cm² of material of atomic number Z_i and atomic weight A_i . Since I_0Z averaged over the components of the mixture is the mean binding energy of the electrons, the ratio ξ / I_0Z is some measure of the extent to which electron binding can be neglected. Landau's treatment, which neglects electron binding, requires $\xi / I_0Z \gg 1$. When the widths are plotted against this ratio (with $I_0 = 13.5$ ev) all the points lie on the same curve as shown in the figure.



The broken curve in the figure gives Landau's values of the widths for argon, and it seems possible that for larger values of ξ / I_0Z than are attained in the present experiments Landau's value may be reached. The points corresponding to methane and the methane plus neon mixture given in the table have not been plotted since the computed mean value of I_0Z for these light gases is extremely sensitive to the small amount of krypton which was added to facilitate calibration.

The ratio $\Delta_0(\text{exp}) / \Delta_0(\text{Landau})$ did not show any systematic variation with ξ / I_0Z . The mean value for all the mixtures was 0.89.

Thanks are due to Dr. P. E. Cavanagh and Mr. J. F. Turner for the use of their β -spectrometer and to Mr. E. F. Bradley for his help with the measurements. Acknowledgment is made to the Director, Atomic Energy Research Establishment, for permission to publish.

Atomic Energy Research Establishment,
Harwell, Didcot, Berks.
30th December, 1952.

D. WEST.

BLUNCK, O., and LEISEGANG, S., 1950, *Z. Phys.*, **128**, 500.

CRANSHAW, T. E., 1952, *Progress in Nuclear Physics*, Vol. II (London: Pergamon Press).

LANDAU, L., 1944, *J. Phys. U.S.S.R.*, **8**, 201.

ROTHWELL, P., 1951, *Proc. Phys. Soc. B*, **64**, 911.

On the Effect of a Strong Electrostatic Field on Scattering

The Raman spectrum, fig. 1 (a), of CCl_4 excited by the mercury line $\lambda 4358 \text{ \AA}$ has been recorded in juxtaposition with the spectrum, fig. 1 (b), obtained when the Raman tube was placed between two cylindrical plates charged to a potential difference of 750 volts. The intensity of the mercury arc, the temperatures of the mercury arc and of the specimen of CCl_4 , and the length of exposure were the same in both cases.

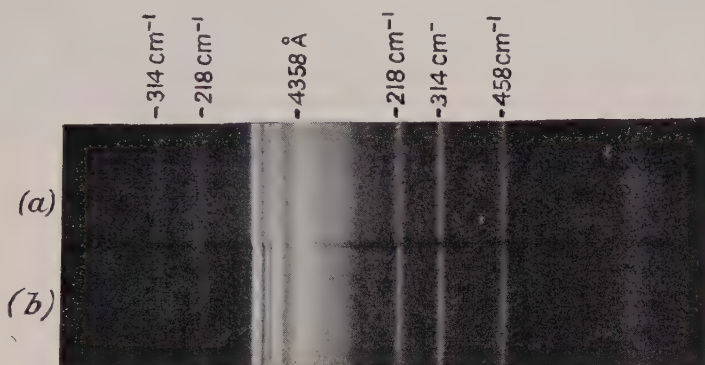


Fig. 1.

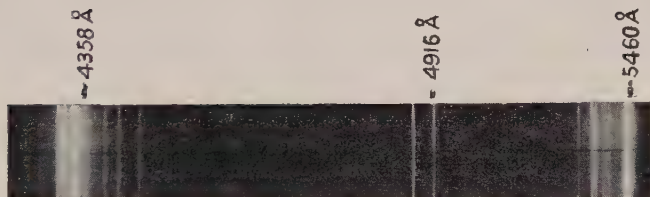


Fig. 2.

It is found that the Rayleigh lines suffer a slight displacement towards the red end of the spectrum on account of the field. The wings accompanying the strong Rayleigh lines 4358 and 5460 \AA are also less broad. At least one Raman line, that representing the fundamental frequency $\nu_2 (=218 \text{ cm}^{-1})$, has also been displaced towards the red end.

Further, the application of the field tends to lower the intensity of the unmodified Hg lines. This change in intensity is very noticeable in case of the group of lines lying between 4916 and 5460 \AA (fig. 2).

The simplest interpretation would be that an electric field produces an ordered orientation of the liquid molecules which modifies the conditions under which scattering normally takes place. It may be pointed out that changes in the frequency and intensity of Raman lines are often noticed when a substance passes from the liquid to the more orderly solid (crystalline) state.

Department of Physics,
Christ Church College, Kanpur.
25th November 1952.

L. SINGH.

The D-³H and D-³He Reactions below 45 kev

The disintegrations which result from bombarding the 'mirror' nuclei ³H and ³He with low energy deuterons have been investigated using thin gas targets and detecting the α -particles in nuclear photographic emulsions. The experimental procedure was based on that used for the D-D reaction by Moffatt, Roaf and Sanders (1952).

The number of ³H atoms in the target was determined by counting directly the β -particles produced by the decay of the tritium in each sample of the target gas.

The concentration of ³He was obtained from mass spectrometer measurements.

The angular distribution in the centre of mass system of the α -particles from D-³H was isotropic within the errors of measurement. Owing to the low yield the D-³He was measured at one angle only and its cross section was calculated assuming an isotropic angular distribution.

The cross sections of both reactions are given in the table.

	D- ³ H			D- ³ He		
Deuteron energy (kev)	19.45	28.97	43.73	28.97	33.68	43.73
Cross section (barns)	0.0733	0.292	0.868	1.76×10^{-5}	4.7×10^{-5}	2.3×10^{-4}

The slope of the Gamow plot, of $\log_{10}(\sigma E)$ against $E^{-1/2}$ for the D-³He was -36.8 and for the D-³H was -18.8 , where the cross section σ is measured in barns and the deuteron energy E is in kev. Hence the difference in yield can be accounted for by the double nuclear charge on the ³He nucleus. The value of the 'Gamow' slope of the D-³H reaction is markedly different from the recently published results of Conner, Bonner and Smith (1952) over this energy range.

The Clarendon Laboratory,
Oxford.
15th December 1952.

R. G. JARVIS.
D. ROAF.

MOFFATT, J., ROAF, D., and SANDERS, J. H., 1952, *Proc. Roy. Soc. A*, **212**, 220.
CONNER, J. P., BONNER, T. W., and SMITH, J. R., 1952, *Phys. Rev.*, **88**, 468.

REVIEWS OF BOOKS

Introduction to Concepts and Theories in Physical Science, by GERALD HOLTON.
Pp. xviii + 650. (Cambridge, Mass.: Addison Wesley Press, 1952.) \$6.50.

The standard university courses in physics as a main or an ancillary subject at British universities have frequently been criticized on the grounds that they lay too much emphasis on imparting a vast amount of factual material to the students instead of concentrating on the thorough teaching of fundamentals. Only at few places does the curriculum include special introductory courses on the fundamental aspects and their historic development, and on scientific method and philosophy of science. The need for such courses has been generally recognized in the U.S.A., and the author, who has great experience in teaching physics and general education

in the physical sciences, has written this book as a guide to teachers and students of courses of this type. To quote from his preface: "At the end of such a course the student will be in a position to know the principal laws and the evolution of key conceptual schemes, but it is then also hoped that he, as a responsible citizen, will understand the criteria of validity in scientific thought, the conditions that aid the fruitful growth of science—and perhaps even the exhilaration that binds his instructor to the scientific profession."

The book is most likely to achieve this aim, as it is written with great skill, care and originality. No previous knowledge of the subject and only the most elementary knowledge of mathematics is required. It contains many interesting problems and at the end of each chapter a carefully selected list of books for further reading. The main emphasis is laid on the development of the fundamental ideas of the dynamics of particles including the laws of planetary motion, and the origins of the atomic theory of physics and chemistry, terminating in the concept of the nuclear atom and the fundamentals of quantum theory. A whole section is devoted to a discourse on structure and method in physical science.

It is perhaps regrettable that the continuum aspect of physical phenomena has been pushed into the background, so much so that the classical physics of electricity and light is confined to the first two chapters of the section on quantum theory and the nuclear atom. After all, the discontinuum and the continuum aspects have vied with each other throughout the whole history of physics, and the current theories are made up of elements from both these concepts in about equal parts. It is also doubtful whether illustrations of the classical conservation principles drawn from atomic and nuclear physics at a stage where the reader has not yet been acquainted with the basic facts of atomic physics are serving a useful purpose unless it is supposed that the students attending the course know a great deal about electrons, protons and nuclear reactions from popular magazines, but practically nothing about Newton's laws. The very casual introduction of the concept of probability and its role in the kinetic theory is also in sharp contrast to the great thoroughness with which the classical concepts of dynamics are discussed.

Notwithstanding these shortcomings the book can be warmly recommended, and it is to be hoped that introductory courses on similar lines will soon be generally available to students in this country.

R. FURTH.

Séries de Fourier régularité, séries divergentes et formulation expérimentale, by PIERRE VERNOTTE. Pp. xvi+105. (Paris: Publications Scientifiques et Techniques du Ministère de l'Air, 1952.) 800 fr.

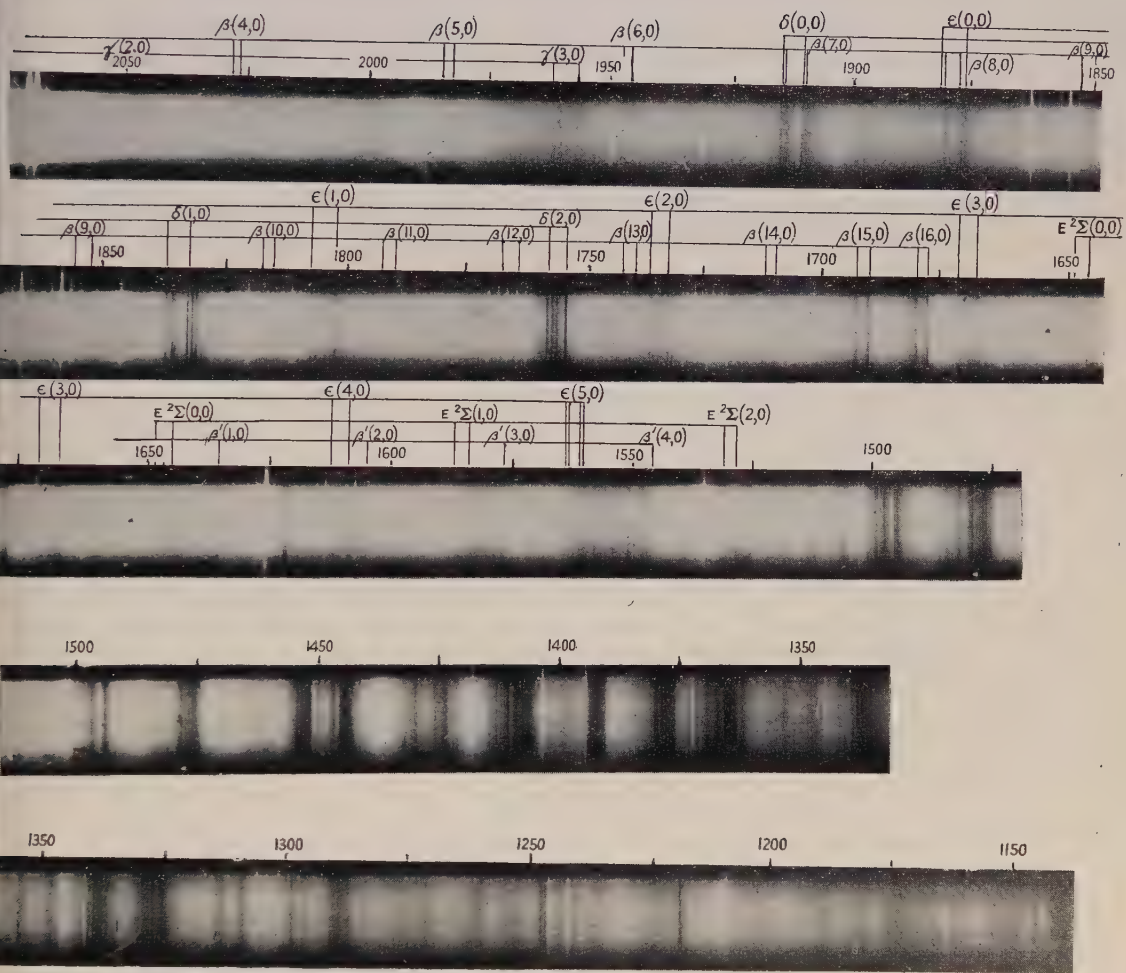
Electrolyse, Report of a conference organized by the Centre National de la Recherche Scientifique. Pp. 147. (Paris: Centre National de la Recherche Scientifique, 1952.) 1,500 fr.

La mécanique rationnelle dans un espace à quatre dimensions et ses applications, by J. LOISEAU. Pp. iii+312. (Paris: Publications Scientifiques et Techniques du Ministère de l'Air (No. 270), 1952.) 2500 fr.

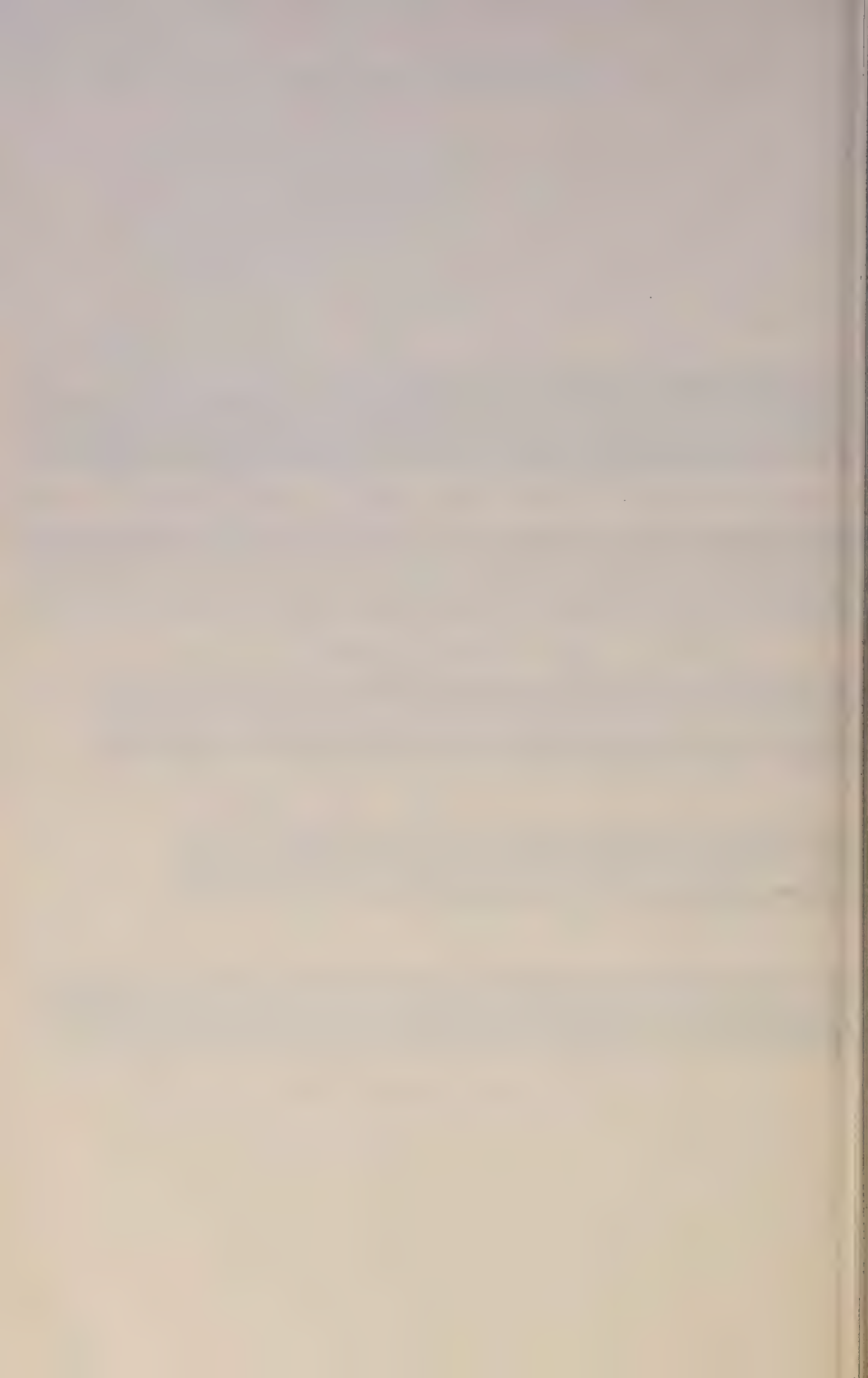
Constantes thermodynamiques des gaz aux températures élevées, by M. G. RIBAUD. Pp. viii+169. (Paris: Publications Scientifiques et Techniques du Ministère de l'Air (No. 266), 1952.) 1500 fr.

CONTENTS OF SECTION B

	PAGE
Mr. L. GRUNBERG. The Formation of Hydrogen Peroxide on Fresh Metal Surfaces	153
Dr. B. V. ROLLIN and Mr. E. L. SIMMONS. Long Wavelength Infra Red Photo-conductivity of Silicon at Low Temperatures	162
Dr. K. S. W. CHAMPION. The Energy Balance Equation for the Positive Columns of High Pressure Arcs	169
Dr. V. I. LITTLE. A Standard Wave Method for Measuring Electromagnetic Absorption in Polar Liquids at Frequencies of the order 3×10^9 c/s	175
Dr. V. I. LITTLE. An Analogue Computer employing the Principle of the Kelvin Bridge	185
Dr. L. ESSEN. The Refractive Indices of Water Vapour, Air, Oxygen, Nitrogen, Hydrogen, Deuterium and Helium	189
Dr. W. PAUL and Prof. R. V. JONES. Absorption Spectra of Lead Sulphide at Different Temperatures	194
Dr. H. CRAIG and Dr. C. F. DIETRICH. Development of a New Method for the Absolute Determination of β -Ray Energies	201
Dr. C. A. HOGARTH. Transistor Action and Related Phenomena in Lead Sulphide Specimens from Various Sources	216
Dr. R. J. WAKELIN and Dr. E. L. YATES. A Study of the Order-Disorder Transformation in Iron-Nickel Alloys in the Region FeNi_3	221
Mr. R. G. WYLIE. The Freezing of Supercooled Water in Glass	241
Letters to the Editor :	
Dr. G. O. JONES and Mr. F. D. STACEY. The Saturation Magnetization of Nickel at High Pressure	255
Dr. H. J. ARNIKAR. The 'Corona Pressure' and Negative Joshi Effect	256
Dr. K. E. SPELLS. Sensitive Bubble Jets	258
Dr. B. V. ROLLIN and Mr. I. M. TEMPLETON. Noise in Semiconductors at Very Low Frequencies	259
Reviews of Books	261
Contents of Section A	264



The ultra-violet spectrum of nitric oxide.



6th Rutherford Lecture

The Atomic Nucleus and Its Constituents

BY R. E. PEIERLS

Department of Mathematical Physics, University of Birmingham

Delivered on 3rd October 1952; MS. received 2nd January 1953

Mr. President, Ladies and Gentlemen,

May I begin by saying how greatly I appreciate being asked to deliver this lecture. There is no name in physics with which it would give greater pleasure to be associated than that of Rutherford. Earlier Rutherford lecturers gave personal reminiscences; while I had the great privilege to spend some years in Cambridge under Rutherford, I did not know him well enough to add to the picture that has there been painted, and I know it is not your wish that I should attempt to do so.

I want to take as my theme tonight our present knowledge of the nucleus, and to show what has been built on the foundations which were laid by Rutherford's work. It may appear perhaps incongruous that the first lecture of this kind should be given by a theoretician, because it has often been said that Rutherford was not interested in theoretical speculations. However, it is evident from his work that he was well aware of the ultimate aim of nuclear studies, which is to extend our knowledge of the basic laws of nature which must be given quantitative form in mathematical terms. His interpretation of the experiment on alpha-ray scattering was a classical example of theoretical reasoning at its best. What he had no patience for was abstruse and complicated speculation, and I shall try tonight to avoid unnecessary complication, and to express simple concepts in simple language. This is an aim that I believe Rutherford would have approved of; to what extent I shall succeed remains to be seen.

The past fifteen years have seen a change of emphasis from what Rutherford liked to call the 'New Chemistry', i.e. the discovery of new nuclear species and their transformations into each other, to the detailed study of the energy levels and other properties of each nucleus, a field which might be called nuclear spectroscopy, or nuclear dynamics.

The difficulties that have to be overcome in this field are very different from those that were encountered in the study of atomic structure. In the atom there was never any serious doubt that the forces between its constituents were electric forces and essentially given by Coulomb's law (with various equally well-known refinements) but the general laws of dynamics and the concepts of position and velocity of a particle, which had served so well to formulate all dynamical problems on larger scale, were found to break down on the atomic scale. One had to develop new dynamical concepts, now embodied in quantum mechanics, before a consistent description of atomic phenomena became possible.

It seems likely that the same dynamical principles are still adequate for a description of the nucleus. At any rate no evidence has so far appeared of their failure, and in all those cases where unique and rigorous predictions could be made on the basis of the general laws of quantum mechanics, such as the existence and properties of angular momentum and other symmetries, they have been borne out by observation. One must evidently keep an open mind on this point until the description of the nucleus is more nearly complete, but for the present we are proceeding on the assumption that the general principles of quantum theory are applicable.

But we cannot use these principles without knowing the nature of the forces between the different parts of a nucleus, and our information about these interactions is still very restricted. Much has been learnt, but many questions still remain open, and I shall try to sketch the features of which we are certain, and the doubts that remain.

Nuclear forces must be of a very different kind from electromagnetic forces. For one thing they are appreciable only for short distances, of the order of a few times 10^{-13} cm. This follows from the fact that the scattering of alpha-particles in Rutherford's original experiment agrees so well with that expected for the electric field of a point charge. More accurate experiments do show deviations, but these occur for fast particles and large deflections, when one is therefore dealing with very close collisions. At very close approach the nuclear forces must be very much stronger than the electric forces. A nucleus is about 10^4 times smaller than an atom, and electric potentials should therefore be 10^4 times larger than typical atomic potentials, say a few times 10^5 volts. On the other hand, a typical binding energy of a particle to a nucleus is of the order of six million electron volts (mev). Hence electric forces can be neglected for many purposes.

How can one obtain information about the law of force? There are essentially two methods available: empirically from observations on nuclear collisions and other data, and theoretically from some simple general principle. Both approaches are being used; both have proved constructive to some extent, but neither is as yet adequate.

Consider first the empirical method. The most important evidence here comes from processes involving only two nucleons (we use the term 'nucleon' to cover both neutrons and protons) since such a two-body process can be described theoretically without much difficulty, so that the relation between the observations and the law of force is straightforward. Further evidence comes from the light nuclei, for which an approximate analysis is possible, and from qualitative and general regularities amongst the nuclei in general.

To analyse the evidence one proceeds by comparing it with some simple hypothesis about the law of force, and where this leads to contradictions one modifies the model so as to make it agree better with the data. It is clear that by this method we go from a simple picture to one that is more and more complicated as more and more evidence is available. We must therefore begin by making a number of simplifying assumptions none of which we shall be able to retain absolutely. However, most of them still appear to be true to a fairly good approximation, so that the initial approach was not far wrong.

It is plausible to start from the assumption that the forces are two-body forces, i.e. that the interaction between any two nucleons in a given state of motion is not influenced by the presence of others. There is so far no evidence

against this assumption, though I shall return to this question later. In any case the point does not arise if we consider processes in which only two particles are involved.

Next we assume that the forces are 'static', i.e. depend only on the positions, and not on the velocities, of the interacting nucleons. Again, there is no evidence against this (though even if the hypothesis were not true, this would not necessarily show up in a very obvious manner).

It is also natural to think of a central force, i.e. a potential energy which depends only on the distance between the particles. This will at once be seen to have only limited validity.

We know that the only stable two-nucleon system, the deuteron, is always found with one unit of angular momentum, and that this is not due to a revolution of the two particles about each other, but to their spins (each of half a unit) being parallel. In quantum theory two such spins may either be parallel (triplet state) or opposite (singlet state). Since no bound singlet state exists it follows that the forces are spin-dependent, and more strongly attractive in the triplet than in the singlet state.

In each state we then require a function which expresses the potential energy as a function of the distance, and if this is of short range, i.e. if the force vanishes for distances greater than a few times 10^{-13} cm, then the results of the mathematical description can be summed up very conveniently.

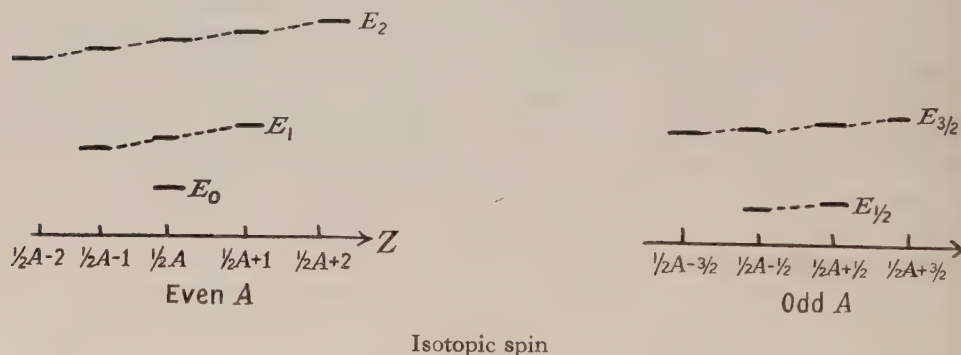
For low-energy problems (energies below, say, 30 meV) the results depend only on two parameters, the 'scattering length' and the 'effective range'. The first is closely related to the scattering cross section for very slow particles. If the interaction potential is of average strength b up to distances of the order a and vanishes at greater distance, then the scattering length depends on the combination ba^2 . The effective range can be obtained from the variation of the scattering cross section with energy and is proportional to the actual range a of the forces.

The energy of the bound state of the deuteron, the cross section for the scattering of neutrons by protons as a function of energy and the cross section for radiative capture of neutrons by protons, can be quite accurately represented for energies below about 30 MeV in terms of four constants, viz. the scattering lengths and the effective ranges for the singlet and triplet interactions. This agreement gives us some confidence in the analysis, but it also shows that those constants are all we can expect to get from this evidence, and that the detailed functional form of the interaction potential is as yet undetermined.

Turning now to the proton-proton interaction, we must remember that we are here dealing with a system of identical particles to which Pauli's exclusion principle applies. If such particles have the same spin direction (triplet state) they must be in different states of motion, and this can be shown to mean that they cannot approach more closely than about their relative de Broglie wavelength. At low energy, when this wavelength exceeds the range of the forces, the collisions in the triplet state are then negligible and we are concerned only with the singlet state. From experiments on the scattering of protons by protons, one can then again fit the interaction length and effective range for this case (the fact that besides nuclear forces we have also electric forces can easily be allowed for) and one finds that to quite a good accuracy they are the same as for the singlet state of the neutron-proton system. One is therefore tempted to postulate that this

is a general symmetry principle, i.e. that the nuclear forces between two protons and between a neutron and a proton are always the same in corresponding states. This is usually stated as the principle of 'charge independence'. It is coupled with another kind of symmetry which says that the nuclear forces do not change if all neutrons are replaced by protons and vice versa. This is usually referred to as 'charge symmetry'. (There is no particular logic in these names.)

The charge symmetry is demonstrated by the properties of 'mirror nuclei', i.e. pairs of nuclei which differ by interchanging the number of neutrons and protons. The simplest cases are a nucleus of charge Z and mass number $A=2Z+1$, containing Z protons and $Z+1$ neutrons, and the adjacent one of charge $Z+1$ and the same mass number, which contains Z neutrons and $Z+1$ protons. If all interactions were strictly charge symmetric, such mirror nuclei should have strictly the same energy levels. In fact, we know that there are weak electric forces present, which violate this symmetry, and so we would expect slight differences, actually in the sense that the energy levels of the nucleus with the greater charge should lie higher, because of the greater electrostatic energy. This is just what is observed, and the states of such mirror pairs have been studied in great detail; one finds that there is a very close correspondence not merely between the positions, but all other properties of the states, such as spins, selection rules and the like.



The effect of charge independence in larger nuclei is not quite as easily described. It means that the interaction remains the same if any one nucleon is changed from a neutron into a proton, thus changing, in general, the number of like and of unlike pairs, provided that the resulting state of motion is not one which violates the exclusion principle. Of all nuclei of mass number A the one with charge $\frac{1}{2}A$, or, if A is odd, the two with charges $\frac{1}{2}(A \pm 1)$ have the least number of like particles of either kind, and are thus least restricted by the exclusion principle. We therefore expect the pattern of the levels of isobars for relatively light elements to look as in the figure. The nucleus with $Z = \frac{1}{2}A$ has levels (like that marked E_0) which have no counterpart in the other isobars. Any level in the isobar $Z = \frac{1}{2}A + 1$ has a counterpart in $\frac{1}{2}A - 1$ (charge symmetry) and in $\frac{1}{2}A$ (charge independence). Such a level may not occur in $\frac{1}{2}A + 2$, as in the case marked E_1 , but any level of $\frac{1}{2}A + 2$ must occur in the four others. Again the positions of the levels will not be quite identical but because of electrostatic forces they will rise towards higher Z . The second part of the figure shows

the same situation for odd A . These patterns are reminiscent of the number of components in the Zeeman effect of an atomic level in a magnetic field. The place of $Z - \frac{1}{2}A$ is then taken by the magnetic quantum number m , and the number of components is $2j+1$, where j is the total angular momentum. For this reason one has introduced a quantity known as 'isotopic spin' T , and each state then occurs in $2T+1$ adjacent isobars. This simple picture is applicable only in very light nuclei, since for heavier ones the electric effects become large enough to confuse the patterns. It is clear that the resemblance of this isotopic spin with a real spin is only very formal and superficial, but it is nevertheless useful in the discussion of such groups of levels, since it often reduces an apparently complicated problem to a familiar statement about composition of spins, or selection rules.

If there were no electrostatic forces, the isotopic spin would, in nuclear reactions and transitions, obey selection rules just like the angular momentum rules. A recent paper by Radicati (1953) has shown that in many cases the effect of the electric forces on these selection rules is quite weak, so that a study of such forbidden transitions would give a fairly sensitive test of the charge independence of the nuclear forces.

It is usually assumed, by way of further simplification, that the forces are attractive at all distances. This raises at once the problem of the so-called 'saturation'. With purely attractive forces one would expect the nucleus to collapse until every nucleon is within the range of force of every other. Hence the density should increase with increasing number of particles, and so should the binding energy per nucleon. In fact, both the binding energy per nucleon and the density are roughly constant, and this is referred to as saturation.

There are three ways of explaining this:

(a) The forces have an 'exchange' character. This means that the elementary process responsible for the force consists of the two particles changing place (either taking their spins with them or otherwise) and it then follows that the force will be of different sign, according as the particles are in the same state of motion or not. Here the state of motion has to be understood to refer to the orbital motion only, or to orbit and spin, according to whether one assumes the particles to exchange their spins as well as their positions, or not. Since Pauli's principle limits the number of nucleons which can be in the same state of motion to one neutron and one proton if the spin is specified, or to two neutrons and two protons otherwise, such exchange forces will show saturation. Exchange forces were first postulated by Heisenberg from the analogy with chemical forces between atoms or ions, and the importance of space exchange without spin exchange was pointed out by Majorana.

(b) The assumption that the force has the same sign at all distances may be at fault, and the forces may be attractive at moderate distances, but repulsive at very close approach. They would then be similar to the interatomic force in a molecule or liquid, and would lead to a constant density and give saturation.

(c) The forces may not be two-body forces, but, when many nucleons come close together, repulsive forces of a new kind may come into play, which could effectively prevent collapse.

For a long time only the first of these possibilities was taken seriously. When experiments on the scattering of neutrons by protons were extended to energies of several hundred mev they gave a direct confirmation of the conjecture

that the forces are, at least in part, of the exchange type. The point is that at these high energies the transfer of momentum between the particles is likely to be small, so that the incident particle will be deflected only through a small angle. Hence with ordinary forces one would expect most of the neutrons to continue forward, with the recoil protons going mainly at right angles to the incident beam. With exchange forces, the particles would, at these high energies just effect one exchange, so that the proton would go forward, and the neutron at right angles. The observed distribution of the recoil protons shows both a maximum forward, and one at right angles, the two being comparable in magnitude. This suggests that the forces are about an equal mixture of exchange and ordinary forces, thus confirming Heisenberg's conjecture. However, 50% exchange force appears to be insufficient to guarantee saturation, and while the exchange effects will help to achieve saturation, some of the other possibilities are also likely to play a vital part.

Of these (b), the 'repulsive core' has been invoked by Jastrow (1951) in an interesting attempt to fit the high-energy neutron-proton and proton-neutron scattering by a charge-independent potential. The question which potential gives the best, and most plausible, fit with the data is still a controversial subject, but more accurate data and more extensive calculations may well show some direct evidence for such a repulsive core. On theoretical grounds, its existence would now seem very reasonable. This is a point to which I shall return.

As regards (c), the many-body forces, there exists no direct evidence either way, except that the general comparison of the binding energy of the three-nucleon problem ${}^3\text{H}$, ${}^3\text{He}$ with the two-body problem seems to show closer agreement than would be likely if many-body forces were of major importance. Theoretically one would be quite prepared to believe in their existence.

The discovery by Rabi's group (Kellogg *et al.* 1940) of the quadrupole moment of the deuteron, which proves that the charge distribution in the deuteron is not spherical but egg shaped, proves that the hypothesis of central forces is also an over simplification. The axis of the 'egg' is aligned with the joint direction of the nucleon spins (which in the deuteron we know to be parallel to each other) and this shows that the potential energy of a neutron and a proton must be lower when the line joining them is parallel to their spin direction than when it is perpendicular to it. Such forces are known as non-central or 'tensor' forces. About their strength we know mainly that it must be such as to explain the magnitude of the deuteron quadrupole moment, but this leaves a considerable uncertainty because we do not know their range. If their range is the same as that of the central force, they would not have to be very strong, and while they would make some contribution to the binding this would not greatly alter the picture that one forms on the basis of central forces only. On the other hand, tensor forces of still shorter range are very inefficient in producing a quadrupole moment, and would thus have to be correspondingly stronger. In that case one would have to allow for them in estimating the central forces from binding energies and low-energy scattering.

From this brief summary it will be evident that we have obtained a good deal of empirical knowledge of nuclear forces, but also that, as more detailed evidence allows us to discuss the problem in greater detail, our picture of the forces becomes more and more complicated. This makes one suspect that a really satisfactory description will not be possible until we succeed in deriving the forces

from some simpler and more fundamental concept. The attempt to do this constitutes the field theory of nuclear forces.

The starting point of this was the idea of Yukawa (1935) who attempted to derive these forces from some field in the same way as we obtain the electric and magnetic forces between charged particles from the electromagnetic field, governed by Maxwell's equations. However, instead of the coulomb potential, which is a solution of the equation

$$\nabla^2 V = 0 \quad \text{.....(1 a)}$$

with a singularity at the centre, we must have short-range force which must therefore obey a different field equation. Now (1 a) is the special form for a static potential of the general wave equation

$$\nabla^2 V - \frac{1}{c^2} \frac{\partial^2}{\partial t^2} V = 0, \quad \text{.....(2 a)}$$

which must then also be modified for the nuclear field. If we want an equation which is still linear and of no higher than second order, the only possible modification compatible with the principle of relativity is

$$\nabla^2 U - \frac{1}{c^2} \frac{\partial^2 U}{\partial t^2} - \kappa^2 U = 0, \quad \text{.....(2 b)}$$

where κ is a constant. A wave equation determines the relation between wavelength and frequency, and hence, using the relations of de Broglie, between momentum and energy. In this way (2 a) leads to the equation

$$E^2 - c^2 p^2 = 0 \quad \text{.....(3 a)}$$

which is the correct relation between energy E and momentum p for a photon. We know that electromagnetic radiation associated with the wave equation (2 a) and the rest of Maxwell's equations consists of such photons. Similarly, (2 b) leads to the relation

$$E^2 - c^2 p^2 - \mu^2 = 0 \quad \text{.....(3 b)}$$

which describes a particle of rest mass $\mu = \hbar\kappa/c$ where $\hbar = h/2\pi$, h being Planck's constant.

On the other hand, the static case of (2 b), viz.

$$\nabla^2 U - \kappa^2 U = 0 \quad \text{.....(1 b)}$$

has a solution analogous to the coulomb potential:

$$U = g e^{-\kappa r}/r, \quad \text{.....(4)}$$

which is a short-range force. g is a constant corresponding to the charge. To obtain a reasonable range for this force, one has to choose the mass μ in (3 b) to be about 300 electron masses.

It is well known that particles of about that mass, known as ' π -mesons', and first discovered by Powell and his group (Lattes *et al.* 1947) do in fact exist, and, as expected, interact strongly with nucleons. One might, then, expect that the interaction of nucleons would be no harder to describe than that of charged particles, if we used the Yukawa potential (4) in place of the coulomb potential. However, this analogy, which had been Yukawa's starting point, turned out to be less close than expected.

The first difference is that, as I have already pointed out, nuclear forces at short distances are much stronger than electrostatic forces would be at the same

distance. Hence, even on the basis of the simple law (4), the constant g must be much larger than the electron charge. Now the fact that atoms can be described to a very good accuracy in terms of static forces only, and that such complications as retardation, relativistic corrections and radiation terms are very small, is due to the small value of the fine structure constant $e^2/\hbar c$ which is about $1/137$. In the case of nuclear forces the corresponding constant $g^2/\hbar c$ must be considerably larger, and even if a picture of static forces may give a reasonable starting point, corrections to it are bound to be much more important than in the atom.

Furthermore, electromagnetic waves are transverse, and can have various states of polarization. Hence photons of a given momentum are not identical but may be differently polarized, and this can be expressed by attributing to the photon a spin of one unit. What is the corresponding spin of a meson? To this question one can now give a certain and unambiguous answer, since high-energy accelerators have permitted the production of mesons in large quantities so that their properties can be studied. From these it can be concluded that both charged and neutral mesons have zero spin, so that the equation (2b) refers only to a single quantity U , not to a vector with four components (vector and scalar potential) as in the electromagnetic case. This still leaves two possible kinds of waves according as the amplitude U stays the same or changes sign if one goes from a left-handed to a right-handed coordinate system. Such quantities are known as scalars or pseudoscalars respectively, and most people have some initial difficulty in visualizing this distinction, since pseudoscalars do not play any important part in classical physics. The similar distinction between vectors and pseudovectors, or in more familiar terminology, polar and axial vectors, is much better known, and there are many important examples of polar vectors (velocity, electric field intensity) and axial vectors (angular momentum, magnetic field intensity). The nature of the coupling between mesons and nucleons depends on the character of the meson wave function U . For example, consider the absorption of a slow meson by a deuteron. The ground state of the deuteron is represented by a wave function which is an even function of the coordinates, as in all states of even angular momentum. If the meson wave function is scalar, then it also is even, and after absorption the system will remain in an even state. The absorption of a pseudoscalar meson, on the other hand would leave the two nucleons in an odd state. Now a careful discussion of this and similar experiments, which is too long to be reproduced here, shows that the meson is, in fact, pseudoscalar.

This result has important consequences for the theory of nuclear forces, because if one works out the analogue of the simple equation (4) for a pseudoscalar field, one finds that this static term is precisely zero. This does not, of course, mean that a pseudoscalar meson field gives no nuclear force, but that this force is due to non-static effects connected mostly with the possibility of creating pairs of nucleons and 'anti-nucleons' in the same way as an electromagnetic field can produce electron and positron pairs. However, such subtle effects tend to be much smaller than the direct static effect, and to get a sufficiently large nuclear force one must make the coupling constant g still larger. This suggests that the fine structure constant $g^2/\hbar c$ may in fact be larger than unity, and perhaps as large as 10 or 20.

With such strong coupling most of the customary methods of describing the interaction of two or more particles through the intermediary of a field become quite useless, and one has to develop quite new mathematical methods for handling such a situation. A step forward was recently made by Lévy (1952) who started from the view that the strong coupling must result in a very strong interaction between two nucleons at close approach. If this were attractive the behaviour of the two-nucleon system would be quite different from what we know it to be. It is therefore reasonable to expect it to be repulsive, and there are also some indications in the mathematics that it should be repulsive. This repulsive core will prevent the nucleons from approaching each other very closely, and therefore the detailed nature of the force at short distances is not important. All we have to know is the minimum distance of approach, and the forces outside this point. Once the region of very short distances is excluded, the interaction is of a more reasonable order of magnitude, and the mathematical problem becomes more manageable. Using in this way only two adjustable parameters, namely the coupling constant g , and the minimum distance, Lévy was able to get satisfactory agreement for all the known data concerning the neutron-proton system at low energies. This encourages the belief that, once we can find a way through the formidable mathematical difficulties, we may find that the meson field theory accounts satisfactorily for the interaction of nucleons.

There is an alternative way in which mesons and nucleons may be coupled. To see this we remember that in solving the Laplace equation (1a) for the static field we might have chosen a solution whose singularity at the centre does not correspond to a point charge, but to a point dipole. This would describe, instead of the electron, a particle with no charge but an intrinsic magnetic moment. Such terms do not occur in the basic law for the interaction of electrons with their field. (The intrinsic magnetic moment of the electron was shown by Dirac to be a consequence of its charge.) Such a particle would have an interaction energy with an external field which is proportional not to the potential, but to the (electric or magnetic) field intensity, which contains the derivatives of the potential. A similar interaction can be postulated between nucleons and the meson field, and it will involve the derivatives of the meson field amplitude U . Such a coupling scheme, which for a pseudoscalar meson is described as 'pseudovector coupling', gives a non-vanishing static part, and therefore does not require as large a coupling constant as the scheme discussed before. However, the new ideas, which have been developed in the past five years or so to avoid the infinities arising in the theory of fields whenever one deals with point particles, are not applicable to such a case of 'pseudovector coupling' and therefore the mathematical analysis fails in this case, too.

I have stressed in this discussion the limitations rather than the successes since the latter are mostly qualitative in nature. But the phenomenon of exchange forces explains itself naturally in terms of charged meson fields, whereas neutral mesons are connected with ordinary forces. One knows what properties the coupling must have to ensure charge independence of all nuclear phenomena, and recent results on the scattering of fast mesons by protons (Fermi *et al.* 1953) are well compatible with this. On the other hand the discovery of several new particles in cosmic radiation raises the possibility that they, too, may belong to fields which contribute to the nuclear forces, so that our picture

would require further modification. However far this may lead us from the original simple law of Yukawa, there is no doubt that his basic idea will remain right and important.

From this account of the somewhat disappointing state of our knowledge of the details of the nuclear forces it might be thought that we could not get much sense out of the study of nuclei until the basic laws were better known. This conclusion would be quite misleading. In fact, for all but the simplest nuclei it would be no immediate help to know the law of force precisely, since the problem of calculating the motion of perhaps 250 particles under given forces is quite outside any practical possibility. Even in the atom, where for several reasons the mathematical problems are rather easier, nobody would attempt to calculate from first principles the absolute values of all the lines in the spectrum, say, of iron. One has to find some simpler approach, based in part on generalizations from empirical data and in part on approximations that can be theoretically justified, and build up a model that contains the essential features of a real nucleus.

For this purpose one can get quite far without knowing the forces in detail, and we feel therefore that we know by now a good deal about what goes on inside a nucleus. Success in this field has been achieved by two quite different methods which appear mutually contradictory, but are really two different idealizations of a situation that lies in fact somewhere between these extremes.

One of these pictures is Bohr's 'liquid drop' model, in which it is assumed that the nucleons interact so strongly that each one has a mean free path quite small with respect to the nuclear dimensions, so that any extra energy given to one of these particles will at once be shared with many others. This picture was first put forward to explain why in a collision of a low-energy neutron with a nucleus the capture of the neutron with the emission of the extra energy in the form of radiation is much more frequent than the re-emission of the neutron. This approach proved very successful in explaining many features of nuclear reactions in great detail. If one takes this model quite seriously, one would expect that the general distribution of energy levels of nuclei should show a predictable behaviour, but that there should be no simple rule for the energy or the properties of the ground state of any particular nucleus.

For this reason all attempts to find and explain simple regularities in the list of stable isotopes, or in their spins or other properties, were regarded with great suspicion. This applied particularly to the picture which regarded the nucleus as analogous to the atom, with each nucleon in a definite state of motion or 'shell'. We argued that whereas the atom was dominated by the strong centre of force and the force due to any particular electron was negligible in comparison with the mean central field, the nucleus had no such centre, and moreover the saturation of the force ensured that each nucleon would interact strongly with a few neighbours, so that one would expect strong correlations between the motions of different nucleons, and therefore could not treat them as approximately independent.

However, the evidence for regularities which suggested the presence of nuclear shells became so strong that it could no longer be ignored, and following the work of Maria Mayer (1950) and Haxel, Jensen and Suess (1950) it is now established beyond doubt that the 'shell model' represents at any rate a very close approximation to the truth, and that many properties of nuclei can be usefully discussed in terms of this model.

Just as in the atom one pictures various quantum states for each electron, which are filled successively as we proceed through the periodic system, and whose order is in the usual notation, 1s, 2s, 2p, 3s, 3p, 3d . . . , the shell model postulates such states in the nucleus. However, one has to assume that the energy of such a state is very different according to whether the spin of the particle is parallel or opposite to its orbital angular momentum. Whether this difference requires the existence of a new kind of force, or whether it may be a consequence of the tensor force which I mentioned earlier, is still an open question. The sequence of levels is then quite insensitive to the average potential in which one assumes each nucleon to move, so that it can be predicted with few ambiguities. It is different from the atomic sequence, because the absence of the attractive centre will make the potential more or less constant over the inside of the nucleus. Specifying each state by the usual symbol for its orbital angular momentum, and the value for the total angular momentum j , so that $d_{3/2}$ means orbital angular momentum 2 and spin antiparallel to it, the sequence is: $s_{1/2}$, $p_{3/2}$, $p_{1/2}$, $d_{5/2}$, $d_{3/2}$, $s_{1/2}$. These levels consist each of $2j+1$ states so that they can take 2, 4, 2, 6, 4, 2 neutrons and the same number of protons respectively. In other words, 2, 6, 8, 14, 18, 20 nucleons of one kind will just fill a number of shells completely, and such nuclei will have greater stability than their neighbours. As a shell is filled successive nucleons go in with opposite directions of their angular momenta, so that the total contribution of the nucleons in a shell of angular momentum j is zero if their number is even, and j if it is odd. (This is the opposite to the rule in atomic spectroscopy where the lowest state has the greatest possible angular momentum, the reason being that the electrons in the atom repel each other whereas the forces between nucleons in the same shell are predominantly attractive.) This leads to simple rules for predicting nuclear spins, which come out correctly in the great majority of cases. I have here over-simplified the rule to avoid the discussion of certain complications which are, however, quite well understood.

Magnetic moments appeared to give some difficulty. The usual discussion assumed that, since, for example, two neutrons in a j shell gave no angular momentum, and three neutrons gave a resultant j , the magnetic moment should just be that of the last neutron. This reasoning is not correct since there are many ways in which three particles, each of angular momentum j can align themselves to give a resultant j , and all these alignments will occur in the stationary state of the nucleus. The correct problem has been solved by Flowers (1952), who finds that the magnetic moments are now in much better agreement than before.

The shell model is a most powerful tool to help in the discussion of data about nuclei. For an understanding of nuclear structure it is important to put it clearly in relation to Bohr's liquid-drop model, and to justify it from first principles in spite of the apparent objections. Some attempts have been made in this direction, but it is a point on which a good deal more thinking has to be done.

On some of these questions evidence is now coming in from experiments involving mesons or high-energy nucleons. A typical instance is the following: To understand the apparent independence of the nucleons of each other which seemed to be demonstrated by the success of the shell model, the hypothesis was put forward that there exist many-body forces of such a kind that each nucleon was, in fact, moving in a uniform field of force which did not depend

much on what the other nucleons were doing. This hypothesis is almost certainly disproved by the observation that, in the capture of positive mesons by nuclei, the most common result is the ejection of two protons in roughly opposite directions. This happens in the deuteron, since the positive meson converts the neutron into a proton. It looks therefore as if in a heavier nucleus the meson interacts with just two nucleons and the rest of the nucleus does not matter much. This is what one expects on the usual picture of strong short-range forces. While a nucleon is not close to any other, it cannot absorb a meson, since it cannot dispose of the excess energy and momentum. The usual theory predicts, and the observation on meson capture confirms, that a nucleon will interact strongly only with one other nucleon at a time, and from the frequency of the phenomenon by comparison with the deuteron case it follows that the number of nucleons which at any time are subject to strong interaction with another, is roughly what one would expect.

I have quoted this example because it provides a nice parallel with Rutherford's experiment on alpha-ray scattering. Even if our only purpose in physics were to understand the structure of the nucleus, it would still pay us to produce mesons and other new particles as tools to explore the nucleus. I am not, of course, suggesting that our investigation should stop there, any more than Rutherford was satisfied with having shown what the atom looked like. If Rutherford were alive today, I am sure he would be in the front line towards the unexplored territory of new energy regions and new particles.

REFERENCES

- FERMI, E., ANDERSON, H. L., and NEAGLE, D. E., 1953, *Phys. Rev.*, in the press.
 FLOWERS, B. H., 1952, *Phil. Mag.*, **43**, 1330.
 HAXEL, O., JENSEN, J. H. D., and SUESS, H. E., 1950, *Z. Phys.*, **128**, 295.
 JASTROW, R., 1951, *Phys. Rev.*, **81**, 636.
 KELLOGG, J., RABI, I., RAMSAY, N., and ZACHARIAS, J., 1940, *Phys. Rev.*, **57**, 677.
 LATTES, C. M. G., MUIRHEAD, M., OCCHIALINI, G. P. S., and POWELL, C. F., 1947, *Nature, Lond.*, **159**, 694.
 LÉVY, M., 1952, *Phys. Rev.*, **88**, 725.
 MAYER, M. G., 1950, *Phys. Rev.*, **78**, 16.
 RADICATI, L. A., 1953, *Proc. Phys. Soc. A*, **66**, 139.
 YUKAWA, H., 1935, *Proc. Phys. Math. Soc., Japan*, **17**, 48.

Boltzmann's Equation in Quantum Mechanics

By H. S. GREEN

University of Adelaide, South Australia

MS. received 4th September 1952

Abstract. This note gives a rigorous derivation of the quantum-mechanical analogue of Boltzmann's equation in gas theory. Assuming that the incidence of multiple encounters, other than binary encounters, between the molecules can be neglected, a closed equation for the phase space distribution of pairs of molecules is derived. The formulation of a boundary condition for this equation requires an independent appeal to statistical principles, and is the only point at which irreversibility enters the theory. A solution of the equation is given which satisfies the boundary condition. Corrections to Boltzmann's equation, which are of quantum-mechanical as well as classical origin, are derived for slightly dense gases.

§ 1. INTRODUCTION

THERE is one fairly obvious way of obtaining a quantum-mechanical generalization of Boltzmann's equation in gas theory: this is simply to modify the 'collision integral' by substituting the quantum-mechanical differential cross section for binary molecular encounters in place of the classical one. This simple procedure has been applied with some success to the theory of the transport phenomena, in the way described in Chapman and Cowling's standard work (1939). But in this way one evades the difficulty of how a molecular phase space distribution function can be defined without violating Heisenberg's uncertainty principle. Although it may be permissible to assume the existence of a velocity distribution in a not too localized region of a gas, the quantitative implications of such an assumption have never been fully discussed.

The concept of a phase space distribution function is not, however, new to quantum mechanics. Wigner (1932) was the first to define and derive the equation satisfied by such a function for an arbitrary molecular assembly. More recently, the significance and general properties of phase space distribution functions have been discussed by Moyal (1949). It is evidently such a phase space distribution function which the quantum-mechanical form of Boltzmann's equation must determine. Accepting this, the only thing which remains is to actually show that the phase space distribution function for a molecule in an assembly satisfies the accepted quantum-mechanical generalization of Boltzmann's equation, or something very much like it. This is attempted in the following note.

The corresponding discussion in the classical theory has been given in alternative forms by Kirkwood (1947) and by Born and Green (1946, 1949). The latter authors pointed out that, in its usual form, Boltzmann's equation incorporates an approximation other than that implied by restricting consideration to binary encounters. It is this other approximation which leads, in the classical theory, to the perfect gas law $\beta p = n$ instead of

$$\beta p = n + \frac{1}{2} n^2 \int [1 - \exp\{-\beta \phi(r)\}] dr \quad \dots\dots (1)$$

for the equation of state, where $\beta kT = 1$, n is the number density, and $\phi(r)$ is the mutual potential energy of two molecules separated by the distance r . The usual quantum-mechanical form of Boltzmann's equation of course incorporates the same approximations as are already present in the classical form. It will be shown that, in addition, it involves an error of purely quantum-mechanical origin. Fortunately all the corrections disappear as the density becomes very small, so that in the application to very rare gases the work of early authors requires no modification. Some deviation is, however, to be expected from their numerical results for gases which are slightly dense.

§ 2. PHASE SPACE DISTRIBUTIONS

The phase space distribution function for a system of N similar molecules may be defined in terms of the corresponding wave function Ψ_N . If \mathbf{x} and ξ represent all the positions $\mathbf{x}^{(i)}$ and velocities $\xi^{(i)}$ respectively ($i = 1, 2, \dots, N$), it is given by the formula (see Moyal 1949)

$$f_N(\mathbf{x}, \xi) = \left(\frac{m}{h}\right)^{3N} \int \Psi_N^*(\mathbf{x} - \frac{1}{2}\mathbf{y}) \Psi_N(\mathbf{x} + \frac{1}{2}\mathbf{y}) \exp\left(im \sum_{i=1}^N \xi^{(i)} \cdot \mathbf{y}^{(i)} / \hbar\right) d^N \mathbf{y} \quad \dots (2)$$

where $\int \dots d^N \mathbf{y}$ denotes integration with respect to all of the N vector variables $\mathbf{y}^{(i)}$, m is the molecular mass, and $h = 2\pi\hbar$ is Planck's constant. The general equation satisfied by f_N has been derived, and solved under equilibrium conditions, by the author (Green 1951, 1952a). Distribution functions in the phase space of only a few of the molecules contained in the gas may be obtained from it by integration, thus :

$$(N-q)! f_q = \int^{2(N-q)} f_N d\mathbf{x}^{(q+1)} d\xi^{(q+1)} \dots d\mathbf{x}^{(N)} d\xi^{(N)}. \quad \dots (3)$$

Then $f_1(\mathbf{x}^{(1)}, \xi^{(1)})$ [denoted hereafter by $f(\mathbf{x}, \xi)$] is the phase space distribution function for a single molecule, which is usually considered in gas theory.

The equations satisfied by f and f_2 are

$$\frac{\partial f}{\partial t} + \xi \cdot \frac{\partial f}{\partial \mathbf{x}} = \iint O^{(12)} f_2 d\mathbf{x}^{(2)} d\xi^{(2)} \quad \dots (4)$$

$$\text{and} \quad \frac{\partial f_2}{\partial t} + \xi^{(1)} \cdot \frac{\partial f_2}{\partial \mathbf{x}^{(1)}} + \xi^{(2)} \cdot \frac{\partial f_2}{\partial \mathbf{x}^{(2)}} = O^{(12)} f_2 + \iint (O^{(13)} + O^{(23)}) f_3 d\mathbf{x}^{(3)} d\xi^{(3)} \quad \dots (5)$$

where $O^{(ij)}$ is the operator

$$O^{(ij)} = \frac{2}{\hbar} \int d\sigma \chi(\sigma) \sin(m\sigma \cdot \mathbf{r}^{(ij)} / \hbar) \exp\left\{\frac{1}{2}\sigma \cdot \left(\frac{\partial}{\partial \xi^{(i)}} - \frac{\partial}{\partial \xi^{(j)}}\right)\right\}, \quad \dots (6)$$

$$\mathbf{r}^{(ij)} = \mathbf{x}^{(j)} - \mathbf{x}^{(i)}, \quad \text{and} \quad \chi(\sigma) = \left(\frac{m}{h}\right)^3 \int \phi(r) \cos(m\sigma \cdot \mathbf{r} / \hbar) d\mathbf{r}. \quad \dots (7)$$

The derivation of these equations has been given in detail by Irving and Zwanzig (1951); they are easily obtained by applying (3) to the equation satisfied by f_N , or by applying a Fourier transform to the equivalent equations satisfied by the density matrix (see Born and Green 1947). From (4), as shown by Irving and Zwanzig (1951) (see also Green 1952b) the equations of continuity, macroscopic motion and energy transport are readily derived in the usual form.

§ 3. TRANSFORMATION OF THE COLLISION INTEGRAL

It is now possible to proceed to the derivation of an analogue of Boltzmann's equation, through the transformation of the integral on the right-hand side of (4). This integral

$$I_1 = \iint O^{(12)} f_2 d\xi^{(2)} d\mathbf{x}^{(2)} \quad \dots (8)$$

is effectively unchanged if the region of integration with respect to $\mathbf{x}^{(2)}$ is limited to a sphere of radius r_0 surrounding the point $\mathbf{x}^{(1)}$, if r_0 is equal to or slightly greater than the range of the intermolecular forces. (The value of r_0 which makes the above assertion true will be defined more precisely later.)

Introducing the assumption of binary encounters, it is assumed that the corresponding integral

$$I_2 = \iint (O^{(13)} + O^{(23)}) f_3 d\mathbf{x}^{(3)} d\boldsymbol{\xi}^{(3)} \quad \dots\dots(9)$$

which appears on the right-hand side of (5), is negligible compared with $O^{(12)}f_2$, for the configurations in which the distance between $\mathbf{x}^{(1)}$ and $\mathbf{x}^{(2)}$ is less than r_0 . The justification of this assumption, for fluids in which the density is sufficiently small, lies in the smallness of the probability, to which f_3 in (9) is proportional, of finding a third molecule in the immediate neighbourhood of the molecules at $\mathbf{x}^{(1)}$ and $\mathbf{x}^{(2)}$. It is a matter of convenience not to neglect I_2 immediately in (5), but to approximate it by the integral

$$I_2' = \iint (f^{(2)} O^{(13)} f_2^{(13)} + f^{(1)} O^{(23)} f_2^{(23)}) d\mathbf{x}^{(3)} d\boldsymbol{\xi}^{(3)} \quad \dots\dots(10)$$

which I_2 approaches when the distance between $\mathbf{x}^{(1)}$ and $\mathbf{x}^{(2)}$ increases, since then either $f_3 = f^{(2)} f_2^{(13)}$ or $f_3 = f^{(1)} f_2^{(23)}$. It will be seen shortly that I_2' is itself negligible compared with $O^{(12)}f_2$, when the density of the fluid is small. With the help of (4), (10) reduces to

$$\begin{aligned} I_2' &= f^{(2)} \left(\frac{\partial}{\partial t} + \boldsymbol{\xi}^{(1)} \cdot \frac{\partial}{\partial \mathbf{x}^{(1)}} \right) f^{(1)} + f^{(1)} \left(\frac{\partial}{\partial t} + \boldsymbol{\xi}^{(2)} \cdot \frac{\partial}{\partial \mathbf{x}^{(2)}} \right) f^{(2)} \\ &= \left(\frac{\partial}{\partial t} + \boldsymbol{\xi}^{(1)} \cdot \frac{\partial}{\partial \mathbf{x}^{(1)}} + \boldsymbol{\xi}^{(2)} \cdot \frac{\partial}{\partial \mathbf{x}^{(2)}} \right) f^{(1)} f^{(2)}, \quad \dots\dots(11) \end{aligned}$$

so that (5) becomes

$$\left(\frac{\partial}{\partial t} + \boldsymbol{\xi}^{(1)} \cdot \frac{\partial}{\partial \mathbf{x}^{(1)}} + \boldsymbol{\xi}^{(2)} \cdot \frac{\partial}{\partial \mathbf{x}^{(2)}} \right) (f_2 - f^{(1)} f^{(2)}) = O^{(12)} f_2. \quad \dots\dots(12)$$

The last equation does not suffice to determine f_2 completely in terms of f ; it has to be supplemented by a boundary condition, which will now be formulated. The sphere $r = r_0$ is divided into two hemispheres S_0 and S , such that, if

$$\mathbf{r} = \mathbf{x}^{(2)} - \mathbf{x}^{(1)}, \quad \boldsymbol{\rho} = \boldsymbol{\xi}^{(2)} - \boldsymbol{\xi}^{(1)}, \quad \dots\dots(13)$$

$\mathbf{r} \cdot \boldsymbol{\rho} \leq 0$ on S_0 and $\mathbf{r} \cdot \boldsymbol{\rho} \geq 0$ on S . A molecule on the hemisphere S_0 is moving towards the one at the centre, and is at such a distance that it can have had no previous interaction with it; one may therefore apply the statistical law for independent events and assert

$$f_2(t, \mathbf{x}^{(1)}, \mathbf{x}^{(2)} \boldsymbol{\xi}^{(1)}, \boldsymbol{\xi}^{(2)}) = f(t, \mathbf{x}^{(1)}, \boldsymbol{\xi}^{(1)}) f(t, \mathbf{x}^{(2)}, \boldsymbol{\xi}^{(2)}), \text{ on } S_0. \quad \dots\dots(14)$$

The same would not be true of the hemisphere S , because a molecule there will, in all probability, have interacted with and been scattered by the one at the centre.

This distinction between the two hemispheres marks the introduction of irreversibility into the theory. The equation (12), and all previous equations, are unchanged when the signs of the time and all velocities are reversed, showing that if they are satisfied by a set of particular distribution functions $f_q(t, \mathbf{x}, \boldsymbol{\xi})$, they must also be satisfied by $f_q(-t, \mathbf{x}, -\boldsymbol{\xi})$; they, by themselves, therefore, have no property which would enable one to predict natural irreversible processes. The condition (14), which defines a unique solution of (12), is not, however, symmetrical with respect to future and past, and is evidently the only premise of the theory which makes possible the prediction of irreversible phenomena.

It is not necessary to introduce any process of time-averaging, such as Kirkwood (1946) employs. Also, irreversibility does not appear to be linked in any special way with the quantum theory. Moyal (1949) points out that Liouville's theorem concerning the conservation of the volume of occupied phase space no longer holds in the quantum theory, but it is doubtful whether this fact has any direct connection with irreversibility. It is the act of observation which introduces the irreversible element into ordinary quantum mechanics, and a more penetrating analysis would doubtless require the correlation of (14) with the pre-requisites of observation.

It should be noticed at this point that (14) is the correct boundary condition only when classical statistics are applicable. With Bose statistics, the density matrix ρ_2 for pairs of particles which have not interacted is of the form

$$\rho_2 = \rho(\mathbf{x}_1^{(1)}, \mathbf{x}_2^{(1)})\rho(\mathbf{x}_1^{(2)}, \mathbf{x}_2^{(2)}) + \rho(\mathbf{x}_1^{(1)}, \mathbf{x}_2^{(2)})\rho(\mathbf{x}_1^{(2)}, \mathbf{x}_2^{(1)}),$$

from which it may be inferred that the functions f_2 and f , defined in terms of ρ_2 and ρ , are related by

$$f_2 = f^{(1)}f^{(2)} + \left(\frac{m}{h}\right)^3 \iint f(\mathbf{x} - \frac{1}{2}\mathbf{r}', \boldsymbol{\xi} - \frac{1}{2}\boldsymbol{\rho}') f(\mathbf{x} + \frac{1}{2}\mathbf{r}', \boldsymbol{\xi} + \frac{1}{2}\boldsymbol{\rho}') \\ \times \exp\{im(\mathbf{r} \cdot \boldsymbol{\rho}' - \boldsymbol{\rho} \cdot \mathbf{r}')/h\} d\mathbf{r}' d\boldsymbol{\rho}' \quad \dots\dots(15)$$

($\mathbf{x} = \frac{1}{2}\mathbf{x}^{(1)} + \frac{1}{2}\mathbf{x}^{(2)}$, $\boldsymbol{\xi} = \frac{1}{2}\boldsymbol{\xi}^{(1)} + \frac{1}{2}\boldsymbol{\xi}^{(2)}$). With Fermi statistics instead of Bose statistics, the additional term is reversed in sign. These formulae were given by Moyal (1949) for non-interacting particles; they apply as a boundary condition on the hemisphere S_0 , but not on S . It has been shown by the author (Green 1951) that deviations from classical statistics are unlikely to be important in any gas, except within a degree or so of absolute zero; for this reason the condition (14) will be used in the following.

The equation (12), in conjunction with the boundary condition (14), suffices to determine f_2 uniquely, provided one makes a further postulate to exclude abnormal situations where the state of the fluid deviates widely from the average, when the macroscopic variation of density, temperature and fluid velocity is assigned—for example, situations in which the molecular velocity distribution differs widely from the Maxwellian distribution. It is assumed that f and f_2 vary with time and position in the fluid only on account of the variation of the local density, temperature and fluid velocity. Thus

$$\frac{\partial}{\partial t}(f, f_2) = \left(\frac{\partial n}{\partial t} \frac{\partial}{\partial n} + \frac{\partial \mathbf{u}}{\partial t} \cdot \frac{\partial}{\partial \mathbf{u}} + \frac{\partial \beta}{\partial t} \frac{\partial}{\partial \beta}\right)(f, f_2) \quad \dots\dots(16)$$

$$\text{and} \quad \frac{\partial}{\partial \mathbf{x}}(f, f_2) = \left(\frac{\partial n}{\partial \mathbf{x}} \frac{\partial}{\partial n} + \frac{\partial \mathbf{u}}{\partial \mathbf{x}} \cdot \frac{\partial}{\partial \mathbf{u}} + \frac{\partial \beta}{\partial \mathbf{x}} \frac{\partial}{\partial \beta}\right)(f, f_2) \quad \dots\dots(17)$$

where, in the case of f_2 , \mathbf{x} denotes the mean centre of the positions $\mathbf{x}^{(1)}$ and $\mathbf{x}^{(2)}$. The time derivatives of n , \mathbf{u} and β can be eliminated with the help of the equations of continuity, macroscopic motion and energy transfer. The most convenient way of solving Boltzmann's equation for non-uniform fluids is to treat the spatial gradients $\partial n/\partial \mathbf{x}$, $\partial \mathbf{u}/\partial \mathbf{x}$, and $\partial \beta/\partial \mathbf{x}$ as small, slowly varying quantities, squares, products and derivatives of which can be neglected in comparison with, or at any rate be separated from, the quantities themselves. This procedure is probably equivalent to Kirkwood's procedure of forming time-averages of quantities derived from 'unsmoothed' distribution functions; however, it is in no way essential to the formulation of Boltzmann's equation itself.

To derive from the integral I_1 of (8) an analogue of Boltzmann's collision integral, f_2 and $f^{(2)}$ should be regarded as functions of $\mathbf{x}^{(1)}$ and $\mathbf{r} = \mathbf{x}^{(2)} - \mathbf{x}^{(1)}$ instead of $\mathbf{x}^{(1)}$ and $\mathbf{x}^{(2)}$; they will then be denoted by \bar{f}_2 and $\bar{f}^{(2)}$, and (12) gives

$$O^{(12)}f_2 = \left(\frac{\partial}{\partial t} + \boldsymbol{\xi}^{(1)} \cdot \frac{\partial}{\partial \mathbf{x}^{(1)}} + \boldsymbol{\rho} \cdot \frac{\partial}{\partial \mathbf{r}} \right) (\bar{f}_2 - f^{(1)}\bar{f}^{(2)}). \quad \dots\dots (18)$$

Substituting this value of $O^{(12)}f_2$ in I_1 , one obtains

$$\left. \begin{aligned} I_1 &= J_1 + K_1, \\ J_1 &= \left(\frac{\partial}{\partial t} + \boldsymbol{\xi}^{(1)} \cdot \frac{\partial}{\partial \mathbf{x}^{(1)}} \right) \iint (f_2 - f^{(1)}f^{(2)}) d\mathbf{r} d\boldsymbol{\xi}^{(2)}, \\ K_1 &= \iint \boldsymbol{\rho} \cdot \frac{\partial}{\partial \mathbf{r}} (\bar{f}_2 - f^{(1)}\bar{f}^{(2)}) d\mathbf{r} d\boldsymbol{\xi}^{(2)}. \end{aligned} \right\} \quad \dots\dots (19)$$

As in (18), the spatial integration may be limited to a sphere of radius r_0 centred at the point $\mathbf{x}^{(1)}$.

The integral J_1 can be evaluated, to a sufficient degree of approximation, by substituting the equilibrium form of the distribution functions f_1 and f_2 , with local values of the density, temperature, and velocity of flow varying with the position $\mathbf{x}^{(1)}$. Under equilibrium conditions, however, one will have (cf. Yvon 1937)

$$\iint (f_2 - f^{(1)}f^{(2)}) d\mathbf{r} d\boldsymbol{\xi}^{(2)} = -2nBf \quad \dots\dots (20)$$

where B is the second virial coefficient. The latter has been calculated, on the basis of quantum theory, down to within a few degrees of absolute zero, and lately (Green 1952c), near absolute zero itself. The integral J_1 , expressed in the form

$$J_1 = \left(\frac{\partial}{\partial t} + \boldsymbol{\xi} \cdot \frac{\partial}{\partial \mathbf{x}} \right) (-2nBf), \quad \dots\dots (21)$$

may therefore be regarded as known, apart from the occurrence of f ; it combines naturally with the terms on the left-hand side of Boltzmann's equation. It is proportional to the square of the density at low densities, and is therefore negligible in very rare gases; at somewhat higher densities, it represents a correction, of purely classical origin, to the usual formulation of Boltzmann's equation.

The remaining part K_1 of I_1 can be transformed to an integral on the surface of the sphere $r = r_0$:

$$K_1 = \iint (f_2 - f^{(1)}f^{(2)}) \boldsymbol{\rho} \cdot d\mathbf{S} d\boldsymbol{\xi}^{(2)} \quad \dots\dots (22)$$

where $d\mathbf{S}$ is a vector element of the surface. On account of the boundary condition (14), the integrand vanishes on the hemisphere S_0 with $\mathbf{r} \cdot \boldsymbol{\rho} \leq 0$; the integration is therefore effectively restricted to the remaining hemisphere S . On this hemisphere, f_2 has to be determined in terms of f from (12) and (14). This is done in the following section. Meanwhile, by collecting the results (4), (8), (19), (21) and (22), one has

$$\left(\frac{\partial}{\partial t} + \boldsymbol{\xi} \cdot \frac{\partial}{\partial \mathbf{x}} \right) \{ (1 + 2n\beta)f \} = \iint (f_2 - f^{(1)}f^{(2)}) \boldsymbol{\rho} \cdot d\mathbf{S} d\boldsymbol{\xi}^{(2)}. \quad \dots\dots (23)$$

§ 4. DETERMINATION OF f_2

In solving the integro-differential equation (12), the term

$$I_2' = \left(\frac{\partial}{\partial t} + \boldsymbol{\xi}^{(1)} \cdot \frac{\partial}{\partial \mathbf{x}^{(1)}} + \boldsymbol{\xi}^{(2)} \cdot \frac{\partial}{\partial \mathbf{x}^{(2)}} \right) f^{(1)}f^{(2)}$$

will be dropped. This may be justified in two virtually equivalent ways. Firstly, it may be noted that this term arose originally from the integral I_2 of (9), which is negligible on the hypothesis of binary encounters. Secondly, on account of the improbability of interaction with a third molecule, $f(t, \mathbf{x}^{(1)}, \xi^{(1)})f(t, \mathbf{x}^{(2)}, \xi^{(2)})$ may be replaced by $f(t_0, \mathbf{x}^{(1)} - \xi^{(1)}(t - t_0), \xi^{(1)})f(t_0, \mathbf{x}^{(2)} - \xi^{(2)}(t - t_0), \xi^{(2)})$, where t_0 is any fixed time somewhat previous to t ; and, when the second expression is substituted for the first in I_2' , the latter vanishes. The equation to be solved will therefore be

$$O^{(12)}f_2 = \left(\frac{\partial}{\partial t} + \xi^{(1)} \cdot \frac{\partial}{\partial \mathbf{x}^{(1)}} + \xi^{(2)} \cdot \frac{\partial}{\partial \mathbf{x}^{(2)}} \right) f_2. \quad \dots\dots (24)$$

This determines the distribution in phase space of two molecules moving only under their mutual interaction. The required solution, which will be verified afterwards, is

$$\begin{aligned} f_2 = & \left(\frac{m}{h} \right)^6 \iiint \int f(t_0, \mathbf{x}_0 - \tfrac{1}{2}\mathbf{r}_0, \xi - \tfrac{1}{2}\boldsymbol{\rho}_0) f(t_0, \mathbf{x}_0 + \tfrac{1}{2}\mathbf{r}_0, \xi + \tfrac{1}{2}\boldsymbol{\rho}_0) \\ & \times \Psi(\mathbf{r} + \mathbf{s}, \boldsymbol{\rho}_0 + \boldsymbol{\sigma}) \Psi^*(\mathbf{r} - \mathbf{s}, \boldsymbol{\rho}_0 - \boldsymbol{\sigma}) \\ & \times \exp \{ m[\boldsymbol{\rho} \cdot \mathbf{s} + \{\mathbf{r}_0 + \boldsymbol{\rho}_0(t - t_0)\} \cdot \boldsymbol{\sigma}] / i\hbar \} d\mathbf{r}_0 d\boldsymbol{\rho}_0 d\mathbf{s} d\boldsymbol{\sigma}, \quad \dots\dots (25) \end{aligned}$$

where $\mathbf{x}_0 = \mathbf{x} - \xi(t - t_0)$, $\mathbf{x} = \tfrac{1}{2}(\mathbf{x}^{(1)} + \mathbf{x}^{(2)})$, $\xi = \tfrac{1}{2}(\xi^{(1)} + \xi^{(2)})$ and $\Psi(\mathbf{r}, \boldsymbol{\rho}_0)$ is a certain solution of the Schrödinger equation

$$-\frac{\hbar^2}{m} \frac{\partial^2 \Psi}{\partial \mathbf{r}^2} + \phi(\mathbf{r}) \Psi = \tfrac{1}{4} m \boldsymbol{\rho}_0^2 \Psi. \quad \dots\dots (26)$$

The verification of the solution proceeds as follows. The operator

$$\left(\frac{\partial}{\partial t} + \xi^{(1)} \cdot \frac{\partial}{\partial \mathbf{x}^{(1)}} + \xi^{(2)} \cdot \frac{\partial}{\partial \mathbf{x}^{(2)}} \right)$$

obviously commutes with \mathbf{x}_0 ; acting on the exponential factor in (25), it introduces a factor $m\boldsymbol{\rho}_0 \cdot \boldsymbol{\sigma} / i\hbar$; and, acting on the product of wave functions, it reduces to

$$\boldsymbol{\rho} \cdot \frac{\partial}{\partial \mathbf{r}}, \quad \text{or to} \quad -\frac{i\hbar}{m} \frac{\partial}{\partial \mathbf{s}} \cdot \frac{\partial}{\partial \mathbf{r}},$$

by virtue of the presence of the exponential factor in the integrand. Now it follows from (26) that

$$\begin{aligned} i\hbar \left(\frac{m\boldsymbol{\rho}_0 \cdot \boldsymbol{\sigma}}{i\hbar} - \frac{i\hbar}{m} \frac{\partial}{\partial \mathbf{s}} \cdot \frac{\partial}{\partial \mathbf{r}} \right) \{ \Psi(\mathbf{r} + \mathbf{s}, \boldsymbol{\rho}_0 + \boldsymbol{\sigma}) \Psi^*(\mathbf{r} - \mathbf{s}, \boldsymbol{\rho}_0 - \boldsymbol{\sigma}) \} \\ = \{ \phi(\mathbf{r} + \mathbf{s}) - \phi(\mathbf{r} - \mathbf{s}) \} \Psi(\mathbf{r} + \mathbf{s}, \boldsymbol{\rho}_0 + \boldsymbol{\sigma}) \Psi^*(\mathbf{r} - \mathbf{s}, \boldsymbol{\rho}_0 - \boldsymbol{\sigma}). \end{aligned}$$

Hence, to prove that (25) is a solution of (24), one requires only to show that the operator $i\hbar O^{(12)}$ also inserts a factor $\{ \phi(\mathbf{r} + \mathbf{s}) - \phi(\mathbf{r} - \mathbf{s}) \}$ in the integrand of (25); and, in fact, one has with the help of (6):

$$i\hbar O^{(12)} \exp(im\boldsymbol{\rho} \cdot \mathbf{s} / \hbar) = 2i \int \chi(\boldsymbol{\sigma}) \sin(m\boldsymbol{\sigma} \cdot \mathbf{r} / \hbar) \exp\{im(\boldsymbol{\rho} - \boldsymbol{\sigma}) \cdot \mathbf{s} / \hbar\} d\boldsymbol{\sigma},$$

which reduces to $\{ \phi(\mathbf{r} + \mathbf{s}) - \phi(\mathbf{r} - \mathbf{s}) \} \exp(im\boldsymbol{\rho} \cdot \mathbf{s} / \hbar)$ on account of (7).

Thus (25) satisfies (24). It will now be supposed further that $\Psi(\mathbf{r}, \boldsymbol{\rho}_0)$ is the particular solution of (26) which corresponds to a monochromatic incident wave $\exp(\tfrac{1}{2}im\boldsymbol{\rho}_0 \cdot \mathbf{r} / \hbar)$, together with scattered waves; then, for sufficiently large values of \mathbf{r} with $\mathbf{r} \cdot \boldsymbol{\rho} \leq 0$, f_2 will reduce to

$$\begin{aligned} & \left(\frac{m}{h} \right)^6 \iiint \int f(t_0, \mathbf{x}_0 - \tfrac{1}{2}\mathbf{r}_0, \xi - \tfrac{1}{2}\boldsymbol{\rho}_0) f(t_0, \mathbf{x}_0 + \tfrac{1}{2}\mathbf{r}_0, \xi + \tfrac{1}{2}\boldsymbol{\rho}_0) \\ & \times \exp \{ m[(\boldsymbol{\rho} - \boldsymbol{\rho}_0) \cdot \mathbf{s} - \{\mathbf{r} - \mathbf{r}_0 - \boldsymbol{\rho}_0(t - t_0)\} \cdot \boldsymbol{\sigma}] / i\hbar \} d\mathbf{r}_0 d\boldsymbol{\rho}_0 d\mathbf{s} d\boldsymbol{\sigma} \\ & = f_1\{t_0, \mathbf{x}^{(1)} - \xi^{(1)}(t - t_0), \xi^{(1)}\} f_1\{t_0, \mathbf{x}^{(2)} - \xi^{(2)}(t - t_0), \xi^{(2)}\}. \end{aligned}$$

The minimum value of r for which this condition is satisfied with sufficient accuracy may be identified with r_0 ; but r_0 is somewhat arbitrary, and a suitable choice of either r_0 or t_0 will make (25) satisfy the boundary condition (14).

By taking the value of f_2 , as given by (25), and substituting in the right-hand side of (23), one obtains a correct quantum-mechanical value for the collision integral. It differs somewhat from that implicit in the pioneer work of Massey and Mohr (1933), which would correspond to the substitution of

$$f_2' = \iint f(t, \mathbf{x}, \boldsymbol{\xi} - \frac{1}{2}\boldsymbol{\rho}_0) f(t, \mathbf{x}, \boldsymbol{\xi} + \frac{1}{2}\boldsymbol{\rho}_0) \Psi^*(\mathbf{r} + \mathbf{s}, \boldsymbol{\rho}_0) \Psi^*(\mathbf{r} - \mathbf{s}, \boldsymbol{\rho}_0) \exp(-im\boldsymbol{\rho} \cdot \mathbf{s}/\hbar) d\boldsymbol{\rho}_0 d\mathbf{s}$$

or

$$f_2' = \iint f\{t_0, \mathbf{x} - \boldsymbol{\xi}_0^{(1)}(t - t_0), \boldsymbol{\xi}_0^{(1)}\} f\{t_0, \mathbf{x} - \boldsymbol{\xi}_0^{(2)}(t - t_0), \boldsymbol{\xi}_0^{(2)}\} \\ \times \Psi^*(\mathbf{r} + \mathbf{s}, \boldsymbol{\rho}_0) \Psi^*(\mathbf{r} - \mathbf{s}, \boldsymbol{\rho}_0) \exp(-im\boldsymbol{\rho} \cdot \mathbf{s}/\hbar) d\boldsymbol{\rho}_0 d\mathbf{s} \quad \dots\dots (27)$$

$$(\boldsymbol{\xi}_0^{(1)} = \boldsymbol{\xi} - \frac{1}{2}\boldsymbol{\rho}_0, \quad \boldsymbol{\xi}_0^{(2)} = \boldsymbol{\xi} + \frac{1}{2}\boldsymbol{\rho}_0)$$

for f_2 . This does not satisfy either (24) or (12) exactly. The difference between f_2 and f_2' is, in fact,

$$\delta f_2 = \left(\frac{m}{\hbar}\right)^6 \iiint \int f(t_0, \mathbf{x}_0^{(1)}, \boldsymbol{\xi}_0^{(1)}) f(t_0, \mathbf{x}_0^{(2)}, \boldsymbol{\xi}_0^{(2)}) \left\{ \boldsymbol{\sigma} \cdot \frac{\partial \Psi^*}{\partial \boldsymbol{\rho}_0}(\mathbf{r} + \mathbf{s}, \boldsymbol{\rho}_0) \Psi^*(\mathbf{r} - \mathbf{s}, \boldsymbol{\rho}_0) \right. \\ \left. - \boldsymbol{\sigma} \cdot \frac{\partial \Psi^*}{\partial \boldsymbol{\rho}_0}(\mathbf{r} - \mathbf{s}, \boldsymbol{\rho}_0) \Psi^*(\mathbf{r} + \mathbf{s}, \boldsymbol{\rho}_0) \right\} \exp\{m[\boldsymbol{\rho} \cdot \mathbf{s} + \{\mathbf{r}_0 + \boldsymbol{\rho}_0(t - t_0)\} \cdot \boldsymbol{\sigma}]/i\hbar\} \\ \times d\mathbf{r}_0 d\boldsymbol{\rho}_0 d\mathbf{s} d\boldsymbol{\sigma}, \quad \dots\dots (28)$$

approximately. This neglects quadratic and higher powers of $\boldsymbol{\sigma}$ under the sign of integration—a procedure which is justified, since, by virtue of the presence of the exponential factor in the integrand, multiplication by $m\boldsymbol{\sigma}/i\hbar$ is equivalent to differentiation with respect to \mathbf{r}_0 . The first approximation, represented by (28), can be transformed to

$$\delta f_2 = \left(\frac{m}{\hbar}\right)^6 \iiint \int \left(\frac{\hbar}{im} \frac{\partial}{\partial \mathbf{r}_0}\right) \{f(t_0, \mathbf{x}_0^{(1)}, \boldsymbol{\xi}_0^{(1)}) f(t_0, \mathbf{x}_0^{(2)}, \boldsymbol{\xi}_0^{(2)})\} \\ \times \left\{ \frac{\partial \Psi^*}{\partial \boldsymbol{\rho}_0}(\mathbf{r} + \mathbf{s}) \Psi^*(\mathbf{r} - \mathbf{s}) - \frac{\partial \Psi^*}{\partial \boldsymbol{\rho}_0}(\mathbf{r} - \mathbf{s}) \Psi^*(\mathbf{r} + \mathbf{s}) \right\} \\ \times \exp\{m[\boldsymbol{\rho} \cdot \mathbf{s} + \{\mathbf{r}_0 + \boldsymbol{\rho}_0(t - t_0)\} \cdot \boldsymbol{\sigma}]/i\hbar\} d\mathbf{r}_0 d\boldsymbol{\rho}_0 d\mathbf{s} d\boldsymbol{\sigma}. \quad \dots\dots (29)$$

So long as one requires only terms linear in the gradients of n , \mathbf{u} , and β , the equilibrium form of f may be substituted in (29). To terms quadratic in the density, or linear in \hbar^2 , this is given by (see Green 1951)

$$f = \left(\frac{\beta m}{2\pi}\right)^{3/2} \exp(-\frac{1}{2}\beta m\xi^2) \left\{ n + \frac{\hbar^2\beta}{24m} \left(\frac{1}{3}\beta\xi^2 - 1\right) \int n_2 \frac{\partial^2 \phi}{\partial \mathbf{r} \cdot \partial \mathbf{r}} d\mathbf{r} \right\}, \quad \left. \vphantom{\int n_2} \right\} \dots\dots (30)$$

$$n_2 = n^2 \exp\{-\beta\phi(r)\}.$$

It is clear that, like J_1 in (21), δf_2 is quadratic in the density for small densities. The quantized form of Boltzmann's equation adopted by earlier authors is therefore verified, apart from corrections proportional to the square of the density. The quantum corrections would be very tedious to evaluate numerically; they may account, in part at least, for the discrepancies which have been noted (cf. Chapman and Cowling 1939) between the predictions of the quantum theory of the transport processes and experiment, at gaseous densities.

REFERENCES

- BORN, M., and GREEN, H. S., 1946, *Proc. Roy. Soc. A*, **188**, 10; 1947, *Ibid. A*, **191**, 168; 1949, *Notes to A General Kinetic Theory of Liquids* (Cambridge : University Press).
- CHAPMAN, S., and COWLING, T. G., 1939, *The Mathematical Theory of Non-Uniform Gases* (Cambridge : University Press).
- GREEN, H. S., 1951, *J. Chem. Phys.*, **19**, 955; 1952 a, *Ibid.*, **20**, 1274; 1952 b, *The Molecular Theory of Fluids* (Amsterdam : North Holland Publishing Co.), Ch. 9; 1952 c, *Proc. Phys. Soc. A*, **65**, 1022.
- IRVING, J. H., and ZWANZIG, R. W., 1951, *J. Chem. Phys.*, **19**, 1173.
- KIRKWOOD, J. G., 1946, *J. Chem. Phys.*, **14**, 180; 1947, *Ibid.*, **15**, 72.
- MASSEY, H. S. W., and MOHR, C. B. O., 1933, *Proc. Roy. Soc. A*, **141**, 434.
- MOYAL, J. E., 1949, *Proc. Camb. Phil. Soc.*, **45**, 99.
- WIGNER, E., 1932, *Phys. Rev.*, **40**, 749.
- YVON, J., 1937, *Actualités Scientifiques et Industrielles*, **542** (Paris : Hermann et Cie).

Anomaly of the $M_{IV,V}$ Absorption in Heavy Elements

By J. FRIEDEL†

H. H. Wills Physical Laboratory, University of Bristol

MS. received 28th October 1952

Abstract. The final state of the observed $M_{IV,V}$ absorption edge in heavy elements has a higher energy than the other (K, L, M) absorption edges. As suggested by Cauchois, this must be because, owing to selection rules, the transition probability of a 3d electron to the top of the conduction band is very small, and a strong absorption begins only when the ejected electron reaches the bottom of the 5f band. The corresponding energy is computed by the Wigner-Seitz method, and is in satisfactory agreement with the experimental data for the anomaly. As the anomaly disappears for the elements Ra to U, the conduction band of these elements must contain a proportion of 5f states. An anomaly of the same type is to be expected for the 4f band in the second long period, and actually seems to be observed.

§ 1. EXPERIMENTAL DATA AND PREVIOUS CONCLUSIONS

WHEN x-ray absorption edges can be observed in a metal corresponding to transitions from two initial states, the difference in the energies $h\nu$ usually corresponds to the energy difference between the two states as shown by the frequency of the emission lines. The $M_{IV,V}$ absorption edges in heavy metals, however, correspond to an energy higher than that deduced from the L_{III} edge and the $M_{IV,V}$ emission by an amount $\delta(h\nu)$ which seems larger than experimental error (Phelps 1934, McGrath 1939, Cauchois 1942, 1952). We give in table 1 the values of $\delta(h\nu)$ obtained by Cauchois, taking the L_{III} absorption edge as a reference (fig. 1):

$$\delta(h\nu) = (M_{IV,V})_{\text{abs}} - \{(L_{III})_{\text{abs}} + (M_{IV,V}, L_{III})_{\text{em}}\} \neq 0.$$

$\delta(h\nu)$ seems to go through a maximum of about 40 eV near W, then decreases regularly down to small negative values for Th, Pa, U. The small discrepancies between M_{IV} and M_V may be due to experimental errors.

Table 1. Experimental Values for $\delta(h\nu)$ in eV according to Cauchois (1952)

	Ta	W	Os	Ir	Pt	Au	Hg	Tl	Pb	Bi	Th	Pa	U
M_{IV}	37.5	42	41	37	32	25	18	20.5	9.5	13	-3	-3.5	-7
									21.7*				
M_V	37	44	38	37	35	29.5	21.5	17.5	9	9	-6.5	-5	-6.5
									20.3*				

* Values from Cauchois (1942).

McGrath and Cauchois conclude that, while the 2p electron ejected in L_{III} absorption may go to the top of the conduction band, the selection rules allow a strong $M_{IV,V}$ absorption only when the 3d electron is thrown into a state of

† Now at the Ecole des Mines, Paris.

the crystal with higher energy but more favourable symmetry. Cauchois suggests in her later paper (1952) that the electron is probably thrown into the bottom of the 5f band. The calculations of this paper will confirm this point of view: in other words, the absorption edge corresponds to a $M_{IV,V}-O_{VI,VII}$ transition.

§ 2. QUALITATIVE INTERPRETATION OF THE $M_{IV,V}$ ABSORPTION EDGE

We first interpret the anomaly in terms of Kronig's elementary theory of x-ray absorption in solids (§2.1). A more refined model given in §2.2 takes into account the screening of the hole created in the x-ray level, and leads to the same conclusions.

§ 2.1. Kronig Structure

As was first pointed out by Kronig (1933) and applied more quantitatively by Jones and Mott (1937), the intensity of x-ray absorption must be a function of the density and symmetry character of the states of the lattice into which the ejected electron is thrown.

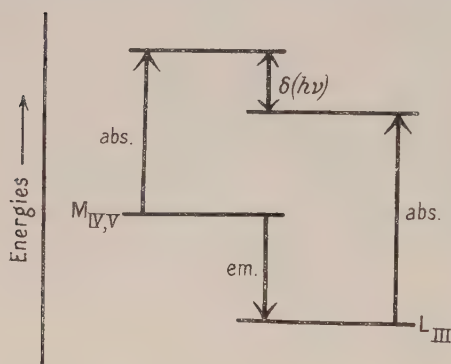


Fig. 1. Comparison of L_{III} and $M_{IV,V}$ absorption edges.

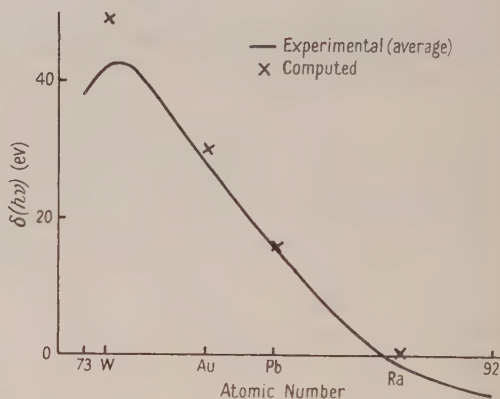


Fig. 2.

In the approximation of tight binding, which can of course give only qualitative indications, even when, as here, we use hybrid wave functions, we write for the wave functions of the electron in its initial and final states

$$\psi_i(\mathbf{r}) \simeq N^{-1/2} \sum_{n=1}^N \exp(i\mathbf{K} \cdot \mathbf{r}_n) \phi_i(\mathbf{r} - \mathbf{r}_n),$$

$$\psi_f(\mathbf{r}) \simeq N^{-1/2} \sum_{n=1}^N \exp(i\mathbf{K} \cdot \mathbf{r}_n) \sum_j a_j(\mathbf{K}) \phi_j(\mathbf{r} - \mathbf{r}_n),$$

where the ϕ_i , ϕ_j are wave functions of electrons in the free atom, and the summation n is over the N atoms of the metal. The momentum \mathbf{K} corresponds to the energy $\frac{1}{2}\hbar^2 K^2$ and is of course the same for ψ_i and ψ_f . The matrix element of the transition is thus

$$T_{ij} = \int \psi_f^* \nabla \psi_i d\tau \simeq N^{-1} \sum_{n=1}^N \sum_j a_j \int \phi_j^*(\mathbf{r} - \mathbf{r}_n) \nabla \phi_i(\mathbf{r} - \mathbf{r}_n) d\tau \simeq \sum_j a_j t_{ij},$$

where $t_{ij} = \int \phi_j^* \nabla \phi_i d\tau$ is the matrix element for transition $i \rightarrow j$ in the free atom, and transitions involving neighbouring atoms have been neglected.

In heavy elements the inner shells are occupied up to at least 5d; we have thus

$$\sum_j a_j \phi_j = a_1 \phi_{5d} + a_2 \phi_{6s} + a_3 \phi_{6p} + a_4 \phi_{6d} + a_5 \phi_{5f} + \dots$$

and, according to the symmetry of the initial state ns, np or nd:

$$T_I \simeq a_3 t_{ns, 6p} + \dots,$$

$$T_{II, III} \simeq a_1 t_{np, 5d} + a_2 t_{np, 6s} + a_4 t_{np, 6d} + \dots,$$

$$T_{IV, V} \simeq a_3 t_{nd, 6p} + a_5 t_{nd, 5f} + \dots$$

The matrix elements t_{ij} are related to the corresponding oscillator strengths f_{ij} by the relation* $|t_{ij}|^2 = f_{ij}(h\nu)_{ij}$ where $(h\nu)_{ij}$ is the energy of transition $i \rightarrow j$. As noted by Bethe (1933) the f_{ij} for a given element and given initial state i are nearly proportional to those of hydrogen (table 2). As $(h\nu)_{ij}$ is nearly the same for

Table 2. Oscillators Strengths f_{ij} for Transitions $i \rightarrow j$ in Hydrogen

i	j	f_{ij}	i	j	f_{ij}	i	j	f_{ij}
2p	5d	0.044	3p	5d	0.139	3d	6p	0.0009
2p	6s	0.0006	3p	6s	0.003	3d	5f	0.156
2p	6d	0.020	3p	6d	0.056			

all these transitions, the t_{ij} are nearly proportional to the square roots of the corresponding f_{ij} .

Now for all elements in table 1 except the last three, the top of the occupied band has mainly 5d and 6sp character, but very little 6d or 5f. In other words, a_1 , a_2 , a_3 are large, a_4 and a_5 small. This is because the 6d, 5f wave functions have definitely higher energies in the free atom, and thus certainly also in the metal: the energy of formation of 5f and 6d states in a neutral atom of gold for instance are respectively 7.4 and 7.7₂ eV, compared with 4.6₂ eV for 6p (Bacher and Goudsmit 1932). Owing to overlap of 5d and 6sp bands, even elements with filled 5d shells like Au, Hg, Pb . . . have of course a large proportion of 5d symmetry at the top of the occupied band.†

A glance at table 2 shows then that $L_{II, III}$ or $M_{II, III}$ absorptions will be large as soon as the 2p or 3p electron is thrown to the top of the conduction band. $M_{IV, V}$ on the contrary will be very weak until the ejected electron is raised to a zone of strong 5f character. There will then be a sudden increase of absorption giving the observed edge.

The additional energy $\delta(h\nu)$ required must therefore be equal to the difference of energy between the top of the conduction band and the bottom of the 5f band. We compute this difference in §3 for tungsten, gold, lead and radium, using the Wigner-Seitz method, and obtain reasonable agreement with Cauchois' data (fig. 2).

Our interpretation indicates that the conduction band of the last elements (Th, Pa, U) must have a strong 5f character. We must point out that the regular contraction of the lattice parameter in this series has been interpreted by Zachariasen (1952) and others as indicating that there are here no 5f electrons analogous to 4f electrons in the rare earth elements. Thus it seems probable that for Th, Pa, U there are no separate '5f electrons' or 'band' with definite properties, but only a complex conduction band with strong 5f character near

* Atomic units used throughout.

† Krutter's computations on 3d and 4sp bands in copper (1935) show the same effect.

some points of the zone structure. The 5f electrons would thus behave in a way similar to d electrons in a transitional metal.

§ 2.2. Screening of the Positive Hole

As pointed out elsewhere (Friedel 1952a), the necessary screening of the hole created, during absorption, in one atom of the metal may be in fundamental or in more excited states, and thus give rise to secondary absorption edges or lines.

A secondary absorption *edge* however, being in general weaker than the main one (Friedel 1952b,c), could not explain the strong anomaly observed. And the energy of the anomaly is too large to be explained by secondary *lines*. In gold, for instance, the K absorption edge would correspond to the excitation of a Au^+ ion from the state $1s^2 2s^2 \dots 5d^{10}$ to $1s 1s^2 \dots 5d^{10} 6s$; 6p and mainly 5f screenings should give absorption lines on the short wavelength side of the main edge, at distances corresponding to the energies of the transitions $6s \rightarrow 6p$ and $6s \rightarrow 5f$ of the Au^+ ion. By analogy with Hg^+ , this is about 6.5 and 15 eV respectively (Bacher and Goudsmit 1932), much less than the value observed (about 30 eV), and cannot explain the anomaly. Furthermore the 5f orbital, owing to its large Bohr radius, overlaps a number of neighbouring atoms and must be strongly perturbed by the lattice. This should reduce the strength of these lines, which have not been observed.

In conclusion, taking the screening into account, we still interpret the anomaly as a Kronig structure.

§ 3. EVALUATION OF THE ENERGY DIFFERENCE BETWEEN THE TOP OF THE CONDUCTION BAND AND THE BOTTOM OF THE 5f BAND IN W, AU, PB AND RA.

Let E_1 be the energy of the top of the conduction band and E_2 that of the bottom of the 5f band. E_1 will be deduced from experimental data; E_2 will be computed by a Wigner-Seitz method. Both are measured from a zero taken as the potential energy of an electron put at infinity outside the metal. $\delta(h\nu)$ will then be given by $\delta(h\nu) = E_2 - E_1$.

§ 3.1. Energy E_1 of the Top of the Conduction Band

If we assume that in a metal the cohesive energy E_s is due to a change in energy of the valency electrons only, E_1 may be deduced from the maximum Fermi energy E_m and the first ionization potential E_i by the approximate relation:

$$-E_1 \simeq E_i + n^{-1}E_s - 0.4E_m, \quad \dots\dots(1)$$

where n is the number of valency electrons per atom. This relation is obtained by assuming that the cohesive energy is due only to a change in energy of the valency electrons, and that the approximations of tight binding are valid. Table 3 gives values of E_1 computed using the cohesive energies given by Kubaschewski and Evans (1951), the first ionization potentials given by Bacher and Goudsmit (1932) and Sommerfeld's values for E_m . Formula (1) is of course not very accurate, either for gold, where an important part of E_s is probably due to van der Waals interactions of the d shells, or for W, Pb and Ra, where the approximation of free electrons is probably not very good for the conduction band.

§3.2. Energy E_2 of the Bottom of the 5f Band

We use here the cellular method of Wigner and Seitz (1933) and Slater (1934) and hence determine the energy $E_2 = \frac{1}{2}k^2$ of the 5f wave function with radial part $\psi = r^{-1}\phi$, such that for $r = r_s$, the radius of an atomic sphere,

$$\psi^{-1} d\psi/dr = \phi^{-1} d\phi/dr - r^{-1} = 0. \quad \dots\dots(2)$$

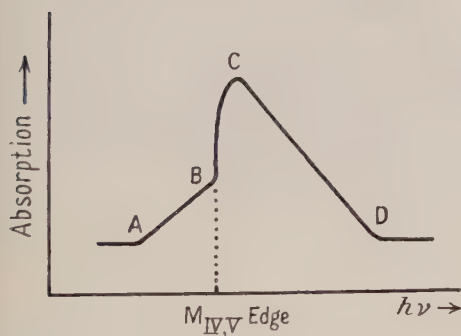
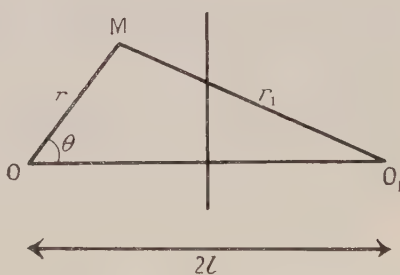
This condition is obtained in Slater's method for r equal to half the interatomic distance. But the 5f wave functions are then continuous only at the centre of the faces of the atomic polyhedra. As shown by Wigner and Seitz for s functions, it is better in this case to equate r to r_s .

Table 3. Computation of $\delta(h\nu)$ in ev. Experimental Data from Table 1

Metal	n	$r_s(\text{\AA})$	$-E_1$	E_2	$-E_0$	$-E_c$	$\delta(h\nu)_{\text{calc}}$	$\delta(h\nu)_{\text{exp}}$	
								M_{IV}	M_V
W	6	1.56	6.2	46.5	1.2	2.3	49.2	42	44
Au	1	1.59	10.9	21.6 ₅	0.6	1.9 ₅	30.0	25	29.5
Pb	4	1.93	4.1 ₅	17.1	2.7	2.1	16.4	9.5	9
								(21.7)	(20.3)
Ra	2	2.6	5.2	2.1 ₅	4.2 ₅	1.7 ₅	1.3 ₅	$\simeq 0$	

E_e =exchange energy, E_c =energy of correlation.

The use of condition (2) seems reasonable for the structures studied here, for none of the three types of 5f wave functions (one of the type xyz , three of the type $x(x^2 - 3y^2)$, three of the type $x(y^2 - z^2)$) is suitable to form bounds in the required directions. We must point out however that, owing to overlap of the so-called '5f band' with 6s, 6p, 6d bands, some of the seven zones starting

Fig. 3. Observed form of the M_{IV} or M_V absorption edge for Os and Pt.Fig. 4. Potential V_3 due to overlap of the d shells.

at energy E_2 have probably another symmetry (6s, 6p, 6d) and consequently some of the bands whose top is at energy E_2 may have 5f symmetry. Also the '5f zones' with 5f symmetry near E_2 may change over to other symmetries for higher energies. Owing to these 'inversions' we must expect in general some absorption on the long wavelength side of the $M_{IV,V}$ edge (AB, fig. 3), and a rapid decrease of absorption on the short wavelength side (CD). An absorption of this type seems to be observed at least in some cases (cf. Rogers 1927 for Os M_{IV} , Pt M_V).

We give now some technical details concerning the method used. Equation (2) was solved for k by the WKB method, as explained in the Appendix. This approximation is sufficient for these wave functions with high quantum number l .

The potential V acting on the 5f electron is made up of several parts:

(a) The potential V_1 of the inner ion (W^{6+} , Au^+ , Pb^{4+} , Ra^{2+}) at the centre of the atomic polyhedron. V_1 was computed by Fermi's approximation of the Thomas-Fermi method (Gombás 1949).

(b) The coulomb potential V_2 of the n Fermi electrons contained in the atomic polyhedron. Assuming they have a uniform density, we have in atomic units $V_2 = n[(r^2/2r_s^3) - (3/2r_s)]$.

(c) In gold, a fraction of the 5d shells of the 12 neighbouring Au^+ ions enters the atomic polyhedron considered. The corresponding potential V_3 was computed by replacing the density ρ of this supplementary charge by an equivalent spherically symmetrical one (fig. 4):

$$\bar{\rho}(r) \simeq 12 \times \frac{1}{2} \int_0^\pi \rho(r_1) \sin \theta d\theta = \frac{3}{2rl} \int_{(2l-r)^2}^{(2l+r)^2} \rho(r_1) d(r_1^2).$$

ρ is deduced from the potential computed for Au^+ and may be approximated by an analytical expression which gives easily $4\pi r^2 \bar{\rho}(r) \simeq 0.02r$, hence $V_3 \simeq 0.140(\frac{1}{2}r - r_s)$. Taking now $V = V_1 + V_2 + V_3$, we found the values of E_2 listed in table 3. For radium, the value taken for r_s corresponds to the density given by Smithells (1949).

V_2 and V_3 are large. They have been included in V and not averaged separately because, contrary to what happens in alkali metals, the 5f wave function treated here cannot be considered as constant over the major part of the atomic polyhedron. Smaller corrective terms due to correlation will now be averaged separately.

§3.3. Corrective Terms Added to E_2

The electron ejected into the bottom of the 5f band is at rest, and we must therefore add to E_2 the energy of correlation E_c of an electron of momentum zero with the conduction electrons of opposite spin. This energy has not been computed, but we can take as an approximation twice the average correlation energy per electron in the conduction band. This is approximately in atomic units (Wigner 1934, Macke 1950) $E_c \simeq -2 \times 0.288(r_s n^{-1/3} + 5.1)^{-1}$. The factor 2 is due to the fact that, in the averaging process used by Wigner, one counts the interaction of the conduction electrons twice.

On the other hand, in computing the exchange energy E_e of the 5f electron with the conduction band, the symmetry of the 5f wave function must be taken into account. It is probably a better approximation to treat the 5f electron here as if it was a free electron of momentum $k_1 = [2(\delta(h\nu) + E_m)]^{1/2}$. E_e is then given by Seitz (1940), $E_e = -2 \times 0.306 n^{1/3} r_s^{-1} [1 + (1 - \alpha^2)(2\alpha)^{-1} \ln \{1 + \alpha / |1 - \alpha|\}]$, where $\alpha = k_1/k_m$ and $k_m = (2E_m)^{1/2}$. The factor 2 is introduced for the same reason as in E_c .

E_c and E_e , computed with the experimental value of $\delta(h\nu)$, are given in table 3. $\delta(h\nu)$ is then obtained from $\delta(h\nu) \simeq E_2 + E_c + E_e - E_1$.

We have neglected in this treatment the correlation between the 5f electron and the inner ions, and the exchange and relativistic corrections in the potential of the inner ion. The values obtained (table 3) compare favourably with the anomaly observed for the $M_{IV,V}$ absorption (fig. 2). For radium the experimental

value obtained by interpolation is near to zero. For lead the agreement is somewhat better with Cauchois' older data.

Finally we expect an anomaly of the same type for the 4f band in the second long period. Rather scanty data, taking the K absorption edge as a reference (Cauchois and Hulubei 1947), seem to confirm this point (table 4).

Table 4. Anomaly $\delta(h\nu)$ in ev. Ag K absorption is measured for AgBr only

$\delta(h\nu)$	Ag	Sn	I
M_{IV}	(34)		
		20	7
M_V	(29)		

ACKNOWLEDGMENTS

The author wishes to thank Professor Y. Cauchois for pointing out the anomaly studied here, and the Direction des Mines for enabling him to stay in Bristol.

APPENDIX

Solution of the Wigner-Seitz Method by the WKB Approximation

Equation (2) of the text must be solved for $\phi(r)$, which is a solution of $d^2\phi/dr^2 + K^2\phi = 0$ with $K^2 = k^2 + 2V(r) - l(l+1)r^{-2}$, where V is the potential acting on the 5f electron. The WKB approximation takes different forms according to the sign of $K^2(r_s)$.

First case: $K^2(r_s) > 0$. One has for r near to r_s the exact system $\phi = a \sin u$; $\phi^{-1} d\phi/dr = K \cot u$, with

$$du/dr = (2K)^{-1}(dK/dr) \sin 2u + K; \quad a^{-1}(da/dr) = -(2K)^{-1}(dK/dr)(1 + \cos 2u).$$

The WKB approximation neglects the oscillating terms in $\sin 2u$, $\cos 2u$ (Friedel 1952 b). Condition (2) thus gives

$$K \cot u = r_s^{-1}, \quad \text{with} \quad u \simeq \int_{r_1}^{r_s} K dr + \frac{1}{4}\pi + \delta. \quad \dots\dots (3)$$

Here r_1 is the last zero of K before r_s :

$$K(r_1) = 0 \quad \text{and} \quad K^2(r) \geq 0 \quad \text{for} \quad r_1 \leq r \leq r_s.$$

δ is a phase shift which depends on the behaviour of K for $r < r_1$.

If r_1 is the only zero of K , $\delta = 0$; this solution was used for tungsten. If on the other hand K^2 has three other zeros r_2, r_3, r_4 and changes its sign each time r crosses one of them, one shows easily (Wu 1933) that

$$\delta = \arctan \left[\frac{1}{4} \exp \left\{ -2 \int_{r_3}^{r_2} |K| dr \right\} \tan \int_{r_4}^{r_s} K dr \right]. \quad \dots\dots (4)$$

The solution (3), (4) was used for lead.

Second case: $K^2(r_s) < 0$. We may write near to r_s

$$\phi \simeq |K|^{-1/2} \left\{ A \exp \left(\int_{r_1}^r |K| dr \right) + B \exp \left(- \int_{r_1}^r |K| dr \right) \right\}, \quad \dots\dots (5)$$

where A and B are two constants and r_1 is the last zero of K before r_s .

We study only the simplest case where K^2 has two other zeros, r_2 , r_3 and changes its sign when r goes through any one of them. Then for $r_2 < r < r_1$ we have

$$\phi_1 \simeq K^{-1/2} \sin \left(\int_{r_2}^r K dr + \frac{1}{4}\pi \right).$$

But as Jeffreys first showed (Mott and Sneddon 1948) the form (5) valid for $r > r_1$ corresponds for $r < r_1$ to

$$\phi_2 \simeq CK^{-1/2} \sin \left(\int_r^{r_1} K dr + \frac{1}{4}\pi + \epsilon \right), \quad \dots\dots(6)$$

with $\tan \epsilon = A/2B$, and C a constant. The condition that ϕ_1 and ϕ_2 are identical gives $\phi_1'/\phi_1 = \phi_2'/\phi_2$; hence

$$\int_{r_1}^{r_2} K dr = (n + \frac{1}{2})\pi - \epsilon \quad (n \text{ integral}). \quad \dots\dots(7)$$

Condition (2) gives then

$$\frac{1}{r_s} = -\frac{1}{2} \frac{d|K|}{|K|dr} + |K| \frac{A \exp \left(2 \int_{r_1}^{r_s} |K| dr \right) - B}{A \exp \left(2 \int_{r_1}^{r_s} |K| dr \right) + B},$$

or, using relations (6), (7),

$$\tan \int_{r_1}^{r_2} K dr = 2 \frac{1-v}{1+v} \exp \left(2 \int_{r_1}^{r_s} |K| dr \right), \quad \dots\dots(8)$$

with

$$v = \frac{1}{|K|} \left(\frac{1}{r_s} + \frac{1}{2} \frac{d|K|}{|K|dr_s} \right).$$

This solution was used for gold and radium.

REFERENCES

- BACHER, R. F., and GOUDSMIT, S., 1932, *Atomic Energy States* (New York: McGraw-Hill).
 BETHE, H. A., 1933, *Handb. d. Phys.*, **24**, 1, p. 469.
 CAUCHOIS, Y., 1942, *Disquisitiones Math. et Phys.*, **2**, 319; 1952, *J. Phys. Radium*, **13**, 113.
 CAUCHOIS, Y., and HULUBEI, H., 1947, *Constantes sélectionnées* (Paris: Hermann).
 FRIEDEL, J., 1952 a, *Phil. Mag.*, [7], **43**, 1115; b, *Ibid.*, [7], **43**, 153; c, *Proc. Phys. Soc. B*, **65**, 769.
 GOMBÁS, P., 1949, *Statistische Theorie des Atoms* (Wien: Springer) p. 47.
 JONES, H., and MOTT, N. F., 1937, *Proc. Roy. Soc. A*, **162**, 49.
 KRONIG, R. de L., 1933, *Handb. d. Phys.*, **24**, 1, p. 290.
 KRUTTER, H. M., 1935, *Phys. Rev.*, **48**, 644.
 KUBASCHEWSKI, O., and EVANS, L. L., 1951, *Metallurgical Thermochemistry* (London: Butterworths Scientific Publications) p. 264.
 MCGRATH, J. W., 1939, *Phys. Rev.*, **56**, 157, 765.
 MACKE, W., 1950, *Z. Naturforsch.*, **5a**, 192.
 MOTT, N. F., and SNEDDON, I. N., 1948, *Wave Mechanics* (Oxford: University Press) p. 21.
 PHELPS, W. D., 1934, *Phys. Rev.*, **46**, 357.
 ROGERS, R. A., 1927, *Phys. Rev.*, **30**, 747.
 SANDSTRÖM, A., 1930, *Z. Phys.*, **65**, 632.
 SEITZ, F., 1940, *Theory of Solids* (New York: McGraw-Hill) p. 340.
 SIEGBAHN, M., 1931, *Spektroskopie der Röntgenstrahlen* (Berlin: Springer).
 SLATER, J. C., 1934, *Phys. Rev.*, **45**, 794.
 SMITHELLS, C. J., 1949, *Metals Reference Book* (London: Butterworths Scientific Publications).
 WIGNER, E., 1934, *Phys. Rev.*, **46**, 1002.
 WIGNER, E., and SEITZ, F., 1933, *Phys. Rev.*, **43**, 804.
 WU, TA-YOU, 1933, *Phys. Rev.*, **44**, 727.
 ZACHARIASEN, W. H., 1952, *Acta Crystallogr.*, **5**, 660.

Internal Pairs in Anisotropic Emission

By G. GOLDRING

Imperial College of Science and Technology, London

Communicated by S. Devons; MS. received 27th October 1952

Abstract. The angular correlation of internally converted pairs is investigated for cases in which the gamma rays are emitted anisotropically. Interference between electric and magnetic multipoles is considered.

§ 1. INTRODUCTION

HORTON (1948) and Rose (1949) have pointed out that the multipolarity of electromagnetic transitions in nuclei can be determined by measurements of the angular correlation of internally converted pairs.

Rose's calculations are valid for cases in which the accompanying gamma radiation is emitted isotropically (for example, transitions following beta decay). The pair emission is then also isotropic in the sense that the probability of emission will not depend on the orientation in space of the triangle formed by \mathbf{p}_+ , \mathbf{p}_- , the momenta of the two electrons. (It will, of course, depend on the size and shape of the triangle.)

Radiations from excited nuclear states produced by bombarding a target with a particle beam, are not in general isotropic. In this paper Rose's results are extended to include radiations of this type.

§ 2. CALCULATIONS

The notation and the units adopted by Rose (1949) will be used throughout. The momenta of the electrons are given by \mathbf{p}_+ , \mathbf{p}_- ; θ , ϕ are the polar angles of $\mathbf{q} = \mathbf{p}_+ + \mathbf{p}_-$ about the axis of quantization \mathbf{z} , and Θ , δ are the polar angles of \mathbf{p}_+ about \mathbf{p}_- (δ is the angle between the $(\mathbf{p}_+, \mathbf{q})$ and (\mathbf{z}, \mathbf{q}) planes).

If the axis of quantization is an axis of symmetry, the component of angular momentum along that axis J_z is a constant of motion, and the probability of a pair being emitted per quantum into solid angles $d\Omega_+$, $d\Omega_-$ and energy interval dW_+ is:

$$F_l(\Theta, \delta, \theta, \phi) d\Omega_+ d\Omega_- dW_+ = \sum_m a_m f_l^m(\Theta, \delta, \theta, \phi) d\Omega_+ d\Omega_- dW_+$$

where $a_m = \sum_{m'} \alpha_{m'} b_{jm', j'm'-m}$; m' are the eigenvalues of J_z , $\alpha_{m'}$ is the fractional population of the m' th initial substate of the emitting nucleus, $b_{jm', j'm'-m}$ is the relative strength of the transition $jm' \rightarrow j'm' - m$ for different m and m' , and f_l^m the probability function for an l, m transition. The coefficients a_m represent the fractional populations of the substates of the radiation field.

If the $\alpha_{m'}$ are all equal the distribution will be isotropic, that is, independent of the spatial orientation angles δ , θ , ϕ . Then also $a_0 = a_{\pm 1} = \dots = 1/(2l+1)$, and we have:

$$F_l(\Theta) = \sum_m a_m f_l^m(\Theta, \delta, \theta, \phi) = \frac{1}{2l+1} \frac{1}{8\pi^2} \sum_m \int f_l^m(\Theta, \delta, \theta, \phi) d\delta \sin \theta d\theta d\phi = \frac{1}{8\pi^2} \gamma_l(\Theta) \dots (1)$$

where $\gamma_l(\Theta)$ is the correlation function integrated over all angles except the angle between the electrons. $\gamma_l(\Theta)$ is independent of m (see Rose 1949).

In this case averaging over m is equivalent to integrating over the orientation angles (principle of spectroscopic stability), and we can say that the significance of the integrated correlation $\gamma_l(\Theta)$ calculated by Rose is that it gives the correct (m averaged) differential distribution for cases in which the radiation is isotropic.

Radiations induced by particle beams are not in general isotropic, and the expression $\Sigma_m a_m f_l^m$ will have to be calculated for each case separately. We still have cylindrical symmetry about the axis of the beam which we shall take as the axis of quantization \mathbf{z} .

The matrix elements of the transition can be written in the following way:

$$\mathcal{H}_i^m = (i|1|f) \bar{V}_i^m + (i|\alpha|f) \bar{\mathbf{A}}_i^m \quad \dots\dots(2)$$

where i, f are the initial and final spin states of the electron (including its description as negatron or positron) and:

$$\left. \begin{aligned} \text{for } M_l \quad \bar{\mathbf{A}}_i^m &= \int e^{-i\mathbf{q}\cdot\mathbf{r}} \mathbf{A}_i^m d\tau = (-i)^{l-1} \left[\frac{2}{\pi l(l+1)} \right]^{1/2} \frac{4\pi}{k} \left(\frac{q}{k} \right)^l \frac{1}{k^2 - q^2} \left\{ \begin{aligned} &\times \mathbf{q} \times \text{grad } \mathbf{q} Y_l^m(\theta, \phi) = \mathbf{q} \times \mathbf{a}_{lM}^m \\ &\bar{V}_i^m = 0, \end{aligned} \right\} \dots\dots(2a) \\ \text{for } E_l \quad \bar{\mathbf{A}}_i^m &= \int e^{-i\mathbf{q}\cdot\mathbf{r}} \mathbf{A}_i^m d\tau = (-i)^{l-1} \left[\frac{2}{\pi l(l+1)} \right]^{1/2} \frac{4\pi}{k} \left(\frac{q}{k} \right)^{l-1} \frac{1}{k^2 - q^2} \\ &\times \left(q \text{grad} + l \frac{\mathbf{q}}{q} \right) Y_l^m(\theta, \phi) = \mathbf{a}_{lE}^m \\ \bar{V}_i^m &= \int e^{-i\mathbf{q}\cdot\mathbf{r}} V_i^m d\tau = (-i)^{l-1} \left[\frac{2l}{\pi(l+1)} \right]^{1/2} \frac{4\pi}{k} \left(\frac{q}{k} \right)^l \frac{1}{k^2 - q^2} Y_l^m(\theta, \phi) = v_l^m \end{aligned} \right\} \dots\dots(2b)$$

\mathbf{A}_i^m, V_i^m are the fields given by Rose (1949, eqns. (1 a) (1 b) (1 d)).

k is the energy of the pair (in units of mc^2).

The probability functions f_l^m can readily be found by taking the matrix elements in this form.

We shall take the directions of both electrons perpendicular to \mathbf{z} . In this way we get particularly simple expressions.

$$\begin{aligned} \text{For } M_l \quad 2\pi l(l+1) F_l(\Theta, \tfrac{1}{2}\pi, \tfrac{1}{2}\pi, \phi) &= \gamma_l(\Theta) \Sigma a_m |q \text{grad } Y_l^m|_{\theta=\pi/2}^2 \\ &+ \frac{2\alpha}{\pi k^3} \frac{p_+ p_-}{(k^2 - q^2)^2} \left(\frac{q}{k} \right)^{2l-2} (\mathbf{p}_+ \times \mathbf{p}_-)^2 \Sigma (-)^{l-m} a_m |q \text{grad } Y_l^m|_{\theta=\pi/2}^2 \dots(3a) \end{aligned}$$

where α is the fine structure constant.

$$\begin{aligned} \text{For } E_l \quad 2\pi l(l+1) F_l(\Theta, \tfrac{1}{2}\pi, \tfrac{1}{2}\pi, \phi) &= \gamma_l(\Theta) l(l+1) \Sigma a_m |Y_l^m|_{\theta=\pi/2}^2 \\ &+ \frac{2\alpha}{\pi k^3} \frac{p_+ p_-}{(k^2 - q^2)^2} \left(\frac{q}{k} \right)^{2l-4} (\mathbf{p}_+ \times \mathbf{p}_-)^2 \Sigma (-)^{l-m-1} a_m |q \text{grad } Y_l^m|_{\theta=\pi/2}^2 \\ &+ \frac{2\alpha}{\pi k^3} \frac{p_+ p_-}{(k^2 - q^2)^2} \left[\left(\frac{q}{k} \right)^{2l-2} \tfrac{1}{2} k^2 (k^2 - q^2) - \left(\frac{q}{k} \right)^{2l-4} (\mathbf{p}_+ \times \mathbf{p}_-)^2 \right] \\ &\times \Sigma a_m (|q \text{grad } Y_l^m|_{\theta=\pi/2}^2 - l(l+1) |Y_l^m|_{\theta=\pi/2}^2) \dots\dots(3b) \end{aligned}$$

$$\begin{aligned} |Y_l^m|_{\theta=\pi/2}^2 &= \begin{cases} \frac{2l+1}{2^{2l+1}} \binom{l-m}{\frac{1}{2}(l-m)} \binom{l+m}{\frac{1}{2}(l+m)} \cdot \frac{1}{2\pi} & \text{for } l+m \text{ even} \\ 0 & \text{for } l+m \text{ odd} \end{cases} \\ |q \text{grad } Y_l^m|_{\theta=\pi/2}^2 &= \begin{cases} m^2 |Y_l^m|_{\theta=\pi/2}^2 & \text{for } l+m \text{ even} \\ \frac{2l+1}{2l+3} (l+m+1)(l-m+1) |Y_{l+1}^m|_{\theta=\pi/2}^2 & \text{for } l+m \text{ odd.} \end{cases} \end{aligned}$$

The $\gamma_l(\Theta)$ are the integrated correlations (Rose 1949, eqns. (8) and (7)). They can be written:

$$\text{for } M_l \quad \gamma_l(\Theta) = \left(\frac{q}{k}\right)^{2l-2} \gamma_{1M}(\Theta) \quad \dots\dots (4a)$$

$$\text{for } E_l \quad \gamma_l(\Theta) = \frac{2l}{l+1} \left(\frac{q}{k}\right)^{2l-2} \gamma_{1E}(\Theta) - \frac{l-1}{l+1} \left(\frac{q}{k}\right)^{2l-4} \gamma_{1M}(\Theta) \quad \dots\dots (4b)$$

where $\gamma_{1M}(\Theta)$, $\gamma_{1E}(\Theta)$ are the integrated magnetic and electric dipole correlation functions respectively:

$$\gamma_{1M}(\Theta) = \frac{\alpha}{2\pi k^3} p_+ p_- \left\{ \frac{4k^2}{(k^2 - q^2)^2} + 2 \frac{p_+^2 + p_-^2}{k^2 - q^2} - 1 \right\}$$

$$\gamma_{1E}(\Theta) = \frac{\alpha}{2\pi k^3} p_+ p_- \left\{ \frac{4k^2}{(k^2 - q^2)^2} + 2 \frac{W_+^2 + W_-^2}{k^2 - q^2} + 1 \right\}.$$

If we put in (3a), (3b) $a_0 = a_{\pm 1} = \dots = 1/(2l+1)$ all terms except the first vanish and we get (1), as expected.

The coefficients a_m will in general be unknown, but if the angular distribution $H(\theta)$ (with respect to the beam) of the gamma-rays emitted in the same transition is known, we must have:

$$H(\theta) \sim \sum_m a_m h_l^m(\theta) \quad \dots\dots (5)$$

where $h_l^m(\theta)$ is the angular distribution of an l, m wave which is known for every l and m .

The a_m are completely determined by (5) for every l with which they are compatible, and when inserted in (3a), (3b) give us a set of unambiguous correlation functions $F_l(\Theta)$ which can then be compared with the measured correlation.

§ 3. EXAMPLES

We shall write down explicitly the three partial correlation functions for the electric dipole:

$$f_{1E}^0(\Theta, \tfrac{1}{2}\pi, \tfrac{1}{2}\pi, \phi) = \frac{\alpha}{k} \frac{3}{16\pi^3} \frac{p_+ p_-}{k^2 - q^2}$$

$$f_{1E}^{\pm 1}(\Theta, \tfrac{1}{2}\pi, \tfrac{1}{2}\pi, \phi) = \frac{\alpha}{k^3} \frac{3}{32\pi^3} p_+ p_- \left\{ \frac{4k^2}{(k^2 - q^2)^2} + \frac{k^2 - 4W_+ W_-}{k^2 - q^2} + 1 \right\}.$$

The correlation function that is most conveniently measured is the integral of $F_l(\Theta)$ over energy. We put:

$$g_l^m(\Theta) = \int_1^{k-1} f_l^m(\Theta, \tfrac{1}{2}\pi, \tfrac{1}{2}\pi, \phi) dW_+$$

$$\Gamma_l(\Theta) = \int_0^{k-1} \gamma_l(\Theta) dW_+$$

In discussing $g_l^m(\Theta)$ or $\Gamma_l(\Theta)$ it is useful to divide the range of angles Θ into 'small' and 'large' angles, the large angles being defined by $1 - \cos \Theta > 1/k$. For the large angles the functions $g_l^m(\Theta)$ are not strongly energy dependent and tend to a limit as $k \rightarrow \infty$. These limiting values which we shall call $g_l^m(\Theta)_\infty$, $\Gamma_l(\Theta)_\infty$, are

easily evaluated, and can serve as a general indication of the behaviour of the correlation functions for large angles and high energies.

For E_1

$$g_{1E}^0(\Theta)_\infty = \frac{\alpha}{8\pi^2} \frac{3}{4\pi} \frac{1}{u}$$

$$g_{1E}^{\pm 1}(\Theta)_\infty = \frac{\alpha}{8\pi^2} \frac{3}{8\pi} \left\{ \frac{1}{3u} + \frac{1}{3} \right\}$$

where $u = 1 - \cos \Theta$.

In the table we give the functions $\Gamma_{lE}(\Theta)_\infty$, $\Gamma_{lM}(\Theta)_\infty$, for $l = 1, 2, 3$ and $\epsilon_l(\Theta)_\infty$, $\eta_l(\Theta)_\infty$, the asymptotic values of the integrals over energy of the 'anisotropic terms' appearing in (3a), (3b):

$$\epsilon_l(\Theta) = \frac{2\alpha}{\pi k^3} \int_1^{k-1} \frac{\mathbf{p}_+ \mathbf{p}_-}{(k^2 - q^2)^2} \left(\frac{q}{k} \right)^{2l-2} (\mathbf{p}_+ \times \mathbf{p}_-)^2 dW_+$$

$$\eta_l(\Theta) = \frac{2\alpha}{\pi k^3} \int_1^{k-1} \frac{\mathbf{p}_+ \mathbf{p}_-}{k^2 - q^2} \left(\frac{q}{k} \right)^{2l-2} \frac{1}{2} k^2 dW_+$$

l	$\frac{2\pi}{\alpha} \Gamma_{lE}(\Theta)_\infty$	$\frac{2\pi}{\alpha} \Gamma_{lM}(\Theta)_\infty$	$\frac{2\pi}{\alpha} \epsilon_l(\Theta)_\infty$	$\frac{2\pi}{\alpha} \eta_l(\Theta)_\infty$
1	$\frac{2}{3u} + \frac{1}{6}$	$\frac{2}{3u} - \frac{1}{6}$	$\frac{1}{3u} - \frac{1}{6}$	$\frac{1}{u}$
2	$\frac{2}{3u} + \frac{1}{90} - \frac{8}{90}u$	$\frac{2}{3u} - \frac{11}{30} + \frac{1}{15}u$	$\frac{1}{3u} - \frac{3}{10} + \frac{1}{15}u$	$\frac{1}{u} - \frac{1}{3}$
3	$\frac{2}{3u} - \frac{1}{6} - \frac{5}{42}u + \frac{3}{70}u^2$	$\frac{2}{3u} - \frac{17}{30} + \frac{22}{105}u - \frac{1}{35}u^2$	$\frac{1}{3u} - \frac{13}{30} + \frac{4}{21}u - \frac{1}{35}u^2$	$\frac{1}{u} - \frac{2}{3} + \frac{2}{15}u$

§ 4. INTERFERENCE

In a mixed M_l , E_{l+1} transition interference terms will appear. If angular correlation measurements are undertaken with the intention of establishing the polarity of a transition, these terms constitute a serious complication, as they add unknown continuous parameters (the ratios of magnetic and electric moments) to an otherwise finite and usually very restricted number of possibilities. It is therefore worth while finding conditions under which the interference terms vanish.

We consider the term: $(\bar{V} + \alpha \bar{\mathbf{A}}_{l+1E}^m) \alpha \bar{\mathbf{A}}_{lM}^{m*}$. From (2), (2a), (2b) we get after summing over the spins:
for M_l , E_{l+1} interference

$$f_{l,l+1}^m = \frac{\alpha k}{32\pi^2} \mathbf{p}_+ \mathbf{p}_- \{ v_{l+1}^m (W_- - W_+) + (\mathbf{p}_- - \mathbf{p}_+, \mathbf{a}_{l+1E}^m) \} (\mathbf{p}_+ \times \mathbf{p}_-, \mathbf{a}_{lM}^{m*}) \dots (6)$$

where v_{l+1}^m , \mathbf{a}_{l+1E}^m , \mathbf{a}_{lM}^m are given by (2a), (2b).

The integral of $f_{l,l+1}^m$ over δ and θ vanishes, so that there is no interference in the isotropic case. In the general case we shall again take the directions of the electrons perpendicular to the axis of quantization. Then the integral of (6) over energy vanishes if the sensitivities of both detectors extend over the same range.

§ 5. CONCLUSION

The angular correlation of internally converted pairs has been investigated for conditions which obtain when the excited state is formed in a nuclear reaction involving a particle beam.

It is advantageous to place the two detectors in the plane through the target perpendicular to the beam, and make them sensitive over the same range of energies. No interference between magnetic and electric transitions will then be observed, and for each particular transition the angular correlation will be given by the integral of (3 *a*), (3 *b*) over the appropriate energy interval.

ACKNOWLEDGMENTS

I would like to express my gratitude to Professor S. Devons for very helpful discussions.

This work has been carried out with the help of a grant from the "Friends of the Hebrew University", London.

REFERENCES

- HORTON, G. K., 1948, *Proc. Phys. Soc.*, **60**, 457.
ROSE, M. E., 1949, *Phys. Rev.*, **76**, 678.

Observations of Extensive Cosmic-Ray Showers Below Ground

BY E. P. GEORGE, J. W. MACANUFF AND J. W. STURGESS

Birkbeck College, University of London

MS. received 13th October 1952

Abstract. The decoherence curve of extensive showers has been studied at a depth of 60 m water equivalent below ground out to a distance of 320 m. The relative frequencies of coincidences in various combinations of counter sets are found to be consistent with the assumption that the frequency of showers containing N particles is proportional to $N^{-\gamma}$ with $\gamma = 3.2 \pm 0.2$. By comparison with observations at other depths it is concluded that the particles in extensive showers are absorbed less rapidly in the earth than the normal particles of the vertical component. The observed showers can be readily understood in terms of the small fraction of penetrating particles (presumed μ -mesons) that is known to exist in extensive showers observed at sea level. At counter separations less than 3 m the observed coincidences are much too frequent to be attributed to extensive showers, indicating a significant contribution from locally produced penetrating particles. The origin of these secondary particles is discussed.

§1. INTRODUCTION

IT has been known for some time that the Auger showers (Auger *et al.* 1938) are not examples of pure electron-photon cascades, since they contain some particles more penetrating than electrons (Auger 1938, Broadbent and Jánosy 1948, Treat and Greisen 1948). At sea level the fraction of penetrating particles is about 2%, 75% of this group consisting of μ -mesons and approximately 25% of more strongly interacting particles (McCusker 1950). When an Auger shower strikes the ground, the electron-photon component and the strongly interacting component should be effectively removed in a few yards of earth, leaving the μ -meson skeleton. At large depths below ground remnants of normal sea-level extensive showers should be found. We decided to look for these events in our underground laboratory in London on the tube railway, and an account of the investigation is given in this paper. Preliminary reports have previously been published by George (1949, 1951).

The observations were begun in 1948, at which time there was some difference of opinion as to the nature and origin of these penetrating particles in Auger showers (Broadbent and Jánosy 1948, Treat and Greisen 1948), and the experiment was intended to clarify some of the points in dispute. In the meantime the situation has become considerably clearer and our results may be regarded as confirming the qualitative picture we now have of the development of cascades of both hard and soft particles from nuclear collisions of great energy.

§2. EXPERIMENTAL

The observations were made at a depth of 30 m below ground in a disused railway tunnel. The density of the local material was 2.0 g cm^{-2} and the equivalent depth was therefore 60 metres of water. Two separate investigations were carried out on 'extensive' and 'local' showers respectively, in the nomenclature of other workers.

(i) *Extensive Showers*

For extensive showers we recorded coincidences between large sets of counters, I, II, III, IV disposed as in fig. 1, the walls of the tunnel necessitating their lying more or less in a single straight line. Sets II and III remained permanently in our underground laboratory, while sets I and IV were moved to various separations up to the limits determined one way by the running trains and the other by a wall blocking the tunnel, the resulting maximum extension between sets I and IV being 320 m. To reduce accidental coincidences each of the sets consisted of either two or three trays of counters placed closely above each other. Each tray had many counters in parallel, coincidences between trays being selected by conventional circuits of microsecond resolving time. Details of the counter sets are given in table 1.

Table 1

Counter set	I	II	III	IV
No. of counter trays	2	3	3	2
No. of counters per tray	12	15	15	15
Sensitive area (m ²)	0.29	0.36	0.36	0.36

The counting rate of each set was close to 2 sec^{-1} , and the coincidence pulses from each of the sets were transmitted by concentric cable back to a multichannel coincidence circuit in the laboratory containing sets II and III, where they were

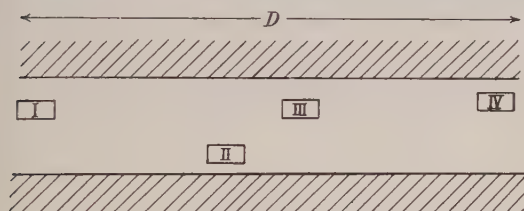


Fig. 1. Layout of extensive shower counter sets.

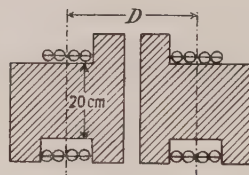


Fig. 2. Apparatus for recording local showers.

lengthened to $10 \mu\text{sec}$ (to allow for the delays incurred by the finite velocity of transmission). Coincidences between various groups were then selected and recorded in a conventional manner.

(ii) *Local Showers*

Other work in our laboratory had shown that low-multiplicity penetrating showers were produced at large underground depths (George and Evans 1950), and Braddick and co-workers had shown the probable existence of additional processes resulting in the production of single penetrating secondaries (Braddick and Hensby 1939, Braddick, Nash and Wolfendale 1951). We therefore expected that, in addition to the extensive showers, there would also be events of low multiplicity produced locally in the earth above the apparatus which would contribute to the observed frequency of extensive showers. Under 30 yards of earth these locally produced showers would only have a width of a few metres. As the counter trays used in the first investigation were too large and clumsy to reveal any fine structure at small separations the apparatus shown in fig. 2 was developed for investigating showers of small extent. Each half of the apparatus

contained two trays of four counters placed one above the other and separated by 20 cm Pb, and one half was mounted on a trolley so that it could be moved easily. Fourfold coincidences were recorded as a function of the distance D separating the centre of each half. The apparatus requires a minimum of two penetrating particles to discharge it and is thus sensitive to locally produced events of the type sought, as well as to Auger shower events. It was one of our objects to determine the relative proportions of each type of event.

§ 3. RESULTS

(i) Extensive Showers

The first observations made were of threefold coincidences between sets I, II and III, with a separation of 6 m between sets I and III, where a coincidence rate of 0.57 ± 0.05 per day was observed. On covering all the sets with 10 cm Pb the coincidence rate dropped to 0.44 ± 0.08 per day. This established the existence of the showers, and that the particles in them were mostly penetrating, as would be expected for μ -mesons. The ratio of the readings with and without lead is 1.3, and this may be contrasted with the ratio of 300:1 observed for the corresponding events at sea level by Cocconi *et al.* (1943), where the showers contain many more electrons than mesons.

The counter set IV (fig. 1) was added to the arrangement, and the frequency of the coincidences between several combinations of the counter sets was recorded for various separations D , the results being given in table 2. The twofold coincidence rates have been corrected for the measured rate of accidental coincidences, no corrections being necessary for coincidences of higher multiplicity. For the larger separations the observed twofold rate was comparable with the accidental rate, and no attempt was made to extend these readings beyond 13 metres.

Table 2. Frequencies per Day of Two, Three and Fourfold Coincidences at 60 m Water Equivalent for Various Separations D between Extreme Counter Sets

Separation D (m)	2.8	3.7	5.8	9.6	13	20	120	200	320
2-fold unscreened	33.5 ± 2.2	15.3 ± 0.3	12.7 ± 1.1	8.5 ± 0.9	9.6 ± 0.6				
2-fold screened 10 cm Pb	23.2 ± 1.5	10.8 ± 1.1	9.4 ± 0.9	— —	8.6 ± 1.3				
2-fold ratio	0.70 ± 0.07	0.71 ± 0.07	0.74 ± 0.10	— —	0.90 ± 0.12				
3-fold			0.57 ± 0.05			0.61 ± 0.06	0.104 ± 0.011	0.073 ± 0.022	0.033 ± 0.01
4-fold							0.027 ± 0.016	— —	0.020 ± 0.01

For the twofold coincidences more observations were made of the effect of covering the trays with 10 cm Pb, and the results are given in the second and third rows of table 2. The ratio of the readings with and without lead increases from 0.7 at 2.8 m to 0.9 at 13 m. We show below that the exponent of the power law which expresses the density spectrum distribution of the showers is close to 3. Thus if x is the proportion of penetrating particles in the showers, $x^2 = 0.7$ to 0.9

(see, for example, Broadbent and Jánossy 1948). Taking the mean value of 0.8, we find $x=0.9$, which means that the soft component is of order 10%, a value consistent with its simple interpretation in terms of knock-on electrons accompanying the μ -mesons forming the main part of the shower. Clearly the knock-on electrons would have a greater effect at small tray separations, their effect becoming smaller as the separation is increased, and this is what the 'ratios' given in table 2 indicate. This is of course all quite trivial; it just shows that the showers behave as expected.

Threefold coincidences were investigated over tray separations varying from 5.8 up to 320 m; at the larger separation the coincidence rate was one per month. The fourfold coincidences given in the last row of table 2 for the larger separations were so low (~ 8 counts per year) that only a few observations were made, and even those were of quite poor statistical accuracy.

(ii) *Local Showers*

The counting rate was observed for various separations of the two halves of the local-shower apparatus (table 3). The distances were measured between the centres of the counter trays, so that 30 cm separation corresponds to the position where the two halves were actually in contact.

Table 3

Separation D (m)	0.30	0.45	1.2	2.0	3.0
2-fold coinc./day	1.23 ± 0.11	1.02 ± 0.10	0.61 ± 0.12	0.32 ± 0.10	0.23 ± 0.06

At the minimum separation we covered the trays with 10 cm Pb placed above the banks of counters, and under this condition the observed counting rate was 1.20 ± 0.11 per day, not significantly different from the rate with no lead over the apparatus.

(iii) *Coincidences between Local and Extensive Showers*

In order to obtain experimental evidence on the degree of association of the local showers with the extensive events a further coincidence unit was constructed to record overall coincidences between the local and the extensive shower trays. The pulses from each of the four large extensive counter sets I, II, III, IV were fed to a hodoscope unit, the master pulse being provided by the local shower set. Thus for every local shower a simultaneous particle passing through any of the other trays distant 1 to 120 m was indicated. Halfway through this run the nearest tray, at 1 m, was moved out to 200 m, the other trays being left in position. Table 4 gives the results.

Table 4

Distance from local shower set (m)	1	3	6	120	200
No. of local showers	50	132	132	132	82
No. of coincidences with extensive trays	6	0	0	0	0

It will be seen that the only coincidences of extensive and local shower sets was at 1 m separation. The decoherence curve results in table 2 show that the extensive showers have a mean radius of approximately 100 m, and a fairly uniform particle density throughout the shower of order 1 particle m^{-2} . This is discussed in more detail in § 4, but these rough figures follow immediately from the observed coincidences at large separations and the ratio of four to threefold

coincidences. Therefore, if the extensive showers contributed significantly to the coincidences recorded as 'local' showers, the sets at 2 and 6 m should have been discharged as frequently as the set at 1 m, and the others a little less frequently. The fact that this was not so indicates that the events were of a local nature.

§4. DISCUSSION

(i) *Lateral Distribution of Shower Particles*

The decoherence curves for twofold events recorded by the two different experimental arrangements overlap at 3 m separation and, therefore, by normalizing at this point, we have been able to combine the two sets of observations, with the result shown in fig. 3. For separations 3.7 m or greater the points all lie on a

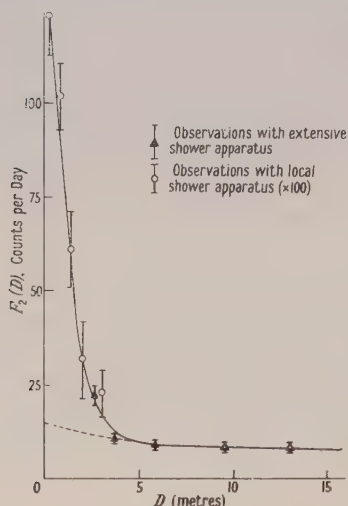


Fig. 3. Decoherence curve for twofold events.

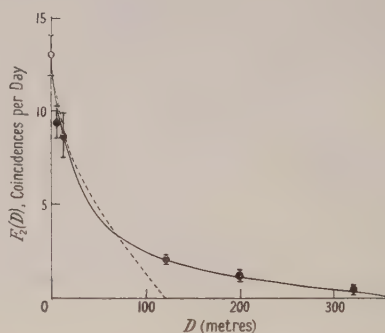


Fig. 4. Decoherence curve for underground showers after subtraction of events of local origin.

slowly falling curve, and this part of the twofold decoherence curve we interpret as being due to the penetrating particles in extensive air showers resulting from energetic nuclear collisions near the top of the atmosphere. In the first place, if secondary particles were produced locally in the overlaying earth, then it is difficult to see how they could cover such a wide region for, suppose a secondary particle is produced, say halfway down from the surface at 15 m above the apparatus, then it must be a μ -meson or some other weakly interacting particle, and would require an energy of at least 6 kmev to arrive at the point of observation. Since the rest energy of the μ -meson is 0.1 kmev, it would move forward at an angle of about 1° to the parent particle, or a slightly larger scale if the secondary is a heavier particle. This means that the separation between the primary and secondary particles would be at the most 1 m at the point of observation. Similar results follow if production at other points is considered, and it follows therefore that the flat portion of the decoherence curve beyond $D = 3.7$ m cannot be explained in terms of locally produced particles. Furthermore, local production would result in a much more steeply falling decoherence curve than is actually observed.

There is a break in the curve at 3.7 m, and the sudden increase for decreasing separations could not be explained in terms of Auger showers: both the theory of

Blatt (1949) and the measurements of Williams (1948) show that the decoherence curve should be extrapolated to zero separation more or less as shown by the dotted line.

Our interpretation of the twofold decoherence curve is that it may be divided into two components, the rapidly falling part from $D=0$ to $D=3.7$ m being due to locally produced secondary particles superimposed on a slowly varying background due to extensive showers. At distances greater than 3.7 m the coincidences are due to extensive showers alone. From the curves of fig. 3 it follows that at small separations the local events are about ten times more frequent than the extensive shower events, and this is consistent with the observations made under § 3 (iii) describing the experimental observations of association between local and extensive events.

In order to see the shape of the decoherence curve beyond 13 m it is necessary to consider the results for threefold coincidences, because of the background of accidental coincidences in the twofold events. Barrett *et al.* (1952, private communication) have shown that the ratio of twofold to threefold events is roughly independent of counter separations; as our two sets of observations of two- and threefold events overlap at 5.8 m, we have normalized the two curves at this point and constructed a composite curve showing the decoherence curve for twofold events out to 320 m (fig. 4). In this graph we have not included the contributions from local showers at small counter separations, and thus fig. 4 should represent the decoherence curve for the twofold coincidences due to extensive showers alone at 60 m water equivalent depth.

(ii) The Number-Frequency Distribution of Shower Particles

If we make the assumption that the frequency of showers containing N mesons is proportional to $N^{-\gamma}$, then the ratios of twofold/single, threefold/two-fold or fourfold/threefold coincidences may be used to determine the value of γ . If the same value of γ accounts simultaneously for all of these ratios then this may be taken as an indication of the validity of the original assumption. Previous analyses (Cocconi, Loverdo and Tongiorgi 1943) have assumed a constant density of particles in a given shower, and the same assumption will be made here. Actually we know that there is a concentration of particles in the vicinity of the shower axis, but we may expect that the picture we deduce on the basis of constant density will get us near the truth. And in any case the radial distribution function is unknown, so that any assumption must be arbitrary to some extent. Thus we assume that the N mesons in a shower are distributed at random over a circle of radius R . Let p be the probability that a counter set of area A will be struck by a given particle so that $p = A/\pi R^2$. Then our purpose is to determine values of R and γ consistent with the observations. Let $P_r(N)$ be the probability that at least one or more particles fall on each of r counter trays. Values of $P_r(N)$ are

$$\left. \begin{aligned} P_1(N) &= 1 - (1-p)^N \\ P_2(N) &= 1 - 2(1-p)^N + (1-2p)^N \\ P_3(N) &= 1 - 3(1-p)^N + 3(1-2p)^N - (1-3p)^N \\ P_4(N) &= 1 - 4(1-p)^N + 6(1-2p)^N - 4(1-3p)^N + (1-4p)^N \end{aligned} \right\} \dots\dots (1)$$

The frequency of r -fold coincidences will then be proportional to

$$F_r = \sum P_r(N) N^{-\gamma} \dots\dots (2)$$

Values of the ratio F_{r+1}/F_r obtained from eqn. (2) are plotted in fig. 5 as a function of γ for $R=30, 60$ and 120 m. The experimental values are also indicated, the relevant twofold rate being the value extrapolated to zero separation as indicated in fig. 3. A consistent set of values of R and γ would be those for which the intersections between the experimental and theoretical lines all give the same value of γ . It is seen that these conditions are satisfied for $R \sim 60$ m, $\gamma = 3.2 \pm 0.2$.

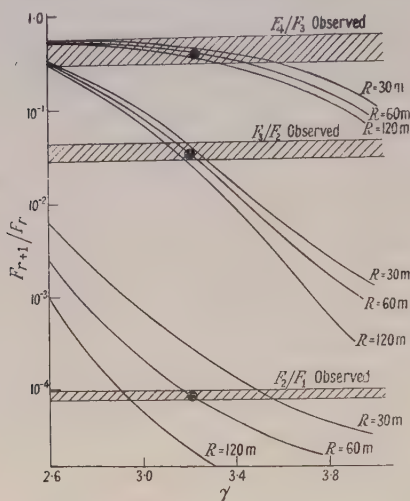


Fig. 5.

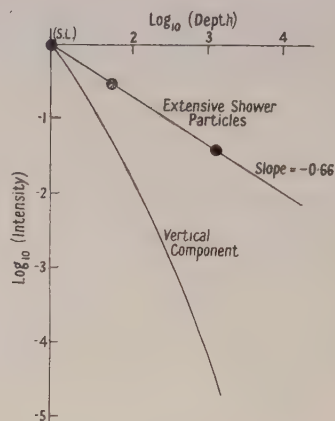


Fig. 6.

Except for the ratio of twofold to single counts, the results are not very sensitive to the choice of R , but γ may be fixed within reasonable limits. The value of R is of order of magnitude indicated by the decoherence curve of fig. 4, good agreement not being expected on account of the simplifying assumption made concerning the density distribution. The value of γ is not dependent on these assumptions.

(iii) The Depth-Intensity Relation for Extensive Shower Particles

Coincidences between three counter trays all shielded with 20 cm Pb have been recorded by McCusker and Millar (1951) at sea level, and by Greisen (1951, private communication) at a depth of 1600 m water equivalent. By comparing these observations with our own it is possible to obtain a preliminary indication of the variation of the frequency of extensive shower particles with depth (table 5).

In comparing the observations at various depths it is the relative densities of the shower particles rather than the actual threefold coincidence rates that are

Table 5

Observer	Depth (m, w.e.)	Area of trays (cm ²)	3-fold rate (d ⁻¹)	Dist. betw. trays (m)	Corrected rate*
McCusker and Millar	10 (S.L.)	1750	2.8 ± 0.1	5	7.85 ± 0.3
George, MacAnuff and Sturgess	60	3500	0.44 ± 0.08	6	0.44 ± 0.08
Greisen	1600	7500	0.013 ± 0.004	6	0.0026 ± 0.001

* The rate which would have been observed if all the trays had been of area 3500 cm², using standard procedures.

of greater physical interest. For example, suppose that of the penetrating shower particles at sea level 1 in 5 survived to a depth of 60 m water equivalent, then the threefold shower frequencies would be in the ratio of $5^{2.2}$ or 35 : 1 (taking our value of γ from §4(ii)), but it is the survival probability 1 in 5, giving the relative absorption, which is of physical interest. Thus from the data of table 5 we have calculated the survival probabilities of the extensive shower particles at 60 and 1600 m water equivalent, see fig. 6, which also shows the depth intensity curve of the single particles. It is clear that the shower particles are absorbed much less than the normal single particles of the penetrating component, indicating that the meson spectrum for the high energy primary particles capable of generating these showers ($\sim 10^{15}$ ev, see below) is flatter than the normal spectrum. This behaviour would be expected from various theories of meson production that have been suggested (Lewis, Oppenheimer and Wouthuysen 1948, Fermi 1951). On the basis of the limited measurements available we may tentatively assign an integral range distribution of the form (range) $^{-0.7}$ to the particles comprising the threefold extensive showers observed underground.*

(iv) *Energy of the Threefold Events*

The observed ratio (3 : 1) of threefold to fourfold events indicates that in the showers recorded the mean particle density must have been of order 1 per tray or 3 particles m^{-2} . The showers cover approximately 10^4 m^2 and must have contained on the average approximately 3×10^4 particles. The energy required for penetration to 60 m water equivalent is 10^{10} ev and, as indicated in §3, the mean energy must be several times this value. Thus the energy in the μ -meson component alone must be on average of order 10^{15} ev, the energy of the primary being greater than this by a factor which is unknown but presumably not large.

By normalizing the observed frequency of single counts in one of the trays to the measured underground flux of single particles the flux of primary particles with energies above this limit is found to be $1.7 \times 10^{-9} \text{ cm}^{-2} \text{ sec}^{-1} \text{ sterad}^{-1}$, in good agreement with the value calculated by extrapolating the integral primary spectrum reported by Kaplon and Ritson (1952).

(v) *Local Showers*

From the rapid rise of the decoherence curve at small separations we have inferred the existence of associated penetrating particles in excess of those accounted for by extensive air shower events, and it is of interest to see to what extent these events can be explained in terms of showers produced underground by fast μ -mesons as observed in nuclear emulsions by George and Evans (1951). Let P be the probability that a μ -meson be accompanied by a further penetrating particle. Then the experimental value of P is given by

$$P = \int_0^\infty \frac{2\pi DF_2(D) dD}{2AF_1} \quad \dots\dots(3)$$

where F_1 is the frequency of recording single particles, $F_2(D)$ the frequency of local twofold events at separation D after subtraction of the background of extensive events, and A is the area of the counter trays.

Using (3) we find the value

$$P_{\text{obs}} = 3 \times 10^{-3}. \quad \dots\dots(4)$$

* Greisen (private communication) has pointed out that the showers at 1600 m are smaller in extent than those at 60 m. Allowance for this brings the last point in fig. 6 nearer to the curve for the vertical component.

We now assume that all the particles emitted in underground hard showers are π -mesons and then calculate the value of P expected from this assumption. If a π -meson is produced in the earth it may, before interacting with another nucleus, decay into a μ -meson which is recorded (it may suffer μ -decay either in the earth or in the air-space between the tunnel roof and our apparatus, a distance of 3 m), or it may escape capture or decay and be recorded as a π -meson. The measured cross section for the production of showers at 60 m water equivalent below ground is $2 \times 10^{-30} \text{ cm}^2/\text{nucleon}$ (George 1951), and the average number of shower particles per event is 3, making a total effective cross section for the production of π -mesons of $6 \times 10^{-30} \text{ cm}^2/\text{nucleon}$. The probability of decay before capture in the earth is $10/E$ (E in mev) and the probability that a μ -meson will be accompanied by a secondary μ -meson via μ -decay of secondary π -mesons in the earth is

$$P_1 = \int_{x=0}^{3000} 6 \cdot 10^{23} \cdot 2 \cdot 6 \cdot 10^{-30} dx \int_{E_0+2x}^{\infty} I(E) \frac{10}{E} dE. \quad \dots\dots(5)$$

E_0 is the minimum energy required for a particle to penetrate our absorber (400 mev) and $I(E)$ is the differential energy spectrum of the emitted shower particles (Camerini *et al.* 1950).

On evaluating (5) we find $P_1 = 7 \times 10^{-6}$. If $L_a \text{ g cm}^{-2}$ is the absorption length for nucleon cascades in the earth, the probability for a π -meson to emerge from the roof is simply $N_\pi = L_a \cdot 6 \cdot 10^{-30} \cdot 6 \cdot 10^{23}$, which, on substituting $L_a = 150 \text{ g cm}^{-2}$, gives

$$N_\pi = 5.4 \times 10^{-4} \text{ per } \mu\text{-meson}. \quad \dots\dots(6)$$

Of these, 10% are calculated to decay in the 3 m path from roof to apparatus, and only 40% will have sufficient energy to discharge the apparatus, giving for the number of secondary μ -mesons from π - μ decay in the air $P_2 = 2.2 \times 10^{-5}$.

Finally, of the remaining 90% of π -mesons, again 40% have sufficient energy to be recorded, while their probability of producing a count is only 0.47 on account of their absorption in lead with an absorption length of the order of 300 g cm^{-2} , the value for nucleon cascade attenuation in lead. Thus for the probability of recording directly one of the secondary π -mesons we find $P_3 = 9.2 \times 10^{-5}$. Adding together P_1 , P_2 and P_3 we get for the total calculated probability

$$P_{\text{calc}} = 1.2 \times 10^{-4}. \quad \dots\dots(7)$$

The observed value (eqn. (5)) is greater than this by an order of magnitude, and the difference cannot be accounted for by uncertainties in factors entering the calculation. All of the required parameters have been measured to a reasonable degree of accuracy, and the overall uncertainty in the calculated value of P is hardly likely to be out by as much as a factor of two. Thus we conclude that there is some additional process taking place underground which leads to the production of secondary penetrating particles over and above the production of nuclear disintegration 'stars' emitting showers of π -mesons as observed in nuclear emulsions. This conclusion lends some support to previous reports by other authors of the anomalous production of secondary penetrating particles underground (George and Trent 1949, Braddick, Nash and Wolfendale 1951).

(vi) Comparison with Other Workers

Associated penetrating particles have been observed recently at a depth of 1600 m water equivalent by Barrett *et al.* (1952, private communication) and at 50 m water equivalent by Amaldi *et al.* (1952, private communication) using

hodoscoped banks of counters separated by lead absorbers. Both local and extensive events were studied by Barrett *et al.*, whereas the events of Amaldi *et al.* were mostly of a local nature. Barrett *et al.* find a similar anomalous rise in the decoherence curve for D less than 3 m, which they attribute to local events. Their twofold decoherence curve falls substantially to zero at 25 m, which may be understood in terms of the greatly increased energy the μ -mesons must have to reach their depth of observation (3×10^{11} ev compared with 1.2×10^{10} ev in our case). For the exponent γ of the power law expressing the number-frequency distribution, Barrett *et al.* find $\gamma = 3.4 \pm 0.1$, and our value (3.2 ± 0.2) is not inconsistent with this. As regards the local events, while we both find the same frequency of associated penetrating particles ($\sim 1/300$ of the frequency of single particles) their conclusions differ from ours in one important respect, in that they argue that the local events can be adequately explained in terms of the photonuclear excitation produced by the virtual quanta of the hard component. In order to do this they have to assume a photonuclear cross section of 10^{-27} cm²/nucleon at $h\nu \geq 5$ kmev, a value ten times greater than the value measured at lower energy (Miller 1951). While such an increase of the cross section cannot be excluded on *a priori* grounds, we are informed by Evans (1952, private communication) that it would appear to be inconsistent with the number of large stars observed in nuclear emulsions exposed below ground. In any case, the discrepancy in our observations is between a measured frequency of shower production and a measured frequency of associated particles, and the discrepancy remains whatever value one assumes for the photonuclear cross section.

Amaldi *et al.* have identified certain of their hodoscope records as examples of the production of penetrating secondary radiation in lead and, assuming the events to be produced by the μ -mesons of the hard component, have deduced a value for the cross section of the order of 1.3×10^{-29} cm² per nucleon for this process. This again is larger than that allowed by the nuclear emulsion observations, and is closer to the figure of 5×10^{-29} cm²/nucleon given by George and Trent and by Braddick, Nash and Wolfendale. Assuming that μ -mesons at this depth do produce penetrating secondary particles with this cross section, there would be no difficulty in accounting for the frequency of associated penetrating particles which we observe at close separations.

The local events could also be understood if the underground showers contained a significant number of particles which decay into μ -mesons with a lifetime appreciably shorter than that of the π -meson (O'Ceallaigh 1951).

§5. CONCLUSIONS

From the observations described in this paper we have drawn the following conclusions concerning the showers at 60 m water equivalent depth:

- (i) 90% of the particles in the underground extensive showers are μ -mesons and the remainder secondary electrons;
- (ii) the frequency of showers containing N particles is proportional to $N^{-3.2 \pm 0.2}$;
- (iii) the showers certainly cover an extent of 320 m and are probably even greater, although their properties can be understood if it is assumed that the showers have a uniform density over a circle of radius of approximately 60 m;
- (iv) in the events recorded with three- and fourfold counter systems the average density of μ -mesons is of order 3 m⁻², indicating the simultaneous passage of 3×10^4 particles at 60 m water equivalent;

(v) the energy of these events is greater than 10^{15} ev, and the flux of primary particles capable of producing them is $1.7 \times 10^{-9} \text{ cm}^{-2} \text{ sec}^{-1} \text{ sterad}^{-1}$;

(vi) at close separation of the counter trays additional events containing two or more particles are recorded which originate locally in the earth overhead;

(vii) the frequency of these local events is higher by an order of magnitude than that calculated in terms of the nuclear showers observed below ground in nuclear emulsions;

(viii) the frequency of local events is not inconsistent with that calculated assuming single secondary penetrating particles to be produced by fast μ -mesons with a cross section of the order of 5×10^{-29} ; such a process has been previously reported by other workers.

ACKNOWLEDGMENTS

We would like to thank Professor J. D. Bernal for tolerating us in his Department at Birkbeck College and for encouraging us with many stimulating discussions. We are grateful to the Transport Executive for permission to work at Holborn Station, and particularly to the Signals Department for their prompt assistance on several occasions. Part of the apparatus was made by Messrs. Cinema Television Ltd. The work was supported by grants from the Department of Scientific and Industrial Research and from the Central Research Fund of the University of London.

REFERENCES

- AUGER, P., 1938, *C. R. Acad. Sci., Paris*, **207**, 907.
 AUGER, P., MAZE, R., and GRIVET-MEYER, T., 1938, *C. R. Acad. Sci., Paris*, **206**, 1721.
 BLATT, J. M., 1949, *Phys. Rev.*, **75**, 1584.
 BRADDICK, H. J. J., and HENSBY, G. S., 1939, *Nature, Lond.*, **144**, 1012.
 BRADDICK, H. J. J., NASH, W. F., and WOLFENDALE, A. W., 1951, *Phil. Mag.*, **42**, 1277.
 BROADBENT, D., and JÁNOSSY, L., 1948, *Proc. Roy. Soc. A*, **192**, 364.
 CAMERINI, U., FOWLER, P. H., LOCK, W. A., and MUIRHEAD, H., 1950, *Phil. Mag.*, **42**, 1241.
 COCCONI, G., LOVERDO, A., and TONGIORGI, V., 1943, *Nuovo Cim.*, **1**, 49.
 FERMI, E., 1951, *Phys. Rev.*, **81**, 683.
 GEORGE, E. P., 1949, *Nuovo Cim.*, **6** (Supplement), 531; 1951, *Progress in Cosmic Ray Physics* (Amsterdam: North Holland Publ. Co.).
 GEORGE, E. P., and EVANS, J., 1950, *Proc. Phys. Soc. A*, **63**, 1248; 1951, *Ibid.*, **64**, 193.
 GEORGE, E. P., and TRENT, P. T., 1949, *Nature, Lond.*, **164**, 838.
 KAPLON, M. E., and RITSON, D. M., 1952, *Phys. Rev.*, **85**, 932.
 LEWIS, H. W., OPPENHEIMER, J. R., and WOUTHUYSEN, S. A., 1948, *Phys. Rev.*, **73**, 127.
 MCCUSKER, C. B. A., 1950, *Proc. Phys. Soc. A*, **63**, 1240.
 MCCUSKER, C. B. A., and MILLAR, D. D., 1951, *Proc. Phys. Soc. A*, **64**, 915.
 MILLER, R. D., 1951, *Phys. Rev.*, **82**, 260.
 O'CEALLAIGH, C., 1951, *Phil. Mag.*, **41**, 1032.
 TREAT, J., and GREISEN, K., 1948, *Phys. Rev.*, **74**, 414.
 WILLIAMS, R. W., 1948, *Phys. Rev.*, **74**, 1689.

The Free Energy of the Double Layer of a Colloidal Particle and the Charging Process

By S. LEVINE

Department of Mathematics, University of Manchester

MS. received 20th June 1952, and in final form 5th November 1952

Abstract. A detailed analysis is given of the alternative charging processes used by Verwey and Overbeek and the author to determine the free energy associated with the electric double layer of a colloidal particle. A general statistical proof of the equivalence of these methods is obtained. It is shown that the use of the different charging processes is equivalent to assuming an additional, hypothetical, thermodynamic variable to describe the colloidal system; this can be simply interpreted as an arbitrary 'chemical' potential of the ions adsorbed on the particle surface. The expression for the free energy derived by Verwey and Overbeek is extended to apply to more general cases, and the treatment by these authors of the so-called chemical energy is clarified.

§ 1. INTRODUCTION

IN this paper various methods of determining the free energy of the double layers of colloidal particles will be examined by employing classical statistical mechanics and thermodynamics. It will be sufficient to examine the model of a single particle with a uniform density of surface ions, immersed in a large volume of electrolyte. Also, for simplicity, we shall neglect the (small) contribution to the free energy of our system from the coulomb interaction of the ions in the interior of the dispersion medium (see Levine 1946, 1951 a, b). Two main results will be obtained. (i) In one of the methods of finding the free energy we introduce an extra, hypothetical, thermodynamic variable to describe the colloidal system at equilibrium. The new variable may be visualized as an arbitrary adsorption potential. Consequently *two* fictitious processes are applied, namely, the familiar Debye-Huckel charging process of the ions and the variation of the adsorption (chemical) potential. (ii) Casimir (see Verwey and Overbeek 1948, p. 63) proved that the charging method of Verwey and Overbeek (1948) (hereafter referred to as V.O.) is equivalent to the use of a Lippmann equation. A generalization of this equivalence theorem will be derived without appealing to the Poisson-Boltzmann equation. The above results lead to a clarification of the charging process of V.O. and of their treatment of the so-called chemical energy of the surface ions (V.O., p. 58).

Since this paper was written, a treatment by Overbeek (see Kruyt 1952) of the same problems has appeared in which different lines of argument are used. For example, in one of the models employed by Overbeek a variable adsorption potential is achieved by changing the electrolyte concentration, as in a completely reversible electrode. However, since the charging process is usually visualized as occurring at constant total electrolyte content, such a process seems to introduce

complications which are avoided in the present paper. Furthermore, the emphasis will be on the derivation of general formulae for the free energy which can be used with a corrected Poisson-Boltzmann equation. This will be illustrated in the following paper (Levine 1953).

§ 2. CHARGING METHOD I

In previous papers (Levine 1946, 1948, 1950, 1951 a), the author derived the Helmholtz free energy of the double layers by charging at constant temperature and volume and under the condition that the number of surface ions remains constant. This method is valid if classical statistical mechanics is assumed and the electrolyte dispersion medium is macroscopic, since we then have a (two-phase) macroscopic system with regard to the ion components.

Suppose that all the ions carry the fraction λ of the normal charge. The charge on the particle is assumed to be due to the adsorption of n ions of type 1, (full) charge e_1 , n being arbitrary. For an *instantaneous* configuration of the ions the electrostatic interaction energy of all the ions is

$$\sum_i e_i \int_0^\lambda \phi_i(\lambda) d\lambda,$$

where $\phi_i(\lambda)$ is the potential at ion i due to all the other ions, and we sum over all the ions; $\phi_i(\lambda)$ includes image terms. Differentiating this energy with respect to λ and then averaging over all configurations of the ions (subject to fixed n), we introduce the quantity

$$\frac{2}{\lambda} E(\lambda, n) = \sum_i e_i [\overline{\phi_i(\lambda)} - \overline{\phi_i^0(\lambda)}], \quad \dots\dots(1)$$

where $\overline{\phi_i^0(\lambda)}$ is the mean potential at an ion i far removed from the particle. To simplify the notation the bar, which denotes the statistical average, will be omitted except in the Appendix. Now let $\psi(\lambda, n)$ be the difference between the average (surface) potential due to other ions at an adsorbed ion and that at a 1 ion in the bulk of the solution; ψ_j will be the corresponding potential at an ion of type j , located at any point in the diffuse outer layer of the particle and ρ_j the charge density of j ions. Then we may write (Levine 1951 a)

$$E(\lambda, n) = \frac{1}{2} n \lambda e_1 \psi(\lambda, n) + \frac{1}{2} \int \left(\sum_{j=1}^s \psi_j \rho_j \right) dv, \quad \dots\dots(2)$$

where the integral is taken over the volume of the diffuse layer, and we now sum over the s ion types. If there is no dielectric saturation in the diffuse layer, $\phi_i(\lambda)$ is proportional to λ and $E(\lambda, n)$ is the average electrostatic energy of the double layer. Otherwise $E(\lambda, n)$ cannot be interpreted in this way.

The part of the free energy of our system which depends on n is now

$$F(\lambda, n) = f_0(n) - n \Delta \chi_1(\lambda) + F_e(\lambda, n), \quad \dots\dots(3)$$

where $f_0(n)$ is the free energy in the completely discharged state, $-\Delta \chi_1(\lambda)$ is the change in the electrical self-energy when a 1 ion is adsorbed, and

$$F_e(\lambda, n) = 2 \int_0^\lambda \frac{1}{\lambda} E(\lambda, n) d\lambda \quad \dots\dots(4)$$

is the so-called electrical term (Levine 1951 a). Let $\Phi(\lambda, n)$ be the potential of the mean force (per unit charge) due to the coulomb interaction and acting on an

adsorbed ion (see Appendix) ; the zero of this potential is taken in the bulk of the solution. Then

$$F_e(\lambda, n) = \lambda e_1 \int_0^n \Phi(\lambda, n) dn, \quad \dots\dots(5)$$

which, like (4), is still valid if there is dielectric saturation.

We now suppose that at each stage λ thermodynamic equilibrium can be attained, and shall refer to such a system as 'normal', hereafter to be abbreviated to N.S. The equilibrium value of n , which we denote by $\bar{n}(\lambda)$, is derived from the condition of minimum free energy,

$$\frac{\partial F(\lambda, n)}{\partial n} = 0 \quad \text{or} \quad \Delta\chi_1(\lambda) = \frac{df_0(n)}{dn} + \lambda e_1 \Phi(\lambda, n), \quad \dots\dots(6)$$

making use of (3) and (5). An alternative derivation of (6) is given in the Appendix. A particularly simple form is obtained for $f_0(n)$ if the adsorbed ions are identical with one of the lattice ion types of the colloidal particle. We now imagine all the lattice ions of the particles and the ions in the dispersion medium are completely discharged and we charge at a uniform rate (at constant volume of each phase). Then

$$f_0(n) = \alpha n, \quad \alpha = -\chi_1^0 + \mu_1, \quad \dots\dots(7)$$

where χ_1^0 and μ_1 are the chemical potentials of a discharged ion in the dispersion medium and in the particle respectively. However, in a previous paper (Levine 1951 c), the author has shown that if (7) applies, then the assumption that equilibrium exists at $\lambda=0$ (and presumably in the vicinity of $\lambda=0$) is contradicted by experiment.

§ 3. CHARGING METHOD II. INTRODUCTION OF GENERALIZED SYSTEM

When $f_0(n)$ has a more complicated form than (7), the N.S. may exist, in which case we shall imagine that during the charging process n takes on its equilibrium value $\bar{n}(\lambda)$. Since $\bar{n}(\lambda)$ is defined by (6), the change in the free energy during an infinitesimal step λ to $\lambda + d\lambda$ can be written as

$$\frac{dF(\lambda, n)}{d\lambda} d\lambda = \frac{\partial F(\lambda, n)}{\partial \lambda} d\lambda, \quad \dots\dots(8)$$

to be evaluated at $n = \bar{n}(\lambda)$. Substituting (3) for $F(\lambda, n)$ integration of (8) yields

$$F[\lambda, \bar{n}(\lambda)] = f_0[\bar{n}(0)] + \int_0^\lambda \left[-\bar{n}(\lambda) \frac{d\Delta\chi_1(\lambda)}{d\lambda} + \frac{2}{\lambda} E[\lambda, \bar{n}(\lambda)] \right] d\lambda. \quad \dots\dots(9)$$

The inverse process of deriving (3) and (4) from (6) and (9) is not possible unless our N.S. is replaced by a fictitious generalized system to be designated as the G.S. We shall increase the number of independent thermodynamic variables by one and regard both λ and n as among such variables. Any path in the (λ, n) plane which passes through fixed end points, say A $[0, \bar{n}(0)]$ and B $[\lambda, \bar{n}(\lambda)]$, will now yield the same change in the free energy. A simple way of choosing the G.S. is to replace $\Delta\chi_1(\lambda)$ by a unique energy term which we shall denote by $M(\lambda, n)$ and which has the following properties :

$$(i) \quad M[\lambda, \bar{n}(\lambda)] = \Delta\chi_1(\lambda), \quad \dots\dots(10)$$

$$(ii) \quad M(0, n) = df_0(n)/dn, \quad \dots\dots(11)$$

(iii) the *inexact* differential $\Delta\chi_1(\lambda) dn + (2/\lambda) E(\lambda, n) d\lambda$ is replaced by the exact differential

$$dV = M(\lambda, n) dn + (2/\lambda) E(\lambda, n) d\lambda. \quad \dots\dots(12)$$

This means (Ince 1927) that a function $V = V(\lambda, n)$ can be found so that

$$\frac{\partial}{\partial n} V(\lambda, n) = M(\lambda, n), \quad \frac{\partial}{\partial \lambda} V(\lambda, n) = \frac{2}{\lambda} E(\lambda, n), \quad \dots\dots (13)$$

and if we choose $V[0, \bar{n}(0)] = 0$

$$V(\lambda, n) = 2 \int_0^\lambda \frac{1}{\lambda} E(\lambda, n) d\lambda + \int_{\bar{n}(0)}^n M(0, n) dn. \quad \dots\dots (14)$$

If we now write (9) as

$$F[\lambda, \bar{n}(\lambda)] = f_0[\bar{n}(0)] - \bar{n}(\lambda) \Delta \chi_1(\lambda) + \int_0^\lambda \left[M[\lambda, \bar{n}(\lambda)] \frac{d\bar{n}(\lambda)}{d\lambda} + \frac{2}{\lambda} E[\lambda, \bar{n}(\lambda)] \right] d\lambda, \quad \dots\dots (15)$$

then the integral expression on the right is precisely

$$V[\lambda, \bar{n}(\lambda)] = \int_0^\lambda \left[M[\lambda, n(\lambda)] \frac{dn(\lambda)}{d\lambda} + \frac{2}{\lambda} E[\lambda, n(\lambda)] \right] d\lambda, \quad \dots\dots (16)$$

and is independent of the path $n = n(\lambda)$ chosen in the (λ, n) plane, the end points A and B being fixed. Making use of (10), (11) and (14), it follows that (15) may be written as

$$F[\lambda, \bar{n}(\lambda)] = f_0[\bar{n}(\lambda)] - \bar{n}(\lambda) M[\lambda, \bar{n}(\lambda)] + F_e[\lambda, \bar{n}(\lambda)], \quad \dots\dots (17)$$

which is identical with (3) at $n = \bar{n}(\lambda)$. The function $F_e(\lambda, n)$ exists and is defined by (4). Also the first relation in (13) defines $M(\lambda, n)$, namely

$$M(\lambda, n) = \frac{df_0(n)}{dn} + \frac{\partial F_e(\lambda, n)}{\partial n} = \frac{df_0(n)}{dn} + \lambda e_1 \Phi(\lambda, n). \quad \dots\dots (18)$$

Up to now we have placed the end points of our arbitrary path on the curve $n = \bar{n}(\lambda)$. However, having introduced the function $M(\lambda, n)$, we may choose these two points anywhere in the first quadrant ($\lambda \geq 0, n \geq 0$) of the (λ, n) plane and repeat the preceding argument; also the N.S. need not exist. Then the free energy of our G.S. is simply

$$F_I(\lambda, n) = f_0(n) - n M(\lambda, n) + F_e(\lambda, n), \quad \dots\dots (19)$$

and the expression (9) is replaced by

$$F_I[\lambda, n(\lambda)] = g[n(0)] + \int_0^\lambda \left[-n(\lambda) \frac{dM[\lambda, n(\lambda)]}{d\lambda} + \frac{2}{\lambda} E[\lambda, n(\lambda)] \right] d\lambda, \quad \dots\dots (20)$$

where the path $n = n(\lambda)$ is quite arbitrary, and where

$$g(n) = f_0(n) - M(0, n) = f_0(n) - n df_0(n)/dn, \quad \dots\dots (21)$$

substituting (11).

§ 4. MODEL OF THE GENERALIZED SYSTEM

A physical interpretation of $M(\lambda, n)$ is provided by a mechanism which is based on the methods of statistical mechanics. It will be sufficient to consider the case where the adsorbed ion is different from the lattice ion types constituting the particle. We shall replace U_0 , the energy of adsorption of a discharged ion of type 1 on the particle surface, by ξU_0 where ξ is a fictitious 'coupling' parameter (cf. Kirkwood 1935) which can be chosen independently of λ . Then the free energy of our system can be written as

$$F_I(\lambda, n) = F(\lambda, n) + n(\xi - 1)U_0. \quad \dots\dots (22)$$

Since we are considering λ and ξ as among the variables defining the equilibrium state of the G.S., n is a function of λ and ξ , say $n = n(\lambda, \xi)$. Suppose now that an

ion of type 1 is transported from the solution phase to the particle surface phase under the condition of *fixed* ξ . The free energy change is zero, i.e. the function $F_I(\lambda, n)$ is a minimum (with respect to n) for given λ and ξ . Hence $n(\lambda, \xi)$ is defined by

$$\Delta\chi_1(\lambda) + (1 - \xi)U_0 = \frac{df_0(n)}{dn} + \lambda e_1 \Phi(\lambda, n) = M(\lambda, n), \quad \dots\dots (23)$$

making use of (3), (5), (18) and (22). It readily follows that the formulae (19) and (22) are identical. In the case of the N.S., $\xi = 1$ and (23) is equivalent to (6).

An alternative mechanism was considered by the author in earlier papers (Levine 1948, 1951 a) and more recently by Overbeek (see Kruyt 1952). It is imagined that an external potential, ψ^* say, is impressed between the interior of the solution and the particle surface, so that the particle behaves as a completely polarized electrode and equilibrium can be attained for any λ and n . If the potential at the particle be taken as the zero, then the term $n(\xi - 1)U_0$ in (22) is replaced by $-\lambda e_1 \psi^*$, making use of the condition of electrical neutrality. Thus there is complete equivalence between the parameters ξ and ψ^* .

§ 5. GENERALIZATION OF CASIMIR EQUIVALENCE THEOREM

To prove this theorem we derive two equivalent forms for the free energy of the G.S. Substituting (18) and (5) into (19) we readily obtain

$$F_I[\lambda, n(\lambda)] = g[n(\lambda)] - \lambda e_1 n(\lambda) \Phi[\lambda, n(\lambda)] + \lambda e_1 \int_0^{n(\lambda)} \Phi(\lambda, n) dn, \quad \dots\dots (24)$$

$$= g[n(\lambda)] - \lambda e_1 \int_{\Phi(\lambda, 0)}^{\Phi[\lambda, n(\lambda)]} n(\lambda, \Phi) d\Phi, \quad \dots\dots (25)$$

where $n = n(\lambda, \Phi)$ is the inverse relation to $\Phi = \Phi(\lambda, n)$; $\Phi(\lambda, 0) \neq 0$ because of the image forces. If we substitute into (20) the expression (2) for $E(\lambda, n)$ and the second form in (18) for $M(\lambda, n)$, then it can be verified that

$$\begin{aligned} F_I[\lambda, n(\lambda)] &= g[n(\lambda)] + e_1 \int_0^\lambda n(\lambda) \frac{d}{d\lambda} \{ \lambda \psi[\lambda, n(\lambda)] - \lambda \Phi[\lambda, n(\lambda)] \} d\lambda \\ &\quad - e_1 \int_0^\lambda \lambda n(\lambda) \frac{d\psi[\lambda, n(\lambda)]}{d\lambda} d\lambda + \int_0^\lambda \frac{d\lambda}{\lambda} \int \left(\sum_j \psi_j \rho_j \right)_{n=n(\lambda)} dv. \quad \dots\dots (26) \end{aligned}$$

The right-hand sides of (25) and (26) must be identical, and this yields a generalization of the formula derived by Casimir (1948). A further generalization which is relevant to the case of spherical particles (Levine 1950) is obtained by replacing the path $n = n(\lambda)$ by the path ACB in the figure, defined by $n = n_0(\epsilon)$, $0 \leq \lambda \leq \epsilon$; $n = n_0(\lambda)$, $\lambda \geq \epsilon$, where the function $n_0(\lambda) \rightarrow \infty$ as $\lambda \rightarrow 0$ and ϵ is small. The range of integration $(0, \lambda)$ on the right of (26) is now divided into two parts $(0, \epsilon)$ and (ϵ, λ) , and we may equate the contributions from $(0, \epsilon)$ to the second term on the right of (25), after replacing λ by ϵ in the latter. If now $\epsilon \rightarrow 0$, it follows that we must add the term

$$- e_1 \lim_{\epsilon \rightarrow 0} \epsilon \int_{\Phi(\epsilon, 0)}^{\Phi[\epsilon, n_0(\epsilon)]} n(\epsilon, \Phi) d\Phi \quad \dots\dots (27)$$

to the right-hand side of (26). This may be described as a 'residual' free energy in the state $\lambda = 0$, which is introduced for mathematical convenience and has no real physical meaning. (We assume that the improper integrals in (26) converge.) The required generalization is obtained on equating (25) to the sum of (26) and (27), with $n(\lambda)$ replaced by $n_0(\lambda)$ (cf. Levine 1951 d).

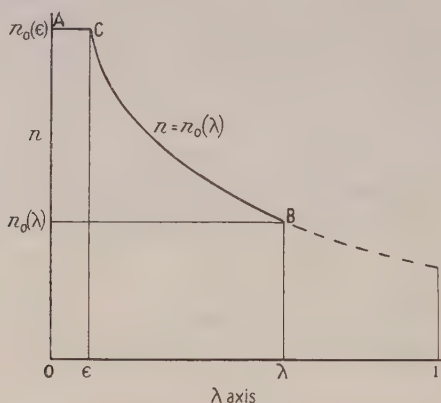
If we ignore a small correction due to short-range forces between the ions then, according to equation (A 10),*

$$e_1 \Phi(\lambda, n) = \int_0^{e_1} \psi(\lambda, n) de_1 \quad \text{or} \quad \Phi(\lambda, n) - \psi(\lambda, n) = -e_1 \frac{\partial \Phi(\lambda, n)}{\partial e_1}. \quad \dots\dots (28)$$

Thus the electrical work of bringing a 1 ion from the solution to the particle surface equals the work of discharging the ion in the solution and then charging it again at the surface. Let $\psi^0(\lambda, n)$ be the mean potential due to the ions at any position on the surface. Adopting the method of Loeb (1951), we write

$$\psi(\lambda, n) = \psi^0(\lambda, n) + \psi'(\lambda, n), \quad \dots\dots (29)$$

where $\psi'(\lambda, n)$ is the difference between the 'perturbation' potential due to the self-atmosphere and image of an adsorbed ion and the corresponding potential in



the interior of the solution. Since $\psi^0(\lambda, n)$ is very nearly independent of e_1 , we obtain from (28) and (29)

$$\Phi(\lambda, n) - \psi^0(\lambda, n) = \frac{1}{e_1} \int_0^{e_1} \psi'(\lambda, n) de_1. \quad \dots\dots (30)$$

If we now use Loeb's approximate result, $\psi'(\lambda, n)$ is proportional to e_1 and then the integral on the right of (30) is equal in magnitude but opposite in sign to the right-hand side of the second equation in (28). This means that the absolute error in the approximation $\Phi(\lambda, n) = \psi^0(\lambda, n)$ on which the Poisson-Boltzmann equation is based approximately equals that in the assumption $\Phi(\lambda, n) = \psi(\lambda, n)$. This result is rather significant for, although $\Phi(\lambda, n)$ and $\psi(\lambda, n)$ are not identical, they both allow for the 'perturbation' potential $\psi'(\lambda, n)$, whereas $\psi^0(\lambda, n)$ does not. It suggests that the 'fluctuation' and image terms neglected in the Poisson-Boltzmann equation are small (cf. Casimir 1944).

Finally we comment on the charging method employed by V.O. These authors employ the Poisson-Boltzmann equation which implies the approximation $\psi'(\lambda, n) = 0$, and hence, according to (28), (29) and (30), $\Phi(\lambda, n) = \psi(\lambda, n) = \psi^0(\lambda, n)$. Identifying the latter quantity with the 'surface potential', ψ_0 say, they charge at constant ψ_0 . Then they assume $\Delta\mu + \lambda e_1 \psi_0 = 0$, where $\Delta\mu$ is the 'chemical potential difference' between the surface phase and the solution phase. In the light of our analysis, the argument of V.O. should be modified as follows. The path of constant surface potential can be chosen for the charging process, but to maintain thermodynamic equilibrium it is necessary to apply some fictitious

* In (28) and (30) λ does not vary and strictly e_1 should be replaced by λe_1 .

mechanism which is equivalent to increasing the degree of freedom of our system by one. The path of constant ψ_0 in the (λ, n) plane is then given by $n = n_0(\lambda)$, which is derived from the equilibrium condition (23) which we write as

$$[df_0(n)/dn]_{n=n_0(\lambda)} - \Delta\chi_1(\lambda) - [1 - \xi\{\lambda, n_0(\lambda)\}]U_0 = -\lambda e_1\psi_0, \quad \dots\dots(31)$$

where the function $\xi = \xi(\lambda, n)$ is the inverse to $n = n(\lambda, \xi)$. Thus $\Delta\mu$ is to be identified with the left-hand side of (31) and it is automatically increased at the same rate as the ionic charges. Also the second and third terms on the right of (26) will vanish. V.O. obtained the last term only on the right of (26), ignoring the first term and the correction (27).

APPENDIX

In deriving (6) and (28) we shall consider a spherical particle and assume that $\lambda = 1$ and that the adsorbed ions differ from the lattice ion types of the particle. If we treat the Gibbs' phase integrals associated with the adsorbed phase and the solution phase for the ions as one integral, then the condition that there are n adsorbed ions is accounted for by properly choosing the configurational sub-space for all ions. Let $W = W_e + W_s$ be the mutual potential energy for all the ions for an instantaneous configuration; W_e is due to the coulomb interaction and W_s to the short-range van der Waals forces. Suppose that a chosen ion of type 1 is fixed at some distance r from the centre of the particle in the solvent or on the particle surface and $n - 1$ adsorbed ions are present on the surface. Let w be the potential of the mean force at the specified ion and w_0 the corresponding potential in the completely discharged state. Then

$$Q \exp(-w/kT) = \int \exp(-W/kT) d\tau, \quad Q_0 \exp(-w_0/kT) = \int \exp(-W_s/kT) d\tau, \quad \dots\dots(A1)$$

where the integrals are taken over the configurations of all the ions except the fixed one at r , with $n - 1$ ions on the particle; Q and Q_0 are constants independent of r , k is Boltzmann's constant and T the absolute temperature. We may write $\exp[\{F(1, n) - F(0, n) - F(1, n - 1) + F(0, n - 1) + \Delta\chi_1(1)\}/kT]$

$$= \frac{\int_V \exp(-w/kT) dv}{\int_V \exp(-w_0/kT) dv} \cdot \frac{\int_{\Delta V} \exp(-w_0/kT) dv}{\int_{\Delta V} \exp(-w/kT) dv}, \quad \dots\dots(A2)$$

where dv is a volume element specifying the position of the chosen ion, V the volume available to this ion in the dispersion medium and ΔV the corresponding volume in the adsorbed phase. Since $w = w_0 = 0$ in the bulk of the solution, the ratio of the two integrals over V on the right of (A2) is very nearly equal to unity if V is sufficiently large. Then if we ignore the amplitude of vibration of an adsorbed ion normal to the particle surface, the right-hand side of (A2) may be equated to $\exp[\{w(n) - w_0(n)\}/kT]$, where $w(n)$ and $w_0(n)$ are the values of w and w_0 respectively, when the specified ion is on the surface. Since

$$F(0, n) - F(0, n - 1) = f_0(n) - f_0(n - 1)$$

and at equilibrium $F(1, n) = F(1, n - 1)$ it follows that (A2) becomes

$$\Delta\chi_1(1) = f_0(n) - f_0(n - 1) + w(n) - w_0(n), \quad \dots\dots(A3)$$

and this is practically identical with (6) at $\lambda = 1$, if we put $e_1 \Phi(1, n) = w(n) - w_0(n)$.

Let ψ be the potential at the given 1 ion, position r , due to the coulomb interaction; for an instantaneous configuration of all the ions. Then, making use of (A 1),

$$Q\bar{\psi} = \exp(w/kT) \int \psi \exp(-W/kT) d\tau, \quad \dots\dots (A 4)$$

where

$$\frac{\partial w}{\partial r} = \frac{\partial \bar{W}}{\partial r} = e_1 \frac{\partial \Phi'}{\partial r}, \quad \dots\dots (A 5)$$

writing $w = e_1 \Phi'$. The bar denotes a statistical average taken over the same configurational sub-space as in (A 1). Differentiating (A 4) with respect to r and substituting (A 5), we readily find that

$$\frac{\partial \bar{\psi}}{\partial r} - \bar{\frac{\partial \psi}{\partial r}} = \frac{1}{kT} \left[\bar{\psi} \frac{\partial \bar{W}}{\partial r} - \bar{\psi} \frac{\partial \bar{W}}{\partial r} \right]. \quad \dots\dots (A 6)$$

We may treat both r and e_1 as parameters of external forces and apply a fluctuation formula for quantities involving external forces as obtained by Gibbs (1928). Since $\psi = \partial W / \partial e_1$ the right-hand side of (A 6) can be written as

$$\frac{1}{kT} \left[\left(\frac{\partial W}{\partial e_1} - \bar{\frac{\partial W}{\partial e_1}} \right) \left(\frac{\partial W}{\partial r} - \bar{\frac{\partial W}{\partial r}} \right) \right] = \frac{\partial^2 \bar{W}}{\partial r \partial e_1} - \frac{\partial}{\partial e_1} \bar{\frac{\partial W}{\partial r}}. \quad \dots\dots (A 7)$$

Then making use of (A 5) and (A 7), the relation (A 6) becomes

$$\frac{\partial \bar{\psi}}{\partial r} = \frac{\partial^2}{\partial r \partial e_1} (e_1 \Phi'). \quad \dots\dots (A 8)$$

On integrating (A 8) first with respect to r ($\Phi' \rightarrow 0$, $\bar{\psi} \rightarrow 0$ as $r \rightarrow \infty$) and then with respect to e_1 , we readily derive a formula already obtained by Kirkwood (1934), namely,

$$w = e_1 \Phi' = \int_0^{e_1} \bar{\psi} de_1 + w_{e_1=0}. \quad \dots\dots (A 9)$$

Here $w_{e_1=0}$ is the potential of the mean force acting on a discharged 1 ion at the position r , when all the other ions carry their full charge. Now if we introduce $e_1 \Phi = e_1 \Phi' - w_0$, where $\Phi = \Phi(1, n)$ when the given 1 ion is on the surface, then (A 9) becomes

$$e_1 \Phi = \int_0^{e_1} \bar{\psi} de_1 + w_{e_1=0} - w_0. \quad \dots\dots (A 10)$$

The difference $w_{e_1=0} - w_0$ is quite small for all r . The above results are still valid in the case of dielectric saturation in the diffuse layer.

REFERENCES

- CASIMIR, H. G. B., 1944, *Tweede symposium over sterke electrolyten en over de electrische dubbellaag* (Utrecht: ed. Ned. Chem. Ver., 6).
 GIBBS, W., 1928, *Collected Works*, Vol. II, Part 1 (London: Longmans), p. 81.
 INCE, E. L., 1927, *Ordinary Differential Equations* (London: Longmans), p. 16.
 KIRKWOOD, J. G., 1934, *J. Chem. Phys.*, **6**, 75; 1935, *Ibid.*, **3**, 300.
 KRUYT, H. R., 1952, *Colloid Science*, I (Amsterdam: Elsevier).
 LEVINE, S., 1946, *Trans. Faraday Soc.*, **42B**, 102; 1948, *Ibid.*, **44**, 833; 1950, *Phil. Mag.*, **41**, 53; 1951 a, *Proc. Camb. Phil. Soc.*, **47**, 217; 1951 b, *Ibid.*, **47**, 230; 1951 c, *J. Coll. Sci.*, **6**, 1 (§ 4); 1951 d, *Proc. Phys. Soc. A*, **64**, 781; 1953, *Ibid.*, **66**, 365.
 LOEB, A. W., 1951, *J. Coll. Sci.*, **6**, 75.
 VERWEY, E. J. W., and OVERBEEK, J. TH. G., 1948, *Theory of the Stability of Lyophobic Colloids* (Amsterdam: Elsevier).

Interaction of Two Parallel Colloidal Plates using a Modified Poisson-Boltzmann Equation

BY S. LEVINE

Department of Mathematics, University of Manchester

MS. received 20th June 1952, and in final form 5th November 1952

Abstract. The application of the general formula for the free energy obtained in the preceding paper is illustrated in the case of two parallel plates by introducing a number of corrections to the Poisson-Boltzmann equation and solving the resulting equation at small potentials. When the surface potential is 50 mv, the total correction to the interaction energy due to the deviations from the Poisson-Boltzmann equation is about 5% or less, except at small separations.

§ 1. INTRODUCTION

The general formulae for the free energy of a single colloidal particle obtained in the preceding paper (Levine 1953), to be referred to as I, can be readily extended to the case of two or more interacting particles with general distribution of surface charge. By way of illustration we have applied the formulae (I, 24) and (I, 25), which are probably the most convenient at small potentials, to the case of two parallel plates (for surface potentials of about 50 mv or less). We have introduced the modifications in the Poisson-Boltzmann (to be abbreviated to P.B.) equation which are due to the fluctuation and image effects, dielectric saturation, electrostriction and finite size of hydrated ions. The first two corrections are treated according to the recent theory of the double layer by Loeb (1951). However, it is demonstrated that in the case of small potentials Loeb's formula for the force between the two plates disagrees with the basic result (I, 25). All undefined symbols have the same meaning as in I.

§ 2. POTENTIAL OF THE MEAN FORCE AT A SURFACE ION

Consider the two plates in the fully charged state $\lambda = 1$ and in the presence of a 1-1 electrolyte; the adsorbed ion, charge e_1 , is univalent. Let each plate be of unit area, R the separation of the plates, x the distance measured from the median plane, D the dielectric constant of the bulk of the electrolyte, κ the Debye-Huckel parameter for the electrolyte and $\psi = \psi(\theta)$ where $\theta = \kappa x$, the mean potential at position x ; if $\Theta = \frac{1}{2}\kappa R$ then in the present notation $\psi^0(1, n) = \psi(\Theta)$. We proceed to set up a modified form for the P.B. equation and then solve it to derive $\psi(\Theta)$ for small n . As a first approximation the 'linear' solution

$$\psi_1 = \psi_1(\theta) = \frac{4\pi n e_1}{D\kappa} \frac{\cosh \theta}{\sinh \Theta} \dots\dots (1)$$

will be chosen.

In his theory of the double layer, Loeb (1951) considers the fluctuation terms neglected in the P.B. equation, and, in fact, his basic equations embody the

relation (I, 28). He then develops an approximate but practicable method of evaluating the quantities in (I, 28), neglecting the dielectric saturation and short-range forces between the ions. Since he examines the limiting case of two interacting plates where the surface potential is very high, we cannot apply (I, 24) to his results. However, it is quite easy to employ his 'intuitive' method (A) at small potentials. Let $\tilde{\kappa}$ be the Debye-Huckel parameter at position x , given as a first approximation by

$$\tilde{\kappa}^2 = \kappa^2 \cosh\left(\frac{e_1\psi}{kT}\right) \simeq \kappa^2 \left[1 + \frac{1}{2}\left(\frac{e_1\psi}{kT}\right)^2\right], \quad \dots\dots(2)$$

neglecting terms of order n^4 . Then according to Loeb's method (A) the correction to ψ_1 due to the self-atmosphere of an ion of charge e_1 is

$$\psi' = -\frac{e_1}{D}(\tilde{\kappa} - \kappa) \simeq -\frac{\kappa e_1}{4D}\left(\frac{e_1\psi}{kT}\right)^2. \quad \dots\dots(3)$$

Loeb also treats the image effect and, using his results for the case of perfectly insulating walls (of infinite thickness), we shall retain only the first four of the infinite set of images associated with an ion at point x between the two walls. This yields an additional correction to ψ_1 which is given approximately by

$$\frac{e_1\kappa}{2D} [g_1(\theta) + g_2(\theta)],$$

$$(\theta)_1 g = \frac{\exp[-2(\Theta + \kappa a - \theta)]}{\Theta + \kappa a - \theta}, \quad g_2(\theta) = \frac{\exp[-2(\Theta + \theta)]}{\Theta + \theta} + \frac{\exp(-4\Theta)}{\Theta}. \quad \dots\dots(4)$$

The form chosen for $g_1(\theta)$ allows for the fact that when the ion is at the wall its nearest image is at a distance $2a$, where a is the ionic radius. This correction has been omitted in $g_2(\theta)$ since it is not important for the other images provided Θ is not too small. To obtain the corresponding correction in the Boltzmann distribution law, we must integrate (3) and (4) with respect to e_1 (keeping $\tilde{\kappa} - \kappa$ fixed), divide by kT and so introduce the quantities

$$\eta' = -\frac{1}{2}\omega(e_1\psi/kT)^2, \quad \eta_1 = \omega g_1(\theta), \quad \eta_2 = \omega g_2(\theta), \quad \dots\dots(5)$$

where $\omega = e_1^2\kappa/4DkT$.

At low electric fields in the diffuse layers, we may account for dielectric saturation by expressing the dielectric constant at position x in the form $D[1 - b\kappa^2(d\psi/d\theta)^2]$, where the constant b has been determined experimentally by Malsch (1928) and theoretically by Booth (1951 a, b) and O'Dwyer (1951). Also we may correct for the hydration shells around each ion by modifying the Boltzmann distribution law in the manner proposed by Grimley and Mott (1947) and Grimley (1950). The final form of the corrected P.B. equation is

$$\kappa^2 \frac{d}{d\theta} \left[D \left\{ 1 - b\kappa^2 \left(\frac{d\psi}{d\theta} \right)^2 \right\} \frac{d\psi}{d\theta} \right] = \frac{8\pi N_0 e_1 \exp\{-(\eta' + \eta_1 + \eta_2)\} \sinh(e_1\psi/kT)}{[1 - 2pc + 2pc \cosh(e_1\psi/kT)]^{1/2}}, \quad \dots\dots(6)$$

where N_0 is the density of ion pairs in the bulk of the electrolyte, p the number of water molecules in the coordination shell of a hydrated ion (assumed to be the same for the two ion types) and $c = N_0/N_m$, where N_m is the density of water molecules. Expanding the right-hand side of (6) in powers of ψ and writing

$$\exp[-(\eta' + \eta_2)] \simeq 1 - \eta' - \eta_2,$$

(6) can be expressed as

$$\frac{d^2\psi}{d\theta^2} - \psi = -\{1 - \exp(-\eta_1)\}\psi - \eta_2\psi + \frac{1}{8}(1 - 3pc + 3\omega)\left(\frac{e_1}{kT}\right)^2\psi^3 + 3b\kappa^2\frac{d^2\psi}{d\theta^2}\left(\frac{d\psi}{d\theta}\right)^2 + \dots, \quad (7)$$

noting that $\kappa^2 = 8\pi N_0 e_1^2 / DkT$; terms of higher order are neglected.

The solution (1) is obtained if the right-hand side of (7) is equated to zero. Substituting (1) into the right-hand side of (7) and denoting the resulting expression for the latter by $h(\theta)$, we obtain an approximate solution of (7) which at $\theta = \Theta$ reads

$$\psi(\Theta) = \psi^0(\Theta) - \frac{1}{\sinh \Theta} \int_0^\Theta (\cosh u) h(u) du. \quad (8)$$

This iteration method, if continued, is equivalent to the use of the Green's function* originally applied in the theory of electrolytes by Gronwall, La Mer and Sandved (1928) and more recently in the theory of colloids by Booth (1951 c). Applying (I, 28), the potential of the mean force at an adsorbed ion (denoted in I by $\Phi(1, n)$) is

$$\Phi(\Theta) = \psi(\Theta) + \frac{kT}{e_1} [\eta'(\Theta) + \eta_1(\Theta - \kappa a) + \eta_2(\Theta)], \quad (9)$$

where we have corrected for the ionic radius when considering the nearest image of the adsorbed ion at distance $2a$. If we now integrate (8) and make use of (4) and (5), (9) can be written as

$$\Phi(\Theta) - A_0(\Theta) = A_1(\Theta)n - A_2(\Theta)n^2 - A_3(\Theta)n^3 - \dots, \quad (10)$$

$$\text{where } A_0(\Theta) = \frac{e_1\kappa}{8D} \left[\frac{\exp(-2\kappa a)}{\kappa a} + 3 \frac{\exp(-4\Theta)}{\Theta} \right], \quad (11)$$

$$A_1(\Theta) = \frac{4\pi e_1}{D\kappa} [\coth \Theta + P(\Theta) + Q(\Theta)], \quad (12)$$

$$P(\Theta) = \frac{1}{\sinh^2 \Theta} \int_0^{\Theta - \kappa a} (\cosh^2 u) \phi(\Theta + \kappa a - u) du, \quad \phi(z) = 1 - \exp\left[-\omega \frac{\exp(-2z)}{z}\right], \quad (13)$$

$$Q(\Theta) = \frac{\omega}{4 \sinh^2 \Theta} \left[2\{\text{Ei}(2\Theta) - \text{Ei}(4\Theta)\} + \exp(2\Theta)\{\text{Ei}(4\Theta) - \text{Ei}(8\Theta)\} + \exp(-2\Theta) \ln 2 + 2 \exp(-4\Theta) \left(1 + \frac{\sinh 2\Theta}{2\Theta}\right) \right], \quad \text{Ei}(z) = \int_z^\infty \frac{\exp(-u)}{u} du, \quad (14)$$

$$A_2(\Theta) = \frac{\omega e_1}{2kT} \left(\frac{4\pi e_1}{D\kappa}\right)^2 \coth^2 \Theta, \quad (15)$$

$$A_3(\Theta) = \left(\frac{4\pi e_1}{D\kappa}\right)^3 \coth^4 \Theta \left[(1 - 3pc + 3\omega) \left(\frac{e_1}{kT}\right)^2 R(\Theta) + \frac{3}{8} b\kappa^2 S(\Theta) \right], \quad (16)$$

$$R(\Theta) = \frac{1}{48} [3\Theta \text{sech}^4 \Theta + (2 + 3 \text{sech}^2 \Theta) \tanh \Theta], \quad (17)$$

$$S(\Theta) = (2 - \text{sech}^2 \Theta) \tanh \Theta - \Theta \text{sech}^4 \Theta. \quad (18)$$

The contributions $P(\Theta)$ and $Q(\Theta)$ are obtained from the first and second terms respectively on the right of (7); we integrate in (13) from $u=0$ to $u=\Theta - \kappa a$ to account for the ionic radius, but this correction is ignored elsewhere. We note

* This function is $-\frac{\cosh(\theta - \Theta)}{\sinh \Theta} \cosh u$, $0 \leq u \leq \theta$; $-\frac{\cosh \theta}{\sinh \Theta} \cosh(u - \Theta)$, $\theta \leq u \leq \Theta$.

that both $\psi(\Theta)$ and $\Phi(\Theta)$ are odd functions of e_1 and, therefore, of the surface charge ne_1 ; this must be so in the case of a 1-1 electrolyte since these potentials change sign with the surface charge.

§ 3. FREE ENERGY EXPRESSION

Suppose that the ions are charged under the condition of constant external pressure p_0 , say, rather than constant volume. Then the work of charging up will be the Gibbs' free energy if the pressure is uniform throughout the dispersion medium and the work done by the external pressure is omitted. But owing to the electrostrictive effect, the internal pressure p at a point x in the double layers is different from p_0 . Consequently, during an infinitesimal increment in the charge on the ions, there is an additional compression work done per unit volume at x . According to Webb (1926), this work is $\beta p' dp'$, where $p' = p - p_0$ and β is the isothermal compressibility at x . For small electric fields β is assumed independent of pressure and we may put

$$p' = \frac{(D-1)}{8\pi} \left(\frac{d\psi_1}{dx} \right)^2. \quad \dots\dots (19)$$

Integrating over the volume between the two plates and making use of (1) and (19), the compression work is

$$2\beta \int_0^{R/2} dx \int_0^{p'} p' dp' = \frac{1}{2} \left(\frac{D-1}{16\pi} \right)^2 \frac{\beta}{\kappa} \left(\frac{4\pi ne_1}{D} \right)^4 (\coth^4 \Theta) T(\Theta) = e_1 n^4 B(\Theta), \quad \text{say,} \quad \dots\dots (20)$$

$$\text{where} \quad T(\Theta) = (2 - 5 \operatorname{sech}^2 \Theta) \tanh \Theta + 3\Theta \operatorname{sech}^4 \Theta. \quad \dots\dots (21)$$

If we consider the form (I, 7), the Gibbs' free energy is conveniently written as

$$\begin{aligned} G &= [\alpha - \Delta\chi_1(1)]n + e_1 \int_0^n \Phi(\Theta) dn + e_1 n^4 B(\Theta) \\ &= [\alpha - \Delta\chi_1(1) + e_1 A_0(\Theta)]n + e_1 \int_0^n \Psi' dn, \quad \dots\dots (22) \end{aligned}$$

$$\text{where} \quad \Psi' = A_1(\Theta)n - A_2(\Theta)n^2 + [4B(\Theta) - A_3(\Theta)]n^3 + \dots \quad \dots\dots (23)$$

The energy (22) is an even function of e_1 , and thus is independent of the sign of the surface charge. The equilibrium value of n is defined by

$$\frac{dG}{dn} = 0 \quad \text{or} \quad e_1 \Psi' = e_1 \psi_0 - \frac{3e_1^2 \kappa}{8D} \frac{\exp(-4\Theta)}{\Theta}, \quad \dots\dots (24)$$

$$\text{where} \quad e_1 \psi_0 = \Delta\chi_1(1) - \alpha - \frac{e_1^2 \kappa}{8D} \frac{\exp(-2\kappa a)}{2\kappa a}.$$

Then the free energy at equilibrium is

$$\bar{G}(\Theta) = -e_1 \int_0^{\Psi'} n d\Psi', \quad \dots\dots (25)$$

where n is expressed as a function of Ψ' by inverting the series (23), and the upper limit of integration in (25) is specified by the relation (24). The energy expression (25) is readily expressed as a power series in Ψ' and, for our present purposes, it is sufficient to put $\Psi' = \psi_0$ and $P(\Theta) = Q(\Theta) = 0$ in the terms in Ψ'^3 and Ψ'^4 .

Making use of (12)–(16) and of (20), this yields the result

$$\begin{aligned} \bar{G}(\Theta) = & -\frac{D\kappa\psi_0^2}{8\pi} \left[\frac{\tanh \Theta \left\{ 1 - \frac{3}{2}\omega \left(\frac{\mathbf{k}T}{e_1\psi_0} \right) \frac{\exp(-4\Theta)}{\Theta} \right\}^2}{1 + \tanh \Theta \{P(\Theta) + Q(\Theta)\}} + \frac{\omega}{3} \left(\frac{e_1\psi_0}{\mathbf{k}T} \right) \tanh \Theta \right. \\ & + \frac{1}{2} \left(\frac{e_1\psi_0}{\mathbf{k}T} \right)^2 \left\{ (1 - 3pc + 3\omega)R(\Theta) + \frac{3}{8}b \left(\frac{\mathbf{k}T\kappa}{e_1} \right)^2 S(\Theta) \right. \\ & \left. \left. - \frac{\beta(D-1)^2}{32\pi D} \left(\frac{\mathbf{k}T\kappa}{e_1} \right)^2 T(\Theta) + \frac{\omega^2 \tanh \Theta}{2} \right\} + \dots \right]. \quad \dots\dots(26) \end{aligned}$$

The limiting form of (26) at infinite separation is readily obtained. For large Θ , the interaction energy is

$$\begin{aligned} \Delta\bar{G}(\Theta) = \bar{G}(\Theta) - \bar{G}(\infty) \\ \simeq \frac{D\kappa\psi_0^2}{8\pi} \exp(-2\Theta) \left[\frac{2(1+\nu)}{(1+P(\infty))^2} + \frac{3}{2}\omega \left(\frac{e_1\psi_0}{\mathbf{k}T} \right) + \frac{1}{2} \left(\frac{e_1\psi_0}{\mathbf{k}T} \right)^2 \left\{ -\frac{1}{6}(1 - 3pc + 3\omega) \right. \right. \\ \left. \left. + 3b \left(\frac{\mathbf{k}T\kappa}{e_1} \right)^2 - \frac{3\beta(D-1)^2}{4\pi D} \left(\frac{\mathbf{k}T\kappa}{e_1} \right)^2 + \omega^2 \right\} + \dots \right], \quad \dots\dots(27) \end{aligned}$$

$$\begin{aligned} \text{since} \quad P(\Theta) \simeq P(\infty) + 2\nu \exp(-2\Theta), \quad P(\infty) = \exp(2\kappa a) \int_{2\kappa a}^{\infty} \exp(-2v)\phi(v) dv, \\ \nu = \int_{2\kappa a}^{\infty} \phi(v) dv + P(\infty). \end{aligned}$$

If we ignore the electrostrictive effect and the various corrections to the P.B. equation considered above, then the interaction energy is

$$\Delta\bar{G}_0(\Theta) = \frac{D\kappa\psi_0^2}{8\pi} \left[1 - \tanh \Theta + \frac{1}{48} \left(\frac{e_1\psi_0}{\mathbf{k}T} \right)^2 \{1 - 24R(\Theta)\} + \dots \right], \quad \dots\dots(28)$$

and the energy at infinite separation is

$$\bar{G}_0(\infty) = -\frac{D\kappa\psi_0^2}{8\pi} \left[1 + \frac{1}{48} \left(\frac{e_1\psi_0}{\mathbf{k}T} \right)^2 + \dots \right], \quad \dots\dots(29)$$

which has already been obtained in an earlier paper by Levine and Suddaby (1951). (Strictly the potential ψ_0 in (28) differs from that in (27) by an image term.) The higher terms in the expansion (28) contribute less than 5% of the energy if $\psi_0 = 50$ mv, and will not be considered here.

Now Verwey and Overbeek (1948) have shown the equivalence of Langmuir's (1938) force equation to (I, 24) if the P.B. equation is used, and Loeb (1951) attempts to extend this force method. Let $\psi_m = \psi_0 \operatorname{sech} \Theta$ be the potential at the median plane between the plates. Then applying the formulae of Langmuir and Loeb, the force between the plates is given by

$$\begin{aligned} 2N_0\mathbf{k}T \left[\cosh \left(\frac{e_1\psi_m}{\mathbf{k}T} \right) - 1 \right] + \frac{\mathbf{k}T}{16\pi} \left[\int_0^{\tilde{\kappa}x=1} \tilde{\kappa}^4 (\tilde{\kappa}^2 x^2 - 1) dx - \int_0^{\kappa x} \kappa^4 (\kappa^2 x^2 - 1) dx \right] \\ \simeq \frac{D\kappa^2\psi_0^2}{2\pi} \exp(-2\Theta) - \frac{8\cdot 4\mathbf{k}T\kappa^3}{64\pi} \left(\frac{e_1\psi_0}{\mathbf{k}T} \right)^2 \exp(-2\Theta). \quad \dots\dots(30) \end{aligned}$$

We have substituted (2) for $\tilde{\kappa}$ with $\psi = \psi_0 \cosh \kappa x / \cosh \Theta$ and expanded in powers of ψ_0 ; Θ is assumed large. The first term on the right of (20) is obtained from Langmuir's force equation and the second term is the correction according to Loeb's theory. However, the force is derived by differentiating (27) partially with respect to R under the condition of constant ψ_0 and then changing sign.

Ignoring the image force, the first two terms on the right of (27) contribute

$$\frac{D\kappa^2\psi_0^2}{2\pi} \exp(-2\Theta) - \frac{kT\kappa^3}{12\pi} \left(\frac{e_1\psi_0}{kT}\right)^3 \exp(-2\Theta) \quad \dots\dots (31)$$

to the force so that, on the basis of the form (3) for ψ' , Loeb's extension is not valid for small ψ_0 .

As a numerical example we choose $T=291^\circ\text{K}$, the electrolyte concentration $\gamma=0.0102\text{ mol/l.}$ and $e_1\psi_0/kT=2$ ($\psi_0 \simeq 50\text{ mv}$), so that $D=81.1$, $\omega=0.0586$, $\kappa=\sqrt{\gamma}/3.06 \times 10^{-8}=3.31 \times 10^6$ and $c=18 \times 10^{-5}$. Also, we shall put $3b=10^{-8}\text{ e.s.u.}$ (the experimental value of Malsch 1928), $\beta=48.5 \times 10^{-12}\text{ c.g.s. units}$, $p=6$ and consider two values of the ionic radius, given by $\kappa a=0.05$ and 0.1 . The integral in the expression for $P(\Theta)$ is evaluated numerically. The quantities $\Delta\bar{G}_0(\Theta)$ and $\bar{G}_0(\infty)$ (divided by $D\kappa\psi_0^2/8\pi$) and their corrections are given for various Θ in the table. The following properties may be noted: (i) the total correction to the energy due to the deviations from the P.B. equation is about 5% or less except at small Θ ; (ii) the image and fluctuation corrections are the main ones: these differ in sign in $\bar{G}_0(\infty)$, but not in $\Delta\bar{G}(\Theta)$; (iii) the saturation and hydration effects are of the same order of magnitude for $\Theta \geq 1$ and have opposite signs in $\bar{G}_0(\infty)$, but the same sign in $\Delta\bar{G}(\Theta)$, also they are approximately proportional to γ , whereas the fluctuation term varies roughly as $\sqrt{\gamma}$; (iv) the electrostrictive effect is very small.

Θ	Interaction energy ($\times 8\pi/D\kappa\psi_0^2$)					Energy at ∞ sep. ($\times 8\pi/D\kappa\psi_0^2$)
	0.5	1.0	1.5	2.0	$\geq 1(\times e^{2\Theta})$	
Equation (28) (P.B. equation)	0.4896	0.1962	0.07609	0.02921	1.6667	-1.0833*
Total						
$\left\{ \begin{array}{l} \kappa a=0.05 \\ \kappa a=0.1 \end{array} \right.$	0.0423 0.0433	0.0105 0.0098	0.00323 0.00287	0.00120 0.00105	0.0716 0.0632	-0.0164 -0.0349
Separate contributions						
Images						
$\left\{ \begin{array}{l} \kappa a=0.05 \\ \kappa a=0.1 \end{array} \right.$	0.0259 0.0269	0.0074 0.0067	0.00236 0.00199	0.00081 0.00067	0.0427 0.0343	0.0392 0.0207
Fluctuations	0.0160	0.0027	0.00075	0.00034	0.0264	-0.0554
Saturation	0.0034	0.0019	0.00077	0.00029	0.0015	-0.0038
Hydration shell	0.0013	0.0014	0.00060	0.00022	0.0011	0.0027
Electrostriction	-0.0023	-0.0018	-0.0010	-0.00045	-0.0014	-0.0012

* Equation (29).

§ 4. DISCUSSION

The above properties apply to small potentials. A preliminary investigation shows that the radius of convergence of the expansion (27) is given approximately (for $\Theta < \pi/2$) by $\psi_0=92, 80$ and 78 mv at $\Theta=0.5, 1.0$ and 1.5 respectively. Although we cannot use (28), and presumably (26), at larger potentials, the form of (26) does suggest that the relative magnitudes of the correction terms will change with ψ_0 in the following manner. The saturation, hydration shell and electrostrictive effects should increase rapidly with ψ_0 , being proportional to ψ_0^2 at small ψ_0 , whereas the fluctuation term does not change so much. The image correction becomes less important at large ψ_0 . Finally, we may expect the overall relative correction to $\Delta\bar{G}_0(\Theta)$ to increase with ψ_0 .

Since the corrections in the expansion (26) are only a first approximation, even at small potentials, further investigations are desirable. For example, the effect of the short-range forces between the ions is only partly accounted for by the hydration shell, and the fluctuation terms should be treated more accurately.

Thus a better approximation than the form (3) is $\psi' = -(e_1/D)(f\tilde{\kappa} - \kappa)$ where $f=f(\theta)$ is a factor which corrects for the fact that when an ion is taken to the vicinity of the plate surface from the interior of the solution its atmosphere is distorted, and consequently $\tilde{\kappa}$ should be replaced by $f\tilde{\kappa}$. For a single unchanged boundary $f=\frac{2}{3}$ when the ion is at the surface and $f=1$ at large distances from the surface (Loeb 1950, 1951). The determination of $f(\theta)$ is equivalent to solving Loeb's equation for ψ' , but this will not be attempted here.

A promising method of deriving alternative expressions to (I, 24) for the free energy suitable for computations at any value of ψ_0 is the following. In an earlier paper (Levine 1951, eqn. 14)) the author integrated the expression (I, 4) for $F_e(\lambda, n)$ with respect to λ , assuming the P.B. equation. Thus in the particular case of a 1-1 electrolyte at $\lambda=1$ and of the single particle model considered in I, we obtain

$$F_e(1, n) = e_1 n \psi(1, n) - \frac{D}{8\pi} \left(\frac{kT}{e_1} \right)^2 \int [|\text{grad } \phi|^2 + 2\kappa^2(\cosh \phi - 1)] dv, \quad \dots\dots(32)$$

where $\phi = e_1 \psi / kT$; ψ is the mean potential at any point in the diffuse layer over which we integrate. The volume integral in (32) has been used by Verwey and Overbeek (1948) in the case of two parallel plates. Now if we turn to the calculus of variations and start from a variational principle, then the expression (32) is precisely the quantity to be made stationary by proper choice of the function ψ . This yields the P.B. equation as the Euler differential equation and also the appropriate boundary conditions at the surface. This suggests that we can arrive at the same generalization of (32) when the modified P.B. equation is used in two ways: (i) the integration of (I, 4) is carried out, (ii) the modified P.B. equation is first set up and then the equivalent variational principle is obtained. It is hoped to consider these problems in later papers.

ACKNOWLEDGMENTS

The author is indebted to Dr. A. S. Coolidge of Harvard University for criticisms of this paper and of the preceding one, and to Mr. D. F. Ferguson of Manchester University for computing $P(\theta)$.

REFERENCES

- BOOTH, F., 1951 a, *J. Chem. Phys.*, **19**, 391; 1951 b, *Ibid.*, **19**, 1327; 1951 c, *Ibid.*, **19**, 821.
 GRIMLEY, T. B., 1950, *Proc. Roy. Soc. A*, **201**, 40.
 GRIMLEY, T. B., and MOTT, N. F., 1947, *Discussions of the Faraday Society*, **1**, 3.
 GRONWALL, T. H., LA MER, V. K., and SANDVED, K., 1928, *Phys. Z.*, **29**, 358.
 LANGMUIR, I., 1938, *J. Chem. Phys.*, **6**, 873.
 LEVINE, S., 1951, *Proc. Phys. Soc. A*, **64**, 781; 1953, *Ibid.*, **66**, 357.
 LEVINE, S., and SUDDABY, A., 1951, *Proc. Phys. Soc. A*, **64**, 287.
 LOEB, A. L., 1950, *Ph.D. Thesis*, University of Harvard; 1951, *J. Coll. Sci.*, **6**, 75.
 MALSCH, J., 1928, *Phys. Z.*, **29**, 770.
 O'DWYER, J. J., 1951, *Proc. Phys. Soc. A*, **64**, 1125.
 VERWEY, E. J. W., and OVERBEEK, J. TH. G., 1948, *Theory of the Stability of Lyophobic Colloids* (Amsterdam: Elsevier).
 WEBB, J., 1926, *J. Amer. Chem. Soc.*, **48**, 2589.

Solution of a Modified Poisson-Boltzmann Equation for a Single Plane Double Layer

By W. E. WILLIAMS

Department of Mathematics, University of Manchester

Communicated by S. Levine; MS. received 22nd October 1952

Abstract. In this paper, a method developed by Loeb to correct the Poisson-Boltzmann equation for the self-atmosphere effect of the ions is applied to the case of a charged plane surface immersed in a binary symmetrical electrolyte. The two limiting cases of a perfectly conducting and a perfectly insulating wall are treated. Numerical values of the correction to the average potential for various distances from the wall are obtained. This correction term is 5% near the wall for a conducting wall and 3% for an insulating one when the wall potential is 100 mv and is larger for higher potentials.

§ 1. INTRODUCTION

CRITICISM has been made of the Debye-Huckel (1923) theory of strong electrolytes on the grounds that certain physical assumptions are made in the derivation of the Poisson-Boltzmann equation which do not agree with the principles of statistical mechanics. Consider, for example, the case of a plate immersed in a large volume of electrolyte. It is assumed that the average potential at an ion near the plate is not affected by the presence of the ion itself, whereas in fact the ion will induce a space charge of opposite sign nearby, with which it interacts, and hence the potential energy is decreased. This decrease may be appreciable near a charged plate owing to the increased ionic concentration.

Kirkwood (1934) has analysed the assumptions made in the Debye-Huckel theory and although he derives a corrected form of the Poisson-Boltzmann equation no practical solution has been obtained. An approximate but practical method of accounting for the self-atmosphere effect of an ion in the neighbourhood of a colloidal particle has been proposed by Loeb (1951), who considers the case of an electrolyte between two parallel plates. Loeb treats the potential at a point as the sum of two terms, one the average potential which is dependent only on the coordinates of the point, and the other a perturbation potential due to the presence of an ion near the point concerned. In the present work the same method is applied to the case of one plate in contact with an electrolyte. In view of the mathematical difficulties which arise in the case of two plates it is certainly desirable to solve the case of one plate. For simplicity Loeb makes Langmuir's (1938) approximation of neglecting all ions whose charge has the same sign as that of the wall; the value of the average potential thus obtained is then used to set up an approximate equation for the perturbation potential and this equation is then solved, although only approximately. Here the case is treated of a binary symmetrical electrolyte and both ion types will be taken into account. The resulting approximate equation for the perturbation potential can be solved exactly for a single plate.

The method used is briefly as follows: (i) two equations are set up, one for the average potential and the other for the perturbation potential; (ii) as a first approximation the perturbation potential is neglected and an expression obtained for the average potential; (iii) the latter expression is introduced into the equation for the perturbation potential which is then solved; (iv) making use of the perturbation potential a more exact equation is set up for the average potential, and this equation is then solved numerically.

§ 2. THE DERIVATION OF THE EQUATION FOR THE PERTURBATION POTENTIAL

The following is the notation used: e charge on an ion, ϵ dielectric constant, k Boltzmann's constant, T absolute temperature, n bulk concentration of each kind of ion, x distance from the plate, x_p coordinate of the central ion, $\psi^0(x)$ average potential at the point x , $\psi'(x, x_p)$ perturbation potential at x due to the presence of the ion at P ; $\psi(x, x_p) = \psi^0(x) + \psi'(x, x_p)$. Loeb's equations for ψ and ψ^0 are:

$$\nabla^2 \psi = \frac{8\pi ne}{\epsilon} \exp \eta' \sinh \frac{e\psi}{kT}, \quad \dots\dots(2.1)$$

$$\frac{d^2 \psi^0}{dx^2} = \frac{8\pi ne}{\epsilon} \exp \eta' \sinh \frac{e\psi^0}{kT}, \quad \dots\dots(2.2)$$

respectively, where η' is given by

$$\eta' = -\frac{1}{kT} \int_0^e \left\{ \lim_{r \rightarrow 0} \left(\psi' - \frac{e}{\epsilon r} \right) - \lim_{r \rightarrow 0} \left(\psi' - \frac{e}{\epsilon r} \right)_{x_p = \infty} \right\} de. \quad \dots\dots(2.3)$$

It is assumed that (i) η' is the same function for both types of ions, (ii) the ionic radius is neglected. It is noted that η' is finite since the infinite self-potential cancels in the integrand of (2.3). The physical significance of the above integral is that it represents the work done, against its own atmosphere, in bringing an ion from infinity to the point x . The equations (2.1)–(2.3) can be derived from Kirkwood's analysis.

Following Loeb it will be assumed that ψ' is small. Hence on subtracting (2.2) from (2.1) and retaining only the first order terms in ψ' we obtain

$$\nabla^2 \psi' = K^2 \exp \eta' \cosh \left(\frac{e\psi^0}{kT} \right) \psi' \quad \dots\dots(2.4)$$

where $K^2 = 8\pi e^2 n / \epsilon kT$.

Equation (2.4) is similar to the one solved by Debye and Huckel, the difference being that here the coefficient of ψ' is not a constant. We first assume $\eta' = 0$, so that (2.2) becomes

$$d^2 \eta^0 / dz^2 = \sinh \eta^0, \quad \dots\dots(2.5)$$

where $z = Kx$ and $\eta^0 = e\psi^0 / kT$. The solution of (2.5) which vanishes as $x \rightarrow \infty$ is known (Verwey and Overbeek 1948) and will be denoted by

$$L = 4 \operatorname{arc} \tanh \{ \exp(-Kx) \tanh \frac{1}{4} \eta_0 \}$$

where η_0 is the first approximation to η^0 at the wall. The equation for ψ' now becomes

$$\nabla^2 \psi' = K^2 \cosh [4 \operatorname{arc} \tanh \{ \exp(-Kx) \tanh \frac{1}{4} \eta_0 \}] \cdot \psi'. \quad \dots\dots(2.6)$$

If we introduce cylindrical polar coordinates x, ρ then (2.6) becomes

$$\frac{1}{\rho} \frac{\partial}{\partial \rho} \left(\rho \frac{\partial \psi'}{\partial \rho} \right) + \frac{\partial^2 \psi'}{\partial x^2} = K^2 \left[1 + \frac{8 \exp(-2Kx) \tanh^2 \frac{1}{4} \eta_0}{\{1 - \exp(-2Kx) \tanh^2 \frac{1}{4} \eta_0\}^2} \right] \psi' = \tilde{K}^2(x) \psi' \text{ say.} \quad \dots\dots(2.7)$$

The azimuthal angle need not be considered because of symmetry.

§ 3. THE SOLUTION FOR THE PERTURBATION POTENTIAL IN THE CASE OF A METALLIC WALL

The boundary conditions are : (i) $\psi' = 0$ when $x = 0$, (ii) $\psi' \rightarrow 0$ as $x \rightarrow \infty$, (iii) $(\psi' - e/\epsilon r)$ is everywhere smooth and continuous. Using the method of separation of variables it is easily seen that the most general solution of (2.7) which is finite on $\rho = 0$ for all x is given by

$$\psi' = \int_0^\infty X(s, x) J_0(s\rho) s ds, \quad \dots\dots(3.1)$$

where $J_0(s\rho)$ is the Bessel function of the first kind, of order zero, and X satisfies

$$\frac{d^2 X}{dx^2} = \left[K^2 \left\{ 1 + \frac{8 \exp(-2Kx) \tanh^2 \frac{1}{4} \eta_0}{\{1 - \exp(-2Kx) \tanh^2 \frac{1}{4} \eta_0\}^2} \right\} + s^2 \right] X. \quad \dots\dots(3.2)$$

Since $\psi' \sim \exp(-Kr)$ as $r \rightarrow \infty$, $\int \psi'(x, \rho) d\rho$ from 0 to ∞ is absolutely convergent and hence Hankel's inversion theorem (Titchmarsh 1937) may be applied to (3.1). This gives

$$X(s, x) = \int_0^\infty \psi'(\rho, x) J_0(s\rho) \rho d\rho, \quad \dots\dots(3.3)$$

X being the Hankel transform of ψ' . Using the fact that the Hankel transform of $1/r$ is $(1/s) \exp(-s|x - x_P|)$ it may be verified from (3.3) that the boundary conditions on ψ' give the following boundary conditions on X : (i) $X(s, 0) = 0$, (ii) $\lim_{x \rightarrow \infty} X(s, x) = 0$, (iii) $(dX/dx)_{x=x_P+0} - (dX/dx)_{x=x_P-0} = -2e/\epsilon$ and X is continuous everywhere. From inspection of (3.2) it is seen that as $x \rightarrow \infty$ there are two solutions X_1, X_2 behaving as $\exp\{\mp x(K^2 + s^2)^{1/2}\}$ and thus $X = AX_1, x > x_P, X = BX_1 + CX_2, x < x_P$, where A, B and C are arbitrary constants.

The boundary condition at $x = 0$ gives $B/C = \lambda$ say, and on applying the boundary conditions at $x = x_P$ we obtain

$$A = \frac{2e}{\epsilon} \left[\frac{X_2 + \lambda X_1}{(X_1 X_2' - X_1' X_2)} \right]_{x=x_P} \quad \dots\dots(3.4)$$

where the prime denotes differentiation with respect to x . If the substitution $y = \exp(-2Kx) \tanh^2 \frac{1}{4} \eta_0$ is made then (3.2) becomes

$$\frac{d^2 X}{dy^2} + \frac{1}{y} \frac{dX}{dy} = \left(\frac{\alpha^2}{y^2} + \frac{2}{y(1-y)^2} \right) X, \quad \dots\dots(3.5)$$

where $\alpha = (1 + s^2/K^2)^{1/2}/2$. Equation (3.5) is of the hypergeometric type and it is easily verified that the solutions are

$$X_1 = y^\alpha (1-y)^{-1} \{2\alpha + 1 - (2\alpha - 1)y\}, \quad X_2 = y^{-\alpha} (1-y)^{-1} \{2\alpha - 1 - (2\alpha + 1)y\}.$$

These solutions are independent except when $\alpha = 1/2$, i.e. $s^2 = 0$. This corresponds to the lower limit of integration in the integral for ψ' , and hence the range of α considered will be from $\frac{1}{2} + \theta$ to ∞ , where $\theta > 0$ and the limit as θ tends to zero will be taken. Using the well-known property of the Wronskian (Copson 1935) it is easily found that

$$A = \frac{e(X_2 + \lambda X_1)_{x=x_P}}{K\epsilon 2\alpha(2\alpha - 1)(2\alpha + 1)},$$

and also

$$\lambda = - \frac{1}{\tanh^{4\alpha} \frac{1}{4} \eta_0} \left[1 - \frac{2(1 + \tanh^2 \frac{1}{4} \eta_0)}{2\alpha \operatorname{sech}^2 \frac{1}{4} \eta_0 + (1 + \tanh^2 \frac{1}{4} \eta_0)} \right]. \quad \dots\dots(3.6)$$

Hence for $x > x_P$ we obtain (after some rearrangement)

$$\begin{aligned} \psi' = & \frac{2Ke}{\epsilon} \lim_{\theta \rightarrow 0} \int_{\frac{1}{2} + \theta}^{\infty} \exp \{-2K\alpha(x - x_P)\} J_0(s\rho) d\alpha \\ & + \frac{2Ke}{\epsilon(1-y)(1-y_P)} \lim_{\theta \rightarrow 0} \int_{\frac{1}{2} + \theta}^{\infty} \left[\frac{2y}{2\alpha + 1} - \frac{2y_P}{2\alpha - 1} \right] \exp \{-2K\alpha(x - x_P)\} J_0(s\rho) d\alpha \\ & - \frac{2Ke}{\epsilon(1-y)(1-y_P)} \lim_{\theta \rightarrow 0} \int_{\frac{1}{2} + \theta}^{\infty} \exp \{-2K\alpha(x + x_P)\} \left[1 - \frac{2(1 + \tanh^2 \frac{1}{4}\eta_0)}{2\alpha \operatorname{sech}^2 \frac{1}{4}\eta_0 + (1 + \tanh^2 \frac{1}{4}\eta_0)} \right] \\ & \times \left[(1-y)(1-y_P) + \frac{2}{2\alpha - 1} - \frac{2yy_P}{2\alpha + 1} \right] J_0(s\rho) d\alpha, \quad \dots\dots(3.7) \end{aligned}$$

where $y_P = \exp(-2Kx_P) \tanh^2 \frac{1}{4}\eta_0$. We require η' and therefore

$$\lim_{r \rightarrow 0} (\psi' - e/\epsilon r) = \phi, \text{ say.}$$

The limit as $\theta \rightarrow 0$ may be taken immediately in the first integral in (3.7), its value being $\exp(-Kr)/2Kr$ (Stratton 1941); hence the contribution of this part to ϕ is $-Ke/\epsilon$. The second integral is uniformly convergent for $x > x_P > 0$; when $x = x_P$ the exponential term in the integrand becomes unity, but since $y = y_P$ this integrand is $O(\alpha^{-2})$ as $\alpha \rightarrow \infty$; hence the integral is uniformly convergent for $x \geq x_P > 0$. Clearly this is also true of the third integral. The coefficient of $(2\alpha - 1)^{-1}$ in the integrands of (3.7) is

$$2 \exp(-2K\alpha x) \tanh^2 \frac{1}{4}\eta_0 [\exp(-2K\alpha x_P) - \exp\{2Kx_P(\alpha - 1)\}].$$

As $\alpha \rightarrow \frac{1}{2}$ this coefficient tends to zero and therefore the integral for $(\psi' - e/\epsilon r)$ exists and is uniformly convergent for $x \geq x_P > 0$. We need to evaluate

$$\lim_{\substack{x \rightarrow x_P \\ \theta \rightarrow 0}} \lim_{\theta \rightarrow 0} \int_{\frac{1}{2} + \theta}^{\infty} f(x, \alpha, \rho) d\alpha,$$

where $f(x, \alpha, \rho)$ is the integrand from the last two terms of (3.7), and because of the existence and uniform convergence of the integral it is permissible to interchange limits and take the limits with respect to x, ρ inside the integral. Therefore if the whole integrand is expanded in partial fractions, we obtain

$$\begin{aligned} \phi = & -\frac{Ke}{\epsilon} + \frac{2Ke}{\epsilon} \left[\lim_{\theta \rightarrow 0} \frac{2}{(1-y)^2} \right. \\ & \times \int_{\frac{1}{2} + \theta}^{\infty} \left\{ \frac{(1 + \tanh^2 \frac{1}{4}\eta_0)[(1-y)^2 - \operatorname{sech}^2 \frac{1}{4}\eta_0 + y^2 \operatorname{cosech}^2 \frac{1}{4}\eta_0]}{2\alpha \operatorname{sech}^2 \frac{1}{4}\eta_0 + (1 + \tanh^2 \frac{1}{4}\eta_0)} \right. \\ & \left. - \tanh^2 \frac{1}{4}\eta_0 \left(\frac{\exp(-4Kx)}{2\alpha + 1} + \frac{1}{2\alpha - 1} \right) \right\} \exp(-4Kx\alpha) d\alpha \left. \right] \\ & + \frac{2Ke}{\epsilon} \lim_{\theta \rightarrow 0} \frac{2}{(1-y)^2} \int_{\frac{1}{2} + \theta}^{\infty} y \left[\frac{1}{2\alpha + 1} - \frac{1}{2\alpha - 1} \right] d\alpha - \frac{e}{\epsilon} \frac{\exp(-2Kx)}{2x} \quad \dots\dots(3.8) \end{aligned}$$

where the suffix on y_P has been dropped and the identity $J_0(0) = 1$ has been used. The limit as $\theta \rightarrow 0$ may be taken immediately for the first integral in (3.8) and there remains to consider

$$\begin{aligned} & \lim_{\theta \rightarrow 0} \frac{2}{(1-y)^2} \tanh^2 \frac{1}{4}\eta_0 \int_{\frac{1}{2} + \theta}^{\infty} \left[\left(\frac{1}{2\alpha + 1} - \frac{1}{2\alpha - 1} \right) \exp(-2Kx) + \frac{\exp(-4Kx\alpha)}{2\alpha - 1} \right] d\alpha \\ & = \frac{y}{(1-y)^2} \lim_{\theta \rightarrow 0} [-\log(2 + 2\theta) + \log 2\theta - \operatorname{Ei}(-4Kx\theta)] \\ & = -\frac{y}{(1-y)^2} (\gamma + \log 4Kx), \quad \dots\dots(3.9) \end{aligned}$$

where $-\operatorname{Ei}(-x) = \int_x^{\infty} \frac{\exp(-t)}{t} dt$ and γ is Euler's constant.

The last identity in (3.9) is obtained by using the following relation (Jeffreys and Jeffreys 1946)

$$\lim_{x \rightarrow 0} [-\text{Ei}(-x) + \log x] = -\gamma.$$

Thus η' is given by

$$\eta' = -\frac{e}{2kT} \left[\phi + \frac{Ke}{\epsilon} \right], \quad \dots\dots (3.10)$$

where

$$\begin{aligned} \phi = & \frac{2Ke}{\epsilon(1-y)^2} [y\{\text{Ei}(-4Kx) - (\gamma + \log 4Kx)\} \\ & - \{(1-y)^2 - \text{sech}^2 \tfrac{1}{4}\eta_0 + y^2 \text{cosech}^2 \tfrac{1}{4}\eta_0\} (\cosh \tfrac{1}{2}\eta_0) \exp(Kx \cosh \tfrac{1}{2}\eta_0) \\ & \times \text{Ei}(-4Kx \cosh^2 \tfrac{1}{4}\eta_0)] - \frac{Ke}{\epsilon} - \frac{e}{2\epsilon x} \exp(-2Kx). \quad \dots\dots (3.11) \end{aligned}$$

There are three types of terms in (3.11): (a) $-Ke/\epsilon$ the contribution from the ordinary Debye-Huckel potential, (b) $-(e/2\epsilon x) \exp(-2Kx)$ the term due to the image of the ion in the plane $x=0$, (c) the remainder, due to the self-atmosphere effect.

§4. THE SOLUTION FOR THE PERTURBATION POTENTIAL IN THE CASE OF AN INSULATING WALL

The only difference in the boundary conditions for this case is that $\partial\psi'/\partial x=0$ for $x=0$, since here the surface charge density is assumed constant (immobile). This gives a new value for λ , namely

$$\begin{aligned} \lambda = & -\left\{ \frac{dX_2}{dy} / \frac{dX_1}{dy} \right\}_{x=0} \quad \dots\dots (4.1) \\ = & \frac{1}{\tanh^{4\alpha} \tfrac{1}{4}\eta_0} \left\{ 1 - \frac{2\alpha(1 + \coth^2 \tfrac{1}{4}\eta_0)}{2\alpha^2 \text{cosech}^2 \tfrac{1}{4}\eta_0 + \alpha(1 + \coth^2 \tfrac{1}{4}\eta_0) + 2 \cosh^2 \tfrac{1}{4}\eta_0} \right\}. \end{aligned}$$

Hence for $x > x_P$

$$\begin{aligned} \psi' = & \frac{e}{\epsilon r} + \frac{2Ke}{\epsilon(1-y)(1-y_P)} \\ & \times \lim_{\theta \rightarrow 0} \int_{\frac{1}{2}+\theta}^{\infty} \left[1 - \frac{2\alpha(1 + \coth^2 \tfrac{1}{4}\eta_0)}{2\alpha^2 \text{cosech}^2 \tfrac{1}{4}\eta_0 + \alpha(1 + \coth^2 \tfrac{1}{4}\eta_0) + 2 \cosh^2 \tfrac{1}{4}\eta_0} \right] \\ & \times \left[(1-y)(1-y_P) + \frac{2}{2\alpha-1} - \frac{2yy_P}{2\alpha+1} \right] \exp\{-2K\alpha(x+x_P)\} J_0(s\rho) d\alpha \\ & + \frac{2Ke}{\epsilon(1-y)(1-y_P)} \lim_{\theta \rightarrow 0} \int_{\frac{1}{2}+\theta}^{\infty} \left[\frac{y}{2\alpha+1} - \frac{y_P}{2\alpha-1} \right] \exp\{-2K\alpha(x-x_P)\} J_0(s\rho) d\alpha. \quad \dots\dots (4.2) \end{aligned}$$

It may be verified as before that the integral for ϕ is uniformly convergent and exists at $\alpha = \frac{1}{2}$, and that the contributions from the terms involving $(2\alpha+1)^{-1}$, $(2\alpha-1)^{-1}$ are exactly the same as in (3.8). The last term in (3.8) is replaced by $(e/2\epsilon x) \exp(-2Kx)$ and on expanding in partial fractions it is seen that the first term of the second integral is replaced by

$$-\frac{2Ke}{\epsilon(1-y)^2} \int_{\frac{1}{2}}^{\infty} \frac{\{[(1-y)^2(1 + \coth^2 \tfrac{1}{4}\eta_0) - (\text{sech}^2 \tfrac{1}{4}\eta_0 + y^2 \text{cosech}^2 \tfrac{1}{4}\eta_0) \text{cosech}^2 \tfrac{1}{4}\eta_0] \alpha + 2 \cosh^2 \tfrac{1}{4}\eta_0 (\text{sech}^2 \tfrac{1}{4}\eta_0 - y^2 \text{cosech}^2 \tfrac{1}{4}\eta_0)\} \exp(-4Kx\alpha) d\alpha}{\alpha^2 \text{cosech}^2 \tfrac{1}{4}\eta_0 + \tfrac{1}{2}\alpha(1 + \coth^2 \tfrac{1}{4}\eta_0) + \cosh^2 \tfrac{1}{4}\eta_0}.$$

After some algebraic manipulation it is found that the final value of ϕ is given by*

$$\begin{aligned}\phi = & -\frac{Ke}{\epsilon} + \frac{2Ke}{\epsilon(1-y)^2} y \{ \text{Ei}(-4Kx) - (\gamma + \log 4Kx) \} + \frac{e}{2\epsilon x} \exp(-2Kx) \\ & - \frac{2Ke}{\epsilon(1-y)^2} \exp(Kx \cosh \tfrac{1}{2}\eta_0) \sinh^2 \tfrac{1}{4}\eta_0 \{ (1 + \coth^2 \tfrac{1}{4}\eta_0)(1-y)^2 \\ & - (\text{sech}^2 \tfrac{1}{4}\eta_0 + y^2 \text{cosech}^2 \tfrac{1}{4}\eta_0) \text{cosech}^2 \tfrac{1}{4}\eta_0 \} I_1 \\ & - \frac{8Ke \exp(Kx \cosh \tfrac{1}{2}\eta_0) \sinh^2 \tfrac{1}{4}\eta_0}{\epsilon(1-y)^2 (2 \cosh^2 \tfrac{1}{4}\eta_0 + 1)} [2 (\text{sech}^2 \tfrac{1}{4}\eta_0 - y^2 \text{cosech}^2 \tfrac{1}{4}\eta_0) \cosh^2 \tfrac{1}{4}\eta_0 \\ & - \tfrac{1}{4} \cosh \tfrac{1}{2}\eta_0 \{ (1 + \coth^2 \tfrac{1}{4}\eta_0)(1-y)^2 - (\text{sech}^2 \tfrac{1}{4}\eta_0 + y^2 \text{cosech}^2 \tfrac{1}{4}\eta_0) \text{cosech}^2 \tfrac{1}{4}\eta_0 \}] I_2 \\ & \dots\dots (4.3)\end{aligned}$$

where

$$I_1 = \int_1^\infty \frac{\exp \{ -Kx(2 \cosh^2 \tfrac{1}{4}\eta_0 + 1)u \} u du}{u^2 + a^2}, \quad I_2 = \int_1^\infty \frac{\exp \{ -Kx(2 \cosh^2 \tfrac{1}{4}\eta_0 + 1)u \} du}{u^2 + a^2}$$

and

$$a^2 = \frac{16 \sinh^2 \tfrac{1}{4}\eta_0}{(2 \cosh^2 \tfrac{1}{4}\eta_0 + 1)^2} (\cosh^2 \tfrac{1}{4}\eta_0 - \tfrac{1}{16} (1 + \coth^2 \tfrac{1}{4}\eta_0)^2 \sinh^2 \tfrac{1}{4}\eta_0).$$

The evaluation of I_1 , I_2 will be considered in the Appendix. It is convenient to introduce the dimensionless quantity $\eta^* = (2\epsilon kT/Ke^2)\eta'$ and in table 1 this is computed for various values of Kx when $\eta_0 = 4$ ($\psi_0 = 100$ mv at room temperature) for both insulating and conducting walls; η^* is written as $\eta_I^* + \eta_{II}^*$ where η_I^* represents the image term.

§ 5. AN APPROXIMATE METHOD OF OBTAINING THE PERTURBATION POTENTIAL

Loeb suggested that a fairly accurate solution could be obtained quite easily by assuming that the coefficient of ψ' on the right-hand side of (2.4) is constant and equal to its value at $x = x_P$. In the present case of a single plate, this implies that we replace the function of x , $K^2(x)$ in (2.7) by $K^2(x_P)$. The solution of (2.7) now becomes

$$\psi' = \frac{e}{\epsilon} \left\{ \frac{1}{r} \exp \{ -\tilde{K}(x_P)r \} \mp \frac{1}{r'} \exp \{ -\tilde{K}(x_P)r' \} \right\}, \quad \dots\dots (5.1)$$

where $r^2 = (x - x_P)^2 + \rho^2$, $r'^2 = (x + x_P)^2 + \rho^2$ and the plus and minus signs refer to insulating and metallic walls, respectively. Table 2 gives the values of η^* for $\eta_0 = 4$ when the expressions (5.1) are used. Comparison of tables 1 and 2 indicates that the approximate method is better for a conducting wall than for an insulating one, the maximum error in the former case being about 10%, whereas in the latter case it is about 40%. For lower potentials the accuracy of (5.1) improves, for example when $\eta_0 = 1$ the error is about 5% for a conducting wall. In view of the laborious numerical work required for the insulating wall, in this case we only estimated the accuracy for $\eta_0 = 1$ and found it to be about 20%. These results seem to indicate that the approximate method does not have the same accuracy for one plate as Loeb claims it to have for two.

*In the limiting case of $\eta_0 = \infty$, the formulae (3.11) and (4.3) for ϕ become identical and are given by the first three terms on the right of (4.3). The author is indebted to Prof. A. S. Coolidge of Harvard University for pointing out that this is to be expected on physical grounds. Consequently, the solutions for the conducting and insulating walls should not differ much when $\eta_0 = 8$.

§ 6. THE SOLUTION FOR THE AVERAGE POTENTIAL

It is convenient to write the solution of (2.2) in the form $\eta^0 = e\psi^0/kT = L + \delta$. If we neglect powers of δ greater than the first, then subtraction of (2.5) from (2.2) yields the following equation for δ :

$$\frac{d^2\delta}{dz^2} = \exp(\eta')(\cosh L)\delta + \{\exp(\eta') - 1\} \sinh L. \quad \dots\dots(6.1)$$

When $z \rightarrow \infty$, $\eta' \rightarrow 0$ and therefore $\delta \rightarrow 0$. The question of the boundary condition at the plate is more difficult. Firstly we observe that the image term in both (3.11) and (4.3) becomes infinite when $x = 0$, and this is due to the neglect of the ionic radius. The expression for ψ' , and therefore η' however is a reasonable approximation provided $\eta' < 1$, say, so that it seems necessary to impose some lower bound $x_0 > 0$ on x . Two possible boundary conditions for δ at $x = x_0$ are

Table 1

$2Kx$	Conducting wall, $\eta_0 = 4$				Insulating wall, $\eta_0 = 4$			
	η^*	η_I^*	η_{II}^*	δ	η^*	η_I^*	η_{II}^*	δ
0.3	3.533	2.469	1.066	-0.19	0.901	-2.469	3.370	-0.113
0.5	2.240	1.213	1.027	-0.18	1.434	-1.213	2.647	-0.111
0.7	1.619	0.709	0.910	-0.176	1.253	-0.709	1.962	-0.106
0.9	1.237	0.452	0.785	-0.15	1.051	-0.452	1.503	-0.099
1.1	0.972	0.303	0.669	-0.14	0.868	-0.303	1.171	-0.092
1.3	0.778	0.210	0.568	-0.12	0.709	-0.210	0.919	-0.084
1.5	0.629	0.149	0.480	-0.11	0.582	-0.149	0.731	-0.077
1.7	0.513	0.108	0.403	-0.10	0.489	-0.108	0.597	-0.070
1.9	0.421	0.079	0.342	-0.090	0.404	-0.079	0.482	-0.064
2.1	0.346	0.058	0.288	-0.081	0.337	-0.058	0.395	-0.058
2.3	0.179	0.022	0.157	-0.057	0.175	-0.022	0.197	-0.040
3.3	0.122	0.011	0.111	-0.044	0.111	-0.011	0.122	-0.031
3.8	0.0703	0.0059	0.0644	-0.035	0.0695	-0.0059	0.0754	-0.025
4.3	0.0441	0.0032	0.0409	-0.027	0.0437	-0.0032	0.0468	-0.020
5.3	0.0172	0.0091	0.0163	-0.016	0.0172	-0.0091	0.0181	-0.012
6.3	0.002667	0.0029	0.00638	-0.0099	0.002661	-0.0029	0.00693	-0.0073
7.3	0.00256	0.0049	0.00247	-0.0060	0.00256	-0.0049	0.00265	-0.0044
8.3	0.003980	0.0043	0.003950	-0.0037	0.003978	-0.0043	0.003101	-0.0025
9.3	0.003372	0.0041	0.003362	-0.0022	0.003371	-0.0041	0.003381	-0.0016
10.3	0.003141	0.0053	0.003138	-0.0014	0.003141	-0.0053	0.003144	-0.0099
when $z > 5.15$				$\delta = -0.238'$	when $z > 5.15$			$\delta = -0.178'$

Table 2

$2Kx$	Conducting wall, $\eta_0 = 4$			Insulating wall, $\eta_0 = 4$		
	η^*	η_I^*	η_{II}^*	η^*	η_I^*	η_{II}^*
0.3	3.603	1.202	2.401	1.199	-1.202	2.401
0.5	2.274	0.499	1.773	1.276	-0.499	1.775
0.9	1.231	0.174	1.057	0.883	-0.174	1.057
1.3	0.757	0.088	0.669	0.581	-0.088	0.669
1.7	0.486	0.051	0.435	0.384	-0.051	0.435
2.1	0.320	0.032	0.288	0.256	-0.032	0.288

(1) $d\delta/dz = 0$ and (2) $\delta = 0$. Now L is a function of η_0 and x and thus the first boundary condition implies that η_0 is so chosen that L has the same slope as the correct potential at $x = x_0$. Similarly the second condition means that η_0 is such that L is equal to the real potential at $x = x_0$. Thus the two boundary conditions imply different values of η_0 , and in principle it should be possible, using either condition, to obtain the same final value for η^0 by means of an

iterative process. We shall choose here the boundary condition $d\delta/dz=0$ for $x=x_0$.

The general solution of (6.1) is given by $\delta=\delta_3+C\delta_1+D\delta_2$ where δ_3 is a particular integral, δ_1, δ_2 are independent solutions of the homogeneous equation

$$d^2\delta/dz^2=\delta \exp \eta' \cosh L \quad \dots\dots (6.2)$$

and C and D are constants. The solutions δ_1, δ_2 may be chosen so that only one of them, δ_1 say, will vanish as $z \rightarrow \infty$ and thus the constant D must be zero. The ratio of the second term to the first on the right-hand side of (6.1) is easily verified to be $O(\exp -2z)$ as $z \rightarrow \infty$, and thus the error in assuming that for z sufficiently large the solution will be given by $C\delta_1$ is negligible. For large z , we may put $\exp \eta' = 1$ and then the solution of (6.2) which vanishes as $z \rightarrow \infty$ becomes

$$C\delta' = Ce^{-z}/\{1 - \exp(-2z) \tanh^2 \frac{1}{4}\eta_0\}. \quad \dots\dots (6.3)$$

This represents the solution of (6.2) for $z > 5$ with an accuracy of at least four figures, and the values of $z=5, 5.15$ were used to integrate (6.2) by means of the Gauss-Jackson method (Jeffreys and Jeffreys 1946). Since it is required that δ be smooth and continuous and we have assumed that for $z > 5.15$, δ is given by $C\delta'$, it follows that the boundary conditions $\delta_3 = d\delta_3/dz = 0$ must be imposed on δ_3 at $z=5.15$. Using these conditions (6.1) is then integrated numerically, again by the Gauss-Jackson method. In table 1 the values of δ as a function of $2Kx$ are given for $\eta_0=4$ for both insulating and conducting walls, and the values for a conducting wall with $\eta_0=8$ are given in table 3.

Table 3

The image term is the same as for Table 1.

Conducting wall $\eta_0=8$

$2Kx$	η^*	η_{II}^*	δ	$2Kx$	η^*	η_{II}^*	δ
0.5	4.272	3.039	-0.32	2.8	0.276	0.254	-0.090
0.7	2.927	2.218	-0.29	3.3	0.173	0.162	-0.068
0.9	2.142	1.690	-0.26	3.8	0.0845	0.0786	-0.053
1.1	1.631	1.298	-0.22	4.3	0.0681	0.0649	-0.041
1.3	1.274	1.064	-0.20	5.3	0.0268	0.0259	-0.025
1.5	1.013	0.864	-0.18	6.3	0.0104	0.0101	-0.015
1.7	0.816	0.708	-0.16	7.3	0.00402	0.00393	-0.0091
1.9	0.662	0.583	-0.14	8.3	0.00154	0.00151	-0.0053
2.1	0.542	0.484	-0.13	9.3	0.000587	0.000577	-0.0033
2.3	0.443	0.401	-0.11	10.3	0.000222	0.000219	-0.0018

when $z > 5.15$ $\delta = -0.32\delta'$

§ 7. CONCLUSIONS

When solving eqn. (2.2) in the case of two parallel plates, Loeb introduced a function δ_L , say, defined by $\eta^0 = L + \delta_L - \eta'$ and then proceeded to neglect powers of δ_L greater than the first. The error in neglecting the higher powers of δ_L will be greatest near the plate since δ_L takes its maximum value there. In our notation $\delta_L = \delta + \eta'$ and we find that for $\eta_0=4$ when x is small δ_L is greater than δ in the ratio of about 3:2, whilst for $\eta_0=8$, δ is greater than δ_L in the ratio of 2:1. The reason for this is that η' and δ are of opposite sign and that, near the plate, as the potential increases, the ratio $|\eta' + \delta|/|\delta|$ decreases. Hence it appears that it is more accurate to solve for δ than for δ_L when $\eta_0=4$ whilst the converse is true for $\eta_0=8$. The solution for δ_L in the latter case has not

been obtained because the complexity of the calculations is greatly increased by the introduction of a term $d^2\eta'/dx^2$ in the equation for δ_L . Since both δ and δ_L decrease rapidly with increasing x , for our present purposes we considered it sufficient to work with the simpler method.

We shall now consider the significance of the lower bound x_0 . If for simplicity we identify x_0 with the ionic radius a , say, then for the value $Kx_0 = 0.15$ chosen in the case of $\eta_0 = 4$, and an electrolyte concentration $\gamma = 0.01$ mole/litre, we have that at 291°K

$$a = 0.15 \times 3.06 \times 10^{-8} \gamma^{-1/2} \text{ cm} = 4.5 \times 10^{-8} \text{ cm}.$$

This value of a is greater than the usual ionic radius of about 1.5×10^{-8} cm, and hence it appears that except for large ions we cannot assume that x_0 is a correction for the ionic radius. For small ions the value of δ will be regarded as a correction to an approximate expression for the average potential, which has the correct slope at $x = x_0$. It would have been more satisfactory to have obtained a correction at the wall, but this is much more difficult since we cannot assume the equation for ψ' to be linear for $x < x_0$.

It should be noted that the ratio $|\delta/L|$ increases slowly with x and has a limiting value as $x \rightarrow \infty$ of $\frac{1}{4} C \tanh \frac{1}{4} \eta_0 = \sigma$, say. In table 4, the values of this

Table 4. Values of $-\delta/L$.

$2Kx$	C, $\eta_0 = 4$	I, $\eta_0 = 4$	I, $\eta_0 = 8$
0.3	0.06	0.033	—
0.5	0.065	0.040	0.083
0.7	0.073	0.044	0.086
1.3	0.073	0.050	0.09
3.3	0.074	0.051	0.091
7.3	0.075	0.052	0.092
∞	0.077	0.053	0.093

C=conducting wall; I=insulating wall.

ratio for various values of x are given for the three cases considered in tables 1 and 3. Loeb obtains similar results in the case of two parallel plates, i.e. his value for $|\delta/L|$ is a maximum at the median plane. This result is rather significant in that it shows that the relative correction to the solution of the Poisson-Boltzmann equation for the average potential is roughly of the same order for all x . For large x , the solution L can be written $L = 4e^{-Kx} \tanh \frac{1}{4} \eta_0$ and the corrected form reads $L = 4(1 + \sigma)e^{-Kx} \tanh \frac{1}{4} \eta_0$. Extrapolation of the ratio $|\delta/L|$ to $x = 0$ suggests that the correction to the average potential at the wall due to the self-atmosphere effect of the ions is not very large. Thus for $\eta_0 = 4$ this correction is 5% for a conducting wall and 3% for an insulating one, and when $\eta_0 = 8$ the correction is 7% for a conducting wall. Such a correction would eventually have to be considered in the equations used when calculating the electrokinetic potential from electrophoretic experiments (Booth 1950), or in the theory of stability of colloidal particles. It should be pointed out that there are other effects which modify the Poisson-Boltzmann equation, such as those of dielectric saturation (Booth 1951) and the hydration shell of an ion (Grimley 1950). Nevertheless in view of the complexity of the problem of obtaining simultaneously all the modifications to the Poisson-Boltzmann equation, particularly at high potentials, the present calculations should be of value in indicating the magnitude of two of these, namely the image and self-atmosphere (or fluctuation) effects.

ACKNOWLEDGMENT

I should like to thank Dr. S. Levine for his advice and encouragement during the preparation of this paper.

APPENDIX

The Evaluation of the Integrals I_1, I_2

We require I_1, I_2 for different values of x . When $Kx > 1.9$ partial integration in the usual manner gave asymptotic expansions for these integrals which were correct to four figures. In the range $0 < Kx < 1$, these integrals were written as $\int_0^\infty - \int_0^1$; the part from 0 to 1 was integrated using a modified form of Simpson's rule (Tranter 1951), which is as follows: If the range (a, b) of the integral

$$I = \int_a^b e^{-\beta u} f(u) du$$

is divided into $2n$ equal parts with an interval h , and $f(u)$ is fitted by parabolic arcs over ranges of width $2h$ then

$$I = h[\{f(b)e^{-\beta b} - f(a)e^{-\beta a}\}\alpha + \mu E_{2S} + \delta E_{2S-1}],$$

where E_{2S} is the sum of all the even ordinates of the integrand less half the first and last ordinates, and E_{2S-1} is the sum of all the odd ordinates. The coefficients α, μ, δ are given by

$$-\theta^3\alpha = \theta^2 + \frac{1}{2}\theta \sinh 2\theta + 1 - \cosh 2\theta, \quad \theta^3\mu = 2 \sinh 2\theta - \theta(3 + \cosh 2\theta),$$

$$\theta^3\delta = 4\theta \cosh \theta - 4 \sinh \theta \quad \text{and} \quad \theta = \beta h.$$

The integrals from 0 to ∞ are given by (Fletcher, Miller and Rosenhead 1946)

$$\int_0^\infty \frac{e^{-\beta u} du}{u^2 + a^2} = \frac{1}{a} \{\sin \beta a \text{Ci}(\beta a) - \cos \beta a \text{Si}(\beta a)\}$$

$$\int_0^\infty \frac{e^{-\beta u} u du}{u^2 + a^2} = -\{\sin \beta a \text{Si}(\beta a) + \cos \beta a \text{Ci}(\beta a)\}$$

where
$$\text{Si}(x) = \int_\infty^x \frac{\sin t}{t} dt \quad \text{and} \quad \text{Ci}(x) = \int_\infty^x \frac{\cos t}{t} dt.$$

When $1 < Kx < 1.9$ the above method does not give the required accuracy and hence for these values of x the range of integration is split up into 1 to 2 and 2 to ∞ . The modified Simpson's rule was used for the first range, and an asymptotic expansion obtained for the second.

REFERENCES

- BOOTH, F., 1950, *Proc. Roy. Soc. A*, **203**, 514; 1951, *J. Chem. Phys.*, **19**, 391.
 COPSON, E. T., 1935, *Theory of Functions of a Complex Variable* (Oxford: University Press), p. 236.
 DEBYE, P., and HUCKEL, E., 1923, *Phys. Z.*, **24**, 305.
 FLETCHER, A., MILLER, J. C. P., and ROSENHEAD, L., 1946, *An Index of Mathematical Tables* (London: Scientific Computing Service).
 GRIMLEY, T. B., 1950, *Proc. Roy. Soc. A*, **201**, 40.
 JEFFREYS, H., and JEFFREYS, B. S., 1946, *Methods of Mathematical Physics* (Cambridge: University Press), p. 442.
 KIRKWOOD, J. G., 1934, *J. Chem. Phys.*, **2**, 767.
 LANGMUIR, I., 1938, *J. Chem. Phys.*, **6**, 875.
 LOEB, A. W., 1951, *J. Coll. Sci.*, **6**, 75.
 STRATTON, J. A., 1941, *Electromagnetic Theory* (New York: McGraw-Hill), p. 576.
 TITCHMARSH, E. C., 1937, *Theory of Fourier Integrals* (Oxford: Clarendon Press), p. 240.
 TRANTER, C. J., 1951, *Integral Transforms in Mathematical Physics* (London: Methuen Monographs), p. 75.
 VERWEY, E. J. W., and OVERBEEK, J. Th. G., 1948, *Theory of Stability of Lyophobic Colloids* (Amsterdam: Elsevier Press).

Absorption Coefficients of Gamma-Rays with Energies between 0.3 and 1.5 Mev*

By S. J. WYARD

Physics Laboratory, University College Hospital, London

MS. received 11th August 1952, and in final form 21st October 1952

Abstract. Accurate measurements have been made of the absorption coefficients of gamma-rays covering the range of quantum energy from 0.3 to 1.5 mev and of atomic number from 6 to 92.

The results verify the Klein-Nishina formula over the whole range of quantum energy. They confirm the calculations of Hulme and co-workers for the photo-electric coefficient at 0.3 mev, but disagree with them at higher energies.

Some improvements have been made in the method of measuring absorption coefficients, and certain errors, previously overlooked, have been noted and corrected.

§ 1. INTRODUCTION

EARLY measurements of the absorption coefficients of gamma-rays were hampered by the difficulty of producing sources of monochromatic radiation. (A full list of references to early work is given in a review article by Davisson and Evans 1952.) This difficulty has recently been overcome by the use of radioactive isotopes, and several workers have made accurate measurements in this way. Cowan (1948) and Davisson and Evans (1951) have published comprehensive measurements which cover a wide range of quantum energy and of atomic number with an accuracy to within 2 or 3%. Most of the measured values of the absorption coefficients agree with the theoretical values within the limits of the experimental errors, but Davisson and Evans reported differences of about 5% in the case of tantalum both at 1.1 and at 1.25 mev. The recent measurements of Shimizu, Hanai and Okamoto (1952) at 1.25 mev differed from the theoretical values in the case of elements with atomic numbers between 73 and 83 by from 1 to 5%.

In the present work, measurements of absorption coefficients have been made as accurately as possible over a wide range of quantum energy and atomic number, using radioactive isotopes as sources of monochromatic radiation. The measurements have then been used to check the values of the absorption coefficients calculated from theory.

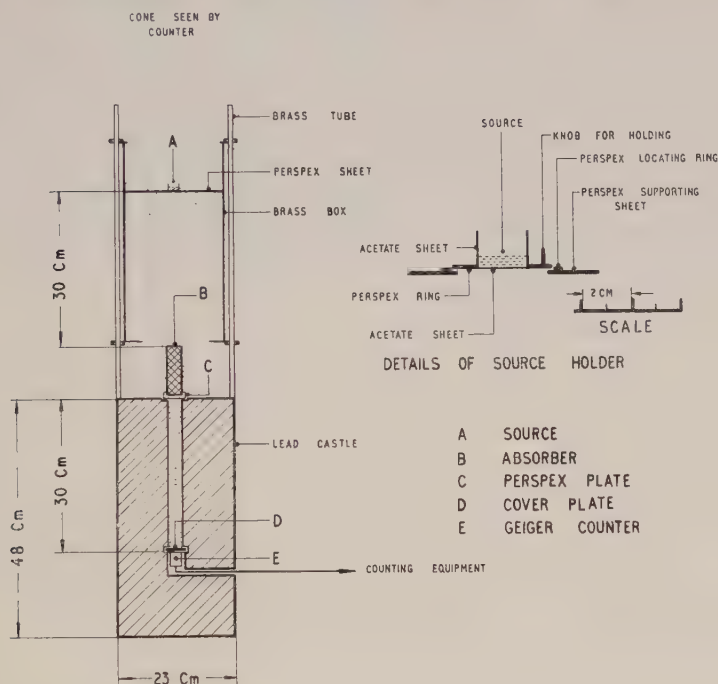
A preliminary note on this work was published earlier (Wyrd 1952 a).

§ 2. EXPERIMENTAL

The standard apparatus for measuring absorption coefficients consists essentially of the source of monochromatic radiation, the detector and the absorbers. The chief problem in arranging the apparatus is that of preventing scattered radiation from affecting the measurements. It is convenient to classify

* This work formed part of a thesis submitted for a Ph.D. degree at the University of London.

the scattered radiation as (i) radiation scattered from the source and its immediate neighbourhood, (ii) radiation scattered from the absorber and (iii) radiation scattered from surrounding objects. The first two classes of radiation will be considered in the next section. The usual method of reducing the effect of radiation scattered from surrounding objects has been to canalize the radiation from the source by means of a lead tunnel. This arrangement has the disadvantage, which in most cases seems to have been overlooked, that scattered radiation from the walls of the tunnel, being softer than the primary radiation, will affect the measurements. Cowan avoided most of the effects of scattered radiation by suspending the whole apparatus in mid-air, as far as possible from any solid objects; but with this arrangement the scatter from the air was sufficient to interfere with the measurements when thick absorbers were being used. In the arrangement shown in the figure, where a lead tunnel is placed *after* the absorber, the effect of



Cross section of apparatus.

scatter is reduced to a minimum. With no absorber the counter receives the direct radiation from the source I_0 , plus a small amount of radiation scattered from the tunnel λI_0 . The absorber reduces the intensity of the direct radiation falling on the counter by a factor $e^{-\mu d}$ and reduces that falling on the walls of the tunnel by the same factor. In addition it scatters on to the counter a small amount of radiation which can be corrected for by the method described in the next section, and scatters on to the walls of the tunnel radiation of which some is scattered back into the counter. The intensity of this doubly scattered radiation will be small, and the resulting error in the measured value of the absorption coefficient is estimated as 1 or 2 parts in 1000 at most. Neglecting the doubly scattered radiation and assuming that a correction has been made for that scattered from the absorber into the counter, the intensity of radiation at the

counter is $I_0 e^{-\mu d} + \lambda I_0 e^{-\mu d}$, compared with $I_0 + \lambda I_0$ with no absorber; so that no error is introduced by singly-scattered radiation from the walls of the tunnel.

Shimizu, Hanai and Okanoto used an arrangement of apparatus similar to that shown in the figure.

The sources used in the present measurements were irradiated in the pile at Harwell. 'Spectroscopically pure' material was used in most cases. In some preliminary experiments where 'chemically pure' materials were used anomalous results were obtained, due to contamination by other radioactive isotopes. In order to reduce the intensity of radiation scattered from the source and its immediate neighbourhood the source and its holder (see figure) were both kept as light as possible. The mass of the source averaged about one gramme. The activity was generally a few millicuries.

The absorbers were manufactured from the purest materials which were commercially available. They were carefully weighed and measured and shown to be of uniform composition and free from holes. The carbon, aluminium, copper, silver and lead absorbers were spectroscopically tested, and the impurities shown to be negligible. The errors due to impurities in the other absorbers are believed to be very small also.

The intensity of radiation was measured with a small end-window Geiger counter. The end-window faced the source of radiation and was covered with an aluminium plate to absorb beta-rays. The aluminium plate was usually backed by a few millimetres of lead in order to reduce the sensitivity of the counter to soft x- or gamma-radiation. The correction for the dead-time of the counter was determined empirically by the method of Kohman (1949). Because of the large mass of lead surrounding the counter the background counting rate was small and constant, averaging about seven counts per minute. The uranium absorbers, when placed in position at the top of the tunnel, added about three counts per minute to the background.

With each source of radiation and each absorbing material the intensity of radiation was measured with no absorber and with a series of absorbers of different thicknesses. The logarithm of the intensity plotted against the thickness of the absorber usually gave a good straight line whose slope was calculated by the method of least squares, and the value of the absorption coefficient was calculated from the slope of this absorption line. This method has the advantage over the use of a single thickness of absorber that inhomogeneity in the radiation will be revealed by curvature in the absorption line. The maximum thickness of absorber was chosen so that the transmission ratio was about 1 to 12, since Rose and Shapiro (1948) have shown that, for a given time spent in counting, the error in the measured value of the absorption coefficient due to statistical fluctuations in the counting rate is at a minimum for this thickness of absorber.

§3. CORRECTIONS

The value of the absorption coefficient, as calculated directly from the slope of the absorption line, must be corrected for two effects: radiation scattered from the absorber, and all x- or gamma-radiation, other than the primary monochromatic radiation, which comes from the source. The latter will be called 'unwanted radiation'.

Tarrant (1932) has calculated the correction due to scatter from the absorber, and has shown how to arrange the apparatus so that the correction is reduced to a

minimum. The value of the correction, $\delta_e\mu$, to the electronic absorption coefficient given by Tarrant is

$$\delta_e\mu = \mu_{\text{true}} - \mu_{\text{obs}} = K(\theta_0) \quad \dots\dots(1)$$

where $K(\theta_0)$ is the fraction of incident energy scattered per electron within a cone of semi-angle θ_0 , and θ_0 is the maximum angle of scattering for radiation entering the centre of the counter. In order to obtain eqn. (1) Tarrant made several simplifying assumptions which, however, do not introduce an error exceeding 5%. Tarrant's formula was checked by measuring absorption coefficients (a) under the conditions shown in the figure where the scatter angle θ_0 is 5° , and (b) with a shorter tunnel giving a scatter angle of 10° . Measurements were made at 1.51 MeV and at 0.325 MeV, and with several different absorbing materials. It was found that eqn. (1) was verified within an experimental error of about 20% provided both Compton and Rayleigh scatter were taken into account when calculating the function $K(\theta_0)$. With the scatter angle of 5° the value of $\delta_e\mu$ given by eqn. (1) was generally about 0.5% of the value of μ , so that an error of 20% in $\delta_e\mu$ meant an error of only one part in 1000 in μ .

Unwanted radiation which comes from the source consists of bremsstrahlung produced by beta-rays, scattered radiation and, in some cases, soft x- or gamma-radiation emitted by the disintegrating nuclei. In order to correct for this radiation it is necessary to know both its total intensity relative to that of the primary radiation and also its intensity distribution as a function of quantum energy. The fraction of the recorded counts which are due to unwanted radiation can then be calculated for each thickness of absorber, taking into account also the absorption in the cover plates on the counter and the variation of counter sensitivity with quantum energy (Renard 1948, down to 0.1 MeV, Saurer 1950, below 0.1 MeV).

The total intensity of bremsstrahlung was calculated for each source from the theory given by Heitler (1944), and the calculation was checked by a preliminary measurement on each source. The intensity distribution of the bremsstrahlung was also calculated from theory, and was checked by means of an absorption measurement using ^{32}P as a source (Wynd 1952 b). Most of the bremsstrahlung is very soft and is filtered out by the lead cover plate on the counter.

The intensity and the intensity distribution of the radiation scattered from the source were calculated from the Klein-Nishina formula. These calculations were also checked by experiment.

The error in the correction for all the unwanted radiation was estimated at not more than 20%, while the value of the correction varied from 0.1 to 1.0% of the value of the absorption coefficient. Thus the error introduced by the correction was never more than two parts in 1000 of the value of the absorption coefficient, and was often negligible.

§ 4. NOTES ON SOME OF THE ISOTOPES USED AS SOURCES

Mercury 203 (gamma-ray energy 0.279 MeV, half life 45.9 days).

The source was allowed to decay for 70 days before absorption measurements were made in order that the isotope ^{197}Hg (half life 64 hours), which is also produced by pile irradiation of mercury, should decay to a negligible amount. The 70 keV characteristic x-radiation which accompanies the disintegration of ^{203}Hg was nearly all filtered out by the lead cover plate on the counter.

Chromium 51 (gamma-ray energy 0.325 mev, half life 26.5 days).

According to Bradt *et al.* (1945) two gamma-rays are emitted at 0.325 and at 0.26 mev, but the lower energy gamma-ray appears to be totally internally converted. From the published data it is only possible to say that the intensity of the lower energy ray is not more than 10% of the intensity of the other, but in the present work it has been assumed that the 0.325 mev gamma-ray is emitted alone.

Ruthenium 103 (gamma-ray energy 0.4979 mev, half life 42 days).

The source was allowed to decay for two weeks before absorption measurements were made, so that the isotopes ^{105}Ru , ^{105}Rh , ^{97}Ru and ^{97}Tc , which are also produced by pile irradiation of ruthenium, should decay to negligible proportions.

Cobalt 60 (gamma-ray energies 1.1715 and 1.3316 mev, half life 5.3 years).

This isotope emits two gamma-rays of slightly different energies, but with the thickness of absorber and accuracy of measurement of the present work the curvature of the absorption line is far too slight to be detected, so that the radiation is effectively monochromatic. The theoretical value of the linear absorption coefficient is given by the formula

$$\mu_{\text{eff}} = \frac{I_1\mu_1 + I_2\mu_2}{I_1 + I_2} - \frac{d}{8}(\mu_1 - \mu_2)^2 + \text{terms of higher orders} \quad \dots\dots (2)$$

where μ_1 and μ_2 are the linear absorption coefficients for the two gamma-rays respectively, I_1 and I_2 are the separate counting rates from the two gamma-rays and d is the thickness of the absorber. For very thin absorbers eqn. (2) reduces to the formula used by Shimizu, Hanai and Okamoto. For the counter used in the present work I_1 and I_2 are proportional to the quantum energies of the two gamma-rays.

§ 5. EXPERIMENTAL RESULTS

Table 1 gives the measured values of the electronic absorption coefficients when all the corrections have been made. The standard deviations were calculated from the least squares analyses of the slopes of the absorption lines, and include an allowance of 20% error in the corrections for scatter from the absorber and for unwanted radiation from the source. The chief source of error was statistical fluctuation in the counting rate. Most of the values of table 1 are the weighted means of two or three separate measurements which agreed within the limits of the experimental errors. The values of the quantum energy assigned to the isotopes are the most likely values taken from the recently published spectroscopic measurements.

§ 6. THEORETICAL VALUES OF THE ABSORPTION COEFFICIENTS

The theoretical values of the absorption coefficients have been calculated as the sum of the Compton effect, the photoelectric effect and pair production. The absorption coefficients for the Compton effect were calculated from the Klein-Nishina formula (1929), using the values of atomic constants given by DuMond and Cohen (1949). The absorption coefficients for the photoelectric effect were obtained by interpolation and extrapolation from the values given by Hulme *et al.* (1935). Extrapolation was required in the case of uranium and also for values at 0.279 and 0.325 mev. The absorption coefficients for pair production were obtained from the calculations of Bethe and Heitler (1934), with alternative values for tungsten, lead and uranium from the calculations of Jaeger and Hulme (1936). The theoretical values of the total electronic absorption coefficients are given in table 1. The errors correspond to the errors of measurement in the values of the energies of the gamma-rays.

Isotope Energy (MeV) Absorber	²⁰³ Hg	⁵¹ Cr	¹⁰³ Ru	⁸⁶ Rb	⁶⁰ Co	⁴² K
H ₂ O	0.279 ± 0.002	0.325 ± 0.005	0.4979 ± 0.0008	1.076 ± 0.003	1.1715 ± 0.001 1.3316	1.51 ± 0.01
$\mu_{\text{exp}}^{\text{H}_2\text{O}}$	3.580 ± 0.080	3.520 ± 0.025	2.920 ± 0.021	2.065 ± 0.019	1.890 ± 0.008	1.701 ± 0.014
$\mu_{\text{theor}}^{\text{H}_2\text{O}}$	3.631 ± 0.005	3.429 ± 0.011	2.897 ± 0.002	2.037 ± 0.003	1.885 ± 0.002	1.713 ± 0.006
% difference	-1.4 ± 2.2	+2.7 ± 0.8	+0.8 ± 0.7	+1.4 ± 0.9	+0.3 ± 0.4	-0.7 ± 0.9
C	3.720 ± 0.040	3.476 ± 0.025	2.879 ± 0.016	2.032 ± 0.013	1.874 ± 0.006	1.697 ± 0.016
$\mu_{\text{exp}}^{\text{C}}$	3.631 ± 0.005	3.429 ± 0.011	2.897 ± 0.002	2.037 ± 0.003	1.885 ± 0.002	1.713 ± 0.006
$\mu_{\text{theor}}^{\text{C}}$	+2.5 ± 1.1	+1.4 ± 0.8	-0.6 ± 0.6	-0.2 ± 0.6	-0.6 ± 0.3	-0.9 ± 1.0
% difference						
Al	3.693 ± 0.081	3.473 ± 0.019	2.876 ± 0.021	2.052 ± 0.013	1.893 ± 0.005	1.714 ± 0.017
$\mu_{\text{exp}}^{\text{Al}}$	3.660 ± 0.005	3.466 ± 0.011	2.903 ± 0.002	2.038 ± 0.003	1.887 ± 0.002	1.717 ± 0.006
$\mu_{\text{theor}}^{\text{Al}}$	+0.9 ± 2.2	+0.8 ± 0.6	-0.9 ± 0.7	+0.7 ± 0.6	+0.3 ± 0.3	-0.2 ± 1.0
% difference						
Cu	4.213 ± 0.063	3.819 ± 0.028	2.972 ± 0.023	2.064 ± 0.016	1.898 ± 0.006	1.717 ± 0.013
$\mu_{\text{exp}}^{\text{Cu}}$	4.151 ± 0.010	3.773 ± 0.018	3.006 ± 0.003	2.055 ± 0.003	1.901 ± 0.002	1.733 ± 0.006
$\mu_{\text{theor}}^{\text{Cu}}$	+1.5 ± 1.5	+1.2 ± 0.9	-1.1 ± 0.8	+0.4 ± 0.8	-0.2 ± 0.3	-0.9 ± 0.8
% difference						
Mo	—	—	3.268 ± 0.019	2.105 ± 0.020	1.945 ± 0.006	—
$\mu_{\text{exp}}^{\text{Mo}}$	—	—	3.288 ± 0.004	2.105 ± 0.003	1.940 ± 0.002	—
$\mu_{\text{theor}}^{\text{Mo}}$	—	—	-0.6 ± 0.6	0.0 ± 1.0	+0.3 ± 0.3	—
% difference						
Ag	6.234 ± 0.078	5.331 ± 0.045	3.454 ± 0.020	2.154 ± 0.013	1.959 ± 0.005	1.766 ± 0.014
$\mu_{\text{exp}}^{\text{Ag}}$	6.383 ± 0.033	5.239 ± 0.048	3.464 ± 0.005	2.138 ± 0.004	1.966 ± 0.002	1.788 ± 0.006
$\mu_{\text{theor}}^{\text{Ag}}$	-2.3 ± 1.3	+1.8 ± 1.2	-0.3 ± 0.6	+0.7 ± 0.7	-0.4 ± 0.3	-1.2 ± 0.8
% difference						
W	—	—	5.336 ± 0.029	2.483 ± 0.022	2.245 ± 0.007	—
$\mu_{\text{exp}}^{\text{W}}$	—	—	5.462 ± 0.013	2.521 ± 0.005	2.264 ± 0.003	—
$\mu_{\text{theor}}^{\text{W}}$	—	—	-2.3 ± 0.6	-1.5 ± 0.9	-0.8 ± 0.4	—
% difference						
* $\mu_{\text{theor}}^{\text{W}}$	—	—	—	2.524 ± 0.005	2.281 ± 0.003	—
% difference*				-1.6 ± 0.9	-1.7 ± 0.4	
Pb	19.05 ± 0.28	14.06 ± 0.08	6.345 ± 0.026	2.704 ± 0.014	2.403 ± 0.006	2.120 ± 0.016
$\mu_{\text{exp}}^{\text{Pb}}$	18.94 ± 0.16	13.76 ± 0.22	6.453 ± 0.019	2.728 ± 0.006	2.425 ± 0.003	2.143 ± 0.011
$\mu_{\text{theor}}^{\text{Pb}}$	+0.6 ± 1.6	+2.2 ± 1.7	-1.7 ± 0.5	-0.9 ± 0.6	-0.9 ± 0.3	-1.1 ± 0.9
% difference						
* $\mu_{\text{theor}}^{\text{Pb}}$	—	—	—	2.732 ± 0.006	2.445 ± 0.003	2.184 ± 0.011
% difference*				-1.0 ± 0.6	-1.7 ± 0.3	-2.9 ± 0.9
U	—	18.10 ± 0.14	8.026 ± 0.032	3.027 ± 0.023	2.641 ± 0.009	2.303 ± 0.012
$\mu_{\text{exp}}^{\text{U}}$	—	18.15 ± 0.30	8.049 ± 0.026	3.061 ± 0.007	2.688 ± 0.003	2.343 ± 0.012
$\mu_{\text{theor}}^{\text{U}}$	—	-0.3 ± 1.8	-0.3 ± 0.5	-1.1 ± 0.8	-1.7 ± 0.3	-1.7 ± 0.7
% difference						
* $\mu_{\text{theor}}^{\text{U}}$	—	—	—	3.066 ± 0.007	2.710 ± 0.003	2.389 ± 0.012
% difference*				-1.3 ± 0.8	-2.5 ± 0.3	-3.6 ± 0.7

* Using Jaeger and Hulme's values of the pair production coefficient; otherwise Bethe and Heitler's values were used.

The percentage differences are the values of $100(\mu_{\text{exp}} - \mu_{\text{theor}})/\mu_{\text{theor}}$. The standard deviations in the percentage differences are the result of combining the standard deviations in the experimental and theoretical values. The experimental and theoretical values differ significantly in the bottom right-hand corner of the table.

Other processes of absorption which were considered were Rayleigh scatter, the effect of nuclear binding on Compton scatter, higher order corrections to the Klein-Nishina formula from the new radiation theory, the double Compton effect, nuclear Thomson scatter, resonant nuclear scatter, pair production in the field of the electron and photodisintegration of the nucleus. However, for the range of energy covered by the present work the first and second and the third and fourth approximately balance each other (Franz 1935, Brown and Feynman 1952), and the last four are zero or negligible (Moon 1950, Levinger 1951, Watson 1947, Sker, Halpern and Mann 1951). The combined effect of all the processes of absorption considered in this paragraph is only one or two parts in 1000 of the value of the total absorption coefficient, and the values given in table 1 should be correct to within these limits.

§ 7. COMPARISON BETWEEN EXPERIMENT AND THEORY

A detailed comparison of the experimental and theoretical values of the total absorption coefficients given in table 1 shows that for light elements at all energies and for heavy elements at low energies there is agreement within the experimental errors of about 0.5%. For heavy elements at the higher energies, however, the experimental values are consistently and significantly smaller than the theoretical values, the maximum difference being about 3%.

§ 8. DISCUSSION

(i) *The Klein-Nishina Formula*

For elements of low atomic number the Compton effect accounts for more than 99% of the theoretical value of the total absorption coefficient between 0.25 and 1.5 mev. If we make the reasonable assumption that the theoretical values of the photoelectric and pair production coefficients are not very greatly in error, then by subtracting these theoretical values from the measured values of the total absorption coefficients we obtain experimental values for the Compton coefficient: it is found that at each quantum energy the values of the Compton coefficient per electron obtained with the different absorbers agree within the limits of the experimental errors. (This is additional evidence for the reliability of the values given for the errors of measurement in table 1.) It is therefore reasonable to calculate the weighted mean of the experimental values of the Compton coefficient at each value of the quantum energy. These mean values are given in table 2, and are compared with the values calculated from the Klein-Nishina formula. The differences of about 1.5% at the lowest energies, shown in table 2, are not regarded as significant, especially in view of the uncertainty about the gamma radiation emitted by ^{51}Cr . Thus the present work confirms the Klein-Nishina formula, at least to within 1.5% at 0.3 mev, to within 0.5% between 0.5 and 1.5 mev, and to within 0.2% at 1.25 mev.

(ii) *The Photoelectric Coefficient*

If we assume that the Klein-Nishina formula, which has been verified for elements of low atomic number, also holds for elements of high atomic number, then the differences between the experimental and theoretical values of the total absorption coefficients for these elements between 0.5 and 1.5 mev must be ascribed to errors in the photoelectric or pair production coefficients; the differences are too large to be due to errors in the pair production coefficient (which in any

case is zero below 1.02 mev), so we must conclude that the theoretical values of the photoelectric coefficient are in error.

Now in order to obtain experimental values of the photoelectric coefficient above 1 mev from the measured values of the total absorption coefficient it is necessary to know the values of the pair production coefficients. A difficulty arises here, since there appears to be no published experimental evidence which will decide conclusively between the values of Bethe and Heitler and those of Jaeger and Hulme. Lawson (1949) has pointed out that between 11 and 88 mev the measured values of the pair production coefficients for heavy elements are in every case about 10% *less* than those calculated by Bethe and Heitler, so that it is surprising that the calculations of Jaeger and Hulme at 1.5 and 2.6 mev give values *greater* than those of Bethe and Heitler. Measurements of the total absorption coefficient at 2.62 mev by Gentner and Starkiewicz (1935) and by Ageno, Chiozzotto and Querzoli (1949) support Bethe and Heitler's values rather than those of Jaeger and Hulme. On the other hand measurements by Hahn, Baldinger and Huber (1951) of the dependence of the pair production coefficient upon atomic number support Jaeger and Hulme's calculations (only relative values of the pair production coefficient were measured). In view of this uncertainty, both Bethe and Heitler's and Jaeger and Hulme's values of the pair production coefficient have been used to obtain alternative experimental values of the photoelectric coefficient.

Table 2. Comparison of Experimental and Theoretical Values of the Electronic Absorption Coefficient corresponding to the Compton Effect $e\sigma$ (all values have been multiplied by 10^{25})

Quantum energy (mev)	$e\sigma(\text{exp})$ (weighted mean)	$e\sigma(\text{K.N.})$	% difference
0.279 ± 0.002	3.685 ± 0.033	3.629 ± 0.005	$+1.5 \pm 0.9$
0.325 ± 0.005	3.478 ± 0.014	3.428 ± 0.011	$+1.4 \pm 0.5$
0.4979 ± 0.0008	2.887 ± 0.011	2.897 ± 0.002	-0.3 ± 0.4
1.076 ± 0.003	2.050 ± 0.007	2.037 ± 0.003	$+0.6 \pm 0.4$
$1.1715 \left. \begin{array}{l} \right\} \pm 0.001$	1.884 ± 0.003	1.884 ± 0.002	0.0 ± 0.2
$1.3316 \left. \begin{array}{l} \right\}$			
1.51 ± 0.01	1.698 ± 0.007	1.710 ± 0.006	-0.7 ± 0.5

It was found that at each quantum energy the percentage differences between the experimental and the theoretical values of the photoelectric coefficient were the same for all absorbers, within the limits of experimental error. Accordingly the weighted mean values of the percentage differences were calculated; these are given in table 3. The calculations of Hulme *et al.* are confirmed at 0.3 mev with an accuracy of within 2%, but at higher energies the measured values are significantly smaller than the theoretical ones. The differences increase with quantum energy, up to 7% at 1.51 mev if Bethe and Heitler's values for the pair production coefficient are correct, or 15% if Jaeger and Hulme's values are correct.

(iii) Comparison with the Measurements of Other Workers

The measured values of the total absorption coefficient, which are given in table 1, agree with all the values of Davisson and Evans and of Shimizu, Hanai and Okamoto if the measurements of these workers are assumed to contain experimental errors of about 2%.

The most accurate measurements of absorption coefficients at energies below 0.3 mev appear to be those of Cuykendall (1936) for light elements and Jones (1936) for heavy elements; in both cases the accuracy of measurement was within about

Table 3. Comparison of Experimental and Theoretical Values of the Photoelectric Absorption Coefficient

Quantum energy (MeV)	0.279	0.325	0.4979	1.076	1.1715 1.3316	1.51
% difference (weighted mean)	-1.5 ± 1.8	$+1.9 \pm 2.1$	-2.0 ± 0.7	-3.5 ± 1.5	-5.0 ± 0.8	-6.8 ± 2.3
% difference*	—	—	—	-4.0 ± 1.5	-8.3 ± 0.8	-15.1 ± 2.3

* Using Jaeger and Hulme's values of the pair production coefficient, otherwise Bethe and Heitler's values were used.

2%. The measurements of the present work agree with those of Cuykendall in confirming the Klein-Nishina formula within the limits of the experimental errors. In the case of the heavy elements the values of the present work agree well with those of Jones, as can be seen from a logarithmic graph of photoelectric coefficient for each absorber plotted against quantum energy.

ACKNOWLEDGMENTS

It is a pleasure to record my gratitude to Professor J. E. Roberts, who suggested this work, for continual help and encouragement in carrying it out.

Acknowledgements are also due to the Atomic Energy Research Establishment, Harwell, for the loan of the uranium absorbers, and for the spectroscopic analyses of some of the other absorbers.

British Acheson Electrodes Ltd. kindly supplied very pure samples of graphite rod.

REFERENCES

- AGENO, M., CHIOZZOTTO, M., and QUERZOLI, R., 1949, *Atti Accad. Naz. Lincei*, **6** (Ser. 8), 319.
 BETHE, H., and HEITLER, W., 1934, *Proc. Roy. Soc. A*, **146**, 83.
 BRADT, H., GUGELOT, P. C., HUBER, O., MEDICUS, H., PREISWERK, P., and SCHERRER, P., 1945, *Helv. phys. Acta*, **18** (No. 4), 259.
 BROWN, L. M., and FEYNMAN, R. P., 1952, *Phys. Rev.*, **85**, 231.
 COWAN, C. L., 1948, *Phys. Rev.*, **74**, 1841.
 CUYKENDALL, T. R., 1936, *Phys. Rev.*, **50**, 105.
 DAVISON, C. M., and EVANS, R. D., 1951, *Phys. Rev.*, **81**, 404; 1952, *Rev. Mod. Phys.*, **24**, 79.
 DUMOND, J. W. M., and COHEN, E. R., 1949, *Rev. Mod. Phys.*, **21**, 651.
 FRANZ, W., 1935, *Z. Phys.*, **98**, 314.
 GENTNER, W., and STARKIEWICZ, J., 1935, *J. Phys. Radium*, **6**, 340.
 HAHN, B., BALDINGER, E., and HUBER, P., 1951, *Helv. phys. Acta*, **24** (No. 4), 324.
 HEITLER, W., 1944, *The Quantum Theory of Radiation* (Oxford: University Press).
 HULME, H. R., McDougall, J., BUCKINGHAM, R. A., and FOWLER, R. H., 1935, *Proc. Roy. Soc. A*, **149**, 131.
 JAEGER, J. C., and HULME, H. R., 1936, *Proc. Roy. Soc. A*, **153**, 443.
 JONES, M. T., 1936, *Phys. Rev.*, **50**, 110.
 KLEIN, O., and NISHINA, Y., 1929, *Z. Phys.*, **52**, 853.
 KOHMAN, T. P., 1949, *Isotopic Carbon* (New York: John Wiley), p. 292.
 LAWSON, J. L., 1949, *Phys. Rev.*, **75**, 433.
 LEVINGER, J. S., 1951, *Phys. Rev.*, **84**, 523.
 MOON, P. B., 1950, *Proc. Phys. Soc. A*, **63**, 1189.
 RENARD, G. A., 1948, *J. Phys. Radium*, **9**, 212.
 ROSE, M. E., and SHAPIRO, M. M., 1948, *Phys. Rev.*, **74**, 1853.
 SAURER, H., 1950, *Helv. phys. Acta*, **23**, 381.
 SHIMIZU, S., HANAI, T., and OKANOTO, S., 1952, *Phys. Rev.*, **85**, 290.
 SKER, R., HALPERN, J., and MANN, A. K., 1951, *Phys. Rev.*, **84**, 387.
 TARRANT, G. T. P., 1932, *Proc. Camb. Phil. Soc.*, **28**, 475.
 WATSON, K. M., 1947, *Phys. Rev.*, **72**, 1060.
 WYARD, S. J., 1952 a, *Phys. Rev.*, **87**, 165; 1952 b, *Proc. Phys. Soc. A*, **65**, 377.

The Polarization of γ -Radiation from Aligned Nuclei

By N. R. STEENBERG

The Clarendon Laboratory, Oxford

MS. received 10th June 1952, and in final form 22nd December 1952

Abstract. Formulae are derived giving the degree of polarization and its angular dependence of γ -radiation anisotropically emitted from nuclei aligned at low temperatures. These are in the form of Legendre series limited by the multipole order or nuclear spin. It is shown how the polarization determines the character of the radiation and the sign of the magnetic moment of the oriented nucleus.

§1. INTRODUCTION

IT is known that γ -radiation is emitted anisotropically from nuclei aligned at low temperature (Daniels *et al.* 1951). Such radiation can be expected to show some degree of polarization. In this paper the magnitude of this effect is given for both the plane and circular components in terms of the polarization vector introduced by Fano (1949). The results are applicable to γ -ray emission of arbitrary multipole order either emitted directly from the oriented nucleus or following a β -emission from the oriented nucleus.

The formulae obtained have a simple form similar to that in which the angular distribution was given in a previous paper, i.e. a series of Legendre functions (Steenberg 1952, to be referred to as I: knowledge of this paper will be assumed). The number of terms in the series is limited by the multipole order or the nuclear spins.

It is shown how the formulae are applicable to any of the four suggested methods (Simon *et al.* 1951) of aligning nuclei. Simple approximate formulae, valid for low degrees of alignment, are also given.

The information of greatest interest which can be gained from a measurement of polarization effects is the character, electric or magnetic, of the radiation and the sign of the magnetic moment of the oriented nucleus. Other information is of the same nature as that derivable from a measurement of the angular distribution, that is, nuclear spins, multipole order and magnitude of the magnetic moment.

§2. THE POLARIZATION VECTOR

Fano (1949) discusses partially polarized radiation in terms of a vector $\mathbf{P} = (p_1, p_2, p_3)$; p_1 and p_2 represent the degree of plane polarization and p_3 the degree of circular polarization, i.e. the excess of right-handed over left-handed circularly polarized radiation. $P^2 = 1$ or < 1 according as the polarization state is pure or partial. For unpolarized radiation $P^2 = 0$.

Consider a radiating quantum system at the origin of a set of spherical polar coordinates. Unit vectors θ, φ and \mathbf{k} are introduced. \mathbf{k} is in the direction of propagation, θ and φ are perpendicular to \mathbf{k} and in the directions of increasing θ and ϕ .

Each individual quantum is characterized by a total angular momentum L (the multipole order) and a z component m , and is emitted in a state of pure polarization, i.e. $(\mathbf{P}^m)^2 = 1$, where \mathbf{P}^m is the polarization vector associated with the quantum. The photon is elliptically polarized, with the axes of the ellipse along θ and φ . The components of \mathbf{P}^m then have the following form:

$$\left. \begin{aligned} p_1^m &= (I_m^\varphi - I_m^\theta) / (I_m^\varphi + I_m^\theta), \\ p_2^m &= 0, \\ p_3^m &= \pm 2(I_m^\varphi I_m^\theta)^{1/2} / (I_m^\varphi + I_m^\theta) \end{aligned} \right\} \dots\dots(1)$$

where I_m^φ and I_m^θ are the intensities of the radiation polarized in the φ and θ directions and the plus or minus refers to right or left circular polarization.

I_m^φ , I_m^θ , p_1^m and p_3^m are obviously functions of the polar angle θ , although this will not generally be indicated. $I_m(\theta)$ is the total intensity irrespective of polarization, $I_m(\theta) = I_m^\theta + I_m^\varphi$.

Photons with all possible z -components m must now be superposed to form a single polarization vector. To do this the transition in which the photon is emitted must be considered. Let us assume that a nucleus of spin J and z component M decays to a nucleus of spin J_1 , ($J \xrightarrow{L} J_1$). The probability that the emitted photon will be characterized by m is proportional to $|C_{M, M-m, m}^J|^2$. Fano shows that two polarization vectors \mathbf{P}' and \mathbf{P}'' are superposed incoherently to form a single polarization vector \mathbf{P} as follows, $I\mathbf{P} = I'\mathbf{P}' + I''\mathbf{P}''$, where I' and I'' are the intensities associated with the first and second vectors and $I = I' + I''$. Thus we can form a polarization vector for all the quanta emitted by nuclei with $J_z = M$ as follows:

$$I_M \mathbf{P}^M = \sum_m |C_{M, M-m, m}^J|^2 I_m \mathbf{P}^m. \dots\dots(2)$$

Then if W_M is the relative population of the initial nuclear sub-state M , the complete polarization vector for radiation from all initial sub-states is

$$I\mathbf{P} = \sum_M W_M I_M \mathbf{P}^M = \sum_{Mm} W_M |C_{M, M-m, m}^J|^2 I_m \mathbf{P}^m. \dots\dots(3)$$

For such a transition as ($J \xrightarrow{j(\beta)} J_1 \xrightarrow{L} J_2$), where a β -emission from the oriented nucleus precedes the γ -emission,

$$I\mathbf{P} = \sum_{MM_1m} W_M |C_{M, M-M_1, M_1}^J C_{M_1, M_1-m, m}^{J_1}|^2 I_m \mathbf{P}^m. \dots\dots(4)$$

j is the total angular momentum of the β - ν system assumed to have one value only.

In I certain functions $\Pi_k(m, L)$ were introduced with the property that

$$\sum_m |C_{M, M-m, m}^J|^2 \Pi_k(m, L) = S_k(J, J_1, L) \Pi_k(M, J). \dots\dots(5)$$

S_k is independent of M and is related to the Racah coefficient (Racah 1943 see also Biedenharn 1952 for a résumé of formulae) as follows:

$$S_k(J, J_1, L) = (2J+1) \left[\frac{(2J-k)! (2L+k+1)!}{(2L-k)! (2J+k+1)!} \right]^{1/2} W(k, L, J, J_1; L, J). \dots\dots(6)$$

$\Pi_k(m, L)$, which is related to $C_{m, 0, m}^{L, k, L}$, has the general form

$$\Pi_k(m, L) = \sum_{\nu=0}^k \frac{(-1)^\nu (L+m)! (L-m)! k!}{[(k-\nu)! \nu!]^2 (L+m-\nu)! (L-m-k+\nu)!}. \dots\dots(7)$$

It is evident that eqns. (3) and (4) could be simplified if $I_m p_1^m$ and $I_m p_3^m$ could be expressed in terms of these functions. Furthermore, a series in

ascending values of k would be cut off by the fact that $\Pi_k(mL)=0$ for $k>2L$, which requires that k satisfy $k \leq 2L, 2J$ (and $2J_1$ in the case of eqn. (4)).

Four methods of nuclear alignment have been discussed by Simon, Rose and Jauch (1951). These are referred to here as (a) direct coupling, (b) Pound's method, (c) Bleaney's method, and (d) the Rose-Gorter method. The relative population W_M for each of these methods is given in another paper by the author (Steenberg 1953, to be referred to as II). It is shown below that in cases (b) and (c) since $W_M = W_{-M}$ these methods can yield no circularly polarized radiation.

§ 3. THE PLANE POLARIZED COMPONENT p_1

We now wish to obtain an expression for $I_m p_1^m$ in terms of the functions $\Pi_k(m, L)$. In § 2 it was given that

$$I_m p_1^m = I_m^\varphi - I_m^\theta = 2I_m^\varphi - I_m(\theta). \quad \dots\dots(8)$$

$I_m(\theta)$ was given in this form in I, that is

$$I_m(\theta) = 1 + \sum_k a_k(L) \Pi_k(m, L) P_k(\cos \theta) \quad \dots\dots(9)$$

irrespective of the character of the radiation.

The intensities of the electric field components in the φ and θ directions are proportional to $|A_\varphi^m|^2$ and $|A_\theta^m|^2$, where A_φ^m and A_θ^m are the φ and θ components of the vector potential. Thus

$$I_m p_1^m = \text{const.} (|A_\varphi^m|^2 - |A_\theta^m|^2). \quad \dots\dots(10)$$

The difference between electric and magnetic radiation is, in effect, that the directions of \mathbf{E} and \mathbf{H} (and so the labels ϕ and θ in eqn. (10)) are interchanged. Thus $p_1^m(\text{el}) = -p_1^m(\text{mag})$.

Furthermore, it follows that we can write for electric radiation

$$I_m^\varphi(\text{el}) = |A_\theta^m(\text{mag})|^2 = |A_z^m(\text{mag})|^2 / \sin^2 \theta. \quad \dots\dots(11)$$

Using for $A_z^m(\text{mag})$ the expression given by Heitler (1936), the following expression is derived in the Appendix:

$$I_m^\varphi(\text{el}) = \frac{1}{2} \left[I_m(\theta) - \sin^2 \theta \sum_{k=2,4,\dots}^{2L} \frac{b_k(L) \Pi_k(mL)}{(k+2)(k-1)} P_k''(\cos \theta) \right], \quad \dots\dots(12)$$

$$\text{where } b_k(L) = \frac{(2k+1)(2L+1)(2L-k)! (k!)^2}{(2L+k+1)!} \Pi_k(0L), \quad \dots\dots(13)$$

$$\Pi_k(0L) = (-1)^{k/2} \frac{(L + \frac{1}{2}k)!}{(\frac{1}{2}k)!^2 (L - \frac{1}{2}k)!}, \quad \dots\dots(14)$$

$$P_k''(z) = \frac{d^2}{dz^2} P_k(z). \quad \dots\dots(15)$$

It is easily verified that this leads to the expressions for $I_m^\varphi(\text{el})$ and $I_m^\theta(\text{el})$ given by Hamilton (1948) for the dipole and quadrupole cases.

We can now give the desired expression for $I_m p_1^m$ from eqns. (8) and (12):

$$I_m p_1^m = -a \sin^2 \theta \sum_k \frac{b_k(L) \Pi_k(mL)}{(k+2)(k-1)} P_k''(\cos \theta). \quad \dots\dots(16)$$

a is ± 1 according as the radiation is electric or magnetic. For the dipole and quadrupole cases this yields

$$L=1, \quad I_m p_1^m = a \frac{3}{4} \sin^2 \theta \Pi_2(m1),$$

$$L=2, \quad I_m p_1^m = a \frac{5}{28} \sin^2 \theta [\Pi_2(m2) - (7 \cos^2 \theta - 1) \Pi_4(m2)].$$

Finally, performing the summations indicated in eqns. (3) and (4), we obtain

$$Ip_1 = \sum_M W_M I_M p_1^M = -a \sin^2 \theta \sum_M W_M \sum_k \frac{b_k(L) \Pi_k(MJ) R_k}{(k+2)(k-1)} P_k''(\cos \theta). \quad \dots\dots (17)$$

If the radiation is observed in the equatorial plane ($\theta = \frac{1}{2}\pi$),

$$P_k''(0) = -(-1)^{k/2} k(k+1)k!/2^k(k/2)!^2.$$

R_k takes one of the following forms according to the indicated transition:

$$\left. \begin{array}{l} \text{(i) } (J \xrightarrow{La} J_1), \quad R_k = S_k(J, J_1, L), \\ \text{(ii) } (J \xrightarrow{j} J_1 \xrightarrow{La} J_2), \quad R_k = S_k(JjJ_1) S_k(J_1 J_2 L). \end{array} \right\} \dots\dots (18)$$

If two γ -rays are emitted in cascade separate polarization vectors describing each γ -ray are required. Ip_1 for either is given by eqn. (17), but if R_k and R_k' refer to the first and second γ -rays respectively these will differ in form. Consider the following transitions in which two γ -rays L and L' are emitted: (iii) $(J \xrightarrow{La} J_1 \xrightarrow{L'a'} J_2)$ and (iv) $(J \xrightarrow{j} J_1 \xrightarrow{La} J_2 \xrightarrow{L'a'} J_3)$. For (iii) and (iv) R_k has the forms given above, eqn. (18) (i) and (ii), for single emission, that is the first γ -ray is unaffected by the emission of the second. R_k' has the forms

$$\left. \begin{array}{l} \text{(iii) } R_k' = S_k(JLJ_1) S_k(J_1 J_2 L'), \\ \text{(iv) } R_k' = S_k(JjJ_1) S_k(J_1 L J_2) S_k(J_2 J_3 L'). \end{array} \right\} \dots\dots (18)$$

The problem of the simultaneous observation of the polarization of both γ -rays by a scattering experiment involves their energies. If the energies are sufficiently different it should be possible to measure p_1 and p_1' separately. It should be noted here that if $J_2 = J_1 - L$ and $J_3 = J_2 - L$ then $R_k = R_k'$, and if further the energies are nearly the same, as in the case of the $(4 \xrightarrow{2+} 2 \xrightarrow{2+} 0)$ cascade in ^{60}Ni , the two emissions can be treated as a single one.

It is not difficult to derive a connection which exists between $p_1(\frac{1}{2}\pi)$ and the anisotropy, $\epsilon = 1 - I(0)/I(\frac{1}{2}\pi)$, discussed in I. This is, that for $L=1$, $p_1(\frac{1}{2}\pi) = -a\epsilon$ and for $L=2$, $p_1(\frac{1}{2}\pi) = a\epsilon$. This is true for all degrees of nuclear alignment, all types of transitions and all methods of nuclear alignment.

In the case of direct coupling (and the Bleaney method where B/A is small, see II) eqn. (17) can be simplified somewhat. Noting that $I_{-M} p_1^{-M} = I_M p_1^M$, eqn. (17) can be written

$$Ip_1 = (\sum_M \cosh \beta M)^{-1} \sum_M \cosh \beta M I_M p_1^M,$$

and since

$$I(\theta) = (\sum_M \cosh \beta M)^{-1} \sum_M \cosh \beta M I_M(\theta), \quad \dots\dots (19)$$

$$p_1 = [\sum_M \cosh \beta M I_M p_1^M] / [\sum_M \cosh \beta M I_M(\theta)]. \quad \dots\dots (20)$$

No such simplification can be made for the other methods of nuclear alignment.

§ 4. THE CIRCULAR COMPONENT, p_3

It was shown previously that

$$I_m p_3^m = \pm 2 [I_m^\varphi I_m^\theta]^{1/2} \quad \dots\dots (21)$$

and that for electric radiation,

$$[I_m^\varphi(\text{el})]^{1/2} = |A_z^m(\text{mag})| / |\sin \theta|. \quad \dots\dots (22)$$

Now for electric radiation

$$[I_m^\theta(\text{el})]^{1/2} = |A_z^m(\text{el})| / |\sin \theta|, \quad \dots\dots (23)$$

where $A_z^m(\text{el})$ is the vector potential for electric multipole radiation given by Heitler (1936). Thus

$$I_m p_3^m = \pm 2 \frac{1}{\sin^2 \theta} |A_z^m(\text{el})| |A_z^m(\text{mag})|, \quad \dots (24)$$

which is obviously independent of the character of the radiation.

The following expression is given without proof*:

$$I_m p_3^m = \sum_{k=1,3,\dots}^{2L-1} C_k(L) P_k(\cos \theta) \Pi_k(mL), \quad \dots (25)$$

$$\text{where } C_k(L) = (-1)^{(k-1)/2} \frac{(k!)^2 (2L+1)(2k+1)(2L-k)!(L+\frac{1}{2}k-\frac{1}{2})!}{[\frac{1}{2}(k-1)]!^2 L(L+1)(2L+k)!(L-\frac{1}{2}k-\frac{1}{2})!}$$

For the dipole and quadrupole cases this reduces to

$$L=1, I_m p_3^m = \frac{3}{4} \Pi_1(m1) P_1(\cos \theta) = -\frac{3}{2} m \cos \theta,$$

$$L=2, I_m p_3^m = \frac{1}{4} P_1(\cos \theta) \Pi_1(m2) - \frac{1}{4} P_3(\cos \theta) \Pi_3(m2).$$

Finally, recalling eqns. (3) and (4),

$$I p_3 = \sum_M W_M I_M p_3^M = \sum_M W_M \sum_{k=1,3,\dots} C_k(L) R_k \Pi_k(MJ) P_k(\cos \theta) \quad \dots (26)$$

where R_k has one of the forms given in eqn. (18).

k takes the odd values 1, 3, ... $2L-1$, or $2J$ (or $2J_1$), whichever is smallest. This permits a finite value for p_3 when the oriented nucleus has $J=\frac{1}{2}$. This is in contrast to the previous results that for $J=\frac{1}{2}$ both p_1 and ϵ vanish.

It was stated earlier that only the direct coupling and R-G methods of nuclear alignment can yield circularly polarized radiation. This is evident from the fact that for the Bleaney and Pound methods $W_M = W_{-M}$, and since $I_{-M} p_3^{-M} = -I_M p_3^M$, $\sum_M W_M I_M p_3^M = 0$.

For direct coupling eqn. (26) can be written

$$I p_3 = (\sum_M \cosh \beta M)^{-1} \sum_M \sinh \beta M I_M p_3^M.$$

Thus, recalling eqn. (19),

$$p_3 = \frac{\sum_M \sinh \beta M I_M p_3^M}{\sum_M \cosh \beta M I_M(\theta)}. \quad \dots (27)$$

For $J=\frac{1}{2}$ and arbitrary multipole order this reduces to

$$p_3 = I p_3 = -\frac{3R_1}{2L(L+1)} \tanh \frac{1}{2} \beta \cos \theta. \quad \dots (28)$$

$p_3 = I p_3$ in this case since the intensity is isotropically distributed, $I(\theta) = 1$.

No such simplifications can be made for nuclear alignment by the R-G method.

§ 5. APPROXIMATIONS

Two approximate forms for W_M were given in II: (a) that giving a finite value for $\sum_M W_M M$, and (b) that giving a finite value for $\sum_M W_M M^2$. These were

$$(a) W_M = \frac{1}{2J+1} \{1 - \frac{1}{2} \alpha \Pi_1(MJ)\}, \quad \dots (29)$$

$$(b) W_M = \frac{1}{2J+1} \{1 + \frac{1}{6} \beta^2 \Pi_2(MJ)\}, \quad \dots (30)$$

where the forms of the parameters α and β^2 were given for the four methods of nuclear alignment.

* The derivation of this expression is along the same lines as that of eqn. (15), but lengthy and tedious.

p_1 and p_3 can be approximated by using the fact that $\sum_M \Pi_k(MJ) \Pi_{k'}(MJ) = 0$ unless $k = k'$. Thus

$$p_1 = Ip_1 = a\beta^2 \frac{J(J+1)(2J+3)(2J-1)}{8(2L+3)(2L-1)} R_2 \sin^2 \theta, \quad \dots\dots (31)$$

$$p_3 = Ip_3 = -\alpha \frac{J(J+1)}{L(L+1)} R_1 \cos \theta. \quad \dots\dots (32)$$

To this order of approximation $p_1 = Ip_1$ since $I(\theta) = 1 + \text{term in } \beta^2$.

§ 6. DISCUSSION

It is useful to review the general behaviour of p_1 and p_3 and to see what information may be derived from their measurement.

Let us first deal with the plane polarized component p_1 as observed in the equatorial plane, $\theta = \frac{1}{2}\pi$. It can be seen that the sign of p_1 at once determines the character of the radiation. For electric radiation $p_1(\frac{1}{2}\pi) > 0$ for all degrees of nuclear alignment, i.e. there is an excess of radiation plane polarized in the φ direction. For magnetic radiation the excess is in the θ direction, $p_1(\frac{1}{2}\pi) < 0$. The behaviour of $p_1(\frac{1}{2}\pi)$ as the degree of nuclear alignment increases from zero gives information similar to that given by a measurement of ϵ . It was stated earlier that $|p_1(\frac{1}{2}\pi)| = \epsilon$ for the dipole and quadrupole cases.

For higher multipoles the behaviour is similar. Thus the slope of the curve of $|p_1(\frac{1}{2}\pi)|$ against $(1/kT)^2$ at the origin will involve the multipole order, nuclear spins and the magnetic moment of the oriented nucleus. In general the magnetic moment can only be determined if the transition is known or vice versa.

As $T \rightarrow 0$, $p_1(\frac{1}{2}\pi)$ tends monotonically to a saturation value. For direct coupling (or the Bleaney method for B/A small) this value is readily predictable. Thus for $(J \xrightarrow{La} J-L)$ or $(J \xrightarrow{j} J-j \xrightarrow{La} J-j-L)$ transitions $p_1(\frac{1}{2}\pi) \rightarrow a$ as $T \rightarrow 0$. For transitions of the type $(J \xrightarrow{La} J+L)$ $|p_1(\frac{1}{2}\pi)|$ at saturation is less than 1; for example,

$$\text{for } (J \xrightarrow{1a} J+1) \quad p_1(\frac{1}{2}\pi) \rightarrow a \frac{J(2J-1)}{(2J^2+7J+4)},$$

$$\text{for } (J \xrightarrow{2a} J+2) \quad p_1(\frac{1}{2}\pi) \rightarrow a \frac{J(2J-1)(2J^2+7J+9)}{(J+1)(4J^3+24J^2+35J+24)}.$$

Let us consider the circular component as observed on the polar axis $\theta = 0$. The first feature to note is the sign of $p_3(0)$. $p_3(0)$ is greater or less than zero according as there is an excess of right or left circularly polarized radiation. It can be seen from eqn. (32) that for $(J \xrightarrow{L} J-L)$ or $(J \xrightarrow{j} J-j \xrightarrow{L} J-j-L)$ transitions, for which $R_1 = L/J$, that $p_3(0)$ depends on the sign of the magnetic moment of the oriented nucleus, thus $p_3(0) < 0$ for a positive moment (α positive), $p_3(0) > 0$ for a negative moment. For $(J \xrightarrow{L} J+L)$ transitions $R_1 = -L/(J+1)$ and $p_3(0)$ has the opposite sign dependence on moment. It should be noted that this is true at the 'north' pole ($\theta = 0$), with the opposite holding at the 'south' ($\theta = \pi$).

Other information which might be obtained is of the same nature as that given by a measurement of the anisotropy ϵ except that some information concerning multipole order and magnetic moment can be obtained for emission from nuclei of spin $\frac{1}{2}$ which is not obtainable from a measurement of ϵ .

Less interest is attached to values of $p_3(0)$ for high degrees of nuclear alignment since they are unlikely to be obtained by direct coupling, and the

behaviour in the R-G case is complex. It can be said however that, in general, for increasing nuclear alignment $p_3(0)$ approaches a saturation value monotonically and rather more rapidly than in the case of ϵ or p_1 .

ACKNOWLEDGMENTS

The work described above was done while the author was an Overseas Scholar of the Royal Commission for the Exhibition of 1851, to whom it is a pleasure for him to express his sincere gratitude. The author is also indebted to Dr. J. A. Spiers for his helpful advice and guidance.

APPENDIX

The Derivation of Equation (12)

It was given in § 3 that

$$I_m^q(\text{el}) = |A_z^m(\text{mag})|^2 / \sin^2 \theta. \quad \text{..... (A 1)}$$

Heitler (1936) gives, in effect, the following expression for $|A_z^m(\text{mag})|^2$:

$$|A_z^m(\text{mag})|^2 = |C_{mm0}^{LL1}|^2 |Y_L^m(\theta\phi)|^2 = \frac{m^2}{L(L+1)} |Y_L^m(\theta\phi)|^2. \quad \text{..... (A 2)}$$

It was shown in I, Appendix I, that

$$|Y_L^m(\theta\phi)|^2 = 1 + \sum_{k=2,4,\dots}^{2L} b_k(L) \Pi_k(mL) P_k(\cos \theta). \quad \text{..... (A 3)}$$

Thus

$$I_m^q(\text{el}) = \frac{m^2}{L(L+1) \sin^2 \theta} \left[1 + \sum_k b_k \Pi_k P_k \right]. \quad \text{..... (A 4)}$$

We write

$$m^2 = \frac{1}{3} [\Pi_2(mL) + L(L+1)] \quad \text{..... (A 5)}$$

and note that $\Pi_k(mL)$ is the matrix element of an operator which behaves under rotation according to the D_k group of space rotations. Thus an expression of the form

$$\Pi_2(mL) \Pi_k(mL) = \sum_{k'=k+2, k, k-2} T_{k'}^{2k}(L) \Pi_{k'}(mL) \quad \text{..... (A 6)}$$

exists. The invariants $T_{k'}^{2k}$ are as follows:

$$\begin{aligned} T_{k+2}^{2k} &= \frac{3(k+2)^2(k+1)^2}{4(2k+3)(2k+1)}, \\ T_k^{2k} &= \frac{k(k+1)[4L(L+1) - 3k(k+1) + 3]}{2(2k+3)(2k-1)}, \\ T_{k-2}^{2k} &= \frac{3(2L+k+1)(2L+k)(2L-k+2)(2L-k+1)}{4(2k+1)(2k-1)}. \end{aligned}$$

To prove the correctness of these invariants it is only necessary to demonstrate the identity

$$\Pi_2(LL) \Pi_k(LL) = \sum_{k'} T_{k'}^{2k}(L) \Pi_{k'}(LL),$$

where

$$\Pi_k(LL) = \frac{(-1)^k (2L)!}{k! (2L-k)!}$$

From eqns. (A 4), (A 5) and (A 6) it follows that

$$I_m^{(el)} = \frac{1}{3L(L+1)\sin^2\theta} \left\{ \Pi_2 + \sum_k b_k P_k \sum_{k'} T_k^{2k} \Pi_{k'} + L(L+1) + L(L+1) \sum_k b_k P_k \Pi_k \right\} \dots\dots (A 7)$$

Gathering terms, the coefficient of Π_k is found to be

$$b_{k-2} T_k^{2k-2} (P_{k-2} - P_k) - b_{k+2} T_k^{2k+2} (P_k - P_{k+2}). \dots\dots (A 8)$$

From the recurrence relations

$$\left. \begin{aligned} P_{k-1}(z) - P_{k+1}(z) &= (1-z^2)(2k+1)P_k'(z), \\ P_{k+1}'(z) &= zP_k' + (k+1)P_k(z) \end{aligned} \right\} \dots\dots (A 9)$$

and Legendre's equation

$$2zP_k'(z) - k(k+1)P_k(z) = (1-z^2)P_k''(z) \dots\dots (A 10)$$

the coefficient of Π_k becomes

$$\frac{3b_k(L)\sin^2\theta}{4} \left\{ [2L(L+1) - k(k+1)]P_k(\cos\theta) - \frac{2L(L+1)\sin^2\theta}{(k-1)(k+2)} P_k''(\cos\theta) \right\}, \dots\dots (A 11)$$

whence eqn. (15) follows.

REFERENCES

- BIEDENHARN, L. C., 1952, *Oak Ridge National Laboratory Report*, 1098.
 DANIELS, J. M., GRACE, M. A., and ROBINSON, F. N. H., 1951, *Nature, Lond.*, **168**, 780.
 FANO, U., 1949, *J. Opt. Soc. Amer.*, **39**, 859.
 HAMILTON, D., 1948, *Phys. Rev.*, **74**, 782.
 HEITLER, W., 1936, *Proc. Camb. Phil. Soc.*, **32**, 112.
 RACAH, G., 1943, *Phys. Rev.*, **63**, 367.
 SIMON, A., ROSE, M. E., and JAUCH, J. M., 1951, *Phys. Rev.*, **54**, 1155.
 STEENBERG, N. R., 1952, *Proc. Phys. Soc. A*, **65**, 791; 1953, *Ibid.*, **66**, 399.

Population Distribution of Nuclei Aligned at Low Temperatures

By N. R. STEENBERG

The Clarendon Laboratory, Oxford

MS. received 1st August 1952, and in final form 22nd December 1952

Abstract. Population distribution functions are given for four suggested methods of nuclear alignment at low temperatures. They are given for arbitrary temperature and in approximate form valid at high temperatures. It is shown how the approximation is related to the approximate angular distribution of γ -radiation.

§ 1. INTRODUCTION

THE alignment of nuclei at low temperatures involves altering the relative populations of the magnetic substates of the nucleus from their normal equilibrium value of $1/(2J+1)$, where J is the nuclear spin. The angular distribution of γ -radiation from nuclei so aligned has been given in a previous paper by the author (Steenberg 1952, to be referred to as I). This was in the form

$$I(\theta) = \sum_M W_M I_M(\theta) \quad \dots\dots(1)$$

where W_M was the temperature dependent relative population of that nuclear substate for which $J_z = M$ and $I_M(\theta)$ is the angular distribution of the radiation originating from that state. It has also been shown (Steenberg 1953) that the polarization distribution of the emitted radiation has a form involving W_M in the same way.

The purpose of this paper is to give W_M for the four methods of nuclear alignment so far suggested. They are given for arbitrary temperature and also for high temperatures in a simple approximate form. The approximate form can be used to obtain simple approximations for the angular distribution and polarization distribution.

§ 2. GENERAL

Four methods of nuclear alignment are discussed by Simon, Rose and Jauch (1951), whose notation is followed here. These are: (a) direct coupling of an external field to the nuclear magnetic moment, (b) coupling of the crystalline electric field to the quadrupole moment (Pound), (c) anisotropic hyperfine structure coupling (Bleaney), (d) hyperfine structure combined with an external field (Rose-Gorter).

In methods (b) and (c) the nuclear spins are aligned in equal numbers along the $+z$ and $-z$ directions, i.e. they are aligned in direction only, $W_M = W_{-M}$. In (a) and (d) the nuclei are aligned in both sense and direction, $W_M \neq W_{-M}$.

In the two simplest cases (a) and (b) the Hamiltonian is diagonal in M ; thus for direct coupling

$$W_M = \exp \frac{g_n \mu_n H}{kT} M \quad \dots\dots(2)$$

and for Pound's method

$$W_M = \exp \left\{ - \frac{3Q}{kT} M^2 \right\} \quad \dots\dots(3)$$

where g_n = nuclear g -factor, μ_n = nuclear magneton, $Q = eq(dE_z/dz)/4J(2J-1)$, and q is the nuclear quadrupole moment.

It is the other two methods however which are of principal interest. These depend on the hyperfine structure interaction between the nucleus and its electronic structure in paramagnetic salts. It is assumed that the lowest ionic state is a Kramers doublet, and is the only one occupied at the experimental temperature. Thus the ionic spin is effectively $S = \frac{1}{2}$. The Hamilton for this interaction is not diagonal in M and the states of the system are, in general, mixtures of nuclear substates.*

§ 3. BLEANEY'S METHOD

Bleaney's method, which is the first to be experimentally successful (Daniels, Grace and Robinson 1951), depends on hyperfine structure which is anisotropic with respect to some crystal axis. The Hamiltonian for this interaction is $AS_zJ_z + B(S_xJ_x + S_yJ_y)$. For $B=0$ there are $2J+1$ uniformly spaced hyperfine doublets, each containing equal numbers of nuclear states with $J_z = \pm M$. W_M is therefore proportional to $\cosh(AM/2kT)$. Since $I_M(\theta) = I_{-M}(\theta)$ this leads to an angular distribution identical to that given in I for the direct coupling method.

For $B > 0$ but $B < A$ the energy levels are altered and the states of the system are mixtures of neighbouring nuclear states (Bleaney 1951). A straightforward perturbation calculation yields

$$W_M = W_{-M} = D \exp\{\gamma(1+q)\} + D' \exp\{\gamma(1-q')\} + E \exp\{\gamma(1-q)\} + E' \exp\{\gamma(1+q')\} \quad \dots\dots(4)$$

where $D(M) = \frac{q+2M-1}{4q}$, $D'(M) = D(M+1)$

$$E(M) = \frac{x^2(J+M)(J-M+1)}{q(q+2M-1)}, \quad E'(M) = E(M+1)$$

$$q(M) = [(2M-1)^2 + 4x^2(J+M)(J-M+1)]^{1/2}, \quad q'(M) = q(M+1)$$

$$x = B/A, \quad \gamma = A/4kT.$$

It is easily confirmed that $W_M \rightarrow \cosh(AM/2kT)$ as $x \rightarrow 0$.

§ 4. THE ROSE-GORTER METHOD

The R-G method depends on an external field to align the electronic system which then, through the hyperfine coupling, orients the nucleus. The Hamiltonian in this case is $g\mu H + A\mathbf{S} \cdot \mathbf{J}$, where g is the ionic g -factor and where we have assumed isotropic hyperfine structure, $A = B$. This leads to

$$W_M = D \exp\{\gamma(1+q)\} + D' \exp\{\gamma(1-q')\} + E \exp\{\gamma(1-q)\} + E' \exp\{\gamma(1+q')\} \quad \dots\dots(5)$$

where $D(M) = \frac{2y+2M-1+q}{4q}$, $D'(M) = D(M+1)$, $\gamma = A/4kT$

$$E(M) = \frac{(J+M)(J-M+1)}{q(2y+2M-1+q)}, \quad E'(M) = E(M+1), \quad y = g\mu H/A$$

$$q(M) = [4y^2 + 4y(2M-1) + (2J+1)^2]^{1/2}, \quad q'(M) = q(M+1).$$

* Interference effects in the angular distribution or polarization distribution are eliminated by the orthonormality of the ionic states.

It is to be noted here that eqns. (2)–(5) do not give population functions which are normalized in the sense that $\sum_M W_M = 1$. An approximation to a given order in $1/kT$, however, must be so normalized.

§ 5. APPROXIMATIONS

For high temperatures where the degree of nuclear alignment is small eqns. (2)–(5) can be approximated by expanding the exponentials and retaining only the relevant terms.

For approximating the angular distribution, since $I_M(\theta) = I_{-M}(\theta)$, only the term in M^2 enters. This is also true for the plane polarization. If $W'_M = W_M / \sum_M W_M$, W'_M is approximately

$$W'_M = \frac{1}{(2J+1)} [1 + \frac{1}{6} \beta^2 \{3M^2 - J(J+1)\}] \quad \dots\dots (6)$$

where the parameter β^2 depends on the method of alignment as follows:

direct coupling,	$\beta^2 = (g_n \mu_n H / kT)^2$
Pound's method,	$\beta^2 = -6Q/kT$,
Bleaney's method,	$\beta^2 = (A/2kT)^2 (1 - B^2/A^2)$,
Rose-Gorter method,	$\beta^2 = \frac{1}{3} \left(\frac{g\mu H}{2kT} \right)^2 \left(\frac{A}{2kT} \right)^2$.

All results to order β^2 given in I can now be used if the proper parameter is substituted for β^2 according to the method of alignment. Equation (6) leads to an anisotropy which is within 10% of the exact anisotropy as long as $\beta^2 < 1/J(J+1)$.

It was suggested in I that the angular distribution for the direct coupling method given there approximated that to be expected for Bleaney's method if B/A was small. In fact, for Bleaney's method the anisotropy $\epsilon = 1 - I(0)/I(\frac{1}{2}\pi)$ is given by $\epsilon = \epsilon'(1 - B^2/A^2)$ where ϵ' is the anisotropy given in I. This is true exactly for low degrees of alignment for all values of B/A , and if $B^2/A^2 \ll 1$ it is very nearly true for all degrees of alignment. Thus, in the experiment on ^{60}Co discussed in I for which $B/A \simeq \frac{1}{6}$ the anisotropy given there is reduced by $1/36 = 2.8\%$.

The distribution of circularly polarized radiation has the form $\sum_M W_M F_M$, where $F_{-M} = -F_M$. Evidently here it is the term in MkT from the expansion which is required. To this order of approximation

$$W'_M = \frac{1}{2J+1} (1 + \alpha M), \quad \dots\dots (7)$$

where α has the forms

direct coupling,	$\alpha = g_n \mu_n H / kT$,
Pound's method	$\alpha = 0$,
Bleaney's method,	$\alpha = 0$,
Rose-Gorter method,	$\alpha = \left(\frac{g\mu H}{2kT} \right) \left(\frac{A}{2kT} \right)$.

The results obtained by Simon, Rose and Jauch (1951) for the parameters $f_N = (\sum_M W_M M)/J$ and $\Delta = [3\sum_M W_M M^2 - J(J+1)]/3J^2$ expressing the degree of nuclear alignment are obtained from eqns. (6) and (7) with the appropriate forms of α and β , recalling that here $S = \frac{1}{2}$ and $G'(S) = 0$.

ACKNOWLEDGMENT

The author is indebted to the Royal Commission for the Exhibition of 1851 for an Overseas Scholarship held while this work was done.

REFERENCES

- BLEANEY, B., 1951, *Phil. Mag.*, **42**, 441.
 DANIELS, J. M., GRACE, M. A., and ROBINSON, F. N. H., 1951, *Nature, Lond.*, **168**, 780.
 SIMON, A., ROSE, M. E., and JAUCH, J. M., 1951, *Phys. Rev.*, **84**, 1155.
 STEENBERG, N. R., 1952, *Proc. Phys. Soc. A*, **65**, 791; 1953, *Ibid.*, **65**, 391.

Neumann Bands in Pure Iron

By A. KELLY

Crystallographic Laboratory, Cavendish Laboratory, Cambridge

Communicated by W. H. Taylor; MS. received 26th June 1952

Abstract. An examination has been made, using an x-ray microbeam method, of Neumann bands in a crystal of pure iron. The lattice in the bands is shown to be twinned with respect to the matrix about a (112) pole.

DEFORMATION by impact at room temperature, or slow deformation at low temperatures, leads to the appearance of narrow lamellae on the surfaces of the crystals of coarse-grained specimens of iron and alloyed ferrites. These are called Neumann bands, and in pure iron are seldom more than 5μ wide. Their orientations are such that they correspond to traces of planes of form (112). The narrowness of the bands makes optical examination difficult, and at one time their nature was the subject of considerable controversy. Most of the work on Neumann bands has been confined to those appearing in alloyed ferrites, where they are usually wider than in pure iron, and for these materials investigations by Mathewson and Edmunds (1928) and McKeehan (1928) showed them to be twins of the parent lattice in planes of the form (112).

The former authors obtained x-ray reflections on Laue photographs which they could attribute to the material occurring within the bands if this were twinned with respect to the matrix. However, the reflections obtained from the twins were extremely weak, and it was only possible to reproduce one spot due to a single twin reflection on the best photograph obtained. Mathewson and Edmunds used silicon ferrite in their experiments, and a proof of the twin nature of the bands has not been given for pure iron. The present note describes the use of the recently developed x-ray microbeam technique (Hirsch and Kellar 1951) to obtain reproducible Laue diagrams from Neumann bands in pure iron, and the determination of the orientation of the material in the bands.

The iron single crystal used contained 0.3% Mn, 0.05% S and 0.05% P. It was strained slowly by approximately 0.1% at the temperature of liquid air, and the bands, which were about 5μ wide, were made visible by electrolytic polishing. Four sets of Neumann bands were visible, and one of these sets was selected for examination. The specimen was mounted on the recently described specimen holder (Gay and Kelly 1952), for use with the microbeam camera, which allows for the precision setting of a particular area of a solid specimen in the x-ray beam. A Laue back-reflection photograph was then taken of an area of the specimen where no bands were visible, using a beam of diameter 150μ . White radiation from an iron target was used and two films were placed in the film holder—the first film served as a very efficient screen to filter out the fluorescent $\text{FeK}\alpha$ radiation from the specimen. The beam was caused to straddle four parallel Neumann bands of the same family, occurring close together, and a second exposure was made. The bands examined are

shown in fig. 1 (Plate) at a magnification of 625. About 14% of the irradiated occurred in the bands.

On comparing the two photographs many extra spots could be seen on that taken of a volume containing the bands. Some of the extra spots are indicated by arrows on fig. 2 (Plate)*.

From the photograph obtained from the matrix crystal alone the orientations of the zones giving the strongest reflections were determined using a Greninger chart (Greninger 1935); these zones were $[1\bar{1}\bar{1}]$, $[0\bar{1}0]$ and $[0\bar{1}1]$. A stereogram giving the matrix orientation is shown in fig. 3. From the second photograph another stereogram was constructed, by the same method, of the orientation of the lattice giving rise to the extra reflections. Only the extra spots were used, and the stereogram is shown in fig. 4. All the extra spots were found to be due to reflections from a single lattice, indicating that the orientation of the lattice in the four bands examined was the same. The main zones identified were of form $[111]$, $[100]$ and $[110]$.

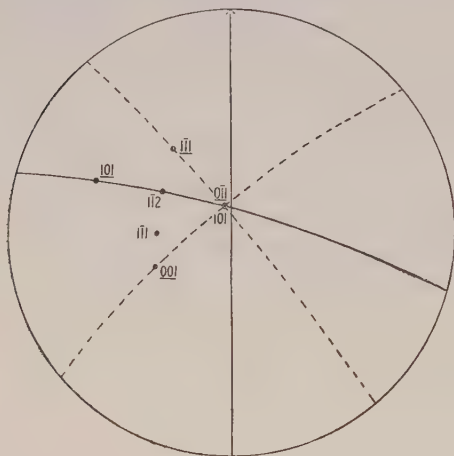


Fig. 3. Orientation of matrix crystal. Underlined indices and dotted zones show orientation of simple 180° twin about $1\bar{1}2$. The arrowed zone is the projection of a fiducial mark made on the film.

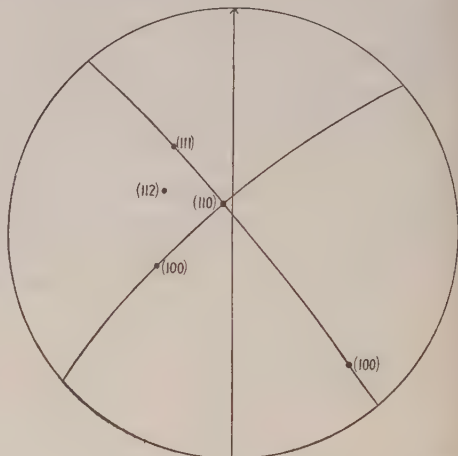


Fig. 4. Orientation of material occurring in the bands.

The orientation of the material within the bands, found from the second photograph, may be slightly less accurate than the determination of the matrix orientation, due to the asterism found in reflections from material in and around the bands. Asterism is not found in reflections from material far from the bands. The radial length of the asterism streaks indicated a range in orientation of the order of $\frac{1}{2}^\circ$. However, the main error in each orientation determination is due to the graphical construction and to the measurement of the specimen to film distance. Within the error of the measurements there is exact coincidence between the orientation of a twin obtained from the matrix by a rotation of 180° about the $(1\bar{1}2)$ pole and that of the lattice in the bands. The Neumann bands occurring both in alloyed ferrites and in pure iron are thus of a similar nature, though the twins found in the latter are of smaller dimensions.

* These spots have been retouched in order to make reproduction possible.—ED.

ACKNOWLEDGMENTS

I should like to thank Professor Sir Lawrence Bragg and Dr. W. H. Taylor, in whose laboratories this work has been carried out. My thanks are also due to Professor A. H. Cottrell (Department of Metallurgy, University of Birmingham) for suggesting this examination and to Mr. W. H. Paxton, of the same department, for supplying the specimen. This investigation was carried out while the author was in receipt of a maintenance allowance from the Department of Scientific and Industrial Research.

REFERENCES

- GAY, P., and KELLY, A., 1952, *J. Sci. Instrum.*, **29**, 287.
GRENINGER, A. B., 1935, *Z. Kristallogr.*, **91**, 424.
HIRSCH, P. B., and KELLAR, J. N., 1951, *Proc. Phys. Soc. B*, **64**, 369.
McKEEHAN, L. W., 1928, *Trans. Amer. Inst. Min. Metall. Engrs.*, **78**, 435.
MATHEWSON, C. H., and EDMUNDS, G. H., 1928, *Trans. Amer. Inst. Min. Metall. Engrs.*, **80**, 311.

RESEARCH NOTES

Calculation of the 1s-2s Electron Excitation Cross Section of Hydrogen by a Variational Method

BY H. S. W. MASSEY* AND B. L. MOISEWITSCH†

* University College, London. † Queen's University, Belfast

MS received 13th January 1953

THE variational methods introduced by Hulthén (1944) and by Kohn (1948) have been applied with considerable success to several atomic elastic scattering problems. A procedure for extending the methods to inelastic collisions has been given by Moiseiwitsch (1951). In order to examine the practicability of this method it has been applied to the calculation of the cross section for the excitation of the 2s level of atomic hydrogen from the ground state by electron impact. Apart from being the simplest inelastic collision which can be examined this choice has the advantage that the results obtained may be compared not only with those given by the Born-Oppenheimer approximation but also by the distorted wave modification of this approximation (Erskine and Massey 1952).

The total wave function Ψ of the system of hydrogen atom and electron satisfies the equation $(H-E)\Psi=0$ where the Hamiltonian H in atomic units is given by

$$H = -\nabla_1^2 - \nabla_2^2 - \frac{2}{r_1} - \frac{2}{r_2} + \frac{2}{r_{12}}, \quad \dots\dots(1)$$

r_1, r_2, r_{12} being the distances of the electrons from the nucleus and from each other respectively.

In order to describe slow collisions in which 1s-2s excitation of a hydrogen atom occurs, it is sufficient to write the total wave function of the system in the form

$$\begin{aligned} \Psi(r_1, r_2) = & r_2^{-1} \{f_0^\pm(r_2)\psi_0(r_1) + f_1^\pm(r_2)\psi_1(r_1)\} \\ & \pm r_1^{-1} \{f_0^\pm(r_1)\psi_0(r_2) + f_1^\pm(r_1)\psi_1(r_2)\}, \quad \dots\dots(2) \end{aligned}$$

the alternate signs depending on whether the electron spins are antiparallel or parallel respectively. ψ_0, ψ_1 are the wave functions of the 1s and 2s states of a hydrogen atom respectively, and $f_0^\pm(r)$ and $f_1^\pm(r)$ proper functions vanishing at $r=0$ which have the asymptotic forms

$$\left. \begin{aligned} f_0^\pm(r) &\sim \sin kr + a^\pm \cos kr, \\ f_1^\pm(r) &\sim d^\pm \exp(ik_1 r). \end{aligned} \right\} \quad \dots\dots(3)$$

In atomic units k^2 is the kinetic energy of the incident electron and k_1^2 of the inelastically scattered electron.

If $a^\pm = x^\pm + iy^\pm$, then the principle of conservation of charge (Mott and Massey 1949) requires that $y^\pm = (k_1/k)|d^\pm|^2$. Hence the cross section for excitation of the 2s level is given by

$$Q_{01} = \frac{1}{4} \{Q_{01}^+ + 3Q_{01}^-\}, \quad \dots\dots(4)$$

$$\text{where } Q_{01}^\pm = \frac{4\pi}{k^2} \frac{k_1}{k} |d^\pm|^2 / |1 - ia^\pm|^2 = \frac{4\pi}{k^2} y^\pm / \{x^{\pm 2} + (1 + y^\pm)^2\}. \quad \dots\dots(5)$$

To apply the variational procedure of Moiseiwitsch, trial functions $f_{0t}^{\pm}, f_{1t}^{\pm}$ are introduced which vanish at $r=0$, are proper functions and have the asymptotic forms (3). The corresponding function Ψ_t can then be regarded as a function not only of r_1, r_2, a and d but also of n parameters c_i . The $n+2$ unknowns a, d and c_i are complex numbers which are determined from the equations

$$L_t=0, \quad \frac{\partial L_t}{\partial a} + 2i \frac{k_1}{k} d^* \frac{\partial L_t}{\partial a} = 0, \quad \frac{\partial L_t}{\partial c_i} = 0, \quad \dots\dots(6)$$

where
$$L_t = \iint \Psi_t^* (H - E) \Psi_t d\tau_1 d\tau_2. \quad \dots\dots(7)$$

With this procedure the approximate cross section Q_{01} obtained will automatically satisfy the condition imposed by conservation of charge.

A correction to the parameter a can be obtained by using the relation

$$\lambda = a - L_t' / 4\pi k, \quad \dots\dots(8)$$

where
$$L_t' = \iint \Psi_t (H - E) \Psi_t d\tau_1 d\tau_2,$$

and λ is the corrected value of the parameter a . This results in a new value for the cross section Q_{01} .

Comparison of Cross Sections for Excitation of the 2s level calculated by Different Methods

Energy of incident electron (ev)	Exchange included														
	Exchange neglected Q_{01}^0														
				Symmetrical Q_{01}^+				Anti-symmetrical Q_{01}^-				Q_{01} $= \frac{1}{4}(Q_{01}^+ + 3Q_{01}^-)$			
	Born	D.W.	V	B.O.	D.W.	B.O.	V	B.O.	D.W.	B.O.	V	B.O.	D.W.	B.O.	V
10.2	0	0	0	0	0	0	0	0	0	0	0	0	0	0	0
13.5	0.198	0.239	0.076	0.287	0.714	0.167	2.02	0.03 ₆	0.002	1.59	0.178	0.043			
19.4	0.127	0.118	0.041	0.011	0.344	0.124	0.668	0.010	0.041	0.503	0.094	0.035			
30.4	0.058 ₅	0.045 ₅	0.020	0.014	0.127	0.057	0.134	0.010	0.007	0.104	0.035	0.020			
54	0.019 ₄	0.014 ₁	0.008	0.018	0.025 ₅	0.016	0.020	0.006	0.005	0.020	0.011	0.008			

B.O. = Born-Oppenheimer, D.W.B.O. = full distorted wave approximation,

V = variational method. Cross sections in units πa_0^2

The great difficulty in applying a procedure of this kind is the complexity of the calculations involved even when using the simplest trial functions. For this reason detailed numerical work was confined to trial functions of the form

$$f_0 = \sin kr + (a + b e^{-r})(1 - e^{-r}) \cos kr, \quad \dots\dots(9)$$

$$f_1 = (1 - e^{-r}) d \exp(ik_1 r), \quad \dots\dots(10)$$

b being the additional variable parameter. These wave functions suffer from the defect that they do not allow for mixing between the incident and scattered waves but it was considered that, in a first application, their relative simplicity was an important advantage. Even so the analysis involved, though elementary, was very extensive, and the determination of a from the equation (6) involved much complex arithmetic. The results obtained for the corrected values of the cross sections Q_{01}^+ , Q_{01}^- and Q_{01} are given in the table which also includes, for purposes of comparison, the corresponding results obtained using the Born-Oppenheimer approximation and the full distorted wave (D.W.B.O.) approximation. The cross

section Q_{01}^0 appearing in the table is the one obtained if exchange effects are completely ignored.

It will be seen that the cross section Q_{01}^+ obtained for the symmetrical case is much greater than Q_{01}^- for the antisymmetrical case. This agrees with the results obtained from the D.W.B.O. approximation and is the reverse of that given by the Born-Oppenheimer approximation. On the other hand, at the lower electron energies the present method gives cross sections considerably smaller than those obtained by the D.W.B.O. method. As the electron energy increases the discrepancy decreases. Because the trial wave function (10) can only be expected to represent the true wave function very crudely, particularly as it does not allow for mixing of elastic and inelastically scattered waves, it is uncertain whether the true cross section is so much less than that given by the D.W.B.O. method at low electron energies. It is to be expected, however, that at these energies the D.W.B.O. results would be somewhat too large. This is because the cross section Q_{01}^+ which it gives for electrons of 13.5 eV energy is already 0.7 of the maximum possible inelastic cross section for such electrons. Such a high value indicates relatively strong coupling between the two states and over-estimation of the cross section by the D.W.B.O. method which assumes this coupling to be small (Massey and Mohr 1952). As it is the cross section near the threshold which is important in most applications more work is clearly required using trial functions of a more elaborate form than those used in the present work. Before undertaking such an extensive calculation it is desirable to examine the effectiveness of the variational formulae (6) or some simpler model equations and this is now being undertaken.

REFERENCES

- ERSKINE, G. A., and MASSEY, H. S. W., 1952, *Proc. Roy. Soc. A*, **212**, 521.
HULTHÉN, L., 1944, *K. Fysiogr. Sällsk. Lund, Förh.*, **14**, No. 21.
KOHN, W., 1948, *Phys. Rev.*, **74**, 1763.
MASSEY, H. S. W., and MOHR, C. B. O., 1952, *Proc. Phys. Soc. A*, **65**, 845.
MOISEWITSCH, B. L., 1951, *Phys. Rev.* **82**, 753.
MOTT, N. F., and MASSEY, H. S. W., 1949, *Theory of Atomic Collisions* (Oxford: Clarendon Press), 2nd ed., Chapter VIII.

LETTERS TO THE EDITOR

X-Ray Scattering from Liquid Helium

We have recently concluded an experimental investigation on the structure of liquid helium as deduced from the x-ray scattering. Observations have been made between 4.2°K and 1.36°K , and since the complete reduction of the angular intensity distributions into atomic distribution functions is a lengthy process we wish to comment briefly on the results at the present time.

The method employed was essentially the same as that adopted in our earlier experiments (Reekie 1940), but, in addition to having an increased resolution, the present camera was circular and able to cover scattering angles up to a 2θ value of nearly 155° . This constituted the major improvement over the previous experimental arrangement and, in addition, allowed considerably more accurate measurements of scattering angles to be made than hitherto. Figure 1

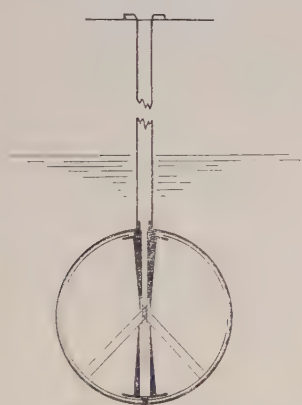


Fig. 1. The x-ray beam enters through the nickel foil at the head of the cryostat and is scattered at the centre of the camera.

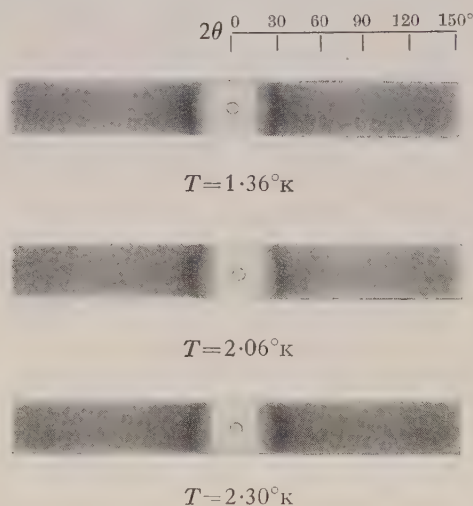


Fig. 2. X-ray diffraction patterns from liquid helium.

illustrates the principle of the method. The x-radiation from a copper target, after passing into the cryostat through a nickel foil, was collimated into a beam approximately 2 mm square. It then traversed the camera and, as shown, was scattered by a small volume of liquid helium at the centre of the camera. The scattering volume remains approximately the same irrespective of the angle of scattering, so that with appropriate small corrections the photographic density recorded on the film can be converted into scattered radiation intensity. In the present experiments exposure times of about 2 hours were adequate when using Kodak No-screen X-ray film and operating the tube at 35 kV and 20 mA. The diameter of the camera was 5.33 cm. It will be noted that the camera remains filled with liquid helium during exposures; this must result in a certain amount of secondary scattering, with consequent additional blackening of the film. However, owing to the very small absorption of x-radiation by liquid helium,

it is easily shown that neglect of this secondary scattering produces an altogether inappreciable error.

Three photographs are shown in fig. 2, taken at temperatures of 1.36°K , 2.06°K and 2.30°K . These latter two temperatures are close to, and on either side of, the λ -point, while the low-temperature exposure corresponds to a T/T_c value of about 0.6 and was the lowest available with the present arrangement.

It will be evident that these results confirm the qualitative findings of the previous experiments, namely, that both helium I and helium II give a typical 'liquid-ring' type diffraction picture, and that there is no outstanding difference between the structure above and below the λ -point (Keesom and Taconis 1938, Reekie 1940, 1947). The angular diameter observed for the main ring (which is much more accurately determined in the present experiments than previously) corresponds to a 2θ value of about 28.5° . This is close to the value obtained by Keesom and Taconis, and does not differ appreciably from that observed by Reekie after applying small geometrical corrections which were omitted in the latter experiments.

Exposures have been made at eight temperatures in all, and microphotometer traces of the films show that, in addition to the main maximum at 28.5° , a subsidiary maximum appears at an angle of about 55° at all temperatures. The traces suggest that this second maximum may be less well-marked in the four exposures made above the λ -point. We are at present reducing the results so as to obtain the atomic distribution function for the liquid over the temperature range from 4.2°K down to 1.36°K . Full details of the calculations and results will be published elsewhere.

Department of Physics,
Royal Military College of Canada,
Kingston, Ontario.
21st January 1953.

J. REEKIE.
T. S. HUTCHISON.
C. F. A. BEAUMONT.

KEESOM, W. H., and TACONIS, K. W., 1938, *Physica*, **5**, 270.

REEKIE, J., 1940, *Proc. Camb. Phil. Soc.*, **36**, 236; 1947, *Ibid.*, **43**, 262.

The Nuclear Electric Quadrupole Moments of Copper 63, 65

The hyperfine structure of the paramagnetic resonance spectrum of $\text{CuK}_2(\text{SO}_4)_2 \cdot 6\text{D}_2\text{O}$ has been studied by Bleaney, Bowers and Ingram (1951), and values of the nuclear electric quadrupole moments of the stable isotopes 63, 65 were deduced using the theory of Abragam and Pryce (1951). Further work on this salt has revealed considerable departures from axial symmetry and a study of the rhombic component of the anisotropy has been made. The results are interpreted in terms of the spin Hamiltonian

$$\mathcal{H} = \beta \mathbf{H} \cdot \mathbf{g} \cdot \mathbf{S} + \mathbf{S} \cdot \mathbf{A} \cdot \mathbf{I} + P \{ I_z^2 - \frac{1}{3} I(I+1) \} + P' (I_x^2 - I_y^2) - \gamma \beta_n \mathbf{H} \cdot \mathbf{I} \quad \dots (1)$$

Here \mathbf{g} and \mathbf{A} are tensors, each with three principal values in directions not *a priori* related to the crystal axes; P is the component of the nuclear electric quadrupole interaction with axial symmetry, while P' represents the departure from this symmetry.

The results for copper potassium sulphate with dilution $\text{Zn}:\text{Cu}=300:1$ at 20°K are given in the table. The relative signs obtained experimentally agree with those given by the theory of Abragam and Pryce (1951), which has been extended by Pryce (private communication) to cover a rhombic component; the theoretical signs are given in the table.

Salt	Isotope	g_z	g_x	g_y	A_z	A_x	A_y	P	P'
Copper Potassium Sulphate	63				- 97	17	+60	+11.3	1.1
	65	2.42	2.16	2.04	-104	18	+64	+10.4	1.0
Copper Lanthanum Nitrate	63				-110	+18	+12	+11.4	0.3
	65	2.470	2.097	2.097	-118	+19	+13	+10.5	0.3

A and P values to be multiplied by 10^{-4} cm^{-1} .

The spectrum is very anisotropic close to the x -axis, and the sign of A_x could not be established. The value of P' has been determined from the spectrum along the y -axis. The ratio of P for the two isotopes agrees with the more accurate ratio obtained from the quadrupole splitting in nuclear resonance (Krüger and Meyer-Berkhout 1952).

In view of the considerable departure from axial symmetry in the sulphate it was felt desirable to make measurements on another type of copper salt, preferably one where the principal axes could be located with greater certainty. It was found by Trenam (1953) that copper bismuth nitrate (whose crystals have trigonal symmetry) shows at low temperatures three Cu^{2+} spectra, each with axial symmetry (cf. Bleaney and Bowers 1952). The most suitable salt of this type when narrow lines are required was found to be $\text{La}_2\text{Cu}_3(\text{NO}_3)_{12} \cdot 24\text{D}_2\text{O}$, with dilution $\text{Mg}:\text{Cu} \simeq 500:1$. This gives lines with a half-width at half intensity of 2 gauss, and the spectrum was examined at 20°K using radiation of wave numbers 0.3 and 0.8 cm^{-1} . It was checked that the three Cu^{2+} spectra are identical in behaviour, but a small rhombic component in the hyperfine structure was found. The principal axes of the three ions appear to be identical, but interchanged so that the z -axis of one is the x -axis of the second and the y -axis of the third. The spectrum is described by the Hamiltonian (1) with the constants given in the table. The signs given are theoretical, but their relative values are checked experimentally. The probable accuracy is ± 0.5 and ± 1 in the values of P for the nitrate and sulphate respectively.

Application of the theory of Abragam and Pryce (1951) to calculate the electric field gradient at the nucleus requires an estimate of the mean value of r^{-3} , where r is the distance from nucleus to electron. From a comparison of the value calculated from Hartree wave functions for $\text{Cu}^+ 3d^{10}$ with that obtained from the $3d^9 4s^2 {}^2\text{D}$ term in the CuI spectrum, Abragam and Pryce adopted the value $\overline{r^{-3}} = 7.2$ atomic units. A more accurate fit between theory and experiment for the magnetic hyperfine structure of the paramagnetic resonance spectrum is obtained, however, if we take the rather lower value of 6.4 atomic units. If there is a difference between the apparent value of $\overline{r^{-3}}$ for the Cu^{2+} ion in the bound and free states, it may be due either to a real change in $\overline{r^{-3}}$, requiring a change in the radial distribution of the $3d$ wave function, or to a migration of the hole from the $3d^9$ copper ion to a position on a water molecule where its

contribution to $\overline{r^{-3}}$ is negligible. In either case the electric field gradient at the copper nucleus would be correspondingly reduced, and we shall accordingly use our empirical value of $\overline{r^{-3}}$ to evaluate the quadrupole moments. This gives -0.157 and $-0.145 \times 10^{-24} \text{ cm}^2$ respectively for the isotopes 63 and 65. Though these values must be regarded as provisional until a full theoretical treatment of the cupric ion in its water complex is available, they are probably correct within about 20%. The difference between these values and those given by Bleaney, Bowers and Ingram is mainly due to the change in the assumed value of $\overline{r^{-3}}$.

Clarendon Laboratory,
Oxford.
23rd January 1953.

B. BLEANEY.
K. D. BOWERS.
R. S. TRENAM.

ABRAGAM, A., and PRYCE, M. H. L., 1951, *Proc. Roy. Soc. A*, **206**, 164.

BLEANEY, B., and BOWERS, K. D., 1952, *Proc. Phys. Soc. A*, **65**, 667.

BLEANEY, B., BOWERS, K. D., and INGRAM, D. J. E., 1951, *Proc. Phys. Soc. A*, **64**, 758.

KRÜGER, H., and MEYER-BERKHOUT, U., 1952, *Z. Phys.*, **132**, 171.

TRENAM, R. S., 1953, *Proc. Phys. Soc. A*, **66**, 118.

Paramagnetic Resonance in some Manganese Salts

The paramagnetic absorption spectra of two salts of manganese were investigated in detail by Bleaney and Ingram (1951) and an analysis made of the five groups of six hyperfine structure lines in terms of the electronic splittings and crystalline field symmetries. Some measurements are reported here on three other salts, and it is hoped to make a systematic survey of various manganese salts as the electronic splittings obtained throw considerable light on the magnitude and symmetry of the crystalline fields.

The Hamiltonian employed in the analysis of the spectra and notation used is the same as that in Bleaney and Ingram (1951). All the measurements were made at room temperature and at a wavelength of 1.25 cm, the standard technique of field modulation and display being used. The magnetic field measurements were made by means of proton resonance, and the cavity wave-meter employed was calibrated against the ammonia inversion spectrum.

The first salt investigated was (Mn-Mg) (CH₃COO)₂.4H₂O. The tetra-hydrates of magnesium and manganese acetate are both monoclinic prismatic with very nearly equal axial angle $\beta = 95^\circ 37'$ and $\beta = 94^\circ 58'$ for the two salts respectively (Groth 1910). They have two ions per unit cell and the magnesium salt has dimensions $a = 8.5 \text{ \AA}$, $b = 11.7 \text{ \AA}$ and $c = 4.7 \text{ \AA}$ (Padmanabhan 1952). The crystal was diluted in a ratio of about one to a hundred, and grows in a form in which the (110) ($\bar{1}\bar{1}0$) ($1\bar{1}\bar{1}$) and ($\bar{1}\bar{1}\bar{1}$) faces are the most prominent.

The crystal was first rotated in the xz (or ac) plane, where the spectra of the two ions coincide, and a maximum separation of the hyperfine groups was obtained at 47° to the z axis, this determining K_1 . The subsidiary maxima at K_2 was slightly smaller than this. Rotation in the K_1K_3 plane ($K_3 \equiv y \equiv b$) then determined the direction of crystalline field axis as at 29° to K_1 , the spectra being symmetrical on either side of K_3 . Rotation in the K_2K_3 plane showed that the spectra of the two ions nearly coincided in all directions in this plane and

the maximum splitting reached was never large (in contrast to the case of (Mn-Mg) $(\text{NH}_4)_2(\text{SO}_4)_2 \cdot 6\text{H}_2\text{O}$ below).

The electronic splittings obtained in the different directions are summarized in table 1. Here the separation between the successive groups of hyperfine structure is given, in gauss. The spectra are very collapsed along all three of the crystallographic axes as these make an angle of about 60° with the crystalline field axis.

Table 1

Direction	Separations of groups (gauss)			
Axis	898	855	862	907
K_1	590	535	547	589
x	368	229	71	0
y	98	86	7	-28
z	306	171	71	-41

A comparison of the spectra obtained perpendicular to the axis in different planes shows that there is a rhombic component present in the field, the separation between extreme centres being 2197, 1240 and 1266 gauss in the xz , xy and K_1K_3 planes respectively.

The hyperfine splitting remains isotropic with a separation between successive lines of 93 gauss. The g value was calculated from the lines in the central group, with the second-order corrections applied, and equals 2.001 ± 0.01 .

From the spectrum along the axis one obtains for the usual Hamiltonian coefficients, in units of 10^{-4} cm^{-1} , $A = B = 87$, $D = 412$, $E = 66$, $a = 8$. It may be noted that the electronic splitting obtained in this salt is considerably greater than that previously observed in any other manganese salt; that obtained in the trihydrate being much smaller (Kumagai *et al.* 1952).

The spectra of (Zn-Mn) $(\text{HCOO})_2 \cdot 2\text{H}_2\text{O}$ is also being investigated. This is a monoclinic prismatic crystal with two ions per unit cell, and appears to have an even larger electronic splitting than the tetrahydrate acetate. The g value is 2.01 ± 0.02 , and the hyperfine splitting is equal to 98 gauss.

The spectra obtained from (Mn-Mg) $(\text{NH}_4)_2(\text{SO}_4)_2 \cdot 6\text{H}_2\text{O}$ has also been analysed in order to see what difference dilution by magnesium instead of zinc ions would have on the spectra. The results are quoted here briefly. Maxima of splitting are obtained in the xz plane at $\psi = +60^\circ$ and 150° . These two directions are labelled K_A and K_B respectively, as the maxima are of nearly equal size (the separation between centres of extreme groups being 1087 and 1396 gauss respectively) and it is not possible to determine directly which is K_1 and which is K_2 .

Rotation in the K_3K_A plane gives a maximum splitting at an angle of 30° to K_A , and rotation in the K_3K_B plane gives a maximum splitting at an angle of 32° to K_B . The fact that in neither planes do the two spectra coincide and that the maximum splittings obtained are of the same order was found previously in the salt diluted with zinc, and shows that there must be a large rhombic component present. This is confirmed by the fact that the maximum separation obtained in the xy plane occurs at 35° to x and is only half that obtained in the other two planes through y . The different splittings along directions perpendicular to the axis are 627, 500 and 1087 gauss in the xy , K_BK_3 and xz planes respectively.

Table 2 gives the successive separations of the hyperfine groups along the maxima obtained in the $K_A K_3$ and $K_B K_3$ planes. From these and the perpendicular measurements one determines for the coefficients of the Hamiltonian,

Table 2

Plane	Separations of Groups			
$K_3 K_A$	471	403	434	489
$K_3 K_B$	505	497	481	502

in units of 10^{-4} cm^{-1} , $A=B=90$ [91], $D=231$ [243], $a=3$ [5], $E \simeq 60$. The figures in brackets are those for the similar salt diluted with zinc, and it is seen that the electronic splitting is slightly reduced in this case. The accuracies are to within ± 2 in the last digit for the constants A , B and D , but that of E is only about 20%.

University of Southampton.
14th February 1953.

D. J. E. INGRAM.

BLEANEY, B., and INGRAM, D. J. E., 1951, *Proc. Roy. Soc. A*, **205**, 336.

GROTH, P., 1910, *Chem. Kristallogr., Lpz.*, **3**, 69.

KUMAGAI, H., ONO, K., HAYASHI, I., and KAMBE, K., 1952, *Phys. Rev.*, **87**, 374.

PADMANABHAN, V. M., 1952, *Curr. Sci.*, **21**, 97.

The Nuclear Magnetic Moment of ^{57}Fe

The paramagnetic resonance spectrum of iron with the isotope ^{57}Fe enhanced to about 40% has been examined at 90°K , using ferric potassium selenate alum. A crystal, grown from heavy water, and containing 0.1% of iron (enhanced in ^{57}Fe) as an impurity in aluminium potassium selenate, gave a spectrum in which the half width at half intensity of the $M = +1/2 \rightarrow M = -1/2$ transition was 2.5 gauss. The differential of this line was plotted using a narrow band phase sensitive detector. Similar line shapes were obtained from five measurements, the maximum variation in shape being $\pm 4\%$ of the line width. A measurement on a similar crystal containing unenhanced iron (2.2% ^{57}Fe) gave the same line shape within the experimental error. The nuclear shell model suggests the value $3/2$ for the nuclear spin of ^{57}Fe and the spin is unlikely to exceed $5/2$. Therefore, using the line shape of the unenhanced iron, curves were constructed showing the expected line shape for the enhanced iron, assuming various hyperfine spacings and the values $1/2$, $3/2$ and $5/2$ for the spin. A comparison of these curves with the experimental line shape enabled an upper limit of six gauss to be set on the overall hyperfine structure of ^{57}Fe .

An estimate of an upper limit for the nuclear magnetic moment of ^{57}Fe may be obtained by comparison with the spectrum of the isoelectronic ion $(3d^5, ^6\text{S})\text{Mn}^{2+}$ (Bleaney and Ingram 1951). Abragam and Pryce (1951) have shown that the main cause of the hyperfine splitting in Mn^{2+} is the configurational interaction with a state in which a $3s$ electron has been promoted to a $4s$ state. This admixture produces a magnetic field at the nucleus which is found to be constant to within 20% in the hydrated salts of the ions V^{2+} , Mn^{2+} , Co^{2+} and Cu^{2+} . Using this empirical fact, Bleaney and Bowers (1951) estimated the nuclear

magnetic moment of ^{53}Cr by comparison with ^{51}V ; and a similar comparison may be made between ^{57}Fe and ^{55}Mn . The overall hyperfine structure splitting of the spectrum of $^{55}\text{Mn}^{2+}$ is about 500 gauss, and the nuclear magnetic moment is 3.47 nuclear magnetons (Sheriff and Williams 1951). Thus an upper limit of 0.05 nuclear magneton may be ascribed to the nuclear magnetic moment of ^{57}Fe .

Schawlow and Townes (1951) predict a nuclear magnetic moment of 0.66 nuclear magneton for ^{57}Fe . However, previous examinations of iron with the isotope 57 enhanced (Gurevitch and Teasdale 1949, Brossel 1949) have shown no structure, broadening or asymmetry of the optical spectral lines. An overall splitting greater than 0.025 cm^{-1} could have been detected, but no upper limit for μ was given.

The author wishes to record his gratitude to Dr. B. Bleaney for generous help and advice, and to the Electromagnetic Separator Group of the Atomic Energy Research Establishment, Harwell, who supplied the iron enhanced in ^{57}Fe .

Clarendon Laboratory,
Oxford.

R. S. TRENAM.

16th February 1953.

ABRAGAM, A., and PRYCE, M. H. L., 1951, *Proc. Roy. Soc. A*, **205**, 135.

BLEANEY, B., and BOWERS, K. D., 1951, *Proc. Phys. Soc. A*, **64**, 1135.

BLEANEY, B., and INGRAM, D. J. E., 1951, *Proc. Roy. Soc. A*, **205**, 336.

BROSSEL, J., 1949, *Phys. Rev.*, **76**, 858.

GUREVITCH, M., and TEASDALE, J. G., 1949, *Phys. Rev.*, **76**, 151.

SCHAWLOW, A. L., and TOWNES, C. H., 1951, *Phys. Rev.*, **82**, 268.

SHERIFF, R. E., and WILLIAMS, D., 1951, *Phys. Rev.*, **82**, 651.

Separation of the Intramolecular and Intermolecular Contributions to the Second Moment of the Nuclear Magnetic Resonance Spectrum

The evaluation of molecular structural parameters from the second moment (mean square width) of the nuclear magnetic resonance spectrum is sometimes impeded by a lack of exact knowledge of the crystal structure at the temperature at which the spectrum is measured. A knowledge of the crystal structure enables the intermolecular contribution to the second moment to be calculated, so that by difference from the measured second moment the intramolecular contribution may be found. The present note describes a method by which in certain cases the intramolecular contribution may be found without the necessity of knowing the crystal structure at all.

The method consists in measuring the second moment for two isotopic species of the same compound; in one species some of the nuclei at resonance are replaced by an isotope of much smaller magnetic moment. Thus in hydrogen compounds some of the protons may be replaced by deuterons. For convenience of discussion it will be assumed that we are in fact dealing with the proton resonance of a hydrogen compound, although the method is in principle capable of wider application. Suppose the second moment of the non-deuterated species is S_a and that of the partially deuterated species is S_b . Suppose also that the deuteration reduces the intramolecular contribution by a factor σ_1 (<1)

and the intermolecular contribution by a factor σ_2 . The intramolecular contribution s_1 for the non-deuterated species is therefore $(\sigma_2 S_a - S_b)/(\sigma_2 - \sigma_1)$. The successful evaluation of s_1 from the measured values of S_a and S_b thus requires that σ_1 and σ_2 be known and that $\sigma_2 - \sigma_1$ be as large as possible.

The method has been applied to benzene. Second moment measurements must be carried out below 100°K since it is known (Andrew 1950) that above this temperature the spectrum is modified by molecular reorientation within the crystal. The crystal structure of benzene has been determined by Cox (1932) at 251°K . In order to calculate the intermolecular contribution at 80°K , it is necessary to guess what contraction of unit cell dimensions accompanies the decrease in temperature from 251°K to 80°K . Since the thermal expansivity of solid benzene is rather large the calculation is subject to considerable uncertainty. This is particularly unfortunate since for this compound the intermolecular contribution is the greater contribution.

The second moment was therefore measured for pure samples of ordinary benzene C_6H_6 and 1.3.5 trideuterobenzene $\text{C}_6\text{H}_3\text{D}_3$. The alternation of protons and deuterons round the benzene ring results in a very small σ_1 . Assuming the hydrogen nuclei are located on the corners of a regular hexagon of side a , σ_1 is found by calculation to be 0.0354. On the other hand σ_2 is 0.5 since it may be assumed that the neighbour of a given proton on a given site in another molecule may equally well be either a proton or a deuteron. The mean value of nine determinations in the range 75 – 85°K of the rigid second moment S_a for C_6H_6 was 9.72 gauss^2 , and of eleven determinations of S_b for 1.3.5 $\text{C}_6\text{H}_3\text{D}_3$ was 3.39 gauss^2 after a small correction had been made for the contribution of the deuterons. The calculated probable error of both means was 0.07 gauss^2 . The intramolecular contribution s_1 for C_6H_6 was thus found to be $3.16 \pm 0.17 \text{ gauss}^2$. The only unknown molecular parameter is the hexagon side a , which was found from s_1 to be $2.487 \pm 0.022 \text{ \AA}$. The geometry of the molecule is such that this distance is the sum of the C–C bond length and the C–H bond length. Our value of this distance is in satisfactory agreement with estimates based on x-ray, electron diffraction and spectroscopic data.

Above 100°K the benzene molecules reorient themselves in the crystal lattice about their hexad axes with sufficient frequency to cause a reduction in the second moment (Andrew 1950). The axis of reorientation is thus perpendicular to the line joining every intramolecular nuclear pair. The contribution of each of these pairs to the second moment is thus reduced by the same factor. It follows then that deuteration should reduce the intramolecular contribution by the same factor σ_1 as in the rigid crystal lattice. σ_2 still has the value 0.5. The separation procedure can therefore also be applied to the spectra of the reorienting system of molecules with the same values of σ_1 and σ_2 .

The mean value of the second moment S_a for C_6H_6 above 130°K , where a steady value has again been reached, was found to be 1.61 gauss^2 ; for 1.3.5 $\text{C}_6\text{H}_3\text{D}_3$ S_b was found to be 0.41 gauss^2 . Hence using the formula given above the intramolecular contribution for the reorienting benzene molecule is found to be 0.85 gauss^2 , with a calculated probable error of 0.07 gauss^2 . The ratio of this reduced intramolecular contribution to the value for the rigid lattice is thus 0.27 ± 0.03 . Gutowsky and Pake (1950) have shown theoretically that if the angle between the axis of reorientation and each intramolecular nuclear pair is 90° , the ratio should be exactly 0.25. Thus, within the limits of experimental error, this reduction factor receives a direct confirmation.

The separation method described here is not restricted in application to benzene and may in principle be applied to all compounds in which all the protons of the non-deuterated molecule are equivalent. In such cases σ_2 can be evaluated directly by statistical argument. Thus, to quote a few examples, the method could be applied to ethylene, cyclopropane, *p*-dichlorobenzene and ammonia.

Full details of the second moment measurements of the benzenes will be published later, together with measurements of spin-lattice relaxation time between 80°K and the melting point, 278.5°K.

We wish to express our thanks to Professor D. H. Everett of University College, Dundee, who supplied the pure sample of C_6H_6 , and to Professor C. K. Ingold and Dr. H. G. Poole of University College, London, who lent us the pure sample of $1.3.5\ C_6H_3D_3$.

Department of Natural Philosophy,
The University,
St. Andrews, Scotland.
9th December 1952.

E. R. ANDREW.
R. G. EADES.

ANDREW, E. R., 1950, *J. Chem. Phys.*, **18**, 607.

COX, E. G., 1932, *Proc. Roy. Soc. A*, **135**, 491.

GUTOWSKY, H. S., and PAKE, G. E., 1950, *J. Chem. Phys.*, **18**, 162.

REVIEWS OF BOOKS

Sir James Jeans—a Biography, by the late E. A. MILNE, with a Memoir by S. C. ROBERTS. Pp. xvi+176. (Cambridge: University Press, 1952.) 21s.

To praise famous men is a pleasant thing, and the biography of James Jeans by the late E. A. Milne is a pleasant book to read. The reviewer in his present capacity praises two great men, for Milne has written a book in spirited, at times sprightly, style, most readable and, as becomes a biography, both revealing and informative.

No more suitable biographer than Professor Milne could have been chosen, for he was himself a great mathematical physicist and, like Jeans, was a reliable contributor to astronomy and astrophysics; moreover, the twain had on more than one occasion crossed swords and fought battles of moment in their time.

Long before Jeans became the interpreter of the Universe to the masses he was, of course, a distinguished scientist, a leader in the first rank, and the manner of his entry—or was it enticement?—into popular exposition is well outlined by Mr. S. C. Roberts of the Cambridge University Press, in a quite delightful 'Memoir' which, in the nature of a preface, precedes chapter 1 of the book.

This Memoir is packed with detail which reveals the man rather than the scientist in Jeans and no one reading these all too few seven pages can doubt that Mr. Roberts was the only man to write them. Jeans was so shy and retiring that few knew him or could pass, or have wished to pass, the barriers which extreme shyness raise. Many will learn for the first time the circumstances of his second romance in later life which led to his second happy marriage to Susi Hoch a young Viennese musician. A charming story well told.

Professor Milne in twelve well-arranged chapters told the story of Jeans' life: from the more personal angle in the first six chapters, and summarizing the contributions to knowledge in fascinating style in the second six.

Jeans was a precocious child, we are told, and could tell the time at the age of three and could read at four; he got full encouragement from his journalist father. The child factorized cab numbers, learned columns of mysterious logarithms by heart, was exercised prodigiously by perpetual motion and wrote a book (bound prophetically in light blue) entitled *Clocks*, by J. Jeans. It is interesting to learn that his contemporaries at Merchant Taylors' School were afterwards astonished at Jeans' vogue as a popular writer in view of his school reputation that "he could never see that anything needed explaining".

The chapter on Cambridge will interest all lovers of that great place of learning, reminding the reader of the old days of the Senior Wrangler and the amount of daily work—in Jeans' estimation—required to win the title!

He—with other distinguished names—took the first part of the Tripos in two years (1898) and after a further two years, interrupted by illness, took Part II.

A Smith's Prize came to him in 1901 for an essay entitled 'The Distribution of Molecular Energy'. Thus early did his genius proclaim itself and its trend.

In 1904 his famous book *Dynamical Theory of Gases* appeared—written incidentally during enforced leisure at sanatoria.

1905 saw publication of his definitive solution of the problem of the partition of energy between matter and radiation; his solution was in utter contradiction to experiment, and so led the way to the acceptance of Planck's quantum theory. Jeans' re-derivation of the Rayleigh formula revealed an error in the constant, so that the formula ($8\pi RT\lambda^{-4}d\lambda$) became known as the Rayleigh-Jeans formula.

Few know how it came about that Jeans went to Princeton in 1905. The manner of his going, the works he published while there and his marriage to a charming American woman have all been duly recounted in this very full biography.

It was during his four years in the States that Jeans, at the early age of 28, was elected a Fellow of the Royal Society, to the pleasure of his friends and the delight of the students, who lightly sang:

Here's to Jimmy Hopwood Jeans,
He tries to make us Math-Machines,
A young and brilliant F.R.S.,
That's going some, we all confess.

Returning to England, Jeans stayed in Cambridge for a few years as Stokes Lecturer but retired in 1912, and at Guildford rapidly made Physical History.

In 1914 appeared his famous Report on *Radiation and the Quantum Theory* (Physical Society) which, after the war, when people had time to read it, did much to establish the theory and help Bohr, in his unorthodoxy, to establish his epoch-making views. A number of pages are devoted to a quite fascinating summary of the Eddington-Jeans controversy—into which Milne himself entered—on the role of radiation pressure in star equilibrium. It is well worth reading. An important decade of Jeans' life was his ten years' tenure of the Secretaryship of the Royal Society, 1919-29, a most influential and time consuming post, but one which did not stop Jeans working and taking interest in atomicity and quanta

(Rouse Bell Lecture 1925) and in general cosmogony (Adams Prize Essay : Problems of Cosmogony and Stellar Dynamics (1919) and Astronomy and Cosmogony (1928)).

It is curious to reflect that this last work in 1928 was his last, or nearly his last, technical contribution, since its final chapter contained such striking sentences as the following, which arrested instantly Mr. Roberts' alert attention :—" Let us, however, reflect that mankind is at the very beginning of its existence ; on the astronomical time-scale it has lived for only a few brief moments and has only just begun to notice the cosmos outside itself. It is perhaps hardly likely to interpret its surroundings aright in the first few moments its eyes are open."

An exciting 'popular book' appeared in 1929, the famous *The Universe Around Us*, followed in 1930 by *The Mysterious Universe*, in the nature of a sequel—books which one hopes are still read ! They are products of a great mind which was no longer concerned with technical detail but preferred to stand back and survey what " he himself and others had accomplished and interpret it for the benefit of the intelligent non-specialist ".

Some 50 pages of the biography are devoted, very suitably, to sketches in " as non-technical language as possible of the topics to which Jeans, as a mathematical physicist, had, in his earlier, productive years, devoted himself ".

Suffice it to say that the biographer, with his special knowledge, has made a very good and entrancingly interesting job of it ! It would be a mistake to do more than mention the chapter headings : Rotating fluid masses, Star clusters, The equilibrium of the stars, and the last chapter entitled Jeans and Philosophy.

Professor Milne was never one to accept *ex cathedra* statements quiescently; his was a critical mind constantly in mesh, so that it is not surprising that the gently critical vein of some of his earlier pages should mount to something like a crescendo in this last chapter on Jeans' philosophy. There are few physicists and, I imagine, no theoretical or mathematical physicists who have never crossed that nebulous and exciting frontier between physics and philosophy. Most return as quickly as may be or say little of their thoughts or feelings. It was otherwise with Jeans, and also, in a different way, Milne. These are some of the things said in the last chapter of the biography : "... Jeans' use of philosophy is disappointing " ; " He never brought his critical powers to bear on the theory of relativity " ; " he wrote facilely of expanding space when it was the fashion . . . without enquiring what in the world this could mean " ; " he wrote of the nebulae as ' straws showing which way the streams of space were following ', a metaphor which, however poetical, is more calculated to darken counsel than to enlighten our minds " ; " his innate reverence for mathematics led him to consider the Creator of the Universe as in essence a mathematician ".

There is a most excellent bibliography, including all Jeans' published scientific papers, books and lectures, and a very helpful index.

No one reading this outstandingly well written biography can fail to have his attention gripped and his interests aroused. There is a good deal of criticism interspersed in its 166 pages, but it is nowhere so bitter as to call to the reader's mind *de mortuis nil nisi bonum*.

R. WHIDDINGTON.

CORRIGENDUM

Photoelectric Absorption in Lithium Vapour, by J. TUNSTEAD (*Proc. Phys. Soc. A*, 1953, **66**, 304).

P. 304. The present address of the author of this Research Note should have been given as the Royal Naval Scientific Service and *not* as the Physics Research Laboratory, University of Reading.

CONTENTS OF SECTION B

	PAGE
Mr. W. P. OSMOND. An Interpretation of the Magnetic Properties of some Iron-Oxide Powders: II	265
Dr. R. W. WRIGHT. Low Temperature Conduction in Extremely Degenerate Semiconductors	273
Mr. A. LEMPICKI. The Origin of Secondary Emission Electrons	278
Mr. A. LEMPICKI. The Electrical Conductivity of MgO Single Crystals at High Temperatures	281
Dr. W. W. H. CLARKE and Dr. L. JACOB. Some Characteristics of a Low Voltage Electron Immersion Objective	284
Mr. P. F. CHESTER and Dr. G. O. JONES. A Miniature Helium Liquefier-Cryostat of Cascade Type	296
Mr. B. W. MOTT and Mr. H. R. HAINES. The Effect of Strain in Objective Lenses used for Microscopical Examination of Metals under Polarized Light	302
Mr. R. P. WALDO LEWIS. The Reflection of Radio Waves from an Ionized Layer having both Vertical and Horizontal Ionization Gradients	308
Dr. A. CHARLESBY. Ionic Current and Film Growth of Thin Oxide Layers on Aluminium	317
Research Notes:	
Mr. J. B. GUNN. Radiative Transitions in Germanium	330
Dr. H. H. HOPKINS. A Note on the Theory of Phase-Contrast Images	331
Letters to the Editor:	
Mr. R. E. BURGESS. Contact Noise in Semiconductors	334
Reviews of Books	335
Contents of Section A	344



Fig. 1. Area of specimen examined. $\times 625$



Fig. 2. X-ray Laue photograph of volume of crystal containing bands, taken with a beam of 150μ diameter.

The Application of Kirkwood's Approximation to the Calculation of Intrinsic Magnetization

By R. H. TREDGOLD

University of Nottingham

Communicated by L. F. Bates; MS. received 9th December 1952

Abstract. The limitations of Opechowski's method of calculating the variation of intrinsic magnetization with temperature are pointed out. An alternative method, based on Kirkwood's treatment of crystallographic ordering, is proposed. It is shown that this method is equivalent to Heisenberg's treatment in the first and second approximations. The third approximation leads to two Curie temperatures which are separated by a smaller interval than in the case of the Heisenberg second approximation. This result is discussed in the light of previous work and the suggestion is put forward that a model in which the exchange interaction is limited to nearest neighbours is incapable of explaining the behaviour of the known ferromagnetic materials.

§ 1. INTRODUCTION

IN view of the remarkable empirical success of the molecular field treatment of ferromagnetism and ferrimagnetism (Néel 1948) it is surprising that a quantum-mechanical justification of this approach has not been forthcoming. The failure of Heisenberg's (1928) treatment of the problem when taken to the second approximation has been attributed to the arbitrary assumption of the gaussian distribution of energy states and it is therefore of interest to attempt to obtain higher approximations based on the same model.

That the application of the Heitler-London approach to solid state phenomena is somewhat artificial is only too apparent. On the other hand the collective electron treatment is unfortunately incapable of giving information as to the effective range of exchange forces.

§ 2. OPECHOWSKI'S TREATMENT OF THE PROBLEM

The essential physical assumptions involved in Heisenberg's first approximation are that $(\bar{\mathbf{S}}_i \cdot \mathbf{S}_j)$ for nearest neighbours (where $\mathbf{S}_i = \frac{1}{2}\boldsymbol{\sigma}_i$, the Pauli spin matrix, and the bar denotes the mean) is the same as $(\bar{\mathbf{S}}_i \cdot \mathbf{S}_j)$ for any two unpaired electrons chosen at random from the lattice and that only nearest neighbour interactions need be considered. The second approximation is an attempt to correct for the error implicit in the first of these assumptions. Higher order approximations have been calculated by Opechowski (1937) for the case of a face-centred cubic lattice having one unpaired electron per lattice site. When an error pointed out by Zehler (1950) has been taken into account, Opechowski's treatment appears to lead to the following conclusions. As successively higher approximations are employed the value of the Curie temperature (in terms of J/k , where J is the

exchange integral) predicted by the theory appears to converge towards a value given approximately by $T_c = 4.25J/k$. An examination of the final stage of the calculation indicates however that little significance can be attached to these results. The expression for the susceptibility above the Curie point is obtained in the form (Opechowski 1937, eqn. (54))

$$\chi t = 1 + \frac{6}{t} + \frac{30}{t^2} + \frac{138}{t^3} + \frac{1193}{t^4} \dots\dots(1)$$

Here t is the reduced temperature and is given by

$$t = kT/J \dots\dots(2)$$

The last term in (1) has since been revised by Zehler but this does not affect the present argument. To find the Curie temperature it is now necessary to find the value of t for which $\chi = \infty$. To do this Opechowski neglects the appropriate number of terms in (1) for the approximation under consideration and then inverts the resultant expression and expands to the highest power in $1/t$ previously retained. The expression for $1/\chi$ so obtained is equated to zero and a solution obtained for t . Since, however, the coefficients of the various powers of $1/t$ in (1) are all positive real constants it is quite evident that the right-hand side of (1) will remain finite for all positive real values of t . Hence the true solution of (1) for $\chi = \infty$ is $t=0$ irrespective of how many terms are taken into account. Thus even the claim made by Opechowski that the theory agrees with that of Heisenberg as far as the term in $1/t^2$ is ill-founded. Bearing this in mind the present writer has attempted to obtain an expression for χ which does not suffer from the defects pointed out above but which can, with sufficient labour, be evaluated to any desired degree of approximation.

§3. THE KIRKWOOD APPROXIMATION

The method used here is based on a method devised by Kirkwood (1938) for treating the problem of crystallographic ordering. The advantage of this method is that it leads directly to an expression for χ , the denominator of which is a polynomial in $1/T$. This denominator can then be equated to zero and solved for the Curie temperature.

It is assumed that there is one unpaired electron per lattice site and that the spin dependent energy of the crystal under consideration may be written

$$E = -2J \sum_{N,Z} \mathbf{S}_i \cdot \mathbf{S}_j \dots\dots(3)$$

where the summation is taken over all pairs of nearest neighbours. Here Z is the coordination number, N is the number of atoms in the crystal, J is the exchange integral and $\mathbf{S}_i = \frac{1}{2}\boldsymbol{\sigma}_i$ where $\boldsymbol{\sigma}_i$ is the Pauli vector matrix representing the spin of the electron located on the i th lattice site. Equation (3) may be written in the form

$$E(\rho) = -2J\rho \dots\dots(4)$$

where ρ is the reduced energy and is proportional to the amount of 'short range order' for the configuration under consideration.

It is assumed that the probability of the total spin of the crystal under consideration coinciding with the direction of an applied magnetic field is overwhelming as compared with the probability of other arrangements. Since

this assumption is implicit in Heisenberg's treatment of the problem it is convenient to introduce it at this stage. Thus for a particular overall crystalline spin having a quantum number S the partition function becomes

$$(PF)_S = \exp(2\beta HS/kT) \sum_{\rho} \omega(S, \rho) \exp x\rho \quad \dots\dots(5)$$

where β is the Bohr magneton, H is the applied magnetic field, $x=2J/KT$ and $\omega(s, \rho)$ is the statistical weight. This expression may be written:

$$(PF)_s = \exp(2\beta HS/KT) g(S) \sum_{\rho} \phi(\rho) \exp x\rho. \quad \dots\dots(6)$$

$$\text{Where} \quad g(S) = \frac{N!}{(\frac{1}{2}N+S)! (\frac{1}{2}N-S)!} \quad \dots\dots(7)$$

$$\text{and} \quad \sum_{\rho} \phi(\rho) = 1. \quad \dots\dots(8)$$

$$\text{Now put} \quad \sum_{\rho} \phi(\rho) \exp x\rho = \exp \left(\sum_{r=0}^{\infty} \lambda_r x^r / r! \right). \quad \dots\dots(9)$$

It may then be shown that the λ 's can be expressed in terms of the moments of the reduced energy ρ . The K th moment is defined as

$$M_K = \sum_{\rho} \rho^K \phi(\rho) \quad \dots\dots(10)$$

and is the mean K th power of the reduced energy for all states characterized by the quantum number S . It is possible to obtain a general relationship between the λ 's and the moments (see Kirkwood 1938) but for the present purposes only the first few λ 's are required.

$$\left. \begin{aligned} \lambda_0 &= 1 \\ \lambda_1 &= M_1 \\ \lambda_2 &= M_2 - M_1^2 \\ \lambda_3 &= M_3 - 3M_1M_2 + 2M_1^3. \end{aligned} \right\} \quad \dots\dots(11)$$

Thus using (6) and the relation

$$F = -kT \log (PF) \quad \dots\dots(12)$$

where F is the configurational free energy, we have

$$-\frac{F}{kT} = \log g(s) + \sum_{r=0}^{\infty} \frac{\lambda_r x^r}{r!} + \frac{2\beta HS}{kT} \quad \dots\dots(13)$$

$g(S)$ being defined by (7).

We now make use of Stirling's formula for large factorials, differentiate with respect to S and equate to zero to find the equilibrium value of S . We then arrive, on rearrangement, at the pair of equations

$$I = \frac{2S}{N} = \tanh y, \quad y = \frac{1}{2} \frac{\partial}{\partial S} \sum_{r=0}^{\infty} \frac{\lambda_r x^r}{r!} + \frac{BH}{kT} \quad \dots\dots(14)$$

where I is the relative intrinsic magnetization. The problem is then reduced to the evaluation of the moments as functions of S . These may be obtained in a convenient form to a very good degree of approximation if it is assumed that N is very large. Bearing in mind the number of atoms known to be involved in one ferromagnetic domain (of the order of 10^{16}) this appears to be a reasonable assumption.

§ 4. THE CALCULATION OF THE MOMENTS

The essential difference between the method used here and the one employed by Opechowski is that in the present method it is the *a priori* moments which are calculated whereas in his method the 'Boltzmann weighted' moments are used.

The method of evaluating the moments is based on the technique employed by Van Vleck (1932) in his treatment of Heisenberg's theory of ferromagnetism. From (3) and (4)

$$\rho = \sum_{N, Z} \mathbf{S}_i \cdot \mathbf{S}_j. \quad \dots\dots(15)$$

It is required to find $\bar{\rho}$, $\bar{\rho}^2$, $\bar{\rho}^3$ (the bar denoting the mean values) in terms of S . To do this it is necessary to find the mean values of such typical terms as $(\mathbf{S}_i \cdot \mathbf{S}_j)$, $(\mathbf{S}_i \cdot \mathbf{S}_j)(\mathbf{S}_i \cdot \mathbf{S}_k)$ etc. obtained on raising ρ to the first, second or third powers and to count the number of times each such term appears in the moment under consideration.

It is not proposed to give the derivation of the first and second moments as these have been given in full by Van Vleck (1932). The derivation of the third moment follows exactly the same method and is given in the Appendix. (The case considered is that of the face-centred cubic lattice having one unpaired electron per lattice site.) Substituting the values obtained for the moments into (11) and neglecting terms which do not increase with the first power of N or S , since these will not contribute to the final result, we arrive at the following expression for the λ 's:

$$\left. \begin{aligned} \lambda_0 &= 1 \\ \lambda_1 &= \frac{S^2 Z}{2N} \\ \lambda_2 &= \left[\frac{3N}{32} - \frac{S^2}{2N} + \frac{S^4}{2N^3} \right] Z \\ \lambda_3 &= \left[-\frac{272}{N^5} S^6 + \frac{5}{4} \frac{S^4}{N^3} - \frac{3}{4N} S^2 \right] Z \end{aligned} \right\} \quad \dots\dots(16)$$

where $Z = 12$.

Substituting these values into (14) and writing $2S/N = I$ and $JZ/KT = \gamma$ we arrive at the equations for the magnetization:

$$I = \tanh y$$

$$y = \frac{BH}{kT} + \frac{\gamma I}{2} + \gamma^2 \left[-\frac{I}{24} + \frac{I^2}{48} \right] + \gamma^3 \left[-\frac{I}{288} + \frac{5I^3}{1728} - \frac{17I^5}{72} \right] \dots\dots(17)$$

The terms in γ and γ^2 are identical respectively with the terms of the first and second approximations of the Heisenberg theory for the case $Z = 12$. To determine the Curie temperature we require the expression for the susceptibility above the Curie point. Since in this region I and hence y are both much less than one we can write $I = \tanh y \simeq y$ and retain only the terms in the first power of I in (17). Hence in this region

$$I = \frac{\beta H}{kT} + \frac{\gamma I}{2} - \frac{\gamma^2 I}{24} - \frac{\gamma^3 I}{288}, \quad \dots\dots(18)$$

giving for the susceptibility per atom

$$\chi = \frac{\beta^2}{kT} / \left(1 - \frac{\gamma}{2} + \frac{\gamma^2}{24} + \frac{\gamma^3}{288} \right). \quad \dots\dots(19)$$

Equating the denominator of the right-hand side of (19) to zero and solving for γ the reduced Curie temperature is obtained.

For the three approximations we have:

- (1) $\gamma_c = 2$, Heisenberg's first approximation.
- (2) $\gamma_c = 6 \pm \sqrt{12}$, Heisenberg's second approximation.
- (3) $\gamma_c = 2.816, 5.192$.

Thus to this degree of approximation the model in question fails to predict ferromagnetism.

§ 5. DISCUSSION

In view of the fact that the more exact methods of Bloch (1930) and Weiss (1948), which are, however, applicable to limited temperature ranges only, predict behaviour which in the low and high temperature regions respectively is in reasonable agreement with the observed behaviour of actual materials, it seems evident that the present treatment would lead to better agreement if taken to a sufficiently high approximation. Nevertheless the fact that the first approximation gives very good agreement with experimental results, the second approximation gives poor agreement, and the agreement in the case of the third approximation is even worse seems to indicate that this model would never lead to anything approaching the agreement with observation obtained from the molecular field hypothesis.

It is to be noted that in the limiting case of every electron having an equal exchange interaction with every other electron in the crystal the molecular field treatment would be reproduced exactly. Therefore in order to obtain agreement with experimental results it is necessary to invoke some mechanism which will allow each electron to interact with a far larger number of other electrons than are provided by the crystallographic nearest neighbours. That this number should not be as great as the total numbers of unpaired electrons in the crystal seems evident since this result would not be arrived at even from the collective electron approach if the correlation correction was taken into account. Moreover, Néel (1934) using an approximation based on the Ising model (wherein the off-diagonal elements of the spin matrices are ignored) has shown that the interaction of each electron with 750 'magnetic nearest neighbours' together with a weaker long range interaction would account very well for observed phenomena in the case of nickel. Although, as Néel himself has pointed out, the number 750 should only be taken as an order of magnitude, these results together with those of the present work seem to indicate that nearest neighbour interactions alone are incapable of explaining the behaviour of known ferromagnetic materials.

An examination of a model involving a compromise between the Heitler-London and collective electron treatments is now being made and it is hoped to publish the results at a later date.

APPENDIX

The Calculation of the Third Moment

On cubing the right-hand side of (15) it is found that eight different kinds of terms are obtained. These have different mean values. These terms, their mean values and the number of times each term appears in M_3 are listed in

table 1 (for the method of obtaining the number of times each term appears see Opechowski 1937).

With the exception of the term $(\mathbf{S}_i \cdot \mathbf{S}_j)(\mathbf{S}_k \cdot \mathbf{S}_l)(\mathbf{S}_p \cdot \mathbf{S}_q)$ all the terms may be expressed as functions of

$$\overline{(\mathbf{S}_i \cdot \mathbf{S}_j)} = \alpha, \quad \overline{(\mathbf{S}_i \cdot \mathbf{S}_j)(\mathbf{S}_p \cdot \mathbf{S}_q)} = \beta. \quad \dots\dots (A 1)$$

These terms may be expressed as functions of S (see Van Vleck 1932) as follows:

$$\begin{aligned} \overline{(\mathbf{S}_i \cdot \mathbf{S}_j)} &= \alpha = \frac{S^2}{N^2} \\ \overline{(\mathbf{S}_i \cdot \mathbf{S}_j)(\mathbf{S}_p \cdot \mathbf{S}_q)} &= \beta = \alpha^2 \left[1 + \frac{4}{N} + \frac{1}{N^2} - \frac{6}{N^3} + \dots \right] \\ &\quad + \alpha \left[-\frac{1}{N} - \frac{2}{N^2} + \frac{5}{N^3} + \dots \right] \\ &\quad - \frac{3}{8} \left[\frac{1}{N^2} + \frac{5}{N^3} + \dots \right] \quad \dots\dots (A 2) \end{aligned}$$

neglecting higher order terms in $1/N$.

Table 1

Typical Term	Number of Occurrences in M_3	Mean Value
$(\mathbf{S}_i \cdot \mathbf{S}_j)^3$	$\frac{ZN}{2}$	$\frac{7\alpha}{16} - \frac{3}{32}$
$(\mathbf{S}_i \cdot \mathbf{S}_j)^2 (\mathbf{S}_i \cdot \mathbf{S}_k)$	$33ZN$	$\frac{\alpha}{16}$
$(\mathbf{S}_i \cdot \mathbf{S}_j)^2 (\mathbf{S}_p \cdot \mathbf{S}_q)$	$-\frac{69NZ}{2} + \frac{3N^2Z^2}{4}$	$\frac{3\alpha}{16} - \frac{\beta}{2}$
$(\mathbf{S}_i \cdot \mathbf{S}_j) (\mathbf{S}_j \cdot \mathbf{S}_k) (\mathbf{S}_k \cdot \mathbf{S}_i)$	$4ZN$	$\frac{3}{64} - \frac{\alpha}{8}$
$(\mathbf{S}_i \cdot \mathbf{S}_j) (\mathbf{S}_i \cdot \mathbf{S}_k) (\mathbf{S}_i \cdot \mathbf{S}_l)$	$110ZN$	$\frac{1}{4}\beta$
$(\mathbf{S}_i \cdot \mathbf{S}_j) (\mathbf{S}_i \cdot \mathbf{S}_k) (\mathbf{S}_k \cdot \mathbf{S}_l)$	$351ZN$	$\frac{\alpha}{16}$
$(\mathbf{S}_i \cdot \mathbf{S}_j) (\mathbf{S}_i \cdot \mathbf{S}_k) (\mathbf{S}_p \cdot \mathbf{S}_q)$	$-1110ZN + \frac{1}{2} \cdot 33Z^2N^2$	$\frac{1}{4}\beta$
$(\mathbf{S}_i \cdot \mathbf{S}_j) (\mathbf{S}_k \cdot \mathbf{S}_l) (\mathbf{S}_p \cdot \mathbf{S}_q)$	$646ZN - \frac{69Z^2N^2}{4} + \frac{Z^3N^3}{8}$	See text

Three further relations, which are readily obtained from the properties of the spin matrices, are required.

$$(\mathbf{S}_i \cdot \mathbf{S}_j)^2 + \frac{(\mathbf{S}_i \cdot \mathbf{S}_j)}{2} - \frac{3}{16} = 0 \quad \dots\dots (A 3)$$

$$[(\mathbf{S}_i \cdot \mathbf{S}_j) + (\mathbf{S}_j \cdot \mathbf{S}_k) + (\mathbf{S}_k \cdot \mathbf{S}_i)]^2 = \frac{9}{16} \quad \dots\dots (A 4)$$

$$4(\mathbf{S}_i \cdot \mathbf{S}_j)(\mathbf{S}_i \cdot \mathbf{S}_k) + 4(\mathbf{S}_i \cdot \mathbf{S}_k)(\mathbf{S}_i \cdot \mathbf{S}_j) = (\mathbf{S}_j \cdot \mathbf{S}_k) + (\mathbf{S}_k \cdot \mathbf{S}_j). \quad \dots\dots (A 5)$$

We now multiply (A 3) by $(\mathbf{S}_i \cdot \mathbf{S}_j)$, $(\mathbf{S}_i \cdot \mathbf{S}_k)$ and $(\mathbf{S}_p \cdot \mathbf{S}_q)$ in turn. On taking mean values we obtain the first three terms listed in table 1. In a similar manner we multiply (A 4) by $(\mathbf{S}_i \cdot \mathbf{S}_j)$, $(\mathbf{S}_p \cdot \mathbf{S}_q)$ and $(\mathbf{S}_i \cdot \mathbf{S}_q)$ and (A 5) by $(\mathbf{S}_i \cdot \mathbf{S}_l)$. On taking

mean values, collecting similar terms and using the values of the first three terms the next four terms may be obtained.

Unfortunately it is not possible to evaluate the term $(\mathbf{S}_i \cdot \mathbf{S}_j)(\mathbf{S}_k \cdot \mathbf{S}_l)(\mathbf{S}_p \cdot \mathbf{S}_q)$ by any direct means.

To obtain this term we note that

$$\left[\sum_{\text{whole crystal}} (\mathbf{S}_i \cdot \mathbf{S}_j) \right]^3 = [S(S+1) - \frac{3}{4}N]^3. \quad \dots\dots (A6)$$

The mean values of the terms obtained by expanding the left-hand side of this equation are all known with the exception of $(\mathbf{S}_i \cdot \mathbf{S}_j)(\mathbf{S}_k \cdot \mathbf{S}_l)(\mathbf{S}_p \cdot \mathbf{S}_q)$. On counting the number of times the various terms appear it is thus possible to obtain the value of this particular term. These numbers are listed in table 2.

Table 2

Typical Term	Number of Occurrences in $[\sum (\mathbf{S}_i \cdot \mathbf{S}_j)]^3$
$(\mathbf{S}_i \cdot \mathbf{S}_j)^3$	$4N(N-1)$
$(\mathbf{S}_i \cdot \mathbf{S}_j)^2 (\mathbf{S}_j \cdot \mathbf{S}_k)$	$24N(N-1)(N-2)$
$(\mathbf{S}_i \cdot \mathbf{S}_j)^2 (\mathbf{S}_p \cdot \mathbf{S}_q)$	$6N(N-1)(N-2)(N-3)$
$(\mathbf{S}_i \cdot \mathbf{S}_j) (\mathbf{S}_j \cdot \mathbf{S}_k) (\mathbf{S}_k \cdot \mathbf{S}_i)$	$8N(N-1)(N-2)$
$(\mathbf{S}_i \cdot \mathbf{S}_j) (\mathbf{S}_i \cdot \mathbf{S}_k) (\mathbf{S}_i \cdot \mathbf{S}_l)$	$8N(N-1)(N-2)(N-3)$
$(\mathbf{S}_i \cdot \mathbf{S}_j) (\mathbf{S}_i \cdot \mathbf{S}_k) (\mathbf{S}_k \cdot \mathbf{S}_l)$	$24N(N-1)(N-2)(N-3)$
$(\mathbf{S}_i \cdot \mathbf{S}_j) (\mathbf{S}_i \cdot \mathbf{S}_k) (\mathbf{S}_p \cdot \mathbf{S}_q)$	$12N(N-1)(N-2)(N-3)(N-4)$
$(\mathbf{S}_i \cdot \mathbf{S}_j) (\mathbf{S}_k \cdot \mathbf{S}_l) (\mathbf{S}_p \cdot \mathbf{S}_q)$	$N(N-1)(N-2)(N-3)(N-4)(N-5)$

Using the information listed in the two tables together with the values of the first and second moments it is now a straightforward though somewhat laborious task to obtain the value of λ_3 to the degree of approximation discussed in the main part of this paper.

REFERENCES

- BLOCH, F., 1930, *Z. Phys.*, **61**, 206.
 HEISENBERG, W., 1928, *Z. Phys.*, **49**, 619.
 KIRKWOOD, J. G., 1938, *J. Chem. Phys.*, **6**, 70.
 NÉEL, L., 1934, *J. Phys. Radium*, **5**, 104; 1948, *Ann. Phys., Paris*, **3**, 137.
 OPECHOWSKI, W., 1937, *Physica* **4**, 181.
 VAN VLECK, J. H., 1932, *The Theory of Electric and Magnetic Susceptibilities* (Oxford: University Press), p. 316-343.
 WEISS, P. R., 1948, *Phys. Rev.*, **74**, 1493.
 ZEHLER, V., 1950, *Z. Naturforsch.*, **5a**, 344.

The Scattering of Fast Positrons by Nuclei

BY L. R. B. ELTON AND K. PARKER

Wheatstone Department of Physics, King's College, London

Communicated by H. S. W. Massey; MS. received 24th October 1952

Abstract. It is shown that the effects of finite nuclear size and radiative correction cause considerable modifications to the Mott formula for the cross sections. An exact calculation of the phase shifts is carried through for a simple nuclear model and 20 mev positrons scattered by gold nuclei. Two approximate phase shift calculations are made and the singularity occurring in the radial wave equation is investigated. The radiative correction for scattering from light nuclei is found to be the same as for electron scattering.

§1. INTRODUCTION

THE object of this paper is to investigate the effects of finite nuclear size and radiative correction on the scattering of very high energy positrons by atomic nuclei. All the experimental investigations so far have been at comparatively low energies (less than 2 mev), and at those energies the results of Lasich (1948), Howatson and Atkinson (1951), Lipkin (1952), Cusack (1952) and Roy and Groven (1952) give fair agreement with the theory of Massey (1942) for point nuclei. At high energies the calculations of Yadav (1952) and Feshbach (1952) give results for point nuclei. Since positron beams of high energy will probably soon be available, it is important now to investigate the effects of finite nuclear size and of the radiative correction, which at the lower energies are negligible. These effects may be expected to furnish information on charge distribution within the nucleus and to indicate a possible experimental test of the new quantum electrodynamics, especially if the results are combined with similar results for electron scattering.

The scattering of fast electrons has been investigated experimentally at 15.7 mev by Lyman, Hanson and Scott (1951) who obtained fair agreement with the theoretical work, in which the effect of finite nuclear size has been considered by Rose (1948, 1951), Elton (1950), Parzen (1950b), Acheson (1951) and Feshbach (1951), and that due to the radiative correction by Schwinger (1949). Here we use methods similar to those developed for electrons by Elton (1950), Elton and Robertson (1952) and Elton (1952). These papers will be referred to as I, II and III respectively and the notation used in them will be followed here.

§2. THE PHASE SHIFT

(i) *Exact Calculation*

The magnitude of the effect of nuclear structure on the scattering can be obtained from a calculation of the phase shifts. The treatment is similar to that of I for electrons. It is shown there that for electrons of energy $40 mc^2$

scattered by gold nuclei only the first phase shifts, i.e. ζ_0 and ζ_{-2} , are significant and that $\zeta_0 \simeq \zeta_{-2}$. This latter fact has been proved to be true quite generally at high energies by Feshbach (1951). For positrons, for which the potential is repulsive, the effect of the finite nucleus is certainly smaller and is, therefore, given entirely by ζ_0 and ζ_{-2} , and ζ_0 can be taken equal to ζ_{-2} . This means that, in the notation of I, β and ν can in general be replaced by α and μ .

The present calculation was carried out for positrons of total energy $W = 40 \text{ mc}^2$ scattered by gold nuclei, on the assumption that the charge is distributed uniformly over the surface of the nucleus (model C of I). Following I, we have to solve the equation

$$\frac{d^2 \mathcal{S}_n}{dr^2} - f_n(r) \mathcal{S}_n = 0, \quad \dots\dots(2.1)$$

where
$$f_n(r) = -\alpha\beta + \frac{n(n+1)}{r^2} - \frac{n+1}{r} \frac{\alpha'}{\alpha} + \frac{3}{4} \frac{\alpha'^2}{\alpha^2} - \frac{1}{2} \frac{\alpha''}{\alpha}$$

and $\mu = (W + \text{mc}^2)/\hbar c$, $\nu = (W - \text{mc}^2)/\hbar c$, $\lambda = Ze^2/\hbar c$, $\alpha = \mu - \lambda/r$, $\beta = \nu - \lambda/r$. For the electron case the regular and irregular solutions, \mathcal{G}_0 and \mathcal{H}_0 respectively, may be computed by solving the differential equation (2.1) numerically, i.e. by expanding the solutions about the origin and extending them outwards by means of a differencing method. This is impossible in the present case, because of the existence of a singularity lying inside the nuclear radius and given by $\alpha = 0$. However, following Mott and Massey (1949 a), we have

$$\begin{aligned} \mathcal{G}_n = \alpha^{-1/2} N_n (2kr)^{\rho_{n+1}} e^{-i\gamma} \{ (n+1-i\gamma') F(-i\gamma + \rho_{n+1} + 1, 2\rho_{n+1} + 1, 2ikr) \\ + (\rho_{n+1} + i\gamma) F(\rho_{n+1} - i\gamma, 2\rho_{n+1} + 1, 2ikr) \}, \quad \dots\dots(2.2) \end{aligned}$$

where
$$N_n = \frac{1}{2} \frac{|\Gamma(\rho_{n+1} + 1 - i\gamma)|}{\Gamma(2\rho_{n+1} + 1)} e^{-\pi\gamma/2} \{(-i\gamma' + n + 1)(\rho_{n+1} + i\gamma)\}^{-1/2},$$

$$\rho_n = (n^2 - \lambda^2)^{1/2}, \quad \gamma = Ze^2/\hbar v, \quad \gamma' = \gamma(1 - v^2/c^2)^{1/2}, \quad k = (\mu\nu)^{1/2}$$

and v is the velocity of the positron. \mathcal{H}_n is obtained from \mathcal{G}_n by replacing ρ_{n+1} by $-\rho_{n+1}$ throughout. Hence \mathcal{G}_0 and \mathcal{H}_0 were evaluated by direct summation of the hypergeometric series at the nuclear radius $r = R$. The values of \mathcal{G}_0 and \mathcal{H}_0 were checked by (a) substitution of the hypergeometric functions in their corresponding hypergeometric equations and (b) calculation of $\mathcal{G}_0''(R)$ and $\mathcal{H}_0''(R)$ and substitution in (2.1).

The numerical value of the phase shift thus obtained was $\zeta_0 = 0.024$, while the phase for the case of the point nucleus was $\eta_0^A = 0.160$.

(ii) Variational Method

As a first check on the calculation an approximate evaluation of ζ_0 was made by a variational method due to Parzen (1950 a). The second radial function \mathcal{R}_n satisfies the equations

$$\left. \begin{aligned} \mathcal{R}_n &= \frac{1}{\alpha} \left(\frac{n+1}{r} \mathcal{S}_n - \frac{1}{2} \frac{\alpha'}{\alpha} \mathcal{S}_n - \mathcal{S}_n' \right), \\ \mathcal{S}_n &= \frac{1}{\beta} \left(\frac{n+1}{r} \mathcal{R}_n + \frac{1}{2} \frac{\alpha'}{\alpha} \mathcal{R}_n + \mathcal{R}_n' \right). \end{aligned} \right\} \quad \dots\dots(2.3)$$

Here of course we have more generally $\alpha = \mu - V(r)/\hbar c$ and $\beta = \nu - V(r)/\hbar c$.

Parzen's notation differs from that followed here, but his method is essentially to consider the variation of the integral

$$I = \frac{\mu}{k} \int_0^\infty \alpha \left\{ \mathcal{S}_n \left[-\beta \mathcal{S}_n + \mathcal{R}_n' + \frac{1}{2} \frac{\alpha'}{\alpha} \mathcal{R}_n + \frac{n+1}{r} \mathcal{R}_n \right] - \mathcal{R}_n \left[\alpha \mathcal{R}_n + \mathcal{S}_n' + \frac{1}{2} \frac{\alpha'}{\alpha} \mathcal{S}_n - \frac{n+1}{r} \mathcal{S}_n \right] \right\} dr, \dots (2.4)$$

which leads to the approximation to the phase

$$\eta_n - \eta_t \simeq - \frac{1}{k\hbar} \int_0^\infty (V - V_t) \left(\frac{\alpha_t \mu^2}{\nu} \mathcal{R}_t^2 + \alpha_t \nu \mathcal{S}_t^2 \right) dr, \dots (2.5)$$

where η_n is the true phase due to the potential V and η_t is the phase due to a trial potential V_t with radial wave functions \mathcal{R}_t and \mathcal{S}_t . In order to get an approximation to ζ_0 we take V_t to be the potential for the extended nucleus and V that for the point nucleus. Thus

$$\zeta_0 \simeq \frac{1}{k\hbar} \int_0^R \left(\frac{Ze^2}{r} - \frac{Ze^2}{R} \right) \left(\frac{\alpha_t \mu^2}{\nu} \mathcal{R}_t^2 + \alpha_t \nu \mathcal{S}_t^2 \right) dr, \dots (2.6)$$

since outside the nuclear radius the potentials V and V_t are identical. Here \mathcal{R}_t and \mathcal{S}_t are the regular solutions for the extended nucleus. Solving the radial equations for this case we find

$$\mathcal{S}_t = A \sin \kappa r, \quad \mathcal{R}_t = A(\sin \kappa r - \kappa r \cos \kappa r)/\alpha_t r$$

where $\kappa^2 = (\mu - \lambda/R)(\nu - \lambda/R)$ and A is a normalizing factor which ensures that \mathcal{R}_t and \mathcal{S}_t have the correct asymptotic form. It is obtained in the course of the numerical calculations in §2(i). After simplification we find

$$\zeta_0 \simeq \frac{2A^2 \lambda \mu^2 \kappa^2}{k\nu \alpha_t} \int_0^{2\kappa R} \left(\frac{1}{x} - \frac{1}{2\kappa R} \right) \left\{ \frac{1 - \cos x - x \sin x}{x^2} + \frac{1}{4}(1 + \cos x) + \frac{\nu^2 \alpha_t^2}{4\mu^2 \kappa^2} (1 - \cos x) \right\} dx. \dots (2.7)$$

This integral was evaluated by taking the integral between ϵ and $2\kappa R$ and letting $\epsilon \rightarrow 0$, using the formula (Magnus and Oberhettinger 1948)

$$\text{Ci}(x) = \int_\infty^x \frac{\cos y}{y} dy = C + \ln x + O(x^2), \dots (2.8)$$

valid for x small and positive; C is Euler's constant. The value obtained was $\zeta_0 = 0.026$, which checks very satisfactorily with the exact calculation, although this method cannot be relied upon to give such good agreement on all occasions, as is shown by the results of Parzen (1950 a).

(iii) *Perturbed Wave Method*

Another method for evaluating ζ_0 is the perturbed wave method developed in III. This has to be modified in the present case because of the singularity at $r = \lambda/\mu = a$, say. It is first necessary to solve the equation

$$y'' + 2py' + qy = f. \dots (2.9)$$

The procedure is analogous to that of Mott and Massey (1949b). If y_1 and y_2 are two independent solutions of eqn. (2.9) with $f=0$, and if $P=\exp\{[p\,dx]\}$, then the general solution of (2.9) is

$$y=y_1\int_{C_1}^z P^2y_2f\,dz-y_2\int_{C_2}^z P^2y_1f\,dz, \quad \dots\dots(2.10)$$

where y_1 and y_2 are so normalized that

$$P^2(y_2y_1'-y_1y_2')=1, \quad \dots\dots(2.11)$$

which is always possible; C_1 and C_2 are any contours in the complex plane which do not pass through any point at which the integrand has a singularity.

We next investigate the behaviour of the functions G_0 and H_0 at the singularity $r=a$. We must use these functions since the corresponding functions \mathcal{G}_0 and \mathcal{H}_0 are clearly infinite at the singularity. For that purpose we transform the equation satisfied by G_0 and H_0 , (I(7)),

$$S''+\left(\frac{2}{r}-\frac{\alpha'}{\alpha}\right)S'+\alpha^2S=0, \quad \dots\dots(2.12)$$

by putting $s=r-a$ and solve it by putting $S=s^\sigma\sum c_n s^n$.

The general solution is then

$$S=c_0\left(1-\frac{\mu^2}{8a^2}s^4+\dots\right)+c_2s^2\left(1-\frac{2s}{a}+\frac{3s^2}{a^2}-\dots\right). \quad \dots\dots(2.13)$$

Thus all solutions of (2.12) are finite and have zero derivatives at the singularity $r=a$. It can easily be shown that the expansion (2.13) is valid for $|s|<a$. A good approximation to (2.13) can be obtained by neglecting terms involving μ^2 , since the coefficients of these terms will be small. For $|s|\ll a$ the expression then reduces to

$$S\simeq c_0+c_2a^2s^2/(s+a)^2. \quad \dots\dots(2.14)$$

It is now possible to find G_0 and H_0 in the form (2.14) by evaluating them and their second derivatives exactly, using (2.2), for $r=a$. These expressions can then be compared with the expansions for G_0 and H_0 , when expanded about $r=0$, the latter expansions being obtained with slight modifications from I, §3 (iii). This gives a valuable check.

We now want to find the general solution of the inhomogeneous equation

$$K_0''+\left(\frac{2}{r}-\frac{\alpha'}{\alpha}\right)K_0'+\alpha^2K_0=F, \quad \dots\dots(2.15)$$

where $F=-(\alpha'/\alpha)K_0'+(\alpha^2-\kappa^2)K_0$ for $r<R$, and $F=0$ for $r>R$. Using (2.10), this solution is

$$K_0=S_1\int_{C_1}^z\frac{z^2}{\alpha}S_2F\,dz-S_2\int_{C_2}^z\frac{z^2}{\alpha}S_1F\,dz, \quad \dots\dots(2.16)$$

where S_1 and S_2 are linearly independent solutions of (2.12) that obey the normalization condition (2.11). They are chosen so that when $z=0$, $zS_1=0$, and when $\text{Re}(z)=r\rightarrow\infty$, $\text{Im}(z)\rightarrow 0$,

$$S_1\rightarrow(1/r)\sin(kr+\gamma\ln 2kr+\eta_0), \quad S_2\rightarrow(\mu/kr)\exp\{i(kr+\gamma\ln 2kr+\eta_0)\};$$

i.e. $S_1=G_0$. Further, K_0 satisfies the boundary conditions $zK_0=0$ when $z=0$; $K_0\rightarrow\text{const.}(kr)^{-1}\exp\{i(kr+\gamma\ln 2kr)\}$, when $\text{Re}(z)=r\rightarrow\infty$, $\text{Im}(z)\rightarrow 0$.

Therefore C_2 must start at the origin and C_1 must start at $+\infty$ on the real axis. In that case, when $\text{Re}(z)=r \rightarrow \infty$, $\text{Im}(z) \rightarrow 0$,

$$K_0 \rightarrow -\frac{1}{kr} \exp \{i(kr + \gamma \ln 2kr + \eta_0)\} \int_{C_1}^{\infty} \frac{z^2}{\alpha} G_0 F dz.$$

C_2 is now further restricted by the requirement that the integral must be real. This is necessary since, in the same way as in III, it follows that

$$\sin \zeta_0 = -\frac{\mu}{k} \int_{C_1}^{\infty} \frac{z^2}{\alpha} G_0 F dz, \quad \dots\dots(2.17)$$

and the phase shift must be real for elastic collisions. Now G_0 , K_0 and K_0' are finite at the singular point, and hence the integrand has a second order pole there. Clearly C_2 is given by either of the two basic paths C_2' or C_2'' , which run along the real axis from 0 to ∞ and go round the singularity in a semicircle either above or below the axis. If the average over the two paths is taken, the imaginary contributions arising from the residue at the singularity cancel. Thus the reality requirement determines the integral uniquely, i.e.

$$\sin \zeta_0 = -\frac{\mu}{2k} \int_{C_1' + C_1''} \frac{z^2}{\alpha} G_0 F dz. \quad \dots\dots(2.18)$$

An approximate formula for ζ_0 is obtained by replacing K_0 in F by G_0 . The integral cannot be evaluated numerically because of the existence of the singularity, but if the closed formula (2.14) is used for G_0 in the neighbourhood of $r=a$, then the integral can be evaluated algebraically in the usual way, the existence of the singularity being simply ignored.

It is not to be expected that this approximation should be very good, since in fact two approximations have been made and, furthermore, over the most important part of the range of integration $G_0' > 0$, while $K_0' < 0$. However, if (2.14) is used for the range $a-R < s < R-a$ (this range is really rather too large for the approximation (2.14) to be good) and a numerical method is used for the remaining range, (2.18) gives $\zeta_0 = 0.020$, which gives a good check on the exact calculation, while the approximate formula obtained by replacing K_0 by G_0 gives $\zeta_0 = 0.0015$.

§ 3. THE DIFFERENTIAL CROSS SECTION

(i) Method of Calculation

In calculating the differential cross section use was made of the results of Feshbach (1952). It is shown there that the differential cross section for the point nucleus is

$$I_A(\theta) = \gamma'^2 |F|^2 \text{cosec}^2(\theta/2) + |G|^2 \sec^2(\theta/2), \quad \dots\dots(3.1)$$

where F and G are complex functions of Z , W and θ . For energies greater than 9 mc^2 the functions F and G are approximately independent of W and are tabulated for both electron and positron scattering over a range of angles and for $Z=13, 29, 47, 62, 80$. The cross sections for gold nuclei (see table) were obtained by interpolation for $Z=79$ and use of the appropriate value of γ' . Additional values for $\theta=15^\circ$ were obtained directly from the results for electrons by Bartlett and Watson (1940) by the method first used by Massey (1942). In the process of this calculation a check was made of Massey's graph for positron scattering, and it was found that this graph was given incorrectly by Massey (1942), but correctly by Mott and Massey (1949 a).

The differential cross section for the extended nucleus is

$$I_C(\theta) = |f_C(\theta)|^2 + |g_C(\theta)|^2, \quad \dots\dots(3.2)$$

where, using the known properties of the phase shifts, we may write, as in I,

$$\left. \begin{aligned} f_C(\theta) &= f_A(\theta) + \frac{1}{2ik} \{ [\exp(2i\eta_0^C) - \exp(2i\eta_0^A)] P_0(\cos \theta) \\ &\quad + [\exp(2i\eta_{-2}^C) - \exp(2i\eta_{-2}^A)] P_1(\cos \theta) \}, \\ g_C(\theta) &= g_A(\theta) + \frac{1}{2ik} [\exp(2i\eta_{-2}^C) - \exp(2i\eta_{-2}^A)] P_1^1(\cos \theta), \end{aligned} \right\} \quad \dots\dots(3.3)$$

with

$$\left. \begin{aligned} kf_A &= G + i\gamma'F, \\ kg_A &= \{G(1 - \cos \theta) - i\gamma'(1 + \cos \theta)F\} \operatorname{cosec} \theta. \end{aligned} \right\} \quad \dots\dots(3.4)$$

(ii) Numerical Results

The results of the calculations are summarized in the table and also in fig. 1, where $I_C(\theta)/I_A(\theta)$ is plotted against θ for both electrons and positrons. The Born approximation is also shown in the figure and, as is easily seen from I § 2, this latter gives identical results for electrons and positrons. In fig. 2 the ratio of electron to positron scattering is shown for the cases of the point nucleus and the extended nucleus. To obtain this ratio for very small scattering angles use is made of the formula (Bartlett and Watson 1940, eqn. (8)), valid for small θ ,

$$I_A^+(\theta) \simeq \frac{1}{4} \cot^4(\theta/2) [\gamma^2 - \pi\lambda^2\gamma \sin(\theta/2) \cos \chi], \quad \dots\dots(3.5)$$

where $\chi = 2[\arg \Gamma(1 - i\gamma) - \arg \Gamma(\frac{1}{2} - i\gamma)]$, and the cross section for electrons is obtained by changing the sign of γ . To this approximation the extended nucleus cross section can easily be shown to be the same. Thus we have for small θ ,

$$I_{A,c}^-(\theta)/I_{A,c}^+(\theta) \simeq 1 + (2\pi\lambda^2/\gamma) \sin(\theta/2) \cos \chi. \quad \dots\dots(3.6)$$

Table

Differential cross sections for the cases of the point nucleus
and the extended nucleus for electrons and positrons
of energy 40 mc^2 being scattered by gold nuclei

θ (deg.)	15	30	45	60	80	90	100	120	135	150	
Electrons	$k^2 I_A$	323	25.6	6.49	2.54	0.945	0.638	0.412	0.186	0.0897	0.0377
	$k^2 I_C$	331	24.7	5.02	1.45	0.330	0.178	0.090	0.031	0.0123	0.0052
Positrons	$k^2 I_A$	265	14.4	2.59	0.75	0.204	0.117	0.069	0.025	0.0110	0.0044
	$k^2 I_C$	265	14.2	2.47	0.68	0.172	0.095	0.054	0.018	0.0075	0.0029

§ 4. RADIATIVE CORRECTION TO POSITRON SCATTERING

The radiative correction to positron scattering in the case of light nuclei can be obtained by slightly modifying the calculations for the corresponding correction to electron scattering. The latter was first evaluated by Schwinger (1949) and later re-calculated on the basis of the Feynman approach in II. This method will again be employed in the present paper.

The first order correction to the matrix element for scattering due to the radiative correction and vacuum polarization is obtained from Feynman (1949 b, eqns. (22) and (33)), on substituting for the scattering potential a the coulomb potential in momentum space. Thus the matrix element to this order is

$$M = M_1 \gamma_4 + M_2 q_\mu (\gamma_\mu \gamma_4 - \gamma_4 \gamma_\mu) + B \gamma_4, \quad \dots (4.1)$$

where

$$M_1 = -\frac{Ze^2 i}{2p^2 \sin^2 \frac{1}{2}\theta} \left\{ 4\phi \coth 2\phi - 2 - \phi \tanh \phi - 4 \coth 2\phi \int_0^\phi x \tanh x dx \right. \\ \left. - 2\left(\frac{1}{3} \coth^2 \phi - 1\right)(\phi \coth \phi - 1) + \frac{2}{9} \right\}$$

and

$$M_2 = -\frac{Ze^2 i}{4mp^2 \sin^2 \frac{1}{2}\theta} \phi \operatorname{cosech} 2\phi.$$

Here $\phi = \sinh^{-1}\{(p/m) \sin (\theta/2)\}$, i.e. Feynman's θ is $i\phi$, \mathbf{p}_1 and \mathbf{p}_2 are the four-vector momenta before and after scattering, $\mathbf{q} = \mathbf{p}_1 - \mathbf{p}_2$ and $p = |\mathbf{p}_1 - \mathbf{p}_1| = |\mathbf{p}_2 - \mathbf{p}_2|$ is

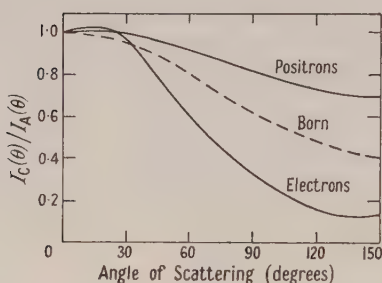


Fig. 1. Angular distribution for the ratio of the differential cross section for the case of the extended nucleus to that for the case of the point nucleus, for electrons and positrons of energy $40 mc^2$ being scattered by gold nuclei.

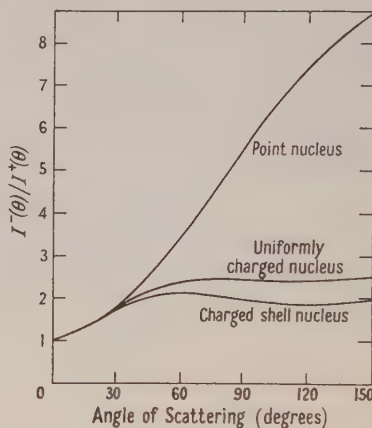


Fig. 2. Angular distribution of the ratio of electron scattering to positron scattering for the case of the point nucleus and two cases of the extended nucleus.

the magnitude of the three-vector momentum, which is unchanged in elastic scattering. Our θ is of course the scattering angle. The infra-red divergence terms which eventually cancel against the bremsstrahlung contribution have been omitted. The rest of the matrix element for scattering to this order is due to the first and second Born approximations. It is easily shown that this is of the form $B\gamma_4$, where B does not contain any γ -matrices. The total scattering cross section is then obtained from the formula (Feynman 1949 a, eqn. (36))

$$I = (32\pi^2)^{-1} \operatorname{Sp} (\mathbf{p}_1 + \mathbf{m}) \bar{M} (\mathbf{p}_2 + \mathbf{m}) M, \quad \dots (4.2)$$

where \bar{M} is M with the operators written in opposite order and explicit appearance of i changed to $-i$.

Now the change from electrons to positrons merely involves the replacement of Z , \mathbf{p}_1 , \mathbf{p}_2 by $-Z$, $-\mathbf{p}_1$, $-\mathbf{p}_2$ (Feynman 1949 a, after eqn. (35)). Of these the change in Z is trivial and, in fact, only changes the sign of the

contribution due to the second Born approximation. Because of the other changes we must now evaluate $\text{Sp}(-\mathbf{p}_1 + \mathbf{m})\gamma_4(-\mathbf{p}_2 + \mathbf{m})\gamma_4$ and

$\text{Sp}\{(-\mathbf{p}_1 + \mathbf{m})\gamma_4(-\mathbf{p}_2 + \mathbf{m})(\gamma_\mu\gamma_4 - \gamma_4\gamma_\mu) + (-\mathbf{p}_1 + \mathbf{m})(\gamma_4\gamma_\mu - \gamma_\mu\gamma_4)(-\mathbf{p}_2 + \mathbf{m})\gamma_4\}$ instead of the corresponding spurs with positive $\mathbf{p}_1, \mathbf{p}_2$. Since $\mathbf{p} = \mathbf{p}_\mu\gamma_\mu$ and spurs of odd numbers of γ -matrices vanish, it is clear that the first spur is unchanged and the second spur is unchanged in magnitude but changed in sign. If the bremsstrahlung term is investigated in the same way it is found that the only spur needed is the first of the above, so that this term is unchanged.

Making use of the formula for electrons given in II we thus obtain the radiative correction for positrons:

$$\delta_{\mathbf{R}}(\text{positron}) = \delta_{\mathbf{R}}(\text{electron}) - \frac{e^2}{\pi} \frac{4\beta^2 \sin^2 \frac{1}{2}\theta}{1 - \beta^2 \sin^2 \frac{1}{2}\theta} \phi \operatorname{cosech} \phi, \dots (4.3)$$

where $\beta = v/c$. However, the last term is quite negligible, being about one per cent of $\delta_{\mathbf{R}}$ unless θ is nearly equal to 180° . Thus the table for $\delta_{\mathbf{R}}$ given in II applies to positrons as well as to electrons.

§ 5. CONCLUSIONS

Our results show that both finite nuclear size and the radiative correction have an appreciable effect on the scattering of high energy positrons by nuclei. As was to be expected, the nuclear size effect is smaller than for electrons, but it is still larger than the radiative correction. Thus any hope that, because of the repulsion of positrons by the nucleus, it might be possible to obtain a pure radiative correction free from any nuclear size effects by using positrons instead of electrons must be abandoned.

More promising conclusions can be reached about the investigation of finite nuclear size. Figure 2 shows that the ratio of the cross sections for electron and positron scattering is particularly sensitive to this effect. In view of this result it seemed worth while to estimate this ratio also for a nucleus with a uniform charge distribution (model B of I), and this has been done by means of an interpolation in the table of cross sections. This is permissible since the ratio is not very sensitive to small errors in the positron cross sections, provided the electron cross sections are correct, and these are known exactly from I. Further, since the radiative correction is the same for positron and electrons—at least this is so for light nuclei, and for heavy nuclei the corrections are likely to be in the same direction and of the same order of magnitude—its effect is much reduced in the ratio of the cross sections, so that here we shall have an almost pure finite nucleus effect. Also, as Lipkin (1952) has shown, it may often be easier to measure the ratio of the cross sections than the cross sections themselves.

Lastly, the calculations show up the danger of the use of approximate methods. The perturbed wave approximation, which gave such good results for electrons in III, gives a value of the phase shift more than ten times too small for positrons, while the variation approximation, which one would expect to be inferior, gives on this occasion almost perfect agreement with the exact calculation. Approximate methods are in fact rarely as good as one thinks they are.

ACKNOWLEDGMENT

Our thanks are due to Professor H. S. W. Massey for many helpful discussions.

REFERENCES

- ACHESON, L. K., 1951, *Phys. Rev.*, **82**, 488.
BARTLETT, J. H., and WATSON, R. E., 1940, *Proc. Amer. Acad. Arts Sci.*, **74**, 53.
CUSACK, N., 1952, *Phil. Mag.*, **43**, 671.
ELTON, L. R. B., 1950, *Proc. Phys. Soc. A*, **63**, 1115; 1952, *Ibid.*, **65**, 481.
ELTON, L. R. B., and ROBERTSON, H. H., 1952, *Proc. Phys. Soc. A*, **65**, 145.
FESHBACH, H., 1951, *Phys. Rev.*, **84**, 1206; 1952, *Ibid.*, **88**, 295.
FEYNMAN, R. P., 1949 a, *Phys. Rev.*, **76**, 749; 1949 b, *Ibid.*, **76**, 769.
HOWATSON, A. F., and ATKINSON, J. R., 1951, *Phil. Mag.*, **42**, 1136.
LASICH, W. B., 1948, *Aust. J. Sci. Res. A*, **1**, 249.
LIPKIN, H. J., 1952, *Phys. Rev.*, **85**, 517.
LYMAN, E. M., HANSON, O. A., and SCOTT, M. B., 1951, *Phys. Rev.*, **84**, 626.
MAGNUS, W., and OBERHETTINGER, F., 1948, *Formeln und Sätze für die speziellen Funktionen der mathematischen Physik* (Berlin: Springer-Verlag), 2nd edn., ch. VI, § 4.
MASSEY, H. S. W., 1942, *Proc. Roy. Soc. A*, **181**, 14.
MOTT, N. F., and MASSEY, H. S. W., 1949 a, *The Theory of Atomic Collisions* (Oxford: University Press), 2nd edn., ch. IV, § 4; 1949 b, *Ibid.*, ch. VII, § 1.
PARZEN, G., 1950 a, *Phys. Rev.*, **80**, 261; 1950 b, *Ibid.*, **80**, 355.
ROSE, M. E., 1948, *Phys. Rev.*, **73**, 279; 1951, *Ibid.*, **82**, 389.
ROY, R. R., and GROVEN, L., 1952, *Phys. Rev.*, **87**, 619.
SCHWINGER, J., 1949, *Phys. Rev.*, **76**, 790.
YADAV, H. N., 1952, *Proc. Phys. Soc. A*, **65**, 672.

The Band-Spectrum of Aluminium Monofluoride

By H. C. ROWLINSON AND R. F. BARROW

Physical Chemistry Laboratory, Oxford University

MS. received 6th October 1952

Abstract. The spectrum of AlF in emission has been examined with moderate dispersion in the range 2000–7500 Å. Four systems have been found: (1) the system $\Lambda^1\Pi-x^1\Sigma^+$ at 2190–2360 Å, already known in absorption, (2) a system of violet-degraded bands, probably $^3\Sigma-^3\Pi$ at 3450–3720 Å, (3) a complex system at 5450–6050 Å, and (4) a system of violet-degraded double-headed bands at 6670–7250 Å. The original vibrational analysis of system (1) has been amended and an analysis of system (2) has been completed. It has so far proved impossible to analyse systems (3) and (4), and it is not certain that AlF is the emitter of these systems. Emission bands previously ascribed to AlF by Yuasa have not been observed: it is suggested that these bands are in fact due to S_2 .

The dissociation energy of AlF is briefly considered: a comparison of the thermochemical and spectroscopic values suggests that there may be a potential maximum in the state $\Lambda^1\Pi$ of AlF.

§ 1. INTRODUCTION

THE present work was prompted by the need for better information about the dissociation energy of AlF. The band spectrum of this molecule was investigated by Rochester (1939) who discovered a system in absorption at 2200–2400 Å. The system was designated $\Lambda^1\Pi-x^1\Sigma^+$ by analogy with AlCl and AlBr. A linear extrapolation of the ground-state vibrational levels using Rochester's constants gives $D_0'' \sim 2.5$ ev. However, the results of thermochemical work by Gross *et al.* (1948) lead to $D_0'' \sim 6.35$ ev. Although it is known (Gaydon 1947) that the Birge-Sponer extrapolation gives dissociation energies which, in the case of molecules possessing appreciable ionic character, may be too low, it seemed that this measure of disagreement was exceptional, and that Rochester's value of $x_e''\omega_e''$ was perhaps too high. This view was confirmed by a consideration of the values of $x_e''\mu^{1/2}$ (μ is the reduced mass) for the members of this group of halides. It has been pointed out (Vago and Barrow 1948) that $x_e''\mu^{1/2}$ is often fairly constant among a set of similar molecules, and indeed varies rather little from group to group. For BF, AlF, GaF, InF and TlF, $x_e''\mu^{1/2} = 2.7_1, 4.2_8, 2.7_2, 2.4_9$ and 2.1_4 respectively. Thus Rochester's value of $x_e''\omega_e''$ although based on measurements of Q heads, is unexpectedly large, suggesting that his vibrational analysis may not be quite correct. We therefore decided to examine the system again, this time in emission.

An emission system in the region 3180–4180 Å has been ascribed to AlF by Yuasa (1938). The bands were produced by a discharge at 12000 v in a silica discharge tube, with neon as carrier gas. The source of AlF was AlF_3 , heated to 700°C in a side-arm. It seems very doubtful that these bands arise from AlF, for the following reasons: (i) as already noted by Pearse and Gaydon (1950), the vibrational analysis given by Yuasa is quite unconvincing (notably, $\omega' \sim \omega''$ and yet the bands are fitted into a scheme with a wide Condon parabola);

(ii) our source of AlF bands, although emitting the 2200–2400 Å system with high intensity, is quite free from the Yuasa bands: instead there appears in this region a new, violet-degraded system with its 0, 0 sequence at about 3600 Å which appears to be a $^3\Sigma^- - ^3\Pi$ system of AlF; (iii) it seems surprising that Yuasa did not observe the 2200–2400 Å system of AlF despite exposures of 4–5 hours on a Hilger E.1 instrument. It is, moreover, possible to suggest the identity of the emitter of Yuasa's bands. A check of their wavelengths against those of other published band-heads gives no agreement except in one case, that of the $^3\Sigma^- - ^3\Sigma^-$ system of S_2 . Of the twenty-eight heads of S_2 listed by Fowler and Vaidya (1931) in the appropriate region, all but four (one of intensity 2, the others of intensity 1) appear on Yuasa's reproduction, while of the fifty-nine bands given by Yuasa, all those of intensity greater than 3, and eight of those of intensity 2 or 1, coincide in wavelength as well as can be expected with S_2 bands. It is suggested, therefore, that Yuasa's bands arise, not from AlF, but from S_2 .

In addition to the new system at 3600 Å ascribed to AlF, two other systems, not apparently hitherto recorded, have been photographed, one in the green, and one in the red region of the spectrum. It has not yet proved possible to establish the vibrational analysis or the emitters of these systems.

§2. EXPERIMENTAL

The emission spectrum of AlF was excited in hollow-cathode discharges using 1000–2000 v d.c. In the first tube (of Pyrex) the cathode, which was made of high-temperature steel, was horizontal and a mixture of Al and AlF_3 was placed in small copper-foil boats inside the cathode. It was necessary to run the tube for some time (using H_2 as carrier gas) until the cathode became hot enough to vaporize sufficient AlF to carry the discharge. This AlF discharge lasted only a short time because of scattering of the powder from the cathode. The spectrograms of the $^1\Pi - ^1\Sigma$ system were however taken with this tube. In an improved design of tube the cathode is vertical; the main tube is of silica, and the cathode can be pre-heated by an external furnace.

The spectrograms of the $^1\Pi - ^1\Sigma$ system were taken on a Hilger E.478 prism instrument with interchangeable glass and quartz optics. The reciprocal dispersion at 2200 Å is about 2 Å/mm. Exposure times were about 10–20 minutes on Ilford Process plates.

Examination of the spectrum at longer wavelengths revealed first a violet-degraded system at 3450–3720 Å. This system was then photographed in first and second orders of a 2.4 m concave grating (Eagle mounting: 15 000 lines/inch) giving about 3.7 Å/mm in a second order, with the vertical tube as source; Ilford Process plates were used.

Other bands were photographed in a first order of the grating at 5600 Å on Ilford H.P.3 plates and at 7000 Å on hyper-sensitized Ilford Special Long Range Panchromatic plates.

§3. THE SYSTEM $A^1\Pi - X^1\Sigma^+$

The bands (Plate (a), (b)) fall into four sequences, of which by far the most intense has its origin at 2275 Å. The sequence at shorter wavelengths has its bands degraded to the red. The appearance of the system in emission is quite similar to that in the high-temperature absorption spectrum, but Rochester observed in addition a fifth sequence at shorter wavelengths. The frequencies of the band-heads (table 1) were obtained from measurements against Cu arc

Table 1. System A¹Π - x¹Σ⁺: Band-Heads and Intensities

λ (Å)	ν _{vac} (cm ⁻¹)	Degradation	v'	v''	O.-C. (cm ⁻¹)	Intensity
2360.47	42351.5	V	0	2 P		2
59.49	368.8	V	1	3 P		2
59.24	373.7	V	0	2 Q	+0.2	3
58.70	383.2	V	2	4 P		2
58.22	391.8	V	1	3 Q	+0.3	4
58.12	393.7	V overlapped	3	5 P		1
57.82	399.1	V	4	6 P		1
57.39	406.9	V	2	4 Q	+0.5	2
56.70	419.2	line	3	5 Q	+1.4	1
56.30	426.4	diffuse	4	6 Q	+1.2	0
18.30	43121.8	V	0	1 P		8
17.92	129.5	V	1	2 P		8
17.24	141.4	overlapped	2	3 P		3
16.44	156.3	V	0	1 Q	0.0	10
15.97	165.1	V	1	2 Q	0.0	10
15.67	170.7	overlapped	2	3 Q	0.0	4
04.81	374.2	R	15	15 Q	-1.9	0
04.24	385.0	R	15	15 R		0
2299.39	476.8	R	14	14 Q	+0.3	0
98.75	488.5	R	14	14 R		0
94.71	565.2	R	13	13 Q	+0.9	1
94.02	578.1	R	13	13 R		0
90.87	638.0	R	12	12 Q	+0.2	1
89.93	656.1	R	12	12 R		1
87.54	701.6	R	11	11 Q	+0.2	2
86.38	724.7	R	11	11 R		1
84.76	754.8	R	10	10 Q	-0.3	2
83.26	783.5	R	10	10 R		1
82.42	797.8	R	9	9 Q	-0.6	3
80.75	831.8	R	9	9 R		1
80.48	836.9	R	8	8 Q	-0.7	3
78.85	868.3	R	7	7 Q	+0.1	4
78.77	869.7	R	8	8 R		2
77.59	892.4	R	6	6 Q	-0.4	7
76.57	912.1	line	5	5 Q	0.0	8
75.80	927.0	V	4	4 Q	+0.2	8
75.25	937.7	V	3	3 Q	+0.1	8
74.90	944.6	V	2	2 Q	+0.1	8
74.67	948.8	V overlapped	{1 0	{1 Q 0 Q}	+0.8 +0.3	10
41.20	44605	R	7	6 Q	-0.3	
39.50	639	R	6	5 Q	-0.1	
38.10	666.9	R	5	4 Q	-0.5	0
36.92	690.6	R	4	3 Q	-0.6	1
35.89	711.2	R	3	2 Q	+0.2	2
35.23	724.2	R	not classified			0
35.08	727.2	R	2	1 Q	0.0	2
34.38	741.3	R	1	0 Q	+1.3	4
09.64	45242	R	9	7 R		
06.67	303	R	8	6 Q	0.0	
05.70	323	R	8	6 R		
04.40	350	R	7	5 Q	-2.0	
03.27	373	R	7	5 R		
02.24	394	R	6	4 Q	-0.2	
01.03	419	R	6	4 R		
00.45	431	R	5	3 Q	-0.8	
2199.05	460	R	5	3 R		
97.36	495	R	3	1 Q	+1.0	
95.76	528	R	3	1 R		
94.27	559	R	2	0 R		

Intensities in tables 1, 3 and 4 are estimated visually on a scale of ten, independently for each system.

In this table the band heads for which no intensities are given are those observed only by Rochester.

lines: they agree well with those of Rochester. However, on the basis of the new spectrograms it is possible to derive an alternative vibrational analysis which is believed to be correct. The main features of the present analysis can be summarized as follows.

(i) *The Position of the 0, 0 Band*

The identification of this band is unequivocal, for on all spectrograms taken while the cathode was hot, it appears self-reversed, and at 800°K, with $\omega \sim 800 \text{ cm}^{-1}$, fewer than 20% of the molecules are in vibrational levels other than the lowest.

(ii) *The 0, 1 Sequence*

This sequence appears on the plate as four violet-degraded heads arranged in two pairs, of which the shorter wavelength, or inner pair, are the most intense. In fact, the inner pair constitute the Q heads, and the outer pair, the P heads, of the 0, 1 and 1, 2 bands, i.e. the P-Q head separation is here greater than the sequence interval.

(iii) *Comparison of Observed and Calculated Band-Head Frequencies*

The frequencies of the heads follow the equation

$$\nu_Q = 43\,947.6 + [803.95u' - 6.14_1u'^2 - 3.9_1 \times 10^{-3}u'^4] \\ - [801.5_2u'' - 4.7_0u''^2 + 0.01_0u''^3], \text{ where } u = v + \frac{1}{2}.$$

The agreement between observed and calculated frequencies for these heads (Table 1) is better than it was on the basis of the previous analysis. In addition, all our measured heads but one (2235.23 Å), and the great majority of Rochester's bands, can be assigned plausible values of v' , v'' .

(iv) *Rotational Constants*

The consideration of head-head separations decided the allocation of the heads in the 0, 1 sequence and enabled the bands of the 2, 0 sequence, which only Rochester observed, to be assigned. From the sixteen bands for which this separation has been measured it is not possible to calculate absolutely the constants B_e' , B_e'' , α_e' and α_e'' . However, by assuming a value for r_e'' it is possible to calculate B_e'' , and from this the other constants with good relative accuracy. The value $r_e'' = 1.67 \text{ Å}$ was obtained by considering similar molecules;

AlF	(1.67)	AlCl	2.13	AlBr	2.30 Å
BF	1.26	BCl	1.72	BBr	1.89
difference			0.41		0.41

This gives $B_e'' = 0.540 \text{ cm}^{-1}$, and the best values to fit the observed separations are: $B_v'' = 0.540 - 0.0037(v'' + \frac{1}{2})$, $B_v' = 0.548 - 0.0054(v' + \frac{1}{2})$. Values of the observed and calculated head-head separations are given in table 2. It can be calculated that the separation of the P and Q heads for the 0, 0 band would be about 50 cm^{-1} , and the P head might be unobservable. In the 1,0 sequence bands, the calculated separations are even larger, around 250 cm^{-1} , and again only Q heads are seen. However, for the 2, 0 band the separation should be about 40 cm^{-1} , and the separation decreases for later members of this sequence. Rochester's measurements on this sequence are seen to fit with this very well (tables 1 and 2).

Table 2. System $A^1\Pi - X^1\Sigma$: Observed and Calculated Band-Head Separations, P-Q or R-Q

$\Delta\nu$ (cm ⁻¹)				$\Delta\nu$ (cm ⁻¹)			
v'	v''	obs	calc	v'	v''	obs	calc
0	2	-22.2	-20.8	11	11	+23.1	+20.1
1	3	-23.0	-22.0	12	12	+18.1	+18.2
2	4	-23.7	-25.4	13	13	+12.9	+15.5
3	5	-26.4	-27.0	14	14	+11.3	+13.4
4	6	-27.5	-29.8	15	15	+10.8	+11.2
0	1	-34.5	-32.5	3	1	+33	+40.2
1	2	-35.1	-33.0	5	3	+29	+30.3
2	3	-29.3*	-35.0	6	4	+25	+25.6
8	8	+32.8	+36.4	7	5	+24	+22.0
9	9	+35.0	+31.3	8	6	+20	+19.8
10	10	+28.2	+24.7				

* Heavily overlapped.

§4. THE 3600 Å SYSTEM

This system appears in emission between 3450 and 3720 Å, and forms three well-defined sequences, which are all degraded to the violet both in rotational and in vibrational structure (Plate (c)). The wavelengths, determined by comparison against internal standards, principally Fe and Mn lines from the hot cathode, and frequencies of the measured bands are given in table 3.

The short-wavelength sequence is the only one to show any obvious regularity of structure: the heads can be arranged in overlapping groups of five with a moderately constant separation of about 92 cm⁻¹. Assuming that this is the sequence difference and that the values of $x_e\omega_e$ are about 5 cm⁻¹, then the sequence differences in the 0, 0 and 0, 1 sequences should be about 102 and 112 cm⁻¹ respectively. The central, most intense, sequence is taken as the 0, 0, and here, as in the 0, 1 sequence, groups of five heads can be arranged with differences of the magnitude expected. Thus the outline of the vibrational analysis is fairly clear, but the rough values of $\Delta G_{0,1}$ so derived, namely 920 cm⁻¹ for the upper state and 820 cm⁻¹ for the lower, show that the transition is not $^3\Pi - X^1\Sigma^-$ as at one time seemed possible, for $\Delta G_{0,1}$ for $X^1\Sigma^+$ is only 794 cm⁻¹. (That this is not the intercombination system is further suggested by its moderate intensity: the system is excited quite strongly in InF, is much less strong in GaF, has not been observed in BF, and might therefore be expected to be very weak in AlF.) By analogy with BF and AlCl, it seems most likely that the system is $^3\Sigma - ^3\Pi$: a definite decision cannot, however, be made without a rotational analysis, which is likely to need very high resolving power.

We may now proceed to examine the conclusions which follow from the suggestion that the system is $^3\Sigma - ^3\Pi$. It is apparent both from table 3 and from Plate (c) that the five heads of each band do not give any constant separations as one might expect in a triplet transition. However, this can be interpreted as arising from the near equality of B' and B'' resulting in head-origin separations of about the same size as the multiplet splitting A in $^3\Pi$. A would be expected to be about 20-40 cm⁻¹, between $A = 64$ cm⁻¹ for AlCl and $A = -2$ cm⁻¹ for BF. This would give $Y = A/B \sim 40-80$, indicating that the $^3\Pi$ state in AlF is probably intermediate in coupling, somewhere between Hund's cases (a) and (b).

Table 3. Measurements of Band-Heads of $^3\Sigma - ^3\Pi$ System

λ (Å)	ν_{vac} (cm $^{-1}$)	Head	v', v''	Intensity	O.-C.	$\Delta\nu$, head-origin
3717.91	26889.2	Q_{13}, P_{23}		2	1.3	13.5
15.97	903.3	—		1		
14.57	13.4	P_{12}	0, 1	2	0.5	36.0
10.94	39.7	P_{22}, Q_{12}		4	-0.2	9.0
06.76	70.1	P_{11}		4	0.5	26.8
04.11	89.4	Q_{11}, P_{21}		3	-0.3	6.7
02.42	27001.7	Q_{13}, P_{23}		2	1.9	13.0
00.61	14.9	—		0		
3699.06	26.2	P_{12}	1, 2	1	-0.1	34.0
95.54	52.0	P_{22}, Q_{12}		4	0.2	8.5
91.43	82.1	P_{11}		3	-0.5	25.2
88.78	101.7	Q_{11}, P_{21}		4	0.2	6.3
87.11	27113.8*	Q_{13}, P_{23}		1	0.7	10.6
84.49	33.1	—		0		
83.50	40.4	P_{12}	2, 3	0	-0.4	30.4
80.33	63.7	P_{22}, Q_{12}		2	0.1	7.6
73.70	212.8*	Q_{11}, P_{21}		0	Obs.	5.9
72.16	27224.2*	Q_{13}, P_{23}		0	0.3	10.2
69.00	47.7*	P_{12}		0	6.0	27.2
65.28	75.3*	P_{22}, Q_{12}	3, 4	0	0.5	6.8
58.75	324.0*	Q_{11}, P_{21}		0	Obs.	5.1
08.17	27707.0	Q_{13}, P_{23}		8	2.0	18.0
05.94	24.1	P_{12}		7	-0.4	46.0
01.41	59.1	P_{22}, Q_{12}	0, 0	10	0.1	11.5
3597.74	87.4	P_{11}		10	3.0	33.6
94.86	809.6	Q_{11}, P_{21}		10	0	8.4
92.71	27826.2	P_{12}		2	-0.8	45.6
88.21	61.5	P_{22}, Q_{12}	1, 1	5	0.3	11.4
84.68	88.6	P_{11}		4	-0.3	31.2
81.59	912.6	Q_{11}, P_{21}		5	0.3	7.8
3492.22	28626.9	Q_{13}, P_{23}		3	1.2	21.0
89.71	47.5	P_{12}		4	1.3	48.0
85.55	81.7	P_{22}, Q_{12}	1, 0	5	-0.5	12.0
82.36	708.0	P_{11}		4	-0.1	33.6
79.31	33.2	Q_{11}, P_{21}		4	-0.1	8.4
80.82	28720.7	Q_{13}, P_{23}		3	2.8	21.0
78.40	40.7	P_{12}		4	-0.2	45.6
74.22	75.3	P_{22}, Q_{12}		4	0.2	11.4
70.95	802.3	P_{11}	2, 1	4	-0.5	31.2
68.06	26.4	Q_{11}, P_{21}		4	0.2	7.8
69.55	28813.9	Q_{13}, P_{23}		0	0.1	17.0
67.15	33.8	P_{12}		3	-2.5	42.0
62.96	68.8	P_{22}, Q_{12}	3, 2	2	1.0	10.5
59.72	95.8*	P_{11}		2	0.4	30.4
57.05	918.1	Q_{11}, P_{21}		2	-0.1	7.6
58.58	28905.5	Q_{13}, P_{23}		1	—	—
55.98	27.1	P_{12}	4, 3	1	-2.1	40.0
51.99	60.7	P_{22}, Q_{12}		0	1.1	10.0

* Indicates a measurement on the 1st order plate only

In a transition, ${}^3\Sigma - {}^3\Pi$ (a), 27 branches are expected: if the spin-splitting in the ${}^3\Sigma$ state is neglected, there appear 15 branches. The rotational energies are to a first approximation:

$${}^3\Sigma : \begin{cases} F_1'(J) = B'K'(K'+1) = B'(J'-1)J' \\ F_2'(J) = B'K'(K'+1) = B'J'(J'+1) \\ F_3'(J) = B'K'(K'+1) = B'(J'+1)(J'+2) \end{cases}$$

$${}^3\Pi : F''(J) = B_{\text{eff}}''J''(J''+1),$$

where $B_{\text{eff}}''({}^3\Pi_0) = B^{(1)} = B_v(1 - 2B_v/A)$

$$B_{\text{eff}}''({}^3\Pi_1) = B^{(2)} = B_v$$

$$B_{\text{eff}}''({}^3\Pi_2) = B^{(3)} = B_v(1 + 2B_v/A).$$

For $B' > B''$, the following are head-forming branches:

$${}^3\Pi_0, \text{ Q-form. } Q_{11}, P_{21}. \quad \nu = \nu_0^{(1)} - (B' + B^{(1)'})J + (B' - B^{(1)'})J^2$$

$$\text{P-form. } P_{11}. \quad \nu = \nu_0^{(1)} + 2B' - (3B' + B^{(1)'})J + (B' - B^{(1)'})J^2$$

$${}^3\Pi_1, \text{ P-form. } P_{22}, Q_{12}. \quad \nu = \nu_0^{(2)} - (B' + B^{(2)'})J + (B' - B^{(2)'})J^2$$

$$\text{O-form. } P_{12}. \quad \nu = \nu_0^{(2)} + 2B' - (3B' + B^{(2)'})J + (B' - B^{(2)'})J^2$$

$${}^3\Pi_2, \text{ O-form. } Q_{13}, P_{23}. \quad \nu = \nu_0^{(3)} - (B' + B^{(3)'})J + (B' - B^{(3)'})J^2$$

$$\text{N-form. } P_{13}. \quad \nu = \nu_0^{(3)} + 2B' - (3B' + B^{(3)'})J + (B' - B^{(3)'})J^2.$$

As the ${}^3\Pi$ state approaches case (b), the branches with $\Delta K = \pm 3$ will disappear, and here the ${}^N P_{13}$ head is not observed: it cannot be far from case (a) for heads apparently corresponding to $\Delta J \neq \Delta K$ are observed, although the ${}^P P_{11}$, ${}^Q Q_{11}$ and ${}^P P_{22}$ are always the strongest. A plausible allocation of the five observed heads in each band to their respective branches may be made following a consideration of head-origin separations. It can easily be shown that when B' and B'' are nearly equal the separation of the longer wavelength head of any sub-band from the origin of the sub-band is four times that of the shorter-wavelength head: e.g. in ${}^3\Pi_0$, $\Delta\nu(P_{11})/\Delta\nu(Q_{11}) \sim 4$. Thus by subtracting the frequency of the outer head from that of the inner, and adding one-third of the difference to the frequency of the inner head, the position of the sub-band origin is obtained. Thus the ${}^3\Pi_0 - {}^3\Pi_1$ origin separation can be found, and if this is constant from band to band, then the allocation of heads should be correct. In fact only the allocation given in table 3 results in constant separations. In this way, the following equation for the band-origins was obtained:

$$\nu = \left. \begin{array}{l} 27766.8 \\ 719.3 \\ 671.8 \end{array} \right\} + [933.5u' - 4.9_0u'^2] - [830.9u'' - 4.5_5u''^2],$$

where $u = v + \frac{1}{2}$. The observed-calculated values given in table 3 have been obtained from these band-origins by subtracting the frequencies of the heads and comparing these differences with those adjusted so that $\Delta\nu(P_{11})/\Delta\nu(Q_{11}) = 4$ and the two O.-C. values are at a minimum.

The O.-C. values for the ${}^3\Pi_2$ heads cannot be obtained in this way as only the $Q_{13} + P_{23}$ head is observed. However the head-origin separations in ${}^3\Pi_2$ can be obtained as follows: let x, y, z , be the head-origin separations of the $(Q_{11} + P_{21})$, $(P_{22} + Q_{12})$ and $(P_{23} + Q_{13})$ heads respectively. Then

$$x = -(B' + B^{(1)'})^2/4(B' - B'' + B''^2/24); \quad y = -(B' + B^{(2)'})^2/4(B' - B''); \\ z = -(B' + B^{(3)'})^2/4(B' - B'' - B''^2/24).$$

We may take the numerators as constant, since $2B/A\lambda \simeq B/24$ affects the terms in $B' - B_{\text{eff}}''$ much more than those in $(B' + B_{\text{eff}}'')^2$. It is then easy to show that $z = xy/(2x - y)$, and so from the head-origin separations in the ${}^3\Pi_0$ and ${}^3\Pi_1$ sub-bands, those for ${}^3\Pi_2$ can be calculated: O.-C. values may then be determined for the ${}^3\Pi_2$ heads from their calculated origins. These results are also included in table 3.

The rather detailed agreement between the heads observed and those expected for a ${}^3\Sigma - {}^3\Pi(a)$ transition, and the values derived of A, ω_e'' and ω_e' combine to suggest strongly that this system is in fact the ${}^3\Sigma - {}^3\Pi$ system of AlF, analogous to those already known in BF (Paul and Knauss 1938) and AlCl (Sharma 1951).

§ 5. OTHER BANDS

Two other band-systems which do not appear to have been recorded before are emitted in the hollow-cathode source, one in the region 5450–6050 Å, the other consisting of violet-degraded double-headed bands at 6670–7250 Å. Measurements of the main heads are given in table 4. The analysis of neither system is obvious. In the case of the yellow-green bands, $B' \sim B''$, and the structure is that of a very complex 0, 0 sequence with weak 1, 0 and 0, 1 sequences. Observations on the red bands are incomplete, for it has not so far proved possible to bring them up with sufficient intensity for a vibrational analysis. Work on these systems is still in progress.

§ 6. THE DISSOCIATION ENERGY OF AlF

With the new and smaller value of $x_e\omega_e$ for $\mathbf{x}^1\Sigma^+$ the linear extrapolation of the vibrational levels now gives $D_0'' \simeq 4.4$ ev. A comparison with the figures for other molecules of this group (see, for example, Welti and Barrow 1952) suggests that this represents about two-thirds of the true value of D_0'' . A better value of D_0'' can be obtained from an extrapolation of the levels in the ${}^1\Pi$ state, whose atomic products of dissociation are most probably $\text{Al}({}^2P_{3/2}) + \text{F}({}^2P_{1/2})$. The excitation energy of the fluorine atom to ${}^2P_{1/2}$ is small (407 cm^{-1}) and may be neglected: that of Al to ${}^2P_{3/2}$ is only 112 cm^{-1} . The graphical extrapolation of the levels in the ${}^1\Pi$ state is fairly short, and we derive $D_0'' = 7.2 \pm 0.3$ ev. It may be remarked here that no pre-dissociation has been observed in the ${}^1\Pi$ state of AlF as, for example, happens for AlCl. A lower limit is obtained through the observation of levels up to $v' = 15$ in ${}^1\Pi$. This gives $D_0'' \geq 6.51$ ev.

The picture is, however, still a little obscure, for the thermochemical value is $D_0'' = 6.3_5$ ev or 147 kcal. This depends upon (i) the heat of formation of gaseous AlF, -49.7 kcal determined by Gross *et al.* (1948), (ii) the heat of dissociation of fluorine, 38 kcal (Evans, Warhurst and Whittle 1950, Doescher 1951), and (iii) on the latent heat of sublimation of aluminium, 77 kcal (from the measurements of Farkas 1931, and of Bauer and Brunner

1934, with specific heat data from Kelley 1949). It seems unlikely that these thermochemical figures are much in error. Gross (private communication) has additional measurements supporting the published figure for the heat of formation of AlF; the value for the heat of dissociation of fluorine appears now to be firmly established; perhaps the least certain is the value of the latent heat of sublimation of aluminium, but it may be noted that the thermochemical and spectroscopic dissociation energies of AlCl are in very fair agreement, supporting $L_{Al} \sim 77$ kcal.* The only way out of the present difficulty seems to be to

Table 4. Other Bands Possibly due to AlF

(a) Yellow-Green System

λ (Å)	ν_{vac} (cm ⁻¹)	Intensity	Degradation	λ (Å)	ν_{vac} (cm ⁻¹)	Intensity	Degradation
6052.43	16517.7	0	?	5758.48	17360.9	4	line
49.83	524.8	2	V	51.10	383.2	5	R
47.90	530.1	1	line ?	41.57	412.0	4	V
45.91	535.5	2	V	37.35	424.8	4	V
42.77	544.1	2	line	30.68	445.1	6	line
41.16	548.4	0	line	27.33	455.3	4	R
37.12	559.5	0	V	10.99	505.3	10	R
35.37	564.4	0	V	09.18	510.8	3	R
28.84	582.4	0	V ?	05.30	522.7	10	V
09.83	634.9	1	V	5696.23	550.6	10	V
05.94	645.6	1	V ?	87.53	577.4	10	V
5988.58	693.8	1	R ?	80.18	600.2	7	V
70.39	744.7	0	V	5492.75	18190.5	2	V
5774.04	17314.1	10	V	88.16	216.0	2	V
70.04	326.1	8	V	67.15	286.0	2	V
				62.83	300.5	1	V

(b) Red System

λ (Å)	ν_{vac} (cm ⁻¹)	Intensity	Degradation
7245.94	13797.2	3	V
40.81	806.8	2	V
6790.07	14723.3	10	V
84.98	734.4	8	V
32.44	849.4	10	V
27.53	860.2	8	V
6678.03	970.3	8	V
74.66	977.9	6	V

postulate a potential maximum in the $^1\Pi$ state of AlF. This may happen elsewhere in this group of molecules, e.g. in AlCl, where it is not easy to give a detailed interpretation of the data without the assumption of a similar, but lower, maximum in the analogous $^1\Pi$ state.

ACKNOWLEDGMENT

One of us (H. C. R.) is glad to acknowledge the award of a maintenance grant from the Department of Scientific and Industrial Research.

* Note added in proof: Recent measurements of the vapour pressure of aluminium lead to $L_{Al} = 77.4 \pm 1.4$ kcal at 298°K (Brewer, L., and Searcy, A. W., 1951, *J. Amer. Chem. Soc.*, **73**, 5308).

REFERENCES

- BAUER, E., and BRUNNER, R., 1934, *Helv. Chim. Acta*, **17**, 958.
DOESCHER, R. N., 1951, *J. Chem. Phys.*, **19**, 1070.
EVANS, M. G., WARHURST, E., and WHITTLE, E., 1950, *J. Chem. Soc.*, 1524.
FARKAS, A., 1931, *Z. Phys.*, **70**, 737.
FOWLER, A., and VAIDYA, W. M., 1931, *Proc. Roy. Soc., A*, **132**, 310.
GAYDON, A. G., 1947, *Dissociation Energies* (London : Chapman and Hall).
GROSS, P., CAMPBELL, C. S., KENT, P. J. C., and LEVI, D. L., 1948, *Discussions of the Faraday Society*, No. **4**, 206.
KELLEY, K. K., 1949, *U.S. Bureau of Mines*, Bulletin No. 476.
PAUL, F. W., and KNAUSS, H. P., 1938, *Phys. Rev.*, **54**, 1072.
PEARSE, R. W. B., and GAYDON, A. G., 1950, *The Identification of Molecular Spectra* (London : Chapman and Hall).
ROCHESTER, G. D., 1939, *Phys. Rev.*, **56**, 305.
SHARMA, D., 1951, *Astrophys. J.*, **113**, 210.
VAGO, E. E., and BARROW, R. F., 1948, *Victor Henri Memorial Volume* (Liège : Desoer), p. 201.
WELTI, D., and BARROW, R. F., 1952, *Proc. Phys. Soc. A*, **65**, 629.
YUASA, T., 1938, *Sci. Rep. Tokyo Bun. Dai.*, **3**, 239.

The Average Number of Neutrons Emitted in the Spontaneous Fission of ^{242}Cm

By F. R. BARCLAY AND W. J. WHITEHOUSE

Atomic Energy Research Establishment, Harwell, Didcot, Berks.

MS. received 24th November 1952

Abstract. The average number of neutrons ν emitted in the spontaneous fission of ^{242}Cm has been measured by a method depending on the device of counting only those neutrons which are detected after the occurrence of a fission. In this way the effect of neutrons from sources other than spontaneous fission is eliminated. The value found for ν is 3.0 neutrons per fission. The estimated standard error is 10–15%.

§ 1. INTRODUCTION

SOON after the discovery of spontaneous fission by Petrzhak and Flerov (1940) the neutrons emitted from natural uranium were detected and quite accurate measurements of the average number per fission (ν) were made. In some experiments the neutrons from kilogramme quantities of uranium were detected by sensitive methods such as boron counters, or absorption in manganese solutions followed by separation of the active ^{56}Mn by the Szilard–Chalmers reaction. The most accurate results are, however, derived by a method initiated by Fermi, which depends upon measurements of the neutron flux in a non-divergent pile. The best value is probably that of Littler (1952), who gives $(1.65 \pm 0.1) \times 10^{-2}$ neutrons per gramme per second. Littler's measurement depends upon a comparison with a neutron source which he had calibrated himself (Littler 1951) and which is also used as the standard in the present experiments. The neutron emission from thorium was more difficult to measure because the spontaneous fission rate is so much lower and the early experiments gave erroneous results. However, Barclay, Galbraith and Whitehouse (1952) compared the rate of emission of neutrons from several kilograms of pure uranium and thorium metals, and found a ratio of 153 ± 10 . Virtually all the spontaneous fission in natural uranium occurs in the isotope ^{238}U . We may therefore combine the results mentioned above with Segrè's (1952) values for the spontaneous fission rates, and deduce that $\nu(^{238}\text{U}) = 2.4 \pm 0.2^*$ and $\nu(^{232}\text{Th}) = 2.6 \pm 0.3$.

All these experiments relied for their accuracy upon the availability of large quantities of pure material and upon the fact that no neutrons are emitted except during the process of fission. Experiments with artificial transuranic elements, such as curium, appear at first sight to be much more difficult. In the first place not more than a few microgrammes of the element are available, the number of neutrons emitted is therefore small, and fluctuations in the background could

* Littler used another value for the spontaneous fission rate (Whitehouse and Galbraith 1950) and therefore finds $\nu(^{238}\text{U}) = 2.5 \pm 0.2$.

introduce large errors. A more serious difficulty arises from the intense α -particle activity. The energetic particles produce neutrons from minute quantities of impurities of low atomic weight, by (α, n) reactions (Roberts 1944), and there is no simple way of deciding what proportion of the neutrons comes from spontaneous fission.

The method described here overcomes both these difficulties. An ionization chamber, containing sufficient curium to give a few spontaneous fissions per minute, is surrounded by a paraffin block containing $^{10}\text{BF}_3$ counters. Neutrons are only counted if detected within about a millisecond of the occurrence of a fission. Since the average time required for a neutron to be slowed down and captured is only about $200\ \mu\text{sec}$, the sensitivity of the arrangement to neutrons originating in fission is not reduced at all. On the other hand the background of neutrons from all causes, including (α, n) reactions, although large compared with the effect which is being measured, gives rise to a negligibly small coincidence rate.

The efficiency of the system of boron counters is necessarily low, and the true neutron counting rate is correspondingly small. It is therefore necessary to count for long periods when using this method (over 200 hours in the present instance). However, as all the apparatus is automatic, and as it had been developed for other purposes, the labour involved in the experiment was not excessive.

§ 2. THE CURIUM SOURCE

The curium used in the experiment was prepared by pile irradiation of ^{241}Am which was believed to be isotopically pure. The irradiation was comparatively short, and only about 2×10^{-3} of the ^{241}Am was converted. Of this about one third eventually appears in the form of a long-lived isomer ^{242}Am ($T_{1/2} \geq 100\ \text{y}$). The short-lived isomer $^{242}\text{Am}^*$ ($T_{1/2} = 16\ \text{h}$) decays mainly to ^{242}Cm , but also to ^{242}Pu . Very small amounts of ^{243}Am may be formed in the original irradiation.

The separation of curium from americium and plutonium was carried out in an ion exchange column, and was not complete. Analysis of the product showed that 99.2–99.7% of its α -particle activity was due to ^{242}Cm , but this does not exclude the possibility that, in terms of mass, the material may have contained 10 times as much americium as curium. The question therefore arises, whether all the fissions observed came from ^{242}Cm . The spontaneous fission rates of the relevant nuclides are:

^{238}Pu	$2.14 \times 10^3\ \text{g}^{-1}\ \text{sec}^{-1}$	Segrè (1952)
^{242}Pu	$\sim 10\ \text{g}^{-1}\ \text{sec}^{-1}$	Estimated from Z^2/A , see Whitehouse and Galbraith (1952)
^{241}Am	$4.6\ \text{g}^{-1}\ \text{sec}^{-1}$	Segrè
^{242}Am	$\leq 10^4\ \text{g}^{-1}\ \text{sec}^{-1}$	Upper limit estimated from Z^2/A
^{242}Cm	$8 \times 10^6\ \text{g}^{-1}\ \text{sec}^{-1}$	Hanna <i>et al.</i> (1951).

The orders of magnitude of the percentages of the various nuclides which are present may be calculated from the cross sections and decay schemes given in the documents AECU 2040 and NBS 499. From these figures it is found that although the source may contain as much as 90% by weight of americium, the proportions of fissions originating from this element will be negligibly small ($\sim 0.01\%$). The fission rate from ^{238}Pu , which accumulates as the ^{242}Cm decays is also negligible. The presence of these impurities therefore has no effect upon either the fission rate or the measured value of ν .

Owing to the small concentration of americium and curium the final source contained a considerable amount of impurity. The film used in the ionization chamber, which was prepared by evaporation on a platinum disc 2 cm in diameter, was thicker than could be desired. Special precautions were therefore taken (§3 (i)) to ensure that nearly all the fission fragments were detected.

The α -particle emission of the specimen was not measured until after the experiment, and no attempt was made to check the published value of the spontaneous fission half-life. However, using this value, the measured spontaneous fission rate and the α -particle count agree within about 5%.

§3. EXPERIMENTAL DETAILS

(i) *General Arrangement*

The arrangement of the apparatus, which was set up under a concrete roof 3 ft. thick, is shown in fig. 1. The specimen was mounted in a simple parallel plate ionization chamber, through which passed a slow stream of hydrogen from a cylinder.* Electron collection was possible in the unpurified gas, though it is doubtless incomplete, and the amplifier operated with a time constant of $1.0\ \mu\text{sec}$. The chance of spurious pulses due to fluctuations in the α -particle background was negligible. The separation of the plates in the ionization chamber is about 1.5 cm while the range of the fission fragments in hydrogen is of the order of 10 cm. Thus only the beginnings of the tracks were measured, and this gives additional discrimination against the α -particles, because the fission fragments ionize most intensely at the beginning of their tracks, while specific ionization of the α -particles is greatest near the end. A denser gas could, of course, have been used at reduced pressure, but this would have complicated the apparatus. The ionization chamber was at the centre of a cube of paraffin, 26 in. across, in which was embedded a ring of eight standard $^{10}\text{BF}_3$ counters, connected to a common h.t. supply, and feeding their pulses to the same amplifier.

A block diagram of the electronic apparatus is shown in fig. 2. It was composed of standard units (the A.E.R.E. reference numbers are quoted under the diagram), with the exception that the coincidence unit was modified so that the fission channel had a long resolving time. This resolving time could be measured by placing a small source in the paraffin to increase the neutron counting rate R_n , and feeding artificial pulses through a small condenser into the head amplifier of the fission channel at such a rate R_f that the accidental coincidence rate R_c was measurable. The equation $R_c = \tau R_f R_n$ then gives the resolving time,† which remained constant at 0.98 msec. (The same equation can be used to show that the background of accidental coincidences in the main experiment is negligible.) The effect is that all the fission pulses and all the neutron pulses are counted by their respective scalers. In addition any neutron pulses which arrive within approximately 1 msec after a fission pulse are counted by the coincidence scaler.

In an experiment of this type it is necessary to take precautions against counting spurious pulses due to electrical breakdown or other causes. For this

* The out-going hydrogen passed through a gas-mask filter, to reduce the risk of contamination by small amounts of americium or curium which might be carried away in the gas.

† The symbol τ really represents the sum of the resolving times of the two channels. However the resolving time of the neutron channel ($\sim 1\ \mu\text{sec}$) is smaller than the error in measurement of that of the fission channel, and may therefore be ignored.

reason the triggered oscilloscope and camera were used from time to time to photograph a number of fission pulses in order to ensure that they were the expected shape and that there were no spurious discharges among them. Every coincidence pulse, every tenth neutron pulse and every hundredth fission pulse was recorded by pen recorder, in order to ensure that the apparatus was running correctly.

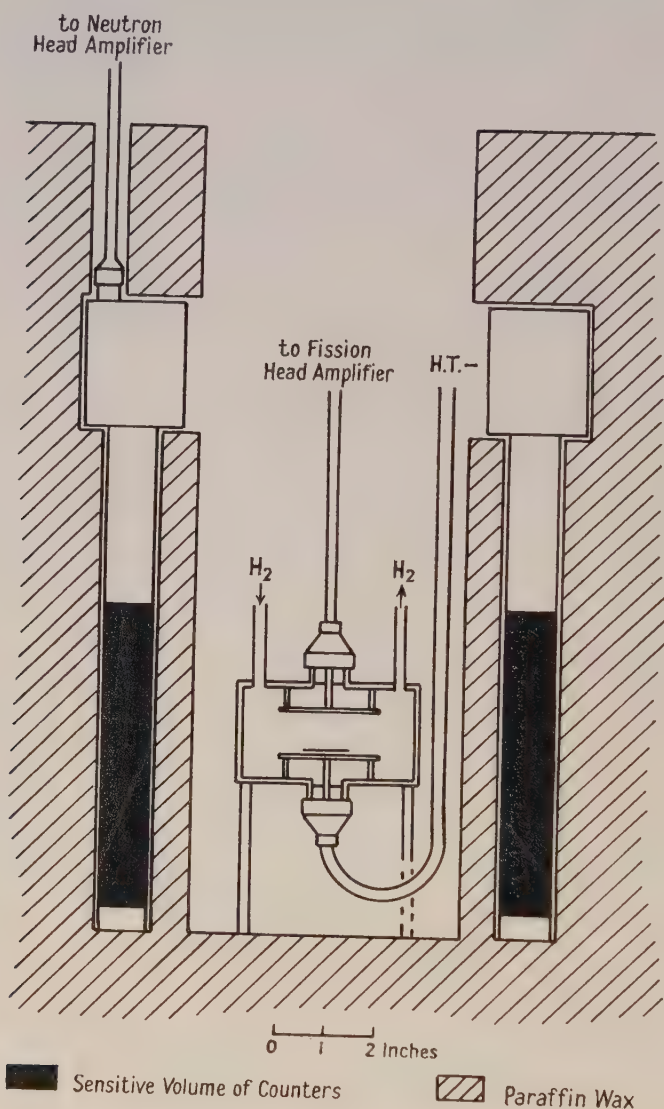


Fig. 1. Arrangement of fission chamber and neutron counters.

(ii) Efficiency of Detection of Fission Fragments

By measuring a number of the photographs of the fission pulses it was possible to construct the differential bias curve shown in fig. 3. This curve is considerably worse than that from a uniform plutonium oxide film of surface density

0.15 mg cm^{-2} , shown for comparison. It is evident, however, that the majority, probably about 88%, of the fission fragments from the curium film were detected, and also that no α -particles were counted as fission fragments. The fact that some fissions were missed does not matter, since this does not affect the measured value of ν . Moreover, it has been shown by Fraser and Milton (1952) that the value of ν varies very little with the total kinetic energy of the fragments. Therefore, even if there were any discrimination in the present experiment against fragments with less than the average kinetic energy, we should not expect the result to be affected.

(iii) Calibration of the Neutron Counters

The sensitivity of the counter system was checked daily by inserting a 1 mc Ra- α -Be source, contained in a chamber identical with the one in use, and remained constant during the greater part of the experiment at 1.10%. Towards the end it became necessary to replace one of the counters and after this the sensitivity was 1.28%. The final result is therefore the statistically weighted mean of the two parts.

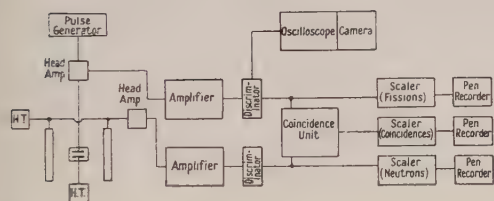


Fig. 2. Block diagram of electronic apparatus. (H.T. supplied by batteries; fission amplifier type 1217; neutron amplifier type 1008; discriminators type 1028; coincidence unit type 1036A modified; scalars type 200; pen recorders Evershed and Vignoles milliammeter; pulse generator type 1013B; recording oscilloscope type 1102A.)

The neutron emission of the source was determined by direct comparison (in the paraffin block, after removing the chamber) with a 215 mc source previously calibrated by Littler, and found to be $(6.8 \pm 0.4) \times 10^3$ neutrons per second. A previous comparison of the same 1 mc source with another calibrated source, using the method of activating indium foils, had yielded a result of $(6.7 \pm 0.7) \times 10^3$ neutrons per second.

Two other experiments had been carried out to ensure that the response of the counter system was independent of the neutron energy. (a) It had been shown that the counting efficiency was constant, within $\pm 10\%$, to photoneutrons from various sources having energies between 30 kev and 1 mev. (b) By placing a uranium bar, surrounded by cadmium sheet, in the central cavity it had been shown that the response to neutrons from spontaneous fission of ^{238}U and Ra- α -Be neutrons was the same within $\pm 9\%$.

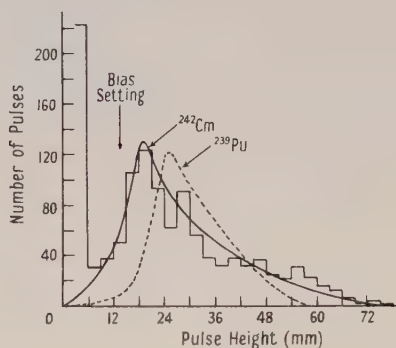


Fig. 3. Differential bias curve of the ionization chamber. (Results with a uniform Pu source of 0.15 mg cm^{-2} are shown for comparison.)

§4. RESULTS

The observed fission rate decreased gradually during the experiment, approximately in accordance with the known half-life of ^{242}Cm . The mean value was approximately 150 per hour. It had previously been shown that the fission rate in this apparatus is the same whether the chamber is surrounded with cadmium or not, and this proves that no significant proportion of the emitted neutrons can be re-absorbed, giving rise to further fissions. Moreover, it had also been shown that the fission counting rate was the same on two scalers, one of which accepted all the pulses, while the other had a dead time of about 20 msec. Any neutron-induced fissions, caused by the re-absorption of neutrons would have occurred within a few hundred microseconds.

The background counting rate in the group of eight counters was about 60 per hour when the curium source was removed from the paraffin castle, and was nearly constant. When the curium source was present the neutron counting rate was about 70 per hour. The difficulties of a straightforward measurement of the neutron emission in spontaneous fission are emphasized by the fact that these rates, in conjunction with the fission rate, would indicate that about six neutrons were emitted per fission. The additional neutrons may, presumably, be ascribed to (α , n) reactions.

The average coincidence rate was about five per hour. A simple statistical test showed that the distribution of time intervals between pulses was consistent with random occurrence.* Several control experiments were made, in which the ionization chamber was removed from the paraffin, and it was found that, in these conditions, no coincidences between a fission and the capture of a neutron occurred in a total of 22 hours. This is to be expected, since the calculated rate of chance coincidences is about 0.003 per hour, but the control experiments served to show that no spurious coincidence pulses were being observed.

The results of the experiment may be summed up as follows

Total hours of counting	157.5	68.7
Number of fissions observed F	24026	9525
Number of neutron-fission coincidences observed N	783	376
Efficiency of counter system ϵ (%)	1.10	1.28

We have $N = F\nu\epsilon$, from which we obtain $\nu = 3.0$.

The standard error on the emission from the neutron source used for calibration of the counter system is approximately 6%. The statistical error on the number of coincidences is 3%. It is more difficult to assess the effect of varying sensitivity of the counter system to neutrons of different energies. There is no proof that this effect exists, and, if it does, the experiments mentioned in §3 indicate that the error introduced is less than 10%. The standard error of the value of ν is therefore of the order of 10–15%.

* The effect of radioactive decay was ignored in this test.

ACKNOWLEDGMENTS

We are indebted to Dr. J. Milstead for preparing the curium source, and for the α -particle counting. Mr. W. Galbraith took part in the preliminary experiments during which the apparatus was developed, and made many valuable suggestions. Our thanks are due to the Director, Atomic Energy Research Establishment, for permission to publish this work, and to Dr. E. Bretscher, head of the Nuclear Physics Division.

REFERENCES

- Atomic Energy Commission Report* No. A.E.C.U. 2040 (1952).
BARCLAY, F. R., GALBRAITH, W., and WHITEHOUSE, W. J., 1952, *Proc. Phys. Soc. A*, **65**, 73.
FRASER, J. S., and MILTON, J. D. C., 1952, Verbal report by G. C. Hanna.
HANNA, G. C., HARVEY, B. G., MOSS, N., and TUNNICLIFFE, P. R., 1951, *Phys. Rev.*, **81**, 466.
LITTLER, D. J., 1951, *Proc. Phys. Soc. A*, **64**, 638; 1952, *Ibid.*, **65**, 203.
National Bureau of Standards Circular No. 499, (1950).
PETRZHAK, K. A., and FLEROV, G. N., 1940, *C.R. Acad. Sci. U.S.S.R.*, **28**, 500; *J. Gen. Physiol.*, **3**, 275.
ROBERTS, J. H., 1944, *Atomic Energy Commission Report* No. MDDC 731.
SEGRÈ, E., 1952, *Phys. Rev.*, **86**, 21.
WHITEHOUSE, W. J., and GALBRAITH, W., 1950, *Phil. Mag.*, **41**, 429; 1952, *Nature, Lond.*, **169**, 494.

The Time Distribution of Delayed Particles in Extensive Air Showers using a Liquid Scintillation Counter of Large Area

BY J. V. JELLEY AND W. J. WHITEHOUSE

Atomic Energy Research Establishment, Harwell, Didcot, Berks.

MS. received 21st November 1952, and in revised form 7th January 1953

Abstract. A liquid scintillation counter, of area 1000 cm^2 and depth 15 cm has been developed for experiments on the delayed particles in extensive air showers. The scintillator was used in conjunction with two trays of Geiger counters to select showers of average density $10/\text{m}^2$; the prompt and delayed particles traversing the scintillator were recorded photographically in an arrangement in which possible sources of spurious delays were eliminated.

The existence of delayed particles has been confirmed and the delay distribution obtained over the range $(3-70) \times 10^{-8} \text{ second}$. This distribution could be represented by an exponential function with half of the delayed particles arriving within $(10 \pm 2) \times 10^{-8} \text{ second}$. The total fraction of shower particles that suffer delays in the above range was found to be $(0.85 \pm 0.05)\%$.

There is evidence that showers with delayed events do not differ in average density from those without such events.

A control experiment was carried out to investigate any spurious effects; this revealed μ -e decay events in the scintillator at approximately the expected rate.

§1. INTRODUCTION

IT has been known for some time (Broadbent and Jánosy 1948, Cocconi *et al.* 1949, McCusker 1950, Mitra and Rosser 1949) that between 1 and 2% of the particles in extensive air showers are penetrating, and further, that of this about three-quarters can be attributed to a non-interacting component (presumed to be μ -mesons) and the remaining quarter to an interacting component (McCusker 1950). We shall henceforward denote the electronic, total penetrating, nucleonic and mesonic components by the symbols e , p , N and μ respectively.

As soon as the presence of the p -component in the showers was demonstrated, it was realized by several workers that the particles composing it might be delayed with respect to the e -component. For if each type of particle has approximately the same average energy, the velocity of the lightest particles will approximate most closely to that of light. If, moreover, a distance of several kilometres, from the higher atmosphere to sea level, is traversed, the difference in time of arrival of electrons and nucleons, or even mesons, can be shown to be measurable.* The e -component itself might arrive over a measurable period of time owing to varying path-lengths due to multiple coulomb scattering and to the fact that it may be secondary to the N or μ components.

* A simple numerical integration showed that a μ -meson which could penetrate 20 cm of lead at sea level would be delayed by $\sim 0.7 \mu\text{sec}$ with respect to a photon if both were created simultaneously in the first 100 g cm^{-2} of the atmosphere. In this calculation only ionization losses were assumed, scattering being neglected. A proton would be delayed by $\sim 4.5 \mu\text{sec}$ but its interaction mean free path of only $\sim 70 \text{ g cm}^{-2}$ would normally prevent it from traversing more than a small fraction of the atmosphere.

A determination of the delay distribution is of interest in throwing light on the theory of the nucleon cascade, which is one of the sources of the normally observed e-component (e.g. Green and Messel 1952). In earlier theories (e.g. Jánosy 1948) it had been assumed that the air showers originated from a single electron at the top of the atmosphere. However, since the discovery of the π^0 -meson in cosmic radiation by Carlson *et al.* (1950) and work on star production (Brown *et al.* 1949), it is necessary (as discussed by Messel) to include nucleon cascades in a rigorous treatment of the air showers.

Previous experimental work on the problem of delayed particles, by McCusker *et al.* (1950), Mezzetti *et al.* (1951) and Officer (1951), has been carried out using Geiger counter detectors.* There are two disadvantages arising from the use of such detectors: (i) because of the rarity of the delayed particles some of the observed effects might be attributed to large fluctuations in the firing times of the counters (e.g. due to negative ion formation) and (ii) owing to the long paralysis time ($\sim 10^{-4}$ sec) of Geiger-Müller counters, an unknown fraction of the detector trays is inoperative after the prompt front of the shower has passed through it. Apart from these objections Geiger counters could only give precise determinations for delays greater than a few times 10^{-7} second at best.

In view of these points it was decided to carry out an experiment using a high efficiency fast liquid scintillation counter of large area, developed for the purpose. If we denote the three detectors used to define the showers by A, B and C, it has been customary to select showers and trigger electronic apparatus by a double coincidence of the type (BC) and to observe the delayed particles in the A-detector, recording events of the type [(BC).A_{del}]. This system has the merit that it is possible to place lead over the A-detector (to eliminate the e-component) if desired, without disturbing the shower selection; it has however the disadvantage that the observed delays must include any electronic delays and their fluctuations in the delay measurements.

In the experiment described here it was considered of paramount importance to observe the prompt and delayed particles simultaneously *in one and the same detector*; it was realized nevertheless that the advantageous feature of the other arrangement was lost. In these experiments the detectors B and C are still composed of Geiger counters and A alone is the scintillator; the showers were detected by triple coincidences of the type (ABC) and the events observed were of the type (AA_{del}).

§ 2. THE LIQUID SCINTILLATION COUNTER AND MEASUREMENTS OF ITS EFFICIENCY

Figure 1 shows the essential features of the scintillation detector. The brass cylindrical container had a cross-sectional area of 1000 cm² and depth 15 cm which corresponded to an energy loss of 23 Mev for a vertically incident singly charged relativistic particle. The container was filled with a solution of para-terphenyl in pure benzene† (of 'Analar' quality), 2 g/litre, and sealed by

* At the time of writing work is being carried out at Manchester University using spark counters. With these a time resolution considerably better than that in the present experiments is achieved but their small size results in a much lower counting rate.

† Benzene was chosen for it was possible to obtain this in a pure form in this laboratory in the necessary quantity, while xylene of the desired purity was only available in small quantities.

a glass plate $\frac{1}{4}$ inch thick, using a polythene gasket $\frac{1}{8}$ inch in diameter. The light from the scintillator was collected by a photomultiplier (EMI type 5311) which was operated throughout the experiment at the low value of h.t. of 1.12 kv to minimize the possibility of 'satellite' pulses (see below).

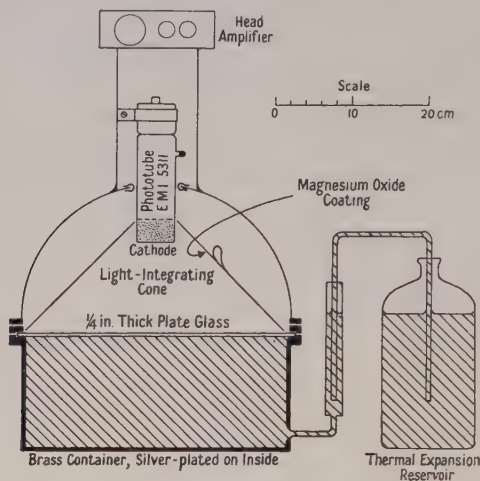


Fig. 1. The liquid scintillation counter.

It was necessary to measure the efficiency of the detector in order to ascertain that the effective area of sensitivity corresponded to the geometrical area. For this purpose the detector was mounted between two trays of counters as shown in fig. 2(a). The incident cosmic-ray particles (predominantly μ -mesons) were selected by the trays B and C and counted in triple coincidence with the detector A. The ratio of coincidences (ABC/BC) was measured at various settings of bias on a discriminator connected to a Type 201 amplifier on the A-channel. The resulting bias curve, shown in fig. 2(b), reveals that the detector has an efficiency in the central region of the container of $(98 \pm 2)\%$ over a range of 0–18 v on the particular bias scale. The bias curve for the scintillator alone is shown in fig. 2(c) from which it is seen that the plateau in the coincidence curve corresponds to a range in the detector's single rate of from $>10^4$ per minute to 900 per minute. By a similar procedure the efficiency at the edge of the scintillator was also measured. In this test the trays B and C were replaced by two small single counters, each of effective length 5 cm, placed one above and one below the container, as shown in fig. 2(d). Values of the efficiency, obtained in the same way as before, were $(91 \pm 6)\%$ and $(91 \pm 7)\%$ at the two bias levels of 12.5 and 5.0 volts respectively, corresponding to single rates in the detector, of 1100 per minute and 2400 per minute respectively.

In order to ensure that the detector was operated in a condition of high efficiency the bias was always set so that the single counting rate never fell below 3000 per minute; under these conditions the efficiency was always known to be greater than about 90%, even at the edge of the detector. The single rate often went considerably *higher* than 3000 per minute for the detector was partially sensitive to local sources of radiation even when the energy of these radiations was much lower than that of approximately 20 mev spent by the cosmic-ray

particles. At no time, however, did the rate go high enough to produce an undesirable contribution to chance triple coincidences in the main experiment.

In order to obtain some idea of the pulse-size distribution from the detector, it was connected up in the coincidence system shown in fig. 2(a) and a recording oscilloscope was triggered by double coincidences AB, with low bias on the amplifier which is connected to A. The resulting pulse-size distribution is shown as a histogram in fig. 3 in which, for comparison, is included the theoretical distribution (Landau 1944) calculated for minimum ionizing μ -mesons and normalized at its maximum to the experimental curve. It will be seen that the general shape of the distribution is similar to the Landau curve in that it has a long 'tail' on the high energy side. That the observed width is greater than

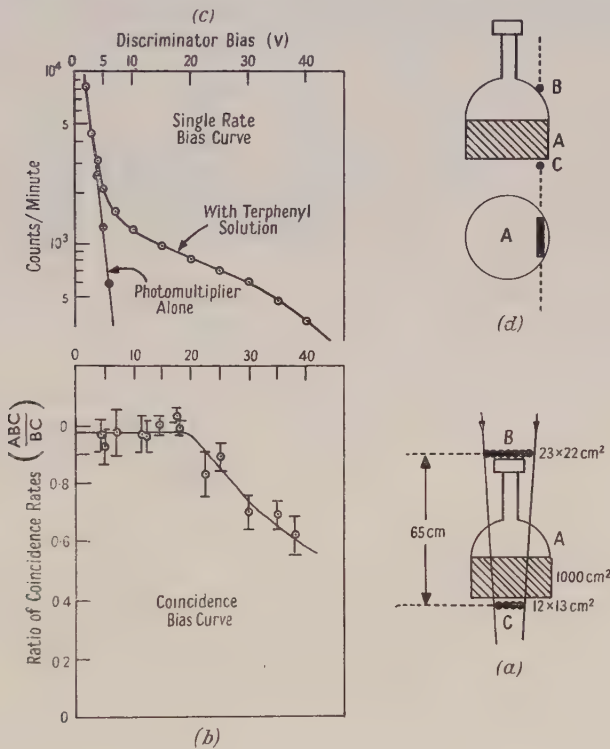


Fig. 2. Bias curves and method of measuring efficiency of scintillator.

the theoretical is expected, and results from the variations in efficiency of gathering the light and from the wide range of energies in the μ -meson spectrum; there is a further contribution from electrons, some of which will come to rest in the liquid. It should be pointed out that in the actual experiment a still greater spread in the distribution is expected, for there is then no collimation of the particles. There is, however, some compensation here, for it is generally accepted that the angular distribution of shower particles varies steeply with the zenith angle θ , being probably $\cos^6 \theta$.

From this curve we can obtain some idea of the overall efficiency of the recording system as it is used, in conjunction with a microfilm reader, in the main experiment. In fig. 3 the abscissa represents the deflection in a microfilm reader measured in millimetres where 18 corresponds to the saturation level of

the amplifier. As will be described later all pulses of amplitude less than 5% of saturation are ignored. From this curve it is seen that of the 606 pulses two fall within the first 1 mm which represents an overall loss of approximately 0.3% of all pulses photographed. Taking the energy spectrum for electrons in air showers from the work of Mitra and Rosser (1949) it is found that approximately

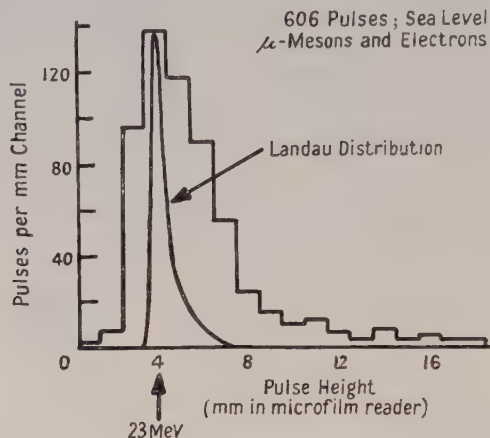


Fig. 3. Pulse-height distribution for sea-level particles selected by a simple telescope.

3% of the particles will not be able to penetrate the glass cover plate of the scintillator, and that of those electrons that do penetrate the plate a further 15% will come to rest in the solution, thus spending less than the maximum transferable energy.

§ 3. ARRANGEMENT OF DETECTORS AND THE ELECTRONIC APPARATUS

A block diagram of the apparatus appears in fig. 4. The detectors, which lie in a horizontal plane, are enclosed in thermostatically controlled housings, situated on a flat roof about 30 metres from the rest of the apparatus in the laboratory; the location is 130 metres above sea level. The counters are standard Cintel units with copper cathodes and an argon-alcohol filling. In the earlier period of the experiment the counter trays had areas of 560 and 1050 cm² respectively while at a later period both trays were of the same area, each 1260 cm².

For purposes of description we will group the various parts of the electronic circuits under two headings: (i) the slow group, operating the trigger mechanism of the recording oscillograph, and (ii) the fast group, serving the deflector plates of the oscillograph, this group comprising the time-delay measuring system. The head amplifier attached to the scintillator had two channels, one slow and one fast.

(i) *The Slow Circuits*

The output from the slow channel of the head amplifier on the scintillator, a simple cathode follower, is fed along a 100 Ω line to a Type 201 amplifier and thence through a discriminator to one channel of a threefold coincidence unit. This amplifier, which has a maximum gain of approximately 10^4 , has gain stabilization and a bandwidth of 5 Mc/s; it was operated with nominal integration and differentiation time constants of 0.032 and 1.6 μ sec respectively. The

outputs of the tray detectors B and C feed the two other channels of the coincidence unit via simple two-stage amplifiers of gain about 300 with blocking-oscillator output stages. The coincidence unit is of simple design employing diode mixers; its resolving time was $0.75 \mu\text{sec}$.

The single rate of the scintillator was monitored continuously on a pen recorder in conjunction with a ratemeter. The single rates of trays B and C were taken twice daily and the coincidence rate ABC was recorded on a mechanical register and another pen recorder.

(ii) *Fast Circuits*

The fast channel of the head-amplifier on the scintillator has been described elsewhere (Wells 1952). The output pulse from this was led along a low-loss 100 Ω cable to a distributed-line amplifier with 23 stages, of gain 200 and a

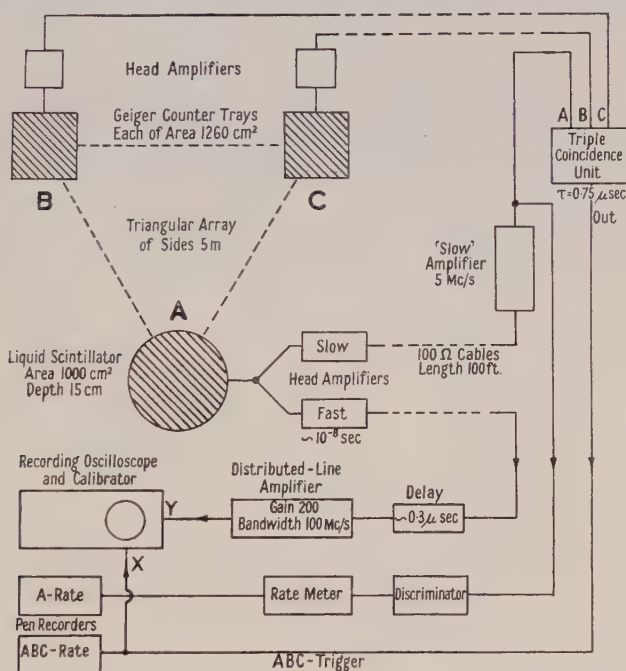


Fig. 4. Arrangement of electronic units.

frequency response sensibly flat to 100 Mc/s; with this amplifier an adequate saturation level, of approximately 35 v, was available for the deflection circuits of the oscilloscope.

The recording oscilloscope was of conventional design. Each time the $1\mu\text{sec}$ time-base was fired by the trigger-pulse a second sweep was made on which was displayed a 10 Mc/s calibration waveform. A small watch was illuminated and photographed for purposes of identification, and the film moved forward one frame after each photograph.

§ 4. RESULTS

Before presenting the results of the experiment it is necessary to mention the method of measuring the delays and pulse amplitudes, and to define and discuss the limiting criteria. The prompt and delayed particles in the A-detector

were displayed on 16 mm film. The measurements were carried out using a microfilm reader with a magnification of 12.5. Of the total length of time-base of $1\mu\text{sec}$, only $0.7\mu\text{sec}$ was on the average available, for $0.3\mu\text{sec}$ was allowed (in the delay circuits) at the start of the time-base for fluctuations as already mentioned. With a pulse-width of the order of 10^{-7} sec at the 'base' of the pulses, the limiting resolution was 3×10^{-8} second. The delay intervals were measured between the peaks of the pulses, in terms of the 10 Mc/s calibration pips present on the frame in question. Pulse amplitudes were also measured in the microfilm reader.

It should here be mentioned that the majority of the recordings showed only a single pulse.

The following criteria of selection of the events were adopted: (i) All showers which had their prompt pulses above saturation were eliminated from the results. (ii) Prompt or delayed pulses of amplitude less than 5% of saturation

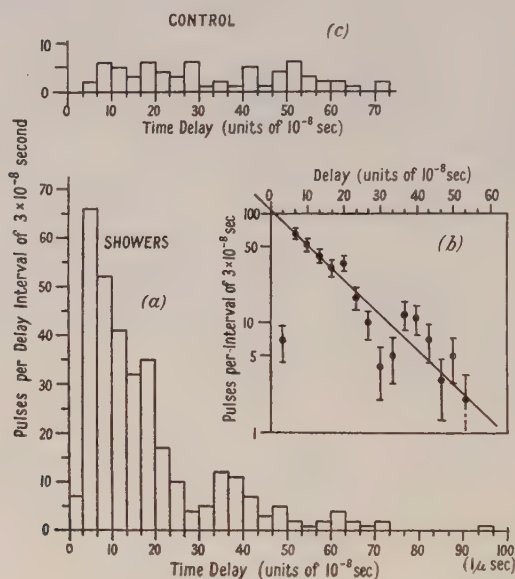


Fig. 5. Time-delay distributions.

were also eliminated. (iii) The counting of the showers which were not followed by delayed events included all pictures in which the prompt pulse was invisible.

We will now briefly discuss these criteria and give estimates of the errors involved through their adoption. Criterion (i) was introduced because large saturating pulses had subsequent ripples on the time-base owing to limits in the fidelity of the fast amplifier. Only about 2% of the showers had their prompt pulses above saturation. This criterion introduces a bias against all showers whose density is very great near A. Criterion (ii) was introduced because this was the smallest deflection that could be reliably read in the microfilm reader. Criterion (iii) was introduced because the slow amplifier channel had a much higher gain than the fast and it was possible for a shower particle to trigger the scintillation detector A by a relatively soft electron (and hence record the shower) though the resulting pulse would be invisible on the oscilloscope trace.

Approximately 10% of the shower photographs had their prompt pulses below 5% of saturation. As a result, it would be possible to mistake the delayed pulse for the prompt, if the initiation of the prompt pulse were a low-energy electron. This effect is unlikely to change the form of the delay distribution curve but will cause some error in the absolute number of delayed events relative to the number of showers; a correction is made for this effect.

With the above criteria, a total of 322 delayed events were recorded in the selected time range in a total recording of 55 500 showers. Figure 5(a) shows a histogram of the delay distribution for these events. The low number of pulses in the first histogram interval is unlikely to be a real effect, but is almost certain to be due to losses arising through the finite time resolution, particularly when the prompt pulse is large and the delayed one small. Assuming the distribution to be exponential, see fig. 5(b), the number of events in this first interval is estimated to be 105, from which it is deduced that half the delayed events fall within $(0.10 \pm 0.02)\mu\text{sec}$ and half outside this figure.

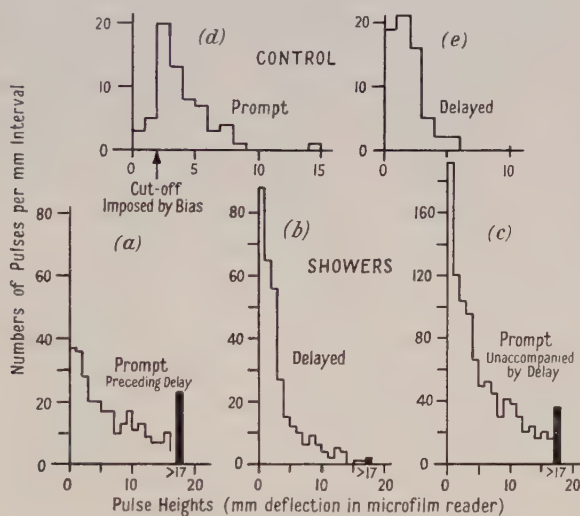


Fig. 6. Pulse-height distributions.

To obtain the true fraction of showers that have associated delayed particles three corrections have to be applied: (a) Correction for the loss of particles in the first interval in the time-delay distribution yields a figure, for the number of delayed events, of $(322 - 7 + 105) = 420$. (This is the total observed number less the observed number in the first interval plus the extrapolated number in this interval.) (b) As 10% of the recorded showers have their prompt pulses below the threshold (criterion (ii) above), 10% of the observed single pulses should have been interpreted as delayed pulses, their corresponding prompt pulses being invisible, raising the number, for this correction, to 467. (c) A further 2% is added for those showers having saturating prompt pulses, (criterion (i)), bringing the total number of delayed events up to 476. The corrected figure for the fraction of showers with associated delays is thus $(476 \pm 26)/55\,500$, i.e. $(0.85 \pm 0.05)\%$. The errors quoted (standard deviations) are only the statistical parts.

In figs. 6(a) and 6(b) are shown the pulse height distributions for the prompt and delayed particles associated with the 322 observed events while fig. 6(c) shows the distribution for 1007 prompt pulses not accompanied by delayed pulses; these will be considered in §6.

There was found to be no significant correlation between pulse height and delay.

§ 5. CONTROL EXPERIMENT; CASUAL RATES

In order to be certain that these delayed events were genuinely associated with the air showers, a control experiment was carried out in which the output of the A-detector was photographed when it was operating on particles not associated with showers, the phototube h.t. voltage, fast-amplifier gain and recording arrangements being unchanged. For this experiment the oscilloscope was triggered directly from the A-channel input to the coincidence unit; the Geiger counter h.t. voltage was removed and the gain of the slow amplifier on the A-channel was very considerably reduced (by about 20 db) so that the oscilloscope was triggering at a reasonable speed and the prompt pulses appeared at an average height corresponding to the average height of those in the air-shower experiment, thus simulating as nearly as possible the normal conditions. Under these conditions of gain the majority of prompt pulses photographed will be due to μ -mesons. In this control experiment the film was run through the camera continuously and in about 10 minutes 9000 time-base traces were recorded, this rate corresponding approximately to the total cosmic-ray flux through the scintillator over the upper hemisphere. Control runs were carried out from time to time and sandwiched between the air-shower runs. The results of this experiment, grouping all the runs together, are summarized in the delay distribution of fig. 5(c). In a total of 33 400 recordings there were 65 delayed events. It will be seen at once that the absolute rate is much lower in the control experiment than in the air-shower experiment and furthermore that the delay distribution is essentially flat over the time region selected. Owing to the absence of Geiger counter delays in the triggering of the oscilloscope in this experiment only $0.5 \mu\text{sec}$ of the time-base is on the average useful. Correcting for a loss of particles in the first channel, as in the shower experiment, a figure of 69 is obtained, and normalizing to a $0.7 \mu\text{sec}$ time-base for comparison with the shower experiment raises this further to 97. The resulting fraction $97/33\,400$, i.e. $(0.29 \pm 0.04)\%$, is seen to be about 0.3 of that obtained in the shower experiment.

§ 6. DISCUSSION

(i) *Origin of the Background*

There are three possible sources of the double pulses in the control experiment: (i) casual rate, (ii) satellite pulses from the phototube and (iii) μ -e decay events in the scintillator. Taking the value quoted by Rossi (1948) for the μ -meson flux at sea level arriving from the upper hemisphere, i.e. 1.27×10^{-2} particles $\text{cm}^{-2} \text{sec}^{-1}$, the calculated rate for casual pulses arriving within $0.7 \mu\text{sec}$ of each other is one double event in approximately 1.1×10^5 single events. From the figure of $(0.29 \pm 0.04)\%$ obtained above, the observed number of double pulses is 1 in (340 ± 50) single events, which is thus about 300 times that calculated on the basis of chance coincidences. From this it is seen that none of the observed double events in the control experiment can be attributed to a casual rate.

There is good evidence that the delayed pulses are not satellite pulses from the phototube because Wells (1952) has shown that, with a tube of the same type as used in the present experiments, there are no observable satellite pulses below an h.t. value of 1.5 kv while in our case we have an h.t. of 1.12 kv. Also it has recently been reported, Müller *et al.* (1952) that satellite pulses correspond in amplitude to the emission of single photo-electrons from the photocathode while we know that in our case the observed pulse heights from the cosmic-ray particles are at least two orders of magnitude larger than noise pulses. Referring to the pulse-height distributions for the prompt and delayed pulses in the control experiment, figs. 6 (*d*) and (*e*), we see that the average height of the prompt pulses is approximately 3.5 mm (extrapolating to zero height) while that for the delayed pulses is approximately 1.5 mm. As the height of the delayed pulses is thus about 0.4 times that of the main pulses (~ 20 mev) the possibility of satellite pulses can be completely eliminated.

The contribution of double events that can be attributed to μ -e decays was calculated from the differential range spectrum of μ -mesons at sea level given by Rossi (1948, fig. 6). Assuming (i) that the rate at which μ -mesons were stopped in the solution was $5.0 \times 10^{-6} \text{ g}^{-1} \text{ sec}^{-1} \text{ sterad}^{-1}$, (ii) a $\cos^3 \theta$ distribution (Kraushaar 1949) where θ is the zenith angle, and (iii) the μ -meson spectrum to be the same at all angles, we obtain after integrating over the upper hemisphere a total rate of 6.1 per minute brought to rest in the 13 kg of benzene. With a mean life of $2.1 \mu\text{sec}$ for μ -mesons in carbon, 0.28 of these events would occur within the $0.7 \mu\text{sec}$ time-base in use. The resultant rate of μ -e decays, i.e. 1.7 per minute, is then compared with the total calculated flux of μ -mesons arriving through the scintillator which is approximately 750 per minute. On this basis the frequency of double events would be 1 in ~ 440 which is consistent within the errors of the above calculation with the experimental figure of 1 in (340 ± 50) . On the basis that all the double pulses observed in the control experiment arise from μ -e decays, it is reasonable to assume that the only background existing in the air-shower experiment, fig. 5 (*a*), is that due to the casual rate, which would be imperceptible on this figure.

(ii) Pulse-Height Distributions

The pulse-height distributions shown in fig. 6 are re-plotted in fig. 7 on a logarithmic scale. Curves *a* and *b* refer, respectively, to the distributions for the delayed and the prompt pulses associated with these delayed particles, for the 322 shower events, while curve *c* refers to the 1007 randomly selected prompt pulses having no associated delayed pulses.

The similarity between the slopes of curves *b* and *c* suggests that the showers with associated delayed events do not differ in average density from those which have no delayed events.

It will be noticed that the size distribution of the delayed pulses, curve *a*, is markedly steeper than that for the prompt pulses. This is easily explained in terms of the relative numbers of prompt and delayed particles.

The delayed particles form such a small proportion of the total number of shower particles that, if they were distributed in a truly random manner, we should not have expected more than about one accidental coincidence between them. In fact, in addition to the 309 cases* in which a single delayed particle

* The figure of 322 quoted earlier includes the cases in which multiple delays were observed.

appeared on the time-base, there were 12 in which two appeared, and one in which three appeared. These figures point to some form of association between the delayed events, but not one which could easily be investigated with the present apparatus. However, it is justifiable to assume that virtually all the delayed pulses are caused by the passage of a single particle into or through the scintillator, and this conclusion is strengthened by the fact that the 'tail' of the distribution for single mesons (fig. 3) is approximately parallel to curve *a* of fig. 7.

The prompt pulses, on the other hand, being associated in fairly dense showers, quite frequently enter the scintillator in groups. A calculation of the relative probabilities of groups of two or more prompt particles is presented in the Appendix. If we take curve *a* of fig. 7 as representing the experimentally determined size distribution of the pulses due to single shower pulses, and calculate the distribution for the prompt particles, allowing for multiple events, we obtain the curve *d* whose slope is much nearer to that of the observed distributions *b* and *c*. Since the difference in the slopes of the size distributions of prompt and delayed events can be satisfactorily explained on statistical grounds, it cannot provide any evidence about the nature of the delayed particles.

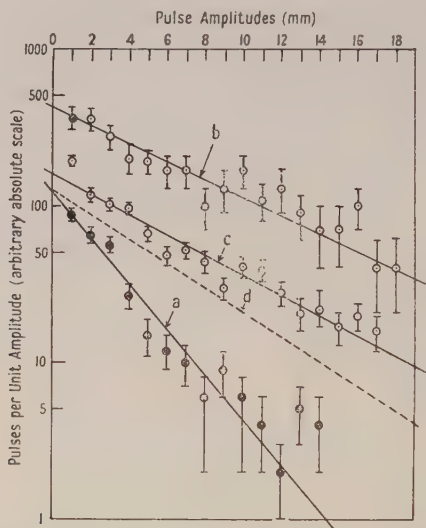


Fig. 7. Logarithmic plot of pulse-height distributions.

It is seen from fig. 6, (*d*) and (*e*), that there is less difference between the distributions for the prompt and delayed events in the control experiment than in the shower experiment. Assuming the μ - e decay process to explain these events this is what would be expected because a μ -meson that stops, say, half-way through the scintillator will spend about 30 mev which is also of the same order of magnitude as the average energy of the decay electrons.

§7. CONCLUSIONS

The existence of delayed particles in extensive air showers has been confirmed, using a scintillation detector in an arrangement in which electronic and counter delays, and possible sources of spurious pulses, have been eliminated. The time-delay distribution could be represented by an exponential function with

half of the delayed particles arriving within $(0.10 \pm 0.02) \mu\text{sec}$. The total fraction of shower particles that suffer delays in the range $(3-70) \times 10^{-8} \text{ sec}$ was found to be $(0.85 \pm 0.05)\%$.

There is evidence that showers having associated delayed events do not differ in average density from those without such events.

ACKNOWLEDGMENTS

The authors would like especially to thank Professor J. G. Wilson of Leeds University for helpful discussions, Mr. F. H. Wells who assisted in the design work of the fast electronic circuits and Mr. E. F. Bradley who helped throughout the work in the construction and maintenance of the equipment. The authors wish to thank Dr. E. Bretscher and the Director of the Atomic Energy Research Establishment for permission to publish this work.

APPENDIX

The Distribution in Height of the Pulses caused by Showers

The probability P_n of n particles entering the scintillator was calculated by numerical integration of a function similar to that introduced by Cocconi, Loverdo and Tongiorgi (1946), namely

$$P_n = c \int_0^\infty x^{-\gamma} (1 - e^{-\alpha x})^2 (x^n e^{-x} / n!) dx$$

where x is the product of the shower density and the scintillator area and c is a constant. The first term takes account of the probability of occurrence of a shower of given density; the value of γ used was 2.5. The second term represents the probability of the two Geiger trays being discharged; the symbol α stands for the ratio of the area of the Geiger trays and the scintillator. The third term represents the probability that n particles from the shower will enter the scintillator in coincidence. The relative numbers of multiple prompt events are as follows:

n	1	2	3	4	5	6	7	8
P_n	1	0.41	0.19	0.12	0.05	0.03	0.014	0.007

The calculations showed, incidentally, that the density of showers which were most likely to be registered was of the order of 4 particles/m² while the mean density selected by the array was of the order of 10 particles/m².

Now, if the size distribution of pulses from single particles is taken from curve (a) of fig. 7 to be $H_1(h) dh = be^{-bh} dh$ where h is the pulse height and b is an empirical constant, it can be shown that the size distribution of pulses caused by n particles is

$$H_n(h) dh = \frac{b^n}{(n-1)!} h^{n-1} e^{-bh}.$$

The size distribution of the pulses from all the showers is accordingly

$$S(h) dh = \sum P_n H_n(h) dh.$$

This, which is plotted in fig. 7 and gives the distribution (d), is discussed in the latter part of the paper.

REFERENCES

- BROADBENT, D., and JÁNOSSY, L., 1948, *Proc. Roy. Soc. A*, **192**, 364.
BROWN, R. H., CAMERINI, U., FOWLER, P. H., HEITLER, H., KING, D. T., and POWELL, C. F., 1949, *Phil. Mag.*, **40**, 862.
CARLSON, A. G., HOOPER, J. E., and KING, D. T., 1950, *Phil. Mag.*, **41**, 701.
COCCONI, G., LOVERDO, A., and TONGIORGI, V., 1946, *Phys. Rev.*, **70**, 846.
COCCONI, G., TONGIORGI, C., and GREISEN, K., 1949, *Phys. Rev.*, **75**, 1063.
GREEN, H. S., and MESSEL, H., 1952, *Proc. Phys. Soc. A*, **65**, 689.
JÁNOSSY, L., 1948, *Cosmic Rays* (Oxford: University Press).
KRAUSHAAR, W. L., 1949, *Phys. Rev.*, **76**, 1045.
LANDAU, L., 1944, *J. Phys. USSR*, **8**, 201.
MCCUSKER, C. B. A., 1950, *Proc. Phys. Soc. A*, **63**, 1240.
MCCUSKER, C. B. A., RITSON, D. M., and NEVIN, T. E., 1950, *Nature, Lond.*, **166**, 400.
MEZZETTI, L., PANCINI, E., and STOPPINI, G., 1951, *Phys. Rev.*, **81**, 629.
MITRA, S. M., and ROSSER, W. G. V., 1949, *Proc. Phys. Soc. A*, **62**, 364.
MÜLLER, D. W., HARRISON, F. B., GODFREY, T. N. K., KEUFFEL, J. W., and DAVISON, P. W., 1952, *Nucleonics*, **10** (3), 32.
OFFICER, V. C., 1951, *Aust. J. Sci. Res.*, **4** (4), 526.
ROSSI, B., 1948, *Rev. Mod. Phys.*, **20**, 537.
WELLS, F. H., 1952, *Nucleonics*, **10** (4), 28.

An Investigation of (d, p) Stripping Reactions III : Results for ^{28}Si and ^{32}S

BY J. R. HOLT AND T. N. MARSHAM

Nuclear Physics Research Laboratory, University of Liverpool

Communicated by H. W. B. Skinner; MS. received 15th December 1952

Abstract. Angular distribution measurements have been carried out on a number of proton groups emitted as a result of the bombardment by 8 mev deuterons of targets of natural SiO_2 and sulphur. Using the theory of the stripping process spins and parities have been assigned to the resulting states of ^{29}Si and ^{33}S . Certain of these states in both nuclei are thought to be produced by simple excitation of the odd neutron. One of the low states in each case probably involves the first excited state of the nuclear core. In the following list the excitation energy of each state in mev is given, together with the suggested shell model term or the possible spin values and parity.

^{29}Si : ground state ($2s_{1/2}$), 1.28($1d_{3/2}$), 2.03($1d_{5/2}^{-1}2s_{1/2}^2$), 3.07($5/2, 3/2+$), 3.62($1f_{7/2}$), 4.93($2p_{3/2}$), 6.38($2p_{1/2}$).

^{33}S : ground state ($1d_{3/2}$), 0.85($2s_{1/2}^{-1}1d_{3/2}^2$), 2.90($1f_{7/2}$), 3.26($2p_{3/2}$), 4.21($3/2, 1/2-$), 4.89($3/2, 1/2-$), 5.72($2p_{1/2}$), 6.48($3/2, 1/2-$).

§ 1. INTRODUCTION

THE apparatus and method of procedure described in Papers I and II of this series (Holt and Marsham 1953 a, b) have been used to study the angular distributions of various groups of protons emitted from targets containing ^{28}Si and ^{32}S under bombardment by 8 mev deuterons. Further comparisons have been made of the theories of the stripping process with experiment, and spins and parities assigned to some of the states of ^{29}Si and ^{33}S . The choice of target nuclei was determined partly by the fact that both have spin zero, which reduces to a minimum the ambiguity in the assignment of spin values to the states produced in the stripping process. Also, both nuclei have equal numbers of protons and neutrons, each group completely filling a sub-shell of the Mayer shell model. States produced solely by the addition of a neutron with little disturbance of the nuclear core might be expected to be prominent in such nuclei.

The spectra of the (d, p) reactions with separated isotopes of silicon have been examined with magnetic analysis by Van Patter and Buechner (1952) at a deuteron energy of 2 mev and we have used these results in the interpretation of the range spectrum from the natural isotopic mixture used in our experiments. Previous work on the (d, p) reaction with sulphur has been carried out mainly by Davison (1949) using the absorption method and deuterons of 3.2 mev.

§ 2. TARGET PREPARATION

Silicon was bombarded in the form of silica, SiO_2 , containing the natural isotopic mixture ^{28}Si , ^{29}Si and ^{30}Si in the proportions 92.3: 4.7: 3.0. A self-supporting target was prepared by blowing a thin bubble of silica from a tube of pure fused quartz in an oxy-hydrogen flame. A suitable flake having a thickness of 1.3 cm air equivalent was broken off from the bubble. The proton groups

emitted from the oxygen in the target did not interfere seriously with the measurements on the groups from silicon. The possibility of contributions to the proton groups from the abundant isotope of silicon by groups from the rare isotopes is considered during the discussion of the angular distributions.

A target of sulphur was prepared by boiling the pure element in a test tube and allowing the vapour to condense on a gold foil stretched across a circular aperture in a brass sheet. During the initial experiments it was found that the sulphur was gradually vaporized during the course of the bombardment. To prevent this a second gold leaf was placed over the target and the temperature raised to the melting point of sulphur. The gold leaf was then drawn into contact with the sulphur by surface tension and a sandwich of sulphur between gold leaves was formed, the air being excluded.

§ 3. RESULTS

(i) Spectra of Proton Ranges

The differential range spectrum of the protons from the silica target is shown in fig. 1 for an angle of observation of 31° . The horizontal scale indicates the total range of the emitted protons in aluminium and the vertical scale shows the proton

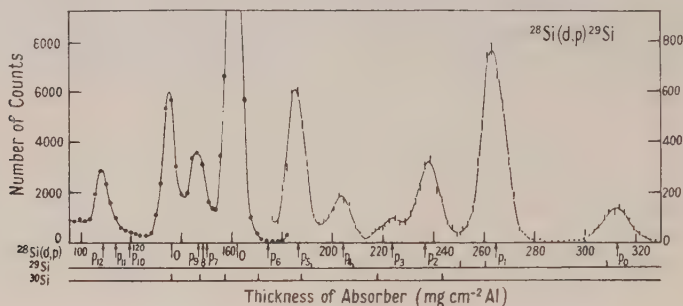


Fig. 1. Range spectrum of protons at an angle of observation of 31° from the deuteron bombardment of a target of natural SiO_2 .

count. The arrows at the bottom of the figure show the expected positions of proton groups as calculated from the Q -values given by Van Patter and Buechner for the reaction $^{28}\text{Si}(d, p)^{29}\text{Si}$. Also indicated are the expected positions of proton groups from the reactions $^{29}\text{Si}(d, p)^{30}\text{Si}$ and $^{30}\text{Si}(d, p)^{31}\text{Si}$. The energy of the bombarding deuterons was 8.21 mev as derived from the measured range and known Q -value of the proton group p_0 . The expected positions of the groups due to oxygen are indicated by the lines marked O. Angular distribution measurements were made on the peaks p_0 , p_1 , p_2 , p_3 , p_4 , p_5 , p_9 and p_{12} . The group p_6 was of small intensity and could be observed only at large angles when the intensity of the neighbouring groups was reduced.

The differential range spectrum of the protons from the sulphur target is shown in fig. 2 for an angle of observation of 16° . The inset shows the region of short ranges at an angle of observation of 26° . The deuteron energy was determined as 8.18 mev from the measured range of the proton group p_0 and the corresponding Q -value of 6.422 mev (Strait *et al.* 1951). Our range spectrum agrees in the main features with that obtained by Davison. The region in our spectrum covering ranges of 230 to 270 $\text{mg cm}^{-2}\text{Al}$ is that expected for groups corresponding to the formation of the second and third excited states of ^{33}S given by Davison. The

intensity and resolving power in our case was not sufficient to verify this, but we have assumed that his analysis is correct and similarly analysed this region into two groups. We did not observe a proton group corresponding to the formation of the eighth excited state of ^{33}S reported by Davison. There was evidence of a proton group corresponding to the formation of the tenth excited state given by Davison, but we were unable to determine its range. The half-width of the peak p_{12} is 30% greater than that of the neighbouring peak p_{11} , suggesting that the former is an unresolved doublet. The peaks p_{13} and p_{14} are outside the range of Davison's observations. Our values for the excitation of the various states, calculated from the mean ranges of the proton peaks indicated by the arrows at the bottom of fig. 2, are collected in table 2, together with the results of Davison. Angular distribution measurements were made on the groups p_0 , p_1 , p_4 , p_5 , p_7 , p_9 , p_{11} and p_{12} .

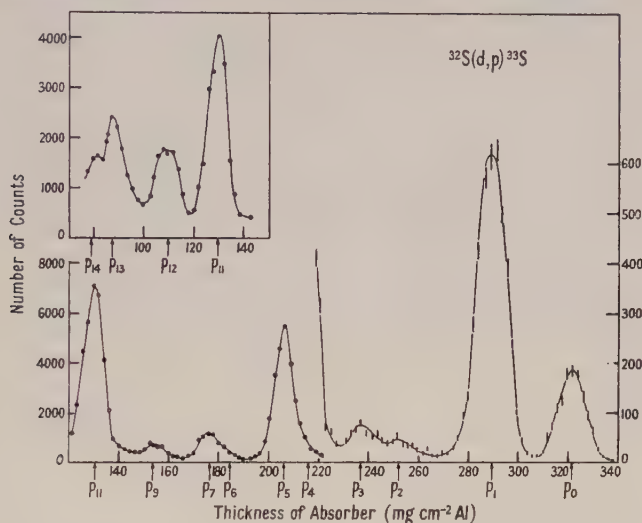


Fig. 2. Range spectrum of protons at an angle of observation of 16° from the deuteron bombardment of a target of natural sulphur. The inset shows a portion of the spectrum at 26° .

(ii) Angular Distributions

The angular distributions of the various groups of protons were obtained from the range spectra as described in I. The resulting angular distributions are shown in figs. 3 to 12 in which the coordinates refer to the centre-of-mass system. The errors shown on the experimental points include the statistical counting error, together with an allowance for any drifts in the apparatus and, where necessary, for the uncertainty introduced by the overlapping of neighbouring peaks. The curves drawn in each case have been calculated using the theory of the stripping process given by Butler (1951) with a radius of interaction given by the formula $(1.7 + 1.22A^{1/3}) \times 10^{-13}$ cm, namely 5.4×10^{-13} cm for silicon and 5.6×10^{-13} cm for sulphur. Comparisons were also made with the theory of Bhatia *et al.* (1952).

The Reaction $^{28}\text{Si}(d, p)^{29}\text{Si}$.

The angular distribution of the proton group p_0 resulting from the formation of the ground state of ^{29}Si is shown in fig. 3. The theoretical curve was drawn using the value 0 for the amount of orbital angular momentum lh , taken into the nucleus by the captured neutron. Figure 4 shows the angular distribution of the proton group p_1 , with a theoretical curve for $l=2$. The distributions of the groups p_2 and

p_3 are shown in fig. 5, the vertical scale being the same for both. The theoretical curve giving the best fit with the experimental points for p_2 is one having $l=2$. The distribution of the group p_3 does not show the pronounced peak characteristic of stripping reactions. At small angles this group was obscured by the rapid increase of a group of slightly shorter range. Van Patter and Buechner report a group of protons from the reaction $^{30}\text{Si}(d, p)^{31}\text{Si}$ corresponding to an excitation of ^{31}Si of 0.757 mev which could be responsible for this if the l -value for the transition were 0. The angular distribution of the protons in peak p_4 is shown in fig. 6. The experimental points could be fitted only by combining together two curves, one having $l=0$ and the other having $l=2$, with their maxima in the ratio 1.4:1. This must mean that the peak p_4 consists of two unresolved groups of protons. According to the magnetic analysis of Van Patter and Buechner the level in ^{29}Si

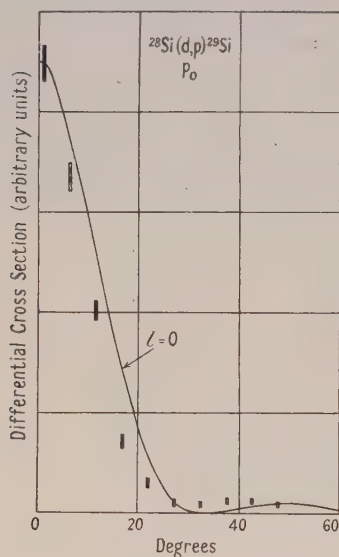


Fig. 3. p_0 from $^{28}\text{Si}(d, p)^{29}\text{Si}$.

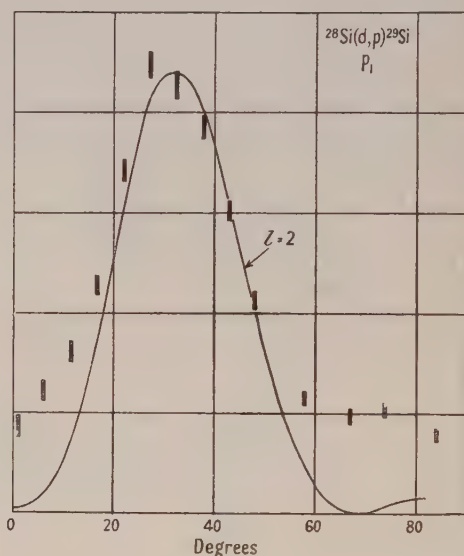


Fig. 4. p_1 from $^{28}\text{Si}(d, p)^{29}\text{Si}$.

corresponding to this proton peak is single. However, these workers find some evidence for a proton group from the reaction $^{29}\text{Si}(d, p)^{30}\text{Si}$ associated with a Q -value close to that for the transition in the reaction $^{28}\text{Si}(d, p)^{29}\text{Si}$. From consideration of the relative intensities of the two components of the measured angular distribution the component having $l=2$ must be due to the group from $^{28}\text{Si}(d, p)^{29}\text{Si}$. The component having $l=0$ is probably due to a proton group from $^{29}\text{Si}(d, p)^{30}\text{Si}$.

The angular distribution of peak p_5 is shown in fig. 7. The best fit with the experimental points was obtained with a theoretical curve constructed by combining a curve having $l=3$ with one having $l=0$. The argument of the previous paragraph can also be applied to this case. The component having $l=3$ must be associated with the transition in $^{28}\text{Si}(d, p)^{29}\text{Si}$. The component having $l=0$ could be due to a transition in $^{29}\text{Si}(d, p)^{30}\text{Si}$ or $^{30}\text{Si}(d, p)^{31}\text{Si}$. A better fit with the experimental angular distribution could be obtained by including a small component having $l=2$, so both the rare isotopes may contribute to this proton peak.

The angular distribution of the prominent peak at a mean range of 147 mg cm^{-2} is shown in fig. 8 (a), together with a theoretical curve having $l=1$. The position of this peak is approximately that expected for the three close groups of protons

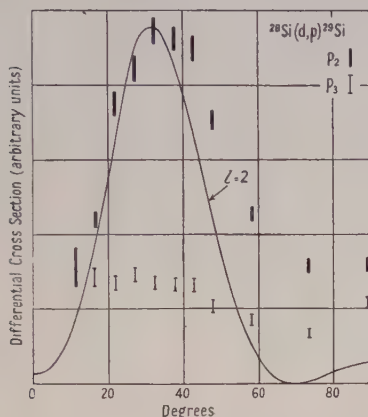


Fig. 5. p_2 and p_3 from $^{28}\text{Si}(d, p)^{29}\text{Si}$.

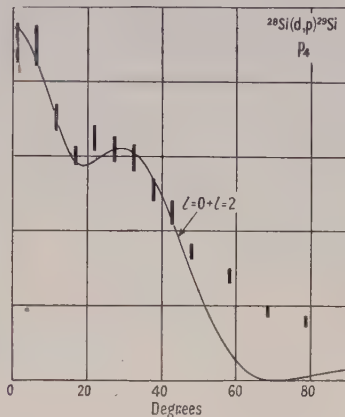


Fig. 6. p_4 from $^{28}\text{Si}(d, p)^{29}\text{Si}$.

associated with the seventh, eighth and ninth excited states of ^{29}Si . The mean range corresponds well with that expected for the group p_9 and it seems likely that this group corresponds to a transition with $l=1$.

The position and half-width of the peak at a mean range of 108 mg cm^{-2} indicate that it is almost entirely due to the proton group p_{12} . The groups p_{10}

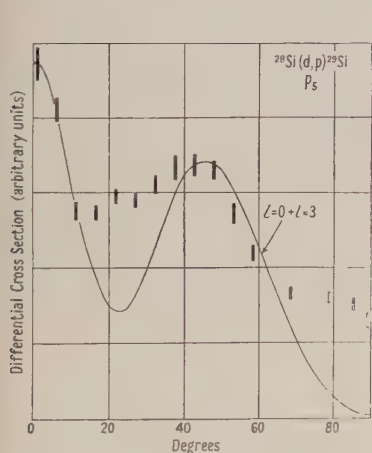


Fig. 7. p_5 from $^{28}\text{Si}(d, p)^{29}\text{Si}$.

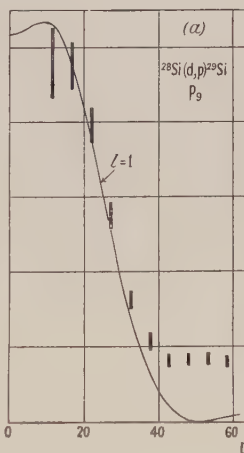


Fig. 8. (a) p_9 from $^{28}\text{Si}(d, p)^{29}\text{Si}$.

(b) p_{12} from $^{28}\text{Si}(d, p)^{29}\text{Si}$.

and p_{11} are much weaker than p_{12} at all angles in the range 10° to 70° . The angular distribution of the group p_{12} is shown in fig. 8 (b) together with a theoretical curve having $l=1$.

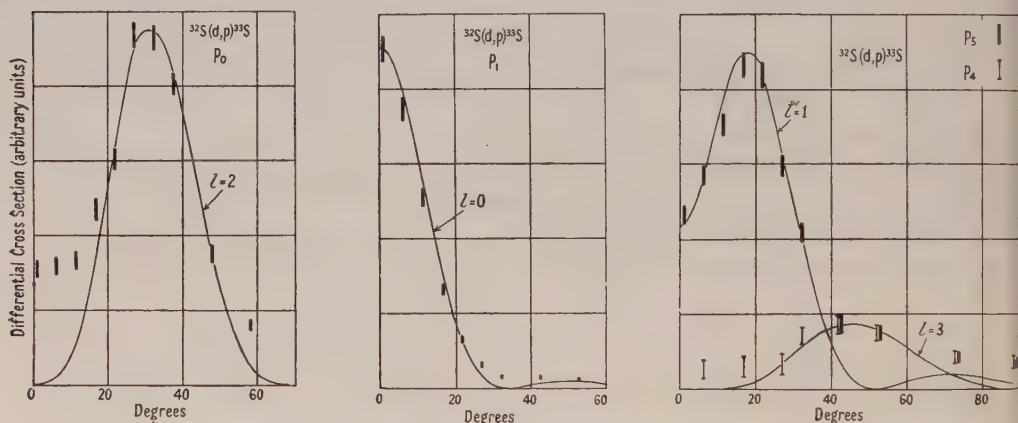
The Reaction $^{32}\text{S}(d, p)^{33}\text{S}$.

The angular distributions of the proton groups p_0 and p_1 are shown in figs. 9 and 10 respectively, the theoretical curves being drawn with $l=2$ and $l=0$.

The region of the spectrum between ranges of 230 and 270 mg cm^{-2} including the proton groups p_2 and p_3 , was measured at a number of angles between 0° and 70° . The shape of the spectrum showed little change and the intensity varied by less than 30% within this angular region.

The proton groups p_4 and p_5 overlapped in the range spectrum and their contributions at each angle were determined graphically by separating the combined peak into two components, each having the known half-width of a single proton peak. The two angular distributions are shown in fig. 11, the vertical scale being the same for both. The points for group p_5 are fitted by a theoretical curve having $l=1$. The errors on the points for group p_4 are rather large, but it appears that a theoretical curve having $l=3$ provides the best fit.

The small intensity of the group p_6 and its proximity to the group p_7 made it impossible to measure the angular distribution.



Angular distributions of proton groups.

Fig. 9. p_0 from $^{32}\text{S}(d, p)^{33}\text{S}$. Fig. 10. p_1 from $^{32}\text{S}(d, p)^{33}\text{S}$. Fig. 11. p_4 and p_5 from $^{32}\text{S}(d, p)^{33}\text{S}$.

The angular distributions of the groups p_7 , p_9 , p_{11} and p_{12} are shown in fig. 12. In the case of the first three groups the best fit is obtained with theoretical curves having $l=1$. The points for p_{12} lie between the curves for $l=1$ and $l=2$. This is probably due to the doublet structure of the group with one component having $l=1$ and the other having $l=2$.

Measurement of Cross Sections

The relative differential cross sections at the maxima of the angular distributions were obtained by comparing the areas beneath the peaks in the range spectrum. In the case of silicon these were converted to the absolute scale by comparison with the differential cross section for the transition to the ground state in the reaction $^{16}\text{O}(d, p)^{17}\text{O}$ using the known proportion of oxygen in the target. The differential cross section for this transition at an angle of 21° was taken to be $4 \times 10^{-26} \text{ cm}^2$ from the previous work with targets of MgO (II) .* This figure could be in error

* Owing to a mistake the values of the absolute cross sections quoted in I and II are all too great by a factor of 4.

by $\pm 50\%$ but the relative cross sections for the transitions in $^{28}\text{Si}(d, p)^{29}\text{Si}$ should be accurate to $\pm 10\%$. In the case of sulphur no such conversion to the absolute scale could be made and the numbers given in table 1 are proportional to the differential cross sections at the maxima of the angular distributions.

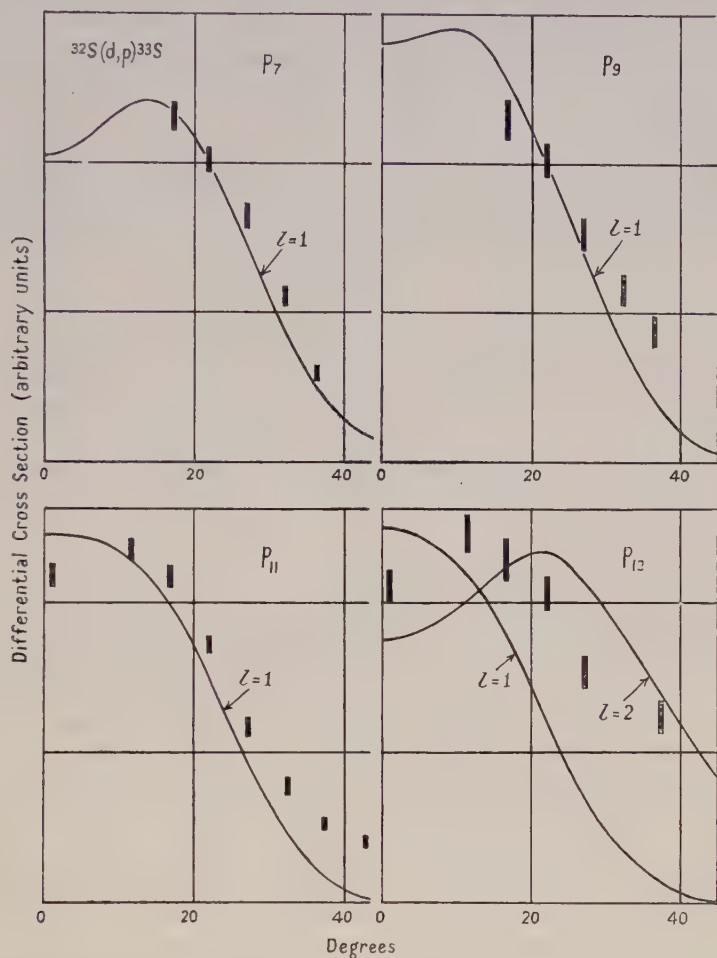


Fig. 12. Angular distributions of the proton groups p_7 , p_9 , p_{11} and p_{12} from $^{32}\text{S}(d, p)^{33}\text{S}$.

§4. DISCUSSION

By comparing the experimental angular distributions with theoretical curves calculated from Butler's theory it has been possible in every case where the measured points were of sufficient accuracy to determine the value of l unambiguously by using a radius of interaction given by the formula $(1.7 + 1.22A^{1/3}) \times 10^{-13}$ cm. Comparisons with the theory of Bhatia *et al.* showed that the best agreement could be obtained by using a value for the radius of interaction which was greater than that given by the above formula by 2×10^{-13} cm in the case of curves having $l=0$ and greater by 1×10^{-13} cm in the case of curves having $l=1$ or $l=2$.

The measured points for the sulphur group p_{11} (fig. 12) with a Q -value of 0.72 MeV and $l=1$ indicate a slight dip in the forward direction not shown by the

theoretical curve. This effect has been observed by Evans *et al.* (1953) in angular distributions for (d, n) transitions with $l=1$ and small Q -values.

In considering the detailed fitting of the experimental curves it was evident that a better fit could be obtained in all cases by subtracting a constant background from the experimental points. This confirms the impression gained from the previous work (II). We have estimated the magnitude of this background in the case of all suitable distributions for which absolute differential cross sections were known. Estimates were made for 15 distributions taken from the work with targets of ^{24}Mg , ^{25}Mg and ^{28}Si .

Although the maximum differential cross section for the various groups of protons varied by a factor of 100, all the values of the differential cross section of the estimated backgrounds lay within the range 4 to $18 \times 10^{-28} \text{ cm}^2$ and 12 of the values lay within the range 6 to $12 \times 10^{-28} \text{ cm}^2$. Included in these results were those for isotropic angular distributions and others for transitions having l -values from 0 to 3. The small range of variation of the differential cross section of the background lends weight to the suggestion that this is due to the competing process in which the transitions take place through the formation of a compound nucleus. All the results relate to nuclei having similar atomic numbers and protons having energies within the range 8 to 15 meV. Since the energy of excitation of the compound nucleus is more than 20 meV there will be many overlapping states and it is reasonable to expect that transitions within the above energy range will have similar probabilities.

The results of the present experiments are collected in tables 1 and 2. The alternative spin values and the parities of the various final states are given using the value 0 for the spin and even parity for both target nuclei. The numbers proportional to the neutron capture probabilities (II) were calculated from the measured differential cross sections after subtracting the estimated cross section of the background. This background is relatively small except for those distributions having $l=3$. Since absolute values of the differential cross sections were obtained only for silicon, the numbers representing the neutron capture probabilities in the two tables are unrelated.

The l -value 0 for the transition to the ground state of ^{29}Si is the same as that found previously for the ground state transition in $^{26}\text{Mg}(\text{d}, \text{p})^{27}\text{Mg}$ and both indicate that the fifteenth neutron goes into the $2s_{1/2}$ level of the Mayer shell model. The l -value 2 for the neutron captured into the ground state of ^{33}S indicates that the seventeenth neutron goes into a d-orbit, again in agreement with the shell model. The spin values $1/2$ and $3/2$ for ^{29}Si and ^{33}S were obtained by Townes *et al.* (1948, 1949) from hyperfine structure measurements.

The values of the neutron capture probability shown in tables 1 and 2 vary by a factor of about 10 in each case. It may be expected that this capture probability will be greatest when the neutron is captured directly into an orbit, that is, into a state of single-particle excitation. In such cases it has been suggested by Bhatia *et al.* that the relative values of the capture probability are governed mainly by a statistical factor $2j_f + 1$ where j_f is the spin of the final state.

In the reaction $^{32}\text{S}(\text{d}, \text{p})^{33}\text{S}$ (table 1) the sequence of l -values of the transitions having the greatest values of capture probability is 2, 3, 1, 1 where the first belongs to the transition to the ground state. In the ground state of ^{33}S the odd neutron is in the $1d_{3/2}$ level of the shell model, and according to this model the higher unfilled levels follow the sequence $1f_{7/2}$, $2p_{3/2}$, $1f_{5/2}$, $2p_{1/2}$. We suggest that the

excited states of ^{33}S corresponding to the proton groups p_4 , p_5 , p_{11} and having *l*-values 3, 1, 1 are states produced by simple excitation of the odd neutron into the levels $1f_{7/2}$, $2p_{3/2}$, $2p_{1/2}$ while the core, consisting of the nucleus ^{32}S , remains unexcited.

Table 1. Reaction $^{32}\text{S}(d, p)^{33}\text{S}$

(1)	(2)	(3)	(4)	(5)	(6)	(7)	(8)	(9)	(10)
P_0	0	0	2	$5/2, 3/2$	Even	7.1	8.0	2.0	$1d_{3/2}$
P_1	0.85 ± 0.03	0.79	0	$1/2$	Even	39	1.5	0.75	$(2s_{1/2})^{-1}(1d_{3/2})^2$
P_2	1.86 ± 0.10	1.90	Isotropic	—	—	0.8	—	—	—
P_3	2.28 ± 0.08	2.17	Isotropic	—	—	1.3	—	—	—
P_4	2.90 ± 0.08	2.85	3	$7/2, 5/2$	Odd	14	20	2.5	$1f_{7/2}$
P_5	3.26 ± 0.04	3.15	1	$3/2, 1/2$	Odd	83	13	3.2	$2p_{3/2}$
P_6	3.91 ± 0.10	3.88	—	—	—	1.5	—	—	—
P_7	4.21 ± 0.05	4.15	1	$3/2, 1/2$	Odd	15	1.6	0.8	—
								or 0.4	
P_8	—	4.42	—	—	—	—	—	—	—
P_9	4.89 ± 0.05	4.70	1	$3/2, 1/2$	Odd	9.4	0.8	0.4	—
								or 0.2	
P_{10}	—	5.11	—	—	—	—	—	—	—
P_{11}	5.72 ± 0.05	5.63	1	$3/2, 1/2$	Odd	100	9	4.5	$2p_{1/2}$
			1	$3/2, 1/2$	Odd	41	2.4	1.2	—
P_{12}	6.48 ± 0.10	6.30	2	$5/2, 3/2$	Even	—	—	—	—
								or 0.6	
P_{13}	7.44 ± 0.07	—	—	—	—	—	—	—	—
P_{14}	7.83 ± 0.12	—	—	—	—	—	—	—	—

(1) Proton group; (2) excitation (mev), present work; (3) excitation (mev), Davison (error ± 0.05); (4) *l*-value; (5) spin; (6) parity; (7) relative differential cross section at maximum; (8) relative neutron capture probability; (9) $(N.C.P.)/(2j_f + 1)$; (10) suggested shell model term.

Table 2. Reaction $^{28}\text{Si}(d, p)^{29}\text{Si}$

(1)	(2)	(3)	(4)	(5)	(6)	(7)	(8)	(9)
P_0	0	0	$1/2$	Even	6.2×10^{-26}	9.0	4.5	$2s_{1/2}$
P_1	1.278	2	$5/2, 3/2$	Even	6.2×10^{-27}	15	3.7	$1d_{3/2}$
P_2	2.027	2	$5/2, 3/2$	Even	2.4×10^{-27}	5.7	0.8	$(1d_{5/2})^{-1}(2s_{1/2})^2$
P_3	2.426	Isotropic	—	—	7.2×10^{-28}	—	—	—
P_4	3.070	2	$5/2, 3/2$	Even	1.2×10^{-27}	1.9	0.5	—
							or 0.3	
P_5	3.623	3	$7/2, 5/2$	Odd	4.0×10^{-27}	19	2.4	$1f_{7/2}$
P_9	4.934	1	$3/2, 1/2$	Odd	5.5×10^{-28}	16	4.0	$2p_{3/2}$
P_{12}	6.380	1	$3/2, 1/2$	Odd	3.2×10^{-26}	5.4	2.7	$2p_{1/2} ?$
							or 1.3	

(1) Proton group; (2) Excitation* (mev); (3) *l*-value; (4) spin; (5) parity; (6) maximum differential cross section (cm^2); (7) neutron capture probability (arbitrary units); (8) $(N.C.P.)/(2j_f + 1)$; (9) suggested shell model term.

* According to Van Patter and Buechner (1952).

If we assume that the spins of the states mentioned above are those given by the shell model and remove the factor $2j_f + 1$ from the relative values of the neutron capture probability, the values of the latter become more nearly equal while remaining larger than the alternative values for the intervening states. These values are given in column (9) of table 1. The fact that no transition having $l=3$ was observed corresponding to the formation of the $1f_{5/2}$ level might

possibly be due to the difficulty of observing a group with such an l -value when there are adjacent groups with smaller values of l .

We suggest that the proton groups associated with low values of the neutron capture probability correspond to states requiring the excitation of one or more particles of the nuclear core. In particular the first excited state having spin $1/2$ and l -value 0 is probably produced by a neutron from the $2s_{1/2}$ level being raised to the $1d_{3/2}$ level. Here, together with the captured neutron, it forms a pair having a resultant spin 0 in accordance with the usual assumption of the shell model. The spin of this excited state is then due solely to the hole in the $2s_{1/2}$ level and has the value $1/2$. In support of this suggestion we note that the first excited state of ^{32}S has an energy of 0.5 ± 0.1 mev (Snowdon 1952) not far from the value 0.85 ± 0.03 mev for this state of ^{33}S . In the last column of table 1 are the shell model terms proposed in the above discussion.

Similar observations can be made concerning the reaction $^{28}\text{Si}(d, p)^{29}\text{Si}$ (table 2). The sequence of l -values associated with the largest values of the neutron capture probability is 0, 2, 3, 1. In the ground state of ^{29}Si the odd neutron is in the $2s_{1/2}$ level and the sequence of unfilled levels according to the shell model is $1d_{3/2}$, $1f_{7/2}$, $2p_{3/2}$, $1f_{5/2}$, $2p_{1/2}$. We suggest as before that the excited states of ^{29}Si corresponding to the proton groups p_1 , p_5 , p_9 and having l -values 2, 3, 1 are states produced by simple excitation of the odd neutron into the levels $1d_{3/2}$, $1f_{7/2}$, $2p_{3/2}$. Also the second excited state, having l -value 2 and spin $5/2$ or $3/2$ is probably produced by a neutron from the $1d_{5/2}$ level being lifted to the $2s_{1/2}$ level to form a pair with the captured neutron, the resultant spin being due to the hole in the $1d_{5/2}$ level. As before we observe that the energy of the first excited state of the ^{28}Si core (1.8 ± 0.2 mev, Peck 1949) is close to that (2.027 mev) of this state of ^{29}Si . The spins of the various states determined on the above assumptions have been again used to remove the factor $2j_f + 1$ from the values of the neutron capture probability and these amended values are given in column (8) of table 2. Comparison of these values makes it appear likely that the twelfth excited state is the $2p_{1/2}$ single-particle state.

ACKNOWLEDGMENTS

We are grateful to Professor H. W. B. Skinner for helpful discussions. One of us (T. N. M.) thanks the Department of Scientific and Industrial Research for a maintenance grant.

REFERENCES

- BHATIA, A. B., HUANG, K., HUBY, R., and NEWNS, H. C., 1952, *Phil. Mag.*, **43**, 485.
 BUTLER, S. T., 1951, *Proc. Roy. Soc. A*, **208**, 559.
 DAVISON, P. W., 1949, *Phys. Rev.*, **75**, 757.
 EVANS, W. H., GREEN, T. S., and MIDDLETON, R., 1953, *Proc. Phys. Soc. A*, **66**, 108.
 HOLT, J. R., and MARSHAM, T. N., 1953 a, *Proc. Phys. Soc. A*, **66**, 249; 1953 b, *Ibid.*, **66**, 258.
 PECK, R. A., 1949, *Phys. Rev.*, **76**, 1279.
 SNOWDON, S. C., 1952, *Phys. Rev.*, **87**, 1002.
 STRAIT, E. N., VAN PATTTER, D. M., BUECHNER, W. W., and SPERDUTO, A., 1951, *Phys. Rev.*, **81**, 747.
 TOWNES, C. H., and GESCHWIND, S., 1948, *Phys. Rev.*, **74**, 626.
 TOWNES, C. H., MAYS, J. M., and DAILEY, B. P., 1949, *Phys. Rev.*, **76**, 700.
 VAN PATTTER, D. M., and BUECHNER, W. W., 1952, *Phys. Rev.*, **87**, 51.

Polarization Effects in (d, p) and (d, n) Reactions

By H. C. NEWNS

Department of Theoretical Physics, University of Liverpool

Communicated by H. Fröhlich; MS. received 6th October 1952

Abstract. The particles emitted from (d, p) and (d, n) reactions are shown to be polarized in a plane perpendicular to the plane of scattering. The direction of polarization is shown to be related to the spin changes involved in the reaction. An estimate of the magnitude of the polarization and the angle at which the maximum occurs is made. The effect of the polarization on the angular correlation of the γ -rays emitted from the product nucleus when measured in coincidence with the outgoing particle is discussed and a comparison made with the result of Satchelor and Spiers.

§ 1. INTRODUCTION

THE angular distribution of particles emitted from (d, p) and (d, n) reactions has been studied theoretically (Butler 1951, Bhatia *et al.* 1952, to be referred to as BH), and in general there is good agreement with the angular distributions obtained experimentally and those predicted by the theory. These treatments show that the spins of the initial and final nuclei (J_A and J_B respectively) are related by the selection rule $\mathbf{J}_B = \mathbf{J}_A + \mathbf{j}$, where j is the total angular momentum of the neutron* entering the nucleus: $j = l \pm \frac{1}{2}$ where l is the orbital angular momentum of the neutron as it enters the nucleus. There is also the parity selection rule that l is even or odd according as the initial and final nuclei have the same parity or not. Fitting the theoretical curves to the experimental angular distributions determines the value of l which has taken part in the reaction. However, except in the cases where J_A and l are both zero, the spin of the final nucleus is not determined uniquely, there being at best two possibilities for the spin. If, however, j could be determined as well as l , the number of possible values for J_B would be reduced and very often a unique result could be obtained.

It is shown here that the protons emitted from a (d, p) reaction are partially polarized, and that if the direction of polarization is measured the value of j is determined if l is known.

The usual treatments of the (d, p) reaction give zero for the polarization. This is due to the fact that the proton is supposed not to interact with the nucleus, and can therefore pass through it without hindrance. In the present calculation protons which would have to pass through the nucleus to reach the observer are assumed to be captured and lost from the beam. It is this screening of some of the protons by the nucleus which is directly responsible for the polarization.

The direction of polarization depends on the value of the total angular momentum j of the neutron as it is captured by the nucleus. It is found that if only one value of j and l can contribute to the reaction, then the outgoing particles

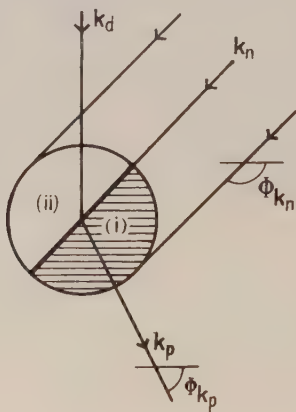
* We assume that we are dealing with a (d, p) reaction throughout this paper. For a (d, n) reaction one simply interchanges the roles of the neutron and proton.

are partially polarized in the direction of $\mathbf{k}_p \times \mathbf{k}_d$ if only $j = l + \frac{1}{2}$ is permitted, and in the opposite direction if only $j = l - \frac{1}{2}$ is permitted. For $l = 0$ the polarization is zero.

If the product nucleus of a (d, p) reaction is formed in an excited state it will emit a γ -ray in falling to the ground state. The angular correlation of these γ -rays with the emitted protons can also lead to information about the spins of the nuclear states involved. The correlation function has been worked out by Biedenharn *et al.* (1952) and Satchelor and Spiers (1952). Both these treatments, however, neglect the interaction of the proton with the nucleus which leads to the polarization. Due to the partial polarization of the nucleus which results, these results will only be strictly correct when the γ -rays are measured in coincidence with protons emitted in the forward direction.

§ 2. A SIMPLE CLASSICAL PICTURE FOR THE POLARIZATION

A simple classical picture can be given to show that one expects protons emitted in (d, p) reactions to be polarized. The reaction can be pictured as follows. We imagine the deuteron to be incident upon the initial nucleus with momentum k_d ; this can break up into a free proton and neutron with conservation of momentum so that $\mathbf{k}_d = \mathbf{k}_p + \mathbf{k}_n$, and the requirement is imposed that the direction of k_n must be such as to allow the neutron to be captured. The neutron is then captured with a certain orbital angular momentum l and the proton emerges, energy being conserved over the whole reaction.



We assume that all the particles are co-planar and suppose that the angular momentum l is the only one with which the neutron is permitted to be captured; let us also suppose that only $j = l + \frac{1}{2}$ is allowed. Then, referring to the figure, in region (i) the neutron is captured with its angular momentum about an axis in the direction of $\mathbf{k}_p \times \mathbf{k}_d$ (i.e. into the paper). Thus to form $j = l + \frac{1}{2}$ the neutron spin must be in this direction, and so therefore must the proton spin, since in a deuteron the neutron and proton have their spins parallel (we neglect for the time being the spin function of the deuteron having zero component along the axis of quantization). Now consider region (ii). The direction of the neutron angular momentum is now in the opposite direction to $\mathbf{k}_p \times \mathbf{k}_d$, i.e. out of the paper. So the neutron and proton spins must both point out of the paper. If the protons are observed at a particular angle of scattering, those liberated by neutrons captured in region (i) will have

their spins in the direction $\mathbf{k}_p \times \mathbf{k}_d$ and the protons liberated by neutrons captured in region (ii) have their spins in the opposite direction. If the interaction of the proton with the nucleus is ignored as in the usual treatments of this reaction, the numbers of protons coming from the two regions will be equal and the net polarization is zero.

Let us now impose the condition that if the proton has to pass through the nucleus to reach the observer, it is captured and lost from the beam. If we bear in mind that an emergent proton originates in the vicinity of its companion neutron, then, for neutrons captured in region (i), most of the protons can emerge without interacting with the nucleus, but, for neutrons captured in region (ii), a number of protons would have to pass through the nucleus in order to reach the observer, and these we suppose are captured and lost from the beam. Thus there will be a predominance of protons with spin in the direction of $\mathbf{k}_p \times \mathbf{k}_d$ over those with spin in the opposite direction. This will result in a net polarization of the proton beam in the direction of $\mathbf{k}_p \times \mathbf{k}_d$. It is obvious that if the selection rules allowed only $j = l - \frac{1}{2}$, there would be a net polarization in the direction opposite to $\mathbf{k}_p \times \mathbf{k}_d$.

The above picture has been described in only two dimensions and has neglected the spin state of the deuteron which has zero component along the axis of quantization. However, if these limitations are removed, the conclusions reached above are still true, namely, that protons emitted from these reactions are polarized, and that the polarization is in the direction of $\mathbf{k}_p \times \mathbf{k}_d$ if the selection rules only allow neutrons to be captured with $j = l + \frac{1}{2}$, and in the opposite direction if the neutrons can be captured only with $j = l - \frac{1}{2}$.

Further consideration of the model shows that the polarization is zero for protons emitted in the forward or backward directions. It is a maximum if the proton is emitted at an angle such that \mathbf{k}_p and \mathbf{k}_n are perpendicular. This is most easily seen if it is assumed that the deuteron is small compared with the nucleus. In this case, for $\mathbf{k}_p \cdot \mathbf{k}_n = 0$, the protons emerging from region (ii) will be completely screened from the observer by the nucleus, whereas those from region (i) can emerge unimpeded. At any other angle of scattering of the proton the screening of region (ii) will not be complete, and the polarization will consequently be reduced.

§ 3. QUANTUM MECHANICAL TREATMENT OF THE POLARIZATION

The Born approximation treatment of BH is used although similar results would be obtained if Butler's (1951) methods were followed.

The differential cross section for the (d, p) reaction for a proton having a given spin direction is given by

$$\sigma(\theta) = A \sum_{M_A, M_B, m_d} |\langle P, J_B, M_B | V | D, J_A, M_A \rangle|^2,$$

where $|J_A, M_A\rangle$ and $|J_B, M_B\rangle$ represent the initial and final nuclei having spin J_A with component M_A , and spin J_B with component M_B respectively. The kets $|P\rangle$ and $|D\rangle$ represent the proton and deuteron wave functions. We average over the spin directions of the initial nucleus and deuteron, and sum over those of the final nucleus but not of the proton since we are interested in its spin directions. A is a general constant into which we absorb all quantities not directly related to the problem.

The matrix element $\langle J_B, M_B | V | J_A, M_A \rangle$ is a function of the neutron coordinates, and this is expressed in a series of eigenfunctions of the total angular momentum j of the neutron, having component μ ,

$$\langle J_B, M_B | V | J_A, M_A \rangle = \sum_{j, \mu, \pm} \langle J_B, M_B | V | J_A, M_A, j, \mu, \pm \rangle \langle j, \mu, \pm |,$$

where \pm denotes the parity of j . It is also assumed as in BH that the neutron is captured on a shell of radius a so that $\langle J_B, M_B | V | J_A, M_A, j, \mu, \pm \rangle$ is independent of the neutron coordinates.

The bra $\langle j, \mu, \pm |$ is further expanded into a sum of eigenfunctions of the orbital and spin angular momenta of the neutron

$$\langle j, \mu, \pm | = \sum_{l, m, m_n} C_{j, \mu; m, m_n}^{l, \frac{1}{2} *} \langle l, m, m_n |,$$

where m is the component of the orbital angular momentum l , and m_n is the component of the spin angular momentum, and the designation of the parity can now be omitted since a particular value of j with a particular parity determines only one value of l .

The remainder of the treatment closely follows BH. Both the deuteron and proton wave functions are resolved into products of space and spin parts, and the summations over M_A and M_B can be performed. One finally obtains

$$\sigma(\theta) = \sum_{\substack{m_d, j, \mu \\ l, m, m_n}} A(j) |C_{j, \mu; m, m_n}^{l, \frac{1}{2} *} C_{l, m_d; m_p, m_n}^{\frac{1}{2}, \frac{1}{2}} \langle p, l, m | d \rangle|^2,$$

where m_p and m_d are components of the proton and deuteron spins respectively.

We now consider in more detail the space matrix element $\langle p, l, m | d \rangle$ which can be written as in BH

$$\langle p, l, m | d \rangle = \int \exp(-i \mathbf{k}_p \cdot \mathbf{R}_p) \cdot Y_l^{m*}(\Theta_n, \Phi_n) \exp\{\frac{1}{2} i \mathbf{k}_d \cdot (\mathbf{R}_n + \mathbf{R}_p)\} \\ \times \psi(|\mathbf{R}_n - \mathbf{R}_p|) d\mathbf{R}_p d\omega_n, \dagger \quad \dots\dots(1)$$

where the axis is now in the direction $\mathbf{k}_p \times \mathbf{k}_d$. This has to be evaluated using the condition that the proton must not pass through the nucleus to reach the observer. This cannot be done in general. If we assume, however, that the deuteron is small compared with the nucleus, i.e. we replace $\psi(|\mathbf{R}_n - \mathbf{R}_p|)$ by $\delta(\mathbf{R}_n - \mathbf{R}_p)$, it has been shown by Huby (see Appendix) that the condition that protons are not allowed to pass through the nucleus becomes a restriction on the values of m (relative to the direction of $\mathbf{k}_p \times \mathbf{k}_d$ as principal axis) for which the matrix element (1) has a non-negligible value. In particular, if the proton is observed at an angle such that $\mathbf{k}_p \cdot \mathbf{k}_n = 0$, then the integral is much larger for positive values of m than for negative. This is essentially the classical result that more of the protons liberated by neutrons captured with a positive component of angular momentum about the axis $\mathbf{k}_p \times \mathbf{k}_d$ are observed than are observed from neutrons captured with a negative component of angular momentum about this axis, since some of the latter are screened from the observer by the nucleus. In fact, the calculation given in the Appendix essentially only demonstrates the well-known fact that quantum mechanics reduces to classical mechanics for large values of the quantum number.

† The spherical harmonics $Y_l^m(\Theta_n, \Phi_n)$ used in this paper are those with the phases defined by Condon and Shortley (1951, chap. 3).

The polarization P is defined as $(N_+ - N_-)/(N_+ + N_-)$, where N_+ and N_- denote the number of protons having $m_p = +\frac{1}{2}$ and $m_p = -\frac{1}{2}$ respectively. If the relative contributions of each value of m to the matrix element $\langle p, l, m | d \rangle$ could be calculated, the magnitude of the polarization could be obtained. This it has not yet been possible to do. However, an *upper limit* can be obtained if we assume that for $m \geq 0$ the Born approximation result holds, and for $m < 0$ the matrix element is zero (these assumptions will evidently be most nearly correct when the proton is scattered through an angle such that $\mathbf{k}_p \cdot \mathbf{k}_n = 0$). If this is assumed, then for only one value of j and l contributing to scattering, the polarization is given by

$$P = \frac{\pm \sum_{m \geq 0} m \frac{(l-m)!}{(l+m)!} \left(\frac{2^m \sqrt{\pi}}{\Gamma[\frac{1}{2}(l-m)+1] \Gamma[\frac{1}{2}(1-l-m)]} \right)^2}{3(j+\frac{1}{2}) \sum_{m \geq 0} \frac{(l-m)!}{(l+m)!} \left(\frac{2^m \sqrt{\pi}}{\Gamma[\frac{1}{2}(l-m)+1] \Gamma[\frac{1}{2}(1-l-m)]} \right)^2}, \dots (2)$$

where the positive sign is taken if $j = l + \frac{1}{2}$, and the negative sign if $j = l - \frac{1}{2}$. For particular values of j and l we obtain the polarizations listed in the table.

l	0	1	2	3
$j = l + \frac{1}{2}$	0	16.67	13.33	18.75
$j = l - \frac{1}{2}$	0	-33.33	-20.00	-25.00

§ 4. ANGULAR CORRELATION OF DECAY γ -RAYS WITH EMITTED PARTICLES

Let us suppose that the product nucleus of a (d, p) reaction is formed in an excited state. This state of the nucleus we now designate by the letter C and we suppose that it has a unique spin J_C and it decays by emitting a γ -ray of multipolarity L to the ground state having spin J_B . The nucleus C will be partially polarized as we have shown, and, therefore, if the γ -rays emitted by C on its decay to the ground state B are measured in coincidence with the outgoing protons, effects due to this partial polarization should be observed.

The axis to which the angular distribution is to be referred, however, is not, as is usually the case in angular correlations, the direction of the outgoing particle, but the chosen axis of quantization, namely $\mathbf{k}_p \times \mathbf{k}_d$. So the angle Θ for the γ -ray is measured from this axis, which is perpendicular to the plane of the scattering, and the angle Φ is in the plane of scattering, $\Phi = 0$ being the direction \mathbf{k}_n . The γ -rays are measured in coincidence with the proton simply to ensure a particular direction of polarization.

The correlation cannot be calculated exactly since the relative contributions of the various matrix elements (1) are not known. However, if we take the extreme case which leads to the result (2) for the polarization, the correlation function can be calculated and is found to be

$$W(\Theta, \Phi) =$$

$$\sum_{\substack{M_A, M_B \\ m_n, \nu}} \left| \sum_{\substack{M_C, l, m \\ j, \mu, L, M}} C_{J_C, M_C; M_B, M}^{J_B, L} C_{J_C, M_C; M_A, \mu}^{J_A, j^*} C_{j, \mu; m, m_n}^{l, \frac{1}{2}^*} A(j, L, l, \theta) G_{L, M}^{\nu}(\Theta, \Phi) \right. \\ \left. \times \left(\frac{(l-m)!}{(l+m)!} \right)^{1/2} \frac{2^m \sqrt{\pi}}{\Gamma[\frac{1}{2}(l-m)+1] \Gamma[\frac{1}{2}(1-l-m)]} \right|^2, \dots (3)$$

where ν can take the values ± 1 . The functions $G_{L,M}^{+1}(\Theta, \Phi)$ and $G_{L,M}^{-1}(\Theta, \Phi)$ refer to different directions of polarization of the γ -ray, and are given by

$$G_{L,M}^{\nu}(\Theta, \Phi) = i^{\alpha(\nu)} \left[\frac{2}{L(L+1)(2L+1)} \right]^{1/2} \left[\frac{\partial}{\partial \Theta} Y_L^M(\Theta, \Phi) - \frac{i\nu}{\sin \Theta} \frac{\partial}{\partial \Phi} Y_L^M(\Theta, \Phi) \right],$$

where $\alpha=0$ for electric multipoles, and $\alpha=\nu$ for magnetic multipoles. The γ -rays are measured in coincidence with the proton simply to ensure a certain energy and direction of polarization.

The result of Satchelor and Spiers (1952) is the same as this when referred to the axis $\mathbf{k}_p \times \mathbf{k}_d$ except that negative values of m are included in the summation. Thus the correlations predicted by the two results are rather different. For example, if the neutron is captured with certain angular momentum $l=1, j=3/2$ and only one value of L is significant, only $m=1$ contributes to (3) and there is no correlation in the plane of scattering. In the case of Satchelor and Spiers, the interference between $m=1$ and $m=-1$ does give a correlation. Thus the experimental correlation should be more isotropic than they predict, and thus affords a means of detecting polarization. Further, for unique l, j , and L , Satchelor and Spiers always obtain complete isotropy in their azimuthal angle ϕ , while for $\Phi=\pi/2$ eqn. (3) often gives a correlation in Θ which is now the same angle as the ϕ of Satchelor and Spiers. This again would be an indication of the presence of polarization.

§ 5. DISCUSSION

The treatment described in this paper differs from the usual treatment of the (d, p) reaction only in the assumption that protons emitted in this reaction cannot pass through the nucleus without being captured and lost from the outgoing beam of particles. If this is granted, polarization of the outgoing particles follows as a direct consequence. The relation between the direction of polarization and the angular momentum of the neutron as it is captured is also dependent only on this assumption, and these results can be relied upon.

The magnitude of the polarization cannot be estimated, but for the purpose of obtaining information about the spins of the nuclear states involved in the reaction it is sufficient to know the direction of polarization only.

The angular correlation, however, depends on the relative contributions of the various values of m to the nuclear matrix element (1), which it has not so far been possible to estimate. It is therefore useless at the moment for the determination of spins and parities. It can serve, however, as a means of detecting the polarization since eqn. (3) indicates the way one would expect the experimental results to deviate from those of Satchelor and Spiers due to the presence of polarization.

ACKNOWLEDGMENTS

It is a pleasure to thank Mr. A. E. Litherland, whose suggestion that particles emitted in these reactions may be polarized led to the present investigation. I am also grateful to Dr. R. Huby for clearing up several difficult points which arose in the course of this work, and who in particular is responsible for the Appendix. I am indebted to Dr. J. A. Spiers for communicating his results before publication.

APPENDIX

Relation of the Quantum Matrix Element to Classical Conditions

By R. HUBY

We shall show that the matrix element (1), in the correspondence limit of large quantum number m , behaves in the same way as would be expected from the classical arguments of § 2.

It is necessary first to modify the factor $\exp(-i\mathbf{k}_p \cdot \mathbf{R}_p)$ belonging to the emergent protons so as to represent the screening effect of the nucleus on the protons. In principle one ought to use a 'distorted wave' representing a plane wave of wave number \mathbf{k}_p , as scattered by a sphere assumed to be either, say, perfectly absorbing or perfectly reflecting. As a crude geometrical approximation to this, for the case of small wavelength (large quantum numbers), we may assume that on the surface of the sphere of radius a the wave has the undistorted value $\exp(-i\mathbf{k}_p \cdot \mathbf{R}_p)$ for $\mathbf{k}_p \cdot \mathbf{R}_p > 0$, and is zero for $\mathbf{k}_p \cdot \mathbf{R}_p < 0$. If further we assume that the deuteron is small, replacing $\psi(|\mathbf{R}_n - \mathbf{R}_p|)$ by $\delta(|\mathbf{R}_n - \mathbf{R}_p|)$, then the matrix element (1) reduces to

$$\langle p, l, m, | d \rangle = \int \exp(-i\mathbf{k}_p \cdot \mathbf{R}_n) \cdot Y_l^{m*}(\Theta_n, \Phi_n) \exp(i\mathbf{k}_d \cdot \mathbf{R}_n) d\omega_n, \quad \dots\dots (4)$$

where $d\omega_n$ is to be taken only over the hemisphere for which $\mathbf{k}_p \cdot \mathbf{R}_n > 0$.

Taking the direction of $\mathbf{k}_p \times \mathbf{k}_d$ as principal axis, let us separate out from this the integration over $d\Phi_n$:

$$\int_{\Phi_{k_p} - \pi/2}^{\Phi_{k_p} + \pi/2} \exp[ik_n a \sin \Theta_n \cos(\Phi_{k_n} - \Phi_n) - im\Phi_n] d\Phi_n. \quad \dots\dots (5)$$

In the limit of large m , the major contribution to this integral will come from a small range of angles near the region where the exponent is stationary, i.e. where

$$ka \sin \Theta_n \sin(\Phi_{k_n} - \Phi_n) = m. \quad \dots\dots (6)$$

This is the classical condition that the particle at the point (a, Θ_n, Φ_n) should have angular momentum $\hbar m$ about the principal axis. Within the range of integration of (4) this can only be satisfied for certain values of m : values of m for which there is no solution will yield small matrix elements. If $\Phi_{k_n} - \Phi_{k_p} = \pi/2$, then all the values of m which satisfy (6) are positive. For other values of $\Phi_{k_n} - \Phi_{k_p}$ negative values of m will also appear until, when $\Phi_{k_n} - \Phi_{k_p} = 0$ or π , both positive and negative values of m are equally important, and polarization will vanish. Although the above criterion for distinguishing between large and small matrix elements has been derived only for large m , it seems reasonable to assume that the same trend will obtain also for smaller m . In the present approximation, the matrix element (4), for those values of m which do satisfy (6), will not be materially altered if we extend the integration over all solid angles, i.e. if we use the same value as when neglecting screening of the protons.

REFERENCES

- BHATIA, A. B., HUANG, K., HUBY, R., and NEWNS, H. C., (BH), 1952, *Phil. Mag.*, **43**, 485.
 BIEDENHARN, L. C., BOYER, K., and CHARPIE, R. A., 1952, *Phys. Rev.*, **88**, 517.
 BUTLER, S. T., 1951, *Proc. Roy. Soc. A*, **208**, 559.
 CONDON, E. U., and SHORTLEY, G. H., 1951, *Theory of Atomic Spectra* (Cambridge: University Press).
 SACHELOR, G. R., and SPIERS, J. A., 1952, *Proc. Phys. Soc. A*, **65**, 980.

The Atomic Position and Size of the Thallium Ions in KCl(Tl) Phosphors

By W. A. RUNCIMAN AND E. G. STEWARD

Research Laboratories, The General Electric Company, Wembley, Middx.

MS. received 25th November 1952

Abstract. A new x-ray investigation has been made of the KCl(Tl) phosphor in view of the discrepancy between the early theory of Fromherz involving formation of complexes in the KCl(Tl) phosphor and the recent theoretical work of Williams, in which substitutional entry of the thallium ions is assumed. The present study has now shown (a) that the expansion of the potassium chloride structure due to the incorporation of thallium is in agreement with Vegard's law and (b) that Tl^+ ions enter the structure substitutionally. The present results differ from those obtained by Stasiw and Saur in a less detailed x-ray study.

The intensities of x-ray reflections have also been used to establish the atomic position of the activator atoms in the phosphor and the results fully confirm the interpretation of the observed lattice expansions.

A new value of 1.42_7 \AA has been obtained for the ionic radius of the Tl^+ ion in six-fold coordination with Cl^- ions. This is of importance in the detailed calculations of the luminescence of KCl(Tl) which have been made by Williams and others.

§ 1. INTRODUCTION

IN most impurity activated solid inorganic phosphors the absorption and emission spectra consist of one or more broad bands. Because of their relative simplicity, the alkali halides activated by heavy metals have been studied with a view to gaining insight into the mechanism of this type of luminescence. In particular, potassium chloride activated by thallium and denoted KCl(Tl) has been investigated extensively both experimentally and theoretically.

Following the earlier theory (Seitz 1938) in which a single average configuration coordinate was used to describe the state of a luminescent centre, a detailed theory has been developed to account for the emission and absorption spectra of KCl(Tl) on the assumption that the thallium enters the lattice substitutionally (Williams 1951, Williams and Hebb 1951, Johnson and Williams 1950, 1952). The absorption spectrum of KCl(Tl) has been measured at 4° , 77° and 298 K (Johnson and Studer 1951) and there is good agreement between the experimental and theoretical half-widths of the absorption band.

Others have taken a different view and have proposed that thallium ions or ions of other heavy metallic activators form complex negative ions with the halides and that these complexes are incorporated at points of lattice defects (Fromherz and Menschick 1929, Fromherz 1931, Pringsheim 1942, 1949). In support of this theory it was observed that the absorption band of aqueous solutions of the phosphors is very similar to the long wavelength absorption band of the solid phosphors (Fromherz and Ku-Hu-Li 1929). In contrast, the emission spectra of the aqueous solution (Pringsheim and Vogels 1940) and of the solid phosphor KCl(Tl) do not exhibit close similarity and this seems a

weak feature of the theory, but it has often been used (e.g. Hilsch 1937 and Antonov-Romanovskii 1943) in the discussion of the properties of $KCl(Tl)$ and other phosphors. Furthermore the theory has had support from an x-ray study of the $KCl(Tl)$ phosphor (Stasiw and Saur 1938) where it was claimed that the expansion of the KCl lattice is only about half the amount predicted on the assumption that the thallium enters the lattice substitutionally.

As the $KCl(Tl)$ phosphor represents the only example of a quantitative theoretical interpretation of an impurity activated phosphor, it is of considerable importance to resolve the discrepancy between the above two theories. The crystal structure of the phosphor has therefore been re-studied.

Where a continuous solid solution range exists between two isomorphous compounds it is comparatively easy to prove by x-ray diffraction that substitutional replacement has taken place. For example, both zinc sulphide and cadmium sulphide can have the hexagonal zinc oxide type structure and it is possible to form the complete solid solution range $ZnS-CdS$ (Kröger 1940, Rooksby 1941). The changes in the structure cell dimensions are found to be closely proportional to the replacement of zinc ions by cadmium ions and Vegard's law therefore operates with reasonable accuracy in such instances.

Potassium chloride has a rock salt face-centred cubic crystal structure whilst thallium chloride has a caesium chloride body-centred cubic structure. A complete solid solution range cannot exist therefore between the two since the end members are not structurally isomorphous. If limited solid solubility of thallium chloride in potassium chloride is possible, however, Vegard's law may be applied over that range, by calculating a theoretical structure cell dimension for thallium chloride having a hypothetical face-centred cubic structure.

Preparations of potassium chloride containing 5, 10 and 15% (molecular) of thallium chloride have been prepared and examined by x-ray diffraction in order to test the correlation between composition and structure cell dimension.

In addition to changes in lattice dimensions of the crystal structure, replacement of potassium ions by thallium ions would also modify the intensities of x-ray reflections. This approach has been used to establish the lattice position of the thallium atoms which have entered the potassium chloride structure.

§ 2. PREPARATION OF SAMPLES

The chemicals used were 'Specpure' potassium and thallos chlorides.

Preliminary experiments were made in which ground mixtures of potassium and thallium chlorides in various proportions were heated in sealed evacuated clear quartz tubes at temperatures in the range 550–750°C. It was considered necessary to seal the tubes to prevent a relative loss of $TlCl$, which has a melting point of 430°C and a high vapour pressure in the above temperature range. KCl has a melting point of 790°C and a relatively low vapour pressure and the substantial differences in the melting points and vapour pressures are largely responsible for the difficulties in preparing uniform samples.

Regrinding and reheating were included in attempts to produce homogeneous products free from excess thallium chloride. These experiments were not completely successful at higher concentrations of thallium chloride. Entry of the thallium was not fully homogeneous and some free thallium chloride was observed. A sample containing 10% (molecular) $TlCl$, however, was quite uniform and was included in the x-ray examination described in § 3.

Although the solubilities of potassium and thallium chlorides in water are very different an aqueous solution of the two chlorides was evaporated to dryness and the residue ground and subjected to a homogenizing heat treatment. This proved to be successful and solutions of potassium chloride containing 5 and 15% (molecular) TlCl were prepared and evaporated to dryness on a steam bath. The powders obtained were then carefully ground in an agate mortar, sealed in evacuated clear quartz tubes and heated for over 12 hours at 425°C , this temperature being just below the melting point of pure TlCl .

In view of the great difference in vapour pressures of potassium and thallium chlorides, the volume of quartz tube not occupied by the powder sample was reduced to a minimum by inserting a length of solid quartz rod above the powder. Sealing-off under vacuum was then accomplished over the section of the tube containing the quartz rod. This technique also avoided excessive heating of the actual powder sample during the sealing-off operation.

§ 3. X-RAY EXAMINATION

A 19 cm diameter Unicam powder camera was used with copper $K\alpha$ radiation, and reflections were recorded over a Bragg angle range θ 5° – 85° ; the photographs obtained are shown in fig. 1, Plate.

(i) Structure Cell Dimensions

With increasing concentration of thallium chloride, an expansion of the potassium chloride structure was observed. This is revealed by the shift of the x-ray reflections, particularly those at high θ values.

Measurements of the shifts of the 622, 640, 642 and 800 reflections enabled the structure cell dimension to be determined for each sample including the 'Specpure' KCl sample. The values obtained after correction (Nelson and Riley 1945) for various camera factors are given in table 1.

Table 1. Observed and Calculated Structure Cell Dimension for KCl-TlCl

Molecular % TlCl	0	5	10	15
Cell dimension (\AA) Obs.*	6.2922	6.2997	6.3085	6.3164
Calc.	(6.2922)	6.3007	6.3091	6.3176

* All values ± 0.0003 .

The value of a_0 obtained for the 'Specpure' KCl is in good agreement with the recorded value of $a_0 = 6.291 \pm 0.002 \text{\AA}$ * (Strukturbericht 1913–1928).

If thallium ions replace potassium ions substitutionally and at random, a change in the dimensions of the potassium chloride structure will result, and if Vegard's law giving a linear relationship is assumed, the change with composition can be calculated.

Because different values have been reported (Goldschmidt 1929, Pauling 1927) for the ionic radius for Tl^+ , it was decided to determine a value from the known lattice parameter of thallium chloride of body-centred cubic structure. Using the value of $a_0 = 3.8417 \text{\AA}$ (Wyckoff 1951), the ionic separation denoted Tl-Cl in the caesium chloride structure is given by $\frac{1}{2}\sqrt{3} \times 3.8417 = 3.327_0 \text{\AA}$.

* This cell dimension and the various ionic radii given in the literature, though described as ångström units, are really kx units (Bragg 1947). A factor of 1.00202 has been used where necessary to correct to ångström unit.

In deducing the $Tl-Cl$ distance in a rock salt type structure from this, the usual correction for coordination number has to be made (Pauling 1945). This correction is

$$\frac{R_{CsCl}}{R_{NaCl}} = \left[\frac{B_{CsCl}}{B_{NaCl}} \frac{A_{NaCl}}{A_{CsCl}} \right]^{1/(n-1)}$$

where B denotes the appropriate repulsive coefficient, A the appropriate Madelung constant and n the Born exponent.

The value of n in this expression is always in the region of 9 but depends upon the ion type. K^+ and Cl^- both have the value of $n=9$ and the value for Tl^+ is approximately 12. In a crystal of mixed ion type, an average value for n is used (Pauling 1945). For $TlCl$ a value of $n=10.5$ is therefore indicated, and the above expression gives a co-ordination number correction of 1.029_8 .

The $Tl-Cl$ interionic distance in a rock salt structure therefore becomes $3.327_0/1.029_8 = 3.230_7 \text{ \AA}$. The lattice constant a_0 is therefore 6.461_4 \AA .

A theoretical relation can now be calculated using Vegard's law, between the cell dimension and the molecular concentration of thallium chloride. This is shown together with the experimental points in fig. 2, and a comparison between observed and calculated values is given in table 1. The slight deviation of the points from the theoretical line may be partly accounted for by small concentrations of free thallium chloride which are detectable in the original x-ray photographs. For example approximately 0.2% (molecular) was detectable in the 15% preparation.

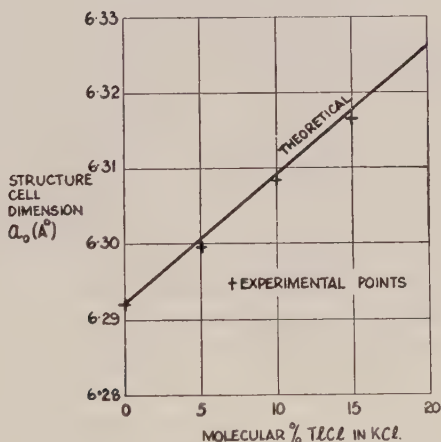


Fig. 2. Structure cell dimensions for $KCl-TlCl$.

These results show that the observed expansion of the potassium chloride structure is in close agreement with the expansion expected from direct substitutional replacement of K^+ ions by Tl^+ ions. Further confirmation of this is to be expected from an examination of the changes with composition in x-ray line intensities.

(ii) Intensities of X-Ray Reflections

In the potassium chloride structure it is well known that those reflections for which h , k and l are all odd, such as 111, 311 and 331 (fig. 1) are very weak on account of the closely similar values of the atomic scattering factors of

potassium and chlorine. The atomic scattering factor for thallium is of course very much greater than that for potassium and if, therefore, thallium ions are situated at the positions normally occupied by potassium ions, the intensities of these reflections are considerably enhanced. This effect is clearly shown by the x-ray photographs in fig. 1.

The intensities of the 111, 311, 331 and 400 reflections have been calculated using a scattering factor which is the appropriate linear combination of the separate scattering factors for K^+ and Tl^+ (International Tables for the Determination of Crystal Structure 1935). Using the 400 reflection as a reference level (unity), the intensities were calculated in the usual way from the expression $I_{calc} = F^2 p(LP)$ where F denotes the crystal structure factor, p denotes the multiplicity of the x-ray reflection concerned, and (LP) denotes the appropriate Lorentz-polarization factor.

Table 2 lists the observed intensities I_{obs} against the calculated values I_{calc} for the various compositions used. The observed intensities of the 311 and 331 reflections were determined from microdensitometer records of the x-ray powder photographs, corrections being made for 'background' and other factors. Only visual estimates are given for the 111 reflections since undiluted x-ray specimens were used to show clearly the line shifts at high θ values, and the consequent absorption at low θ values makes quantitative measurement of the intensity of the 111 reflection unreliable.

Table 2. KCl-TlCl: Calculated and Observed Intensities of x-ray Reflections

Reflection	Composition mol.% TlCl	Intensities*	
		I_{obs}	I_{calc}
331	0	≤ 0.1	0.01
	5	0.1	0.08
	10	0.2	0.18
	15	0.3	0.29
311	0	< 0.1	0.04
	5	0.2	0.22
	10	0.5	0.48
	15	0.7	0.75
111†	0	very weak	0.05
	5	weak	0.36
	10	weak-medium	0.80
	15	medium	1.29

* Intensities relative to the 400 reflection.

† The observed intensities given for this reflection are visual estimates, high absorption at low angles making quantitative measurements unreliable.

Within the limits of experimental error, the observed and calculated intensities are in complete agreement, and it should be noted that this proof of the location of the Tl^+ ions is independent of any consideration of either the validity of Vegard's law or the values of the ionic radii.

(iii) The Size of the Tl^+ Ion

A value of the size of the Tl^+ ion in sixfold co-ordination in a chloride structure can be calculated from the inter-ionic distance which has received substantial confirmation by the x-ray results.

Using the hypothetical cell dimension of $a_0 = 6.461 \text{ \AA}$ determined above and an ionic radius of 1.810 \AA for Cl^- in sixfold co-ordination (Pauling 1945) the ionic radius for Tl^+ may be calculated, allowance being made for the radius ratio effect (Pauling 1945).

Using a provisional radius for Tl^+ and approximating successively to self-consistency, a value of 1.42_7 \AA has been obtained. The final calculation was as follows:

$$\text{Assume } R_{Tl^+} = 1.42_7 \text{ \AA}$$

$$\text{Radius ratio} = 1.42_7 / 1.810 = 0.788$$

$$\text{Correction factor } F(\rho) = 0.998.$$

Therefore in the rock salt type chloride,

$$R_{Tl^+} + R_{Cl^-} = \frac{6.461_4}{2 \times 0.998} = 3.237_2 \text{ \AA}.$$

With $R_{Cl^-} = 1.810 \text{ \AA}$, the value of $R_{Tl^+} = 1.42_7 \text{ \AA}$.

The size of the thallium ion would vary, of course, with the particular halogen on account of the high polarizability of the thallium ion. The above value, however, would appear to be an accurate assessment for a Tl^+ ion in sixfold co-ordination with Cl^- .

A useful confirmation of the above calculation is provided by determining the value of the ionic radius of K^+ in potassium chloride ($a_0 = 6.292 \text{ \AA}$) from the value used above for Cl^- . The result of 1.333 \AA is in exact agreement with the size given by Pauling (1945).

§ 4. DISCUSSION

If substitutional entry in $KCl(Tl)$ phosphors is assumed, it is known that there is good agreement between the theoretical and experimental luminescent properties for thallium concentrations of less than 0.1% (Cornell Symposium 1948, p. 14). Since the experiments described here have established that substitutional entry does occur at higher concentrations of thallium, it is reasonable to infer that the thallium ions enter the structure substitutionally over the whole range from very small concentrations of the order of 0.002 (Johnson and Williams 1950, 1952) to 15% (molecular) $TlCl$. This is supported by the recent theoretical calculations (Brauer 1952) which have shown, by considering the energy changes involved, that substitutional entry of Tl^+ ions is possible.

There is always the possibility that a few thallium atoms will be interstitially incorporated either randomly or at points of lattice irregularities, but the number of such atoms can be only a small fraction of those occupying substitutional positions. It is suggested therefore that upon excitation by ultra-violet radiation the fluorescent emission of samples of KCl containing different concentrations of $TlCl$ is probably capable of explanation on the basis of complete substitutional entry of the Tl^+ ions into the crystal lattice. For instance, it has been proposed that the emission in the band with a peak at 3050 \AA is favoured by excitation in the absorption band at 2470 \AA and that the blue emission at 4750 \AA is favoured by excitation in the absorption band at 1960 \AA (Johnson and Williams 1952). These emission bands are attributed to single substitutional Tl^+ ions having $^3P_1 \rightarrow ^1S_0$ and $^1P_1 \rightarrow ^1S_0$ transitions respectively. The only electronic transition is believed to be in the thallium ion, the neighbouring ions undergoing an adjustment in position which affects the average equilibrium inter-ionic distances.

When excited by the short ultra-violet radiation from a low vapour pressure mercury discharge in quartz, the three specimens containing 5, 10 and 15% (molecular) of TlCl all have a visible yellow-white fluorescence, which becomes rather deeper with increasing thallium concentration. This yellow emission band (Cornell Symposium 1948, p. 398), the phosphorescence (Seitz 1938) and an emission band at 3775 \AA (Johnson and Williams 1952) all occur in samples with high thallium concentration and have all been attributed to pairs of Tl^{+} ions which are situated in adjacent positive ion locations.

§ 5. CONCLUSION

Our results have demonstrated that the lattice expansion of potassium chloride on solid solution with thallium chloride is proportional to the concentration of TlCl and is in very good agreement with a generalized form of Vegard's law. Intensity changes of the x-ray reflections agree with the values predicted on the assumption that Tl^{+} ions occupy K^{+} positions. Furthermore, it appears very improbable that the intensity results can be explained by any theory other than that of random substitutional replacement by at least a very high percentage of the Tl^{+} ions which enter the KCl lattice.

The theory of the formation of negative complexes in solid KCl(Tl) was based (i) on the x-ray evidence (Stasiw and Saur 1938), (ii) on the similarity of the absorption and emission spectra of the solid phosphors and of the aqueous solutions, and (iii) on some indirect evidence of the results obtained in halides activated with silver, antimony, tin or lead. None of these arguments seems convincing in the light of the present more complete x-ray investigation.

Any similarities between the properties of the solid phosphors and of the aqueous solutions can probably be explained by the similarity in the surroundings of a thallium ion in a positive ion location in the crystal lattice and in a concentrated aqueous solution of KCl . The activation by other metallic elements is certainly not completely analogous to the activation by thallium and it is not intended to suggest that the entry is both random and substitutional in these instances without a detailed investigation of each case.

With reference to the size of the thallium ion, a new value of 1.427 \AA has been obtained for sixfold co-ordination with Cl^{-} . There has not been general agreement in the literature and a value of 1.49 \AA has been used, for example, in a recent calculation of the luminescence of KCl(Tl) (Williams 1951).

Finally, the examination has included the first known application in the study of phosphors, of the intensities of x-ray reflections to the determination of the atomic positions of the activator atoms in the crystal structure of a phosphor. This method is of general applicability and is especially suitable for the many cases where there is activation by a heavy metallic ion.

REFERENCES

- ANTONOV-ROMANOVSKII, V. V., 1943, *J. Phys. USSR*, **7**, 153.
BRAGG, W. L., 1947, *J. Sci. Instrum.*, **24**, 27.
BRAUER, P., 1952, *Z. Naturforsch.*, **7a**, 372.
CORNELL SYMPOSIUM, 1948, *Solid Luminescent Materials* (New York: John Wiley).
FROMHERZ, H., 1931, *Z. Phys.*, **68**, 233.
FROMHERZ, H., and KU-HU-LI, 1929, *Z. Phys. Chem. A*, **153**, 321.
FROMHERZ, H., and MENSCHICK, W., 1929, *Z. Phys. Chem. B*, **3**, 1.
GOLDSCHMIDT, V. M., 1929, *Trans. Faraday Soc.*, **25**, 253.

- HILSCH, R., 1937, *Proc. Phys. Soc.*, **49**, 40 (Supplement).
- INTERNATIONAL TABLES FOR THE DETERMINATION OF CRYSTAL STRUCTURE, 1935 (Berlin : Borntraeger).
- JOHNSON, P. D., and STUDER, F. J., 1951, *Phys. Rev.*, **82**, 976.
- JOHNSON, P. D., and WILLIAMS, F. E., 1950, *J. Chem. Phys.*, **18**, 1477; 1952, *Ibid.*, **20**, 124.
- KRÖGER, F. A., 1940, *Z. Kristallogr.*, **102**, 132.
- NELSON, J. B., and RILEY, D. P., 1945, *Proc. Phys. Soc.*, **57**, 160.
- PAULING, L., 1927, *J. Amer. Chem. Soc.*, **49**, 765; 1945, *The Nature of the Chemical Bond* (Cornell : University Press).
- PRINGSHEIM, P., 1942, *Rev. Mod. Phys.*, **14**, 133; 1949, *Fluorescence and Phosphorescence* (New York : Interscience), p. 524.
- PRINGSHEIM, P., and VOGELS, H., 1940, *Physica*, **7**, 225.
- ROOKSBY, H. P., 1941, *J. Sci. Instrum.*, **18**, 89.
- SEITZ, F., 1938, *J. Chem. Phys.*, **6**, 150.
- STASIW, O., and SAUR, E., 1938, *Verh. Dtsch. Phys. Ges.*, **19**, 4.
- Strukturbericht*, 1913–1928 (Edited by Ewald, P. P., and Hermann, C.).
- WILLIAMS, F. E., 1951, *J. Chem. Phys.*, **19**, 457.
- WILLIAMS, F. E., and HEBB, M., 1951, *Phys. Rev.*, **84**, 1181.
- WYCKOFF, R. W. G., 1951, *Crystal Structures* (New York : Interscience).

RESEARCH NOTES

On a Minimum Property of the Free Energy

BY A. B. LIDIARD

Department of Physics, University of Illinois, Urbana, U.S.A.

MS. received 23rd December 1952

RECENTLY Wohlfarth (1950), correcting some calculations made by Koppe (1947), has discussed the influence of the exchange energy on the thermal properties of free electrons in metals. This discussion has been refined in a note by the author (Lidiard 1951 a) and an extension of it used to calculate ferromagnetic properties (Lidiard 1951 b). However, the starting point of all these papers has been the assumption of a plausible approximation for the Helmholtz free energy of the electrons, F . This expresses F in terms of the distribution function $n_{\mathbf{k}}$ which gives the average probability that the one electron state \mathbf{k} is occupied.

By first drawing attention to a certain minimal property of the free energy, we shall now derive this approximate free energy expression in a way which shows a strong analogy with the approximate Hartree method of quantum mechanics (see, for example, Seitz 1940, particularly §49). This same minimal property has been previously employed by Mayer and Careri (1952) to calculate approximately the equation of state of a gas.

Let us assume that we know the energy levels $E_1, E_2, \dots, E_n, \dots$ of a system. We then observe that the function

$$F = \sum_n a_n E_n + kT \sum_n a_n \ln a_n, \quad \dots\dots(1)$$

where*

$$a_n \equiv a(E_n), \text{ and } \sum_n a_n = 1, \quad \dots\dots(2)$$

has its least value of $-kT \ln \sum_n \exp(-E_n/kT)$ when

$$a_n = \frac{\exp(-E_n/kT)}{\sum_n \exp(-E_n/kT)}. \quad \dots\dots(3)$$

The set of a_n 's given by (3) is thus the 'best' possible set. However, in certain cases the calculation of the true free energy is impossibly difficult. It may nevertheless be possible to obtain approximations to the free energy by assuming arbitrary but manageable forms for the function $a(E_n)$. For this purpose it is convenient to remove the condition (2) on the a_n 's by writing,

$$a_n = \eta_n / \sum_n \eta_n \quad \dots\dots(4)$$

where the set $\{\eta_n\}$ is now quite unrestricted. Then (1) becomes

$$F = -kT \ln \sum_n \eta_n + \frac{\sum_n \eta_n (E_n + kT \ln \eta_n)}{\sum_n \eta_n}. \quad \dots\dots(5)$$

* By this equation we indicate that a_n depends principally on E_n . Through (2) it will, of course, depend also on all the energy levels of the system, but only in a way which is the same for all the a_n 's.

We now wish to apply this result to discuss the metallic valence electron system, assuming the total wave function to be a single determinant of one-electron functions, each of which is the product of a spin function and a space function ('orbital'). If we introduce the upwards spin occupation number $n_{\mathbf{k}}$ (equal to 0 or 1) and likewise the downwards spin occupation number $m_{\mathbf{k}}$ (equal to 0 or 1) for the orbital \mathbf{k} , then the total energy calculated using such a wave function will be of the form

$$E = \sum_{\mathbf{k}} (n_{\mathbf{k}} + m_{\mathbf{k}}) \epsilon_{\mathbf{k}} + \sum_{\mathbf{k} < \mathbf{k}'} (n_{\mathbf{k}} + m_{\mathbf{k}})(n_{\mathbf{k}'} + m_{\mathbf{k}'}) J_{\mathbf{k}\mathbf{k}'} - \sum_{\mathbf{k} < \mathbf{k}'} (n_{\mathbf{k}} n_{\mathbf{k}'} + m_{\mathbf{k}} m_{\mathbf{k}'}) K_{\mathbf{k}\mathbf{k}'}, \quad \dots (6)$$

where $\epsilon_{\mathbf{k}}$ is a one-electron energy which can be described as the kinetic energy of orbital \mathbf{k} , plus its potential energy in the field of the ion cores. $J_{\mathbf{k}\mathbf{k}'}$ is the coulomb integral and $K_{\mathbf{k}\mathbf{k}'}$ is the exchange integral between the two orbitals \mathbf{k} and \mathbf{k}' . We now take as our approximate ensemble distribution function η the following product,

$$\eta = \prod_{\mathbf{k}} \phi_{\mathbf{k}}^{n_{\mathbf{k}}} \psi_{\mathbf{k}}^{m_{\mathbf{k}}}, \quad \dots (7)$$

where the two sets of numbers $\{\phi_{\mathbf{k}}\}$ and $\{\psi_{\mathbf{k}}\}$ can be placed in a one-to-one correspondence with the available orbitals. (In the special case where the exchange and coulomb interactions can be neglected and the problem reduced to that of simple Fermi-Dirac statistics, the best sets of $\phi_{\mathbf{k}}$ and $\psi_{\mathbf{k}}$ become equal to one another and to the set $\{\exp(-\epsilon_{\mathbf{k}}/kT)\}$.) Using (6) and (7) together with the two subsidiary conditions

$$\sum_{\mathbf{k}} n_{\mathbf{k}} = N_1 = \text{No. of upwards spins} \quad \dots (8)$$

$$\text{and} \quad \sum_{\mathbf{k}} m_{\mathbf{k}} = N_2 = \text{No. of downwards spins}, \quad \dots (9)$$

we can evaluate the free energy F in the way generally used for Fermi-Dirac statistics (cf. Schrödinger 1946, particularly chap. VII). If we neglect, as is legitimate, the difference between the mean value of $n_{\mathbf{k}} n_{\mathbf{k}'}$ and the product of the mean values $\bar{n}_{\mathbf{k}}$ and $\bar{n}_{\mathbf{k}'}$, we get

$$\begin{aligned} F = & \sum_{\mathbf{k}} (\bar{n}_{\mathbf{k}} + \bar{m}_{\mathbf{k}}) \epsilon_{\mathbf{k}} + \sum_{\mathbf{k} < \mathbf{k}'} (\bar{n}_{\mathbf{k}} + \bar{m}_{\mathbf{k}})(\bar{n}_{\mathbf{k}'} + \bar{m}_{\mathbf{k}'}) J_{\mathbf{k}\mathbf{k}'} - \sum_{\mathbf{k} < \mathbf{k}'} (\bar{n}_{\mathbf{k}} \bar{n}_{\mathbf{k}'} + \bar{m}_{\mathbf{k}} \bar{m}_{\mathbf{k}'}) K_{\mathbf{k}\mathbf{k}'} \\ & + kT \sum_{\mathbf{k}} \{ \bar{n}_{\mathbf{k}} \ln \bar{n}_{\mathbf{k}} + (1 - \bar{n}_{\mathbf{k}}) \ln (1 - \bar{n}_{\mathbf{k}}) \} \\ & + kT \sum_{\mathbf{k}} \{ \bar{m}_{\mathbf{k}} \ln \bar{m}_{\mathbf{k}} + (1 - \bar{m}_{\mathbf{k}}) \ln (1 - \bar{m}_{\mathbf{k}}) \}. \quad \dots (10) \end{aligned}$$

In this expression $\bar{n}_{\mathbf{k}}$ is the mean value of $n_{\mathbf{k}}$ and $\bar{m}_{\mathbf{k}}$ is the mean value of $m_{\mathbf{k}}$ with respect to the distribution function (7). Explicitly they are

$$\bar{n}_{\mathbf{k}} = \lambda_1 \phi_{\mathbf{k}} / (\lambda_1 \phi_{\mathbf{k}} + 1), \quad \dots (11)$$

$$\text{and} \quad \bar{m}_{\mathbf{k}} = \lambda_2 \psi_{\mathbf{k}} / (\lambda_2 \psi_{\mathbf{k}} + 1), \quad \dots (12)$$

where λ_1 and λ_2 are determined in terms of N_1 and N_2 from eqns. (8) and (9). However, on account of the form of the free energy (10) it is convenient to regard $\bar{n}_{\mathbf{k}}$ and $\bar{m}_{\mathbf{k}}$ as the arbitrary functions. If we now seek the 'best' possible set of $\bar{n}_{\mathbf{k}}$'s and $\bar{m}_{\mathbf{k}}$'s by setting the variation δF equal to zero for all variations $\delta \bar{n}_{\mathbf{k}}$ and $\delta \bar{m}_{\mathbf{k}}$ consistent with the conditions (8) and (9), we easily obtain two implicit equations from which to determine $\bar{n}_{\mathbf{k}}$ and $\bar{m}_{\mathbf{k}}$. However in practice, as for example in the calculations made by Koppe (1947) and Wohlfarth (1950), it may not be possible to use this 'best' set of distribution functions and it is then

convenient to use some special form for $\bar{n}_{\mathbf{k}}$ and $\bar{m}_{\mathbf{k}}$ and to minimize the resulting free energy F with respect to any undetermined parameters which it may contain as a result.

There is an interesting analogy between our derivation of the free energy expression (10) (which was simply assumed by Koppe 1947) and the use of the Hartree product wave function to describe the states of atoms. The true ensemble distribution function is

$$\eta = \exp(-E/kT) \quad \dots\dots(13)$$

where E is given by (6). Now the coulomb and exchange interactions in E have the form of interactions between pairs of particles in \mathbf{k} -space. Therefore since these occur in the ensemble distribution function (13) we may speak of correlations in \mathbf{k} -space which would be taken into account in a rigorous calculation of the free energy. Such correlations are however neglected when we use the ensemble distribution function (7), just as the Hartree product wave function completely neglects positional correlations between electrons in configuration space.

REFERENCES

- KOPPE, H., 1947, *Z. Naturforsch.*, **2a**, 429.
 LIDIARD, A. B., 1951 a, *Phil. Mag.*, **42**, 1325; 1951 b, *Proc. Phys. Soc. A*, **64**, 814.
 MAYER, J. E., and CARERI, G., 1952, *J. Chem. Phys.*, **20**, 1001.
 SCHRÖDINGER, E., 1946, *Statistical Thermodynamics* (Cambridge : University Press).
 SEITZ, F., 1940, *Modern Theory of Solids* (New York : McGraw-Hill).
 WOHLFARTH, E. P., 1950, *Phil. Mag.*, **41**, 534.

LETTERS TO THE EDITOR

Nuclear Reactions Produced by Fast Nitrogen Ions

The beam of high energy $^{14}\text{N}^{6+}$ ions, produced by the 60-inch fixed-frequency cyclotron at the University of Birmingham (Walker and Fremlin 1953), has been used to bombard internal targets. Work has been concentrated mainly on aluminium targets from which a number of radioactive products have been separated chemically and identified.

As was pointed out in the communication quoted above, the $^{14}\text{N}^{6+}$ ions are not accelerated directly from the gas-discharge ion source of the cyclotron, which is fed with nitrogen or nitrous oxide. Rather, the nitrogen ions undergo a preliminary harmonic acceleration in the doubly charged state which aids in stripping the ions to the six-charged state. This leads to the final $^{14}\text{N}^{6+}$ ions having a continuous distribution in energy extending up to a maximum possible energy which corresponds roughly to a $^{14}\text{N}^{6+}$ ion revolving around the centre of the cyclotron. Our targets have been bombarded at a radius of 25 inches where the maximum possible energy is about 125 mev. Some measurements have been made, at this radius, of the current of ions reaching the target with energies exceeding 50 mev, the best beams at present being about 10^{10} nitrogen ions per second. With these beams we have obtained counting rates well in excess of 10^4 per minute from freshly bombarded targets.

The following radioactive nuclei have been identified so far in the reaction products from aluminium: ^{38}K (half-life 7.5 minutes, β^+ -emitter), ^{34}Cl 33 minutes, β^+), ^{32}P (14.3 days, β^-), ^{31}Si (157 minutes, β^-), ^{24}Na (14.8 hours, β^-).

The mechanisms by which these nuclei are produced have not yet been established. One possible mode of formation involves the evaporation of particles from an excited compound nucleus (^{41}Ca) formed by the fusion of ^{27}Al and ^{14}N . This process may account for the heavier products, particularly ^{38}K and ^{34}Cl . On the other hand it seems likely that the lighter nuclei, especially ^{24}Na , which is lighter even than the target nucleus, are produced by a different type of reaction. The evaporation process in the case of ^{24}Na would involve the emission of four alpha-particles and a proton



Since this investigation was started, Wyly and Zucker (1953), working at the Oak Ridge National Laboratory, have reported observing a number of activities produced by bombarding deuterium, beryllium, carbon, nitrogen, and oxygen targets with 25 mev $^{14}\text{N}^{3+}$ ions. In the case of these lighter target nuclei, the Coulomb barrier is substantially lower than that of aluminium. It is worth mentioning that at Birmingham we have produced both α - and β -activities in platinum and gold targets by bombardment with the nitrogen beam. This confirms that a useful fraction of the particles in our beam can penetrate the Coulomb barrier (about 70 mev) of these heavy elements.

Further details of our work will be published later.

Physics Department,
The University, Birmingham, 15.
11th March 1953.

K. F. CHACKETT.
J. H. FREMLIN.
D. WALKER.

REVIEWS OF BOOKS

Electronic Analog Computers, by GRAMINO A. KORN and THERESA M. KORN.
Pp. xv + 378. (New York, London : McGraw-Hill, 1952.) \$7.00, 59s. 6d.

This book will form a useful addition to the literature of analogue computing. It is perhaps unfortunate that the authors have confined themselves almost exclusively to the problem of the design of differential analysers but, even with this limitation, the book contains many ideas which will be useful in other fields of computation.

In the first chapter the fundamental computing elements are considered in a general way. Networks suitable for the operations of addition and subtraction are given and multiplication by means of a servo driven potentiometer is shown to be an applicable technique at low frequencies. The differentiation and integration of a function is next taken up and it is indicated that differentiating circuits have not been much used in serious analogue computation.

The second chapter discusses the set-up procedure favoured by the authors and is mostly devoted to the questions of scale factors and the replacement of the differential operation by integrations. Several equations of interest of physicists are discussed in detail and solutions obtained on a computer are shown for the equations of Mathieu, Legendre and van der Pol.

For the physicist more interested in applications than in computer design, the third chapter will be most stimulating. Practical problems discussed include dynamic vibration dampers, the simple servo, the spherical cannon ball with air resistance and the equations of flight. Flight simulators receive considerable attention and it is shown how a suitable computer can be used in the design and testing of automatic pilots. The chapter concludes with an all too brief discussion of simultaneous equations, integral transforms and boundary and eigenvalue problems.

Chapter four sees the start of the really practical part of the book. The setting of constants and the multiplication of functions by constants are discussed, chiefly with reference to simple potentiometers. This is followed by a detailed analysis of the R.C. integrator and of the improvement of its characteristics by feedback. The chapter concludes with a discussion of the stabilization of amplifiers by feedback.

At the start of the fifth chapter the statement appears (p. 167) "... an exhaustive treatment of amplifier design is entirely beyond the scope of this book". This is surprising since the remainder of the chapter contains an exhaustive account of the design of d.c. amplifiers. The reviewer found the account of drift compensation particularly valuable especially as no other comprehensive treatment appears to be readily available. An omission, which might well be remedied in any future edition, is that of all mention of magnetic amplifiers.

Chapter six discusses techniques for multiplication and for function generation. There does not appear to be anything of particular novelty in any of the circuits given but it is satisfactory to have the various techniques gathered together in one place.

Auxiliary circuits for setting initial conditions and available output mechanisms form the chief subjects of chapter seven, and a brief description of power supply design and of checking procedures ends the chapter.

The final chapter describes some complete computer installations which are available in the United States of America. A sound discussion of design considerations for future machines is followed by a somewhat sketchy discussion of accuracy. Those concerned with the actual building of computers, especially in this country, will sympathize with the statement that the computer room should be a 'showplace'.

An appendix gives a mathematical discussion of the properties of parallel feedback type operational amplifiers. There is a reasonably complete bibliography and good author and subject indexes.

The reviewer noticed a few errors, the penultimate line of p. 12 should have R_0 instead of R_1 . The footnote on p. 130 appears to refer to a further appendix which has not, in fact, been included, and, in the reviewer's experience, it seems most unlikely that electro-mechanical relays are available for operation at 1500 c/s as stated on p. 228.

A. D. BOOTH.

International Tables for X-Ray Crystallography, Volume I. *Symmetry Groups*.

Edited by N. F. M. HENRY and KATHLEEN LONSDALE. Pp. xi+558.

(Birmingham: Kynoch Press, 1952.) £5 5s. (£3 to Members of the Physical Society.)

This book, which is the first volume of three to appear and which collectively will be known as the *International Tables for X-Ray Crystallography*, deals with symmetry groups. This volume has as its counterpart Volume I of the original *International Tables for Crystal Structure Determination*, which appeared in 1935. Much of the material contained in the latter has been incorporated into the present volume, but the editors have compiled the tables in such a manner (and this would of course apply to all three volumes) as to widen their scope and thus to meet the needs "of three categories of scientists: those who are actually engaged in the determination of crystal structure, those who are using x-ray methods in the study of crystals in general, and students of x-ray crystallography".

In preparing this volume the editors have rewritten and carefully re-arranged the topics in a more systematic manner, and furthermore have introduced brief discussions on subjects that might prove to be of general use in the future. There is no attempt made at theoretical completeness, but in spite of this limitation the basic information has been so well sifted and presented that it can be regarded, especially to the advantage of students, as something more than a reference book. One noticeable difference from the older Tables is that these volumes are written entirely in English with a dictionary at the end of each volume giving crystallographic terms used in English, French, German, Russian, and Spanish.

There are seven sections to this first volume, which dealing, as it does, with symmetry groups, forms the basis for the successful interpretation of the x-ray diffraction patterns of crystals. The first section contains an admirable and appropriate historical introduction on x-ray crystallography by von Laue, part of which is subscribed to by Sir Lawrence Bragg himself. In starting the tables with such an introduction the editors have put the subject matter following it into better perspective than was the case with the older Tables.

Section 2 introduces the subject matter of crystal lattices. Within 16 pages the following topics are discussed:—One- and Two-Dimensional Lattices, the 14 Three-Dimensional Bravais Lattices, Crystal Axes and System, the Reciprocal Lattice and Unit Cell Transformations. Section 3 deals with the symmetry of the crystal classes (point group symmetry) both with respect to the external morphology of the crystals and their corresponding Laue x-ray diffraction patterns. Sub- and super-groups among the point groups are also considered. There follows an appropriate discussion dealing briefly with such physical properties of crystals, as pyro- and piezo-electricity, optical activity and optical refractions, etch-figures and morphology in relation to their point group symmetries. Concluding this section is a revised table giving the different names and symbols of the 32 crystal classes.

Perhaps the most noticeable change in this volume, from that of its predecessor, is to be found in section 4 which deals with space group symmetry and related topics. There are changes in nomenclature and layout that are more in line with present-day usage—for instance, the old H setting in trigonal and hexagonal systems has been dropped in favour of more systematic descriptions, where the primitive hexagonal lattice is now called P and not C. Similar changes have been carried out in the tetragonal system—P and I lattices have replaced the old C and F. All this has meant redrawing a large number of tetragonal, trigonal and hexagonal lattice diagrams. The geometrical structure factor and electron density expressions are grouped in a separate subsection with an excellent introduction, and somewhat reminiscent of the methodical way in which these mathematical expressions were set out in Lonsdale's *Structure Factor Tables*. Quite logically there next follows a list of the Patterson and Patterson-Harker Functions for the seven crystal systems. Lastly there is subsection on the transformation of coordinates of equivalent points where this is necessary if the unit cell origin has been changed or the cell size altered. This fourth section occupies 485 pages and comprises the major portion of this book.

Section 5 deals with notes on special topics. Here we find descriptions of methods that are likely to form the basis of future developments in x-ray crystallography. The topics include (1) the correct choice of a Bravais lattice from Powder and Rotation photographs, (2) the determination of sub- and super-groups of space groups, (3) space group determinations outside Friedel's Law and (4) the use of inequalities arising from symmetry elements. The last two subsections deal with techniques that are gradually gaining more recognition in x-ray crystal structure determination. This is particularly true (subsection 3) where, for instance, the statistical methods for the examination of x-ray intensities, devised by Wilson and his school, are applicable for space group determinations where centres of symmetry are not easily distinguished, or where the crystals are very small. In this same subsection there is a discussion of the breakdown of Friedel's Law and its recent very successful use by Bijvoet and his school in the determination of the absolute configuration of tartaric acid. The potentialities of the breakdown of this law have obviously not as yet been fully exploited in crystal structure determination. Lastly, there is a brief discussion (subsection 4) on the limitation of the signs of $|F|$ values using the Harker-Kasper method of inequality relationships involving the $|F|$ values of a crystal. This method of phase determination (together with the very recent developments in

this field by Sayre, Cochran and Zachariasen which are not referred to in this volume) does not pretend to yield unique answers, but it has been shown that of all relationships established between significantly strong $|F|$ values in a given crystal, there is a fair chance that a large number will be correct. The method has so far only been successful for crystals with small unit cells. The development of the inequality method of phase determination, however, does reflect, in one sense, the same trends in crystallography that permeated the work of the Braggs and their schools, viz. the attempt to determine the structure of a crystal as directly as possible from the x-ray data. The difference now is that more complex crystal structures are being studied, and still necessitating techniques involving the minimum of chemical assumption.

Section 6, the last but one, deals with Index Symbols of space groups for various crystal settings, and section 7 gives a dictionary of the basic crystallographic terms used in the different languages, already referred to in the introduction to this review.

It is not merely the inclusion of the newer topics that makes this volume of the *International Tables for X-Ray Crystallography* different from the older Tables, but it is the careful thought which the editors have exercised in layout and presentation that makes it a valuable reference book. The excellent cross references between sections, the references to fundamental papers, the examples given to elucidate the many difficult points, all go towards making the book a welcome guide to the struggling newcomer to this subject. One sees in this volume the long-standing experiences of the two editors as teachers in x-ray crystallography, and they are to be commended on having produced a book of such high standard. The publishers, in their turn, are also to be commended on having produced an excellently printed book.

Lastly the Editorial Commission have done a great service by making this volume available to individual workers at a reduced price on signing a declaration involving two conditions: firstly that the purchaser will not resell the volume, and secondly that he (or she) belongs to a learned scientific society. These are small restrictions and should make it possible for many to obtain this highly recommendable book.

C. H. CARLISLE.

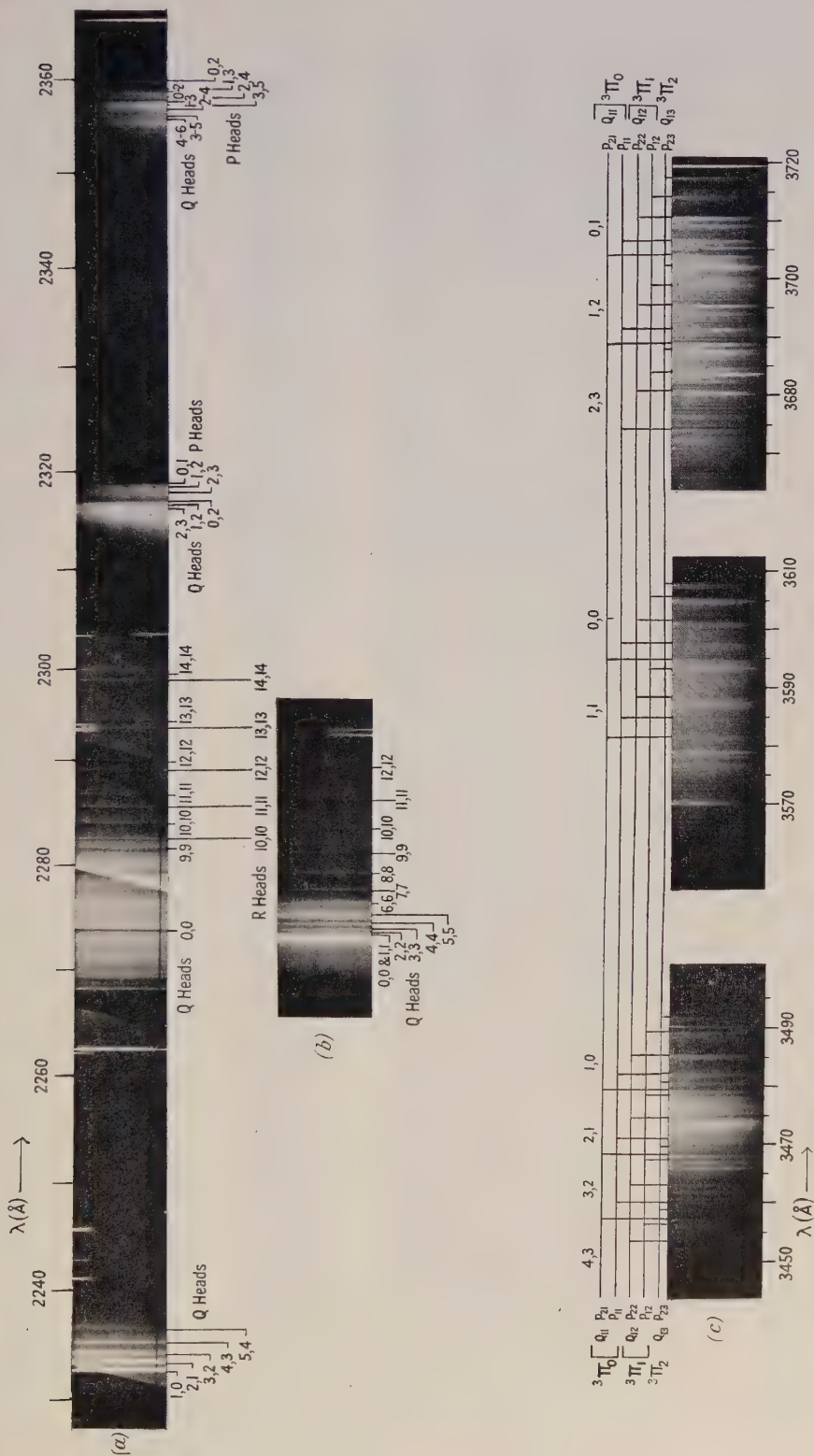
X-Ray Crystallography, by R. W. JAMES. 5th edition. Pp. x+101. (London: Methuen and Co., 1952.) 7s. 6d.

The first edition of this book published in 1930 had become severely out of date. A number of advanced treatises on x-ray crystallography have appeared during the last few years, but no work of an introductory character. This new edition fills this gap admirably. It would be an understatement to say that the old book has been brought up to date: James' monograph has now become a masterpiece, leading the reader smoothly from the law of rational indices to Fourier projections and Harker-Kasper inequalities: it shows how much information can be conveyed in 100 small pages. The book sets a new high standard in the Methuen Monograph series.

W. E.

CONTENTS OF SECTION B

	PAGE
Prof. F. LLEWELLYN JONES and Dr. G. C. WILLIAMS. The Electrical Breakdown of Gases in Non-Uniform Fields at Low Pressure	345
Dr. H. R. HEATH. The Viscosity of Gas Mixtures	362
Dr. S. PARTHASARATHY and Mr. N. N. BAKHSI. Relation between Velocity of Sound and Viscosity in Liquids	368
Prof. H. N. BOSE and Mr. J. SHARMA. Decay of Long Period Afterglow of Alkali Halides under Cathode Ray Excitation	371
Dr. R. MANSFIELD and Mr. S. A. SALAM. Electrical Properties of Molybdenite .	377
Dr. A. SCHALLAMACH. The Velocity and Temperature Dependence of Rubber Friction	386
Dr. HUNTER ROUSE, Dr. W. D. BAINES and Mr. H. W. HUMPHREYS. Free Convection over Parallel Sources of Heat	393
Dr. S. WAGENER. Sorption of Gases at Very Low Pressures by Thorium Powder	400
Dr. AJIT RAM VERMA and Miss P. M. REYNOLDS. Interferometric Studies of the Growth of Stearic Acid Crystals and their Optical Properties	414
Research Notes :	
Mr. M. O. BRYANT and Dr. G. O. JONES. Direct Measurement of the Specific Heat at Constant Volume of Pentane and Alcohol	421
Dr. P. A. LINDSAY and Mr. G. D. SIMS. Application of the Thermodynamics of Irreversible Processes to the Theory of the Magnetron	423
Dr. T. J. LEWIS. The Dependence of the Dielectric Strengths of Pure Liquids on Cathode Material	425
Letters to the Editor :	
Dr. J. W. GRANVILLE and Dr. W. BARDSLEY. Some Properties of Silicon Point-Contact Transistors	429
Mr. R. E. BURGESS. The Influence of Mobility Variation in High Fields on the Diffusion Theory of Rectifier Barriers	430
Mr. O. P. DOGRA, Mr. M. G. BHATAWDEKAR and Mr. N. A. RAMAIAH. A Note on Secondary Processes in a Low-Frequency Electrodeless Discharge .	431
Reviews of Books	433
Contents of Section A	440



(a), (b) $^1\Pi-^1\Sigma^+$ system of AlF : E 478 Hilger Littrow spectrograph. (c) $^3\Sigma-^3\Pi$ system of AlF : 2nd order 2.4 m grating.

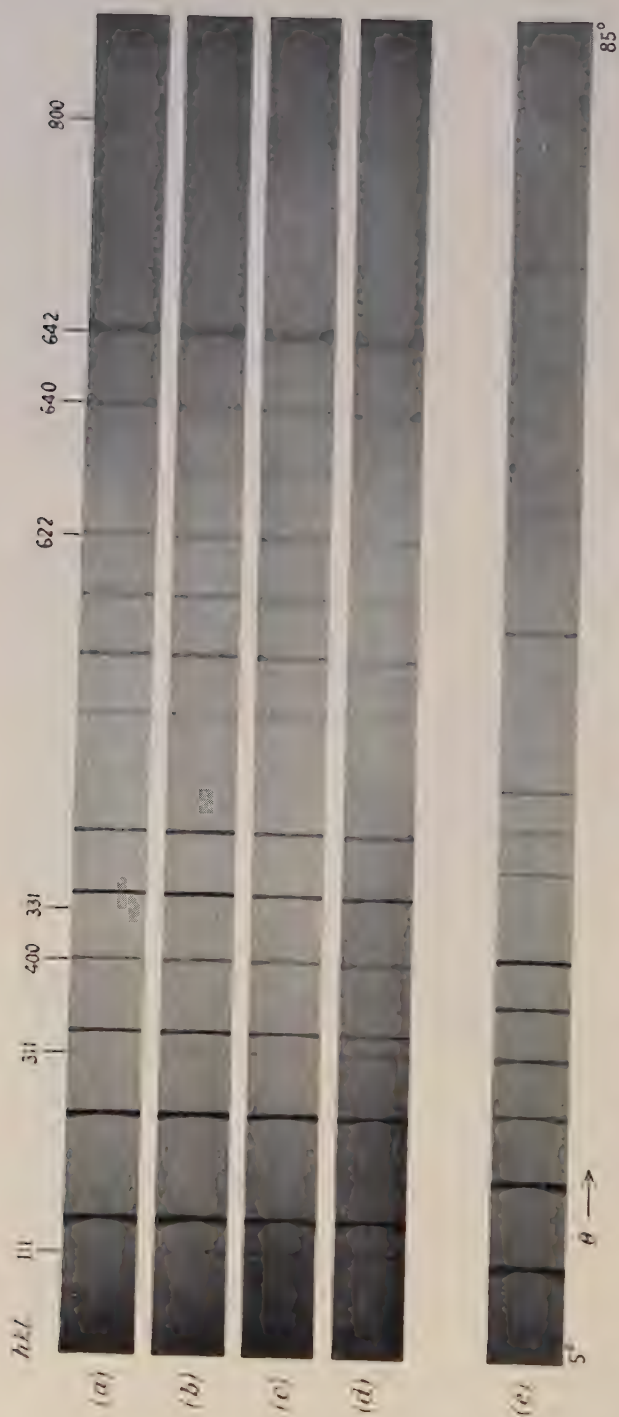


Fig. 1. X-ray powder diffraction photographs of KCl-TiCl₃ preparations, (a) KCl, (b) KCl-TiCl₃: 5% (molecular) TiCl₃, (c) KCl-TiCl₃: 10% (molecular) TiCl₃, (d) KCl-TiCl₃: 15% (molecular) TiCl₃, (e) TiCl₃ (19 cm diameter camera, CuK α radiation).

37th Guthrie Lecture

The Conceptual Situation in Physics and the
Prospects of its Future Development

BY MAX BORN

Department of Mathematical Physics, University of Edinburgh

37th Guthrie Lecture, delivered 13th March 1953; MS. received 13th March 1953

LET me begin with a personal remark. Fifty years ago I was a young student of science, in my second academic year. At that time Planck's radiation formula and the quantum hypothesis were already more than two years old. But I was ignorant of those momentous events. We were taught Newton's mechanics and its applications, and we were cautiously introduced to Maxwell's theory of the electromagnetic field.

Today the situation may be similar. A great discovery may be made somewhere by somebody of which I have heard nothing or whose importance I do not see. With increasing age it becomes more and more difficult to keep step with contemporary research. My knowledge of what is going on in the laboratories and studios all over the world is now almost as scanty as it was half a century ago. Yet the years have not passed without trace. They have left an accumulation of experience over a wide horizon, and this encourages me to speak to you about my impressions of the present situation in theoretical physics and the direction in which it is moving. A forecast about the future may appear presumptuous, for science has always been full of surprises, unexpected experimental results which changed the structure of the theory. Yet I venture certain guesses because of a phenomenon which might be called the 'stability of the principles'. I do not suggest that, apart from mathematics, there are any principles which are unchangeable, *a priori* in the strictest sense. But I think that there are general attitudes of the mind which change very slowly and constitute definite philosophical periods with characteristic ideas in all branches of human activities, science included. Pauli, in a recent letter to me, has used the expression 'styles', styles of thinking, styles not only in art, but also in science. Adopting this term, I maintain that physical theory has its styles and that its principles derive from this fact a kind of stability. They are, so to speak, *relatively a priori* with respect to that period. If you are aware of the style of your own time you can make some cautious predictions. You can at least reject ideas which are foreign to the style of your time.

I shall not attempt a historical review of physics from this standpoint, nor an investigation of the question whether the style of science, in particular of physics, depends on other conditions, for instance economic ones. I shall just begin with the modern era, with Galileo and Newton, and stress solely one characteristic point, namely, the separation of subject and object in the description of natural phenomena. For the Greek philosophers the cause of motion, the force producing the motion, was inseparable from a living being, man or god, who felt the exertion. Moreover they used ideas of value as a principle of

explanation. The planets moved in circular (or epicyclic) orbits because the circle is the most perfect curve. Perfection reigned in the celestial spheres, corruption on the terrestrial level; law and order among the stars, chaos and strife on earth. The Christian era introduced new ideas and is certainly a separate period with its own style, but in regard to science it relied on the ancients and preserved the anthropocentric, subjective attitude. The idea of perfection was now personified in God. Natural phenomena happen to glorify Him, to punish the wicked, to reward the good ones. This motive is still strong in Kepler.

The break came with Galileo and Newton. They introduced the disinterested, objective description and explanation which is characteristic for the modern epoch. But the ancient style did not disappear at once. Traces survived a long time, for instance in the metaphysical interpretation of the minimum principles of mechanics. Maupertuis certainly believed that the minimum of action was the expression of a purpose of Nature or the Creator. Even Euler's writing, where the first rigorous formulation of the principle of least action is given, is not free from this metaphysical attitude. It finally disappears in Lagrange's work.

From now on the world is a mechanism, ruled by strict deterministic laws. Given the initial state, all further development can be predicted from the differential equations of mechanics. The minimum principles are not due to nature's parsimony but to human economy of thinking, as Mach said; the integral of action condenses a set of differential equations into one simple expression.

The supposition is that the external world, the object of natural science, and we, the observing, measuring, calculating subjects, are perfectly separated, that there is a way of obtaining information without interfering with the phenomena.

This is the philosophy of science in which we, of the older generation, have grown up. It can be called the Newtonian style, as it is modelled on Newton's celestial mechanics. It was extremely successful also in terrestrial matters, even when it was extended from mechanics of material systems to electrodynamic phenomena *in vacuo* and in matter. Maxwell's theory takes the polarity between subject and object for granted and is strictly deterministic.

A new era, a new style, commenced in 1900, when Planck published his radiation formula and the idea of the quantum of energy. Its way was prepared by a long development which revealed the inadequacy of classical mechanics to deal with the behaviour of matter. The differential equations of mechanics do not determine a definite motion, but need the fixation of initial conditions. For instance, they explain the elliptic orbits of the planets, but not why just the actual orbits exist. But there are regularities concerning the latter: Bode's well known rule. This is regarded as a question of the prehistory of the system, a problem of cosmogony, and still highly controversial. In the realm of atomistics the incompleteness of the differential equations is even more important. The kinetic theory of gases was the first example to show that new assumptions had to be made about the distribution of the atoms at a fixed instant, and these assumptions turned out to be more important than the equations of motions; the actual orbits of the particles do not matter at all, only the total energy which determines the observable averages. Mechanical motions are reversible, therefore the explanation of the irreversibility of physical and chemical processes needed new assumptions of a statistical character. Statistical mechanics paved the way for the new quantum era.

With the quantum came a new attitude to the polarity subject-object. It is neither essentially subjective, as the ancient and mediaeval doctrines, nor wholly objective, as the post-Newtonian philosophy.

The change was due to the breakdown of all attempts to understand atomic phenomena from the standpoint of ordinary mechanics. A new atomic mechanics had to be found, and the way leading to it proceeded in steps. The most important of these was Bohr's idea of stationary states and transitions between them. The states are certain mechanical orbits picked out by simple quantum rules, and the energies lost or gained by the transition are connected with frequencies of emission and absorption by Planck's quantum law $E = h\nu$. The amazing success of this theory in explaining the stability of atoms, the structure of atomic and molecular spectra, the periodic system of elements and of many other properties of matter did not delude Bohr into believing that this was a final solution. He stressed, from the very beginning, the new features of the scheme, namely the indeterministic character of the transitions, the appearance of chance in the elementary processes. This means the end of the sharp separation of the object observed and the subject observing. For chance can be understood only in regard to expectations of a subject.

After 25 years of struggle a satisfactory theory was obtained, from different sources. One approach, which expresses Bohr's ideas in a logically consistent way, is due to Heisenberg, the so-called matrix mechanics. Another quite independent approach was found by de Broglie and developed in Schrödinger's wave mechanics. In the form given to the theory by Dirac it is a structure of great beauty and perfection, but rather abstract. It has been supplemented by a doctrine of measurement, due to Heisenberg and Bohr, which connects the formalism with the experimental reality.

The essential feature is that the physical quantities or, in Dirac's terminology, 'observables', like coordinate, momentum, energy of a particle, components of field strength, etc., are not represented by variables, but by symbols with a non-commuting multiplication law, or, more concretely, by operators A , which operate on a quantity ψ , transforming it into another quantity $A\psi$. This function ψ is a generalization of de Broglie's and Schrödinger's wave amplitude and defines the state of the system. It satisfies an equation of the deterministic type current in classical theory. Nevertheless it does not allow deterministic predictions about the observables, but only statistical ones: $|\psi|^2$ is the probability of the state represented by ψ , and the expectation value of an observable A in this state can be expressed in terms of ψ . In particular, the accuracy δq of a measurement of a coordinate q (properly defined through the expectation value of the mean square deviation) and the accuracy δp for the corresponding momentum p are found to satisfy Heisenberg's uncertainty relation $\delta q \delta p > h$, where h is Planck's constant h divided by 2π . Similar relations hold for other pairs of 'conjugate' variables.

In this abstract formulation the words particle, coordinate, momentum etc. are used, but obviously with a different meaning from ordinary language. A dust particle is supposed to have at a given instant a certain position and velocity. An electron or other particle obeying the laws of quantum mechanics behaves differently; for according to the uncertainty rule a definite position (δq very small) demands a large δp ($> h/\delta q$), hence a large uncertainty of velocity. This question has been discussed so often that I need not dwell upon it. The further development of quantum mechanics has revealed more features of strange

behaviour, for instance the lack of individuality of particles, which has very direct and decisive consequences for statistical thermodynamics.

Therefore the question arises how these new conceptions of particles and their properties can be handled without coming into conflict with the obvious fact that the instruments used in experimenting with them and observing them are ordinary bodies which obey Newtonian laws. This is the object of Bohr's theory of measurement. The essence of quantum mechanics, stripped of all mathematical refinement, are the laws of Planck and of Einstein-de Broglie, namely $E = h\nu$, $p = h\kappa$; here E , p are the energy and momentum of a particle, ν , κ the frequency and wave number of the 'corresponding' wave. If one tries to visualize the meaning of this correspondence in space and time, one finds a paradoxical situation. For E , p refer to an extensionless particle, ν , κ to a harmonic wave which by its very definition is infinitely extended in time and space. The solution of the paradox must therefore be found in an analysis of the use of the concepts of location and duration in connection with a train of waves.

One is accustomed to apply the idea of a definite time interval or duration to any ordinary pair of events (e.g. the fall of a stone from my hand to the earth). Yet there are seemingly harmless cases where this is not justified. The sentence 'a musical tone lasts a definite time' has no rigorous meaning. That is not a purely logical statement, but one of fact. Indeed, a sharp *staccato* on the low pipes of an organ sounds badly. For a wave train starting harmonically but broken off at a time not large compared with the period of vibration is not actually harmonic but a superposition of harmonic waves of different frequencies, a wave packet: acoustically a noise. This fact is also well known in optics, where it is the basis of the theory of the resolving power of instruments, and it has recently become most important in the theory of information (obtained by transmitting electromagnetic or other waves).

Elementary considerations lead for the mutual limitation of δt and $\delta\nu$, δx and $\delta\kappa$, to the relations $\delta t \delta\nu > 1$, $\delta x \delta\kappa > 1$. They are the root of the uncertainty rules of Heisenberg; for if they are multiplied by h and the Planck-de Broglie relations used, the result is $\delta t \delta E > h$, $\delta x \delta p > h$. This consideration in no way mitigates the paradoxical, almost irrational, character of the Planck-de Broglie correspondence. But it helps to handle it in such a way that contradictions between the results of measurement cannot occur.

Location and duration can be measured only with the help of rigid scales and clocks; energy and momentum only with the help of mobile parts, which react according to the conservation laws. Thus the reciprocal uncertainty can be traced to two types of mutually exclusive but complementary experiments. Bohr has illustrated this "complementarity" by many instructive examples, some of these in response to attacks made by Einstein, who hoped to disprove the uncertainty rules by ingenious experimental arrangements. I think that attempts against the uncertainty laws will cease in time. The lasting result of Bohr's endeavours is the simple consideration given above, which shows with irrefutable logic that the Planck-de Broglie laws of necessity imply the duality particles-waves and the complementary quality of experimental arrangements set up to measure 'conjugate' pairs of quantities, like energy-time, momentum-location.

Intimately connected with this duality is the polarity subjective-objective. For if an experiment must be set up in a definite way to investigate one or the

other of a conjugate pair of quantities, it is impossible to obtain information of the system considered as such; the observer has to decide beforehand which kind of answer he wants to obtain. Thus subjective decisions are inseparably mixed with objective observations. The same can be seen from the mathematical description with the help of the state-function ψ , which is only determined by the whole system, including the means of observation which depend on the subject.

This is a sketch of the modern style of physics which is accepted by practically the whole community of experimental and theoretical physicists. It fits exactly to the practice of electronics, spectroscopy, radioactivity, nuclear physics and also chemistry and astrophysics. The questions for which the theory offers answers are just those which the experimentalist wants to be answered. He is entirely indifferent to orbits of electrons in atoms, of atoms in gases, of nucleons in nuclei; he is quite content with stationary states and collision cross sections which the theory supplies.

I think that this mode of scientific thought is also in conformity with the general trend of contemporary philosophy. We have lost confidence in the possibility of separating knowledge from decision, we are aware of being at every moment spectators and actors in the drama of life. Bohr himself has indicated generalizations of his 'complementary' idea to biology and psychology; ancient problems like that of the relation of matter and mind, freedom and necessity, are thus seen from a new angle. I cannot enter into these deep questions, but may mention some fascinating books by von Weizsäcker (1949, 1951), where they are treated with competence and good taste.

I venture the prediction that this style of thinking will last, and that a future change, when it comes, will not lead back to the past, so-called classical, style but to something more removed from it. My confidence in this forecast rests not only on the success of the present theory but in my personal affinity for its philosophy.

However, this view is strongly contested, just by some of those who have done most to develop quantum theory. Planck himself was sceptical. For instance, when he, as President of the Berlin Academy, inaugurated Schrödinger (who was his successor to his chair), he praised him as the man who had re-established determinism through his wave equation. Einstein, who renewed the corpuscular idea in optics, who introduced the transition probabilities between two stationary states and is guilty of other anti-classical deviations, has turned with a kind of passion against the statistical interpretation of quantum mechanics. I have already mentioned his attempts to disprove the uncertainty laws by ingenious contraptions and Bohr's refutations of these attacks. When Einstein could not maintain the existence of logical flaws in quantum mechanics he declared it to be an 'incomplete' description of nature. I have used the same expression before in regard to the differential equations of classical mechanics which are incomplete without initial values for which classical theory gives no law and which, in my opinion, lead to absurd consequences. Imagine N particles fixed in random positions and another particle fired amongst them, colliding and recoiling, according to classical laws. It is obvious that for large N the tiniest deviations of the initial motion produce not small changes in the final position, but an enormous variety of large effects. If all particles are moving like gas atoms this would hold *a fortiori*. Thus the supposed determinism is an illusion.

This group of distinguished men, to whom von Laue may be added, may be called philosophical objectors, or, to use a less respectful expression, general grumblers.

There are those who, aware of the unavoidable consequences of the Planck-de Broglie relations $E = h\nu$, $p = h\kappa$, want to sacrifice these and preserve only one side of the picture. There are the particle defenders or p-totalers, and the ψ -wave defenders or ψ -totalers. They are of course all theoretical physicists, and you find them well represented in a recently published book* dedicated to de Broglie on the occasion of his 60th birthday (1952). De Broglie himself, though the discoverer of the electron waves, has made serious attempts to save determinism by introducing concealed parameters. One of his suggestions (de Broglie 1926, 1927) was to write a complex ψ -function in the form $\psi = Re^{i\Phi}$; then Schrödinger's wave equation is equivalent to a set of classical equations of motion of particles under the action of two forces, one with the potential Φ , the other with a supplementary potential U . The latter depends on R and is subject to strong fluctuations due to the interaction of the particles, thus producing the same effect as the uncertainty in the current interpretation. A similar suggestion has been independently made by Madelung (1927). Recently such considerations have been renewed and refined by Frenkel (1950, 1951) and Blokhintzev (1950, 1951) in Russia, and by Bohm (1952) in America. Already in 1932 von Neumann had shown that it is impossible to introduce concealed parameters without conflict with confirmed results of the current theory. Therefore Bohm is anxious to show that in the frame of present knowledge his concealed parameters cannot be determined by experiment; he hopes that future discoveries will make this possible. But Pauli, in the de Broglie volume mentioned, has shown that this attitude leads to contradictions; for in problems of statistical thermodynamics the concealed parameters must necessarily show their existence and produce secular distortions of the Bose- or the Fermi-Dirac distribution.

Thus the reactionary p-totaller movement can be discarded.

Schrödinger has, right from the beginning, taken the opposite standpoint: the whole of physics is wave theory, there are no particles, no stationary states and no transitions, only waves. I have already mentioned that Planck welcomed this idea; but the majority of physicists continued to use the particle image and to speak of atoms, electrons, nuclei, mesons etc.

Recently Schrödinger (1952) has taken up his purification campaign and pleaded passionately for ejecting not only particles, but also stationary states, transitions, etc., from physics. The motive for his discovery of wave mechanics was his violent dislike of Bohr's instantaneous 'quantum jumps', and we can understand his triumph when he could represent all these 'absurdities' in terms of well-known and innocuous resonance phenomena of waves.

I myself might have a similar motive to declare matrices as the only real thing. Allow me to indulge in a personal reminiscence. When Heisenberg published the fundamental paper in which he cleared quantum theory from classical remnants and formulated it in terms of transition amplitudes, he was my assistant, very brilliant but very young, and not very learned. In fact he did not exactly know what a matrix was, and as he felt stuck he asked my help. After some effort I found the connection with the matrix calculus, and I remember my

* This book contains the literature in more complete form than is given here. In the list of references at the end of this article papers are mentioned which are quoted in the text only by 'and others'.

surprise when Heisenberg's quantum condition turned out to be the matrix equation $qp - pq = i\hbar$. If Heisenberg were here instead of myself he would tell you the same story. The matrix form of quantum mechanics was first published by myself in collaboration with my pupil Jordan.*

However, I have not, and never had, a particular preference for the matrix method. When Schrödinger's wave mechanics appeared I felt at once that it demanded a non-deterministic interpretation, and I guessed that $|\psi|^2$ was the probability density; but it took some time before I had found physical arguments in favour of this suggestion, namely collision phenomena and transitions under external forces. Now the strange thing happened that Heisenberg first disagreed and accused me of treason against the spirit of matrix mechanics. But he soon came round and produced the wonderful reconciliation of particles and waves with the help of his uncertainty relation.

But now I have to return to Schrödinger's attack against particles and quantum jumps. It cannot be proved wrong, for the ψ -function which can be represented as a wave in a multi-dimensional space contains all physical information—provided you know how to connect it with experience. And there is the difficulty. We have no other language to describe what we do and what we see in experimenting than in terms of bodies and their movements. Schrödinger himself cannot avoid the particle language even when he tries to demonstrate the supremacy of the wave language. I have dealt with this question in detail at another place (1953) and need not repeat it. I think Schrödinger's suggestion is impracticable and against the spirit of the time.

Yet I do not wish to create the impression that I believe the present interpretation of quantum theory to be final. I only think that a return to Newtonian determinism is impossible.

I have now arrived at the point where I have to make good my promise to try some forecast of the future.

The fundamental problems of contemporary physics are concerned with elementary particles and the corresponding fields, in particular the explanation of stability or instability, masses, spin character, interactions, etc. This is a wide programme which includes the whole of nuclear physics and the study of cosmic rays, and it leads definitely beyond the scope of current quantum mechanics, for the problem of the elementary masses is connected with the difficulty of the self-energy of particles. It is well known that the self-energy of an electron is infinite even in the classical theory of Maxwell-Lorentz. In quantum theory this primary infinity of the type e^2/a (e charge, a radius, limit $a \rightarrow 0$) is superposed by a variety of other divergent integrals. I have followed these investigations only from afar, but my impression is that through the work initiated by Tomonaga (1946) and Schwinger (1948) a kind of solution has been found: By a profound mathematical method called 'renormalization' the actual, intrinsic singularities can be separated out and, if infinite, omitted in a way which is uniquely fixed by postulating relativistic invariance, and the remaining formulae give definite, finite results. Dirac (1951) wrote about this theory: "it is an ugly and incomplete one, and cannot be considered as a satisfying solution of the problem of the electron", and he suggests an alternative theory. I think the first part of his judgment too hard, for it is a great achievement to have a

* The early phase of quantum mechanics is misquoted nearly everywhere in the literature. I have given a few more examples in my book *Natural Philosophy of Cause and Chance* (Oxford: Clarendon Press, 1949), App. 27, p. 188.

working formalism which in the hands of the initiated leads to the explanation of such delicate effects as the Lamb-Retherford shift (1947) in the hydrogen terms and deviations from Landé's magnetic factors, etc. But I subscribe to the view that this theory is incomplete and circumvents, instead of attacking, the actual problem. Dirac has suggested an alternative theory whose main idea is that the occurrence of charge in finite quanta, electrons, must be a quantum effect; hence the corresponding classical theory should be a pure wave theory. By a slight modification of the current formulae he obtains such a wave theory, but so far he has not succeeded in quantizing it. It is quite possible that a satisfying theory of the electromagnetic field and its charges can never be obtained because photons and electrons cannot be treated without regard to other particles.

The most conspicuous feature of modern physics is the discovery of more and more unstable particles, called mesons. For practical purposes linear wave equations for each type of particle are established with non-linear coupling terms between them. It is clear that this is a preliminary approach which one day will have to be superseded by a coherent theory of matter, in which the different masses of the particles appear as eigenvalues of operators or solutions of equations. It is now generally accepted that this theory will contain an absolute length a , or an absolute momentum $b = \hbar/a$, and that in domains of the dimension a geometry may become meaningless. A remarkable attempt to formulate such a situation is due to Yukawa (1949); he regards a field component ϕ not as a function of the space coordinates and time, x, y, z, t , but both ϕ and x, y, z, t as non-commuting quantities, and postulates certain commutation laws between them which are generalizations of the current differential equations and go over into them if all distances are large compared with the absolute length a . Yukawa, Møller (1951), Rayski (1951) and others have shown that the divergences of the self-energy and other such difficulties can thus be avoided.

The first who clearly saw the necessity of uniting the theories of different particles was Eddington. But at his time there were only two kinds known, protons and electrons. Thus the discoveries of mesons have made his attempt rather obsolete, quite apart from the rather fantastic foundations. [His main assumptions led to the integral value 137 of the reciprocal fine structure constant $1/\alpha = \hbar c/e^2$, which is almost but not quite in agreement with the latest observations, from which the value $1/\alpha = 137.0364 \pm 0.0009$ is derived (Du Mond and Cohen 1951).]

I cannot deal with the many attempts to unify the different fields. Most of them can be reduced to the following scheme:

The wave equation $(\square + m^2)\psi = 0$ (\square is the d'Alembertian operator) is replaced by $f(\square)\psi = 0$, where $f(\xi) = (\xi - \xi_1)(\xi - \xi_2) \dots (\xi - \xi_n)$ is a polynomial of degree n ; it describes the motion of n independent particles with masses $m_1 = \sqrt{\xi_1} \dots m_n = \sqrt{\xi_n}$. By using instead of \square Dirac's operator one can take account of the spin. Theories of this type have been derived by Bhabha (1945) and others from considerations of particles with higher spin. I have suggested another way to determine the function $f(\xi)$ which connects this problem with that of the infinities. One can add to $f(\xi)$ a transcendental factor without zeros. If one has, for instance, the differential operator in the domain of one variable $q, p^2 - m^2$, where $p = -i\hbar\partial/\partial q$, one can add the factor $\exp(-\frac{1}{2}p^2)$ (where $b = \hbar/a$ is taken as unit for p). This has, in the first place, the consequence that the possible momenta are cut off, thus removing infinities. And secondly, one can determine

the mass m by giving the expression $(p^2 - m^2) \exp(-\frac{1}{2}p^2)$ a proper meaning; it is the second Hermitian function of p for $m^2=2$, hence identical with its Fourier transform. This remark suggests the application of the general principle that the whole of physics can be formulated in terms of transformation groups and their invariants. By postulating reciprocal invariance (i.e. against Fourier transformation) it seems to be possible to determine a set of masses as the roots of (Hermitian) polynomials. However, Schrödinger has shown that in the four-dimensional space-time serious difficulties appear.

Quite independently from these considerations, the elimination of the infinities with the help of the factor $\exp(-\square)$ has been investigated by Pais and Uhlenbeck (1950) and others.

The most radical change in the structure of the theory has been proposed by Heisenberg (1943). Convinced of the existence of an absolute length $a \sim 10^{-13}$ cm or an absolute time $\tau = a/c \sim 10^{-24}$ sec, he doubts that the usual description of a physical system with the help of a Hamilton function has a meaning at all for space- and time-intervals smaller than a and τ . What we really can observe are only alterations in time-intervals long compared with τ . If the state of the system at a time t_1 is described by $\psi(t_1)$, that at t_2 by $\psi(t_2)$, it is legitimate to assume that in the equation

$$\psi(t_2) = S(t_1, t_2)\psi(t_1)$$

the transition operator $S(t_1, t_2)$ has a physical meaning for $t_2 - t_1 > \tau$, in particular its value $S(-\infty, \infty)$. This operator is usually called S -matrix. For instance, in a collision process we observe particles before and after the collision, and we are interested only to know the distribution after the collision if that before is known. Heisenberg maintains that all attempts to describe the collision process itself should be abandoned.

The postulate of relativistic invariance introduces strange paradoxes in this theory. The temporal order of events, and thus the cause-effect relation, breaks down for short time intervals; for instance, a particle may be absorbed before the creating collision has taken place. But Heisenberg (1951) has made it plausible that these anomalies may be unobservable in principle because of the atomistic structure of the instruments.

According to the principle of correspondence the S -matrix theory must go over into an ordinary Hamiltonian theory for cases where the absolute length or time play no important part. Heisenberg comes to the conclusion that very likely the current assumptions about interactions are not sufficient. These lead to Hamiltonians which can be re-normalized in the sense described above. Actually there are indications that a more thorough non-linearity is needed. In a recent paper (1952) he discusses the process of meson showers from this standpoint and uses a type of non-linear field theory which I found about 20 years ago and published in collaboration with Infeld (1933, 1934). It is a modification of Maxwell's electrodynamics in which the self-energy of the electron is finite. Mie had shown already in 1912 that the equations of the electromagnetic field can be formally generalized by replacing the linear relations between the two pairs of field vectors \mathbf{E}, \mathbf{B} and \mathbf{D}, \mathbf{H} by non-linear ones. Yet he did not specify these relations, and thus his formalism remained empty.

The idea which I applied to it is a special case of what Whittaker (1949) has called the principle of impotence. If research leads to an obstacle which in spite of all efforts cannot be removed, theory declares it as insurmountable in principle.

Well-known examples are the first and second theorems of thermodynamics which are derived from the impossibility of perpetual motion of the first and second kind. Other examples are relativity, where the impossibility of material and signal velocities larger than the velocity of light is declared, and the uncertainty relations of quantum mechanics, which forbid the simultaneous determination of position and velocity and of similar pairs.

In the case of the electromagnetic field the self-energy can be made finite by prohibiting the increase of \mathbf{E} the electric vector beyond a certain limit, the absolute field. This can be done by imitating relativity where the classical Lagrangian of a free particle $\mathcal{L} = \frac{1}{2}mv^2$ is replaced by $m\mathbf{c}^2[1 - (1 - v^2/\mathbf{c}^2)^{1/2}]$, from which $v < \mathbf{c}$ follows. In a similar way the Lagrangian density of Maxwell's electrodynamics can be replaced by a square root expression. Thus a finite self-energy of a point charge is obtained which represents not only the inertial mass but also, as Schrödinger has shown, the gravitational mass.

A more important asset of this theory seems to me the estimate of the fine structure constant, obtained by Heisenberg and his pupils Euler and Kockel (1935, 1936) and confirmed by Weisskopf (1936), by comparing the lowest non-linear terms of it with the corresponding terms of Dirac's theory of holes, which are due to what is called a 'polarization of the vacuum'. The result is $1/\alpha = \hbar\mathbf{c}/e^2 = 82$, which, though still much too small, is of the right order of magnitude. This method appears to me the only rational attempt to derive the number $1/\alpha = 137$.

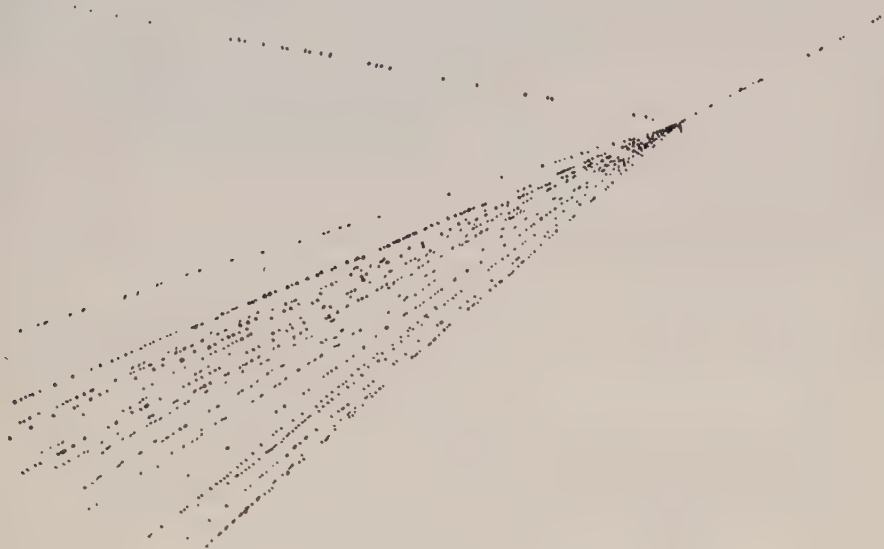
That the non-linear theory has not found favour is partly due to the difficulty of quantization, partly to an objection raised by Heitler which at the time seemed to me convincing. He said that a classical theory of the electron, which takes Planck's constant \hbar as negligible but the charge e as finite, is meaningless because $1/\alpha = \hbar\mathbf{c}/e^2 = 137$ is a large number.

Now Heisenberg, in search of a non-linear field theory as limiting case of his S -matrix formalism, took over that square root method and applied it to the meson field produced by a nucleon. But he applied it to quite a different type of problem, namely the meson showers produced by a nuclear collision. Here Heitler's objection becomes insignificant. If Heisenberg's procedure is analysed, it is seen that it does not rest on the limit $\hbar \rightarrow 0$, but $N \rightarrow \infty$, where N is the number of quanta involved. In fact Bohr had both these cases in mind right from the beginning when he formulated the transition from quantum theory to its classical limit. (The same consideration justifies the estimate of the fine structure constant, mentioned above.)

Heisenberg considers the collision of two nucleons, each being the source of a meson field, obeying his non-linear field equations. For a very high collision energy the number of meson quanta will be very large, hence the application of a classical wave equation permitted. The total energy carried by this wave ψ can be represented by an integral over all wave vectors \mathbf{k} of a function $u(\mathbf{k})$; if $u(\mathbf{k})$ is divided by the energy quantum $\hbar\nu$, where $\nu = \mathbf{c}|\mathbf{k}|$ is the frequency of the wave \mathbf{k} , and the result integrated over all \mathbf{k} one obtains the total number N of quanta emitted. In this way it can be shown that for a non-linear theory of the type described multiple meson production is possible and the value of N can be estimated.

Now this idea of multiple showers is sharply contradicted, in particular by Heitler, who thinks that the observations can be explained in terms of plural

production. The experiments are made not with two colliding nucleons but with one nucleon hitting a nucleus; then a cascade of nucleons and mesons will develop and thus a shower of mesons mixed with nucleons or larger splinters appear. Heitler, in a letter to me, quotes experimental investigations by Terreaux (1951, 1952) as confirming the cascade theory, and some unpublished work by McCusker. Showers were produced in layers of carbon and of a paraffin containing equal numbers of C atoms; thus the effect of the H atoms (proton-proton collisions) can be deduced, and the result was that up to 3×10^{10} ev no multiple production was observed. This is, however, in strict contradiction to experiments made by Haxel and collaborators, of which I have learned through my correspondence with Heisenberg; here layers of carbon and paraffin of equal mass (equal number of nucleons) were investigated with the help of counters which recorded showers of three or more penetrating particles.



Meson shower without tracks of heavy particles.

(Photograph taken by Frä. Chr. Schriell, reproduced from Teucher, *Naturwissenschaften*, 1952, **39**, 68)

"The result is that the H atoms have their full share in the multiple production. Heisenberg has further sent me a photograph, which is reproduced here, of a shower containing about 16 mesons, but no heavy track. He interprets it as evidence for multiple production, but it might just as well be a nuclear cascade in which the heavy particles are by chance all neutrons.

Just a few days ago my attention was directed to a paper by Vidale and Schein (1951) which, if confirmed, would settle the dispute. Self-registering instruments were carried by balloons to more than 90 000 feet altitude and showers in liquid hydrogen observed with counters. The results seemed to be in favour of multiple production, but the assumption made that the primary particles are nucleons (protons) is not certain at all. I have the impression that Heisenberg's audacious ideas are in the right direction, and this direction is obviously not backwards, but forward to new abstractions, to a new style of thinking.

I have so far only considered the conceptual problems arising from the microscopic world of elementary particles. Of equal importance are the problems of

the macrocosmos which are intimately connected with general relativity. However, as I am not an expert in astrophysics and cosmology, I wish to make only a few remarks about this vast subject.

Since Eddington's time we have been aware of the intimate relation between the atomistic world and the universe. Einstein himself has made incessant attempts to understand the existence of particles and quanta as singularities of a united gravitational electromagnetic field. But I cannot believe that by singling out these two types of field a real unification can be achieved, quite apart from my conviction that quantum theory cannot be reduced to classical concepts. The most important idea, due to astrophysics, is the suggestion of spontaneous creation of matter. There are two versions of it, one by Hoyle, Bondi and Gold (1948), who assume the permanent creation of hydrogen atoms uniformly in space, the other by Jordan (1944), who assumes the instantaneous creation of whole stars or even galaxies, which then appear as super-novae. Both theories have in common that they oppose the idea of a history of the universe, as suggested by the simplest interpretation of the recession of the nebulae (Hubble effect), namely an expanding universe, beginning, about 2000 million years ago, in a highly concentrated state. Instead, both theories aim at describing the world as being in a steady state, where just as much matter is created as disappears in infinity (that is when it reaches the velocity of light).

Both authors have suggested modifications of Einstein's field equations. Hoyle's original theory did not follow the usual Lagrangian pattern, which secures the compatibility of the cause-effect relation and of general relativity. Thus he, strangely enough, seemed to be prepared to sacrifice general relativity. McCrea (1951) has recently shown that this is not necessary, and that by assuming the existence of a kind of universal cosmic pressure (apart from that due to ordinary matter and energy) the relativistic equations can be preserved.

Jordan's theory is based on an idea of Dirac (1937) according to which the gravitational constant κ is actually not a constant, but a (slowly changing) eleventh field variable, in addition to the 10 components $g_{\mu\nu}$ of the gravitational field. This suggestion is not at all arbitrary, but based on strong arguments concerning the order of magnitude of the cosmic constants. Jordan has further shown that from the standpoint of group theory his equations are preferable to those with constant κ , and that the creation of matter in bulk, as suggested by him, does not mean a violation of the conservation law of energy, but only a transformation of gravitational energy into material substance.

Both types of hypotheses are supported by a considerable amount of empirical evidence which consists, of course, not so much in direct observations, but in developing a coherent and rational picture of the universe in agreement with the facts. I am unable to decide who may be nearer to the truth.

I have mentioned these ideas because the future theory of matter cannot bypass the cosmological point of view. Very likely I have omitted to mention other important suggestions, for which I apologize.

Returning to the first sentences of this lecture, I may say that much has been achieved during the 50 years since my student days; many problems have been solved which about 1900 had not even been formulated. But the present time seems to offer still more puzzles, and perhaps harder ones. My aim was to show that our conceptual armoury will be capable of dealing with them, provided we do not look back to the good old times, but forward to new adventures of discovery and explanation.

REFERENCES

- BHABHA, H. J., 1945, *Rev. Mod. Phys.*, **17**, 200; 1948, *Report of 1946 International Conference, I: Fundamental Particles* (London: The Physical Society), 22; 1949, *Rev. Mod. Phys.*, **21**, 451; 1951, *Phys. Rev.*, **77**, 665.
- BLOKHINTZEV, D., 1950, *Upsekkii fisick nauk*, **42**, 76; 1951, *Ibid.*, **44**, 104.
- BOHM, D., 1952, *Phys. Rev.*, **85**, 166, 180.
- BONDI, H., and GOLD, T., 1948, *Mon. Not. R. Astr. Soc.*, **108**, 252.
- BORN, M., 1933, *Nature, Lond.*, **132**, 282; 1934, *Proc. Roy. Soc. A*, **143**, 410; 1953, *Brit. J. Phil. Sci.*, **4**, in the press.
- BORN, M., and GREEN, H. S., 1949, *Proc. Roy. Soc. Edinb. A*, **62**, 470.
- BORN, M., and INFELD, L., 1933, *Nature, Lond.*, **132**, 970, 1004; 1934, *Proc. Roy. Soc. A*, **144**, 425.
- DE BROGLIE, L., 1926, *C. R. Acad. Sci., Paris*, **188**, 447; 1927, *Ibid.*, **184**, 273; **185**, 380; 1952, see *De Broglie, Physicien et Penseur* (Paris: A. Michel).
- DIRAC, P. A. M., 1937, *Nature, Lond.*, **139**, 323; 1951, *Proc. Roy. Soc. A*, **209**, 291; 1952, *Ibid.*, **212**, 330.
- DU MOND, J. W. M., and COHEN, E. R., 1951, *Phys. Rev.*, **82**, 555.
- EDDINGTON, A., 1928, *Proc. Roy. Soc. A*, **121**, 524; **122**, 358; see also *Relativity Theory of Protons and Electrons* (Cambridge: University Press, 1936).
- EULER, H., 1936, *Ann. Phys., Lpz.*, **26**, 398.
- EULER, H., and HEISENBERG, W., 1936, *Z. Phys.*, **98**, 714.
- EULER, H., and KOCKEL, B., 1935, *Naturwiss.*, **23**, 246.
- FIERZ, M., 1939, *Helv. Phys. Acta*, **12**, 3.
- FIERZ, M., and PAULI, W., 1939, *Proc. Roy. Soc. A*, **173**, 211.
- FRENKEL, J., 1950, *Upsekkii fisick nauk*, **42**, 69; 1951, *Ibid.*, **44**, 110.
- HEISENBERG, W., 1943, *Z. Phys.*, **120**, 313, 673; 1951, *Festschrift Akad. d. Wiss. Göttingen*, p. 50; 1952, *Z. Phys.*, **133**, 65.
- HOYLE, F., 1948, *Mon. Not. R. Astr. Soc.*, **108**, 252.
- JORDAN, P., 1944, *Phys. Z.*, **45**, 183; 1947, *Die Herkunft der Sterne* (Stuttgart: Hirzel); 1949, *Nature, Lond.*, **164**, 637; 1952, *Schwerkraft und Weltall* (Braunschweig: Vieweg).
- KARPLUS, R., and KLEIN, A., 1952, *Phys. Rev.*, **85**, 972.
- KOCKEL, B., 1937, *Z. Phys.*, **107**, 153.
- LAMB, W. E., Jr., and RETHERFORD, R. C., 1947, *Phys. Rev.*, **72**, 241; 1949, *Ibid.*, **75**, 1325, 1332; 1950, *Ibid.*, **79**, 549.
- MCCREA, W. H., 1951, *Proc. Roy. Soc. A*, **206**, 562; 1951, *J. Trans. Victoria Inst.*, **83**, 105.
- MADLUNG, E., 1927, *Z. Phys.*, **40**, 322.
- MIE, G., 1912, *Ann. Phys., Lpz.*, **37**, 511; **39**, 1; 1913, *Ibid.*, **40**, 1.
- MØLLER, G., 1951, *D. Kgl. Danske Vidensk. Selskab, Mat-fys. Medd.*, Nos. 21 and 22.
- VON NEUMANN, J., 1932, *Mathematische Grundlagen der Quanten mechanik* (Berlin: Springer Verlag), pp. 167–171.
- PAIS, A., and UHLENBECK, G. E., 1950, *Phys. Rev.*, **79**, 145.
- PEIERLS, R., and McMANUS, H., 1948, *Proc. Roy. Soc. A*, **195**, 323.
- RAYSKI, J., 1951, *Proc. Roy. Soc. A*, **206**, 575; 1951, *Phil. Mag.*, **42**, 1289.
- SCHRÖDINGER, E., 1952, *Brit. J. Phil. Sci.*, **3**, 109, 233.
- SCHWINGER, J., 1948, *Phys. Rev.*, **74**, 1439; 1949, *Ibid.*, **75**, 651, **76**, 790.
- STÜCKELBERG, E. C. G., and PETERMANN, A., 1951, *Phys. Rev.*, **82**, 548; 1951, *Helv. Phys. Acta*, **24**, 317.
- TERREAUX, CH., 1951, *Helv. Phys. Acta*, **24**, 551; 1952, *Nuovo Cim.*, **9**, 1029.
- TOMANAGA, S., 1946, *Prog. Theor. Phys.*, **1**, 27, and subsequent papers.
- VIDALE, M. L., and SCHEIN, M., 1951, *Nuovo Cim.*, **8**, 1.
- WEISSKOPF, V., 1936, *Kgl. Danske Vidensk. Selskab, Mat-fys. Medd.*, **14**, 6.
- VON WEIZSÄCKER, K. F., 1949, *Die Geschichte der Natur* (Stuttgart: Hirzel); 1951, *Zum Weltbild der Physik* (Stuttgart: Hirzel).
- WHITTAKER, E. T., 1949, *From Euclid to Eddington* (Cambridge: University Press).
- YUKAWA, H., 1949, *Phys. Rev.*, **77**, 219.

Analytical Wave Functions for Methane and the Ammonium Ion

By M. J. M. BERNAL

University College, London

Communicated by H. S. W. Massey; MS. received 24th October 1952 and in final form 26th January 1953

Abstract. Analytical antisymmetric wave functions for the ground states of CH_4 and NH_4^+ , and the corresponding C—H and N—H bond lengths have been obtained. These were calculated by a method which is essentially an application of the variational principle to the procedure used by Buckingham, Massey and Tibbs in their calculation of a self-consistent field for methane. The calculated C—H bond length is in good agreement with the experimental value. No experimental value for the N—H bond length in the free ammonium ion is available. However, the calculated value differs by only about 5% from the experimental value of the N—D bond length in ND_4Cl . The wave functions should form useful first approximations in future calculations of the physical and chemical properties of CH_4 and NH_4^+ . The NH_4^+ function has already been used as a first approximation in a self-consistent field calculation at present in progress.

§ 1. INTRODUCTION

A METHOD for calculating the wave functions of molecules possessing a high degree of spherical symmetry, such as CH_4 , has been described by Buckingham, Massey and Tibbs (1941). They suggested that the wave function of the electrons moving in the field formed by averaging the proton charge over all orientations about the central nucleus would be a wave function of the corresponding molecule of sufficient accuracy to be of value. The spherical symmetry of the averaged nuclear field makes possible the use of the usual methods of solution of the central field problem. Buckingham, Massey and Tibbs applied their method to methane, using the Hartree self-consistent field method to solve the central field problem. They concluded from their calculations of the properties of CH_4 that the electron distribution was too diffuse, but that the method was not otherwise less satisfactory than the usual self-consistent method for atoms. Use of the Hartree-Fock method would improve the results since it would reduce the diffuseness of the electron distribution. The success of the methane calculations suggested using the method for other molecules and ions. However, one of the major obstacles in the way of using the method is that a fairly good first approximation is required for the solution of the self-consistent field equations. The primary aim of the present calculations was to obtain such an approximation for the ammonium ion. Since no experimental value for the N—H bond length in the free ammonium ion was available the determination of this quantity was an important part of the calculations. The usual units and notation employed for self-consistent field calculations (Hartree and Black 1933) will be used throughout.

§ 2. THE VARIATION CALCULATIONS

Since both the NH_4^+ and CH_4 wave functions were calculated by the same method only the NH_4^+ calculations will be described. The NH_4^+ wave function was obtained by applying the variation method to a system of ten electrons moving in the potential field of a nitrogen nucleus at the centre of a uniformly charged spherical shell, the total charge on the shell being that of four protons. The system may be thought of as an ammonium ion in which the proton distribution has been averaged over all orientations about the central nucleus.

The variation function for the NH_4^+ calculations was of the type used by Fock and Petraschen (1934) for Na^+ , which when applied to methane gave results which were in fairly good agreement with the calculations of Buckingham, Massey and Tibbs. This variation function, which involves only three arbitrary parameters is a ten-electron Slater determinant Ψ with configuration $(1s)^2(2s)^2(2p)^61S$, where the radial factors $R(nl|r)$ of the orthogonal one-electron functions nl are

$$\begin{aligned} R(1s|r) &= 2\alpha^{3/2} e^{-\alpha r}, \\ R(2s|r) &= \left\{ \frac{12\beta^5}{\alpha^2 - \alpha\beta + \beta^2} \right\}^{1/2} [1 - \frac{1}{3}(\alpha + \beta)r] e^{-\beta r}, \\ R(2p|r) &= \left(\frac{4\gamma^5}{3} \right)^{1/2} r e^{-\gamma r} \end{aligned}$$

The total energy of the ion was taken to be the sum of the electronic energy E and the classical nuclear interaction energy N :

$$E = \int \Psi^* H \Psi / \int \Psi^* \Psi, \quad N = [4Z + 3(3/2)^{1/2}] / r_0,$$

where H is the Hamiltonian of the averaged nuclear field, Z the charge on the central nucleus ($Z=7$ for NH_4^+), and r_0 the radius of the spherical shell, which is identified with the N—H bond length.

$$H = \sum_{i=1}^{10} (K_i + V_i) + \sum_{i,j=1}^{10} 1/r_{ij}$$

$$\text{where} \quad K_i = -\frac{1}{2} \nabla_i^2, \quad V_i = \begin{cases} -Z/r_i - 4/r_0, & r_i \leq r_0 \\ -(Z+4)/r_i, & r_i \geq r_0 \end{cases}$$

and where the second summation in H is to exclude those terms for which $i \leq j$.

In calculating the formulae for E and N , r_0 and the central nuclear charge Z were left arbitrary so that the formulae obtained apply to any ten-electron tetrahydride molecule or ion.

The expression for E in terms of one- and two-electron integrals† is

$$\begin{aligned} E = & 2I(1s) + 2I(2s) + 6I(2p) + F_0(1s, 1s) + F_0(2s, 2s) - 2G_0(1s, 2s) + 4F_0(1s, 2s) \\ & + 12F_0(1s, 2p) + 12F_0(2s, 2p) - 2G_1(1s, 2p) - 2G_1(2s, 2p) + 15F_0(2p, 2p) \\ & - 1.2F_2(2p, 2p). \end{aligned}$$

† The quantities I , F and G are defined by

$$\begin{aligned} I(\alpha) &= \int_0^\infty R(\alpha|r) \left[-\frac{1}{2} \frac{d^2}{dr^2} + V_n + \frac{l_\alpha(l_\alpha+1)}{2r^2} \right] R(\alpha|r) r^2 dr \\ F_k(\alpha\beta) &= \int_0^\infty \int_0^\infty R^2(\alpha|r_1) R^2(\beta|r_2) \{r_1, r_2\}^k dr_1 dr_2 \\ G_k(\alpha\beta) &= \int_0^\infty \int_0^\infty R(\alpha|r_1) R(\alpha|r_2) R(\beta|r_1) R(\beta|r_2) \{r_1, r_2\}^k dr_1 dr_2 \end{aligned}$$

$$\text{where} \quad \{r_1, r_2\} = \begin{cases} r_1^{k+2}/r_2^{k-1}, & r_2 \geq r_1, \\ r_2^{k+2}/r_1^{k-1}, & r_2 \leq r_1. \end{cases}$$

Taking

$$\begin{aligned}\sigma &= 2\alpha r_0 & \sigma/(\sigma + \omega) &= x \\ \omega &= 2\beta r_0 & \omega/(\omega + \mu) &= y \\ \mu &= 2\gamma r_0 & \mu/(\mu + \sigma) &= z\end{aligned}$$

and

$$\begin{aligned}B_0 &= \sigma^2 - \sigma\omega + \omega^2 \\ B_1 &= 7\omega^4 - \sigma\omega^3 + \sigma^2\omega^2 \\ B_2 &= 3\omega^3 - 2\sigma\omega^2 + \sigma^2\omega \\ B_3 &= \omega^5 - 2\omega^4(\sigma - 3) + \omega^3(\sigma^2 + 6) + 6\omega^2(\sigma^2 - 2\sigma + 4) + 6\sigma\omega(3\sigma - 4) + 24\sigma^2 \\ B_4 &= \mu^3 + 6\mu^2 + 18\mu + 24\end{aligned}$$

the formulae obtained for the integrals were

$$\begin{aligned}I(1s) &= [2e^{-\sigma}(\sigma + 2) - (Z\sigma/2) - 4]/r_0 + (\sigma^2/8)/r_0^2 \\ I(2s) &= [e^{-\omega}(B_3/6B_0) - (ZB_2/B_0) - 4]/r_0 + (B_1/24B_0)/r_0^2 \\ I(2p) &= [e^{-\mu}(B_4/6) - (Z\mu/4) - 4]/r_0 + (\mu^2/8)/r_0^2 \\ r_0 F_0(1s, 1s) &= (5/16)\sigma \\ r_0 F_0(1s, 2s) &= \sigma(2x^5 - 7x^4 + 5x^3 + 4x^2 - 6x + 2)/4(3x^2 - 3x + 1) \\ r_0 F_0(2s, 2s) &= \omega(245\omega^4 - 420\omega^3\sigma + 438\omega^2\sigma^2 - 244\omega\sigma^3 + 93\sigma^4)/512B_0^2 \\ r_0 F_0(1s, 2p) &= \sigma(-2z^5 + z^4 + z^3 + z^2 + z)/4 \\ r_0 F_0(2s, 2p) &= y\mu[\omega^2 T(y) - \omega(\sigma + \omega)U(y) + (\sigma + \omega)^2 V(y)]/B_0\end{aligned}$$

where

$$\begin{aligned}T(y) &= \frac{3}{4}(-2y^4 + 7y^3 - 8y^2 + 2y + 2) \\ U(y) &= \frac{1}{4}(-10y^5 + 32y^4 - 31y^3 + 4y^2 + 4y + 4) \\ V(y) &= \frac{1}{4}(-5y^6 + 15y^5 - 13y^4 + y^3 + y^2 + y + 1) \\ r_0 F_0(2p, 2p) &= (93/512)\mu \\ r_0 F_2(2p, 2p) &= (45/512)\mu \\ r_0 G_0(1s, 2s) &= 2\sigma^3(1 - x)^5/B_0 \\ r_0 G_1(1s, 2p) &= 14\sigma^3\mu^5/(\mu + \sigma)^7 \\ r_0 G_1(2s, 2p) &= \omega^5\mu^5[126(\omega + \mu)^2 - 294(\omega + \mu)(\sigma + \omega) + 185(\sigma + \omega)^2]/3(\omega + \mu)^9 B_0.\end{aligned}$$

Following the usual variation method the total energy ϵ of the ion would be minimized with respect to the parameters σ , ω and μ , r_0 being taken to be the N—H bond length. However, as no experimental value for this quantity was available the procedure adopted was to minimize the total energy with respect to this quantity also and take the value of r_0 at the minimum as the bond length.

The methane calculations of Buckingham, Massey and Tibbs show that the 1s function for the central atom does not differ much from the corresponding function in the molecule. For this reason the minimization with respect to σ was not formally carried out, the value of σ being chosen so that the 1s function was a good approximation to the 1s function for nitrogen. Since ϵ may be written $\epsilon = V/r_0 + T/r_0^2$ where V and T (which may be determined by inspection from the above formulae) are functions of σ , ω and μ only, the minimization with respect to r_0 may be performed at once. Differentiating ϵ with respect to r_0 and equating the result to zero gives $r_0 = -2T/V$ and hence the minimum value of ϵ with respect to r_0 is $\epsilon = -V^2/4T$. The values of ω and μ may thus be determined by minimizing

this expression where the value of σ is determined as indicated above. r_0 is then determined by the formula given above. The final values obtained for the parameters α , β , γ and the bond length r_0 are given in the following table where the corresponding results for CH_4 are also given.

	2α	2β	2γ	ϵ	r_0	r_0 (exp)
NH_4^+	13.43	4.34	3.24	-55.684	1.836 ± 0.002	—
CH_4	11.12	3.5	2.6	-39.33	1.975 ± 0.025	2.0

The error terms in the bond lengths are given to indicate the numerical accuracy to which the minimization process was performed. As can be seen the NH_4^+ calculation was performed to a greater accuracy than the CH_4 calculation.

To conclude this section it will be shown how the procedure described here follows by the variation method when the variation function has the form Ψ . By the variation method the total energy of the molecule (or ion, as the case may be) is calculated as the minimum value of $N + \int \Psi^* H_T \Psi$ where $H_T = H + \sum_i (v_i - V_i)$, where v_i is the electron-proton interaction energy of the tetrahedral proton distribution, and where H , V_i and N have the meanings given above. Detailed examination shows that $\int \Psi^* \sum_i (v_i - V_i) \Psi = 0$ for functions of the type Ψ with configuration $(1s)^2 (2s)^2 (2p)^6$. Thus $\int \Psi^* H_T \Psi = \int \Psi^* H \Psi$ and in calculating the electron-proton contribution to the total energy in the variation calculation, the field of the proton distribution may be taken to be that of a spherical shell as described above.

§ 3. DISCUSSION OF THE RESULTS

The remarkably good agreement between the calculated and observed values of the C—H bond length suggest that the calculated N—H bond length is not seriously in error. The N—D bond length in ND_4Cl has recently been determined experimentally (Goldschmidt and Hurst 1951), the value being 1.03 \AA ($= 1.95 a_H$) which differs by only about 5% from the value predicted above for the ion. The total energy of methane obtained by Buckingham, Massey and Tibbs was $-40.37 e^2/a_H$. Thus they obtained a deeper energy than that obtained here, and hence on the basis of the energy criterion a more accurate wave function for the spherically averaged nuclear distribution. By pre-selecting α in the present calculation the variation function Ψ was effectively reduced to a two-parameter function. A deeper value for the total energy could be obtained by allowing α to vary also.

The results obtained here, taken together with those of Buckingham, Massey and Tibbs, indicate that the present method of calculation provides bond lengths and energies of tolerable accuracy. Though it is not to be expected that the same will be true of other properties calculated from the wave functions, the functions are of sufficient accuracy to form useful first approximations in calculations of molecular and ionic properties, and their simple analytical form makes them eminently suitable for such calculations.

Horváth (1948) has made a calculation for the ammonium ion of the charge distribution, N—H bond length and the energy difference between N^{5+} and NH_4^+ . Since he calculates these quantities by a method radically different from that used here, and since there is great lack of experimental data, it is difficult to make a comparison of the respective methods.

The value he obtains for the N—H bond length is $1.6 a_H$ which may be compared with the value $1.84 a_H$ obtained here and the value $1.95 a_H$ for the

N—D bond length in ND_4Cl . The value he obtains for the energy difference between N^{5+} and NH_4^+ is $12.57 e^2/a_{\text{H}}$. Using the total binding energy of nitrogen given by Coulson and Duncanson (1949) and the first five ionization potentials of nitrogen (Horváth 1948), to calculate the binding energy of N^{5+} , the energy difference calculated for the present wave function is $10.41 e^2/a_{\text{H}}$. Horváth has also calculated this energy difference by the Born–Haber process, using Madelung's formula to calculate the lattice energy of NH_4Cl , and obtains the value $11.95 e^2/a_{\text{H}}$.

§ 4. CONCLUDING REMARKS

The approximate wave function for the ammonium ion obtained here has been used as a first approximation in a self-consistent field calculation for the ion. When this calculation is complete it is proposed to calculate physical and chemical properties of the ion and the ammonium molecule. In particular it is proposed to calculate the lattice constants and compressibility of ammonium metal, a substance which Ramsey (1951) has suggested may be an influential constituent of the major planets.

ACKNOWLEDGMENTS

This work has been carried out at the suggestion of Professor H. S. W. Massey to whom the author has been acting as Research Assistant. Thanks are due to the Department of Scientific and Industrial Research whose financial assistance has made this post available. Acknowledgment is also made of the assistance rendered by Dr. R. A. Buckingham in several discussions. The author also wishes to thank Miss Turner for computing assistance.

REFERENCES

- BUCKINGHAM, R. A., MASSEY, H. S. W., and TIBBS, E. R., 1941, *Proc. Roy. Soc. A*, **178**, 119.
 COULSON, C. A., and DUNCANSON, W. E., 1949, *Nature, Lond.*, **164**, 1003.
 FOCK, V., and PETRASCHEN, MARY J., 1934, *Phys. Z. Sowjet*, **6**, 368.
 GOLDSCHMIDT, G. H., and HURST, D. G., 1951, *Phys. Rev.*, **83**, 88.
 HARTREE, D. R., and BLACK, M. M., 1933, *Proc. Roy. Soc. A*, **139**, 311.
 HORVÁTH, J. I., 1948, *J. Chem. Phys.*, **16**, 851.
 RAMSEY, W. H., 1951, *Mon. Not. R. Astr. Soc.*, **111**, 427.

An Investigation of the β -Particle Spectrum of Mesothorium 2

By J. KYLES, C. G. CAMPBELL AND W. J. HENDERSON *

Department of Natural Philosophy, University of Edinburgh

Communicated by N. Feather; MS. received 10th February 1953

Abstract. Using a permanent magnet double β -ray spectrometer, the β -particle spectrum of mesothorium 2 has been examined, and partial spectra with end points at 2.18, 1.85, 1.70, 1.11, 0.64 and 0.45 Mev have been found. A list of conversion lines is given with an analysis in terms of γ -rays. A level scheme is put forward which is consistent with the β - β , β - γ and γ - γ coincidence measurements made. The ground-to-ground state transition is unobserved, the partial spectrum of highest energy corresponding to an excited state at 57 keV which is metastable with a half-life greater than 10^{-2} second.

§1. INTRODUCTION

A DETAILED magnetic analysis of the β -particle spectrum of mesothorium 2 has not been made since the investigations by Black (1924), using a semicircular focusing spectrograph, and Yovanovitch and d'Espine (1927), using the direct deviation method. These measurements were important chiefly in establishing the presence of a large number of internal conversion lines, some of which were of high intensity.

More recently cloud chamber studies by Lecoin, Perey and Teillac (1929) and absorption measurements by Lecoin, Perey and Riou (1949) showed that on the average 1.1 secondary electrons were emitted per disintegration and provided evidence of a time delay between the emission of a primary β -particle and a conversion electron of less than 60 keV energy. The half-life of the delayed emission was estimated as greater than 0.01 second. Earlier measurements of the maximum energy of the primary β -particles, made by Lecoin (1935, 1938) with a cloud chamber, by Libby and Lee (1939) with a screen cathode spectrometer, and by Feather (1930, 1938) using absorption methods, showed considerable disagreement.

The presence of an intense γ activity suggests that the disintegration spectrum is complex, and coincidence experiments were therefore made in an effort to determine the end points of the partial spectra and to study time-correlations between the γ radiations. A preliminary report of this work has been published (Campbell, Henderson and Kyles 1952) confirming the complexity of the spectrum and fixing the ultimate end point at 2.16 ± 0.02 MeV.

§2. APPARATUS

A detailed description of the double β -ray spectrometer used in this work has been given by Feather, Kyles and Pringle (1948). The Geiger counters, with which a resolving time of 2×10^{-7} sec was then obtained, were replaced for

* On leave from the National Research Council of Canada. Present address: Atomic Energy of Canada Ltd., Chalk River, Ontario.

the present investigation by scintillation counters, and the resolving time in this way reduced by a factor of 20. Figure 1 shows the spectrometer box in its present form, and illustrates the arrangement of the scintillation counters. Rotation of the handle A moves the crystal unit carrying the detector slit B to and fro, the slit moving in the plane of focusing and thus altering the radius of curvature of the spectrometer. The β -particles, selected by the slit, fall upon an anthracene crystal which is placed on a polished shelf cut in a Perspex rod of 1 in. diameter. Light, emitted by the phosphor, is transmitted to the Perspex guide by a thin layer of white petroleum jelly and, after reflection at the polished plane surface cut at 45° to the shelf, passes along the rod to the photomultiplier (E.M.I. type 5045). Even with a double-walled 'mu-metal' can in position it was necessary to use a light guide 18 in. long to ensure that the performance of the multiplier was not influenced by the stray field of the permanent magnet. A block diagram of the electronic accessories is shown in fig. 2. The coincidence unit was designed and constructed at the Atomic Energy Research Establishment, Harwell, and has been described in detail by Wells (1951).

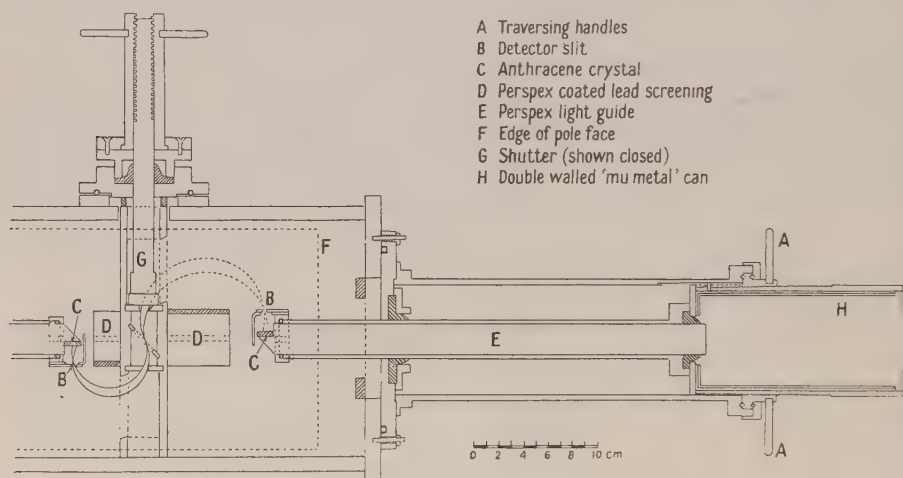


Fig. 1. The spectrometer.

§3. COUNTER PERFORMANCE

Because the discriminators in the coincidence set had a fixed bias of 5 volts, the efficiency of the scintillation counters, for mono-energetic β -particles, was studied by plotting the β -particle counting rate against the multiplier voltage. For β -particles of energies greater than 90 kev the curves showed plateaux with slopes of the order of 0.03% per volt, starting at a voltage which decreased as the energy of the β -particles increased. For particles of energy less than 90 kev no plateaux were obtained, although it was still possible to count β -particles of 30 kev energy with low efficiency. Loss of efficiency in this energy range was clearly due to the limited light collection of the optical system, and no sustained effort was made to improve it since a separate study of the low-energy end of the β -particle spectrum was being undertaken in Edinburgh on another spectrometer (Brodie, thesis, to be published later).

For γ -counting the detector was moved as close as possible to the source, and the counter slit was screened from β -particles by a shutter, shown closed in fig. 1. When the counters were tested with sources emitting γ -rays of known energy, peaks were obtained in the (differential counting rate, multiplier voltage) curves. These were attributed to the most intense γ -radiations of the sources used. By assuming that the counter ceased to record any γ -ray when the applied voltage was somewhat less than that corresponding to the appropriate peak, a rough calibration of the minimum multiplier voltages required for the counting of γ -rays of various energies was established.

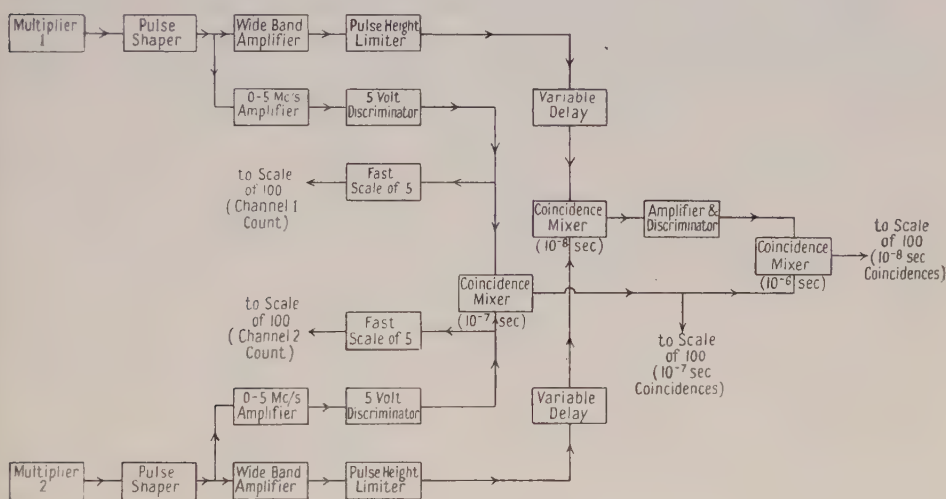


Fig. 2. Block diagram of electronic circuits.

The counting rate of genuine coincidences from a source of ^{60}Co was plotted against the relative time delay between pulses in the two channels, and correct matching of the channels was obtained corresponding to the flat-topped peak of the curve. That the genuine coincidence counting rates obtained from the 10^{-7}sec and the 10^{-8}sec coincidence mixers were in agreement confirmed both that the channels were properly matched and that the 10^{-8}sec mixer recorded coincidences with 100% efficiency.

§4. PREPARATION OF SOURCES OF MESOTHORIUM 2

From a stock solution containing mesothorium 1 and its decay products associated with an appreciable activity of radium and its daughter elements, the mesothorium 2 was extracted chemically by a method based on that of Haissinsky (1933). When separations were made daily it was found that more than 1 mc activity due to MsTh_2 could be obtained from the solution at each extraction. In these separations the grown MsTh_2 (and other decay products) were precipitated as hydroxide with as little as 0.015 mg iron as carrier. The precipitate was dissolved in dilute HCl and approximately 1 mg each of bismuth and lead carriers was added. Hydrogen sulphide was bubbled through this solution and the resulting sulphide precipitate carried activities due to isotopes of polonium, bismuth, lead and thallium. After filtering and washing the precipitate, the

total filtrate was boiled to remove any excess H_2S , approximately 1 mg of barium was added as hold-back carrier, and the MsTh_2 and iron were reprecipitated. This procedure ensured that any remaining MsTh_1 or radium was removed. The iron- MsTh_2 precipitate was next dissolved in 1N nitric acid, and after the solution had been evaporated to dryness the residue was taken up in the minimum quantity of N/10 nitric acid. No attempt was made to separate radiothorium although a method for doing so was available (McLane and Peterson 1948) since, after the first extraction of MsTh_2 (which was not used as a source), the contamination of the stock solution by radiothorium, resulting from about 24 hours' growth, was of negligible proportions.

The mesothorium 2 may also be carried with cerium, and in this case a method of obtaining carrier-free sources has been outlined by Peterson (1948). The method was used initially but was later abandoned in view of the fact that the iron-carrier method was shorter, and still capable of good yield when as little as 15 μg iron was used.

The final solution of MsTh_2 with carrier was deposited in drops over a length of approximately 1 cm of aluminium foil of thickness 1 mg cm^{-2} cut into a strip of width 2 mm, each drop being evaporated to dryness before the next drop was applied. The ends of the strip were then cemented to a rectangular aluminium frame which was set in the spectrometer at an angle of 45° to the plane of the focusing slit. In this way the effective breadth of the source was reduced to give better resolution. For β - β coincidence work, and for the investigation of the low energy region of the spectrum, aluminium foil of 0.2 mg cm^{-2} thickness was used. The acid solution required to take up the activity almost completely dissolved this foil, which was therefore supported on a thin collodion film. Sources of total effective thickness approximately 0.7 mg cm^{-2} (in the backwards direction, and after allowing for the emission angle at which they were set) and of strength of the order of 1 mc were thus regularly obtained.

To check the purity of the sources, observations of their decay were made at various β -particle energies over periods exceeding two half-lives. In all cases the observed half-life was within 1% of the accepted value. In addition no evidence was found in any of the spectra for the F line of $\text{ThB} \rightarrow \text{C}$ or of the strong F, G and H lines of $\text{RaB} \rightarrow \text{C}$.

§ 5. THE RADIATIONS OF MESOTHORIUM 2

(i) *Investigations with a Single Counter*

Using one half of the spectrometer, a survey was made of the spectrum over the range of $H\rho$ values from 600 to 10 000 gauss cm. Table 1 shows the $H\rho$ values of the lines found, with the corrected* values of Black listed for comparison. The intensities quoted have been computed from the absolute intensities of the six strongest lines recently determined by Brodie (private communication) taken together with some relative intensities as given by Black.

We made no attempt to check systematically the relative intensities of these lines, since many occur in the range of energy below 100 keV, in which our counter is not 100% efficient.

* Black based his measurements on the $H\rho$ values for the lines of Ra(B+C) obtained by Ellis and Skinner (1924). We have altered Black's values to agree with the later measurements on Ra(B+C) made by Ellis (1934).

Table 1

(1)	(2)	(3)	(4)	(5)	(6)
1	—	652	36.34	—	44
2	665	659	36.91	9.4	
3	696	690	40.33	8.0	
4	—	715	43.14	—	
5	—	750	47.28	—	Weak
6	—	776	50.47	—	Weak
7	790	789	52.16	6.1	15
8	816	815	55.41	4.2	
9	836	—	58.19	0.56	—
10	864	872	61.91	0.38	Weak
11	900	901	66.97	1.5	0.1
12	—	929	71.03	—	Weak
13	946	948	73.76	4.7	8.0
14	975	977	77.98	3.3	
15	—	1000	81.49	—	Weak
16	1069	1072	92.66	1.5	1.3
17	—	1099	97.04	—	
18	1162	1166	108.1	3.3	5.6
19	1183	1185	111.3	2.3	
20	—	1205	114.8	—	Weak
21	1248	1247	122.2	2.1	1.8
22	1267	—	125.8	0.56	
23	1299	—	131.6	0.38	—
24	1336	1357	140.3	1.7	Weak
25	—	1376	145.8	—	Weak
26	—	1435	157.0	—	Weak
27	1459	1475	164.9	1.9	1.3
28	1528	1545	178.7	0.56	
29	1681	1660	202.4	1.5	Weak
30	—	1721	212.0	—	Weak
31	1770	1771	225.9	0.75	Weak
32	2081	2102	300.5	0.56	Weak
33	2159	2168	315.9	0.19	Weak
34	2303	2305	348.6	0.75	Weak
35	2663	—	437.0	0.38	—
36	2722	—	451.9	0.19	—
37	4012	4013	796.4	0.56	Weak
38	4214	4237	858.5	0.28	Weak
39	4347	4345	888.6	0.19	Weak
40	—	4475	925.1	—	Weak
41	4530	—	940.4	0.19	—
42	—	4689	985.1	—	Weak
43	6430	6406	1477	0.09	Weak
44	6564	6588	1530	0.09	Weak

(1) Line; (2) H_p (Black); (3) H_p (observed); (4) energy (kev); (5) Black's intensities per 100 disintegrations; (6) intensity observed per 100 disintegrations.

In the momentum range above 1500 gausscm the normalized β -particle counting rates were plotted on a Fermi diagram using the Fermi functions of Feister (1950). Figure 3 shows the final portion of this plot, which has been analysed into partial β -spectra of the allowed form with end points at energies of 2.18 ± 0.02 , 1.85 ± 0.05 and 1.70 ± 0.10 mev respectively (cf. 2.16 ± 0.03 , 1.85 ± 0.10 and 1.60 ± 0.10 mev of Campbell, Henderson and Kyles (1952)). The straight lines were fitted by the method of least squares. Forbidden correction factors calculated from the formulae given by Konopinski and Uhlenbeck (1941) did not alter the linearity of the curves sufficiently over the range of energies involved to change the analysis significantly. The three partial spectra above mentioned appeared to account for no more than one-third of the total β -emission of the source, and it was concluded that the main component of the radiation has maximum energy of approximately 1.2 mev.

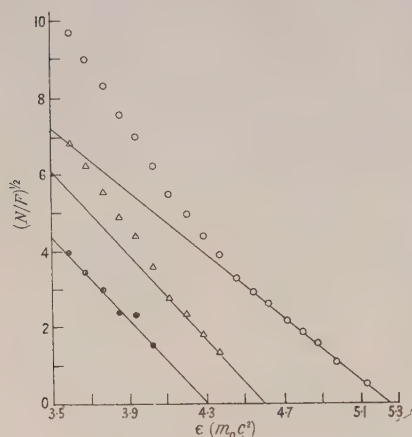


Fig. 3. Analysis of Fermi plot of the high energy portion of the MsTh_2 spectrum.

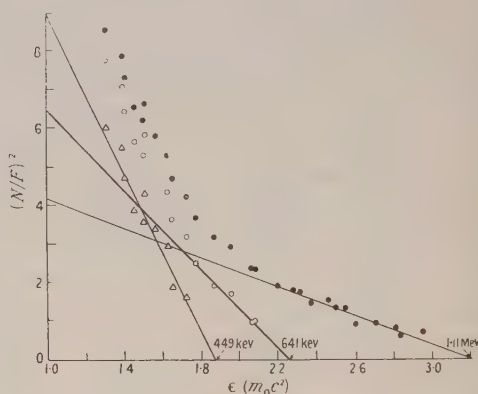


Fig. 4. Analysis of Fermi plot of coincidences between γ -rays of energy greater than 900 kev and β -particles of the continuous spectrum.

(ii) β - γ Coincidence Studies

To investigate further the end points of less energetic partial spectra, coincidence experiments were made between the β -particles of various energies entering one counter and the γ -rays of energies above a chosen minimum recorded by the other.

With the multiplier voltage adjusted so that the γ -counter was sensitive to all radiations of energy greater than 50 kev, genuine coincidences were recorded with β -particles of energy up to 1.80 mev only, at resolving times of 10^{-8} and 10^{-7} second. The straight line of a least squares fit to the points on a Fermi diagram showed a coincidence end point at 1.82 mev, but no great reliance should be placed on this value, the statistical errors being large. Moreover the β -particle counter could not be completely screened from γ -radiation, and the estimated correction for γ - γ coincidences was considerable. For these reasons it was not expected that the two partial spectra with end points at 1.85 and 1.70 mev, suggested by the experiments with a single counter, would be resolved, but it can be claimed that the end point found should not be identified with the single counter end point at 2.18 mev.

When the multiplier voltage was adjusted so that the γ -counter was sensitive only to radiations of energy greater than about 900 kev, β - γ coincidences were recorded only with β -particles of energy less than about 1.1 mev. Detailed observations were made and, after correcting these for γ - γ coincidences, a Fermi plot was obtained which is shown in fig. 4. On analysis into components of allowed shape, this plot yielded end points of partial spectra at 1.11, 0.64 and 0.45 mev. Since it is unlikely that the β -particles of each partial spectrum will be in coincidence with the same γ -radiations of energy greater than about 900 kev it should be noted that the relative intensities of these partial spectra cannot be deduced from the relative slopes of the Fermi lines. That this conclusion was valid was shown by reducing the voltage of the γ -counter still further so that only radiations of energy greater than about 1.1 mev were counted. Coincidences between β -particles and these γ -rays disappeared at a β -particle energy between 0.6 and 0.7 mev. The statistical errors in this case did not permit the determination of an accurate value for an end point, but a tentative identification with the former 0.64 mev seems plausible.

Assuming the end point energies of the six partial spectra deduced at this stage, and an allowed shape for each, relative intensities of the low energy spectra were adjusted so that the composite spectrum agreed most closely with the continuous spectrum as obtained with a single counter. The line shown in fig. 5 results from our assuming the intensities given in table 2; the points represent the actual observations. The agreement appears close enough to lend general support to our assumptions and to the conclusions drawn from them.

Table 2. Classification of Partial Spectra

		Sargent diagram		<i>ft</i> values		
(1)	(2)	(3)	(4)	(5)	(3)	(6)
2.18	10.1	2nd or 3rd	3	8.9	1st	2 (Yes)
1.85	9.6	2nd or 3rd	3	8.7		
1.70	6.7	2nd or 3rd	2 or 3	8.6		
1.11	53.0	1st	2	7.1	Either Allowed (<i>l</i> -forbidden) or 1st	Either 1 (No) or 0 or 1 (Yes)
0.64	7.6	1st	1	7.2		
0.45	13.0	1st	1	6.4		

(1) End point of partial spectrum (mev); (2) intensity (%); (3) degree of forbiddenness; (4) spin change; (5) log *ft*; (6) spin and parity change.

Apart from these conclusions, the following features of the disintegration of $MsTh_2$ are established by the experiments already described :

(i) If the β -particles of maximum energy 2.18 mev are followed by γ -radiation then the characteristic half-value period is greater than 10^{-7} second.

(ii) The excited states of the daughter nucleus $^{228}_{90}RdTh$ which are fed by β -particles of end point energies 1.85 and 1.70 mev are de-excited by γ -rays of which none has energy greater than 900 kev.

(iii) De-excitation of the state fed by β -particles of end point energy 1.11 mev involves one or more γ -rays of energy between approximately 0.9 mev and 1.1 mev, but not γ -rays of energy greater than 1.1 mev.

(iv) γ -rays of energy greater than 1.1 mev are involved in the de-excitation of one or both of the states fed by β -particles of end point energies 0.64 and 0.45 mev.

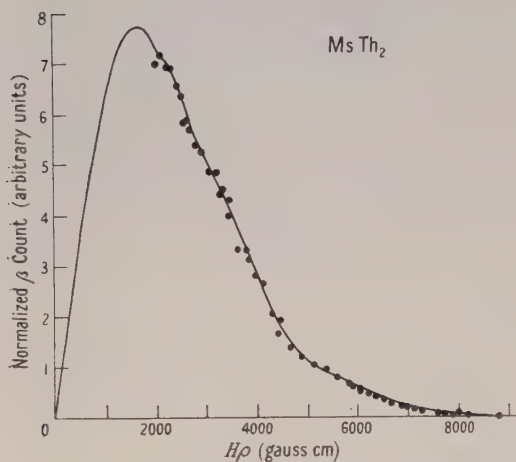


Fig. 5. The continuous β -particle spectrum of MsTh_2 .

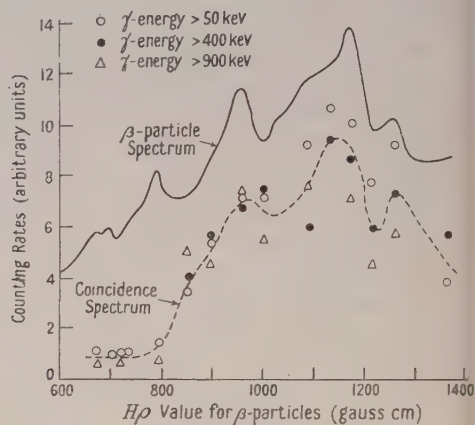


Fig. 6. Coincidences between internal conversion electrons and γ -rays per γ -ray recorded.

(iii) Coincidences between γ -Radiations and Internal Conversion Electrons

Only the more intense conversion electron lines could be studied in experiments of this type, without recourse to excessively long periods of counting, owing to the presence of a considerable background of coincidences between the electrons of the continuous spectrum and the γ -rays. Furthermore, even with the stronger lines it was necessary to open the focusing slit to provide a comparatively large collection angle for the β -particle counter, although this necessarily resulted in a loss of resolution and increased the background correction. Because of this fact and the complexity of the spectrum the lines studied were in several instances only partially separated, but in many cases the overlapping lines belonged to the conversion of a single γ -ray in different shells, and the effect was not so serious.

The results of experiments made with γ -radiations in the three energy ranges as indicated are shown in fig. 6. The shape of the spectrum observed with the β -particle counter is given together with the corresponding plots of the β - γ coincidence rate per γ -count recorded. This method of presenting the results allows an estimate to be made of the relative importance in producing coincidences of the γ -rays in each additional energy range made effective as the voltage on the multiplier is progressively increased.

Figure 6 shows the following features:

(a) The γ -ray of energy 57 keV as converted in the L_{II} and L_{III} shells to give the unresolved lines at 659 and 690 gauss cm and in the M and N shells to give the unresolved lines at 789 and 815 gauss cm shows no coincidences with any other γ -radiation, the coincidence resolving time being 10^{-8} second. (When the resolving time was increased to 10^{-7} sec a similar negative result was obtained.)

(b) The K shell conversion electrons of the 184 keV γ -ray form a line at 948 $H\rho$ which overlaps that due to $L_{I,II}$ conversions of the 98 keV γ -ray. The considerable coincidence counting rate at this β -particle energy and resolving time of 10^{-8} sec, which is obtained for all ranges of γ -radiations recorded by the γ -counter, shows that one or both of the low energy γ -rays (184 and 98 keV) is in coincidence with some of the other γ -radiations. (That these coincidences should be attributed, at least partly, to the 184 keV radiation has been checked by repeating a similar experiment with the line at 1475 $H\rho$, which represents the L conversion of this γ -ray. However, the situation regarding the 98 keV γ -ray remains undecided.)

(c) Observations on the unresolved lines at 1166 and 1185 $H\rho$, which are attributed to the $L_{I,II}$ and the L_{III} conversions of the 127 keV γ -ray, show that this radiation is also in coincidence with some of the other γ -rays within a resolving time of 10^{-8} second.

(iv) Coincidences between Internal Conversion Electrons of Different Lines

Here, again, for reasons similar to those given in the last section, only the strong lines could be studied.

With one counter set to receive the L conversion electrons (at an $H\rho$ value of ~ 1175 gauss cm) of the 127 keV γ -ray, the second counter was moved to receive electrons over the range 700 to 1200 gauss cm. No evidence was found for prompt coincidences between the 127 keV γ -ray and the 57 keV or the 184 keV γ -rays. Similar negative results in respect of coincidences over the same momentum range were also obtained with the first counter set to receive the conversion electrons of the 184 keV γ -ray.

Since the earlier observations of coincidences between conversion electrons and γ -radiations suggest that the lifetimes of the excited states emitting the 127 and 184 keV γ -rays are each shorter than 10^{-8} sec, it was concluded from the last results that these rays are not in cascade.

With regard to the 57 keV γ -ray, the new results do not violate the previous conclusion that the excited state from which this radiation is emitted has a lifetime greater than 10^{-7} second.

(v) γ - γ Coincidence Studies

Observations of the γ - γ coincidence rates recorded when various voltages were applied to the multipliers may be summarized as follows: (1) with both counters sensitive only to γ -radiations of energy greater than 900 keV, no coincidences were observed. (2) Coincidences were recorded between γ -radiations of energies between 400 and 500 keV and radiations of energies between 900 and 1100 keV. No coincidences were found between γ -rays of energy greater than 1.1 MeV and the 400–500 keV γ -rays. (3) There are further coincidences between γ -rays of energy of the order of 900 keV and γ -rays of energy less than approximately 400 keV. This statement cannot be made more precise because of the limited resolution of the scintillation counter method at low energies.

(vi) An Attempt to Measure the Lifetime of the State Emitting the 57 keV γ -Radiation

A very weak source of MsTh_2 was evaporated on to the cathode of a Geiger counter in order to obtain a geometry of about 50% for counting β -particles. The pulses from the counter were fed via a probe unit (type 1014) into two scalers (type 1009A) connected in parallel.

The paralysis times corresponding to the various settings of the input circuits of the scalers were measured to 0.5%. With the paralysis time of one scaler set to a nominal 500 μ sec, that of the second scaler was varied up to 10 msec. In this way the average number of counts occurring in a known interval starting 500 μ sec after the arrival of a triggering pulse could be obtained. Any excess in this number, above that to be expected if the impulses were occurring randomly in the counter, must be due to a pairing of events in which the first event is the emission of a β -particle leading to the excited state from which the 57 keV γ -ray is emitted, and the second event the emission of an internal conversion electron produced by this γ -ray. Although the 57 keV γ -ray gives rise to conversion electrons in at least 60% of the disintegrations, no departure from randomness was observed in a time interval as long as 10 msec after the triggering pulse.

To test if much shorter paralysis times would show pairing of events, the experiment was repeated with a scintillation counter using anthracene as the phosphor. The same negative result was obtained.

It was therefore concluded that the lifetime of the 57 keV γ -ray was considerably greater than 10 msec. This is in accordance with the results of Lecoïn, Perey and Teillac.

§6. DISCUSSION

The classification of the observed partial spectra* depends on whether use is made of a Sargent diagram such as that given by Feather (1948) and discussed by Feather and Richardson (1948), or whether the criteria based on ft values adopted by Mayer, Moszkowski and Nordheim (1951) are employed. A comparison of the predictions of the two methods is included in table 2. The two methods would show better agreement if the present first forbidden line of the former authors were allotted to the allowed (L -forbidden) transitions of the latter, with a corresponding reduction of one in the degree of forbiddenness of the succeeding lines.

The γ -rays suggested from an analysis of the conversion lines are shown in table 3. In some cases, where the interpretation of the lines is not unique, both values of the deduced γ -ray energy have been included. To fit the transitions responsible for these γ -radiations into the energy levels of the radiothorium nucleus in a manner which does not violate the experimental results already outlined appears to require four extra levels in addition to those suggested by the end points of the β -spectra listed in table 2. Figure 7 illustrates the tentative scheme put forward. Clearly the problem is one of considerable complexity, and alternative schemes may be equally valid. The spins and parities used in this level scheme have been based on the predictions of the ft values of the β -modes, which have been found to yield more plausible γ -ray intensities than the predictions of the Sargent diagram.

The intensities given in table 3 for the weaker conversion lines should be regarded as indications of order of magnitude only; nevertheless we have used these conversion line intensities in many cases, in conjunction with the K conversion coefficients of Rose *et al.* (1951), to determine the quantum intensities of the γ -rays, and have chosen the type of radiation to give γ -ray intensities which conform to the level scheme suggested. Columns (6), (7) and (8) of table 3 summarize these deductions, which are corroborated to some extent by the observed K:L ratios and by the early work of Thibaud (1926), which is discussed later. On the basis of

* Recently results of Jenkins and O'Kelley (1951, unpublished) have been quoted by Hollander, Perlman and Seaborg (*Table of Isotopes*, 1952—draft copy). Partial spectra with end point energies 2.03, 1.74 and 1.10 mev are given by these authors.

Table 3

(1)	(2)	(3)	(4)	(5)	(6)	(7)	(8)
1	Weak	L _I	56.80				
2	23.8	L _{II}	56.60				
3	20.2	L _{III}	56.63	56.75	E2	—	60
7	8.9	M _{II}	56.98				
8	7.1	N _I	56.73				
9	0.1	L _{II}	77.88	78.05	E2+M1	—	—
10	0.1	L _{III}	78.21				
14	3.3	L _{II}	97.67				
15	—	L _{III}	97.79	97.77	E2+M1	—	—
16*	—	M _I	97.84				
16*	—	L _{II}	112.4				
17	—	L _{III}	113.3	113.0	E2+M1	—	—
18†	—	M _I	113.3				
18†	3.3	L _{II}	127.8				
19	2.3	L _{III}	127.6	127.5	E2+M1	0.6 (E2)	6 (see text)
21‡	—	M _I	127.4				
22	0.56	N _I	127.1				
12	—	K	180.6	179.0	E2+M1	—	—
26	—	L _I	177.5				
13	4.7	K	183.4				
27	1.0	L _I	185.4	184.2	M1	4.0	7.2
28	0.3	M _I	183.9				
21‡	—	K	231.8	232.2	E2+M1	—	—
30	—	L _I	232.5				
31	0.75	K	335.5	336.0	E2+M1	0.8 (M1)	1.9 (M1)
33	0.19	L _I	336.4			0.06 (E2)	13.4 (E2)
32	0.56	K	410.1	410.1	E2+M1	0.49 (M1)	1.7 (M1)
						0.044 (E2)	13.3 (E2)
34	0.75	K	458.2			0.36 (M1)	3.4 (M1)
35	0.38	L _I	457.5	457.6	E2+M1		
36	0.19	M _I	457.1			0.035 (E2)	22.8 (E2)
37	0.56	K	905.9	907.1	E3+M2	0.10 (M2)	6.4 (M2)
39	0.19	L _I	908.3			0.023 (E3)	25.1 (E3)
38	0.28	K	968.1	964.5	E3+M2	0.086 (M2)	3.7 (M2)
41	0.19	L _I	960.9			0.021 (E3)	13.8 (E3)
40	—	K	1035	1035	E1	—	—
42	—	K	1095	1095	E3	—	—
43	0.69	K	1587	1587	E3	0.0075	12
44	0.09	K	1640	1640	E2+M1	0.014 (M1)	6.5 (M1)
						0.0036 (E2)	25.1 (E2)

Lines which are capable of double interpretation are marked with *, † or ‡ in column 1. Line 11 of table 1 is interpreted as an Auger line.

Lines 4, 5, 6, 20, 23, 24, 25 and 29 have not been assigned to γ -rays.

(1) Line; (2) intensity of line per 100 disintegrations; (3) conversion shell; (4) γ -ray energy (keV); (5) mean γ -ray energy (keV); (6) type of radiation; (7) K conversion coefficient (after Rose *et al.*); (8) total transition probability (%).

these tentative identifications, spins and parities have been assigned to the levels, assuming that the ground state of radiothorium ($^{228}_{90}\text{RdTh}$), an even-even nucleus, has zero spin and even parity. Any more direct information regarding intensities, or new and more accurate theoretical values for the L-shell conversion coefficients, may well lead to revision of the scheme suggested.

Further remarks regarding individual γ -rays are now added.

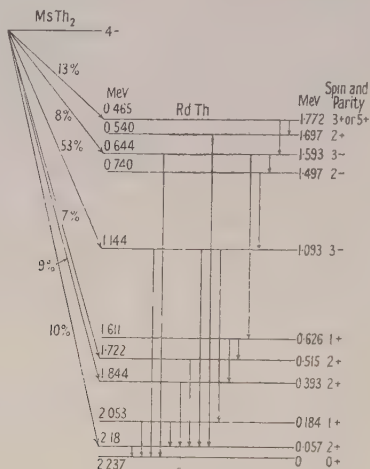


Fig. 7. Suggested level scheme.

(i) The 57, 127, and 184 keV Radiations

The predominant conversions of the 57 keV radiation occur in the L_{II} and L_{III} shells, with a relatively small L_I conversion. The 'relativistic but unscreened' L conversion coefficients calculated by Gellman, Griffith and Stanley (1952) suggest that the transition is not electric or magnetic dipole. Since it occurs in at least 60% of the disintegrations and is of relatively long lifetime, it is unlikely to be in competition with other transitions of higher energy. If it is to be assigned to radiothorium it is highly probable that it comes from the first excited state. To account for the lifetime of this state the transition should be either electric or magnetic quadrupole or of still higher order (see Goldhaber and Sunyar 1951).

Study of the 127 keV and 184 keV γ -radiations imposes further restrictions on the classification of the 57 keV transition. The relative intensities of 127 keV γ -ray conversions in the L subshells suggest that this radiation is to be classified as E2. A K:L ratio of the order of 1/40 has been found by Brodie (thesis, to be published later) and, taking the K threshold conversion coefficients of Spinrad and Keller (1951) and the L shell coefficients of Gellman *et al.* (1952), optimum agreement with this value is obtained if this γ -ray is assumed to be predominantly electric quadrupole.

With regard to the 184 keV radiation, the strong L_I conversion with no L_{II} or L_{III} conversions found, and the short lifetime, suggest that the radiation is magnetic dipole although the K:L ratio is rather low. Quantum emission of this energy was detected by Thibaud, but he quotes no intensities for the photo-electron lines excited in lead, and we must assume that the lines were too weak to

measure. This agrees to some extent with the estimate that the quantum intensity is of the order of 0.01 per disintegration, the radiation being classified as M1.

Assuming that the 184 keV γ -ray is a cross-over for the 127 and 57 keV γ -rays in cascade, the 57 keV radiation must then be classed as either E2 or M3. We are inclined to favour E2, as M3 should give a lifetime long enough to be detected by ordinary decay methods. In addition, the statistical evidence is strongly in favour of the first excited state of an even-even nucleus having a spin of two and even parity.

The possibility of the emission of the 57 keV γ -radiation from an excited state of MsTh_2 could not at first be ruled out, but recent study of the α -particle activity of $^{232}_{92}\text{U}$ by Dunlavey and Seaborg (1952) has shown the existence of an excited state of $^{228}_{90}\text{RdTh}$ at an energy of about 60 keV. It seems plausible to identify this energy level with that at 57 keV shown in the decay scheme suggested.

(ii) *The 336, 410, 458, 907 and 964 keV Radiations*

These radiations have all been observed by Thibaud using the method of the 'excited' photoelectron spectrum. He gives the relative intensities of lines obtained for a source of MsTh_1 in equilibrium with its decay products. A comparison with the results obtained for the thorium active deposit by Martin and Richardson (1950) has allowed us to make a very rough estimate of the absolute quantum intensities of the five γ -rays listed above. The rough values 9%, 4%, 3%, 25% and 20% respectively show reasonable agreement with those quoted in table 3.

The possibility that the 2.18 MeV β -transition feeds the ground state may now be excluded. The argument depends on the suggestion that the γ -transition of 336 keV energy occurs between the levels fed by the partial spectra with end points at energies of 1.85 and 2.18 MeV. These modes of β -decay are clearly forbidden to the same degree (see table 2), and should therefore excite states of RdTh of identical spin and parity. If one of these states is the ground state of RdTh , then both states should have zero spin and even parity (since RdTh is an even-even nucleus). In this case, quantum emission for a transition between two states of zero spin will be prohibited by selection rules. Since Thibaud has detected such emission, then if the 336 keV γ -radiation is correctly placed, the 2.18 MeV β -transition feeds an excited state of RdTh of non-zero spin.

(iii) *The Possibility of Additional γ -Rays*

The decay scheme suggests the possibility of several γ -radiations not yet observed, and examination of the spectrum with an instrument of very high resolution would almost certainly reveal lines at present undetected or unresolved.

ACKNOWLEDGMENTS

We have to thank Dr. N. Miller for much helpful advice in source preparation and Dr. W. D. Brodie for allowing us to use some of his results, at present unpublished. We are also indebted to Professor N. Feather for much stimulating discussion and to Mr. Headridge and the technical staff of the Natural Philosophy Department for valuable assistance in the construction of apparatus.

REFERENCES .

- BLACK, D. H., 1924, *Proc. Roy. Soc. A*, **106**, 632.
CAMPBELL, C. G., HENDERSON, W. J., and KYLES, J., 1952, *Phil. Mag.*, **43**, 126.
DUNLAVEY, D. C., and SEABORG, G. T., 1952, *Phys. Rev.*, **87**, 165.
ELLIS, C. D., 1934, *Proc. Roy. Soc. A*, **143**, 350.
ELLIS, C. D., and SKINNER, H. W. B., 1924, *Proc. Roy. Soc. A*, **105**, 165.
FEATHER, N., 1930, *Phys. Rev.*, **35**, 1559; 1938, *Proc. Camb. Phil. Soc. I*, **34**, 115; 1948, *Nature, Lond.*, **161**, 431.
FEATHER, N., KYLES, J., and PRINGLE, R. W., 1948, *Proc. Phys. Soc.*, **61**, 466.
FEATHER, N., and RICHARDSON, H. O. W., 1948, *Proc. Phys. Soc.*, **61**, 452.
FEISTER, I., 1950, *Phys. Rev.*, **78**, 375.
GELLMAN, H., GRIFFITH, B. A., and STANLEY, J. P., 1952, *Phys. Rev.*, **85**, 944.
GOLDHABER, M., and SUNYAR, A. W., 1951, *Phys. Rev.*, **83**, 906.
HAISSINSKY, M., 1933, *C. R. Acad. Sci., Paris*, **196**, 1778.
KONOPINSKI, E. J., and UHLENBECK, G. E., 1941, *Phys. Rev.*, **60**, 308.
LECOIN, M., 1935, *C. R. Acad. Sci., Paris*, **200**, 1931; 1938, *J. Phys. Radium*, **9**, 81.
LECOIN, M., PEREY, M., and RIOU, M., 1949, *J. Phys. Radium*, **10**, 390.
LECOIN, M., PEREY, M., and TEILLAC, J., 1949, *J. Phys. Radium*, **10**, 33.
LIBBY, W. F., and LEE, D. D., 1939, *Phys. Rev.*, **55**, 245.
MCLANE, C. K., and PETERSON, S., 1948, Declassified Document No. MDCC 1742, U.S. Atomic Energy Commission.
MARTIN, D. G. E., and RICHARDSON, H. O. W., 1950, *Proc. Phys. Soc. A*, **63**, 223.
MAYER, M. G., MOSZKOWSKI, S. A., and NORDHEIM, L. W., 1951, *Rev. Mod. Phys.*, **23**, 315.
PETERSON, S., 1948, Declassified Document No. MDCC 1709, U.S. Atomic Energy Commission.
ROSE, M. E., GOERTZEL, G. H., and PERRY, C. L., 1951, *Oak Ridge National Laboratory, Report No. 1023*.
SPINRAD, B. I., and KELLER, L. B., 1951, *Phys. Rev.*, **84**, 1056.
THIBAUD, J., 1926, *Ann. Phys., Paris*, **5**, 73.
WELLS, F. H., 1951, *J. Brit. Instn. Radio Engrs.*, **11**, 491.
YOVANOVITCH, D. K., and D'ESPINE, J., 1927, *J. Phys. Radium*, **8**, 276.

Cloud Chamber Observations of the Cosmic Radiation Underground

By E. P. GEORGE*, J. L. REDDING AND P. T. TRENT

Birkbeck College, University of London

MS. received 20th February 1953

Abstract. In a study of the passage of fast charged particles through a cloud chamber containing two Pb plates at a depth below ground equivalent to 60 m water, examples of associated pairs of penetrating particles and of large angle scattering of single particles have been observed. If these events are interpreted as the production of secondary particles by μ -mesons, and as anomalous scattering of μ -mesons in Pb, the following cross sections per nucleon result: for penetrating secondary particles 4×10^{-29} cm², and for anomalous large angle scatter 2×10^{-28} cm².

§ 1. INTRODUCTION

THE experiments described in this paper were carried out as a continuation of earlier experiments made with heavily shielded counter systems operated in our Holborn Underground laboratory.

These experiments, reported earlier in this journal (George and Trent 1951), led us to conclude that a proportion of the radiation observed to traverse large thicknesses of lead was subject to anomalous scatter, inexplicable in terms of coulomb interaction. Additionally, we reported further on the presence of pairs of penetrating particles, presumed similar to those first reported by Braddick and Hensby (1939) and later investigated by other workers (Braddick, Nash and Wolfendale 1951).

In order to carry these investigations further we have made observations with a cloud chamber, operated in our same underground laboratory, at a depth equivalent to 60 m water, and the results obtained so far, and such conclusions as may be drawn, are given in this paper.

§ 2. APPARATUS

The cloud chamber was of conventional type, cylindrical in shape, and with the sensitive volume containing two lead plates each 2 cm thick. Expansions were triggered by a simple counter telescope, in the position shown in fig. 1. This figure also indicates the three different experimental arrangements used. With arrangement (a) a total of 1071 photographs was taken, with arrangement (b) the total was 1628, and with arrangement (c) 1492.

The intention behind these different arrangements was to investigate the variation in the numbers of large angle scatters observed with reference to the energy of the particles on emergence from the chamber. In the analysis of the photographs precise measurements of the scatter of tracks traversing the chamber were made in only 2000 cases: approximately 1000 in arrangement (a) and

* Now at University of Sydney, N.S.W., Australia.

1000 in arrangement (b). In the remaining cases the scatter was only measured and recorded if it was found to be greater than 6° . In all cases the results cited below are in terms of the projected angle of scatter in the plane of illumination of the chamber. The method of measurement adopted enabled observations to be made to within 0.2° , and the chamber distortions were rather smaller than this limit.

In the observations of pairs of particles traversing the chamber the criteria adopted were that two particles only should be observed to traverse either one or both of the lead plates in the chamber, and that both should emerge unaccompanied by any other, secondary, particle. Photographs in which any other contemporaneous track was visible in the chamber were discarded.

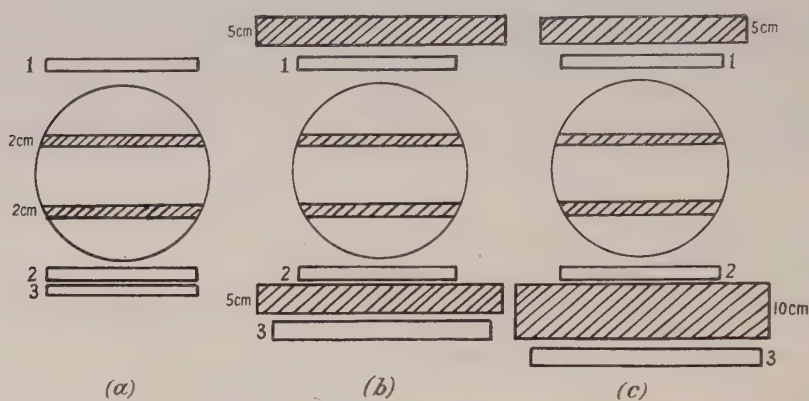


Fig. 1. Layout of apparatus in the three different arrangements used. Lead absorbers are shown cross-hatched. The Geiger-counter telescope controlling the expansions is shown as 1, 2, 3.

The resolving time of the chamber was estimated as being approximately one-fortieth of a second, and under the conditions of experiment it is most improbable that more than one of the pairs observed could have been the result of an accidental coincidence.

§ 3. RESULTS

(i) Results of Scattering Measurements

The results obtained may be divided into two parts: firstly, those in which the scatter of all tracks was measured, and secondly, those in which only scatters greater than 6° were measured. The results in the former case are displayed in table 1 together with the scatter to be expected, computed as described below.

For the purposes of this comparison results obtained with both arrangements (a) and (b) are grouped together, since the distributions in angle observed with these arrangements were substantially identical over this range of angles.

Table 1

Angle of scatter ($^\circ$)	0-1.2	1.2-1.7	1.7-2.3	2.3-2.9	2.9-3.4	3.4-4.0	4.0-4.6	4.6-5.2
No. of tracks observed	1965	65	43	30	14	11	6	5
No. of tracks computed (no correction)	1932	85	46	30	18	13	9	6

The results for the second case, in which scatters greater than 6° are being considered, are displayed in fig. 2 for each of the three different experimental arrangements used. In fig. 2 the distributions expected from coulomb scattering under various assumptions about the arrangement of the charge in lead nuclei are shown. In computing this expected distribution account was taken of the geometrical correction, obtained in the manner described below. Further, for the purpose of obtaining the expected distribution given in fig. 2, due allowance was made for the different levels of low energy cut-off required by the three different experimental arrangements.

(ii) Results of Measurements on Pairs

In the series of 3870 photographs examined for pairs of penetrating particles only eight definite cases were observed. Of these, three were produced in the chamber itself, originating in the upper lead plate, and the remaining five appeared to be produced in the lead absorber situated immediately above the chamber. Of these five, in two cases both of the particles penetrated both of the lead plates in the chamber without producing secondaries, in the remaining three cases one member passed through both plates but the other passed through only one plate before leaving the chamber.

In fig. 3 (Plate) is shown one of the examples of the apparent production of a single secondary penetrating particle in the top plate in the chamber.

§ 4. DISCUSSION OF RESULTS

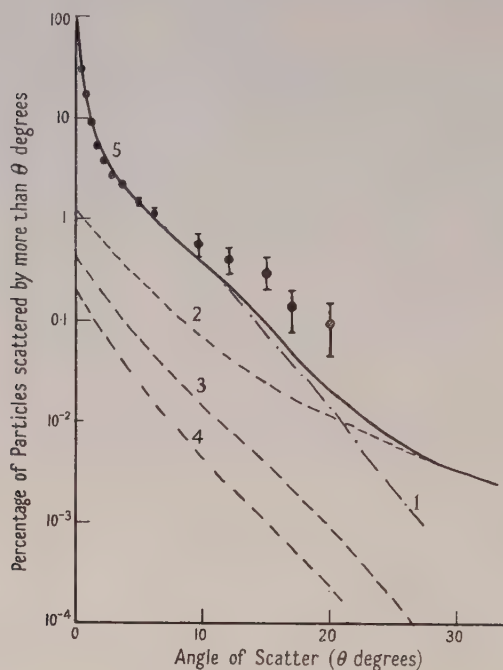
(i) Scattering

The results given in table 1 are compared with the expected distribution calculated on the basis of the Williams multiple scattering formula, averaged over the energy spectrum of the underground radiation. The energy spectrum assumed was of the customary form, viz. $N(E)dE = dE/(E + E_0)^{2.7}$, where $E_0 = 1.2 \times 10^{10}$ ev. The choice of the value 2.7 as exponent is based on the data given by Barrett *et al.* (1952).

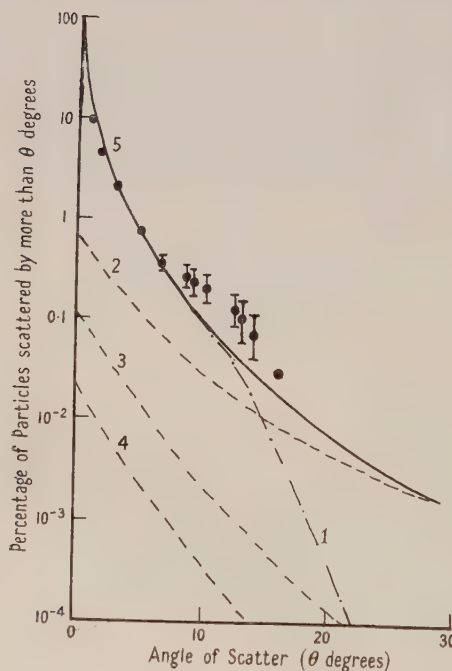
The comparison between experimental and theoretical values over this energy range appears reasonable. The fact that the observed distribution is slightly lower than that calculated may be attributed to some degree of non-uniformity in the illuminated region. This is borne out by the fact that the total number of scatters observed in the top plate of the chamber was slightly larger than the number observed in the bottom plate, presumably as a result of the depth of illumination in the central portion of the chamber being greater than that in the upper and lower portions (by about 1 cm in 5 cm).

The calculated probabilities of scatter shown in fig. 2 are presented in the usual way as a superposition of the effects of multiple scattering, which predominates at small angles, and of single scattering, which becomes more important at large angles. The values for the contribution from multiple scatter were derived in a manner similar to those of table 1.

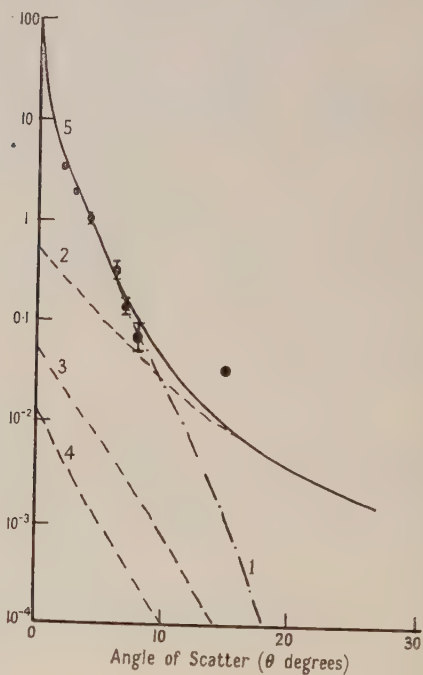
In computing the values for large angle single scatter some allowance must be made for the distribution of charge in the scattering nucleus (Williams 1938), as shown experimentally by Lyman, Hanson and Scott (1951) for 15.7 mev electrons. We have computed the expected single scatter distribution by averaging over the underground energy spectrum the Born-approximation formulae given by Rose (1948) for the following cases: point nuclei, a uniform



(a)



(b)



(c)

Fig. 2. Observed and calculated frequencies of scatter. 1, calculated multiple scatter; 2, 3 and 4, calculated single scatter for point, uniformly charged and superficially charged nuclei; 5, sum of 1 and 2. Figures 2 (a), (b) and (c) are the results for arrangements 1 (a), (b) and (c) respectively.

charge distribution and a spherical shell charge distribution of radius equal to the nuclear radius of Pb. A correction factor has been introduced for the geometric loss of large angle scatters resulting from the telescope system used. The method of evaluating this factor is indicated in the Appendix. The results are shown in fig. 2.

The experimental observations are seen to depart significantly from the curves calculated for point nuclei at angles greater than 15° , and the discrepancy is even greater for those based on some form of nuclear structure.

Amaldi, Fidecaro and Mariani (1950) have pointed out that, in addition to the coherent scattering considered above, account should also be taken of the incoherent scattering resulting from collisions with individual protons in the nucleus, the recoiling proton exciting the parent nucleus. We have evaluated this effect for Pb and find that it turns out to be very small, about 1 to 2% of the observed cross sections. Hence we conclude that the observed frequency of large angle scatter is significantly greater than can be explained in terms of either multiple or single coulomb scattering of μ -mesons.

(a) *Nature of scattered particles.*

From the known frequency of nuclear disintegration 'stars' (George and Evans 1950) we know that strongly interacting charged particles such as π -mesons and protons form less than 0.05% of the cosmic-ray flux at this depth. Assuming such particles to be scattered with a nuclear geometric cross section, they would account for 2% of the observed scatters at the most, and the true number is certainly much less than this figure.

Since the scattered particles are observed to pass through two 2 cm Pb plates without being accompanied by secondary particles on emerging, and since their deflection in the lead plate not showing the large angle scatter was always small, we can safely assume that the particles scattered through large angles were not electrons. The rapidly falling energy spectrum of such electrons, characteristic of their origin in knock-on collisions, strengthens this argument. Also, the extra absorbers in the second and third runs all help to reduce the possible influence of electrons.

So far no singly charged particles other than electrons, π - and μ -mesons and protons have been identified in the underground component, and we therefore conclude that the scattered particles are μ -mesons, and that the observed frequency of scatters with angles greater than 15° cannot be attributed to coulomb effects. If we interpret the results as examples of non-electrical scatter of μ -mesons, the results of the first run give a cross section for this process, averaged over the energy spectrum of the underground particles, of 2×10^{-28} cm² per nucleon, in agreement with our results reported earlier (George and Trent 1951).

(b) *Energy dependence of scattering cross section.*

From fig. 2 the introduction of Pb absorbers in the counter telescope is seen to produce a large decrease in the frequency of large angle scatters, suggesting that the majority of μ -mesons scattered had kinetic energies between 100 and 300 MeV, although the statistical weight of the results does not merit a refined analysis. Since only about 5% of the underground particles lie in this energy band, this would imply a cross section of 4×10^{-27} cm² per nucleon for μ -mesons of energies between 100 and 300 MeV. In this respect our results are similar to

those of Amaldi and Fidecaro (1950), who made observations at sea level and gave 4.5×10^{-29} cm² per nucleon as an upper limit for the scattering cross section in the band 200 to 320 mev, and about 2.3×10^{-30} cm² per nucleon for the energy band 320 mev to infinity. Our results are larger, and an explanation of the discrepancy may presumably be found in the differing techniques, energy limits and geometries used.

After our observations were completed, Whittemore and Shutt (1952) gave an account of cloud chamber observations at sea level and mountain altitude of scattering of cosmic-ray particles in Pb. Magnetic curvature indicated the sign of charge of the scattered particles, and in this way they were able to eliminate the possible contribution from protons, obtaining a cross section for the scattering of μ -mesons of about 10^{-25} cm² per lead nucleus, or 5×10^{-28} cm² per nucleon. This value is similar to that observed by other workers at sea level (Wilson 1940, Code 1941, Shutt 1942). The complexity of the cosmic-ray beam at sea level or mountain altitudes renders difficult the interpretation of observations of scattering. By working at large depth below ground, where only the μ -meson component survives, we have been able to overcome this particular difficulty.

Barrett *et al.* (1952) studied the lateral distribution in the showers of μ -mesons detected at a depth equivalent to 1600 m water, and concluded that there was no evidence for anomalous scatter of μ -mesons. If, in fact, the anomalous scatter is only significant for μ -mesons of a few hundred mev, no evidence of large angle scatters would be expected under their conditions of observations on account of the high value of the mean energy of the μ -mesons at this depth, and also because of the low energy cut-off produced by the absorbers in their telescopes.

(ii) Pairs

From measurements of the knock-on rate carried out in these experiments we may estimate that, in the course of our observations, approximately 80 cases should have occurred in which a penetrating particle was incident on the chamber together with a single electron of energy greater than about 40 mev.

The probability of a knock-on electron produced by an energetic meson traversing 2 cm of lead without scatter greater than 2° , and without producing a secondary particle, may be estimated as of the order of 0.01 or less, and we therefore conclude that any contribution to the effect observed from this source is negligible.

Consequently we may conclude that a minimum number of seven events was observed in which penetrating pairs of particles were produced, either in the lead in the chamber or in that above. Because the experiments varied in the amount of lead above the chamber, it is not possible to obtain an accurate cross section, but it seems reasonable to conclude that the cross section for this process is of the same order as that previously reported both by other workers and ourselves, i.e. 4×10^{-29} cm² per nucleon, corresponding to a mean free path of 40 m of lead. This cross section is too large to be accounted for in terms of the known probability for nuclear interaction of μ -mesons involving star production, as observed in photographic plates.

Recently Lovati *et al.* (1953) observed no certain examples of penetrating pairs in a track length of 350 m of lead, using a multiplate cloud chamber underground, indicating that the cross section for this process may be appreciably smaller than that given above. A value of between 1 and 2×10^{-29} cm² per

nucleon would not be inconsistent with all the underground investigations of this process, including that of Lovati. Further observations are required to clarify this situation, and we have an additional experiment in progress.

Hayakawa (1952) has suggested that the anomalous scatters and the pair events might be attributed to K-mesons existing in the underground radiation. The experimental observations are as yet too meagre to say anything about this possibility.

§5. CONCLUSIONS

From the experiments reported in this paper we have drawn the following conclusions:

(i) The frequency of anomalous large angle scatter of more than 15° of energetic μ -mesons indicates a cross section of 2×10^{-28} cm² per nucleon, averaged over the energy spectrum of particles with energy above 100 mev at a depth of 60 m water.

(ii) Most of the observed large angle scatters refer to particles with energies between 100 and 300 mev.

(iii) Previous results on the production of pairs of penetrating particles in the cosmic radiation underground are confirmed, with a cross section of approximately 4×10^{-29} cm² per nucleon. These events are not explicable in terms of star production by μ -mesons.

ACKNOWLEDGMENTS

We are grateful to Professor J. D. Bernal for the excellent facilities placed at our disposal, and we are indebted to Professor A. Lovati for communicating his results prior to publication. The cloud chamber was bought with a grant from the Royal Society, and the rest of the equipment with a grant from the Central Research Fund of London University. Our thanks are due to the London Transport Executive for permission to work on Holborn Underground Station.

REFERENCES

- AMALDI, E., and FIDECARO, G., 1950, *Nuovo Cim.*, **7**, 537.
 AMALDI, E., FIDECARO, G., and MARIANI, F., 1950, *Nuovo Cim.*, **7**, 553.
 BARRETT, P. H., BOLLINGER, L. M., COCCONI, G., EISENBERG, Y., and GREISEN, K., 1952, *Rev. Mod. Phys.*, **24**, 133.
 BRADDICK, H. J. J., and HENSBY, G., 1939, *Nature, Lond.*, **144**, 1012.
 BRADDICK, H. J. J., NASH, W. F., and WOLFENDALE, A. W., 1951, *Phil. Mag.*, **42**, 1277.
 CODE, F. L., 1941, *Phys. Rev.*, **59**, 229.
 GEORGE, E. P., and EVANS, J., 1950, *Proc. Phys. Soc. A*, **63**, 1248.
 GEORGE, E. P., and TRENT, P. T., 1951, *Proc. Phys. Soc. A*, **64**, 1134.
 HAYAKAWA, S., 1952, *Proc. Phys. Soc. A*, **65**, 215.
 LOVATI, A., MURA, A., SUCCI, C., and TAGLIAFERRI, G., 1953, *Nuovo Cim.*, **10**, 105.
 LYMAN, E. M., HANSON, A. O., and SCOTT, M. B., 1951, *Phys. Rev.*, **84**, 626.
 ROSE, M. E., 1948, *Phys. Rev.*, **73**, 279.
 SHUTT, R. P., 1942, *Phys. Rev.*, **61**, 6.
 WHITTEMORE, W. L., and SHUTT, R. P., 1952, *Phys. Rev.*, **88**, 1312.
 WILLIAMS, E. J., 1938, *Proc. Roy. Soc. A*, **169**, 531.
 WILSON, J. G., 1940, *Proc. Roy. Soc. A*, **174**, 73.

APPENDIX

The effect of considering all particles to be incident in a vertical plane (the plane of observation) was calculated to produce a negligible error. This is due to the depth of the illuminated region being small (~ 6 cm).

If ϕ and ψ are the angle of scatter of a particle, projected on to the plane of observation and a perpendicular vertical plane, respectively, then the probability of a projected angle of scatter between ϕ and $\phi + d\phi$ is

$$P(\phi) d\phi = 4 d\phi \int_0^{\psi_0} \frac{\exp \{-(\phi^2 + \psi^2)/4\alpha^2\} \sec^2 \phi \sec^2 \psi d\psi}{\{\tan^2 \phi + \sec^2 \psi\}^{3/2}}$$

(assuming the scattering angle θ is small and therefore approximately $\theta^2 = \phi^2 + \psi^2$), where ψ_0 is an upper limit on ψ imposed by the chamber and α is a function of the energy of the particle and the thickness of the lead plates, as given by Williams.

However, this expression does not allow for the fact that a particle scattered through an angle (ϕ, ψ) will not always be observed, depending on its initial direction and that part of the chamber on which it is incident. If $C_2(\psi)$ is the fraction, of all incident particles scattered with a projected angle ψ , which can be observed, and $C_1(\phi)$ is the fraction, of all incident particles scattered with a projected angle ϕ , which can be observed, then

$$P_2(\phi) d\phi = \frac{4C_1(\phi) \sec^2 \phi d\phi \exp(-\phi^2/4\alpha^2)}{\alpha^2 \pi} \int_0^{\psi_0} \frac{\exp(-\psi^2/4\alpha^2) C_2(\psi) \sec^2 \psi d\psi}{\{\tan^2 \phi + \sec^2 \psi\}^{3/2}}$$

is the probability of observing a scatter between ϕ and $\phi + d\phi$, allowing for the geometry of the chamber.

Functions $C_1(\phi)$ and $C_2(\psi)$ can be obtained by calculating, with the aid of a scale diagram of the chamber, particular values for a series of values ϕ and ψ , and then fitting an appropriate polynomial.

Note added in proof. We have been informed by Dr. A Wolfendale that he has studied the scattering of cosmic-ray particles in a multi-plate cloud chamber operated under 1 m of lead at Manchester, and that he also finds evidence for anomalous scatter of μ -mesons with a cross section in good agreement with that reported in this paper.

Ionization of Cosmic Ray Mesons in Argon

By J. K. PARRY, H. D. RATHGEBER AND J. L. ROUSE

Department of Physics, University of Melbourne

Communicated by L. H. Martin; MS. received 2nd December 1952

Abstract. The ionization of cosmic ray mesons with momentum in the range 3×10^8 to 7×10^{10} ev/c is investigated using an argon-filled proportional counter. The results obtained are in agreement with theoretical calculations and show evidence of a polarization effect.

§ 1. INTRODUCTION

THE rate at which fast particles lose energy by ionization processes is of considerable importance in the identification of tracks in cloud chambers and nuclear emulsions. Although the theory of the variation of ionization with the momentum of the particle was developed some time ago (Bohr 1915, Bethe 1930), until quite recently there were no satisfactory measurements in the region of relativistic particle velocities.

Theory predicts an initial decrease of ionization with increasing momentum until a minimum is reached, at an energy of the order of the rest energy of the particle, whereupon the ionization increases logarithmically. At higher momenta depending on the density of the medium, polarization effects (Halpern and Hall 1948) limit this rise, and the ionization approaches a constant value. In a dispersed substance such as a gas this rise should be readily observable. A preliminary measurement made in this laboratory (Goodman, Nicholson and Rathgeber 1951), however, showed no evidence for such a rise. In view of this discrepancy and the unsatisfactory hypotheses required to explain it, immediate plans were formulated for further measurements with increased precision and improved methods of analysis. A critical study of the preliminary measurements published showed that the accuracy was insufficient to justify the conclusions reached. The results of the experiment described in this paper agree well with the theoretical expressions.

Since the experiment commenced, there have been several other measurements (Ghosh, Jones and Wilson 1952, Becker *et al.* 1952, Kupperian and Palmatier 1952, Carter and Whittemore 1952), notably by Ghosh, Jones and Wilson (1952) using cloud chamber techniques and Becker *et al.* (1952) using proportional counters. The results of these experiments are in good agreement with the theoretical curve, but with the exception of the work of Ghosh, Jones and Wilson (1952) do not extend to sufficiently high momenta to show polarization effects.

In the experiment described in this paper, the particles are separated into a number of momentum ranges by means of a magnetic spectrometer, and the ionization of each particle is recorded with a proportional counter. Due to the low stopping power of the counter large fluctuations in the ionization are observed. If a histogram of the ionization readings in any particular range is plotted the familiar asymmetrical distribution curve calculated by Landau (1944) is obtained.

The quantity measured in this experiment is the peak of the distribution, which corresponds to the most probable ionization. The measurements extend over the momentum range 3×10^8 ev/c to 7×10^{10} ev/c.

In the preliminary measurements reported by Goodman, Nicholson and Rathgeber (1951), the limited number of results (400 tracks) made it impracticable to use a curve fitting method to obtain the most probable ionization. In each range the mean value of the ionization was computed. Since the amplifier used in the preliminary experiments had a low overload point, the tail of the fluctuation distribution was truncated. The effect of this was more serious in the region of high ionization and resulted in the mean being insensitive to changes in ionization. Further, due to the neglect of overloads, the experimental errors given were far too optimistic.

§ 2. EXPERIMENTAL METHOD

(i) Description of Equipment

The spectrometer as used here for momentum measurements on cosmic ray particles has been described elsewhere (Caro, Parry and Rathgeber 1951). The path of the particle through the magnetic field is established by trays of Geiger counters (fig. 1), the track through the spectrometer being recorded on a punched

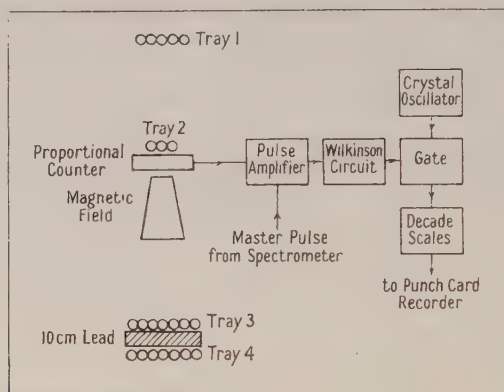


Fig. 1.

card. Tray 4 records particles which pass through 10 cm of lead, thus defining the penetrating component. An estimate based on the work of Mylroie and Wilson (1951) shows that less than 0.5% of the particles penetrating the lead are protons. Electrons may be excluded since the probability of a high energy electron penetrating the lead without producing a shower is negligible. Thus, in this experiment, all particles which penetrate the lead without producing showers are assumed to be mesons.

The proportional counter is placed in the spectrometer immediately below tray 2. The counter which is constructed of brass, has a square cross section with 7.5 cm side and an active length of 10 cm. Aluminium windows 7.5 cm square and 0.25 mm thick allow the particles to pass through the counter with little scattering. A tungsten wire of 0.1 mm diameter is used and the counter filled with argon and ethylene at partial pressures of 774 and 46 mm of mercury (0°C) respectively. The linear pulse amplifier has a stabilized gain of about 10^4 and a stabilized rise time. The height of the pulse from the amplifier is measured by means of a circuit due to Wilkinson (1950) which has been modified to record only

when the spectrometer registers a coincidence. This circuit converts the amplifier pulse into a rectangular pulse whose time duration is proportional to the peak of the input pulse. This rectangular pulse gates a crystal oscillator, the oscillations transmitted being counted by a pair of decade scales and recorded on the punched card. The linearity of the complete pulse height recording circuit is excellent.

(ii) Calibration of Proportional Counter

The proportional counter was calibrated using the filtered characteristic $K\alpha$ radiation of Cu and Mo. The pulse height distribution at the amplifier output was obtained with a single channel analyser. A graph of the peak of the pulse height distribution against energy in kev showed that the Mo and Cu $K\alpha$ points and the origin lay closely on a straight line indicating true proportionality of the counter. The width at half height of the distributions was approximately 20%. The absolute value of the energy loss for particles traversing the counter was obtained from the Mo $K\alpha$ calibration.

Using the Cu $K\alpha$ radiation, pulse distributions were obtained for various counter potentials V ranging from 2100 to 2400 v corresponding to gas gains A of about 600 to 4000. In this range $\log A = \text{constant}$. V .

A study of the active region of the counter was made by passing the Mo $K\alpha$ radiation into the counter at various positions along the wire. A small end effect was observed, which necessitated a correction of 2% between measurements taken with the counter in the spectrometer, where the tracks were distributed over a 4-cm square, and measurements taken in the calibration when the tracks all lay very close to the centre of the counter.

(iii) Operation

Since the results were obtained over many months of continuous operation, a regular check on the stability and constancy of the equipment was necessary. Daily checks were made on the stabilized proportional counter h.t. supply, the calibration of the Wilkinson pulse height circuit and the Geiger counters. In the absence of a suitable K capture source, self-excited x-rays from a Po source were used for weekly checks on the proportional counter and amplifier. Both the peak and half width of the pulse distribution were measured. It was found necessary to increase the proportional counter h.t. by approximately 0.1% per week to keep the gas gain constant. The half width of the distribution remained constant throughout.

The results were obtained in two runs:

Run 1. Field 1900 gauss. Zenith angle 0° . No. of mesons 3958

Run 2. Field 13500 gauss. Zenith angle 30° East. No. of mesons 2430

Run 2 was made at a zenith angle of 30° so that the momentum results could be included in another experiment.

Before and after each run the counter was calibrated with Cu and Mo x-rays. The amplifier gain was measured and found to remain constant. The single channel analyser and the Wilkinson pulse height circuit were compared using a pulse generator.

(iv) The Determination of the Fluctuation Curve

An experiment was performed primarily to obtain an accurate fluctuation curve for this particular proportional counter, which could be fitted to the histograms obtained in the two meson runs.

Electrons of momentum 1.3 MeV/c were passed centrally through the proportional counter and then through a Geiger counter. These two counters were arranged in coincidence so that scattered electrons which failed to pass through the central region of the proportional counter were not recorded. The pulse height distribution from the proportional counter was recorded by the Wilkinson pulse height circuit for 9000 electrons. From the histogram, a distribution function was obtained which is shown in fig. 2 together with the Landau curve for comparison, where Δ , Δ_0 and ξ are defined in § 4. The experimental distribution is broader than the Landau curve, an effect which is in agreement with the measurements of Rothwell (1951).

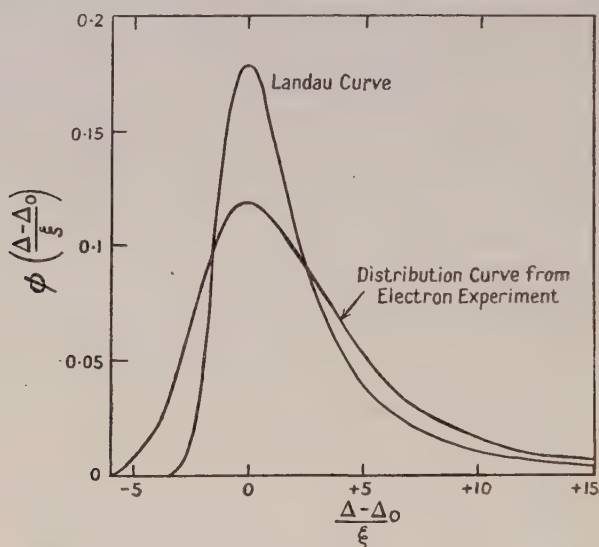


Fig. 2. Comparison of Landau curve with measured fluctuation curve.

§ 3. RESULTS

(i) Method of Analysis

The results obtained for the meson component in the two runs were divided into a number of momentum intervals, selected so that within an interval the ionization was little dependent on the momentum, and the number of particles was not too small. The distribution function obtained for electrons was fitted to each of the histograms representing the energy loss distribution for a particular momentum interval, using Behrens method of curve fitting as described recently by Becker *et al.* (1952), and thus obtaining the mode, scale factor and their r.m.s. errors. Examples are shown in fig. 3 of histograms and the fitted distribution functions omitting the tail at large values of energy loss. These histograms are not those used in the curve-fitting process, but show the results grouped into large intervals suitable for display on a diagram. The results obtained in the two meson runs and the electron experiment are given in the table.

In the meson runs (see table) the positively and negatively charged particles are taken together. No significant difference is observed when each charge is considered separately.

The width w at half height of the distribution varies little for different momentum intervals, the mean values being run 1: $w=57 \pm 2\%$; run 2: $w=57 \pm 4\%$; 1.3 Mev/c electrons: $w=59 \pm 2\%$.

The errors associated with the most probable energy loss (last column of table) are errors due to the process of curve-fitting only, and do not include experimental errors. The effect of the experimental errors is negligible when comparing values of the most probable energy loss obtained in either one of the runs, but

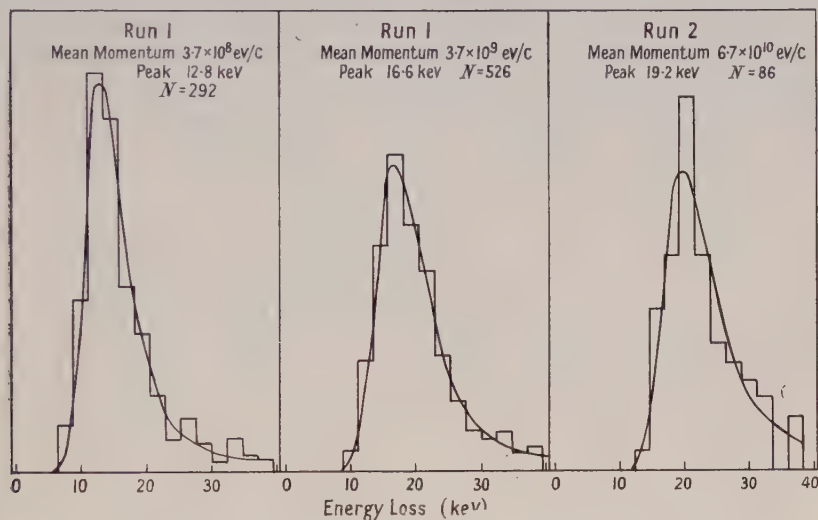


Fig. 3.

	Momentum range (ev/c)	Mean momentum (ev/c)	No. of particles	Most probable energy loss in counter (kev)
Run 1	$> 1.5 \times 10^{10}$	$\sim 3.0 \times 10^{10}$	290	17.7 ± 0.3
	$4.9-15.0 \times 10^9$	7.4×10^9	602	17.1 ± 0.2
	$3.0-4.9 \times 10^9$	3.7×10^9	526	16.6 ± 0.2
	$2.1-3.0 \times 10^9$	2.5×10^9	479	15.8 ± 0.1
	$1.3-2.1 \times 10^9$	1.7×10^9	655	15.4 ± 0.1
	$8.7-13.0 \times 10^8$	1.1×10^9	572	14.2 ± 0.1
	$4.8-8.7 \times 10^8$	6.4×10^8	542	13.8 ± 0.2
	$2.4-4.8 \times 10^8$	3.7×10^8	292	12.8 ± 0.1
Run 2	$> 3.5 \times 10^{10}$	$\sim 6.7 \times 10^{10}$	86	19.2 ± 0.7
	$1.5-3.5 \times 10^{10}$	2.0×10^{10}	160	19.3 ± 0.6
	$8.1-15.0 \times 10^9$	1.0×10^{10}	316	18.1 ± 0.3
	$5.0-8.1 \times 10^9$	5.8×10^9	401	17.4 ± 0.3
	$3.0-5.0 \times 10^9$	3.8×10^9	571	16.5 ± 0.2
	$2.1-3.0 \times 10^9$	2.5×10^9	483	15.6 ± 0.3
	$1.3-2.1 \times 10^9$	1.7×10^9	413	14.9 ± 0.2
Electron				
Run	$1.2-1.4 \times 10^6$	1.3×10^6	9000	12.5 ± 0.1

must be taken into account when comparing the most probable energy loss between meson runs or between a meson run and the electron experiment.

The estimated absolute experimental errors are:

(a) $\pm 6\%$ error in the absolute value of the most probable energy loss affecting the results as a whole.

(b) $\pm 2\%$ error in the energy loss when comparing the two meson runs.

(c) $\pm 4\%$ error in the energy loss between either meson run and the electron experiment.

The meson results are plotted in fig. 4 as a function of momentum, where the errors shown are those due to curve-fitting only.

The results for the meson component given in the table exclude particles deflected away from trays 3 and 4, particles which failed to fire a counter in tray 4, and particles which produced a shower beneath the lead firing two non-adjacent counters or more than two counters in tray 4. These three cases, which contain only a relatively small number of particles, gave no significant results, because the particles could not be identified with certainty.

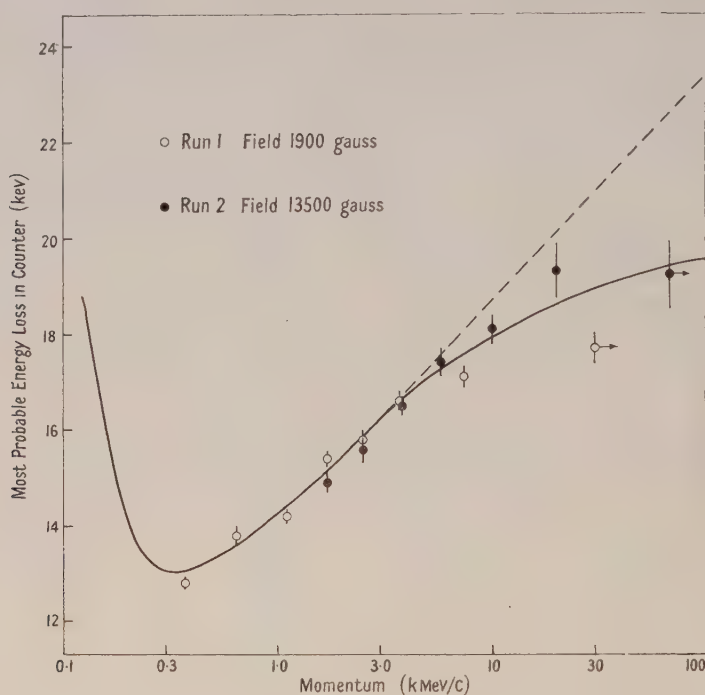


Fig. 4. The most probable energy loss of mesons in argon as a function of momentum. The errors shown are due to curve-fitting only.

(ii) Comparison with Theory

The proportional counter is essentially an instrument which measures the ionization within the gas volume, but since the calibration was carried out using the known energy loss of x-ray photo-electrons, it was considered more satisfactory to treat the measurement as one of energy loss. This entails the assumption that the number of electron volts required to produce one ion-pair in the gas remains constant from x-ray energies to cosmic-ray energies. This assumption has some theoretical justification (Williams 1932).

It was emphasized earlier in the paper that the method of analysis gives the most probable energy loss in the counter. To calculate this quantity it is necessary to use the equation derived by Landau. If Δ is the energy lost by the ionizing

particle in travelling a distance x , and Δ_0 the most probable value, then

$$\Delta_0 = \xi \{ \ln(\xi/\epsilon') + 0.37 \},$$

$$\text{where } \xi = x \frac{2\pi N e^4}{m c^2 \beta^2} \rho \frac{\Sigma Z}{\Sigma A} \quad \text{and} \quad \epsilon' = \frac{I^2(Z)}{2 m c^2 \beta^2} (1 - \beta^2) \exp \beta^2,$$

N is Avogadro's number, e and m the electronic charge and mass, Z and A the atomic number and atomic weight of the medium of density ρ , $\beta = v/c$ where v is the velocity of the ionizing particle and $I(Z)$ the average excitation potential given by Bloch's approximation $I(Z) = 13.5Z$.

From this equation the most probable energy loss was calculated for a number of points over the range of the measurements, and the energy loss-momentum curve obtained. At high values of the momentum, the Landau expression must be modified to allow for polarization effects. These corrections were calculated for the mixture of argon and ethylene using the theory of Halpern and Hall (1948). The continuous curve in fig. 4 shows the modified expression for the most probable energy loss, while the broken portion represents that obtained without taking account of polarization corrections.

The calculated value of the energy loss was on the average 2% lower than that obtained experimentally. This is well within the 6% uncertainty in the absolute value of the experimental results. In order to ascertain the experimental variation in energy loss with momentum, the theoretical curve has been normalized to the meson results.

It can be seen that the points from the two meson runs agree well over the range where the two runs overlap, with the possible exception of the high momentum points in each run. The highest momentum group in each run is unresolved by the spectrometer, this is indicated by a small horizontal arrow. Since these points are at the limit of resolution of the equipment they contain an appreciable contamination of mesons from the lower adjacent group. This effect lowers the unresolved points, particularly that in run 1, where the contamination from the adjacent group is larger and more effective than in run 2. A calculation shows that the contamination is sufficient to make these points lie below the curve by approximately the amount obtained in the experiment.

Despite the large errors of the points above 10^{10} ev/c the results indicate a polarization effect of the same order as that calculated by Halpern and Hall (1948).

§ 4. CONCLUSION

The results obtained in this experiment show that within the limit of theoretical and experimental uncertainty the absolute value and variation with momentum of energy loss of mesons in argon agree with the theoretical calculations over the momentum range 10^8 to 10^{10} ev/c. These results agree well with the measurements of Ghosh, Jones and Wilson, and Becker *et al.*, and do not confirm the report of a preliminary experiment performed in this laboratory.

ACKNOWLEDGMENTS

The authors wish to thank Professor L. H. Martin for his continued interest in the project, Associate Professor C. B. O. Mohr for his helpful discussion and Mr. J. R. Moroney for his assistance with the measurement. The construction and operation of the equipment was made possible by a grant from the Commonwealth Scientific and Industrial Research Organisation.

REFERENCES

- BECKER, J., CHANSON, P., NAGEOTTE, E., TRIELLE, P., PRICE, B. T., and ROTHWELL, P., 1952, *Proc. Phys. Soc. A*, **65**, 437.
- BETHE, H. A., 1930, *Ann. Phys., Lpz.*, **5**, 325.
- BOHR, N., 1915, *Phil. Mag.*, **30**, 581.
- CARO, D. E., PARRY, J. K., and RATHGEBER, H. D., 1951, *Aust. J. Sci. Res.*, **4**, 16.
- CARTER, R. S., and WHITTEMORE, W. L., 1952, *Phys. Rev.*, **87**, 494.
- GHOSH, S. K., JONES, G. M. D. B., and WILSON, J. G., 1952, *Proc. Phys. Soc. A*, **65**, 68.
- GOODMAN, P., NICHOLSON, K. P., and RATHGEBER, H. D., 1951, *Proc. Phys. Soc. A*, **64**, 96.
- HALPERN, O., and HALL, H., 1948, *Phys. Rev.*, **73**, 477.
- KUPPERIAN, J. E., and PALMATIER, E. D., 1952, *Phys. Rev.*, **85**, 1043.
- LANDAU, L., 1944, *J. Phys. USSR*, **8**, 201.
- MYLROI, M. G., and WILSON, J. G., 1951, *Proc. Phys. Soc. A*, **64**, 404.
- ROTHWELL, P., 1951, *Proc. Phys. Soc. B*, **64**, 911.
- WILKINSON, D. H., 1950, *Proc. Camb. Phil. Soc.*, **46**, 508.
- WILLIAMS, E. J., 1932, *Proc. Roy. Soc. A*, **135**, 108.

The Lateral Structure of Cosmic Ray Extensive Air Showers at Sea Level

BY S. R. HADDARA* AND D. JAKEMAN†

The Physical Laboratories, The University, Manchester

Communicated by J. G. Wilson; MS. received 16th October 1952

Abstract. The axes or cores of extensive air showers have been selected by observing in a cloud chamber cascade showers produced by a single high-energy ($> 5 \times 10^9$ ev) electron or photon, and an upper limit of 5 m for the spread of such particles has been found. By placing trays of hodoscoped counters at various distances from this core selector it has been possible to determine the relation between density of ionizing particles and distance from the axis for showers of approximately 10^4 – 10^5 particles. The experimental arrangement and method of analysis used have certain advantages over those employed by other workers. It is concluded that although the results of the present experiment and those of other workers are consistent with the Molière structure function, not too much weight should be placed on this agreement.

§ 1. INTRODUCTION

THE lateral development of an extensive air shower is determined by the mechanism of growth of the shower; it is important because a study of it is expected to give information about the processes through which the shower has grown, and because a knowledge of the lateral structure is necessary if the size and energy of the shower, important with particular reference to the energy spectrum of cosmic-ray primaries in the high energy region, are to be determined. The relation between density of ionizing shower particles and distance measured from the axis of the shower is described as the 'lateral structure function'. This has been derived theoretically for showers developing through the atmosphere from a single primary electron or photon, by Molière (1946) for the parts of the shower near maximum development and more recently by Nishimura and Kamata (1951) at two different stages of shower growth.

Experiments at high altitude, by Williams (1948) using ion chambers, and by Cocconi, Tongiorgi and Greisen (1949) using Geiger counters, have shown close agreement with the calculations of Molière, although Blatt (1949), using Williams' data, and Hazen (1952), who uses a cloud chamber, both conclude that the structure within a metre or so of the shower axis is flatter than predicted. Recent experiments at sea level by Campbell and Prescott (1952) using ion chambers with small separations also support this latter conclusion.

It seemed of interest to make structure measurements over large distances upon the relatively older showers which reach sea level, and to test a procedure which appears to be a decided improvement upon that developed by Cocconi

* Now at the Fouad I University, Cairo, Egypt. † Now at the National Research Council, Ottawa, Canada.

and his colleagues. The examination of the lateral structure is greatly helped if the shower axis can be located with confidence, and the design of an efficient 'core selector' is an important step in the investigation of shower structure. The selector used in our work appears to have great advantages compared with those used by other workers.

When the shower axis is determined, the structure function follows immediately from density measurements at a series of distances from it. However, the measurements of local density are not straightforward, and even in the elaborate arrangement used by Cocconi, in which 27 independently recorded counters were used at each point, the density at a point could only be determined to a factor of two in favourable cases. We have made no attempt to measure the densities of individual showers, and instead make use of a procedure which allows the data from all recorded showers to be analysed as a whole.

§ 2. THE DETERMINATION OF SHOWER CORES

(i) *General Discussion*

We define the axis of an extensive shower as the line of motion of the primary producing it, and for a pure cascade developing from a single electron or photon there is a high density of particles near to the axis which falls off continuously with increasing distance. It is the region of high density in the immediate neighbourhood of the shower axis which has come to be called the 'core' of the shower.

It is by no means clear that an actual extensive shower, derived from the decay electrons of neutral mesons formed in the nuclear cascade which is initiated by a cosmic-ray primary, will have such a well-defined core. Indeed, it might be expected that several cores, defined by the direction of individual neutral mesons of high energy, would occur. The treatment of nuclear interaction by Lewis, Oppenheimer and Wouthuysen (1948) suggests this conclusion, but a qualitative model due to Bethe (1949) is consistent with an extremely close superposition of the subsidiary cores to be expected in the process. The evidence of experiments by Williams (1948) and Cocconi *et al.* (1949) all support the existence of a single core from which the particle density falls away smoothly with increasing distance.

(ii) *Methods of Selection*

Ise and Fretter (1949) and Milone, Tamburino and Villari (1950) have calculated how given close arrangements of unshielded counters in coincidence respond with regard to the position of a shower axis, and conclude that most of the recorded showers have axes close to the selecting apparatus. Milone *et al.* estimated that 80% of showers recorded at sea level have axes within 10 metres of the selector, but Singer (1951) has shown that this result arises on account of the numerous small showers which only have appreciable probability of operating the selector when their axes fall in the region immediately surrounding this selector. If, however, additional counters are placed some distance away, supposedly to investigate the properties of showers away from the core, it must be remembered that the 20% of showers having their axes at greater than 10 metres from the selector have a very much greater probability of discharging these additional counters than the remaining 80%. The bias which the additional counters introduce depends on many factors, and great care has to be

taken in the analysis of experiments of this kind. For this reason the curve of Milone *et al.* relating the density of electrons at a detector distant from a group of unshielded counters is not simply related to the structure function.

It can be shown, assuming that all showers have a similar structure, that the efficacy of core selection of a system of unshielded counters is independent of the size of counters used: high density at a point in general indicates a large shower, and not the immediate neighbourhood of a shower core. Thus coincidences between a number of small counters, large bursts in ion chambers, heavy ionization in proportional counters, large numbers of particles in a cloud chamber and so on, do not indicate the proximity of a shower core, as has sometimes been supposed.

A characteristic of cascade development is that high energy electrons and photons show less lateral spread than those of lower energy. This is the principle of the core selectors first used by Cocconi and his co-workers and by the present authors. In showers from an electron or photon primary, cascade theory indicates that electrons of energy 5×10^9 eV will have a root mean square spread from the axis, at sea level, of about 1.5 metres, while the spread of photons of the same energy will not be larger. The spread of these energetic electrons and photons will depend to some extent on the age of the shower (Eyges and Fernbach 1951), but the changes in spread are not large.

In actual extensive showers the distribution of energetic electrons and photons will clearly be more complicated. But the details of development of the nuclear cascade and the numbers, height of formation and geometry of projection of the neutral mesons through which the shower is born are all too little understood for any estimate of the modification of structure to be of value at the moment. The results of the experiments will allow some conclusions on the actual spread of energetic electrons to be made.

To detect energetic electrons and photons, Cocconi *et al.* (1949) used the fivefold coincidence of four counters under 9 cm of lead with a single unshielded counter a small distance away, the latter counter ensuring that the selected events were associated with extensive showers. A single incident electron would on average require an energy of at least 6×10^9 eV to discharge all four shielded counters. However, it is clear that this device can be triggered by other phenomena not necessarily associated with a shower core. For example, the four counters could be discharged by particles not all belonging to the same cascade, consequently some of the recorded events may arise from a high density of relatively low energy particles. Further, many workers have shown the presence of penetrating particles in extensive air showers, and a high density of these could discharge the selector. Finally, nuclear interacting particles associated with showers may produce an interaction in the shielding above the counters, which would then be discharged. Greisen (private communication) has pointed out that for small thicknesses of lead above the selector events produced by a high density of relatively low energy particles will predominate, whilst for large thicknesses events produced by penetrating particles will predominate. Consequently, an intermediate thickness of 9 cm of lead is such that events produced by incident high energy electrons or photons might be expected to predominate.

Anticipating the operation of the selector by such processes, Cocconi *et al.* argued from a measured decoherence curve that most of the events arose from particles situated within a few metres of the core. However, for the largest

showers recorded, the results certainly indicate that the core selection was relatively poor, and it appears likely that in such showers high energy electrons will not be the predominant factors discharging the counters. In analysing the results for trays placed at large distances from the core selector it is these large showers which have the greatest influence, and consequently some systematic error is introduced into the experiment. It is extremely difficult to determine how large this error is, and consequently how reliable is the structure function given by Cocconi *et al.* It is suggested that the errors given by these authors could be considerably underestimated.

In the present work high energy electrons and photons are recognized by the characteristic cascades emerging from a 5 cm lead shield placed immediately over a cloud chamber. A cascade of nine or more electrons diverging from a point at the lower surface of the lead is taken to establish the entry into the lead of an electron or photon of energy 5×10^9 ev (or greater), which, according to cascade theory, would have a root mean square spread of 1.5 metres (or less) at sea level from the axis of the extensive air shower. The entry of an electron having energy of 10^9 ev would, on the average, only produce one shower particle in the cloud chamber, and although the fluctuations of this number are considerably larger than that given by a Poisson distribution (Messel 1951), the chance of producing at least nine shower particles is very small. The fluctuations in the size of a cascade produced by a 5×10^9 ev electron, however, are near the minimum and do not differ appreciably from a Poisson distribution.

Using this selector, the presence of a high energy particle incident in the chamber is easily distinguished from a high density of relatively low energy particles since the latter will produce electrons in the chamber which are clearly not associated. A visual inspection of the photographs indicated that this occurred frequently as expected under 5 cm of lead.

There must be a few nuclear interactions occurring near the lower surface of the lead shield which lead to events not readily distinguished from electron cascades in our cloud chamber. The application of a magnetic field would make the identification still more certain, but we consider that our apparatus already selects the products of high energy electrons with great efficiency. Certainly in our selector the relative contribution from nuclear interactions will be less than that in the selector of Cocconi *et al.* since a minimum of nine particles is chosen in our experiment, whereas a minimum of three particles is necessary to discharge their selector, but the number of 5×10^9 ev electrons or photons associated with showers recorded per unit area of selector should be the same in both experiments.

The disadvantage of the present selector is that with the size of chamber used the rate of observed 'cores' was approximately one per two days, and the collection of data was very slow. With much larger cloud chambers such a core selector could be used very effectively.

§ 3. EXPERIMENTAL ARRANGEMENT AND RESULTS

The experiment was performed at Manchester, 50 metres above sea level, and the showers analysed here were recorded during the summer of 1950.

The cloud chamber, 27 cm diameter and 13 cm deep, closely shielded by 5 cm of lead and placed with the cylindrical axis horizontal, was placed symmetrically, as shown in fig. 1, with respect to the counter array. For the present purpose this array consists of four pairs of counter trays on opposite

sides of the cloud chamber at distances 2.5 m, 11 m, 23 m, and 44 m respectively. The basic composition of each counter tray was of ten 220 cm² counters and one 10 cm² counter, but variations from this composition for certain trays were made for part of the work in the manner indicated in table 1. Events were selected by coincidence combinations from the two trays located 2.5 m from the cloud chamber, and for selected events the behaviour of every counter of the whole array was recorded. This paper discusses those events for which the incidence of an electron or photon of high energy in the cloud chamber, triggered by the counter coincidences, was indicated in the manner already described.

Thirty-six showers were recorded which were accompanied by a cascade of nine or more particles proceeding from the lower surface of the lead shield which covered the cloud chamber, and the counter discharges in these events are given in table 1. Each row refers to one of the recorded showers. The columns headed by L refer to the counters of area 220 cm² and those headed by M to counters of area 30 cm². An italic figure indicates that the small counter associated with a particular counter tray was discharged.

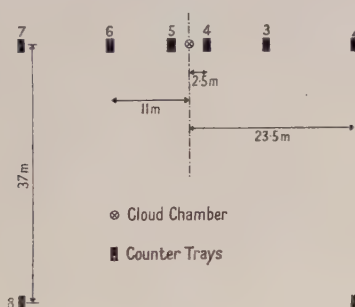


Fig. 1. Experimental arrangement showing position of the counter trays and location of the cloud chamber.

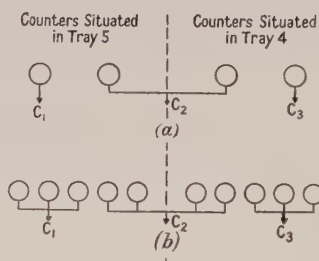


Fig. 2. Counters connected to the three channels C_1 , C_2 , C_3 of coincidence circuit. (a) 1st series; (b) 2nd series.

The data given in this table are clearly very limited, and more extensive material would be valuable, but there is already information which suffices to exhibit the method of treatment of data.

As far as may be judged by inspection, the recorded showers show the expected features, maximum density at the counter units nearest to the core-detecting cloud chamber and a continuous fall of density to the more distant counter arrays. An interesting feature is that the largest showers recorded still have their maximum density near to the core selector, and this we believe indicates an improvement over previous selectors. Only for three records out of thirty-six does inspection suggest that the shower core in fact fell nearer to any counter arrays other than those adjacent to the chamber, and these examples can readily be attributed to the fluctuations inherent in the operation of arrays of relatively small numbers of counters. We discuss information about the shower structure in the first place using the assumption that the shower core is strictly located at the cloud chamber, and we afterwards consider the effect of displacement of the shower core from this central point.

Table 1. Counter discharges in 36 showers for which an electron or photon of high energy was detected at the cloud chamber

		1st Series							
Distance of unit from cloud chamber (m)		44	23	11	2.5	2.5	11	23	44
		L	L	L	L	L	L	L	L
Composition of unit		10	10	10	10	10	10	10	10
		6	8	10	10	10	10	9	5
		1	8	10	10	10	10	9	3
		1	1	1	5	7	3	—	—
		3	7	9	10	10	8	2	4
		1	7	10	10	10	10	7	1
		3	6	10	10	9	9	6	4
		2	5	10	10	10	10	7	3
		—	7	10	10	9	6	7	3
		6	8	8	10	10	10	10	8
Number of counters discharged at each unit for each of the recorded showers		2	2	5	9	10	8	8	2
		1	—	4	10	7	2	—	—
		1	5	9	10	8	4	4	—
		—	8	10	9	10	7	1	—
		5	9	10	10	10	10	8	8
		1	6	10	10	10	9	4	—
		4	4	3	5	7	6	7	—
		—	1	4	9	10	4	3	—
		—	2	9	10	10	9	3	2
		10	9	10	10	10	10	10	10
		2nd Series							
Distance of unit from cloud chamber (m)		44	23	11	2.5	2.5	11	23	47
		L	L	L M	L M	L M	L M	L	L
Composition of unit		10	10	7 3	6 3	6 3	7 3	10	10
		—	—	1 —	2 —	1 1	— —	1	—
		7	10	7 2	6 3	6 3	7 3	9	4
		—	2	2 —	6 —	4 —	1 —	—	—
		7	4	4 —	4 1	5 —	6 —	8	10
		3	3	5 1	5 1	5 2	5 —	6	1
		1	1	2 —	2 1	3 —	4 —	3	—
		5	10	6 2	6 3	6 1	6 —	9	1
		1	2	4 —	5 2	6 1	2 —	4	—
		—	2	5 1	5 2	6 2	7 1	9	3
Number of counters discharged at each unit for each of the recorded showers		1	1	3 —	5 1	6 2	4 —	3	—
		3	5	3 1	5 1	5 1	7 —	7	6
		2	1	1 —	4 —	4 —	3 —	—	—
		—	—	2 —	4 —	2 2	7 1	6	—
		1	3	6 1	6 1	6 1	1 —	2	1
		6	9	6 1	6 3	6 3	7 1	5	6
		1	—	1 1	2 —	2 —	— —	—	—
		6	7	7 1	4 2	5 1	4 —	2	—

§ 4. DETERMINATION OF LATERAL STRUCTURE

The data in table 1 refer to showers which we now assume to have axes reaching the surface at the point occupied by our cloud chamber. They are showers selected by the particular counter arrays indicated in fig. 2, and hence are of a range of sizes which are characteristic of these counter arrays and of the unselected size spectrum of showers incident upon the apparatus.

We write the size spectrum of *selected* showers $F(N) dN$, and then the density spectrum of the selected showers at a tray distant r from the shower axis is

$$\frac{1}{f(r)} F[\rho/f(r)] d\rho, \quad \dots\dots(1)$$

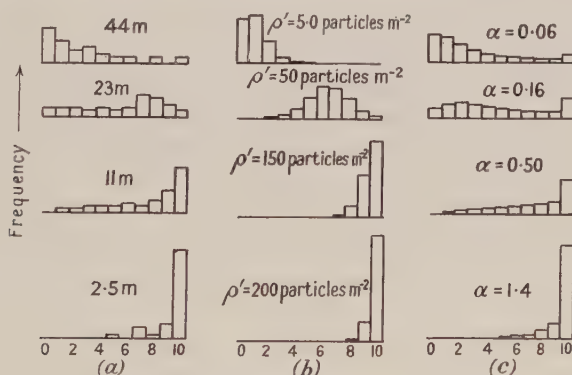
where $f(r)$ is the lateral structure function, assumed the same for all selected showers.

The frequency of showers discharging n out of 10 counters of area A at a given point (we refer here particularly to the first series of results and neglect the discharges of the small counters of area 10 cm^2) is therefore

$$R(n, 10) = \text{const. } {}^nC_{10} \int_0^\infty [1 - \exp(-A\rho)]^n \exp[-(10-n)A\rho] F\left(\frac{\rho}{\alpha}\right) d\rho \quad \dots\dots(2)$$

where α is a parameter depending only on the distance of the counter tray considered from the shower axis. If the size distribution F of showers is known, the frequency R for various n can be computed as a function of α , and the value of α determined for each counter tray from which the computed values of R , for $0 \leq n \leq 10$, best fit the observed distributions summed over all showers. The method adopted for determining the best fit is essentially a least squares method, and for problems of this type has been discussed by Broadbent, Kellermann and Hakeem (1950). These authors indicate how the standard deviation of the parameter giving the best fit can be found, and also give the criteria for a good or bad fit.

The function F is not, in fact, known; since very small showers have a vanishingly small probability of detection by the selecting array, while large showers are absolutely rare, it clearly has some maximum value corresponding to a most probable shower size which is selected. As a first approximation the function F may be assumed single-valued at this optimum shower size. In fig. 3(a) the



Figures refer to number of counters discharged
Frequency scale \square equals one event

Fig. 3. (a) Observed distribution.
(b) Calculated distribution for a single density ρ' at each tray.
(c) Calculated distribution for a spectrum of densities at each tray.

observed distribution of $R(n, 10)$ for trays at four distances from the core selecting chamber in the first series showers is shown, and in fig. 3(b) the calculated distribution making this approximation of constant shower size is shown for the value of size yielding the best fit. The fit is not a good one.

A more realistic approximation to F can readily be made, and within reasonable limits the result is not sensitive to the assumed form. We have used the form

$$F(\rho) = [1 - \exp(-2A\rho)][1 - \exp(A\rho)]^2 [1 - \exp(-\delta A\rho)] \rho^{-\gamma+1} \dots\dots (3)$$

with $\delta = 0.012$ and $\gamma = 1.5$. With this form of the selected incident shower spectrum a good fit with the observed frequencies $R(n, 10)$ is attained as shown in fig. 3 (c), and the values of α for best fit are given in table 2.

Table 2. First Series: α as a function of r (m)

r	2.5	11	23	44
α	1.42 ± 0.31	0.53 ± 0.15	0.16 ± 0.06	0.059 ± 0.021

The quantity α is proportional to $f(r)$, the lateral structure function, at each point of observation; over the restricted range of the experiment we write

$$f(r) = \text{const. } r^{-n} \dots\dots (4)$$

and for the data of table 2, $n = 1.09 \pm 0.16$.

The treatment of data of the second series is basically similar to that of the first, but since in some of the trays not all the counters have equal areas, expressions for the rates of different types of possible events are more complicated than those given by eqn. (2) for the first series. To ease the analysis of the data, counters of a particular area were considered as a single counter having an area equal to the sum of the individual areas; thus we are no longer interested in how many of the large counters are discharged but only in whether at least one is discharged or none.

Using the spectrum of density given by (3), a good fit between experiment and calculation was found for values of α given in table 3.

Table 3. Second Series: α as a function of r (m)

r	2.5	11	23	44
α	0.71 ± 0.15	0.23 ± 0.056	0.092 ± 0.030	0.021 ± 0.007

These values are about half the values of those obtained in the first series; this indicates that the sizes of shower in each of the two series differ by this factor and is due to the fact that more low density showers were recorded in the second series because of the larger areas used in the selection trays. It is emphasized that the fact that the same form for $F(\rho)$ gave agreement in both series arises from the poor statistics and that, if the data were extended, different forms for $F(\rho)$ would have had to be used in the two series.

Again the values of α are proportional for $f(r)$, and lead to the expression (4), where $n = 1.14 \pm 0.18$, in agreement with the value obtained previously. Combining the two series we obtain a value of $n = 1.11 \pm 0.12$, where the uncertainty is the statistical one due to the limited amount of data, and does not take account of a possible displacement of the shower axis relative to the cloud chamber.

The existing data are not extensive enough to enable an actual estimate of the average distance of the true shower axis of selected showers from the cloud chamber to be made, but inspection of the data suggests that it cannot be as great as 5 metres. We accordingly calculated as an extreme correction to the result obtained above the value of the structure function which would be obtained if

the shower axis were always 5 metres from the chamber and in a direction to give the maximum effect. These conditions require $n = 1.42 \pm 0.12$, but this figure is certainly an extreme value, and consequently we take the value of $n = 1.2 \pm 0.2$ as indicating the form of the structure function in the region $r = 5$ m to 50 m. Although in fact the axes of the showers are situated over a finite region, it can be shown that the error introduced in assuming a single fixed position is included in the extreme correction. In fig. 4 the derivation of the index of the structure function is shown for what we consider to be the two extreme assumptions, namely an exactly located core at the cloud chamber and a core displaced up to 5 metres: the results of the two series have been combined.

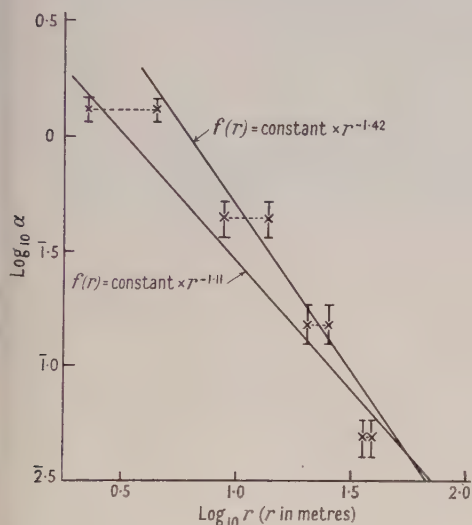


Fig. 4. α as a function of r on a logarithmic scale.

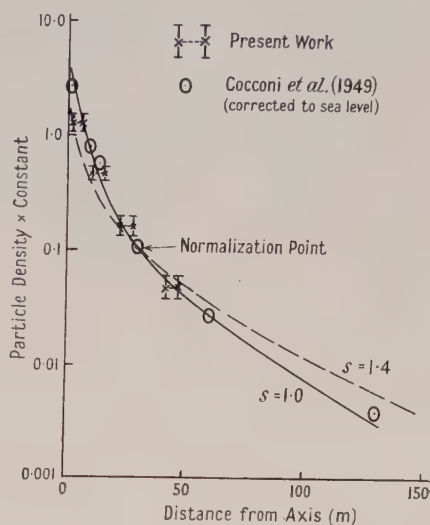


Fig. 5. Experimental and theoretical lateral structure functions at sea level.

§ 5. DISCUSSION

The results of our experiment, together with those of Cocconi *et al.* (1949), are shown in fig. 5, which also shows the theoretical curves (for showers developing from single electrons or photons incident at the top of the atmosphere) of Molière (1946), $s = 1$, and of Nishimura and Kamata (1951), $s = 1.4$. The quantity s is the well-known cascade parameter defined by Rossi and Greisen (1941), and the condition $s = 1$ refers to showers at maximum development, while $s = 1.4$ refers to 'older' showers. Over the distances covered in our work there is no significant difference to be anticipated between $s = 1$ showers and those for which the later value, $s = 1.4$, obtains. The results given by Cocconi and his co-workers appear to follow the curve $s = 1$ rather closely in spite of the fact that for the conditions of these experiments the appropriate value is probably about $s = 1.3$. The uncertainties in this work, however, make any interpretation of this difference of doubtful validity. In particular, the interpretation laid upon their results by Borsellino (1950) that, since they conform more nearly to $s = 1$ than to the anticipated flatter distribution $s = 1.3$, the observed showers cannot arise from a single primary electron does not follow, however likely from other evidence this conclusion may be.

§ 6. CONCLUSIONS

A cloud chamber core selector has been used and an upper limit of 5 metres is found for the spread of electrons or photons of energy greater than 5×10^9 ev in the air showers to which the apparatus responds. The lateral structure function is obtained by placing Geiger counters at different distances from the selector, and it is shown to be of the form $f(r) = \text{const. } r^{-n}$, where $n = 1.2 \pm 0.2$ for the region $r = 5$ m to 50 m. A comparison of the results with the theoretical curves of Molière, and Nishimura and Kamata indicate agreement subject to the large statistical errors. However, it is concluded that this agreement and the agreement which Cocconi *et al.* obtained should not be given too much weight and provide little information on the processes of development of an extensive air shower.

ACKNOWLEDGMENTS

The authors are greatly indebted to Professor P. M. S. Blackett for his encouragement and for providing facilities for this research. They wish to express their gratitude to Dr. J. G. Wilson for valuable criticisms during the course of the experiment. In particular the authors wish to acknowledge the guidance received from Mr. D. Broadbent, with whom they have had many valuable discussions.

One of us (D. J.) wishes to acknowledge grants from the Department of Scientific and Industrial Research (1948–49) and the Ministry of Education (1949–51) whilst this research was in progress.

REFERENCES

- BETHE, H. A., 1949, *Echo Lake Symposium*.
 BLATT, J. M., 1949, *Phys. Rev.*, **75**, 1584.
 BORSELLINO, A., 1950, *Nuovo Cim.*, **7**, 638.
 BROADBENT, D., KELLERMANN, E. W., and HAKEEM, M. A., 1950, *Proc. Phys. Soc. A*, **63**, 864.
 CAMPBELL, I. D., and PRESCOTT, J. R., 1952, *Proc. Phys. Soc. A*, **65**, 258.
 COCCONI, G., TONGIORGI, V. T., and GREISEN, K., 1949, *Phys. Rev.*, **76**, 1020.
 EYGES, L., and FERNBACH, S., 1951, *Phys. Rev.*, **82**, 23.
 HAZEN, W. E., 1952, *Phys. Rev.*, **85**, 455.
 ISE, J., and FRETTER, W. B., 1949, *Phys. Rev.*, **76**, 933.
 LEWIS, H. W., OPPENHEIMER, J. R., and WOUTHUYSEN, S. A., 1948, *Phys. Rev.*, **73**, 127.
 MESSEL, H., 1951, *Proc. Phys. Soc. A*, **64**, 807.
 MILONE, C., TAMBURINO, S., and VILLARI, G., 1950, *Nuovo Cim.*, **7**, 207.
 MOLIÈRE, G., 1946, *Cosmic Radiations*, ed. W. Heisenberg (New York: Dover Publications).
 NISHIMURA, J., and KAMATA, K., 1951, *Prog. Theor. Phys.*, **6**, 628.
 ROSSI, B., and GREISEN, K., 1941, *Rev. Mod. Phys.*, **13**, 240.
 SINGER, F., 1951, *Phys. Rev.*, **76**, 701.
 WILLIAMS, R. W., 1948, *Phys. Rev.*, **74**, 1689.

The Thermal Conductivity of Gold at Low Temperatures

By G. K. WHITE

Division of Physics, National Standards Laboratory, Commonwealth Scientific and Industrial Research Organisation, Sydney, Australia

Communicated by G. H. Briggs; MS. received 14th January 1953

Abstract. Measurements of thermal conductivity at temperatures between 2 and 150°K for several specimens of gold of differing physical and chemical purity are reported. A brief description is given of the cryostat and the experimental technique. Below 35°K the total thermal resistance is given approximately by $R = A/T + BT^2$; apparent small departures from this equation are discussed. The experimental values of B lead to a value of $C \simeq 15$ in the equation for the ideal resistance $R_i = R_\infty CN^{2/3}(T/\Theta)^2$. At temperatures above $\Theta/2$ the conductivity is sensibly constant and no minimum is observed.

§ 1. INTRODUCTION

FOR many metallic elements at room temperature the Lorentz number $K/\sigma T$ approximates to a universal constant indicating that heat is conducted in these elements by electrons. It may be inferred that the lattice component of the conduction in such elements is relatively insignificant, partly because of the scattering of the phonons by the conduction electrons. The electron conduction is limited by two major processes: impurity scattering, and scattering due to the thermal vibrations of the lattice. The former arises from small scale lattice defects, strains and impurity atoms which produce a thermal resistance R_0 , and the latter give rise to an 'ideal' resistance R_i .

Wilson (1937) suggested that these resistances should be additive, in which case the total conductivity and total thermal resistance R would be given by

$$1/K = R = R_0 + R_i, \quad \dots\dots (1)$$

where R_0 and the residual electrical resistivity ρ_0 are related by

$$\rho_0/R_0 T = L_0, \text{ the Lorentz number,} \quad \dots\dots (2)$$

$$\text{i.e.} \quad R_0 = A/T.$$

The theories of thermal conductivity of Wilson (1937) and Makinson (1938) indicate that at low temperatures, where $T \ll \Theta$, the ideal resistance R_i is given by

$$R_i = BT^2, \quad \dots\dots (3)$$

$$\text{where} \quad B = C R_\infty N^{2/3}/\Theta^2; \quad \dots\dots (4)$$

N is the number of free electrons per atom and R_∞ is the limiting value of the ideal thermal resistance at high temperatures. Whereas the Wilson-Makinson solution of the transport equation gave a value of 95.3 for the numerical constant C , more recent solutions give values of 71.7 (third approximation by Sondheimer 1950) and 27 (Bremmer 1934).

Recent experiments of Berman and MacDonald (1951, 1952) shed considerable light on the temperature dependence of the thermal conductivity of the monovalent metals copper and sodium, showing, for example, no trace of the minimum in the conductivity at a temperature of about 0.25θ predicted by Makinson.

The results reported in this paper are part of an investigation of monovalent metals designed to give information about the following: (a) the validity of the additive resistance hypothesis expressed in eqn. (1), (b) the strict proportionality of the impurity conductivity K_0 with temperature, (c) the validity of the T^2 law of eqn. (3) for the ideal thermal resistance R_i , (d) the numerical value of C in eqn. (4).

The work of Mendelssohn and Rosenberg (1952), published before the completion of the investigations reported here, indicates the general character of the conductivity of a large number of metals of groups 1, 2 and 3 and the transition elements. Their results for gold taken over a temperature interval up to 20°K agree with our figures on a similar type of specimen.

§ 2. EXPERIMENTAL DETAILS

The thermal conductivity measurements extend over the range from 2° to 150°K using liquid helium and liquid oxygen as the cooling agents. Liquid helium for the cryostat (fig. 1) is produced in a liquefier of the Collins (1947) type constructed in the laboratory.

The brass vessel *a* is maintained at either 4.2 or 90°K according to the range being investigated, and the inner metal shield *b* is temperature controlled by either of two methods. In the ranges 2 to 4.2°K and 55 to 90°K the vapour pressure of liquid in the chamber *C* is controlled by pumping through a simple glass cartesian manostat (Gilmont 1951). Outside these temperature ranges *b* is maintained within 0.01° of any desired temperature by the electrical heater H_1 ; R_1 is a 1000 ohm manganin resistor in one arm of an a.c. bridge, the amplified out-of-balance e.m.f. from which is supplied to the heater H_1 (Wylie 1948).

R_2 is a glass-sheathed platinum resistance thermometer of the coiled filament type (Meyers 1932) attached to the shield *b*.

The thermal conductivity measurements are made with the helium-filled gas thermometers *A* and *B* attached to a differential butyl phthalate manometer (Hulm 1950, Berman 1951). The random experimental error in the conductivity is estimated to be less than 1% .

§ 3. SPECIMENS

Measurements were made on two different samples of gold. The first sample, termed Au1 before and Au2 after annealing, was a 2 mm diameter rod of commercial purity (99.9%) obtained from Messrs. Garrett, Davidson and Matthey of Sydney. Analysis of this sample by the Defence Research Laboratories, Victoria, showed silver to be the major impurity with a trace of platinum and faint traces of iron, lead, copper and tin.

Au3 was a 1.5 mm diameter rod drawn by Garrett, Davidson and Matthey from a 3 mm rod, JM 3226, of purity greater than 99.999% ; spectrographic examination of the 3 mm rod by Johnson Matthey showed lines of silver and

copper, faintly visible lines of cadmium, iron, magnesium and sodium and very faintly visible lines of calcium and zinc.

Au4 was the same high purity rod after annealing. Both Au2 and Au4 were annealed *in vacuo* at 700°C for about 3 hours and cooled slowly to 200°C over a period of 6 hours.

When measurements on the fully annealed rod Au4 were completed it was reduced by drawing from 1.5 mm to 1.3 mm diameter, and its conductivity re-determined in the unannealed state. In this form it is termed Au5.

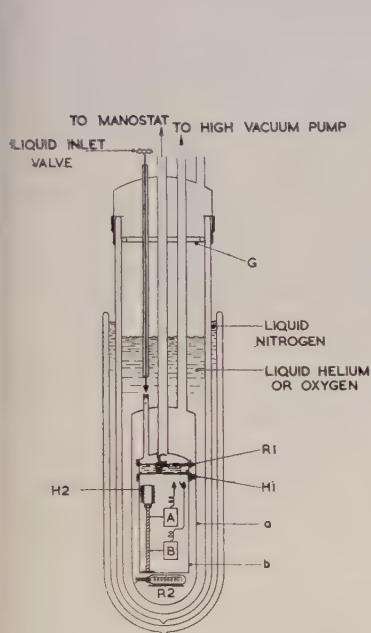
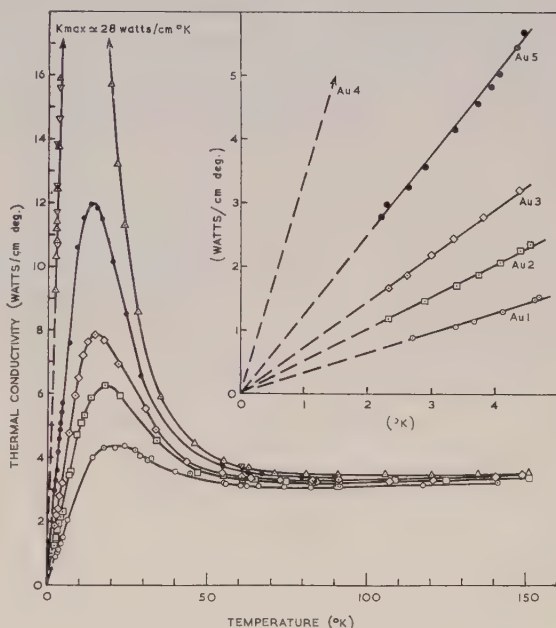


Fig. 1. Cryostat for thermal conductivity measurements.



○	Au1	99.9% purity (unannealed)
□	Au2	99.9% purity (annealed)
◇	Au3	JM 3226 (freshly drawn)
△	Au4	JM 3226 (annealed)
▽	Au4	JM 3226 (annealed) — 2nd RUN
●	Au5	JM 3226 (redrawn)

Fig. 2. Thermal conductivity of gold.

§ 4. RESULTS

The results for the five specimens are shown in figs. 2 and 3, together with calculated curves, which are discussed in § 5.

The results indicate that the conductivity is practically temperature independent above 75°K, and below this temperature it rises to a maximum. As the degree of physical and chemical purity increases from Au1 to Au4, the height of this maximum increases from 4.4 to 28 watts/cm deg and the temperature at which the maximum occurs decreases from 22 to 10°K. At temperatures in the liquid helium range the conductivity varies nearly linearly with temperature; the measurements on Au4 (second set) and Au5 were made specifically to examine whether there is any systematic departure from linearity. The small increase with temperature of the measured conductivities at temperatures above 90°K can probably be ascribed to lack of correction for heat loss by radiation, which may reach 3% at 150°K.

§ 5. DISCUSSION

An analysis of the results shown in figs. 2 and 3 indicates that the relations $1/K = R = R_0 + R_i = A/T + BT^2$ are at least approximately valid below 30°K. Using approximate values of A , deduced from the slopes of the lines shown in the inset of fig. 2, the ideal resistance R_i at, say, 20°K may be calculated, and hence R_0 may be obtained for temperatures in the low temperature region. The figures for R_0 obtained allow us to examine the constancy of $A = R_0T$ and subsequently to calculate more precise values of $R_i = R - R_0$.

5.1 Impurity Thermal Resistance

The initial measurements on Au4 gave the value 0.228 ± 0.004 cm deg² per watt for RT . Further measurements with increased accuracy were made from 2.5 to 5.0°K and the result was 0.232 ± 0.002 cm deg per watt with no apparent systematic variation.

For specimens Au1, Au2, and Au3 the values of R_0T obtained were 3.08, 1.93 and 1.35 respectively. In each of these an increase in R_0T of approximately 3% was observed as the temperature fell from about 4.5 to 2°K. This increase appeared to lie outside the range of experimental error.

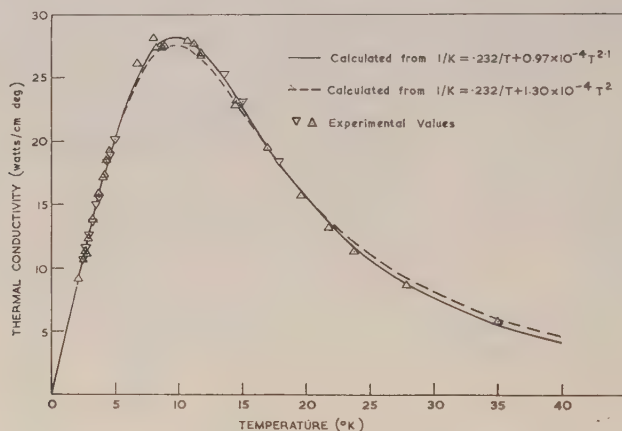


Fig. 3. Thermal conductivity of Au4.

The fully annealed sample Au4 was redrawn to become Au5, and observations of higher accuracy were made in the low temperature region. The redrawn rod, however, has a physical impurity content less than Au3 and its conductivity shown in fig. 2 lies between Au3 and Au4. For Au5 R_0T is 0.792 ± 0.010 , with no apparent systematic deviation from constancy, indicating that any such deviation which might be related to changing residual electrical resistance appears at temperatures below 2°K.

5.2 Ideal Thermal Resistance

Since it has been shown, particularly for Au4, that the variation in R_0T is small, the ideal resistance has been calculated for each specimen by assuming that it is equal to $(RT - A)/T$.

The logarithmic plot of the ideal resistance for Au4 (fig. 4) indicates that R_i is proportional to T^n , where n is equal to 2.1 in the range 5 to 30°K, i.e. from the lowest temperature for which an accurate estimate of R_i is available up to $T \simeq \Theta/5$. Curves for the total conductivity are shown in fig. 3 for $n=2.1$ and $n=2.0$, assuming $A=0.232$ and using values for B from the experimental data at 18°K. The logarithmic plot indicates that $n=2.1$ fits the observations better than $n=2.0$.

Figure 4 shows the ideal resistance of Au1, Au2, Au3 and Au4 against temperature. Logarithmic plots for the latter three specimens do not give a uniform power n over such a wide temperature range as for the pure annealed Au4, presumably because below 15°K uncertainty in the larger impurity resistance affects the accuracy of R_i .

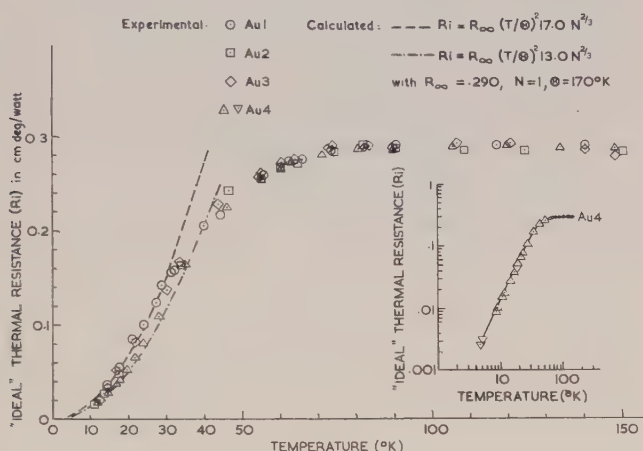


Fig. 4. 'Ideal' thermal resistance $R_i = R - R_0$ as a function of temperature. Inset shows logarithmic graph of R_i against temperature for Au4 (pure annealed gold).

The most significant points that emerge from fig. 4 are the following:

- (i) The ideal resistances R_i for specimens Au1, Au2 and Au3 lie on a common curve.
- (ii) For $T < 30^\circ\text{K}$ this curve follows an equation of the form $R_i = BT^2$.
- (iii) R_i approaches a constant value at a temperature $T \simeq \Theta/2$, and there appears no evidence of any distinct maximum in the resistance corresponding to the minimum in the conductivity predicted by Makinson (1938).
- (iv) Specimen Au4 has values of R_i which, over the range 10 to 30°K, are about 20% lower than those for the less chemically and/or physically pure specimens. This suggests that the additive resistance law of eqn. (1) is not strictly valid.
- (v) Values of C were calculated from eqn. (4), taking R_∞ from fig. 4 to be 0.290 cm deg/watt, $N=1$ electron per atom and $\Theta=170^\circ\text{K}$. From the specific heat data of Clusius and Harteck (1928) and the electrical resistance measurements of de Haas and Van den Berg (1936) it is concluded that Θ lies between 163 and 180°K. We obtain $C=13.0$ for Au4 and $C=17.0$ for Au1, Au2, Au3. The maximum error arising from uncertainty in N and Θ is estimated to be not more than 20%.

ACKNOWLEDGMENTS

The author wishes to thank Dr. G. H. Briggs and Mr. A. F. A. Harper for their interest and encouragement. He is indebted also to Mr. W. R. G. Kemp and his assistants, who produced liquid helium for these experiments, and to Dr. P. G. Klemens for many valuable suggestions and discussions.

REFERENCES

- BERMAN, R., 1951, *Proc. Roy. Soc. A*, **208**, 90.
BERMAN, R., and MACDONALD, D. K. C., 1951, *Proc. Roy. Soc. A*, **209**, 368; 1952, *Ibid.*, **211**, 122.
BREMMEER, H., 1934, *Thesis*, University of Leiden.
CLUSIUS, K., and HARTECK, P., 1928, *Z. Phys. Chem.*, **134**, 243.
COLLINS, S. C., 1947, *Rev. Sci. Instrum.*, **18**, 157.
GILMONT, R., 1951, *Analyt. Chem.*, **23**, 157.
DE HAAS, W. J., and VAN DEN BERG, G. J., 1936, *Physica*, **3**, 440.
HULM, J. K., 1950, *Proc. Roy. Soc. A*, **204**, 98.
MAKINSON, R. E. B., 1938, *Proc. Camb. Phil. Soc.*, **34**, 474.
MENDELSSOHN, K., and ROSENBERG, H. M., 1952, *Proc. Phys. Soc. A*, **65**, 385, 388.
MEYERS, C. H., 1932, *Bur. Stand. J. Res., Wash.*, **9**, 807.
SONDHEIMER, E. H., 1950, *Proc. Roy. Soc. A*, **203**, 75.
WILSON, A. H., 1937, *Proc. Camb. Phil. Soc.*, **33**, 371.
WYLIE, R. G., 1948, *C.S.I.R.O. Division of Physics Report*, PA-2.

An Investigation of (d, p) Stripping Reactions IV : Results for ^{40}Ca and ^{88}Sr

By J. R. HOLT AND T. N. MARSHAM

Nuclear Physics Research Laboratory, University of Liverpool

Communicated by H. W. B. Skinner; MS. received 12th February 1953

Abstract. Angular distributions have been measured of some of the proton groups emitted from targets of natural calcium and strontium under bombardment by 8 mev deuterons. The theory of the stripping process has been used to enable assignments of spin and parity to be made to the corresponding states of ^{41}Ca and ^{89}Sr . The first and second excited states of ^{41}Ca are thought to be states of single-particle excitation of the odd neutron. In the following list the excitation energies in mev are accompanied by the shell model term or the possible spin values and the parity in brackets :

^{41}Ca : ground state ($1f_{7/2}$), 1.90 ($2p_{3/2}$), 2.42 ($2p_{1/2}$), 3.96 ($5/2, 3/2+$), 4.76 ($5/2, 3/2+$), 5.72 ($5/2, 3/2+$).

^{89}Sr : ground state ($9/2, 7/2+$), 1.07 ($7/2, 5/2-$).

The Q -value of the transition to the ground state of ^{89}Sr is 4.18 ± 0.08 mev, and this nucleus has excited states at 1.07 ± 0.08 , 2.09 ± 0.08 , 2.66 ± 0.08 , 4.73 ± 0.1 and 5.46 ± 0.08 mev.

§ 1. INTRODUCTION

THE methods of the previous papers of this series (Holt and Marsham 1953 a, b, c, to be referred to as I, II, III respectively) have been applied to the nuclei ^{40}Ca and ^{88}Sr . Range spectra of emitted protons and angular distributions of certain of the proton groups have been measured when the nuclei were bombarded with 8 mev deuterons. These nuclei were chosen for reasons similar to those which governed the choice of ^{28}Si and ^{32}S . Both nuclei have zero spin, which limits the ambiguity in the assignment of the spins of the resultant nuclear states. Both have closed neutron shells, and ^{40}Ca has a closed proton shell while ^{88}Sr has a closed proton sub-shell. Such target nuclei should be favourable to the identification of states of single-particle excitation of the odd neutron added in the (d, p) stripping process (III).

The range spectrum of the reaction $^{40}\text{Ca}(d, p)^{41}\text{Ca}$ has previously been investigated by Sailor (1949) using 3.9 mev deuterons. A magnetic analysis of the reaction $^{88}\text{Sr}(d, p)^{89}\text{Sr}$ with 10 mev deuterons has been reported by McFarland and Shull (1953).

§ 2. TARGET PREPARATION

A small piece of calcium metal containing the natural proportion 96.96% of ^{40}Ca was beaten out into a thin flake having an area of about 0.3 cm^2 and a mass of about 0.6 mg. This was held at one corner by a clip and suspended at the centre of the target chamber. There was some surface oxidation, but this did not interfere seriously with the measurements.

The target of strontium was prepared in a similar way except that it had to be kept wetted with mineral oil during the beating process to prevent excessive oxidation. The oil was removed with benzene just before the target was inserted into the chamber. The target had a thickness of about 6 mg cm^{-2} and contained

the natural mixture of mass numbers 88, 87, 86 and 84 in the proportions 82.6:7.0:9.9:0.6. Oxygen and carbon were present as contaminants.

§ 3. RESULTS

Spectra of Proton Ranges

The differential range spectrum of the protons from the calcium target is shown in fig. 1 for an angle of observation of 26° . The energy of the bombarding deuterons was 8.13 mev and was derived from the range and known Q -value of the proton group corresponding to the formation of the ground state of ^{17}O . The lines marked O and C in fig. 1 indicate the positions of the groups due to oxygen

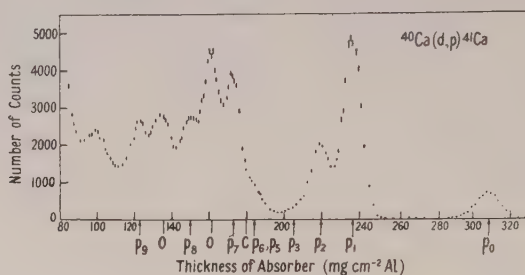


Fig. 1. Range spectrum of protons at an angle of observation of 26° from the deuteron bombardment of a target of calcium.

and carbon. The arrows indicate the estimated mean ranges of the groups attributed to calcium. The Q -value of the transition to the ground state of ^{41}Ca was found to be 6.14 ± 0.05 mev, in good agreement with Sailor's value of 6.17 ± 0.05 mev. In the table are given our values for the energies of the excited

$^{40}\text{Ca}(d, p)^{41}\text{Ca}$								
(1)	(2)	(3)	(4)	(5)	(6)	(7)	(8)	(9)
p_0	0	0	3	$7/2, 5/2-$	3.8×10^{-27}	25	3.1 ± 0.3	$1f_{7/2}$
p_1	1.9 ± 0.05	1.95 ± 0.07	1	$3/2, 1/2-$	2.3×10^{-26}	14	3.5 ± 0.3	$2p_{3/2}$
p_2	2.42 ± 0.05	2.41 ± 0.07	1	$3/2, 1/2-$	1.0×10^{-26}	5.3	2.6 ± 0.2	$2p_{1/2}$
p_3	2.9 ± 0.1	3.0 ± 0.1						
p_4		3.3 ± 0.1						
p_5	3.6 ± 0.1	3.5 ± 0.1						
p_6		3.7 ± 0.1						
p_7	3.96 ± 0.05	3.86 ± 0.07	2	$5/2, 3/2+$	6.0×10^{-27}	8.8	1.5 ± 0.7 or 2.2 ± 1.0	
p_8	4.76 ± 0.08		2	$5/2, 3/2+$	7.2×10^{-27}	8.4	1.4 ± 0.3 or 2.1 ± 0.4	
p_9	5.72 ± 0.08		2	$5/2, 3/2+$	7.8×10^{-27}	6.9	1.1 ± 0.2 or 1.7 ± 0.3	

(1) Proton group; (2) excitation energy (mev), present work; (3) excitation energy (mev), Sailor; (4) l -value; (5) spin and parity; (6) maximum differential cross section (cm^2) ($\pm 20\%$); (7) neutron capture probability (arbitrary units); (8) $(N.C.P.)/(2j_f + 1)$; (9) suggested shell model term.

states of ^{41}Ca , together with those obtained by Sailor. We find no definite evidence for the state of ^{41}Ca at 3.3 mev. The groups labelled p_8 and p_9 in fig. 1 correspond to states at 4.76 and 5.72 mev, which were outside the range of Sailor's observations. Angular distribution measurements were made on the groups p_0, p_1, p_2, p_7, p_8 and p_9 .

The differential range spectrum of the protons from the target of strontium is shown in fig. 2 for an angle of observation of 90° . From observations at different angles the groups indicated by the arrows p_0 , p_1 , p_2 , p_3 , p_4 and p_5 have been ascribed to strontium. The groups due to oxygen and carbon are also indicated. The energy of the deuteron beam was found from the ranges of the oxygen groups and was 8.01 mev. The Q -value of the transition to the ground state of ^{89}Sr was calculated to be 4.18 ± 0.08 mev. This agrees with the value 4.33 ± 0.1 mev obtained by McFarland and Shull. The excitation energies corresponding to the

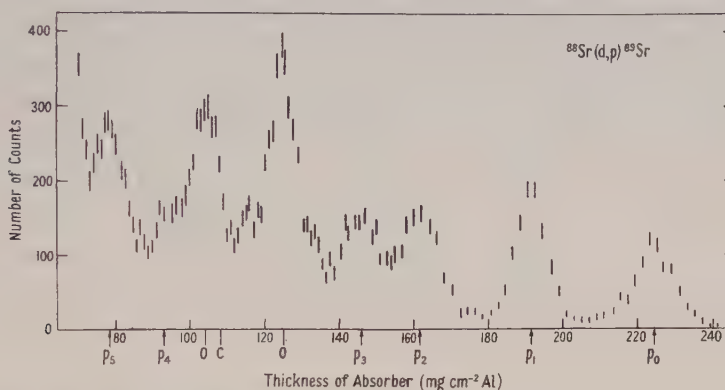


Fig. 2. Range spectrum of protons at an angle of observation of 90° from the deuteron bombardment of a target of strontium.

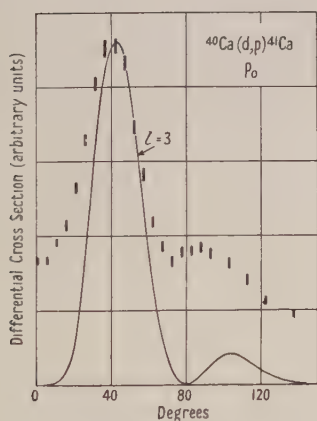


Fig. 3. Angular distribution of the proton group p_0 from $^{40}\text{Ca}(d, p)^{41}\text{Ca}$.

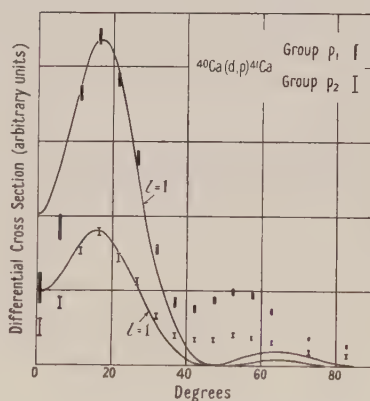


Fig. 4. Angular distributions of the proton groups p_1 and p_2 from $^{40}\text{Ca}(d, p)^{41}\text{Ca}$.

proton groups p_1 to p_5 are 1.07 ± 0.08 , 2.09 ± 0.08 , 2.66 ± 0.08 , 4.73 ± 0.1 and 5.46 ± 0.08 mev, of which the first three agree with the values 1.07, 2.07 and 2.54 mev reported by these workers. Angular distribution measurements were made on the groups p_0 and p_1 .

Angular Distributions

The angular distributions of the various groups of protons are shown in figs. 3 to 8. The curves drawn in each case have been calculated using the theory of the stripping process due to Butler (1951) with a radius given by the formula

$(1.7 + 1.22A^{1/3}) \times 10^{-13}$ cm, that is 5.87×10^{-13} cm for calcium and 7.13×10^{-13} cm for strontium. Practically identical curves were obtained with the theory of Bhatia *et al.* (1952) using a radius greater than this by 1×10^{-13} cm in each case.

The reaction $^{40}\text{Ca}(d, p)^{41}\text{Ca}$.

The angular distribution of the proton group p_0 is shown in fig. 3. The theoretical curve which gave the best fit with the experimental points is shown, and was obtained using the value 3 for the number of units of orbital angular momentum l taken into the nucleus by the captured neutron.

In fig. 4 are shown the angular distributions of the groups p_1 and p_2 , the vertical scales being the same for both. Each theoretical curve is drawn for $l=1$. The experimental curves in both cases show a larger dip in the forward direction than the theoretical curves. This effect has been observed previously for curves having $l=1$ both for (d, p) reactions (III) and for (d, n) reactions (Evans *et al.* 1953).

The intensities of the groups p_3 and p_6 were too small to allow their angular distributions to be measured. They remained less intense than the neighbouring groups p_2 and p_7 at all angles investigated.

The angular distribution of the prominent group p_7 is shown in fig. 5. At

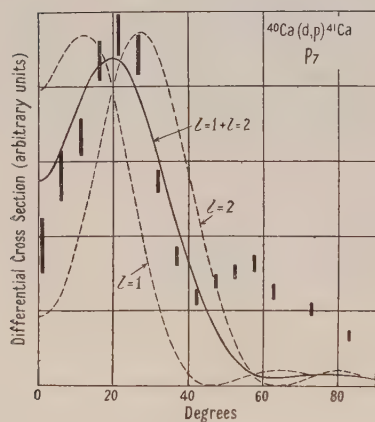


Fig. 5. Angular distribution of the proton group p_7 from $^{40}\text{Ca}(d, p)^{41}\text{Ca}$.

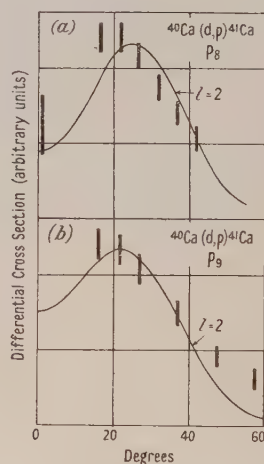


Fig. 6. (a) Angular distribution of the proton group p_8 from $^{40}\text{Ca}(d, p)^{41}\text{Ca}$. (b) Angular distribution of the proton group p_9 from $^{40}\text{Ca}(d, p)^{41}\text{Ca}$.

angles below 20° , where the neighbouring oxygen group became very close, the angular distribution of the combined oxygen and calcium groups was measured and the oxygen contribution subtracted by making use of its known angular distribution. The resulting experimental points could not be fitted by any single theoretical curve. In fig. 5 theoretical curves having $l=1$ and $l=2$ are shown and also a composite curve constructed by adding together curves having $l=1$ and $l=2$, with the same maximum height in both cases. This agrees reasonably well with the experimental points.

Measurements on the groups p_8 and p_9 (fig. 6) were rather inaccurate because of the proximity of the two oxygen groups. In the case of group p_9 measurements

were not made at angles less than 15° because the range of the protons was too small. In spite of the large errors on the experimental points it seems reasonably certain that both transitions have $l=2$.

The reaction $^{88}\text{Sr}(d, p)^{89}\text{Sr}$.

The angular distributions of the groups p_0 and p_1 are shown in figs. 7 and 8.

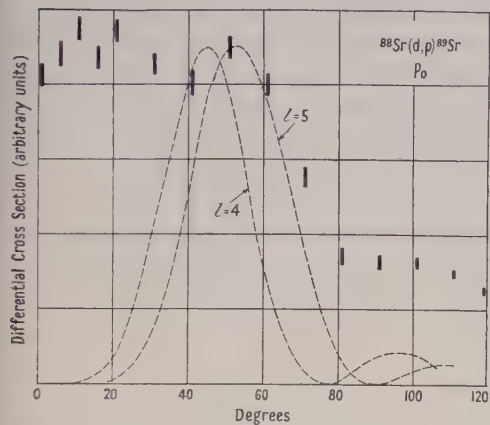


Fig. 7. Angular distribution of the proton group p_0 from $^{88}\text{Sr}(d, p)^{89}\text{Sr}$.

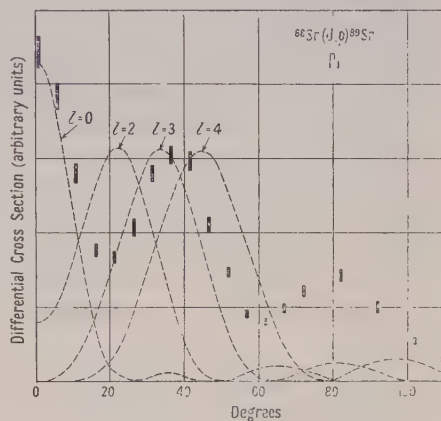


Fig. 8. Angular distribution of the proton group p_1 from $^{88}\text{Sr}(d, p)^{89}\text{Sr}$.

Both are complex. A fair agreement with experiment can be obtained in the case of the group p_1 (fig. 8) by combining theoretical curves having $l=0$ and $l=3$. As the proton spectra from the less abundant strontium isotopes are not known it is not possible to say whether groups from these having ranges close to the groups from ^{88}Sr have contributed to the measured angular distributions. Neither is it known whether the groups from ^{88}Sr are single or multiple. In the case of the group p_0 at least three theoretical curves would have to be combined to give a tolerable fit with the measured points. The main component would seem to have an l -value of 4 or 5.

§4. DISCUSSION

The results for ^{40}Ca are collected in the table. The maximum differential cross sections in column (6) were obtained by comparing the intensities of the proton groups with that of the deuterons scattered elastically from the target at an angle of 21° and using the Rutherford formula for the cross section in the latter case. The differential cross section of the assumed isotropic background was estimated from the angular distribution curves as in (III). The values lay within the range 7 to $11 \times 10^{-28} \text{ cm}^2$. The neutron capture probabilities shown in column (7) of the table were calculated from the theory of Bhatia *et al.* using the cross sections for the stripping process obtained by subtracting this background from the measured cross sections.

The value $l=3$ for the transition to the ground state of ^{41}Ca is consistent with the Mayer shell model since this predicts that the added neutron should go into the $1f_{7/2}$ orbit.

Following the same arguments which were applied to the results obtained with targets of ^{28}Si and ^{32}S (III), we have tried to pick out those states of ^{41}Ca which might be produced by single-particle excitation. The sequence of unfilled orbits

available to the odd neutron is $1f_{7/2}$, $2p_{3/2}$, $1f_{5/2}$, $2p_{1/2}$, $1g_{9/2}$, $2d_{5/2}$ (Klinkenberg 1952*). We suggest that the prominent proton groups p_1 and p_2 , both having $l=1$, are associated with the capture of the neutron directly into the orbits $2p_{3/2}$ and $2p_{1/2}$. If this is so, then the spins j_f of the corresponding excited states of ^{41}Ca are $3/2$ and $1/2$. States of single-particle excitation are expected to be associated with neutron capture probabilities whose relative values are determined mainly by the statistical weight $2j_f+1$. The neutron capture probabilities for the transitions to the ground state and to the above two excited states of ^{41}Ca when divided by the factor $2j_f+1$ become nearly equal as shown in column (8) of the table. This lends support to the assumption that these are single-particle states. The numbers in column (8) are expressed in the same units as those for the single-particle states of ^{29}Si (III), and it is noteworthy that the values are very similar in the two cases.

Proton groups associated with the $1f_{5/2}$ and $1g_{9/2}$ single-particle states would have l -values of 3 and 4 respectively. The intensities of these groups would be of the order of 10% of that of the group p_1 . Such a group corresponding to the $1f_{5/2}$ level could not have been observed between the two groups p_1 and p_2 , and the $1g_{9/2}$ level might be associated with the groups p_3 or p_6 or some other weak group in that region of the spectrum.

The group p_7 seems to have a double value of l which suggests that it is an unresolved doublet. However, since the range of the carbon group p_0 is close to that of this calcium group, the component having $l=1$ may possibly be due to carbon contamination. Thus the three groups p_7 , p_8 and p_9 probably all have $l=2$ and values of the neutron capture probability similar to those of single-particle states. It is likely that two of these groups correspond to the $2d_{5/2}$ and $2d_{3/2}$ single-particle states, but the large errors on the values of the capture probabilities make it impossible to suggest which they might be.

No definite conclusions can be drawn from the angular distributions of the groups p_0 and p_1 from $^{88}\text{Sr}(d, p)^{89}\text{Sr}$. Some uncertainty is introduced by our lack of knowledge of any fine structure of the proton spectrum, due either to the presence of close levels of ^{89}Sr or to contributions from the less abundant isotopes of strontium. Further uncertainty is introduced by the fact that no previous test of the stripping theory has been made when the deuterons have an energy less than the height of the coulomb barrier, and the theory in its present form neglects the effect of the coulomb field. Possible effects of this field are a shift in position of the maximum of the angular distribution and a change in the relative intensities of groups with different values of l but the same neutron capture probability. The results obtained with ^{40}Ca , which has a barrier height 5.4 Mev compared with 8.2 Mev for ^{88}Sr , show no deviations from theoretical predictions greater than those shown by our results for nuclei with much smaller barrier heights. Simple considerations of the effect of the coulomb field indicate that the position of the maximum in the angular distribution is shifted to larger angles, and that the shift in the case of Sr should not be greater than twice that in the case of Ca. Thus the peak at 37° in the angular distribution of the group p_1 from ^{88}Sr is probably consistent with the l -value 3, and the steep decrease at large angles in the case of the group p_0 is probably consistent with the presence of a large component having $l=4$. According to the shell model the odd neutron of ^{89}Sr should occupy the $2d_{5/2}$ level in the ground state. There is support for this from the β -decay $^{89}\text{Sr} \rightarrow ^{89}\text{Y}$ (Langer and Price 1949), which indicates that there is a

* The notation differs slightly from ours.

change of spin in the process of two units, together with a change of parity, and the spin of ^{89}Y is known to be $\frac{1}{2}$ (Crawford and Olson 1949). The l -value for p_0 should therefore be 2. Instead, the main component of the angular distribution appears to have an l -value of 4, although there are components with lower values of l .

The shell model suggests that the $1g_{7/2}$ level is very close to the $2d_{5/2}$ level (Klinkenberg 1952), so that the ground state of ^{89}Sr could be a doublet giving rise to an unresolved proton group having components with $l=4$ and $l=2$. The difficulty would then be to account for the fact that the component with $l=2$ is not the most intense component, as should be the case according to the stripping theory if the values of the neutron capture probability are similar.

ACKNOWLEDGMENTS

We are grateful to Professor H. W. B. Skinner for helpful discussions. One of us (T.N.M.) thanks the Department of Scientific and Industrial Research for a maintenance grant.

REFERENCES

- BHATIA, A. B., HUANG, K., HUBY, R., and NEWNS, H. C., 1952, *Phil. Mag.*, **43**, 485.
BUTLER, S. T., 1951, *Proc. Roy. Soc. A*, **208**, 559.
CRAWFORD, M. F., and OLSON, N., 1949, *Phys. Rev.*, **76**, 1528.
EVANS, W. H., GREEN, T. S., and MIDDLETON, R., 1953, *Proc. Phys. Soc. A*, **66**, 108.
HOLT, J. R., and MARSHAM, T. N., 1953 a, *Proc. Phys. Soc. A*, **66**, 249; 1953 b, *Ibid.*, **66**, 258; 1953 c, *Ibid.*, **66**, 467.
KLINKENBERG, P. F. A., 1952, *Rev. Mod. Phys.*, **24**, 63.
LANGER, L. M., and PRICE, H. C., 1949, *Phys. Rev.*, **76**, 641.
McFARLAND, C. E., and SHULL, F. B., 1953, *Phys. Rev.*, **89**, 489.
SAILOR, V. L., 1949, *Phys. Rev.*, **75**, 1836.

On the Theory of Internal Friction in Metals*

BY B. V. PARANJAPE

Department of Theoretical Physics, University of Liverpool

Communicated by H. Fröhlich; MS. received 22nd December 1952

Abstract. The absorption and emission of vibrational quanta by the conduction electrons in metals leads to a contribution $\pi^2 \nu F \sigma / K_0 (10^{-3})$ to the internal friction per cycle independent of frequency. This holds only for longitudinal vibrations whose wavelength is sufficiently small compared with the dimensions of the sample. In the above ν is the number of free electrons per atom; σ / K_0 is twice the ratio of the velocity of sound to that of the fastest electron and is of the order 10^{-3} . F is a constant of the order unity; its exact value can be found from the temperature coefficient of the electrical resistivity at high temperatures.

§ 1. INTRODUCTION

THE origin of internal friction has been studied by several authors, in particular by Zener (1948) and his collaborators, who suggest that it is largely due to the plastic flow associated with the oscillatory motion of dislocations in crystals. This suggestion should hold whenever the frequency of vibration is sufficiently low. At very high frequencies this type of friction may be expected to vanish. At such high frequencies, however, another type of internal friction appears, owing to the interaction between the elastic vibrations of the lattice and the conduction electrons. This interaction leads to an energy exchange between the electrons and the lattice, which has been extensively studied in the theory of conductivity. In the present paper it will be shown that the contribution arising out of this interaction may be considerable. Application of this theory requires, however, that the vibrations be longitudinal and that their wavelength be sufficiently small compared with the linear dimensions of the specimen, i.e. that the frequency be at least 10^6 c/s (assuming a linear dimension of 1 cm).

As usual, internal friction is defined as

$$I = \Delta E / E, \quad \dots\dots(1)$$

where E denotes the total vibrational energy and ΔE the energy dissipated within the body in one cycle.

To calculate ΔE the theory of metals in its simplest form will be used. Here the lattice vibrations are described in terms of their quantized normal modes. The energy of a quantum is then $\hbar \mathbf{w} s$, where \mathbf{w} is the wave vector and s is the velocity of sound in the metal. The conduction electrons are considered to be free except for occasional scattering through absorption or emission of longitudinal quanta.

* Based on Report, L/T 288 of the British Electrical and Allied Industries Research Association (E.R.A.).

It is well known that in thermal equilibrium a system of normal modes follows Bose-Einstein statistics, whereas a system of free electrons satisfies Fermi-Dirac statistics, and that if the temperatures of the two systems are equal the distributions are not disturbed by the interaction. The various processes of emission and absorption of lattice quanta by electrons are in a state of detailed balance.

If, however, equilibrium is upset through the excitation of additional quanta in mode \mathbf{w} by external means, the electron gas will at first absorb more quanta of this mode than it emits. The excess energy gained by the electrons is then passed on through further interactions, and is eventually shared in the appropriate way by all the degrees of freedom of the system.

§ 2. CALCULATIONS

In order to simplify the problem, the calculations presented are for the absolute zero of temperature, but it can be shown that the formulae which are valid even up to room temperature are very little different.

According to the theory of free electrons a scattering process satisfies conservation of wave vector and energy, i.e. an electron in the state \mathbf{K} can go into the state \mathbf{K}' by absorbing (emitting) a lattice quantum $\hbar\omega$ provided

$$\mathbf{K}' = \mathbf{K} \pm \mathbf{w}, \quad \dots\dots(2)$$

$$K'^2 = K^2 \pm \frac{2msw}{\hbar}. \quad \dots\dots(3)$$

Eliminating K' in equations (2) and (3),

$$K = (w \mp 2ms/\hbar)/2 \cos \theta, \quad \dots\dots(4)$$

where θ is the angle between \mathbf{K} and \mathbf{w} . The Pauli principle imposes the additional condition that, while the state \mathbf{K} must be occupied, the state \mathbf{K}' must be empty.

It is convenient to introduce polar coordinates K, θ, ϕ in K -space with the principal axis parallel to the lattice wave vector \mathbf{w} . The polar angle θ is equal to the angle between \mathbf{K} and \mathbf{w} . One can specify a possible final state of the system, if the selection rule (2) is taken into account, by either the initial wave vector \mathbf{K} or the final \mathbf{K}' of the electron which absorbs a quantum. The energy difference between such a final state of the system and the initial state is

$$E_{K'} = \frac{\hbar^2}{2m} [|\mathbf{K} + \mathbf{w}|^2 - |\mathbf{K}|^2] - \hbar s w. \quad \dots\dots(5)$$

The probability that electrons in the solid angle $d \cos \theta d\phi$ absorb a lattice quantum of vibration \mathbf{w} can be written as

$$P d\Omega = \frac{2\pi}{\hbar} \rho |M_{KK'}|^2 f_K (1 - f_{K'}), \quad \dots\dots(6)$$

where

$$\rho = \frac{2V}{8\pi^3} K^2 \frac{dK}{dE_{K'}} d \cos \theta d\phi \Big|_{E_{K'}=0}$$

is an appropriately defined density of energy levels. V is the volume of the crystal, and the matrix element as given by Bloch (1928) is

$$|M_{KK'}|^2 = \frac{2C^2 \hbar w}{9nV\bar{M}s} n_w, \quad \dots\dots(7)$$

where C is an interaction constant with the dimension of energy, n the number

of atoms per unit volume, M the atomic mass, and n_w the number of quanta of mode w ; f_K and $f_{K'}$ are the probability distribution factors for the states K and K' to be occupied.

In eqn. (6) K and K' have to satisfy conditions (2) and (3). Eliminating K by substituting its value from eqn. (4) and writing [from (5)]

$$\frac{dE_{K'}}{dK} = \frac{\hbar^2}{2m} 2w \cos \theta, \quad \dots\dots(8)$$

one finds

$$P d\Omega = \frac{2\pi}{\hbar} \frac{2V}{8\pi^3} \frac{m}{\hbar^2} \frac{d\Omega}{w \cos \theta} \left[\frac{w - 2ms/\hbar}{2 \cos \theta} \right]^2 \frac{2C^2 \hbar w}{9nVMs} f_K (1 - f_{K'}) n_w. \quad \dots\dots(9)$$

Integrating with respect to ϕ , one gets a factor 2π . The limits of integration with respect to $\cos \theta$ have now to be found. At absolute zero of temperature the electrons fill a sphere of radius K_0 . The factor $f_K (1 - f_{K'})$ can then have only the values 0 or 1. For the latter it is required that in the initial state $K < K_0$ and in the final state $K' > K_0$. The conditions, in conjunction with (2), (3) and (4), lead to the following limits for $\cos \theta$:

$$\cos \theta_1 = (w/2 - ms/\hbar) / (K_0^2 - 2msw/\hbar)^{1/2}, \quad \dots\dots(10)$$

$$\cos \theta_2 = (w/2 - ms/\hbar) / K_0. \quad \dots\dots(11)$$

Integration of (9) then yields

$$P = \frac{2C^2 m^2 w}{9\pi \hbar^3 n M} n_w. \quad \dots\dots(12)$$

Thus the energy absorbed by the electrons in one cycle is

$$\Delta E = (2\pi \hbar s w / s w) P = 2\pi \hbar P.$$

Hence

$$I = \frac{\Delta E}{E} = \frac{2\pi \hbar P}{s w \hbar n_w} = \frac{4C^2 m^2}{9\hbar^3 n M s}. \quad \dots\dots(13)$$

§ 3. DISCUSSION

The above calculations clearly hold only if the wavelength of the vibrations is sufficiently small compared with the linear dimensions of the specimen. From expression (13) it follows that, for longitudinal vibrations, internal friction due to lattice-electron interaction is independent of frequency at sufficiently high frequencies. It is convenient to express this dimensionless quantity in terms of constants defined by Fröhlich (1950, eqns. (2.2) and (2.6)):

$$\sigma = 2ms/\hbar, \quad \dots\dots(14)$$

$$F = \frac{C^2 2m}{3\hbar^2 K_0^2 M s^2}. \quad \dots\dots(15)$$

Also, by expressing n as

$$\nu n = \frac{1}{8\pi^3} \frac{8\pi}{3} K_0^3, \quad \dots\dots(16)$$

where ν is the number of free electrons per atom, one finds from (13)

$$I = \pi^2 \nu F \sigma / K_0. \quad \dots\dots(17)$$

In expression (17) the factor F is of the order unity; σ/K_0 is twice the ratio of the velocity of sound to the highest velocity of an electron, and is of the order 10^{-3} ; ν , although it cannot be determined precisely, is generally less than one. Thus internal friction through lattice-electron interaction is of the order 10^{-3} .

In expression (17) the constant F can be expressed in terms of the temperature coefficient of the resistivity $\rho(T)$ at high temperatures for which $\rho(T) \propto T$. Thus (Sommerfeld and Bethe 1933, p. 523, eqn. (36.12))

$$\frac{1}{k} \frac{\partial \rho(T)}{\partial T} = \frac{\pi^3}{\nu(6\pi^2 n)^{2/3} e^2 s} \frac{3}{4} F \frac{\sigma}{K_0}, \quad \dots\dots(18)$$

if use is made of our equations (14) and (15). Introducing this into eqn. (17) leads to

$$I = \frac{4(6\pi^2)^{2/3}}{3\pi} \frac{s\nu^2 n^{2/3} e^2}{k} \frac{\partial \rho(T)}{\partial T}. \quad \dots\dots(19)$$

Here internal friction is expressed in terms of quantities that are known experimentally except for the number of free electrons per atom, ν .

Thus, for high-frequency longitudinal vibrations, the present theory predicts a frequency-independent internal friction whose magnitude is given by equation (17) or (19). At these high frequencies internal friction for transverse vibrations should be considerably less.

Lack of suitable experimental data on the internal friction of high-frequency longitudinal vibrations does not at present permit a comparison with experiment.

ACKNOWLEDGMENTS

The present work was supported by the British Electrical and Allied Industries Research Association, to whom the writer is indebted for permission to publish this paper.

He also wishes to express his gratitude to Professor H. Fröhlich for help and guidance in all stages of the work, and to Dr. R. Huby for his advice in the preparation of the manuscript.

REFERENCES

- BLOCH, F., 1928, *Z. Phys.*, **52**, 555.
 FRÖHLICH, H., 1950, *Phys. Rev.*, **79**, 845.
 SOMMERFELD, A., and BETHE, H., 1933, *Handbuch der Physik*, **24**, 523.
 ZENER, C., 1948, *Elasticity and Anelasticity of Metals* (Chicago: University of Chicago Press).

RESEARCH NOTES

Electronic Thermal Conduction in Superconductors

BY P. G. KLEMENS

Division of Physics, Commonwealth Scientific and Industrial Research Organization,
Sydney, Australia*MS. received 30th December 1952, and in amended form 18th March 1953*

WHILE Hulm (1950) has interpreted his measurements of thermal conductivities of superconductors by a decrease in the electronic thermal conduction and an increase in the lattice thermal conduction as compared with the metal in the normal state at the same temperature, Mendelssohn and Olsen (1950) have postulated a third mode of heat transport, first suggested by Ginsburg (1944). This is a circulation process in which a supercurrent flows to the warmer end, and is compensated by a normal current in the opposite direction. At the warm end electrons are raised from the superfluid to the normal state with the absorption of energy. The reverse process takes place at the cool end, resulting in heat transport. We shall estimate here the order of magnitude of the resulting additional heat flow.

In an ordinary metal in the presence of an electric field \mathbf{F} and a temperature gradient ∇T , the electric current j and the energy flow Q are given by

$$j/e = \left[e\mathbf{F} + \nabla T \left(\frac{\zeta}{T} - \frac{d\zeta}{dT} \right) \right] K_0 - \frac{1}{T} \nabla T K_1 \quad \dots\dots(1)$$

$$Q = \left[e\mathbf{F} + \nabla T \left(\frac{\zeta}{T} - \frac{d\zeta}{dT} \right) \right] K_1 - \frac{1}{T} \nabla T K_2 \quad \dots\dots(2)$$

where ζ is the Fermi energy, and K_n are transfer coefficients defined by Mott and Jones (1936, p. 306, eqn. (99)). The thermal conductivity is $-Q/\nabla T$ under the supplementary condition $j=0$, and turns out to be

$$\kappa_0 = (K_2 - K_1^2/K_0)/T. \quad \dots\dots(3)$$

In a superconductor we have the possibility of a flow of superfluid electrons (current j_s) from the cold to the warm end, to be compensated by a normal current j_n , so that

$$j = j_n + j_s = 0. \quad \dots\dots(4)$$

Thus no restriction is placed on the magnetic flux inside the superconductor. Consequently heat transport by circulation is not restricted to alloys or other non-ideal superconductors, as stated by Mendelssohn and Olsen.

In the static case the electric field must vanish inside a superconductor. Thus in contrast to the supplementary conditions in a normal metal, where $j_n=0$, but $F \neq 0$, we now have $F=0$, but $j_n \neq 0$. Ginsburg (1944) assumes $F - \nabla\zeta = 0$, but the order of magnitude of the additional heat flow will be independent of which assumption is made.

Treating the electron-gas on a two-fluid model, in which the superconducting electrons cannot transport thermal energy, we can assume that (1) and (2) hold for the normal component, except that all K 's must be multiplied by the fraction

of electrons on the Fermi surface which are in the normal state, and that $F=0$. Thus from (1) and (2)

$$Q_n = \nabla T \left[\left(\frac{\zeta}{T} - \frac{d\zeta}{dT} \right) K_1 - \frac{K_2}{T} \right] = \frac{j K_1}{K_0 e} - \kappa_0 \nabla T. \quad \dots\dots(5)$$

In addition to the energy current Q_n there is also an effective heat transfer by the circulation process. If ϕ is the energy required to raise one electron from the superconducting to the normal state, the circulation process can be described by saying that every superconducting electron carries energy $\zeta - \phi$, so that

$$Q_s = (\zeta - \phi) j_s / e. \quad \dots\dots(6)$$

Thus the additional conductivity due to the circulation process is

$$\kappa_c = - \frac{Q_n + Q_s}{\nabla T} - \kappa_0 = - \left[\phi - \zeta + \frac{K_1}{K_0} \right] \left[\left(\frac{\zeta}{T} - \frac{d\zeta}{dT} \right) K_0 - \frac{K_1}{T} \right]. \quad \dots\dots(7)$$

Expanding the integrand of K_n about ζ we find that $K_1/K_0 - \zeta$ is of the order $(\hbar T)^2/\zeta$, while $(\zeta/T - d\zeta/dT)K_0 - K_1/T$ is of the order $(\hbar T)^2/T\zeta$. Also ϕ is of the order $\hbar T_s$, where T_s is the transition temperature, while κ_0 is of the order $(\hbar T)^2/T$. Hence κ_c/κ_0 is of the order $\hbar T_s/\zeta$, and κ_c is thus quite negligible compared with κ_0 .

We therefore conclude that the circulation process postulated by Mendelssohn and Olsen (1950) should exist in all superconductors, but cannot contribute appreciably to the total heat conduction. These authors postulated the process to account for a conductivity, larger in the superconducting than in the normal state, for such substances as lead-bismuth alloys. The alternative explanation, that the lattice conductivity is enhanced, was examined by Olsen (1952), who showed that the results for lead-bismuth alloys could be interpreted along these lines, although not without some difficulties.

The author is grateful to Dr. G. K. White for several helpful discussions.

REFERENCES

- GINSBURG, V. L., 1944, *J. Phys. U.S.S.R.*, **8**, 148.
 HULM, J. K., 1950, *Proc. Roy. Soc. A*, **204**, 98.
 MENDELSSOHN, K., and OLSEN, J. L., 1950, *Proc. Phys. Soc. A*, **63**, 2 and 1182, *Phys. Rev.*, **80**, 859.
 MOTT, N. F., and JONES, H., 1936, *Properties of Metals and Alloys* (Oxford: University Press).
 OLSEN, J. L., 1952, *Proc. Phys. Soc. A*, **65**, 518.

The Wavelengths of Nitrogen First Positive Bands

By D. SAYERS AND P. K. CARROLL

Physics Department, Queen's University, Belfast

Communicated by K. G. Emeléus; MS. received 11th March 1953

WHILE investigating the excitation conditions of some of the weaker triplet systems of nitrogen (N_2), photographs of the first positive bands in the infra-red region $\lambda=8900-10\,500\text{ \AA}$ were obtained. The spectrum was recorded on Kodak IQ plates using a glass Littrow spectrograph with a dispersion of 80 \AA/mm at $10\,000\text{ \AA}$. Xenon and argon arc lines, whose

wavelengths were taken from the measurements of Meggers and Humphreys (1933) and Humphreys and Meggers (1933) were used as references.

Poetker (1927), working at low resolution, gave wavelengths of two intensity maxima for each of the bands in the $\Delta v = 0$ sequence. The wavelengths of neither set of maxima agree well with those calculated from the vibrational formula given by Herman-Montagne (1945). However, it is evident from the new plates that the maxima recorded by Poetker lie in the neighbourhood of the P_2 and Q_3 heads in each band, whereas the vibrational formula, derived from the bands with wavelengths less than 8920 \AA , refers to the P_1 head. In view of the importance of having accurate data for the identification of auroral and other spectra, the measured P_1 heads are given in the accompanying table. It is intended to give fuller details of this investigation, including a recalculation of the vibrational constants, in another publication.

(v', v'')	(0, 0)	(6, 7)*	(2, 2)	(3, 3)	(4, 4)	(5, 5)
$\lambda_{\text{obs}} (\text{\AA})$	10508.3	10129.1	9939.9	9680.4	9435.0	9201.9

* Identified as the (1, 1) band by Poetker. The (1, 1) band was not recorded on our plates.

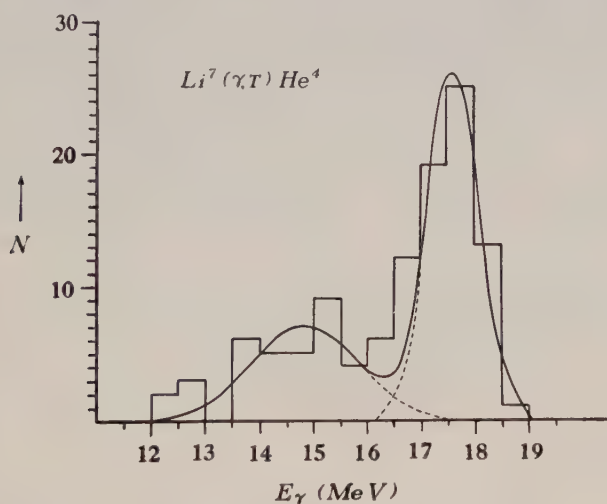
REFERENCES

- HERMAN-MONTAGNE, R., 1945, *Thesis*, University of Paris.
 HUMPHREYS, C. J., and MEGGERS, W. F., 1933, *J. Res. Nat. Bur. Stand., Wash.*, **10**, 139.
 MEGGERS, W. F., and HUMPHREYS, C. J., 1933, *J. Res. Nat. Bur. Stand., Wash.*, **10**, 427.
 POETKER, A. H., 1927, *Phys. Rev.*, **30**, 812.

LETTERS TO THE EDITOR

Cross Sections for the Reaction ${}^7\text{Li}(\gamma\text{T}){}^4\text{He}$ at 6.13, 14.8 and 17.6 Mev

The reaction ${}^7\text{Li}(\gamma\text{T}){}^4\text{He}$ was first observed using the γ -rays from the 440 kev ${}^7\text{Li}(p\gamma)$ resonance (Titterton 1950). Recently the variation of cross section with energy has been determined for the reaction from threshold to 24 Mev (Titterton and Brinkley 1953). To establish values of the cross section as a function of energy it is necessary to measure the cross section at some suitable energy, and this can be done using the lines at 17.6 and 14.8 Mev in the ${}^7\text{Li}(p\gamma)$ spectrum at the 440 kev resonance. Ilford 200 μ type E1 lithium-loaded plates were exposed to the γ -radiation resulting when thick lithium metal targets were bombarded with a proton beam of 250 μA at 490 kev using the Canberra H.T. Set. To minimize irradiation time the experiment was carried out in poor geometry. The plates were searched for ${}^7\text{Li}(\gamma\text{T}){}^4\text{He}$ and ${}^{12}\text{C}(\gamma 3\alpha)$ events, identification being made by energy and momentum balances and the scattering characteristics of the tracks. A total of 110 complete (γT) events was observed in the work, and a histogram of the energy distribution is shown in the figure. The



fitted curve is calculated assuming a line at 17.6 Mev of negligible width, a broad line at 14.8 Mev of width 2 Mev and an experimental half width of 1 Mev. As the cross section varies only slowly over the width of the 14.8 Mev line, no correction has been made for this factor. After making appropriate geometrical corrections for escape of events from the emulsion, the cross section at 17.6 Mev can be calculated in terms of the ${}^{12}\text{C}(\gamma 3\alpha)$ cross section at the same energy, and is

$$\frac{\sigma_{17.6}({}^7\text{Li}(\gamma\text{T}))}{\sigma_{17.6}({}^{12}\text{C}(\gamma 3\alpha))} = (1.94 \pm 0.25).$$

The ratio of the (γT) cross sections at 14.8 and 17.6 Mev can also be obtained assuming the intensity of these lines to be in the ratio 1 : 2.5. It is

$$\frac{\sigma_{14.8}({}^7\text{Li}(\gamma\text{T}))}{\sigma_{17.6}({}^7\text{Li}(\gamma\text{T}))} = (1.04 \pm 0.25),$$

which compares with the value of 1.20 taken from the excitation function of Titterton and Brinkley (1953).

There have been several measurements of the $^{12}\text{C}(\gamma 3\alpha)$ cross section for Li γ -rays, and agreement among them is not good. The most recent is by Glättli, Seippel and Stoll (1952), and we shall adopt their value of

$$\sigma_{17.6}^{12}\text{C}(\gamma 3\alpha) = 2.4 \times 10^{-28} \text{ cm}^2.$$

We then find

$$\sigma_{17.6}^7\text{Li}(\gamma\text{T}) = (4.7 \pm 0.8) \times 10^{-28} \text{ cm}^2, \quad \dots\dots(1)$$

$$\sigma_{14.8}^7\text{Li}(\gamma\text{T}) = (4.9 \pm 0.8) \times 10^{-28} \text{ cm}^2. \quad \dots\dots(2)$$

The small group of events in the figure centring about 12.5 mev appear to be due to a γ -ray of this energy first reported in the $^7\text{Li}(\text{p}\gamma)$ spectrum by Nabholz, Stoll and Wäffler (1952); this result is discussed elsewhere (Titterton 1953).

In the course of experiments on the reaction $^6\text{Li}(\gamma\text{d})^4\text{He}$, Titterton and Brinkley (1952) have also measured the cross section of the $^7\text{Li}(\gamma\text{T})^4\text{He}$ reaction for the γ -ray group 6.13, 6.9 and 7.1 mev which results from proton bombardment at 950 kev of a thick CaF_2 target. The γ -ray flux was determined using the data of Chao *et al.* (1950). In all, 33 events were observed which could definitely be assigned to the reaction, although the resolution was not good enough for them to be sorted into the appropriate γ -ray groups. The cross section obtained is

$$\sigma_{(6.1, 6.9, 7.1)}^7\text{Li}(\gamma\text{T})^4\text{He} = (1.5 \pm 0.5) \times 10^{-29} \text{ cm}^2. \quad \dots\dots(3)$$

This is larger than the value of approximately $0.5 \times 10^{-29} \text{ cm}^2$ obtained from the excitation function when this is normalized with results (1) and (2), but the excitation function is expected to be inaccurate in this region owing to the corrections which have to be made in deriving it to allow for the presence of slow neutron events from the reaction $^6\text{Li}(\text{n}\alpha)^3\text{H}$. However the value obtained is considerably smaller than the value $(2.65 \pm 0.8) \times 10^{-29} \text{ cm}^2$ given by Nabholz *et al.* (1952) for the 6.13 mev γ -ray.

Research School of Physical Sciences,
Australian National University,
Canberra.

E. W. TITTERTON.
T. A. BRINKLEY.

20th February 1953.

CHAO, C. Y., TOLLESTRUP, A. V., FOWLER, W. A., and LAURITSEN, C. C., 1950, *Phys. Rev.*, **79**, 108.

GLÄTTLI, H., SEIPPEL, O., and STOLL, P., 1952, *Helv. Phys. Acta*, **25**, 491.

NABHOLZ, H., STOLL, P., and WÄFFLER, H., 1952, *Helv. Phys. Acta*, **25**, 701.

TITTERTON, E. W., 1950, *Proc. Phys. Soc. A*, **63**, 915; 1953, *Aust. J. Sci.*, **15**, 174.

TITTERTON, E. W., and BRINKLEY, T. A., 1952, *Proc. Phys. Soc. A*, **65**, 1052; 1953, *Ibid.*, **66**, 194.

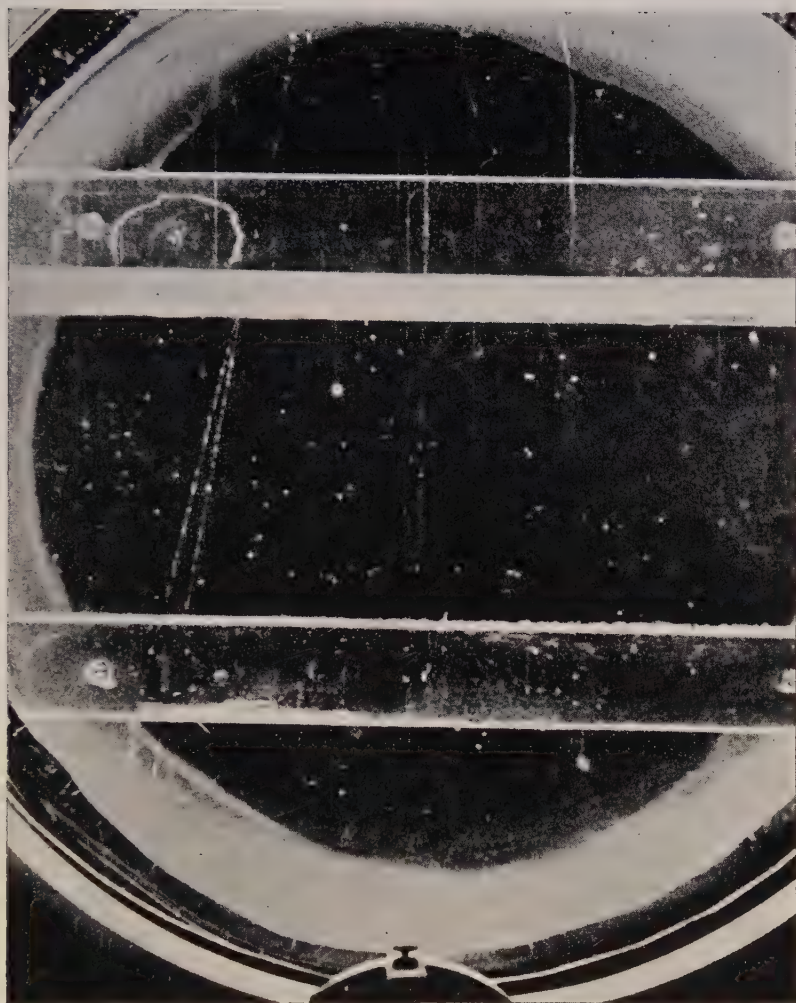


Fig. 3. An example of the production of a single penetrating secondary particle in the top lead plate, at a depth of 60 m water equivalent.

REVIEWS OF BOOKS

Numerical Analysis, by D. R. HARTREE. Pp. xiv+287. (Oxford: University Press, 1952.) 30s.

Most physics research laboratories are now equipped with some type of desk calculating machine. Unfortunately many physicists have never received any instruction in their use and they either avoid using the machines altogether or else fail to use them in the most efficient manner. One reason for this failure to exploit the full possibilities of numerical calculations has been the lack of any single book which indicated clearly the steps required to carry through the work. Professor Hartree's book satisfies this need very successfully. It provides a practical guide to computing the solutions of the most frequently arising types of numerical problem, ranging from the solution of quadratic equations to the inversion of matrices.

The early chapters explain simply the characteristics of the main types of desk machine and the most efficient ways of using them for the basic arithmetical operations. The subject of finite differences is then treated in a concise but satisfactory manner by making use of the method of finite difference operators. This leads to the derivation of the various formulae of interpolation and numerical integration, which are stated in such a manner that they can be referred to without the necessity of following their derivation. The following chapters deal with the solution of simultaneous linear equations, non-linear algebraic equations and the solution of both ordinary and partial differential equations. Finally there is an introductory account to the preparation of calculations for large electronic calculating machines. This last chapter seems rather out of place; all the rest of the book is designed to be of immediate practical value, whereas this one is only a general descriptive account. The author considers that the analysis of observations and statistics are not part of numerical analysis and does not discuss these topics, except for short sections on smoothing and harmonic analysis.

One of the most valuable features of this book is the large number of examples which are set out and worked in detail. Great attention is paid to questions of accuracy and the location of errors, again with many illustrations. There is also a set of examples on which the reader may practise. The author does not attempt to give all the special techniques which are used by professional computers. Throughout he concentrates on the more commonly used methods and is particularly helpful in showing under what circumstances any one method is to be preferred. The book will provide an excellent basis for a short course in computing for students of mathematics or physics, in addition to providing research workers with a useful reference book.

J. C. B.

Advanced Experiments in Practical Physics, 2nd edn, by J. E. CALTHROP. Pp. xvi+142. (London: Heinemann, 1952.) 10s 6d.

The first edition of this book was reviewed in 1939 (*Proc. Phys. Soc.*, **51**, 894). The main alterations in the present edition are in the section on Electricity and Magnetism, where some experiments on the use of a resonance circuit are described.

This book should be useful to a lecturer or demonstrator in charge of a practical class designed for students who have just taken the intermediate degree examination. He will find therein brief but useful descriptions of a considerable number of suitable experiments, and while few will wish to accept the course as a whole, many will find something to use. All students at this stage would gain by reading the introductory pages entitled 'Instructions to Students', though few students will accept the advice given until they have experienced the results of ignoring it!

The reviewer would prefer to see a larger proportion of experiments on accurate electrical measurements. The buzzer excited resonance circuit has long been obsolete. Some indication should be given as to which of the different methods described for finding the cardinal points of a lens system is intended for a given class of system.

This (and some other books on practical physics) would be improved by a few carefully thought out paragraphs on safety precautions instead of occasional remarks on this matter, which are not very helpful.

Not the least of the merits of this useful book is its low price.

R. W. DITCHBURN.

Charbons activés, by C. COURT. Pp. ix+534. (Paris: Gauthier-Villars, 1952.) 4500 fr. (In French.)

This book is a treatise of 514 pages on the adsorptive properties of activated charcoal. An admirable balance is attained between the description of experimental work, a thorough account of the underlying physics and chemistry, and a mathematical treatment of the theories of adsorption. The author admits that neither the investigations nor the theories are by any means complete, but he makes a valuable contribution towards a full understanding by offering a very careful and critical survey of what has so far been achieved. One of the main problems is the mechanism of the chemical sorption of gases and vapours, and here M. Courty's own researches have played an important part in the progress which has been made in recent years. It is evident throughout that he is writing with authority.

The book opens with an account of surface tension and capillarity, and a critical discussion of the various theories of adsorption. A similarly careful survey follows, dealing with the types of heat of adsorption and the kinetics of adsorption. While these treatments are quite general, special attention is naturally given to those theories which can be applied to highly activated porous surfaces, and to charcoal in particular. The remainder of the book is more concerned with experiment. Measurements of the sorption of various gases and gas mixtures are described, followed by the properties of charcoal relevant to its use in respirators. These include studies of the desorption processes, and the correlation between sorption and numerous physical properties, such as grain size, density and porosity. The book concludes with a detailed account of work on chemical sorption, and on methods of testing the efficiency of sorption and the degree of activation of the charcoal.

The standard of production is reasonable as regards legibility of type, mathematics and diagrams. The book is, however, paper covered, which does not offer a high degree of permanence. Moreover, it is very irritating to the

purchaser to be supplied with a book in which almost all the pages are uncut. The writer estimates that he spent almost two hours in page-cutting. This standard of production does not seem consistent with the price of the book, and compares unfavourably with standards in this country. D. A. WRIGHT.

Metallurgical Equilibrium Diagrams, by W. HUME-ROTHERY, J. W. CHRISTIAN and W. B. PEARSON. Physics in Industry Series. Pp. 311. (London: Institute of Physics, 1952.) 50s.

The equilibrium diagrams of alloy systems occupy a very important position in metallurgical knowledge and an increasing need has been felt in recent years for a comprehensive account of the methods available for their determination. The present book meets this need and will be especially welcome as coming from the laboratory in which Dr. Hume-Rothery has built up a tradition of work of the highest quality in this field. Although written primarily for metallurgists it contains much that could be read with profit by anyone—physicist, chemist, or engineer—who is concerned with measurements of the properties of alloys. The days are fortunately past when physicists would report the values of some property across an alloy system and discuss its variation without reference to changes of constitution, but many papers still reveal a lack of appreciation of the precautions required in the preparation and heat treatment of alloys if measurements on them are to have real significance.

The book opens with a survey of the general principles and thermodynamic basis of phase diagrams, which includes a brief consideration of the status to be assigned to order-disorder changes, without, however, showing the forms that can be taken by superlattice phase fields. The discussion of general experimental procedure that follows includes a useful chapter on refractory materials, and a table showing the appropriate crucible materials and atmospheres for the melting of different metals, which should prove invaluable to a wide range of workers. The chapters on thermal analysis are remarkable in being the only description of these methods known to the reviewer in which there are no errors in the diagrams illustrating the interpretation of heating and cooling curves. The application of x-ray methods to the determination of diagrams is discussed critically, and attention is drawn to possible sources of error; the authors recognize the usefulness of such methods, properly applied, and it is to be hoped that one has heard the last echoes of the 'x-ray versus microscope' controversy. Other physical methods that can be used in this type of work are discussed only briefly. The section on ternary systems that follows is an excellent exposition of this involved subject and draws much of its strength from the remarkably well produced diagrams which make clear many of the points which are difficult to visualize.

The book is described as being intended for fourth-year honours students and research students in metallurgy, but much of the subject matter is appropriate to the earlier stages of metallurgy degree courses. In addition the sections on the preparation and heat treatment of alloys and the emphasis laid on the need for chemical analysis of actual specimens should prove useful to any scientist concerned with the properties of alloys.

It should be made clear (for the title fails to do so) that the observed phase diagrams of actual alloy systems do not lie within the scope of this book.

B. R. COLES.

CONTENTS OF SECTION B

	PAGE
Mr. T. MULVEY. The Magnetic Circuit in Electron Microscope Lenses	441
Dr. G. LIEBMANN. The Effect of Pole Piece Saturation in Magnetic Electron Lenses	448
Dr. O. H. WYATT. Transient Creep in Pure Metals	459
Dr. N. THOMPSON. Dislocation Nodes in Face-Centred Cubic Lattices	481
Dr. H. P. MYERS. A Simple Varying Capacitor Method for the Measurement of Contact Potential Difference in High Vacuum	493
Mr. R. D. CRAIG and Dr. J. D. CRAGGS. Some Properties of Hydrogen Spark Channels	500
Letters to the Editor :	
Dr. D. G. AVERY and Dr. P. L. CLEGG. The Optical Constants of a Single Crystal of Germanium	512
Dr. K. N. OGLE: Prof. W. D. WRIGHT. The Role of Convergence in Stereoscopic Vision	513
Dr. H. L. WAIN and Mr. F. HENDERSON. Room Temperature Brittleness of Chromium	515
Reviews of Books	517
Corrigendum (VERMA and REYNOLDS)	523
Contents of Section A	524

Resonant Nuclear Scattering of ^{198}Hg Gamma-Rays

By P. B. MOON AND A. STORRUSTE *

Department of Physics, University of Birmingham

MS. received 15th January 1953

Abstract. The resonant scattering has been measured using the original principle of Doppler shift produced by mechanical motion, but with a quite different experimental arrangement. The intrinsic width of the 0.411 MeV excited state is estimated to be about 5×10^{-6} eV, corresponding to a half-life of about 8×10^{-11} second. The difference from the first estimate ($T \sim 10^{-11}$ sec) is mainly due to the statistical weight factor of 5 resulting from the now well-established spin (2) of the excited state. This factor causes the resonant-scattering values to differ considerably from the most recent direct measurement of the half-life, $(1.0 \pm 1.7) \times 10^{-11}$ sec, and possible causes of the discrepancy are discussed.

§ 1. INTRODUCTION

PREVIOUS experiments (Moon 1951) on the scattering in liquid mercury of the 0.411 MeV gamma-rays of ^{198}Hg showed a small increase of intensity when the source, carried on a high-speed rotor, approached the scatterer at a speed such that Doppler effect compensated for energy lost to nuclear recoils and so restored resonance between the energy available from the gamma-ray and the energy required for resonant excitation of the scattering nucleus.

We here describe the confirmatory experiments briefly mentioned in the former paper, and discuss them in the light of more recent information about the nuclear levels.

§ 2. METHOD OF EXPERIMENT

In the earlier experiments a Geiger-Müller counter surrounded by $\frac{1}{8}$ in. of lead detected the radiation scattered at an average angle of 115° ; the background due to Compton scattering was several times the irreducible background of elastic electronic (Rayleigh) scattering.

In the present experiments the Compton background was reduced in two alternative ways: by increasing the angle to about 135° and, at a smaller angle of about 106° , by using a lead-shielded scintillation counter suitably biased against soft gamma-rays. (With the scintillation counter the Compton background was less than that of Rayleigh scattering, which is a more direct standard against which to measure the resonant scattering; having the same energy, they are equally attenuated in emerging from the scatterer and passing through the shielding, and they are detected with equal efficiency.)

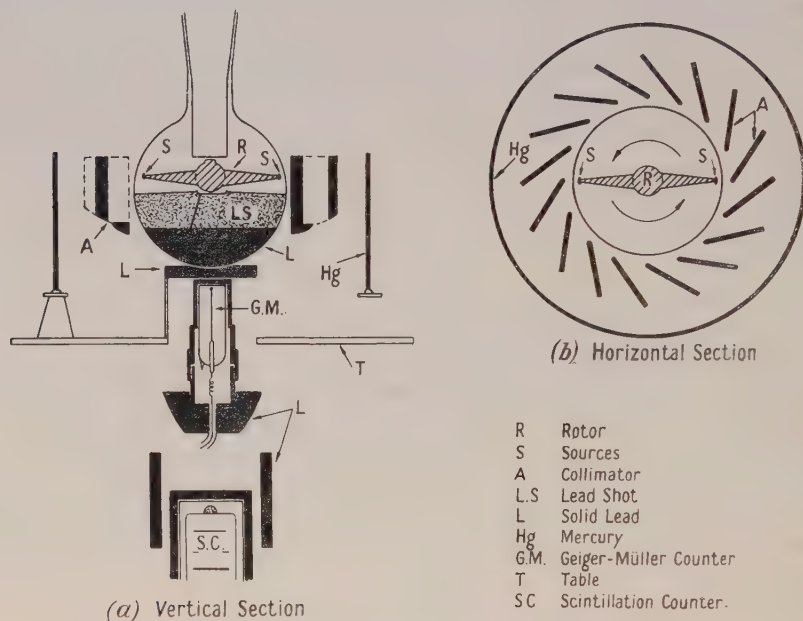
At the same time a drastic change was made in the geometry of the apparatus, primarily to verify that the effect observed by Moon was not peculiar to his arrangement.

The new arrangement (see figure) had the following advantages: (i) continuous irradiation of the scatterer, which in the old apparatus could 'see' the source for only a fraction of the time; (ii) symmetry about the axis of rotation, a drift of

* Now at Fysisk Institutt, Universitetet, Blindern, pr. Oslo, Norway.

which could give only a second-order change in the mean intensity of irradiation; (iii) the possibility of using, at the same time, two detectors at different angles of scattering.

These advantages were offset by the following disadvantages: (iv) greater distance of detector from scatterer; (v) greater sensitivity to changes of length of the rotor; (vi) greater scattering from the coils with which the rotor was electromagnetically driven. This prevented observations during acceleration; when full speed was reached, the coils were removed by remote control and readings were taken as the rotor slowly decelerated.



Vertical and horizontal sections of the apparatus are shown, arrangements for driving and stabilizing the rotor being omitted. The gamma-rays travel obliquely to the planes shown in the figure.

After some preliminary tests in which only the Geiger counter was used, three runs were made with both counters in use, interspersed with blank runs in which either the direction of rotation was reversed or the mercury scatterer was replaced by a geometrically similar scatterer of lead. To counteract any effects due to diurnal drifts of temperature or of counter voltages, care was taken to distribute 'forward' and 'blank' runs evenly between morning and afternoon, the photomultiplier case was water-cooled and extra stabilization of mains voltage was provided.

§3. RESULTS

Detailed plots of the variation of counting rate with speed have been given by Storruste (1951).

Table 1 shows the percentage excess of the average counting rate at speeds above 4×10^4 cm sec⁻¹ over the counting rate at lower speeds. It is seen that a positive effect occurs even with the 'reverse' and 'dummy' experiments. Much of this is due to stretching of the rotor at high speeds, as was shown by an experiment in which a stationary rotor with a source at one end only was set up

in the normal position and then given various radial displacements. The background of the scintillation counter increased by 10% for each millimetre of outward displacement. Calculation showed that the half-length of the rotor was 0.2 mm greater at an average 'high' speed than at an average low speed, so that a 2% change of counting rate is to be expected. Thermal contraction of the lead shot as the apparatus cools during deceleration, giving improved shielding against direct rays, accounts for about 0.2%; the remainder, if real, may be due to a temperature coefficient of the phosphor (CaWO_4).

Table 1. Ratio of Mean Counting Rates at Source Speeds
above and below $4 \times 10^4 \text{ cm sec}^{-1}$

	Hg forward (a.m.)	Hg backward (p.m.)	Hg forward (p.m.)	Pb forward (a.m.)	Hg forward (p.m.)	Hg backward (a.m.)
Scintillation counter (106°)	1.048	1.023	1.043	1.028	1.068	1.035
Geiger counter (135°)	1.038	1.019	1.077	1.053	1.055	1.034

Next it will be seen that for each of the six pairs of results the 'forward' one shows a greater effect than the 'reverse' or 'dummy'. The same was true of the two pairs taken with the earlier apparatus, and of the three pairs that constituted the preliminary tests of the present apparatus. These eleven pairs, involving two kinds of counter, two forms of 'blank' experiment and two quite different geometrical arrangements, leave no doubt of the existence of the resonant scattering.

§4. ANALYSIS OF RESULTS

In estimating the actual intensity of the resonant scattering, the measurements with the scintillation counter should be superior because of the higher rate of counting as well as for the reasons given in §2. The method of analysis will therefore be illustrated with reference to these results rather than those obtained with the Geiger counter.

An experimental analysis was first made of the various contributions to the low-speed counting rate. The percentages were as follows: counter background, 8%; radiation penetrating directly through shielding, 24%; scattering from collimator, walls and floor of room, etc., 34%; scattering from mercury, 34%.

A theoretical analysis was then made of the various components of scattering from the mercury, including that due to the weak high energy gamma-rays from ^{198}Hg . Each entry of table 2 shows the cross section per unit solid angle (at the mean angle of 106°) for the process in question, multiplied by its relative chance of penetrating the lead shield and being detected by the scintillation counter, this chance being taken as unity for elastic scattering.

Table 2. Effective Cross Sections for Various Components of
Secondary Radiation

Primary γ -ray (mev)	Process	Effective cross section ($\text{cm}^2 \text{ sterad}^{-1}$ at 106°) $\times 10^{-27}$
0.41	Elastic scattering (Rayleigh and Thomson)	10
0.41	Compton scattering	5.9
0.41	Bremsstrahlung from photoelectrons	0.4
0.67	Compton scattering	1.3
1.08	Compton scattering	1.4
	Total	19.0

The total of $19 \times 10^{-27} \text{ cm}^2 \text{ sterad}^{-1}$ thus represents the cross section for a fictitious elastic scattering process that would give the same counting rate as all the actual processes (except resonant scattering) that occur in the scatterer. These, as stated above, were responsible for 34% of the total background, so if the resonant scattering at some particular rotor speed is $x\%$ of the background, its equivalent cross section is $(x/34) \times 19 \times 10^{-27} \text{ cm}^2 \text{ sterad}^{-1}$.

Taking the detailed plots of counting rate against rotor speed, averaging the 'real' and 'blank' experiments separately and subtracting their ordinates, we obtained the experimental resonant-scattering cross section as a function of rotor speed. It is not, of course, a nuclear constant, but it may be useful to mention that at the highest speed ($7.5 \times 10^4 \text{ cm sec}^{-1}$) it was found to be about $2 \times 10^{-27} \text{ cm}^2 \text{ sterad}^{-1}$, which may be compared with Compton and Rayleigh cross sections of about 10^{-24} and $10^{-26} \text{ cm}^2 \text{ sterad}^{-1}$ respectively.

If the Doppler shift added to the energy E of the γ -ray by the velocity u of the rotor tip were simply Eu/c , the cross section should theoretically be

$$\sigma = 3.6 \times 10^{-3} \frac{f(\theta)}{4\pi} \frac{I\Gamma}{E^3} \frac{g_a}{g_b} \left(\frac{A}{T}\right)^{1/2} \exp \left[-3.0 \times 10^{-9} \frac{A}{T} (u - u_m)^2 \right], \quad \dots (1)^*$$

where I is the isotopic abundance of the resonantly scattering isotope, A its (conventional) atomic weight, g_a and g_b the multiplicities of the excited and ground states respectively, and T the mean of the temperatures of the source and the scatterer; u is the actual speed of approach of source to scatterer, u_m is the optimum speed of approach (for ^{198}Hg , $6.7 \times 10^4 \text{ cm sec}^{-1}$) and $f(\theta)$ is the angular distribution factor, normalized so as to be equal to unity for isotropic scattering. Γ is the width of the excited state and, like E , is measured in electron volts.

However, the velocity component of the source towards the scatterer is equal to the speed of the source only for those gamma-rays which leave the source exactly in the direction of its motion; the coarse structure of the collimator and the incomplete opacity of its fins to the gamma-rays together allow a considerable spread of angle in the horizontal plane, while in the vertical plane the considerable height of the cylindrical scatterer has to be taken into account. An estimate of the corrections to be applied was first made (Storruste 1951) by calculations in which the scatterer was imagined split into several sections. The correction has since been determined experimentally by placing a scintillation counter at various heights representing the various sections of the scatterer and, for each of these positions, placing a stationary ^{198}Hg source in a series of positions round the circle described by the rotor tip. From the measured relative intensities and the angles, combined with the theoretical variation of resonant scattering with velocity of approach, it was found (for example) that at the rotor tip speed nominally corresponding to resonance ($6.7 \times 10^4 \text{ cm sec}^{-1}$) the spread of velocity components would reduce the actual resonant scattering to 0.30 of the ideal maximum. Correcting in this manner the cross sections observed at various source speeds, and comparing them with eqn. (1), we find the mean value, in electron volts, for $\theta = 106^\circ$:

$$\Gamma = 1.9 \times 10^{-5} \frac{g_b}{g_a} \frac{1}{f(\theta)}. \quad \dots (2)$$

The Geiger counter at 135° gave an identical result.

* The expression given by Moon (1951, eqn. (7)) was for the *total* cross section without statistical weights; the factor 3.0×10^{-9} was accidentally omitted from this equation only.

§ 5. DISCUSSION

Owing to the smallness of the effect and the complexity of the corrections, the above result might easily be in error by a factor of two; it is in reasonable agreement with Moon's estimate of 3×10^{-5} and with the 3.9×10^{-5} obtained recently by Malmfors (1952), who has observed resonant scattering by raising the source of gamma-rays to a high temperature.

It is now almost certain from internal conversion measurements (Siegbahn and Hedgran 1949, Elliott and Wolfson 1951) that the transition in question is an electric quadrupole one between a ground state of spin zero and an upper state of spin 2, and this agrees with the general rule for even-even nuclei (Goldhaber and Sunyar 1951). If so, the factor g_b/g_a is $\frac{1}{5}$ and $f(\theta)$ at 106° is close to unity, while at 135° $f(\theta)$ is $\frac{5}{8}$. The width Γ as obtained from the scintillation counter would then be about 4×10^{-6} eV, corresponding to a half-life of about 10^{-10} sec, while the Geiger counter gives $\Gamma = 6 \times 10^{-6}$ eV, $T_{1/2} = 6 \times 10^{-11}$ second.

Graham and Bell (1951) have looked for the half-life directly, finding $(1.0 \pm 1.7) \times 10^{-11}$ second. Though the various experimental results might be strained to fit a value of $T_{1/2}$ in the neighbourhood of 4×10^{-11} sec, it is necessary to consider whether the discrepancy may be due to the use of eqn. (1). The basic equation for resonant scattering, including the statistical factor g_a/g_b , is securely linked to Einstein's detailed-balancing derivation of Planck's law, but eqn. (1) involves the additional assumptions that the β -ray recoil has been dissipated by collisions before the γ -ray is emitted, and that the initial velocity of γ -ray recoil is to be calculated for free nuclei unaffected by their surrounding electrons and neighbouring atoms, but having thermal velocities as in a gas.

In support of the first assumption it may be mentioned that the mean delay between β and γ emission is much greater than the time required for the recoiling nucleus to travel an interatomic distance, while the Debye frequency ν_m for gold corresponds to an energy $h\nu_m$ of about 1.5×10^{-2} eV, so there should be little quantum restriction upon transfer of energy to the lattice. The low Debye temperature (175°K) makes 'gaseous' thermal velocities a good approximation.

The assumption of free γ -ray recoil rests upon the conception of emission, absorption and re-emission of the photon as three separate instantaneous acts, collisions made by the scattering nucleus while in the excited state affecting the exact energy of the scattered photon but not retrospectively affecting the process of excitation. More experimental evidence—particularly a test of whether the maximum scattering occurs at the predicted relative velocity of source and scatterer—is needed to determine whether recoil is, in fact, free.

ACKNOWLEDGMENTS

The authors are grateful to Mr. T. H. Bull for controlling and measuring the speed of the rotor during the experiments. Part of the apparatus was obtained with the aid of a Royal Society Government Grant.

REFERENCES

- ELLIOTT, L. G., and WOLFSON, J. L., 1951, *Phys. Rev.*, **82**, 333.
 GOLDBABER, M., and SUNYAR, A. W., 1951, *Phys. Rev.*, **83**, 906.
 GRAHAM, R. L., and BELL, R. E., 1951, *Phys. Rev.*, **84**, 380.
 MALMFORS, K. G., 1952, *Ark. Fys.*, **6**, 49.
 MOON, P. B., 1951, *Proc. Phys. Soc. A*, **64**, 76.
 SIEGBAHN, K., and HEDGRAN, A., 1949, *Phys. Rev.*, **75**, 523.
 STORRUSTE, A., 1951, *Thesis*, University of Oslo.

Ionization and Excitation Losses of Charged Particles of Intermediate Energies

By J. NEUFELD

Oak Ridge National Laboratory

*Communicated by P. Howard-Flanders; MS. received 20th August 1952,
and in amended form 9th February 1953*

Abstract. A method has been outlined for determining energy losses of charged particles of intermediate energies, i.e. which do not carry bound electrons and have velocities lower than the K shell velocity of the stopping atom. The 'free collisions' and the 'resonance effects' have been separately evaluated.

The number of electrons participating in free collisions has been determined by using the Thomas-Fermi model for the stopping atom, and the energy loss has been evaluated by means of the Rutherford formula. The resonance effects have been calculated by means of an expression derived by Fermi which represents a much better approximation than the usual logarithmic formula.

The stopping power of a few elements has been computed and the results compared with experimental data.

§ 1. INTRODUCTION

THE stopping power formula of Bohr (1913), Bethe (1930) and Bloch (1933) is based on the assumption that the velocity v of the moving particle exceeds the velocity of the electron in the K shell of the stopping substance (having atomic number Z), i.e. $v > Ze^2/\hbar$.

The present procedure in determining the stopping power for lower velocities consists in evaluating separately the contribution of each electronic shell. The effectiveness of the K shell in stopping particles of various velocities has been determined by Livingston and Bethe (1937) and Brown (1950). Their results are applicable for particle velocities that are greater than the electron velocities for all electron shells except the K shell. The effectiveness in stopping due to shells other than the K shell has not been determined. A semi-empirical method has been used by Hirschfelder and Magee (1948) to determine the effectiveness of other shells for substances such as C, H, O, A and Xe. This method requires in each particular case the knowledge of an experimental value for each substance, such as the range of an alpha-particle.

The purpose of the present investigations is to determine the stopping power for lower velocities at which the effectiveness of electron shells other than the K shell has to be taken into account. The proposed method may be applied with some advantage to those elements for which the experimental data required by Hirschfelder and Magee are not available.

It should be considered, however, that for very low velocities the moving particle undergoes a recurrent process of capturing and losing orbital electrons, and no adequate theory seems to exist at present for dealing with such a case. In our present discussion we shall assume that the moving particle does not

carry with it any bound electrons and is, therefore, essentially an atomic nucleus having a constant charge Z_1e . Thus, in the case of protons, our results will be applicable for $E_p > 0.3$ mev, since at these energies the proton does not carry any bound electrons (Hall 1950).

It is of importance to realise here that the proposed procedure is not based on an exact theory of stopping phenomena and, in view of several simplifying assumptions, the results should be considered merely as a method of approximating to experimental values.

§ 2. CALCULATIONS

Let various electrons in the stopping atom be specified by an index r , and the energy which is necessary to remove the r th electron from the atom be denoted by I_r . We associate with each electron a quantity b_r , which represents the 'radius' of the r th orbit. We take (see, for instance, Bohr 1948)

$$b_r \simeq u_r / \omega_r \quad \dots\dots(1)$$

where ω_r is the cyclic frequency of each electron defined by

$$I_r = \hbar \omega_r \quad \dots\dots(2)$$

and u_r is an 'orbital' velocity defined by

$$I_r = \frac{1}{2} m u_r^2 \quad \dots\dots(3)$$

When the velocity of the particle is high, all the electrons in the stopping atom have their maximum effect in stopping. As the velocity of the particle decreases, the inner shells become gradually less effective and when the velocity becomes low, the moving field is unable to excite any electrons except the outermost. It is convenient to consider separately the contribution of the r th electron in stopping the particle and then sum over r to determine the total effect. We apply the usual procedure of separating the 'free collisions' from the 'resonance effects' (Bohr 1948). For the free collisions the influence of the binding forces of the orbital electrons is neglected, and for the resonance effects the mechanism of the energy transfer is analogous to that of absorption of radiation with wavelengths large compared with the atomic dimensions.

(i) Free Collisions

The maximum energy transfer from the moving particle to a free electron is $2mv^2$, and we shall consider those electrons as free that have binding energies I_r smaller than $2mv^2$. Let $r=1$ represent the outermost electron and $r=2, 3, 4, \dots$, etc., represent electrons having correspondingly increasing binding energies. The number n of the electrons in each atom that behave as if they were free can be determined from the relation

$$I_n \simeq 2mv^2 \quad \dots\dots(4)$$

For the remaining $Z-n$ electrons the interaction is assumed to be adiabatic, i.e. the binding forces will prevent their removal from the atom.

The values I_r may in some instances be determined from spectroscopic measurements. It is desirable to establish a general basis for computing the values I_r , and in that connection we may adopt a rough theoretical approach based on the Thomas-Fermi model of the atom.

The various binding energies can be expressed as

$$I_r = Q_r - Q_{r-1} \quad \dots\dots(5)$$

where Q_r is the energy required to strip a neutral atom of its r external electrons. The amounts Q_r have been evaluated (Sommerfeld 1932, 1933, see also Gombás 1949) and are as follows:

$$\text{for } r \ll Z \quad Q_r = 1.27 \frac{r^{7/3}}{1 - 0.903(r/Z)^{1/4}} \text{ ev} \quad \dots\dots(6)$$

and for larger values of r

$$Q_r = 13.18Z^{7/3} \left\{ \frac{r}{Z^2 x_r} + [\phi_r'(0) - \phi_0'(0)] \right\} \text{ ev} \quad \dots\dots(7)$$

where $\phi_0'(0) = -1.5880464$ and $\phi_r'(0)$ is the solution of the Thomas-Fermi equation corresponding to an ion having charge $-re$ and, therefore, satisfying the boundary condition

$$\phi_r(0) = 1; \phi_r(x_r) = 0; x_r \phi_r'(x_r) = -r/Z, \quad \dots\dots(8)$$

which also determine the radius x_r of the ion.

No published data seem to be available regarding x_r and $\phi_r'(0)$ when r is not small compared with Z . To evaluate (7) would require, therefore, a relatively large amount of computation. It is known, however, that for $r = Z$

$$Q_Z = 20.94Z^{7/3} \text{ ev}, \quad \dots\dots(9)$$

which represents the internal energy of a Thomas-Fermi atom. We may, therefore, evaluate Q_r by using (6) for $r \ll Z$ and (9) for $r = Z$ and, subsequently, determine the intermediate values of Q_r by a rough interpolation.

An example of such interpolation is given in fig. 1, illustrating these computations for gold ($Z=79$). The curve designated ' Q_r (calculated)' represents (6), which is assumed to be valid for $r < 11$. The value Q_r for $r = 79$ has been determined from (9) and the curve ' Q_r (interpolated)' extends the values of r for $11 < r < 79$. Figure 1 shows also the curve I_r determined from (5).

The contribution of each of the n electrons having binding energy smaller than $2mv^2$ can be expressed by means of the Rutherford formula

$$-\left(\frac{\Delta E}{\Delta z}\right) = \frac{2\pi N Z_1^2 e^4}{mv^2} \log \frac{Q_{\max}}{Q_{\min}} \quad \dots\dots(10)$$

where N is the number of atoms per cm^3 and Q_{\max} and Q_{\min} represent, respectively, the maximum and the minimum energy transferred to the electron, i.e. $Q_{\max} = 2mv^2$ and $Q_{\min} = I_r$.

In order to evaluate the total energy loss in free collisions, we add the contributions of all the n electrons and obtain

$$-\left(\frac{\Delta E}{\Delta z}\right)_A = \frac{2\pi N n Z_1^2 e^4}{mv^2} \log \frac{2mv^2}{I_{\text{mean}}} \quad \dots\dots(11)$$

where

$$n \log I_{\text{mean}} = \sum_{r=1}^n \log I_r \quad \dots\dots(12)$$

The value of n can be determined from the graph I_r of fig. 1, since it represents the abscissa having the ordinate given by (4). The values I_r for $r < n$ can be determined directly from the graph of fig. 1, and the value I_{mean} can be subsequently evaluated from (12).

(ii) Resonance Effects

We disregard the finer details of atomic structure and, as is known to be quite reasonable, we compare each electron of the stopping atom with an

isotropic oscillator having frequency ω_r . Then the contribution of each electron to the energy loss of the moving particle can be expressed as

$$-\left(\frac{\Delta E}{\Delta z}\right)_B^{(r)} = \frac{4\pi N Z_1^2 e^4}{m v^2} B_1 \quad \dots\dots(13)$$

where
$$B_1 = \left(\frac{\omega_r b_r}{v}\right) K_0\left(\frac{\omega_r b_r}{v}\right) K_1\left(\frac{\omega_r b_r}{v}\right). \quad \dots\dots(14)$$

K_0 and K_1 are modified Bessel functions of the second kind, having the order of 0 and 1 respectively.

The above relationship was obtained by Fermi (1940). A somewhat simpler method of deriving the result is shown in the Appendix.

The expression (14) represents a modification of the commonly used expression

$$B_1 = \log(v/\omega_r b_r). \quad \dots\dots(15)$$

The expression (15) is based on the existence of a 'maximum impact parameter', $X_{\max} = v/\omega_r$, beyond which the interaction is adiabatic and, therefore, causes no transfer of energy. On the other hand, (14) results from the contribution of oscillators with impact parameters distributed over the unlimited range from b_r to infinity.

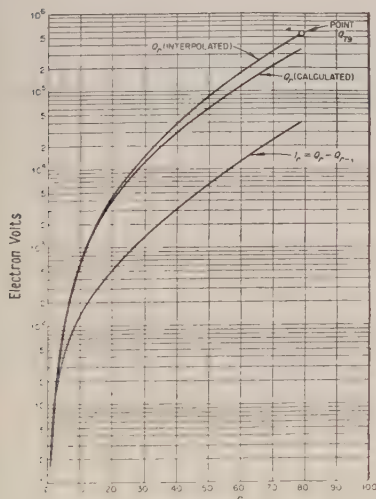


Fig. 1.

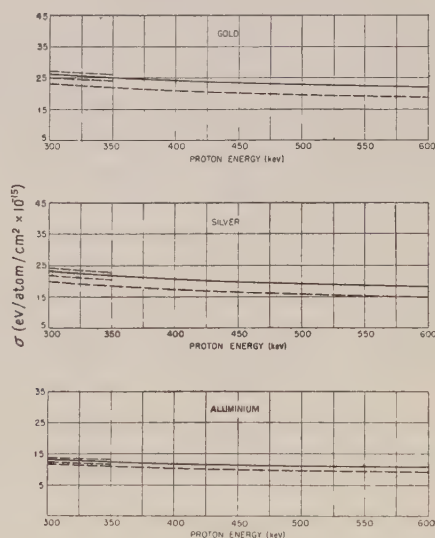


Fig. 2.

The values given by (14) and (15) are substantially equal one to another for $v \gg \omega_r b_r$. For $v < \omega_r b_r$ (15) becomes negative. This accounts for the paradoxical result that for sufficiently slow particles the energy loss is negative. In the same range of abscissae, (14) remains positive and represents actual energy losses.

Using (13), (14) and (1), the energy loss due to resonance effects can be expressed as

$$-\left(\frac{\Delta E}{\Delta z}\right)_B = \frac{4\pi N Z_1^2 e^4}{m v^2} \sum_{r=1}^Z \frac{u_r}{v} K_0\left(\frac{u_r}{v}\right) K_1\left(\frac{u_r}{v}\right), \quad \dots\dots(16)$$

In order to evaluate (16) we need u_r for all the electrons in the stopping atom. We refer then again to a curve I_r , such as the one shown in fig. 1, and determine u_r by means of this curve and (3).

§ 3. NUMERICAL RESULTS

The literature on measurements of stopping powers for heavy particles of intermediate energies is not abundant since most of the measurements have been made in the high energy region in which the Bethe-Bloch formula is valid.

The numerical values obtained with the present method are compared with the measurements of Warshaw (1949), Madsen and Venkateswarlu (1948), Huus and Madsen (1949) and Wenzel and Whaling (1952).

Figure 2 shows stopping powers for protons in Au, Ag and Al within the energy range from 300 to 600 kev. The results obtained by means of (11) and (16), plotted in broken lines, are compared with similar results by Warshaw. The measurements of Warshaw were made for energies below 350 kev. Beyond this range the results of Warshaw were extrapolated to a high enough energy so that the Livingston-Bethe formulae would be valid. In the case of gold, extrapolation was considerably facilitated by the data of Huus and Madsen. The instrumental errors reported by Warshaw are about $\pm 4.5\%$.

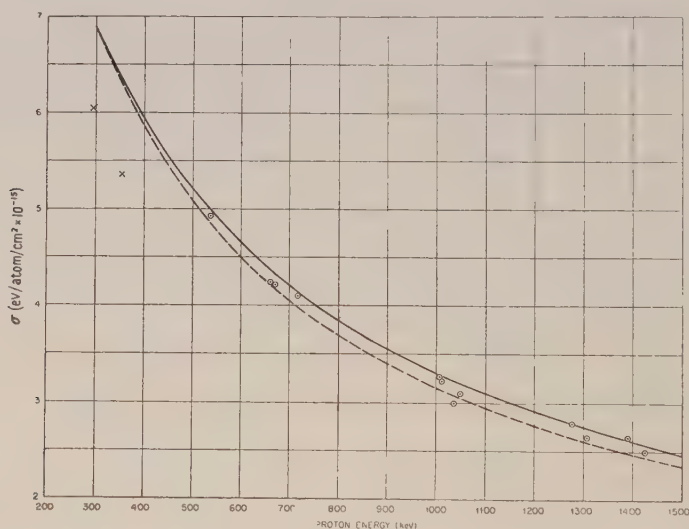


Fig. 3.

Figure 3 shows stopping powers for protons in Be within the energy range from 300 kev to 1500 kev. The crosses represent measurements of Warshaw and the circles the measurements of Madsen and Venkateswarlu. The broken line represents the sum of the formulae (11) and (16) and the solid curve represents the Livingston and Bethe (1937) formula:

$$\sigma = \frac{4\pi e^4 Z}{mv^2} \left(\log \frac{2mv^2}{I} - \frac{C_K}{Z} \right). \quad \dots (17)$$

In (17) I is the average excitation potential of the electrons in the Be atom and C_K is the deficiency in the stopping power due to the fact that the velocity of the

proton is not considerably larger than the velocity of electrons in the K shell. The Livingston-Bethe curve is based on the value $I = 64$ ev determined from the experimental data of Madsen and Venkateswarlu and should be valid in the energy range considered since $E \gg (M/m)E_L$, where E and M represent the energy and the mass of the proton and $E_L = 18.12$ ev is the highest ionization potential of an electron in the L shell of the Be atom. The curve obtained from the sum of formulae (11) and (16) appears to be in better agreement with results of Madsen and Venkateswarlu and with the formula of Livingston and Bethe than with the results of Warshaw.

Figure 4 shows the stopping power for protons in a molecule of D_2O ice as measured by Wenzel and Whaling (indicated by circles) and the stopping power of two atoms of H + one atom of O as calculated by means of the sum of formulae (11) and (16) (solid line). The measured values were determined with an accuracy within 4.5%. In comparing the calculated and measured stopping powers the following assumptions should be considered: (a) that the atomic stopping power of H and D are identical, (b) that the stopping power of D_2O is independent of its physical state, and (c) that Bragg's law for the addition of stopping power is valid. This matter has been discussed by French and Seidl (1951) and Platzmann (1952), and on the basis of the existing evidence we may assume that in fig. 4 the values calculated may differ from the measured values by several per cent.

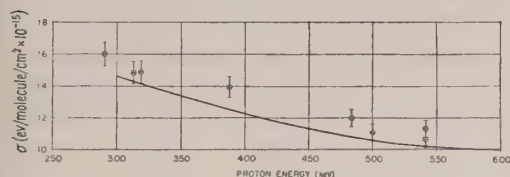


Fig. 4.

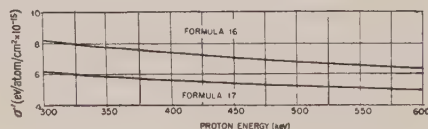


Fig. 5.

In the above calculations the resonance effects have been evaluated by means of (16), which represents a much better approximation than the approximate logarithmic formula

$$-\left(\frac{\Delta E}{\Delta z}\right)_B = \frac{4\pi NZ_1^2 e^4}{mv^2} \sum_{r=1}^Z \log \frac{v}{u_r}. \quad \text{.....(18)}$$

It may be of interest to compare (16) and (18) by means of a specific example. Such a comparison for protons in gold is shown in fig. 5. It appears, therefore, that the stopping power due to resonance effects would be about 25% too small if (18) were used and, consequently, the use of (16) is fully justified.

The energy losses in free collisions have been evaluated by means of (11), which represents a rough approximation. It is to be expected that the values obtained by means of (11) are not as accurate as those obtained by means of (16).

ACKNOWLEDGMENTS

The computations have been performed by M. R. Ford and Carl Perhacs. The author wishes to express his thanks to Dr. T. A. Welton for his criticisms and very valuable suggestions.

APPENDIX

We consider a particle $Z_1\mathbf{e}$ moving along the z axis with velocity v and assume that an isotropic oscillator having an angular frequency ω_r is located on the x axis at a distance x_1 from the origin. The value x_1 is the impact parameter and $t=0$ corresponds to the instant at which the particle passes through the origin.

Since $v \ll c$ we consider the scalar potential only, i.e.

$$V_x = \mathbf{e}(\partial\phi/\partial x)_{x=x_1}(x-x_1) \quad \text{and} \quad V_y = \mathbf{e}(\partial\phi/\partial z)_{z=0}z \quad \dots\dots(19)$$

where

$$\phi = Z_1\mathbf{e}/(x_1^2 + v^2t^2)^{1/2}. \quad \dots\dots(20)$$

Let $a^{(r)}_x(t)$ and $a^{(r)}_z(t)$ represent the transition probabilities for excitation of the oscillator along axis x and z due to the moving particle at the instant t . We have

$$a^{(r)}_x(t) = i\hbar \int_{-\infty}^t \langle 1 | V_x | 0 \rangle \exp(i\omega_r t) dt \quad \dots\dots(21)$$

and a similar expression for $a^{(r)}_z(t)$.

We are concerned here with the transition probability after the particle went to infinity. The energy $e^{(r)}(x_1)$ absorbed by the oscillator at $t = \infty$ comprises two terms corresponding to vibrations along x and z axis, i.e.

$$e^{(r)}(x_1) = |a^{(r)}_x(\infty)|^2 \hbar\omega_r + |a^{(r)}_z(\infty)|^2 \hbar\omega_r. \quad \dots\dots(22)$$

Substituting (20) and (19) in (21) we obtain

$$a^{(r)}_x(\infty) = \frac{-2i\pi^{1/2}\omega_r^{1/2}Z_1\mathbf{e}^2}{m^{1/2}v^2\hbar^{1/2}} K_1\left(\frac{\omega_r x_1}{v}\right) \quad \dots\dots(23)$$

$$a^{(r)}_z(\infty) = \frac{2i\pi^{1/2}\omega_r^{1/2}Z_1\mathbf{e}^2}{m^{1/2}v^2\hbar^{1/2}} K_0\left(\frac{\omega_r x_1}{v}\right) \quad \dots\dots(24)$$

where K_0 and K_1 are modified Bessel functions of the second kind having the order 0 and 1 respectively.

Assume that the medium contains N oscillators per cm^3 . Then the total energy loss is

$$-\left(\frac{\Delta E}{\Delta z}\right)^{(r)} = \int_{b_r}^{\infty} 2\pi x N e^{(r)}(x) dx. \quad \dots\dots(25)$$

Substituting (23), (24) in (22), and subsequently in (25), we obtain (13).

REFERENCES

- BETHE, H. A., 1930, *Ann. Phys., Lpz.*, **5**, 325.
 BLOCH, F., 1933, *Ann. Phys., Lpz.*, **16**, 285.
 BOHR, N., 1913, *Phil. Mag.*, **25**, 10; 1948, *The Penetration of Atomic Particles through Matter* (Copenhagen: Det Kgl. Danske Videnskabernes Selskab).
 BROWN, L. M., 1950, *Phys. Rev.*, **79**, 297.
 FERMI, E., 1940, *Phys. Rev.*, **57**, 485.
 FRENCH, A. F., and SEIDL, F. G. P., 1951, *Phil. Mag.*, **42**, 537.
 GOMBÁS, P., 1949, *Die Statistische Theorie des Atoms* (Vienna: Springer-Verlag), p. 172.
 HALL, T., 1950, *Phys. Rev.*, **79**, 504.
 HIRSCHFELDER, J. O., and MAGEE, J. L., 1948, *Phys. Rev.*, **73**, 207.
 HUUS, T., and MADSEN, C. B., 1949, *Phys. Rev.*, **76**, 323.
 LIVINGSTON, M. S., and BETHE, H. A., 1937, *Rev. Mod. Phys.*, **9**, 263.
 MADSEN, C., and VENKATESWARLU, P., 1948, *Phys. Rev.*, **74**, 648.
 PLATZMAN, R. L., 1952, *Symposium on Radiobiology: The Basic Aspects of Radiation Effects on Living Systems* (New York: John Wiley), p. 139.
 SOMMERFELD, A., 1932, *Z. Phys.*, **78**, 283; 1933, *Ibid.*, **80**, 415.
 WARSHAW, S. D., 1949, *Phys. Rev.*, **76**, 1763.
 WENZEL, W. A., and WHALING, W., 1952, *Phys. Rev.*, **87**, 499.

On the Ionization Loss of a Fast Particle in a Dielectric Medium

BY G. N. FOWLER AND THE LATE G. M. D. B. JONES

University of Manchester

Communicated by L. Rosenfeld; MS. received 13th March 1953

Abstract. A difficulty which has arisen in the physical interpretation of the theory of the ionization loss by fast particles on passing through matter is discussed and it is shown how it is resolved by using a more general expression for the dielectric constant.

§ 1. INTRODUCTION

RECENT measurements on particles of relativistic energies by Ghosh *et al.* (1952) and Daniel *et al.* (1952) have revealed a logarithmic increase in ionization loss with increasing energy which reaches a saturation value at the highest energies. It is important to note that these measurements necessarily refer to loss at short distances from the path of the particle. The observations are in general agreement with the results of the theory of Fermi (1940), it being understood that an upper limit is imposed on the maximum transferable energy observed. However, it has been pointed out by Schönberg (1950) and Messel and Ritson (1950) that the increase given by the theory would seem to be made up of Čerenkov radiation which should not be appreciably absorbed at short distances from the track. The theory gives the energy loss outside a cylinder of radius b about the path of the particle by calculating the Poynting vector flux out of this cylinder. The expression for the Poynting vector as a Fourier integral is given by

$$\frac{dW_b}{dx} = \frac{2e^2b}{\pi v^2} \mathcal{R} \int_0^\infty \left(\frac{1}{\epsilon} - \beta^2 \right) i\omega k^* K_1(k^*b) K_0(kb) d\omega, \quad \dots\dots(1)$$

$$\left. \begin{aligned} \text{where} \quad \epsilon(\omega) &= 1 + \frac{4\pi ne^2}{m(\omega_0^2 - \omega^2 - 2ip\omega)}, \\ k(\omega) &= \frac{\omega}{v} \{1 - \beta^2 \epsilon(\omega)\}, \end{aligned} \right\} \quad \dots\dots(2)$$

and the K functions are the Hankel functions of imaginary argument. The energy loss with p small is then given by

$$-\frac{dW_b}{dx} = \frac{2\pi ne^4}{mv^2} \left\{ \frac{2b\omega_a}{v} K_0\left(\frac{b\omega_a}{v}\right) K_1\left(\frac{b\omega_a}{v}\right) - \frac{v^2}{c^2} - \log\left(1 - \frac{v^2}{c^2}\right) \right\} \text{ for } v < \frac{c}{\epsilon_0^{1/2}}, \quad \dots\dots(3)$$

and

$$-\frac{dW_b}{dx} = \frac{2\pi ne^4}{mv^2} \left\{ \frac{2b\omega_a}{v} K_0\left(\frac{b\omega_a}{v}\right) K_1\left(\frac{b\omega_a}{v}\right) - \frac{(1 - v^2/c^2)}{\epsilon_0 - 1} + \log \frac{\epsilon_0}{\epsilon_0 - 1} \right\} \text{ for } v > \frac{c}{\epsilon_0^{1/2}}, \quad \dots\dots(3')$$

ω_a is given by $\epsilon(\omega_a) = 0$ and $\epsilon_0 = \epsilon(0)$.

With $b \sim 10^{-8}$ cm these expressions reduce to

$$-\frac{dW_b}{dx} = \frac{2\pi ne^4}{mv^2} \left\{ \log \left(\frac{mv^2}{3 \cdot 17 \pi ne^2 b^2} \right) + \log \left(\frac{\epsilon_0 - 1}{\epsilon_0(1 - v^2/c^2)} \right) - \frac{v^2}{c^2} \right\} \text{ for } v < \frac{c}{\epsilon_0^{1/2}},$$

and (4)

$$-\frac{dW_b}{dx} = \frac{2\pi ne^4}{mv^2} \left\{ \log \left(\frac{mv^2}{3 \cdot 17 \pi ne^2 b^2} \right) - \frac{(1 - v^2/c^2)}{\epsilon_0 - 1} \right\} \text{ for } v > \frac{c}{\epsilon_0^{1/2}}. \text{ (4')}$$

The part of the loss due to Čerenkov radiation is given by the limiting value of dW_b/dx for $b \rightarrow \infty$:

$$-\frac{dW_\infty}{dx} = \frac{2\pi ne^4}{mv^2} \left\{ -\frac{v^2}{c^2} - \log \left(1 - \frac{v^2}{c^2} \right) \right\} \text{ for } v < \frac{c}{\epsilon_0^{1/2}}, \text{ (5)}$$

$$\text{and } -\frac{dW_\infty}{dx} = \frac{2\pi ne^4}{mv^2} \left\{ -\frac{(1 - v^2/c^2)}{\epsilon_0 - 1} + \log \frac{\epsilon_0}{\epsilon_0 - 1} \right\} \text{ for } v > \frac{c}{\epsilon_0^{1/2}}. \text{ (5')}$$

To find the energy transferred to the medium, as excitation and ionization, one must subtract (5) from (4). The result is

$$W_I = \frac{2\pi ne^4}{mv^2} \left\{ \log \frac{mv^2}{3 \cdot 17 \pi ne^2 b^2} + \log \frac{\epsilon_0 - 1}{\epsilon_0} \right\}, \text{ (6)}$$

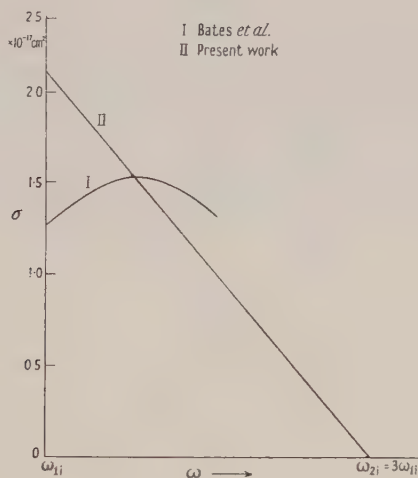
which is essentially the same as the loss calculated with neglect of relativistic effects in (4). By reference to (1) and (3) it may be seen that this term is produced by the Fourier component of frequency ω_a satisfying $\epsilon(\omega_a) = 0$. A detailed discussion of this aspect of the result is given by Schönberg (1950).

§ 2. DIELECTRIC CONSTANT

In order to remove this discrepancy Huybrechts and Schönberg (1952) have suggested that for distances from the track smaller than R (where $R = 10^{-4}$ cm) the medium might not behave like a dielectric. The reason given for this is that the proper interaction of the particles forming the medium is in general so strong as to make the usual quantum theory of dispersion (see for example Heitler 1947) inapplicable. It is suggested that owing to this strong interaction for very short collision times, i.e. for short distances from the track, it is impossible to describe the medium in terms of a dielectric constant with definite resonance frequencies. Accordingly they attempt to estimate the order of magnitude of R mentioned above and they calculate the loss neglecting interference effects from electrons at distances from the track less than R . In this way they find good agreement with experiment. However, the main interaction term between atoms in condensed media is in any case the electrostatic interaction and for optical frequencies one should not expect that this would affect the dielectric character of the medium as such, though it would certainly affect the parameters occurring in the expression for the dielectric constant. One may also expect that the velocity dependent interaction between the electrons is small except for those in the inner shells which, however, one knows are little affected by the proximity of other atoms. In the case of gases at normal pressures one may show that the static interaction between atoms gives rise to a perturbation in their energy states which is small compared with the energies of these states when the atoms are isolated. Thus it does not seem that this explanation of the absorption of energy close to the path of the particle is correct, and one must conclude that for distances from the path larger than atomic dimensions the medium should be regarded as a homogeneous dielectric.

In the following work it is shown that the difficulty disappears if one includes in the dielectric constant the terms due to the continuous spectrum of states of the atomic electron. Since we are interested in the ionization produced by the incident particle this part of the dielectric constant might indeed be expected to play an important role. In fact it is found that when such a term is introduced into the dielectric constant the resonance at $\epsilon = 0$ which has been noted no longer occurs. Instead one finds a dielectric constant which is essentially complex over the range of frequencies corresponding to the continuous spectrum and this gives rise to a heavily damped Čerenkov radiation of these frequencies which is absorbed inside a cylinder about the path of the particle of radius $b \sim 10^{-4}$ cm.

The expression for the dielectric constant is obtained by using the theory of Kallmann and Mark (1926, 1927), in which the continuous spectrum of states is represented as a continuum of harmonic oscillators over which an integration replaces a summation. To obtain the distribution of virtual oscillators over the continuum for oxygen, the calculated photo-ionization cross section of Bates *et al.* (1939) has been replaced, for the present calculation, by an approximate value (curves I and II respectively). Included in the dielectric constant are contributions from the first excited level and the continuum of the 2p electrons



Dependence of ionization cross section on frequency

and the continuum of the 2s electrons. The cross section for photo-ionization of a 2s electron has been taken to be the same as that for a 2p electron (Jones 1952). The final expression for ϵ is

$$\epsilon = 1 + K \sum_{i=s,p} (\omega_{2i} - \omega) \log \left| \frac{\omega_{2i} - \omega}{\omega - \omega_{1i}} \right| - (\omega_{2i} + \omega) \log \left| \frac{\omega_{2i} + \omega}{\omega_{1i} + \omega} \right| + \frac{i\pi K}{\omega} (\omega_{2i} - \omega) \delta_1 + \frac{8\pi n e^2}{m(\omega_0^2 - \omega^2)},$$

where $\delta_{s,p} = 1$ for $\omega_{1s} \leq \omega \leq \omega_{2s}$, $\omega_{1p} \leq \omega \leq \omega_{2p}$, respectively, and $|\gamma| \ll 1$
 $= 0$ otherwise,

and $K = \frac{nc \cdot 2 \cdot 2 \times 10^{-17}}{2\pi}$. For ω_{1i} , ω_{2i} see figure.

$\hbar\omega_{1s}$ and $\hbar\omega_{1p}$ are the ionization thresholds of the 2s and 2p electrons respectively, and $\hbar\omega_0$ is the energy of the first excited state of the 2p electrons. The total oscillator strength for the continuum using curve II is approximately 1.7. This compares with a total oscillator strength of four for the 2p electrons and two for the 2s electrons.

The calculation of the ionization loss proceeds on standard lines using the method of Williams (1933, 1935) modified to take into account the polarization*. One finds for the energy loss

$$W = \frac{2e^2c}{v^2} \sum_{i=s,p} n_i \int_{\omega_{1i}}^{\omega_{2i}} \frac{1}{|\epsilon|^2} \left\{ \log \frac{4v^2}{(3.17)^2 b_0^2 |1 - \beta^2 \epsilon| \omega^2} - \theta \cot \theta + |1 - \beta^2 \epsilon| \theta \operatorname{cosec} \theta \right\} \sigma_i(\omega) d\omega, \quad \dots\dots (7)$$

where $\theta = \arg(1 - \beta^2 \epsilon)^{1/2}$ and $b_0 \sim 10^{-8}$ cm.

Approximate evaluation of the integral (7) gives agreement with the observed increase in ionization loss and also with the observed value of $(1 - \beta^2)^{-1/2}$ at which the plateau begins. More accurate numerical evaluation of (7) is proceeding.

Since this work was completed it was found that a similar suggestion had been made by Wick (1941) though without application to the present problem.

ACKNOWLEDGMENTS

The completion of this work was interrupted by the death of one of the authors, at the beginning of his career. He would have wished to join in thanking Professors Rosenfeld and Wilson for their interest and encouragement. Mr. J. R. Maddox also gave us valuable assistance in many interesting discussions.

Thanks are also due to the Department of Scientific and Industrial Research for financial assistance during the time that this work was carried out.

REFERENCES

- BATES, D. R., BUCKINGHAM, R. A., MASSEY, H. S. W., and UNWIN, J. J., 1939, *Proc. Roy. Soc. A*, **170**, 322.
 BUDINI, P., and POIANI, G., 1952, *Nuovo Cim.*, **9**, 199.
 DANIEL, R. R., DAVIES, J. H., MULVEY, J. W., and PERKINS, D. H., 1952, *Phil. Mag.*, **43**, 753.
 FERMI, E., 1940, *Phys. Rev.*, **57**, 485.
 GHOSH, S. K., JONES, G. M. D. B., and WILSON, J. G., 1952, *Proc. Phys. Soc. A*, **65**, 68.
 HEITLER, W., 1947, *The Quantum Theory of Radiation*, Second Edn. (Oxford: University Press).
 HUYBRECHTS, M., and SCHÖNBERG, M., 1952, *Nuovo Cim.*, **9**, 764.
 JONES, G. M. D. B., 1952, *Thesis*, University of Manchester.
 KALLMAN, W., and MARK, H., 1926, *Naturwissenschaften*, **14**, 648; 1927, *Ann. Phys., Lpz.*, **82**, 385.
 MESSEL, H., and RITSON, D. M., 1950, *Phil. Mag.*, **41**, 1139.
 SCHÖNBERG, M., 1950, *Bull. Cent. Phys. Nucl., Bruxelles*, 20.
 WICK, G. C., 1941, *Ric. Scia.*, **19**, 858.
 WILLIAMS, E. J., 1933, *Proc. Roy. Soc. A*, **139**, 163; 1935, *K. Danske Vidensk. Selsk.*, **13**, No. 4.

* Budini and Poiani (1952) have used a similar procedure but with a dielectric constant so approximate as to conceal the difficulty discussed here.

The Interaction of Electrons with Lattice Vibrations : Radiation by a Fast Electron

By M. J. BUCKINGHAM

Department of Theoretical Physics, University of Liverpool

Communicated by H. Fröhlich; MS. received 12th February 1953

Abstract. The interaction of a single electron with the field of the lattice vibrations is examined classically and the rate of radiation of energy by an electron moving faster than the velocity of sound is calculated. This agrees in the high velocity limit with a simple perturbation theory result. The interaction between a pair of electrons, due to this field, is also discussed.

§ 1. INTRODUCTION

IN the free electron theory of metals one considers the conduction electrons as free except for their interaction with the lattice vibrations. This interaction was first treated on the basis of quantum mechanics by Bloch (1928) and Houston (1928), in connection with the theory of metallic conductivity. Bloch described it in terms of the emission and absorption of vibrational quanta, and Fröhlich (1950) has shown that an effective interaction between electrons arises as the result of virtual emission and absorption of phonons. This may be described in terms of a field theory, the electrons acting as sources of the field. If the coupling between the electrons and the field is sufficiently strong there is a possibility for the existence of a ground state different from the normal one. The identification of this state with the superconducting state is supported by the experimental verification of the isotope effect.

In a field with a characteristic velocity s of free vibrations, a source moving with velocity greater than s excites vibrations in the form of a 'wake', giving rise to phenomena analogous to conical flow in hydrodynamics. An example of this behaviour in the case of the electromagnetic field is the Čerenkov radiation produced by an electron moving through a medium at a speed greater than the velocity of light in the medium.

The field of the lattice vibrations has a characteristic velocity equal to the velocity of sound in the metal, and this is nearly a thousand times less than the velocity of the electrons at the top of the Fermi distribution. The field of a fast electron has the form of a very narrow wake, so that the interaction of a pair of electrons would be greatest when one lies in the wake of the other. This fact has led Bohm and Staver (1951) and Singwi (1952) to suggest models for the superconducting state in which electrons are held in chains, each being in the wake of the one before it. In this paper we examine further the interaction of a fast electron with the acoustic field, and calculate the rate of loss of energy to the wake by an electron moving with uniform velocity. The constancy of the velocity implies that the recoil is neglected, so that the results will only apply to an electron in a metal which has an energy much greater than the Fermi energy,

so that the momentum is large compared with that of the phonons. At zero temperature the conduction electrons cannot, of course, lose energy, because of the operation of the Pauli principle.

§ 2. FIELD EQUATIONS

Consider a Hamiltonian for the free longitudinal vibrations of a crystal lattice in a form similar to that employed by Fröhlich (1952):

$$H_f = \frac{1}{2} \int \{ M \dot{\mathbf{P}}^2 + Ms^2 \sum_{i,k} (\partial P_i / \partial x_k)^2 \} n d\tau, \quad \text{curl } \mathbf{P} = 0. \quad \dots\dots(2.1)$$

Here \mathbf{P} represents a longitudinal displacement of the lattice, M is the mass of an ion, and ρ their density; s is the velocity of sound. Now the short range interaction with the electrons depends on the relative displacement, and we introduce as the interaction term $\int C\rho \text{div } \mathbf{P} d\tau$, where C is a constant with the dimension of an energy and ρ is the electron density. We can now set up a Lagrangian density function from which the Hamiltonian with interaction and the equations of motion for the field can be obtained. Thus, regarding the components of \mathbf{P} as independent variables, we assume

$$L = nMs^2 \left\{ \frac{1}{2} \frac{1}{s^2} \dot{\mathbf{P}}^2 - \frac{1}{2} \sum_{i,k} \left(\frac{\partial P_i}{\partial x_k} \right)^2 - \frac{C}{nMs^2} \rho \text{div } \mathbf{P} \right\}. \quad \dots\dots(2.2)$$

The equation of motion for the P_i component is then

$$\frac{1}{s^2} \ddot{P}_i - \nabla^2 P_i = \frac{C}{nMs^2} \frac{\partial \rho}{\partial x_i}. \quad \dots\dots(2.3)$$

Since $\text{curl } \mathbf{P} = 0$, we may introduce a potential function χ such that

$$\mathbf{P} = (C/nMs^2) \text{grad } \chi, \quad \dots\dots(2.4)$$

so that

$$\frac{1}{s^2} \ddot{\chi} - \nabla^2 \chi = \rho - \rho_0, \quad \dots\dots(2.5)$$

where $\text{grad } \rho_0 = 0$. Forming the energy momentum tensor

$$T_{\mu\nu} = - \sum \frac{\partial P_i}{\partial x_\nu} \frac{\partial L}{\partial (\partial P_i / \partial x_\mu)} + L\delta_{\mu\nu}, \quad \dots\dots(2.6)$$

where $\mu, \nu = 1, 2, 3, 4$ and $x_4 = it$, the conservation laws of energy and momentum are expressed by $\partial T_{\mu\nu} / \partial x_\mu = 0$ and the energy current density is given by

$$S_k = -isT_{k4} = (C^2/nMs^2)u_k, \quad \dots\dots(2.7)$$

where

$$u_k = - \frac{\partial \dot{\chi}}{\partial x_i} \frac{\partial^2 \chi}{\partial x_i \partial x_k}.$$

We note that anywhere where the electron density ρ is zero the tensor $T_{\mu\nu}$ is symmetric.

§ 3. SOLUTION FOR SINGLE NON-ACCELERATED ELECTRON

Taking ρ to represent a single electron with constant velocity \mathbf{v} , and passing through the origin of coordinates at $t=0$,

$$\rho = \delta(\mathbf{r} - \mathbf{v}t) = \frac{1}{(2\pi)^3} \int \exp \{ i\mathbf{k} \cdot (\mathbf{r} - \mathbf{v}t) \} d\mathbf{k}.$$

Expanding χ in momentum space, we set

$$\chi = \frac{1}{(2\pi)^3} \int \chi(\mathbf{k}, t) \exp(i\mathbf{k} \cdot \mathbf{r}) d\mathbf{k}$$

and obtain as the equation of motion for $\chi(\mathbf{k}, t)$, with $k = |\mathbf{k}|$,

$$\frac{1}{s^2} \ddot{\chi}(\mathbf{k}, t) + k^2 \chi(\mathbf{k}, t) = \exp(-i\mathbf{k} \cdot \mathbf{v}t) \quad \dots\dots(3.1)$$

whose general solution is

$$\chi(\mathbf{k}, t) = \frac{1}{k^2 - (\mathbf{k} \cdot \mathbf{v})^2/s^2} \exp(-i\mathbf{k} \cdot \mathbf{v}t) + A(\mathbf{k}) \exp(\pm isk t). \quad \dots\dots(3.2)$$

We note here that there is a natural cut-off in the wave-number spectrum of the lattice vibrations, corresponding to a wavelength of the order of the lattice distance; in fact, if w_0 is the maximum wave number,

$$2w_0^3/3(2\pi)^2 = n, \quad \dots\dots(3.3)$$

and in what follows we use this cut-off whenever necessary to ensure a finite result.

Taking cylindrical polar coordinates (x, ρ, ϕ) with the direction of \mathbf{v} as axis, and taking (l, q, θ) as coordinates of \mathbf{k} , we have

$$\chi = -\frac{1}{(2\pi)^3} \int \frac{\exp\{il(x-vt)\} \exp(iq\rho \cos \theta) q d\theta dq dl}{(\alpha^2 - 1)l^2 - q^2}$$

where $\alpha = v/s$. Performing the integration over θ ,

$$\chi = -\frac{1}{(2\pi)^2(\alpha^2 - 1)} \iint \frac{\exp\{il(x-vt)\} J_0(q\rho) q dq dl}{l^2 - \beta^2 q^2}, \quad \dots\dots(3.4)$$

in which J_0 is the Bessel function of order zero and $\beta^2 = (\alpha^2 - 1)^{-1}$. The paths of integration are chosen so that χ corresponds to the retarded solution. In the case that $v < s$ the poles of the integrand in (3.4) are on the imaginary axis, and choosing the path of integration along the real axis one has

$$\chi = \frac{1}{4\pi} \frac{1}{\{(x-vt)^2 + (1-\alpha^2)\rho^2\}^{1/2}}. \quad \dots\dots(3.5)$$

When $v > s$ the poles are on the real axis, and choosing as path the real axis indented with small semicircles in the positive imaginary half-space around the poles, one has

$$\begin{aligned} \chi &= -\frac{\beta}{2\pi} \int J_0(q\rho) \sin \beta q(vt-x) dq, & vt-x > 0; \\ &= 0 & vt-x < 0. \end{aligned} \quad \dots\dots(3.6)$$

Taking for the moment the upper limit in the q -integration as infinity one obtains

$$\begin{aligned} \chi &= \frac{1}{2\pi} \{(vt-x)^2 - (\alpha^2 - 1)\rho^2\}^{-1/2}, & \rho \leq \beta(vt-x); \\ &= 0 & \text{otherwise.} \end{aligned} \quad \dots\dots(3.7)$$

This solution has the expected conical 'shock front' at the surface $(vt-x)^2 = (\alpha^2 - 1)\rho^2$, on which χ diverges. The solution obtained when q is restricted by the cut-off w_0 is similar but remains finite on the front.

§ 4. LOSS OF ENERGY BY RADIATION

We will now calculate the rate of energy loss by radiation, assuming that the velocity of the electron is maintained constant and greater than s . The rate of radiation equals the energy crossing in unit time the boundary of a cylinder concentric with and parallel to the path of the electron, in the limit as the radius of the cylinder tends to infinity.

The component of the energy current density normal to this cylindrical surface is given by $(C^2/nMs^2)u_e$, where

$$\begin{aligned} u_e &= -\frac{\partial \dot{\chi}}{\partial x} \frac{\partial^2 \chi}{\partial x \partial \rho} - \frac{\partial \dot{\chi}}{\partial \rho} \frac{\partial^2 \chi}{\partial \rho^2} \\ &= v \frac{\partial^2 \chi}{\partial x \partial \rho} \left\{ \frac{\partial^2 \chi}{\partial x^2} + \frac{\partial^2 \chi}{\partial \rho^2} \right\} \\ &= \alpha^2 v \frac{\partial^2 \chi}{\partial x \partial \rho} \left\{ \frac{\partial^2 \chi}{\partial x^2} - \frac{1}{\rho} \frac{\partial \chi}{\partial \rho} \right\}, \end{aligned}$$

where we have used the equation of motion (2.5) and the fact that χ is a function only of ρ and $vt-x$.

The term in $\rho^{-1}\partial\chi/\partial\rho$ will give zero contribution when integrated over the surface, so that, for $\alpha > 1$,

$$\begin{aligned} u_e &= -\alpha^2 \beta^5 v / (2\pi)^2 \int_0^{w_0} q^2 q'^2 J_0(q\rho) J_1(q'\rho) \\ &\quad \times \sin \beta q(vt-x) \cos \beta q'(vt-x) dq dq', \quad vt-x > 0; \\ &= 0, \quad vt-x < 0. \end{aligned} \quad \dots\dots (4.1)$$

We require the value of the integral

$$2\pi\rho \int_{-\infty}^{\infty} u_e dx = \alpha^2 \beta^4 v \rho / 2\pi \int_0^{w_0} q^3 q'^2 (q^2 - q'^2)^{-1} J_0(q\rho) J_1(q'\rho) dq dq';$$

interchanging q and q' and taking half the sum, this equals

$$\begin{aligned} &\frac{\alpha^2 \beta^4 v}{4\pi} \iint_0^{w_0} \frac{q^2 q'^2}{\rho} \left\{ \frac{q\rho J_0(q\rho) J_1(q'\rho) - q'\rho J_0(q'\rho) J_1(q\rho)}{q^2 - q'^2} \right\} dq dq' \\ &= \frac{\alpha^2 \beta^4 v}{4\pi} \int_0^{w_0} q^2 q'^2 \left\{ \int_0^e \rho J_1(q\rho) J_1(q'\rho) d\rho \right\} dq dq', \end{aligned}$$

using a property of Bessel functions.

Now

$$\lim_{R \rightarrow \infty} \int_0^R x J_n(\alpha x) J_n(\beta x) dx = \frac{1}{\alpha} \delta(\alpha - \beta),$$

so that, in the limit as the radius $\rho \rightarrow \infty$,

$$2\pi\rho \int u_e dx = \frac{\alpha^2 \beta^4 v}{4\pi} \iint_0^{w_0} qq'^2 \delta(q - q') dq dq' = \frac{\alpha^2 \beta^4 w_0^4 v}{16\pi}. \quad \dots\dots (4.2)$$

The loss of energy by radiation per unit time is then R , say, where

$$\begin{aligned} R &= \lim_{\rho \rightarrow \infty} \frac{2\pi\rho C^2}{nMs^2} \int_{-\infty}^{\infty} u_e dx, \\ &= \frac{1}{16\pi} \left(\frac{\alpha^2}{\alpha^2 - 1} \right)^2 \frac{C^2 w_0^4}{nMv}, \end{aligned} \quad \dots\dots (4.3)$$

by (2.7) and (4.2).

In the case $\alpha < 1$, that is, for velocities less than the velocity of sound, one would expect R to be zero, and this can easily be verified. It is apparent from (4.3) that the radiation would diverge strongly but for the cut-off at w_0 , and that in any case there is a singularity at $\alpha = 1$. For very large velocities the rate of radiation is inversely proportional to the velocity.

For an electron with velocity corresponding to a wave vector \mathbf{k} in a metal we can write R in the form

$$R = \pi(1 - \sigma^2/k^2)^{-2}(\sigma/k)\zeta F w_0 s, \quad \dots\dots(4.4)$$

where F is the factor proportional to C^2 introduced by Fröhlich (1952), and defined by $3C^2 = 8\zeta Ms^2 F$; ζ is the Fermi energy and $\sigma = ms/\hbar$ the wave number of an electron moving with the velocity of sound. In (4.4) we have introduced the value of n given by (3.3). We may note that the energy loss in travelling one lattice distance is $\pi(1 - \sigma^2/k^2)^{-2}(\sigma/k)^2 F \zeta$ and for the fastest electrons in a metal this is of the order of 10^{-4} eV per lattice distance. For high energy electrons in metals this loss is small compared with that from other causes, principally coulomb interaction with other electrons. The results of experiments by Ruthemann (1948) and Lang (1948) on the energy loss of electrons with energy about 1 keV indicate that the total loss is about 10^5 times that due to this acoustic interaction alone.

§ 5. QUANTUM MECHANICAL CALCULATION

In the case of an electron moving fast enough for the recoil due to its interaction with the field to be neglected we can easily calculate the rate of loss of energy to the field.

Considering an electron with wave number $k \gg w_0$ we note that the probability of its emitting a quantum the magnitude of whose wave number lies between w and $w + dw$ is

$$P(w) = (2\pi/\hbar)\rho(w) |M_w|^2 dw, \quad \dots\dots(5.1)$$

where M_w is the matrix element for the emission of a quantum of wave number \mathbf{w} , and where $\rho(w) dE dw$ is the number of final states within the energy range dE near resonance. If θ is the angle between \mathbf{k} and \mathbf{w} , the energy difference between the initial and final states is $(\hbar^2/2m)(w^2 - 2kw \cos \theta + \sigma w)$, and since there are $V/(2\pi)^3$ levels per unit volume in \mathbf{w} -space, the number of levels

$$\rho(w) dE dw = \frac{V}{2(\pi)^3} \frac{2m}{2\hbar^2 kw} 2\pi w^2 dE dw$$

provided energy can be conserved, i.e. provided $w \leq 2(k - \sigma)$. Thus

$$\rho(w) = mVw/4\pi^2 \hbar^2 k. \quad \dots\dots(5.2)$$

Now the energy lost by emitting a quantum \mathbf{w} is $\hbar w s$, so the loss of energy per unit time by the electron is

$$R = \int_0^{w_0, 2(k-\sigma)} P(w) \hbar w s dw,$$

where the upper limit is the smaller of the two values given.

Inserting (5.1) and (5.2) and using the fact that $|M_w|^2 = C^2 \hbar w / 2nVMs$, we obtain

$$R = mC^2 w_0^4 / 16\pi n M \hbar k, \quad w_0 < 2(k - \sigma). \quad \dots\dots(5.3)$$

This is identical with the limit of the classical value (4.3) for large v/s , since $v = \hbar k/m$.

For values of k in the range $0 < 2(k - \sigma) < w_0$, R is given by

$$R = \frac{mC^2 w_0^4}{16\pi n M \hbar k} \left(\frac{2(k - \sigma)}{w_0} \right)^4, \quad 0 < 2(k - \sigma) < w_0;$$

and

$$R = 0 \quad k < \sigma.$$

Comparing these results with those obtained classically, we see that in both cases the radiation is zero for subsonic velocities ($v/s = k/\sigma < 1$), and that they agree in the limit of very large velocity. At speeds just above the speed of sound, however, the classical expression diverges, whereas the expression above approaches zero.

§ 6. INTERACTION BETWEEN PAIR OF ELECTRONS

To estimate the interaction energy of one electron in the 'wake' of another we will calculate the value of the term $\int C \rho \operatorname{div} \mathbf{P} d\tau$, describing the interaction of the electron density ρ of one with the field \mathbf{P} due to the other.

Provided that the electron is at a distance great compared with w_0^{-1} from the 'shock cone', we can ignore the cut-off w_0 in the momentum space representation of the field and use the simple expression (3.7).

Thus we have, for the interaction energy,

$$E_{\text{int}} = \frac{C^2}{nMs^2} \int \rho \nabla^2 \chi d\tau = \frac{C^2}{nMs^2} \nabla^2 \chi(\mathbf{r}), \quad \dots\dots(6.1)$$

where $\nabla^2 \chi(\mathbf{r})$ represents the value of $\nabla^2 \chi$ at the position \mathbf{r} of the electron. From (3.7), then,

$$\nabla^2 \chi = - \frac{\beta(1 + \beta^2)}{2\pi} \frac{2\beta^2 x^2 + \rho^2}{(\beta^2 x^2 - \rho^2)^{5/2}} = - \frac{\alpha^2}{\pi x^3} \quad \dots\dots(6.2)$$

on the axis distant x from the source.

Thus

$$E_{\text{int}} \sim - \frac{\alpha^2 C^2}{\pi n Ms^2 x^3} = - \frac{16\pi \zeta \alpha^2 F}{(w_0 x)^3}. \quad \dots\dots(6.3)$$

Recently Singwi (1952) has discussed the 'wake' character of the electron lattice interaction. Using an expression for the interaction energy, obtained by Bardeen (1951) by means of a Bloch-Nordsieck transformation, Singwi found for the energy of one electron in the wake of another an expression equivalent to (6.1), making the approximation that the wave numbers of the phonons are small compared with those of the electrons. Under these conditions, as we have seen, the perturbation theory results should approach the classical ones. It appears that Singwi, in performing the calculation corresponding to our (6.2), has omitted the factor α^2 . In addition, for the theory to apply, the position of the second electron should be more than w_0^{-1} distant from the 'shock cone', not only from the other electron. Thus taking x_{min} to be a few times αw_0^{-1} one finds

$$E_{\text{int}}(x_{\text{min}}) \sim - \zeta F / \alpha \sim - 10^{-2} \text{ eV},$$

a value 10^2 greater than that given by Singwi and of about the same order as the interaction energy per electron calculated by Fröhlich (1950) using perturbation theory.

ACKNOWLEDGMENTS

The author wishes to express his thanks to Professor H. Fröhlich for many helpful discussions. This work was carried out during the tenure of a scholarship from the Australian National University.

REFERENCES

- BARDEEN, J., 1951, *Rev. Mod. Phys.*, **23**, 268.
BLOCH, F., 1928, *Z. Phys.*, **52**, 555.
BOHM, D., and STAUER, T., 1951, *Phys. Rev.*, **84**, 836.
FRÖHLICH, H., 1950, *Phys. Rev.*, **79**, 845; 1952, *Proc. Roy. Soc. A*, **215**, 291.
HOUSTON, W. V., 1928, *Z. Phys.*, **48**, 449.
LANG, W., 1948, *Optik*, **3**, 233.
RUTHEMANN, G., 1948, *Ann. Phys., Lpz.*, **2**, 113.
SINGWI, K. S., 1952, *Phys. Rev.*, **47**, 1044.

The Absolute Standardization of the 2.615 Mev γ -Rays of ThC'' and the Cross Section for the Photodisintegration of the Deuteron at this Energy

BY P. MARIN, G. R. BISHOP AND H. HALBAN

The Clarendon Laboratory, Parks Road, Oxford

MS. received 11th February 1953

Abstract. The absolute number of short and long range α -particles from a source of active deposit of RdTh (0.6 mc) has been determined by counting, with an ionization chamber, in low geometry. This measurement gives a new value for the branching ratio (0.354 ± 0.004) and at the same time the absolute number of 2.615 Mev γ -rays emitted by this source (0.384 ± 0.009 mc per mg radium equivalent of active deposit). The same source has then been compared with a standard radium source on a Curie-type ionization chamber. The procedure for future absolute calibration is in this way simplified. The increased precision of these measurements leads to a revision of former determinations of the cross section for the photodisintegration of the deuteron at 2.615 Mev. This new cross section is $(13.80 \pm 0.38)10^{-28} \text{ cm}^2$.

§ 1. INTRODUCTION

THE absolute standardization of the 2.615 Mev γ -rays of ThC'' is of interest particularly for the determination of the cross section for the photodisintegration of the deuteron (Bishop *et al.* 1950). The disintegration scheme of ThC'' is now sufficiently well understood to allow the conclusion that one 2.615 Mev γ -ray is emitted for at least 99.7% of all disintegrations of ThC''. Thus an absolute standard of ThC'' would be also an absolute standard of the 2.615 Mev γ -rays.

In the past absolute standardizations of RdTh active deposit sources have been done by Ricoux (1937) and by Winand (1939) in terms of the number of disintegrations of ThB nuclei. These can be converted into standards of ThC'' by multiplying with the branching ratio of ThC, known at the time to an accuracy of within 4%. The accuracy of Ricoux's and Winand's measurements were within the order of 2%, to which we should add a possible systematic error of 3% for Ricoux's method and 1.5% for Winand's method.* The standards of ThC'' were then known with an accuracy of the order of 6%.

We have carried out a new absolute standardization based on the counting of the individual α -particles of the active deposit of RdTh. As Ricoux and Winand, we have compared the γ -ray activity of our standardized sources of active deposit with a radium standard on a Curie-type ionization chamber. In this way any

* The systematic errors are compounded of 1% for the absolute standardization of radium sources and 0.5% due to the fact that the branching ratio is used for determining the average energy of an α -particle emitted by either ThC or ThC' in both methods of standardization. Another systematic error of 1.5% enters in Ricoux's measurements due to the uncertainty of the absolute average energy required to form an ion pair.

new source of active deposit can now be standardized by measuring the equivalent in milligrams of radium of the ionization of its γ -rays on a similar Curie chamber.

§ 2. EQUALITY OF THE NUMBER OF α -PARTICLES EMITTED BY ThC AND OF THE NUMBER OF 2.615 MeV γ -RAYS EMITTED BY ThC''

The branching scheme of ThC and the decay scheme of ThC'' are shown in fig. 1.

A difference between the number of ThC'' disintegrations and the number of 2.615 MeV γ -rays emitted could arise from the cross-over γ -rays of 3.2, 3.48, 3.71 MeV, or from the direct β decay to the ground state of ThD . The intensity of the cross-over γ -rays has been found altogether to be less than 0.001 per disintegration of ThC'' (Bishop, Halban and Wilson 1950). The direct β decay to the ground state of ThD has been investigated by Cavanagh (private communication). He found no 5 MeV β -particles to a limit of one in 500. We can therefore say that one 2.615 MeV γ -ray is emitted for at least 99.7% of all the disintegrations of ThC'' . By counting the number of short range α -particles emitted by the source of active deposit we then obtain the number of ThC'' disintegrations and, therefore, the number of 2.615 MeV γ -rays.

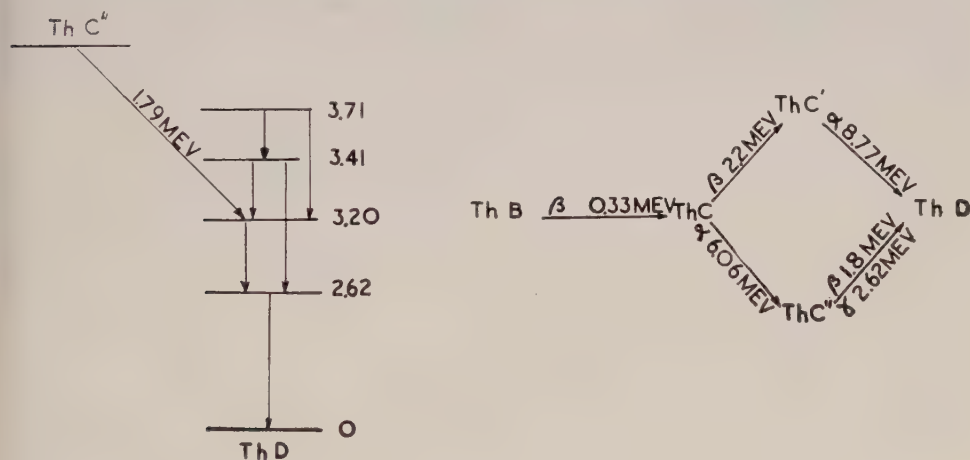


Fig. 1. Decay scheme of ThC'' and branching scheme of ThC .

§ 3. METHOD USED FOR THE COUNTING OF THE α -PARTICLES

For the counting of the α -particles we decided to use a low geometry arrangement and rejected 2π counters. These require low intensity sources, which could not be compared accurately with radium standards of one mc or above, on the Curie chamber. Furthermore, corrections of the order of several per cent must be applied to the counting rates for the back-scattering of the sources. These corrections are difficult to calculate and could not be easily verified in our case, since there are two groups of α -particles. In the case of a low geometry arrangement none of these troubles occurs. The strength of the source is

$$S = \text{counting rate} \times \frac{4\pi}{\text{solid angle subtended by the window}}.$$

Figure 2 shows the arrangement used. The source was placed at one end of an evacuated tube of 50 cm length. A small fraction of the α -particles (0.5×10^{-6}) entered through a mica window a cylindrical chamber of one inch diameter, with a central wire of 2×10^{-3} inch diameter. The use of a guard ring at an intermediate potential defines accurately the sensitive volume and avoids the 'end effect'.

The electronic apparatus included a linear amplifier type 1008, a discriminator, two scalers and an oscilloscope. A single channel kicksorter, with a channel width of one volt stable to ± 0.05 volt, was used to give at the same time the differential and the integral bias curves. From the differential curve and the value of the channel width we deduced the slope of the plateaux on the integral curve.

Figures 3 and 4 show typical integral and differential bias curves for a gas filling of 63 cm of methane (670 volts on the cathode). The curves were corrected for the decay of the source and the non-secular equilibrium.

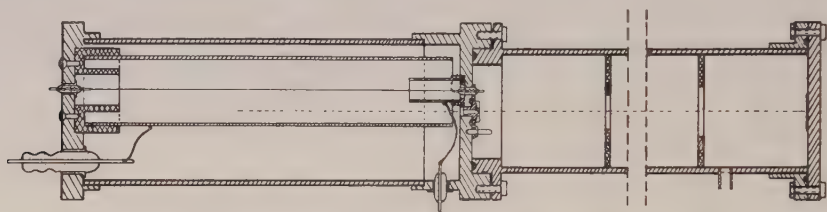


Fig. 2. Ionization chamber and collimating system used for the counting of the α -particles.

§ 4. LOSS IN α -PARTICLE COUNTING

In order to count the number of short range α -particles emitted by the source of active deposit we have to achieve a good discrimination between the two main groups of α -particles from ThC and ThC'. Furthermore, all the α -particles which enter the window within the solid angle, and only those, must be counted. In the following paragraphs we shall deal with the effects which can produce a loss of counts.

(a) *Loss of Particles due to the Differential Absorption*

All particles of a group must suffer the same average loss of energy by absorption before entering the sensitive volume. This can be achieved by having a perfectly clean 'infinitely thin' source and a homogeneous mica window. The sources of RdTh active deposit were obtained by activation of a carefully cleaned gold foil, by an emanating source of RdTh. The window was made with a foil of freshly cleaved mica of thickness 1 cm air equivalent. Differences of thickness of the mica foil as small as 0.2 cm air equivalent could have been easily detected under a microscope. Since the range of the ThC α -particles inside the sensitive volume of the counter is 1.8 cm air equivalent at S.T.P., such irregularities could not reduce their energy below the lowest bias voltage used.

However, we usually found that particles of dust were deposited on the surface of the mica, but it was estimated, with the help of a microscope, that the area covered by those particles was less than 0.1%.

(b) *Loss of Counts due to Electron Capture*

The capture of some of the electrons produced in an α -particle track by electro-negative gases present in the counter has two effects: it reduces the

average pulse height and increases the spread of the pulse height distribution. The ThC α -particle tracks at the edges of the collimated beam have an average radial separation inside the sensitive volume of 0.5 mm. Thus electrons from such tracks travel distances varying from 7.5 to 8.5 mm before reaching the central wire, and therefore have different probabilities for capture by electro-negative

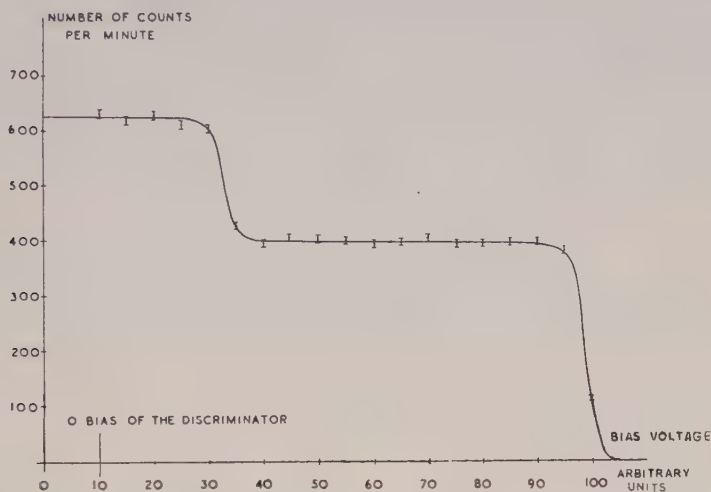


Fig. 3. Integral count of the two groups of α -particles from ThC and ThC' .

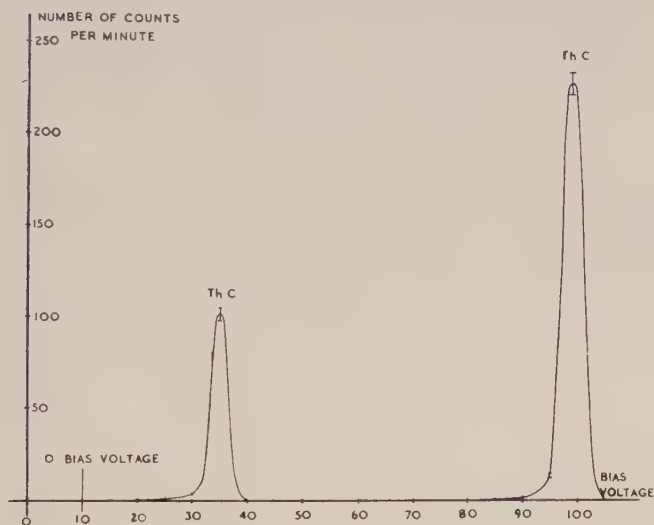


Fig. 4. Differential count of the two groups of α -particles from ThC and ThC' .

gases. If a sufficient number of electrons of one track is captured, the resulting pulse may fall below the lowest bias voltage used and not be recorded. Various gas fillings were tried. Pure argon gave a spread of the pulse height which was ten or twelve times greater than the total spread to be expected from the straggling in the source, the window, the dead volume of the counter and from the positive ion effect. We believe this to be due to the slow outgassing of the chamber

materials. Fillings of argon with 1 cm of alcohol and with pure methane gave a marked reduction of the observed pulse height spread. The polyatomic gases give a much lower 'electron temperature' than pure noble gases. This might produce a strong decrease of the probability of electron capture, which would explain the reduction of the spread of the pulse height distribution.

The calculated spread for the ThC' α -particle group is 1% and the spread of the pulse height distribution deduced from the bias curve was found to be 4% for the final measurements. This is reduced to 2.5% after correction for the channel width of the discriminator. The discrepancy can be attributed to electron attachment and irregularities of the central wire. From the small value of the spread of the pulse height distribution we can expect that all particles which enter the sensitive volume, within the solid angle, are counted.

(c) Loss of Particles due to Scattering

Some of the α -particles are scattered by parts of the apparatus. If they are stopped by the walls of the counter they lose a fraction of their energy and then contribute to a tail on the low energy side of the pulse height distribution.

Table 1

(1)	(2)		(3)	
	(a)	(b)	(a)	(b)
Window	0.04	0.02	0.07	0.29
Holder	0.03	0.015	0.03	0.03
Gas (methane)	0.02	0.01	0.45	0.84
Window + holder + gas	0.09	0.045	0.55	1.16

- (1) Scatterer; (2) particles scattered outside sensitive volume (%): (a) ThC group, (b) ThC' group; (3) ThC' group, scattered particles (%) with energy E :
(a) $E < 6.06$ mev, (b) 6.06 mev $< E < 8.77$ mev.

The particles scattered by the walls of the collimating tube before the counter were stopped by Perspex diaphragms of decreasing aperture. However, it is impossible to avoid the scattering by the window, the support of the window and the gas filling of the counter. Since the particles are scattered mostly at small angles, we must put the outside electrode as far as possible from the axis of the α -particle beam. Since the scattering cross section is proportional to Z^2 , gases with low atomic number will be the most suitable. We actually found the plateaux to be better with methane than with an argon-alcohol mixture by a factor between 3 and 4.

The ThC'' disintegration rate of the source is obtained from the observed counting rates a and b on the plateaux of the integral bias curve by multiplying the difference $a - b$ by the factor $4\pi/\text{solid angle}$. Errors, therefore, are of two classes:

(i) Those due to particles which never reach the sensitive volume, because they are scattered out of it. We have calculated the percentage of particles from ThC and ThC' scattered outside the sensitive volume (see table 1, column (2) a and b), for a methane gas filling. The correction to the counting rate a is 0.13%.

(ii) Those due to particles which are scattered but reach the sensitive volume and are stopped by the walls of the counter. They contribute a pulse of less than

average height. For the ThC' group some of those α -particles fall below the lowest bias voltage on the second plateau. The percentage of those particles has been calculated (column (3 a)), and the correction to the counting rate b amounts to 0.55%.

We have verified the validity of these corrections by comparing the experimental tail between the ThC and ThC' groups with the percentage of the ThC' α -particles which are scattered and give rise to a pulse greater than the lowest bias voltage used on the second plateau (see column (3 b)). The agreement was good, respectively 1.3% and 1.16%. The correction to the branching ratio arose to 0.9% and we can expect the error due to this correction to be less than 0.3%.

§ 5. SPURIOUS EFFECTS

Investigations have been made to determine the importance of some spurious effects. Since the source is in vacuum, the recoils from the β disintegration and the ejection of aggregates of ThC nuclei from the source by α -disintegration might shorten the half lifetime of the active deposit. The correction applied for the decay during the measurements would then be too small. Another spurious effect would arise if ThX nuclei reached the foil during the activation. A weak group of α -particles emitted by ThX, Th and ThA might be confused with those from the ThC group since the difference in energy is small (5.7, 6.28, 6.77 mev respectively, compared with 6.06 mev for ThC' α -particles).

A comparison, carried out over 80 hours, of the γ -ray intensity of two sources, one covered and the other kept in vacuum, showed that these effects were negligible. In particular, an upper limit of 0.5×10^{-3} times the initial strength of the source was found for the amount of ThX collected with the RdTh active deposit.

§ 6. RESULTS

Our measurements really yield two data:

- (1) The branching ratio of ThC which is defined as

$$R = \frac{\text{number of } \alpha\text{-particles emitted by ThC}}{\text{number of } \alpha\text{-particles emitted by ThC + C'}} = \frac{a - b}{a}.$$

- (2) The absolute number of α -particles emitted in the branch ThC-C'-D.

(a) Branching Ratio of ThC

Table 2 shows the values obtained for the branching ratio, for several measurements, corrected for the tail of the pulse height distribution. We give the value of the probable error on the branching ratio $\Delta R/R = (P_a^2 + P_b^2)^{1/2}$, P_a

Table 2

Curves	3	4	5	6
Branching ratio	0.355	0.3536	0.3524	0.3554
Statistical error (%)	1.4	1.4	1.55	1.45

and P_b being the probable error on the counting rates a and b . Though the counts on each plateau were of the order of 35 to 40 thousand for each of the four measurements, we still have a large statistical error on R . This is because one has to measure separately a and b to obtain the difference $a - b$.

The combined statistical error of the branching ratio is 0.72%. Since the error on the extrapolation is certainly less than 0.3%, the value of the branching ratio is given to an accuracy of within 1%. We can then say that $R = 0.354 \pm 0.004$.

Previous results were 0.35 ± 0.012 , obtained by Meitner and Freitag (1926) using a cloud chamber and 0.377 ± 0.007 by Kovarik and Adams (1939). The latter authors, using an ionization chamber, measured the α -particles from a RdTh source in secular equilibrium with the daughter substances. The method suffered from lack of resolution and the quoted accuracy (within 2%) seems overestimated.

(b) Number of 2.615 MeV γ -Rays Emitted by 1 mg Radium Equivalent of RdTh Active Deposit on the Curie Chamber

The milligram radium equivalent of RdTh active deposit on the Curie chamber is defined as the quantity of ThB in secular equilibrium with all the daughter substances, which gives the same ionization current as 1 mg of radium. We shall call τ the number of the ThC'' disintegrations taking place in 1 mg radium equivalent of RdTh active deposit.*

The Curie chamber (Curie 1912) has already been discussed elsewhere (Wilson and Bishop 1949). It permits the comparison of two sources with great accuracy by means of their emitted γ -rays. Several improvements of the chamber itself and the electronic apparatus are embodied in the new design. It is now possible to compare sources of one millicurie to an accuracy of within 0.25%. The instrument was tested by following the decay of RdTh active deposit sources over 30 hours. A value of 10.64 ± 0.03 hours was found. This is in agreement with the accepted value 10.60 h (International Radium Standard Commission Report, 1931).

Sources 3, 4, 5 and 6 were compared with a radium standard of 1.01 mc (N.P.L. certificate). The standard is contained in platinum (0.5 mm wall thickness) and was measured at the National Physical Laboratory on their substandard ionization chamber. This chamber is of different geometry from the Curie chamber; in particular the γ -rays are absorbed by 5 mm of lead in the N.P.L. geometry and by 10 mm on the Curie chamber. The radiation of the source is not homogeneous and the absorption of the soft components is different from that of the hard components in the two geometries. We must therefore correct the effective value of the standard obtained at the National Physical Laboratory for use with measurements on our Curie chamber. The correction is estimated from the results of Kaye *et al.* (1934), who measured the relative absorption of the radiation in the walls of the source as a function of the thickness of lead in front of the N.P.L. ionization chamber. They found that the relative absorption is less with a thickness of 12 mm of lead than with 5 mm by a factor of 0.81. The figure for a thickness of 12 mm of lead is used because the γ -rays pass obliquely through the 10 mm thick plate of the Curie chamber. For the N.P.L. geometry there is a correction of 6.2% to the effective value of the standard. The radium standard therefore has the value $1.01 \times 1.062/1.050 = 1.021$ mc on our geometry.

* It would not be correct to call this quantity a milligram radium equivalent of ThC'' since the contribution of the γ -rays of ThB, C to the ionization current is not negligible.

Table 3 shows the results. The value of the milligram radium equivalent of RdTh active deposit was found to be 1.083 ± 0.016 mc.

The total error (1.5%) is the sum of 1% inaccuracy for the radium standard and 0.5% for the combined standard deviation on the measurements of the counting rate (0.3%), the comparison of the sources on the Curie chamber (0.3%) and the measurement of the solid angle subtended by the window (0.2%).

The value of τ was found to be 0.384 ± 0.009 mc. The standard deviation on the counting rate is now 1.3%, so that the total error is 2.35%. The value of the milligram radium equivalent of RdTh active deposit agrees, within the limit of the error, with the value found by Ricoux (1938, 1.10) and Winand (1939, 1.11).

For work in this laboratory the 1% inaccuracy of the radium standard cancels out, since we can always compare our sources with this standard.

Table 3

Curves	3	4	5	6
mg radium equiv. of RdTh active dep. (mc)	1.075	1.084	1.078	1.094
Stand. deviation on counting rate (%)	0.65	0.7	0.6	0.7
τ (mc)	0.3816	0.3833	0.380	0.3888
Stand. deviation on counting rate (%)	2.05	2.1	2.25	2.15

§ 7. NEW VALUE OF THE CROSS SECTION FOR THE PHOTODISINTEGRATION OF THE DEUTERON AT 2.615 MeV

Adopting the new value for the number of 2.615 MeV γ -rays emitted by 1 mg radium equivalent of RdTh active deposit, one can correct the value of the cross section measured before (Bishop *et al.* 1950). With the notations used by these authors, the cross section is given by the ratio S/T where S is a factor which reduces the observed photo-proton counting rate, in the counting geometry adopted, to that expected from a RdTh source equivalent, on the Curie chamber, to the radium standard used, and T is the number of γ -rays emitted per unit time by this fictitious RdTh source.

Our measurements deal with the value of T and provide a correction to the value adopted in the previous paper.

The radium standard used in the cross section determination was calibrated by the National Physical Laboratory and was 226 mc on their ionization chamber. The present radium standard was 1.01 mc on the same ionization chamber. The quoted inaccuracy for these determinations is 1% (N.P.L. certificates R.9467, C.2521). In order to decrease this 2% inaccuracy we have compared these radium sources on our Curie chamber and found a ratio of 229.4 ± 2.0 instead of the value 225.50 obtained from the N.P.L. quotations after correction for the difference of geometry. Since the strengths of the sources were widely different, the comparison was made via an intermediate substandard (8.7 mc). Thus the error of two successive comparisons (0.9%) enters in the ratio found.

The connection with the cross section measurements is made in the following way. The number of 2.615 MeV γ -rays emitted per second by the RdTh source

was in the previous estimation:

$$N_1 = T_1 \times \frac{I(\text{RdTh})}{I(\text{Ra}_1)} = \frac{I(\text{RdTh})}{I(\text{Ra}_1)} \times S(\text{Ra}_1) \times \frac{1.101}{1.0818} \times R_1 \times B_1$$

where $I(\text{RdTh})/I(\text{Ra}_1)$ is the ratio of the ionization currents of the RdTh source to the radium standard used.

$S(\text{Ra}_1)$ is the strength of this radium standard on the N.P.L. geometry. The factor $1.101/1.0818$ takes account of the difference between the N.P.L. geometry and our geometry. R_1 is the milligram radium equivalent of RdTh active deposit on the basis of Ricoux's and Winand's measurements (1.11 mc). B_1 is the value of the branching ratio used (0.34).

The number of the 2.615 mev γ -rays in the new estimation is

$$N_2 = T_2 \times \frac{I(\text{RdTh})}{I(\text{Ra}_1)} = \frac{I(\text{RdTh})}{I(\text{Ra}_1)} \times \frac{I(\text{Ra}_1)}{I(\text{Ra}_2)} \times S(\text{Ra}_2) \times \frac{1.062}{1.050} \times \tau$$

where $I(\text{Ra}_1)/I(\text{Ra}_2)$ is the ratio of the two radium standards measured on our Curie chamber and corrected for the slight decay during the period between the two measurements, $S(\text{Ra}_2)$ the strength of the new radium standard on the N.P.L. geometry, $1.062/1.050$ the correction factor for the difference between the two geometries and τ the number of γ -rays emitted by 1 mg radium equivalent of RdTh active deposit (evaluated in mc) in the new estimation.

The new value of the cross section is found by multiplying the previous value by the ratio N_1/N_2 . The previous value of the cross section was quoted to be $(13.9 \pm 0.4) \times 10^{-28} \text{ cm}^2$. The inaccuracy was the sum of an 0.5% inaccuracy in the value of S , and 2.4% in the value of T . This did not include a possible systematic error between 3 or 4% for the milligram radium equivalent of RdTh active deposit and the branching ratio.

The new value of the cross section is $(13.80 \pm 0.38) \times 10^{-28} \text{ cm}^2$. The factor

$$T = \frac{I(\text{Ra}_1)}{I(\text{Ra}_2)} \times S(\text{Ra}_2) \frac{1.062}{1.050} \times \tau,$$

so that the total error on it is the sum of 0.9% for the error in $I(\text{Ra}_1)/I(\text{Ra}_2)$ and 1.35% for the error in the product $S(\text{Ra}_2) \times \tau$. The total inaccuracy in the value of the cross section is now 2.75%.

ACKNOWLEDGMENT

We thank Lord Cherwell for extending to us the facilities of the Clarendon Laboratory.

REFERENCES

- BISHOP, G. R., COLLIE, C. H., HALBAN, H., HEDGRAN, A., SIEGBAHN, K., DU TOIT, S., and WILSON, R., 1950, *Phys. Rev.*, **80**, 15.
 BISHOP, G. R., HALBAN, H., and WILSON, R., 1950, *Phys. Rev.*, **77**, 416.
 CURIE, Mm̄e. P., 1912, *J. Phys. Radium*, Ser. 5, **11**, 795.
 International Radium Standards Commission Report, 1931, *Rev. Mod. Phys.*, **3**, 427.
 KAYE, G. W. H., ASTON, G. H., PERRY, W. E. T., 1934, *Brit. Inst. Rad.*, **7**, 540.
 KOVARIK, A. F., and ADAMS, W. I., 1939, *Phys. Rev.*, **34**, 413.
 MEITNER, L., and FREITAG, K., 1926, *Z. Phys.*, **37**, 481.
 RICOUX, A., 1937, *J. Phys. Radium*, Ser. 7, **8**, 388.
 WILSON, R., and BISHOP, G. R., 1949, *Proc. Phys. Soc. A*, **62**, 457.
 WINAND, L., 1939, *J. Phys. Radium*, Ser. 7, **10**, 361.

The ${}^2\Sigma^+ - {}^2\Pi_1$ Band System of HBr^+

BY R. F. BARROW AND A. D. CAUNT

Physical Chemistry Laboratory, University of Oxford

MS. received 27th March 1953

Abstract. Rotational analyses of the 1, 1 and 0, 1 bands of the ${}^2\Sigma^+ - {}^2\Pi_1$ system of HBr^+ have been made from spectrograms of moderate dispersion. The value of $\Delta G_{1/2}''$ is found to be 2348.3 cm^{-1} . Estimates of the equilibrium vibrational constants for the ground state are: $\omega_e'' \sim 2450$, $x_e''\omega_e'' \sim 50 \text{ cm}^{-1}$.

§ 1. INTRODUCTION

A MANY-LINED spectrum observed in hollow-cathode discharges in hydrogen in the presence of potassium fluoride was recently analysed (Caunt and Barrow 1952) and ascribed to a hydride of a first-row element. It has however not yet been possible to identify the emitter of this spectrum. The possibility that it is HF^+ led us to consider the spectrum of HBr^+ with a view to predicting as far as possible the spectroscopic behaviour of HF^+ .

The spectrum of HBr^+ was obtained by Norling (1935) using a hollow-cathode discharge in HBr gas. A rotational analysis of what were assumed to be the 0, 0 and 1, 0 bands was carried out, and the system shown to arise from a ${}^2\Sigma \rightarrow {}^2\Pi_1$ transition analogous to that in HCl^+ . No direct information about the ground-state vibrational constants was obtained.

The purpose of the present note is to summarize the rotational analyses of the 0, 1 and 1, 1 bands: the results confirm Norling's analysis and enable values of the ground-state vibrational constants to be derived.

§ 2. EXPERIMENTAL

We have found that the ${}^2\Sigma \rightarrow {}^2\Pi_1$ system is conveniently excited by a high-frequency electrodeless discharge in HBr gas, operating at about 3 Mc/s. The spectrum was photographed in a first order of a 2.4 m grating in an Eagle mounting giving a reciprocal dispersion of about 7.4 \AA/mm .

Our measurements of the lines of the 1, 0 and 0, 0 bands agree well with those of Norling, but his were made using a grating instrument of considerably higher dispersion than ours, and Norling's measurements of the lines of these bands have been used in the analysis below. The wave numbers of the lines of the 0, 1 and 1, 1 bands are given in table 1.

Table 1. Wave Numbers of the 0, 1 and 1, 1 Bands of HBr⁺

0, 1 Band. $^2\Sigma \rightarrow ^2\Pi_{3/2}$						
J	$^sR_{21}$	R_1	$^RQ_{21}$	Q_1	$^oP_{21}$	P_1
$1\frac{1}{2}$	26931.45	26902.5*	26897.35	26878.25	26875.1	26865.45
$2\frac{1}{2}$	938.65	900.25	892.9	864.3	859.1	839.75
$3\frac{1}{2}$	941.95*	894.2	884.7*	846.55	—	810.55
$4\frac{1}{2}$	941.95*	884.7*	873.05	825.15	815.4	777.55
$5\frac{1}{2}$	937.75	871.1	857.4	800.2	788.45*	740.9
$6\frac{1}{2}$	929.6	853.85	838.2	771.55	757.7*	700.55
$7\frac{1}{2}$	917.8	832.85	815.4*	738.9	723.1*	656.6
$8\frac{1}{2}$	902.5*	807.8	788.45*	702.9	684.9*	609.25
$9\frac{1}{2}$	882.85	779.35	757.7*	662.8	642.95	557.55*
$10\frac{1}{2}$	—	746.9	723.1*	619.45	597.65	503.35
$11\frac{1}{2}$	—	710.3	684.9*	572.0	548.25	444.7
$12\frac{1}{2}$	—	—	642.55	—	—	—
0, 1 Band. $^2\Sigma \rightarrow ^2\Pi_{1/2}$						
J	R_2	$^oR_{12}$	Q_2	$^RQ_{12}$	P_2	$^oP_{12}$
$1\frac{1}{2}$	—	—	—	—	—	—
$1\frac{1}{2}$	—	24239.95	24234.5	24210.95*	24208.35	—
$2\frac{1}{2}$	—	238.25	231.1	196.4	190.95	—
$3\frac{1}{2}$	—	232.95	223.5*	177.1	169.65	—
$4\frac{1}{2}$	—	223.5*	212.2	154.6	144.8	—
$5\frac{1}{2}$	—	210.95*	197.15	—	116.2	—
$6\frac{1}{2}$	—	193.95	177.8	097.5*	083.8	—
$7\frac{1}{2}$	—	172.85	155.4	063.3*	047.45	—
$8\frac{1}{2}$	—	148.4	—	025.1*	007.35	—
$9\frac{1}{2}$	—	119.9	097.5*	23983.4	23963.7	—
$10\frac{1}{2}$	—	087.3	063.3*	—	915.7	—
$11\frac{1}{2}$	—	050.75	025.1*	888.55	864.55	—
$12\frac{1}{2}$	—	010.5	23982.6	835.4	809.15	—
$13\frac{1}{2}$	—	23966.2	936.4	—	750.05	—
1, 1 Band. $^2\Sigma \rightarrow ^2\Pi_{3/2}$						
J	$^sR_{21}$	R_1	$^RQ_{21}$	Q_1	$^oP_{21}$	P_1
$1\frac{1}{2}$	28257.4	—	28224.8	28206.3*	28203.3	28194.45*
$2\frac{1}{2}$	262.85	—	218.55*	191.45	186.3	168.15
$3\frac{1}{2}$	263.55	28218.55*	208.8	172.35	165.1	137.7
$4\frac{1}{2}$	260.35	206.3*	194.45*	148.85	139.95	—
$5\frac{1}{2}$	252.85	189.2	175.9	121.35	—	064.5
$6\frac{1}{2}$	—	—	153.1	089.35	076.25	021.8
$7\frac{1}{2}$	—	143.2	126.1	—	038.2	27974.9*
$8\frac{1}{2}$	—	—	094.5	013.45	27996.0	923.75
$9\frac{1}{2}$	—	—	058.9	27969.0	949.7	—
$10\frac{1}{2}$	—	—	019.2	920.4	—	—
1, 1 Band. $^2\Sigma \rightarrow ^2\Pi_{1/2}$						
J	R_2	$^oR_{12}$	Q_2	$^RQ_{12}$	P_2	$^oP_{12}$
$1\frac{1}{2}$	—	25566.1	25562.45*	25551.75	—	—
$1\frac{1}{2}$	—	567.25	562.45*	539.45	25536.35	—
$2\frac{1}{2}$	—	564.1	556.65*	523.4	—	25505.85
$3\frac{1}{2}$	—	556.65*	547.45	502.7	495.45	476.15
$4\frac{1}{2}$	—	—	533.35	478.0	468.75	—
$5\frac{1}{2}$	—	528.6	—	448.6	437.65	—
$6\frac{1}{2}$	—	508.4	493.2	—	401.95	—
$7\frac{1}{2}$	—	483.45	466.4	377.75	362.25	—
$8\frac{1}{2}$	—	454.35	435.35	335.65	318.4	—
$9\frac{1}{2}$	—	421.0	399.6	289.35	269.95	—
$10\frac{1}{2}$	—	382.55	—	238.55	217.15	—
$11\frac{1}{2}$	—	—	—	183.8	160.8	—

* indicates a line used more than once in the analysis.

§ 3. ANALYSIS

The theory of $^2\Sigma \rightarrow ^2\Pi_1$ transitions has been treated by Mulliken (1930) and by Herzberg (1950). The method of analysis and the nomenclature used here are essentially the same as those used by Ramsay (1952) in his analysis of bands of SH and SD.

(i) *The Upper State*

The upper-state term-values were obtained from Norling's measurements of the 0, 0 and 1, 0 bands.

Spin-Splitting. Values of γ_K were evaluated from combination differences such as $^PQ_{12}(J+1) - P_2(J+1) = ^Q R_{12}(J) - Q_2(J)$. The small variation of γ_K with K was assumed to follow the relation $\gamma_K = \gamma_0/[1 + (D_e'/B_e')K(K+1)]$ from which γ_0 was derived.

B_v' and D_v' . The rotational constants were calculated from combination differences such as

$$\begin{aligned} R_1(J) - P_1(J) - \gamma_K &= ^S R_{21}(J-1) - ^Q P_{21}(J-1) + \gamma_K \\ &= ^R Q_{21}(J) - P_1(J) + J\gamma_{K-1} = ^S R_{21}(J-1) - Q_1(J-1) + J\gamma_{K-1} \\ &= (4B_v' - 6D_v')(K + \tfrac{1}{2}) - 8D_v'(K + \tfrac{1}{2})^3, \text{ where } K = J - \tfrac{1}{2}, \end{aligned}$$

using graphical methods.

$\Delta G_{1/2}'$ and α_e' . Values of $\Delta G_{1/2}'$ and of α_e' were derived using formulae such as

$$\tfrac{1}{2}\{Q_1(J) + Q_2(J)\}^{(1,0)} - \tfrac{1}{2}\{Q_1(J) + Q_2(J)\}^{(0,0)} = \Delta G_{1/2}' + (B_1' - B_0')(J - \tfrac{1}{2})(J + \tfrac{1}{2}),$$

neglecting terms in $(D_1' - D_0')$ and $(\gamma_0^{(1)} - \gamma_0^{(0)})$. The value of α_e' obtained in this way (0.249 cm^{-1}) agrees well with that derived from the values of $\Delta_2 F'(K)$ (0.247_6 cm^{-1}).

(ii) *The Lower State*

Term formulae for $^2\Pi$ states have been given by Hill and Van Vleck (1923), Mulliken and Christy (1931) and Almy and Horsfall (1937). The ground-state constants were obtained using upper-state term values, F_1' and F_2' derived as above: for example,

$$P_1(J) - F_1'(J - \tfrac{3}{2}) = ^R Q_{21}(J) - F_2'(J + \tfrac{1}{2}) = R_1(J) - F_1'(J + \tfrac{1}{2}) = \nu_0^{(1)} - F''_{1,d}(J).$$

B_v'' and D_v'' . The average values of $\Delta_2 F''(J)$ are related, according to Hill and Van Vleck, to the ground-state rotational constants, B_v'' and D_v'' , by the expression

$$\frac{\Delta_2 F''_{1,c}(J) + \Delta_2 F''_{1,d}(J) + \Delta_2 F''_{2,c}(J) + \Delta_2 F''_{2,d}(J)}{4J + 2} = (2B_v'' - 7D_v'')(J + \tfrac{1}{2})^2.$$

(Almy and Horsfall give $2D''$ in place of $7D''$: the difference here is negligible.) B_v'' and D_v'' were evaluated graphically from the average values of $\Delta_2 F''(J)$ in the usual way.

The Coupling Constant A. The Hill and Van Vleck formulae lead to

$$\left\{ \frac{F''_{1c,d}(J) - F''_{2c,d}(J) - D_v''[(J+1)^4 - J^4]}{B_v''} \right\}^2 - 4(J + \tfrac{1}{2})^2 = Y(Y-4),$$

where $Y = A/B_v$, and $F''_{1c,d} = (F''_{1c} + F''_{1d})/2$ and similarly for F''_2 . Values of A were derived for each value of J , and these values were then plotted against $(J - \frac{1}{2})^2$ and extrapolated to $(J - \frac{1}{2})^2 = 0$.

Λ -Doubling. The following approximation formulae, applicable to states near Hund's case a , were used:

$$\begin{aligned} \text{For } {}^2\Pi_{1/2} \quad \Delta\nu_{dc}/(J + \tfrac{1}{2}) &= p + 2q, \\ \text{for } {}^2\Pi_{3/2} \quad \Delta\nu_{dc}/(J + \tfrac{1}{2}) &= -(p/4Y^2 + 2q/Y)(J - \tfrac{1}{2})(J + \tfrac{3}{2}), \end{aligned}$$

with $\Delta\nu_{dc} = F''_d(J) - F''_c(J)$. (These formulae differ from those of Mulliken and Christy only in the term $p/4Y^2$, for which they give p/Y^2 .) $\Delta\nu_{dc}$ were negative and very small for ${}^2\Pi_{3/2}$, positive and large in ${}^2\Pi_{1/2}$. A rough value, $q \sim -10^{-2} \text{ cm}^{-1}$, was derived from the ${}^2\Pi_{3/2}$ sub-bands, the term $p/4Y^2$ being quite small compared with $2q/Y$. Values of p for each J -value were calculated from the lines of the ${}^2\Pi_{1/2}$ sub-bands, from which p_0 was obtained using $p = p_0/\{1 + (D_v''/B_v'')J(J+1)\}$. The approximate equality $p({}^2\Pi) \simeq \gamma({}^2\Sigma)$ (see table 3) shows that these two states stand not far from the relation of pure precession (Mulliken and Christy 1931); in this case we should have $q \sim p/Y = -0.6 \times 10^{-2} \text{ cm}^{-1}$, a little smaller than the experimental estimate.

The Band-Origins. Values of ν_0 were obtained for all four bands using the expression

$$\begin{aligned} Q_1(J) + Q_2(J) + D_v'[(J - \tfrac{1}{2})^2(J + \tfrac{1}{2})^2 + (J + \tfrac{1}{2})^2(J + \tfrac{3}{2})^2] - D_v''[J^4 + (J+1)^4] \\ + \phi_1(J) - \phi_2(J) = 2\nu_0 + 2(B_v' - B_v'')J(J+1) + \tfrac{1}{2}B_v' + \tfrac{3}{2}B_v'' - \gamma \end{aligned}$$

where $\phi_1(J) = -\frac{1}{2}\Delta\nu_{1dc}$ and $\phi_2(J) = \frac{1}{2}\Delta\nu_{2dc}$ are Λ -doubling terms. The analysis is confirmed by the Deslandres scheme of band-origins, given in table 2.

Table 2. Deslandres Scheme of Band-Origins

$v' = 0$	29233.2	2348.2	26885.0
	1328.6		1328.7
	27904.6	2348.3	25556.3
	$v'' = 0$		I

A further check on the calculation of the ground-state constants $\Delta G_{1/2}''$ and α_e'' followed from use of the expression

$$\tfrac{1}{2}[Q_1(J) + Q_2(J)]^{(0,0)} - \tfrac{1}{2}[Q_1(J) + Q_2(J)]^{(0,1)} = \Delta G_{1/2}'' + (B_1'' - B_0'')(J - \tfrac{1}{2})(J + \tfrac{3}{2}),$$

in which terms in $(D_1 - D_0)$ and $(\Delta\nu_{dc}^{(1)} - \Delta\nu_{dc}^{(0)})$ are neglected. We obtain $\alpha_e'' = 0.240 \text{ cm}^{-1}$, $\Delta G_{1/2}'' = 2348.4$ as compared with $\alpha_e'' = 0.236_3$ from $\Delta_2 F''(J)$ and $\Delta G_{1/2}'' = 2348.2_5$ from ν_0 . The constants derived in this work are collected together in table 3.

§ 4. DISCUSSION

It is of interest to estimate the equilibrium vibrational constants. For the upper state, $x_e'\omega_e'$ can be derived in two ways: (i) using the relation of Pekeris (see, for example, Herzberg 1950) $x_e'\omega_e' = \{\frac{1}{6}(\alpha_e'\omega_e' + 6B_e'^2)\}^2/B_e'^3$, $x_e'\omega_e' = 41 \text{ cm}^{-1}$; (ii) using Kratzer's relation, $\omega_e'^2 = 4B_e'^3/D_e'$, $\omega_e' \simeq 1407 \text{ cm}^{-1}$, and with

$$\Delta G_{1/2}' = 1328.7, \quad x_e'\omega_e' = 39 \text{ cm}^{-1}.$$

We conclude $\omega_e' \simeq 1409$, $x_e'\omega_e' \simeq 40 \text{ cm}^{-1}$.

For the lower state, the agreement between the two estimates is much less good: $x_e''\omega_e'' \simeq 51 \text{ cm}^{-1}$ (Pekeris), 80 cm^{-1} (Kratzer), using $D_e'' = 3.34_2 \times 10^{-4} \text{ cm}^{-1}$. It is probable that the latter value of $x_e''\omega_e''$ is too high, for the value expected by comparison with HCl^+ , assuming constancy of $x_e\mu^{1/2}$ (with μ = reduced mass) is 50 cm^{-1} , supporting the Pekeris estimate. The poor value obtained from the use of Kratzer's relation arises most probably from an error in the value of D_e'' ,

Table 3. Spectroscopic Constants for HBr^+

Upper State : $^2\Sigma^+$						
	B	r (Å)	D	α	β	γ_0
$v'=1$	5.598 ₈	1.739	$4.27_9 \times 10^{-4}$			2.03 ₇
$v'=0$	5.846 ₄	1.702	4.29 ₃			2.10 ₅
$(v'=-\frac{1}{2})$	5.970 ₂	1.684	4.30 ₀	0.247 ₆	-2.4×10^{-6}	
$\Delta G_{1/2}' = 1328.7 \text{ cm}^{-1}$						
Lower State : $^2\Pi_1$						
	B	r (Å)	D	α		
$v''=1$	7.717 ₅	1.482	$(3.74_7) \times 10^{-4}$			
$v''=0$	7.953 ₈	1.459	3.47 ₇			
$(v''=-\frac{1}{2})$	8.072 ₀	1.448	3.48 ₅ *	0.236 ₃		
	A		Y	p_0	} $\simeq -0.01$	
$v''=1$	-2649.2 ₅		-343.2 ₈	2.05 ₅		
$v''=0$	-2651.6 ₅		-333.9 ₁	2.07 ₀		
$\Delta G_{1/2}'' = 2348.2_5 \text{ cm}^{-1}$						

$$* \text{ From } D_0'', \text{ using } \beta = D_e \left[\frac{8x_e\omega_e}{\omega_e} - \frac{5\alpha_e}{B_e} - \frac{\alpha_e^2\omega_e}{24B_e^3} \right].$$

which is based on values of $\Delta_2 F''(J)$ extending to not very high values of J . Indeed it may be guessed that the value of D_0'' is a little low, that of D_1'' a little high, in agreement with the fact that the value of α_e'' derived from the values of $\Delta_2 F''(J)$ is slightly smaller than that obtained directly from the Q lines. This

Table 4. Values of $\Delta G_{1/2}$

		X=Cl	X=Br	X=I
HX ⁺	$A^2\Sigma^+$	1527	1329	—
HX ⁺	$x^2\Pi_1$	2568	2348	—
HX	$c^1\Pi$	2670	2448	1970
HX	$x^1\Sigma^+$	2886	2559	2330

The values for the c states are from Price (1938); the other values are from Herzberg (1950).

is confirmed by the fact that the experimental value of $(D_0'' - D_1'')$ is considerably greater than the theoretical value (see table 3). We therefore reject the Kratzer estimate, and conclude $\omega_e'' \simeq 2450$, $x_e''\omega_e'' \simeq 50 \text{ cm}^{-1}$.

The close similarity in the behaviour of the vibrational intervals for HCl , HBr and the ionized molecules is illustrated in table 4, and it may be predicted that $\Delta G_{1/2}$ for $x^2\Pi$ of HI^+ is about 90% of 2330, i.e. about 2100 cm^{-1} . Price (1938) has already suggested that the coupling constant A in the ground state

of HI^+ should be about 5500 cm^{-1} , so that the spectrum of this molecule should be identifiable without difficulty. However the attempts of Norling (1937) and of the authors to excite this spectrum have met with no success.

In the case of HF^+ , the change in order of the ionization potentials, the ionization potential of the halogen here being greater than that of hydrogen, may lead to a breakdown of these simple regularities, and, as Norling suggested, it seems most probable that the $^2\Sigma \rightarrow ^2\Pi$ or $^2\Pi \rightarrow ^2\Sigma$ system of HF^+ is to be sought in the red region of the spectrum. The possibility that the many-line spectrum which prompted the present investigation is a $^2\Sigma \rightarrow ^2\Sigma$ transition in HF^+ remains.

ACKNOWLEDGMENT

One of the authors (A. D. C.) wishes to thank Imperial Chemical Industries Limited for the award of a Research Fellowship.

REFERENCES

- ALMY, G. M, and HORSFALL, R. B., 1937, *Phys. Rev.*, **51**, 491.
CAUNT, A. D., and BARROW, R. F., 1952, *Proc. Phys. Soc. A*, **65**, 373.
HERZBERG, G., 1950, *Molecular Spectra and Molecular Structure*, Vol. I (New York: Van Nostrand).
HILL, E. L., and VAN VLECK, J. H., 1923, *Phys. Rev.*, **32**, 250.
MULLIKEN, R. S., 1930, *Rev. Mod. Phys.*, **2**, 60.
MULLIKEN, R. S., and CHRISTY, A., 1931, *Phys. Rev.*, **38**, 87.
NORLING, F., 1935, *Z. Phys.*, **95**, 179; 1937, *Ibid.*, **106**, 177.
PRICE, W. C., 1938, *Proc. Roy. Soc. A*, **167**, 216.
RAMSAY, D. A., 1952, *J. Chem. Phys.*, **20**, 1920.

The Influence of Domain Structure on the Magnetization Curves of Single Crystals

By E. W. LEE

University of Nottingham

Communicated by L. F. Bates; MS. received 13th February 1953

Abstract. It is pointed out that the lack of agreement between theoretical and experimental magnetization curves found for single crystals in low fields is probably caused, not by residual internal strains, but by neglect of the domain structure of the crystal in the theoretical calculations. Using Néel's model for the domain structure of a single crystal of iron in the form of a strip parallel to the $[110]$ direction, magnetization curves have been calculated taking the domain structure into proper account. It is found that the (I, H) curves depend explicitly on the width of the crystal. Comparison is made between the calculated curves and the experimental results of Williams. The agreement between the two is good.

§ 1. INTRODUCTION

IT is well known that the simple domain theory may be used to calculate the magnetization curves of ferromagnetic single crystals. Formally, such calculations are carried out by setting down the free energy of the system in terms of the known variables and seeking to make this a minimum. This free energy of unit volume of a single domain is, for a cubic crystal, given by

$$E = -HI_s \cos \theta + K_1(\alpha_1^2\alpha_2^2 + \alpha_2^2\alpha_3^2 + \alpha_3^2\alpha_1^2) + K_2\alpha_1^2\alpha_2^2\alpha_3^2, \dots\dots(1)$$

where the first term represents the magnetic potential energy and the second and third terms together represent the crystal anisotropy energy, and in which θ is the angle between the direction of the spontaneous magnetization I_s in the domain and H , and K_1 and K_2 are the crystal anisotropy constants and $\alpha_1, \alpha_2, \alpha_3$, the direction cosines of the spontaneous magnetization with respect to the cubic crystal axes. In this way (I, H) curves have been calculated for single crystals magnetized along the three principal directions by Akulov (1931) and others, and these calculations have been extended by Lawton and Stewart (1948) to cover arbitrary directions of H . In most cases the agreement between theory and experiment is very good, particularly in high fields. In very low fields, however, small but definite discrepancies are found, namely in that the calculated curves possess sharp corners which are not found by experiment. For example, the calculated curve for a single crystal magnetized along the $[110]$ direction shows that the magnetization rises to a value $I/\sqrt{2}$ in substantially zero effective field. As the field is increased the magnetization increases slowly from this value until saturation is reached at a field strength which, for iron, is approximately 600 oersteds. The experimental points lie beneath the theoretical curve for all field strengths below about 30 oersteds.

Such discrepancies between theory and experiment are usually attributed to internal strains. In other words, a term should be added to eqn. (1) which

may not possess the same symmetry as the second and third terms. However, in spite of such careful annealing that only magnetostrictive stresses may reasonably be supposed to remain, discrepancies still persist. Now, the free energy associated with pure magnetostrictive stresses is of the order $\frac{1}{2}E_{100}\lambda_{100}^2$, or some 500 erg cm^{-3} , i.e. smaller than K_1 by a factor of about 10^3 . It seems desirable therefore to seek elsewhere for the cause of the differences. One likely suggestion is that, in applying eqn. (1) to an actual single crystal, no account has been taken of the detailed domain structure. In any actual single crystal the domain structure may be complicated; in particular, closure domains exist whose purpose it is to lower the free energy of the system, and the direction of the magnetization in these domains is in general not the same as that given by minimizing eqn. (1). Equation (1) is therefore applicable only to an infinite crystal in which the volume of the closure domains may be neglected in comparison with the main (primary) domains; but in any actual crystal the domain structure should be taken into account. The effect of the closure domains on the (I, H) curve is calculated below for an actual crystal, and the results are compared with experiment.

§2. CALCULATION OF MAGNETIZATION CURVES

On the above considerations it is evident that to calculate magnetization curves for an actual single crystal an accurate knowledge of its domain structure is required. This may in principle be obtained from observation of Bitter patterns on the surfaces of single crystals, but apart from the fact that such observations may not always be easily and reliably interpreted, except in a few simple cases, the patterns themselves may be somewhat indistinct and the domain width difficult to measure accurately in low fields where the chief divergences between theoretical and experimental (I, H) curves are found.

The calculations are therefore confined to the single case of a crystal in the form of a strip parallel to the (100) plane with the long axis of the strip parallel to the $[110]$ direction. This case has been extensively investigated by Néel (1944), who showed that the domain structure is relatively simple. The structure predicted by Néel is shown in fig. 1; it has been confirmed in essentials by Bates and Neale (1949, 1950), Bates and Mee (1952), and by Williams, Bozorth and Shockley (1949) by the Bitter pattern technique.* In a very small, almost zero, effective field the primary domains are packed like the leaves of a book with their planes perpendicular to the $[011]$ axis and the magnetization vectors are directed equally along $[001]$ and $[0\bar{1}0]$. In addition, there are certain so-called antiparallel closure domains or q domains. These prismatic domains have their magnetization vectors parallel or antiparallel to the $[100]$ direction, and help to reduce the magnetostatic energy associated with free poles which would appear if the primary domains extended to the edge of the strip. Under a small (effective) field the magnetization vectors of the primary domains are rotated towards the $[110]$ direction and at the same time an additional set of closure domains, the p domains, appears. The p domains have their magnetization vectors directed approximately along the $[110]$ direction. As the field is increased the magnetization is increased by the rotation of the magnetization vectors of the primary domains towards the $[110]$ direction. At the same time

* According to Williams (private communication) there is considerable evidence to show that in very low fields the domain structure is that proposed by Lawton (1950). The difference between the Lawton and Néel schemes is, however, not great enough to alter the present results appreciably.

the volumes of the primary and the q domains decrease whilst that of the p domains increases.

At any value of the field the angle θ made by the magnetization vector of the primary domain with the $[110]$ direction is given by eqn. (1) which now reduces to

$$HI_s = 2K_1 \cos \theta (2 \cos^2 \theta - 1). \quad \dots\dots(2)$$

Following Néel's treatment, we readily find that the volumes of the p and q closure domains are given by

$$V_p = \frac{d^2}{4} \frac{W_q}{W_p + W_q} \frac{\sin \theta}{1 - \cos \theta}, \quad \dots\dots(3)$$

$$V_q = \frac{d^2}{4} \frac{W_p}{W_p + W_q} \tan \theta, \quad \dots\dots(4)$$

where d is the distance between successive p or q domains as indicated in fig. 1. The quantities W_p and W_q are the energies of formation of the p and q closure domains respectively, and represent the difference between the energies of the primary and closure domains, viz.

$$W_p = K_1 \sin \theta \cos \theta (2 + 3 \cos \theta) (1 - \cos \theta),$$

$$W_q = K_1 \tan \theta (6 \cos^2 \theta + 1) (2 \cos^2 \theta - 1).$$

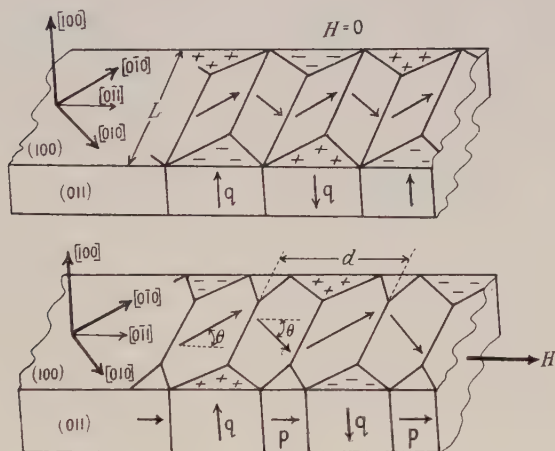


Fig. 1. Domain structure proposed by Néel. Easy direction $[100]$.

The derivation of these expressions (during the process of which it is shown that the p and q domains have their magnetization vectors directed approximately as in fig. 1) is quite straightforward, and for further details reference should be made to the original paper. According to Néel d is given by

$$d^2 W_p W_q = \gamma L (W_p + W_q), \quad \dots\dots(5)$$

where γ is the energy per cm^2 of the wall between adjacent primary domains and L is the width of the strip. Using this value for d , the expressions for V_p and V_q may be put in the simpler forms

$$V_p = \frac{\gamma L}{4W_p} \frac{\sin \theta}{1 - \cos \theta}, \quad \dots\dots(6)$$

$$V_q = \frac{\gamma L}{4W_q} \tan \theta. \quad \dots\dots(7)$$

The variation of V_p , V_q and d with H is shown in fig. 2, from which it is evident that the volume of q closure domains may be quite an appreciable fraction of the total volume in very low fields.

Assuming that the p and q domains have their magnetization vectors set exactly as indicated in fig. 1, the resultant magnetization is

$$I = \frac{I_s V \cos \theta + V_p I_s}{V + V_p + V_q}, \quad \dots\dots(8)$$

where V is the volume of primary domains, and $V + V_p + V_q = Ld/2$.

Magnetization curves in low fields calculated from eqns. (2), (6), (7) and (8) are shown in fig. 3 for several widths of a single crystal of iron strip. It may be noted that as H is reduced d increases and eventually becomes equal to L . For lower field strengths the postulated domain structure must therefore break down, and consequently no attempt has been made to carry the calculations down to $H = 0$.

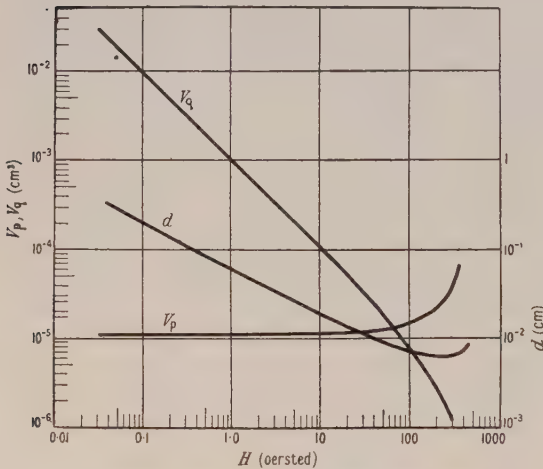


Fig. 2. Variation with applied field strength of the line spacing d and the volumes of the p and q closure domains for a single crystal strip of iron 1 cm wide. The primary domain width is equal to $d/2$.

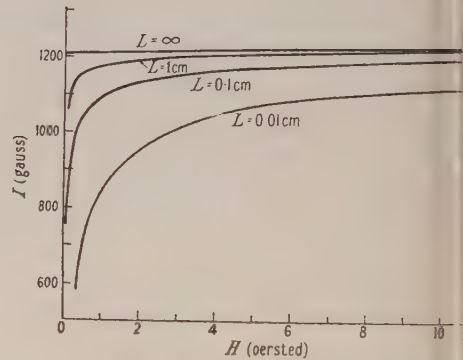


Fig. 3. Theoretical magnetization curves for a single crystal strip of iron in the [100] direction for various crystal widths.

In small fields the closure domains are predominantly of the antiparallel (q) type, and so the magnetization becomes smaller the greater their volume. The volume of primary domains is not very different from $Ld/2$ (actually it is rather less). The volume of the closure domains is proportional to L and so the ratio of the volumes of closure to primary domains is proportional to $L^{-1/2}$. Thus the influence of the closure domains on the magnetization curve becomes greater the smaller the width of the strip. The simple case in which domain structure is neglected is therefore seen to correspond to the limiting case of $L = \infty$. The effect of the q domains is thus to reduce the magnetization in low fields from that given by eqn. (2), the reduction becoming smaller as H is increased. For H greater than 40 oersteds the effect of the closure domains for $L = 1$ cm is less than 1%, and it is gratifying to note that there is in general good agreement between simple theory and experiment for higher values of H . In large fields of the order 200–300 oersteds, the p domains grow at the expense of the q domains and soon

become appreciable compared with the volumes of the primary domains, which in this field range are very small. The magnetization therefore rises above the value calculated from eqn. (2). This effect is too small to be visible on a graph and appears to be too small to be detected by experiment.

§3. COMPARISON WITH EXPERIMENT

Néel's treatment applies to a single crystal in the form of a strip of infinite length where demagnetization effects are non-existent. Unfortunately single crystals in the form of very long strips are not easy to make, and so it is necessary to measure (I, H) curves on crystals which have relatively large demagnetizing factors. This entails measuring the effective field either by assuming a value for the demagnetization factor, in which case the effective field is given by the difference between two relatively large quantities, or by the use of a magnetic potentiometer. However, in the region of greatest interest for which $H < 5$ oersteds, and with only small specimens available, this cannot be done with any accuracy, and there appear to be no data for strips in the literature which are either relevant or of sufficient reliability. The calculations have therefore been compared with the experimental results of Williams (1937) for a picture-frame crystal of 3.85% silicon-iron cut so that each leg lies along a $[110]$ direction. With a specimen of this shape the applied field may be found however small it may be. Moreover, with the closed magnetic circuit existing in such a crystal the actual conditions are likely to approach the case of an infinite strip more closely than those existing in a strip of finite length. The dimensions of Williams' crystal are given as (1.49×1.17) cm—area of cross section 0.0670 cm²—and so the only regions where the behaviour of the picture frame may be expected to differ from that of a long strip, namely the corners, amount to only 5% of the whole and may be neglected for the present purpose. Accordingly the (I, H) curve has been calculated as in the preceding section for a strip of 3.85% Si-Fe using the values of K_1 and I_s found by Williams, i.e. $K_1 = 2.80 \times 10^5$ erg cm⁻³, $I_s = 1625$. The results are shown in fig. 4 together with Williams' experimental points*. The agreement between theory and experiment is quite good in fields greater than about 1 oersted. For very low fields the experimental points lie well below the calculated curve, and this is in agreement with the observations of Williams, Bozorth and Shockley (1949) that in such fields the primary domains become split into two antiparallel domains by the formation of a 180° wall, a possibility not considered in the simple treatment of Néel. It is true that the Bitter patterns were observed by Williams, Bozorth and Shockley on a strip with non-negligible demagnetization factor, whereas the crystal under consideration here is a picture frame in which the flux is closed. There is no *a priori* reason why the break up of the primary domains should be the same here as for the strip, but it is clear that the Néel structure breaks down in very low fields, and the appearance of antiparallel primary domains is not unlikely (cf. Bates and Martin 1953). In high fields, too, the simple Néel structure is known to break down (Bates and Mee 1952). In particular the p domains are much more complicated in structure than simple theory suggests. However, in such fields the line spacing, and hence the volume of closure domains, is small and the inadequacy of the theoretical model becomes unimportant.

* In Williams' original paper no figures are given. Those shown in fig. 4 have been kindly supplied to the author by Dr. H. J. Williams.

It is to be noted that the experimental points in fig. 4 consistently lie below the calculated curve. Now the value of I_s used, namely 1625, although somewhat greater than the accepted value for 3.85% Si-Fe, is in fact the lowest value consistent with Williams' (I, H) curve. Using the accepted value for I_s would in fact bring the calculated curve exactly on the experimental points but there is clearly little justification for this procedure. On the other hand there is good reason to expect the calculated curve to lie above the experimental one for the following reason. Observations by Bates and Neale (1949, 1950) and Bates and Mee (1952) indicate that whereas the variation of primary domain width with field is as predicted by Néel, the actual magnitude of the line spacing d is greater than the theoretical value. The experiments of Williams, Bozorth and Shockley show that the observed and theoretical domain widths are equal only for crystals less than 1 mm wide. For a crystal whose width (as here) is 2.3 mm the observed domain width is about twice the theoretical value. Thus for the crystal used here the effects of closure domains are likely to be about twice as great as those given by our calculations. It is reasonable to assume therefore that by using the correct (i.e. observed) values for the domain width the calculated and experimental behaviours would be brought closer together. Moreover no account has been taken of the closure domains that exist inside the crystal around inclusions and imperfections. The importance of such domains has recently been demonstrated by Bates and Martin (1953).

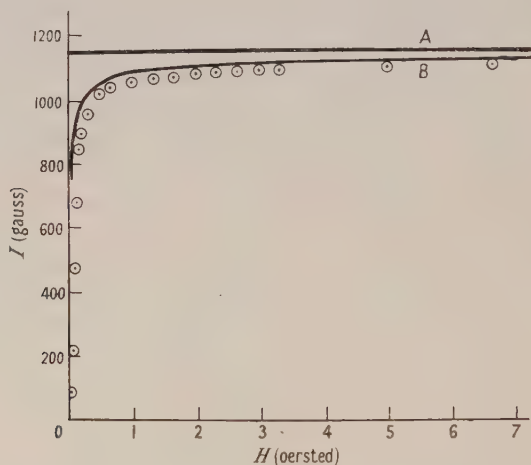


Fig. 4. Theoretical magnetization curves for a 3.85% Si-Fe single crystal. A: calculated from eqn. (2) neglecting the domain structure. B: calculated from eqn. (8) taking the effects of the closure domains into account. Experimental points due to Williams (1937).

§ 4. DISCUSSION AND CONCLUSIONS

The considerations presented above indicate that even a perfect crystal will not possess a sharp-cornered (I, H) curve unless the crystal is very large, and that the curves of fig. 3 represent the most rapid variation of I with H that is possible for an actual crystal. In terms of the mechanism elaborated here the shape of the (I, H) curve, i.e. the susceptibility, is a function of the crystal size and shape since the effect of the closure domains is proportional to $L^{-1/2}$. A disc may be

regarded to a first approximation as a strip in which L varies continuously, and so the permeability of a single crystal in the form of a disc may be quite different from that of a strip.

Although the calculations have been carried out for iron and silicon-iron, it is easy to see that similar results would be obtained for other materials, for the operative quantity, the ratio of the volumes of closure to primary domains, is proportional to $d/2L$ and hence to $K^{-1/4}$. In view of the very good agreement between calculated and experimental (I, H) curves obtained in §3 it seems reasonable to suppose that, at least for strips, the deviations of the experimental (I, H) curves from those predicted by simple theory are due almost entirely to closure domains, and that in a well annealed crystal the effect of magnetostrictive strains, lattice imperfections etc. are small in comparison. This is reasonable since there is no magnetostrictive energy associated with the primary domains, but only with the p and q domains. This energy for iron is much smaller than the crystal anisotropy energy. Now, owing to the fact that in the p domains the magnetization is not in an easy direction, there is considerable anisotropy energy associated with them. The effect of the magnetostrictive energy may therefore be neglected in comparison. In the case of the q domains there is no anisotropy energy and the magnetostrictive energy may be of importance. In high fields where the closure domains are small this energy equals $\frac{1}{4}\lambda_{100}^2(c_{11} + c_{12})$ approximately, or about 400 ergs cm^{-3} for iron. The magnetostatic energy that would exist if the primary domains extended right up to the edge of the crystal is $0.85 I_s \sin^2 \theta d'$ per unit area, d' being half the domain width (Kittel 1949). For an iron strip with $L = 1 \text{ cm}$, calculation shows that this energy is always considerably greater than the magnetostrictive energy, which may thus be neglected in comparison.

In very low fields the magnetostrictive energy of the q domains may become comparable with the field energy. Unfortunately it is almost impossible to estimate the magnetostriction energy in this field range. The usual assumption, that the closure domains are held by the deformation of the primary domains, is obviously not valid when the volume of the closure domains becomes appreciable compared with that of the primary domains. Under these conditions the strain is shared by the primary and closure domains, and although it is clear that the energy will depend on the boundary surface area between two such domains, the depth over which the strain may be supposed to exist cannot be estimated. All that can be said is that the energy of a q domain will remain finite even in zero field, and hence that the primary domain width will not become infinite. It may nevertheless become quite large. It is possible that for nickel the effects of magnetostriction may be appreciable especially since K_1 and I_s are so much smaller than for iron.

The fact that, contrary to simple theory, the (I, H) curves of single crystals are anisotropic in low fields was first observed by Williams (1937). This is readily understood since the closure domain structure will be different for different crystallographic directions. In zero field the volume occupied by closure domains will presumably be greater the greater the area of the surface of the crystal which has no direction of easy magnetization lying in it. Thus closure domains may be expected to occupy a greater volume for an iron crystal strip when the axis is along the $[111]$ direction than one for which it is along the $[110]$ direction. Similarly the closure domain volume would be greater for a $[110]$

strip than for a [100] strip. This is in agreement with the observations of Williams that the maximum permeability of an iron picture frame crystal is greatest for a [100] crystal where there are no closure domains and least for a [111] crystal. For crystals other than those in the form of strips, e.g. discs, oblate spheroids, the closure structure is much more complicated, but some variation with crystal plane, and hence some low field anisotropy of the (I, H) curves, is to be expected, though on account of the large demagnetization factor of such crystals this anisotropy would be very difficult to observe.

Possibly the most important conclusion to be drawn from this work is that the permeability in a given direction in a single crystal is no longer to be regarded as characteristic of the material but depends explicitly on crystal shape and size. The bearing of this fact on the behaviour of polycrystalline materials, in which the crystallite size may be very small, will be discussed in a later paper.

ACKNOWLEDGMENTS

The author wishes to record his thanks to Professor L. F. Bates for his interest in this work. He is indebted to Mr. D. H. Martin for numerous illuminating discussions and for many useful comments on this paper. Thanks are also due to Dr. H. J. Williams of the Bell Telephone Laboratories, U.S.A., for supplying numerical data used in § 3.

REFERENCES

- AKULOV, N., 1931, *Z. Phys.*, **67**, 794.
BATES, L. F., and MARTIN, D. H., 1953, *Proc. Phys. Soc. A*, **66**, 162.
BATES, L. F., and MEE, C. D., 1952, *Proc. Phys. Soc. A*, **65**, 129.
BATES, L. F., and NEALE, F. E., 1949, *Physica*, **15**, 220; 1950, *Proc. Phys. Soc. A*, **63**, 374.
KITTEL, C., 1949, *Rev. Mod. Phys.*, **21**, 541.
LAWTON, H., 1950, *E.R.A. Report* No. N/T. 58.
LAWTON, H., and STEWART, K. H., 1948, *Proc. Roy. Soc. A*, **193**, 72.
NÉEL, L., 1944, *J. Phys. Radium*, **5**, 241.
WILLIAMS, H. J., 1937, *Phys. Rev.*, **52**, 747.
WILLIAMS, H. J., BOZORTH, R., and SHOCKLEY, W., 1949, *Phys. Rev.*, **75**, 155.

Ionization in Liquids due to Alpha Particles

By E. W. T. RICHARDS*

Department of Natural Philosophy, University of Glasgow

MS. received 12th February 1953

Abstract. The ionization current produced by polonium alpha-particles in liquid hexane has been studied using a collimated beam so that it has been possible to determine the direction of the alpha-particles with respect to the collecting electrostatic field. Measurements of the ionization current have been made with various collecting field strengths and experiments conducted in which the attempts were made to measure the specific ionization.

The ion currents measured were of the same order of magnitude as those obtained by earlier experimenters but no dependence on the angle between the direction of the alpha-particles and the field was observed. This was in contradiction to results as calculated using Jaffé's columnar theory. The experimental values of the specific ionization do not conform to the Bragg curve as in the case of gases, but all the experimental results obtained are consistent with a calculation assuming that the only ions which can be collected are formed by δ -rays at some distance from the alpha-particle track.

§ 1. INTRODUCTION

THE effect of bombarding a liquid with alpha-particles was first studied about 1906 by Jaffé. Since that date a considerable amount of work has been carried out on the various problems connected with this subject. From 1906 until 1913 (Jaffé 1913) Jaffé and his associates investigated the purely physical side, connected with the primary ionization. Since that period comparatively little work has been effected on this aspect (Stockland 1924).

It has been shown that the chief method by which an alpha-particle loses energy in a gas is by the formation of ions, and it is thought that this is also the case in liquids. However, unlike the gaseous case, no direct evidence has been obtained that this is in fact the mechanism involved. For fast electrons, generated in a liquid by means of x-rays, about 80% of the ion current which would be expected, from the assumptions that all the electron energy was used to form ions and that 32 electron volts were required to liberate an ion pair, has been collected by the application of electric fields (Mohler and Taylor 1934). For alpha-particles only about 1/500 of the ion current, calculated in a similar manner, has been similarly collected. In order to explain this result, Jaffé proposed the 'columnar theory of ionization' (Jaffé 1913). Jaffé assumed that the initial ionization was confined to a small cylindrical volume surrounding the path of the ionizing particle. The slowness of normal diffusion was considered to give rise to a high probability of recombination and Jaffé estimated that recombination would proceed very rapidly (half period $\sim 10^{-7}$ sec) leaving very few ions available for collection even when strong collecting fields were used (Stockland 1924).

In more recent years, experiments have been carried out in which liquefied gases have been subjected to bombardment with alpha-particles. In general

* Now at Atomic Energy Research Establishment, Harwell, Didcot, Berks.

there is no evidence of electron currents being collected in liquids. Kramers (see Gerritsen 1949) has pointed out, that if ion columns exist, as suggested by Jaffé, internal field strengths of the order of 10^7 v cm⁻¹ must be present. Such fields will have a far greater effect on the rate of recombination than the normal diffusion processes. It should be noted that the field strength so generated is at least of the same order as the dielectric strength of the liquids used, and that in consequence such configurations would be extremely unstable.

According to Jaffé's theory, the relationship between the strength of the collecting field and the ion current should depend markedly upon the angle between the direction of the applied field and the direction of the alpha-particles. In the case of gases under considerable pressure this has been investigated experimentally and found to be in fair agreement with the theoretical prediction. In liquids, however, owing to the shortness of the alpha-particle ranges, no such evidence was available to establish the validity of the columnar theory. The experiments described in this paper were therefore undertaken in an attempt to obtain information upon the behaviour of ions formed by the passage of alpha-particles through a liquid.

§ 2. EXPERIMENTS

Two types of experiment were performed, one to establish the ion current field strength relationships when the angle between the collecting field and the particles was varied, and the other to determine the dependence of the collectable ionic current on the primary ionic density. In the former case the relationship was determined when the field was applied first along the alpha-particle tracks and then perpendicular to the tracks, as these cases should give the largest variation. The second investigation was carried out by utilizing the variation in specific ionization along the track of an alpha-particle.

Apparatus

Two types of ionization chamber were designed for these experiments. For the case in which the collecting field was applied at right angles to the path of the ionizing particles the electrode assembly was as shown in fig. 1. Provision was made to adjust both the height and the spacing of the electrodes which were mounted on Perspex blocks. Electrical connections were made by means of coaxial screened cables and great care was taken to ensure that at no point could the inner conductors act as ion collectors. The entire electrode assembly was mounted in a vessel made of Perspex which was chosen because of its good insulation properties. To reduce the danger of 'leakage currents' between the electrodes two guard electrodes were placed as shown in fig. 1, so that no field was applied across the Perspex insulating blocks. With this arrangement it was found possible to maintain an interelectrode resistance which was large compared with 10^{12} ohms.

Electrode spacings of between 0.5 mm and 2 mm were used, the exact distances being measured by means of feeler gauges. Owing to the extreme shortness of the range of the alpha-particles in liquids the collimation was carried out in air prior to the entry of the alpha-particles into the liquid. It was found that if the alpha-particles were allowed to pass through a gas which was in direct contact with the liquid surface ions formed in the gas were dissolved in the liquid, and gave the effect of liquid ionization current. This phenomenon was presumably enhanced by the image forces set up at the interface of the dielectrics. The

currents due to this phenomenon were found to be up to 1000 times as great as those due to the ions produced directly in the liquid. Various systems of earthed screens and protective electrodes were tried unsuccessfully to eliminate this effect. As the liquid chosen for most of these experiments was hexane it was not possible to maintain a vacuum above the liquid. A successful solution of this difficulty was obtained by covering the liquid surface with a thin glass layer, supported on the Perspex blocks. The blocks were mounted directly on the electrodes and formed the collimator having a 0.5 mm slit. Experiments were carried out to determine the protective effects of the window by measuring the ionization current produced in 'Apiezon oil' first with the window in place, and then without a window, but with a vacuum above the oil surface. In the latter

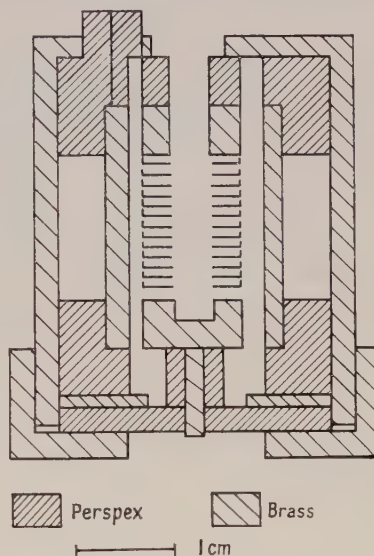
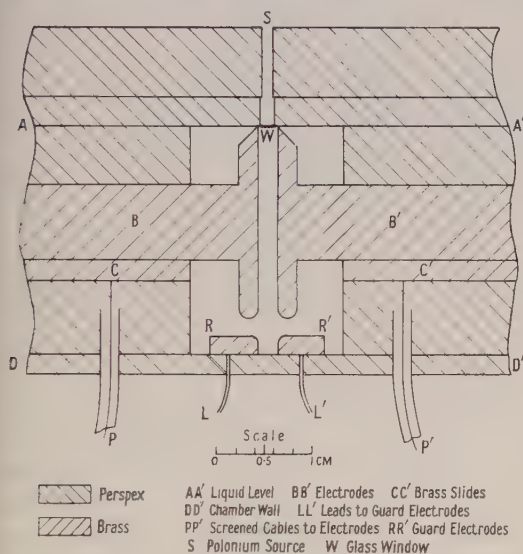


Fig. 1. Electrode assembly for first type of ionization chamber.

Fig. 2. Electrode assembly for second type of ionization chamber.

case the oil level was maintained at the same height as the two electrodes and two guard electrodes placed 1 mm above the surface of the liquid. No difference was detected in the current collected in the two cases, after allowance had been made for the thickness of the window.

In order to protect the entire system from the influence of any stray electric fields, the outside of the chamber was coated with graphite. This served also to protect the liquid from light, thus reducing the dark current flowing when the liquid was subjected to electric fields without the presence of radiation.

The second type of ionization chamber was designed on the principle of two concentric cylindrical electrodes (fig. 2). These were spaced 2 mm apart by means of Perspex rings. As in the former case, guard rings were used to ensure that the insulators which supported the electrodes were not subjected to any electrical fields. The central portion of the inner electrode was fabricated from a series of rings and spacers. These formed a collimator for the alpha-particles, the source being suspended along the centre of the inner cylinder. This collimator was sealed by means of thin aluminium foil having a thickness equivalent to 2 mm of air. The whole electrode structure was enclosed in a brass cylinder which protected the system from the effects of any stray electric fields.

The alpha-particle sources used in these experiments were 20 mc of polonium. These were mounted on silver foils 2 thousandths of an inch thick, 2 cm long and 2 mm wide. The sources were tested for contamination with other decay products of radium and found to be free from beta-particle emitting materials.

The current measurements were made by means of a d.c. amplifier. This choice was mainly determined by the comparatively large random current pulses which were observed when a liquid was subjected to high electric fields. These current pulses appear to be due either to the occurrence of local 'break down' in the liquid or to the presence of very small quantities of impurity in the liquid which may become ionized at the electrode surfaces and then act as current carriers. The conducting particles responsible appear to travel with velocities

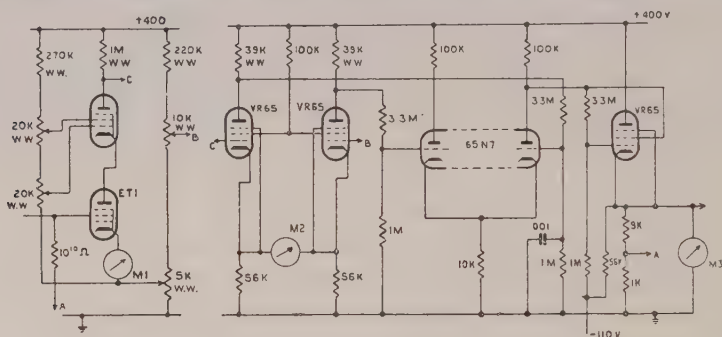


Fig. 3. Circuit of d.c. amplifier.

similar to those of the normal liquid ions and give rise to pulses having a duration of the order of 100 milliseconds. The frequency of occurrence of these pulses increases rapidly with the applied field. In these investigations it was found that an upper limit of about 5 kv cm^{-1} was set by this phenomenon to the applied field strength.

The circuit of the d.c. amplifier used is shown in fig. 3. The electrometer valve was an ET1 manufactured by the General Electric Company. The anode load of this valve consisted of a valve type 52 connected in series with a $1 \text{ M}\Omega$ resistance. In this manner it was possible to maintain a constant voltage across the electrometer valve and at the same time to obtain a large voltage amplification. The output of this system was further amplified in a two stage push-pull amplifier of conventional design. The signals so produced were fed back to a top point on the input resistance of the electrometer valve after being passed through a cathode follower. The gain of the entire system was controlled by the proportion of the signal which was fed back to the input circuit. Using this apparatus and an input resistance of 10^{12} ohms it was found possible to measure currents of 10^{-15} ampere. However, due to the random currents in the liquid discussed previously, it was found impracticable to use resistances of more than 10^{10} ohms with a corresponding reduction of the sensitivity of the amplifier. The power supplies for the amplifier were obtained from two stabilized power packs of conventional design.

Hexane was chosen as the liquid for most of these experiments primarily because it was one of the liquids used in the earlier published work on the subject and also because of its good insulation properties. It was found necessary to purify carefully the liquid used in the ionization chambers (Plumby 1941).

Commercially pure hexane was obtained and purified in the usual manner, special care being taken to ensure that no moisture was present in the resulting liquid. It was found that the presence of even small quantities of water greatly increased the noise level of the liquid when subjected to electric fields.

Experimental Procedure

In order to obtain absolute values of the measured ionic currents the amplifier system was calibrated using a gas ionization chamber and an alpha-particle source of known strength. This procedure was found necessary owing to the difficulty of measuring the value of the high resistances used in the input to the electrometer valve and to the variation in value of these resistances with time. The alpha-particle sources together with their associated collimators were also calibrated using a gas ionization chamber.

The liquid ionization chambers were filled with the pure dry hexane, care being taken that no bubbles of gas were trapped between the electrodes. In some of the experiments the cells were filled directly from a vacuum distillation plant, but this process was abandoned as no improvement in performance could be detected compared with chambers filled with freshly purified dried hexane in the ordinary way. The liquid was first subjected for several minutes to a field strength considerably greater than that required in the experiment, the field was then reduced to the required value for the experiment, and the apparatus maintained under experimental conditions for 10 minutes prior to reading the value of current flowing. (This procedure was adopted before each reading as it was found to reduce the random current pulses flowing in the liquid.) The value of the current was measured both with the source in position and then with the source removed for each value of the applied field. Taking these precautions it was found possible to obtain reproducible results for the field applied both parallel and perpendicular to the path of the ionizing particles.

Experiments were also carried out to investigate the relationship between the ionic density and the percentage of ions which could be collected. For this investigation use was made of the variation in the specific ionization along the path of an alpha-particle. (In these experiments the cylindrical ionization chambers were employed since the insertion of absorbers between the source and the liquid would result in field distortion in the other type of chamber.) The primary ionization in a liquid was assumed to obey the same law with respect to the energy of the ionizing particle as that which applies in a gaseous medium. Therefore by reducing the energy of the incident particles, the average ion density should be increased, and indicated by the integrated 'Bragg' curve. The absorbers used in these experiments were thin cylinders of aluminium leaf, having a stopping power equivalent of 0.8 mm of air. Readings of the ionization current were taken for various thicknesses of absorber. The same precautions as have been mentioned earlier were necessary in order to obtain reproducible results.

§ 3. RESULTS

The order of magnitude of the ion currents measured in the experiments was in general agreement with those obtained by previous experiments. However, the relationship between the field strength and the percentage of the ions which could be collected appeared to be independent of the angle between the path of the ionizing

particle and the direction of the collecting field (figs. 4, 5, 6). Moreover, the relationship between the field strength and the proportion of the ions which can be generated appeared to obey a logarithmic law (fig. 6). These results are in direct contradiction to those predicted by Jaffé's theory of ionization and also to those obtained experimentally for gases under high pressures. However, they are

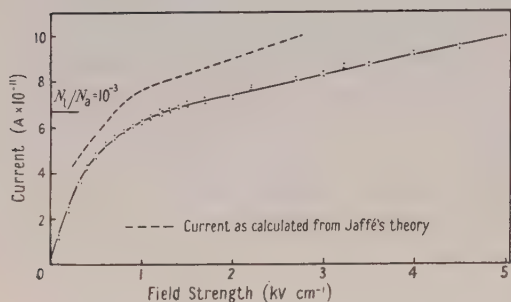


Fig. 4. Field applied perpendicular to alpha-particle tracks.

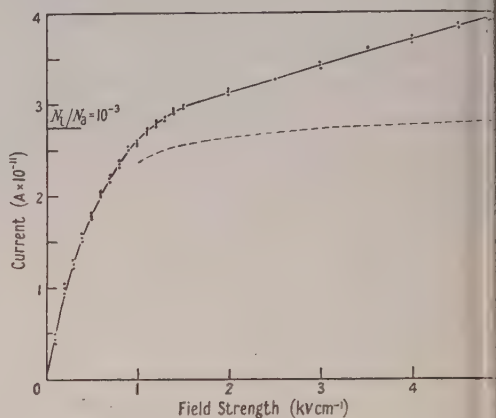


Fig. 5. Field applied parallel to alpha-particle tracks.

$N_I(N_a)$ = ionization current in liquid (air).

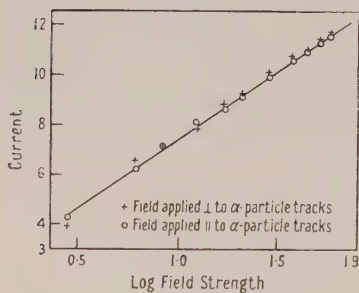


Fig. 6. Ionic current plotted against field strength.

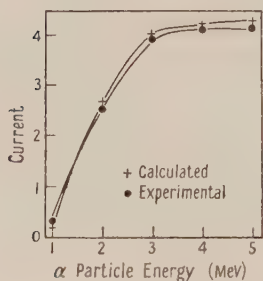


Fig. 8. Specific ionization (the δ -ray current is normalized for the collection efficiency of the electrodes). The calculated results assume ionization from δ -rays of energy greater than 1 kv.

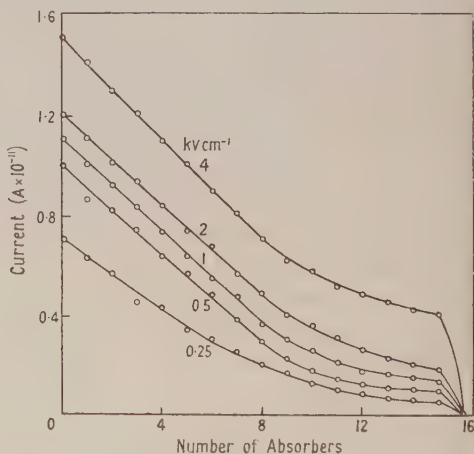


Fig. 7. Absorber thickness plotted against ionic current.

in approximate agreement with the experimental measurements made in hexane by Jaffé, who had no method of collimating his alpha-particles. The results of the experiments in which the specific ionization was investigated are shown in figs. 7 and 8. It will be seen that the current which can be collected per unit length of the

track decreases with decreasing energy of the ionizing particle. This is in disagreement with the results obtained in gases. If, however, it is assumed that only those ions produced by secondary δ -rays outside the track of the primary ionization can be collected, then the results agree within experimental error with the current which would be theoretically predicted. Thus fig. 8 shows the ion current measured compared with that calculated if only the ions formed by δ -rays of an energy in excess of 1 kv contributed to the ion current.

The results of the other experiments described in this paper could be explained on the basis of the same theory. Thus since the ions created by fast δ -rays may be regarded as being distributed at random around the path of the alpha-particle and have no angular dependence on the direction of the alpha-particle, then there should be no angular dependence between the path of the ionizing particle and the collecting field on the ion current. An estimate of the width of primary ion columns in a liquid can be obtained from the value of the lowest energy δ -rays contributing to the collectable ion current. Although owing to the difficulty of calculating paths of such particles no accurate estimate can be obtained, a value of 0.05μ appears to be reasonable in the light of these experiments.

§ 4. CONCLUSION

From the results of these experiments it would appear that the 'columnar theory of ionization' does not adequately explain the ionization effects of the passage of an alpha-particle through a liquid. From consideration of the diameter of the ion tracks and of the density of the ions per unit length of track the strength of the electric fields which so result must be at least of the same order of magnitude as the dielectric strength of the liquid. This would lead to an extremely unstable configuration of ions in which the vast majority must recombine before they can be affected by collecting electric fields. Assuming a column width of 0.05μ as suggested from the experimental results and an effective ionization potential of 30 ev per ion pair, the field strength inside the primary ion column would be of the order of 10^7 v cm^{-1} . It is therefore not surprising that the experimental result shows that little or no current is contributed by the primary ionization to the ion current that can be collected. No dependence of the ionic current is therefore to be expected upon the angle between the collecting field and the path of the alpha-particle. Further, if it be assumed that only the ions produced by outside δ -rays outside the primary ionic column contribute to the current, then the results of the experiments upon the specific ionization can also be explained.

ACKNOWLEDGMENTS

The author wishes to thank Professor P. I. Dee for his continued interest and many useful discussions in connection with this work, also the Nuffield Trust whose generosity made the work possible.

REFERENCES

- JAFFÉ, G., 1906, *J. Phys. Radium*, **5**, 263; 1913, *Ann. Phys., Lpz.*, **42**, 303.
GERRITSEN, A. N., 1949, *Comm. Kamerlingh Onnes Lab.* No. 275.
MOHLER, F. L., and TAYLOR, L. S., 1934, *Bur. Stand. J. Res., Wash.*, **13**, 659.
PLUMBY, H. J., 1941, *Phys. Rev.*, **59**, 200.
STOCKLAND, H., 1924, *Handbuch der Physik*, **14**, 27.

A Formula for Thick Target Bremsstrahlung

By RICHARD WILSON*

Stanford University, U.S.A.

MS. received 6th March 1953

Abstract. Corrections to the Bethe-Heitler formula for thin target bremsstrahlung are calculated for the degradation of the electrons in a thick target by ionization and radiative losses. The calculations apply only to the cross section integrated over all angles, and the accuracy of the formulae is discussed.

THE radiation of fast electrons in a coulomb field has been calculated using the Born approximation (Bethe 1934, Bethe and Heitler 1934, Heitler 1935). The calculations make several assumptions.

(A) The source of the coulomb field (a nucleus) must not recoil appreciably, an assumption satisfied in all applications so far (Drell 1952).

(B) The quantities $Ze^2/\hbar v = Zc/137v$, where v is the velocity of the incoming or outgoing electron, must be small compared with unity for the Born approximation to be valid. The deviations from the Born approximation result have been calculated for high Z and low energies of both electrons for the inverse process—the production of electron-positron pairs (Hulme and Jaeger 1936). The deviations have also been calculated assuming high energy for both electrons but a high Z (Maximon and Bethe 1952, Davies and Bethe 1952). The deviations are not calculated in the important region where the incident electron has high energy and the outgoing electron has low energy. In this region it seems likely (Heitler 1935, p. 171) that the main correction will arise from the normalization of the wave function. A naïve calculation has been performed using Sommerfeld's non-relativistic wave functions to evaluate the correction. It is found that the cross section for producing photons with an energy $\frac{1}{2}$ mev less than the electron kinetic energy is 20% higher than the Bethe-Heitler value for $Z=29$. The deviation is greater at higher Z .

(C) The effect of the screening of the coulomb field by the atomic electrons was calculated on the Thomas-Fermi statistical model of the atom. Wheeler and Lamb (1939) have calculated the screening correction for hydrogen and nitrogen using exact wave functions; for nitrogen the errors involved in the assumption of Thomas-Fermi screening are not great, and are expected to be less for higher atomic number. More recently Fraser (1952) has calculated the screening for mercury using the Hartree approximation, which is likely to be more accurate than the Thomas-Fermi model. A negligible difference was found.

(D) At first the bremsstrahlung in the field of an electron was neglected. This gives an important correction for low atomic number elements; the screening is slightly different from the nuclear case; the correction due to recoil is unknown, but is expected to be small. It will probably reduce the

* Now at Clarendon Laboratory, Oxford.

cross section for radiating high energy photons. The calculations (Wheeler and Lamb 1939) may be approximated by multiplying the Bethe-Heitler cross section by $1 + 1/Z$.

The Bethe-Heitler equations, as modified to take account of the above correction, have been verified extensively for the inverse process—pair production (Rosenblum *et al.* 1952 and earlier references). The formula for bremsstrahlung has also been verified (Lanzl and Hanson 1952, DeWire and Beach 1951). Since the theory describes the experimental results so well for high Z , where deviations might be expected, it is safe to regard the theoretical formulae as well known for $13 < Z < 30$, with the exception of the high energy limit discussed in (C) above.

This theoretical spectrum applies, however, only to a thin target. The thin target formula shows that even for an infinitesimal target thickness there is an overwhelming probability of radiating a low energy photon. This means that we must derive a thick target formula in order to discuss bremsstrahlung in any experimental situation. The aim and purpose of this paper is to derive a thick target formula which is convenient to use in numerical work and to discuss its validity.

After an electron has once radiated a photon in a target the energy is reduced. The probability of radiating subsequent photons is now reduced. The first attempt to calculate this is due to Eyges (1951). Eyges writes down the equations for a shower initiated by an electron and takes the first order expansion in powers of the radiator thickness. Eyges then makes an approximation to the bremsstrahlung spectrum which is only valid at high energies.

Since the notations used by various authors differ, we define ours here: E_0 = incident electron energy including rest energy, E = scattered electron energy, k = momentum of radiated photon in energy units, μ = rest energy of the electron, $\bar{\phi}$ = unit of cross section for bremsstrahlung = $Z^2 r_0^2 / 137$ where r_0 is the classical electron radius = $Z^2 e^4 / 137 m^2 c^4$; $\gamma = 100 \mu k / E E_0 Z^{1/3}$; $\sigma(k)$ = absorption cross section for photons of energy k , $\sigma_{\pi}(k)$ = pair production cross section for photons of energy k , $\sigma_c(k)$ = Compton scattering cross section for photons of energy k . $\phi_1(E_0, k) dk$ is the cross section per nucleus for an electron of energy E_0 for radiating a photon of energy between k and $k + dk$. In the high energy limit $E_0 \gg \mu$, $E \gg \mu$ and

$$\phi_1(E_0, k) dk = 2\bar{\phi} \frac{dk}{k} \left\{ 1 + \left(\frac{E}{E_0} \right)^2 - \frac{2}{3} \left(\frac{E}{E_0} \right) \right\} \left\{ 2 \log \frac{2E_0 E}{\mu k} - 1 - 2c(\gamma) \right\} \dots\dots(1)$$

where $c(\gamma)$ is the numerical correction for screening computed by Bethe or Wheeler and Lamb. This formula can still be used for $\gamma > 0.8$ although $c(\gamma)$ is only tabulated by Bethe for $\gamma > 2$. For $\gamma < 0.8$ it is necessary to use a different formula. For the regions of interest this formula is adequate.

We define $\phi_2(E_0, k, t) dk$ as the 'effective' cross section per nucleus for a target of thickness t , where t is measured in gm cm^{-2} .

It should be noted that $\phi_1(E_0, k) dk$ has the dimensions of a cross section. $\phi_1(E_0, k)$ has the dimensions of a cross section divided by an energy; this is similar to the notation used by Wheeler and Lamb (1939) but in distinction to that used by Heitler (1935) or Rossi and Greisen (1941).

This calculation is, like Eyges', calculated to first order in thickness, and is divided into four parts: firstly, the effect of radiation of high energy photons

—which occurs with low probability—is calculated to first order in $\phi_1(E_0, k)t$; secondly, the absorption of the photons produced in the front of the radiator by the rest of the radiator; this is also calculated to first order in $\sigma(k)t$. Thirdly, we calculate separately ionization losses and the cumulative effects of small radiative losses. For these, although it is still possible to calculate to first order in t , it is no longer valid to calculate to first order in $\phi_1(E_0, k)t$. Fourthly, we take into account the increased path length of the electrons in the foil due to multiple scattering (Yang 1951).

CALCULATION

(i) *Attenuation of Primary Electron Beam due to Radiation of High Energy Photons*

Once an electron has radiated a photon of energy $m > E_0 - k - \mu$ it can never again radiate a photon of energy k because there is not the available energy. We can correct for this loss of electrons from the beam to first order in t to obtain

$$\phi_2(E_0, k, t) dk = \phi_1(E_0, k) dk \left[1 - \frac{Nt}{2A} \int_{E_0 - k - \mu}^{E_0 - \mu} \phi_1(E_0, m) dm \right]. \quad \dots\dots(2)$$

(ii) *Absorption of Photons of Energy k*

This may also be treated to first order to obtain

$$\phi_2(E_0, k, t) dk = \phi_1(E_0, k) dk \left[1 - \frac{Nt}{2A} \sigma(k) \right]. \quad \dots\dots(3)$$

The absorption cross section $\sigma(k)$ is composed of two parts for the energy region in which we are concerned. The part given by pair production effectively removes the photons from the beam and the re-radiation by the electrons is a second order process which is negligible except for low energy quanta. The part which is due to Compton effect, however, merely degrades the quanta.

According to the Klein-Nishina formula (Heitler 1935) approximately one-half of the Compton scattering leaves degraded quanta of only about $\frac{1}{2}$ Mev energy. The rest degrades the quanta, leaving a uniform distribution of energies. An approximation, adequate for many purposes, is to set

$$\sigma(k) = \sigma_\pi(k) + \sigma_C(k). \quad \dots\dots(4)$$

(iii) *Effect of Ionization Loss and of the Low Energy Photons Radiated; Increased Path Length*

We define as Δ the total electron energy loss up to the point considered. Here we take Δ to be the sum of ionization losses I in the radiator, and small radiative losses. We have already considered the large losses.

Then to obtain $\phi_2(E_0, k, t)$ we take $\phi_1(E_0 - \Delta, k)$ and average over all values of Δ in the radiator with the appropriate weighting factors. The averaging is easily carried out by expanding, by Taylor's theorem,

$$\phi_1(E_0 - \Delta, k) - \phi_1(E_0, k) = -\Delta \left(\frac{\partial \phi_1}{\partial E_0} \right)_{k=\text{const}} + \frac{\Delta^2}{2} \left(\frac{\partial^2 \phi_1}{\partial E_0^2} \right)_{k=\text{const}} + \dots\dots\dots(5)$$

If we neglect, for the moment, the second order terms we may average Δ instead of averaging ϕ_1 to obtain

$$\phi_2(E_0, k, t) = \phi_1(E_0 - \frac{1}{2}\bar{\Delta}, k) = \phi_1(E_0, k) - \frac{\bar{\Delta}}{2} \frac{\partial \phi_1}{\partial E_0} \quad \dots\dots\dots(6)$$

where $\bar{\Delta}$ is the average of small energy losses of an electron in traversing a thickness of radiator t .

$$\bar{\Delta} = I + \frac{Nt}{A} \int_0^{E_0 - k - \mu} m \phi_1(E_0, m) dm. \quad \dots\dots(7)$$

I may be taken from the calculations including the density effect (Halpern and Hall 1948, Sternheimer 1952).

By differentiation we find

$$\begin{aligned} \frac{k}{2\bar{\phi}} \left(\frac{\partial \phi_1}{\partial E_0} \right) = & \left\{ 1 - \frac{2}{3} \frac{E}{E_0} + \left(\frac{E}{E_0} \right)^2 \right\} \left\{ \frac{1}{E} + \frac{1}{E_0} \right\} \left\{ 2 + 2 \frac{dc(\gamma)}{d\gamma} \right\} \\ & + \frac{2}{3E_0} \left\{ 4 \left(\frac{E}{E_0} \right) - 3 \left(\frac{E}{E_0} \right)^2 - 1 \right\} \left\{ 2 \log \frac{2EE_0}{\mu k} - 1 - 2c(\gamma) \right\}. \end{aligned} \quad \dots\dots(8)$$

The contribution of the second order terms can be found by noticing that the dominant term comes from differentiating the logarithm in the equation for $\phi_1(E_0, k)$. Thus we easily find

$$\frac{k}{2\bar{\phi}} \frac{\partial^2 \phi_1}{\partial E_0^2} = \left\{ 1 - \frac{2}{3} \left(\frac{E}{E_0} \right) + \left(\frac{E}{E_0} \right)^2 \right\} \left\{ \frac{1}{2E^2} + \frac{1}{2E_0^2} \right\} \left\{ 2 + 2 \frac{dc(\gamma)}{d\gamma} \right\}. \quad \dots\dots(9)$$

The error involved in neglecting second order terms can be deduced from this for any special case.

The fourth effect, that of the increased path length due to multiple scattering, is, to our approximation, found by multiplying our cross section by a factor $(1 + Bt)$ (Yang 1951).

(iv) Sum of Effects

Thus we find, combining all our effects,

$$\phi_2(E_0, k, t) = \phi_1(E - \frac{1}{2}\bar{\Delta}, k) \left\{ 1 + Bt - \frac{Nt}{2A} \left[\int_{E_0 - k - \mu}^{E_0 - \mu} \phi_1(E_0, m) dm + \sigma_\pi(k) + \frac{1}{2}\sigma_C(k) \right] \right\} \quad \dots\dots(10)$$

$$\text{where } \bar{\Delta} = I + \frac{Nt}{A} \int_0^{E_0 - k - \mu} m \phi_1(E_0, m) dm.$$

For convenience we may also express this in terms of the concept of a radiation length (Rossi and Greisen 1941). We may define a radiation length X_0 of a material by the equation

$$\frac{1}{X_0} = 4 \frac{N}{A} \bar{\phi} \log(183Z^{-1/3}). \quad \dots\dots(11)$$

We define the probability per unit radiation length of emitting a photon of energy between k and $k + dk$

$$\Phi_3(E_0, k) dk = \frac{X_0 N}{A} \phi_1(E_0, k) dk$$

and similarly

$$\Phi_4(E_0, k, t) dk = \frac{X_0 N}{A} \phi_2(E_0, k, t) dk,$$

$$\Sigma_\pi(k) = \frac{X_0 N}{A} \sigma_\pi(k),$$

$$\Sigma_C(k) = \frac{X_0 N}{A} \sigma_C(k), \quad \dots\dots(12)$$

where it should be noted that Φ_3 , Φ_4 and Σ have not the same dimensions as ϕ_1 , ϕ_2 and σ . The constant B now equals E_s^2/E_0^2 , where $E_s=21$ mev (Yang 1951). Then we have

$$\Phi_4(E_0, k, t) = \Phi_3(E_0 - \frac{1}{2}\bar{\Delta}, k) \left\{ 1 + \frac{E_s^2 t}{E_0^2} - \frac{t}{2X_0} \left[\int_{E_0-k-\mu}^{E_0-\mu} \Phi_3(E_0, m) dm + \Sigma_\pi(k) + \frac{1}{2}\Sigma_C(k) \right] \right\}. \quad \dots\dots(13)$$

In the high energy limit $E_s/E_0 \rightarrow 0$ and $k\Phi_3(E_0, k) = 1$ to a fair approximation. Then $\partial\Phi_3/\partial E_0 = 0$ and we get

$$\Phi_4(E_0, k, t) = \Phi_3(E_0, k) \left\{ 1 - \frac{t}{2X_0} \left[\Sigma(k) + \frac{1}{2}\Sigma_C(k) - \log \left(1 - \frac{k}{E_0} \right) \right] \right\}, \quad \dots\dots(14)$$

which is Eyges' formula.

On inspection of the Bethe-Heitler formula we see that the approximation $k\Phi_3(E_0, k) = 1$ is approximately true for small k even when it is not true for large k . Then it is reasonable to use this approximation for calculating $\bar{\Delta}$ and $\bar{\Delta}^2$ without assuming $\partial\Phi_3(E_0, k)/\partial E_0 = 0$. Then

$$\bar{\Delta}^n = I^n + \frac{t}{X_0} \frac{E^n}{n} + \text{cross terms}, \quad \dots\dots(15)$$

where we can neglect as small cross terms of higher order than the first in I . This then gives us the second and higher order corrections which are not negligible.

If we accept our approximation of eqn. (9) for $\partial^2\phi_1/\partial E_0^2$ we can take into account our higher order corrections by using eqns. (10) or (13) and writing

$$\bar{\Delta} = -E \log \left(1 - \frac{I}{E} \right) + 1.6 \frac{Nt}{A} \int_0^{E_0-k-\mu} m\phi_1(E_0, m) dm$$

or

$$\bar{\Delta} = -E \log \left(1 - \frac{I}{E} \right) + 1.6 \frac{t}{X_0} E.$$

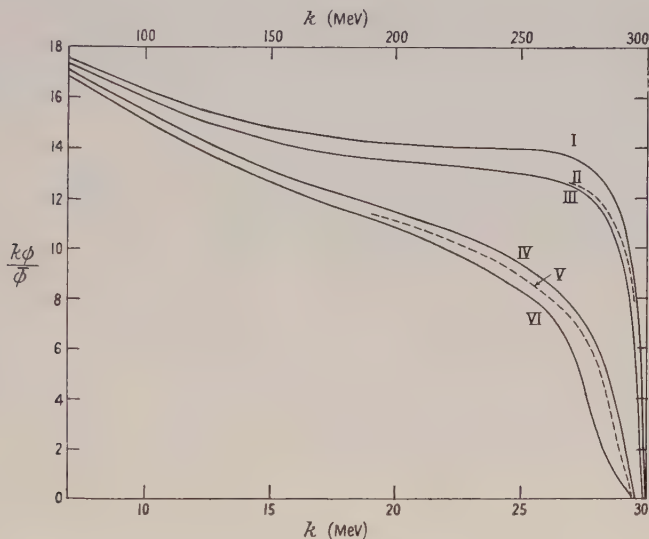
The accuracy of this formula should be to within 2% for $t/X_0 = 0.05$ except when $E - \mu < I$. When this occurs, the part of the radiator remote from the electron beam does not radiate photons contributing to our cross section. The extreme relativistic formula (1) for the bremsstrahlung may no longer be used, but a simple averaging is possible. The accuracy of the formula obtainable for $\partial\phi_1(E_0, k)/\partial E_0$ which is usually used for analysing photonuclear reactions is of the same order.

Example

To exemplify the use of our equations the corrections to thin target bremsstrahlung have been calculated and are shown in the figure for two cases, $E_0 = 30$ mev, $E_0 = 300$ mev, each with a copper target of thickness $t = X_0/20$. The ionization loss assumed is that given by Halpern and Hall. No allowance has been made for pair production by electrons, since these effects can be included in the factor $\bar{\phi}$ to our accuracy by putting $\bar{\phi} = (Z^2 + Z)r_0^2/137$.

It is to be emphasized that these formulae apply to the photon spectrum integrated over all angles. With a synchrotron the target is often placed in the centre of the beam. Multiple scattering in targets of the thickness we are

considering will tend to make the photon spectrum in the forward direction nearly equal to the integrated spectrum. Calculations of this type have been made by Schiff (1951) and by Lawson (1950, 1952), neglecting the effect considered here. The accuracy of calculations of the angular distribution do not compare with the accuracy of the integrated Bethe-Heitler formula. It is therefore desirable for any detector to cover a large angular proportion of the gamma-ray beam so that the angular distribution calculations enter only as corrections.



Curves I and IV are the thin target bremsstrahlung spectra for $E_0 = 300$ mev and 30 mev respectively; curves II and V (dotted) are Eyges' approximations to the thick target spectra, and curves III and VI are the approximations as derived in this paper. For curves I, II and III the upper scale should be used; for curves IV, V and VI the lower scale should be used.

It is perhaps worth mentioning that the shape of both the modified and unmodified bremsstrahlung curves are dependent primarily on E at the high energy end and little on E_0 or k . Thus the effect of neglecting the thick target corrections is similar for all E_0 and k . For the case calculated, the effect is approximately equivalent to a 1 mev shift in the peak energy. In analysing photonuclear yield curves this could give rise to a 1 mev shift in peak position. For a tungsten target of 5% of a radiation length the shift would be 0.3 mev.

ACKNOWLEDGMENTS

These calculations were made while the author was at Stanford University, U.S.A., to aid in a programme of the study of photonuclear reactions. The author has had the pleasure of many interesting discussions with Professors Lamb, Panofsky and Schiff.

This work was supported by the joint programme of the Office of Naval Research and the Atomic Energy Commission.

REFERENCES

- BETHE, H., 1934, *Proc. Camb. Phil. Soc.*, **30**, 524.
BETHE, H., and HEITLER, W., 1934, *Proc. Roy. Soc. A*, **146**, 83.
DAVIES, H., and BETHE, H. A., 1952, *Phys. Rev.*, **87**, 156.
DEWIRE, J. W., and BEACH, L. A., 1951, *Phys. Rev.*, **83**, 476.
DRELL, S. D., 1952, *Phys. Rev.*, **87**, 753.
EYGES, L., 1951, *Phys. Rev.*, **81**, 981.
FRASER, P. A., 1952, *Phys. Rev.*, **87**, 523.
HALPERN, O., and HALL, H., 1948, *Phys. Rev.*, **73**, 477.
HEITLER, W., 1935, *Quantum Theory of Radiation* (Oxford : University Press).
HULME, H. R., and JAEGER, J. C., 1936, *Proc. Roy. Soc. A*, **153**, 443.
LANZL, L. H., and HANSON, A. D., 1952, *Phys. Rev.*, **83**, 959.
LAWSON, J. D., 1950, *Proc. Phys. Soc. A*, **63**, 653; 1952, *Phil. Mag.*, **43**, 306.
MAXIMON, L. C., and BETHE, H. A., 1952, *Phys. Rev.*, **87**, 156.
ROSENBLUM, E. S., SHRADER, E. F., and WARNER, R. M., 1952, *Phys. Rev.*, **88**, 612.
ROSSI, B., and GREISEN, K., 1941, *Rev. Mod. Phys.*, **13**, 240.
SCHIFF, L. I., 1951, *Phys. Rev.*, **83**, 252.
STERNHEIMER, R. M., 1952, *Phys. Rev.*, **88**, 851.
WHEELER, J., and LAMB, W., 1939, *Phys. Rev.*, **55**, 858.
YANG, C. N., 1951, *Phys. Rev.*, **84**, 599.

Analysis of Photonuclear Reactions

By RICHARD WILSON*

Stanford University, U.S.A.

MS. received 6th March 1953

Abstract. A method is described which enables photonuclear cross section curves to be derived from the appropriate yield curve with little ambiguity about assigning of errors.

IN experiments on photonuclear processes it is common to use as the source of photons a synchrotron or betatron. In these circumstances there is a continuous distribution of photon energies and there has to be some method of disentangling the data in order to find the cross section for a photonuclear process at any given energy.

In a common type of experiment, artificial radioactivity is induced in a foil, and the foil activity measured by a Geiger counter. The electron energy in the synchrotron is varied and the foil activity is plotted as a function of the electron energy. The response of the monitor will, in general, change, so that there is the additional problem of relating the monitor response, as a function of energy, to the incident electron current.

Here it is assumed that, in some way, a graph of activity yield against electron energy is available, suitably normalized to a constant electron current. It is also assumed that the spectrum of photon energies is known theoretically or from other experiments.

Mathematically the problem is simple. If the yield curve and the photon spectrum are known precisely, the curve of cross section versus energy may be found in a number of ways, which must each give the same answers. Thus Johns *et al.* (1950) and Katz and Cameron (1951) both describe numerical methods. Also an analytical method is possible (Spencer 1952). In practice it is difficult to know how the experimental errors in the measured yield curve are to be brought into the final answer. All these methods described necessitate a 'smoothing' of the yield curve. This means that it is impossible to assign errors to the final curves and they differ appreciably according to the smoothing procedure used. The only cross section curves to which errors have been attached are those of Krohn and Shrader (1952) and Goward and Wilkins (1952). It is the purpose of this note to explain a consistent method for analysing the data which enables errors to be assigned to the final results.

METHOD

We shall define the yield curve as a series of measured activities $Y(E_0)$ normalized to a unit electron current incident on the radiator. The number of photons incident on the target of energies between k and $k + dk$ we define as

* Now at Clarendon Laboratory, Oxford.

$N(E_0, k) dk$. If photons from all angles are to be collected, this is related to the thick target bremsstrahlung curve discussed by Wilson (1953) by a constant A :

$$N(E_0, k) = A\phi(E_0, k).$$

The constant A will depend upon the beam normalization and upon the radiator.

It is assumed that a series of calculated values are available for $N(E_0, k)$ for a series of values of E_0 and k . It is not considered that an analytical approach has any merit, since neither the photon spectrum nor the yield curve are given analytically.

Then if the yield of the photonuclear reaction is measured at a series of values of E_0 differing by an interval δE_0 we define as follows

$$\delta Y(E_0) = Y(E_0) - Y(E_0 - \delta E_0), \quad \delta N(E_0, k) = N(E_0, k) - N(E_0 - \delta E_0, k).$$

To a first approximation, the function $\delta N(E_0, k)$ is treated as a δ function $C\delta(k-m)$; this is equivalent to the assumption that when the electron energy is increased the effect on the photon spectrum is to add a certain number of photons of an energy m . The number we take is clearly

$$B = \int_{E_t}^{E_0 - \mu} \delta N(E_0, k) dk$$

where E_t is any convenient limit below the threshold energy for the reaction and the average energy m we take according to the formula

$$\int_{E_t}^{E_0 - \mu} (k - m) \delta N(E_0, k) dk = 0.$$

m is a function principally of E_0 and δE_0 .

Then the cross section $\sigma(m)$ for the photonuclear process is taken in first approximation to be

$$\sigma_1(m) = C \frac{\delta Y(E_0)}{\int_{E_t}^{E_0 - \mu} \delta N(E_0, k) dk}$$

where C is a constant incorporating the counter efficiency, thickness of target and so forth.

So far, in our calculation, no smoothing of the yield curve has been performed and errors in $Y(E_0)$ can be introduced directly as errors in $\delta Y(E_0)$. It remains to be shown that in all cases of practical interest this first approximation is not in error by more than 10%. We may then 'smooth' the resulting first approximation to obtain the correction. The details of the smoothing procedure are no longer important.

Then

$$\sigma(m) = \sigma_1(m) + \frac{\int_{E_t}^{E_0 - \mu} [\sigma_1(m) - \sigma_1(k)] \delta N(E_0, k) dk}{\int_{E_t}^{E_0 - \mu} \delta N(E_0, k) dk}$$

where in the correction term we have taken the first approximation. The errors in $\sigma(m)$ are effectively the errors in $\sigma_1(m)$.

The computational procedure for a series of photodisintegration experiments could proceed as follows.

An energy E_t is chosen below the threshold energy of all the reactions studied. A choice is also made of the intervals δE_0 at which the yield curve should be measured. Then tables are made of

$$N(E_0, k), \quad \delta N(E_0, k), \quad \int_{E_t}^{E_0 - \mu} \delta N(E_0, k) dk \quad \text{and} \quad m$$

as a function of E_0 . These tables will be independent of the experimental data and of the element.

Then from the measured yield curve $Y(E_0)$, the values of $\sigma_1(m)$ may be deduced easily.

VALIDITY

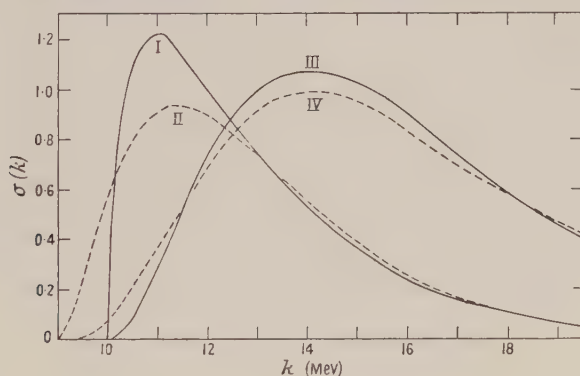
In order to check the validity of the method, several analytical curves for the cross section have been assumed and the correction term calculated. The Bethe-Heitler thin target formula for $Z = 82$ was used for $N(E_0, k)$ and a lower limit for the definite integral $E_t = 8$ Mev was used.

Firstly it is obvious that when $\sigma(k) = \alpha k$ where α is a constant, $\sigma(m) = \sigma_1(m)$ exactly. Thus we can see that the correction is small if $d\sigma(k)/dk$ varies slowly over the region where $\delta N(E_0, k)$ is finite.

Then cross section curves have been assumed of the shape

$$\sigma(k) = \frac{C}{x} (k - 10)^x \exp \{ -(k - 10)/2 \} \quad k > 10 \text{ Mev}$$

where k is in Mev and x is given successively the values $\frac{1}{2}$ and 2. The curves are plotted in the figure together with the appropriate first approximation. It is seen that the error is more than 10% near threshold and for the sharp peak $x = \frac{1}{2}$.



Curves I and III show the assumed cross section curves $\sigma = 1/x(k - 10)^x \exp \{ -(k - 10)/2 \}$ where $x = \frac{1}{2}$ and 2 respectively; curves II and IV show the first approximation evaluated as described in the text.

It should be noted that it is not possible to include estimated errors in the assumed bremsstrahlung curves directly. It may be seen that there are two main possible errors. The first is due either to neglect of finite target thickness or to the assumption of the Born approximation in the doubtful region near the high energy limit. The principal effect here will be to change the value of m by a constant amount. This error can conveniently be specified as an error in the origin. The other type of error might be caused by using a limited angular portion of the bremsstrahlung in an uncertain way. This will primarily lead to an

uncertainty in the slope of the curve of $kN(k)$ against k , and hence an error in low energy tail of the curve of $k\delta N(k)$ against k . This will affect any attempt to prove or disprove that the photo cross section goes to zero above some energy. The best method to introduce these errors will be to evaluate the cross sections for two assumed extreme bremsstrahlung curves using the methods described in this paper.

ACKNOWLEDGMENTS

This method was developed while the author was at Stanford University, U.S.A., to aid in a programme of study of photonuclear reactions. The work was supported by the joint programme of the Office of Naval Research and the Atomic Energy Commission; to them and to Stanford University the author is greatly indebted for support and hospitality.

REFERENCES

- GOWARD, F. K., and WILKINS, J. J., 1952, *Proc. Phys. Soc. A*, **65**, 671.
JOHNS, H. E., KATZ, L., DOUGLAS, R. A., and HASLAM, R. N. H., 1950, *Phys. Rev.*, **80**, 1062.
KATZ, L., and CAMERON, A. G. W., 1951, *Canad. J. Res.*, **28**, 518.
KROHN, V. E., and SHRADER, E. F., 1952, *Phys. Rev.*, **87**, 685.
SPENCER, L. V., 1952, *Phys. Rev.*, **87**, 196.
WILSON, R., 1953, *Proc. Phys. Soc. A*, **66**, 638.

RESEARCH NOTES

Many-Particle Systems : Derivation of a Shell Model

By H. R. POST

Department of Physics, Chelsea Polytechnic, London

MS. received 17th March 1953

In order to compare empirical binding energies and angular momenta of nuclei with those resulting from various pair-force interactions, it is necessary to find these values for stationary-state solutions of many-body problems in quantum mechanics. The actual many-body problem in physics is greatly simplified by the fact that it involves identical particles. A general study of this 'many identical particle' problem may provide some general rules concerning saturation (a phenomenon encountered in all systems of strongly interacting identical particles occurring in nature) and shell structure.

We shall first solve a particular many-body problem exactly: the case of N identical particles moving in three dimensions, interacting by ordinary harmonic-oscillator pair-forces. The separation into the x , y and z dimensions is immediate.

In suitable units, the Schrödinger equation in the x -dimension is

$$\left[\frac{\partial^2}{\partial x_1^2} + \frac{\partial^2}{\partial x_2^2} + \dots + \frac{\partial^2}{\partial x_N^2} + E - (x_2 - x_1)^2 - (x_3 - x_1)^2 - \dots - (x_i - x_j)^2 - \dots - (x_N - x_{N-1})^2 \right] \psi = 0$$

i.e.
$$\left[\Delta + E - (N-1) \sum_{i=1}^N x_i^2 + \sum_{i=1}^N x_i \sum_{j=1}^N x_j \right] \psi = 0. \quad \dots\dots(1)$$

Let us consider only those ψ solutions not involving the centre of gravity coordinates (i.e. the general solution apart from a factor $\exp(ipx)$ where p is the total momentum). If we now consider the solution of the equation

$$[\Delta + E' - (N-1)\sum x_i^2 + \sum x_i \sum x_j - (\sum x_i)^2] \phi = 0 \quad \dots\dots(2)$$

it is clear that there is a solution ϕ of the form

$$\phi = \psi_E \exp \left(- \frac{(x_1 + x_2 + \dots + x_N)^2}{2\sqrt{N}} \right). \quad \dots\dots(3)$$

We have simply added an external potential $(\sum x_i)^2$ acting on the centre of gravity, and a solution of this new problem is then any of the products $\psi_E \exp(-X^2/2\sqrt{N})$ where $X = x_1 + x_2 + x_3 + \dots + x_N$ and the energies add such that

$$E' = E + \sqrt{N}. \quad \dots\dots(4)$$

But (2) can be rewritten

$$[\Delta + E' - N \sum (x_i^2)] \phi = 0$$

which is simply the problem of N independent particles moving in an external harmonic oscillator potential well and hence has as general solution a superposition of solutions of the form

$$\phi_{ab\dots r} = C_{ab\dots r} H_a(N^{1/4}x_1) H_b(N^{1/4}x_2) \dots H_r(N^{1/4}x_N) \quad \dots\dots(5)$$

(where H_k is the k th order Hermite function and $C_{ab\dots r}$ is some constant depending on the indices $a, b, \dots r$ but not on the x 's) subject to the condition that

$$\{2(a+b+\dots+r)+N\}\sqrt{N}=E'. \quad \dots\dots(6)$$

But a solution ϕ was found to be $\phi=\psi_E \exp(-X^2/2\sqrt{N})$ where ψ_E is any solution ψ for energy E . Therefore

$$\psi_E \exp(-X^2/2\sqrt{N}) = \Sigma C_{ab\dots r} H_a(N^{1/4}x_1) H_b(N^{1/4}x_2) \dots H_r(N^{1/4}x_N) \quad \dots\dots(7)$$

$$\text{where} \quad \{2(a+b+\dots+r)+N-1\}\sqrt{N}=E. \quad \dots\dots(8)$$

Since this holds for any ψ_E , the most general solution ψ_E is given by

$$\psi_E = \exp(+X^2/2\sqrt{N}) \Sigma C_{ab\dots r} H_a(N^{1/4}x_1) H_b(N^{1/4}x_2) \dots H_r(N^{1/4}x_N).$$

It remains to find the weight factors $C_{ab\dots r}$.

Not every ϕ corresponds to a solution ψ . We have only shown that every ψ corresponds to a solution ϕ . The necessary and sufficient condition is that $\phi \exp(X^2/2\sqrt{N})$ be translation invariant. It is a necessary condition by definition of our ψ 's. That it is also sufficient follows from the fact that the ψ 's are a complete set in the remaining $N-1$ dimensions. (The sufficiency is proved in the Appendix.)

For E having the lowest possible value $(N-1)\sqrt{N}$ we have necessarily $a=b=r=0$. This solution is translation invariant and represents the ground state for bosons (apart from an arbitrary total momentum factor).

This solution could have been obtained directly using normal coordinates. There are, however, two points of advantage in this form of the solution: (a) the particle symmetry of a given solution is more clearly shown, particularly in the more complex case of fermions below, (b) it shows the relation to the independent particle model.

The lowest ϕ that fulfils the total antisymmetry requirement is given by

$$H_0(N^{1/4}x_1)H_1(N^{1/4}x_2)\dots H_{N-1}(N^{1/4}x_N) \text{ antisymmetrized.}$$

This is the only possible partition of different $a, b, \dots r$ to add to this lowest energy. Thus this ground state solution is 'unmixed'. It is a solution since

$$\psi_0 = \exp(X^2/2\sqrt{N}) A H_0(N^{1/4}x_1) H_1(N^{1/4}x_2) \dots H_{N-1}(N^{1/4}x_N)$$

is translation invariant. A here represents the antisymmetrization operator. The gaussian part of the solution is always translation invariant, and in the polynomial part all terms containing a in the transformation $x \rightarrow x+a$ are antisymmetrized out, since a only enters into the lower power terms.

Thus the ground state of a system of fermions moving under the influence of mutual harmonic oscillator pair-forces is given by

$$\psi_0 = A H_{N-1}(N^{1/4}x_1) H_{N-2}(N^{1/4}x_2) \dots H_0(N^{1/4}x_N) \exp(+X^2/2\sqrt{N})$$

where A is the antisymmetrizing operator $\Sigma(-1)^i \Pi^i P_{ij}$.

The interesting point about this solution is that it agrees with the independent particle model for an overall harmonic oscillator well, both as regards angular momentum and number of particles in a given shell.

In three dimensions the total energy of successive ground states is given by

$$\sqrt{N}(3+5+5+5+7+7+7+7+7+7\dots)-3\sqrt{N}$$

to N terms in the bracket. We have successive 'shells' of $\frac{1}{2}k(k+1)$ terms of the same energy (apart from the factor \sqrt{N} increasing steadily with increasing N ,

the total number of particles), $\frac{1}{2}k(k+1)$ being the number of different partitions of the k excitation quanta corresponding to an energy $(2k+3)\sqrt{N}$ over the three dimensions. (These different partitions of the minimum energy correspond to allowable solutions, since these are shown to be translation invariant by the same argument as before.)

Similarly, the angular momentum is just that required by the 'harmonic oscillator side' of the shell model of Jensen and Mayer (Haxel, Jensen and Suess 1950, Mayer 1950) (before introducing spin and spin-orbit coupling; the introduction of spin doubles the degeneracy without changing the spatial functions being invariant to translation and allowed).

The total energy does not, of course, exhibit saturation (we must remember that we are measuring energy here from a zero level corresponding to all particles coinciding, i.e. from an effective depth that is increasing as $\frac{1}{2}n(n-1)$).

This model should be extended to the case of finite well depth and by introducing exchange forces to produce saturation. The more interesting problem remains to cover all possible interaction potentials by considering the class of functions that can arise as correlation functions of a problem symmetrical in N particles.

REFERENCES

- HAXEL, O., JENSEN, J. H. D., and SUESS, H. E., 1950, *Z. Phys.*, **128**, 295.
MAYER, M. G., 1950, *Phys. Rev.*, **78**, 16.

APPENDIX

Sufficiency of Translation-Invariance Condition

It is required to prove:

$$\nabla^2 \phi \gamma = -E \phi \gamma + |N(x_1^2 + \dots + x_N^2) - (x_1 + \dots + x_N)^2| \phi \gamma$$

provided (a) $\nabla^2 \phi = -\epsilon \phi + N(x_1^2 + \dots + x_N^2) \phi$ (A1)

(b) $\gamma = \exp(X^2/2\sqrt{N})$, hence

$$D\gamma = N \frac{\partial \gamma}{\partial X} = +\sqrt{N} X \gamma, \quad \text{..... (A2)}$$

where $X = x_1 + x_2 + \dots + x_N$ and $D \equiv \frac{\partial}{\partial x_1} + \frac{\partial}{\partial x_2} + \dots + \frac{\partial}{\partial x_N}$,

(c) $\frac{\partial}{\partial X}(\phi \gamma) = 0 \dots$ (translation invariance). (A3)

Proof: $\nabla^2(\phi \gamma) = N \frac{\partial^2}{\partial X^2}(\phi \gamma) + \gamma \left(\frac{\partial^2}{\partial \xi_1^2} + \dots + \frac{\partial^2}{\partial \xi_N^2} \right)$

where the ξ 's are the $N-1$ coordinates orthogonal to X ;

then $\nabla^2(\phi \gamma) = \gamma \sum \frac{\partial^2 \phi}{\partial \xi_i^2}$, from (A3),

$$= \gamma \nabla^2 \phi - \gamma N \frac{\partial^2}{\partial X^2} \phi \quad \text{..... (A4)}$$

but, from (A3), $\frac{\partial}{\partial X}(X\phi\gamma) = \phi\gamma$

i.e. $\frac{\partial}{\partial X}\left(\phi\sqrt{N}\frac{\partial\gamma}{\partial X}\right) = \phi\gamma$, from (A2),

i.e. $\phi\frac{\partial^2\gamma}{\partial X^2} + \frac{\partial\phi}{\partial X}\frac{\partial\gamma}{\partial X} = \frac{\phi\gamma}{\sqrt{N}}$(A5)

Now $\frac{\partial^2(\phi\gamma)}{\partial X^2} = \phi\frac{\partial^2\gamma}{\partial X^2} + \gamma\frac{\partial^2\phi}{\partial X^2} + 2\frac{\partial\phi}{\partial X}\frac{\partial\gamma}{\partial X} = 0$.

Therefore, substituting in (A5),

$$\phi\frac{\partial^2\gamma}{\partial X^2} - \gamma\frac{\partial^2\phi}{\partial X^2} = \frac{2\phi\gamma}{\sqrt{N}}, \quad \text{.....(A6)}$$

and substituting (A6) in (A4):

$$\begin{aligned} \nabla^2(\phi\gamma) &= \gamma\nabla^2\phi + 2\sqrt{N}\phi\gamma - N\phi\frac{\partial^2\gamma}{\partial X^2} \\ &= \gamma\nabla^2\phi + 2\sqrt{N}\phi\gamma - X^2\phi\gamma - \sqrt{N}\phi\gamma \text{ from definition of } \gamma \\ &= -(\epsilon - \sqrt{N})\phi\gamma + |N(x_1^2 + x_2^2 \dots + x_n^2) - X^2|\phi\gamma \\ &= -E\phi\gamma + |N(x_1^2 + x_2^2 + \dots + x_n^2) - (x_1 + x_2 + \dots + x_n)^2|\phi\gamma \end{aligned}$$

where $E = \epsilon - \sqrt{N}$.

Free-Electron Wave Functions for Conjugated Molecules

By C. A. COULSON

Mathematical Institute, Oxford

MS. received 2nd April 1953

IN view of the considerable importance now attached to the free-electron model of conjugated hydrocarbon compounds it is interesting to see that in many respects the wave functions suggested by this approximation are closely similar to those obtained in a more conventional LCAO molecular-orbital treatment (for terminology see for example Coulson 1952). Hückel (1937), Kuhn (1948 a, b), Herzfeld (1947), Bayliss (1948), Simpson (1948), Nikitine (1950), Jaffé (1952) and Griffith (1953) have shown how, for a polyene chain, the LCAO coefficients c_r in the expansion of a molecular orbital ψ in terms of its component atomic orbitals ϕ_r ($r = 1, 2, \dots, n$), viz.

$$\psi = \sum c_r \phi_r, \quad \text{.....(1)}$$

are precisely those to be found by supposing that the electron could move freely along the chain under no potential except that which confined it to the molecule at the two ends of the chain. Substantially this equivalence results from the fact (Coulson 1939) that for any one of the allowed molecular orbitals (the j th one, say)

$$c_r \propto \sin [rj\pi/(n+1)]. \quad \text{.....(2)}$$

This shows that the c_r are equally spaced ordinates along the curve

$$y = \text{constant} \times \sin \{j\pi x/(n+1)a\}, \quad \text{.....(3)}$$

where a is the C-C distance, and x is measured along the chain from an origin such that the n atoms have coordinates $x = a, 2a, \dots na$. The curve (3) is precisely the free-electron (FE) wave function. The fact that this agreement between the LCAO and FE wave functions requires us to place the first atom at $x = a$ and not $x = 0$ implies that the electron is free to move a further distance a at each end of the chain. We could call this the free-electron extension of the molecule. Some such extension is physically necessary. If we choose a value less than a —as might be considered rather more plausible on physical grounds—the complete identity of the coefficients c_r with the FE amplitudes at the nuclei no longer holds in an exact, but in an approximate, manner.

This similarity between LCAO and FE wave functions can be established in an alternative way, which is more general since it pays no attention to the size of the molecule, as follows. Let us first consider the polyene chain of fig. 1, in



Figure 1

which the direction of increasing x is shown by an arrow. Then according to the LCAO approximation (see for example Coulson 1952) the coefficients c_r in (1) satisfy a set of equations, of which a typical one (the r th) is:

$$(\alpha - E)c_r + \beta(c_{r-1} + c_{r+1}) = 0. \quad \dots\dots(4)$$

Here α and β are the conventional coulomb and resonance integrals, supposed constant for each atom and each bond. Now at nucleus r the only element in the wave function (1) which is of significant size is $c_r\phi_r$ so that $\psi(x_r) \propto c_r$. Thus (4) may be written

$$(\alpha - E)\psi(x_r) + \beta\{\psi(x_{r-1}) + \psi(x_{r+1})\} = 0. \quad \dots\dots(5)$$

This is a difference equation. But if we regard its solution $\psi(x)$ as a continuous function of x , we can replace (5) by an equivalent differential equation. Thus

$$\psi(x_{r+1}) = \psi(x_r) + a\psi'(x_r) + \frac{1}{2}a^2\psi''(x_r) + \dots \quad \dots\dots(6)$$

where a prime denotes differentiation with respect to x . It follows that (5) may be rewritten as

$$\frac{d^2\psi}{dx^2} + k^2\psi = 0, \quad \dots\dots(7)$$

where

$$k^2 = (\alpha - E + 2\beta)/\beta a^2. \quad \dots\dots(8)$$

Now eqn. (7) is precisely the Schrödinger wave equation for a free electron moving along the molecular chain. Thus the FE wave function (7) would be expected to resemble closely the LCAO wave function (1). Disagreement would arise when the omitted terms in the Taylor expansion (6) were not negligible. The first such terms would lead to a more correct form of (7) :

$$\frac{d^2\psi}{dx^2} + k^2\psi = -\frac{a^2}{12} \frac{d^4\psi}{dx^4}. \quad \dots\dots(9)$$

The term on the right-hand side of (9) is small if

$$a^2k^2/12 \ll 1. \quad \dots\dots(10)$$

This condition is well satisfied with the lower levels, for which k is small (at the bottom of the band of levels which arises with the infinite chain $k=0$). However, at the top occupied level in the ground state, $a^2k^2/12$ is just less than $\frac{1}{6}$, so that the equivalence is still reasonably good: but for more highly excited levels it begins to break down, a conclusion already reached on energy considerations by Platt (1949).

An interesting feature of this analysis is that it may be extended to branched chains, and it suggests that the FE model should now be one in which the electron moves not just in a one-dimensional motion along the lines of the bonds, as has hitherto been usually supposed (Griffith 1953, Platt 1949), but in a two-dimensional motion similar to that put forward several years ago by Schmidt (1940).

Consider an inner region of a branched chain, or condensed ring, molecule as shown in fig. 2.

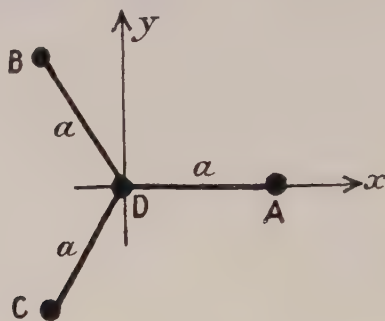


Figure 2

Then the secular equation associated with atom D is

$$(\alpha - E)c_D + \beta(c_A + c_B + c_C) = 0. \quad \dots\dots(11)$$

This is equivalent to

$$(\alpha - E)\psi(D) + \beta\{\psi(A) + \psi(B) + \psi(C)\} = 0.$$

A Taylor series expansion in xy coordinates similar to that used in (6) allows us to transform this to

$$\frac{\partial^2 \psi}{\partial x^2} + \frac{\partial^2 \psi}{\partial y^2} + k^2 \psi = 0 \quad \dots\dots(12)$$

where, now,

$$k^2 = 4(\alpha - E + 3\beta)/3\beta a^2. \quad \dots\dots(13)$$

Equation (12) is a FE Schrödinger equation, in the two coordinates xy . We may therefore anticipate that for molecules where the number of internal (or tertiary)

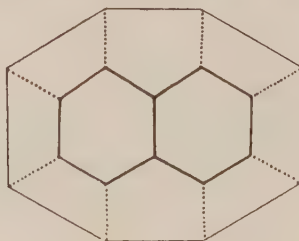


Figure 3

atoms such as D is large, the best FE model is that of a two-dimensional box. But provided that this number is small compared with the outer (primary or secondary) atoms, the one-dimensional, or peripheral, model may suffice. This no

doubt explains the considerable agreement for the wave functions found by Platt (1949) and Kuhn (1948 a, b).

In conclusion it may be stated that in a condensed system such as naphthalene (fig. 3), if we extend the space over which the free electron can move in the same way that it was extended earlier in the case of the polyene chains, then all the carbon atoms of the framework become effectively tertiary atoms; eqn. (12) applies throughout the space occupied by the molecule, and the correct free electron area would be something like that shown by the outer contour line of the figure. Presumably this could be replaced by a rectangle without much loss of accuracy.

REFERENCES

- BAYLISS, N. S., 1948, *J. Chem. Phys.*, **16**, 287.
COULSON, C. A., 1939, *Proc. Roy. Soc. A*, **169**, 413; 1952, *Valence* (Oxford: University Press), p. 239.
GRIFFITH, J. E., 1953, *J. Chem. Phys.*, **21**, 174.
HERZFELD, K. F., 1947, *Chem. Rev.*, **41**, 233.
HÜCKEL, E., 1937, *Z. Elektrochem.*, **43**, 752, 827.
JAFFÉ, H., 1952, *J. Chem. Phys.*, **20**, 1646.
KUHN, H., 1948a, *Helv. Chim. Acta*, **31**, 1441 and later papers in the same journal; 1948b, *J. Chem. Phys.*, **16**, 840.
NIKITINE, S., 1950, *J. Chim. Phys.*, **47**, 614.
PLATT, J. R., 1949, *J. Chem. Phys.*, **17**, 484.
SCHMIDT, O., 1940, *Chem. Ber.*, **73A**, 97.
SIMPSON, W. T., 1948, *J. Chem. Phys.*, **16**, 1124.

The Continuous Absorption of Light in Magnesium Vapour

BY R. W. DITCHBURN AND G. V. MARR

The Physics Research Laboratory, University of Reading

MS. received 7th April 1953

THE apparatus used in the vacuum ultra-violet experiments on sodium (Ditchburn, Jutsum and Marr 1953) has been employed to investigate the absorption cross section for magnesium vapour in the region of the series limit. Slight modifications were required to enable the apparatus to be used at the higher temperatures needed for magnesium. About 5 g of 'specpure' magnesium was introduced into each nickel reservoir. Calibration spectra were taken using grids which transmitted 100, 50 and 25% of the incident beam. The operation and mounting of the grids have been described in the above paper.

Absorption spectra were taken over a range of vapour pressures from 0.5 to 1.3 mm. The equation for the variation of pressure with temperature was taken from a paper by Ditchburn and Gilmour (1941), who give an estimate of $\pm 20\%$ for the probable error of the pressure in this region.

The method of separating atomic and molecular absorption by plotting the total absorption cross section against concentration and extrapolating to zero concentration (Ditchburn, Tunstead and Yates 1943) was employed. No trace of molecular absorption was detected. If only atomic absorption is present, then $\beta = \sigma C$, where β is the total absorption, σ is the atomic absorption cross

section and C is the concentration. Plots of this equation for various wavelengths should reveal any spurious effects. Figure 1 shows curves at the limit, at 1610 Å, and at 1500 Å. The slopes are in agreement with the mean absorption cross sections taken over the range of pressures employed.

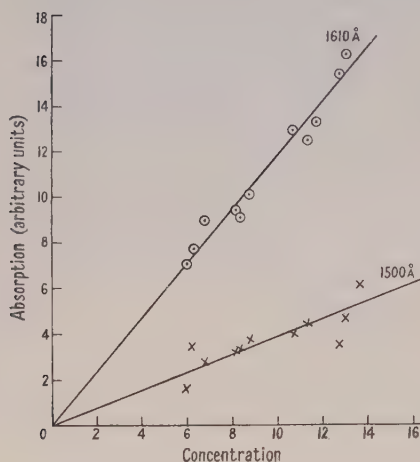


Fig. 1. Total absorption as a function of concentration.

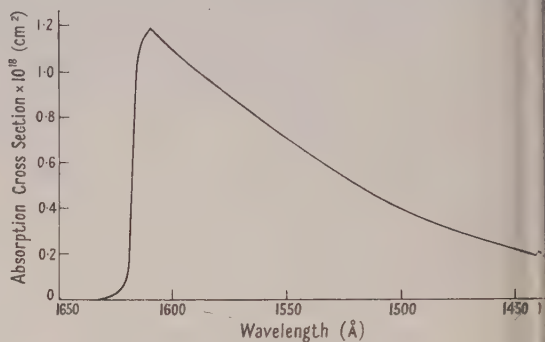


Fig. 2. Photoionization cross section of magnesium as a function of wavelength.

The error introduced in the photography and photometry is estimated at $\pm 5\%$, while that due to uncertainty in the temperature of the furnace and effective path length is $\pm 1\%$. Taking into account the probable error in the vapour pressure, the value for the maximum atomic absorption cross section is $1.18 \pm 0.25 \times 10^{-18} \text{ cm}^2$.

No theoretical calculations have been made for magnesium, but Bates (1946) gives a value of $8.2 \times 10^{-18} \text{ cm}^2$ for beryllium at the limit, and Bates and Massey (1941) give a value of $2.5 \times 10^{-17} \text{ cm}^2$ for calcium. The calculations for calcium require the atomic absorption cross section to fall off as λ^3 on the short-wavelength side of the limit, while those for beryllium require it to fall off rather more rapidly. Figure 2 shows the variation of atomic cross section with wavelength for magnesium. Near the limit the absorption falls off much more rapidly than is predicted for beryllium and calcium, and a variation of cross section with λ^{15} would be more appropriate. The low value at the limit, and the rapid decrease of the atomic cross section, indicate a much lower value than that predicted for the f -value of the continuum as a whole, unless the absorption curve has a minimum at a wavelength below the range of the measurements. If this is so then the curve would be similar to that found for potassium (Ditchburn, Tunstead and Yates 1943).

One of us (G. V. Marr) wishes to acknowledge receipt of a maintenance grant from the Department of Scientific and Industrial Research.

REFERENCES

- BATES, D. R., 1946, *Mon. Not. R. Astr. Soc. A*, **106**, 423.
 BATES, D. R., and MASSEY, H. S. W., 1941, *Proc. Roy. Soc. A*, **177**, 329.
 DITCHBURN, R. W., and GILMOUR, J. C., 1941, *Rev. Mod. Phys.*, **13**, 310.
 DITCHBURN, R. W., JUTSUM, P. J., and MARR, G. V., 1953, *Proc. Roy. Soc. A*, in the press.
 DITCHBURN, R. W., TUNSTEAD, J., and YATES, J. G., 1943, *Proc. Roy. Soc. A*, **181**, 386.

LETTERS TO THE EDITOR

The Quantum Mechanical Equations of Motion
and the Commutation Relations

Some time ago Wigner (1950) raised the question whether the postulate that the quantum mechanical operators obey the classical equations of motion determines the commutation rules uniquely. He examined the case of the harmonic oscillator and, taking a representation in which the Hamiltonian was diagonal, showed that there was an ambiguity in the commutator $[q, p]$. He found a more general relation to hold* :

$$([q, p] - i)_{nn'} = ia(-1)^n \delta_{nn'} \quad \dots\dots (1)$$

$$\text{where} \quad a = 2E_0 - 1 \quad \dots\dots (2)$$

E_0 being the lowest energy of the oscillator, not necessarily equal to $\frac{1}{2}$.

Yang (1951) has shown by working in the q -representation that the validity of the eigenfunction expansion theorem in the case of a harmonic oscillator requires that the right-hand side of (1) must be zero. This needs however an explicit calculation of the eigenfunctions, which is not always possible and is, in any case, rather tedious.

In view of the importance of this question, it seems worth while to point out that there is a much simpler way of looking at the problem based on correspondence to the classical theory. Now, in classical mechanics the PB relations are invariant under contact transformations. It is therefore pertinent to demand that the quantum analogue of these brackets, viz. the commutators, ought to be invariant under unitary transformations.

One sees immediately that if one makes the transformations

$$Q = S^{-1}qS \quad \dots\dots (3a) \quad P = S^{-1}pS, \quad \dots\dots (3b)$$

(1) gives

$$([Q, P] - i)_{nn'} = ia \sum_{n''} (S^{-1})_{nn''} (-1)^{n''} S_{n''n'} \quad \dots\dots (4)$$

and the right-hand side is not independent of the arbitrary unitary matrix S unless $a = 0$.

The argument can be easily extended to the general non-relativistic case with an arbitrary potential $V(q)$. The Hamiltonian in that case is

$$H = \frac{1}{2}p^2 + V(q) \quad \dots\dots (5)$$

and one of the classical equations of motion which holds independently of V is

$$dq/dt = p. \quad \dots\dots (6)$$

Inserting this in the quantum mechanical equation of motion

$$i \, dq/dt = [q, H] \quad \dots\dots (7)$$

we get

$$ip = [q, H] = [q, \frac{1}{2}p^2 + V] = \frac{1}{2}[q, p^2] = \frac{1}{2}p[q, p] + \frac{1}{2}[q, p]p. \quad \dots\dots (8)$$

$$\text{Writing} \quad A = [q, p] - i \quad \dots\dots (9)$$

the identity (8) can be written as

$$pA + Ap = 0. \quad \dots\dots (10)$$

* For simplicity we take $\hbar = 1$, $m = 1$, $\omega = 1$.

Here we observe that only the multiple of a unit matrix on the right-hand side of (1) can preserve the invariance of the commutation rules under canonical transformations. Equation (10) now shows that the multiplying factor must be zero, i.e. $A=0$. Therefore we get the usual commutation rule $[q, p]=i$ which, we conclude, is valid generally in non-relativistic quantum mechanics.

Physical Research Laboratory,
Navrangpura,
Ahmedabad 9, India.
22nd April 1953.

VACHASPATI.

WIGNER, E. P., 1950, *Phys. Rev.*, **77**, 711.

YANG, L. M., 1951, *Phys. Rev.*, **84**, 788.

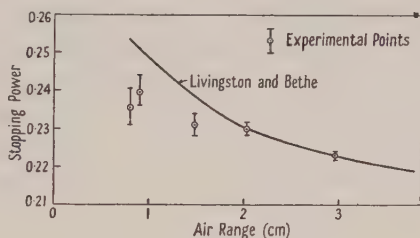
The Relative Stopping-Power of Hydrogen and of Helium for Slow α -Particles

When finding the air-ranges of nuclear particles it is often convenient to make the actual measurement in a gas other than air and then convert to air-ranges by use of the stopping-power of the particular filling. The stopping-power is usually obtained during the experiment by calibration with α -particles of known range (e.g. from polonium or thorium C). Gilbert (1948) has pointed out that in this procedure it is necessary to consider the variation of relative stopping-power with the velocity of the particle, otherwise appreciable errors will result. He was interested particularly in the ranges of the α -particles from the slow neutron reaction $^{10}\text{B}(n, \alpha)^7\text{Li}$ as measured in a Wilson cloud chamber; this reaction is valuable as it provides a point on the range-energy curve for slow α -particles. The main group of particles has a range of about 0.7 cm (1.47 mev) whereas the α -particles which Gilbert used for calibration have ranges 8.63 cm (8.78 mev) and 4.79 cm (6.04 mev). He calculated the range correction due to the change of stopping-power with velocity to be about 10%, i.e. the uncorrected ranges had to be increased by this amount. This is almost certainly an overestimate of the correction even if the full ranges of the calibrating particles were in the chamber. The cloud chamber filling used by Gilbert was helium with the vapour of ethyl borate ($\text{B}(\text{OCH}_3)_3$) as a target. He used the curves given by Livingston and Bethe (1937) to obtain the stopping-power of H_2 and C at different ranges and interpolated for He and B. This procedure gives a difference of about 10% in the atomic stopping-power of He relative to air for α -particles of 8 mev and 1.5 mev, a result which contradicts the early experimental results of Gurney (1925) which gave a variation of 3%. A contradiction of this sort makes not only the relative stopping-power for He uncertain but also throws suspicion on the values for H_2 and C. Of the latter two elements, H_2 is the more important to consider because the variation of stopping-power with velocity is much greater than for C and, indeed, in the boron experiment the variation due to hydrogen contributes by far the major part of the total variation.

Because of charge-exchange uncertainties it is very unlikely that the difficulties mentioned can be resolved by theoretical analysis, and we have therefore investigated experimentally the stopping-power variation by

performing careful range measurements in a Wilson cloud chamber. Stereo-photographs were taken with a large angle (about 25°) between the views, and range measurements were made on the reprojected images.

The helium stopping-power was first investigated by means of an air absorber cell attached to the wall of the cloud chamber and separated from the chamber filling by a thin mica window (about $\frac{1}{2}$ cm air equivalent). A known portion of the range of polonium alpha-particles was absorbed in the air-cell and the window and the residual range was measured in the chamber. From the chamber conditions the relative stopping-power of helium at S.T.P. was found for each track measured, the residual range being corrected for those particles not passing through the cell normally. The stopping-power measurements were made for residual ranges from 2.5 cm to 0.65 cm and the results were as follows: 0.181 ± 0.002 (2.3 cm), 0.178 ± 0.004 (1.8 cm), 0.181 ± 0.004 (1.1 cm), 0.183 ± 0.004 (0.65 cm). These disagree strongly with the large variation of stopping-power with velocity estimated by Gilbert, but are compatible with the early measurements of Gurney and the value (3%) used by Bethe (1950) in his work on the new range-energy curves. The results can also be compared with the 0.175 quoted by Livingston and Bethe (1937) from Mano's work for a range of 4.6 cm (6 MeV α -particles). Again, it can be seen that the 3% velocity correction is favoured rather than the higher value. Moreover, we feel that our results suggest that Mano's figure is itself a little low and that a value of 0.180 at 4.6 cm would be more in keeping with the expected trend in stopping-power variation.



Stopping-power of hydrogen relative to air.

The variation of the relative stopping-power of hydrogen with particle velocity was also studied with the air-cell technique, and the results obtained are shown in the figure together with the relevant part of Livingston and Bethe's curve. The experimental points suggest that the Livingston and Bethe curve gives an excessive variation in stopping-power; this may be due to small errors in the estimation of the K-shell contribution to the average ionization potential or to differences in charge-exchange between air and hydrogen.

Physics Department,
University of Birmingham.
27th March 1953.

P. N. COOPER.
V. S. CROCKER.
J. WALKER.

BETHE, H. A., 1950, *Rev. Mod. Phys.*, **22**, 213.

GILBERT, C. W., 1948, *Proc. Camb. Phil. Soc.*, **44**, 447.

GURNEY, R. W., 1925, *Proc. Roy. Soc. A*, **107**, 332.

LIVINGSTON, M. S., and BETHE, H. A., 1937, *Rev. Mod. Phys.*, **9**, 245.

Range-Energy Data from the $^{10}\text{B}(\text{n}, \alpha)^7\text{Li}$ and $^6\text{Li}(\text{n}, \text{t})^4\text{He}$ Reactions

The stopping-power information given by the authors (Cooper *et al.* 1953) has been used to obtain accurately the mean air-ranges of the particles emitted in the slow neutron reactions $^{10}\text{B}(\text{n}, \alpha)^7\text{Li}$ and $^6\text{Li}(\text{n}, \text{t})^4\text{He}$. Both reactions have been investigated in a 9 in. diameter Wilson cloud chamber, using the slow neutrons passing through the shielding of the Birmingham cyclotron when deuterons were being accelerated. For the boron reaction hydrogen and helium were used as the chamber gas, whereas air was used for the lithium work.

The boron reaction has been studied by several workers using both solid and gaseous targets (see Bethe (1950) for earlier work). In an attempt to improve on the accuracy of the range measurements we have used gaseous targets (boron ester $\text{B}(\text{OCH}_3)_3$) and have pulsed the cyclotron (neutron source) in synchronism with the operation of the cloud chamber. The operating time of the clearing field and the light flash on the chamber were also carefully controlled in order to give good tracks for a photometric study of the density. As in the work of Bower, Bretscher and Gilbert (1938), the discontinuity in the grain density gave the common origin of the α and ^7Li tracks. For our work a standard Hilger microphotometer, as used in spectroscopy, has proved very satisfactory for density measurements which were always made on plate photographs of the tracks with a magnification of $\frac{1}{4}$ rather than the usual film photographs with a magnification of $\frac{1}{9}$.

The result of the density measurements was a value of 1.62 ± 0.01 for the ratio of α -particle to ^7Li ranges, which agrees exactly with the result of Bower *et al.* (1938) but with a smaller error. This result, together with the total track length, which was measured relative to polonium α -particles, gave the uncorrected air-range for the boron α -particles. These were then corrected for the variation with particle velocity of the stopping-power of the chamber filling and the final range for the boron α -particles was 0.725 ± 0.007 cm.

From the new range-energy data the associated energy for this range is 1.47 ± 0.01 mev, in excellent agreement with the 1.474 mev given by Tollestrup, Fowler and Lauritsen (1949) from magnetic analysis measurements. In the lithium reaction we used a thick source of $^6\text{Li}_2\text{SO}_4 \cdot 2\text{H}_2\text{O}$ on nickel and concentrated on measuring the triton range. The extrapolated range was measured from the number-range curve and, as shown by Livingston and Bethe (1937), this gives directly the mean range of the particles from the surface if the incident particle is a neutron. By comparison with polonium α -particles the mean range of the tritons was found to be 5.97 ± 0.05 cm, no velocity correction for stopping-power being needed. This result agrees with that of Bøggild and Minnhagen (1949), who found a range of 6.00 ± 0.06 cm, but is higher than earlier measurements which show no agreement with each other. The equivalent proton range is 1.99 ± 0.02 cm with an associated energy of 0.915 ± 0.005 mev on the new range-energy curves. The comparison figure from the data of Tollestrup, Fowler and Lauritsen is 0.910 ± 0.004 mev, again giving agreement within the experimental error.

Physics Department,
University of Birmingham.
27th March 1953.

P. N. COOPER.
V. S. CROCKER.
J. WALKER.

- BETHE, H. A., 1950, *Rev. Mod. Phys.*, **22**, 213.
 BØGGILD, J. K., and MINNHAGEN, L., 1949, *Phys. Rev.*, **75**, 782.
 BOWER, J. C., BRETSCHER, E., and GILBERT, C. W., 1938, *Proc. Camb. Phil. Soc.*, **34**, 290.
 COOPER, P. N., CROCKER, V. S., and WALKER, J., *Proc. Phys. Soc. A*, **66**, 658.
 LIVINGSTON, M. S., and BETHE, H. A., 1937, *Rev. Mod. Phys.*, **9**, 245.
 TOLLESTRUP, A. V., FOWLER, W. A., and LAURITSEN, C. C., 1949, *Phys. Rev.*, **76**, 428.

Alpha-Emitting Levels of ^8Be with Isotopic Spin $T=1$

A recent communication (Wilkins and Goward 1951) reported the existence of a 16.9 mev level of ^8Be which decays by emission of alpha-particles. Ajzenburg and Lauritsen (1952) point out that both the excitation energy and narrow width of this level suggest that it is the isotopic spin $T=1$ ($T_z=0$) analogue of the ground states of ^8Li and ^8B , and its properties are therefore of special interest. The present communication gives a preliminary account of further work which confirms the (predominantly) $T=1$ character of the level, and demonstrates that the total angular momentum J is 2 (both parity and J must be even, to permit decay into alpha-particles). The existence of a further alpha-emitting level at 17.6 mev excitation is also reported.

Analysis of over 200 $^{12}\text{C}(\gamma, 3\alpha)$ stars produced in nuclear emulsions by gamma-rays of energy greater than 26 mev has indicated transitions to ^8Be levels in approximately the following proportions: 2% to the ground state, 10% to the 3 mev level and other levels below 16 mev excitation, and 88% to a group of levels near 17 mev. The latter group was originally reported as a single level, but has now been clearly resolved into two levels at 16.8 ± 0.2 mev and 17.6 ± 0.2 mev excitation, having real widths $\Gamma < 0.3$ mev. There is some evidence for a third (unresolved) level at about 16.4 mev, the three levels occurring in the approximate proportions 56 : 20 : 12 respectively.

Writing the $^{12}\text{C}(\gamma, 3\alpha)$ reaction more fully as $^{12}\text{C}(\gamma, \alpha_1)^8\text{Be}^*(\alpha_2\alpha_3)$, both the J value of the ^8Be level and the multipole nature of the gamma-ray absorption may be deduced from the angular distributions of α_1 and α_2 (or α_3), and from the $(\alpha_1\alpha_2)$ angular correlation. Results to be expected theoretically have been calculated by M. J. Brinkworth (to be published), assuming $J=0, 2$ or 4 (the possibility $J>4$ may reasonably be neglected) and any mixture of electric dipole (E.D.), electric quadrupole and magnetic dipole absorption. The experimental statistics available for the 16.8 mev level are adequate to point conclusively to the combination $J=2$ and E.D. absorption (with interference between $l=1$ and $l=3$ outgoing α_1 waves). For the 17.6 mev level, statistics do not permit such a definite conclusion, although E.D. absorption combined with $J=2$ or 4 yields the best agreement; it may be remarked that $J=4$ seems more likely than $J=0$ or 2 , since the level has not been observed in the $^7\text{Li}(p, \alpha)$ reaction (Ajzenburg and Lauritsen 1952).

The following additional evidence now supports the suggested $T=1$ character of the 16.8 mev level. According to isotopic spin selection rules (Radicati 1952), E.D. absorption can excite only $T=1$ states in ^{12}C . Provided, therefore, that mixing of states of different T (by coulomb forces, etc.) is not too great, it is very probable that the ^{12}C states involved here have mainly $T=1$ character. Transitions to $T=1$ states in ^8Be should thus be favoured. It has been observed, however, that transitions to the 16.8 mev level occur with at least six times the frequency of (energy-favoured) transitions to the 3 mev, $T=0$ level, although both levels are 2^+ . Thus assignment of $T=1$ to

the 16.8 mev level gives complete accord with the experimental results. Similar (though weaker) evidence, combined with the observed narrow width, makes it likely that the 17.6 mev level also has $T=1$.

Some admixture of $T=0$ in both the 16.8 and 17.6 mev levels must of course be present, in order to allow emission of alpha-particles rather than gamma-rays. Emission of gamma-rays would imply the occurrence of $^{12}\text{C}(\gamma, \gamma'3\alpha)$ reactions, and special analyses for detecting such reactions are described by Goward and Wilkins (1953). An upper limit of about $\frac{1}{4}$ may be set in this way to the ratio of gamma-rays to alpha-particle emission from the two levels. The same methods show that the well known 17.7 mev (1^+) gamma-emitting level of ^8Be is not excited by the $^{12}\text{C}(\gamma, \alpha)$ reaction as frequently as the 17.6 mev (possibly 4^+) level reported here. Differing T values may again be the explanation.

The above results show that the 16.8 mev level of ^8Be has $J=2$, even parity, $\Gamma < 0.3$ mev, and a predominantly $T=1$ character. Its excitation energy is just that predicted (Lauritsen 1952) for the analogue of the ^8Li and ^8B ground states, but considerably more evidence is required to make such an identification certain. The most pressing requirement is a determination of spin and parity for ^8Li and ^8B . In addition, neighbouring $T=1$ levels of ^8Be must be looked for (e.g. the suspected 16.4 mev level mentioned above), preferably with techniques which do not limit the search to alpha-emitting (0^+ , 2^+ , 4^+ . . .) levels.

We are indebted to Mr. M. J. Brinkworth for many helpful discussions, and for making his theoretical results on angular distributions and correlations available before publication.

Atomic Energy Research Establishment,
Harwell, Didcot, Berks.
22nd April 1953.

J. J. WILKINS.
F. K. GOWARD.

AJZENBURG, F., and LAURITSEN, T., 1952, *Rev. Mod. Phys.*, **24**, 321.

GOWARD, F. K., and WILKINS, J. J., 1953, *Proc. Roy. Soc. A*, **217**, 357.

LAURITSEN, T., 1952, *Annual Review of Nuclear Science*, **1**, 67.

RADICATI, L. A., 1952, *Phys. Rev.*, **87**, 521.

WILKINS, J. J., and GOWARD, F. K., 1951, *Proc. Phys. Soc. A*, **64**, 1056.

Semiconductor Statistics

It has been usual to obtain the number of electrons in impurity centres by using simply the Fermi-Dirac distribution function

$$1/\{1 + \exp [(E - E_F)/kT]\}. \quad \dots\dots (1)$$

The approach which uses (1) (referred to as 'approach B') was recently shown to be inadequate (Landsberg 1952) by a free energy argument (referred to as 'approach A') which yielded

$$1/\{1 + \frac{1}{2} \exp [(E - E_F)/kT]\} \quad \text{or} \quad 1/\{1 + 2 \exp [(E - E_F)/kT]\}, \quad \dots (2)$$

depending on whether the bound electron states are 'unpaired' or 'paired' respectively. These more correct functions can also be derived by using the grand canonical ensemble (James, unpublished*, Guggenheim 1953), and there are other methods. Guggenheim has inadvertently mistaken our approach B

* The author is indebted to Dr. K. Lark-Horovitz for informing him of this work. It is described in a report on semiconductor research issued in 1952 by the Department of Physics, Purdue University, to the United States Signal Corps.

to stand for all 'direct' statistical mechanical approaches, and this has led him to misinterpret our statement 'approach A is to be preferred to approach B', and similar statements. It is clear that all valid treatments must be equivalent to approach A, and lead to (2). Which of them is preferred is a matter of choice, but they are all superior to approach B. There is therefore no difference of principle between Guggenheim's point of view and our own.

Department of Natural Philosophy,
The University, Aberdeen.

P. T. LANDSBERG.

16th February 1953.

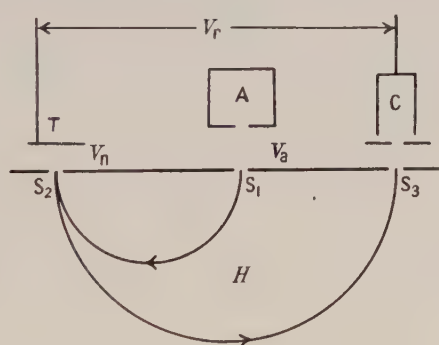
GUGGENHEIM, E. A., 1953, *Proc. Phys. Soc. A*, **66**, 121.

LANDSBERG, P. T., 1952, *Proc. Phys. Soc. A*, **65**, 604.

The Liberation of Positive Ions by Negative Ion Bombardment of Surfaces

It is well known that bombardment of an untreated metal surface by positive ions of one species can result in the liberation of an extensive spectrum of negative ions, and that some of these negative ions leave the surface with appreciable initial energy (Sloane and Press 1938, Arnot and Beckett 1938). This was shown directly using a double mass spectrometer (Sloane and Press 1938) in which the bombarding positive ion beam was selected in a primary arc and the resulting negative ions analysed in a secondary arc. We have now used essentially the same instrument, with suitable modifications and improvements, to investigate the converse process, namely, the liberation of positive ions under negative ion bombardment.

The arrangement used is shown in the figure. Negative ions from a



discharge in lithium chloride vapour were drawn off from the source A, and accelerated by a variable potential difference V_a . These passed through the slit S_1 , and were deflected in a preset magnetic field H . By varying V_a (usually between 100 and 400 volts) a negative ion beam of given kind could be made to pass through the slit S_2 , and after acceleration through the potential difference V_n (usually between 300 and 2800 volts) bombard the target T. Positive ions liberated on T under this bombardment were in turn accelerated in the reverse direction by V_n , to pass through the slit S_2 and be deflected in the magnetic field H . By varying V_n one positive ion beam after another could be made to enter the slit S_3 and be detected by the valve electrometer connected to the Faraday cylinder C. The mass scale was calibrated by using a potassium Kunsman positive ion source behind a small hole in the target T. The Faraday

cylinder could be held at any desired potential V_r with respect to the target, and a retarding potential curve, which on differentiation yielded an energy distribution curve, could be obtained by varying V_r and plotting electrometer current against V_r .

It was found, for example, that on bombarding the target with a single negative ion beam consisting of the unresolved isotopic combinations in LiCl_2^- (mass numbers 76, 77, 78, 79, 80 and 81, with 77 and 79 the more intense) an extensive positive ion spectrum could be recorded by gradually varying V_n . Several positive ion peaks corresponding to mass to charge ratios M/e in the range 12 to 95 were detected. The most prominent of these formed a group with M/e values 47, 48, 49, 50 and 51, whose relative intensities were in the ratios to be expected from the different combinations of the isotopes of lithium and chlorine in the alkali halide ion Li_2Cl^+ . However, only two very small peaks with M/e values 77 and 79, which might possibly be attributable to LiCl_2^+ , could be detected. The peak due to 77 was only about one half of one per cent of that due to 49. This is interesting since, whether or not the small peaks at 77 and 79 are due to LiCl_2^+ , the observations show that in this case the most intense alkali halide positive ion group is not that corresponding to the bombarding negative ion. This, together with the presence of other positive ion peaks, shows that the liberated positive ions can result from a process other than a simple charge transfer, as was in fact found in the case of negative ion formation under positive ion bombardment (Sloane and Press 1938). However, in contrast to the latter process, we have not in this preliminary investigation detected liberated positive ions showing excess energies; in all the retarding curves examined so far the current had fallen to zero before the potential of the Faraday cylinder became appreciably positive with respect to the target T. On the other hand, though the retarding runs revealed no excess energies, they did show that most of the ions possessed energies consistent with their having been formed on the target surface. Confirmation that these positive ions resulted from the negative ion bombardment was furnished by the fact that a small change in V_a which caused an alteration in the radius of the LiCl_2^- beam sufficient to swing it off the slit S_2 , but not to replace it by another beam, resulted in a reduction to zero of the intensity of the positive ion spectrum. This reduction took place gradually as the negative ion beam was slowly swept off the slit.

These preliminary direct experiments seem to leave little room for doubt that bombardment of a surface by negative ions of one kind can result in the liberation of positive ions of a different kind. This process had previously been suspected (Sloane, Watt, Cole and Love, unpublished) as being at least partly responsible for certain reverse currents observed during retarding potential runs on negative ions, and has also been suggested by Timoshenko (1941) as being a possible explanation of some effects observed during sputtering measurements by Johnson and Harris (1934).

Queen's University,
Belfast.

4th May 1953.

R. H. SLOANE.
R. M. HOBSON.

ARNOT, F. L., and BECKETT, C., 1938, *Proc. Roy. Soc. A*, **168**, 103.

JOHNSON, E. A., and HARRIS, L., 1934, *Phys. Rev.*, **45**, 630.

SLOANE, R. H., and PRESS, R., 1938, *Proc. Roy. Soc. A*, **168**, 284. (See also Sloane, R. H., and Watt, C. S., 1948, *Proc. Phys. Soc.*, **61**, 217, for detailed identifications.)

TIMOSHENKO, G., 1941, *J. Appl. Phys.*, **12**, 69.

Charge Independence and Nuclear Reactions

Several writers (Adair 1952, Kroll and Foldy 1952, Trainor 1952, Radicati 1953) have recently discussed the significance of charge independence or charge symmetry of nuclear forces, and the relative insignificance of coulomb forces, in relation to reactions involving light nuclei. This is usually expressed by ascribing to a nuclear system the quantity \mathbf{T} (total 'isotopic spin' vector) which, in so far as electromagnetic forces are neglected, is conserved in any process. Previous discussions have emphasized the application of this conservation rule to systems involving charge-symmetrical nuclei (i.e. equal numbers of neutrons and protons), where $\mathbf{T}=0$ for the initial, and therefore also for 'allowed' final states. It is the purpose of this note to draw attention to the application of this rule to a type of reaction which has been extensively studied, namely, one in which the initial nuclei are not charge-symmetrical, the final nuclei are, and the reaction proceeds through well-defined (resonance) states of a compound nucleus. In particular, for the reaction type (p, α) with an initial nucleus having one more neutron than proton (e.g. $^{11}\text{B} + p \rightarrow ^{12}\text{C}^* \rightarrow ^8\text{Be} + \alpha$), both initial nuclei have $\mathbf{T}=\frac{1}{2}$, so that the states of the compound nucleus can be $\mathbf{T}=0$ or 1, but the final states usually involve only low lying states of symmetrical nuclei for which $\mathbf{T}=0$. One might then expect the partial widths for the second stage of these reactions to be unusually small, but not zero, in the case of some resonance levels, involving transitions of the type $\mathbf{T}=1 \rightarrow \mathbf{T}=0$.

Relevant information is available for (p, α) reactions with ^7Li , ^8Be , ^{11}B , ^{15}N , ^{19}F , ^{23}Na and ^{27}Al . One interesting case is the resonance with ^{11}B (165 keV proton energy) for which the α -particle width for the most energetic group seems to be about 0.1 eV although the energy available for the break-up of the compound nucleus is nearly 9 MeV (Ajzenberg and Lauritsen 1952). The total α -particle width of this level is only a few volts. The absence of some transitions in the reaction $^9\text{Be}(p, \alpha)^6\text{Li}$ might, as suggested by Adair, be similarly interpreted, but complete absence may also be due to rigorous conservation rules (J and parity). There is some evidence of partial widths reduced by a factor 100 or more in the $^{19}\text{F}(p, \alpha)^{16}\text{O}$ reaction, but the interpretation here is not unambiguous, particularly in the absence of resonance-scattering measurements. One may also note that $\mathbf{T}=1$ states of the compound nucleus which have small widths for particle emission, should, if J and parity are appropriate, have normal widths for electric dipole emission to the low ($\mathbf{T}=0$) states of the compound nucleus and conversely (Radicati 1952). There is no clear experimental evidence which exemplifies this correlation.

Comparison of level density at typical excitations of the compound nucleus with that of corresponding regions of the neighbouring isobaric nuclei, indicates that, in many cases, the large level density observed is mainly composed of $\mathbf{T}=0$ states, and the ' \mathbf{T} -forbidden' transitions will be relatively rare. The effect of the conservation rule might also be weakened by the high density of $\mathbf{T}=0$ states. In a recent examination of the application of the similar imperfect conservation rule for mechanical spin S , Christy (1953) finds good evidence for the validity of S -conservation in reactions involving comparable excitation energies.

Department of Physics,
Imperial College, London.
19th May 1953.

S. DEVONS.

- ADAIR, R. K., 1952, *Phys. Rev.*, **87**, 1041.
 AJZENBERG, F., and LAURITSEN, T., 1952, *Rev. Mod. Phys.*, **24**, 321, and references therein.
 CHRISTY, R. F., 1953, *Phys. Rev.*, **89**, 839.
 KROLL, N. M., and FOLDY, L. L., 1952, *Phys. Rev.*, **88**, 1177.
 RADICATI, L. A., 1952, *Phys. Rev.*, **87**, 521; 1953, *Proc. Phys. Soc. A*, **66**, 139.
 TRAINOR, L. E. H., 1952, *Phys. Rev.*, **85**, 962.

Paramagnetic Resonance in an Argentic Compound

An extensive study has been made of the paramagnetic resonance spectrum of the cupric ion in crystalline solids (e.g. Bleaney, Penrose and Plumptre 1949). The ground state configuration of the free ion is $3d^9$, and the experimental results have been interpreted with considerable success by Abragam and Pryce (1951) on the assumption of a single electron hole localized on the copper ion. Although there is some evidence that this assumption is not fully justified (Bleaney, Bowers and Trenam 1953) it nevertheless seems to represent a reasonable first approximation. For comparison the paramagnetic resonance spectrum of a compound of the argentic ion $Ag^{2+}(4d^9)$ has been investigated.

To obtain the argentic ion in a stable form a complex with a nitrogenous base may be used (Sidgwick 1950). The spectrum has been examined of argentic di-o-phenanthroline persulphate $(Ag(phn)_2)_2S_2O_8$, and also that of the corresponding cupric compound. Unfortunately it did not prove possible to grow single crystals and, as the interpretation of the spectrum of a powder is somewhat hazardous, the conclusions must be accepted with some reserve.

The spectrum of the powder of the argentic compound has been examined at 290°K, 90°K and 20°K, using radiation of wave numbers 0.8 and 0.3 cm^{-1} . In each case the spectrum consisted of a continuous absorption band whose ends were sharply defined, and the intensity reached a sharp peak close to the end corresponding to the lower g -value. The results may be interpreted by assuming the g -value to have approximately axial symmetry, with $g_{||} = 2.18$ and $g_{\perp} = 2.04$. The hyperfine structure splitting due to the two naturally abundant isotopes $^{107}, ^{109}Ag$ appears to be small, as would be expected from the small nuclear magnetic moments ($\simeq -0.12$ n.m.) of these isotopes.

The spectrum of the powder of the cupric compound was similar, except that the boundaries of the absorption band were not so sharply defined, and the apparent g -values depended on the wave number of the radiation. This effect may be ascribed to the hyperfine structure due to the two naturally abundant isotopes $^{63}, ^{65}Cu$, and on allowing for this the g -values are found to be $g_{||} = 2.3_0$, $g_{\perp} = 2.05$.

On the assumption that the electron hole remains localized on the paramagnetic ion, one obtains the relation (see Polder 1942): $g_{||} = 2 - 8\lambda/\Delta$ where λ is the spin-orbit coupling coefficient of the free ion, and Δ is the splitting of the levels of the 2D term by the crystalline electric field. Taking for the cupric ion $\lambda = -828$ cm^{-1} (Shenstone, unpublished: see Abragam and Pryce 1951), the experimentally determined g -value gives Δ to be 22 000 cm^{-1} . In view of the bluish-green colour of the compound, this value is perhaps somewhat high, but it is of a reasonable order of magnitude. For the argentic ion $\lambda = -1840$ cm^{-1} (Gilbert 1935), and this gives for Δ the improbably large value of 82 000 cm^{-1} . Thus the relatively small departure of $g_{||}$ from the free spin value indicates that

the contribution from the orbital angular momentum is unduly low, and it seems likely that the hole in the 4d subshell is not localized on the silver ion, but migrates to the surrounding atoms (cf. Owen and Stevens 1953).

The author wishes to record his gratitude to Drs. B. Bleaney and K. W. H. Stevens for helpful discussion, and to Dr. P. F. D. Shaw for the preparation of the compounds.

Clarendon Laboratory,
Oxford.

20th May 1953.

K. D. BOWERS.

ABRAGAM, A., and PRYCE, M. H. L., 1951, *Proc. Roy. Soc. A*, **206**, 164.

BLEANEY, B., BOWERS, K. D., and TRENAM, R. S., 1953, *Proc. Phys. Soc. A*, **66**, 410.

BLEANEY, B., PENROSE, R. P., and PLUMPTON, B. I., 1949, *Proc. Roy. Soc. A*, **198**, 406.

GILBERT, W. P., 1935, *Phys. Rev.*, **48**, 338.

OWEN, J., and STEVENS, K. W. H., 1953, *Nature, Lond.*, **171**, 836.

POLDER, D., 1942, *Physica*, **9**, 709.

SIDGWICK, N. V., 1950, *Chemical Elements and their Compounds*, Vol. I (Oxford: University Press), p. 176.

REVIEWS OF BOOKS

Schwerkraft und Weltall, by PASCUAL JORDAN. Pp. viii + 204. (Braunschweig: Vieweg, 1952.) DM. 1580.

This book will be of interest to all students of relativity because it gives Dr. Pascual Jordan's views. He begins with a brief account of the red-shift observed in the spectral lines of external galaxies and appears to take it for granted that the relationship of red-shift with distance has been shown empirically to be a linear one. Whilst this may be approximately true for those nearer galaxies, whose red-shifts have so far been measured, there is no means of knowing *a priori* that the linearity persists for the more remote ones and there are theoretical reasons for doubting that it does. Dr. Jordan then passes on to the tensor calculus where he departs from the traditional treatment of covariant differentiation. Instead of defining it through the geodesics of a Riemannian space, he assumes without proof that a geodesic coordinate system exists at every point of such a space. There then follows an interesting chapter on general relativity and the Schwarzschild solution of Einstein's equations, followed by one on the cosmology of general relativity in which the cosmological constant is rejected. The second part of the book begins with a chapter on projective relativity and then Dr. Jordan turns to his own ideas on the modification that he believes ought to be made in Einstein's field equations. Essentially this consists in taking the gravitational 'constant' to be a scalar function of the space and time coordinates. He obtains field equations by means of a variational principle that contain two constants which are dimensionless pure numbers, one of which is arbitrarily set equal to unity whilst the other is believed to have some value greater than thirty. In view of his rejection of the cosmological constant—which appears as a constant of integration in Einstein's equations—the introduction of these two constants in

Dr. Jordan's theory may strike the reader as strange: their presence is defended on the ground that they are dimensionless whilst the cosmological constant is not. A solution of the new field equations corresponding to the Schwarzschild solution in general relativity is given and cosmological models are also worked out. The model most favoured by Dr. Jordan is one in which the expansion is a linear function of the time and the last forty pages of the book are devoted to a statement of the author's views on the development of stars, on the comparison of theory and observation in cosmology and on the geological history of the Earth, in support of this linearity and also in defence of his postulate that the 'constant' of gravitation is in fact a variable. As with Hoyle's version of the creation of matter theory, it appears to this reviewer that Dr. Jordan's new field equations (p. 141 (8) and (9)) are reducible to those of general relativity by altering the definition of the energy-tensor of matter and of the electromagnetic field.

G. C. MCVITTIE.

Molecular Theory of Fluids, by H. S. GREEN. Pp. viii+264. (Amsterdam: North-Holland Publishing Co., 1952.) 20s.

This volume is one of a series of monographs (entitled 'Deformation and Flow') on the *Rheological Behaviour of Natural and Synthetic Products*, edited by J. M. Burgers (Delft), J. J. Hermans (Groningen) and G. W. Scott Blair (Reading). The author is professor of mathematical physics at the University of Adelaide, and is probably best known for his work with Professor Max Born on the kinetic theory of liquids.

The book gives an authoritative summary of the present state of the theory of fluids (which includes gases, liquids and non-crystalline solids), both at rest and in motion, both simple and complex, including the theory of diffusion. The final chapters deal with the kinetic theory and the quantum theory of fluids, the bearing of the latter on fluids at very low temperatures and the remarkable flow properties of liquid helium. The preceding chapter discusses elasticity, surface tension, the Brownian motion, the second virial coefficient, gravity and boundary forces and the dielectric constant.

A rigorous quantitative treatment of this wide field necessarily involves much mathematics, which is concisely presented, but nearly a third of the book is non-mathematical text, in which the essential features of the physics of the subject are explained in a very clear and attractive way. The book is a highly valuable addition to the literature of physics.

S. CHAPMAN.

Atomic Energy Levels as derived from the Analyses of Optical Spectra: Vol. II. 24 Cr to 41 Nb, by C. E. MOORE. Circular 467 of the National Bureau of Standards. Pp. xxxi+227. (Washington, D.C.: U.S. Department of Commerce, 1952.) \$2.25.

The first volume of this work, covering the elements hydrogen to vanadium was published in 1949. The second volume follows the plan of the first. It corresponds essentially to a greatly enlarged version of Bacher and Goudsmit's *Atomic Energy States* which appeared in 1932. The earlier work was able to include some 231 spectra of 69 elements: there are now known more than 500 spectra of 85 elements, and many of the spectra summarized in 1932 have subsequently been much revised and extended.

The typical entry for a given spectrum includes an introductory paragraph of general information, with a classified bibliography, followed by a list of energy levels, with their electron configurations, designations, J -values, heights above the ground-state in cm^{-1} and multiplet intervals. Hyperfine structure data ascribed to atomic nuclei have been omitted (with the exception of H, D). The tables have been prepared with the close collaboration of many experts in the field, and contain a good deal of material in advance of publication.

This will inevitably become the acknowledged authority on the subject, and it must be said that it is worthy in every way of that position. The many users of the work will have great cause to be thankful to the author and to all concerned in this notable production, and will wish them success in the completion of their task.

R. F. B.

Rechenmethoden der Quantenmechanik, Part I, by S. FLÜGGE and H. MARSCHALL. Pp. viii + 272. 2nd Edition. (Berlin : Springer-Verlag, 1952.) DM. 29.80.

The aim of the authors of this book is to exemplify the mathematical techniques used in quantum theory; this is achieved by stating a series of problems and giving detailed answers. A wide range of problems is discussed, and the type of approach allows a degree of flexibility which gives this book a novel character.

The subject matter falls into two main divisions: one particle and many particle problems. The first part of the book deals *inter alia* with the determination of eigenvalues (both exact and approximate methods being discussed), with various forms of collision theory and with perturbation theory. In the second part the topics considered include the algebra of spin operators, the formulation of expressions for spin coupling, and exchange interaction.

The problems are arranged in a series of increasing complexity, are carefully compiled and annotated. Some are standard examples to be found in textbooks on quantum mechanics, many have been taken from original papers and, where necessary, suitably simplified. The references to original papers form a useful feature of the book.

A certain amount of mathematical background is required of the reader—in particular some acquaintance with the properties of Bessel, Hankel, and hypergeometric functions. In general, however, the knowledge required would already be possessed by an advanced student of mathematical physics, or could easily be acquired by suitable reading.

The book would be a useful addition to a departmental library and should prove valuable to teachers and students alike.

M. BLACKMAN.

Anfangswertprobleme bei partieller Differentialgleichungen, by R. SAUER. Pp. xiii + 239. (Berlin : Springer-Verlag, 1952.) DM. 29.

For information on the mathematical theory of the partial differential equations they encounter, most physicists consult Courant's *Methoden der mathematischen Physik—II*. When this appeared in the thirties much of the extensive material in it on hyperbolic problems, and especially on non-linear ones, may have seemed unnecessary to working physicists. Since then, however, the spectacular expansion of the science of high speed gas flow has provided a

wide field of application of this material, and its systematic exposition by Courant certainly facilitated the progress in that field. The same mathematics has been used in modern developments in the theories of plastic flow and of hydraulics.

Now Professor Sauer of München, who has himself made valuable contributions to gas dynamics, has brought out a short self-contained account of the mathematical theory of hyperbolic problems, with detailed specialization of each aspect of the theory for the different branches of physics mentioned above. The book is in four chapters, respectively on (i) classification of problems into elliptic and hyperbolic, (ii) first order partial differential equations, (iii) higher order hyperbolic systems with two independent variables, (iv) systems with three or more. Broadly speaking, the same mathematical material as in Courant's book is covered. There is somewhat more information on the finite difference approach to calculating solutions, using a characteristic network, but no details of computational technique. Little of the more recent work by the Courant school on existence theorems for non-linear hyperbolic problems is included. The Hadamard theory for the linear equation is not abandoned in favour of the streamlined approach due to Marcel Riesz; nor is the theory of 'distributions' used much to simplify Hadamard's arguments, not at least as much as the preface would lead one to expect.

But the student will find the book pleasantly concise, systematic and easy to follow, and all workers in fields where the material is relevant should find it convenient to use as a work of reference.

M. J. LIGHTHILL.

Applied Nuclear Physics, by E. POLLARD and W. L. DAVIDSON. Pp. ix+352. (London: Chapman and Hall, 1951.) 40s.

This book is both readable and authoritative. In making it readable the authors have gone to considerable length; whenever the going gets rough the reader is patted on the shoulder and assured that things will presently get easier; dull bits are periodically enlivened with suitable humorous touches. This is in striking contrast to the traditional kind of textbook which called for strong coffee to keep the student awake. But joking aside, this is a clever piece of writing, readable, easygoing, and yet full of useful information.

Despite its popular style, the book is authoritative; the authors clearly know their subject. There are various slips and inaccuracies, such as the statement on p. 22 "even in a solid the centres of the atoms are separated by distances a million times greater than the atoms themselves" (which probably ought to read "... than the nuclei themselves", and not "a million times" but "about 20000 times"). On p. 15 kinetic energy is identified with $m\mathbf{c}^2$ instead of $(m-m_0)\mathbf{c}^2$. I have discovered about two dozen errors of that kind, but that is perhaps not much in a book dealing with such a large range of material.

How far does the book take the reader? Not very far. In scope, as in style, it is half way between a popular book for laymen and a textbook. Only the simplest of formulae are used; matters of nuclear theory are only briefly and vaguely touched on, as, of course, one would expect from the title. Also the breezy style is not conducive to precision; sometimes it is confusing (as in the explanation of spin on p. 269), or misleading (as in the description of the Rabi method on p. 272).

All the same this is probably one of the best books for getting an introduction into nuclear physics in all its aspects. It contains, as the title would indicate, all that a man may need to know of nuclear physics in order to apply it without becoming a fully fledged nuclear physicist. And the freshness and human approach of the writing may well stimulate readers to go further and study the subject more deeply.

O. R. FRISCH.

Mesons—A Summary of Experimental Facts, by A. M. THORNDIKE. Pp. viii+242. (London: McGraw-Hill, 1952.) 47s.

This book consists of an uncritical survey of the experimental data concerning mesons up to early 1952. It is suitable for students reading for an honours physics degree and might be useful as an introduction to the subject for research students. The data are mostly taken from cosmic-ray mesons, but material on artificially produced mesons is included where appropriate.

The facts as reported are substantially correct, but their reciting is so deadly dull. The quest for the properties of these new and unstable forms of matter has been and still is an exciting one. One would not have gathered this from Mr. Thorndike's book. This might perhaps be due to the author not having made any contribution in this field. The book would hardly inspire students with a burning zeal to take part in the quest themselves.

No mention is made of the fact that the sigma meson was discovered by D. H. Perkins, and it is interesting to note that the author is one of the few remaining people who still believe that there is a sudden break, or 'knee' in the cosmic ray depth intensity curve at a depth below water of 300 m. The book is well produced but much too expensive.

E. P. GEORGE.

Wavelength Tables of Emission and Absorption Bands of Diatomic Molecules, edited by B. ROSEN. Tables de Constantes et Données Numériques. Constantes Sélectionnées, 5. Pp. 389. (Paris: Hermann, 1952.) 5,600 fr.

Le Point de Vue du Physicien dans le Problème du Lissage des Courbes Expérimentales, by PIERRE VERNOTTE. Pp. ii+23. (Paris: Publications Scientifiques et Techniques du Ministère de l'Air (No. N.T. 46), 1953.) 400 fr.

Viscosité sous pression rapidement variable, by F. CHARRON. Pp. 30. (Paris: Publications Scientifiques et Techniques du Ministère de l'Air, No. 268, 1952. 550 fr.

Values of some Physical Functions and Constants used in Meteorology.—Functions and Specifications of Water Vapour in the Atmosphere. Publication No. 79 of Organisation Météorologique Internationale. Pp. 92. (Lausanne: Organisation Météorologique Mondiale, 1951.) 2 Sw. Fr.

CONTENTS OF SECTION B

	PAGE
Dr. A. J. GOSS. Heat Flow and the Growth of Metal Single Crystals from the Melt	525
Dr. A. CHARLESBY. Electron Currents in Thin Oxide Films on Aluminium . . .	533
Dr. K. M. POOLE. Electrode Contamination in Electron Optical Systems . . .	542
Dr. P. W. TREZONA. Additivity of Colour Equations	548
Dr. R. CADE. Some Electrostatic and Steady-Current Problems Involving Anisotropic Bodies	557
Miss A. D. STUCKES. Electro-Thermal Behaviour of Point Contacts to Semiconductors	570
Dr. A. F. GIBSON. Injected Absorption in Germanium	588
Dr. W. CULSHAW. The Fabry-Perot Interferometer at Millimetre Wavelengths .	597
Research Note :	
Prof. L. F. BATES and Mr. N. P. R. SHERRY. Thermal Effects accompanying Magnetization of a Ferrimagnetic Material	609
Letters to the Editor :	
Mr. S. H. M. EL-SABEH and Dr. J. B. HASTED. The Dielectric Constant of a Liquid containing Spherical Particles	611
Dr. R. MANSFIELD. The Electrical Conductivity and Thermoelectric Power of Magnesium Oxide	612
Mr. J. W. BREMNER. The Variation of Transverse Viscosity with Shear Rate	614
Reviews of Books	615
Contents for Section B	616

The Effect of Interactions in a Paramagnetic on the Entropy and Susceptibility

By J. M. DANIELS

The Clarendon Laboratory, Oxford

MS. received 2nd March 1953

Abstract. Van Vleck's theory of magnetic dipole interaction is extended to take into account magnetic anisotropy of the individual ions, and hyperfine splitting. The entropy and susceptibility are expressed as power series in $1/T$ as far as the term in $1/T^4$. Explicit formulae are found for the term in $1/T^2$ in the entropy, the important term at high temperatures, and for the Curie-Weiss Δ 's; for paramagnetics with one ion in the unit cell and axial symmetry, and for the Tutton salts. This is done both in the case of a general interaction and also for pure magnetic dipole-dipole interaction. It is shown that the contributions of interactions and of hyperfine splitting to both the entropy and the susceptibility are additive as far as the term in $1/T^3$, and that hyperfine splitting introduces into the susceptibility shape-dependent terms which cannot be included in the Curie-Weiss Δ . This is followed by a review of the properties of cerium magnesium nitrate, the rare earth ethylsulphates, and the Tutton salts in relation to this theory.

§ 1. INTRODUCTION

IN a well known paper (Van Vleck 1937) formulae are derived for the entropy and susceptibility of paramagnetic salts at temperatures large compared with the splittings of the ground level of the paramagnetic ions. These are obtained by expanding the partition function in powers of $1/T$, where T is the absolute temperature, the coefficient of the terms being obtained from the energy matrix of the whole crystal. The cases treated are : (i) Where the ions can be treated as free magnetic dipoles interacting through their own magnetic fields, and where there is an isotropic exchange coupling between adjacent ions (i.e. an energy which depends only on the angle between the two spin axes). (ii) Where there is, in addition, a crystalline field acting on the ions. In this case the energy of the crystal is considered to be predominantly that of the individual ions in this field, and the effect of interactions is obtained by using perturbation theory.

Since this paper was written important advances have taken place in the detailed knowledge of the properties of paramagnetic salts, particularly the discovery of the hyperfine splitting of the ground state of the paramagnetic ions, the fact that most ions are anisotropic in their properties and cannot be represented by free magnetic dipoles, and the idea of indirect exchange interaction. These discoveries have made it desirable that Van Vleck's original theory should be extended to cover these cases, and this is the purpose of this paper.

An extension to take into account anisotropic indirect exchange was made by Opechowski (1948), who obtained eqn. (8) of this paper and also an expression for the mean Curie-Weiss Δ in terms of a general interionic interaction. However, Opechowski never considered in detail the effect of magnetic anisotropy on dipole-dipole interaction, nor did he consider the effect of hyperfine splitting,

which had not then been discovered in solid paramagnetics. His application of his theory is limited to a discussion of copper potassium sulphate, which was largely invalidated by the subsequent discovery of hyperfine splitting.

The anisotropic properties of an ion come about in the following way. An ion, with an odd number of electrons subjected to a crystalline field, experiences a Stark splitting so large that any normally occurring external influence (e.g. a magnetic field) causes only very small admixtures of higher states with the ground state. In this case the ground state of the ion can be put into 1:1 correspondence with the states of a spin 1/2, provided that the magnetic moment associated with this spin is supposed to depend on its orientation (Pryce 1950). Thus the energy E of such a spin in a field \mathbf{H} is $\mathbf{H} \cdot \mathbf{g} \cdot \mathbf{S}$ where \mathbf{S} is the spin vector, and \mathbf{g} is a dyadic (or a tensor of rank 2). Writing this in the more usual form $E = -\mathbf{H} \cdot \boldsymbol{\mu}$ where $\boldsymbol{\mu}$ is the magnetic moment, we can equate $\boldsymbol{\mu}$ to $-\mathbf{g} \cdot \mathbf{S}$.

Going over to a tensor notation and using the dummy suffix summation convention, this can be written $\mu_\epsilon = -\frac{1}{2}\beta g_{\epsilon\eta}\sigma_\eta$ where μ_ϵ is the component of the magnetic moment along the ϵ th (cartesian) axis, σ_η is twice the component of the spin along the η th axis, and β is the Bohr magneton. $g_{\epsilon\eta}$ is a tensor of rank 2 called the g -tensor, and is a generalization of the gyromagnetic ratio which is appropriate to the case of free ions. When such a system is treated quantum mechanically, the components σ_η are the Pauli matrices

$$\sigma_x = \begin{pmatrix} 0 & 1 \\ 1 & 0 \end{pmatrix} \quad \sigma_y = \begin{pmatrix} 0 & -i \\ i & 0 \end{pmatrix} \quad \sigma_z = \begin{pmatrix} 1 & 0 \\ 0 & -1 \end{pmatrix}.$$

In this picture the ion is said to have an 'effective spin 1/2' and an 'anisotropic g '. At temperatures where only the ground doublet is occupied it is mathematically simpler to treat the ion as though it were such a spin 1/2 than to treat the real ion exactly.

Examples of substances containing such ions are all the rare earth ethylsulphates with even atomic number, except gadolinium ethylsulphate, and many of the sulphates and double sulphates of divalent ions of the iron transition series, e.g. $\text{Co}(\text{NH}_4)_2(\text{SO}_4)_2 \cdot 6\text{H}_2\text{O}$.

In some of these substances the ions may have a hyperfine splitting of the ground level; e.g. in Co^{2+} all the ions have a hyperfine splitting since the only naturally occurring isotope is ^{59}Co with nuclear spin 7/2. On the other hand, naturally occurring cerium ions have no hyperfine splitting, while some naturally occurring neodymium ions have a hyperfine splitting and others have not. The effect of a hyperfine splitting is similar to that of a Stark splitting in Van Vleck's theory: it restricts the orientations which the electron spin can assume at low temperatures, and hence modifies the interaction specific heat (or entropy) and the susceptibility. This is in addition to the Schottky anomaly which it introduces into the specific heat. Most hyperfine splittings are very small (i.e. less than $0.1^\circ\text{K} \times k$ overall), and can thus be treated by the method of series expansion in powers of $1/T$ just like the interactions, instead of requiring the perturbation procedure which Van Vleck used for Stark splittings.

PART I. GENERAL THEORY

§ 2. GENERAL CONSIDERATIONS

Suppose the partition function Z for the crystal, an assembly of N ions, can be written (assuming for the time being no hyperfine splitting)

$$Z = 2^N (1 + A/T + B/T^2 + C/T^3 + D/T^4 + E/T^5 + \dots). \quad \dots\dots(1)$$

It will be shown later that $A=0$.

Hence the entropy S is given by

$$\begin{aligned} S &= \frac{\partial}{\partial T} (kT \ln Z) \\ &= Nk \ln 2 - \frac{kB}{T^2} - \frac{2kC}{T^3} - 3k \left\{ D - \frac{B^2}{2} \right\} T^4 - \dots, \quad \dots\dots(2) \end{aligned}$$

and the susceptibility χ is given by

$$\begin{aligned} \chi &= \lim_{H \rightarrow 0} \frac{kT}{H} \frac{\partial}{\partial H} (\ln Z) \\ &= \lim_{H \rightarrow 0} \frac{k}{H} \left\{ \frac{1}{T} \frac{\partial B}{\partial H} + \frac{1}{T^2} \frac{\partial C}{\partial H} + \frac{1}{T^3} \frac{\partial}{\partial H} \left(D - \frac{B^2}{2} \right) + \frac{1}{T^4} \frac{\partial}{\partial H} (E - BC) + \dots \right\}. \end{aligned} \quad \dots\dots(3)$$

Now if W is the energy matrix for the whole assembly

$$\begin{aligned} Z &= \text{Spur} \left[\exp \left(-\frac{W}{kT} \right) \right] \\ &= \text{Spur} \left\{ 1 - \frac{W}{kT} + \frac{W^2}{2k^2 T^2} - \frac{W^3}{6k^3 T^3} + \frac{W^4}{24k^4 T^4} - \frac{W^5}{120k^5 T^5} + \dots \right\}. \end{aligned}$$

$$\text{Hence} \quad \left. \begin{aligned} A &= -\frac{\text{Spur}(W)}{k \text{ Spur}(1)} & B &= \frac{\text{Spur}(W^2)}{2k^2 \text{ Spur}(1)} \\ C &= -\frac{\text{Spur}(W^3)}{6k^3 \text{ Spur}(1)} & D &= \frac{\text{Spur}(W^4)}{24k^4 \text{ Spur}(1)} \\ E &= -\frac{\text{Spur}(W^5)}{120k^5 \text{ Spur}(1)} \end{aligned} \right\} \quad \dots\dots(4)$$

Since the spur of a matrix does not depend on the representation chosen, any convenient representation can be used. In general, we shall use a representation with σ_z diagonal, where the z -axis is chosen to simplify the working by invocation of symmetry arguments. It is necessary to calculate only the principal values of the susceptibility, since its value in any other direction can be obtained from its well known transformation law, that of a tensor of rank 2.

§ 3. NOTATION

Let Latin suffixes i, j , etc., refer to individual ions, and a pair of suffixes in brackets (ij) refer to a pair of ions counted once, e.g. $\sum_{(ij)} W_{ij}$ is the total interaction energy of the crystal, if W_{ij} is the interaction energy of ions i and j .

Let Greek suffices α, β, \dots refer to cartesian axes; i.e. they are tensor suffices. The dummy suffix summation convention will be used for Greek suffices. Since in cartesian coordinates there is no distinction between co-variance and contra-variance, all tensor indices will be written in the lower position. Although tensor notation is unnecessary for the first term of the expressions for the entropy and susceptibility, and even makes the working look cumbersome, it is retained throughout since its use simplifies enormously the more complicated later terms.

The following well known property of the Pauli matrices for the *same* ion will be used:

$$\sigma_{j\alpha} \sigma_{j\beta} = \delta_{\alpha\beta} + i\epsilon_{\alpha\beta\gamma} \sigma_{j\gamma},$$

where $\delta_{\alpha\beta}$ is the Kronecker delta symbol, i.e.

$$\delta_{\alpha\beta} = \begin{cases} 0 & \alpha \neq \beta \\ 1 & \alpha = \beta \end{cases}$$

and $\epsilon_{\alpha\beta\gamma}$ are the antisymmetric symbols, i.e.

$$\epsilon_{\alpha\beta\gamma} = \begin{cases} 0 & \text{if any two of } \alpha, \beta, \gamma \text{ are the same} \\ +1 & \text{if } \alpha\beta\gamma \text{ is an even permutation of } xyz \\ -1 & \text{if } \alpha\beta\gamma \text{ is an odd permutation of } xyz \end{cases}$$

Using this relation, products of the σ 's referring to the same ion can be reduced to sums of the σ 's.

In the 2^N -dimensional product space for the whole crystal it is seen that

$$\left. \begin{aligned} \text{Spur}(1) &= 2^N; & \text{Spur}(\sigma_{j\alpha}) &= 0 \\ \text{Spur}(\sigma_{j\alpha}\sigma_{i\beta}) &= \begin{cases} 0 & i \neq j \\ 2^N \delta_{\alpha\beta} & i = j \end{cases} \end{aligned} \right\} \dots\dots(5)$$

etc.

§ 4. INTERACTION WITHOUT HYPERFINE SPLITTING

Now the σ 's, and the products of σ 's for the same ion, are components of a vector, and as the interaction energy W_{ij} between two ions i and j is a scalar which depends on the σ_i 's and the σ_j 's, the most general form for W_{ij} is

$$W_{ij} = P_{ij\alpha\beta} \sigma_{i\alpha} \sigma_{j\beta}$$

where $P_{ij\alpha\beta}$ is a tensor of rank 2.

This includes both the case of isotropic exchange, where $W_{ij} = -(2/\hbar^2) J_{ij} \mathbf{S}_i \cdot \mathbf{S}_j$ (or $P_{ij\alpha\beta} = -J_{ij} \delta_{\alpha\beta} / 2\hbar^2$ in tensor notation) where J_{ij} is the exchange integral between ions i and j , and also the case of pure magnetic dipole-dipole interaction where

$$W_{ij} = \frac{\boldsymbol{\mu}_i \cdot \boldsymbol{\mu}_j}{r_{ij}^3} - \frac{3(\boldsymbol{\mu}_i \cdot \mathbf{r}_{ij})(\boldsymbol{\mu}_j \cdot \mathbf{r}_{ij})}{r_{ij}^5}$$

or, in tensor notation,

$$P_{ij\alpha\beta} = \frac{\beta^2}{4} \left[\frac{g_{i\alpha} g_{j\beta}}{r_{ij}^3} - \frac{3g_{i\alpha} g_{j\beta} r_{ij\lambda} r_{ij\lambda}}{r_{ij}^5} \right]$$

where r_{ij} is the distance between the ions i and j , and $r_{ij\lambda}$ is the component of r_{ij} along the λ -axis.

In a similar manner, the energy of the p th ion in an external magnetic field H directed along the τ -axis can be written $W_p = +HR_{p\tau} \sigma_{p\tau}$ where $R_{p\tau} = \frac{1}{2} g_{p\tau} \beta$. Then the total energy

$$\begin{aligned} W &= \sum_{(ij)} W_{ij} + \sum_p W_p \\ &= \sum_{(ij)} P_{ij\alpha\beta} \sigma_{i\alpha} \sigma_{j\beta} + H \sum_p R_{p\tau} \sigma_{p\tau} \end{aligned} \dots\dots(6)$$

In the previous expression the effect of induced magnetic dipoles (diamagnetism and temperature independent paramagnetism) has been ignored. This is because they usually contribute only some 1% to the susceptibility at 1°K, the theory being applicable at temperatures near this, and can be expected to contribute even less to the entropy, which in Van Vleck's theory depends on the square of the Curie constant at 'high' temperatures. Induced moments can therefore be reasonably neglected.

Applying the results of (5), it follows that

$$\text{Spur}(W) = 0 \quad \dots\dots(7)$$

and hence A vanishes, as was anticipated in (2).

$$\text{Spur}(W^2) = \text{Spur} \left(\sum_{(ij)} P_{ij\alpha\beta} \sigma_{i\alpha} \sigma_{j\beta} + H \sum_p R_{p\varrho} \sigma_{p\varrho} \right) \cdot \left(\sum_{(kl)} P_{kl\gamma\delta} \sigma_{k\gamma} \sigma_{l\delta} + H \sum_q R_{q\tau} \sigma_{q\tau} \right).$$

In this the term independent of H is

$$\text{Spur} \left(\sum_{(ij)(kl)} P_{ij\alpha\beta} P_{kl\gamma\delta} \sigma_{i\alpha} \sigma_{j\beta} \sigma_{k\gamma} \sigma_{l\delta} \right)$$

which equals $2^N \sum_{(ij)} P_{ij\alpha\beta} P_{ij\alpha\beta}$ since $\text{Spur}(\sigma_{i\alpha} \sigma_{j\beta} \sigma_{k\gamma} \sigma_{l\delta}) = 0$ unless $i=k$ and $j=l$, when it is $2^N \delta_{\alpha\gamma} \delta_{\beta\delta}$. The term of degree one in H ,

$$\text{Spur} \left\{ H \sum_{(ij)p} P_{ij\alpha\beta} R_{p\varrho} (\sigma_{i\alpha} \sigma_{j\beta} \sigma_{p\varrho} + \sigma_{p\varrho} \sigma_{i\alpha} \sigma_{j\beta}) \right\},$$

is zero, since $\text{Spur}(\sigma_{i\alpha} \sigma_{j\beta} \sigma_{p\varrho}) = 0$, as is easily seen since $i \neq j$ by definition. Physical intuition demands that this term should vanish, since the square of the energy cannot intuitively be expected to depend on the sign of the applied magnetic field. Finally, the term of degree two in H in $\text{Spur}(W^2)$ is

$$H^2 \text{Spur} \left(\sum_{p,q} R_{p\varrho} R_{q\tau} \sigma_{p\varrho} \sigma_{q\tau} \right) = H^2 2^N \sum_p R_{p\varrho} R_{p\varrho}$$

since $\text{Spur}(\sigma_{p\varrho} \sigma_{q\tau}) = 0$ unless $p=q$, when it is $2^N \delta_{\varrho\tau}$. Hence

$$\text{Spur}(W^2) = 2^N \left\{ \sum_{(ij)} P_{ij\alpha\beta} P_{ij\alpha\beta} + H^2 \sum_p R_{p\varrho} R_{p\varrho} \right\}. \quad \dots\dots(8)$$

Other spurs can be worked out in a similar manner, for instance

$$\text{Spur}(W^3) = 2^N 6 \sum_{\substack{(ij)(il) \\ (jl)}} P_{ij\alpha\beta} P_{il\alpha\delta} P_{jl\beta\delta} + 2^N 6 \sum_{(ij)} P_{ij\alpha\beta} R_{i\alpha} R_{j\beta}. \quad \dots\dots(9)$$

Of $\text{Spur}(W^4)$ only the term of degree two in H will be evaluated here. A typical term of W^4 of degree two in H is

$$H^2 P_{ij\alpha\beta} \sigma_{i\alpha} \sigma_{j\beta} P_{kl\gamma\delta} \sigma_{k\gamma} \sigma_{l\delta} R_{p\varrho} \sigma_{p\varrho} R_{q\tau} \sigma_{q\tau}$$

and up to 24 permutations of the factors of each term are to be summed to give W^4 . Only products of two or four σ 's of the same ion survive the summation over the permutations: hence the spur of this term is found, after some manipulation, to be

$$H^2 2^N \left[\begin{aligned} & 24 \sum_{\substack{(ij)(jl) \\ i \neq l}} P_{ij\alpha\beta} P_{jl\beta\delta} R_{i\alpha} R_{l\delta} \\ & + 6 \sum_{(ij)} P_{ij\alpha\beta} P_{ij\alpha\beta} \cdot \sum_p R_{p\varrho} R_{p\varrho} \\ & + 8 \sum_{(ij)} (P_{ij\alpha\beta} P_{ij\gamma\beta} R_{i\alpha} R_{i\gamma} + P_{ij\alpha\beta} P_{ij\alpha\delta} R_{j\beta} R_{j\delta}) \\ & - 4 \sum_{(ij)} P_{ij\alpha\beta} P_{ij\alpha\beta} (R_{i\alpha} R_{i\alpha} + R_{j\beta} R_{j\beta}) \\ & - 4 \sum_{(ij)} P_{ij\alpha\beta} P_{ij\alpha\beta} (R_{i\epsilon} R_{i\epsilon} + R_{j\eta} R_{j\eta}) \end{aligned} \right] \quad \dots\dots(10)$$

§ 5. THE EFFECT OF HYPERFINE SPLITTING

The energy of an isolated ion in zero external magnetic field, but with hyperfine splitting, can be written

$$W_j = F_{j\alpha\beta} \sigma_{j\alpha} I_{j\beta} + Q_{j\gamma\delta} I_{j\gamma} I_{j\delta}$$

where $F_{j\alpha\beta}$ and $Q_{j\gamma\delta}$ are tensors appropriate to the ion, and \mathbf{I}_j is the nuclear spin vector, represented by a $(2I+1) \times (2I+1)$ matrix in a single particle representation

(Abragam and Pryce 1951). The the energy of the crystal becomes

$$W = \sum_{(ij)} P_{ij\alpha\beta} \sigma_{i\alpha} \sigma_{j\beta} + H \sum_p R_{pe} \sigma_{pe} + \sum_r Q_{re\eta} I_{re} I_{r\eta} + \sum_q F_{q\gamma\delta} \sigma_{q\gamma} I_{q\delta}. \quad \dots\dots (11)$$

Q can be, and usually is, chosen so that $\text{Spur}(Q_{re\eta} I_{re} I_{r\eta}) = 0$, and this convention is adopted in the rest of this paper.

The partition function can be written $Z = \text{Spur}[\exp\{-(W_e/kT + W_n/kT)\}]$, where W_n is the hyperfine part of the energy and W_e is the rest. Z can be factorized into two parts, one depending entirely on the hyperfine splitting tensors and the other independent of them, only if W_e and W_n commute. This is not the case unless $F=0$. It is thus not possible in general to consider the effects of hyperfine splitting separately from the effects of interaction, and the contribution to the energy from hyperfine splitting must be treated along with the rest of the energy in the expansion in powers of $1/T$.

One effect of nuclear spin is to increase the multiplicity M of the states of the crystal. If there are K_r nuclei with nuclear spin I_r , where $\sum_r K_r = N$, the multiplicity M is increased from 2^N to $2^N (2I_1 + 1)^{K_1} (2I_2 + 1)^{K_2} \dots$.

Hence $\text{Spur}(1) = M$. Also $\text{Spur}(W) = 0$, and hence $A=0$ as before.

It is not necessary to evaluate all the terms which occur in the spurs of powers of W ; since those terms which do not contain the interaction tensor $P_{ij\alpha\beta}$ lead to the entropy and susceptibility without interaction, and are more easily and exactly calculated using a single particle model (see for example Bleaney 1950, 1951); while those terms which contain the interaction tensor but no hyperfine splitting tensor (F or Q) have already been evaluated apart from allowance for the increased multiplicity. Hence only terms of degree zero and two in H , containing both the interaction tensor and the hyperfine splitting tensors need now to be evaluated. Such terms will be called 'mixed terms'.

There are no such terms in the coefficients of $1/T^2$ and $1/T^3$. In the expression for the entropy, when $H=0$, the coefficient of $1/T^4$,

$$D - \frac{B^2}{2} = \frac{1}{24k^4} \left[\frac{\text{Spur}(W^4)}{\text{Spur}(1)} - 3 \left\{ \frac{\text{Spur}(W^2)}{\text{Spur}(1)} \right\}^2 \right] \quad \dots\dots (12)$$

contains two mixed terms.

Let $\text{Spur}(W^2)/\text{Spur}(1)$ be denoted by $Y_n + Y_e$ when $H=0$, where Y_n depends on the hyperfine splitting tensors, and Y_e does not. Then the second part of (12), $-3\{\text{Spur}(W^2)/\text{Spur}(1)\}^2$, has one mixed term, $-6Y_e Y_n$.

For the first part of (12) which comes from $\text{Spur}(W^4)$ the only mixed terms in W^4 with non-zero spur are of the type

$$P_{ij\alpha\beta} \sigma_{i\alpha} \sigma_{j\beta} P_{kly\delta} \sigma_{ky} \sigma_{ld} Q_{qe\eta} I_{qe} I_{q\eta} Q_{r\lambda\mu} I_{r\lambda} I_{r\mu} + P_{ij\alpha\beta} \sigma_{i\alpha} \sigma_{j\beta} P_{kly\delta} \sigma_{ky} \sigma_{ld} F_{q\lambda\mu} \sigma_{q\lambda} I_{q\mu} F_{re\eta} \sigma_{re} I_{r\eta}$$

together with up to 23 other permutations of the factors in each term. The detailed evaluation of the spurs of these terms is very similar to the derivation of eqn. (10), and it is found that the mixed term of $\text{Spur}(W^4)/\text{Spur}(1)$ has a part $6Y_e Y_n$ which cancels the mixed term from $-3\{\text{Spur}(W^2)/\text{Spur}(1)\}^2$. Multiplying the remainder by $(-3k/T^4)(1/24k^4)$ it follows that the first mixed term which occurs in the expression for the entropy S is

$$- \frac{3k}{T^4} \frac{1}{24k^4} \left[\begin{aligned} & 8 \sum_{(ij)} \left\{ \frac{1}{3} I_i(I_i + 1) P_{ij\alpha\beta} P_{ij\gamma\delta} F_{i\alpha\eta} F_{i\gamma\delta} + \frac{1}{3} I_j(I_j + 1) P_{ij\alpha\beta} P_{ij\alpha\delta} F_{j\beta\eta} F_{j\delta\eta} \right\} \\ & - 4 \sum_{(ij)} P_{ij\alpha\beta} P_{ij\alpha\beta} \left\{ \frac{1}{3} I_i(I_i + 1) F_{i\alpha\eta} F_{i\alpha\eta} + \frac{1}{3} I_j(I_j + 1) F_{j\beta\eta} F_{j\beta\eta} \right\} \\ & - 4 \sum_{(ij)} P_{ij\alpha\beta} P_{ij\alpha\beta} \left\{ \frac{1}{3} I_i(I_i + 1) F_{i\epsilon\eta} F_{i\epsilon\eta} + \frac{1}{3} I_j(I_j + 1) F_{j\epsilon\eta} F_{j\epsilon\eta} \right\} \end{aligned} \right] \quad \dots\dots (13)$$

The first mixed term in the expression for the susceptibility is part of the term in $1/T^4$, i.e.

$$\lim_{H \rightarrow 0} \frac{k}{H} \frac{1}{T^4} \frac{\partial}{\partial H} (E - BC) = \frac{2k}{T^4} \times (\text{coefficient of } H^2 \text{ in } E - BC).$$

Write $B = \frac{1}{2k^2} \{Y_e + Y_n + H^2 X_e\}$ and $C = \frac{-1}{6k^3} \{Y_e' + Y_n' + H^2 X_e'\}$,

where, as before, the suffix n denotes a quantity depending on the hyperfine splitting tensors, and the suffix e denotes a quantity independent of these tensors. Then the coefficient of H^2 in $-BC$ is

$$\frac{1}{12k^5} \{Y_n X_e' + Y_n' X_e\} + \text{terms independent of } F \text{ and } Q.$$

The only mixed terms in W^5 of degree two in H and with non-zero spur are of the type

$$H^2 P_{ij\alpha\beta\sigma_{i\alpha}\sigma_{j\beta}} R_{pe}\sigma_{pe} R_{q\tau}\sigma_{q\tau} Q_{s\lambda\mu} I_{s\lambda} I_{s\mu} Q_{re\eta} I_{re} I_{r\eta} \\ + H^2 P_{ij\alpha\beta\sigma_{i\alpha}\sigma_{j\beta}} R_{pe}\sigma_{pe} R_{q\tau}\sigma_{q\tau} F_{s\lambda\mu} \sigma_{s\lambda} I_{s\mu} F_{re\eta} \sigma_{re} I_{r\eta}$$

together with up to 119 other permutations of the factors in each term.

The evaluation of the spurs of these terms is again similar to the derivation of eqn. (10), and it is found that the mixed term in E proportional to H^2 contains a part $-(1/12k^5)Y_n X_e'$ which cancels part of $-BC$. Finally, the first mixed term in the expression for the susceptibility χ is

$$\frac{2k}{T^4} \frac{1}{12k^5} \left[Y_n' X_e \right. \\ \left. + 4 \sum_{(ij)} \left\{ \frac{1}{3} I_i(I_i + 1) P_{ij\alpha\beta} R_{i\gamma} R_{j\beta} F_{i\alpha\eta} F_{i\gamma\eta} + \frac{1}{3} I_j(I_j + 1) P_{ij\alpha\beta} R_{i\alpha} R_{j\delta} F_{j\beta\eta} F_{j\delta\eta} \right\} \right. \\ \left. - 4 \sum_{(ij)} P_{ij\alpha\beta} R_{i\alpha} R_{j\beta} \left\{ \frac{1}{3} I_i(I_i + 1) F_{i\epsilon\eta} F_{i\epsilon\eta} + \frac{1}{3} I_j(I_j + 1) F_{j\epsilon\eta} F_{j\epsilon\eta} \right\} \right] \\ \dots\dots (14)$$

In the case of magnetic dipole-dipole interaction, the sums in eqn. (14) give a shape-dependent contribution to the susceptibility. (Shape dependence of terms in the susceptibility is discussed in more detail in § 7.)

PART II. APPLICATIONS OF THE GENERAL THEORY

§ 6. THE ENTROPY IN ZERO MAGNETIC FIELD

It follows from eqns. (2a), (4) and (8) that for one gram ion

$$\frac{S}{R} = \ln 2 - \frac{1}{2Nk^2 T^2} \sum_{(ij)} P_{ij\alpha\beta} P_{ij\alpha\beta} - \dots$$

The first term, $\ln 2$, is merely the entropy of the crystal in the absence of interactions, i.e. in complete disorder. It is the term in $1/T^2$, the dominant term at high temperatures, which is usually the most interesting, and several particular cases will now be considered. It is easily seen that hyperfine splitting has two effects: to increase the constant term on account of the increased multiplicity, and to introduce an extra term in $1/T^2$ which is a term in the expansion of the entropy in the absence of interactions. The sum $\sum_{(ij)} P_{ij\alpha\beta} P_{ij\alpha\beta}$ is essentially positive, being a sum of squares, and so can never vanish unless the interaction between all pairs of ions is identically zero, in which case $S/R = \ln 2$ independent of temperature. Thus all interacting assemblies of this type have a $1/T^2$ term in the entropy.

(i) *All Ions Identical*

Here the sum over all pairs,

$$\sum_{(ij)} P_{ij\alpha\beta} P_{ij\alpha\beta} = \frac{1}{2} N \sum_j P_{ij\alpha\beta} P_{ij\alpha\beta},$$

where the latter sum is taken for one typical ion i over all the other ions j in the crystal. This is valid only if all the ions have the same interaction tensors, i.e. if each ion is situated in the same position relative to its neighbours, and if the sum $\sum_j P_{ij\alpha\beta} P_{ij\alpha\beta}$ converges so that it does not depend on the position of the ion i in the crystal. Then the entropy becomes

$$\frac{S}{R} = \ln 2 - \frac{1}{4k^2 T^2} \sum_j P_{ij\alpha\beta} P_{ij\alpha\beta} - \dots \quad \dots (15)$$

Now consider pure magnetic dipole-dipole interaction. Then

$$P_{ij\alpha\beta} = \frac{\beta^2}{4} \left[\frac{g_{i\alpha} g_{j\beta}}{r_{ij}^3} - \frac{3g_{i\alpha} g_{j\beta} r_{ij\lambda} r_{ij\mu}}{r_{ij}^5} \right].$$

Now choose the coordinate axes to be the principal axes of the g -tensor; and further suppose that $g_{xx} = g_{yy} = g_{\perp}$, $g_{zz} = g_{\parallel}$ say, i.e. the ions have z -axial symmetry. (Axial symmetry of the g -tensor is very common, occurring at least to a first approximation in most of the paramagnetic salts already investigated.) Substituting this tensor in the formula for the entropy, and eliminating $x^2 + y^2$ by the relation $x^2 + y^2 = r^2 - z^2$, it follows that

$$\frac{S}{R} = \ln 2 - \frac{\beta^4}{64k^2 T^2} \left[(g_{\parallel}^4 + 5g_{\perp}^4) \sum_j \frac{1}{r_{ij}^6} - 6(g_{\parallel}^2 - g_{\perp}^2)(g_{\parallel}^2 - 2g_{\perp}^2) \sum_j \frac{z_{ij}^2}{r_{ij}^8} + 9(g_{\parallel}^2 - g_{\perp}^2)^2 \sum_j \frac{z_{ij}^4}{r_{ij}^{10}} \right]. \quad \dots (16)$$

Let $k \ln M - S = S'$. Then $S' T^2 / R$ is, at high temperatures, a dimensionless constant whose value depends on the substance chosen*.

It is seen that the sums in (16) are like $\int^\infty dr/r^4$, and hence rapidly convergent. If $g_{\parallel} = g_{\perp} = g$, (16) reduces to

$$\frac{S}{R} = \ln 2 - \frac{3g^4 \beta^4}{32k^2 T^2} \sum_j \frac{1}{r_{ij}^6} - \dots,$$

which is Van Vleck's formula for an isotropic spin 1/2.

Example (i). Cerium Magnesium Nitrate $Ce_2 Mg_3 (NO_3)_{12} \cdot 24H_2O$.

This salt crystallizes in the trigonal system. The cerium ions are situated in a simple rhombohedral lattice, and the long diagonal of the rhombohedra coincides with the trigonal axis of the crystals. If the crystal is described by the alternative hexagonal unit cell, the unit cell dimensions are $a = 10.92 \text{ \AA}$, $c = 17.22 \text{ \AA}$, where c is the cell axis parallel to the crystal trigonal axis.† Using these data, we find

$$\left. \begin{aligned} \sum_j 1/r_{ij}^6 &= 38.63 \\ \sum_j z_{ij}^2/r_{ij}^8 &= 14.76 \\ \sum_j z_{ij}^4/r_{ij}^{10} &= 7.13 \end{aligned} \right\} \times 10.92^{-6} \text{ \AA}^{-6}.$$

In the evaluation of these sums the contribution of the 296 ions inside a sphere of radius $a\sqrt{10}$ was worked out directly, and the contribution of all the

* The specific heat C at these temperatures is also proportional to $1/T^2$, and $CT^2/R = 2S'T^2/R$. Most of the published experimental results are given in terms C rather than S .

† The positions of the cerium ions in the salt have been determined for me by Mr. H. M. Powell, to whom I am indebted. The detailed crystal structure is not known.

ions outside was estimated by replacing the sum by an integral, i.e.

$$\sum_{\substack{j \\ r > a}} \frac{1}{r_{ij}^6} \simeq \int_a^\infty \frac{4\pi r^2 dr}{V r^6} = \frac{4\pi}{3V\rho^3} = \frac{0.132}{V} \quad \text{if } \rho = \sqrt{10}$$

where V is the volume occupied by one ion on the average, and

$$\sum_{\substack{j \\ r > \sqrt{10}}} \frac{z_{ij}^2}{r_{ij}^8} \simeq \frac{0.0442}{V} \quad \text{and} \quad \sum_{\substack{j \\ r > \sqrt{10}}} \frac{z_{ij}^4}{r_{ij}^{10}} \simeq \frac{0.0265}{V}.$$

The contribution from the integral is quite small, for example it contributes 0.29 to the total of 38.63 for $\sum_j r_{ij}^{-6}$.

Measurements on this substance by Cooke, Duffus and Wolf (1953) give $g_{\perp} = 1.84$, $g_{\parallel} \leq 0.1$. Putting $g_{\parallel} = 0$, it follows that $S'T^2/R = 3.30 \times 10^{-6}$. This is in good agreement with two experimental determinations: 3.20×10^{-6} from experiments on adiabatic demagnetization (Daniels and Robinson 1953) and 3.75×10^{-6} from experiments on paramagnetic relaxation (Cooke, Duffus and Wolf 1953). It seems that the specific heat of cerium magnesium nitrate can be explained entirely on the assumption of magnetic dipole-dipole interaction.

Example (ii). The Ethylsulphates of the Rare Earths: $M(\text{C}_2\text{H}_5\text{SO}_4)_3 \cdot 9\text{H}_2\text{O}$

These salts, where M is a rare earth metal, scandium or yttrium, form an isomorphous series, and crystallize from aqueous solution in hexagonal prisms. The crystal structure has been described by Ketelaar (1937). The hexagonal unit cell dimensions vary slightly from one salt to another; typical values are, e.g. for cerium ethylsulphate, $a = 14.048 \text{ \AA}$, $c = 7.11 \text{ \AA}$, $c/a = 0.506$. The value of c/a is the same for all salts of the series, to within the limits of experimental error. Taking this value of c/a and taking the z -axis to be the crystalline hexagonal axis, or c -axis, we find

$$\left. \begin{aligned} \sum_j 1/r_{ij}^6 &= 245.53 \\ \sum_j z_{ij}^2/r_{ij}^8 &= 144.32 \\ \sum_j z_{ij}^4/r_{ij}^{10} &= 128.07 \end{aligned} \right\} \times a^{-6} \text{ \AA}^{-6}.$$

As before, these sums have been evaluated by direct summation over the ions inside a sphere radius $a\sqrt{10}$, and by an integration for the ions outside. The g -values of many of the rare earth ions in the ethylsulphates have been measured, and the results of fitting these values into the formula for the entropy (eqn. (16)) are given in table 1.

Table 1

Ion	a (Å)	g_{\parallel}	g_{\perp}	$S'T^2/R$	Reference for g -values
Ce	14.048	3.80	0.2	9.67×10^{-5}	Cooke, Whitley and Wolf 1953
Nd	13.992	3.535	2.073	8.95×10^{-5}	Bleaney, Scovil and Trenam 1952
Sm	13.961	0.602	0.587	1.5×10^{-7}	Bogle 1952
Er	13.91*	1.47	8.85	3.2×10^{-3}	Bleaney and Scovil 1951

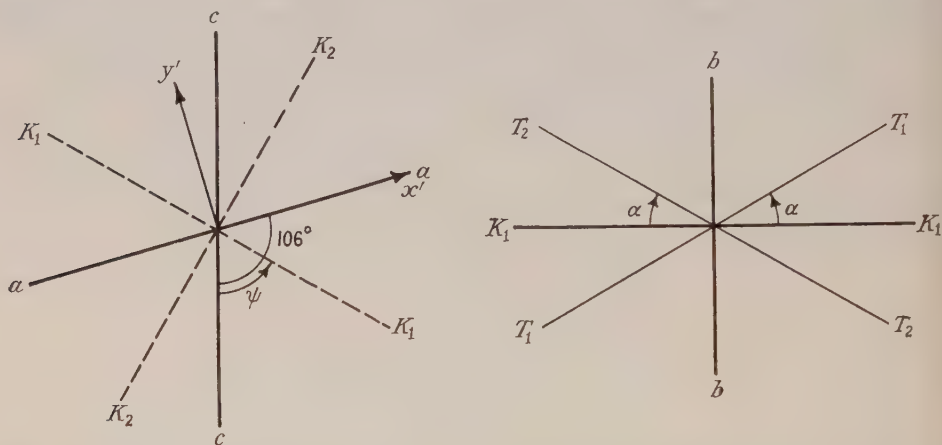
* Value obtained by interpolation from the measured values for the other ions.

$S'T^2/R$ has been measured for only two of these salts, cerium ethylsulphate and neodymium ethylsulphate. The method of de Haas and du Pré (1939) was used in each case. The value for cerium ethylsulphate (Cooke, Whitley and Wolf 1953), 56×10^{-5} , is far too large to be explained on the basis of this theory of magnetic dipole-dipole interaction. On the other hand, the contribution of interactions to $S'T^2/R$ in neodymium ethylsulphates has been deduced, from measurements on samples made from neodymium of unnatural isotopic

composition, to be $8.85 \pm 0.25 \times 10^{-5}$ (Roberts, Sartain and Borie 1952). This is in agreement with the calculated value of 8.95×10^{-5} .

(ii) *Two Dissimilar Ions in the Unit Cell—the Tutton Salts*

This isomorphous series of salts has the formula $M''XO_4 \cdot M_2'XO_4 \cdot 6H_2O$, where M'' is a divalent metal, one of Mg, Ti, V, Cr, Mn, Fe, Co, Ni, Cu, Zn, Cd, and is responsible for the magnetism of the salt; M' is a monovalent metal, one of K, Rb, Cs, Tl, (NH_4) , and X is one of S, Se, Cr. The external morphology has been described in a series of papers by Tutton (1905, 1913, 1916) and the structure has been evaluated by Hofmann (1931). The unit cell is monoclinic, and its dimensions vary slightly from one salt to another; however, the lattices of all the salts of the series approximate very closely to one with $a:b:c = 1.47:2:1$, the b -axis perpendicular to the ac plane, and the angle β between the a and c axes 106° . This representative lattice will be used throughout, and the length of the c -axis, 6.20 \AA , will be taken as the unit of length. The paramagnetism of the salt is due to the divalent ions, of which there are two dissimilar kinds, type A at $(0, 0, 0)$ and type B at $(\frac{1}{2}, \frac{1}{2}, 0)$. The three mutually perpendicular principal axes of susceptibility are denoted by K_1 , K_2 and K_3 : K_3 coincides with the b -axis and K_1 and K_2 lie in the ac plane. The angle between c and K_1 is denoted by ψ (see figure). In the K_1K_3 (i.e. K_1b) plane lie two axes T_1 and T_2 which each



make an angle α with K_1 ; the angles ψ and α vary considerably from one salt to another. The g -tensor of each ion has (at least to a first approximation) axial symmetry, the axis being T_1 for the ions situated at $(0, 0, 0)$ say, and T_2 for those at $(\frac{1}{2}, \frac{1}{2}, 0)$. The principal values of g are the same for all ions, and will be denoted by g_{\parallel} along the appropriate T axis and by g_{\perp} at right angles to this axis (Bleaney, Penrose and Plumptre 1949).

Take as axes (x, y, z) the principal axes of susceptibility (K_1, K_2, K_3) respectively. The values of the non-vanishing elements of the g -tensor referred to these axes are*

$$\begin{aligned} g_{xx} &= g_{\parallel} \cos^2 \alpha + g_{\perp} \sin^2 \alpha & g_{zz} &= g_{\parallel} \sin^2 \alpha + g_{\perp} \cos^2 \alpha \\ g_{yy} &= g_{\perp} & g_{xz} &= g_{zx} = \pm (g_{\parallel} - g_{\perp}) \cos \alpha \sin \alpha, \end{aligned}$$

* The symbol g is commonly used also for the spectroscopic splitting factor. When an external magnetic field is applied along a principal axis of the g -tensor, the spectroscopic splitting factor has the same numerical value as the appropriate principal value of the g -tensor. The spectroscopic splitting factor has, however, a different transformation law, $g^{\theta 2} = g_{\parallel}^2 \cos^2 \theta + g_{\perp}^2 \sin^2 \theta$.

the \pm sign depending on whether the ion is type A or type B. The elements $P_{ij\alpha\beta}$ of the interaction tensor between ions i and j can be written down, assuming for the time being that the interaction is pure magnetic dipole-dipole interaction and using these g -values. It is then found that

$$\begin{aligned} P_{ij\alpha\beta}P_{ijx\beta} = & \frac{1}{r_{ij}^6} \{g_{xx}^4 + g_{yy}^4 + g_{zz}^4 + 2g_{xz}^4 + 2g_{xz}^2(g_{xx}^2 + g_{zz}^2) \pm 2g_{xz}^2(g_{xx} + g_{zz})^2\} \\ & - 6 \frac{1}{r_{ij}^8} \{x_{ij}^2[(g_{xx}^2 + g_{zz}^2)^2 \pm g_{xz}^2(g_{xx} + g_{zz})^2] + y_{ij}^2 g_{yy}^4 \\ & + z_{ij}^2[(g_{zz}^2 + g_{xx}^2)^2 \pm g_{xz}^2(g_{xx} + g_{zz})^2]\} + \frac{9}{r_{ij}^{10}} \{x_{ij}^2(g_{xx}^2 + g_{zz}^2) \\ & + y_{ij}^2 g_{yy}^2 + z_{ij}^2(g_{zz}^2 + g_{xx}^2)\}^2 \pm 36 \frac{x_{ij}^2 y_{ij}^2}{r_{ij}^{10}} g_{xz}^2(g_{xx} + g_{zz})^2. \end{aligned}$$

In the expression above, the positive sign is to be used if the ions i and j are of the same type, and the negative sign if the ions are of different types. Terms containing z or z^3 as a factor have been omitted since, on account of the crystal symmetry, these vanish when the summation over pairs of ions is made. This expression is independent of the sign of g_{xz} , and thus depends on whether the ions i and j are of the same or different types, but not on the type of the ion i .

When this is summed over all pairs of ions, various lattice sums occur,

$$\text{e.g. } \sum_{(ij)} \frac{1}{r_{ij}^6}; \quad \sum_{(ij)} \frac{1}{r_{ij}^6} \text{ etc.,}$$

where the suffices A and B indicate the type of ion i and j , the first referring to ion i and the second to ion j . It is seen that, owing to the symmetry of the lattice, $\Sigma_{AA} = \Sigma_{BB}$ and $\Sigma_{AB} = \Sigma_{BA}$. Hence the sums over two sets of pairs can be replaced by $N/2$ times the same sum for a typical ion i over the same range of values of j , e.g.

$$\sum_{(ij)} \frac{1}{r_{ij}^6} + \sum_{(ij)} \frac{1}{r_{ij}^6} = \frac{N}{2} \sum_j \frac{1}{r_{ij}^6}.$$

Substituting also for g_{xx} , g_{yy} , g_{zz} and g_{xz} the formula for the entropy then becomes

$$\begin{aligned} \frac{S'T^2}{R} = & \frac{\beta^4}{64k^2} \left[\{g_{\parallel}^4 + 2g_{\perp}^4 - 2(g_{\parallel}^2 - g_{\perp}^2)^2 \cos^2 \alpha \sin^2 \alpha\} \Sigma_+ \frac{1}{r_{ij}^6} \right. \\ & + (g_{\parallel}^2 \cos^2 \alpha + g_{\perp}^2 \sin^2 \alpha)^2 \left(9 \Sigma_+ \frac{x_{ij}^4}{r_{ij}^{10}} - 6 \Sigma_+ \frac{x_{ij}^2}{r_{ij}^8} \right) \\ & + g_{\perp}^4 \left(9 \Sigma_+ \frac{y_{ij}^4}{r_{ij}^{10}} - 6 \Sigma_+ \frac{y_{ij}^2}{r_{ij}^8} \right) \\ & + (g_{\parallel}^2 \sin^2 \alpha + g_{\perp}^2 \cos^2 \alpha)^2 \left(9 \Sigma_+ \frac{z_{ij}^4}{r_{ij}^{10}} - 6 \Sigma_+ \frac{z_{ij}^2}{r_{ij}^8} \right) \\ & + 18(g_{\parallel}^2 \cos^2 \alpha + g_{\perp}^2 \sin^2 \alpha) g_{\perp}^2 \Sigma_+ \frac{x_{ij}^2 y_{ij}^2}{r_{ij}^{10}} \\ & + 18(g_{\parallel}^2 \sin^2 \alpha + g_{\perp}^2 \cos^2 \alpha) g_{\perp}^2 \Sigma_+ \frac{y_{ij}^2 z_{ij}^2}{r_{ij}^{10}} \\ & + 18(g_{\parallel}^2 \cos^2 \alpha + g_{\perp}^2 \sin^2 \alpha) (g_{\parallel}^2 \sin^2 \alpha + g_{\perp}^2 \cos^2 \alpha) \\ & \times \Sigma_+ \frac{x_{ij}^2 z_{ij}^2}{r_{ij}^{10}} + (g_{\parallel}^2 - g_{\perp}^2)^2 \sin^2 \alpha \cos^2 \alpha \\ & \times \left\{ 2 \Sigma_- \frac{1}{r_{ij}^6} - 6 \Sigma_- \frac{x_{ij}^2}{r_{ij}^8} - 6 \Sigma_- \frac{z_{ij}^2}{r_{ij}^8} + 36 \Sigma_- \frac{x_{ij}^2 z_{ij}^2}{r_{ij}^{10}} \right\} \left. \right] \dots (17) \end{aligned}$$

where Σ_{\pm} denotes $\Sigma_{AA} \pm \Sigma_{AB}$.

It is not convenient to evaluate these sums directly, since neither the x -axis nor the y -axis coincides with one of the crystallographic axes; and since the sums evaluated for one particular salt would be inapplicable to any other salt with a different value of ψ . Instead, various lattice sums are evaluated with respect to a new set of axes (x', y', z') where x' and z' coincide with a and b respectively. The sums referred to the (x, y, z) set of axes can be obtained from these using the transformation:

$$\left. \begin{aligned} x &= x' \cos(\psi - 106^\circ) + y' \sin(\psi - 106^\circ) \\ y &= y' \cos(\psi - 106^\circ) - x' \sin(\psi - 106^\circ) \\ z &= z' \end{aligned} \right\} . \quad \dots\dots(18)$$

The 14 sums listed in table 2 are needed; only nine of these are independent for there are several relations based on Pythagoras' theorem, e.g.

$$\Sigma x^2/r^8 + \Sigma y^2/r^8 + \Sigma z^2/r^8 = \Sigma 1/r^6. \quad \dots\dots(19)$$

Table 2

Function summed \ Type of sum	Σ_{AA}	Σ_{AB}	Σ_+	Σ_-
$1/r^6$	2.505	1.798	4.303	0.708
y'^2/r^8	1.958	0.287	2.245	1.671
z'^2/r^8	0.086	0.990	1.075	-0.904
y'^4/r^{10}	1.763	0.123	1.886	1.541
z'^4/r^{10}	0.073	0.583	0.656	-0.510
$y'^2 z'^2/r^{10}$	0.008	0.112	0.121	-0.104
$x' y'/r^8$	0.454	-0.038	0.416	0.492
$x' y' z'^2/r^{10}$	0.013	-0.023	-0.010	0.036
$x' y'^3/r^{10}$	0.465	-0.021	0.445	0.486
x'^2/r^8	0.461	0.520	0.982	-0.059
$x'^3 y'/r^{10}$	-0.024	0.006	-0.019	-0.030
x'^4/r^{10}	0.271	0.174	0.444	0.097
$x'^2 y'^2/r^{10}$	0.186	0.052	0.238	0.134
$x'^2 z'^2/r^{10}$	0.004	0.295	0.299	-0.290

The unit of length in these sums is the length of the c -axis which may be taken to be 6.20 Å.

Using the unit cell described at the beginning of this section, the various lattice sums can be worked out. These are given in table 2; those in the rectangle at the top left-hand corner have been worked out directly, and the rest deduced using the relations such as (19) between the sums. No account has been taken of the ions outside a sphere of radius $c\sqrt{10}$ in the evaluation of these sums. The error introduced into the specific heat by neglecting these ions is about 3%. It is hardly justifiable to attempt greater accuracy, on account of the other uncertainties in the problem. The procedure is now to calculate from these, using the transformation (18), the actual sums required in any particular case, and then to substitute these into eqn. (17) for $S'T^2/R$.

Now it is known that exchange plays an important part in the properties of the Tutton salts; evidence for this lies in the 'anomalously' large specific heats of some salts, coupled with considerable 'exchange narrowing' of the lines of

the paramagnetic resonance spectrum. Equation (17) can be expected to give a good estimate of the entropy only for salts where there is evidence that the exchange interaction is small. This is so for two salts: copper caesium sulphate (Bleaney, Penrose and Plumpton 1949) and cobalt ammonium sulphate (Bleaney and Ingram 1951). The results of these calculations, and experimental values for comparison, are given in table 3.

Table 3

	CuCs ₂ (SO ₄) ₂ · 6H ₂ O		Co(NH ₄) ₂ (SO ₄) ₂ · 6H ₂ O	
ψ	114°	(1)	130°	(2)
α	40°	(1)	34°	(2)
g_{\parallel}	2.43	(1)	6.45	(2)
g_{\perp}	2.07	(1)	3.06	(2)
S^2T^2/R calculated	0.62×10^{-4}		6.14×10^{-4}	
hyperfine measured	0.6×10^{-4}	(3)	8.6×10^{-4}	(4)
total measured	1.26×10^{-4}	(3)	19.2×10^{-4}	(4)

(1) Bleaney, Penrose and Plumpton 1949

(2) Bleaney and Ingram 1951

(3) Benzie, Cooke and Whitley 1953

(4) Cooke, Whitley and Wolf 1953

§ 7. THE SUSCEPTIBILITY

The susceptibility is obtained from eqn. (3), the values of the coefficients in this equation being given by (4), (8), (9), (10) and (14). The coefficient of $1/T$ in (3) comes from the second term of (8), and does not contain the interaction tensor; it is the familiar Langevin–Brillouin expression for the Curie constant. If the term in $1/T^2$ is also considered, (3) is equivalent (to this degree of approximation) to a Curie–Weiss formula, for

$$\chi = \frac{c}{T - \Delta} = \frac{c}{T} + \frac{c\Delta}{T^2} + \dots$$

is equivalent to

$$\chi = \frac{c}{T} + \frac{d}{T^2} + \dots$$

if

$$\Delta = \frac{d}{c} = -\frac{1}{3k^2} \cdot \frac{\text{Coefficient of } H^2 \text{ in Spur}(W^3)}{\text{Curie constant} \times \text{Spur}(1)} \dots\dots\dots (20)$$

Hyperfine splitting contributes neither to the Curie constant c nor to the Curie–Weiss Δ , neither in the absence of interactions (Bleaney 1950) nor in their presence, since mixed terms do not occur in $\text{Spur}(W^2)$ or $\text{Spur}(W^3)$. The first term which indicates a departure from a Curie–Weiss law is that in $1/T^3$; its coefficient contains an interaction term (10) and, in general, a hyperfine splitting term. These terms will not be considered further.

The Curie–Weiss Δ

For simplicity we will first consider the case §6.1; i.e. all ions identical and a g -tensor with symmetry about the z -axis. Let there be pure magnetic dipole–dipole interaction, and let the susceptibility be measured along the z -axis. Then

$$\begin{aligned} \Delta &= -\frac{1}{3k^2c} \sum_{(ij)} 6P_{ij\alpha\beta} R_{iz} R_{j\beta} \\ &= -\frac{\beta^4 g_{\parallel}^4}{8k^2c} \sum_{(ij)} \left\{ \frac{1}{r_{ij}^3} - 3 \frac{z_{ij}^2}{r_{ij}^5} \right\}. \end{aligned}$$

Now it is possible to replace $\Sigma_{(ij)}$ by $\frac{1}{2}N\Sigma_j$ only if Σ_j for each i is the same. This is certainly so if Σ_j is rapidly convergent (as in the case of sums occurring in the expression for the entropy, eqn. (15)), but here $\Sigma(r^2 - 3z^2)/r^5$ converges like $\int(r^2 - 3z^2)dr/r^3$, i.e. it is only conditionally convergent since both $\int dr/r$ and $\int z^2 dr/r$ are each divergent. Thus the finite sum $\Sigma_j(r_{ij}^2 - 3z_{ij}^2)/r_{ij}^5$ is not, in general, independent of the ion i ; but it is for certain shaped specimens, namely spheres, spheroids, and ellipsoids (Van Vleck 1937), and for these $\Sigma_{(ij)} = \frac{1}{2}N\Sigma_j$. We shall consider only spherical specimens, and shall consider the ion i to be the ion at the centre. Let the sum $\Sigma_j(1/r_{ij}^3 - 3z_{ij}^2/r_{ij}^5)$ be computed by adding consecutive spherical shells centred on i . Then for shells of large radius the contribution of each shell can be replaced by an integral over the shell, and is

$$\frac{N}{V} \frac{dr}{r} \iint (1 - 3 \cos^2 \theta) \sin \theta \, d\theta \, d\phi = 0$$

where V is the gram ionic volume and θ and ϕ are spherical polar coordinates for the shell. Hence

$$\Delta_{\parallel} = \frac{g_{\parallel}^2 \beta^2}{4k} \sum_j \frac{3z_{ij}^2 - r_{ij}^2}{r_{ij}^5} \quad \dots\dots (21)$$

where the sum is taken over the inside of a sphere so large that the contribution of the next spherical shell is negligible. The Curie-Weiss Δ in the perpendicular direction Δ_{\perp} is given by a similar expression. The value of Δ in any other direction can be obtained from the fact that the transformation law for $c\Delta$ is exactly the same as that for the susceptibility. In this particular case it is easily seen that

$$\frac{\Delta_{\parallel}}{g_{\parallel}^2} + 2 \frac{\Delta_{\perp}}{g_{\perp}^2} = 0,$$

and that for a powder

$$\Delta = \Delta_{\parallel} \frac{g_{\parallel}^4 - g_{\perp}^4}{g_{\parallel}^2(g_{\parallel}^2 + 2g_{\perp}^2)}.$$

It is well known that $\Delta = 0$ for a specimen with a cubic lattice—this is the basis of the derivation of the Lorentz interaction field—but this is not so in general for a specimen with a non-cubic lattice.

In the case of the Tutton salts, using the notation of § 6 (ii), it is found by similar reasoning that

$$\left. \begin{aligned} \Delta_x &= \frac{\beta^2}{4k} \left\{ (g_{\parallel}^2 \cos^2 \alpha + g_{\perp}^2 \sin^2 \alpha) \Sigma_+ \frac{3x_{ij}^2 - r_{ij}^2}{r_{ij}^5} \right. \\ &\quad \left. + \frac{(g_{\parallel}^2 - g_{\perp}^2)^2 \cos^2 \alpha \sin^2 \alpha}{(g_{\parallel}^2 \cos^2 \alpha + g_{\perp}^2 \sin^2 \alpha)} \Sigma_- \frac{3z_{ij}^2 - r_{ij}^2}{r_{ij}^5} \right\} \\ \Delta_y &= \frac{\beta^2}{4k} g_{\perp}^2 \Sigma_+ \frac{3y_{ij}^2 - r_{ij}^2}{r_{ij}^5} \\ \Delta_z &= \frac{\beta^2}{4k} \left\{ (g_{\parallel}^2 \sin^2 \alpha + g_{\perp}^2 \cos^2 \alpha) \Sigma_+ \frac{3z_{ij}^2 - r_{ij}^2}{r_{ij}^5} \right. \\ &\quad \left. + \frac{(g_{\parallel}^2 - g_{\perp}^2)^2 \cos^2 \alpha \sin^2 \alpha}{(g_{\parallel}^2 \sin^2 \alpha + g_{\perp}^2 \cos^2 \alpha)} \Sigma_- \frac{3x_{ij}^2 - r_{ij}^2}{r_{ij}^5} \right\} \end{aligned} \right\} \dots\dots (22)$$

where the sums are again taken over the inside of a large enough sphere.

In order to check these formulae against experimentally measured values, comparison should be made only for salts where it is reasonable to suppose that the interaction is predominantly due to magnetic dipole-dipole coupling. This appears to be so for cerium magnesium nitrate, neodymium ethylsulphate, and

copper caesium sulphate, of the salts yet investigated. The Curie-Weiss Δ would be expected to be quite small and tedious to compute in the case of cerium magnesium nitrate, since the lattice of this salt is simple cubic only slightly distorted. Although copper caesium sulphate exhibits very nearly the specific heat to be expected on the basis of pure magnetic dipole-dipole interaction, its susceptibility temperature curve does not follow Curie's law (Benzie and Cooke 1950), and thus it is not the most suitable substance to use as a test of theory. In addition, Benzie and Cooke were unable to measure the Curie-Weiss Δ for this substance. The relevant lattice sum, $\sum_j (3z_{ij}^2 - r_{ij}^2)/r_{ij}^5$, has therefore been evaluated for the ethylsulphate lattice. The value obtained is $18.7 \times a^{-3}$ taken over the inside of a sphere radius $a\sqrt{10}$. The values obtained for the Curie-Weiss Δ for neodymium ethylsulphate are as follows:

$$\Delta_{\parallel} = 0.013^{\circ}\text{K}, \quad \Delta_{\perp} = -0.002^{\circ}\text{K}, \quad \Delta_{\text{powder}} = 0.007^{\circ}\text{K}.$$

A value of Δ for a spherical powder sample of neodymium ethylsulphate has been obtained by Roberts, Sartain and Borie (1953) and is $0.013 \pm 0.005^{\circ}\text{K}$.

§ 8. CONCLUSIONS

This theory, which is an extension of Van Vleck's original theory of dipole-dipole interaction, provides formulae for calculating the entropy and susceptibility of a paramagnetic provided the nature of the interaction between the dipoles is known. In particular, it is shown that the contribution to each of these quantities from interaction and hyperfine splitting are additive as far as the term in $1/T^3$, and that there are contributions to the susceptibility from hyperfine splitting which are shape dependent and yet are not included in the Curie-Weiss Δ .

In the case of magnetic dipole-dipole interaction, detailed formulae are given for the entropy (eqns. (16) and (17)) and for the Curie-Weiss Δ (eqns. (21) and (22)) for salts with one ion in the unit cell, and for the Tutton salts.

When comparison is made between the calculated and experimental values of the specific heat (or entropy) assuming pure magnetic dipole-dipole interaction, it is found that, although some salts (e.g. $\text{Ce}_2\text{Mg}_3(\text{NO}_3)_{12} \cdot 24\text{H}_2\text{O}$, $\text{Nd}(\text{C}_2\text{H}_5\text{SO}_4)_3 \cdot 9\text{H}_2\text{O}$, $\text{CuCs}_2(\text{SO}_4)_2 \cdot 6\text{H}_2\text{O}$) fit the theory well enough, the majority of salts show a much larger specific heat than can be accounted for only by magnetic dipole-dipole interaction. Exchange interaction is undoubtedly an important factor in most salts, as is shown by other evidence, such as the narrowing of paramagnetic resonance absorption lines, and a large Curie-Weiss Δ . In hydrated salts like those considered here, the exchange interaction is most likely to occur through the intermediary of intervening atoms as suggested by Kramers (1934), and is not necessarily isotropic in character. It should be noted that, although the contributions to the specific heat from isotropic magnetic dipole interaction and isotropic exchange are additive in the $1/T^2$ term, this is not so for anisotropic exchange, nor for anisotropic magnetic dipole interactions (Opechowski 1948).

Although the entropy and susceptibility can be calculated if the interaction tensors are known, it is not possible to calculate the elements of these tensors from measurable quantities such as the specific heat and the Curie-Weiss Δ 's. In particular, complete information about the exchange interaction between ions cannot be determined. This is because the unknown elements are more numerous than the measurable quantities, even though the number of independent tensor

elements is reduced on account of crystal symmetry (Opechowski 1948). Any other assumptions (e.g. isotropic exchange, or nearest neighbour interaction only) would require careful justification in the light of present knowledge.

Finally, this theory can be applied to nuclear paramagnetics in the appropriate temperature range, when the interaction is due to magnetic dipole coupling. The analogue of the Stark effect in a nuclear paramagnetic is the interaction between the nuclear electric quadrupole moment and the orbital electrons. This can be so large as to leave only the lowest hyperfine doublet populated over a range of temperatures for which this theory is applicable. As an example, many covalent iodine compounds have a quadrupole splitting which, for ^{127}I , is of the order of $0.02^\circ\text{K} \times k$ between the lowest two hyperfine doublets. This theory should then apply at temperatures of the order of 0.001°K .

ACKNOWLEDGMENTS

I wish to acknowledge gratefully the interest taken in this work by Dr. K. W. H. Stevens of the Clarendon Laboratory, and the valuable advice given by him. I am indebted to Dr. Betty Hunt for assistance with the numerical calculations.

REFERENCES

- ABRAGAM, A., and PRYCE, M. H. L., 1951, *Proc. Roy. Soc. A*, **205**, 135.
 BENZIE, R. J., and COOKE, A. H., 1950, *Proc. Phys. Soc. A*, **63**, 1366.
 BENZIE, R. J., COOKE, A. H., and WHITLEY, S., 1953, in course of publication.
 BLEANEY, B., 1950, *Phys. Rev.*, **78**, 214; 1951, *Phil. Mag.*, **42**, 441.
 BLEANEY, B., and INGRAM, D. J. E., 1951, *Proc. Roy. Soc. A*, **208**, 143.
 BLEANEY, B., PENROSE, R. P., and PLUMPTON, B. I., 1949, *Proc. Roy. Soc. A*, **198**, 406.
 BLEANEY, B., and SCOVIL, H. E. D., 1951, *Proc. Phys. Soc. A*, **64**, 204.
 BLEANEY, B., SCOVIL, H. E. D., and TRENAM, R. S., 1952, *Phil. Mag.*, **43**, 995.
 BOGLE, G. S., 1952, *Thesis*, University of Oxford.
 COOKE, A. H., DUFFUS, J. H., and WOLF, W. P., 1953, *Phil. Mag.*, **44**, 623.
 COOKE, A. H., WHITLEY, S., and WOLF, W. P., 1953, in course of publication.
 DANIELS, J. M., and ROBINSON, F. N. H., 1953, *Phil. Mag.*, **44**, 630.
 DE HAAS, W. J., and DU PRÉ, F. K., 1939, *Physica*, **6**, 705.
 HOFMANN, W., 1931, *Z. Kristallogr.*, **78**, 279.
 KETELAAR, J. A. A., 1937, *Physica*, **4**, 619.
 KRAMERS, H. A., 1934, *Physica*, **1**, 182.
 OPECHOWSKI, W., 1948, *Physica*, **14**, 237.
 PRYCE, M. H. L., 1950, *Proc. Phys. Soc. A*, **63**, 25.
 ROBERTS, L. D., SARTAIN, C. C., and BORIE, B., 1952, *Phys. Rev.*, **87**, 192; 1953, *Rev. Mod. Phys.*, **25**, 170.
 TUTTON, A. E. H., 1905, *J. Chem. Soc. Trans.*, **87**, 1123; 1913, *Proc. Roy. Soc. A*, **88**, 361; 1916, *Phil. Trans. Roy. Soc. A*, **216**, 1.
 VAN VLECK, J. H., 1937, *J. Chem. Phys.*, **5**, 320.

Photodisintegration Processes in Light Even-Even Nuclei yielding Alpha-Particles

By D. L. LIVESEY* AND C. L. SMITH†

* Oundle School, Northants.

† Department of Radiotherapeutics, Cambridge

MS. received 25th March 1953

Abstract. The photodisintegration processes splitting the nuclei $^{12}_6\text{C}$ and $^{16}_8\text{O}$ completely into alpha-particles have been studied in some detail by the photographic plate method. It is found that, for energies below about 25 mev resonances occur in the excitation functions, indicating that a compound nucleus interpretation may be valid. These results, and also certain data of Green and Gibson concerning the inelastic scattering of neutrons in carbon, are related to excited states of the nuclei $^{12}_6\text{C}$ and ^8_4Be as intermediate stages in the various processes. Levels in $^{12}_6\text{C}$ at 9.6 mev and 11.3 ± 0.3 mev occur and these yield first an alpha-particle and ^8_4Be in the ground state, while a third level in $^{12}_6\text{C}$ near 12 mev is found to yield ^8_4Be in the broad 3 mev excited state. Other levels in ^8_4Be at 4.1 mev and 17 mev, disintegrating into two alpha-particles, are found as intermediate stages in these reactions.

§ 1. INTRODUCTION

DISINTEGRATION of those light even-even nuclei which consist of multiples of the extremely stable α -particle unit ^4_2He may be expected to proceed in some cases by the emission of one or more α -particles. The nucleus ^8_4Be is, in fact, unstable in the ground state with respect to dissociation into two α -particles. The excited states of ^8_4Be also lead to the production of two α -particles where the levels are characterized by even parity and even total angular momentum. Other levels in ^8_4Be are believed to lose their energy either by emission of γ -rays (as in the case of the well-known level 17.6 mev above the ground state) or by emission of protons or neutrons.

The next stable even-even nucleus is $^{12}_6\text{C}$, and experiments with fast neutrons and energetic γ -rays have shown that this can be split into three α -particles. It remains to be determined whether this is a process of direct tripartition (as suggested by Chastel 1951) or via various even-parity, even-momentum levels of ^8_4Be , as suggested by Goward, Telegdi and Wilkins (1950).

The nucleus $^{16}_8\text{O}$ can also be split up by energetic γ -rays to give four α -particles (Goward and Wilkins 1950). It is conceivable that this reaction may proceed (a) by direct quadripartition, (b) by the creation of two unstable ^8_4Be nuclei, or (c) via excited levels in $^{12}_6\text{C}$ and possibly ^8_4Be also.

Experimental methods used in the study of these disintegrations include the inelastic scattering of light particles and direct photodisintegration, either by monoergic γ -rays from a lithium + proton source or by bremsstrahlung from a betatron target. Most of the published results have been obtained by using

photographic plates to record the tracks of particles produced when γ -rays split up carbon and oxygen nuclei present in the photographic emulsion. These tracks form 'stars' apparently radiating from the points of disintegration, because all the processes under investigation occur within a very short interval (less than 10^{-14} second). This fact introduces certain difficulties into the task of identifying intermediate stages in the reactions.

The following reactions are discussed in ensuing sections:

- (1) ${}^8_4\text{Be} \rightarrow 2 {}^4_2\text{He} + 0.1 \text{ Mev}$
- (2) ${}^{12}_6\text{C} + h\nu \rightarrow 3 {}^4_2\text{He} - 7.3 \text{ Mev}$
- (3) ${}^{12}_6\text{C} + {}^1_0\text{n} \rightarrow {}^1_0\text{n}' + 3 {}^4_2\text{He} - 7.3 \text{ Mev}$
- (4) ${}^{16}_8\text{O} + h\nu \rightarrow 4 {}^4_2\text{He} - 14.4 \text{ Mev.}$

Information about reaction (1) is summarized in the review by Ajzenberg and Lauritsen (1952).

Reaction (2) has been studied in detail by Goward, Telegdi and Wilkins (1950), by Chastel (1951) and by Eder and Telegdi (1952). Some of their results are compared with our own in §2 of this paper.* Reaction (3) was studied by Green and Gibson (1949)†, whose results have been re-examined and re-calculated by the present authors, and certain new deductions from their data appear in §3. Reaction (4) was investigated by Goward and Wilkins (1950, 1952), by Millar and Cameron (1950), and by Livesey and Smith (1952); a fuller discussion of the available results is presented in §4.

The theoretical treatment of these reactions has not proceeded very far, although Haefner (1951) has recently discussed the excited states of ${}^8_4\text{Be}$ and ${}^{12}_6\text{C}$. A major problem is to decide whether the compound nucleus interpretation of such high-energy processes is valid. A great deal of experimental information is required concerning the nature of the excitation function of each reaction and the angular momenta and parities of the various nuclear levels involved. Some of this information may be obtained from simple experiments of the type described here. This paper summarizes the results obtained from a series of photographic plates exposed to bremsstrahlung of maximum energies between 26 Mev and 32 Mev, produced by the beta-synchrotron in the Department of Radiotherapeutics at Cambridge. The plates used were of the Ilford C2 and E1 types, developed in the usual way, and examined by two observers using microscope magnifications between $\times 750$ and $\times 1500$.

§ 2. PHOTODISINTEGRATION OF ${}^{12}_6\text{C}$ INTO THREE ALPHA-PARTICLES

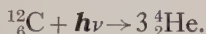
This reaction was established by Hänni, Telegdi and Zünti (1948), who used monoergic 17.6 Mev γ -rays from a lithium + proton source. At higher energies, bremsstrahlung may be used, but these x-rays have a continuous spectrum extending from zero energy to the maximum energy of electrons striking the target. The energy of the photon responsible for a particular triple α -star in a photographic plate may be calculated by adding 7.3 Mev to the sum of the α -particle energies, provided that there is no loss of energy by re-emission of a γ -ray or other processes. That such energy loss is very unlikely in the x-ray region

* Later results by Goward and Wilkins in Atomic Energy Research Establishment Report G/M 127 (1952) became available after this paper was prepared for publication.

† We are very grateful to Drs. Green and Gibson for permission to use their experimental results.

investigated is shown by the following considerations: (a) one can examine the variation of yield in plates irradiated with bremsstrahlung of different maximum energies: in every case the maximum calculated photon energy agrees closely with the energy of electrons striking the target; (b) the calculated lifetimes of excited nuclei with respect to γ -ray emission are long compared with those for disintegrations into separate particles, where such disintegrations are possible; (c) in those stars which can be measured most accurately, the vector sum of the α -particle momenta always agrees in magnitude and direction with the calculated momentum of the incident photon, within the limits of experimental error.

The latter condition has been used as a criterion for acceptance of stars as due to a particular reaction (cf. Goward and Wilkins 1950). In these experiments the plates were exposed at right angles to the bremsstrahlung, so in the directions OX, OY (in the plane of the plate) the net momentum should be zero, while the excess momentum in the OZ direction should agree with the calculated photon momentum. In 146 observed triple stars, the excess momentum* was within 2 mass-mev units of the expected values in the three directions, and these stars were ascribed to the reaction:



About half of the stars satisfied the more rigid criterion of having a net excess momentum within 1 mass-mev unit of zero, and these stars only were used for detailed analysis. The accuracy of the estimated photon energies is limited by errors in range measurements, by uncertainties in the range-energy relation for low-energy α -particles (see Rotblat 1951, Catala and Gibson 1951), and by other factors. A very complete treatment of this problem has been given by Wilkins (1951, 1952). We estimate that the calculated photon energies should not be in error by more than 0.5 mev.

The total yield curve for the 146 stars is shown in fig. 1, which represents numbers plotted against photon energy at intervals of 0.5 mev, so that in this

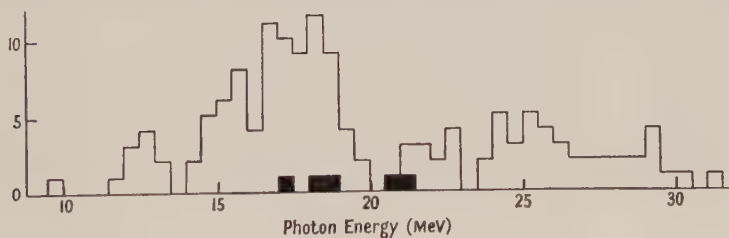


Fig. 1. Yield Curve for $^{12}\text{C} \rightarrow 3^4\text{He}$. 146 stars.

histogram no corrections have been applied to obtain the true shape of the excitation function. Nevertheless, the chief feature of the curve may be distinguished as a broad peak, between marked minima near 14 mev and 20 mev, similar to that reported by other authors. Goward and Wilkins (1952) have given evidence that the peak actually consists of overlapping resonance peaks. We find in fig. 1 that there is also a suggestion of a subsidiary peak between 11.5 and 13.5 mev. Small peaks occur in the same region in histograms published by Wilkins and Goward (1951 a) and by Eder and Telegdi (1952). In the light of

* Momentum calculated as $(2mE)^{1/2}$ with mass number m and energy E in mev.

evidence presented in §§ 3 and 4, this may be very important in helping to settle the question whether the observed peaks in the excitation function correspond to definite excited states in $^{12}_6\text{C}$.

We find from these results that the excitation function for this reaction probably exhibits resonance effects in the region below 20 mev, and that there is some evidence for a peak at 12.5 ± 0.5 mev. These resonance effects are important in attempts to elucidate the actual mode of disintegration of the excited $^{12}_6\text{C}$ nucleus because different excited levels may give rise to different modes of disintegration. However, until the various peaks can be more clearly resolved (as is possible with the data for $^{16}_8\text{O}$ in § 4), the behaviour of each group cannot be determined with any certainty.

The problem of identifying particular modes of disintegration is rendered difficult, not only by non-resolution of resonance peaks, but also by the quasi-instantaneous nature of the process and the fact that the three products are similar particles. Experiments with 17.6 mev γ -rays by Hänni, Telegdi and Züti (1948) have shown that, at this energy, most of the disintegrations proceed via the broad excited level at 3 mev in ^8_4Be . The stars produced by bremsstrahlung can be analysed by taking the α -particle tracks in pairs and calculating, for each pair, the excitation energy (denoted here by f) of a possible intermediate ^8_4Be nucleus. For each star three values of f are obtained, and of these only one may be significant, i.e. the 'significance ratio' S is 1:3 at the most. If a histogram of all possible f -values be plotted, as in fig. 2, we shall expect to find a continuous distribution due to non-significant values with superimposed peaks corresponding to any states of ^8_4Be operative in the reaction.

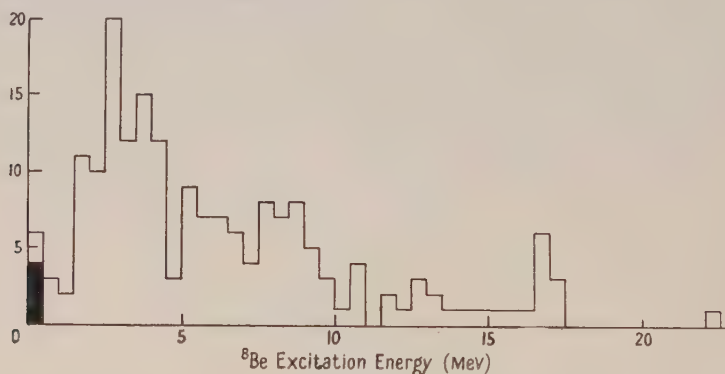


Fig. 2. Excitation energies of ^8Be in ^{12}C stars. $S=1:3$. 65 stars.

From fig. 2, the following deductions may be drawn concerning the occurrence of intermediate ^8_4Be nuclei in the reaction:

(a) A small group of stars with f -values below 0.5 mev presumably involved ^8_4Be nuclei in the ground state. Such f -values could arise by chance, but we have ascribed four stars out of the 65 stars analysed to the ground state after studying their mode of occurrence, and these four stars are shown shaded in figs. 1 and 2.

(b) A major peak occurs in the region between 2 mev and 4 mev, and this is too large to be a chance effect. It seems certain that the broad 3 mev level is responsible for many of these stars, and it is possible that the level already reported at 4.09 mev in ^8_4Be (see Ajzenberg and Lauritsen 1952) may also be involved, as the peak is not symmetrical about 3.0 mev.

(c) At higher energies, a third definite peak occurs at 17 mev and it is known that there is probably an even-momentum, even-parity level in this region, apart from the well-known odd-momentum level at 17.6 mev.

The three principal peaks mentioned here agree closely with the results of Wilkins and Goward (1951 b).

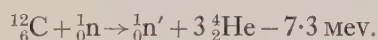
A further consistency test can be applied to these experimental results, provided that the f -value histogram exhibits definite peaks. One can test a given interpretation of the disintegration by seeing whether it accounts for every star in a suitable energy group. With this criterion we find that 57 out of the 65 stars analysed give at least one f -value in the ranges 0–0.5 mev, 2.0–4.5 mev, 16.0–18.0 mev. The remaining eight stars yield 24 f -values, a number insufficient for full analysis.

One may also attempt to relate different modes of disintegration to the different peaks occurring in the yield curve, fig. 1. The four shaded stars do not, however, occur at a single energy. The 3 mev level in ${}^8_4\text{Be}$ occurs over a wide energy range of fig. 1, up to about 25 mev. Above this energy, it becomes energetically possible for the ${}^8_4\text{Be}$ to be formed in the 17 mev excited state, and this mode accounts for most of the stars between 25 mev and 30 mev. It is difficult to draw definite conclusions concerning the small group of stars near 12.5 mev in fig. 1, but all these stars show evidence of the 3 mev level in ${}^8_4\text{Be}$.

Another approach to the problem of identifying modes of disintegration lies in plotting the angular distribution of the product particles. Unfortunately it is difficult to obtain significant distributions unless one can certainly identify the particle first emitted in each star, and this is only possible for a very small number of the stars considered here.

§ 3. DISINTEGRATION OF CARBON BY INELASTIC SCATTERING OF NEUTRONS

Green and Gibson (1949) have reported measurements on triple stars observed in photographic plates exposed to the high-energy neutrons from a lithium target bombarded with deuterons. These stars are ascribed to the reaction:



More detailed analyses have been carried out to discover the mode of disintegration. The compound nucleus ${}^{13}_6\text{C}$ formed by the incident neutron may break up by emitting first a neutron, or an α -particle, or the unstable nucleus ${}^5_2\text{He}$. Of these only the re-emission of a neutron, corresponding to inelastic scattering, gave new results of significance. The excitation energy of the ${}^{12}_6\text{C}$ nucleus left behind was calculated for 84 stars, and the histogram obtained is shown in fig. 3. These calculations should give a random distribution unless definite levels in ${}^{12}_6\text{C}$ are involved. In fact, two peaks are observed, and the first of these is close to the known level at 9.6 mev, which is known to yield an α -particle and ${}^8_4\text{Be}$ in the ground state. That this is the correct interpretation of the first group of stars (group A) is shown by calculating the possible ${}^8_4\text{Be}$ excitation energies for the 14 most accurately measured stars in this group. Figure 4(a) is a histogram of such f -values derived from the α -particles taken in pairs. It is seen that, in addition to a broad peak due to non-significant pairs, there is a sharp group with $f \leq 0.5$ mev, corresponding to the ground state in ${}^8_4\text{Be}$. Moreover, 12 of these stars have one f -value ≤ 0.2 mev, and the two remaining stars each have one f -value at 0.5 mev.

The second peak observed in fig. 3 (group B) is less well defined than the 9.6 mev peak, and it may be part of a continuous distribution due to non-significant

values. Analysis of the possible ${}^8\text{Be}$ f -values calculated for 14 stars in this group (fig. 4(b)) shows that the ground state ${}^8\text{Be}$ nuclei do not occur in appreciable numbers, and no definite peaks occur in the histogram. It may be that the broad level at 3 mev in ${}^8\text{Be}$ is involved, but is masked by the continuous distribution of non-significant values. One can only tentatively conclude that a possible mode of disintegration of these stars is via a level in ${}^{12}\text{C}$ at 11.8 ± 0.6 mev and the broad level at 3 mev in ${}^8\text{Be}$.

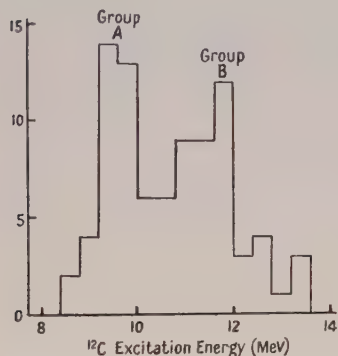


Fig. 3. Excitation energies of ${}^{12}\text{C}$ in the reaction ${}^{12}\text{C}(n, n') {}^{34}\text{He}$. 84 stars.

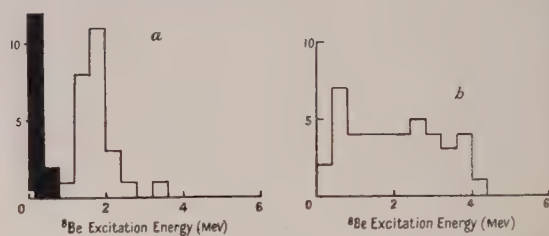


Fig. 4. Excitation energies of ${}^8\text{Be}$ in stars from the reaction ${}^{12}\text{C}(n, n') {}^{34}\text{He}$. (a) Group A, (b) Group B. $S=1:3$. 14 stars in each.

§ 4. PHOTODISINTEGRATION OF ${}^{16}\text{O}$ INTO FOUR ALPHA-PARTICLES

This reaction has been studied in some detail by Goward, Titterton and Wilkins (1949), by Goward and Wilkins (1950 and 1952), also by Millar and Cameron (1950); and the present authors have published a brief report on resonance effects in the yield curve (Livesey and Smith 1952). In a series of plates exposed to bremsstrahlung of maximum energy 32 mev we have observed 79 quadruple stars which are ascribed to this reaction after calculations of the momentum balance as in § 2. The yield curve is shown in histogram form in fig. 5, and this is seen to display at least three peaks. A broad group occurs in the energy range 19–23.5 mev, a sharper peak occurs close to 25 mev, and there are possibly two peaks in the region 27–30 mev. Rather similar results have been published by Goward and Wilkins (1952). The good resolution of the groups in fig. 5 enables one to divide the data easily for further analysis.

A notable feature of these stars is the frequent occurrence of pairs of α -particles apparently derived from ${}^8\text{Be}$ in the ground state, as shown by f -values of less than 0.5 mev. In this category 22 stars have been observed: they all belong to the first peak in the yield curve, and they are shown shaded in fig. 5. These stars have been analysed in detail and, as Goward and Wilkins have reported, there is no evidence that the process involves the creation of two unstable ${}^8\text{Be}$ nuclei. We have therefore calculated the possible ${}^{12}\text{C}$ excitation energies, which are shown in histogram form in fig. 6, where only one half of the data can be significant. In this diagram there is some slight indication of a group near 9.6 mev, and, allowing for experimental error, 16 of the 22 stars could be explained as being due to the known level at 9.6 mev. But, as fig. 6 shows, there are rather stronger indications of an excited state at 11.3 ± 0.3 mev, and this is certainly required to explain the remaining six stars. One can also calculate theoretically the possible

α -particle energies, taking a typical photon energy of 22 mev, and disintegrations involving two possible excited states of ^{12}C at 9.6 mev and 11.3 mev, both yielding ^8Be in the ground state. Facsimiles of such stars, with different angles of emission of the α -particles, are shown in fig. 7, where in every case α_1 refers to the α -particle first emitted. The distinguishing feature is that in the 9.6 mev case the energy of α_1 exceeds the total energy of the other three α -particles, and the α_1 track is therefore very prominent, whereas in the 11.3 mev case α_1 is less energetic and more symmetrical stars can occur. Stars of both types have been observed, and we find that each of the two ^{12}C levels considered accounts for approximately half of the stars involving ^8Be in the ground state.

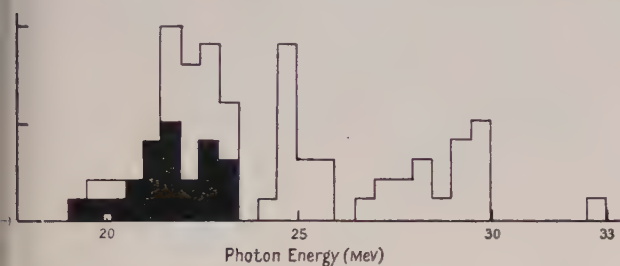


Fig. 5. Yield Curve for $^{16}\text{O} \rightarrow 4^4\text{He}$. 79 stars.

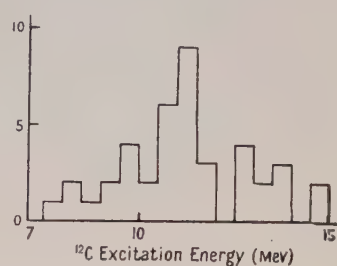


Fig. 6. Oxygen stars involving ground state ^8Be : ^{12}C excitation energies.

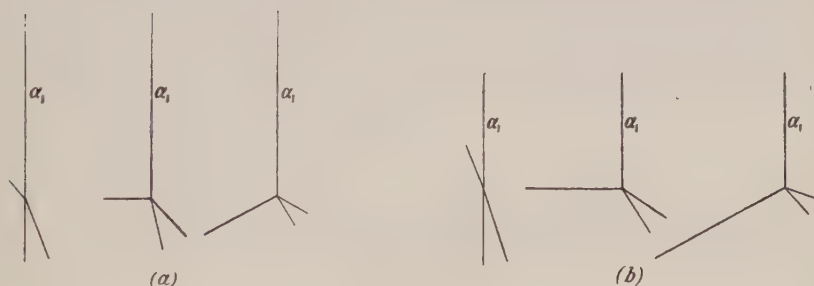


Fig. 7. Star facsimiles produced via excited levels in ^{12}C at (a) 9.6 mev and (b) 11.3 mev.

Proceeding to a consideration of the remaining stars, we found it advisable to apply detailed analysis only to those which satisfied the more rigorous criterion mentioned in § 2, namely, that the net excess momentum was within 1 mass-mev unit of zero in each of the three directions OX, OY, OZ. In the low-energy group of fig. 5, nine stars satisfied this condition, and for these all the possible ^{12}C excitation energies were calculated. The results are plotted in fig. 8 (a), where the significance ratio is 1:4, and the average non-significant value for random events is shown by an arrow. There are indications of a peak at 12.0 ± 0.3 mev and the consistency test shows that all the nine stars have at least one value between 11.0 and 13.0 mev. The ^8Be f -values were also calculated and are shown in fig. 9 (a), but here the significance ratio is only 1:6 if the process occurs via ^{12}C and ^8Be excited nuclei, and the average random f -value is 2.5 mev, which is close to the broad 3 mev level in ^8Be . We can only conclude that the 3 mev level is probably involved, derived from the presumed ^{12}C level at 12.0 ± 0.3 mev.

The sharp peak at 25 Mev in the yield curve of fig. 5 consists of 16 stars, and nine of these satisfied the criterion for detailed analysis. The calculated excitation energies for a possible intermediate $^{12}_6\text{C}$ nucleus are shown in fig. 8(b), and the f -values for ^8_4Be in fig. 9(b). There is no indication of a definite level in $^{12}_6\text{C}$, but the ^8_4Be f -values display a distinct peak at 4.3 ± 0.2 Mev. The consistency test shows that all these stars possess one f -value between 3.9 and 4.7 Mev, and it is probable that the reported level at 4.09 Mev (see Ajzenberg and Lauritsen 1952) is responsible for this result. We conclude that the stars produced by photons of energy 25.0 ± 0.3 Mev are formed via an intermediate ^8_4Be nucleus with an excitation energy of 4.3 ± 0.2 Mev.

Finally the high-energy group in the yield curve, fig. 5, may possibly consist of two peaks at 28 Mev and 30 Mev, but for detailed analysis we have regarded this as one group, and the $^{12}_6\text{C}$ excitation energies and the ^8_4Be f -values are shown in figs. 8(c) and 9(c) respectively. There is no clear evidence of a $^{12}_6\text{C}$ level here, but a peak near 3.5 Mev in fig. 9(c) may be due to the broad 3 Mev level in ^8_4Be . The results would be consistent with a disintegration scheme via $^{12}_6\text{C}$ levels near 16 Mev and the 3 Mev level in ^8_4Be .

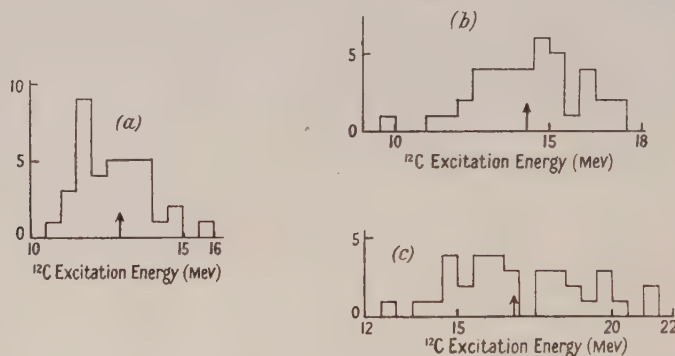
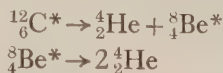


Fig. 8. Excitation energies of ^{12}C in oxygen stars: (a) low energy group (excluding stars involving ground state ^8Be), (b) medium-energy group, (c) high-energy group. $S=1:4$. 9 stars in each.

§ 5: SUMMARY OF EXPERIMENTAL RESULTS

Despite the limited number of stars examined in these experiments, the foregoing analyses show how the modes of disintegration of excited $^{12}_6\text{C}$ and $^{16}_8\text{O}$ nuclei may be related to the properties of ^8_4Be and $^{12}_6\text{C}$ as intermediate products.

In § 2 we showed that a considerable proportion of $^{12}_6\text{C}$ photodisintegrations proceed according to the scheme:

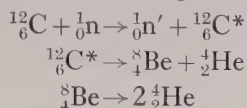


Assuming that peaks in the yield curve, fig. 1, correspond to levels in the compound nucleus $^{12}_6\text{C}$, we may tentatively summarize the results as follows:

$^{12}_6\text{C}$ level	^8_4Be level (even parity and momentum)
12.5 ± 0.5 Mev \rightarrow	3 Mev
One or more levels $\left\{ \begin{array}{l} 15.0 \\ \text{to} \\ 19.0 \end{array} \right.$	\rightarrow 3 Mev
Excitation > 25 Mev \rightarrow	17 Mev

A few stars include ${}^8\text{Be}$ in the ground state as an intermediate product, and the 4.09 mev level in ${}^8\text{Be}^*$ may also occur.

In § 3 the following scheme was investigated:



About half of the analysed stars were formed via the 9.6 mev level in ${}^{12}_6\text{C}$ and the ground state of ${}^8_4\text{Be}$; the remainder may involve a ${}^{12}_6\text{C}$ level at 11.8 ± 0.6 mev and the 3 mev level in ${}^8_4\text{Be}^*$.

In § 4 we found evidence for the following modes of disintegration of ${}^{16}_8\text{O}^*$:

${}^{16}_8\text{O}$ level	${}^{12}_6\text{C}$ level	${}^8_4\text{Be}$ level
	9.6 Mev	→ ground state
22.5 ± 1.0 Mev	11.3 ± 0.3 Mev	→ ground state
	12.0 ± 0.3 Mev	→ (3 Mev)
25.0 ± 0.3 Mev	-----	→ 4.3 ± 0.2 Mev
27–30 Mev	→ (16 Mev)	→ 3 Mev

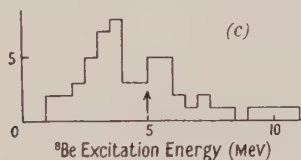
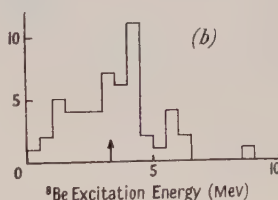
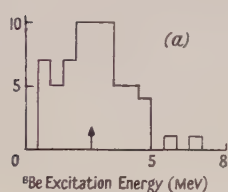


Fig. 9. Excitation energies of ${}^8\text{Be}$ (other than ground state) in oxygen stars: (a) low-energy group, (b) medium-energy group, (c) high-energy group. $S=1:6$ for single ${}^8\text{Be}$ occurrence. 9 stars in each.

§ 6. DISCUSSION

Experiments of this type have shown that the disintegration of these even-even nuclei by high-energy γ -rays proceeds in most cases by successive emission of α -particles rather than by direct partition. The presence of well-defined resonance peaks in the yield curve indicates that the compound nucleus interpretation is valid, to some extent, for excitations not exceeding 25 mev. Unfortunately the experimental conditions do not allow of great accuracy in resolving these peaks, so that identification of a given peak with a known level of the nucleus concerned is somewhat hazardous. Nevertheless, the successive stages of each disintegration process may be related to well-defined excited states of the intermediate nuclei, ${}^8_4\text{Be}$ and ${}^{12}_6\text{C}$.

The ${}^8_4\text{Be}$ levels concerned in these processes are those of types 0^+ , 2^+ , 4^+ etc., which can give two α -particles by quasi-instantaneous disintegration. The ground state is almost certainly 0^+ , and various nuclear reactions indicate that the broad

level at 3 mev is 2^+ . The high-energy photodisintegration processes in ^{12}C yield the 17 mev level in ^8Be , the existence of which had been deduced from the experiments of Wilkins and Goward (1951b). A fourth level of ^8Be operative in photodisintegration is that at 4.09 mev, which occurs in the disintegration of ^{16}O by 25.0 mev photons, and which must have even parity and even total angular momentum.

These experiments have provided interesting evidence concerning excited states of ^{12}C between the known level at 9.6 mev and those near 16 mev. There are clear indications of a level at 11.3 ± 0.3 mev yielding an α -particle and ^8Be in the ground state. Apart from this, the levels reported at 12.5 ± 0.5 mev in § 2, at 11.8 ± 0.6 mev in § 3 and at 12.0 ± 0.3 mev in § 4 may be considered as the same level, or a group of similar levels close together, since they all apparently yield $^8\text{Be}^*$ in the 3 mev state. Recently, Titterton† has reported levels at 10.3 ± 0.25 mev, at 11.3 ± 0.25 mev, and at 13.0 ± 0.25 mev as the results of experiments on the inelastic scattering of neutrons in ^{12}C , but it will be seen that these figures do not agree with the results of § 3 which relate to similar experiments. Johnson (1952) reports several new levels in ^{12}C , at 10.8, 11.1, 11.7, 12.8 and 13.3 mev, but examination of his neutron spectra for the reaction $^{11}\text{B}(d, n)^{12}\text{C}$ shows that more detailed work is required in this region. We conclude that there is at least one ^{12}C level close to 12 mev which yields $^8\text{Be}^*$ in the 3 mev state. Assuming that the latter state is 2^+ , it is a plausible contention that the ^{12}C level is also 2^+ , in order to explain the preferred mode of disintegration as emission of an s-wave α -particle. Transition to the 0^+ ground state of ^8Be would then require emission of a d-wave α -particle. In this connection, it is relevant to point out that the work of Telegdi (1951) on photodisintegration of ^{12}C by 17.6 mev γ -rays leads to the conclusion that the ^{12}C levels involved are probably 1^+ or 2^+ , again yielding the excited $^8\text{Be}^*$ preferentially.

The most remarkable feature of the ^{16}O data in § 4 is the fact that the yield curve (fig. 5) shows fewer peaks than the ^{12}C yield curve (fig. 1), although the excitation energy is higher and a heavier nucleus is involved. It may be that the extra degree of symmetry possessed by the ^{16}O makes certain forms of photon absorption improbable, even at high energies. If the first broad level at 22.5 mev in fig. 5 represents a single ^{16}O level, it must have three alternative modes of transition to levels in ^{12}C , of comparable probability. On the other hand, further experiments may resolve the 22.5 mev group into separate peaks. The peak at 25.0 mev is more sharply defined than the others, and this may be due to photon absorption of a higher multipole type. It is possible that this group also differs from the others in its mode of disintegration, which may be of the type



The two ^8Be nuclei would then be in different excited states, one of which is found at 4.3 ± 0.2 mev.

ACKNOWLEDGMENTS

Our acknowledgments are due to Professor J. S. Mitchell, the Director of the Department of Radiotherapeutics, and to Mr. C. M. Rawlings for skilled technical assistance both in the operation of the beta-synchrotron and in processing the photographic plates.

† We are grateful to Professor Titterton for sending us his results before publication.

REFERENCES

- AJZENBERG, F., and LAURITSEN, T., 1952, *Rev. Mod. Phys.*, **24**, 321.
CATALA, J., and GIBSON, W. M., 1951, *Nature, Lond.*, **167**, 550.
CHASTEL, R., 1951, *C.R. Acad. Sci., Paris*, **233**, 1440.
EDER, M., and TELEGDI, V. L., 1952, *Helv. Phys. Acta*, **25**, 55.
GOWARD, F. K., TELEGDI, V. L., and WILKINS, J. J., 1950, *Proc. Phys. Soc. A*, **63**, 402.
GOWARD, F. K., TITTERTON, E. W., and WILKINS, J. J., 1949, *Proc. Phys. Soc. A*, **62**, 460.
GOWARD, F. K., and WILKINS, J. J., 1950, *Proc. Phys. Soc. A*, **63**, 1171; 1952, *Ibid.*, **65**, 671.
GREEN, L. L., and GIBSON, W. M., 1949, *Proc. Phys. Soc. A*, **62**, 296.
HAEFNER, R. R., 1951, *Rev. Mod. Phys.*, **23**, 228.
HÄNNI, H., TELEGDI, V. L., and ZÜNTI, W., 1948, *Helv. Phys. Acta*, **21**, 203.
JOHNSON, V. R., 1952, *Phys. Rev.*, **86**, 302.
LIVESEY, D. L., and SMITH, C. L., 1952, *Proc. Phys. Soc. A*, **65**, 758.
MILLAR, C. H., and CAMERON, A. G. W., 1950, *Phys. Rev.*, **78**, 78.
ROTLAT, J., 1951, *Nature, Lond.*, **167**, 550.
TELEGDI, V. L., 1951, *Phys. Rev.*, **84**, 600.
WILKINS, J. J., 1951, *Atomic Energy Research Establishment Report G/R*, 664; 1952, *Ibid.*, Report G/R, 1020.
WILKINS, J. J., and GOWARD, F. K., 1951 a, *Proc. Phys. Soc. A*, **64**, 201; 1951 b, *Ibid.*, **64**, 1056.

The Pile Neutron Absorption Cross Sections of Bismuth

By D. J. LITTLER AND E. E. LOCKETT

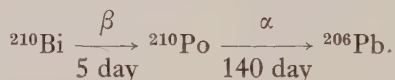
Atomic Energy Research Establishment, Harwell, Berks.

MS. received 6th March 1953

Abstract. The pile neutron absorption cross section of bismuth has been measured as 30.8 ± 2.2 millibarns. Also the activation cross section of bismuth for the production of ^{210}Po has been measured as 20.5 ± 1.1 millibarns. The difference between these two values, namely 10.3 ± 2.5 millibarns, is claimed to be the activation cross section for the production of a long-lived alpha-particle emitting state of ^{210}Bi .

§ 1. INTRODUCTION

NATURAL bismuth has only a single isotope of mass number 209. Neutron capture by bismuth leads, therefore, to the production of ^{210}Bi , which is radioactive. ^{210}Bi decays by two methods, one being the well-known decay scheme of RaE, namely



The other, more recently discovered, mode of decay (Newman, Howland and Perlman 1950) is by the chain



The neutron capture (n, γ) cross section of bismuth will be the sum of the activation cross sections for the production of these two activities. We have measured the pile neutron absorption cross section of bismuth and the activation cross section for the production of ^{210}Po . Since it can be shown that, in a pile neutron spectrum, the (n, γ) cross section must be very much greater than the (n, p), (n, α) and ($n, 2n$) cross sections, it follows that the pile absorption cross section is almost identical with the (n, γ) cross section. The difference between the pile absorption cross section and the activation cross section for the production of ^{210}Po must therefore be the activation cross section for the production of the long lived alpha-particle emitting state in ^{210}Bi (unless, of course, there are other undiscovered α or β modes of decay of ^{210}Bi).

§ 2. THE PILE NEUTRON ABSORPTION CROSS SECTION OF BISMUTH

The pile absorption cross section of bismuth was measured using the pile oscillator method, which has been extensively described in the published literature (Colmer and Littler 1951, Benoist *et al.* 1951, Langsdorf 1951, Littler 1950).

The G.L.E.E.P. oscillator was used, and the absorption cross section of bismuth was compared with that of boron. (We have consistently used an

assumed value of 710 barns for the absorption cross section of boron, and all the bismuth cross section values quoted herein are based on this value.)

Oscillation of any sample in the pile causes changes in the pile reproduction constant due to (Anderson *et al.* 1947) (a) the absorption of neutrons, (b) the scattering of neutrons, (c) the 'slowing down' or moderating effect on the neutrons.

The scattering of neutrons affects the reproduction constant whilst the sample is in motion, but not when the sample is outside or at the centre of the pile. Its effect can therefore be reduced by reducing the fraction of the total oscillation period during which the sample is in motion. By this means we were able to make the scattering effect negligible compared with the absorption effect of the bismuth.

To estimate the 'slowing down' effect on the reproduction constant for any substance, the assumption was made that the effect is proportional to $\sigma_s \xi$ (Anderson *et al.* 1947), where σ_s is the scattering cross section for resonance neutrons and ξ is the average logarithmic energy loss per collision. For heavy water $\sigma_s \xi$ is large compared with its absorption cross section σ_a . Knowing σ_s , ξ , and σ_a for heavy water we were therefore able to measure the change in reproduction constant as a function of $\sigma_s \xi$. From this and a knowledge of σ_s and ξ for bismuth we thus obtained the correction for 'slowing down' to be applied to the measured cross section for the bismuth. The correction was such as to increase the measured cross section by 0.7 millibarn.

A further correction was applied to allow for the displacement of air by the sample when it moved to the centre of the pile. Taking the cross section of nitrogen as 1.76 barns (Colmer and Littler 1950), the correction was computed to be 2.6 millibarns.

After applying these corrections the value found for the absorption cross section of bismuth was 38.5 ± 1.5 millibarns.

After the pile measurements were completed, the bismuth sample was sent to the Chief Chemical Inspectorate, Ministry of Supply, Woolwich. A full chemical analysis was made of the sample and the following table shows the impurities with large absorption cross sections which were found.

Impurity	Quantity*	Impurity	Quantity*	Impurity	Quantity*
Gadolinium	<0.02	Dysprosium	<0.02	Sodium	2 ± 0.3
Boron	0.05 ± 0.005	Lead	15 ± 2	Nickel	1.5 ± 0.3
Cadmium	0.25 ± 0.025	Zinc	8 ± 1	Tin	1 ± 0.1
Lithium	<0.1	Antimony	5 ± 0.25	Iron	<5
Samarium	<0.03	Silicon	5 ± 0.5	Arsenic	<1
Europium	<0.01	Calcium	5 ± 1	Manganese	<1
Silver	10 ± 1	Copper	4 ± 0.4	Cobalt	<1
Indium	<1	Molybdenum	4 ± 0.2	Chromium	<0.5
Chlorine	20 ± 4				

* in parts per million.

The total absorption cross section of these impurities per atom of bismuth comes to $6.9^{+2.4}_{-0.8}$ millibarns. For the sake of convenience, and without introducing any serious error, we can rewrite this as 7.7 ± 1.6 millibarns. Therefore, correcting for the impurities in the sample, we obtain for the pile absorption cross section of bismuth a value of 30.8 ± 2.2 millibarns.

We have also measured a sample of bismuth which was lent to us by Dr. B. B. Kinsey of Atomic Energy of Canada, Ltd., and was believed to be of very much higher purity than our sample. From this the value obtained for the bismuth absorption cross section was 34.3 millibarns. No correction has been applied for impurities, since we were not able to have a chemical analysis made of the sample.

§ 3. (n, p), (n, α) AND (n, 2n) REACTIONS IN BISMUTH

Besides radiative capture of neutrons by the bismuth (n, γ process) there may also be neutron absorption giving (n, p), (n, α) and (n, 2n) reactions. We will now investigate the relative probabilities of these different processes when bismuth is irradiated in a pile neutron spectrum.

To begin with, we will consider the Q values for the (n, p), (n, α) and (n, 2n) processes. Starting with the (n, 2n) process, it is known, from the measurements of Parsons and Collie (1950), that the threshold for this reaction is 7.2 ± 0.1 mev. Since there will be a negligible number of neutrons in the pile with energies greater than 7.2 mev, there will be no contribution to the absorption cross section from the (n, 2n) process.

The reactions $^{209}\text{Bi}(n, p)^{209}\text{Pb}$ and $^{209}\text{Bi}(n, \alpha)^{206}\text{Tl}$ are both exothermic, the energies released by thermal neutrons in the two reactions being 0.147 ± 0.01 mev and 9.23 ± 0.02 mev respectively. The first figure is derived from the known β decay energy of ^{209}Pb (Wapstra 1952), and the second one by combining the known energy release in the β, α decay from ^{210}Bi to ^{206}Pb with the values for the energy of the capture gamma-rays in the reaction $^{209}\text{Bi}(n, \gamma)^{210}\text{Bi}$ (Kinsey *et al.* 1951) and the β decay energy of ^{206}Tl (Alburger and Friedlander 1951).

Now the cross section for an (n, p) or (n, α) reaction at a given neutron energy is equal to the product of the cross section for forming a compound nucleus and the probability of emitting the charged particle. We will assume that, at a neutron energy of 3 mev, the cross section for the production of the compound nucleus is of the same order as the geometrical cross section of the nucleus, that is about 3 barns.

Since the potential barrier heights for proton and alpha-particle emission are about 12 and 24 mev respectively, the penetrability factor for both proton and alpha-particle emission (Bethe 1937) is of the order of 10^{-7} when the energy of the incident neutrons is 3 mev.

Thus the (n, p) and (n, α) cross sections are of the order of 3×10^{-7} barn for a neutron energy of 3 mev, and will be less at thermal energies. Since the pile neutron spectrum is predominantly a thermal one, we can therefore say that the (n, p) and (n, α) cross sections are negligible compared with the (n, γ) cross section and that the radiative capture cross section of bismuth is 30.8 ± 2.2 millibarns.

§ 4. ACTIVATION CROSS SECTION OF BISMUTH FOR THE PRODUCTION OF ^{210}Po

Three thin discs of bismuth (~ 0.4 mg cm^{-2}) were mounted on aluminium, and were irradiated in the G.L.E.E.P. together with a sample of sodium carbonate. After the irradiation, the ^{24}Na activity of the sodium carbonate was counted absolutely by the coincidence method (Putman 1950). The bismuth discs were kept for several weeks (to allow all the ^{210}Bi to decay to ^{210}Po) and were then counted in an argon-filled 2π alpha-counter. The total counting rates were

determined in the usual way from extrapolated bias curves. The three discs gave results which were in good agreement, and measurements made at intervals showed that the activity decayed with a half-life of about 140 days. A measurement made on unirradiated bismuth showed that there was negligible α -activity in the original sample.

From these measurements a value was obtained of the ratio of the cross sections of bismuth and sodium, which was 0.0410 ± 0.0027 . Taking the cross section of sodium as 0.50 ± 0.015 barns (Colmer and Littler 1950), we have for the activation cross section of bismuth for polonium production 20.5 ± 1.5 millibarns. This value has been quoted previously by Colmer and Littler (1950).

Two further measurements have been made of the ratio of the bismuth and sodium cross sections. For these measurements sodium carbonate and bismuth were irradiated together in B.E.P.O. The β -disintegration rates from ^{24}Na and ^{210}Bi were then compared in a 4π counter (Putman 1950) by the Isotopes Standardization Group of the Atomic Energy Research Establishment. Small corrections were applied for the contribution to the counting rate for each bismuth sample from the activation of impurities in the bismuth. The corrections were roughly determined by following the decay of some of the bismuth on a β -electroscope. Using the same value as before for the sodium cross section, the mean of these two measurements gave for the activation cross section of bismuth for polonium production a value of 20.4 ± 1.6 millibarns.

The two determinations of the activation cross section obtained from observing both the β and α decay in the chain



agree very well together, and from them we obtain a final value for the activation cross section of 20.5 ± 1.1 millibarns.

§ 5. DISCUSSION

Unless there are any other, as yet undiscovered, β or α modes of decay of ^{210}Bi , the difference between the (n, γ) cross section and the activation cross section for polonium production, namely 10.3 ± 2.5 millibarns, must be the activation cross section for the production of the α -emitting state in ^{210}Bi .

This α -emitting state is long lived (Newman, Howland and Perlman 1950), and hitherto its half-life has not been determined. If its activation cross section is 10.3 millibarns, however, it is possible to determine the half-life by comparing the rate of α -emission from ^{210}Bi with that from ^{210}Po in pile-irradiated bismuth, using as the ratio of the activation cross sections

$$(10.3 \pm 2.5)/(20.5 \pm 1.1) = 0.50 \pm 0.12.$$

ACKNOWLEDGMENTS

We would like to thank the members of the Counters Group and the Isotopes Standardization Group at the Atomic Energy Research Establishment for their assistance in the absolute counting experiments, the members of the Chief Chemical Inspectorate, Woolwich, for making the chemical analysis on the bismuth sample, and Dr. T. H. R. Skyrme for his advice on the method of calculating the (n, p) and (n, α) cross sections. Finally we would like to thank the Director of the Atomic Energy Research Establishment for permission to publish this paper.

REFERENCES

- ALBURGER, D. E., and FRIEDLANDER, G., 1951, *Phys. Rev.*, **82**, 977.
ANDERSON, H. L., FERMI, E., WATTENBERG, A., WEIL, G. L., and ZINN, W. H., 1947, *Phys. Rev.*, **72**, 16.
BENOIST, P., KOWARSKI, L., and NETTER, F., 1951, *J. Phys. Radium*, **12**, 584.
BETHE, H. A., 1937, *Rev. Mod. Phys.*, **9**, 69.
COLMER, F. C. W., and LITTLER, D. J., 1950, *Proc. Phys. Soc. A*, **63**, 1175 ; 1951, *Nucleonics*, **8**, 3.
KINSEY, B. B., BARTHOLOMEW, G. A., and WALKER, W. H., 1951, *Phys. Rev.*, **82**, 380.
LANGSDORF, A., 1951, *Atomic Energy Commission Declassified Report* 3194.
LITTLER, D. J., 1950, *Atomics*, **1**, 189.
NEWMAN, H. M., HOWLAND, J. J., and PERLMAN, I., 1950, *Phys. Rev.*, **77**, 720.
PARSONS, R. W., and COLLIE, C. H., 1950, *Proc. Phys. Soc. A*, **63**, 839.
PUTMAN, J. L., 1950, *Brit. J. Radiol.*, **23**, 46.
WAPSTRA, A. H., 1952, *Phys. Rev.*, **86**, 562.

A Method of Calculating Critical Size in Multi-Group Neutron Transport Theory for Some Simple Systems

By E. R. WOODCOCK

Ministry of Supply

MS. received 17th March 1953

Abstract. A simple method is developed for obtaining a good approximation to the critical size of some simple nuclear reactors when neutrons of all relevant energies are allowed for by dividing them into a number of energy groups. The method is applicable for any number of energy groups.

§ 1. INTRODUCTION

IN an assembly containing fissile material the neutron population will tend to increase as the result of neutron induced fissions but will tend to decrease because of loss of neutrons over the boundaries and by capture. There is a critical size of the assembly in which these two effects just balance, for smaller sizes the neutron population would steadily die away and for larger sizes it would increase without limit. The critical size is therefore an important parameter of such an assembly.

It is not difficult to calculate a critical size for an assembly of simple geometry in which all the neutrons can be treated as of the same energy. In general, however, neutrons will be present of a wide range of energies. One way of allowing for such a spectrum of energies is to divide the neutrons into a number of energy groups and use mean values of the necessary nuclear parameters for neutrons in each group. By increasing the number of groups it is then possible to approximate as near as we like to the true neutron spectrum.

Unfortunately standard methods, such as the spherical harmonics method, of calculating critical sizes in multi-group theory lead to a considerable amount of rather complicated numerical computation. In some cases, it is possible, however, by means of a method developed by Professor Feynman and his team during the war to reduce the problem to the solution of a series of one-group problems. Using such methods a comparatively simple formula can be deduced which gives a good approximate answer for critical size.

We will first make such a reduction for one-component systems.

§ 2. THE INTEGRAL EQUATION

We define a one-component system as a system in which the nuclear parameters α and β have values which are independent of position at every point at which they are not zero.

The integral equation for a one-component critical system in t -group theory is then

$$n_i(\mathbf{r}) = \sum_{j=1}^t \beta_{ji} \int \int n_j(\mathbf{r}') K_i(\mathbf{r}, \mathbf{r}') d\tau' \quad \dots (1)$$

where* $K_i(\mathbf{r}, \mathbf{r}') = \exp \{ -|\mathbf{r} - \mathbf{r}'| \alpha_i \} / 4\pi |\mathbf{r} - \mathbf{r}'|^2. \dots\dots(2)$

$n_i(\mathbf{r})$ is the density of neutrons in energy group i at the point \mathbf{r} .

$\alpha_i dx$ is the probability that a neutron in energy group i has a collision in distance dx .

$V_i \beta_{ji} dx / V_j$ is the probability that a neutron of group i is generated by a neutron of group j in distance dx .

V_i is the mean velocity of neutrons in energy group i .

§ 3. REDUCTION BY FEYNMAN'S METHOD

This method has also been described by Davison (1950).

Define $q_i(\mathbf{r}) = \sum_{j=1}^t \beta_{ji} n_j(\mathbf{r}), \dots\dots(3)$

then (1) becomes $n_i(\mathbf{r}) = \int \int q_i(\mathbf{r}') K_i(\mathbf{r}, \mathbf{r}') d\tau' \dots\dots(4)$

and eliminating n between (4) and (3)

$$q_i(\mathbf{r}) = \sum_{j=1}^t \beta_{ji} \int \int q_j(\mathbf{r}') K_j(\mathbf{r}, \mathbf{r}') d\tau', \dots\dots(5)$$

which is a similar equation to (1) but with K_i replaced by K_j .

Now consider the equation

$$f(\mathbf{r}) = C_i \int \int f(\mathbf{r}') K_i(\mathbf{r}, \mathbf{r}') d\tau'. \dots\dots(6)$$

There is a set of eigenvalues C_{mi} of C_i for each of which the equation has a solution $f_m(\mathbf{r})$ which is finite and not everywhere zero. From experience of one-group theories it is known that the dependence of $f_m(\mathbf{r})$ on i is small for any given value of m and so for our present purpose we will assume that $f_m(\mathbf{r})$ is independent of i .

The functions $f_m(\mathbf{r})$ form a set of orthogonal functions and if, as is almost certain, they are a complete set we can express any other well-behaved function in terms of them. In particular

$$q_i(\mathbf{r}) = \sum_{m=1}^{\infty} P_{mi} f_m(\mathbf{r}). \dots\dots(7)$$

Substituting (7) in (5) and using (6) we obtain

$$\sum_m P_{mi} f_m(\mathbf{r}) = \sum_{j=1}^t \beta_{ji} \sum_k \frac{P_{kj}}{C_{kj}} f_k(\mathbf{r}). \dots\dots(8)$$

Normalizing the f 's so that

$$\int \int f_m(\mathbf{r}) f_n(\mathbf{r}) d\tau = \delta_{mn} \dots\dots(9)$$

(where $\delta_{mn} = 0$ if $m \neq n$; $\delta_{mm} = 1$) we obtain from (8) by multiplying by $f_m(\mathbf{r}) d\tau$ and integrating

$$P_{mi} = \sum_{j=1}^t \beta_{ji} \frac{P_{mj}}{C_{mj}}. \dots\dots(10)$$

* It is assumed here that the system is convex. Other systems will need a more general definition of K similar to that given in a later section on tamped cores.

§4. CONDITION FOR CRITICAL SIZE

The condition for critical size is that not all the P_{mj} 's should be zero, that is

$$\begin{vmatrix} \beta_{11} - C_{m1} & \beta_{21} \dots \dots \dots \beta_{t1} \\ \beta_{12} & \beta_{22} - C_{m2} \dots \dots \dots \\ \vdots & \vdots \\ \beta_{1t} & \vdots & \beta_{tt} - C_{mt} \end{vmatrix} = 0 \quad \dots \dots (11)$$

for at least one value of m .

There is also another condition that we must satisfy and that is that the neutron density should be nowhere negative. That is, all the n_i must be equal to or greater than zero and therefore the q_i should be everywhere positive.

The only everywhere positive functions $f_m(\mathbf{r})$ are those corresponding to the lowest eigenvalue C_{1i} . Consequently if we satisfy equation (11) with $m=1$ we have found a critical size.

Now, suppose we have satisfied the condition (11) for critical size with $m>1$. The function $f_m(\mathbf{r})$ is negative at some points in the interior of the system and so must vanish on a certain surface S . If S were the boundary of the active part of the system we would have a smaller size than that for which we have satisfied the critical condition. This smaller system would also satisfy the criticality condition (11) with C_{mi} as its lowest eigenvalues and $f_m(\mathbf{r})$ the corresponding eigenfunction.

Consequently to obtain critical size we put $m=1$ in equation (11) leading to the criticality condition:

$$\begin{vmatrix} \beta_{11} - C_{11} & \beta_{21} \dots \dots \dots \beta_{t1} \\ \beta_{12} & \beta_{22} - C_{12} \dots \dots \dots \\ \vdots & \vdots \\ \beta_{1t} & \vdots & \beta_{tt} - C_{1t} \end{vmatrix} = 0 \quad \dots \dots (12)$$

The C_{1i} can be obtained from equation (6) which is a one-group equation for a system with the same boundaries and so can be solved to any desired approximation by standard methods.

§5. ILLUSTRATIVE EXAMPLES

If $t=1$ eqn. (12) reduces, as it should, to $C_{11} = \beta_{11}$.

If $t=2$ we get

$$(\beta_{11} - C_{11})(\beta_{22} - C_{12}) = \beta_{12}\beta_{21}. \quad \dots \dots (13)$$

The infinite medium solution for eqn. (6) which vanishes at a radius b in spherical symmetry and is finite at the origin leads to

$$\left. \begin{aligned} C_{1i} &= \frac{\theta}{\tan^{-1}(\theta/\alpha_i)} \\ \theta &= \pi/b \end{aligned} \right\} \quad \dots \dots (14)$$

where

With these values of C_{1i} eqn. (13) becomes

$$\{\beta_{11} \tan^{-1}(\theta/\alpha_1) - \theta\} \{\beta_{22} \tan^{-1}(\theta/\alpha_2) - \theta\} = \beta_{12}\beta_{21} \tan^{-1}(\theta/\alpha_1) \tan^{-1}(\theta/\alpha_2). \quad \dots (15)$$

The particular approximation used in this illustration to obtain the one-group solution, eqn. (14), is however most accurate when radius b is not at the boundary of the system but at a distance Z beyond the boundary, where the extrapolated

distance Z is roughly one half to three quarters of a mean free path for neutrons. Consequently the number b obtained from eqn. (15) is an overestimate of the critical radius though the percentage error in b is small for systems large compared to the mean free path.

§ 6. EXTENSION TO MORE GENERAL SYSTEMS

(i) *Systems with α and β as Functions of \mathbf{r}*

The most general system is one in which both the α_i and the β_{ji} are functions of \mathbf{r} . In this case the function K_i is defined by

$$K_i(\mathbf{r}, \mathbf{r}') = \exp \{ - |\mathbf{r} - \mathbf{r}'| \bar{\alpha}_i \} / 4\pi |\mathbf{r} - \mathbf{r}'|^2, \quad \dots\dots (16)$$

where $\bar{\alpha}_i$ is the average value of α_i on the line joining \mathbf{r} to \mathbf{r}' .

If α_i is a function of \mathbf{r} therefore, the developments set out in the previous sections are unaffected except that K is defined by eqn. (16) instead of eqn. (2).

However, if β_{ji} are functions of \mathbf{r} the reduction by Feynman's method is in general not possible. There is however one case of interest for which we can use Feynman's method and that is when we can write

$$\beta_{ji} = \lambda_{ji} \rho(\mathbf{r}), \quad \dots\dots (17)$$

where $\rho(\mathbf{r})$ depends on \mathbf{r} but not on i or j , and λ_{ji} is independent of \mathbf{r} .

Such a case arises, for example, when the system consists of one material only but the density of the material varies from point to point.

The integral equation is now

$$n_i(\mathbf{r}) = \sum_{j=1}^t \int \int \beta_{ji} n_j(\mathbf{r}') K_i(\mathbf{r}, \mathbf{r}') d\tau'. \quad \dots\dots (18)$$

This equation can be reduced in a manner exactly similar to the simpler case, but now we have, instead of eqn. (6)

$$f(\mathbf{r}) = C_i \int \int \rho(\mathbf{r}') f(\mathbf{r}') K_i(\mathbf{r}, \mathbf{r}') d\tau' \quad \dots\dots (19)$$

with (9) replaced by

$$\int \int \rho(\mathbf{r}) f_m(\mathbf{r}) f_n(\mathbf{r}) d\tau = \delta_{mn}. \quad \dots\dots (20)$$

Equation (12) with β_{ji} replaced by λ_{ji} is now the condition for critical size but we must interpret C_{1i} as the lowest eigenvalue of equation (19).

(ii) *Fissile Core in a Reflector*

Another problem that arises is to find the critical size of a fissile core in a reflector. This can be solved by similar methods provided that neutrons are not transferred from one energy group to another while they are travelling in the reflector.

To do this we must define $K_i(\mathbf{r}, \mathbf{r}')$ in a different way.

Let $K_i(\mathbf{r}, \mathbf{r}')$ be the probability that a neutron in energy group i leaving at point \mathbf{r}' in the core will reach the point \mathbf{r} in the core without having a collision in the core. The track of the neutron from \mathbf{r}' to \mathbf{r} may, of course, pass into the reflector, where it can have any number of collisions. This definition retains the essential symmetry of K in \mathbf{r} and \mathbf{r}' since it is just as easy for a neutron to travel on the reverse track.

Equation (1) is now an equation for neutron densities in the core where the volume integral is over the core only.

This equation can now be manipulated exactly as before leading to eqn. (12) as the condition for criticality, but with C_{1i} the lowest eigenvalue of the equation

$$f(\mathbf{r}) = C_i \int \int \int_{\text{core only}} f(\mathbf{r}') K_i(\mathbf{r}, \mathbf{r}') d\tau'. \quad \dots\dots(21)$$

ACKNOWLEDGMENT

I am indebted to the Chief Scientist, Ministry of Supply, for permission to publish this paper.

REFERENCE

DAVISON, B., 1950, *Atomic Energy Research Establishment Report*, T/R 590.

The Decay of the τ -Meson

By R. H. DALITZ

Department of Mathematical Physics, University of Birmingham

MS. received 7th April 1953

Abstract. The applicability of the hypothesis of charge independence is discussed for the τ -meson. One consequence of this hypothesis is that the frequency of charged τ -meson decay leading to a single charged π -meson must exceed one-quarter of that of the established decay into three charged π -mesons.

THE existence of a τ -meson of mass approximately $975 m_e$ is now well established in consequence of its characteristic decay (Brown *et al.* 1949), $\tau^\pm \rightarrow \pi^\pm + \pi^+ + \pi^-$, of which about ten clear examples are now available. The preference for this mode of decay is most simply understood if the τ -meson is a pseudoscalar boson, as simpler decay processes would then be forbidden by requirements of angular momentum and parity conservation. It is of interest to enquire next whether an isotopic spin may be defined for the τ -meson in such a way that the major interactions of the τ -meson are charge independent (i.e., more precisely, invariant for rotations in the isotopic spin space). If the τ -meson may be understood in terms of the known interaction between nucleon and π -meson, the charge independence of this interaction implies that, in general, the τ -meson would have a definite isotopic spin and that the total isotopic spin of systems involving τ -mesons would be conserved. Since no τ -meson of charge exceeding e has yet been observed, the present data would suggest strongly that the τ -meson would then have unit isotopic spin. On the other hand, the τ -meson may require representation by some new meson field coupled directly with the nucleon and meson fields. It is usually argued that the charge independence of nuclear forces requires the charge independence of all mesons responsible for nuclear forces. However, this argument may not be relevant here since the slow rate of decay of the charged τ -meson suggests that the τ -meson-nucleon interaction may be weak, and since, in any case, such a heavy meson would modify nuclear forces only at short distances, where little is known of the charge independence of nuclear forces.

If the τ -meson does have unit isotopic spin and the interactions responsible for its decay satisfy charge independence, there will exist restrictions on the relationship between the possible modes of decay of the τ -meson, so that experimental data on the branching ratios would be of considerable interest. For the τ^\pm meson the decay (Pais 1952) $\tau^\pm \rightarrow \pi^\pm + \pi^0 + \pi^0$ may be expected to compete with the established decay $\tau^\pm \rightarrow \pi^\pm + \pi^+ + \pi^-$. Such a decay event in an emulsion would be difficult to distinguish from the π -decay of other heavy mesons, owing to the difficulty of detecting π^0 -mesons, and some heavy meson decay events may possibly be examples† of this process. In cloud chambers

† In this decay process, the π^\pm meson has energy less than about 60 mev, so that it will not be confused with χ -meson decay, where the product meson has about 110 mev. Of the other heavy mesons, only K5 (Menon and O'Ceallaigh 1953) and (just possibly) KM3 (Levi Setti and Tomasini 1952), could be interpreted as examples of this τ -meson decay process. I am glad to acknowledge Dr. W. O. Lock's guidance in the K-meson data.

containing lead plates, such a decay event may become apparent by the existence of four cascade showers related to the τ -decay event, due to the decay γ -rays from the π^0 -meson, though no events of this kind have yet been reported.

The relation between these processes may be discussed simply, following the method of Van Hove (1952) and Van Hove *et al.* (1952). Consider first the differential probability of emitting π -mesons into three particular states f, g, h of spatial motion—since the meson charges are specified the probability $P(\tau^+ \rightarrow \pi^+ \pi^+ \pi^-)$ is distinct from $P(\tau^+ \rightarrow \pi^+ \pi^- \pi^+)$ and $P(\tau^+ \rightarrow \pi^- \pi^+ \pi^+)$. The isotopic spins of the first two particles may be added to form isotopic spin $t=0, 1$ or 2 , and, by adding to this the isotopic spin of the third particle, three functions $\chi_0^{m_T}, \chi_1^{m_T}, \chi_2^{m_T}$ may be formed for total isotopic spin $T=1$ and component m_T . That part of the totally symmetric wave function which contains the spatial states f, g, h is then a linear superposition:

$$\frac{1}{6} \Sigma_P (F_0 \chi_0^{m_T} + F_1 \chi_1^{m_T} + F_2 \chi_2^{m_T}) f(1) g(2) h(3) \quad \dots\dots (1)$$

where Σ_P indicates summation over all permutations of (123), and the coefficients F_0, F_1, F_2 are dependent on the set (f, g, h). For $m_T = \pm 1$, then, assuming f, g, h to be approximately normalized,

$$\left. \begin{aligned} P(\tau^+ \rightarrow \pi^+ \pi^+ \pi^-) &= 3F_2^2/5, \\ P(\tau^+ \rightarrow \pi^+ \pi^- \pi^+) &= (F_0/\sqrt{3} + F_1/2 + F_2/\sqrt{60})^2, \\ P(\tau^+ \rightarrow \pi^- \pi^- \pi^+) &= (F_0/\sqrt{3} - F_1/2 + F_2/\sqrt{60})^2, \\ P(\tau^+ \rightarrow \pi^+ \pi^0 \pi^0) &= (F_1/2 + \sqrt{3}F_2/\sqrt{20})^2, \\ P(\tau^+ \rightarrow \pi^0 \pi^+ \pi^0) &= (F_1/2 - \sqrt{3}F_2/\sqrt{20})^2, \\ P(\tau^+ \rightarrow \pi^0 \pi^0 \pi^+) &= (F_2/\sqrt{15} - F_0/\sqrt{3})^2, \end{aligned} \right\} \dots\dots (2)$$

so that the total probabilities for emission of mesons into the spatial state f, g, h are

$$\left. \begin{aligned} P(\tau^+ \rightarrow 2\pi^+ + \pi^-) &= \frac{2}{3} F_0^2 + \frac{1}{2} F_1^2 + \frac{19}{30} F_2^2 + \frac{2}{3\sqrt{5}} \mathcal{R}(F_0 * F_2); \\ P(\tau^+ \rightarrow \pi^+ + 2\pi^0) &= \frac{1}{3} F_0^2 + \frac{1}{2} F_1^2 + \frac{11}{30} F_2^2 - \frac{2}{3\sqrt{5}} \mathcal{R}(F_0 * F_2). \end{aligned} \right\} \dots\dots (3)$$

[The appearance of three parameters F_0, F_1, F_2 here contrasts with the result of Gamba (1952) for the total triple π -emission in nucleon-nucleon collisions. Gamba notes that for similar particles there are just two independent states of isotopic spin $T=1$ formed from three states of unit isotopic spin, and his result has just two constants. In fact our results (3) may be written in terms of two constants α, β where $\alpha = F_1^2 + (\sqrt{5}F_2 - 2F_0)^2/9$, $\beta = (2F_2 + \sqrt{5}F_0)^2/9$, though the three constants are necessary for more detailed considerations, as eqns. (2) show. For a given spatial state f, g, h two totally symmetric wave functions may be formed in addition to that totally symmetric in charge and space. If $[A, B]$ is the basis of a two-dimensional representation of the symmetric group S_3 on the isotopic spin variables, and $[X, Y]$ that on the space variables, the wave function which is totally symmetric for the interchange of both spatial and isotopic spin variables of the mesons is $AY + BX$. However, we may now permute f, g, h and, as $[X, Y]$ is a two-dimensional representation of S_3 , there must therefore be just two linearly independent symmetric wave functions of this type $[21] \times [21]$ (Littlewood 1950). Corresponding to these three totally symmetric wave functions, the general wave function for the final state requires three coefficients, as Van Hove's

method indicates. Each of the wave functions of type $[21] \times [21]$ contribute to the branching ratio in the same way, so that only two constants appear there.]

If x denotes the ratio $x = P(\tau^+ \rightarrow 2\pi^+ + \pi^-) / P(\tau^+ \rightarrow \pi^+ + 2\pi^0)$, then

$$\frac{x-1}{x+1} = \frac{1}{3} \frac{F_0^2 + 4F_2^2/5 + 4\mathcal{R}(F_0^* F_2)/\sqrt{5}}{F_0^2 + F_1^2 + F_2^2} = \frac{3}{5} \frac{\beta}{\alpha + \beta}. \quad \dots\dots (4)$$

This quantity is always positive and attains its greatest value of $\frac{3}{5}$ when $F_0 = \frac{1}{2}\sqrt{5}F_2$, $F_1 = 0$, so that $\dagger 1 \leq x \leq 4$. The total decay probability is obtained by integrating over all such spatial states allowed by energy and momentum conservation, and therefore the total decay probability for $\tau^+ \rightarrow \pi^+ + 2\pi^0$ is not less than one quarter of the total decay probability for $\tau^+ \rightarrow 2\pi^+ + \pi^-$, though it cannot exceed it. If no evidence can be found for a neutral π -meson decay of the τ -meson \ddagger , the hypothesis of charge independence for the τ -meson decay would then be untenable.

The charge independence hypothesis necessitates the existence of a τ^0 -meson, which will have competing decay processes $\tau^0 \rightarrow \pi^+ + \pi^- + \pi^0$ and $\tau^0 \rightarrow \pi^0 + \pi^0 + \pi^0$. With the same notation as before $P(\tau^0 \rightarrow \pi^0 + \pi^0 + \pi^0) = (\sqrt{5}F_0 + 2F_2)^2/30$, which may possibly vanish. As for the τ^\pm meson,

$$P(\tau^0 \rightarrow 3\pi^0) + P(\tau^0 \rightarrow \pi^+ + \pi^- + \pi^0) = F_0^2 + F_1^2 + F_2^2,$$

as charge independence requires, and $0 \leq P(\tau^0 \rightarrow 3\pi^0) \leq \frac{3}{7}P(\tau^0 \rightarrow \pi^+ + \pi^- + \pi^0)$.

The considerations above have neglected effects arising from the existence of the weak electromagnetic interactions which violate the charge independence hypothesis. In general, these will introduce small corrections so that conservation of isotopic spin would hold only as a good approximation, but, if the decay processes discussed above depended on the electromagnetic interaction for their very existence, isotopic spin conservation may be a very bad approximation, even though all other τ -meson interactions may be charge independent. However, such a situation would be suspected only if the decay processes could not proceed through charge independent interactions (e.g. the decay $B^0 \rightarrow \pi^0 + \pi^0$ for a scalar boson B^0 of unit isotopic spin, as discussed by Pais (1952)). Further, if such were the situation, one would expect that the process $\tau^\pm \rightarrow \pi^\pm + \pi^+ + \pi^- + \gamma$ would have higher probability than the process $\tau^\pm \rightarrow \pi^\pm + \pi^+ + \pi^-$, whereas the data show energy and momentum conservation to be satisfied by the three charged particles alone. \S The existence of the electromagnetic interactions does imply the possibility of competing γ -ray processes, such as $\tau^\pm \rightarrow \pi^\pm + 2\gamma$ or $\tau^\pm \rightarrow \pi^\pm + \pi^0 + \gamma$, with probabilities comparable with the established decay.

\dagger The part of χ_t^{mT} which is symmetric in (123) may be extracted by the operation of $\Sigma_p/6$ on χ_t^{mT} alone. After carrying this out, it may be seen that $\beta=0$ is the condition that (2) does not contain any of the wave function with symmetry $[3] \times [3]$. The other extreme value of x corresponds to $\alpha=0$ which, as one may easily check from the normalization of (2), occurs when (2) contains only this wave function.

\ddagger It is of interest to note that the ratios $P(\tau^+ \rightarrow 2\pi^+ + \pi^-) / P(\tau^+ \rightarrow \pi^+ + 2\pi^0)$ are given uniquely to be 1 or $\frac{1}{4}$ should the τ -meson have isotopic spin $T=2$ or 3 respectively, contrary to the present evidence.

\S These remarks would not be applicable if some intermediate heavy meson essential for the decay process was responsible for a failure of isotopic spin conservation, even with charge independent τ -meson couplings, as energy conservation would forbid appearance of this particle in a competing decay process; such a situation may in fact be the explanation of the contrast between the slow decay rate of the τ -meson and its high rate of production in cosmic rays, which Pais (1952) has recently emphasized.

In principle, these decay processes may be identified in cloud chamber observations from the number and orientation of the resulting cascade showers, but for the present purpose it is sufficient to note that these are additional to the process $\tau^\pm \rightarrow \pi^\pm + \pi^0 + \pi^0$, and increase the frequency of τ -decay events giving a single charged π -meson. Similar remarks apply even more strongly for the τ^0 -meson since, as for the decay of the π^0 -meson, the process $\tau^0 \rightarrow 2\gamma$ may possibly be the major mode of decay. However, apart from the special case noted above, these competing processes do not imply appreciable modification of the branching ratios given above for the π -meson processes. One definite conclusion can be stated: if the major interactions responsible for charged τ -meson decay are charge independent, the frequency of τ -meson decay giving rise to a single charged π -meson cannot be less than one-quarter of that for the established decay into three charged π -mesons.

ACKNOWLEDGMENTS

In conclusion, I wish to remark that the importance of this branching ratio came to my notice in consequence of a question put by Dr. E. P. George, and to thank Professor R. E. Peierls for his comments on the manuscript.

REFERENCES

- BROWN, R., CAMERINI, U., FOWLER, P. H., MUIRHEAD, H., POWELL, C. F., and RITSON, D. M., 1949, *Nature, Lond.*, **163**, 82.
 GAMBA, A., 1952, *Nuovo Cim.*, **9**, 1032.
 LEVI SETTI, R., and TOMASINI, G., 1952, *Nuovo Cim.*, **9**, 1244.
 LITTLEWOOD, D. E., 1950, *Group Characters*, 2nd edn. (Oxford : University Press).
 MENON, M. G. K., and O'CEALLAIGH, C., 1953, *Proc. Roy. Soc. A*, in the press.
 PAIS, A., 1952, *Phys. Rev.*, **86**, 663.
 VAN HOVE, L., 1952, *Rochester Report*, NYO 3074, unpublished.
 VAN HOVE, L., MARSHAK, R., and PAIS, A., 1952, *Phys. Rev.*, **88**, 1211.

The Diamagnetic Anisotropy of Large Aromatic Systems V: Interpretation of the Results

By R. McWEENY

Laboratories of Physical Chemistry and Coke Research, King's College,
University of Durham

MS. received 30th March 1953

Abstract. Calculated values of $\Delta\chi$ of a large number of molecules have been carefully examined: the diamagnetic anisotropy of a molecule is clearly related to certain features of its structure. A preliminary interpretation of this relationship is attempted, in the light of a revised valence bond theory at present being developed by the author. The observed effects of structural change are then discussed at a more fundamental level in terms of the system of bond orders.

Certain features of the work which are of importance in the study of carbon blacks and cokes are briefly pointed out.

§ 1. SOME GENERAL CONCLUSIONS

IN previous papers (McWeeny 1951 a, b, 1952, Berthier *et al.* 1951, 1952) calculations of the diamagnetic anisotropy $\Delta\chi$ (i.e. the π -electron susceptibility) have been made for a large number of aromatic molecules. The object of this final note is to point out how the dependence of $\Delta\chi$ upon structural characteristics may be interpreted.

A careful analysis of calculated $\Delta\chi$ values for nearly forty molecules indicates that in building up large aromatic systems from a central benzene ring the following principles are observed:

(i) Addition of a $=CH_2$ group to a ring always leads to a reduction in the original $\Delta\chi$. The addition of a number of groups may be almost equivalent in effect to removing the ring from the molecule.

(ii) Addition of either of the groups $-C\equiv CH$ or $-CH=CH_2$ has little effect on $\Delta\chi$.

(iii) Addition of complete rings, joined to the original system by *single* links (e.g. as in the polyphenyls) gives an increase in $\Delta\chi$ slightly less than would be expected in the absence of any conjugation across the bonds.

(iv) Addition of complete rings by condensation (at least one side of each added ring being present in the original system, e.g. as in the polyacenes) leads invariably to an increase in $\Delta\chi$ which (in units of $\Delta\chi_{\text{benzene}}$) is never appreciably less than unity per added ring and is often much greater. The increment per added ring may depend on the geometry of the molecule as a whole: if the added ring is in an 'exposed' position the increment is near to unity, but if it 'fits into' the original system, completing a roughly circular path round the periphery, the increment may be very much greater.

It will be remembered that (i) and (ii) were originally put forward as essentially empirical rules, based on the calculated susceptibilities of a small

number of systems (McWeeny 1951b): further calculations (Berthier *et al.* 1951) on styrene, α , α -diphenylethylene and a series of eight quinodimethanes suggest that these rules are indeed rather generally applicable. (iii) may be regarded as an extension of (i) and (ii), while (iv) is plausible on general grounds when we remember that, physically, the diamagnetic anisotropy arises from induced π -electron currents and that the larger the area of the available 'circuits' the larger will be the induced magnetic dipole. An essentially classical approach (Pauling 1936), however, leads to results in conflict both with experiment and with the predictions of wave mechanics (cf. McWeeny 1951b), and it is clearly desirable that any pictorial interpretation we may seek should emerge from a wave mechanical scheme.

§ 2. INTERPRETATION

All the results under discussion have been obtained using the molecular orbital (MO) method, but when attention is turned from numerical calculations to physical interpretation this method proves less attractive. This is hardly surprising when we remember that an individual MO has no direct pictorial significance; the MOs may be freely transformed among themselves without any effect on the complete many-electron wave function, and 'orbital' quantities (e.g. one-electron energies, charge distributions, susceptibility contributions etc.) arise simply from a convenient mathematical resolution of corresponding quantities associated with the system as a whole. In particular (cf. London 1937), the one-electron contributions to $\Delta\chi$ appear to be physically quite meaningless, showing an irregular variation of both magnitude and sign. The other main method of discussing electrons in

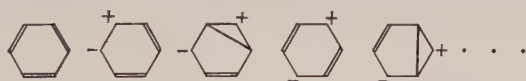


Fig. 1. Motion of free electron and 'hole' in the VB description of a ring current.

molecules, the valence bond (VB) method, is on the other hand more closely associated with a pictorial scheme, for the wave function is built up from many-electron 'structures' which correspond to states (though not eigenstates) of the system as a whole, and each such structure shows an accumulation of charge in certain regions and may consequently be represented by a diagram. In particular, we may set up structures which show a negative charge (excess electron) on one atom and a positive 'hole' on another: it is evident that a time-dependent process such as a current flow, may then be pictured as the time development of a superposition of such structures, e.g. a shift of emphasis from one structure to another in such a way that the negative charge goes in one direction while the positive hole goes in the opposite direction (see fig. 1).

Unfortunately the conventional VB method is fundamentally less satisfactory than the MO. Indeed, recent work by the author (a full account of which will appear elsewhere) shows that the theory may be put in a fundamentally satisfactory form only by complete reformulation;* but the whole interpretation of valence bond 'structures' and of bonding must then undergo a profound

* The VB calculations of $\Delta\chi$ by Brooks (1940) are open to the same criticism, but the revised theory substantiates, as we shall see, his general picture of 'hopping' currents.

change. It is not our intention to give here any account of the revised VB method, but for our present purpose it is desirable to mention the following features of the theory.

(a) VB 'structures', though indicated by the usual diagrams (showing links between atoms with 'paired' spins), are mathematically re-defined and acquire a new significance.

(b) A wave function corresponding to a bond between two atoms *must* contain *pairs* of structures which show a 'charge hop' across the bond (e.g. $\bullet=\bullet$ and $\overset{+}{\bullet}-\overset{-}{\bullet}$ *). Polar structures thus occur not as a *refinement* (e.g. Craig 1949) but as an integral part of the theory.

(c) A bond order may be defined which is large when structures associated with 'charge hopping' across the bond feature prominently in the wave function and which is small when they are less prominent, i.e. when they are energetically inhibited. Preliminary calculations show that the bond orders so calculated are in substantial agreement with those given by MO theory.

This formulation is novel in so far as bonding can be explained only by making *explicit* provision for an electron to 'hop' from one atom to another. The theory is particularly attractive in our present discussion because it provides a link between the properties of a system with and without an applied magnetic field: both the magnetic perturbation energy and the *bond orders* depend upon the relative importance of certain polar structures. Put very naïvely, the electrons responsible for bonding would normally hop back and forth across a bond with equal facility, but application of a field favours hopping in one direction, producing a net effect in the form of an induced ring current (cf. fig. 1). The description should not, of course, be taken too literally, but a formal solution of the appropriate secular problem, along the lines indicated by Brillouin (1933) and Wigner (1935), lends support to this picture and suggests a useful corollary to (c), namely:

(d) Magnetic perturbation terms occur which correspond to (generally) each π -electron circuit in the molecule (such terms containing certain integrals associated with the bonds comprising the circuit). The weight of a given term is determined essentially by the product of the orders of the bonds comprising the corresponding circuit.

Now direct numerical calculations of $\Delta\chi$ for polycyclic systems, comparable with those made in previous papers by the MO method, appear to be quite out of the question in VB theory, for the VB approach must recognize *explicitly* all the polar structures which are implicit in an MO treatment (and there may be millions of these: even for naphthalene there are several thousand). For the same reason a rigorous and general discussion of (d) presents considerable difficulty and cannot be entered upon here, but we shall make considerable use of (d) and, therefore, first confirm its approximate validity by examination of a number of one-ring systems whose bond orders are progressively changed by structural modifications.

Figure 2 shows four molecules in which the bond orders in the benzene ring are increasingly affected by substitution of external groups. Taking the product of orders of the ring bonds as a measure of the π -electron susceptibility we may

* The wave function for the first structure involves orbitals on both atoms, but in the second case the left-hand orbital is missing while the right-hand is doubly occupied.

predict $\Delta\chi$ (in units $\Delta\chi_{\text{benzene}}$); the results are given beneath each molecule. The numerical values obtained by the full MO analysis (Berthier *et al.* 1951, McWeeny 1951 b) are shown in brackets. The accuracy of our predictions is quite surprising, but the agreement may be substantiated by considering other molecules possessing two or more *non-overlapping* circuits, which might be expected to give independent contributions to $\Delta\chi$. In fig. 3 the comparison is extended to four such molecules, again with satisfactory results; the same general effect explains the somewhat unusual behaviour of the whole series of polyphenyls (McWeeny 1951 a). It is interesting to note that the classical approach of Pauling would give $\Delta\chi = 1.0$ for the molecules of fig. 2 and $\Delta\chi = 2.0$ for those of fig. 3. It is also worth noting that the π -electron susceptibility may be suppressed almost completely without any real approach to 'bond fixation'; even in the last molecule of fig. 2 (which, of course, is hypothetical) the ring (π -) bond order is still 0.385 (as compared with 0.667 for benzene).

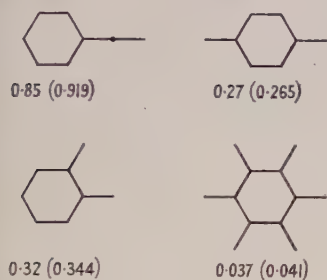


Fig. 2. Estimates of $\Delta\chi$ (one-ring molecules). (Bracketed values give the results of the complete MO calculation.)

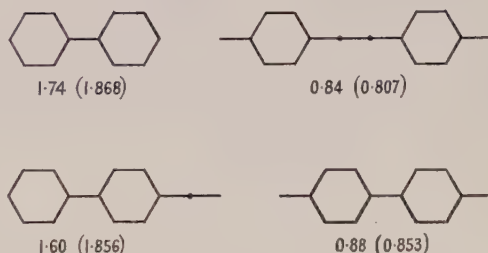


Fig. 3. Estimates of $\Delta\chi$ (two-ring molecules). (Bracketed values give the results of the complete MO calculation.)

Now the effect of structural modification upon the orders of bonds is fairly well understood, both from direct experience and from general theoretical considerations (cf. Coulson and Longuet-Higgins 1947, 1948). The success of our approach in simple cases encourages us to believe that the effect upon magnetic properties may be discussed with equal confidence. Indeed, in passing to highly condensed systems, we find a pleasing continuity of interpretation for, although numerical estimates are no longer feasible, the observations embodied in (i), (ii) and (iii) show that the lowering of ring bond orders, resulting from conjugation *outside* the ring, is accompanied *generally* by a depression of $\Delta\chi$, the effect upon both bond order and susceptibility being most marked when the external bonds are classically 'double'.

The actual growth of highly condensed polycyclic systems (cf. McWeeny 1951 b), by addition of complete rings, obviously presents a rather less clear-cut situation. But the obscurity arises only from the diversity of possible electron paths introduced by each modification and from the mathematical intractability of the problem; there is no reason to suppose that the underlying picture which accounts successfully for (i), (ii) and (iii) should be invalid in discussing (iv). Now the addition of a ring to an existing polycyclic system creates not only a new *one-ring* circuit but a variety of *many-ring* circuits: the first inference from (iv) is that when the ring is in an 'exposed' position the net effect is the addition of one new benzene-like ring current, new *many-ring* currents, or modifications

of those already present, being of secondary importance. Two examples of additions of this kind are shown in fig. 4(a), the $\Delta\chi$ increments per added ring being shown in each case and being near to unity. In contrast, fig. 4(b) shows the effect of adding rings in such a way that 'gaps' are filled, the systems thereby acquiring a regular peripheral circuit of large area. The very much greater increment per ring is presumably associated with the realization of many-ring paths of large area and *regularity*, for paths of large area are introduced also in the examples of fig. 4(a), without making any apparent contribution, but they are very irregular in form. This is intuitively satisfactory, and, moreover, is consistent with our theoretical picture, for the perturbation energy associated with a molecular circuit, whilst depending on the square of the circuit area (in

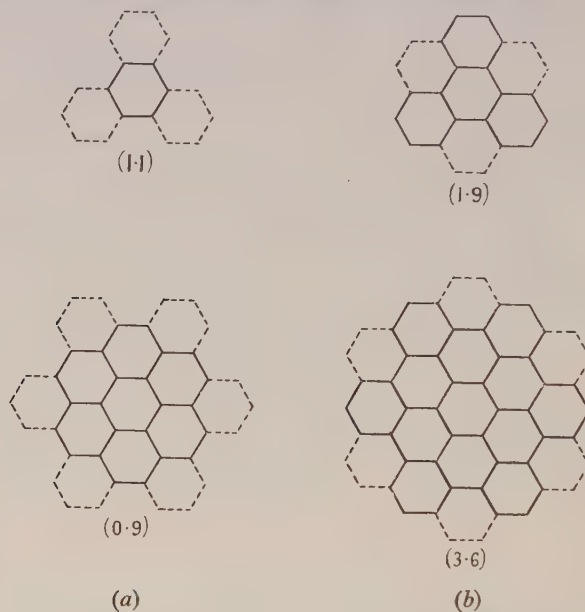


Fig. 4. Effect of ring additions. (Added rings are indicated by broken lines. The figure in brackets gives the $\Delta\chi$ increment per added ring.)

MO and VB theory alike), will be reduced, according to (d), by an increasing number of bond order factors; the most significant contributions would thus be associated with the roughly circular paths for which this number is least.

§ 3. CONCLUSION

We have now seen how the 'empirical' rules suggested by a large number of numerical results admit a qualitative theoretical interpretation in terms of the picture provided by a revised VB theory. It is useful to put our conclusions in the following form:

(i) Addition of side groups to a polycyclic conjugated system is accompanied by a depression of $\Delta\chi$ which is greater the greater the reduction in ring bond orders. For single rings (or systems of singly connected rings) the final $\Delta\chi$ may be quantitatively estimated, being proportional (for each ring) to the product of orders of the ring bonds. For more complex systems the effect may be qualitatively discussed: if the bond orders in a ring are seriously depressed

(e.g. by addition of a classically 'double-bonded' group) the effect is likely to be somewhat less than would arise from striking out the affected ring; if they are not seriously changed (e.g. by a 'single-bonded' group) the magnetic effect is correspondingly smaller.

(ii) Addition of further rings by condensation (i.e. *not* by single linkages) is accompanied by an increase in $\Delta\chi$ near to unity for each added ring provided no large roughly circular π -electron circuits are thereby realized (i.e. for 'exposed' rings). But when such circuits *are* realized the increase must be supplemented by many-ring contributions which play an increasing part with increasing circuit area. For all known hydrocarbons upper limits to this effect are almost certainly indicated by the results for the system of nearly circular molecules of up to nineteen rings (McWeeny 1951 b).

For reasons which are well appreciated, the calculations in this series of papers have been confined to a particular class of molecule ('alternant' hydrocarbons). There seems to be no fundamental objection to the application of our qualitative picture to other types of molecules (containing for example odd-membered rings and hetero-atoms), but the simple MO treatment is open to considerable suspicion in such cases, and it would be difficult to justify an extension of the discussion. Berthier *et al.* have, however, made calculations in this field: they give, for example, the result $\Delta\chi \sim 0.1$ for fulvene, and it is satisfying to note that a low value, $\Delta\chi \sim 0.3$, is also predicted using the (equally uncertain) bond order values.

Finally it is worth mentioning the bearing of this work upon the properties of cokes and carbon blacks (see McWeeny 1951 a) which consist largely of graphite fragments of 'molecular' dimensions (often much less than 100 Å in diameter).^{*} In discussing such systems interest centres upon $\Delta\chi/n$, n being the number of carbon atoms in a particle, for an average value of this quantity becomes (as n becomes large) a measure of the mass susceptibility of the material. Our results indicate beyond reasonable doubt that increasing condensation of the 'molecules' to a disc-like form favours a high mass susceptibility. In particular we may cite two examples in which first 42 and then 54 atoms condense by rearrangement, from an open polyphenyl chain to a hexagonal disc. These processes and the accompanying values of $\Delta\chi/n$ (in units of $(\Delta\chi/n)_{\text{benzene}}$) are set out below:

7-ring polyphenyl	→ 10-ring polyacene	→ 13-ring hexagonal molecule
0.89	1.90	2.19
9-ring polyphenyl	→ 13-ring polyacene	→ 19-ring hexagonal molecule
0.88	1.96	4.07

The increase is due partly to an increase in number of rings, by more 'efficient' arrangement of atoms, and, particularly in the second case, to the simultaneous formation of regular circuits of large area. A tentative estimate, based on the $\Delta\chi$ values of the first three molecules of the 'disc-like' series, suggests that growth of such particles to a diameter of 20–25 Å might account for up to a quarter of the susceptibility value associated with complete graphitization. On the other hand *linear* growth, as of the polyphenyl and polyacene chains, might proceed without significant increase of the mass susceptibility.

^{*} A broader discussion of structure and magnetic properties, including temperature dependence etc., will be given elsewhere.

REFERENCES

- BERTHIER, G., *et al.*, 1951, *J. Phys. Radium*, **12**, 717 ; 1952, *Ibid.*, **13**, 15.
BRILLOUIN, L., 1933, *J. Phys. Radium*, **4**, 1.
BROOKS, H., 1940, *J. Chem. Phys.*, **8**, 939.
COULSON, C. A., and LONGUET-HIGGINS, H. C., 1947, *Proc. Roy. Soc. A*, **191**, 39 ; 1948, *Ibid.*, **192**, 16, **193**, 447, **195**, 188.
CRAIG, D. P., 1949, *Proc. Roy. Soc. A*, **200**, 272.
LONDON, F., 1937, *J. Phys. Radium*, **8**, 397.
MCWEENY, R., 1951 a, *Proc. Phys. Soc. A*, **64**, 261 ; 1951 b, *Ibid.*, **64**, 921 ; 1952, *Ibid.*, **65**, 839.
PAULING, L., 1936, *J. Chem. Phys.*, **4**, 673.
WIGNER, E. P., 1935, *Math. naturw. Anz. ungar. Akad. Wiss.*, **53**, 477.

A Search for Polarization of High Energy Neutrons

By J. M. DICKSON AND D. C. SALTER

Atomic Energy Research Establishment, Harwell, Didcot, Berks.

Communicated by J. M. Cassels; MS. received 24th March 1953

Abstract. An attempt has been made to detect polarization effects in n-p scattering. A beryllium target bombarded by protons was used to produce 'polarized' neutrons, and a search was made for asymmetry when these neutrons were scattered by hydrogen. A polarization effect of $-1.6\% \pm 2.1\%$ was observed, which is to be compared with a predicted effect of $+6\%$. It is concluded that either (i) little polarization is produced in n-p scattering or (ii) the polarization effect is smeared out in some way when the elementary collision takes place inside a beryllium nucleus.

§ 1. INTRODUCTION

THE results of high energy n-p scattering experiments all show approximate forward-backward symmetry in the scattering, with a broad minimum near 90° (Hadley, Kelly, Leith, Segrè, Wiegand and York (1949) at 40 and 90 mev, Fox (1950) at 90 mev, Brueckner, Hartsough, Hayward and Powell (1949) at 90 mev, Randle, Taylor and Wood (1952) at 156 mev, Guernsey, Mott and Nelson (1952) at 220 mev and Kelly, Leith, Segrè and Wiegand (1950) at 260 mev). Potential models using only central forces tend to predict angular distributions which are too flat in the 90° region, and the introduction of tensor forces (Christian and Hart 1950) or spin-orbit coupling (Case and Pais 1950) results in a better fit with the experimental angular distribution. The interference terms in the scattering produced by these non-central potentials give rise to polarization effects (Wolfenstein 1949, 1951) which should be detectable in a double scattering experiment. Figure 1 is a schematic plan of such an 'n-n-n'

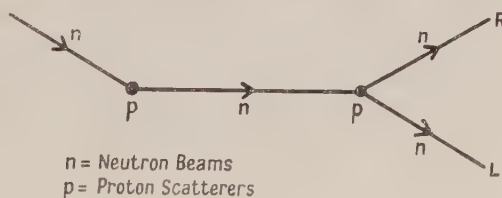


Fig. 1. Schematic n-n-n experiment.

experiment. The initially unpolarized neutrons which are scattered twice to the right by the proton targets and counted at R, should be greater in number than those which are scattered first to the right and then to the left, and counted at L. The percentage polarization effect in this type of experiment is conveniently defined as $W = 100 (R/L - 1)$, where R and L are the counting rates at R and L respectively. Central forces alone produce no polarization, so an experimentally observed effect would be clear evidence for the existence of non-central forces in the n-p interaction.

Unfortunately a true double scattering experiment involving two n-p events is very difficult, if not impossible, with present experimental resources. However, it seemed possible that polarized neutrons could be obtained by high energy proton bombardment of, for example, a beryllium target. In some respects neutron production at high energies can be regarded as the result of elementary n-p collisions inside a relatively 'transparent' nucleus. Wouters (1951) used lithium deuteride and lithium hydride targets in the Berkeley 184-in. cyclotron as neutron sources and observed a polarization effect of $+6.5 \pm 3.6\%$ with LiD and $+1.4 \pm 4.9\%$ with LiH for scattering angles of 30° in laboratory space (all errors quoted in this paper are standard deviations). The effect predicted by Swanson (1951) from the Christian and Hart tensor force model, was $+12^\circ$ for a true double n-p scattering at the energies and the angles of scattering in Wouters' experiment.

This paper describes an attempt to measure the polarization of neutrons produced by the bombardment of a beryllium target by protons in the Harwell cyclotron.

§ 2. METHOD AND APPARATUS

Principle

An attempt was in fact made to observe a true double n-p scattering, with the apparatus shown in fig. 2. The first scatterer was placed close to the target inside the cyclotron magnet gap. Neutrons scattered at 30° and collimated through a

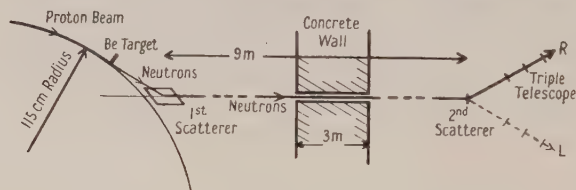


Fig. 2. Attempted double scattering experiment (not to scale).

hole in a concrete wall 3 m thick underwent a second scattering in a polyethylene scatterer, at a distance of about 9 m from the cyclotron. The protons produced at 30° to the secondary neutron beam were counted in a triple coincidence scintillation counter telescope. The experiment was not successful because the triple coincidence counting rates with and without the first scatterer in position were practically equal. Some improvement might have been achieved by increased shielding, better geometry and faster electronic circuits, but the chance of success was rather small.

The experiment was then entirely redesigned (fig. 3). Two beryllium targets were set up in the cyclotron in line with one of the collimating holes in the 1.8 m thick shielding wall, so that the neutrons selected by the collimator were emitted at 20° to the circulating proton beam bombarding one target and at 0° for the other target. Either a 'polarized' neutron beam from the 20° target or an unpolarized beam from the 0° target could be selected. The polarization of the neutron beam was analysed by scattering protons into two double coincidence telescopes at $\pm 30^\circ$ to the neutron beam. The plane of the second scattering could be rotated relative to the plane of the first scattering. The maximum effect should occur when the two planes coincide and the effect should be zero when the angle between the two planes is 90° .

When the second scattering is in a horizontal plane, the scattering of protons into the telescope R corresponds to Swanson's $\phi_2 = 0$ and into L to $\phi_2 = \pi$. The right/left ratio for the 20° target is then given by

$$\left(\frac{R}{L}\right)_{20} = k \frac{1 + P_1 P_2}{1 - P_1 P_2} \simeq k(1 + 2P_1 P_2)$$

where P_1, P_2 are the coefficients defined by Swanson. The factor k , which is equal to $(R/L)_0$, takes account of unintentional angular misalignments or differences in solid angles of the counter telescopes. The normalized right/left asymmetry is then

$$\left(\frac{R}{L}\right)' = \left(\frac{R}{L}\right)_{20} / \left(\frac{R}{L}\right)_0 = 1 + 2P_1 P_2 = 1 + \frac{W}{100}$$

where W is the percentage polarization effect.

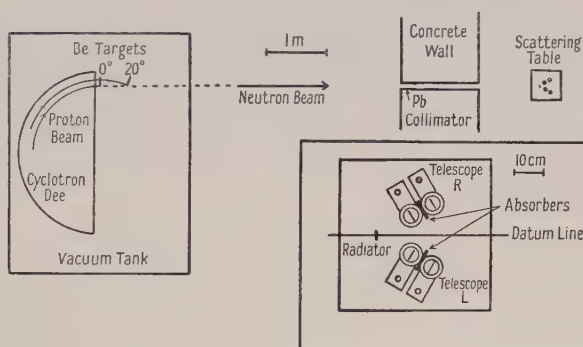


Fig. 3. Final experimental set up. The details of the scattering geometry are to scale, and the inset shows the layout of the counter heads on the scattering table.

When the second scattering is in a vertical plane, scattering upwards corresponds to $\phi_2 = \frac{1}{2}\pi$ and downwards to $\phi_2 = -\frac{1}{2}\pi$. The up/down ratios for the 0° and 20° targets should then be equal and hence $W = 0$ in this case.

Scattering Geometry

Figure 3 also shows the scattering geometry in detail. The axis of the collimating hole in the 1.8 m thick shielding wall was taken as the datum line for the visual alignment of the apparatus by means of a theodolite. The bombarded edges of the targets were set on the datum line and adjusted in position to obtain the required first scattering angles of 0° and 20° . Both targets could be moved accurately in and out of the proton beam by a simple electrical device.

The second scatterer or radiator and the two counter telescopes were mounted on an adjustable table, which could be rotated round the datum line as axis. Cross wires could be fitted in order to align the table by means of the theodolite. The radiator was mounted between two thin aluminium rods and was adjustable in position. The counter telescopes each consisted of two scintillation counters which were rigidly mounted on the scattering table, so that the centre of scintillators, the centre of the radiator and the datum line were all in the same plane. The angles between the datum line and the lines joining the centres of the scintillators to the centre of the radiator were fixed at 30° .

The defining aperture in the collimator consisted of a 2.54 cm diameter hole in a cylinder of lead 45 cm long, which fitted inside a brass tube in the shielding wall. The neutron beam striking the radiator was 3.5 cm in diameter and nearly circular; the slight departure from a true circle was due to the finite height of the neutron source.

The visual alignment was checked by exposing an x-ray film (with polyethylene intensifier) in the neutron beam at the position of the radiator. Small misalignments were discovered with the first films and these were corrected and checked. The radiator was situated centrally in the neutron beam from both the 0° and 20° targets for all the films exposed before, during, and after, the main experiments.

Targets, Radiators, Scintillators and Absorbers

The targets were rectangles of beryllium, 2.54 cm \times 5.08 cm, and were bombarded on one of the 2.54 cm edges. The thickness of the 0° target was 1.1 gm cm⁻² and the 20° target was 0.25 g cm⁻².

The hydrogen for the second scattering was obtained by using polyethylene and carbon radiators of equal stopping power and correcting for the inequality of the number of carbon atoms in the two radiators. The ratio of the molecular stopping powers of polyethylene and carbon was taken as 1.4. Both radiators were cylinders of 2.54 cm diameter, the polyethylene being 0.82 g cm⁻² thick and the carbon 0.98 g cm⁻².

The scintillators were machined from plastic scintillator (1.5% tetraphenyl-butadiene in polystyrene, decay time 6×10^{-9} sec) to the dimensions 4 cm \times 4 cm \times 0.4 cm and were carefully polished. They remained undisturbed on the photomultiplier cathodes during the whole course of the experiment. The distances between the centre of the radiator and the first and second scintillators were 13 cm and 21 cm respectively. The aperture of the telescopes was defined by the second scintillator, which accepted protons scattered at angles between 24.5° and 35.5° from the centre of the radiator. The total variation in azimuthal scattering angle for all parts of the radiators was 22° to 38°.

The total absorber in each counter telescope (including half the radiator thickness) was equivalent to 6.7 g cm⁻² of aluminium.

Proton and Neutron Energies

The proton and neutron energies used in this experiment are summarized in table 1. The energy loss of the highest energy protons in the first scintillator was about 3 mev and the minimum detectable proton energy in the second scintillator was estimated as 10 mev (corresponding to a proton of 77 mev entering the first scintillator). The effective energy of the internal proton beam was calculated from the previously measured single traversal spectrum (Dickson and Salter 1953) and the calculated number of traversals of the targets (Cassels, Dickson and Howlett 1951, Dickson 1951).

Scintillation Counters and Coincidence Units

The counting system was designed for simplicity in construction and tolerance in operation together with a short resolving time. The counter heads and coincidence units have already been described (Dickson, Salter, Gunnill, Dolley and Cassels 1952). The resolving time of the coincidence units was 8×10^{-9} second.

The counter telescopes were set on counting rate plateaux by adjusting the gain of each photomultiplier so that all protons which produced a coincidence gave a certain minimum output pulse from the photomultiplier anodes. The photomultiplier e.h.t. voltages were then raised by 50 v above this threshold level. Electron transit time delays in the photomultipliers and other incidental unbalanced delays in the inputs to the coincidence units were balanced by introducing additional delay cables between the counter heads and the coincidence units. Counting rate plateaux were plotted with constant differences in the e.h.t. voltages of each pair of counters and were found to be flat up to 200 to 300 v above the threshold voltages.

Table 1

		0°	20°
Proton energy, internal cyclotron beam (mev)	max.	134	150
	effective	120	135
Neutron energy, if the production process is assumed to be equivalent to free n-p scattering (mev)	max.	134	132
	min.	87	87
	mean	121	120
Recoil proton energy (mev)	max.	116	114
	min.	77	77
	mean	91	90

Beam Monitor

The cyclotron beam current was monitored by a boron trifluoride counter which was immersed in a block of paraffin wax and placed in a position shielded from the cyclotron targets by about 3 m of concrete. The counting rate of this monitor was known to be linear with beam current.

Random Counting Rate

The random coincidence counting rate was measured by delaying the pulses from one counter head to its coincidence unit by an additional time which was an integral number of radio-frequency periods. Equal random rates were observed for 50 and 200×10^{-9} sec delays (radio-frequency ~ 20 Mc/s). Since the random rate depends on the product of the single channel rates (i.e. the square of the beam current), while the real rate is proportional to the beam current, then the ratio of the random to real rates is also proportional to the beam current. The measured ratio of the random to real counting rates was 0.025 at the normal full beam and was proportional to the monitor counting rate within the experimental errors. The beam was maintained at about 30% of the full beam during the main experiment, thus reducing the random rate to less than 1% of the real rate.

Collection of Data

The experiment consisted essentially of the measurement of the ratio of the number of proton recoils counted in the telescope R (see fig. 3) to the number in telescope L. The carbon effect was cancelled out in the usual way using the counting rates observed for the carbon radiator and background.

One cycle of the experiment consisted of twelve observations of the coincidence counting rates for the polyethylene and carbon radiators and background for 0° and 20° targets and second scattering angles of right 30° and

left 30° , together with six observations of the monitor counting rate. The results of one cycle are set out in full in table 2. R and L are the normalized hydrogen counting rates for the right and left telescopes respectively and the subscripts 0 and 20 refer to the angle of the first scattering.

Table 2

Radiator	Target	Time (min)	Monitor	Right	Left	Right Monitor	Left Monitor
Polyethylene	0	15	23744	5766	5543	242.8 ± 3.6	233.4 ± 3.5
Polyethylene	20	25	61370	5404	5088	88.1 ± 1.25	82.9 ± 1.21
Carbon	0	7	10887	1035	1023	95.1 ± 3.1	94.0 ± 3.1
Carbon	20	12	26412	1071	964	40.5 ± 1.26	36.5 ± 1.20
Background	0	2	3452	118	138	34.2 ± 3.2	40.0 ± 3.5
Background	20	4	9506	190	177	20.0 ± 1.46	18.6 ± 1.43

$$\begin{aligned}
 R_0 &= 165.1 \pm 2.6\% & R_{20} &= 53.5 \pm 3.0\% \\
 L_0 &= 154.8 \pm 2.8\% & L_{20} &= 51.5 \pm 3.0\% \\
 \left(\frac{R}{L}\right)_0 &= 1.067 \pm 3.8\% & \left(\frac{R}{L}\right)_{20} &= 1.039 \pm 4.2\% \\
 \left(\frac{R}{L}\right)' &= 0.974 \pm 5.7\% & W &= -2.6 \pm 5.6\%
 \end{aligned}$$

§ 3. RESULTS

Second Scattering Horizontal

The counting cycle just described was repeated 29 times with exactly the same target, radiator and counter positions in each cycle. The polarization effect W was calculated for each cycle, giving 29 values whose average was -1.6° . The internal consistency of the counting errors was checked by three calculations of the standard deviation σ of this result: (i) the total number of counts gave $\sigma = 1.02\%$, (ii) the average R_0 , etc. and the variance of each (from the 29 values of R_0 etc.) were calculated giving $\sigma = 1.4\%$ and (iii) the 29 values of W gave $\sigma = 0.90\%$. The high value obtained by method (ii) shows that some systematic errors cancelled out when R/L ratios were calculated.

The asymmetry of the scattering from the carbon radiator was calculated for each cycle, giving 29 values of W_c whose average was $+2.8 \pm 3\%$ (standard deviation calculated from the 29 results).

Second Scattering Vertical

With the scattering table rotated to the vertical scattering position the up/down ratio for the 0° target was 1.025 ± 0.015 and for the 20° target 1.006 ± 0.017 . The 'polarization' effect was $-1.9 \pm 2\%$. These are the averages for nine counting cycles. These measurements were performed as a check on the behaviour of the counting system in conditions where no polarization was expected.

Misalignment Tests

The alignment of the targets, radiators and counters was carried out carefully before the main experiment and there was no reason to believe that any part of the apparatus was displaced at any time during the experiment. To obtain an estimate of the systematic errors due to small misalignments of various parts of the apparatus, four series of counting cycles were performed with the counter

telescope and the 20° target misaligned by known small amounts. The four tests were:

(i) The radiators were placed at 80° to the neutron beam, that is in 10° misalignment, while retaining the correct alignment of the telescope.

(ii) The second scattering angles were changed by 1° each, to 29° right and 31° left, by rotating the scattering table through 1° about a vertical axis through the centre of the radiator. The radiators were placed at 90° to the neutron beam.

(iii) The scattering table was moved 0.5 cm to one side so that the axis of the table was still parallel with the neutron beam, but one edge of the radiator coincided with the edge of the neutron beam.

(iv) The 20° target was moved 0.5 cm away from the datum line; a misalignment of 0.1 cm was easily detectable by the theodolite.

The results are summarized in table 3.

Table 3

Misalignment	No. of cycles	$\left(\frac{R}{L}\right)_0$	$\left(\frac{R}{L}\right)_{20}$	$\left(\frac{R}{L}\right)'$
None	29	1.061	1.043	0.984 ± 0.010
(i)	4	1.019	1.042	1.022 ± 0.027
(ii)	6	1.410	1.481	1.050 ± 0.022
(iii)	6	1.082	1.104	1.021 ± 0.022
(iv)	6	1.098	1.054	0.960 ± 0.022

The change in $(R/L)'$ per unit of misalignment can be conveniently expressed: (i) 0.0038/degree, (ii) 0.066/degree, (iii) 0.074/cm, (iv) 0.048/cm. The errors in alignment of these four sections of the apparatus are estimated to have standard deviations of (i) $\pm 2^\circ$, (ii) $\pm 0.2^\circ$, (iii) ± 0.1 cm and (iv) ± 0.1 cm which give errors in $(R/L)'$ of (i) ± 0.0076 , (ii) ± 0.0132 , (iii) ± 0.0074 and (iv) ± 0.0048 . The square root of the sum of the squares of these errors is ± 0.0176 , which was regarded as the systematic error of the experiment and combined with the counting error. The final value of $(R/L)'$ then becomes 0.984 ± 0.021 .

§ 4. DISCUSSION

The polarization effect $W = -1.6 \pm 2.1\%$ measured in this experiment is consistent with the view that the neutrons produced at 20° from a beryllium target by high energy protons are not polarized. The negative sign of the result is not regarded as having any real significance since it would imply that P_1 and P_2 are of opposite sign, which is not very likely. The probability that the result could be positive is 0.2, and the probability that it is greater than $+1\%$ is 0.1, greater than $+2\%$ is 0.05, and greater than $+3\%$ is 0.01. The experimental value of W is therefore significantly different from the value of $+6\%$ which Swanson's theory suggests for the energies and the angles of scattering used in this experiment.

There are two possible explanations of this result. Either the polarization produced in free n-p scattering (at about 130 mev) is less than Swanson's theory predicts, or the polarization is smeared out in some way when the n-p scattering takes place inside a beryllium nucleus. The latter conclusion would be interesting in view of the work of Mandl and Skyrme (1952) and Strauch and Hofmann (1952). The neutron yield and spectrum from a beryllium target bombarded by protons, as calculated by Mandl and Skyrme for a 'transparent' nucleus, gave very

tolerable agreement with the experimental results (Randle, Cassels, Pickavance and Taylor 1953). Strauch and Hofmann have shown that the peak in the neutron spectrum produced by the bombardment of beryllium by 112 mev protons behaves in a way that suggests that it arises from essentially free n-p scattering in the beryllium nucleus.

The present result is not in very direct conflict with that of Wouters who, as mentioned earlier, observed an effect of $6.5 \pm 3.6\%$ with a lithium deuteride target, under conditions such that a 12% effect was expected. Wouters attributed his apparently low result to the fact that the majority of his neutrons came from the lithium component of the target. He suggests that neutrons from lithium are unpolarized, because of internal smearing, and this is given some support, though of small statistical significance, by his results for a lithium hydride target.

It seems clear that further progress in deciding between the two explanations can only be made by an experiment to determine accurately the effect of a deuterium target alone.

ACKNOWLEDGMENTS

We are indebted to Professors R. E. Peierls and M. H. L. Pryce for bringing this problem to our attention, and to Drs. T. G. Pickavance and R. H. Dalitz for helpful discussions. We are especially grateful to Dr. J. M. Cassels for his guidance throughout the experiment. We also wish to thank the cyclotron operating crew for their willing co-operation. This paper is published by permission of the Director of the Atomic Energy Research Establishment, Harwell.

REFERENCES

- BRUECKNER, K., HARTSOUGH, W., HAYWARD, E., and POWELL, W. M., 1949, *Phys. Rev.*, **75**, 555.
CASE, K. M., and PAIS, A., 1950, *Phys. Rev.*, **80**, 203.
CASSELLS, J. M., DICKSON, J. M., and HOWLETT, J., 1951, *Proc. Phys. Soc. B*, **64**, 590, 719.
CHRISTIAN, R. S., and HART, E. W., 1950, *Phys. Rev.*, **77**, 441.
DICKSON, J. M., 1951, *Proc. Phys. Soc. B*, **64**, 615.
DICKSON, J. M., and SALTER, D. C., 1953, *Brit. J. Appl. Phys.*, **4**, 175.
DICKSON, J. M., SALTER, D. C., GUNNILL, O., DOLLEY, P. E., and CASSELLS, J. M., 1952, *Atomic Energy Research Establishment Report G/R 1039*.
FOX, R. H., 1950, *University of California Radiation Laboratory Report*, UCRL 867.
GUERNSEY, G., MOTT, G., and NELSON, B. K., 1952, *Phys. Rev.*, **88**, 15.
HADLEY, J., KELLY, E., LEITH, C., SEGRÈ, E., WIEGAND, C., and YORK, H., 1949, *Phys. Rev.*, **75**, 351.
KELLY, E., LEITH, C., SEGRÈ, E., and WIEGAND, C., 1950, *Phys. Rev.*, **79**, 96.
MANDL, F., and SKYRME, T. H. R., 1952, *Proc. Phys. Soc. A*, **65**, 101.
RANDLE, T. C., CASSELLS, J. M., PICKAVANCE, T. G., and TAYLOR, A. E., 1953, *Phil. Mag.*, **44**, 425.
RANDLE, T. C., TAYLOR, A. E., and WOOD, E., 1952, *Proc. Roy. Soc. A*, **213**, 392.
STRAUCH, K., and HOFMANN, J. A., 1952, *Phys. Rev.*, **86**, 563.
SWANSON, D. R., 1951, *Phys. Rev.*, **84**, 1068.
WOLFENSTEIN, L., 1949, *Phys. Rev.*, **76**, 541 ; 1951, *Ibid.*, **82**, 308.
WOUTERS, L. F., 1951, *Phys. Rev.*, **84**, 1069.

Matrix Elements in Radiative Transitions

By R. J. BLIN-STOYLE

The Clarendon Laboratory, Oxford

MS. received 31st March 1953

Abstract. The matrix elements occurring in the theory of radiative transitions of electrons and positrons for a case of spherical symmetry are expanded in the general case as a series of radial integrals with known coefficients.

§ 1. INTRODUCTION

THE treatment of problems dealing with the radiative transitions of electrons and positrons generally involves the evaluation of a matrix element having the form $\mathfrak{M} = \int \Psi^* (V + \boldsymbol{\alpha} \cdot \mathbf{A}) \Phi d\tau$, where Ψ and Φ are Dirac wave functions, $\boldsymbol{\alpha}$ is the usual Dirac operator and V and \mathbf{A} are the scalar and vector potentials of the electromagnetic field (Heitler 1936a). In a case of spherical symmetry† Ψ , Φ , V and \mathbf{A} are decomposed into spherical waves and \mathfrak{M} then reduces to a complicated series of angular and radial integrals.

It has been found possible to write \mathfrak{M} for all types of process in the general form $\mathfrak{M} = \sum_n a_n R_n$ where the R_n are radial integrals and the coefficients a_n are known. Writing \mathfrak{M} in this form at once simplifies the setting up of a problem for detailed computational purposes since no account has to be taken of the angular integrations (which have, in fact, already been performed) and the form of the radial integrations can be seen immediately.

§ 2. CALCULATION

The method of calculation is similar to that set out by Spiers and Blin-Stoyle (1952) in a paper dealing with the theory of β -decay.

The Dirac wave function for a particle with total angular momentum quantum numbers j, m can be expressed in spherical polar form in the following way

$$\Psi_{ja}^m(\mathbf{r}, \sigma, \beta) = c \begin{smallmatrix} j & j - \frac{1}{2} & a & \beta \\ m & m & \sigma & \sigma \end{smallmatrix} f_{j+\frac{1}{2}a\beta}^{\beta a}(r) Y_{j+\frac{1}{2}a\beta}^m(\theta\phi). \quad \dots\dots(1)$$

Here c is a vector addition coefficient (Racah 1942) and the spherical harmonic is defined with the Condon and Shortley (1935) choice of phase factors. The four components of each wave function are characterized by the variables $\beta = \pm 1$, $\sigma = \pm \frac{1}{2}$ and a takes the values ± 1 corresponding to the two possible types of solution. The radial function f is determined by the particular problem under consideration.

The electromagnetic potential can also be decomposed into spherical waves each corresponding to the total angular momentum quantum numbers j, m (Heitler 1936b). Inspection shows that each spherical wave can be written in the form

$$A_j^m(\mathbf{r}, s, \lambda) = \sum_l a_l(j, s) c_{m+\lambda-\lambda}^{jls} g_l(r) Y_l^{m+\lambda}(\theta\phi), \quad \dots\dots(2)$$

† Such cases are, for example, internal conversion, internal pair creation, inner bremsstrahlung, atomic transitions, etc.

where $s=0, 1$ corresponds to the scalar and vector potentials respectively.† $\lambda=0$ for $s=0$ whilst for $s=1$, $\lambda=-1, 0, 1$ and refers to the three components of the vector potential.

The matrix element for a given transition then has the following form

$$\mathcal{M}_{j_1 m_1 a_1; j_2 m_2 a_2}^{jm} = -\sqrt{3} \sum_{\sigma_1 \sigma_2 \lambda s \beta_1 \beta_2} \int \Psi_{j_1 a_1}^{* m_1} c_{\lambda}^{011} [\alpha_{\lambda}(s)]_{\beta_1 \beta_2}^{\sigma_1 \sigma_2} A_j^m(\mathbf{r}, s, -\lambda) \Psi_{j_2 a_2}^{m_2} d\tau, \quad \dots (3)$$

where $\alpha_{\lambda}(1)$ represents the three components of the Dirac operator α and $\alpha_{\lambda}(0) = \delta_{\lambda 0}$.

In order to simplify the above matrix element it is convenient to deal with the emission (or absorption) of both Dirac particles and to characterize the created (or absorbed) two particle system by the total angular momentum quantum numbers J, M . This can be achieved by introducing the operator $D(= -i\beta\alpha_y)$ defined by Furry (1937, 1938) together with an appropriate vector addition coefficient. Thus

$$\mathcal{M}_{j_1 a_1; j_2 a_2}^{JM*} = -\sqrt{3} \sum_{m_1 \sigma_1 \sigma_2 \lambda s \beta_1 \beta_2} c_{m_1 M - m_1}^{J j_1 j_2} \int \Psi_{j_1 a_1}^{m_1} c_{\lambda}^{011} [D\alpha_{\lambda}(s)]_{\beta_1 \beta_2}^{\sigma_1 \sigma_2} A_j^{M*}(\mathbf{r}, s, -\lambda) \Psi_{j_2 a_2}^{m_2 \dagger} d\tau, \quad \dots (4)$$

where \dagger indicates that the positive and negative energy levels have been interchanged.

Substituting from (1) into (4) and using the following relation between vector addition coefficients and spherical harmonics (Spiers and Blin-Stoyle 1952)

$$\begin{aligned} \sum_{m_1} c_{m_1 M - m_1}^{J j_1 j_2} c_{m_1 - \sigma_1}^{j_1 l_1 \frac{1}{2}} c_{M - m_1 - \sigma_2}^{j_2 l_2 \frac{1}{2}} Y_{l_1}^{m_1 - \sigma_1}(\theta\phi) Y_{l_2}^{M - m_1 - \sigma_2}(\theta\phi) \\ = \sum_{S=0,1} A_{j_1 j_2}^{l_1 l_2}(JLS) c_{M - \sigma_1 - \sigma_2}^{JLS} c_{\sigma_1 \sigma_2}^{S \frac{1}{2} \frac{1}{2}} Y_L^{M - \sigma_1 - \sigma_2}(\theta\phi) \quad \dots (5) \end{aligned}$$

$L = l_1 + l_2, \dots |l_1 - l_2|$

gives

$$\begin{aligned} \mathcal{M}_{j_1 a_1; j_2 a_2}^{JM*} = -\sqrt{3} \sum_{\lambda \sigma_1 \sigma_2 \beta_1 \beta_2 s L} a_l(j_s) A_{j_1 j_2}^{l_1 l_2}(JLS) c_{M - \sigma_1 - \sigma_2}^{JLS} c_{\sigma_1 \sigma_2}^{S \frac{1}{2} \frac{1}{2}} c_{\lambda - \lambda}^{011} c_{m - \lambda \lambda}^{jls} [D\alpha_{\lambda}(s)]_{\beta_1 \beta_2}^{\sigma_1 \sigma_2} \\ \times \int f_{l_1}^{\beta_1 a_1}(r) g_l^*(r) f_{l_2}^{\beta_2 a_2 \dagger}(r) r^2 dr \int Y_L^{m - \lambda*}(\theta\phi) Y_L^{M - \sigma_1 - \sigma_2}(\theta\phi) d\omega. \quad \dots (6) \end{aligned}$$

The coefficients $A_{j_1 j_2}^{l_1 l_2}(JLS)$ are given in the Appendix and for brevity we have written $j_1 + \frac{1}{2} a_1 \beta_1 = l_1$; $j_2 + \frac{1}{2} a_2 \beta_2 = l_2$.

Performing the angular integrations and using various summation properties of the vector addition coefficients, the matrix element (6) for the creation (or absorption) of the two particle system in the state $(JM; j_1 a_1, j_2 a_2)$ and the absorption (or creation) of a photon in the state (jm) reduces to

$$\mathcal{M}_{j_1 a_1; j_2 a_2}^{jm; JM} = \delta_{jJ} \delta_{mM} \sum_{L S \beta_1 \beta_2} a_L(JS) A_{j_1 j_2}^{l_1 l_2}(JLS) \gamma_{\beta_1 \beta_2}(S) R_{l_1; l_2}^{\beta_1 a_1; \beta_2 a_2}(L), \quad \dots (7)$$

the summation extending over $L = l_1 + l_2, \dots |l_1 - l_2|$, $S = 0, 1$; $\beta_1, \beta_2 = \pm 1$, with $l_1 = j_1 + \frac{1}{2} a_1 \beta_1$, $l_2 = j_2 + \frac{1}{2} a_2 \beta_2$ and where

$$R_{l_1; l_2}^{\beta_1 a_1; \beta_2 a_2}(L) = \int f_{l_1}^{\beta_1 a_1}(r) g_L^*(r) f_{l_2}^{\beta_2 a_2 \dagger}(r) r^2 dr$$

and

$$\begin{aligned} \gamma_{11}(1) &= -\gamma_{-1-1}(1) = 1; & \gamma_{1-1}(1) &= \gamma_{-11}(1) = 0; \\ \gamma_{11}(0) &= \gamma_{-1-1}(0) = 0; & \gamma_{1-1}(0) &= -\gamma_{-11}(0) = 1. \end{aligned}$$

† In the conventional gauge there is no longitudinal potential and for magnetic radiation $s=1$, $l=j$ whilst for electric radiation $s=1$, $l=j \pm 1$ and $s=0$, $l=j$.

§ 3. DISCUSSION

Expression (7) is perfectly general and a particular problem is characterized by the form chosen for the radial functions.

Thus, for internal conversion and internal pair formation g_L is chosen to represent an outward flux of photons and will therefore have the form $g_L(r) = iH_{L-1}^{(1)}(kr)(kr)^{1/2}$ which corresponds to the emission of $1/\pi^2 k$ quanta per second. In addition the values of J and L to be used are restricted by the multipolarity and character ('electric' or 'magnetic') of the transition considered. For internal conversion, $f_l^{\beta a_1}(r)$ is the radial function for an electron in an appropriate bound atomic state; e.g. for K-conversion (Rose 1951), $a_1 = +1$, $j_1 = \frac{1}{2}$ and $f_1^{11} = -(1-\gamma)^{1/2} Dr^{\gamma-1} e^{-\alpha Zr}$, $f_0^{-11} = (1+\gamma)^{1/2} Dr^{\gamma-1} e^{-\alpha Zr}$ where $\gamma = (1-\alpha^2 Z^2)^{1/2}$ and $D = (2\alpha Z)^{\gamma+1/2} [2\Gamma(2\gamma+1)]^{-1}$ whilst $f_{l_2}^{\beta a_2}(r)$ is the radial function for a positron (since positive and negative energy levels have been interchanged) moving in the coulomb field of the nucleus. These functions have been given by Rose (1937) and in his notation $f_l^{11} = if_{l-1}$, $f_l^{-11} = g_l$; $f_l^{1-1} = if_{-l-2}$, $f_l^{-1-1} = g_{-l-1}$. On the other hand, for internal pair formation, both f_1 and f_2 are positive energy functions for particles moving in a coulomb field.

For transitions involving the emission of radiation, only the transverse components of the electromagnetic field contribute and the term with $S=0$ is therefore dropped. Further $g_L = J_{L-1}(kr)/(kr)^{1/2}$ and the functions f_1 and f_2 will generally be of the type which are non-singular at the origin. As shown by Knipp and Uhlenbeck (1936), however, it is for instance permissible to treat inner bremsstrahlung resulting from an allowed β -transition as a first order process if f_1 , say, is replaced by an appropriate radial function representing a source at the origin.

ACKNOWLEDGMENT

The author would like to express his thanks to the Pressed Steel Company Ltd. for a research fellowship.

APPENDIX

The coefficients $a_l(js)$ occurring in the expression for the electromagnetic potential are given by

$$\begin{aligned} a_j(j0) &= [j(j+1)]^{1/2} & a_{j+1}(j1) &= -[j/(2j+1)]^{1/2} \\ a_j(j1) &= 1 & a_{j-1}(j1) &= [(j+1)/(2j+1)]^{1/2}. \end{aligned}$$

The coefficients $A_{j_1 j_2}^{l_1 l_2}(JLS)$ can be written in the following way

$$A_{j_1 j_2}^{l_1 l_2}(JLS) = C_{L l_1 l_2} \langle j_1 j_2 J | JLS \rangle.$$

$C_{L l_1 l_2}$ has been given explicitly by Carlson and Rushbrooke (1950 eqn. 17):

$$C_{L l_1 l_2} = (-)^{g-L} g! \left\{ \frac{(2l_1+1)(2l_2+1)}{4\pi(2g+1)!} \right\}^{1/2} \frac{\{(2g-2l_1)!(2g-2l_2)!(2g-2L)!\}^{1/2}}{(g-l_1)!(g-l_2)!(g-L)!}$$

if $2g = l_1 + l_2 + L$ is even and $C_{L l_1 l_2} = 0$ if $l_1 + l_2 + L$ is odd.

$\langle j_1 j_2 J | JLS \rangle$ is the matrix element for a transformation from jj to LS coupling. The amplitudes of these matrix elements have been given by Pryce (1952) but, to the author's knowledge, the phases have not been published. For completeness the full formulae for these matrix elements are given below.

If $j_1 = l_1 + \frac{1}{2}$, $j_2 = l_2 + \frac{1}{2}$

$$\langle j_1 j_2 J | JJ0 \rangle = \epsilon \left\{ \frac{(J + l_1 + l_2 + 2)(l_1 + l_2 + 1 - J)}{2(2l_1 + 1)(2l_2 + 1)} \right\}^{1/2}$$

$$\langle j_1 j_2 J | JJ1 \rangle = \epsilon(l_1 - l_2) \left\{ \frac{(J + l_1 + l_2 + 2)(l_1 + l_2 + 1 - J)}{2(2l_1 + 1)(2l_2 + 1)J(J + 1)} \right\}^{1/2}$$

$$\langle j_1 j_2 J | JJ + 1 \ 1 \rangle = \epsilon \left\{ \frac{(J + 1 + l_1 - l_2)(J + 1 + l_2 - l_1)(l_1 + l_2 - J)(l_1 + l_2 + 1 - J)}{2(2l_1 + 1)(2l_2 + 1)(J + 1)(2J + 1)} \right\}^{1/2}$$

$$\langle j_1 j_2 J | JJ - 1 \ 1 \rangle = \epsilon \left\{ \frac{(J + l_1 - l_2)(J + l_2 - l_1)(J + l_1 + l_2 + 1)(J + l_1 + l_2 + 2)}{2(2l_1 + 1)(2l_2 + 1)J(2J + 1)} \right\}^{1/2}$$

The expressions for the other matrix elements can be obtained from the above by replacing l_1 by $-l_1 - 1$ if $j_1 = l_1 - \frac{1}{2}$ and l_2 by $-l_2 - 1$ if $j_2 = l_2 - \frac{1}{2}$.

The phase factors ϵ are given for all cases in the table.

Phases of the Transformation Matrix Elements $\langle j_1 j_2 J | JLS \rangle$

j_1	j_2	(JLS)			
		$(JJ0)$	$(JJ1)$	$(JJ + 1 \ 1)$	$(JJ - 1 \ 1)$
$l_1 + \frac{1}{2}$	$l_2 + \frac{1}{2}$	+1	+1	-1	+1
$l_1 + \frac{1}{2}$	$l_2 - \frac{1}{2}$	+1	+1	-1	-1
$l_1 - \frac{1}{2}$	$l_2 + \frac{1}{2}$	-1	-1	+1	+1
$l_1 - \frac{1}{2}$	$l_2 - \frac{1}{2}$	+1	+1	+1	-1

REFERENCES

- CARSLON, B. C., and RUSHBROOKE, G. S., 1950, *Proc. Camb. Phil. Soc.*, **46**, 626.
 CONDON, E. U., and SHORTLEY, G. H., 1935, *The Theory of Atomic Spectra* (Cambridge : University Press).
 FURRY, W. H., 1937, *Phys. Rev.*, **51**, 125; 1938, *Ibid.*, **54**, 36.
 HEITLER, W., 1936 a, *The Quantum Theory of Radiation* (Oxford : University Press); 1936 b, *Proc. Camb. Phil. Soc.*, **32**, 112.
 KNIPP, J. K., and UHLENBECK, G. E., 1936, *Physica*, **3**, 425.
 PRYCE, M. H. L., 1952, *Proc. Phys. Soc. A*, **65**, 773.
 RACAH, G., 1942, *Phys. Rev.*, **62**, 438.
 ROSE, M. E., 1937, *Phys. Rev.*, **51**, 484; 1951, *Ibid.*, **83**, 79.
 SPIERS, J. A., and BLIN-STOYLE, R. J., 1952, *Proc. Phys. Soc. A*, **65**, 801.

Intensity Distribution among Bands of the Herzberg System of O₂

By M. E. PILLOW

Northern Polytechnic, London

MS. received 26th January 1953

Abstract. Using Herzberg's revised measurements, relative band-intensities in the system are calculated, first in absorption, and compared qualitatively with laboratory observations, and then in emission, when they are compared with Barbier's measurements on the emission from the night sky.

§ 1. INTRODUCTION

CALCULATIONS on the Herzberg system of O₂ have until recently been of doubtful value because of the lack of agreed data on the bands, which in the laboratory can be observed only in absorption.* Here they are represented only by the $v''=0$ progression and the bands corresponding to lower v' values are extremely faint, so that the existence of some of them has been in doubt. Herzberg's latest measurements (1952) however, made at much greater dispersion than before and with very long absorbing paths, give much more reliable rotational data than were hitherto available, and establish with considerable probability the position of the system origin. These data, then, have been used for a new calculation of relative band intensities in the system. The method used is the most recent modification of the distortion process for wave functions (Pillow 1951, 1952).

The lower state of the system is the same as that of the Schumann-Runge bands, and these give

$$\omega_e'' = 1580, \quad x\omega_e'' = 12.07, \quad r_e'' = 1.207 \times 10^{-8} \text{ cm.}$$

Herzberg's measurements for the vibrational levels of the excited state cannot, unfortunately, be represented exactly by a quadratic expression in $v' + \frac{1}{2}$, but such a formula has been fitted to them by the method of least squares, and appears to be sufficiently accurate for the purpose. Herzberg's rotational measurements give r_e' . The values used, then, are $\omega_e' = 836.4$, $x\omega_e' = 27.18$, $r_e' = 1.534 \times 10^{-8} \text{ cm.}$

§ 2. INTENSITIES IN ABSORPTION

No measurements on the intensities of the bands in absorption have as yet been made with any accuracy. The microphotometer traces of Chalonge and Vassy (1934) and Morguleff and Vassy (1939) were made for purposes of wavelength measurement, and are not calibrated for intensity, and the same applies to the plate taken by Stopes-Roe (1948), and examined by the writer. All that can be fairly stated at present is that the intensities in the progression are small at the red end ($\lambda = 2795 \text{ \AA}$), so that these bands did not appear on any of the earlier exposures, increase rapidly in the middle of the progression, and approach a maximum in the last two bands at the violet end ($\lambda = 2443, 2429 \text{ \AA}$) where the system probably terminates in a continuum. Calculation gives a

* Since this paper was written, Drs. H. P. Broida and A. G. Gaydon have observed the Herzberg bands in emission in an afterglow of helium.

very wide range of absolute intensities, but the order in which they are arranged agrees well with experiment, as is shown by fig. 1, in which $\log_{10} I$ (probably bearing a roughly proportional relation to plate blackening) is plotted against v' .

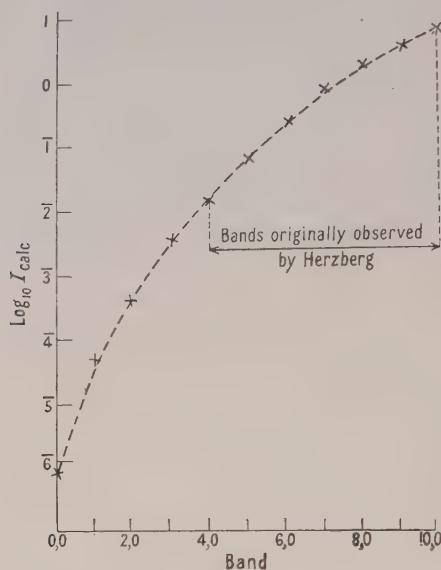


Fig. 1.

§ 3. INTENSITIES IN EMISSION

Now the astrophysical interest of the Herzberg system lies in its probable presence in the emission from the night sky. Tentative identification of many of the bands observed in this radiation with those of the Herzberg system have been made by Dufay and Déjardin (1946), Déjardin (1948), Barbier (1947) and others. The dispersion of the spectrograms is necessarily small, being of the order of 100 Å per mm, so that identification can be made only to an accuracy within several ångströms. Within the range 3000–5000 Å it is possible to identify, to this accuracy, a very large proportion of the observed bands with those of either the Vegard–Kaplan system of N_2 or the Herzberg system of O_2 , and the latter predominate in the range 3000–4000 Å. Plates showing this region have been studied very fully by Barbier, and it is of interest to discover whether the theoretical intensity distribution in the Herzberg system is at all closely related to that obtaining among the observed bands. The comparison is complicated by the fact that for many wavelengths there are likely to be two or more Herzberg bands superposed, and the total observed intensity will be a combination of overlapping components. Failing fuller resolution of the observed bands, a direct band-by-band comparison cannot therefore be made; a fairly close check is nevertheless possible.

The table shows the intensities in the system as found by calculation, on an arbitrary scale, together with wavelengths. Wavelengths below 3100 Å were not registered by Barbier, and above about 4050 Å the Vegard–Kaplan bands occur prominently, so that no comparison has been attempted here. In the intervening range an asterisk indicates that Barbier has observed a strong band

within a few ångströms of the wavelength given, and it can be seen that in all these cases, with one exception (3484 Å), there is according to theory at least one strong band there.

Table

τ''	0	1	2	3	4	5	6	7	8	9	10
0	2794	2921	3059	3208	3369	3544	3756	3945	4176	4430	4713
					2	7*	17*	30*	43	51	54
1	2737	2859	2991	3143	3287	3453	3635	3833	4050	4284	4554
			1	4	12	26*	43*	60*	52*	40	21
2	2685	2802	2929	3064	3211	3371	3543	3731	3937	4162	4411
		1	3	13	31*	56*	70*	65*	33*	7	7
3	2637	2750	2872	3002	3143	3295	3460	3639	3835	4048	4283
		3	10	30	57*	79*	75*	46*	9*	1	19
4	2593	2703	2820	2947	3082	3228	3386	3557	3743	3947	4169
	1	8	23	53	84*	98*	66*	20*		14	22
5	2554	2660	2774	2896	3026	3167	3319	3484	3662	3857	4069
	6	24	49	93	138	100*	43*	4*	7	25	15
6	2519	2622	2733	2851	2977	3114	3260	3419	3591	3777	3981
	23	42	91	132	139	80	15		20	25	5

The comparison can, however, be made more precise. The calculated intensities have been arranged in order of wavelength, and where two bands have heads lying within 10 Å their intensities have been added together. The upright lines in fig. 2(a) show these total intensities plotted against wave number. This has been done in order that comparison may be made with a graph published by Barbier and reproduced approximately, with his permission, in fig. 2(b). This shows the intensities of the night sky bands, obtained from photometric data. It will be seen that the peaks occur for almost exactly the same wavelengths in the two cases.

In comparing the heights of the peaks in the two diagrams several points may be noted:

(a) The calculations have been made on the assumption of uniform distribution of molecules among the vibrational levels of the excited state. Even in the night sky this condition is unlikely to hold, and it can be seen from the table that peak values in the short wave part of the range considered would be somewhat lower if allowance were made for a smaller population of the higher levels.

(b) In Barbier's graph the background intensity is falling for ν greater than $30\,000\text{ cm}^{-1}$. For comparison with theoretical values, therefore, his last few peaks might be raised somewhat.

(c) There is nothing in the theoretical distribution to account for the sudden drop in the heights of Barbier's maxima for wavelengths above 3600 \AA . Error in calculation, whether accidental or due to the method used, could not be

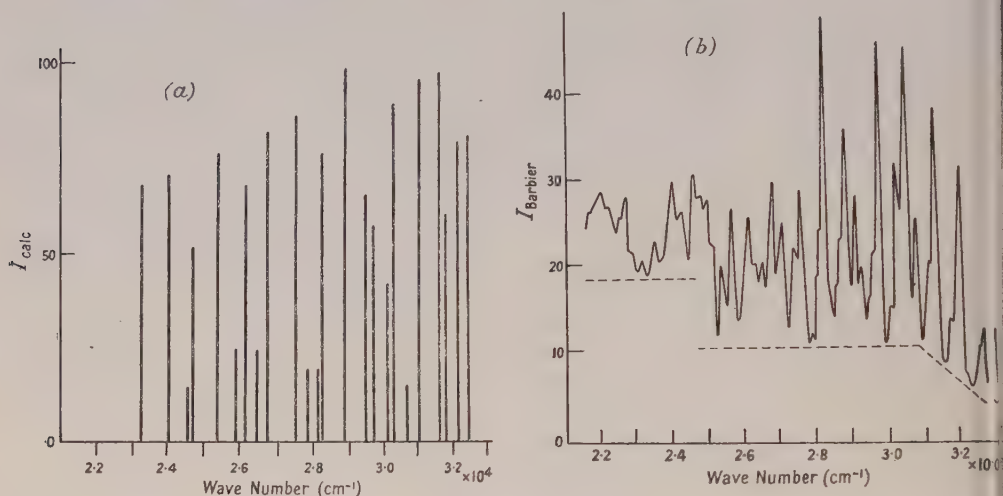


Fig. 2.

dependent on wavelength in any consistent way, and Barbier's method of calibration seems to allow fully for variations in plate sensitivity. A very tentative suggestion of absorption in the night sky may be put forward.

§ 4. CONCLUSION

The observational data are not yet sufficient for a fully quantitative comparison of intensities in this system with theoretical values, but with the latest vibrational and rotational measurements the calculations appear to afford a reliable standard of comparison, which can be used in examining the emission of the system from remote sources.

ACKNOWLEDGMENTS

The writer's thanks are due to Dr. G. Herzberg for the use of his data prior to publication, and to Dr. D. Barbier for permission to reproduce the graphical representation of his results.

REFERENCES

- BARBIER, D., 1947, *Ann. Astrophys.*, **10**, 141.
- CHALONGE, D., and VASSY, E., 1934, *Rev. Opt. (Théor. Instrum.)*, **13**, 113.
- DÉJARDIN, G., 1948, *Emission Spectra of the Night Sky and Aurora* (London: Physical Society).
- DUFAY, J., and DÉJARDIN, G., 1946, *Ann. Geophys.*, **2**, 249.
- HERZBERG, G., 1952, *Canad. J. Phys.*, **30**, 185.
- MORGULEFF, N., and VASSY, A., 1939, *Ann. Astrophys.*, **1**, 427.
- PILLOW, M. E., 1951, *Proc. Phys. Soc. A*, **64**, 722; 1952, *Thesis*, University of London.
- STOPES-ROE, H. V., 1948, *Thesis*, University of London.

Band Intensities in the CN Violet System

By M. E. PILLOW

Northern Polytechnic, London

MS. received 28th January 1953

Abstract. Relative intensities for the bands of the CN violet system are calculated, and compared graphically with the experimental values of Ornstein and Brinkman, and of Tawde.

IN a contribution to the 1951 Conference on Auroral Physics Pearse (1953) suggested that a graphical comparison between calculated and measured band intensities for a system might lead to useful information. Such a comparison was carried out for the Swan bands of C_2 , and reported at the Colloquium on the Physics of Comets, at Liège (Pillow 1952b). A similar study of the CN system is made briefly here.

Transition probabilities for this system have already been published (Pillow 1951), but at the end of the same paper a further improvement in the method of calculation was suggested. The earlier results are here slightly modified, using this method, and extended, and the relative transition probabilities are shown in the table. Intensities calculated from these are now compared with the

Transition Probabilities: CN Violet System

Band		Probability	Band		Probability
0, 0	3883	0.89	3, 2	3584	0.16
0, 1	4216	0.09	3, 3	3855	0.63
0, 2	4606	0.02	3, 4	4168	0.16
			3, 5	4532	0.04
			3, 6	4959	0.01
1, 0	3590	0.08	4, 2	3348	0.01
1, 1	3871	0.74	4, 3	3583	0.21
1, 2	4197	0.11	4, 4	3851	0.56
1, 3	4578	0.02	4, 5	4158	0.21
			4, 6	4515	0.06
2, 1	3586	0.18	5, 3	3351	0.02
2, 2	3862	0.64	5, 4	3584	0.27
2, 3	4181	0.14	5, 5	3849	0.51
2, 4	4553	0.03	5, 6	4152	0.19
			5, 7	4502	0.06

measured values of Ornstein and Brinkman (1931) for the same system, made on the intensities in the band heads, which were taken by those workers and by others as giving the same ratios as the corresponding lines of bands, owing to the very similar structure of all the bands. The source was a carbon arc in air.

Now if P represents the vibrational transition probability $[\int \psi_v \psi_{v'} dr]^2$ for a band whose origin has wave number ν we may, by making certain well-known

assumptions not discussed here, take the intensities of corresponding lines in bands, and therefore the total band-intensities, to be proportional to $Z^{-1}P\nu^4$, where Z is a factor determined by the distribution of the molecules among the vibrational levels of the excited state. If the distribution were purely thermal Z^{-1} would be the Boltzmann factor $\exp(-hc\omega_e\nu'/kT)$ to a very good approximation.

For $P\nu^4$ we write I_{calc} and this represents the intensity to be expected 'at infinite temperature', that is, for uniform population of the excited levels. Then if the measured intensity is I ,

$$\log I = \log I_{\text{calc}} - \log Z.$$

$\log Z$ should be constant for all the bands of one ν'' progression, and for a thermal distribution it should be proportional to ν' . Therefore if $\log I$ be plotted against $\log I_{\text{calc}}$, we shall expect to obtain a series of parallel straight lines, which for a thermal type of distribution will be equally spaced. In this case it will be

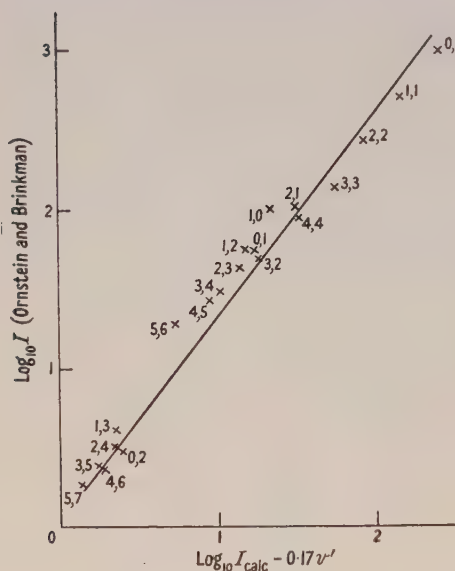


Fig. 1.

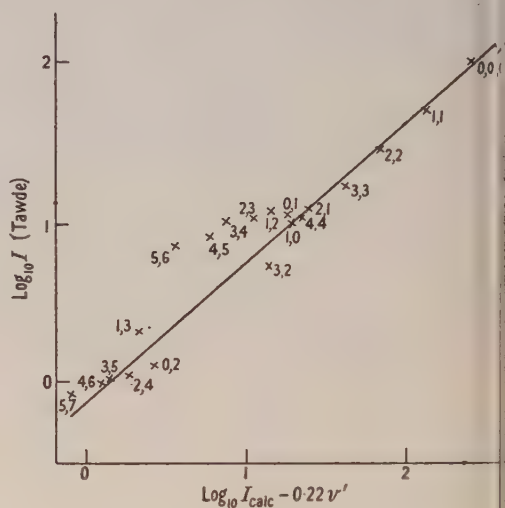


Fig. 2.

possible to plot $\log I$ against $\log I_{\text{calc}} - Av'$, where A is a suitably chosen constant, and to obtain a single straight line. From such a plot we can determine whether the excitation is thermal in type, and the corresponding 'vibrational temperature', and we can examine discrepancies between theory and experiment and between measured values obtained from different sources, or under different conditions. I and I_{calc} may be on any arbitrary scale, the slope and spacing of the lines being unaffected by this.

Figure 1 shows the comparison between calculated values and those measured by Ornstein and Brinkman. From consideration of space the original plot of $\log I$ against $\log I_{\text{calc}}$ is omitted, as well as the table of values plotted, but the graph of $\log I$ against $\log I_{\text{calc}} - 0.17\nu'$ may be claimed to be very nearly linear. The vibrational distribution appears to correspond to a temperature T given by $hc\omega_e\nu'/2.303kT = 0.17 \pm 0.01$, i.e. $T = 8000 \pm 500^\circ\text{K}$. It may be noted that the very small departures from the line that do occur tend to be connected with

sequences; that is, they are associated with certain small ranges of wavelength. It is difficult to see how errors in the calculations, whether accidental or due to the approximations made, could be systematically dependent upon wavelength. We shall return to this point after considering Tawde's results.

Tawde (1936) made measurements on the same system, also using a carbon arc as source. A direct comparison of his published results with those of Ornstein and Brinkman shows good agreement except in the 0, 1 sequence, where his results are all higher than those of the other workers. Figure 2 shows that Tawde's results, when plotted against the calculated values, give an almost exactly linear graph, this time with a lateral shift of $0.22\nu'$, corresponding to a temperature of about 6200°K , except for the points belonging to that particular sequence, which are all too high. Since the sources used by the two sets of workers were similar, the differences between their results, as well as the small discrepancies noted in the first case, are most probably a matter of plate calibration, and it would appear that the Ornstein and Brinkman values are the more reliable. Other explanations of discrepancies between theory and experiment, and between various sets of observations, have been suggested in the work on C_2 , but they are unlikely to be relevant here.

The calculations made here, then, seem to give results sufficiently reliable for comparison with observed values, and the method of comparison can equally well be used when calculations are made by other methods. The use of such calculated values in comparing measurements made on different sources is indicated here, and the use of such comparisons in astrophysical work is discussed elsewhere.

REFERENCES

- ORNSTEIN, L. S., and BRINKMAN, H., 1931, *Proc. K. Ned. Akad. Wet.*, **34**, 33.
PEARSE, R. W. B., 1953, *Geophysical Research Papers, Proceedings of 1951 Conference on Auroral Physics*, in the press.
PILLOW, M. E., 1951, *Proc. Phys. Soc. A*, **64**, 772; 1952 a, *Thesis*, University of London; 1952 b, *Mem. Soc. Roy. Sci., Liège*, **13**, 105.
TAWDE, N. R., 1936, *Proc. Indian Acad. Sci. A*, **3**, 140.

The Elastic Scattering of Neutrons by Tritons and of Protons by ^3He

By P. SWAN

Department of Physics, University College, London

Communicated by H. S. W. Massey; MS. received 19th February 1953

Abstract. The theory of the elastic collisions of neutrons with tritons which was given in an earlier paper by the author and applied to an energy of 14 mev. is here extended to cover a number of neutron energies between 2.5 and 14 mev. The scattering phases are evaluated using the variational methods of Hulthén and Kohn. The corresponding angular distributions for proton- ^3He scattering are obtained by treating the coulomb field as a perturbation on the neutron-triton scattering, as both cases have the same symmetry properties.

§ 1. INTRODUCTION

DETAILED calculations and comparison with experiment (Buckingham, Hubbard and Massey 1952) of the elastic scattering of neutrons by deuterons, using Wheeler's resonating group structure method, have strongly favoured an exchange type of nuclear force. It therefore becomes of interest to see if exchange forces are also necessary to explain neutron-triton and proton- ^3He scattering, and if the resonating group structure method is capable of giving reasonable results for the interaction of four nucleons.

In a previous paper (Swan 1953) the theory of neutron-triton collisions was worked out and applied to an incident neutron energy of 14 mev. The calculations were based upon the following assumptions:

(a) The nuclear potential acting between two nucleons at a distance apart is given by the gaussian form

$$V(r) = V_0(mM + hH + bB + w) \exp(-\mu r^2) \quad \dots\dots(1)$$

where M , H and B are the Majorana, Heisenberg and Barlett operators which interchange the spatial, spatial and spin, and spin coordinates respectively of the interacting particles, and m , h , b and w are constants chosen so as to determine the exchange character of the interaction, while satisfying the condition that the ratio between the neutron-proton singlet and triplet well-depths $x \sim 0.6$.

The well dimensions used are those derived by Breit, Hoisington and Shore (1939) from analysis of low energy proton-proton scattering: $V_0 = -45$ mev $\mu = 2.669 \times 10^{25}$, range $r_0 = 1/\sqrt{\mu} = 1.936 \times 10^{-13}$ cm.

The well dimensions derived from proton-proton scattering have been used because the neutron-triton interaction involves neutron-neutron and neutron-proton interactions in the ratio 2:1. The equality of proton-proton and neutron-neutron forces is assumed.

Calculations were carried out for four types of exchange force given by:

$$\left. \begin{array}{l} \text{I Ordinary forces (WB case): } m=h=0, w=\frac{1}{2}(1+x), b=\frac{1}{2}(1-x). \\ \text{II Majorana-Heisenberg forces (MH case):} \\ \qquad w=b=0, m=\frac{1}{2}(1+x), h=\frac{1}{2}(1-x). \\ \text{III Symmetric forces (MHWB case):} \\ \qquad m=2b=\frac{1}{3}(1+3x), h=2w=\frac{1}{3}(1-3x). \\ \text{IV The Serber mixture: } m=w=\frac{1}{4}(1+x), h=b=\frac{1}{4}(1-x). \end{array} \right\} \dots (2)$$

(b) The ground state wave function $\psi(123)$ of the triton is given approximately by the product of three two-body wave functions of gaussian form:

$$\psi(123) = 3^{3/4}(\lambda/\pi)^{3/2} \exp \left[-\frac{1}{2}\lambda(r_{12}^2 + r_{23}^2 + r_{31}^2) \right]. \dots (3)$$

Estimation of the binding energy E_T of the triton by the variational method leads to the result $\lambda = 1.436 \times 10^{25}$, $E_T = -5.49$ mev, the latter value comparing with the experimental value of -8.3 mev. As scattering calculations are insensitive to small variations in binding energy, no appreciable error should be introduced by the use of the theoretical binding energy.

(c) The total wave function of the four-body system can be adequately represented by the resonating group formalism of Wheeler employing approximate gaussian wave functions for the triton.

The only groups taken into account are the triton and neutron groups, as by the application of the variational method it may be shown that the deuteron plus two neutron groups have a negligible probability of occurrence.

(d) The polarization of the triton by the neutron is small and may be neglected, as the triton with its binding energy of 8.3 mev is a more compact structure than the deuteron (binding energy 2.2 mev), and consequently the polarization of the triton by neutrons should be much smaller than in the case of deuterons. As calculations on n - d scattering have hitherto neglected this effect, yet obtain good agreement with experiment for energies above about 3 mev, below which the polarization effect is believed to be large, it follows we are fairly safe in neglecting polarization for neutron-triton collisions.

Just as in the deuteron case, the size of the triton results in neutrons with several mev energy and with one unit of quantized angular momentum passing close enough to interact quite strongly, resulting in an appreciable P phase contribution to scattering at a low energy where neutron-proton scattering is quite isotropic.

(e) For the energy range considered below 14 mev the non-central component of force may be represented by an equivalent central force, so that it is assumed that the tensor interaction leads to no appreciable deviation from the results obtained using purely central forces.

§ 2. GENERAL FORMULAE AND METHODS OF CALCULATION

The angular distribution for the elastic scattering of neutrons by tritons into a solid angle $d\Omega$ at an angle between θ and $\theta + d\theta$ with the incident beam direction is given by $d\sigma = I(\theta) d\Omega$ where $I(\theta) = \frac{3}{4}I_T(\theta) + \frac{1}{4}I_S(\theta)$; $I_T(\theta)$ represents triplet scattering with the spin quantum number $S=1$, and $I_S(\theta)$ the singlet scattering, $S=\frac{1}{2}$.

$I_T(\theta)$ and $I_S(\theta)$ are expressed in terms of the phases δ_l by the usual scattering formula

$$I_{T,S}(\theta) = (1/4k^2) |\Sigma_l (2l+1) \{\exp(2i\delta_l^{T,S}) - 1\} P_l(\cos \theta)|^2. \quad \dots\dots (4)$$

It was shown in a previous paper (Swan 1953) that the radial wave equation describing the scattering is of the form

$$\left[\frac{d^2}{dr^2} + k^2 - \frac{l(l+1)}{r^2} \right] f_l(r) = \alpha U_n(r) f_l(r) + \int_0^\infty K_n^l(r, r') f_l(r') dr', \quad \dots\dots (5)$$

where

$$K_n^l(r, r') = \beta q_l(r, r') + \gamma t_l(r, r') + \left(\frac{E_n}{E_T} - \frac{5}{4} \right) n_l(r, r') + p_l(r, r') + \beta s_l(r, r') + \delta r_l(r, r'). \quad \dots\dots (6)$$

α, β, γ and δ are numbers depending on the spin state and exchange character of the interaction, and are given in table 1. If expressions (1) and (3) are used

Table 1

Nuclear force law	Spin state	α	β	γ	δ
(I) WB	triplet	$\frac{3}{4}(5+x)$	$\frac{3}{16}(1+x)$	$\frac{3}{4}(-3+x)$	$\frac{15}{16}(1+x)$
	singlet	$\frac{9}{4}(1+x)$	$\frac{3}{8}x$	$\frac{3}{4}(-3+x)$	$\frac{15}{32}(3-x)$
(II) MH	triplet	$\frac{3}{4}(-3+x)$	$\frac{3}{16}(1+x)$	$\frac{3}{4}(5+x)$	$\frac{15}{16}(1+x)$
	singlet	$\frac{3}{4}(-3+x)$	$\frac{3}{8}x$	$\frac{9}{4}(1+x)$	$\frac{15}{32}(3-x)$
(III) MHWB	triplet	$\frac{3}{8}(-1+3x)$	$\frac{3}{16}(1+x)$	$\frac{1}{4}(-1+27x)$	$\frac{15}{16}(1+x)$
	singlet	$\frac{3}{4}(-1-x)$	$\frac{3}{8}x$	$\frac{3}{4}(1+5x)$	$\frac{15}{32}(3-x)$
(IV) Serber	triplet	$\frac{3}{4}(1+x)$	$\frac{3}{16}(1+x)$	$\frac{3}{4}(3x-1)$	$\frac{15}{16}(1+x)$
	singlet	$\frac{3}{2}x$	$\frac{3}{8}x$	$\frac{3}{2}x$	$\frac{15}{32}(3-x)$

for the potential and the ground-state wave function of the triton respectively, and we denote the constituent nucleons of the triton by 1, 2, 3 and the incident neutron by 4, then

$$U_n(r) = (9/8)^3 (M/\hbar^2) \iint \psi^2(123) V(14) d\mathbf{R} d\mathbf{r}'. \quad \dots\dots (7)$$

$$\left. \begin{matrix} q_l(r, r') \\ t_l(r, r') \\ n_l(r, r') \\ p_l(r, r') \\ s_l(r, r') \\ r_l(r, r') \end{matrix} \right\} = 2\pi r r' \int_0^\pi P_l(\cos \theta) \sin \theta d\theta \left\{ \begin{matrix} Q(\mathbf{r}, \mathbf{r}'), \\ T(\mathbf{r}, \mathbf{r}'), \\ N(\mathbf{r}, \mathbf{r}'), \\ P(\mathbf{r}, \mathbf{r}'), \\ S(\mathbf{r}, \mathbf{r}'), \\ R(\mathbf{r}, \mathbf{r}'). \end{matrix} \right. \quad \dots\dots (8)$$

$$\left. \begin{aligned}
 \text{where } Q(\mathbf{r}, \mathbf{r}') &= (9/8)^3 (M/\hbar^2) \int \psi(123) \psi(234) V(12) d\mathbf{R}, \\
 T(\mathbf{r}, \mathbf{r}') &= (9/8)^3 (M/\hbar^2) \int \psi(123) \psi(234) V(14) d\mathbf{R}, \\
 N(\mathbf{r}, \mathbf{r}') &= \frac{3}{2} E_T (9/8)^3 (M/\hbar^2) \int \psi(123) \psi(234) d\mathbf{R}, \\
 P(\mathbf{r}, \mathbf{r}') &= \frac{3}{8} (9/8)^3 \int \psi(123) \psi(234) \\
 &\quad \times \left[9 \left(\frac{\mathbf{u} \cdot \mathbf{t}}{ut} \right) \frac{v'(u)v'(t)}{v(u)v(t)} - 5 \frac{\nabla_R^2 \{v^3(R)\}}{v^3(R)} \right] d\mathbf{R}, \\
 S(\mathbf{r}, \mathbf{r}') &= (9/8)^3 (M/\hbar^2) \int \psi(123) \psi(234) V(24) d\mathbf{R}, \\
 R(\mathbf{r}, \mathbf{r}') &= (9/8)^3 (M/\hbar^2) \int \psi(123) \psi(234) V(23) d\mathbf{R}.
 \end{aligned} \right\} \dots\dots (9)$$

$$\left. \begin{aligned}
 \mathbf{r} &= \frac{1}{3}(\mathbf{r}_1 + \mathbf{r}_2 + \mathbf{r}_3) - \mathbf{r}_4, & \mathbf{r}' &= \frac{1}{3}(\mathbf{r}_2 + \mathbf{r}_3 + \mathbf{r}_4) - \mathbf{r}_1, \\
 R &= \mathbf{r}_2 - \mathbf{r}_3, & v(R) &= \exp(-\frac{1}{2}\lambda R^2).
 \end{aligned} \right\} \dots\dots (10)$$

By employing (1) and (3) we may evaluate analytically the integrals in (7) and (8), thus obtaining

$$\left. \begin{aligned}
 U_n(r) &= A_0 \exp(-\gamma_0 r^2), \\
 q_l(r, r') &= A_1 \exp(-\gamma_1 r^2 - \gamma_5 r'^2) \mathcal{J}_{l+1/2}(\kappa_1 r r'), \\
 t_l(r, r') &= A_2 \exp\{-\gamma_2(r^2 + r'^2)\} \mathcal{J}_{l+1/2}(\kappa_2 r r'), \\
 n_l(r, r') &= A_3 \exp\{-\gamma_3(r^2 + r'^2)\} \mathcal{J}_{l+1/2}(\kappa_3 r r'), \\
 p_l(r, r') &= A_4 \exp\{-\gamma_4(r^2 + r'^2)\} \\
 &\quad \times \left[\left(3r^2 + 3r'^2 + \frac{160}{27\lambda} \right) \mathcal{J}_{l+1/2}(\kappa_4 r r') - 10 r r' \mathcal{J}'_{l+1/2}(\kappa_4 r r') \right], \\
 s_l(r, r') &= A_5 \exp\{-\gamma_5 r^2 - \gamma_1 r'^2\} \mathcal{J}_{l+1/2}(\kappa_5 r r'), \\
 r_l(r, r') &= A_6 \exp\{-\gamma_6(r^2 + r'^2)\} \mathcal{J}_{l+1/2}(\kappa_6 r r')
 \end{aligned} \right\} \dots\dots (11)$$

$$\dots\dots (12)$$

where the constants A , γ and κ are simple functions of V_0 , μ and λ , and $A_1 = A_5$, $\kappa_1 = \kappa_5$. $\mathcal{J}_{l+1/2}(x)$ is defined in terms of the half-integral Bessel function for unreal argument: $i^{l+1/2} \mathcal{J}_{l+1/2}(x) = (\pi x/2)^{1/2} J_{l+1/2}(ix)$. $\dots\dots (13)$

From (13) it follows that the kernels have opposite signs for even and odd l , being attractive and repulsive respectively.

The kernels t_l , n_l , p_l , r_l and the kernel sum $q_l + s_l$ are all symmetrical in r and r' , thus satisfying the condition for Hulthén's variational method to be applicable. This symmetry condition is also necessary if a formula of the Blatt-Jackson (1949) type is to describe the S phase shifts for low energy scattering in many-body problems:

$$k \cot \delta = -\frac{1}{a} + \frac{1}{2} r_0 k^2. \dots\dots (14)$$

Kernels which could not be symmetrized would not, if they occurred, correspond to a physical solution to a problem.

The asymptotic solution of the wave equation (5) is the usual form:

$$f_l(r) \sim \sin(kr - \frac{1}{2}l\pi + \delta_l). \dots\dots (15)$$

The total elastic cross section Q for scattering is then

$$Q = \frac{4\pi}{k^2} \sum_l (2l+1) \left(\frac{3}{4} \sin^2 \delta_l^T + \frac{1}{4} \sin^2 \delta_l^S \right). \dots\dots (16)$$

For proton-³He collisions the coulomb field introduces small modifications to the scattering. One may expect these modifications in the phases to be about double those for proton-deuteron collisions.

If we take the Rutherford scattering in the centre-of-mass system as

$$I_e(\theta) = \left(\frac{e^2}{2E} \right)^2 \frac{1}{\sin^4 \frac{1}{2}\theta}, \quad \dots\dots (17)$$

where E is the proton energy in the centre-of-mass system, the ratio R of the scattering through angles θ and $\theta + d\theta$ to that given by the Rutherford scattering formula (17) is then

$$R = \frac{3}{4}R_T + \frac{1}{4}R_S, \quad \dots\dots (18)$$

$$\text{where } R_{T,S} = \left| 1 + \frac{i}{\alpha_1} \sin^2 \frac{1}{2}\theta \exp(i\alpha_1 \ln \sin^2 \frac{1}{2}\theta) \Sigma(2l+1) \right. \\ \left. \times \exp[2i(\zeta_l - \zeta_0)] (\exp 2i\eta_l^{T,S} - 1) P_l(\cos \theta) \right|^2. \quad \dots\dots (19)$$

$\alpha_1 = e^2/\hbar v$, where v is the velocity of the incident protons, and

$$\zeta_l = \arg \Gamma(l+1+i\alpha_1).$$

The phases η_l are found from the asymptotic solution of a wave equation of the same type as (5), but with U_n and K_n^l replaced by U_p and K_p^l , where

$$\left. \begin{aligned} U_p &= U_n + 2C(r), \\ K_p^l &= K_n^l + \frac{1}{8}g_l(r, r') - h_l(r, r'), \\ C(r) &= \frac{3}{2}(9/8)^3(M/\hbar^2) \int \int \psi^2(123) \frac{e^2}{r_{14}} d\mathbf{r} d\mathbf{r}', \\ \left. \begin{aligned} g_l(r, r') \\ h_l(r, r') \end{aligned} \right\} &= 2\pi r r' \int_0^\pi P_l(\cos \theta) \sin \theta d\theta \begin{cases} G(\mathbf{r}, \mathbf{r}'), \\ H(\mathbf{r}, \mathbf{r}'). \end{cases} \\ G(r, r') &= \frac{3}{2}(9/8)^3(M/\hbar^2) \int \psi(123) e^2 \left(\frac{1}{r_{12}} + \frac{1}{r_{24}} \right) \psi(234) d\mathbf{R}, \\ H(r, r') &= \frac{3}{2}(9/8)^3(M/\hbar^2) \int \psi(123) \frac{e^2}{r_{14}} \psi(234) d\mathbf{R}. \end{aligned} \right\} \quad \dots\dots (20)$$

In this case the asymptotic solution of the integral equation is

$$f_l(r) \sim \sin(kr - \alpha_1 \ln 2kr - \frac{1}{2}l\pi + \zeta_l + \eta_l). \quad \dots\dots (21)$$

The same modification of U_n and K_n^l occurs for both triplet and singlet interactions. The integral $C(r)$ and the kernels may be evaluated on substitution of (1) and (3) in (20); one thus obtains

$$\left. \begin{aligned} C(r) &= B_0 \frac{e^2}{r} \Phi(\omega_0 r), \\ g_l(r, r') &= B_1 r r' \exp \{ -a(r^2 + r'^2) \} \int_{-1}^1 \exp(-brr'z) P_l(z) \\ &\quad \times [r^2 + 9r'^2 + 6rr'z]^{-1/2} \Phi\{\omega_1(r^2 + 9r'^2 + 6rr'z)^{1/2}\} \\ &\quad + (9r^2 + r'^2 + 6rr'z)^{-1/2} \Phi\{\omega_1(9r^2 + r'^2 + 6rr'z)^{1/2}\} dz, \\ h_l(r, r') &= \frac{4}{3} B_1 r r' \exp \{ -a(r^2 + r'^2) \} \\ &\quad \times \int_{-1}^1 \exp(-brr'z) P_l(z) (r^2 + r'^2 - 2rr'z)^{-1/2} dz, \end{aligned} \right\} \quad \dots\dots (22)$$

$$\text{where } \left. \begin{aligned} B_0 &= (3M/2\hbar^2), & \omega_0 &= 3(\lambda/2)^{1/2}, \\ B_1 &= 6(2/\pi)^{1/2}(9/8)^3(M/\hbar^2)\lambda^{3/2}e^2, & \omega_1 &= \frac{3}{8}(6\lambda)^{1/2}, \\ a &= (45/32\lambda), & b &= (27/16\lambda). \end{aligned} \right\} \dots\dots(23)$$

Here $\Phi(r)$ is the error integral

$$\Phi(r) = \frac{2}{\sqrt{\pi}} \int_0^r \exp(-t^2) dt. \dots\dots(24)$$

The kernels $g_l(r, r')$ and $h_l(r, r')$ are again symmetrical in r and r' . For $r > 1/\omega_0$ the ordinary force potential $C(r)$ behaves like a coulomb potential $B_0 e^2/r$; the latter is thus a coulomb potential cut off at the origin, and as we know the scattering contribution to come chiefly from the long range part of the field, the departure from the coulomb law for $r < 1/\omega_0$ may be ignored to a good approximation.

§ 3. CALCULATION OF THE PHASES δ_l AND η_l

The phases δ_l for $l=0, 1$ were obtained by use of the variational principles due to Hulthén (1944) and Kohn (1948), but the phases δ_2, δ_3 were found by use of the Born approximation. The phases η_0, η_1 were evaluated from δ_0, δ_1 , respectively, by treating the coulomb field in the proton- ^3He interaction as a perturbation on the nuclear interaction, the latter being identical by charge symmetry with the neutron- ^3H interaction.

The phases δ_0, δ_1 .

The kernels $q_0, q_1; t_0, t_1; n_0, n_1; p_0, p_1; s_0, s_1; r_0, r_1$ were plotted numerically, and the triplet and singlet wave equations solved numerically by variation methods. The variational wave function for S-wave scattering was chosen as

$$f_0(r) = \{1 - A \exp(-0.3r^2)\} \sin kr + \{M - B \exp(-0.3r^2)\} \{1 - \exp(-0.3r^2)\} \cos kr. \dots\dots(25)$$

For P-wave scattering the corresponding function is

$$f_1(r) = \{1 - A \exp(-0.3r^2)\} \left(\frac{\sin kr}{kr} - \cos kr \right) + \{M - B \exp(-0.3r^2)\} \{1 - \exp(-0.3r^2)\} \left(\frac{\cos kr}{kr} + \sin kr \right), \dots\dots(26)$$

where A and B are two arbitrary parameters and $M = \tan \delta_l$.

The factor 0.3 in (25) corresponds to a 'mean range' of the kernels. (25) and (26) satisfy the necessary boundary conditions:

$$\left. \begin{aligned} f_0(r) &= f_1(r) = 0, \\ f_0(r \rightarrow \infty) &\sim \sin kr + M \cos kr, \\ f_1(r \rightarrow \infty) &\sim \left(\frac{\sin kr}{kr} - \cos kr \right) + M \left(\frac{\cos kr}{kr} + \sin kr \right). \end{aligned} \right\} \dots\dots(27)$$

In Hulthén's method one evaluates the integral

$$I = \int_0^\infty f^* Lf dr, \dots\dots(28)$$

$$\text{where } Lf = \left[\frac{d^2}{dr^2} + k^2 - \frac{l(l+1)}{r^2} - \alpha U_n(r) \right] f_l(r) - \int_0^\infty K_n^l(r, r') f_l(r') dr' \dots\dots(29)$$

and $K_n^l(r, r')$ is symmetrical in r and r' .

The function $f(r)$ is obtained from the conditions

$$I(A, B, M) = 0, \quad \frac{\partial I}{\partial A} = \frac{\partial I}{\partial B} = 0. \quad \dots\dots(30)$$

Equation (30) leads to a quadratic equation in $M = \tan \delta$. Kohn's linear method is based on the alternative conditions

$$\frac{\partial I}{\partial A} = \frac{\partial I}{\partial B} = 0, \quad \frac{\partial I}{\partial M} = -k, \quad \delta = \arctan (M + I/k). \quad \dots\dots(31)$$

Although Hulthén's method has hitherto proved more accurate than Kohn's method, the former, when used together with the latter, enables us to choose the correct M from the pair of solutions of the quadratic equation in Hulthén's method.

Kato (1950) showed that if (30) and (31) are satisfied, then Hulthén's and Kohn's methods are exactly equivalent, but this holds only for a good choice of the wave functions $f_0(r)$ and $f_1(r)$. Consequently the two methods were worked out by integration for each of the four alternative trial wave functions corresponding to $A=B=0$, $A \neq 0$, $B=0$, $A=0$, $B \neq 0$, $A \neq B \neq 0$, and the result accepted which gave good agreement, say within 2%, between the two methods.

For the evaluation of the integral I in (28), steps of 0.4×10^{-13} cm were used in the numerical integration when applied to n - ^3H scattering at 14 mev, but at the lower energies of 8 mev and 2.5 mev steps of 0.8×10^{-13} cm were found to give sufficient accuracy. The kernels were found to extend appreciably to a distance of about five times the well range, that is about 10×10^{-13} cm.

The phases δ_0 , δ_1 at 11 mev and 5 mev were obtained from the results at 14, 8 and 2.5 mev by interpolation.

A check on the accuracy of the phases was carried out in several cases by iterating the trial function, and the phases were found to be altered by not more than two per cent. A feature of the variational method is that the phase is given to an order better than the wave function itself from small r .

The Phases η_0 , η_1 .

The values of η_l were found from those of δ_l in two distinct steps:

(a) The kernel term $[\frac{1}{8}g(r, r') - h(r, r')]$ was plotted numerically for $l=0, 1$ and its contribution to η_l found using the formula

$$\delta_l'' \simeq -\frac{1}{k} \int_0^\infty \int dr (\frac{1}{2}\pi kr)^{1/2} J_{l+1/2}(kr) [\frac{1}{8}g(r, r') - h(r, r')] f_l(r') dr', \quad \dots\dots(32)$$

where $f_l(r)$ is the solution of (5) for neutron-triton scattering. $f_l(r')$ turns out to be less than 0.05 in all cases, so that the use of the formula (32) is a reasonable approximation.

(b) The potential $C(r)$ of (22) was treated as a coulomb term, although it is actually cut off at the origin. This approximation is valid as the scattering contribution comes mainly from the long range nature of the field.

The treatment of a coulomb potential term as a small perturbation on the nuclear field has been given by Chew and Goldberger (1949). For S-wave scattering the phase δ_0' for the combined nuclear and coulomb field is given in terms of the phase δ_0^0 for the nuclear field alone by the formula

$$\beta Q + C_0^2 k \cot \delta_0' = k \cot \delta_0^0 - \beta(W_0 + \ln \gamma^2 \beta r_0) + \beta^2 W_1 - \beta^4 W_2 + \dots \dots(33)$$

where β is the coefficient of the coulomb potential $C(r)$ of (22).

$$\left. \begin{aligned} Q &= \mathcal{R} \frac{\Gamma'(-i\alpha)}{\Gamma(-i\alpha)} - \ln \alpha, & \alpha &= \beta/2k, \\ C_0^2 &= 2\pi\alpha/(e^{2\pi\alpha} - 1), & \ln \gamma &= 0.5772 \dots \text{(Euler's constant)}, \\ W_0 &= \int_0^\infty \frac{1}{r} [Y_I^2(r) - v_R^2(r)] dr. \end{aligned} \right\} \dots \dots (34)$$

Here $Y_I(r)$ is the solution of (5) for $l=0$, and $v_R = \sin(kr + \delta_0)$.

As $\beta \sim 0.1$, the higher order terms W_1 and W_2 may be neglected. For P-wave scattering the corresponding expression becomes

$$\begin{aligned} (1 + \alpha^2)C_0^2\kappa^3 \cot \delta_1' + \beta k^2(Q_1 - 2) + \beta^3 Q_1/4 = k^3 \cot \delta_1^0 - \beta \left[W_0 + \ln \gamma^2 \beta r_0 - \frac{1}{2r_0^2} \right] \\ + \beta^2 \left[W_1 - \frac{1}{2r_0} \right] - \beta^3 \left[W_2 + \frac{1}{4} \ln \gamma^2 \beta r_0 + \frac{3}{8} \right] + \beta^4 W_3 + \dots \dots \dots (35) \end{aligned}$$

$$\text{where } Q_1 = R_1 P_1 \frac{\Gamma'(2-i\alpha)}{\Gamma(2-i\alpha)} - \ln \alpha, \quad W_0 = \int_0^\infty \frac{1}{r} [Y_I^2(r) - v_R^2(r)] dr.$$

The scattering phases η_l for proton- ^3He scattering are then found from (32), (33) and (34):

$$\eta_l = \delta_l' + \delta_l'' \dots \dots (36)$$

W_0 turns out to be difficult to compute, owing to the influence of the $1/r$ factor in the integrand on numerical integration, but as the effect of the coulomb field on the scattering phases is comparatively small, a rough value of W_0 suffices. In the calculations, the value $(W_0 + \ln r_0) = 0.40 \times 10^{-13} \text{ cm}$ was used for the S-wave scattering and $(W_0 + \ln r_0 - \frac{1}{2}r_0^{-2}) = 0.10 \times 10^{-13} \text{ cm}$ for the P-wave scattering.

The phases for l greater than 1 were taken unchanged as for n-T scattering, as they are negligible in the energy region of a few mev where the coulomb field produces important changes in the n-T phases.

Table 2. Calculated Phases*

(1) Neutron-Triton Collisions

Total spin	E_n	Phase	(I) WB	(II) MH	(III) MHWB	(IV) Serber
1	14	δ_0	1.22	1.29	1.27	1.13
		δ_1	-0.59	-0.60	-0.54	-0.49
		δ_2	0.144	0.044	0.037	0.096
		δ_3	-0.031	-0.016	-0.005	-0.023
0	14	δ_0	1.28	1.25	1.24	1.24
		δ_1	-0.64	-0.52	-0.62	-0.45
		δ_2	0.108	0.026	0.038	0.061
		δ_3	-0.017	-0.012	-0.002	-0.014
1	11	δ_0	1.36	1.41	1.42	1.39
		δ_1	-0.36	-0.42	-0.41	-0.42
		δ_2	0.105	0.047	0.045	0.075
		δ_3	-0.021	-0.017	-0.009	-0.019

* Values in heavy type have been obtained by variational methods for solving the integro-differential equations. Other phases have been interpolated or calculated using the Born approximation, as indicated in the text.

Table 2 (*cont.*)

0	11	δ_0	1.47	1.18	1.38	1.36
		δ_1	-0.41	-0.36	-0.37	-0.37
		δ_2	0.079	0.047	0.045	0.050
		δ_3	-0.012	-0.016	-0.012	-0.012
1	8	δ_0	1.50	1.57	1.64	1.57
		δ_1	-0.18	-0.26	-0.23	-0.24
		δ_2	0.068	0.051	0.052	0.052
		δ_3	-0.010	-0.017	-0.012	-0.013
0	8	δ_0	1.71	1.51	1.58	1.62
		δ_1	-0.23	-0.21	-0.20	-0.19
		δ_2	0.052	0.030	0.031	0.041
		δ_3	-0.008	-0.017	-0.010	-0.010
1	5	δ_0	1.99	1.86	1.94	1.81
		δ_1	-0.089	-0.134	-0.105	-0.122
		δ_2	0.040	0.040	0.040	0.040
		δ_3	—	—	—	—
0	5	δ_0	1.82	1.81	1.83	1.87
		δ_1	-0.112	-0.091	-0.087	-0.105
		δ_2	0.034	0.034	0.034	0.034
		δ_3	—	—	—	—
1	2.5	δ_0	2.08	2.22	2.35	2.19
		δ_1	-0.036	-0.049	-0.040	-0.044
		δ_2	0.014	0.014	0.014	0.014
		δ_3	—	—	—	—
0	2.5	δ_0	2.28	2.28	2.09	2.21
		δ_1	-0.044	-0.044	-0.027	-0.031
		δ_2	0.012	0.012	0.012	0.012
		δ_3	—	—	—	—

(2) Proton-³He Collisions

Total spin	E_p	Phase	WB	MH	MHWB	Serber
1	14	η_0	1.38	1.47	1.45	1.25
		η_1	-0.55	-0.57	-0.49	-0.43
0	14	η_0	1.46	1.42	1.40	1.40
		η_1	-0.61	-0.45	-0.59	-0.38
1	11	η_0	1.59	1.66	1.67	1.62
		η_1	-0.33	-0.41	-0.39	-0.41
0	11	η_0	1.74	1.32	1.62	1.59
		η_1	-0.39	-0.33	-0.34	-0.34
1	8	η_0	1.79	1.89	1.98	1.88
		η_1	-0.14	-0.23	-0.19	-0.21
0	8	η_0	2.07	1.81	1.91	1.95
		η_1	-0.19	-0.17	-0.15	-0.15
1	5	η_0	2.41	2.27	2.35	2.21
		η_1	-0.069	-0.12	-0.085	-0.10
0	5	η_0	2.22	2.21	2.24	2.28
		η_1	-0.092	-0.070	-0.067	-0.085
1	2.5	η_0	2.54	2.67	2.76	2.65
		η_1	-0.024	-0.037	-0.027	-0.031
0	2.5	η_0	2.77	2.72	2.56	2.66
		η_1	-0.026	-0.022	-0.017	-0.016

§ 4. RESULTS OF CALCULATION

Figure 1 (a) compares the theoretical angular distribution for the several types of exchange forces with the experiments of Coon, Bockelman and Barschall (1951) at 14 meV neutron energy, and it is seen that good general agreement is obtained

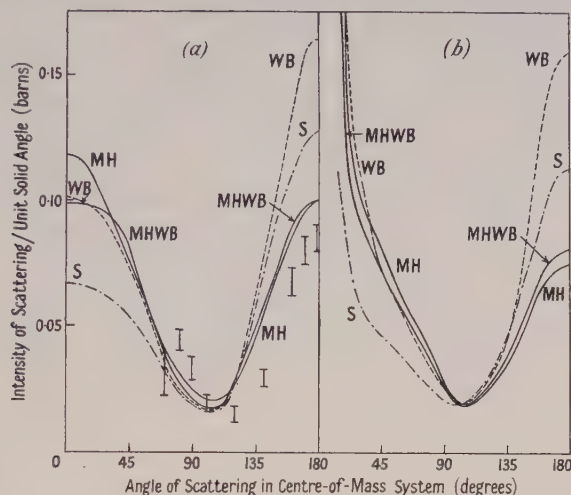


Fig. 1. Calculated angular distributions at 14 meV for (a) neutron-triton collisions, (b) proton- ^3He collisions, assuming WB, MH, MHWB and Serber forces. In (a) the experimental points are due to Coon, Bockelman and Barschall (1951).

for exchange forces of MH and MHWB type. Ordinary forces of WB type result in too high a peak of back-scattering, and Serber forces yield a result intermediate between ordinary and exchange forces in the experimental angular range $70\text{--}180^\circ$ (centre-of-mass system).

In fig. 1(b) the calculated angular distributions at 14 meV for proton- ^3He collisions are seen to differ little from those for neutron- ^3H collisions except for small angles.

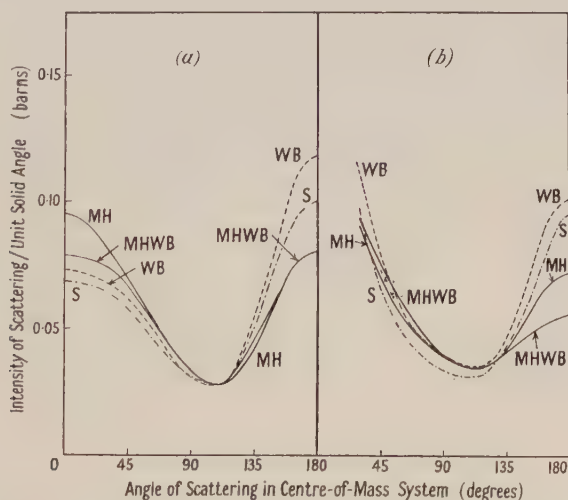


Fig. 2. Calculated angular distributions at 11 meV for (a) neutron-triton collisions, (b) proton- ^3He collisions, assuming WB, MH, MHWB and Serber forces.

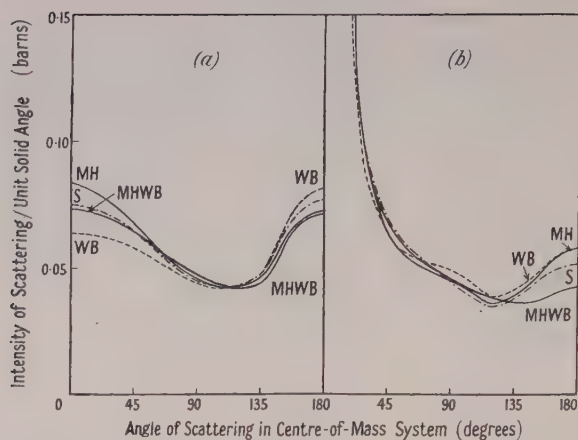


Fig. 3. Calculated angular distributions at 8 mev for (a) neutron-triton collisions, (b) proton- ^3He collisions, assuming WB, MH, MHWB and Serber forces.

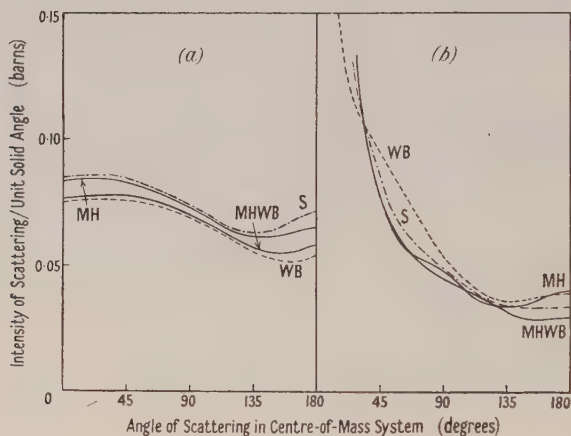


Fig. 4. Calculated angular distributions at 5 mev for (a) neutron-triton scattering, (b) proton- ^3He collisions, assuming WB, MH, MHWB and Serber forces.

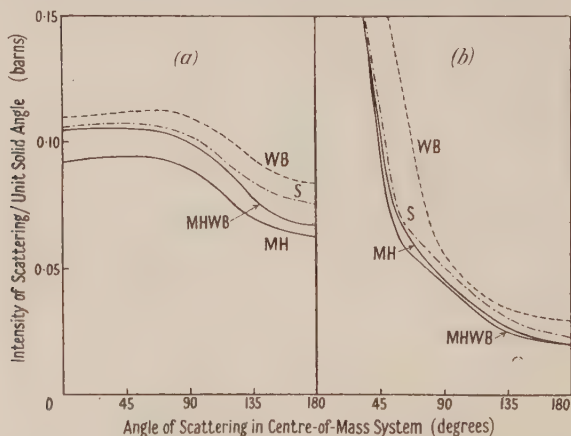


Fig. 5. Calculated angular distributions at 2.5 mev for (a) neutron-triton scattering, (b) proton- ^3He collisions, assuming WB, MH, MHWB and Serber forces.

Figures 2(a), 2(b), 3(a), 3(b), 4(a), 4(b), 5(a), 5(b) show the corresponding differential cross sections for neutron- ^3H and proton- ^3He scattering at incident nucleon energies of 11, 8, 5 and 2.5 mev respectively. As the incident energy decreases from 14 to 8 mev the peak of back-scattering diminishes in importance, particularly for proton- ^3He scattering, but the scattering distributions maintain their general character. However, at lower energies the situation changes, for at 5 mev the back scattering peak almost vanishes, while at 2.5 mev there is actually a back-scattering minimum, and the various alternative theoretical distributions do not differ appreciably in general shape. The proton scattering distributions give a much lower amount of back-scattering and a greater amount of forward scattering than the corresponding neutron- ^3H calculations at 5 mev and 2.5 mev.

The minimum of back-scattering at low energies is due to the occurrence of an S-phase considerably in excess of $\pi/2$ together with a small negative P-phase. The fact that the triplet and singlet S-phases approach π for $k \rightarrow 0$ may be understood if we note that the values of the coefficients α , β , γ , δ in table 1 are predominantly positive, and the summed effect of the ordinary potential $U(r)$ and the kernels in the wave equation (5) is equivalent to a strong attractive potential. Thus the S-phase must be positive, and the equivalent potential is strong enough to 'pull in' the incident wave, producing a phase π .

The total elastic cross section for n-T scattering is illustrated in fig. 6 as a

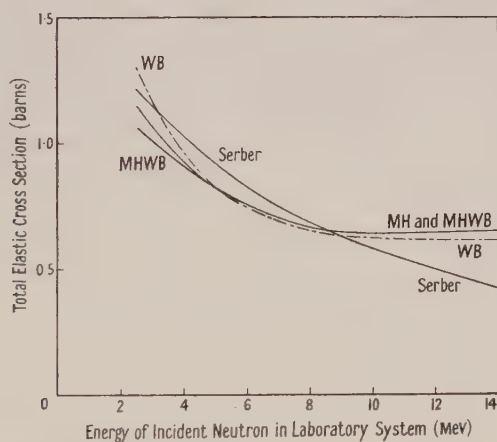


Fig. 6. Calculated total cross sections for neutron-triton collisions as a function of neutron energy, assuming WB, MH, MHWB and Serber forces.

function of neutron energy. Little difference exists between the predictions of the WB, MH and MHWB forces; in fact the Serber force appears to differ more in that it yields a lower cross section for scattering at 14 mev. As for neutron-triton angular distributions at energies other than 14 mev, no total cross section measurements yet exist to enable a comparison of theoretical predictions with experiment.

§ 5. CONCLUSION

A comparison of the predictions of resonating group structure, as applied to four-body collision problems, with neutron-triton scattering experiments at 14 mev favours nuclear forces of exchange type as against ordinary forces.

Theoretical predictions of the scattering distribution of neutrons by tritons and protons by ^3He are made over a range of energies 2.5–14 mev, but no other experimental data are available for comparison.

ACKNOWLEDGMENTS

The writer would like to thank Professor H. S. W. Massey for his interest in this problem, and the Department of Scientific and Industrial Research for a Research Assistantship.

REFERENCES

- BLATT, J. M., and JACKSON, J. D., 1949, *Phys. Rev.*, **76**, 18.
BREIT, G., HOISINGTON, L. E., and SHARE, S. S., 1939, *Phys. Rev.*, **56**, 884.
BUCKINGHAM, R. A., HUBBARD, S. J., and MASSEY, H. S. W., 1952, *Proc. Roy. Soc. A*, **211**, 183.
CHEW, G. F., and GOLDBERGER, M. L., 1949, *Phys. Rev.*, **75**, 1637.
COON, J. H., BOCKELMAN, C. K., and BARSCHALL, H. H., 1951, *Phys. Rev.*, **81**, 33.
HULTHÉN, L., 1944, *K. Fysiogr. Sällsk. Lund, Förh.*, **14**, no. 21.
KATO, T., 1950, *Phys. Rev.*, **80**, 475.
KOHN, W., 1948, *Phys. Rev.*, **74**, 1763.
SWAN, P., 1953, *Proc. Phys. Soc. A*, **66**, 238.

On the Theory of the Isothermal Hall Effect in Semiconductors

By P. C. BANBURY, H. K. HENISCH AND A. MANY*

Physics Department, University of Reading

Communicated by R. W. Ditchburn; MS. received 8th April 1953

Abstract. The theory of the isothermal Hall effect is re-examined taking into account the finite dimension of the specimen in the direction of the Hall e.m.f. This involves consideration of concentration gradients, space charges, recombination processes and floating potentials at the Hall electrodes. The analysis leads to recommendations concerning experimental technique.

§ 1. INTRODUCTION

THE conventional treatments of the isothermal Hall effect in semiconductors are based on the important assumption that effects due to the finite breadth of the specimen can be neglected. This implies that the concentration of free charge carriers (electrons and positive holes) does not vary throughout the specimen in the direction of the Hall e.m.f., so that the specimen contains no space charges. These assumptions represent a simplification of the problem which is often permissible. It will be shown, in particular, that in the case of a one-carrier system the conventional approximation is a very good one. In two-carrier systems, however, concentration gradients are more important, and a full treatment, taking into account finite breadth, must allow for variations of carrier concentration, and hence also for recombination processes and the presence of floating potentials at the electrodes.

§ 2. FORMULATION OF THE PROBLEM

The relations which govern the behaviour of electrons and holes in the presence of a transverse magnetic field can be formulated as follows. Let the longitudinal electric field E_x , the magnetic field H and the Hall field E_z be in the x , y and z directions respectively. Then the hole and electron currents in the z direction are given respectively by

$$I_{pz} = e\mu E_z p + \frac{1}{c} H e \mu^2 E_x p - eD \frac{dp}{dz} \quad \dots\dots(1)$$

$$I_{nz} = eb\mu E_z n - \frac{1}{c} H eb^2 \mu^2 E_x n + ebD \frac{dn}{dz} \quad \dots\dots(2)$$

where μ is the mobility of holes, b the ratio of electron to hole mobility, D the diffusion constant for holes, and n and p the electron and hole concentrations in the presence of a sweeping field and magnetic field. The generation and recombination of carriers in the bulk is neglected compared with surface recombination processes. This will be justified later. The effect of space charge barriers at the surfaces, arising from the presence of surface states, is not

* At present on leave of absence from the Hebrew University, Jerusalem.

considered here. Uniform carrier velocity due to the longitudinal electric field is assumed and the usual correction can be made for a velocity distribution. Since the Hall e.m.f. is measured under zero current conditions, $-I_{nz} = I_{pz} = I_z$. Owing to surface generation and recombination, these currents will not separately vanish. Assuming complete ionization of impurity centres, the Hall field is given by

$$\frac{dE_z}{dz} = \frac{4\pi e}{\kappa} (p - n + n_0 - p_0) \quad \dots\dots(3)$$

where n_0 and p_0 are the equilibrium values of electron and hole concentrations. In these equations, the electron and hole concentrations n and p are functions of z (c.g.s. units are used).

Two of the boundary conditions to be imposed on the above equations may be taken as follows:

$$E_z(a) = E_z(-a) = 0 \quad \dots\dots(4)$$

$$\int_{-a}^a (p - n + n_0 - p_0) dz = 0 \quad \dots\dots(5)$$

where $z = a$ and $z = -a$ are the boundary planes. The first of these equations involves the neglect of edge effects due to the finite extension of the specimen in the x and y dimensions; eqn. (5) imposes total neutrality over the whole cross section. A further condition is required to ensure that there is no continuously increasing accumulation or deficit of carriers at the surfaces $z = \pm a$. In the simplest case, for $p \ll n_0$, this would be expressed as

$$I_z/e = s_a[p(a) - p_0] = -s_{-a}[p(-a) - p_0] \quad \dots\dots(6)$$

where s_a and s_{-a} are the surface recombination velocities at $z = a$ and $z = -a$ respectively. In the present case this formulation is not necessarily adequate, since the above inequality may not be satisfied. In the case when it is not valid, e.g. in near-intrinsic cases, a more general expression must be used, the form of which will depend on the recombination mechanism envisaged. For example, a trapping process on the surface similar to that considered in the bulk by Shockley and Read (1952) could be employed.

The conventional expression for the Hall field of a two-carrier system is obtained by regarding the specimen as infinite. The concentration gradients then vanish, and the condition is obtained that $dE_z/dz = 0$ everywhere. For a finite specimen, E_z must in fact be determined from eqns. (1), (2) and (3), and cannot be constant, as this would require a surface charge giving rise to infinite values of concentration gradients at the surfaces. The fact that E_z varies with z indicates that the Hall angle, which is defined as $\tan^{-1}(E_z/E_x)$, has no unique meaning in a specimen of finite breadth.

§ 3. SOLUTION FOR ONE-CARRIER SYSTEM

In the case of a one-carrier system (e.g. $p_0 = 0$), eqns. (2) and (3) reduce to

$$\frac{d^2 V}{dz^2} = \frac{4\pi e}{\kappa} n_0 [\exp(AV + bBz) - 1] \quad \dots\dots(8)$$

where V is the Hall potential, $E_z = -dV/dz$, $A = \mu/D$ and $B = \mu^2 H E_x / cD$. The boundary conditions imposed are

$$V(0) = 0, \quad (dV/dz)_{z=a} = 0. \quad \dots\dots(9)$$

The condition $n(0) = n_0$ follows from (5) from considerations of symmetry. It is sufficient to consider only positive values of z .

By using the substitution $U = AV + bBz$, the first integration of (8) is easily carried out. For the second integration, the approximation $\exp U = 1 + U + \frac{1}{2}U^2$ is used. This is justified by the fact that U is small compared with unity, for all values of z . This can be verified from the solution using this approximation. In fact, $U=0$ in the conventional treatment.

The integration yields

$$V(z) = V_c(z) \left\{ 1 - \frac{L}{z} \frac{\sinh(z/L)}{\cosh(a/L)} \right\} \quad \dots\dots(10)$$

where $V_c(z)$ is the conventional Hall potential: $V_c(z) = -(bB/A)z$, and $L = (\kappa D / 4\pi e \mu n_0)^{1/2} = (\kappa kT / 4\pi e^2 n_0)^{1/2}$. The Hall e.m.f. in a finite specimen is thus given in terms of the conventional e.m.f. by

$$2V(a) = 2V_c(a)[1 - (L/a) \tanh(a/L)]. \quad \dots\dots(11)$$

It is seen that as the breadth $2a$ is increased the correction term is reduced, which is consistent with the fact that the conditions in an infinite specimen are more nearly approached. Taking for example a specimen with $n_0 = 10^{15}$ (p_0 negligible), $\kappa = 16$ and $2a = 0.1$ cm, the correction amounts to only 0.03%. Even for the lowest carrier concentrations and smallest crystal sizes encountered in practice, the departure from the accepted value will scarcely be appreciable. The correction might be significant, however, in polycrystalline material.

It should be pointed out that the departure of the Hall field from the accepted value (and hence the departure from neutrality) is appreciable only near the surfaces; the difference in the Hall potentials in the two models reduces from $V_c(a)L/a$ at the surface to $1/e$ of this value at a distance of L from the surfaces. The region of space charge is thus confined to two layers of effective thickness L near the surfaces $z = \pm a$. The expression for L is similar in form to the Debye-Hückel length, referred to in Shockley's theory of p-n junctions (Shockley 1949). It may be shown that if the total space charge is regarded as distributed uniformly over each of these layers, the effective average electron concentrations will be $n(a)$ and $n(-a)$. These charges establish the Hall field, the specimen being regarded as a parallel plate condenser system. From eqns. (8) and (11) it can be shown that $n(a) \simeq n_0(1 + bBL)$. For ordinary values of E_x and H the space charge, and hence the value of $[n(a) - n_0]e$, will be a small fraction of en_0 . (In the example considered above for $E_x = 1$ v cm⁻¹ and $H = 5000$ gauss, $n(a) - n_0 \simeq 10^{11}$ compared with $n_0 = 10^{15}$.) Thus concentration gradients will be small, which is consistent with the fact that the correction term in eqn. (11) is generally trivial. These considerations suggest that the system may legitimately be regarded as a single carrier one only if the condition $p_0 \ll n(a) - n_0$ is satisfied.

§ 4. DISCUSSION OF A TWO-CARRIER SYSTEM

For two-carrier systems, the conventional assumptions are less justified because of the larger concentration gradients encountered. The associated recombination processes at the surfaces must also be considered. A general solution of eqns. (1), (2) and (3) for this case is difficult and may have to be carried out numerically. An approximate solution will now be discussed.

The results obtained in the single carrier case suggest that it is reasonable to expect the departure from neutrality, and hence the value of dE_z/dz , to be

negligible far inside the specimen, e.g. near the centre $z=0$. For such a region, integration of eqns. (1) and (2) for the case E_z constant, gives

$$p = \frac{I_z}{eD(AE_z + B)} + \left[p_0 - \frac{I_z}{eD(AE_z + B)} \right] \exp [(AE_z + B)z], \quad \dots\dots(12)$$

$$n = \frac{I_z}{ebD(-AE_z + bB)} + \left[n_0 - \frac{I_z}{ebD(-AE_z + bB)} \right] \exp [(-AE_z + bB)z]. \quad \dots\dots(13)$$

It follows from eqns. (12) and (13) that the assumption of neutrality is strictly self-consistent only if the coefficients of the exponential terms vanish, which implies that p and n each have their equilibrium values (p_0 and n_0) throughout the region considered. The vanishing of these coefficients is realized only if

$$I_z = eD(AE_z + B)p_0 = ebD(-AE_z + bB)n_0. \quad \dots\dots(14)$$

The right-hand equality here leads to the accepted value of the Hall field (near the centre)

$$E_z^0 = \frac{b^2 n_0 - p_0}{bn_0 + p_0} \frac{B}{A}.$$

The left-hand equality in (14) then requires that I_z should have the particular value

$$I_z = I_z^0 = eBD \left[\frac{b^2 n_0 - p_0}{bn_0 + p_0} + 1 \right] p_0 \quad \dots\dots(15)$$

which is the value characteristic of an infinite specimen. There is, however, another condition imposed on I_z , namely that I_z/e must be equal to the rate of generation and recombination of carriers at the two surfaces. Only if the surface generation rate is large enough to allow I_z to attain the value I_z^0 can eqns. (14) and (15) be satisfied. If this condition is not satisfied I_z is limited to a value less than I_z^0 , and is dependent on surface conditions. It is thus possible to divide the problem into two ranges according to whether the generation rate is sufficient to establish $I_z = I_z^0$ or not. These two cases will now be discussed, and the range of generation rates in which each treatment is valid will be indicated.

(i) $I_z < I_z^0$

In this case, corresponding to low surface generation rate, the coefficients of the exponentials in eqns. (12) and (13) cannot vanish and therefore neutrality cannot be satisfied to as good an approximation as when eqns. (14) and (15) hold. However, the discussion can be confined to a very small region of the specimen near the centre, in which the exponential terms in eqns. (12) and (13) can be expanded with the neglect of second and higher order terms in z . The condition of neutrality is then approximately satisfied in this region if $dn/dz = dp/dz$ at $z=0$, which leads to

$$E_z = \frac{bn_0 - p_0}{n_0 + p_0} \frac{B}{A} + \frac{(1 - 1/b)}{e\mu(n_0 + p_0)} I_z \quad \dots\dots(16)$$

in the centre. This value of the Hall field may be appreciably different from the accepted value. In the extreme case of no recombination $I_z=0$ and the departure from the accepted expression is then greatest: for example, for $n_0 = p_0$ the Hall field at the centre is half the accepted value. This case has been considered by Fowler (1935). As more generation and recombination are allowed

I_z], and hence the Hall field in the centre, increases, until finally when $I_z = I_z^0$ the accepted value is obtained.

$$(ii) \quad I_z = I_z^0$$

In this case neutrality is effectively maintained in the bulk, and the situation is somewhat analogous to that in a single-carrier system. Solutions in this range will be discussed in more detail, as most of the specimens encountered in practice are believed to come within this category, as will be explained below.

For the sake of simplicity a case will be considered where p_0 is small compared with n_0 . For such a specimen, the neglect of p_0 with respect to n_0 in eqn. (15) gives

$$I_z^0/e = (b+1)BDp_0. \quad \dots\dots(17)$$

The use of the boundary condition expressed in eqn. (6) is now permissible, and the hole concentrations at $z = \pm a$ are obtained, namely

$$p(a) = \left[1 + \frac{(b+1)BD}{s_a}\right] p_0; \quad p(-a) = \left[1 - \frac{(b+1)BD}{s_{-a}}\right] p_0. \quad \dots\dots(18)$$

Thus for given surface recombination velocities s_a and s_{-a} , $p(a)$ and $p(-a)$ are determined. Also the limits of the validity of the assumption $I_z = I_z^0$ can be found. Obviously $p(-a)$ cannot be negative and hence for $s_{-a} < (b+1)BD$, I_z cannot attain the value I_z^0 ; the rate of carrier generation at $z = -a$ is lower than I_z^0/e . Values of s_{-a} in the neighbourhood of that given by the right-hand side of the above inequality thus correspond to the transition between range (i) and range (ii). These transition values depend on the value of B , which is proportional to HE_x . For example, in the case of a measurement on germanium in which $H = 5000$ gauss, $E_x = 1 \text{ v cm}^{-1}$, the transition occurs for values of s_{-a} in the neighbourhood of 500 cm sec^{-1} . Thus, except for extremely well etched surfaces or high B values, most practical cases will be covered by the present treatment.

§ 5. CONCLUSION

Approximate solutions have been obtained in ranges (i) and (ii) for the Hall field in the centre of the specimen. This field falls away in the space-charge region to zero at the two boundaries. In cases within range (i) the departure from neutrality has been shown to extend further into the specimen than for those in range (ii), and hence the field is constant over a larger proportion of the specimen in the latter cases. For the simple interpretation of experimental results, therefore, it is desirable to ensure that specimens fall within range (ii), since the field is then more uniform throughout the specimen. This is readily achieved in practice.

In these cases it can now be seen that, since the departures from equilibrium carrier concentration are effectively limited to narrow regions near the surfaces, bulk recombination processes can safely be neglected. The time of transit for a carrier across the region where concentrations are disturbed can be estimated and is usually less than a microsecond.

Regarding the values of the concentration gradients in range (ii), it is seen first that as both positive and negative charge carriers are deflected to the same surface, it is only the difference in added carrier concentration, and not the added concentration of each, which is limited to that required to establish the Hall field. Thus the concentration gradients near the surface may be very large

compared with those encountered in one-carrier systems. This may be confirmed numerically by inserting appropriate values for B and s_a in eqn. (18).

It also follows from eqn. (18) that the larger the values of s_a and s_{-a} , the smaller will be the departures of the hole concentrations at $z = \pm a$ from p_0 . This suggests that the average hole concentration gradients will be reduced by further increasing surface recombination rates. It thus appears that the conditions under which diffusion currents may be neglected, and under which the accepted Hall effect treatment may be applied, are approached more nearly as surface recombination rates are made larger. In practice this means that the specimens used for Hall measurements should have roughened rather than etched surfaces, so as to make the approximation of the accepted expressions more legitimate.

It should be noted that the e.m.f. actually measured between the Hall probes is not only $V_H = - \int_{-a}^a E_z dz$, but also involves contribution from the two 'floating potentials' (Bardeen 1950) $V_f(a)$ and $V_f(-a)$ at the Hall electrodes. The latter will in general arise if the Hall electrodes are associated with rectifying barriers. The polarity of these floating potentials will be in opposition to the Hall potentials. This can be seen, for example, by consideration of the case of an n-type specimen with rectifying barriers at the Hall contacts. Both types of carriers are deflected by the magnetic field towards the same surface $z = a$, and this surface develops a negative Hall potential. At the same time, the added hole concentration at this surface produces a positive floating potential across the contact barrier.

In order that the floating potentials shall be small, it is desirable that the electrodes shall be free from rectifying barriers, a condition which is in any case favourable for sensitive measurement of the total voltage. The roughening of the surface, which has already been found advantageous above, will also tend to reduce the floating potentials, by reducing $p(a) - p_0$.

Two-carrier systems of the kind here discussed are now under experimental investigation, and it is hoped to publish a further report in due course. The preliminary results so far available provide support for the present conclusions.

Since the preparation of this paper it has come to our notice that some aspects of the present problem have also been considered by Welker (1951) and by Landauer and Swanson (1953).

ACKNOWLEDGMENTS

We wish to thank Professor R. W. Ditchburn for his interest and encouragement, and also Mr. L. A. G. Dresel for his help. Thanks are also due to the Humanitarian Trust and to the Friends of the Hebrew University for a grant to one of us (A. M.).

REFERENCES

- BARDEEN, J., 1950, *Bell Syst. Tech. J.*, **29**, 469.
- FOWLER, R. H., 1935, *Statistical Mechanics* (Cambridge: University Press).
- LANDAUER, R., and SWANSON, J., 1953, *Bull. Amer. Phys. Soc.*, **28**, No. 2, 9.
- SHOCKLEY, W., 1949, *Bell Syst. Tech. J.*, **28**, 435.
- SHOCKLEY, W., and READ, W. T., 1952, *Phys. Rev.*, **87**, 835.
- WELKER, H., 1951, *Z. Naturforsch.*, **6a**, 184.

By H. G. HOWELL

The British Rayon Research Association, Urmston, Manchester

MS. received 1st April 1953

Abstract. The vibrational analysis of the spectrum of Cl_2^+ proposed by Elliott and Cameron is criticized. The magnitude of the vibrational and electronic constants to be expected from considerations of the electron configurations is discussed and it is shown that these are probably such as to make any analysis extremely difficult.

§ 1. INTRODUCTION

THE high-frequency emission spectrum of chlorine consists of ultra-violet continua and red-degraded bands stretching from 3400 to at least 5500 Å. According to Elliott and Cameron (1937) a prominent feature under low dispersion is a series of strong bands from 5100 Å towards the red, grouped in pairs, having a separation of roughly 140 K^* , at intervals of approximately 300 K. These show no marked heads in contrast with the rest of the spectrum where the band heads are well defined.

These bands were first studied by Ota and Uchida (1928) who arranged them into three systems. Elliott and Cameron (to be referred to as EC) remeasured them obtaining much more accurate data, with which they were able to show that certain discrepancies in the values of Ota and Uchida were greater than any experimental error and that consequently their analysis could not be accepted. In their first paper they were unable to offer an alternative analysis but they definitely established the commonly-occurring differences of 627 and 600 K, and also showed from isotopic considerations that there were probably two systems present, with system origins at approximately 21 000 and 21 340 K.

In a later paper (1938) they extended their study by analysing the rotational structure of 18 bands, as a result of which they concluded that most of these belonged to a $^2\Pi - ^2\Pi$ transition with the system origins at 20 800 and 20 600 K approximately, a slight alteration from the values given from their previous study of the isotope effect. They gave a vibrational analysis of this system and suggested that the four bands which could not be fitted belonged to another whose origin is near to the $^2\Pi - ^2\Pi$, although they did not rule out the possibility that a $^4\Delta - ^4\Delta$ transition might be involved. From the even multiplicity of the systems they pointed out that the emitting molecule could not be the normal halogen but must rather be the ionized molecule Cl_2^+ .

More recently Deo (1948) has reported the occurrence of a number of these bands in a weak discharge in chlorine using a Siemens' ozonizer. The work was done under low dispersion and the measurements cannot compare in accuracy with those of EC. No attempt was made to assess their conclusions concerning this spectrum.

* K (after Kayser) is here used for wave number instead of cm^{-1} on the recommendation of the International Commission of Spectroscopy (Rome 1952).

§ 2. COMMENTS ON THE VIBRATIONAL ANALYSIS

Examination of the Deslandres scheme for the sub-systems of $^2\Pi - ^2\Pi$ given by EC shows that the proposed analysis is far from satisfactory. There are an extraordinary number of gaps in the scheme, for, as they point out, in sub-system I the bands which have odd v' values are rarely observed whilst in sub-system II the bands from even v' values are occasionally missing. The number of gaps is emphasized by the fact that certain bands appear in both sub-systems. It is noted that bands may be present to fill such gaps but may be overlaid by other bands. Next, the intensity distribution of the bands seems in conflict with the given ω_e values, for this follows an open Franck-Condon parabola, characteristic of bands having widely different ω_e values, whereas the values derived from the analysis are actually 645 K and 572 K . Although EC claim that their allocation of vibrational quantum numbers is justified from the isotope measurements, they admit that the agreement between observed and calculated isotope separations is not very satisfactory with three of the bands. If these are considered doubtful, and omitted from the analysis, the aforementioned gaps in the quantum array become larger and suggest a fundamental weakness in the scheme.

Yet another difficulty in the proposed analysis arises from the value of the dissociation energy derived from a Birge-Sponer extrapolation. This is found to be 4.4 eV as against 2.23 which is obtained indirectly from the values of the ionization potentials I of Cl and Cl_2 and the dissociation energy D of Cl_2 . In the face of this difficulty EC suggested that one or more of these normally accepted values may be in error. A critical survey of these data, however, does not support such a view. Whilst the ionization potential of Cl is not now in question, the value for Cl_2 might well be regarded as the possible source of error, but this was determined by Mackay (1924) and Mulliken (1934) observes that Mackay's values of I for the halogens have been found by him to be unusually reliable. The other factor, the dissociation energy of Cl_2 , is now accepted as 2.47 eV—the value used by EC. It is inconceivable that this is in error by as much as 2.2 eV which is the discrepancy between the expected value of $D(\text{Cl}_2^+)$ and that obtained from the Birge-Sponer extrapolation. A more reasonable view is that this extrapolation has given a poor result.

This could occur if either the use of the Birge-Sponer method is unsound (as often is the case) or the values of ω_e and $x_e\omega_e$ used in the extrapolation are faulty. Now Gaydon (1946) in a survey of the methods used in determining dissociation energies finds that the Birge-Sponer extrapolation gives reliable results with ionized molecules, and so we should not complain of its use in the present case. Accordingly, it is reasonable to explain the discrepancy between the two calculated D'' values as being due to incorrect vibrational constants, particularly in view of the presence of the other discordant features in the analysis already mentioned. This point will be further discussed in a later section. These comments indicate the need for a re-evaluation of the spectrum of this important molecule.

§ 3. PREDICTIONS FOR Cl_2^+

In view of the foregoing remarks, attempts were made to rearrange the data of EC into a vibrational scheme which seemed more satisfactory to the writer, using their excellent reproduction of the spectrum as a guide, but without any success. The main difficulty in testing possible alternative arrangements is that there are too many heads or structures which may be heads, and consequently

some sort of agreement can be obtained for a number of possibilities none of which is consequently really satisfying. Accordingly it was decided to attack the problem from quite a different angle, viz. is it possible to anticipate certain features of the spectrum of Cl_2^+ before actually studying it? In particular, it was reasoned that a consideration of the electron configuration of the molecule might lead to the prediction of the type of electron transitions involved, and also to the vibrational properties of the levels so that some sort of order in the mass of heads might suggest itself.

3.1. Ground State

The electron configuration of the normal state of the halogen molecule X_2 is now accepted as being $\sigma^2\pi^4\pi^4, {}^1\Sigma_g$ giving as the most probable ground state of the ion X_2^+ , $\sigma^2\pi^4\pi^3, {}^2\Pi_g$. The σ and π orbitals are in the case of Cl_2 , $3p\sigma$ and $3p\pi$ in type Mulliken points out that the state $\sigma^2\pi^3\pi^4, {}^2\Pi_u$ which could be expected to have the same energy as the $\sigma^2\pi^4\pi^3, {}^2\Pi_g$ will resonate quantum mechanically with it, a π electron oscillating between the two shells, so that the configuration of each could actually be represented as $\sigma^2\pi^{3\frac{1}{2}}\pi^{3\frac{1}{2}}$. Both of these ${}^2\Pi$ states will be inverted, having a doublet separation of the same order as a for the X^+ ion or atom X which, in the present case for Cl , amounts to 610 κ . The mean separation of the two ${}^2\Pi$ states would depend upon the magnitude of the resonance between the π^4 shells and may be small enough to permit of overlapping of the doublet components, thus

$${}^2\Pi_{1\frac{1}{2}g}, {}^2\Pi_{1\frac{1}{2}u}, {}^2\Pi_{\frac{3}{2}g}, {}^2\Pi_{\frac{3}{2}u}.$$

Since the bonding σ electrons are not concerned, the r value for both states should be the same as in neutral Cl_2 and consequently the ω_e'' values can be expected to be of the same order, viz. 600 κ . It is worth noting that Mulliken has ascribed some bromine bands for which $\omega_e'' = 362 \kappa$ to the ion Br_2^+ . If this is correct then the ratio $\omega(\text{Br}_2^+)/\omega(\text{Br}_2) = 1.12$ and using this same value for Cl_2^+ , ω_e'' should be 630 κ .

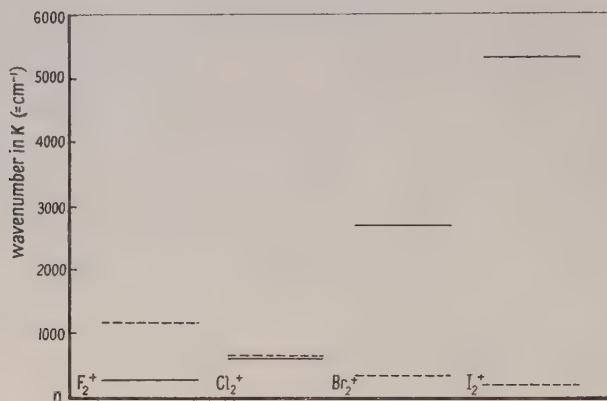
Thus to summarize, we can expect to find for Cl_2^+ four low-lying levels comprising two ${}^2\Pi$ states with an unknown separation but with each having a doublet splitting of about 600 κ and each component of each doublet having an ω_e value of the same order. It is therefore suggestive that EC emphasize the recurring differences of 627 and 632 κ . It is also evident how this near equality of the ω_e and $\Delta\nu$ values can confuse and present difficulties in any analysis. A similar case arose with the β bands of SiF where a satisfactory analysis was delayed until Eyster (1937) recognized that the sequence difference was almost the same as the ground state doublet separation (161 κ).

In the figure the probable magnitudes of the doublet separation and vibrational frequency are shown for all the halogen ions and it will be seen that the coincidence for Cl_2^+ makes it a particularly unfortunate choice for analysis. This diagram does not show the additional complication of the other ${}^2\Pi$ resonance state.

3.2. Excited States

There is a large number of states which can be excited from the ground state configuration to give $\pi^3\pi^3\sigma$ where σ is the anti-bonding orbital ($3p\sigma - 3p\sigma$, σ_u) corresponding to the main bonding orbital ($3p\sigma + 3p\sigma$, σ_g) and these are ${}^2\Sigma^+(2)$, ${}^2\Sigma^-(2)$, ${}^2\Delta$, ${}^2\Delta_u$, ${}^4\Sigma^+$, ${}^4\Sigma^-$ and ${}^4\Delta$. The corresponding transition, bonding-antibonding orbital in neutral Cl_2 reduces the vibrational frequency from

$\omega_e'' = 565 \text{ K}$ to $\omega_e'' = 239 \text{ K}$ and there is no *a priori* reason why the same order of reduction should not occur in Cl_2^+ as the transition is essentially the same. Hence all of these levels should have an ω_e value of about half of ω_e'' , i.e. about 300 K . Another indication of the expected order of magnitude of the upper state or states is obtained from a study of the B values found by EC from their rotational analysis of some of these bands. In the halogens, the ratio B^2/ω_e for a pair of states is found to be approximately constant and it is reasonable to expect the same to be true for Cl_2^+ . Assuming a value of 630 K for ω_e'' the value of ω_e' comes to 310 K .



Comparison between probable values of ω_e'' (-----) and $^2\Pi$ separation $\Delta\nu$ (———).

Now it is obvious that in a progression type of band system or systems when one of the vibrational frequencies is about half the other many coincidences or near coincidences of band heads will occur, thus giving a deceptive appearance of simplicity, which will increase the difficulty of analysis. Such a state of affairs occurred with the absorption spectrum of I_2 and a satisfactory solution was only obtained when Warren (1935) recognized this property of the vibrational frequencies. Indeed with these halogens, coincidence may not be confined to the band heads but may occur between branches of the same band giving a more deceptive appearance of simplicity which may ultimately lead to an incorrect interpretation of the type of transition.

With these predictions in mind it would appear that the spectrum of Cl_2^+ should have an exceptional number of pitfalls for the investigator. With this particular molecule Nature seems to have arranged the vibrational and electronic constants to be of such magnitudes as to present very heavy odds against an easy analysis, and perhaps even against any satisfactory final solution. It may be that a study of Br_2^+ would be more helpful in that at least one of the difficulties mentioned would be removed, viz. the equality of ω_e and $\Delta\nu$. It might then be possible to determine how many systems were involved, and this information could be carried back to the Cl_2^+ case with some confidence.

§ 4. DISSOCIATION ENERGY

The foregoing arguments are in favour of rejecting the proposed vibrational constants of EC and hence the value of 4.4 eV for D'' . In the absence of other evidence, then, the value for this constant is now left open and it would appear

more reasonable to accept the 2.23 eV which is obtained from the data on Cl and Cl_2 which has already been discussed. There is however other evidence which, if accepted, leads to a higher value than 2.23 eV with the consequent implication that the data referred to above are in error as suggested by EC in their discussion of their 4.4 eV value. This evidence is the selection of 20 600 and 20 800 K as system origins. These values are determined from isotope separations and if the identification of the isotopic heads is correct then it is most probable that $D'' > 2.23$ eV, for the excited states must dissociate into one or other combinations of the ground states of the atom-ion; assuming the most favourable case of dissociation—the excited state into $^2\text{P}_{1/2} + ^3\text{P}_0$ with even a flat potential energy curve giving, say, only 0.5 eV for D' and the ground state into $^2\text{P}_{3/2} + ^3\text{P}_2$ —a value of 2.83 eV is obtained for D'' .

Rather than accept this value however, it seems more reasonable to suspect that, owing to the richness and profusion of vibrational structure expected, and also observed, certain of the heads may have been incorrectly assigned as isotopic heads thus raising doubt as to the validity of the extrapolation which yields the values quoted as system origins.

§ 5. ROTATIONAL ANALYSIS

There remains now a need to examine how far these views on the vibrational analysis affect the analysis of the rotational structure made by EC and also the resulting interpretation of the measured bands as belonging to a $^2\Pi - ^2\Pi$ transition.

The use of the B values of EC in § 3.2 of the present paper implicitly states the writer's own conviction of the correctness of the rotational analysis as far as the quantitative work goes. These values are just of the order to be expected when compared with those established for neutral Cl_2 . It was the failure of the B^2/ω constancy rule which led to the doubt as to the accuracy of the proposed ω_e' value.

However the absence of a $^2\Pi$ state from the list arising from the excited configuration throws doubt on EC's interpretation of their analysis. The relevant facts in this connection are (a) the bands do not possess a Q branch giving a choice of transitions from $^2\Sigma - ^2\Sigma$, $^2\Pi - ^2\Pi$ and $^2\Delta - ^2\Delta$, (b) the absence of alternating intensities in the lines. The suggested explanation of (b) given by Kronig was that $^2\Sigma$ states are not involved and that the Λ -type doubling is not resolved so that each line would consist of an unresolved strong and weak component. This argument leaves only $^2\Pi - ^2\Pi$ and $^2\Delta - ^2\Delta$ as probable transitions and because the ground state is expected to be $^2\Pi$ the former was selected.

Now this leaves out of consideration the type of coupling which occurs. The corresponding transition in the case of neutral Cl_2 is $^3\Pi_0 - ^1\Sigma$ when described in terms of normal $\Lambda - \Sigma$ coupling but it is recognized that the coupling is nearer case c , with the transition being better represented as 0-0. On the same coupling scheme (case c) with Cl_2^+ , a transition $^2\Sigma - ^2\Pi_{1/2}$ becomes $\frac{1}{2} - \frac{1}{2}$ and will give a two-branch band system similar to a $^2\Sigma - ^2\Sigma$. Further, Kronig's argument about the alternating intensities still applies but now involves Ω -type doubling instead of Λ -type and this now does not rule out the case c equivalent of $^2\Sigma - ^2\Pi_{1/2}$. Consequently it is suggested that the two systems studied by EC are both case c $\frac{1}{2} - \frac{1}{2}$ transitions with a common lower state deriving from $^2\Pi$ and the upper states deriving from separate $^2\Sigma$ -type levels.

REFERENCES

- DEO, P. G., 1948, *Phil. Mag.*, **39**, 978.
ELLIOTT, A., and CAMERON, W. H. B., 1937, *Proc. Roy. Soc. A*, **158**, 681; 1938, *Ibid.*, **164**, 531.
EYSTER, E. H., 1937, *Phys. Rev.*, **51**, 1078.
GAYDON, A. G., 1946, *Dissociation Energies* (London : Chapman and Hall).
MACKAY, C. A., 1924, *Phys. Rev.*, **24**, 319.
MULLIKEN, R. S., 1934, *Phys. Rev.*, **46**, 549.
OTA, Y., and UCHIDA, Y., 1928, *Jap. J. Phys.*, **5**, 53.
WARREN, D. T., 1935, *Phys. Rev.*, **47**, 1.

RESEARCH NOTES

Ferromagnetic Resonance in Colloidal Suspensions

BY D. M. S. BAGGULEY

The Clarendon Laboratory, Oxford

MS. received 16th April 1953

SINCE the first report of ferromagnetic resonance absorption at microwave frequencies (Griffiths 1946) a number of workers have extended the investigations to other metals and the results have been reviewed by Kittel (1951). The experiments have been made using plane samples with the mutually perpendicular static and high-frequency magnetic fields in the plane of the specimen, so that in order to derive the spectroscopic splitting factor g a knowledge of the saturation intensity of magnetization under the actual experimental conditions is necessary. This is not always easy to determine accurately and it is the purpose of this note to suggest an alternative technique using colloidal suspensions for which the ferromagnetic particles apparently behave like small spheres.

The experiments reported here have been carried out at 290°K and wavelengths of 3.14 cm and 1.20 cm. A few measurements have been made at 20°K and these will be discussed separately. The colloids were obtained as suspensions in paraffin wax either from the reduction of chemical salts at temperatures less than 350°C (e.g. formates, oxalates or carbonyls) or from a high-frequency arc discharge in hydrogen at one atmosphere pressure. The particles remaining after centrifuging the molten wax are believed to be nearly spherical and about 50–100 Å in diameter (Weil 1951, Svedberg 1928) so that their dimensions are much less than the skin depth at these frequencies and they may well be expected to behave like single domains (Kittel 1949).

The formula relating the frequency ν_0 of maximum power absorption to the static magnetic field H has been derived by Kittel (1948) and should be rigorously applicable to such small particles. For a sphere the relation is

$$h\nu_0 = g\beta H \quad \dots \dots (1)$$

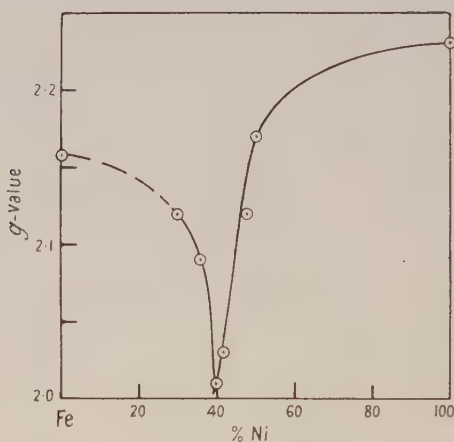
where β is the Bohr magneton and h is Planck's constant. To check that this relation is applicable to the experiments described here measurements were made using colloidal suspensions of iron, cobalt and nickel for which metals the g -values are well known. The measurements were made at two wavelengths under very different experimental conditions, those at 3 cm wavelength involving magnetic fields of about 3000 gauss used a technique analogous to the Bloch induction method of nuclear resonance whilst the measurements at 1.20 cm wavelength in fields of about 8000 gauss measured the microwave absorption using the method of magnetic field modulation. Using eqn. (1) very good agreement with previous results was obtained at both of these wavelengths and in the table we give the g -values and half line widths for the colloidal suspensions together with typical values obtained by previous methods (Kittel 1951). These

results make it seem reasonably clear that the particles which we have obtained are spherical in so far as microwave resonance is concerned and the g -value, which is found to be independent of wavelength, can be obtained directly without making any assumptions about the value of the saturation intensity of magnetization.

Substance		Iron	Cobalt*	Nickel
Colloidal suspension	half-width (gauss)	1200	450	550
	g	2.16	2.23	2.23
Previous measurements of g		2.12-2.17	2.22	2.2-2.3

* This cobalt colloid was obtained from a d.c. arc discharge within the paraffin wax which was then centrifuged.

We have therefore a useful method allowing the investigation of ferromagnetic alloy systems over a range of electron concentrations and at various temperatures. As an example we give some results obtained for a series of nickel-iron alloys which form a single phase solid solution in the range 30% to 100% nickel. The colloids were obtained from the high-frequency arc discharge in hydrogen and the results of the measurements at 3.14 cm wavelength (which have been confirmed at 1.20 cm) are given in the figure, where



the experimental error is expected to be not more than $\pm 1\%$ in either the g -value or nickel-iron concentration. It can be seen that the g -value changes rapidly for the range of alloys 30% to 50% nickel falling sharply to a value of 2.01 at 40% nickel. We have checked that the g -value for this alloy is definitely greater than 2.0 by comparison with an organic free radical. The width of the absorption line also changes rapidly for this range of alloys, half the width between the half power points decreasing from about 1000 gauss at 30% nickel to about 250 gauss at 50% nickel. It appears that the minimum width may occur for an alloy having about 65% nickel.

It is well known that the nickel-iron alloys have anomalous properties in the region of 40% nickel; thus there are maxima in the electrical resistance at 30% and in the lattice spacing at 38% nickel whilst the Curie point has a minimum value at about 26% nickel and the coefficient of expansion is a

minimum for the 36% alloy. Although the Bohr magneton value per atom has a sharp anomaly in the region of 40% Ni at 290°K this anomaly appears to diminish and almost disappear at the absolute zero. In order to see whether this last anomaly is connected with our results and to see whether the g -value is sensitive to the atomic spacing we have made measurements using the 36% Ni and 40% Ni alloys at 20°K and 1.20 cm wavelength. There did not appear to be any change in either the g -value or the line width although the resonance absorption was more intense than at 290°K suggesting an increase in the saturation magnetization.

Gyromechanical measurements giving g' have been reported (Barnett and Kenny 1952) but there does not appear to be an anomaly comparable with that reported here although such might be expected to occur if the relation $g-2=2-g'$ suggested by Kittel (1949) and Van Vleck (1950) is applied to our results.

A full account of these experiments is being prepared for publication. The author wishes to express his indebtedness to the Mond Nickel Co., Ltd., for the gift of the nickel-iron alloys and to Dr. J. H. E. Griffiths and Mr. J. Owen for helpful discussions and assistance with the experimental techniques.

REFERENCES

- BARNETT, S. J., and KENNY, G. S., 1952, *Phys. Rev.*, **87**, 723.
GRIFFITHS, J. H. E., 1946, *Nature, Lond.*, **158**, 670.
KITTEL, C., 1948, *Phys. Rev.*, **73**, 155; 1949, *Rev. Mod. Phys.*, **21**, 541; 1951, *J. Phys. Radium*, **12**, 291.
SVEDBERG, T., 1928, *Colloid Chemistry* (New York: Reinhold).
VAN VLECK, J. H., 1950, *Phys. Rev.*, **78**, 266.
WEIL, L., 1951, *J. Phys. Radium*, **12**, 437.

Light Output of Potassium Iodide Crystals under Bombardment by Heavy Charged Particles

BY W. T. LINK AND D. WALKER

Physics Department, University of Birmingham

MS. received 27th April 1953

§ 1. INTRODUCTION

ALKALI halide crystals, containing a small thallium impurity, have now become well established as detectors of energetic charged particles (Hofstadter 1948, 1949, Franzen *et al.* 1950, Lovberg 1951, Taylor *et al.* 1951, Likely and Franzen 1952). The individual scintillations produced in a crystal are recorded by means of a photomultiplier. The purpose of this communication is to report some measurements of the relative light output of KI(Tl) crystals as a function of incident particle energy for protons of up to 10 mev, for deuterons of up to 20 mev, and for α -particles of up to 40 mev. The relation between light output and particle energy has been found to be noticeably non-linear in all cases.

§ 2. EXPERIMENTAL PROCEDURE

Freshly cleaved and optically clear crystals, containing about 0.1% of thallium, were used in the experiments. The crystals were exposed to weak external beams of protons, deuterons and α -particles from the Birmingham 60-inch cyclotron. The energy of the charged particles incident on the crystal could be varied in a known fashion by inserting aluminium foils in the beam. The scintillations were recorded by means of an E.M.I. photomultiplier type 6260, the amplitudes of the electrical pulses on the collector being measured by means of a calibrated amplifier and discriminator. Special care was taken to ensure that, within our working range, the overall amplification, including that of the multiplier itself, was independent of the amplitude of the output pulse. The decay time of scintillations in KI(Tl) is about 1.5×10^{-6} second. The integrating time constant of our recording system was 6×10^{-7} sec so that the shape of the output pulse tended to be determined by the *rate* of emission of light from the crystal. This may be important in comparing our results with those of other authors who have not always stated what integration time constant they used.

§ 3. RESPONSE CURVES

Figures 1 and 2 show the relative amplitudes of the light pulses for protons and deuterons, and for α -particles, plotted as functions of the energy of the particles incident on the crystal. These results are typical examples chosen from

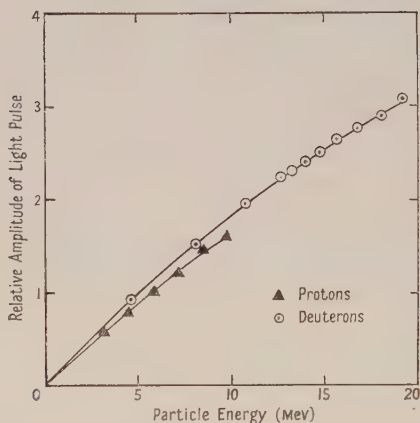


Fig. 1. Response of a KI(Tl) crystal to protons and to deuterons.

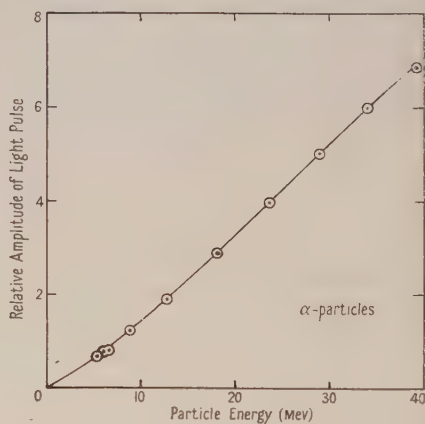


Fig. 2. Response of a KI(Tl) crystal to α -particles.

a number of consistent runs with different crystals. For all energies at which measurements were made, the distribution of pulse heights observed from the multiplier was sufficiently narrow to enable the mean pulse height to be fixed with an accuracy of within 2% or better. Various checks, including a comparison of the pulse heights due to low energy α -particles with those due to α -particles from natural α -emitters (ThC, ThC', RaF), confirmed that the energy scales are accurate to within 1% of the highest energy indicated. It is clear that, at low energies, the amplitude of the light pulse produced by protons and by deuterons is closely proportional to the total energy dissipated in the crystal, whereas for α -particles the relative light output increases more rapidly than proportionally

with the energy. At the higher energies, the curves for protons and deuterons show a definite drop below the line representing strict proportionality. By contrast the curve for α -particles becomes linear.

§ 4. DISCUSSION

The slight but definite deviation from linearity which we find for protons of up to 10 mev contrasts with the result of Franzen *et al.* (1950) who reported linearity up to 17 mev. It may be noted that the same authors, as well as Likely and Franzen (1952), have reported that NaI(Tl) displays linearity under bombardment by protons of up to 18 mev. There are no published data with which to compare our results from the bombardment of KI(Tl) with deuterons, but Taylor *et al.* (1951) have reported that NaI(Tl) displays linearity under bombardment by deuterons of up to 10 mev. Our results for α -particles incident on KI(Tl) overlap and extend the observations of Raffle and Robbins (1952) in the region up to 8.8 mev. In the common energy range the results are similar. At the lower energies, our results for KI(Tl) also show a close similarity to the response curves reported for NaI(Tl) under bombardment by α -particles of up to 8 mev (Lovberg 1951), and by α -particles of up to 20 mev (Taylor *et al.* 1951).

Figure 3 shows dL/dE , the light output per unit energy dissipated in the KI(Tl) crystal (the arbitrary scale corresponds to those of figs. 1 and 2), plotted as a function of dE/dx , the energy loss per unit length of particle path in the

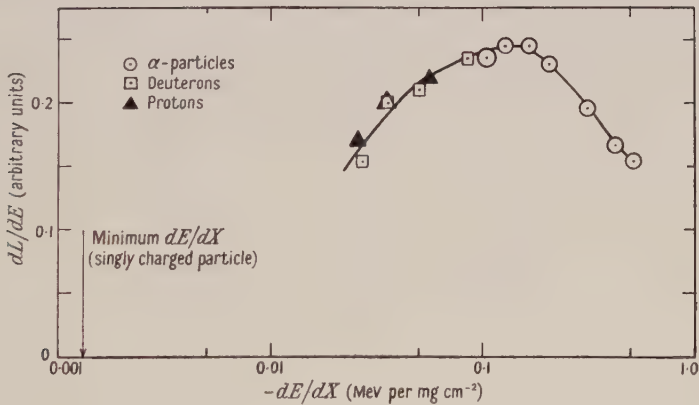


Fig. 3. Efficiency of a KI(Tl) crystal as a function of specific energy loss. (The arrow indicates the minimum dE/dx for a singly charged particle.)

crystal. The points obtained from the slopes of the smoothed proton, deuteron and α -particle curves of figs. 1 and 2 are shown distinctively. dL/dE exhibits a maximum at a value of dE/dx equal approximately to that of a 30-mev α -particle. The fall in dL/dE for large values of dE/dx is consistent with the picture of a limited number of luminescent centres in the crystal (Broser and Warminsky 1951, Wright and Garlick 1953). When the density of ionization electrons becomes very large the number of electrons which can be captured by luminescent centres tends to a limit. It does not seem profitable on the basis of the present measurements, however, to speculate on the mechanism responsible for the fall in efficiency of the crystal which we observe also at the lower values of dE/dx , since there remains a large unexplored range of dE/dx lying between our smallest

value and the minimum dE/dx of a particle carrying one electron charge. (This minimum dE/dx occurs when the kinetic energy of a charged particle is equal to approximately twice its rest mass.) Our smallest value of dE/dx is about 20 times the minimum dE/dx of a singly charged particle.

ACKNOWLEDGMENTS

We are indebted to Mr. K. Stephens for assistance with experiments and to Mr. R. B. Owen of the Atomic Energy Research Establishment, Harwell, for the supply of the KI(Tl) crystals.

REFERENCES

- BROSER, I., and WARMINSKY, R., 1951, *Z. Naturforsch.*, **6a**, 85.
FRANZEN, W., PEELLE, R. W., and SHERR, R., 1950, *Phys. Rev.*, **79**, 742.
HOFSTADTER, R., 1948, *Phys. Rev.*, **74**, 100, 628; 1949, *Ibid.*, **75**, 796.
LIKELY, J. G., and FRANZEN, W., 1952, *Phys. Rev.*, **87**, 666.
LOVBERG, R. H., 1951, *Phys. Rev.*, **84**, 852.
RAFFLE, J. E., and ROBBINS, E. J., 1952, *Proc. Phys. Soc. B*, **65**, 320.
TAYLOR, C. J., JENTSCHKE, W. K., REMLEY, M. E., EBY, F. S., and KRUGER, P. G., 1951, *Phys. Rev.*, **84**, 1034.
WRIGHT, G. T., and GARLICK, G. F. J., 1953, *Brit. J. Appl. Phys.*, in the press.

LETTERS TO THE EDITOR

The Absorption Spectrum of Aluminium Monofluoride in the Schumann Region

The existence of a number of band systems observed in the emission spectrum of AlF between 2500 and 8700 Å, not all of which involve the ground state, $x^1\Sigma^+$ (Rowlinson and Barrow 1953, Naudé and Hugo 1953), suggested that the absorption spectrum of this molecule in the Schumann region would be of interest. Preliminary observations of this spectrum have now been made.

AlF was obtained conveniently by heating mixtures of aluminium with aluminium trifluoride to temperatures of the order of 800°C; suitable experimental conditions were determined by Mr. N. C. Harris by observations on the $A^1\Pi-x^1\Sigma^+$ system. So far, the region 1300 to 2000 Å has been explored, using a normal incidence 1 m vacuum spectrograph of reciprocal dispersion about 8.6 Å mm⁻¹. Six band systems, all degraded to shorter wavelengths, have been found. The constants of the states are given in the table, which includes all the singlet states of AlF now known.

Constants of the Singlet States of AlF

State	$\nu_{0,0}$	ω_e	$x_e\omega_e$	Intensity*
H	67392	958	7.0	3
G	66398	948	8.0	6
F	65864	955	5.0	6
E	63739	>800	—	1
D ¹ Δ	61275	902.6	7.5	not observed
C ¹ Σ ⁺	57750	938.4	5.18	1
B	54273	862	7.0	10
A ¹ Π	43949	803.9 ₅	6.14	?7
x ¹ Σ ⁺		800.5	4.9	

* The figures given for intensities are rough visual estimates for the transitions from $x^1\Sigma^+$ on a scale of 10.

Notes. The state C¹Σ⁺ is known only through the transition C-A (system (7) of Naudé and Hugo).

The state D¹Δ is known only through the transition D-A (system (6) of Naudé and Hugo); we are grateful to Dr. Hugo for letting us have the conclusions of his rotational analysis of this system in advance of publication.

Apart from the systems summarized above, a number of violet degraded bands have also been observed in the region 71000 to 80000 cm⁻¹, of which the strongest are 71390, 72103 and 73028 cm⁻¹; it is not yet certain that they are to be attributed to AlF.

No intercombination system of AlF has yet been identified; the heights of the triplet states (Rowlinson and Barrow 1953) with respect to the singlets are therefore unknown.

The strongest feature of the absorption spectrum is the system B-x, which has its 0,0 band at 1842.6 Å, and to which about 30 bands have been assigned. In contrast, the C¹Σ⁺-x¹Σ⁺ system, with 0,0 band at 1731.6 Å, expected from Naudé and Hugo's analysis of the emission system (7), is very much weaker, and only three bands, the 0,0, 0,1 and 1,2 appear.

It seems probable that transitions from the upper states F, G, H are responsible for the bands of Naudé and Hugo's system (4), while their system (8) may tentatively be identified with the transition B-A $^1\Pi$. The 0,0 band of this system should lie at about 9685 Å.

Physical Chemistry Laboratory,
Oxford University.
29th May 1953.

H. C. ROWLINSON.
R. F. BARROW.

NAUDÉ, S. M., and HUGO, T. J., 1953, *Phys. Rev.*, **90**, 318.

ROWLINSON, H. C., and BARROW, R. F., 1953, *Proc. Phys. Soc. A*, **66**, 437.

The Electrostatic Energy of Boron Nitride

Boron nitride crystallizes in a layer structure very similar to that of graphite, the observed structure (Pease 1952) being one in which any atom is surrounded as closely as the layer structure allows by atoms of the opposite kind, so maximizing the electrostatic binding energy. Pease (1952) and Coulson and Taylor (1952) have both suggested that the difference in packing of the hexagonal layers in the two cases is due to the electrostatic interactions in the boron nitride.

A calculation of the electrostatic energy of the actual boron nitride lattice, and of a lattice geometrically the same as the graphite lattice has been carried out (Morton 1953). A direct application of Ewald's (1921) method is inconclusive, as it does not allow the direct evaluation of the energy difference between the two structures. A high degree of accuracy in the total binding energy of the structures is thus necessary, but is difficult to obtain in any case in which the unit cell edges are far from equal, since it is then not possible to obtain rapid convergence in all the lattice sums which occur. The method was modified by considering the potential at a given atomic position as being made up of contributions from the charges in each separate layer: that arising from the layer in which the point lies takes the same form as the sums in Ewald's method, but now only in two dimensions, and since the edges of the plane unit cell are now equal, the convergence of these sums is rapid. The potential from any other layer can be expressed, as far as variation parallel to the layer is concerned, as a sum of Fourier components with wavelength a/n , where a is the interatomic distance in the layer, and n may take a series of values greater than unity and characteristic of the lattice. These components decrease with z , the distance from the layer, as $\exp(-2\pi n z/a)$; the least value of $n z/a$ for boron nitride is 1.5 so that the contributions from all but the first layer are negligible. The first contribution is the same for the two structures being considered, but those arising from layers other than that in which the point lies give directly the difference in electrostatic energy due to different stacking of the layers. This method of calculation is clearly useful for any layer structure, even when $n z/a$ is not as large as in this instance.

The final result is that the difference in energy between the two lattices is only 0.077 kg cal mole⁻¹ if we assume unit charge on each atom. This is very small, in fact only $RT/10$ at room temperature.

It is, however, unlikely that the net electrostatic charge carried by each atom is as great as one electronic unit, since this would imply that the electron density round the boron atoms is as great as that round the more electronegative nitrogen atoms. An estimate of the mean net charge can be made from Coulson and Taylor's (1952) figures, and these appear to point to a value of about 0.5 electron per atom, making the electrostatic energies smaller by a factor four.

The electrostatic contribution then becomes only about 0.02 kg cal mole⁻¹ and there may well be other interlayer interactions which give larger energy differences than this.

We wish to thank Mr. R. S. Pease for raising the problem, and for his many helpful suggestions.

Theoretical Physics Division,
Atomic Energy Research Establishment,
Harwell, Didcot, Berks.
10th June 1953.

W. M. LOMER.
K. W. MORTON.

COULSON, C. A., and TAYLOR, R., 1952, *Proc. Phys. Soc. A*, **65**, 834.

EWALD, P. P., 1921, *Ann. Phys., Lpz.*, **64**, 253.

MORTON, K. W., 1953, *Atomic Energy Research Establishment Report T/R 1110*.

PEASE, R. S., 1952, *Acta Crystallogr.*, **5**, 356.

The Born-Yang Nuclear Model for High Energy Electron Scattering

Employing the nuclear model with a uniform density distribution and characterized by the radius $R = \bar{r}A^{1/3}$ cm reasonable correlations of the theoretical and the experimental angular distributions of 15.7 mev electrons scattered by heavy nuclei (Lyman, Hanson and Scott 1951) can be obtained by taking $\bar{r} = 1.16 \times 10^{-13}$ cm. This is close to the value $\bar{r} = 1.2 \times 10^{-13}$ cm for heavy nuclei obtained by investigating the nuclear scattering of 345 mev protons (Gatha and Riddell 1952) on the basis of a similar model. On the other hand, it is well-known that $\bar{r} \simeq 1.4 \times 10^{-13}$ cm is required to account for the nuclear scattering of nucleons of lower energy. This inconsistency in the effective magnitude of \bar{r} may perhaps be explained on the basis of nuclear models with non-uniform density distributions giving a greater concentration towards the centre. An interesting model of this type (Born and Yang 1950, Yang 1951) is described by the density distribution:

$$\left. \begin{aligned} \rho(r) &= \rho_0 & \text{for } r \leq R_0 \\ &= \rho_0 \exp[-\{(r - R_0)/a\}^2] & \text{for } r > R_0 \end{aligned} \right\} \dots\dots(1)$$

On the basis of a correlation between the nuclear shell structure and the above density distribution Born and Yang have determined that, for heavy nuclei, $R_0 = 0.673 r_0 A^{1/3}$ cm and $a = 0.327 r_0 A^{1/3}$ cm while on the basis of density normalization they have obtained $\rho_0 = 1.04/\frac{4}{3}\pi r_0^3$. This does not fix r_0 but they have suggested that it would be of the order of magnitude 1.5×10^{-13} cm. A better estimate of r_0 has been obtained in the present investigation by considering the nuclear scattering of 15.7 mev electrons on the basis of this model.

The Born approximation has been employed to compare the uniform density model with the Born-Yang model. The scattering amplitude* for a spherically symmetric potential in this approximation is given by

$$f(\theta) = \frac{2m}{\hbar^2 K} \int_0^\infty V(r) \sin(Kr) r dr \quad \dots\dots(2)$$

where $K = 2k \sin \frac{1}{2}\theta$ while the other symbols have the usual meanings. For an electrostatic $V(r)$ which varies as $1/r$ for large values of r and where $V(r)$ and dV/dr are regular at $r=0$ one obtains through partial integrations

$$f(\theta) = -\frac{8\pi mZe^2}{A\hbar^2 K^3} \int_0^\infty \rho(r) \sin(Kr) r dr. \quad \dots\dots(3)$$

Using this expression one gets for the uniform density model

$$f_u(\theta) = -(6mZe^2/A\hbar^2 K^3 \bar{r}^3) \{\sin(KR) - KR \cos(KR)\}/K^2. \quad \dots\dots(4)$$

and for the Born-Yang model

$$f_B(\theta) = -(6.24mZe^2/A\hbar^2 K^3 r_0^3) [\{\sin(KR_0) - KR_0 \cos(KR_0)\}/K^2 \\ - (\sqrt{\pi a/2})(\partial/\partial K)\{P \cos(KR_0) - Q \sin(KR_0)\}] \quad \dots\dots(5)$$

where

$$P = \exp\left(-\frac{K^2 a^2}{4}\right), \quad Q = \frac{2}{\pi} - \frac{4}{\pi} \sum_{n=1}^{\infty} \frac{\exp(-n^2 K^2 a^2)}{4n^2 - 1}.$$

A numerical comparison of the scattering amplitudes given by eqns. (4) and (5) with $\bar{r} = 1.16 \times 10^{-13}$ cm was made for Au, and it was found that the two would be very close for all angles if $r_0 = 1.06 \times 10^{-13}$ cm. The same value of r_0 gives good agreement also for Ag. Therefore on the basis of the above experiment we may conclude that $r_0 \simeq 1 \times 10^{-13}$ cm within the approximations employed. It remains to be seen whether this value of r_0 would explain both low and high energy nucleon scattering data.

A detailed study of the usefulness of the Born-Yang nuclear model for the various scattering processes has been undertaken, the results of which will be published later.

Physical Research Laboratory,
Navrangpura, Ahmedabad 9, India.

A. L. MATHUR.

M.G. Science Institute,
Navrangpura, Ahmedabad 9, India.

K. M. GATHA.

26th May 1953.

BORN, M., and YANG, L. M., 1950, *Nature, Lond.*, **166**, 399.

GATHA, K. M., and RIDDELL, R. J., 1952, *Phys. Rev.*, **86**, 1035.

LYMAN, E. M., HANSON, A. O., and SCOTT, M. B., 1951, *Phys. Rev.*, **84**, 626.

YANG, L. M., 1951, *Proc. Phys. Soc. A*, **64**, 632.

* The relativistic term drops out when comparing the scattering amplitudes.

REVIEWS OF BOOKS

Superconductivity, 2nd edn., by D. SHOENBERG. Pp. x+256. Cambridge Monograph on Physics. (Cambridge: University Press, 1952.) 30s.

Although the phenomenon of superconductivity has until now maintained its position as an unsolved mystery of science, so much new experimental and theoretical evidence has accumulated since the publication in 1938 of the first edition of Dr. Shoenberg's monograph that in its second edition the book has had to be greatly enlarged and revised. An introductory chapter deals with the discovery of the effect (it was a happy thought to include the delightful portrait sketch of the discoverer) and rapidly surveys the outlines of the subject. The account which follows of the magnetic and thermal properties of macroscopic superconductors reproduces the main topics of the first edition, but has been rearranged and expanded to include recent results on thermal conductivity and thermoelectric effects. The next chapter gives an account of the recent investigations, experimental and theoretical, which have elucidated the structure of the intermediate state; of particular interest here are the remarkable Russian experiments which have demonstrated directly that the metal in the intermediate state is broken up into a complicated mixture of superconducting and normal regions. A further chapter describes the various methods which have been used to study the depth of penetration of a magnetic field into a superconductor and which have provided much important information, not only on the absolute value of the penetration depth, but also on its variation with temperature, crystal orientation and magnetic field strength. The last chapter, which is of great interest, discusses the extent to which the phenomenological theories of superconductivity, the thermodynamic theory of Gorter and Casimir and the electrodynamic theory of F. and H. London have been successful in correlating the experimental facts, and emphasizes that recent experiments, particularly the important work of Pippard on the behaviour at high frequencies, have revealed phenomena which seem to lie beyond the grasp of these theories. A brief sketch follows of the various attempts at a fundamental theory of superconductivity which have lately been appearing in regular succession; although it seems fairly certain now that superconductivity is in some way connected with the interaction between the electrons and the lattice vibrations in a metal, no convincing demonstration has yet been given of the way in which this interaction can lead to the characteristic properties of a superconductor. An appendix gives an extensive list of numerical data on superconducting transition temperatures and critical fields.

It is a pleasure to read Dr. Shoenberg's clear and critical account of the present state of our knowledge of what is surely among the most remarkable of all physical phenomena. The book can be strongly recommended to the general reader interested in the subject, and will be indispensable to the specialist. It is evident that, between the first and second editions of the book, the plot of the story has greatly thickened; will the third edition be able to announce that it has at last been unravelled?

E. H. SONDHEIMER,

CONTENTS OF SECTION B

	PAGE
Mr. J. E. H. BRAYBON. The Mechanism of Stress Birefringence in Amorphous Solids	617
Mr. J. LEES. Cuprous Oxide Rectifier Characteristics	622
Dr. R. S. TEBBLE and Dr. V. L. NEWHOUSE. The Barkhausen Effect in Single Crystals	633
Dr. O. M. WHITE. Oscillations in Space Charge Detectors and the Ultra-Ionization Potentials of Mercury	642
Dr. N. FUSCHILLO. Thermoelectric Effects due to Stationary and Moving Asymmetrical Temperature Gradients in Mercury	649
Dr. C. HENDERSON, Mr. F. F. HEYMANN and Dr. R. E. JENNINGS. The Design and Operation of a 4.5 mev Microtron	654
Dr. C. GREY MORGAN and Mr. D. HARCOTBE. Fundamental Processes of the Initiation of Electrical Discharges	665
Mr. I. M. TEMPLETON and Dr. D. K. C. MACDONALD. The Electrical Conductivity and Current Noise of Carbon Resistors	680
Mr. E. K. BIGG. The Supercooling of Water	688
Mr. D. E. WESTON. The Theory of the Propagation of Plane Sound Waves in Tubes	695
Research Notes :	
Prof. S. CHAPMAN. Note on the Grazing-Incidence Integral $Ch(x, \chi)$ for Monochromatic Absorption in an Exponential Atmosphere	710
Mr. D. H. MARTIN. Ferromagnetic Domain Processes in Single Crystal Disc Specimens of Silicon Iron	712
Letters to the Editor:	
Dr. D. A. BELL. Johnson Noise and Equipartition	714
Dr. R. COOPER and Mr. D. T. GROSSART. The Influence of Cathode Material on the Electric Strength of Potassium Bromide Crystals	716
Mr. R. P. AGARWALA and Dr. H. WILMAN. The Surface Deformation caused on Iron Crystals by Unidirectional Abrasion	717
Book Notices	719
Contents of Section A	720

Fluorescence Characteristics of Mixed Organic Crystals

By G. T. WRIGHT*

Department of Physics, University of Birmingham

MS. received 5th March 1953

Abstract. Experiments with mixed crystals of anthracene in naphthalene are described. A fluorimeter technique is used to measure crystal concentrations, and it is found that considerable purification of the melt occurs during crystallization. No significant difference is observed in the relative fractional intensity of each fluorescence component for excitation with 2540 Å radiations and with alpha-particles. A simple theory is formulated and agrees well with the experimental data.

The equations obtained are used to explain the decrease in radioluminescence efficiency of organic phosphors due to radiation damage, and it is estimated that for anthracene each 5 Mev alpha-particle absorbed produces approximately 2×10^4 effective non-radiative dissipative centres.

§ 1. INTRODUCTION

THE transfer of electronic excitation energy between molecules in organic crystals is demonstrated in many cases by the fluorescence properties of dilute solid solutions. Measurements by Bowen, Mikiewicz and Smith (1949) for photon excitation and Birks (1950) for particle excitation have shown that energy absorbed by the host molecules can be transferred with high efficiency to the solute molecules, especially in systems composed of the benzene homologues and related compounds.

A general criticism, however, of these results and of others, e.g. decay time measurements by Liebson (1952), is that crystal concentrations are given as those of the melts from which they were grown, whereas in all probability some purification will occur on crystallization.

This paper describes some further measurements with mixed crystals in which this source of error was eliminated by developing a fluorimeter technique enabling crystal constitutions to be determined after they had been grown. These results are described in § 2 together with some observations of fluorescence quenching produced in pure anthracene by radiation damage and compared with a simple theory which is formulated in § 3.

§ 2. EXPERIMENTAL RESULTS

2.1. *Fluorescence of Mixed Crystals*

Large, clear crystals of anthracene-in-naphthalene were grown from the melt by slow cooling in a thermostat bath. The anthracene concentrations were determined by dissolving a known mass of the crystal in a known mass of pure benzene, irradiating the solution with 3650 Å radiation and, with an RCA type 931-A photomultiplier, comparing the intensity of the anthracene emission with that from a series of standard solutions. Exhaustive experiments were performed

* Now at Physics Department, Rhodes University, Grahamstown, South Africa.

to verify that the presence of the naphthalene in the solution did not affect the fluorescence of the anthracene. With this fluorimeter it was found possible to measure as little as one part of anthracene in 10^8 parts naphthalene. Because of the small concentrations involved great care was taken to ensure purity of the materials used. Several crystals were grown and their concentrations determined in this manner; in all cases purification of the mixture was found to occur during crystallization. A melt containing 1% of anthracene gave a crystal containing about 0.001% anthracene. With the comparatively crude thermostat bath available large, clear crystals containing greater concentrations of anthracene could not be grown.

To measure the relative fractional intensities of the naphthalene and anthracene emissions excited by 5 mev alpha-particles, small crystals approximately 1 mm thick were cleaved from the large blocks and placed on the photocathode window of an EMI type 5311 photomultiplier. The naphthalene emission was observed through a thick Wood's glass filter and the anthracene emission through a Wratten

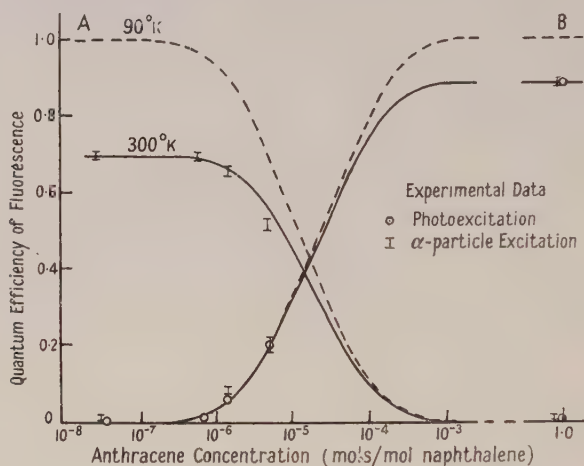


Fig. 1. Fractional intensity of each fluorescence component for mixed anthracene-naphthalene crystals.

Theoretical curves : A, naphthalene emission; B, anthracene emission.

2A filter. For the photoluminescence measurements the crystals were coarsely powdered and spread on a glass slide placed at a fixed distance from an RCA type 931-A photomultiplier. A circular diaphragm was then placed over the powdered layer so that a standard area of this was exposed. The powder was illuminated with 2540 Å radiations and the anthracene emission selected with a Wratten 2A filter. The results of these measurements, which were made at room temperature, are illustrated in fig. 1 and compared with theoretical curves drawn from the equations developed in §3. The emission intensities for both photon and particle excitation are normalized to give 0.7 and 0.9 for pure naphthalene and anthracene respectively. Although they do not cover a very wide range of concentrations the experimental data show good agreement with theory and do not indicate any appreciable difference in the relative fractional intensities of emission for the two modes of excitation. It is unfortunate that crystals could not be grown with a greater anthracene content so as to test these observations more stringently.

2.2. Quenching of Fluorescence by Radiation Damage

Although not conclusive, the above results indicate that the energy transfer mechanism operates in the same manner and with the same relative effects whether the fluorescence is excited with photons or particles. If so we would expect that the decrease in radioluminescence efficiency of organic phosphors due to radiation damage would be described by a curve similar to that shown in fig. 1 for the naphthalene emission, for we may consider the production of non-radiative dissipative centres by the absorbed particle to be analogous to the insertion in the host lattice of impurity molecules in so far as quenching of the host emission is concerned.

This is found by Birks and Black (1951) for anthracene irradiated with 5 mev alpha-particles, using a particle flux of 1.1×10^9 per cm^2 per minute. The relative scintillation efficiency L is given by $L = (1 + KD)^{-1}$ where D is the particle dose and K , determined empirically, is 1.0×10^{-11} . A similar experiment was performed by the author using a particle flux of 1.73×10^6 per cm^2 per minute and a value of 4.8×10^{-11} found for K (Wright 1952); the difference can be attributed only to the different intensities of radiation used. One measurement was made of the decrease in photoluminescence efficiency using 2540 Å radiations; this was found to be reduced by the same extent as the radioluminescence efficiency.

§ 3. THEORETICAL STUDIES

In the following section we shall derive first the equations describing the fluorescence characteristics of mixed crystals without reference to any particular method of energy transfer, using the suffices X and Y to denote consideration of solvent and solute molecules respectively. We shall consider that the whole of the incident energy is absorbed by the host molecules and that, because of their lower electronic levels, energy acquired by the solute molecules is retained by them until it is lost by luminescence emission or thermal dissipation.

If at time t there are S_X excited molecules remaining of S_0 formed initially at time $t = 0$ the number losing their energy in the interval t to $t + dt$ will be

$$dS_X = -(p_X + k_X + P) S_X dt = -a S_X dt \quad \dots\dots(1)$$

where p , k , P are the probabilities in unit time of luminescence emission, thermal dissipation or transfer to a solute molecule. The number of transferences to solute molecules in this interval is

$$Q_0 = -PS_X dt = -PS_0 e^{-at} dt. \quad \dots\dots(2)$$

Fixing attention on these molecules, if at a total time T (where $T \geq t$) there are Q_Y remaining in the excited state, the number removed in the interval T to $T + dT$ is

$$dQ_Y = -(p_Y + k_Y) Q_Y dT = -b Q_Y dT \quad \dots\dots(3)$$

and the number which are lost as luminescence emission is

$$dI_Y = -p_Y Q_Y dT = -p_Y Q_0 e^{-b(T-t)} dt. \quad \dots\dots(4)$$

The total amount of luminescence emission from the solute molecules in the interval T to $T + dT$ is evidently

$$I_Y = \int_0^T dI_Y = p_Y P S_0 e^{-bT} (1 - e^{-aT}) dT/a. \quad \dots\dots(5)$$

The whole emission from the solute molecules is given by

$$L_Y = \int_0^\infty I_Y = p_Y P S_0 / (p_Y + k_Y)(p_X + k_X + P). \quad \text{.....(6)}$$

From eqn. (1) it is evident that

$$I_X = p_X S_0 e^{-at} dt; \quad \text{.....(7)}$$

hence

$$L_X = \int_0^\infty I_X = p_X S_0 / (p_X + k_X + P). \quad \text{.....(8)}$$

Apart from P the constants in the last four equations are all known, for p and k may be evaluated from measurements of photoluminescence decay times and efficiencies. The actual mechanism by which the electronic energy is transported through the crystal lattice is not known with certainty, hence a definite value for P cannot be adopted. We may consider two possibilities.

Energy transfer in organic crystals is considered by Bowen and Mikiewicz (1947) and by Franck and Livingstone (1949) to be due to a resonance exchange process. If this is so it is unlikely that the excitation energy will do more than move from an excited molecule to one of its neighbours, for not only will these be sufficiently near for direct interaction to occur between their outer electrons and the expanded orbital of the excited molecule but, in addition, they will almost certainly screen this molecule to some extent from those further away. If we accept this description of the excitation energy moving through the crystal lattice by transfer between adjacent molecules with a mean frequency of transfer ν , we have $P = \nu n / N$ where there are N molecules, of which n are impurity molecules, in unit volume of the crystal. Further, we might expect ν to be similar in value to the mean frequency of thermal vibrations of the molecules, for the probability of transfer is greatest when these are nearest (Mott and Massey 1950); by identifying ν with this frequency it may be evaluated from Raman spectra, compressibility data or the Lindemann melting point theory.

An alternative method has been proposed by Birks (1953) in terms of photon absorption and emission processes. A fluorescence photon emitted by an excited solvent molecule may be reabsorbed by a solvent molecule, absorbed by a solute molecule or escape from the crystal. However, the constants involved in the expression for P depend upon absorption coefficients and crystal size and cannot be readily computed, so that a quantitative comparison cannot be made.

Accordingly the theoretical curves illustrated are drawn only for the case $P = \nu n / N$. The technical decay time of anthracene has been measured as 1.3×10^{-8} sec (Liebson 1952) and the efficiency is about 0.9 (Bowen *et al.* 1949). The technical decay time of naphthalene has not been measured, but since in general photoluminescence decay times seem to be about half of the radioluminescence decay times (Liebson, Bishop and Elliot 1950), a value of 3.5×10^{-8} sec has been used together with an efficiency of 0.7 (Bowen *et al.* 1949). From compressibility data the mean frequency of thermal vibrations is deduced to be 1.5×10^{12} . This value is calculated by supposing the crystal to be an isotropic solid and determining from bulk modulus measurements the mean force constant between adjacent molecules. Assuming these to be independent harmonic oscillators, their frequency can thus be obtained. From the Lindemann melting point theory a value of 7.2×10^{11} is given, but the former value is considered more reliable and is used here. Inserting these numerical values in eqns. (6) and

(8), we obtain respectively the curves for the anthracene and naphthalene emissions which are shown in fig. 1.

From eqn. (5) the intensity of the anthracene emission at times after the initial excitation may be calculated for different anthracene concentrations. If we define an effective decay time τ by the equation

$$L_Y - \int_0^\tau I_Y dt = L_Y/e$$

this may be evaluated graphically. Figure 2 shows how the decay times of the anthracene and naphthalene emissions are expected to depend upon the anthracene concentration.

In the previous section it was noted that quenching of the host emission by radiation damage was similar to that produced by insertion of impurity molecules into the host lattice. If the effective number of non-radiative dissipative centres produced by each particle is s , then the number of these produced in unit volume of the lattice after a total dose of D particles is Ds/R , where R is the particle range.

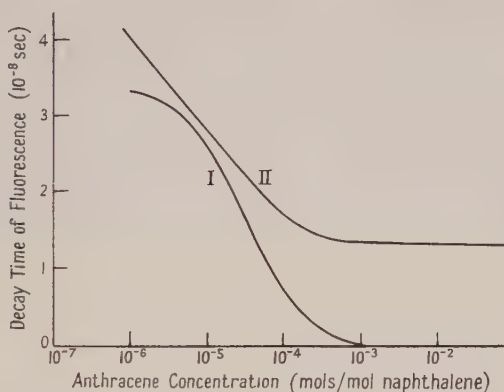


Fig. 2. Calculated decay time of each fluorescence component as a function of anthracene concentration. I, naphthalene emission; II, anthracene emission.

Substitution of this for n in eqn. (8), using $P = \nu n_i N$, should thus give the curve for quenching by radiation damage. Comparison with the experimental results will then enable s to be determined. Those described in § 2 for anthracene give $s \simeq 2 \times 10^4$ for each 5 mev alpha-particle absorbed.

§ 4. DISCUSSION AND REMARKS

Complete quantitative comparison of the equations obtained with experimental observations is not possible because of the dubious nature of published data. Thus Liebson and Keller (1950) find that stilbene dissolved in naphthalene gives a lower intensity emission than anthracene at the same apparent concentration, whereas according to eqn. (6) any solute material should give the same intensity emission apart from variations due to differences in the luminescence efficiency of the molecules involved.

However, as with other workers, their quoted crystal concentrations actually refer to concentrations in the mother liquor and cannot therefore be made the basis of quantitative discussions. The enhancement of the solute emission at low temperatures, as found by Bowen *et al.*, is in accord with the theory (fig. 1), as is

the result found by Liebson *et al.* (1950) that the decay time of an anthracene-naphthalene crystal was the same as that of pure anthracene. Hence from a qualitative aspect, which is the only form of comparison possible, theory and experiment are in agreement. The apparent discrepancy between the results of Birks and Black for excitation with alpha-particles, and Bowen *et al.* for photofluorescence, is removed by the results illustrated in fig. 1, which show no differences for either form of excitation. This similarity in results for the two modes of excitation is also observed in the case of radiation damaged crystals. Unpublished studies by the author show that this similarity is in general to be expected, for the majority of the additional quenching in the case of particle excitation occurs within the first 10^{-10} sec, during which time a very small part of the total fluorescence is emitted and subsequent processes occur in the same manner as under conditions of photoexcitation.

Due to their relative ease of preparation and the higher sensitivity of photomultiplier tubes for the anthracene emission, crystals of naphthalene containing anthracene have been extensively used for detection of ultra-violet and ionizing radiations. Equation (5) shows that such crystals may be unsuitable for use when a rapid initial rise of luminescence is required as for particle coincidence experiments. However, extremely rapid decay times may be obtained by utilizing the emission of the host material. Providing that the accompanying decrease in intensity is not too disadvantageous, phosphor decay times of the order of 3×10^{-10} sec may be obtained. A system such as stilbene containing naphthacene, with suitable filters to eliminate the naphthacene emission, might prove suitable for this purpose.

A further point of interest, also illustrated by eqn. (5), concerns the assumption of an exponential decay of luminescence for the purpose of decay time measurements; this may not be always justifiable. For the case of particle excitation, when time-varying quenching mechanisms are operative and such processes as ion recombination times may contribute to the ultimate decay time, this assumption seems even less justifiable.

§ 5. CONCLUSIONS

By accepting the process of resonance exchange for the mechanism of energy transfer between molecules in organic crystals an adequate explanation can be given of all the observed data. The frequency with which the energy is transferred shows that before it is emitted or thermally dissipated it passes through an average of about ten thousand molecules ($M = \nu\tau$); due to the random nature of its motion the distance of migration will thus be of the order of \sqrt{M} .

Complete acceptance of this or any other proposed mechanism, however, is not possible until more accurate experimental data are available.

ACKNOWLEDGMENTS

The experimental work described in this paper was performed during the author's stay at the University of Birmingham, and he wishes to thank Dr. G. F. J. Garlick for the original suggestion of the fluorimeter technique used. Thanks are also due to the Department of Scientific and Industrial Research for a maintenance grant during this period.

The author also wishes to thank Professor J. B. Birks and Mr. W. A. Little of Rhodes University for many informative and stimulating discussions.

REFERENCES

- BIRKS, J. B., 1950, *Proc. Phys. Soc. A*, **63**, 1044; 1953, *Scintillation Counters* (London : Pergamon Press).
- BIRKS, J. B., and BLACK, F. A., 1951, *Proc. Phys. Soc. A*, **64**, 511.
- BOWEN, E. J., and MIKIEWICZ, E., 1947, *Nature, Lond.*, **159**, 706.
- BOWEN, E. J., MIKIEWICZ, E., and SMITH, F. W., 1949, *Proc. Phys. Soc. A*, **62**, 26.
- FRANCK, J., and LIVINGSTONE, R., 1949, *Rev. Mod. Phys.*, **21**, 505.
- LIEBSON, S. H., 1952, *Nucleonics*, **10**, 41.
- LIEBSON, S. H., BISHOP, M. E., and ELLIOT, J. O., 1950, *Phys. Rev.*, **80**, 907.
- LIEBSON, S. H., and KELLER, J. W., 1950, *Phys. Rev.*, **78**, 305.
- MOTT, N. F., and MASSEY, H. S. W., 1950, *Theory of Atomic Collisions* (Oxford : Clarendon Press).
- WRIGHT, G. T., 1952, *Thesis*, University of Birmingham.

Properties of the Hydrogen Molecular Ion I: Quadrupole Transitions in the Ground Electronic State and Dipole Transitions of the Isotopic Ions

BY D. R. BATES AND G. POOTS

Department of Applied Mathematics, Queen's University, Belfast

MS. received 23rd April 1953

Abstract. The Einstein spontaneous emission coefficients and the oscillator strengths due to the quadrupole moment connecting the vibrational-rotational levels of H_2^+ are evaluated using two-centre wave functions. All $(v', J') - (v'', J'')$ lines arising from combinations of the following values of the quantum numbers are treated: $v' = 0, 1, 2$ or 3 ; $v'' = 0$; J' and $J'' = 0, 2, 4, 6$ or 8 (with $\Delta J = 0 \pm 2$). In the case of the higher harmonics serious cancellation occurs in certain of the integrations, but the results should be reliable as the calculations do not involve approximations. The dipole transitions of the isotopic ions are also investigated, though less fully.

§ 1. INTRODUCTION

OWING to the comparative complexity of the wave functions concerned, the hydrogen molecular ion has not been studied in the same detail as the hydrogen atom. The purpose of this series of papers is to remedy the omission as far as possible. In general the calculations will be performed with exact two-centre electronic wave functions; but for comparison some use will also be made of approximate wave functions based for example on a linear combination of atomic orbitals. It is hoped that the proposed investigation of the simplest molecular system, besides being of interest in itself, will give insight into other molecular systems and the methods employed in treating them.

The present paper is devoted to the investigation of the quadrupole transitions in the $x^2\Sigma_g^+$ ground electronic state, and to the investigation of the corresponding dipole transitions of systems isotopic with the hydrogen molecular ion. These transitions may be of importance in certain astrophysical problems.

§ 2. QUADRUPOLE TRANSITIONS

2.1. The Einstein spontaneous emission coefficient $A(P, Q)$ and the oscillator strength $f(Q, P)$ for the quadrupole transition connecting an upper level P with a lower level Q are given by the formulae

$$A(P, Q) = \frac{32\pi^6\nu^5 S}{5c^5 h \omega_P}; \quad f(Q, P) = \frac{4\pi^4 m \nu^3 S}{5c^2 e^2 h \omega_Q}; \quad \dots\dots(1)$$

in which c is the velocity of light, h is Planck's constant, m and e are the electronic mass and charge respectively, ν is the frequency of the radiation emitted or absorbed, ω_P and ω_Q are the statistical weights, and S is the strength of the line, that is

$$S = \sum_{ij} S(p_i, q_j), \quad \dots\dots(2)$$

$S(p_i, q_j)$ being the strength of the component joining state p_i of one level to state q_j of the other, and the summation being carried out over all components (cf. Condon and Shortley 1935). It has been shown (James and Coolidge 1938) that

$$S(p, q) = \left| \int \Psi_p^* \mathcal{M} \Psi_q d\tau \right|^2, \quad \dots\dots(3)$$

$$\text{with} \quad \mathcal{M} = \mathcal{N} - \frac{1}{3} \mathcal{N}_s \mathcal{I}, \quad \dots\dots(4)$$

where Ψ_p and Ψ_q are the normalized wave functions of the two states, \mathcal{N} is the quadrupole moment operator, \mathcal{N}_s is its scalar, \mathcal{I} is the idemfactor, and the modulus squared indicates the double dot product of the enclosed tensor with its complex conjugate. If the position vector \mathbf{r} of the electron is represented by $x\mathbf{i} + y\mathbf{j} + z\mathbf{k}$, where \mathbf{i} , \mathbf{j} and \mathbf{k} are an orthogonal set of unit vectors the last of which is parallel to the internuclear line, and if all quantities are expressed in atomic units, then

$$\mathcal{M} = \frac{1}{3} \{ (y^2 + z^2 - 2x^2 - \frac{1}{2}R^2)\mathbf{ii} + (z^2 + x^2 - 2y^2 - \frac{1}{2}R^2)\mathbf{jj} + (x^2 + y^2 - 2z^2 + R^2)\mathbf{kk} - 3xy(\mathbf{ij} + \mathbf{ji}) - 3yz(\mathbf{jk} + \mathbf{kj}) - 3zx(\mathbf{ki} + \mathbf{ik}) \}, \quad \dots(5)$$

R being the distance between the protons.

The complete wave functions Ψ_p and Ψ_q of H_2^+ may be written in the product form

$$\left. \begin{aligned} \Psi_p &= \chi(\mathbf{r}|R) P_{v', J'}(R) Y_{J', M'}(\Theta, \Phi), \\ \Psi_q &= \chi(\mathbf{r}|R) P_{v'', J''}(R) Y_{J'', M''}(\Theta, \Phi), \end{aligned} \right\} \quad \dots\dots(6)$$

where χ is the $1s\sigma_g$ electronic wave function, and P and Y respectively are the relevant vibrational and rotational wave functions. Using (5) and taking account of symmetry it can readily be seen that

$$\int \chi^*(\mathbf{r}|R) \mathcal{M} \chi(\mathbf{r}|R) d\mathbf{r} = \frac{1}{3} M(R) \{ -\mathbf{ii} - \mathbf{jj} + 2\mathbf{kk} \}, \quad \dots\dots(7)$$

$$\text{with} \quad M(R) = (\frac{1}{2}R^2 + \overline{\rho^2} - \overline{z^2}), \quad \dots\dots(8)$$

$$\overline{\rho^2} = \int \chi^*(\mathbf{r}|R) x^2 \chi(\mathbf{r}|R) d\mathbf{r} = \int \chi^*(\mathbf{r}|R) y^2 \chi(\mathbf{r}|R) d\mathbf{r}, \quad \dots\dots(9)$$

$$\overline{z^2} = \int \chi^*(\mathbf{r}|R) z^2 \chi(\mathbf{r}|R) d\mathbf{r}. \quad \dots\dots(10)$$

$$\text{Hence} \quad \int \Psi_p^* \mathcal{M} \Psi_q d\tau = \overline{M}(v', J'; v'', J'') \int_0^{2\pi} \int_0^\pi Y_{J', M'}^*(\Theta, \Phi) \frac{1}{3} \{ -\mathbf{ii} - \mathbf{jj} + 2\mathbf{kk} \} \times Y_{J'', M''}(\Theta, \Phi) \sin \Theta d\Theta d\Phi \quad \dots\dots(11)$$

$$\text{where} \quad \overline{M}(v', J'; v'', J'') = \int_0^\infty P_{v', J'}^*(R) M(R) P_{v'', J''}(R) R^2 dR. \quad \dots\dots(12)$$

The angular integration in (11), together with the summation in (2), has been discussed fully by James and Coolidge (1938) in connection with the quadrupole transitions of the neutral molecule. Their analysis, which can be taken over without modification, yields

$$S = |\overline{M}|^2 \times \left\{ \begin{aligned} &(J' + 1)(J' + 2)/(2J' + 3) && (J'' = J' + 2) \\ &2J'(J' + 1)(2J' + 1)/3(2J' - 1)(2J' + 3) && (J'' = J') \\ &J'(J' - 1)/(2J' - 1). && (J'' = J' - 2) \end{aligned} \right\} \quad \dots(13)$$

Transitions in which the change in the rotational quantum number is not 0 or ± 2 , are of course forbidden.

2.2. The Schrödinger equation for the motion of the electron in the field of the two protons can be solved exactly by using the confocal elliptical coordinates defined by the equations

$$\lambda = (r_1 + r_2)/R, \quad \mu = (r_1 - r_2)/R, \quad \dots\dots(14)$$

r_1 and r_2 being the radial distances (cf. Burrau 1927, Mott and Sneddon 1948).

For the $1s\sigma_g$ state the wave function may be expressed as

$$\chi = M(\mu)\Lambda(\lambda), \quad \dots\dots(15)$$

where

$$M(\mu) = \sum_{s=0}^{\infty} a_{2s} P_{2s}(\mu), \quad \dots\dots(16)$$

the P 's being the Legendre polynomials, and where

$$\Lambda(\lambda) = (1+\lambda)^{\sigma} \exp(-p\lambda) \sum_{t=0}^{\infty} b_t \left(\frac{\lambda-1}{\lambda+1} \right) \quad \dots\dots(17)$$

Tables of a , b , σ and p (all of which depend parametrically on R) are now available (Bates, Ledsham and Stewart 1953) and with their aid $\bar{\rho}^2$ and \bar{z}^2 can be computed without difficulty. We have

$$\bar{\rho}^2 = \int_0^{2\pi} \int_{-1}^{+1} \int_1^{\infty} M(\mu)^2 \Lambda(\lambda)^2 (\lambda^2 - 1)(1 - \mu^2)(\lambda^2 - \mu^2)(R/2)^5 \cos^2 \phi \, d\lambda \, d\mu \, d\phi, \quad \dots\dots(18)$$

$$\text{and} \quad \bar{z}^2 = \int_0^{2\pi} \int_{-1}^{+1} \int_1^{\infty} M(\mu)^2 \Lambda(\lambda)^2 \lambda^2 \mu^2 (\lambda^2 - \mu^2)(R/2)^5 \, d\lambda \, d\mu \, d\phi; \quad \dots\dots(19)$$

$$\text{that is} \quad \bar{\rho}^2 = \pi(R/2)^5 [A_0(B_4 - B_2) - A_2(B_4 - 1) + A_4(B_2 - 1)], \quad \dots\dots(20)$$

$$\text{and} \quad \bar{z}^2 = 2\pi(R/2)^5 [A_2 B_4 - A_4 B_2], \quad \dots\dots(21)$$

$$\text{where} \quad A_n = \int_{-1}^{+1} M(\mu)^2 \mu^n \, d\mu, \quad B_n = \int_1^{\infty} \Lambda(\lambda)^2 \lambda^n \, d\lambda. \quad \dots\dots(22)$$

On substituting for $M(\mu)$ from (16) we obtain

$$\left. \begin{aligned} A_0 &= \sum_{s=0}^{\infty} \frac{2a_{2s}^2}{4s+1}, \\ A_2 &= \sum_{s=0}^{\infty} \frac{2}{4s+3} \left\{ \frac{(2s+1)a_{2s}}{4s+1} + \frac{(2s+2)a_{2s+2}}{4s+5} \right\}^2, \\ A_4 &= \sum_{s=0}^{\infty} \frac{2}{4s+1} \left\{ \frac{2s(2s-1)a_{2s-2}}{(4s-3)(4s-1)} + \left(\frac{(2s+1)^2}{4s+3} + \frac{4s^2}{4s-1} \right) \frac{a_{2s}}{4s+1} \right. \\ &\quad \left. + \frac{(2s+1)(2s+2)a_{2s+2}}{(4s+3)(4s+5)} \right\}^2, \end{aligned} \right\} \quad \dots\dots(23)$$

which, since the series converge rapidly, may readily be evaluated. The B 's must be determined by numerical integration.

For comparison it is interesting to calculate $\bar{\rho}^2$ and \bar{z}^2 from the standard l.c.a.o. wave function

$$\chi = \{\exp(-r_1) + \exp(-r_2)\} / \{2\pi(1+S)\}^{1/2}, \quad S = e^{-R}(1+R+\frac{1}{3}R^2). \quad \dots\dots(24)$$

Using this approximation in (9) and (10) we find after some elementary analysis that

$$\bar{\rho}^2 = \frac{1}{1+S} \left[1 + \frac{e^{-R}}{15} (15 + 15R + 6R^2 + R^3) \right], \quad \dots\dots(25)$$

$$\bar{z}^2 = \frac{1}{1+S} \left[1 + \frac{1}{4}R^2 + \frac{e^{-R}}{60} (60 + 60R + 27R^2 + 7R^3 + R^4) \right]. \quad \dots\dots(26)$$

Table 1 gives the values of $\bar{\rho}^2$, \bar{z}^2 and $M(R)$ based on the exact and on the l.c.a.o. wave functions for a range of R centred around R_e the equilibrium internuclear separation (which is almost exactly twice the radius of the first Bohr orbit). As can be seen the agreement in the case of $\bar{\rho}^2$ and \bar{z}^2 is poor; but, partly because of fortuitous cancellation of the errors in these two quantities, and partly because of the presence of the $\frac{1}{2}R^2$ term (cf. formula (8)) the agreement in the case of

$M(R)$ is quite good. It may be remarked in parenthesis that the instantaneous static quadrupole moment

$$\mathbf{N}(R) = -\overline{\rho^2}(\mathbf{ii} + \mathbf{jj}) + (\frac{1}{2}R^2 - \overline{z^2})\mathbf{kk}, \quad \dots\dots(27)$$

can be obtained at once from the figures in the table: for example we have

$$\mathbf{N}(2a_0) = -0.6416(\mathbf{ii} + \mathbf{jj}) + 0.8890\mathbf{kk} \quad (\text{atomic units}).$$

Buckingham and Reid (1953) have obtained the vibrational wave functions, $P_{v,J}(R)$, for various v and J by solving the appropriate differential equations numerically. Using these the integral expression for $\overline{M}(v', v''; J', J'')$ in (12) was

Table 1. Data relating to the Quadrupole Moment of the Hydrogen Molecular Ion in the Ground Electronic State
(in atomic units)

R	$\overline{\rho^2}$		$\overline{z^2}$		$M(R)$	
	exact	l.c.a.o.	exact	l.c.a.o.	exact	l.c.a.o.
1.0	0.4236	1.0264	0.5204	1.1840	0.4033	0.3424
1.2	0.4678	1.0352	0.6125	1.2666	0.5753	0.4886
1.4	0.5120	1.0441	0.7168	1.3657	0.7752	0.6584
1.6	0.5562	1.0528	0.8341	1.4825	1.0021	0.8503
1.8	0.5995	1.0609	0.9652	1.6177	1.2543	1.0632
2.0	0.6416	1.0682	1.1110	1.7725	1.5307	1.2957
2.2	0.6826	1.0746	1.2729	1.9479	1.8296	1.5467
2.4	0.7220	1.0799	1.4522	2.1449	2.1497	1.8150
2.6	0.7595	1.0840	1.6501	2.3643	2.4894	2.0997
2.8	0.7949	1.0869	1.8676	2.6070	2.8473	2.3999
3.0	0.8281	1.0886	2.1064	2.8734	3.2217	2.7152

computed. It will be observed from the results, presented in table 2, that contrary to the assumption of earlier workers this quantity is far from independent of the rotational quantum numbers of the connected levels. As would be expected

Table 2. Values of $\overline{M}(v', v''; J', J'')$
(in atomic units)

$v', v''=0, 0$		$v', v''=1, 0$		$v', v''=2, 0$			$v', v''=3, 0$		
$\Delta J=+2$	$\Delta J=+2$	$\Delta J=0$	$\Delta J=-2$	$\Delta J=+2$	$\Delta J=0$	$\Delta J=-2$	$\Delta J=+2$	$\Delta J=0$	$\Delta J=-2$
1.644	0.314	—	—	0.029	—	—	0.005	—	—
1.663	0.279	0.346	0.375	0.032	0.027	0.023	0.006	0.004	0.003
1.697	0.245	0.352	0.419	0.034	0.028	0.019	0.007	0.004	0.002
1.745	0.209	0.357	0.462	0.034	0.028	0.012	0.008	0.004	+0.000
		0.364	0.511		0.029	0.005		0.004	-0.001

$$\Delta J = J' - J''.$$

dash signifies that the transition does not occur, and a blank space that the transition has not been treated.

its magnitude falls off rapidly with increased change in the vibrational quantum number. The cancellation within the integral, which is responsible for the fall off, naturally causes the dependence of the value of \overline{M} on the form of $P(R)$ and $M(R)$ to be rather critical for the higher harmonics. The sensitivity to $P(R)$ is demonstrated sufficiently by the influence of rotation (cf. table 2) to which attention has just been directed. To examine the sensitivity to $M(R)$ it was found convenient to fit the function to a cubic

$$M(R) = M_0 + M_1(R - R_e) + M_2(R - R_e)^2 + M_3(R - R_e)^3, \quad \dots\dots(28)$$

using the method of least squares to find the best values of the coefficients. If $P(R)$ is represented by the Morse approximation, the integration in (13) can now

be done analytically (cf. Rosenthal 1935, James and Coolidge 1938, and Ishiguro, Arai, Mizushima and Kotani 1952). It yields

$$\begin{aligned} \bar{M}(v', v'') = & M_0 g_0(v', v'' | \omega_e, x_e) + M_1 g_1(v', v'' | \omega_e, x_e) + M_2 g_2(v', v'' | \omega_e, x_e) \\ & + M_3 g_3(v', v'' | \omega_e, x_e), \dots\dots (29) \end{aligned}$$

where, for a given reduced mass, the g 's are known functions of ω_e and x_e , the standard spectroscopic constants. Computations were carried out with these

Table 3. Values of Successive Terms in the Expansion of $\bar{M}(v', v'')$ (in atomic units)

Quantum numbers		$M_0 g_0$	$M_1 g_1$	$M_2 g_2$	$M_3 g_3$	Sum.
$v''=0$	$v'=0$	1.526 ₇	0.085 ₀	0.016 ₂	-0.000 ₄	1.627
	$v'=1$	0	0.330 ₈	0.013 ₀	-0.001 ₄	0.342
	$v'=2$	0	0.040 ₉	-0.019 ₂	0.000 ₈	0.022
	$v'=3$	0	0.008 ₄	-0.006 ₀	-0.000 ₈	0.002

Table 4. Wave Numbers σ (in cm^{-1}), Einstein Spontaneous Emission Coefficients A (in sec^{-1}), and Oscillator Strengths f of some Quadrupole Transitions of the Hydrogen Molecular Ion

J''	σ	$A \times 10^8$	$f \times 10^{15}$	σ	$A \times 10^8$	$f \times 10^{15}$	σ	$A \times 10^8$	$f \times 10^{15}$
$v', v''=0, 0$									
$\Delta J = +2$									
0	176	0.0010	2.5						
2	400	0.091	15						
4	615	0.90	51						
6	816	4.0	120						
8									
$v', v''=1, 0$									
$\Delta J = +2$				$\Delta J = 0$			$\Delta J = -2$		
0	2357	16	220	—	—	—	—	—	—
2	2562	28	110	2181	19	60	2014	52	39
4	2745	33	95	2162	17	55	1782	18	48
6	2900	33	77	2130	16	52	1547	9.6	42
8				2084	15	51	1314	5.0	33
$v', v''=2, 0$									
$\Delta J = +2$				$\Delta J = 0$			$\Delta J = -2$		
0	4411	3.1	12	—	—	—	—	—	—
2	4595	6.6	8.5	4235	3.2	2.6	4079	6.8	1.2
4	4747	9.8	9.4	4195	2.9	2.5	3835	1.7	0.94
6	4860	11	9.4	4132	2.7	2.4	3580	0.44	0.36
8				4044	2.6	2.4	3316	0.050	0.052
$v', v''=3, 0$									
$\Delta J = +2$				$\Delta J = 0$			$\Delta J = -2$		
0	6343	0.5	1	—	—	—	—	—	—
2	6508	1.5	1	6168	0.4	0.2	6020	0.6	0.05
4	6629	2	1	6108	0.4	0.2	5768	0.1	0.03
6	6700	3	1.5	6014	0.4	0.2	5493	< 0.01	< 0.01
8				5885	0.4	0.2	5198	0.03	0.01

$$\Delta J = J' - J''.$$

A dash signifies that the transition does not occur and a blank space that the transition has not been treated.

The wave numbers may be in error by several units. In the first three cases there are *two* significant figures in the A and f columns but in the last case there is only *one* significant figure.

constants taken as 2321.4 cm^{-1} and 2.89×10^{-2} respectively.* Inspection of the results in table 3 shows that the latter terms of expression (29) give an important contribution when the vibration quantum numbers of the connected levels differ by more than unity. Now these terms depend on the detailed variation of $M(R)$ —they are in fact measures of the *second and higher* derivatives of the function at the equilibrium internuclear separation. This makes the treatment of complex molecules very difficult, for the usefulness of approximate calculations, based even on the most accurate wave functions at present available, would clearly be severely limited.

The Einstein spontaneous emission coefficients and oscillator strengths due to the quadrupole moment were finally obtained by numerical substitution in formulae (1), the frequencies of the lines being taken from the calculations of Buckingham and Reid (1953). Table 4 gives the results. It will be observed that the transitions generally become progressively weaker as Δv increases beyond unity, but that the spread for any one harmonic is so great that there is a certain amount of overlap, some of the transitions being actually stronger than some of those in the preceding harmonic. The values of A and f naturally present a rather complex pattern since they are controlled by several independent factors (the matrix elements, the frequencies and the statistical weights of the connected levels).

§ 3. DIPOLE TRANSITIONS

3.1. Consider a representative ion isotopic with H_2^+ , the heteronuclear ion whose nuclei A and B are λ_1 and λ_2 times the mass M of the proton. It can be seen that the dipole moment operator is

$$\left\{ \frac{\lambda_1 - \lambda_2}{2(\lambda_1 + \lambda_2)} \right\} R - z \quad \dots\dots(30)$$

in atomic units, R being the internuclear separation and z the coordinate of the electron with respect to an axis along AB with origin at the mid-point of this line. Wu (1952) has pointed out that the associated matrix element is controlled almost entirely by the R -term (which arises because of excess positive charge on the system). Taking it alone into account, and adopting the Morse approximation, he was able to express $D(v', v'')$, the dipole moment connecting the vibration levels v' and v'' , as a function of known molecular parameters. Expansion of his formulae in powers of the anharmonic constant x_e yields

$$\left. \begin{aligned} D(0, 1) &\simeq K(1 + \tfrac{1}{2}x_e), \\ D(0, 2) &\simeq 2^{-1/2} K x_e^{1/2} (1 + 3x_e/2), \\ D(0, 3) &\simeq 2^{1/2} 3^{-1/2} K x_e (1 + 3x_e), \end{aligned} \right\} \quad \dots\dots(31)$$

with

$$K = \frac{\lambda_1 - \lambda_2}{2^{1/2} \lambda_1 \lambda_2 (\lambda_1 + \lambda_2)^{1/2}} \left(\frac{mR}{M\omega_e} \right)^{1/2},$$

where R is Rydberg's constant. Both ω_e and x_e are of course $\{(\lambda_1 + \lambda_2)/2\lambda_1\lambda_2\}^{1/2}$ times the corresponding parameters of the ordinary hydrogen molecular ion.

* The values cited were obtained by the application of Dunham's formulae (1932) to the electronic potential energy curve calculated by Bates, Ledsham and Stewart (1953). They are in accord with the earlier theoretical values of Sandeman (1935) ($\omega_e = 2321.5 \text{ cm}^{-1}$, $x_e = 2.92 \times 10^{-2}$) and with the admittedly imprecise experimental values of Richardson (1938) ($\omega_e = 2297 \text{ cm}^{-1}$, $x_e = 2.72 \times 10^{-2}$).

The Einstein spontaneous emission coefficients and the oscillator strengths may now be found from the standard relations

$$A(v', v'') = \frac{64\pi^4\nu^3}{3c^3h} D(v', v'')^2, \quad f(v'', v') = \frac{8\pi^2 m\nu}{3e^2h} D(v', v'')^2. \quad \dots\dots (32)$$

Results obtained for $^1\text{H}^2\text{H}^+$ are displayed in table 5. Comparison with table 4 shows that the dipole transitions are very much more rapid than are the quadrupole transitions. The high absolute magnitudes should not of course be regarded

Table 5. Einstein Spontaneous Emission Coefficients $A(v', v'')$ and Oscillator Strengths $f(v'', v')$ due to the Dipoles connecting the Vibrational Levels (v', v'')

Transition	v''	v'	A (sec $^{-1}$)	f
$^1\text{H } ^2\text{H}^+, x^2\Sigma_g^+$	0	1	1.8×10^1	7.3×10^{-6}
	0	2	1.7	1.9×10^{-7}
	0	3	2.0×10^{-1}	1.0×10^{-8}
$^{14}\text{N } ^{15}\text{N}^+, x^2\Sigma_g^+$	0	1	2.2×10^{-2}	7.4×10^{-9}
	0	2	6.4×10^{-4}	5.3×10^{-11}
	0	3	2.1×10^{-5}	7.8×10^{-13}

as typical of dipole transitions of the type under discussion since, as is obvious from the formulae, the small values of λ_1 and λ_2 and the rather large value of x_e cause the ions isotopic with H_2^+ to favour such transitions. To illustrate the position the results of similar computations on $^{14}\text{N}^{15}\text{N}^+$ are included in the table. In carrying out the computations the values of the spectroscopic constants recommended by Herzberg (1950) were used.

Though the z -term of (30) is relatively unimportant the contribution from it is nevertheless of general interest since the dipole moment operator of *neutral* systems contains no other term.

First order perturbation theory enables the wave functions, Φ , of a heteronuclear ion to be obtained from the wave functions X of the corresponding homonuclear ion. Noting that the Hamiltonians differ by approximately

$$\mathcal{W} = \frac{\hbar^2(\lambda_1 - \lambda_2)}{8\pi^2 M \lambda_1 \lambda_2} \cdot \frac{\partial^2}{\partial z \partial R},$$

it is apparent that the dipole moment connecting the states of collective quantum numbers n' and n'' is

$$D(n', n'') = \left| \sum_{m \neq n'} \frac{W(n', m) Z(m, n'')}{E_{n'} - E_m} + \sum_{m \neq n''} \frac{W(m, n'') Z(n', m)}{E_{n''} - E_m} \right|,$$

where $W(s, t) = \int X_s^* \mathcal{W} X_t d\tau$, $Z(s, t) = \int X_s^* z X_t d\tau$,

the E 's are the unperturbed eigen-energies and all quantities are now in atomic units. Wick (1935) has discussed the reduction to a form suitable for numerical evaluation. Writing

$$R(s, t) = \int X_s^* R X_t d\tau,$$

and introducing $f^z(s, t) = \frac{2(E_t - E_s)}{3} Z(s, t) Z(t, s)$

the oscillator strength for the *parallel* transition ($s-t$) it may be shown by a trivial generalization of his final result that if n' and n'' refer to states of the same

electronic and rotational quantum numbers and neighbouring vibrational quantum numbers then

$$D(n', n'') = \frac{3(\lambda_1 - \lambda_2)}{4(\lambda_1 + \lambda_2)} (E_{n''} - E_{n'})^2 R(n', n'') \left\{ \sum_m \frac{f^z(n', m) + f^z(n'', m)}{(E_{n'} - E_m)(E_{n''} - E_m)} \right\}, \quad \dots (33)$$

the summation being over all allowed transitions. This is the expression most convenient in the present problem but it is usually preferable to replace the term in curly brackets by $\frac{2}{3}\alpha_p$ where α_p is the polarizability along the internuclear line.

We will consider specifically the calculation of the dipole moment connecting the zeroth and first vibrational levels of the ground electronic state. To indicate this limitation the collective quantum numbers n' and n'' will be replaced by 0 and 1 respectively.

As far as the oscillator strengths are concerned the nuclear part of the wave functions may be ignored and the sum for each electronic transition may be taken as the value $f^z(s, t | R_e)$ at the equilibrium internuclear separation. It is known that $f^z(1\sigma_g, 2p\sigma_u | R_e)$ is 0.32₀ (Bates 1951), and hence from the Thomas-Kuhn sum rule it follows that

$$\sum_{m \neq 2p\sigma_u} f^z(1\sigma_g, m | R_e) = 0.01_3. \quad \dots (34)$$

Reference to tables of eigen-energies (Bates, Ledsham and Stewart 1953) shows that the effective value of $(E_0 - E_m)(E_1 - E_m)$ is about 0.185 atomic units in the case of the $1\sigma_g - 2p\sigma_u$ transition. It is much greater for other transitions from the ground electronic state.* In view of their low oscillator strengths these may, therefore, be neglected.

Using the figures just cited and taking

$$R(0, 1) = \left\{ \frac{\lambda_1 + \lambda_2}{\lambda_1 \lambda_2} \left(\frac{mR}{M\omega_e} \right) \right\}^{1/2} (1 + \frac{1}{2}x_e), \quad \dots (35)$$

as given by the Morse approximation, we find on numerical substitution in (32) and (33) that the z -term of (30) gives the spontaneous transition probability $A(1, 0)$ and oscillator strength $f(0, 1)$ of the fundamental vibrational band of $^1\text{H}^2\text{H}^+$ to be $2.7 \times 10^{-6} \text{ sec}^{-1}$ and 1.1×10^{-12} respectively. These values, though still larger than the values for the quadrupole transition (cf. table 4) are 1.5×10^{-7} times smaller than the values given by the R -term (which is in reasonable agreement with Wu's estimate that they should be about 10^{-6} times smaller).

ACKNOWLEDGMENTS

We wish to thank Dr. R. A. Buckingham and Mr. S. Reid for allowing us to use the results of their calculations on the vibrational wave functions prior to their publication.

REFERENCES

- BATES, D. R., 1951, *J. Chem. Phys.*, **19**, 1122.
 BATES, D. R., LEDSHAM, K., and STEWART, A. L., 1953, *Phil. Trans. Roy. Soc. A*, in the press.
 BUCKINGHAM, R. A., and REID, S., 1953, *Proc. Roy. Soc. A*, in the press.
 BURRAU, O., 1927, *Kgl. Danske Videnskab. Selskab*, **7**, 1.

* Some calculations carried out in another connection show that the main contribution to the summation in (34) comes from high in the $f\sigma_u$ photoionization continuum.

- CONDON, E. U., and SHORTLEY, G. H., 1935, *Theory of Atomic Spectra* (Cambridge : University Press).
- DUNHAM, J. L., 1932, *Phys. Rev.*, **41**, 721.
- HERZBERG, G., 1950, *Spectra of Diatomic Molecules*, 2nd edn. (London : Macmillan).
- ISHIGURO, E., ARAI, T., MIZUSHIMA, M., and KOTANI, M., 1952, *Proc. Phys. Soc. A*, **65**, 178.
- JAMES, H. M., and COOLIDGE, A. S., 1938, *Astrophys. J.*, **87**, 444.
- MOTT, N. F., and SNEDDON, I. N., 1948, *Wave Mechanics and its Applications* (Oxford : Clarendon Press).
- RICHARDSON, O. W., 1938, *Nuovo Cim.*, **15**, 293.
- ROSENTHAL, J. E., 1935, *Proc. Nat. Acad. Sci., Wash.*, **21**, 281.
- SANDEMAN, I., 1935, *Proc. Roy. Soc. Edinb.*, **55**, 73.
- WICK, G. C., 1935, *Atti R. Accad. dei Lincei*, **21**, 708.
- WU, TA-YOU, 1952, *Canad. J. Phys.*, **30**, 291.

Nuclear Binding Energies and the *jj*-Coupling Shell Model

By A. R. EDMONDS

University of Manchester

Communicated by L. Rosenfeld; MS. received 4th May 1953

Abstract. Variations with N and Z of nuclear binding energies in the radioactive region are compared with calculations of the energies of the lowest states of configurations of neutrons and protons suggested by the *jj*-coupling shell model and experimental data on spins and magnetic moments. Attention is given to the variations of neutron-proton interaction among the 'outer' nucleons which are indicated by the experimental binding energies.

§ 1. INTRODUCTION

THE occurrence of discontinuities in the binding energy of the 'last' nucleon at the magic numbers is well known (Glueckauf 1948, Pryce 1950, Harvey 1951, etc.). These, and other regularities in nuclear properties have been explained by the *jj*-coupling shell model of Mayer (1950).

The success of calculations of energy level schemes using a quasi-atomic method based on this model (Pryce 1952, Edmonds and Flowers 1952a, b) has suggested that some agreement may be reached between the experimental binding energies and theoretical values obtained from similar calculations of ground state energies of appropriate configurations of neutrons and protons.

This paper describes an attempt to analyse in this way the data in the tables of nuclear binding energies in the radioactive region compiled by Way and Wood (1951).

The method of Harvey† (1951) has been followed, in which the discontinuities in binding energies which may be attributed to shell structure are isolated from variations due to bulk effects (e.g. coulomb energy) by subtracting from the experimental binding energies values derived from a semi-empirical mass formula, which describes the slower variations in nuclear masses with N and Z .

Attention has been concentrated on the variation of the binding of the last *proton* with the number of *neutrons* and vice versa; this gives us information on the interactions of the protons and neutrons in the unclosed shells of the nuclei considered.

§ 2. DISCUSSION OF EXPERIMENTAL RESULTS

We denote binding energies as follows:

$$E_n(N, Z) = E(N+1, Z) - E(N, Z) - E(1, 0)$$

$$E_p(N, Z) = E(N, Z+1) - E(N, Z) - E(0, 1)$$

where $E(N, Z)$ is the energy equivalent of the nucleus (N, Z) . The quantities discussed are $\epsilon_n(N, Z)$ and $\epsilon_p(N, Z)$ where

$$\epsilon_n(N, Z) = E_n(N, Z) - E_n^*(N, Z)$$

$$\epsilon_p(N, Z) = E_p(N, Z) - E_p^*(N, Z)$$

† This method was proposed earlier by Podolanski and used by Wapstra (1948) in his discussion of nuclear masses.

and the E_n^* , E_p^* are calculated from masses given in the U.S. Atomic Energy Commission *Table of Atomic Masses*, computed from the following semi-empirical formula, due to Fermi:

$$M(A, Z) = 1.01464A + 0.014A^{2/3} - 0.041905Z_A + \frac{0.041905}{Z_A}(Z - Z_A)^2 + \frac{0.036}{A^{3/4}}\lambda$$

where $Z_A = A/(1.980670 + 0.0149624A^{2/3})$ and $\lambda = +1$ if A is even and Z odd

$= 0$ if A is odd

$= -1$ if A is even and Z even.

The values of E_n and E_p have been taken from the tables of Way and Wood, and the corresponding ϵ_n and ϵ_p are given in figs. 1 and 2. In fig. 1 $\epsilon_n(N, Z)$ is plotted as a function of N for various fixed values of Z ; in fig. 2 $\epsilon_p(N, Z)$ is plotted in the same way as a function of N . This method of display has been chosen because there are in this part of the N, Z plane long rows of nuclei with a fixed Z and different N , but only short rows with a fixed N and different Z .

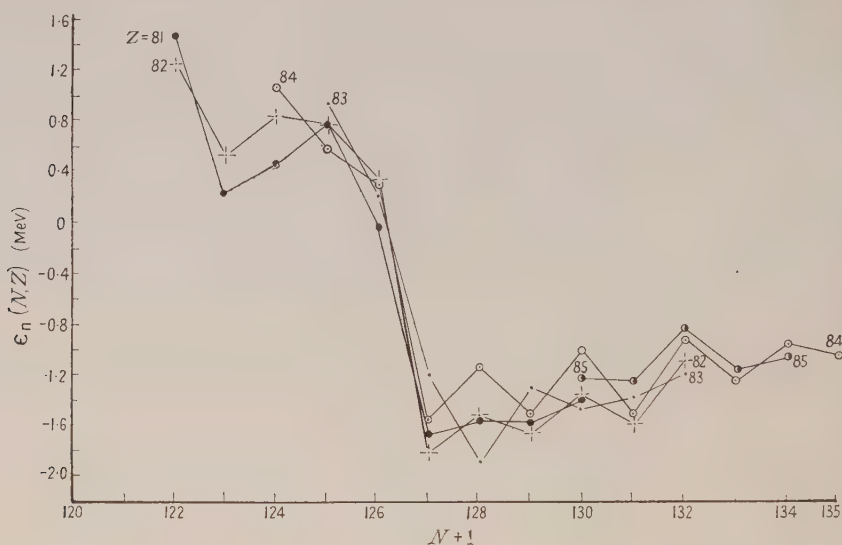


Fig. 1.

We consider first the behaviour of ϵ_n shown in fig. 1. The sharp drop of ϵ_n at the magic number 126 of N has already been remarked by Harvey. Above $N=126$ there is a systematic even-odd variation of ϵ_n with N . This is small for $Z=81, 82$; for $Z=83$, ϵ_n is larger for N even, and for $Z=84, 85$, ϵ_n is larger for N odd. Thus for the nuclei with $Z \geq 83$ the λ term in the semi-empirical formula does not account for the whole of the even-odd spacing. These effects will be discussed later in connection with the variations of the n - p interaction.

In fig. 2 we discuss first the average variation of ϵ_p with N —i.e. ignoring the even-odd effects—and then consider separately these even-odd differences. We see that for $Z=81$ ϵ_p increases with N when $N < 126$, but decreases slightly with N when $N \geq 126$. On the other hand, for $Z=82$ and 83 , ϵ_p increases with N when $N \geq 126$; since there are only two points in each of these cases for $N < 126$, we say with less confidence that ϵ_p remains constant (for $Z=82$) and decreases (for $Z=83$) with N for values of $N < 126$.

The even-odd variations of ϵ_p with N for $N \geq 126$ are regular and well marked. We notice first that for $Z=81$ they are much smaller than for $Z \geq 82$. The even-odd variations have the common feature that for Z even ϵ_p is greater for odd N , and for Z odd ϵ_p is greater for even N . For $N < 126$ we can say little; the even-odd variations for $Z=82$ and 83 appear to be less than for $N \geq 126$, and those for $Z=81$ are greater than for $N \geq 126$. The irregular behaviour of the points for $N \leq 123$ is discussed later.

§ 3. BINDING ENERGIES AND THE SHELL MODEL

From the viewpoint of the *jj*-coupling shell model, a typical nucleus in this region consists of a core of 126 neutrons and 82 protons plus a number of neutrons and protons moving in orbits whose quantum numbers are arrived at partly from the original Mayer scheme (1950) and partly from experimental values of spins and magnetic moments (Klinkenberg 1952). A nucleus with less than 126 neutrons or 82 protons is equivalent to a core with the appropriate

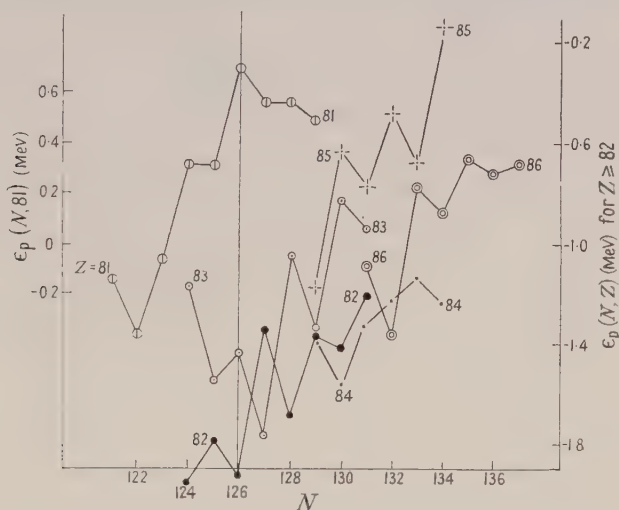


Fig. 2.

number of 'holes', the energy of a hole being taken as minus the energy of a particle in the same state. The variations of, say, ϵ_n with N have been interpreted by Harvey and others as being due to the filling of successive orbits of neutrons in analogy with the cause of the variations of electron binding energy in atoms. However the variations of ϵ_p with N point to an interaction between the neutrons and protons (or holes) outside the core, the strength of which depends upon the states in which these particles lie. Now since the range of nuclear forces is small compared with the diameters of nuclei in this region (about one-tenth) we can get an indication of the amount of the *n p* interaction energy for a given choice of states for the neutron and proton by computing the correlation between the respective wave functions. It is assumed that, if we neglect for the moment the even-odd variation of ϵ_p with N , the interaction energy between a proton in one orbit and n neutrons in another orbit is n times that between the proton and one neutron in that orbit. This assumption is supported by more refined calculations which are described later.

Thus a large rate of increase of ϵ_p with N in a certain region of N and Z should correspond to a large correlation between the neutron and proton wave functions with the quantum numbers which are assigned to that region of N and Z , and similarly a small rate of increase or a decrease of ϵ_p with N should correspond to a small correlation of the relevant wave functions.

The correlation between neutron and proton wave functions is given by

$$\int |\psi(n_n l_n j_n, \mathbf{r}) \psi(n_p l_p j_p, \mathbf{r})|^2 d\mathbf{r}.$$

Calculations of this quantity have been carried out for the values of $n_n l_n j_n$, $n_p l_p j_p$ given by Klinkenberg (1952). The 82nd proton is given to be in the state $3s_{1/2}$, and the 83rd, 84th, ... in $6h_{9/2}$. The neutron holes for $N < 126$ correspond to the states $4p_{1/2}$ or $4p_{3/2}$, and the 127th, 128th, ... neutrons are in the state $6g_{9/2}$. The radial dependence of the wave functions was assumed to be of the harmonic oscillator type, for ease of computation. This assumption is a poor one for heavy nuclei, but it has been found that the variation in the radial integral contribution to the correlation for different choices of quantum numbers is unimportant. The method of calculation followed exactly that of Pryce (1952) in a similar problem, that of an approximate calculation of energy level schemes in the region of ^{208}Pb . Use was made of his result that the levels of the neutron-proton system with smallest total J lie lowest.

The results of calculation of the correlation of neutron and proton wave functions are as follows: †

$4p_{1/2}, 3s_{1/2}$	1.23	($N \leq 126, Z \leq 82$)
$4p_{3/2}, 3s_{1/2}$	0.96	($N \leq 126, Z \leq 82$)
$6g_{9/2}, 3s_{1/2}$	0.016	($N > 126, Z \leq 82$)
$4p_{1/2}, 6h_{9/2}$	0.28	($N \leq 126, Z > 82$)
$6g_{9/2}, 6h_{9/2}$	1.92	($N > 126, Z > 82$)

Thus these results agree qualitatively with the behaviour of $\epsilon_p(N, Z)$. Agreement was not obtained when some other assignments of nlj consistent with the Mayer scheme were taken, for instance if the neutron holes were given the state $7i_{13/2}$. These correlation calculations can, of course, only distinguish between states whose quantum numbers differ considerably.

It was hoped to reproduce the even-odd variation of ϵ_p with N in a simple jj -coupling model representing the nucleons outside the closed shells. The original intention was to calculate the energies of the lowest states of systems $(n_n l_n j_n)^x (n_p l_p j_p)^y$ for various x and y and various types of central interaction between pairs of nucleons. The results would give the binding energies of the 'last' nucleon in systems of this kind. However, this type of calculation is extremely laborious for values of x or y greater than 3, and a simplification was therefore introduced. It was assumed that the neutrons and protons moved in the same orbit, making possible the use of the group theoretical methods of calculation of energies described by Edmonds and Flowers (1952a) for configurations of identical particles in jj -coupling. This is perhaps plausible

† The numbers given are 4π times the probability per unit volume that the neutron and proton coincide; the singlet and triplet states have, however, been weighted according to the strengths of singlet and triplet interaction assumed by Pryce (1952).

for $N > 126$, $Z > 82$, where the relevant neutron and proton configurations are $6g_{9/2}$ and $6h_{9/2}$ respectively. Calculations of the energies of the lowest states of systems consisting of one or two protons and a variable number of neutrons have been carried out. The configurations considered were $d_{5/2}$ and $f_{7/2}$ (since these were dealt with in the above-mentioned paper). Central interactions of various ranges and exchange types were used. Details of the methods of calculation are given in the Appendix.

Figure 3 shows a typical result of calculations of this kind. It is for the configuration $f_{7/2}$ and shows, for systems of (a) one proton and N neutrons, and (b) two protons and N neutrons, the binding energy of the last proton as a function of N . The interaction assumed is a central force of δ -function radial dependence. It was found that a central interaction of finite range with a range parameter corresponding to the accepted values of the range of nuclear forces and nuclear radius, and with a large Majorana exchange component gave a very similar dependence of binding energy on N to that given by a δ -function interaction.

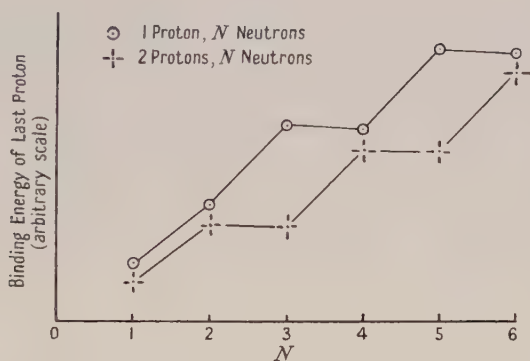


Fig. 3. Binding energy of last proton in configuration $(f_{7/2})^n$, δ -function interaction.

It will be seen that the sign of the even-odd variation with N of the binding energy of even and odd protons agrees with the variation of ϵ_p with N . However, the amount of this even-odd variation, when compared with the average rate of rise of binding energy with N , is appreciably smaller than that observed in practice. This fact has not yet been accounted for; no special choice of central force gives an even-odd variation of binding energy with N appreciably greater than that for a δ -function interaction.

The irregular behaviour of ϵ_p with N for $Z=81$ and $N \leq 123$ may be attributed to the possibility that the $4p_{3/2}$ and $4p_{1/2}$ neutron levels are being filled together in this region of N (cf. Klinkenberg 1952).

The even-odd variations of ϵ_n with N may also be attributed to variations in n - p interactions; however they are really superimposed on the normal even-odd variations in binding energy (taken account of by the λ -term in the semi-empirical formula) and are hence of doubtful significance. The situation when we consider ϵ_p is different; when n - p interactions may be expected to be small, as between the 82nd proton and the neutrons above 126, we see that ϵ_p varies only slightly with N , and this implies, when we consider just the even-odd variations, that E_p also varies only slightly with N .

§ 4. CONCLUSION

The discontinuities of the binding energy of the last nucleon in nuclei in the region of ^{208}Pb have been shown to be partially explained by a quasi-atomic model of the jj -coupling type. This consists of closed shells of 82 protons and 126 neutrons plus the appropriate number of nucleons in higher orbits or holes in the closed shells.

The influence of the number of neutrons in the nucleus on the binding energy of the last proton has been interpreted as reflecting the variation of interaction between the neutrons and protons in unclosed shells or neutron and proton holes in the closed shells. Some success has been achieved in correlating this information with the results obtained by calculating the ground state energies of these systems of extra-core nucleons, assuming wave functions suggested by the Mayer scheme and by experimental evidence on spins, etc., and short range central interactions.

Application of these methods to other parts of the N, Z plane is difficult, due to lack of accurate binding energy data. However some remarks may be made about the results of Harvey (1951). He demonstrates a large ($\sim 2\text{ MeV}$) discontinuity in neutron binding energy at $N=50$. This should not be attributed solely to the difference in energy of neutron levels above and below the magic number, for at $N=50$, as at other magic numbers, there is an unusual number of isotones, and nuclei exist with Z values higher than would be expected otherwise for that number of neutrons. It seems possible that there is a strong interaction between protons in the higher levels and neutron holes in the closed shell in this region, giving the nuclei with higher than normal Z a bigger neutron binding energy than might otherwise occur. But there are too few binding energy data in this region to be sure.

APPENDIX

*Methods of Calculation of Lowest States of Configurations $(lj)^n$
of Neutrons and Protons*

The group theoretical classification of the states of configurations $(lj)^n$ of neutrons and protons has been made by Flowers (1952). Methods of calculation of the energy matrices for these configurations are given by Edmonds and Flowers (1952a) and the lowest states for various central interactions by Edmonds and Flowers (1952b) (these two papers will be referred to as EF).

It is shown that the energy of a state of $(lj)^n$ is given by

$$E = e_0 E^{(0)} + e_1 E^{(1)} + e_2 E^{(2)} + \dots$$

where the $E^{(i)}$ are linear combinations of the Slater integrals $F^{(k)}$ and are given in table 8 of EF (1952a). The $F^{(k)}$ are determined by the radial dependence of the wave functions and central interaction assumed, and the e_i depend on the quantum numbers n, T, s, t, J, α of the state concerned.

We are concerned with configurations of (a) all neutrons, (b) one proton, the rest neutrons, and (c) two protons, the rest neutrons. Using the notation of Flowers (1952), (a) includes states of type [11] 1(0000)(00)0 and [111] $3/2(1000)(1, \frac{1}{2})7/2$. (b) includes those of type [21] $\frac{1}{2}(1000)(1, \frac{1}{2})7/2$ and [211] 1(1100)(2, 1)2 and (c) includes [221] $\frac{1}{2}(1000)(1, \frac{1}{2})7/2$ and [2211]

1(0000)(00)0. j has been taken equal to $7/2$ for definiteness. For nearly all these states e_2 and e_3 are identically zero, and e_0 and e_1 are given by EF 1952 a, eqn. (28). Only for those of type [211] 1(1100)(2,1)2 (i.e. those of seniority 2) are e_2 and e_3 non-zero. However, calculations show that e_2 and e_3 in these cases are of the same order as for the two-particle configuration state [11] (1100)2. The values of the matrix elements of e_2 and e_3 are given in EF 1952 a, table 8. The contribution from $e_2 E^{(2)} + \dots$ is in any case small for short range forces. For a δ -function interaction we have $E^{(1)} = 2E^{(0)}$.

ACKNOWLEDGMENTS

The author wishes to thank Professors R. E. Peierls and L. Rosenfeld for several discussions during the course of the work.

REFERENCES

- EDMONDS, A. R., and FLOWERS, B. H., 1952 a, *Proc. Roy. Soc. A*, **214**, 515; 1952 b, *Ibid.*, **215**, 120.
 FLOWERS, B. H., 1952, *Proc. Roy. Soc. A*, **212**, 248.
 GLUECKAUF, E., 1948, *Proc. Phys. Soc.*, **61**, 25.
 HARVEY, J. A., 1951, *Phys. Rev.*, **81**, 353.
 KLINKENBERG, P. F. A., 1952, *Rev. Mod. Phys.*, **24**, 63.
 MAYER, M. G., 1950, *Phys. Rev.*, **78**, 16.
 PRYCE, M. H. L., 1950, *Proc. Phys. Soc. A*, **63**, 692; 1952, *Ibid.*, **65**, 773.
 U. S. ATOMIC ENERGY COMMISSION, 1950, *Table of Atomic Masses* (NP-1980).
 WAPSTRA, A. H., 1948, *Nature, Lond.*, **161**, 529.
 WAY, K., and WOOD, M., 1951, *Neutron and Proton Binding Energy Map* (National Bureau of Standards, Washington).

Excitation Curves of the Reactions $^{27}\text{Al}(\text{p}, \alpha)^{24}\text{Mg}$ and $^{27}\text{Al}(\text{p}, \gamma)^{28}\text{Si}$

By J. G. RUTHERGLEN AND R. D. SMITH

Department of Natural Philosophy, Glasgow University

MS. received 16th March 1953

Abstract. New data are presented on the excitation curve of the reaction $^{27}\text{Al}(\text{p}, \alpha)^{24}\text{Mg}$ in the range of proton energies from 400 kev to 750 kev. Resonances are found which coincide with the previously known gamma-ray resonances at 503, 630 and 728 kev. No alpha-emission is detected from the gamma-ray resonances at 652, 677 and 733 kev. The results are discussed in terms of some possible spin and parity assignments of the corresponding levels in ^{28}Si .

§ 1. INTRODUCTION

THE alpha-particles from the reaction $^{27}\text{Al}(\text{p}, \alpha)^{24}\text{Mg}$ were first observed by Freeman and Baxter (1948), who measured the Q -value and also gave an excitation curve with low resolution for proton energies from 500 kev to 900 kev. An excitation curve showing resonances above 800 kev has been reported by Shoemaker *et al.* (1951). In this paper we report on some rather more precise determinations of the excitation curves in the range of proton energies from 400 kev to 750 kev. The Q -value of the reaction has also been measured and is in agreement with the recent determination of Van Patter *et al.* (1952). The excitation curve of the reaction $^{27}\text{Al}(\text{p}, \gamma)^{28}\text{Si}$ has also been measured for comparison purposes.

§ 2. EXPERIMENTAL ARRANGEMENTS

Proton Accelerator

The Glasgow H.T. set was used as a source of protons. The output voltage from the cascade generator was stabilized by an electronic feedback circuit with a time constant of $\frac{1}{10}$ second which maintained the average voltage constant to within about 100 volts. The energy spread of the proton beam was mainly due to small irregularities of striking of the mercury vapour rectifiers and to the 400 c/s ripple of the cascade generator. The ripple was reduced by a resistance-condenser smoothing circuit. The total energy spread of the beam was estimated to be about 1.5 kev at a proton energy of 600 kev.

Spectrometer and Target Arrangements

Since the alpha-particles from the reaction have a range which is less than that of the bombarding protons it was necessary to use a magnetic spectrometer to separate them (fig. 1). The proton beam passed through slit S and struck the target T, which was surrounded by a tube A maintained at a negative potential of 100 v to prevent secondary emission. An electronic current integrator was

used to record the total charge reaching the target during a run. The alpha-particles from the target traversed tube B and those of the correct energy were deflected through 45° with a radius of curvature of 15 cm in tube C lying between the magnetic poles. The target was at a distance of 15 cm from the edge of the magnet poles, so that, to a first order, the particles of the correct energy emerged from the magnetic field in planes parallel to the axis of the tube D and perpendicular to the plane of the diagram. These particles were selected by a collimator E, which consisted of thin sheets of mica 10 cm long with a spacing of 0.36 cm. Thus only particles travelling within $\pm 2^\circ$ of the plane of the sheets were able to reach the proportional counter F. The counter window was a thin collodion film supported on a grid. The counter was filled to a pressure of 5 cm Hg with pure methane and operated at about 1200 v. The pulses were amplified, passed through a discriminator and recorded on a scaling unit.

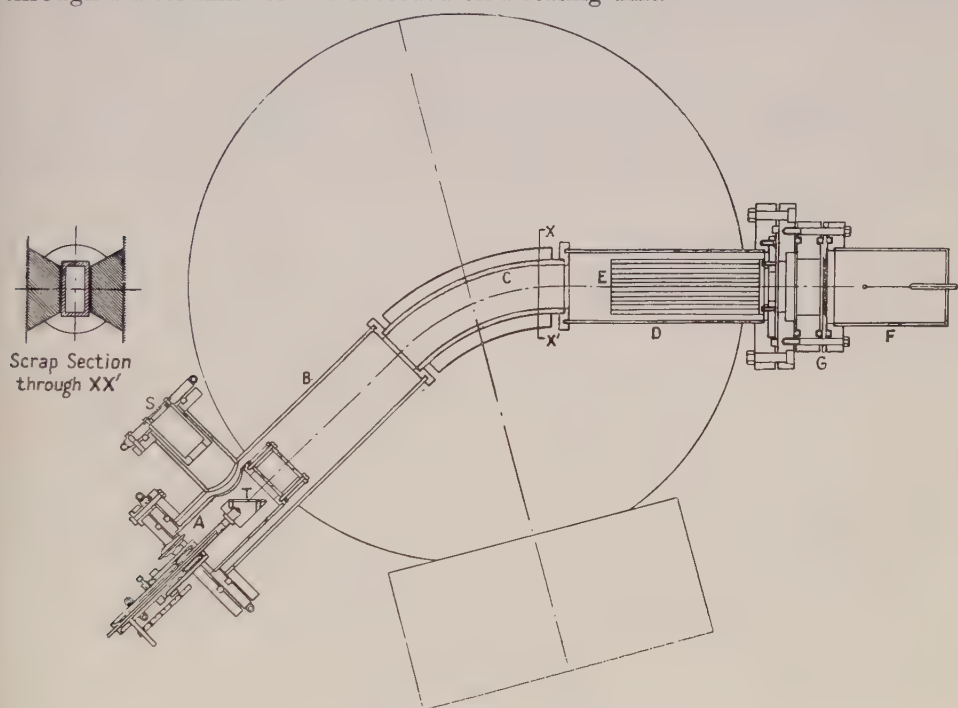


Fig. 1. Sectional diagram of spectrometer.

Because of the small angle of deflection of the spectrometer there was an appreciable background at all magnetic fields due to multiple scattering of protons from the spectrometer walls. However, the pulses due to alpha-particles with energies above 1.5 MeV were about three times as large as any due to scattered protons and were constant to better than 20%. It was thus possible to eliminate the effect of scattered protons by suitable setting of the discriminator bias.

The magnet current was supplied from a generator and was stabilized and controlled to an accuracy within about 0.1%. A careful calibration of the magnetic field as a function of the magnet current was made with a fluxmeter. This calibration remained constant provided that the field was always cycled in the same way so as to avoid hysteresis effects. The calibration was made absolute by measuring the alpha-particle group of energy 1.837 MeV from the reaction

$^{19}\text{F}(\text{p}, \alpha)^{16}\text{O}^*$. The Q -value for this reaction was taken to be 1.977 MeV (Hornyak *et al.* 1950). These alpha-particles were also used as an intensity calibration since their absolute yield at the 340 keV resonance has been accurately measured by Chao *et al.* (1950) to be 1.5 alpha-particles per 10^8 protons.

Gamma Counter

A thick walled aluminium Geiger counter was placed close to the target to detect the gamma-rays. The curve published by Fowler *et al.* (1948) was used to estimate the relative efficiency of this counter for the 12.1 MeV radiation from $^{27}\text{Al}(\text{p}, \gamma)^{28}\text{Si}$ and the 6.13 MeV radiation from $^{19}\text{F}(\text{p}, \alpha, \gamma)^{16}\text{O}$ which was used for the intensity calibration. The fact that the radiation from aluminium is complex due to cascade transitions (Rutherglen *et al.* 1951) is not important because the counter efficiency varies approximately linearly with energy.

Targets

The aluminium targets were prepared by evaporating spectroscopically pure aluminium *in vacuo* on to brass plates. Preliminary experiments had shown that aluminium of commercial purity gave rise to spurious particle groups.

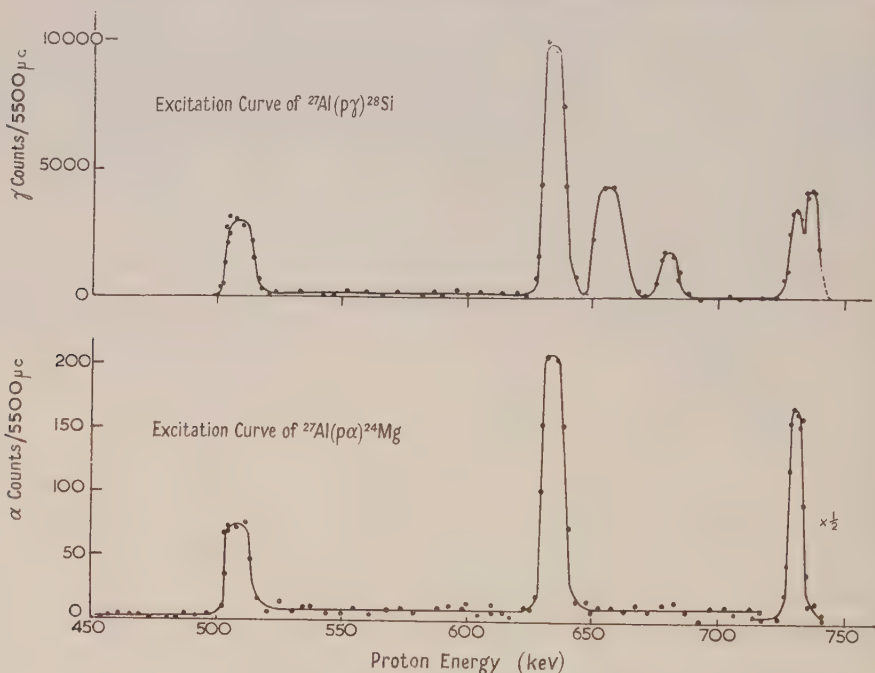


Fig. 2. Excitation curves for $^{27}\text{Al}(\text{p}, \gamma)^{28}\text{Si}$ and $^{27}\text{Al}(\text{p}, \alpha)^{24}\text{Mg}$.

§ 3. EXPERIMENTAL RESULTS

The excitation curves for the alpha-particles and gamma-rays are shown in fig. 2. Measurements were made at 5 keV intervals from 350 keV to 750 keV and at 1 keV intervals in the neighbourhood of resonance peaks. No alpha-particle resonances were detected at bombarding energies below 500 keV. The target thickness was 10 keV for the measurements below 700 keV and 5 keV for the measurements between 700 keV and 750 keV so that the resonances at 728 keV

and 733 kev could be resolved. The widths of the peaks in the excitation curves are almost entirely due to target thickness and the peaks are approximately flat-topped, as would be expected in this case. The slope of the front edge of the peak is due to the ripple and voltage fluctuations on the H.T. set and it is, therefore, only possible to say that the true widths of the nuclear resonances are less than 1.5 kev. The magnet current of the spectrometer was adjusted during the runs so that the magnetic field was always at the value corresponding to the peak of the energy spectrum. The counting rate at each peak, therefore, gives a measure of the 'thick-target' yield of the resonance.

The energy spectrum of the alpha-particles was measured at the resonances corresponding to bombarding energies of 503 kev, 630 kev and 728 kev. These spectra are shown in fig. 3. In order to reduce the effects of target deterioration,

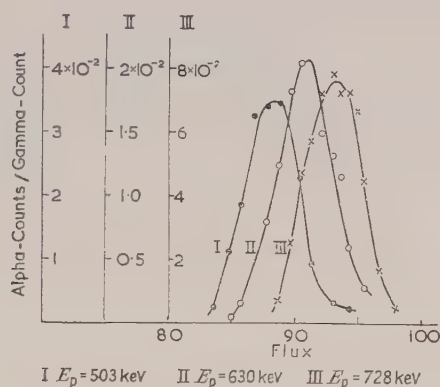


Fig. 3. Spectra of alpha-particles from $^{27}\text{Al}(p, \alpha)^{24}\text{Mg}$.

the Geiger counter was used as a monitor rather than the current integrator and the ordinates of fig. 3 are, therefore, the ratio of alpha-counts to gamma-counts. From the position of the peaks, the alpha-particle energies were calculated to be 1.79 mev, 1.89 mev and 1.98 mev at the 503 kev, 630 kev and 728 kev resonances respectively. The Q -values calculated from these results are 1.62 mev, 1.60 mev and 1.61 mev. We estimate the total probable error of these measurements to be $\pm 1\%$, and thus obtain a final Q -value of 1.61 ± 0.02 mev. This is in reasonable agreement with the value of 1.585 ± 0.015 mev found by Freeman (1950) and the value of 1.595 ± 0.007 mev of Van Patter *et al.* (1952).

The results of the yield measurements are summarized in the table. The yield measurements of Broström *et al.* (1947) are also included for comparison purposes. It will be seen that our yield measurements are uniformly lower than those of Broström *et al.* by a factor of about two. Part of this discrepancy is due to the use by Broström *et al.* of the earlier value of 1.8 disintegrations per 10^8 protons for the $^{19}\text{F}(p, \alpha, \gamma)^{16}\text{O}$ reaction (Van Allen and Smith 1941). A further difference of about 20% may be attributed to slightly different assumptions made as to the relative efficiency of their gamma-counter for radiation from fluorine and aluminium. However, there remains a discrepancy of about 50% for which it is difficult to account.

The ratios of the alpha-particle to gamma-ray yields are also given in the table for the various resonances. It will be seen that the three resonances at

503 kev, 630 kev and 728 kev give alpha- and gamma-yields of the same order of magnitude, whereas alpha-particle emission appears to be forbidden from the three gamma-ray resonances at 652 kev, 677 kev and 733 kev. No resonances are observed which emit only alpha-particles.

Thick Target Yields of $^{27}\text{Al} + p$

E_p (kev)	Yields per 10^{10} protons Y_α	Y_γ	Broström Y_γ	$\frac{Y_\alpha}{Y_\gamma}$
503	1.2	0.95	1.7	1.3
630	3.6	3.3	7.0	1.1
652	< 0.15	1.4	2.7	< 0.1
677	< 0.15	0.55	1.1	< 0.3
728	4.8	1.15	2.5	4.2
733	< 0.35	1.4	3.5	< 0.25

§ 4. DISCUSSION

On the basis of these results we can infer possible values for the angular momentum and parity of the levels in the ^{28}Si compound nucleus involved in these transitions, but we shall see that a unique determination cannot be made without further information.

The ground state of ^{27}Al is known to have an angular momentum of $5/2$, and it seems plausible from the nuclear shell model that it is a D-state and, therefore, has even parity. We can also assume that the ground states of ^{28}Si and ^{24}Mg are both $0, (+)$.

If we first assume that the incoming protons have zero angular momentum (S-wave), then the compound states of ^{28}Si will be either $2, (+)$ or $3, (+)$. But it is clear that only the former will be allowed to emit alpha-particles to the ground state of ^{24}Mg . Hence, on the basis of this assumption, we could say that those resonances which are observed to emit alpha-particles correspond to $2, (+)$ states and those which only emit gamma-rays correspond to $3, (+)$ states. If we assume incoming P-wave protons, then a similar argument shows that the alpha-emitting states could be either $1, (-)$ or $3, (-)$ and the other states could be either $2, (-)$ or $4, (-)$. Choice of higher l -values would, of course, lead to further possibilities, but at such low proton energies the effect of the potential barrier should make the formation of such states rather improbable.

It should be possible to obtain further information on the properties of the states of ^{28}Si by a study of the gamma-radiation. For example, the selection rules for gamma-ray transitions would only allow electric quadrupole radiation from a $2, (+)$ state to the ground state of ^{28}Si , and magnetic octupole radiation from a $3, (+)$ state. Now the spectrum of the total gamma-radiation from all resonances below 750 kev (Rutherglen *et al.* 1951) shows that cascade transitions to the 1.8 mev and 4.5 mev states are more favoured than the ground state transition, as might be expected if electric dipole radiation is allowed to these states. Gamma-ray spectra from the separate resonances would be of some interest. For example, if all the states were formed by S-wave protons one would expect to observe one type of spectrum from the alpha-emitting resonances and a different one from the others, with the first type containing most of the ground state radiations. Preliminary measurements of these spectra have been made in this laboratory with a scintillation spectrometer, and these show considerable

differences between the different resonances, suggesting that at least some of the states are not formed by S-wave protons. It should be possible to obtain further information by angular distribution measurements, and it is proposed to make these measurements in the near future.

REFERENCES

- BROSTRÖM, K. J., HUUS, T., and TANGEN, R., 1947, *Phys. Rev.*, **71**, 661.
 CHAO, C. V., TOLLESTRUP, A. V., FOWLER, W. A., and LAURITSEN, C. C., 1950, *Phys. Rev.*, **79**, 108.
 FOWLER, W. A., LAURITSEN, C. C., and LAURITSEN, T., 1948, *Rev. Mod. Phys.*, **20**, 236.
 FREEMAN, J. M., 1950, *Proc. Roy. Soc. A*, **63**, 668.
 FREEMAN, J. M., and BAXTER, A. S., 1948, *Nature, Lond.*, **162**, 696.
 HORNYAK, W. F., LAURITSEN, T., MORRISON, P., and FOWLER, W. A., 1950, *Rev. Mod. Phys.*, **22**, 291.
 RUTHERGLEN, J. G., RAE, E. R., and SMITH, R. D., 1951, *Proc. Phys. Soc. A*, **64**, 906.
 SHOEMAKER, F. C., FALKNER, J. E., BOURICUS, G. M. B., KAUFMANN, S. G., and MOORING, F. P., 1951, *Phys. Rev.*, **73**, 1011.
 VAN ALLEN, J. A., and SMITH, N. M., 1941, *Phys. Rev.*, **59**, 501.
 VAN PATTTER, D. M., SPERDUTO, A., ENDT, P. M., BEUCHNER, W. W., and ENGE, H. A., 1952, *Phys. Rev.*, **85**, 142.

Elastic Scattering of Electrons

By L. R. B. ELTON

Wheatstone Department of Physics, King's College, London

Communicated by H. S. W. Massey; MS. received 20th May 1953

Abstract. It is shown that, to a high degree of accuracy, the scattering of fast electrons by atomic nuclei is independent of the model chosen for the charge structure of the nucleus, even if the energy of the electrons is sufficiently high for several of the partial scattered waves to be modified by the finite extent of the nucleus.

§ 1. INTRODUCTION

FESHBACH (1951) has shown that it is possible to adjust the nuclear radius R to different models of charge distribution in the nucleus so that the scattering of fast electrons by nuclei is the same to a high degree of accuracy for the different models, provided the energy E of the incident electrons is comparatively low. The effect of a finite size of a nucleus on the scattering of fast electrons is thus by itself insufficient to determine both the charge distribution in the nucleus and the nuclear radius. He finds that this is so provided that the dimensionless quantity $ER/\hbar c$ is much less than unity. For a heavy nucleus ($A \simeq 200$) this means that the energy is much less than $50 mc^2$. For such energies only the partial scattered wave of zero angular momentum is modified by the finite nucleus. The problem arises as to whether at higher energies, when the next partial scattered wave becomes important, it might be possible to determine both the charge distribution and the nuclear radius. A further problem is the fact that Feshbach's result, which is based on an approximation to the wave function and small $ER/\hbar c$, is astonishingly correct even for values of $ER/\hbar c$ as high as 0.9, where deviations might certainly be expected.

It is the purpose of this paper to deal with these two problems. In the course of the investigation the energy at which the second partial scattered wave becomes important will be calculated by a semi-classical method, and an approximate method for calculating the variation of the scattering phases with energy and nuclear radius will also be outlined. Natural units ($\hbar = m = c = 1$) will be employed, so that distances are measured in units of the Compton wavelength \hbar/mc and energies in units of the electron rest-energy mc^2 .

§ 2. DISTANCE OF CLOSEST APPROACH (SEMI-CLASSICAL)

A particular partial scattered wave for scattering of electrons by a nucleus of finite size will be different from the corresponding wave for a point nucleus if the classical path of the electrons passes through the nucleus.

At the distance of closest approach d , the energy of a classical electron in a potential $V(r)$ is

$$E = (1 - v^2)^{-1/2} + V(d), \quad \dots\dots (2.1)$$

and the angular momentum is

$$I = vd(1 - v^2)^{-1/2}, \quad \dots\dots (2.2)$$

where v is the velocity of the electron at that distance. The angular momentum must be quantized in the usual way,

$$I = \{n(n+1)\}^{1/2}. \quad \dots\dots(2.3)$$

Eliminating v from these equations, we obtain, for $V(r) = -Ze^2/r$,

$$E + \lambda/d = \{1 + n(n+1)/d^2\}^{1/2}, \quad \dots\dots(2.4)$$

where we have written $\lambda = Ze^2$. Now $E^2 \gg 1$. Hence

$$Ed = -\lambda + \{n(n+1)\}^{1/2}. \quad \dots\dots(2.5)$$

Thus the critical quantity is not the energy, but the dimensionless quantity ER , where R is the nuclear radius.

Equation (2.5) can be checked against the numerical calculations of Elton (1950) and Parzen (1950). This is done in the table. The energy required for gold nuclei ($Z=79$, $A=196$) so that the $n=2$ wave is just negligible, can also be calculated from (2.5) and is 88 mc^2 , corresponding to $ER=1.87$.

Z	A	R	E	ER	n (from (2.5))	Partial wave negligible for :
79	196	0.0212	40	0.85	1.01	$n=1$ (Elton)
82	208	0.0216	197	4.25	4.36	$n=5$ (Parzen)

§ 3. MODEL INDEPENDENCE

The radial wave equations for the scattering of electrons by a central potential are the well-known equations

$$\left. \begin{aligned} [E - V(r) + 1]F_n + \frac{dG_n}{dr} - \frac{n}{r}G_n &= 0, \\ -[E - V(r) - 1]G_n + \frac{dF_n}{dr} + \frac{n+2}{r}F_n &= 0. \end{aligned} \right\} \quad \dots\dots(3.1)$$

We put $Er=y$ and transform to $f_n=yF_n$, $g_n=yG_n$. Following Feshbach, we write the potential as

$$V(r) = -\frac{\lambda}{r} \left[1 - q\left(\frac{r}{R}\right) \right], \quad \dots\dots(3.2)$$

where $q(r/R)$ gives the deviation from pure coulomb scattering inside the nucleus. For $r > R$, $q \rightarrow 0$ very rapidly. Since $E \gg 1$, (3.1) can then be written

$$\left. \begin{aligned} g_n' - \frac{n+1}{y}g_n + \left\{ 1 + \frac{\lambda}{y} \left[1 - q\left(\frac{y}{Y}\right) \right] \right\} f_n &= 0, \\ f_n' + \frac{n+1}{y}f_n - \left\{ 1 + \frac{\lambda}{y} \left[1 - q\left(\frac{y}{Y}\right) \right] \right\} g_n &= 0, \end{aligned} \right\} \quad \dots\dots(3.3)$$

where primes denote differentiation with respect to y and $Y=ER$. This shows that the phase shift ζ_n due to the deviation from coulomb scattering depends only on Y . The coulomb radial functions, which are the solutions of (3.3) for $q=0$, will be denoted by f_{cn} and g_{cn} .

To obtain an expression for ζ_n we note that the asymptotic expressions for f_n and g_n are

$$\left. \begin{aligned} f_n &\sim -\cos(y + \lambda \ln 2y - \tfrac{1}{2}n\pi + \eta_n + \zeta_n), \\ g_n &\sim \sin(y + \lambda \ln 2y - \tfrac{1}{2}n\pi + \eta_n + \zeta_n), \end{aligned} \right\} \quad \dots\dots(3.4)$$

where the corresponding expressions for f_{cn} and g_{cn} are obtained by putting

$\zeta_n = 0$. With this definition, f_n , g_n , f_{cn} and g_{cn} all vanish for $y=0$. From (3.3) and the corresponding equations with $q=0$ we then have

$$\left. \begin{aligned} g_n' f_{cn} - f_n g_{cn}' - \frac{n+1}{y} (g_n f_{cn} - f_n g_{cn}) - \frac{\lambda q}{y} f_n f_{cn} &= 0, \\ f_n' g_{cn} - g_n f_{cn}' + \frac{n+1}{y} (f_n g_{cn} - g_n f_{cn}) + \frac{\lambda q}{y} g_n g_{cn} &= 0. \end{aligned} \right\} \dots\dots(3.5)$$

Subtracting,

$$\frac{\lambda q}{y} (f_n f_{cn} + g_n g_{cn}) = g_n' f_{cn} + g_n f_{cn}' - f_n' g_{cn} - f_n g_{cn}'.$$

Hence
$$\int_0^\infty \frac{\lambda q}{y} (f_n f_{cn} + g_n g_{cn}) dy = \left[g_n f_{cn} - f_n g_{cn} \right]_0^\infty.$$

Using (3.4), we have

$$\sin \zeta_n = -\lambda \int_0^\infty q \left(\frac{y}{Y} \right) (f_n f_{cn} + g_n g_{cn}) \frac{dy}{y}. \dots\dots(3.6)$$

Feshbach's approximate equation (17) is obtained from (3.6) by replacing f_{cn} and g_{cn} by f_n and g_n . We shall, however, use the approximation in which f_n and g_n are replaced by f_{cn} and g_{cn} .

For a particular energy, ζ_n can always be made model independent by a correct choice of Y for each model, but this choice will, in general, be dependent on the energy. For the scattering to be model independent at all energies, both ζ_n and $\partial \zeta_n / \partial E$ must be independent of the choice of $q(y/Y)$. In the approximation mentioned above, which is valid if the effect of q is small,

$$\sin \zeta_n = -\lambda \int_0^\infty q \left(\frac{y}{Y} \right) (f_{cn}^2 + g_{cn}^2) \frac{dy}{y} \dots\dots(3.7)$$

and

$$\cos \zeta_n \frac{\partial \zeta_n}{\partial E} = -\frac{\lambda Y}{E} \int_0^\infty \frac{\partial q}{\partial Y} (f_{cn}^2 + g_{cn}^2) \frac{dy}{y}, \dots\dots(3.8)$$

since $E \partial \zeta_n / \partial E = Y \partial \zeta_n / \partial Y$. But $Y \partial q / \partial Y = -y \partial q / \partial y$. Hence, on integrating by parts, we obtain

$$\cos \zeta_n \frac{\partial \zeta_n}{\partial E} = \frac{\lambda}{E} \int_0^\infty q \left(\frac{y}{Y} \right) \frac{d}{dy} (f_{cn}^2 + g_{cn}^2) dy, \dots\dots(3.8')$$

as the integrated part vanishes at both limits. Thus for model independence we must have simultaneously

$$\int_0^\infty q (f_{cn}^2 + g_{cn}^2) \frac{dy}{y} \quad \text{and} \quad \int_0^\infty q \frac{d}{dy} (f_{cn}^2 + g_{cn}^2) dy \dots\dots(3.9)$$

model independent. This is possible if inside the nucleus

$$f_{cn}^2 + g_{cn}^2 \propto y^t, \quad t > 0. \dots\dots(3.10)$$

(The argument in the above paragraph is essentially due to Feshbach (1951).)

To investigate the validity of (3.10) we expand f_{cn} and g_{cn} in power series,

$$f_{cn} = y^s \sum b_m y^m, \quad g_{cn} = y^s \sum a_m y^m. \dots\dots(3.11)$$

These expressions are substituted into (3.3) with $q=0$ and yield in the usual way

$$s = \pm \rho_n = \pm \{(n+1)^2 - \lambda^2\}^{1/2}, \dots\dots(3.12)$$

and the recurrence relations

$$\left. \begin{aligned} (s+m-n-1)a_m + \lambda b_m + b_{m-1} &= 0, \\ (s+m+n+1)b_m - \lambda a_m - a_{m-1} &= 0. \end{aligned} \right\} \dots\dots(3.13)$$

As $f_{cn}(0) = g_{cn}(0) = 0$, we must take the positive sign in (3.12). In that case,

$$\left. \begin{aligned} m(m+2\rho_n)a_m &= -\lambda a_{m-1} - (\rho_n + m + n + 1)b_{m-1}, \\ m(m+2\rho_n)b_m &= -\lambda b_{m-1} - (\rho_n + m - n - 1)a_{m-1}, \end{aligned} \right\} \dots\dots(3.14)$$

and, from (3.13),

$$b_0 = \frac{\lambda}{\rho_n + n + 1} a_0 = -\frac{\rho_n - n - 1}{\lambda} a_0. \dots\dots(3.15)$$

From (3.14) we then obtain

$$a_1 = -\frac{2\rho_n + 2n + 3}{(\rho_n + n + 1)(2\rho_n + 1)} \lambda a_0 \quad \text{and} \quad b_1 = -\frac{a_0}{2\rho_n + 1}. \dots\dots(3.16)$$

Hence, to order y^{2e_n+}

$$f_{cn}^2 + g_{cn}^2 = a_0^2 y^{2e_n} \left\{ \frac{2(n+1)(n+1-\rho_n)}{\lambda^2} - \frac{4(\rho_n + n + 2)(n+1-\rho_n)}{\lambda(2\rho_n + 1)} y \right\} \dots\dots(3.17)$$

Therefore (3.10) can be satisfied provided

$$Y \ll \frac{(n+1)(2\rho_n + 1)}{2\lambda(\rho_n + n + 2)}. \dots\dots(3.18)$$

Since $\rho_n \simeq n + 1$, this reduces to

$$Y \ll (n+1)/2\lambda. \dots\dots(3.19)$$

If $E \ll 40mc^2$ then, as can be seen from the table, the $n=1$ wave is negligible even for heavy nuclei, and (3.19) is satisfied for $n=0$. Equation (3.7) then reduces to

$$\sin \zeta_0 \simeq -\frac{2(1-\rho_0)}{\lambda} a_0^2 \int_0^\infty q\left(\frac{y}{Y}\right) y^{2e_0-1} dy. \dots\dots(3.20)$$

Hence if two models are given by (q_a, Y_a) and (q_b, Y_b) the only quantity that can be determined from the scattering is

$$I = \int_0^\infty q_a\left(\frac{y}{Y_a}\right) y^{2e_0-1} dy = \int_0^\infty q_b\left(\frac{y}{Y_b}\right) y^{2e_0-1} dy. \dots\dots(3.21)$$

This is Feshbach's main result.

If the two models are the surface and homogeneous models of charge distribution, then

$$\left. \begin{aligned} q_s &= 1 - \frac{y}{Y_s}, \quad y < Y_s; \quad q_s = 0, \quad y > Y_s; \\ q_h &= 1 - \frac{y}{2Y_h} \left(3 - \frac{y^2}{Y_h^2} \right), \quad y < Y_h; \quad q_h = 0, \quad y > Y_h. \end{aligned} \right\} \dots\dots(3.22)$$

In that case the two integrals in (3.21) reduce to

$$\frac{Y_s^{2e_0}}{2\rho_0(2\rho_0+1)} \quad \text{and} \quad \frac{3Y_h^{2e_0}}{2\rho_0(2\rho_0+1)(2\rho_0+3)}, \dots\dots(3.23)$$

so that for model independence

$$\frac{Y_s}{Y_h} = \left(\frac{3}{2\rho_0+3} \right)^{1/2e_0}. \dots\dots(3.24)$$

For $Z=1$ to 82, ρ_0 varies from 1.0 to 0.8, but (3.24) stays remarkably constant at 0.77. This is the value obtained by Feshbach for the ratio Y_s/Y_h , using his approximation which makes $Y_s/Y_h = \sqrt{(3/5)}$, independent of Z . Since Feshbach's approximation and the one used here are likely to err in opposite directions,

the ratio Y_s/Y_h will probably be the same for an exact calculation. This is borne out by the excellent agreement between Feshbach's result and the exact calculations of Acheson (1951).

At higher energies, when the $n=1$ wave is significant, it would seem that model independence could not be achieved, since on the one hand (3.19) will no longer be satisfied, and on the other ρ_0 in (3.23) has to be replaced by ρ_1 , which will lead to different values for Y_s/Y_h for model independence for the $n=0$ and $n=1$ waves. This latter fact will not make any appreciable difference, since (3.24) is such a slowly varying function of ρ_0 . If ρ_0 is replaced by $\rho_1=1.9$ to 2.0 , then $Y_s/Y_h=0.81$, and if by $\rho_2=2.9$ to 3.0 , then $Y_s/Y_h=0.83$. The inclusion of higher order partial waves will thus not lead to improved differentiation between models.

It remains to see whether the $n=0$ wave remains model independent for $Y \gtrsim 1/2\lambda$. For this part of the investigation we shall use Feshbach's approximation since it is easier to deal with, and we have already shown that the two approximations lead to the same results. We therefore replace f_{c0} and g_{c0} in (3.6) by f_0 and g_0 , where we use the radial wave functions for the shell model which inside the nucleus are

$$f_0 = A \left(\frac{2}{u} \sin \frac{1}{2}u - \cos \frac{1}{2}u \right) \quad \text{and} \quad g_0 = A \sin \frac{1}{2}u, \quad \dots (3.25)$$

where we have put $u=2y(1+\lambda/Y_s)$, and A is a constant which is determined from the amplitude of the asymptotic wave. With this notation,

$$\left. \begin{aligned} q_s &= 1 - \frac{u}{U_s}, \quad u < U_s; \quad q_s = 0, \quad u > U_s; \quad U_s = 2(1 + \lambda/Y_s)Y_s; \\ q_h &= 1 - \frac{3u}{2U_h} + \frac{u^3}{2U_h^3}, \quad u < U_h; \quad q_h = 0, \quad u > U_h, \quad U_h = 2 \left(1 + \frac{\lambda}{Y_s} \right) Y_h. \end{aligned} \right\} \dots (3.26)$$

After some simplification we obtain

$$\sin \zeta_{0s} = -\lambda A^2 \left\{ -\frac{3}{2} + \frac{\sin U_s}{U_s} + \frac{1 - \cos U_s}{U_s^2} + C + \ln U_s - \text{Ci}(U_s) \right\}, \quad \dots (3.27)$$

$$\sin \zeta_{0h} = -\lambda A^2 \left\{ -\frac{11}{6} + \frac{\sin U_h}{U_h} + \frac{3 - \cos U_h}{U_h^2} - \frac{2 \sin U_h}{U_h^3} + C + \ln U_h - \text{Ci}(U_h) \right\}, \quad \dots (3.28)$$

$$\cos \zeta_{0s} \frac{\partial \zeta_{0s}}{\partial E} = -\frac{\lambda}{E} A^2 \left\{ 1 - \frac{2(1 - \cos U_s)}{U_s^2} \right\}, \quad \dots (3.29)$$

$$\cos \zeta_{0h} \frac{\partial \zeta_{0h}}{\partial E} = -\frac{\lambda}{E} A^2 \left\{ 1 - \frac{6}{U_h^2} + \frac{6 \sin U_h}{U_h^3} \right\}, \quad \dots (3.30)$$

where C is Euler's constant and $\text{Ci}(x)$ is the integral cosine. (3.29) and (3.30) are most easily obtained directly from (3.8) and not from (3.8'). Clearly it will not be possible to find a value for the ratio U_s/U_h which will make the phases and their derivatives exactly the same for the two models, but if we put $U_h = U_s + c$ in (3.28) and (3.30) and equate the expressions for the phases and those for their derivatives, then, to the first power in c/U_s , we obtain from both equations

$$c/U_s = \frac{1}{3}, \quad \text{i.e. } U_s/U_h = \frac{3}{4}. \quad \dots (3.31)$$

This is a most unexpected result, since in general the ratio U_s/U_h which gives model independence at one energy will not do so at another energy. With the

value of the ratio given by (3.31) the values of ζ_0 and $\partial\zeta_0/\partial E$ for the two models differ by two to three per cent in the region $Y < 2$.

To sum up. At low energies (about 40 mc^2 for heavy nuclei) the scattering is model independent and the shell and homogeneous models give the same scattering for $R_s/R_h = 0.77$. At high energies (about 80 mc^2 for heavy nuclei), when the $n=1$ wave is important, the scattering is not quite model independent since for the two models considered the $n=0$ wave is model independent for $R_s/R_h = 0.75$ and the $n=1$ wave for $R_s/R_h = 0.81$.

§ 4. VARIATION OF PHASE SHIFT WITH ENERGY AND NUCLEAR RADIUS

Once an exact value of a phase shift for a particular energy and nuclear radius has been obtained, it is desirable that neighbouring phase shifts should be obtained with less labour. All past experience shows that approximate values of the phase shifts calculated from variation principles or perturbation methods are too inaccurate to be useful. It is quite definitely necessary, when calculating a range of phase shifts, to calculate the first one exactly. The quickest way to do this is probably to compute the various radial functions at the nuclear radius, as was done by Elton (1950). The work can however be simplified by using $v = Er$ as variable and by using coupled recurrence relations, such as (3.13). For small changes in E and R in the neighbourhood of the exactly calculated phase shift the approximate expression (3.8) for $\partial\zeta_n/\partial E$ and the corresponding one for $\partial\zeta_n/\partial R$ can be employed. Alternatively, (3.29) can be used, since the constant A will have been determined in the course of the calculation of the exact phase shift.

As an illustration we shall use the scattering of electrons of energy 40 mc^2 by gold nuclei according to the surface model. The exact phase shift is $\zeta_0 = -0.27$, and the approximate values of $\partial\zeta_0/\partial E$ at this point are -0.0063 from (3.8) and -0.0078 from (3.29). Hence ζ_0 at 30 mc^2 is -0.21 or -0.19 , according to which approximation is chosen. This compares satisfactorily with the exact value $\zeta_0 = -0.20$ (Acheson 1951). On the other hand, if ζ_0 at 40 mc^2 is calculated from (3.7) or (3.27) directly, the respective results are -0.20 and -0.17 , and these are clearly not accurate enough.

§ 5. CONCLUSION

As Feshbach has pointed out, the assumption of a charge density in the nucleus which is constant in time is justified only if the wavelength of the incident electron is considerably larger than interparticle distances in the nucleus, so that we must have $E \ll 274 \text{ mc}^2$. For heavy nuclei this corresponds to $Y \ll 6$. Since the $n=3$ wave is not important until $Y \approx 4$, we must restrict ourselves to energies where only the first three partial scattered waves are important. As was shown in § 3, these waves are separately model independent for different values of the ratio R_s/R_h . However, these ratios differ by so little from each other that an average value of R_s/R_h is likely to exist which will give practically model independent scattering. Nuclear radii are in any case not known with very great accuracy (Blatt and Weisskopf 1952) and, furthermore, any difference between models will almost certainly be masked by the radiative correction (Schwinger 1949), the size of which is not known for large Z . There is then at present little hope that experiments on electron scattering at energies of the order of 80 mc^2 will give any information about the charge structure inside the nucleus.

Lastly, the question arises whether a ratio $R_s/R_h \simeq 0.8$ is physically reasonable, and whether independent measurements of nuclear radii confirm or contradict this ratio. Of all the methods for measuring nuclear radii that based on the theory of mirror nuclei (Lu 1950) is the only one which depends directly on the charge distribution in the nucleus and not on the internuclear forces. Lu finds that $R_s/R_h = 0.83$, which lends strong support to the hypothesis that electron scattering, at least to a high degree of accuracy, is model independent.

REFERENCES

- ACHESON, L. K., 1951, *Phys. Rev.*, **82**, 488.
BLATT, J. M., and WEISSKOPF, V. F., 1952, *Theoretical Nuclear Physics* (New York : John Wiley), p. 15.
ELTON, L. R. B., 1950, *Proc. Phys. Soc. A*, **63**, 1115.
FESHBACH, H., 1951, *Phys. Rev.*, **84**, 1206.
LU, H., 1950, *Phys. Rev.*, **77**, 416.
PARZEN, G., 1950, *Phys. Rev.*, **80**, 355.
SCHWINGER, J., 1949, *Phys. Rev.*, **76**, 790.

A Comparison of the Powder Patterns on a Sample of Grain-Orientated Silicon-Iron with those obtained on a Single Crystal

BY L. F. BATES AND A. HART

Department of Physics, University of Nottingham

MS. received 28th May 1953

Abstract. A comparison is made of the powder patterns observed on grains within the surface of a polycrystalline specimen of silicon-iron with those found on the surfaces of a single crystal of the same material. A new pattern not hitherto recorded with a single crystal is described, and the conditions for the appearance of three different sets of patterns on polycrystalline and single crystal specimens are noted; data concerning domain boundary spacings are presented.

§1. INTRODUCTION

FEW measurements with the Bitter figure technique have so far been made with the object of comparing the powder patterns obtained on single crystals of a ferromagnetic metal with the patterns obtained on a polycrystalline specimen of the metal. It is obvious, if such comparison is to be at all profitable, that the polycrystalline specimen must possess a grain structure of size adequate for reasonably undisturbed patterns to be formed, and that individual grains chosen for examination must have a definite crystal plane located in the surface of the polycrystalline specimen.

Among recent experiments may be mentioned those of Martius, Gow and Chalmers (1951), who photographed the behaviour of domain boundaries, as manifested by powder deposits, in the neighbourhood of grain boundaries in a bicrystal of nickel. Dijkstra and Martius (1953) examined the changes in the domain pattern of grain-oriented silicon-steel with large grain size when the specimen was put under tensions within the elastic range of the material. The grain on which observations were made had a (110) plane in the surface of the specimen and the [110] direction was parallel to the specimen axis along which the tension was applied. They found that at a load of approximately 1 kg mm^{-2} the original domain pattern vanished, and that after a transition stage with increasing load a new stress-induced domain pattern appeared. Nesbitt and Williams (1950) obtained patterns on alnico V (Alcomax), which is, of course, polycrystalline, in an attempt to explain the mode of action of a magnetic field applied during heat treatment of such materials. In the present communication an attempt has been made to see how far patterns found on polycrystalline surfaces have their counterpart in patterns on single crystal surfaces.

§2. EXPERIMENTS ON A POLYCRYSTALLINE DISC

A preliminary survey of powder patterns on a specimen of polycrystalline grain-oriented silicon-iron provided many interesting patterns. The orientation of the grains in the sheet specimen was such that many of them intersected the sheet surface in a plane near to a (110) plane, and some of the patterns obtained

were very similar to patterns previously observed on single crystal specimens; e.g. when in the demagnetized state many of the grains were crossed by 180° boundaries, while others carried characteristic 'dagger' structures. Examples are given in figs. 1 and 2 (*a*) (Plate I) respectively.

Three types of pattern which occurred frequently in applied fields were as follows:

(*a*) Patterns hereafter called type (*a*) were in effect normal 'lace' patterns very similar to those obtained by Bates and Mee (1952) on the (110) surface of a Néel block during Mode III magnetization, cf. fig. 2 (*b*) (Plate I).

(*b*) Patterns hereafter called type (*b*), which were present at the same field values as type (*a*) patterns, or at field values between those required for type (*a*) patterns and those for saturation. The type (*b*) patterns, like those on the single crystal specimen shown in fig. 5 (Plate III), were really made up of short lengths of type (*a*) or 'lace' patterns all having very nearly the same orientation, but not formed into continuous lines. In the cases where type (*b*) patterns were produced from type (*a*) patterns by increasing the applied field, the orientations of the two types of pattern were not necessarily the same.

(*c*) A third type of pattern, which has not hitherto been observed on a single crystal, was usually obtained in lower fields than those required to produce types (*a*) and (*b*). The new pattern, called type (*c*), consisted of short lines of colloid ending in small 'blobs', the lines being arranged in columns. This type of pattern is clearly shown in fig. 3 (Plate II). The columns formed by these so-called 'tadpoles' usually appeared at angles of about 30° to the [100] direction. The type (*c*) pattern started as a dagger structure, characteristic of the demagnetized state, broke up, and later gave way to normal lace-type patterns. The fact that such patterns appear between the demagnetized (6-phase) state and the lace structure (2-phase state) indicates that they are present in a field whose value is suitable for the production of a 3-phase state. However, as the patterns persist, in some cases even after the lace structure is established, they cannot in fact be 3-phase patterns. The patterns always appeared near to the edge of the crystal, and it is probable that they are a special type of closure structure, masking a more simple elementary domain structure. Since the individual lines of the pattern end in well defined 'blobs', an arrangement of domains giving rise to sharply localized stray fields is indicated.

§ 3. EXPERIMENTS ON A SINGLE CRYSTAL DISC

A single crystal disc of silicon-iron with its main surfaces parallel to the (110) plane was prepared. With this disc, attempts were made to obtain patterns similar to types (*b*) and (*c*) above. A comparison was also made between the spacing of the lines of type (*a*) patterns with applied field in the cases of the single and polycrystalline specimens.

The dimensions of the specimens used were: single crystal: diameter of disc = 0.755 cm, depth = 0.125 cm; polycrystal: diameter of disc = 1.015 cm, depth = 0.032 cm. The approximate size of the grains viewed was $1\text{--}2\text{ mm}^2$. It was found that by altering the orientation of the specimen in the applied field, and also the value of the field, it was possible to reproduce practically all the types of patterns observed on the polycrystal. Type (*c*) patterns were formed at the lateral edge of the single crystal as a stage in a transition from a dagger pattern in

the demagnetized state to a lace pattern structure. This is clearly shown in fig. 3 (Plate II), where the lace pattern lines are just appearing in a broken form. In this case the lines of the type (c) structure are at an angle of about 30° to the lace pattern lines, i.e. at 30° to the [100] direction; in this photograph the [100] direction was perpendicular to the applied field. In all photographs the external field is applied along a direction approximately parallel to the long edge of the photograph. A further example of the type (c) structure forming striations between adjacent lace-pattern lines is visible in the lower half of fig. 7 (b) (Plate IV), where between the main lace patterns running upwards from left to right there are sets of ' tadpoles ' running upwards from right to left.

Patterns of type (b) occurred on the single crystal at field values intermediate between those required for lace patterns and those for saturation. The patterns appeared for a range of orientations of the crystal with respect to the applied field, and their orientation with respect to the field was not fixed, fig. 5 (Plate III). These, and later experiments on a thinner crystal, indicate that this type of pattern is obtained when there is a component of the applied magnetic field perpendicular to the plane of the specimen surface, the (110) plane.

§ 4. VARIATION OF LINE SPACING WITH APPLIED FIELD FOR PATTERNS OF TYPE (a).

(i) *Single Crystal*

The crystal was mounted on a cylindrical brass holder, and fitted between the pole-pieces of an electromagnet, with air gaps about 0.1 cm separating it from either pole-piece. The specimen was always set, by means of the zero-field daggers, so that its [100] direction was perpendicular to the applied field. The patterns on the specimen surface were projected on to a ground-glass screen, and the spacing of the pattern lines measured directly. The measurements were all made on parts of the specimen near its centre. Measurements were recorded as soon as the lines of the pattern were sufficiently well developed, and continued to be made for increasing field values until the colloid line deposits became so thick as to preclude accurate measurement. The specimen was always taken through several cycles of magnetization before measurements were taken. After several sets of results had been obtained, the specimen and holder were rigidly fixed in position between the pole-pieces, and field measurements were made near the centre of the crystal. The mean separation of the feet of the magnetic potentiometer used for field measurements was only 0.4 cm.

A curve of average line spacing d against field H was now drawn, fig. 10, curve B. It showed an initial sharp fall in d with increasing H followed by a region in which d approached an asymptotic value as H reached large values. The curve was compared with a theoretical curve B' calculated for a Néel block whose width was equal to the depth of the specimen used. The experimental curve had a shape similar to the theoretical curve, but differed from it in two respects: (i) the experimental field values for the region where d depended sharply on H were several times larger than the theoretical field values given by the Néel theory, (ii) the limiting value of d in high fields was about three times the theoretical value (say $70\ \mu$ instead of $24\ \mu$), and the value of field at which this limiting value of d was reached was about twice that required theoretically.

Series of photographs showing the appearance of the patterns for several field strengths are given in figs. 4 (a)–(c) (Plate II).

(ii) *Polycrystal Specimen*

The procedure used in the case of the polycrystal specimen was very similar to that outlined above for the single crystal. In this case it was not usually possible to obtain lace patterns on grains whose [100] direction was perpendicular to the applied field. This was probably due to the demagnetizing field in the neighbourhood of the grain under observation causing the effective field to be out of alignment with the external field. Normal lace patterns were obtained for angles between the [100] direction and the perpendicular to the applied field of up to 45° . The patterns obtained at low fields, when d was relatively large, were observed to be much better defined on the polycrystal specimen than on the single crystal.

A (d, H) curve (fig. 10, curve A) was drawn, and compared with a theoretical curve A' for a Néel block of roughly the same dimensions. Again, the curve had a similar shape to the theoretical curve, and the limiting value of d reached in high fields was about three times the theoretical value (35μ instead of 12μ). In this case, however, the field at which this limiting value of d was reached was of the same order as the theoretically predicted field. A series of pictures of the patterns on the polycrystal specimen is shown in figs. 2 (a)–(c) (Plate I). It is perhaps desirable to point out that we measured an average field extending over several grains as distinct from the field on one individual grain.

(iii) *Experiments on Change of Thickness*

It was thought that better agreement between the results for the single crystal and the polycrystal specimens might be obtained if the thickness of the single crystal specimen were reduced to that of the polycrystal. The thickness of the single crystal was therefore reduced in acid, so that its final dimensions were diameter 0.675 cm and depth 0.035 cm. The measurement of line spacing on this specimen now proved to be more difficult, due to the very 'broken' nature of the patterns at the large d values (fig. 6 (a), Plate III). At higher field values the lines of the patterns tended to turn away from the [110] direction, even in the centre of the crystal; perhaps it would therefore be wise to call them abnormal lace patterns. At fields of about 200 oersteds the patterns near the centre of the crystal were as shown in fig. 5 (Plate III). The general trend of the lines of this pattern appears to be more nearly parallel to the applied field than perpendicular to it.

However, a (d, H) curve (fig. 10, curve B'') was drawn; it was mainly restricted to higher field values where d was already approaching a limiting value. Readings were taken around the centre of the crystal, and the curve obtained was very similar, and close to, the curve for the polycrystal specimen. The limiting value of d was the same as that for the polycrystal, i.e. almost three times the theoretical value. The field at which this value of d was reached was larger than that required for the polycrystal and was about 3.2 times the theoretical value. A set of pictures of the patterns at the centre of the specimen is given in figs 5–6 (Plate III). The patterns (Plate IV) obtained at the edges of this thin single crystal specimen showed certain interesting features. It was noted that, at any fixed value of the applied field, the patterns on the lateral edges of the disc were of a type which had previously appeared near the centre of the crystal at a lower field value. This was attributed to the presence of a larger demagnetizing field at the lateral edge of the crystal than at the centre. The orientation of the lace patterns at the edge of the crystal was as shown in the diagram. At points XX, fig. 9, the

patterns had an orientation nearly parallel to the applied field, as shown in fig. 7 (c) (Plate IV) for which fig. 8 provides a key. Some examples of the orientations of these patterns at various fields are given in figs. 7 (a) to (d) inclusive.

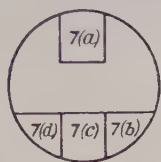


Fig. 8. Relative positions of figs. 7 (a) to (d).

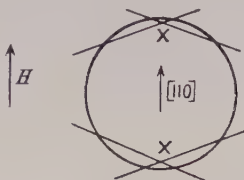


Fig. 9. Lines showing direction of lace patterns (type (a)) near crystal edges.

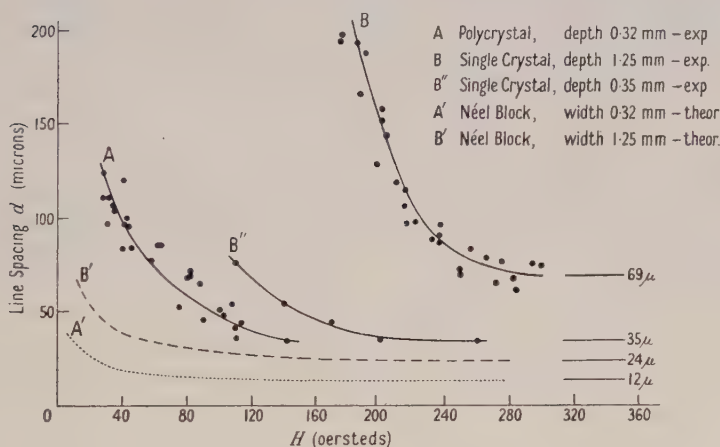


Fig. 10. (d , H) curves for poly- and single crystal specimens.

§ 5. CONCLUSIONS

We therefore see that as far as line spacing with applied field is concerned the agreement is not good in either the case of the polycrystal or that of the single crystal. But owing to the shape of the specimens used, as compared with the perfect block postulated in the theory, very good agreement was not to be expected. The main fact of importance is that the results for the single crystal and polycrystalline specimens agree with the theory to within the same limits, particularly when the thicknesses are comparable.

In general the patterns gave clear indication of the relative orientations of adjacent grains, for in the case of adjacent grains of almost the same orientation the pattern lines often crossed the grain boundaries, whereas adjacent grains between which there was a larger difference in orientation carried patterns which changed abruptly at the grain boundary (cf. figs. 2 (b), (c) (Plate I)). As the applied field was increased, the colloid deposits on the grain boundaries themselves became thicker, those on boundaries between grains of widely different orientation being very dense.

In the case of all three types of pattern considered above, patterns on the polycrystal can be reproduced on a single crystal by adjusting the specimen

orientation and the applied field. In the case of type (a) patterns the good agreement between the experimental (d , H) curves for the two specimens is an indication of the close similarity of the patterns on the poly- and single crystals. It is interesting to note that the orientation of the (a) patterns on the polycrystal indicates that the demagnetizing fields of the grains surrounding the one under observation are such that the effective internal field is considerably out of alignment with the external applied field, even at applied field strengths of about 60 oersteds (fig. 2 (c) (Plate I)). The general results obtained, of course, give further support to the view that magnetization processes in polycrystalline materials may be explained by consideration of results for aggregates of suitably orientated single crystals.

ACKNOWLEDGMENTS

One of us (A. H.) is indebted to the Department of Scientific and Industrial Research for a maintenance allowance, and our thanks are due to Mr. I. Williams of the British Thomson-Houston Research Laboratories for the polycrystalline specimens used, and to Dr. D. Shoenberg for the single crystal.

REFERENCES

- BATES, L. F., and MEE, C. D., 1952, *Proc. Phys. Soc. A*, **65**, 129.
DIJKSTRA, L. J., and MARTIUS, U. M., 1953, *Rev. Mod. Phys.*, **25**, 146.
MARTIUS, U. M., GOW, K. V., and CHALMERS, B., 1951, *Phys. Rev.*, **82**, 106.
NESBITT, E. A., and WILLIAMS, H. J., 1950, *Phys. Rev.*, **80**, 112.

A Study of Bitter Figures on the (110) Plane of a Single Crystal of Nickel

BY L. F. BATES AND G. W. WILSON*

Department of Physics, University of Nottingham

MS. received 8th June 1953

Abstract. Experiments were made by the powder pattern technique to determine the magnetic domain structure of a single crystal of nickel cut so that two easy directions of magnetization lay in the plane of each main surface. The closure domain structure is a very simple one, and from the experimental evidence a model is proposed which is similar to that investigated theoretically by Néel in the case of a single crystal of iron.

§1. PREPARATION OF THE CRYSTAL AND EXPERIMENTAL PROCEDURE

IN this communication we report some measurements made on the powder patterns formed on a (110) plane of a single crystal of nickel. The crystal was cut from an ingot into the form of a rectangular slab measuring 11 mm × 8 mm × 4 mm. The surface was prepared for examination by the methods reported in a previous paper (Bates and Wilson 1951). After electrolytic polishing of the main surface and sides, their orientations with respect to the {011} and {0 $\bar{1}1$ } planes were measured with an x-ray goniometer. Photographs showed that the surfaces made an angle of about 5° with the (110) planes. Before regrinding, the crystal was annealed to remove strains and was examined for evidence of domain structures. Later it was reground until from x-ray examination the angles between its surfaces and (110) planes were less than 1½°. It was then annealed once more at a temperature of 1000°C.

The magnetic colloid was prepared according to the Elmore recipe (cf. Bates and Neale 1950). The specimen was placed between the poles of an electromagnet and photographs were taken by normal light-field illumination of the crystal surface of the patterns formed thereon. Measurements of the spacing of the deposits were made, and the corresponding effective magnetic fields were measured with a very small magnetic potentiometer. For each measurement the crystal was brought to the appropriate value of the applied magnetic field several times. The magnetization curve for the crystal was measured using a coil in the usual way, together with the magnetic potentiometer. Curves connecting the intensity of magnetization I with the effective magnetic field H , and the spacing of the colloid deposits d with H , are drawn in figs. 1 (a) and 1 (b).

§2. EXPERIMENTAL RESULTS

Upon the application of a field along the $\langle 100 \rangle$ axis a system of colloid deposits formed. When the crystal surface under examination was inclined at 5° to the {011} plane, these deposits appeared as thick heavy lines perpendicular to the

* Now at H.M. Underwater Countermeasures and Weapons Establishment, Havant.

quaternary axis. Such inclination would, as predicted by Néel (1944), accentuate the stray magnetic fields attracting the colloid particles to alternate domain boundaries. Some photographs of these patterns are shown in plate I together with a picture of a peculiar maze pattern formed before annealing.

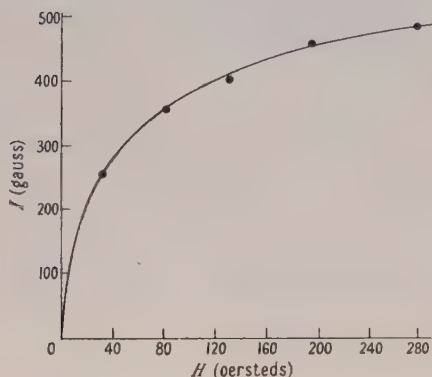


Fig. 1 (a). Magnetization curve for nickel crystal of section shown in fig. 2.

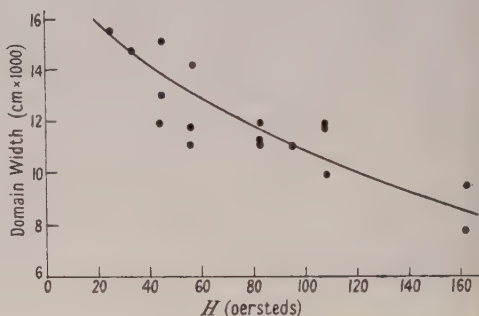


Fig. 1 (b). Domain spacings on (110) plane of a nickel crystal.

After the crystal had been reground, polished and annealed, regular line deposits were observed upon the two planes examined (plates II and III). Slight overpolishing of the side which was parallel to the $\{01\bar{1}\}$ plane produced an orange-peel effect which did not, however, appear to affect the regularity of the deposits. Close to the edge of the crystal the lines observed on the top surface parallel to the $\{01\bar{1}\}$ plane became denser and frequently split into two components. This splitting is probably due to a slight rounding at the edge enhancing the stray fields and causing colloid agglomeration at the intersection of each domain boundary with the crystal surface and not at every alternate one as is usually observed.

The photographs of plate I show colloid striations 'springing' from the sides of the main deposits. At first it was thought that these might be 'tree patterns' similar to those observed by Yamamoto and Iwata (1951). As the effective field was increased, however, the striations rotated in the opposite direction to that expected if they were tree patterns. They may thus be assumed to be formed perpendicular to the direction of magnetization of the underlying domain on which they are deposited. The lines observed upon the crystal surface after regrounding were rather more weak and diffuse.

Reversal of the direction of the applied field did not cause any displacement of the deposits. The lines merely broke up and reformed in the same positions. This fact, together with the directions of the striations observed before regrounding, suggests that the change in direction of the resultant induction of the crystal was accomplished by 180° rotations of the domain magnetization vectors.

On the side of the crystal, deposits were observed at somewhat lower fields than upon the main surface; plate III (a) shows the patterns observed for an effective field, over the whole crystal, of about 10 oersteds, applied parallel to the $\langle 100 \rangle$ axis. Some boundaries running from left to right can be seen which make an angle of 50° to 55° with the $\langle 100 \rangle$ direction. One of the 'easy' directions of

magnetization, a $[111]$ axis, makes an angle of 55° with this direction. Elsewhere on III (a) domain boundaries which are perpendicular to the direction of the applied magnetic field can be seen. Apparently this photograph shows the transition from one mode of magnetization to the simpler two-phase mode which persisted right up to saturation. A slight increase in the applied field resulted in the complete disappearance of the oblique lines, when the straight lines perpendicular to the $\langle 100 \rangle$ axis covered the surface.

The straight lines usually consisted of doublets as shown in plate III, (b), (c) and (f). If it is assumed, on the basis of plates I and II, that the magnetization vectors of the fundamental domains lie along two directions making equal angles with the $\langle 100 \rangle$ axis and lying in the $\{011\}$ plane, then from magneto-crystalline anisotropy energy considerations these magnetizations at the beginning of the two-phase state will be parallel to the $\langle 111 \rangle$ and $\langle \bar{1}\bar{1}1 \rangle$ directions, as depicted in fig. 2. Magnetization therefore proceeds by rotation of these vectors towards the $\langle 100 \rangle$ direction.

Small prismatic closure domains required to close the flux at the edges of the crystal are shown in fig. 2. Calculation shows that flux closure parallel and anti-

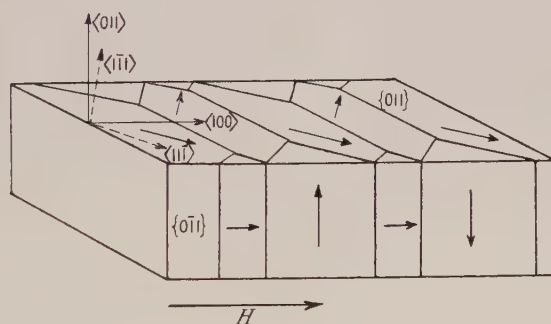


Fig. 2. Domain structure of nickel crystal.

parallel to the overall induction of the crystal should be achieved by means of domains magnetized almost parallel to the $\langle 011 \rangle$ and $\langle 100 \rangle$ axes. Thus the appearance of doublets on the $\{011\}$ plane having a separation equal to the width of two fundamental, or f , domains on the $\{011\}$ plane suggests that these mark the boundaries of closure domains at their intersections with the side of the crystal as in fig. 2. It is interesting to contrast these figures and their explanation with those of Bates and Mee (1952) for the case of the $\{011\}$ plane of a silicon-iron crystal.

It is emphasized that the observations strongly support the above model, which approximates to the domain structure postulated by Néel (1944) for a specially shaped crystal of iron even more closely than do the sections of crystals of silicon-iron examined by Bates and Mee (1952), Bozorth, Williams and Shockley (1949) and others, because of the absence of really complicated closure domains on the sides. Any attempted calculation of the dependence of d , the width of a fundamental domain, upon the effective field H will, however, be merely approximate unless it takes into account the magnetostriction strain energy associated with the closure domains.

ACKNOWLEDGMENTS

We are indebted to the Electrical Research Association for the financial help and encouragement which made this work possible and for permission to publish the paper. We are also indebted to Dr. Rohn Truell of Brown University, Rhode Island, U.S.A., for the gift of the ingot from which the crystal was cut.

REFERENCES

- BATES, L. F., and MEE, C. D., 1952, *Proc. Phys. Soc. A*, **65**, 129.
BATES, L. F., and NEALE, F. E., 1950, *Proc. Phys. Soc. A*, **63**, 374.
BATES, L. F., and WILSON, G. W., 1951, *Proc. Phys. Soc. A*, **64**, 691.
BOZORTH, R. M., WILLIAMS, H. J., and SHOCKLEY, W., 1949, *Phys. Rev.*, **75**, 155.
NÉEL, L., 1944, *J. Phys. Radium*, **5**, 241.
YAMAMOTO, M., and IWATA, T., 1951, *Phys. Rev.*, **81**, 887.

Microwave Resonance Absorption in some Ferromagnetic Manganese Compounds

BY G. D. ADAM AND K. J. STANDLEY

Department of Physics, Nottingham University

Communicated by L. F. Bates ; MS. received 21st April 1953

Abstract. Microwave resonance absorption has been investigated at a wavelength of 1.26 cm in powdered samples of manganese arsenide (MnAs), manganese antimonide (MnSb) and manganese bismuthide (MnBi). Experiments were performed over a range of temperatures from -180°C to $+300^{\circ}\text{C}$, and detailed results are given, including where possible the calculated values of the spectroscopic splitting factor g and the measured resonance line widths.

With manganese arsenide a g -value of 3.2 was found at room temperature, and this remained sensibly constant from -180°C to $+45^{\circ}\text{C}$; above the latter temperature only a very small resonance absorption was detected. For the case of manganese antimonide the g -value ranged from 2.2 at -180°C to 2.6 at $+20^{\circ}\text{C}$ and decreased to about 2.1 near the Curie point, 315°C ; in this material a marked decrease in line width with increase in temperature was found above 100°C . With manganese bismuthide a resonance absorption was detected only near -180°C and above $+240^{\circ}\text{C}$. The g -value at -180°C was estimated to be 2.4.

A comparison is made with other published results and their significance briefly discussed in the light of existing theories.

§ 1. INTRODUCTION

SINCE the first description of ferromagnetic resonance in iron, cobalt and nickel (Griffiths 1946) there has been a number of investigations of the effect in various materials. The experimental method is to measure the high frequency power loss in the material at constant frequency ν as a function of an applied steady magnetic field H_z which is perpendicular to the high frequency field H_x . The loss rises to a maximum at a field H_z^{max} and the phenomenon shows the usual characteristics of a resonance effect. It has been shown classically (Kittel 1948) and quantum mechanically (Kittel and Luttinger 1948, Van Vleck 1950) that the resonance condition for polycrystalline material is given by

$$\nu = \frac{ge}{4\pi mc} \{ [H_z^{\text{max}} + (N_y - N_z)I] [H_z^{\text{max}} + (N_x - N_z)I] \}^{1/2} \quad \dots\dots (1)$$

where g is the spectroscopic splitting factor, N_x , N_y , N_z are the demagnetizing factors of the specimen in the three coordinate directions, and the other symbols have their usual significance. It will be seen that this equation permits the determination of a value for g for the material used from measurements of the resonance field H_z^{max} at a known frequency. For free electron spins this value should be 2.00, whereas the results of previously reported measurements with various ferromagnetic materials have given g -values between 2.0 and 2.3 (for a summary see Kittel 1949). The reason for the relatively large differences from the free spin value is not clearly understood and is discussed with reference to the results of the present investigation in § 4.

The experiments to be described were performed at a wavelength of 1.26 cm with the materials manganese arsenide (MnAs), antimonide (MnSb) and bismuthide (MnBi). These compounds are similar, since in all of them manganese, which is the ferromagnetic ion, occurs with metalloids of similar electronic configurations in NiAs-type crystal lattices (Ofstedal 1928, Halla and Nowotny 1936). In addition, the saturation intensities of magnetization of the three compounds are similar (Guillaud 1951).

Polycrystalline specimens were examined in the temperature range -180°C to 300°C , and the width of the absorption line and the g -value were calculated whenever the absorption was sufficiently large. The results of these measurements are given in detail in § 3 and are discussed in § 4.

§ 2. EXPERIMENTAL APPARATUS AND PROCEDURE

2.1. General Arrangement of Apparatus

The general form of the apparatus is sketched in fig. 1. The output from the VX 302 klystron was fed to the cavity resonator located between the poles of an electromagnet in such a way that the steady field of the electromagnet was at right angles to the high-frequency magnetic field at the bottom face of the resonator. The power transmitted through the cavity was measured by a silicon tungsten crystal detector connected to a sensitive galvanometer.

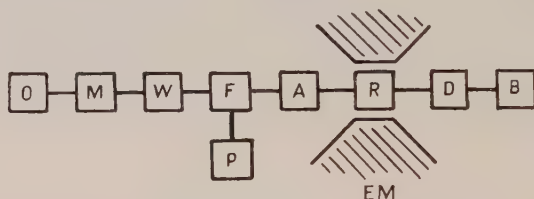


Fig. 1. Block diagram of the apparatus.

O, klystron oscillator; M, matching unit; W, wavemeter; F, directive feed; P, power monitor; A, attenuator; R, cavity resonator; EM, electromagnet; D, detector; B, backing plunger.

The steady field in the magnet gap was determined as a function of the exciting current using a fluxmeter and standardized search coils, and it is estimated that the fields were determined with an error not greater than 1%.

Cylindrical cavities oscillating in the H_{111} mode were used. That employed at room temperature and above was of the usual transmission type. It was silver plated internally and was tuned by means of a micrometer-driven plunger. The specimen under examination was carried on a copper head which screwed into the resonator body to form the lower end of the cavity. A nichrome heater wire was wound over the length of the resonator, insulated from it by mica, and the temperature was measured by means of a copper-constantan thermocouple which was screwed into the specimen holder. Heat insulation was provided by fabricating 3 in. sections of input and output waveguide from German silver and by carrying the micrometer tuning arrangement in a brass block at the end of a stainless steel tube. A second cavity, semi-fixed in its tuning, was used at low temperatures. Its body was machined from a copper block and the input and output German silver waveguides were filled with polystyrene so that a smaller cross section could be employed. The guides were iris-coupled to the cavity through small holes in

its upper wall, and fine tuning was provided by means of a quartz rod extending axially into the resonator. The cavity was surrounded by a Dewar vessel in which either liquid oxygen or a mixture of solid carbon dioxide and butyl alcohol were placed.

2.2. Experimental Method

A complete account of the theory of the method has been given by Standley (1949), and therefore only an outline is included here.

As already described, the ferromagnetic material formed part of the bottom of a cylindrical resonating cavity. It may be demonstrated experimentally that, of the energy lost in such a cavity, only that dissipated in the ferromagnetic specimen is dependent on the strength of the applied magnetic field H_z . This energy may be shown to be proportional to $(\mu_R \rho)^{1/2}$ where ρ is the electrical resistivity of the material and $\mu_R = (\mu_1^2 + \mu_2^2)^{1/2} + \mu_2$ the complex permeability being written as $\mu = \mu_1 - i\mu_2$. Since the Q of the resonator may be defined as the ratio of the energy stored in the cavity to the energy lost per radian, it follows that the magnification of the cavity may be expressed in the form $1/Q = a + b(\mu_R \rho)^{1/2}$, where a and b are constants for a given cavity at a constant temperature.

If Q_0 is the magnification in some reference field H_0 , far removed from the resonance peak, and Q is the same quantity in a field H_z , the relative energy loss in this latter field is proportional to $(Q_0/Q - 1)$. In the experimental arrangement used, the rectified current from the detector D, which was found to follow closely a square law characteristic, is proportional to Q^2 . Thus if θ and θ_0 are the galvanometer deflections which correspond to Q and Q_0 , the energy lost in the specimen in the field H_z relative to that lost in the field H_0 is proportional to $(\theta_0/\theta)^{1/2} - 1$.

When absolute values of μ_R are required, it is desirable that H_0 should be a very high field where it may be assumed that $\mu_R \rightarrow 1$. In the present experiments, values of μ_R were not required, and, in fact, the width of the absorption curve was such that μ_R was clearly very different from unity in the greatest field which could be applied. Hence, in the sequel, θ_0 and Q_0 refer to these quantities measured in the remanent field of the magnet (~ 50 oersteds), and all the absorption curves have been plotted relative to this point. From each curve the width of the half power absorption and the value of H_z^{max} were found, and the corresponding g -value obtained, using eqn. (1).

2.3. Preparation of Specimens

Samples of manganese arsenide, which had been prepared from constituents of high purity (Bates 1927), were kindly given to the authors by Professor L. F. Bates. As a precaution, before using these specimens in the present series of experiments, they were digested with hydrochloric acid, washed with alcohol, and finally repeatedly sorted with a permanent magnet. Colorimetric analysis of the final product showed that manganese and arsenic were present in equal atomic proportions, within 3%, which was the limit of accuracy attainable with the colorimeter.

Manganese antimonide was prepared from pure constituents ($\text{Mn} > 99.99\%$; $\text{Sb} > 99.9\%$) by heating the correct proportions of these elements in powder form in an atmosphere of dry argon at a temperature of 850°C for 30 hours. After cooling, the residue was finely powdered and purified as above. Again, colorimetric

analysis was used to check the composition of the final product. X-ray powder photographs of this material were also obtained.

The preparation of manganese bismuthide was effected in a similar way, by heating powdered manganese and bismuth ($\text{Bi} > 99.95\%$) for 6 hours at a temperature of 370°C . Since the resulting product reacted vigorously with all strong acids, mechanical sorting of the powdered material with a permanent magnet had to be relied upon for its purification, the process being continued until a satisfactory colorimetric analysis was obtained.

The specimens used in the resonance experiments were prepared in the following way. A small piece of copper foil, about $\frac{1}{4}$ in. square and $1/2000$ in. thick, was stuck with Durofix on the head which formed the lower end of the cavity. A thin layer of the same adhesive was placed on the foil and a small quantity of the ferromagnetic powder was shaken upon it and moulded into disc-like form, about 3 mm across and 0.1 mm deep. A specimen of greater size could not be used owing to the losses introduced into the cavity with consequent reduction in Q and hence in sensitivity. On completion of the resonance experiment the copper foil, still carrying the specimen, was removed from the head and used for the magnetometer measurements described below.

2.4. Measurement of $(N_y - N_z)I$

Griffiths (1951) and MacDonald (1951) have shown that the resonance equation (1) is altered when anisotropic strains are present in the ferromagnetic material. The form of the equation remains unaltered, however, if the terms accounting for strain anisotropy are included with the demagnetizing terms of the form $(N_y' - N_z')I$ and $(N_x' - N_z')I$. The primed quantities are not readily calculated but, by means of the oscillation magnetometer devised by Griffiths and MacDonald (1951), the quantity $(N_y' - N_z')I$ may be measured directly. In the resonance experiments described, no change in the value of H_z^{\max} could be found when the specimen was rotated in the xz plane. Thus it was concluded that N_x' and N_z' were sufficiently close to equality for the term $(N_x' - N_z')I$ to be negligible, the resonance equation (1) then reducing to

$$\nu = \frac{ge}{4\pi mc} \{H_z^{\max} [H_z^{\max} + (N_y' - N_z')I]\}^{1/2}. \quad \dots\dots(2)$$

As only small ferromagnetic specimens were used in the resonance experiment, a magnetometer of small moment of inertia and small natural restoring torque was required. The final form of magnetometer used is shown in fig. 2. The body was a Pyrex glass rod, 5 in. long and $\frac{1}{4}$ in. diameter at the top, tapering to $\frac{1}{8}$ in. diameter at the foot. Near its upper end it carried a small wooden rectangular block and a mirror. Fine nylon threads, attached to each end of the body, suspended it between the poles of the electromagnet, so that the specimen, fixed by Durofix on a flat near the lower end, was in a homogeneous field. For high temperature measurements the body passed through a small furnace, indicated by the dotted line in fig. 2, the temperature being measured by a thermometer, the bulb of which was placed as near to the specimen as possible. The free period of the magnetometer alone was of the order of 10 seconds, and the periods with specimen present of the order of 1 second, so that the correction due to the natural restoring torque was small.

The procedure was to measure the period of oscillation τ in a series of known fields H . Then, since it may be shown that

$$k\tau^2 = \frac{1}{H} + \frac{1}{(N_y' - N_z')I}$$

where k is a constant for a given magnetometer and specimen, a plot of τ^2 against $1/H$ gives $-1/(N_y' - N_z')I$ as the intercept when $\tau^2 = 0$.

Individual measurements were reproducible to within about 2 to 3%, and an overall error of the order of 5% in $(N_y' - N_z')I$ is probable.

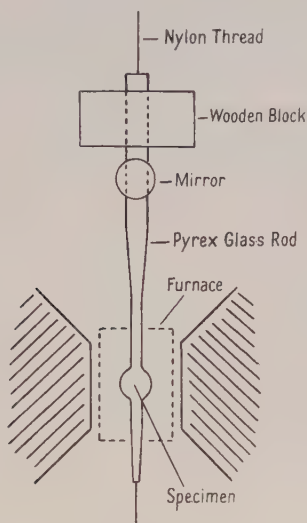


Fig. 2. The oscillation magnetometer.

§ 3. EXPERIMENTAL RESULTS

3.1. Manganese Arsenide

Manganese arsenide exists in the ferromagnetic state up to about 45°C. At this temperature its crystal lattice undergoes a sudden decrease in size, and this transition is accompanied by the rapid disappearance of its ferromagnetic properties (Ofteidal 1928, Bates 1932, 1933). In addition, it exhibits temperature hysteresis since, on cooling, the ferromagnetic state is regained at a lower temperature (Bates 1927, Guillaud 1951). Susceptibility measurements indicate (Bates 1929, Guillaud 1951) that at temperatures between 45°C and 126°C manganese arsenide is probably antiferromagnetic, whereas above 126°C it is paramagnetic.

At room temperature (18°C) absorption measurements on powdered specimens of this material showed that, at a wavelength of 1.26 cm, the applied magnetic field for maximum absorption was between 2900 and 2950 oersteds, the mean value for five specimens being 2920 oersteds. As can be seen from fig. 3 the absorption curve is broad and relatively flat, and it was therefore estimated that the location of the resonance field was subject to an uncertainty of about ± 75 oersteds. Magnetometer measurements on the specimens used yielded values of $(N_y' - N_z')I$ between 6900 and 7300 oersteds resulting in a mean value of 7000 oersteds for this quantity. Hence the g -value, calculated from (2), is 3.2 with a probable error of $\pm 3\%$.

Results published earlier (Adam and Standley 1950) reported a higher value for g , due to the use of a lower value of I . It has since been found that the low magnetic moment per unit volume was due to free manganese and arsenic in the rod sample used at that time.

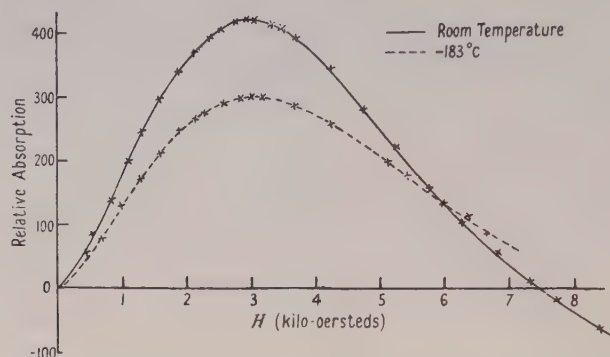


Fig. 3. Typical absorption curves obtained with samples of MnAs.

Table 1 gives typical results which show that, up to 45°C , the g -value does not change within experimental error. The values of I used in the results above room temperature were obtained using a ballistic method on the material in bulk, since it was considered impossible, in using the magnetometer, to keep the temperature steady enough to measure the rapid and irreversible decrease in I on approaching the transition point. It was observed that I decreased slowly between room temperature and about 40°C , and then fell rapidly to zero in the next 4° , indicating a transition point close to 45°C . Above about 39°C the absorption diminished considerably, and the curve became very broad and flat, so that the resonance field in this temperature region could only be estimated to about ± 400 oersteds. Hence, taking into account also the possible error due to the rapid change in I , the g -value would be expected to be susceptible to an error of the order of $\pm 10\%$ at temperatures in the neighbourhood of the transition temperature.

Table 1. Manganese Arsenide Data. $\lambda_a = 1.26 \text{ cm}$

Temp. ($^{\circ}\text{C}$)	$(N_y' - N_z')I$	H_z^{max} (Oe)	g	Width (Oe)
-183	9150	3030	2.8	4200
-73	8400	3000	2.9	4000
18	6950	2920	3.2	4100
32.2	6880	2910	3.2	4000
39	6500	2950	3.2	4400
41.7	4700	3500	3.2	4000
42.3	3600	3690	3.3	3800
43.5	1400	4150	3.5	
45.4	—	4700-5100	3.3-3.6	Uncertain

Observations were extended into the antiferromagnetic region, where a small absorption, which corresponded to a change in galvanometer deflection of $\frac{1}{2}$ to 1 cm in 60 cm was detected up to 65°C . As far as could be judged, the position of the absorption peak did not alter from its position at 45°C . Thereafter, up to 250°C (that is, in the remainder of the antiferromagnetic region and in the paramagnetic

region), no absorption was detected which corresponded to a change in galvanometer deflection of more than 2 mm in 60 cm.

The resonance absorption in manganese arsenide was also examined at temperatures below room temperature—at about 200°K and at about 90°K. These low temperature measurements revealed absorption curves similar to that at room temperature, as shown in fig. 3. The width of the resonance curve did not change appreciably down to 90°K, but the resonance field shifted slightly towards higher values as the temperature was lowered. (The curve width is defined as the separation in oersteds between the two fields at which the absorption is half maximum absorption.) At 200°K the mean value of the field for maximum absorption was found to be 3000 oersteds, and at 90°K 3030 oersteds. In order to obtain an estimate of the g -value at these temperatures it was assumed that, in the term $(N_y' - N_z')I$, the demagnetizing factor $N_y' - N_z'$ did not alter appreciably from its room temperature value, and that the intensity of magnetization alone changed. Using a corresponding states curve for $j = 3/2$, the values of $(N_y' - N_z')I$ at 200°K and at 90°K were thus calculated to be 8400 and 9150 oersteds respectively. Hence, from eqn. (2), the estimated g -value at 200°K is 2.9, and at 90°K, 2.8.

3.2. Manganese Antimonide

The results obtained from absorption measurements on manganese antimonide differ from those obtained from similar measurements on the arsenide. This may be due in part to the fact that the magnetic behaviour of the two compounds is different, in that the ferromagnetic phase of the antimonide is terminated by a true Curie point at 315°C and not, as in the arsenide, by a crystallographic phase change at a temperature below its true Curie point (Serres 1947).

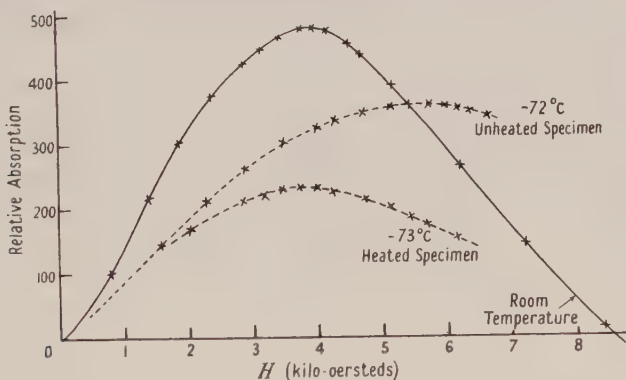


Fig. 4. Typical absorption curves obtained with samples of MnSb.

In our experiments, the purified manganese antimonide was used, either directly or after a further heating in air to about 250°C for periods up to two hours; these specimens will be referred to as 'unheated' and 'heated' respectively. It was not possible to detect any change in the chemical composition as a result of the heating: x-ray powder photographs were identical, and the saturation intensity of magnetization was unchanged within experimental error. A different temperature dependence of the behaviour at microwave frequencies was found, however, as described below.

At room temperature, the absorption curve is broad, having a width about 1000 oersteds greater than that of the arsenide, with a peak in the region of 3900 oersteds (fig. 4). As the temperature is raised, the peak moves progressively to higher fields, and the width at first increases slightly and then decreases appreciably. Very close to the Curie point there is an indication that the width increases again markedly, but here the total absorption is too small for a reliable estimate of the width to be made. Both heated and unheated specimens showed this general behaviour, but between 50°C and 225°C the resonance field value increased more rapidly in the unheated than in the heated specimens. The values of $(N_y' - N_z')I$ were measured by the oscillation magnetometer method at temperatures from room

Table 2. Manganese Antimonide Data. $\lambda_a = 1.26$ cm

Heated Specimens				
Temp. (°C)	$(N_y' - N_z')I$	H_z^{\max} (Oe)	g	Width (Oe)
-183	7550	4950	2.2	~6500
-78	7450	4050	2.5	~6700
-73	7450	3780	2.6	~6700
20	6800	3910	2.6	4850
68	5860	4330	2.5	5350
117	5400	5190	2.3	5700
175	3890	6160	2.1	4800
200	3190	6610	2.1	3900
250	1790	7340	2.1	2600
292	550	7990	2.0	1100

Unheated Specimens				
Temp. (°C)	$(N_y' - N_z')I$	H_z^{\max} (Oe)	g	Width (Oe)
-183	7550	6360	1.8	Uncertain
-78	7450	6210	1.8	
-72	7450	5650	2.0	
-62	7420	4780	2.2	
-45	7350	4110	2.4	4950
20	6800	3900	2.6	
67	5880	4900	2.3	
117	5400	5470	2.2	
150	4600	6180	2.1	5650
180	3740	6680	2.0	4500
222	2550	7070	2.1	3100

to about 210°C, at which temperature the value of I had become too small to be measured with any degree of certainty by this method. The results are given in detail in table 2, and represent average results of several different specimens.

Using eqn. (2), the g -value for manganese antimonide was calculated at various temperatures, and the results are given in fig. 5. It will be seen that the g -value falls from a value of 2.6 at 20°C to a value of about 2.1 as the Curie point is approached, the fall in g -value with temperature being more rapid for an unheated specimen than for a heated one. An error of not more than $\pm 3\%$ in the g -values is expected.

When absorption measurements were extended to low temperatures, the difference in behaviour of the two types of specimen became more marked. In

the region of -75°C , the unheated specimen undergoes a change of some kind, while the heated specimen does not. This is apparent both from the change in resonance field indicated in table 2, and from the change in curve shape (fig. 4). The nature of the change has not been established, for while rough measurements at liquid air temperature indicate that the intensity of magnetization in the two types of specimen does not differ markedly, some difference cannot be ruled out. It has not been found possible to carry out an x-ray diffraction examination of the specimens at low temperatures to investigate the possibility of a crystal structure change in the unheated specimens. It is to be noted that the g -values quoted in table 2 are calculated using approximate values of $(N_y' - N_z')I$, obtained by extrapolating the room temperature values using a corresponding states curve.

In the discussion, however, reference is made only to results obtained at temperatures above about 20°C and to the results obtained with heated specimens at low temperature.

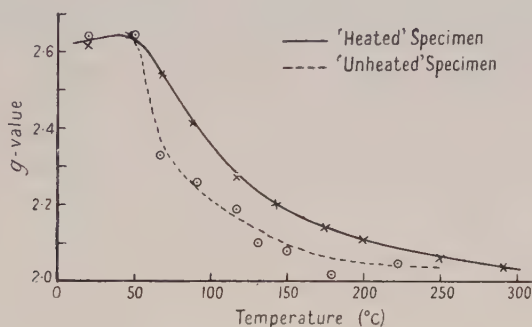


Fig. 5. Curves showing the variation of the calculated g -value with temperature in 'heated' and 'unheated' specimens of MnSb .

3.3. Manganese Bismuthide

Manganese bismuthide exhibits pronounced ferromagnetic properties up to 360°C , at which temperature the substance undergoes a crystallographic phase change, accompanied by a rapid transition to probably an antiferromagnetic state. This transition is marked by temperature hysteresis. The antiferromagnetic state persists to 445°C where a second transition, to a paramagnetic state, takes place (Guillaud 1951). The general magnetic behaviour of manganese bismuthide is therefore similar to that of the arsenide.

Specimens of this material were examined at temperatures between liquid air and 300°C . Only at liquid air temperatures was there a measurable absorption; at -75°C , and from room temperature to 240°C no resonance absorption was detected, while at 250°C a small absorption was found amounting to an overall change in galvanometer deflection of about 1 cm in 60 cm. The magnetic field for maximum power absorption could not be located with sufficient accuracy, however, for a calculation of the splitting factor to be made at this temperature, and the magnitude of the absorption did not increase appreciably up to 300°C .

At 90°K and with a wavelength of 1.26 cm the observed resonance field for several specimens ranged from 4050 to 4200 oersteds. The resonance curve was always broad, of the order of 5500 to 6000 oersteds. The actual value of $(N_y' - N_z')I$ was not determined experimentally, but an order of magnitude of the g -value was obtained by assuming an intensity of magnetization at 90°K of 655 c.g.s.

units and a demagnetizing factor of 4π . The intensity was calculated from the saturation moment at 0°K (Guillaud 1951) using a corresponding states curve.

With these assumptions the splitting factor at 90°K was found to be 2.4.

§ 4. DISCUSSION

Certain features of interest emerge from the results presented in the previous section. Firstly, it is seen that in manganese arsenide the line width remains sensibly constant with change in temperature, whereas in manganese antimonide it shows a definite temperature dependence. Secondly, in the case of manganese arsenide the g -value does not vary with temperature within experimental error, while in the case of the antimonide a marked variation of g -value with temperature is found. Thirdly, anomalously high g -values are obtained for each of the three materials examined.

It may at once be pointed out that the temperature dependence of the g -value and line width in manganese arsenide and in manganese antimonide cannot be compared directly since, as has been stated earlier, manganese antimonide possesses a true Curie point whereas manganese arsenide does not. Therefore the resonance phenomena in manganese antimonide at temperatures approaching its Curie temperature (315°C) cannot be studied in a similar way to those in manganese arsenide at temperatures in the region of its critical point (45°C). However, assuming that the true Curie point of manganese arsenide would occur at 126°C (Guillaud 1951), a comparison of the resonance absorption in the two substances may be made from liquid air temperature to the same reduced temperature, $T/\theta = 0.78$; that is to approximately 40°C in the case of the arsenide and to approximately 190°C in the case of the antimonide. In addition, since it was not found practicable to measure the quantity $(N_y' - N_z')I$ accurately at low temperatures, the possibility of a greater error in the g -values quoted at such temperatures must not be excluded.

With reference to resonance line widths, results obtained on certain ferrites show that the line width decreases with increase in temperature, the decrease being more rapid at low than at high temperatures (Okamura *et al.* 1952, Okamura and Torizuka 1951, Healy 1952). In nickel, on the other hand, while there is evidence that at low temperatures the line width is greater than at room temperature, observations from 24°C to 358°C indicate an increase in line width with increase in temperature (Bloembergen 1950). The line widths in manganese arsenide and manganese antimonide do not follow a temperature dependence of either of these forms, although there is some resemblance between the behaviour of the antimonide and that of the ferrites.

From Bloembergen's work, it is evident that surface imperfections affect the measured width of the resonance line. Using a nickel specimen which had been annealed and electrolytically polished, he found at room temperature a line width of the order of 1000 oersteds. Standley (1949) found, for a nickel specimen which had been annealed but not polished in any way, that the same quantity was about 2000 oersteds while, for a specimen of coarse nickel powder, we have obtained a line width of 5000 oersteds. In nickel, then, the apparent width is decreased by a factor of about 5 in changing from a powdered specimen to one whose surface is plane and free from blemishes. Hence, in view of the fact that all the specimens used in the present experiments were in powder form, a considerable amount of the line width would be expected to result from the irregular nature of the surface. At

the same time it does not seem likely that this contribution to the line width will be markedly temperature dependent.

In addition to the surface condition, the use of polycrystalline material causes a further experimental broadening of the line of the order of $2K_1/I$ oersteds, where K_1 is the first order anisotropy constant. While for manganese arsenide and manganese antimonide neither the value nor the variation with temperature of K_1 is known, it is to be expected that K_1 will decrease towards zero at the Curie point. Hence the observed decrease in line width with temperature in manganese antimonide as its Curie temperature is approached might be explained by a more rapid rate of decrease in K_1 than in I , but the magnitude of the observed change seems too great for this to yield, by itself, a complete explanation. On the other hand, the fact that a resonance absorption cannot be detected around room temperature in manganese bismuthide is readily explained by this anisotropy broadening. At room temperature, K_1 for manganese bismuthide is 10^7 erg cm⁻³ (Guillaud 1949) and hence the width from this cause alone would be of the order of 3×10^4 oersteds. Around 90°K, the anisotropy constant is sufficiently small for the line width to be of a reasonable value, while the small absorption detected above 250°C points to the fact that here too the anisotropy constant is small, but the total absorption has also decreased owing to the decrease in I .

It will be seen that the observed line widths in manganese arsenide and manganese antimonide are of the same order of magnitude as that in powdered nickel. Therefore, since the intensities of magnetization of the three materials are approximately the same, and K_1 is likely to be greater for manganese arsenide and manganese antimonide than for nickel, the line widths in good single crystals of these manganese compounds are expected to be quite small.

Moreover, a contribution to the line width in the arsenide and the antimonide due to eddy current damping (Kittel and Herring 1950) cannot be ruled out since these materials have conductivities of the same order of magnitude as those of metals. This effect, which should be absent in the non-conducting and semi-conducting ferrites, gives the right kind of temperature dependence, since it will be greatest at low temperatures.

To sum up, it would appear that the observed variation in line width with temperature in manganese arsenide and manganese antimonide cannot readily be explained by one mechanism alone, but might be accounted for in terms of an anisotropy contribution in addition to a contribution arising from the conduction electrons. However, it can at least be said that spin-lattice interaction does not appear to play an important part in determining the line width in these manganese compounds, for this interaction should result in an increase in line width with increase in temperature.

Turning to the question of g -values, there seems at present to be no satisfactory reason which might account for the fact that eqn. (2) yields anomalously high g -values for the materials examined and, in addition, for the temperature dependent g -value in the case of manganese antimonide.

A basic assumption made in deriving eqn. (1) is that the static magnetic field H_z is sufficient to magnetize the specimen to saturation. Since the resonance field for manganese arsenide is only about 3000 oersteds and that for the antimonide about 4000 oersteds, it seemed possible that this condition might not be fulfilled for these materials. However, in the measurement of $(N_y' - N_z')I$ by the oscillation magnetometer, a linear relationship between τ^2 and $1/H$ exists only if I

has a constant (i.e. saturation) value (Griffiths and MacDonald 1951). Thus the occurrence of a non-linear relationship at low fields may be construed as indicating lack of magnetic saturation of the material. We have found that there is no departure from linearity of the $(\tau^2, 1/H)$ graph, within experimental error, for either manganese arsenide or manganese antimonide in fields greater than about 2500 oersteds, and therefore conclude that in each case the material is saturated at resonance.

The use of the resonance equation (1) may also be questioned on the grounds that it holds strictly only for an undamped system. Although the mechanism of relaxation is not yet understood, considerable success has been achieved in representing the experimental curve shapes by empirical damping terms in the equations of motion (Kittel 1947, 1948, Bloembergen 1950, Yager *et al.* 1950). Bloembergen's equations, based on the nuclear work of Bloch, introduce a relaxation time T_2 to account for the damping, and yield

$$\omega^2 = \gamma^2 \{H_z^{\max} + (N_y - N_z)I\} \{H_z^{\max} + (N_x - N_z)I\} + \frac{1}{T_2^2} \dots\dots (3)$$

as the condition for maximum absorption, where $\omega = 2\pi\nu$ and $\gamma = ge/2mc$. This equation reduces to eqn. (1) when $1/T_2^2 \ll \omega^2$. For nickel, Bloembergen finds $1/T_2^2 \sim \omega^2/400$, so that his use of eqn. (1) is correct within the limits of experimental error. It has been found for the three nickel specimens already discussed that, although the surface of the specimen affected the line width, the resonance field was unaltered. Comparison of Bloembergen's resonance curve for nickel with that for manganese arsenide shows that if a fivefold broadening due to the surface of the specimen is allowed for in the latter case, agreement between the two curve widths is obtained. It is therefore concluded that T_2 for manganese arsenide, and hence also T_2 for manganese antimonide will be of the same order of magnitude as for nickel. The calculated g -values do not therefore appear to be affected by neglecting the damping term in eqn. (3).

In addition, in his discussion of ferromagnetic resonance absorption, Van Vleck (1950, 1951) has pointed out that the interaction between spin-orbit coupling and orbital valence will give rise to non-magnetic pseudo-dipolar forces which might influence the resonance frequency, particularly in the case of non-cubic crystals. Such forces, which are of comparatively short range, also give rise to magnetic anisotropy, and hence a correlation might be expected between the g -value and the anisotropy of the material. It may therefore be significant that the high g -values found in this investigation occur in materials whose anisotropy is known or expected to be high, and that the decrease in the g -value with increase in temperature in manganese antimonide follows the expected decrease in the anisotropy as the Curie point is approached. However, the published experimental evidence on the connection between anisotropy and g -value is at present inconclusive. Temperature dependent g -values which might be correlated with changes in anisotropy have been found in copper and cobalt ferrites (Okamura *et al.* 1951, Okamura and Kojima 1952), but Healy (1952) has found no such correlation possible in nickel ferrite.

Finally it is of interest to draw attention to the measurements which have now been made by various authors on materials in which the manganese ion is presumably the ferromagnetic carrier. Some of these are recorded in table 3, and it will be noted that in all these materials it is reasonable to deduce from their various magnetic data that the manganese ion is in an S state spectroscopically. Thus it is clear that, in the absence of any orbital contribution, a g -value close to the free spin

value is obtained, but in manganese arsenide, antimonide and bismuthide where an S state is not postulated (Guillaud 1951) a spectroscopic splitting factor differing markedly from 2.00 is found.

§ 5. CONCLUSION

This investigation was undertaken in an attempt to determine parameters upon which the experimental value of the spectroscopic splitting factor depends. The crystallographically similar series of materials manganese arsenide, antimonide and bismuthide was chosen for this purpose, since certain factors (§ 1) remain constant or change only slightly through the series. From the results obtained it can be stated that (a) the g -values differ markedly from the spin only value 2.00, (b) in manganese antimonide the g -value found varies with temperature, and (c) there may be a connection between the g -values in the three materials and the known or inferred (manganese arsenide) high crystalline anisotropy.

Table 3. Spectroscopic Splitting Factors for Various Ferromagnetic Materials containing Manganese

Material	g	λ (cm)	Author
Manganese ferrite	2.05	1.25	Yager <i>et al.</i> (1951)
Manganese zinc ferrites	2.01–2.06	1.25	Yager <i>et al.</i> (1951)
Heusler alloy	2.01	1.25	Yager and Merritt (1949)
Manganese nitride Mn_4N	2.00	1.26	Adam and Standley (unpublished)

In connection with points (b) and (c) further experiments with material of high anisotropy would be of interest, and it is hoped to carry out similar measurements with cobalt, whose K values are high and reasonably well known.

ACKNOWLEDGMENT

The authors wish to record their thanks to Professor L. F. Bates for his interest and advice during the course of this work.

REFERENCES

- ADAM, G. D., and STANDLEY, K. J., 1950, *Proc. Phys. Soc. B*, **63**, 820.
 BATES, L. F., 1927, *Proc. Roy. Soc. A*, **117**, 680; 1929, *Phil. Mag.*, **8**, 714; 1932, *Ibid.*, **13**, 393; 1933, *Ibid.*, **16**, 657.
 BLOEMBERGEN, N., 1950, *Phys. Rev.*, **78**, 572.
 GRIFFITHS, J. H. E., 1946, *Nature, Lond.*, **158**, 670; 1951, *Physica*, **17**, 253.
 GRIFFITHS, J. H. E., and MACDONALD, J. R., 1951, *J. Sci. Instrum.*, **28**, 56.
 GUILLAUD, C., 1949, *J. Rech., Cent. Nat. Rech. Sci.*, **9**, 267; 1951, *J. Phys. Radium*, **12**, 223.
 HALLA, F., and NOWOTNY, H., 1936, *Z. phys. Chem. B*, **34**, 141.
 HEALY, D. W., 1952, *Phys. Rev.*, **86**, 1009.
 KITTEL, C., 1947, *Phys. Rev.*, **71**, 270; 1948, *Ibid.*, **73**, 155; 1949, *Ibid.*, **76**, 743.
 KITTEL, C., and HERRING, C., 1950, *Phys. Rev.*, **77**, 725.
 KITTEL, C., and LUTTINGER, J. M., 1948, *Helv. Phys. Acta*, **21**, 480.
 MACDONALD, J. R., 1951, *Proc. Phys. Soc. A*, **64**, 968.
 OFTEDAL, I., 1928, *Z. phys. Chem.*, **132**, 208.
 OKAMURA, T., and KOJIMA, Y., 1952, *Phys. Rev.*, **86**, 1040.
 OKAMURA, T., and TORIZUKA, Y., 1951, *Nature, Lond.*, **168**, 872.
 OKAMURA, T., TORIZUKA, Y., and KOJIMA, Y., 1951, *Phys. Rev.*, **84**, 372; 1952, *Ibid.*, **85**, 693.
 SERRES, A., 1947, *J. Phys. Radium*, **8**, 146.
 STANDLEY, K. J., 1949, *Thesis*, University of Oxford.
 VAN VLECK, J. H., 1950, *Phys. Rev.*, **78**, 266; 1951, *Physica*, **17**, 234.
 YAGER, W. A., GALT, J. K., MERRITT, F. R., and WOOD, E. A., 1950, *Phys. Rev.*, **80**, 744.
 YAGER, W. A., and MERRITT, F. R., 1949, *Phys. Rev.*, **75**, 318.
 YAGER, W. A., MERRITT, F. R., and GUILLAUD, C., 1951, *Phys. Rev.*, **81**, 476.

The Ultra-Violet Band Spectrum of Carbon Monoselenide

By R. K. LAIRD AND R. F. BARROW

Physical Chemistry Laboratory, University of Oxford

MS. received 18th May 1953

Abstract. An improved source of the CSe band system in emission has been discovered which has enabled a partial rotational analysis of seven bands to be made. The value derived for r_e'' is 1.67 \AA . No evidence against the view that the main system is $^1\Pi-^1\Sigma$, in which the $^1\Pi$ state is greatly perturbed, has been obtained.

§1. INTRODUCTION

THE ultra-violet spectra of CS and of CSe present a number of problems of some interest, since although their strong band-systems appear at first sight to be analogous to the $A^1\Pi-X^1\Sigma^+$ system of CO, there exist marked irregularities in the vibrational and rotational constants derived by Crawford and Shurcliff (1934) for CS, and in the vibrational constants of CSe (Barrow 1939). These irregularities have been attributed to strong perturbations of the $^1\Pi$ states, as happens in the case of CO (Coster and Brons 1934, Schmidt and Gerö 1935, Budó and Kovács 1938), of SiO (Lagerqvist and Uhler 1953) and of SiS (Lagerqvist, Nilheden and Barrow 1952). However, Howell (1947) has suggested that the CS and CSe systems are really $^3\Pi-^1\Sigma$, analogous to the Cameron bands of CO. This view is not supported by later work on CS: thus the extended rotational analysis made by Laird (1952), using high dispersion plates most kindly placed at our disposal by Professor F. H. Crawford, shows that it would be very difficult to interpret the system as other than $^1\Pi-^1\Sigma$, and the apparent strength of the system in absorption (Laird 1952, Dyne and Ramsay 1952) also favours this interpretation. The present work is concerned with some further observations on the transition in CSe.

§2. EXPERIMENTAL

The spectrum of CSe was first excited by Rosen and Désirant (1935), who used an electrodeless discharge in a silica tube containing selenium and deposited carbon. Barrow (1939) used a positive column discharge in a silica capillary to which were admitted pellets of aluminium and selenium with a small amount of hydrocarbon grease. Following the preparation of CSe₂ by Ives, Pittman and Wardlaw (1947), a much improved source of the CSe spectrum has now been obtained. This consists of an electrodeless discharge excited by an oscillator running at about 30 m through methylene chloride and selenium vapour. CO impurity was effectively cut down by working at as high a pressure of methylene chloride as possible, and apart from the CSe bands, the only other bands excited with any strength arose from the $^2\Sigma-^2\Pi$ system of HCl⁺.

Satisfactory spectrograms were taken on a Hilger quartz Littrow instrument (E.478) in about 100 minutes on Ilford Process plates. The region 2000 to 6000 Å was examined for other systems of CSe, but none was found.

The CSe system was also sought in absorption by the methods which had proved successful for CS, NS and CF₂ (Barrow 1950, Laird, Downie and Barrow 1952, Laird, Andrews and Barrow 1950). However, it is evidently more difficult to set up an adequate stationary concentration of CSe than of CS, for no trace of the CSe system appeared in absorption.

§3. VIBRATIONAL ANALYSIS

We were able to make somewhat more certain measurements of the band-heads than was possible on the 1939 plates. The list given in table 1 therefore replaces

Table 1. Band-Heads of CSe

v', v''	ν (cm ⁻¹)	Intensity	v', v''	ν (cm ⁻¹)	Intensity
—	36194.3	2	0, 1	34114.4	5
1, 0	35960.9	4	1, 2	33916.6	5
2, 1	769.4	3	2, 3	745.8	3
3, 2	571.7	3	—	641	2
4, 3	392.6	0	3, 4	570.3	2
5, 4	191.8	2	—	313.5	2
0, 0	141.1	10	—	207.7	1
1, 1	34934.3	5	0, 2	101.9	2
2, 2	751.2	1	1, 3	32911.0	3
—	660.6	4	2, 4	752.6	2
—	326.7	1	—	230.5	2
			1, 4	31918.6	1

In addition to these bands, there appear to be inner heads to the 0, 0 and 1, 1 bands and to the unidentified band at 34661 cm⁻¹ at about 35080, 34870 and 34620 cm⁻¹ respectively. These change in appearance somewhat according to resolving power, and it is not certain that they are other than fortuitous groupings of perturbed lines.

the earlier table. However, the main outline of the vibrational analysis, in which, although the upper state vibrational intervals vary quite irregularly, the ground state intervals and the intensity distribution run normally, is unaltered. There remain a number of unassigned bands of considerable intensity which do not appear to fit into the main Deslandres scheme. Some of these heads may perhaps arise from large perturbations of the main system rotational levels as in CS, but the band at 2884 Å is so strong as to suggest that there is more than one system of CSe in this region.

§4. ROTATIONAL ANALYSIS

The rotational structure of many of the bands is fairly open, and a partial analysis of seven bands, the 0, 0, 0, 1, 1, 0, 1, 1, 1, 2, 2, 1 and 3, 2, has been carried out, although the resolving power was equivalent to not more than about 1 cm⁻¹. For these bands it was fairly easy to pick out an intense branch, presumed to be the Q branch and, since these branches could be followed to quite small J values, generally in the region of 5 to 10, the numbering of the branches could be established without difficulty. The analysis then proceeded as follows:

(i) Values of $\Delta G_{0,1}$, $\Delta G_{1,2}$ and of α'' were obtained from the differences $Q(J)_{0,0} - Q(J)_{0,1}$, $Q(J)_{1,0} - Q(J)_{1,1}$ and $Q(J)_{1,1} - Q(J)_{1,2}$. Thus were found $\Delta G_{0,1} = 1026.1$, $\Delta G_{1,2} = 1016.4$, $\alpha'' = 0.004_0$ cm⁻¹.

(ii) The values of the band-origins and of $B'' - B'$ were then obtained by fitting the Q lines to formulae

$$Q(J) \simeq \nu_0 - (B'' - B')J(J+1).$$

The results of these calculations are summarized in table 2.

(iii) The determination of the absolute values of B presents of course much greater difficulty. The R lines form heads at $J \sim 5$ to 6, and the returning lines are for the most part not well resolved. However, a number of fragments of what appeared to be P-branch lines could be detected, especially in the range $J \sim 20$ to $J \sim 40$. The usual combination differences could then be formed, and the assignments checked by comparison between appropriate bands. Finally the values of B'' were determined by averaging values of $\Delta_1 F''(J)/(J+1)$ and of $\Delta_2 F''(J)/(J+\frac{1}{2})$, and using a value of D'' calculated from Kratzer's relation. The results are given in table 3. From these figures, $B_v'' = 0.580 - 0.004(v'' + \frac{1}{2})$, and, with the values of ΔB given in table 2, we derive the values of B' given in table 4.

Table 2. Constants for Q lines (cm^{-1})

v', v''	Range of J	ν_0	$B'' - B'$	$B_0'' - B_v''^*$
0, 0	7-43	35134.6	0.091	0.091
0, 1	7-30	34108.5	0.087	0.091
1, 0	13-33	35954.6	0.082	0.082
1, 1	8-32	34928.0	0.077	0.081
1, 2	6-25	33911.2	0.072	0.080
2, 1	12-35	35761.4	0.092	0.096
3, 2	19-44	(35573.1)	0.123	0.131

* Calculated with $\alpha'' = 0.004$.

Table 3. Values of B'' (cm^{-1})

v''	B_v''	$B_e''^*$	B_e'' (mean)
0	0.577	0.579	
1	0.574	0.580	0.580
2	0.571 ₅	0.581 ₅	

* with $\alpha'' = 0.004$.

Table 4. Values of B' (cm^{-1})

v'	0	1	2	3
B'	0.487	0.497	0.482	0.447

There must exist lines arising from the less abundant molecule CSe^{78} , which should be about half as intense as those from CSe^{80} . However, the separations expected in these bands are quite small (about 1 cm^{-1} or less for all the bands whose rotational structure has been examined, except for the 0, 1 and 1, 2) and a search for isotopic lines and heads was unsuccessful.

§ 5. DISCUSSION

The molecular constants derived in the present work are collected in table 5.

Table 5. Molecular Constants of CSe

State	T_0	ω_e	$x_e \omega_e$	B_e	α	r_e (\AA)
($^1\Pi$)	35134.6	840	—	0.50	—	1.80
$^1\Sigma^+$	0	1035.9	4.8 ₈	0.58 ₀	0.004	1.66 ₉

In this table the vibrational constants have been derived from the values of ν_0 given in table 2. It is not possible, nor indeed has it meaning, to give precise values for the upper state constants, for the values neither of B' nor of $\Delta G'$ (which are 819.6, 833.4 and, less certainly, 828.9 cm^{-1} for 0-1, 1-2, and 2-3 respectively) run smoothly. Thus the analysis indicates that there are large perturbations, both of the vibrational and of the rotational levels in the upper state, and the simplest assumption about the upper state remains that it is $^1\Pi$, heavily perturbed by interaction with other states yet to be identified.

It remains to see what independent checks of the rotational analysis outlined here can be made. First the value of α'' may be compared with that calculated from the Pekeris relation (Herzberg 1950), $\alpha = 6(x_e\omega_e B_e^3)^{1/2}/\omega_e - 6 B_e^2/\omega_e$. This gives $\alpha'' = 0.0037$, in good agreement with the experimental value of 0.004 cm^{-1} . Next the value of r_e'' may be considered. The best comparison seems to be with OSe: here the length of the C-Se bond is found to be 1.709 \AA . In OCS, the C-S distance is 1.559 \AA , 0.025 \AA longer than in CS (the distances in OCS and OSe are from microwave spectra: see Crawford and Mann 1950). This suggests that the value of r_e'' for CSe should be about $1.709 - 0.025 = 1.684 \text{ \AA}$, about 1% bigger than the value derived from the rotational analysis. The agreement is satisfactory.

Thus it may be concluded that the original vibrational scheme for the CSe system is supported by rotational analysis: a number of complexities remain, however, which are likely to be unravelled only after a detailed study of high dispersion spectrograms.

ACKNOWLEDGMENT

One of us (R. K. L.) is glad to acknowledge the award of a maintenance grant from the Department of Scientific and Industrial Research.

REFERENCES

- BARROW, R. F., 1939, *Proc. Phys. Soc.*, **51**, 989; 1950, *Discussions of the Faraday Society*, **9**, 81.
 BUDÓ, A., and KOVÁCS, I., 1938, *Z. Phys.*, **109**, 393.
 COSTER, D., and BRONS, F., 1934, *Physica*, **1**, 634.
 CRAWFORD, B. L., and MANN, D. E., 1950, *Ann. Rev. Phys. Chem.*, **1**, 151.
 CRAWFORD, F. H., and SHURCLIFF, W. A., 1934, *Phys. Rev.*, **45**, 860.
 DYNE, P. J., and RAMSAY, D. A., 1952, *J. Chem. Phys.*, **20**, 1055.
 HERZBERG, G., 1950, *Molecular Spectra and Molecular Structure: I. Spectra of Diatomic Molecules* (New York: van Nostrand).
 HOWELL, H. G., 1947, *Proc. Phys. Soc.*, **59**, 107.
 IVES, D. L. G., PITTMAN, R. W., and WARDLAW, W., 1947, *J. Chem. Soc.*, 1080.
 LAGERQVIST, A., NILHEDEN, G., and BARROW, R. F., 1952, *Proc. Phys. Soc. A*, **65**, 419.
 LAGERQVIST, A., and UHLER, U., 1953, *Ark. Fys.*, **6**, 95.
 LAIRD, R. K., 1952, *Thesis*, University of Oxford.
 LAIRD, R. K., ANDREWS, E. B., and BARROW, R. F., 1950, *Trans. Faraday Soc.*, **46**, 803.
 LAIRD, R. K., DOWNIE, A. R., and BARROW, R. F., 1952, *Proc. Phys. Soc. A*, **65**, 70.
 ROSEN, B., and DÉsirANT, M., 1935, *C.R. Acad. Sci., Paris*, **200**, 1659.
 SCHMID, R., and GERÖ, L., 1935, *Z. Phys.*, **94**, 386.

RESEARCH NOTES

A Proposed Structure for Certain Domain Configurations on a Single Crystal of Nickel*

By G. W. WILSON†

Department of Physics, University of Nottingham

Communicated by L. F. Bates; MS. received 8th June 1953

EXPERIMENTAL observations have recently been reported (Bates and Wilson 1951) of Bitter figures observed upon the surface of a crystal of nickel cut as a rectangular parallelepiped having its main surface parallel to a (111) plane and two of its sides parallel to (112) planes. It was suggested that the fundamental domains, occupying the main fraction of the volume of the crystal, would take the form of sheets perpendicular to the direction of the applied magnetic field, i.e. to the $\langle 01\bar{1} \rangle$ direction. In this case they would, in the condition of zero internal magnetic field, be magnetized alternately parallel to the two [111] axes making angles of approximately 35° with the $\langle 01\bar{1} \rangle$ direction. Neither of these [111] axes is parallel to the {111} surface on which the regular straight line colloid deposits were observed. Alternatively, it was proposed that the fundamental domains could be magnetized along the two [110] axes, making angles of 60° with the applied field direction, but calculation shows that the second structure is unlikely on account of the increased magnetic energy associated with it due to the magneto-crystalline anisotropy and the magnetic field.

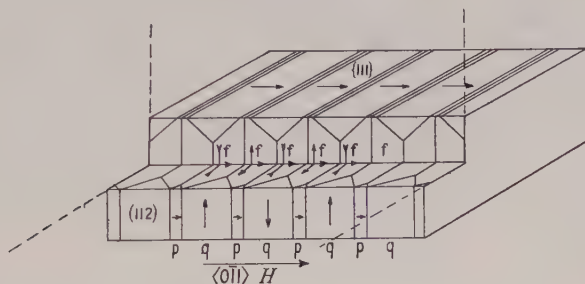
Referring to Bates and Wilson (1951) and comparing the patterns formed upon the (111) and (112) planes, i.e. upon the top and sides of the crystal, it can be seen that whereas the lines on the latter planes exhibit a fine structure and appear relatively broad, those on former planes do not, and indeed appear much narrower. If we postulate a model based upon fundamental domains whose magnetization vectors initially lie parallel to [111] axes, and assume that these vectors symmetrically approach the direction along which the magnetic field is applied as the latter is increased, then we need also to have a closure domain structure which does not allow the formation of free magnetic poles upon the surface of the crystal, for the presence of such free poles would mean instability in the structure.

As pointed out by Néel, satisfactory flux closure may be accomplished by two sets of closure domains. Each set serves to provide a closed path for the component of magnetization perpendicular to the surface, one set in a direction parallel to the applied field—p domains—and the other partly *antiparallel* to this direction—q domains. They may be revealed by the powder pattern technique as a series of bands having a fine structure (Bates and Mee 1952) or as lines of unequal spacing, e.g. doublets, as shown in a paper by Bates and Wilson (1953).

* The work described in this Note is part of a thesis approved by the University of Nottingham for the degree of Ph.D.

† Now at H.M. Underwater Countermeasures and Weapons Establishment, Havant.

The nature and regularity of the lines observed upon the (111) plane of the crystal suggests that one set of these closure domains is absent. On the (112) plane both sets appear to be present. The domain structure, which appears to be correct, is drawn in the figure. A section of the crystal is cut away in the figure



Proposed domain structure.

to reveal the magnetization of the fundamental domains, marked *f*. The magnetization of each of these is resolved into three components in the diagram. One is parallel to the direction of the applied field representing the magnetization *I*, which is measured by a coil wound round the crystal, while the second and third components are respectively perpendicular to the (111) and (112) planes.

Only *p*-type closure domains are present on the {111} surface. Magnetic colloid collects in the stray fields set up by the thin lines of free poles occurring on the surface in the place of antiparallel closure domains. These stray fields act in opposition to the applied field, and it was observed that as the latter was increased the deposits of colloid particles grew weaker.

Both *p* and *q* closure domains are present on the (112) plane, and their directions of magnetization are marked in the figure. Calculations similar to those performed by Néel (1944) show that antiparallel closure may be effected along directions as drawn, only slightly inclined to the $\langle 111 \rangle$ axis perpendicular to the direction of the applied magnetic field. Magnetization of the crystal occurs by rotation of the magnetization vectors of the fundamental domains towards the direction of the applied field. This takes place in the (110) plane containing the directions of magnetization of the fundamental domains and the direction of the applied field, and is accompanied by an increase in the ratio of the relative volumes occupied by the *p* and *q* domains.

The above model appears to fit the observed facts very well but, as pointed out elsewhere, the desired confirmation by determining the direction of magnetization of the surface domains is very difficult in the case of nickel.

This work was carried out in the Physics Department of the University of Nottingham under the supervision of Professor L. F. Bates as part of a programme sponsored by the Electrical Research Association, to whom I am indebted for permission to publish.

REFERENCES

- BATES, L. F., and MEE, C. D., 1952, *Proc. Phys. Soc. A*, **65**, 129.
 BATES, L. F., and WILSON, G. W., 1951, *Proc. Phys. Soc. A*, **64**, 691; 1953, *Ibid.*, **66**, 819.
 NÉEL, L., 1944, *J. Phys. Radium*, **5**, 241.

A Note on the $^{10}\text{B}(\alpha, p)^{13}\text{C}$ Reaction

BY G. MANNING AND B. SINGH

Department of Physics, Imperial College, London

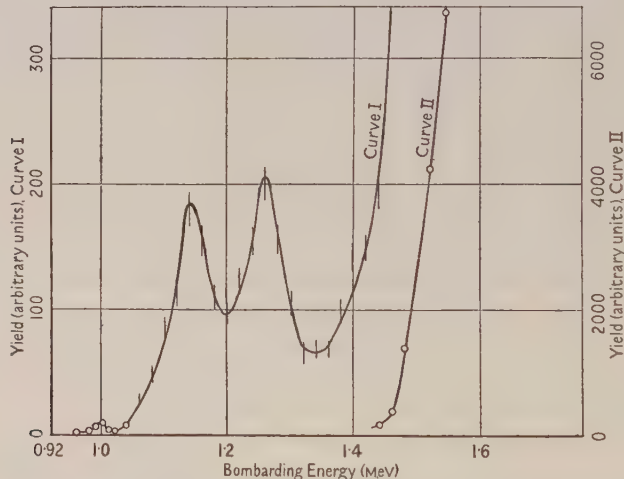
Communicated by S. Devons; MS. received 30th June 1953

A POSSIBLE level of ^{13}C at about 0.7 MeV has been reported by Perkins (1950) and several other authors (see Hornyak *et al.* 1950) from studies of the $^{10}\text{B}(\alpha, p)^{13}\text{C}$ reaction, the α -particles being obtained from natural radioactive sources. Creagan (1949), using 7 MeV helium ions from a cyclotron, but with poor energy resolution, failed to find the level.

No conclusive evidence has been found of a 0.7 MeV level in ^{13}C from any of the following reactions: $^{12}\text{C}(\text{d}, \text{p})^{13}\text{C}$, $^{12}\text{C}(\text{n}, \gamma)^{13}\text{C}$, $^{13}\text{C}(\text{p}, \text{p}')^{13}\text{C}$, $^{13}\text{N}(\beta^+)^{13}\text{C}$, although it is energetically possible and no γ -ray of 0.7 MeV has been observed from ^{13}C (Ajzenberg *et al.* 1952).

Confirmation of this level is of considerable theoretical interest since there is no known corresponding level in the mirror nucleus ^{13}N . It was therefore decided to restudy the $^{10}\text{B}(\alpha, p)^{13}\text{C}$ reaction with better energy resolution.

A thin electromagnetically separated ^{10}B target of $5 \mu\text{g cm}^{-2}$ on a copper backing was bombarded with a few microamperes of singly charged helium ions from the electrostatic generator. An excitation curve (see figure) was taken for



the ground state proton group, detected with a proportional counter at 90° in the laboratory frame, for bombarding energies in the range 0.5–1.5 MeV with energy resolution better than 4 keV. The excitation curve shows two peaks corresponding to levels in ^{14}N at 12.47 ± 0.03 MeV and 12.39 ± 0.03 MeV, which agree well with known levels. A third peak corresponding to a level of ^{14}N at 12.29 ± 0.03 MeV confirms a suspected level. Above 1.4 MeV the excitation function follows the same trend as that given by Heydenberg (1953).

An Ilford C2 nuclear emulsion plate, 200 microns thick, was used to study the proton groups emitted from the target at a bombarding energy of 1.5 MeV.

Four proton groups were found. Three of these corresponded to transitions to the ground state of ^{13}C and to known levels at 3.68 and 3.89 MeV. The fourth group was due to the $^{11}\text{B}(\alpha, p)^{14}\text{C}$ reaction (see table). No indication was found

(1)	(2)	(3)
^{13}C ground state	1	1
^{13}C 3.68 MeV level	2	2
^{13}C 3.89 MeV level	5	15
^{14}C ground state	0.25	0.5

Bombarding energy 1.5 MeV ; (1) groups corresponding to transitions to following levels ; (2) relative intensity at 90° ; (3) relative intensity at 150° .

of groups corresponding to a level in ^{13}C at 0.7 MeV, or to the known level at 3.08 MeV, either at 90° or 150° in the laboratory frame. A little but not violent anisotropy was indicated.

The amount of labour necessary to obtain a small upper limit to the yield of a group corresponding to a level at 0.7 MeV by the above method is prohibitive. Therefore, greater statistical accuracy was obtained by examining the energy distribution of the emitted protons at 90° in the laboratory frame, using a proportional counter biased to count differentially, with aluminium absorbing foils. This simple technique allowed a large solid angle to be used with adequate energy resolution. Bombarding energies of 1.14 MeV and 1.54 MeV were used and no indication was found in either case of a level at 0.7 MeV: the upper limit to the intensity of a proton group associated with such a level is less than 2% that of the ground state intensity for 1.14 MeV bombarding energies, and less than 0.5% for 1.54 MeV bombarding energies.

We should like to thank Professor S. Devons for suggesting the problem and for many helpful discussions, and Dr. P. E. Hodgson for assistance in searching the plates. One of us (G. M.) is indebted to the Department of Scientific and Industrial Research for financial assistance, and the other (B. S.) wishes to thank Patna University for study leave.

REFERENCES

- AJZENBERG, F., and LAURITSEN, T., 1952, *Rev. Mod. Phys.*, **24**, 321.
 CREAGAN, R. J., 1949, *Phys. Rev.*, **76**, 1769.
 HEYDENBERG, N. P., 1953, *Phys. Rev.*, **90**, 186.
 HORNYAK, W. F., LAURITSEN, T., MORRISON, P., and FOWLER, W. A., 1950, *Rev. Mod. Phys.* **22**, 291.
 PERKINS, J. L., 1950, *Phys. Rev.*, **79**, 175.

LETTERS TO THE EDITOR

Thermal Conductivity of Silver at Low Temperatures

The theories of Wilson (1937) and Makinson (1938) indicate that the thermal resistance R of a metallic element in which conduction is by electrons may be expressed as the sum of an impurity resistance R_0 and an 'ideal' resistance R_i . Scattering of the electrons by small scale lattice imperfections can be expressed by the term $R_0 = A/T$, and thermal vibration scattering by R_i , which for $T \ll \Theta$ is given by BT^n . Experiments previously reported on gold (White 1953) indicate that n lies between 2.0 and 2.1, in support of the theoretical value $n = 2$ suggested by Wilson and Makinson.

The thermal conductivity of silver in various states of physical purity has been determined at temperatures between 2 and 160°K with experimental methods similar to those used for gold. Silver of purity greater than 99.999% was supplied as a 2 mm diameter rod by Messrs. Johnson, Matthey, and measurements were made on the following specimens:

Ag1 JM4606, 2 mm diameter rod.

Ag2 JM4606, 2 mm diameter rod, annealed at 650°C, grain size ~ 0.1 mm.

Ag3 JM4606, 1.16 mm diameter rod, drawn from Ag2.

Ag4 JM4606, 1.16 mm diameter rod, annealed at 650°C.

Ag5 JM4606, Ag4 after being removed and replaced in cryostat.

The results (fig. 1) indicate the remarkable decrease in R_0 produced by annealing, the constant A falling from 8.4 to 0.03 cm deg² per watt. This is equivalent to reducing the residual electrical resistance by a factor of nearly 300. Whereas Ag1 shows no maximum in the thermal conductivity, measurements on Ag2, rendered difficult by very high conductivity and comparatively large diameter, indicate a maximum of almost 200 w cm⁻¹ deg⁻¹ at about 7°K. The effect of drawing to a smaller diameter has probably introduced additional chemical impurities into Ag3, Ag4 and Ag5, accounting for the reduction of the maximum in the annealed specimens to a little over 100 w cm⁻¹ deg⁻¹. The random experimental error in the majority of the results is estimated to be less than 1%, but the very high values of conductivity may be in error by as much as 3% owing to the difficulty of measuring the very small temperature gradients along the specimen.

As with gold, the specimens in the higher state of purity, i.e. with lower impurity resistance R_0 , have an ideal resistance $R_i = R - R_0$, appreciably smaller than for the less 'pure' specimens. Figure 2 indicates this clearly, showing that for temperatures below $\Theta/5 \simeq 40^\circ\text{K}$ the ideal resistance may be expressed by the relations

$$R_i = 2.86 \times 10^{-5} T^{2.3} \text{ for Ag1, Ag3 (unannealed).}$$

$$R_i = 1.06 \times 10^{-5} T^{2.5} \text{ for Ag2, Ag4, Ag5 (annealed).}$$

The Wilson-Makinson theory indicates that B is related to the Debye characteristic temperature Θ , the number of free electrons per atom N and the limiting value of the ideal thermal resistance R_∞ by the equation $B = CR_\infty N^{2/3}/\Theta^2$. Experimental evidence that, for silver, n differs from 2, makes it of little value to

calculate the constant C . If, however, a T^2 relation is fitted to the experimental data at 25°K , then substituting $\Theta = 220^\circ\text{K}$ (MacDonald 1952), $R_\infty = 0.220 \text{ cm deg } \Omega^{-1}$ and $N=1$, C is found to be approximately 12 for the annealed specimens and 16 for the unannealed specimens. These values are in agreement with those found for gold, but considerably lower than the value 95.3 of Wilson and Makinson and 71.7 predicted by Sondheimer (1950).

The results for silver and gold indicate that : (a) $R_0 T$ is sensibly constant for a particular specimen ; the small systematic variations occurring with some gold specimens may be related to the minimum in the residual electrical resistance. (b) Doubt is cast on the validity of the Wilson-Makinson prediction that B is a constant for an element and that $n=2$. Experiments indicate that a large

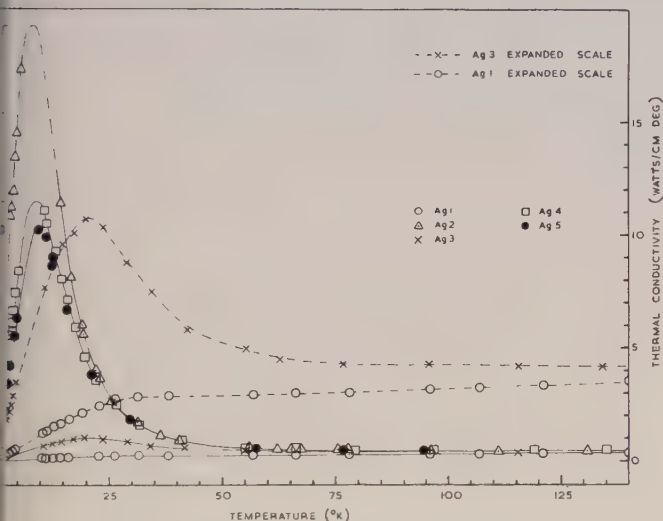


Fig. 1. Thermal conductivity of silver.

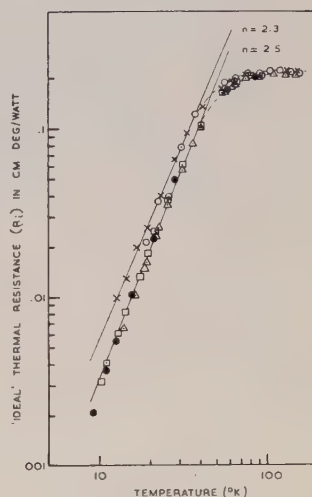


Fig. 2. 'Ideal' thermal resistance of silver.

increase in purity, i.e. in $A = R_0 T$, introduces a decrease of up to 30% in B . This may be interpreted as a departure from the additive resistance hypothesis in the direction of, but of greater magnitude than, that predicted by Sondheimer. In addition a value of n greater than 2 may be required to express the experimental results.

The author is grateful to Mr. W. R. G. Kemp and his assistants for supplying liquid helium and to Dr. P. G. Klemens for helpful discussion.

Division of Physics,
National Standards Laboratory,
Commonwealth Scientific and Industrial Research
Organization, Sydney, Australia.

G. K. WHITE.

18th May 1953.

- MACDONALD, D. K. C., 1952, *Progress in Metal Physics*, **3**, 42.
MAKINSON, R. E. B., 1938, *Proc. Camb. Phil. Soc.*, **34**, 474.
SONDHEIMER, E. H., 1950, *Proc. Roy. Soc. A*, **203**, 75.
WHITE, G. K., 1953, *Proc. Phys. Soc. A*, **66**, 559.
WILSON, A. H., 1937, *Proc. Camb. Phil. Soc.*, **33**, 371.

On the Geometry of Angular Correlation Experiments

Church and Kraushaar (1952) have recently indicated a fairly general method to correct angular correlation data for the finite angular resolution of the counters. They obtain the correction coefficients by numerical calculation from the experimentally determined angular resolution of the apparatus for annihilation radiation. The calculations are somewhat laborious; moreover, the counters will in general have different detection areas for annihilation quanta and the rays relevant in the actual experiment so that the procedure is not always applicable.

In this laboratory, we use the more satisfactory *direct* evaluation of the expected coincidence rates. In the important case of two circular detectors looking at a perfectly centred point source (for the practical realization of these two ideal conditions see the original study by Walter, Huber and Züti (1950), or the reviews by Frauenfelder (1952), and Deutsch (1951)) it leads to simple and rigorous formulae which we report here for the convenience of other workers.

If the correlation function is $W(\theta) = \sum a_n P_n(\cos \theta)$, the coincidence rate becomes

$$K(\delta) = A \sum a_n C_n(\alpha) C_n(\beta) P_n(\cos \delta), \quad \dots\dots (1)$$

where δ is the angle between the two vectors from the source to the counter centres, A is a constant containing detection efficiencies etc., and α, β are the angular radii of the first and second counters respectively. The correction factors C_n are given by

$$C_n(x) = \int_0^x P_n(\cos \theta) \sin \theta d\theta.$$

The P_n are employed in the usual normalization $P_n(1) = 1$. The proof of (1) is substantially that of Frankel (1951) and needs no comment.

Explicit expressions for the $C_n(x)$ in a form suitable for computation are:

$$C_0(x) = 2 \sin^2(x/2)$$

$$C_1(x) = C_0(x)(1 + \cos x)/2$$

$$C_2(x) = C_0(x)(1 + 2 \cos x + \cos 2x)/4$$

$$C_3(x) = C_0(x)(6 + 11 \cos x + 10 \cos 2x + 5 \cos 3x)/32$$

$$C_4(x) = C_0(x)(9 + 18 \cos x + 16 \cos 2x + 14 \cos 3x + 7 \cos 4x)/64$$

$$C_5(x) = C_0(x)(30 + 58 \cos x + 56 \cos 2x + 49 \cos 3x + 42 \cos 4x + 21 \cos 5x)/256$$

$$C_6(x) = C_0(x)(50 + 100 \cos x + 95 \cos 2x + 90 \cos 3x + 78 \cos 4x + 66 \cos 5x + 33 \cos 6x)/512$$

$$C_8(x) = C_0(x)(1225 + 2450 \cos x + 2380 \cos 2x + 2310 \cos 3x + 2156 \cos 4x + 2002 \cos 5x + 1716 \cos 6x + 1430 \cos 7x + 715 \cos 8x)/16384$$

The expressions for odd n have been included in the list because they are needed in experiments on correlations following a nuclear reaction; there the transformation from the centre-of-mass system to laboratory angles introduces odd terms in (1). In angular distribution experiments odd terms may also appear because of interference (in such an experiment only one C_n appears in (1), since there is

only one counter). The adaptation of these formulae to detectors whose sensitivity is not uniform over their faces, or to annular detectors, such as β -spectrometers, will be obvious.

Cavendish Laboratory,
Cambridge.
27th June 1953.

E. BREITENBERGER.

- CHURCH, E. L., and KRAUSHAAR, J. J., 1952, *Phys. Rev.*, **88**, 419.
 DEUTSCH, M., 1951, *Reports on Progress in Physics*, **14** (London : Physical Society), p. 196.
 FRANKEL, S., 1951, *Phys. Rev.*, **83**, 673.
 FRAUENFELDER, H., 1952, *Ann. Rev. Nucl. Sci.*, **2**, 129.
 WALTER, M., HUBER, O., and ZÜNTI, W., 1950, *Helv. Phys. Acta*, **23**, 697.

The Second Virial Coefficient near Absolute Zero

Under the above title Green (1952) has published in this journal an account of calculations of the second virial coefficient of gases obeying an intermolecular force law of the Lennard-Jones (1924) type with cut-off. It is claimed by him that "this is, so far as the author is aware, the first rigorous theoretical calculation of any physical quantity at liquid helium temperatures". Moreover, Green states that "Massey and Buckingham (1938), Gropper (1939), de Boer (1940) and Kahn (1938) later attempted to extend calculations (of the second virial coefficient) to lower temperatures, but their method also fails in the interesting region below 2°K ". I feel that the second statement is incorrect, and that thus Green's claim is not justified.

Green expands the second virial coefficient in terms of a quantity $\beta (=1/kT)$ and obtains a power series in inverse powers of β . The expression given by Green for the second virial coefficient B holds only up to a temperature slightly less than 1°K , but according to Green extended calculations could probably make the development useful up to the λ -point (2.2°K).

On the other hand, de Boer (1940, especially pp. 40-52, see also de Boer and Michels (1939), Massey and Buckingham (1938)) made numerical evaluations of the *exact* general quantum mechanical expressions for B given by Uhlenbeck and Beth (1936), Beth and Uhlenbeck (1937) and Kahn (1938) in the temperature range from the absolute zero up to 5°K . This method consists in expressing B in terms of the phase shifts η_l of the wave function at infinity. These phase shifts are calculated numerically for all values of l , but it turns out that only η_0 contributes to B up to about 0.7°K , while even at 5°K one only needs to take $l=0, 2, 4, 6$. At higher temperatures the calculations become rather too cumbersome. Instead of an expansion in terms of β , we have here an expansion in terms of l but it can be shown (de Boer 1940, p. 47) that this is also essentially an expansion in terms of $1/\beta$.

It seems thus to me that not only do the expressions of B given by Kahn, Massey and Buckingham, and de Boer hold near the absolute zero, but they also extend upwards to higher temperatures than can be reached by Green's method.

From correspondence with Professor Green, I have learned that his claim is based on the fact that earlier writers use the so-called phase-shift formula which, according to him, depends on the equation

$$\pi[N_l(k) - N_l^0(k)] = \eta_l^{(k)}, \quad \dots\dots(1)$$

where $N_l(k)$ and $N_l^0(k)$ are the number of energy levels corresponding to l with wave numbers less than k for the case with, and the case without, interaction. Equation (1) should then be an approximation, since the left-hand side is a discrete, and the right-hand side a continuous, function of k .

It seems to me that eqn. (1) is incorrect, since one is dealing with a continuous spectrum, so that one must apply instead of (1) the equation

$$\pi[\rho_l(k) - \rho_l^0(k)] = \partial \eta_l / \partial k, \quad \dots\dots(2)$$

where $\rho_l(k)$ and $\rho_l^0(k)$ are the level densities (see de Boer 1940, p. 45, ter Haar 1953).

The misunderstanding may be due to the fact that in order to take the continuity of the spectrum into account, one first assumes the pair of molecules to be present in a finite volume and then lets the volume go to infinity, thus coming back to the continuous spectrum and at the same time going over from the number of levels to the level density.*

In conclusion, I may add that Professor de Boer has given me permission to say that he entirely agrees with the remarks of this note. I should also like to thank Professor R. E. Peierls for a discussion on the subject of this letter.

Department of Natural Philosophy,
The University, St. Andrews.
18th June 1953.

D. TER HAAR.

BETH, E., and UHLENBECK, G. E., 1937, *Physica*, **4**, 915.

DE BOER, J., 1940, *Thesis*, University of Amsterdam.

DE BOER, J., and MICHELS, A., 1939, *Physica*, **5**, 409.

GREEN, H. S., 1952, *Proc. Phys. Soc. A*, **65**, 1022.

GROPPER, L., 1939, *Phys. Rev.*, **55**, 1095.

TER HAAR, D., 1953, *Elements of Statistical Mechanics* (New York: Rinehart), in the press, § VIII. 6, especially equation (8.629).

KAHN, B., 1938, *Thesis*, University of Utrecht.

LENNARD-JONES, J. E., 1924, *Proc. Roy. Soc. A*, **106**, 463.

MASSEY, H. S. W., and BUCKINGHAM, R. A., 1938, *Proc. Roy. Soc. A*, **168**, 378.

UHLENBECK, G. E., and BETH, E., 1936, *Physica*, **3**, 729.

* One might ask whether one should not take into account the fact that the system is enclosed in a finite volume. Apart from the fact that this would only affect the results at temperatures of the order of $\hbar^2/mV^{2/3}k$, that is, about 10^{-11}°K , the difficulty arises that the wave function of a pair of molecules can no longer, without enormous complications, be split into two factors, one pertaining to the movement of the centre of gravity, the other pertaining to the relative motion. Moreover, from the expression at the top of p. 1026 of Green's paper, and from other similar expressions, it appears that Green himself is also making the usual assumption of an infinite volume, that is, using a boundary condition at infinity.

Observation of the 4050 Å Band Group in a King Furnace

Much interest currently attaches to the production and origin of a group of bands around 4050 Å, which occur in emission in cometary spectra. Bands appearing to be identical with the comet features have been produced in the laboratory by Herzberg (1942) and other workers. Study of rotational structure and isotope effects in the strongest band, at 4049 Å, led Douglas (1951) to the conclusion that the emitter was possibly the linear triatomic C_3 . In a recent paper Rosen and Swings (1953) review existing knowledge, and discuss the

sources and conditions in which the bands have been observed, for instance, discharges, flames, photolysis. It therefore seems worth reporting observation of the stronger bands of the group, during initial trials of a new King-type vacuum furnace recently erected in this laboratory.

In these trials, graphite tubes of 13 in. length, $\frac{1}{2}$ in. bore, $\frac{1}{8}$ in. wall, have been heated by passage of currents of up to 1100 A, to temperatures above 2800°C; this limit has been set by rapid volatilization of the graphite. Initial heating of a new graphite tube is accompanied by the appearance of a number of emission lines, but a short run at high temperature suffices to drive off the responsible impurities. The only emission features then remaining, with the tube above 2500°C, are the Swan system of C₂, which appears very strongly, and the five strongest bands listed in table 1 of the paper by Rosen and Swings. In spite of the fact that the photographs so far obtained suffer from a good deal of background continuum coming from the wall of the furnace-tube, much of the rotational structure of the 4050 Å group is plainly visible. For the first exposures, the furnace-chamber was pumped continuously, the pressure of residual gas being below 0.05 mm Hg. Repetition, with a slow current of hydrogen at 5 mm pressure passing through the furnace, did not appear to affect sensibly the intensities of either Swan or 4050 Å bands.

Another relevant detail is that when, after prolonged running, a furnace-tube fails, the spectrum of the resulting arc shows no sign of CH. Bands of the latter radical are notoriously easy to excite, and these details suggest that, in distinction to what has previously appeared the case, the 4050 Å bands can occur in the absence of appreciable hydrogen.

Rosen and Swings have emphasized that appearance of the bands seems to be connected with the process of formation of solid carbon particles. It is very probable that this is the case also when the bands are generated in the furnace. The reason for this statement is that if the temperature of the graphite tube is raised above about 2650°C, then, accompanying rapid volatilization, a sort of 'horizontal rain' of incandescent particles is observed to proceed from the interior of the tube and impinge on the end windows. The fine dust which thus accumulates appears to be carbon.

Department of Astrophysics,
Imperial College, London.
16th July 1953.

W. R. S. GARTON.

DOUGLAS, A. E., 1951, *Astrophys. J.*, **114**, 466.

HERZBERG, G., 1942, *Astrophys. J.*, **96**, 314.

ROSEN, B., and SWINGS, P., 1953, *Ann. d'Astrophys.*, **16**, 82.

Galvano-Magnetic Effects at High Frequencies

Although the magneto-resistance effect in metals has been investigated thoroughly in the case of direct currents, comparatively few measurements have been made at high frequencies. For bismuth Blunt (1948) found no appreciable departure from the d.c. value for frequencies up to 3.5 Mc/s. Measurements of the reflectivity of bismuth in the visible and infra-red regions (Heaps 1926, McLennan *et al.* 1932, Englert and Schuster 1932) have led to the conclusion

that the change in resistivity is zero for wavelengths less than about 8μ . More recently Heaps (1950) has obtained results with a bismuth cavity which indicate that at 3000 Mc/s the magneto-resistance change is of the order of half the d.c. value.

As a first step towards a theoretical interpretation of these results we have investigated the effect for the free-electron model, taking into account relaxation effects but excluding 'anomalous' effects (Reuter and Sondheimer 1948) and terms involving the displacement current. We consider a semi-infinite metal, with the h.f. electric field $(\mathcal{E}_x(z), \mathcal{E}_y(z), 0)e^{i\omega t}$ parallel to the surface and a constant magnetic field H perpendicular to the surface. The current density $(J_x(z), J_y(z), 0)$ is calculated in the usual way (cf. Sondheimer and Wilson 1947), except that the Boltzmann equation includes a term containing the angular frequency ω (cf. Reuter and Sondheimer 1948). Combination with Maxwell's equations leads to a pair of simultaneous differential equations which may be solved for $\mathcal{E}_x(z)$ and $\mathcal{E}_y(z)$. The quantity of interest is the surface impedance defined by

$$Z = \mathcal{E}_x(0) / \int_0^\infty J_x(z) dz, \quad \text{with} \quad \int_0^\infty J_y(z) dz = 0,$$

and a straightforward calculation gives

$$Z(H) = \frac{(1+i)}{\sqrt{2}} \left(\frac{2\pi\omega}{c^2\sigma_0} \right)^{1/2} (1+i\omega\tau)^{1/2} \left[1 + \left\{ 1 + \left(\frac{\alpha\tau}{1+i\omega\tau} \right)^2 \right\}^{1/2} \right]^{1/2}, \quad \dots\dots(1)$$

where $\alpha = eH/mc$, σ_0 is the d.c. conductivity and τ is the time of relaxation of the conduction electrons.

The real part of (1) gives the surface resistance $R(H)$ which is proportional to the absorption coefficient, and the relative change in resistance is given by $\Delta R/R(0)$, where $\Delta R = R(H) - R(0)$. It is of interest that the free-electron model leads to a non-zero change in R at high frequencies, in view of its prediction of a zero d.c. magneto-resistance effect.

For low frequencies ($\omega\tau \ll 1$) (1) reduces to

$$Z(H) = \frac{(1+i)}{\sqrt{2}} \left(\frac{2\pi\omega}{c^2\sigma_0} \right)^{1/2} [1 + \{1 + (\alpha\tau)^2\}^{1/2}]^{1/2}, \quad \dots\dots(2)$$

and $\Delta R/R(0)$ tends to a *constant* value as $\omega \rightarrow 0$. (This appears to be inconsistent with the zero d.c. magneto-resistance change obtained for free electrons, but it must be remembered that our result is valid only if the penetration depth is small compared with the dimensions of the specimen. For the same reason the expression for $Z(0)$ must itself break down in the limit $\omega \rightarrow 0$; it predicts that $Z \propto \omega^{1/2}$ whereas for a specimen of finite dimensions Z is non-zero at $\omega = 0$.)

For high frequencies ($\omega\tau \gg 1$) the behaviour of (1) is determined by $(\alpha/\omega)^2$, and $\Delta R/R(0)$ will be negligibly small when $\omega \gg \alpha$. Since, for the highest magnetic fields obtainable, $\alpha \sim 5 \times 10^{12}$ it is clear that no magneto-resistance effect is to be expected at optical frequencies. Detailed calculations show that $\Delta R/R(0)$ drops rapidly to zero in the frequency range $\omega\tau \sim \frac{1}{2}$ to $\omega\tau \sim 4$. For sodium $\tau \sim 3 \times 10^{-14}$ sec, and the region of rapidly diminishing magneto-resistance occurs in the far infra-red, roughly between 100μ and 10μ . The experimental results of Heaps (1950) suggest that these orders of magnitude may be entirely different for bismuth. Although the above simple model would not be expected to apply to bismuth, we may infer tentatively that the relaxation time in bismuth is abnormally long (cf. Sondheimer 1952).

Finally, to describe the Hall effect at high frequencies we may introduce the 'surface Hall constant' defined by

$$Y = \mathcal{E}_y(0) / \left(H \int_0^\infty J_x(z) dz \right).$$

Corresponding to (1) we find that

$$Y(H) = - \frac{(1+i)}{H \sqrt{2}} \left(\frac{2\pi\omega}{c^2\sigma_0} \right)^{1/2} (1+i\omega\tau)^{1/2} \left[-1 + \left\{ 1 + \left(\frac{\alpha\tau}{1+i\omega\tau} \right)^2 \right\}^{1/2} \right]^{1/2} \dots (3)$$

In general Y , like Z , is a complex quantity, so that there is a phase difference between the Hall field and the current. Y is independent of H only in weak fields; in this region Y varies as $\omega^{1/2}$ at low frequencies and rises to a constant value when $\omega\tau \gg 1$. In strong fields Y tends to zero as $H^{-1/2}$ for a given frequency and varies as $\omega^{1/2}$ for a given field.

A full account of the calculations, including a discussion of the behaviour of the two-band model and the consequences for the properties of bismuth, will be published shortly by one of us (B.D.).

Department of Physics,
Northern Polytechnic, London.

B. DONOVAN.

Department of Mathematics,
Imperial College, London.

E. H. SONDHEIMER.

20th July 1953.

BLUNT, R. F., 1948, *Phys. Rev.*, **73**, 654.

ENGLERT, E., and SCHUSTER, K., 1932, *Z. Phys.*, **79**, 194.

HEAPS, C. W., 1926, *Phys. Rev.*, **27**, 764; 1950, *Ibid.*, **80**, 892.

MCLENNAN, J. C., ALLIN, E. J., and BURTON, A. C., 1932, *Phil. Mag.*, **14**, 508.

REUTER, G. E. H., and SONDHEIMER, E. H., 1948, *Proc. Roy. Soc. A*, **195**, 336.

SONDHEIMER, E. H., 1952, *Proc. Phys. Soc. A*, **65**, 561.

SONDHEIMER, E. H., and WILSON, A. H., 1947, *Proc. Roy. Soc. A*, **190**, 435.

REVIEWS OF BOOKS

Electronic and Ionic Impact Phenomena, by H. S. W. MASSEY and E. H. S. BURHOP.
Pp. xviii + 699. (Oxford: Clarendon Press, 1952.) 70s.

The subject matter of this book lies at the root of our understanding of electrical phenomena in gases. The varied aspects of ionization and electrical discharges are only explicable in terms of the dynamical theory of the motions of electrons and ions in gases, and the study of discharge phenomena has been, and is, an important means of investigating elementary electronic and ionic collisional processes. In turn, knowledge thus gained has been of the greatest importance in the elucidation of problems of the extra-nuclear structure of the atom: this is particularly the case in regard to spectroscopy. Consequently, a modern book which gives a comprehensive account of most aspects of impact phenomena for particles of comparatively low energies is bound to be welcome. It can be said at once that *Electronic and Ionic Impact Phenomena* by Professor H. S. W. Massey and Dr. E. H. S. Burhop has succeeded most excellently in doing this, and this work is likely to be the standard reference book on the subject for some time to come.

The mathematical methods and the general theory of collisions has been treated previously in *The Theory of Atomic Collisions* by Mott and Massey (a second edition of which, with cross references to the present book, has appeared), and the present book deals with the subject more from the experimental side, but wherever possible the experimental data are discussed and interpreted in terms of the modern theory of collisions. It is not possible within the confines of a brief review to deal in detail with such a comprehensive volume of nearly 700 pages, but the scope of the treatment can be seen from the chapter headings: The passage of electrons through gases, cross section; The experimental analysis of the cross section of the impact of electrons with atoms; Electron collisions with atoms—theoretical description (this is a particularly helpful and useful chapter for the experimental physicist); Collisions of electrons with molecules; Reflection and secondary emission from surfaces due to electron bombardment; Electron collisions involving emission of radiation; Collisions under gas kinetic conditions; The passage of homogeneous electrons through gases; The collision of positive and neutral atoms with surfaces; Recombination. The preparation of a work of this magnitude, involving as it does a highly detailed survey of a vast number of published papers, must have required considerable time, but by the inclusion of a short appendix with notes the authors have been able to include the most recent work on the decay of electron density and on the nature of the various ions in discharges.

The relevant experiments are considered in some detail, and the actual results of the various authors are given rather than their conclusions. This procedure is an admirable feature of the book, greatly enhancing its value for reference purposes. For example, in discussing the question of ionization of gas atoms in collisions with positive ions, the enormous amount of published experimental work on this particular aspect is reviewed in some detail in Chapter 8, where all the elementary data on cross sections for ionization are given. Such an analysis would perhaps be even more valuable to the reader if set against the background of a critical assessment of the various experimental techniques employed, as there is considerable variation in the published values of the cross sections found by different observers; this is all the more important today in view of the work of Horton and Millest in 1946. While on the subject of positive ions, it may perhaps be worth pointing out that in the account on page 547 of the calculation of the secondary emission coefficient γ for various metals from the Townsend expression for the growth of an ionization current, or from the resulting breakdown criterion, it should have been noted that the procedure is only valid provided that some test does show that the electron emission was actually due only to impact of positive ions; this is necessary because a precisely similar expression for the growth of ionization current (and therefore for the static breakdown criterion) is obtained if the emission were due to the incidence of photons, but a knowledge of the shape of the $(\gamma, X/p)$ curve is usually sufficient to establish which of the processes in fact predominated.

Considering the comprehensiveness of the work, the number of misprints in this book is extraordinarily small, but it is perhaps worth pointing out one because this is not immediately obvious from the text. In Appendix 1 on page 649 the sentence saying that Biondi measured the recombination coefficient of electrons containing 1% of argon states that he found the coefficient to be less than 10^{-3} of that observed in pure helium; this should read *pure argon*.

The indexes and references are, however, insufficiently detailed for so valuable a book. The authors deserve every congratulation for undertaking the preparation of an up-to-date account of work in this field and for succeeding so admirably in producing a book which is indispensable to those interested in fundamental collisional processes of electrical phenomena in gases. The general production of the book by the Oxford University Press is excellent.

F. LLEWELLYN JONES.

Advanced Mathematics in Physics and Engineering, by A. BRONWELL.
Pp. xvi+475. (London: McGraw-Hill, 1953.) 51s.

There is at present no lack of books on mathematics written specifically for engineers and physicists. Professor Bronwell, writing in language familiar to the engineer, gains much by avoiding the more ambitious and formal nature of many of these, and his book is, on balance, a worthwhile addition. The author does claim "a moderate balance of mathematical rigour", but this seems to rest mainly on a liberal use of such terms as "continuous", "differentiable", "regular", and "assuming it exists". Since these are not particularly well defined in the text, if at all, it is unlikely that the average reader will take much notice of them.

Choice of material is interesting and varied and the presentation is very clear apart from a certain looseness of language (e.g. "we can put $\partial/\partial z = 0$ "). Layout and typography are excellent and only a few minor misprints were noted. Many problems are worked out in the text and a set of examples, with answers, is provided after each chapter. The main topics discussed are infinite series, Fourier series and integrals, solution of differential equations including Bessel's equation and Legendre's equation, vector analysis, functions of a complex variable, Laplace transforms, vibrations, hydrodynamics, heat flow, electromagnetic theory and roots of polynomials and stability criteria.

The work on convergence of series leaves much to be desired. Little is given in the way of proofs and, in the course of the proof that absolute convergence implies convergence, the author implicitly assumes what he is supposed to be proving. Other weaknesses are the statement of Taylor's theorem given, and the suggestion that convergence of series of complex terms should be examined by separation into real and imaginary parts. In fact nowhere in the book is the convergence of complex series treated on its own merits and nothing is said about even the simplest of tests for convergence of integrals although the need for such convergence is frequently mentioned later on. The various cases that arise in the series solution of differential equations are very clearly explained and the account of Bessel functions is particularly good. Legendre functions, however, receive much less attention and only one recurrence relation is given.

The chapter on vector analysis is, in general, quite adequate. The cartesian components of the curl of a vector are defined by means of a certain line integral, but the question as to whether the quantity so defined is in fact a vector (i.e. that the components retain their form on change of axes) is not raised. The section on Gauss' theorem is not very convincing. In the next chapter, equation (4) is certainly not Schrödinger's equation, as stated.

The chapters on hydrodynamics, heat flow and electromagnetic theory constitute attractive introductions to these subjects, but time differentiation following the motion, which students usually find difficult, is dismissed too lightly and there is a mistake on p. 283 where it is stated that, in steady irrotational flow, the constant in Bernoulli's equation varies from one streamline to another. The section on functions of a complex variable is clearly presented. It consists mainly of the theory of residues, contour integration and simple conformal transformations. This chapter ends with the Schwarz-Christoffel transformation, proved for a closed polygon. In the example given on a semi-infinite strip the reader is left to wonder what happens to the vertex at infinity.

The final chapter contains an elementary account of Laplace transforms and the Mellin inversion integral. An example of the latter involving a branch point would not have been out of place.

A. N. GORDON.

Thermal Diffusion in Gases, by K. E. GREW and T. L. IBBS. Pp. xi+143. (Cambridge: University Press, 1952.) 22s. 6d.

Thermal diffusion has become well known, largely as a result of the application made of it by Clusius and Dickel to the separation, or partial separation, of isotopes in the years just before the war. Readers of Chapman and Cowling's book on the theory of gases will know that it has the additional interest of being the manifestation of a rather obscure term in the higher approximations of gas theory.

This Cambridge Monograph treats the matter from both points of view, beginning with an historical outline which shows that, in gases, the theory preceded observation of the effect, although this had been noted experimentally in liquids before the theory for gases was developed. The treatment is naturally not as deep as that of Chapman, but it is enough to give the general physicist an understanding of the theory. There is a chapter on the effect in liquids, and on the converse effect, first observed by Dufour in 1873.

J. H. A.

Colloque sur la Sensibilité des Crystaux et des Émulsions Photographiques, Paris, 1951, Mémoires et Discussions. Pp. xii+380. (Paris: Éditions de la Revue d'Optique théorique et instrumentale, 1953.)

In September 1951, the fourth of the recent series of photographic conferences was held in Paris, following meetings in preceding years at Liège, Zurich and Bristol. These conferences, with their pleasantly informal atmosphere, attracted large numbers of research workers from the photographic industry and the universities all over the world, mainly from amongst those who are interested in the fundamental problems of photographic sensitivity, and in the properties of nuclear research emulsions.

The present volume contains all the papers submitted to the conference, and much of the discussions which followed the presentation of the papers. The number of communications was large, sixty-eight, and the range of subjects covered extended from crystal physics via the properties of the latent image and the mechanism of development to the photographic aspects of work with nuclear research emulsions—a wide range indeed, giving a good indication of the state of non-secret research into these subjects at the time of the conference.

All the papers are printed in French, original or translation as the case may be, and whether or not this is a good thing is very much a matter of personal taste. Whatever one's opinion, however, the question of language is not such an important one here, for this is not a book for the private bookshelf: it is a collection of papers which should find its place in the reference libraries both because of the intrinsic value of the matter it contains, and as a record of the state of fundamental photographic research in 1951.

A. J. HERZ.

Calculus of Variations with Applications to Physics and Engineering, by ROBERT WEINSTOCK. Pp. x + 326. (London: McGraw-Hill, 1952.) 55s. 6d.

Many of the laws of mathematical physics can be set up in two alternative ways; a law may be formulated either as a partial differential equation or as the necessity for a definite integral to have its extreme value. The first approach is the more common one, so much so that it has often been said that the aim of physics is to express all its laws in this form. The second method is less easy to understand but has the advantage of including the boundary conditions directly. Also, where a solution in terms of known functions is impossible, it leads to approximate methods which are often useful and are particularly appropriate for use with high-speed computing machines.

This book deals with both the mathematical theory of the calculus of variations and its application to a selection of problems in physics. These include examples on the dynamics of particles, electrostatics and geometric optics, but the main emphasis is on eigenvalue problems for which the associated differential equation is of the Sturm-Liouville type. The general treatment is clear and the amount of prior mathematical knowledge required by the reader is reasonably limited. A set of examples at the end of each chapter, with hints on their solution, fill in the details of proofs which are curtailed in the text and apply the results to further problems.

The physics student might be slightly misled at a few places. Thus the author gives the impression that Schrödinger originally formulated his equation independently of de Broglie's work. Also in the application of the Ritz method to the helium atom no physical explanation is given for the device of treating the nuclear charge as an adjustable parameter. These minor criticisms will not reduce the value of the book, especially to students of theoretical physics.

J. C. B.

Température et équilibre thermique dans une flamme de diffusion, by PIERRE BARRET. Pp. iii + 114. (Paris: Publications Scientifiques et Techniques du Ministère de l'Air (No. 273), 1952.) 1200 fr.

Contribution à la théorie des ondes liquides de gravité en profondeur variable, by MAURICE ROSEAU. Pp. ii + 89. (Paris: Publications Scientifiques et Techniques du Ministère de l'Air (No. 275), 1952.) 1300 fr.

CONTENTS OF SECTION B

Dr. D. F. DENNY. The Influence of Load and Surface Roughness on the Friction of Rubber-Like Materials	721
Dr. R. F. KING and Dr. D. TABOR. The Effect of Temperature on the Mechanical Properties and the Friction of Plastics	728
Dr. K. LANDECKER and Mr. B. J. ROBINSON. Study of High-Frequency Fluctuations from Light Sources using Phototubes and Tuned Radio-Frequency Amplifiers	737
Dr. T. S. MOSS, Dr. L. PINCHERLE and Mrs. A. M. WOODWARD. Photoelectromagnetic and Photodiffusion Effects in Germanium	743
Prof. K. ALEXOPOULOS and Dr. A. THEODOSSIOU. On the Nature of Ferromagnetism in Pyrrhotite.	753
Dr. D. E. CARO and Prof. L. H. MARTIN. The Velocity of Sound in Air at Low Pressures	760
Mr. D. E. WESTON and Mr. I. D. CAMPBELL. Experiments on the Propagation of Plane Sound Waves in Tubes—I: The Adiabatic Region, by D. E. WESTON. II: The Transition Region, by D. E. WESTON and I. D. CAMPBELL	769
Dr. J. C. BURFOOT. Correlation of Electrostatic Lenses by Departure from Rotational Symmetry	775
Dr. A. K. HEAD. Edge Dislocations in Inhomogeneous Media	793
Research Notes :	
Mr. J. S. BELL. Vertical Focusing in the Microtron	802
Mr. A. W. SIMPSON and Mr. R. H. TREDGOLD. Magnetic Viscosity in Platinum Cobalt	805
Letters to the Editor :	
Mr. T. F. JOHNS. Vapour Pressure Ratio of $^{12}\text{C}^{16}\text{O}$ and $^{13}\text{C}^{16}\text{O}$	808
Reviews of Books	810
Corrigendum	815
Contents of Section A	816



Fig. 1. 180° boundaries in zero field.



Fig. 2 (a). Daggertags on both sides of grain boundary in zero field.

0.1 mm
|—|



Fig. 2 (b). $H=15$ Oe.

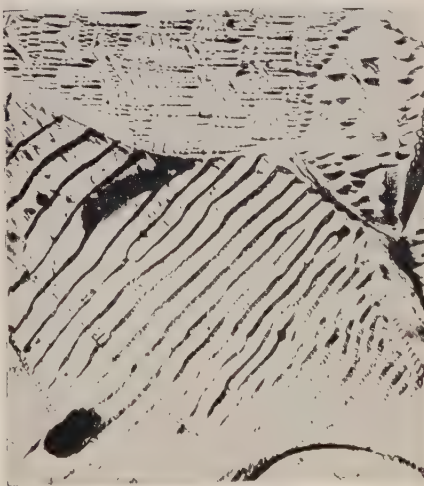


Fig. 2 (c). $H=58$ Oe.

Patterns on polycrystalline disc.



Fig. 3. Type (c) patterns at edge of crystal.

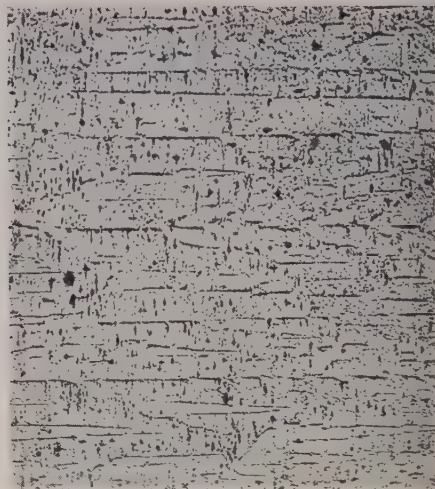


Fig. 4 (a). Zero field pattern.

0.1 mm
—

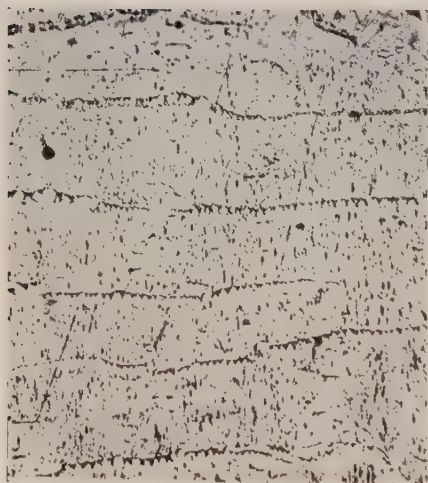


Fig. 4 (b). $H=190$ Oe.

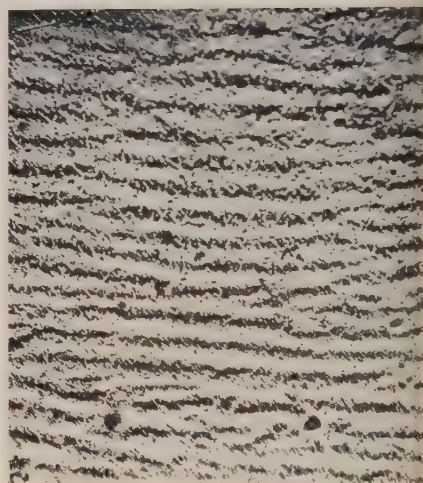


Fig. 4 (c). $H=310$ Oe.

Patterns on single crystal disc; applied field along [110].



Fig. 5. $H=180$ Oe. Type (b) patterns.

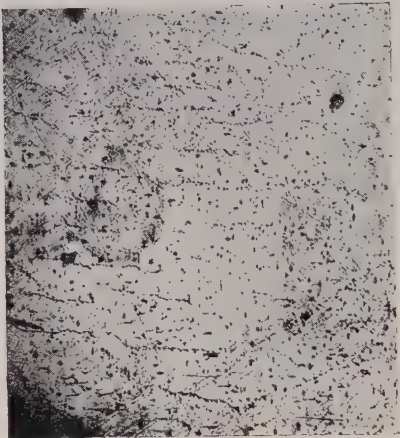


Fig. 6 (a). $H=110$ Oe.

0.1 mm
|—|

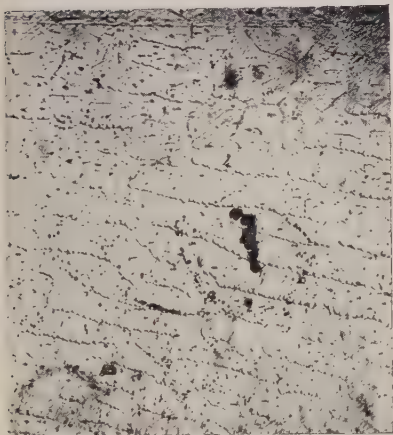


Fig. 6 (b). $H=140$ Oe.

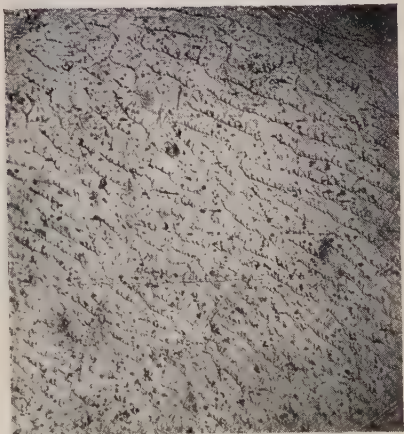


Fig. 6 (c). $H=260$ Oe.

↑
 H

Patterns near centre of thin single crystal; applied field along $[110]$.



Fig. 7 (a). $H=110$ Oe.

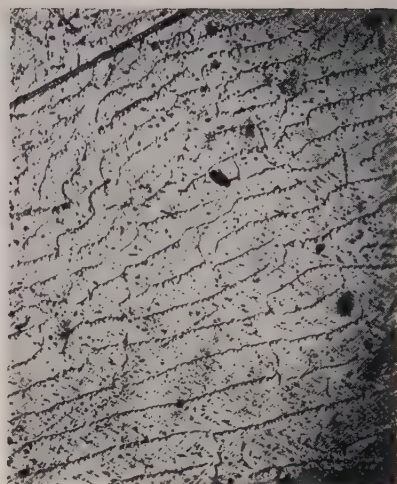


Fig. 7 (b). $H=140$ Oe.

0.1 mm
|—|



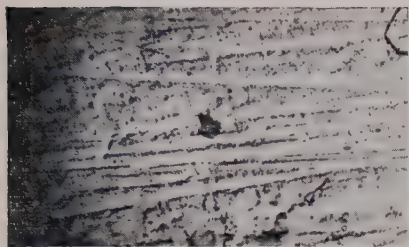
Fig. 7 (c) $H=140$ Oe.



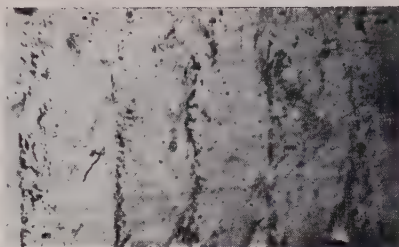
Fig. 7 (d). $H=250$ Oe.

↑
 H

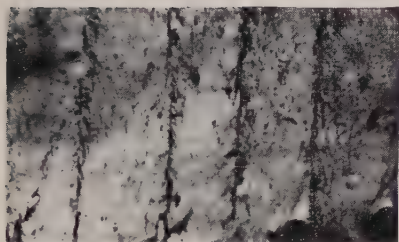
Field strengths measured at centre of disc. Patterns at edges of thin single crystal; applied field along $[110]$.



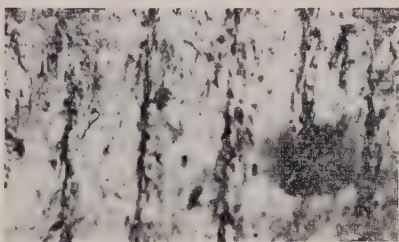
(a) Maze pattern.



(b) 43 Oe.



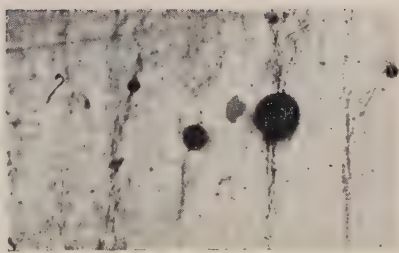
(c) 55 Oe.



(d) 55 Oe.



(e) 131.5 Oe.

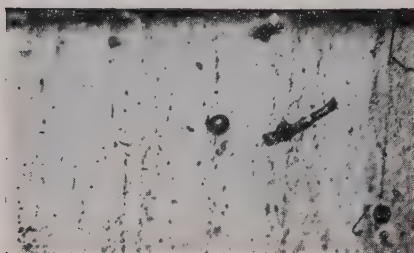


(f) 161.6 Oe.

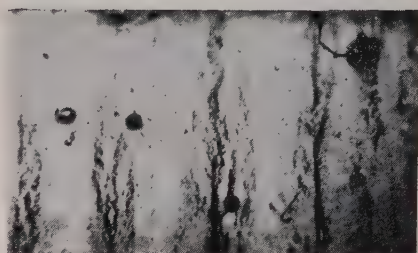
PLATE I.

Bitter figures obtained on crystal surface 5° away from the (110) plane.

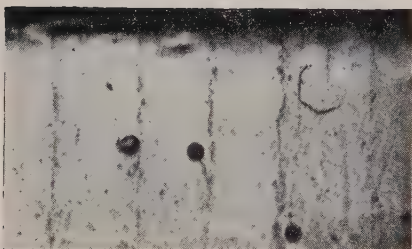
Magnification $\times 43.5$. $H \rightarrow [100]$.



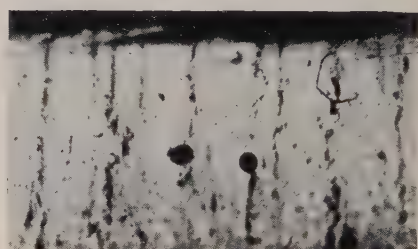
(a) 44 Oe.



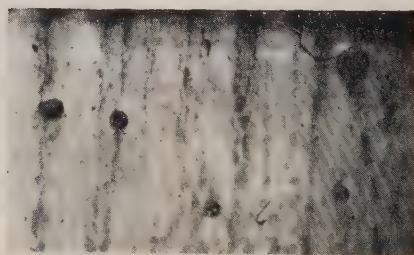
(b) 56 Oe.



(c) 82 Oe.



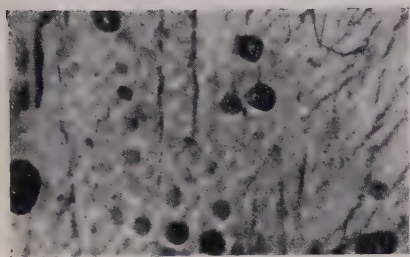
(d) 94.5 Oe.



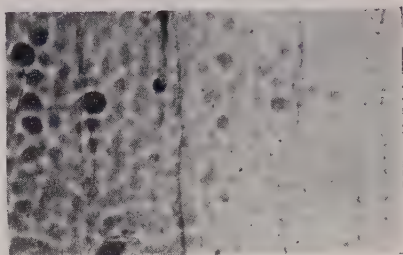
(e) 107 Oe.

PLATE II.

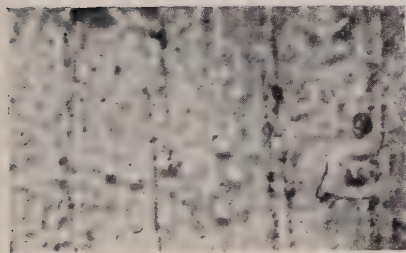
Crystal surface within 1° of the (110) plane. Magnification $\times 43.5$. $H \rightarrow [100]$.



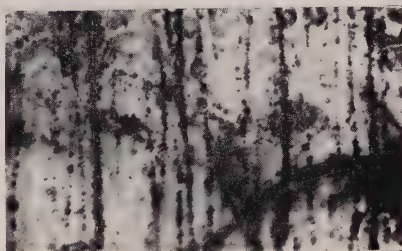
(a) Small field. Change of mode.



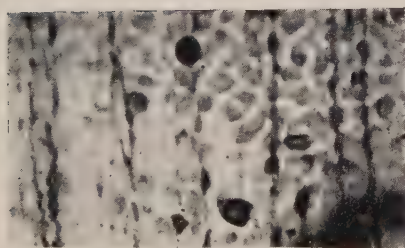
(b) 24 Oe.



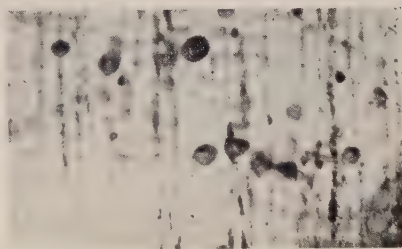
(c) 32 Oe.



(d) 56 Oe.



(e) 82 Oe.



(f) 107 Oe.

PLATE III.

Bitter figures observed on the side of the crystal shown on plates I and II. (110) plane.
Magnification $\times 43.5$. $H \rightarrow [100]$.

On Perturbation and Variation Methods

By R. E. B. MAKINSON AND J. S. TURNER

School of Physics, University of Sydney, Sydney, Australia

Communicated by H. S. W. Massey; MS. received 13th March 1953, and in final form 11th June 1953

Abstract. It is pointed out that the notation of the theory of functionals and the theorem in it analogous to Taylor's theorem facilitates a compact discussion of perturbation and variation methods in quantum mechanics, both for bound state and scattering problems.

With this aid it is shown (i) how stationary expressions required for variation methods may be sought and found, (ii) that the perturbation and variation methods are virtually identical, (iii) that second order perturbations and expressions stationary to the second order may be found similarly, though these are complicated. The form found for the second order perturbation of bound states differs from that commonly used in that it does not explicitly involve the eigenfunctions of states other than that perturbed.

§ 1. INTRODUCTION

IT would seem that the theory of functionals (Volterra 1930) is not well known among physicists, although the notions of a functional and a functional derivative find some place in current literature. It is felt by the authors that those notions and a few of the theorems from that theory greatly clarify the derivation and presentation of well-known results in the perturbation and variation methods of dealing with wave equations, and facilitate their extension as is shown in §§ 3–6.

Discussions similar to that following may be given of any physical problem in which we are interested in eigenvalues which depend on a given function (as functionals of it) or, for example, in diffraction problems where the field at a distance depends on the function specifying the shape of the diffracting body. The transmission coefficient of a potential barrier as a functional of the function defining the barrier may be discussed similarly (cf. di Francia 1950 a, b).

In Appendix I a brief summary is given of the notation and some results required in the present discussion.

§ 2. FUNCTIONAL EXPANSIONS FOR ASYMPTOTIC PHASES

Consider the differential equation

$$LG \equiv \{L_0 + \phi(r)\}G \equiv G'' + \{k^2 - l(l+1)/r^2 + \phi(r)\}G = 0 \dots\dots (2.1)$$

which arises when an electron is in the field of a centre of short-range force with potential function given by $-2m\phi(r)/\hbar^2$, $l=0, 1, 2, \dots$

(a) If $k^2 > 0$ the problem is one of scattering (Mott and Massey 1949, p. 19), and we have to find the value of η_l in the asymptotic form for large r of the solution G which vanishes at $r=0$. Various normalizations of G are possible:

$$G \sim \text{const.} \sin(kr + \eta_l) \dots\dots (2.2)$$

$$G \sim \sin kr + \tan \eta_l \cos kr \dots\dots (2.3)$$

$$G \sim \cot \eta_l \sin kr + \cos kr \dots\dots (2.4)$$

We will adopt (2.3) in the following and regard $\tan \eta_l$ as a functional of $\phi(r)$, depending as a function also on the parameters k, l , and write it as $\tan \eta_l[\phi(x); k]$. (If (2.4) had been adopted the most convenient functional to consider would have been $\cot \eta_l$, and if (2.2), η_l .)

(b) If $k^2 \equiv -K^2 < 0$ the electron is bound and the problem of interest is to find the values K_n^2 of K^2 (which then give the binding energy $E_n = \hbar^2 K_n^2 / 2m$) for which solutions G_n are zero at the origin and at infinity. We write K_n^2 as the functional $K_n^2[\phi(x); l]$. We may put this problem in a form similar to that of (a) by noting that for large r

$$G \sim \text{const. } e^{-Kr} = \sinh Kr + \tanh \xi \cosh Kr \quad \dots\dots (2.5)$$

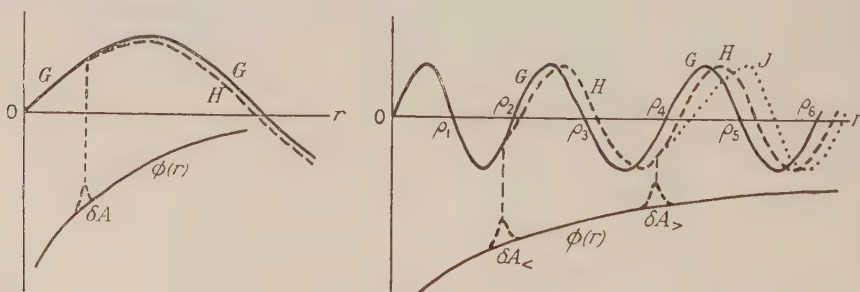
with suitable normalization, and we have to determine the values of K^2 for which $\tanh \xi = -1$, i.e. an imaginary phase angle has to be infinite. We write $\tanh \xi$ as $\tanh \xi[\phi(r); l]$.

In both cases we shall be interested in the changes of the functionals when the function $\phi(r)$ is varied by, say, $\delta\phi(r)$, and we may, using the analogue of Taylor's theorem (Appendix I, eqn. (A 1)), put

$$\begin{aligned} \tan \eta_l[\phi(r) + \delta\phi(r); k] &= \tan \eta_l[\phi(r); k] \\ &+ \int_0^\infty \tan \eta_l'[\phi(r); r_1; k] \delta\phi(r_1) dr_1 \\ &+ \frac{1}{2!} \int_0^\infty \int_0^\infty \tan \eta_l''[\phi(r); r_1, r_2; k] \delta\phi(r_1) \delta\phi(r_2) dr_1 dr_2 \\ &+ \dots\dots \end{aligned} \quad \dots\dots (2.6)$$

The expansion for $\tanh \xi[\phi(r); l]$ is formally the same. In less simple scattering and bound state problems $\tan \eta$ and $\tanh \xi$ are functionals of more than one function, each of the latter depending on more than one variable, but we would proceed on similar lines.

It is necessary next to find expressions for the functional derivatives of $\tan \eta_l$ which appear in (2.6).



Illustrating the calculation of the first and second functional derivatives of $\tan \eta [\phi(r)]$.

§ 3. SCATTERING PERTURBATION OF POTENTIAL

The first functional derivative, $\tan \eta_l'[\phi(r); r_1, k]$, is given by $\delta \tan \eta_l / \delta A$, where $\delta \tan \eta_l$ is the small change in $\tan \eta_l$ resulting from a small bump in $\phi(r)$, localized at $r = r_1$, of area $\delta A = \int \delta\phi(r) dr$ (see figure). If the solution $G + \delta G$

of (2.1) is being integrated out from its zero value at $r=0$, it follows the unperturbed form G until it suffers at r_1 a change in gradient

$$-G(r_1) \int_{r-\Delta}^{r+\Delta} \delta\phi(r) dr$$

to the first order, i.e. $-G(r_1)\delta A$, its magnitude being unchanged to the same order. Supposing the integration is continued from r_1 outwards, $G+\delta G$ will follow some solution $H(r)$ of (2.1) which is linearly independent of G and whose asymptotic form (cf. (2.3)) is

$$H(r) \sim (1 + \alpha\delta A + \dots)(\sin kr + \text{const.} \cos kr). \quad \dots\dots(3.1)$$

Thus
$$G(r_1) = H(r_1), \quad G'(r_1) - \delta AG(r_1) = H'(r_1). \quad \dots\dots(3.2)$$

The Wronskian of these two solutions is independent of r ; thus, equating its values at r_1 and at large r , we have

$$G(r_1)H'(r_1) - H(r_1)G'(r_1) = -k\delta \tan \eta_l, \quad \dots\dots(3.3)$$

neglecting second order terms on the right. Hence

$$\delta A = \frac{k\delta \tan \eta_l}{G^2(r_1)}, \quad \dots\dots(3.4)$$

so
$$\tan \eta_l'[\phi(r); r_1, k] = k^{-1}G^2(r_1), \quad \dots\dots(3.5)$$

and (2.6) gives for the first order perturbation of $\tan \eta_l$ the well-known* expression

$$\tan \eta_l[\phi(r) + \delta\phi(r); k] = \tan \eta_l[\phi(r); k] + \frac{1}{k} \int_0^\infty G^2(r_1) \delta\phi(r_1) dr_1. \quad \dots\dots(3.6)$$

The second order perturbation requires calculation of the second functional derivative $\tan \eta_l''[\phi(r); r_1, r_2, k]$, which involves calculating the term proportional to $\delta A_1 \delta A_2$ in the $\delta \tan \eta_l$ produced by two bumps in $\phi(r)$ at r_1 and r_2 of areas δA_1 and δA_2 respectively. That term, divided by $\delta A_1 \delta A_2$, is the required derivative.

Let $r_<, r_>$ be the lesser and greater of r_1, r_2 . We use the equations (see figure):

$$G(r_<) = H(r_<), \quad G'(r_<) - \delta A_< G(r_<) = H'(r_<) \quad \dots\dots(3.7)$$

$$H(r_>) = J(r_>), \quad H'(r_>) - \delta A_> H(r_>) = J'(r_>) \quad \dots\dots(3.8)$$

arising from the changes in slope at $r_<$ and $r_>$. Also, from the condition that the Wronskians are independent of r ,

$$G(r_<)H'(r_<) - H(r_<)G'(r_<) = G(r_>)H'(r_>) - H(r_>)G'(r_>) \quad \dots\dots(3.9)$$

and
$$G(r_>)J'(r_>) - J(r_>)G'(r_>) = -kB^{-1}\delta \tan \eta_l, \quad \dots\dots(3.10)$$

the value of the Wronskian for large r . Here B is the constant appearing in

$$J(r) \sim B^{-1}\{\sin kr + (\tan \eta_l + \delta \tan \eta_l) \cos kr\}.$$

These equations give

$$k\delta \tan \eta_l = B\{G^2(r_<)\delta A_< + G(r_>)H(r_>)\delta A_>\}. \quad \dots\dots(3.11)$$

If
$$H(r) = G(r) + \delta A_< G(r_<)h(r_<, r) \quad \dots\dots(3.12)$$

then, from the constancy of the Wronskian, h is that solution of

$$G(r)h'(r_<, r) - h(r_<, r)G'(r) = -G(r_<), \quad \dots\dots(3.13)$$

viz.
$$h(r_<, r) = -G(r_<)G(r) \int_{r_<}^r \frac{dr}{G^2(r)} + CG(r), \quad \dots\dots(3.14)$$

* cf. Mott and Massey (1949), p. 28, where small changes from $\phi=0$ are considered.

with the constant of integration C fixed by the boundary condition $h(r_<, r_<) = 0$. When zeros of $G(r)$ lie between $r_<$ and $r_>$ a different lower limit of integration and a different constant are required in each range of r between successive zeros, as discussed in Appendix II. (The second order calculation thus becomes involved if the potential is appreciable over many half-periods of G .)

In terms of this solution, picking out the terms in $\delta A_< \delta A_>$ on the right-hand side of (3.11),

$$k \tan \eta_l [\phi(r); r_<, r_>, k] = \alpha(r_>) G^2(r_<) + \alpha(r_<) G^2(r_>) + G(r_<) G(r_>) h(r_<, r_>) \quad \dots (3.15)$$

where we have put $B = 1 + \alpha(r_<) \delta A_< + \alpha(r_>) \delta A_> + \text{higher powers}$. Here $\alpha(r_<)$ and $\alpha(r_>)$ are given by

$$H(r) \sim (1 - \alpha(r_<) \delta A_<) \{\sin kr + \text{const.} \cos kr\} \\ J(r) \sim (1 - \alpha(r_>) \delta A_>) \{\sin kr + \text{const.} \cos kr\}$$

where the latter is calculated supposing $\delta A_<$ to be zero, using equations corresponding to (3.12), (3.13) and (3.14). Explicitly, $-\alpha(r_<)/G(r_<)$ is equal to the coefficient, P say, of $\sin kr$ in $h(r_<, r)$ for any r , say R , large enough for H to have reached its asymptotic form $P \sin kr + Q \cos kr$. We may choose R to be a zero, ρ_n say, of G ; then $h(r_<, \rho_n)$, $h'(r_<, \rho_n)$ calculated as shown in Appendix II fix P . Similarly $\alpha(r_>)$ may be found. We note that (3.15) vanishes if either or both of $r_<, r_>$ is a zero of G .

To the second order* then

$$\tan \eta_l [\phi(r) + \delta \phi(r); k] = \tan \eta_l [\phi(r); k] + \frac{1}{k} \int_0^\infty G^2(r_1) \delta \phi(r_1) dr_1 \\ + \frac{1}{2!k} \int_0^\infty \int_0^\infty [\alpha(r_2) G^2(r_1) + \alpha(r_1) G^2(r_2) + G(r_1) G(r_2) h(r_<, r_>)] \\ \times \delta \phi(r_1) \delta \phi(r_2) dr_1 dr_2. \quad \dots (3.16)$$

A physical interpretation of the various terms of (3.16) is that in the first order each increment $\delta \phi$ of potential in a spherical shell gives rise to an elementary scattered wave proportional to the square of the wave function $G(r)$ on that shell. The second order terms arise from successive scattering from pairs of such shells.

§ 4. BOUND STATES. PERTURBATION OF POTENTIAL

In calculating the first functional derivative of $\tanh \xi[\phi(r), l]$ we have again eqns. (3.2) and, instead of (3.3),

$$G(r_1) H'(r_1) - H(r_1) G'(r_1) = -K \delta \tanh \xi \quad \dots (4.1)$$

to the first order. So

$$\tanh \xi'[\phi(r), l] - \frac{\delta \tanh \xi}{\delta A} = \frac{1}{K} G^2(r_1) \quad \dots (4.2)$$

$$\text{and} \quad \tanh \xi[\phi(r) + \delta \phi(r); l] = \tanh \xi[\phi(r); l] + \frac{1}{K} \int_0^\infty G^2(r_1) \delta \phi(r_1) dr_1. \quad \dots (4.3)$$

We now require the change in energy ΔE which will bring $\tanh \xi$ back to its original value of -1 . Since a change ΔK^2 is equivalent to a constant ΔK^2 added to ϕ we have

$$0 = \frac{1}{K} \int_0^\infty G^2(r_1) \{\delta \phi(r_1) + \Delta K^2\} dr_1$$

* A form for the second order terms can also be arrived at on the same lines as the first order calculation by Mott and Massey (1949), p. 28.

i.e.
$$\frac{2m}{\hbar^2} \Delta E_n = +\Delta K^2 = - \int_0^\infty G_n^2(r_1) \delta\phi(r_1) dr_1 / \int_0^\infty G_n^2(r_1) dr_1 \dots\dots (4.4)$$

which is the well-known expression.

The same result is contained in the statement : "regarding an energy level E_n of a one-particle system as a functional of the potential $V(r)$, the first functional derivative of E_n at r is equal to the electron density there".

Calculation of the second order perturbation proceeds as for unbound states except that we replace (3.10) by

$$G(r_>)J'(r_>) - J(r_>)G'(r_>) = -K(a+b) \dots\dots (4.5)$$

$$\text{where } J(r) \sim a \sinh Kr + b \cosh Kr, \dots\dots (4.6)$$

and arrive at

$$-K(a+b) = \delta A_1 G^2(r_1) + \delta A_2 G^2(r_2) + \delta A_1 \delta A_2 G(r_1) G(r_2) h(r_<, r_>), \dots\dots (4.7)$$

where $h(r_<, r)$ is again given by (3.14), with the constant C fixed in the same way. Thus

$$-K(a+b) = \int_0^\infty G^2(r) \delta\phi(r) dr + \frac{1}{2!} \int_0^\infty \int_0^\infty G(r_1) G(r_2) h(r_<, r_>) \delta\phi(r_1) \delta\phi(r_2) dr_1 dr_2. \dots\dots (4.8)$$

If in (4.8) we replace $\delta\phi(r)$ by $\{\delta\phi(r) + \Delta K^2\}$ and require the left side to be zero, we have a quadratic equation giving ΔK^2 correctly to the second order, viz.

$$\begin{aligned} 0 = & \int_0^\infty G^2(r) \{\delta\phi(r) + \Delta K^2\} dr \\ & + \frac{1}{2!} \int_0^\infty \int_0^\infty G(r_1) G(r_2) h(r_<, r_>) \{\delta\phi(r_1) + \Delta K^2\} \{\delta\phi(r_2) + \Delta K^2\} dr_1 dr_2, \text{ i.e.} \\ \Delta K_n^2 \int_0^\infty G_n^2(r) dr = & - \int_0^\infty G_n^2(r) \delta\phi(r) dr \\ & - \frac{1}{2!} \int_0^\infty \int_0^\infty G_n(r_1) G_n(r_2) h(r_<, r_>) \delta\phi(r_1) \delta\phi(r_2) dr_1 dr_2 \\ & - \Delta K_n^2 \int_0^\infty \int_0^\infty G_n(r_1) G_n(r_2) h(r_<, r_>) \delta\phi(r_2) dr_1 dr_2 \\ & - \frac{1}{2!} (\Delta K_n^2)^2 \int_0^\infty \int_0^\infty G_n(r_1) G_n(r_2) h(r_<, r_>) dr_1 dr_2 \dots (4.9) \end{aligned}$$

and in the terms on the right ΔK^2 may be replaced by its first order approximation (4.4).

This expression differs in the second order term from that usually given in that it does not involve wave functions of any state other than that perturbed.

The second functional derivative $E_n''[\phi(r); r_1, r_2]$ is not directly obtainable from (4.9).

§ 5. SCATTERING. VARIATION METHODS

In such methods of finding approximate solutions of (2.1) with the boundary conditions (a) of §2 some expression F for $\tan \eta_l$ (or η_l , $\sin \eta_l$ etc.) is discovered which is stationary for small deviations of G from the actual solution. We guess a suitable trial function $G_t(\lambda, \mu, \nu \dots)$ containing parameters $\lambda, \mu, \nu \dots$, and with asymptotic form (2.2), (2.3) or (2.4) select the 'best' values of the parameters according to some criterion (which may involve F but need not), then calculate F using those 'best' values.

Any particular trial function G_t which we choose is not in general a solution of (2.1), though LG_t is small, but does satisfy

$$\{L_0 + \phi_t(r)\} G_t \equiv G_t'' + \{k^2 - l(l+1)/r^2 + \phi_t(r)\} G_t = 0 \quad \dots\dots (5.1)$$

where ϕ_t is a potential function differing little from ϕ , namely $\phi_t = -L_0 G_t / G_t = \phi + \delta\phi$ say, where

$$\delta\phi(r, \lambda, \mu, \nu \dots) = -LG_t / G_t. \quad \dots\dots (5.2)$$

Thus we are in effect choosing a potential function differing from that given by a small function containing several parameters. We can find a stationary expression for $\tan \eta_l$ in the case where G_t has the asymptotic form (2.3) as follows:

Perturb the trial potential ϕ_t by $-\delta\phi$ into the given potential ϕ . Then to the first order, from (3.6) and (5.2),

$$\tan \eta_l[\phi(r)] = \tan \eta_l[\phi_t(r) - \delta\phi(r)] = \tan \eta_l[\phi_t(r)] + \frac{1}{k} \int_0^\infty G_t LG_t dr, \quad \dots\dots (5.3)$$

i.e., the expression on the right is stationary, to the first order, at the true value of $\tan \eta_l$ for the given potential (Kohn 1948, Kato 1950).

The close relationship or virtual identity of the perturbation and variation methods is apparent from the above.

An expression stationary to the *second* order comes similarly from (3.16), giving an additional term on the right of (5.3):

$$\frac{1}{2!k} \int_0^\infty \int_0^\infty \left\{ 2\alpha(r_1) \frac{G_t(r_2)}{G_t(r_1)} LG_t(r_1) LG_t(r_2) + h(r_<, r_>) LG(r_1) LG(r_2) \right\} dr_1 dr_2 \quad (5.4)$$

where α and h are supposed calculated as in § 3 with ϕ_t, G_t replacing ϕ, G there.

However ϕ_t , hence also $\delta\phi$, has an infinity at each zero of G_t unless we happen to have chosen G_t so that each zero is also a point of inflection. The necessary elaboration of the argument of § 3 is slight in justifying (5.3), but is more extensive for the second order term (5.4). This is outlined in Appendix II.

Any expression differing from (5.3) only by terms of the second order in LG_t is of course equivalent to it for first order calculations. Such an expression might be sought which would leave the second order terms always of one sign, making the stationary expression always a maximum or always a minimum.

The foregoing exemplifies a manner in which forms for a functional of a function, stationary against small variations in the function, may be sought and found, rather than discovered by trial.

Various criteria for selection of the 'best' values of the parameters $\lambda, \mu, \nu \dots$ have been proposed. That of Hulthén (1944) includes the condition upon them that

$$\mathcal{L} \equiv \int_0^\infty G_t L G_t dr = 0. \quad \dots\dots (5.5)$$

From the present point of view this amounts to choosing the trial potential ϕ_t (fixed by the trial function G_t) so that the first order perturbation is zero when ϕ_t is varied into the given potential ϕ .

The other relations used in Hulthén's procedure to give the parameters are determined from the requirements that, if the phase η_l is independent of $\mu, \nu \dots$, $\partial \mathcal{L} / \partial \mu, \partial \mathcal{L} / \partial \nu$ are all zero. Kohn, instead of using (5.5), regards $\lambda = \tan \eta_l$ as an additional parameter in the trial function and requires $\partial F / \partial \lambda = 0$, where F is given by (5.3).

The above conditions are reasonable but not of course essential or necessarily the best to choose; they merely make the trial function imitate *one* property of the exact wave function. One might alternatively select some or all of the parameters by fitting G_t to the differential equation (2.1) at selected points, or one might make use of an integral equation known to be satisfied by η_t . These various alternative procedures differ simply in their effectiveness in keeping second and higher order terms small. Some of these alternatives will be discussed elsewhere.

Having arrived by any means at suitable values for the parameters, which fixes an approximate $\tan \eta_t$, these are used in calculating the value of the stationary expression (5.3), which gives a closer value for $\tan \eta_t$ (unless (5.5) has been used following Hulthén, in which case the correction is zero). As pointed out by Kato (1950), the various procedures give results which differ by second order terms only, and it is not easy to see any reason why one should consistently give better results than another, though it would seem likely that Hulthén's condition (5.5) would in general assist in keeping second order terms (5.4) small.

§ 6. BOUND STATES. VARIATION METHODS

Let H be the given Hamiltonian, E the energy level and ψ the corresponding eigenfunction of a system. If some trial function ψ_t (approximating to ψ), which is 'well-behaved' and normalized, is selected, this will satisfy the equation $H_t \psi_t = E_t \psi_t$ for some corresponding Hamiltonian† H_t differing from H by a small term $\delta V(q)$ in the potential energy function, E_t being a constant close to E , and q the coordinates of the particles in the system.

Perturb H_t into H . Then the change in energy

$$\begin{aligned} E - E_t &= - \int \psi_t^* \delta V(q) \psi_t d\tau \text{ to the first order} \\ &= \int \psi_t^* (H - H_t) \psi_t d\tau = \int \psi_t^* H \psi_t d\tau - E_t, \quad \dots\dots(6.1) \end{aligned}$$

so $E - \int \psi_t^* H \psi_t d\tau$ differs from zero by second order quantities, i.e. is stationary, which is the well-known result. An expression stationary in the second order would be found by using a second order perturbation formula on the right of (6.1).

Again we see the virtual identity of perturbation and variation methods, the latter amounting to choice of an approximately correct trial potential function containing parameters which are (usually though not necessarily) selected by the condition that the first order change in energy is zero on perturbing the trial potential into that given.

The variation method of Kohn (1952) for energies in a periodic lattice potential requires, for a similar discussion, the first order perturbation formula appropriate to perturbed boundary conditions.

ACKNOWLEDGMENTS

One of us (J.S.T.) was the holder of a Research Studentship from the University of Sydney while this work was carried out. The other is indebted to Professor H. S. W. Massey and Mr. B. I. Moiseiwitsch for stimulating discussion.

† Explicit expressions for H_t and E_t are not needed, but could be found as follows. Since $H_t \psi_t = \{H + \delta V(q)\} \psi_t - E_t \psi_t$, $\delta V(q) = (E_t \psi_t - H \psi_t) \psi_t$. In the last expression we insert for E_t some approximation to the value of E . Then $\delta V(q)$ may be calculated, and if ψ_t was well chosen the perturbation considered in the next paragraph will be small.

REFERENCES

- DI FRANCIA, G. T., 1950a, *Phys. Rev.*, **78**, 298; 1950b, *Nuovo Cim.*, **7**, 255.
 HULTHÉN, L., 1944, *K. Fysiogr. Sällsk. Lund. Förhandl.*, **14**, 257.
 JEFFREYS, H., and JEFFREYS, B. S., 1946, *Methods of Mathematical Physics* (Cambridge : University Press).
 KATO, J., 1950, *Phys. Rev.*, **80**, 475.
 KOHN, W., 1948, *Phys. Rev.*, **74**, 1763; 1952, *Phys. Rev.*, **87**, 472.
 MOTT, N. F., and MASSEY, H. S. W., 1949, *The Theory of Atomic Collisions*, 2nd edn. (Oxford : University Press).
 VOLTERRA, V., 1930, *Theory of Functionals*, (London : Blackie).

APPENDIX I

A quantity F which depends on the form of a function $\phi(x)$ over a whole range of x from a to b , say, is called a functional of that function and may be written, in Volterra's notation, $F[\phi(x); \lambda, \mu \dots]$, where $\lambda, \mu \dots$ are any parameters upon which the quantity also depends. We may regard F as a function of the infinite number of variables $\phi(x_1), \phi(x_2) \dots$ which are all the successive values ϕ takes in the range (a, b) of x .

The functional derivative of F at the point x_1 may be written as

$$\left. \frac{\delta F}{\delta \phi} \right|_{x=x_1} \quad \text{or as} \quad F'[\phi(x); x_1]$$

if we omit the limits a, b as being understood in a particular case. This is defined as the limit obtained by making a small perturbation $\delta\phi(x)$ of $\phi(x)$, localized near the point x_1 , calculating the resulting change δF of the quantity F and taking the limit of the ratio $\delta F / \int \delta\phi(x) dx$ as $\delta\phi$ is reduced to zero in magnitude and width; F' is at the same time a functional of $\phi(x)$ and a function of x_1 .

The second functional derivative $F''[\phi(x); x_1, x_2]$ is defined as the functional derivative at x_2 of $F'[\phi(x), x_1]$, regarding the latter as a functional of $\phi(x)$ containing the parameter x_1 . It may be shown that

$$F''[\phi(x); x_1, x_2] \equiv F''[\phi(x); x_2, x_1].$$

The form taken by Taylor's theorem for a functional (i.e. for a function of a number of variables which tends to infinity) is

$$\begin{aligned} F[\phi(x) + \delta\phi(x)] &= F[\phi(x)] + \int_a^b F'[\phi(x), x_1] \delta\phi(x_1) dx_1 \\ &+ \frac{1}{2!} \int_a^b \int_a^b F''[\phi(x); x_1, x_2] \delta\phi(x_1) \delta\phi(x_2) dx_1 dx_2 \\ &+ \dots \end{aligned} \quad \dots\dots (A1)$$

A functional equation is one of the form

$$F[\phi(x); \lambda, \mu \dots] = g(\lambda, \mu \dots) \quad \dots\dots (A2)$$

where g is a given function, the way in which F depends on all the values assumed by $\phi(x)$ is known and we have to determine the unknown function ϕ . A problem of this kind is to determine the potential function for a centre of force given the asymptotic phases for various energies and angular momenta of scattered particles. Solutions in terms of the solutions of a series of integral equations may be found.

APPENDIX II

The Solutions h of Equation (3.13)

If ρ_s , $s=1, 2, 3 \dots$, are the successive values of r where $G(r)$ vanishes and $r_<, r_>$ both lie between an adjacent pair of these, we take $r_<$ as the lower limit of integration and C is then zero.

Writing $h(r_<, r)$ as $h(r)$,

$$h(r_>) = -G(r_<)G(r_>) \int_{r_<}^{r_>} \frac{dr}{G^2(r)}. \quad \dots\dots (A\ 3)$$

At any of the ρ_s it follows directly from (3.13) that

$$h(\rho_s) = G(r_<)/G'(\rho_s). \quad \dots\dots (A\ 4)$$

If, however, one or more zeros of G lie between $r_<$ and $r_>$, let ρ_m be the zero next above $r_<$. In the interval between $r_<$ and ρ_m

$$h(r) = -G(r_<)G(r) \int_{r_<}^r \frac{dr}{G^2(r)} \quad \dots\dots (A\ 5)$$

$$h'(r) = -G(r_<)G'(r) \int_{r_<}^r \frac{dr}{G^2(r)} - \frac{G(r_<)}{G(r)}. \quad \dots\dots (A\ 6)$$

The limit of (A 5) as $r \rightarrow \rho_m$ agrees with (A 4), and from (A 6) the limit of $h'(r)$ may be found. In the next interval, ρ_m to ρ_{m+1} , we take as the solution

$$h(r) = -G(r_<)G(r) \int_{R_m}^r \frac{dr}{G^2(r)} + C_m G(r),$$

$$\text{so} \quad h'(r) = -G(r_<)G'(r) \int_{R_m}^r \frac{dr}{G^2(r)} - \frac{G(r_<)}{G(r)} + C_m G'(r) \quad \dots\dots (A\ 7)$$

where R_m is some point within this interval.

The limit of $h(r)$ as $r \rightarrow \rho_m$ from above is again (A 4), and we determine C_m by equating the limit of $h'(r)$ to that found from the first interval. Proceeding in this way, we may calculate the constants C in each interval between zeros $\rho_m, \rho_{m+1} \dots \rho_{m+q}$. The solution in the last interval, ρ_{m+q} to $r_>$,

$$h(r) = -G(r_<)G(r) \int_{R_{m+q}}^r \frac{dr}{G^2(r)} + C_{m+q} G(r)$$

may thus be found, and $h(r_>)$ determined from this.

Explicitly

$$-G'(\rho_m)C_m/G(r_<) = \int_{r_<}^{R_m} \frac{G'(\rho_m) - G'(\xi)}{G^2(\xi)} d\xi + \frac{1}{G(r_<)} - \frac{1}{G(R_m)} \quad \dots\dots (A\ 8)$$

$$\begin{aligned} & -G'(\rho_{m+p})(C_{m+p} - C_{m+p-1})/G(r_<) \\ &= \int_{R_{m+p-1}}^{R_{m+p}} \frac{G'(\rho_{m+p}) - G'(\xi)}{G^2(\xi)} d\xi + \frac{1}{G(R_{m+p-1})} - \frac{1}{G(R_{m+p})} \quad \dots\dots (A\ 9) \end{aligned}$$

where $p=1 \dots q$ and, in the last of these equations, $R_{m+q} = r_>$. The integrals in these expressions are all finite since each zero of G is a point of inflection when $\phi(r)$ is finite at those points.

If, however, as in § 5, we have a potential ϕ_t which is infinite like $\text{const}/(r-\rho)$ at the points ρ , the integrands are infinite in the same way, but it can easily be shown that the above expressions for the constants C still apply, provided we understand the integral signs to denote the principal values (e.g. Jeffreys and Jeffreys 1946, p. 348) of the integral.

A Comparison of Various Methods of Solving the Central Force Scattering Problem

BY J. S. TURNER AND R. E. B. MAKINSON

School of Physics, University of Sydney, Sydney, Australia

Communicated by H. S. W. Massey; MS. received 13th March 1953, and in final form 11th June 1953

Abstract. The variational methods employed by several writers are discussed, and their methods of choosing parameters in a trial wave function examined. It is pointed out that the parameters may be obtained in other ways, while still using the variation principle to compute an improved value of the asymptotic phase. The essentially equivalent process of perturbing a simple potential into the given form and evaluating the first order perturbation is also considered. The advantages and limitations of several methods proposed are examined numerically in a particular case of scattering by a Yukawa potential.

§ 1. INTRODUCTION

THE well-known variational procedures for finding the solution, zero at $r=0$, of

$$LG \equiv \frac{d^2 G}{dr^2} + \{k^2 - l(l+1)/r^2 + \phi(r)\}G = 0 \quad \dots\dots(1.1)$$

which arises in calculating cross sections for scattering of a beam of particles by a central field of force consist in finding an expression F for a function λ of the asymptotic phase η_l of G , which is stationary for small deviations of the wave function from the true solution. A trial function $G_t(\lambda, \mu, \nu \dots)$ is chosen, the 'best set' of parameters $(\lambda, \mu, \nu \dots)$ determined and F calculated using these 'best' values. It is pointed out in an accompanying paper (Makinson and Turner 1953, to be referred to as I), that the selection of the parameters and the use of the stationary property are quite independent processes.

In much of the literature on the application of the variational methods, however, the condition that a functional of the form

$$F \equiv k\lambda + \int_0^\infty GLG dr \quad \dots\dots(1.2)$$

is stationary for the correct wave function has been used for *both* these purposes. The parameters in $G_t(\lambda, \mu, \nu)$ are determined through the conditions

$$\partial F / \partial \lambda = 0 \quad \text{and} \quad \partial F / \partial \mu = 0, \quad \partial F / \partial \nu = 0 \quad \dots\dots(1.3)$$

used by Kohn (1948) or

$$\left. \begin{aligned} \mathcal{L} &\equiv \int_0^\infty G_t LG_t dr = 0 \\ \partial F / \partial \mu &= 0, \quad \partial F / \partial \nu = 0 \end{aligned} \right\} \quad \dots\dots(1.4)$$

and

as proposed by Hulthén (1944). These parameters are then used to find an improved value for the asymptotic phase using equations of the type

$$\lambda = \lambda_t + \frac{1}{k} \int_0^\infty G_t LG_t dr. \quad \dots\dots(1.5)$$

The most convenient functional to take for λ will depend on the normalization of G_t which we adopt. The relation (1.5), given by Kohn, also arises directly in the perturbation method described in 1, where the virtual identity of the variational and perturbation methods is demonstrated; it is independent of the conditions (1.3) and (1.4).

It is the object of the present discussion firstly to examine more closely, with reference to a particular example, exactly what is being done when conditions of the form (1.3) or (1.4) are used to find the parameters, and secondly to investigate the approach which uses (1.5) without reference to (1.3) or (1.4). It is pointed out that (1.5) also gives a means of correcting a calculation of the phase shift carried out using as a first approximation a simplified potential such as a step function.

For a one-dimensional scattering problem we can always of course obtain a solution by direct numerical integration, and often nothing is saved by using other approximate methods. However, the present methods, although discussed here for a simple case, may be of interest for more complicated problems where non-central forces are considered.

§ 2. THE VARIATIONAL METHODS

We treat a problem which has been solved by the Hulthén and Kohn methods, and for which an accurate numerical solution is available (Löwdin and Sjölander 1951). This is the problem of S wave scattering by a potential of the Yukawa type, described by

$$LG = \frac{d^2G}{dr^2} + (k^2 + be^r/r)G = 0 \quad \dots\dots(2.1)$$

with $k = 0.8$, $b = 1.5$.

The corresponding value of η is known to be 0.837 082.

Take a two-parameter trial function of a form used by Hulthén:

$$G_t = C\{\cos \eta_t \sin kr + \sin \eta_t(1 - e^{-r})(1 + he^{-r}) \cos kr\}. \quad \dots\dots(2.2)$$

This may be normalized in various ways to give the asymptotic forms

$$G_t \sim \sin(kr + \eta_t), \quad \dots\dots(2.3)$$

$$G_t \sim \sin kr + \tan \eta_t \cos kr, \quad \dots\dots(2.4)$$

$$G_t \sim \cot \eta_t \sin kr + \cos kr, \quad \dots\dots(2.5)$$

and the corresponding variational principles are found by putting λ_t respectively equal to η_t , $\tan \eta_t$ and $-\cot \eta_t$ in (1.2) and (1.5) as shown by Kato (1950).

Various methods of choosing parameters, followed by the application of the several forms of (1.5), will lead to slightly different values for the asymptotic phase, which will differ from each other and the correct value by second order quantities. When the parameters have been chosen by some means it is worth while to compare the results using two or more of these forms of (1.5), to get some idea of the size of the second order quantities.

Using (2.3) and the corresponding form of (1.5), it is possible to calculate the values of η for various η_t and h , regardless of how these parameters have been chosen. This has been done using the analytic expression for \mathcal{L} given by Hulthén (1944), and the results are presented as a contour plot of differences from the exact value, i.e. $(\eta_{\text{exact}} - \eta)$, in fig. 1(a). The conditions (1.3) and (1.4)

are represented on the plot by the intersection of pairs of the curves $\partial F/\partial h=0$, $\partial F/\partial \eta_t=0$, $\mathcal{L}=0$. It can be seen that Kohn's condition (1.3) leads to a saddle point of the plot in this case and that the Hulthén method gives a better numerical result. Notice that there are sets of parameters which give the exact phase shift, because the difference from the exact value can change sign, but that these are not chosen by either (1.3) or (1.4).

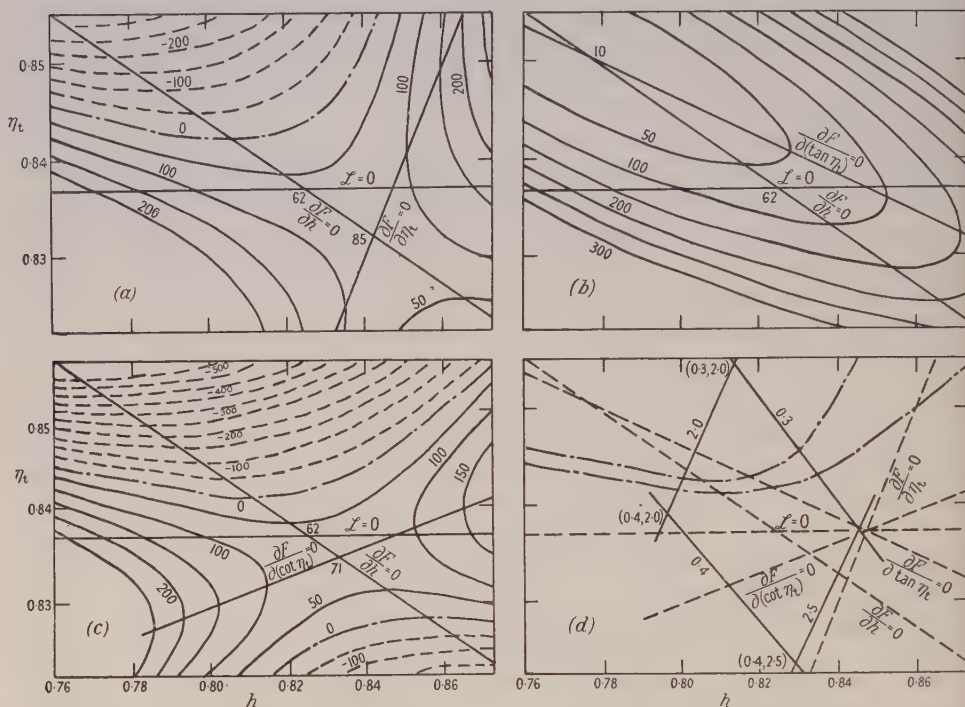


Fig. 1. (a), (b), (c): Contour plots of $(\eta_{\text{exact}} - \eta) \times 10^6$ for various η_t and h , using the trial function (2.2) with the normalizations (2.3), (2.4) and (2.5) respectively, and the corresponding forms of (1.5). (d): The parameters resulting from fitting to the differential equation at one fixed point and one other point are shown by the full lines, which are labelled according to the fixed point. Also plotted are the zero contours from (a) and (c) and the curves used to find parameters by the Hulthén and Kohn methods.

Similarly, using (2.4) and (2.5) and the corresponding forms of (1.5), we may calculate differences of η from the exact value for various sets of parameters. These are presented in figs. 1(b) and 1(c) with the relations corresponding to (1.3) and (1.4) again marked. In the latter case we again have a saddle point chosen by the Kohn condition, but in the former this gives a minimum which, since the difference does not change sign, is in fact the best value of the phase for the trial function used. All the plots have the same cross section along $\mathcal{L}=0$ and therefore give the same value of η according to the Hulthén condition.

It is clear then that Kohn's condition can sometimes give better and sometimes worse values for the phase than Hulthén's, according to the form of trial function chosen and the particular expression used of all those which are stationary to the first order. There is of course no means of knowing which is the better when a problem is treated without an exact solution being available for comparison.

§ 3. FITTING TO THE DIFFERENTIAL EQUATION

In using the conditions (1.3) and (1.4) we are making the trial function imitate one condition which holds for the true wave function, but this is not the only property we can use. The exact wave function must of course satisfy (2.1), and a suitable trial function G_t will be one which keeps LG_t small everywhere. One way to secure this is to make LG_t *exactly* zero at a number of points (as many as there are parameters), so chosen that the oscillations of $G_t LG_t$ in between are small. This will keep the first order terms (i.e. the integral \mathcal{L}) small, and thus give a set of parameters likely to be close to Hulthén's values. One might select fitting points distributed over the region in which $\phi(r)$ is comparable with k^2 (see fig. 2).

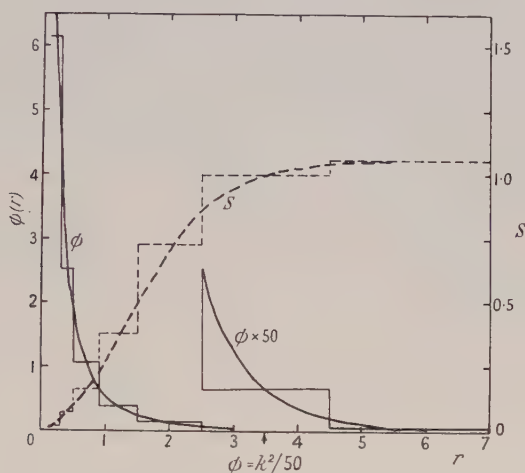


Fig. 2. Showing the step function used to approximate to the Yukawa potential and the resulting approximation to the function S .

First, taking the trial function (2.2) we have computed the parameters corresponding to fitting at various pairs of points. Those which fall in the region near Hulthén's values have been marked in fig. 1(d), where the solid curves represent the range of parameters obtainable when one fitting point is kept fixed at the values shown. Also plotted in fig. 1(d) are the curves used in fig. 1(a), (b) and (c) to give the values of parameters in the Hulthén and Kohn methods, and the contours of zero ($\eta_{\text{exact}} - \eta$) taken from figs. 1(a) and 1(c).

It is impossible to obtain parameters close to the Hulthén values for a fit at zero and one other point, but other combinations may do so. Very good values of the phase could be obtained if *any* point were chosen, even zero, if the second fitting point were taken by chance to give a pair of parameters near the zero contour for the particular form of (1.5) we apply.

This dependence of the parameters on the fitting points is the weakness of the method, and the criterion given for selecting them does not reliably lead in this case to errors as small as those given by the Kohn and Hulthén procedures.

One would expect that the choice of fitting points would not be so important if a trial function containing many parameters is used, provided these are reasonably distributed. We consider the four-parameter form of trial function

used by Hulthén in the above problem:

$$G_t = \cos \eta_t f(r) \sin kr + \sin \eta_t g(r) \cos kr \quad \dots\dots(3.1)$$

with $f(r) = 1 + c_1 e^{-r} + c_2 e^{-2r}$, $g(r) = (1 - e^{-r})(1 + h e^{-r})$. Fitting at the two sets of points $r=0, 0.4, 0.7$, and 1.0 , $r=0, 1.0, 2.0$, and 3.0 , the latter of which is preferred according to the rather vague criterion given above, one finds $\mathcal{L} = -0.010389$, $\mathcal{L} = -0.014541$, and using the form of (1.5) corresponding to (2.3), $\eta = 0.83868$, $\eta = 0.83691$. The latter value is in error by 1 in 10^4 , about twice the error of the previous methods. In these evaluations the parameters obtained by solving the four linear equations given by the fitting procedure have been substituted in the expression (28, III) given for \mathcal{L} in Hulthén's paper (1944).

Again there is a variation with fitting points chosen, and no adequate guide in choosing them. The 'best' fitting points will depend also on the form of trial function taken, so no criterion of selection based only on the form of $\phi(r)$ and the magnitude of k^2 can be always reliable.

A plot of the integrand $G_t L G_t$ as a function of r is informative and shows that with the first set of fitting points the integrand is very small and oscillatory in the range $r < 1$ but becomes large in the range $1 < r < 4$. Taking fitting points in this latter range reduces the size of the integrand here.

An advantage of the fitting method would be that we need not restrict ourselves to trial functions for which the integral \mathcal{L} may be evaluated analytically. The parameters can be found using the simpler expression $L G_t = 0$, and the correction term calculated numerically.*

When applied to *linear* trial functions the fitting procedure is simpler than Hulthén's in that it leads to linear equations for the parameters, but this is also so with Kohn's procedure and there is no saving of labour.

§ 4. MODIFICATIONS OF THE POTENTIAL

The methods discussed so far have dealt with the replacement of the exact wave function by a trial wave function. We will now show how the perturbation theory can be applied when the *potential* is replaced directly by a simple form; that is, we perturb from a form of potential for which the asymptotic phase can easily be calculated and evaluate correction terms. As shown in I, this procedure is essentially the same as the variation method since in the latter the choice of trial function in effect selects a trial potential, and the 'improvement' formula (1.5) gives just the first order perturbation.

The simplest function which suggests itself is a series of potential steps. We will treat the same problem as before, replacing the Yukawa potential in a narrow interval of r by its value at some point in it, say the midpoint. That is, in the interval I_n put $k^2 - l(l+1)/r^2 + \phi(r) = k_n^2$, say. $\dots\dots(4.1)$

The solution over this interval will be

$$G_t = a_n \sin k_n r + b_n \cos k_n r. \quad \dots\dots(4.2)$$

The successive solutions are joined by the conditions that the ordinate and

* A referee has drawn our attention to a procedure of selecting the parameters by minimizing $\int_0^\infty (L G_t)^2 dr$. This avoids the difficulty of selecting suitable fitting points but is inapplicable if the integral cannot be evaluated analytically. If the latter is possible no advantage over the Hulthén or Kohn procedures is evident.

slope of G_t should be continuous. The initial conditions will be $b_t=0$ and a_t arbitrary = 1, say. We could avoid any difficulties which may be associated with the infinite potential at the origin by integrating out for a short distance.

The value of b_t/a_t , the required $\tan \eta_t$ in the final interval I_t , will be obtained by solving the $2n$ simultaneous equations for the coefficients a_n and b_n . The process of solution is most conveniently carried out on a desk calculator using a systematic self-checking method described for example by Milne (1949), p. 19. This is particularly simple here since only terms near the diagonal of the 'auxiliary matrix' are non-zero.

Using the steps shown in fig. 2, we have found $\eta_t = 0.815984$ for the problem described by eqn. (2.1). This could of course be improved directly by taking more steps. It is of interest to look at the progressive phase shift b_n/a_n as drawn in fig. 2, which may be regarded as an approximation to the function S used by Kynch (1952). It is clear that the potential out as far as $x=4$ has a great influence on the phase shift even though it is there small compared to k^2 ($< k^2/50$). This incidentally indicates that a good set of fitting points in §3 would have been distributed over the range 0.3 to 4.0, where the rate of increase of S is greatest.

The value of η_t just obtained may be improved using one of the forms of (1.5) and evaluating \mathcal{L} numerically. \mathcal{L} may be put in the form $\mathcal{L} = \int_0^\infty \delta\phi G_t^2 dr$ (I, eqn. (3.6)), where $\delta\phi$ is the difference between the two potentials, i.e.

$$\delta\phi = \frac{be^{-r}}{r} - c. \quad \dots\dots(4.3)$$

All the parts of the integrand have already been tabulated at the fitting points, and it is zero at the midpoints of the intervals, so the separate contributions to the integral may be found simply using Simpson's rule. To test the accuracy of this approximation additional values of the integrand were computed and Simpson's rule again used. The agreement was found to be satisfactory only so long as the number of intervals in each half cycle of G is about 8 or 10, and more tabulation was necessary over the larger steps.

Finally we obtained the value 0.0044053 for \mathcal{L} , and the values for η corrected for first order terms according to the several forms of (1.5) are $\tan \eta = 1.104639$, $\eta = 0.83508$; $\cot \eta = 0.903892$, $\eta = 0.83583$; $\eta = 0.83547$. The differences between these values, which are equivalent in the first order, give some idea of the size of second order terms and the number of figures we should keep in the answer.

Forms other than the staircase approximating to the given potential were tried in the hope of reducing second order terms. Replacement by chords for example does not look at first sight very much more difficult, but it leads to a solution in terms of Bessel functions of fractional order with arguments rather complicated functions of r , which is much more difficult to handle numerically.

Attempts to perturb from continuous potentials for which the phase shift may be found exactly are also difficult because of the complexity of the wave function, which must be evaluated in obtaining the correction terms. That is, in applying the perturbation theory it is an advantage to have the wave function as simple as possible, since it is this which must occur explicitly in the correction term. The usual approach using a trial wave function is therefore more satisfactory except in a special case where both the potential and wave function are simple, as with the potential steps.

ACKNOWLEDGMENT

One of us (J. S. T.) was the holder of a Research Studentship from the University of Sydney while this work was carried out.

REFERENCES

- HULTHÉN, L., 1944, *K. Fysiogr. Sällsk. Lund Förhandl.*, **14**, 257.
KATO, T., 1950, *Phys. Rev.*, **80**, 475.
KOHN, W., 1948, *Phys. Rev.*, **74**, 1763.
KYNCH, G. J., 1952, *Proc. Phys. Soc. A*, **65**, 83.
LÖWDIN, P.-O., and SJÖLANDER, A., 1951, *Ark. Fys.*, **3**, 155.
MAKINSON, R. E. B., and TURNER, J. S., 1953, *Proc. Phys. Soc. A*, **66**, 857.
MILNE, W. E., 1949, *Numerical Calculus* (Princeton : University Press).

A Pre-Renormalized Quantum Electrodynamics

BY H. S. GREEN

University of Adelaide, South Australia

MS. received 13th July 1953

Abstract. A pair of integral equations is derived, which, together with a well-defined mathematical procedure, will automatically generate the elements of the S-matrix in their accepted renormalized form.

§ 1. INTRODUCTION

AN unsatisfactory feature of quantum electrodynamics in its present state is that, in order to obtain finite expressions for physically measurable quantities, it is necessary to start with a set of equations which contain infinities, and to manipulate these infinities as though they were ordinary numbers. Dyson (1949) pointed this out near the end (pp. 1754–5) of his classical paper on the renormalization procedure (see also Dyson 1951), and suggested that it should be possible to reformulate the theory in such a way that no infinity ever appeared. In such a reformulation, only the physical (renormalized) charge and mass of the electron should appear, and not the corresponding ‘bare’ quantities, which are in fact unobservable. Källén (1952) has demonstrated that this is possible within the framework of the Lagrangian formalism only at the expense of putting infinities into the Lagrangian density.

However, Schwinger (1951, see also Edwards 1953) has recently proposed an alternative formalism, which is clearly an advance on the earlier one, since the emphasis is on the actual propagation functions $G(x)$ [Dyson’s $S_F'(x)$] and $D(x)$ [Dyson’s $D_F'(x)$] for the electron and photon, rather than on the hypothetical functions to which they would reduce if there were no interaction. Schwinger’s new formulation is quite equivalent to its predecessors, and still requires renormalization for the elimination of the infinities. The transparent reason for this is the survival of some of the old symbols which represent unobservables, notably γ_λ in a context which corresponds to a simple vertex in the Feynman diagrams. The principal object of this paper is to show how to eliminate these residual unphysical abstractions and thus to obtain a theory which requires no renormalization.

A pair of closed equations is derived which, together with a well-defined mathematical procedure, can be used to obtain exactly elements of the S-matrix in their accepted renormalized form. Questions of regularization, or whether all terms of the S-matrix are present with their correct coefficients—which are a source of practical, if not theoretical difficulty with existing methods—never arise.

§ 2. PRELIMINARIES

To those unfamiliar with Schwinger’s formalism, it should be explained that $G(x-x_0)$ is the probability amplitude for the propagation of an electron from the point x_0 (with coordinates $x_{01}, x_{02}, x_{03}, x_{04}$) of space-time to any other point x ; and $D(x-x_0)$ is the corresponding function for the photon. Full coupling

is assumed from the outset between the electron and photon fields, so that self-energy effects are already accounted for by these functions. The object in view is to set up a system of equations sufficient to determine $G(x)$ and $D(x)$, from which any desired element of the S-matrix is easily derived.

We shall find it convenient to work mostly in the momentum representation, and accordingly define

$$\left. \begin{aligned} G(p) &= \int G(x) e^{ip \cdot x} dx, \\ D(k) &= \int D(x) e^{ik \cdot x} dx, \end{aligned} \right\} \dots\dots(1)$$

where $p = p^\lambda \gamma_\lambda = p_4 \gamma_4 - \mathbf{p} \cdot \boldsymbol{\gamma}$, $p \cdot x = p^\lambda x_\lambda = p_4 x_4 - \mathbf{p} \cdot \mathbf{x}$, etc., and the integrations extend over the large region of space and time considered. We shall suppose that these functions are the renormalized ones; they are, therefore (provided certain power series in e^2 converge!) well defined and finite. When there is no external field $G(p)$ has one pole, for $p = m$, where m is the observed electron mass; also, $D(k)$ is a function of $k^2 = k^\lambda k_\lambda$ with one pole, for $k^2 = \mu^2$, where μ represents the photon mass and must ultimately be made to vanish. The physical requirements of causality are most easily met by assigning a small imaginary part to both m and μ in evaluating integrals over momentum space; and μ is conveniently regarded as small but finite for the analysis of the infra-red catastrophe. Thus the form of $G(p)$ and $D(k)$ may be expressed by

$$\{G(p)\}^{-1} = (p - m)f(p), \dots\dots(2)$$

and

$$\{D(k)\}^{-1} = (k^2 - \mu^2)g(k^2). \dots\dots(3)$$

It turns out that the normalization of $f(p)$ and $g(k^2)$ for $p = m$ and $k^2 = \mu^2$ respectively has no observable significance, so that it may be assumed that

$$f(m) = 1, \dots\dots(4)$$

and

$$g(\mu^2) = 1. \dots\dots(5)$$

The function $G(p)$ represents all Feynman diagrams describing the propagation of an electron with momentum p . We shall wish to construct from $G(p)$, or any other function representing Feynman diagrams of a particular type, a second function which represents a new set of diagrams, obtainable from the former by the insertion of a simple vertex, in all possible ways. The function $G_*(p; k)$ obtained from $G(p)$ in this way will then represent an electron line containing a vertex for the emission of a photon with momentum k and direction of polarization parallel to the x_* axis. Thus one will have

$$G_*(p; k) = -ieG(p)\Gamma_*(p; k)G(p - k), \dots\dots(6)$$

where e is the observed electronic charge and $\Gamma_*(p; k)$ represents the vertex (Dyson and Schwinger use the same notation).

The operation which enables one to pass from $G(p)$ to $G_*(p; k)$, or more generally from any function F representing a type of Feynman diagrams to $F_*(k)$, obviously corresponds to Schwinger's functional differentiation with respect to the external field potential A_* . Here no external field is contemplated, and anyway something more explicit will be required. It may be noticed, however, that F will always be the same functional of the electron momentum p , when no external field is present, as of $p - eA$ in the more general (but less physical) case.

Suppose, then, that F is regarded as a functional of an electron momentum p . Then $F_\lambda(l)$ can be defined inductively by the rules

$$\left. \begin{aligned} F_\lambda(l) &= ie\gamma_\lambda \quad \text{when} \quad F=p, \\ F_\lambda(l) &= F_\lambda^{(1)}(l) + F_\lambda^{(2)}(l) \quad \text{when} \quad F=F^{(1)} + F^{(2)}, \\ F_\lambda(l) &= F^{(1)}(p)F_\lambda^{(2)}(p; l) + F_\lambda^{(1)}(p; l)F^{(2)}(p-l) \quad \text{when} \quad F=F^{(1)}(p)F^{(2)}(p). \end{aligned} \right\} \dots\dots(7)$$

For example, when $F=p^2$, $F_\lambda(l)=ie\{p\gamma_\lambda + \gamma_\lambda(p-l)\}$; and when $F=(p-m)^{-1}$, $F_\lambda(l)=-ie(p-m)^{-1}\gamma_\lambda(p-l-m)^{-1}$. The above rules are sufficient for our present purpose; their extension to cases where more than one electron is involved is given in the Appendix to this paper, where a general proof is also given that the operation of forming $F_\lambda(l)$ from F corresponds to the insertion of a simple vertex, in every possible way, in the Feynman diagrams represented by F .

From (7) it follows by induction that

$$ie\{F(p) - F(p-l)\} = l^\lambda F_\lambda(p; l); \quad \dots\dots(8)$$

hence, for the limit $l=0$, one has

$$ie \frac{\partial F(p)}{\partial p^\lambda} = F_\lambda(p; 0). \quad \dots\dots(9)$$

The vertex function which appears in (6) can be derived from

$$\Gamma(p) = \{ieG(p)\}^{-1}, \quad \dots\dots(10)$$

in accordance with the above rules. From the present point of view, therefore, the identity

$$\Gamma_\lambda(p; 0) = \frac{\partial}{\partial p^\lambda} \{G(p)\}^{-1}, \quad \dots\dots(11)$$

due to Ward (1950, 1951, see also Thirring 1950) is a special case of (9).

§ 3. THE INTEGRAL EQUATIONS

In his paper on the renormalization procedure (1949), Dyson described two integral equations which are also fundamental in Schwinger's formalism. They may be expressed in the form

$$\{G(p)\}^{-1} = \{G_0(p)\}^{-1} + e^2 \int \Gamma_\kappa(p; k)G(p-k)D(k)\gamma_0^* dk \quad \dots\dots(12)$$

$$\text{and} \quad \{D(k)\}^{-1} = \{D_0(k)\}^{-1} + e^2 \text{Spur} \int G(p)\Gamma_\kappa(p; k)G(p-k)\gamma_0^* dp \quad \dots\dots(13)$$

where $G_0(p)$ and $D_0(k)$ represent electron and photon lines without self-energy processes, and γ_0^* a vertex without radiative processes. These equations express elementary facts concerning the structure of the Feynman diagrams: for example, (12) can be decomposed into two equations

$$\left. \begin{aligned} G(p) &= G_0(p) + G_0(p)\Sigma(p)G(p), \\ \Sigma(p) &= -e^2 \int \Gamma_\kappa(p; k)G(p-k)D(k)\gamma_0^* dk, \end{aligned} \right\} \dots\dots(14)$$

of which the first states that all diagrams represented by $G(p)$, except the one represented by $G_0(p)$, consist of one or more self-energy insertions in a simple electron line; and the second states that any self-energy insertion can be constructed from a vertex by joining an electron line and a photon line, the other ends of which are made to meet at a simple vertex.

In an unrenormalized theory, $G_0(p)$, $D_0(k)$ and γ_0^* would be finite, and $G(p)$, $D(k)$ and $\Gamma_\kappa(p; k)$ would contain the infinities. But in the pre-renormalized

theory which we shall consider, the physically meaningful functions $G(p)$, $D(k)$ and $\Gamma_{\lambda}(p; k)$ are finite, and it is the unphysical abstractions $G_0(p)$, $D_0(k)$ and γ_0^* which contain the infinities. However, one may always write formally

$$\left. \begin{aligned} \{G_0(p)\}^{-1} &= a(p-m) + a' \\ \{D_0(k)\}^{-1} &= b(k^2 - \mu^2) + b' \\ \gamma_0^* &= a\gamma^* \end{aligned} \right\} \dots\dots(15)$$

and, within certain limitations, treat a , a' , b and b' as though they were ordinary numbers.

It should be admitted at once that the equations (12) and (13) cannot be considered as a satisfactory basis for quantum electrodynamics. They are equally objectionable from the mathematical point of view, and from the point of view of their physical interpretation. For electron and photon lines without self-energy processes, and vertices without radiative processes do not exist; and it is such things that $G_0(p)$, $D_0(k)$ and γ_0^* are supposed to represent. However, if one can eliminate these quantities from (12) and (13), one will be left with equations which are invariant against renormalization, and which make sense both mathematically and physically. That is what will now be attempted.

The function $G_0(p)$, expressed as in (15), can be eliminated by taking (12) and applying the operation, defined in the previous section, which corresponds to the insertion of a vertex. Anticipating the well-known fact that $D_{\lambda}(l; k)$ vanishes numerically (though not as a functional of electron momenta, which explains why $D_{\lambda Q}(l; k, r)$ does not), one has

$$\Gamma_{\lambda}(p; k) = \gamma_{0\lambda} - ie \int \{ \Gamma_{\lambda\lambda}(p; l, k) - ie \Gamma_{\lambda}(p; l) G(p-l) \Gamma_{\lambda}(p-l; k) \} G(p-k-l) D(l) \gamma_0^{\lambda} dl. \dots\dots(16)$$

This is another equation of Schwinger's formalism, written in the momentum representation and formally renormalized. Setting for convenience

$$B_{\lambda}(p, l) = -ie \Gamma_{\lambda}(p; l) G(p-l) D(l), \dots\dots(17)$$

it may also be written

$$\Gamma_{\lambda}(p; k) = \gamma_{0\lambda} + \int B_{\lambda\lambda}(p, l; k) \gamma_0^{\lambda} dl. \dots\dots(18)$$

After a second operation representing vertex insertion, one has

$$\Gamma_{\lambda Q}(p; k, r) = \int B_{\lambda\lambda Q}(p, l; k, r) \gamma_0^{\lambda} dl. \dots\dots(19)$$

If, now, γ_0 were eliminated between (18) and (19), a completely meaningful and divergence-free equation would result, which is actually common to the unrenormalized and pre-renormalized theories. The result would not, however, be very useful, since one requires the function $G(p)$, which appears only in a gravely mutilated form in (18) and (19). We shall show, however, that with the help of (2) and (4), the renormalized $G(p)$ can be reconstructed.

It should be noticed in advance, concerning the substitution, in a function $\phi(p)$ of $p = p' \gamma_{\lambda}$, of an argument m' such that $m'^2 = m^2$, it does not follow in general from an equation $(m' + m)\phi(m')(m' + m) = 0$ that $\phi(m') = 0$. But in such cases we shall find it convenient to write simply $\phi(m') = 0$, meaning in effect $(m' + m)\phi(m')(m' + m) = 0$.

With this convention, it follows from (2) that

$$\{G(m')\}^{-1} = 0 \dots\dots(20)$$

when $m'^2 = m^2$. Also, with the help of (10) and (8)

$$\begin{aligned}\{G(p)\}^{-1} &= \{G(m')\}^{-1} + (p - m')_\lambda \Gamma^\lambda(p; p - m') \\ &= (p - m')_\lambda \Gamma^\lambda(p; p - m').\end{aligned}\quad \dots\dots(21)$$

Further, it follows from (4) that

$$\Gamma_\lambda(m'; 0) = \gamma_\lambda. \quad \dots\dots(22)$$

Therefore, if one takes (18) and subtracts the same equation with $p = m'$ and $k = 0$, one obtains

$$\Gamma_\kappa(p; k) = \gamma_\kappa + \int \{B_{\lambda\kappa}(p, l; k) - B_{\lambda\kappa}(m', l; 0)\} \gamma_0^\lambda dl. \quad \dots\dots(23)$$

From (21) and (23) one has finally

$$\{G(p)\}^{-1} = (p - m) + (p - m')_\kappa \int \{B_{\lambda\kappa}(p, l; p - m') - B_{\lambda\kappa}(m', l; 0)\} \gamma_0^\lambda dl. \quad \dots\dots(24)$$

From this equation γ_0^λ still has to be eliminated; this can be done with the help of the equation

$$\gamma_{0\kappa} = \gamma_\kappa - \int B_{\lambda\kappa}(m', l; 0) \gamma_0^\lambda dl \quad \dots\dots(25)$$

obtained by subtracting (18) from (23).

The eliminant of γ_0 from (24) and (25) is the final form of our integral equation for $G(p)$; it is unnecessary, however, for practical purposes actually to carry out the elimination. The equations are easily solved to obtain power series in e^2 for $\{G(p)\}^{-1}$ and $\gamma_{0\kappa}$, and at each stage a convergent expression is obtained for $\{G(p)\}^{-1}$, though not for $\gamma_{0\kappa}$. The procedure is as follows.

In the first approximation, one sets $e^2 = 0$ and has

$$(i) \quad \{G(p)\}^{-1} = p - m; \quad \gamma_{0\kappa} = \gamma_\kappa; \quad \Gamma_\kappa(p; k) = \gamma_\kappa.$$

These expressions are then used to obtain, correct to order e^2 ,

$$\begin{aligned}(ii) \quad \{G(p)\}^{-1} &= (p - m) + e^2 \int \gamma_\lambda \{ (p - l - m)^{-1} - (m' - l - m)^{-1} \} \\ &\quad \times (p - m')(m' - l - m)^{-1} \gamma^\lambda D(l) dl, \\ \gamma_{0\kappa} &= \gamma_\kappa + e^2 \int \gamma_\lambda (m' - l - m)^{-1} \gamma_\kappa (m' - l - m)^{-1} \gamma^\lambda D(l) dl, \\ \Gamma_\kappa(p; k) &= \gamma_\kappa - e^2 \int \gamma_\lambda \{ (p - l - m)^{-1} \gamma_\kappa (p - k - l - m)^{-1} \\ &\quad - (m' - l - m)^{-1} \gamma_\kappa (m' - l - m)^{-1} \} \gamma^\lambda D(l) dl.\end{aligned}$$

This process can be continued indefinitely. At each stage one obtains $\Gamma_\kappa(p, k)$ from $\{G(p)\}^{-1}$ by using (7) and (10), and computes $B_{\lambda\kappa}(p, l; k)$ for the next stage with the help of (7) and (17). At no stage beyond the first does $\gamma_{0\kappa}$ have any independent meaning; it is intended only for substitution in (24), where its divergences are removed exactly by Dyson's 'b-divergences' which (cf. Salam 1951) arise from overlapping self-energy insertions in the Feynman diagrams.

The relation between the present considerations and the ordinary renormalization procedure can be seen most easily by using (8) and (9) to express (24) in the equivalent form

$$\{G(p)\}^{-1} = (p - m) + ie \int \left\{ B_\lambda(p, l) - B_\lambda(m', l) - (p - m')_\kappa \frac{\partial B_\lambda(m', l)}{\partial m'_\kappa} \right\} \gamma_0^\lambda dl, \quad \dots\dots(26)$$

and, secondly, noticing that the constant a which appears in the relation $\gamma_0^\kappa = a\gamma^\kappa$ of (15), is equivalent to Dyson's renormalization constant Z_1 .

An almost identical treatment can be given of the equation (13) for $D(k)$. One can perform the elimination of the unphysical and divergent $D_0(k)$ by a

mathematical procedure corresponding to vertex insertion in the Feynman diagrams, such as was used to eliminate $G_0(p)$. However, such a procedure reduces essentially to the derivation of

$$\{D(k)\}^{-1} - \{D(\mu')\}^{-1} - (k - \mu')_e (k + \mu')_\sigma \frac{\partial^2 \{D(\mu')\}^{-1}}{\partial \mu'_e \partial \mu'_\sigma} \\ = ie \text{ Spur} \int \left\{ G_\pi(p, k) - G_\pi(p, \mu') - (k - \mu')_e (k + \mu')_\sigma \frac{\partial^2 G_\pi(p, \mu')}{\partial \mu'_e \partial \mu'_\sigma} \right\} \gamma_0^* dp \quad \dots (27)$$

from (13), where μ' is any momentum vector satisfying $\mu'^2 = \mu^2$, and $G_\pi(p, k)$ may be expressed as in (6). Equation (27), when γ_0 is eliminated by means of (25), is one which holds whether the theory is pre-renormalized or not; but (3) and (5) are needed to determine the renormalized $D(k)$ completely. In fact, with the help of (3) and (5), (27) reduces to

$$\{D(k)\}^{-1} = (k^2 - \mu^2) \\ + ie \text{ Spur} \int \left\{ G_\pi(p, k) - G_\pi(p, \mu') - (k - \mu')_e (k + \mu')_\sigma \frac{\partial^2 G_\pi(p, \mu')}{\partial \mu'_e \partial \mu'_\sigma} \right\} \gamma_0^* dp \quad \dots (28)$$

The eliminant of γ_0 between (25) and (28) is our final equation for $D(k)$.

In this way the theory is reduced essentially to two equations, which automatically ensure the fulfilment of eqns. (2)–(5), and express in addition certain facts about the structure of Feynman diagrams without allusion to simple lines and vertices. They involve only physically significant quantities and are free of all divergences. When $G(p)$ and $D(k)$ have been determined by the solution of these equations, other elements of the S-matrix are readily constructed by the process corresponding to vertex insertion, and joining the elementary diagrams thus obtained.

§4. ADDITIONAL REMARKS

It is interesting to notice that the mathematical steps involved in proceeding from (12) to (26), or from (13) to (28), correspond to the insertion of two vertices in the diagrams for electron and photon transmission, respectively. The final equations are therefore disguised statements about processes which are in principle observable, such as Compton scattering or the scattering of light by light. It would, of course, be very unsatisfactory if irreducible elements of the S-matrix corresponding to such processes were not finite; this nevertheless is the case for several varieties of meson theory.

The question naturally arises whether the methods of this paper can be used to obtain finite results for meson field theories. In those cases (see Matthews and Salam 1951) where it is known that renormalization is possible, this is certainly so. In other cases it would also be possible to eliminate the infinities, but whether the procedure could be justified on physical grounds is doubtful.

The expression of the fundamental results of quantum electrodynamics in the form of closed integral equations such as (26) and (28) of this paper could have more than theoretical importance if an alternative could be found to the method of solution in powers of e^2 . Reasons have been given (Dyson 1952) for believing that these power series are at best only semiconvergent, and recent work by Edwards (1953) has pointed to the possibility of solving the integral equations in other ways. Edwards' method was hardly systematic, and it is therefore perhaps worth pointing out that there is at least one practicable and

systematic alternative to the e^2 expansion: the expansion of $\{G(p)\}^{-1}$ and $\{D(k)\}^{-1}$ in powers of $(p-m)$ and $(k^2-\mu^2)$ respectively. The fact that the coefficients need not be developed as power series in e^2 is encouraging. The radius of convergence of such power series is of course unknown, and analytical continuation might be required; but, as in a renormalized theory, at least at low energies, one does not expect wide departures from free particle states to be very important, the procedure is physically plausible.

ACKNOWLEDGMENT

The author is indebted to Professor Max Born for several suggestions which led to a material improvement of this paper in manuscript.

APPENDIX

We wish here to justify the assumption that the mathematical procedure, formulated in the rules (7), represents the insertion of vertices in electron lines; and also to generalize the rules for applications beyond those required in the text.

A typical Feynman diagram (see Feynman 1949) can be represented by an expression involving the momentum of each segment of the electron and photon lines which it contains, thus:

$$\left. \begin{aligned} F_0 &= \iint (\Pi_i A_i)(\Pi_j B_j) dk' dp', \\ A_i &= (p_i - m)^{-1} \delta(p_{i+1} - p_i \pm k_j)(ie\gamma_i), \\ B_j &= (\text{Spur } F_j)(k_j^2 - \mu^2)^{-1}, \end{aligned} \right\} \dots\dots (29)$$

where the integrations extend only over the momenta p_i' and k_j' of the internal segments of the particle lines; and F_j is an expression similar in form to F_0 . It should be noticed first that the rules (7) can be applied straightforwardly to (29), if supplemented by an additional rule

$$\left. \begin{aligned} F_\lambda(l) &= F_\lambda^{(1)}(p_i; l) F^{(2)}(p_j) + F^{(1)}(p_i) F_\lambda^{(2)}(p_j; l) \quad \text{when} \\ F &= F^{(1)}(p_i) F^{(2)}(p_j) \quad \text{and} \quad i \neq j, \end{aligned} \right\} \dots\dots (30)$$

necessitated by the fact that more than one electron momentum is involved. One obtains, in fact, from (29)

$$F_{0\lambda}(l) = \iint \{ \Sigma_i (\Pi_{n < i} A_n) A_{i\lambda}(l) (\Pi_{n > i} A_n) (\Pi_j B_j) + \Sigma_j (\Pi_i A_i) (\Pi_{n < j} B_n) B_{j\lambda}(l) (\Pi_{n > j} B_n) \} dk' dp', \dots\dots (31)$$

where

$$\left. \begin{aligned} A_{i\lambda}(l) &= -ie(p_i - m)^{-1} \gamma_\lambda (p_i - l - m)^{-1} \delta(p_{i+1} - p_i \pm k_j + l)(ie\gamma_i), \\ B_{j\lambda}(l) &= \{ \text{Spur } F_{j\lambda}(l) \} (k_j^2 - \mu^2)^{-1}. \end{aligned} \right\} \dots\dots (32)$$

This is a sum representing all diagrams which can be obtained from that represented by F_0 by the insertion of a simple vertex.

The effect has now to be considered of eliminating the factors $\delta(p_{i+1} - p_i \pm k_j)$ by performing the integrations over p_i' in (29) and (31). The number of independent electron momenta is thereby reduced to one for each complete electron line, but the rules (7) and (30) are still applicable to those which survive.

The only complication arises from the self-energy insertions in the photon lines, which are represented by the factors $(\text{Spur } F_j)$ in (29). These can be

accounted for as follows. Suppose the position of the factors B_j in (29), and of B_j and $B_{j\lambda}(l)$ in (31) is changed, so that each stands before the factor

$$\delta(p_{i+1} - p_i - k_j)(ie\gamma_j)$$

representing the vertex at which the photon momentum k_j is absorbed. (It is left at the end if it corresponds to an externally emitted photon.) Considering a sequence of factors $(k_a^2 - \mu^2)^{-1}(\text{spur } F_j)(k_j^2 - \mu^2)^{-1}\delta(p_{i+1} - p_i - k_j)$ in (29), or $(k_a^2 - \mu^2)^{-1}\{\text{spur } F_{j\lambda}(l)\} \cdot (k_j^2 - \mu^2)^{-1}\delta(p_{i+1} - p_i - k_j)$ in the relevant term of (31), one finds that by integrations over electron momenta all the δ -functions appearing in F_j and $F_{j\lambda}(l)$ can be removed except one, which reduces to $\delta(k_a - k_j)$ in F_j and $\delta(k_a - l - k_i)$ in $F_{j\lambda}(l)$. Because of these δ -functions, the sequence of factors $(\text{spur } F_j)(k_j^2 - \mu^2)^{-1}\delta(p_{i+1} - p_i - k_j)$ can be written

$$(\text{Spur } F_j)(k_a^2 - \mu^2)^{-1}\delta(p_{i+1} - p_i - k_a),$$

and $\{\text{Spur } F_{j\lambda}(l)\}(k_j^2 - \mu^2)^{-1}\delta(p_{i+1} - p_i - k_j)$ can be written

$$\{\text{Spur } F_{j\lambda}(l)\}\{(k_a - l)^2 - \mu^2\}^{-1}\delta(p_{i+1} - p_i - k_a + l).$$

The practical result is therefore as follows. Given an expression F which involves $D(k)$, $D_\lambda(k; l)$, $D_{\lambda\mu}(k; l, r)$ etc., one should apply the rule

$$F_\lambda(l) = F^{(1)}(k)F_\lambda^{(2)}(k; l) + F_\lambda^{(1)}(k; l)F^{(2)}(k - l) \quad \text{when} \quad F = F^{(1)}(k)F^{(2)}(k). \quad \dots\dots(33)$$

From this it follows in particular [by substituting

$$F^{(1)}(k) = \{D(k)\}^{-1}, \quad F^{(2)}(k) = D(k)] \quad \text{that} \\ D_\lambda(k; l) = -ieD(k)P_\lambda(k; l)D(k - l), \quad \dots\dots(34)$$

where

$$P(k) = \{ieD(k)\}^{-1}. \quad \dots\dots(35)$$

The last two formulae may be compared with (6) and (10) respectively. In evaluating $P_\lambda(k; l)$ one naturally regards $P(k)$ as a functional of the electron momentum which survives in the self-energy integral.

REFERENCES

- DYSON, F. J., 1949, *Phys. Rev.*, **75**, 1736; 1951, *Proc. Roy. Soc. A*, **207**, 395; 1952, *Phys. Rev.*, **85**, 631.
 EDWARDS, S. F., 1953, *Phys. Rev.*, **90**, 284.
 FEYNMAN, R. P., 1949, *Phys. Rev.*, **76**, 769.
 KÄLLÉN, G., 1952, *Helv. Phys. Acta*, **25**, 417.
 MATTHEWS, P. T., and SALAM, A., 1951, *Rev. Mod. Phys.*, **23**, 311.
 SALAM, A., 1951, *Phys. Rev.*, **82**, 217.
 SCHWINGER, J. S., 1951, *Proc. Nat. Acad. Sci., Wash.*, **37**, 452, 455.
 THIRRING, W., 1950, *Phil. Mag.*, **41**, 1193.
 WARD, J. C., 1950, *Phys. Rev.*, **78**, 182; 1951, *Proc. Phys. Soc. A*, **64**, 54.

The Effect of Nuclear Multipole Moments on Electron Scattering

BY K. PARKER

Wheatstone Department of Physics, King's College, London

Communicated by H. S. W. Massey; MS. received 20th May 1953

Abstract. It is shown that possible effects of nuclear multiple moments on electron scattering are too small for measurement with the present experimental technique.

EARLY experiments on the scattering of fast electrons (with kinetic energies greater than about 0.1 mev) gave contradictory results, but the experimental results of Van de Graaff *et al.* (1946), Buechner *et al.* (1947) and Sigrist (1943) are in quite good agreement with the calculations of Bartlett and Watson (1940), McKinley and Feshbach (1948) and Feshbach (1952) based on the theory of Mott (1929, 1932). Recent experiments by Kinzinger and Bothe (1952), Paul and Reich (1952) and Kinzinger (1953) lead to cross sections which show a definite deviation from the calculated values of McKinley and Feshbach for $Z > 40$, especially at high angles. Improvement in the technique of high-angle measurement might lead to better agreement with the theory, but meanwhile it is of interest to investigate any possible corrections to the theoretical calculations. Here we consider the effect on the scattering of the perturbation of the coulomb field of the nucleus by the nuclear electric and magnetic multipole moments.

Any treatment of the problem will be approximate since non-central forces are involved. The distribution of charge and current inside the finite nucleus gives rise to electric and magnetic multipole moments, and it is easy to calculate the scalar and vector potentials for points outside a sphere enclosing the nucleus. We now suppose that these potentials are correct at all distances r , measured from the centre of the nucleus; in other words, we approximate the potentials by those due to a series of point multipoles situated at the centre of the nucleus.

The theory of nuclear multipole moments is given by Blatt and Weisskopf (1952) and it is easily shown that if the nucleus has an axis of symmetry, as we shall assume, then the scalar potential at \mathbf{r} is

$$\phi(\mathbf{r}) = \sum_{n=0}^{\infty} \left(\frac{4\pi}{2n+1} \right)^{1/2} Q_{n0} r^{-n-1} P_n(\cos \Theta), \quad \dots\dots(1)$$

where Θ is the angle between the axis of symmetry and the direction of \mathbf{r} . Under normal physical conditions the axis of symmetry will have a completely random direction in space, and observable physical effects will be obtained by averaging over λ and μ , the polar and azimuthal angles of the direction of the axis of symmetry. Q_{nm} is an electric multipole moment and we have the relations $Z\mathbf{e} = (4\pi)^{1/2} Q_{00}$, $Q\mathbf{e} = (16\pi/5)^{1/2} Q_{20}$, where \mathbf{e} is the proton charge, Z the atomic number of the nucleus, and Q the experimentally measured quadrupole moment. The dipole term is absent from parity considerations.

The usual integral equation treatment (Mott and Massey 1949) gives the cross section on averaging over λ and μ as

$$I(\theta, \phi) = \frac{m^2}{4\pi^2\hbar^4} \iint \frac{\sin \lambda \, d\lambda \, d\mu}{4\pi} \iint \exp \{ik\mathbf{n} \cdot (\mathbf{r}'' - \mathbf{r}')\} \times \psi(\mathbf{r}', \lambda, \mu) \psi^*(\mathbf{r}'', \lambda, \mu) \epsilon^2 V(\mathbf{r}', \lambda, \mu) V^*(\mathbf{r}'', \lambda, \mu) d\tau' d\tau'' \quad \dots\dots (2)$$

where we write $\epsilon V = -e\phi$; ϵ is some suitable expansion parameter. If we assume the existence of a convergent Born expansion, we may take $\epsilon = Ze^2/\hbar v = eQ_{00}/\hbar v$, v being the incident velocity, and expand $I(\theta, \phi)$ as a power series in ϵ ; $\psi(\mathbf{r}, \lambda, \mu)$ is the wave function for the scattering and \mathbf{n} a unit vector in the direction of \mathbf{r} . Electrons of momentum $\hbar\mathbf{k}$ are supposed to be incident along the polar axis. The problem is here considered non-relativistically for simplicity; the extension to Dirac's equation is straightforward. The wave function may be written in the form (Jost and Pais 1951, eqns. (6), (7))

$$\psi(\mathbf{r}, \lambda, \mu) = \exp(i\mathbf{k}_0 \cdot \mathbf{r}) + \sum_{n=1}^{\infty} \epsilon^n \int \underset{n \text{ integrals}}{F(\mathbf{r}; \mathbf{r}', \mathbf{r}'', \dots \mathbf{r}^{(n)})} \times V(\mathbf{r}', \lambda, \mu) V(\mathbf{r}'', \lambda, \mu) \dots V(\mathbf{r}^{(n)}, \lambda, \mu) d\tau' d\tau'' \dots d\tau^{(n)} \quad \dots\dots (3)$$

where the λ, μ dependence is solely in the terms in V ; $\mathbf{k}_0 = k\mathbf{n}_0$ where \mathbf{n}_0 is a unit vector in the direction of the incident beam. A typical term in $\epsilon V(\mathbf{r}', \lambda, \mu)$ is

$$-eQ_{n0}(r')^{-n-1} P_n(\cos \Theta') = -e(r')^{-n-1} Q_{n0} \sum_{m=-n}^n \{4\pi/(2n+1)\} Y_{nm}^*(\lambda, \mu) Y_{nm}(\theta', \phi'), \quad \dots\dots (4)$$

where

$$Y_{mn}(\theta, \phi) = \left\{ \frac{(2n+1)(n-|m|)!}{4\pi(n+|m|)!} \right\}^{1/2} P_n^m(\cos \theta) \exp(im\phi), \quad \dots\dots (5)$$

and such expressions completely determine the dependence of ϵV on λ, μ . Combining (1), (2) and (3) the cross section is given as a sum of terms depending on the Q_{n0} and the terms in Q_{00} represent the Born expansion for a coulomb potential. We can now show that terms in $Q_{00}^s Q_{r0}$ (r, s positive integers) will not arise because of the averaging over λ, μ . Terms in $Q_{00}^s Q_{r0}$ arise as follows:

(a) We take the Q_{r0} from one of the potentials in (2). We must then take the Q_{00} terms in the other potential and the two wave functions. These are independent of λ, μ . Integration over λ, μ then gives zero by the orthogonality relations for the $Y_{nm}(\lambda, \mu)$.

(b) We take the Q_{r0} from one of the wave functions. By a similar procedure we again get zero on averaging.

For all actual nuclei $Q_{10}=0$ and Q_{r0} is negligible for $r>2$. The largest perturbation term is then that in Q_{20}^2 which comes from the $\exp\{i\mathbf{k}_0 \cdot \mathbf{r}\}$ part of ψ taken with the Q_{20} term in V , so that as a first approximation to the cross section we have

$$I(\theta, \phi) = \frac{m^2}{16\pi^3\hbar^4} \iint \sin \lambda \, d\lambda \, d\mu \iint \exp \{ik\mathbf{n} \cdot (\mathbf{r}'' - \mathbf{r}')\} \exp \{ik\mathbf{n}_0 \cdot (\mathbf{r}' - \mathbf{r}'')\} \times \left[-\frac{Ze^2}{r'} - \frac{Qe^2}{4r'^3} (3 \cos^2 \Theta' - 1) \right] \left[-\frac{Ze^2}{r''} - \frac{Qe^2}{4r''^3} (3 \cos^2 \Theta'' - 1) \right] d\tau' d\tau'' \quad \dots\dots (6)$$

$$= I_0(\theta, \phi) + \frac{Q^2 e^4 m^2}{256\pi^3\hbar^4} \iint \sin \lambda \, d\lambda \, d\mu \iint (r')^{-3} (r'')^{-3} \exp \{ik(\mathbf{n}_0 - \mathbf{n}) \cdot (\mathbf{r}' - \mathbf{r}'')\} \times (3 \cos^2 \Theta' - 1)(3 \cos^2 \Theta'' - 1) d\tau' d\tau'' \quad \dots\dots (7)$$

since the terms in Q average to zero.

$I_0(\theta, \phi)$ is the first Born approximation for coulomb scattering which, as is well known, is equal to the exact coulomb cross section.

Since $\cos \Theta = \cos \lambda \cos \theta' + \sin \lambda \sin \theta' \cos(\mu - \phi')$, with a similar formula for $\cos \Theta''$, we may carry out the averaging over λ, μ with the help of the addition theorem for Legendre functions. This gives

$$\iint \sin \lambda d\lambda d\mu P_n(\cos \Theta') P_n(\cos \Theta'') = \{4\pi/(2n+1)\} P_n(\cos \omega), \quad \dots\dots (8)$$

where ω is the angle between \mathbf{r}' and \mathbf{r}'' . Hence the second term of (6) may be written

$$I_2(\theta, \phi) = \frac{Q^2 e^4 m^2}{80\pi^2 \hbar^4} \iint (r')^{-3} (r'')^{-3} \exp \{ik(\mathbf{n}_0 - \mathbf{n}) \cdot (\mathbf{r}' - \mathbf{r}'')\} P_2(\cos \omega) d\tau' d\tau''. \quad (9)$$

If we take a new coordinate system with polar axis along $\mathbf{n}_0 - \mathbf{n}$ given by (r, α, β) then

$$I_2(\theta, \phi) = \frac{Q^2 e^4 m^2}{80\pi^2 \hbar^4} \iint (r')^{-3} (r'')^{-3} \exp \{ik(\mathbf{n}_0 - \mathbf{n}) \cdot (\mathbf{r}' - \mathbf{r}'')\} \\ \times \sum_{m=-2}^2 \frac{(l-|m|)!}{(l+|m|)!} P_2^m(\cos \alpha') P_2^m(\cos \alpha'') \exp \{im(\phi' - \phi'')\}, \quad \dots\dots (10)$$

where the addition theorem for Legendre functions has again been used. Terms with $m \neq 0$ vanish on performing the β' and β'' integrations. Hence

$$I_2(\theta, \phi) = \frac{Q^2 e^4 m^2}{20\hbar^4} \left| \iint (r')^{-1} \exp(iKr' \cos \alpha') P_2(\cos \alpha') \sin \alpha' d\alpha' dr \right|^2 \quad \dots\dots (11)$$

where $K = 2k \sin(\theta/2)$. The integral over α' is evaluated by writing $x = \cos \alpha'$ and integrating by parts. Finally,

$$I_2(\theta, \phi) = \frac{Q^2 e^4 m^2}{5\hbar^4} \left\{ \int_0^\infty \left(\frac{\sin y}{y^2} + \frac{3 \cos y}{y^3} - \frac{3 \sin y}{y^4} \right) dy \right\}^2 \quad \dots\dots (12)$$

and the integral is evaluated by integrating between ϵ and ∞ and letting ϵ tend to zero. This leads to a finite value of $-\frac{1}{3}$ for the integral and therefore

$$I_2(\theta, \phi) = \frac{Q^2 e^4 m^2}{45\hbar^4} \quad (\text{non-relativistic}). \quad \dots\dots (13)$$

Calculations with the relativistic wave equation are essentially similar and lead to

$$I_2(\theta, \phi) = \frac{Q^2 e^4 m^2}{45\hbar^4} \frac{1 - (v/c)^2 \sin^2(\theta/2)}{1 - (v/c)^2} \quad (\text{relativistic}). \quad \dots\dots (14)$$

This correction term has a maximum value of about $2 \times 10^{-30} \text{ cm}^2$, which is negligible compared with the cross section for pure coulomb scattering, this latter quantity being of the order of 10^{-23} cm^2 . Even if it were possible to align nuclei so that all axes of symmetry were parallel the effect would still be small. The unaveraged term in Q_{20} is approximately 10^{-26} cm^2 .

Similar results may be obtained by considering the magnetic moment of the nucleus, and here we find the largest correction term is approximately $2 \times 10^{-31} \text{ cm}^2$ if we average over λ, μ ; without averaging, the largest term is of order 10^{-26} cm^2 . This problem has been previously investigated by Massey (1930) who, using a somewhat different method for the evaluation of the first Born approximation, arrives at similar results.

Thus, our calculations show that the nuclear magnetic and electric quadrupole moments may be ignored in experiments on the scattering of fast electrons by nuclei. The perturbations to the cross section are so small as to be well inside the experimental error. Even with aligned nuclei we need an accuracy of one part in a thousand to detect any effect and, as experiments with aligned nuclei must be performed at temperatures of less than 1°K , this is most unlikely to be attained. In view of the numerical values obtained it does not seem worth while to take into account the correction to the effect due to the finite size of the nucleus.

ACKNOWLEDGMENTS

I should like to express my gratitude to Dr. L. R. B. Elton for suggesting this problem and for many helpful discussions. My thanks are also due to London University for the award of a postgraduate scholarship and to King's College for the award of the Layton Research Studentship, during the tenure of which this investigation was made.

REFERENCES

- BARTLETT, J. H., and WATSON, R. E., 1940, *Proc. Amer. Acad. Arts Sci.*, **74**, 53.
 BLATT, J. M., and WEISSKOPF, V. F., 1952, *Theoretical Nuclear Physics* (New York: Wiley), chap. 1, § 7.
 BUECHNER, W. W., VAN DE GRAAFF, R. J., SPERDUTO, A., BURRILL, E. A., Jr., and FESHBACH, H., 1947, *Phys. Rev.*, **72**, 678.
 FESHBACH, H., 1952, *Phys. Rev.*, **88**, 295.
 JOST, R., and PAIS, A., 1951, *Phys. Rev.*, **82**, 840.
 KINZINGER, E., 1953, *Z. Naturforsch.*, **8a**, 312.
 KINZINGER, E., and BOTHE, W., 1952, *Z. Naturforsch.*, **7a**, 390.
 MASSEY, H. S. W., 1930, *Proc. Roy. Soc. A*, **127**, 666.
 MCKINLEY, W. A., Jr., and FESHBACH, H., 1948, *Phys. Rev.*, **74**, 1759.
 MOTT, N. F., 1929, *Proc. Roy. Soc. A*, **124**, 426; 1932, *Ibid.*, **135**, 429.
 MOTT, N. F., and MASSEY, H. S. W., 1949, *The Theory of Atomic Collisions*, 2nd Edn. (Oxford: University Press), chap. vii, § 1.
 PAUL, W., and REICH, H., 1952, *Z. Phys.*, **131**, 326.
 SIGRIST, W., 1943, *Helv. Phys. Acta*, **16**, 471.
 VAN DE GRAAFF, R. J., BUECHNER, W. W., and FESHBACH, H., 1946, *Phys. Rev.*, **69**, 452.

The Absorption Spectrum of SnS Vapour in the Ultra-Violet and Schumann Regions

By R. F. BARROW, G. DRUMMOND AND H. C. ROWLINSON

Physical Chemistry Laboratory, Oxford University

MS. received 1st July 1953

Abstract. New spectrograms of the E-X system of SnS have been taken, and additional bands have been assigned to the short wavelength end of this system. A fairly short extrapolation leads to a dissociation limit at about 40850 cm^{-1} above $v''=0$. The energy of dissociation of SnS is found to be $110\text{ kcal mole}^{-1}$, and this value is shown to be consistent with thermochemical information. The absorption spectrum in the Schumann region has also been examined; two band systems and a region of continuous absorption have been observed.

§1. THE E-X SYSTEM OF SNS

THE ultra-violet band systems E-X of GeS, GeSe (Drummond and Barrow 1952b), SnO (Eisler and Barrow 1949) and SnSe (Vago and Barrow 1946) exhibit long $v''=0$ progressions from which fairly sharp dissociation limits have been obtained. Although the E-X system of SnS has already been the subject of careful study by Rochester (1935), it was thought possible that the existing vibrational analysis might be capable of extension to higher values of v' . Earlier spectrograms taken by Mrs. E. E. Richards of the system in emission in a heavy current, positive column discharge enabled Rochester's analysis to be confirmed, but led to no extension of the system. New pictures have now been taken of the system in absorption. Mixtures of stannous sulphide and tin were heated to temperatures around 1350°C , and the system was photographed on a Hilger Medium Quartz spectrograph. Measurements on the main part of the E-X system are in good agreement with those of Rochester, but new bands which—on grounds of appearance, intensity, and the occurrence of the ground state intervals for SnS—appear to constitute an extension of this system have been found in the region $2500\text{--}2620\text{ \AA}$. Details of the bands are given in table 1. The upper-state vibrational intervals do not vary regularly with v' , and there appears to be a perturbation with a maximum at about $v'=21$ or 22 . As a result, the numbering of bands with $v'\geq 23$ may not be quite correct.

§2. THE ABSORPTION SPECTRUM OF SNS IN THE SCHUMANN REGION

The absorption spectrum of SnS has also been examined in the region $1500\text{--}2000\text{ \AA}$, using a 1 m vacuum grating spectrograph of reciprocal dispersion about 8.6 \AA mm^{-1} . SnS vapour was obtained by heating SnS+Sn to temperatures between $1150\text{--}1250^\circ\text{C}$: the addition of Sn metal effectively removed S_2 impurity, so that the strong S_2 band at 1796.9 \AA was not visible, but SnO bands were more persistent and were never entirely removed.

Three features ascribed to SnS have been observed: (i) a weak system of red-degraded bands in the region $1860\text{--}1935\text{ \AA}$, (ii) a $v'=0$ progression of three

strong bands at 1788.0, 1803.5 and 1819.2 Å, (iii) a region of continuous absorption, sharply bounded on the short-wavelength side with a more diffuse long-wavelength edge. Details are given in tables 2 and 3, where these features are given the non-committal designations p, q and r, respectively.

Table 1. Band Heads of the E-X System of SnS

v', v''	λ (Å)	ν (cm ⁻¹)	Intensity
20, 0	2612.8	38262	5
21, 0	00.1	449	4
22, 0	2592.6	560	3
25, 1	81.9	720	1
28, 2	78.4	772	1
26, 1	69.2	911	1
24, 0	62.8	39008	0
27, 1	57.8	084	1
25, 0	49.8	207	0
28, 1	46.6	256	1
26, 0; 29, 1	36.5	413	1
30, 1	27.2	558	0
27, 0	26.7	565	0
28, 0	15.6	740	0
29, 0	06.1	891	0

Table 2. Absorption Bands Attributed to SnS

λ_{vac} (Å)	ν_{vac} (cm ⁻¹)	Degradation	Intensity	Assignment
1933.1	51732	R	0	p. 0, 1
18.3	52128	R	0	p. 1, 1
04.0	522	R	0	p. 2, 1
1892.4	844	R	0	—
86.5	53009	R	1	p. 2, 0
75.6	317	R	0	—
73.2	386	R	1	p. 3, 0
60.0	762	R	0	p. 4, 0
19.2	54969.6	R	5	q. 0, 2
03.5	55449	R	8	q. 0, 1
1788.0	928	R	8	q. 0, 0
70.9	56470	V	8	r
57.9	887	R	10	r

Table 3. States of SnS

State	T_0	ω	Notes
r	56890–56470	—	continuum
q	55928	—	$v'=0$ progression only
p	(52220)	(395)	—

Constants for the lower-lying states of SnS are given by Rochester (1935) and Shawhan (1935).

The most interesting point about the present observations is the evidence that there is at least one repulsive state of SnS at about 56 000 cm⁻¹. From the absence of bands with $v'=1$ in the transition $q-x^1\Sigma$ we may infer $D_0'' \simeq 56\,100 - E_A$, and from the continuous absorption, $D_0'' \leq 56\,890 - E_A$. If the apparent strength of these transitions is interpreted as meaning that they are singlet-singlet transitions, then the only likely products are

$\text{Sn}(^1\text{D}_2) + \text{S}(^1\text{D}_2)$, and, from the lower limit, $D_{\text{SnS}}'' \simeq 109.4$ kcal, a figure which, as will be seen, fits in well with other evidence about the dissociation energy of this molecule.

§3. THE DISSOCIATION ENERGY OF SnS

A short graphical extrapolation of the levels in the E state leads to a limit at 40850 cm^{-1} above $v''=0$, which should be reliable, provided only that the vibrational levels do not follow an unexpected course after the perturbation. The corresponding limit has also been observed for SnO (Eisler and Barrow 1949), and thermochemical evidence is clear that this limit corresponds to dissociation into $\text{Sn}(^3\text{P}) + \text{O}(^3\text{P})$: which ^3P sub-level of Sn is involved is not however certain, although the figures given by Drummond and Barrow (1952a) suggested that Sn is in the $^3\text{P}_2$ state. The present extrapolation for SnS thus corresponds to $D_0'' = 111 \pm 6$ kcal, where the limits represent the spread of the ^3P levels of Sn + S.

A value of $D_0'' \simeq 110$ kcal is supported in two ways. First, a long extrapolation of the ground-state vibrational intervals, using the mean of the constants derived by Rochester (1935) and by Shawhan (1935), gives $D_0'' \simeq 120$ kcal. The justification for attaching any weight to this value comes from a study of the oxides of this group (see, for example, Brewer 1953), from which evidence has accumulated that the linear ground-state extrapolations give dissociation energies which are in very fair agreement with the thermochemical values, provided, of course, that the values of $x_e''\omega_e''$ are accurately known.

Secondly, there is the thermochemical evidence on SnS itself. The boiling point of SnS is given as 1513°K (Biltz and Mecklenburg 1909). If then it is assumed that the heat-capacity equation of Kelley (1949) for SnS_c can be extrapolated to the melting point (1153°K), that the heat capacity of the liquid is $20\text{ cal mol}^{-1}\text{ }^\circ\text{C}$, and that the entropy of fusion is $3\text{ cal mol}^{-1}\text{ }^\circ\text{C}$ (as for PbS), we find that the heat of sublimation at 298°K is $52.6\text{ kcal mole}^{-1}$, using $S_{298}^0 = 18.2$ for SnS_c (Kireev 1946) together with values of S^0 and of $H_{1513} - H_{298}$ for SnS_{gas} tabulated by Kelley (1949). Combining $L_{\text{SnS}} = 52.6$ kcal with the values of $L_{\text{Sn}} = 65$ kcal (the mean of the values proposed by Baughan and by Brewer, private communications), of $Q_f(\text{SnS}) = -18.6$ kcal and of $Q_f(\frac{1}{2}\text{S}_2) = 14.9$ kcal (National Bureau of Standards 1952), we obtain $D_{298}''(\text{SnS}) = 97$ or 84 kcal according as to whether the value of $\frac{1}{2}D(\text{S}_2)$ is taken as 51 or 38 kcal, corresponding to the limiting values of $D(\text{S}_2)$, 4.4 or 3.3 eV (Gaydon 1953). Clearly this estimate is of no great precision, but it may be taken as supporting a value of $D_0''(\text{SnS})$ of about 100 kcal, and as an indication that the high value of $D(\text{S}_2)$ is the most likely one. This question will be clarified when vapour pressure figures become available for SnS(crystal).

It should be noted that a much lower value, $D(\text{SnS}) \leq 68.5$ kcal, is suggested by the work of Shawhan (1935) on the basis of a supposed predissociation in the A-x system. However, no adequate analysis of all the SnS bands in the region of the A-x system has yet been put forward, and it seems probable that transitions to more than one upper electronic state are involved. A similar state of affairs arises in the long-wavelength bands of SnO and SnSe: in SnTe, what appear to be the corresponding bands are resolvable into two overlapping systems (Barrow and Vago 1944). Thus the explanation of Shawhan's

observations may well lie in an interaction between the neighbouring states, and the predissociation cannot be regarded as established.

We therefore conclude that the best value of $D_0''(\text{SnS})$ that can be derived with the information available at present is 110 kcal.

ACKNOWLEDGMENTS

Two of us (G. D. and H. C. R.) are glad to acknowledge the award of maintenance grants from the Department of Scientific and Industrial Research.

REFERENCES

- BARROW, R. F., and VAGO, E. E., 1944, *Proc. Phys. Soc.*, **56**, 78.
BILTZ, W., and MECKLENBURG, W., 1909, *Z. anorg. Chem.*, **64**, 226.
BREWER, L., 1953, *Chem. Rev.*, **52**, 1.
DRUMMOND, G., and BARROW, R. F., 1952 a, *Proc. Phys. Soc. A*, **65**, 148; 1952 b, *Ibid.*, 277.
EISLER, B., and BARROW, R. F., 1949, *Proc. Phys. Soc. A*, **62**, 740.
GAYDON, A. G., 1953, *Dissociation Energies* (London: Chapman and Hall).
KELLEY, K. K., 1949, *U.S. Bureau Mines Bull.*, Nos. 476, 477.
KIREEV, V. A., 1946, *J. Gen. Chem., U.S.S.R.*, **16**, 1569.
NATIONAL BUREAU OF STANDARDS, 1952, Circular 500.
ROCHESTER, G. D., 1935, *Proc. Roy. Soc. A*, **150**, 668.
SHAWHAN, E. N., 1935, *Phys. Rev.*, **48**, 521.
VAGO, E. E., and BARROW, R. F., 1946, *Proc. Phys. Soc.*, **58**, 707.

The Energy Band Structure of a Linear Metal

By E. P. WOHLFARTH

Department of Mathematics, Imperial College, London

MS. received 27th May 1953

Abstract. A tight binding calculation of the one-electron energy as a function of wave number is described for a linear chain of hydrogen atoms in the ground state. The calculation is accurate to the order of $\exp(-2a)$, where a is the interatomic distance (in atomic units), all non-orthogonality and energy integrals of this order of magnitude being included in the energy expression. A closed expression for the band width is derived and compared with expressions corresponding in their approximations to those usually made in tight binding calculations for actual metals.

§ 1. INTRODUCTION

IN a recent paper Fletcher (1952, see also Fletcher and Wohlfarth 1951) has carried out a calculation of the energy band structure of metallic nickel on the basis of the tight binding method. The approximations made in this calculation include the following: (i) neglect of non-orthogonality of the atomic wave functions based on different atoms in the crystal; (ii) use of a particular approximate potential field for the electrons in the crystal and in the free atom; (iii) neglect of contributions to the matrix elements of the one-electron Hamiltonian operator H_1 other than those arising from the overlap of the atomic wave functions of neighbouring atoms in the crystal.

A complete investigation of the effects of these approximations on the numerical results of Fletcher's calculation would be extremely laborious in view of the complexity of the calculation even in its simplest form. It is proposed, therefore, to describe an accurate tight binding calculation for the simplest possible case, a linear chain of hydrogen atoms in the ground state, for which these effects may be examined. Here it is possible (i) to include non-orthogonality integrals to any order of magnitude (in the present calculation the final expressions are accurate to the order of $\exp(-2a)$, where a is the interatomic distance in atomic units); (ii) to use an exact expression for the potential field; (iii) to include matrix elements of H_1 to the same order of magnitude as in (i).

Since the various energy and non-orthogonality integrals which occur in the calculation may be evaluated analytically, it is, in fact, possible to obtain a closed expression for the width of the energy band. Comparison may then be made with approximate expressions for the band width, corresponding to the nearest neighbour assumption with or without inclusion of the nearest neighbour non-orthogonality integral. The calculation also shows that the consistent inclusion of all the terms in the energy expression leads to the exact cancellation of all divergent terms of the form $\exp(-na) \ln N$, where N is the number of atoms, assumed large, and $n = 1, 2$. As shown below, these terms arise through the use of the expression (6) for the potential field. This effect does not seem to have been noted previously.

Earlier work on the band structure of a linear metal on the basis of the tight binding approximation includes the calculation of Hoffmann and Kónya (1948,

1951), who included the effects of non-orthogonality integrals for neighbouring atoms and demonstrated the effects of their inclusion in distorting the density of states curve from its familiar U-shaped form. Here matrix elements of H_1 for non-neighbouring atoms were neglected. Further, the values of the integrals included were left unspecified. Calculations for the linear molecule H_4 to give the total energy, including exchange and coulomb terms, have been carried out by Taylor (1951). In this work account was also taken of configurational interactions, a difficult task even for this simple molecule. The effects of including non-orthogonality integrals and matrix elements of the total Hamiltonian operator for atoms more widely separated than nearest neighbours have been considered by Löwdin (1951) in his work on metallic sodium. This work is based on a modified tight binding approximation; clearly this method must be taken to a much higher degree of approximation for an alkali metal, where the s electrons are almost free, than in d band calculations for a transition metal like nickel, the d electrons being here much more 'tightly bound'. In Löwdin's calculation interactions between neighbours up to order nine are included. The calculations are complicated, and it is difficult to assess the effects of including or omitting terms of different orders of magnitude in the total energy expression. Other tight binding calculations which include non-orthogonality integrals to some extent include those of Coulson *et al.* (Coulson and Taylor 1952, Duncanson and Coulson 1952, Taylor and Coulson 1952) on graphite and related compounds. The general non-orthogonality problem has been discussed by Löwdin (1950).

§ 2. CALCULATION OF THE ONE-ELECTRON ENERGY. DISCUSSION

It is required to calculate the one-electron energy of the linear metal as a function of the wave number k . A general expression for the total energy on the basis of the tight binding approximation has been given by Wohlfarth (1953). It is noted that the one-electron energy, there denoted by F_i , diverges (the divergence being of the form $\ln N$ for a linear metal containing N atoms, see relations (1), (2) and (8) below), so that it is convenient to supplement F_i by a term $2K/N$, where K is the total interaction energy of the ion cores. Since K is independent of wave number this effective re-definition of the energy zero has no influence on the band width. A similar redefinition is necessary in obtaining a convergent expression for the coulomb energy of the metal; this situation had been discussed previously by Seitz (1940, p. 360 ff.) in deriving an expression for the total energy on the basis of the cellular method.

It is convenient to denote the term $2K/N$ by D , so that for a linear metal of hydrogen atoms, using atomic units,

$$D = 4 \sum_{n=1}^G (an)^{-1}, \quad \dots\dots(1)$$

where $N = 2G + 1$ is the number of atoms, assumed large, and a the interatomic distance; the term D diverges as $\ln N$ as $N \rightarrow \infty$, but, as already pointed out, the final energy expression is free of all terms involving D .

The energy expression it is required to evaluate is, with the re-definition of the energy zero discussed above,

$$E = E(k) = E_0 + D - \left\{ J_0 + 2 \sum_{n=1}^G J_n \cos(ank) \right\} / \left\{ S_0 + 2 \sum_{n=1}^G S_n \cos(ank) \right\}, \dots\dots(2)$$

expressed in atomic units. Here k is the wave number, defining the 'Brillouin zone' by $-\pi/a \leq k \leq \pi/a$, and E_0 is the energy of an isolated atom. Also

$$J_n = - \int \phi(r)(V-U)\phi(r-an) d\tau(\mathbf{r}), \quad \dots\dots(3)$$

$$S_n = \int \phi(r)\phi(r-an) d\tau(\mathbf{r}), \quad \dots\dots(4)$$

where $\phi(r-an)$ is the atomic 1s function of the H atom based on the nucleus having position an in the chain; i.e.

$$\phi(r) = \pi^{-1/2} \exp(-r). \quad \dots\dots(5)$$

In (3) U is the potential for an electron in the field of an isolated nucleus and V the potential in the field of all the nuclei of the metal, so that, in atomic units,

$$-(V-U) = 4 \sum_{n=1}^G r_n^{-1}, \quad \dots\dots(6)$$

where $r_n = |r-an|$ is the distance of the electron at r from the nucleus at an .

In the present calculation the interatomic distance a is taken to be so large that $\exp(-3a)$ is negligible. Then only integrals J_n , S_n for $n \leq 2$ need be included in (2), since, in effect, J_n and S_n are both of order $\exp(-an)$. Using (4) and (5) it is easy to show that

$$S_n = S(an), \text{ where } S(x) = \exp(-x)(1+x+\frac{1}{3}x^2), \quad \dots\dots(7)$$

Also, correct to $O\{\exp(-2a)\}$,

$$J_0 = 4 \sum_{n=1}^G \int r_n^{-1} \phi^2(r_0) d\tau(\mathbf{r}) = D - 4 \exp(-2a)(1+a)/a, \quad \dots\dots(8)$$

where D is given by (1).

The integral J_1 may be written, using (5),

$$J_1 = 2\pi^{-1} \int r_1^{-1} \exp\{-(r_0+r_1)\} d\tau(\mathbf{r}) + 4\pi^{-1} \sum_{n=2}^G \int r_n^{-1} \exp\{-(r_0+r_1)\} d\tau(\mathbf{r}).$$

The integrals in the second term are one-electron three-centre integrals for which a general formula has been given by Hirschfelder, Eyring and Rosen (1936), giving, correct to $O\{\exp(-2a)\}$,

$$J_1 = 2 \exp(-a)(1+a) + 12a^{-1}S(a) \sum_{n=1}^G f(n),$$

$$\left. \begin{aligned} \text{where } f(n) &= (2n+1) - 2n(n+1) \ln \{(n+1)/n\} \\ &= \frac{1}{3}n^{-1} - 2 \sum_{p=2}^{\infty} \frac{(-1)^p}{(p+1)(p+2)} n^{-p}. \end{aligned} \right\} \quad \dots\dots(9)$$

$$\text{Hence } J_1 = 2 \exp(-a)(1+a) + S(a)D - 24a^{-1}S(a)\beta_1, \quad \dots\dots(10)$$

where D is given by (1) and

$$\beta_1 = \sum_{p=2}^{\infty} \frac{(-1)^p \zeta(p)}{(p+1)(p+2)} = 0.098693, \quad \dots\dots(11)$$

where $\zeta(x)$ is the Riemann function (tabulated by Dwight 1941).

The integral J_2 may be written

$$\begin{aligned} J_2 &= 2\pi^{-1} \int r_1^{-1} \exp\{-(r_0+r_2)\} d\tau(\mathbf{r}) + 2\pi^{-1} \int r_2^{-1} \exp\{-(r_0+r_2)\} d\tau(\mathbf{r}) \\ &\quad + 4\pi^{-1} \sum_{n=3}^G \int r_n^{-1} \exp\{-(r_0+r_2)\} d\tau(\mathbf{r}). \end{aligned} \quad \dots\dots(12)$$

The first term in (12) may be evaluated using the general formula of Hirschfelder *et al.* (1936) and is given by

$$\frac{3}{2}a^{-1}\{(\gamma + \ln 4a)S(2a) - \text{Ei}(-4a)S(-2a)\} - 2 \exp(-2a)(2+a), \quad \dots\dots(13)$$

where γ is Euler's constant and $-\text{Ei}(-x)$ the exponential integral. The second term in (12) is given by

$$2 \exp(-2a)(1+2a), \quad \dots\dots(14)$$

and the third term becomes

$$6a^{-1}S(2a) \sum_{n=2}^G f\left(\frac{n-1}{2}\right),$$

where the function f has been defined in (9), i.e. it becomes

$$12a^{-1}S(2a) \sum_{n=2}^G \sum_{p=1}^{\infty} \frac{1}{4p^2-1} n^{-(2p-1)} = S(2a)D - 12a^{-1}S(2a)\beta_2, \quad \dots\dots(15)$$

$$\text{where } \beta_2 = \frac{1}{2} - \sum_{p=2}^{\infty} \left\{ \frac{\zeta(2p-1)}{4p^2-1} \right\} = 0.318\,651. \quad \dots\dots(16)$$

The complete expression for J_2 is given as the sum of the three terms (13), (14) and (15). Inspection shows that $J_1 \sim O\{\exp(-a)\}$, $J_2 \sim O\{\exp(-2a)\}$.

The expression (2) for the energy may be written in the form $E = E_0 - J$, where J may be expanded to give

$$J = \{(J_0 - D) - 2(J_2 - J_0 S_2)\} + \kappa\{J_1 - J_0 S_1\} + \kappa^2\{(J_2 - J_0 S_2) - S_1(J_1 - J_0 S_1)\} + O\{\kappa^3 e^{-3a}\}, \quad \dots\dots(17)$$

where $\kappa = 2 \cos(ak)$. The appearance of terms of the form $J_n - J_0 S_n$ in expressions for the energy of molecules and crystals has been noted by Löwdin (1950), and the properties of such terms have been studied by him. On inserting the values of the integrals the following conclusions may be drawn:

(i) The constant term in the energy expression (2) is free of all terms involving D , which have cancelled out; it may be written in the form $E_0 + O\{\exp(-2a)\}$.

(ii) Similarly the term in κ^2 in (17) is free of all terms involving D and is $O\{\exp(-2a)\}$. This term gives a measure of the distortions of the curve of E against k , and hence of the density of states curve, from symmetrical shape.

(iii) Of greatest interest is the final expression for the energy band width E_B . This is given by

$$E_B = E(k=\pi/a) - E(k=0) = 4\{J_1 - J_0 S_1\}. \quad \dots\dots(18)$$

The expression (18) is accurate to the order of $\exp(-2a)$; explicitly

$$E_B = 8 \exp(-a)\{a(1-4\beta_1) + (1-12\beta_1) - 12a^{-1}\beta_1\}, \quad \dots\dots(19)$$

again free of all terms involving D . Inserting the value of β_1 given by (11),

$$E_B = 4.84a \exp(-a)\{1 - 0.30a^{-1} - 1.96a^{-2}\} + O\{\exp(-3a)\}. \quad \dots\dots(20)$$

The exact relation (20) for the band width may now be compared with approximate expressions corresponding to (i) neglect of all non-orthogonality integrals, and neglect of all energy integrals except those involving overlap between nearest neighbours (equivalent to the approximations of Fletcher's calculation); (ii) inclusion of the non-orthogonality integral as well as of the

energy integral for nearest neighbours and neglect of all other terms. The corresponding expressions are, respectively,

$$(i) E_B = 8a \exp(-a)(1 + a^{-1}), \quad \dots\dots(21)$$

$$(ii) E_B = 2.67a \exp(-a)(1 - 3a^{-1} - 6a^{-2}). \quad \dots\dots(22)$$

It is of interest to note, comparing (20), (21) and (22), that the exact band width is intermediate between the values given by the first and second approximations, in the sense indicated.

It is hoped to extend the calculations given in this paper to two- and three-dimensional lattices at a later stage. It should be pointed out, however, that in d-band calculations the various effects considered here may enter in quite a different way, partly since atomic d-functions have pronounced nodal properties. There are reasons for believing that, with d-functions, the value of the band width corresponding to approximation (i) above (i.e. Fletcher's approximation) lies even closer to the exact value corresponding to the relation (20).

REFERENCES

- COULSON, C. A., and TAYLOR, R., 1952, *Proc. Phys. Soc. A*, **65**, 815.
 DUNCANSON, W. E., and COULSON, C. A., 1952, *Proc. Phys. Soc. A*, **65**, 825.
 DWIGHT, H. B., 1941, *Mathematical Tables* (New York : McGraw-Hill).
 FLETCHER, G. C., 1952, *Proc. Phys. Soc. A*, **65**, 192.
 FLETCHER, G. C., and WOHLFARTH, E. P., 1951, *Phil. Mag.*, **42**, 106.
 HIRSCHFELDER, J., EYRING, H., and ROSEN, N., 1936, *J. Chem. Phys.*, **4**, 121.
 HOFFMANN, T. A., and KÓNYA, A., 1948, *J. Chem. Phys.*, **16**, 1172 ; 1951, *Acta Phys. Hungar.*, **1**, 5.
 LÖWDIN, P. O., 1950, *J. Chem. Phys.*, **18**, 365 ; 1951, *Ibid.*, **19**, 1579.
 SEITZ, F., 1940, *The Modern Theory of Solids* (New York : McGraw-Hill).
 TAYLOR, R., 1951, *Proc. Phys. Soc. A*, **64**, 249.
 TAYLOR, R., and COULSON, C. A., 1952, *Proc. Phys. Soc. A*, **65**, 834.
 WOHLFARTH, E. P., 1953, *Rev. Mod. Phys.*, **25**, 211.

The Scattering of 10 and 14 Mev Neutrons by Deuterons

By T. C. GRIFFITH

University College, London

Communicated by H. S. W. Massey; MS. received 4th April 1953 and in final form 3rd July 1953; read before the Society 1st February 1952

Abstract. The angular distributions of scattering of 10 and 14 mev neutrons by deuterons have been investigated using photographic emulsions. 1540 deuteron recoils entering the emulsion from a thin target of heavy wax placed in contact with its surface were measured. The results are shown to be in good agreement with the recent theoretical curves of Buckingham, Hubbard and Massey. The errors to which the measurements are subject have been carefully considered and give a clear indication of the limitations of the photographic emulsion technique in an experiment of this nature.

§ 1. INTRODUCTION

THE problem of determining the angular distribution of neutrons scattered by deuterons has been extensively investigated by several workers. The work has, however, been mainly concerned with neutrons of energies below 6 mev. At higher energies only two determinations have been reported: Griffith, Remley and Kruger (1950) used a pressure cloud chamber to investigate the angular distribution of 12 to 13 mev neutrons scattered by deuterons, whilst Coon and Taschek (1949) used a proportional counter telescope for a similar measurement with 14 mev neutrons.

These results have been compared with the recent theoretical calculations of Buckingham, Hubbard and Massey (1952). In these calculations the effects of d-wave scattering, which make appreciable contributions to the scattering at higher energies, have been taken into account. There is reasonable agreement between the shapes of the angular distributions found by experiment and those calculated on the assumption of symmetrical exchange forces. At higher energies, however, there is ample room for further confirmation of the experimental results available at present, especially for neutrons of energies between 6 and 12 mev.

In the experiment described here neutrons of energies 10 and 14 mev were considered and the angular distributions were determined by observations on the recoil deuterons detected in nuclear emulsions.

The method employed has been essentially the same in principle as the one described in detail by Martin, Burhop, Alcock and Boyd (1950). In their experiment neutrons of energy about 3 mev were used and deuterons at recoil angles between 0° and 40° in the laboratory system could be measured with reasonable accuracy.

With the higher energy neutrons employed in the present experiment it has been possible to measure the recoil deuterons at all angles between 5° and 57° in the laboratory system.

§2. DETAILS OF THE EXPERIMENTAL ARRANGEMENT

The neutrons were produced by the bombardment of an unseparated boron target by deuterons from the Cavendish Laboratory high tension generator. Gibson(1949) has shown that several homogeneous groups of neutrons are produced in this manner. Only the higher energy neutrons, the 9.4 and 13.5 mev groups (when emitted at right angles to the deuteron beam), have been accepted for analysis in the present experiment.

The boron target employed had dimensions 2 cm by 1 cm and was bombarded by a $60\mu\text{A}$ deuteron beam of mean energy 930 kev.

Nuclear emulsions with a layer of deuterium wax (99% of the hydrogen content being deuterium), of thickness 20μ , in contact with the surface of the emulsion were enclosed in thin light-tight metal cassettes and arranged radially around the target as shown in fig. 1. Four plates were exposed with their leading edges 10 cm

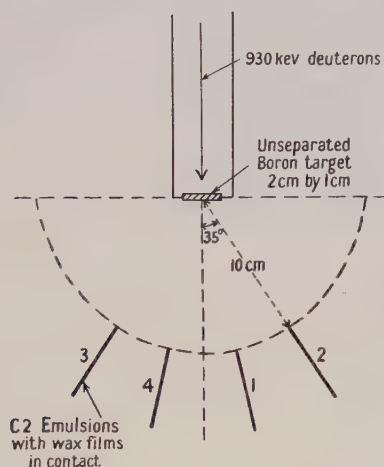


Fig. 1. Experimental arrangement.

from the centre of the target; plates 1 and 4 were at an angle of 5° to the deuteron beam, plates 2 and 3 at 35° . With this arrangement it was hoped that the background of stray neutrons, not coming directly from the target, would be very small.

Ilford C2 emulsions, of thickness 200μ , were employed and were processed using the temperature cycle of Dilworth, Occhialini and Payne (1948).

§3. THE MEASUREMENT AND SELECTION OF THE DEUTERON RECOILS

With the plates arranged radially around the target the neutrons travelled through the wax film parallel to the surface of the emulsion. All deuteron recoils entering the emulsion at the surface and travelling forward at an angle to the direction of the incident neutrons were examined.

The measurements were all taken from plate No. 2. It was estimated that the mean energies of the higher energy neutron groups incident on this plate were 9.7 and 13.9 mev. About 3000 deuteron recoils were measured, 1540 of which were accepted in the final analysis.

Four measurements were taken on each track: L the total projected length of the track on the plane of the surface of the emulsion; l the projected length of the first straight portion of the track; α the angle between l and the direction of the

incident neutrons in the region of the plate under consideration; δ the dip of the track over the length l . The measurements of α and δ were confined to the first straight portion l of the tracks in order to ensure that the errors arising from the scattering of the particles in the emulsion would not be significant.

The angle of dip ϕ was calculated from δ and l , δ being corrected for the shrinkage* suffered by the emulsion during fixing. θ the angle of recoil of the deuteron in the laboratory system is given by $\cos \theta = \cos \alpha \cos \phi$. The range of the deuterons R_d is given by $R_d = L_d / \cos \phi$, and the corresponding energy E_d was deduced from the range-energy relationships of Lattes, Fowler and Cier (1947), Rotblat (1951), and Catala and Gibson (1951) for protons in C 2 emulsions. The energies of the neutrons responsible for the deuteron recoils were calculated from the relationship $E_n = \frac{8}{9} E_d \cos^2 \theta$.

Only deuterons resulting from collisions with the 7, 10 and 14 MeV neutrons were required, and therefore energy-angle criteria were defined which could be employed to reject many of the deuterons resulting from collisions with neutrons of lower energy.

With wax films of thickness 20μ , deuterons of small dip into the emulsion could lose a considerable amount of energy in the wax. This loss of energy was investigated for deuterons of different energies at various angles of dip. It was concluded that straight tracks ending nearer than 13μ from the surface of the emulsion (unprocessed) should be excluded for all recoil angles.

§4. ANALYSIS OF THE RESULTS

The recoils selected for analysis were divided into seven groups according to their recoil angles, each group consisting of the recoils observed in equal intervals of $\cos \Theta$ where $\Theta = \pi - 2\theta$ is the angle of scattering of the neutron in the centre-of-mass system. Histograms of the distribution in energy of the incident neutrons for each of the seven intervals are shown in fig. 2(a). At large scattering angles peaks in the distributions corresponding to the higher energy neutron groups are very prominent, but at smaller angles of scattering the peaks are not so clearly defined.

Three factors contribute towards the broadening and overlapping of the peaks: (i) errors in the measurements of L , l , α and δ ; (ii) uncertainty in the direction of the incident neutrons because of the finite size of the target; (iii) loss in energy of the deuterons in the wax film.

To determine the number of deuteron recoils belonging to each neutron group (in each range of recoil angles) the extent of the overlapping between neighbouring peaks had to be determined. The spread dE_n arising from (i) and (ii) for the 7, 10 and 14 MeV groups was calculated and combined with the spread ΔE_n due to the loss of energy in the wax.

dE_n was calculated from the relationship

$$\left(\frac{dE_n}{E_n}\right)^2 = \left(\frac{dE_d}{E_d}\right)^2 + 4[\tan^2 \alpha (d\alpha)^2 + \tan^2 \phi (d\phi)^2]$$

where $d\alpha$ and $d\phi$ include the mean errors arising from (i) and (ii), and dE_d includes the mean errors arising from (i) and from the straggling of the range of the deuterons in the emulsion.

* The shrinkage factor s was estimated to be 2.1 ± 0.15 . A change in s from 1.9 to 2.3 was not found to produce a significant change in the energy distributions shown in fig. 2(a), and consequently the mean value of 2.1 has been used in all the calculations.

In the region of the plate where the measurements were taken a mean error of $\pm 1.8^\circ$ has been assumed in the direction of the incident neutrons, l could be measured to within 1.5μ and δ to within 2.5μ (after allowing for the shrinkage of the emulsion); L was measured to within 1.5μ for short tracks, the error increasing to about 5μ for the longest tracks measured; α was measured to within 0.5° .

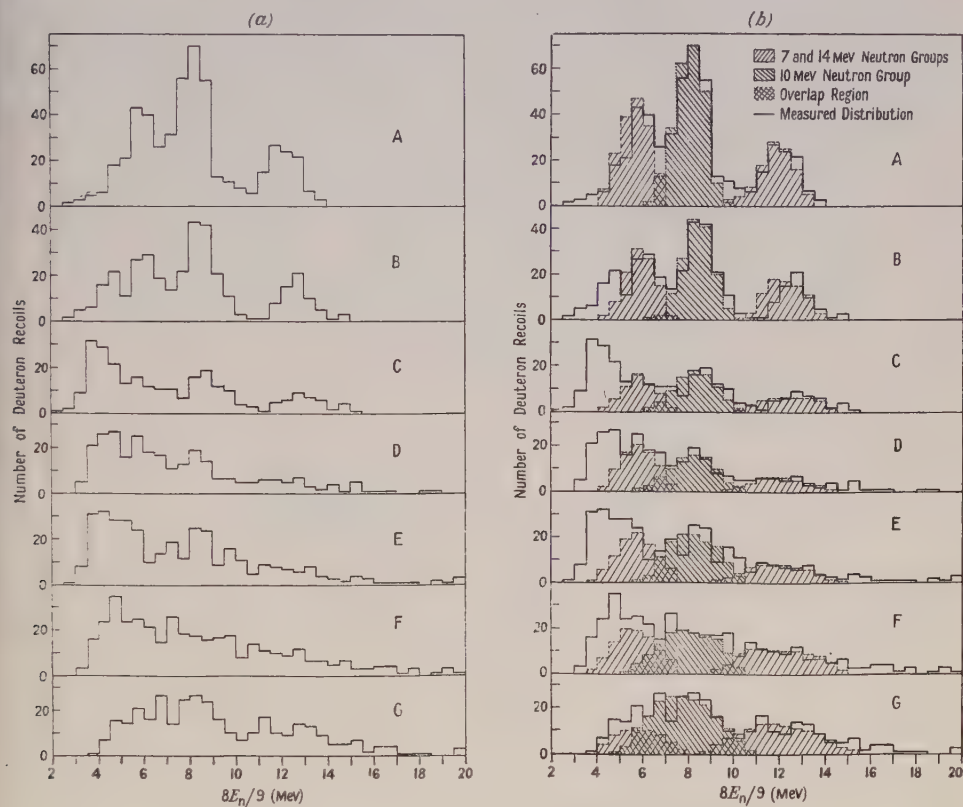


Fig. 2 (a). Apparent energy distributions of the incident neutrons deduced from the observed energy of the deuterons in the seven ranges of recoil angles considered.

Fig. 2 (b). Comparison of the experimental distributions with the distributions calculated assuming definite values for the various errors of measurements.

Range of recoil angles (laboratory system): A, 5.0° to 19.1° ; B, 19.1° to 27.1° ; C, 27.1° to 33.7° ; D, 33.7° to 39.7° ; E, 39.7° to 45.4° ; F, 45.4° to 51.2° ; G, 51.2° to 57.3° .

dE_n was calculated for the three neutron groups in each range of recoil angles. Corresponding to the mean angle θ , in each range, several values of α and ϕ were considered. The value of dE_n corresponding to the mean values of α and ϕ (for given θ) was used in the subsequent calculations.

The spread due to the loss of energy in the wax was estimated by considering deuteron recoils with different dip angles originating at various depths in the wax. Deuteron recoils, at angle θ , produced at a depth t in the wax by monoenergetic neutrons, have the same initial energies (ranges R_d) and can be represented by the generators of a cone of angle θ with vertex O, as shown in fig. 3. For given θ the path d of the deuterons in the wax increases as the dip ϕ decreases. An increase in d is accompanied by a decrease in the observed range $L_d = R_d - d$ of the deuterons

in the emulsion, which in turn leads to an apparent decrease in the neutron energy deduced from the measurements made on the tracks. If OA and OB are tracks such that the apparent neutron energies are E_n and $E_n + \Delta E_n$, then the number n of recoils between these two limits will be proportional to $d\psi$ (see fig 3). The fraction f of the total number of recoils N at angle θ can be calculated for this interval ΔE_n of neutron energy, f being defined as n/N .

For a given depth in the wax regular intervals ΔE_n can be considered over a range of neutron energies from E_{n1} to E_{n2} , where E_{n1} is the apparent neutron energy computed from a deuteron track ending 13μ from the surface of the emulsion, viz. a deuteron having the longest acceptable path in the wax, and E_{n2} corresponds to a deuteron having the shortest path in the wax, viz. at an angle $\phi = \theta$. The fractions f for each interval ΔE_n between E_{n1} and E_{n2} can be calculated. These calculations were carried out for ten different values of t between 0 and 20μ , f being found in the same intervals ΔE_n for each value of t . The sum $F = f_1 + f_2 + \dots + f_{10}$, where f_1, f_2, \dots, f_{10} are the fractions in the same interval ΔE_n for different values of t , was then found for each interval between the extreme limits (viz. E_{n1} corresponding to $t = 19\mu$ and E_{n2} corresponding to $t = 1\mu$) of neutron energies expected.

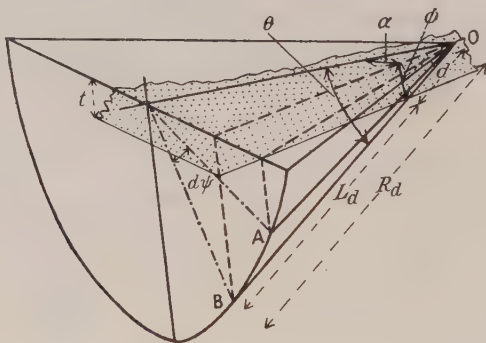


Fig. 3.

A histogram of F against E_n with intervals $\Delta E_n = 0.5$ mev was constructed and represents, to a fair degree of accuracy, the distribution of energies for a homogeneous group of neutrons due to loss in the wax. The histograms were constructed for the mean value of θ in each angular range for the three neutron groups under consideration.

On each step of these histograms the spread dE_n resulting from (i) and (ii) had to be superimposed. Each interval ΔE_n was extended to $\Delta E_n + 2dE_n$ and the height of the step was reduced so as to leave a rectangle of the same area as before. The final histograms were then constructed by adding the overlapping areas of each rectangle falling in the original 0.5 mev steps. The shape of these histograms, representing the expected distribution in energy of each neutron group, could be directly compared with the measured distributions.

The calculated distributions were normalized to fit the measured distributions, for each neutron group, in the region of least overlap, viz. for the steps of the histograms directly under the peaks. A comparison of the measured and calculated (normalized) distributions, for each angular range, is shown in fig. 2(b).

After obtaining the best fit between the calculated and measured distributions the total number of deuteron recoils under each peak was estimated. Steps in the histograms were considered individually and the extent of the overlap between neighbouring peaks in each step was expressed as the ratio of the calculated number of recoils from one group to the calculated number of recoils from the other group in that step. The observed number of recoils in the step was then divided between the groups in this ratio. Table 1 shows a typical example of the application of this method in estimating the total number of recoils under the peaks.

Table 1. Extraction of the Deuteron Recoils under the Peak for the 10 mev Neutron Group in the Angular Range 33.7° to 39.7°

E_n	N	G	S	NS/G
5.5 to 6.0	25	21	1	1
6.0 to 6.5	18	20	3	3
6.5 to 7.0	17	17	6	6
7.0 to 7.5	11	13	10	11
				[7]
7.5 to 8.0	13	15	15	13
8.0 to 8.5	19	16	16	19
8.5 to 9.0	14	15	15	14
9.0 to 9.5	8	10	10	8
9.5 to 10.0	7	5	4	6
10.0 to 10.5	5	4	2	3
				[14]
Total number of recoils: 82				84

E_n —range of neutron energy (mev); N —observed number of tracks; G —calculated total number of tracks (from all groups); S —calculated number from the 10 mev group; NS/G —estimated number from the 10 mev group; [7], [14]—overlap with 7, 14 mev group.

Since deuterons ending within 13μ of the surface of the emulsion were excluded, a correction factor for this loss had to be applied in each range of recoil angles. The observed number of recoils under each peak was multiplied by a loss correction factor which was estimated from the histograms calculated for the loss of energy in the wax. The loss factor changes rapidly for small recoil angles (5° to 19.1°) and consequently the first range of recoil angles was divided into two groups for which different correction factors were applied.

§ 5. BACKGROUND TRACKS

There were three possible sources of background tracks that could be included amongst the accepted deuteron recoils: (a) deuteron recoils from neutrons not coming directly from the target; (b) proton recoils originating within 1μ of the surface of the emulsion could be confused with deuterons entering at the surface; (c) protons from inelastic collisions of neutrons with deuterons.

Examination of the experimental distributions for small recoil angles (where the most accurate measurements were taken) shows that very few tracks lie outside the expected distributions. It was therefore concluded that the contribution from (a) could be neglected.

With wax films of thickness 20μ the ratio of protons originating within 1μ of the surface of the emulsion to deuterons entering the emulsion from the wax should be very small. This background was estimated by counting the number of protons originating inside the emulsion and travelling in the same direction as the

deuterons accepted for analysis (viz. forward and downwards), in a known volume of emulsion. The number originating in a known area, within 1μ of the surface of the emulsion, was then obtained and can be compared with the average number of deuterons observed in the same area. It was found that the greatest contribution from (b) would be no more than 4% in any range of recoil angles.

Several authors, notably Coon and Taschek (1949), Ageno, Amaldi, Bocciarelli and Trabacchi (1947), and Griffith Remley and Kruger (1950), have estimated that the cross section for inelastic collisions, $d(n, 2n)p$ (threshold 3.3 mev), yielding protons of energy greater than 2 mev, is about 10% to 15% of the total cross section for n - d elastic scattering. It is not unreasonable to assume that the disintegration protons have a continuous energy spectrum and that therefore some of them will undoubtedly be included amongst the deuteron recoils. The three groups of neutrons with energies 7, 10 and 14 mev and intensities in the ratios of 4:18:9 respectively (used in the present experiment) may each be expected to yield disintegration protons with cross section increasing by a factor of about 2 from 7 to 14 mev. Protons from each group will be present under the peaks (figs. 2(a) and 2(b)) from which the deuteron recoils are extracted and, since the protons from the different groups overlap, it becomes extremely difficult to estimate the magnitude of the correction that should be applied. At recoil angles greater than 20° the ranges of the particles in the emulsion were less than 300μ , and therefore it was not possible to identify the protons and deuterons satisfactorily by grain counting. Some of the tracks on the higher energy side of the 14 mev peak are probable due to protons; at large recoil angles (where most of these tracks are observed) the errors in measurement may, for some tracks, be much greater than the average and consequently estimates of the proton backgrounds based on these observations will not be reliable.

Some indication of the magnitude of the contribution from disintegration protons may be obtained from calculations based on arguments similar to those used by Griffith, Remley and Kruger (1950). Very approximate upper limits to the ratio of protons to acceptable deuteron recoils in some ranges of recoil angles can be estimated. After allowing for the overlapping of protons from the different groups (contributions from the 7 mev group being neglected) upper limits to the percentage contribution of protons amongst the deuterons may be as high as 4% to 7% for recoil angles less than 20° , increasing to 25% for the 14 mev group and 20% for the 10 mev group at recoil angles between 30° and 40° (minima of the angular distribution curves). At recoil angles greater than 40° the percentage contribution probably decreases; estimates of the upper limits could not be made in this region because of the serious overlapping between the peaks.

These figures suggest that the number of protons in the distributions may be quite large. The method of estimating the contributions has been, however, very approximate and almost certainly overestimates the proton contribution. There are two reasons for believing that the contribution is appreciably less than indicated: (a) for recoil angles up to 33.7° the higher energy groups are fairly well resolved (fig. 2(a)); this would be unlikely if a high background of protons had been present, (b) if 25% of the tracks in the angular range 27.1° to 33.7° were due to protons, then more neutrons of apparent energies greater than 15 mev would be expected due to the disintegration protons of ranges greater than the deuterons elastically scattered by 14 mev neutrons.

§6. DISCUSSION OF THE RESULTS

The results of the measurements are shown in table 2.

Table 2. The Number of Scattered Neutrons in each Angular Range from the 10 and 14 MeV Neutron Groups

	Interval of θ (deg)	Interval of $\cos \Theta$	10 mev neutron group			14 mev neutron group		
			(1)	(2)	(3)	(1)	(2)	(3)
A	5.0 to 12.5	-0.985 to -0.906	100	2.11		45	1.37	
					396			144
	12.5 to 19.1	-0.906 to -0.785	145	1.28		72	1.14	
B	19.1 to 27.1	-0.785 to -0.585	152	1.185	180	67	1.102	74
C	27.1 to 33.7	-0.585 to -0.385	81	1.170	95	45	1.085	49
D	33.7 to 39.7	-0.385 to -0.185	84	1.195	101	50	1.095	55
E	39.7 to 45.4	-0.185 to +0.015	113	1.270	143	69	1.115	77
F	45.4 to 51.2	+0.015 to +0.215	133	1.38	184	107	1.160	124
G	51.2 to 57.3	+0.215 to +0.415	158	1.63	254	119	1.245	148

(1) observed number of recoils; (2) loss correction factor; (3) total number of recoils.

A, B . . . G correspond with lettering of fig 2.

In figs. 4 and 5 the corrected numbers of recoils from the 10 and 14 mev groups, in each angular range, are plotted against the angle of scattering of the neutrons in the centre-of-mass system. No corrections other than those for the loss in the wax

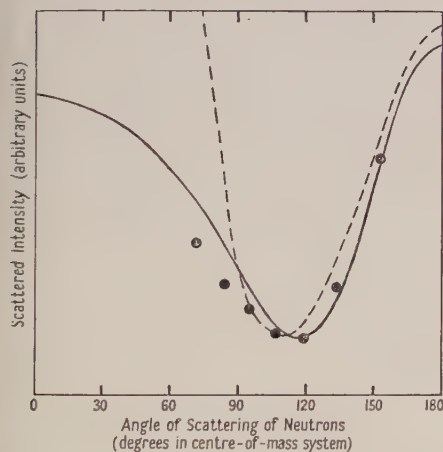


Fig. 4. Angular distribution of 966 scattered neutrons from the 10 MeV group.

● experimental points.
— exchange force curve for 10 MeV neutrons.
----- ordinary force curve for 11.5 MeV neutrons.

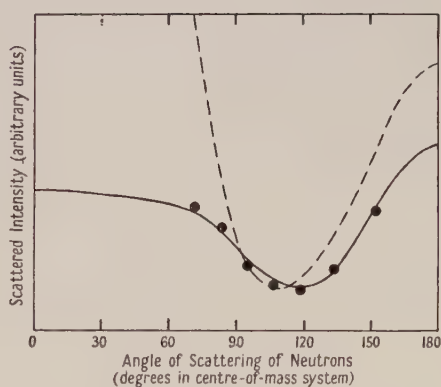


Fig. 5. Angular distribution of 574 scattered neutrons from the 14 MeV group

● experimental points.
— exchange force curve for 14 MeV neutrons.
----- ordinary force curve for 11.5 MeV neutrons.

have been applied to the measurements because the methods of estimating the contribution from disintegration protons was not considered to be sufficiently reliable. For this reason the angular distributions cannot be regarded as being

strictly those for n - d elastic scattering. The approximate estimates of the corrections for the $d(n, 2n)p$ reaction suggest that the shape of the distributions at the minima of the curves (where the ratio of protons to acceptable deuteron recoils is a maximum) will be slightly altered if such corrections are applied. The contributions from the proton backgrounds (*a*) and (*b*) are small enough to be insignificant in comparison with the statistical fluctuations of the measurements.

At large recoil angles the uncertainties in the measurements are rather large because of the difficulties involved in estimating the overlap between the peaks. Especially is this so for the 10 mev group, where an overlap exists on both sides of the peak. The error $\Delta E_n + 2dE_n$ in the determination of E_n is large for some recoil angles, but the corresponding error in $\cos \theta$ is much less. Consequently, within the errors discussed, the angular distribution between 70° and 155° in the centre-of-mass system for the scattered neutrons can be considered as significant. It is found that there is very close agreement between the angular distribution for the 14 mev neutrons, measured in this experiment, and that obtained by Griffith, Remley and Kruger (1950) for 12 to 13 mev neutrons.

The angular distributions determined experimentally are compared with those calculated by Buckingham, Hubbard and Massey (1952), the former being normalized to fit the theoretical curves at large angles of scattering. The shape of the measured distributions, both for the 10 and 14 mev neutrons, compare favourably with the distributions calculated on the assumption of symmetrical exchange forces. Calculations assuming ordinary forces are only available for 11.5 mev neutrons, but this energy is sufficiently close to 10 and 14 mev to indicate that the shapes of the distributions are in better agreement with the exchange force curve than with the ordinary force one. This, however, is not conclusive because the angular range covered in this experiment is the range where there is the least difference between the theoretical curves. Experiments extending the observations over a wider range of angles and with provisions for estimating more accurately the background of disintegration protons amongst the deuterons will have to be performed to obtain conclusive information about the nature of the forces.

The method employed to obtain the above results has suffered from rather severe limitations. The large spread in the apparent energy distribution of the incident neutrons (fig. 2(*a*)) at large recoil angles indicates the limitation of the nuclear emulsion technique in an experiment of this nature, especially when an attempt is made to obtain all the data from one plate. If, however, an intense beam of monoenergetic neutrons were available some improvement in the resolution of the peaks could be achieved by employing thinner wax films and a smaller boron target. It should be possible, under these conditions, to extend the measurements to larger recoil angles and also to obtain some indication of the background due to the disintegration protons.

ACKNOWLEDGMENTS

The author wishes to thank Professor W. E. Burcham, then at the Cavendish Laboratory, Cambridge, for arranging the exposures, Dr. E. H. S. Burhop for suggesting the problem and for his continued interest shown throughout the progress of the work, and Professor H. S. W. Massey and Dr. R. A. Buckingham for many useful discussions. Thanks are also extended to Mrs. M. Brown for her invaluable assistance in measuring the tracks.

REFERENCES

1. AGENO, M., AMALDI, E., BOCCIARELLI, D., and TRABACCI, G. C., 1947, *Phys. Rev.*, **71**, 20.
2. BUCKINGHAM, R. A., HUBBARD, S. J., and MASSEY, H. S. W., 1952, *Proc. Roy. Soc. A*, **211**, 183.
3. CATALA, J., and GIBSON, W. M., 1951, *Nature, Lond.*, **167**, 551.
4. COON, J. H., and TASCHEK, R. F., 1949, *Phys. Rev.*, **76**, 710.
5. DILWORTH, C. C., OCCHIALINI, G. P. S., and PAYNE, R. M., 1948, *Nature, Lond.*, **162**, 102.
6. GIBSON, W. M., 1949, *Proc. Phys. Soc. A*, **62**, 586.
7. GRIFFITH, G. L., REMLEY, M. E., and KRUGER, P. G., 1950, *Phys. Rev.*, **79**, 443.
8. LATTES, C. M. G., FOWLER, P. H., and CUER, P., 1947, *Proc. Phys. Soc.*, **59**, 883.
9. MARTIN, S. L., BURHOP, E. H. S., ALCOCK, C. B., and BOYD, R. L. F., 1950, *Proc. Phys. Soc. A*, **63**, 884.
10. ROTBLAT, J., 1951, *Nature, Lond.*, **167**, 550.

The Calculation of Auto-Ionization Probabilities—I: Perturbation Methods with Application to Auto-Ionization in Helium

BY B. H. BRANSDEN* AND A. DALGARNO†

* Department of Physics, Queen's University of Belfast

† Department of Applied Mathematics, Queen's University of Belfast

Communicated by D. R. Bates ; MS. received 4th June 1953

Abstract. Earlier calculations for auto-ionization probabilities using time-dependent perturbation methods are critically reviewed and improved methods are developed. These are applied to the calculation of the auto-ionization probabilities for certain doubly excited states of helium. The calculated probabilities lie in general between 10^{14} and 10^{15} sec $^{-1}$, confirming previous results. The evaluation of certain integrals involving coulomb functions is described in an appendix.

§ 1. INTRODUCTION

IF an energy level of an atom lies above the lowest ionization potential and certain selection rules are satisfied, a radiationless transition into the adjacent continuum may take place. This phenomenon of auto-ionization, by reducing the lifetime of the level, will broaden the corresponding emission lines. Apart from its significance in the interpretation of atomic spectra (Shenstone 1939, Burhop 1952, Garton 1952) and certain types of collision problems (Fox, Hickam and Kjeldaas 1953), a knowledge of the lifetime of an atomic state towards auto-ionization is needed in estimating the rate of dissociative recombination (Bates 1950, Massey 1952), a process of importance in the upper atmosphere and in other connections.

Time-independent perturbation theory has been used in all the published work. In this paper a method is developed to remove certain internal inconsistencies occurring in the earlier calculations and is applied to the calculation of auto-ionization probabilities for some doubly excited states of helium. The evaluation of certain integrals involving coulomb functions which are required is described in an appendix.

A discussion of the identification of some helium lines in the vacuum ultra-violet, in the light of our results, is deferred to the following paper (Bransden and Dalgarno 1953 b).

§ 2. THEORY

2.1. General

If Ψ_i is the wave function of the initial discrete state, normalized to unity, and Ψ_f that of the final continuum state, normalized to have the asymptotic form

$$\Psi_f(r_1) = \left(\frac{2}{\pi k}\right)^{1/2} r_1^{-1} \{\cos(kr_1 + k^{-1} \log 2kr_1 + \eta)\} \phi(2, \dots, n) \quad \dots\dots (1)$$

where $\phi(2, \dots, n)$ is the core wave function and the energy of the ejected

electron is k^2 rydbergs, then Wentzel (1928) has shown by applying the method of variation of parameters (Dirac 1926) that the probability of auto-ionization from the state Ψ_i to the state Ψ_f is given by

$$\gamma = 2\pi \left| \int \Psi_i^* \left(\sum \frac{1}{r_{jk}} \right) \Psi_f d\tau \right|^2 \text{ per atomic unit of time}^\dagger \quad \dots\dots(2)$$

in which r_{jk} is the distance between the j th and k th electrons and the integration is over the coordinates of all the electrons of the system. In the case of $L-S$ coupling γ vanishes unless the initial and final states have the same values of the total orbital angular momentum L and of the total spin S . If β is the probability of transitions from the state Ψ_i to lower discrete states, the mean life of the state Ψ_i is $(\beta + \gamma)^{-1}$, so that the width of the corresponding spectral line is proportional to $\beta + \gamma$: $\Delta E \sim 5 \times 10^{-12}(\beta + \gamma) \text{ cm}^{-1}$, where $(\beta + \gamma)^{-1}$ is measured in seconds.

2.2. Discussion of the Theory

Calculations of γ for some doubly excited states of helium have been carried out by Kreisler (1935), Kiang, Ma and Wu (1936 a, b) and Wu (1944). Similar calculations for beryllium have been carried out by Wu and Ourom (1950). For the continuum, Kiang, Ma and Wu, considering the $(2s \ 3s)^3S$ state of helium, chose a wave function $\mathcal{F}(r)$ given by

$$\mathcal{F}(r) = \left(\frac{2}{\pi k} \right)^{1/2} r^{-1} \cos(kr - \alpha) \quad \dots\dots(3)$$

though, as Wu (1944) has pointed out, this is not accurate at any radial distance. The discrete wave function was of the form

$$\Psi_i(\mathbf{r}_1, \mathbf{r}_2) = (1 - \alpha r_1) \exp(-\alpha r_1) (2\beta^2 r_2^2 - 6\beta r_2 + 3) \exp(-\beta r_2) \quad \dots\dots(4)$$

(properly normalized and symmetrized), the parameters and the energy of the state being determined by a variational method in which the Hamiltonian was that of the helium atom (Ma and Wu 1936),

$$H = -\frac{1}{2}(\nabla_1^2 + \nabla_2^2) - \frac{1}{r_{12}} + \frac{2}{r_1} + \frac{2}{r_2} \quad \dots\dots(5)$$

where $\mathbf{r}_1, \mathbf{r}_2$ are the position vectors of electrons 1 and 2 relative to the nucleus and $r_{12} = |\mathbf{r}_1 - \mathbf{r}_2|$. In a later investigation, covering a number of transitions, Wu (1944) employed discrete wave functions of similar type, but for the continuum wave functions he solved the corresponding integro-differential equation for a free electron in the field of a positive helium ion, normalization being effected by fitting to the function (3) at large radial distances that given by expression (1). Unfortunately the error caused by not using the correct function (1) cannot be easily estimated. A more serious objection which may be raised lies in the choice by Wu and his collaborators of the discrete wave functions. These are essentially products of hydrogenic wave functions modified by scale factors adjusted to allow for the influence of the electron interaction r_{12}^{-1} ; yet, the perturbation which causes the transition they also take as r_{12}^{-1} (cf. eqn. (2)). This procedure is clearly inconsistent; the use of wave functions determined by a variational method in which the Hamiltonian

[†] The atomic unit of time is 2.42×10^{-17} sec.

is given by (5) implies a different perturbation for the auto-ionization process. If the perturbation is taken to be as in formula (2) then products of hydrogen-like wave functions must be used. Kreisler (1935), in a calculation of γ for the $(2s\ 3s)^3S$ state of helium, represented Ψ_i by such a product, but he also is inconsistent in that he took for $\mathcal{F}(r)$ the wave function of a free electron in the field of a *screened* helium nucleus.

2.3. A Suggested Improvement to the Usual Theory

The adoption of hydrogen-like wave functions is not ideal since the corresponding perturbation Σr_{jk}^{-1} can scarcely be regarded as small in view of the fact that it makes a very considerable difference to the energy levels. It would seem better to use less crude wave functions and to replace Σr_{jk}^{-1} in formula (2) by the smaller perturbation associated with these, which is of course the difference between the true Hamiltonian \mathcal{H} and the artificial Hamiltonian \mathcal{H}' , which yields the *approximate* wave function *exactly*.

If Ψ_i^v is a normalized variational wave function depending upon n parameters α_m corresponding to an energy E , then α_m, E are determined by minimization of

$$E = \int \Psi_i^{v*} \mathcal{H} \Psi_i^v d\tau.$$

The equation of which Ψ_i^v is an exact solution may be written

$$(\mathcal{H}' - E)\Psi_i^v = 0 \quad \dots\dots(6)$$

where

$$\mathcal{H}' = \mathcal{H} + V' \quad \text{and} \quad V' = [(E - \mathcal{H})\Psi_i^v]/\Psi_i^v. \quad \dots\dots(7)$$

The function Ψ_i^v is then consistent with the perturbation V' and the probability of auto-ionization from state Ψ_i to a state Ψ_f is given by

$$\gamma = 2\pi \left| \int \Psi_i^{v*} V' \Psi_f d\tau \right|^2 \quad \text{per atomic unit of time} \quad \dots\dots(8)$$

provided that V' is small; otherwise Ψ_i will be ill-defined and the perturbation theory inapplicable. It may be noted that there is no possibility of obtaining an exact bound eigenfunction of \mathcal{H} with the consequent reduction of V' and therefore γ to zero, for Ψ_i represents a state that is not completely closed.

To avoid the so-called 'post-prior' discrepancy, the perturbation V' must be the same for both the initial and final states. It is therefore necessary to use continuum wave functions Ψ_f that satisfy the same wave equation as Ψ_i^v , thus

$$(\mathcal{H}' - E)\Psi_f = 0, \quad \dots\dots(9)$$

If the core wave function ϕ is a solution of the equation $(\mathcal{H}' - \epsilon)\phi = 0$, the continuum wave function $\mathcal{F}(r)$ satisfies

$$(\mathcal{H}' - \mathcal{H}_1 - E + \epsilon)\mathcal{F}(r) = 0. \quad \dots\dots(10)$$

The asymptotic form of $\mathcal{F}(r)$ is of the type (1) and may be conveniently written

$$\mathcal{F}(r) = \left(\frac{2}{\pi k}\right)^{1/2} r^{-1}(1+a^2)^{-1/2} \{F_l(kr) + aG_l(kr)\} \quad \dots\dots(11)$$

where k^2 equals the effective energy occurring in (10) and F_l, G_l are the regular and irregular coulomb functions for an attractive field corresponding to an electron with azimuthal quantum number l and energy k^2 . In any particular

instance one must use wave functions Ψ_i^v ; Ψ_f possessing the correct symmetry properties, an extension that produces no theoretical difficulty.

§ 3. AUTO-IONIZATION IN HELIUM

3.1. Using Hydrogenic Wave Functions

In order to provide a comparison for the method described in the previous paragraph and for the results of Wu *et al.* γ has been computed for a number of helium auto-ionizations using hydrogenic wave functions in the formula (2).

The Hamiltonian of the system is given by (5), so that the discrete wave function Ψ_i satisfies the equation

$$\left(\nabla_1^2 + \nabla_2^2 - \frac{4}{r_1} - \frac{4}{r_2} + E\right) \Psi_i(\mathbf{r}_1, \mathbf{r}_2) = 0, \quad \dots\dots(12)$$

which is separable in r_1 and r_2 . Writing the final wave function in the form

$$\Psi_f(\mathbf{r}_1, \mathbf{r}_2) = \frac{1}{\sqrt{2}} \{ \phi(r_1) \mathcal{F}(r_2) \pm \phi(r_2) \mathcal{F}(r_1) \}, \quad \dots\dots(13)$$

the upper sign referring to a singlet and the lower to a triplet state, the functions ϕ, \mathcal{F} are determined by the equations

$$\left(\nabla^2 - \frac{4}{r} + \epsilon\right) \phi(r) = 0, \quad \left(\nabla^2 - \frac{4}{r} - \epsilon + E\right) \mathcal{F}(r) = 0,$$

$\mathcal{F}(r)$ having the asymptotic form (1). $\phi(r)$ is simply the helium ion wave function whilst $\mathcal{F}(r)$ is given by

$$\mathcal{F}(r) = r^{-1} F_l(r) P_l(\cos \theta). \quad \dots\dots(14)$$

With these forms for Ψ_i and Ψ_f , γ may be evaluated analytically. The details of the calculations are described in an appendix. The values of γ obtained for the various transitions investigated are given in the table.

3.2. Using Variational Wave Functions

The method of §2.3 has been applied to a number of states but will be described in detail only for the $(2s^2)^1S - (1sks)^1S$ transition. The discrete variational wave functions were taken from the work of Ma and Wu (1936), the wave function of the $(2s^2)^1S$ state being

$$\Psi_i^v(\mathbf{r}_1, \mathbf{r}_2) = \frac{\alpha^3}{\pi} (1 - \alpha r_1)(1 - \alpha r_2) \exp \{ -\alpha(r_1 + r_2) \}$$

corresponding to a binding energy ϵ . This function satisfies $(H + V' - E)\Psi_i^v = 0$ with

$$V' = \frac{4(\alpha - 1)}{r_1} + \frac{4(\alpha - 1)}{r_2} - \frac{2}{r_{12}} + \epsilon - 2\alpha^2.$$

The final wave function $\Psi_f = (8/\pi)^{1/2} \{ \exp(-2r_1) \cdot \mathcal{F}(r_2) + \exp(-2r_2) \cdot \mathcal{F}(r_1) \}$, so that $\mathcal{F}(r)$ satisfies

$$\begin{aligned} & \left[\nabla^2 + \frac{4\alpha}{r} + (8\alpha - 4 - 2\alpha^2) \right] \mathcal{F}(r) \\ &= -32 \int_0^\infty [\exp\{-2\alpha(r+r')\} r'^2] \left\{ \frac{4\alpha-4}{r'} + \frac{4\alpha-4}{r} + 8 - 2\alpha^2 \right\} \mathcal{F}(r') dr' \\ & \dots\dots(15) \end{aligned}$$

and has the asymptotic form (11) with $k^2 = (8\alpha - 4 - 2\alpha^2)$. Equation (15) was solved using Hulthén's variational method (1944) with trial functions of the form selected by Bransden and Dalgarno (1953 a) for a variational treatment of the elastic scattering of slow electrons by helium ions. It was found for the $(2s)^2\ ^1S$ and $(2s3s)^{1,3}S$ states that γ , given by (8), was affected only slightly by the inclusion of the irregular part G_l of \mathcal{F} (cf. (11)) and of a polarization term in the final wave function so that they were ignored for the $(2s2p)^{1,3}$ states. With neglect of the G_l term it becomes possible to evaluate γ analytically.

An attempt was made to apply the method taking account of polarization in the initial wave function

$$\Psi_i^\vee(\mathbf{r}_1, \mathbf{r}_2) = (1 - 2\alpha_1)(1 - 2\alpha_2) \exp\{-\alpha(r_1 + r_2)\} + \lambda r_{12} \exp\{-4(r_1 + r_2)\}, \quad \dots\dots(16)$$

but the resulting equation (10) for $\mathcal{F}(r)$ was too complicated to admit of ready solution. To obtain some idea of the possible importance of polarization formula (2) was used with Ψ_i as given by (16) and it was found that the effect was negligible for any reasonable value of λ .

§ 4. RESULTS AND DISCUSSION

The results for the various transitions are given in the table. Apart from the $(2s3s)^3S - (1sks)^3S$ transition, for which great cancellation occurs (so that the value of γ must be considered unreliable), the results obtained by the two methods are in fair agreement with each other and, apart from the $(2s2p)^3P - (1skp)^3P$ transition, also in fair agreement with the results of Wu. This latter transition was also evaluated using Wu's method with a hydrogenic continuum wave function giving a value of γ equal to $2 \times 10^{15} \text{ sec}^{-1}$ compared with his $5 \times 10^{13} \text{ sec}^{-1}$. This unfortunate discrepancy is again probably due to the effect of cancellation.

Probability of Auto-Ionization γ (in sec^{-1})

Transition	Energy of ejected electron (rydbergs)	Wu's results	Hydrogenic results	Improved results
$(2s^2)^1S - (1sks)^1S$	2.56	4×10^{14}	4×10^{14}	7×10^{14}
$(2s3s)^1S - (1sks)^1S$	2.84		7×10^{13}	1.5×10^{14}
$(2s3s)^3S - (1sks)^3S$	2.86	$10^{14} - 10^{15}$	2×10^{12}	1×10^{14}
$(2s2p)^1P - (1skp)^1P$	2.69		4×10^{15}	1×10^{15}
$(2s2p)^3P - (1skp)^3P$	2.50	5×10^{13}	2×10^{15}	8×10^{14}
$(2p^2)^1D - (1skd)^1D$	2.67	1×10^{14}	3×10^{14}	
$(3d^2)^1G - (1skg)^1G$	3.13	4×10^{11}	2×10^{11}	
$(3d^2)^1G - (2skg)^1G$	0.13	5×10^{13}	1×10^{14}	

The general rule that the probability of auto-ionization decreases with increasing separation from the ionization limit is obeyed. It is generally of the order of 10^{14} sec^{-1} to 10^{15} sec^{-1} so that lines originating from these levels have widths of the order of $10^3 - 10^4 \text{ cm}^{-1}$. In order to examine the applicability of the time-dependent perturbation theory, the transition $(2s^2)^1S - (1sks)^1S$ has been investigated using an entirely different approach which has been briefly described elsewhere (Bransden and Dalgarno 1952). The procedure followed and the results obtained are described in detail in the following paper (Bransden and Dalgarno 1953 b).

ACKNOWLEDGMENT

The authors wish to thank Professor D. R. Bates for many stimulating discussions concerning possible improvements to the usual theory. The method finally adopted was suggested by him.

APPENDIX

The integrals whose evaluation is required are of the form

$$\int_0^{\infty} e^{-\beta r} r^n f(r) dr$$

where $f(r)$ is a coulomb function defined as the regular solution $F_l(r)$ of the equations

$$\left(\frac{d^2}{dr^2} + k^2 + \frac{2\alpha}{r} - \frac{l(l+1)}{r^2} \right) F_l(r) = 0 \quad \dots\dots (17)$$

such that $F_l(0) = 0$ with asymptotic behaviour given by

$$F_l(r) \sim \sin(kr + \alpha k^{-1} \log 2kr - l\pi/2 + \eta_l)$$

where $\eta_l = \arg \Gamma(l+1 - i\alpha k^{-1})$. It is well known (Gordon 1928) that the regular coulomb function can be expressed as

$$F_l(r) = \exp(\frac{1}{2}\pi\alpha k^{-1}) \frac{|\Gamma(l+1 - i\alpha k^{-1})|}{(2l+1)!} k(2k)^l r^{l+1} e^{-ikr} \\ \times {}_1F_1(l+1 + i\alpha k^{-1}, 2l+2; 2ikr) \quad \dots\dots (18)$$

where ${}_1F_1(a, b; x)$ is the confluent hypergeometric series

$${}_1F_1(a, b; x) = 1 + \frac{a}{b} \cdot \frac{x}{1} + \frac{a(a+1)}{b(b+1)} \cdot \frac{x^2}{2} + \dots \quad \dots\dots (19)$$

Defining $\mathcal{F}_l(\beta, n) = \int_0^{\infty} e^{-\beta r} r^n F_l(r) dr$,

it is easily shown by term by term integration that

$$\mathcal{F}_0(\beta, 0) = (2\pi |\alpha| k)^{1/2} \{ |1 - \exp(-2\pi\alpha k^{-1})| \}^{-1/2} (k^2 + \beta^2)^{-1} \\ \times \exp(-2|\alpha| k^{-1} \arctan k/\beta) \quad \dots\dots (20)$$

or, more generally,

$$\mathcal{F}_l(\beta, l) = k(2k)^l [(l^2 + \alpha^2 k^{-2}) \{ (l-1)^2 + \alpha^2 k^{-2} \} \dots (1^2 + \alpha^2 k^{-2}) \\ \times (2\pi |\alpha| k^{-1}) \{ |1 - \exp(-2\pi\alpha k^{-1})| \}^{-1}]^{1/2} (k^2 + \beta^2)^{-(l+1)} \\ \times \exp(-2|\alpha| k^{-1} \arctan k/\beta).$$

The following recurrence relations may be immediately established by formal integration of the differential equation (17):

$$(k^2 + \beta^2) \mathcal{F}_l(\beta, -l) = (2l+1) \lim_{r \rightarrow 0} (r^{-l-1} F_l(r)) - 2(l\beta + \alpha) \mathcal{F}_l(\beta, -l-1)^\dagger \\ (k^2 + \beta^2) \mathcal{F}_l(\beta, 1-l) = -2\{(l-1)\beta + \alpha\} \mathcal{F}_l(\beta, -l) + 2l \mathcal{F}_l(\beta, -l-1) \\ (k^2 + \beta^2) \mathcal{F}_l(\beta, n) = 2(n\beta - \alpha) \mathcal{F}_l(\beta, n-1) + \{l(l+1) - n(n-1)\} \mathcal{F}_l(\beta, n-2) \\ \text{for } n > 1-l. \quad \dots\dots (21)$$

$\lim_{r \rightarrow 0} \{r^{-l-1} F_l(r)\}$ can be written down immediately (Breit, Yost and Wheeler 1936):

$$^\dagger \mathcal{F}_l(\beta, n) \text{ diverges for } n < -(l+1).$$

$$\lim_{r \rightarrow 0} \{r^{-l-1} F_l(r)\} = \frac{(l^2 + \alpha^2 k^{-2})^{1/2}}{l(2l+1)} \lim_{r \rightarrow 0} \{r^{-l} \mathcal{F}_{l-1}(r)\}$$

$$\lim_{r \rightarrow 0} \{r^{-1} F_0(r)\} = (2\pi |\alpha| k)^{1/2} |1 - \exp(-2\pi \alpha k^{-1})|^{-1/2}.$$

The recurrence formula (21) can be used to evaluate $\mathcal{F}_l(\beta, n)$ for all n once any two are known, or if we restrict ourselves to integral values of n once any one is known, except that integrals for which $n < l+1$ cannot be connected with those for which $n \geq l+1$. This limitation may be most easily surmounted by use of the formula (Powell 1947, Infeld 1947)

$$(l+1)F_l'(r) = \left(\frac{(l+1)^2}{r} - \alpha\right) F_l(r) - \{(l+1)^2 k^2 + \alpha^2\}^{1/2} F_{l+1}(r), \quad \dots\dots (22)$$

from which follows, on multiplication by $e^{-\beta r} r^l$ and integrating

$$\{(l+1)^2 k^2 + \alpha^2\}^{1/2} \mathcal{F}_{l+1}(\beta, l) = -(m[l+1] + \alpha) \mathcal{F}_l(\beta, l)$$

$$+ (l+1)(2l+1) \mathcal{F}_l(\beta, l-1). \quad \dots\dots (23)$$

It follows that, once $\mathcal{F}_0(\beta, 0)$ and $\mathcal{F}_0(\beta, -1)$ are known, $\mathcal{F}_l(\beta, n)$ can be obtained by repeated application of (23) or by the combined use of (23) and (21). Since $\mathcal{F}_0(\beta, -1)$ is given in terms of $\mathcal{F}_0(\beta, 0)$ by (21) and $\mathcal{F}_0(\beta, 0)$ is known analytically from (20), the evaluation of the integrals is completed.

Formulae similar to (21) and (23) hold for integrals involving the irregular solution $G_l(r)$ of (17), so that all integrals of the form $\int_0^\infty G_l(r) e^{-\beta r} r^n dr$ may be obtained in terms of the single integral $\int_0^\infty G_0(r) e^{-\beta r} dr$.

REFERENCES

- BATES, D. R., 1950, *Phys. Rev.*, **78**, 492.
 BRANSDEN, B. H., and DALGARNO, A., 1952, *Phys. Rev.*, **88**, 148; 1953 a, *Proc. Phys. Soc. A*, **66**, 268; 1953 b, *Ibid.*, **66**, 911.
 BREIT, G., YOST, F. L., and WHEELER, J. A., 1936, *Phys. Rev.*, **49**, 174.
 BURHOP, E. H. S., 1952, *Auger Effect* (Cambridge: University Press).
 DIRAC, P. A. M., 1926, *Proc. Roy. Soc. A*, **112**, 661.
 FOX, R. E., HICKAM, W. M., and KJELDAAS, T., Jr., 1953, *Phys. Rev.*, **89**, 555.
 GARTON, W. R. S., 1952, *Proc. Phys. Soc. A*, **65**, 268.
 GORDON, W., 1928, *Z. Phys.*, **48**, 180.
 HULTHÉN, L., 1944, *K. fysiogr. Sällsk. Lund. Förh.*, **14**, No. 21.
 INFELD, L., 1947, *Phys. Rev.*, **72**, 626.
 KIANG, A. T., MA, S. T., and WU, T. Y., 1936 a, *Phys. Rev.*, **50**, 673; 1936 b, *Chin. J. Phys.*, **2**, 117.
 KREISLER, J., 1935, *Acta Phys. Polon.*, **4**, 15.
 MA, S. T., and WU, T. Y., 1936, *J. Chin. Chem. Soc.*, **4**, 345.
 MASSEY, H. S. W., 1952, *Advances in Physics* (Phil. Mag. Suppl.), **1**, 395.
 POWELL, J. L., 1947, *Phys. Rev.*, **72**, 1125.
 SHENSTONE, A. G., 1939, *Rep. Prog. Phys.*, **5** (London: Physical Society), p. 210.
 WENTZEL, G., 1928, *Phys. Z.*, **29**, 321.
 WU, T. Y., 1944, *Phys. Rev.*, **66**, 291.
 WU, T. Y., and OUROM, L., 1950, *Canad. J. Res. A*, **28**, 542.

The Calculation of Auto-Ionization Probabilities—II : A Variational Method for Radiationless Transitions with Application to the $(2s)^2\ ^1S-(1sks)^1S$ Transition of Helium

BY B. H. BRANSDEN* AND A. DALGARNO†

* Department of Physics, Queen's University of Belfast

† Department of Applied Mathematics, Queen's University of Belfast

Communicated by D. R. Bates; MS. received 4th June 1953

Abstract. A variational method is developed for the calculation of radiationless transition probabilities, and applied to the $(2s)^2\ ^1S-(1sks)^1S$ transition of helium. The calculated probability of 1.5 or $1.1 \times 10^{14}\ \text{sec}^{-1}$ agrees well with the values 7 or $4 \times 10^{14}\ \text{sec}^{-1}$ found by previous perturbation calculations. The identification of certain helium lines in the vacuum ultra-violet is discussed.

§ 1. INTRODUCTION

RADIATIONLESS transitions may occur wherever an atomic system has been excited to a level whose energy is overlapped by a continuous spectrum. Such processes occur as the Auger effect, auto-ionization and molecular predissociation, and similar transitions are of great importance in various nuclear phenomena, ranging from α decay to the break-up of a compound nucleus formed by a collision.

Radiationless transitions may be divided, roughly, into two classes. If the mean lifetime of the excited state is of the same order as the time in which it is formed, then we may speak of the radiationless decay as forming part of a 'collision of the second kind'. The other class of transition is that for which the mean lifetime of the excited state is long compared with its time of formation and for which the wave function is nearly closed. The various phenomena listed in the previous paragraph belong to the latter class and the probability of the decay of such states is usually determined by the application of time-dependent perturbation theory (Dirac 1926, Wentzel 1928). In the present paper a variational method is employed (Bransden and Dalgarno 1952) which avoids the difficulties associated with the perturbation method (cf. Bransden and Dalgarno 1953 b (preceding paper, to be referred to as I)). Although the method is applicable only to the decay of states belonging to the second class and for which the transition probability is small, this limitation‡, unlike the perturbation method, does not involve the consideration of the 'strength' of the potential terms.

§ 2. GENERAL THEORY

The auto-ionization of an excited atomic system may be described by a wave function $\Phi(1, 2, \dots, n)$ which is a linear combination of a properly

‡ Extension of the method to cover transitions which depend on the mode of formation of the excited state is straightforward but is unnecessary for the discussion of auto-ionization and similar effects.

antisymmetrical normalized and closed wave function $\Psi_c(1, 2, \dots, n)$, representing the excited state and an antisymmetrical wave function $\Psi_f(1, 2, \dots, n)$ describing the final continuum state

$$\Phi(1, 2, \dots, n) = c\Psi_c(1, 2, \dots, n) + d\Psi_f(1, 2, \dots, n). \quad \dots\dots(1)$$

The asymptotic form of Ψ_f is required to be that of a product of a core wave function $\chi(2, \dots, n)$ and an outgoing spherical wave

$$\Psi_f(1, 2, \dots, n) \sim \chi(2, \dots, n)\phi(1)\sigma(1, 2, \dots, n) \quad \dots\dots(2)$$

where $\sigma(1, 2, \dots, n)$ is the appropriate spin wave function and

$$\phi(1) = r_1^{-1} \exp[i(kr_1 + k^{-1}\alpha \log 2kr_1)] P_l^m(\cos \theta) e^{im\varphi}, \quad \dots\dots(3)$$

k^2 being the energy of the ejected electron[†], and the parameter α taking the values zero, one or two according to whether the excited system is a negative ion, a neutral atom or positive ion. In general the expression (2) has to be suitably symmetrized, but for the sake of clarity this simple extension is omitted from the equations. If the Hamiltonian of the system is H and we write $E = \epsilon + k^2$, ϵ being the core binding energy, then $\Phi(1, 2, \dots, n)$ cannot be an exact solution of the wave equation

$$(H - E)\Psi(1, 2, \dots, n) = 0 \quad \dots\dots(4)$$

since $\Phi(1, 2, \dots, n)$ contains only outgoing waves and has no source. Two equivalent procedures are possible: we may modify the Hamiltonian H by the inclusion of a small imaginary potential representing the source, so that

$$H' = H + iV \text{ and } (H' - E)\Phi(1, 2, \dots, n) = 0 \quad \dots\dots(5)$$

or we may write the correct wave function for the system as

$$\Psi = \Psi_i + \Phi \quad \dots\dots(6)$$

where Ψ_i is some wave function that describes the process by which the excited level is formed. (For example if the level were formed by electron impact, Ψ_i would contain terms corresponding to incoming plane waves, thus allowing the solution of eqn. (4).)

In order that the concept of a definite excited state represented by $\Psi_c(1, 2, \dots, n)$, may have significance, the lifetime of this state must be so long that its mode of decay is not influenced by its mode of formation.[‡] This implies that the direct coupling between the states represented by Ψ_i , Ψ_c is negligible and that between the pairs Ψ_i , Ψ_c and Ψ_c , Ψ_f is small. If this is the case, then it is justifiable to ignore terms deriving from Ψ_i or depending on the structure of iV when calculating the transition probability c-f.

If the core wave function $\chi(2, \dots, n)$ is normalized to unity then from eqn. (3) it follows that

$$\int \Psi_f^*(k') \Psi_c(k) d\tau = \frac{4\pi^2}{(2l+1)} \delta(k-k') \quad \dots\dots(7)$$

and that the probability γ of auto-ionization is given by

$$\gamma = \frac{8\pi k}{(2l+1)} \left(\frac{d^2}{c^2 + d^2} \right).$$

For the state Ψ_c to be well defined $|d/c|$, which is a measure of the coupling between states Ψ_c and Ψ_f , must be small compared with unity, so that

$$\gamma = \frac{8\pi k}{(2l+1)} \left| \frac{d}{c} \right|^2. \quad \dots\dots(8)$$

[†] Atomic units are employed throughout.

[‡] Compare with the theory of the compound nucleus, cf. Mott and Massey 1949, p. 157.

Define $L=H-E$ and let $\Phi_t(1, 2, \dots, n)$ be a trial function depending on p constants $a_m, m=1, 2, \dots, p$, the boundary conditions of Φ_t being those of Φ with the exception that d_t replaces d . Writing $\Psi_t = \Psi_i + \Phi_t$ and $\omega = \Psi_t - \Psi$, we have in the notation of Kato (1950)

$$I(a_m, d_t) = \sum_{\text{spin}} \int \Psi_t^* L[\Psi_t] d\tau = \frac{4\pi i}{(2l+1)} [k_0 y - 2kd^* d_t] + O(\omega^2) \dots\dots (9)$$

where it is assumed that the initial state Ψ_i (which is supposed to be exact) contains a continuum term of asymptotic form

$$P_l(\cos \theta) [(\pi k_0 r/2)^{1/2} \{J_{l+1/2}(k_0 r) + (-1)^l J_{-l-1/2}(k_0 r) \cdot (x + iy)\}].$$

As for the correct function Ψ , $I(a_m, d) = 0$ (or by consideration of particle conservation, cf. Mott and Massey 1949) so it follows that

$$y = (k/k_0) d^* d. \dots\dots (10)$$

In accordance with the requirement that Ψ_c shall represent a well-defined state, the approximation is now made that

$$\sum_{\text{spin}} \int \Psi_i^* L[\Phi] d\tau$$

and its complex conjugate can be neglected and that the only contribution retained from

$$\sum_{\text{spin}} \int \Psi_i^* L[\Psi_i] d\tau$$

is the imaginary source component $4\pi i k_0 y / (2l+1)$. Thus

$$I(a_m, d_t) \simeq \sum_{\text{spin}} \int \Phi_t^* L[\Phi_t] d\tau + \frac{4\pi i k_0 y}{(2l+1)} = \frac{8\pi i k}{(2l+1)} d^* (d - d_t) + O(\omega^2).$$

The imaginary term in $\sum_{\text{spin}} \int \Phi_t^* L[\Phi_t] d\tau$ can be shown to be $-\{4\pi i k / (2l+1)\} d_t d_t^*$ and this can be separated by defining

$$I_1(a_m, d_t) = \sum_{\text{spin}} \int \Phi_t^* L[\Phi_t] d\tau + \frac{4\pi i k}{(2l+1)} d_t^* d_t.$$

To the first order†

$$I_1(a_m, d_t) = \frac{4\pi i}{(2l+1)} k (d d_t^* - d^* d_t). \dots\dots (11)$$

I_1 is a stationary expression for the following variational methods of determining the constants $|d/c|$ and a_m . Following Hulthén (1944) we require that δI_1 be zero and hence

$$\partial I_1 / \partial a_m = 0; \quad I_1(a_m, d_t) = 0. \dots\dots (12)$$

Alternatively following Hulthén (1948), Kohn (1948) and Hulthén and Olsson (1950), we obtain‡

$$\frac{\partial I_1}{\partial a_m} = 0; \quad \frac{\partial I_1}{\partial d^*} = - \frac{4\pi i k d}{(2l+1)}. \dots\dots (13)$$

† If the excited state is formed by other means than that of electron impact, we may obtain eqn. (11) by using the concept of a source potential iV . Thus

$$I(a_m, d_t) = \sum_{\text{spin}} \int \Phi_t^* L[\Phi_t] d\tau + i \int \Phi_t^* V \Phi_t d\tau = - \frac{4\pi i k}{(2l+1)} d^* d_t + O(\omega^2) + i \int \Phi_t^* V \Phi_t d\tau.$$

Since for the correct Φ , $I=0$ and as

$$\int \Phi^* L[\Phi] d\tau = - \frac{4\pi k}{(2l+1)} d^* d \quad \text{we have} \quad i \int \Phi^* V \Phi d\tau = + \frac{4\pi i k}{(2l+1)} d^* d$$

and eqn. (11) follows.

‡ From the form of I_1 it can be shown that the auto-ionization obeys the same selection rules as are indicated by the perturbation method.

§ 3. INTEGRAL EQUATIONS

As a check on the value of $|d/c|$ found by the variational method and also as the starting point for the variational principle derived by Schwinger (cf. Lippman and Schwinger 1950, Kohn 1948), it is interesting to construct an integral equation for Ψ and $|d/c|$. Although general formulae are readily obtained for a system with any angular momentum, it is instructive to fix attention on the example of auto-ionization of helium from a doubly excited state, of zero angular momentum neglecting exchange.

The exact wave function $\Psi = \Psi_i + \Psi_c + \Psi_f$ satisfies

$$(\nabla_1^2 + \nabla_2^2 + 4/r_1 + 4/r_2 - 2/r_{12} + \epsilon + k^2)\Psi(\mathbf{r}_1, \mathbf{r}_2) = 0 \quad \dots\dots(15)$$

in which $\mathbf{r}_1, \mathbf{r}_2$ are the position vectors of electrons 1 and 2 with respect to the nucleus and $r_{12} = |\mathbf{r}_1 - \mathbf{r}_2|$.

It can be shown that if $\Psi_f(\mathbf{r}_1, \mathbf{r}_2)$ is written as

$$\Psi_f(\mathbf{r}_1, \mathbf{r}_2) = \chi(r_2)\mathcal{F}(r_1) \quad \dots\dots(16)$$

where
then

$$(\nabla^2 + 4/r + \epsilon)\chi(r) = 0$$

$$\begin{aligned} \mathcal{F}(r_1) = 4\pi \int_0^\infty \int_0^\infty K(r_1, r_1') \chi^*(r_2') \left\{ \frac{2}{r_1'} - 2\gamma_0(r_1', r_2') \right\} \\ \times \Psi(r_1', r_2') r_1'^2 r_2'^2 dr_1' dr_2' \quad \dots\dots(17a) \end{aligned}$$

with $\gamma_0(r_1', r_2') = r_1'^{-1}; r_1' > r_2'$
 $= r_2'^{-1}; r_2' > r_1'$

$$\dots\dots(17b)$$

$$\begin{aligned} K(r, r') = \frac{1}{kr r'} F(r) \{G(r') + iF(r')\}; r' > r \\ = \frac{1}{kr r'} \{G(r) + iF(r)\} F(r'); r > r', \quad \dots\dots(17c) \end{aligned}$$

$F(r)$ and $G(r)$ being the regular and irregular coulomb functions appropriate to the attractive potential $2/r$ and energy k^2 .

The Green's function $K(r, r')$ is chosen so that the asymptotic form of $\mathcal{F}(r)$ is $\mathcal{F}(r_1) \sim r_1^{-1} \exp [i\{kr_1 + \alpha k^{-1} \log 2kr_1\}] \exp(i\eta_0)$

$$\times 4\pi \int_0^\infty \int_0^\infty \left\{ \frac{F(r_1')}{kr_1'} \right\} \chi^*(r_2') \left\{ \frac{2}{r_1'} - 2\gamma_0(r_1', r_2') \right\} \Psi(r_1', r_2') r_1'^2 r_2'^2 dr_1' dr_2'$$

where $\eta_0 = \arg \Gamma(1 + i\alpha k^{-1})$.

Hence

$$d = 4\pi k^{-1} \exp(i\eta_0) \int_0^\infty \int_0^\infty F(r_1) \chi^*(r_2) \left\{ \frac{2}{r_1} - 2\gamma_0(r_1, r_2) \right\} \Psi(r_1, r_2) r_1 r_2^2 dr_1 dr_2. \quad \dots\dots(18)$$

From (17) and (18) the following integral equation for Ψ may be obtained in a homogeneous form:

$$\Psi(r_1, r_2) = 4\pi \int_0^\infty \int_0^\infty G'(r_1, r_2; r_1', r_2') \left\{ \frac{2}{r_1'} - 2\gamma_0(r_1', r_2') \right\} \Psi(r_1', r_2') r_1'^2 r_2'^2 dr_1' dr_2' \quad \dots\dots(19)$$

with $G'(r_1, r_2; r_1', r_2') = G(r_1, r_2; r_1', r_2')$

$$+ k^{-1} d^{-1} \exp(i\eta_0) F(r_1') \chi^*(r_2') \{\Psi_i(r_1, r_2) + \Psi_c(r_1, r_2)\}$$

and

$$G(r_1, r_2; r_1', r_2') = K(r_1, r_1') \chi(r_2) \chi^*(r_2').$$

In accordance with our approximation the function Ψ_i is to be neglected on the right-hand side of eqns. (17) and (19). Following Schwinger, it is observed that if any trial function Ψ_t is inserted in the right-hand side of eqn. (19), the resulting Ψ has the correct asymptotic form and may be inserted in the integral

$$I = \int \Psi(H-E)\Psi \, d\mathbf{r}_1 \, d\mathbf{r}_2 = 0$$

to give a stationary expression for d^{-1} (cf. Kohn 1948):

$$d^{-1}\{4\pi \exp(i\eta_0)/k\} = A/B \quad \dots\dots(20)$$

with

$$A = \int_0^\infty \int_0^\infty \int_0^\infty \int_0^\infty \Psi(r_1, r_2) \left\{ \frac{2}{r_1} - 2\gamma_0(r_1, r_2) \right\} G(r_1, r_2; r_1', r_2') \\ \times \left\{ \frac{2}{r_1'} - 2\gamma_0(r_1', r_2') \right\} \Psi(r_1', r_2') r_1'^2 r_2'^2 r_1^2 r_2^2 \, dr_1' \, dr_2' \, dr_1 \, dr_2$$

$$B = \int_0^\infty \int_0^\infty \int_0^\infty \int_0^\infty \Psi(r_1, r_2) \left\{ \frac{2}{r_1} - 2\gamma_0(r_1, r_2) \right\} F(r_1') \chi^*(r_2') \\ \times \left\{ \frac{2}{r_1'} - 2\gamma_0(r_1', r_2') \right\} \Psi_c(r_1, r_2) \Psi(r_1', r_2') r_1^2 r_2^2 r_1'^2 r_2'^2 \, dr_1' \, dr_2' \, dr_1 \, dr_2.$$

It is interesting to notice that the substitution $\Psi \simeq \Psi_c$ (the equivalent of Born's approximation) in the integral equation (18) for d gives the first order perturbation formula discussed in paper I. In particular, if Ψ_c is represented by $\phi(r_1)\phi(r_2)$, ϕ being the excited state of a *helium ion* then Ψ_c is orthogonal to $\chi(r_2)$ and

$$d = -8\pi k^{-1} \exp(i\eta_0) \int_0^\infty \int_0^\infty F(r_1) \chi(r_2) \gamma_0(r_1, r_2) \phi(r_1) \phi(r_2) r_1 r_2^2 \, dr_1 \, dr_2. \quad \dots\dots(21)$$

To correspond to the choice of the unperturbed function $\phi(r_1)\phi(r_2)$ for Ψ_c , $F(r_1)$ must be taken to be a coulomb function appropriate to the potential $4/r_1$ rather than $2/r_1$; (21) is then exactly the matrix element given by the perturbation method with hydrogenic wave functions.†

§ 4. THE $(2s)^2 \, ^1S - (1sks) \, ^1S$ HELIUM TRANSITION

The excited $(2s)^2 \, ^1S$ state of helium may be represented by the simple function (Ma and Wu 1936):

$$\Psi_c = \frac{\beta^3}{\pi} (1 - \beta r_1) \exp(-\beta r_1) (1 - \beta r_2) \exp(-\beta r_2),$$

β being a variable parameter, and the continuum trial function Ψ_t by a form suggested by the variational calculations of the elastic scattering of electrons by helium ions (Bransden and Dalgarno 1953 a):

$$\Psi_t = \chi(r_2) \mathcal{F}(r_1) + \chi(r_1) \mathcal{F}(r_2) \quad \text{with} \quad \chi(r) = (8/\pi)^{1/2} e^{-2r}$$

and

$$r \mathcal{F}(r) = [F(id + ge^{-2r}) + (d + be^{-2r})(1 - e^{-2r})G],$$

where F and G are the appropriate regular and irregular coulomb functions, and where d, g, b are to be determined by the variational procedure.

As the trial function is not linear in the parameter β and the total energy of the system (that is the energy of the excited state) is not known from experiment,

† This remains true, of course, when exchange is taken into account.

this energy and the parameter β were taken to be the values computed by Ma and Wu. The evaluation of the expression (9) is rather laborious since many of the auxiliary integrals must be computed numerically.

§ 5. RESULTS AND DISCUSSION

The results obtained for γ using the two sets of eqns. (12), (13), were $1.1 \times 10^{14} \text{ sec}^{-1}$, $1.5 \times 10^{14} \text{ sec}^{-1}$ respectively. These are to be compared with the results 4 to $7 \times 10^{14} \text{ sec}^{-1}$ obtained in paper I, using the time-dependent perturbation theory. In view of the approximate nature of the calculations in paper I, the agreement between the results must be considered extremely good, which suggests that the calculated auto-ionization probabilities are of the correct order of magnitude, if serious cancellation does not occur.

§ 6. IDENTIFICATION OF HELIUM LINES IN THE VACUUM ULTRA-VIOLET

Compton and Boyce (1928) have observed emission lines with wave numbers 279 715, 312 118 and 323 206 cm^{-1} whilst Kruger (1930) has observed the first *two* of these together with lines with wave numbers 310 061, 311 346 cm^{-1} the additional pair appearing on only one of the two spectrographs that he used. The emissions occurred when a discharge was maintained in helium gas at low pressure, care being taken to ensure that they did not arise from impurities. Kruger found the lines to be of comparable intensity.

Although many tentative identifications have been suggested (Fender and Vinti 1934, Cady 1934, Wu 1934, Wilson 1935, Wu 1944) none can be considered certain. The upper levels of these lines (if they are due to atomic helium) must be doubly excited and as Wu (1944) has pointed out, all doubly excited levels other than the $(2pnp)^3P$, $(3dnd)^3D$ etc. series, are subject to auto-ionization; and if the calculations are correct, lines originating from them must, in general, be broadened to at least 1 Å. Although Kruger does not specify the widths of the observed lines it appears not unreasonable to assign to them a *maximum* width of 0.05 Å* requiring the auto-ionization probability to be *less* than $2 \times 10^{12} \text{ sec}^{-1}$. The theoretical probabilities for the various doubly excited states of helium are of the order 10^{14} sec^{-1} (paper I) apart from that for the $(2s3s)^3S$ term for which, because of the occurrence of cancellation, there is some doubt as to the correct value, which might conceivably be so small that detectable broadening would not ensue. The decrease in intensity due to auto-ionization is normally very considerable, the probability of a discrete emission being of the order of 10^8 sec^{-1} (Kreisler 1935)†, some 10^6 times less than that of auto-ionization. There is thus a conflict between the experimental data and the theoretical predictions unless the upper levels are the $(2s3s)^3S$ and the $(2pnp)^3P$, $(3dnd)^3D$ etc. series.

Wilson (1935), Ma and Wu (1936) and Wu (1934, 1944) have computed the energies of some of the levels of interest. Their results are presented in the table together with the energies of the upper levels of the observed lines, various assumptions regarding the identity of the lower levels being made.

* We are indebted to Dr. P. K. Carroll for discussion of this point.

† Kreisler computed the probability of a discrete transition from only one doubly excited level, but it seems unlikely that other discrete emissions from doubly excited levels are much more probable.

It is seen that no single upper level can be the origin of more than one of the observed lines unless one admits the possibility of optically forbidden transitions* ; it then becomes difficult to reconcile the observed intensities and to believe that each level gives rise to only one allowed line. Even if the theoretical probabilities are incorrect, the problem of identification is still not easily resolved. Thus, unless the calculated energies are grossly in error the 279 715 line must correspond to one of the transitions $(2s2p)^3P-(1s4s)^3S$, $(2s2p)^3P-(1s5s)^3S$ and $(2s2p)^3P-(1s4d)^3D$; all of these involve double electron jumps but the unobserved line $(2s2p)^3P-(1s2s)^3S$ will be expected to be more intense. It is not easy to estimate the error involved in the theoretical energies. Some recent rather elaborate calculations by Hylleraas (1950) of the energy of the $(2s2p)^3P$ term yield a value 58.50 eV differing by only 0.05 eV from the value obtained by Wilson (1935) using self-consistent field wave functions which encourages the belief that they are quite accurate. However, Whiddington and Priestley (1934) and Swift and Whiddington (1936) have reported that electron collision experiments show a weak transition in helium causing an energy loss of 59.73 ± 0.12 eV and a still weaker transition causing an energy loss of 63.25 ± 0.13 eV (cf. table) and have shown that they are due to double excitation of helium atoms. On the basis of their calculations of the excitation cross sections in helium, Massey and Mohr (1935) identify the energy loss of 59.73 eV as due to the transition $(1s^2)^1S-(2s2p)^1P$ and the 63.25 eV loss as due to $(1s^2)^1S-(3s2p)^1P$. The first identification requires an error of 1.49 eV in the theoretical energy.†

If errors of about 2 eV (1 eV is equivalent to 8068 cm^{-1}) do indeed occur, all the observed lines could be attributed to the $(2pnp)^3P$ series, but in spite of the collision experiments such errors appear rather unlikely.

However, the theoretical auto-ionization probabilities receive some support from the small number of lines found and from the fact that attempts by Kiang, Ma and Wu (1936) and by Bundy (1937) to detect a visible spectrum due to transitions between pairs of doubly excited states met with failure. Again high auto-ionization probabilities undoubtedly sometimes occur: for example, Shenstone (1940) has observed silver lines of widths corresponding to auto-ionization probabilities of some 10^{14} sec^{-1} .

Though the position is far from satisfactory, the experimental evidence cannot be said to disprove the theory; but it is admittedly disturbing to note that Wu and Ourom (1950) were unable to reconcile the theoretical auto-ionization probabilities of some apparently well identified beryllium lines with the spectroscopic observations.

ACKNOWLEDGMENT

It is a pleasure to record our indebtedness to Professor D. R. Bates. The discussion of the identification of the helium lines has benefited greatly from his readily given advice.

* Coincidences such as $(1s2s)^3S$ (159 850) \rightarrow x(469 911) \rightarrow 310 061 and $(1s4s)^3S$ (190 292) \rightarrow x(470 007) \rightarrow 279 715 are excluded unless $(1s3s)^3S$ (183 231) \rightarrow x \rightarrow 286 769 is also observed.

† The energy of the $(3s2p)^1P$ state has not been computed.

(2p ²) ¹ S	62.22	501 988	508 366	He ⁺ (1s) ² S	509 651	He ⁺ (1s) ² S	509 661	(1s12d) ³ D	509 410	(1s3p) ¹ P
			503 402	(1s5s) ³ S	502 281	(1s4s) ¹ S	502 410	(1s4s) ³ S	506 437	(1s3s) ³ S
(2s2p) ¹ P	61.22	493 900	501 548	(1s4p) ¹ P	501 638	(1s4s) ³ S	498 322	(1s3p) ¹ P		
			494 920	(1s3s) ¹ S	494 577	(1s3s) ³ S	495 349	(1s3s) ³ S	494 335	(1s2p) ¹ P
(2p ²) ¹ D	60.79	490 432	493 292	(1s3s) ³ S					492 287	(1s2p) ³ P
(2p ²) ³ P	59.92	483 387							489 478	(1s2s) ¹ S
Whiddington's level (i)	59.73	481 896							483 056	(1s2s) ³ S
(2s ²) ¹ S	59.35	478 843	481 190	(1s2p) ¹ P						
			479 142	(1s2p) ³ P	480 427	(1s2p) ³ P	481 199	(1s2p) ³ P		
He(2s2p) ³ P	58.55	472 370	478 020	He ⁺ (1s) ² S						
			473 056	(1s5s) ³ S	476 333	(1s2s) ¹ S	477 618	(1s2s) ¹ S	478 390	(1s2s) ¹ S
He ⁺ (1s) ³ S	24.58	198 305	471 202	(1s4p) ¹ P					471 968	(1s2s) ³ S
			439 565	(1s2s) ³ S	469 911	(1s2s) ³ S				

* All energies are measured relative to that of the ground state of the neutral atom.

(a) Term; (b) Computed energy (eV); (c) Computed energy (cm⁻¹); (d) Energy of upper level of 279 715 cm⁻¹; (e) Assumed lower level of 279 715 cm⁻¹; (f) Energy of upper level of 310 061 cm⁻¹; (g) Assumed lower level of 310 061 cm⁻¹; (h) Energy of upper level of 311 346 cm⁻¹; (i) Assumed lower level of 311 346 cm⁻¹; (j) Energy of upper level of 312 118 cm⁻¹; (k) Assumed lower level of 312 118 cm⁻¹; (l) Energy of upper level of 323 206 cm⁻¹; (m) Assumed lower level of 323 206 cm⁻¹.

REFERENCES

- BRANSDEN, B. H., and DALGARNO, A., 1952, *Phys. Rev.*, **88**, 148; 1953 a, *Proc. Phys. Soc. A*, **66**, 268; 1953 b, *Ibid.*, **66**, 904.
- BUNDY, F. P., 1937, *Phys. Rev.*, **52**, 452.
- CADY, W. M., 1934, *Phys. Rev.*, **46**, 439.
- COMPTON, K. T., and BOYCE, J. C., 1928, *J. Franklin Inst.*, **205**, 497.
- DIRAC, P. A. M., 1926, *Proc. Roy. Soc. A*, **112**, 661.
- FENDER, F. G., and VINTI, G. P., 1934, *Phys. Rev.*, **46**, 77.
- HULTHÉN, L., 1944, *K. Fysiogr. Sällsk. Lund Forhandl.*, **14**, No. 21; 1948, *Arkiv. Mat. Astr. Fys.*, **35 A**, 25.
- HULTHÉN, L., and OLSSON, P. O., 1950, *Phys. Rev.*, **79**, 532.
- HYLLERAAS, E. A., 1950, *Astrophys. J.*, **113**, 209.
- KATO, T., 1950, *Phys. Rev.*, **80**, 475.
- KIANG, A. T., MA, S. T., and WU, T. Y., 1936, *Phys. Rev.*, **50**, 673, *Chin. J. Phys.*, **2**, 117.
- KOHN, W., 1948, *Phys. Rev.*, **74**, 1763.
- KREISLER, J., 1935, *Acta Phys. Polon.*, **4**, 15.
- KRUGER, P. G., 1930, *Phys. Rev.*, **36**, 853.
- LIPPMAN, B. A., and SCHWINGER, J., 1950, *Phys. Rev.*, **79**, 469.
- MA, S. T., and WU, T. Y., 1936, *J. Chin. Chem. Soc.*, **4**, 345.
- MASSEY, H. S. W., and MOHR, C. B. O., 1935, *Proc. Camb. Phil. Soc.*, **31**, 604.
- MOTT, N. F., and MASSEY, H. S. W., 1949, *Theory of Atomic Collisions*, 2nd Edn. (Oxford: University Press).
- SHENSTONE, A. G., 1940, *Phys. Rev.*, **57**, 894.
- SWIFT, W., and WHIDDINGTON, R., 1936, *Proc. Leeds Phil. Lit. Soc.*, **3**, 262.
- WENTZEL, G., 1928, *Phys. Z.*, **66**, 291.
- WHIDDINGTON, R., and PRIESTLEY, H., 1934, *Proc. Roy. Soc. A*, **145**, 462.
- WILSON, W. S., 1935, *Phys. Rev.*, **48**, 536.
- WU, T. Y., 1934, *Phys. Rev.*, **46**, 239; 1944, *Ibid.*, **66**, 291.
- WU, T. Y., and OUROM, L., 1950, *Canad. J. Res. A*, **28**, 542.

Photo-Fluorescence Decay Times of Organic Phosphors

BY J. B. BIRKS AND W. A. LITTLE

Physics Department, Rhodes University, Grahamstown, South Africa

MS. received 27th February 1953, and in amended form 6th July 1953

Abstract. A method for measuring photo-fluorescence decay times to approximately 10^{-9} sec is described. Observations are made of the phase and modulation of the light from a 7.5 Mc/s air discharge tube, and of the fluorescence excited by this light, using a photomultiplier modulated at 15 Mc/s. The decay times of anthracene, stilbene, terphenyl and diphenylacetylene crystals of various thicknesses have been measured. Due to the overlap of the emission and absorption spectra, the technical decay time t_f of a thick crystal is greater than the molecular decay time $(t_f)_0$ observed for a microcrystalline specimen. For anthracene $t_f = 14 \pm 2$ m μ sec and $(t_f)_0 = 3.5 \pm 1.0$ m μ sec. This value of t_f agrees with that derived from $(t_f)_0$ and the comparative technical and molecular emission spectra. For each of the compounds studied the molecular decay time $(t_f)_{00}$, in the absence of internal quenching, is of the order of 3–4 m μ sec.

§ 1. INTRODUCTION

THE decay time of the fluorescence from the organic crystals and solutions, used in scintillation counting, is of the order of 10^{-8} second. Many observations have been reported of the decay time t_1 of the fluorescence excited by ionizing radiations for the more important phosphors. Few direct measurements are available however of the decay time t_f of the photo-fluorescence excited by ultra-violet radiation, apart from those of Liebson *et al.* (1950), who found that t_1 was greater than t_f , and approximately equal to $2t_f$ for most of the organic crystals investigated.

Previous measurements by Bowen and Lawley (1949) and Little and Birks (1952) have shown that the spectrum of the photo-fluorescence observed in transmission through an organic crystal is critically dependent on crystal thickness, due to the overlap of the absorption and emission spectra. Only a fraction of the molecular emission occurs in a spectral region to which the crystal is transparent, the remainder being absorbed. The absorbed radiation will be re-emitted as fluorescence, this process of emission and absorption recurring until all the initial excitation energy either escapes from the crystal as fluorescence in the transparent region, or is dissipated thermally by internal conversion. Due to this 'photon cascade' process, the technical decay times t_1 and t_f observed for thick crystals would be expected to correspond to the sum of the decay times of several molecular emissions (Birks 1953). This distinction between the technical and molecular decay times appears to have been overlooked by previous observers.

An experimental method has therefore been developed for the measurement of photo-fluorescence decay times, and it has been used to study the effect of crystal size on t_f , and to determine the molecular decay time $(t_f)_0$ for various organic compounds of interest.

§ 2. PRINCIPLE OF THE METHOD

When a phosphor of photo-fluorescence decay time t_f is excited by light, whose intensity

$$I = I_c + I_0 \sin^2 \omega t \quad \dots\dots(1)$$

is modulated at a high angular frequency 2ω , the fluorescence emission is also modulated in intensity, but its phase lags behind that of the exciting light, and its degree of modulation differs from that of the exciting light.

The decay of the fluorescence emission from an organic molecule is exponential (Pringsheim 1949). It is shown subsequently that the technical decay process, consisting of several such monomolecular decays, is also exponential. This is confirmed by the shape of the observed modulation curves, and it is in agreement with the exponential scintillation decay pulses, excited in organic crystals by fast electrons and recorded by other observers. A non-exponential scintillation decay may occur with heavy particle excitation, due to bimolecular quenching processes in the primary ionization column (Wright 1953).

The rate of emission of light by a phosphor, excited by a light pulse of intensity I at the time $t=0$, is at a time t given by

$$\frac{dS}{dt} = \frac{qI}{t_f} \exp(-t/t_f) \quad \dots\dots(2)$$

where q is the photo-fluorescence efficiency. Hence the intensity of the fluorescence emission, excited by a modulated light source whose intensity is given by (1), is at a time t_0

$$S = \int_{-\infty}^{t_0} \frac{q}{t_f} (I_c + I_0 \sin^2 \omega t) \exp\{- (t_0 - t)/t_f\} dt \\ = qI_c + \frac{1}{2} qI_0 [1 - \cos \phi \cos (2\omega t_0 - \phi)] \quad \dots\dots(3)$$

where

$$\tan \phi = 2\omega t_f \quad \dots\dots(4)$$

and ϕ is the phase lag between the exciting light and the fluorescence emission.

The degree of modulation of the source is

$$m_s = \frac{I_{\max} - I_{\min}}{I_{\max} + I_{\min}} = \frac{I_0}{2I_c + I_0} \quad \dots\dots(5)$$

and of the fluorescence emission is

$$m_f = \frac{S_{\max} - S_{\min}}{S_{\max} + S_{\min}} = m_s \cos \phi. \quad \dots\dots(6)$$

Hence the fluorescence decay time t_f can be obtained from observations of either the phase lag ϕ or the relative modulation m_f/m_s of the fluorescence emission.

§ 3. EXPERIMENTAL APPARATUS

3.1. General Description

A diagram of the apparatus is shown in fig. 1. The power from a 40 watt 7.5 Mc/s 807 Hartley oscillator is fed via a concentric cable to a resonant circuit across the high-frequency discharge tube, whose light output is thus modulated at 15.0 Mc/s. The oscillator also feeds a frequency doubler stage, and the 15 Mc/s signal is fed via a 'coil line' phase changer, to a constant-output tuned

amplifier. The amplifier output, which is of constant amplitude and of variable phase, is applied between the photo-cathode and the first dynode of an RCA 931-A photomultiplier tube, thus modulating the sensitivity of the tube at a frequency of 15 Mc/s. The integrated current i from the photomultiplier is measured with a sensitive galvanometer. The magnitude of i depends on the relative phase of the cathode-first dynode modulating potential and the incident

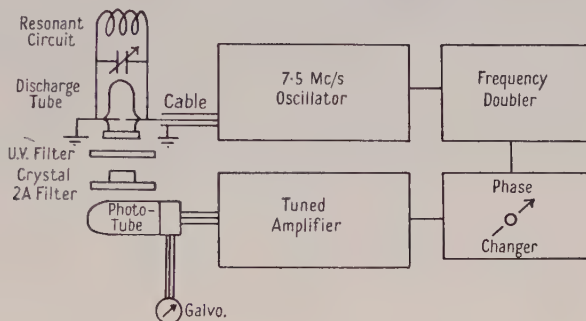


Fig. 1. Schematic design of apparatus.

modulated light. The current is measured as a function of the phase difference between the potential applied to the discharge tube and that applied to the photomultiplier tube, and hence the degree of modulation and the relative phase of the incident light are obtained. Similar measurements on the fluorescence emission excited in the phosphor by the light from the discharge tube enable ϕ , the phase lag, and m_f/m_s , the relative degree of modulation, to be determined.

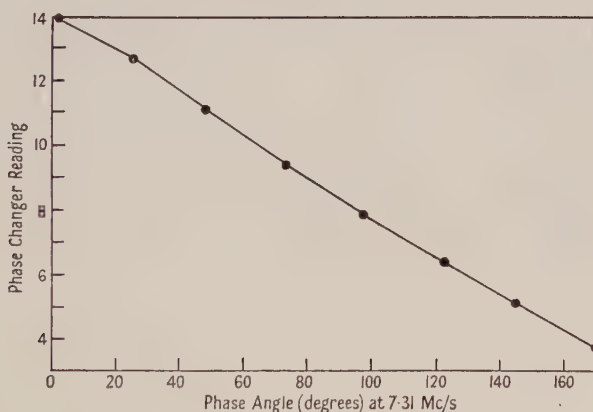


Fig. 2. Calibration of phase changer.

3.2. The Design and Calibration of the Phase Changer

The phase changer (Hund 1936) is an artificial line which consists of ten $2\mu\text{H}$ inductances wound on a single bakelite former with each inductance shunted to earth with a 50 pF condenser, and the line is terminated in a matched resistive load. A movable pick-up coil is mounted inside the coil former on a graduated, adjustable screw. The phase changer was calibrated by comparison with a short length of cable of known electrical length. The 15 Mc/s signal

from the phase changer was fed to the X deflection plates of a fast oscilloscope, and the 15 Mc/s signal from the frequency doubler was fed via an amplifier through a concentric cable to the Y deflection plates. The phases of the two signals were adjusted to give a linear trace on the oscilloscope screen. The introduction of a short known additional length of cable in the Y-plate channel caused a phase change. The resultant elliptical oscilloscope trace was reduced to a linear trace again by an adjustment of the phase changer, whose reading was equated to the calculated phase change introduced by the cable. The calibration curve of the phase changer is shown in fig. 2. Different calibration runs agreed to within less than 1° of phase, i.e. approximately 2×10^{-10} second. The signal from the phase changer is variable over 300° and is approximately constant in amplitude. It is fed through a limiting tuned amplifier giving an output constant in amplitude to better than 0.1% over the whole range of phase.

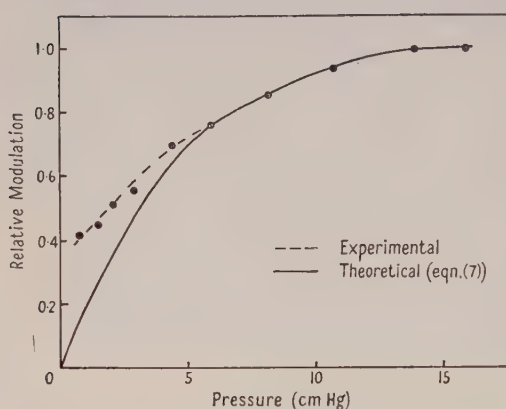


Fig. 3. Degree of modulation plotted against pressure for discharge tube.

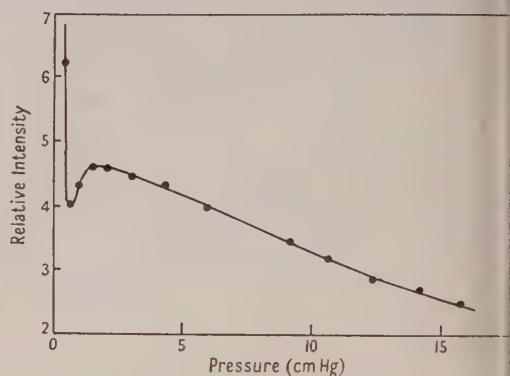


Fig. 4. Light intensity plotted against pressure for discharge tube.

3.3. Design and Studies of Modulated Discharge Tube

The high-frequency gas discharge tube operates at pressures of up to 15 cm Hg. Air is found to be the most satisfactory and convenient gas. The discharge tube has two needle-point tungsten electrodes with 1 mm separation, sealed into a Pyrex tube which has a flat quartz window. The unperturbed decay times of the excited states of the O_2 and N_2 molecules are relatively long, of the order of 5×10^{-8} sec (Frey 1936), so that at very low pressures the degree of modulation of the light output from the discharge is low though the intensity is high. An increase in the pressure p causes collisional quenching of the excited gas molecules, giving a reduction in intensity, but an increase in the degree of modulation due to the reduced decay time. If it is assumed that the decay time of the excited state of the gas molecule is inversely proportional to the pressure, then the degree of modulation m_s is given theoretically by an equation of the form

$$m_s = (1 + a/p^2)^{-1/2}. \quad \dots\dots(7)$$

The relative degree of modulation of the 7.5 Mc/s air discharge has been measured as a function of p . These measurements are plotted in fig. 3, and they are in good agreement with the theoretical relation (7) for values of p from approximately 3 cm to 15 cm Hg for $a=35$. The relative intensity of the light output as a function of p is plotted in fig. 4. The large increase in intensity at low pressures is due to a sudden increase in the volume of the discharge.

Although these measurements on the high-frequency gas discharge were primarily conducted to establish the optimum conditions of the modulated light source for the photo-fluorescence studies, the results obtained indicate that the experimental method should be useful in studies of the decay times of the excited states of gas molecules. The degree of modulation of the discharge is simply related to the decay time, and different spectral bands can be isolated and studied by the use of appropriate filters. For the photo-fluorescence studies an air pressure of about 5 cm Hg was used, since this gave a high degree of modulation combined with an adequate intensity.

§ 4. EXPERIMENTAL RESULTS

4.1. Decay Times

A Wood's glass filter, transmitting only ultra-violet radiation, was placed over the window of the discharge tube, and the photomultiplier output current i was measured as a function of the phase difference between the discharge tube potential and the cathode-first dynode potential (fig. 5, curve a). A Wratten 2A

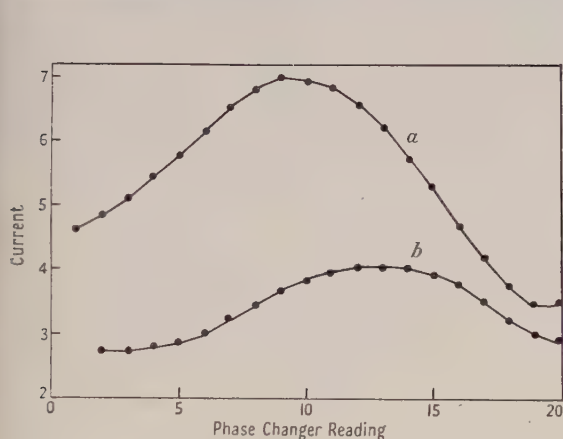


Fig. 5. Photomultiplier current i plotted against phase changer reading; a , light source; b , anthracene crystal.

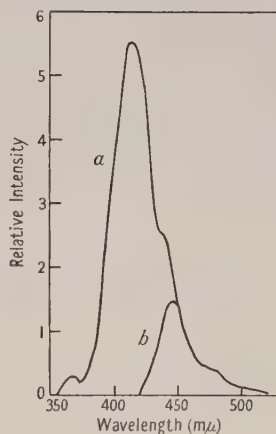


Fig. 6. Fluorescence spectra of anthracene; a , microcrystals (molecular spectrum); b , 1 cm thick crystal (technical spectrum).

filter placed between the Wood's glass filter and the photomultiplier was found to absorb almost all the radiation from the discharge tube. When an anthracene crystal, 1 cm thick, was introduced between the two filters, a strong photo-multiplier signal was obtained due to the anthracene photo-fluorescence, which is transmitted by the Wratten 2A filter. The current i (corrected for the small background current present in the absence of the crystal) was observed as before as a function of phase difference (fig. 5, curve b). The phase lag $\phi = 53^\circ \pm 3^\circ$, corresponding to $t_f = 14.4 \pm 1.5 \text{ m}\mu\text{sec}$. A similar value of $\phi = 55^\circ \pm 1.2^\circ$, corresponding to $t_f = 15.5 \pm 0.7 \text{ m}\mu\text{sec}$, is obtained from the relative degree of modulation m_f/m_g .

Similar measurements of t_f at room temperature were made on other anthracene single crystals, and also on single crystals of *trans*-stilbene, diphenylacetylene and *para*-terphenyl. In addition, observations were made on thin powdered specimens of anthracene and *para*-terphenyl, prepared by grinding,

and on microcrystalline layers of each of the four materials formed on a thin glass plate, by evaporation of a dilute solution of the compound in xylene. In the latter case it was only found possible to excite the photo-fluorescence of anthracene and stilbene with sufficient intensity to observe t_f , since the absorption spectra of the other two compounds lie further into the ultra-violet region, where the emission of the source is weak. The mean observed values of t_f for the various specimens studied are listed in the table.

Compound	Description of specimen	t_f (m μ sec)	t_f (L) (m μ sec)
Anthracene	1 cm cube	14 ± 2	17
	Powder	4.8 ± 1.5	—
	Microcrystals	3.5 ± 1.0	—
	$\frac{1}{2}\%$ solution in benzene	—	2.0 ± 0.5
Stilbene	2 mm thick	3.0 ± 0.8	3.1
	Microcrystals	1.7 ± 0.6	—
Diphenylacetylene	2 mm thick	3.0 ± 0.8	2.5
Terphenyl	2 mm thick	3.8 ± 1.0	11
	Fine powder	3.5 ± 1.0	—
	$\frac{1}{2}\%$ solution in benzene	—	2.5 ± 0.5

The values of t_f reported by Liebson (1952) (t_f (L)) for crystals of unspecified size (probably >1 mm thickness) and other specimens are shown in the last column of the table for comparison.

4.2. Fluorescence Spectra

The emission spectra of the different anthracene specimens, excited by monochromatic radiation of 254 m μ wavelength, have been measured. The spectra were observed by transmission through the specimens using a modified Cenco-Sheard 'spectrophotometer' with an EMI 6262 photomultiplier tube as the radiation detector. The intensity readings were corrected for the variation of the sensitivity of the photomultiplier and of the transmission coefficient of the 'spectrophotometer' with wavelength. The fluorescence spectra from (a) a microcrystalline specimen, and (b) a single crystal, of 1 cm thickness, normalized at a wavelength of 450 m μ , are plotted in fig. 6. The absence of vibrational structure is due to the low resolution of the experimental arrangement.

The spectra of the anthracene powders were intermediate between (a) and (b), extending from a wavelength of about 390 m μ , with an intensity peak at about 425 m μ , and coinciding with the other two spectra at wavelengths greater than 450 m μ . These powder spectra, like the corresponding decay time measurements, are critically dependent on the grain size. For crystal thicknesses greater than 1 mm the spectrum is practically independent of thickness, and similar to that shown in fig. 6, curve b.

The emission spectrum of a 2 mm thick mixed crystal of naphthalene, containing 0.01% of anthracene by weight, and excited by the 254 m μ radiation, was observed to contain two spectral components characteristic of the naphthalene and anthracene molecules respectively. The spectrum of the anthracene emission was found to be similar to that from the pure anthracene microcrystals (fig. 6, curve a). For mixed crystals of greater thickness and higher anthracene concentration, the anthracene emission spectra were intermediate between

(a) and (b), and similar to those from pure anthracene powders. Certain of these spectral measurements have been reported previously (Little and Birks 1952) but have not been published.

§ 5. DISCUSSION

The dependence of the fluorescence spectra of the anthracene specimens on crystal size is due to the overlap of the absorption and emission spectra. For the microcrystalline specimens the self-absorption is practically eliminated, and the observed spectrum corresponds to the true molecular fluorescence of anthracene in the crystalline state. It is similar to that of anthracene in dilute solid solution in naphthalene, and it also agrees closely with that of anthracene in solid solution in polystyrene, observed by Koski (1951). In each case the complete molecular spectrum is observed because the surrounding medium is transparent to the emission.

In a large crystal, a fraction of the fluorescence emitted by the molecules initially excited by the incident radiation is reabsorbed. This absorbed radiation is subsequently re-emitted as molecular fluorescence, which hence includes both Stokes and anti-Stokes radiation. The process recurs until all the fluorescence emission is in the spectral region to which the crystal is transparent. The spectrum observed (fig. 6, curve *b*) corresponds to the technical emission spectrum of an anthracene crystal of thickness greater than 1 mm. The probability k_e of the escape of the molecular emission is given by the ratio of the area under the technical spectrum to the area under the molecular spectrum. For the thick anthracene crystals $k_e = 0.2$ from fig. 6. The probability of absorption $k = 1 - k_e = 0.8$.

The effect of the self-absorption on the observed value of t_f may be calculated. Let N be the number of excited molecules at time t , $1/(t_f)_{00}$ be the probability per unit time of molecular emission, and $1/t_i$ be the probability per unit time of internal conversion. Then

$$-\frac{dN}{dt} = N [1/(t_f)_{00} + 1/t_i - k/(t_f)_{00}] = N\lambda, \quad \dots\dots (8)$$

$$N = N_0 e^{-\lambda t}. \quad \dots\dots (9)$$

The intensity of the fluorescence emission escaping from the crystal is

$$J = (1 - k)N/(t_f)_{00} = J_0 e^{-\lambda t}. \quad \dots\dots (10)$$

Hence the decay of the emission is exponential, and of technical decay time

$$t_f = \frac{1}{\lambda} = \frac{(t_f)_{00}}{k_e + (t_f)_{00}/t_i}. \quad \dots\dots (11)$$

The molecular decay time ($k = 0$, $k_e = 1$) is

$$(t_f)_0 = \frac{(t_f)_{00}}{1 + (t_f)_{00}/t_i} = q_0(t_f)_{00} \quad \dots\dots (12)$$

where q_0 is the molecular photo-fluorescence quantum efficiency. In the absence of internal quenching ($q_0 = 1$)

$$t_f = (t_f)_0/k_e. \quad \dots\dots (13)$$

Bowen, Mikiewicz and Smith (1949) have observed $q_0 = 0.9$ for small anthracene crystals at room temperature. This represents a minimum value for q_0 , since it is not certain that their specimens were sufficiently thin to eliminate self-absorption completely. Substituting $q_0 = 0.9$, $k_e = 0.2$, $(t_f)_0 = 3.5 \pm 1.0$ m μ sec

in the equations above, we obtain $(t_f)_{00} = 3.9 \pm 1.2 \text{ m}\mu\text{sec}$, $t_i = 35 \pm 10 \text{ m}\mu\text{sec}$, and $t_f = 12.6 \pm 3.5 \text{ m}\mu\text{sec}$. This value of t_f agrees, within the experimental error, with that of $t_f = 14 \pm 2 \text{ m}\mu\text{sec}$ observed directly.

The photo-fluorescence quantum efficiency q_0 of a solution of anthracene in benzene is ~ 0.65 (Bowen 1949). Since self-absorption will be negligible in a relatively dilute solution, we may equate Liebson's value of $t_f = 2.0 \pm 0.5 \text{ m}\mu\text{sec}$ to $(t_f)_0$, giving $(t_f)_{00} = 3.1 \pm 0.8 \text{ m}\mu\text{sec}$ in agreement with the value obtained from the crystal measurements.

The smaller difference in the values of t_f observed for thick crystals and microcrystals of *trans*-stilbene is due to the reduced overlap of the absorptino and emission spectra. The reduced self-absorption of stilbene compared with anthracene is confirmed by the observations of Koski (1951), who compared the emission spectrum of a stilbene crystal with that of a dilute solution of stilbene in polystyrene. The data on t_f for stilbene, diphenylacetylene and terphenyl indicate that $(t_f)_{00}$ for each of these materials is of the order of $3\text{--}4 \text{ m}\mu\text{sec}$. This is to be expected since the oscillator strengths of the optical transition from the first electronic excited state to the ground state, responsible for the fluorescence emission, are similar to that of anthracene.

Liebson's value of $t_f = 11 \text{ m}\mu\text{sec}$ for terphenyl appears anomalous, and disagrees with his value of $t_i = 6 \text{ m}\mu\text{sec}$ for the same material. Since $t_i \sim 2t_f$ we may estimate $t_f \sim 3 \text{ m}\mu\text{sec}$ from this latter measurement, in agreement with the general results.

§ 6. CONCLUSION

The results indicate that the photo-fluorescence molecular decay time $(t_f)_{00}$, in the absence of internal quenching, of the organic compounds studied is of the order of $3\text{--}4 \text{ m}\mu\text{sec}$. This is reduced to $(t_f)_0$ for microcrystals, due to internal conversion, and increased to t_f for large crystals, due to self-absorption. The spectral and decay time measurements on anthracene crystals show clearly that intermolecular energy exchange occurs by photon emission and reabsorption, as proposed by Birks (1953).

ACKNOWLEDGMENT

We wish to thank the South African Council for Scientific and Industrial Research for a research grant in support of this work, and for a bursary awarded to one of us (W. A. L.).

REFERENCES

- BIRKS, J. B., 1953, *Scintillation Counters* (London : Pergamon Press; New York : McGraw-Hill).
- BOWEN, E. J., 1949, *The Chemical Aspects of Light* (Oxford : University Press).
- BOWEN, E. J., and LAWLEY, P. D., 1949, *Nature, Lond.*, **164**, 572.
- BOWEN, E. J., MIKIEWICZ, E., and SMITH, F. W., 1949, *Proc. Phys. Soc. A*, **62**, 26.
- FREY, A. R., 1936, *Phys. Rev.*, **49**, 305.
- HUND, A., 1936, *Phenomena in High Frequency Systems* (New York : McGraw-Hill).
- KOSKI, W. S., 1951, *Phys. Rev.*, **82**, 230.
- LIEBSON, S. H., BISHOP, M. E., and ELLIOT, J. O., 1950, *Phys. Rev.*, **80**, 907.
- LIEBSON, S. H., 1952, *Nucleonics*, **10**, 41.
- LITTLE, W. A., and BIRKS, J. B., 1952, South African Association for the Advancement of Science Congress, Cape Town, South Africa (July 1952).
- PRINGSHEIM, P., 1949, *Fluorescence and Phosphorescence* (New York : Interscience).
- WRIGHT, G. T., 1953, *Phys. Rev.*, in the press.

Interpretation of Cosmic Ray Jets

By W. HEITLER AND CH. TERREAUX

Department of Theoretical Physics, University of Zürich, Switzerland

MS. received 4th June 1953

Abstract. Cosmic-ray jets are interpreted as being due to the creation of a more or less cylindrical penetration tunnel in the nucleus. An estimate of the energy transfer to the residual nucleus is made and it is shown that this arises mainly from the surface energy of the tunnel. The order of magnitude found accounts for the relatively small number of heavy tracks N_H observed. The fluctuations of N_H are also in rough agreement with the observations. The variation of the shower size n_s is largely due to the variation of the tunnel length d , but there are also substantial fluctuations of n_s for a given d . The upper limit of n_s is due to the maximum tunnel length in AgBr, and is, above a certain energy, independent of the primary energy. The values of n_s can be obtained (in agreement with the facts) from a purely plural or a suitable mixed plural-multiple model for meson production.

§ 1. GENERAL SURVEY

THE cosmic-ray jets have recently been the subject of several investigations (Daniel *et al.* 1952, Kaplon and Ritson 1952, and various publications describing individual events, for example, Pickup and Voyvodic 1951). Although the statistical material is still not very great enough appears to be known to attempt a theoretical explanation, at least on broad and more qualitative lines. The characteristic features of these jets are the following: (i) The shower particles are emitted within a very small angle which indicates that the primary nucleon must have had a very high energy, ≥ 50 kmev say.* The number of shower particles n_s ranges from a few up to about 30 in AgBr. (ii) The number of heavy tracks N_H is surprisingly small, ranging from 0 to 5, say, if we except a few events near the lower end of the energy region considered. This is in contrast to the showers observed at lower energies where large values of N_H are quite frequent. As far as could be ascertained, the shower particles are mostly mesons. The number of protons may be estimated to be 10–20%. A considerable fraction of the mesons appear to be κ -mesons. But as the energies are so high, we shall not, in the following, distinguish between the various types of mesons.

On account of the small value of N_H these jets, in particular those with $N_H = 0, 1$ or 2 , have often been interpreted as due to glancing collisions. This, we shall show, is quite unjustified.

The energy of the primary cannot be inferred directly from the angular spread Φ of the jet. This would be the case if only one collision with a single nucleon in the nucleus took place. But as will be shown, there is no justification for such an assumption. In the case of a single collision the primary energy would be given by approximately $2/\Phi^2$, in units of $Mc^2 \sim 1$ kmev. Thus $2/\Phi^2$ is a lower limit to the primary energy (in kmev) which is, in most cases, much

* Showers initiated by primary heavy nuclei will not be considered in this paper, but a few α -initiated jets are included in fig. 1. For these n_s has been divided by four but N_H is the measured value.

higher. We therefore use $\overline{\Phi^2}$, which is the quantity actually measured, to characterize the showers.

In fig. 1 we have plotted the individual events observed by Daniel *et al.* and by Kaplon and Ritson according to the number of jet particles n_s and as a function of $\log_{10} \overline{\Phi^2}$. The first measurements are made in the photographic plate and refer to AgBr; a few of the smaller events may actually be due to C, N, O, but they cannot be identified as such and as their number is certainly not large we disregard this possibility. The second set of experiments refer to Cu and are made with an alternating set of Cu and photographic plates set horizontally (the direction of the jet is more or less vertical). Since the diameter of the Cu nucleus is only slightly smaller ($\frac{6}{7}$) than that of Ag we may plot both measurements in the same diagram. The first set comprises showers with $2/\overline{\Phi^2} \geq 50$, the second set only those with $2/\overline{\Phi^2} \geq 480$. There is, of course, no statistical relationship between the two sets of experiments. The number of heavy tracks is indicated for each event of the first set, but could not be measured in the second set.

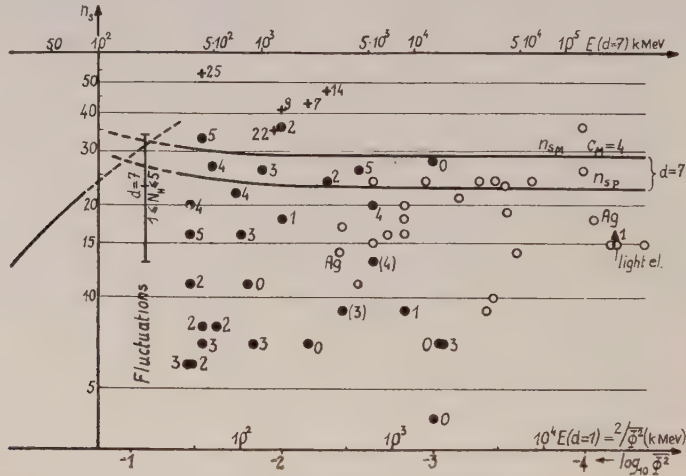


Fig. 1. Plot of cosmic-ray jets with n_s shower particles as function of the average half-angle ϕ . Full circles and crosses according to Daniel *et al.* (1952), open circles according to Kaplon and Ritson (1952). One event (triangle) by Lord *et al.* (1950). The number of heavy tracks N_H is attached for the first set of experiments. When this is bracketed, the event is initiated by an α -particle and n_s (but not N_H) is divided by four. The theoretical curves for plural model (n_{sP}) and mixed plural-multiple model (n_{sM}) refer to a maximum tunnel length in Ag. The curve to the left from Terreaux (1951) applies to smaller energies. The upper energy scale applies to a maximum tunnel length, the lower scale to glancing collisions. Fluctuations of n_s and N_H are marked on the left for maximum tunnel length.

A substantial advance in the understanding of the jets has been made in a recent paper by Roesler and McCusker (1953). The picture used is this: At the very high energies with which we are concerned the primary nucleon will penetrate right through the nucleus sweeping out all nuclear matter along its path, together with the mesons created in the collisions. Thus a more or less clear-cut penetration tunnel is made through the nucleus. This, of course, is only true in a large nucleus (a light nucleus could not keep together) and if the collision is not a glancing, or near glancing, one.

The energy of the jet particles will degrade along the tunnel with a corresponding increase in the angles. So in general the shape will be that of a trumpet. At the entrance the radius of the tunnel will be equal to the nucleon-nucleon distance in the nucleus. If the primary energy is sufficiently high the angular spread is small and the shape will be a cylinder. Actually, we shall see that this phenomenological treatment of the tunnel begins to fail just when the shape begins to deviate from a cylinder.

We shall accept this general picture in the following but deviate in the actual application. Our conclusions will also be different. We shall use the following unit of length: let the nuclear diameter be $d_A = 2.8 \times 10^{-13} A^{1/3}$ cm; if the cross section in a collision with a nucleon is geometric, i.e.

$$\sigma = \pi \left(\frac{\hbar}{\mu_n c} \right)^2 = \pi (1.4 \times 10^{-13})^2 \text{ cm}^2 = 6.15 \times 10^{-26} \text{ cm}^2,$$

our unit of length shall be the average distance between two collisions in a nucleus, i.e.

$$d_0 = \frac{1}{\sigma N} = \frac{\pi d_A^3}{6 \sigma A} = 1.87 \times 10^{-13} \text{ cm}.$$

In these units, the nuclear diameters are $d_A = 7.2$ (Ag), 6.0 (Cu), 3.8 (O). This is the average number of collisions in a tunnel of maximum length. The average distance between two nucleons in the nucleus is, in these units, $1.2 d_0$.

Consider now showers created by a central hit and with an energy so high that the tunnel is cylindrical. The number of nucleons hit is then determined by the diameter of the nucleus and independent of the primary energy. We expect then that n_s also remains constant and does not change substantially with energy. This will be the maximum shower size. A glance at fig. 1 shows that such an upper limit really exists, namely $n_s \simeq 30$, if we except a few cases in the upper left-hand corner, which are characterized by a large N_H as well as a large n_s and a comparatively small $2/\overline{\Phi}^2$. These exceptional cases will be discussed below (§ 5). Considering the large range in energy (more than a factor 100) the constancy of the maximum is rather striking. Thus we interpret the upper boundary of the events in fig. 1 as due to a penetration tunnel along the diameter d_A . We shall see in § 4 that the actual value of n_s is in agreement with the plural theory.

If we disregard the fluctuations of n_s , the smaller values of n_s should be due to impact parameters corresponding to a tunnel length less than d_A . Theoretically, the lower boundary should be due to glancing collisions and would give the actual multiplicity in a nucleon-nucleon collision. However, it is doubtful whether this theoretical lower boundary is that of the experimental points in fig. 1. In the photographic plate a certain bias exists against small showers. We see from fig. 1 that N_H decreases as n_s decreases. Showers with $N_H = 0$ and $n_s = 2$ or 3 have certainly not been recorded at all and when $N_H = 1$ and $n_s \leq 3$ probably the majority of the events have been missed. It is therefore impossible to say where the true lower boundary lies.*

§ 2. ENERGY TRANSFER TO RESIDUAL NUCLEUS, EVAPORATION NUCLEONS

When the tunnel is created a certain amount of energy is transferred to the residual nucleus. We shall try to estimate this energy. It is quite clear that only a very rough estimate can be given for this quantity.

* From the portion of fig. 1 where both sets of experiments overlap it appears that an even stronger bias against small jets must have existed in the Kaplon and Ritson experiment. Thus we attribute no significance to the lower bound of the latter experiment.

We consider the residual nucleus immediately after the passage of the primary. The energy transferred consists then of two contributions:

(i) *Friction*. Energy is directly transferred by the primary and the jet particles to the neighbouring nucleons which remain part of the residual nucleus. This contribution will be very small.

(ii) *Surface energy*. When the tunnel is created the nucleus has an additional surface due to the tunnel. This will be the main contribution.

First we show that (i) is very small. Consider a nucleon 1 bound to a nucleon 2 with a potential $V(r_{12})$. Let the nucleon 1 be in the jet line and be hit by the jet developed up to that point. Owing to the very high energy of the jet the nucleon 1 will acquire almost immediately a velocity \mathbf{c} . The force acting on nucleon 2 is

$$\mathbf{K}_2 = -\text{grad } V = d\mathbf{p}_2/dt.$$

Thus after the collision the momentum of nucleon 2 will be of the order

$$p_2 = \int \frac{(\text{grad } V \cdot d\mathbf{r}_{12})}{\mathbf{c}} \simeq \frac{V}{\mathbf{c}}.$$

Hence the energy transferred to nucleon 2 is of the order

$$E \sim V^2/2M\mathbf{c}^2. \quad \dots\dots(1)$$

If we assume $V \sim 30$ mev, $E \simeq 0.5$ mev. Even if we assume that each nucleon, originally situated in the tunnel, has four neighbours, each of which receives the energy (1) and if the number of nucleons along the tunnel is seven (Ag, maximum tunnel length) we obtain a total energy transfer of only

$$U_1 \sim 14 \text{ mev}. \quad \dots\dots(2)$$

This is far too small to account for the observed numbers N_H . The estimate is only correct if the nucleons, when they emerge from the tunnel, have still energies very much greater than $M\mathbf{c}^2$. Otherwise the energy transfer is much larger near the end of the tunnel.

The surface energy is much larger than (2). It will be reasonable to lay the surface of the tunnel through the centres of the bordering nucleons. Then the diameter of the tunnel is twice the average distance between two nucleons or 2.4 in our units.* The surface of the maximal tunnel in Ag is then $2.4\pi \times 7.2$ and the ratio of the tunnel surface to the outer surface of the Ag nucleus is

$$\frac{\sigma_T}{\sigma_{\text{Ag}}} = \frac{2.4\pi \times 7.2}{4\pi(3.6)^2} = \frac{1}{3}.$$

The surface energy of a nucleus is usually given as (Rosenfeld 1948) $15.4A^{2/3}$ mev = 350 mev for Ag. We calculate the energy transfer from the difference of the surfaces of the original nucleus (Ag) pierced by the tunnel and the smaller spherical nucleus which has seven nucleons less and is in its ground state, assuming that the surface energy per unit area is the same for the tunnel and a spherical nucleus. Since the density of the nucleons is constant no change in volume energy occurs. This gives an energy transfer of

$$U_2 \sim 105 \text{ mev}. \quad \dots\dots(3)$$

* U_2 depends, of course, on what is assumed for the radius of the tunnel but roughly the same result is obtained by counting the number of nucleon-nucleon bonds broken by the tunnel.

Both estimates are very crude but we shall probably not be far wrong if we assume that the energy transfer to the residual nucleus in a diametral passage through an Ag nucleus at extreme energies is of the order of magnitude of

$$U \sim 80-150 \text{ MeV} \quad \dots\dots(4)$$

We shall assume now that, after this excitation, a thermal equilibrium is established before any further particles are ejected by evaporation. This is, no doubt, an idealization: immediately after the creation of the tunnel, no significant heat energy exists; this arises only through the gradual reconstitution of the nucleus in forming a new spherical nucleus, and the heat thus created is distributed more or less uniformly over the nucleus.* Relatively fast non-relativistic nucleons (grey tracks) may occur, and have also been observed, as border line cases between the creation of the tunnel and the subsequent evaporation, but the sharp distinction we are making seems to be a justified simplification.

The evaporation process for a given excitation energy has been the subject of an extensive theoretical investigation by Le Couteur (1950, 1952). The average number of heavy tracks is very nearly proportional to U in the region in question. According to Le Couteur

$$\bar{N}_H = 2.5 \times 10^{-2} U(\text{MeV}) - 0.7 \quad \dots\dots(5)$$

(for U not too small). From fig. 1 we find that \bar{N}_H for showers with $n_s = 25-30$ is $\bar{N}_H = 3$, excepting again the group with large N_H and n_s . The corresponding excitation energy of 148 MeV is in remarkable agreement with the crude estimate (4).† That our estimate is in fact somewhat lower is not surprising because the tunnel is not exactly cylindrical but has certain irregularities due to the accidental distribution of the nucleons.

Next we consider the dependence of the surface energy on the impact parameter y (in units of d_0), or the tunnel length d , defined as the length of the central line of the cylinder through the nucleus ($d^2 = d_A^2 - 4y^2$). For small y , the surface energy is nearly proportional to d . This changes when y is so large (>2.3 say) that no tunnel proper is created but merely a piece of the nucleus is knocked off. The surface of a nucleus thus mutilated is almost the same as that of the original nucleus. Thus we expect the energy transfer to decrease very rapidly when $y > 2.3$, say. The calculation gives the following results (for Ag):

y	0	1	2.3	3.1	3.6
d	7.2	6.8	5.6	3.6	0
U_2 (MeV)	105	100	55	20	15

The case $y = 3.6$ means glancing collisions with just one or two nucleons knocked off from the surface. We see that the energy transfer has decreased to half its maximum value at $y = 2.3-2.5$ (if we include U_1), and there we expect \bar{N}_H to have decreased to 1.5 or so.

* The case of π^- -capture, where the energy transfer is of the same order as (4), differs in this respect from our case. Here the whole rest energy is first given to a single nucleon creating a very hot local region (see Menon *et al.* 1950). Moreover, there is an excess of one neutron after the capture, whereas in our case this is, on the average, not the case. Owing to the neutron excess the number of evaporation tracks is smaller by about one.

† Le Couteur has shown that his results agree with the observations of stars due to π^- -capture.

We shall see in § 4 that for $d = 5.5$ we expect \bar{n}_s to be of the order of 14. For still smaller jets \bar{N}_H is expected to decrease rather rapidly.

From fig. 1 we see indeed that, broadly speaking, \bar{N}_H decreases as n_s decreases and we would thus attribute the smaller jets to larger impact parameters. However, for several reasons, a quantitative comparison with the experiments can hardly be made at the present stage: (i) It will be seen (§ 4) that the fluctuations of n_s are rather large so that events with the same n_s may be due to a rather large range of tunnel lengths. (ii) Showers with small N_H and small n_s are likely to be missed in the scanning and therefore the statistical material presented in fig. 1 becomes somewhat unreliable when n_s is small and may therefore indicate too large a value for the average \bar{N}_H . Also the fluctuations of N_H become relatively large for small N_H . (iii) The above estimate of U only holds as long as all jet nucleons emerging from the tunnel have energies much greater than Mc^2 . We shall see in § 5 that this is only true for sufficiently small $\bar{\Phi}^2$. The events furthest to the left in fig. 1 are situated not far from the limits where this theory ceases to hold. When the energy of the emerging nucleons is not very large compared with Mc^2 the energy transfer U_1 is larger.* If we except the events with fairly large $\bar{\Phi}^2$ the statistical material is too small for a value of \bar{N}_H to be derived. (iv) A number of the smaller events are no doubt due to collisions with C, N, O nuclei. For these our theory cannot be applied at all because these nuclei are disrupted entirely in the collision and in this case N_H may be larger.

As the main result of this section we can state: There is no difficulty in understanding that in the *creation of a jet the number of heavy tracks is small*, even in a *diametral passage through the nucleus*.

Finally a remark about real glancing collisions: In this case there is little change in surface energy (~ 15 mev). The direct energy transfer U_1 is quite negligible. Although it is doubtful whether Le Couteur's theory holds for such small U , \bar{N}_H is certainly less than one. A further effect is the disturbance of the proton-neutron equilibrium. If a neutron/proton is knocked out this favours somewhat the evaporation of a proton/neutron but also leads in many cases to β -decay.

We conclude that in a true glancing collision it is improbable that more than one heavy track appears. Only cases $N_H = 0$, or at most 1, can be glancing collisions (in contrast to some publications where stars with small N_H are interpreted as glancing collisions).

§ 3. FLUCTUATIONS OF N_H

The fluctuations of N_H appear to be rather large. Near the upper limit where $\bar{N}_H = 3$, N_H ranges from 0 to 5. There are several causes for these fluctuations:

(i) The fluctuations of the evaporation process with given U have also been studied by Le Couteur (1952). When $\bar{N}_H = 3$, he finds $\Delta_1 N_H = 0.8$.

(ii) If d nucleons are ejected from the tunnel half of them will on the average be protons, half neutrons. The chance that, in reality, n ejected particles are protons is

$$\frac{1}{2^d} \binom{d}{n}.$$

The expected mean square deviation from the proton-nucleon equilibrium in the residual nucleus is then $\Delta n = \sqrt{d/2}$. For $d = 7$ this gives $\Delta n = 1.3$. If such

* A slight increase of N_H towards the left of fig. 1 can perhaps be discerned from the diagram.

a proton or neutron excess exists, this will show in the number of heavy tracks. The excess of one neutron is likely to reduce the number of evaporation protons by ~ 1 (Le Couteur 1952). We may therefore not be far wrong if we assume a fluctuation of N_H of approximately Δn , due to a possible neutron or proton excess. Thus $\Delta_2 N_H \sim 1.3$.

(iii) The true number of nucleons ejected deviates from the average number d , depending on the accidental distribution of nucleons in the nucleus (even if this is assumed to be uniform; not every nucleon receives a central hit). A similar problem was considered by Terreaux (1951) in the theory of plural meson production when no secondary effects are considered (i.e. if only one meson is produced for each nucleon hit by the primary). It was found that the deviation of the number of nucleons hit was $\Delta k \sim 2$ when $d = 7$ (independent of the primary energy if this is ≥ 100 mkev). Accordingly the tunnel is not really cylindrical in shape and therefore also U_2 fluctuates. We may, very roughly, assume that U_2 is proportional to the actual number of nucleons ejected. This gives a fluctuation $\Delta U_2 \simeq U_2 \Delta k / d$. For $d = 7$, this gives $\Delta U_2 \simeq 40$ mev. Accordingly, $\Delta_3 N_H \sim \bar{N}_H \Delta k / d \sim 0.9$.

Combining all these sources we obtain an expected fluctuation

$$\Delta N_H = \{(\Delta_1 N_H)^2 + (\Delta_2 N_H)^2 + (\Delta_3 N_H)^2\}^{1/2} \simeq 1.7. \quad \dots\dots(6)$$

This quite accounts for the observed fluctuations.

§ 4. NUMBER OF SHOWER PARTICLES n_s

We shall see in the following section that for all the jets under consideration the tunnel is nearly cylindrical and that the widening out of the tunnel into a trumpet form begins to become significant just at the lower end of the $E(d=1) = 2/\Phi^2$ scale, i.e. for $2/\Phi^2 < 100$ say. We shall therefore in this section assume a cylindrical shape.

The number of shower particles to be found depends, of course, on what is assumed for the process of meson production. We shall see that both purely plural production and mixed plural-multiple production can account for the observations, as far as n_s is concerned.*

If we consider the problem as continuous along the tunnel rather than as a complicated statistical problem of collisions with individual nucleons, the calculation becomes very simple.

Let t be the variable distance along the tunnel in our units. The number of shower particles in the jet will then increase as t increases and the characteristics of the process will be given by $dn_s(t)/dt$.

(a) Plural Production

We shall use the model first suggested by Heitler and Jánosy (1950) namely, only one meson is produced in a nucleon-nucleon collision. If, however, t fast nucleons all moving in the same direction hit simultaneously one nucleon at rest

* The plural interpretation of penetrating showers has received support through the experiments of McCusker, Porter and Wilson (1953) in carbon and paraffin, for primary energies up to 30 mkev. The hydrogen in paraffin contributes nothing to showers $n_s > 2$ within the statistical errors, which are very much smaller than the rate to be expected if the showers in carbon were due to multiple processes. Thus, for $E \leq 30$ mkev, multiple processes must be comparatively rare. For higher energies nothing definite is known yet and we shall therefore also discuss briefly the case of a mixed plural-multiple production.

(in a many body collision) t mesons (but only one recoil nucleon) are produced.* We assume that the jet mesons do not produce further mesons in colliding with nucleons. We shall also assume the cross section to be geometric ($\pi(\hbar/\mu_\pi c)^2$). At a depth t , just $t+1$ fast nucleons are present including the primary. Assuming that two thirds of the mesons and half of the nucleons are charged we have

$$dn_{sP}/dt = \frac{2}{3}(t+1) + \frac{1}{2}$$

and

$$n_{sP} = \int_0^d dt \left(\frac{2}{3}(t+1) + \frac{1}{2} \right) = \frac{1}{3}d^2 + \frac{5}{6}d + \frac{1}{2}. \quad \dots\dots(7)$$

The last term $\frac{1}{2}$ corresponds to the primary. For $d=7.2$, we therefore obtain $n_{sP}=23$, and for $d=d_A/2=3.6$, $n_{sP}=8$.

The number of protons in these jets is $\frac{1}{2}(d+1)$; n_{sP} is independent of the primary energy (provided that this is large enough for our considerations to be valid) and increases more or less like d^2 .

First we see that the value $n_s=23$ for $d=d_A$ is in fair agreement with the upper boundary of the observed jets, considering that n_s also fluctuates. (7) is the average.

The fluctuation of the number of shower particles n_s is largely due to the fluctuation of the number of nucleons hit by the primary (see §3, third cause of fluctuations). We are here, of course, dealing not with a single primary passing through the nucleus but with a jet developing along the tunnel. Tentatively we assume that the fluctuations of the number of nucleons hit is the same if the single primary is replaced by the jet. Thus Δk (§3) is the fluctuation of the number of nucleons hit. The fluctuations of n_s thus obtained (as well as those of N_H) are marked on the left-hand side of fig. 1 for $d=7$. We see that the fluctuations are quite large but still smaller than the variation of n_s due to the variation of the tunnel length, say by a factor 2. We also see that the observed upper limit of n_s (~ 30 or so) is just within the fluctuation of n_s for a maximum tunnel length.

The assumption of an energy independent geometrical cross section is, of course, purely phenomenological, supported by the fact that fig. 1 shows no noticeable energy dependence whatsoever. There is no theoretical basis for it. Pseudoscalar meson theory (unreliable though the calculations are) would give a decrease of the cross section with E . However, we are in the region where mesons of all kinds contribute and we know too little about the heavy mesons to venture any theoretical prediction.

(b) *Mixed Plural-Multiple Production*

McCusker and Roesler have considered the following simple model:

$$\frac{dn_{sM}}{dt} = c_M \quad \dots\dots(8)$$

where c_M is assumed constant. This may be regarded as a model for multiple production in a single jet-nucleon encounter. In the usual theories of multiple production the multiplicity is regarded as increasing with energy (see, for example,

* This is not an arbitrary assumption but follows from the basic idea of plural production. We can transform the centre of gravity of the t fast nucleons to rest, thus obtaining an assembly of t nucleons arranged along a line and these are hit by one fast nucleon. Then t mesons are produced.

Heisenberg 1952). However, for our more phenomenological considerations, one simple model may suffice. The assumption c_M independent of t means that it is the total energy E of the jet which is responsible for the multiplicity. E is constant along the tunnel and equals the primary energy. To account for the observed independence of n_s on E we must also assume that c_M is, for the very high energies in question, independent of E . It follows that

$$n_{sM} = c_M d + \frac{1}{2} \quad \dots\dots(9)$$

and to reach agreement for $d = d_A$ we have to put $c_M \simeq 4$. The fluctuations would be $c_M \Delta k (\Delta k \simeq 2 \text{ for } d = 7)$ which is also quite large. While there is no particular justification for this model it should be clear that no decision in favour of a definite model can be derived from the jet experiments extant.

§ 5. CONDITION FOR CYLINDRICAL TUNNEL, SHOWERS WITH LARGE N_H

So far we have assumed that the penetration tunnel is cylindrical and we must find out under which conditions this is true. Roesler *et al.* have derived the condition from their diffusion equation. Without going into details of the diffusion problem the condition can be derived very simply. The tunnel is cylindrical if the angle Φ of a shower particle is so small that, when it originates from the tunnel entrance, it remains within the tunnel. Let r be the radius of the tunnel, then $\Phi \leq r/d$. On our units $r = 1.2$. Hence

$$\bar{\Phi}^2 \ll (1.2/d)^2. \quad \dots\dots(10)$$

For $d = 7$, this means $\bar{\Phi}^2 \leq 3 \times 10^{-2}$.

We can now also estimate the primary energy E ; the jet energy at each stage is also E . We may assume that the square of the average angle in a jet-nucleon collision is of the order of $2Mc^2/E$, as is generally true for relativistic collisions. Thus in each collision Φ^2 increases by an amount $\Delta\Phi^2 \sim 2Mc^2/E$. According to the theory of Brownian movement $\bar{\Phi}^2$ then increases proportionally to the number of collisions. Thus

$$\bar{\Phi}^2 \simeq 2Mc^2 d/E. \quad \dots\dots(11)$$

The energy scale attached to fig. 1 depends then on d . For the upper boundary, when $d = d_A = 7$, the energy scale is given at the top of fig. 1. When $d = 1$ (glancing collisions) the scale at the bottom applies (this is the scale usually applied in the experimental literature, but we see that for most of the showers the energies are higher, by a factor d , for the largest showers about 7 times larger).

The limit where the cylindrical tunnel widens is marked in fig. 1 by the slight rise of the theoretical curves n_{sp} and n_{sM} . This has been calculated as follows: The sideways extension of the tunnel is $x > r$ and a factor x^2/r^2 is inserted in the integral (7) and in (8). For x^2 the results of Roesler *et al.* have been used but the increase for the showers in question is so insignificant that we refrain from a detailed account.

There is another limit of interest, namely the energy E_t at which the emerging jet nucleons have an energy of order Mc^2 . This is the region where meson production rapidly decreases. When $E < E_t$ no tunnel in the above sense is created, or at least meson production ceases in the lower parts of the tunnel. Then also the direct energy transfer U_1 will be much larger than (2). The limit can only be derived from a more detailed model. If we accept Terreaux's theory (1951, 1952) we obtain for $E < E_t$, for example, the curve furthest to the left

for one particular choice of the parameters. For the curve in fig. 1 the critical energy for meson production $E_c = 1.5 Mc^2$; E_t is then the energy where the dotted curves intersect. We see that $E_t \sim 150$ kmev, whereas $E_{cyl} \sim 500$ kmev (E_{cyl} is the limit given by (10) and (11)). It also follows that when $E \sim E_{cyl}$ the average energy of the jet nucleons is about $5 Mc^2$.

We can now also understand the comparatively few 'jets with large N_H ' (marked by crosses in fig. 1), at least qualitatively.* These are all situated in the neighbourhood of $E \sim E_{cyl}$.

Φ is the *average* angle of the jet particles which means that roughly half of the particles lie inside, half outside this angle. It must then happen occasionally that a fast jet nucleon forms an angle substantially larger than the average. In this case much more nuclear matter is drawn into the process, or in other words a *second penetration tunnel* is created (fig. 2). Since n_s is sensitive to d , n_s will be raised considerably above the curves calculated for a tunnel whose shape is determined by the *average* Φ^2 . Also the surface energy will be increased.

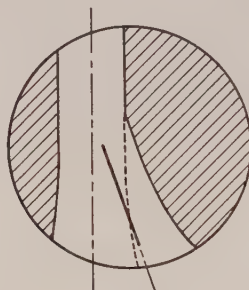


Fig. 2. Penetration tunnel with sideways track for moderate energies.

Moreover, we have seen that in this region the average energy of the emerging nucleons is no longer very large compared with Mc^2 . This means that also the direct energy transfer U_1 will be larger, and in addition the chance is quite appreciable that a recoil nucleon with energy only of the order of Mc^2 is formed. This also goes sideways and transfers a large amount of energy to the residual nucleus.

It follows from these considerations that the tunnel idea breaks down as soon as the theoretical tunnel begins to widen. Then the fate of the individual nucleons must be considered. The tunnel idea can only be applied when Φ^2 is so small that *all* particles remain well inside the tunnel.

While it is difficult to give a quantitative account of the events described there is no difficulty in understanding the jets with large n_s and N_H in the region where they are observed, namely where the tunnel idea becomes substantially invalid.

ACKNOWLEDGMENTS

We should like to thank Dr. K. Bleuler for interesting discussions. One of us (Ch. T.) is indebted to the 'Stiftung zur Förderung des Akademischen Nachwuchses' for a research grant.

* It is significant that, in the energy region considered here, showers with large N_H are not very frequent (Perkins, private communication), whereas at lower energies where Φ^2 is larger, large N_H are the rule rather than an exception.

REFERENCES

- DANIEL, R. R., DAVIES, J. H., MULVEY, J. H., and PERKINS, D. H., 1952, *Phil. Mag.*, **43**, 753.
 HEISENBERG, W., 1952, *Z. Phys.*, **133**, 65.
 HEITLER, W., and JÁNOSSY, L., 1950, *Helv. Phys. Acta*, **23**, 417.
 KAPLON, M. F., and RITSON, D. M., 1952, *Phys. Rev.*, **88**, 386.
 LE COUTEUR, K. J., 1950, *Proc. Phys. Soc. A*, **63**, 259; 1952, *Ibid.*, **65**, 718.
 LORD, J. J., FAINBERG, J., and SCHEIN, M., 1950, *Phys. Rev.*, **80**, 970.
 MCCUSKER, C. B. A., PORTER, N. A., and WILSON, B. G., 1953, *Phys. Rev.*, **91**, 384.
 MENON, M. G. K., MUIRHEAD, H., and ROCHAT, O., 1950, *Phil. Mag.*, **41**, 583.
 PICKUP, E., and VOYVODIC, L., 1951, *Phys. Rev.*, **82**, 265.
 ROESLER, F. C., and MCCUSKER, C. B. A., 1953, *Nuovo Cim.*, **10**, 127.
 ROSENFELD, L., 1948, *Nuclear Forces* (Amsterdam : North Holland Publishing Co.).
 TERREAUX, CH., 1951, *Helv. Phys. Acta*, **24**, 551; 1952, *Nuovo Cim.*, **9**, 1029.

RESEARCH NOTES

The Efficiency of the Anthracene Scintillation Counter

By D. K. BUTT

Physics Department, Birkbeck College, London

MS. received 19th January 1953, and in final form 30th March 1953

INTRODUCTION

A SCINTILLATION counter has been constructed for use as a detector in a lens β -spectrometer, with the purpose of obtaining a large counting efficiency for low energy electrons. An anthracene crystal of dimensions approximately 1 cm² by 2 mm was placed directly on the end of an uncooled EMI 5060 photomultiplier tube, optical contact being achieved with white vaseline.

RESULTS

To calibrate the instrument, electrons of a known incident energy from a thorium active deposit were focused on to a spot of 2 mm diameter on the crystal and integral pulse amplitude curves were taken for various energies of the incident electrons. Integral pulse amplitude curves were also taken for very weak sources of light incident on the photo-cathode. These curves are shown in fig. 1. For their interpretation their absolute intensities are of no importance; the intensity marked on the figure therefore represents only that of the background curve of the photomultiplier (curve G).

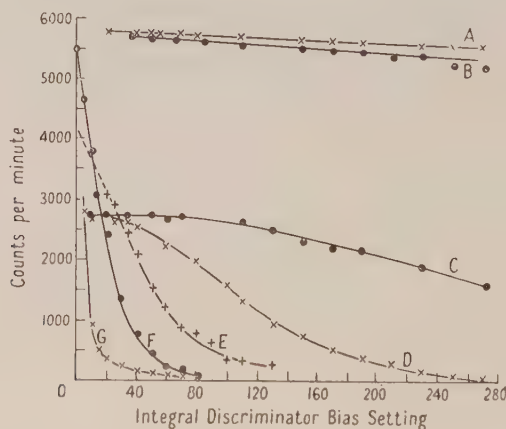


Fig. 1.

- | | | | | | |
|---|------------------|------------|---|------------------------------|------------|
| A | 25 keV electrons | $V=1500$. | E | 4 keV electrons | $V=1300$. |
| B | 25 keV electrons | $V=1300$. | F | pulses due to single photons | $V=1300$. |
| C | 8 keV electrons | $V=1500$. | G | photomultiplier noise | $V=1300$. |
| D | 8 keV electrons | $V=1300$. | | | |

N.B. The counting rate scale applies only to curve G.

Curves A and B are for 25 kev electrons with overall multiplier voltages of 1500 and 1300 v respectively. They represent only a part of the integral pulse curves, since the discriminator scale was not large enough to deal with the full pulse amplitude range. The slight slope of the curves down to almost zero pulse height is probably due to the back-scattering of some of the incident electrons from the crystal. From these curves it can be assumed that for a bias of 40 divisions practically every pulse is counted.

Curves C and D are for 8 kev electrons. These become almost horizontal at small discriminator settings. The comparison of curve D with the noise curve G (taken at the same multiplier voltage) shows that at the smallest workable bias (~ 20 divisions) practically all the pulses will be counted.

By comparing the average pulse heights of curves D and F, it has been calculated that on an average 5.0 photo-electrons are produced by each 8 kev incident electron.

Curve E is for 4 kev electrons. Extrapolating this curve to zero pulse height it will be seen that at least 90% of the pulses produced in the photomultiplier are counted at a bias of 20 divisions.

INTERPRETATION OF RESULTS

Statistics of the counting process.

Seitz and Muller (1950) derived the expression

$$P = 1 - (1 - \Omega p)^N \quad \dots\dots (1)$$

for the probability that a particle, incident on the crystal of a scintillation counter, produces at least one photo-electron at the photo-cathode. N is the number of photons generated by the incident electron in the crystal, Ω is the fraction of these which reach the photo-cathode and p the average probability that a photon, hitting the photo-cathode, will eject a photo-electron.

If N is the average number of photons produced by electrons of a given energy which are completely absorbed in the crystal, the number produced by any one electron will fluctuate about N . It is reasonable to suppose that this fluctuation can be approximately represented by a Poisson distribution

$$P_n = \frac{N^n}{n!} e^{-N},$$

where P_n is the probability that n photons are emitted, the average number being N .

The average probability \bar{P} is thus

$$\bar{P} = 1 - \exp(-N\Omega p). \quad \dots\dots (2)$$

Unless the photo-cathode of the scintillation counter is cooled, it will not be possible to count all the pulses due to single photo-electrons owing to the presence of thermal emission from the photo-cathode and cold emission from the dynodes, etc. If the multiplier pulses are 'biased off' so that only a small fraction of the pulses due to single photo-electrons is passed, eqn. (2) will no longer apply.

In this case the probability can be expected to be somewhere between the probability of eqn. (2) and that of counting pulses due to at least two photo-electrons. This latter probability is given by

$$\bar{P} = 1 - (1 + N\Omega p) \exp(-N\Omega p). \quad \dots\dots (3)$$

Ramler and Freedman (1950) found that the counting efficiency of their scintillation counter was approximately 15% for 10 kev and 50% for 20 kev incident electrons. Since they were using a cooled photo-cathode eqn. (2) will apply. It can be deduced that their efficiencies would be obtained if the Ωp they were employing was about 0.0025. Their value of Ω was about 0.1, and if the p value of their photo-cathode was about 0.025 for the radiation from anthracene—not an unreasonably small value—the relatively low counting efficiency for this energy region is not surprising.

If allowance is made for internal reflection occurring at the bottom surface of the crystal and if the light emission occurs inside the crystal (i.e. greater than a wavelength of light from the top surface, in order that internal reflection may occur at the top surface)*, for anthracene, which has refractive indices between 1.959 and 1.556 (Winchell 1943), a value of approximately 0.6 is obtained for Ω of the present apparatus.

The photo-cathode sensitivity of the photomultiplier employed is 35 microamps per lumen for light from a standard tungsten filament lamp of colour temperature 2848°K. This, together with the Sb-Cs photo-cathode sensitivity curve, leads to the quantum yield curve shown in fig. 2.

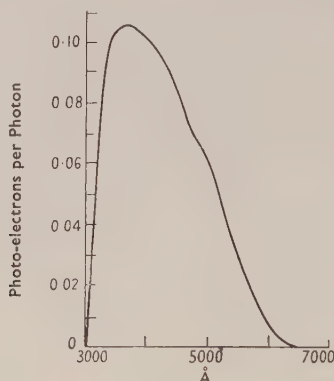


Fig. 2.

The emission spectrum of anthracene has peaks at 4240 Å, 4440 Å, and 4700 Å, the most intense one being at 4440 Å (Roth 1949). It can be deduced then that p for this combination is of the order of 0.09, giving a value of Ωp of about 0.05.

Taking Ωp as 0.05 and using the fact, previously established, that an 8 kev electron produces on the average 5.0 photo-electrons, we obtain the figure of 80 ev as the energy expended by the electron in producing one photon in the crystal.† This figure compares with 90 ev for high energy deuterons in anthracene (Wouters 1949), 64 ev for electrons in naphthalene (Kallman 1949) and 140 ev for electrons in anthracene (Hopkins 1951).

It should perhaps be mentioned that Hopkins' estimate was for electron energies greater than 30 kev. Since the average pulse-height-energy curve is not linear below this energy, the value obtained in the present work for 8 kev electrons is not strictly comparable with Hopkins' value.

* This is only just the case for 5 kev electrons in anthracene.

† Assuming that all the photo-electrons produced reach the first dynode.

From the figure of 80 ev per photon it can be deduced from eqn. (2) that, if all the energy of the incident electrons is absorbed in the crystal, 100% of the 25 kev electrons, 99.3% of the 8 kev electrons and 92% of the 4 kev electrons should produce pulses.

The effect of electron back-scattering from the crystal.

From the results of Schonland (1923, 1925) and Palluel (1947) it can be expected that for a material of the average atomic number of anthracene, about 10% of normally incident electrons will be back-scattered. In the case at present under consideration, the electrons are incident at a mean angle of about 10° to the normal, so that it is reasonable to expect this 10% still to apply.

The important question that arises now is whether or not these back-scattered electrons will lose enough energy in the crystal, before leaving it, to be counted. To answer this fully, the energy spectrum of back-scattered electrons leaving the crystal at all angles from the normal would be required. These data are not available and the only relevant data which are known to the author are those of Wagner (1930) and Chylinski (1932) for electrons incident and back-scattered at an angle $\frac{1}{2}\pi$ to the normal (as in reflection).

The shape of this energy distribution does not vary markedly with energy for electrons incident with energies between 2 and 30 kev, or with atomic number Z between 13 and 79. Hence, it is reasonable to assume that the back-scattered electrons from anthracene under similar circumstances would have this type of distribution.

The larger assumption will be made however that the energy spectrum of back-scattered electrons, from the problem in hand, will also be represented approximately by this distribution. Since this is a case of multiple scattering, it is not expected that this energy distribution will change sharply with back-scattered electron angle.

From fig. 1 it can be assumed that electrons which lose 6 kev or more of their energy in the crystal will be counted. In the case of the 25 kev electrons (curves A and B) the results of Wagner and Chylinski show that about 95% of the back-scattered electrons will have lost more than this amount of energy in the crystal. Thus, assuming a total of 10% have been back-scattered, at least 95% of these will be counted. This figure is a minimum value because a number of electrons losing less than 6 kev in the crystal will still be counted. Thus more than 99.5% of the 25 kev electrons will be counted.

For 8 kev electrons, similar reasoning will give an overall counting efficiency of 98% or more for a discriminator bias of 20 divisions.

The 4 kev curve E is more difficult to interpret. It has been seen from fig. 1 that 90% of the pulses produced by these electrons are counted at the minimum workable bias of 20 divisions. It has also been calculated from eqn. (2) that 92% of the electrons when completely absorbed will produce a pulse. Hence, assuming that the 10% of the incident electrons which are back-scattered produce no pulses at all for this low energy, a resultant counting efficiency of 70% is obtained. Of course, many of these back-scattered electrons will be counted, so this is a minimum value. Equation (3) gives an efficiency of 71.3% for electrons of this energy.

Experimentally it has been found that the counter has a workable efficiency down to an energy of 0.5 kev.

ACKNOWLEDGMENTS

My thanks are due to Professor Bernal for the laboratory facilities he provided for me. The research was financed by a grant made to Mr. R. E. Siday by the Department of Scientific and Industrial Research.

REFERENCES

- CHYLINSKI, S., 1932, *Phys. Rev.*, **42**, 393.
 HOPKINS, J. I., 1951, *Rev. Sci. Instrum.*, **22**, 29.
 KALLMAN, H., 1949, *Scintillation Counter Symposium*, Oak Ridge, Tennessee.
 RAMLER, W. J., and FREEDMAN, M. S., 1950, *Rev. Sci. Instrum.*, **21**, 784, 922.
 ROTH, L., 1949, *Phys. Rev.*, **75**, 983.
 SCHONLAND, B. F. J., 1923, *Proc. Roy. Soc. A*, **104**, 235; 1925, *Ibid.*, **108**, 187.
 SEITZ, F., and MULLER, D. W., 1950, *Phys. Rev.*, **78**, 605.
 PALLUEL, F., 1947, *C.R. Acad. Sci., Paris*, **224**, 1492.
 WAGNER, P. B., 1940, *Phys. Rev.*, **35**, 98.
 WINCHELL, A. N., 1943, *Optical Properties of Organic Compounds* (Wisconsin: University of Wisconsin Press).
 WOUTERS, L., 1949, *University of California Radiation Laboratory* (American Atomic Energy Commission declassified report), **116**, 11.

The Half-Life of $^{181}\text{Ta}^m$ and the Delayed Coincidence Method

BY H. S. MURDOCH

School of Physics, University of Sydney, Australia

Communicated by R. E. B. Makinson; MS. received 27th May 1953

§ 1. INTRODUCTION

TWO methods have been used for the measurement of half-lives in the range 10^{-3} to 10^{-6} second. In either case the source is placed between two counters, the pulses from which are suitably sharpened or lengthened and fed to a coincidence circuit. In the integral method the pulse width in one channel is kept fixed while that in the other channel is progressively increased. In the differential method the pulses in both channels are of fixed width, but the pulses in one channel are progressively delayed with respect to those in the other channel.

Two metastable excited states of ^{181}Ta occur in the β -decay of ^{181}Hf (Barber 1950). The half-life of the upper (610 kev) excited state of ^{181}Ta has been measured as 22 μsec by De Benedetti and McGowan (1946), using the differential method, and as $20.1 \pm 0.7 \mu\text{sec}$ by Bunyan *et al.* (1948), using the integral method. The half-life has been approximately verified by Madansky and Wiedenbeck (1947), Lundby (1949) and Barber (1950). The experiment described here was undertaken to determine the half-life more accurately. Both methods were used.

§ 2. THEORY OF THE METHOD

The delayed coincidence rate is given by

$$C_D = N[e_1' e_2 \{1 - \exp(-\lambda \tau_2)\} + e_1 e_2' \{1 - \exp(-\lambda \tau_1)\}], \quad \dots\dots(1)$$

where e_1 and e_2 are the respective net efficiencies of counters 1 and 2 for the initial radiation, e_1' and e_2' have similar meanings for the delayed radiation, τ_1 and τ_2 are the respective pulse widths in channels 1 and 2, λ is the decay constant of the delayed radiation and N the number of disintegrations per second.

In the integral method τ_2 is progressively increased, and we may write

$$C_D = A[1 - \exp(-\lambda \tau_2)] + B, \quad \dots\dots(2)$$

where A and B are constants. The decay constant λ may be obtained by fitting the experimental points to a curve of this form. There may also be a considerable constant background of instantaneous coincidences due to the presence of other radiation. For the decay of ^{181}Hf to ^{181}Ta instantaneous coincidences between the various γ -rays following the upper excited state were found to represent about 50% of the maximum delayed coincidence rate.* If the pulses in channel 2 are delayed by a time $t_d > \tau_1$, eqn. (1) becomes

$$\begin{aligned} C_D &= A \exp[-\lambda(t_d - \tau_1)][1 - \exp\{-\lambda(\tau_1 + \tau_2)\}] \\ &= A_1[1 - \exp\{-\lambda(\tau_1 + \tau_2)\}]. \end{aligned} \quad \dots\dots(3)$$

The use of a suitable delay line† eliminates the instantaneous coincidence background and reduces from three to two the number of parameters for which the experimental points must be fitted. Furthermore, if the pulse widths are determined by counting chance coincidences, $\tau_1 + \tau_2$ is obtained more readily than either τ_1 or τ_2 . The value of the time delay need not be known accurately, as it does not affect the form of the curve.

In the differential method t_d is varied but τ_1 and τ_2 are both fixed. For $t_d > \tau_1$ eqn. (3) may be rearranged as

$$C_D = A_2 \exp(-\lambda t_d). \quad \dots\dots(4)$$

For this method it is of interest to calculate the most suitable value of the width τ_2 of the delayed pulses. We take as a criterion that, for a given true coincidence rate, the chance rate should be a minimum. The ratio of chance to true coincidences is given by

$$R = K \frac{N(\tau_1 + \tau_2)}{1 - \exp[-\lambda(\tau_1 + \tau_2)]} = K_1 \frac{C_D(\tau_1 + \tau_2)}{[1 - \exp\{-\lambda(\tau_1 + \tau_2)\}]^2 [\exp\{-\lambda(t_d - \tau_1)\}]}, \quad \dots\dots(5)$$

where K and K_1 are constants.

Differentiation with respect to $\tau_1 + \tau_2$, keeping C_D constant, yields the following condition for a minimum value of R :

$$\exp[\lambda(\tau_1 + \tau_2)] = 1 + 2\lambda(\tau_1 + \tau_2).$$

The required solution is

$$\lambda(\tau_1 + \tau_2) = 1.26. \quad \dots\dots(6)$$

* The decay of the 10^{-8} sec excited state of ^{181}Ta may be considered as instantaneous for the purpose of the measurements described here.

† A time delay was used by Burson *et al.* (1951) to eliminate instantaneous coincidences for a coincidence absorption study of the delayed radiation.

If an approximate value of λ is known the optimum value of $\tau_1 + \tau_2$ can be chosen by means of eqn. (6). The value selected for τ_1 should be less than the smallest delay used in the experiment.

§ 3. EFFECT OF COUNTER TIME-LAGS

The simple considerations of §2 must be somewhat modified for small delays and pulse widths because of time-lags in the counters. Assuming a normal distribution of counter time-lags, Bunyan, Lundby and Walker (1949) derived an expression for the probability of a coincidence being recorded. They considered only the case where $\tau_1 = \tau_2$, and where counter 1 records only the delayed radiation. Extending their calculations to the case where each counter may record either radiation (cf. Nag, Sen and Chatterjee 1950), and further, where the pulse widths are not necessarily equal, we obtain for the coincidence rate

$$C_D = N[e_1' e_2 \psi_1 + e_1 e_2' \psi_2], \quad \dots\dots (7)$$

where

$$\begin{aligned} \psi_1 = & \frac{1}{2} \left[\phi \left(\frac{\tau_2 + t_d - \theta}{t_0 \sqrt{2}} \right) + \phi \left(\frac{\tau_1 - t_d + \theta}{t_0 \sqrt{2}} \right) \right] \\ & + \frac{1}{2} \exp \left[-\lambda(t_d - \theta - \frac{1}{2}\lambda t_0^2) \right] \left[\exp(\lambda\tau_1) \left\{ 1 + \phi \left(\frac{t_d - \tau_1 - \theta - \lambda t_0^2}{t_0 \sqrt{2}} \right) \right\} \right. \\ & \left. - \exp(-\lambda\tau_2) \left\{ 1 + \phi \left(\frac{t + \tau_2 - \theta - \lambda t_0^2}{t_0 \sqrt{2}} \right) \right\} \right], \\ \psi_2 = & \frac{1}{2} \left[\phi \left(\frac{\tau_2 + t_d - \theta}{t_0 \sqrt{2}} \right) + \phi \left(\frac{\tau_1 - t_d + \theta}{t_0 \sqrt{2}} \right) \right] \\ & + \frac{1}{2} \exp \left[-\lambda(\theta - t_d - \frac{1}{2}\lambda t_0^2) \right] \left[\exp(\lambda\tau_2) \left\{ 1 + \phi \left(\frac{-\tau_2 - t_d + \theta - \lambda t_0^2}{t_0 \sqrt{2}} \right) \right\} \right. \\ & \left. - \exp(-\lambda\tau_1) \left\{ 1 + \phi \left(\frac{\tau_1 + \theta - t_d - \lambda t_0^2}{t_0 \sqrt{2}} \right) \right\} \right], \\ \phi(x) = & (2/\sqrt{\pi}) \int_0^x \exp(-z^2) dz, \\ \theta = & \bar{t}_1 - \bar{t}_2, \end{aligned}$$

\bar{t}_1 and \bar{t}_2 are the respective mean time-lags in counters 1 and 2 and $t_0/\sqrt{2}$ is the standard deviation of counter time-lags (assumed the same for each counter).

In the integral method, as only τ_2 is varied, terms not involving τ_2 are constant. If we impose the condition

$$\tau_2 + t_d \geq \theta + t_0 \sqrt{2} + \lambda t_0^2, \quad \dots\dots (8)$$

the term in $\exp(-\lambda\tau_2)$ is multiplied by a constant factor and the other terms in τ_2 are either zero or constant, hence

$$C_D = A'[1 - \exp(-\lambda\tau_2)] + B'. \quad \dots\dots (9)$$

This is equivalent to eqn. (2). If condition (8) is not satisfied the coincidence rate will fall below that given by eqn. (9). If we also impose the condition

$$t_d \geq \tau_1 + \theta + t_0 \sqrt{2} + \lambda t_0^2 \quad \dots\dots (10)$$

the term in B' is eliminated from eqn. (9) and we have an equation of the form (3). Where τ_1 is of the same order as the counter time-lags it is not sufficient to merely make t_d greater than τ_1 as suggested in §2.

The inequality (10) also gives the condition for the minimum delay to be used in the differential method. For smaller values of t_d eqn. (3) is not valid.

§ 4. EXPERIMENTAL ARRANGEMENT

The ^{181}Hf source consisted of hafnium oxide irradiated for one week in the atomic pile at the Atomic Energy Research Establishment, Harwell. The source was deposited on aluminium foil which was placed between two G.E.C. β counters, with the active side facing the counter used to detect the delayed radiation, in order to minimize the absorption of the low energy delayed conversion electrons.

The pulse width in channel 1 was $0.12\ \mu\text{sec}$ obtained by means of a shorted delay line. For the integral method the pulses in channel 2 were delayed by $0.65\ \mu\text{sec}$. This was not quite sufficient to eliminate all instantaneous coincidences, but reduced the instantaneous coincidence rate from 50% to 4% of the maximum delayed rate. Pulse widths in channel 2 of from $1\ \mu\text{sec}$ upwards were obtained by means of a selector switch which varied the width of a univibrator pulse. For the differential method these univibrator pulses were differentiated to produce corresponding delays, and the width of the delayed pulse was fixed at $32\ \mu\text{sec}$, this value being close to the optimum value given by eqn. (6) for a half-life of about $20\ \mu\text{sec}$.

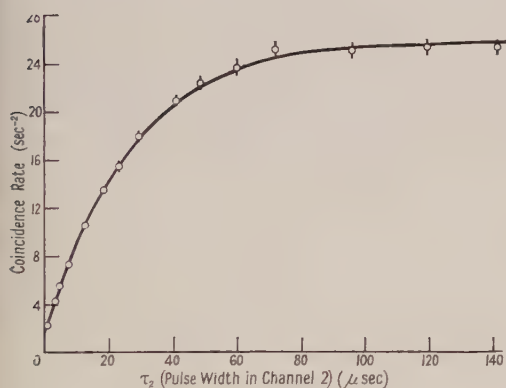


Fig. 1. Integrated decay curve of $^{181}\text{Ta}^m$. Least squares fit to experimental points.

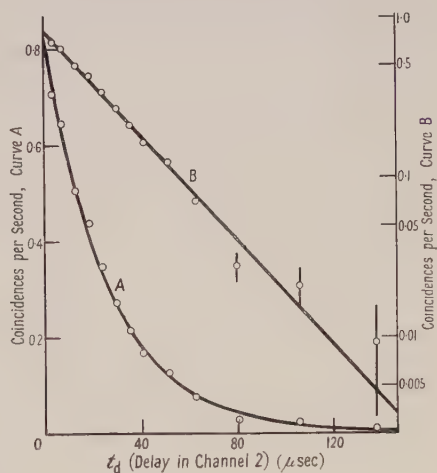


Fig. 2. Differential decay curve of $^{181}\text{Ta}^m$. Least squares fit to experimental points.

The pulse widths were obtained by counting chance coincidences, and were checked by measurement with a calibrated oscilloscope, the calibration of which was in turn checked against a crystal oscillator. This oscilloscope was also used to measure the delays.

§ 5. EXPERIMENTAL RESULTS

5.1. Integral Method

A sufficiently weak source was used for the chance coincidence rate to be only a few per cent of the true rate at the maximum value of the pulse width τ_2 . The latter was varied from 1 to $141\ \mu\text{sec}$. The experimental results are plotted in fig. 1, the vertical lines indicating standard errors. The coincidence rates have

been corrected for the decay of ^{181}Hf . A least squares fit with appropriate weighting of the experimental points yields for the half-life $19.1 \pm 0.4 \mu\text{sec}$. As the point at $1 \mu\text{sec}$ falls on the curve, there do not appear to be any coincidence losses due to counter time-lags at this value of τ_2 . We assume, therefore, that condition (8) holds, and the inclusion of this point is justified.

5.2. Differential Method

Delays in channel 2 of from 3.2 to $138 \mu\text{sec}$ were used, and the experimental results are plotted in fig. 2. A least squares fit yields for the half-life $18.6 \pm 0.2 \mu\text{sec}$. The minimum delay of $3.2 \mu\text{sec}$ is sufficient to ensure the validity of eqn. (3) and to eliminate any instantaneous coincidences. A test experiment was carried out with a ^{60}Co source to verify that the coincidence rate was no greater than the expected chance coincidence background for this value of the delay.

5.3. Half-Life of ^{181}Hf

In the course of the integral experiment the counting rate in one of the counters was plotted over a period of 30 days. The value obtained for the half-life of ^{181}Hf was 46 ± 4 days. In assessing the half-life allowance was made for a small progressive decrease in the efficiency of the counter, obtained by plotting the counting rate for a ^{60}Co source over a period of three weeks and allowing for the known decay of ^{60}Co .

§ 6. CONCLUSION

The results obtained from the integral and differential methods agree within the limits of their standard errors, and we conclude that the half-life of the 610 kev excited state of ^{181}Ta is $18.8 \mu\text{sec}$, with an error unlikely to exceed $0.5 \mu\text{sec}$. This value is barely consistent with the result of Bunyan *et al.* (1948), and rules out the value obtained by De Benedetti and McGowan (1946).*

The value obtained for the half-life of ^{181}Hf is consistent with recent determinations (Cork *et al.* (1950) 45 days, Seren, Friedlander and Turkel (1947) 46 ± 3 days). Because of contamination with ^{175}Hf (Hedgran and Thulin 1951), which has a half-life of 70 days (Wilkinson and Hicks 1949), all determinations of the half-life of ^{181}Hf probably yield a value which is slightly too high. The observed value of the half-life would depend on the age of the sample, and also, to some extent, on the period of neutron irradiation in the pile and the period over which the half-life determination was made. The present determination was commenced about six weeks after irradiation. There is a need for a half-life determination of the separated isotope ^{181}Hf .

ACKNOWLEDGMENTS

The author would like to thank Drs. R. E. B. Makinson and K. Landecker for their interest in this work and for many helpful suggestions. Mr. J. Webb assisted with readings and calculations.

* Note added in proof. Brown, H. N., and Becker, H. A. (*Phys. Rev.*, 1953, **90**, 328), have produced $^{181}\text{Ta}^{\text{m}}$ by γ -ray bombardment of tantalum. They report a half-life of $16 \pm 3 \mu\text{sec}$, which is consistent with our value.

REFERENCES

- BARBER, W. C., 1950, *Phys. Rev.*, **80**, 332.
 BUNYAN, D. E., LUNDBY, A., and WALKER, D., 1949, *Proc. Phys. Soc. A*, **62**, 253.
 BUNYAN, D. E., LUNDBY, A., WARD, A. H., and WALKER, D., 1948, *Proc. Phys. Soc. A*, **61**, 300.
 BURSON, S. B., BLAIR, K. W., KELLER, H. B., and WEXLER, S., 1951, *Phys. Rev.*, **83**, 62.
 CORK, J. M., STODDARD, A. E., RUTLEDGE, W. C., BRANYON, C. E., and LE BLANC, J., 1950, *Phys. Rev.*, **78**, 299.
 DE BENEDETTI, A., and MCGOWAN, F. K., 1946, *Phys. Rev.*, **70**, 569.
 HEDGRAN, A., and THULIN, H. G., 1951, *Phys. Rev.*, **81**, 1072.
 LUNDBY, A., 1949, *Phys. Rev.*, **76**, 1809.
 MADANSKY, L., and WIEDENBECK, M. L., 1947, *Phys. Rev.*, **72**, 185.
 NAG, B. D., SEN, S., and CHATTERJEE, S., 1950, *Indian J. Phys.*, **24**, 261.
 SEREN, L., FRIEDLANDER, N., and TURKEL, S. H., 1947, *Phys. Rev.*, **72**, 888.
 WILKINSON, G., and HICKS, H. G., 1949, *Phys. Rev.*, **75**, 696.

The Compressibility of Metallic Aluminium

BY S. RAIMES

Department of Mathematics, Imperial College, London

MS. received 29th June 1953

GÁSPÁR (1952) has recently calculated the lattice parameter, compressibility, and cohesive energy of metallic aluminium, using a method which relies greatly upon the assumption that the valence electrons in the metal are almost free; and his results are in good agreement with experiment. It may therefore be of some interest to give a brief account of a different calculation of these quantities, which also makes use of the approximation of free electrons, but which is in some respects simpler and less laborious than that of Gáspár. Although the treatment is essentially approximate, and does not yield a good value for the cohesive energy, it leads with great facility to a curve of compression against pressure which accords very well with observation over a range of pressures up to $100\,000\text{ kg cm}^{-2}$, and it has the advantage that it does not require the use of an ion-core field of the Hartree type.

The method is a formal extension to trivalent metals of that applied to the divalent metals by Raimès (1952), to which paper reference must be made for details omitted here. The energy of the lowest state of a valence electron in the metal is obtained by a procedure which is essentially that of Wigner and Seitz (1933, 1934), but reasonable assumptions regarding the approximate constancy of the wave function for the lowest state, together with the use of the experimental value of the third ionization potential of a free atom, permit the work to be carried out analytically without the explicit computation of an ion-core field. Assuming, in addition, that the valence electrons are very nearly free, the total energy per electron of a trivalent metal is found, as a function of the atomic radius r_s , to be

$$E(r_s) = 3 \left(\frac{r_0^2}{r_s^3} - \frac{3}{r_s} \right) + \frac{3.60}{r_s} + \frac{4.60}{r_s^2} - \frac{1.321}{r_s} - \frac{0.831}{r_s + 7.36}, \quad \dots\dots(1)$$

the terms having been kept separate for identification. The first term is the eigenvalue ϵ_0 of the Schrödinger equation for the lowest state, when, as for the divalent metals, the self-consistent field of the valence electrons is ignored and only the potential function of the ion-core appears in the equation. The second term compensates for the neglect of the self-consistent field of the valence electrons, and is one third of the self-potential energy of the valence-electron charge distribution, taking this to be uniform, within an atomic sphere. The third and fourth terms are the Fermi and exchange energies, calculated according to the free-electron approximation; and the final term is the expression obtained by Wigner (1934, cf. Seitz 1940, p. 343) for the correlation energy, suitably modified for a trivalent metal. The constant r_0 , which is the atomic radius corresponding to the minimum of the curve of ϵ_0 against r_s , is given by the equation

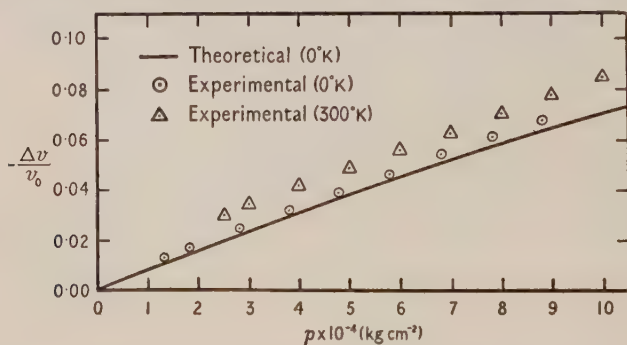
$$r_0^2 - \frac{3(3+\omega)}{2\omega^3} r_0 + \frac{3(3-\omega)^2}{2\omega^5} + \left[\frac{r_0}{\omega} - \frac{3(3-\omega)}{2\omega^4} \right] \xi \cot \xi = 0, \quad \dots (2)$$

where $\xi = (6r_0 - \omega^2 r_0^2)^{1/2}$, and $\omega^2 = I_3$, the negative of the *third* ionization potential of a free neutral atom (the *second* ionization potential had to be used for the divalent metals). In both equations (1) and (2) energies are in Rydberg units and lengths in Bohr units.

Using the value of 28.44 eV (Moore 1949) for I_3 , r_0 is found to be 2.13 Bohr units. The resulting values of the lattice parameter a , compressibility κ , cohesive energy S , and total energy E are compared with the experimental values in the following table, the experimental values of κ and S being those quoted by Gáspár as correct at 0°K.

	a (Å)	$\kappa \times 10^{12}$ (cm ² dyn ⁻¹)	S (kcal mole ⁻¹)	$-E$ (kcal mole ⁻¹)
Calculated	4.36	0.82	9	1237
Experimental	4.04	0.95	60	1288

The agreement between theoretical and experimental values is reasonable except for the cohesive energy; and a large error in the calculated S is to be expected in an approximate calculation of the present type, for this quantity



is the small difference between two large energies, one calculated and one empirical. There are two principal sources of error in this work—the approximate analytical method of calculating the eigenvalue ϵ_0 of the Schrödinger equation for the lowest state, and the free-electron approximation used in evaluating the remaining terms of $E(r_s)$ —and it may be worth mentioning that

an error of only 2% in ϵ_0 , for instance, would result in the observed error of 80% in the calculated cohesive energy; the possibility of compensating errors, however, must not be disregarded.

Of greater interest, perhaps, although not computed by Gáspár, is the curve, shown in the figure, of compression as a function of pressure. The *compression* is defined as $-\Delta v/v_0$, that is, the magnitude of the change in volume divided by the volume v_0 at zero pressure; and the *pressure* p corresponding to an atomic volume $4\pi r_s^3/3$, at the absolute zero of temperature, is given by

$$p = - \frac{3}{4\pi r_s^2} \frac{dE}{dr_s},$$

and can be obtained directly from eqn. (1). Also shown in the figure are the experimental values of Bridgman (1948), at room temperature, together with the points resulting from a rough correction of these to absolute zero by a method due to Bardeen (1938). The theoretical curve corresponds very well with the latter set of points.

Although the possibility of mutual cancellation of errors must always be borne in mind, it is fairly safe to conclude from the results that, for certain limited purposes at least, the valence electrons in metallic aluminium may be considered to be approximately free.

REFERENCES

- BARDEEN, J., 1938, *J. Chem. Phys.*, **6**, 372.
 BRIDGMAN, P. W., 1948, *Proc. Amer. Acad. Sci.*, **76** (3), 55.
 GÁSPÁR, R., 1952, *Acta Phys. Hungarica*, **2** (1), 31.
 MOORE, C. E., 1949, *Atomic Energy Levels* (National Bureau of Standards, Circular 467, Washington, D.C.), Vol. 1.
 RAIMES, S., 1952, *Phil. Mag.*, **43**, 327.
 SEITZ, F., 1940, *Modern Theory of Solids* (New York: McGraw-Hill).
 WIGNER, E., 1934, *Phys. Rev.*, **46**, 1002.
 WIGNER, E., and SEITZ, F., 1933, *Phys. Rev.*, **43**, 804; 1934, *Ibid.*, **46**, 509.

LETTERS TO THE EDITOR

**The Influence of Combined Electric and Magnetic
Interaction on Gamma-Gamma Directional Correlation**

The influence of an external magnetic field on the gamma-gamma directional correlation of ^{111}Cd has been shown in earlier work (Aeppli *et al.* 1951, 1952). The anisotropy was measured as a function of the strength of the magnetic field applied perpendicular to the plane of the two counters. From this measurement—which showed decreasing anisotropy with increasing field strength—the magnetic moment of the first excited state of ^{111}Cd was obtained by comparison with theory (Alder 1951, 1952, Alder *et al.* 1953). A measurement of the phase shift occurring in the case where the counters were not equally sensitive yielded the sign of the moment.

Recently (Albers-Schönberg, Hänni *et al.* 1953, to be referred to as I) we have shown that it is also possible to measure the quadrupole moment of the same nuclear level by studying the effect of the inhomogeneous electric crystalline field in a tetragonal indium single crystal. Since in this case it is not possible to vary the field strength one has to measure the anisotropy as a function of the direction of the crystal axis with respect to the counters (e.g. experiment 1 or 2 of I). By comparing the experimental curve with theory (Alder *et al.* 1953) one gets the magnitude of the quadrupole coupling (Albers-Schönberg, Alder *et al.* 1953, to be referred to as II). The sign cannot be determined in this way even if the counters are not equally sensitive.

In this letter we will discuss the interesting effects which occur if both a magnetic and an electric interaction are present. This case has recently been treated in a detailed theoretical paper on the measurement of nuclear moments by angular correlation methods (Alder *et al.* 1953). The theory is until now restricted to fields with axial symmetry and, furthermore, to parallel magnetic and electric fields. These conditions are fulfilled if one applies a magnetic field parallel to the symmetry axis of a suitable single crystal. The angular correlation function may then be calculated and depends upon the orientation of the field axis with respect to the counters and upon both interaction energies individually.

One gets especially simple expressions if the fields are applied in the direction perpendicular to the plane of the two counters. If the undisturbed correlation can be written as

$$W(\theta) = 1 + A_{22}P_2(\cos \theta) \quad \dots\dots(1)$$

one obtains for the disturbed correlation

$$W(\theta) = 1 + B_2 \cos 2\theta \quad \dots\dots(2)$$

$$B_2 = (\frac{3}{4}G_2^{22}A_{22} - \sqrt{15/8}G_2^{24}A_{24})/(1 + \frac{1}{4}A_{22}) \quad \dots\dots(3)$$

$$G_2^{22} = \frac{9}{28} \left(\frac{1}{1+(x-2y)^2} + \frac{1}{1+(x+2y)^2} \right) + \frac{5}{28} \left(\frac{1}{1+(3x-2y)^2} + \frac{1}{1+(3x+2y)^2} \right) \quad \dots\dots(4)$$

$$G_2^{24} = -\frac{3}{28} \sqrt{5} \left(\frac{1}{1+(x-2y)^2} + \frac{1}{1+(x+2y)^2} \right) + \frac{3}{28} \sqrt{5} \left(\frac{1}{1+(3x-2y)^2} + \frac{1}{1+(3x+2y)^2} \right). \quad \dots\dots(5)$$

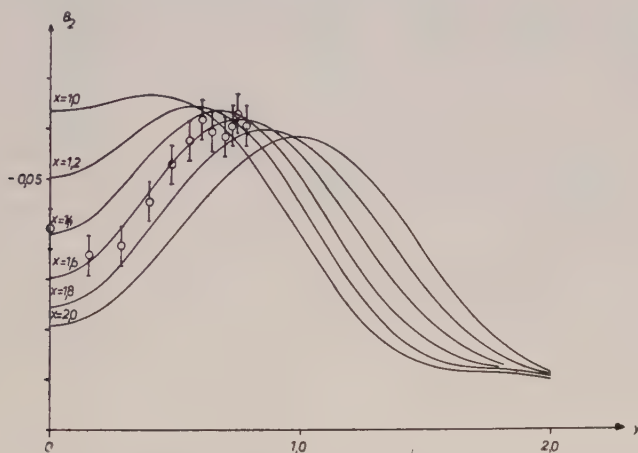
This formula must be corrected for finite resolving time and is only valid for equally sensitive counters. The figure shows the coefficient B_2 in the case of ^{111}Cd as a function of the strength of the magnetic interaction

$$y = \omega_y \tau = \frac{g\mu_k H \tau}{\hbar} \quad \dots\dots(6)$$

for various values of the electric interaction

$$x = \omega_x \tau = \frac{eQ}{2\hbar} \frac{\partial E_z}{\partial z} \frac{6}{(2I-1)I} \tau. \quad \dots\dots(7)$$

The coefficient B_2 , which is related to the anisotropy $\epsilon = W(\pi)/W(\pi/2) - 1$ by $B_2 = \epsilon/(2 + \epsilon)$, shows a maximum at a value of $y = x/2$.



The coefficient B_2 of the angular correlation function $W(\theta) = 1 + B_2 \cos 2\theta$ plotted against the magnetic interaction y for various electric interactions x . The curves are corrected for finite resolving time of the coincidence circuit. The points show the results of one preliminary measurement with an indium single crystal source.

This behaviour may be qualitatively understood by a semiclassical picture. The electric interaction causes the nuclei to precess around the symmetry axis with both directions of precession equally probable. The magnetic interaction on the other hand causes a unidirectional precession. If one superimposes these two precessions and chooses the magnetic field so that $\omega_y = \omega_x/2$ a maximum cancellation of the precession is obtained which gives rise to a maximum in the anisotropy.

Preliminary experiments were carried out with a single crystal source of metallic indium containing active ^{111}In . The crystal was grown and oriented by x-ray methods (I). A measurement of the type of experiment 1 of I was performed to test the orientation. In the figure the coefficients B_2 obtained are plotted against the strength of the applied magnetic field. The values are corrected for finite solid angle and for scattering at the pole faces of the magnet and can directly be compared with the theoretical curves which are corrected for finite resolving time of the coincidence circuit. For the strength of the electric interaction we obtain from this preliminary experiment $x = 1.6 \pm 0.2$, which is in agreement with the value obtained from other experiments (II). From this value the quadrupole moment of the first excited state of ^{111}Cd may be calculated (II). The figure shows that it is possible to measure in one

experiment the magnetic moment as well as the quadrupole moment of a short-lived nuclear level. At least in principle one may obtain by a least squares fit x and y simultaneously.

The growth and x-ray orientation of a single crystal is rather difficult and the measurement is therefore only possible if the activity has a suitably long lifetime. It is however possible to obtain the same information by using a polycrystalline source together with an axial magnetic field. Since this case (where the fields are no longer parallel) has not yet been treated theoretically our experiments with polycrystalline indium metal sources cannot yet be interpreted.

We thank F. Hänni and O. Braun for the help with the measurements and the calculations.

Swiss Federal Institute of Technology,
Zürich, Switzerland.
13th July 1953

H. ALBERS-SCHÖNBERG.
K. ALDER.*
E. HEER.
T. B. NOVEY.†
P. SCHERRER.

* C.E.R.N., European Council for Nuclear Research, Theoretical Study Group at the Institute for Theoretical Physics, University of Copenhagen.

† U.S.A. National Science Foundation Postdoctoral Fellow, on leave from Argonne National Laboratory.

AEPPLI, H., ALBERS-SCHÖNBERG, H., BISHOP, A. S., FRAUENFELDER, H., and HEER, E., 1951, *Phys. Rev.*, **84**, 370.

AEPPLI, H., ALBERS-SCHÖNBERG, H., FRAUENFELDER, H., and SCHERRER, P., 1952, *Helv. Phys. Acta*, **25**, 339.

ALBERS-SCHÖNBERG, H., ALDER, K., BRAUN, O., HEER, E., and NOVEY, T. B., 1953, *Phys. Rev.*, in the press.

ALBERS-SCHÖNBERG, H., HÄNNI, F., HEER, E., NOVEY, T. B., and SCHERRER, P., 1953, *Phys. Rev.*, **90**, 322.

ALDER, K., 1951, *Phys. Rev.*, **84**, 369; 1952, *Helv. Phys. Acta*, **25**, 235.

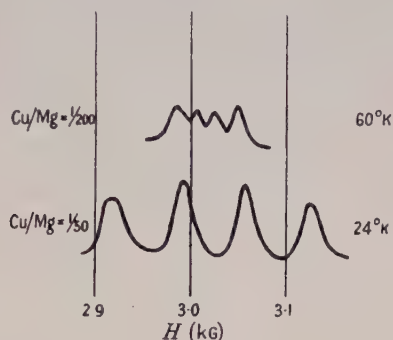
ALDER, K., ALBERS-SCHÖNBERG, H., HEER, E., and NOVEY, T. B., 1953, *Helv. Phys. Acta*, **26**, in the press.

Temperature Change in the Paramagnetic Resonance Spectrum of Copper Lanthanum Nitrate

A radical change in the paramagnetic resonance spectra of certain cupric salts at low temperatures has been reported by Bleaney and Bowers (1952) and Trenam (1953). In dilute copper bismuth nitrate (the copper diluted with magnesium) the spectrum at the temperature of liquid oxygen is that of one paramagnetic ion per unit cell. The g -value is nearly isotropic, $g = 2.22$. We shall call this the 'H.T.' type of spectrum. At liquid hydrogen temperature, however, the spectrum was that of three ions per unit cell. The symmetry axes of the three ions lie parallel to the three mutually perpendicular edges of a cube whose body diagonal is parallel to the trigonal axis of the crystal. The g -value of each ion is anisotropic, $g_{\parallel} = 2.45$, $g_{\perp} = 2.10$. We shall call this the 'L.T.' form. The constants A and B in the spin Hamiltonian are different in the two cases, giving a much larger hyperfine structure splitting in the L.T. spectrum. Typical spectra for the two cases are shown in the figure.

In the apparatus of the above authors it was not possible to maintain temperatures intermediate to those of the liquefied gases. Hence they could only say that transitions from the L.T. to H.T. form took place between 20°K and 60°K.

With our apparatus paramagnetic resonance measurements can be made at any temperature between 6°K and room temperature and we have made a more detailed study of this transition. We have investigated the change in the spectrum of copper lanthanum nitrate, both in the concentrated salt and with the Cu^{2+} ions diluted with magnesium.



H.T. (60°K) and L.T. (24°K) forms of spectra. The constant magnetic field is parallel to the trigonal axis of the crystal.

The dilute salt.

We made measurements over a range of temperatures on three single crystals of the dilute nitrate $3(\text{Cu},\text{Mg})(\text{NO}_3)_2 \cdot 2\text{La}(\text{NO}_3)_3 \cdot 24\text{H}_2\text{O}$:

- (i) a crystal grown from a solution where the ratio of copper to magnesium atoms was 1 : 200;
- (ii) a crystal grown from a solution where the ratio was $\text{Cu} : \text{Mg} = 1 : 50$;
- (iii) a very dilute crystal grown from a heavy water solution (kindly lent by Dr. K. D. Bowers). This gave very narrow lines. The change from the L.T. to the H.T. kind of spectrum was similar for all three specimens and occurred at about 38°K.

To measure the temperature at which the change takes place we cooled the crystal to 20°K and then rotated it until the trigonal axis was parallel to the splitting field. The three ions in the unit cell are then equivalent and their spectra overlap to give four strong hyperfine structure lines (nuclear spin of copper = $3/2$), apart from weak lines due to quadrupole effect etc. The temperature was then raised (slowly, to make sure of thermal equilibrium) and the appearance of the spectrum and the fields of the lines noted at intervals.

As the temperature was raised from 20°K, the spectrum remained as the L.T. spectrum up to about 33°K. As the temperature was raised further, the intensity fell off and by 37°K it was very weak though still of the L.T. form. At 38°K the weak spectrum appeared to be a mixture of the L.T. and H.T. kinds. As the temperature continued to rise, the intensity of the H.T. spectrum increased while that of the L.T. fell. By 45°K the spectrum was essentially of the H.T. form except that its g -value was higher. It seems that the g -value approaches Bleaney, Bowers and Trenam's value (1953) as the temperature rises towards 90°K. Thus we have: $T = 90^\circ\text{K}$, $g = 2.218 \pm 0.003$ (Bleaney *et al.* 1953); $T = 45^\circ\text{K}$, $g = 2.235 \pm 0.005$ (our value).

Concentrated copper lanthanum nitrate.

We have examined the spectrum of this salt and found that the transition occurs above 90°K. Because of the concentration of the Cu^{2+} ions, the lines

are so wide that the hyperfine structure is not resolved. One can, however, distinguish the H.T. and L.T. types of spectrum by the g -values of the lines.

The g -values measured at 90°K showed that the spectrum was of the L.T. type with anisotropic g -values, $g_{||}=2.41$, $g_{\perp}=2.10$, which, considering the width of the lines (about 100 G), agree well with the g -values for the L.T. form of the dilute salt. As a check, the g -values were measured at 20°K and identical values were obtained. Thus it appeared that the transition takes place above 90°K and we therefore heated the salt above this temperature. At room temperature the spectrum consisted of a single line whose g -value was isotropic ($g=2.22$), which is the value of the H.T. form. The gas thermometers used were not designed to work at such a high temperature and hence temperature readings in this range are not accurate. However, it seems that the transition takes place gradually over the range 0 to -100°C.

At sufficiently high temperatures the Jahn-Teller effect causes distortions of the octahedron of water molecules surrounding the cupric ion. There is a continuous set of configurations all giving the same energy. The system resonates between these and consequently the H.T. form of spectrum is isotropic (Abragam and Pryce 1950). At lower temperatures the rapidly fluctuating distortions are replaced by a static distortion which gives rise to the L.T. form of spectrum. The nature of this transition is not understood.

We propose to investigate the similar transitions which occur in the fluosilicate and bromate of copper.

We wish to thank Dr. B. Bleaney and his group for drawing our attention to this phenomenon and for their helpful discussion. Acknowledgment is also due to the University for the award of a Pressed Steel Co., Ltd. research fellowship (D. B.) and the Department of Scientific and Industrial Research for a maintenance grant (A. C. R.-I.).

Clarendon Laboratory,
Oxford.
24th June 1953.

D. BIJL.
A. C. ROSE-INNES.

ABRAGAM, A., and PRYCE, M. H. L., 1950, *Proc. Phys. Soc. A*, **63**, 409.

BLEANEY, B., and BOWERS, K. D., 1952, *Proc. Phys. Soc. A*, **65**, 667.

BLEANEY, B., BOWERS, K. D., and TRENAM, R. S., 1953, *Proc. Phys. Soc. A*, **66**, 410.

TRENAM, R. S., 1953, *Proc. Phys. Soc. A*, **66**, 118.

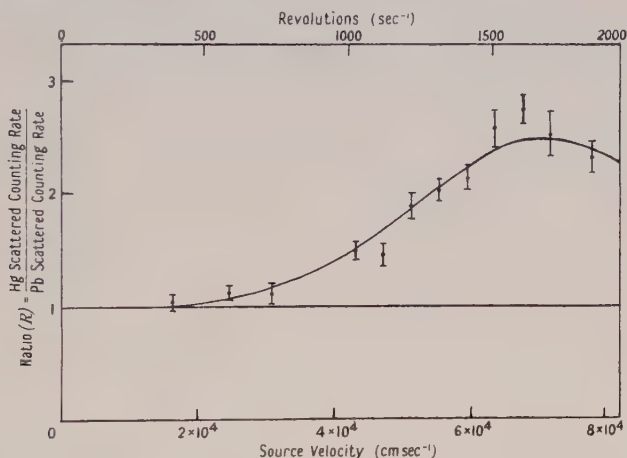
The Resonant Scattering of ^{198}Hg Gamma Rays

The scattering of ^{198}Hg γ -rays (0.411 MeV) from liquid mercury has been studied with an improved technique that greatly increased the ratio of resonant scattering to background. About 50 millicuries of ^{198}Au was carried by a steel rotor on a circular path six inches in diameter at speeds up to 8×10^4 cm sec $^{-1}$. Gamma-rays leaving the source in the forward direction fell upon interchangeable scatterers of mercury and lead, and the radiation scattered through about 90° was detected by a NaI(Tl) scintillation counter well shielded against direct rays. A discriminator circuit (E. C. Park 1953, to be published) limited the response of the counter to the photoelectric peak of the elastically scattered gamma-rays.

The elastic scattering from mercury at low source speeds, and from lead at any speed, should be due to the Rayleigh and nuclear Thomson processes alone. At high speeds the Doppler effect compensates for the energy lost to

nuclear recoils and permits resonant scattering from the (10% abundant) ^{198}Hg isotope. The optimum source speed is $6.7 \times 10^4 \text{ cm sec}^{-1}$ if the nuclei recoil freely, but the experimental spread of angles about the forward direction, in the apparatus used, should shift this optimum to about $7 \times 10^4 \text{ cm sec}^{-1}$.

The width of the resonance is calculable (on the assumption that β -ray recoil is completely dissipated before the γ -ray is emitted) from the temperatures of source and scatterer. The intensity of the resonance is proportional to the intrinsic width of the excited state; it involves also the statistical weights of the excited state and the ground state and, as regards the angular distribution, the multipole order of the transition.



Variation of the elastic scattering from mercury with the source velocity.

The figure shows the ratio of counting rates with Hg and Pb scatterers, after subtraction of background, as a function of source speed. The curve is calculated for a quadrupole transition between a ground state of spin 0 and an excited state of spin 2 having a width of $2.1 \times 10^{-5} \text{ eV}$, the Rayleigh plus Thomson elastic scattering cross section from mercury at 90° being taken as $1.32 \times 10^{-26} \text{ cm}^2 \text{ sterad}^{-1}$ on the basis of Franz's theory of Rayleigh scattering (Franz 1935) and Storruste's (1950) measurements of the total elastic scattering from lead.

Apart from any uncertainty as to the correctness of the Rayleigh plus Thomson cross section, we believe our value for the intrinsic width to be accurate to about 25%; it corresponds to a half-life of $(2.2 \pm 0.5) \times 10^{-11} \text{ second}$. This lies between the delayed-coincidence value of $(1.0 \pm 1.7) \times 10^{-11} \text{ sec}$ (Graham and Bell 1951) and the previous Doppler effect measurements which (allowing for the statistical weight factor) give half-lives of about $5 \times 10^{-11} \text{ sec}$ (Moon 1951), $8 \times 10^{-11} \text{ sec}$ (Moon and Storruste 1953) and $6 \times 10^{-11} \text{ sec}$ (Malmfors 1952), the last value being obtained from the thermal Doppler effect.

The principal result of the present measurements, however, is that the shape of the response curve and the optimum speed are approximately as predicted on the basis of free γ -ray recoils and no β -ray recoil.

Department of Physics,
The University,
Edgbaston, Birmingham 15.
26th May 1953.

W. G. DAVEY.
P. B. MOON.

FRANZ, W., 1935, *Z. Phys.*, **98**, 314.

GRAHAM, R. L., and BELL, R. E., 1951, *Phys. Rev.*, **84**, 380.

MALMFORS, K. G., 1952, *Ark. Fys.*, **6**, 49.

MOON, P. B., 1951, *Proc. Phys. Soc. A*, **64**, 76.

MOON, P. B., and STORRUSTE, A., 1953, *Proc. Phys. Soc. A*, **66**, 585.

STORRUSTE, A., 1950, *Proc. Phys. Soc. A*, **63**, 1197.

Accidental Degeneracy of Hydrogen

Fock (1935) gave an interesting explanation of the accidental degeneracy of hydrogen by showing that the Schrödinger equation can be transformed into an integral equation satisfied by four-dimensional spherical harmonics. This suggests that there must be a vector integral of the system which forms with the angular momentum vector a four-dimensional angular momentum tensor. This vector integral is shown here to be essentially the quantal analogue of Hamilton's integral (Milne 1948). By using it the possible negative energy levels can be obtained in an algebraic way.

Let \mathbf{p} and \mathbf{r} denote the momentum and displacement from the nucleus of the electron, so that the Hamiltonian H and the angular momentum \mathbf{m} are given by

$$H = \frac{1}{2m} \mathbf{p}^2 - \frac{e^2}{r}, \quad \mathbf{m} = \mathbf{r} \times \mathbf{p}.$$

Then the Hermitian vector $\mathbf{k} = (2m)^{-1}(\mathbf{p} \times \mathbf{m} - \mathbf{m} \times \mathbf{p}) - (e^2/r)\mathbf{r}$ can be shown to satisfy the following Poisson bracket relations :

$$[H, \mathbf{k}] = 0, \quad [k_r, m_s] = \epsilon_{rst} k_t, \quad \mathbf{k} \times \mathbf{k} = -\frac{2H}{m} i\hbar \mathbf{m}.$$

Similarly it can be shown that

$$\mathbf{k} \cdot \mathbf{m} = 0, \quad \mathbf{k}^2 = \frac{2H}{m} (\mathbf{m}^2 + \hbar^2) + e^4.$$

Consequently \mathbf{k} is a vector integral of the motion, known in classical mechanics as Hamilton's integral (Milne 1948). If we put

$$\mathbf{n} = \left(-\frac{2H}{m} \right)^{-1/2} \mathbf{k},$$

then we see that \mathbf{m} and \mathbf{n} together have the commutation relations of four-dimensional angular momentum, and that

$$\mathbf{m} \cdot \mathbf{n} = 0, \quad H(\mathbf{m}^2 + \mathbf{n}^2 + \hbar^2) = -\frac{1}{2} m e^4.$$

If H' is a negative characteristic value of H , \mathbf{n} is Hermitian in the corresponding characteristic subspace, which therefore carries a unitary representation of the four-dimensional rotation group. The equation $\mathbf{m} \cdot \mathbf{n} = 0$ shows that only the (j, j) representations of dimension $(2j+1)^2$, $j=0, \frac{1}{2}, 1, \dots$ can occur. These are the representations determined by the spherical harmonics of order $l=2j$, in which $\mathbf{m}^2 + \mathbf{n}^2$ has the characteristic value $l(l+2)\hbar^2$. Consequently the negative characteristic values of H are $-me^4/\{2(l+1)^2\hbar^2\}$, and these are $r(l)(l+1)^2$ fold degenerate, where $l=0, 1, 2, \dots$ and $r(l)$ takes integral non-negative values. To show that $r(l)=1$ we may rely on Fock's result that the wave functions are continuous functions on a three sphere.

In the positive continuous spectrum \mathbf{in} is Hermitian, and we obtain infinite dimensional unitary representations of the Lorentz group in which $\mathbf{m}^2 + \mathbf{n}^2$ has arbitrary negative values.

Note added in proof. It has come to my notice that Hamilton's integral is used by Born and Jordan in their book *Elementare Quantenmechanik*, pp. 177-190, but its connection with Fock's work is not given.

Department of Applied Mathematics,
University of Liverpool.
19th May 1953.

T. A. S. JACKSON.

FOCK, V. I., 1935, *Bull. Acad. Sci., U.S.S.R.*, Series 7, No. 2, 179.

MILNE, E. A., 1948, *Vectorial Mechanics* (London: Methuen).

REVIEWS OF BOOKS

The Dynamical Character of Adsorption, by J. H. DE BOER. Pp. xv+239, 45 figs. (Oxford: Clarendon Press, 1953.) 30s.

Although this book is written by a leading authority on the subject, it is by no means of interest to the specialist only. To many not actively engaged in similar work, and therefore unfamiliar with the literature, it will come as a surprise to learn how much is known of the processes of adsorption and the extent of the experimental work already performed in this difficult field. The author sets out to give a picture of what occurs during the processes of adsorption and to create in the mind of the reader a clear conception of the numerical magnitudes involved. To do this, striking use is made in the first chapter of a magnified picture for a gas in which the molecules are replaced by super bees, the dimensions of the container and the time scale also being suitably adjusted. The first three chapters give a careful exposition of the fundamentals of kinetic theory, particularly those parts of importance to an understanding of the mechanism by which adsorption occurs. Following these are discussions of the number of molecules adsorbed, unimolecular and multimolecular adsorption being considered. The Langmuir adsorption isotherm is obtained by a kinetic argument and compared with the experimental results. For multimolecular adsorption the isotherm is derived by a method different from that of the originators and its form considered under various conditions. Considerable attention is given to the elaboration of van der Waals' theory for a two-dimensional gas to which the movements of adsorbed molecules which have maintained a free translation may be likened. The scope of the book is deliberately circumscribed, detailed discussions of the energy of adsorption and the origin and magnitude of the forces involved being excluded, since these have been dealt with elsewhere. The emphasis throughout is physical, the mathematical results being closely related at all stages to the picture of adsorption being drawn. Because of this, and the useful summary of our present knowledge that it contains, the book is sure to find many interested readers and in the words of the author "... may stimulate further research and lead to much new experimental evidence of the real equation of state of adsorbed matter".

F. E. H.

CONTENTS OF SECTION B

	PAGE
Dr. A. SCHALLAMACH. Surface Condition and Electrical Impedance in Rubber Friction	817
Mr. P. M. TIPPLe and Dr. H. K. HENISCH. Thermal Effects at Point Contact Diodes	826
Dr. P. C. BANBURY. Theory of the Forward Characteristic of Injecting Point Contacts	833
Dr. H. K. HENISCH and Mr. F. D. MORTEN. Forward Characteristic of Injecting Area Contacts on Germanium	841
Dr. C. A. HOGARTH. A Study of Carrier Injecting Properties of Emitter Contacts and Light Spots at Normal and Moderately Elevated Temperatures	845
Dr. W. CULSHAW and Mr. D. S. JONES. Effect of a Metal Plate on Total Reflection	859
Dr. P. FELTHAM. The Plastic Flow of Iron and Plain Carbon Steels above the A ₃ -Point	865
Miss S. M. CRAWFORD. The Relation between Stress, Strain and Birefringence in some High Polymers	884
Dr. E. V. VERNON and Mr. S. WEINTROUB. The Measurement of the Thermal Expansion of Single Crystals of Indium and Tin with a Photoelectric Recording Dilatometer	887
Research Notes :	
Mr. F. J. HEWITT. The Study of Lightning Streamers with 50 cm Radar	895
Letters to the Editor :	
Dr. L. W. DAVIES. Spectroscopic Study of Caesium Discharges in a Magnetic Field	898
Dr. W. N. REYNOLDS. Surface Recombination in Germanium	899
Reviews of Books	901
Contents of Section A	904

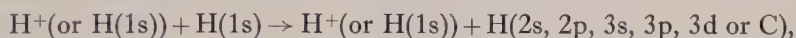
Inelastic Collisions between Heavy Particles
I: Excitation and Ionization of Hydrogen Atoms in Fast
Encounters with Protons and with other Hydrogen Atoms

By D. R. BATES and G. GRIFFING *

Department of Applied Mathematics, Queen's University, Belfast

MS. received 10th June 1953

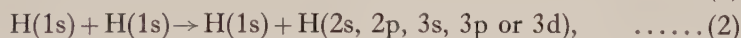
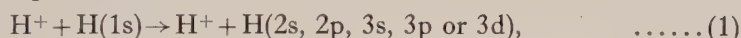
Abstract. Born's approximation is used to calculate the cross sections of the following processes :



where C represents the continuum. The results are presented mainly in graphical form. In the case of the ionizing collisions the energy distribution of the ejected electrons is also given.

§ 1. INTRODUCTION

THOUGH inelastic collisions between heavy particles are of importance in aurorae and in many other phenomena few detailed calculations on them have been performed. The present paper is devoted to the investigation of some of the simpler of such collisions:



Born's approximation is used, no account being taken of exchange. Results for relatively low impact energies are included to enable the range of validity of the approximation to be assessed should proper comparison data become available. This range is still very uncertain. Charge transfer between hydrogen atoms and protons has recently been studied (cf. Bates and Dalgarno 1952, Dalgarno and Yadav 1953, Jackson and Schiff 1953) and for it Born's approximation appears to be quite satisfactory when the energy of the incident particle is above about 25 kev; but the process is of course dissimilar from those under discussion.

§ 2. THEORY

2.1. Consider an encounter between the atomic system A, comprised of a nucleus of charge $Z_a e$ and an electron, and another atomic system B, comprised either of a bare nucleus of charge $Z_b e$, or of such a nucleus and an electron. These two cases can be treated together, the symbols for corresponding quantities being distinguished, when this is necessary, by superscripts + and \pm (as in eqns. (9) and (10) below). According to the simple Born approximation

* Affiliated to the Cambridge Geophysics Research Directorate of the United States Air Force.

(cf. Mott and Massey 1949) the cross section associated with the reaction in which A is excited from state p to state q , B remaining unchanged, is

$$Q(p \rightarrow q) = \frac{8\pi^3 M^2}{K_p^2 h^4} \int_{K_{\min}}^{K_{\max}} |\mathcal{N}|^2 K dK \quad \dots\dots(5)$$

where h is Planck's constant, M is the reduced mass $M_a M_b / (M_a + M_b)$;

$$\mathbf{K} = \mathbf{K}_p - \mathbf{K}_q, \quad \dots\dots(6)$$

$$\mathbf{K}_p = 2\pi M \mathbf{v}_p / h, \quad \mathbf{K}_q = 2\pi M \mathbf{v}_q / h; \quad \dots\dots(7)$$

\mathbf{v}_p and \mathbf{v}_q are the initial and final velocities of relative motion; and, assuming that at least one of the colliding systems is neutral,

$$\mathcal{N} = \iint \chi_p(\mathbf{r}_a) \chi_q^*(\mathbf{r}_a) \exp(i\mathbf{R} \cdot \mathbf{K}) V(\mathbf{R}, \mathbf{r}_a) d\mathbf{r}_a d\mathbf{R}, \quad \dots\dots(8)$$

$\chi_p(\mathbf{r}_a)$ and $\chi_q(\mathbf{r}_a)$ being the wave functions of the electron bound to nucleus A, \mathbf{R} being the relative position vector of the heavy particles, and $V(\mathbf{R}, \mathbf{r}_a)$ being the interaction potential. If B is a bare nucleus this interaction potential is

$$V^+(\mathbf{R}, \mathbf{r}_a) = e^2 \left[\frac{Z_a Z_b}{R} - \frac{Z_b}{|\mathbf{R} - \mathbf{r}_a|} \right], \quad \dots\dots(9)$$

and if there is an electron of wave function $\phi_n(\mathbf{r}_b)$ attached it is

$$V^\pm(\mathbf{R}, \mathbf{r}_a) = e^2 \int \phi_n(\mathbf{r}_b) \left[\frac{Z_a Z_b}{R} - \frac{Z_a}{|\mathbf{R} + \mathbf{r}_b|} - \frac{Z_b}{|\mathbf{R} - \mathbf{r}_a|} + \frac{1}{|\mathbf{R} + \mathbf{r}_b - \mathbf{r}_a|} \right] \phi_n^*(\mathbf{r}_b) d\mathbf{r}_b. \quad \dots\dots(10)$$

The first two terms within the curly brackets of integral (10) give no contribution to \mathcal{N} owing to the fact that χ_p and χ_q are orthogonal. On neglecting them it may be seen that if ϕ_n represents the 1s state (which is the only case which will be considered) then effectively

$$V^\pm(\mathbf{R}, \mathbf{r}_a) = -e^2 \left[\frac{Z_b - 1}{|\mathbf{R} - \mathbf{r}_a|} + \left\{ \frac{Z_b}{a_0} + \frac{1}{|\mathbf{R} - \mathbf{r}_a|} \right\} \exp\left(\frac{-2Z_b}{a_0} |\mathbf{R} - \mathbf{r}_a|\right) \right], \quad \dots\dots(11)$$

where a_0 is the radius of the first orbital of hydrogen. Substitution of (9) and (11) in (8) and application of the integration formula of Bethe (1930) yields

$$|\mathcal{N}^+| = \frac{4\pi e^2 a_0^2}{t^2} Z_b |\mathcal{J}|, \quad \dots\dots(12)$$

$$|\mathcal{N}^\pm| = \frac{4\pi e^2 a_0^2}{t^2} Z_b \left\{ 1 - \frac{16Z_b^3}{(4Z_b^2 + t^2)^2} \right\} |\mathcal{J}|, \quad \dots\dots(13)$$

in which

$$\mathbf{t} = \mathbf{K} a_0 \quad \dots\dots(14)$$

and

$$|\mathcal{J}| = \left| \int \chi_p(\mathbf{r}_a) \chi_q^*(\mathbf{r}_a) \exp(i\mathbf{t} \cdot \mathbf{r}_a) d\mathbf{r}_a \right|, \quad \dots\dots(15)$$

\mathbf{r}_a being now in atomic units. From (5) it hence follows that

$$Q^+(p \rightarrow q) = \left[\frac{8Z_b^2}{s^2} \int_{t_{\min}}^{t_{\max}} |\mathcal{J}|^2 t^{-3} dt \right] \pi a_0^2 \quad \dots\dots(16)$$

(which is of course a standard result, cf. Mott and Massey 1949) and

$$Q^\pm(p \rightarrow q) = \left[\frac{8Z_b^2}{s^2} \int_{t_{\min}}^{t_{\max}} |\mathcal{J}|^2 t^{-3} \left\{ 1 - \frac{16Z_b^3}{(4Z_b^2 + t^2)^2} \right\}^2 dt \right] \pi a_0^2, \quad \dots\dots(17)$$

where

$$s^2 = \frac{1}{2} m v_p^2 / I_H, \quad \dots\dots(18)$$

I_H being the ionization potential of hydrogen. If $\Delta E(p, q)$ is the difference between the energies of the two states in units of I_H , then

$$t_{\min} = (K_p - K_q)a_0 \quad \dots\dots(19)$$

$$\simeq \frac{\Delta E(p, q)}{2s} \left[1 + \frac{m\Delta E(p, q)}{4Ms^2} \right] \quad \dots\dots(20)$$

since $m\Delta E(p, q)/Ms^2$ is small compared with unity except in the region immediately above the threshold (where in any event Born's approximation is invalid). As is usual in the treatment of heavy particle collisions, it is sufficient to take t_{\max} as infinite. Comparison of (16) and (17) shows that if the energy of relative motion E is much less than $[EZ_b^{1/2} + M\Delta E(p, q)^2/16mZ_b^{3/2}]$ then $Q^+(p \rightarrow q|E)$ and $Q^\pm(p \rightarrow q|E)$ are approximately equal.

Before proceeding to the detailed calculations it may be noted from (15) that $|\mathcal{J}|$ is a function of t/Z_a (or the more convenient equivalent $t/\Delta E(p, q)^{1/2}$), so that the cross sections may be expressed in the form

$$Q^+(p \rightarrow q|E) = \{Z_b^2/\Delta E(p, q)^2\} f_{pq}(M\Delta E(p, q)/E) \quad \dots\dots(21)$$

$$Q^\pm(p \rightarrow q|E) = Q^+(p \rightarrow q|E) - \{1/\Delta E(p, q)^2\} [Z_b g_{pq}\{M\Delta E(p, q)/E, \Delta E(p, q)/Z_b^2\} - h_{pq}\{M\Delta E(p, q)/E, \Delta E(p, q)/Z_b^2\}] \quad \dots\dots(22)$$

where for any given pair of quantum numbers p and q the functions f_{pq} , g_{pq} and h_{pq} depend only on the variables indicated and the region immediately above the threshold is again excluded. These scaling relations give the results which will be presented later a rather wider applicability than they would otherwise have.

2.2. For discrete transitions $|\mathcal{J}|$ can be got from (15) by elementary methods. If t/Z_a is denoted by τ then

$$\left. \begin{aligned} |\mathcal{J}(1s \rightarrow 2s)| &= 2^{17/2} \tau^2 / (4\tau^2 + 9)^3 \\ |\mathcal{J}(1s \rightarrow 2p)| &= 2^{15/2} \times 3\tau / (4\tau^2 + 9)^3 \\ |\mathcal{J}(1s \rightarrow 3s)| &= 2^4 \times 3^{7/2} (27\tau^2 + 16) \tau^2 / (9\tau^2 + 16)^4 \\ |\mathcal{J}(1s \rightarrow 3p)| &= 2^{11/2} \times 3^3 (27\tau^2 + 16) \tau / (9\tau^2 + 16)^4 \\ |\mathcal{J}(1s \rightarrow 3d)| &= 2^{17/2} \times 3^{7/2} \tau^2 / (9\tau^2 + 16)^4 \end{aligned} \right\} \quad \dots\dots(23)$$

On substituting in (16) and (17) and resolving the integrands into partial fractions analytical expressions for the cross sections can readily be obtained. These have little interest and need not be displayed here: for they are, in general, cumbersome and, owing to very severe cancellation between the individual terms, are awkward to evaluate, so that except in a few instances it is easier to perform the necessary integrations numerically. However, in the case of slow collisions we may expand in powers of $1/\tau$, and if we retain only the leading term we get the following formulae in which the cross sections are in units of $\pi a_0^2 (8.8 \times 10^{-17} \text{ cm}^2)$, the reduced mass is measured on the scale on which the proton mass is unity, and the energies of relative motion and excitation are in electron volts:

$$\left. \begin{aligned} Q(1s \rightarrow 2s) &= 1.3 \times 10^{-6} Z_b^2 E^4 / M^4 \Delta E(1s - 2s)^6 \\ Q(1s \rightarrow 2p) &= 7.4 \times 10^{-9} Z_b^2 E^5 / M^5 \Delta E(1s - 2p)^7 \\ Q(1s \rightarrow 3s) &= 2.0 \times 10^{-7} Z_b^2 E^4 / M^4 \Delta E(1s - 3s)^6 \\ Q(1s \rightarrow 3p) &= 1.1 \times 10^{-9} Z_b^2 E^5 / M^5 \Delta E(1s - 3p)^7 \\ Q(1s \rightarrow 3d) &= 6.1 \times 10^{-13} Z_b^2 E^6 / M^6 \Delta E(1s - 3d)^8 \end{aligned} \right\} \quad \dots\dots(24)^*$$

* The distinguishing superscripts are omitted since at the low energies concerned Q^+ and Q^\pm are of almost equal magnitude. For some purposes it is convenient to replace E and M , respectively, by the energy and mass of the incident particle.

with

$$\Delta E \ll E \ll \sim 100 M \Delta E. \quad \dots\dots(25)$$

To be sure the range of energies covered is not one over which the treatment can be expected to give reliable results; but it is to be noted that the formulae show that the Born approximation is successful in predicting the extremely rapid fall off in the cross section at low impact energies, and the other main features characteristic of near-adiabatic heavy particle collisions (cf. Bates and Massey, 1954).

2.3. In the calculations on transitions into the continuum the free wave function was taken as

$$\chi_{\kappa}(\mathbf{r}_a) = [Z_a \kappa^{1/2} [2\pi a_0 \{1 - \exp(-2\pi/\kappa)\}^{1/2} \Gamma(1 - i/\kappa)]^{-1} \times \exp(iZ_a \kappa \mathbf{r}_a / a_0) \int_0^\infty u^{-i/\kappa} \exp(-u) I_0([4iZ_a \kappa u(z_a + r_a)/a_0]^{1/2}) du \quad \dots(26)$$

where \mathbf{x} denotes $2\pi m \mathbf{v} a_0 / h Z_a$, \mathbf{v} is the velocity of ejection of the electron, z_a is its coordinate, with respect to nucleus A, along a line parallel to the direction of ejection, and I_0 is the usual Bessel function (Sommerfeld 1931). The rather lengthy analysis involved in the integration of (15) is essentially the same as that described by Massey and Mohr (1933) in their work on ionization by electron collision. It is therefore only necessary to give the result:

$$|\mathcal{J}(1s \rightarrow \kappa)|^2 = \frac{2^8 \kappa \tau^2 (1 + 3\tau^2 + \kappa^2) \exp[(- 2/\kappa) \tan^{-1}\{2\kappa/(1 + \tau^2 - \kappa^2)\}]}{3\{1 + (\tau - \kappa)^2\}^3 \{1 + (\tau + \kappa)^2\}^3 \{1 - \exp(-2\pi/\kappa)\}}. \quad \dots(27)$$

Substitution of this expression in (16) and (17) gives $Q(1s \rightarrow \kappa)$, which is such that $Q(1s \rightarrow \kappa) d\kappa$ is the cross section of an ionizing collision in which the κ value of the liberated electron lies between κ and $\kappa + d\kappa$, all angles of ejection being included. The completion of the calculation must in general be carried out by numerical methods. If condition (25) is satisfied we can however obtain simple approximate formulae: thus, proceeding as in the case of excitation and using the same units, we find that the cross section associated with the ejection of an electron with energy between ϵ and $\epsilon + d\epsilon$ ev is

$$Q(1s \rightarrow \epsilon) d\epsilon = \{1.7 \times 10^{-6} Z_b^2 E^4 \Delta E (1s - c)^3 / M^4 [\Delta E (1s - c) + \epsilon]^{10}\} d\epsilon, \quad \dots\dots(28)$$

and so the total cross section,

$$\int_0^\infty Q(1s \rightarrow \epsilon) d\epsilon = 1.9 \times 10^{-7} Z_b^2 E^4 / M^4 \Delta E (1s - c)^6, \quad \dots\dots(29)$$

E being again the energy of relative motion and $\Delta E(1s - c)$ being the ionization potential.

2.4. If the velocities of relative motion are the same, and are sufficiently high, the cross sections Q^+ for proton-atom collisions are of course equal to the cross sections Q for the corresponding electron-atom collisions (cf. Mott and Massey 1949). It is worth noting that a more general relation between the two exists. The inequality of the cross sections at moderate and low velocities of relative motion arises because both t_{\max} and t_{\min} are different. Thus with protons t_{\max} is $(M/m)\Delta E/t_{\min}$, which enables the upper integration limit in (16) to be treated as infinite except for extremely slow collisions; but with electrons this

simplification only becomes valid at much higher velocities since here t_{\max} is $\Delta E/t_{\min}$. Again with protons (20) is a good approximation to (19), and indeed it is generally sufficient to take t_{\min} as $\Delta E/2s$; but with electrons it is necessary to use the more accurate formula

$$(\Delta E + t_{\min}^2)/2t_{\min} = s, \quad (t_{\min} \leq \Delta E^{1/2}). \quad \dots\dots(30)$$

Suppose now that in corresponding proton-atom and electron-atom collisions the energies $E^+(x)$ and $E^-(x)$ are such that t_{\min} in both cases is equal to x , and denote the cross sections at these energies by $Q^+(E^+(x))$ and $Q^-(E^-(x))$ respectively. From (16) and (18) it is apparent that we can write

$$Q^+(E^+(x)) = (M/m)w(x)/E^+(x) \quad \dots\dots(31)$$

and

$$Q^-(E^-(x)) = \{w(x) - w(\Delta E/x)\}/E^-(x), \quad (x \leq \Delta E^{1/2}), \quad \dots\dots(32)$$

where w is a function of only the variable indicated. Noting that

$$E^-(x) = (\gamma m/M)E^+(x), \quad (E^+(x) \geq M\Delta E/4m) \quad \dots\dots(33)$$

with

$$\gamma = \left\{1 + \frac{M\Delta E}{4mE^+(x)}\right\}^2, \quad \dots\dots(34)$$

it may be seen from (31) and (32) that

$$Q^-(E^-(x)) = \gamma^{-1} \left\{ Q^+(E^+(x)) - \frac{E^+(y)}{E^+(x)} Q^+(E^+(y)) \right\}, \quad \dots\dots(35)$$

where

$$E^+(y) = M^2\Delta E^2/16m^2E^+(x), \quad \dots\dots(36)$$

which expresses the electron-atom cross section at energy $E^-(x)$ in terms of the proton-atom cross sections at the related energies $E^+(x)$ and $E^+(y)$. As the Born approximation has been evaluated for numerous electron-atom cross sections (cf. Bates, Fundaminsky, Leech and Massey 1950, Massey and Burhop 1952) the formula provides a useful check on the computation of the proton-atom cross sections. Clearly the electron-atom cross sections are smaller than the corresponding proton-atom cross sections.

2.5. Finally we will consider briefly the kinetic energy

$$T = (m/M_A)t^2 \quad \dots\dots(37)$$

given to a stationary atom suffering excitation or ionization. For a fixed impact energy the integrands in (16) and (17) fall off extremely rapidly as t increases beyond some value t_M so that transitions in which T is more than several times

$$T_M = (m/M_A)t_M^2 \quad \dots\dots(38)$$

are very rare. In any particular case t_M can of course easily be found from the expression for the matrix element.

The general position is illustrated sufficiently by the 1s-2s and 1s-2p transitions of atomic hydrogen. If the incident particle is a proton it is immediately apparent from (16) and (23) that for both transitions t_M is simply

t_{\min} ; if the incident particle is a hydrogen atom it may be shown from (17) and (23) that for the 1s–2s transition

$$\begin{aligned} t_M &= t_{\min}, & (t_{\min} \geq 0.877) \\ &= 0.877, & (t_{\min} \leq 0.877) \end{aligned}$$

and for the 1s–2p transition

$$\begin{aligned} t_M &= t_{\min}, & (t_{\min} \geq 0.577) \\ &= 0.577, & (t_{\min} \leq 0.577). \end{aligned}$$

On substituting in (38) it is found that if \mathcal{E} is the energy of the incident hydrogen ion or atom in kev then according to the Born approximation

$$\begin{aligned} T_M &= (0.026/\mathcal{E}) \text{ ev} & \begin{cases} \text{H}^+ \text{ ion impact, 1s–2s, 1s–2p transitions, all } \mathcal{E} \\ \text{H atom impact, 1s–2s transition, } \mathcal{E} \leq 4.6 \text{ kev} \\ \text{H atom impact, 1s–2p transition, } \mathcal{E} \leq 10.5 \text{ kev} \end{cases} \\ &= 0.0057 \text{ ev} & \{ \text{H atom impact, 1s–2s transition, } \mathcal{E} \geq 4.6 \text{ kev} \\ &= 0.0025 \text{ ev} & \{ \text{H atom impact, 1s–2p transition, } \mathcal{E} \geq 10.5 \text{ kev.} \end{aligned}$$

The kinetic energy transferred is thus minute. Qualitative verification of this well-known characteristic of inelastic collisions is provided by the recent experiments of Keene (1949).

§ 3. RESULTS

3.1. The cross sections associated with the processes mentioned in the introduction were computed from the formulae that have been given. Figures 1 to 6 show the values obtained. It should be noted that a log–log scale is used,

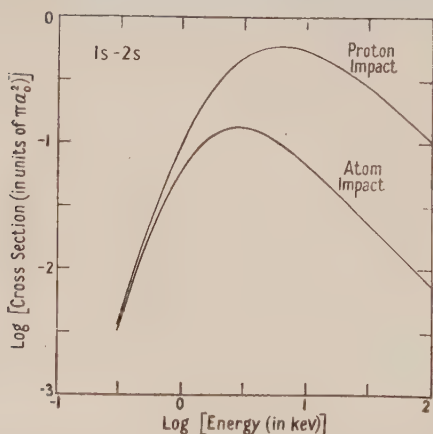


Fig. 1. $\text{H}^+ + \text{H}(1s) \rightarrow \text{H}^+ + \text{H}(2s)$ and $\text{H}(1s) + \text{H}(1s) \rightarrow \text{H}(1s) + \text{H}(2s)$.

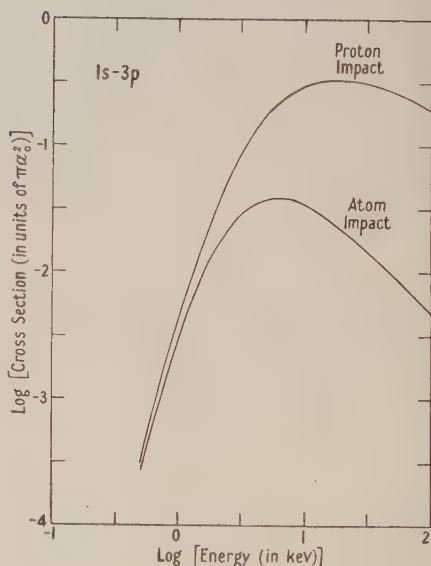


Fig. 4. $\text{H}^+ + \text{H}(1s) \rightarrow \text{H}^+ + \text{H}(3p)$ and $\text{H}(1s) + \text{H}(1s) \rightarrow \text{H}(1s) + \text{H}(3p)$.

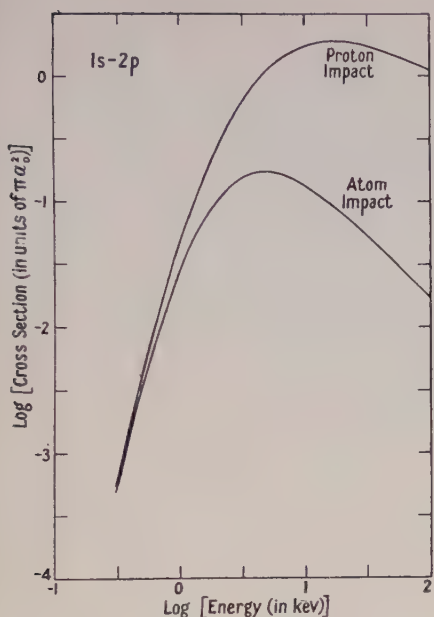


Fig. 2. $H^+ + H(1s) \rightarrow H^+ + H(2p)$ and $H(1s) + H(1s) \rightarrow H(1s) + H(2p)$.

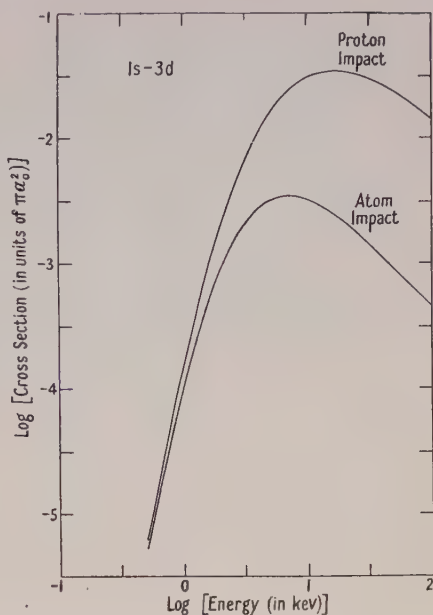


Fig. 5. $H^+ + H(1s) \rightarrow H^+ + H(3d)$ and $H(1s) + H(1s) \rightarrow H(1s) + H(3d)$.

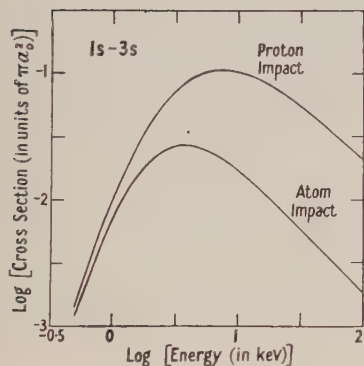


Fig. 3. $H^+ + H(1s) \rightarrow H^+ + H(3s)$ and $H(1s) + H(1s) \rightarrow H(1s) + H(3s)$.

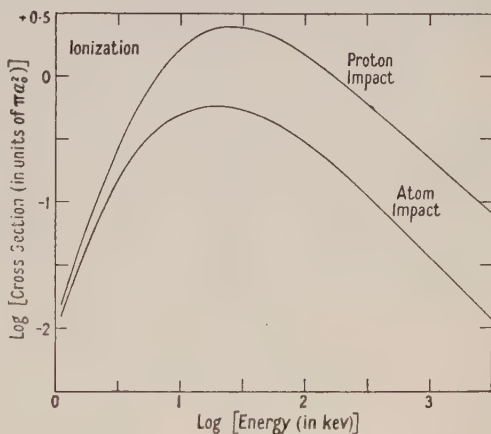


Fig. 6. $H^+ + H(1s) \rightarrow H^+ + H^+ + e$ and $H(1s) + H(1s) \rightarrow H(1s) + H^+ + e$.

Figs. 1-6. Cross-section-energy curves.

and that the independent variable chosen is *not* E , the energy of relative motion, but is instead \mathcal{E} , the energy of the incident particle, the atom undergoing the transition being taken to be at rest. In the case of the excitations the results for energies above 100 kev (the upper limit in the figures) can most conveniently be

presented algebraically: thus by expanding in inverse powers of \mathcal{E} (which we measure in kev) we find that

$$\left. \begin{aligned} Q^+(1s \rightarrow 2s) &= 11.1 \mathcal{E}^{-1} \{1 - 7.8 \mathcal{E}^{-1}\}, \\ Q^\pm(1s \rightarrow 2s) &= 0.721 \mathcal{E}^{-1} \{1 - 123 \mathcal{E}^{-3}\}, \\ Q^+(1s \rightarrow 2p) &= 128 \mathcal{E}^{-1} \{\log \mathcal{E} - 1.185 + 4.1 \mathcal{E}^{-1}\}, \\ Q^\pm(1s \rightarrow 2p) &= 1.78 \mathcal{E}^{-1} \{1 - 48 \mathcal{E}^{-2}\}, \\ Q^+(1s \rightarrow 3s) &= 2.20 \mathcal{E}^{-1} \{1 - 7.5 \mathcal{E}^{-1}\}, \\ Q^\pm(1s \rightarrow 3s) &= 0.186 \mathcal{E}^{-1} \{1 - 180 \mathcal{E}^{-3}\}, \\ Q^+(1s \rightarrow 3p) &= 20.5 \mathcal{E}^{-1} \{\log \mathcal{E} - 1.104 + 2.4 \mathcal{E}^{-1}\}, \\ Q^\pm(1s \rightarrow 3p) &= 0.478 \mathcal{E}^{-1} \{1 - 57 \mathcal{E}^{-2}\}, \\ Q^+(1s \rightarrow 3d) &= 1.69 \mathcal{E}^{-1} \{1 - 19.4 \mathcal{E}^{-1} + 162 \mathcal{E}^{-2}\}, \\ Q^\pm(1s \rightarrow 3d) &= 0.0453 \mathcal{E}^{-1} \{1 - 1473 \mathcal{E}^{-3}\}, \end{aligned} \right\} \dots\dots (39)$$

the unit of cross section being πa_0^2 as usual. The final term in each of the expressions is very small, and is included mainly to demonstrate how rapidly the asymptotic form is approached.

On comparing a Q^+ curve with the corresponding Q^\pm curve it will be observed that the former lies close to, but above, the latter at low energies, that its maximum is much larger and occurs at much higher energies, and that its final rate of fall off is the same for optically forbidden transitions but is slightly slower for optically allowed transitions. It will be noted also that the curves for each spectral series (such as $1s \rightarrow ns$) are almost identical in shape, any one curve approximating to the preceding curve displaced downwards and to the right, the latter displacement being far greater than the difference between the excitation potentials.

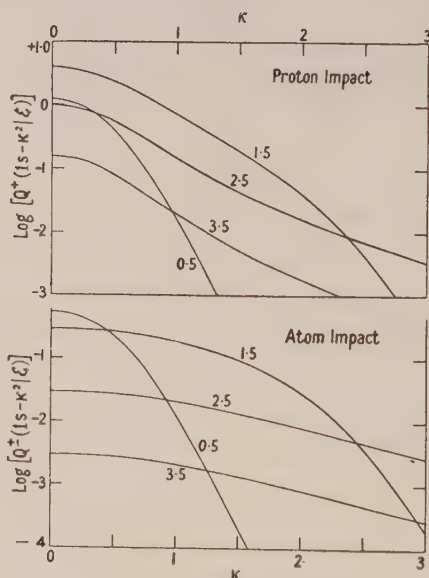


Fig. 7. Energy distribution of the ejected electrons. The upper set of curves refers to process (3) and the lower set to process (4). The numbers on the individual curves give the logarithm of the energy of the incident particle (expressed in kev).

In the case of ionization information is often required on the energy distribution of the ejected electrons. One convenient way of representing the distribution is by the function $Q(1s \rightarrow \kappa^2 | \mathcal{E})$, which is such that $Q(1s \rightarrow \kappa^2 | \mathcal{E}) d\kappa^2$ is the cross section for a collision in which an incident particle of energy \mathcal{E} ejects an electron with energy between κ^2 and $\kappa^2 + d\kappa^2$ times the ionization potential.* Figure 7 shows the variation of $\log \{Q^+(1s \rightarrow \kappa^2 | \mathcal{E})\}$ and of $\log \{Q^\pm(1s \rightarrow \kappa^2 | \mathcal{E})\}$ with κ for some selected impact energies. Attention is drawn to the rapidity of the fall off when \mathcal{E} is small, to the change in the form of the distribution as \mathcal{E} is increased, and to the great difference between the proton and atom cases when \mathcal{E} is large. It should perhaps be mentioned that the rather abrupt changes of slope which occur are real, and are associated with passage through the maximum of a curve of $Q(1s \rightarrow \kappa^2 | \mathcal{E})$ plotted against \mathcal{E} .

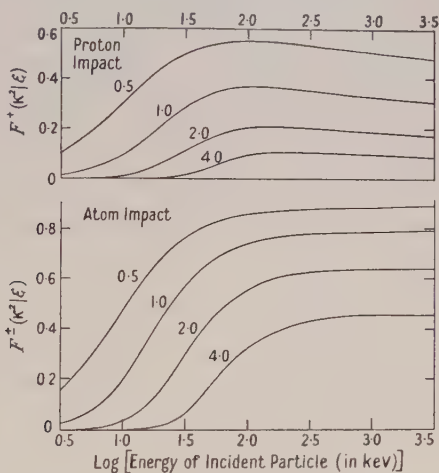


Fig. 8. Fraction of ejected electrons which have more than a certain amount of energy κ^2 . The upper set of curves refers to process (3) and the lower set to process (4). The numbers on the individual curves give κ^2 (expressed in units of I_H , the ionization potential of hydrogen).

Instead of the actual energy distribution it is sometimes more useful to know

$$F(\kappa^2 | \mathcal{E}) = \int_{\kappa^2}^{\infty} Q(1s \rightarrow \kappa^2 | \mathcal{E}) d\kappa^2 / \int_0^{\infty} Q(1s \rightarrow \kappa^2 | \mathcal{E}) d\kappa^2, \quad \dots (40)$$

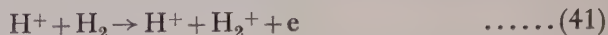
that is the fraction of the ejected electrons which have energy greater than κ^2 times the ionization potential. The results of some relevant calculations are displayed in fig. 8. As can be seen, F increases rapidly until \mathcal{E} is some 100 kev, and thereafter is approximately constant. The value of F on what may be called the plateau is quite large: thus when κ^2 is unity, F is about 0.3 in the proton case, and is about 0.8 in the atom case. This is of considerable interest in connection with aurorae.

3.2. Experimental work on collisions between heavy particles is extremely difficult as is evidenced by the contradictory results that have been reported

* For corresponding values of \mathcal{E} the energy of the incident particle and E the energy of relative motion we have of course that $Q(1s \rightarrow \kappa^2 | \mathcal{E})$ is equal to $Q(1s \rightarrow \kappa | E)/2\kappa$ where $Q(1s \rightarrow \kappa | E)$ is the function introduced in § 2.3.

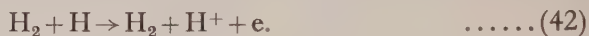
(cf. Massey and Burhop 1952). The only relevant data at present available refer to ionization, which is naturally simpler to study than is excitation.

Keene (1949) has conducted a careful investigation of the process



over an energy range of from 2 to 36 kev. The agreement with theory is rather poor: for example, the observed cross section at the upper limit of the energy range covered is $1.5(\pm 0.2)\pi a_0^2$, whereas the predicted cross section* is $3.4\pi a_0^2$; and again the observed cross section curve is still increasing steadily at this energy, whereas the predicted cross section curve is passing through its maximum. There is thus apparently a discrepancy of the type characteristic of the Born approximation (cf. Bates, Fundaminsky, Leech and Massey 1950). At an impact energy of 36 kev the velocity of the proton is about equal to the orbital velocity of the bound electrons, so it would not be surprising if the theory should prove to be inadequate. However, it would be premature to conclude that the error is as great as is indicated by Keene's experiments, for the charge transfer cross sections he obtained with the same apparatus are significantly different from those of some later workers (cf. Jackson and Schiff 1953).

By studying the passage of a beam of hydrogen atoms through hydrogen gas Bartels (1932), Montague (1951) and Ribe (1951) have determined the cross section associated with



Their results are mutually consistent, and when combined cover the 20 to 300 kev energy range. The calculated variation over this energy range (cf. fig. 6) is essentially identical with that observed. However, Born's approximation gives the absolute magnitude of the cross section for process (4) to be only half the measured cross section (per hydrogen atom).† Part of the difference may arise from the fact that a small fraction of the hydrogen atoms in the beam must have been in excited states, for judging from the work of Yavorsky (1945) on ionization by electron impact the cross section of excited atoms is very many times that of normal atoms. Another, and probably much more important, factor is that in the process studied in the laboratory the neutral molecule causing the transition is not necessarily left in the initial state but may itself be excited or ionized, so that process (4) represents only one of the possible reaction paths. Calculations on the contributions from simultaneous ionization and excitation and double ionization are in progress.

ACKNOWLEDGMENTS

We wish to thank {Drs. A. Dalgarno and A. L. Stewart for several helpful discussions.

* In predicting the cross section one molecule was assumed to be equivalent to two atoms and scaling formula (21) was used to allow for the fact that the *vertical* ionization potential of molecular hydrogen is $1.2 I_{\text{H}}$.

† In contrast, the semi-classical treatment of Bohr (1948) gives a cross section which is about thrice too large. This treatment assumed that only close collisions are effective and that in these the ionizing effects of the individual particles constituting the perturbing atom or molecule are additive.

REFERENCES

- BARTELS, H., 1932, *Ann. Phys., Lpz.*, **13**, 373.
BATES, D. R., and DALGARNO, A., 1952, *Proc. Phys. Soc. A*, **65**, 919.
BATES, D. R., FUNDAMINSKY, A., LEECH, J. W., and MASSEY, H. S. W., 1950, *Phil. Trans. Roy. Soc. A*, **243**, 117.
BATES, D. R., and MASSEY, H. S. W., 1954, *Phil. Mag.*, in the press.
BETHE, H. A., 1930, *Ann. Phys., Lpz.*, **5**, 325.
BOHR, N., 1948, *Kgl. Danske Videnskab. Selskab, Mat-fys. Medd.*, **18**.
DALGARNO, A. and YADAV, H. N., 1953, *Proc. Phys. Soc. A*, **66**, 173.
JACKSON J. D. and SCHIFF, H., 1953, *Phys. Rev.* **89**, 359.
KEENE, J. P., 1949, *Phil. Mag.*, **40**, 369.
MASSEY, H. S. W., and BURHOP, E. H. S., 1952, *Electronic and Ionic Impact Phenomena* (Oxford: Clarendon Press).
MASSEY, H. S. W., and MOHR, C. B. O., 1933, *Proc. Roy. Soc. A*, **140**, 613.
MONTAGUE, J. H., 1951, *Phys. Rev.*, **81**, 1026.
MOTT, N. F., and MASSEY, H. S. W., 1949, *Theory of Atomic Collisions*, 2nd Edn. (Oxford: Clarendon Press).
RIBE, F. L., 1951, *Phys. Rev.*, **83**, 1217.
SOMMERFELD, A., 1931, *Ann. Phys., Lpz.*, **11**, 257.
YAVORSKY, B., 1945, *C. R. Acad. Sci., U.R.S.S. (Doklady)*, **49**, 250.

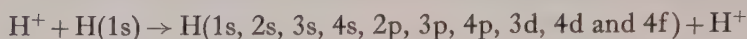
Electron Capture—III : Capture into Excited States in Encounters between Hydrogen Atoms and Fast Protons

BY D. R. BATES AND A. DALGARNO

Department of Applied Mathematics, Queen's University, Belfast

MS. received 26th June 1953

Abstract. The cross sections associated with the electron capture processes



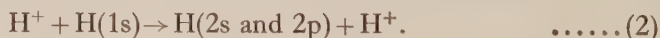
are calculated. They are used in the evaluation of f_α and f_β , the fractions of the total number of captures which result in H_α and H_β emission. It is found that f_α and f_β are very small, being only about 0.050 and 0.015 respectively even at the most favourable impact energy (approximately 70 kev).

§ 1. INTRODUCTION

IN the first paper of this series (Bates and Dalgarno 1952) it was pointed out that in their treatment of electron capture Oppenheimer (1928) and Brinkman and Kramers (1930) had erroneously omitted one of the terms of the interaction potential so that their approximation is not a form of the Born approximation as was supposed. Calculations were carried out on the resonance process



using the full interaction potential but otherwise making the same basic assumptions (which are valid only at high impact energies). These revealed that the adoption of the O.B.K. approximation causes the cross sections to be seriously over-rated. The second paper (Dalgarno and Yadav 1953) verified the correctness of the proper Born approximation by showing the revised cross section curve to be in harmony with the cross section curve given by the perturbed stationary state method (which should yield reliable results at low impact energies). Since the calculated cross sections were found to be considerably smaller than the measured cross sections of Ribe (1951) it was suggested that captures into excited states might be comparable in importance with captures into the ground state, and it was intended to extend the treatment to include these. However Jackson and Schiff (1953), who were working on the same problem quite independently, have now published the Born approximation not only to the cross section for process (1) (for which their results agree with those obtained by us), but also to the cross sections for the processes



Their estimated total capture cross section curve is closely the same as that observed. While this removes one of the reasons for the calculations which had been planned, it is still desirable to determine the cross sections associated with captures into the states with principal quantum number three and higher so as to derive f_α and f_β , the fractions of the number of captures which give rise to the emission of the H_α and H_β lines. The labour involved in using the

full interaction potential would be extremely formidable, but fortunately Jackson and Schiff have advanced evidence that the ratio of the cross section obtained by the O.B.K. approximation to the corresponding cross section obtained by the Born approximation is almost independent of the final state. This enables some calculations based on the former approximation, which had been carried out in connection with the original programme, to be utilized. The results are presented briefly in the present paper.

§ 2. CALCULATIONS

2.1. Consider the re-arrangement collision in which an electron is transferred from an orbital around a nucleus A described by a wave function $\phi_i(\mathbf{r})$, to an orbital around a nucleus B described by a wave function $\phi_f(\mathbf{s})$, letting M_A and M_B be the masses of the nuclei and $Z_A e$ and $Z_B e$ be their charges. On the O.B.K. approximation the cross section of the process is given by

$$\left. \begin{aligned} Q(i \rightarrow f) &= \frac{8\pi^3 M^2 v_f}{h^4 v_i} \int_{-1}^{+1} |\mathcal{M}|^2 d(\cos \theta) \\ |\mathcal{M}| &= \left| \iint \phi_i(\mathbf{r}) \phi_f^*(\mathbf{s}) \{Z_A e^2 / r\} \exp[i(\boldsymbol{\alpha} \cdot \mathbf{r} + \boldsymbol{\beta} \cdot \mathbf{s})] d\mathbf{r} d\mathbf{s} \right|, \end{aligned} \right\} \dots\dots(3)$$

where M is the reduced mass of the system; v_i and v_f are the magnitudes of the initial and final velocities of relative motion; θ is the angle between unit vectors \mathbf{n}_i and \mathbf{n}_f parallel to these velocities; and

$$\boldsymbol{\alpha} = k_f \mathbf{n}_f + k_i \mathbf{n}_i M_A / (M_A + m), \quad \boldsymbol{\beta} = -k_i \mathbf{n}_i - k_f \mathbf{n}_f M_B / (M_B + m), \quad \dots\dots(4)$$

$$\text{with} \quad k_i = \frac{2\pi v_i}{h} \frac{(M_A + m) M_B}{M_A + M_B + m}, \quad k_f = \frac{2\pi v_f}{h} \frac{(M_B + m) M_A}{M_A + M_B + m}.$$

From the form of the hydrogenic wave functions, ϕ_i and ϕ_f , it is apparent that in any particular case $|\mathcal{M}|/Z_A e^2$ may be expressed as the sum of a number of terms of the type

$$\iint \frac{r^{l_1} s^{l_2} \mu_r^{l_3} \mu_s^{l_4}}{r} \exp[i(\boldsymbol{\alpha} \cdot \mathbf{r} + \boldsymbol{\beta} \cdot \mathbf{s}) - (ar + bs)/a_0] d\mathbf{r} d\mathbf{s},$$

in which μ_r and μ_s are the cosines of the angles between \mathbf{r} and $\boldsymbol{\alpha}$ and between \mathbf{s} and $\boldsymbol{\beta}$ respectively, l_1, l_2, l_3 and l_4 are positive integers or zero, a_0 is the radius of the first Bohr orbit and

$$a = Z_A / n_i, \quad b = Z_B / n_f, \quad \dots\dots(5)$$

n_i and n_f being the principal quantum numbers of the states concerned. Such terms may be evaluated by a suitable sequence of differentiations of

$$\iint r^{-1} \exp[i(\boldsymbol{\alpha} \cdot \mathbf{r} + \boldsymbol{\beta} \cdot \mathbf{s}) - (ar + bs)/a_0] d\mathbf{r} d\mathbf{s} = \frac{32\pi^2 b a_0^5}{(\alpha^2 a_0^2 + a^2)(\beta^2 a_0^2 + b^2)^2}.$$

The integration over $\cos \theta$ can readily be carried out, it being noted that at the positive limit $(\alpha^2 a_0^2 + a^2)$ and $(\beta^2 a_0^2 + b^2)$ may be taken as infinite, and that at the negative limit they may be taken as

$$x = \{p^2 + (a+b)^2\} \{p^2 + (a-b)^2\} / 4p^2 \quad \dots\dots(6)$$

where

$$p = (2\pi m v_i / h) a_0. \quad \dots\dots(7)$$

In the system in which nucleus A is stationary p^2 is m/M_B times the initial kinetic energy of nucleus B measured in units of the ionization potential of hydrogen.

The final formulae† are cumbersome and their pattern is obscured. Compactness and clarity may, however, be achieved by expressing them in terms of a set of elementary integrals: thus

$$Q(n_i l_i - n_f l_f) = \left\{ \frac{1}{p^2} C(n_i l_i - n_f l_f) \int_x^\infty F(n_i l_i - n_f l_f) dx \right\} \pi a_0^2 \dots (8)$$

with

$$C(1s-1s) = 2^8 Z_A^5 Z_B^5$$

$$C(1s-2s) = 2^5 Z_A^5 Z_B^5$$

$$C(1s-3s) = 2^8 \times 3^{-3} Z_A^5 Z_B^5$$

$$C(1s-4s) = 2^2 Z_A^5 Z_B^5$$

$$C(1s-3d) = 2^{15} \times 3^{-9} Z_A^5 Z_B^9$$

$$C(1s-4d) = Z_A^5 Z_B^9$$

$$C(2s-n_f l_f) = 2^{-3} C(1s-n_f l_f)$$

and

$$F(1s-1s) = x^{-6}$$

$$F(1s-2s) = x^{-8}(x-2b^2)^2$$

$$F(1s-3s) = x^{-10} \left(x^2 - \frac{16b^2x}{3} + \frac{16b^4}{3} \right)^2$$

$$F(1s-4s) = x^{-12}(x-2b^2)^2 \times (x^2 - 8b^2x + 8b^4)^2$$

$$F(1s-3d) = x^{-10}(x-b^2)^2$$

$$F(1s-4d) = x^{-12}(x-b^2)^2(x-2b^2)^2$$

$$F(2s-n_f l_f) = x^{-2}(x-2a^2)^2 F(1s-n_f l_f)$$

$$C(1s-2p) = 2^5 Z_A^5 Z_B^7$$

$$C(1s-3p) = 2^{13} \times 3^{-6} Z_A^5 Z_B^7$$

$$C(1s-4p) = 5 Z_A^5 Z_B^7$$

$$C(1s-4f) = 2^{-2} \times 5^{-1} Z_A^5 Z_B^{11}$$

$$C(2p-n_f l_f) = 2^{-3} \times 3^{-1} Z_A^2 C(1s-n_f l_f);$$

$$F(1s-2p) = x^{-8}(x-b^2)$$

$$F(1s-3p) = x^{-10}(x-b^2)(x-2b^2)^2$$

$$F(1s-4p) = x^{-12}(x-b^2) \left(x^2 - \frac{24b^2x}{5} + \frac{24b^4}{5} \right)^2$$

$$F(1s-4f) = x^{-12}(x-b^2)^3$$

$$F(2p-n_f l_f) = x^{-2}(x-a^2) F(1s-n_f l_f).$$

It should be noted that a and b are as defined in (5) so that their values depend on the principal quantum numbers of the connected states.

For collisions between normal hydrogen atoms and protons the Jackson-Schiff correction factor (by which the cross sections given by the formulae based on the O.B.K. approximation must be multiplied) is

$$\left\{ \frac{1}{192} (127 + 56p^{-2} + 32p^{-4}) - \frac{(\tan^{-1} p/2)}{48p} (83 + 60p^{-2} + 32p^{-4}) + \frac{(\tan^{-1} p/2)^2}{24p^2} (31 + 32p^{-2} + 16p^{-4}) \right\}. \dots (9)$$

2.2. The $H-H^+$ electron-capture cross sections were computed from the combination of (8) and (9) for a wide range of impact energies. The results are displayed in the table, a log-log form of presentation being adopted. As can be seen the cross section associated with the resonance $1s-1s$ transition, which is of course the largest, falls off monotonically with increasing impact

† The formula for $Q(1s-1s)$ was first derived by Brinkman and Kramers (1930), and that for $Q(1s-2p)$ by Saha and Basu (1945).

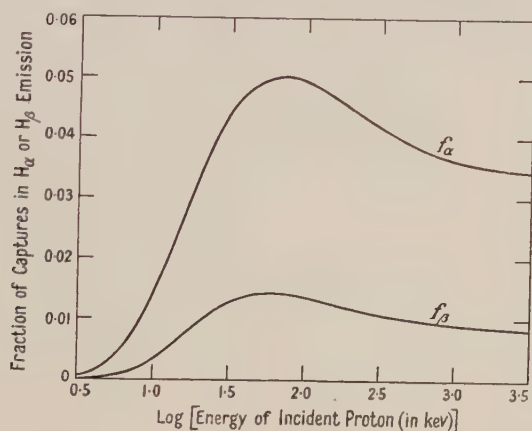
energy whereas the other cross sections pass through maxima at impact energies of some 10 to 20 kev. For a given l_f the cross sections are decreasing functions of n_f^i ; and for a given n_f they are decreasing functions of l_f except for impact energies between about 0.5 and 100 kev where the optically allowed s—p transitions are the most probable.

Electron Exchange between Normal Hydrogen Atoms and Protons

log (capture cross section in units of πa_0^2)

p^{2*}	Final state	1s	2s	3s	4s	2p	3p	4p	3d	4d	4f
1.0		1.73	— 0.88	— 1.86	— 2.39	— 1.12	— 2.18	— 2.73	— 3.43	— 3.90	— 5.67
0.9		1.62	— 0.69	— 1.62	— 2.14	— 0.84	— 1.85	— 2.39	— 3.02	— 3.47	— 5.16
0.8		1.51	— 0.54	— 1.42	— 1.92	— 0.60	— 1.55	— 2.08	— 2.65	— 3.08	— 4.69
0.7		1.39	— 0.42	— 1.25	— 1.73	— 0.40	— 1.30	— 1.80	— 2.31	— 2.73	— 4.27
0.6		1.27	— 0.34	— 1.11	— 1.58	— 0.24	— 1.08	— 1.57	— 2.03	— 2.43	— 3.90
0.5		1.14	— 0.29	— 1.02	— 1.47	— 0.13	— 0.91	— 1.38	— 1.80	— 2.17	— 3.59
0.4		1.00	— 0.28	— 0.96	— 1.39	— 0.07	— 0.79	— 1.24	— 1.63	— 1.98	— 3.35
0.3		0.86	— 0.30	— 0.94	— 1.36	— 0.05	— 0.72	— 1.15	— 1.52	— 1.85	— 3.18
0.2		0.71	— 0.35	— 0.96	— 1.36	— 0.08	— 0.70	— 1.11	— 1.48	— 1.79	— 3.09
0.1		0.54	— 0.43	— 1.01	— 1.40	— 0.15	— 0.74	— 1.13	— 1.50	— 1.79	— 3.08
0.0		0.36	— 0.54	— 1.10	— 1.48	— 0.28	— 0.82	— 1.21	— 1.58	— 1.86	— 3.14
0.1		0.17	— 0.68	— 1.22	— 1.60	— 0.45	— 0.97	— 1.34	— 1.74	— 2.00	— 3.30
0.2	—	0.05	— 0.86	— 1.38	— 1.75	— 0.67	— 1.16	— 1.52	— 1.96	— 2.21	— 3.53
0.3	—	0.28	— 1.06	— 1.57	— 1.94	— 0.93	— 1.40	— 1.76	— 2.25	— 2.49	— 3.84
0.4	—	0.54	— 1.30	— 1.80	— 2.17	— 1.24	— 1.70	— 2.05	— 2.59	— 2.82	— 4.22
0.5	—	0.82	— 1.57	— 2.07	— 2.44	— 1.59	— 2.04	— 2.39	— 2.99	— 3.22	— 4.67
0.6	—	1.13	— 1.88	— 2.38	— 2.74	— 1.98	— 2.43	— 2.77	— 3.44	— 3.67	— 5.18
0.7	—	1.46	— 2.21	— 2.72	— 3.08	— 2.41	— 2.85	— 3.20	— 3.94	— 4.17	— 5.75
0.8	—	1.82	— 2.59	— 3.09	— 3.45	— 2.88	— 3.31	— 3.66	— 4.49	— 4.71	— 6.36
0.9	—	2.21	— 2.99	— 3.49	— 3.86	— 3.37	— 3.81	— 4.16	— 5.07	— 5.29	— 7.02
1.0	—	2.62	— 3.41	— 3.92	— 4.29	— 3.90	— 4.33	— 4.68	— 5.68	— 5.90	— 7.72
1.1	—	3.06	— 3.86	— 4.37	— 4.74	— 4.44	— 4.88	— 5.23	— 6.32	— 6.54	— 8.44
1.2	—	3.52	— 4.33	— 4.85	— 5.22	— 5.01	— 5.46	— 5.80	— 6.98	— 7.20	— 9.20
1.3	—	3.99	— 4.83	— 5.34	— 5.71	— 5.60	— 6.05	— 6.40	— 7.67	— 7.89	— 9.98
1.4	—	4.49	— 5.33	— 5.85	— 6.22	— 6.21	— 6.66	— 7.00	— 8.37	— 8.59	— 10.77
1.5	—	5.00	— 5.85	— 6.37	— 6.74	— 6.83	— 7.28	— 7.63	— 9.09	— 9.31	— 11.58
1.6	—	5.52	— 6.38	— 6.90	— 7.28	— 7.46	— 7.91	— 8.26	— 9.82	— 10.04	— 12.41
1.7	—	6.06	— 6.93	— 7.45	— 7.82	— 8.10	— 8.55	— 8.90	— 10.56	— 10.78	— 13.25
1.8	—	6.60	— 7.48	— 8.00	— 8.37	— 8.75	— 9.20	— 9.55	— 11.31	— 11.53	— 14.09
1.9	—	7.15	— 8.03	— 8.56	— 8.93	— 9.41	— 9.86	— 10.21	— 12.06	— 12.28	— 14.95
2.0	—	7.71	— 8.60	— 9.12	— 9.50	— 10.08	— 10.53	— 10.88	— 12.83	— 13.05	— 15.81
2.1	—	8.28	— 9.17	— 9.69	— 10.07	— 10.74	— 11.20	— 11.55	— 13.60	— 13.82	— 16.68
2.2	—	8.85	— 9.74	— 10.27	— 10.64	— 11.42	— 11.87	— 12.22	— 14.37	— 14.59	— 17.55
2.3	—	9.42	— 10.32	— 10.85	— 11.22	— 12.10	— 12.55	— 12.90	— 15.15	— 15.37	— 18.43
2.4	—	10.00	— 10.90	— 11.43	— 11.80	— 12.78	— 13.23	— 13.58	— 15.93	— 16.15	— 19.31
2.5	—	10.58	— 11.48	— 12.01	— 12.38	— 13.46	— 13.91	— 14.26	— 16.71	— 16.93	— 20.19

* The energy of the incident proton is $24.97 p^2$ kev.



Since the relevant Einstein spontaneous emission coefficients are known (cf. Condon and Shortley 1935), and since the cross sections associated with transitions into states with $n_f \geq 5$ can be estimated with sufficient accuracy by extrapolation, it is a simple task to calculate the fractions of the captures yielding the H_α and H_β lines, either directly or following downward cascading. The figure shows these two fractions, f_α and f_β , as functions of the logarithm of the energy of the incident proton. It will be observed that their maximum values are only about 0.050 and 0.015 respectively. Electron capture by protons entering the Earth's upper atmosphere is also likely to be a very inefficient source of the Balmer series. This adds to the significance of the fact that not only do the H_α and H_β lines appear in the spectra of aurorae but so too does the weaker H_γ line (Vegard 1940, Gartlein 1950, Meinel 1951), for these features could scarcely be as prominent as they sometimes are if protons did not form a major part of the incoming corpuscular stream.

REFERENCES

- BATES, D. R., and DALGARNO, A., 1952, *Proc. Phys. Soc. A*, **65**, 919.
BRINKMAN, H. C., and KRAMERS, H. A., 1930, *Proc. Acad. Sci., Amsterdam*, **33**, 973.
CONDON, E. U., and SHORTLEY, G. H., 1935, *The Theory of Atomic Spectra* (Cambridge : University Press).
DALGARNO, A., and YADAV, H. N., 1953, *Proc. Phys. Soc. A*, **66**, 173.
GARTLEIN, C. W., 1950, *Trans. Amer. Geophys. Union*, **31**, 18.
JACKSON, J. D., and SCHIFF, H., 1953, *Phys. Rev.*, **89**, 359.
MEINEL, A. B., 1951, *Reports on Progress in Physics*, **14**, 121 (London : Physical Society).
OPPENHEIMER, J. R., 1928, *Phys. Rev.*, **31**, 349.
RIBE, F., 1951, *Phys. Rev.*, **83**, 1217.
SAHA, M. N., and BASU, D., 1945, *Indian J. Phys.*, **19**, 121.
VEGARD, L., 1940, *Geofys. Publ., Oslo*, **12**, No. 14.

Studies in Intermediate Coupling: the Energy States of ^{13}C and ^{13}N belonging to the Configuration $1p^9$

By A. M. LANE*

Department of Mathematical Physics, University of Birmingham

MS. received 6th July 1953

Abstract. The nuclear shell-model and the theory of fractional parentage are used to derive theoretical formulae for certain observable features of nuclear energy levels that are not expected to be sensitive to the choice of the nucleon interaction potential. These features comprise: (i) the magnetic dipole transition strengths, (ii) the magnetic moments, (iii) the reduced widths for nucleon emission. Intermediate coupling, besides extreme L - S and extreme j - j coupling, is discussed, and the resulting formulae are applied to the low-lying odd-parity states of ^{13}C and ^{13}N in an attempt to explain all the relevant experimental data. It is found that the extreme coupling models give generally poor agreement of theory with experiment. On the other hand, all the data are consistent with an intermediate coupling model and quite a small range of values of the intermediate coupling parameter.

§ 1. INTRODUCTION

ATTEMPTS to explain certain features of the energy states of light nuclei by use of the nuclear shell-model have recently been extensively reviewed (Inglis 1953). A general conclusion of this review is that neither of the extreme types of perturbing coupling forces (L - S or j - j), experienced by nucleons moving in their orbits, can give an adequate explanation of all the experimental data that are discussed. For instance, for nuclei belonging to the nuclear $1p$ -shell, the L - S coupling scheme appears to give a better account of nuclei in the lower half of the shell (corresponding to mass-number A lying between 4 and 10), whereas the j - j scheme seems to be the better one in the upper half (A between 11 and 16). The situation is not a simple one, however, and there is no steady increase in preference for j - j coupling with increasing A . This is especially so for nuclei in the region of $A=12$ (i.e. with 8 nucleons in the $1p$ -shell). The spin, $\frac{3}{2}^-$, of the ground state of ^{11}B suggests that j - j coupling forces are beginning to predominate already with only seven $1p$ -nucleons present (the L - S model predicts a spin $\frac{1}{2}$). On the other hand, the fairly equal spacing of the lower excited levels of ^{12}C is only consistent with L - S coupling (the j - j model predicts a large gap above the ground state, followed by relatively closely spaced levels).

The obvious way to make further progress towards clarifying the situation is to consider the shell-model with intermediate coupling, i.e. a shell-model in which the central forces between the nucleons (giving rise to L - S coupling) and the spin-orbit forces (giving rise to j - j coupling) are of comparable strengths.

* On leave of absence from the Cavendish Laboratory, Cambridge.

Such considerations lead to calculations that are always more unpleasant and complicated than those encountered with an extreme coupling model. The reason is that there is no simple classification of states in intermediate coupling to correspond to those existing for $L-S$ or $j-j$ coupling. Consequently we must work with a complete set of wave functions of one extreme coupling scheme, and evaluate the interaction matrix of the other coupling scheme in this complete set. Diagonalization of the total interaction matrix then determines the eigenfunctions of the intermediate coupling situation as a superposition of eigenfunctions of the complete set. For large complete sets (say with more than six components), these calculations may become lengthy and tedious.

In the previously mentioned review (Inglis 1953) the intermediate coupling situation was investigated mainly by the approximate method of interpolation between the two extreme modes of coupling (for which exact calculations were done) with smoothly drawn curves. The main interest in these investigations lay in the ordering and spacing of nuclear energy levels. Since theoretical predictions about these depend not only upon the usual shell-model assumptions, but also directly upon the (unknown) detailed nature of nuclear interactions, exact calculations would not seem to be worth the effort in this case. Nevertheless it is significant that, when this approximate method is applied to the low states of ^{10}B , it makes it uncertain where the 3^+ level should be depressed below the 1^+ level in the intermediate region. Exact calculations, on the other hand (Zeldes 1953), show that the 3^+ level does, in fact, come lower (in agreement with the observed spin 3^+ of ^{10}B) when the two types of coupling forces are of comparable strengths.

In the present investigation we restrict ourselves to examining observed magnitudes that are not expected to depend very strongly on the detailed nature of the interaction forces, but only upon the mode of coupling. Such magnitudes should thus provide a good test for the predominant mode of perturbing coupling forces (always provided that the basic shell-model concepts are themselves correct). Consequently an exact treatment of the intermediate coupling situation is desirable. The magnitudes to be discussed are: (i) magnetic dipole transition strengths, (ii) magnetic dipole moments, (iii) reduced level-widths for nuclear emission.

Magnetic dipole (M1) transition strengths have been listed for light nuclei (Wilkinson 1953). It is observed in this compilation that electric dipole (E1) transition strengths show much less fluctuation from their mean value than do the M1 cases. This would follow from the fact that E1 transitions must lead to a change in configuration involving one nucleon because a change in parity is implied, whereas M1 transitions usually take place between states of the same configuration (at least for light nuclei). In the former case the transition is more likely to be approximately a one-particle one (for example, for nuclei of the $1p$ -shell, $(1p)^n 2s \rightarrow (1p)^{n+1}$ or $(1p)^n 1d \rightarrow (1p)^{n+1}$). In the latter case the transition generally involves many equivalent particles and so a severe rearrangement of the nuclear state may be implied, in which case the transition strength will be strongly inhibited. It is clear, then, that M1 transition strengths should furnish much more delicate tests of the finer features of the shell-model (such as the mode of coupling) than the E1 transitions. In §2 we derive theoretical expressions for the magnitudes of the M1 transition probabilities in terms of the various coupling schemes.

Magnetic moments have long been examined in the light of the shell-model but not always correctly. It has been shown (Flowers 1952) that the Schmidt model, which attributes all the magnetic moment of an odd-even nucleus to the odd nucleon, is not implied by a 'good' shell-model in which the nuclear states are correctly constructed. Just as with M1 transition strengths (to which they are closely related), magnetic moments should be a sensitive guide to the mode of coupling existing in a nucleus. In § 3 expressions are derived for the magnetic moment by simple specialization of those for the transition strengths.

Reduced widths for nucleon emission have rarely been used as evidence for the shell-model. In fact, it is the (small) size of the reduced widths of energy levels found in thermal neutron capture and scattering that has inspired the opposing 'compound-nucleus' model. It is very important to note that 'small' reduced widths for nucleon emission do not, in themselves, imply a breakdown of any shell-model ideas or necessarily lead to a picture of a compound nucleus in which the motion of the nucleons is exceedingly complex with all degrees of freedom excited. Just as M1 transition strengths can be severely reduced for transitions between states of the same configuration so can the reduced widths for nucleon emission of the type $l^n \rightarrow l^{n-1} + l$ be diminished or even reduced to zero in certain circumstances. In § 4 these remarks are discussed after presenting formulae for the reduced nucleon widths in the various coupling schemes.

The remainder of this paper is devoted to a close analysis of the low odd-parity states of ^{13}C and ^{13}N in the light of the general coupling model developed in the earlier sections.

§ 2. THE STRENGTH OF MAGNETIC DIPOLE TRANSITIONS

The width of a nuclear energy level of spin J for an M1 transition to another level of spin J' (where J' must be $J-1$, J or $J+1$ of course) and energy E below the first level, can be written in the form

$$\Gamma = \frac{e^2 E^3}{3\mu^2 \hbar c^5} \sum_{M'} \langle JM | \mathcal{M}_{M-M'} | J'M' \rangle^2 \quad \dots\dots(1)$$

where e , \hbar , c have their usual meaning, μ is the reduced nucleon mass, M is the (fixed) component of J , M' is the (variable) component of J' , and $\mathcal{M}_{M-M'}$ is the magnetic dipole operator in nuclear magnetons for a change in magnetic quantum number of $M-M'$.

There are, at most, three terms in the sum over M' . To evaluate the matrix elements separately as they stand is an unnecessary labour. Instead we shall introduce 'reduced matrix elements', which do not depend on magnetic quantum numbers. For any vector or tensor operator we can separate off the dependence of a matrix element on magnetic quantum numbers (spatial directions) as follows:

$$\langle JM | \mathcal{M}_{M-M'} | J'M' \rangle = C_{M'(M-M')M}^{J'} \langle J | \mathcal{M} | J' \rangle \quad \dots\dots(2)$$

where the second quantity is the reduced matrix element (into which a factor $(2J+1)^{1/2}$ that is usually written explicitly is incorporated for convenience) and the first quantity is a Wigner vector-coupling coefficient. In the following sections extensive use will be made of the properties of the coefficients and also

of the related Racah functions. All the relevant properties, along with tables of Racah functions, have been conveniently compiled recently* (Biedenharn 1952).

Substitution of (2) into (1) immediately gives

$$\Gamma = \frac{e^2 E^3}{3\mu^2 \hbar c^5} \langle J | \mathcal{M} | J' \rangle^2. \quad \dots\dots(3)$$

The problem is now to find expressions for the reduced matrix element $\langle J | \mathcal{M} | J' \rangle$. First we rewrite (2) in the form

$$\langle J | \mathcal{M} | J' \rangle = \frac{3}{2J+1} \sum_M C_{M0M}^{J'1J} \langle JM | \mathcal{M}_0 | J'M \rangle \quad \dots\dots(4)$$

where \mathcal{M}_0 is the operator for zero change in magnetic quantum number in nuclear magnetons, and can be written as

$$\mathcal{M}_0 = \sum_{\text{all nucleons}} \{ [g_n(\frac{1}{2} + m_t) + g_p(\frac{1}{2} - m_t)] \sigma_z + (\frac{1}{2} - m_t) l_z \}. \quad \dots\dots(5)$$

In (5) m_t is the isotopic spin component ($+\frac{1}{2}$ for a neutron, $-\frac{1}{2}$ for a proton), g_n and g_p are the gyromagnetic ratios for a neutron and a proton in Bohr magnetons (-3.83 and $+5.58$ respectively), and σ_z , l_z are the components of angular momentum operators (in units of \hbar) for intrinsic spin and orbital motion respectively.

In order to express the matrix elements of \mathcal{M}_0 we must assume some kind of nuclear model. We shall consider a j - j coupling, an L - S coupling and an intermediate coupling model in that order.

(i) j - j Coupling

\mathcal{M}_0 is a single particle operator, and so, in order to find its matrix elements with a shell-model, we use the fractional parentage coefficients (Flowers and Edmonds 1952) for expressing a given j - j coupling state $\langle JT[\lambda]MM_T |$ of n nucleons in terms of the parent states $\langle J_p T_p[\lambda_p]M_p M_{T_p} |$ of $n-1$ nucleons vector-coupled up to the odd nucleon $\langle jm_j | \langle tm_t |$:

$$\begin{aligned} \langle JT[\lambda]MM_T | &= \sum_{J_p T_p \lambda_p} \langle JT[\lambda] | \rangle J_p T_p [\lambda_p] \rangle \\ &\times \left(\sum_{M_{T_p} + m_t} C^{T_p 1 T} \langle T_p M_{T_p} | \langle tm_t | \right) \left(\sum_{M_p + m_j} C^{J_p 1 J} \langle J_p M_p | \langle jm_j | \right). \quad \dots\dots(6) \end{aligned}$$

By specifying the j -value of the odd nucleon we have implicitly assumed that we are only concerned with the nucleons in the last (unfilled) shell, i.e. with the configuration j^n , for some value of $n \leq 2(2j+1)$. Using (5) and (6), we have

$$\begin{aligned} \langle JM | \mathcal{M}_0 | J'M \rangle &= n \sum_{J_p T_p \lambda_p} \langle JT | \rangle J_p T_p \langle J'T' | \rangle J_p T_p \\ &\times \{ [g_n(\frac{1}{2} + \mathcal{T}_p) + g_p(\frac{1}{2} - \mathcal{T}_p)] \mathcal{S}_p + (\frac{1}{2} - \mathcal{T}_p) \mathcal{L}_p \} \quad \dots\dots(7) \\ \text{where} \quad &\left\{ \begin{aligned} \mathcal{T}_p &= \sum C^{T_p 1 T} C^{T_p 1 T'} m_t \\ \mathcal{S}_p &= \sum C^{J_p 1 J} C^{J_p 1 J'} (C^{1\sigma j})^2 m_\sigma \\ \mathcal{L}_p &= \sum C^{J_p 1 J} C^{J_p 1 J'} (C^{1\sigma j})^2 m_l \end{aligned} \right. \end{aligned}$$

In order to economize in notation the following conventions have been adopted: (i) the symmetry symbols $[\lambda]$ are omitted in the fractional parentage coefficients,

* Attention should be drawn to an error in formula 1 on page 5. In the summation the magnetic quantum number of c should be held constant, and not that of d , as implied by the notation.

(ii) a 'bare' summation sign preceding Wigner coefficients and the omission of the magnetic quantum numbers of these coefficients implies summation over all magnetic quantum numbers, except that of J or T as the case may be. Insertion of (7) into (4) leads, after use of the properties of Wigner coefficients and the relations between Wigner coefficients and Racah functions (Biedenharn 1952), to the final expression for the reduced matrix elements:

$$\begin{aligned} \langle J(j'') | \mathcal{H} | J'(j'') \rangle \\ = (-)^{j+1} 3n \left(\frac{2J'+1}{j(j+1)(2j+1)} \right)^{1/2} \sum_{J_p T_p \lambda_p} \langle JT | \{ J_p T_p \} \langle J' T' | \{ J_p T_p \} \rangle \\ \times (-)^{J_p} W(JJ'jj, 1J_p) \{ [g_n(\frac{1}{2} + \mathcal{T}_p) + g_p(\frac{1}{2} - \mathcal{T}_p)] \mathcal{S}'_p + (\frac{1}{2} - \mathcal{T}_p) \mathcal{L}'_p \} \quad \dots (8) \end{aligned}$$

where

$$\begin{cases} \mathcal{S}'_p = \sum_{m_\sigma m_j} m_j m_\sigma (C_{m_p m_\sigma m_j}^{l\sigma j})^2 \\ \mathcal{L}'_p = \sum_{m_l m_j} m_j m_l (C_{m_l m_\sigma m_j}^{l\sigma j})^2. \end{cases}$$

(ii) L - S Coupling

The method of derivation of the expression for the reduced matrix elements is very similar to that used for j - j coupling. We use a fractional parentage relation corresponding to (6) (Jahn and van Wieringen 1951). This relates the L - S state $\langle LST[z] M_L M_S M_T |$ to its parent states $\langle L_p S_p T_p [\alpha_p] M_{L_p} M_{S_p} M_{T_p} |$ and the single particle states $\langle l m_l | \langle \sigma m_\sigma | \langle t m_t |$ of a nucleon in the unfilled l -shell being considered:

$$\begin{aligned} \langle LST[z] M_L M_S M_T | = \sum_{L_p S_p T_p \alpha_p} \langle LST[z] | \{ L_p S_p T_p [\alpha_p] \} \left(\sum_{M_{T_p} + m_t} C_{T_p T' T}^{T_p T' T} \langle T_p M_{T_p} | \langle t m_t | \right) \\ \times (\sum C_{L_p L' L}^{L_p L' L} C_{S_p S' S}^{S_p S' S} \langle L_p M_{L_p} | \langle l m_l | \langle S_p M_{S_p} | \langle \sigma m_\sigma |). \quad \dots (9) \end{aligned}$$

Use of relation (4) and the introduction of Racah functions enables the reduced matrix element to be written

$$\begin{aligned} \langle J(LS) | \mathcal{H} | J'(L'S') \rangle = (-)^{L-J'-\sigma-S-S'} 3n \delta_{LL'} \left(\frac{(2J'+1)(2S+1)(2S'+1)}{\sigma(\sigma+1)(2\sigma+1)} \right)^{1/2} \\ \times W(JJ'SS', 1L) \sum_{T_p} \left[\frac{g_n + g_p}{2} + (g_n - g_p) \mathcal{T}_p \right] \\ \times \mathcal{S}''_p \sum_{S_p \alpha_p} (-)^{S_p} \langle LST | \{ L_p S_p T_p \} \langle L'S'T' | \{ L_p S_p T_p \} \rangle \\ \times W(SS'\sigma\sigma, 1S_p) \\ + (-)^{S-J-L'} 3n \delta_{SS'} \left(\frac{(2J'+1)(2L+1)(2L'+1)}{l(l+1)(2l+1)} \right)^{1/2} \\ \times W(JJ'LL', 1S) \sum_{T_p} (\frac{1}{2} - \mathcal{T}_p) \\ \times \mathcal{L}''_p \sum_{L_p \alpha_p} (-)^{L_p} \langle LST | \{ L_p S_p T_p \} \langle L'S'T' | \{ L_p S_p T_p \} \rangle \\ \times W(LL'LL, 1L_p) \quad \dots (10) \end{aligned}$$

where

$$\begin{cases} \mathcal{S}''_p = \sum_{m_\sigma} m_\sigma^2 = \frac{1}{2} \\ \mathcal{L}''_p = \sum_{m_l} m_l^2 \end{cases}$$

and convention (i) of eqn. (7) has been used for the symmetry symbols $[\alpha]$.

(iii) *Intermediate Coupling*

When the intermediate coupling situation exists, we shall express the eigenfunction $\langle JM|$ in terms of the complete set of L - S eigenfunctions:

$$\begin{aligned}\langle JM| &= \sum_{LS\alpha} \langle J||J(LS)\rangle \langle J(LS)M| \\ &= \sum_{LS\alpha} \langle J||J(LS)\rangle \left(\sum_{M_L+M_S} C_{M_L M_S}^{L S J} \langle LM_L| \langle SM_S| \right) \dots\dots (11)\end{aligned}$$

where $\langle J||J(LS)\rangle$ are the transformation coefficients. The expression for the reduced matrix elements is then simply

$$\langle J|\mathcal{M}|J'\rangle = \sum_{\substack{LS\alpha \\ L'S'\alpha}} \langle J||J(LS)\rangle \langle J'||J'(L'S')\rangle \langle J(LS)|\mathcal{M}|J'(L'S')\rangle. \dots\dots (12)$$

In all three modes of coupling it is clear that the magnitude of the reduced matrix element depends on the number of 'parents' that the two states have in common. For two states of the same configuration that are otherwise quite different (belonging to different symmetries for instance) there may be very few or even no common parent-states. In this sense we may say that the M1 transition probability may be greatly lessened if a severe reorganization of the nucleon state is implied.

One feature of magnetic dipole transitions and moments is that the radial wave function (which will depend on the precise type of potential well assumed in the shell-model) does not enter the theoretical expressions (and neither does the nuclear size), and so there is no source of uncertainty in this respect.

§ 3. MAGNETIC MOMENTS

The formulae for magnetic moment in the various coupling schemes follow immediately from the above formulae for the M1 matrix elements. By definition, the magnetic moment of a state is $\langle JJ|\mathcal{M}_0|JJ\rangle$ nuclear magnetons and so, from (2), it is equal to

$$C_{J0J}^{JJ} \langle J|\mathcal{M}|J\rangle = \frac{J}{\{J(J+1)\}^{1/2}} \langle J|\mathcal{M}|J\rangle. \dots\dots (13)$$

Equations (8), (10) and (12) give the necessary expressions for $\langle J|\mathcal{M}|J\rangle$ on putting $J=J'$.

§ 4. REDUCED WIDTHS FOR NUCLEON EMISSION

Given any nuclear state $\langle JM| = \Psi^{JM}$ (the latter notation will be rather more convenient for the present), we can label all possible modes of two-particle disintegration by the symbol (s, l) , where s identifies the intrinsic nature of the two particles and also their combined spin j_s , and lh is their relative orbital angular momentum. To each such mode of disintegration there corresponds an 'escape channel' in the configuration space of all the nucleons, and a channel surface Σ_{sl} defined for each mode (s, l) by specifying that the separation distance r_s of the pair is equal to their interaction radius a_s .

The reduced width of the state for the disintegration mode (s, l) is a measure of the *intrinsic* probability of the state splitting into the pair s with relative orbital angular momentum lh , i.e. it is proportional to the square amplitude of the wave function Ψ^{JM} on the channel surface Σ_{sl} . To be more explicit, the state Ψ^{JM} can be expanded upon the 'nuclear surface' Σ (the sum of all surfaces Σ_{sl})

in terms of the normalized states Φ_{sl}^{JM} of the product pairs (s, l) and certain coefficients β_{sl} :

$$\Psi^{JM}(\Sigma) = \sum_{sl} \beta_{sl} \Phi_{sl}^{JM}. \quad \dots\dots(14)$$

The function Φ_{sl}^{JM} is actually the product of the internal wave functions of the pair, coupled up to give a spin j_s which is, in turn, coupled to l to give a resulting spin J :

$$\Phi_{sl}^{JM} = \sum C^{j_s l J} \langle j_s m_s | \langle l m_l | \quad \dots\dots(15)$$

where again the bare summation sign means summing over all magnetic quantum numbers except that of J . Provided that Ψ^{JM} is normalized to unity over the interior of the nucleus, the reduced width for process (s, l) is simply $\hbar^2 \beta_{sl}^2 / 2M_s$, where M_s is the reduced mass of the pair s . It is usually denoted by the symbol γ_{sl}^2 . Equation (14) may be rewritten as

$$\beta_{sl} = \int_{\Sigma_{sl}} \Psi^{JM} \Phi_{sl}^{JM}, \quad \dots\dots(16)$$

and this is the formula we use to find expressions for the reduced widths for nucleon emission.

§5. j - j COUPLING

In extreme j - j coupling the state Ψ^{JM} of n equivalent nucleons can be decomposed into its 'parental' states of $n-1$ equivalent nucleons vector-coupled to the odd nucleon as in (6). The states $\langle j_s m_s |$ of a product pair s can be written as

$$\langle j_s m_s | = \sum C^{J_0 \sigma J} \langle J_0 M_0 | \langle \sigma m_\sigma | \quad \dots\dots(17)$$

where the bare summation sign has the same meaning as in (7) and σ, J_0 are the spins of the component particles (nucleon and residual nucleus respectively). Insertion of (17) into (15) gives

$$\Phi_{sl}^{JM} = \sum C^{j_s l J} C^{J_0 \sigma j_s} C^{l \sigma j} \langle J_0 M_0 | \langle j m_j | \quad \dots\dots(18)$$

where l and σ have been vector-coupled to give j . Using the orthogonality of the parental states, eqn. (16) gives:

$$\beta_{nl} = n^{1/2} \chi_l(a) \langle JT | \rangle J_0 T_0 \rangle \sum C^{J_0 j J} C^{j_n l J} C^{J_0 \sigma j_n} C^{o l j} \quad \dots\dots(19)$$

where the subscript n means that one of the two disintegration products is a nucleon, and the 'bare summation sign' convention is used. $\chi_l(a)$ is the radial part of Ψ^{JM} evaluated on the surface $r = a$, i.e. it is the surface value of the one-body radial wave function corresponding to the potential well $V(r)$ assumed in the shell-model (and normalized over $r \leq a$ where a is the radius of the well). The sum in (19) is, by definition, a Racah function, so

$$\beta_{nl} = n^{1/2} \chi_l(a) \langle JT | \rangle J_0 T_0 \rangle (2j+1)^{1/2} (2j_n+1)^{1/2} W(J_0 \sigma J l, j_n j). \quad \dots\dots(20)$$

There are certain sum rules for reduced widths that follow from the properties of the Racah functions and the fractional parentage coefficients. Summing the square of (20) over all possible spin combinations j_n yields

$$\sum_{j_n} \gamma_{nl}^2 = n \frac{\hbar^2}{2M_n} \chi_l^2(a) \langle JT | \rangle J_0 T_0 \rangle^2 \quad \dots\dots(21)$$

where M_n is the reduced nucleon mass. For convenience we define a dimensionless quantity x_l as $\frac{1}{2} a \chi_l^2(a)$, so that

$$\sum_{j_n} \gamma_{nl}^2 = n x_l \frac{\hbar^2}{M_n a} \langle JT | \rangle J_0 T_0 \rangle^2. \quad \dots\dots(22)$$

Further summation over all possible parent states of the configuration j^{n-1} gives

$$\sum_{j_p T_p j_p} \sum_{j_n} \gamma_{nl}^2 = n x_l \frac{\hbar^2}{M_n a}. \quad \dots\dots (23)$$

§ 6. L - S COUPLING

Just as in the case of j - j coupling, we decompose the Ψ^{JM} and Φ_{sl}^{JM} into eigenstates of the coupling mode we are considering. In L - S coupling we have, then, corresponding to (19),

$$\beta_{nl} = n^{1/2} \chi_l(a) \langle LST | \rangle L_0 S_0 T_0 \rangle (\sum C^{LSJ} C^{L_0 L} C^{S_0 S} C^{j_n l J} C^{J_0 j_n} C^{L_0 S_0 J_0}). \quad \dots\dots (24)$$

Introducing Racah functions gives

$$\beta_{nl} = n^{1/2} \chi_l(a) (-)^{j_n + L_0 - J - L} \langle LST | \rangle L_0 S_0 T_0 \rangle [(2j_n + 1)(2J_0 + 1)(2L + 1)(2S + 1)]^{1/2} \\ \times W(L_0 S_0 j_n \sigma, J_0 S) W(l L_0 J S, l j_n). \quad \dots\dots (25)$$

Summing the square over all J_0 belonging to the L - S state $\langle L_0 S_0 T_0 [\alpha_0] \rangle$, for given L_0, S_0 :

$$\sum_{J_0} \gamma_{nl}^2 = n x_l \frac{\hbar^2}{M_n a} \langle LST | \rangle L_0 S_0 T_0 \rangle^2 (2L + 1)(2j_n + 1) W^2(l L_0 J S, l j_n). \quad \dots\dots (26)$$

Summing (26) over all spin combinations j_n for given $\langle L_0 S_0 T_0 [\alpha_0] \rangle$,

$$\sum_{j_n} \sum_{J_0} \gamma_{nl}^2 = n x_l \frac{\hbar^2}{M_n a} \langle LST | \rangle L_0 S_0 T_0 \rangle^2. \quad \dots\dots (27)$$

Finally, summing over all possible parent states $\langle L_p S_p T_p [\alpha_p] \rangle$ of the configuration l^{n-1} :

$$\sum_{L_p S_p T_p} \sum_{j_p} \sum_{j_n} \gamma_{nl}^2 = n x_l \frac{\hbar^2}{M_n a}. \quad \dots\dots (28)$$

§ 7. INTERMEDIATE COUPLING

Expressing the intermediate coupling eigenfunction in the L - S representation as in (11), and denoting the β_{nl} of (25) by $\beta_{nl}(LS, L_0 S_0)$, we have for β_{nl} in intermediate coupling

$$\beta_{nl} = \sum_{\substack{LS\alpha \\ L_0 S_0 \alpha_0}} \langle J \| J(LS) \rangle \langle J_0 \| J_0(L_0 S_0) \rangle \beta_{nl}(LS, L_0 S_0). \quad \dots\dots (29)$$

The orthogonality properties of the transformation coefficients enables us to derive a sum-rule for disintegration to all possible parent states of the configuration l^{n-1} :

$$\sum_{j_p j_n} \gamma_{nl}^2 = n x_l \frac{\hbar^2}{M_n a}. \quad \dots\dots (30)$$

As a check to the correctness of the various equations for β_{nl} , we can regard j - j coupling as a special case of intermediate coupling, in which case eqn. (29) when combined with (25) must be equivalent to (20) (see Appendix I).

The terminology 'reduced width' is not an ideal one. In the first place the term 'reduced' has no connection with the sense in which it is used to describe a matrix element (see (2)). It implies, in this case, that the 'reduced width' of a mode of decay is associated with an actual energy level width for that mode, and is obtained from it by removing a factor corresponding to the penetrability of any extra-nuclear barrier (coulomb or angular momentum) that may inhibit the decay outside the nucleus. This method of extracting reduced widths from

observed level widths has been well discussed (Thomas 1952). The second objection to the terminology is that the 'reduced width' for a process need not be associated with an observed width at all. Equation (16), which defines 'reduced widths', can be applied to all processes and to all levels, whether bound or free. For energetically impossible ('bound') processes the observed widths vanish of course, but the 'reduced widths' do not. The latter are, in fact, quite independent of whether the escape channel is open or closed.

The theory of deuteron stripping reactions and its success (Butler 1951) have made it possible to determine the reduced widths for nucleon emission of bound as well as free energy levels. The stripping theory treats deuteron reactions and extra-nuclear phenomena in which a neutron or a proton is captured into the 'tail' of the final state wave function protruding beyond the range of nuclear forces. The amplitude of the wave function in this tail is determined by the reduced width of the final state for the nucleon. Consequently the absolute stripping cross section must be proportional to the reduced width of the captured nucleon in the final state, and so the measurement of these cross sections furnishes a valuable method of determining the values of reduced widths. This method will be applied and related to the standard method for free levels in a later section.

In the formulae for the reduced widths that we have given, the only indefinite quantity is the dimensionless factor x_l . As defined, x_l depends upon the value of l , the shape of the potential well in the shell-model, and the external potential. The dependence upon the latter is an indirect one and is due to the fact that the internal radial wave function $\chi_l(r)$ must join on to the appropriate external wave function at the nuclear boundary $r=a$. This can be expressed by defining the logarithmic derivatives of the two wave functions at the boundary, and equating them. Define, then, a dimensionless quantity f_l as $[r(d\chi_l/dr)/\chi_l]_{r=a}$ for the internal wave function and a similar quantity g_l for the external wave function. For bound states g_l corresponds to the unique bound state solution that goes to zero for large r . For free states (resonance levels) it corresponds to the real part of the solution for outgoing waves (Thomas 1952). In all cases of physical interest g_l is negative or zero. It is zero for free S-neutron waves, and is most negative for heavily bound processes, in which it may attain a value of -3 or so.

In order to have some idea of the magnitude of f_l (and so of x_l) we consider the instance of a square well. The wave functions inside the nucleus are then Bessel functions of argument $\rho = \kappa r$, where κ is the wave number corresponding to energy E measured from the base of the well. The formulae for the wave functions, for f_l and for x_l as functions of ρ for $l=0, 1, 2$ are given in table 1.

Table 1

l	Radial wave function (not normalized)		x_l
0	$\sin \rho$	$\rho \cot \rho$	$\frac{1}{\rho} \cot \rho - \operatorname{cosec}^2 \rho$
1	$\frac{\sin \rho}{\rho} - \cos \rho$	$\frac{\rho^2}{1 - \rho \cot \rho} - 1$	$\frac{2 - \rho(\cot \rho + \rho \operatorname{cosec}^2 \rho)}{(1 - \rho \cot \rho)^2}$
2	$\left(\frac{3}{\rho^2} - 1\right) \sin \rho - \frac{3}{\rho} \cos \rho$	$\frac{\rho^4}{3(3 - \rho^2 - 3\rho \cot \rho)} + \frac{\rho^2}{3} - 2$	$\frac{6(1 - \rho \cot \rho)^2 + \rho^3(\cot \rho - \rho \operatorname{cosec}^2 \rho)}{(3 - \rho^2 - 3\rho \cot \rho)^2}$

The expressions for x_l are derived from the equation (Thomas 1952)

$$x_l^{-1} = \frac{1}{\rho} \frac{df_l}{d\rho}. \quad \dots\dots(31)$$

In figs. 1 and 2 the quantities f_l and x_l are plotted as functions of ρ . Imposing the condition $0 \geq f_l \geq -3$ (which follows when the logarithmic derivatives are equated at the boundary) restricts the ranges of values of x_l considerably. These ranges are indicated by heavy lines in fig. 2, and we see that the mean values of x_l are 0.8 for 1s and 2s waves, 1.0 for 1p waves, and 1.2 for 1d waves. The possible variations are about 50%. Consequently, if we always assumed $x_l=1$, the error so introduced would probably not be larger than the uncertainty in the experimental value of the reduced width due to the ambiguous choice of a nuclear radius (to which the penetrability factor is sensitive). Since the experimental values of the reduced widths (for nucleon emission) of different levels in the same nucleus can vary by a factor of thirty or more, this error is not usually serious.

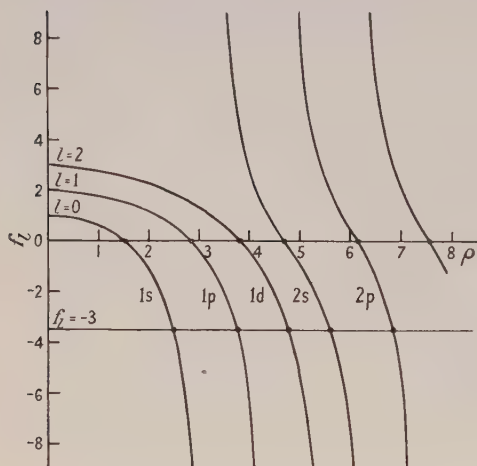


Fig. 1. f_l as a function of ρ .

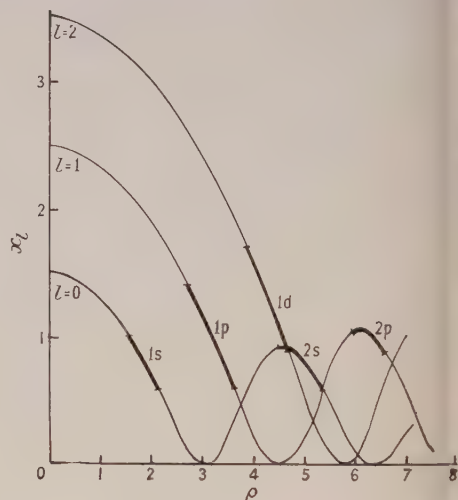


Fig. 2. x_l as a function of ρ for $l=0, 1, 2$.

So far no mention has been made of the effect upon the values of x_l of varying the well shape. Trial numerical calculations indicate that the above remarks hold for any reasonable shape and that x_l is fairly insensitive to such changes. Unfortunately it seems impossible to handle analytically any type of well other than a square well over a continuous range of energy values, and so this statement cannot be made more specific.

§ 8. ^{13}C AND ^{13}N AND THE EXTREME COUPLING MODELS

The isobaric pair of nuclei ^{13}C and ^{13}N should be especially useful for explaining the mode of coupling of nucleons in nuclei in the region $A=12$. Since ^{12}C is a closed-shell nucleus in $j-j$ coupling, but is open in $L-S$ coupling, the addition of an extra 1p nucleon will give rise to different situations in the two instances, and this will be reflected in the values of certain experimental magnitudes of ^{13}C and ^{13}N . The level schemes of the two nuclei are given in fig. 3. Up to 4 Mev excitation there are two odd-parity states (configuration $1p^9$ on the shell-model) and two even-parity ones ($1p^8 2s$ and $1p^8 1d$). Throughout

the following discussion we shall take the correspondence of mirror levels for granted. The only levels that will be examined in detail are odd-parity ones, i.e. the ground and second-excited states.

The even-parity first-excited level has already been investigated (Thomas 1952). This level has the configuration $1p^8 2s$, and so the disintegration of the level into the ground state of ^{12}C plus an S-wave nucleon is essentially a one-particle process in which the remaining eight nucleons do not participate. The reduced width for the process will be the 'one-particle reduced width' $x_0 \hbar^2 / M_n a$, and no insight will be afforded into the mode of coupling inside the eight $1p$ nucleons. Unpublished calculations by the author show that all the observable features of the interaction of an S-wave nucleon with ^{12}C can be represented by a simple potential well model in which the nucleus ^{12}C is replaced by a square well. (There was some indication in these calculations that a rounded well would give a rather better account of the data. This is also suggested by the fact that the $2s$ level comes below the $1d$ levels in ^{13}C and ^{13}N , in contrast to the level ordering for a square well.)

The two odd-parity levels have the configuration $1p^9$ (at least in L - S coupling), and any disintegration of the levels must be considered as a process in which all nine (equivalent) particles are concerned. The values of the reduced widths will thus be sensitive to the mode of coupling between the nine particles. The

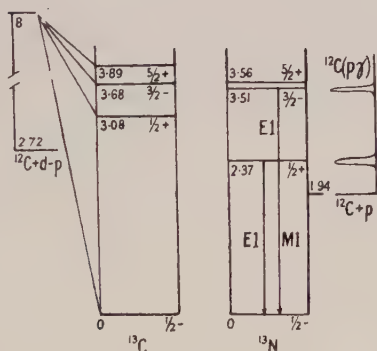


Fig. 3. The low-lying states of the mirror nuclei ^{13}C and ^{13}N .

situation with regard to break-up of the even- and odd-parity levels is very similar to that found in electric and magnetic dipole transitions respectively, as discussed in the Introduction.

There are four available data on the odd-parity levels:

- (i) the magnetic dipole moment of ^{13}C (Poss 1949),
- (ii) the magnetic dipole transition width between the two odd-parity levels in ^{13}N (Seagrave 1951),
- (iii) the reduced width of the excited state in ^{13}N (Jackson and Galonsky 1953),
- (iv) the reduced width of the ground state (Thomas 1952, Holt and Marsham 1953 b).

In order to predict theoretical values for these magnitudes with the extreme coupling models, we must first identify the levels involved in the two coupling schemes. The two levels in ^{13}C and ^{13}N must both be ^{22}P in L - S coupling, whereas, in j - j coupling, the lower one is $p_{3/2}^8 p_{1/2}$ and the upper one $p_{3/2}^7 p_{1/2}^2$.

The ground state of ^{12}C is ^{11}S in L - S coupling, and $p_{3/2}^8$ in j - j coupling. In j - j coupling it is clear from elementary considerations that the reduced width of the excited state of ^{13}C and ^{13}N is zero for the production of ^{12}C in its ground state. On the other hand the reduced width of the ground state of ^{13}C and ^{13}N in j - j coupling has the uninhibited one-particle value x_1 (in units of $\hbar^2/M_n a$). The value of the M1 transition width in j - j coupling is found to be zero by treating j - j coupling as a special case of intermediate coupling (see later). Presumably this vanishing is due to the operation of some symmetry selection rule (Gamba *et al.* 1952).

In table 2 the experimental data are listed together with the theoretical values.

Table 2

Type of data	Experimental value	Predicted value	
		from L - S model	from j - j model
Magnetic moment of ^{13}C (nucl. magnetons)	0.70	1.08	0.64
Width of the transition (ev)	0.70	1.34	0
Reduced width, excited state (units of $\hbar^2/M_n a$)	0.047	$0.33x_1$	0
Reduced width, ground state (units of $\hbar^2/M_n a$)	0.03 or 0.70	$0.33x_1$	x_1

There are two sources for the value of the ground state reduced width. Unfortunately there is serious disagreement between the two values obtained. One source uses the existence of the extra-nuclear thermal-neutron capture process (Thomas 1952) to arrive at a value of approximately $0.03\hbar^2/M_n a$. The other source uses the relative absolute yields of the $^{12}\text{C}(d, p)^{13}\text{C}$ stripping reaction (Holt and Marsham 1953 b). That such data can be used to derive values for the reduced widths has been pointed out in an earlier section. After correction for the statistical factor $2J+1$ and the angular distribution (Holt and Marsham 1953 a), the yields to the ground and first three excited states of ^{13}C are in the ratios 1.0:1.2:0.07:1.8. These ratios are expected to correspond to the ratios of the reduced widths of the levels for neutron emission since the other factors occurring in the deuteron stripping cross section (Butler 1951) will not vary greatly from level to level provided that fast deuterons are used (8 Mev in this case). The ratios of the reduced widths for proton emission of the upper three levels of the mirror nucleus ^{13}N are (Jackson and Galonsky 1953): 1.2:0.07:0.6. There is excellent agreement between the first ratios in the two cases. The discrepancy in the last ratio may well be explained by the fact that the experimental value of the reduced width of the d-wave proton, corresponding to the third excited $5/2^+$ level, is hypersensitive to the choice of radius and much more so than that for s- and p-wave protons. Jackson and Galonsky used the rather large radius of 4.77×10^{-13} cm in their analysis. Calculation shows that, if an unmodified external coulomb field is always used, the value of the reduced width of the level in question actually becomes infinite at a radius of 4.0×10^{-13} cm. Consequently the disagreement of the last ratio is not a serious objection to the suggestion that absolute deuteron stripping cross sections can be used to estimate reduced widths. Indeed, in such cases as the $5/2^+$ level referred to, it may even afford a better value than a direct resonance reaction. Acceptance of the

suggestion leads to a value of $0.70 \hbar^2/M_0 a$ for the ground state width of ^{13}C , in serious disagreement with the value 0.03 from thermal neutron capture. The source of this discrepancy is not known.

The figures given in table 2 show that both extreme L - S and extreme j - j coupling give poor accounts of the experimental data. The striking feature of all four data (accepting the larger value of the ground state reduced width) is that they always lie *between* the extreme coupling values. This fact immediately suggests an exploration of the intermediate coupling region.

§9. ^{13}C AND ^{13}N IN INTERMEDIATE COUPLING

Before attempting to express intermediate coupling eigenfunctions in an L - S representation, we must establish the complete sets of L - S eigenfunctions. These are given in table 3 for the three states in which we are interested. The

Table 3

State	Complete set				
^{13}C , ^{13}N ground. $J=\frac{1}{2}^-$, $T=\frac{1}{2}$	^{22}P [441]	^{22}P [432]	^{24}P [432]	^{24}D [432]	^{22}S [333]
^{13}C , ^{13}N excited. $J=\frac{3}{2}^-$, $T=\frac{1}{2}$	^{22}P [441]	^{22}P [432]	^{24}P [432]	^{22}D [432]	^{24}D [432]
^{12}C ground. $J=0^+$, $T=0$	^{11}S [44]	^{13}P [431]	^{11}S [422]	^{15}D [422]	^{13}P [332]

members of the complete sets are identified by the usual L - S symbol and their symmetry character. There are (by coincidence) five members in each set. Consequently the spin-orbit interaction matrices (Appendix II) are all fifth-order ones. In Appendix II we derive a general formula (A 6) for the elements of a spin-orbit matrix. In the case of n nucleons in the $1p$ shell this formula becomes

$$\begin{aligned} \langle J(LS) | \alpha \sum_i \mathbf{l}_i \cdot \boldsymbol{\sigma}_i | J(L'S') \rangle &= 3\alpha n \hbar^2 (-)^{L+L'-J-\frac{1}{2}} \\ &\times [(2S+1)(2L+1)(2S'+1)(2L'+1)]^{1/2} W(LSL'S', J1) \sum_{L_p S_p T_p} (-)^{L_p+S_p} \\ &\times \langle LST | \rangle_{L_p S_p T_p} \langle L'S'T' | \rangle_{L_p S_p T_p} W(LIL'L', L_p 1) W(S\sigma S'\sigma', S_p 1). \quad (32) \end{aligned}$$

where $l=l'=1$, $\sigma=\sigma'=\frac{1}{2}$ and we have taken the spin-orbit interaction of the i th nucleon as $\alpha \mathbf{l}_i \cdot \boldsymbol{\sigma}_i$. The spin-orbit matrices of ^{13}N , ^{13}C (ground), ^{13}N , ^{13}C (excited) and ^{12}C (ground) are found to be

$$\alpha \begin{bmatrix} \frac{1}{3} & -\frac{\sqrt{10}}{3} & \frac{\sqrt{10}}{6} & -\frac{\sqrt{2}}{2} & 0 \\ -\frac{\sqrt{10}}{3} & \frac{1}{3} & -\frac{1}{6} & \frac{\sqrt{5}}{2} & 1 \\ \frac{\sqrt{10}}{6} & -\frac{1}{6} & \frac{5}{6} & 0 & -1 \\ -\frac{\sqrt{2}}{2} & \frac{\sqrt{5}}{2} & 0 & \frac{3}{2} & 0 \\ 0 & 1 & -1 & 0 & 0 \end{bmatrix}, \alpha \begin{bmatrix} \frac{1}{6} & -\frac{1}{3}\sqrt{\frac{5}{2}} & -\frac{5}{6} & \frac{1}{\sqrt{2}} & \frac{1}{2} \\ -\frac{1}{3}\sqrt{\frac{5}{2}} & \frac{1}{6} & \frac{1}{6}\sqrt{\frac{5}{2}} & 0 & -\frac{1}{2}\sqrt{\frac{5}{2}} \\ -\frac{5}{6} & \frac{1}{6}\sqrt{\frac{5}{2}} & -\frac{1}{3} & \frac{1}{2\sqrt{2}} & 0 \\ \frac{1}{\sqrt{2}} & 0 & \frac{1}{2\sqrt{2}} & -\frac{1}{2} & \frac{1}{2\sqrt{2}} \\ \frac{1}{2} & -\frac{1}{2}\sqrt{\frac{5}{2}} & 0 & \frac{1}{2\sqrt{2}} & -1 \end{bmatrix},$$

$$\alpha \begin{bmatrix} 0 & -\frac{2\sqrt{6}}{3} & 0 & 0 & 0 \\ -\frac{2\sqrt{6}}{3} & \frac{3}{4} & -\frac{\sqrt{15}}{3} & \frac{7\sqrt{6}}{12} & \frac{\sqrt{15}}{4} \\ 0 & -\frac{\sqrt{15}}{3} & 0 & 0 & -1 \\ 0 & \frac{7\sqrt{6}}{12} & 0 & \frac{3}{2} & \frac{\sqrt{10}}{4} \\ 0 & \frac{\sqrt{15}}{4} & -1 & \frac{\sqrt{10}}{4} & \frac{5}{4} \end{bmatrix}.$$

To obtain the total interaction matrices, diagonal terms must be added for the central interaction energies in the various L - S states. To evaluate these energies we use the Rosenfeld prescription for the nucleon interaction potential V_{ij} (Rosenfeld 1948):

$$V_{ij} = -0.13V_W + 0.93V_M + 0.46V_B - 0.26V_H$$

(where the subscripts W , M , B , H denote Wigner, Majorana, Bartlett and Heisenberg exchange forces), and we also use the convenient formulae of Racah (Racah 1950) for the diagonal matrix elements of a general central force mixture. The matrix elements are given in table 4, and are expressed, as is usual, in terms

Table 4

State	Interaction matrix elements				
^{13}C , ^{13}N ground	$9.54L$ $+16.18K$	$6.75L$ $+19.75K$	$8.13L$ $+16.61K$	$8.13L$ $+14.61K$	$3.96L$ $+24.12K$
^{13}C , ^{13}N excited	$9.54L$ $+16.18K$	$6.75L$ $+19.75K$	$8.13L$ $+16.61K$	$6.75L$ $+18.15K$	$8.13L$ $+14.61K$
^{12}C ground	$9.56L$ $+12.92K$	$6.76L$ $+14.02K$	$3.98L$ $+20.06K$	$6.74L$ $+10.78K$	$3.04L$ $+19.38K$

of the $1p$ -shell direct integral L and exchange integral K . Making the assumption $L = 6K$ we can express the total interaction matrix in terms of the intermediate coupling parameter $\zeta = \alpha/K$, which is a measure of the relative sizes of the two types of coupling. When $\zeta = 0$, the matrix is diagonal and pure L - S coupling is represented. When $\zeta = \infty$ pure j - j coupling is represented. It is a useful check against mistakes to evaluate the eigenvectors and eigenvalues in the latter extreme and compare their implications with what we know intuitively. These eigenvalues and eigenvectors of the states in which we are interested are given in table 5.

Table 5

State	Eigenvalue	Eigenvector components				
^{13}C , ^{13}N ground	3α	$\sqrt{\frac{5}{27}}$	$-\sqrt{\frac{8}{27}}$	$\sqrt{\frac{2}{27}}$	$-\sqrt{\frac{10}{27}}$	$-\sqrt{\frac{2}{27}}$
^{13}C , ^{13}N excited	$\frac{3\alpha}{2}$	$\frac{2}{3}$	$-\frac{1}{3}\sqrt{\frac{5}{2}}$	$-\frac{1}{3}$	$\frac{1}{3\sqrt{2}}$	$\frac{1}{3}$
^{12}C ground	4α	$\frac{\sqrt{5}}{9}$	$-\frac{\sqrt{30}}{9}$	$\frac{\sqrt{8}}{9}$	$-\frac{\sqrt{20}}{9}$	$-\frac{\sqrt{18}}{9}$

The intermediate coupling region was covered by evaluating the eigenvalues and vectors for the four ratios $\zeta = 3, 6, 10$ and 30 . This enables graphs to be drawn giving the theoretical values of the four observed data (table 2) for any coupling mixture. These graphs are presented in figs. 4-7. The abscissa in each case has been chosen to be $y = \zeta/(5 + \zeta)$ for convenience in plotting. The horizontal lines are the experimental values (assuming for the reduced widths that $x_1 = 1$).

§ 10. DISCUSSION OF RESULTS

It is very satisfying to find that all four experimental magnitudes can be explained with the shell-model in intermediate coupling. It would be even more satisfying to find that all the magnitudes were consistent with the same value

of the intermediate coupling parameter. An inspection of figs. 4-7 shows that the experimental magnitudes indicated correspond to a small but definite spread of values of y . However, there are several sources of uncertainty to be taken

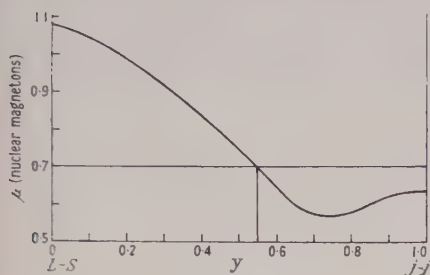


Fig. 4. The magnetic moment of ^{13}C .

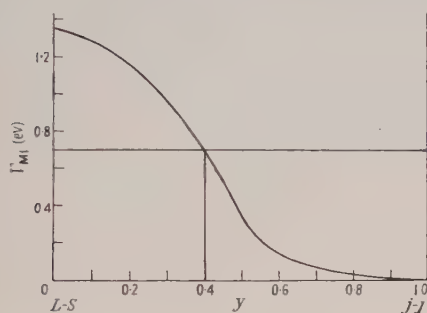


Fig. 5. The magnetic dipole transition width (in eV).

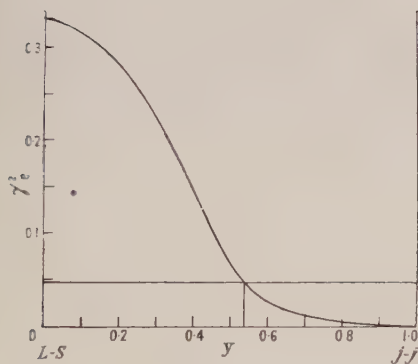


Fig. 6. The reduced width of the excited state in units of \hbar^2/Ma .

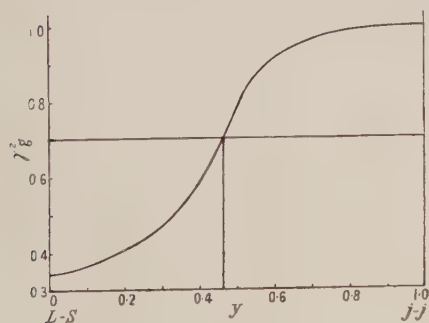


Fig. 7. The reduced width of the ground state in units of \hbar^2/Ma .

into account. It is generally estimated that magnetic moments (and so presumably magnetic dipole matrix elements) may be changed to the extent of

something like 0.1 nuclear magneton by relativistic and exchange current effects (Blatt and Weisskopf 1952). Thus we may say that all values of y within about 0.05 of those selected by the experimental values in figs. 4 and 5 are permissible. The line drawn to represent the experimental values of the reduced width in fig. 6 is almost certainly too low because quite a large value of the nuclear radius (4.77×10^{-13} cm) was used in extracting the reduced width of the excited level from the observed width (much larger, for instance, than that which gives the best analysis of the angular distribution in the $^{12}\text{C}(\text{d}, \text{p})^{13}\text{C}$ reaction, viz. 4.2×10^{-13} cm (Holt and Marsham 1953 b). This means that we should allow values of y corresponding to values of the reduced width of up to twice the indicated magnitude. The result of the considerations is that all the various experimental magnitudes are indeed consistent with one value of the intermediate coupling parameter ζ to within the uncertainty mentioned. The most likely value of y seems to be about 0.47, and this means a value of ζ of 4.4. It may be significant that this value is near that used to explain the spins of the ground states of ^6Li and ^{10}B (Zeldes 1953), viz. 3.7. It should be pointed out, however, that this search for a very accurate value of ζ does not take into account errors introduced by the wrong choice of force mixture used in evaluating the intermediate eigenfunctions and values. Such errors could also be a contributory cause of the spread in values of y . The general impression one gets from the calculations is that the qualitative form of the curves in figs. 4-7 is not sensitive to variations in the force mixture, but that quantitative results may have some such dependence. Similar remarks apply to deviations from the assumption $L=6K$ for the relation between the direct and exchange integrals.

In this paper we have developed methods for examining the shell-model and its mode of coupling and applied them to one pair of nuclei. Other experimental data are being subjected to similar treatment. Preliminary investigations are encouraging, and it is hoped that a full report will be incorporated in a forthcoming review article (Thomas and Lane 1954).

ACKNOWLEDGMENTS

I would like to express my deep gratitude to Professor R. E. Peierls for the facilities he has afforded me at Birmingham where much of this work was done. My thanks are due to him and many colleagues for their helpful criticism and advice, and also to the Department of Scientific and Industrial Research for a maintenance award.

APPENDIX I: THE CONSISTENCY OF EQUATIONS (20), (25) AND (29)

Equations (20) and (25) give expressions for $\beta_{nl} (2M_n/\hbar^2)^{1/2}$ times the reduced width amplitude γ_{nl} in $j-j$ and $L-S$ coupling respectively. Equation (29) gives the corresponding quantity in intermediate coupling using an $L-S$ representation. By considering $j-j$ coupling as a special case of intermediate coupling it should be possible to show the consistency of (25) and (29) with (20). Denote the transformation amplitudes of the $j-j$ wave functions in terms of the $L-S$ wave functions by $\langle J(j'') || J(LS) \rangle$ and $\langle J_0(j''-1) || J_0(L_0S_0) \rangle$. If we combine (25) with (29)

for j - j wave functions, then equate the result to (20), we have, after multiplying by $U(J_0\sigma J l, j_n j)$ and adding over j_n ,

$$\begin{aligned} \langle J T | J_0 T_0 \rangle = & \sum_{\substack{LSz \\ L_0 S_0 z_0}} \langle J(j^n) || J(LS) \rangle \langle J_0(j^{n-1}) || J_0(L_0 S_0) \rangle \langle LST || L_0 S_0 T_0 \rangle \\ & \times \sum_{j_n} (-)^{j_n + L_0 - J - L} U(L_0 S_0 j_n \sigma, J_0 S) U(L_0 J S, L j_n) U(J_0 \sigma J l, j_n j), \\ & \dots\dots (A1) \end{aligned}$$

where $U(abcd, ef)$ is defined as $(2e+1)^{1/2}(2f+1)^{1/2}W(abcd, ef)$ and is used to shorten the formula. This relation is a general one between the fractional parentage coefficients of the extreme coupling modes, and the transformation coefficients between the modes. It can be proved as follows: consider (11) in the case when $\langle JM |$ represents a j - j coupled wave function, and expand the wave functions on both sides of the equation in terms of their parent states. Equation (11) can again be used to express the *parent* j - j wave functions in terms of L - S wave functions. After some manipulation of the Wigner coefficients involved and the elimination of the wave functions we have

$$\begin{aligned} \langle J T | J_0 T_0 \rangle = & \sum_{\substack{LSz \\ L_0 S_0 z_0}} \langle J(j^n) || J(LS) \rangle \langle J_0(j^{n-1}) || J_0(L_0 S_0) \rangle \langle LST || L_0 S_0 T_0 \rangle \\ & \times \sum C^{LSJ} C^{L_0 L} C^{S_0 \sigma S} C^{L_0 S_0 J_0} C^{J_0 j J} C^{\sigma l j} \\ & \dots\dots (A2) \end{aligned}$$

where, as in the text, the bare summation sign and absence of magnetic quantum numbers implies summation over all magnetic quantum numbers except that of J . The second sum is just that encountered in the theory of transformation amplitudes in the two-particle problem (Flowers and Edmonds 1952), and is written $\langle J_0 j J M | LSJM \rangle$. It can be shown to reduce to the sum over the U -functions in (A1), and so the consistency of (20), (25) and (29) is proved.

APPENDIX II: THE SPIN-ORBIT INTERACTION MATRIX

Insertion of the expansion (11) of the intermediate coupling eigenfunction $\langle JM |$ (in the L - S representation) into the Hamiltonian equation for all nucleons gives the following eigenvalue problem:

$$E \langle J || J(LS) \rangle = \sum_{L'S'z'} \langle J || J(L'S') \rangle \langle J(L'S') | \sum_{i < j} V_{ij} + \alpha \sum_i \mathbf{1}_i \cdot \boldsymbol{\sigma}_i | J(LS) \rangle$$

..... (A3)

for the energies of the intermediate coupling states. The nucleon central interaction energy $\sum_{i < j} V_{ij}$ is diagonal in the L - S representation, but the spin-orbit energy $\alpha \sum_i \mathbf{1}_i \cdot \boldsymbol{\sigma}_i$ is not, and its matrix must be evaluated before the eigenvalue calculation can be commenced.

Expansion of the L - S states of n particles into the parent states of $n-1$ particles coupled to the odd particle enables a typical element of the spin-orbit matrix to be written as

$$\begin{aligned} \langle J(LS) | \alpha \sum_i \mathbf{1}_i \cdot \boldsymbol{\sigma}_i | J(L'S') \rangle \\ = \alpha n \sum_{L_p S_p T_p \alpha_p} \langle L'S'T' || L_p S_p T_p \rangle \langle LST || L_p S_p T_p \rangle \\ \times \sum C^{LSJ} C^{L'S'J} C^{L_1 l_1 L} C^{L_p l_p L'} C^{S_p \sigma S} C^{S_p \sigma' S'} \langle l \sigma m_l m_\sigma | \mathbf{1} \cdot \boldsymbol{\sigma} | l' \sigma' m_l m_{\sigma'} \rangle. \dots\dots (A4) \end{aligned}$$

The last matrix element can be expressed as

$$\langle l\sigma m_l m^\sigma | \mathbf{1} \cdot \boldsymbol{\sigma} | l'\sigma' m_l' m_{\sigma'}' \rangle = \hbar^2 \sum C_{m_l m_\sigma}^{l \sigma j} C_{m_l' m_{\sigma'}'}^{l' \sigma' j} \left[\frac{j(j+1) - l(l+1) - \sigma(\sigma+1)}{2} \right] \dots \dots \dots (\text{A } 5)$$

where j takes the values $l + \frac{1}{2}$, $l - \frac{1}{2}$. When this is substituted into (A 4) a sum over eight Wigner coefficients results. This can be reduced to a sum over four Racah functions, and the final expression for the spin-orbit matrix element is

$$\begin{aligned} & \langle J(LS) | \alpha \Sigma \mathbf{1}_i \cdot \boldsymbol{\sigma}_i | J(L'S') \rangle \\ &= \frac{\alpha \hbar^2}{2} (-)^{L'+L-J+1} \sum_{L_p S_p T_p \alpha_p} \langle L'S'T' | \rangle_{L_p S_p T_p} \langle LST | \rangle_{L_p S_p T_p} \\ & \times [j(j+1) - l(l+1) - \sigma(\sigma+1)] \\ & \times \left(\frac{(2j+1)(2L+1)(2S+1)(2L'+1)(2S'+1)}{(2L_p+1)(2S_p+1)} \right)^{1/2} \\ & \times \sum_f \frac{1}{2f+1} U(SLS'L', Jf) U(LlL'l', L_p f) U(S\sigma S\sigma', S_p f) U(\sigma'l'\sigma l, jf), \quad (\text{A } 6) \end{aligned}$$

where U is the function defined in Appendix I and f is a summation dummy.

REFERENCES

- BLATT, J., and WEISSKOPF, V., 1952, *Theoretical Nuclear Physics* (New York: John Wiley), p. 251.
 BIEDENHARN, L. C., 1952, *Tables of the Racah Coefficients*, O.R.N.L., 1098.
 BUTLER, S. T., 1951, *Proc. Roy. Soc. A*, **208**, 559.
 FLOWERS, B. H., 1952, *Phil. Mag.*, **43**, 1330.
 FLOWERS, B. H., and EDMONDS, A. R., 1952, *Proc. Roy. Soc. A*, **214**, 515.
 GAMBA, A., MALVANO, R., and RADICATI, L. A., 1952, *Phys. Rev.*, **87**, 440.
 HOLT, J. R., and MARSHAM, T. N., 1953 a, *Proc. Phys. Soc. A*, **66**, 249; 1953 b, *Ibid.*, **66**, 1032.
 INGLIS, D. R., 1953, *Rev. Mod. Phys.*, **25**, 390.
 JACKSON, H. A., and GALONSKY, A. I., 1953, *Phys. Rev.*, **89**, 370.
 JAHN, H. A., and VAN WIERINGEN, H., 1951, *Proc. Roy. Soc. A*, **214**, 502.
 POSS, H. L., 1949, *Phys. Rev.*, **75**, 600.
 RACAH, G., 1950, *Helv. Phys. Acta*, **23** (Supplement), 229.
 ROSENFELD, L., 1948, *Nuclear Forces* (Amsterdam: North Holland Publishing Co.), p. 234.
 SEAGRAVE, J. D., 1951, *Phys. Rev.*, **84**, 1219.
 THOMAS, R. G., 1952, *Phys. Rev.*, **88**, 1109.
 THOMAS, R. G., and LANE, A. M., 1954, "The Theory of Nuclear Reactions," *Rev. Mod. Phys.*, to be published.
 WILKINSON, D. H., 1953, *Phil. Mag.*, **44**, 542.
 ZELDES, N., 1953, *Phys. Rev.*, **90**, 416.

A New Theory of Liquid Helium : Further Treatment

BY H. N. V. TEMPERLEY

King's College, Cambridge

MS. received 10th April 1953, and in final form 30th June 1953

Abstract. A treatment of liquid helium is given that is a simplified version of that in a former paper. The assembly, consisting of vapour and liquid, is treated as an equilibrium mixture of aggregates of all sizes, an aggregate being defined as a number of atoms which together form a bound quantum-mechanical state. By making plausible assumptions about the energy levels of these aggregates a model is found which shows both liquefaction and a generalized Bose condensation. The model seems to be a satisfactory compromise between the points of view of Landau and of London and Tisza, and leads to a synthesis of their two explanations of the appearance of superfluidity. It also provides a physical basis for the model assumed by F. London in 1939.

§1. INTRODUCTION

IN two previous papers (1952 a, b, to be referred to as I and II) two existing theories of liquid helium, corresponding to the 'nearly free' and 'tight-binding' approximations in the theory of metals, were compared critically, and it was pointed out that neither of them could be expected to be a particularly good approximation. The difficulty in finding a satisfactory 'intermediate' model may be traced to the fact that quite a number of the non-dimensional quantities that can be built up out of the physically relevant parameters are neither large nor small, but are of the order of unity. For example:

(a) For almost any quasi-lattice arrangement, consistent with the actual density of liquid helium, the mean distance between the repulsive 'cores' of neighbouring atoms is comparable with the core diameter itself. This means that the 'cell' model of a liquid is unlikely to lead to useful results, because the probability of escape of an atom from its cell cannot be treated as 'small'.

(b) The mean de Broglie wavelength of helium atoms is comparable with the lattice spacing. This means that an attempt to begin with a classical model and then to apply 'quantum corrections' is unlikely to be satisfactory.

(c) The temperatures are comparable with one-tenth of the Debye temperature. In I it was shown that large deviations from a theory of Landau-Debye type are then to be expected, even if we could treat the liquid as a 'perfect' crystal lattice, obeying Hooke's law.

(d) The attractive force between two helium atoms is about that required to form a bound state. This means that most of the known perturbation methods in quantum mechanics break down.

In II it was suggested that a satisfactory compromise between the two extreme types of theory might be arrived at by developing the cluster theory of Mayer and Mayer (1940), and a possible behaviour of the cluster-integrals, as

a function of the number of atoms involved, was suggested that seems to account for many of the observed facts. In view of the obscurity associated with the concept of cluster integrals in a quantum-mechanical assembly, and the fact that explicit calculations of them, taking proper account of the symmetry properties of the wave functions, are unlikely to be available for some time, it seems worth while to put on record the consequences of a model that is admittedly a somewhat crude approximation, but is nevertheless less drastic than the approximations implied by either of the two models discussed in I. The results are fairly encouraging: it is, for example, possible to describe both evaporation and the λ -transition within the framework of a single theory. Comparison of its consequences with experiment seem to give clues enabling the model to be improved. In its improved form it provides a physical basis for the suggestions of F. London (1939).

§2. DESCRIPTION OF THE MODEL

We suppose that our assembly, consisting of imperfect gas, plus liquid if present, can be regarded as an equilibrium mixture of aggregates of all sizes, where an n -aggregate is to be thought of as n atoms which together form a bound quantum-mechanical state. The whole assembly will contain a certain equilibrium number of aggregates of a given size, individual aggregates being constantly broken up and re-formed by collisions. We now make the assumption that, apart from this effect of collisions in keeping these numbers near the equilibrium values, the effect of interactions between aggregates can be neglected. This approximation is of the same type as those which lead to Dalton's law of partial pressures in a mixture of gases, or to the 'perfect' solution in a liquid or solid phase. Since these are useful first approximations, it seems reasonable to examine the consequences of an analogous assumption in a one-component assembly, cf. A. Bijl (1934), Frenkel (1939) and ter Haar (1953). The fact that we are envisaging the formation of bound states does mean that we are taking *some* account of interactions, so that our approximation is better than that of a 'perfect gas' type of theory. On the other hand, we are allowing for the presence of aggregates of all sizes, instead of merely considering very large aggregates, so that the approximation should be better than that made in a 'solid-like' theory of Landau-Debye type (Landau 1941).

We are purposely using the term 'aggregate' rather than 'cluster' in this paper to emphasize the difference between the two concepts, namely that it is rigorously correct to neglect interactions between clusters in the Mayer (1940) theory, whereas the neglect of interactions between aggregates is an approximation. It may well be that a quantity $\phi(n)$ that we shall introduce shortly, the partition function formed by summing over the bound states of an n -aggregate, is closely allied to the n th cluster integral, but the two are certainly not identical.

§3. CONSEQUENCES OF THE MODEL

To make progress, we really need the results of a quantum-mechanical calculation on n interacting atoms in an enclosure. Such a calculation does not seem to be available for the case we are interested in, namely that in which the interactions between two atoms are of about the strength needed to form a bound state, the atoms being described by symmetrical wave functions. A not dissimilar problem is that of the formation of atomic nuclei, where the mutual

interaction is also near this critical strength, but the nucleons have to be described by antisymmetrical wave functions. Here it is well known that useful results can be obtained from comparatively crude assumptions about the actual form of the force-field, and even from still more crude treatments based on a common potential field for all the particles in a nucleus. The properties of antisymmetrical wave functions guarantee a small probability of configurations in which two particles are very near one another, therefore the results are insensitive to the finer details of the interaction function. If, however, we use symmetrical wave functions, it becomes necessary to take proper account of the repulsive fields between the atoms in order to get a physically sensible result, and this greatly complicates the calculations. However, it seems not unreasonable to guess that an attraction of about the critical strength, together with a repulsive core, should lead to results broadly similar to those of a similar attraction together with the effect of antisymmetrical wave functions, and we make such a working hypothesis until better methods of calculation become available. We therefore assume the following behaviour as we add more and more atoms to an aggregate:

(a) The *total* binding energy increases steadily as the aggregate becomes larger, and is zero or small for a pair of atoms.

(b) The *binding energy per atom* passes through a maximum (probably a rather shallow one) as the aggregate becomes larger. For a very large aggregate we may suppose that the binding energy per atom approaches a limiting value, a fair approximation to which should be given by F. London's calculations (1936), in which he assumed various types of quasi-lattice arrangements.

(c) The small aggregates have but one bound state, but, as we add more and more atoms, there will come a time when excited states become possible. *A priori*, we cannot say whether this will occur for values of n smaller or larger than that corresponding to the maximum binding energy per atom.

The analogy with the atomic nucleus is, of course, very rough, and the accepted explanation of the maximum that occurs in the binding energy per nucleon (saturation of exchange forces together with coulomb repulsion) certainly cannot be applied in the present case, where there is no analogue of the coulomb repulsion. No minimum of the kind assumed in (b) for helium is to be expected for ordinary liquids, where the binding energy per atom should increase steadily as more atoms are added, zero-point effects being negligible.

It is not immediately obvious that the existence of zero-point energy in liquid helium modifies this situation. As a rough model of an n -aggregate we might take a drop of liquid of radius a . On the basis of van der Waals forces between helium atoms, it is to be expected that the attractive energy will be of the form $-An^3/a^6$ and the surface tension correction of the form Bn^2/a^4 . If now we assume some simple power laws, such as $Cn^l a^{-m}$ for the variation of zero-point energy with n and a , and first suppose a so chosen that the total of these three terms is a minimum, it is readily shown that no reasonable choice of the indices l and m can lead to a minimum in the energy per atom of the aggregate as a function of n . If n is small, it probably remains sufficiently accurate to describe the van der Waals forces by means of the volume and surface terms introduced above, but the zero-point energy per atom in the aggregate is no longer likely to be a *smooth* function of n and a . As we add more and more atoms to an aggregate, there will come a stage when more than one bound state is possible and, although the zero-point energy refers to the *lowest* bound state,

it seems plausible that the formula describing the variation of zero-point energy with n and a changes its form abruptly at this value of n at which a second bound state appears. If so, it is possible to understand qualitatively the postulated minimum in the energy per atom as a function of n . (We shall see later that only a very shallow minimum is needed to account for the experimental facts.) This argument suggests that this minimum occurs, if at all, at, or near, the value of n at which the aggregate first has more than one bound state.

We suppose, therefore, that we know the energy-levels of an n -aggregate, denoting them by $E_{l,n}$ where $l=1$ corresponds to the ground state. We now develop the statistical mechanical consequences of postulates (a), (b), (c) above, and show that they lead to a model which shows two types of transition, one corresponding to ordinary liquefaction, the other to a generalization of Bose-Einstein condensation. In addition to these energy levels, we have to allow for the kinetic energy of each n -aggregate moving as a whole (the motion of the centre of gravity can always be allowed for separately in the wave equation of the n -aggregate). According to the assumption that the effect of interactions of aggregates with one another is negligible, the energy levels for an aggregate of mass nm , moving freely in an enclosure of side d , are simply $(p^2 + q^2 + r^2)h^2/8nmd^2$ (p, q, r positive integers), i.e. an n -aggregate having any of the energies $E_{l,n}$ may, in addition, have a kinetic energy of translation corresponding to any of these values. Thus, the grand partition function for such assemblies is

$$f = \prod_{p,q,r} \prod_n \prod_l \left[1 - \lambda^n \exp(-E_{l,n}/kT) \exp\left\{-\frac{h^2(p^2 + q^2 + r^2)}{8nmd^2 kT}\right\} \right]^{-1} \dots\dots (1)$$

the partition function for an assembly of exactly N atoms being the coefficient of λ^N in this product. This formula is the obvious generalization of that for cases in which only 'single-particle' levels are considered, the factor λ^n occurring simply because an n -aggregate contributes n , and not unity, to the total number of atoms present. We may transform expression (1) by the technique used in discussing the perfect gas; we take logarithms, expand the logarithms in ascending powers of λ , and then replace the sums over p, q, r by integrals, remembering that the terms for which $p=q=r=1$ are not necessarily all negligible and retaining them explicitly. This gives

$$\begin{aligned} \log f \sim & (2\pi m k T)^{3/2} V h^{-3} \sum_n \sum_{l=1}^{\infty} n^{3/2} S^{-5/2} \lambda^{Sn} \exp(-SE_{l,n}/kT) \\ & - \sum_n \sum_l \log\{1 - \lambda^n \exp(-E_{l,n}/kT)\} \end{aligned} \dots\dots (2)$$

where, in the second series, we have omitted the factor $\exp(3h^2/8nmd^2 kT)$, which tends to unity as $d \rightarrow \infty$.

Equation (2) represents the rigorous consequence of the assumption that the aggregates can be treated as non-interacting. We now examine it in the light of the assumptions about the energy-levels that we have already introduced, namely that $E_{1,n}/n$ passes through a (negative) minimum for a certain value of n , say z , and that for all smaller values of n there is, at most, one bound state per aggregate. We first show that the double series in (2) can, in practice, be replaced by a very few terms. The triple series is multiplied by the factor $Vh^{-3}(2\pi m k T)^{3/2}$, which will be written N^* and is of the order of N at 'helium' temperatures. A given term in the double series is therefore negligible compared with the sum of the corresponding terms in the triple series unless the argument of the

logarithm is $O(1/N)$. (In this case the presence of the factor $S^{-5/2}$ in the triple series ensures that the sum of the corresponding terms converges.) As in the perfect gas, all the arguments of the logarithms must be positive, so that λ can never exceed the value $\exp(E_z/kT)$, where we write E_z for $E_{1,z}/z$. In the perfect gas these two conditions can only be satisfied for *one* level, the very lowest. In this more general model there *may* be a few values of n , near z , for which $E_{1,n}/n$ is sufficiently nearly constant for the corresponding terms in the double series to give comparable contributions. (The effect on the mathematics of the problem is comparable with what occurs in a 'one-particle' Bose-Einstein model if the lowest level is degenerate. For clearness, we shall suppose, in what follows, that there is only one term contributing effectively to the double series, but this assumption can readily be dropped.)

We split the triple series up into

(a) The contribution for $n < z$.

(b) The contribution for $n = z$.

(c) The contribution for $n > z$.

We are assuming that aggregates smaller than z have no more than one bound state (an assumption that could also be dropped if the levels for $l > 1$ were known). The contribution (a) then reduces to

$$N^* \sum_{n=1}^{z-1} \sum_{S=1}^{\infty} \lambda^{S_n} n^{3/2} S^{-5/2} \exp(-SE_{1,n}/kT). \quad \dots\dots(3)$$

For $n=1$ the binding and zero-point energies vanish, so $E_{1,1}=0$ and the corresponding terms represent simply the log (grand partition function) of a perfect gas. The terms for n greater than 1 but less than z specify the probabilities of finding small aggregates in the vessel, that is, are a measure of the departure of the vapour phase from perfection. Now we know experimentally that vapours, including helium, can safely be treated as nearly perfect, for example for the purpose of predicting vapour pressure curves (except in the region of the critical point). To a first approximation we neglect these terms in comparison with the terms for $n=1$. This approximation could also be removed if we had definite knowledge of the variation of $E_{1,n}/n$ with n . The summation over S is easily shown to converge for physically permissible values of λ , an upper limit to which is set by (8 b) below.

We now consider the contribution (b) to (2). For $n=z$, it reduces to

$$N^* z^{3/2} \sum_{S=1}^z S^{-5/2} \{\lambda \exp(-E_z/kT)\}^{S_z} - \log\{1 - \lambda^z \exp(-zE_z/kT)\} \quad \dots\dots(4)$$

after adding in the one significant term from the double series. This expression differs in form from the logarithmic term corresponding to the lowest state in a 'one-particle' model. The presence of the series is a consequence of the fact that the z -aggregates are not necessarily at rest, but each can acquire kinetic energy as a whole without leaving the ground state $E_{1,z}$. For high temperatures λ is small and the series in (4) is small compared with expression (3), which implies that only a few z -aggregates are present in the assembly. If, however, λ is comparable with $\exp(E_z/kT)$, condensation of Bose-Einstein type is approaching, and simultaneously series (4) becomes large compared with series (3). This means that, as we gradually lower the temperature, first we get an increase in the numbers of aggregates of various sizes present at the expense of the number of

free atoms; secondly, a finite fraction of all the atoms drops into the z -state with a translational energy of effectively zero. The existence of a minimum in the function $E_{1,n}/n$ thus leads to an analogue of Bose-Einstein condensation in an assembly of interacting atoms.

Since the departure of a gas from perfection heralds also the ordinary process of liquefaction, we must examine the conditions for the latter phenomenon. We shall show that the model predicts liquefaction in a manner quite analogous to Mayer's theory (1940) in spite of the fact that the complexion of lowest energy for this model would be one in which all the atoms are in z -aggregates. (For clearness we make the convention that the word condensation is always to be understood to refer to the generalized Bose-Einstein process.) We have still to examine the contribution (c) to expression (2) for $n > z$. This can further be split into

(c i) The contribution for $s = 1$.

(c ii) The contribution for $s > 1$.

The contribution (c i) may be written

$$N^* \sum_{n>z} \lambda^n n^{3/2} \phi(n) \dots\dots\dots (5)$$

where $\phi(n)$ is the sum $\sum_l \exp(-E_{l,n}/kT)$, which is the classical sum-over-states for an n -aggregate. The sum is taken over bound states only because energy of translation is allowed for through the contribution (c ii) and the factor N^* in (5). The appearance of large aggregates in the assembly will, in the same way as in Mayer's (1940) theory, correspond to the higher-order terms in expression (5) becoming important, that is, the series (5) is 'just about' to diverge. The criterion for this is, by the ratio test,

$$\frac{\partial}{\partial n} [n \log \lambda + \frac{3}{2} \log n + \log \phi(n)] \rightarrow 0 \dots\dots\dots (6)$$

where the differentiation has to be taken keeping the volume of the aggregate constant. Thus

$$\log \lambda + \frac{3}{2n} + \left(\frac{\partial \log \phi(n)}{\partial n} \right)_{v,T} \rightarrow 0. \dots\dots\dots (7)$$

In the limit of large n the negligible term $3/2n$ can be dropped. Because of the definition of $\phi(n)$ we may write $-kT \log \phi(n) = F_n$ where F_n is the free energy associated with the bound levels in an n -aggregate. As n becomes large (7) reduces to the ordinary relationship between λ and the partial potential of an atom in a large aggregate.

We have still not considered the contribution (c ii) explicitly. For n large it is negligible compared with (c i) because the typical term for $S=2$ contains the factor $\lambda^{2n} \exp(-2E_{l,n}/kT)$, which is negligible compared with the corresponding term for $S=1$, and the summation over S converges rapidly, because the factor $\lambda \exp(-E_{l,n}/n kT)$ is appreciably less than unity unless $n \simeq z$. For the large aggregates the omission of contribution (c ii) is practically equivalent to neglecting their translational energy, which is only of order kT , and therefore small compared with $E_{l,n}$ in any case. For $n \simeq z$, (c ii) implies the presence of appreciable numbers of aggregates of size of the order of z with finite translational energy. This adds nothing physically to what we have already considered under contribution (b).

We have thus shown that expression (2) can be split into the contributions (3), (4) and (5), corresponding respectively to vapour, z -aggregates and large aggregates, without sensible error. We have given reasons for thinking that the terms we have omitted, and the assumptions we have made (some of which can be removed when more information about the energy levels of aggregates of He atoms becomes available) do not essentially alter the physical consequences of the model. The discussion of the various contributions to (2) can be extended without difficulty to the corresponding contributions to the series for $N = \lambda \partial (\log f) / \partial \lambda$, obtained by differentiating (2), the corresponding numbers of atoms in the aggregates of the three types being obtained by differentiating expressions (3), (4) and (5). The condition of equilibrium between two types of aggregate is that they should correspond to the same value of λ . This is readily shown to be equivalent to equating partial potentials.

The vapour phase is described approximately by expression (3), and the partial potential of the vapour is given by the usual expression

$$g_{\text{vap}} = kT \log \lambda. \quad \dots\dots(8a)$$

Our discussion has shown that appreciable numbers of z -aggregates are present only if

$$E_z = kT \log \lambda \quad \dots\dots(8b)$$

while Mayer's criterion (7) for liquefaction has been shown to be equivalent to

$$g_{\text{liq}} = \lim_{n \rightarrow \infty} \frac{\partial F_n}{\partial n} \simeq kT \log \lambda \quad \dots\dots(8c)$$

where g_{liq} is the partial potential associated with a large aggregate. As a first approximation, we may represent the large aggregates as quasi-crystalline lattices, which can be described by means of a Debye function. Thus

$$g_{\text{liq}} \simeq E_0 - \frac{\pi^4}{5} kT \left(\frac{T}{\Theta} \right)^3 + Pv \quad \dots\dots(9)$$

where E_0 is $\lim_{n \rightarrow \infty} (E_{1,n}/n)$, the energy per atom of the lowest state of a large aggregate, which is made up of the interaction energy of the atoms together with the zero-point energy. These are two large quantities of opposite sign that nearly cancel. F. London (1936) has estimated them, using various quasi-lattice models, and it turns out that the theoretical E_0 is of the order of -15 calories per mole, this figure not being particularly sensitive to the precise lattice type assumed.

If we start with the vapour phase, we obtain an equation for λ in terms of the density by differentiating expression (3). The condition for the equilibrium between the vapour and liquid is obtained simply by equating expressions (8a) and (8c). This is consistent with the observed latent heat of vaporization, but we know experimentally that expression (9) ceases to be valid for the liquid above about 0.6°K , so the vapour-pressure curve is only predicted semi-quantitatively. The condition that the vapour phase should form itself into z -aggregates instead of into large ones is given by equating expressions (8a) and (8b). The resulting condition is (see I) the same as the condition for Bose-Einstein condensation of a gas, provided that we assume that a state of energy E_z per atom is available for the atoms to condense into. (According to our model, this gain in energy is associated with the interaction between the atoms in the z -aggregates.) We have assumed that E_z lies slightly below E_0 ,

which means that, at very low temperatures, the vapour prefers to form z -aggregates. However, there will be a point on the vapour-pressure curve at which g_{liq} becomes equal to E_z , because of the effect of the entropy term in expression (9), and above this the vapour will prefer to form itself into large aggregates. We identify this point with the λ -point of liquid helium. To predict a λ -point at 'helium' temperatures $E_0 - E_z$ must be no more than a few hundredths of a calorie per mole, in which case the curve obtained by equating (8a) and (8b) is practically identical with that obtained by equating (8a) and (8c). Physically this must mean that in much of the 'liquid' region expressions (4) and (5) are comparable, so that both z -aggregates in their state of lowest kinetic energy and large aggregates are present together. In an ordinary liquid the postulated minimum in $E_{1,n}/n$ is probably absent, and large aggregates will always be more probable than ones of intermediate size. (Ordinarily, we should expect $E_{1,n}/n$ to decrease steadily with increasing n .) In the present model the relative probability of large aggregates and z -aggregates is expected to vary with temperature because of the entropy term in (9). This term arises because we have supposed z -aggregates to possess one bound state only, whereas large aggregates have a great many possible bound states, and transitions between them are represented, on the Debye picture, by the emission and absorption of sound quanta, giving rise to the entropy term.

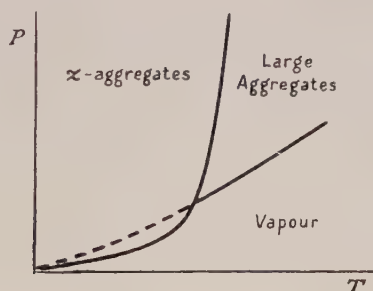
We can examine this point further by attempting to determine the equilibrium line in the liquid region between z -aggregates and large ones. This involves the tacit assumption that a theory of Mayer type is valid in part of the liquid region. The validity of assuming that the liquid can be described by a constant value of Mayer's parameter Z has been discussed by the author elsewhere (to be published shortly), and the assumption seems to be reasonably valid as long as one is not too far from the vapour region. On this basis, the equilibrium between z -aggregates and large aggregates is described by equating expressions (8b) and (8c). (The role of the parameter λ in the present theory is similar to that of Mayer's parameter Z .) If we assume that E_z is constant, this condition is that the partial potential of the liquid is constant, which implies

$$\frac{dP}{dT} = - \left(\frac{\partial g}{\partial T} \right)_P / \left(\frac{\partial g}{\partial P} \right)_T = \rho s. \quad \dots\dots(10)$$

This would imply a positive slope for the λ -line at which z -aggregates begin to appear in the liquid in large numbers. Inserting observed values of ρ and s leads to a slope of the order of 3 atmospheres per degree, in contrast with the observed negative and large slope. The predictions of the model are summarized in the figure, the equilibrium diagram between small aggregates (expression (3)), z -aggregates (expression (4)) and large aggregates (expression (5)) being not unlike that of an ordinary one-component assembly with three possible phases. The dotted curve indicates how the vapour pressure curve would run if there were no minimum in the curve for $E_{1,n}/n$ as a function of n . The difference between this and the full-line curve is nowhere more than a few per cent if we choose $E_z - E_0$ so as to get a λ -temperature of 2°K . The following fact should also be mentioned. If we had a nearly perfect gas, of density corresponding to that of He vapour at the λ -point ($1.2 \times 10^{-3} \text{ g cm}^{-3}$), this would be on the point of Bose-Einstein condensation provided that there existed a level of negative energy E_z of the order of -15 calories per mole into which condensation

could take place. As is well known, a perfect gas of atoms of mass equal to that of helium atoms would, at a density of 0.15 g cm^{-3} , have a condensation temperature of 3.1°K . The factor arising from the formation of z -aggregates, $\exp(-E_z/kT)$, is of the right order of magnitude to compensate for the smaller density of the vapour, if E_z is of the order of -15 calories per mole. The observed partial potential of the liquid is also consistent with such a value of E_z , together with the suggested criterion $g_{\text{liq}} = E_z$ for the λ -line.

The relative numbers of atoms in z - and large aggregates can be estimated by comparing the contributions of expressions (4) and (5) after differentiating with respect to λ . It will be noticed that the singularities in these expressions, considered as functions of λ , are of somewhat different types, that in (4) arising from the argument of a logarithmic term approaching zero, while that in (5) arises because a series is at its limit of convergence. The asymptotic behaviour of series (5) can be estimated if we make the assumption, customary in discussing crystal lattices, that $\phi(n)$ behaves asymptotically as κ^n , where κ is the partition function per atom associated with the interactions in a large aggregate. This assumption has been discussed by Fowler and Guggenheim (1939), and amounts simply to saying that the energy and partial potential per atom approach limiting



values as $n \rightarrow \infty$. Making this assumption, we obtain from (4) for N_z , the probable number of atoms in z -aggregates:

$$N_z \sim 2.612 z^{3/2} N^* + [z \lambda^z \exp(-z E_z/kT)] / [1 - \lambda^z \exp(-z E_z/kT)]. \quad \dots (11)$$

(The series in (4), and its differential coefficient with respect to λ , both converge for all physically relevant values of λ .) The asymptotic behaviour of N_{large} is intermediate between that of

$$3N^* \lambda \kappa (1 - \lambda \kappa)^{-4} \quad \text{and} \quad 2N^* \lambda \kappa (1 - \lambda \kappa)^{-3}, \quad \dots (12)$$

these two expressions being obtained by replacing $n^{3/2}$ in (5) by n^2 and n respectively. We have defined the λ -line by a condition practically equivalent to $\kappa = \exp(-E_z/kT)$ as long as the pressure is not too large. (If we used the latter relation to define the λ -line, it would be equivalent to writing $E_z = f_{\text{liq}}$ instead of g_{liq} .)

The asymmetry between expressions (11) and (12) stems basically from the fact that, in estimating the relative probabilities of large aggregates and z -aggregates, we have to allow for the fact that there are many different possible sizes of large aggregate, but only one size of z -aggregate. On the λ -line, comparison of (11) and (12) shows that the number of atoms in z -aggregates is

very small compared with the number in large aggregates, but that the proportion may be expected to increase rapidly as we go to the low temperature side of the λ -line. At absolute zero all the atoms will be in z -aggregates. Thus, helium II is described on this model as an equilibrium mixture of z -aggregates and large aggregates. Since we are neglecting interactions between aggregates, the picture is one of a 'perfect' mixture or solution of these two types of aggregate. The first term in (11) arises from the z -aggregates with finite kinetic energy. This term only varies slowly with λ and corresponds to z -aggregates in the vapour phase. The second term corresponds to z -aggregates at rest.

We shall discuss a few further consequences of this model as it stands, and then indicate how it might be improved. First, it seems to be a natural generalization of the criterion of Bose-Einstein condensation proposed in I for a many-particle type of assembly. The assumption that the liquid represented, e.g. by a Debye type of partition function, was in equilibrium with *free* atoms was found to call for $g_{\text{liq}} = 0$, whereas, if it is in equilibrium with z -aggregates, it is possible for g_{liq} to be negative, as experiment requires.

The connection with the two-fluid picture seems to be given by a treatment on exactly the same lines as that given in II, clusters being replaced by aggregates. From this treatment, making the assumption that, for any large aggregate, the velocity v_{ph} associated with the phonons it contains is substantially the same as the velocity V_l with which the centre of gravity of the aggregate is moving, it can be concluded that $v_n - v_s$ is proportional to ρ_c , the effective mass of the small clusters, or z -aggregates, per unit volume of liquid. Accordingly 'superfluid' effects are only possible with finite ρ_c , and we thus seem to have established a link between the two suggested criteria for superfluid effects. According to Landau's original picture (1941) some highly artificial assumption seems to be necessary, for example that the coupling between the degrees of freedom V_l and v_{ph} is strong in all liquids but helium, and that, in this one liquid, the coupling suddenly jumps from being strong to weak at the λ -temperature. If z -aggregates are present, no such assumption need be made.

§4. HELIUM 3

It remains to consider what predictions the present model makes about this liquid. Since aggregates with an even number of He_3 atoms may be expected to behave as Bose particles, the possibility of a condensation effect cannot be completely excluded; indeed it would occur in much the same way if the variation of binding energy with n were of the same type as that postulated for He_4 . If there is *no* minimum in $E_{1,n}/n$ we expect, as we have already seen, an ordinary liquefaction. It is too early to say whether such a minimum is likely to be present or not. It can be stated with certainty that the distribution of energy levels $E_{l,n}$ of the aggregates will be entirely different for the two isotopes. Quite apart from the difference in statistics, the binding energies will be smaller in He_3 than in He_4 for comparable aggregates of all sizes because of the larger zero-point energy, which is already a major factor in He_4 , and is now increased by a factor $4/3$. Another question that remains unsettled is whether large aggregates of He_3 atoms (liquid He_3) can be described by a Debye model, or whether they are better described as an 'imperfect Fermi gas', the interactions

being allowed for by some smoothed field. A determination of the specific heat and compressibility of the liquid He_3 might help to decide some of these points. At the present time we do not know whether to expect a condensation effect, nor how the excitations in a large aggregate of He_3 atoms can best be described. If a Debye treatment is applicable to the liquid, Landau's theory (1941) would predict superfluidity at some temperature. The present theory would predict superfluidity only if $E_{1,n}/n$ had a minimum.

Some very recent experiments (Hammel and Schuch 1952 and private communication) suggest that, in certain circumstances, He_3 atoms in an He_3 - He_4 mixture can take part in superfluid flow, though there is still no evidence of such effects in pure He_3 . On the present model such a result, if confirmed, can be interpreted in a way not open to theories invoking Bose-Einstein condensation into 'one-particle' type levels. It is, in principle, entirely possible that a few of the He_4 atoms in a z -aggregate can be replaced by He_3 atoms without removing the postulated minimum in the binding energy per atom, and yet that this minimum is absent in aggregates consisting entirely of He_3 atoms.

§5. POSSIBLE IMPROVEMENT OF THE MODEL

Various pieces of evidence show that the model in which interactions between aggregates are completely neglected is too crude. For example, just as in II, we find that no possible choice of the parameter $E_z - E_0$ can lead to a specific heat anomaly whose position and height both agree with observed values. This could be remedied if, for example, we attempted to take account of the interactions between aggregates by supposing that E_z and E_0 were effectively functions of density and possibly of the number N_z of atoms in z -aggregates. It is well known that one can get a quantitatively correct specific heat curve by various *ad hoc* assumptions along such lines. For example, Bijl, de Boer and Michels (1941) postulated that the 'condensed' states are separated from the remaining liquid states by an energy-gap, an assumption that resembles our model. F. London (1939) gets the correct curve by assuming arbitrarily that about one sixth of the atoms are in 'gas-like' states, the remainder in Debye-like states, an assumption that also resembles the consequences of our model.

The failure of equation (10) to predict the λ -line properly can also be remedied by supposing that E_z varies strongly with density. Numerically, we should have to postulate a value of the order of -15 calories per mole near the vapour-pressure curve, rising to nearly zero as we approach the top of the λ -line. Such an effect of the mutual interactions of aggregates seems very plausible. Further support is given to this idea by the following circumstance. A curious property of the perfect gas model was pointed out independently by several writers (Lamb and Nordsieck 1941, Halpern 1951, Temperley 1952 a), namely, that the wave function of the lowest state is profoundly modified by the effect of gravity, and would extend only to a distance of the order of 10^{-4} cm above the floor of the vessel, so that the *condensed* Bose-gas would show a very strong 'sedimentation' effect which would be almost absent above the transition temperature. A result of this type is just what seems to be needed to help interpret the *non-classical* behaviour of liquid helium under extremely small

pressure gradients. (It is *not* sufficient to postulate *absence of viscosity* in part of the liquid: one has also to account for the fact that the rate of flow in films and narrow capillaries can be greater than the velocity of free fall associated with the pressure head, i.e. Torricelli's theorem does not hold.) Also, the circumstance that the percentage of condensed atoms within a given volume is a function of pressure as well as of temperature is what is needed to account for the thermo-mechanical effects. If the condensed atoms or aggregates carry no entropy, then H. London's (1939) formula $dP/dT = \rho s$ follows thermodynamically. However the very violence of the effect predicted in the perfect gas tends to make one think that the picture becomes meaningless in the liquid. A very similar criticism can be levelled at our crude model (the figure of 10^{-4} cm would not be significantly changed by any reasonable choice of the number z), but the situation becomes entirely different if we postulate that E_z varies with density, and possibly also with the number of z -aggregates present. Our theory requires that E_z should be a small fraction of a calorie per mole more negative than $E_0 + Pv$. (If the difference were greater than this the condensation effect would persist to higher temperatures, while if E_z becomes less negative than $E_0 + Pv$ the condensation process becomes thermodynamically unprofitable at any temperature.)

We now consider our improved model of a liquid under gravity. According to our crude model, the condensation process would lead to the appearance of a large number of z -aggregates at the very bottom of the vessel and thus to an absurdly large density gradient. If, however, we suppose that E_z is a function of the density, it is clear that while, under gravity, we may still have a larger number of z -aggregates near the bottom, the density of the liquid as a whole can nowhere be changed appreciably. We have introduced the assumption that E_z is raised from -15 calories per mole to zero as we travel along the λ -line, that is by a change of 0.03 g cm^{-3} in the density, so that, if the density of any particular region of the liquid were increased by a few ten-thousandths, E_z would increase by a few hundredths of a calorie per mole and it would no longer be thermodynamically profitable for further z -aggregates to appear there—they would prefer instead to appear in the other regions of the liquid where no increase in the local density had taken place. In this way it is possible to predict that the number of z -aggregates in the liquid may depend slightly on the pressure at each point, while avoiding the very drastic predictions of the cruder model. (If E_z varies with the density, it no longer necessarily follows that the assembly consists entirely of z -aggregates at $T=0$, and the relative numbers of large and z -aggregates would depend on the pressure. The T^3 law for specific heat strongly suggests that large aggregates do persist down to absolute zero.) Thus our improved model provides a physical basis for the suggestion of F. London (1939), that, in helium II, the atoms can assume both 'Debye-like' and 'gas-like' states.

One more feature of interest may be referred to briefly. A z -aggregate has been supposed to have a lower binding energy per atom than any other type. It will therefore require work either to break up such an aggregate, or to induce two or more such aggregates to join together. Presumably this means that the z -aggregates must be destroyed before the solid state becomes possible, and rough estimates of g_{liq} suggest that E_z does indeed become approximately zero at pressures of the order of 20–30 atmospheres.

We may sum up this discussion by saying that the crude model, in which interactions between aggregates are neglected altogether, predicts a vapour-pressure-temperature curve of quite normal type, but a λ -line that slopes in the wrong direction. It also predicts an absurdly large density gradient in liquid helium II under gravity. These considerations seem to require that E_z be a function of density, a result that also seems to be required by the behaviour of the λ -line. A variation of E_z with density, and possibly with N_z also, is a very plausible consequence of taking interactions between aggregates properly into account, cf. A. Bijl (1934). It would not be difficult to invent *ad hoc* a variation of E_z with N_z to give a specific heat anomaly of the observed magnitude and type (cf. Bijl, de Boer and Michels 1941).

While such ideas are physically reasonable, there seems little point in pursuing them further until more reliable indications about the behaviour of the energies $E_{l,n}$ become available. Assumptions of the kind we have arrived at would lead, as in other theories of co-operative phenomena, to the appearance of several adjustable constants, and numerical comparison with experiment ceases to be a conclusive test. Moreover, we should also have available the resource of supposing that the liquid (large aggregates) is not completely described by a Debye model, cf. Landau (1941). The introduction of 'rotons' leads to at least two further adjustable constants.

§ 6. CONCLUSION

Our crude model represents a first approximation to a Mayer type theory of liquid helium, if we suppose that the binding energy per atom in an n -aggregate passes through a maximum as a function of n . A plausible argument suggests that such a hypothesis is reasonable for a weak interaction, just about sufficient to bind two atoms together, and the absence of superfluidity in other liquids can accordingly be understood. Tentative accounts of the behaviour of He_3 and He_3 - He_4 mixtures are also possible.

In II we discussed whether the transition of liquid helium was more closely allied to ordinary liquefaction (formation of 'large' aggregates or clustering in coordinate space) or to the behaviour of a perfect Bose gas (assumption of the same velocity by a finite fraction of the atoms, or 'clustering in momentum space'). Our investigation suggests that z -aggregates, rather than free atoms, are responsible for the condensation process. If so, no clear distinction between the two types of clustering can be made in any actual assembly of *light* molecules.

It seems certain that a quantum-mechanical study of an assembly in which the interactions are near the critical value should lead to worth-while results.

ACKNOWLEDGMENTS

This work was carried out during my stay at Yale for part of the academic year 1952/3, and I wish to thank the Chemistry Department for hospitality and the United States Congress and King's College, Cambridge, for research grants. I also wish to thank very many friends in the United States for their helpful discussions of the points in this paper, which resulted in several errors being detected.

REFERENCES

- BIJL, A., 1934, *Physica*, **1**, 1125.
BIJL, A., DE BOER, J., and MICHELS, A., 1941, *Physica*, **8**, 655.
FOWLER, R. H., and GUGGENHEIM, E. A., 1939, *Statistical Thermodynamics* (Cambridge University Press).
FRENKEL, J., 1939, *J. Phys.*, U.S.S.R., **1**, 315.
TER HAAR, D., 1953, *Proc. Camb. Phil. Soc.*, **49**, 130.
HALPERN, O., 1951, *Phys. Rev.*, **87**, 520.
HAMMEL, E. F., and SCHUCH, A. F., 1952, *Report of Schenectady Cryogenics Conference*, p. 7.
LAMB, W. E., and NORDSIECK, A., 1941, *Phys. Rev.*, **59**, 677.
LANDAU, L., 1941, *J. Phys.*, U.S.S.R., **5**, 71.
LONDON, F., 1936, *Proc. Roy. Soc. A*, **153**, 576; 1939, *J. Phys. Chem.*, **43**, 49.
LONDON, H., 1939, *Proc. Roy. Soc. A*, **171**, 484.
MAYER, J. E., and MAYER, M. G., 1940, *Statistical Mechanics* (New York : Wiley).
TEMPERLEY, H. N. V., 1952 a, *Proc. Phys. Soc. A*, **65**, 490, referred to as I; 1952 b, *Ibid.*, **65**, 619, referred to as II.

The General Three-Dimensional Theory of Cascade Processes

BY H. MESSEL* AND H. S. GREEN†

* School of Physics, University of Sydney, Sydney, Australia

† University of Adelaide, Adelaide, South Australia

MS. received 7th May 1953

Abstract. A mathematical treatment is given of the general three-dimensional theory of a cascade shower developing in a medium in which the number density of the constituent atoms may vary from point to point. This treatment reduces the work of obtaining all angular and radial moments to a drill. The case of the soft component developing in an extensive air shower initiated by a primary nucleon is worked out as an illustration.

§ 1. INTRODUCTION

THE distribution function

$$Q_n^{(j,i)}\{E_0; (E_1, r_1, c_1), \dots, (E_n, r_n, c_n); z\} dE_1 dr_1 dc_1 \dots dE_n dr_n dc_n,$$

representing the probability of finding exactly n particles of the i th type at an absorber depth z , with energies, angles (cosines) and radial distances measured with respect to the shower axis in the specified intervals $E_i, E_i + dE_i; r_i, r_i + dr_i; c_i, c_i + dc_i; i = 1, \dots, n$, due to a primary particle of the j th type with energy E_0 , describes the behaviour of the cascade throughout its lifetime. If adequate expressions could be found for the $Q_n^{(j,i)}$ for any given theory, and if the experimentalists were able to measure completely the various properties of a given shower, then it would be a straightforward matter to check any theory from the measurements made on a single shower. However, to realize this end theoretically appears to be even more difficult than it is experimentally; both the mathematical and the experimental difficulties involved are immense. For this reason the experimentalist is usually concerned with accumulating data on a large number of showers—he deals with the ‘average’ shower. The theoretician, likewise, is forced to deal with averages, special functions derived from the $Q_n^{(j,i)}$. To illustrate this consider the distribution function

$$R_n^{(j,i)}\{E_0; (E_1, r_1, c_1), \dots, (E_n, r_n, c_n); z\} dE_1 dr_1 dc_1 \dots dE_n dr_n dc_n$$

representing the probability of finding n particles of the i th type at an absorber depth z , with energies, angles (cosines) and radial distances measured with respect to the shower axis in the specified intervals $E_i, E_i + dE_i; r_i, r_i + dr_i; c_i, c_i + dc_i; i = 1, \dots, n$, due to a primary particle of the j th type with energy E_0 , and any number of particles of the i th type with arbitrary energies, angles and radial distance. The $R_n^{(j,i)}$ are given by

$$R_n^{(j,i)} = \sum_{a=0}^{\infty} \frac{1}{a!} \int_0^{\infty} dE_{n+1} \int_0^{\infty} dr_{n+1} \int_{-1}^1 dc_{n+1} \dots \int_0^{\infty} dE_{n+a} \int_0^{\infty} dr_{n+a} \int_{-1}^1 dc_{n+a} Q_{n+a}^{(j,i)} \dots (1)$$

$R_1^{(j,i)}$ corresponds, for instance, to the angular-radial distribution function $f^{(i)}(E, r, c, z)$ used by Green and Messel (1952, to be referred to as GM) in treating the spread of the soft component of the cosmic radiation. The

well-known angular and radial distribution functions appearing in cascade theory are obtained from $R_1^{(j,i)}$ by integrating over the radial or angular variable respectively, thus

$$\Theta^{(j,i)}(E, c, z) = \int_0^\infty r R_1^{(j,i)} dr \quad \dots\dots (2)$$

$$R^{(j,i)}(E, r, z) = \int_{-1}^1 R_1^{(j,i)} dc. \quad \dots\dots (3)$$

The differential average number of particles at a given depth z may be obtained from either (2) or (3) by integrating over the angular or radial variable respectively. To appreciate what state the theoretical development of the subject is in one should recall that even in the case of the differential average numbers solutions of the integral equations have been obtained under special conditions only (homogeneous type of cross section). Recently, Messel and his collaborators (Messel and Potts 1952 a, b, Messel 1953) were successful in solving the fluctuation problem in cascade theory. The diffusion equations for the functions obtained from $Q_n^{(j,i)}$ and $R_n^{(j,i)}$, after integrating over the angular and radial variables, were completely solved for the cases of the nucleon and electron-photon cascade. About the same time Green and Messel (Green and Messel 1952, Messel and Green 1952, Messel 1953) were successful in developing the theory for the angular and radial distribution functions defined in (2) and (3). The mathematical methods used by the authors were effective but cumbersome. Lately we have been successful in developing new techniques which will allow one to solve a broad field of related problems. The purpose of this paper is to develop these techniques for the general problem of the three-dimensional development of cascades. To illustrate the power of the method we will apply it to the case of the electron-photon cascade developing as part of an extensive air shower, initiated by a nucleon.

§2. GENERAL THREE-DIMENSIONAL THEORY

The purpose of this section is to give the general three-dimensional theory of a cascade shower, in a medium in which the number density of the constituent atoms may vary from point to point. The theory is independent of the particular assumptions made concerning the interactions of the elementary particles, and may therefore be applied to test the consequences of any special set of hypotheses. However, only particles with ultra-relativistic energies will be considered.

The probability distributions of the various kinds of particles which may be present (nucleons, various types of mesons, electrons, photons) will be described by a set of functions $f^{(i)}(\mathbf{p}, \mathbf{r})$ such that $f^{(i)}(\mathbf{p}, \mathbf{r})(2\pi p^2)^{-1} dp_1 dp_2 dp_3 dr_1 dr_2$ is the differential probability of finding a particle of the i th kind, and of momentum \mathbf{p} at a vector displacement \mathbf{r} from the foot of the shower axis. It is supposed that the x_3 axis is parallel to the shower axis, so that $z = -r_3$ is the distance of the point considered along the shower axis. The differential cross section for the collision of a particle of the j th kind and of momentum \mathbf{p}' , with an atom (or nucleus) of the medium to generate a particle of the i th kind and of momentum \mathbf{p} , will be denoted by $w^{(j,i)}(\mathbf{p}', \mathbf{p})(2\pi p^2)^{-1} dp_1 dp_2 dp_3$. The total cross section for such a collision will be denoted by $\alpha^{(j)}(\mathbf{p}')$. The probability per unit path length that a particle of the j th kind and of momentum \mathbf{p}' should decay to generate a particle of the i th kind and of momentum \mathbf{p} will be represented by $y^{(j,i)}(\mathbf{p}', \mathbf{p})(2\pi p^2)^{-1} dp_1 dp_2 dp_3$; the total probability per unit path length for

the decay of a particle of the j th kind will be represented by $\gamma^{(j)}(\mathbf{p}')$. [If $m^{(j)}$ is the mass, and $\tau^{(j)}$ the mean lifetime of the particle, $\gamma^{(j)}(\mathbf{p}') = m^{(j)}/(\tau^{(j)}\mathbf{p}')$.] If $\nu(\mathbf{r})$ is the number density of the atoms of the medium, the total probability per unit path length that a particle j of momentum \mathbf{p}' will generate a particle i of momentum \mathbf{p} is $x^{(j,i)}(\mathbf{p}', \mathbf{p})(2\pi p^2)^{-1} dp_1 dp_2 dp_3$, where

$$x^{(j,i)}(\mathbf{p}', \mathbf{p}, \mathbf{r}) = y^{(j,i)}(\mathbf{p}', \mathbf{p}) + \nu(\mathbf{r})w^{(j,i)}(\mathbf{p}', \mathbf{p}) \quad \dots\dots(4)$$

and the total probability per unit path length that a particle j of momentum \mathbf{p}' should suffer an interaction is

$$\zeta^{(j)}(\mathbf{p}', \mathbf{r}) = \gamma^{(j)}(\mathbf{p}') + \nu(\mathbf{r})\alpha^{(j)}(\mathbf{p}'). \quad \dots\dots(5)$$

Hence
$$\frac{\mathbf{p}}{p} \cdot \frac{\partial f^{(i)}(\mathbf{p})}{\partial \mathbf{r}} = \sum_j \int x^{(j,i)}(\mathbf{p}', \mathbf{p}) f^{(j)}(\mathbf{p}') d\bar{\mathbf{p}}' - \zeta^{(i)}(\mathbf{p}) f^{(i)}(\mathbf{p}) \quad \dots\dots(6)$$

where $d\bar{\mathbf{p}}' = (2\pi p'^2)^{-1} dp'_1 dp'_2 dp'_3$.

It will henceforth be assumed that $\nu(\mathbf{r})$ depends only on $z = -r_3$, and not on r_1 or r_2 ; this is the case in all situations of physical interest. Put $p_3 = Cp$, $p_1 = pS\theta_1$, $p_2 = pS\theta_2$ where $S = (1 - C^2)^{1/2}$, so that $\theta_1^2 + \theta_2^2 = 1$ and

$$\frac{\mathbf{p}}{p} \cdot \frac{\partial f^{(i)}}{\partial \mathbf{r}} = -C \frac{\partial f^{(i)}}{\partial z} + S\boldsymbol{\theta} \cdot \frac{\partial f^{(i)}}{\partial \mathbf{r}}. \quad \dots\dots(7)$$

As only particles of very high energy are considered, the angle whose cosine is C is very small, and one may set $C = 1$ (see Messel and Green 1952 for the justification of this). Then

$$-\frac{\partial f^{(i)}}{\partial z} + S\boldsymbol{\theta} \cdot \frac{\partial f^{(i)}}{\partial \mathbf{r}} = \sum_j \int x^{(j,i)}(\mathbf{p}', \mathbf{p}) f^{(j)}(\mathbf{p}') d\bar{\mathbf{p}}' - \zeta^{(i)}(\mathbf{p}) f^{(i)}(\mathbf{p}). \quad \dots\dots(8)$$

Introducing the double Fourier transform

$$g^{(i)}(\mathbf{p}, k, z) = \frac{1}{2\pi} \iint f^{(i)}(\mathbf{r}) \exp(i\mathbf{k} \cdot \mathbf{r}) d\mathbf{r}_1 d\mathbf{r}_2 \quad \dots\dots(9)$$

this gives

$$-\left\{ \frac{\partial g^{(i)}(\mathbf{p})}{\partial z} + iS\boldsymbol{\theta} \cdot \mathbf{k} g^{(i)}(\mathbf{p}) \right\} + \zeta^{(i)}(\mathbf{p}) g^{(i)}(\mathbf{p}) = \sum_j \int x^{(j,i)}(\mathbf{p}', \mathbf{p}) g^{(j)}(\mathbf{p}') d\bar{\mathbf{p}}' \quad \dots\dots(10)$$

and further, if one writes $\boldsymbol{\theta} \cdot \mathbf{k} = k \cos \beta$, $T_1 = (S \cos \beta)/C$, $T_2 = (S \sin \beta)/C$, so that $\mathbf{p}' \cdot \mathbf{p}/(p'p) = 1 - \frac{1}{2}\{(T_1' - T_1)^2 + (T_2' - T_2)^2\}$ very nearly and

$$\begin{aligned} \int d\bar{\mathbf{p}}' &= \frac{1}{2\pi} \int_p^\infty dp' \int_{-\infty}^\infty dT_1' \int_{-\infty}^\infty dT_2' = \frac{1}{2\pi} \int_p^\infty dp' \int d\mathbf{T}', \\ -\left\{ \frac{\partial g^{(i)}}{\partial z} + ikT_1 g^{(i)} - \zeta^{(i)}(p) g^{(i)} \right\} &= \sum_j \frac{1}{2\pi} \int_p^\infty dp' \int d\mathbf{T}' x^{(j,i)}(p', p, \mathbf{T}' - \mathbf{T}) g^{(j)}(p', \mathbf{T}'). \end{aligned} \quad \dots\dots(11)$$

Now we introduce the further double transform

$$h^{(i)}(\mathbf{l}, \mathbf{k}) = \frac{1}{2\pi} \iint g^{(i)}(k, \mathbf{T}) \exp(i\mathbf{l} \cdot \mathbf{T}) dT_1 dT_2 \quad \dots\dots(12)$$

and the equation becomes

$$-\left\{ \frac{\partial h^{(i)}}{\partial z} + k \frac{\partial h^{(i)}}{\partial l_1} - \zeta^{(i)}(p) h^{(i)} \right\} = \sum_j \int_p^\infty dp' h^{(j)}(p') \tau^{(j,i)}(p', p) \quad \dots\dots(13)$$

where
$$\tau^{(j,i)}(p', p, \mathbf{l}) = \frac{1}{2\pi} \iint x^{(j,i)}(p', p, \boldsymbol{\tau}) \exp(i\mathbf{l} \cdot \boldsymbol{\tau}) d\boldsymbol{\tau}, \quad \dots\dots(14)$$

Since $x^{(j,i)}$ depends only on the magnitude $(\tau_1^2 + \tau_2^2)^{1/2}$ of the vector $\boldsymbol{\tau} = \mathbf{T}' - \mathbf{T}$, $\tau^{(j,i)}$ will depend only on the magnitude of \mathbf{l} . Thus (14) may be written

$$v^{(j,i)}(\mathbf{p}', \mathbf{p}, l) = \int_0^\infty x^{(j,i)}(\mathbf{p}', \mathbf{p}, \tau) J_0(l\tau) \tau d\tau. \quad \dots\dots(15)$$

The angular and radial moments of the original distribution functions are obtained very easily from the expansion of the functions $h^{(i)}$ as power series in l_1 and k . In the first place it is clear from (9) that if one sets $k=0$, $g^{(i)}(\mathbf{T}, k=0)$ is simply the angular distribution function, which is a function of $T = (T_1^2 + T_2^2)^{1/2}$ alone. One has, therefore, from (12)

$$\begin{aligned} h^{(i)}(\mathbf{l}, 0) &= \int_0^\infty g^{(i)}(\mathbf{T}, 0) J_0(lT) T dT \\ &= \sum_{m=0}^\infty (-l^2/4)^m (m!)^{-2} \int_0^\infty g^{(i)}(\mathbf{T}, 0) T^{2m+1} dT \\ &= \sum_{m=0}^\infty (-l^2/4)^m (m!)^{-2} \Omega_m^{(i)}. \end{aligned} \quad \dots\dots(16)$$

Since T , the tangent, does not differ appreciably for the small values which are important, from the angle itself, the coefficients in the expansion of $h^{(i)}(\mathbf{l}, 0)$ in powers of l^2 are clearly the angular moments, apart from the factor $\{(-4)^m (m!)^2\}^{-1}$. In the second place, if one sets $\mathbf{l}=0$, one has

$$\begin{aligned} h^{(i)}(0, k) &= \int_0^\infty \left\{ \frac{1}{2\pi} \int_0^{2\pi} g^{(i)}(k, \beta) d\beta \right\} T dT \\ &= \int_0^\infty \left\{ \frac{1}{2\pi} \int \int f^{(i)}(\mathbf{r}) J_0(kr) dr_1 dr_2 \right\} T dT \\ &= \sum_{n=0}^\infty (-k^2/4)^n (n!)^{-2} \int \int \int f^{(i)}(\mathbf{r}) r^{2n} dr_1 dr_2 T dT \\ &= \sum_{n=0}^\infty (-k^2/4)^n (n!)^{-2} R_n^{(i)}. \end{aligned} \quad \dots\dots(17)$$

Thus, apart from a factor $\{(-4)^n (n!)^2\}^{-1}$, the coefficients of the expansion of $h^{(i)}(0, k)$ in powers of k^2 are the radial moments of the original distribution functions.

It follows from the above that if $h^{(i)}(\mathbf{l}, \mathbf{k})$ with $l_2=0$ is expanded as a double power series in l_1 and k , thus:

$$h^{(i)}(l_2=0) = \sum h_{m,n}^{(i)} l_1^m k^n \quad \dots\dots(18)$$

the coefficients $h_{2m,0}^{(i)}$ and $h_{0,2n}^{(i)}$ give the angular and radial moments respectively of the angular and radial distribution functions obtained from the original distribution function $f^{(i)}$, by integrating over the radial and angular variables respectively. These coefficients can be obtained by substituting (18) in (13) and equating coefficients of $l_1^m k^n$. The result is

$$\begin{aligned} - \left\{ \frac{\partial h_{m,n}^{(i)}}{\partial z} + (m+1) h_{m+1,n-1}^{(i)} - \zeta^{(i)}(\mathbf{p}) h_{m,n}^{(i)} \right\} \\ = \sum_j \int_p^\infty d\mathbf{p}' \sum_{r=0}^m h_{m-r,n}^{(j)}(\mathbf{p}') v_r^{(j,i)}(\mathbf{p}', \mathbf{p}) \end{aligned} \quad \dots\dots(19)$$

where $v_r^{(j,i)}(\mathbf{p}', \mathbf{p})$ is the appropriate coefficient in the power series expansion

$$x^{(j,i)}(\mathbf{p}', \mathbf{p}) = \sum_r v_r^{(j,i)}(\mathbf{p}', \mathbf{p}) l_1^r. \quad \dots\dots(20)$$

From (14) it can be seen that, apart from a numerical factor, $v_r^{(j,i)}(\mathbf{p}', \mathbf{p})$ is a moment of the distribution function $x^{(j,i)}(\mathbf{p}', \mathbf{p}, \tau)$ for individual interactions.

Assuming that (19) can be solved for $m=n=0$ (the differential average number of particles), with $h_{m,-1}^{(i)}=0$ and suitable boundary conditions, the values of all the $h_{m,n}^{(i)}$ can be obtained by a straightforward iteration process. For instance if in $\Sigma_j, j \neq i$, one determines in succession $h_{2,0}^{(i)}, h_{4,0}^{(i)}$, etc., and then $h_{1,1}^{(i)}, h_{0,2}^{(i)}; h_{3,1}^{(i)}, h_{2,2}^{(i)}, h_{1,3}^{(i)}, h_{0,4}^{(i)}$, etc. If the summation contains the case $j=1$ then one determines in succession $h_{0,0}^{(i)}; h_{1,0}^{(i)}, h_{0,1}^{(i)}; h_{2,0}^{(i)}, h_{1,1}^{(i)}, h_{0,2}^{(i)}$, etc. In this way the angular and radial moments of all the distribution functions are properly obtained. Note that the inversion of the two double transforms (9) and (12) is not required, and that the problem has been reduced essentially to the determination of expressions of the average number type, $h_{0,0}^{(i)}$.

If one applies the method outlined above to solve the problem of the electron-photon cascade considered previously by Green and Messel (GM) then the work becomes short and straightforward. The final results obtained are naturally the same. Rather than apply our new method to the electron-photon case, we shall in the next section consider the more complex problem of an electron-photon cascade, in an extensive air shower, developing in the atmosphere. This example contains the development of a pure electron-photon cascade as a special case.

§ 3. THE MIXED CASCADE

The three-dimensional development of an electron-photon cascade in an extensive air shower in the atmosphere will now be given, based on the following model: it is assumed that the primary radiation consists of nucleons; the nucleons generate the meson component by collision with nuclei; the charged π -mesons decay into μ -mesons; the neutral π -mesons decay into photons which initiate the soft component. The contribution to the high-energy soft component by μ -mesons is neglected. The theory is first developed for a single incident nucleon and can then be applied to any given initial spectrum of nucleons.

The equations for the nucleons and mesons have been considered in previous papers (Messel and Green 1952, Green, Messel and Chartres 1952) and will not be given here. We shall, however, freely use the notation and results developed in these papers. It should be stressed at this point that since the theory for nucleons and mesons is based on a number of assumptions (see the above references), the results for the electrons and photons given below are tentative and are presented only for purposes of comparison with future experimental data.

Let the suffix $i=1$ refer to electrons and $i=2$ to photons. The ratio of the radiation length to the nucleon interaction mean free path will be denoted by η . The function $f(\mathbf{p}, \mathbf{r})$ is the angular-radial distribution function for nucleons and $\frac{1}{3}P(\mathbf{p}', \mathbf{p})$ is the nucleon-nucleus cross section for the production of neutral π -mesons. If we measure energies in proton mass units and set the momentum equal to the energy $|P|=U$, then the equation corresponding to (8) is

$$\begin{aligned} & \frac{-1}{q'(z)} \left\{ -\frac{\partial f^{(i)}}{\partial z} + S\theta \cdot \frac{\partial f^{(i)}}{\partial \mathbf{r}} \right\} + (\alpha^{(i)} + \alpha\delta_{i,1})f^{(i)} \\ &= \int_U^\infty \{w^{(3-i)}(U/U')f^{(3-i)}(U') + w^{(i)}(1-U/U')f^{(i)}(U')\delta_{i,1}\}dU'/U' \\ &+ \frac{1}{2\pi} \int_U^\infty dU' \int d\mathbf{T}' w(U', U, \mathbf{T}' - \mathbf{T})f^{(i)}(U', \mathbf{T}')\delta_{i,1} \\ &+ \frac{2\eta}{3} \int_U^\infty \frac{dU'}{U'} \int_{U'}^\infty dU'' \int d\mathbf{T}' f(U'', \mathbf{T}', \eta q)P(U'', U', \mathbf{T}' - \mathbf{T})\delta_{i,2} \dots (21) \end{aligned}$$

where for an isothermal atmosphere $q = (p_0/43g) \exp(-g\delta_0 z/p_0)$, $q'(z) = (-g\delta_0/p_0)q$ and p_0, δ_0 are the surface pressure and density, and g the acceleration due to gravity. Equation (21) is identical with that used in GM for the exception of the addition of the last term. This term expresses the spread of the photons arising from the spread of the neutral π -mesons before they decay. The angle between the decay photons is neglected since it is negligible compared with the two scattering processes considered in (21).

Introducing the double transform defined by (9), eqn. (21) becomes

$$\begin{aligned} & \left\{ \frac{\partial}{\partial q} + iS\mathbf{0} \cdot \mathbf{k}/q'(z) + (\alpha^{(i)} + \alpha\delta_{i,1}) \right\} g^{(i)} \\ &= \int_U^\infty \{ w^{(3-i)}(U/U') g^{(3-i)}(U') + w^{(i)}(1 - U/U') g^{(i)}(U') \delta_{i,1} \} dU'/U' \\ &+ \frac{1}{2\pi} \int_U^\infty dU' \int d\mathbf{T}' w(U', U, \mathbf{T}' - \mathbf{T}) g^{(i)}(U', \mathbf{T}') \delta_{i,1} \\ &+ \frac{2\eta}{6\pi} \int_U^\infty \frac{dU'}{U'} \int_{U'}^\infty dU'' \int d\mathbf{T}' g(U'', \mathbf{T}', \eta q) P(U'', U', \mathbf{T}' - \mathbf{T}) \delta_{i,2}. \\ &\dots\dots(22) \end{aligned}$$

On applying the second twofold transform defined by (12) we find

$$\begin{aligned} & \left\{ \frac{\partial}{\partial q} + \frac{k}{q'(z)} \frac{\partial}{\partial l_1} + (\alpha^{(i)} + \alpha\delta_{i,1}) \right\} h^{(i)} \\ &= \int_U^\infty \{ w^{(3-i)}(U/U') h^{(3-i)}(U') + w^{(i)}(1 - U/U') h^{(i)}(U') \delta_{i,1} \} dU'/U' \\ &+ \int_U^\infty dU' h^{(i)}(U') v^{(1)}(U', U, \mathbf{l}) \delta_{i,1} \\ &+ \frac{2\eta}{3} \int_U^\infty \frac{dU'}{U'} \int_{U'}^\infty dU'' h(U'', \mathbf{l}, \eta q) v^{(2)}(U'', U', \mathbf{l}) \delta_{i,2} \\ &\dots\dots(23) \end{aligned}$$

$$\begin{aligned} \text{where } v^{(1)}(U', U, l) &= \int_{\tau'}^{\tau''} J_0(l\tau) w(U', U, \tau) \tau d\tau \\ &= \sum_{m=0}^{\infty} (-l^2/4)^m (m!)^{-2} \int_{\tau'}^{\tau''} \tau^{2m+1} w(U', U, \tau) d\tau \\ &= \sum_{m=0}^{\infty} (-l^2/4)^m (m!)^{-2} U^{-2m} w_m \delta(U' - U) \dots\dots(24) \end{aligned}$$

where w_m is the m th moment in proton mass units of the elastic scattering cross section w . The explicit value of w_m may be found in GM. $v^{(2)}$ is given by

$$\begin{aligned} v^{(2)}(U'', U', l) &= \int_0^\infty J_0(l\tau) P(U'', U', \tau) \tau d\tau \\ &= P_0(U'', U') \exp \left\{ \frac{l^2}{2\beta} \left(\frac{1}{U''} - \frac{1}{U'} \right) \right\}. \dots\dots(25) \end{aligned}$$

$$\text{Now writing } h^{(i)}(l_2=0) = \sum_{m,n} h_{m,n}^{(i)} l_1^m k^n \dots\dots(26)$$

$$h(l_2=0) = \sum_{m,n} h_{m,n} l_1^m k^n \dots\dots(27)$$

and substituting in (23), we find

$$\begin{aligned} \frac{\partial h_{m,n}^{(i)}}{\partial q} + \frac{m+1}{q'(z)} h_{m+1,n-1}^{(i)} + \alpha^{(i)} h_{m,n}^{(i)} \\ = \int_U \{ w^{(3-i)} (U/U') h_{m,n}^{(3-i)}(U') + w^{(i)} (1 - U/U') h_{m,n}^{(i)}(U') \delta_{i,1} \} dU'/U' \\ + \sum_{r=1}^{\infty} (-4)^{-r} (r!)^{-2} w_r U^{-2r} h_{m-2r,n}^{(i)}(U) \delta_{i,1} \\ + \frac{2\eta}{3} \int_U \frac{dU'}{U'} \int_{U'}^{\infty} dU'' P_0(U'', U') \sum_{r=0}^{\infty} (2\beta)^{-r} (r!)^{-1} \left(\frac{1}{U''} - \frac{1}{U'} \right)^r h_{m-2r,n}^{(i)}(U'', \eta q) \delta_{i,2}. \end{aligned} \quad \dots\dots (28)^*$$

The equations for $h_{m,n}^{(i)}$ are simplified considerably on applying the Mellin transform defined by

$$g_{m,n}^{(i)}(v) = \int_0^{\infty} U^v h_{m,n}^{(i)}(U) dU \quad \dots\dots (29)$$

$$\begin{aligned} \frac{\partial g_{m,n}^{(i)}}{\partial q} + \frac{m+1}{q'(z)} g_{m+1,n-1}^{(i)} - B^{(i)}(v) g_{m,n}^{(3-i)} + D^{(i)}(v) g_{m,n}^{(i)} \\ = \sum_{r=1}^{\infty} (-4)^{-r} (r!)^{-2} w_r g_{m-2r,n}^{(i)}(v-2r) \delta_{i,1} \\ + \frac{2\eta}{3(v+1)} \sum_{r=0}^{\infty} (2\beta)^{-r} \sum_{s=0}^r \frac{(-1)^s}{s!(r-s)!} P_0(v-s) g_{m-2r,n}^{(i)}(v-r, \eta q) \delta_{i,2} \end{aligned} \quad \dots\dots (30)$$

where
$$P_0(v) = \int_0^1 (U/U')^v P_0(U', U) dU \quad \dots\dots (31)$$

and
$$g_{m,n}(v) = \int_0^{\infty} U^v g_{m,n}(U) dU. \quad \dots\dots (32)$$

The functions $B^{(i)}(v)$ and $D^{(i)}(v)$ are the known (GM) Mellin transforms of the Bethe-Heitler cross sections. The solution of the simultaneous set of equations (30) is readily shown to be

$$g_{m,n}^{(i)}(v, q) = \int_0^q \exp \{ a_{\theta}(v)(t-q) \} G_{\theta}^{(j,i)}(v) Q^{(j)}(v, t) dt \quad \dots\dots (33)$$

where the repeated affixes j and θ are summed over the values 1 and 2, as in relativity theory. The $G_{\theta}^{(j,i)}(v)$ are combinations of $B^{(i)}$ and $D^{(i)}$; their explicit values are given in GM. Furthermore

$$\begin{aligned} Q^{(1)}(v, t) &= -\frac{m+1}{t'(z)} g_{m+1,n-1}^{(1)} + \sum_{r=1}^{\infty} (-4)^{-r} (r!)^{-2} w_r g_{m-2r,n}^{(1)}(v-2r), \\ Q^{(2)}(v, t) &= -\frac{m+1}{t'(z)} g_{m+1,n-1}^{(2)} \\ &+ \frac{2\eta}{3(v+1)} \sum_{r=0}^{\infty} (2\beta)^{-r} \sum_{s=0}^r \frac{(-1)^s}{s!(r-s)!} P_0(v-s) g_{m-2r,n}^{(2)}(v-r, \eta t) \end{aligned} \quad \dots\dots (34)$$

and hence

$$\begin{aligned} g_{m,n}^{(i)}(v, q) &= \int_0^q G_{\theta}^{(1,i)}(v) \exp \{ a_{\theta}(v)(t-q) \} \left\{ \frac{-(m+1)}{t'(z)} g_{m+1,n-1}^{(1)}(v) \right. \\ &+ \sum_{r=1}^{\infty} (-4)^{-r} (r!)^{-2} w_r g_{m-2r,n}^{(1)}(v-2r) \Big\} dt \\ &+ \int_0^q G_{\theta}^{(2,i)}(v) \exp \{ a_{\theta}(v)(t-q) \} \left\{ \frac{-(m+1)}{t'(z)} g_{m+1,n-1}^{(2)}(v) \right. \\ &+ \frac{2\eta}{3(v+1)} \sum_{r=0}^{\infty} (2\beta)^{-r} \sum_{s=0}^r \frac{(-1)^s}{s!(r-s)!} P_0(v-s) g_{m-2r,n}^{(2)}(v-r, \eta t) \Big\} dt. \end{aligned} \quad \dots\dots (35)$$

* Where \sum signifies summation from the lower limit to $m/2$. If m is odd then the summation extends to $(m-1)/2$.

For the average number $g_{0,0}^{(i)}$ we find from (35)

$$g_{0,0}^{(i)}(v, q) = \frac{2\eta P_0(v)}{3(v+1)} \int_0^q G_\theta^{(2,i)}(v) \exp \{a_\theta(v)(t-q)\} g_{0,0}(v, \eta t) dt \quad \dots\dots (36)$$

and since (see Messel and Green 1952)

$$g_{0,0}(v, \eta t) = U_0^v \exp \{-h(v)\eta t\} \quad \dots\dots (37)$$

for a single incident nucleon of energy U_0 at the top of the atmosphere,

$$g_{0,0}^{(i)}(v, q) = \frac{2\eta U_0^v P_0(v) G_\theta^{(2,i)}(v)}{3(v+1) \{a_\theta(v) - \eta h(v)\}} [\exp \{-\eta h(v)q\} - \exp \{-a_\theta(v)q\}]. \quad \dots (38)$$

All other $g_{m,n}^{(i)}$ may now be found by a straightforward iteration process. For instance, in the case of the second angular moment

$$\begin{aligned} g_{2,0}^{(i)}(v, q) &= \int_0^q G_\theta^{(1,i)}(v) \exp \{a_\theta(v)(t-q)\} \left\{ -\frac{w_1}{4} g_{0,0}^{(1)}(v-2) \right\} dt \\ &\quad + \frac{2\eta}{3(v+1)} \int_0^q G_\theta^{(2,i)}(v) \exp \{a_\theta(v)(t-q)\} \\ &\quad \times \left\{ P_0(v) g_{2,0}(v, \eta t) + \frac{[P_0(v) - P_0(v-1)]}{2\beta} g_{0,0}(v-1, \eta t) \right\} dt \\ &= -\frac{\eta U_0^{v-2} w_1 P_0(v-2)}{6(v-1)} \frac{G_\theta^{(1,i)}(v) G_\mu^{(2,1)}(v-2)}{a_\mu(v-2) - \eta h(v-2)} \exp \{-a_\theta(v)q\} \\ &\quad \times \left[\frac{\exp [\{a_\theta(v) - \eta h(v-2)\}q] - 1}{a_\theta(v) - \eta h(v-2)} - \frac{\exp [\{a_\theta(v) - a_\mu(v-2)\}q] - 1}{a_\theta(v) - a_\mu(v-2)} \right] \\ &\quad + \frac{\eta U_0^{v-1}}{3(v+1)} G_\theta^{(2,i)}(v) \exp \{-a_\theta(v)q\} \left[P_0(v) \frac{\exp [\{a_\theta(v) - \eta h(v)\}q] - 1}{a_\theta(v) - \eta h(v)} \right. \\ &\quad \left. - P_0(v-1) \frac{\exp [\{a_\theta(v) - \eta h(v-1)\}q] - 1}{a_\theta(v) - \eta h(v-1)} \right] \quad \dots\dots (39) \end{aligned}$$

where we have used

$$g_{2,0}(v, t) = \frac{U_0^{v-1}}{2\beta} [\exp \{-h(v)t\} - \exp \{-h(v-1)t\}]. \quad \dots\dots (40)$$

Similarly for the second radial moment

$$\begin{aligned} g_{0,2}^{(i)}(v, q) &= \int_0^q G_\theta^{(1,i)}(v) \exp \{a_\theta(v)(q_1-q)\} \{-z'(q_1) g_{1,1}^{(1)}(v)\} dq_1 \\ &\quad + \int_0^q G_\theta^{(2,i)}(v) \exp \{a_\theta(v)(q_1-q)\} \{-z'(q_1) g_{1,1}^{(2)}(v)\} dq_1 \\ &\quad + \frac{2\eta P_0(v)}{3(v+1)} \int_0^q G_\theta^{(2,i)}(v) \exp \{a_\theta(v)(q_1-q)\} g_{0,2}(v, \eta q_1) dq_1. \quad \dots\dots (41) \end{aligned}$$

Using the fact that

$$\begin{aligned} g_{0,2}(v, q) &= \frac{U_0^{v-1}}{\beta} \exp \{-h(v)q\} \int_0^q z'(q_1) dq_1 \int_0^{q_1} z'(q_2) \\ &\quad \times \{1 - \exp [\{h(v) - h(v-1)\}q_2]\} dq_2 \quad \dots\dots (42) \end{aligned}$$

$$g_{1,1}(v, q) = -\frac{U_0^{v-1}}{\beta} \exp \{-h(v)q\} \int_0^q z'(q_1) \{1 - \exp [\{h(v) - h(v-1)\}q_1]\} dq_1 \quad \dots\dots (43)$$

and

$$G_\theta^{(j,i)}(v) G_\mu^{(k,i)}(v) = G_\theta^{(k,i)}(v) \delta_{\theta,\mu} \quad \dots\dots (44)$$

we find

$$\begin{aligned}
 g_{0,2}^{(i)}(v, q) = & -\frac{v_1}{2} G_{0,0}^{(1,i)}(v) \exp \{-a_0(v)q\} \int_0^q dq_1 z'(q_1) \int_0^{q_1} dq_2 z'(q_2) \\
 & \times \int_0^{q_2} dq_3 \exp \{a_0(v)q_3\} g_{0,0}^{(1)}(v-2, q_3) + \frac{2\eta U_0^{v-1}}{3\beta(v+1)} G_{0,0}^{(2,i)}(v) \exp \{-a_0(v)q\} \\
 & \times \int_0^q dq_1 z'(q_1) \int_0^{q_1} dq_2 z'(q_2) \int_0^{q_2} dq_3 \exp \{a_0(v)q_3\} \\
 & \times [P_0(v) \exp \{-\eta h(v)q_3\} - P_0(v-1) \exp \{-\eta h(v-1)q_3\}] \\
 & + \frac{2\eta P_0(v) U_0^{v-1}}{3\beta(v+1)} G_{0,0}^{(2,i)}(v) \exp \{-a_0(v)q\} \int_0^q dq_1 \exp [\{a_0(v) - \eta h(v)\}q_1] \\
 & \times \int_0^{\eta q_1} z'(q_2) dq_2 \int_0^{q_2} dq_3 z'(q_3) \{1 - \exp [\{h(v) - h(v-1)\}q_3]\} \\
 & + \frac{2\eta P_0(v) U_0^{v-1}}{3\beta(v+1)} G_{0,0}^{(2,i)}(v) \exp \{-a_0(v)q\} \int_0^q dq_1 z'(q_1) \int_0^{q_1} dq_2 \\
 & \times \exp [\{a_0(v) - \eta h(v)\}q_2] \int_0^{\eta q_2} dq_3 z'(q_3) \{1 - \exp [\{h(v) - h(v-1)\}q_3]\}. \quad \dots (45)
 \end{aligned}$$

On taking the inverse Mellin transform and multiplying by (-4) , the expressions (39) and (45) give the second angular and radial moment respectively, as defined in (16) and (17), thus

$$\Omega_2^{(i)}(U_0, U, q) = \frac{-4}{2\pi i} \int_{v_0-i\infty}^{v_0+i\infty} U^{-(v+1)} g_{2,0}^{(i)}(v, q) dv \quad \dots\dots (46)$$

and

$$R_2^{(i)}(U_0, U, q) = \frac{-4}{2\pi i} \int_{v_0-i\infty}^{v_0+i\infty} U^{-(v+1)} g_{0,2}^{(i)}(v, q) dv. \quad \dots\dots (47)$$

Repeating the above procedure will thus yield all the required moments.

§ 4. DISCUSSION AND CONCLUSION

It is interesting to note that the expressions for the second angular and radial moments contain terms in $1/U$ and $1/U^2$. The terms in $1/U$ arise from the spread of the nucleons and neutral π -mesons, the terms in $1/U^2$ from the coulomb scattering of the electrons. This means that at high energies the spread of the soft component is governed by the spread of the nucleons, but at low energies the spread is governed by the coulomb scattering of the electrons.

We have not troubled to carry out the lengthy numerical evaluation of expressions (39) and (45) since it does not appear justifiable at the present moment. When more experimental data become available to substantiate the model we have used as an illustration, the calculations may be carried out.

The present paper has given a method whereby the long standing problem of angular and radial moments has been reduced to a mathematical drill. The methods outlined here should be of value when considering neutron diffusion problems in pile theory.

Messel and Green (1952) and Green and Messel (1953) have shown that the distribution functions themselves may be reconstructed from a knowledge of the first few lower movements and from the n th moment as $n \rightarrow \infty$. In practice it becomes very difficult to evaluate numerically moments above the sixth, although the asymptotic behaviour of the n th moments as $n \rightarrow \infty$ may easily be

found. In many instances the use of only the first few lower moments and the asymptotic behaviour of the n th moment for large values of n may lead to a considerable error in the distribution functions near the origin. If one could determine the behaviour of the distribution functions near the origin and know the behaviour of the n th moment as $n \rightarrow \infty$ then only the second and fourth moments would be required to get an exceedingly fine approximation to the actual distribution function. We are at present considering the problem of determining the exact behaviour of the radial distribution function for very small distances from the shower axis.

REFERENCES

- GREEN, H. S., and MESSEL, H., 1952, *Phys. Rev.*, **88**, 331; 1953, *Quart. J. Maths.*, **4**, in the press.
GREEN, H. S., MESSEL, H., and CHARTRES, B. A., 1952, *Phys. Rev.*, **88**, 1277.
MESSEL, H., 1953, *Progress in Cosmic Ray Physics*, Vol. II (Amsterdam: North Holland Publishing Company), chap. IV.
MESSEL, H., and GREEN, H. S., 1952, *Phys. Rev.*, **87**, 738.
MESSEL, H., and POTTS, R. B., 1952 a, *Phys. Rev.*, **86**, 847; 1952 b, *Ibid.*, **87**, 759.

The Production of Delta-Rays in Nuclear-Research Emulsions

By D. A. TIDMAN*, E. P. GEORGE* AND A. J. HERZ*

Imperial College, London

MS. received 4th June 1953

Abstract. Theoretical formulae are derived which give the δ -ray density as function of the velocity and charge of the primary particle, taking into consideration the fact that the electrons in the emulsion are both bound and in motion. The two main types of convention used in deciding which configurations of grains are to be accepted as δ -rays are investigated: those in which the δ -rays must contain more than a specified number of grains, and those in which they must reach a specified distance from the primary track. Account is taken, where necessary, of straggling, multiple scattering, and the fluctuations in the numbers of grains in electron tracks. The theory is compared with the results of δ -ray counts on the tracks of singly charged particles of known velocity. The agreement is very good in the case of the conventions based on range, and fairly satisfactory for the grain-number conventions. The range conventions are found to be preferable in practice as they are more easily learnt and more objective than those in which numbers of grains have to be estimated.

§ 1. INTRODUCTION

FOLLOWING the discovery of the existence of heavy nuclei in the primary cosmic radiation (Freier, Lofgren, Ney, Oppenheimer, Bradt and Peters 1948 a) many workers have used nuclear-research emulsions to determine their charge. The charge has usually been deduced from observations of (a) the frequency of occurrence per unit length of track N_δ of knock-on electrons or δ -rays with energies in excess of a certain minimum value, together with (b) the residual ranges of the particles (Freier, Lofgren, Ney and Oppenheimer 1948 b, Bradt and Peters 1948) or (c) their multiple scattering (Dainton, Fowler and Kent 1951). By making observations at such low geomagnetic latitudes that the primary particles must be moving with relativistic velocities, Bradt and Peters (1950 a, b) dispensed with the need for observing a second parameter of the track, such as (b) or (c) above, making the assumption that for such particles N_δ depends only on the square of their charge Z^2 and is independent of energy.

Using these methods, the charge spectrum of the primary radiation has been determined by Bradt and Peters (1950 a, b) and by Dainton *et al.* (1951, 1952). Both these groups of workers agreed that the charge distribution of the primary cosmic rays was roughly similar to that of the matter in the universe as a whole, but disagreed strongly on the amount of lithium, beryllium and boron present in the primary radiation. Bradt and Peters concluded that negligible amounts of these elements were present in the primary rays, for such small amounts as they found at a depth of 5 to 10 g cm⁻² in the atmosphere

* Now at the University of Sydney, Sydney, N.S.W., Australia.

could be attributed to the break-up of heavier nuclei in the overlying air, whereas Dainton *et al.* reported that the frequency with which lithium, beryllium and boron nuclei occurred in the primary radiation was greater than that of all the heavier elements put together. A careful study of their experimental observations reveals that the disagreement is one of interpretation: from similar observational material different conclusions have been drawn.

Neither Bradt and Peters nor Dainton *et al.* used in their interpretations the theoretical relations which were, at that time, believed to describe the production of δ -rays by heavy nuclei—indeed, Dainton *et al.* (1952) state explicitly that their experimental data do not agree with calculations based on the Rutherford scattering formula. However, as both these groups of workers, in common with many others, used δ -ray densities in part or all of their charge determinations, we thought that it would be useful and worth while to derive complete theoretical relations giving the δ -ray densities to be expected, and to compare the results with the densities found experimentally along the tracks of particles of known charge and velocity.

Briefly, our observations are in very reasonable agreement with those of the Bristol workers, and they agree with the theoretical formulae which we have been able to derive. We have also come to the conclusion that the convention most commonly employed at the present time in deciding which configurations of grains are to be counted as δ -rays (the counting convention, for short) is a highly subjective one, and, when we discuss this matter in more detail below, we shall suggest a convention which we have found to give reproducible results more easily.

§ 2. STATEMENT OF THE PROBLEM

2.1. Initial State of the Electrons

Considering only forces of electrostatic repulsion or attraction, and assuming the electrons to be free, the classical treatment of the problem gives the following expression, known as the Rutherford formula, for the number of δ -rays per cm with energies between W and $W + dW$:

$$N_{\delta}'(\beta_p, W) = 2\pi\mathcal{N}_t \left(\frac{e^2}{mc^2} \right)^2 \frac{Z^2}{\beta_p^2} mc^2 \frac{dW}{W^2} \quad \dots\dots (1)$$

where \mathcal{N}_t is the total number of electrons per unit volume, and β_p is the velocity of the primary particle ($c=1$).

Integrating this over W gives for N_{δ} ,

$$N_{\delta} = 2\pi\mathcal{N}_t \left(\frac{e^2}{mc^2} \right)^2 \frac{Z^2}{\beta_p^2} \left(\frac{mc^2}{W_{\min}} - \frac{mc^2}{W_{\max}} \right). \quad \dots\dots (2)$$

For large energies of the primary particle and for very close collisions, other forces, connected with spin, need to be taken into consideration (Bhabha 1938), and eqn. (1) becomes replaced by

$$N_{\delta}'(\beta_p, W) = 2\pi\mathcal{N}_t \left(\frac{e^2}{mc^2} \right)^2 \frac{Z^2}{\beta_p^2} mc^2 [1 + f(W, \sigma, \beta_p, Z)] \frac{dW}{W^2} \quad \dots\dots (3)$$

but for the present problem $f(W, \sigma, \beta_p, Z) \ll 1$, and this term is usually dropped, use being made only of eqns. (1) and (2). A further refinement was introduced by Ashkin (1949), who took Mott's (1929) expression for the cross section for the scattering of electrons by atomic nuclei and transformed it into the rest frame

of the electrons, using relativistic kinematics. This is still an approximation, however, as it is assumed that the electrons are initially free and at rest, whereas in a real solid they are both bound and in motion. On working it out we found that allowance for these two conditions made a significant difference to the theoretical expression for N_δ , improving the agreement between theory and observation. Further improvement was obtained by allowing for the effects of straggling.

2.2. Value of W_{\min}

In formula (2) W_{\min} is the minimum energy corresponding to the convention used for accepting a track as a δ -ray, and W_{\max} is the smaller of the two quantities (a) the maximum energy considered in the counting convention and (b) the maximum possible energy for ejected electrons. W_{\max} is usually much greater than W_{\min} , so that, because of the $1/W$ dependence, the calculated value of N_δ is very sensitive only to changes in W_{\min} . For the same reason the observed values of N_δ depend strongly on the convention used. Thus, if we are to compare observations of N_δ with the results of calculations, we must first consider the problem of what numerical values are to be inserted into the formulae.

§ 3. ENERGY LIMITS CORRESPONDING TO δ -RAY COUNTING CONVENTIONS

Two different counting conventions have so far been employed. In the first, used by Bradt and Peters, by Dainton *et al.*, and by many others, all those electron tracks originating in the track of the primary particle which contain not less than a stated number G of grains outside the primary track are accepted as δ -rays. The convention $G \geq 4$ is often used.

In the second, used by Freier *et al.* (1948b) and by Hoang (1951), the criterion is based on range: if a δ -ray is to be accepted, the projection on the plane of the emulsion of the perpendicular distance from some point on the δ -ray to the track of the primary particle must exceed a minimum value of the order of 2 microns. For the sake of brevity these two criteria will henceforth be called the 'grain criterion' and the 'range criterion' respectively.

As anyone with experience in δ -ray counting will easily appreciate, one frequently meets doubtful cases, and in order to eliminate personal judgments as far as possible some further conventions must be employed. We believe that it would be useful if all workers in this field adopted the same conventions, but as yet no such general agreement exists, and it becomes important for individual laboratories at least to state their δ -ray conventions. Those which we found it useful to adopt are given in the Appendix.

Now let $P(W)$ be the probability that a δ -ray of energy W satisfies a certain criterion. Then it is clear that, owing to the statistical nature of the many processes involved in track formation, $P(W)$ is a continuous function which vanishes for small values of W , and approaches unity asymptotically at high δ -ray energies. In previous comparisons with theory it has been tacitly assumed that $P(W)$ has the form of a unit step function. The manner in which we have estimated values of $P(W)$ for the grain and the range criteria will now be stated.

3.1. Grain Criterion

In calculating the probability that a δ -ray track will contain G grains, we make the simplifying assumption that the track is straight, and that it can be

divided up into cells, all of the same size d (see fig. 1), each of which contains a silver bromide crystal which can become a developed grain. For d we take the value of 0.6 micron, the mean diameter of the developed grains in our emulsions. Now let p_i be the probability that a crystal will be developed into a grain in the i th cell, counting from the end of the track. Then two problems arise whose influence will be investigated: (a) the purely statistical problem of determining the distribution in numbers of developed grains given the values of p_i as a function of cell number i and (b) the effect of fluctuations in p_i . The effects of scattering, variations in grain size and grain sensitivity are considered to be of secondary importance and will be ignored.

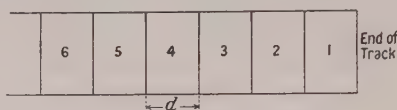


Fig. 1.

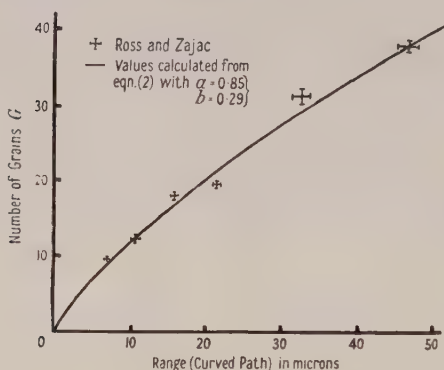


Fig. 2. Grain-number-range relation for electrons. The points (with standard deviations) are experimental results by Ross and Zajac, modified for G5 emulsion. The curve was calculated from formula (5).

In our laboratory we have sometimes found it useful to adopt a relation of the following form (Herz 1952):

$$p_i = a - b \log_{10} R_i \quad \dots\dots (4)$$

where p_i is the probability that the i th grain, at a residual range of R_i microns, will be developed. This, of course, is a purely empirical interpolation formula whose only justification lies in the agreement it gives with experimental data. The average number of grains in a track of range $R_k = kd$ then follows from (4):

$$G_{av} = ka - b \sum_{i=1}^k \log R_i \quad \dots\dots (5)$$

In fig. 2, the experimental results of Ross and Zajac (1949), modified so as to apply to G5 emulsion (Ross 1952, private communication), are compared with formula (5), in which the values $a = 0.85$, $b = 0.29$ have been inserted. It is seen that the agreement is satisfactory.

The probability of finding just G developed grains in a track of k cells is then given by the coefficient of t^G in the expansion of

$$\prod_{i=1}^k (p_i t + 1 - p_i) \quad \dots\dots (6)$$

This completes the solution of the purely statistical problem.

To account for straggling we now assume that the actual ranges of mono-energetic electrons are distributed normally about the mean with standard deviation $\sigma_R = 0.25R$ (cf. Ross and Zajac 1949) and split the distribution into three groups containing one-third of the tracks each, and with ranges equal to the arithmetic mean values of the three groups. The new values of a and b (eqn. (4)) were determined for the shorter and longer tracks from the modified values of ionization loss for these groups. From eqns. (4) and (6) the probability of finding G grains was calculated separately for the three straggling groups for values of k from 1 to 15, i.e. for residual ranges between 0.3 micron and 8.7 microns. The results for these three groups have been summed over G and averaged together to give $P_G(W)$, the probability that a δ -ray of energy W will contain G or more developed grains. The results are displayed in fig. 3 for four- and five-grain δ -rays. In computing $P_G(W)$ allowance has been made for the fact that, depending on the orientation of the first few grains in the δ -ray track, one or more of these will be obscured by the track of the primary particle, and thus will not be counted. It has been assumed that the track of the primary is one grain diameter (0.6μ) wide: the calculation does not, therefore, apply to δ -rays produced by very heavy nuclei.

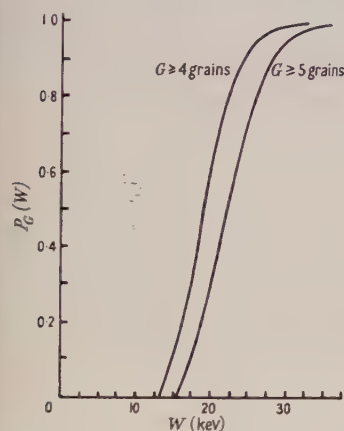


Fig. 3. The probability $P_G(W)$ that a δ -ray of energy W will contain G or more grains.

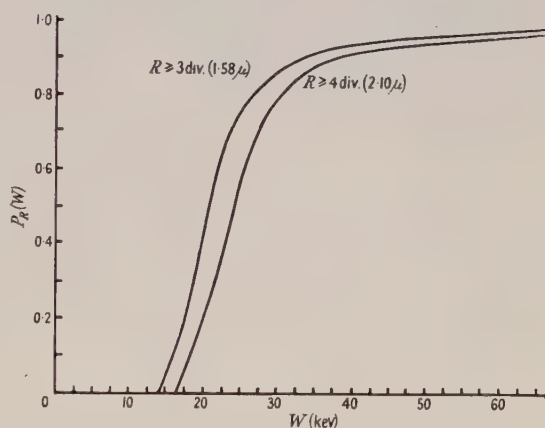


Fig. 4. The probability $P_R(W)$ that a δ -ray of energy W will reach a projected distance of R or more from the primary track.

3.2. Range Criterion

Most of the δ -ray electrons move off initially in a direction at right angles to the path of the primary particle, but, because of scattering, the directions of the first portion of the tracks of low-energy δ -rays are very nearly isotropically distributed about their points of origin. Owing to scattering, also, the maximum distance which an electron reaches from its point of origin will be less than its true or curved-path range.

The relation between the curved-path range and the maximum distance reached was studied by Williams (1931) for 20-keV electrons. He found ratios of 1.24 for oxygen and 1.48 for argon, and he deduced from this a ratio of 1.35 for aluminium, an element very similar in its ionization and scattering properties to nuclear-research emulsion. This relation has been confirmed experimentally by R. H. Herz (1949) for 25- and 50-keV electrons in nuclear-research emulsion, and we may safely assume that it can be applied to the present problem.

Taking these considerations into account, we have calculated values of the probability $P_R(W)$ that a δ -ray of energy W should at least reach a projected distance R from the path of the primary particle. The effect of straggling was dealt with in the same way as in the previous calculation of the grain-criterion probabilities. The results are given in fig. 4 for values of R of 1.58μ and 2.10μ , corresponding to three and four divisions on our eyepiece scales. These results are independent of the thickness of the track of the primary particle.

§4. CALCULATION OF N_δ

It is convenient to consider the problem under the usual separate headings of 'close' and 'distant' collisions. A collision is considered to be 'close' if the impact parameter is less than the mean orbital radius of the electron, and 'distant' if it is greater than this radius.

4.1. Notation

Let S denote the laboratory rest frame, S' the rest frame of the incident particle. Then all symbols for quantities measured in S' have also been given a prime, e.g. β_e' . Symbols referring to the primary particle, the electron with which it collides (before collision), and the resulting δ -ray have been given the suffixes p , e and δ respectively.

All velocities are measured in units of c , and denoted by β . We also use the notation $\gamma \equiv (1 - \beta^2)^{-1/2}$.

4.2. Close Collisions

We found it most convenient to solve this problem by Ashkin's (1949) procedure, i.e. to make a Lorentz transformation of Mott's (1929) formula for the nuclear scattering of electrons, with the difference that we consider the electron to be initially in motion in some arbitrary direction. This makes the arithmetic somewhat tedious, although the fundamental ideas are quite simple and straightforward.

Consider the collision of a heavy particle of charge $Z|e|$ and velocity β_p , with an atomic electron of binding energy ϵ and moving at the time of collision with a velocity β_e in a direction (θ, ϕ) to the line of motion of the heavy particle. In the rest frame S' of the charged primary the electron will have the following velocity components:

$$-\frac{\beta_p - \beta_e \cos \phi}{1 - \beta_p \beta_e \cos \phi}, \quad \frac{\beta_e \sin \phi \sin \theta}{\gamma_p(1 - \beta_p \beta_e \cos \phi)}, \quad \frac{\beta_e \sin \phi \cos \theta}{\gamma_p(1 - \beta_p \beta_e \cos \phi)}. \quad \dots\dots(7)$$

We first calculate the number of electrons scattered into the solid angle $d\omega'$ at (Θ', Φ') . It is

$$dN = \mathcal{N}_\omega \sigma(\psi', \beta_e') d\omega' \quad \dots\dots(8)$$

where \mathcal{N}_ω denotes the number of electrons per cm^3 in the laboratory frame, moving with velocity β_e in the solid angle $\sin \phi d\theta d\phi$ at (θ, ϕ) , $\sigma(\psi', \beta_e')$ is the Mott cross section, and ψ' is the angle of scattering in S' , given by

$$\cos \psi' = \frac{1}{\beta_p'} \left\{ -\frac{\cos \Phi' (\beta_p - \beta_e \cos \phi)}{1 - \beta_p \beta_e \cos \phi} + \frac{\sin \Theta' \sin \Phi' \beta_e \sin \theta \sin \phi}{\gamma_p(1 - \beta_p \beta_e \cos \phi)} + \frac{\cos \Theta' \sin \Phi' \beta_e \cos \theta \sin \phi}{\gamma_p(1 - \beta_p \beta_e \cos \phi)} \right\}. \quad \dots\dots(9)$$

In S' these electrons retain their velocity β_e' after the (elastic) collision, but this is not the case in S . We require the number of electrons which have a velocity greater than a given value β_δ in S , and in S' all these are found within the solid angle between $\Phi' = 0$ and $\Phi' = \pi - \Phi_0'$ where

$$\cos \Phi_0' = \frac{1}{\beta_p \beta_p'} \left\{ 1 - \frac{\gamma_\delta}{\gamma_p \gamma_p'} \right\}. \quad \dots\dots(10)$$

Integrating expression (8) over this solid angle we find the number of electrons which originally moved as stated above and give δ -rays of velocities greater than β_δ :

$$\begin{aligned} \int_{\Theta'=0}^{2\pi} \int_{\Phi=0}^{\pi-\Phi_0'} dN &= \mathfrak{N}(\theta, \phi, \beta_e) \sin \phi \, d\theta \, d\phi \\ &= \frac{\mathcal{N}_\omega \kappa B^2}{(\gamma_e^2 + \gamma_\delta^2)(B^2 - \gamma_e^{-2} \gamma_p^{-2})} \left\{ \frac{\gamma_\delta^2 + \beta_p^2 \gamma_p^2}{\gamma_e^2 \gamma_p^2} + B^2 - 2B \frac{\gamma_\delta}{\gamma_e} \right\} \\ &\quad - \frac{\mathcal{N}_\omega \kappa}{\beta_p^2 \gamma_p^2} \ln \frac{2\beta_p^2 \gamma_p^2}{\gamma_\delta - 1} \quad \dots\dots(11) \end{aligned}$$

where $B = 1 - \beta_p \beta_e \cos \phi$ and κ is a numerical constant.

We now replace \mathcal{N}_ω and B by the expressions they represent and integrate (11) over all admissible values of θ and ϕ to get the contribution to the δ -ray density of all the electrons which originally moved with velocity β_e :

$$N_n(\beta_e, \beta_\delta, \beta_p) = \int_{\theta=0}^{2\pi} \int_{\phi_1}^{\phi_2} \mathfrak{N}(\theta, \phi, \beta_e) \sin \phi \, d\theta \, d\phi. \quad \dots\dots(12)$$

The limits ϕ_1 and ϕ_2 must be chosen in such a way that only positive values of \mathfrak{N} are accepted.

The velocity β_e depends on the binding energy of the shell in which the electron moves, and β_δ is determined by the low-energy limit W_{\min} . On summing over the shells we obtain the total density of δ -rays with energies greater than W_{\min} in the laboratory frame, and due to close collisions:

$$N_{\text{el}} = \sum N_n(\epsilon_n, W_{\min}, \beta_p) \quad \dots\dots(13)$$

where ϵ_n is the binding energy in the n th shell, and the density of n th-shell electrons has already been introduced through the value of \mathcal{N}_ω . The spin term s (a few per cent) has been approximated by the positive values of

$$\frac{Z^2 e^4 \pi}{m^2 c^4} \frac{1}{\beta_p^2 \gamma_p^2} \ln \frac{2\beta_p^2 \gamma_p^2}{\gamma_\delta - 1}.$$

In explicit form the integral (12) can be written

$$N_n = \frac{Z^2 e^4 \pi}{m^2 c^4} (I_1 + I_2 + I_3) \frac{1}{(\gamma_\delta^2 - \gamma_e^2) \gamma_e \beta_p \beta_e} - s \quad \dots\dots(14a)$$

where

$$I_1 \equiv \frac{1}{2} \gamma_p \left\{ 1 + \frac{2 + \gamma_\delta^2}{\gamma_p^2} \right\} \{ \coth^{-1} \gamma_p x_2 - \coth^{-1} \gamma_p x_1 \}$$

$$I_2 \equiv \gamma_\delta \ln \frac{x_2^2 - \gamma_p^{-2}}{x_1^2 - \gamma_p^{-2}}$$

$$I_3 = \gamma_p^2 \frac{x_1 - x_2}{4} \left\{ \frac{(1 - \gamma_\delta / \gamma_p)^2 + \gamma_\delta / \gamma_p + 1}{1 - \gamma_p(x_1 + x_2) + x_1 x_2 \gamma_p^2} + \frac{1}{\gamma_p^2} \right\} \quad \dots\dots(14b)$$

and

$$\begin{aligned} x_1 &\equiv \gamma_e(1 + \beta_p\beta_e) \\ x_2 &\equiv \begin{cases} \gamma_\delta(1 - \beta_p\beta_\delta) & \text{for } \beta_+ < \beta_p < \beta_0 \\ \gamma_e(1 - \beta_p\beta_e) & \text{for } \beta_p > \beta_0 \end{cases} \\ \beta_0 &\equiv \frac{\gamma_\delta - \gamma_e}{\beta_\delta\gamma_\delta - \beta_e\gamma_e}, \quad \beta_+ \equiv \frac{\gamma_\delta - \gamma_e}{\beta_\delta\gamma_\delta + \beta_e\gamma_e}. \end{aligned} \quad \text{.....(14 c)}$$

Equations (13) and (14) are the solution of the close-collision problem. In obtaining them, the effect on the Mott formula of the field of the parent nucleus of an electron in a particular shell has been neglected. We investigated this effect, using the Born approximation, and found it to be negligible for the collisions in which we are interested.

Values computed from eqns. (13) and (14) will be discussed in §5 after we have considered the distant collisions.

4.3. Distant Collisions

Following Williams (1934) and von Weizsäcker (1934), the distant collisions may be treated as the photoelectric absorption of the virtual quanta of the incident particle. The number of virtual photons with frequencies in the range $(\nu, \nu + d\nu)$ for collisions with impact parameter greater than p_n is well known:

$$N_{h\nu}(\nu, p_n) d\nu = \frac{2\alpha}{\pi} \frac{Z^2}{\beta_p^2} \frac{d\nu}{\nu} \ln \frac{c\beta_p\gamma_p}{2\pi\nu p_n}. \quad \text{.....(15)}$$

The experimentally determined cross section for photoelectric absorption from the n th shell of atoms of atomic number Z' may be expressed as

$$\sigma'(n, Z', \nu) = F(n, Z')\nu^{-3}. \quad \text{.....(16)}$$

From (15) and (16) it follows that the total cross section for the photoelectric emission of an electron from a given shell may be calculated in the usual manner:

$$\sigma(n, Z') = \int_{\nu_{\min}}^{\nu_{\max}} N_{h\nu}(\nu, p_n) \sigma'(n, Z', \nu) d\nu \quad \text{.....(17)}$$

where $h\nu_{\min} = \epsilon_n + W_{\min}$. Formula (17) must then be summed over the various shells of the constituent atoms of the emulsion. In practice we found that only the K and L shells of silver and bromine were of importance. In evaluating (17), the value of p_n in (15) was taken as the radius of the particular shell, and numerical values of $F(n, Z')$ in (16) were taken from Compton and Allison (1935).

The proportion of δ -rays resulting from distant collisions depends on the lower limit, as the energy distributions of the produced electrons are different, being proportional to W^{-2} for close and W^{-4} (eqns. (15), (16), (17)) for distant collisions.

For $W_{\min} = 20$ kev, and at high values of β_p , the distant collisions contribute about 6% of the total number of δ -rays. It may be seen from the occurrence of γ_p inside the logarithm in eqn. (15) that the distant-collision contribution shows a logarithmic rise, which would in practice be masked by the much larger close-collision contribution which does not show any such rise. Saturation of the distant-collision contribution at extreme energies due to polarization effects would be expected to follow a similar course to the known saturation of grain density in similar emulsions.

4.4. Theoretical Results

Adding together the contributions from the close and distant collisions, we obtain $N'(\beta_p, W)$ the density of δ -rays in the energy range $(W, W + dW)$ produced by a singly charged particle of velocity β_p . This still refers to electrons of a certain energy, whereas the quantity observed is the density of δ -rays $N_\delta(\beta_p, G)$ containing a minimum number G of grains, or the density of those exceeding the range criterion, $N_\delta(\beta_p, R)$. These latter quantities are clearly to be obtained from:

$$N_\delta(\beta_p, G) = \int_0^{W_{\max}} P_G(W) N'_\delta(\beta_p, W) dW$$

$$N_\delta(\beta_p, R) = \int_0^{W_{\max}} P_R(W) N'_\delta(\beta_p, W) dW. \quad \dots\dots(18)$$

The differential densities $N'_\delta(\beta_p, W)$ were obtained by computing the integral densities for several energies and then differentiating with respect to W .

Values of $P_G(W)$ and $P_R(W)$ have been given in figs. 3 and 4. The theoretical values of the δ -ray density, obtained by inserting in eqn. (18) values of $P(W)$ from figs. 3 or 4, are plotted as a function of β_p in fig. 5 for two different values of the minimum grain number G , and for two different values of the minimum range R .

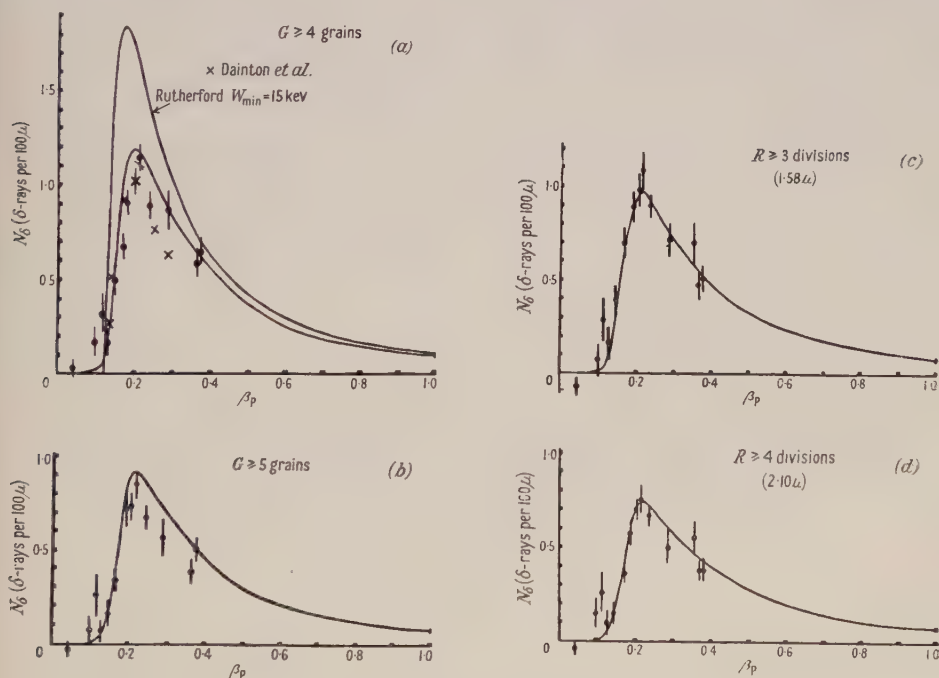


Fig. 5. Comparison between experimental results and theory. The errors shown are statistical standard deviations.

§ 5. EXPERIMENTAL RESULTS

In order to test the theory, observations were made of the density of δ -rays on the tracks of protons ending in the emulsion, and of length greater than 3 mm. That they were reasonably classified as protons was checked by determining

their masses by a multiple-scattering method developed by Tennent (1953). For values of β_p around 0.4 the δ -ray density was measured on long tracks of μ -mesons, all of which came to rest in the emulsion and had a decay-electron track at the ends of their ranges. For values of β_p near unity the δ -ray density was measured on long tracks of particles at 'plateau' grain density.

The emulsions used were Ilford type G5 of thickness 400μ which had been exposed at a depth of three metres in the glacier at the Jungfraujoch.

The δ -rays accepted were those which satisfied the following criteria: (a) containing 4 or more grains, (b) 5 or more grains, (c) reaching a projected distance from the primary track greater than 1.58μ (3 eyepiece-scale divisions), (d) greater than 2.1μ (4 eyepiece-scale divisions).

5.1. Comparison with Theory

The experimental results for each of the four criteria are given in figs. 5(a)–(d). These results have been corrected for background in a manner described below. There is seen to be a marked disagreement with values calculated using the

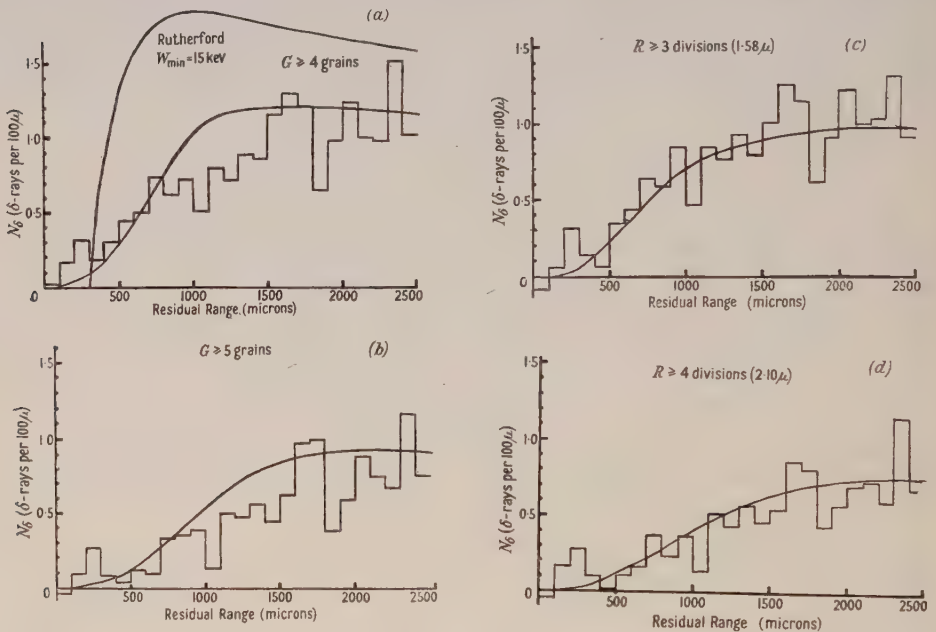


Fig. 6. Comparison between experimental results and theory. δ -ray densities on tracks of protons ending in the emulsion.

Rutherford formula, particularly at low values of β_p . The results for values of β_p up to 0.2, derived from δ -ray counts on proton tracks, are given on a more open scale, and as a function of range, in figs. 6(a)–(d). The agreement will be seen to be very good in the case of the range criteria, but the calculated values still lie slightly above the observed ones when the grain criterion is used.

It might be worth emphasizing that both the calculated curves and the observed values in figs. 5 and 6 are drawn on an absolute scale. The theory contains no adjustable parameters and, apart from the background correction, the observations have not been adjusted or normalized in any way. The difference between the two criteria will be discussed further below.

5.2. The Background Correction

The background of low-energy electrons distributed throughout the emulsion contributes to the observed density of δ -rays, and a correction to the observed values is therefore necessary. We have attempted to determine the background by counting the apparent δ -rays satisfying our various criteria when scanning along a straight line in the emulsion in an arbitrary direction, not connected with the track of an ionizing particle. We found that in every case the background density obtained was equal within the statistical limits of accuracy to the difference between the experimental and the theoretical δ -ray densities we had obtained at $\beta_p = 1$.

We then found that if we subtracted the difference between the experimental and theoretical densities at $\beta_p = 1$ from *all* our experimental points the agreement between theory and experiment for the whole range of β_p from 0 to 1 became excellent in the case of the range criterion, and that it was much improved for the grain criterion.

We concluded that this difference is a good estimate of the background, and we have subtracted it from the observed δ -ray densities to obtain the results given in figs. 5 and 6. The values of these corrections are given in the table.

Background δ -Ray Densities

	Criterion			
	Grains (G)		Range (div.)	
	≥ 4	≥ 5	≥ 3	≥ 4
$N_\delta/100\mu$	0.07	0.07	0.15	0.11

§ 6. DISCUSSION

As we have shown in fig. 5(a), our experimental results for the four-grain criterion are in very reasonable agreement with those of Dainton *et al.* (1952). A small discrepancy remains, but this is most likely due to slight differences in the conventions used. Our results are also similar to those obtained by Fowler (1953, unpublished) by counting δ -rays along the tracks of slow protons. We are confident, therefore, that our experimental methods and conventions are sufficiently similar to those of other workers to make direct comparisons of results meaningful.

Because of the good agreement between theory and experiment in the case of the range criterion, we believe that our methods of attacking the problem were, in the main, correct. There is still some disagreement, however, between the grain-criterion theory and our experimental results, especially at low values of the velocity of the primary particle, and this we think to be due to the approximations we have made in our statistical treatment of this convention. It would be very difficult to make further refinements in the theory in order to give a more adequate theoretical account of the very complex experimental situation, and we do not think that a more elaborate treatment would be justified at present, especially as we have found that the range criterion is preferable in practice to the grain criterion.

The advantage of the range criterion is that it is basically an objective one, for personal judgments are required only in a few cases, and even then a set of conventions such as the one we have used (see Appendix) will do a great deal to promote uniformity of judgment. With the grain criterion, on the other

hand, one constantly has to estimate the numbers of grains in clusters, and one has to decide whether or not grains belong to the tracks of the primary. This makes it difficult to maintain consistency over long periods of time or between different observers. In practice we have found that the range criterion is easy to learn, and, once an observer has learnt it, his results are consistent with those of others without further difficulty. Proper care must, of course, be taken with the measurements; good optical definition in particular is necessary. The grain criterion we found hard to learn, and consistency could be achieved only by constant comparison of results and discussion between the observers concerned. A further disadvantage of the grain criterion is that the number of grains visible in the track of a δ -ray of given energy depends on the thickness of the primary track. It is thus not possible to compare grain-criterion δ -ray counts on the thick tracks of very heavy nuclei with those on the tracks of lighter particles without making a correction for obscuration. With the range criterion this difficulty does not, of course, occur as long as the limiting range is chosen sufficiently great.

ACKNOWLEDGMENTS

We should like to thank Mr. P. H. Fowler for a number of helpful discussions, and him and Dr. M. A. S. Ross for giving us their unpublished results. We are grateful to Dr. R. M. Tennent for providing us with many identified protons, and to Mr. N. C. Barford for a number of stimulating discussions and suggestions during the early stages of this work. The computations were carried out by Messrs. Scientific Computing Services, Ltd., whose help we gladly acknowledge. One of us (D. A. T.) is indebted to the Department of Scientific and Industrial Research for a maintenance grant.

REFERENCES

- ASHKIN, J., 1949, quoted by Bradt and Peters in *Cosmic Radiation*, 1949 (London: Butterworths Scientific Publications), p. 9.
- BHABHA, H. J., 1938, *Proc. Roy. Soc. A*, **164**, 257.
- BRADT, H. L., and PETERS, B., 1948, *Phys. Rev.*, **74**, 1828; 1950 a, *Phys. Rev.*, **80**, 943; 1950 b, *Ibid.*, **77**, 54.
- COMPTON, A. H., and ALLISON, S. K., 1935, *X-Rays in Theory and Experiment* (London: Macmillan).
- DAINTON, A. D., FOWLER, P. H., and KENT, D. W., 1951, *Phil. Mag.*, **42**, 317; 1952, *Ibid.*, **43**, 729.
- FREIER, P., LOFGREN, E. J., NEY, E. P., OPPENHEIMER, F., BRADT, H. L., and PETERS, B., 1948 a, *Phys. Rev.*, **74**, 213.
- FREIER, P., LOFGREN, E. J., NEY, E. P., and OPPENHEIMER, F., 1948 b, *Phys. Rev.*, **74**, 1818.
- HERZ, A. J., 1952, *Thesis*, University of London.
- HERZ, R. H., 1949, *Phys. Rev.*, **75**, 478.
- HOANG TCHANG-FONG, 1951, *J. Phys. Radium*, **12**, 739.
- MOTT, N. F., 1929, *Proc. Roy. Soc. A*, **124**, 425.
- ROSS, M. A. S., and ZAJAC, B., 1949, *Nature, Lond.*, **164**, 311.
- TENNENT, R. M., 1953, *Thesis*, University of London.
- VON WEIZSÄCKER, C. F., 1934, *Z. Phys.*, **88**, 612.
- WILLIAMS, E. J., 1931, *Proc. Roy. Soc. A*, **130**, 310; 1934, *Phys. Rev.*, **45**, 729.

APPENDIX—CONVENTIONS

(i) General

Perhaps the most difficult of the decisions one has to make is whether or not a particular electron track originates in the track of the primary. This decision is especially difficult for electron tracks which contain only a few grains, widely spaced. For this we have adopted the following convention (fig. 7(a)):

(a) if doubtful δ -ray contains 5 grains or less, count only if $a + b \leq 4$ grain widths,

(b) apply personal judgment if there are more than 5 grains: there is not usually any difficulty in these cases.



Fig. 7 (a).



Fig. 7 (b)



Fig. 7 (c).

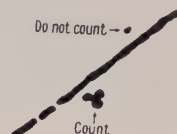


Fig. 7 (d).

Frequently, doubtful cases of the kind shown in fig. 7(b) occur: here we have found no really satisfactory alternative to 'personal judgment'. As an example, however, fig. 7(c) shows a type of configuration which we would always count as one, not two, δ -rays if it is otherwise acceptable according to the criterion in force.

(ii) Grain Criterion

Only those grains are to be counted which lie entirely outside the primary track. They may, however, touch it: they need not be separated completely. Thin-filament connections between grains do not count as grains. Grains above or below the primary track are counted if they are otherwise acceptable.

(iii) Range Criterion

Clusters of grains, completely separated from the primary track, but acceptable according to the range criterion, are to be counted only if they contain three or more grains (fig. 7(d)).

An Investigation of (d, p) Stripping Reactions V : Results for some of the Light Elements and Conclusions

BY J. R. HOLT AND T. N. MARSHAM

Nuclear Physics Research Laboratory, University of Liverpool

Communicated by H. W. B. Skinner; MS. received 15th June 1953

Abstract. Angular distribution measurements have been carried out on proton groups emitted under bombardment by 8 mev deuterons from targets of ${}^6\text{Li}$, ${}^7\text{Li}$, ${}^9\text{Be}$, ${}^{10}\text{B}$ and ${}^{11}\text{B}$. The theory of the stripping process has been applied to determine in each case the orbital angular momentum l of the captured neutron. In the following list the values of l are shown in brackets after the excitation energy of the product nucleus (in mev):

${}^6\text{Li} \rightarrow {}^7\text{Li}$, ground state (1), 0.478(1); ${}^7\text{Li} \rightarrow {}^8\text{Li}$, ground state (1); ${}^9\text{Be} \rightarrow {}^{10}\text{Be}$, ground state (1); ${}^{10}\text{B} \rightarrow {}^{11}\text{B}$, ground state (1); ${}^{11}\text{B} \rightarrow {}^{12}\text{B}$, ground state (1), 0.95(1), 1.67(0), 3.38(1), 4.53(2).

Similar measurements have been made on triton groups from ${}^7\text{Li}$ and ${}^9\text{Be}$ and the results compared with the theory of Newns.

The results of this and previous work on stripping are discussed.

§ 1. INTRODUCTION

IN the previous papers of this series (Holt and Marsham 1953 a, b, c, d, to be referred to as I, II, III, IV) angular distribution measurements have been reported on the protons emitted under bombardment by 8 mev deuterons from a variety of elements having values of atomic number in the range 12 to 38. The results of similar measurements with the light elements lithium, beryllium and boron are reported here. Measurements have also been made on groups of tritons from beryllium and lithium and the angular distributions compared with the theory of Newns (1952). Previous measurements of angular distributions of proton groups from beryllium have been reported by El Bedewi (1952) with 7.7 mev deuterons, by Black (1952) with 14.5 mev deuterons, and by Fulbright *et al.* (1952) with 3.6 mev deuterons. Measurements have been made at lower energies by de Jong and Endt (1952), Resnick and Hanna (1951) and Canavan (1952). El Bedewi and Fulbright *et al.* also made measurements on a group of tritons from beryllium.

§ 2. TARGET PREPARATION

Natural lithium contains the isotopes ${}^7\text{Li}$ and ${}^6\text{Li}$ in the proportions 92.5 : 7.5. Separated isotopes were available in the form of the carbonate and the target of ${}^6\text{Li}$ was prepared by dissolving some of this in a drop of water and allowing the solution to evaporate on a thin gold foil. The resulting layer had a thickness of about 2.5 mg cm^{-2} . To avoid interference from oxygen and carbon the more abundant isotope was investigated in the form of a self-supporting foil of natural lithium made by squeezing a small piece of the metal between polished steel plates. This had a thickness of about 3 mg cm^{-2} .

The target of ^9Be was a self-supporting foil having a thickness of about 1 mg cm^{-2} prepared by evaporation.

Natural boron contains the isotopes ^{11}B and ^{10}B in the proportions 81.6:18.4. Separated isotopes were available as deposited layers on thick platinum. It was found possible to cleave a flake of ^{11}B from the platinum having an area of about 10 mm^2 and a thickness of about 8 mg cm^{-2} . This was cemented at one corner to a gold support and used as a target. Measurements on ^{10}B were carried out with a layer of natural boron powder deposited on gold foil from an aqueous suspension.

§ 3. ANGULAR DISTRIBUTIONS

The reactions $^6\text{Li}(d, p)^7\text{Li}$ and $^7\text{Li}(d, p)^8\text{Li}$.

Angular distribution measurements were made on the two proton groups from $^6\text{Li}(d, p)^7\text{Li}$ leading to the ground state of ^7Li and the first excited state at 0.478 mev. The results are shown plotted in the centre-of-mass system in fig. 1, the vertical scale being the same for both distributions. The full curves

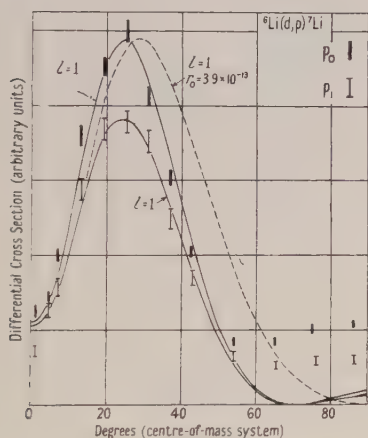


Fig. 1. Angular distributions of the proton groups p_0 and p_1 from $^6\text{Li}(d, p)^7\text{Li}$.

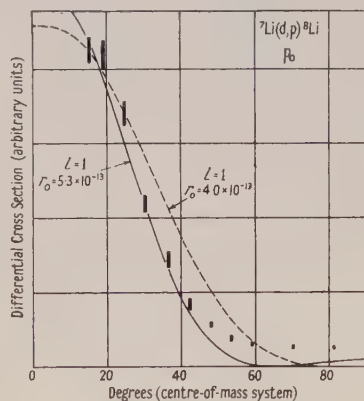


Fig. 2. Angular distribution of the proton group p_0 from $^7\text{Li}(d, p)^8\text{Li}$.

were drawn according to the theory of Butler (1951) with a radius parameter $r_0 = 4.9 \times 10^{-13}\text{ cm}$ and $l=1$ in both cases. The broken curve was drawn using a value for r_0 given by the usual formula $(1.7 + 1.22A^{1/3}) \times 10^{-13}\text{ cm}$, namely $3.9 \times 10^{-13}\text{ cm}$.

Owing to the small Q -value for the reaction $^7\text{Li}(d, p)^8\text{Li}$ measurements could be made only on the proton group corresponding to the ground state of ^8Li , and it was not possible to make observations on this group at small angles. The resulting angular distribution is shown in fig. 2, where the measured points are fitted by a theoretical curve having $r_0 = 5.3 \times 10^{-13}\text{ cm}$ and $l=1$. The broken curve was drawn for $r_0 = 4.0 \times 10^{-13}\text{ cm}$, the value given by the above formula. As in the case of ^6Li the use of this formula for the radius did not give such good agreement with experiment as in the previously reported work on heavier elements. The differential cross section of this transition was obtained by comparison with the intensity of deuterons scattered elastically from the target at an angle of 16° and assuming the Rutherford formula to hold for the elastic cross section.

The reaction ${}^9\text{Be}(d, p){}^{10}\text{Be}$.

As noted in § 1 the reaction ${}^9\text{Be}(d, p){}^{10}\text{Be}$ has been studied by several workers. We have re-measured the angular distribution of the protons from the transition to the ground state of ${}^{10}\text{Be}$. This is shown in fig. 3 in which the full curve was drawn from Butler's theory using $l=1$ and $r_0=5.7 \times 10^{-13}$ cm. The broken curve was drawn using the value 4.24×10^{-13} cm for r_0 obtained from the empirical formula.

The reactions ${}^{10}\text{B}(d, p){}^{11}\text{B}$ and ${}^{11}\text{B}(d, p){}^{12}\text{B}$.

With the target of natural boron, measurements could be made only on the protons corresponding to the formation of the ground state of ${}^{11}\text{B}$. Other proton groups from ${}^{10}\text{B}(d, p){}^{11}\text{B}$ were too weak for the angular distributions to be measured. The result is shown in fig. 4. The theoretical curve which gives the best agreement with experiment has $l=1$ and $r_0=4.8 \times 10^{-13}$ cm. The radius given by the empirical formula is 4.33×10^{-13} cm.

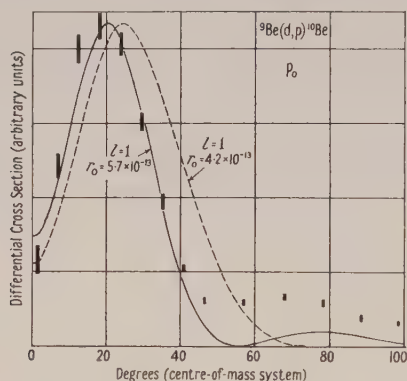


Fig. 3. Angular distribution of the proton group p_0 from ${}^9\text{Be}(d, p){}^{10}\text{Be}$.

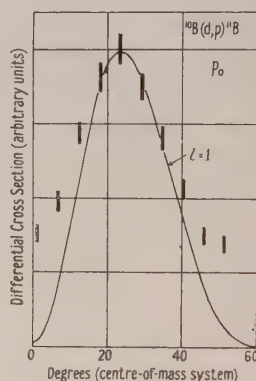


Fig. 4. Angular distribution of the proton group p_0 from ${}^{10}\text{B}(d, p){}^{11}\text{B}$.

The reaction ${}^{11}\text{B}(d, p){}^{12}\text{B}$ has been investigated by Buechner *et al.* (1950) using 1.5 mev deuterons and magnetic analysis. They determined the Q -value for the transition to the ground state to be 1.136 ± 0.004 mev and observed the formation of an excited state of ${}^{12}\text{B}$ at 0.947 ± 0.005 mev. Recent measurements of the same kind by Elkind and Sperduto (1953) point to excited states at 0.95, 1.67, 2.62, 2.72 and 3.38 mev. Our range spectrum for this reaction at an angle of observation of 31° is shown in fig. 5. The arrows p_1 , p_2 , p_3 , p_4 and p_5 indicate the expected positions of proton groups as calculated from the excitation energies given by Elkind and Sperduto, using the value of the deuteron energy (7.95 mev) derived from the Q -value given by Beuchner for the group p_0 . The arrows p_6 and p_7 indicate the expected positions of groups having excitation energies of 3.76 and 4.53 mev which were observed by Bockelman *et al.* (1951, amended by Ajzenberg and Lauritsen 1952) through the resonance scattering of neutrons by ${}^{11}\text{B}$. States p_1 , p_2 and p_6 were also observed in (α, p) experiments by McMinn *et al.* (1951). The intense group indicated by the arrow d is due to elastically scattered deuterons.

The angular distributions of the five proton groups p_0 , p_1 , p_2 , p_5 and p_7 from ${}^{11}\text{B}(d, p){}^{12}\text{B}$ are shown in figs. 6 to 9. The theoretical curves for p_0 , p_1 and p_2

were drawn in each case with $r_0 = 4.4 \times 10^{-13}$ cm, which is the value given by the empirical formula and the agreement with the measured points is in general very

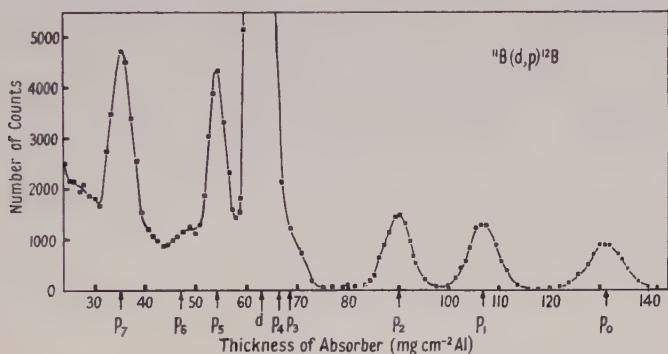


Fig. 5. Range spectrum of particles from deuteron bombardment of a target of ^{11}B at an angle of observation of 31° .

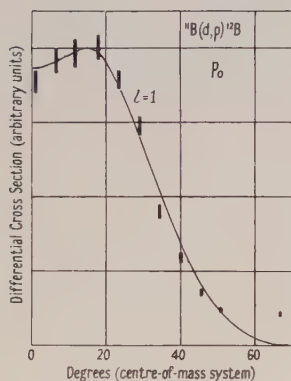


Fig. 6.

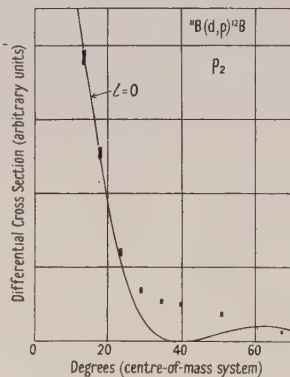


Fig. 8.

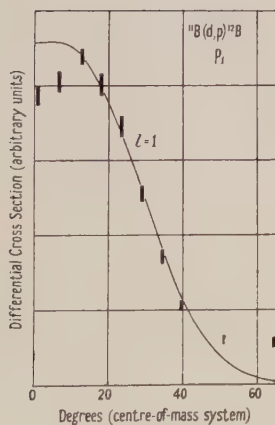


Fig. 7.

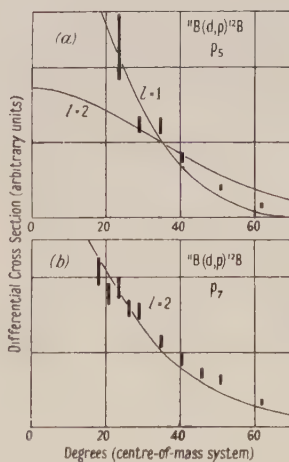


Fig. 9.

Fig. 6-9. Angular distribution of proton groups p_0, p_1, p_2, p_5, p_7 from $^{11}\text{B}(d, p)^{12}\text{B}$.

good. The theoretical curves for p_5 and p_7 were drawn using the theory of Bhatia *et al.* (1952) and a radius $R = 5.4 \times 10^{-13}$ cm, the value required on this theory to give good agreement with the other distributions. The Q -values of these two groups are -2.3 and -3.4 MeV and are in the region where Butler's theory appears to be unreliable (Bhatia *et al.*). The measured angular distribution of the group p_5 is rather inaccurate because it has a range close to that of the elastically scattered deuterons. Theoretical curves with $l=1$ and $l=2$ are shown in fig. 9(a) and it appears, in view of the fact that the theoretical curves in general lie below the experimental points at large angles, that $l=1$ provides the best agreement. The measured points for the group p_7 are fitted by a theoretical curve having $l=2$ (fig. 9(b)).

Differential cross sections for the transitions in $^{11}\text{B}(d, p)^{12}\text{B}$ were determined by comparison with the intensity of the deuterons scattered elastically at an angle of 16° .

The reactions $^{12}\text{C}(d, p)^{13}\text{C}$ and $^{16}\text{O}(d, p)^{17}\text{O}$.

The angular distributions of proton groups from targets of carbon and oxygen bombarded with 8 MeV deuterons have been measured by Burge *et al.* (1951) and Rotblat (1951 a, b). During the course of the present investigation we have re-measured the angular distributions of the protons associated with the transitions to the ground states of ^{13}C and ^{17}O . The parameters in Butler's theory which gave the best fit with the results were $l=1$ and $r_0 = 4.2 \times 10^{-13}$ cm for carbon and $l=2$ and $r_0 = 5.1 \times 10^{-13}$ cm for oxygen.

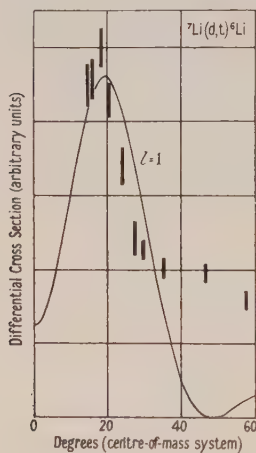


Fig. 10. Angular distribution of the triton group from $^7\text{Li}(d, t)^6\text{Li}$.

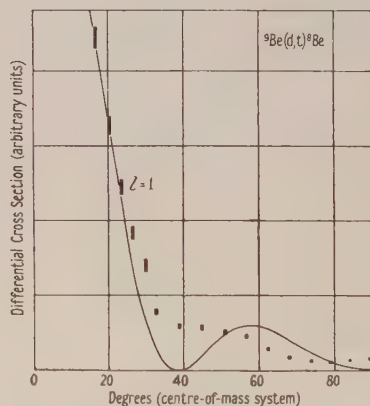


Fig. 11. Angular distribution of the triton group from $^9\text{Be}(d, t)^8\text{Be}$.

The reactions $^7\text{Li}(d, t)^6\text{Li}$ and $^9\text{Be}(d, t)^8\text{Be}$.

Theories of the inverse stripping or 'pick-up' reactions in which a proton or deuteron picks up a neutron from the target nucleus have recently been published by Newns (1952) and Butler and Salpeter (1952). We have measured the angular distributions of the triton groups from the targets of ^7Li and ^9Be leading to the ground states of ^6Li and ^8Be and the results are shown in figs. 10 and 11. The curves were drawn according to the theory of Newns (non-perturbation method) to give the best agreement with experiment by suitable choice of the

orbital momentum l of the picked-up neutron and the radius parameter r_0 . In the case of ${}^7\text{Li}$ these were $l=1$ and $r_0=7\times 10^{-13}\text{ cm}$ and in the case of ${}^9\text{Be}$ they were $l=1$ and $r_0=4.7\times 10^{-13}\text{ cm}$.

§ 4. DISCUSSION

The results of the measurements on the (d, p) reactions are summarized in the table. The neutron capture probabilities $\Lambda/(2j_f+1)$ from the theory of Bhatia *et al.* were obtained by using the measured cross sections after subtracting the estimated values of an approximately isotropic background. In column (9) of the table the values of the capture probability have been divided by the statistical weight $(2j_f+1)$ where j_f is the spin of the final state.

The results indicate differences in parity between the ground states of ${}^6\text{Li}$ and ${}^7\text{Li}$, ${}^7\text{Li}$ and ${}^8\text{Li}$, ${}^{10}\text{B}$ and ${}^{11}\text{B}$ and between ${}^{11}\text{B}$ and ${}^{12}\text{B}$. The parity changes and l -values for the various transitions are all consistent with the Mayer shell model.

The spin of the ground state of ${}^{12}\text{B}$ is probably 1 (Nordeim 1951) and that of the excited state associated with p_7 is 3 according to the neutron resonance absorption measurements of Bockelman *et al.* (1951). Using these values for j_f the amended values of the neutron capture probability for these states are 3.4 and 3.8. If we take these as being characteristic of neutron capture into a single-particle state, then much larger values should not occur and we may eliminate some of the possible spin values of the other excited states. Thus 0 is not a likely value for the spin of the first or the fifth excited state, and the spin of the second excited state is probably 2.

(1)	(2)	(3)	(4)	(5)	(6)	(7)	(8)	(9)	(10)
${}^6\text{Li}$	1+	p_0 p_1	0 0.478	1 1	3/2— 5/2, 3/2, 1/2—		∞ 0.73x		
${}^7\text{Li}$	3/2—	p_0	0	1	3, 2, 1, 0+	8.3(0°)	7.1	1.0, 1.4, 2.4, 7.1	
${}^9\text{Be}$	3/2—	p_0	0	1	0+				
${}^{10}\text{B}$	3+	p_0	0	1	3/2—				
${}^{11}\text{B}$	3/2—	p_0 p_1 p_2 p_5 p_6 p_7	0 0.95 1.67 3.38 3.76 4.53	1 3 0 1 [1] 2 2	1+ 3, 2, 1, 0+ 2, 1— 3, 2, 1, 0+ 2+ 3—	7.0(15°) 11(0°) 54(0°) 25(0°) 1(35°) 29(0°)	10 10 17 11 2 27	3.4 1.5, 2.1, 3.5, 10 3.5, 5.8 1.6, 2.2, 3.7, 11 0.4 3.8	0.036 0.28
${}^{12}\text{C}$	0+	p_0 p_1 p_2 p_3	0 3.08 3.68 3.89	1 0 1 2	1/2— 1/2+ 3/2, 1/2— 5/2, 3/2+	32(20°) 100(20°) 11(20°) 75(30°)	19 22 2.7 102	9.5 11 0.7, 1.3 17, 25	0.54 0.031 0.21
${}^{16}\text{O}$	0+	p_0 p_1	0 0.875	2 0	5/2+ 1/2+	36(30°) 270(0°)	62 26	10 13	

(1) Target nucleus, (2) spin of target nucleus and its parity according to the shell model, (3) proton group, (4) excitation (MeV), (5) l -value, (6) spin of final state when known or the alternative values from stripping and the parity, (7) differential cross section ($\times 10^{27}\text{ cm}^2$) at the angle shown, (8) neutron capture probability, (9) N.C.P./ $(2j_f+1)$, (10) reduced level width from resonance scattering (after Ajzenberg and Lauritsen).

Groups p_6 and p_7 correspond to virtual states of ${}^{12}\text{B}$ and it is of interest to compare the neutron capture probabilities for these states with their reduced widths determined from neutron resonance scattering (Bockelman *et al.*) since theory indicates that there should be a close connection between these two quantities (Huby 1952). Group p_6 is relatively weak and difficult to separate

from neighbouring groups in the spectrum. However, we have estimated its differential cross section and calculated the neutron capture probability using the l -value 1 obtained from the known spin and parity of the resultant state. The reduced widths (Ajzenberg and Lauritsen 1952) are shown in the last column of the table.

The results of all the measurements on ^{12}C and ^{16}O are included in the table, the cross sections for the transitions in $^{12}\text{C}(\text{d}, \text{p})^{13}\text{C}$ being taken from the work of Rotblat. The target nuclei ^{12}C and ^{16}O are strongly bound and are expected to be favourable to the formation of single-particle states of the extra neutron which is added in the stripping process (cf. the results for ^{28}Si , ^{32}S and ^{40}Ca in III and IV). The values of the amended capture probability for the transitions to the ground states and first excited states of ^{13}C and ^{17}O are very similar, while the alternative values for the second excited state of ^{13}C are much smaller. These values suggest that the first excited states in both nuclei are single-particle states, whereas the second excited state of ^{13}C is not.

On the basis of the shell model the odd neutron in ^{13}C is in the $1\text{p}_{1/2}$ level in the ground state and the l -value 1 is in accord with this. The next available levels are $1\text{d}_{5/2}$ and $2\text{s}_{1/2}$. The l -value 0 for the first excited state indicates that the $2\text{s}_{1/2}$ level is lower in ^{13}C than the $1\text{d}_{5/2}$ level. The third excited state has a value of the capture probability which suggests that this is also a single-particle state. The spin $5/2$ gives an amended value of the capture probability nearer to those of the other single-particle states than does the alternative possibility $3/2$. The former spin is in agreement with the neutron being in the $1\text{d}_{5/2}$ level and also agrees with the known spin of the corresponding level in the mirror nucleus ^{13}N (Ajzenberg and Lauritsen 1952). The second excited state of ^{13}C is possibly formed by the excitation of a neutron from the $1\text{p}_{3/2}$ level of the core into the $1\text{p}_{1/2}$ level to pair with the captured neutron, as suggested in III for a state in ^{29}Si and one in ^{33}S . The above results may be compared with those from the resonant scattering of protons by ^{12}C . These show that the first and third excited states of ^{13}N have large values of the reduced level width, suggesting that they are single-particle states, while the second has a small value (Jackson and Galonsky 1951). These values are shown in the last column of the table for comparison with the capture probabilities of the corresponding states in the mirror nucleus ^{13}C .

This paper concludes the present series on (d, p) stripping reactions. With 8 mev deuterons and target elements within the region of the periodic table below calcium good agreement with the main features of the measured angular distributions has been obtained using both the theories of Butler and of Bhatia *et al.* The agreement could always be improved by subtracting from the measured distribution an isotropic background which probably represents the contribution of the alternative mode of transition through the formation of a compound nucleus. The differential cross section of this background in most cases lay between 5×10^{-28} and $13 \times 10^{-28} \text{ cm}^2$. Several groups were observed whose angular distributions did not show the well-defined maximum characteristic of the stripping process. The differential cross sections of these lay within the limits mentioned above, and it is likely that in these cases the differential cross section for stripping was smaller than that for the compound nucleus process.

In the determination of the values of l from the comparison of theoretical angular distributions with experiment we have used the formula

$$r_0 = (1.7 \times 1.22 A^{1/3}) \times 10^{-13} \text{ cm}$$

for the radius parameter in Butler's theory. This gave good agreement with experiment for the nuclei between Mg and Ca, but discrepancies appeared for some of the light elements. These were not sufficient to give rise to any ambiguity in the assignment of the l -value. However, we have determined, for each element investigated, the value of r_0 which gave the best agreement between theory and experiment. For any particular element the same value of r_0 gave good agreement for all the states investigated except that curves having $l=0$ required a value greater by about 1×10^{-13} cm. In fig. 12 the best values of r_0 , determined from distributions having $l=1$ or 2, are plotted against $A^{1/3}$ for the various elements. The point for ^{14}N was estimated by fitting curves to the distributions measured by Gibson and Thomas (1951). Also shown are the values of the nuclear radius derived from measurements by Coon *et al.* (1952) of the total cross section of each element for 14 mev neutrons. These were obtained by using the expression $r = \sqrt{(\sigma/2\pi)}$ and making a correction for the wavelength of the neutrons (Blatt and Weisskopf 1952). The trend of the variation with mass

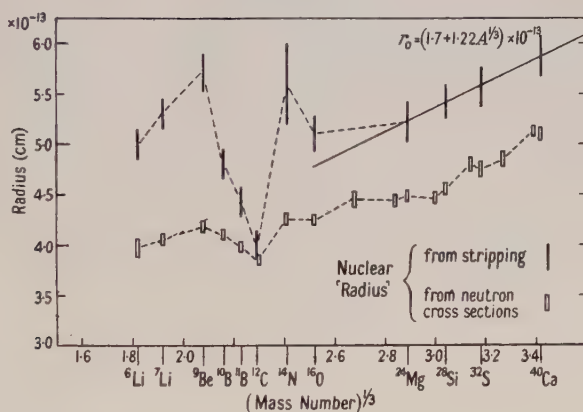


Fig. 12. Variation with mass number of the radius parameter used in stripping theory and of the nuclear radius determined from fast neutron total cross sections.

number is similar for the two sets of points, although the value obtained from stripping is always the greater of the two for a particular element. Thus starting with ^6Li the radius increases to a maximum at ^9Be and then decreases to a minimum at ^{12}C followed by a rapid increase to ^{14}N and then more gradual changes. These variations are more marked in the radii determined from the stripping reactions.

From comparisons with the theory of Bhatia *et al.* it appears that this theory yields angular distributions which are practically identical for positive Q -values with those derived from Butler's theory provided that the radius parameter R is given a value greater than that of r_0 by 1×10^{-13} cm. Thus the variations of this parameter for different target nuclei are the same on both theories.

From the relative differential cross sections of the various proton groups in the spectrum from each element we have derived relative values of the neutron capture probability $\Lambda/(2j_i + 1)$ according to the theory of Bhatia *et al.* In cases where the differential cross sections were determined absolutely the capture probabilities for different nuclei have been expressed in the same units. To convert the tabulated values to the c.g.s. system they should be multiplied by

8.94×10^{-50} . This applies to the values given in all the papers, including I and II, although in these two papers the differential cross sections are quoted incorrectly and should be divided by 4.

The largest values of the capture probability, amended for the spin of the final state, are expected to be associated with the formation of single-particle levels. We have found in general that the corrected values for transitions to ground states are among the largest values for a given nucleus and moreover these largest values are fairly constant, at about 3, for most nuclei between which comparisons could be made. Carbon and oxygen appeared to be exceptional in having values considerably larger at about 12.

In cases where the target nucleus forms a closed shell of protons and neutrons, e.g. ^{40}Ca , ^{32}S , ^{28}Si , ^{16}O and ^{12}C (III, IV, V), we have found evidence that it is possible to select, on the basis of the values of the capture probability, those final states which are states of single-particle excitation of the captured neutron.

ACKNOWLEDGMENTS

We are grateful to Professor H. W. B. Skinner for helpful discussions. One of us (T. N. M.) thanks the Department of Scientific and Industrial Research for a maintenance grant.

We wish also to thank the Director and Dr. R. H. Dawton of the Atomic Energy Research Establishment, Harwell, for the supply of separated isotopes.

REFERENCES

- AJZENBERG, F., and LAURITSEN, T., 1952, *Rev. Mod. Phys.*, **24**, 321.
 BHATIA, A. B., HUANG, K., HUBY, R., and NEWNS, H. C., 1952, *Phil. Mag.*, **43**, 485.
 BLACK, C. T., 1952, *Phys. Rev.*, **87**, 205A.
 BLATT, J. M., and WEISSKOPF, V. F., 1952, *Theoretical Nuclear Physics* (New York : Wiley), p. 348.
 BOCKELMAN, C. K., MILLER, D. W., ADAIR, R. K., and BARSCHALL, H. H., 1951, *Phys. Rev.*, **84**, 69.
 BUECHNER, W. W., VAN PATTTER, D. M., STRAIT, E. N., and SPERDUTO, A., 1950, *Phys. Rev.*, **79**, 262.
 BURGE, E. J., BURROWS, H. B., GIBSON, W. M., and ROTBLAT, J., 1951, *Proc. Roy. Soc. A*, **210**, 534.
 BUTLER, S. T., 1951, *Proc. Roy. Soc. A*, **208**, 559.
 BUTLER, S. T., and SALPETER, E. E., 1952, *Phys. Rev.*, **88**, 1331.
 CANAVAN, F. L., 1952, *Phys. Rev.*, **87**, 136.
 COON, J. H., GRAVES, E. R., and BARSCHALL, H. H., 1952, *Phys. Rev.*, **88**, 562.
 EL BEDEWI, F., 1952, *Proc. Phys. Soc. A*, **65**, 64.
 ELKIND, M. M., and SPERDUTO, A., 1953, *Bull. Amer. Phys. Soc.*, **28**, 39.
 FULBRIGHT, H. W., BRUNER, J. A., BROMLEY, D. A., and GOLDMAN, L. M., 1952, *Phys. Rev.*, **88**, 700.
 GIBSON, W. M., and THOMAS, E. E., 1951, *Proc. Roy. Soc. A*, **210**, 543.
 HOLT, J. R., and MARSHAM, T. N., 1953 a, *Proc. Phys. Soc. A*, **66**, 249; 1953 b, *Ibid.*, **66**, 258; 1953 c, *Ibid.*, **66**, 467; 1953 d, *Ibid.*, **66**, 565.
 HUBY, R., 1952, *Proc. Roy. Soc. A*, **215**, 385.
 JACKSON, H. L., and GALONSKY, A. I., 1951, *Phys. Rev.*, **84**, 401.
 DE JONG, D., and ENDT, P. M., 1952, *Physica*, **18**, 407.
 McMINN, W. O., SAMPSON, M. B., and RASMUSSEN, V. K., 1951, *Phys. Rev.*, **84**, 963.
 NEWNS, H. C., 1952, *Proc. Phys. Soc. A*, **65**, 916.
 NORDEIM, L. W., 1951, *Rev. Mod. Phys.*, **23**, 322.
 RESNICK, I., and HANNA, S. S., 1951, *Phys. Rev.*, **82**, 463.
 ROTBLAT, J., 1951 a, *Nature, Lond.*, **167**, 1027; 1951 b, *Phys. Rev.*, **83**, 1271.

Nuclear Scattering of Electrons and Isotope Shift*

By A. R. BODMER

Physical Laboratories, University of Manchester

Communicated by L. Rosenfeld; MS. received 8th July 1953

Abstract. The volume dependent isotope shift and the elastic scattering of electrons by nuclei are treated by a method with which they can be simply related.

The result already obtained by Feshbach that the s-wave scattering due to the finite nuclear size depends only on the volume integral of the potential due to the nuclear charge distribution is derived in a simple manner with a clear indication of the limitations. It is shown that this is then the only information which can be obtained for energies at which only the s-wave scattering is important.

The isotope shift is calculated taking into account the distortion of the electronic wave function by the nuclear charge distribution using a non-perturbation method due to Broch and is reduced considerably below that obtained with the simple perturbation method. It is shown by the same method as that used for the electron scattering that the isotope shift depends essentially only on the above volume integral and on its difference between two isotopes. Using the results obtained from the scattering of electrons by Ag and Au by Lyman, Hanson and Scott and assuming that the nuclear radius increases proportionally to $A^{1/3}$ the isotope shift is brought into considerably better agreement with the experimental data.

PART I. THE ELASTIC SCATTERING OF ELECTRONS BY NUCLEI

§ 1. INTRODUCTION

THE scattering of electrons by nuclei deviates from pure coulomb scattering, i.e. that due to point charges, for energies at which the electron wavelength λ becomes of the same order of magnitude as the nuclear dimensions. If for the nuclear radius we take $R_0 = (e^2/2mc^2) A^{1/3}$, then for energies considerably in excess of the rest mass $R_0/\lambda = \epsilon A^{1/3}/137$, where $\epsilon = E/mc^2$ is the energy in relativistic units. For heavier nuclei the scattering at large angles can then be expected to be influenced by the finite nuclear size at energies greater than about 5 mev. For lighter nuclei, observable effects will be at somewhat higher energies. For such energies, which must not be so great that the wavelength becomes of the same order as the internucleon distance, the scattering will be almost wholly elastic, and can be considered as due to the charge distribution of the nucleus as a whole. The scattering process will be adequately described by considering the electrons to move in the potential of the nuclear charge distribution. In the following we restrict ourselves to energies for which such a description of the scattering can be considered as valid. Radiative effects are quite appreciable and must be allowed for in order that the scattering may be interpreted in terms of the nuclear charge distribution.

* This paper forms part of work submitted to the University of Manchester as a thesis for the degree of Ph.D.

Calculations using the Born approximation, which, however, is only valid for very light elements, have been made by Rose (1948), Elton (1950) and Parzen (1950). Detailed calculations of the differential cross section making a phase shift analysis have been made for a uniform and a surface charge distribution by Elton for the scattering by Au at an energy of 40 mc^2 and by Acheson (1951) for $Z = 13$, 29, 50, 79 and energies between 15 and 35 mev.

Feshbach (1951) has derived some general properties of the phase shifts for the extreme relativistic case when the rest mass of the electron can be neglected. In particular, he has shown that for not too high energies the additional s-wave phase shift due to the finite nuclear size, which for energies up to about 30 mev is sufficient to describe the deviation from pure coulomb scattering, depends essentially only on

$$\int_0^r V r'^2 dr'$$

where V is the potential due to the nuclear charge distribution and r is sufficiently far outside this distribution for the potential to be coulomb. It follows that scattering experiments can then determine only this volume integral of the nuclear potential giving one condition for the nuclear charge distribution. Feshbach assumes the condition $\epsilon R_0/(\hbar/\text{mc}) \ll 1$ for his proof. However, for the extreme relativistic case this is just equal to R_0/λ , which as we have seen must be of the order of unity for finite nuclear size effects to be appreciable. In fact, for heavier nuclei for energies somewhat greater than 20 mev this expression will actually become greater than one. Hence it is of importance to see exactly what are the limitations of the above dependence of the phase shift on the volume integral of the potential. In the following a method is developed with which Feshbach's result may be derived in a simple manner. It will be shown that the above volume integral of the potential is then effectively the first term of what is essentially an expansion in powers of $\epsilon R_0/(\hbar/\text{mc})$, which above about 50 mev ceases to converge. When, however, only the comparison of two charge distributions is of interest, it will be shown that it is sufficient to use only the volume integral of the potential up to about 50 mev.

The method can also be applied to higher phase shifts which can be expected to become important at energies above about 35 mev.

All the conclusions obtained remain essentially unchanged for the scattering of positons.

§ 2. CALCULATION OF PHASE SHIFTS

We consider an electron, energy E , moving in a central field with potential energy V . On separating out the angular dependence, the small and large radial functions f_k/ξ , g_k/ξ , may be obtained from the solutions of the equations

$$\begin{aligned} \frac{df_k}{d\xi} &= \frac{kf_k}{\xi} - (\epsilon - 1 - U)g_k \\ \frac{dg_k}{d\xi} &= (\epsilon + 1 - U)f_k - \frac{k}{\xi}g_k \end{aligned} \quad \dots\dots(1)$$

where

$$\begin{aligned} k &= -(j + \tfrac{1}{2}) = -(l + 1), \quad \text{for } j = l + \tfrac{1}{2} \\ k &= +(j + \tfrac{1}{2}) = l, \quad \text{for } j = l - \tfrac{1}{2}. \end{aligned}$$

We use relativistic units, $\hbar = \text{mc} = 1$, and $\epsilon = E/\text{mc}^2$, $U = V/\text{mc}^2$, $\xi = r/(\hbar/\text{mc})$. For the scattering of an electron by the field of a finite size nucleus, charge Ze , the

asymptotic expressions for the regular solutions of f_k, g_k , in the form given by Feshbach, are

$$\begin{aligned} f_k &\sim (\epsilon - 1)^{1/2} \sin \left\{ p\xi + \frac{a\epsilon}{p} \log 2p\xi - (l+1) \frac{\pi}{2} + \eta_k \right\} \\ g_k &\sim (\epsilon + 1)^{1/2} \cos \left\{ p\xi + \frac{a\epsilon}{p} \log 2p\xi - (l+1) \frac{\pi}{2} + \eta_k \right\} \end{aligned} \quad \dots\dots(2)$$

where $a = Z\alpha$, $\alpha = e^2/\hbar c$ and p is the electron momentum in relativistic units.

In the more usual notation (Mott and Massey 1949), the phase shift for the state $j = l + \frac{1}{2}$ is denoted by η_l and that for $j = l - \frac{1}{2}$ by $\eta_{-(l+1)}$.

We may write

$$\eta_k = \eta_{k,R}^{(c)} + \delta_k; \quad \dots\dots(3)$$

$\eta_{k,R}^{(c)}$ is the phase shift for pure coulomb scattering, the corresponding regular solutions being denoted by $f_{k,R}^{(c)}, g_{k,R}^{(c)}$, while δ_k is the extra phase shift due to the finite nuclear size and gives the deviation from pure coulomb scattering. The irregular coulomb functions are denoted by $f_{k,I}^{(c)}, g_{k,I}^{(c)}$, and have the same asymptotic forms as the regular solutions except for a different phase shift $\eta_{k,I}^{(c)}$. Explicit expressions for $\eta_{k,R}^{(c)}, \eta_{k,I}^{(c)}$, and also for the differential cross section in terms of the phase shifts, are given by Parzen and Elton, but are not necessary for our purpose.

For the extreme relativistic case, $\epsilon \gg 1$, where the rest mass may be neglected in the above equations, Acheson and Feshbach have pointed out the following relation between the phase shifts:

$$\eta_k = \eta_{-k}. \quad \dots\dots(4)$$

Since this holds separately for the coulomb phase shifts, also $\delta_k = \delta_{-k}$. Thus for extreme relativistic energies states with the same j but opposite spin orientations with respect to the orbital angular momentum have the same phase shifts. The numerical analysis of Elton and Parzen using the accurate equation (1) are in good agreement with this result. In addition for energies up to about 35 mev, the calculations of Acheson show that only the phase shifts δ_{-1}, δ_1 for the $s_{1/2}, p_{1/2}$ states differ appreciably from zero. Thus he finds that at 35 mev, δ_{-2} is about 3% of δ_{-1} . It is therefore only necessary to calculate δ_{-1} for energies less than this. However, for an energy of 100 mev, Parzen's results show that the phase shifts up to δ_{-5}, δ_5 must be included. As an approximate criterion we may take δ_k to become important for $R_0/\lambda > l$. Thus δ_{-2}, δ_2 , i.e. the $p_{3/2}, d_{3/2}$ states may be expected to become significant at energies above about 35 mev, for heavier elements. Convenient expressions for the cross section in terms of the phase shifts for $\epsilon \gg 1$ have been given by Acheson.

Feshbach has brought attention to the special class of potentials

$$V = \frac{F(r/r_0, \beta)}{r_0} \quad \dots\dots(5)$$

where r_0, β are parameters describing the charge distribution, r_0 being a length of the order of the nuclear dimensions and β any additional parameters needed to specify the potential. From Poisson's equation it is seen that the corresponding charge density must have the form

$$\rho = \frac{G(r/r_0, \beta)}{r_0^3}. \quad \dots\dots(6)$$

For this type of charge distribution Feshbach has proved that for $\epsilon \gg 1$ the phase shifts depend on ϵ , r_0 only through ϵr_0 . This may be seen by rewriting eqns. (1) with the rest mass neglected. The importance of this result is in extending calculations already made to other radii or energies.

In order to calculate δ_k we consider the regular solutions of the radial functions at a point r_1 , sufficiently far outside the nuclear charge distribution for the potential to be coulomb,

$$\begin{aligned} f_k(r_1) &= C_1 f_{k,R}^{(c)}(r_1) + C_2 f_{k,I}^{(c)}(r_1) \\ g_k(r_1) &= C_1 g_{k,R}^{(c)}(r_1) + C_2 g_{k,I}^{(c)}(r_1). \end{aligned} \quad \dots\dots(7)$$

C_2/C_1 measures the admixture of the irregular to the regular solution due to the deviation from a coulomb field in the nuclear interior. From (7) and using the asymptotic forms (2),

$$\tan \delta_k = \frac{C_2/C_1 \sin(\eta_{k,I}^{(c)} - \eta_{k,R}^{(c)})}{C_2/C_1 \cos(\eta_{k,I}^{(c)} - \eta_{k,R}^{(c)}) - 1} \quad \dots\dots(8)$$

C_2/C_1 is obtained using both eqns. (7),

$$\frac{C_2}{C_1} = \frac{K_{k,\epsilon}(r_1) g_{k,R}^{(c)}(r_1) - f_{k,R}^{(c)}(r_1)}{f_{k,I}^{(c)}(r_1) - K_{k,\epsilon}(r_1) g_{k,I}^{(c)}(r_1)} \quad \dots\dots(9)$$

where $K_{k,\epsilon}(r_1) = f_k(r_1)/g_k(r_1)$.

K_k is written with the suffix ϵ when we specially wish to emphasize that it depends on the energy. For our purpose it is sufficient to note that for a given energy δ_k depends on the nuclear charge distribution only through $K_{k,\epsilon}(r_1)$. As is evident from the above derivation C_2/C_1 , and hence δ_k , are independent of r_1 so long as this is outside the charge distribution. Thus two different charge distributions will give the same scattering if the $K_{k,\epsilon}(r_1)$ for all the important δ_k are the same for both. In particular at energies for which the phase shifts $\delta_{-1} = \delta_1$ are sufficient, two distributions will give the same scattering at a given energy if $K(r_1)$ is the same, where for the s-state the suffix -1 will for convenience be omitted.

§ 3. METHOD FOR OBTAINING K_k

By differentiating $K_k = f_k/g_k$ with respect to ξ and using the equation (1), the following Riccati equation* is obtained for K_k ,

$$\frac{dK_k}{d\xi} = \frac{2k}{\xi} K_k - (\epsilon + 1 - U) K_k^2 - (\epsilon - 1 - U). \quad \dots\dots(10)$$

For the extreme relativistic case, $\epsilon \gg 1$, this becomes

$$\frac{dK_k}{d\xi} = \frac{2k}{\xi} K_k - (\epsilon - U)(1 + K_k^2). \quad \dots\dots(11)$$

For the potential (5), it is then seen by rewriting this equation that for $\epsilon \gg 1$,

$$K_{k,\epsilon} = K_k(\epsilon\xi, \epsilon\xi_0, \beta) \quad \dots\dots(12)$$

which is in agreement with Feshbach's result that for potentials of this type, the phase shift depends on ϵ , ξ_0 only through $\epsilon\xi_0$. We may then for future reference note that for the charge distributions (6), which in addition are such that the

* Rose and Newton (1951) have used this equation in a discussion of the nodal properties of the radial functions.

charge density is zero outside r_0 , where r_0 can now be considered as the nuclear radius, the total differential of K_k with respect to ξ_0 , using (12), is given by

$$\frac{dK_{k,\epsilon}(\xi_0)}{d\xi_0} = \left[\frac{\partial K_{k,\epsilon}}{\partial \xi} \right]_{\xi=\xi_0} + \left[\frac{\partial K_{k,\epsilon}}{\partial \xi_0} \right]_{\xi=\xi_0} = \frac{\epsilon}{\xi_0} \left[\frac{\partial K_{k,\epsilon}}{\partial \epsilon} \right]_{\xi=\xi_0} \dots \dots (13)$$

The required solution of K_k is determined by the behaviour near the origin. We require those solutions of (10) which correspond to the regular solutions for f_k, g_k . For potentials less rapidly divergent at the origin than a coulomb potential it is seen from eqns. (1) that the indicial behaviour of K_k corresponding to these regular solutions is

$$\left. \begin{aligned} \lim_{\xi \rightarrow 0} K_k &= \frac{\epsilon - 1 - U(0)}{2k - 1} \xi; & k < 0 \\ \lim_{\xi \rightarrow 0} K_k &= \frac{2k + 1}{\epsilon + 1 - U(0)} \frac{1}{\xi}; & k > 0. \end{aligned} \right\} \dots \dots (14)$$

We consider first the case $k < 0$. If we rewrite (10) in the form

$$(1 - K_k^2) + (U - \epsilon)(1 + K_k^2) = \frac{dK_k}{d\xi} - \frac{2k}{\xi} K_k$$

this may be transformed into an integral equation by multiplying by the integrating factor ξ^{-2k} ,

$$K_k(\xi) = \xi^{2k} \int_0^\xi \{ (U - \epsilon + 1) + (U - \epsilon - 1) K_k^2 \} \xi'^{-2k} d\xi'. \dots \dots (15)$$

If $K_k \ll 1$, this may be solved by successive iteration starting with $K_k = 0$. The solution obtained in this way is then seen to have the appropriate indicial behaviour corresponding to $k < 0$.

For $k > 0$, if we put $K_k = 1/X_k$ we obtain a Riccati equation for X_k similar to that for K_k . As above this may be transformed into the integral equation

$$X_k(\xi) = \frac{1}{\xi^{2k}} \int_0^\xi \{ (\epsilon + 1 - U) + (\epsilon - 1 - U) X_k^2 \} \xi'^{2k} d\xi'. \dots \dots (16)$$

The solution which corresponds to solving this by successive iteration starting with $X_k = 0$ gives then the correct indicial behaviour for K_k when $k > 0$. From the Riccati equations for X_k, K_k it is readily seen that for $\epsilon \gg 1$, the solutions as obtained above satisfy $K_k K_{-k} = -1$, which is of course the counterpart of the result $\delta_{-k} = \delta_k$. In what follows we shall then restrict ourselves to $k < 0$.

The first iteration of (15) is

$$K_k^{(1)}(\xi) = \xi^{2k} \int_0^\xi \xi'^{-2k} U d\xi' + \frac{\epsilon - 1}{2k - 1} \xi. \dots \dots (17)$$

Thus within the validity of the first iteration we just obtain Feshbach's result that δ_{-1} and hence also δ_1 , depend only on the volume integral of the potential. By integrating by parts twice and using Poisson's equation, the integral in (17) may be expressed in terms of an integral over the charge density. Thus

$$\int_0^r V r'^{-2k} dr' = \frac{2\pi}{k(2k-1)} \int_0^\infty \rho r'^{-2k+2} dr' + \frac{Ze^2 r^{-2k}}{2k}. \dots \dots (18)$$

The upper limit in the integral on the right is actually r but may be replaced by ∞ since for the calculation of the phase shift r must be effectively outside the charge distribution. Thus if the first iteration gives a sufficiently good approximation for K_k , then δ_k will be the same for two charge distributions if $\int_0^\infty \rho r^{-2k+2} dr$ is the same for both. For the s-wave this integral just becomes $\int_0^\infty \rho r^4 dr$.

§ 4. CALCULATION OF K_ϵ FOR $\epsilon \gg 1$

We now consider in more detail the case of the s-wave, $k = -1$, for $\epsilon \gg 1$. Equation (15) then becomes

$$K_\epsilon(\xi) = \frac{1}{\xi^2} \int_0^\xi \xi'^2 (U - \epsilon)(1 + K_\epsilon^2) d\xi'. \quad \dots\dots(19)$$

For the first iteration we have

$$K_\epsilon^{(1)}(\xi) = \frac{1}{\xi^2} \int_0^\xi U \xi'^2 d\xi' - \frac{\epsilon \xi}{3} \quad \dots\dots(20)$$

and for the second

$$K_\epsilon^{(2)}(\xi) = K_\epsilon^{(1)}(\xi) + \frac{1}{\xi^2} \int_0^\xi (U - \epsilon) [K_\epsilon^{(1)}(\xi')]^2 \xi'^2 d\xi'. \quad \dots\dots(21)$$

This process converges rapidly if $K_\epsilon^2 \ll 1$, and we may then write

$$K_\epsilon(\xi) = K_\epsilon^{(1)}(\xi) + \sum_{n=2}^{\infty} X_\epsilon^{(n)}(\xi) \quad \dots\dots(22)$$

where $X^{(n)}$ is the extra term given by the n th iteration. If the potential is of the type (5) and proportional to a , then the above iteration process will also give an expansion in homogeneous polynomials in a and $\epsilon \xi_0$ of increasing degree. Thus the first iteration will contain terms in a , $\epsilon \xi_0$, the second terms in a^3 , $a^2(\epsilon \xi_0)$, $a(\epsilon \xi_0)^2$, $(\epsilon \xi_0)^3$. Such successive homogeneous polynomials do not, however, correspond to successive iterations after the second since K_ϵ occurs as the square in the iteration.

We may expect that above a certain energy the iteration procedure for calculating $K(\xi_1)$ where ξ_1 is of the order of the nuclear radius will no longer converge and the basis for Feshbach's result will break down. This will occur when $K^{(1)}(\xi_1)$ which, since U is proportional to a , is of the order of $a + \epsilon \xi_1$, becomes of the order of unity.

In order to obtain a more precise idea of the convergence and of the importance of the additional term given by the second iteration, we consider the charge distribution used by Rosenthal and Breit (1932),

$$\left. \begin{aligned} \rho &= \frac{n+1}{4\pi} \frac{Ze}{r_0^3} \left(\frac{r}{r_0}\right)^{n-2} ; & r < r_0 \\ \rho &= 0 ; & r > r_0. \end{aligned} \right\} \quad \dots\dots(23)$$

The corresponding potential energy of the electron is

$$\left. \begin{aligned} V &= -\frac{n+1}{n} \left[1 - \frac{1}{n+1} \left(\frac{r}{r_0}\right)^n \right] \frac{Ze^2}{r_0} ; & r < r_0 \\ V &= -\frac{Ze^2}{r} ; & r > r_0. \end{aligned} \right\} \quad \dots\dots(24)$$

n can vary from -1 for a point charge through $n=2$ for a uniform charge distribution to $n=\infty$ when all the charge is on the surface. For the first iteration we have

$$K_\epsilon^{(1)}(\xi) = \left(\frac{\xi_0}{\xi}\right)^2 K_{\epsilon=0}^{(1)}(\xi_0) - \frac{a}{2} \left[1 - \left(\frac{\xi_0}{\xi}\right)^2 \right] - \frac{\epsilon \xi}{3} ; \quad \xi > \xi_0 \quad \dots\dots(25)$$

$$K_{\epsilon=0}^{(1)}(\xi) = -\frac{a}{3} \frac{n+4}{n+3}. \quad \dots\dots(26)$$

For the second iteration ($\xi > \xi_0$),

$$K_\epsilon^{(2)}(\xi) = K_\epsilon^{(1)}(\xi) + \left(\frac{\xi_0}{\xi}\right)^2 X_\epsilon^{(2)}(\xi_0) + \frac{1}{\xi^2} \int_{\xi_0}^\xi (U - \epsilon) [K_\epsilon^{(1)}(\xi')]^2 d\xi' \quad \dots\dots(27)$$

$$X_{\epsilon}^{(2)}(\xi_0) = -\frac{a^3}{9} \left(\frac{n+1}{n}\right)^3 A_0 - \frac{(\epsilon\xi_0)a^2}{9} \left(\frac{n+1}{n}\right)^2 A_1 - \frac{(\epsilon\xi_0)^2 a}{9} A_2 - \frac{(\epsilon\xi_0)^3}{45} \dots \quad (28)$$

$$A_0 = \frac{1}{5} - \frac{n+9}{(n+1)(n+3)(n+5)} + \frac{3(2n+9)}{(n+1)^2(n+3)^2(2n+5)} - \frac{9}{(n+1)^3(n+3)^2(3n+5)}$$

$$A_1 = \frac{3}{5} - \frac{2(n+9)}{(n+1)(n+3)(n+5)} + \frac{3(n+9)}{(n+1)^2(n+3)^2(2n+5)}$$

$$A_2 = \frac{3n+2}{5n} - \frac{6}{n(n+3)(n+5)} - \frac{1}{(n+1)(n+5)}$$

$$\frac{1}{\xi^2} \int_{\xi_0}^{\xi} (U - \epsilon) [K_{\epsilon}^{(1)}(\xi')]^2 \xi'^2 d\xi' = -\frac{a^3}{4} B_0 - \frac{(\epsilon\xi)a^2}{18} B_1 - \frac{(\epsilon\xi)^2 a}{9} B_2 - \frac{(\epsilon\xi)^3}{45} B_3 \dots \quad (29)$$

$$B_0 = \frac{1}{2} \left[1 - \left(\frac{\xi_0}{\xi}\right)^2 \right] + \frac{2}{3} \left(\frac{n+1}{n+3}\right) \left(\frac{\xi_0}{\xi}\right)^2 \log \frac{\xi_0}{\xi} + \frac{1}{18} \left(\frac{n+1}{n+3}\right)^2 \left(\frac{\xi_0}{\xi}\right)^2 \left[1 - \left(\frac{\xi_0}{\xi}\right)^2 \right]$$

$$B_1 = \frac{1}{2} \left(\frac{n+1}{n+3}\right)^2 \left(\frac{\xi_0}{\xi}\right)^3 \left[1 - \left(\frac{\xi_0}{\xi}\right) \right] - 5 \left(\frac{n+1}{n+3}\right) \left(\frac{\xi_0}{\xi}\right)^2 \left[1 - \left(\frac{\xi_0}{\xi}\right) \right] + \frac{7}{2} \left[1 - \left(\frac{\xi_0}{\xi}\right)^3 \right]$$

$$B_2 = \left[1 - \left(\frac{\xi_0}{\xi}\right)^4 \right] - \frac{1}{2} \left(\frac{n+1}{n+3}\right) \left(\frac{\xi_0}{\xi}\right) \left[1 - \left(\frac{\xi_0}{\xi}\right)^2 \right]$$

$$B_3 = \left[1 - \left(\frac{\xi_0}{\xi}\right)^5 \right].$$

For constant density, $n=2$, we have from the above formulae

$$K_{\epsilon}^{(2)}(\xi_0) = -\left\{ \frac{2}{5} a + \frac{\epsilon\xi_0}{3} \right\} - \{0.042 a^3 + 0.102 (\epsilon\xi_0) a^2 + 0.074 (\epsilon\xi_0)^2 a + 0.022 (\epsilon\xi_0)^3\} \dots \quad (30)$$

For a surface charge distribution, $n=\infty$, the solution for $K(\xi_0)$ may be obtained explicitly:

$$K(\xi_0) = -\frac{1}{a + \epsilon\xi_0} \left[1 - (a + \epsilon\xi_0) \cot(a + \epsilon\xi_0) \right]; \quad \epsilon \gg 1.$$

Expanding $\cot(a + \epsilon\xi_0)$ this becomes

$$K(\xi_0) = -\frac{1}{3} (a + \epsilon\xi_0) \left[1 + \frac{1}{15} (a + \epsilon\xi_0)^2 + \frac{2}{315} (a + \epsilon\xi_0)^4 + \dots \right] \dots \quad (31)$$

The first two terms of this expression are identical with those derived from the first two iterations, while the third term can easily be obtained from the third iteration. We see that above about 50 mev the second iteration increases very rapidly and the method ceases to be reliable. Thus even at 15 mev the second iteration contributes almost 10% to $K(\xi_0)$ for a surface charge distribution.

§ 5. COMPARISON OF CHARGE DISTRIBUTIONS

Although it would appear from the above that the first iteration is not a very good approximation for K even at rather lower energies, and breaks down completely at higher energies, nevertheless when the equivalence of two charge distributions is being considered it is sufficient to use only the first iteration.

We consider as an example the equivalent radii, r_s and r_c , of a surface and a uniform charge distribution respectively which give the same s-wave scattering. The simplest way to obtain the relation between r_s and r_c is to equate the expressions (27) for $n=2$ and $n=\infty$ with $\xi=\xi_c$,

$$\left(\frac{r_s}{r_c}\right)^2 = \frac{3}{5} \{1 - [0.012a^2 + 0.023(\epsilon\xi_c)a + 0.012(\epsilon\xi_c)^2]\}. \quad \dots\dots(32)$$

The first term is due to the first iteration and can immediately be obtained by equating

$$\int_0^\infty \rho r^4 dr = \frac{Ze}{4\pi} \frac{n+1}{n+3} r_0^2$$

for $n=2$ and $n=\infty$. The remaining terms from the second iteration make only a very small contribution. Thus for energies for which the iteration procedure does not break down entirely, i.e. up to energies of about 50 mev, the use of the first iteration is a very good approximation when the equivalence between the two charge distributions and not the actual value of K is being considered. Since the difference between a uniform and a surface charge distribution can be considered as an extreme, the magnitude of the terms in (32) due to the second iteration may be regarded as in the nature of an upper limit to these terms in the expression for the radius of the uniform charge distribution equivalent to some actual distribution. The reason for the near cancellation of the terms from the second iteration is seen from (21). Thus if $K^{(1)}(\xi_1)$ is equal for two charge distributions, $K^{(1)}(\xi)$ and $U(\xi)$ will not be very different for $0 < \xi \leq \xi_1$, and hence the integrand occurring in $X_\epsilon^{(2)}(\xi_1)$, and hence $X_\epsilon^{(2)}(\xi_1)$ itself, will not differ very much for the two distributions. We see then that for any given charge distribution ρ , the radius of the equivalent uniform charge distribution will be given with good accuracy by

$$\frac{3}{5} \frac{Ze}{4\pi} r_c^2 = \int_0^\infty \rho r^4 dr. \quad \dots\dots(33)$$

Of course for purposes of comparison any of the charge distributions (23), and more especially a surface charge distribution, could have been used; however, it seems most natural to use a uniform one.

§ 6. SIGNIFICANCE FOR THE INTERPRETATION OF THE EXPERIMENTAL RESULTS

The significance of the result just obtained is in the interpretation of the experiments. The calculations of Acheson and Elton extended by using Feshbach's result that the scattering depends only on ϵr_0 may be used to determine the radius $r_c(\epsilon)$ of the equivalent uniform charge distribution for the $s_{1/2}$, $p_{1/2}$ phase shifts from the scattering at an energy ϵ . Because of the near cancellation of terms in the second iteration, this equivalent radius for the actual but unknown distribution will only be very slightly energy dependent. Thus from (32) for Pb the ratio between the equivalent radii for a surface and a uniform charge distribution, r_s/r_c , differs by less than 0.25% from that given by the first iteration for $\epsilon=0$, and by less than 4% for an energy of 50 mev. Since for energies at which r_c can be expected to become appreciably energy dependent, higher phase shifts will be important, the equivalent radius may be taken as energy independent for the energies of interest since variations of the above amount would hardly be experimentally significant. This implies that for energies at which only the $s_{1/2}$, $p_{1/2}$ phase shifts are appreciably influenced by the finite nuclear size, the only information which can

be deduced from scattering experiments at different energies is the equivalent radius r_c for $\epsilon=0$. From (33) knowledge of r_c then implies knowledge of

$$\int_0^\infty \rho r^4 dr.$$

More detailed information about the form of the nuclear charge distribution could be obtained from the scattering at somewhat higher energies when the $p_{3/2}$, $d_{3/2}$ states become important ($k=-2$ and $k=2$ respectively). In a similar way, as above, it can be expected that for energies up to about 50 mev the phase shifts for these states would depend on the charge distribution only through $\int_0^\infty \rho r^6 dr$.

This could again be expressed in terms of the radius of an equivalent uniform charge distribution which would not of course in general be the same as that for the $s_{1/2}$, $p_{1/2}$ states. It should be possible for energies in the region of 35–50 mev to determine this additional moment of the charge distribution since the phase shifts for the $d_{3/2}$, $g_{5/2}$ states ($k=-3$ and $k=3$ respectively) can be expected to become important only at energies somewhat above 50 mev.

For the scattering of positons it is only necessary to change the sign of the charge in all the above considerations. In the Born approximation, which is only valid for very light elements, the cross section will be the same as for electrons; however, for heavier elements there will be large differences. Recently Elton and Parker (1953) have made detailed calculations of the phase shifts for the scattering of positons by Au for an energy of $40 mc^2$. They find that again only the $s_{1/2}$, $p_{1/2}$ phase shifts are significantly affected by the finite nuclear size and that the reduction from coulomb scattering, although quite appreciable, is considerably less than for electrons, as is to be expected because of the repulsive potential. Since ϵ and U have the same sign for positons, $\epsilon - U$ may be quite small in the nuclear region and may even become negative for not too high energies, and thus in general the second iteration will be rather less important relative to the first than for electrons. More explicitly K for the potential (24) is obtained from (25)–(29) by changing the sign of a , the various terms now no longer having all the same sign. In particular it is seen from (32) that for the relation between the equivalent radii for a surface and a uniform charge distribution there is now a partial cancellation in the terms due to the second iteration. Thus, also, for positons the scattering for the $s_{1/2}$, $p_{1/2}$ states depends only on the volume integral of the potential, and the radius of the equivalent uniform charge distribution should be the same as for electrons.

The only relevant experiments so far available are those of Lyman, Hanson and Scott (1951) with 15.7 mev electrons. For the heavier elements Ag and Au they find that the radius of the equivalent uniform charge distribution needed to fit their results is about $1.15 \times 10^{-13} A^{1/3}$ cm, i.e. about 20% smaller than a value of the order of magnitude $1.45 \times 10^{-13} A^{1/3}$ cm, which might have been expected. These results must be considered as somewhat uncertain as the radiative correction was allowed for using the result of Schwinger (1949). This is of uncertain accuracy for heavy elements since the radiative scattering is calculated for a coulomb field using the Born approximation, and is given relative to the Born approximation expression for the elastic scattering.

For the lighter elements C, Al, Cu the reduction from coulomb scattering is small and of the same order of magnitude as the uncertainties in the measurements which are not incompatible with either of the above values for the radius of the equivalent uniform charge distribution.

Independent evidence about nuclear radii of light elements is given by the discussion of energy differences of mirror nuclei. This is rather strongly in favour of a larger value of $1.4 \times 10^{-13} A^{1/3}$ cm. Thus the total evidence would seem to indicate a trend in the direction of a greater concentration of charge for heavier nuclei. As we shall see, this inference seems further to be confirmed by the isotope shift of heavy elements; however, more accurate scattering experiments, especially for lighter nuclei, are needed before this conclusion can be considered as well established. Such a concentration of charge would have to be considered as indicating a corresponding concentration in the nuclear density.

PART II. THEORY OF THE ISOTOPE SHIFT

§ 7. INTRODUCTION

In the usual derivation of the volume dependent isotope shift (I.S.) the change in binding energy of an electron due to the difference in its electrostatic interaction with a point charge and the same charge spread over the nuclear volume is calculated using a simple perturbation method. With this the difference between two isotopes of the potential energy of the electron in the nuclear region is averaged over the relativistic charge density when the electron is moving in the field of a point nucleus. For comparison with the data Brix and Kopfermann (1949) used a model which assumes a uniform charge distribution of radius $1.4 \times 10^{-13} A^{1/3}$ cm and such that the increase in volume between two isotopes is proportional to the increase in mass. Using the simple perturbation theory, they found that the experimental I.S. was smaller by a factor of 2–3 except in the region of $Z=60$ (Ce, Sm, Eu) where the I.S. is anomalously large.

It might be expected, however, that the spreading of the charge would strongly distort the wave function of the electron from its coulomb form just inside the nuclear region where the perturbation takes place, and thus considerably affect the I.S. Hence it is of some interest to investigate whether a more accurate calculation taking into account this distortion of the wave function might not remove some of the discrepancy. An estimate of the effect of the distortion when all the charge is on the surface was made by Rosenthal and Breit (1932). The fundamental expressions for an accurate treatment of the I.S. which have been used in subsequent discussions, including the present one, were given by Broch (1945). Crawford and Schawlow (1949) made a calculation for a uniform and a surface charge distribution. Their results are, however, not quite in agreement with ours, the discrepancy being probably due to some numerical error. They do not examine other charge distributions or the dependence on Z , and their method cannot be extended to an arbitrary charge distribution. Since the completion of the present work there has appeared a paper by Humbach (1952) who has also made calculations of the distortion effect. Our results are in agreement with those of Humbach who, in addition to Broch's method, has also used a more accurate perturbation treatment. However, he does not give any simple procedure for calculating the I.S. for any given charge distribution such as will be given in the following, nor does he discuss the relation between the I.S. and the electron scattering.

Brix and Kopfermann (1951) in their most recent presentation, in which they give the ratio of the experimentally determined I.S. to the I.S. of their standard

model, have already allowed for the influence of distortion using Humbach's results. The previous discrepancy is however only very partially reduced (see § 11, formula (57) and discussion).

In the following, we take up the discussion with a method similar to the one used in Part I for the electron scattering. It will be shown that the I.S. of an s electron depends on the charge distribution only through $K_{\epsilon=0}$, $\delta K_{\epsilon=0}$ where the latter is the change in $K_{\epsilon=0}$ between the two isotopes. The method developed in Part I may then be applied to calculate the I.S. of any given charge distribution. It is then also possible to establish a simple connection with the elastic scattering of electrons by nuclei.

§ 8. PERTURBATION THEORY OF THE I.S.

Before proceeding to a more accurate calculation of the I.S. we give a brief account of the simple perturbation theory given by Rosenthal and Breit (1932) and Racah (1932), as it is convenient to use this for comparison and to give a measure of the effect of distortion. With this the I.S. due to a change in potential energy δV is then

$$\delta(\Delta E)_{\text{pert}} = \int_0^\infty \delta V (f_{k,R}^{(c)^2} + g_{k,R}^{(c)^2}) dr \quad \dots\dots(34)$$

where ΔE is the term shift due to the effect of the finite nuclear size. Since δV is only different from zero in a region of the dimensions of the nuclear radius, we may for the wave functions of optical terms in this region neglect the binding energy as compared with the rest mass.*

It is then convenient for the present purpose to write the radial equations in the form

$$\frac{df_k}{dx} = \frac{k}{x} f_k + \frac{U}{2a} g_k, \quad \frac{dg_k}{dx} = \frac{2-U}{2a} f_k - \frac{k}{x} g_k \quad \dots\dots(35)$$

where

$$x = 2Zr/a_H = 2a\xi$$

and $a_H = \hbar^2/me^2$ is the Bohr radius. With $U = -2a^2/x$ the functions $f_{k,R}^{(c)}$, $g_{k,R}^{(c)}$ are then given by (43) with $C_2 = 0$. It is sufficiently accurate to retain only the lowest power of x since the value of x corresponding to the nuclear radius is approximately equal to $\alpha^2 Z A^{1/3}$. It is seen that the errors involved in making this approximation will be of the same order of magnitude as those involved in neglecting the binding energy. We have then

$$f_{k,R}^{(c)^2} + g_{k,R}^{(c)^2} = \frac{2C^2}{\Gamma^2(1+2\sigma)} k(k-\sigma) x^{2\sigma} \quad \dots\dots(36)$$

where $\sigma = (k^2 - a^2)^{1/2}$. Thus

$$\delta(\Delta E)_{\text{pert}} = N \frac{k(k-\sigma)}{\Gamma^2(1+2\sigma)} \int_0^\infty \frac{\delta U}{2a} x^{2\sigma} dx \quad \dots\dots(37)$$

with

$$N = 8\pi Z e^2 C^2. \quad \dots\dots(38)$$

The normalization is that used by Rosenthal and Breit:

$$4\pi \int_0^\infty (f_k^2 + g_k^2) dr = 1. \quad \dots\dots(39)$$

* For electrons in the innermost shells this approximation would no longer be justified.

C^2 is determined from the normalization by putting g_k/r asymptotically equal to the radial Schrodinger wave function for larger r . In this way Rosenthal and Breit obtain for an s electron

$$C^2 = \frac{R}{2Z^2 e^2} a_H^3 \psi^2(0). \quad \dots\dots(40)$$

where R is the Rydberg constant and $\psi(0)$ the value of the Schrödinger wave function at the origin. In order to obtain from the I.S. of an optical s electron the part independent of N , i.e. that part which depends only on the nuclear charge distribution, it is seen that it is essential to have a reliable knowledge of $\psi^2(0)$ for the state in question. Any effects due to screening will be included in $\psi(0)$. For alkali-like terms this quantity may be determined by means of the semi-empirical formula of Goudsmit and Fermi-Segrè. Since the hyperfine splitting of such terms also depends on $\psi^2(0)$ the proportionality of the I.S. to this may be tested if one of the isotopes has a nuclear spin by observing whether the ratio of the hyperfine splitting to the I.S. is approximately the same for different terms. This has actually been found to be the case (Crawford and Schawlow 1949, Brix and Kopfermann 1951). With nuclear magnetic moments independently and accurately available from nuclear resonance experiments it then becomes possible to determine $\psi^2(0)$ from the hyperfine splitting and thus to avoid many uncertainties in the determination of this quantity. It should be mentioned that there is some uncertainty in obtaining the I.S. due to only the optical s electron from the observed I.S. due to the transitions of this, since it is necessary to allow for the change in the I.S. of all the inner electrons arising from the difference in the shielding of these by the optical electron in its initial and final state. Such shielding effects have been considered by Crawford and Schawlow (1949) and more recently by Humbach (1952), whose calculations indicate that the part of the observed I.S. due to the optical s electron only is slightly greater for an important class of electronic configurations than the observed I.S. itself.

With the charge density (23) Rosenthal and Breit then obtain for the I.S. of an s electron

$$\delta(\Delta E)_{\text{pert}} = N \frac{1+\sigma}{\Gamma^2(1+2\sigma)} \frac{n+1}{(2\sigma+n+1)(2\sigma+1)} x_0^{2\sigma} \frac{\delta x_0}{x_0}. \quad \dots\dots(41)$$

§ 9. NON-PERTURBATION METHOD FOR THE I.S.

By a method avoiding the use of simple perturbation theory Broch obtains for the difference in energy between an electron in the field of a finite size nucleus and a point nucleus

$$\Delta E = -N \left(\frac{C_2}{C_1} \right) \frac{1}{2\Gamma(2\sigma)\Gamma(1-2\sigma)} \quad \dots\dots(42)$$

where N is given by (38) with C_1 instead of C . C_1, C_2 are the coefficients of the regular and irregular solutions respectively in the general solution for the two radial functions in the region exterior to the charge distribution where the electron is moving in a coulomb field. For this region, and where r is still sufficiently small that the binding energy may be neglected,

$$\left. \begin{aligned} f_k(x) &= a[C_1 J_{2\sigma}(2x^{1/2}) + C_2 J_{-2\sigma}(2x^{1/2})] \\ g_k(x) &= C_1 A_{2\sigma}(2x^{1/2}) + C_2 A_{-2\sigma}(2x^{1/2}) \end{aligned} \right\} \quad \dots\dots(43)$$

where

$$\begin{aligned} A_{2\sigma} &= (k-\sigma)J_{2\sigma} + x^{1/2}J_{2\sigma+1} \\ A_{-2\sigma} &= (k+\sigma)J_{-2\sigma} + x^{1/2}J_{-2\sigma+1}. \end{aligned}$$

For a point nucleus $C_2 = 0$. Following Broch, the condition for the continuity of $K_k = f_k g_k$ at a point x_1 , where the potential is coulomb, then gives the admixture of the irregular relative to the regular solution due to the deviation from a coulomb field in the region $x < x_1$,

$$\frac{C_2}{C_1} = \frac{aJ_{2\sigma}(2x_1^{1/2}) - K_k(x_1)A_{2\sigma}(2x_1^{1/2})}{K_k(x_1)A_{-2\sigma}(2x_1^{1/2}) - aJ_{-2\sigma}(2x_1^{1/2})} \quad \dots\dots (44)$$

where $K_k(x_1)$ is now assumed evaluated neglecting the binding energy and is determined from the solution interior to x_1 . It must be emphasized that the only condition on x_1 is that the potential is coulomb at x_1 . Thus if the charge density does not fall abruptly to zero, x_1 must be sufficiently far out to satisfy this condition. As is evident from the derivation, C_2/C_1 is then independent of x_1 . Expanding the Bessel functions and retaining only the lowest power of x_1 ,

$$\frac{C_2}{C_1} = - \frac{\Gamma(1-2\sigma)}{\Gamma(1+2\sigma)} \frac{a - (k-\sigma)K_k(x_1)}{a - (k+\sigma)K_k(x_1)} \quad \dots\dots (45)$$

In this approximation it can easily be verified directly that C_2/C_1 is independent of x_1 by showing that $(d/dx)(C_2/C_1) = 0$ using eqn. (49) together with $U = -2a^2/x_1$. All the results derived below from (45) are then independent of x_1 . Substituting (45) in (42),

$$\Delta E = N \frac{1}{4\sigma\Gamma^2(2\sigma)} \frac{a - (k-\sigma)K_k(x_1)}{a - (k+\sigma)K_k(x_1)} \quad \dots\dots (46)$$

The normalization is given by (39). For an s electron C_1^2 is again given by (40), since the part of the normalization integral extending to x_1 may be neglected because of the smallness of x_1 , and outside x_1 that part due to C_2 can also be neglected again as a result of the smallness of x_1 . The problem of determining N is therefore again that of determining $\psi^2(0)$, and the same remarks as in § 8 apply.

The I.S. is

$$\delta(\Delta E) = N \frac{1}{2\Gamma^2(2\sigma)} \frac{a\delta K_k(x_1)}{[a - (k+\sigma)K_k(x_1)]^2} x_1^{2\sigma} \quad \dots\dots (47)$$

Thus for two charge distributions to give the same I.S. $K_k(x_1)$, $\delta K_k(x_1)$ must be the same for both.

In order to obtain K_k , the same method may be used as in Part I. If the binding energy is neglected, i.e. with $\epsilon = 1$, the Riccati equation for K_k becomes

$$\frac{dK_k}{dx} = \frac{2k}{x} K_k + \frac{U-2}{2a} K_k^2 + \frac{U}{2a} \quad \dots\dots (48)$$

The indicial behaviour of the required solutions is obtained from (14) by putting $\epsilon = 1$. If in the nuclear region it is also permissible to write $U/2a$ instead of $(U-2)/2a$ for the factor multiplying K_k^2 , (48) becomes

$$\frac{dK_k}{dx} = \frac{2k}{x} K_k + \frac{U}{2a} (1 + K_k^2) \quad \dots\dots (49)$$

This is formally equivalent to the equation for the extreme relativistic case if in this we put $\epsilon = 0$. The approximation just made is equivalent to assuming $x_0/a^2 \ll 1$ for the factor multiplying K_k^2 . This is somewhat more stringent, especially for lighter elements, than the condition $x_0 \ll 1$ assumed previously. However, for $k < 0$ we see from the iteration procedure for obtaining K_k that the term neglected only affects K_k in the second iteration, the error involved in the

additional term due to this being less than 10%. The only important case for the I.S. is in fact that of an s electron, $k = -1$, and since, as we shall see, the additional term due to the second iteration makes only a relatively small contribution for this, the error in K due to the above approximation is very small. For $k > 0$ we see from (16) that the approximation made above would cause an error in K_k already in the first iteration. Thus for $p_{1/2}$ states, which are the only other states for which the I.S. is at all appreciable, it would be necessary to use eqn. (48) if we wish to obtain a more accurate value of K_1 . However, even in this case, if we are only interested in comparing charge distributions which give the same K_1 , it is again only necessary to compare the volume integrals of the potentials as for $k = -1$, since the term neglected would only give a contribution independent of the potential in the first iteration.

In what follows we shall consider only s states and assume that it is sufficiently accurate to use (49). If we assume the potential has the form (5), then by rewriting (49) it is seen that

$$K = K\left(\frac{x}{x_0}, \beta\right). \quad \dots\dots(50)$$

From this it follows that

$$\frac{\partial K}{\partial x_0} = -\frac{x}{x_0} \frac{\partial K}{\partial x}$$

and therefore, using (49),

$$\frac{\partial K}{\partial x_0} = -\frac{x}{x_0} \left\{ -\frac{2K}{x} + \frac{U}{2a} (1 + K^2) \right\}. \quad \dots\dots(51)$$

With x_1 outside the charge distribution where $U = -2a^2/x_1$,

$$\frac{\partial K}{\partial x_0} = \frac{1}{x_0} [a(1 + K^2) + 2K] = \frac{1}{ax_0} [a + (1 + \sigma)K][a + (1 - \sigma)K]. \quad \dots\dots(52)$$

If we now consider a charge distribution of the form (6), but depending only on x_0 , then using (52) and substituting for $\delta K = (\partial K / \partial x_0) \delta x_0$ in (47),

$$\delta(\Delta E) = N \frac{1}{2\Gamma^2(2\sigma)} \frac{a + (1 + \sigma)K(x_1)}{a + (1 - \sigma)K(x_1)} x_1^{2\sigma} \frac{\delta x_0}{x_0}. \quad \dots\dots(53)$$

Thus if $V = F(r/r_0)/r_0$ for both isotopes (with different values of r_0) then the I.S. depends on the change in charge distribution between the two isotopes only through $\delta r_0/r_0$.

It is of particular interest to consider the special class of charge distributions (6), but in addition such that the charge density is zero outside x_0 , where x_0 can now be considered as the nuclear radius. The distribution (23) is of this type. An alternative way of obtaining the I.S. in this case is by evaluating C_2/C_1 at $x_1 = x_0$ for the lighter isotope and at $x_1 = x_0 + \delta x_0$ for the heavier, i.e. we do not keep x_1 fixed. $\delta(\Delta E)$ is then obtained by taking the total differential with respect to x_0 of (46) with $x_1 = x_0$. From (13) we have with $\epsilon = 0$, $dK(x_0)/dx_0 = 0$ and we immediately obtain (53) with $x_1 = x_0$. For this type of charge distribution $K(x_0)$ is then independent of x_0 and the I.S. depends on the radius x_0 only through $x_0^{2\sigma}$ in addition to the relative change of radius $\delta x_0/x_0$.

§ 10. EVALUATION OF K

Since for the I.S. of an s electron K can be considered as satisfying the same equation as for the extreme relativistic case with $\epsilon = 0$, all the results obtained in Part I for $k = -1$, $\epsilon \gg 1$ can immediately be used for the I.S. if we put $\epsilon = 0$.

Since with relativistic units the potential U is proportional to a , the iteration procedure will also give K as an expansion in powers of a ,

$$K = \lim_{n \rightarrow \infty} K_{(n)}; \quad K_{(n)} = K^{(1)} \left[1 + \sum_{m=2}^n \gamma_m a^{2(m-1)} \right]. \quad \dots\dots(54)$$

As already pointed out in Part I, successive $K_{(n)}$, γ_n do not correspond to successive iterations above the second. For the potentials (24), $K^{(1)}$, γ_2 are given by (25)–(29) with $\epsilon = 0$. $\gamma_3(r_0)$ is obtained from the third iteration and can be calculated without too much difficulty; the general expression for any n is, however, rather long. We give some special cases:

$$\left. \begin{aligned} n=0: \quad K_{(2)}(r_0) &= K^{(2)}(r_0) = -\frac{4a}{9} (1 + 0.15a^2) \\ n=1: \quad K_{(3)}(r_0) &= -\frac{5a}{12} (1 + 0.12a^2 + 0.021a^4) \\ n=2: \quad K_{(3)}(r_0) &= -\frac{2a}{5} (1 + 0.106a^2 + 0.0105a^4) \\ n=3: \quad K_{(3)}(r_0) &= -\frac{7a}{18} (1 + 0.097a^2 + 0.014a^4) \\ n=4: \quad K_{(3)}(r_0) &= -\frac{8a}{21} (1 + 0.092a^2 + 0.0135a^4) \\ n=\infty: \quad K_{(3)}(r_0) &= -\frac{a}{3} \left(1 + \frac{a^2}{15} + \frac{2a^4}{315} \right), \end{aligned} \right\} \quad \dots\dots(55)$$

$n=0$ is a limiting case; the potential becomes logarithmic and the calculations must be carried out separately. In figs. (1) and (2), $-K(r_0)/a$ is shown plotted

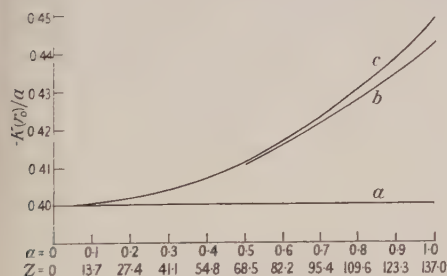


Fig. 1.

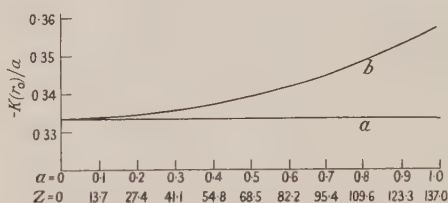


Fig. 2.

Figs. 1 and 2. $-K(r_0)/a$ as a function of a or Z for a uniform and a surface charge distribution respectively. Curves a , b , c represent $-K^{(1)}(r_0)/a$, $-K^{(2)}(r_0)/a$ and $-K_{(3)}(r_0)/a$ respectively.

against a for $n=2$ and $n=\infty$. The straight line in each case represents the first iteration and the upper curve the result when $\gamma_3(r_0)$ has also been included. It is seen that this last term makes only a very small contribution to $K(r_0)$ for all elements, i.e. $Z \leq 92$. We may thus consider the second iteration to be a very good approximation for all elements. Since also the additional term due to the second iteration is only a relatively minor part of K , the use of the equation (49) from K is seen to be justified.

It is of interest to compare the above results for K with those obtained by solving the radial equations directly. These calculations were made before the above iteration method was devised. The equations (35) are transformed into

second order linear equations each involving only one of the functions f_k, g_k . Thus for f_k

$$\frac{d^2 f_k}{dx^2} = \left[\frac{k(k-1)}{x^2} - \frac{U(U-2)}{4a^2} - \frac{k}{x} \frac{1}{U} \frac{dU}{dx} \right] f_k + \frac{1}{U} \frac{dU}{dx} \frac{df_k}{dx} \dots (56)$$

If this is solved g_k may be obtained from the first of the equations (35) and K_k may be found. For the potentials (24) with n an integer greater than zero, the singularity at the origin is regular and a series solution in x is possible. Owing to the smallness of x_0 it is found that the terms in x_0 in $K(x_0)$ may be neglected and that hence $dK(x_0)/dx_0 = 0$ as already proved more generally above. For $k = -1$ the term in $K(x_0)$ in a is just (26). Successive terms in ascending powers of a^2 may be obtained from the recurrence relations. The coefficient of each power in a is now a not very rapidly converging series. The terms up to a^5 were calculated for $n = 1, 2, 3, 4, \infty$ and are in agreement with the ones given above. This is essentially the method used by Crawford and Schawlow to investigate the cases of uniform and surface distributions. It is seen that the iteration method is much less tedious and can be applied to any charge distribution, whereas only in exceptional cases can a series solution in x be found for eqn. (56).

§ 11. EVALUATION OF I.S.

The I.S. for the potentials (24) is obtained if the appropriate value of $K(r_0)$ is substituted in (53) with $x_1 = x_0$. The ratio of this is to the I.S. as calculated using the simple perturbation method (41) with the same value of r_0 in both cases is

$$P = \frac{\delta(\Delta E)}{\delta(\Delta E)_{\text{pert}}} = \frac{2\sigma^2(1+2\sigma)}{1+\sigma} \frac{2\sigma+n+1}{n+1} \frac{a+(1+\sigma)K(r_0)}{a+(1-\sigma)K(r_0)} \dots (57)$$

P was calculated using (55) for $n = 1, 2, 3, 4, \infty$, and in figs. (3) and (4) is shown plotted against K for $n = 2$ and $n = \infty$. For the lower curve in each case the terms

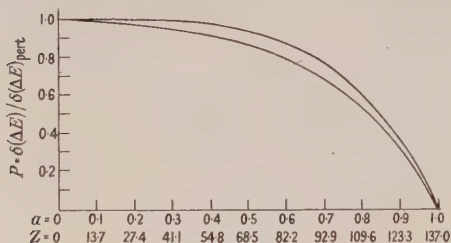


Fig. 3.

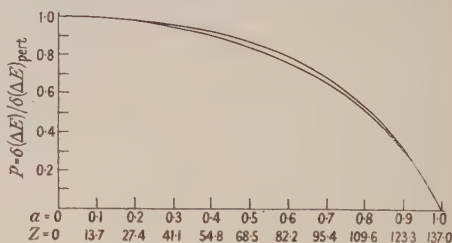


Fig. 4.

Figs. 3 and 4. $P = \delta(\Delta E) / \delta(\Delta E)_{\text{pert}}$ as a function of a or Z for a uniform and surface charge distribution respectively. The upper curve in each case corresponds to the use of the first iteration $K^{(1)}(r_0)$ for $K(r_0)$ and the lower to the use of $K^{(2)}(r_0)$. The curves obtained using $K^{(2)}(r_0)$ and $K^{(3)}(r_0)$ are almost identical.

up to a^5 have been included in $K(r_0)$, while the upper curve corresponds to the use of the first iteration only. The effect of $\gamma_3(r_0)$ is very small, and on the scale used the curve for P , using only the second iteration, is almost identical with that obtained if $\gamma_3(r_0)$ is also included.

It is seen that the effect of the distortion of the wave function is to decrease the I.S. below its value as calculated by the simple perturbation method and that this difference increases with Z , as is to be expected. P varies only slightly with n , i.e. with the concentration of charge. Thus for $Z = 82$, $P = 0.78$ for a uniform charge distribution and 0.76 when all the charge is on the surface. The use of the

first iteration is already a considerable improvement on the perturbation treatment and becomes a progressively better approximation as the charge moves outward.

Thus the effect of distortion, although appreciable and in the right direction, could explain only a part of the discrepancy between the standard model of Brix and Kopfermann and the experimental data so long as we keep to the fixed value $1.4 \times 10^{-13} A^{1/3}$ cm for the radius.

With the help of the results just obtained the I.S. may be calculated for any given charge distribution. Thus the uniform charge distribution which gives the same I.S. must have the same values of $K(r_1)$, $\delta K(r_1)$ as the given distribution, and the problem is then just to calculate this equivalent uniform charge distribution. The equivalence of K considered in Part I was seen to be conveniently specified by the radius r_c of this equivalent distribution. It was shown that if r_c is obtained from (33) it has almost the same value as if the second iteration is used for its determination. Similarly, using only the first iteration $\delta r_c/r_c$ may be determined from

$$\frac{3}{5} \frac{Ze}{2\pi} r_c^{2\sigma} \frac{\delta r_c}{r_c} = \int_0^\infty \delta \rho r^4 dr \quad \dots\dots (58)$$

and will again be almost as accurate as if obtained using the second iteration.

It may be noted that for the charge distributions (6), which in addition do not depend on further parameters β , we have from (46) and (53) that

$$\delta(\Delta E) = 2\sigma(\delta x_0/x_0)\Delta E$$

and that therefore $\delta r_c/r_c = \delta x_0/x_0$ for these distributions. This also follows from (33) and (58).

The I.S. for the given distribution may now be obtained from (53) with $x_1 = x_c$ and $\delta x_0/x_0 = \delta r_c/r_c$ and using for $K(r_0)$ the values already obtained for a uniform charge distribution. Alternatively we may use the results obtained for P , which depends only on K , together with the I.S. as calculated by the perturbation method with the values r_c and $\delta r_c/r_c$.

The important point is that, using only the first iteration to determine r_c , $\delta r_c/r_c$ for a given charge distribution, the I.S. for this may be calculated with almost the same accuracy as using the second iteration if the results for a uniform charge distribution already obtained with the second iteration are used. The I.S. of the given charge distribution will then depend besides on Z only on $r_c^{2\sigma} \delta r_c/r_c$. For a uniform charge distribution of radius $1.4 \times 10^{-13} A^{1/3}$ cm and with $\delta r_0/r_0 = 2/3 A$ Humbach, including the correction due to distortion, has tabulated the quantity $C_{th} = (4R/N)\delta(\Delta E)$ introduced by Brix and Kopfermann. These values may then be used to obtain the I.S. for any other charge distribution if only $r_c^{2\sigma} \delta r_c/r_c$ has been calculated for this.

§ 12. RELATION WITH ELECTRON SCATTERING

It was shown in Part I that the radius r_c of the uniform charge distribution needed to describe the s-wave scattering was almost independent of energy and in particular equal to r_c for $\epsilon = 0$. Thus r_c as obtained from experiments on electron scattering can be used for the I.S. in a way which follows immediately from the discussion at the end of the previous paragraph. The data on the I.S. will then give effective values of $\delta r_c/r_c$ which are related to the change in the charge distribution between the two isotopes by (58). If the charge distribution is of the type (6) and also does not depend on β , then $\delta r_c/r_c$ would have the direct interpretation as the relative charge of the parameter occurring in the potential. Any such information

would be a valuable test for theories of nuclear structure. Thus on the basis of an extended individual particle model, the change in charge distribution would have to be ascribed to a change in the range and strength and also of the shape of the collective potential in which the nucleons move. The addition of any neutrons must change in some way the extent and depth of this potential and hence also the proton distribution. On the other hand, there would also, according to Rainwater (1950) be a change in the shape of the individual nucleon potential and consequently a change in deformation of the nucleus. Any such difference in deformation between two isotopes would then, according to Brix and Kopfermann (1949), also give rise to an I.S.

Since Ag and Au are near the lighter and heavier end respectively of the elements for which the volume dependent I.S. is known, we take as a tentative value for the equivalent radius r_c of these elements the value $1.15 \times 10^{-13} A^{1/3}$ cm as determined from the scattering of electrons by Ag and Au by Lyman, Hanson and Scott. The I.S. will then be reduced by a factor $(1.15/1.4)^{2\sigma}$ from the value obtained if a radius of $1.4 \times 10^{-13} A^{1/3}$ cm is used. This is equal to 0.7 for $Z=55$ and to 0.74 for $Z=82$. This further reduction accounts for a considerable part of the remaining discrepancy (except of course for the anomalous region). Although the agreement with experiment is by no means perfect, this further reduction may be taken, as already mentioned in Part I, as an indication of a greater concentration of charge in heavier nuclei. It should be emphasized that this discussion depends on the assumption that the radius increases proportionally to $A^{1/3}$. This may be insufficient to specify the change in the charge distribution between two isotopes, especially if deformation effects are likely to be important, as is, for instance, strongly suggested for the exceptionally large I.S. of Sm and Eu (Brix and Kopfermann 1949).

ACKNOWLEDGMENTS

I would like to express my gratitude to Professor L. Rosenfeld for suggesting the subject of the isotope shift, for his constant interest and encouragement, and many helpful discussions.

I am indebted to the British Rayon Research Association for a grant which made this investigation possible.

REFERENCES

- ACHESON, L. K., 1951, *Phys. Rev.*, **82**, 488.
 BRIX, P., and KOPFERMANN, H., 1949, *Z. Phys.*, **126**, 344; 1951, *Festschrift Akad. Wiss. Göttingen, Math.-Phys. Kl.*, 17.
 BROCH, E. K., 1945, *Arch. Mat. Naturvidensk.*, **48**, 25.
 CRAWFORD, M. F., and SCHAWLOW, A. L., 1949, *Phys. Rev.*, **76**, 1310.
 ELTON, L. R. B., 1950, *Proc. Phys. Soc. A*, **63**, 1115.
 ELTON, L. R. B., and PARKER, K., 1953, *Proc. Phys. Soc. A*, **66**, 428.
 FESHBACH, H., 1951, *Phys. Rev.*, **84**, 1206.
 HUMBACH, W., 1952, *Z. Phys.*, **133**, 589.
 LYMAN, E. M., HANSON, A. C., and SCOTT, M. B., 1951, *Phys. Rev.*, **84**, 626.
 MOTT, N. F., and MASSEY, H. S. W., 1949, *The Theory of Atomic Collisions*, 2nd Edn. (Oxford: University Press), p. 75.
 PARZEN, G., 1950, *Phys. Rev.*, **80**, 261, 355.
 RACAH, G., 1932, *Nature, Lond.*, **129**, 723.
 RAINWATER, J., 1950, *Phys. Rev.*, **79**, 432.
 ROSE, M. E., 1948, *Phys. Rev.*, **73**, 279.
 ROSE, M. E., and NEWTON, R. R., 1951, *Phys. Rev.*, **82**, 470.
 ROSENTHAL, J. E., and BREIT, G., 1932, *Phys. Rev.*, **41**, 459.
 SCHWINGER, J., 1949, *Phys. Rev.*, **76**, 790.

The Elastic Scattering of 1.33 mev and 2.76 mev Gamma Rays by Lead

By W. G. DAVEY

Department of Physics, University of Birmingham

Communicated by P. B. Moon; MS. received 26th May 1953

Abstract. A report is given of measurements of the elastic-scattering cross section of lead for gamma-rays of 1.33 mev and 2.76 mev at scattering angles between 40° and 120° . With 1.33 mev γ -rays good agreement was obtained with the theoretical predictions on the basis of Rayleigh and Thomson scattering alone. The Rayleigh scattering cross section was calculated from Franz's formulae which are non-relativistic and based on the Thomas-Fermi approximation to the electron distribution in the atom. With 2.76 mev γ -rays the experimental cross sections were compared with an unpublished curve given by Bethe calculated for the K electrons alone, in addition to the values given by Franz's formulae. These theoretical curves are calculated only for Rayleigh and nuclear Thomson scattering, and at all angles in the range investigated the measured cross sections were found to be greater than those predicted. The discrepancy is possibly due either to secondary effects, or the occurrence of Delbruck scattering.

§ 1. INTRODUCTION

THE theoretical information on Rayleigh, nuclear Thomson and resonant nuclear scattering of γ -rays has been summarized by Moon (1950), Franz's (1935) formulae, which are non-relativistic and based on the Thomas-Fermi approximation to the electron distribution in the atom, having been used for the calculation of the Rayleigh cross section. Above 1 mev the scattering due to virtual creation of positron-electron pairs in the nuclear coulomb field (Delbruck 1933) should become appreciable. Some theoretical aspects of Delbruck scattering were investigated by Rohrllich and Gluckstern (1952) and Bethe and Rohrllich (1952), but the differential cross section at large angles of scattering is not calculated. This scattering is primarily at small angles and, in addition, the cross section increases greatly with increasing γ -ray energy so that this scattering should be the dominant form at very high energies.

The scattering by Rayleigh, Thomson and Delbruck processes from an individual atom will be coherent with each other, the relative phases of the scattered waves determining whether the interference is constructive or destructive. Rayleigh and Thomson scattering should have the same phase (Moon 1950), but Delbruck scattering may have the opposite phase (Bethe 1951, private communication to Professor Moon).

The elastic-scattering cross section of lead for 0.411 mev γ -rays has been measured over an angular range of 3° to 150° by Storruste (1950). His results show that elastic scattering at this energy is due entirely to Rayleigh and Thomson scattering.

The object of the present work was to extend these measurements to higher energies to check the theoretical formulae and to see if the Delbruck scattering indicated by Wilson's (1950, private communication to Professor Moon, and 1951) measurements could be observed. The scatterers used in the present experiments covered narrower ranges of scattering angles than those used by Wilson.

§ 2. EXPERIMENTS WITH COBALT 60

The source used was a cobalt cylinder 1.2 cm in diameter and 1.2 cm in height which had been irradiated at Harwell to an activity of 100 mc.

Figure 1(a) shows the general arrangement of the apparatus. A lead double cone was suspended above the counter which rested on a table in the centre of

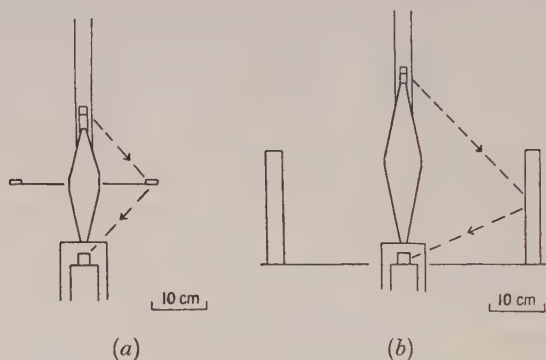


Fig. 1. General arrangement of the scattering apparatus for (a) 1.33 mev gamma-rays, and (b) 2.76 mev gamma-rays.

a large room. The scatterers for angles of 40° , 60° , 75° and 90° were in the form of annuli of the appropriate diameter and were suspended in the horizontal plane mid-way between source and phosphor. They each covered an angular range of about 12° , and weighed respectively 120 g, 730 g, 1100 g and 1700 g. The 120° scatterer was part of the appropriate solid of revolution and weighed 1500 g.

The detector was a cylindrical, thallium-activated, sodium iodide crystal 2 cm in diameter and 2 cm in height, mounted directly on the photo-cathode of an E.M.I. photomultiplier, aluminium foil being used around the crystal as reflector. The output pulses from the photomultiplier were then fed to a linear amplifier, and a single-channel pulse-height analyser designed by Mr. E. C. Park.

Measurements could not be made at angles less than 40° , as at these angles the energy of a photon scattered by the Compton effect is not greatly different from that of an elastically scattered photon, and the scintillation counter could not discriminate adequately between them.

First the pulse-height distribution was determined with the direct radiation from a small ^{60}Co source, and then the bias and width of the channel were set to record the 1.33 mev photopeak. Under these conditions somewhat less than 5% of the counts were due to 1.17 mev γ -rays.

The experiment consisted of the measurement of the counting rates in the channel with and without each scatterer in position. For each scattering angle ten such measurements were made. The source strength was measured by removing the double cone and scatterers and determining the counting rate in the channel with the source placed two metres from the phosphor. Thus, as

the geometry and weights of the scatterers were known, the absolute cross section for scattering at each angle was calculated.

Due to the presence of a great number of photons scattered by the Compton effect, on occasion two or more of these photons were detected simultaneously by the phosphor, and hence they appeared to be a single, elastically scattered photon. This effect only occurred to any detectable extent at 40° , 60° and 75° , the effect decreasing due to the decrease in the energy of the Compton-scattered photons as the scattering angle increased. At 40° the cross section was corrected for this effect by taking an absorption curve of the scattered radiation with lead absorbers around the phosphor. The counting rates at 60° and 75° were too low to apply this method of correction, and hence the measured cross sections at these angles are certainly too large.

The experimental results are shown in fig. 2, in comparison with a theoretical

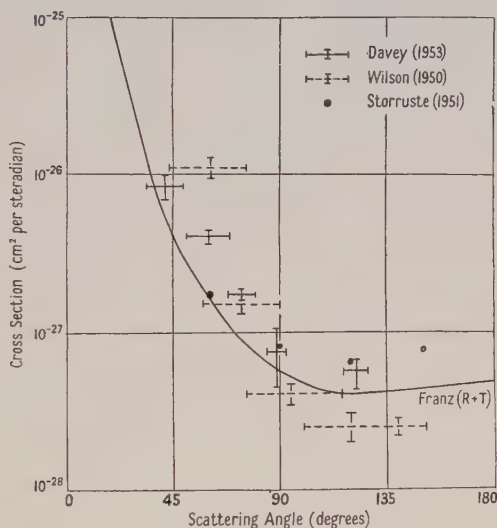


Fig. 2. Experimental variation of the cross section per atom for the elastic scattering of 1.33 mev gamma-rays from lead. The curve is based on the theoretical predictions of Franz.

curve assuming constructive interference between Rayleigh scattering, as calculated by Franz, and Thomson scattering. As the scattered counting rate and the background were always comparable and as low as 0.2 sec^{-1} , the errors are large.

§ 3. EXPERIMENTS WITH SODIUM 24

The source was 100 mc of ^{24}Na prepared by the $^{24}\text{Mg}(d, 2p)^{24}\text{Na}$ reaction in the 60 in. cyclotron of this Department. The face of the target was sawn off, and the pieces placed in a small test-tube.

Figure 1(b) shows the general arrangement of the apparatus, which closely resembled that used in the ^{60}Co experiment. The scatterers, for 40° , 60° , 85° and 109° , were, however, much more massive, weighing 690 g, 1000 g, 40 kg and 64 kg respectively. Those for 40° and 60° were annuli, whilst those for 85° and 109° were approximately cylindrical in form, being composed of lead blocks placed on edge on a tin-plate platform built around the counter.

^{24}Na emits only two γ -rays of 1.38 mev and 2.76 mev in cascade, and the channel was set to record the 2.76 mev photopeak. The technique used was similar to that used in the ^{60}Co experiment. Due to the higher energy of these gamma-rays, no effect due to the simultaneous detection of two Compton-scattered photons was experienced, and it was not necessary to use lead absorbers around the phosphor. The scattered counting rate and background were again each about 0.2 sec^{-1} .

The experimental results are shown in fig. 3, together with theoretical curves

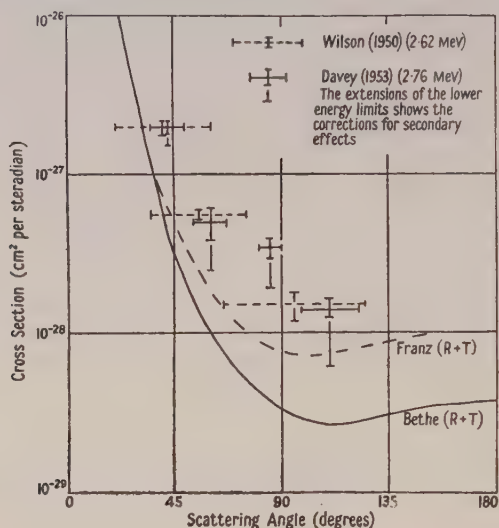


Fig. 3. Experimental variation of the cross section per atom for the elastic scattering of 2.76 mev gamma-rays from lead. The full and broken curves are based respectively on the theoretical predictions of Bethe (for 2.6 mev) and Franz (for 2.76 mev).

for the Rayleigh plus Thomson scattering cross section. The curve calculated by Bethe (1951, private communication to Professor Moon) for 2.6 mev γ -rays may, in spite of the fact that the energy used was 2.76 mev, be more accurate than the 2.76 mev curve based on Franz's formula.

§ 4. SECONDARY CONTRIBUTIONS TO THE SCATTERED COUNTING RATE

There are three phenomena which produce high-energy photons which register as elastically scattered γ -rays. These occur in the scatterer and are (i) bremsstrahlung from photo-electrons, (ii) bremsstrahlung from Compton electrons, (iii) photons produced by the single-quantum annihilation of positrons formed by pair production.

On the assumption of isotropic distribution of these photons, the total effective cross sections per unit solid angle for these effects are, for 1.33 mev and 2.76 mev γ -rays, $4 \times 10^{-29} \text{ cm}^2 \text{ sterad}^{-1}$ and $2 \times 10^{-28} \text{ cm}^2 \text{ sterad}^{-1}$ respectively. It is, however, doubtful if the assumption of isotropic distribution is justified, as isotropy would only be obtained if the electrons and positrons in the scatterer were scattered through very large angles with little loss of energy.

For the 1.33 mev γ -rays the correction of $4 \times 10^{-29} \text{ cm}^2 \text{ sterad}^{-1}$ makes very little difference to the experimental results, and the degree of anisotropy of the photons has not been estimated.

Secondary effects are more important at 2.76 mev, and the work of Petrauskas *et al.* (1943) has been used to estimate the degree of anisotropy of the bremsstrahlung. The effective cross sections per steradian were estimated to be $2.3 \times 10^{-28} \text{ cm}^2$, $1.5 \times 10^{-28} \text{ cm}^2$, $8.8 \times 10^{-29} \text{ cm}^2$ and $6.1 \times 10^{-29} \text{ cm}^2$ at 40° , 60° , 85° and 109° respectively. The lower energy limits in fig. 3 have been extended downwards to take account of this correction.

§ 5. DISCUSSION OF THE RESULTS

(a) 1.33 MeV.

As has already been stated, the values obtained at 60° and 75° are certainly too high owing to insufficient discrimination against the γ -rays scattered by the Compton process.

Nevertheless, fig. 2 shows that the present measurements agree reasonably well with those of Wilson (1950, private communication to Professor Moon) and Storruste (1951), and run closely parallel to, if somewhat above, the curve calculated from Franz's theory. The experimental errors are somewhat large, and the theory, which is non-relativistic and based on the Thomas-Fermi electron distribution, is open to doubt for the energy and atomic number in question.

(b) 2.76 MeV.

The experimental results are in good agreement with those of Wilson for 2.6 mev, and lie above Bethe's curve (for 2.6 mev) and the curve based on Franz's formulae (for 2.76 mev).

The excess scattering observed, although substantial when compared with the theoretical Rayleigh-Thomson scattering, corresponds to a quite small absolute cross section and might perhaps be attributable to some secondary effects. For a positive identification with Delbruck scattering, one would wish to compare theory and experiment in respect of some characteristic property such as the angular distribution at a fixed energy, or variation with energy at a fixed angle. The experiments suggest a rapid increase with energy, and provide a rough angular distribution for comparison with future calculations. One should note that if the excess scattering at 2.76 mev is due to the Delbruck process, and if its phase is opposite to that of the Rayleigh-Thomson component, its amplitude must be substantially greater.

ACKNOWLEDGMENTS

The author wishes to thank Professor P. B. Moon for guidance throughout this work, and to thank Dr. W. I. B. Smith and the cyclotron team for preparation of the ^{24}Na source. He also wishes to acknowledge a maintenance grant from the Department of Scientific and Industrial Research.

REFERENCES

- BETHE, H. A., and ROHRlich, F., 1952, *Phys. Rev.*, **86**, 10.
DELBRUCK, M., 1933, *Physik*, **84**, 144.
FRANZ, W., 1935, *Z. Phys.*, **98**, 314.
MOON, P. B., 1950, *Proc. Phys. Soc. A*, **63**, 1189.
PETRAUSKAS, A. A., VAN ATTA, L. C., and MYERS, F. E., 1943, *Phys. Rev.*, **63**, 389.
ROHRlich, F., and GLUCKSTERN, R. L., 1952, *Phys. Rev.*, **86**, 1.
STORRUSTE, A., 1950, *Proc. Phys. Soc. A*, **63**, 1197; 1951, *Thesis*, University of Oslo.
WILSON, R. R., 1951, *Phys. Rev.*, **82**, 295.

RESEARCH NOTES

Intensities in the Herzberg System of O₂

By M. E. PILLOW

Northern Polytechnic, London

MS. received 27th July 1953

VERY recent calculations on the relative intensities of bands in the Herzberg system of O₂ (Pillow 1953, to be referred to as I) were based on Herzberg's latest measurements on the absorption spectrum (1952), and assumed the system origin to be at $\lambda = 2794 \text{ \AA}$, that being the band of longest wavelength yet observed in absorption. While these results were in course of publication Broida and Gaydon (1953) obtained, in the emission from an afterglow of oxygen, an extensive system of bands with wavelengths appropriate to the Herzberg system, this being the first known appearance of these bands in emission under laboratory conditions. Their observations include several bands which appear to belong to a further progression, thus necessitating the extrapolation of the system origin to $\lambda = 2856 \text{ \AA}$, and the increase by 1 of all the values of v' . This change shifts the main Franck-Condon parabola in the vibrational scheme somewhat to the left, and the wave functions have therefore been plotted again, and the relative intensities calculated in accordance with the new numbering. Rotational data for the new vibrational level are not available, but extrapolation from the values previously used gives $\omega_e' = 890.8$, $x\omega_e' = 27.18$, $r_e' = 1.521 \times 10^{-8} \text{ cm}$. (It may here be observed that, as in I, a formula of the form $\omega_e(v + \frac{1}{2}) - x\omega_e(v + \frac{1}{2})^2$ is fitted by least squares to the energy levels, and that while the constants used appear very different from the first two in Herzberg's suggested polynomial form, the energy levels given by the formula are in very good agreement with those observed, and the corresponding potential curve is likely to be reasonably correct.)

Table 1 shows the new vibrational intensity scheme up to $v' = 7$, together with visual estimates of intensity made by Broida and Gaydon. The agreement is seen to be good, especially when allowance is made for overlapping of the bands with one another and with the afterglow continuum. In view of this agreement it appears unlikely that there is yet a further vibrational level to be found. (The wavelengths quoted here have been modified to agree with the latest estimates.)

Reference was made in I to the possible identification of a number of bands in the night-sky spectrum with those of the Herzberg system. When allowance is made for the overlapping of close bands at the small dispersion used, it is found that the peaks of intensity still occur in the appropriate positions, and that agreement in magnitude with Barbier's values is, if anything, rather better than before; so that the change of numbering leaves unaltered the probability that many of the night-sky bands can be attributed to this system, though some of the individual assignments are doubtful.

Table 1. Herzberg System of O₂. Calculated Intensities and Wavelengths

v''	0	1	2	3	4	5	6	7	8	9	10
0	2856	2988	3132	3287	3457 3	3641 7	3842 16 [5?]	4064 26 [5]	4308 34 [7]	4579 37 [5]	4881 35 [2]
1	2794	2921	3058	3206 4	3367 11	3541 25 [a8]	3731 37 [8]	3940 43 [7]	4169 33 [6]	4422 17	4703 3
2	2737	2859	2990 3	3131 12	3284 28 [7]	3450 45 [8]	3631 48 [8]	3827 36 [8]	4044 13 [?]	4281 0	4544 4
3	2685	2802 3	2928 9 [1]	3063 26 [b5?]	3209 46 [10]	3367 58 [10]	3539 44 [a8]	3726 18	3930 1	4155 5	4401 14
4	2637 1	2750 7	2871 21 [2]	3001 46 [5]	3141 65 [7]	3293 62 [4?]	3456 30 [?]	3635 1	3829 3	4041 16	4274 11
5	2593 3	2703 17	2819 38 [b3?]	2945 68 [5]	3079 74 [b?]	3225 54	3382 11	3553 1	3738 15	3940 18	4161 2
6	2554 16	2660 36	2773 65 [3]	2894 90 [6]	3025 76 [b3]	3164 31	3316 2	3479 7	3657 21	3849 11	4061 0
7	2519 37	2622 62 [3]	2732 102 [5]	2850 107 [5]	2976 70	3111 15	3257 1	3415 16	3586 21	3771 4	3973 2

Numbers in brackets represent intensities estimated visually by Broida and Gaydon. A few weak bands, whose assignment is doubtful, have not been included. *a*: bands overlapping each other; *b*: bands overlapped by OH in afterglow.

In absorption, the $v''=0$ progression alone has been observed. Because of the small overlap of most of the wave functions involved only the order of these intensities can safely be claimed as a result of calculation. The form of their distribution is not changed by the new numbering, and agrees qualitatively with such observations as are available, which are discussed in I. Relative, and very approximate, values for the transition probabilities in this progression are given in table 2.

Table 2

0, 0 2856 1.2×10^{-6}	0, 1 2794 1×10^{-5}	0, 2 2737 8.5×10^{-5}	0, 3 2685 7×10^{-4}	0, 4 2637 2.5×10^{-3}		
Bands originally observed by Herzberg						
0, 5 2593 1×10^{-2}	0, 6 2554 3.2×10^{-2}	0, 7 2519 8×10^{-2}	0, 8 2489 1.6×10^{-1}	0, 9 2463 3.2×10^{-1}	0, 10 2443 6.3×10^{-1}	0, 11 2429 1

Thanks are due to Drs. Gaydon and Broida for access to their results in advance of publication.

REFERENCES

- BROIDA, H. P., and GAYDON, A. G., 1953, private communication; also reported at Congrès de Spectroscopie, Paris, June 1953.
 HERZBERG, G., 1952, *Canad. J. Phys.*, **30**, 185.
 PILLOW, M. E., 1953, *Proc. Phys. Soc. A*, **66**, 733.

On the Existence of a Bound State of ${}^4\text{H}$

By P. SWAN

Physics Department, University College, London

Communicated by H. S. W. Massey; MS. received 17th July 1953

IN view of recent experiments and calculations (Breit and MacIntosh 1951, McNeill and Rall 1951) on the possible existence of ${}^4\text{H}$, it is of interest to examine whether a bound state can exist in which the third neutron is an excited state relative to the component triton group. Denoting the neutrons by 1, 2 and 4, and the proton by 3, the appropriate resonating group structure wave function has the anti-symmetric form for triplet and singlet spin functions:

$$\Psi_{s,T}(123, 4) = \sigma_{s,T}(1234)\phi(123, 4) + \sigma_{s,T}(2431)\phi(243, 1) + \sigma_{s,T}(4132)\phi(413, 2).$$

The resonating group spin functions are

$$\sigma_T(1234) = 2^{-1/2}(\alpha_1\beta_2 - \beta_1\alpha_2)\alpha_3\alpha_4, \quad \sigma_s(1234) = \frac{1}{2}(\alpha_1\beta_2 - \beta_1\alpha_2)(\alpha_3\beta_4 - \beta_3\alpha_4) \quad \dots (2)$$

for triplet and singlet spin states respectively.

It is simplest to use spatial wave functions of gaussian type:

$$\begin{aligned} \phi(123, 4) &= \exp[-\alpha(r_{12}^2 + r_{23}^2 + r_{31}^2) - \beta(r_{14}^2 + r_{24}^2 + r_{34}^2)] \\ &= \exp[-(\frac{3}{2}\alpha + \frac{1}{2}\beta)R^2 - (2\alpha + \frac{2}{3}\beta)u^2 - 3\beta x^2], \end{aligned} \quad \dots (3)$$

where \mathbf{R} , \mathbf{u} and \mathbf{x} are the natural coordinates:

$$\mathbf{R} = \mathbf{r}_3 - \mathbf{r}_2, \quad \mathbf{u} = \mathbf{r}_1 - \frac{1}{2}(\mathbf{r}_2 + \mathbf{r}_3), \quad \mathbf{x} = \mathbf{r}_4 - \frac{1}{3}(\mathbf{r}_1 + \mathbf{r}_2 + \mathbf{r}_3). \quad \dots (4)$$

Here α is found by applying the variational principle to the ground state of the triton. We take the nuclear potential of the form

$$(M/\hbar^2)\bar{V}(r) = -(mM + hH + bB + w)U(r), \quad \dots (5)$$

where m , h , b , w are the coefficients of Majorana, Heisenberg, Bartlett and Wigner force respectively; M , H , B , 1 are the corresponding exchange operators, and $U(r) = U_0 \exp(-\lambda r^2)$. Taking $U_0 = 45 \text{ MeV}$, $\lambda = 0.267 \times 10^{26}$, then $\alpha = 0.0718$ corresponds to a variational energy for the triton of 5.49 MeV .

Four alternative types of nuclear force were considered:

$$\left. \begin{aligned} \text{I Ordinary force: } m=h=0, w=\frac{1}{2}(1+x), b=\frac{1}{2}(1-x), \\ \text{II Majorana-Heisenberg force: } w=b=0, m=\frac{1}{2}(1+x), h=\frac{1}{2}(1-x), \\ \text{III Symmetric force: } m=b=0, w=\frac{1}{2}(1+x), h=\frac{1}{2}(1-x), \\ \text{IV Serber force: } m=w=\frac{1}{4}(1+x), h=b=\frac{1}{4}(1-x), \end{aligned} \right\} \quad \dots (6)$$

where $x=0.6$ is the ratio of the singlet to the triplet neutron-proton interaction.

After elementary but tedious calculation, one obtains for the binding energy E of ${}^4\text{H}$:

$$\begin{aligned} (M/\hbar^2)E &= 12\beta + 72\beta^2 N [\int x^2 \phi(123, 4)\phi(243, 1) d\tau - \int x^2 \phi^2(123, 4) d\tau] \\ &\quad + N[A \int \phi^2(243, 1) U(12) d\tau + B \int \phi(123, 4)\phi(234, 1) d\tau \\ &\quad + C \int \phi(123, 4)\phi(234, 1) U(12) d\tau], \end{aligned} \quad \dots (7)$$

where $1/N = \int \Psi^2(123, 4) d\tau$

$$\text{Triplet} \begin{cases} A = (-3m - 6h + 6b + 9w), \\ B = (9m + 6h - 6b - 3w), \\ C = (-6m - 6w), \end{cases} \quad \text{Singlet} \begin{cases} A = (-3m - 6h + 9w), \\ B = (9m - 6b - 3w), \\ C = (-6m + 6h + 6b - 6w). \end{cases}$$

One finds that not only does no bound state of ${}^4\text{H}$ exist for any of the force types I, II, III and IV, but that the expectation energy is positive for all positive values of β in (3). Now ${}^4\text{H}$ is composed essentially of the ${}^3\text{H}$ group plus a spare neutron, all other groupings being of negligible importance, so that if we put the ${}^3\text{H}$ group into the 1s level and the neutron into the lowest state compatible with the Pauli principle, then the neutron is actually repelled by the triton group. This negative conclusion is in agreement with the experiments of McNeill and Rall (1951), in which a tritium target was bombarded with deuterons.

The fact that wave functions antisymmetric in identical particles, (1) being an example, describe excited states may be seen by considering the simpler case of excited atoms. The binding energies of 1s2s states of two electron systems may be found using only wave functions of 1s type, provided that the total wave function is antisymmetric. The same method could be applied to 2p3p or 3d4d states by using only wave functions of 2p or 3d type respectively. If the total wave function Ψ is formulated according to resonating group theory or the usual Slater determinant, and Ψ turns out to be antisymmetric, then if the 1s state is already occupied by one or more electrons, the next electron must be in an excited state (as they have parallel spins). If both electrons are placed in the 1s state, Ψ is zero, although by normalizing and going to the limit a function may be found which has the wrong form for a bound S state. The method has two features:

(a) The 2s state is described by a simple function of 1s type, and yet the Pauli principle ensures that the 1s2s state and not the $(1s)^2$ state is described.

(b) The usual Feenberg orthogonality terms cancel out identically in the total wave function, thus greatly simplifying the calculation of energy levels.

The 1s2s ${}^3\text{S}$ state of helium provides a suitable test of the method. Denoting the electrons by 1 and 2 respectively and using atomic units, the simplest wave function is

$$\begin{aligned} \Psi = & \exp(-2r_1) \left(\exp(-br_2) - \frac{1}{\pi} \exp(-2r_2) \int \exp[-(2+b)r_1] d\tau_1 \right) \\ & - \exp(-2r_2) \left(\exp(-br_1) - \frac{1}{\pi} \exp(-2r_1) \int \exp[-(2+b)r_2] d\tau_2 \right) \\ = & [\exp(-2r_1 - br_2) - \exp(-2r_2 - br_1)]. \end{aligned} \quad \dots\dots(8)$$

This yields a 1s2s ${}^3\text{S}$ energy for He of -58.47 ev for $b=0.32$, compared with the experimental value of -58.82 ev. The agreement to within 0.6% is achieved with a 2s function having the incorrect form $\exp(-br)$, thus illustrating the effectiveness of the approximation.

Unfortunately the method cannot be used to investigate possible excited states of the alpha particle, as the appropriate wave function is symmetric, thus describing the ground state.

REFERENCES

- BREIT, G., and MACINTOSH, J. S., 1951, *Phys. Rev.*, **83**, 1245.
MCNEILL, K. G., and RALL, W., 1951, *Phys. Rev.*, **83**, 1244.

Ionization and Fragmentation of Molecules by Bombardment with Atomic Ions

By E. LINDHOLM

Department of Physics, Chalmers Institute of Technology, Gothenburg, Sweden

MS. received 15th June 1953

THE exchange of charge in the collisions between ions and molecules has been investigated by several authors (Massey and Burhop 1952, Hasted 1951, 1952). In such experiments it has been difficult to determine the collision process exactly as, usually, the reaction products have not been analysed.

In the present work atomic ions have been sent into H_2S gas and the collision products have been analysed in a mass spectrometer, according to a method used by Keene (1949) for hydrogen and helium. The reasons for using H_2S in these preliminary experiments are: the ionized fragments from this molecule when subjected to electron bombardment are of approximately equal intensity (H_2S^+ : 100, HS^+ : 42.7, S^+ : 45.6), and the mass numbers of these fragments are almost equal (34, 33, 32). It is therefore possible to analyse them with electrostatic scanning in a permanent magnet without any appreciable discrimination due to the voltage effect. The appearance potentials are known (Neuert and Clasen 1952). As they lie relatively far apart from each other (H_2S^+ : 10.5 ± 0.2 eV; HS^+ : 15.2 ± 0.5 eV; S^+ : 14.0 ± 0.7 eV and 18.5 ± 1.0 eV), the process during the collision may be determined.

All the parts of the apparatus are placed inside a large vacuum container. The atomic ions (marked A) are produced in an ion source of Nier type with an electron accelerating voltage of 80 v, are analysed in a semicircular inhomogeneous permanent magnet A with a radius of 75 mm (Snyder, Rubin, Fowler and Lauritsen 1950), enter the collision chamber that is filled with H_2S gas at a pressure of 2×10^{-3} mm Hg, and after leaving the collision chamber they are collected and measured. In the collision chamber ionized fragments (marked B) are obtained from H_2S . The ions B are drawn out through one side of the collision chamber, are accelerated and analysed in a permanent magnet B similar to magnet A, and are finally collected and measured.

During the measurements the potentials of the ion source and the collision chamber were usually +2000 v and +1500 v, which meant that the energy of the ions A during the collision was 500 eV. For the analysis of the ions A and B the potentials of the magnets were varied. As the collector A must have earth potential and the collision chamber has a high positive potential, secondary electrons that are ejected from collector A when hit by the ions A might enter the collision chamber and might ionize the gas there. To prevent this a negative plate with a rather wide slit is placed between the collector A and the collision chamber. Between magnet A and the collision chamber there is a similar slit. These slits act as strong electrostatic lenses and cause defocusing of the ion beam. As this defocusing increases rapidly for decreasing energy of the ions A, it has been impossible to determine the dependence of the cross section on the collision energy in the

present apparatus. During the measurements a constant collision energy of 500 ev has therefore been used.

The results of the measurements of the ionization of H_2S are given in the table. The first column gives the incident ions, the second their ionization potential (I.P.) and the third the corresponding transition, where the first symbol denotes the state of the ion and the second symbol the state of the atom after the charge-exchange. In columns (4), (5) and (6) the cross sections Q for formation of fragments from H_2S are given. The unit of the cross section has been estimated roughly in the following manner: Argon gas was bombarded with argon ions with an energy of 500 ev. The cross section for this case is given by Hasted (1951) to be 80 cm^{-1} , and with this value the apparatus could be calibrated. The values in the table are in

(1)	(2)	(3)	(4)	(5)	(6)	(7)	(8)	(9)	(10)	(11)	(12)
Kr^{++}	24.45		0.5	3	6	0	0.5	2			Kr
Ne^+	21.56		0	2	6	0	0.3	3			Ne
F^+	17.43		1.5	7	9	0	0.7	1			KHF_2
Sb^{++}	17?		2	1	2						SbF_3
A^+	15.76	$^2\text{P}-^1\text{S}$	0.5	16	5	0	3	0.3	doublet	15.94	A
N^+	14.55	$^3\text{P}-^4\text{S}$	75						$^3\text{P}-^2\text{P}$	10.97	$\text{N}_2, \text{N}_2\text{O}, \text{NH}_3$
				20					$^1\text{S}-^3\text{P}$	15.03	
					25				$^3\text{P}-^4\text{S}$	14.55	
Kr^+	14.0	$^2\text{P}-^1\text{S}$	3	11	24	0.1	0.4	1.7	doublet	14.7	Kr
O^+	13.62	$^4\text{S}-^3\text{P}$	41			0.7			?	?	$\text{CO}_2, \text{CO}, \text{N}_2\text{O}$
				18			0.2				
					52			0.9	$\begin{cases} ^2\text{D}-^1\text{D} \\ ^2\text{P}-^1\text{S} \end{cases}$	$\begin{cases} 14.98 \\ 14.45 \end{cases}$	
Cl^+	12.90	$^3\text{P}-^2\text{P}$	22	10	10	1	0.3	0.3			CCl_4
Br^+	11.76	$^3\text{P}-^2\text{P}$	3	4	14	0.2	0.2	2	$^1\text{S}-^2\text{P}_{1/2}$	14.88?	CuBr_2
C^+	11.27	$^2\text{P}-^3\text{P}$	180	12	8	9	0	0	$^2\text{P}-^1\text{D}$	10.00	$\text{CO}_2, \text{CO}, \text{CCl}_4$
P^+	10.99	$^3\text{P}-^4\text{S}$	260	1.5	1.5	87	0	0	$^1\text{D}-^2\text{D}$	10.66	P_4S_3
S^+	10.36	$^4\text{S}-^3\text{P}$	140	4	2.5	22	0	0	$^2\text{P}-^1\text{S}$	10.65	H_2S
Se^+	9.73	$^4\text{S}-^3\text{P}$	70	2.5	0.6	22	0	0	$^2\text{D}-^1\text{D}$	10.25	SeO_2
Zn^+	9.39	$^2\text{S}-^1\text{S}$	0	0	0						Zn
B^+	8.28	$^1\text{S}-^2\text{P}$	8	0	2.5	3	0	0.3	$^3\text{P}-^2\text{P}$	12.91	BF_3
Cu^+	7.72		0	0	0						CuF
H_2S^+	10.5		150	0	0						H_2S
Electrons			100	44	46						

(1) Ion; (2) I.P.; (3) transition; (4) $Q_{\text{H}_2\text{S}}$; (5) Q_{HS} ; (6) Q_{S} ; (7) $Q_{\text{H}_2\text{S}}/(Q_{\text{HS}}+Q_{\text{S}})$; (8) $Q_{\text{HS}}/(Q_{\text{H}_2\text{S}}+Q_{\text{S}})$; (9) $Q_{\text{S}}/(Q_{\text{H}_2\text{S}}+Q_{\text{HS}})$; (10) probable transition; (11) E ; (12) material.

the same units (cm^{-1}), but it is evident that there is a high degree of uncertainty, and the error may be different for different atomic ions. In columns (7), (8) and (9) the ratios between the cross sections are given. For these the degree of accuracy is probably high. Column (10) gives the transition of the atomic ion that probably is responsible for the charge exchange, and column (11) the corresponding recombination energy E . Column (12) gives the materials from which the ions are obtained. The bottom row gives the mass spectrum of H_2S that was obtained by electron bombardment.

It is evident from the table that the mass spectrum of H_2S is sometimes simpler when the molecule is hit by ions than when an ordinary ion source with electrons is used. The reason for this is that ionization and fragmentation take place in the

main only when there is resonance between the energies of the ion and of the fragments of the molecule. Consequently we obtain large H_2S^+ peaks only when the recombination energy of the ion approximately coincides with the appearance potential 10.5 eV for this fragment. Using ions with higher recombination energies, we obtain in the main HS^+ and S^+ fragments. For the formation of HS^+ fragments the cross section has a maximum at about 15.2 eV (Ar^+) and for the formation of S^+ fragments there are two weak maxima at about 14.0 eV (Kr^+) and 18.5 eV (Ne^+). These maxima are more evident in columns (7), (8) and (9), where the ratios between the cross sections are given. From these ratios the collision process may reliably be judged even though the cross sections are uncertain owing to the defocusing mentioned above.

For some ions we must take into consideration that the transition of the ion may end in an excited atomic state. With N^+ we obtain large cross sections for the formation of H_2S^+ . The reason for this is, probably, that $\text{N}^+(\text{}^3\text{P})$ goes over to $\text{N}(\text{}^2\text{P})$, and in this transition the recombination energy is 10.97 eV.

The large cross section for the formation of H_2S^+ in collisions with Se^+ is probably caused by the transition ${}^2\text{D} - {}^1\text{D}$, for which the recombination energy is 10.25 eV. It seems to be improbable that the ionization potential of Se (9.73 eV) contributes to this cross section as it is much smaller than the appearance potential for H_2S^+ (10.5 ± 0.2 eV). Therefore we must presume that the ion is in a metastable state before the collision and goes over to an excited atomic state.

For C^+ , P^+ and S^+ alternative transitions and energies are given in columns (10) and (11) for the formation of H_2S^+ . Both explanations seem to be possible. No explanation can be given of the large cross section for the formation of H_2S^+ with O^+ ions.

The cross section for the formation of S^+ is large in collisions with Br^+ , Kr^+ , O^+ and N^+ . According to Neuert and Clasen 14.0 \pm 0.7 eV is necessary. With Br^+ several transitions are possible with the following energies: 15.3, 14.9, 13.4 and lower. Kr^+ gives only two energies: 14.0 and 14.7. This shows that Neuert and Clasen's value is probably too low and should be increased to about 14.7 eV. This value agrees approximately with the recombination energies for O^+ and N^+ in column (11).

By means of similar experiments with other molecules with known appearance potentials it will be possible to investigate the states of the ions that are produced in an ion source of this kind. After that the method may possibly be of value for the investigation of molecules.

REFERENCES

- HASTED, J. B., 1951, *Proc. Roy. Soc. A*, **205**, 421; 1952, *Ibid.*, **212**, 235.
KEENE, J. P., 1949, *Phil. Mag.*, **40**, 369.
MASSEY, H. S. W., and BURHOP, E. H. S., 1952, *Electronic and Ionic Impact Phenomena* (Oxford: Clarendon Press).
NEUERT, H., and CLASEN, H., 1952, *Z. Naturforsch.*, **7a**, 410.
SNYDER, C. W., RUBIN, S., FOWLER, W. A., and LAURITSEN, C. C., 1950, *Rev. Sci. Instrum.*, **21**, 852.

LETTERS TO THE EDITOR

**The Surface Resistance of Normal and Superconducting Tin
at 36 000 Mc/s**

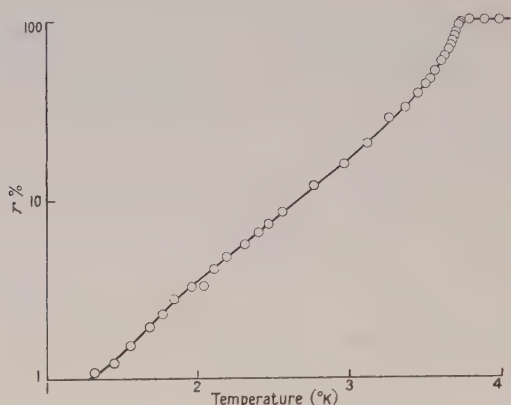
An apparatus has been constructed to investigate the surface resistance at 36 000 Mc/s of metals at liquid helium temperatures. Previous investigations at 1500 Mc/s (Pippard 1947), 9400 Mc/s (Pippard 1950 a), and 25 000 Mc/s (Greibenkemper and Hagen 1952) have thrown some light on the frequency dependence of the surface resistance of tin in its normal and superconducting states. Pippard (1950 b) has shown that in the superconducting state the frequency dependence of the resistance and the form of its variation with temperature are inconsistent with a simple form of the two-fluid model of superconductivity, and has also found a non-tensorial anisotropy in both the normal and superconducting states. In the present work, plane single crystals of tin are used, with the current flow in one direction in the plane, so that the anisotropy can be further studied, and detailed comparison made with Pippard's results at 9400 Mc/s. The residual resistance at the lowest temperatures is of particular interest, since Ramanathan (1952) has found that at infra-red frequencies there is no change in the surface resistance at the transition to the superconducting state, while at lower microwave frequencies there is a sharp discontinuity of gradient at the transition temperature, and the resistance tends to very low values, probably zero, at the absolute zero.

Because of the relatively low frequency stability of the VX357 klystron used, a calorimetric rather than a resonance technique was adopted. A rectangular brass cavity, operated in an H_{10} mode, is closed at one end by a copper plate, and at the other by a plane single crystal of tin, also in the form of a plate; to ensure thermal isolation, the plates are not in physical contact with the rest of the cavity, but microwave leakage is prevented by the choking action of suitable circular grooves. The cavity is fed through a T-junction, and the dimensions of the coupling hole are designed to give adequate power amplification without too high a selectivity. The apparatus is enclosed within an evacuated chamber, and each of the tin and copper plates is connected to the helium bath through the thermal resistance of a copper-nickel rod, so that the power absorbed by the plate raises its temperature. The rise in temperature is measured by a resistance thermometer, and the power absorption determined by substituting an equivalent d.c. joule heating in an attached heating coil. In this way, the ratio of the surface resistances of the two plates is found, and since, in this range, the surface resistance of copper is independent of temperature, the variation with temperature of the resistance of the tin surface may be obtained.

Typical results are plotted in the figure, which shows the variation with temperature of the ratio r of the superconducting to the normal surface resistance of an electropolished plane single crystal of tin.

The residual value of r , obtained by a suitable extrapolation, is about 0.4%, but this represents an upper limit, since there is a possibility of a spurious heat leak on to the tin specimen from the cavity, where considerable heat is generated by the microwaves in the low conductivity brass walls. This low

value may be compared with that observed at infra-red frequencies, where the surface resistance in the superconducting state remains equal to that in the normal state down to 2°K (Ramanathan 1952); this suggests that a frequency of 36 000 Mc/s is still not high enough to produce an appreciable absorption by the mechanism responsible for the absorption in the superconducting state at infra-red frequencies.



Temperature variation of superconducting resistance of a plane single crystal of tin (dyad axis in the plane, tetrad axis inclined at about 60° to the normal, current flow perpendicular to the dyad axis).

The curves may be described by the same functions as used by Pippard (1950 a) to reduce his results at 9400 Mc/s. A more detailed comparison, to deduce the frequency dependence in the normal and superconducting states, must be postponed until the anisotropy has been thoroughly investigated, since Pippard's results represent the mean resistance of a cylindrical single crystal with current flow parallel to the axis, and other work has been on polycrystalline specimens. The non-tensorial form of the anisotropy has, however, already been confirmed by measurements on single crystals of tin of several orientations. A more complete picture of the anisotropy in the normal state may give some insight into the form of the Fermi surface.

The author's thanks are due to Dr. A. B. Pippard for suggesting the problem and his continued advice and encouragement, and to the Chief Superintendent, Telecommunications Research Establishment, Malvern, for the loan of microwave equipment.

Royal Society Mond Laboratory,
Cambridge.
29th July 1953.

E. FAWCETT.

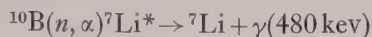
GREBENKEMPER, C. J., and HAGEN, J. P., 1952, *Phys. Rev.*, **86**, 673.

PIPPARD, A. B., 1947, *Proc. Roy. Soc. A*, **191**, 370; 1950 a, *Ibid.*, **203**, 98; 1950 b, *Ibid.*, **203**, 195.

RAMANATHAN, K. G., 1952, *Proc. Phys. Soc. A*, **65**, 532.

A Scintillation Detector for Neutrons of Intermediate Energy

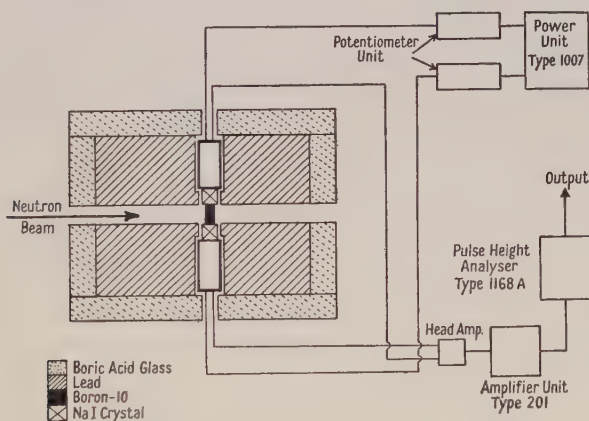
Following up the work of Duckworth, Merrison and Whittaker (1950), a detector has been built in which the γ -rays from the reaction



are detected in a sodium iodide scintillation spectrometer. This device has now been in use for some time with the time-of-flight equipment of the Harwell linear accelerator.

One of the difficulties with this type of neutron detector is that it depends on counting the relatively soft γ -rays from $^7\text{Li}^*$, and hence tends to have a large background of accidental counts due to the presence of radioactive sources, cosmic rays and so on. In our case this background has been minimized by very thorough lead screening and by the use of sodium iodide scintillators of high resolution in conjunction with a single-channel kicksorter set to count the total-energy peak of the $^7\text{Li}^*$ radiation.

The arrangement of the apparatus is shown schematically in the diagram. The collimated neutron beam from the accelerator strikes a thin-walled aluminium cylinder 3 in. in diameter and $1\frac{1}{4}$ in. deep, filled with amorphous boron-10. Two large sodium iodide crystals ($1\frac{3}{4}$ in. diam. \times 2 in. deep) which are attached to photomultipliers (E.M.I. Type 6260), are placed one on each side of the boron-10



container, on opposite ends of a diameter. The high tension supply for the multipliers is stabilized to within 0.1% and set separately by two potentiometer units. The outputs are fed into a fast amplifier (upper frequency limit 5 Mc/s) and thence, at a level of about 20 v, to a single-channel pulse height analyser. The boron-10 crystals and multipliers are enclosed in a lead 'castle' approximately 2 ft cube which is surrounded by a 4 in. shield of boric acid glass for protection against stray slow neutrons.

With the kicksorter set to accept those pulses which occur when the crystal has absorbed all the energy of the $^7\text{Li}^*$ radiation and with the channel-width adjusted to about 25% of the corresponding pulse height, the detector has an efficiency of approximately 2.6%, and this efficiency should be very nearly constant up to neutron energies of around 1000 ev. Above this energy this thickness of boron-10 ceases to be 'black' and losses of the order of 15% at 5 kev and 50% at 50 kev are to be expected. It should also be noted that the

power unit and amplifier used with a detector of this type must be very stable since a shift of 10% in pulse height produces a drop of 30% in counting rate. The units used, with selected neon tubes in the power unit, have given very stable results, drifting being very slow and not more than 5% in pulse height in a week. With daily monitoring, this drift is not serious and produces a variation in the efficiency of not more than a few per cent.

This detector has been used to replace a $^{10}\text{BF}_3$ proportional counter of effective length 10 cm and filled to a pressure of 60 cm Hg with $^{10}\text{BF}_3$. This counter has an efficiency which varies as $1/\sqrt{E}$ where E is the neutron energy, except at very low values of E . The efficiency of the $^{10}\text{BF}_3$ counter is equal to that of the scintillation counter at a neutron energy of 10 eV (E_0). Above this energy the scintillation counter is more efficient by the factor $\sqrt{E/E_0}$. Hence from the point of view of efficiency its main usefulness is in the region 10 to 10^5 eV.

When the scintillation detector is used in the time-of-flight spectrometer, the higher efficiency obtained makes possible the use of longer flight-paths. Now the resolution of such a spectrometer, other things being equal, is inversely proportional to the length of the flight-path, and so the increased efficiency makes possible improved resolution, especially at the higher energies. For example, at 10^5 eV the theoretical improvement in resolution which is possible without loss in counting rate is by a factor of 4.6. The use of solid boron-10 makes a further contribution to improved resolution in that the physical length of the new counter is only 3 cm as compared with the 10 cm of the $^{10}\text{BF}_3$ counter. Lastly, the rise-time of the scintillation pulses is much shorter than that of the pulses from the $^{10}\text{BF}_3$ counter ($0.1 \mu\text{sec}$ as against 1 or $2 \mu\text{sec}$) thus reducing errors in timing caused by varying levels of discrimination. This makes possible a further improvement in the resolution of the spectrometer by the use of narrower timing channels.

We must express our gratitude to the Atomic Energy Commission of the United States for the loan of the boron-10 used in the detector.

Atomic Energy Research Establishment,
Harwell, Didcot, Berks.
28th July 1953.

E. R. RAE.
E. M. BOWEY.

DUCKWORTH, J. C., MERRISON, A. W., and WHITTAKER, A., 1950, *Nature, Lond.*, **165**, 69.

The Internal Conversion Electrons Emitted in the Decay of Ionium and Radio-Thorium

In the course of a previous investigation (Jarvis and Ross 1951) of the α -decay of ionium by the nuclear emulsion technique, it was observed that in a small percentage of the disintegrations two electron tracks had a common origin with an α -track. The number of these events examined was too small to allow the energies of the associated γ -rays to be determined with any precision, but certain suggestions were put forward as to likely values. The suggestion that two transitions indistinguishable in energy (~ 70 keV) are involved in the ionium disintegration formed part of an interpretative scheme in which the first (67 keV) excited state of the daughter nucleus ^{226}Ra was regarded as non-radiative, of spin 0 and even parity. Since it has been shown conclusively that this state,

like the first excited states of almost all even-even nuclei, is a 2^+ state, and therefore feebly quantum-emitting, this suggestion is now unnecessary.

A more extensive search for these rare events is at present being made using, as before, Kodak NT4 emulsion impregnated in a neutral solution of ammonium ionium oxalate. Although this investigation is as yet incomplete, it is already evident from the results that at least one of the conversion electrons in each pair cannot be attributed to a nuclear transition of about 70 keV.

A preliminary investigation has also been made by the same technique of the modes of disintegration of radio-thorium. In this case, 241 α -tracks out of a total of 569 (42%) were associated with conversion electron tracks. These electrons fall roughly into three groups. The two groups of highest energy can be identified as the L and M conversion electrons of the 84 keV γ -radiation (Rosenblum, Valadares and Guillot 1952) and these were found to be emitted in 27% of the disintegrations. The difference in mean range (0.5μ) between the α -tracks associated with these conversion electrons and those not associated with electron tracks indicates that the difference in energy of the two α -groups is 87 ± 24 keV.

The group of electrons of lowest energy, emitted in 15% of the disintegrations, is associated with α -tracks of mean range 1.2μ less than normal. This indicates that these conversion electrons are chiefly emitted following α -disintegration to an excited state differing in energy from the ground state by 209 ± 28 keV. This result is consistent with the report of γ -rays of energies 216 ± 3 and 172 ± 4 keV (Bouissières *et al.* 1953), since the low-energy electrons can be attributed either to the L-conversion of a γ -radiation of energy about 44 keV (216–172 keV), or to the K-conversion of the γ -radiation of energy 133 ± 2 keV also reported (Bouissières *et al.* 1953) and assumed to arise in transition from the 216 keV to the 84 keV state. In addition to events in which a single conversion electron was found, a few events were observed in which two electron tracks had a common origin with an α -track. A further analysis of these will be given in a later publication when more information has been obtained.

It is a pleasure to thank Professor N. Feather and Dr. M. A. S. Ross for their continued interest in these investigations originally started in Edinburgh.

University of London,

Royal Holloway College,

Englefield Green, Surrey.

24th August 1953.

C. J. D. JARVIS.

BOUSSIÈRES, G., FALK-VAIRANT, P., RIOU, M., TEILLAC, J., and VICTOR, C., 1953, *C.R. Acad. Sci., Paris*, **236**, 1874.

JARVIS, C. J. D., and ROSS, M. A. S., 1951, *Proc. Phys. Soc. A*, **64**, 535.

ROSENBLUM, S., VALADARES, M., and GUILLOT, M., 1952, *C.R. Acad. Sci., Paris*, **235**, 238.

Jastrow's Nuclear Model for High Energy Electron Scattering

In a previous note (Mathur and Gatha 1953) we have pointed out the inadequacy of the nuclear model with a uniform density distribution arising from an inconsistency in the magnitudes of nuclear radii required to account for the nuclear scattering of low and high energy nucleons. This model has also been found to be unsuitable (Born and Yang 1950, Yang 1951) from the point of view of a reasonable correlation between the nuclear density distribution and shell

structure. On this basis, Born and Yang have proposed a semi-gaussian nuclear density distribution wherein one parameter remained undetermined. In our previous investigation we have obtained that parameter on the basis of the nuclear scattering of high energy electrons.

To account for the nuclear scattering of nucleons Jastrow has proposed another interesting nuclear model (Jastrow and Roberts 1952), with the density distribution given by

$$\left. \begin{aligned} \rho &= \rho_0 & \text{for } r \leq R_0 \\ \rho &= \rho_0 \exp \{-(r-R_0)/a\} & \text{for } r > R_0 \end{aligned} \right\} \dots\dots(1)$$

where a indicates the range of nuclear forces and $R_0 \propto A^{1/3}$ approximately. Following the method of Born and Yang we have correlated this density distribution with the nuclear shell structure for $l \geq 3$ and found that the model must be modified so that both R_0 and a must be proportional to $A^{1/3}$. In particular we obtained $R_0 = 0.792r_0A^{1/3}$ cm and $a = 0.208r_0A^{1/3}$ cm while the normalization of density gives $\rho_0 = 0.87/\frac{4}{3}\pi r_0^3$. This, however, leaves the parameter r_0 undetermined.

To determine r_0 we have used the same procedure as employed by us in the determination of a similar parameter for the Born-Yang nuclear model. We have used the Born approximation to compare the scattering amplitudes for the nuclear scattering of 15.7 Mev electrons for the uniform density model and Jastrow's model. These are given respectively by

$$f_U(\theta) = -(6mZe^2/A\hbar^2K^3\bar{r}^3)\{\sin(KR) - KR \cos(KR)\}/K^2, \dots\dots(2)$$

where $R = \bar{r}A^{1/3}$ is the nuclear radius, and

$$\begin{aligned} j(\theta) = & -\frac{5.22mZe^2}{A\hbar^2K^3r_0^3} \left[\{\sin(KR_0) - KR_0 \cos(KR_0)\}/K^2 \right. \\ & + \frac{a^2}{1+a^2K^2} \left\{ \left(\frac{R_0}{a} + \frac{1-a^2K^2}{1+a^2K^2} \right) \sin(KR_0) + \left(KR_0 + \frac{2aK}{1+a^2K^2} \right) \cos(KR_0) \right\} \Big] \\ & \dots\dots(3) \end{aligned}$$

wherein the relativistic corrections are not considered as they drop out during the required comparison.

In a numerical comparison of these scattering amplitudes at various angles for Ag and Au with $\bar{r} = 1.16 \times 10^{-13}$ cm (Lyman, Hanson and Scott 1951) a close agreement is obtained with $r_0 = 0.95 \times 10^{-13}$ cm. Thus within the approximations employed one can take $r_0 \simeq 1 \times 10^{-13}$ cm on the basis of the above experimental data. One of us is now examining the utility of the Born-Yang and the Jastrow nuclear models for the nuclear scattering of nucleons. The results of this investigation will be published later.

Physical Research Laboratory,
Navrangpura, Ahmedabad, 9.
M.G. Science Institute,
Navrangpura, Ahmedabad, 9.
17th July 1953.

A. L. MATHUR.

K. M. GATHA.

BORN, M., and YANG, L. M., 1950, *Nature, Lond.*, **166**, 399.

JASTROW, R., and ROBERTS, J. E., 1952, *Phys. Rev.*, **85**, 757.

LYMAN, E. M., HANSON, A. O., and SCOTT, M. B., 1951, *Phys. Rev.*, **84**, 626.

MATHUR, A. L., and GATHA, K. M., 1953, *Proc. Phys. Soc. A*, **66**, 773.

YANG, L. M., 1951, *Proc. Phys. Soc. A*, **64**, 632.

The Thermal Conductivity of Magnesium at Low Temperatures

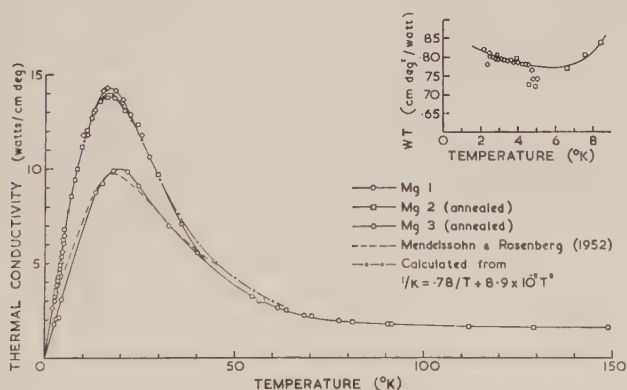
Recently Mendelssohn and Rosenberg (1952) determined the thermal conductivity of a number of metallic elements in the range 2°K to about 40°K . With the exception of magnesium, these metals behaved as expected from earlier experiments (cf. Andrews, Webber and Spohr 1951, Berman and MacDonald 1951); for temperatures below about $\theta/10$ the conductivity K or resistance W could be expressed fairly well as the sum of two terms

$$1/K = W \simeq A/T + BT^n \quad \text{where } n \simeq 2, \quad \dots\dots(1)$$

the terms being attributed to scattering of electrons by impurities and by lattice vibrations respectively.

For magnesium they reported that the extrapolated linear portion of the conductivity curve did not pass through zero, and Mendelssohn (1952) suggested this might be related to the minimum in the electrical resistance (MacDonald and Mendelssohn 1950). As similar minima in the cases of gold and copper have been found (White 1953 a, b) to result in a barely observable change in slope, or variation of a few per cent in the product WT in the region where $A/T \gg BT^n$ ($T < 5^{\circ}\text{K}$), it seemed worth while making further measurements on the thermal conductivity of this metal. At the same time opportunity was taken to extend the measurements to higher temperatures to permit a better determination of the values of B and n .

Our measurements were carried out with an apparatus and method described previously (White 1953 a) on specimens drawn by Messrs. Johnson, Matthey from a sample JM1848 of purity greater than 99.98%, for which Messrs. Johnson, Matthey quote the following impurities: iron 0.013%, manganese 0.0023%, lead 0.0013%, and faintly visible spectral lines of silicon, copper, silver, calcium and sodium. Mg 1 was a 3 mm diameter rod, measured in the 'as drawn' condition, Mg 2 was Mg 1 after annealing *in vacuo* at 350°C for 3 hours, Mg 3 was similar to Mg 2.



The thermal conductivity of magnesium. Inset shows variation of the product WT at very low temperatures.

The figure indicates that annealing only increases the maximum conductivity from 10.0 watt/cm deg at 19°K to 14.3 watt/cm deg at 17°K ; the conductivity shows no sign of the theoretically predicted minimum at $T \simeq \theta/4$ (Wilson 1937, Makinson 1938, Sondheimer 1950) and attains a sensibly constant value of about 1.61 watt/cm deg at $T \simeq \theta/2$.

The figure and inset show the result of fairly extensive measurements, made on Mg 2 and repeated on Mg 3, to reveal any anomalies in the impurity resistance. Although rather scattered, the values of WT below 5°K suggest a slight increase with falling temperature rather than the marked decrease observed by Mendelssohn and Rosenberg.

Using values for $A = W_0T$ of 1.36 (Mg 1) and 0.78 (Mg 2, Mg 3), the ideal resistance W_i has been calculated, assuming the additive resistance hypothesis $W = W_0 + W_i$ to be valid. A logarithmic graph of W_i against T gave $n = 2.0 \pm 0.1$, and $B = 8.9 \times 10^{-5}$ for $T < \theta/5$, the index n tending to the higher value of about 2.1 in the range 30° to 60°K ; this latter effect is reflected in the departure of the experimental from the calculated curve above 30°K .

The theoretical work of Wilson, Makinson and Sondheimer has predicted that eqn. (1) should be reasonably correct, although Sondheimer pointed out that small departures from additivity should occur in the region where the effect of the two resistance mechanisms are comparable. They indicated that the constant B should be given by

$$B = C W_\infty N^{2/3} / \theta^2$$

where C is a constant having a value 71.7 on the Sondheimer theory. For magnesium θ from specific heat data (cf. Estermann, Friedberg and Goldman 1952) is about 330°K , W_∞ from the figure is 0.62 cm deg/watt and the effective number of free electrons per atom N is not known. Our results therefore lead to a value of 15.8 for $CN^{2/3}$.

We wish to thank Dr. P. G. Klemens for discussions and other members of the low temperature group for their assistance. One of us (A.K.S.) gratefully acknowledges the assistance of the Australian Government for a Colombo Plan Fellowship.

Commonwealth Scientific and Industrial
Research Organisation, Division of Physics,
National Standards Laboratory,
Sydney, Australia.

W. R. G. KEMP.
A. K. SREEDHAR.
G. K. WHITE.

31st August 1953.

- ANDREWS, F. A., WEBBER, R. T., and SPOHR, D. A., 1951, *Phys. Rev.*, **84**, 994.
BERMAN, R., and MACDONALD, D. K. C., 1951, *Proc. Roy. Soc. A*, **209**, 368.
ESTERMANN, I., FRIEDBERG, S. A., and GOLDMAN, J. E., 1952, *Phys. Rev.*, **87**, 582.
MACDONALD, D. K. C., and MENDELSSOHN, K., 1950, *Proc. Roy. Soc. A*, **202**, 523.
MAKINSON, R. E. B., 1938, *Proc. Camb. Phil. Soc.*, **34**, 474.
MENDELSSOHN, K., 1952, *Proceedings Commissions 1 et 2, Institut International du Froid*, Louvain, p. 69.
MENDELSSOHN, K., and ROSENBERG, H. M., 1952, *Proc. Phys. Soc. A*, **65**, 385.
SONDHEIMER, E. H., 1950, *Proc. Roy. Soc. A*, **203**, 75.
WHITE, G. K., 1953 a, *Proc. Phys. Soc. A*, **66**, 559 ; 1953 b, *Aust. J. Phys.*, **6**, No. 4.
WILSON, A. H., 1937, *Proc. Camb. Phil. Soc.*, **33**, 371.

REVIEWS OF BOOKS

Fundamentals of Engineering Electronics, by W. G. Dow. Pp. xviii + 627. 2nd Edn. (New York : John Wiley; London : Chapman and Hall, 1952.) 68s.

It is becoming more and more difficult to define the scope of *electronics*. The subject today is concerned with the motions of electrons and ions under electric fields *in vacuo*, in gases, and also in metals, as well as with the important surface or boundary phenomena occurring at the electrodes. The fundamentals of electronics therefore involves a great deal of modern extra-nuclear statistical physics. The vast borderland between physics and light electrical engineering is of equal interest to the physicist and electrical engineer, and some knowledge of the fundamental physics of the phenomena of electronics is of very great importance to the modern electrical engineer. *The Fundamentals of Engineering Electronics* by William G. Dow was written primarily with the view of providing students of electrical engineering with a reasonably complete and satisfactory account of the fundamental physical processes required for the understanding of the operation of electronic devices, and it appears to the reviewer that this object is achieved. This volume is a revised and modified edition of the author's book published in 1937, and it certainly provides the electrical engineering student with an excellent introduction to basic physical principles and the more elementary quantum and statistical aspects of electronics.

The first three chapters are concerned with the mathematical treatment of the motion of electrons *in vacuo* under electric and magnetic fields, with applications of the analysis to ultra-high frequency systems, magnetrons and cathode-ray tubes. The next four chapters are devoted to a treatment of electrostatic fields and space charge currents by means of conformal transformation. Considerable use is made of potential energy diagrams throughout. The short seventh chapter is devoted to thermionic cathodes and thermionic emission; no mention is made of the decay characteristics of pulsed thermionic emission.

The quantum and statistical concepts in the modern theory of metals are introduced in a clear and simple manner in Chapter VIII, and extended to the case of semiconductors. This second edition contains an excellent account of the energy level behaviour of semiconductors. After this the author returns to deal with thermionic emission in the presence of high fields (Schottky effect) and field emission of electrons is dealt with briefly : a more systematic treatment of the subject would perhaps have been desirable and the account of field emission is not really adequate in view of its great importance in discharge phenomena. The influence of these effects and of contact potentials in electronic valves is discussed. Mention should certainly be made of the excellent elementary account given of the ionization and excitation of atoms, and the electronic structure of atoms. This covers the ground necessary for introduction to the more specialist treatment of these subjects. Chapters IX and X deal with the design of amplifiers; as here a knowledge of fundamentals is not strictly necessary, there seems no very great justification for the inclusion of this matter in the book, since this aspect is adequately treated in many others which are devoted solely to the properties of electrical circuits. Chapters XII and XIII are of a more fundamental character and deal with Maxwell-Boltzmann statistics with applications to electron emission and noise.

Photoelectric devices and the amplification of currents by ionizing collisions between electrons and gas molecules are treated in Chapter XIV. It is perhaps unfortunate that the definition of Townsend's α given on p. 439 is incomplete: the words "in the direction of the applied field" should be added. Chapter XV treats qualitatively the development of the Townsend type discharge, glow and arc discharges, and is a good introduction to the subject.

In a volume which attempts such a comprehensive survey of the basic physical processes of the motions of electrons and ions in gases, it is unfortunate that it was not possible to bring up-to-date the comparatively short treatment of electrical breakdown on pages 510-513. The account given here is short and entirely qualitative, and, in the light of experimental work published since 1950, completely misleading to the student. The MKS system is used throughout. A highly pleasing feature of the book is the inclusion of a list of problems at the end of each chapter. A student who works through all these can certainly feel that he has understood the subject-matter. From the choice of question it would appear that the author is an accomplished teacher.

The book of 627 pages is well presented and bound, and apart from one or two printing errors (e.g. 'lies' for 'lines' on page 8) is up to the usual high standard of publication by Wiley. It will be found a most useful addition to the library of both physicists and electrical engineers as well as to production engineers, and it can be strongly recommended.

F. LL. J.

CONTENTS OF SECTION B

	PAGE
Dr. H. P. MURBACH and Dr. H. WILMAN. The Origin of Stress in Metal Layers Condensed from the Vapour in High Vacuum	905
Dr. C. G. CAMPBELL and Mr. J. KYLES. The Variable-Radius Semicircular Magnetic Focusing β -Ray Spectrometer	911
Dr. J. M. DANIELS. The Design and Construction of a 1000 kw Water Cooled Solenoid intended for Experiments on Nuclear Alignment and Adiabatic Nuclear Demagnetization	921
Dr. E. RABINOWICZ. A Quantitative Study of the Wear Process	929
Mr. M. K. BANERJEE and Dr. A. K. SAHA. Investigations on a Short Magnetic Lens Spectrometer	937
Prof. G. I. FINCH, Dr. H. C. LEWIS and Dr. D. P. D. WEBB. The Diffraction of 150 kv Electrons	949
Miss S. M. CRAWFORD. An Optical Method of Observing Stress Relaxation in Transparent Solids	954
Mr. J. C. BURRIDGE, Dr. H. KUHN and Lady ANNE PERY. Reflectivity of Thin Aluminium Films and their Use in Interferometry	963
Dr. T. S. ROBINSON and Dr. W. C. PRICE. The Determination of Infra-Red Absorption Spectra from Reflection Measurements	969
Mr. L. R. BAKER. The Effect of Source Size on the Coherence of an Illuminating Wave	975
Research Notes:	
Dr. F. W. G. ROSE and Mr. E. W. TIMMINS. A Method of Estimating Impurity Concentrations in Germanium	984
Mr. R. N. BRACEWELL. A Microwave Computing Problem	987
Letters to the Editor:	
Dr. A. R. VERMA and Miss P. M. REYNOLDS. A Further Note upon the Growth and Optical Properties of Stearic Acid Crystals	989
Reviews of Books	990
Contents of Section A	992

Angular Distribution of γ -Radiation Following a Deuteron Stripping Reaction

By G. R. SATCHLER

Clarendon Laboratory, Oxford

MS. received 9th July 1953

Abstract. The angular distribution of γ -radiation from a deuteron stripping reaction is given as a Legendre series $W(\theta) = \sum_v A_v P_v(\cos \theta)$. The coefficients are given in terms of the total angular momentum (orbital plus spin) of the captured nucleon and fully tabulated. Analysis of observed distributions can then test j - j shell model assumptions.

Cascades are discussed and a general theorem for the angular distribution of the n th radiation of a cascade is stated in an Appendix.

Formulae are given relating the parameters of this paper to those used in the channel spin formulation. Their values when the nuclei obey L - S coupling rules are also given.

Some other applications of the theory are indicated and results of interest to experimentalists are summarized.

§ 1. INTRODUCTION

THE angular distribution of γ -radiation following a deuteron stripping reaction may be expected to give additional information about the spins of the nuclear states involved. This problem has been treated both in terms of the total angular momentum \mathbf{j} (orbital plus spin) of the captured particle (Satchler and Spiers 1952) and in terms of the channel spin \mathbf{s} of the capture process (Biedenharn *et al.* 1952, Gallaher and Cheston 1952).

The purpose of the present paper is twofold:

- (i) to extend the former formulation with the aid of Racah techniques to include mixtures of j -values and to tabulate numerical correlation coefficients,
- (ii) to discuss the relation between the ' j ' formulation and that in terms of channel spin: in particular we have derived the form of the mixture parameters when the nuclear states obey L - S coupling rules.

In stripping reactions nucleons can be captured directly into low-lying excited states where the Mayer j - j coupling model is expected to be a good approximation. Then the extent to which the actual angular distribution can be analysed in terms of one j -value tests the validity of this model.

A similar analysis in terms of unique L and S values for the initial and excited nuclear states would test the validity of the L - S coupling scheme.

These two extremes and the analysis in terms of channel spin differ only in the angular momenta coupling assumed. Hence they are related by the corresponding change-of-coupling transformation coefficients. These are given.

The theoretical treatment of an earlier paper (Satchler and Spiers 1952) shows that the capture process in stripping is formally the same as that from a plane wave incident along the recoil axis. Thus the formulae and tables given below apply quite generally to the formation of an excited state of sharp spin by the absorption or emission of a spin- $\frac{1}{2}$ particle. They can be applied immediately to the analysis of measurements on, for example, (p, γ) reactions, and include the results of Christy (1953) as special cases.

Finally, in the course of this work it was noted that there was a quite general expression for the angular distribution of the n th radiation of a cascade. This is given in Appendix IV.

§2. ANGULAR DISTRIBUTION OF GAMMA-RAYS

The γ -radiation is to be measured in coincidence with the outgoing nucleon. It is then azimuthally symmetrical about the recoil axis, $\mathbf{K}_d - \mathbf{K}_p$, where \mathbf{K}_d , \mathbf{K}_p are the linear momenta (laboratory system) of deuterons and outgoing particles respectively.* The angular distribution about this axis (Satchler and Spiers 1952, eqn. (6)) may readily be extended to cover mixtures.† We sum over j and L with appropriate amplitudes $B(j)$ and $C(L)$ which are proportional to the (real) reduced matrix elements for the capture and emission processes respectively, so that $B^2(j)$ is the fraction captured with j , etc.

Expressed as a series of even Legendre polynomials it becomes

$$W(\theta) = \sum_{jj'LL'} B(j)B(j')C(L)C(L')\eta_\nu(jj'J_iJ_e)\lambda_\nu(LL'J_fJ_e)P_\nu(\cos\theta) \quad \dots\dots(1)$$

where J_i = spin of initial nucleus, J_e = spin of excited state, J_f = spin of final state, j = total angular momentum of captured nucleon, L = multipole order of gamma-ray. The radiation parameters are given in terms of Wigner (vector-addition) and Racah coefficients (Biedenharn 1952):

$$\begin{aligned} \eta_\nu(jj'J_iJ_e) &= \eta_\nu(j'jJ_iJ_e) \\ &= [(2J_e+1)(2j+1)(2j'+1)]^{1/2}(-)^{J_i-J_e-1/2}C_{0\frac{1}{2}\frac{1}{2}}^{\nu j j'}W(J_eJ_ejj'\nu J_i) \\ \lambda_\nu(LL'J_fJ_e) &= \lambda_\nu(L'LJ_fJ_e) \quad \dots\dots(2) \\ &= [(2J_e+1)(2L+1)(2L'+1)]^{1/2}(-)^{J_f-J_e-1}C_{01-1}^{\nu L L'}W(J_eJ_eLL'; \nu J_f), \end{aligned}$$

with $\eta_0 = \delta_{jj'}$, and $\lambda_0 = \delta_{LL'}$.

The λ_ν have been tabulated by Biedenharn and Rose (1953); in their notation

$$\begin{aligned} \lambda_\nu &= F_\nu(LJ_fJ_e) \text{ if } L' = L, \text{ or} \\ &= [(2J_e+1)(2L+1)(2L+3)]^{1/2}(-)^{J_f-J_e-1}G_\nu(LJ_fJ_e) \text{ if } L' = L+1. \end{aligned}$$

Tables 4(a) and (b) contain values of η_ν for $j = \frac{1}{2}, \frac{3}{2}, \frac{5}{2}$; the layout of Biedenharn and Rose is adopted for ease of reference. The usual limitations on ν apply, $\nu \leq (j+j')$, $(L+L')$, or $2J_e$, and even only.

* Any effect of interaction of the outgoing particle with the nucleus (which may lead to compound nucleus formation) is neglected in the present paper, as its magnitude is uncertain. Newns (1953) uses a semi-classical model of the stripping process to suggest upper limits for this effect; we feel, however, that only experiment can decide whether it is important.

† Contrary to the letter of Gallaher and Cheston (1952), the summation over j and hence L is coherent and interference terms do appear.

Since the Racah functions have not been tabulated with more than 3 arguments half-integer, a relation between η_ν and the γ -ray parameters λ_ν has been found of value for computation. Using recurrence properties of the Wigner and Racah functions given in Appendix I and elsewhere we obtain

$$\eta_\nu(jj'J_1J_e) = \rho_\nu(jj')(2J_1+1)^{-1}[\phi(+)\lambda_\nu(j+\frac{1}{2}j'+\frac{1}{2}J_1+\frac{1}{2}J_e) + \phi(-)\lambda_\nu(j+\frac{1}{2}j'+\frac{1}{2}J_1-\frac{1}{2}J_e)], \quad \dots\dots(3)$$

Explicit expressions for ρ_ν and $\phi(\pm)$ are given in Appendix I.

Of course, for unique angular momenta (1) reduces to

$$W(\theta) = \Sigma_\nu \eta_\nu(jj'J_1J_e) F_\nu(LJ_fJ_e) P_\nu(\cos\theta), \quad \dots\dots(4)$$

We see that the j - j model predicts isotropy for $p_{1/2}$ capture, although in general p waves would give a $\cos^2\theta$ term.

If it is desired to use a polarization sensitive detector for the photons we may apply the formulae of Lloyd (1952), which simplify greatly in this case. Changing his notation a little, for a pure multipole

$$W(\theta, \beta) = \Sigma_\nu A_\nu [P_\nu(\cos\theta) \pm \kappa_\nu(L) \cos 2\beta P_\nu^2(\cos\theta)], \quad \dots\dots(5)$$

where A_ν is the coefficient in the directional distribution. We take $+$ or $-$ as the radiation is electric or magnetic; β is the angle between the polarization axis of the counter and the 'reaction plane' (containing $\mathbf{K}_d - \mathbf{K}_p$ and the emission direction). $\kappa_\nu(L)$ is given in table 1.

Table 1. $\kappa_\nu(L)$

ν	$L=1$	$L=2$	$L=3$
2	-0.500	+0.500	+0.333
4	—	-0.083	+0.333
6	—	—	-0.033

§3. GAMMA-RAY CASCADE

The triple correlation of three γ -rays has been treated by Biedenharn and Rose (1953). The corresponding triple coincidence correlation when stripping leads to a cascade of two photons is obtained from their equation (138) by replacing $F_{\nu_0}(L_0J_0J_1)$ for the first transition by our $\Sigma_{jj'}B(j)B(j')\eta_{\nu_0}(jj'J_1J_e)$, (see Appendix III). If $j = \frac{1}{2}$ or $J_e = 0, \frac{1}{2}$, the first excited state is formed isotropically and the triple correlation reduces to the ordinary γ - γ correlation for a $J_e(L_1)J_e'(L_2)J_f$ cascade, and is independent of observation of the stripped nucleon.

Since in many cases there will be no summation variable $\nu > 2$ (e.g. $j = \frac{3}{2}$ and two dipole photons) it was thought worth while to give explicitly the coefficients for $\nu = 0$ and 2 (Appendix III).

Again, by analogy with eqn. (141) of Biedenharn and Rose (1953), if the first photon is unobserved the coefficient of $P_\nu(\cos\theta)$ in the angular distribution about the recoil axis of the second becomes

$$\Sigma_{jj'}B(j)B(j')\eta_{\nu}(jj'J_1J_e)F_\nu(L_2J_fJ_e')(-)^{J_e'+J_e-L_1} \\ \times [(2J_e+1)(2J_e'+1)]^{1/2}W(J_e'J_e'J_eJ_e; \nu L_1).$$

The unobserved radiation L_1 does not restrict ν , but the conditions $\nu \leq 2J_e, 2J_e'$ remain.

It is interesting to note that this is a special case of a general theorem, given in Appendix IV, for the angular distribution of the n th radiation of a cascade.

§ 4. CHANNEL SPIN AND L-S COUPLING

If the channel spin s (vector sum of initial spins, $\mathbf{s} = \mathbf{J}_i + \frac{1}{2}\boldsymbol{\sigma}$) is used for the capture process and only one orbital l is involved*, we must replace the η_v in (1) by (cf. Biedenharn *et al.* 1952, eqn. (3))

$$\Sigma_s |A(s)|^2 C_{000}^{v \frac{1}{2} l} (2J_e + 1)^{1/2} (2l + 1) (-)^{s-J_e} W(J_e J_e l l; v s) \\ = [1 - v(v+1)/2l(l+1)]^{-1} [x F_v(l J_i + \frac{1}{2} J_e) + (1-x) F_v(l J_i - \frac{1}{2} J_e)] \dots\dots (6)$$

where x is the proportional contribution of channel $s = J_i + \frac{1}{2}$, i.e. $x = |A(J_i + \frac{1}{2})|^2$ if $\Sigma_s |A(s)|^2 = 1$.

When a unique j -value describes the capture, comparison of (6) with (3) shows the corresponding channel-spin mixture for $j = l - \frac{1}{2}$ is given by

$$x = (J_i + J_e + l + \frac{3}{2})(J_i - J_e + l + \frac{1}{2}) / (2J_i + 1)(2l + 1). \dots\dots (7)$$

Similar analysis when $j = l + \frac{1}{2}$ shows

$$x = 1 - (J_i + J_e + l + \frac{3}{2})(J_i - J_e + l + \frac{1}{2}) / (2J_i + 1)(2l + 1). \dots\dots (8)$$

An alternative derivation could be given on noting that the two descriptions differ only in the order of coupling of the three vectors \mathbf{J}_i , \mathbf{l} , and $\frac{1}{2}\boldsymbol{\sigma}$. The basic states of each are then connected by the transformation coefficients for the change of representation from $(J_e M_e; J_i j)$ to $(J_e M_e; s l)$. Then for single j we have: j - j model: $A(s) = [(2j+1)(2s+1)]^{1/2} (-)^{l-j-1/2} W(\frac{1}{2} l J_i J_e; j s). \dots\dots (9)$

This is equivalent to (7) and (8).

If the initial and excited nuclear states are correctly described by L - S coupling quantum numbers $(J_i L_i S_i)$ and $(J_e L_e S_e)$ respectively, the $B(j)$ are the transformation coefficients for the change of representation from

$$[L_e(L_i l) S_e(S_i \frac{1}{2}); J_e M_e] \text{ to } [J_i(L_i S_i) j(l \frac{1}{2}); J_e M_e].$$

For a single l -transfer,

$$L\text{-}S \text{ model: } B(j) \sim (2j+1)^{1/2} X(J_i L_i S_i; j l \frac{1}{2}; J_e L_e S_e), \dots\dots (10)$$

X is the recoupling symbol introduced by Fano (1951) (see Appendix II. Since one argument is $\frac{1}{2}$, there are only two terms in this case). $B(j)$ is no longer normalized to $\Sigma_j B^2(j) = 1$.

Similar analysis with the channel spin gives

$$L\text{-}S \text{ model: } A(s) \sim (2s+1)^{1/2} W(S_e s L_e l; L_i J_e) W(L_i S_i s \frac{1}{2}; J_i S_e). \dots\dots (11)$$

§ 5. OTHER APPLICATIONS

The γ -ray may be replaced by some other radiation X (conversion electron, alpha- or beta-ray, etc.). We obtain the corresponding correlation in the usual way, multiplying each term in (1) by the appropriate parameter $b_v(X, L)$ as given by Biedenharn and Rose (1953). If a nucleon is re-emitted, and the intermediate state is still characterized by a single J_c , λ_v in (1) is replaced by the η_v appropriate for the emission.

As pointed out in the Introduction the results given above apply equally well to (n, γ) , $(p, \gamma\gamma)$ reactions, etc. (the reference axis now being the direction of the incident beam), or the inverse processes, when proceeding through an intermediate state of sharp J_c . The results of Feld (1953) for photo-meson production

* This condition will be satisfied if measurements are made in coincidence with nucleons of a definite ' l peak'.

are immediately obtained in this way. Similarly the scattering of π mesons by nucleons via an isobaric nucleonic state of spin j may be written, for example, $\pi^-(p, n)\pi^0$, where both J_i and J_f are zero. Then

$$W(\theta) = \sum_v \eta_v^2 (jj0j) P_v(\cos \theta).$$

In general, the formation of a state J_e by the absorption or emission (along \mathbf{k}_i) of spin- $\frac{1}{2}$ radiation with total angular momentum j gives a density matrix:

$$\rho_{M_e M_e'}(\mathbf{k}_i) = \sum_{jj'} B(j) B(j') \eta_v(jj' J_i J_e) C_{M_e}^{J_e} C_{M_e'}^{J_e} D_{M_e' - M_e, 0}^{(v)}(\mathbf{k}_i) (-)^{J_e - M_e} (2J_e + 1)^{1/2},$$

where $D^{(v)}$ is a $(2\nu + 1)$ -dimensional representation of the rotation group.

§ 6. CONCLUSIONS

The angular distribution of γ -radiation following a stripping reaction has been given as a series of even Legendre polynomials in $\cos \theta$, where θ is the polar angle of emission with $\mathbf{K}_d - \mathbf{K}_p$ as axis. The coefficients factorize into quantities depending on the capture and emission processes separately. The formula intended for numerical use when there is a mixture of two total angular momenta j, j' involved in the capture, and pure multipole emission, is

$$W(\theta) = \sum_v [\eta_v(jj J_i J_e) \pm 2\delta \eta_v(jj' J_i J_e) + \delta^2 \eta_v(j'j' J_i J_e)] F_v(L J_f J_e) P_v(\cos \theta).$$

The ratio of the number captured with j' to that with j is δ^2 ; ν takes even values only, $\leq 2j_{\max}, 2J_e, 2L$. η_v is tabulated here, and F_v by Biedenharn and Rose (1953). Choice of \pm depends on the relative phase of the matrix elements $B(j), B(j')$. The value of $\delta = B(j')/B(j)$ for L - S coupled nuclei is given by eqn. (10) above. The j - j coupling model suggests we should find δ zero. Some other tentative predictions may be made.

(i) Initial nucleus even-even, final even-odd: $J_i = 0$, and $j_e = J_e$ uniquely. If the ground and excited states form a doublet we have $J_e = l + \frac{1}{2}$, $J_f = l + \frac{1}{2}$, and $L = 1$ (or possibly an $M1 + E2$ mixture).

(ii) Even-odd to even-even: $j = J_i$ if the captured nucleon enters the same orbit as the original 'odd' one and forms an excited state by coupling with it to give $J_e = 2$ (or 4) and $J_f = 0$ (or 2) with $L = 2$.

Some explicit angular distributions relevant to these have been given in a letter (Satchler 1953).

ACKNOWLEDGMENTS

The author is indebted to Dr. J. A. Spiers for advice on this problem, and to Drs. Biedenharn and Rose for a preprint of their review paper on angular correlations.

APPENDIX I

Explicitly the coefficients in (3) are:

$$\phi(\pm) = \psi(\pm; j)\psi(\pm; j'),$$

where $\psi(\pm; j) = [(J_e + J_i + 1) \pm (j + 1)][(J_e - J_i) \mp (j + 1)]$, and

$$\rho_v(jj') = [(2j + 1)(2j' + 1)(2j + 3)(2j' + 3)/(j + 1)(j' + 1)] \xi_v(jj'),$$

where

$$\xi_v(jj') = [(2j + 1)(2j + 3) + (2j' + 1)(2j' + 3) - 4\nu(\nu + 1)]^{-1}, \quad j + j' \text{ odd},$$

or

$$= [4(j + j' + \nu + 2)(j + j' - \nu + 1)]^{-1}, \quad j + j' \text{ even}.$$

Some new relations between Wigner coefficients with half-integer indices appeared during the derivation of (3). If ν is even,

$$(2j+1)C_{0\frac{1}{2}-\frac{1}{2}}^{\nu j \frac{j}{2}} = \mp [(2l+1)(2l+1 \mp 1) - \nu(\nu+1)]^{1/2} C_{000}^{\nu l l}, \quad \text{as } l = j \pm \frac{1}{2},$$

and

$$(2j+3)^{1/2} C_{0\frac{1}{2}-\frac{1}{2}}^{\nu j \frac{j+1}{2}} = -[\nu(\nu+1)(2j+1)/(2j+2)(2j+1) - \nu(\nu+1)]^{1/2} C_{0\frac{1}{2}-\frac{1}{2}}^{\nu j \frac{j}{2}} \\ = [(\nu-1)(\nu+2)(2j+5)/(2j+3)(2j+2) - \nu(\nu+1)]^{1/2} C_{0\frac{1}{2}-\frac{1}{2}}^{\nu j \frac{j+2}{2}}.$$

The values of $C_{0\frac{1}{2}-\frac{1}{2}}^{\nu j \frac{j'}{2}}$ in table 2 may be required for transitions not covered by our tabulation of η_{ν} .

Table 2. $C_{0\frac{1}{2}-\frac{1}{2}}^{\nu j \frac{j'}{2}}$

ν	$(jj') = (\frac{1}{2} \frac{3}{2})$	$(\frac{1}{2} \frac{5}{2})$	$(\frac{1}{2} \frac{7}{2})$	$(\frac{3}{2} \frac{3}{2})$	$(\frac{3}{2} \frac{5}{2})$	$(\frac{3}{2} \frac{7}{2})$	$(\frac{5}{2} \frac{5}{2})$	$(\frac{5}{2} \frac{7}{2})$	$(\frac{5}{2} \frac{9}{2})$
2	+0.707	+0.707	—	+0.500	-0.267	-0.567	—	-0.436	+0.169
4	—	—	+0.707	—	+0.655	+0.423	-0.301	+0.378	-0.313
6	—	—	—	—	—	—	+0.640	—	+0.616

APPENDIX II

The recoupling symbol X of Fano (1951) used in (10) occurs in the transformation coefficient from a coupling scheme $[j_1(l_1s_1)j_2(l_2s_2); JM]$ to one $[L(l_1l_2)S(s_1s_2); JM]$

$$\langle j_1 j_2 | LS \rangle = [(2j_1+1)(2j_2+1)(2L+1)(2S+1)]^{1/2} X(JLS; j_1 l_1 s_1; j_2 l_2 s_2),$$

where

$$X(abc; def; ghi) = \sum_{\alpha} (2\alpha+1) W(bgcd; \alpha a) W(gbie; \alpha h) W(dcei; \alpha f).$$

Values of $\langle jj | LS \rangle$ for $j = \frac{3}{2}, \frac{5}{2}, \frac{7}{2}$ are given by Edmonds and Flowers (1952).

Fano's presentation

$$X \begin{pmatrix} a & b & c \\ d & e & f \\ g & h & i \end{pmatrix}$$

more clearly shows its symmetries, but is less convenient typographically. We briefly reiterate its properties:

(i) Interchange of any two rows or columns multiplies X by $(-)^{a+b+\dots+i}$. It is invariant under interchange of rows and columns.

(ii) The elements of each row or column must satisfy triangular inequalities.

(iii) α is limited by the triangular inequality of the triads $(bg\alpha)$, $(cd\alpha)$, $(ie\alpha)$. Since in (10) $f = \frac{1}{2}$, the sum reduces to two terms, $\alpha = L_e \pm \frac{1}{2}$.

(iv) If any element is zero, the sum reduces to one term, e.g.

$$X(abc; def; gh0) = \delta_{gh} \delta_{ef} (-)^{c+g-a-e} [(2c+1)(2g+1)]^{-1/2} W(abde; cg).$$

APPENDIX III

Gamma-Ray Cascade

Adaptation of eqn. (138) of Biedenharn and Rose (1953) gives the triple correlation formulae:

$$W(\theta_1 \theta_2 \phi) = \sum_{jj' \nu_0 \nu_1 \nu_2} B(j) B(j') \eta_{\nu_0} (jj' J_1 J_c) F_{\nu_2} (L_2 J_1 J_c') R_{\nu_0 \nu_1 \nu_2} (J_c L_1 J_c') S_{\nu_0 \nu_1 \nu_2} (\theta_1 \theta_2 \phi),$$

where

$$R_{\nu_0 \nu_1 \nu_2} = (-)^{L_1-1} [(2J_c+1)(2J_c'+1)]^{1/2} (2L_1+1) C_{01-1}^{\nu_0 L_1 L_1} X(J_c J_c' \nu_0; L_1 L_1 \nu_1; J_c' J_c' \nu_2)$$

and

$$S_{\nu_0 \nu_1 \nu_2} = 4\pi \sum_m C_{0m-m}^{\nu_0 \nu_1 \nu_2} Y_{\nu_1}^m(\theta_1 0) Y_{\nu_2}^{-m}(\theta_2 \phi).$$

The Y_{ν}^m are Condon and Shortley spherical harmonics, ϕ is the difference in azimuth of the two emission directions and θ_1, θ_2 their polar angles. The following triads have to satisfy triangular inequalities: $(\nu_0\nu_1\nu_2)$, $(\nu_0j'j)$, $(\nu_0J_eJ_e)$, $(\nu_1L_1L_1)$, $(\nu_2L_2L_2)$, $(\nu_2J_e'J_e')$, and the ν 's take even values only.

In many cases where $L_1=1$ the angular momenta allow no $\nu>2$. R and S then assume fairly simple forms:

$$R_{000}S_{000}=1,$$

$$R_{0\nu\nu}S_{0\nu\nu}=F_{\nu}(L_1J_eJ_e')P_{\nu}(\cos\gamma); \cos\gamma=\cos\theta_1\cos\theta_2+\sin\theta_1\sin\theta_2\cos\phi,$$

$$R_{\nu\nu0}S_{\nu\nu0}=F_{\nu}(L_1J_e'J_e)P_{\nu}(\cos\theta_1),$$

$$R_{\nu0\nu}S_{\nu0\nu}=[(2J_e+1)(2J_e'+1)]^{1/2}(-)^{J_e'+J_e-L_1}W(J_e'J_e'J_eJ_e; \nu L_1)P_{\nu}(\cos\theta_2),$$

$$S_{222}=0.668[3\sin^2\theta_1\sin^2\theta_2\cos 2\phi-\frac{3}{2}\sin 2\theta_1\sin\theta_2-(3\cos^2\theta_1-1)(3\cos^2\theta_2-1)]$$

$R_{222}(J_e1J_e')$ is given in table 3.

Table 3. $R_{222}(J_e1J_e')$

$J_e \backslash J_e'$	$\frac{3}{2}$	$\frac{5}{2}$	$\frac{7}{2}$	$\frac{9}{2}$	$J_e \backslash J_e'$	1	2	3	4
3/2	+0.150	-0.040	—	—	1	+0.187	-0.032	—	—
5/2	-0.040	+0.125	-0.047	—	2	-0.032	+0.134	-0.034	—
7/2	—	-0.047	+0.136	-0.049	3	—	-0.034	+0.117	-0.048
9/2	—	—	-0.049	+0.113	4	—	—	-0.048	+0.115

APPENDIX IV

*A Theorem for Radiation Cascades**

Consider a series of n transitions represented by $J_1(L_1)J_2(L_2)\dots(L_n)J_{n+1}$, where L is the total angular momentum of the radiation emitted or absorbed at each step and the J are nuclear spins. Take the angular correlation of the first and n th radiations with the rest unobserved. Then the only effect of each unobserved radiation L_r is to introduce an extra (normalized) Racah function $U(J_{r+1}\nu L_r J_r; J_{r+1}J_r)=(-)^{J_r+J_{r+1}-L_r}[(2J_r+1)(2J_{r+1}+1)]^{1/2}W(J_{r+1}J_{r+1}J_rJ_r; \nu L_r)$ into the correlation coefficients, quite independently of the nature of the radiation. Thus if two photons are observed, the coefficient of $P_{\nu}(\cos\theta)$ is

$$F_{\nu}(L_1J_1J_2)F_{\nu}(L_nJ_nJ_{n+1})U(J_3\nu L_2J_2; J_3J_2)\dots U(J_n\nu L_{n-1}J_{n-1}; J_nJ_{n-1});$$

if either is a nucleon we replace its parameter by η_{ν} ; if a conversion electron or alpha- or beta-ray, we multiply by the corresponding $b_{\nu}(L)$ given by Biedenharn and Rose (1953).

The unobserved L_r do not restrict the complexity of the angular distribution, but the intervening nuclear spins still act as 'gates' for angular information and the conditions $\nu\leq 2J_2, \dots, 2J_n$ remain.

If any radiation is mixed we have to sum over the L with appropriate amplitudes, but the sum over any unobserved radiation is incoherent and interference terms do not appear.

* A special case of this theorem has been given by Steenberg (1952). It follows from his work that in directional correlation problems a nuclear alignment axis is equivalent to detection of a radiation for defining a direction. Then in the correlation coefficients we just replace the parameter for the first radiation observed by the alignment parameter $B_{\nu}(T)$, given by him, to give the angular distribution of the n th radiation about this axis.

Table 4(a). $\eta_v(jj'J_1J_e)$ for half-odd J_e

$\eta_2(\frac{1}{2}\frac{3}{2}J_1J_e)$					
$J_e \backslash J_1$	1	2	3	4	5
3/2	-0.894	+0.400	—	—	—
5/2	—	-0.800	+0.478	—	—
7/2	—	—	-0.756	+0.516	—
9/2	—	—	—	-0.730	+0.540

$\eta_2(\frac{1}{2}\frac{5}{2}J_1J_e)$					
$J_e \backslash J_1$	1	2	3	4	5
3/2	+0.447	+0.917	—	—	—
5/2	—	+0.600	+0.878	—	—
7/2	—	—	+0.655	+0.856	—
9/2	—	—	—	+0.683	+0.842

$\eta_2(\frac{3}{2}\frac{3}{2}J_1J_e)$						
$J_e \backslash J_1$	0	1	2	3	4	5
3/2	-1.000	-0.2000	+0.600	-0.200	—	—
5/2	—	-0.748	+0.107	+0.588	-0.267	—
7/2	—	—	-0.655	+0.218	+0.567	-0.306
9/2	—	—	—	-0.606	+0.275	+0.551

$\eta_2(\frac{3}{2}\frac{5}{2}J_1J_e)$					
$J_e \backslash J_1$	1	2	3	4	5
3/2	-0.400	-0.262	+0.280	—	—
5/2	-0.343	-0.367	-0.112	+0.324	—
7/2	—	-0.374	-0.324	-0.041	+0.343
9/2	—	—	-0.383	-0.294	—

$\eta_2(\frac{3}{2}\frac{7}{2}J_1J_e)$					
$J_e \backslash J_1$	1	2	3	4	5
3/2	—	+0.642	+0.939	—	—
5/2	+0.192	+0.505	+0.798	+0.849	—
7/2	—	+0.324	+0.620	+0.832	+0.798
9/2	—	—	+0.391	+0.675	+0.842

Table 4(b). $\eta_v(jj'J_iJ_e)$ for integral J_e

		$\eta_2(\frac{1}{2}\frac{3}{2}J_iJ_e)$				
$J_e \backslash J_i$		$\frac{1}{2}$	$\frac{3}{2}$	$\frac{5}{2}$	$\frac{7}{2}$	$\frac{9}{2}$
1		-1.000	+0.316	—	—	—
2		—	-0.837	+0.447	—	—
3		—	—	-0.775	+0.500	—
4		—	—	—	-0.742	+0.529
5		—	—	—	—	-0.721

		$\eta_2(\frac{1}{2}\frac{5}{2}J_iJ_e)$			
$J_e \backslash J_i$		$\frac{3}{2}$	$\frac{5}{2}$	$\frac{7}{2}$	$\frac{9}{2}$
1		+0.949	—	—	—
2		+0.548	+0.894	—	—
3		—	+0.633	+0.816	—
4		—	—	+0.671	+0.849
5		—	—	—	+0.693

		$\eta_2(\frac{3}{2}\frac{3}{2}J_iJ_e)$				
$J_e \backslash J_i$		$\frac{1}{2}$	$\frac{3}{2}$	$\frac{5}{2}$	$\frac{7}{2}$	$\frac{9}{2}$
1		-0.707	+0.566	-0.141	—	—
2		-0.837	—	+0.598	-0.239	—
3		—	-0.693	+0.173	+0.577	-0.289
4		—	—	-0.627	+0.251	+0.558
5		—	—	—	-0.589	+0.294

		$\eta_2(\frac{3}{2}\frac{5}{2}J_iJ_e)$				
$J_e \backslash J_i$		$\frac{1}{2}$	$\frac{3}{2}$	$\frac{5}{2}$	$\frac{7}{2}$	$\frac{9}{2}$
1		—	-0.424	+0.227	—	—
2		-0.293	-0.391	-0.171	+0.307	—
3		—	-0.364	-0.343	-0.071	+0.335
4		—	—	-0.380	-0.308	-0.018
5		—	—	—	-0.385	-0.283

		$\eta_2(\frac{3}{2}\frac{7}{2}J_iJ_e)$			
$J_e \backslash J_i$		$\frac{3}{2}$	$\frac{5}{2}$	$\frac{7}{2}$	$\frac{9}{2}$
1		—	+1.014	—	—
2		+0.383	+0.753	+0.887	—
3		+0.271	+0.575	+0.821	+0.821
4		—	+0.362	+0.652	+0.839
5		—	—	+0.414	+0.693

Table 4(a)—continued

		$\eta_2(\frac{5}{2} \frac{5}{2} J_i J_e)$					
$J_e \backslash J_i$		0	1	2	3	4	5
3/2		—	-0.800	+0.114	+0.629	-0.286	—
5/2		-1.069	-0.703	-0.107	+0.443	+0.535	-0.382
7/2		—	-0.935	-0.436	+0.125	+0.524	+0.461
9/2		—	—	-0.865	-0.299	+0.236	+0.550

		$\eta_4(\frac{1}{2} \frac{7}{2} J_i J_e)$			
$J_e \backslash J_i$		2	3	4	5
5/2		-0.943	+0.356	—	—
7/2		—	-0.873	+0.444	—
9/2		—	—	-0.832	+0.492

		$\eta_4(\frac{3}{2} \frac{5}{2} J_i J_e)$				
$J_e \backslash J_i$		1	2	3	4	5
5/2		+0.990	-0.793	+0.324	-0.062	—
7/2		—	+0.716	-0.827	+0.432	-0.100
9/2		—	—	+0.595	-0.822	+0.492

		$\eta_4(\frac{3}{2} \frac{7}{2} J_i J_e)$				
$J_e \backslash J_i$		1	2	3	4	5
5/2		-0.553	-0.450	+0.484	-0.164	—
7/2		—	-0.620	-0.180	+0.510	-0.232
9/2		—	—	-0.607	-0.045	+0.503

		$\eta_4(\frac{5}{2} \frac{5}{2} J_i J_e)$					
$J_e \backslash J_i$		0	1	2	3	4	5
5/2		+0.926	-0.133	-0.463	+0.419	-0.152	+0.022
7/2		—	+0.537	-0.418	-0.239	+0.456	-0.222
9/2		—	—	+0.403	-0.476	-0.110	+0.454

Table 4(b)—continued

		$\eta_2(\frac{5}{2} \frac{5}{2} J_i J_e)$				
$J_e \backslash J_i$		$\frac{1}{2}$	$\frac{3}{2}$	$\frac{5}{2}$	$\frac{7}{2}$	$\frac{9}{2}$
1		—	-0.566	+0.646	-0.202	—
2		-0.956	-0.341	+0.342	+0.581	-0.342
3		-0.990	-0.544	+0.033	+0.495	+0.495
4		—	-0.895	-0.358	+0.189	+0.541
5		—	—	-0.841	-0.252	+0.272

		$\eta_4(\frac{1}{2} \frac{7}{2} J_i J_e)$			
$J_e \backslash J_i$		$\frac{3}{2}$	$\frac{5}{2}$	$\frac{7}{2}$	$\frac{9}{2}$
2		-1.000	+0.272	—	—
3		—	-0.903	+0.408	—
4		—	—	-0.850	+0.471
5		—	—	—	-0.817

		$\eta_4(\frac{3}{2} \frac{5}{2} J_i J_e)$				
$J_e \backslash J_i$		$\frac{1}{2}$	$\frac{3}{2}$	$\frac{5}{2}$	$\frac{7}{2}$	$\frac{9}{2}$
2		-1.310	-0.700	+0.229	-0.038	—
3		—	+0.821	-0.821	+0.387	-0.083
4		—	—	+0.646	-0.826	+0.466
5		—	—	—	+0.556	-0.817

		$\eta_4(\frac{3}{2} \frac{7}{2} J_i J_e)$			
$J_e \backslash J_i$		$\frac{3}{2}$	$\frac{5}{2}$	$\frac{7}{2}$	$\frac{9}{2}$
2		-0.714	+0.416	-0.110	—
3		-0.612	-0.288	+0.505	-0.202
4		—	-0.616	-0.103	+0.508
5		—	—	-0.598	—

		$\eta_4(\frac{5}{2} \frac{5}{2} J_i J_e)$				
$J_e \backslash J_i$		$\frac{1}{2}$	$\frac{3}{2}$	$\frac{5}{2}$	$\frac{7}{2}$	$\frac{9}{2}$
2		+0.535	-0.611	+0.344	-0.102	+0.013
3		+0.670	-0.335	-0.335	+0.447	-0.193
4		—	+0.457	-0.457	-0.166	+0.457
5		—	—	+0.364	-0.486	-0.065

REFERENCES

- BIEDENHARN, L. C., 1952, *Tables of Racah Functions* (Oak Ridge National Laboratory Report 1098).
- BIEDENHARN, L. C., BOYER, K., and CHARPIE, R. A., 1952, *Phys. Rev.*, **88**, 517.
- BIEDENHARN, L. C., and ROSE, M. E., 1953, *Rev. Mod. Phys.*, **25**, 729.
- CHRISTY, R. F., 1953, *Phys. Rev.*, **89**, 839.
- EDMONDS, A. R., and FLOWERS, B. H., 1952, *Proc. Roy. Soc. A*, **214**, 515.
- FANO, U., 1951, *National Bureau of Standards Report* 1214.
- FELD, B. T., 1953, *Phys. Rev.*, **89**, 330.
- GALLAHER, L. J., and CHESTON, W. B., 1952, *Phys. Rev.*, **88**, 684.
- LLOYD, S. P., 1952, *Phys. Rev.*, **88**, 986.
- NEWNS, H. C., 1953, *Proc. Phys. Soc. A*, **66**, 477.
- SATCHLER, G. R., 1953, *Phys. Rev.*, **90**, 722.
- SATCHLER, G. R., and SPIERS, J. A., 1952, *Proc. Phys. Soc. A*, **65**, 980.
- STEENBERG, N. R., 1952, *Proc. Phys. Soc. A*, **65**, 791.

The Decay Scheme of Krypton-83

By P. SWINBANK AND J. WALKER

Department of Physics, University of Birmingham

Communicated by P. B. Moon; MS. received 12th June 1953, and in final form 19th August 1953

Abstract. The occurrence of a nuclear level preceding the 1.9 hour metastable state in ^{83}Kr has been confirmed. The associated transition has been shown to be of magnetic dipole type, of energy 51 kev and half-life less than 5×10^{-8} second.

§ 1. INTRODUCTION

INFORMATION on the decay scheme of ^{83}Kr has recently been given by Barrett (1952), Bergström (1952) and Walker (1952). It has been well established that ^{83}Br decays by a 1 mev β -transition to a 1.9 h metastable state in ^{83}Kr , and Walker suggested the presence of a nuclear level preceding the 1.9 h state as shown in fig. 1. The existence of this level has now been confirmed by coincidence measurements, and data obtained from coincidence absorption and cloud chamber experiments suggest a magnetic dipole character for the decay transition.

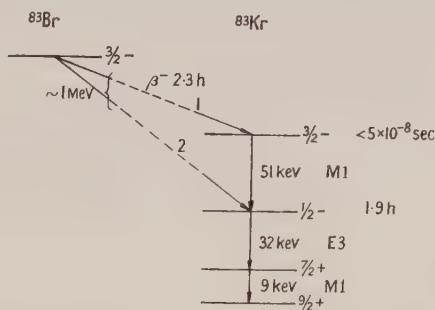


Fig. 1. Decay scheme of ^{83}Kr .

§ 2. SOURCE PREPARATION

Bromine-83 was prepared by the deuteron bombardment of a thick target of selenium in the Birmingham 60 in. cyclotron. An incident energy of 10 mev was used, and a double chemical separation gave the required isotope in extremely pure form.

The bombarded selenium, together with a little potassium bromide carrier, was boiled in concentrated nitric acid to expel the bromine isotopes formed directly by (d, n) and (d, 2n) reactions. The residue was left for about 30 minutes to generate ^{83}Br by the 25 min β^- decay of ^{83}Se produced originally by the (d, p) reaction. This bromine, again with a little carrier, was distilled into silver nitrate solution and the resulting bromide collected. This was dissolved in ammonia, and a drop of the solution evaporated on a collodion foil to give a very

thin source of ^{83}Br . Measurements of the half-life of the beta-activity of sources prepared in this way gave 2.3 ± 0.05 h, in agreement with the reported values of 2.4 h (Katcoff *et al.* 1951) and 2.3 h (Langsdorf and Segrè 1940).

§ 3. COINCIDENCE MEASUREMENTS

The coincidence of the β -particle and the γ -ray required by the decay scheme of fig. 1 was investigated by means of a delayed coincidence equipment with resolving time 3×10^{-7} sec, using two Geiger counters (G.E.C. type GM4). It was found that the instantaneous coincidence rate from a ^{83}Br source was reduced from 42 coincidences per minute to 4 coincidences per minute when a magnetic field was applied to deflect 1 mev β -particles from the counters. This result, coupled with the knowledge that conversion electrons of the expected energy could not penetrate the counter windows, points conclusively to the coincidence of the β -particle with the γ -ray. One of us (Walker 1952) has already pointed out that the β -particle must precede the γ -ray if the established relation between energy and half-life is to be followed for the β -transition.

Using the delayed coincidence system, an attempt has been made to measure the half-life of the krypton state by direct comparison of the curves of log (coincidence rate) plotted against delay time for a bromide source and for cobalt-60 (half-life less than 2×10^{-9} sec). No difference could be detected between these curves, and it is therefore concluded that the half-life of the state in krypton must be less than 5×10^{-8} sec. For an energy of about 50 kev and this half-life the single particle theory of Weisskopf (1951) suggests a magnetic dipole transition. Information has been obtained on the K/L conversion ratio and the conversion coefficient to test this conclusion.

§ 4. K/L CONVERSION RATIO

The investigation of K/L ratio was made by an absorption method because of the lack of a suitable spectrometer. Apparatus designed and described by Fuller (1950) was found suitable for this work. It consists of two windowless counters in a glass vessel with arrangements for mounting a source and absorbing foils between them.

Coincidence absorption results are shown in fig. 2. For this diagram the component of the coincidence rate due to β - γ coincidences has been subtracted from the experimental results, so that only coincidences between β -particles and soft electrons are represented. Our interpretation of these results is that part A is due to conversion electrons from the upper level, and part B due to radiations following the 1.9 h level. Part B was only obtained when the short range measurements were made after a time sufficient for the appearance of activity from the 1.9 h level, and the maximum range agrees, within the limits of error, with that expected for conversion electrons from the 32 kev transition.

Thus, in considering the new level, part B is to be ignored, and only part A examined. There is no evidence for conversion electrons from the L-shell, and the end-point of the line A may be compared with that for K-electrons of 35 kev from ^{80}Br (obtained in a subsidiary experiment), as shown. The results of the main experiment could not be confused by the presence, in the ^{83}Br source, of ^{80}Br , since this isotope was completely eliminated by the double separation used. The energy obtained for ^{83}Kr (38 kev) corresponds to K-conversion of a 51 kev

γ -ray. Assuming this value for the energy to be correct and that absorption of monoenergetic electrons in this region is linear, absorption lines corresponding to $K/L = 1$ and 8 have been drawn. It can be seen that the experimental results favour a high value for this ratio and hence a magnetic transition. These results differ from those of Helmholtz (1941), who found an energy of 46 keV and a K/L ratio of unity using a spectrometer, but these observations were made with a thick source.

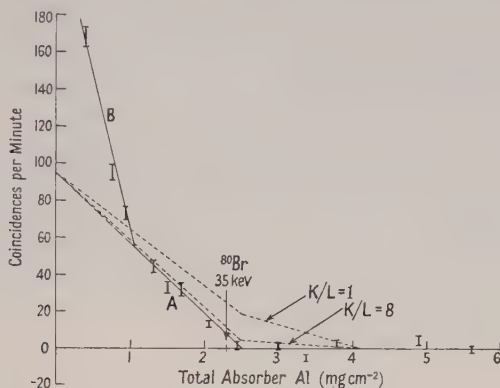


Fig. 2. Beta-electron coincidence absorption.

§ 5. TOTAL CONVERSION COEFFICIENT

An estimate of the total conversion coefficient has been made by comparing the numbers of β -particle tracks with and without conversion electrons in a Wilson cloud chamber with a magnetic field. ^{83}Br was injected as ethyl bromide vapour, and stereoscopic pairs of photographs were taken. A check on the absence of unwanted activities was provided by a rough β -spectrum and the absence of positron tracks.

The accuracy of the cloud-chamber method for conversion coefficients is limited by the large correction that has to be made to allow for the presence in the illuminated zone of β -particles which have their origin outside this zone and which therefore do not show conversion electrons even if they exist. This correction has been carefully calculated and enables the results to be compared with the theoretical conversion coefficients of Rose *et al.* (1951) extrapolated in conjunction with figure 8 of Segrè and Helmholtz (1949). 64 out of a total of 510 observed events were found to involve slow electron- β -particle pairs. This result (12%) is to be compared with the theoretical values of 13% for M1 and 33% for E2 transitions if the probabilities of β -decay by paths 1 and 2 of fig. 1 are assumed equal (these β -decays differ in energy by only 5% and are both allowed), and 9% (M1) and 20% (E2) in the case of the probability of decay by path 2 being twice that by path 1. It is felt that the experimental result definitely favours the magnetic transition.

§ 6. CONCLUSION

The existence of a level 51 keV above the 1.9 h level and decaying by an M1 transition has thus been established, and the decay scheme of fig. 1 verified. Duffield and Langer (1951) found the β -decay of ^{83}Br to be simple, whereas the present scheme requires it to be complex. However, they were clearly not considering differences in decay energy as small as 50 keV,

ACKNOWLEDGMENTS

The authors wish to thank Professors P. B. Moon and W. E. Burcham for providing facilities for this work and for much valuable discussion. They also wish to thank Dr. P. T. Barrett for his generous co-operation in preliminary experiments. One of us (P. S.) gratefully acknowledges a grant from the Department of Scientific and Industrial Research.

REFERENCES

- BARRETT, P. T., 1952, *Proc. Phys. Soc. A*, **65**, 450.
BERGSTRÖM, I., 1952, *Ark. Fys.*, **5**, 191.
DUFFIELD, R. B., and LANGER, L. M., 1951, *Phys. Rev.*, **81**, 203.
FULLER, E. W., 1950, *Proc. Phys. Soc. A*, **63**, 1348.
HELMHOLZ, A. C., 1941, *Phys. Rev.*, **60**, 415.
KATCOFF, S., FINKLE, B., and SUGARMAN, N., 1951, *National Nuclear Energy Series*, **9**,
Radiochemical Studies : The Fission Products, paper 59.
LANGSDORF, A., and SEGRÈ, E., 1940, *Phys. Rev.*, **57**, 105.
ROSE, M. E., GOERTZEL, G. H., and SPINRAD, B. I., 1951, *Phys. Rev.*, **83**, 79.
SEGRÈ, E., and HELMHOLZ, A. C., 1949, *Rev. Mod. Phys.*, **21**, 271.
WALKER, J., 1952, *Proc. Phys. Soc. A*, **65**, 449.
WEISSKOPF, V. F., 1951, *Phys. Rev.*, **83**, 1073.

The Application of Variational Methods to Scattering by Ions

II: The Distorted Wave Approximation and the 1s-2s Excitation of Helium Ions by Electron Impact

BY B. H. BRANSDEN*, A. DALGARNO† AND N. M. KING*

* Department of Physics, Queen's University of Belfast

† Department of Applied Mathematics, Queen's University of Belfast

Communicated by D. R. Bates; MS. received 22nd July 1953

Abstract. Wave functions determined by the variational methods of Hulthén and Kohn are employed in the calculation of the zero order partial cross section for the process $\text{He}^+(1s) + e \rightarrow \text{He}^+(2s) + e$ by the distorted wave, the Born and the Oppenheimer approximations. The inadequacy of the latter approximation near the threshold is disclosed.

§ 1. INTRODUCTION

THE excitation of neutral atoms by electron impact has been extensively studied using either Born's approximation, for which the wave functions of the initial and final states are assumed to be products of the wave functions of the target atom and the plane waves describing the unperturbed motion of the incident electron, or the Oppenheimer approximation, which differs from the Born approximation only in that it uses properly symmetrized wave functions (cf. Mott and Massey 1949), both approximations being equivalent to a first order perturbation theory calculation. Little attention has been directed to the excitation of ions for which in the Born and Oppenheimer approximations the plane waves appropriate to neutral atoms must be replaced by coulomb waves with consequent increase in analytical complexity. However, the recent discussion by Bates, Fundamirsky, Leech and Massey (1950) has emphasized that for electron energies near the threshold of a transition first order perturbation theory may be quite inadequate, often leading to partial cross sections which exceed the maximum allowed by the conservation theorem of Mott (1931) and of Bohr, Peierls and Placzek (cf. Mott and Massey 1949). This is the case for the few calculations on excitation of ions that have been carried out (Hebb and Menzel 1940, Aller 1949, Aller and White 1950).

An improvement to the first order perturbation theory may be made by allowing for the distortion of the incident wave and the outgoing inelastically scattered wave by the interaction. In the distorted wave method (Mott and Massey 1949) this is achieved by replacing the unperturbed plane (or coulomb) waves by the wave functions appropriate to elastic scattering by the initial and final states of the target atom (or ion). Although this procedure may be expected to give quite accurate results provided the coupling between the initial and final states is weak (Massey and Mohr 1952), it has been followed only infrequently for neutral atoms and never for ions. In paper I of this series (Bransden and Dalgarno 1953) the variational methods developed by Hulthén (1944, 1948) and by Kohn (1948) were employed to obtain analytical wave functions describing the elastic scattering of electrons by

helium ions in the ground $(1s)^2S$ state. These methods are employed here to obtain wave functions describing the elastic scattering by helium ions in the excited $(2s)^2S$ state which together with those of paper I are substituted into the distorted wave approximation. A comparison is made of the partial cross section for zero angular momentum derived using the Born, Oppenheimer and distorted wave approximations.

§ 2. THEORY

The equations of the distorted wave approximation have been presented for the case of neutral atoms by Mott and Massey (1949), Erskine and Massey (1952). Slight modifications are necessary in the case of ions. The Schrödinger equation for the complete system may be written in Hartree units as

$$\left(\nabla_1^2 + \nabla_2^2 + \frac{4}{r_1} + \frac{4}{r_2} - \frac{2}{r_{12}} \right) \Psi(\mathbf{r}_1, \mathbf{r}_2) = E \Psi(\mathbf{r}_1, \mathbf{r}_2) \quad \dots\dots(1)$$

where $\mathbf{r}_1, \mathbf{r}_2$ are the position vectors of electrons 1 and 2 relative to the nucleus, $r_{12} = |\mathbf{r}_1 - \mathbf{r}_2|$ and the total energy $E = k_0^2 + \epsilon_0 = k_1^2 + \epsilon_1$, ϵ_0 and ϵ_1 being respectively the energies of the $(1s)^2S$ and $(2s)^2S$ states of the helium ion. The total wave functions Ψ is now expanded in terms of the complete set of helium ion wave functions $X_n(\mathbf{r})$:

$$\Psi(\mathbf{r}_1, \mathbf{r}_2) = \sum_n \{ X_n(\mathbf{r}_2) \Phi_n^{+-}(\mathbf{r}_1) \pm X_n(\mathbf{r}_1) \Phi_n^{+-}(\mathbf{r}_2) \}, \quad \dots\dots(2)$$

the plus sign referring to the singlet state and the minus sign to the triplet state. The distorted wave approximation assumes that the only significant terms in (2) are those involving the initial and final states of the ion. We assume further that for incident energies just above the threshold the scattering in states of non-zero angular momentum may be neglected with the consequence that $\Phi_n^{+-}(\mathbf{r}) = \Phi_n^{+-}(r)$. The justification for this latter assumption will be examined in a later paper. Equation (2) then becomes

$$\Psi(r_1, r_2) = \{ X_0(r_2) \Phi_0^{+-}(r_1) + X_1(r_2) \Phi_1^{+-}(r_1) \} \\ \pm \{ X_0(r_1) \Phi_0^{+-}(r_2) + X_1(r_1) \Phi_1^{+-}(r_2) \} \quad \dots\dots(3)$$

where $X_0(r)$, $X_1(r)$ are the 1s and 2s wave functions of the helium ion and Φ_0, Φ_1 , behave asymptotically as

$$\left. \begin{aligned} \Phi_0^{+-}(r) &\sim \exp(i\rho_0^{+-})(k_0 r)^{-1} \sin(k_0 r + k_0^{-1} \log 2 k_0 r + \rho_0^{+-}) \\ \Phi_1^{+-}(r) &\sim y^{+-} r^{-1} \exp\{i(k_1 r + k_1^{-1} \log 2 k_1 r)\}. \end{aligned} \right\} \quad \dots\dots(4)$$

The partial cross sections Q^{+-} corresponding to the singlet and triplet states of the whole system are

$$Q^{+-} = 4\pi \frac{k_1}{k_0} |y^{+-}|^2 \quad \dots\dots(5)$$

and the mean partial cross section for an unpolarized beam of electrons is

$$Q = \frac{\pi k_1}{k_0} \{ |y^+|^2 + 3 |y^-|^2 \}. \quad \dots\dots(6)$$

y^+ and y^- are determined from (3) and (1) (cf. Mott and Massey 1949) which, when combined, yield the coupled integro-differential equations

$$\left[\frac{d^2}{dr^2} + V_{00}(r) + \frac{2}{r} + k_0^2 \right] \Phi_0^{+-}(r) \pm \int_0^\infty K_{00}(r, r') \phi_0^{+-}(r') dr' \\ = -V_{01}(r) \phi_1^{+-}(r) \mp \int_0^\infty K_{01}(r, r') \phi_1^{+-}(r') dr', \quad \dots\dots(7a)$$

$$\left[\frac{d^2}{dr^2} + V_{11}(r) + \frac{2}{r} + k_1^2 \right] \phi_1^{+,-}(r) \pm \int_0^\infty K_{11}(r, r') \phi_1^{+,-}(r') dr' \\ = -V_{10}(r) \phi_0^{+,-}(r) \mp \int_0^\infty K_{10}(r, r') \phi_0^{+,-}(r') dr' \quad \dots\dots (7b)$$

where

$$\phi_0^{+,-}(r) = r \Phi_0^{+,-}(r), \quad \phi_1^{+,-}(r) = r \Phi_1^{+,-}(r), \\ V_{nm}(r) = V_{mn}^*(r) = 8\pi \int_0^\infty X_m^*(r') \left(\frac{1}{r} - \gamma_0(r, r') \right) X_n(r') r'^2 dr',$$

and

$$K_{nm}(r, r') = K_{mn}^*(r, r') = 4\pi [-2\gamma_0(r, r') + k_n^2 - E_m] X_n^*(r) X_m(r') r r'$$

with

$$\gamma_0(r, r') = r^{-1} \quad \text{for } r > r' \\ = r'^{-1} \quad \text{for } r < r'.$$

In the distorted wave approximation, the terms involving $\phi_1^{+,-}$ on the right-hand side of (7a) are neglected and the solution of the resulting equation

$$\left(\frac{d^2}{dr^2} + V_{00}(r) + \frac{2}{r} + k_0^2 \right) \phi_0^{+,-}(r) \pm \int_0^\infty K_{00}(r, r') \phi_0^{+,-}(r') dr' = 0, \quad \dots\dots (8)$$

which satisfies the boundary conditions

$$\phi_0^{+,-}(0) = 0, \\ \phi_0^{+,-}(r) \sim k_0^{-1} \exp(ip_0^{+,-}) \sin(k_0 r + k_0^{-1} \log 2k_0 r + \rho_0^{+,-}),$$

is substituted into the right-hand side of (7b). The solution of the consequent inhomogeneous integro-differential equation which satisfies the boundary condition

$$\phi_1^{+,-}(r) \sim y^{+,-} \exp \{ i(k_1 r + k_1^{-1} \log 2k_1 r) \}$$

is easily shown (cf. Mott and Massey 1949) to be

$$\phi_1^{+,-}(r) = - \int_0^\infty G^{+,-}(r, r'') [V_{01}(r'') \phi_0^{+,-}(r'') \pm \int_0^\infty K_{01}(r'', r') \phi_0^{+,-}(r') dr'] dr'', \quad \dots\dots (9)$$

where

$$G^{+,-}(r, r'') = -k_1^{-1} \mathcal{L}^{+,-}(r) \mathcal{M}^{+,-}(r'') \quad \text{for } r'' > r \\ = -k_1^{-1} \mathcal{L}^{+,-}(r'') \mathcal{M}^{+,-}(r) \quad \text{for } r > r''$$

and $\mathcal{L}^{+,-}(r)$, $\mathcal{M}^{+,-}(r)$ satisfy the equation

$$\left[\frac{d^2}{dr^2} + V_{11}(r) + \frac{2}{r} + k_1^2 \right] \mathcal{L}^{+,-}(r) \pm \int_0^\infty K_{11}(r, r') \mathcal{L}^{+,-}(r') dr' = 0, \quad \dots\dots (10)$$

with $\mathcal{L}^{+,-}(0) = 0$, $\mathcal{L}^{+,-}(r) \sim \exp(ip_1^{+,-}) \sin(k_1 r + k_1^{-1} \log 2k_1 r + \rho_1^{+,-})$,

$$\text{and } \mathcal{M}^{+,-}(r) \sim \exp \{ i(k_1 r + k_1^{-1} \log 2k_1 r + \rho_1^{+,-}) \}.$$

From eqns. (9) and (10) it follows that

$$\phi_1^{+,-}(r) \sim \frac{1}{k_0 k_1} \exp \{ i(\rho_0^{+,-} + \rho_1^{+,-}) \} \exp \{ i(k_1 r + k_1^{-1} \log 2k_1 r) \} J_{10}^{+,-} \quad \dots\dots (11)$$

where $J_{mn}^{+,-} = \int_0^\infty g_m^{+,-}(r) [V_{nm}(r) g_n^{+,-}(r) \pm \int_0^\infty K_{nm}(r, r') g_n^{+,-}(r') dr'] dr$

with

$$g_1^{+,-}(r) = \exp(-ip_1^{+,-}) \mathcal{L}^{+,-}(r), \quad g_0^{+,-}(r) = \exp(-ip_0^{+,-}) k_0 \phi_0^{+,-}. \quad \dots\dots (12)$$

Comparing eqn. (11) with (4), we deduce

$$y^{+,-} = \frac{1}{k_0 k_1} \exp \{ i(\rho_0^{+,-} + \rho_1^{+,-}) \} J_{10}^{+,-}. \quad \dots\dots (13)$$

Using (10) and (12), we have that $g_0^{+,-}$ and $g_1^{+,-}$ are the solutions of (8) and (10) respectively satisfying the conditions

$$\left. \begin{aligned} g_0^{+,-} &\sim \frac{1}{\{1+(a^{+,-})^2\}^{1/2}} \{F_0(k_0, r) + a^{+,-}G_0(k_0, r)\} \\ g_1^{+,-} &\sim \frac{1}{\{1+(d^{+,-})^2\}^{1/2}} \{F_0(k_1, r) + d^{+,-}G_0(k_1, r)\}, \end{aligned} \right\} \dots\dots (14)$$

where F_0 , G_0 are the regular and irregular coulomb functions appropriate to an attractive potential $2/r$ and zero angular momentum.

Thus $g_0^{+,-}(r)$ is simply the wave function describing the elastic scattering of electrons by $\text{He}^+(1s)$ (cf. paper I), and $g_1^{+,-}(r)$ is the wave function describing the elastic scattering of electrons by $\text{He}^+(2s)$.

The 'one-body' cross sections, Q^0 , found by neglecting exchange effects arising from the identity of the two electrons, is of interest and may be calculated from eqns. (5) and (13) by the omission of the kernel K_{10} and the replacement of $g_0^{+,-}(r)$, $g_1^{+,-}(r)$ by the solutions $g_0^0(r)$, $g_1^0(r)$ of eqns. (8) and (10), omitting the kernels K_{00} and K_{11} .

§ 3. CALCULATION OF THE WAVE FUNCTIONS $g_{0,1}^{+,-}$ AND $g_{0,1}^0$

Solutions $g_0^{+,-}(r)$ of eqn. (8) have been calculated previously (paper I) by the application of the Hulthén and Kohn-Hulthén variational methods employing trial functions of the form

$$g_0^{+,-}(r) = \frac{1}{\{1+(a^{+,-})^2\}^{1/2}} [F_0(k_0r) + (a^{+,-} + b^{+,-}e^{-2r})(1 - e^{-2r})G_0(k_0r)], \quad \dots (15)$$

the constant $a^{+,-}$ being related to the zero order phase shift for the elastic scattering of electrons by the helium ion in the ground state by the equations

$$\rho_0^{+,-} = \mu_0^{\text{H}^{+,-}} + \eta_0; \quad \mu_0^{\text{H}^{+,-}} = \tan^{-1} a^{+,-} \quad \dots\dots (16)$$

$$\text{or} \quad \rho_0^{+,-} = \mu_0^{\text{K}^{+,-}} + \eta_0; \quad \mu_0^{\text{K}^{+,-}} = \tan^{-1} \left\{ a^{+,-} - \frac{J_{00}(a^{+,-})}{k_0} \right\}$$

in the Hulthén and Kohn-Hulthén methods respectively, where $\eta_0 = \arg \Gamma(1 + ik_0^{-1})$ is the zero order phase shift at energy k_0^2 due to an attractive coulomb potential $2/r$. The 'one-body' wave function $g_0^0(r)$, which is the solution of eqn. (8) with K_{00} and K_{11} set equal to zero, was determined by the same methods with a^0 , b^0 replacing $a^{+,-}$, $b^{+,-}$ in (15) and μ_0^0 , ρ_0^0 replacing $\mu_0^{+,-}$, $\rho_0^{+,-}$ in (16).

The wave functions $g_1^{+,-}(r)$, $g_1^0(r)$ may be obtained by these variational methods, if suitable trial functions are inserted in the integral J_{11} . Trial functions of the form (15) were found to be unsatisfactory and were replaced by a form indicated by the work of Erskine and Massey (1952):

$$g_1^{+,-,0}(r) = \frac{1}{\{1+(d^{+,-,0})^2\}^{1/2}} [F_0(k_1r)(1 + c^{+,-,0}e^{-r}) + d^{+,-,0}(1 - e^{-r})G_0(k_1r)]. \quad \dots\dots (17)$$

Here the parameter $d^{+,-,0}$ is related to the zero order phase shift $\rho_1^{+,-,0}$ for elastic scattering of electrons by the helium ion in the (2s) state, by the equations

$$\left. \begin{aligned} \rho_1^{+,-,0} &= \mu_1^{\text{H}^{+,-,0}} + \eta_1; \quad \mu_1^{\text{H}^{+,-,0}} = \tan^{-1} d^{+,-,0} \\ \text{or} \quad \rho_1^{+,-,0} &= \mu_1^{\text{K}^{+,-,0}} + \eta_1; \quad \mu_1^{\text{K}^{+,-,0}} = \tan^{-1} \left\{ d^{+,-,0} - \frac{J_{11}(d^{+,-,0})}{k_1} \right\} \end{aligned} \right\} \dots\dots (18)$$

in the Hulthén and Kohn-Hulthén methods respectively and where $\eta_1 = \arg \Gamma(1 + ik_1^{-1})$ is the zero order phase shift due to an attractive coulomb potential $2/r$ and energy k_1^2 .

An indication of the accuracy of the Hulthén wave functions is given by observing how closely these functions satisfy the integral equation

$$\tan \mu_1^{\text{H}+, -} = d^{+, -} = \frac{\{1 + (d^{+, -})^2\}^{1/2}}{k_1} \int_0^\infty F_0(k_1 r) \left[V_{11}(r) g_1^{+, -}(r) \pm \int_0^\infty K_{11}(r, r') g_1^{+, -}(r') dr' \right] dr. \quad \dots\dots(19)$$

(The 'one-body' wave functions $g_1^0(r)$ should satisfy eqn. (19) with K_{11} omitted.) The Kohn-Hulthén wave functions are constructed so as to satisfy automatically the integral equation, but their accuracy may be tested by noting that the relation $J_{11}/k_1 \ll d$ should be satisfied. (The Hulthén wave functions automatically satisfy $J_{11} = 0$.) A comparison of the phases calculated in the Hulthén and Kohn-Hulthén methods together with those found from the integral equation (19) is made in table 1, where the quantities J_{11}/k_1 and d for the Kohn-Hulthén method are also given.*

§ 4. THE OPPENHEIMER AND BORN APPROXIMATIONS

If the kernels V_{00} , K_{00} and V_{11} , K_{11} are set equal to zero in eqns. (8) and (10) respectively, the Oppenheimer approximation is obtained for which the wave functions $g_0^{+, -}$ and $g_1^{+, -}$ reduce to regular coulomb functions appropriate to an attractive potential $2/r$ and zero angular momentum

$$g_0^{+, -}(r) = F_0(k_0 r); \quad g_1^{+, -}(r) = F_0(k_1 r), \quad \dots\dots(20)$$

and eqn. (13) for the scattering amplitude $y^{+, -}$ becomes

$$y_{B0}^{+, -} = \frac{\exp \{i(\eta_0 + \eta_1)\}}{k_0 k_1} \int_0^\infty F_0(k_1 r) \left[V_{10} F_0(k_0 r) \pm \int_0^\infty K_{10}(r, r') F_0(k_0 r') dr' \right] dr. \quad \dots\dots(21)$$

The corresponding 'one-body' scattering amplitude y_B is obtained in Born's approximation by putting K_{10} equal to zero in (21),

$$y_B = \frac{\exp \{i(\eta_0 + \eta_1)\}}{k_0 k_1} \int_0^\infty F_0(k_1 r) V_{10} F(k_0 r) dr. \quad \dots\dots(22)$$

Although the Born approximation is not expected to be qualitatively accurate at low energies, it gives the correct variation of cross section with energy at the threshold of the transition (cf. Wigner 1948). It can be shown directly from eqns. (21) and (22) that as $k_1^2 \rightarrow 0$, Q^+ , Q^- and Q^0 all tend to constant values, so that there is a finite transition probability even at the threshold.

§ 5. RESULTS AND DISCUSSION

The partial cross sections Q^0 , Q^+ , Q^- and Q determined by the distorted wave approximation, using wave functions derived by the Hulthén and Kohn-Hulthén variational methods, are compared in table 2 with those resulting from the Born and Oppenheimer approximations. The excellent agreement between the values

* Only slightly better results were obtained using more complicated functions of the form $g_1(r) = F_0(k_1 r)(1 + ce^{-r}) + (d + fe^{-r})(1 - e^{-r})G(k_1 r)$, so that it was considered unnecessary to retain the additional parameter f .

Table 1. (i) Tangents of the phase shifts for the scattering of electrons of zero angular momentum by the 2S state of the helium ion

Electron (energy ev)	$d = \tan \mu$					
	One-body d^0		Singlet d^+		Triplet d^-	
	(a)	(b)	(a)	(b)	(a)	(b)
43.7	-10.16	-10.13	5.18	5.18	-3.40	-3.92
48.7	2.51	2.40	1.33	1.32	35.9	34.7
65.3	1.76	1.63	1.48	1.33	2.09	1.98

(a) d as determined by the Kohn-Hulthén method.(b) d as determined by the Hulthén method.(c) d as given by the integral equation with the Hulthén wave function (eqn. (19)).(ii) Comparison of d with J_{11}/k_1

Electron energy (ev)	One-body		Singlet	Triplet
	d^0	J_{11}/k_1	d^+	d^-
43.7	-10.75	+0.58	6.11	-3.40
48.7	3.00	-0.49	1.46	42.40
65.3	2.19	-0.43	1.89	2.54

 J_{11}/k_1
-0.60
-6.50
-0.45Table 2. Zero order partial cross sections for the 1^2S - 2^2S excitation of the helium ion by electron impact
Cross sections in units of a_0^2 *

Energy of incident electron (ev)	One-body Q^0				Singlet Q^+				Triplet Q^-				Mean Q		π/k_0^2
	(a)	(c)	(d)		(b)	(c)	(d)		(b)	(c)	(d)		(b)	(c)	(d)
40.5 (threshold)	0.064	—	—		0.0032	—	—		0.317	—	—		0.238	—	—
41.8	0.062	—	—		0.0021	—	—		0.295	—	—		0.222	—	—
43.7	0.056	0.041	0.044		0.0001(4)	0.120	0.104		0.236	0.0010	0.0011		0.177	0.031	0.027
48.7	0.046	0.021	0.025		0.0014	0.064	0.049		0.156	0.0009	0.0001		0.117	0.017	0.012
65.3	0.028	0.011	0.014		0.0108	0.023	0.021		0.053	0.0015	0.0013		0.042	0.0063	0.0060

(a) Cross sections determined by the Born approximation.

(b) Cross sections determined by the Oppenheimer approximation.

(c) Cross sections determined by the distorted wave approximation employing Hulthén wave functions.

(d) Cross sections determined by the distorted wave approximation employing Kohn-Hulthén wave functions.

* $a_0^2 = 2.80 \times 10^{-17} \text{ cm}^2$.

derived using the Hulthén and Kohn–Hulthén wave functions shows that the use of variationally determined wave functions in the distorted wave approximation is satisfactory although, of course, it does not mean that the distorted wave approximation as such is satisfactory. However, at no energy is the theoretical maximum πk_0^2 exceeded, and in fact Q is always much less than π/k_0^2 . In these circumstances the coupling between the initial and final states is probably small, and it appears likely that the distorted wave method is accurate (Massey and Mohr 1952). The failure of the Oppenheimer approximation is striking. It overestimates by large factors the triplet and mean partial cross sections and underestimates by a large factor the singlet cross section. Distortion of the waves is thus of great importance even when, as in the case here, the coupling may be regarded as small. (Similar behaviour was found by Erskine and Massey (1952) in the case of excitation of the $^2S(2s)$ level of hydrogen, although there the coupling is strong.) As is frequently the case (cf. Bates, Fundamirsky, Leech and Massey 1950), the less refined Born approximation is, when applicable, much superior to the Oppenheimer approximation.

Attention may be drawn to the fact that there is some cancellation within the transition integrals, it being especially severe in the triplet case. Because of this the cross sections are small and, in addition, may be rather sensitive to the details of the wave functions.

For the triplet the cancellation is actually complete when the incident energy is slightly less than 43.7 eV, so that the associated partial cross section towards an appropriately polarized electron beam is zero. The effect on the form of the total cross-section–energy curve will of course be masked to at least some extent by the contributions from the higher order partial cross sections. Nevertheless it is apparent that there may be exceptions to the general rule that the cross section for the excitation of an ionic system is a monotonically decreasing function of the energy of the colliding electrons. The position is closely analogous to that arising in the case of photoionization.

ACKNOWLEDGMENT

The authors are indebted to Professor D. R. Bates for reading this paper and for helpful discussions of the results.

REFERENCES

- ALLER, L. H., 1949 (quoted by Bates *et al.* 1950).
 ALLER, L. H., and WHITE, M. L., 1950 (quoted by Bates *et al.* 1950).
 BATES, D. R., FUNDAMIRSKY, A., LEECH, J. W., and MASSEY, H. S. W., 1950, *Phil. Trans. Roy. Soc. A*, **243**, 93.
 BRANSDEN, B. H., and DALGARNO, A., 1953, *Proc. Phys. Soc. A*, **66**, 268.
 ERSKINE, G. A., and MASSEY, H. S. W., 1952, *Proc. Roy. Soc. A*, **212**, 521.
 HEBB, M. H., and MENZEL, D. H., 1940, *Astrophys. J.*, **92**, 408.
 HULTHÉN, L., 1944, *K. fysiogr. Sällsk. Lund. Förh.*, **14**, No. 21; 1948, *Ark. Mat. Astr. Fys. A*, **35**, 25.
 KOHN, W., 1948, *Phys. Rev.*, **74**, 1763.
 MASSEY, H. S. W., and MOHR, C. B. O., 1952, *Proc. Phys. Soc. A*, **65**, 845.
 MOTT, N. F., 1931, *Proc. Roy. Soc. A*, **133**, 228.
 MOTT, N. F., and MASSEY, H. S. W., 1949, *The Theory of Atomic Collisions*, 2nd Edn. (Oxford: Clarendon Press).
 WIGNER, E., 1948, *Phys. Rev.*, **73**, 1002.

Note on the Spin Paramagnetism of a Free Electron Gas

BY N. H. MARCH* AND B. DONOVAN†

* Department of Physics, The University, Sheffield

† Department of Physics, Northern Polytechnic, London

MS. received 15th June 1953, and in amended form 28th July 1953

Abstract. The effect of exchange on the spin paramagnetism of a free electron gas is discussed. It is shown that in general the exchange terms have a marked effect on the susceptibility and can be legitimately neglected only at extremely high temperatures. A comparison is made with the results of a simple treatment due to Stoner, and qualitative similarities are apparent.

§ 1. INTRODUCTION

As is well known, the first application of Fermi-Dirac statistics to the electrons in metals was made by Pauli (1927) when he calculated the spin paramagnetism due to a system of free electrons. Pauli's result applied to absolute zero and was subsequently extended to all temperatures by Bloch (1929), Stoner (1935) and Mott (1936).

However, in these treatments exchange effects were neglected, and the purpose of this work is to show how the results are modified when exchange is introduced and the simple Fermi-Dirac statistics therefore no longer applicable. The first discussion of the modifications introduced by exchange was given by Wilson (1936), whose considerations were, however, confined to absolute zero. Recent work by Koppe (1947), Wohlfarth (1950) and Lidiard (1951) now enables the dependence of susceptibility on temperature to be found for all temperatures.

§ 2. METHOD OF CALCULATION OF SUSCEPTIBILITY

Using Lidiard's notation, the free energy of a system of n_1 electrons with spin parallel to the field H , and n_2 with antiparallel spin, can be written

$$F = \frac{3}{8}n_1^2\epsilon_0 A(x_1) + \frac{3}{8}n_2^2\epsilon_0 A(x_2) - \frac{3}{4}n_1\epsilon_j B(x_1) - \frac{3}{4}n_2\epsilon_j B(x_2) - \frac{3}{2}n_1\hbar TC(x_1) - \frac{3}{2}n_2\hbar TC(x_2) - (n_1 - n_2)\mu H, \quad \dots\dots(1)$$

where μ is the Bohr magneton and A , B and C are complicated functions of x , with simple forms only at very small and very large values of x . Minimizing the free energy with respect to n_1 , subject to the condition that

$$n_1 + n_2 = N, \quad \dots\dots(2)$$

where N is the total number of electrons, we obtain the basic equation of our treatment:

$$2\mu H = [^1\epsilon_0 A(x_1) - ^2\epsilon_0 A(x_2)] - [^1\epsilon_j B(x_1) - ^2\epsilon_j B(x_2)] - \frac{3kT}{2} [C(x_1) - C(x_2)]. \quad \dots(3)$$

Putting $n_1 = \frac{1}{2}(N + \delta), \quad n_2 = \frac{1}{2}(N - \delta), \quad \dots\dots(4)$

it is easily shown that

$$\left. \begin{aligned} x_1 &= x + a\delta + O(\delta^2), \\ x_2 &= x - a\delta + O(\delta^2), \end{aligned} \right\} \quad \dots\dots(5)$$

where

$$3Na = \frac{5(\epsilon_j/\epsilon_0)B'(x) - 8A'(x)}{4A''(x) - 5(\epsilon_j/\epsilon_0)B''(x) - 10(kT/\epsilon_0)C''(x)}. \quad \dots\dots(6)$$

Developing eqn. (3), neglecting terms of order δ^2 and introducing the susceptibility χ defined by

$$\chi = \delta\mu/H, \quad \dots\dots(7)$$

we obtain the relation

$$\frac{\mu^2 N}{\chi\epsilon_0} = \frac{1}{2} \left[\left\{ 2aNA'(x) + \frac{4}{3}A(x) \right\} - \frac{\epsilon_j}{\epsilon_0} \left\{ 2aNB'(x) + \frac{2}{3}B(x) \right\} - 3aN \frac{kT}{\epsilon_0} C'(x) \right]. \quad \dots\dots(8)$$

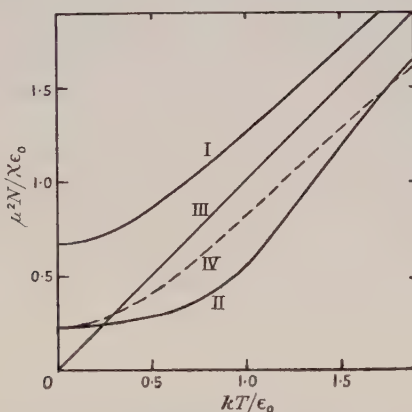
The equations (6) and (8), together with the equation

$$\frac{3}{5}A'(x) - \frac{3}{4}\frac{\epsilon_j}{\epsilon_0}B'(x) - \frac{3}{2}\frac{kT}{\epsilon_0}C'(x) = 0, \quad \dots\dots(9)$$

connecting x and T , completely define the susceptibility as a function of temperature when ϵ_j/ϵ_0 is given.

§ 3. RESULTS

In the figure we have plotted the results obtained from eqns. (6), (8) and (9) for $\epsilon_j/\epsilon_0 = 1.32$ (the value for sodium) together with the well-known results for



Variation of susceptibility with temperature.

- Curve I: Without exchange ($\epsilon_j = 0$).
- Curve II: With exchange ($\epsilon_j/\epsilon_0 = 1.32$).
- Curve III: Classical.
- Curve IV: Stoner treatment ($k\theta'/\epsilon_0 = 0.44$).

$\epsilon_j = 0$ (Mott 1936), in order to illustrate the general effect of exchange on the paramagnetic susceptibility. To facilitate calculations for other values of ϵ_j/ϵ_0 we have recorded in the table the values of the functions used in the calculations for $\epsilon_j/\epsilon_0 = 1.32$.

Strictly it is not permissible to expand $B(x)$ in a Taylor series about the origin since B'' becomes negatively infinite there. To obtain the susceptibility at $T = 0$ it is therefore best to go back to eqn. (3) and to use the fact that $x_1 = x_2 = 0$ when $T = 0$. From the table, $A(0) = B(0) = 1$, and retaining only terms of order δ , we have

$$\frac{\mu^2 N}{\chi\epsilon_0} = \frac{2}{3} - \frac{1}{3}\frac{\epsilon_j}{\epsilon_0}, \quad \dots\dots(10)$$

in agreement with Wilson's result. No difficulties arise in applying eqns. (6), (8) and (9) as the origin is approached. It follows from eqn. (10) that the spin paramagnetic susceptibility at $T=0$ is always increased by exchange. For example, it can be seen from the figure that the susceptibility for sodium is increased by a factor of about 3. Sampson and Seitz (1940) have shown, however, that at $T=0$ correlation effects will oppose the exchange terms and tend to bring the value back towards the Pauli result. Unfortunately it is not possible at the moment to take account of correlation at all satisfactorily except at $T=0$.

x	$A(x)$	$A'(x)$	$A''(x)$	$B(x)$	$B'(x)$	$B''(x)$	$C'(x)$	$C''(x)$
0	1	0	0.8333	1	0	$-\infty$	1	1
0.5	1.160	0.7365	1.859	0.8555	-0.5160	-0.5985	1.391	0.1285
1	1.680	1.120	-0.3733	0.5965	-0.3977	0.6628	0.8889	-1.333
2	2.667	0.8889	-0.1481	0.3758	-0.1253	0.1044	0.3738	-0.2118
3	3.494	0.7765	-0.08628	0.2868	-0.06373	0.03540	0.2390	-0.08599
4	4.233	0.7055	-0.05879	0.2367	-0.03945	0.01644	0.1758	-0.04644

For very high temperatures it can be shown that

$$\frac{\mu^2 N}{\chi \epsilon_0} = \frac{kT}{\epsilon_0} \left[1 + \frac{64}{75(15)^{1/2}} \left(\frac{\epsilon_0}{kT} \right)^{3/2} - \frac{8}{225} (28 - 16 \ln 2) \frac{\epsilon_j}{\epsilon_0} \left(\frac{\epsilon_0}{kT} \right)^2 + \dots \right], \quad \dots\dots(11)$$

and we see that the exchange effects become negligible as the temperature becomes sufficiently high, curve II in the figure becoming asymptotic to the classical line from above, exactly as in the case when exchange is neglected. Thus for higher temperatures than those shown in the figure curve II crosses the classical line again.

As an indication of the accuracy of the susceptibility calculated from the approximate free energy expression (1) it is of interest to consider briefly the results for $\epsilon_j=0$.

For low temperatures our equations lead to the result

$$\frac{\mu^2 N}{\chi \epsilon_0} = \frac{2}{3} \left[1 + \frac{1}{12} \left(\frac{3kT}{\epsilon_0} \right)^2 + \dots \right], \quad \dots\dots(12)$$

whereas the exact result (Stoner 1935) is

$$\frac{\mu^2 N}{\chi \epsilon_0} = \frac{2}{3} \left[1 + \frac{1}{12} \left(\frac{\pi kT}{\epsilon_0} \right)^2 + \dots \right]. \quad \dots\dots(13)$$

The replacement of π by 3 is the usual modification at low temperatures due to the use of the approximate free energy (see Wohlfarth 1950).

When the temperature is very high, the result derived from the approximate free energy is given by putting $\epsilon_j=0$ in eqn. (11) whilst the exact result (Stoner 1935) is

$$\frac{\mu^2 N}{\chi \epsilon_0} = \frac{kT}{\epsilon_0} \left[1 + \frac{2}{3(2\pi)^{1/2}} \left(\frac{\epsilon_0}{kT} \right)^{3/2} + \dots \right]. \quad \dots\dots(14)$$

The coefficient of $(\epsilon_0/kT)^{1/2}$ from the approximate expression (11) is 0.220, whilst the exact value from (14) is 0.266.

For intermediate temperatures the susceptibility can be easily obtained numerically from the results given in the table, and the deviations from the exact results over the range of kT/ϵ_0 shown in the figure are no more than a few per cent.

It should be added that the results presented here for $\epsilon_j \neq 0$ are only valid when there is no ferromagnetism (see Lidiard 1951).

§ 4. COMPARISON WITH TREATMENT DUE TO STONER

Stoner (1936, see also 1948) has discussed in a simple way the effect of exchange on the paramagnetism of metals. This treatment is quite different from the one given here, but it is of obvious interest to compare the results. Stoner assumes a particular form for the exchange interaction which is independent of temperature.

For purposes of comparison we can identify Stoner's parameter $k\theta'$ with $\frac{1}{3}\epsilon_j$, and curve IV in the figure shows the result of Stoner's treatment, curve I simply being displaced parallel to itself. It can be seen that over the range plotted the curves are qualitatively similar though quantitative differences occur.

First of all, at low temperatures, there is no simple form such as (12) for the susceptibility due to the presence of a term $x^2 \ln x$ in the function $B(x)$. This is similar to the situation found by Wohlfarth (1950) when discussing the specific heat of free electrons using the same basic assumptions. Also the temperature dependence at low temperatures is even weaker than that given when exchange is neglected or by Stoner's treatment. The major differences between curves II and IV of the figure lie in the region where $kT/\epsilon_0 \sim 1$, and it seems probable that Lidiard's distribution function is less satisfactory in this region than at very high or very low temperatures. It is thus not impossible that in this region the true results could lie somewhat nearer to Stoner's curve than is indicated by curve II.

However, at high temperatures the results become quite different, due to the fact that Stoner has assumed an exchange interaction independent of temperature, whilst in the free electron theory there is a strong temperature dependence. Thus, whereas in our calculations the form of the susceptibility is given at very high temperatures by eqn. (11), in which the coefficient of ϵ_j/ϵ_0 is proportional to $(\epsilon_0/kT)^2$, in Stoner's treatment the coefficient is proportional to (ϵ_0/kT) , and hence curve IV does not tend asymptotically to curve I.

§ 5. CONCLUSIONS

The results presented here show that exchange effects can be of decided importance in determining the paramagnetic susceptibility of a free electron gas at all temperatures except extremely high ones; the actual deviations from the results when exchange is ignored depending on the strength of the exchange interaction as measured by ϵ_j/ϵ_0 . Even though correlation effects will most probably oppose the exchange terms, it can hardly be expected that the cancellation will be at all complete.

A comparison of the results with those of a simple treatment due to Stoner leads to qualitative agreement, except at the highest temperatures, even though the two approaches differ very considerably.

It is, however, not possible to obtain from experiment reliable estimates of the spin paramagnetic contributions to the total susceptibilities of any metals to which the free electron theory is at all applicable unless the diamagnetic contribution from the free electrons is also known. Since very little attention has been paid to the influence of exchange and correlation effects on free electron diamagnetism we are now considering this problem before attempting any analysis of experimental results.

Note added in proof. Dr. A. B. Lidiard (private communication) has recently informed us that he has made similar calculations independently and that the use of a smaller interval than we have worked with reveals a relatively small anomaly in curve II of the figure around $\hbar T/\epsilon_0 \sim 0.8$, which, however, increases with increasing ϵ_j/ϵ_0 . As he points out, this is almost certainly due to the approximate distribution function used in this work and therefore has no physical significance. In view of this, we are giving attention to an improved distribution function for calculation of the susceptibility more accurately in this region. The main conclusions of our paper remain quite unchanged. We wish to thank Dr. Lidiard for informing us of the results of his work.

ACKNOWLEDGMENT

We would like to acknowledge the very helpful remarks of a referee, who also drew our attention to Stoner's treatment of exchange.

REFERENCES

- BLOCH, F., 1929, *Z. Phys.*, **53**, 216.
 KOPPE, H., 1947, *Z. Naturforsch.*, **2a**, 429.
 LIDIARD, A. B., 1951, *Proc. Phys. Soc. A*, **64**, 814.
 MOTT, N. F., 1936, *Proc. Camb. Phil. Soc.*, **32**, 108.
 PAULI, W., 1927, *Z. Phys.*, **41**, 81.
 SAMPSON, J. B., and SEITZ, F., 1940, *Phys. Rev.*, **58**, 633.
 STONER, E. C., 1935, *Proc. Roy. Soc. A*, **152**, 672; 1936, *Ibid.*, **154**, 656; 1948, *Rep. Progr. Phys.*, **11**, 43 (London: Physical Society).
 WILSON, A. H., 1936, *The Theory of Metals* (Cambridge: University Press).
 WOLHFARTH, E. P., 1950, *Phil. Mag.*, **41**, 534.

Absorption Bands of SbSe and SbTe in the Quartz Ultra-Violet Region 3650 to 2200 Å

By C. B. SHARMA*

Department of Physics, Imperial College, London

MS. received 16th April 1953

Abstract. Several new band systems have been observed in the absorption spectra of SbSe and SbTe molecules in the vapour state at high temperatures (1000° to 1300°C). All the systems lie in the ultra-violet region. The systems have been analysed and the following constants obtained:

Molecule system	Å	ν_e	ω_e''	$\omega_e''x_e''$	ω_e'	$\omega_e'x_e'$
SbSe I	3685–3289	28965	326.1	1.04	221.8	1.00
SbSe II	2870–2620	36041	326.1	1.04	418.9	0.48
SbSe III	2456–2360	—	326.1	1.04	—	—
SbSe IV	2335–2222	43756	326.1	1.04	365.74	0.76
SbTe I	2383–2260	43553	284.4	0.20	314.5	0.48

§ 1. INTRODUCTION

THE oxides, sulphides, selenides and tellurides of antimony and bismuth form a group of substances interesting for spectroscopic study. Some similar molecules—SnO, SnS, SnSe, SnTe, PbSe and PbTe—have been studied in detail by Mahanti (1931), Connelly (1933), Jevons (1938), Barrow and Vago (1943), D. Sharma (1944), and others. The author has studied the absorption spectra of SbSe and SbTe molecules in the vapour state at high temperatures. No previous data are available on these molecules. Several new band systems have been observed and analysed.

In some of these measurements the absorption bands of the diatomic molecule Sb₂ also appeared prominently. These, however, are easily identified since they are well known from the detailed studies made by Nakamura and Shidei (1935), Almy and Sparks (1933). Fortunately they do not interfere with the present measurements. Se₂ bands were observed when selenium was in excess, but when equal amounts of selenium and antimony were taken selenium bands were not observed. In the case of SbTe banded absorption of Te₂ was not observed.

§ 2. EXPERIMENTAL

The experimental arrangement was essentially the same as used by D. Sharma (1944) in the study of some similar diatomic molecules.

A silica tube containing a mixture of pure antimony and selenium or tellurium was placed inside the graphite tube of a vacuum furnace which could give temperatures up to 2000°C. Nitrogen at a pressure of 20 cm Hg was introduced inside the furnace to prevent rapid diffusion of the vapour from the silica tube.

* Now at University of Lucknow, India.

The source of continuum was a water-cooled hydrogen discharge tube. Photographs were taken on a medium quartz spectrograph using copper arc for comparison.

The band systems were well developed between 1000° and 1300°c. No rotational structure was resolved.

§ 3. RESULTS

SbSe Molecule

Four new band systems have been observed and the band-heads measured.

System I (table 1).

The system lies between 3685 and 3289 Å and is degraded to the red. The wave numbers fit well with the formula

$$\nu(\text{cm}^{-1}) = 28965 + (221.8u' - 1.0u'^2) - (326.1u'' - 1.04u''^2)$$

where $u = v + \frac{1}{2}$.

Table 1

$\lambda(\text{\AA})$	Int.	v'	v''	$\lambda(\text{\AA})$	Int.	v'	v''
3289.8	2	10	2	3483.5	8	2	2
3304.0	2	11	3	3496.7	8	0	1
3313.0	2	9	2	3509.3	8	1	2
3325.6	4	10	3	3522.0	6	2	3
3335.4	2	8	2	3537.2	8	0	2
3347.1	6	9	3	3549.3	10	1	3
3358.3	2	7	2	3561.2	6	2	4
3370.0	6	5	1	3577.7	6	0	3
3382.6	2	6	2	3588.3	10	1	4
3394.2	6	4	1	3602.9	6	2	5
3406.3	8	2	0	3616.6	6	0	4
3419.1	6	3	1	3630.0	10	1	5
3431.6	10	1	0	3644.3	10	2	6
3444.3	4	2	1	3659.3	9	0	5
3457.6	10	0	0	3672.3	9	1	6
3470.1	8	1	1	3685.6	9	2	7

System II (table 2).

This system lies in the region 2827 to 2620 Å and is degraded to the violet. The band-heads correspond to the formula

$$\nu(\text{cm}^{-1}) = 36041 + (418.0u' - 0.48u'^2) - (326.1u'' - 1.04u''^2)$$

Table 2

$\lambda(\text{\AA})$	Int.	v'	v''	$\lambda(\text{\AA})$	Int.	v'	v''
2872.5	3	0	4	2732.0	6	2	1
2846.1	4	0	3	2728.0	3	6	6
2839.0	0	1	4	2724.5	1	3	2
2821.0	3	0	2	2718.0	1	4	3
2813.5	1	1	3	2712.0	3	5	4
2795.6	3	0	1	2708.2	5	2	0
2788.0	2	1	2	2704.0	4	6	5
2780.5	0	2	3	2701.0	2	3	1
2770.3	10	0	0	2694.0	1	3	2
2766.4	1	4	5	2687.5	1	5	3
2763.0	4	1	1	2681.5	3	6	4
2755.5	2	2	2	2678.0	1	3	0
2742.5	3	4	4	2648.0	1	4	0
2739.0	7	1	0	2641.0	1	5	1
2735.0	2	5	5	2620.0	0	5	0

System III (table 3).

This system lies in the region 2450 to 2351 Å and is degraded to the violet.

Table 3

$\lambda(\text{\AA})$	Int.	$\lambda(\text{\AA})$	Int.	$\lambda(\text{\AA})$	Int.
2455.8	5	2396.0	10	2363.6	1
2436.4	8	2377.5	3	2361.3	4
2417.4	9	2374.6	4	2351.5	2

System IV (table 4).

System IV lies in the region 2335 to 2222 Å and is degraded to the violet. The band-heads correspond to the formula

$$\nu(\text{cm}^{-1}) = 43\,756 + (365.74u' - 0.76u'^2) - (326.1u'' - 1.04u''^2)$$

Table 4

$\lambda(\text{\AA})$	Int.	v'	v''	$\lambda(\text{\AA})$	Int.	v'	v''
2335.4	2	0	3	2261.0	6	3	2
2333.0	2	1	4	2258.9	3	4	3
2317.9	5	0	2	2256.6	3	5	4
2315.3	5	1	3	2254.5	1	6	5
2313.0	4	2	4	2246.4	8	2	0
2300.8	7	0	1	2244.5	3	3	1
2298.5	4	1	2	2242.6	3	4	2
2296.0	3	2	3	2240.4	4	5	3
2283.7	8	0	0	2238.5	3	6	4
2281.5	7	1	1	2228.5	2	3	0
2279.3	7	2	2	2226.5	2	4	1
2277.0	6	3	3	2224.5	4	5	2
2264.8	10	1	0	2222.6	6	6	3
2262.8	6	2	1				

SbTe Molecule

Only one band system was observed lying in the region 2384 to 2260 Å; it is degraded to the violet (table 5).

The band-heads correspond to the formula

$$\nu(\text{cm}^{-1}) = 43\,553 + (314.5u' - 0.48u'^2) - (284.4u'' - 0.20u''^2)$$

Table 5

$\lambda(\text{\AA})$	Int.	v'	v''	$\lambda(\text{\AA})$	Int.	v'	v''
2383.8	6	2	8	2318.4	5	4	6
2382.1	6	3	9	2309.6	10	0	1
2368.2	7	2	7	2307.9	10	1	2
2366.4	4	3	8	2306.4	8	2	3
2364.6	3	4	9	2304.7	8	3	4
2354.1	7	1	5	2294.6	8	0	0
2352.4	3	2	6	2293.0	8	1	1
2350.7	3	3	7	2291.5	8	2	2
2340.3	6	0	3	2290.0	8	3	3
2338.5	3	1	4	2278.2	8	1	0
2336.9	5	2	5	2276.8	8	2	1
2335.3	2	3	6	2275.2	7	3	2
2324.8	10	0	2	2273.8	6	4	3
2323.2	3	1	3	2272.4	5	5	4
2321.5	3	2	4	2260.5	7	3	1
2319.9	5	3	5				

§ 4. DISCUSSION

The conditions of formation of these molecules appear to be very critical. An attempt was made to obtain the band systems of SbSe and SbS in emission by placing a mixture of Sb and Se or SbS inside a constricted discharge tube in which hydrogen or nitrogen served as the carrier of discharge. A dense vapour was produced, the emission spectrum of which comprised strong antimony lines and CS bands as impurity. It is thought that either the molecule was not formed at all or it readily dissociated because of the electron impact. This is supported by the observation that, in the case of SbS beyond a certain temperature, bands of SO appear strongly, indicating that the molecule was dissociated.

ACKNOWLEDGMENTS

I take pleasure in expressing my thanks to Sir K. S. Krishnan for his guidance and encouragement in the work at the University of Allahabad and to Dr. D. Sharma for his helpful suggestions. Thanks are also due to Dr. R. W. B. Pearse for advice and interest during the course of my stay at the Imperial College of Science and Technology, London, where the work in emission was done.

REFERENCES

- ALMY, G. M., and SPARKS, F. M., 1933, *Phys. Rev.*, **44**, 365.
BARROW, R. F., and VAGO, E. E., 1943, *Proc. Phys. Soc.*, **55**, 326.
CONNELLY, C. F., 1933, *Proc. Phys. Soc.*, **45**, 780.
JEVONS, W., 1938, *Proc. Phys. Soc.*, **50**, 910.
MAHANTI, P. C., 1931, *Z. Phys.*, **68**, 144.
NAKAMURA, G., and SHIDEI, T., 1935, *Jap. J. Phys.*, **10**, 11.
SHARMA, D., 1944, *Proc. Nat. Acad. Sci., India*, **14**, 133.

Properties of the Hydrogen Molecular Ion II: Photo-Ionization from the $1s\sigma_g$, $2s\sigma_g$ and $3s\sigma_g$ States*

BY D. R. BATES, U. ÖPIK AND G. POOTS

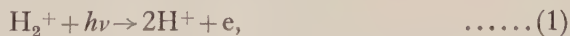
Department of Applied Mathematics, Queen's University of Belfast

MS. received 20th July 1953

Abstract. The cross sections associated with transitions from the bound $1s\sigma_g$, $2s\sigma_g$ and $3s\sigma_g$ states of H_2^+ to the free $p\sigma_u$, $p\pi_u$, $f\sigma_u$ and $f\pi_u$ states are calculated using exact two-centre electronic wave functions. They are tabulated for various values of the energy of the ejected electron and of the distance between the protons (which are treated as fixed in position). In the case of the $1s\sigma_g$ state (which, alone of the three, is stable) the investigation is carried further: the vibration and rotation of the molecule are taken into account and curves showing true photo-ionization cross section plotted against wave number are obtained.

§ 1. INTRODUCTION

INFORMATION on molecular photo-ionization cross sections is required in many fields. The need for such information arises, for example, in investigations on the formation of the ionized layers of the Earth's upper atmosphere and in theoretical studies of comets and of inter-stellar matter. Unfortunately it is not easy to obtain quantitative data. Direct measurements are difficult in that the spectral region involved is usually an awkward one; moreover, complications may be introduced by other continua and by superimposed band systems. The value of quantal methods is also as yet rather limited since, though many calculations have been carried out on the photo-ionization of atoms, similar work for molecules has been prevented by the lack of satisfactory wave functions. For the heavier systems the problem of obtaining such wave functions is formidable. However, in the case of the hydrogen molecular ion the relevant Schrödinger equation can be solved accurately, and the results should illustrate some of the general trends. The present paper is devoted to the determination of the cross section associated with



the bound electron being in either the $1s\sigma_g$, $2s\sigma_g$ or $3s\sigma_g$ state.†

§ 2. BASIC FORMULAE

Letting \mathbf{r} be the position vector of the electron relative to the centre of mass, and \mathbf{R} be that of one proton relative to the other, denote the normalized wave functions of the degenerate initial and final states of H_2^+ by $X(A|\mathbf{r}, \mathbf{R})$ and

* Part I of this paper, by D. R. Bates and G. Poots, was published in the *Proceedings*, A, 1953, **66**, 784.

† The separated-atoms designation for $1s\sigma_g$ is $\sigma(1s)$, that for $2s\sigma_g$ is $\sigma(2s, 2p_z)$ and that for $3s\sigma_g$ is $\sigma(3s, 3p_z, 3d_z)$, where as usual the symbols within the brackets represent the atomic orbitals (all of which are associated with both nuclei).

$X(B(\epsilon_e, \epsilon_p)|\mathbf{r}, \mathbf{R})$ respectively, where A and B represent groups of quantum numbers, ϵ_e is the energy of the ejected electron and ϵ_p is the energy of the separated protons. From standard quantum theory (cf. Dirac 1947) the cross section for the photo-ionization transition in which ϵ_e is definite and ϵ_p lies within an interval of width $d\epsilon$, or in which ϵ_p is definite and ϵ_e lies within this interval, is $Q_A(\epsilon_e, \epsilon_p) d\epsilon$, where

$$Q_A(\epsilon_e, \epsilon_p) = \frac{8\pi^3 e^2 \nu}{3c \omega_A} \sum_A \sum_B \left| \iint X^*(A|\mathbf{r}, \mathbf{R}) \mathbf{r} X(B(\epsilon_e, \epsilon_p)|\mathbf{r}, \mathbf{R}) d\mathbf{r} d\mathbf{R} \right|^2, \quad \dots\dots (2)$$

ω_A being the total statistical weight of the initial states, ν the frequency of the radiation absorbed, and e and c having their customary significance. In practice it is more useful to have the cross section for ν definite. This is given by

$$Q_A(\nu) = \int Q_A(\epsilon_e, \epsilon_p) d\epsilon, \quad \dots\dots (3)$$

the integration being carried over all combinations of positive values of ϵ_e and ϵ_p consistent with the conservation of energy relation.

On writing the complete wave functions in the usual product form (cf. Herzberg 1950) the integration over the angular coordinates of the internuclear axis, and the summations over the magnetic quantum numbers M_a and M_b associated with the rotational quantum numbers J_a and J_b , can be carried out analytically (cf. Kronig 1930). Formula (2) becomes

$$Q_{n, n_a, J_a}(\epsilon_e, \epsilon_p) = \frac{8\pi^3 e^2 \nu}{3c \omega_A} \sum_a \sum_{b, J_b} \left\{ \mathcal{S}(J_a, J_b) \left| \int P^*(a, v_a, J_a | R) \mathfrak{M}(a, b(\epsilon_e) | R) \right. \right. \\ \left. \left. \times P(B(\epsilon_p, J_b) | R) dR \right|^2 \right\} \quad \dots\dots (4)$$

$$\mathfrak{M}(a, b(\epsilon_e) | R) = \int \Psi^*(a, R | \mathbf{r}) \mathbf{r} \Psi(b(\epsilon_e), R | \mathbf{r}) d\mathbf{r}, \quad \dots\dots (5)$$

where the P 's are the vibrational wave functions, v_a is a vibrational quantum number, the Ψ 's are the electronic wave functions, a and b are groups of electronic quantum numbers, and $\mathcal{S}(J_a, J_b)$ is a factor which depends only on J_a, J_b and the type of the transition. Rademacher and Reiche (1927) and others have shown that for σ - σ transitions

$$\begin{aligned} \mathcal{S}(J_a, J_b) &= J_a + 1, & (J_b - J_a = +1), \\ &= J_a, & (J_b - J_a = -1), \\ &= 0, & (J_b - J_a \neq \pm 1); \end{aligned}$$

and that for σ - π transitions

$$\begin{aligned} \mathcal{S}(J_a, J_b) &= \frac{1}{2}(J_a + 2), & (J_b - J_a = +1), \\ &= \frac{1}{2}(2J_a + 1), & (J_b - J_a = 0), \\ &= \frac{1}{2}(J_a - 1), & (J_b - J_a = -1), \\ &= 0, & (J_b - J_a \neq 0, \pm 1). \end{aligned}$$

A useful simplification can be effected by representing the vibrational wave functions of the continua by the δ -function of Winans and Stueckelberg (1928) which in spite of its apparent crudeness is, in fact, a remarkably successful approximation (cf. Coolidge, James and Present 1936). Thus if the difference

between J_a and J_b is ignored,* and the δ -function corresponding to the effective potential energy (including the nuclear centrifugal term) is adopted, then

$$Q_{a,v_a,J_a}(\epsilon_e, \epsilon_p) = \frac{8\pi^3 e^2 \nu}{3c\omega_a} \left| P(a, v_a, J_a | R) \right|^2 \mathcal{M}_a(\epsilon_e, R)^2 \times \left| \frac{dR}{d\epsilon_p} \right|, \quad \dots\dots(6)$$

where ω_a denotes $\omega_a/(2J_a+1)$, the electronic contribution to the statistical weight;

$$\mathcal{M}_a(\epsilon_e, R)^2 = \sum_a \sum_b \left| \mathfrak{M}(a, b(\epsilon_e) | R) \right|^2, \quad \dots\dots(7)$$

the summations being over the degenerate electronic states; and

$$\epsilon_p = \frac{e^2}{R} + \frac{h^2 J_a(J_a+1)}{8\pi^2 M R^2}, \quad \dots\dots(8)$$

M being the reduced mass. Substitution of (6) in (3) with change of variable from R to ϵ_p yields

$$Q_{a,v_a,J_a}(\nu) = \frac{8\pi^3 e^2 \nu}{3c\omega_a} \int \left| P(a, v_a, J_a | \epsilon_p) \right|^2 \mathcal{M}_a(\epsilon_e, \epsilon_p)^2 \times \left| \frac{dR}{d\epsilon} \right| d\epsilon \quad \dots\dots(9)$$

$$\text{with} \quad \epsilon_e + \epsilon_p = h\nu + E_{a,v_a,J_a} \quad \dots\dots(10)$$

where E_{a,v_a,J_a} is the sum of the initial electronic, vibrational and rotational energies.

Instead of $Q_{a,v_a,J_a}(\epsilon_e, \epsilon_p)$ it is often instructive to consider

$$q(a, b(\epsilon_e) | R) = \frac{8\pi^3 e^2 \nu}{3c} \left| \mathfrak{M}(a, b(\epsilon_e) | R) \right|^2, \quad \dots\dots(11)$$

which is the fictitious cross section corresponding to the electron being ejected with definite energy ϵ_e , the protons being supposed held at a fixed distance R apart.† We will therefore treat this cross section in some detail.

§ 3. ELECTRONIC WAVE FUNCTIONS

If \mathbf{r} is expressed in terms of λ and μ , the standard elliptical coordinates, and ϕ , the azimuthal angle, then (cf. Mott and Sneddon 1948) the Schrödinger equation governing the wave function describing the motion of the electron in the field of the two protons may be separated. Using Hartree units (I_H , the ionization potential of atomic hydrogen, for energy; a_0 , the radius of the Bohr orbit, for length) and omitting the quantum numbers (where this does not cause confusion) we have

$$\Psi(R | \lambda, \mu, \phi) = \Phi(\phi) M(R | \mu) \Lambda(R | \lambda) \quad \dots\dots(12)$$

$$\text{where} \quad \Phi = \frac{\cos}{\sin} (m\phi) \{m=0 (\sigma \text{ states}), 1 (\pi \text{ states}), \text{etc.} \} \quad \dots\dots(13)$$

and M and Λ satisfy

$$\frac{d}{d\mu} \left\{ (1-\mu^2) \frac{dM}{d\mu} \right\} + \left\{ -A - \frac{1}{4} R^2 \epsilon_e \mu^2 - \frac{m^2}{1-\mu^2} \right\} M = 0 \quad \dots\dots(14)$$

$$\frac{d}{d\lambda} \left\{ (\lambda^2-1) \frac{d\Lambda}{d\lambda} \right\} + \left\{ A + 2R\lambda + \frac{1}{4} R^2 \epsilon_e \lambda^2 - \frac{m^2}{\lambda^2-1} \right\} \Lambda = 0 \quad \dots\dots(15)$$

in which A is a separation constant and the symbol ϵ_e is now used for negative, as well as positive, electronic energies.

* As can be seen from the expressions for $\mathcal{S}(J_a, J_b)$ the best mean value to take for J_b is not precisely J_a but is instead rather greater. However, the effect on the final result is small even when J_a is zero; and in view of the nature of the δ -function approximation the refinement does not seem to be justified.

† In (11) the frequency is of course such that $h\nu$ is the change in the electronic energy.

The solutions of (14) and (15) for the lower bound states have been obtained by Bates, Ledsham and Stewart (1953) following the work of Jaffe (1934) and others. In the case of the $ns\sigma_g$ states, with which we are concerned,

$$M = \sum_{s=0}^{\infty} a_{2s} P_{2s}(\mu), \quad \dots\dots (16)$$

the P 's being the Legendre polynomials. The coefficients a_{2s} , which fall off rapidly when s is greater than n , the principal quantum number, have been tabulated as functions of R for the $1s\sigma_g$, $2s\sigma_g$ and $3s\sigma_g$ states. An expression for Λ is also known and the parameters occurring in it have been tabulated similarly. As all integrations with respect to λ had to be carried out by numerical methods the explicit form of the expression need not be displayed.

The bound wave function $\Phi M \Lambda$ was of course normalized so that

$$\left(\frac{R}{2}\right)^3 \int_1^{\infty} \int_{-1}^1 \int_0^{2\pi} \Phi^2 M^2 \Lambda^2 (\lambda^2 - \mu^2) d\lambda d\mu d\phi = 1. \quad \dots\dots (17)$$

This could readily be effected since the triple integral entailed reduces to

$$2\pi \left(\frac{R}{2}\right)^3 \left[\left\{ \sum_{s=0}^{\infty} \frac{2}{4s+1} a_{2s}^2 \right\} \left\{ \int_1^{\infty} \Lambda^2 \lambda^2 d\lambda \right\} - \left\{ \sum_{s=0}^{\infty} \frac{2}{4s+3} \left(\frac{2s+1}{4s+1} a_{2s} + \frac{2s+2}{4s+5} a_{2s+2} \right)^2 \right\} \left\{ \int_1^{\infty} \Lambda^2 d\lambda \right\} \right]. \quad \dots\dots (18)$$

The treatment of the continuum is facilitated by the comprehensive study of (14) which has been carried out by Stratton, Morse, Chu and Hutner (1941). Because of the dipole selections rules only odd σ and odd π states contribute to the photo-ionization cross section. For the former

$$M = \sum_{t=0}^{\infty} b_{2t+1} P_{2t+1}(\mu) \quad \dots\dots (19)$$

and for the latter

$$M = \sum_{t=0}^{\infty} b_{2t} P_{2t+1}^1(\mu). \quad \dots\dots (20)$$

Stratton *et al.* have tabulated the coefficients involved and separation constants A taking the independent variable as p , where

$$p^2 = \frac{1}{4} R^2 \epsilon_e. \quad \dots\dots (21)$$

Their results thus give M for any chosen pair of values of R , the internuclear separation, and ϵ_e , the electronic energy. Moreover, knowing A it is possible to compute Λ from (15) by numerical methods. For λ close to unity it is convenient to write

$$\Lambda = (\lambda^2 - 1)^{m/2} F(\xi) \quad \text{with} \quad \xi = \lambda - 1 \quad \dots\dots (22)$$

and obtain F by integrating the transformed equation

$$\xi(\xi+2)F'' + 2(m+1)(\xi+1)F' + \{p^2\xi^2 + 2(p^2+R)\xi + p^2 + 2R + A + m(m+1)\}F = 0, \quad \dots\dots (23)$$

using a power series expansion near the origin. Throughout the main range of λ it is, however, simpler to make the substitution

$$\Lambda = (\lambda^2 - 1)^{-1/2} G(\lambda), \quad \dots\dots (24)$$

and solve

$$G'' + \left\{ \frac{p^2\lambda^2 + 2R\lambda + A}{\lambda^2 - 1} + \frac{1 - m^2}{(\lambda^2 - 1)^2} \right\} G = 0 \quad \dots\dots (25)$$

by the method recommended by Fox and Goodwin (1949), which was found to be extremely efficient. Such calculations were carried out, using various values of R and ϵ_e , for the free $p\sigma_u$, $p\pi_u$, $f\sigma_u$ and $f\pi_u$ states.

The normalization condition for the continuum is that

$$\lim_{\tau_0 \rightarrow \infty} \int_{\tau_0}^{\infty} d\epsilon_e' \int_{\tau_0}^{\infty} \Psi^*(\epsilon_e') \Psi(\epsilon_e) d\tau = 1 \quad \dots\dots(26)$$

(Dirac 1947). Applying Green's theorem to transform from integration over the volume τ_0 to over its bounding surface σ_0 we obtain

$$\int_{\tau_0}^{\infty} \Psi^*(\epsilon_e') \Psi(\epsilon_e) d\tau = \frac{1}{\epsilon_e' - \epsilon_e} \int_{\sigma_0} \mathbf{n} \cdot \{ \Psi^*(\epsilon_e') \nabla \Psi(\epsilon_e) - \Psi(\epsilon_e) \nabla \Psi^*(\epsilon_e') \} d\sigma \quad \dots\dots(27)$$

\mathbf{n} being the outward drawn unit normal. If we choose σ_0 to be given by λ constant and equal to λ_0 then on it

$$\mathbf{n} \cdot \nabla = \left(\frac{2}{R} \right) \left\{ \frac{\lambda_0^2 - 1}{\lambda_0^2 - \mu^2} \right\}^{1/2} \left(\frac{\partial}{\partial \lambda} \right)_{\lambda=\lambda_0} \quad \dots\dots(28)$$

Substitution of (12), (24) and (28) in (27) yields

$$\int_{\tau_0}^{\infty} \Psi^*(\epsilon_e') \Psi(\epsilon_e) d\tau = \frac{R}{2(\epsilon_e' - \epsilon_e)} \int_{-1}^{+1} \int_0^{2\pi} \Phi^* \Phi M^*(\epsilon_e') M(\epsilon_e) d\mu d\phi \times \left\{ G^*(\epsilon_e') \frac{dG(\epsilon_e)}{d\lambda} - G(\epsilon_e) \frac{dG^*(\epsilon_e')}{d\lambda} \right\}_{\lambda=\lambda_0} d\mu d\phi. \quad \dots\dots(29)$$

Letting λ_0 tend to infinity and noting from (25) that the asymptotic form of G is $C \sin(p\lambda + \delta_p)$, where δ_p includes the characteristic coulomb logarithmic phase, we hence see that the integration over ϵ_e' is essentially the same as that which arises in the normalization of wave functions expressed in spherical polar coordinates. This integration has been treated by Hargreaves (1929). From his analysis and (29) we find that condition (26) requires that

$$C = 2(\pi p R Y)^{-1/2}, \quad \dots\dots(30)$$

where

$$Y = \int_0^{2\pi} \Phi^* \Phi d\phi \int_{-1}^{+1} M^*(\epsilon_e) M(\epsilon_e) d\mu \quad \dots\dots(31)$$

$$= \begin{cases} 4\pi \sum_{t=0}^{\infty} \frac{b_{2t+1}^2}{4t+3} & (\sigma_u \text{ states}) \\ 4\pi \sum_{t=0}^{\infty} \left\{ \frac{(t+1)(2t+1)}{4t+3} \right\} b_{2t}^2 & (\pi_u \text{ states}) \end{cases}$$

In order to apply (30) it is of course first necessary to determine D , the asymptotic amplitude of the unnormalized G functions. This can readily be done by the well-known method of Strömberg (1941) based on the Jeffreys approximation (cf. Bates and Seaton 1949). We obtain

$$D = (1/2p^{1/2}) \{ [a(\lambda_1) + a(\lambda_2)]^2 \sec^2 \alpha(\lambda_1, \lambda_2) + [a(\lambda_1) - a(\lambda_2)]^2 \operatorname{cosec}^2 \alpha(\lambda_1, \lambda_2) \}^{1/2} \quad \dots\dots(32)$$

where

$$a(\lambda) = U(\lambda)^{1/2} G(\lambda), \quad \alpha(\lambda_1, \lambda_2) = \frac{1}{2} \int_{\lambda_1}^{\lambda_2} U(\lambda) d\lambda,$$

$$U(\lambda)^2 = v(\lambda) + w(\lambda),$$

$$v(\lambda) = (p^2 \lambda^2 + 2R\lambda + A)(\lambda^2 - 1)^{-1} + (1 - m^2)(\lambda^2 - 1)^{-2},$$

$$w(\lambda) = \frac{5}{16\tau^2} \left(\frac{dv}{d\lambda} \right)^2 - \frac{1}{4\tau} \frac{d^2 v}{d\lambda^2},$$

and λ_1 and λ_2 are two arbitrary values of λ sufficiently large to make w small compared with v in the range concerned.

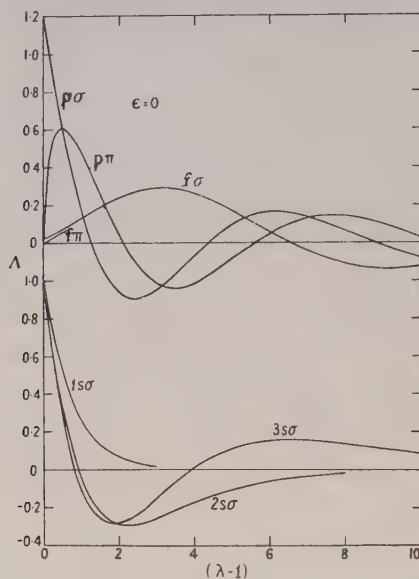


Fig. 1. The Λ parts of the free ($\epsilon_0=0$) and bound wave functions when the internuclear separation is $2a_0$. In the free case the multiplying factor is such that the corresponding G functions have an asymptotic amplitude of $p^{-1/2}$ (cf. eqn. (32)); and in the bound case it is such as to make the Λ 's unity at the origin.

§ 4. TRANSITION MATRIX ELEMENTS

On resolving \mathbf{r} into components along and perpendicular to the internuclear axis we see that for $\sigma_g-\sigma_u$ transitions

$$\mathcal{M}(a, b(\epsilon_c) | R) = \left(\frac{R}{2}\right)^4 \int_1^\infty \int_{-1}^{+1} \int_0^{2\pi} \Psi^*(a, R | \lambda, \mu, \phi) \times \Psi(b(\epsilon_c), R | \lambda, \mu, \phi) \lambda \mu (\lambda^2 - \mu^2) d\lambda d\mu d\phi, \quad \dots (33)$$

and that for $\sigma_g-\pi_u$ transitions

$$\mathcal{M}(a, b(\epsilon_c) | R) = 2^{1/2} \left(\frac{R}{2}\right)^4 \int_1^\infty \int_{-1}^{+1} \int_0^{2\pi} \Psi^*(a, R | \lambda, \mu, \phi) \Psi(b(\epsilon_c), R | \lambda, \mu, \phi) \times (\lambda^2 - 1)^{1/2} (1 - \mu^2)^{1/2} (\lambda^2 - \mu^2) \frac{\cos \phi}{\sin \phi} d\lambda d\mu d\phi, \quad \dots (34)$$

the degeneracy factor for these latter being included. After substituting from (12), (16), (19) and (20) we can carry out the integration over ϕ and μ analytically to obtain

$$\mathcal{M}_{(\sigma_g-\sigma_u)}(a, b(\epsilon_c) | R) = 2\pi \left(\frac{R}{2}\right)^4 \left[\mathcal{A}_1 \int_1^\infty \Lambda^*(a, R | \lambda) \Lambda(b(\epsilon_c), R | \lambda) \lambda^3 d\lambda - \mathcal{A}_2 \int_1^\infty \Lambda^*(a, R | \lambda) \Lambda(b(\epsilon_c), R | \lambda) \lambda d\lambda \right], \quad \dots (35)$$

and $\mathcal{M}_{(\sigma_g-\pi_u)}(a, b(\epsilon_c) | R) = 2^{1/2} \pi \left(\frac{R}{2}\right)^4 \left[\mathcal{A}_3 \int_1^\infty \Lambda^*(a, R | \lambda) \Lambda(b(\epsilon_c), R | \lambda) \lambda^2 (\lambda^2 - 1)^{1/2} d\lambda - \mathcal{A}_4 \int_1^\infty \Lambda^*(a, R | \lambda) \Lambda(b(\epsilon_c), R | \lambda) (\lambda^2 - 1)^{1/2} d\lambda \right], \quad \dots (36)$

with

$$\begin{aligned}
 \mathcal{A}_1 &= 2 \sum_{t=0}^{\infty} \frac{a_{2t}}{4t+1} \left[\left(\frac{2t+1}{4t+3} \right) b_{2t+1} + \left(\frac{2t}{4t-1} \right) b_{2t-1} \right], \\
 \mathcal{A}_2 &= 2 \sum_{t=0}^{\infty} \frac{a_{2t}}{4t+1} \left[\left(\frac{(2t+1)(2t+2)(2t+3)}{(4t+3)(4t+5)(4t+7)} \right) b_{2t+3} \right. \\
 &\quad + \frac{2t+1}{4t+3} \left(\frac{(2t+2)^2}{(4t+3)(4t+5)} + \frac{(2t+1)^2}{(4t+1)(4t+3)} + \frac{4t^2}{(4t-1)(4t+1)} \right) b_{2t+1} \\
 &\quad + \frac{2t}{4t-1} \left(\frac{(2t+1)^2}{(4t+1)(4t+3)} + \frac{4t^2}{(4t-1)(4t+1)} + \frac{(2t-1)^2}{(4t-3)(4t-1)} \right) b_{2t-1} \\
 &\quad \left. + \left(\frac{(2t-2)(2t-1)(2t)}{(4t-5)(4t-3)(4t-1)} \right) b_{2t-3} \right], \\
 \mathcal{A}_3 &= 2 \sum_{t=0}^{\infty} \frac{a_{2t}}{4t+1} \left[\left(\frac{(2t+1)(2t+2)}{4t+3} \right) b_{2t} - \left(\frac{(2t-1)(2t)}{4t-1} \right) b_{2t-2} \right], \\
 \mathcal{A}_4 &= 2 \sum_{t=0}^{\infty} \frac{a_{2t}}{4t+1} \left[\left(\frac{(2t+1)(2t+2)(2t+3)(2t+4)}{(4t+3)(4t+5)(4t+7)} \right) b_{2t+2} \right. \\
 &\quad + \frac{(2t+1)(2t+2)}{(4t+3)^2} \left(\frac{(2t+1)(2t+3)}{4t+5} + \frac{2t}{4t-1} \right) b_{2t} + \frac{(2t-1)(2t)}{(4t-1)^2} \\
 &\quad \times \left(\frac{2t+1}{4t+3} - \frac{(2t-2)(2t)}{4t-3} \right) b_{2t-2} - \left(\frac{(2t-3)(2t-2)(2t-1)(2t)}{(4t-5)(4t-3)(4t-1)} \right) b_{2t-4} \left. \right].
 \end{aligned}$$

§ 5. CROSS SECTIONS FOR FIXED NUCLEI

Having determined $\mathcal{M}(a, b(\epsilon_e) | R)$ from (35) and (36), the cross sections $q(a, b(\epsilon_e) | R)$ defined in (11) can be obtained at once. It is apparent that the states of the continua whose azimuthal quantum number is 5 or higher are utterly unimportant in the present connection. The transitions treated were therefore limited to

$$1s\sigma_g, 2s\sigma_g, 3s\sigma_g \rightarrow \epsilon_e p\sigma_u, p\pi_u, f\sigma_u, f\pi_u.$$

Table 1 gives the calculated cross sections for various values of ϵ_e , the energy of the ejected electron, when R , the internuclear separation, is $2a_0$; and table 2 gives them for various values of R when ϵ_e is zero. The electronic energies of the bound states are displayed in table 3.

As will be observed, the dependence of the different q 's on ϵ_e and on R are quite dissimilar. In commenting on the reasons for this we will, for the sake of definiteness, confine ourselves to transitions from the $1s\sigma_g$ state.

(i) $b \equiv p\sigma_u$. There is essentially complete cancellation between the positive and negative portions of the integrands in the matrix element when $\epsilon_e = 0$ and $R = 2a_0$ so that q passes through a zero minimum; thus the variations exhibited in tables 1 and 2, which might at first seem peculiar, are in fact simple in origin. The situation is closely analogous to that occurring in the photo-ionization of potassium (Bates 1947).

(ii) $b \equiv p\pi_u$. When ϵ_e is small the value of λ at which the Λ part of the free wave function first changes sign is well beyond the region where the corresponding part of the bound wave function is near its maximum (cf. fig. 1); moreover even when R is as great as $4a_0$ the M parts of the free and bound wave functions retain much of the character of atomic p and s states respectively. Consequently cancellation is important in neither the radial nor the angular integrations. Since, in addition, the wave functions overlap to a considerable extent, the cross sections

Table 1. Cross Section $q(a, b(\epsilon_e)|R)$ in units of 10^{-20} cm^2 for the Combinations $a \equiv 1s\sigma_g$, $2s\sigma_g$ and $3s\sigma_g$; $b \equiv p\sigma_u$, $p\pi_u$, $f\sigma_u$ and $f\pi_u$, $\epsilon_e = 0.00, 0.04, 0.16, 0.36, 0.64$ and $1.00 I_H$; $R = 2a_0$

(The degeneracy factor of 2 which occurs in transitions to the π states is included)

ϵ_e	$a \equiv 1s\sigma_g$ $b \equiv p\sigma_u$	$p\pi_u$	$f\sigma_u$	$f\pi_u$	Total
0.00	0.00	92	0.52	0.66	93
0.04	0.00	86	0.56	0.72	88
0.16	0.05	73	0.64	0.82	74
0.36	0.17	54	0.77	0.97	56
0.64	0.46	37	0.87	1.12	39
1.00	0.54	25	0.94	1.19	27

ϵ_e	$a \equiv 2s\sigma_g$ $b \equiv p\sigma_u$	$p\pi_u$	$f\sigma_u$	$f\pi_u$	Total
0.00	6.6	244	0.27	0.37	251
0.04	2.2	214	0.22	0.25	216
0.16	0.60	141	0.10	0.14	142
0.36	0.01	79	0.02	0.03	79
0.64		39			39
1.00		19			

ϵ_e	$a \equiv 3s\sigma_g$ $b \equiv p\sigma_u$	$p\pi_u$	$f\sigma_u$	$f\pi_u$	Total
0.00	9.3	439	0.14	0.19	448
0.04	4.6	334	0.11	0.13	338
0.16	1.0	169	0.06	0.09	170
0.36	0.06	69	0.02	0.02	69
0.64		29			29
1.00		12			

Table 2. Cross Section $q(a, b(\epsilon_e)|R)$ in Units of 10^{-20} cm^2 for the Combinations $a \equiv 1s\sigma_g$, $2s\sigma_g$ and $3s\sigma_g$; $b \equiv p\sigma_u$, $p\pi_u$, $f\sigma_u$ and $f\pi_u$; $\epsilon_e = 0$; $R = 0, 1, 2, 3$ and $4a_0$

(The degeneracy factor of 2 which occurs in transitions to the π states is included)

R	$a \equiv 1s\sigma_g$ $b \equiv p\sigma_u$	$p\pi_u$	$f\sigma_u$	$f\pi_u$	Total
0	53	105	0.000	0.000	158
1	26	103	0.015	0.019	129
2	0.0	92	0.52	0.66	93
3	7.9	83	4.7	5.5	101
4	20	75	22	23	141

R	$a \equiv 2s\sigma_g$ $b \equiv p\sigma_u$	$p\pi_u$	$f\sigma_u$	$f\pi_u$	Total
0	123	246	0.000	0.000	369
1	82	265	0.032	0.043	347
2	6.6	244	0.27	0.37	251
3	6.4	218	0.36	0.59	225
4	25	203	0.00	0.10	228

R	$a \equiv 3s\sigma_g$ $b \equiv p\sigma_u$	$p\pi_u$	$f\sigma_u$	$f\pi_u$	Total
0	210	419	0.000	0.000	629
1	158	469	0.008	0.010	627
2	9.3	439	0.14	0.19	448
3	4.1	399	0.45	0.64	404
4	28	373	0.38	0.84	402

are large. As ϵ_e increases, the vital node of the free wave function moves inwards, cancellation grows in importance, and q becomes smaller. The decrease with R is associated with the decrease of the vertical ionization potential (cf. formula (11) and table 3).

Table 3. Electronic Energies in units of I_H (all are of course negative)

R	$1s\sigma_g$	$2s\sigma_g$	$3s\sigma_g$
0	4.00000	1.00000	0.44444
1	2.90356	0.84585	0.39687
2	2.20525	0.72173	0.35536
3	1.82178	0.63777	0.32519
4	1.59216	0.57703	0.30198

(iii) $b \equiv f\sigma_u$ and $f\pi_u$. The Λ parts of the free wave functions are very diffuse (cf. fig. 1), and even when ϵ_e is unity they do not change sign in the region where the Λ part of the bound wave function is appreciable. Mainly because of this, q at first increases with ϵ_e , for the rise in the overlap between the wave functions is not compensated by any significant rise in the cancellation. It may be remarked that a similar effect controls the form of the photo-ionization curve of atomic oxygen (Bates and Seaton 1949). The extremely rapid growth of q with R is entirely different in origin, being due to the increase in the amount of combining Legendre polynomials in the M parts of the wave functions.

The same general considerations apply to the transitions from the $2s\sigma_g$ and $3s\sigma_g$ states. Owing to the greater diffuseness of the wave functions (cf. fig. 1) cancellation effects are more pronounced, arising even with the $f\sigma_u$ and $f\pi_u$ continua; but in spite of this complication it is apparent that the changes in the q 's in going from one bound state to the next show a definite pattern.

Complete cancellation along a line in (ϵ_e, R) space is clearly of common occurrence, and q is of course very small for some distances on either side of such a line. Nevertheless instances in which the total photo-ionization cross section is extremely low are probably quite rare, for transitions can take place into several* states of the continua, and all the zero lines are unlikely to lie in close proximity.

Molecules other than H_2^+ can only be treated by approximate methods. Caution must be exercised in accepting any results obtained since they are rather sensitive to the form of the wave functions even if the extent of the cancellation is not serious. It is perhaps worth recalling here that the errors in the calculated atomic photo-ionization cross sections were often sadly underestimated in the early investigations.

§ 6. FINAL RESULTS

As the $2s\sigma_g$ and $3s\sigma_g$ states are unstable, the determination of the photo-ionization cross sections for ν definite was confined to the case in which the system is initially in the $1s\sigma_g$ state.

Direct computations on $\mathcal{M}_{1s\sigma}(\epsilon_e, R)^2$ (defined in (7)) were only done for the lines $R=0$ (which is of course the He^+ limit), $R=2a_0$ and $\epsilon_e=0$; but in spite of this

* It should be noted that the number of contributing transitions involving *basically different* matrix elements is greater for molecules than it is for atoms. Table 2 illustrates the position. In the true molecular cases ($R>0$) there are four contributing transitions each having a basically different matrix element, whereas in the atomic case ($R=0$) there are only two contributing transitions, and they have what is essentially a *common* matrix element. The hydrogen molecular ion is not, of course, an ideally representative system.

a sufficiently accurate and extensive double-entry table of the function could readily be constructed. Thus the variation with frequency along the lines $R=0$ and $R=2a_0$ is closely the same, so that the corresponding variation along any parallel line in the region of interest can be predicted with confidence, and the known value on the intersecting line $\epsilon_e=0$ gives the absolute scale. It was found convenient to replace the variable R by ϵ_p (cf. (8)) and to tabulate at the points of an equi-spaced (ϵ_e, ϵ_p) lattice. Having converted the vibrational wave functions $P(|R|)$ of Buckingham and Reid (1954) into the form $P(|\epsilon_p|)$ it was then a simple matter to carry out the integrations in (9) for a selection of lines on which the sum of ϵ_e and ϵ_p is constant. The derived cross sections for transitions from the (v, J) vibrational-rotational levels $(0, 0)$, $(0, 4)$ and $(0, 8)$ are shown in fig. 2, in which the independent variable is taken as the wave number. According to the calculations of Buckingham and Reid the thresholds of these three photo-ionizations lie at 1.310×10^5 , 1.305×10^5 and $1.290 \times 10^5 \text{ cm}^{-1}$ respectively. It will be observed that the cross sections remain extremely small until much higher wave

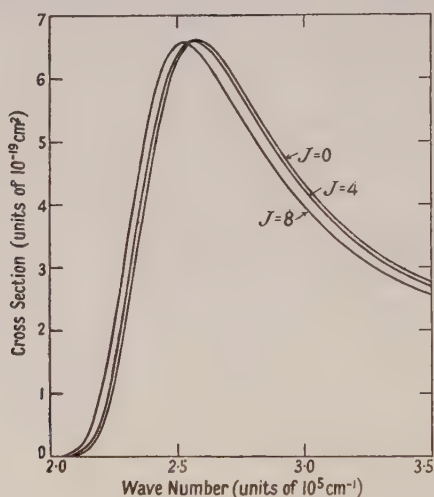


Fig. 2. The calculated photo-ionization cross section curves of $\text{H}_2^+(\text{x}^2\Sigma_g)$ in the (v, J) vibrational-rotational levels $(0, 0)$, $(0, 4)$ and $(0, 8)$.

numbers are reached. This is of course an immediate consequence of the Franck-Condon principle. The three curves are clearly very similar in shape, the main effect of rotational excitation being to cause a general displacement towards lower wave numbers by an amount which is less than the difference between the thresholds.

ACKNOWLEDGMENTS

We wish to thank Dr. R. A. Buckingham and Mr. S. Reid for supplying us with their vibrational wave functions in advance of publication.

REFERENCES

- BATES, D. R., 1947, *Proc. Roy. Soc. A*, **188**, 350.
 BATES, D. R., LEDSHAM, K., and STEWART, A. L., 1953, *Phil. Trans. Roy. Soc. A*, **246**, 215.
 BATES, D. R., and SEATON, M. J., 1949, *Mon. Not. Roy. Astr. Soc.*, **109**, 698.
 BUCKINGHAM, R. A., and REID, S., 1954, *Proc. Roy. Soc. A*, in the press.

- 2 COOLIDGE, A. S., JAMES, H. M., and PRESENT, R. D., 1936, *J. Chem. Phys.*, **4**, 193.
- 1 DIRAC, P. A. M., 1947, *Principles of Quantum Mechanics*, 3rd Edn. (Oxford : Clarendon Press).
- 1 FOX, L., and GOODWIN, E. T., 1949, *Proc. Camb. Phil. Soc.*, **45**, 373.
- 3 HARGREAVES, J., 1929, *Proc. Camb. Phil. Soc.*, **25**, 75.
- 3 HERZBERG, G., 1950, *Spectra of Diatomic Molecules*, 2nd Edn. (New York : van Nostrand).
- 1 JAFFE, G., 1934, *Z. Phys.* **87**, 535.
- 1 KRONIG, R. DE L., 1930, *Band Spectra and Molecular Structure* (Cambridge : University Press).
- 7 MOTT, N. F., and SNEDDON, I. E., 1948, *Wave Mechanics and Its Applications* (Oxford : Clarendon Press).
- 1 RADEMACHER, H., and REICHE, F., 1927, *Z. Phys.*, **41**, 453.
- 2 STRATTON, J. A., MORSE, P. M., CHU, L. J., and HUTNER, R. A., 1941, *Elliptic Cylinder and Spheroidal Wave Functions* (London : Chapman and Hall).
- 2 STRÖMGREN, B., 1941, unpublished (cited by M. Rudkjöbing in *Publ. Kbh. Obs.*, **18**, 1).
- 7 WINANS, J. G., and STUECKELBERG, E. C. G., 1928, *Proc. Nat. Acad. Sci., Wash.*, **14**, 867.

Properties of the Hydrogen Molecular Ion
III : Oscillator Strengths of the $1s\sigma_g-2p\pi_u$, $2p\sigma_u-3d\pi_g$
and $2p\pi_u-3d\pi_g$ Transitions

By D. R. BATES, R. T. S. DARLING, S. C. HAWE AND A. L. STEWART
 Department of Applied Mathematics, Queen's University of Belfast

MS. received 13th August 1953

Abstract. The oscillator strengths of the $1s\sigma_g-2p\pi_u$, $2p\sigma_u-3d\pi_g$ and $2p\pi_u-3d\pi_g$ transitions of H_2^+ are calculated from the exact two-centre wave functions. A comparison is made with results obtained from the l.c.a.o. approximation, both the dipole length and the dipole velocity formulae being used. The polarizability of the normal ion perpendicular to the molecular axis is discussed briefly.

§ 1. INTRODUCTION

THE experimental determination of molecular oscillator strengths is extremely difficult and consequently few measurements have in fact been made. Though numerous theoretical studies have been carried out since the publication of Mulliken's first paper on the subject (1939) the wave functions generally used have been of necessity, rather crude so that there is very little reliable information either on the absolute magnitudes of the relevant matrix elements or on how they vary with the internuclear separation (which is of importance in connection with calculations on the relative intensities of the individual bands of a system). It is the purpose of the present paper to provide precise results for some representative cases, and in addition to investigate the accuracy of results based on the simple l.c.a.o. approximation. The following transitions are treated: H_2^+ , $1s\sigma_g-2p\pi_u$; $2p\sigma_u-3d\pi_g$; $2p\pi_u-3d\pi_g$. In the separated atoms designation, favoured in chemical literature, these transitions are $\sigma(1s)-\pi(2p_x)$, $\sigma^*(1s)-\pi^*(2p_x)$ and $\pi(2p_x)-\pi^*(2p_x)$ respectively.

§ 2. CALCULATIONS

2.1. Regarding the nuclei as held at a fixed distance R apart, and using the dipole length formula, we have that the oscillator strength associated with the transition from a lower electronic state, A, to an upper electronic state, B, is given by

$$f(A \rightarrow B | R) = \frac{1}{3} E(A-B | R) G(A-B) \left| \int \chi_A^*(\mathbf{r} | R) \mathbf{r} \chi_B(\mathbf{r} | R) d\mathbf{r} \right|^2 \quad \dots (1)$$

where $E(A-B | R)$ is the photon energy of the radiation absorbed measured in rydbergs, $G(A-B)$ is the orbital degeneracy factor and χ_A and χ_B are the wave functions expressed in atomic units (Mulliken 1939). Alternatively using the dipole velocity formula (Chandrasekhar 1945) we have that

$$f(A \rightarrow B | R) = \frac{4}{3} \frac{G(A-B)}{E(A-B | R)} \left| \int \chi_A^*(\mathbf{r} | R) \nabla \chi_B(\mathbf{r} | R) d\mathbf{r} \right|^2 \quad \dots (2)$$

In discussing the results of the calculations it is convenient to compare the transition integrals $Q^L(A-B|R)$ and $Q^V(A-B|R)$, defined by

$$Q^L(A-B|R)\mathbf{t} = \int \chi_A^*(\mathbf{r}|R)\mathbf{r}\chi_B(\mathbf{r}|R) d\mathbf{r}, \quad \dots\dots(3)$$

and

$$Q^V(A-B|R)\mathbf{t} = -\frac{2}{E(A-B|R)} \int \chi_A^*(\mathbf{r}|R)\nabla\chi_B(\mathbf{r}|R) d\mathbf{r}, \quad \dots\dots(4)$$

\mathbf{t} being some unit vector. These two quantities should of course be equal.

2.2. The exact two-centre wave functions of the hydrogen molecular ion may be written in the form

$$\chi(\mathbf{r}|R) = \Lambda(\lambda|R)M(\mu|R)\Phi(\phi), \quad \dots\dots(5)$$

where λ and μ are the usual elliptical coordinates and ϕ is the azimuthal angle (cf. Mott and Sneddon 1948). Bates, Ledsham and Stewart (1953) have recently published tables from which Λ and M can be obtained; and Φ is simply unity for σ states, and $\sin\phi$ or $\cos\phi$ for π states. The normalization is of course such that

$$(R/2)^3 \int_1^\infty \int_{-1}^{+1} \int_0^{2\pi} \Lambda^2 M^2 \Phi^2 (\lambda^2 - \mu^2) d\lambda d\mu d\phi = 1. \quad \dots\dots(6)$$

Since the wave functions are true solutions of the Schrödinger equation Q^L and Q^V are identical. The superscripts may therefore be omitted. Using formula (3) (which is rather simpler than (4)) we see that in the case of σ - π transitions

$$Q(A-B|R) = \pi(R/2)^4 \left[\int_1^\infty \lambda^2 (\lambda^2 - 1)^{1/2} \Lambda_A \Lambda_B d\lambda \int_{-1}^{+1} (1 - \mu^2)^{1/2} M_A M_B d\mu \right. \\ \left. - \int_1^\infty (\lambda^2 - 1)^{1/2} \Lambda_A \Lambda_B d\lambda \int_{-1}^{+1} \mu^2 (1 - \mu^2)^{1/2} M_A M_B d\mu \right], \quad \dots\dots(7)$$

and that in the case of π - π transitions

$$Q(A-B|R) = \pi(R/2)^4 \left[\int_1^\infty \lambda^3 \Lambda_A \Lambda_B d\lambda \int_{-1}^{+1} \mu M_A M_B d\mu \right. \\ \left. - \int_1^\infty \lambda \Lambda_A \Lambda_B d\lambda \int_{-1}^{+1} \mu^3 M_A M_B d\mu \right]. \quad \dots\dots(8)$$

These expressions may readily be evaluated, the integrations over λ being carried out numerically, and those over μ being carried out analytically (cf. Bates, Öpik and Poets 1953, the second of this series of papers).

2.3. On the l.c.a.o. approximation (cf. Eyring, Walter and Kimball 1944)

$$\left. \begin{aligned} \chi_{1s\sigma_g} &= [\exp(-r_1) + \exp(-r_2)] / \{2\pi(1+S)\}^{1/2} \\ \chi_{2p\sigma_u} &= [\exp(-r_1) - \exp(-r_2)] / \{2\pi(1-S)\}^{1/2} \\ \chi_{2p\pi_u} &= \left[r_1 \exp(-r_1/2) \sin\theta_1 + r_2 \exp(-r_2/2) \sin\theta_2 \right] \frac{\sin\phi}{\cos\phi} / \left\{ 64\pi(1+T) \right\}^{1/2} \\ \chi_{3d\pi_g} &= \left[r_1 \exp(-r_1/2) \sin\theta_1 - r_2 \exp(-r_2/2) \sin\theta_2 \right] \frac{\sin\phi}{\cos\phi} / \left\{ 64\pi(1-T) \right\}^{1/2} \end{aligned} \right\} \quad \dots\dots(9)$$

where

$$S = (1 + R + \frac{1}{3}R^2) \exp(-R), \quad T = (1 + \frac{1}{2}R + \frac{1}{10}R^2 + \frac{1}{120}R^3) \exp(-R/2),$$

r_1 and r_2 are the distances of the electron from the two protons, θ_1 and θ_2 are the corresponding polar angles (measured in the same sense from the molecular axis),

and ϕ is, as before, the azimuthal angle. Substituting in (3) and (4) we obtain

$$\left. \begin{aligned} Q^L(1s\sigma_g - 2p\pi_u | R) &= [I_1 + I_2] / \{(1+S)(1+T)\}^{1/2} \\ Q^L(2p\sigma_u - 3d\pi_g | R) &= [I_1 - I_2] / \{(1-S)(1-T)\}^{1/2} \\ Q^L(2p\pi_u - 3d\pi_g | R) &= [R/2] / \{1 - T^2\}^{1/2} \end{aligned} \right\} \dots\dots (10)$$

$$\left. \begin{aligned} Q^V(1s\sigma_g - 2p\pi_u | R) &= [J_1 + J_2] / \{(1+S)(1+T)\}^{1/2} E(1s\sigma_g - 2p\pi_u | R) \\ Q^V(2p\sigma_u - 3d\pi_g | R) &= [J_1 - J_2] / \{(1-S)(1-T)\}^{1/2} E(2p\sigma_u - 3d\pi_g | R) \\ Q^V(2p\pi_u - 3d\pi_g | R) &= [K] / \{1 - T^2\}^{1/2} E(2p\pi_u - 3d\pi_g | R) \end{aligned} \right\} \dots\dots (11)$$

with

$$\begin{aligned} I_1 &= 2^{15/2} \times 3^{-5}, & I_2 &= 2^{15/2} \times 3^{-4} \{3x + 16(4 + 3R)y\} \exp(-3R/4), \\ J_1 &= 2^{11/2} \times 3^{-4}, & J_2 &= 2^{11/2} \times 3^{-3} \{x + (16 + 12R - R^2)y\} \exp(-3R/4), \\ x &= 3 \sinh(R/4) + \cosh(R/4), & y &= 2R^{-3} \{4 \sinh(R/4) - R \cosh(R/4)\}, \\ K &= \frac{R}{120} (12 + 6R + R^2) \exp(-R/2). \end{aligned}$$

The remarkable simplicity of the formula for $Q^L(2p\pi_u - 3d\pi_g | R)$ arises from the fact that the transition concerned is of the so-called *charge-transfer* type (cf. Mulliken 1939).

§ 3. RESULTS

Figures 1, 2 and 3 show the calculated values of the $1s\sigma_g - 2p\pi_u$, $2p\sigma_u - 3d\pi_g$ and $2p\pi_u - 3d\pi_g$ transition integrals, Q being obtained from the exact wave functions and Q^L and Q^V from the l.c.a.o. approximation.† It will be observed that Q^L and Q^V differ greatly from each other and from Q , the exact transition integral; that at small R , Q^V is the better, that at large R , Q^L is the better, and that at intermediate R , the mean, $\frac{1}{2}(Q^L + Q^V)$, is generally rather better than either. Essentially the same behaviour was found in earlier work on the $1s\sigma_g - 2p\sigma_u$ transition (Bates 1951). It is clear therefore that the l.c.a.o. approximation often yields results which are seriously in error. Owing to cancellation effects many transition integrals are of course much more sensitive to the detailed form of the wave functions than are the four transition integrals which have been investigated.

The oscillator strengths are given in the table. They were obtained by substituting the values of Q derived from the exact wave functions in formula (1), taking

$$G(1s\sigma_g - 2p\pi_u) = G(2p\sigma_u - 3d\pi_g) = 2, \quad G(2p\pi_u - 3d\pi_g) = 1 \quad \dots\dots (12)$$

(cf. Mulliken 1939).

As would be expected of the oscillator strength of a charge-transfer transition, $f(2p\pi_u - 3d\pi_g | R)$ is large—when R is $5a_0$ it is actually almost $1/3$ which is the maximum permitted by the Thomas-Kuhn sum rule.‡ Both $f(1s\sigma_g - 2p\pi_u | R)$ and $f(2p\sigma_u - 3d\pi_g | R)$ are also large but the result is again as would be expected since the two transitions concerned are optically allowed, and indeed intense, in the united-atom limit and in the separated-atoms limit. It may be noted too that

† In computing Q^V from formulae (11) the exact value of the photon energy E was used rather than an approximate value.

‡ It is of interest to note that the maximum is likewise almost reached in the case of $1s\sigma_g - 2p\sigma_u$ (Bates 1951) which is another transition of the charge-transfer type.

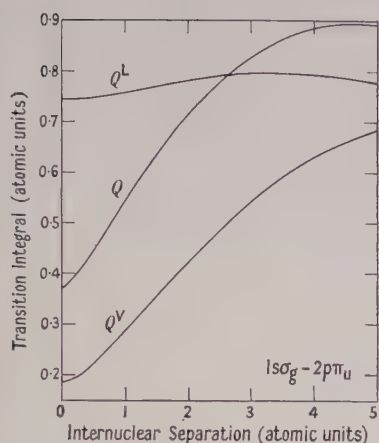


Fig. 1. $1s\sigma_g-2p\pi_u$ transition integral: Q calculated from exact wave functions; Q^L and Q^V from l.c.a.o. approximation using the dipole length (3) and dipole velocity (4) formulae respectively.

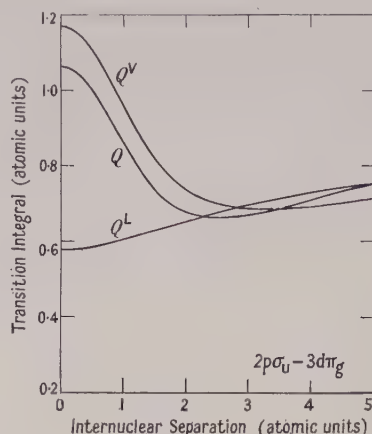


Fig. 2. $2p\sigma_u-3d\pi_g$ transition integral: Q calculated from exact wave functions; Q^L and Q^V from l.c.a.o. approximation using the dipole length (3) and dipole velocity (4) formulae respectively.

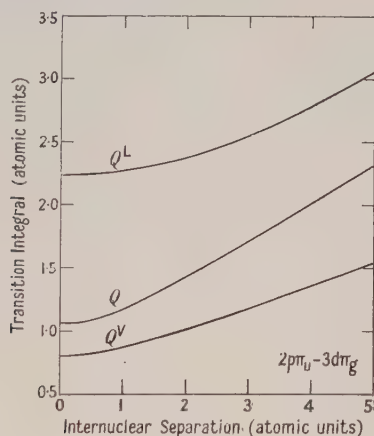


Fig. 3. $2p\pi_u-3d\pi_g$ transition integral: Q calculated from exact wave functions; Q^L and Q^V from l.c.a.o. approximation using the dipole length (3) and dipole velocity (4) formulae respectively.

Photon Energies E and Oscillator Strengths f of some Transitions of the Hydrogen Molecular Ion

R	$1s\sigma_g-2p\pi_u$		$2p\sigma_u-3d\pi_g$		$2p\pi_u-3d\pi_g$	
	E	f	E	f	E	f
0.0	3.0000	0.27 ₇	0.5556	0.41 ₇	0.5556	0.20 ₉
0.4	2.6116	0.31 ₉	0.5767	0.40 ₂	0.5450	0.21 ₁
0.8	2.1446	0.37 ₂	0.6393	0.36 ₁	0.5182	0.22 ₅
1.2	1.7938	0.41 ₂	0.7290	0.31 ₂	0.4826	0.24 ₁
1.6	1.5376	0.44 ₁	0.8165	0.28 ₁	0.4435	0.25 ₆
2.0	1.3477	0.46 ₀	0.8817	0.26 ₈	0.4041	0.27 ₅
3.0	1.0489	0.47 ₉	0.9435	0.28 ₃	0.3135	0.30 ₈
4.0	0.8905	0.46 ₅	0.9292	0.31 ₃	0.2397	0.32 ₃
5.0	0.8061	0.43 ₀	0.8944	0.33 ₇	0.1825	0.32 ₇

The internuclear separation R is in units of a_0 , the radius of the first Bohr orbit, and the photon energy E is in rydbergs.

certain other transitions of the $1s\sigma_g - nl\pi_u$ and $2p\sigma_u - nl\pi_g$ series must have considerable oscillator strengths to enable the sum for each series to be $2/3$ as is required. Some further information is available on the series associated with the ground state. Bates, Öpik and Poots (1953) have carried out calculations on the photo-ionization cross section. By extending these to higher energies the last named author has shown that the total oscillator strength of the $(1s\sigma_g - \epsilon l\pi_u)$ continua is 0.11 when the internuclear separation is $2a_0$ (which is approximately the equilibrium value).† Hence

$$\sum_{nl}' f(1s\sigma_g - nl\pi_u | 2a_0) = 0.10 \quad \dots\dots(13)$$

where \sum_{nl}' denotes a summation over all discrete states of the species indicated other than the $2p\pi_u$ state.

Finally we shall estimate $\alpha^\perp(1s\sigma_g | 2a_0)$ the polarizability of the normal ion in a direction at right angles to the molecular axis. The standard quantal formula relating this quantity to the oscillator strengths (cf. Mott and Sneddon 1948) may be written

$$\alpha^\perp(1s\sigma_g | 2a_0) = 6 \left[\frac{f(1s\sigma_g - 2p\pi_u | 2a_0)}{E(1s\sigma_g - 2p\pi_u | 2a_0)^2} + \sum_{nl}' \frac{f(1s\sigma_g - nl\pi_u | 2a_0)}{E(1s\sigma_g - nl\pi_u | 2a_0)^2} + \sum_l \int_{\epsilon} \frac{df(1s\sigma_g - \epsilon l\pi_u | 2a_0)}{E(1s\sigma_g - \epsilon l\pi_u | 2a_0)^2} \right] a_0^3. \quad \dots\dots(14)$$

From the data given in the table and from the photo-ionization cross section curves it may be shown that the first and third terms equal $1.52a_0^3$ and $0.07_1a_0^3$ respectively. Moreover from (13) it is apparent that the second term may be expressed as $(0.60/\bar{E}^2)a_0^3$ where \bar{E} is some mean energy which must be greater than $E(1s\sigma_g - 3p\pi_u | 2a_0)$, the photon energy for the excitation of the first state of the series, and must be smaller than $E(1s\sigma_g - \mathcal{C} | 2a_0)$, the photon energy for ionization. Since $E(1s\sigma_g - 3p\pi_u | 2a_0)$ is approximately 1.80 rydbergs (Gilbert 1933) and since $E(1s\sigma_g - \mathcal{C} | 2a_0)$ is 2.21 rydbergs (cf. Bates, Ledsham and Stewart 1953) we see that $\alpha^\perp(1s\sigma_g | 2a_0)$ lies between $1.71a_0^3$ and $1.78a_0^3$, and is probably closer to the upper limit since the main contribution to the term causing the uncertainty presumably comes from the lower of the $nl\pi_u$ states. This is in harmony with the variational calculations of Rahman (1953) which give the value to be $1.758a_0^3$.

REFERENCES

- BATES, D. R., 1951, *J. Chem. Phys.*, **19**, 1122.
 BATES, D. R., LEDSHAM, K., and STEWART, A. L., 1953, *Phil. Trans. Roy. Soc. A*, **246**, 215.
 BATES, D. R., ÖPIK, U., and POOTS, G., 1953, *Proc. Phys. Soc. A*, **66**, 1113.
 CHANDRASEKHAR, S., 1945, *Astrophys. J.*, **102**, 223.
 EYRING, H., WALTER, J., and KIMBALL, G. E., 1944, *Quantum Chemistry* (London: Chapman and Hall).
 GILBERT, G., 1933, *Phil. Mag.*, **26**, 929.
 MOTT, N. F., and SNEDDON, I. N., 1948, *Wave Mechanics and Its Applications* (Oxford: Clarendon Press).
 MULLIKEN, R. S., 1939, *J. Chem. Phys.*, **7**, 14, 20.
 RAHMAN, A., 1953, *Physica*, **19**, 145.

† We wish to thank Mr. G. Poots for allowing us to quote this result.

A Scalar Representation of Electromagnetic Fields

BY H. S. GREEN† AND E. WOLF

Department of Mathematical Physics, University of Edinburgh

Communicated by Max Born; MS. received 16th June 1953, and in amended form 31st August 1953

Abstract. It is shown that in a region which is free of currents and charges, any electromagnetic field may be rigorously derived from a single, generally complex, scalar wave function $V(\mathbf{x}, t)$. In terms of this function the momentum density $\mathbf{g}(\mathbf{x}, t)$ and the energy density $w(\mathbf{x}, t)$ of the field may be defined in such a way that they are represented by expressions analogous to the formulae for the probability current and the probability density in quantum mechanics; in a homogeneous isotropic medium

$$\mathbf{g}(\mathbf{x}, t) = -\frac{1}{8\pi\mu_0 c} [\dot{V}^* \nabla V + \dot{V} \nabla V^*],$$

$$w(\mathbf{x}, t) = \frac{1}{8\pi} \left[\frac{\epsilon_0}{c^2} \dot{V} \dot{V}^* + \frac{1}{\mu_0} \nabla V \cdot \nabla V^* \right].$$

The densities defined in this way differ from those given by the usual expressions, but the choice is justified since the differences disappear on integration over any arbitrary macroscopic domain. (The corresponding Lagrangian densities differ by a four divergence.) When V is of the form $V_0(\mathbf{x})e^{-i\omega t}$, \mathbf{g} is found to form a solenoidal field which is orthogonal to the co-phasal surfaces $\arg V_0 = \text{constant}$.

§ 1. INTRODUCTION

IN a region of space which is free of charges and currents an electromagnetic field is fully specified by the magnetic vector potential \mathbf{A} . From it the electric and the magnetic field vectors may be derived by means of well-known relations.

In a wide class of problems, particularly in those encountered in optics, the actual behaviour of the field vectors is of little interest. What one primarily wishes to know is the average energy or the average flux, and one is led to wonder whether for such purposes the derivation from a vector potential is really the most suitable one. Except in the so-called 'rigorous' diffraction theory, one does in fact often employ in optical considerations of energy a single, generally complex, scalar wave function (usually called the disturbance, or the complex amplitude), whose squared modulus is taken as the measure of the light intensity. This simple procedure has been employed in optics since about the time of Fresnel (the disturbance then being considered to be the displacement of a particle in an 'elastic ether') and has been the subject of much criticism, in spite of the fact that under fairly general conditions it gives results which are found to be in excellent agreement with experiment. The validity of the scalar

† On leave of absence from the University of Adelaide, Adelaide, South Australia.

theory has been justified, at least as an approximation or as a time average, for a number of special cases only: (a) for certain two-dimensional problems and for monochromatic fields with rotational symmetry (cf. Braunkbek 1951), (b) in applications to diffraction problems encountered in optical instruments of usual design and working with non-polarized and almost monochromatic light (Picht 1931, Luneberg 1947-8, Theimer, Wassermann and Wolf 1952).

Now it is well known that the energy density and the momentum density (and consequently the light intensity) are not uniquely defined by the electric and the magnetic field vectors. One may always add to the Lagrangian density a four divergence which gives no contribution to the field equations, though it may alter the local (unobservable) values of the densities of the energy and the momentum. Such alteration must of course lead to no observable changes in the *total* amount of energy and momentum contained in any extended (macroscopic) domain. The question is therefore open as to whether one could not define the energy and momentum densities in such a way that they would always be expressible in a simple manner in terms of a single complex scalar wave function, the field vectors remaining unchanged. In the present paper it is shown that this in fact is possible.

We find that in regions where no currents or charges are present the magnetic potential may be rigorously derived from a single, generally complex, scalar wave function $V(\mathbf{x}, t)$, which we call the *complex potential*. In terms of this function the momentum density $\mathbf{g}(\mathbf{x}, t)$ and the energy density $w(\mathbf{x}, t)$ in a homogeneous isotropic medium may be defined by means of formulae analogous to the expressions for the probability current and the probability density in quantum mechanics:

$$\text{and} \quad \left. \begin{aligned} \mathbf{g}(\mathbf{x}, t) &= -\frac{1}{8\pi\mu_0 c} [\dot{V}^* \nabla V + \dot{V} \nabla V^*], \\ w(\mathbf{x}, t) &= \frac{1}{8\pi} \left[\frac{\epsilon_0}{c^2} \dot{V} \dot{V}^* + \frac{1}{\mu_0} \nabla V \cdot \nabla V^* \right]; \end{aligned} \right\} \quad \dots\dots(1.1)$$

these quantities satisfy a conservation law of the usual form:

$$\frac{1}{c} \frac{dw}{dt} + \nabla \cdot \mathbf{g} = 0. \quad \dots\dots(1.2)$$

The corresponding Lagrangian density L is

$$L(\mathbf{x}, t) = \frac{1}{8\pi} \left\{ \frac{\epsilon_0}{c^2} \dot{V} \dot{V}^* - \frac{1}{\mu_0} \nabla V \cdot \nabla V^* \right\}; \quad \dots\dots(1.3)$$

here ϵ_0 , μ_0 are the dielectric constant and the magnetic permeability and c is the vacuum velocity of light.

An interesting consequence of the present analysis is the result that in the case when the time enters V only through the factor $e^{-i\omega t}$, i.e. when V is of the form

$$V(\mathbf{x}, t) = v(\mathbf{x}) \exp \{i[k\mathcal{L}(\mathbf{x}) - \omega t]\} \quad (v \text{ and } \mathcal{L} \text{ real}) \quad \dots\dots(1.4)$$

(ω = frequency, $k = \omega/c$), \mathbf{g} and w become independent of time and (1.1) reduces to

$$\mathbf{g}(\mathbf{x}) = \frac{k^2}{4\pi\mu_0} v^2 \nabla \mathcal{L}. \quad \dots\dots(1.5)$$

The conservation law now becomes

$$\nabla \cdot \mathbf{g}(\mathbf{x}) = 0. \quad \dots\dots(1.6)$$

Equation (1.5) shows that the energy flow is orthogonal to the surfaces of constant phase of the complex potential and (1.6) expresses the fact that the vector field \mathbf{g} is solenoidal. One is thus led rigorously to the concept of 'electromagnetic rays', and one obtains for a class of electromagnetic fields a simple model which may be regarded as a natural generalization of geometrical optics.

§ 2. DEFINITION OF THE COMPLEX POTENTIAL

We consider an electromagnetic field in a homogeneous, isotropic medium. In regions free of currents and charges the field quantities may be derived from a single vector potential $\mathbf{A}(\mathbf{x}, t)$ which satisfies the homogeneous wave equation and also the divergence condition

$$\nabla \cdot \mathbf{A} = 0. \quad \dots\dots (2.1)$$

In general, currents and charges will, of course, be present in some parts of the \mathbf{x} space. It will be convenient to imagine these enclosed in boxes and to consider in place of \mathbf{A} the function \mathbf{A} defined by

$$\begin{aligned} \mathbf{A}(\mathbf{x}, t) &= \mathbf{A}(\mathbf{x}, t) \text{ outside and on the boxes} \\ &= 0 \quad \text{inside the boxes.} \end{aligned}$$

\mathbf{A} is formally defined over the whole \mathbf{x} space and may be represented by a Fourier integral

$$\mathbf{A}(\mathbf{x}, t) = \int [\mathbf{a}(\mathbf{k}, t) \cos(\mathbf{k} \cdot \mathbf{x}) + \mathbf{b}(\mathbf{k}, t) \sin(\mathbf{k} \cdot \mathbf{x})] d\mathbf{k}, \quad \dots\dots (2.2)$$

where, since \mathbf{A} is real, the integration is carried over half of \mathbf{k} space (e.g. $k_x \geq 0$). On account of (2.1) the (real) vectors $\mathbf{a}(\mathbf{k}, t)$ and $\mathbf{b}(\mathbf{k}, t)$ are orthogonal to \mathbf{k} ,

$$\mathbf{a} \cdot \mathbf{k} = \mathbf{b} \cdot \mathbf{k} = 0. \quad \dots\dots (2.3)$$

With each \mathbf{k} we associate two unit vectors $\mathbf{l}_1(\mathbf{k})$ and $\mathbf{l}_2(\mathbf{k})$ such that \mathbf{l}_1 , \mathbf{l}_2 and \mathbf{k} form a right-handed orthogonal triad. This may be done for example by choosing a constant vector \mathbf{n} and taking as \mathbf{l}_1 a unit vector perpendicular to the (\mathbf{k}, \mathbf{n}) plane and as \mathbf{l}_2 a unit vector perpendicular to \mathbf{k} and \mathbf{l}_1 :

$$\left. \begin{aligned} \mathbf{l}_1(\mathbf{k}) &= \frac{\mathbf{n} \wedge \mathbf{k}}{|\mathbf{n} \wedge \mathbf{k}|}, \\ \mathbf{l}_2(\mathbf{k}) &= \frac{\mathbf{k} \wedge \mathbf{l}_1}{|\mathbf{k} \wedge \mathbf{l}_1|} = \frac{k^2 \mathbf{n} - (\mathbf{n} \cdot \mathbf{k}) \mathbf{k}}{|k^2 \mathbf{n} - (\mathbf{n} \cdot \mathbf{k}) \mathbf{k}|}. \end{aligned} \right\} \quad \dots\dots (2.4)$$

Equations (2.3) show that \mathbf{a} and \mathbf{b} lie in the plane of \mathbf{l}_1 and \mathbf{l}_2 and may therefore be resolved along these vectors:

$$\left. \begin{aligned} a_1 &= \mathbf{a} \cdot \mathbf{l}_1, & a_2 &= \mathbf{a} \cdot \mathbf{l}_2, \\ b_1 &= \mathbf{b} \cdot \mathbf{l}_1, & b_2 &= \mathbf{b} \cdot \mathbf{l}_2. \end{aligned} \right\} \quad \dots\dots (2.5)$$

Next we form the complex combinations

$$\left. \begin{aligned} \alpha(\mathbf{k}, t) &= a_1(\mathbf{k}, t) + ia_2(\mathbf{k}, t), \\ \beta(\mathbf{k}, t) &= b_1(\mathbf{k}, t) + ib_2(\mathbf{k}, t), \end{aligned} \right\} \quad \dots\dots (2.6)$$

and regard α and β as Fourier coefficients of a function V :

$$V(\mathbf{x}, t) = \int [\alpha(\mathbf{k}, t) \cos(\mathbf{k} \cdot \mathbf{x}) + \beta(\mathbf{k}, t) \sin(\mathbf{k} \cdot \mathbf{x})] d\mathbf{k}. \quad \dots\dots (2.7)$$

We call $V(\mathbf{x}, t)$ the *complex potential* of the field.

We have now replaced the magnetic vector potential by a complex scalar function. Conversely it is easily seen that from the complex potential V , the

magnetic vector potential \mathbf{A} and consequently the field vectors may be uniquely derived. For in the first place, from the knowledge of V the quantities α and β may be obtained by applying the Fourier inversion formula. Then a_1, a_2, b_1 and b_2 may be determined from (2.6). From them the Fourier components \mathbf{a} and \mathbf{b} of the complex potential are obtained:

$$\mathbf{a} = a_1 \mathbf{l}_1 + a_2 \mathbf{l}_2, \quad \mathbf{b} = b_1 \mathbf{l}_1 + b_2 \mathbf{l}_2. \quad \dots\dots (2.8)$$

Finally, if one forms the combinations $\mathbf{a} \cos(\mathbf{k} \cdot \mathbf{x}) + \mathbf{b} \sin(\mathbf{k} \cdot \mathbf{x})$ and integrates over all \mathbf{k} , one obtains the vector potential \mathbf{A} . Hence the scalar $V(\mathbf{x}, t)$ completely specifies the field.*

It is easily seen that in a homogeneous isotropic medium of dielectric constant ϵ_0 and magnetic permeability μ_0 the complex potential satisfies the wave equation

$$\nabla^2 V - \frac{\epsilon_0 \mu_0}{c^2} \ddot{V} = 0. \quad \dots\dots (2.9)$$

For, since the vector potential \mathbf{A} satisfies the wave equation

$$\nabla^2 \mathbf{A} - \frac{\epsilon_0 \mu_0}{c^2} \ddot{\mathbf{A}} = 0, \quad \dots\dots (2.10)$$

one must have, for each component,

$$\mathbf{A}_{\mathbf{k}} = \mathbf{a}(\mathbf{k}, t) \cos(\mathbf{k} \cdot \mathbf{x}) + \mathbf{b}(\mathbf{k}, t) \sin(\mathbf{k} \cdot \mathbf{x}) \quad \dots\dots (2.11)$$

of \mathbf{A} ,

$$\ddot{\mathbf{A}}_{\mathbf{k}} + \frac{k^2 c^2}{\epsilon_0 \mu_0} \mathbf{A}_{\mathbf{k}} = 0. \quad \dots\dots (2.12)$$

It then follows from (2.12), (2.5) and (2.6) that the corresponding terms $V_{\mathbf{k}}$ of V , i.e.

$$V_{\mathbf{k}} = \alpha(\mathbf{k}, t) \cos(\mathbf{k} \cdot \mathbf{x}) + \beta(\mathbf{k}, t) \sin(\mathbf{k} \cdot \mathbf{x}), \quad \dots\dots (2.13)$$

must satisfy the scalar wave equation

$$\ddot{V}_{\mathbf{k}} + \frac{k^2 c^2}{\epsilon_0 \mu_0} V_{\mathbf{k}} = 0. \quad \dots\dots (2.14)$$

Consequently the complex potential satisfies the homogeneous wave equation (2.9).

§ 3. THE MOMENTUM DENSITY AND THE ENERGY DENSITY

3.1. We now derive expressions for the momentum density and the energy density of the field in terms of the complex potential. We restrict our discussion to a homogeneous isotropic medium.

In terms of the vector potential, the electric and the magnetic field vectors are given by

$$\mathbf{E} = -\frac{1}{c} \dot{\mathbf{A}}, \quad \mu_0 \mathbf{H} = \nabla \wedge \mathbf{A}, \quad \dots\dots (3.1)$$

and the total momentum \mathbf{G} of the field is

$$\mathbf{G}(t) = \frac{1}{4\pi} \int (\mathbf{E} \wedge \mathbf{H}) d\mathbf{x} = -\frac{1}{4\pi\mu_0 c} \int \dot{\mathbf{A}} \wedge (\nabla \wedge \mathbf{A}) d\mathbf{x}, \quad \dots\dots (3.2)$$

the integration being taken throughout the \mathbf{x} space.

* Note added in proof. Since this paper was written our attention has been drawn to a paper by E. T. Whittaker (*Proc. Lond. Math. Soc.*, 1904, **1**, 367), where it is shown that *in vacuo* at points not occupied by electrons a field produced by any number of electrons moving in any arbitrary manner may be derived from two real scalar wave functions.

The connection between Whittaker's analysis and that of the present section is being investigated and it is hoped to publish the results in a later communication.

To express \mathbf{G} in terms of V we first substitute into (3.2) from (2.2). We have

$$\left. \begin{aligned} \dot{\mathbf{A}} &= \int [\dot{\mathbf{a}} \cos(\mathbf{k} \cdot \mathbf{x}) + \dot{\mathbf{b}} \sin(\mathbf{k} \cdot \mathbf{x})] d\mathbf{k}, \\ \nabla \wedge \mathbf{A} &= \int \mathbf{k} \wedge [-\mathbf{a} \sin(\mathbf{k} \cdot \mathbf{x}) + \mathbf{b} \cos(\mathbf{k} \cdot \mathbf{x})] d\mathbf{k}. \end{aligned} \right\} \dots\dots (3.3)$$

Hence

$$\mathbf{G} = -\frac{1}{4\pi\mu_0 c} \int d\mathbf{x} \int \int [\dot{\mathbf{a}}(\mathbf{k}', t) \cos(\mathbf{k}' \cdot \mathbf{x}) + \dot{\mathbf{b}}(\mathbf{k}', t) \sin(\mathbf{k}' \cdot \mathbf{x})] \wedge [\mathbf{k} \wedge (-\mathbf{a}(\mathbf{k}, t) \sin(\mathbf{k} \cdot \mathbf{x}) + \mathbf{b}(\mathbf{k}, t) \cos(\mathbf{k} \cdot \mathbf{x}))] d\mathbf{k} d\mathbf{k}'. \dots\dots (3.4)$$

This becomes, with the help of the Fourier integral theorem,

$$\mathbf{G} = -\frac{\pi^2}{2\mu_0 c} \int \dot{\mathbf{a}}(\mathbf{k}, t) \wedge [\mathbf{k} \wedge \mathbf{b}(\mathbf{k}, t)] - \dot{\mathbf{b}}(\mathbf{k}, t) \wedge [\mathbf{k} \wedge \mathbf{a}(\mathbf{k}, t)] d\mathbf{k}, \dots\dots (3.5)$$

or, using (2.8),

$$\begin{aligned} \mathbf{G} &= \frac{\pi^2}{2\mu_0 c} \int [(a_1 \dot{b}_1 + a_2 \dot{b}_2) - (b_1 \dot{a}_1 + b_2 \dot{a}_2)] \mathbf{k} d\mathbf{k} \\ &= \frac{\pi^2}{2\mu_0 c} \int [(\alpha^* \dot{\beta} + \alpha \dot{\beta}^*) - (\dot{\alpha}^* \beta + \dot{\alpha} \beta^*)] \mathbf{k} d\mathbf{k} \\ &= -\frac{1}{8\pi\mu_0 c} \int (\dot{V}^* \nabla V + \dot{V} \nabla V^*) d\mathbf{x}. \end{aligned} \dots\dots (3.6)$$

Hence the density \mathbf{g} of the momentum may be defined as

$$\mathbf{g}(\mathbf{x}, t) = -\frac{1}{8\pi\mu_0 c} [\dot{V}^* \nabla V + \dot{V} \nabla V^*]. \dots\dots (3.7)$$

The electric and the magnetic energy densities may also easily be defined in terms of the complex potential. The total *electric energy* W_e is

$$\begin{aligned} W_e(t) &= \frac{\epsilon_0}{8\pi} \int E^2 d\mathbf{x} \\ &= \frac{\epsilon_0}{8\pi c^2} \int d\mathbf{x} \int \int \{ \dot{\mathbf{a}}(\mathbf{k}, t) \cos(\mathbf{k} \cdot \mathbf{x}) + \dot{\mathbf{b}}(\mathbf{k}, t) \sin(\mathbf{k} \cdot \mathbf{x}) \} \\ &\quad \cdot \{ \dot{\mathbf{a}}(\mathbf{k}', t) \cos(\mathbf{k}' \cdot \mathbf{x}) + \dot{\mathbf{b}}(\mathbf{k}', t) \sin(\mathbf{k}' \cdot \mathbf{x}) \} d\mathbf{k} d\mathbf{k}' \\ &= \frac{\pi^2 \epsilon_0}{2c^2} \int (\dot{a}^2 + \dot{b}^2) d\mathbf{k} \\ &= \frac{\pi^2 \epsilon_0}{2c^2} \int (\dot{a}_1^2 + \dot{a}_2^2 + \dot{b}_1^2 + \dot{b}_2^2) d\mathbf{k} \\ &= \frac{\pi^2 \epsilon_0}{2c^2} \int (\dot{\alpha} \dot{\beta}^* + \dot{\beta} \dot{\alpha}^*) d\mathbf{k} \\ &= \frac{\epsilon_0}{8\pi c^2} \int (\dot{V} \dot{V}^*) d\mathbf{x}. \end{aligned} \dots\dots (3.8)$$

The total *magnetic energy* W_m is

$$W_m(t) = \frac{\mu_0}{8\pi} \int \mathbf{H}^2 d\mathbf{x},$$

and one finds, by a similar calculation as above,

$$W_m(t) = \frac{1}{8\pi\mu_0} \int (\nabla V \cdot \nabla V^*) d\mathbf{x}. \dots\dots (3.9)$$

Equations (3.8) and (3.9) show that one may define the electric and magnetic densities w_e and w_m by the expressions

$$w_e(\mathbf{x}, t) = \frac{\epsilon_0}{8\pi c^2} \dot{V} \dot{V}^*, \quad w_m(\mathbf{x}, t) = \frac{1}{8\pi\mu_0} (\nabla V \cdot \nabla V^*). \quad \dots\dots(3.10)$$

It is easily verified, with the help of the wave equation (2.9), that the total energy density $w = w_e + w_m$ and the energy flux $\mathbf{S} = c\mathbf{g}$ satisfy the conservation law

$$\frac{dw}{dt} + \nabla \cdot \mathbf{S} = 0. \quad \dots\dots(3.11)$$

3.2. V is in general a complex function. Let v denote its amplitude and ϕ its phase:

$$V(\mathbf{x}, t) = v(\mathbf{x}, t) \exp \{i\phi(\mathbf{x}, t)\}. \quad \dots\dots(3.12)$$

If one substitutes from (3.12) into the wave equation (2.9) and separates real and imaginary parts, one obtains the following two equations:

$$\nabla^2 v - v(\nabla\phi)^2 - \frac{\epsilon_0\mu_0}{c^2} (\ddot{v} - v\dot{\phi}^2) = 0, \quad \dots\dots(3.13)$$

$$2(\nabla v) \cdot (\nabla\phi) + v\nabla^2\phi - \frac{\epsilon_0\mu_0}{c^2} (2\dot{v}\dot{\phi} + v\ddot{\phi}) = 0. \quad \dots\dots(3.14)$$

In terms of v and ϕ the momentum density \mathbf{g} and the energy densities w_e and w_m are

$$\left. \begin{aligned} \mathbf{g}(\mathbf{x}, t) &= -\frac{1}{4\pi\mu_0 c} (\dot{v}\nabla v + v^2\dot{\phi}\nabla\phi), \\ w_e(\mathbf{x}, t) &= \frac{\epsilon_0}{8\pi c^2} (\dot{v}^2 + \dot{\phi}^2 v^2), \\ w_m(\mathbf{x}, t) &= \frac{1}{8\pi\mu_0} \{(\nabla v)^2 + v^2(\nabla\phi)^2\}. \end{aligned} \right\} \quad \dots\dots(3.15)$$

Of particular interest is the case when the time enters only through a factor† $e^{-i\omega t}$. Then v is independent of time and ϕ is of the form

$$\phi(\mathbf{x}, t) = k\mathcal{S}(\mathbf{x}) - \omega t \quad \dots\dots(3.16)$$

($k = \omega/c$). The eqns. (3.13) and (3.14) reduce to

$$(\nabla\mathcal{S})^2 - \frac{1}{k^2 v} \nabla^2 v = n^2, \quad \dots\dots(3.17)$$

$$\nabla v \cdot \nabla\mathcal{S} + \frac{1}{2} v \nabla^2\mathcal{S} = 0, \quad \dots\dots(3.18)$$

where

$$n^2 = \epsilon_0\mu_0. \quad \dots\dots(3.19)$$

The expressions (3.7) and (3.10) for the momentum densities and the energy densities become

$$\mathbf{g}(\mathbf{x}) = \frac{\epsilon_0 k^2}{4\pi n^2} v^2 \nabla\mathcal{S}, \quad \dots\dots(3.20)$$

$$w_e(\mathbf{x}) = \frac{\epsilon_0 k^2}{8\pi} v^2, \quad \dots\dots(3.21)$$

$$w_m(\mathbf{x}) = \frac{\epsilon_0 k^2}{8\pi n^2} v^2 \left[(\nabla\mathcal{S})^2 + \frac{1}{k^2} (\nabla \log v)^2 \right]. \quad \dots\dots(3.22)$$

† Note added in proof: A general monochromatic wave must be represented by a V function of the form

$$V(\mathbf{x}, t) = V_1(\mathbf{x})e^{-i\omega t} + V_2(\mathbf{x})e^{i\omega t},$$

where V_1 and V_2 are complex functions of positions. It appears that the case here considered ($V_2 \equiv 0$) represents a monochromatic wave of arbitrary shape but circularly polarized, at least in the sense of a space average over a macroscopic domain.

Equation (3.20) shows that the energy flow is orthogonal to the surfaces

$$\mathcal{S}(\mathbf{x}) = \text{constant}. \quad \dots\dots(3.23)$$

Moreover, (3.18) may be written in the form

$$\nabla \cdot (v^2 \nabla \mathcal{S}) = 0; \quad \dots\dots(3.24)$$

this relation (which also follows from the conservation law (3.11)) shows that the vector field \mathbf{g} is solenoidal.

The two results which we have just established show a close analogy with the model presented by geometrical optics. The surfaces $\mathcal{S} = \text{constant}$ may be regarded as generalized wave fronts and the energy may be considered as being propagated along the curves (rays) orthogonal to these surfaces.

To determine the wave fronts $\mathcal{S} = \text{constant}$ one must in general solve two equations (3.17) and (3.18). But we note that the second term in (3.17) contains as multiplicative factor the second power of the small quantity $1/k$. Except in special regions this term will be very small in comparison with $n^2 = \epsilon_0 \mu_0$ and may therefore be neglected. This implies that the geometrical wave fronts given by the solution of the eikonal equation

$$(\nabla \mathcal{S})^2 = n^2 \quad \dots\dots(3.25)$$

are in general a very good approximation to the waves associated with the complex potential.† Better approximations may be obtained by the application of the W.K.B. method, or with the help of Huygens' principle (or Kirchhoff's integral formula).

One can also easily write down an expression for the variation of the amplitude along each 'electromagnetic ray' (orthogonal trajectory to the \mathcal{S} surfaces). For if $\partial/\partial\tau$ denotes differentiation along a particular ray, $\partial/\partial\tau = \nabla \mathcal{S} \cdot \nabla$, and (3.18) gives $\partial v/\partial\tau + \frac{1}{2}(\nabla^2 \mathcal{S})v = 0$; hence

$$v(\tau) = v(\tau_0) \exp \left[-\frac{1}{2} \int_{\tau_0}^{\tau} \nabla^2 \mathcal{S} d\tau \right]. \quad \dots\dots(3.26)$$

§ 4. A COMPARISON WITH THE CLASSICAL THEORY

The energy and the momentum of the electromagnetic field may be derived by a variational principle from a Lagrangian density L' which is Lorentz invariant:

$$L' = \frac{1}{8\pi} \left\{ \frac{\epsilon_0}{c^2} \dot{\mathbf{A}}^2 - \frac{1}{\mu_0} (\nabla \wedge \mathbf{A})^2 \right\}. \quad \dots\dots(4.1)$$

The variational principle leads to the vector wave equation (2.10) for the vector potential \mathbf{A} .

In the present theory we have, in place of (2.10), the scalar wave equation (2.9) for the complex potential V . This equation may also be derived from the variational principle by replacing L' by the Lagrangian density‡

$$L = \frac{1}{8\pi} \left\{ \frac{\epsilon_0}{c^2} \dot{V} \dot{V}^* - \frac{1}{\mu_0} \nabla V \cdot \nabla V^* \right\}. \quad \dots\dots(4.2)$$

† In this connection mention must be made of recent researches of Luneberg (cf. 1949, particularly pp. 55-56), which have shown that for small wavelengths geometrical optics, in its extended form, including also description of vectorial properties of the field, gives a very good first approximation to a steady state field.

‡ It is of interest to note the analogy with the Lagrangian density for a scalar meson with zero rest mass.

Since L' and L lead to the same field equations, their difference must be of the form

$$L - L' = \dot{P} + \text{div } \mathbf{Q}. \quad \dots\dots(4.3)$$

In consequence, the momentum density \mathbf{g} and the energy density w of the present theory will differ from the usual expressions \mathbf{g}' and w' associated with (4.1). In fact one has relations of the type

$$\mathbf{g} - \mathbf{g}' = \text{grad } \hat{P}, \quad w - w' = -\text{div } \hat{\mathbf{Q}}, \quad \dots\dots(4.4)$$

where $\hat{P} = P$ and $\hat{\mathbf{Q}} = \mathbf{Q}$ if P and \mathbf{Q} do not involve the field variables. The effect of these differences will be negligible on integration over an arbitrary domain which is large compared with the wavelength.

That the usual definition of energy flow, based on the Poynting vector, is not the only possible one is of course well known.* Our present definition has several advantages. We saw, for example, that in a field represented by a complex potential of the form

$$V(\mathbf{x}, t) = V_0(\mathbf{x})e^{-i\omega t} \quad \dots\dots(4.5)$$

\mathbf{g} , w_e and w_m are independent of time and \mathbf{g} is orthogonal to the surfaces of constant phase of the complex potential. But even in more complicated fields the densities as defined by the present theory seem to lead to simpler results. To illustrate this point we consider an example (essentially due to Braunbek 1951):

Suppose that the vector potential of a field *in vacuo* ($\epsilon_0 = \mu_0 = 1$) is

$$\mathbf{A}(\mathbf{x}, t) = C\{\mathbf{n}_2 \cos[k(\mathbf{n}_1 \cdot \mathbf{x} - ct)] + \mathbf{n}_3 \cos[k(\mathbf{n}_2 \cdot \mathbf{x} - ct)]\}, \quad \dots\dots(4.6)$$

where C is a constant and \mathbf{n}_1 , \mathbf{n}_2 , \mathbf{n}_3 is a right-handed orthogonal triad of unit vectors. A straightforward calculation gives for the time average

$$\langle \mathbf{S}' \rangle = \left\langle \frac{c(\mathbf{E} \wedge \mathbf{H})}{4\pi} \right\rangle$$

of the Poynting vector:

$$\langle \mathbf{S}' \rangle = \frac{ck^2C}{8\pi} [(\mathbf{n}_1 + \mathbf{n}_2) - \mathbf{n}_2 \cos[k(\mathbf{n}_1 - \mathbf{n}_2) \cdot \mathbf{x}]]. \quad \dots\dots(4.7)$$

This expression does not satisfy the relation $\langle \mathbf{S}' \rangle \cdot \text{curl } \langle \mathbf{S}' \rangle = 0$ which would obtain if $\langle \mathbf{S}' \rangle$ possessed orthogonal trajectories (cf. Weatherburn 1930, p. 217). On the other hand one easily finds that the average energy flux $\mathbf{S} = c\mathbf{g}$ as defined by (3.7) possess orthogonal trajectories. For one has in this case (taking $\mathbf{n} = \mathbf{n}_1 + \mathbf{n}_2$)

$$V(\mathbf{x}, t) = C \left\{ \frac{1}{\sqrt{2}} (1 - i) \cos[k(\mathbf{n}_1 \cdot \mathbf{x} - ct)] + i \cos[k(\mathbf{n}_2 \cdot \mathbf{x} - ct)] \right\}. \quad \dots\dots(4.8)$$

From (4.8) and (3.7) one obtains, by a straightforward calculation,

$$\langle \mathbf{S} \rangle = \langle c\mathbf{g} \rangle = \frac{ck^2C}{8\pi} [\mathbf{n}_1 + \mathbf{n}_2] \left[1 - \frac{1}{\sqrt{2}} \cos(k(\mathbf{n}_1 - \mathbf{n}_2) \cdot \mathbf{x}) \right], \quad \dots\dots(4.9)$$

and it follows from (4.9) that $\langle \mathbf{S} \rangle$ satisfied the required condition for the existence of orthogonal trajectories: $\langle \mathbf{S} \rangle \cdot \text{curl } \langle \mathbf{S} \rangle = 0$.

It is seen that $\langle \mathbf{S}' \rangle$ and $\langle \mathbf{S} \rangle$ differ by a space-periodic function, to which clearly no physical meaning can be attached. For $\text{div } \{\langle \mathbf{S}' \rangle - \langle \mathbf{S} \rangle\} = 0$, and consequently the (time-averaged) energy which crosses any closed surface in the field, will be the same whether \mathbf{S} or \mathbf{S}' is taken to define the energy flow.

* cf. Stratton 1941, p. 134; also Hines 1952.

Finally we give a summary of our main formula and the corresponding formulae of the classical theory:

	Usual definition	Present definition
Basic field quantity	\mathbf{A}	V
	$\left(\mathbf{E} = -\frac{1}{c} \dot{\mathbf{A}}, \mu_0 \mathbf{H} = \nabla \wedge \mathbf{A} \right)$	
Lagrangian density	$\frac{1}{8\pi} \left\{ \frac{\epsilon_0}{c^2} \dot{\mathbf{A}}^2 - \frac{1}{\mu_0} (\Delta \wedge \mathbf{A})^2 \right\}$	$\frac{1}{8\pi} \left\{ \frac{\epsilon_0}{c^2} \dot{V} \dot{V}^* - \frac{1}{\mu_0} \nabla V \cdot \nabla V^* \right\}$
Field equation	$\nabla^2 \mathbf{A} - \frac{\epsilon_0 \mu_0}{c^2} \ddot{\mathbf{A}} = 0$	$\nabla^2 V - \frac{\epsilon_0 \mu_0}{c^2} \ddot{V} = 0$
Momentum density	$\frac{1}{4\pi} (\mathbf{E} \wedge \mathbf{H})$	$-\frac{1}{8\pi \mu_0 c} (\dot{V}^* \nabla V + \dot{V} \nabla V^*)$
Electric energy density	$\frac{\epsilon_0}{8\pi} \mathbf{E}^2$	$\frac{\epsilon_0}{8\pi c^2} \dot{V} \dot{V}^*$
Magnetic energy density	$\frac{\mu_0}{8\pi} \mathbf{H}^2$	$\frac{1}{8\pi \mu_0} \nabla V \cdot \nabla V^*$

ACKNOWLEDGMENT

In conclusion we wish to thank Professor Max Born for his interest in this work and for stimulating discussions.

REFERENCES

- BRAUNBEK, W., 1951, *Z. Naturforsch.*, **6a**, 12.
HINES, C. O., 1952, *Canad. J. Phys.*, **30**, 123.
LUNEBERG, R. K., 1947-8, *Propagation of Electromagnetic Waves* (mimeographed notes of lectures delivered at New York University); 1949, *Asymptotic Development of Steady State Electromagnetic Fields*, New York University, Mathematics Research Group, Report No. EM-14.
PICHT, J., 1931, *Optische Abbildung* (Braunschweig: Vieweg).
STRATTON, J. A., 1941, *Electromagnetic Theory* (New York: McGraw-Hill).
THEIMER, O., WASSERMANN, G. D., and WOLF, E., 1952, *Proc. Roy. Soc. A*, **212**, 426.
WEATHERBURN, C. E., 1930, *Differential Geometry of Three Dimensions*, Vol. II (Cambridge: University Press).

The Band Spectrum of Nitrogen : New Studies of the Triplet Systems

By P. K. CARROLL AND N. D. SAYERS

Physics Department, Queen's University of Belfast

Communicated by K. G. Emeléus; MS. received 21st July 1953

Abstract. Using three different sources the molecular spectrum of nitrogen has been investigated in the visible and near infra-red. A new infra-red system recently reported by Herman has been studied in greater detail and the vibrational analysis revised. It has been shown that the bands do not arise from the singlet transition $v \rightarrow q$ but that states of higher multiplicity are involved. Extensions of the second positive system and the Gaydon-Herman bands in the green are reported. Improved measurements for bands of the First Positive system are given and a new vibrational formula has been derived. A new unassigned band at 8311 Å is reported.

§ 1. INTRODUCTION

FOR the purposes of interpreting auroral and night-sky observations it is essential that the spectra of the atmospheric gases be investigated as thoroughly as possible in the laboratory. The present experiments were undertaken with a view to obtaining some further information about the molecular spectrum of nitrogen. Three sources were investigated under moderate dispersion, and much improved plates were obtained of the new infra-red system reported by Herman (1951), as well as of the $\Delta v = 0$ sequence of the First Positive system. Some further information on the Gaydon-Herman Green bands and the Second Positive system was secured, while a complex band at 8310.6 Å, the emitter of which is most probably N_2 , was also discovered.

§ 2. EXPERIMENTAL ARRANGEMENTS

A conventional π -shaped positive column tube, of radius 5 mm and length 20 cm, containing nitrogen, was used. Purity of the gas was ensured by preliminary torching of the apparatus under vacuum and by the use of liquid air traps. In some instances the electrodes were degassed *in situ* by inductive heating. The nitrogen was prepared by exploding small charges of sodium azide. Pressures between 2 and 20 mm Hg were used.

Three methods of excitation were employed. In the first the spectrum was excited by a Tesla oscillator, with a secondary of 120 turns of diameter 7 cm and length 17 cm, and a primary of ten turns of stout wire in series with a spark gap and condenser of capacity 0.12 μ F. The condenser was charged by a 25 000 v transformer with input adjustable by a Variac transformer. In the other sources the transformer voltage was applied directly to the discharge tube. With moderate pressures of nitrogen a rather feeble blue or pink discharge was obtained. This form of discharge will be referred to as subnormal as it had anomalous properties in that, as the voltage was raised, the current and light intensity decreased until a

sufficient voltage was applied to maintain a normal bright discharge, which set in discontinuously. The latter discharge gave the third source. It was intensely yellow and its spectrum in the visible region consisted of the negative and the First Positive bands, while the Second Positive system was almost entirely absent. It appeared to be very similar to the 'auroral' discharge described by Kaplan (1932).

§ 3. HERMAN'S INFRA-RED BANDS

Herman (1951), using low current discharges through nitrogen in a tube cooled by liquid air, found eight new bands in the near infra-red which she attributed to the N_2 molecule. These bands were first observed in this laboratory in the Tesla source. On the original plates the First Positive bands were strong, so that a satisfactory study of the new system was not possible. The subnormal discharge, however, although weaker than the Tesla source, gave the new bands with an intensity comparable with that of the adjacent First Positive bands. Plate I(a) shows the spectrum of the latter source recorded on Kodak IIN plates using a Hilger D 187 spectrograph, which gave a dispersion of 185 \AA mm^{-1} at 8000 \AA .

From the spectrograms at her disposal Herman concluded that the bands had a simple structure, and assigned them to the transition between the high energy singlet states v and q of Worley (1943). There are, however, objections to this assignment. In the first place, the agreement between the vibrational intervals is poor. In the second place, the levels v and q are reached readily in absorption from the ground state $x^1\Sigma_g^+$. Consequently they are both of u symmetry, and the transition $v \rightarrow q$ is forbidden. In the present work the bands, although not readily excited, were obtained with greater ease and intensity than one would expect for a forbidden transition.

At the dispersion of plate I(a) the bands appear to have a simple structure, but at greater dispersion six close heads are resolved. Plate I(b) shows the system photographed on a glass Littrow spectrograph, with a dispersion of 50 \AA mm^{-1} at 8000 \AA , using the subnormal discharge. It is evident from the complexity of the structure that the bands result from a triplet, or possibly a quintet, transition.

Table 1. Wavelengths of New Infra-Red Bands (\AA)

(0, 1)	—	(0, 0)	8101.1 (1)	(1, 0)	7558.3 (1)	(2, 0)	7094.4 (1)
	—		8094.1 (2)		7550.0 (2)		7087.5 (2)
	—		8084.7 (3)		7541.4 (3)		7080.8 (3)
	—		8077.6 (4)		7536.5 (4)		7076.3 (4)
	—		8070.9 (5)		7530.7 (5)		7069.8 (5)
	8549 (6)		8057.6 (6)		7521.0 (6)		7061.7 (6)
(1, 2)	—	(2, 2)	7868.5 (1)	(2, 1)	7471.8 (1)	(3, 1)	7033.3 (1)
	—		7862.0 (2)		—		7025.8 (2)
	—		7853.7 (3)		—		7019.3 (3)
	—		7846.7 (4)		—		7014.6 (4)
	—		7840.7 (5)		—		7009.2 (5)
	8397 (6)		7828.5 (6)		7435.0 (6)		7001.2 (6)

The heads of the bands were measured against A, Ne and Xe reference lines. Their wavelengths are shown in table 1. For convenience the heads of each band have been numbered 1 to 6 in order of decreasing wavelength. The (0, 0), (2, 2), (2, 0) and (3, 1) bands could be measured accurately as they were strong and free

from overlapping. The (1, 0) band was strong enough for its heads to be separated from First Positive structure, but heads 1 and 6 alone could be measured for the (2, 1) band. The (1, 2) band was very weak, while the (0, 1) band was heavily masked by First Positive bands, so that in both cases it was possible only to make an estimate of the position of the strongest head.

Table 2. Deslandres Scheme for the New Infra-Red System

v'	v''	0	1	2
0		12407.2 (10)	713.1 11694.1 (2)	
		885.4		
1		13292.6 (4)		11905.7 (1)
		864.5		864.6
2		14157.1 (6)	710.9 13446.2 (5)	665.9 12770.3 (8)
			833.2	
3			14279.4 (4)	

The general appearance of the bands can be judged from the (2, 0) and (3, 1) bands in plate I(b). The strongest heads are those of shortest wavelength. A tentative Deslandres scheme for the No. 6 heads, corresponding to the v' values used above, is given in table 2. The intensity estimates are visual and subject to all the usual limitations in such assessments. In particular the intensity figures for the bands which overlap First Positive bands are subject to considerable error. The vibrational scheme differs from Herman's in that the v' values have been decreased by unity. This revision seems desirable, as on Herman's scheme, which was drawn up on the assumption that the transition involved was $v \rightarrow q$, the $v' = 0$ progression is absent. From Herman's analysis it follows that the heads of the (0, 0) band of the new system should lie in the region 8742–8692 Å, but failure to observe any new structure here is rather inconclusive as the (2, 1) First Positive band is very strong in this wavelength range. However, the new scheme has the advantage of identifying the strongest band of the entire system as the (0, 0) band, and is generally in better accord with the observed intensity distribution. The absence of the (1, 1) band could be due to an almost complete cancellation of the (1, 1) overlap integral. This effect, i.e. strong (0, 0) and (2, 2) bands with the (1, 1) band weak, is not unusual and is observed in the case of the First Positive system (§ 7). The absence of the (2, 1) band required by Herman's analysis is not so readily explained.

It was thought that the new system might have the same upper state as the Gaydon–Herman Green bands. This interpretation is attractive, since all the present work shows that the two systems are excited under identical conditions. Furthermore, in general appearance the bands are not unlike, while the vibrational

structure of the two systems is very similar. The relevant vibrational intervals are shown in table 3. The present measurements were used in both cases and the values in table 3 were obtained by averaging the differences between the wave numbers of corresponding heads. The discrepancies are individually outside the limit of experimental error and the ΔG values for the Green bands are all somewhat greater than those for the infra-red bands. It therefore seems that the two systems are unrelated.

Table 3. Mean Vibrational Intervals for the Green and Infra-Red Systems (cm^{-1})

	v	0	1	2
$\Delta G'(v + \frac{1}{2})$	Green	896.0	872.0	843.8
	Infra-red	888.1	864.3	833.7

§4. THE GAYDON-HERMAN GREEN SYSTEM

As very little is known about this system some time was spent in studying its excitation conditions. The bands were excited in the Tesla and subnormal discharges already described, and again the subnormal source, although the weaker of the two, was the more satisfactory for the production of the bands in relative isolation; it was difficult to control conditions in the Tesla discharge so that the First Positive bands were sufficiently suppressed to permit the observations of the Green system. In view of the possible relationship with the new infra-red system (§3) fresh measurements were made of the bands from plates taken with a Hilger D 187 spectrograph, which gives a dispersion of 55 \AA mm^{-1} at 5100 \AA . The complete measurements are not given, as they agree with Gaydon's (1944) to better than 1 \AA . However, two further bands were measured, the (2, 0) band with heads at 5090.2 , 5084.2 , 5080.2 , 5077.7 and 5073.0 \AA (for which Gaydon gives one head), and the (3, 1) band with heads at 5062.7 , 5057.5 , 5054.0 , 5050.7 , and 5046.8 \AA .

Tentative vibrational analyses of the system were made by Gaydon (1944) and Herman (1945a). Herman's scheme was essentially the same as Gaydon's, with v' and v'' interchanged on the grounds that at the temperature of liquid air the (0, 1) and (0, 2) bands on Gaydon's assignment were suppressed. The effect is not very marked in the reproduction of Herman's spectrograms due to the strength of the First Positive bands in the same region. In this laboratory the system was also observed in a subnormal discharge in a tube immersed in liquid air with the First Positive bands almost completely absent from the region in question. Our spectrograms show that the effect of cooling on the relative intensities is slight and, if anything, such that the $v' = 0$ progression is somewhat enhanced. It would therefore appear that whatever inference can be made about the vibrational structure from the effect of temperature favours Gaydon's scheme. This interpretation is supported by the fact that the bands degrade to shorter wavelengths, so that one would expect to find $\omega_e' > \omega_e''$, which follows from Gaydon's scheme, whereas Herman's requires that $\omega_e' < \omega_e''$.

Both the Green system and the new infra-red system are always accompanied by strong Negative and Second Positive bands, while in the near ultra-violet the Fourth Positive system and the singlet bands of Herman and Gaydon are also observed. The First Positive bands, although sometimes strong enough to be troublesome in observing the Green and infra-red bands, are relatively weak. The sources used therefore excite states of high rather than of low energy. Hence it

seems likely that the levels involved in the Green and infra-red systems lie at fairly high energies.

§ 5. SECOND POSITIVE BANDS

In the course of the present work several bands were observed in the green, which although not recorded by Pearse and Gaydon (1950), or Kayser and Konen (1934) obviously belong to the Second Positive system. To substantiate this the spectrum of a vigorous Tesla discharge through air was photographed, it being common knowledge that in discharges through oxygen-nitrogen mixtures, the Second Positive bands are strongly enhanced. Plate I(c) shows the spectrum of this discharge photographed with the Hilger D 187 spectrograph. The bands were measured from plates taken with the Littrow glass spectrograph. The wavelengths and vibrational numbering of the bands are as follows: (0, 6) 5031.5; (3, 10) 5066.0; (2, 9) 5179.3; (1, 8) 5309.3; and (0, 7) 5452.0 Å. The wavelengths recorded refer to the strongest (i.e. short wavelength) head and are in good agreement with the values calculated from Birge's formula (1929). It should be noted that the (1, 8) band lies exactly on top of the strongest head of the (1, 0) Green band and tends to give the latter an abnormally large intensity in the Tesla source.

The strong development of the visible Second Positive bands does not involve any departure from a normal intensity distribution. It is due simply to the strong excitation of the system as a whole under vigorous discharge conditions.

§ 6. A NEW INFRA-RED BAND

The infra-red spectrum of the transformer discharge was dominated by bands of the First Positive system. However, in the middle of the $\Delta v = 1$ sequence, where the intensity of the First Positive bands is not so great, a new band of moderate strength was observed. Plate I(d) shows the spectrum photographed on the Littrow glass spectrograph. The band is degraded to longer wavelengths and its structure is complicated. It has at least four heads at 8265.5, 8283.8, 8293.3 and 8310.6 Å, of which the last is the strongest. No other band which could be correlated with this band was observed although the spectrum was investigated down to 10600 Å. Nevertheless, some such bands could be present but escape detection due to overlapping First Positive bands.

It was not possible to assign the band at 8310.6 Å to a transition between any of the known triplet levels of N_2 . In general appearance it is not unlike a First Positive band, so that the transition may be of the ${}^3\Pi \rightarrow {}^3\Sigma$ type. There is no direct evidence that the emitter is N_2 , but this seems most probable as the source was remarkably free from impurity spectra.

§ 7. THE FIRST POSITIVE SYSTEM

In the course of studying the band at 8310.6 Å some plates of the First Positive system in the region 8900–10500 Å were obtained. Plate I(e) shows the spectrum recorded on a Kodak I Q plate, using the glass Littrow spectrograph, which has a dispersion of 80 Å mm⁻¹ at 10000 Å. The bands were measured against Xe and A arc lines.

Previous measurements of these bands were made by Poetker (1927), who worked at low resolution and gave the wavelengths of two intensity maxima for each band of the $\Delta v = 0$ sequence. The wavelengths of neither set of maxima agree well with those calculated from Birge's vibrational formula (Rosen 1951).

However, it is evident from our plates that the maxima recorded by Poetker lie near the P_2 and Q_3 heads in each band, whereas the vibrational formula refers to the P_1 heads. Table 4 gives the new measurements, together with the quantity termed $p(v', v'')$ by Jarman and Nicholls (1952), which is approximately proportional to the transition probability. (For transition probabilities of bands of small v values see also Bates (1949).) The (1, 1) band should lie at about 10214 Å, but was not recorded. The feeble band at 10133.3 Å, which is presumably what Poetker assumed to be the (1, 1) band, is undoubtedly the (6, 7) band. This is in agreement with Jarman and Nicholls' calculations, which show that the (1, 1) band should be very weak while the (6, 7) band should be one of the strongest of the $\Delta v = -1$ sequence in the spectral region under consideration. It is seen from plate I (e) that the intensities of the other bands in the region are in good qualitative agreement with what one would expect from the calculated $p(v', v'')$ values.

Table 4. Wavelengths of Infra-Red First Positive Bands (Å)

v', v''	(0, 0)	(1, 1)	(6, 7)	(2, 2)	(3, 3)	(4, 4)	(5, 5)
$\lambda(\text{Å})$	10508.3	—	10133.3*	9939.9	9680.4	9435.0	9201.9
$p(v', v'')$	0.340	0.002	0.084	0.113	0.161	0.113	0.044

* This wavelength differs slightly from that previously given for the (6, 7) bands in a preliminary publication (Sayers and Carroll 1953). The present measurement, made from a more intense plate, is believed to be more accurate.

It was mentioned in §2 that in the yellow transformer discharge the First Positive and Negative systems were strongly developed, while the Second Positive bands were almost entirely absent. It was therefore possible to photograph on the Littrow spectrograph the higher members of the $\Delta v = 6$ sequence of the First Positive system in the blue. These bands have previously been observed only in an afterglow (Herman 1945 b) in which the higher vibrational levels were enhanced. The wavelengths of the P_1 heads are given in table 5, as the new measurements, made from plates of larger dispersion, are probably more accurate than those given by Herman.

Table 5. Wavelengths of the Blue Bands of the First Positive System

	$\lambda(\text{Å})$		$\lambda(\text{Å})$		$\lambda(\text{Å})$
(13, 7)	5008.9	(18, 12)	4907.9	(23, 17)	4822.9
(14, 8)	4987.4	(19, 13)	4889.5	(24, 18)	4808.4
(15, 9)	4966.6	(20, 14)	4872.0	(25, 19)	4794.6
(16, 10)	4946.3	(21, 15)	4854.9	(26, 20)	4782.4
(17, 11)	4926.8	(22, 16)	4838.4		

To represent the blue bands Herman added terms in v^3 and v^4 to Birge's vibrational formula. Both Birge's and Herman's formulae show a small systematic error when applied to the infra-red bands, and in addition Herman's formula does not give good agreement with the vibrational intervals for the higher v values. A recalculation of the vibrational constants therefore seemed worth while. For the blue bands and the $\Delta v = 0$ sequence the present measurements were used, while for the visible and infra-red bands the measurements of Birge (1914) and Birkenbeil (1934) respectively were used. The formula obtained is

$$v = 9514.8 + (1720.35 v' - 14.913 v'^2 + 0.048423 v'^3 - 0.0022079 v'^4) \\ - (1446.26 v'' - 13.846 v''^2 + 0.008933 v''^3 - 0.0022667 v''^4).$$

Wavelengths calculated from this formula are in good agreement with all observations of the system. The discrepancy between calculated and observed wave numbers is nowhere greater than 3 cm^{-1} (except in the case of the (26,20) band, whose measurement was doubtful due to overlapping structure of the Goldstein-Kaplan band at 4728 \AA) and for most bands is less than 1 cm^{-1} . The vibrational constants derived from the formula are

$$\begin{aligned}\omega_e' &= 1735.30, & \omega_e x_e' &= 14.989, & \omega_e y_e' &= 0.052839, & \omega_e z_e' &= 0.0022079 \\ \omega_e'' &= 1460.11, & \omega_e x_e'' &= 13.863, & \omega_e y_e'' &= 0.013466, & \omega_e z_e'' &= 0.0022667\end{aligned}$$

§ 8. CONCLUSION

The states involved in the Green system and the new infra-red system have notable features in common. The ω_e values are all small and the r_e values correspondingly large for N_2 , while the energies are probably fairly high. The difficulty in observing the systems is undoubtedly due, at least in part, to the considerable increase in r_e required in exciting the upper states. Certainly the best excitation conditions of the systems are still obscure. It seems that considerably more work is required on the development of novel techniques which provide conditions not obtaining in the more conventional sources.

It is worthy of note that there are now three sets of levels whose positions on the energy level diagram are not known, viz. the states involved in the Fifth Positive and related systems, and the states giving rise to the Green system and the new infra-red system. A thorough search of all spectral regions should yield some transitions between the Fifth Positive or associated levels and some of the many known singlet states. Transition between states involved in the Green or infra-red systems and known triplet states are not so likely, due to the large discrepancy in r_e values. Furthermore, if the states of the former systems are quintet states they will be metastable with respect to both the singlet and triplet levels, thus rendering the determination of their energy doubly difficult.

ACKNOWLEDGMENT

In conclusion the authors would like to thank Professor K. G. Emeléus for his keen interest in the experiments and for helpful discussions at all stages in the work.

REFERENCES

- BATES, D. R., 1949, *Proc. Roy. Soc. A*, **196**, 217.
 BIRGE, R. T., 1914, *Astrophys. J.*, **39**, 50; 1929, *Int. Critical Tables*, **5**, 415.
 BIRKENBEIL, H., 1934, *Z. Phys.*, **88**, 1.
 GAYDON, A. G., 1944, *Proc. Phys. Soc.*, **56**, 85.
 HERMAN, R., 1945 a, *J. Phys. Radium*, **6**, 183; 1945 b, *Ann. Phys., Paris*, **20**, 241; 1951, *C.R. Acad. Sci., Paris*, **233**, 738.
 JARMAIN, W. R., and NICHOLLS, R. W., 1952, University of Western Ontario, Dept. of Physics, *Scientific Report No. 4*.
 KAPLAN, J., 1932, *Phys. Rev.*, **42**, 807.
 KAYSER, H., and KONEN, H., 1934, *Handbuch der Spektroskopie*, Vol. 7.
 PEARSE, R. W. B., and GAYDON, A. G., 1950, *The Identification of Molecular Spectra* (London: Chapman & Hall).
 POETKER, A. H., 1927, *Phys. Rev.*, **30**, 812.
 ROSEN, B., 1951, *Données spectroscopiques concernant les molécules diatomiques* (Paris: Hermann).
 SAYERS, N. D., and CARROLL, P. K., 1953, *Proc. Phys. Soc. A*, **66**, 577.
 WORLEY, R. E., 1943, *Phys. Rev.*, **64**, 207.

Vibrational Transition Probabilities of Diatomic Molecules : I

By P. A. FRASER AND W. R. JARMAN

Department of Physics, University of Western Ontario, London, Canada

Communicated by R. W. Nicholls; MS. received 16th July 1953

Abstract. An approximation is made which allows analytic integration of the 'overlap', and other, integrals of vibrational wave functions in Morse potentials that arise in the study of the electronic spectra of diatomic molecules. The heavy and lengthy work that goes into numerical integration is thus avoided for many bands of many systems. The necessity for the type of approximation made is discussed from the point of view of the extensive cancellation that occurs in any method of evaluating these integrals. An indication is given of the validity and applicability of the approximation and the formulae thus derived.

In this paper p -values (i.e. overlaps squared) calculated on this approximation are presented for the transitions N_2 , $B^3\Pi_g \rightarrow A^3\Sigma_u^+$ (First Positive) and N_2 , $C^3\Pi_u \rightarrow B^3\Pi_g$ (Second Positive), and compared with values calculated with Morse wave functions by numerical methods. The agreement is excellent.

§ 1. INTRODUCTION

IN the well-known formulae for the intensities of diatomic molecular bands in emission or absorption occur squares of integrals of the form

$$\int_0^\infty \psi_1^{(v')} R_e \psi_2^{(v'')} dr. \quad \dots\dots (1)$$

$\psi_1^{(v')}(r)$ and $\psi_2^{(v'')}(r)$ are respectively the vibrational wave functions in the v' and v'' levels in the electronic states 1 and 2 between which the transition $1 \rightarrow 2$ takes place; $R_e(r)$ is the matrix element of the appropriate multipole moment of the electrons (electronic transition integral); r is the internuclear separation.

The dependence of $R_e(r)$ on r is generally unknown, and as a first approximation $R_e(r)$ is replaced by a mean value \bar{R}_e for the band system. Thus

$$\int_0^\infty \psi_1^{(v')} R_e \psi_2^{(v'')} dr \simeq \bar{R}_e \int_0^\infty \psi_1^{(v')} \psi_2^{(v'')} dr. \quad \dots\dots (2)$$

The so-called overlap integral

$$\int_0^\infty \psi_1^{(v')} \psi_2^{(v'')} dr \equiv (v', v'') \quad \dots\dots (3)$$

is thus of importance when considering relative intensities within a band system. We define p -values by $p(v', v'') = (v', v'')^2$, these being a measure of the vibrational transition probabilities.

Further, if the dependence of $R_e(r)$ on r is either known, or sought, in a linear or quadratic form, then the integrals

$$\int_0^\infty \psi_1^{(v')} r \psi_2^{(v'')} dr \equiv (v', r v'') \quad \dots\dots(4)$$

$$\int_0^\infty \psi_1^{(v')} r^2 \psi_2^{(v'')} dr \equiv (v', r^2 v'') \quad \dots\dots(5)$$

become of interest.

Many methods have been suggested in the literature for evaluating overlap integrals. Most suffer from being either inaccurate or long and tedious, or both. An approximate method is presented here that uses wave functions in Morse potentials, which are relatively both accurate and simple representations of the vibrational potential. The method gives p -values rapidly, and the results are as reliable and useful, in view of the approximate nature of the Morse potential, as those derived by long and tedious numerical methods. To show the validity of the method two tables of p -values calculated on this approximation are shown and the results are compared with those of numerical integration of Morse wave functions. The agreement is excellent. Transitions for which tables are presented are:

$$N_2, B^3\Pi_g \rightarrow A^3\Sigma_u^+ \quad (\text{First Positive})$$

$$N_2, C^3\Pi_u \rightarrow B^3\Pi_g \quad (\text{Second Positive}).$$

Similar tables for band systems mainly of astrophysical interest are available and are in process of publication (Jarman, Fraser and Nicholls 1953).

§ 2. THE OVERLAP INTEGRAL

When a Morse function,

$$U_i(r) = D_i[1 - \exp\{-\alpha_i(r - r_{ei})\}]^2, \quad \dots\dots(6)$$

represents the potential of nuclear vibration in the electronic state i , the vibrational wave function for level v is given by (Morse 1929), ignoring a phase factor,

$$\begin{aligned} \psi_i^{(v)} &= \left[\frac{\alpha_i(K_i - 2v - 1)}{v! \Gamma(K_i - v)} \right]^{1/2} \{\exp(-z_i/2)\} z_i^{(K_i - 2v - 1)/2} (-1)^v \sum_{k=0}^v (-1)^k \binom{v}{k} \\ &\quad \times \frac{\Gamma(K_i - v)}{\Gamma(K_i - v - k)} z_i^{v-k} \\ &= N_i^{(v)} \{\exp(-z_i/2)\} z_i^{(K_i - 2v - 1)/2} L_{K_i - v - 1}^{K_i - 2v - 1}(z_i), \end{aligned} \quad \dots\dots(7)$$

where $L_{K_i - v - 1}^{K_i - 2v - 1}(z_i)$ is the associated Laguerre polynomial of degree v in z_i ,

$$z_i = K_i \exp\{-\alpha_i(r - r_{ei})\} = \lambda_i \exp(-\alpha_i r), \quad \dots\dots(8)$$

and K_i and D are related to the constants in the expression for the vibrational energy

$$\begin{aligned} E_i^{(v)} &= (\omega_e)_i(v + \tfrac{1}{2}) - (\omega_e x_e)_i(v + \tfrac{1}{2})^2; \\ K_i &= \frac{(\omega_e)_i}{(\omega_e x_e)_i}, \quad D_i = \frac{(\omega_e)_i^2}{4(\omega_e x_e)_i}. \end{aligned} \quad \dots\dots(9)$$

We note that

$$(\omega_e x_e)_i = \frac{\hbar}{4\pi c \mu_i} \alpha_i^2, \quad \dots\dots(10)$$

where μ_i is the reduced mass of the molecule in state i .

The overlap integral is given by (3):

$$(v', v'') = \int_0^\infty \psi_1^{(v')} \psi_2^{(v'')} dr.$$

Negligible error is introduced by integrating from $-\infty$ to ∞ (Morse 1929, ter Haar 1946). Then

$$\begin{aligned} (\tau', \tau'') &= \int_{-\infty}^\infty \psi_1^{(v')} \psi_2^{(v'')} dr \\ &= (-1)^{(v'+v'')} N_1^{(v')} N_2^{(v'')} \lambda_1^{(K_1-1)/2} \lambda_2^{(K_2-1)/2} \sum_{k=0}^{v'} \sum_{l=0}^{v''} (-1)^{k+l} \binom{v'}{k} \binom{v''}{l} \\ &\quad \times \frac{1}{\lambda_1^k \lambda_2^l} \frac{\Gamma(K_1 - v') \Gamma(K_2 - v'')}{\Gamma(K_1 - v' - k) \Gamma(K_2 - v'' - l)} J(k, l) \quad \dots\dots (11) \end{aligned}$$

$$\begin{aligned} \text{where } J(k, l) &= \int_{-\infty}^\infty dr \exp\{-\frac{1}{2}[\lambda_1 \exp(-\alpha_1 r) + \lambda_2 \exp(-\alpha_2 r)]\} \\ &\quad \times \exp[-(\{\frac{1}{2}(K_1 - 1) - k\}\alpha_1 r + \{\frac{1}{2}(K_2 - 1) - l\}\alpha_2 r)]. \quad \dots\dots (12) \end{aligned}$$

The $J(k, l)$ cannot be evaluated exactly, in general, since $\alpha_1 \neq \alpha_2$, and if it is desired to obtain a general formula for an overlap it is necessary to resort to a valid approximation.

Because of the very large cancellation that occurs on performing the double sum in the expression for (v', v'') , an individual approximation to each $J(k, l)$ would be difficult to make consistently. In fact, the number of figures lost on summing can be shown to be of the order of $(v' + v'') + m - n$ where $(0, 0) \sim 10^{-n}$ and $|(\tau', \tau'')| \sim 10^{-m}$. This cancellation is, of course, an intrinsic property of the Laguerre polynomials. For $v' + v'' \lesssim 2$ or 3, approximation to each $J(k, l)$ would be adequate, but for greater $v' + v''$ such a procedure would break down (e.g. Bouigue 1951, Wu 1952). Therefore, the approximation adopted here is one which covers consistently all vibrational levels of the two states and allows analytic integration of the $J(k, l)$, and hence the (v', v'') .

It was noted above that the $J(k, l)$ are not integrable because $\alpha_1 \neq \alpha_2$. The approximation is to replace $U_1(r)$ and $U_2(r)$ by two new potentials, $U_1'(r)$ and $U_2'(r)$. The new potentials each have their α -values equal to some mean of the original α_1 and α_2 . It is easiest to take the arithmetic mean $\alpha = \frac{1}{2}(\alpha_1 + \alpha_2)$, though it is sometimes convenient to choose another α that will make final computations easier and yet not affect the result.* Compensating adjustments are made in the constants of the two states that depend on the α -value for the state. Thus normalization and closure properties are maintained.

The adjusted molecular constants, adjusted to correspond to the new α , and indicated for the present by primes, are:

$$\begin{aligned} K_1' &= K_1(\alpha_1/\alpha)^2, \quad K_2' = K_2(\alpha_2/\alpha)^2, \quad \lambda_1' = K_1' \exp \alpha r_{e1}, \quad \lambda_2' = K_2' \exp \alpha r_{e2}, \quad N_1^{(v')'}, \quad N_2^{(v'')'} \\ &\dots\dots (13) \end{aligned}$$

Assuming $\alpha = \frac{1}{2}(\alpha_1 + \alpha_2)$ and writing $\alpha_1 = \alpha + \delta\alpha$, $\alpha_2 = \alpha - \delta\alpha$, it is readily seen that errors introduced by the approximation will be proportional to $|\delta\alpha/\alpha|$, and that the errors will be less the smaller the overlapping of the two potentials. Small values of $|\delta\alpha/\alpha|$, i.e. $\lesssim 5\%$, imply slight change in the description of the

* e.g. sometimes an α between α_1 and α_2 can be found that makes $\lambda_1' = \lambda_2'$ (λ_1' and λ_2' are defined in (13)).

states (e.g. a small change in the second term in the energy), and one would expect that the wave functions in the new potentials would be quite adequate for the calculation of such quantities as overlap integrals.*

The adjustment of state constants having been made, and dropping the primes on all the new quantities, (v', v'') takes on the same form as (11) with $J(k, l)$ now given by

$$J(k, l) = \int_{-\infty}^{\infty} dr \exp\{-[\lambda \exp(-\alpha r)]\} \exp\{-(K-1)-(k+l)]\alpha r\} \\ = J(k+l)$$

$$\text{where} \quad K = \frac{1}{2}(K_1 + K_2); \quad \lambda = \frac{1}{2}(\lambda_1 + \lambda_2). \quad \dots\dots(14)$$

$J(k+l)$ can now be integrated exactly:

$$J(k+l) = \frac{1}{\alpha} \left(\frac{1}{\lambda}\right)^{(K-1)-(k+l)} \Gamma(K-1-[k+l]). \quad \dots\dots(15)$$

It is natural to take the ratio of (v', v'') to $(0, 0)$, and also to introduce $\sigma = k+l$. Then

$$\frac{(v', v'')}{(0, 0)} = (-1)^{v'+v''} \frac{N_1^{(v')} N_2^{(v'')}}{N_1^{(0)} N_2^{(0)}} \sum_{\sigma=0}^{v'+v''} (-1)^{\sigma} \frac{\Gamma(K-1-\sigma)}{\Gamma(K-1)} C(v', v''; \sigma) \quad \dots\dots(16)$$

where

$$C(v', v''; \sigma) \equiv \sum_{k=0}^{\sigma} \binom{v'}{k} \binom{v''}{\sigma-k} \rho_1^k \rho_2^{\sigma-k} \frac{\Gamma(K_1-v') \Gamma(K_2-v'')}{\Gamma(K_1-v'-k) \Gamma(K_2-v''-\sigma+k)}; \dots\dots(17)$$

$$\rho_1 \equiv \lambda/\lambda_1; \quad \rho_2 \equiv \lambda/\lambda_2; \quad \dots\dots(18)$$

with

$$(0, 0) = \frac{N_1^{(0)} N_2^{(0)}}{\alpha} \left(\frac{1}{\rho_1}\right)^{(K_1-1)/2} \left(\frac{1}{\rho_2}\right)^{(K_2-1)/2} \Gamma(K-1) \\ = \left(\frac{1}{\rho_1}\right)^{(K_1-1)/2} \left(\frac{1}{\rho_2}\right)^{(K_2-1)/2} \frac{\Gamma(K-1)}{\{\Gamma(K_1-1) \Gamma(K_2-1)\}^{1/2}}. \quad \dots\dots(19)$$

It will be noticed that for $\sigma \geq 1$

$$\frac{\Gamma(K-1-\sigma)}{\Gamma(K-1)} = \frac{1}{(K-2)(K-3) \dots (K-1-\sigma)}.$$

Similar reduction is possible in the ratios of gamma functions appearing in $C(v', v''; \sigma)$. A few of the $(v', v'')/(0, 0)$ are displayed explicitly in the Appendix.

§ 3. THE OTHER INTEGRALS

The integrals (v', rv'') , eqn. (4), and (v', r^2v'') , eqn. (5), may be evaluated on the above approximation. Straightforward analysis leads to:

$$\frac{(v', rv'')}{(0, r0)} = (-1)^{v'+v''} \frac{N_1^{(v')} N_2^{(v'')}}{N_1^{(0)} N_2^{(0)}} \sum_{\sigma=0}^{v'+v''} (-1)^{\sigma} \frac{\Gamma(K-1-\sigma)}{\Gamma(K-1)} C(v', v''; \sigma) g(K-1-\sigma) \quad \dots\dots(20)$$

$$\frac{(v', r^2v'')}{(0, r^20)} = (-1)^{v'+v''} \frac{N_1^{(v')} N_2^{(v'')}}{N_1^{(0)} N_2^{(0)}} \sum_{\sigma=0}^{v'+v''} (-1)^{\sigma} \frac{\Gamma(K-1-\sigma)}{\Gamma(K-1)} C(v', v''; \sigma) h(K-1-\sigma) \quad \dots\dots(21)$$

$$\text{with} \quad (0, r0) = \alpha^{-1}(0, 0)f(K-1) \quad \dots\dots(22)$$

$$\text{and} \quad (0, r^20) = \alpha^{-2}(0, 0)F(K-1), \quad \dots\dots(23)$$

* An improvement that gives excellent results when $|\delta\alpha/\alpha| \gtrsim 5\%$ is described elsewhere (Jarman and Fraser 1953 b).

$$\left. \begin{aligned} \text{where } f(K-1) &= \ln \lambda - \phi(K-1), \quad F(K-1) = f^2(K-1) + \phi'(K-1) \\ g(K-1-\sigma) &= \frac{\ln \lambda - \phi(K-1-\sigma)}{f(K-1)} \\ h(K-1-\sigma) &= \frac{[\ln \lambda - \phi(K-1-\sigma)]^2 + \phi'(K-1-\sigma)}{F(K-1)} \end{aligned} \right\} \dots\dots(24)$$

$$\text{and} \qquad \qquad \qquad \phi(x) = \frac{d}{dx} \ln \Gamma(x). \qquad \qquad \qquad \dots\dots(25)$$

Expressions can be found for f , F , g and h using the expansion and properties of the logarithmic derivative of the gamma function (e.g. Jahnke and Emde 1938). Details are given elsewhere (Fraser and Jarman 1953). It will be noticed that g and h multiply terms in the σ -sum that appear in the expression for the overlap integral and would thus be available.

The expressions (20), (21) for $(v',rv'')/(0,r0)$ and $(v',r^2v'')/(0,r^20)$ are of course directly applicable to the calculation of intensities in pure vibration

Table 1. Molecular Constants of N₂ (Herzberg 1950)

State	α (Å ⁻¹)	K	r_e (Å)
c ³ Π _u	2·6636	119·15	1·1482
B ³ Π _g	2·4517	119·84	1·2123
A ³ Σ _u ⁺	2·4021	105·13	1·293
Transition	Chosen mean α (Å ⁻¹)		
B → A	2·4269		
C → B	2·5619		

spectra. There is no approximation involved in this case, for $\alpha_1=\alpha_2$, and $K_1=K_2=K$, $\lambda_1=\lambda_2=\lambda$, $\rho_1=\rho_2=1$. The expressions for $(v',r^2v'')/(0,r^20)$, after obvious simplification arising from the above equalities and the orthogonality of the wave functions in this case, are perhaps in a form more suited for computation than those previously published for pure vibration spectra (Buckmaster 1952), though otherwise completely equivalent.

§ 4. RESULTS

To show the validity of the approximation two tables of p -values are presented, and compared with values obtained earlier by numerical integrations of Morse wave functions (Jarman and Nicholls 1952). Table 1 shows the basic molecular constants for the three states, c³Π_u, B³Π_g, A³Σ_u⁺ of N₂ (Herzberg 1950), and the mean α -values chosen for the two transitions. p -values for the First and Second Positive systems of N₂ are shown in tables 2 and 3.

For the First Positive system $|\delta\alpha/\alpha|$ is small, and the agreement between the two methods of computation is excellent. Table 1 shows that for the Second Positive system $|\delta\alpha/\alpha|$ is somewhat larger and the agreement is satisfactory.

The limitation of tables 2 and 3 is dictated only by the use of a ten-digit desk computing machine, and results from the extensive cancellation mentioned above. The limit is given approximately by $v'+v''\leq 6+n$, where $(0,0)\sim 10^{-n}$. Work is in progress on the performance of this cancellation algebraically. Results to the present time, important in themselves in that they allow calculation of overlaps for the first four progressions to high quantum numbers, are reported elsewhere (Jarman and Fraser 1953 b).

Table 2. $N_2, B^3\Pi_g \rightarrow A^3\Sigma_u^+$ (First Positive)

$$p(v', v'') = (v', v'')^2$$

(Results from numerical integration (Jarman and Nicholls 1952) are shown in parentheses)

$v' \backslash v''$	0	1	2	3	4	5	6
0	0.33 ₇ (0.34 ₀)	0.32 ₄ (0.32 ₃)	0.19 ₀ (0.19 ₀)	0.08 ₉ (0.08 ₈)	0.03 ₇ (0.03 ₆)	0.01 ₄ (0.01 ₄)	0.00 ₅ (0.00 ₅)
1	0.40 ₆ (0.40 ₆)	0.00 ₃ (0.00 ₂)	0.10 ₂ (0.10 ₃)	0.17 ₇ (0.17 ₇)	0.14 ₅ (0.14 ₈)	0.08 ₇ (0.08 ₉)	
2	0.19 ₈ (0.20 ₀)	0.20 ₉ (0.21 ₃)	0.11 ₅ (0.11 ₃)	0.00 ₁ (0.00 ₂)	0.07 ₄ (0.07 ₄)		
3	0.05 ₁ (0.05 ₀)	0.29 ₉ (0.30 ₁)	0.03 ₆ (0.03 ₉)	0.15 ₉ (0.16 ₁)			
4	0.00 ₇ (0.00 ₆)	0.13 ₄ (0.13 ₄)	0.27 ₀ (0.27 ₃)				
5	0.00 ₁ (0.00 ₀)	0.02 ₉ (0.02 ₇)					
6	0.00 ₀ (0.00 ₀)						

Table 3. $N_2, c^3\Pi_u \rightarrow B^3\Pi_g$ (Second Positive)

$$p(v', v'') = (v', v'')^2$$

(Results from numerical integration (Jarman and Nicholls 1952) are shown in parentheses)

$v' \backslash v''$	0	1	2	3	4	5	6
0	0.44 ₄ (0.44 ₈)	0.32 ₈ (0.32 ₈)	0.14 ₉ (0.14 ₆)	0.05 ₄ (0.05 ₃)	0.01 ₈ (0.01 ₆)	0.00 ₅ (0.00 ₅)	0.00 ₂ (0.00 ₁)
1	0.38 ₉ (0.39 ₃)	0.01 ₅ (0.01 ₉)	0.19 ₆ (0.20 ₃)	0.19 ₉ (0.19 ₅)	0.11 ₆ (0.11 ₅)	0.05 ₂ (0.04 ₇)	
2	0.13 ₈ (0.13 ₅)	0.31 ₂ (0.32 ₃)	0.04 ₁ (0.03 ₂)	0.04 ₉ (0.06 ₂)	0.15 ₂ (0.15 ₈)		
3	0.02 ₆ (0.02 ₂)	0.25 ₆ (0.25 ₆)	0.14 ₃ (0.16 ₃)	0.13 ₁ (0.11 ₆)			
4	0.00 ₃ (0.00 ₂)	0.07 ₆ (0.07 ₀)	0.29 ₆ (0.30 ₃)				

ACKNOWLEDGMENTS

The authors wish to acknowledge the encouragement and support given to them by Dr. R. W. Nicholls during the course of this work. They wish also to thank Dr. Ta-You Wu for a recent profitable discussion of the subject, and for drawing their attention to the work of Bouigue.

The research reported in this paper has been sponsored by the Geophysics Research Directorate, Air Force Cambridge Research Centre, Air Research and Development Command, under Contract No. AF19 (122)-470.

APPENDIX

Explicit Formulae

A few of the formulae resulting from (16) are shown below, and the ease of computation from them is clear. The formulae for (v', rv'') and (v', r^2v'') integrals are, of course, similar.

$$\frac{(0, 1)}{(0, 0)} = - \frac{N_2^{(1)}}{N_2^{(0)}} \left\{ 1 - \rho_2 \frac{(K_2 - 2)}{(K - 2)} \right\},$$

$$\frac{(0, 2)}{(0, 0)} = \frac{N_2^{(2)}}{N_2^{(0)}} \left\{ 1 - 2\rho_2 \frac{(K_2 - 3)}{(K - 2)} + \rho_2^2 \frac{(K_2 - 3)(K_2 - 4)}{(K - 2)(K - 3)} \right\},$$

$$\frac{(1, 1)}{(0, 0)} = \frac{N_1^{(1)} N_2^{(1)}}{N_1^{(0)} N_2^{(0)}} \left\{ 1 - \left[\rho_1 \frac{(K_1 - 2)}{(K - 2)} + \rho_2 \frac{(K_2 - 2)}{(K - 2)} \right] + \rho_1 \rho_2 \frac{(K_1 - 2)(K_2 - 2)}{(K - 2)(K - 3)} \right\},$$

$$\begin{aligned} \frac{(0, 3)}{(0, 0)} = - \frac{N_2^{(3)}}{N_2^{(0)}} \left\{ 1 - 3\rho_2 \frac{(K_2 - 4)}{(K - 2)} + 3\rho_2^2 \frac{(K_2 - 4)(K_2 - 5)}{(K - 2)(K - 3)} \right. \\ \left. - \rho_2^3 \frac{(K_2 - 4)(K_2 - 5)(K_2 - 6)}{(K - 2)(K - 3)(K - 4)} \right\}, \end{aligned}$$

$$\begin{aligned} \frac{(1, 2)}{(0, 0)} = - \frac{N_1^{(1)} N_2^{(2)}}{N_1^{(0)} N_2^{(0)}} \left\{ 1 - \left[\rho_1 \frac{(K_1 - 2)}{(K - 2)} + 2\rho_2 \frac{(K_2 - 3)}{(K - 2)} \right] \right. \\ \left. + \left[2\rho_1 \rho_2 \frac{(K_1 - 2)(K_2 - 3)}{(K - 2)(K - 3)} + \rho_2^2 \frac{(K_2 - 3)(K_2 - 4)}{(K - 2)(K - 3)} \right] \right. \\ \left. - \rho_1 \rho_2^2 \frac{(K_1 - 2)(K_2 - 3)(K_2 - 4)}{(K - 2)(K - 3)(K - 4)} \right\}. \end{aligned}$$

The ratios of normalizing constants, $N_i^{(v)}$, are best built up from the ratios of adjacent normalizing constants. From (7) it is observed that

$$\frac{N_i^{(v)}}{N_i^{(v-1)}} = \left[\frac{K_i - v}{v} \cdot \frac{K_i - 2v - 1}{K_i - 2v + 1} \right]^{1/2};$$

and then, for example,

$$\frac{N_2^{(2)}}{N_2^{(0)}} = \frac{N_2^{(2)}}{N_2^{(1)}} \cdot \frac{N_2^{(1)}}{N_2^{(0)}}, \text{ etc.}$$

The formula for $(m, n)/(0, 0)$ is obtained from that for $(n, m)/(0, 0)$ by interchanging subscripts 1 and 2.

A method of computation that avoids explicit writing down of the formulae for other than the $v' = 0$, $v'' = 0$ progressions is based on the observation that $(m, n)/(0, 0)$ resembles closely the product of $(m, 0)/(0, 0)$ and $(0, n)/(0, 0)$, differing only in the K denominators. Compensation with tabulated factors may then be made in individual terms of such a product while computing. This is discussed more fully elsewhere (Jarman and Fraser 1953 a).

REFERENCES

- BOUIGUE, R., 1951, *C. R. Acad. Sci., Paris*, **232**, 2401.
BUCKMASTER, H. A., 1952, *Canad. J. Phys.*, **30**, 314.
FRASER, P. A., and JARMAN, W. R., 1953, *Scientific Report* No. 5,* Contract No. AF 19 (122)-470 (London, Canada : Dept. of Physics, University of Western Ontario).
TER HAAR, D., 1946, *Phys. Rev.*, **70**, 222.
HERZBERG, G., 1950, *Spectra of Diatomic Molecules* (New York : Van Nostrand).
JAHNKE, E., and EMDE, F., 1938, *Tables of Functions*, 3rd Edn. (New York : Stechert).
JARMAN, W. R., and FRASER, P. A., 1953 a, *Scientific Report* No. 7,* Contract No. AF 19 (122)-470 (London, Canada : Dept. of Physics, University of Western Ontario); 1953 b, *Proc. Phys. Soc. A*, **66**, 1153.
JARMAN, W. R., FRASER, P. A., and NICHOLLS, R. W., 1953, *Astrophys. J.* **118**, 228.
JARMAN, W. R., and NICHOLLS, R. W., 1952, *Scientific Report* No. 4,* Contract No. AF 19 (122)-470 (London, Canada : Dept. of Physics, University of Western Ontario).
MORSE, P., 1929, *Phys. Rev.*, **34**, 57.
WU, TA-YOU, 1952, *Proc. Phys. Soc. A*, **65**, 965.

* Available from the authors on request.

Vibrational Transition Probabilities of Diatomic Molecules : II

BY W. R. JARMAIN AND P. A. FRASER

Department of Physics, University of Western Ontario, London, Canada

Communicated by R. W. Nicholls; MS. received 16th July 1953

Abstract. Two improvements in the method of calculating vibrational overlap integrals presented in a previous paper are given here.

The first improvement allows the treatment of cases where $|(\alpha_1 - \alpha_2)/(\alpha_1 + \alpha_2)|$ is so large ($\geq 5\%$) that the results using the technique of the previous paper are merely indicative of trends. α_1 and α_2 are the parameters in the Morse potentials whose adjustment is the basis of the approximation in the previous paper.

The second improvement is a method of overcoming algebraically the heavy cancellation (intrinsic in the wave functions) that limits the extent of tables of p -values (i.e. overlaps squared). Formulae for the 0, 1, 2 and 3 progressions in either direction are given that allow the overlaps to be calculated for much higher quantum numbers than was previously possible.

§ 1. INTRODUCTION

IN a previous paper (Fraser and Jarmain 1953, to be referred to as I) whose notation is used here, a rapid approximate method of calculating overlap, and other, integrals of vibrational wave functions in Morse potentials was presented. Two difficulties with the application of the formulae of I were indicated: (i) the limited reliability of the results when $|(\alpha_1 - \alpha_2)/(\alpha_1 + \alpha_2)| = |\delta\alpha/\alpha|$ is large, say $\geq 5\%$, where α is the arithmetic mean of α_1 and α_2 , and (ii) the limitation on the extent of a table of overlaps due to the large cancellation originating from the Laguerre polynomials in the wave functions. Methods of overcoming these difficulties are presented here.

§ 2. THE ' r_e -SHIFT'

The formulae in I for the overlap integrals give results in excellent agreement with those derived by numerical integration of Morse wave functions when $|\delta\alpha/\alpha| \leq 5\%$.^{*} For larger $|\delta\alpha/\alpha|$ the results are satisfactory or, at worst, indicative of trends. The improvement described below applies to such cases and raises the 'satisfactory' class to the 'excellent' class, and the 'indicative of trends' class to either of the two higher classes.

One of the distortions introduced by the approximation (the basis of which, one recalls, is the replacement of the 'old' Morse potentials by two 'new' ones, which allow analytic integration of the overlaps) is a displacement of the vibrational wave functions slightly to larger or smaller values of r , the internuclear distance, depending on the directions of change of α_1 and α_2 . This displacement increases

^{*} This restriction on $|\delta\alpha/\alpha|$ covers most cases. When the difference between the equilibrium internuclear distances is less than ~ 0.05 Å, the tolerance on $|\delta\alpha/\alpha|$ is less, and when the difference is larger, the tolerance is greater.

with the changes in α_1 and α_2 . An improvement would be to shift the 'new' potentials either to the right or to the left, necessarily a different amount for each band, by changing the r_e values, so that the 'new' wave functions are approximately in the position of the 'old'. The best ' r_e -shift' to make for each vibrational level has been found empirically by requiring the best over-all agreement with values calculated by numerical methods. This procedure led to the following very reasonable expression for the shift:

$$\delta r_{ei}^{(v)} = -\frac{1}{2} \left\{ \frac{1}{2} (\delta r_{+i}^{(v)} + \delta r_{-i}^{(v)}) + \delta r_{0i}^{(v)} \right\}, \quad \dots\dots (1)$$

where $\delta r_{+i}^{(v)}$ is the change in the r coordinate of the right-hand classical turning point caused by the approximation, for the v th level in the electronic state i , $\delta r_{-i}^{(v)}$ is the similar change in the left-hand classical turning point, and $\delta r_{0i}^{(v)}$ is the change in the r coordinate of the central node or maximum of the wave function $\psi_i^{(v)}$.

Calculation using a formula given by Pillow (1951) for $\delta r_{0i}^{(v)}$ gives

$$\delta r_{ei}^{(v)} = \left(\frac{3v+2}{2K_i} \right) \left(\frac{\delta \alpha_i}{\alpha^2} \right) \quad \dots\dots (2)$$

to first order in $|\delta \alpha_i / \alpha|$ and $1/K_i$, where $\alpha = \alpha_i - \delta \alpha_i$, and where K_i is the *adjusted* parameter. The required change in the difference ($r_{e1} - r_{e2}$) for the [v' , v''] band is given by

$$\delta(r_{e1} - r_{e2})^{(v', v'')} = \delta r_{e1}^{(v')} - \delta r_{e2}^{(v'')}. \quad \dots\dots (3)$$

In the case that $\alpha = \frac{1}{2}(\alpha_1 + \alpha_2)$, $\delta \alpha = \frac{1}{2}(\alpha_1 - \alpha_2) = \delta \alpha_1 = -\delta \alpha_2$, this reduces to

$$\delta(r_{e1} - r_{e2})^{(v', v'')} = \left(\frac{\delta \alpha}{\alpha^2} \right) \left\{ \frac{3v' + 2}{2K_1} + \frac{3v'' + 2}{2K_2} \right\}. \quad \dots\dots (4)$$

The quantities in the formulae that depend on $(r_{e1} - r_{e2})$ are ρ_1 and ρ_2 . However, it is not necessary to work out a set of ρ_1 and ρ_2 , a pair for each band, and a set of (0, 0) integrals with the consequent loss of the valuable multiplication technique of computing (Appendix of I). The value of an overlap depends linearly to a high degree of approximation on any small change in the difference $r_{e1} - r_{e2}$. Hence two tables of overlaps are computed using the multiplication technique: one table with no ' r_e -shift', the other with the ' r_e -shift' appropriate to some particular band, the (2, 2) band, say. Interpolation or extrapolation with these two tables, making use of the appropriate ' r_e -shift' for the band given by (2) or (4), will lead to the improved values for the overlaps.

§ 3. RESULTS OF APPLYING ' r_e -SHIFT'

The band system used to establish the amount of ' r_e -shift' for each band was the violet system of CN, $B^2\Sigma^+ \rightarrow X^2\Sigma^+$. The technique was then applied to the Second Positive system of N_2 , $c^3\Pi_u \rightarrow B^3\Pi_g$, as a check. In I results were reported for the Second Positive system of N_2 (I, table 3) without this shift. Applying the ' r_e -shift' gave even better agreement with the results of numerical integration. For example, the technique changed $p(3, 2)$ to 0.163, and $p(3, 3)$ to 0.120, both in much better agreement with the results from numerical methods. A very few bands were slightly worsened, but there was an overall improvement throughout the table.

Table 1 shows the basic constants of the two states $B^2\Sigma^+$ and $X^2\Sigma^+$ of CN (Herzberg 1950), and the mean α chosen for the transition. Table 2 presents p -values (overlaps squared) for this transition computed by three methods: (a) approximate method, no ' r_e -shift', (b) approximate method with ' r_e -shift', and (c) numerical integration of the 'true' wave functions. It is clear from the table

that the well-defined shift (1) will give results in excellent agreement with those of numerical integration. It should be noted that the property of p -values, $\sum_{v'} p(v', v'') = 1$ and $\sum_{v''} p(v', v'') = 1$, is lost to a certain extent after applying ' r_e -shift ' . The difference from unity is not serious.

Table 1. Molecular Constants of CN (Herzberg 1950)

State	α (\AA^{-1})	K	r_e (\AA)
B $^2\Sigma^+$	2.7863	106.87	1.1506
X $^2\Sigma^+$	2.2448	157.39	1.1718

Mean $\alpha = 2.5156 \text{ \AA}^{-1}$

Table 2. CN, $B^2\Sigma^+ \rightarrow X^2\Sigma^+$ (Violet)

$$p(v', v'') = (v', v'')^2$$

v'	0	1	2	3
0	0.91 ₂ 0.91 ₇ (0.92 ₀)	0.08 ₁ 0.07 ₃ (0.07 ₄)	0.00 ₆ 0.00 ₅ (0.00 ₅)	0.00 ₁ 0.00 ₀ (0.00 ₀)
1	0.08 ₆ 0.07 ₇ (0.07 ₉)	0.75 ₂ 0.78 ₅ (0.78 ₇)	0.14 ₃ 0.12 ₁ (0.12 ₁)	0.01 ₇ 0.01 ₁ (0.01 ₄)
2	0.00 ₂ 0.00 ₁ (0.00 ₁)	0.16 ₂ 0.13 ₄ (0.13 ₇)	0.61 ₂ 0.69 ₂ (0.69 ₁)	0.18 ₈ 0.15 ₀ (0.14 ₇)
3	0.00 ₀ 0.00 ₀ (0.00 ₀)	0.00 ₅ 0.00 ₃ (0.00 ₂)	0.22 ₉ 0.17 ₄ (0.18 ₀)	0.49 ₀ 0.62 ₇ (0.62 ₅)

The three lines in each group indicate respectively : approximate method, no ' r_e -shift ' ; approximate method, with ' r_e -shift ' ; numerical integration.

§ 4. ' REMAINDER ' FORMULAE

The procedure presented in I for evaluating overlap integrals is very rapid compared with other available methods, with the exception of an approximation offered by Bates (1953). However, Bates' method is limited by the small number of bands for which tables are given, apparently because of the dubious validity of the approximation for higher quantum numbers. As noted in I, there is a limitation due to the intrinsic cancellation in the Laguerre polynomials on the extent of a table of $p(v', v'')$ computed by the formulae of I. The limit on the sum of the quantum numbers using a ten-digit desk calculating machine is given approximately by $v' + v'' \leq 6 + n$ where $(0, 0) \sim 10^{-n}$. This cancellation accounts for many more figures (the full capacity of the machine) having to be used in the computations than are apparently justified by the molecular data. One must assume the data exact for computation purposes.

From the formulae resulting from the present approximation, this cancellation may be carried out algebraically, and a quantity is left which exhibits none of this large cancellation*, and which could be evaluated on a slide-rule if necessary, giving accuracy to two decimal places.

* Any cancellation left would be due to the smallness of the integral being evaluated, and would rarely amount to more than 2 or 3 figures.

Such 'remainder' formulae have been found for progressions in which one of the quantum numbers is 0, 1, 2 or 3, the other not restricted. These are the progressions usually of greatest experimental interest. Work is continuing on this problem with the hope of finding a general result (there is a clear pattern in the progressions so far treated) or of extending to higher progressions.

It is convenient to define quantities ΔK and δ by

$$\Delta K = \frac{1}{2}(K_1 - K_2); \quad \delta = 1 - \frac{1}{\rho_1} = \frac{1}{\rho_2} - 1. \quad \dots\dots(5)$$

Then expansion of the expression for (0, 0) gives

$$(0, 0) = \exp \left[- \left\{ \frac{(\Delta K)^2}{2} \left[\frac{1}{(K-1)} + \frac{1}{2(K-1)^2} \right] + \frac{(\Delta K)^4}{12} \frac{1}{(K-1)^3} \right. \right. \\ \left. \left. + \frac{1}{2}(K-1)(\delta^2 + \frac{1}{2}\delta^4) + (\Delta K)(\delta + \frac{1}{3}\delta^3) \right\} \right], \quad \dots\dots(6)$$

which holds if $|\Delta K| \lesssim 10$, $|\delta| \lesssim \frac{1}{10}$. Further terms are easily found for larger $|\Delta K|$ and $|\delta|$.

For the $v' = 0$ progression the following are obtained:

$$\frac{(0, 1)}{(0, 0)} = - \frac{N_2^{(1)}}{N_2^{(0)} \rho_2} \left\{ \frac{\Delta K}{K-2} + \delta \right\}, \quad \dots\dots(7)$$

$$\frac{(0, 2)}{(0, 0)} = \frac{N_2^{(2)}}{N_2^{(0)} \rho_2^2} \left\{ \frac{(\Delta K)(\Delta K+1)}{(K-2)(K-3)} + 2\delta \frac{(\Delta K+1)}{(K-2)} + \delta^2 \right\}, \quad \dots\dots(8)$$

$$\frac{(0, 3)}{(0, 0)} = - \frac{N_2^{(3)}}{N_2^{(0)} \rho_2^3} \left\{ \frac{(\Delta K)(\Delta K+1)(\Delta K+2)}{(K-2)(K-3)(K-4)} + 3\delta \frac{(\Delta K+1)(\Delta K+2)}{(K-2)(K-3)} \right. \\ \left. + 3\delta^2 \frac{(\Delta K+2)}{(K-2)} + \delta^3 \right\}. \quad \dots\dots(9)$$

The formulae for higher quantum numbers in this progression follow the same pattern. The replacement of ΔK by $-\Delta K$ and δ by $-\delta$ within the braces and the subscript 2 by 1 outside the braces gives the formulae for the $v'' = 0$ progression.

The method of obtaining formulae for the 1, 2 and 3 progressions follows from the relation:

$$\frac{(v', v'')}{(0, 0)} - \frac{(v', 0)}{(0, 0)} \cdot \frac{(0, v'')}{(0, 0)} = \frac{N_1^{(v')} N_2^{(v'')} \sum_{\sigma=0}^{v'+v''} (-1)^\sigma \frac{\Gamma(K-1-\sigma)}{\Gamma(K-1)}}{N_1^{(0)} N_2^{(0)}} \\ \sum_{k=0}^{\sigma} \gamma(v', v''; \sigma, k) \left[1 - \frac{\Gamma(K-1-k) \Gamma(K-1-\sigma+k)}{\Gamma(K-1) \Gamma(K-1-\sigma)} \right], \quad \dots\dots(10)$$

where

$$\gamma(v', v''; \sigma, k) \equiv \binom{v'}{k} \binom{v''}{\sigma-k} \rho_1^k \rho_2^{\sigma-k} \frac{\Gamma(K_1-v') \Gamma(K_2-v'')}{\Gamma(K_1-v'-k) \Gamma(K_2-v''-\sigma+k)}$$

$$\text{i.e.} \quad \sum_{k=0}^{\sigma} \gamma(v', v''; \sigma, k) = C(v', v''; \sigma) \quad [\text{eqn. (17) of I}].$$

Manipulation of the indices of summation for the special cases $v' = 1$, $v' = 2$, $v' = 3$ leads to considerable simplification of this expression. Let $\{(0, v'')/(0, 0)\}_{K-n}$ stand for the part within the braces of the formula for $(0, v'')/(0, 0)$, with K replaced by $K-n$, e.g.

$$\left\{ \frac{(0, 2)}{(0, 0)} \right\}_{K-4} = \frac{(\Delta K)(\Delta K+1)}{(K-6)(K-7)} + \frac{2\delta(\Delta K+1)}{(K-6)} + \delta^2.$$

Then, for $v'' \geq v'$,

$$\frac{(1, v'')}{(0, 0)} = (-1)^{1+v''} \frac{N_1^{(1)} N_2^{(v'')}}{N_1^{(0)} N_2^{(0)}} \rho_1 \rho_2^{v''} \left[\left\{ \frac{(1, 0)}{(0, 0)} \right\}_K \left\{ \frac{(0, v'')}{(0, 0)} \right\}_K \right. \\ \left. + \frac{v''(K_1 - 2)(K_2 - 1 - v'')}{(K - 2)^2(K - 3)} \left\{ \frac{(0, v'' - 1)}{(0, 0)} \right\}_{K-2} \right], \quad \dots\dots(11)$$

$$\frac{(2, v'')}{(0, 0)} = (-1)^{v''} \frac{N_1^{(2)} N_2^{(v'')}}{N_1^{(0)} N_2^{(0)}} \rho_1^2 \rho_2^{v''} \left[\left\{ \frac{(2, 0)}{(0, 0)} \right\}_K \left\{ \frac{(0, v'')}{(0, 0)} \right\}_K \right. \\ \left. + \frac{2v''(K_1 - 3)(K_2 - 1 - v'')}{(K - 2)^2(K - 3)} \left\{ \frac{(1, 0)}{(0, 0)} \right\}_{K-2} \left\{ \frac{(0, v'' - 1)}{(0, 0)} \right\}_{K-2} \right. \\ \left. + \frac{v''(v'' - 1)(K_1 - 3)(K_1 - 4)(K_2 - 1 - v'')(K_2 - 2 - v'')}{(K - 2)(K - 3)^2(K - 4)^2(K - 5)} \left\{ \frac{(0, v'' - 2)}{(0, 0)} \right\}_{K-4} \right], \\ \dots\dots(12)$$

$$\frac{(3, v'')}{(0, 0)} = (-1)^{1+v''} \frac{N_1^{(3)} N_2^{(v'')}}{N_1^{(0)} N_2^{(0)}} \rho_1^3 \rho_2^{v''} \left[\left\{ \frac{(3, 0)}{(0, 0)} \right\}_K \left\{ \frac{(0, v'')}{(0, 0)} \right\}_K \right. \\ \left. + \frac{3v''(K_1 - 4)(K_2 - 1 - v'')}{(K - 2)^2(K - 3)} \left\{ \frac{(2, 0)}{(0, 0)} \right\}_{K-2} \left\{ \frac{(0, v'' - 1)}{(0, 0)} \right\}_{K-2} \right. \\ \left. + \frac{3v''(v'' - 1)(K_1 - 4)(K_1 - 5)(K_2 - 1 - v'')(K_2 - 2 - v'')}{(K - 2)(K - 3)^2(K - 4)^2(K - 5)} \left\{ \frac{(1, 0)}{(0, 0)} \right\}_{K-4} \left\{ \frac{(0, v'' - 2)}{(0, 0)} \right\}_{K-4} \right. \\ \left. + \frac{v''(v'' - 1)(v'' - 2)(K_1 - 4)(K_1 - 5)(K_1 - 6)(K_2 - 1 - v'')(K_2 - 2 - v'')(K_2 - 3 - v'')}{(K - 2)(K - 3)(K - 4)^2(K - 5)^2(K - 6)^2(K - 7)} \left\{ \frac{(0, v'' - 3)}{(0, 0)} \right\}_{K-6} \right] \\ \times \left\{ \frac{(0, v'' - 3)}{(0, 0)} \right\}_{K-6}. \quad \dots\dots(13)$$

For the $v'' = 1, 2, 3$ progressions obvious exchanges are made in the formulae. These formulae, it must be emphasized again, exhibit none of the very large cancellation. Great simplification results if it is possible to choose the mean α that such $\lambda_1 = \lambda_2$ (see a footnote of I), and thus $\delta = 0$, or such that δ is so small that only 2 or 3 terms in the 0-progression braces need to be retained. Otherwise the work with these formulae is heavy, but still very much less than that required to do the calculation of the overlaps numerically. Elimination of the cancellation is accompanied by the loss of a convenient check on the correctness of computation. Using the formulae of I, one knows how much cancellation to expect and can immediately sense a mistake if there is not as much as there should be. If one is interested in a few bands of low quantum number, the formulae of I are easier to apply, with the exception of that for (0, 0).

ACKNOWLEDGMENTS

The authors wish to acknowledge the encouragement and support given to them by Dr. R. W. Nicholls during the course of this work. They also wish to acknowledge Prof. D. R. Bates' communication to Dr. Nicholls of a pre-publication copy of his paper referred to above.

The research reported in this paper has been sponsored by the Geophysics Research Directorate, Air Force Cambridge Research Centre, Air Research and Development Command under Contract No. AF 19(122)-470.

REFERENCES

- BATES, D. R., 1953, *Mon. Not. R. Astr. Soc.*, **112**, 614.
FRASER, P. A., and JARMAIN, W. R., 1953, *Proc. Phys. Soc. A*, **66**, 1145.
HERZBERG, G., 1950, *Spectra of Diatomic Molecules* (New York: Van Nostrand).
PILLOW, M. E., 1951, *Proc. Phys. Soc. A*, **64**, 772.

The Magnetic Moments of Spin $\frac{1}{2}$ Nuclei

BY R. J. BLIN-STOYLE

Clarendon Laboratory, Oxford

MS. received 11th August 1953

Abstract. It is shown that the deviations of the magnetic moments of all spin $\frac{1}{2}$ nuclei from the Schmidt limits can be adequately accounted for by simple interconfigurational mixing.

§ 1. INTRODUCTION

MANY attempts have been made to explain the deviations of the magnetic moments of odd A nuclei from the Schmidt limits obtained for the single particle model (SPM) of the nucleus.* In this paper the particular case of spin $\frac{1}{2}$ nuclei is considered, and it is shown that for all such nuclei the value of the magnetic moment is adequately accounted for by simple interconfigurational mixing.

It is convenient to describe such mixing for a nucleus of spin j in terms of a wave function of the form

$$\Psi_j = \chi_j + \sum_p \alpha_p \phi_{p,j} \quad \dots\dots(1)$$

where χ_j corresponds to the SPM configuration and the $\phi_{p,j}$ represent admixed configurations, such configurations being characterized by the variable p . χ_j can be written as the product of a single particle wave function Ψ_j and a wave function ω_0 for a core with zero spin; thus $\chi_j = \Psi_j \omega_0$ and both ω_0 and $\phi_{p,j}$ can be expressed as a superposition of single particle functions (in jj -coupling).

The magnetic moment of the nucleus (in nuclear magnetons) is obtained by calculating the expectation value of the operator $\sum_{n=1}^A (g_s^n \sigma^n + g_l^n \mathbf{L}^n)$ using the above wave function, the summation being taken over all nucleons in the nucleus. g_s^n and g_l^n are the spin and orbital g -factors for the n th nucleon and σ^n and \mathbf{L}^n are the appropriate spin and orbital angular momentum operators. Thus

$$\mu = \frac{j}{m} \langle \Psi_j^m | \sum_{n=1}^A (g_s^n \sigma_z^n + g_l^n L_z^n) | \Psi_j^m \rangle, \quad \dots\dots(2)$$

where it is supposed that the nuclear wave function is constructed to represent a state in which the angular momentum j has a component m along the axis of quantization.

If all the α_p are zero then the SPM value is obtained for the magnetic moment. On the other hand a large deviation from this value is to be expected if terms linear in the α_p are non-vanishing. The condition for this is that χ_j and $\phi_{p,j}$ must differ at most by one single particle state and that then the orbital state must be the same. For nuclei with spin greater than $\frac{1}{2}$ there are many ways in which wave functions

* A review of such attempts and detailed references are given, for instance, by Ross (1952).

satisfying this condition can be constructed, but if $j = \frac{1}{2}$ the exclusion principle and angular momentum considerations restrict such admixed wave functions to one type only, namely that in which a single nucleon in the core is excited from the state $l'_{j'} = l' + \frac{1}{2}$ to $l'_{j''} = l' - \frac{1}{2}$.

In the following calculations an estimate is made of the values of the α_p for this type of interconfigurational mixing assuming a delta function interaction between nucleons.

§ 2. CALCULATIONS

The calculation is formulated in terms of three particles, two of which in the SPM are in the same state coupled to give zero spin and one of which is excited to a different state in the admixed configuration.* Also for purposes of generality j is not at present restricted to the value $\frac{1}{2}$. Then symbolically,

$$\chi_j \sim [(l_j)_j (l'_{j'})_0^2]_j \quad \text{and} \quad \phi_{J,j} \sim [(l_j)_j \{ (l'_{j'}) (l'_{j''}) \}_J]_j$$

where $j' = l' + \frac{1}{2}$, $j'' = l' - \frac{1}{2}$ and the admixed configuration is now characterized by the angular momentum J to which j' and j'' are coupled.

Consider first the case in which the odd nucleon (1 say) differs from the core nucleons (2 and 3). Suitably antisymmetrized wave functions are then

$$\chi_j^m(1, 2, 3) = \sum_{m'} c_{0m'}^{0j'j''} \psi_{j'}^{m'}(2) \psi_{j''}^{-m'}(3) \psi_j^{m'}(1) \quad \dots\dots (3)$$

$$\phi_{J,j}^m(1, 2, 3) = \frac{1}{\sqrt{2}} \sum_{m'm''\mu\sigma} c_{\mu m'}^{Jj'j''} c_{\mu m''}^{Jj} (\psi_{j'}^{m'}(2) \psi_{j''}^{m''}(3) \psi_j^{m'}(3) - \psi_{j''}^{m''}(2) \psi_j^{m'}(1)) \quad \dots\dots (4)$$

where the c 's are Wigner coefficients and both wave functions are normalized to unity.

Denoting the inter-nucleon interaction by

$$V = V(|\mathbf{r}_1 - \mathbf{r}_2|) + V(|\mathbf{r}_2 - \mathbf{r}_3|) + V(|\mathbf{r}_1 - \mathbf{r}_3|)$$

the matrix element to be calculated is

$$\mathcal{M}_J = \int \chi_j^{m*}(1, 2, 3) V \phi_{J,j}^m(1, 2, 3) d\tau_1 d\tau_2 d\tau_3.$$

Substituting for $\chi_j^m(1, 2, 3)$ and $\phi_{J,j}^m(1, 2, 3)$ and using various relations between Wigner and Racah coefficients, \mathcal{M}_J reduces to

$$\mathcal{M}_J = (-)^J \left[\frac{2(2J+1)}{(2j+1)(2j'-1)} \right]^{1/2} \sum_i (2i+1) W(j'Jij; j''j) \mathfrak{A}_{i:jj'j''} \quad \dots\dots (5)$$

where $\mathfrak{A}_{i:jj'j''} = \int \xi_{i:jj'}^*(p, q) V(|\mathbf{r}_p - \mathbf{r}_q|) \xi_{i:jj''}(p, q) d\tau_p d\tau_q$.

$\xi_{i:jj'}(p, q)$ is a wave function representing nucleons p and q in the single particle states $\psi_j(p)$ and $\psi_{j'}(q)$ coupled to give a total spin i and similarly for $\xi_{i:jj''}(p, q)$. Rewriting these wave functions in an LS coupling scheme, using a delta function for the inter nucleon interaction and taking account of the singlet and triplet interactions in the manner set out by Pryce (1952) gives

$$\mathfrak{A}_{i:jj'j''} = \epsilon_s \langle jj'i | ii0 \rangle \langle jj''i | ii0 \rangle P(i; ll') + \epsilon_t \sum_{y=i-1, i, i+1} \langle jj'i | iy1 \rangle \langle jj''i | iy1 \rangle P(y; ll') \quad \dots\dots (6)$$

where the $\langle jj'i | iLS \rangle$ are jj - LS transformation coefficients for spin $\frac{1}{2}$ particles (Blin-Stoyle 1953). ϵ_s and ϵ_t are singlet and triplet interaction energies, and these, together with the coefficients $P(i; ll')$, are defined and discussed by Pryce (1952).

* Note added in proof. The results obtained are unchanged if one of the core particles is replaced by a 'hole'.

If the nucleons 1, 2 and 3 are all of the same type, an expression identical with (5) is obtained for \mathcal{H}_J , but now, because of the complete antisymmetrization of the wave functions,

$$\mathcal{H}_{i: jj'j''} = 2\sqrt{2}\epsilon_s \langle jj'i | \ddot{u}0 \rangle \langle jj''i | \ddot{u}0 \rangle P(i; l''). \quad \dots\dots(7)$$

α_J is then given in terms of \mathcal{H}_J by $\alpha_J = -\mathcal{H}_J/\Delta E$, where ΔE (always positive) is the energy difference between the SPM and admixed configurations.

§ 3. CONTRIBUTION TO THE MAGNETIC MOMENT

Using (1), (2), (3) and (4), a straightforward calculation gives for the contribution of the term linear in α_J to the magnetic moment (i.e. the approximate deviation of the moment from the Schmidt limit)

$$\mu' = 2\alpha_1(g_1 - g_s) \left[\frac{2jl'}{3(j+1)(2l'+1)} \right]^{1/2} \text{ for } J=1 \quad \dots\dots(8)$$

and $\mu' = 0$ for $J \neq 1$.

Here g_s and g_l are the spin and orbital g -factors for the core nucleons.

§ 4. APPLICATION TO SPIN $\frac{1}{2}$ NUCLEI

For the particular case $j = \frac{1}{2}$ only \mathcal{H}_1 is non-vanishing, and in (5) the summation over i reduces to a single term, namely that for which $i = l'$.

$s_{1/2}$ odd-neutron nuclei.

The first non-trivial spin $\frac{1}{2}$ nucleus is ^{29}Si . In this instance the only possible interconfigurational mixing of the type required is that in which either or both of a $d_{5/2}$ proton or neutron is excited to the $d_{3/2}$ state. By (5), (6), (7) and (8) it is found that for neutron excitation $\mu' = -2.9\epsilon_s/\Delta E$ and for proton excitation $\mu' = 1.2(\epsilon_s - \epsilon_t)/\Delta E$. Taking $\epsilon_t = 1.5\epsilon_s$ (Pryce 1952) and noting that ϵ_s is negative, it is seen that the deviation of the magnetic moment has the right sign in both cases (experimental deviation = 1.4 n.m.). Further, very roughly estimating $\Delta E = 3$ mev and $\epsilon_s = -1.0$ mev (for a light nucleus $|\epsilon_s|$ will be larger than the value 0.85 mev suggested by Pryce (1952) for nuclei in the region of lead) gives a total correction to the magnetic moment of 1.2 n.m. which is of the required order of magnitude.

Exactly similar arguments can be applied to the $s_{1/2}$ nuclei ^{111}Cd , ^{113}Cd , ^{115}Sn , ^{117}Sn , ^{119}Sn , ^{123}Te , ^{125}Te and ^{129}Xe . In every case there can be neutron excitation from the $d_{5/2}$ to the $d_{3/2}$ state, and this will give a deviation in the magnetic moment of the right sign (+) and magnitude (~ 1 n.m.).

$s_{1/2}$ odd-proton nuclei.

^{19}F is particularly interesting. There can be no proton interconfigurational mixing since the $d_{5/2}$ proton shell is empty. On the other hand Klinkenberg's (1952) tables of nuclear shell structure would suggest that there are two neutrons in the $d_{5/2}$ state, and this should cause the magnetic moment to deviate considerably from the SPM value. Experimentally there is found to be little deviation (~ 0.16 n.m.). A likely explanation for this is that the two neutrons prefer to pair off in the neighbouring $2s_{1/2}$ state: this hypothesis is in fact supported by calculations due to Hitchcock (1953) and ideas on 'stabilization' energy put forward by Goldhaber and de Shalit (1953).

The deviation of the magnetic moment of ^{31}P from the SPM value by 1.48 n.m. can be explained in exactly the same way as for ^{29}Si .

^{203}Tl and ^{205}Tl are the only other two odd proton nuclei in an $s_{1/2}$ state whose magnetic moments are known. Here proton interconfigurational mixing is unlikely since the $d_{5/2}$ and $d_{3/2}$ states are both filled. In this region, however, there can be neutron excitation from the $p_{3/2}$ to the $p_{1/2}$ state, and calculation shows that the deviation of the magnetic moment from this cause should be $\mu' = +1.8(\epsilon_t - \epsilon_s)/\Delta E$. Taking $\epsilon_s = -0.85 \text{ Mev}$ and estimating $\Delta E = 0.6 \text{ Mev}^*$ gives $\mu' = -1.2 \text{ n.m.}$, which is in good agreement with the experimentally observed deviations of -1.18 n.m. and -1.17 n.m.

$p_{1/2}$ nuclei.

Using (5), (6) and (7) it can be shown for $p_{1/2}$ nuclei that μ_1 is always identically zero for any value of l' and for excitation of either a proton or a neutron from the core. Thus, the magnetic moments of $p_{1/2}$ nuclei should not deviate very much from the SPM values. This is confirmed by experiment, the maximum deviation of the magnetic moment of a $p_{1/2}$ nucleus from the SPM value being 0.19 n.m. (for ^{171}Yb) compared with 1.48 n.m. (for ^{31}P) for $s_{1/2}$ nuclei.

ACKNOWLEDGMENT

The author would like to express his thanks to the Pressed Steel Company Limited for a research fellowship during the tenure of which this work was completed.

REFERENCES

- BLIN-STOYLE, R. J., 1953, *Proc. Phys. Soc. A*, **66**, 729.
 GOLDBABER, M., and DE SHALIT, A., 1953, *Phys. Rev.*, in the press.
 HITCHCOCK, A. J. M., 1953, *Phil. Mag.*, **44**, 766.
 KLINKENBERG, P. F. A., 1952, *Rev. Mod. Phys.*, **24**, 63.
 MAYER, M. G., 1950, *Phys. Rev.*, **78**, 16.
 PRYCE, M. H. L., 1952, *Proc. Phys. Soc. A*, **65**, 773.
 ROSS, M., 1952, *Phys. Rev.*, **88**, 935.

* This value is obtained by assuming that $\Delta E \sim (2l' + 1)$ and that in this region for $l' = 5$, $\Delta E \simeq 2 \text{ Mev}$ (Mayer 1950).

The Electronic Structure of some Body-Centred Cubic Metals

By G. G. HALL

Department of Theoretical Chemistry, University of Cambridge

MS. received 20th May 1953, and in amended form 4th August 1953

Abstract. The electronic structure of a body-centred cubic metal is considered using the standard excited state extension of the equivalent orbital method. The form of the energy surfaces for both the standard excited state and the ground state is deduced in terms of a small number of parameters using the transformation properties of a determinant wave function. The energy expressions thus found do not depend on any analytical approximation to the wave functions nor on any arbitrary simplification of the theory. Values of the parameters for lithium and sodium are found by fitting the theoretical energies to energies calculated by other methods.

§1. INTRODUCTION

THE orbital theory of the electronic structure of a crystal is founded on the one basic postulate that a wave function in the form of a single determinant is an adequate approximation to the true eigenfunction of the electronic ground state. Each element of this determinant is an orbital multiplied by one of the two spin functions. To give the most accurate wave function the orbitals must satisfy certain differential equations. These equations can be interpreted in terms of a Hamiltonian operator for the motion of one electron in the field of the nuclei and the averaged field of the other electrons.

The orbitals are not determined uniquely by these equations. An arbitrary unitary transformation of the orbitals leaves the determinant unaltered both in magnitude and in form and so leads to differential equations of exactly the same form. It is possible, therefore, to define different kinds of orbitals by adding different restrictions and to transform one kind to another by a unitary transformation. In most previous discussions of the orbital equations the solutions were made unique by restricting the orbitals so that their matrix elements with the effective Hamiltonian operator were zero except on the diagonal. Such orbitals have been called crystal orbitals by Löwdin (1951). For many purposes this choice of orbitals is not the most convenient and equivalent orbitals, which are defined as identical with each other except for their position and orientation, may be used instead with equal accuracy (Lennard-Jones 1949). It follows that the equations for a set of equivalent orbitals reduce to one equation when referred to suitable axes. The utility of equivalent orbitals is, however, due to the localization which they are found to possess.

In an ionic crystal the equivalent orbitals can be localized around single atoms and so are modified atomic orbitals. The equivalent orbital method reduces

then to the Heitler–London method provided that in the latter the atomic orbitals are the best possible ones. Wannier (1937) has found it useful to define orthogonal orbitals for ionic crystals as transforms of the crystal orbitals of a single zone. These orbitals are equivalent under the translation subgroup of the crystal and so may sometimes coincide with the equivalent orbitals. Equivalent orbitals, however, are equivalent under the full symmetry group and so are, in general, transforms of the crystal orbitals of all the occupied zones.

In a valence crystal not all the equivalent orbitals can be localized around single nuclei; some are localized around single nuclei and some around pairs of neighbouring nuclei. Diamond, for example, has electrons in inner shell orbitals around each carbon nucleus and in two-centre equivalent orbitals which are tetrahedrally oriented at each nucleus and form the C—C bonds. It has already been shown (Hall 1952a) that because these can be transformed to crystal orbitals by a unitary transformation the energies of the crystal orbitals can be very simply expressed in terms of parameters which represent the energies of interaction of the equivalent orbitals.

Equivalent orbitals which cannot be effectively localized around one or two nuclei, as for the conduction electrons of a metal, are more difficult to visualize and are so much more dependent on their environment that their practical value is small. To meet these difficulties another method of studying mobile electrons in terms of equivalent orbitals has been developed (Hall 1952b). The object of this paper is to apply this method to metals and in particular to the body-centred alkali metals.

§2. THE STANDARD EXCITED STATE METHOD

The standard excited state method is a method of defining localized equivalent orbitals in terms of which the ground state and its properties can be discussed. The standard excited state is a highly excited state in which the conduction electrons are all in singly occupied orbitals with parallel spins and the inter-nuclear distances are kept the same as in the ground state. Although it cannot be realized experimentally it can be discussed theoretically using a single determinant wave function. The standard equivalent orbitals are then defined as transforms of these singly occupied orbitals which are equivalent to one another. In the standard excited state of sodium, for example, the inner shell equivalent orbitals corresponding to the 1s, 2s and 2p atomic shells remain doubly occupied and so need not be considered further. The singly occupied orbitals transform among themselves to give equivalent orbitals which permute under the various operations of the space group in the same way as the nuclei do. This result depends on the fact that, in the standard excited state, there are as many singly occupied orbitals as unit cells in the lattice so that one Brillouin zone can be completely spanned with occupied orbitals. Equivalent orbitals can therefore be associated with each nucleus and, since the net coulomb attraction towards the nucleus is the principal term in the equation determining an equivalent orbital, they may be pictured as modified 3s orbitals. The orbitals are, however, strictly orthonormal and are not necessarily spherically symmetrical, so that this picture is oversimplified.

The equivalence and localization of these orbitals make them a particularly suitable starting point in studying the electronic structure of the crystal. The significant quantities are the matrix elements, with respect to these equivalent

orbitals, of the effective Hamiltonian operator for the standard excited state, viz.

$$e_{rs} = \int \bar{\chi}_r \left\{ \left(-\frac{1}{2} \nabla^2 - \sum_{\alpha} \frac{Z_{\alpha}}{r_{\alpha}} + 2 \sum_i \int \bar{\chi}_i \chi_i / r_{12} dV_2 + \sum_e \int \bar{\chi}_e \chi_e / r_{12} dV_2 \right) \chi_s \right. \\ \left. - \sum_i \int \bar{\chi}_i \chi_s / r_{12} dV_2 \chi_i - \sum_e \int \bar{\chi}_e \chi_s / r_{12} dV_2 \chi_e \right\} dV_1, \quad \dots (2.1)$$

where α refers to the nuclei, i to the inner shell equivalent orbitals and e to the standard equivalent orbitals. Since the orbitals are equivalent a large number of these matrix elements are equal and, since they are localized, the matrix elements of widely separated orbitals will be negligible. The matrix elements will therefore be taken as

$$\left. \begin{aligned} e_{rr} &= a \\ e_{rs} &= b \text{ for nearest neighbours,} \\ &= c \text{ for second neighbours,} \\ &= 0 \text{ otherwise.} \end{aligned} \right\} \quad \dots (2.2)$$

It would be straightforward to allow for higher order interactions between orbitals and so obtain a more detailed account of the structure, but it is sufficient for present purposes to include only the major terms.

According to the theory of equivalent orbitals the crystal orbitals and their energies are defined as the eigenvectors and eigenvalues of this matrix (Hall and Lennard-Jones 1950). The matrix T_{ts} , which reduces e_{rs} to diagonal form and so transforms equivalent orbitals to crystal orbitals, is determined by the equations

$$\sum_s e_{rs} T_{ts} - E_{tt} T_{tr} = 0 \quad (r = 1, 2, \dots), \quad \dots (2.3)$$

where E_{tt} is an eigenvalue of the matrix. This infinite set of equations is most easily solved by using the symmetry of the body-centred lattice.

The unit cell of a body-centred cubic lattice is a parallelepiped of half the volume of the cube. Its three basic vectors $\mathbf{r}_1, \mathbf{r}_2, \mathbf{r}_3$ have components, referred to the cubic axes, of (d, d, d) , $(d, -d, -d)$ and $(-d, -d, d)$ respectively, where the shortest internuclear distance is $d\sqrt{3}$. The atoms may be placed at the corners of the cells so that the atom (l, m, n) is at the position $\mathbf{r} = l\mathbf{r}_1 + m\mathbf{r}_2 + n\mathbf{r}_3$ (l, m, n integers).

The translational symmetry of the lattice suggests that there might be periodic solutions to the eigenvalue equations of the form

$$T_{\mathbf{k}, \mathbf{r}} = T_{\mathbf{k}} e^{i\mathbf{k} \cdot \mathbf{r}}, \quad \dots (2.4)$$

where \mathbf{k} is a vector in the reciprocal space

$$\mathbf{k} = f\mathbf{k}_1 + g\mathbf{k}_2 + h\mathbf{k}_3 \quad \dots (2.5)$$

and the vectors \mathbf{k}_i are determined by the equations

$$\mathbf{k}_i \cdot \mathbf{r}_j = \delta_{ij}, \quad \dots (2.6)$$

Since there is only one orbital to each unit cell of the lattice, this substitution reduces the set of equations to the single equation

$$\{ce^{-i(g+h)} + ce^{-i(f+h)} + ce^{-i(f+g)} + be^{-if} + be^{-ig} + be^{-ih} + be^{-i(f+g+h)} \\ + (a - E) + be^{if} + be^{ig} + be^{ih} + be^{i(f+g+h)} + ce^{i(g+h)} + ce^{i(f+h)} + ce^{i(f+g)}\} T_{\mathbf{k}} = 0.$$

The eigenvalues are therefore determined as functions of \mathbf{k} by the equation

$$E_{\mathbf{k}} = a + 2b\{\cos f + \cos g + \cos h + \cos(f+g+h)\} \\ + 2c\{\cos(g+h) + \cos(f+h) + \cos(f+g)\}. \quad \dots (2.7)$$

The corresponding crystal orbital $\psi_{\mathbf{k}}$ has the form

$$\psi_{\mathbf{k}} = T_{\mathbf{k}} \sum_{\mathbf{r}} e^{i\mathbf{k} \cdot \mathbf{r}} \chi(\mathbf{r}), \quad \dots\dots(2.8)$$

where $\chi(\mathbf{r})$ is the equivalent orbital localized around the position \mathbf{r} and $T_{\mathbf{k}}$ is a normalization constant which need not be specified further. Since $E_{\mathbf{k}}$ is a triply periodic function of \mathbf{k} , it is sufficient to consider its form inside a single Brillouin zone. The form of this zone is shown as fig. 1 in the paper by Howarth and Jones (1952).

§ 3. THE FORM OF THE ENERGY CONTOURS

The energy of the crystal orbitals can be plotted in reciprocal space as a function of the wave vector \mathbf{k} . The result is most easily visualized by considering cross sections. The cross section by the plane $h = -g$ is particularly useful because there are two other cross sections exactly similar and because it intersects the Brillouin zone in a square.

Over the plane $h = -g$, $E_{\mathbf{k}}$ takes the form

$$E = a + 2bE_1 + 2cE_2, \quad \dots\dots(3.1)$$

where

$$E_1 = 2 \cos f + 2 \cos g, \quad \dots\dots(3.2)$$

$$E_2 = 1 + \cos(f - g) + \cos(f + g). \quad \dots\dots(3.3)$$

Since the energy is the sum of a number of terms each term can be discussed separately. This has the advantage that the discussion is then applicable whatever values are subsequently assigned to the parameters. The functions E_1 and E_2 are shown in figs. 1 and 2.

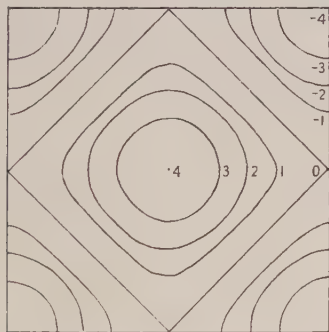


Fig. 1. Cross section by the plane $h = -g$ of the energy contours for nearest neighbours.

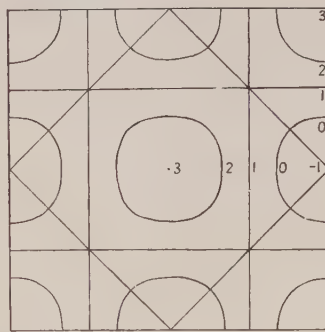


Fig. 2. Cross section by the plane $h = -g$ of the energy contours for second nearest neighbours.

These two functions are of very similar form. The inner contours are closely circular but there is a gradual change to the square contour at $E_1 = 0$ or $E_2 = 1$, followed by a return to circular contours but around different centres. Thus, in the three-dimensional space, the inner contours are spherical and the outer contours are portions of spheres with transition contours, sometimes consisting of planes, between the extremes. For $E_1 = 0$ the transition contour is a cube inscribed in the zone and having half the volume of the zone.

Since the first and second neighbours are at comparable distances it is to be expected that the parameters b and c would be of similar magnitude but that $|b| > |c|$. It is also clear that both will be negative. Over the plane $h = -g$ the inner contours of E_1 and E_2 are similar but the outer contours have opposing

maxima and minima, so that E will have circular inner contours but its outer contours will be smoother than those either of E_1 or of E_2 . If b and c are approximately equal the outer minima disappear and E rises steadily from the centre to the surface of the zone. In three dimensions the effect of combining E_1 and E_2 is similar. The inner contours are more nearly spheres and the outer become smoother and flatter. These results would be reversed if it were possible to have b and c of opposite sign. The inner contours would cease to be spherical and instead become flat while the outer maxima would become more and more pronounced.

§4. THE GROUND STATE

The crystal orbitals of the ground state and their energies can be deduced from those of the standard excited state. There are only half as many occupied crystal orbitals, since, at absolute zero, each is doubly occupied, but these may be taken as equal to the corresponding crystal orbitals of the ground state, for the equations which determine them are almost the same. Since the number of orbitals is proportional to the volume in reciprocal space the ground state orbitals will occupy half the volume of the Brillouin zone. The Fermi surface, which divides the occupied from the unoccupied orbitals, will be the energy contour whose volume is half that of the zone.

For $c=0$ the Fermi surface is the inscribed cube for which $E_1=0$. The shape of this contour is of some importance, for the ground state orbitals then occupy an integral number of zones of a cubic lattice. It follows, using group theoretical arguments (cf. Hall 1950), that the ground state orbitals can be transformed into bond equivalent orbitals each localized mainly around two first neighbours and such that all the bonds are parallel. This is one of the structures considered by Pauling (1949), except that the bonds are equivalent orbitals rather than electron pair bonds. The transformation to equivalent orbitals is not unique, however, and the same crystal orbitals can be transformed into the equivalent orbitals of any one of the eight structures in which all the bonds are parallel. A similar result holds for the benzene molecule, where both Kekulé structures can be obtained by different transformations of the orbitals of the same determinantal wave function. If $c \neq 0$ the Fermi surface is more nearly a sphere than a cube and the ground state orbitals cease to have these simple transformation properties.

As a first rough approximation the energies of the ground state crystal orbitals are equal to those of the standard excited state crystal orbitals. A more accurate approximation is obtained by adding corrections to allow for the difference between the effective Hamiltonians for the two states (Hall 1952b). Thus the energy of a ground state crystal orbital $\psi_{\mathbf{k}}$ is

$$E_{\mathbf{k}} = \int \bar{\psi}_{\mathbf{k}} \left\{ \left(-\frac{1}{2} \nabla^2 - \sum_{\alpha} \frac{Z_{\alpha}}{r_{\alpha}} + 2 \sum_1 \int \bar{\psi}_1 \psi_1 / r_{12} dV_2 \right) \psi_{\mathbf{k}} - \sum_1 \int \bar{\psi}_1 \psi_{\mathbf{k}} / r_{12} dV_2 \psi_1 \right\} dV_1, \quad \dots (4.1)$$

where 1 denotes the crystal orbitals of the inner shells and the conduction electrons. If these crystal orbitals are equal to those of the standard excited state, this energy can be written in the form

$$E_{\mathbf{k}} = E_{\mathbf{k}}^0 + \int \bar{\psi}_{\mathbf{k}} \psi_{\mathbf{k}} \left\{ \int \left(\sum_o \bar{\psi}_o \psi_o - \sum_u \bar{\psi}_u \psi_u \right) / r_{12} dV_2 \right\} dV_1 \\ + \sum_u \int \bar{\psi}_{\mathbf{k}}(1) \bar{\psi}_u(2) r_{12}^{-1} \psi_u(1) \psi_{\mathbf{k}}(2) dV_{12}, \quad \dots (4.2)$$

where E_k^0 is the energy of the orbital in the standard excited state, viz.

$$E_k^0 = \int \bar{\psi}_k \left\{ \left(-\frac{1}{2} \nabla^2 - \sum_{\alpha} \frac{Z_{\alpha}}{r_{\alpha}} + 2 \sum_i \int \chi_i \chi_i / r_{12} dV_2 + \sum_e \int \bar{\chi}_e \chi_e / r_{12} dV_2 \right) \psi_k \right. \\ \left. - \sum_i \int \bar{\chi}_i \psi_k / r_{12} dV_2 \chi_i - \sum_e \int \bar{\chi}_e \psi_k / r_{12} dV_2 \chi_e \right\} dV_1, \dots\dots(4.3)$$

and o refers to the crystal orbitals occupied in the ground state and u to the unoccupied. With these two corrections the energy expression has the correct form but the orbitals are not exactly optimum.

Before discussing the form of these energy corrections further it is convenient to extend to crystals the idea of alternants, introduced for molecules by Coulson and Rushbrooke (1940). A monatomic crystal will be called an alternant if it is possible to divide its atoms into two classes so that no two members of the same class are first neighbours. For a body-centred lattice these two classes are the two interpenetrating cubic lattices of which it is composed, so that these crystals will be alternants. If first neighbour interactions only are allowed, it can be proved that the electron density of the occupied orbitals of an alternant has the full symmetry of the lattice. This introduces many simplifications into the theory (Hall 1952 b), and in particular the first correction to E_k becomes very small. When second neighbour interactions are allowed it can no longer be proved that the electron distribution is the same around each atom even though, on physical grounds, it may be expected to be still a good approximation. For body-centred metals these second neighbour interactions are of importance but it will be assumed that the distribution remain symmetrical.

When the electron distribution is periodic, the energy of the ground state crystal orbitals becomes

$$E_k = E_k^0 + \sum_u \int \bar{\psi}_k(1) \bar{\psi}_u(2) r_{12}^{-1} \psi_u(1) \psi_k(2) dV_{12}, \dots\dots(4.4)$$

The significance of this correction is more obvious when it is expressed in terms of integrals over the standard equivalent orbitals by using (2.8):

$$E_k = E_k^0 + \sum_{rs} \bar{T}_k T_k e^{i\mathbf{k} \cdot (\mathbf{s} - \mathbf{r})} \left\{ \sum_n (rn | G | ns) - \frac{1}{2} \sum_{mn} Q_{mn} (rm | G | ns) \right\} \\ = E_k^0 + \frac{1}{2} \sum_{rs} \bar{T}_k T_k e^{i\mathbf{k} \cdot (\mathbf{s} - \mathbf{r})} \left\{ \sum_n (rn | G | ns) - \sum_{m \neq n} Q_{mn} (rm | G | ns) \right\}, \dots\dots(4.5)$$

where s, r, m, n refer to equivalent orbitals and Q_{mn} is the bonding matrix defined as

$$Q_{mn} = 2 \sum_o \bar{T}_o T_o e^{i\mathbf{o} \cdot (\mathbf{n} - \mathbf{m})} = Q_{m-n} \dots\dots(4.6)$$

so that $Q_{nn} = 1$. The values of Q_{m-n} for a body-centred lattice have been calculated by Löwdin (1951). If integrals involving equivalent orbitals further apart than second neighbours are neglected, except for the coulomb third neighbour interaction, then (4.5) becomes

$$E_k = E_k^0 + A + 2B \{ \cos f + \cos g + \cos h + \cos (f + g + h) \} \\ + 2C \{ \cos (g + h) + \cos (f + h) + \cos (f + g) \} \\ + 2D \{ \cos (2f - g - h) + \cos (2g - h - f) + \cos (2h - f - g) \\ + \cos (g - h) + \cos (h - f) + \cos (f - g) \}, \dots\dots(4.7)$$

where

$$A = \frac{1}{2}(11|G|11) - 8Q_1(11|G|12) + 4(12|G|21) - 6Q_2(11|G|13) - 12Q_2(12|G|23) \\ - 24Q_1(12|G|31) + 3(13|G|31),$$

$$B = -\frac{1}{2}Q_1(12|G|12) + (11|G|12) - \frac{1}{2}Q_2(12|G|13) - \frac{1}{2}Q_1(12|G|21) \\ - 3Q_1(12|G|23) - \frac{1}{2}Q_1(12|G|32) + 3(1 - Q_2)(12|G|31),$$

$$C = -\frac{1}{2}Q_2(13|G|13) - 2Q_1(12|G|13) + 2(12|G|23) + (11|G|13) - 4Q_1(12|G|31) \\ - \frac{1}{2}Q_2(13|G|31),$$

$$D = -\frac{1}{2}Q_3(14|G|14)$$

or, using (2.7),

$$E_k = a + A + 2(b + B)\{\cos f + \cos g + \cos h + \cos(f + g + h)\} \\ + 2(c + C)\{\cos(g + h) + \cos(f + h) + \cos(f + g)\} \\ + 2D\{\cos(2f - g - h) + \cos(2g - h - f) + \cos(2h - f - g) + \cos(g - h) \\ + \cos(h - f) + \cos(f - g)\}. \quad \dots\dots(4.8)$$

Thus the main effect of the correction is to change the values of the parameters in the energy expression without changing the dependence on reciprocal space. The final term implies some alteration in the shape of the energy contours.

§ 5. COMPARISON WITH PREVIOUS RESULTS

There is a strong superficial resemblance between the equivalent orbital method when applied to a metal and the Bloch tight-binding method, but they rest on quite different foundations and give different results. The Bloch theory assumes that the crystal orbitals can be expressed as a linear combination of atomic orbitals and that their energies, and the coefficients of the atomic orbitals, can be found by minimizing the energy of a crystal orbital with respect to these coefficients. This is assumed to lead to a determinantal equation for the crystal orbital energies very similar in form to the equivalent orbital one. This equation is then simplified by using the crystal symmetry. The overlap integrals between the atomic orbitals are usually ignored. Unfortunately the overlap integrals are frequently large and the equations for the coefficients, when derived rigorously by minimizing the total energy (Hall 1951), are not usually linear but cubic. It is therefore difficult to justify the simple Bloch method. It may be possible to modify the method to allow for overlapping and non-linearity by, for example, Roothaan's self-consistent field procedure (1951), but its simplicity will thereby be lost. The equivalent orbital method has the advantage that it is based on orthogonal orbitals and that its equations, though rigorously deduced, are of the simple linear form.

It should be noted that the crystal orbital equations cannot be solved as one-electron equations by the usual variational method. For a fixed known potential it is possible to find an integral which is stationary (Kohn 1952), but here the orbitals themselves enter into the potential function and destroy the stationary property. Thus there is a fundamental theoretical objection to the usual derivation of the tight-binding equations and a restriction on the use of Kohn's variational principle.

Löwdin (1951) has discussed sodium by a modification of the Bloch tight-binding method which takes the overlapping of the atomic orbitals and the non-linearity of the equations into account. His calculated cohesive energy and inter-nuclear distance are in very good agreement with experiment. He has not discussed the energies of the crystal orbitals, however, so that his results cannot be compared with the present ones, but his orthogonal atomic orbitals may be regarded as approximate standard equivalent orbitals.

The Wigner-Seitz method is also concerned with finding approximate solutions of the crystal orbital equations. In it the potential in the one-electron Hamiltonian is replaced by an ion core potential and the resulting equation solved inside a suitable cell around each nucleus with appropriate boundary conditions. The crystal orbitals obtained should be close to the true crystal orbitals but there are approximations involved in using the ionic potential and in applying the boundary conditions.

Wigner and Seitz (1933) used sodium as an illustration of their cellular method, and its energy contours were discussed by Slater (1934) in his extension of their work. Millman (1935) has applied Slater's method to lithium. More recently von der Lage and Bethe (1947) have shown that some of the main features of the energy surfaces of sodium can be investigated, with greater accuracy than Slater achieved, by considering only a few crystal orbitals of high symmetry. Howarth and Jones (1952) have extended this treatment by considering more orbitals and by investigating the cellular boundary conditions.

A comparison of the energy contours predicted here with those obtained by these methods reveals some interesting features. There is an immediate contrast between the large number of unoccupied orbitals which other methods discuss and the small number mentioned above. The equivalent orbital method is restricted to occupied orbitals, since these alone appear in the determinantal wave function, so that, in the standard excited state, orbitals are defined for the whole of the conduction zone, while in the ground state only half of these orbitals can be defined. There are, of course, other solutions of the orbital equations and, although they correspond to the motion of a negative test charge in the field of the neutral crystal (Hall and Lennard-Jones 1950), they may be good approximations to the optimum orbitals to be used in setting up wave functions for various excited states of the crystal. The excitation energies are taken as the difference in energies of the orbitals occupied and vacated in the transition. It is not yet clear, however, that these unoccupied zones will retain their properties when the excitation is large. The crystal orbitals of the standard excited state which are unoccupied in the ground state should also be good approximations to the orbitals occupied on excitation, but their energies are not simply related to the excitation energies. It is not easy to decide whether the energies found by other methods should be compared with those of the standard excited state or the ground state, but it is simpler to use the standard excited state orbitals and their energies (2.7).

The energy contours for sodium and lithium found by Slater and Millman are qualitatively similar and both have features in common with those predicted above for the first zone, notably the almost circular contours of low energy around the origin and the maxima at the corners of the zone. This agreement seems to be largely accidental, however, for they have determined the energies by boundary conditions which imply fitting together the wave functions of nearest

neighbours only. Disagreement also appears when attempts are made to find values of a , b , c to fit their results. From their graphs the energies of five crystal orbitals were estimated and fitted to the expression (2.7) by a least squares method giving equal weight to each. The values of the parameters are shown in table 1 with the standard deviation of each in parentheses. The fit is not very good and the values of the parameters, especially c , are subject to large standard deviations.

Table 1. Parameters Determined by Fitting Previous Calculations
(atomic energy units)

	a	b	c
Lithium (Millman)	-0.251 (0.016)	-0.0076 (0.009)	-0.0063 (0.008)
Sodium (Slater)	-0.222 (0.021)	-0.0099 (0.011)	-0.0032 (0.010)
Sodium (Howarth and Jones)	-0.125 (0.056)	-0.0186 (0.008)	-0.002 (0.013)

The energies of certain sodium orbitals, calculated by Howarth and Jones (1952), can also be fitted by finding suitable parameters. The result is given in table 1. They have found the energy only at isolated points in the Brillouin zone, and interpolated the results with a free electron parabola. There is little reason for assuming this particular function and it would be better to use (2.7). The value of c is surprisingly small in view of the much greater accuracy of these calculations and their choice of boundary conditions which make allowance for second neighbour interactions. The fitting too is not very good, as table 2 shows.

Table 2. Fitting of Calculated Energies (atomic energy units)

	Howarth and Jones	Fitted from eqn. (2.7)
Γ_s	-0.304	-0.286
N_s	-0.158	-0.121
H_p	-0.0068	0.012
P_s	-0.055	-0.129

It may be significant that a lower eigenvalue for the point P_s (using their notation) would improve both the value of c and the fitting. The remaining error is probably due to the inherent inaccuracies of any cellular method.

§ 6. LIMITATIONS OF THE EQUIVALENT ORBITAL METHOD

In contrast to other methods of studying the electronic structure of crystals, the equivalent orbital method does not set out to find wave functions in an explicit analytical or numerical form but rather to deduce, from the known form of the crystal, as much as possible about its electronic structure. Although this makes the method more accurate and easier to apply it sets severe limits on the amount of quantitative results it can give. Thus the form of the energy contours is determined qualitatively from the crystal structure, but the parameters which fix the energy uniquely must be found otherwise. Comparison with experiment or approximate calculation may give estimates of the parameters but, without these, the equivalent orbital method yields no quantitative result. It may be possible to find approximate solutions of the equivalent orbital equations directly and so estimate the parameters, but this would be another independent development of the theory.

A more serious limitation of the equivalent orbital method and its extension is that it requires the crystal to have at least as many electrons as there are orbitals occupied in the state being considered. This condition raises little difficulty for molecules, but there are many metals which cannot be discussed because their crystal orbitals occupy some zones so partially that many more electrons than are available would be required to span all the zones completely and so make possible a transformation to localized equivalent orbitals.

ACKNOWLEDGMENTS

The author wishes to thank Sir John Lennard-Jones and Professor H. Jones for reading this paper and giving him the benefit of their comments.

REFERENCES

- COULSON, C. A., and RUSHBROOKE, G. S., 1940, *Proc. Camb. Phil. Soc.*, **36**, 193.
 HALL, G. G., 1950, *Proc. Roy. Soc. A*, **202**, 336; 1951, *Ibid.*, **205**, 541; 1952 a, *Phil. Mag.*, **43**, 338; 1952 b, *Proc. Roy. Soc. A*, **213**, 102, 113.
 HALL, G. G., and LENNARD-JONES, J. E., 1950, *Proc. Roy. Soc. A*, **202**, 155.
 HOWARTH, D. J., and JONES, H., 1952, *Proc. Phys. Soc. A*, **65**, 355.
 KOHN, W., 1952, *Phys. Rev.*, **87**, 472.
 VON DER LAGE, F. C., and BETHE, H. A., 1947, *Phys. Rev.*, **71**, 612.
 LENNARD-JONES, J. E., 1949, *Proc. Roy. Soc. A*, **198**, 1.
 LÖWDIN, P. O., 1951, *J. Chem. Phys.*, **19**, 1570, 1579.
 MILLMAN, J., 1935, *Phys. Rev.*, **47**, 286.
 PAULING, L., 1949, *Proc. Roy. Soc. A*, **196**, 343.
 Roothaan, C. C. J., 1951, *Rev. Mod. Phys.*, **23**, 69.
 SLATER, J. C., 1934, *Phys. Rev.*, **45**, 794.
 WANNIER, G. H., 1937, *Phys. Rev.*, **52**, 191.
 WIGNER, E., and SEITZ, F., 1933, *Phys. Rev.*, **43**, 804.

The Multiple Scattering of 7.5 MeV Deuterons in Metals

BY A. ASHMORE AND A. V. CREWE

Nuclear Physics Research Laboratory, University of Liverpool

Communicated by H. W. B. Skinner; MS. received 30th July 1953

Abstract. Measurements have been made of the multiple scattering of 7.5 MeV deuterons in a range of metallic elements from aluminium to gold. Satisfactory agreement was obtained between the experimental distributions and those calculated from Molière's theory. The heavy elements do not show discrepancies similar to those observed in the multiple scattering of electrons and μ -mesons with relativistic velocities in lead.

§ 1. INTRODUCTION

THERE is some evidence that the mean angle of multiple scattering of relativistic particles in heavy elements is less than the theoretical value. Thus experiments with lead scatterers by Sheppard and Fowler (1940), Kulchitsky and Latishev (1942), and Sinha (1945) have all shown this discrepancy. More recently Crewe (1951a) has obtained a mean angle of scattering in lead for μ -mesons of energy 184 ± 12 MeV which is 65% of that calculated from Williams' theory. A repetition of the experiment using a steel scatterer (Crewe 1951b) shows agreement with theory within the experimental error. The discrepancy is, however, absent from the measurements of Skyrme (1953) on the scattering of 147 MeV protons in silver, platinum and photographic emulsion.

For non-relativistic particles the available evidence is contradictory. Measurements with α -particles by Geiger (1910) and Mayer (1913) both suggest a discrepancy between experiment and theory for heavier elements but in opposite senses. The experiments of Gottstein *et al.* (1951) on the multiple scattering of protons in the energy range 9–35 MeV in nuclear emulsions show agreement with Molière's theory within the experimental error. In this case, however, silver is the heaviest nucleus involved.

We have, therefore, investigated the multiple scattering of 7.5 MeV deuterons from the Liverpool 37 in. cyclotron in a range of metals from aluminium to gold and compared the results obtained with those calculated from Molière's theory.

§ 2. EXPERIMENTAL METHOD

A vertical section through the scattering camera is shown in fig. 1. The deuteron beam from the cyclotron was almost parallel in the vertical plane and about 1 cm in height, while in the horizontal plane it was brought to a focus on the entrance window W of the camera. Measurements were made of the scattering in the vertical plane, the beam being defined by passing between two brass blocks A and B, separated by shim steel 0.002 in. thick. The angular spread was thereby limited to $\pm 0.043^\circ$. Horizontally, in the direction perpendicular to the plane of the diagram, the hole between the blocks was $\frac{1}{2}$ in. wide. The scattering foil F

was placed over the end of the collimator and the scattered particles detected by the blackening produced in the photographic plate P. A microphotometer was used to measure this blackening. To reduce the effect of scattering from the inside faces of the brass plates, serrations were cut in them. An exposure without a foil indicated a negligible 'tail' due to this on the expected geometrical width of the image.

The relation between the microphotometer readings and the intensity of the scattered particles was determined by exposure of the plates *in vacuo* to a collimated beam of α -particles from polonium. These exposures ranged from 1 to 65 hours compared with values from 0.2 to 2 sec used in the experiment. There is, however, ample evidence (Kinoshita 1910, Svedberg and Anderson 1921, Wilkins and Wolfe 1933) that the reciprocity law is obeyed by α -particles and it seems safe to assume its validity for deuterons.

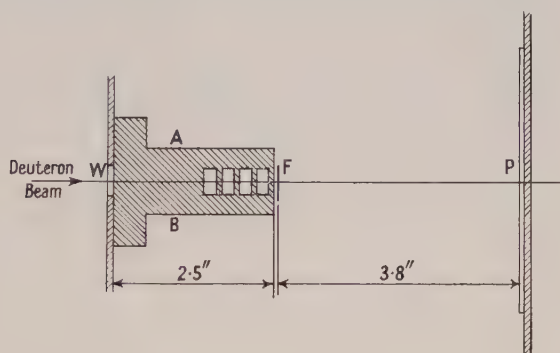


Fig. 1. Vertical section through scattering camera.

In order to obtain convenient angles of scattering, foils have to be used in which the deuterons lose a considerable fraction of their energy. In making the theoretical calculations it is therefore necessary to use the average momentum of the particle in the foil. For this purpose the rate of loss of energy of the deuterons was either taken from the tables of Aron, Hoffman and Williams (1949) or calculated on the same basis as they employed.

§ 3. EXPERIMENTAL RESULTS AND COMPARISON WITH THEORY

The experimental distributions were compared with that given by Moliere (1948) :

$$p(\phi) \delta\phi = \left[\frac{2}{\sqrt{\pi}} \exp(-\phi^2) + \frac{1}{B} f^{(1)}(\phi) + \frac{1}{B^2} f^{(2)}(\phi) \right] \delta\phi$$

in which ϕ is a constant multiple of the projected angle of scattering. As the initial portion of this distribution is approximately gaussian, it is convenient to plot graphs of the logarithm of the equivalent exposure, obtained from the calibration curve, against the square of the scattering angle. Good agreement was obtained with all the foils up to the largest angles measured, which are limited by considerations of intensity to about three times the mean angle of the gaussian term. As an example the theoretical curve for tantalum (115.4 mg cm^{-2}) with the experimental points marked is shown in fig. 2. The maximum disagreement in this case is less than 5% in the intensity of the scattered particles. To indicate

the extent of the agreement for all the foils, the table gives the theoretical and experimental values of the mean angle of the gaussian term. The experimental value was calculated from the slope of the almost linear portion of the graphs up to twice the mean angle. A small correction has to be made since this slope is a few per cent higher than that of the gaussian term owing to the effect of $f^{(1)}(\phi)$ and $f^{(2)}(\phi)$.

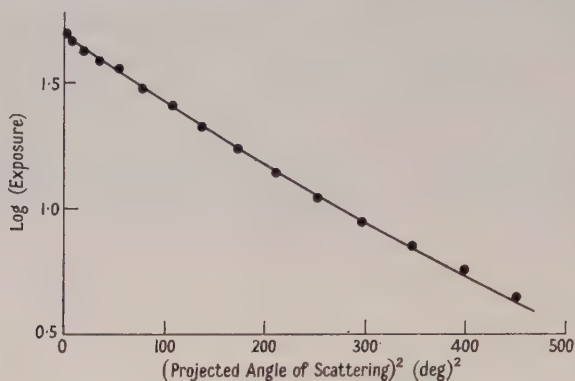


Fig. 2. Theoretical curve and experimental points for tantalum (115.4 mg cm^{-2}).

Note. Ordinates are \log_{10} (exposure).

The rather large discrepancy for aluminium may be associated with the value of $\gamma = Zz/137\beta$ (Z and z being the atomic numbers of the scattering and scattered nuclei). Moliere's theory is most accurate for values of γ very much less than or very much greater than 1 and least accurate (but sufficiently so) for γ of the order of 1. It can in any case be concluded that there is satisfactory agreement between theory and experiment, both as regards the values of the mean scattering angles and the shape of the distribution, over the range of elements we have employed.

Table of Results

Metal	Thickness (mg cm^{-2})	γ	Mean angle of gaussian term		Exptl. value
			Exptl.	Theor.	Theor. value
Aluminium	51.4	1.18	2.41	2.63	0.92
Steel	53.2	2.29	3.15	3.03	1.04
Steel	43.4	2.26	2.45	2.51	0.98
Nickel	41.2	2.43	2.40	2.52	0.95
Copper	70.3	2.64	4.50	4.31	1.04
Niobium	75.9	3.68	4.65	4.66	1.00
Tantalum	115.4	6.64	7.55	7.65	0.99
Tantalum	57.7	6.26	3.95	3.90	1.01
Gold	109.8	7.11	7.30	7.25	1.01
Mean value					0.99

ACKNOWLEDGMENTS

The authors wish to express their appreciation of the help and co-operation they received from the cyclotron crew, and their gratitude to the Department of Inorganic and Physical Chemistry for the loan of the microphotometer. They would like to acknowledge the benefit from discussions with Professor H. W. B. Skinner and Dr. G. D. Rochester.

REFERENCES

- ARON, W. A., HOFFMAN, B. G., and WILLIAMS, F. C., 1949, *University of California Radiation Laboratory Report*, UCRL 121.
- CREWE, A. V., 1951 a, *Proc. Phys. Soc. A*, **64**, 660; 1951 b, *Thesis*, University of Liverpool.
- GEIGER, H., 1910, *Proc. Roy. Soc. A*, **83**, 492.
- GOTTSTEIN, K., MENON, M. G. K., MULVEY, J. H., O'CEALLAIGH, C., and ROCHAT, O., 1951, *Phil. Mag.*, **42**, 708.
- KINOSHITA, A., 1910, *Proc. Roy. Soc. A*, **83**, 432.
- KULCHITSKY, L. A., and LATISHEV, D. G., 1942, *Phys. Rev.*, **61**, 254.
- MAYER, M. G., 1913, *Ann. Phys., Lpz.*, **41**, 931.
- MOLIERE, G., 1948, *Z. Naturforsch.*, **3a**, 78.
- SHEPPARD, C. W., and FOWLER, W. A., 1940, *Phys. Rev.*, **57**, 273.
- SINHA, M. S., 1945, *Phys. Rev.*, **68**, 153.
- SKYRME, D. M., 1953, *Phil. Mag.*, **44**, 191.
- SVEDBERG, T., and ANDERSON, H., 1921, *Photogr. J.*, **65**, 325.
- WILKINS, T. R., and WOLFE, R. N., 1933, *J. Opt. Soc. Amer.*, **23**, 324.

RESEARCH NOTES

The Reaction $^{13}\text{C}(\alpha n)^{16}\text{O}$

BY G. A. JONES AND D. H. WILKINSON

Cavendish Laboratory, Cambridge

MS. received 7th April 1953, and in amended form 23rd July 1953

§ 1. INTRODUCTION

SOME time ago we reported our observation of the reaction $^{13}\text{C}(\alpha n)^{16}\text{O}$ (Jones and Wilkinson 1951); the neutrons from a thick target were detected at 0° to the alpha-particle beam of energy 1.05 mev in an ionization chamber filled with deuterium at high pressure. Their energy of 2.68 ± 0.15 mev was in reasonable accord with that expected from the mass values ($Q = 2.20$ mev; thin target neutron energy = 2.82 mev) and their abundance increased as expected on using a target of separated ^{13}C rather than one of the natural mixture of isotopes.

The energy range of ^{17}O accessible to this reaction (above 6.344 mev) is perhaps more powerfully covered by the reactions $^{16}\text{O}(\text{nn})^{16}\text{O}$, $^{16}\text{O}(\text{dp})^{17}\text{O}$ and $^{19}\text{F}(\text{d}\alpha)^{17}\text{O}$, while the excited states of ^{16}O may certainly be investigated more profitably by the reactions $^{19}\text{F}(\text{p}\alpha)^{16}\text{O}$, $^{12}\text{C}(\alpha\alpha)^{12}\text{C}$ and $^{12}\text{C}(\alpha\gamma)^{16}\text{O}$. The present reaction is, however, still of interest in that it permits the most accurate location of certain levels in ^{17}O and may give information concerning alpha-particle and neutron penetrabilities. It is also a very great nuisance in that it takes place in the ^{13}C of the deposits formed on targets during bombardment, and its neutrons tend to obscure the gamma-rays from the less prolific ($\alpha\gamma$) reactions if certain types of detectors are used. It is therefore of importance to have available a thin-target excitation function of this reaction in order that the sharp resonances that it displays may not be taken for genuine ($\alpha\gamma$) resonances. We have pursued the excitation function as far as 2 mev, and this Note presents the results.

§ 2. THE TARGET AND NEUTRON DETECTOR

The neutrons were detected in a NaI(Tl) crystal (1 in. cube) biased at 0.8 mev and placed at 0° to the alpha-particle beam almost in contact with a target of natural carbon, whose stopping power was about 10 kev for alpha-particles of 1 mev when the experiment began. During the course of the experiment the target became noticeably thicker owing to the familiar deposition of ill-identified carbonaceous materials; this effect was not of great importance and, in any case, we must interpret the general shape of the excitation function with some reserve since the neutron energy changes as a function of alpha-particle energy and hence the efficiency of the crystal detector must itself be presumed to be a function of alpha-particle energy. We did not examine the pulse-spectrum from the crystal with very great care; it rose more or less exponentially to low energies and was wholly different from that produced by monochromatic gamma-rays. The upper limit of the spectrum—which was fairly well defined—increased with increasing neutron energy and, indeed, agreed in energy with that of the neutrons to within a few per cent; it is probable that it derives from inelastic scattering of

neutrons in the room and apparatus and in the iodine and thallium of the crystal, followed by detection of the many and complex gamma-rays of de-excitation. This accounts both for the 'exponential' character of the pulse distribution and for the rough correspondence of the high-energy limit of that distribution with the energy of the neutrons. Such detection of fast neutrons by NaI(Tl) crystal has been remarked before (Grace, Lemmer and Halban 1952) and is certainly more of a nuisance than otherwise.

§ 3. THE EXCITATION FUNCTION AND LEVELS OF ^{17}O

In our earlier communication we reported that the neutron yield rose slowly and monotonically to 1.2 Mev in alpha-particle energy. That measurement was not well adapted to the detection of sharp resonances because a thick target was used and the alpha-particle beam had a large spread in energy (about 30 kev). The present excitation function, which is displayed in fig. 1, was made on the thin target described above and used alpha-particles whose energy spread was less than 1 kev. It is seen from fig. 1 that the main feature of the excitation

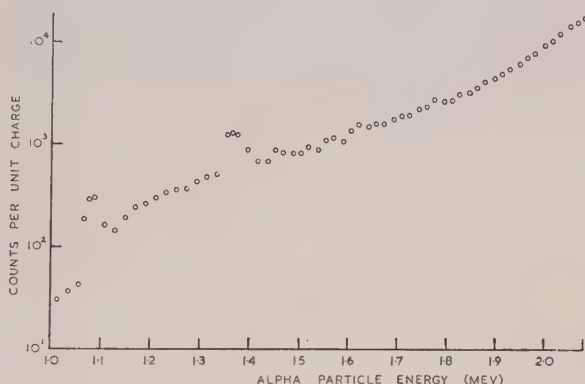


Fig. 1. Thin target excitation function of the reaction $^{13}\text{C}(\alpha n)^{16}\text{O}$ taken with an NaI(Tl) crystal as neutron detector. The neutron yield may not be taken as linear in the ordinate of this plot—see text.

function as we reported it before is again observed and, indeed, persists to the highest energies we have used. In addition to the gradual rise there appear two well-defined resonances at alpha-particle energies of 1066 ± 5 and 1344 ± 10 kev. These correspond to states of ^{17}O at 7.158 ± 0.009 and 7.372 ± 0.011 mev. (We arrive at the value 6.344 ± 0.008 mev for the excitation produced in ^{17}O on adding an alpha-particle to ^{13}C by using the Q -values of the reactions $^{16}\text{O}(\text{dp})^{17}\text{O}$, $^{16}\text{O}(\text{d}\alpha)^{14}\text{N}$, $^{13}\text{C}(\text{dp})^{14}\text{C}$, $^{14}\text{C}(\beta^-)^{14}\text{N}$, $\text{D}(\gamma n)\text{p}$ and $\text{n}(\beta^-)\text{p}$ taken from the compilation of Li, Whaling, Fowler and Lauritsen (1951).) For the rest there appears to be little else than a yield that rises exponentially towards 2 mev.

That such sharp resonances should appear in a compound nucleus unstable by 3 mev to neutron emission is interesting, and we have studied the lower resonance more carefully (with a semi-thick target) in order to ascertain its true width. The result is shown in fig. 2, where it appears that the resonance shows a genuine width of about 3 kev. So small a width demands that neutrons of high angular momentum be emitted; it appears from the usual expression for the neutron transmission coefficient (see, for example, Blatt and Weisskopf 1952) that neutrons of $l=4$ or more may be involved, since the broad levels found at about the same

energy by the elastic scattering of neutrons in ^{16}O have a width of 200–800 keV for neutrons of $l=1$ or 2 (Freier, Fulk, Lampi and Williams 1950, Baldinger, Huber and Proctor 1952). This, in turn, implies that the alpha-particles that form the level should have $l=3$ or more and would therefore be expected to show a width considerably less than 1 keV. We have not been able to make an estimate of the absolute cross section in the present work because of the nature of the detector but if such a measurement were made and the character of the resonance established by angular distribution measurements on the emitted neutrons the resulting information on the width for alpha-particles of high angular momentum would be of considerable interest.

The sharpness of these levels shows that they may indeed simulate $(\alpha\gamma)$ resonances as was mentioned above and that for $(\alpha\gamma)$ studies in which scintillation detection is used a clean target is essential.

That there exist levels of width 10 keV or less in this region of excitation is known from the work of Watson and Buechner (1952) on the reaction $^{19}\text{F}(d\alpha)^{17}\text{O}$. These authors were prevented from discovering the level at 7.16 MeV by an obscuring group of alpha-particles from the reaction $^{16}\text{O}(d\alpha)^{14}\text{N}$; they observed, however, an alpha-particle group that they tentatively assigned to the reaction $^{19}\text{F}(d\alpha)^{17}\text{O}$ of an energy that implied a level of ^{17}O at 7.371 ± 0.015 MeV which agrees very well with our higher resonance.

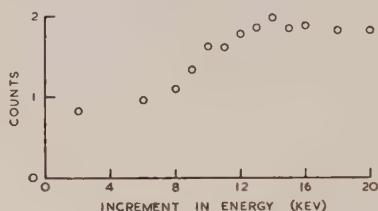


Fig. 2. Detailed semi-thick target excitation function near the 1066 keV resonance.

Burrows, Powell and Rotblat (1952) have reported a state in ^{17}O at 7.53 ± 0.05 MeV from the reaction $^{16}\text{O}(dp)^{17}\text{O}$ and at 7.51 ± 0.03 MeV from the reaction $^{19}\text{F}(d\alpha)^{17}\text{O}$; these measurements may refer to the same state as ours of 7.37 MeV, but appear to be incompatible with them. These workers did not observe the state at 7.16 MeV in either reaction. The inverse reaction $^{16}\text{O}(n\alpha)^{13}\text{C}$ has not revealed any narrow levels in the range of excitation studied by us (Wilhelmy 1937). The broad levels at 7.28 and 7.72 MeV in ^{17}O of width 220 and 800 respectively found by fast neutron scattering in ^{16}O (Freier, Fulk, Lampi and Williams 1950, Baldinger, Huber and Proctor 1952) should, in the absence of the coulomb barrier, be centred at alpha-particle energies of 1.23 and 1.81 MeV respectively, but the alpha-particle width changes so rapidly across them that it is not unreasonable that they should not appear in the present excitation function.

§ 4. THE REACTION $^{12}\text{C}(\alpha\gamma)^{16}\text{O}$

Throughout the present work the pulse distribution from the NaI(Tl) crystal was that appropriate to fast neutrons and not to gamma-rays; this has been particularly carefully checked at the two sharp resonances. We must now ask what are the chances that we should have detected a level in ^{16}O by radiative capture had it existed in the range of excitation (7.88 to 8.70 MeV) under investigation.

If we neglect statistical factors then the expected counting rate under our experimental conditions is of the order $20\Gamma\text{sec}^{-1}$, where Γ is the smaller of Γ_α and Γ_γ measured in ev. This corresponds to an increment of 2000 Γ counts per unit charge in fig. 1. We must note that only those states whose characteristics may be represented as $n(-)^n$ can be excited by our method. M1 transitions would be available from hypothetical $(2+)$ or $(3-)$ states to those of the same characteristics at 6 and 7 mev as would E2 transitions to the ground state of ^{16}O from a hypothetical $(2+)$ state (these characteristics are taken from the compilation of Ajzenberg and Lauritsen 1952). E1 transitions from hypothetical states of suitable properties would be discouraged by a large factor by the isotopic spin rule (Radicati 1952, 1953, Wilkinson and Jones 1953). The single particle estimates of the radiative widths (Weisskopf 1951) are probably reliable to an order of magnitude (Wilkinson 1953), and it appears from them that we can make no firm statement about the possible existence of states of ^{16}O in the range of excitation covered here. It is clear that a target depleted in ^{13}C is needed for a study of radiative capture.

ACKNOWLEDGMENTS

We should like to thank Mr. E. S. Shire for allowing us the use of the electrostatic generator and Messrs. G. Lindsay Jones and J. Wormald for operating the machine.

REFERENCES

- AJZENBERG, F., and LAURITSEN, T., 1952, *Rev. Mod. Phys.*, **24**, 321.
 VON BALDINGER, E., HUBER, P., and PROCTOR, W. G., 1952, *Helv. Phys. Acta*, **25**, 142.
 BLATT, J. M., and WEISSKOPF, V. F., 1952, *Theoretical Nuclear Physics* (New York: Wiley).
 BURROWS, H. B., POWELL, C. F., and ROTBLAT, J., 1952, *Proc. Roy. Soc. A*, **209**, 478.
 FREIER, G., FULK, M., LAMPI, E. E., and WILLIAMS, J. H., 1950, *Phys. Rev.*, **78**, 508.
 GRACE, M. A., LEMMER, H. R., and HALBAN, H., 1952, *Proc. Phys. Soc. A*, **65**, 456.
 JONES, G. A., and WILKINSON, D. H., 1951, *Proc. Phys. Soc. A*, **64**, 756.
 LI, C. W., WHALING, WARD, FOWLER, W. A., and LAURITSEN, C. C., 1951, *Phys. Rev.*, **83**, 512.
 RADICATI, L. A., 1952, *Phys. Rev.*, **87**, 521; 1953, *Proc. Phys. Soc. A*, **66**, 139.
 WATSON, H. A., and BUECHNER, W. W., 1952, *Phys. Rev.*, **88**, 1324.
 WEISSKOPF, V. F., 1951, *Phys. Rev.*, **83**, 1073.
 WILHELMY, E., 1937, *Z. Phys.*, **107**, 769.
 WILKINSON, D. H., 1953, *Phil. Mag.*, **44**, 450.
 WILKINSON, D. H., and JONES, G. A., 1953, *Phil. Mag.*, **44**, 542.

The Production of a Short-Lived Activity by Irradiation of Pb with X-Rays

BY J. M. REID AND K. G. MCNEILL

Department of Natural Philosophy, University of Glasgow

Communicated by P. I. Dee; MS. received 28th September 1953

THERE is a well-established isomer of ^{207}Pb , of half-life 0.8 sec, which has been produced by neutron irradiation of lead (Campbell and Goodrich 1950), and by the radioactive decay of a bismuth isotope (Grace and Prescott 1951). Pryce (1952) has assigned spins to energy levels of ^{207}Pb on a

shell model basis. We find evidence of a 0.8 sec half-life on irradiation of lead by bremsstrahlung x-rays from a 23 mev synchrotron.

The Pb target was $\frac{1}{4}$ in. thick and 6 in. long, and lay at a small angle to the x-ray beam. One inch below the target was placed a 1 in. cube of NaI(Tl) crystal, mounted on an E.M.I. photomultiplier. By means of a rotary switch, based on cold cathode discharge tubes and short suppressor base pentodes (more fully described elsewhere by Reid and Telfer (1953)), the following sequence was cyclically repeated: Irradiation for t_1 seconds, followed by counting in three scalers during three successive periods of t_2 seconds each. Experiments were performed with various values of t_1 and t_2 to minimize systematic errors. The combined results gave a half-life of 0.8 ± 0.1 second.

A further experiment was carried out to determine the integrated cross section for the formation of the $^{207}\text{Pb}^*$ relative to the cross section for the well-known $^{63}\text{Cu}(\gamma, n)^{62}\text{Cu}$ process. In this experiment the Pb target and a Cu target of similar dimensions were irradiated in turn. The rotary switch was used to measure the intensity of the short-lived Pb activity, but in order to increase the counting efficiency only two counting channels, of lengths 1.2 seconds each, were used. The yield of ^{62}Cu was measured using the same detector and amplifier, but the pulses were fed directly to a scaler. Allowance was made for the fact that the NaI crystal had a comparatively long-lived background (of half-life approximately 30 minutes), an effect which is being further investigated.

It was found that the integrated cross section for the formation of $^{207}\text{Pb}^*$ was of the order of 0.07 mev barn, accepting the value for the $^{63}\text{Cu}(\gamma, n)^{62}\text{Cu}$ reaction to be 0.7 mev barn (Johns, Katz, Douglas and Haslam 1950).

There are two possible modes of production of $^{207}\text{Pb}^*$ by the irradiation of natural lead with x-rays, viz. $^{208}\text{Pb}(\gamma, n)^{207}\text{Pb}^*$ and $^{207}\text{Pb}(\gamma, \gamma')^{207}\text{Pb}^*$, and accepting the spin values assigned by Pryce, the overall spin changes are 0 to $13/2$ for the former reaction and $1/2$ to $13/2$ for the latter. These results may be compared with those of Goldemberg and Katz (1953) on ^{115}In . They find that the probability of a (γ, γ') reaction is one-twentieth of that of a (γ, n) reaction in which there is a similar overall spin change. It therefore appears likely that the Pb isomer is formed by a (γ, n) process.

A comparison with other (γ, n) cross sections is useful only if the spin changes involved are known. In the case of $^{115}\text{In}(\gamma, n)^{114}\text{In}$, where the total spin change is $9/2 \rightarrow 1$, the integrated cross section is 0.5 mev barn.

REFERENCES

- CAMPBELL, E. C., and GOODRICH, M., 1950, *Phys. Rev.*, **78**, 640.
 GOLDEMBERG, J., and KATZ, L., 1953, *Phys. Rev.*, **90**, 308.
 GRACE, M. A., and PRESCOTT, J. R., 1951, *Phys. Rev.*, **84**, 1059.
 JOHNS, H. E., KATZ, L., DOUGLAS, R. A., and HASLAM, R. N. H., 1950, *Phys. Rev.*, **80**, 1062.
 PRYCE, M. H. L., 1952, *Proc. Phys. Soc. A*, **65**, 773.
 REID, J. M., and TELFER, J. C. W., 1953, in the press.

The Effect of Variation of the Dipole Moment with Internuclear Separation on the Relative Intensities of the Second Negative Band System of Oxygen

By G. POOTS

Department of Applied Mathematics, Queen's University of Belfast

Communicated by D. R. Bates; MS. received 8th July 1953

§1. INTRODUCTION

IN calculations on the relative intensities of the members of a band system of a diatomic molecule it is generally assumed for the sake of simplicity that D , the transition dipole moment, is independent of R , the internuclear separation; for in this case the Einstein spontaneous emission coefficients connecting the vibrational levels v' and v'' can be taken proportional to the easily evaluated expression

$$\nu(v', v'')^3 p(v', v'')^2, \quad \dots\dots(1)$$

in which ν is the frequency of the emitted radiation and

$$p(v', v'') = \int_0^\infty P(v'|R)P(v''|R) dR, \quad \dots\dots(2)$$

$P(v'|R)$ and $P(v''|R)$ being the vibrational wave functions of the electronic states concerned. However, the transition dipole moment is in fact a function of R , and it may indeed be quite a rapidly varying function (cf. Bates 1951, Bates, Darling, Hawe and Stewart 1953). It is therefore of importance to investigate the errors likely to be introduced by the usual treatment. Bates (1949) has shown that they are actually quite small in the case of a compact band system but the position regarding diffuse band systems has not yet been examined. It is the purpose of the present paper to provide information on the subject by presenting the results of some calculations on the Second Negative system of oxygen. Wu (1952) has recently developed a procedure for evaluating nuclear overlap integrals and has applied it to the same system. In addition to their main use, the new results enable an assessment to be made of the accuracy he achieves.

§2. CALCULATIONS

The best simple representation of vibration wave functions is that of Morse (1929):

$$P(v|R) = N(v)S(v|R) \exp \left\{ -\frac{1}{2x_e} [(1-x_e)\delta + \exp(-\delta)] \right\} \quad \dots\dots(3)$$

with

$$N(v) = \left[\frac{ak^{k-1}(k-2v-1)}{v! \Gamma(k-v)} \right]^{1/2},$$

$$S(v|R) = v! \Gamma(k-v) \sum_{s=0}^v \frac{(-1)^s e^{s\delta}}{s! (v-s)! k^s \Gamma(k-v-s)}$$

$\delta = a(R - R_e)$, $k = 1/x_e$, the standard spectroscopic notation (cf. Herzberg 1950) being used. This representation was therefore adopted. The values of the molecular constants involved were taken from a recent paper by Feast (1950).

Unfortunately integrals such as (2) cannot be determined analytically so that resort must be had to numerical methods. The labour incurred is considerable. Thus in the case of the Second Negative system the range of the dimensionless independent variable δ that is of importance is from -0.660 to $+0.990$; and throughout this range it is necessary to tabulate the wave functions at intervals of 0.015 to enable them to be adequately checked by differencing.* Again, owing to cancellation effects, the individual terms in the expression for $S(v|R)$ have in some cases to be computed to 9 figures to be certain of $P(v|R)$ to 5 figures.

Having determined the wave functions for the seven lower vibrational levels, the nuclear overlap integrals, $p(v', v'')$, and the auxiliary integrals

$$q(v', v'') = \int_0^\infty P(v'|R)P(v''|R)R dR, \quad \dots\dots(4)$$

were evaluated using the quadrature formulae of Newton-Cotes. The results were shown to be free from error by differencing the ratios of the successive members of the various progressions.

Table 1. Franck-Condon Factors for $O_2^+(A^2\Pi_u - x^2\Pi_g)$

$v' \backslash v''$	0	1	2	3	4	5	6
0	2.4×10^{-6} (3.0×10^{-6})	4.2×10^{-5} (5.8×10^{-5})	3.6×10^{-4} (4.5×10^{-4})	1.9×10^{-3} (2.2×10^{-3})	7.4×10^{-3} (8.0×10^{-3})	2.1×10^{-2} (1.6×10^{-2})	4.9×10^{-2} (8.8×10^{-2})
1	1.9×10^{-5} (2.8×10^{-5})	2.9×10^{-4} (3.9×10^{-4})	2.1×10^{-3} (2.5×10^{-3})	9.3×10^{-3} (9.8×10^{-3})	2.8×10^{-2} (2.8×10^{-2})	6.1×10^{-2} (2.7×10^{-2})	9.5×10^{-2} (—)
2	8.1×10^{-5} (1.2×10^{-4})	1.1×10^{-3} (2.3×10^{-3})	6.5×10^{-3} (7.3×10^{-3})	2.3×10^{-2} (2.4×10^{-2})	5.4×10^{-2} (3.2×10^{-2})	8.3×10^{-2} (—)	8.0×10^{-2} (—)
3	2.5×10^{-4} (3.5×10^{-4})	2.8×10^{-3} (3.5×10^{-3})	1.4×10^{-2} (1.4×10^{-2})	4.1×10^{-2} (4.8×10^{-2})	7.1×10^{-2} (7.0×10^{-2})	7.0×10^{-2} (—)	2.9×10^{-2} (—)
4	5.9×10^{-4} (8.1×10^{-4})	5.8×10^{-3} (7.0×10^{-3})	2.4×10^{-2} (1.9×10^{-2})	5.5×10^{-2} (13.5×10^{-2})	6.7×10^{-2} (—)	3.6×10^{-2} (—)	9.0×10^{-2} (—)
5	1.2×10^{-3} (1.6×10^{-3})	1.0×10^{-2} (1.2×10^{-2})	3.5×10^{-2} (—)	6.1×10^{-2} (—)	4.8×10^{-2} (—)	8×10^{-5} (—)	8.6×10^{-3} (—)
6	2.1×10^{-3} (1.9×10^{-3})	1.5×10^{-2} (—)	4.4×10^{-2} (—)	5.7×10^{-2} (—)	2.5×10^{-2} (—)	2×10^{-6} (—)	2.9×10^{-2} (—)

* The upper figure is that obtained in the present investigation; the lower figure (in parentheses) is that obtained by Wu.

Table 1 gives the derived values of $p(v', v'')^2$ the so-called Franck-Condon factors † (cf. Bates 1952), together with the corresponding values found by Wu. These latter are also based on the Morse approximation, but were got by an approximate analytical method. It will be observed that Wu's results, while in general satisfactory, are occasionally wrong by a factor 2 or more.

An indication of the errors that might be caused by the assumption that the transition dipole moment D is independent of the internuclear distance (and is equal to, say, unity) may be obtained by supposing that

$$D = (a + bR)/(a + b\bar{R}_e), \quad \dots\dots(5)$$

* The check provided by verifying that $\int_0^\infty P(v|R)^2 dR$ is unity, though useful, is not sufficiently exacting.

† Wu actually tabulates what appears to be 10^3 times the Franck-Condon factors.

in which a and b are constants, and \bar{R}_e is the mean of the equilibrium internuclear separations. With this linear dependence it is apparent that the relative transition probabilities, instead of being controlled by the quantity $p(v', v'')^2$, are controlled by the quantity $p(v', v'')^2 t(v', v'')^2$, where

$$t(v', v'') = \{a + b(q/p)\} / (a + b\bar{R}_e). \quad \dots\dots (6)$$

For any chosen a and b the quantity $t(v', v'')^2$, which may be termed the *correction factor*, can be got from table 2 which gives the computed values of q/p for the various transitions. The possibilities can best be seen from the variation of $t(v', v'')^2$ with the parameter

$$\alpha = \left(\frac{1}{D} \frac{dD}{dR} \right)_{R=\bar{R}_e} = \frac{b}{a + b\bar{R}_e}, \quad \dots\dots (7)$$

Table 2. Calculated Values of $q(v', v'')/p(v', v'')$ in units of \AA^{-1}

$v' \backslash v''$	0	1	2	3	4	5	6
0	1.25	1.26	1.28	1.29	1.31	1.33	1.34
1	1.24	1.25	1.27	1.28	1.30	1.32	1.33
2	1.23	1.25	1.26	1.28	1.29	1.31	1.33
3	1.23	1.24	1.25	1.27	1.29	1.30	1.31
4	1.22	1.23	1.25	1.26	1.28	1.29	1.29
5	1.21	1.23	1.24	1.26	1.27	1.6*	1.3*
6	1.21	1.22	1.24	1.25	1.26	1.1*	1.3*

* Cancellation is here severe in both p and q .

Table 3. Dependence of Correction Factor $t(v', v'')^2$ on α (eqn. 6),
for $\text{O}_2^+(\text{A}^2\Pi_u - \text{X}^2\Pi_g)$

Transition		α (in units of \AA^{-1})										
v'	v''	-2.0	-1.6	-1.2	-0.8	-0.4	0.0	0.4	0.8	1.2	1.6	2.0
0	6	1.25	1.19	1.14	1.10	1.05	1.00	0.95	0.91	0.87	0.82	0
1	5	1.16	1.13	1.10	1.06	1.03	1.00	0.97	0.94	0.91	0.88	0.85
2	4	1.09	1.07	1.05	1.03	1.02	1.00	0.98	0.97	0.95	0.94	0.92
3	3	0.99	0.99	0.99	1.00	1.00	1.00	1.00	1.01	1.01	1.01	1.01
4	2	0.90	0.92	0.94	0.96	0.98	1.00	1.02	1.04	1.06	1.09	1.11
5	1	0.81	0.84	0.88	0.92	0.96	1.00	1.04	1.08	1.13	1.17	1.22
6	0	0.71	0.77	0.82	0.88	0.94	1.00	1.06	1.13	1.20	1.27	1.34

that is, with the fractional change in D per unit change in R at the mean equilibrium internuclear separation. Table 3 shows this variation for some representative bands. It is apparent from the entries that in general gross errors should not be caused by the customary procedure of taking D to be constant: thus the correction factor lies between 0.77 and 1.27 even if the modulus of α is

as much as 1.6 \AA^{-1} (which corresponds to a very rapidly varying transition dipole moment).^{*} For some individual bands $p(v', v'')$ may be almost zero due to cancellation so that $q(v', v'')/p(v', v'')$, and hence the correction factor, may be abnormally large; but such bands are of course very feeble, and it is usually not a serious matter if their relative intensities are not known reliably.

ACKNOWLEDGMENT

I should like to thank Professor D. R. Bates for suggesting this problem, and for his interest and help during its progress.

REFERENCES

- BATES, D. R., 1949, *Proc. Roy. Soc. A*, **196**, 217; 1951, *J. Chem. Phys.*, **19**, 1122; 1952, *Mon. Not. Roy. Astr. Soc.*, **112**, 614.
BATES, D. R., DARLING, R. T. S., HAWE, S. C., and STEWART, A. L., 1953, *Proc. Phys. Soc. A*, **66**, 1124.
FEAST, M., 1950, *Proc. Phys. Soc. A*, **63**, 557.
HERZBERG, G., 1950, *Spectra of Diatomic Molecules*, 2nd Edn. (New York: Van Nostrand).
MORSE, P., 1929, *Phys. Rev.*, **34**, 57.
WU, TA-YOU, 1952, *Proc. Phys. Soc. A*, **65**, 965.

* It should be noted, however, that even a slight variation of D causes appreciable errors. Some workers, while assuming D to be constant, give the Franck-Condon factors to three decimal places, which is quite unrealistic. There is no justification for such elaborate calculations.

LETTERS TO THE EDITOR

Predissociations and CO Dissociation Energy

In his book on dissociation energies Gaydon (1953) deals in some detail with the predissociation observations and CO dissociation energy scheme of Schmid and Gerö. We want here neither to enter into a criticism of the foundations of the 'non-crossing rule' (see Valatin 1946 a), which is Gaydon's leading principle for the determination of dissociation energies, nor to discuss our different appreciation of the available experimental material on which our views have been expressed on several occasions. We think that in the present state of the discussion on CO additional experimental information is needed in order to make the discussion fruitful. We feel confident as to the outcome of future experiments from the point of view of the scheme of Schmid and Gerö, including the graphite sublimation heat measurements, where a better knowledge of the secondary processes involved will probably clarify the different observations on the vapour pressure of carbon.

It seems, however, desirable to rectify a few of the statements in Gaydon's book on the occasion of its revised second edition. According to the CO dissociation scheme of Schmid and Gerö (1936, 1937 a, b, 1938), which is based on spectroscopic observations (and is attributed to Gerö in the rather misleading Table 14 of the book), the energy distance of the $\text{CO}(x^1\Sigma)$ ground level from the $\text{C}(^3\text{P}) + \text{O}(^3\text{P})$ atomic term combination is 6.90 eV. The scheme leads to a value $L_2 = 169.735 \text{ kcal mole}^{-1}$ for the heat of sublimation of carbon into ^5S atoms (Gerö 1948, Valatin 1948). Contrary to the statement on p. 180 of Gaydon's book, the levels of the $x^1\Sigma$ ground state of the divalent CO molecule are not believed to tend to the $\text{C}(^5\text{S}) + \text{O}(^3\text{P})$ atomic term combination, but to the $\text{C}(^1\text{D}) + \text{O}(^1\text{D})$ combination at 10.13 eV, with a more reasonable bond energy.

The observed predissociation limit at $89620 \pm 47 \text{ cm}^{-1} \sim 11.11 \text{ eV}$ is identified with the position of the atomic term combination $\text{C}(^5\text{S}_2) + \text{O}(^3\text{P}_0)$, the predissociation limit at $77497 \pm 44 \text{ cm}^{-1} \sim 9.61 \text{ eV}$ with that of $\text{C}(^1\text{S}) + \text{O}(^3\text{P}_0)$. According to Gaydon, this identification does not give a good numerical agreement between the difference of the predissociation limits and the difference of the energies of the atomic products. His opinion is based probably on the estimated value of the $\text{C}(^5\text{S})$ energy given in Table 15 of the first edition of the book. Actually, on adding the 21648 cm^{-1} excitation energy of the $\text{C}(^1\text{S})$ state to the difference of the two predissociation energies, the obtained $33771 \pm 91 \text{ cm}^{-1}$ value is in excellent agreement with the measured 33735.2 cm^{-1} excitation energy of the ^5S state given by Shenstone (1947), and is the best value proposed for the ^5S state before Shenstone's direct observation (Long and Norrish 1946, Valatin 1946 b, Edlén 1947, Goudsmit 1947).

Schmid and Gerö (1938) reported the observation of a predissociation at the $\text{A}^1\Pi$ final level of the ångström bands at about $71500 \text{ cm}^{-1} \sim 8.87 \text{ eV}$ (and not at 8.42 eV as given in Gaydon's book). The coordination of this

new observation resulted in a slight shift of the atomic term combinations with respect to their position previously supposed, with the value of approximately 220 cm^{-1} of the $\text{O}(^3\text{P}_0) - \text{O}(^3\text{P}_2)$ energy difference. (This is partly the reason for the slightly different value 6.90 eV of the dissociation energy with respect to the 6.92 eV value quoted by Gaydon.) Gaydon writes that he is "quite unable to see how predissociation in the final levels of an emission band could cause a sudden falling off in intensity". For the benefit of the reader, however, it might be remarked that according to the quantum theory of radiation (Heitler 1936, p. 114) the breadth of a spectral line depends on the lifetime of both the initial and the final state, and the mixing of the wave functions of the initial or final states with those of a third state affects equally the transition probabilities. In the case when the predissociation takes place in the initial state of an emission band, the weakening of the intensity of the emission lines might be partly due to the decrease in the number of molecules in the initial state, and this is often the main effect. The effect of predissociation on the mixing of wave functions and the broadening of energy levels might, however, become equally important, and a sufficiently strong predissociation in the final levels might even lead to a complete missing of the corresponding lines. For more details the paper by Schmid and Gerö (1938) and that of Holst (1934) should be consulted, the latter dealing with the breaking off of emission lines in AlH through predissociation in the final levels.

According to the comments by Schmid and Gerö (1938), the low pressure part of the absorption spectrogram of Hopfield and Birge, reproduced in the book of Bonhoeffer and Harteck (1933, p. 132), also shows a definite intensity minimum of the $\text{A}^1\Pi \leftarrow \text{x}^1\Sigma$ absorption bands near the 8.87 eV energy height of the $\text{A}^1\Pi$ levels. Herman and Herman (1948) have reported independently a predissociation of the $\text{d}^3\Pi$ initial levels of the triplet bands at this energy height. The levels of the $\text{d}^3\Pi$ state were previously observed only up to the supposed predissociation limit at 8.87 eV . Gaydon's remark on 'wishful thinking' obviously does not apply to this later observation.

Department of Mathematical Physics,
University of Birmingham.
4th September 1953.

J. G. VALATIN.

- BONHOEFFER, K. F., and HARTECK, P., 1933, *Grundlagen der Photochemie* (Dresden and Leipzig : Steinkopff).
EDLÉN, B., 1947, *Nature, Lond.*, **159**, 129.
GAYDON, A. G., 1953, *Dissociation Energies and Spectra of Diatomic Molecules*, 2nd (revised) Edn. (London : Chapman and Hall.) (1st Edn, 1947.)
GERÖ, L., 1948, *J. Chem. Phys.*, **16**, 1011.
GOUDSMIT, S., 1947, *Nature, Lond.*, **159**, 742.
HEITLER, W., 1936, *The Quantum Theory of Radiation* (Oxford : University Press).
HERMAN, R., and HERMAN, L., 1948, *J. Phys. Radium*, **9**, 160.
HOLST, W., 1934, *Z. Phys.*, **90**, 735.
LONG, L. H., and NORRISH, R. G. W., 1946, *Nature, Lond.*, **157**, 486, **158**, 237.
SCHMID, R., and GERÖ, L., 1936, *Z. Phys.*, **99**, 281; 1937 a, *Z. Phys. Chem. B*, **36**, 105; 1937 b, *Z. Phys.*, **106**, 205; 1938, *Phys. Z.*, **39**, 460.
SHENSTONE, A. G., 1947, *Phys. Rev.*, **72**, 411.
VALATIN, J. G., 1946 a, *Proc. Phys. Soc.*, **58**, 695; 1946 b, *Nature, Lond.*, **158**, 237; 1948, *J. Chem. Phys.*, **16**, 1018.

Proton Magnetic Resonance Evidence for the Planar Structure of the Urea Molecule

It is well known from x-ray analysis that the four heavy atoms of the urea molecule, $\text{OC}(\text{NH}_2)_2$, lie in a plane (Hendricks 1928, Wyckoff 1930, 1932, Wyckoff and Corey 1934, Vaughan and Donohue 1952). In carrying out an analysis of the vibrations of the molecule Kellner (1941) assumed that the hydrogen atoms do not lie in this plane, but lie symmetrically above and below the plane as indicated in figure 1 (a). On the other hand, analyses of infra-red spectroscopic measurements on monocrystalline urea (Keller 1948, Waldron and Badger 1950) have suggested that the whole molecule is planar, the hydrogen atoms lying in the positions shown in figure 1 (b). This note shows that a study of the anisotropy of the second moment (mean square width) of the proton magnetic resonance spectrum for a single crystal of urea yields strong support for the planar structure.

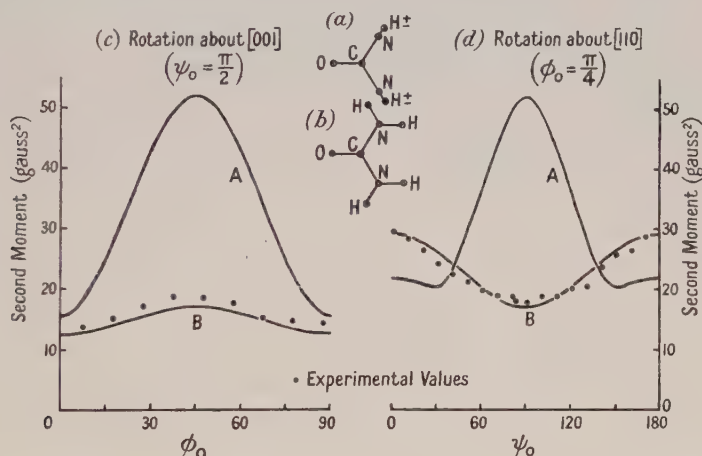


Figure 1. Experimental values of second moment, and theoretical curves, A for non-planar model (a) and B for planar model (b).

Measurements were made at room temperature on a single crystal of mass about 1 g, using apparatus similar to that of Bloembergen, Purcell and Pound (1948). The crystal was first mounted with its tetrad [001] axis perpendicular to the steady magnetic field; the azimuth angle ϕ_0 of the field (measured from the [100] direction) was varied by rotation of the crystal about this axis. The experimental values of second moment for one quadrant of the fourfold symmetrical pattern are shown as closed circles in figure 1 (c). The crystal was then mounted with its [110] axis perpendicular to the field, and the polar angle ψ_0 of the field (measured from the [001] direction) was varied by rotation of the crystal about this axis. Experimental values for half of the twofold symmetrical pattern are shown in figure 1 (d).

Theoretical values of the second moment have been calculated for both planar and non-planar structures using the formula of Van Vleck (1948); the expected behaviour of the theoretical second moment is shown in the figure (curves A for the non-planar structure, curves B for the planar structure).

The calculation made use of the accurate determination by Vaughan and Donohue (1952) of the positions in the unit cell of the O, C and N atoms. The length of the N—H bond was taken as 1.00 Å, and the C—N—H angle as 120°. These values, which are unlikely to be far wrong, suffice to determine the planar model. For the non-planar model it was further assumed that the plane defined by each NH₂ group also included the carbon atom of the molecule. Any incorrectness in this last assumption leads only to small changes in curves A since, for both structures, the form of variation of the second moment is mainly determined by the contribution of the proton pairs of the NH₂ groups.

It is seen from the figure that the experimental points are in good accord with the theoretical curves for the planar model, while there is no agreement with the markedly different curves for the non-planar model; indeed, for rotation about the [110] axis even the qualitative form of variation is quite different. When we have obtained experimental values of the second moment more accurate than the preliminary values shown in the figure, it should be possible to improve upon the assumed parameters of the planar model. The fairly good quantitative agreement of the experimental values with curves A does however suggest that they are not much in error.

Department of Natural Philosophy,
The University,
St. Andrews, Scotland.
14th September 1953.

E. R. ANDREW.
D. HYNDMAN.

- BLOEMBERGEN, N., PURCELL, E. M., and POUND, R. V., 1948, *Phys. Rev.*, **73**, 679.
HENDRICKS, S. B., 1928, *J. Amer. Chem. Soc.*, **50**, 2455.
KELLER, W. E., 1948, *J. Chem. Phys.*, **16**, 1003.
KELLNER, L., 1941, *Proc. Roy. Soc. A*, **177**, 456.
VAN VLECK, J. H., 1948, *Phys. Rev.*, **74**, 1168.
VAUGHAN, P., and DONOHUE, J., 1952, *Acta Cryst., Camb.*, **5**, 530.
WALDRON, R. D., and BADGER, R. M., 1950, *J. Chem. Phys.*, **18**, 566.
WYCKOFF, R. W. G., 1930, *Z. Kristallogr.*, **75**, 529; 1932, *Ibid.*, **81**, 102.
WYCKOFF, R. W. G., and COREY, R. B., 1934, *Z. Kristallogr.*, **89**, 462.

Antiferromagnetism in Metals*

The qualitative success of the Heitler London–Heisenberg theory of ferromagnetism as applied to the metals Fe, Co and Ni, has led to the suggestion (Néel 1936, Zener 1951) that the remaining 3d transition metals can be treated as antiferromagnetics. On this basis we would expect each to possess a critical, or Curie, temperature T_c below which the atomic moments would be arranged alternately parallel and antiparallel, but above which they would be oriented at random. Such an antiferromagnetic order should be detectable by neutron diffraction experiments, and the order–disorder transition at the Curie point should be marked by clearly defined maxima in the magnetic susceptibility and specific heat. However, recent measurements of specific heats and susceptibilities of a number of metals have failed to provide any conclusive evidence for the existence of such transitions (see, for example, Kriessman 1953, McGuire and Kriessman 1952 and Armstrong and Grayson-Smith 1950). On the other hand

* This research has been supported in part by the U.S. Office of Naval Research.

the neutron diffraction studies of Shull and Wilkinson (1953) have clearly demonstrated the occurrence of antiferromagnetic order in both chromium ($T_c = 475^\circ\text{K}$) and α -manganese ($T_c = 100^\circ\text{K}$). A notable feature of their results is the very small magnetic moments (about half a Bohr magneton) which are located on the atoms. These small moments and the absence of any recognizable anomalies in the susceptibility and specific heat present considerable difficulties for the Néel-Zener theory.

These difficulties may be resolved by abandoning the Heitler-London theory and using instead the collective electron approach in a way recently suggested by Slater (1951). In the usual way let us divide the atomic lattice into two interlocking sub-lattices (A, B) such that in the ordered state A sites have positive spins and B sites have negative spins. Then Slater showed how the non-localized solutions of the Hartree-Fock equations for such a system will divide into two groups, those that are mainly concentrated about the A atoms and those that are mainly around the B atoms. The stable arrangement is obtained by assigning positive spins to the electrons in A orbitals and negative spins to the electrons in the B orbitals. However, it is not necessary for all the electrons in the A (B) orbitals to have $+$ ($-$) spin. The actual proportion is determined so as to strike a balance between the exchange energy, which favours all $+$ ($-$) in A (B), and the Fermi energy which favours equal numbers and thus no antiferromagnetism. Such a situation is familiar from the band theory of ferromagnetism (Stoner 1938 a), so that the occurrence of small non-integral moments in the antiferromagnetic metals Cr and Mn should occasion no surprise. As to the absence of anomalies in the specific heats and susceptibilities, we have now obtained a semi-quantitative formulation of Slater's ideas which enables us to correlate this absence with the small moments.

Let us denote by N the total number of 3d ('antiferromagnetic') electrons and let us also define relative magnetizations ζ_A and ζ_B such that $N\zeta_A/2$ is the total spin moment of the A sub-system in the *positive* direction and $N\zeta_B/2$ is the total moment of the B sub-system in the *negative* direction. Our principal assumption is that the total energy of the whole system contains, in addition to the Fermi energy (energy of motion in the periodic electrostatic field of the ions and the other electrons), an exchange term

$$-\frac{1}{4}N\mathbf{k}\theta_1(\zeta_A^2 + \zeta_B^2) - \frac{1}{2}N\mathbf{k}\theta_{12}\zeta_A\zeta_B, \quad \dots\dots(1)$$

where θ_1 and θ_{12} are constants. The first part of (1) represents a ferromagnetic interaction between electrons in like orbitals (AA or BB), while the second part describes the tendency for the moments of the A and B sub-systems to be antiparallel. In the presence of an external magnetic field H there will be a third term in the total energy, namely $-\beta HN(\zeta_A - \zeta_B)/2$. Application of Fermi-Dirac statistics to this system now leads to implicit equations for ζ_A and ζ_B as functions of temperature and applied field strength. Let us assume that the 3d band is parabolic, i.e. $n(\epsilon) = 3N\epsilon^{1/2}/8\epsilon_0^{3/2}$, where $n(\epsilon)$ is the density of states of one spin and one kind (A or B) and ϵ_0 is a constant. In the absence of H the equations for $\zeta_A = \zeta_B = \zeta$ then become formally identical with those obtained by Stoner (1938 a) in his theory of ferromagnetism. In particular the system is not antiferromagnetic unless $\mathbf{k}\theta'/\epsilon_0 > \mathbf{k}(\theta_1 + \theta_{12})/\epsilon_0 > \frac{2}{3}$; the relative moment ζ_0 at $T=0$ lies between 0 and 1 if $\frac{2}{3} < \mathbf{k}(\theta_1 + \theta_{12})/\epsilon_0 < 2^{-1/3}$. Furthermore, the excess specific heat will be exactly as calculated by Stoner (1939)

in his second paper. The formula for the magnetic susceptibility $\chi(T)$ is different however. We find that

$$\frac{\beta^2 N}{\chi(T)\epsilon_0} = \left[3 \left(\frac{\mathbf{k}T}{\epsilon_0} \right)^{1/2} F'_{1/2} \left(\frac{\eta + \mathbf{k}\theta'\zeta}{\mathbf{k}T} \right) \right]^{-1} + \left[3 \left(\frac{\mathbf{k}T}{\epsilon_0} \right)^{1/2} F'_{1/2} \left(\frac{\eta - \mathbf{k}\theta'\zeta}{\mathbf{k}T} \right) \right]^{-1} - \frac{\mathbf{k}(\theta_1 - \theta_{12})}{\epsilon_0} \dots (2)$$

where β is the Bohr magneton and η and ζ are given by

$$(1 \pm \zeta) = \frac{3}{2} \left(\frac{\mathbf{k}T}{\epsilon_0} \right)^{3/2} F_{1/2} \left(\frac{\eta \pm \mathbf{k}\theta'\zeta}{\mathbf{k}T} \right).$$

The function (2) in general has an angular minimum at the Curie point where ζ vanishes. Above T_c the system is paramagnetic (Stoner 1938 b). The susceptibility at $T=0$ is zero if $\zeta_0=1$, but for $0 < \zeta_0 < 1$ it is non-zero and less than $\chi(T_c)$. In fact,

$$\frac{\chi(0)}{\chi(T_c)} = \frac{\mathbf{k}(\theta_1 + \theta_{12})/\epsilon_0 - \mathbf{k}(\theta_1 - \theta_{12})/\epsilon_0}{\frac{1}{3}(1 + \zeta_0)^{-1/3} + \frac{1}{3}(1 - \zeta_0)^{-1/3} - \mathbf{k}(\theta_1 - \theta_{12})/\epsilon_0} \dots (3)$$

As $\zeta_0 \rightarrow 0$, $\chi(0)/\chi(T_c) \rightarrow 1$; the Heitler-London model gives $\chi(0)/\chi(T_c) = \frac{2}{3}$ (Van Vleck 1941).

For chromium Shull and Wilkinson's data give $\zeta_0 = 0.08$ and $T_c = 475^\circ\text{K}$. Hence from Stoner's (1938 a) equation (5.13) we get $\epsilon_0 \sim 20\,000^\circ\text{K}$. The measured susceptibility at the Curie point (McGuire and Kriessman 1952) gives, on the assumption of five 3d electrons per atom, $\mathbf{k}\theta_{12}/\epsilon_0 \sim 0.25$ and hence $\mathbf{k}\theta_1/\epsilon_0 \sim 0.42$. Substitution of these values into (3) shows that the difference between $\chi(0)$ and $\chi(T_c)$ amounts to only 0.1% of $\chi(T_c)$. Stoner's (1938 a) equation (4.9) predicts that the height of the specific heat peak is only $0.0016 \text{ cal deg}^{-1} \text{ mole}^{-1}$. Both 'anomalies' are therefore too small to be observable.

Department of Physics,
University of California,
Berkeley 4, California, U.S.A.

A. B. LIDIARD.

21st September 1953.

- ARMSTRONG, L. D., and GRAYSON-SMITH, H., 1950, *Canad. J. Res. A*, **28**, 51.
 KRIESSMAN, C. J., 1953, *Rev. Mod. Phys.*, **25**, 122.
 MCGUIRE, T. R., and KRIESSMAN, C. J., 1952, *Phys. Rev.*, **85**, 452.
 NÉEL, L., 1936, *C. R. Acad. Sci., Paris*, **203**, 304.
 SHULL, C. G., and WILKINSON, M. K., 1953, *Rev. Mod. Phys.*, **25**, 100.
 SLATER, J. C., 1951, *Phys. Rev.*, **82**, 538.
 STONER, E. C., 1938 a, *Proc. Roy. Soc. A*, **165**, 372; 1938 b, *Proc. Leeds Phil. Soc.*, **3**, 403;
 1939, *Proc. Roy. Soc. A*, **169**, 339.
 VAN VLECK, J. H., 1941, *J. Chem. Phys.*, **9**, 85.
 ZENER, C., 1951, *Phys. Rev.*, **81**, 440.

OBITUARY NOTICES

WILLIAM DAMPIER

By the death of Sir William Dampier (formerly William Cecil Dampier Whetham) on 11th December 1952 the Physical Society has lost a senior Fellow and Cambridge one of its oldest and best loved sons, who was recently described by Sir Lionel Whitby as "a most distinguished scientist, agriculturalist and sociologist" (*Cambridge University Reporter*, October 1953). Dampier, son of the late C. L. Whetham, was born in London in 1867, and one of his grandfathers was Lord Mayor of London in 1878. He was educated at Trinity College, Cambridge, and took his B.A. degree in 1889. He held both the Coutts Trotter Studentship and the Clerk Maxwell Scholarship, and in 1891 was elected to a Fellowship which he retained throughout his long life. For many years he held a College lectureship, and gave courses in Heat and Electricity for students working for Part I of the Natural Sciences Tripos. In the earlier years these lectures were delivered in Trinity, but were later transferred to the Cavendish Laboratory, where more accommodation and better facilities for lecture experiments were available. Many of those who attended his lectures in the days before the First World War must still have vivid memories of his habit of pacing slowly backwards and forwards behind the lecture table, his deliberate but admirably clear delivery, the charm and lucidity of his exposition, and his gift for arousing interest in physics as an exciting and rapidly advancing subject. His elegant treatment of the basic principles of thermodynamics is preserved for us in the first chapter of his *Theory of Solution*, published in 1902. In more popular vein was his *Recent Development of Physical Science* (1904), which gave him full scope for the display of his considerable literary gifts, and revealed a sense of humour that prompted him to preface a chapter on Atoms and Aether with the quotation: "Oh, dear! What can the matter be?—*Old Song*." His characteristic pleasing style is to be found even in his textbooks, such as *Theory of Experimental Electricity* (1905), a work that was deservedly popular in its day, but which may have resulted in some loss of freshness and spontaneity in the lectures on which it was based, and so caused some of the later students to complain that what they listened to was "all in the book".

From 1889 onwards Dampier worked in the Cavendish Laboratory under J. J. Thomson, and between 1890 and 1905 he produced a long series of important papers published in the *Philosophical Transactions*, the *Proceedings of the Royal Society* and the *Philosophical Magazine*. Some of his earlier experimental work was concerned with the flow of liquids through tubes, but most of his researches were directed towards the elucidation of the properties of electrolytic ions in solution, a subject which he made his own and on which he wrote authoritatively in his *Theory of Solution*. Part of this work was done in collaboration with E. H. Griffiths. Dampier's eminence in his chosen field led to his election in 1901 to the Fellowship of the Royal Society. After he became Tutor and, later, Senior Tutor of Trinity, an office which he held until 1917, he found that the heavy burden of administrative duties left him little time for original research, but though his experimental work ceased his interest remained, and he began gradually to collect material for his *History of Science*, which was not published until 1929.

Though a Londoner by birth, Dampier was always greatly interested in country life, and this led him to purchase an estate in Devonshire, and to turn his attention to problems of agriculture. Later (1917) he inherited a family estate. During the First World War he worked in the Food Production Department of the Ministry of Agriculture, and from that time onwards he began to be recognized as an authority on agricultural matters and was frequently consulted by the Government. He played a leading part in preparing the ground for the setting up of the Agricultural Research Council, of which he became first secretary, and to which was entrusted the administration of public funds devoted to agricultural research. In 1927 he published his book *Politics and the Land*. In 1931 he was knighted in recognition of his public services, and in the same year he was awarded the Gold Medal of the Royal Agricultural Society, of which he became Vice-President in 1945. He was also a member of the Agricultural Wages Board, and was a Fellow of Winchester College from 1917-47.

In 1897 Dampier married Catherine Holt, daughter of the late R. D. Holt of Liverpool, and they had five daughters. He was a man of quiet charm, kindly nature and friendly disposition, and his success both as College Tutor and also in his public relations was due in no small measure to his deep understanding of human nature. It was characteristic of him that when he had to ask a junior to give a lecture for him he would never offer detailed instructions. "Treat the subject in your own way" he would say "and you will make a success of it". He will be much missed by all who knew him.

G. STEAD.

ROBERT DONALDSON

By the sudden death, on 5th November 1953, of Robert Donaldson, Head of the Colorimetry Section of the Light Division of the National Physical Laboratory since 1933, his many friends and colleagues suffered a great personal loss, and the branch of science which he had made his own was deprived of one of its leading exponents in the fullness of his career.

Donaldson was born on 8th June 1904, in the fishing village of Port-Seton on the Firth of Forth, and was the oldest of three brothers, all of whom were later to gain distinction as students at the University of Edinburgh. His principal studies were Physics and Mathematics—under Professor C. G. Darwin, who was later to become Director of the National Physical Laboratory. After graduation he remained at the University for two years as Demonstrator in the Department of Natural Philosophy.

He joined the staff of N.P.L. on 3rd July 1928, and was first employed as an assistant in the work which culminated in the adoption by the Commission Internationale de L'Eclairage, in 1931, of the first internationally agreed system of colorimetric standardization. It is a curious coincidence that the quantitative basis of that system, having stood the tests of twenty years, is only now being rechecked and extended with the greatly improved resources of modern equipment and technique, and that Donaldson, in collaboration with Dr. W. S. Stiles, was engaged on this work at the time of his death: so in one sense his first job was also his last. But much happened in the intervening years. When he joined us at N.P.L. his interest was more in the mathematical aspects of physics than the experimental; and though, as events showed, he had a natural flair

for experiment he had no special leaning to any particular field. However, he quickly mastered the apparent complexities of colorimetry and heterochromatic photometry and became fascinated by the interesting problems, physical, physiological, and mathematical, which he could foresee would arise in the course of their development to meet the ever-increasing requirements of industry. Just when useful investigation in any field of this kind ends depends on the imagination and foresight of those working in it. To Donaldson colorimetry had no end, and except during the war, when he participated in the general optical work of the Light Division, he has been primarily occupied, by his own choice, with this subject and its ramifications, gaining for himself an international reputation.

But he avoided the narrowness often found in the expert. He always retained his interest in mathematics and was a keen follower of all significant developments in relativity and quantum physics, bringing a balanced philosophical judgment to discussions of these matters or others of fundamental scientific import. This width of interest helped his work as a specialist by keeping his feet on the ground and his eyes on essentials. Like most of us he may sometimes have failed to see the most direct solution of some problem of theory or design, but if so the writer knows of no instance.

His many contributions to his subject are too well known to all workers in the field to need recapitulation, especially here where we are more concerned with what we have lost of future promise than with what we have had from him.

He enjoyed the respect and esteem not only of his colleagues in N.P.L., but also of the many with whom he was associated on committees of other organizations. Normally of a cheerful—and cheering—disposition, which was often a source of help and encouragement to others, he nevertheless suffered from shyness which showed itself as a dislike, sometimes amounting to a dread, of personal prominence. For example, he could not be induced to accept nomination for Chairmanship of the Society's Colour Group, of which he has been an enthusiastic member from its inception, though strongly pressed to do so on several occasions. He was loath to give lectures, or to participate in discussions among unfamiliar groups, if he could possibly avoid doing so; but if it could not be avoided, when he had forgotten his audience in the interest of his subject there could be no clearer exponent of whatever he had to say.

He had little interest in outdoor sports of the more intense varieties, such as football or tennis, but was an enthusiastic golfer. He was fond of music, being an efficient pianist and a fair violinist. The writer has memories of many pleasant musical evenings in his home during the pre-war years.

In 1934, he married Miss Kathleen Edwards, who was at that time a colleague on the Laboratory staff. They had one son, Ian, now 12 years of age.

J. GUILD.

LEONARD BELLINGHAM

We record with regret the death of Leonard Bellingham who had been a Member of the original Optical Society since 1918 and continued his Membership with the Physical Society and its Optical and Colour Groups. Mr. Bellingham was a founder of the firm Messrs. Bellingham and Stanley, Ltd., having gained his skill in the making of sensitive apparatus with Messrs. Adam Hilger, Ltd.

EDWARD FELIX HERROUN

We record with regret the death of Edward Felix Herroun who had been a Member of the Physical Society since 1885. Herroun was born in 1862 and was educated at Greenwich and King's College, London. In 1881 he gained the Daniell Scholarship in chemistry. His main interest was in research on magnetites, and this work he continued for many years after his retirement.

W. H. TOWNS

We record with regret the death of W. H. Towns who had been a member of the original Optical Society since 1918 and continued his Membership with the Physical Society and its Optical Group. He maintained his interest in optics throughout his very long life and died on 3rd September 1953 at the age of 92.

LEWIS FRY RICHARDSON

Lewis Fry Richardson was born in 1881, the youngest of the seven children of David Richardson, who was the owner of an old-established leather works in Newcastle-on-Tyne. All the children of this well-to-do Quaker family showed unusual ability, not least of them Lewis.

He was educated at Bootham School, York, and at the Universities of Durham and Cambridge, where he gained a First Class in the Natural Sciences Tripos in 1903. He was for a few years at the National Physical Laboratory, but his interests gradually changed to geophysics and meteorology: he was for a time Superintendent of Eskdalemuir Geophysical Observatory and was elected a Fellow of the Royal Society in 1926. The last twelve years of Richardson's professional life were spent as Principal of Paisley Technical College.

Richardson had been a Fellow of the Physical Society since 1922, and from 1921 to 1924 was Honorary Secretary of the Royal Meteorological Society. During the First World War he served with the Friends' Ambulance Unit in France. He was a man always popular with his students, and always gave an impression of youth despite his white hair.

REVIEWS OF BOOKS

Logic for Mathematicians, by J. BARKLEY ROSSER. Pp. xiv + 530. (London : McGraw-Hill, 1953.) 85s.

It is related of the late Professor Hardy that, when lecturing on the theory of divergent series, he came to a point in a proof where he said "Now, it is obvious that ...". He stopped. There was a long, silent pause. Then he said "But is it obvious?". After another long pause he left the room. Ten minutes later he came back, said "Yes, it *is* obvious" and went on with the lecture. Another story, the characters in which must remain anonymous, because they are fortunately still with us, is told of the professors of the leading University of the United States of America. It is, that when Professor C says a thing is obvious, it means that the class already saw the point hours ago, and are impatiently waiting for the next step; when Professor B says a thing is obvious, it is just obvious. When Professor SB says a thing is obvious, if you go away and think about it for a week, you will probably succeed in proving it. But when Professor L says a thing is obvious, you know it is false.

Professor Rosser defines the object of his book as that of giving a formal definition of the word 'obvious', or, rather, of the phrase 'immediate consequence of', so that we can tell, by means of a mechanical checking procedure, whether one statement is, or is not, an 'obvious' consequence of another. He claims no absolute or intrinsic justification for his definition, only that its results seem to coincide with those of the 'judgement of careful mathematicians'. His programme is thus the same as that of Russell and Whitehead, in *Principia Mathematica*, except perhaps that these latter laid claim to an absolute validity which Rosser explicitly disclaims. The present volume is considerably shorter than the three volumes of *Principia Mathematica*, partly because some topics, no longer of great mathematical interest, are omitted, but mainly because Professor Rosser makes use of the powerful results that have been obtained in symbolic logic since 1912 when *Principia* was first published. In fact the present work goes further than did *Principia Mathematica*, in that a detailed discussion is given of the various forms of the axiom of choice, and its modern equivalent, Zorn's lemma. And illustrations of the various forms of argument used are drawn from current mathematical texts, ranging from textbooks of elementary geometry to advanced works on the theory of functions.

In course of his development, from the calculus of statements, through the restricted predicate calculus, to the theory of classes, relations and functions, and finally to the theories of cardinal and of ordinal numbers, Professor Rosser has many illuminating remarks to make about mathematicians' use of symbols. One of the most valuable distinctions to which he calls attention is that between a function f and a function value $f(x)$. The equation (or 'identity') $x^2 - 2x + 1 = (x - 1)^2$ is a statement that two functions are equal, while the equation $x^2 - 2x + 1 = 0$ is a statement that two numbers, one of which is a function value, are equal. Current mathematical notation is unable to distinguish between the function x^2 and the function value x^2 , and Rosser shows how Church's notation can be used to overcome this difficulty. Church would write $\lambda x . x^2$ for the function, reserving x^2 for the function value. The x in $\lambda x . x^2$ is a 'bound variable', like the x in $\int_0^1 x^2 dx$, and it can be changed

to another letter y , for example, without altering the meaning. So that, for example, we have, for all values of x , $(\lambda y . y^2)(x) = x^2$. There is no doubt in the reviewer's mind that attention to this point of notation alone would save many a student great difficulty in the understanding of the theory of partial differentiation, of Laplace transforms, and especially thermodynamics. Church's notation has long deserved to be better known, and Professor Rosser's book would be worth while if it did no more than bring this about.

But besides helping to do this, and helping to clarify many similar points of difficulty for the aspiring mathematician, Professor Rosser has much to say of mathematical interest to the mature mathematician, aside from his main logical thesis. In particular, his treatment of the theory of sets, cardinals, ordinals and the axiom of choice supersedes the accounts in current books, which are either too old-fashioned, or too brief (as, for example, the modern account given by M. Bourbaki).

The one point of criticism which occurs to the reviewer is that too little attention is given to the outstanding results in metamathematics associated mainly with the name of Gödel. Gödel's theorem about the impossibility of a consistency proof for a formal system of mathematics is mentioned briefly only once, and his main theorem, of which this is a corollary, on the existence of undecidable arithmetical propositions, is not mentioned explicitly at all. Nor is his result about the completeness of the predicate calculus mentioned. Tarski's work on the concept of truth in formal systems is also not mentioned, nor is the Skolem-Löwenheim theorem and its associated paradox concerning the real numbers.

But the author could well answer this criticism by saying that his book does not purport to be a book on metamathematics. A book on this latter subject has just been published by the author's former colleague, S. C. Kleene. And it is certainly true that in his method of presenting symbolic logic, Professor Rosser takes full account of these metamathematical results by explicitly disclaiming finality and completeness for his system. He says:

"Our symbolic logic is not intended as a model for how mathematicians should think but only as a model of how at the present time they do indeed think. Indeed it is desirable that new and more potent and flexible principles of reasoning be devised and generally accepted, so that distant portions of the mathematical edifice will become more readily accessible. One advantage of a symbolic logic is that it can be made very precise, but an even greater advantage is that it can be changed to fit the circumstances."

Such a forward-looking attitude, welcoming the possibility of change in our modes of thinking, is most refreshing at a time when so many people still cling to the discredited notion that the principles of mathematical thinking are absolute, and that the 'inductive' and other modes of thinking used in physics and elsewhere are in some sense 'inferior' to mathematical deduction in its 'immutable glory'.

This book should be read by everyone concerned with the teaching of mathematics, and by every mathematics undergraduate at some stage in his career. It ought also to be in the library of any grammar school, where it can be read by the mathematics master and dipped into by the mathematics scholarship candidates. Anyone who does read it, with some knowledge of first-year University mathematics, can be guaranteed a feast of entertainment as well as instruction.

G. A. BARNARD.

The Mathematical Theory of Non-Uniform Gases, 2nd Edn., by S. CHAPMAN and T. G. COWLING. Pp. xxiii+431. (Cambridge: University Press, 1952.) 60s.

The first edition of this book appeared in 1939 and was out of print for some time. The new edition, with some alterations and corrections and a number of additional notes, will be greatly welcomed. The notes are also obtainable separately in the form of a booklet, costing 5s., which will be appreciated by the owners of the first edition.

Although the book is entirely devoted to a comparatively narrow subject it is of fundamental importance because it is the only treatise in which the theory of non-uniform gases is developed from its basic principles, as laid down by Maxwell, Boltzmann, Hilbert, Chapman and Enskog, in all its intricacies and to all its consequences, including its application to electromagnetic phenomena in ionized gases and electron gases in metals. It is not an easy book to read, but the more experimentally minded physicists working in this field, who are either not able or not willing to follow the mathematical argument in detail, can in most instances find the answers to their queries in the form of formulae which can be understood out of their context because each symbol used has a unique meaning. Another feature of the book which makes it valuable to both theorist and experimenter is the elaborate and clear comparison of theory with experiment.

The first of the new additional notes deals with the great improvement introduced by the assumption of an inter-molecular force law, representing attractive and repelling forces by inverse powers of the mutual distance; many inconsistencies, previously unaccountable, have thus been cleared up. Other notes deal with the so-called 'volume viscosity', self diffusion, and higher approximations for the velocity distribution which may be significant in highly non-uniform gases, e.g. in the presence of shock waves. New theoretical and experimental work on thermal diffusion and the more recently discovered diffusion thermo effect is presented in some further notes, and a sketch is given of the main principles of the new theories of Kirkwood and Born and Green, who approach the problem of the kinetic theory of liquids from the direction of dense gases. It is to be regretted that these and some other recent developments in the theory of fluids could not be elaborated in more detail and notes added on other related subjects, for example the theory of the ionic 'plasma' and the transfer phenomena in semiconductors.

R. FURTH.

Vorlesungen über theoretische Physik, Band V, *Thermodynamik und Statistik*, by A. SOMMERFELD. Pp. xiv+374. (Wiesbaden: Dieterich'sche Verlagsbuchhandlung, 1952.) 24.80 DM. (gbd.).

This book completes the series of six volumes containing the lectures which Sommerfeld used to give to his students. The present volume deals with thermodynamics, kinetic theory and statistical mechanics. As the number of satisfactory textbooks on thermodynamics or on statistical mechanics is extremely small, the publication of this volume must have been awaited with great expectations in view of the excellence of the earlier volumes. Unfortunately, before Sommerfeld could finish the manuscript of this last part he was killed in an accident and, in accordance with his own wish, F. Bopp and J. Meixner have

finished and edited it. Sommerfeld had finished parts I to III, dealing respectively with thermodynamics, its applications, and kinetic theory, and also most of part IV, dealing with statistical mechanics. The concluding sections of part IV and part V, which deals with irreversible processes and the transport equation, have been contributed by Bopp and Meixner. It would have been in any case an extremely difficult and nearly impossible task to complete a book started by Sommerfeld, but the character of the subject matter made it even more impossible, and parts IV and V are as a result rather disappointing. The first three parts can be used as lecture notes as they stand, and it is surprising how teachable they are, but I would hesitate before using all the methods of parts IV and V in a lecture course.

In parts I and II Sommerfeld stresses especially the technical aspects of thermodynamics, and wherever possible the historical development is discussed. The second law is discussed in the way introduced by Clausius, but Caratheodory's method is discussed and it is stated that the main content of the second law is the statement that the 'entropy' exists and under certain well-defined conditions never decreases. The introduction of the four thermodynamic potentials is extremely clear and beautiful.

The classical statistical mechanics in part IV is still Sommerfeld's, and he uses in his discussion Boltzmann's enumeration method and only obliquely mentions Gibbs' ensemble theory. The treatment of the quantum statistics is to my mind the least satisfactory part of the volume. Apparently Sommerfeld had not yet decided how to introduce the Bose-Einstein and Fermi-Dirac statistics before he died, and Bopp and Meixner do this by using the Darwin-Fowler method instead of Boltzmann's enumeration method (what Kramers called the elementary method) or, even better, Gibbs' ensembles.

In part V the moments method of solving the transport equation is discussed in detail, but Lorentz's assumptions leading to the elementary electron theory of metals are nowhere clearly stated.

Apart from a few minor infelicities—which as far as can be seen are mainly due to Sommerfeld's untimely death—this volume can be highly recommended, and with the five other volumes of the same series will for a long time to come be a handbook for the teaching of classical theoretical physics. D. TER HAAR.

The Annual Review of Nuclear Science, Vol. II, 1953. Pp. ix + 429. (Stanford : Annual Reviews Inc.; London : H. K. Lewis (agent).) \$6.00.

The first volume of *The Annual Review of Nuclear Science* was published last year (see *Proc. Phys. Soc. A*, 1952, **65**, 1068) and covered a very wide range of subjects, including those aspects of Physics, Chemistry, Metallurgy and the Biological and Medical Sciences which either contribute towards or receive benefits from research into Atomic Energy. The form and quality of the articles in the second volume are much the same as in the first, but it happens, apparently by chance, that all are on physical subjects, and that there is even a movement away from laboratory science towards cosmology and similar grand themes. Judging from the table of contents announced for Volume III, this is only a temporary departure from catholicity.

In the present volume articles on the Origin and Abundance of the Elements by Alpher and Herman, on Energy Production in Stars by Salpeter, and on the

Origin and Propagation of Cosmic Rays by Biermann, apart from their intrinsic interest, contain much material which is important for nuclear physicists. For instance, the first discusses possible thermodynamical equilibria between the nuclides at temperatures and pressures much higher than can be contemplated on earth, and also the systematic behaviour of neutron cross sections in relation to the possible formation of the elements in a primitive neutron-rich universe. The second article contains a discussion not only of the well-known carbon cycle, the separate stages of which can be reproduced in the laboratory, but also of the proton-proton reaction ($p + p = {}^2\text{H} + e + \nu$) which has not been observed on earth. An article on the Production and Distribution of Radio-Carbon, by E. C. Anderson, touches upon nearly all the facets of this exciting subject, including cosmic-ray neutrons, counting techniques, geophysics and isotope effects in chemical reactions, but omits the results of archeological dating, which is a most interesting application of the technique.

The article on Subnuclear Particles by Blair and Chew deals briefly with the heavy mesons discovered in the cosmic radiation but concentrates mostly on the properties of π -mesons as studied in the laboratory. Other branches of physics which depend on large machines are served by articles on Recent Progress in Accelerators by Chu and Schiff, on Nuclear Reactions Induced by High Energy Particles by Templeton, on Recent Studies of Photonuclear Reactions by Strauch, and on Advances in Nucleon-Nucleon Scattering Experiments and their Theoretical Consequences by Breit and Gluckstern.

Angular Correlation of Nuclear Radiation is reported upon by Frauenfelder, who both summarizes the theory and gives very practical advice on experimental procedures. There are articles on Nuclear Moments by Feld, on The Experimental Clarification of the Theory of β -Decay by Konopinski and Langer, and on β -Decay Energetics by Coryell. Feld and Coryell both make use of the nuclear shell model as an aid towards classification.

Radiation Effects in Solids by Dienes summarizes a subject which contributes both to the theoretical understanding of the solid state and to the practical design of power reactors. Bigeleisen writes on Isotopes, and, besides dealing very briefly with measurements of isotopic masses and abundances, has written the only few pages of chemistry to be found in the volume, when he describes the isotope effects on phase equilibria and on chemical kinetics. The volume ends with an article on High Energy Fission by Spence and Ford.

From such authors the reader will expect contributions of consistently high quality, and will not often be disappointed. He should, however, be warned that the articles are short, ranging from ten to forty pages, and that in this space it has seldom been possible to do much more than provide a guide to the literature. Those who are accustomed to longer reviews, in which there is room for some recapitulation of older knowledge and for some explanations of principles, may find these articles more difficult to read and may be more often driven to the original sources.

W. J. WHITEHOUSE.

CONTENTS OF SECTION B

	PAGE
Dr. T. S. MOSS. Photoelectromagnetic and Photoconductive Effects in Lead Sulphide Single Crystals	993
Dr. A. R. LANG. Extinction in X-Ray Diffraction Patterns of Powders	1003
Dr. U. W. ARNDT, Mr. W. A. COATES and Dr. D. P. RILEY. A Proportional-Counter Technique for Measuring X-Ray Scattering from Powders, Fibres and Liquids	1009
Mr. F. J. HYDE. Measurements of Noise Spectra of a Point Contact Germanium Rectifier	1017
Mr. T. L. ECKERSLEY. Recombination and Diffusion and Spread Echoes from the Ionosphere	1025
Dr. A. POWELL. On the Mechanism of Choked Jet Noise	1039
Dr. W. EHRENBERG and Dr. J. FRANKS. The Penetration of Electrons into Luminescent Material	1057
Dr. G. N. LANCE and Dr. R. L. PERRY. Water Bells	1067
Mr. D. A. WRIGHT and Dr. J. WOODS. The Decomposition of Thin Films on Bombardment with Slow Electrons	1073
Dr. N. L. ALLEN. An Experiment on the Radial Motion of Charged Particles from a Pulsed Arc Discharge	1087
Dr. J. M. COWLEY. A New Microscope Principle	1096
Prof. J. REEKIE, Dr. T. S. HUTCHISON and Mr. F. E. HETHERINGTON. Precipitation Processes in Copper-Iron Alloys	1101
Letters to the Editor :	
Dr. R. COOPER and Mr. A. A. WALLACE. Plastic Deformation and the Electric Strength of Alkali Halide Crystals	1113
Dr. F. A. CUNNELL, Dr. E. W. SAKER and Mr. J. T. EDMOND. A Note on the Semiconducting Compound InSb	1115
Mr. Y. KLINGER and Dr. E. W. SAKER. The Dielectric Constant of Amorphous Selenium at Wavelengths of 1 cm and 3 cm	1117
Dr. J. W. GRANVILLE and Dr. A. F. GIBSON. The Reduction of Rectifier Noise by Illumination	1118
Obituary Notices :	
WILLIAM DAMPIER	1120
ROBERT DONALDSON	1121
LEONARD BELLINGHAM	1122
EDWARD FELIX HERROUN	1123
W. H. TOWNS	1123
LEWIS FRY RICHARDSON	1123
Reviews of Books	1124
Contents of Section A	1128
Subject Index, Section B, Vol. 66	1129
Index of Authors (with Titles), Section B, Vol. 66	1137
Index to Reviews of Books, Section B, Vol. 66	1143

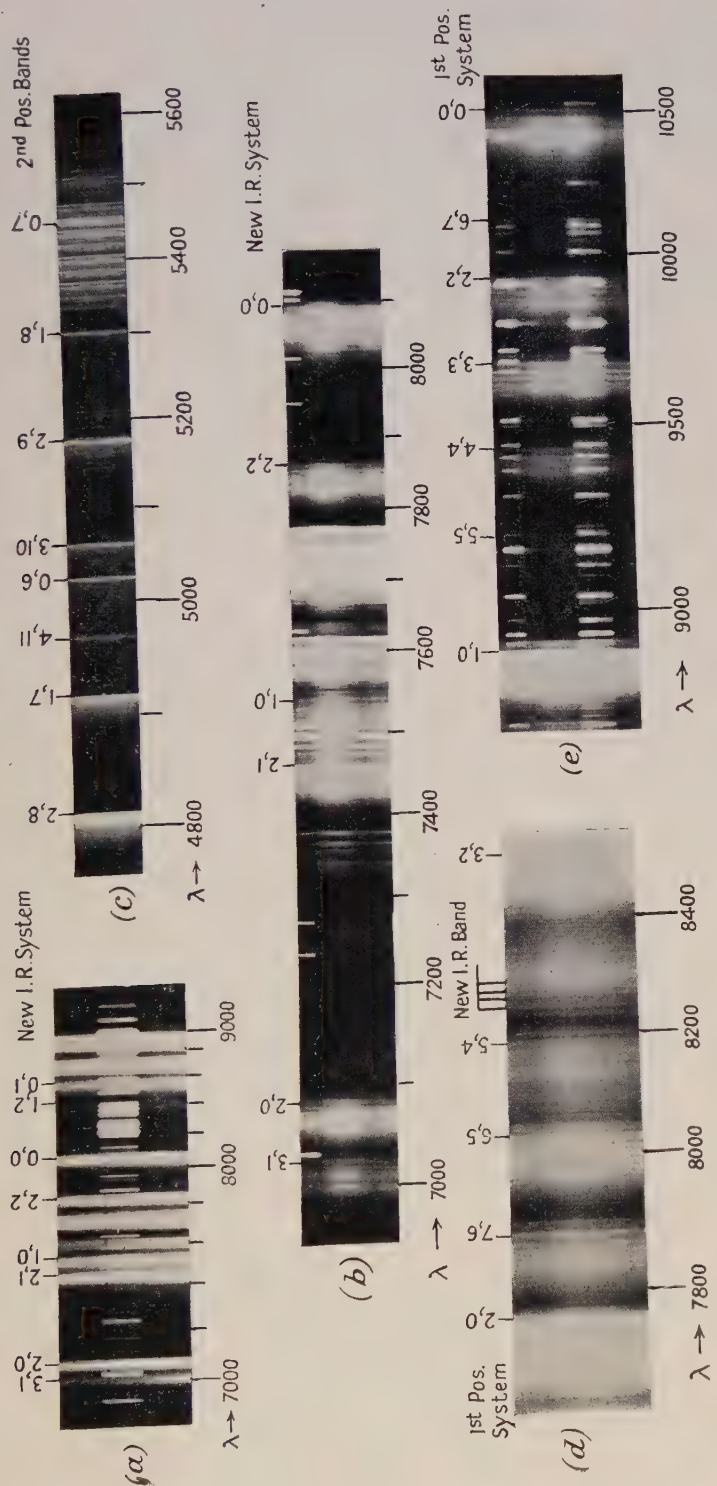


PLATE I.

(a) Spectrum of blue subnormal discharge through nitrogen at pressure of 15 mm Hg recorded with a Hilger D 187 spectrograph on Kodak II N plate. Exposure time 30 minutes.
(b) Discharge conditions as in (a). Spectrum recorded with glass Littrow spectrograph on Kodak II N plate. Exposure time 3 hours.
(c) Spectrum of vigorous Tesla discharge through air at 5.5 mm Hg taken with the Hilger D 187 spectrograph on Kodak I F plate. Exposure time 30 minutes.
(d) Spectrum of bright yellow transformer discharge through pure nitrogen at 2.5 mm Hg recorded with glass Littrow spectrograph on Kodak II N plate. Exposure time 20 minutes.
(e) Discharge conditions as in (d). Spectrum photographed with glass Littrow spectrograph on Kodak I Q plate. Exposure time 6 hours.

PROCEEDINGS OF THE PHYSICAL SOCIETY

SECTION A, 1953—VOLUME 66

SUBJECT INDEX

	PAGE
Absorption bands of SbSe and SbTe in quartz ultra-violet region 3650 to 2200 Å .	1109
Absorption coefficients of gamma-rays with energies between 0.3 and 1.5 mev .	382
Absorption, continuous, of light in Mg vapour (R)	655
Absorption of cosmic rays in lead, search for irregularities	33
Absorption, M_{IV} , v , in heavy elements, anomaly of	333
Absorption, neutron, <i>see under</i> Cross sections.	
Absorption, photoelectric, in lithium vapour (R)	304, corr. 420
Absorption, resonance, microwave, in ferromagnetic manganese compounds .	823
Absorption spectrum of aluminium monofluoride in Schumann region (L) .	771
Absorption spectrum of SnS vapour in ultra-violet and Schumann regions .	885
Absorption spectrum, ultra-violet, of nitric oxide	209
Air showers, extensive, altitude variation	49
Air showers, extensive, penetrating particles	65
Air showers, extensive, time distribution of delayed particles in	454
Alpha-emitting levels of ^8Be with isotopic spin $T=1$ (L)	661
Alpha-particles, in diluted Ilford G5 emulsions, range-energy relations .	13
Alpha-particles, effect of tensor force on binding energy	17
Alpha-particles, ionization in liquids due to	631
Alpha-particles, photodisintegration in light even-even nuclei yielding .	689
Alpha-particles, slow, relative stopping-power of hydrogen and helium for (L) .	658
Altitude variation of extensive air showers	49
Aluminium, metallic compressibility (R)	949
Aluminium monofluoride, absorption spectrum in Schumann region (L) .	771
Aluminium monofluoride band spectrum	437
Angular correlation experiments, geometry of (L)	846
Angular correlation of protons and γ -radiation from reaction $^6\text{Li}(d, p)^7\text{Li}^*\gamma^7\text{Li}$.	297
Angular distribution of gamma-radiation following deuteron stripping reaction .	1081
Anisotropy, diamagnetic, of large aromatic systems: V—interpretation of results	714
Antiferromagnetism in metals (L)	1188
Antiferromagnetism by spin wave method:	
III—Application to more complex systems.	89
Argent compound, paramagnetic resonance in (L)	666
Argon, ionization of cosmic-ray mesons in	541
Aromatic systems, large, diamagnetic anisotropy:	
V—Interpretation of results	714
Asymmetry, east-west, of moderate-energy neutrons in the cosmic radiation .	160
Asymptotic solution of equation occurring in scattering theory (L)	123
Atomic nucleus and its constituents	313
Atomic position and size of thallium ions in KCl(Tl) phosphors	484
Auto-ionization probabilities, calculation:	
I—Perturbation methods with application to auto-ionization in He	904
II—Variation at method for radiationless transitions with application to $(2s)^2\ ^1S-(1s^k)^1S$ transition of He	911
Band intensities in CN violet system	737
Band spectrum of aluminium monofluoride	437
Band spectrum of nitrogen: new studies of triplet systems	1138
Band spectrum 4050 Å, observation in King furnace (L)	848
Band spectrum, ultra-violet, of carbon monoselenide	836
Band system, Second Negative, of O_2 , effect of variation of dipole moment with internuclear separation on relative intensities of (R)	1181
Band system $^2\Sigma^+-^2\Pi_1$ of HBr^+	617
Bands, First Positive of nitrogen, wavelengths (R)	577
Bands, Neumann, in pure iron	403
Bands, ultra-violet, <i>see</i> Ultra-violet bands.	

	PAGE
Beryllium 8, alpha-emitting levels of, with isotopic spin $T=1$ (L)	661
Beta-particle spectrum of mesothorium 2	519
Binding energy, <i>see</i> Energy, binding.	
Bismuth, pile neutron absorption cross sections	700
Bitter figures on (110) plane of single crystal of Ni	819
Boltzmann's equation in quantum mechanics	325
Boltzmann's H-theorem, statistical aspect	153
Born-Yang model for high energy electron scattering (L)	773
Boron nitride, electrostatic energy (L)	772
Bound state of ^4H , existence of (R)	1066
Bremsstrahlung, production in electron-electron collisions (L)	196
Bremsstrahlung, thick target, formula for	638
 Carbon 13, energy states belonging to configuration $1p^2$: studies in intermediate coupling	 977
Carbon monoselenide, ultra-violet band spectrum	836
Carbon nitride violet system, band intensities	737
Cascade processes, general three-dimensional theory	1009
Cascades, note on fluctuation problem (L)	117
Central force scattering problem, comparison of methods of solving	866
Charge independence and nuclear reactions (L)	665
Charged particles, heavy, light output of potassium iodide crystals under bombardment by (R)	767
Charged particles of intermediate energies, ionization and excitation losses	590
Chlorine ⁺ , visible emission spectrum	759
Cloud chamber observations of cosmic radiation underground	533
Cobalt 57, radioactive, nuclear spin and magnetic moment (L)	305
Coincidence method, delayed, and half-life of $^{181}\text{Ta}^m$ (R)	944
Collisions, electron-electron, production of bremsstrahlung (L)	196
Collisions, inelastic, of electrons in helium and Townsend's ionization coefficient	288
Collisions, inelastic, between heavy particles:	
I—Excitation and ionization of hydrogen atoms in fast encounters with protons and with other hydrogen atoms.	961
Colloidal particle, free energy of double layer of, and charging process	357
Colloidal plates, two parallel, interaction, using modified Poisson-Boltzmann equation	365
Colloidal suspensions, ferromagnetic resonance (R)	765
Commutation relations, and quantum mechanical equations of motion (L)	657
Compressibility of metallic aluminium (R)	949
Conceptual situation in physics and prospects of its future development (37th Guthrie Lecture).	501
Conduction, thermal, <i>see</i> Thermal conduction.	
Conductivity, thermal, <i>see</i> Thermal conductivity.	
Conjugated molecules, free-electron wave functions for (R)	652
Copper 63, 65, nuclear electric quadrupole moments of (L)	410
Cosmic mesons, <i>see</i> Mesons, cosmic.	
Cosmic radiation, east-west asymmetry of moderate-energy neutrons in	160
Cosmic radiation underground, cloud chamber observations	533
Cosmic-ray absorption in lead, search for irregularities.	33
Cosmic-ray extensive air showers at sea level, lateral structure	549
Cosmic-ray jets, interpretation	929
Cosmic-ray mesons in argon, ionization	541
Cosmic-ray μ -mesons, ionization by, further measurements.	167
Cosmic-ray particles, pairs of associated, short time interval measurements	79
Cosmic-ray showers, extensive, below ground	346
Cosmic-rays, short time interval measurements, spark counters for	73
Coulomb forces, isotopic spin and	139
Counter, <i>see</i> Proportional counter, Scintillation counter, Spark counter,	

Coupling, intermediate, studies : energy states of ^{13}C and ^{13}N belonging to configuration $1p^0$	977
Critical size in multi-group neutron transport theory for some simple systems	705
Cross section excitation, 1s-2s electron of hydrogen, calculation by variational method (R)	406
Cross section for photodisintegration of deuteron at 2.615 mev, and absolute standardization of γ -rays of ThC''	608
Cross sections, pile neutron absorption, of bismuth	700
Cross sections for reaction $^7\text{Li}(\gamma\text{T})^4\text{He}$ at 6.13, 14.8 and 17.6 mev (L)	579
Crystal, single, influence of domain structure on magnetization curves of	623
Crystal, single, Ni, Bitter figures on (110) plane	819
Crystal, single, Ni, domain configuration structure on (R)	840
Crystals, organic, mixed, fluorescence characteristics	777
Crystals, potassium iodide, light output under bombardment by heavy charged particles (R)	767
Curium 242, average number of neutrons emitted in spontaneous fission	447
Damping corrections in the photo-meson process	233
Decay scheme of krypton 83	1093
Decay of τ -meson	710
Degeneracy, accidental, of hydrogen (L)	958
Delta-rays, production in nuclear-research emulsions	1019
Density, electron, <i>see</i> Electron density.	
Deuteron energy, investigation of reactions $^{14}\text{N}(\text{d}, \text{n})^{15}\text{O}$ at 8 mev	108
Deuteron stripping process, some features	28
Deuteron stripping reaction, angular distribution of gamma-radiation following	1081
Deuterons, 7.5 mev, in metals, multiple scattering	1172
Deuterons, scattering of 10 and 14 mev neutrons by	894
Deuterons, <i>see also</i> Cross section, Stripping reaction.	
Diamagnetic anisotropy of large aromatic systems : V—Interpretation of results	714
Diatomic molecules, vibrational transition probabilities : I	1145
Diatomic molecules, vibrational transition probabilities : II	1153
Dielectric medium, ionization loss of fast particle in	597
Diffusion, thermal, <i>see</i> Thermal diffusion.	
Dipole moment, effect of variation with internuclear separation on relative intensities of Second Negative band system of O_2 (R)	1181
Dissociation energy, CO, and predissociations (L)	1185
Distorted wave approximation and 1s-2s excitation of He by electron impact	1097
Distortion, reduction in nuclear research emulsion (R)	115
Distribution, angular, <i>see</i> Angular distribution.	
Domain configuration structure on single crystal of Ni (R)	840
Domain structure, influence on magnetization curves of single crystals	623
Domains of reverse magnetization	162
Double layer of a colloidal particle and the charging process, free energy of	357
Double layer, single plane, solution of modified Poisson-Boltzmann equation for	372
Editorial	1
Elastic scattering of electrons by helium ions, application of variational methods to	268
Elastic scattering of neutrons by tritons at 14 mev	238
Elastic scattering of 1.33 mev and 2.76 mev gamma-rays by lead	1059
Electric spin in semiconductors (L)	121
Electrodynamics, quantum, <i>see</i> Quantum electrodynamics.	
Electromagnetic fields, scalar representation	1129
Electron capture : II—Resonance capture from hydrogen atoms by slow protons III—Capture into excited states in encounters between hydrogen atoms and fast protons,	173 972

	PAGE
Electron density, Thomas-Fermi, theory of	178
Electron gas, free, spin paramagnetism	1104
Electron scattering, effect of nuclear multipole moments	881
Electronic structure of some body-centred cubic metals	1162
Electrons, elastic scattering of	806
Electrons, elastic scattering by helium ions, application of variational methods.	268
Electrons, inelastic collisions in helium and Townsend's ionization coefficient	288
Electrons, interaction with lattice vibrations : radiation by fast electron.	601
Electrons, internal conversion, emitted in decay of ionium and radio-thorium (L)	1074
Electrons, motion of, in non-sinusoidal periodic fields (L)	197
Electrons, nuclear scattering of, and isotope shift	1041
Electrostatic field, and certain exact solutions of equations of general relativity	145
Electrostatic field, effect on scattering (L)	309
Emission, anisotropic, internal pairs in	341
Emission spectrum, visible, of Cl_2^+	759
Emulsion, Ilford G5 diluted, range-energy relations for protons and α -particles	13
Emulsion, nuclear research, production of delta rays in	1019
Emulsion, nuclear research, reduction of distortion (R)	115
Energy band structure of linear metal	889
Energy, binding, of α -particle, effect of tensor force	17
Energy, binding, nuclear, and jj -coupling shell model	793
Energy, electrostatic, of boron nitride (L)	772
Energy, free, of double layer of colloidal particle and the charging process	357
Energy, free, minimum property of (R)	492
Energy loss distribution for minimum ionizing electrons in proportional counter, measurements (L)	306
Energy, surface, of a metal, determination by molecular orbits	2
Energy, <i>see also</i> Deuteron energy, Fermi energy, Range-energy.	
Excitation functions for (γp) and (γT) reactions in ^7Li for energies up to 24 mev (L)	194
Excitation and ionization of hydrogen atoms in fast encounters with protons and with other hydrogen atoms	961
Excitation and ionization losses of charged particles of intermediate energies	590
Excited states, capture into, in encounters between hydrogen atoms and fast protons	972
Extensive air showers, <i>see under</i> Cosmic ray.	
Fermi energy, effect on stability of superlattices	201
Ferromagnetic resonance in colloidal suspensions (R)	765
Fields, auxiliary, quantum electrodynamics with	129
Fields, electrostatic, <i>see</i> Electrostatic fields.	
Fields, non-sinusoidal periodic, motion of electrons in (L)	197
Fission, spontaneous, of ^{242}Cm , average number of neutrons emitted	447
Fluctuation problem of cascades, note (L)	117
Fluorescence characteristics of mixed organic crystals	777
Force, tensor, <i>see</i> Tensor force.	
Fragmentation and ionization of molecules by bombardment with atomic ions (R)	1068
Free-electron wave functions for conjugated molecules (R)	652
Free energy, <i>see</i> Energy, free.	
Friction, internal in metals, theory	572
Furnace, King, for observation of 4050 Å band group (L)	848
Galvano-magnetic effects at high frequencies (L)	849
Gamma-gamma directional correlation, influence of combined electric and magnetic interaction on (L)	952
Gamma-radiation, angular distribution of, following deuteron stripping reaction	1081
Gamma-radiation, polarization from aligned nuclei	391
Gamma-rays, absorption coefficients of, with energies between 0.3 and 1.5 mev	382
Gamma-rays, ^{198}Hg , resonant nuclear scattering	585

	PAGE
Gamma-rays, ^{198}Hg , resonant scattering (L)	956
Gamma-rays, of ThC'' , 2.615 mev, absolute standardization and photodisintegration cross section of deuteron	608
Gamma-rays, 1.33 mev and 2.76 mev, elastic scattering by lead	1059
Gas mixtures, thermal diffusion, and forces between unlike molecules	278
Germanium, ultra-violet bands associated with (L)	191
Gold, thermal conductivity at low temperatures	559
Guthrie Lecture, 37th: The conceptual situation in physics and the prospects of its future development	501
Half-life of $^{181}\text{Ta}^m$ and delayed coincidence method (R)	944
Hall effect, isothermal, in semiconductors, theory	753
Heavy elements, anomaly of $M_{IV, V}$ absorption in	333
Helium, inelastic collisions of electrons in, and Townsend's ionization coefficient	288
Helium, liquid, <i>see</i> Liquid helium.	
Helium, 1s-2s excitation by electron impact, and distorted wave approximation	1097
Herzberg system of O_2 , intensities in (R)	1064
Herzberg system of O_2 , intensity distribution among bands.	733
Hydrogen, accidental degeneracy (L)	958
Hydrogen atoms, excitation and ionization of, in fast encounters with	961
Hydrogen atoms, and fast protons, capture into excited states in encounters between	972
Hydrogen atoms, resonance capture from, by slow protons	173
Hydrogen bromide $^+$, $^2\Sigma^+-^2\Pi_1$ band system	617
Hydrogen, calculation of the 1s-2s electron excitation cross section of, by a variational method (R)	406
Hydrogen 4, existence of bound state of (R)	1066
Hydrogen molecular ion, properties:	
I—Quadrupole and dipole transitions	784
II—Photo-ionization from $1s\sigma_g$, $2s\sigma_g$ and $3s\sigma_g$ states	1113
III—Oscillator strengths of $1s\sigma_g-2p\pi_u$, $2p\sigma_u-3d\pi_g$, and $2p\pi_u-3d\pi_g$ transitions	1124
Inelastic neutron scattering in iron (L)	120
Intensity distribution among bands of Herzberg system of O_2	733
Interaction, combined electric and magnetic, influence on γ - γ directional correlation (L)	952
Interactions in paramagnetic, effect on entropy and susceptibility	673
Internal pairs in anisotropic emission	341
Internuclear separation, and variation of dipole moment, effect on relative intensities of Second Negative band system of O_2 (R)	1181
Intrinsic magnetization, <i>see</i> Magnetization, intrinsic.	
Ion bombardment, negative, of surfaces, liberation of positive ions by (L)	663
Ionium, internal conversion electrons emitted in decay of (L)	1074
Ionization coefficient, Townsend's, and inelastic collisions of electrons in helium	288
Ionization of cosmic-ray mesons in argon	541
Ionization and excitation of hydrogen atoms in fast encounters with protons and with other hydrogen atoms	961
Ionization by energetic cosmic-ray μ -mesons, further measurements	167
Ionization and excitation losses of charged particles of intermediate energies	590
Ionization and fragmentation of molecules by bombardment with atomic ions (R)	1068
Ionization loss of fast particle in dielectric medium	597
Ionization in liquids due to α -particles	631
Ions, atomic, ionization and fragmentation of molecules by bombardment with (R)	1068
Ions, helium, and elastic scattering of electrons, variational methods	268
Iron, pure, Neumann bands in	403
Iron 57, nuclear magnetic moment of (L)	414
Irradiation of Pb with x-rays, production of short-lived activity by (R)	1179

	PAGE
Isotope shift, and nuclear scattering of electrons	1041
Isotopic spin and coulomb forces	139
Isotopic spin $T=1$, alpha-emitting levels of ^8Be with (L)	661
 Jastrow's nuclear model for high energy electron scattering (L)	 1075
 Kirkwood's approximation, application to the calculation of intrinsic magnetization	 421
Krypton 83, decay scheme	1093
 Lattice vibrations, interaction of electrons with : radiation by fast electron	 601
Lead, absorption of cosmic rays in, some irregularities	33
Lead, elastic scattering of 1.33 mev and 2.76 mev gamma-rays by	1059
Lead, irradiation with x-rays, production of short-lived activity by (R)	1179
Light, continuous absorption in Mg vapour (R)	655
Light output of potassium iodide crystals under bombardment by heavy charged particles (R)	767
Line width transition, nuclear magnetic resonance, in aluminium	85
Liquid helium, new theory : further treatment	995
Liquid helium, x-ray scattering from (L)	409
Liquids, ionization in, due to α -particles	631
Lithium 7, reactions (γp) and (γT), excitation functions for energies up to 24 mev (L)	194
Lithium vapour, photoelectric absorption in (R)	304, corr. 420
Low temperatures, population distribution of nuclei aligned at	399
Low temperatures, thermal conductivity of gold at	559
Low temperatures, thermal conductivity of Mg at (L)	1077
Low temperatures, thermal conductivity of silver at (L)	844
 Magnesium isotopes, investigation of (d, p) stripping reactions	 258
Magnesium, thermal conductivity at low temperatures (L)	1077
Magnesium vapour, continuous absorption of light in (R)	655
Magnetic moment and nuclear spin of radioactive ^{57}Co (L)	305
Magnetic moment of spin $\frac{1}{2}$ nuclei	1158
Magnetic resonance, proton, evidence for planar structure, of urea molecule (L)	1187
Magnetic resonance spectrum, nuclear, separation of the intra-molecular and inter-molecular contributions to second moment (L)	415
Magnetic resonance, <i>see also</i> Nuclear magnetic resonance.	
Magnetization curves of single crystals, influence of domain structure	623
Magnetization, intrinsic, application of Kirkwood's approximation to calculation of	421
Magnetization, reverse domains of	162
Manganese compounds, ferromagnetic, microwave resonance absorption in	823
Manganese salts, paramagnetic resonance in (L)	412
Many-particle systems : derivation of shell model (R)	649
Matrix elements in radiative transitions	729
Meson, cosmic, up to 6 kmev/c, momentum distribution	40
Meson, μ , energetic, measurements of ionization by	167
Meson, tau, decay	710
Meson, <i>see also under</i> Cosmic ray.	
Mesothorium 2, β -particle spectrum.	519
Metals, antiferromagnetism in (L)	1188
Metals, body-centred cubic, electronic structure	1162
Metals, determination of surface energy by molecular orbits	2
Metals, linear, energy band structure	889
Metals, multiple scattering of 7.5 mev deuterons in	1172
Metals, theory of internal friction in	572
Microwave resonance absorption in ferromagnetic manganese compounds	823

	PAGE
Molecular ion, hydrogen, properties :	
I—Quadrupole and dipole transitions	784
II—Photo-ionization from $1s\sigma_g$ and $2s\sigma_g$ and $3s\sigma_g$ states	1113
III—Oscillator strengths of $1s\sigma_g-2p\pi_u$, $2p\sigma_u-3d\pi_g$, and $2p\pi_u-3d\pi_g$ transitions.	1124
Molecular orbits, determination of surface energy of metal, by	2
Molecules, ionization and fragmentation of, by bombardment with atomic ions (R)	1068
Molecules, unlike, forces between, and thermal diffusion of gas mixtures	278
Moment, magnetic, <i>see</i> Magnetic moment.	
Moment, nuclear electric quadrupole, of copper 63, 65 (L)	410
Moment, nuclear magnetic, of ^{57}Fe (L)	414
Moment, second, of nuclear magnetic resonance spectrum, separation of intra-molecular and intermolecular contributions (L)	415
Momentum distribution for cosmic mesons up to 6 kmv/c	40
Motion, quantum mechanical equations of, and the commutation relations (L)	657
Neutron absorption, <i>see</i> Cross sections.	
Neutron groups, investigation form the reactions $^{12}\text{C}(\text{d}, \text{n})^{13}\text{N}$, $^{16}\text{O}(\text{d}, \text{n})^{17}\text{F}$ and $^{32}\text{S}(\text{d}, \text{n})^{33}\text{Cl}$	95
Neutron scattering, inelastic, in iron (L)	120
Neutron transport theory, calculation of critical size for some simple systems	705
Neutron, <i>see also</i> Scattering.	
Neutrons, average number emitted in spontaneous fission of ^{242}Cm	447
Neutrons, elastic scattering by tritons	740
Neutrons, elastic scattering by tritons at 14 mev	238
Neutrons, high energy, polarization	721
Neutrons of intermediate energy, scintillation detector for (L)	1073
Neutrons, moderate-energy, east-west asymmetry in the cosmic radiation	160
Nitrogen, band spectrum : new studies of triplet systems	1138
Nitrogen 13, energy states belonging to configuration $1p^9$: studies in intermediate coupling	977
Nitrogen First Positive bands, wavelengths (R)	577
Nitrogen ions, fast, nuclear reactions produced by (R)	495
Nuclear binding energies and jj -coupling shell model	793
Nuclear magnetic resonance line width transition in aluminium	85
Nuclear magnetic resonance spectrum, separation of the intramolecular and inter-molecular contributions to second moment (L)	415
Nuclear model, Jastrow's, for high energy electron scattering (L).	1075
Nuclear multipole moments, effect on electron scattering	881
Nuclear reactions, charge independence and (L)	665
Nuclear reactions produced by fast nitrogen ions (R)	495
Nuclear research emulsion, <i>see</i> Emulsion.	
Nuclear scattering, <i>see</i> Scattering.	
Nuclear spin and magnetic moment of radioactive ^{57}Co (L)	305
Nuclei aligned at low temperatures, population distribution of	399
Nuclei, aligned, polarization of γ -radiation from	391
Nuclei, light even-even, photodisintegration in, yielding alpha-particles	689
Nuclei, scattering of fast positrons by	428
Nuclei, spin $\frac{1}{2}$, magnetic moment	1158
Nucleus, atomic, and its constituents	313
Orbits, molecular, <i>see</i> Molecular orbits.	
Oxygen, Herzberg system, intensities in (R)	1064
Oxygen, Herzberg system, intensity distribution among bands	733
Oxygen, Second Negative band system, effect of variation of dipole moment with internuclear separation on relative intensities of (R)	1181
Paramagnetic, effect of interactions on entropy and susceptibility	673
Paramagnetic resonance in an argentic compound (L)	666
Paramagnetic resonance in four double nitrate salts (L).	118

	PAGE
Paramagnetic resonance in some manganese salts (L)	412
Paramagnetic resonance spectrum of copper lanthanum nitrate, temperature change in (L)	954
Paramagnetism, spin, <i>see</i> Spin paramagnetism.	
Particle, colloidal, <i>see</i> Colloidal particle.	
Particles, delayed, in extensive air showers, time distribution of	454
Particles, <i>see also</i> Cosmic-ray particles, Penetrating particles.	
Penetrating particles in extensive air showers	65
Perturbation and variation methods	857
Perturbation methods with application to auto-ionization in He	904
Phosphors, KCl(Tl), atomic position and size of thallium ions in	484
Phosphors, organic, photo-fluorescence decay times	921
Photodisintegration processes in light even-even nuclei yielding alpha-particles	689
Photodisintegration, <i>see also</i> Cross section.	
Photo-fluorescence decay times of organic phosphors	921
Photo-ionization from $1s\sigma_g$, $2s\sigma_g$ and $3s\sigma_g$ states: properties of hydrogen molecular ion	1113
Photo-meson process, damping corrections	233
Photonuclear reactions, analysis	645
Physics, conceptual situation and prospects of its future development (37th Guthrie Lecture)	501
Pile neutron absorption cross sections of bismuth	700
Poisson-Boltzmann equation, modified, interaction of two parallel colloidal plates using	365
Poisson-Boltzmann equation, modified, solution for a single plane double layer	372
Polarization effects in (d, p) and (d, n) reactions	477
Polarization of γ -radiation from aligned nuclei	391
Polarization of high energy neutrons	721
Positrons, fast, scattering by nuclei	428
Powder patterns, comparison of grain-orientated and single crystal Si-Fe	813
Predissociations and CO dissociation energy (L)	1185
Probabilities, transition, <i>see</i> Transition probabilities.	
Proportional counters, measurements of energy loss distribution for minimum ionizing electrons (L)	306
Protons, in diluted Ilford G5 emulsions, range-energy relations	13
Protons, elastic scattering by ^3He	740
Protons, excitation and ionization of hydrogen atoms in fast encounters with	961
Protons, fast, and hydrogen atoms, capture into excited states in encounters between	972
Protons, slow, resonance capture from hydrogen atoms by	173
Quantum electrodynamics with auxiliary fields	129
Quantum electrodynamics, pre-renormalized	873
Quantum mechanical equations of motion and the commutation relations (L)	657
Quantum mechanics, Boltzmann's equation in	325
Radiation by fast electron: interaction of electrons with lattice vibrations	601
Radiation, <i>see also</i> Cosmic radiation.	
Radiative transitions, matrix elements in	729
Range-energy data from $^{10}\text{B}(\text{n}, \alpha)^7\text{Li}$ and $^6\text{Li}(\text{n}, \text{t})^4\text{He}$ reactions (L)	660
Range-energy relation for protons and α -particles in diluted Ilford G5 emulsions	13
Radio-thorium, internal conversion electrons emitted in decay of (L)	1074
Reaction $^{10}\text{B}(\alpha, \text{p})^{13}\text{C}$ (R)	842
Reaction $^{13}\text{C}(\alpha, \text{n})^{16}\text{O}$ (R)	1176
Reaction $^6\text{Li}(\text{d}, \text{p})^7\text{Li}^*\gamma^7\text{Li}$, angular correlation of protons and γ -radiation	297
Reaction $^{14}\text{N}(\text{d}, \text{n})^{15}\text{O}$ at 8 mev deuteron energy, investigation	108
Reactions $^{27}\text{Al}(\text{p}, \alpha)^{24}\text{Mg}$ and $^{27}\text{Al}(\text{p}, \gamma)^{28}\text{Si}$, excitation curves	800
Reactions $^{10}\text{B}(\text{n}, \alpha)^7\text{Li}$ and $^6\text{Li}(\text{n}, \text{t})^4\text{He}$, range-energy data from (L)	660

	PAGE
Reactions $^{12}\text{C}(\text{d}, \text{n})^{13}\text{N}$, $^{16}\text{O}(\text{d}, \text{n})^{17}\text{F}$ and $^{32}\text{S}(\text{d}, \text{n})^{33}\text{Cl}$, investigation of neutron groups from	95
Reactions $\text{D}-^3\text{H}$ and $\text{D}-^3\text{He}$, below 45 kev (L)	310
Reactions (d, p) and (d, n), polarization effects in	477
Reactions (γp) and (γT) in ^7Li , excitation functions for energies up to 24 mev (L)	194
Reactions, <i>see also under</i> Cross sections, Nuclear, Photonuclear, Stripping.	
Relativity, general, certain exact solutions of equations of, with electrostatic field	145
Resistance, surface, of normal and superconducting tin at 36000 Mc/s (L)	1071
Resolution of scintillation spectrometers (L)	192
Resonance absorption, microwave, in ferromagnetic manganese compounds	823
Resonance, <i>see also under</i> Ferromagnetic, Magnetic, Nuclear magnetic, Paramagnetic.	
Resonant scattering of ^{198}Hg gamma-rays (L)	956
Rutherford Lecture, 6th : The atomic nucleus and its constituents	313
Scalar representation of electromagnetic fields	1129
Scattering, effect of strong electrostatic field on (L)	309
Scattering, elastic, of electrons	806
Scattering, elastic, of neutrons by tritons and of protons by ^3He	740
Scattering, elastic, of 1.33 mev and 2.76 mev gamma-rays by lead	1059
Scattering of fast positrons by nuclei	428
Scattering, high energy electron, Born-Yang model for (L)	773
Scattering, high energy electron, Jastrow's nuclear model for (L)	1075
Scattering, inelastic neutron, in iron (L)	120
Scattering, multiple, of 7.5 mev deuterons in metals	1172
Scattering of 10 and 14 mev neutrons by deuterons	894
Scattering, nuclear, of electrons, and isotope shift	1041
Scattering, nuclear resonant, of ^{198}Hg gamma-rays	585
Scattering problem, central force, comparison of methods of solving	866
Scattering, resonant, of ^{198}Hg gamma-rays (L)	956
Scattering theory, asymptotic solution of an equation in (L)	123
Scattering, x-ray, from liquid helium (L)	409
Schumann region, absorption spectrum of aluminium monofluoride in (L)	771
Schumann region and ultra-violet region, absorption spectrum of SnS vapour in	885
Scintillation counter, anthracene, efficiency (R)	940
Scintillation detector for neutrons of intermediate energy (L)	1073
Scintillation spectrometers, resolution of (L)	192
Second Negative band system, <i>see</i> Band system, Second Negative.	
Semiconductor, electric spin (L)	121
Semiconductor statistics (L)	662
Semiconductor, theory of isothermal Hall effect in	753
Shell model, derivation in many-particle systems (R)	649
Shell model, <i>jj</i> -coupling, and nuclear binding energies	793
Showers, cosmic-ray, <i>see</i> Cosmic-ray showers.	
Silicon 28, investigation of (d, p) stripping reactions	467
Silicon-iron, comparison of powder patterns of grain-orientated and single crystal	813
Silver, thermal conductivity at low temperatures (L)	844
Spark counters for short time interval measurements	73
Specific heat, anomalous, of ferrous ammonium sulphate	228
Spectrometers, scintillation, <i>see</i> Scintillation spectrometers.	
Spectrum, <i>see under</i> Absorption, Band, Emission, Nuclear magnetic resonance, β -particle.	
Spin, electric, in semiconductors (L)	121
Spin $\frac{1}{2}$ nuclei, magnetic moment	1158
Spin paramagnetism of free electron gas	1104
Spin wave method, antiferromagnetism by : III—Application to more complex systems.	89
Spin, <i>see also</i> Isotopic spin, Nuclear spin.	
Spontaneous fission, <i>see</i> Fission, spontaneous.	
Statistical aspect of Boltzmann's H-theorem	153

	PAGE
Stopping-power, relative, of hydrogen and helium for slow α -particles (L)	658
Stripping process, deuteron, some features	28
Stripping reactions, (d, p), investigation :	
I—Results and apparatus for aluminium	249
II—Results for the isotopes of magnesium	258
III—Results for ^{28}Si and ^{32}S	467
IV—Results for ^{40}Ca and ^{88}Sr	565
V—Results for some light elements and conclusions	1032
Stripping reactions, <i>see also under</i> Deuteron.	
Superconductors, electronic thermal conduction in (R)	576
Superlattices, effect of Fermi energy on stability	201
Surface energy, <i>see</i> Energy, surface.	
Surface resistance, <i>see under</i> Resistance.	
Temperature change in paramagnetic resonance of copper lanthanum nitrate (L)	954
Tensor force, effect on binding energy of α -particle	17
Thallium ions, atomic position and size in KCl(Tl) phosphors	484
Thermal conduction, electronic, in superconductors (R)	576
Thermal conductivity of gold at low temperatures	559
Thermal conductivity of Mg at low temperatures (L)	1077
Thermal conductivity of silver at low temperatures (L)	842
Thermal conductivity of superconducting tin below 1°K	217
Thermal diffusion of gas mixtures and forces between unlike molecules	278
Thomas-Fermi electron density, theory of	178
Time distribution of delayed particles in extensive air showers	454
Tin, normal and superconducting, surface resistance at 36000 Mc/s (L)	1071
Tin, superconducting, thermal conductivity below 1°K	217
Transition, line width, nuclear magnetic resonance, in aluminium	85
Transition probabilities, vibrational, of diatomic molecules : I	1145
Transition probabilities, vibrational, of diatomic molecules : II	1153
Transitions, quadrupole and dipole, in hydrogen molecular ion	784
Transitions, radiative, matrix elements in	729
Triplet systems, new studies in band spectrum of nitrogen	1138
Ultra-violet absorption spectrum, <i>see under</i> Absorption.	
Ultra-violet bands associated with germanium (L)	191
Ultra-violet region between 3650 and 2200 Å, absorption bands of SbSe and SbTe in.	1109
Urea molecule, planar structure, proton magnetic resonance evidence for (L)	1187
Variation and perturbation methods.	857
Variational method, application to scattering by ions :	
I—Elastic scattering of electrons by helium ions	268
II—Distorted wave approximation and 1s-2s excitation of He by electron impact	1097
Variational method, calculation of 1s-2s electron excitation cross section of hydrogen (R)	406
Variational method for radiationless transitions with application to He	911
Vibrational transition probabilities of diatomic molecules : I	1145
Vibrational transition probabilities of diatomic molecules : II	1153
Vibrations, lattice, <i>see</i> Lattice vibrations.	
Virial coefficient, second, near absolute zero (L)	847
Wave functions, analytical, for methane and ammonium ion	514
Wave functions, free-electron, for conjugated molecules (R)	652
X-rays, <i>see also under</i> Scattering.	
X-rays, irradiation of Pb with, production of short-lived activity (R)	1179

INDEX OF AUTHORS (WITH TITLES)

	PAGE
Abdelnabi, I., and Massey, H. S. W. : Inelastic collisions of electrons in helium and Townsend's ionization coefficient	288
Adam, G. D., and Standley, K. J. : Microwave resonance absorption in some ferromagnetic manganese compounds	823
Albers-Schönberg, H., Alder, K., Heer, E., Novey, T. B., and Scherrer, P. : The influence of combined electric and magnetic interaction on gamma-gamma directional correlation (L)	952
Alder, K., <i>see</i> Albers-Schönberg, H.	
Allcock, G. R. : Damping corrections in the photo-meson process	233
Andrew, E. R., and Eades, R. G. : Separation of the intramolecular and intermolecular contributions to the second moment of the nuclear magnetic resonance spectrum (L)	415
Andrew, E. R., and Hyndman, D., Proton magnetic resonance evidence for the planar structure of the urea molecule (L)	1187
Ashmore, A., and Crewe, A. V. : The multiple scattering of 7.5 mev deuterons in metals	1172
Bagguley, D. M. S. : Ferromagnetic resonance in colloidal suspensions (R)	765
Baker, J. M., Bleaney, B., Bowers, K. D., Shaw, P. F. D., and Trenam, R. S. : Nuclear spin and magnetic moment of radioactive cobalt 57 (L)	305
Baldock, G. R. : Determination of the surface energy of a metal by molecular orbitals	2
Banbury, P. C., Henisch, H. K., and Many, A. : On the theory of the isothermal Hall effect in semiconductors	753
Barclay, F. R., and Whitehouse, W. J. : The average number of neutrons emitted in the spontaneous fission of ^{242}Cm	447
Barrow, R. F., <i>see</i> Laird, R. K., Rowlinson, H. C.	
Barrow, R. F., and Caunt, A. D. : The $2\Sigma^{+}-2\Pi_1$ band system of HBr^{+}	617
Barrow, R. F., Drummond, G., and Garton, W. R. S. : Ultra-violet bands associated with germanium (L)	191
Barrow, R. F., Drummond, G., and Rowlinson, H. C. : The absorption spectrum of SnS vapour in the ultra-violet and Schumann regions	885
Barton, J. C. : East-West asymmetry of moderate-energy neutrons in the cosmic radiation	160
Bates, D. R., Darling, R. T. S., Hawe, S. C., and Stewart, A. L. : Properties of the hydrogen molecular ion : III—oscillator strengths of the $1s\sigma_g-2p\pi_u$, $2p\sigma_u-3d\pi_g$ and $2p\pi_u-3d\pi_g$ transitions	1124
Bates, D. R., and Dalgarno, A. : Electron capture : III—capture into excited states in encounters between hydrogen atoms and fast protons	972
Bates, D. R., and Griffing, G. : Inelastic collisions between heavy particles : I—excitation and ionization of hydrogen atoms in fast encounters with protons and with other hydrogen atoms	961
Bates, D. R., Öpik, U., and Poots, G. : Properties of the hydrogen molecular ion : II—photoionization from the $1s\sigma_g$, $2s\sigma_g$ and $3s\sigma_g$ states	1113
Bates, D. R., and Poots, G. : Properties of the hydrogen molecular ion : I—quadrupole transitions in the ground electronic state and dipole transitions of the isotopic ions	784
Bates, L. F., and Hart, A. : A comparison of the powder patterns on a sample of grain-orientated silicon-iron with those obtained on a single crystal	813
Bates, L. F., and Martin, D. H. : Domains of reverse magnetization	162
Bates, L. F., and Wilson, G. W. : A study of Bitter figures on the (110) plane of a single crystal of nickel	819
Beaumont, C. F. A., <i>see</i> Reekie, J.	
Becker, J., <i>see</i> Price, B. T.	

	PAGE
Bernal, M. J. M. : Analytical wave functions for methane and the ammonium ion	514
Bijl, D., and Rose-Innes, A. C. : Temperature change in the paramagnetic resonance spectrum of copper lanthanum nitrate (L)	954
Birks, J. B., and Little, W. A. : Photo-fluorescence decay times of organic phosphors	921
Bishop, G. R., <i>see</i> Marin, P.	
Bleaney, B., <i>see</i> Baker, J. M.	
Bleaney, B., Bowers, K. D., and Trenam, R. S. : The nuclear electric quadrupole moments of copper 63, 65 (L)	410
Blin-Stoyle, R. J. : Matrix elements in radiative transitions	729
Blin-Stoyle, R. J. : The magnetic moments of spin $\frac{1}{2}$ nuclei	1158
Bodmer, A. R. : Nuclear scattering of electrons and isotope shift.	1041
Bonnor, W. B. : Certain exact solutions of the equations of general relativity with an electrostatic field	145
Born, Max : The conceptual situation in physics and the prospects of its future development (37th Guthrie Lecture)	501
Bowers, K. D. : Paramagnetic resonance in an argentic compound (L)	666
Bowers, K. D., <i>see also</i> Baker, J. M., Bleaney, B.	
Bowey, E. M., <i>see</i> Rae, E. R.	
Bransden, B. H., and Dalgarno, A. : The application of variational methods to scattering by ions : I—the elastic scattering of electrons by helium ions	268
Bransden, B. H., and Dalgarno, A. : The calculation of auto-ionization probabilities : I—perturbation methods with application to auto-ionization in helium	904
Bransden, B. H., and Dalgarno, A. : The calculation of auto-ionization probabilities : II—a variational method for radiationless transitions with application to the $(2s)^2\ ^1S-(1sks)\ ^1S$ transition of helium	911
Bransden, B. H., Dalgarno, A., and King, N. M. : The application of variational methods to scattering by ions : II—the distorted wave approximation and the $1s-2s$ excitation of helium by electron impact	1097
Breitenberger, E. : On the geometry of angular correlation experiments (L)	846
Brinkley, T. A., <i>see</i> Titterton, E. W.	
Buckingham, M. J. : The interaction of electrons with lattice vibrations : radiation by a fast electron	601
Butt, D. K. : The efficiency of the anthracene scintillation counter (R)	940
Campbell, C. G., <i>see</i> Kyles, J.	
Carroll, P. K., <i>see</i> Sayers, N. D.	
Carroll, P. K., and Sayers, N. D. : The band spectrum of nitrogen : new studies of the triplet systems	1138
Caunt, A. D., <i>see</i> Barrow, R. F.	
Chackett, K. F., Fremlin, J. H., and Walker, D. : Nuclear reactions produced by fast nitrogen ions	495
Chanson, P., <i>see</i> Price, B. T.	
Cooper, P. N., Crocker, V. S., and Walker, J. : Range-energy data from the $^{10}\text{B}(n, \alpha)^7\text{Li}(n, t)^4\text{He}$ reactions (L)	660
Cooper, P. N., Crocker, V. S., and Walker, J. : The relative stopping-power of hydrogen and of helium for slow α -particles (L)	658
Coulson, C. A. : Free-electron wave functions for conjugated molecules (R)	652
Crewe, A. V., <i>see</i> Ashmore, A.	
Crocker, V. S., <i>see</i> Cooper, P. N.	
Dalgarno, A., <i>see</i> Bates, D. R., Bransden, B. H.	
Dalgarno, A., and Yadav, H. N. : Electron capture : II—resonance capture from hydrogen atoms by slow protons	173
Dalitz, R. H. : Some features of the deuteron stripping process	28
Dalitz, R. H. : The decay of the τ -meson.	710
Daniels, J. M. : The effect of interactions in a paramagnetic on the entropy and susceptibility	673
Darling, R. T. S., <i>see</i> Bates, D. R.	

	PAGE
Davey, W. G. : The elastic scattering of 1.33 mev and 2.76 mev gamma-rays by lead	1059
Davey, W. G., and Moon, P. B. : The resonant scattering of ^{193}Hg gamma-rays (L)	956
Devons, S. : Charge independence and nuclear reactions (L)	665
Dickson, J. M., and Salter, D. C. : A search for polarization of high energy neutrons	721
Ditchburn, R. W., and Marr, G. V. : The continuous absorption of light in magnesium vapour (R)	655
Donovan, B., <i>see</i> March, N. H.	
Donovan, B., and Sondheimer, E. H. : Galvano-magnetic effects at high frequencies	849
Drummond, G., <i>see</i> Barrow, R. F.	
Duncanson, W. E., <i>see</i> Heyland, G. R.	
Eades, R. G., <i>see</i> Andrew, E. R.	
Edgar, M., <i>see</i> Herz, A. J.	
Edmonds, A. R. : Nuclear binding energies and the <i>jj</i> -coupling shell model	793
El-Bedewi, F. A., <i>see</i> Middleton, R.	
Elton, L. R. B. : Elastic scattering of electrons	806
Elton, L. R. B., and Parker, K. : The scattering of fast positrons by nuclei	428
Erskine, G. A., and Seaton, M. J. : The asymptotic solution of an equation occurring in scattering theory (L)	123
Evans, W. H., Green, T. S., and Middleton, R. : An investigation of the reaction $^{14}\text{N}(\text{d}, \text{n})^{15}\text{O}$ at 8 mev deuteron energy	108
Fawcett, E. : The surface resistance of normal and superconducting tin at 36000 Mc/s (L)	1071
Fowler, G. N., and Jones, G. M. D. B., the late : On the ionization loss of a fast particle in a dielectric medium	597
Fraser, P. A., <i>see</i> Jarman, W. R.	
Fraser, P. A., and Jarman, W. R. : Vibrational transition probabilities of diatomic molecules : I	1145
Freeman, J. M., <i>see</i> Rose, B.	
Fremlin, J. H., <i>see</i> Chackett, K. F.	
Friedel, J. : Anomaly of the $\text{M}_{\text{IV}, \text{V}}$ absorption in heavy elements	333
Garton, W. R. S. : Observations of the 4050Å band group in a King furnace	848
Garton, W. R. S., <i>see also</i> Barrow, R. F.	
Gatha, K. M., <i>see</i> Mathur, A. D.	
George, E. P., <i>see</i> Tidman, D. A.	
George, E. P., MacAnuff, J. W., and Sturgess, J. W. : Observations of extensive cosmic-ray showers below ground	346
George, E. P., Redding, J. L., and Trent, P. T. : Cloud chamber observations of the cosmic radiation underground	533
Goldring, G. : Internal pairs in anisotropic emission	341
Goodman, B. B. : The thermal conductivity of superconducting tin below 1°K	217
Goward, F. K., <i>see</i> Wilkins, J. J.	
Green, C. D., <i>see</i> ter Haar, D.	
Green, H. S. : A pre-renormalized quantum electrodynamics	873
Green, H. S. : Boltzmann's equation in quantum mechanics	325
Green, H. S., <i>see also</i> Messel, H.	
Green, H. S., and Wolf, E. : A scalar representation of electromagnetic fields	1129
Green, T. S., <i>see</i> Evans, W. H.	
Griffing, G., <i>see</i> Bates, D. R.	
Griffith, T. C. : The scattering of 10 and 14 mev neutrons by deuterons	894
Guggenheim, E. A. : Electric spin in semiconductors (L)	121
Gupta, Suraj N : Quantum electrodynamics with auxiliary fields	129

	PAGE
ter Haar, D. : The second virial coefficient near absolute zero (L)	847
ter Haar, D., and Green, C. D. : The statistical aspect of Boltzmann's H-theorem	153
Haddara, S. R., and Jakeman, D. : The lateral structure of cosmic ray extensive air showers at sea level	549
Halban, H., <i>see</i> Marin, P.	
Hall, G. G. : The electronic structure of some body-centred cubic metals	1162
Hart, A., <i>see</i> Bates, L. F.	
Hawe, S. C., <i>see</i> Bates, D. R.	
Heer, E., <i>see</i> Albers-Schönberg, H.	
Heitler, W., and Terreaux, Ch. : Interpretation of cosmic ray jets	929
Henderson, W. J., <i>see</i> Kyles, J.	
Henisch, H. K., <i>see</i> Banbury, P. C.	
Herz, A. J., <i>see</i> Tidman, D. A.	
Herz, A. J., and Edgar, M. : The reduction of distortion in nuclear-research emulsion (R)	115
Heyland, G. R., and Duncanson, W. E. : A search for irregularities in the absorption of cosmic rays in lead	33
Heyland, G. R., and Duncanson, W. E. : Momentum distribution for cosmic ray mesons up to 6 kmev/c	40
Hill, R. W., and Smith, P. L. : The anomalous specific heat of ferrous ammonium sulphate	228
Hobson, R. M., <i>see</i> Sloane, R. H.	
Hodson, A. L. : Penetrating particles in extensive air showers	65
Hodson, A. L. : Some aspects of the altitude variation of extensive air showers	49
Holt, J. R., and Marsham, T. N. : An investigation of (d, p) stripping reactions : I—apparatus and results for aluminium	249
Holt, J. R., and Marsham, T. N. : An investigation of (d, p) stripping reactions : II—results for the isotopes of magnesium	258
Holt, J. R., and Marsham, T. N. : An investigation of (d, p) stripping reactions : III—results for ^{28}Si and ^{32}S	467
Holt, J. R., and Marsham, T. N. : An investigation of (d, p) stripping reactions : IV—results for ^{40}Ca and ^{88}Sr	565
Holt, J. R., and Marsham, T. N. : An investigation of (d, p) stripping reactions : V—results for some of the light elements and conclusions	1032
Howell, H. G. : The visible emission spectrum of Cl_2^+	759
Hutchison, T. S., <i>see</i> Reekie, J.	
Hyndman, D., <i>see</i> Andrew, E. R.	
Inall, E. K., <i>see</i> Salmon, A. J.	
Ingram, D. J. E. : Paramagnetic resonance in some manganese salts (L)	412
Irving, J. : The effect of the tensor forces on the binding energy of the alpha-particle	17
Jackson, T. A. S. : Accidental degeneracy of hydrogen (L)	958
Jakeman, D., <i>see</i> Haddara, S. R.	
Jánosy, L. : Note on the fluctuation problem of cascades (L)	117
Jarmain, W. R., <i>see</i> Fraser, P. A.	
Jarmain, W. R., and Fraser, P. A. : Vibrational transition probabilities of diatomic molecules : II	1153
Jarvis, C. J. D. : The internal conversion electrons emitted in the decay of ionium and radio-thorium (L)	1074
Jarvis, R. G., and Roaf, D. : The $\text{D}-^3\text{H}$ and $\text{D}-^3\text{He}$ reactions below 45 kev (L)	310
Jelley, J. V., and Whitehouse, W. J. : The time distribution of delayed particles in extensive air showers using a liquid scintillation counter of large area	454
Jones, G. A., and Wilkinson, D. H. : The reaction $^{13}\text{C}(\alpha, n)^{16}\text{O}$ (R)	1176
Jones, G. M. B. D., the late, <i>see</i> Fowler, G. N.	
Kelly, A. : Neumann bands in pure iron	403
Kemp, W. R. G., Sreedhar, A. K., and White, G. K. : The thermal conductivity of magnesium at low temperatures (L)	1077

- King, N. M., *see* Bransden, B. H.
- Klemens, P. G. : Electronic thermal conduction in superconductors 576
- Kouvelites, J. S. : On the motion of electrons in non-sinusoidal periodic fields (L) 197
- Kyles, J., Campbell, C. G., and Henderson, W. J. : An investigation of the β -particle spectrum of mesothorium 2 519
- Laird, R. K., and Barrow, R. F. : The ultra-violet band spectrum of carbon monoselenide 836
- Landsberg, P. T. : Semiconductor statistics (L) 662
- Lane, A. M. : Studies in intermediate coupling : the energy states of ^{13}C and ^{13}N belonging to the configuration $1p^9$ 977
- Lee, E. W. : The influence of domain structure on the magnetization curves of single crystals. 623
- Lees, C. F., Morrison, G. C., and Rosser, W. G. V. : The range-energy relation for protons and alpha-particles in diluted Ilford G5 emulsions 13
- Levine, S. : Interaction of two parallel colloidal plates using a modified Poisson-Boltzmann equation 365
- Levine, S. : The free energy of the double layer of a colloidal particle and the charging process 357
- Lidiard, A. B. : Antiferromagnetism in metals (L) 1188
- Lidiard, A. B. : On a minimum property of the free energy 492
- Lindholm, E. : Ionization and fragmentation of molecules by bombardment with atomic ions (R) 1068
- Link, W. T., and Walker, D. : Light output of potassium iodide crystals under bombardment by heavy charged particles (R) 767
- Little, W. A., *see* Birks, J. B.
- Littler, D. J., and Lockett, E. E. : The pile neutron absorption cross sections of bismuth 700
- Livesey, D. L., and Smith, C. L. : Photodisintegration processes in light even-even nuclei yielding alpha-particles 689
- Lockett, E. E., *see* Littler, D. J.
- Lomer, W. M., and Morton, K. W. : The electrostatic energy of boron nitride (L) 772
- MacAnuff, J. W., *see* George, E. P.
- McNeill, K. G., *see* Reid, J. M.
- McWeeny, R. : The diamagnetic anisotropy of large aromatic systems : V—interpretation of the results 714
- Madan, M. P., *see* Srivastava, B. N.
- Makinson, R. E. B., *see* Turner, J. S.
- Makinson, R. E. B., and Turner, J. S. : On perturbation and variation methods 857
- Manning, G., and Singh, B. : A note on the $^{10}\text{B}(\alpha, p)^{13}\text{C}$ reaction (R) 842
- Many, A., *see* Banbury, P. C.
- March, N. H., and Donovan, B. : On the spin paramagnetism of a free electron gas 1104
- Marin, P., Bishop, G. R., and Halban, H. : The absolute standardization of the 2.615 mev γ -rays of ThC'' and the cross section for the photodisintegration of the deuteron at this energy 608
- Marr, G. V., *see* Ditchburn, R. W.
- Marshsm, T. N., *see* Holt, J. R.
- Martin, D. H., *see* Bates, L. F.
- Massey, H. S. W., *see* Abdelnabi, I.
- Massey, H. S. W., and Moiseiwitsch, B. L. : Calculation of the 1s–2s electron excitation cross section of hydrogen by a variational method (R) 406
- Mathur, A. L., and Gatha, K. M. : Jastrow's nuclear model for high-energy electron scattering (L) 1075
- Mathur, A. L., and Gatha, K. M. : The Born–Yang model for high-energy electron scattering (L) 773
- Messel, H., and Green, H. S. : The general three-dimensional theory of cascade processes 1009
- Middleton, R., *see* Evans, W. H.

	PAGE
Middleton, R., El-Bedewi, F. A., and Tai, C. T. : An investigation of the neutron groups from the reactions $^{12}\text{C}(\text{d}, \text{n})^{13}\text{N}$, $^{16}\text{O}(\text{d}, \text{n})^{17}\text{F}$ and $^{32}\text{S}(\text{d}, \text{n})^{33}\text{Cl}$.	95
Moiseiwitsch, B. L., <i>see</i> Massey, H. S. W.	
Moon, P. B., <i>see</i> Davey, W. G.	
Moon, P. B., and Storruste, A. : Resonant nuclear scattering of ^{198}Hg gamma-rays	585
Morrison, G. C., <i>see</i> Lees, C. F.	
Morton, K. W., <i>see</i> Lomer, W. M.	
Murdoch, H. S. : The half-life of $^{181}\text{Ta}^{\text{m}}$ and the delayed coincidence method (R)	944
Nageotte, E., <i>see</i> Price, B. T.	
Neufeld, J. : Ionization and excitation losses of charged particles of intermediate energies.	590
Newns, H. C. : Polarization effects in (d, p) and (d, n) reactions	477
Nicholas, J. F. : Effect of the Fermi energy on the stability of superlattices .	201
Novey, T. B., <i>see</i> Albers-Schönberg, H.	
Öpik, U., <i>see</i> Bates, D. R.	
Paranjape, B. V. : On the theory of internal friction in metals .	572
Parker, K. : The effect of nuclear multipole moments on electron scattering .	881
Parker, K., <i>see also</i> Elton, L. R. B.	
Parry, J. K., Rathgeber, H. D., and Rouse, J. L. : Ionization of cosmic-ray mesons in argon	541
Peierls, R. E. : The atomic nucleus and its constituents (6th Rutherford Lecture)	313
Pillow, M. E. : Band intensities in the CN violet system .	737
Pillow, M. E. : Intensities in the Herzberg system of O_2 (R) .	1064
Pillow, M. E. : Intensity distribution among bands of the Herzberg system of O_2	733
Plaskett, J. S. : The theory of the Thomas-Fermi electron density .	178
Poots, G. : The effect of variation of the dipole moment with internuclear separation on the relative intensities of the Second Negative band system of oxygen (R)	1181
Poots, G., <i>see also</i> Bates, D. R.	
Post, H. R. : Many-particle systems : derivation of a shell model (R) .	649
Price, B. T., West, D., Becker, J., Chanson, P., Nageotte, E., and Treille, P. : Further measurements of the ionization by energetic cosmic-ray μ -mesons .	167
Radicati, L. A. : Isotopic spin and coulomb forces .	139
Rae, E. R., and Bowey, E. M. : A scintillation detector for neutrons of intermediate energy (L)	1073
Raimes, S. : The compressibility of metallic aluminium (R)	949
Rathgeber, H. D., <i>see</i> Parry, J. K.	
Redding, J. L., <i>see</i> George, E. P.	
Redhead, M. L. G. : The production of bremsstrahlung in electron-electron collisions (L) .	196
Reekie, J., Hutchison, T. S., and Beaumont, C. F. A. : X-ray scattering from liquid helium (L)	409
Reid, J. M., and McNeill, K. G. : The production of a short-lived activity by irradiation of Pb with x-rays (R)	1179
Richards, E. W. T. : Ionization in liquids due to alpha particles .	631
Roaf, D., <i>see</i> Jarvis, R. G.	
Roberts, P. W. : Some comments on the resolution of scintillation spectrometers (L)	192
Robinson, E. : Short-time interval measurements on pairs of associated cosmic-ray particles	79
Robinson, E. : Spark counters for short-time interval cosmic-ray measurements	73
Rose, B., and Freeman, J. M. : Inelastic neutron scattering in iron (L) .	120
Rose-Innes, A. C., <i>see</i> Bijl, D.	
Rosser, W. G. V., <i>see</i> Lees, C. F.	
Rouse, J. L., <i>see</i> Parry, J. K.	
Rowlinson, H. C., <i>see</i> Barrow, R. F.	

Rowlinson, H. C., and Barrow, R. F. : The absorption spectrum of aluminium monofluoride in the Schumann region (L)	771
Rowlinson, H. C., and Barrow, R. F. : The band-spectrum of aluminium monofluoride	437
Runciman, W. A., and Steward, E. G. : The atomic position and size of the thallium ions in KCl(Tl) phosphors	484
Rutherglen, J. G., and Smith, R. D. : Excitation curves of the reactions $^{27}\text{Al}(\text{p}, \alpha)^{24}\text{Mg}$ and $^{27}\text{Al}(\text{p}, \gamma)^{28}\text{Si}$	800
Salmon, A. J., and Inall, E. K. : The angular correlation of the protons and γ -radiation from the reaction $^6\text{Li}(\text{d}, \text{p})^7\text{Li}^*\gamma^7\text{Li}$	297
Salter, D. C., <i>see</i> Dickson, J. M.	
Satchler, G. R. : Angular distribution of gamma-radiation following a deuteron stripping reaction	1081
Sayers, N. D., <i>see</i> Carroll, P. K.	
Sayers, N. D., and Carroll, P. K. : The wavelengths of nitrogen First Positive bands (R)	577
Scherrer, P., <i>see</i> Albers-Schönberg, H.	
Seaton, M. J., <i>see</i> Erskine, G. A.	
Seymour, E. F. W. : Nuclear magnetic resonance line width transition in aluminium	85
Sharma, C. B. : Absorption bands of SbSe and SbTe in the quartz ultra-violet region between 3650 and 2200 Å	1109
Shaw, P. F. D., <i>see</i> Baker, J. M.	
Singh, B., <i>see</i> Manning, G.	
Singh, L. : On the effect of a strong electrostatic field on scattering (L)	309
Sloane, R. H., and Hobson, R. M. : The liberation of positive ions by negative ion bombardment of surfaces (L)	663
Smith, C. L., <i>see</i> Livesey, D. L.	
Smith, P. L., <i>see</i> Hill, R. W.	
Smith, R. D., <i>see</i> Rutherglen, J. G.	
Sondheimer, E. H., <i>see</i> Donovan, B.	
Sreedhar, A. K., <i>see</i> Kemp, W. R. G.	
Srivastava, B. N., and Madan, M. P. : Thermal diffusion of gas mixtures and forces between unlike molecules.	278
Standley, K. J., <i>see</i> Adam, G. D.	
Steenberg, N. R. : Population distribution of nuclei aligned at low temperatures	399
Steenberg, N. R. : The polarization of γ -radiation from aligned nuclei	391
Steward, E. G., <i>see</i> Runciman, W. A.	
Stewart, A. L., <i>see</i> Bates, D. R.	
Storruste, A., <i>see</i> Moon, P. B.	
Sturgess, J. W., <i>see</i> George, E. P.	
Sutcliffe, L. H., and Walsh, A. D. : The ultra-violet absorption spectrum of nitric oxide	209
Swan, P. : The elastic scattering of neutrons by tritons and of protons by ^3He	740
Swan, P. : The elastic scattering of neutrons by tritons at 14 mev	238
Swan, P. : On the existence of a bound state of ^4H (R)	1066
Swinbank, P., and Walker, J. : The decay scheme of krypton 83	1093
Tai, C. T., <i>see</i> Middleton, R.	
Temperley, H. N. V. : A new theory of liquid helium : further treatment	995
Terreaux, Ch., <i>see</i> Heitler, W.	
Tidman, D. A., George, E. P., and Herz, A. J. : The production of delta-rays in nuclear-research emulsions	1019
Titterton, E. W., and Brinkley, T. A. : Cross sections for the reaction $^7\text{Li}(\gamma\text{T})^4\text{He}$ at 6.13, 14.8 and 17.6 mev	579
Titterton, E. W., and Brinkley, T. A. : Excitation functions for the (γp) and (γT) reactions in lithium-7 for energies up to 24 mev (L)	194
Tredgold, R. H. : The application of Kirkwood's approximation to the calculation of intrinsic magnetization.	421

	PAGE
Treille, P., <i>see</i> Price, B. T.	
Trenam, R. S. : Paramagnetic resonance in four double nitrate salts (L)	118
Trenam, R. S. : The nuclear magnetic moment of ^{57}Fe (L)	414
Trenam, R. S., <i>see also</i> Baker, J. M. <i>see also</i> Bleaney, B.	
Tunstead, J. : Photoelectric absorption in lithium vapour (R)	304, corr. 420
Trent, P. T., <i>see</i> George, E. P.	
Turner, J. S., <i>see</i> Makinson, R. E. B.	
Turner, J. S., and Makinson, R. E. B. : A comparison of various methods of solving the central force scattering problem	866
Vachaspati : The quantum mechanical equations of motion and the commutation relations (L)	657
Valatin, J. G. : Predissociations and CO dissociation energy (L)	1185
Walker, D., <i>see</i> Chackett, K. F. <i>see</i> Link, W. T.	
Walker, J., <i>see</i> Cooper, P. N. <i>see</i> Swinbank, P.	
Walsh, A. D., <i>see</i> Sutcliffe, L. H.	
West, D. : Measurements of the energy loss distribution for minimum ionizing electrons in a proportional counter (L)	306
West, D., <i>see also</i> Price, B. T.	
White, G. K. : The thermal conductivity of gold at low temperatures	559
White, G. K. : The thermal conductivity of silver at low temperatures (L)	844
White, G. K., <i>see also</i> Kemp, W. R. G.	
Whitehouse, W. J., <i>see</i> Barclay, F. R. <i>see</i> Jelley, J. V.	
Wilkins, J. J., and Goward, F. K. : Alpha-emitting levels of ^8Be with isotopic spin $T=1$ (L)	661
Wilkinson, D. H., <i>see</i> Jones, G. A.	
Williams, W. E. : Solution of a modified Poisson-Boltzmann equation for a single plane double layer	372
Wilson, G. W. : A proposed structure for certain domain configurations on a single crystal of nickel (R)	840
Wilson, G. W., <i>see also</i> Bates, L. F.	
Wilson, R. : A formula for thick target bremsstrahlung	638
Wilson, R. : Analysis of photonuclear reactions	645
Wohlfarth, E. P. : The energy band structure of a linear metal	889
Wolf, E., <i>see</i> Green, H. S.	
Woodcock, E. R. : A method of calculating critical size in multi-group neutron transport theory for some simple systems	705
Wright, G. T. : Fluorescence characteristics of mixed organic crystals	777
Wyard, S. J. : Absorption coefficients of gamma-rays with energies between 0.3 and 1.5 Mev	382
Yadav, H. N., <i>see</i> Dalgarno, A.	
Ziman, J. M. : Antiferromagnetism by the spin wave method : III—application to more complex systems	89

INDEX TO REVIEW OF BOOKS

	PAGE
Annual Reviews Inc.: <i>The Annual Review of Nuclear Science</i> , Vol. II, 1953	1198
de Boer, J. H.: <i>The Dynamical Character of Adsorption</i>	959
Bondi, H.: <i>Cosmology</i>	124
Bronwell, A.: <i>Advanced Mathematics in Physics and Engineering</i>	853
Bückner, H.: <i>Die praktische Behandlung von Integralgleichungen</i>	125
Calthrop, J. E.: <i>Advanced Experiments in Practical Physics</i>	581
Centre National de la Recherche Scientifique: <i>Oeuvres scientifiques de Jean Perrin</i>	126
Chapman, S., and Cowling, T. G.: <i>The Mathematical Theory of Non-Uniform Gases</i>	1197
Courty, C.: <i>Charbons activés</i>	582
Dow, W. G.: <i>Fundamentals of Engineering Electronics</i>	1079
Flügge, S., and Marschall, H.: <i>Rechenmethoden der Quantenmechanik</i> , Part I	669
Green, H. S.: <i>Molecular Theory of Fluids</i>	668
Grew, K. E., and Ibbs, T. L.: <i>Thermal Diffusion in Gases</i>	854
Hartree, D. R.: <i>Numerical Analysis</i>	581
Henry, N. F. M., and Lonsdale, K. (Ed.): <i>International Tables for X-Ray Crystallography</i> , Volume 1, <i>Symmetry Groups</i>	497
Holton, G.: <i>Introduction to Concepts and Theories in Physical Science</i>	310
Houston, W. V.: <i>The Principles of Quantum Mechanics</i>	199
Hume-Rothery, W., Christian, J. W., and Pearson, W. B.: <i>Metallurgical Equilibrium Diagrams</i>	583
James, R. W.: <i>X-Ray Crystallography</i>	499
Jordan, Pascual: <i>Schwerkraft und Weltall</i>	667
Korn, G. A., and Korn, T. M.: <i>Electronic Analog Computers</i>	496
Lindsay, R. B.: <i>Concepts and Methods of Theoretical Physics</i>	125
Massey, H. S. W., and Burhop, E. H. S.: <i>Electronic and Ionic Impact Phenomena</i>	851
Milne, E. A., the late: <i>Sir James Jeans—a Biography</i>	417
Moore, C. E.: <i>Atomic Energy Levels as derived from the Analyses of Optical Spectra</i> , Vol. II, 24 Cr to 41 Nb	668
Nehari, Z.: <i>Conformal Mapping</i>	124
Pollard, E., and Davidson, W. L.: <i>Applied Nuclear Physics</i>	670
Revue d'Optique théorique et instrumentale: <i>Colloque sur la Sensibilité et des Émulsions Photographiques</i> , Paris 1951, <i>Mémoires et Discussions</i>	854
Rosser, J. Barkley: <i>Logic for Mathematicians</i>	1195
Sauer, R.: <i>Anfangswertprobleme bei partieller Differentialgleichungen</i>	669
Shoenberg, D.: <i>Superconductivity</i>	775
Sommerfeld, A.: <i>Vorlesungen über theoretische Physik</i> , Band V, <i>Thermodynamik und Statistik</i>	1197
Thorndike, A. M.: <i>Mesons—A Summary of Experimental Facts</i>	671
U.S. Department of Commerce: <i>Mechanical Properties of Metals at Low Temperature</i>	127
Weinstock, Robert: <i>Calculus of Variations with Applications to Physics and Engineering</i>	855

